McGRAW-HILL PUBLICATIONS IN AERONAUTICAL SCIENCE

Jerome C. Hunsaker, Consulting Editor

INSTRUMENT ENGINEERING

VOLUME III

APPLICATIONS OF THE INSTRUMENT ENGINEERING METHOD

PART 1

MEASUREMENT SYSTEMS

McGRAW-HILL PUBLICATIONS IN AERONAUTICAL SCIENCE

Jerome C. Hunsaker, Consulting Editor

Draper, McKay, and Lees

INSTRUMENT ENGINEERING

VOL. I. METHODS FOR DESCRIBING THE SITUATIONS OF INSTRUMENT ENGINEERING.

VOL. II. METHODS FOR ASSOCIATING MATHEMATICAL SOLUTIONS WITH COMMON FORMS.

VOL. III. APPLICATIONS OF THE INSTRUMENT ENGINEERING METHOD.

Part 1. Measurement Systems

Part 2. Control Systems

Küchemann and Weber

AERODYNAMICS OF PROPULSION

Shapiro

PRINCIPLES OF HELICOPTER ENGINEERING

Shaw and Macks

ANALYSIS AND LUBRICATION OF BEARINGS

Streeter

FLUID DYNAMICS

von Mises

THEORY OF FLIGHT

INSTRUMENT ENGINEERING

VOLUME III

APPLICATIONS OF THE INSTRUMENT ENGINEERING METHOD

PART 1

MEASUREMENT SYSTEMS

CHARLES STARK DRAPER
Head, Department of Aeronautical Engineering
Director, Instrumentation Laboratory

WALTER McKAY
Associate Professor of Aeronautical Engineering

SIDNEY LEES
Assistant Professor of Aeronautical Engineering

Massachusetts Institute of Technology

First Edition

New York Toronto London

McGRAW-HILL BOOK COMPANY, INC.

1955

INSTRUMENT ENGINEERING

Copyright © 1955 by McGraw-Hill Book Company, Inc. Printed in the United States of America. All rights reserved. This book, or parts thereof, may not be reproduced in any form without permission of the publishers.

LIBRARY OF CONGRESS CATALOG CARD NUMBER 52-7438

OBAL LIBRARY

629.107
D792I

JAMMU & KASHMIR UNIVERSITY
LIBRARY
No. 22745
Date 12.5.58
SRINAGAR

STG
RG1

Text and illustrations prepared for offset reproduction by Jackson & Moreland, Boston, Massachusetts

To LESTER EARL PAYNE

Until his untimely passing in September of 1953, Earl Payne poured his energy into a wide variety of activities with a zest that few could help but admire. This seemingly boundless drive was given direction by a rigid code of service to his fellow man and was marked by a spirit of contagious enthusiasm. In memory of his friendship and unstinting assistance in the preparation of this book – as well as many other publications – we dedicate these chapters.

PREFACE

Instrument Engineering describes and illustrates methods for finding solutions to measurement and control problems. These methods are drawn together into a generalized pattern of procedures, plots, and tables designed to reduce greatly the time and effort required to produce effective results in practical situations. The material is intended for engineers who are concerned with working "gadgets" of all degrees of complexity, at any point from the initial stages of preliminary design through all the succeeding steps until production and successful use are accomplished facts. To this end, elegance in mathematical analysis and the forced application of any particular method are subordinated to the goal of providing a maximum amount of help on typical problems.

The organization of the material in Instrument Engineering is primarily for reference purposes, but the book is also well suited for use as a text by students and teachers. Principles and procedures are illustrated by means of examples, but no practice exercises are included. In any given situation, this omission leaves the instructor free to build up his own set of problems in those areas that hold the greatest interest for his students.

Instrument Engineering describes several commonly used mathematical procedures for finding solutions to practical problems, and stresses the equivalence of the information available in all cases. For the purpose of mathematical manipulation, working variables with the simplest possible symbols are used. These working variables are associated with the operations of formal reasoning without being specifically connected with physical quantities of any kind.

The necessary physical associations for particular situations are made in terms of self-defining symbols that are adapted for transferring information rather than for use in the manipulations of analysis. Self-defining symbols are more cumbersome than working-variable symbols, but they do convey complete physical information directly, without forcing the reader to consult a glossary of symbols. It undoubtedly requires more effort to set up equations and plots in self-defining symbols than in the simpler working-variable notation. On the other hand, it is just as evident that the sense and meaning of equations written in self-defining notation is more readily grasped and remembered. The difference in

usefulness between self-defining symbols and working-variable notation in transferring information becomes more important as the situation under consideration becomes more complex.

By presenting all formal reasoning in terms of nondimensional variables, Instrument Engineering makes available to the reader much useful quantitative information in the form of equations and curve families. The information is easily interpreted for specific physical situations by means of equivalent definitions in working variables and in self-defining symbols. The equivalent definitions are repeated frequently in the text. The object is to eliminate the need for reviewing previous material when the information on any particular page is to be applied to a given problem. This repetition of symbols increases the effort required in the original preparation of the text and may appear unnecessary to a superficial reader. However, the repeated material can be disregarded if the definitions are already familiar, and it saves time and effort when Instrument Engineering is used for reference purposes.

Formal results in generalized terms are useful in practice only if the mathematical relationships upon which they are based actually correspond to the physical facts of the situation under consideration. When such a correspondence exists, engineering results are immediately available by a simple association of working variables with the symbols that represent physical quantities. In this method of attack, employed in Instrument Engineering, there is no advantage in using an intermediate set of analogous quantities once the necessary associations are established for describing the solution of any given situation. In fact, the use of analogs is likely to hinder the search for solutions to complex problems; it is often more difficult to prove the validity of analogs than to find the desired results directly in terms of the physical quantities actually involved.

Instrument Engineering is comprised of three volumes. The subject matter of Volume I is concerned with the description of physical situations by means of mathematical and graphical forms. Volume II gives the theoretical background for generating solutions for these forms. Volume III contains examples in which the theory, methods, and techniques described in the first and second volumes are applied to typical cases. Part 1 of Volume III covers measurement system applications, while Part 2 deals with control system applications.

Useful methods for solving measurement problems are built up in Part 1 of Volume III by means of typical examples, beginning with thermometers that have the simplest possible performance equations. The discussions that follow deal with instruments and measuring systems of increasing complexity, including electromechanical measuring devices, pressure-measuring systems, integrators and differentiators, analog computers, and vibration-measuring equipment. The concepts, symbols, and methods developed in this pattern are equally effective

for handling the theory of systems that include feedback loops. Applications of this type naturally follow the measurement examples of Part 1, and make up the subject matter of Part 2 of Volume III.

As in the case of the two earlier volumes of Instrument Engineering, many students and colleagues have helped with the preparation of Part 1, Volume III. The contribution of Mr. Henry B. Brainerd is acknowledged by placing his name on Chapter 30. In a similar fashion, Dr. Yao T. Li is given credit for his work on Chapters 33 and 35. Credit is also due to two others who were kind enough to contribute individual sections: Dr. Morton Finston wrote the section on temperature measurement in high-speed flow at the end of Chapter 31. Dr. Robert K. Mueller wrote the section on the Microsyn angular displacement receiver in Chapter 35.

The assistance of Mr. Lawrence H. McNeill in preparing some of the material in Chapter 34 is also appreciated and gratefully acknowledged. Similar credit is due to Mr. James E. Forbes and Mr. Theodore Kaslow for their work on the test data of Chapter 32, as well as Mr. James L. Stockard for the test reports of Chapter 35. Mr. John Barley, Mr. Arnold I. Klayman and Mr. George W. Masters, Jr., were invaluable in assembling and maintaining the test setups. The curves and data associated with displaced cosine pulse functions and corresponding system responses in Chapters 32 and 35 were computed by Dr. Jeremiah M. Stark and Mr. Richard C. Hutchinson.

Part 1, Volume III, of Instrument Engineering is a textbook and reference for students and engineers interested in the theory and applications of measuring systems. Since Volume III is written with considerable repetition of the fundamentals of Volume I and the mathematical principles of Volume II, this makes Part 1 of Volume III useful as a self-contained text and reference book on measuring instruments and systems. The necessary information is presented in the form of mathematical results plotted as nondimensional curve families. In every case, references are given to the more extended treatments of Volumes I and II.

In preparing Volume III, stress has been placed on the complete treatment of fundamentals, supplemented by numerical data in nondimensional plots. Lack of time has prevented the development of polished examples of all the possible applications that exist for the material. However, these applications will appear naturally as the available information is applied to problems encountered in teaching and engineering.

Cambridge, Massachusetts
January, 1955

C. S. Draper
W. McKay
S. Lees

CONTENTS

Illustrations, Tables and Summaries xvii

INTRODUCTION 1

CHAPTER 28

CONCEPTS, DEFINITIONS, DIAGRAMS AND NOTATION FOR DESCRIBING OPERATING COMPONENTS AND OPERATING SYSTEMS

Operating Components 4
Transducers and Coducers. 4
Representation of Transducers and Coducers 5
Representation of Operating Components 8
Representation of Systems Formed by Combinations of Operating Components 8
Concepts, Terminology, and Symbols for Describing Static Performance of Operating Components 10
Tangent, Chord, and Secant Definitions of Sensitivity 15
Working Variable Symbols for Describing Static Performance 17
Representation of Generalized Performance of Operating Components 18
Representation of Steady-State Sinusoidal Performance for Operating Components 20
Diagrams for Describing Operating Systems 22
Illustrative Schematic and Functional Diagrams for a Liquid Heater 31

CHAPTER 29

INDICATION AND MEASUREMENT

Introduction. 38
Indicating Instruments 39
Measuring Instruments 42
Calibration 43
Perfect, Ideal, and Actual Measuring Instruments 43
Relationship between Scale Sensitivity and Mechanism Sensitivity for Ideal Measuring Instruments 46
Performance-Quality-Describing Concepts for Actual Measuring Instruments; Inaccuracy, Uncertainty, and Error 47
Terminology for Describing the Quality of Measuring Instrument Performance 53
Actual Measuring Instruments; Actuating Inputs, Interfering Inputs and Modifying Inputs . . . 58
Calibration Conditions 59
Scales 60
Concepts, Terminology, and Notation for Describing Uncertainty Components 63
Error and Correction Components of Scale Reading 70

CHAPTER 29 (Cont.)

Error Analysis Example 71
Indication Errors and Indication Corrections. 71
Scale Reading Error and Scale Reading Correction. 72
Nondimensional Measures of Performance Quality. 78
Accuracy and Precision. 79
Summary of Performance-Describing Concepts. 85
Specification of Measuring Instruments 85

CHAPTER 30

ELEMENTS AND COMPONENTS ASSOCIATED WITH INSTRUMENT SYSTEMS
H. B. Brainerd

Introduction 102
Elements 103
Components. 125

CHAPTER 31

TEMPERATURE-MEASURING INSTRUMENTS

Introduction. 161
Essential Features of Temperature-Measuring Instruments. 162
Liquid-in-Glass Thermometers 162
Bimetal Thermometers. 163
Fluid-Pressure-Coupled Thermometers 163
Resistance-Coupled Thermometers. 168
Thermocouple Thermometers. 168
Optical Pyrometers 169
Radiation Pyrometers 170
Temperature Indicators for Recording and Control. 170
Relationship of Temperature Receiver Performance to Temperature-Measuring Instrument Performance 171
Performance Equation for a Typical Temperature Receiver. 171
Convective Heat Flow into a Receiver 178
Radiation Heat Flow into a Receiver 178
Conduction Heat Flow into a Receiver 180
Temperature Receiver Performance Equation 180
Response Characteristics for Ideal Thermometers. 180
Step Function Response of a Thermometer 181
Ramp Function Response of a Thermometer 183
Thermometer Response to a Parabolic Input Temperature Change 186
Steady-State Response to Sinusoidal Input Temperature Change 188
Impulse Function Response of a First-Order Thermometer. 193
Semilogarithmic Plots of Thermometer Response to Step Changes of Input Temperature . . . 193
Determination of Characteristic Time from Semilogarithmic Plots of Step Function Response . 194
Dimensional Analysis of Factors Controlling Thermometric Characteristic Time 194
Test Arrangement for Producing Step Function Changes of Thermometer Input 199
Illustrative Results from a Step Function Survey of Thermometer Performance 201
Temperature Measurement in High-Speed Flow. 204
Conclusion 216

CHAPTER 32
ELECTROMECHANICAL MEASURING INSTRUMENTS

Introduction 218
Generalized Functional Diagram for Electromechanical Measuring Instruments 223
Derivation of Performance Coefficients and Parameters in Terms of Design Factors For Moving-Coil Instruments 232
Performance Characteristics of Electromechanical Measuring Instruments 234
Impulse Function Response 236
Step Function Response 238
Ramp Function Response 244
Parabolic Response 252
Ramp-Followed-By-Step Response 252
Steady-State Sinusoidal Response: Performance Functions 252
Linear Complex Plane Performance Function Plots 261
Linear Scale Sensitivity and Dynamic Response Angle Plots 263
Logarithmic Scale Sensitivity and Dynamic Response Angle Plots 263
Sensitivity and Dynamic Response Angle Deviation Curves 267
Applications of Performance-Describing Equations and Curves to Engineering Problems Associated with Measuring Instruments 271
Determination of (−;0,1, 2) System Performance Parameters from Oscillatory Step Function Transients 276
Determination of (−;0, 1, 2) System Performance Parameters from Nonoscillatory Transients in the Critically Aperiodic Damping Ratio Region 277
Determination of (−;0, 1, 2) System Parameters from Nonoscillatory Response Transients in the High Damping Ratio Region 281
Determination of (0;0, 1, 2) System Performance Parameters from Steady-State Sinusoidal Response Information 282
Interpretation of Response Information Not Compatible with the Theoretical Response of (0;0, 1, 2) Systems 284
Moving-Coil Oscillographs 284
Determination of Optical Oscillograph Performance Characteristics from Oscillatory Step Function Response 285
Oscillograph Performance Characteristics from Aperiodic Step Function Response 286
Oscillograph Performance Characteristics from Steady-State Sinusoidal Response 289
Measurement of Instrument Performance Parameters by Stroboscopic Observations 298
Pulse Testing 301
Rectangular Pulse Functions 301
Displaced Cosine Pulse Functions 303
Evaluation of Performance Functions from Pulse Function Responses 306
Response Functions of (0;0, 1, 2) Measuring Instruments 307
Displaced Cosine Pulse Function Test of a Recording Oscillograph 313

CHAPTER 33
PRESSURE-MEASURING SYSTEMS
Y. T. Li

Introduction 319
Pressure-Measuring Units 319
Pressure-Measuring Systems 320
Methods of Performance Analysis 320
Static-Functional Diagrams for Pressure-Measuring Units and Systems 321

Typical Pressure-Measuring Instruments . . . 324
Pressure-Measuring Systems as Open-Chain Systems . . . 333
Performance Problems Associated with Pressure-Measuring Systems . . . 334
Performance Functions for Open-Chain Systems . . . 335
Graphical Manipulation of Component Performance Functions to Produce Open-Chain System Performance Functions . . . 339
First- and Second-Order Logarithmic-Scale Performance Function Profiles . . . 339
Dynamic Error Effects in Terms of Sinusoidal Response Characteristics . . . 340
Indicator Cards from a Spring-and-Piston-Type Indicator . . . 352
Electrical Pressure-Recording System . . . 361
Over-all Measuring-System Performance when Component Performance Functions are Expressed as Equations . . . 365
Cutoff Frequencies and Band Widths . . . 370
Measuring-System Performance Requirements for Satisfactory Internal Combustion Engine Cylinder-Pressure Records . . . 377
Internal Combustion Engine Cylinder-Pressure Record from an Electrical Measuring System . . . 378
Turbine-Nozzle-Chamber Pressure Measurement in a Turbojet Engine . . . 385
Interfering and Modifying Effects in Pressure-Measuring Systems . . . 391
Pressure-Receiving-Element Performance Equations . . . 393
Modifying Input Effects . . . 398
Reduction of Pressure-Receiving-Element Interference Effects due to Modifying Inputs . . . 398
Component Performance Functions for Pressure Receiving Elements . . . 399
Expressions for Dynamic Deviation Effects and Interference Effects in Pressure Receiving Elements . . . 403
Reduction of Pressure-Receiving-Element Interference Effects due to Interfering Inputs . . . 406
Selection of Design Features and Materials . . . 407
Mechanical and Electrical Filtering Techniques . . . 410
Isolation of System Components . . . 410
Compensation . . . 410
Practical Factors of Pressure-Receiving-Element Design . . . 411
Determination of Performance Characteristics for Pressure-Measuring Instruments . . . 412
Determination of Dynamic Performance Parameters . . . 413
Shock Tube for Determining Characteristics of High-Natural-Frequency Pressure-Measuring Instruments . . . 416
Typical Pressure Record from Shock-Tube Test . . . 416
Conclusion . . . 421

CHAPTER 34
INTEGRATORS AND DIFFERENTIATORS

Introduction . . . 422
Ideal Integrators . . . 422
Ideal Differentiators . . . 427
Typical Integrators and Differentiators . . . 427
Ball-and-Disc Mechanical Integrator . . . 432
Eddy-Current-Drag-Disc Watt-Hour-Meter-Type Integrator . . . 437
Viscous-Shear-Drag-Generator-Type Integrator . . . 441
Liquid-Flow Integrator . . . 443
Thermal Integrator . . . 447

Pneumatic Pressure Integrator 450
Resistance-Capacitance Electrical Integrator 453
Resistance – Amplifier – Feedback-Capacitance Integrator. 456
Motor – Amplifier – Feedback-Tachometer Integrator 463
Ball-and-Disc Mechanical Differentiator 471
Tachometers as Differentiators 473
Centrifugal Tachometer. 478
Rotating-Magnet Drag-Cup Tachometer 478
Direct-Current Electrical Tachometer. 478
Alternating-Current Drag-Cup Electrical Tachometer 482
Resistance-Inductance Electrical Differentiator. 482
Resistance – Amplifier – Feedback-Inductance Differentiator 484
Resistance-Capacitance Electrical Differentiator 486
Capacitance – Amplifier – Feedback-Resistance Differentiator 489
Integrator and Differentiator Performance Equation Forms. 489
Relating Function Deviations 490
Relating Functions for Integrator and Differentiator Performance Equation Forms 493
Step Function Response Deviations from Ideal Integration 495
Nondimensional Dynamic Amplitude Ratio and Dynamic Response Angle Deviations 497
Viscous Shear Integrator Example 508
Viscous Shear Integrator with Uncertainty Torque 524
Motor – Amplifier – Feedback-Tachometer Integrator with Zero Uncertainty. 527
Analog Computers 536
Operation of Analog-Computer Components 542
Solution of the General Linear Differential Equation with Constant Coefficients by an Analog Computer. 551
Solution of the (0;0, 1) Differential Equation by an Analog Computer 555
Solution of the (0;0, 1, 2) Differential Equation by an Analog Computer 560
Numerical Example of Scaling a Problem for Analog-Computer Solution 567

CHAPTER 35

VIBRATION MEASUREMENT AND VIBRATION ISOLATION

Y. T. Li

Introduction. 601
The Generalized Problem of Single-Degree-of-Freedom Vibration Measurements 602
The Seismographic System. 605
Seismographic System Operation in the Accelerometer Range 606
Seismographic System Operation in the Velocimeter Range 606
Seismographic System Operation in the Vibrometer Range 607
Vibration Receivers 607
External-Reference Vibration Receivers 607
Self-Contained Vibration Receivers. 610
Electrical-Signal-Generating Vibration Receivers 610
Relative Motion Receivers and Indicators. 613
Dial Gage Displacement Indicator 613
Optical Displacement Indicator 615
Electrical-Signal-Generating Relative Motion Receivers. 615
Unbonded Resistance Wire Displacement Receiver. 616

Bonded Resistance Wire Displacement Receiver. 617
Electronic Tube Displacement Receiver 624
Electrostatic Capacity Relative Motion Receivers 625
Electromagnetic Generator Relative Velocity Receivers 626
Variable-Air-Gap Linear Velocity Receiver 628
Magnetostrictive Linear Velocity Receiver 630
E-Magnet Differential Transformer Linear Displacement Receiver 630
E-Magnet Differential Transformer Angular Displacement Receiver 632
Microsyn Angular Displacement Receiver. 632
Concentric-Coil Inductance-Bridge Displacement Receiver 633
Concentric-Coil Differential Coupling Transformer Displacement Receiver 635
Piezoelectric Displacement Receiver 635
Factors Determining Selection of Relative Motion Receivers 637
Vibratory Motion Receivers and Indicators 641
Typical Vibratory Motion Receivers and Indicators 642
Self-Contained Vibratory Motion Indicators 642
Self-Contained Vibratory Motion Receivers with Electrical Outputs 648
Selection of Vibration Receivers. 658
Generalized Theory of the Single-Degree-of-Freedom Seismographic System. 658
Generalized Performance Function for the Single-Degree-of-Freedom Seismographic System with Viscous Damping Only 664
Performance Characteristics of the Seismographic System as an Operating Component for Receiving Vibration 664
Seismographic System Performance in the Displacement-Receiving (Vibrometer) Range . . . 678
Vibratory Frequency-Receiving Characteristics of the Lightly Damped Seismographic System . . 682
Seismographic System Performance in the Velocity-Receiving (Velocimeter) Range. 688
Seismographic System Performance in the Acceleration-Receiving (Accelerometer) Range . . 696
Summary of Vibration-Receiving Characteristics of the Seismographic System with Viscous Damping Only 704
Seismographic System with Both Viscous Damping and Coulomb Damping 704
Transient Response of the Seismographic System with Combined Viscous Damping and Coulomb Damping 708
Steady-State Response of the Seismographic System with Combined Viscous Damping and Coulomb Damping 722
Single-Degree-of-Freedom Vibration Isolation 726
Vibratory Force Isolation System 742
Illustrative Test Report on the Experimental Calibration of a Linear Vibration Receiver . . . 751
Illustrative Test Report on the Experimental Calibration of a Torsional Vibration Receiver . . 773
Illustrative Test Report on the Calibration of an Integrating Amplifier 782
Illustrative Test Report on the Calibration of a Linear Acceleration Recording System. . . . 794
The Performance Function Deviation Function Concept for Describing Instrument Performance. . 803
Application of the Deviation Method to the Performance of a Typical Recording System . . . 808
Vibration Measurement for a Rigid Body Moving in Space 819
Typical Example of Angular Vibration Measurement with Linear Vibration Receivers 822
Displaced Cosine Pulse Forcing Functions 832
Illustrative Examples of Isolation Systems Associated with (1, 0;0, 1, 2) Performance Equations 837
Recording Oscillograph Vibratory Motion Isolation System 837
Aircraft Engine Vibratory Torque Isolation System 840

BIBLIOGRAPHY 845

INDEX 861

ILLUSTRATIONS, TABLES AND SUMMARIES

ILLUSTRATIONS

28-1 Tangent, chord, and secant definitions of sensitivity for an operating component with a curved input-output characteristic 16

28-2 Sensitivity definitions for a linear input-output characteristic passing through the origin . . 17

28-3 Features of the generalized control problem 26

28-4 Diagram of the control loop 27

28-5 Analysis diagram for a controlled system. 28

28-6 Controlled system diagram 28

28-7 Closed-loop control system 29

28-8 Block diagram for a feedback control system containing all basic elements. 30

28-9 Diagram for a feedback control system 31

28-10 Functional diagram for a controlled system and a single feedback control system 32

28-11 Generalized functional diagram for a controlled system with multiple feedback control systems 33

28-12 Functional-schematic diagram for a liquid heater with proper names for operating components 34

28-13 Functional diagram for the liquid heater of Fig. 28-12 with functional names for operating components 35

29-1 Definitions for inaccuracy, uncertainty, and error of indicated quantity and scale reading when repeated observations are possible 48

29-2 Summary of definitions and symbols for concepts associated with the description of measuring instrument static performance quality 50-1

29-3 Summary of definitions and symbols for concepts associated with the description of measuring instrument performance quality when the input quantity and scale readings vary with time 52

29-4 Functional diagram for an actual measuring instrument with multiple inputs 59

29-5 Calibration by means of a primary standard and by means of a secondary standard 61

29-6 Scale characteristics 62

29-7 The normal probability frequency function for scale reading in terms of various uncertainty-describing concepts 64

31-1 Step function response of an ideal thermometer with first-order performance characteristics and a constant characteristic time 183

31-2 Ramp function response of an ideal thermometer with first-order performance characteristics and a constant characteristic time 184

31-3 Parabolic function response of an ideal thermometer with first-order performance characteristics and constant characteristic time 187

31-4 Steady-state sinusoidal response of an ideal thermometer with first-order performance characteristics and constant characteristic time: linear-scale plots 190

31-5 Steady-state sinusoidal response of an ideal thermometer with first-order performance characteristics and constant characteristic time: linear-scale plots, low-frequency range . . . 191

ILLUSTRATIONS (Cont.)

31-6 Steady-state sinusoidal response of an ideal thermometer with first-order performance characteristics and constant characteristic time: logarithmic-scale plots 192

31-7 Test apparatus for step function response of air temperature thermometer 200

31-8 Semilog plots of step function response of vapor-pressure thermometer with various air speeds 204

31-9 Linear and log-log plots of air temperature characteristic time as a function of air velocity at bulb 205

31-10 Typical velocity profiles, greatly enlarged in the vertical direction 207

31-11 Receiver – free-stream static temperature ratio as a function of Mach number and recovery factor for the case of air flow. 209

31-12 Views showing tip of shielded thermocouple probe 210

31-13 Typical illustrative temperature probe calibration of recovery factor as a function of Mach number and Reynolds number 211

31-14 Distortion of a velocity profile by the presence of a probe 214

31-15 Illustrative plot showing recovery factor as a function of Reynolds number at a nominal Mach number of 2.0 215

31-16 Vortex tube 215

31-17 Results of flight tests of a vortex thermometer 216

32-1 Impulse function response curves for measuring instruments with (0;0,1,2) performance equations when the time – undamped natural frequency product is the running variable . . 238

32-2 Impulse function response curves for measuring instruments with (0;0,1,2) performance equations when the time – high damping ratio characteristic time sum ratio is the running variable 239

32-3 Measuring instrument performance deviation curves for second-order impulse function response with respect to first-order impulse function response 240

32-4 Step function response of measuring instruments with (0;0,1,2) performance equations when the time – undamped natural frequency product is the running variable 241

32-5 Step function response of measuring instruments with (0;0,1,2) performance equations when the time – low damping ratio characteristic time ratio is the running variable 242

32-6 Step function response of measuring instruments with (0;0,1,2) performance equations when the time – high damping ratio characteristic time sum ratio and time – first-order characteristic time ratio are running variables 243

32-7 Measuring instrument performance deviation curves for second-order step function response with respect to first-order step function response 245

32-8 Indication time – undamped natural period ratio as a function of damping ratio for measuring instruments with (–;0,1,2) performance equation 246

32-9 Illustrative critically damped ramp function response curve for measuring instruments with (0;0,1,2) performance equations when the time – low damping ratio characteristic time ratio is the running variable 247

32-10 Ramp function response for measuring instruments with (0;0,1,2) performance equations when the time – low damping ratio characteristic time ratio is the running variable . . . 248

32-11 Ramp function response for measuring instruments with (0;0,1,2) performance equations when the time – high damping ratio characteristic time sum ratio and time – first-order characteristic time ratio are running variables. 249

32-12 Measuring instrument performance deviation curves for second-order ramp function response with respect to first-order ramp function response 250

32-13 Ramp function response – forcing function ratio for measuring instruments with (0;0,1,2) performance equations when the time – low damping ratio characteristic time ratio is the running variable 251

32-14 Parabolic response for measuring instruments with (0;0,1,2) performance equations when the time – low damping ratio characteristic time ratio is the running variable 253

32-15 Ramp-followed-by-constant response for measuring instruments with (0;0,1,2) performance equations when the time – low damping ratio characteristic time ratio is the running variable 254

32-16 Linear-scale complex plane performance function plots for measuring instruments with (0;0, 1, 2) performance equations 260

32-17 Linear-scale over-all sensitivity and dynamic response angle curves for the steady-state sinusoidal response of measuring instruments with (0;0, 1, 2) performance equations . . . 262

32-18 Linear-scale dynamic response angle curves for the steady-state sinusoidal response of measuring instruments with (0;0, 1, 2) performance equations 264

32-19 Expanded linear-scale over-all sensitivity and dynamic response angle curves for the steady-state sinusoidal response of measuring instruments with (0;0, 1, 2) performance equations 265

32-20 Logarithmic-scale over-all sensitivity curves for the steady-state sinusoidal response of measuring instruments with (0;0, 1, 2) performance equations 266

32-21 Semilogarithmic-scale dynamic response angle curves for the steady-state sinusoidal response of measuring instruments with (0;0, 1, 2) performance equations 268

32-22 Semilogarithmic-scale over-all sensitivity deviation curves for the steady-state sinusoidal response of measuring instruments with (0;0, 1, 2) performance equations 269

32-23 Semilogarithmic-scale dynamic response angle deviation curves for the steady-state sinusoidal response of measuring instruments with (0;0, 1, 2) performance equations 270

32-24 Frequency ratio for maximum steady-state sinusoidal over-all sensitivity as a function of damping ratio 274

32-25 Maximum steady-state sinusoidal over-all sensitivity as a function of damping ratio . . . 274

32-26 Transient peak ratio as a function of damping ratio for step function oscillatory response of measuring instruments with (0;0, 1, 2) performance equations 278

32-27 Logarithmic-scale curves of maximum over-all sensitivity as a function of step function transient peak ratio for instruments with (0;0, 1, 2) performance equations 279

32-28 Time ratio and undamped angular natural frequency – time product as a function of damping ratio for the step function response of measuring instruments with (0;0, 1, 2) performance equations 280

32-29 Damping ratio as a function of high damping ratio characteristic time ratio for measuring instruments with (0;0, 1, 2) performance equations 283

32-30 Pictorial schematic diagram for a photographic recording oscillograph with a moving-coil galvanometer 285

32-31 Step function response record from moving-coil oscillograph with oscillatory characteristics . 287

32-32 Step function response record from moving-coil oscillograph with nonoscillatory characteristics 288

32-33 Arrangement for determining dynamic response angle of oscillograph 290

32-34 Linear-scale experimental data plots of dynamic response angle as a function of frequency and frequency ratio for an optical oscillograph 293

32-35 Logarithmic-scale plots of experimental data on variation of an optical oscillograph indicator sensitivity with frequency for steady-state sinusoidal input variation. 296

32-36 Relationship between damping ratio and sensitivity at dynamic response angle = −90° for instruments with (0;0, 1, 2) performance equations 297

32-37 Arrangement for making stroboscopic light photographs of instrument response 298

32-38 Drawing of a stroboscopic light photograph and data summary for step function response of special heavily damped voltmeter X-1 299

32-39 Semilogarithmic plot of step function response of special heavily damped voltmeter X-1 . . 300

32-40 Fourier transform of a rectangular pulse function 304

32-41 Fourier transform of a displaced cosine pulse function 307

32-42 First response peak – pulse height ratio for the displaced cosine pulse function response of (0;0, 1, 2) measuring instruments. 308

32-43 Peak response delay – pulse duration ratio for the displaced cosine pulse function response of (0;0, 1, 2) measuring instruments. 309

32-44 Nondimensional first response peak characteristics associated with (0;0, 1, 2) measuring instruments. 310

32-45 Typical displaced cosine pulse function responses of a measuring instrument with a very low damping ratio and a (0;0, 1, 2) performance equation. Pulse duration is long compared with the undamped natural period 313

32-46 Pictorial schematic diagram showing the setup for making displaced cosine pulse tests on an optical recording oscillograph with a moving-coil galvanometer 314

32-47 Displaced cosine pulse function response records from an optical recording oscillograph . . 315

32-48 Plot of first response peak characteristics from displaced cosine pulse tests of an optical recording oscillograph 316

32-49 Plot of first response peak – pulse height ratios from displaced cosine pulse tests of an optical recording oscillograph 317

32-50 Plot of peak response delay – pulse duration ratios from displaced cosine pulse tests of an optical recording oscillograph 318

33-1 Illustrative static-functional diagrams of pressure-measuring instruments and systems . . 322

33-2 Essential features of two commonly used pressure-measuring instruments 324

33-3 Typical automobile-engine oil-pressure gages 326

33-4 Illustrative pictorial, static-functional, and basic electrical circuit diagrams for seven typical pressure receivers. 328-30

33-5a Illustrative logarithmic-scale plot of the Fourier-series amplitude ratios for the cylinder pressure record from an internal combustion engine given in Figs. 12-8 and 12-10. 356

33-5b Illustrative semilogarithmic-scale plot of the Fourier-series component phase angles for the cylinder pressure record from an internal combustion engine given in Figs. 12-8 and 12-10. 357

33-6a Illustrative logarithmic-scale plot of the Fourier-series amplitude ratios for the cylinder pressure variation of an internal combustion engine at 2400 rpm, and the corresponding amplitude ratios for the pressure record from a spring-and-piston indicator 358

33-6b Illustrative semilogarithmic-scale plot of the Fourier-series component phase angles for the cylinder pressure variation of an internal combustion engine at 2400 rpm, and the corresponding phase angles for the pressure record from a spring-and-piston indicator . . . 359

33-7 Illustrative theoretical plot for the cylinder pressure variation of an internal combustion engine at 2400 rpm and the corresponding pressure record from a spring-and-piston indicator 360

33-8a Illustrative logarithmic-scale plot of the Fourier-series amplitude ratios for the cylinder pressure variation of an internal combustion engine at 800 rpm, and the corresponding amplitude ratios for the pressure record from a spring-and-piston indicator 362

33-8b Illustrative semilogarithmic-scale plot of the Fourier-series component phase angles for the cylinder pressure variation of an internal combustion engine at 800 rpm, and the corresponding phase angles for the pressure record from a spring-and-piston indicator . . . 363

33-9 Illustrative theoretical plot for the cylinder pressure variation of an internal combustion engine at 800 rpm and the corresponding pressure record from a spring-and-piston indicator 364

33-10 Pictorial diagram for a typical pressure-measuring system with electrical components . . 366

33-11a Illustrative logarithmic-scale plot of the Fourier-series amplitude ratios for the cylinder pressure variation of an internal combustion engine at 800 rpm, and the corresponding amplitude ratios for the pressure record from a pressure-measuring system using electrical components. 380

33-11b Illustrative semilogarithmic-scale plot of the Fourier-series component phase angles for the cylinder pressure variation of an internal combustion engine at 800 rpm, and the corresponding phase angles for the pressure record from a pressure-measuring system using electrical components 381

33-12 Illustrative theoretical plot for the cylinder pressure variation of an internal combustion engine at 800 rpm and the corresponding pressure record from a pressure-measuring system with inadequate low-frequency performance 382

33-13 Pictorial diagram for an electrical pressure-measuring system applied to the turbine nozzle chamber of a jet engine. 386

33-14a Dimensionless sensitivity ratio performance characteristic for pressure-measuring system of Fig. 33-13 389

33-14b Dynamic response angle performance characteristic for pressure-measuring system of Fig. 33-13 390

33-15 Static-functional diagram for a typical pressure-measuring system showing interfering inputs and modifying inputs 392

33-16 Static-functional diagram for the pressure receiving element of the pressure receiver of Fig. 33-15, showing interfering inputs. 393

33-17 Shock tube for exciting transients in high-natural-frequency pressure-measuring instruments. 417

34-1 Illustrative pictorial diagram of a ball-and-disc mechanical integrator 433

34-2 Illustrative pictorial-functional diagram of a ball-and-disc mechanical integrator 434

34-3 Illustrative pictorial diagram of an eddy-current-drag-disc watt-hour-meter integrator . . 438

34-4 Illustrative pictorial diagram for a viscous-shear-drag-generator-type integrator 442

34-5 Illustrative pictorial diagram for a liquid-flow integrator 447

34-6 Illustrative pictorial diagram for a thermal integrator 451

34-7 Illustrative pictorial diagram for a pneumatic integrator 451

34-8 Illustrative pictorial and circuit diagrams for a resistance-capacitance electrical integrator . 457

34-9 Illustrative pictorial and electrical circuit diagrams for a resistance – amplifier – feedback-capacitance integrator 460

34-10 Illustrative pictorial diagram for a motor – amplifier – feedback-tachometer integrator . . 464

34-11 Illustrative pictorial diagram for a ball-and-disc differentiator 472

34-12 Illustrative pictorial-functional diagram for a ball-and-disc differentiator 474

34-13 Illustrative pictorial diagram for a centrifugal tachometer 479

34-14 Illustrative pictorial-functional diagram for a centrifugal tachometer 479

34-15 Illustrative pictorial diagram for a rotating-magnet drag-cup tachometer 480

34-16 Illustrative pictorial-functional diagram for a rotating-magnet drag-cup tachometer . . . 480

34-17 Illustrative pictorial diagram for a direct-current electrical tachometer 481

34-18 Illustrative pictorial-functional diagram for a direct-current electrical tachometer. . . . 481

34-19 Illustrative pictorial diagram for an alternating-current drag-cup electrical tachometer . . 483

34-20 Illustrative pictorial-functional diagram for an alternating-current drag-cup electrical tachometer 483

34-21 Illustrative pictorial and circuit diagrams for a resistance-inductance electrical differentiator 484

34-22 Illustrative pictorial and circuit diagrams for a resistance – amplifier – feedback-inductance differentiator 486

34-23 Illustrative pictorial and circuit diagrams for a resistance-capacitance electrical differentiator 488

34-24 Illustrative pictorial and electrical circuit diagrams for a capacitance – amplifier – feedback-resistance differentiator 490

34-25 Diagram illustrating the deviation of the step function response of an integrator with a (0;0,1) performance equation with respect to the step function response of an ideal integrator. . . 498

34-26 Deviation of the (0;0, 1) equation increasing step function response with respect to the corresponding (0;1) equation response 500

34-27 Diagram illustrating the definition of the [(0;1) – (0;0, 1)] dimensionless dynamic amplitude ratio deviation 501

34-28 Diagram illustrating the definition of the [(1;0) – (1;0, 1)] dimensionless dynamic amplitude ratio deviation 502

34-29 Dimensionless dynamic amplitude ratio and dynamic response angle deviation plots for the (0;1,2) and (1;0,1) differential equations with respect to the (0;1) and (1;0) differential equations, respectively 506

34-30 Dimensionless dynamic amplitude ratio and dynamic response angle deviation plots for the (0;0, 1) and (1;1, 2) differential equations with respect to the (0;1) differential equations . . 507

34-31 Pictorial representation of the relationship between physical problem time and analog computer time in terms of the solution time ratio 541

34-32 General arrangement of Computer No. 1 599

34-33 General arrangement of Computer No. 2 600

ILLUSTRATIONS (Cont.)

35-1 Generalized six-degree-of-freedom displacement of a moving body with respect to a reference position of the body. 602

35-2 Essential features of the vibration measurement problem 604

35-3 Essential features of single-degree-of-freedom seismographic systems for receiving vibration 608

35-4 Diagrams illustrating the essential features of external-reference vibration receivers and self-contained vibration receivers 611-2

35-5 Illustrative diagrams of typical relative motion receivers and indicators 618-23

35-6 Functional diagram showing the self-contained vibration receiver or indicator formed by combining a seismographic system and a relative motion receiver or indicator 643

35-7 Typical single-degree-of-freedom vibration-measuring systems 644-8

35-8 Linear-scale plots of the forcing displacement input – relative displacement output dimensionless sensitivity ratio for the seismographic system with viscous damping only 674

35-9 Linear-scale plots of the forcing displacement input – relative displacement output dynamic response angle for the seismographic system with viscous damping only 675

35-10 Logarithmic-scale plots of the forcing displacement input – relative displacement output dimensionless sensitivity ratio for the seismographic system with viscous damping only . . 676

35-11 Logarithmic-scale abscissa – linear-scale ordinate plots of the forcing displacement input – relative displacement output dynamic response angle for the seismographic system with viscous damping only 677

35-12 Forcing displacement input – relative displacement output sensitivity performance ratio deviation for the seismographic system with viscous damping only 681

35-13 Forcing displacement input – relative displacement output dynamic response angle deviation for the seismographic system with viscous damping only. 683

35-14 Frequency ratio for maximum forcing displacement input – relative displacement output dimensionless sensitivity ratio as a function of damping ratio for the seismographic system with viscous damping only 685

35-15 Maximum forcing displacement input – relative displacement output dimensionless sensitivity ratio as a function of damping ratio for the seismographic system with viscous damping only 685

35-16 Logarithmic-scale plot of maximum forcing displacement input – relative displacement output dimensionless sensitivity ratio as a function of damping ratio for the seismographic system with viscous damping only 686

35-17 Dimensionless sensitivity ratio – maximum dimensionless sensitivity ratio ratio as a function of frequency ratio deviation for the seismographic system with viscous damping only . 687

35-18 Logarithmic-scale curves of forcing velocity input – relative displacement output dimensionless sensitivity ratio for the seismographic system with viscous damping only 693

35-19 Semilogarithmic-scale curves of forcing velocity input – relative displacement output dynamic response angle for the seismographic system with viscous damping only 694

35-20 Semilogarithmic-scale curves of forcing velocity input – relative displacement output sensitivity performance ratio deviation for the seismographic system with viscous damping only 695

35-21 Semilogarithmic-scale curves of forcing velocity input – relative displacement output dynamic response angle deviation for the seismographic system with viscous damping only . . 697

35-22 Linear-scale curve families of forcing acceleration input – relative displacement output dimensionless sensitivity ratio and dynamic response angle for the seismographic system with viscous damping only 702

35-23 Semilogarithmic-scale curves of forcing acceleration input – relative displacement output sensitivity performance ratio deviation of the seismographic system with viscous damping only 703

35-24 Semilogarithmic-scale curves of forcing acceleration input – relative displacement output dynamic response angle deviation of the seismographic system with viscous damping only. . 705

35-25 Illustrative step function transient response curves for the seismographic system with Coulomb damping and no viscous damping; step function transient response equations for the seismographic system with combined viscous damping and Coulomb damping 716-7

35-26 Illustrative step function transient response curves for the seismographic system with zero viscous damping and various maximum Coulomb friction displacement – initial peak maximum magnitude ratios 719

35-27 Illustrative step function transient response curves for the seismographic system with the damping ratio component due to viscous damping equal to 0.1 and various maximum Coulomb friction displacement – initial peak maximum magnitude ratios 720

35-28 Illustrative step function transient response curves for the seismographic system with the damping ratio component due to viscous damping equal to 0.2 and various maximum Coulomb friction displacement – initial peak maximum magnitude ratios 721

35-29 Maximum Coulomb friction displacement – forcing displacement amplitude ratio as a function of breakaway frequency ratio for the seismographic system 724

35-30 Linear-scale plots of the forcing displacement input – relative displacement output dimensionless sensitivity ratio as a function of frequency ratio for the seismographic system with Coulomb damping only 725

35-31 Linear-scale plots of the forcing displacement input – relative displacement output dynamic response angle as a function of frequency ratio for the seismographic system with Coulomb damping only 727

35-32 Linear-scale plots of the forcing displacement – isolated member displacement dimensionless dynamic amplitude ratio as a function of frequency ratio for the single-degree-of-freedom vibratory motion isolation system with viscous friction only. 733

35-33 Linear-scale plots of the forcing displacement – isolated member displacement dynamic response angle as a function of frequency ratio for the single-degree-of-freedom vibratory motion isolation system with viscous friction only 734

35-34 Frequency ratio for maximum dimensionless dynamic amplitude ratio as a function of damping ratio for the single-degree-of-freedom vibratory motion isolation system. 735

35-35 Maximum dimensionless dynamic amplitude ratio as a function of damping ratio for the single-degree-of-freedom vibratory motion isolation system 735

35-36 Logarithmic-scale plot of forcing displacement – isolated member displacement dimensionless dynamic amplitude ratio as a function of frequency ratio for the single-degree-of-freedom vibratory motion isolation system 737

35-37 Maximum Coulomb friction displacement – forcing displacement amplitude ratio as a function of breakaway frequency ratio for the vibratory motion isolation system 738

35-38 Linear-scale plots of the forcing displacement – isolated member displacement dimensionless dynamic amplitude ratio as a function of frequency ratio for the single-degree-of-freedom vibratory motion isolation system with Coulomb damping only 739

35-39 Linear-scale plots of the forcing displacement – isolated member displacement dynamic response angle as a function of frequency ratio for the single-degree-of-freedom vibratory motion isolation system with Coulomb damping only 743

35-40 Linear-scale plots of the force-applied-to-vibrating-member – force-applied-to-support dimensionless dynamic amplitude ratio for the single-degree-of-freedom vibratory force isolation system with viscous damping only 749

35-41 Linear-scale plots of the force-applied-to-vibrating-member – force-applied-to-support dynamic response angle for the single-degree-of-freedom vibratory force isolation system with viscous damping only 750

35-42 Calibration of linear and torsional vibration receivers 767

35-43 Calibration of an integrating amplifier. 783

35-44 Calibration of a linear acceleration recording system. 795

35-45 Plot of linear vibration recording system sensitivity ratio fractional deviation 817

35-46 Plot of linear vibration recording system dynamic response angle deviation 818

35-47 Displacement of a body coordinate system X_b, Y_b, Z_b with respect to a fixed reference coordinate system $X_{(ref)}$, $Y_{(ref)}$, $Z_{(ref)}$ by a combination of translational and rotational motion . . 820

35-48 Test setup for determining the angular vibration of an aircraft engine 829

35-49 Functional diagram of the aircraft-engine-torsional-vibration recording system. 830

35-50 Dynamic response characteristics of the combined receiver-integrator-oscillograph system used to measure the vibratory motion of an 18-cylinder, radial aircraft engine 833

35-51 Actual test record of the torsional oscillation of a Pratt & Whitney R-2800-79 aircraft engine on its mount with one cylinder misfiring 834

35-52 First response peak – pulse height ratio for the displaced cosine pulse function response for (1, 0; 0, 1, 2) systems. 835

35-53 Peak response delay – pulse duration ratio for the displaced cosine pulse function response for (1, 0; 0, 1, 2) systems. 836

35-54 Nondimensional first response peak characteristics associated with (1, 0;0, 1, 2) systems . . 838
35-55 Typical installation of an instrument for vibratory motion isolation 839
35-56 Typical installation of an aircraft engine for vibratory torque isolation 841
35-57 Approximation of a typical internal combustion engine cylinder gas torque by a displaced cosine pulse function. 842

TABLES

28-1 Corresponding components, names, and symbols used in Figs. 28-13, 28-9, and 28-8 . . 37

29-1 Names, symbols and defining equations for description of measuring instrument operations . 80-4

30-1 Dimensions and units 110-1

31-1 Step function response data for a vapor-pressure thermometer at various air speeds . . 202-3
31-2 Characteristic times of temperature-measuring instruments 216

32-1 Definitions and relationships associated with parameters and coefficients of second-order performance equations for measuring instruments. 237
32-2 Relationships and procedures for determination of (0;0, 1, 2) performance equation coefficients and parameters from experimental step function response curves 275

33-1 Characteristics of several pressure-receiving-element types 408

34-1 Relating function information for first- and second-order differential equation forms associated with integration and differentiation 499
34-2 Dimensionless dynamic amplitude ratio and dynamic response angle deviations for first- and second-order differential equation forms associated with integration and differentiation. 504-5
34-3 Cutoff frequencies and band widths for specified values of dimensionless dynamic amplitude ratio and dynamic response angle tolerance limits for the (0;1, 2) and (1;0,1) differential equation relating functions with respect to the (0;1) and (1;0) differential equation relating functions. 509
34-4 Cutoff frequencies and band widths for specified values of dimensionless dynamic amplitude ratio and dynamic response angle tolerance limits for the (1;1, 2) and (0;0, 1) differential equation relating functions with respect to the (0;1) differential equation relating function 510

35-1 Summary of seismographic system performance characteristics in various operating ranges when the system has viscous damping only 706
35-2 Cutoff frequencies and band widths for the linear vibration recording system corresponding to specified values of dimensionless sensitivity ratio fractional deviation tolerance limits and dynamic response angle deviation tolerance limits 819

DATA SUMMARIES

32-1 Steady-state sinusoidal dynamic response angle for an optical oscillograph with two damping shunt resistances. 292
32-2 Steady-state sinusoidal indication sensitivity for an optical oscillograph with two damping shunt resistances. 295

DATA ANALYSIS SUMMARIES

32-1 Analysis of step function data for an optical oscillograph with oscillatory response 287

32-2 Analysis of step function data for an optical oscillograph with aperiodic response 288

32-3 Analysis of displaced cosine pulse function response data for an optical recording oscillograph 317

33-1 Experimental determination of the damping ratio and undamped natural frequency of a pressure receiver from a transient response record 418-20

35-1 Displaced cosine pulse response to data for a typical aircraft engine. 843

DEFINITION SUMMARIES

28-1 Defining diagrams for transducers and coducers 6

28-2 Conventional diagrams for transducers and coducers 6

28-3 Transducer and coducer examples 7

28-4 Comparison of conventions for operating component diagrams 9

28-5 Conventions for representing measuring instruments 11-2

28-6 Description of operating component static performance in physical representation terms and in corresponding working variable terms 14-5

28-7 Description of operating component generalized performance in physical representation terms and in the corresponding working variable terms; performance functions and relating functions. 19

28-8 Description of operating component steady-state sinusoidal performance in physical representation terms and in corresponding working variable terms 21-2

28-9 Various conventions for describing steady-state sinusoidal performance of operating components 23

28-10 Definitions, symbols, and terms for feedback control systems. 24-5

29-1 Representation and performance description for an indicating instrument mechanism . . . 40-2

29-2 Functional diagram and performance description for measuring instruments 44-6

29-3 Summary of dictionary definitions for terms associated with descriptions of the quality of measuring instrument performance. 54-5

29-4 Concepts, definitions and symbols for uncertainty measures associated with measuring instrument operation 65-8

29-5 Error and correction components associated with indications and scale readings from measuring instruments 74-7

33-1 Definitions, symbols and names for concepts used in describing essential features of dimensionless sensitivity ratio and dynamic response angle plots: cutoff frequency and band width 371-4

34-1 Concepts and notation for describing differences between relating functions in terms of dynamic amplitude ratio and dynamic response angle deviations 492-3

DERIVATION SUMMARIES

31-1 Performance functions for the generalized temperature-measuring instrument 172-3

31-2 Temperature receiver performance equation under idealized conditions. 175-7

31-3 Semilogarithmic plot representations for the step function response of an ideal thermometer with first-order performance characteristics and a constant characteristic time . . . 195-6

31-4 Application of dimensional analysis to the development of a generalized functional expression for thermometric characteristic time 198

31-5 Relationships associated with high-speed-flow temperature measurement 212-3

DERIVATION SUMMARIES (Cont.)

32-1 Functional diagram and performance equations for electromechanical measuring instruments 225-31

32-2 Fourier transform for rectangular pulse functions 303

32-3 Fourier transform for displaced cosine pulse functions 305

33-1 (0;0,1) equation performance function as the steady-state sinusoidal response for operating components with (0;0, 1) characteristics: expressed in terms of reference frequency ratio and break point 341-5

33-2 (0;0,1,2) equation performance function as the steady-state sinusoidal response for operating components with (0;0,1,2) characteristics: expressed in terms of reference frequency ratio and break point 347-52

33-3 Functional diagram, frequency response information in performance function form, and indicated pressure record of a pressure-measuring system when the input pressure is described in Fourier series terms 367-9

33-4 Pressure-receiving-element performance equation forms with the effects of interfering inputs and modifying inputs included 394-7

33-5 Performance functions of a flat-diaphragm pressure receiving element for a pressure input and for a linear acceleration input 400-2

33-6 Equations for dynamic deviation effects and interference effects in pressure receiving elements. 404-6

34-1 Performance equation and performance function for the ideal integrator 423-6

34-2 Performance equation and performance function for the ideal differentiator 428-30

34-3 Performance equation for a ball-and-disc mechanical integrator 435-6

34-4 Functional diagram and generalized performance equations for an eddy-current-drag-disc watt-hour-meter integrator 440-1

34-5 Functional diagram and generalized performance equations for a viscous-shear-drag-generator-type integrator 444-6

34-6 Functional diagram and performance equation for a liquid-flow integrator 448-50

34-7 Functional diagram and performance equations for a thermal integrator 452-3

34-8 Functional diagram and performance equations for a pneumatic pressure integrator . . 454-5

34-9 Functional diagram and performance equation for a resistance-capacitance electrical integrator 458-9

34-10 Functional diagram and performance equation for a resistance – amplifier – feedback-capacitance integrator 461-2

34-11 Functional diagram and performance equations for a motor – amplifier – feedback-tachometer integrator 466-9

34-12 Functional diagram and performance equations for a ball-and-disc differentiator . . . 475-7

34-13 Performance equations for a resistance-inductance electrical differentiator 485

34-14 Performance equations for a resistance – amplifier – feedback-inductance differentiator. . 487

34-15 Performance equations for a resistance-capacitance electrical differentiator 489

34-16 Performance equations for a capacitance – amplifier – feedback-resistance differentiator . 491

34-17 Relating function for the (0;1, 2) linear differential equation with constant coefficients . . 494-5

34-18 Relating function for the (1;1, 2) linear differential equation with constant coefficients . . 496-7

34-19 Illustrative performance analysis for a viscous shear integrator 512-23

34-20 Illustrative performance analysis for a motor – amplifier – feedback-tachometer integrator . 528-36

34-21 Basic concepts and relationships associated with an electrical analog computer in which voltages represent the dependent and independent variables of a physical problem 540

34-22 Performance relationships associated with the components of a linear-system electrical analog computer 543-50

34-23 Transformation of an nth-order linear differential equation with constant coefficients to a form suitable for solution by an electrical analog computer 552-4

34-24 Functional diagram and performance equations for an analog-computer arrangement based on the "least number of components" connection and representing a general n^{th}-order linear system 556-60

DERIVATION SUMMARIES (Cont.)

34-25 Analog-computer arrangements for solving a first-order linear differential equation with constant coefficients 561-7

34-26 Analog-computer arrangements for solving a second-order linear differential equation with constant coefficients 568-76

34-27 Component analysis and performance equation of a typical positional servo system; derivation of the corresponding analog-computer equation and the equivalent analog-computer arrangement; determination of the coefficient settings 577-96

35-1 Pictorial diagram, functional diagram, and performance equation for the single-degree-of-freedom seismographic system that has combined viscous damping and Coulomb damping . 660-2

35-2 The (2;0,1,2) relating function and the performance function for the single-degree-of-freedom seismographic system that has viscous damping only 666-9

35-3 Line schematic diagram, functional diagram, performance equation, performance function and performance deviation equations for the seismographic system that has viscous damping only and operates in the displacement-receiving range 670-3

35-4 Line schematic diagram, functional diagram, performance equation, performance function and performance deviation equations for the seismographic system that has viscous damping only and operates in the velocity-receiving range 689-91

35-5 Line schematic diagram, functional diagram, performance function and performance deviation equations for the seismographic system that has viscous damping only and operates in the acceleration-receiving range 699-701

35-6 Performance equation, performance functions and breakaway frequency ratios for seismographic systems with Coulomb damping 709-15

35-7 The (1, 0;0, 1, 2) relating function and the performance function for the single-degree-of-freedom vibratory motion isolation system with viscous damping only 728-31

35-8 Performance equation, performance function and breakaway frequency ratio for the single-degree-of-freedom vibratory motion isolation system with Coulomb damping only . . . 740-2

35-9 Pictorial diagram, differential equation, performance functions and transmissibility equations for the single-degree-of-freedom vibratory force isolation system 745-8

35-10 Sensitivity ratio fractional deviations for an open-chain system 805-7

35-11 Performance function of a typical recording system expressed in terms of component deviations 809-10

35-12 Schematic diagram showing use of six linear vibration receivers for the generation of signals to determine the generalized motion of a vibrating member; equations for expressing the vibration components in terms of linear displacements of the receivers 823-8

DESCRIPTION SUMMARY

31-1 Illustrative pictorial-functional and pictorial diagrams for common temperature-measuring instruments. 164-7

INFORMATION SUMMARIES

30-1 Elements of translational mechanics 112

30-2 Elements of rotational mechanics 113

30-3 Elements of electric circuits 114-5

30-4 Elements of magnetic circuits 116-8

30-5 Elements of heat flow 119-20

30-6 Elements of fluid mechanics 121-4

30-7 Mechanism components. 136-40

30-8 Electromagnetic components 141-9

30-9 Electronic components 150-4

30-10 Thermometric components 155-6

30-11 Fluid components. 157-60

problems and that the confusion and lack of coherence among references is primarily due to variations in terminology, symbols, mathematical procedures, and presentation of results. These variations stem from differences among the educational backgrounds and personalities of individual writers rather than from basic characteristics of the physical situations to be handled.

3. A considerable effort by individuals and engineering organizations* to establish a common system of concepts, terminology, and notation began some years ago and is still in progress. The difficulties that must exist in the path of a project of this kind are apparent when it is noted that definite proposals for standard systems are just now appearing in engineering journals. This amount of progress is certainly a great step forward, but it is also probable that much discussion remains before any scheme of terminology and notation wins the same universal acceptance that is accorded, for example, to the symbols of electrical circuit analysis. In any case, it is only possible to establish a general pattern for representing physical situations that has sufficient flexibility to be applied easily in cases with any degree of complexity. One of the objectives of Instrument Engineering is to develop a pattern of this kind and to show in a general way the relationships of this pattern to other schemes for representing the behavior of measurement and control systems.

4. Volume III of Instrument Engineering is made up of two parts. Part 1 illustrates the problems of indication and measurement by self-contained unit instruments and by systems formed of open chains of operating components. Part 2 is concerned with applications of feedback, including servomechanisms, process controllers, and systems for the control of the motion of platforms and vehicles with respect to inertial space.

5. Both parts of Volume III are made up of chapters that individually deal with a single phase of instrument engineering. In effect, the "case method" of presentation is used, with the individual cases treated as particular applications of the generalized pattern described in Volumes I and II. The methods and quantitative results from these volumes are used freely in all the chapters of Parts 1 and 2 of Volume III. The sequence of subjects chosen not only brings out information on particular problems but also develops the pattern for working out solutions to situations with all levels of complexity.

6. The first chapter of Volume III, Chapter 28, contains a review of the concepts and notation used by various authors to describe operating components and operating systems. The agreements and differences among commonly used terms and symbols are discussed with particular reference to the self-defining symbols and working variables of the comprehensive pattern developed for the purposes of Instrument Engineering.

* See AIEE (A3), ASME (A4), (A5), Behar (B2), Ivanoff (I2), Philbrick (P1), Porter (P2), and Trimmer (T1).

7. Chapter 29 gives a discussion of the generalized concepts of indication and measurement. Particular attention is paid to concepts and symbols for describing the static and dynamic performance of measuring instruments.

8. Chapter 30 is a summary of information about many of the physical principles and devices that may play important roles in measurement and control equipment. For convenience, this information is presented in readily available tabular form.

9. Chapter 31 is an engineering treatment of temperature-measuring instruments. It is shown that typical thermometric instruments have performance functions matching the relating function form of the first-order differential equation. This makes it possible to use thermometer theory as the vehicle for developing practical applications of the first-order nondimensional curve families derived in Chapter 18.

10. Chapter 32 builds up the theory of electromechanical measuring instruments to show that typical examples have second-order performance functions. The background for applying the nondimensional curve families of Chapter 19 is developed for use with electrical instruments as well as all other instruments associated with second-order performance equations. Nondimensional plots for instrument response to displaced cosine pulse forcing functions are also included.

11. Chapter 33 uses pressure measuring as the engineering problem for developing the theory of open-chain systems. Specific examples are treated in terms of component performance functions and the frequency response method described in Chapter 24.

12. Chapter 34 describes and develops the theoretical background for a number of typical integrators and differentiators. These results are reduced to specific nondimensional curves that may be immediately applied to actual components. Chapter 34 also includes a theoretical discussion of analog computers.

13. Chapter 35 describes and discusses the theory of instruments and systems for measuring mechanical vibrations. Because of the close relationship between the theory of vibration-measuring instruments and the theory of vibration isolation, the latter subject is included as a part of the discussion. Nondimensional curves from Chapters 19 and 26 are given specific applications to vibration problems in Chapter 35. The information provided includes not only transient and frequency spectrum results but also pulse function response data. A number of examples based on actual tests are included to demonstrate applications of the theoretical results.

14. An outline of the subject matter covered in Part 2 of Volume III, which starts with Chapter 36, is given in the introduction to that part.

CHAPTER 28

CONCEPTS, DEFINITIONS, DIAGRAMS AND NOTATION FOR DESCRIBING OPERATING COMPONENTS AND OPERATING SYSTEMS

OPERATING COMPONENTS

28.1. Operating components under the definition of Chapter 1 establish functional relationships among physical quantities. In the generalized situation, some of the physical quantities involved are inputs, in the sense that their variations are independent of the action of the operating component, while others are outputs, in the sense that their variations are dependent on the operating component. The concept of the operating system is identical with the concept of the operating component except that the entity considered is some combination of operating components. Because of this similarity, discussions carried out in terms of operating components may also be applied to operating systems.

TRANSDUCERS AND CODUCERS

28.2. Operating components may be classified in many ways. One of the basic characteristics that may be used for classification purposes is the energy flow involved. When the essential input variations are associated with energy that is "carried over" so that (except for losses) it appears as the output, the operating component falls into the class known as transducers.* The essential feature of the transducer is that all the energy in the output actually comes from the input, although certain ambiguities may appear in connection with devices that require excitation power. For example, a loud-speaker that uses direct-current excitation for its field receives power from a source other than the input. However, because the excitation power does not go directly into the output and is actually unnecessary when a permanent magnet field is used, the loud-speaker – which receives electrical power as its input and (except for losses) produces sound-wave power as its output – is definitely a transducer.

28.3. Any device that depends not upon the input but upon an auxiliary source of energy for the power associated with the output may be classified as a coducer.**

---

* Webster's New Collegiate Dictionary gives for transducer: "[Latin transducere to lead across.] Physics. A device actuated by power from one system and supplying power to a second system." (By permission. From Webster's New Collegiate Dictionary, copyright, 1949, 1951, by G.&C. Merriam Co.) The Latin roots are trans, over or across, and ducere, to lead.

** Coducer is from the Latin co-, combining form of cum, with; and ducere, to lead. Compare with Webster's

Although the input determines the output, the power associated with the output comes from a supplied power source that either is free from variations or has variations that do not have a primary effect on the power output. In the coducer concept, some part of the output power may be derived from the input, but it is implied that power from this source is relatively unimportant.

REPRESENTATION OF TRANSDUCERS AND CODUCERS

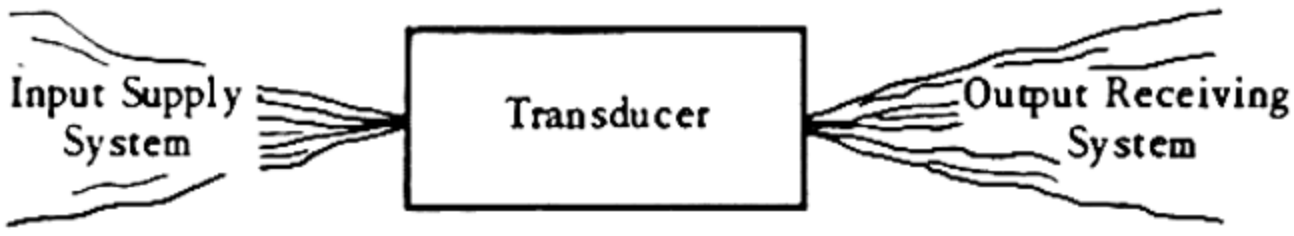
28.4. Section a of Definition Summary 28-1 represents the transducer as receiving energy from an input supply system and delivering this energy to an output receiving system. As shown in section b of the summary, the coducer receives its input (without regard to the energy involved), together with energy from an energy supply system, and produces an output functionally determined by the input and supplied with the necessary energy by the energy supply system.

28.5. Definition Summary 28-2 gives conventional block diagrams that may be used to represent transducers and coducers. In each case, arrows drawn from left to right show the direction from the independent variable toward the dependent variable so far as the operating component is concerned. The input quantity, or input, is represented by the lower-case letter q, for quantity, with (in) as its subscript. Similarly, the output quantity, or output, is represented by q with the subscript (out). Supplied power for the coducer is represented by an arrow drawn toward the rectangle of the diagram in a direction at right angles to the input-output direction. The symbol for supplied power is the capital letter P, for power, with (sup), for supplied, as its subscript. Because the important characteristics of the coducer are normally determined by the input-output relationships it establishes, rather than by its power consumption, the arrow representing supplied power is generally omitted from coducer diagrams. This means that, from the standpoint of representation, the conventional operating component diagram (similar to that in Fig. 1-2b of Chapter 1) may be used for either the transducer or the coducer, with no necessity for specifying which is involved.

28.6. Section a of Definition Summary 28-3 represents a telephone receiver as a transducer that receives an electrical voice signal as its input and produces sound energy as its output. The symbol for the input is (S_g), for signal, with (voice) as its identifying subscript. The output symbol is (E), for energy, with (sound) as its subscript. These two representations are simple illustrations of the conventions described in Chapter 1 for using self-defining symbols.

28.7. Section b of Definition Summary 28-3 shows the amplifier as a coducer.

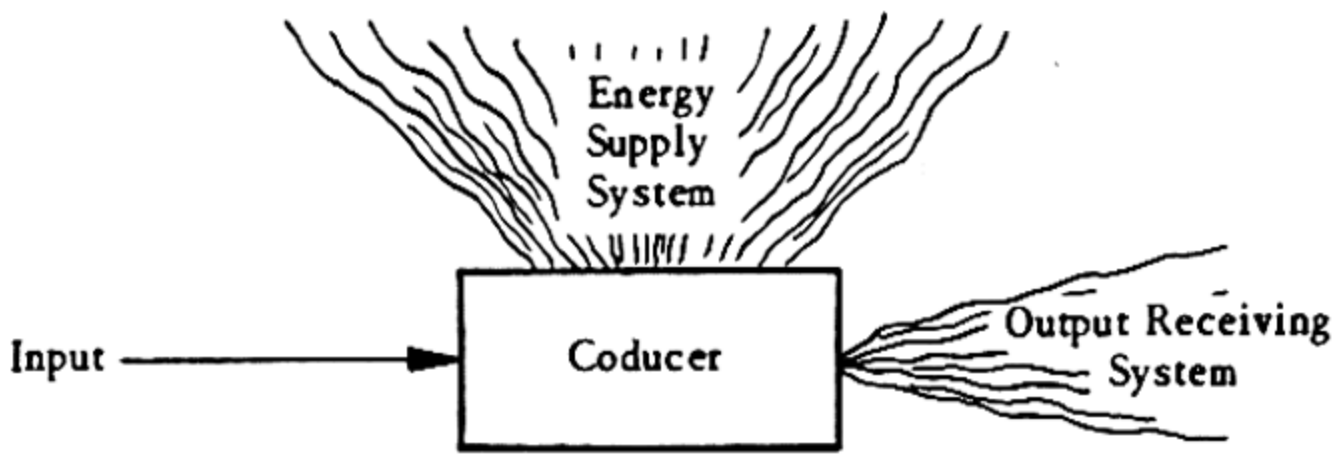
New Collegiate Dictionary: co-"... signifies in general with, together, in conjunction, jointly." (By permission. From Webster's New Collegiate Dictionary, copyright, 1949, 1951, by G.&C. Merriam Co.) The word "coducer" is based on a suggestion by Henry B. Brainerd of the Instrumentation Laboratory, Massachusetts Institute of Technology.



The transducer receives an input associated with energy from one system and supplies its output associated with this energy (or this energy reduced by losses in the transducer) to a second system.

Note: Energy that is supplied to maintain transducer operation but does not directly appear in the output is immaterial as far as the transducer definition is concerned.

a) Defining diagram for transducers

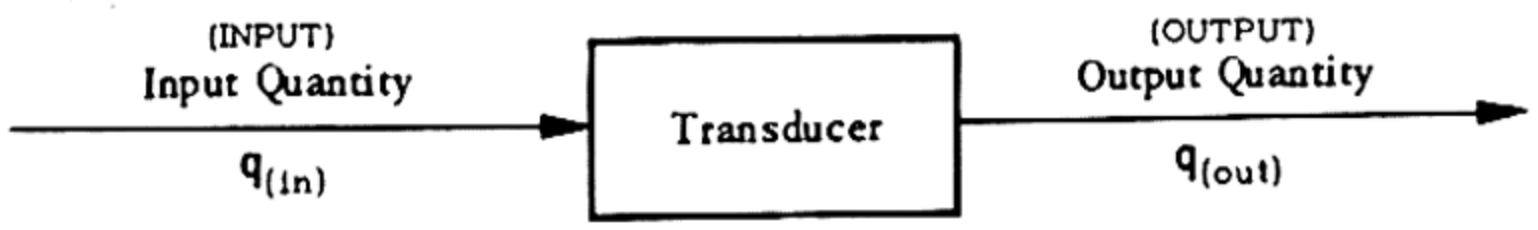


The coducer receives energy from an energy supply system. This energy is supplied with the output to the output receiving system. Output variations are determined by input variations.

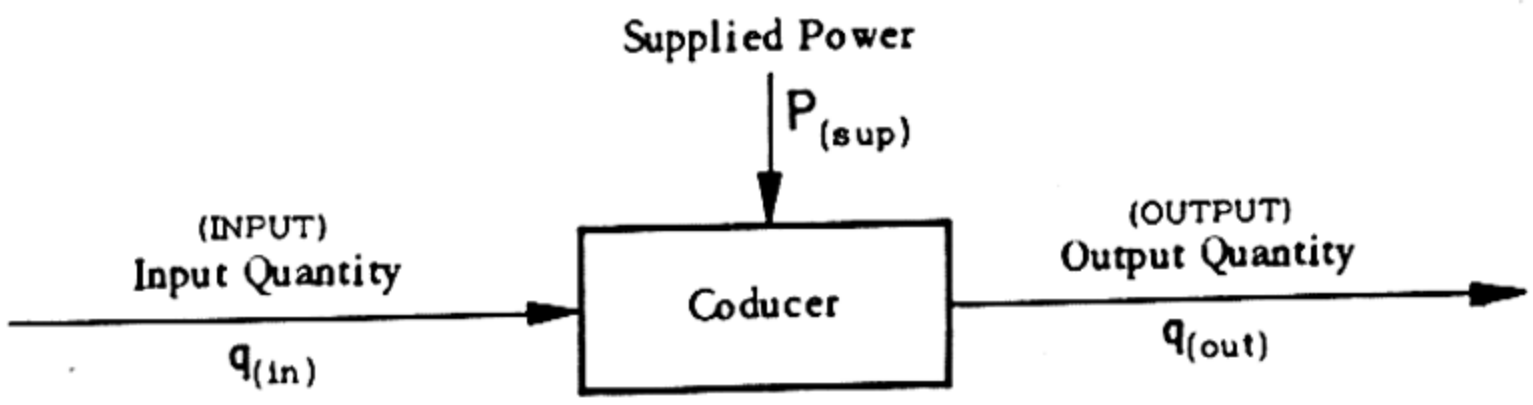
Note: Relatively small amounts of energy supplied to the output from the input are immaterial as far as the coducer definition is concerned.

b) Defining diagram for coducers

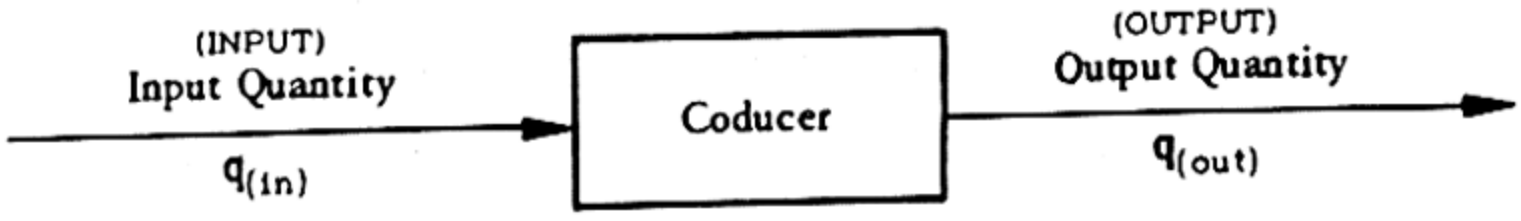
Definition Summary 28-1. Defining diagrams for transducers and coducers.



a) Conventional diagram for transducers



or

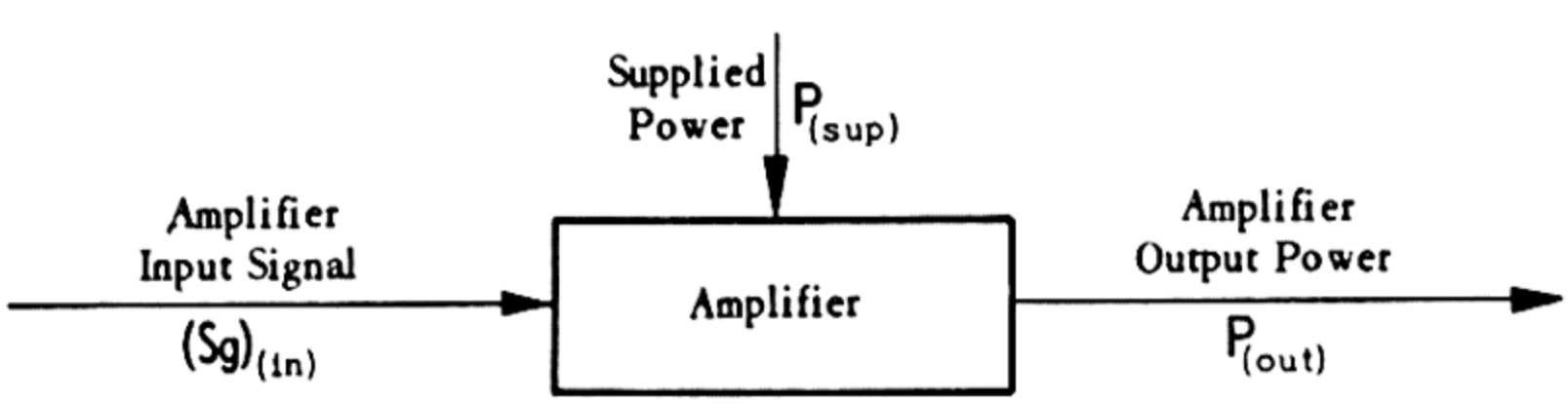


b) Conventional diagrams for coducers

Definition Summary 28-2. Conventional diagrams for transducers and coducers.

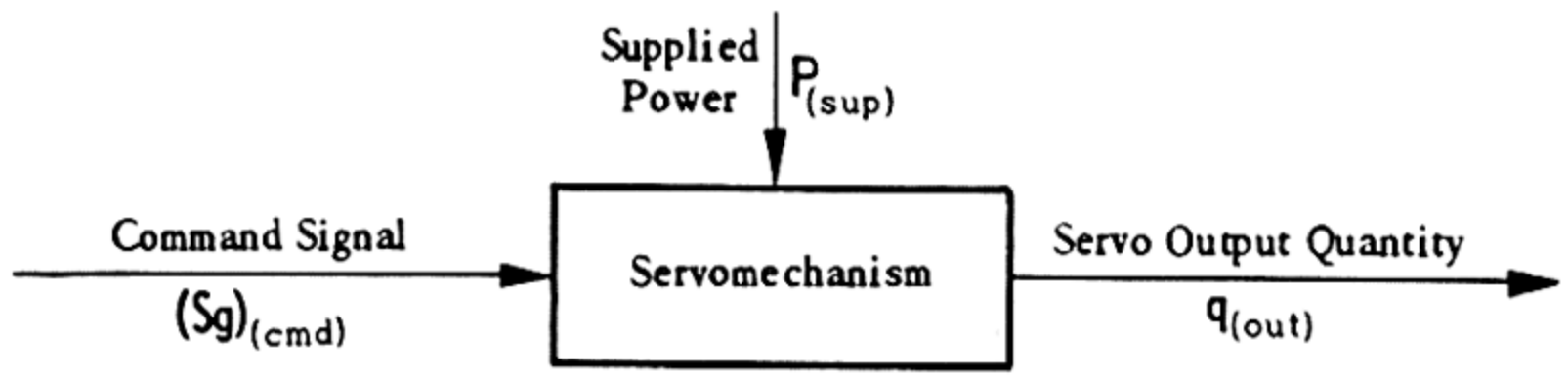


a) The telephone receiver as a transducer



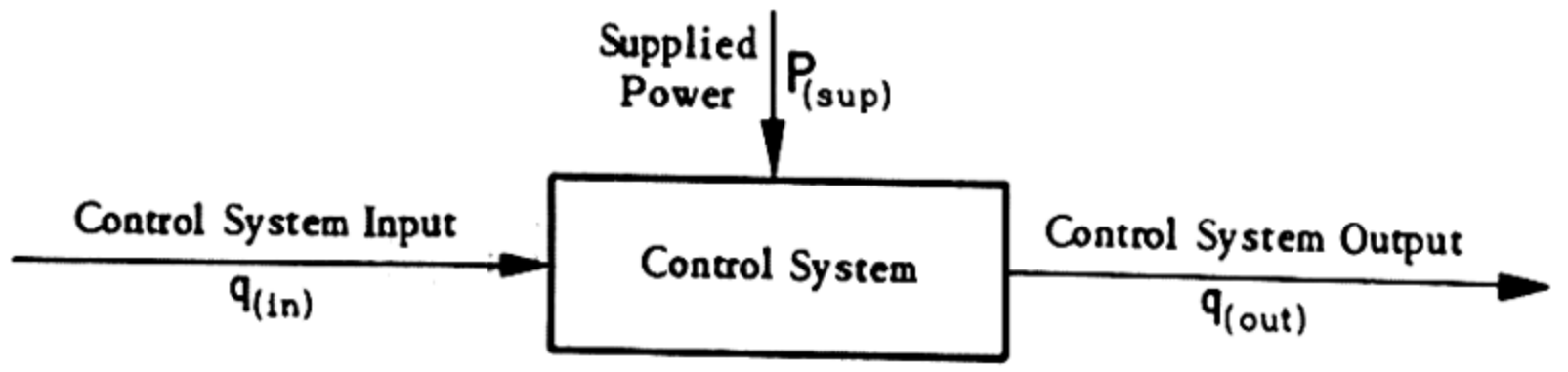
The energy components associated with the input, the supplied power, and the output power of the amplifier have the same physical form.

b) The amplifier as a coducer



The servo output quantity is a mechanical position (A4). The command signal is either a mechanical position or some quantity that may be associated with a mechanical position. The supplied power may be mechanical power or any other suitable form of energy.

c) The servomechanism as a coducer



Input, supplied power, and output are (except for special cases) different physical quantities.

d) The control system as a coducer

Definition Summary 28-3. Transducer and coducer examples.

The noteworthy characteristic of the amplifier is that the input, the supplied power, and the output have the same physical form. Section c of the summary shows the servomechanism as a coducer whose output quantity is mechanical position. The control system of section d is a coducer in which (except for special cases) the input, the supplied power, and the output are all different physical quantities.

REPRESENTATION OF OPERATING COMPONENTS

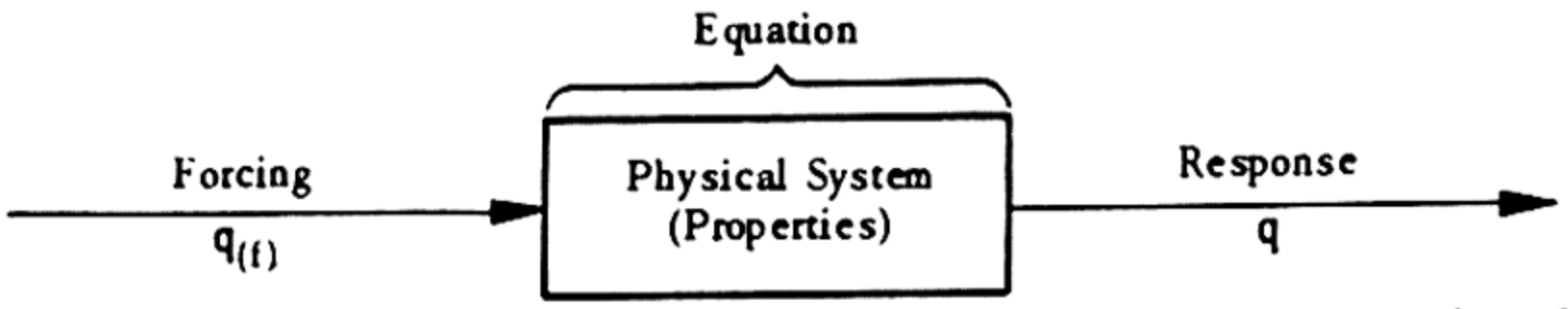
28.8. Definition Summary 28-4 gives eight block diagrams that represent essentially similar physical situations. The first seven diagrams illustrate the operating component concept as it is used by various authors in the field of measurement and control. Eckman,[E2] Oldenbourg and Sartorius,[O1] Ahrendt and Taplin,[A1] Behar,[B2] and the authors of this book either leave the rectangle of the block diagram blank or write in a name. On the other hand, Brown and Campbell[B4] and Chestnut and Mayer[C1] identify the block with mathematical symbols.

28.9. Section h of Definition Summary 28-4 is a functional diagram for the diaphragm-type pressure receiver of the pressure gage described in Chapter 2. In this special case of the generalized operating component diagram of section g, the input symbol $q_{(in)}$ becomes $p_{(in)}$ for input pressure, and the output symbol $q_{(out)}$ becomes $d_{(pr)}$ for pressure receiver output displacement. The name within the block is accompanied by (pr) for pressure receiver, as the identifying symbol.

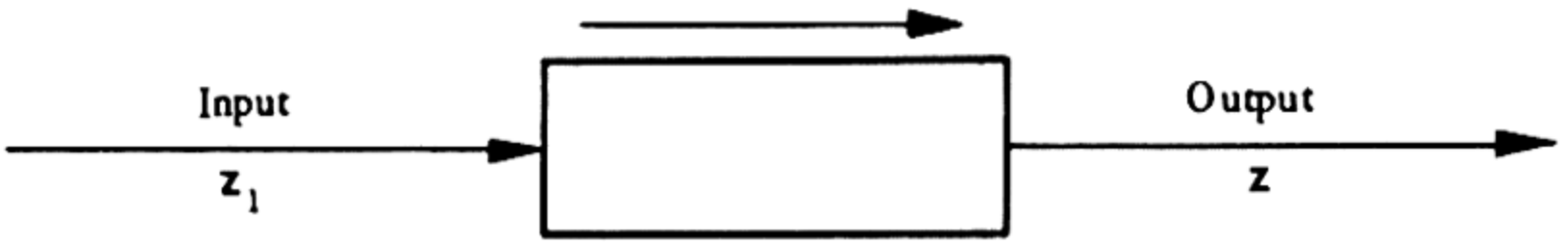
REPRESENTATION OF SYSTEMS FORMED BY COMBINATIONS OF OPERATING COMPONENTS

28.10. Operating systems are made up of combinations of operating components that form either open-chain or closed-chain patterns as these concepts are defined in Chapter 1. As noted in the previous section, the rectangles of the functional diagram for an operating system may be labeled with names or mathematical expressions. When names are used, several methods for generating terminology may be applied:

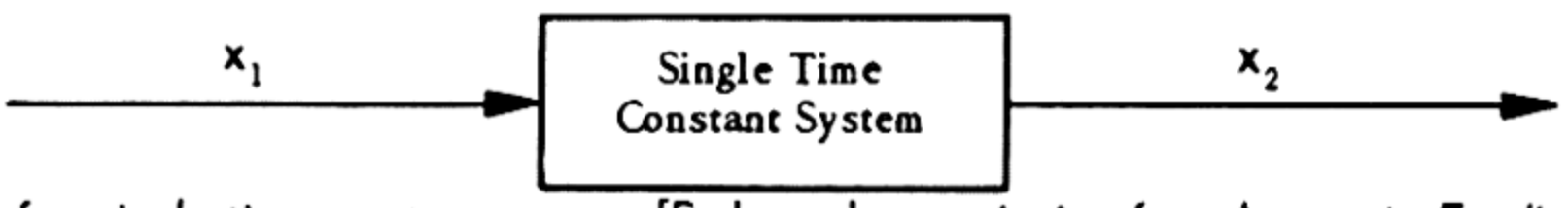
1) Operating components may be named on the basis of their importance in the system. When this plan is used, one component may be called the primary component; another, the secondary component; etc.
2) Operating components may be named on the basis of their position in the chains of the system. When this plan is used, one component may be the initial component, while another is the final component or the end component.
3) Operating components may be given descriptive proper names. For example, the pressure receiver of the pressure gage of Fig. 2-2 in Chapter 2 is also called the diaphragm unit.
4) Operating components may be given functional names that describe their action in relating outputs to inputs. For example, the diaphragm unit of



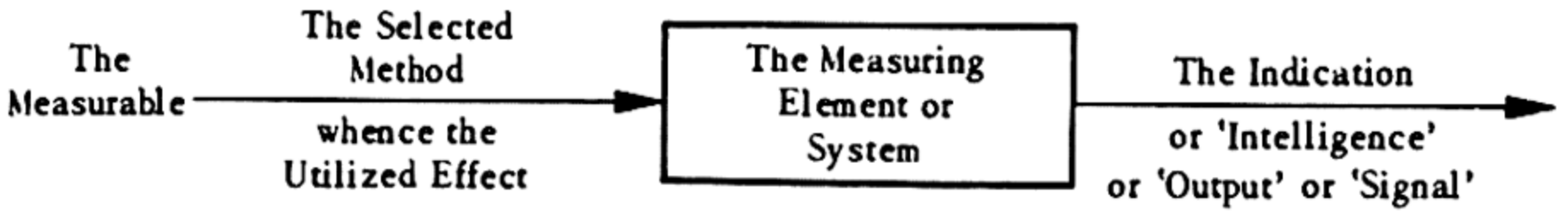
a) *Physical system representation.* [Redrawn by permission from D.P. Eckman, *Principles of Industrial Process Control*, 1945, John Wiley & Sons, Inc. (E2).]



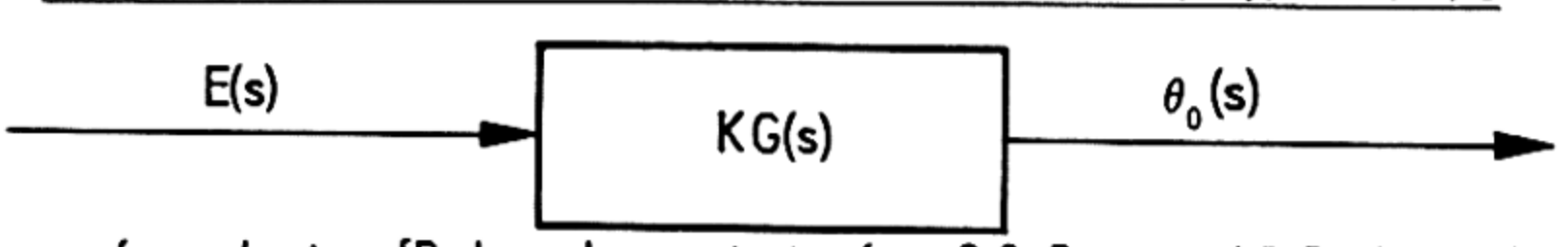
b) *Diagram of a linear transfer system.* [Redrawn by permission from R. C. Oldenbourg and H. Sartorius, *The Dynamics of Automatic Controls*, 1948, The American Society of Mechanical Engineers (01).]



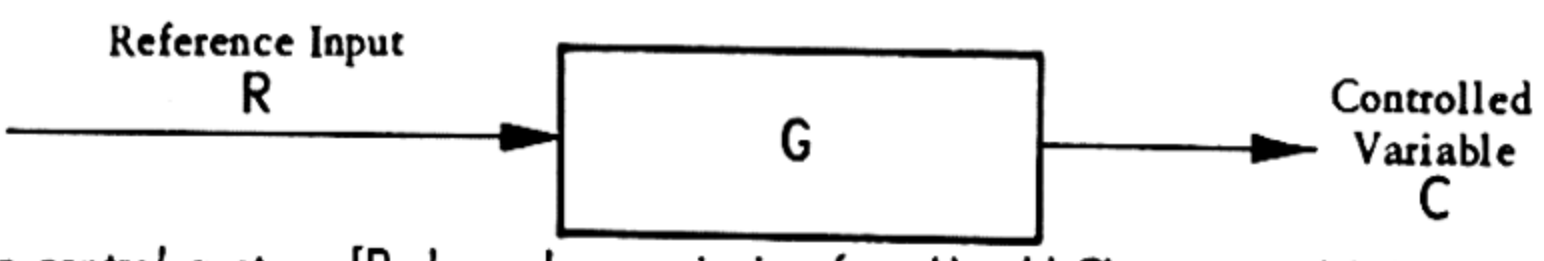
c) *Diagram of a single time constant system.* [Redrawn by permission from *Automatic Feedback Control* by W.R. Ahrendt and J.F. Taplin. Copyright, 1951. McGraw-Hill Book Company, Inc. (A1).]



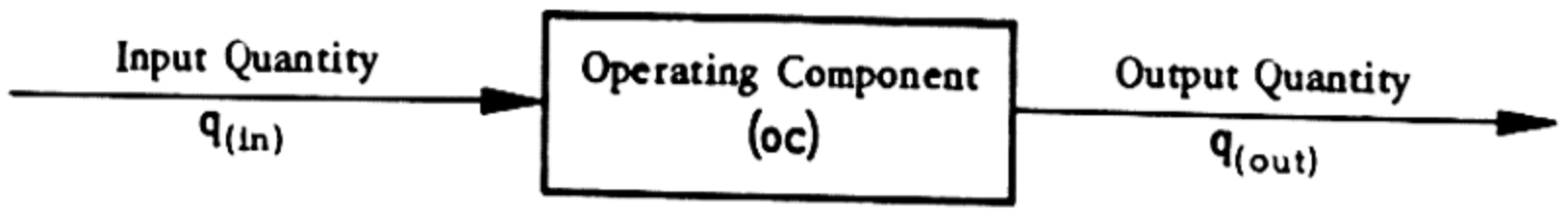
d) *Diagram of a measuring system.* [Redrawn by permission from M.F. Behar et al, *The Handbook of Measurement and Control*, 1951, The Instruments Publishing Company, Inc. (B2).]



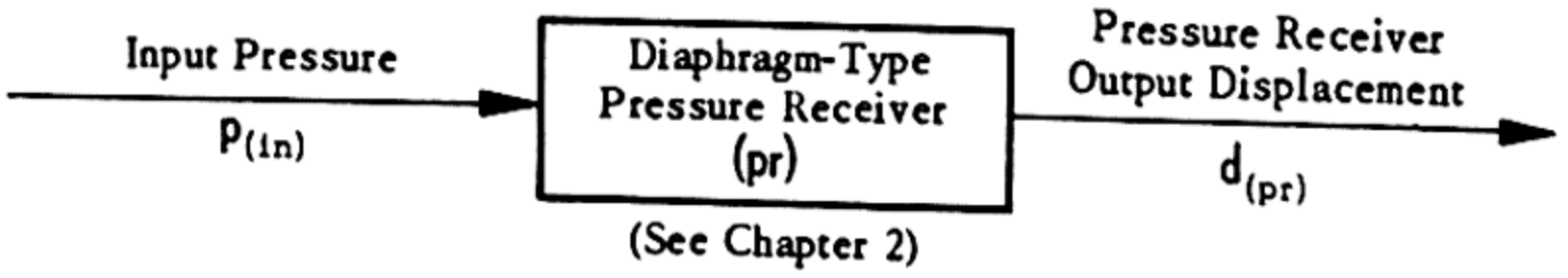
e) *Block diagram of a mechanism.* [Redrawn by permission from G.S. Brown and D.P. Campbell, *Principles of Servomechanisms*, 1948, John Wiley & Sons, Inc. (B4).]



f) *Open-loop control system.* [Redrawn by permission from Harold Chestnut and R.W. Mayer, *Servomechanisms and Regulating System Design*, 1951, John Wiley & Sons, Inc. (C1).]



g) *Operating component diagram using the conventions of Instrument Engineering*



h) *Diaphragm-type pressure receiver as an operating component*

Definition Summary 28-4. Comparison of conventions for operating component diagrams.

Fig. 2-2 is a pressure input – deflection output transducer, or a pressure receiver.

28.11. Section a of Definition Summary 28-5 is the functional diagram for an open-chain system after Behar.[B2] It will be noted that a combination of methods 1 and 2 is used, with the first component of the open chain called the primary element, and the last component called the final element. Section b of Definition Summary 28-5 shows the combination of a block diagram and a schematic diagram as given by Eckman.[E2] The schematic diagram is labeled with descriptive proper names, while a combination of "importance" names and "functional" names is used on the block diagram. Sections c, d, e and f of Definition Summary 28-5 are based on Figs. 2-2, 2-3, 2-6 and 2-8 to illustrate the use of proper names and functional names, with the corresponding symbols, to describe the essential features of a diaphragm-type pressure gage as an operating system. A further discussion of this example is omitted here because of the detailed treatment available in Chapter 2.

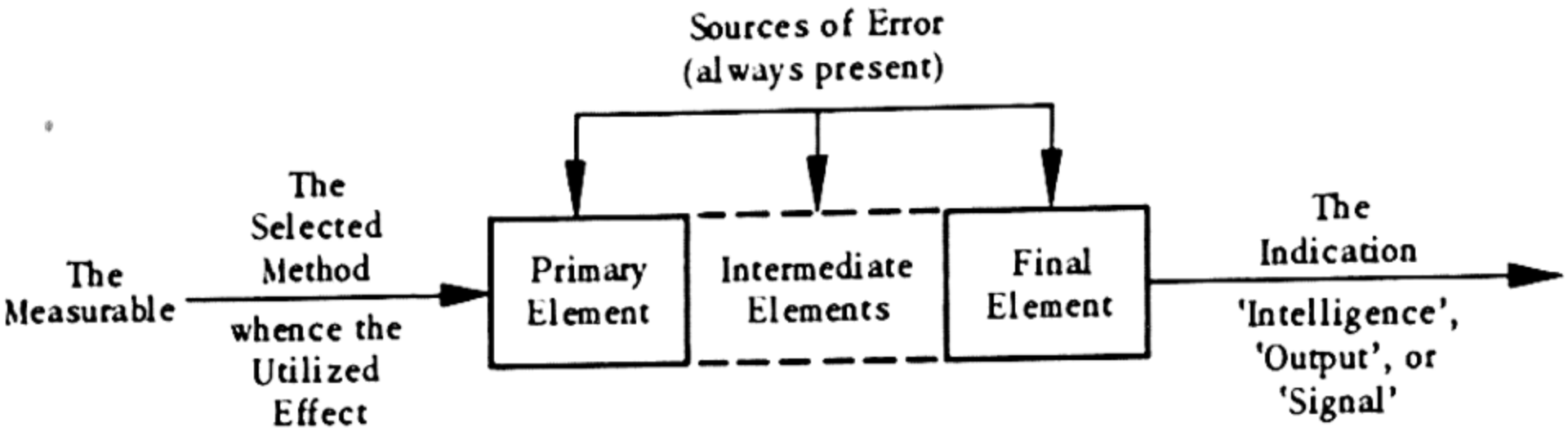
CONCEPTS, TERMINOLOGY, AND SYMBOLS FOR DESCRIBING STATIC PERFORMANCE OF OPERATING COMPONENTS

28.12. The concepts of static and dynamic operating conditions are defined and discussed in Chapter 4. By definition, static conditions exist for an operating component when both its input and its output are constant. Under static conditions, the concept of static sensitivity defined and discussed in Chapters 4 and 5 describes the performance of an operating component.* Static sensitivity for an operating component is defined in Chapter 4 as the ratio of a small change between constant output levels to the corresponding small change between constant input levels. This definition follows the context of the definition given for sensitivity by Webster's New Collegiate Dictionary: "sensitivity . . . 1. Quality or state of being sensitive. 2. Psychol. The capacity of an organism or of a sense organ to respond to stimulation; irritability; also the degree of such responsiveness. 3. Radio. The degree to which a receiving set responds to incoming waves."** Thus, sensitivity, as the term is used in Instrument Engineering, implies that the component or system to which it is applied has the "capacity of responding" to inputs (corresponding to stimulation in psychology). Quantitatively, the numerical measure of sensitivity for a given instrument describes the "degree of responsiveness" of the instrument. For example, if under static conditions one indicator has an index angle of ten degrees for the same input that gives twenty degrees index angle on a second indicator, the second indicator has a sensitivity twice as great as the sensitivity of the first indicator.

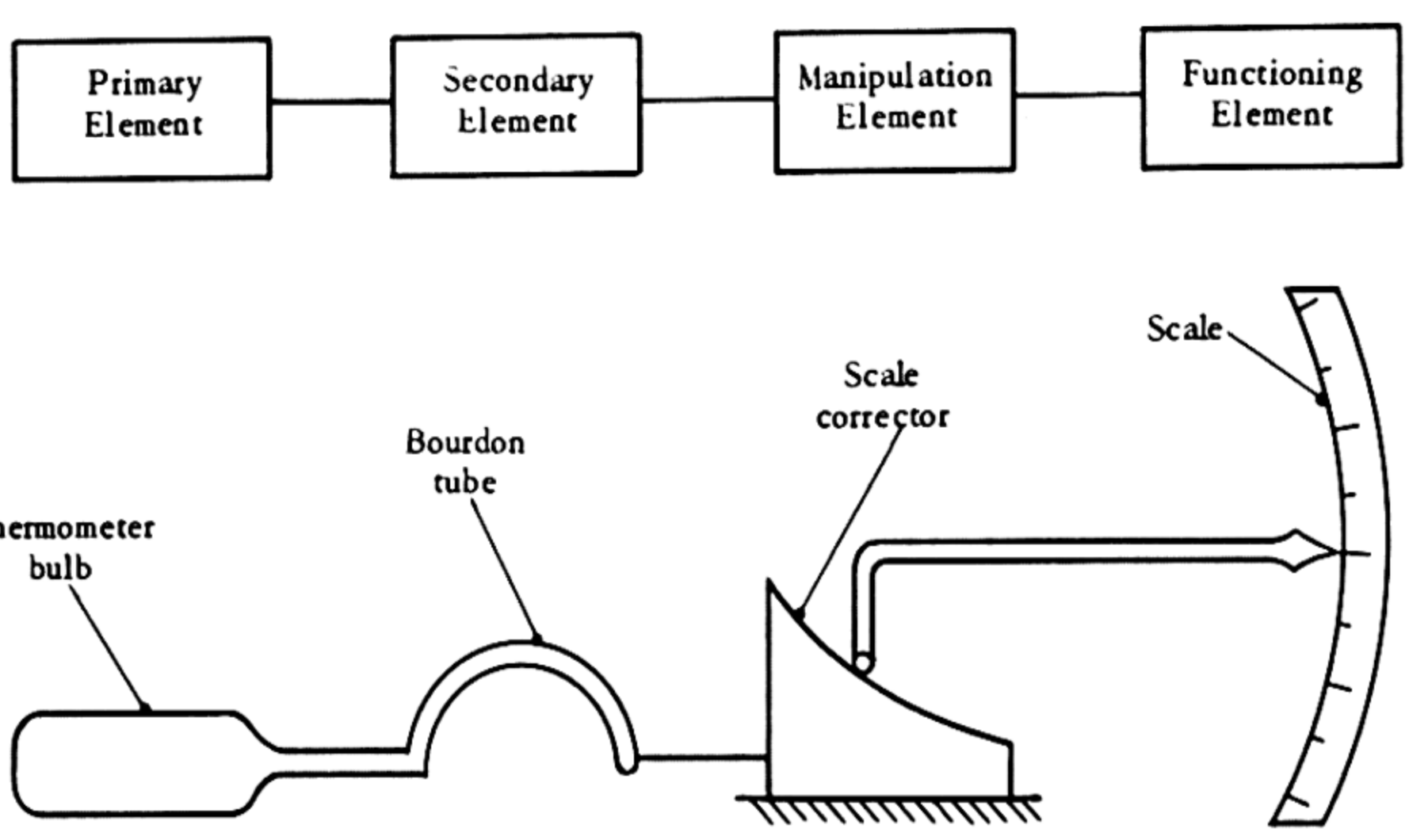
---

* Actually, static sensitivity does not completely describe static performance unless the operating component considered is an ideal component. This matter is discussed in later chapters.

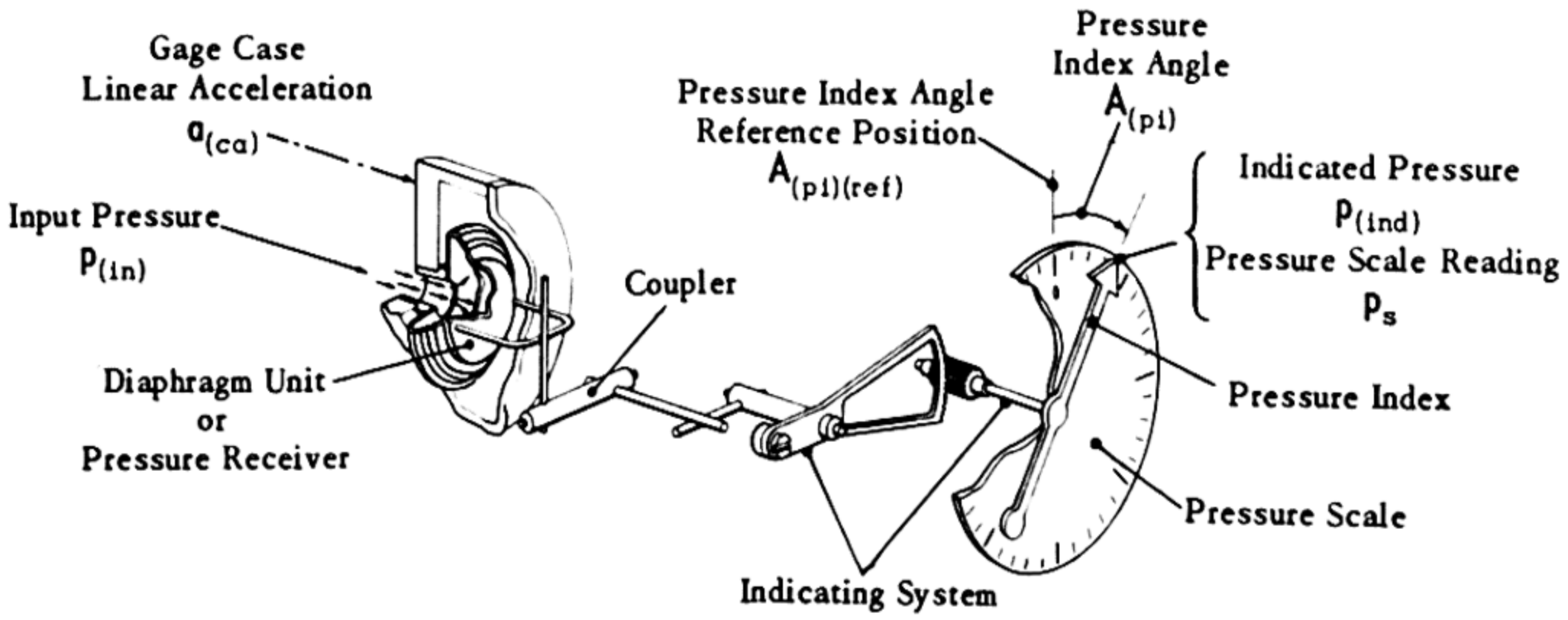
** By permission. From Webster's New Collegiate Dictionary, copyright, 1949, 1951, by G.&C. Merriam Co.



a) *The self-operating measuring instrument.* [Redrawn by permission from M.F. Behar et al, *The Handbook of Measurement and Control*, 1951, The Instrument Publishing Company, Inc. (B2).]



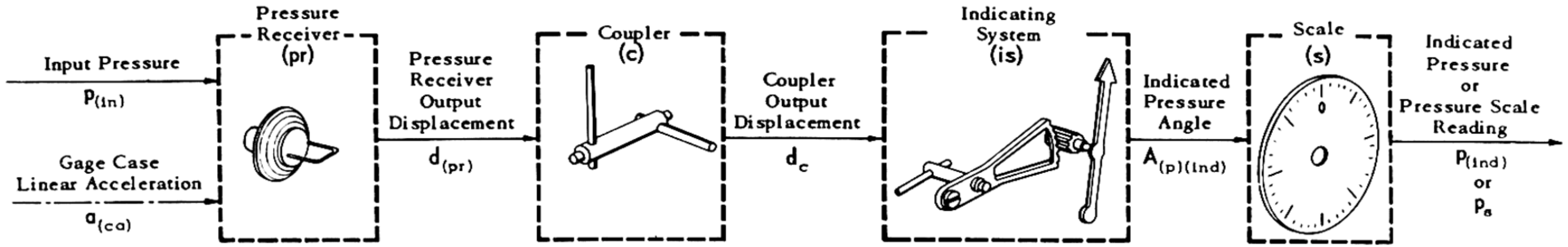
b) *Elements of an instrument.* [Redrawn by permission from D. P. Eckman, *Principles of Industrial Process Control*, 1945, John Wiley & Sons, Inc. (E2).]



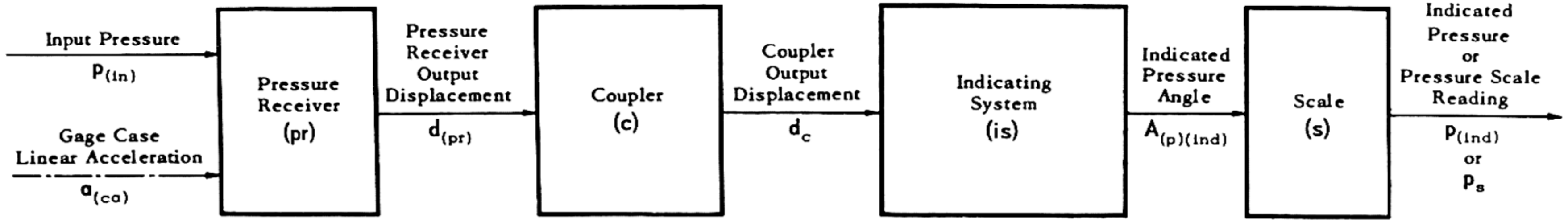
Note: Actuating inputs are represented by full lines. Interfering inputs are represented by dot-and-dash lines. Modifying inputs (none appear in this diagram) are represented by dashed lines.

c) *Illustrative pictorial schematic diagram for a diaphragm-type pressure gage*

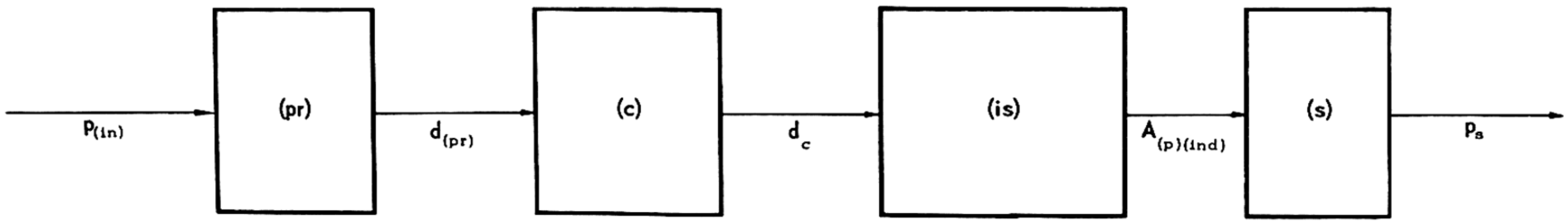
Definition Summary 28-5. Conventions for representing measuring instruments. (Page 1 of 2)



d) Illustrative pictorial-functional diagram for a diaphragm-type pressure gage



e) Illustrative functional diagram for a diaphragm-type pressure gage



f) Illustrative symbol diagram for a diaphragm-type pressure gage

Definition Summary 28-5. Conventions for representing measuring instruments. (Page 2 of 2)

28.13. The definition of static sensitivity given in Chapter 4 is in complete agreement with the definition of the same term listed among the basic terms in "Automatic Control Terminology,"[A5][A6] the report of the Terminology Committee of the Industrial Instrument and Regulators Division of the American Society of Mechanical Engineers (ASME). This reference states:

> SENSITIVITY *is the ratio of output response to a specified change in the measured variable.* For example, an automatic temperature controller having a net output pressure of 15 psi and a full scale range of 0 degree to 150 degrees F would have a sensitivity of 0.1 psi per degree F. Where nonlinear relationships are involved, the point or points at which the sensitivity is given should be stated.

28.14. Definition Summary 28-6 gives the basic defining equation for static sensitivity in physical representation terms and also in working variable terms. In this summary, information on the physical representation terms is placed above the conventional functional diagram for an operating component, and the same information in corresponding working variable terms is placed in a "mirror image" position below the diagram.

28.15. The basic equation of static performance in section a of Definition Summary 28-6 states that the input multiplied by a coefficient b_0 is equal to the output multiplied by another coefficient a_0. The definition of static sensitivity given in section b shows that this concept is the ratio of small changes between static levels of the output to the associated small input changes. The corresponding equation in section a shows that the sensitivity reduces to the ratio of b_0 to a_0. Section b also summarizes the conventions used to form identifying subscripts for the main symbol S, used to represent sensitivity. The subscript (id) associates the sensitivity with a given operating component, the input-output bracket shows the input and the output considered, and the subscript (st) associates the sensitivity with static conditions.

28.16. As already described, the sensitivity symbol makes it possible to read off immediately the component with which the sensitivity is associated, the input-output combination on which the sensitivity is based, and the operating conditions considered. This information is only part of the data that may be supplied by a generalized performance-describing symbol formed under the conventions described in Chapter 10. These conventions make it possible to write self-defining symbols for any characteristic of an operating component, subsystem or system, however complex, by the application of a few simple rules and a properly drawn functional diagram with names and symbols assigned to the essential parts and quantities. For example, the pressure input – displacement output static sensitivity for the pressure receiver of section f of Definition Summary 28-5 has the symbol $S_{(pr)[p;d](st)}$. In physical terms, this sensitivity is the ratio of the diaphragm output displacement to the corresponding pressure input.

PHYSICAL REPRESENTATION TERMS

Under static conditions (i.e., all derivatives of $q_{(in)}$ and $q_{(out)}$ are zero), the static performance equation is

$$a_0 q_{(out)} = b_0 q_{(in)}$$

$$\left[\frac{dq_{(out)}}{dq_{(in)}}\right]_{(st)} = \frac{b_0}{a_0} = S_{(id)[q_{(in)};q_{(out)}](st)}$$

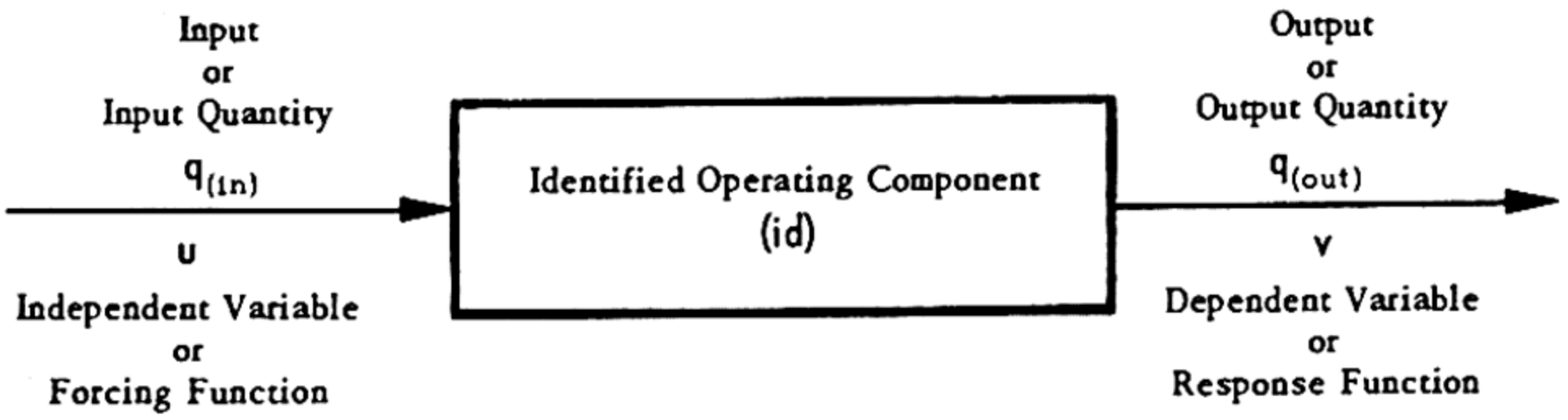
where

$S_{(id)[q_{(in)};q_{(out)}](st)}$ = input quantity – output quantity static sensitivity

(See Chapters 3 and 4.)

The concept of static sensitivity is similar to

Gain, (symbol G) (T1)(B4)(A1)(C1)
Scale Factor, (symbol SF) (Z1)
Gradient, (symbol Gr)*
Sensitivity Factor, (symbol K) (B4)
Proportionality Factor, (symbol $1/\zeta$) (O1)



(See Volume II: Introduction, Chapter 14, and Chapter 17)

(See Volume II: Introduction, Chapter 14, and Chapter 17)

WORKING VARIABLE TERMS

The static performance equation in working variable terms is

$$\gamma_0 V = \sigma_s \nu_{(0-0)} \gamma_0 U$$

(See Definition Summaries 14-1 and 18-1.)

When $\nu_{(0-0)} = 1$ and $\sigma_s = \sigma$,

$$V = \sigma U$$

where

σ = dimensional similarity factor

(See Definition Summary 14-1.)

a) Diagram, symbols and forms for describing operating component performance

* In field theory, the symbol for gradient is grad or ∇ (F2).

Definition Summary 28-6. Description of operating component static performance in physical representation terms and in corresponding working variable terms. (Page 1 of 2)

Note:

1. By definition, static sensitivity (see Fig. 4-1 of Chapter 4) is the ratio of small changes between constant levels of the output quantity to the corresponding small changes between constant levels of the input quantity.
2. This relationship is a special case in which the output is a linear function of the input.
3. a) The main symbol S represents sensitivity.
   b) The first subscript parenthesis symbol identifies the operating component whose static performance is described by the complete symbol.
   c) The square subscript bracket is the input-output bracket.
   d) The subscript symbol inside the square bracket nearest the main symbol represents the input quantity.
   e) The subscript symbol inside the square bracket separated from the input quantity symbol by a semicolon represents the output quantity.
   f) The subscript (st) following the input-output bracket identifies the sensitivity as being associated with static conditions.
4. The present application of the term sensitivity is a special case of a much broader definition given later in the book.

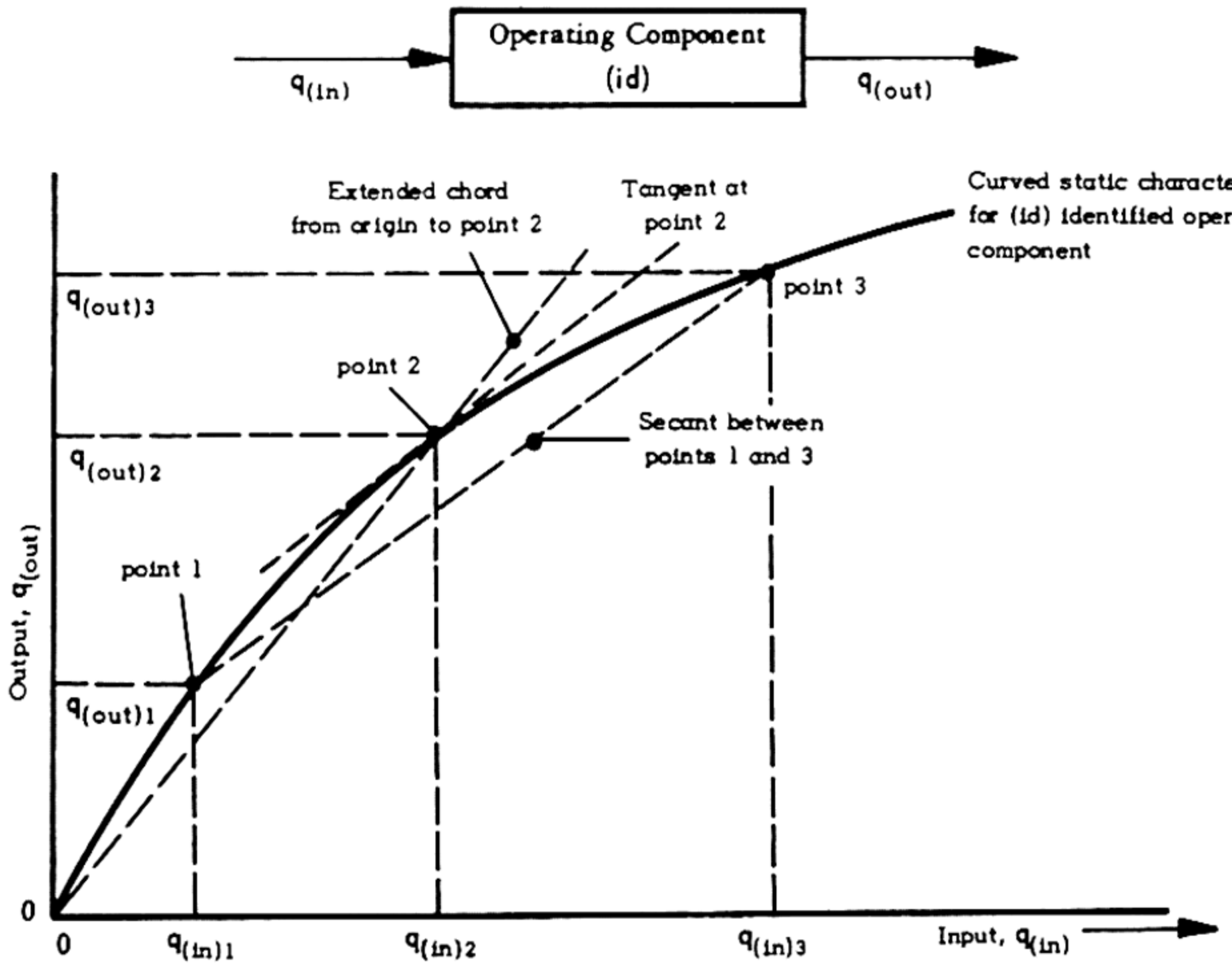
b) Definition of static sensitivity

Definition Summary 28-6. Description of operating component static performance in physical representation terms and in corresponding working variable terms. (Page 2 of 2)

TANGENT, CHORD, AND SECANT DEFINITIONS OF SENSITIVITY

28.17. The concept of sensitivity may be generalized so that it applies under dynamic conditions by defining sensitivity (without the qualifying word "static") as the ratio of the time rate of change of the output to the corresponding time rate of change of the input. This interpretation of sensitivity is illustrated in Fig. 4-2. In Chapter 13, sensitivity is identified with the input-output dynamic amplitude ratio for steady-state sinusoidal variations. When it is considered that sensitivity describes only the magnitude effect associated with sinusoidal response, it appears that the representation illustrated in Fig. 4-2 is consistent with the dynamic amplitude ratio definition given in Chapter 13.

28.18. For engineering applications, several sensitivity definitions are useful, depending on the nature of the relationship that exists between small output changes and the corresponding small input changes for various input levels. When the input-output relationship is linear in the sense that it may be represented by a single straight line passing through the origin, sensitivity may be represented by a single constant. On the other hand, when the input-output characteristic is a curved line, three definitions of sensitivity are possible. These three definitions are illustrated in Fig. 28-1. In this diagram, tangent sensitivity corresponds to the slope of the input-output characteristic at the point for which the sensitivity is specified. When the characteristic is a curve passing through the origin, the chord sensitivity is represented by the slope of the chord drawn from the origin through the point at which the sensitivity is defined. For any type of input-output



Tangent definition of sensitivity: Tangent sensitivity at point 2

$$S_{(id)[q_{(in)};q_{(out)}](tan)2} = \frac{dq_{(out)2}}{dq_{(in)2}} = \text{slope of curved static characteristic at point 2}$$

Chord definition of sensitivity: Chord sensitivity at point 2

$$S_{(id)[q_{(in)};q_{(out)}](ch)2} = \frac{q_{(out)2}}{q_{(in)2}} = \text{slope of chord from origin to point 2}$$

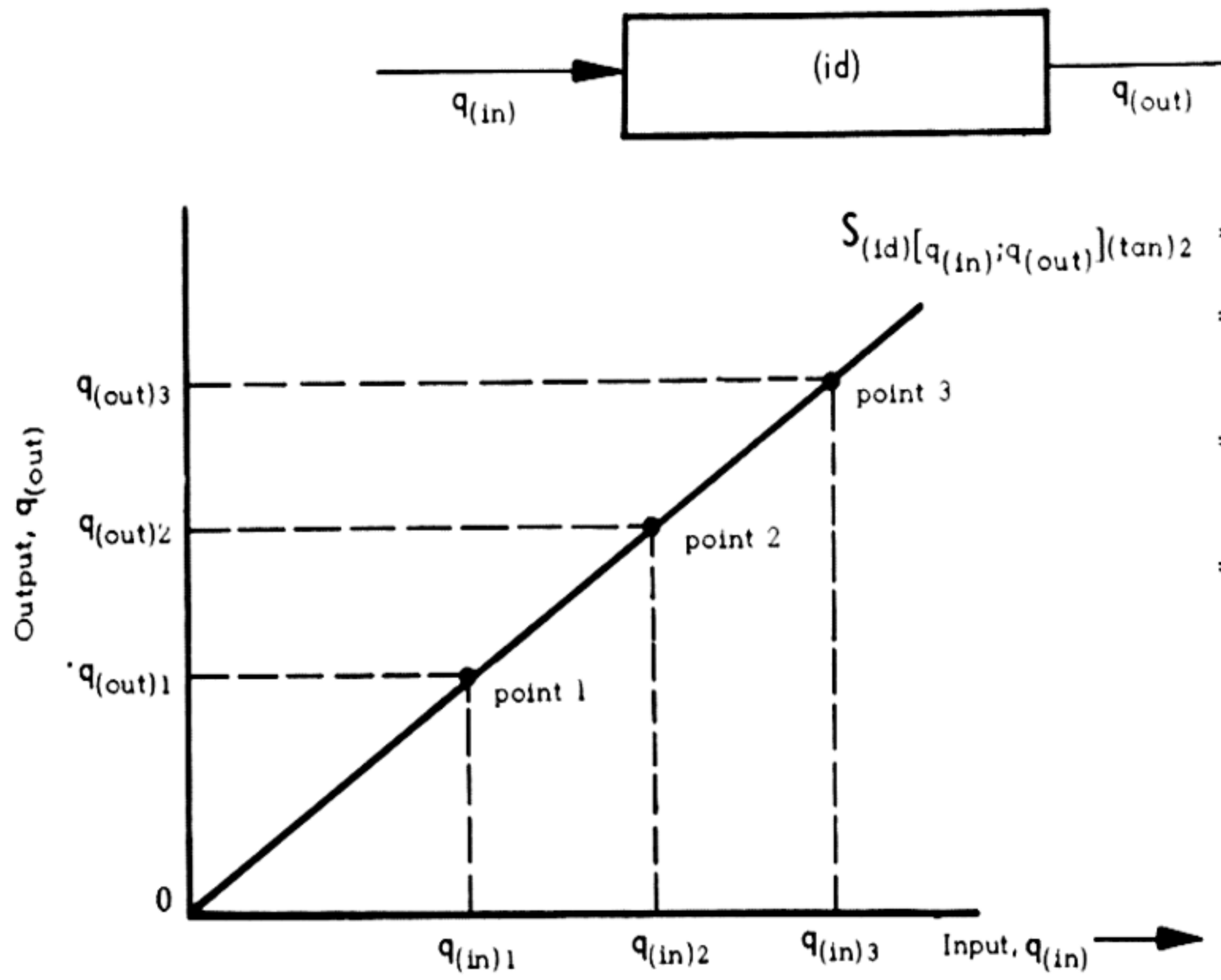
Secant definition of sensitivity: Secant sensitivity between points 1 and 3

$$S_{(id)[q_{(in)};q_{(out)}](sec)1,3} = \frac{q_{(out)3} - q_{(out)1}}{q_{(in)3} - q_{(in)1}} = \text{slope of secant between points 1 and 3}$$

Fig. 28-1. Tangent, chord, and secant definitions of sensitivity for an operating component with a curved input-output characteristic.

characteristic curve, the secant sensitivity associated with the region in the vicinity of two points on the curve is defined as the slope of the secant drawn between the two points. It is obvious that the secant sensitivity approaches the tangent sensitivity as the two points approach a single point. Similarly, the secant sensitivity approaches the chord sensitivity when one of the two defining points approaches the origin of the characteristic.

28.19. Figure 28-2 illustrates the simplifications that appear when the input-output characteristic becomes a straight line passing through the origin. In this situation, the tangents, chords, and secants for any point on the characteristic reduce to the same single line that is coincident with the characteristic itself. This means that a single constant may be used to represent sensitivities of all three types.



Straight line input-output characteristic passing through zero gives constant sensitivity.

Chord sensitivity, tangent sensitivity and secant sensitivity are identical and are constant, if input-output characteristic is a straight line.

When sensitivity is constant the subscript designations (ch), (tan), or (sec) are unnecessary and can be omitted, so the symbol for sensitivity becomes

$$S_{(id)[q_{(in)};q_{(out)}]}$$

where

$$S_{(id)[q_{(in)};q_{(out)}]} = \frac{q_{(out)}}{q_{(in)}} = \text{constant}$$

Fig. 28-2. Sensitivity definitions for a linear input-output characteristic passing through the origin.

28.20. The illustrations of Figs. 28-1 and 28-2 have been drawn in terms of generalized input and output quantities. It is obvious that the sensitivity definitions may be applied to any given operating component or operating system by substituting the proper identifying subscripts in the sensitivity symbols.

WORKING VARIABLE SYMBOLS FOR DESCRIBING STATIC PERFORMANCE

28.21. In section a of Definition Summary 28-6, working variable terms are placed below the functional diagram to show the correspondence with the physical representation terms discussed above. The symbol u for the independent variable corresponds to the input, $q_{(in)}$; the symbol v for the dependent variable corresponds to the output, $q_{(out)}$; and the symbol σ for the dimensional similarity factor corresponds to the static sensitivity. For any given practical case, all mathematical procedures would be carried out in the working variable symbols, which are deliberately chosen to be as simple as possible. In general, only one set of working variables appears in the formal procedures for finding solutions to any given problem.

A few loosely applied conventions are used to give some assistance in identifying patterns that may appear in solutions. When mathematical reasoning is to be employed for any given physical situation, a necessary step is to set up a table showing the working variable symbols that correspond to the physical representation symbols used in the formation of performance equations and the interpretation of results. For example, the working variable equation for the pressure receiver illustration would have u corresponding to $p_{(in)}$, v corresponding to $d_{(pr)}$, and σ corresponding to the pressure-deflection static sensitivity. For convenience in relating the concept of static sensitivity to the terminology used by various authors in the field of measurement and control, a list of equivalent names and symbols, with references to the Bibliography, is included with the physical representation terms in section a of Definition Summary 28-6.

REPRESENTATION OF GENERALIZED PERFORMANCE OF OPERATING COMPONENTS

28.22. The concepts and methods for representing the generalized performance of operating systems in physical terms are discussed in Chapters 3, 4, 5, 6 and 10. The working variable terms corresponding to these physical terms and the mathematical procedures for associating solutions with the common forms in which they appear are the subject matter of Volume II. Definition Summary 28-7 gives a simplified picture of the basic relationships among physical representation terms and working variable terms. The pattern used is generally similar to that of Definition Summary 28-6 for static performance, with the simple algebraic performance equation forms replaced by generalized integro-differential equations. In physical representation terms, the static sensitivity corresponds to the input quantity – output quantity performance function, which under proper restrictions completely represents the meaning of the performance equation in describing the input-output functional relationships established by the operating component. The performance function symbol is [PF], with identifying subscripts formed by conventions identical with those used in writing static sensitivity symbols. In practice, the performance function is especially useful for describing operating component behavior because it appears as a coefficient of the input in an expression that is easily combined with similar forms. The application of performance functions is subject to certain restrictions that are discussed in detail in Chapter 17. As noted in Definition Summary 28-7, when no misunderstanding is possible, all subscripts except those required to identify the operating component involved may be omitted.

28.23. In working variable terms, an integro-differential equation with $q_{(in)}$ and $q_{(out)}$ replaced by u and v and with a_i and b_j replaced by Greek-letter coefficients corresponds to the performance equation. It is a general procedure to reduce the working variable equation coefficients to dimensionless forms and to give the product $\sigma_s u$ the dimensions of v before mathematical processes are started.

PHYSICAL REPRESENTATION TERMS

The performance equation is:

$$\sum_{i=-r}^{i=n} a_i \frac{d^i(q_{(out)})}{dt^i} = \sum_{j=-s}^{j=m} b_j \frac{d^j(q_{(in)})}{dt^j}$$

(See Chapters 7 and 14.)

Under proper restrictions, the relationships established by the performance equation may be represented by the input quantity – output quantity performance function:

$$[PF]_{(id)}[q_{(in)};q_{(out)}]$$

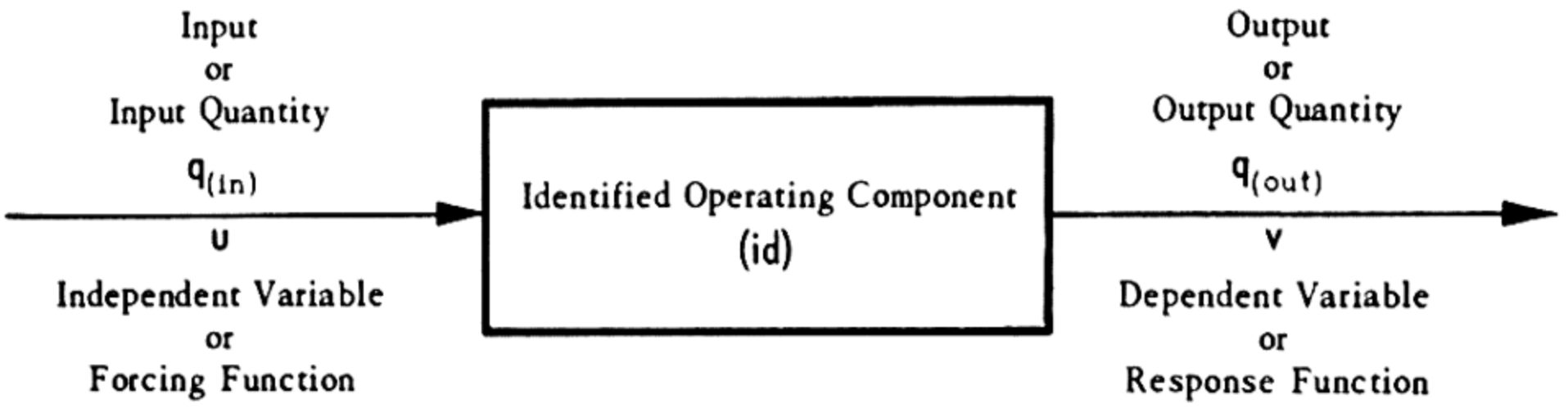
where

$$q_{(out)} = [PF]_{(id)}[q_{(in)};q_{(out)}]q_{(in)}$$

When no misunderstanding is possible, the performance function may be written as

$$[PF]_{(id)}$$

(See Chapters 3, 10, 13, 17, 18 and 19.)



(See Volume II: Introduction, Chapter 14, and Chapter 17.)

(See Volume II: Introduction, Chapter 14, and Chapter 17.)

WORKING VARIABLE TERMS

The working variable integro-differential equation is:

$$\sum_{i=-r}^{i=n} \gamma_i v^{(i)} = \sigma_s \sum_{j=-s}^{j=m} \eta_j u^{(j)}$$

(See Chapters 14, 15, 16 and 17.)

Under special conditions, the relating function

$$\eta \approx [RF]$$

may be used to represent the effect of the working variable equation so that

$$v = \eta u$$

(See Chapters 17, 18 and 19.)

When the working variable differential equation is nonlinear, the procedure discussed in Chapter 27 may be applied.

Note: The performance function and the relating function may be functions either of frequency or of the Laplace transform variable (see Chapter 17).

Definition Summary 28-7. Description of operating component generalized performance in physical representation terms and in the corresponding working variable terms; performance functions and relating functions.

A system of conventions for making this reduction and for transforming performance equations into working variable equations is described in Chapter 14. The relating function (whose working variable symbol is the lower-case Greek letter eta, η) is the working variable form that corresponds to the performance function. The theoretical background of the relating function and the conditions under which it may be used to represent the relationships established by integro-differential equations are discussed in Chapter 17. Chapters 14 through 25 discuss methods for associating response functions with forcing functions when the working variable integro-differential equation is linear and has constant coefficients. Chapter 26 describes procedures for finding solutions for a special nonlinear form of the working variable equation. Chapter 27 gives a number series procedure that may be used with equations that are nonlinear and have nonconstant coefficients.

REPRESENTATION OF STEADY-STATE SINUSOIDAL PERFORMANCE FOR OPERATING COMPONENTS

28.24. Because of its general usefulness for forming Fourier series or integral representations for arbitrary functions (see Chapter 12), the sinusoidal variation is a very important forcing function form. The corresponding steady-state response function may be conveniently expressed as the product of the sinusoidal performance function and the sinusoidal input variation. The corresponding steady-state sinusoidal relating functions are derived and discussed in Chapters 17, 18 and 19.

28.25. Section a of Definition Summary 28-8 lists several forms of the steady-state sinusoidal performance function in physical representation terms and in working variable terms. Section b of Definition Summary 28-8 gives interrelations and definitions for the symbols appearing in section a. A more complete tabulation of sinusoidal performance function expressions is given in Chapter 13. That chapter also contains a discussion of the physical and geometrical interpretations that may be associated with the various sinusoidal performance function forms.

28.26. The use of steady-state sinusoidal response to describe the action of operating components was originated and developed to a high level of effectiveness by scientists and engineers* working in the fields of electrical circuit analysis, communications, and servomechanisms. The literature on this subject has produced several names and symbols for a concept that is generally identical with the steady-state sinusoidal performance function or the sinusoidal relating function. Section a of Definition Summary 28-9 shows the sinusoidal performance function representation of operating component action. Section b of this summary lists the names and symbols associated with sinusoidal performance-describing concepts by a number of writers in the fields of communications, servomechanisms, and controls.

* See Ahrendt and Taplin (A1), (A2), Bode (B3), Brown and Campbell (B4), Chestnut and Mayer (C1), Gardner and Barnes (G1), James, Nichols and Phillips (J1), Lauer, Lesnick and Matson (L1), MacColl (M1), and Porter (P2).

Acc No 22745

PHYSICAL REPRESENTATION TERMS

Under steady-state sinusoidal conditions (see Chapters 13, 17, 18 and 19),

1) $q_{(out)} = [PF]_{(id)[q_{(in)};q_{(out)}]}\, q_{(in)}$

2) $q_{(out)} = S_{(id)[q_{(in)};q_{(out)}](ref)}\, (FF)_{(id)(q_{(in)};q_{(out)})}\, q_{(in)}$

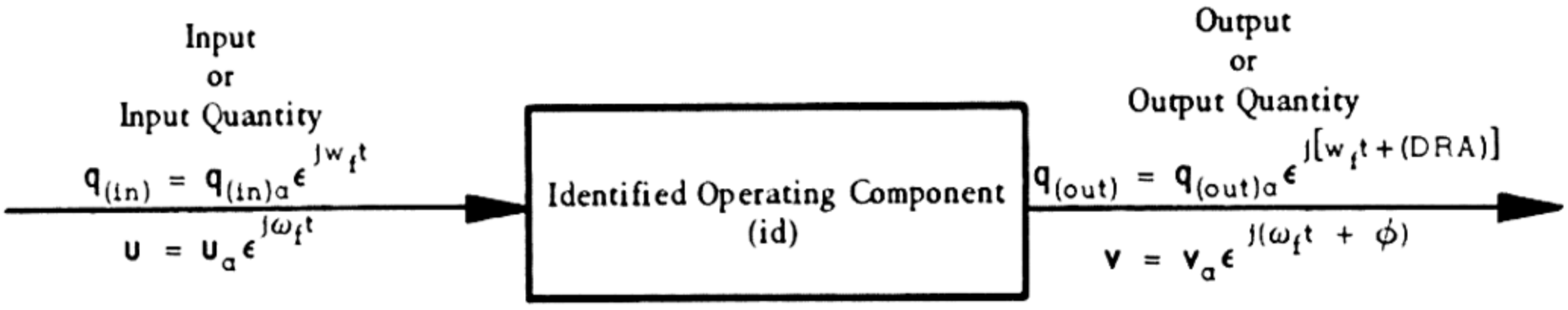
3) $q_{(out)} = S_{(id)[q_{(in)};q_{(out)}]} \epsilon^{\,j(DRA)_{(id)(q_{(in)};q_{(out)})}}\, q_{(in)}$

4) $q_{(out)} = S_{(id)[q_{(in)};q_{(out)}](ref)}\, [S(RS)R]_{(id)(q_{(in)};q_{(out)})} \epsilon^{\,j(DRA)_{(id)(q_{(out)};q_{(in)})}}\, q_{(in)}$

When no misunderstanding is possible, input-output brackets may be omitted; i.e., 4 may be written*

$$q_{(out)} = S_{(id)(ref)}\, [S(RS)R]_{(id)} \epsilon^{\,j(DRA)_{(id)}}\, q_{(in)}$$

(See Definition Summary 13-6 and Chapter 13.)



WORKING VARIABLE TERMS

The steady-state sinusoidal response forms in working variable terms are:

1) $v = \eta u$; in Laplace transform terms $v(\lambda) = \eta(\lambda)u(\lambda)$ (see Chapter 16)

2) $v = \rho_r \eta_f u$

3) $v = \rho \epsilon^{j\phi} u$

4) $v = \rho_r \mu \epsilon^{j\phi} u$

} (See Definition Summary 13-6 and Chapters 17, 18 and 19.)

where

η = relating function

η_f = frequency function

ρ = dynamic amplitude ratio

ρ_r = reference dynamic amplitude ratio

μ = dimensionless amplitude ratio

ϕ = dynamic response angle

a) Steady-state sinusoidal response characteristics

---

* For convenience, [S(RS)R] may be represented by $'(SR)$ ≡ dimensionless sensitivity ratio.

Definition Summary 28-8. Description of operating component steady-state sinusoidal performance in physical representation terms and in corresponding working variable terms. (Page 1 of 2)

$\eta \approx [PF]_{(id)} = [PF]_{(id)[q_{(in)}\,;\,q_{(out)}]}$ = input-output performance function of the (id) identified operating component

$\rho \approx (DAR)_{(id)} = (DAR)_{(id)[q_{(in)}\,;\,q_{(out)}]}$ = input-output dynamic amplitude ratio of the (id) identified operating component (this symbol appears on the dimensionless curves of Volume II)

$\rho \approx S_{(id)} = S_{(id)[q_{(in)};q_{(out)}]}$ = input-output sensitivity of the (id) identified operating component

$\rho_r \approx (RAR)_{(id)} = (RAR)_{(id)[q_{(in)}\,;\,q_{(out)}]}$ = input-output reference amplitude ratio of the (id) identified operating component (this symbol appears on the dimensionless curves of Volume II)

$\rho_r \approx S_{(id)(ref)} = S_{(id)[q_{(in)};q_{(out)}](ref)}$ = input-output reference sensitivity of the (id) identified operating component

$\eta_f \approx (FF)_{(id)} = (FF)_{(id)(q_{(in)};q_{(out)})}$ = input-output frequency function of the (id) identified operating component

$$\mu \approx [S(RS)R]_{(id)} = [S(RS)R]_{(id)(q_{(in)}\,;\,q_{(out)})} = \frac{S_{(id)[q_{(in)};q_{(out)}]}}{S_{(id)[q_{(in)};q_{(out)}](ref)}}$$

= input-output sensitivity – reference sensitivity ratio of the (id) identified operating component

$\mu \approx {}'(SR)_{(id)} = {}'(SR)_{(id)(q_{(in)};q_{(out)})}$ = dimensionless sensitivity ratio

$$\mu \approx [(DAR)(RAR)R]_{(id)} = [(DAR)(RAR)R]_{(id)(q_{(in)};q_{(out)})} = \frac{(DAR)_{(id)[q_{(in)};q_{(out)}]^{*}}}{(RAR)_{(id)[q_{(in)};q_{(out)}](ref)}}$$

= input-output dynamic amplitude ratio – reference amplitude ratio ratio of the (id) identified operation component (this symbol appears on the dimensionless curves of Volume II)

$\phi \approx (DRA)_{(id)} = (DRA)_{(id)(q_{(in)}\,;\,q_{(out)})}$ = input-output dynamic response angle of the (id) identified operating component (this symbol appears on the dimensionless curves of Volume II)

(See Chapter 13.)

Note: The sinusoidal performance function and the corresponding relating function are generally expressed as functions of frequency ratio or forcing frequency (see Chapter 17).

b) Definitions of symbols for steady-state sinusoidal response representation

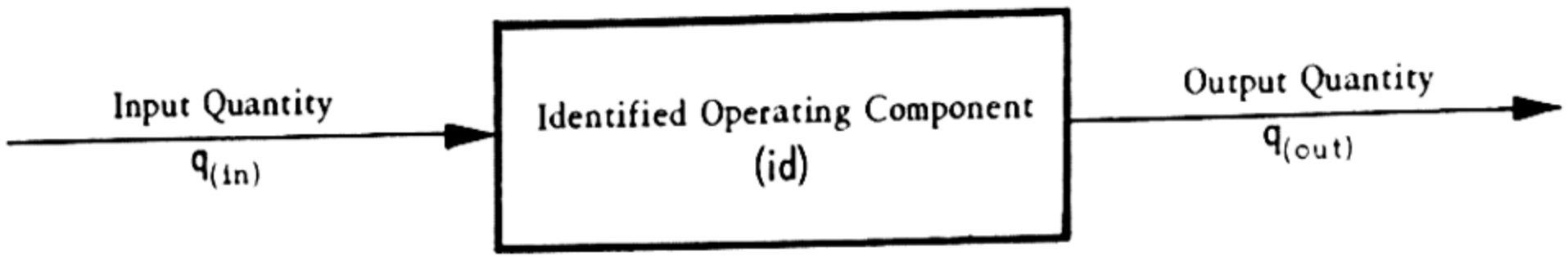
* For convenience, [(DAR)(RAR)R] may be represented by ${}'(DAR) \equiv$ dimensionless amplitude ratio.

Definition Summary 28-8. Description of operating component steady-state sinusoidal performance in physical representation terms and in corresponding working variable terms. (Page 2 of 2)

From the standpoint of practice, all of the symbol conventions are satisfactory if the involved concept and its applications are clearly understood and properly used.

DIAGRAMS FOR DESCRIBING OPERATING SYSTEMS

28.27. Concepts, terminology, and notation for describing systems made up of operating components have received considerable attention during the past few years. In particular, organizations within the American Institute of Electrical Engineers,[A3] The American Society of Mechanical Engineers,[A5] and the American Standards Association have submitted reports proposing standard systems for general adoption. Definition Summary 28-10, which is included here for reference purposes, is a reproduction of terminology and symbol lists prepared by the AIEE Committee on Feedback Control Systems and published in Electrical Engineering for October, 1951.[A3] Although certain differences do exist, the definitions given in these tabulations are generally similar to the corresponding definitions presented in the report of the Terminology Committee, Industrial Instruments and Regulators



The performance function form of the performance equation for the identified operating component is

$$q_{(out)} = [PF]_{(id)[q_{(in)};q_{(out)}]}(FR)\ q_{(in)} \tag{1}$$

where

$[PF]_{(id)[q_{(in)};q_{(out)}]}(FR)$ = input quantity – output quantity sinusoidal performance function for the identified operating component (see Chapter 3) as a function of the frequency ratio

or

$$q_{(out)} = [PF]_{(id)}(FR)\ q_{(in)} \tag{2}$$

The corresponding working variable form is

$$v = \eta(\beta)\ u \tag{3}$$

The performance function corresponds mathematically to the relating function discussed in Chapter 17. The sinusoidal form for the performance function may be written as a function of the frequency ratio (see Derivation Summary 17-3), where the frequency ratio is given by

$$\beta = FR = \frac{\omega_f}{\omega_{(ref)}} = \frac{2\pi \times (\text{forcing frequency})}{2\pi \times (\text{reference frequency})} \tag{4}$$

a) Steady-state sinusoidal performance function in terms of the conventions used in Instrument Engineering

Relationships similar to Eq. (1) are applied by many writers using various names for the input and output quantities and for the concept corresponding to the performance function; e.g.,

$[PF] =$

- $Y(p)$ = transmission ratio; MacColl (M1)
- G = transfer function; Chestnut and Mayer (C1), Ahrendt and Taplin (A1)
- $G = G\epsilon^{j\phi}$ = gain ratio (for steady-state sinusoidal response); Trimmer (T1)
- $F(i\omega)$ = complex frequency – dependent transference or transference (for steady-state sinusoidal response); Oldenbourg and Sartorius (O1)
- $KG(j\omega)$ = transfer function (for steady-state sinusoidal response)
  - where K = constant or frequency-invariant portion of transfer function
  - $G(j\omega)$ = frequency-variant portion of transfer function; Brown and Campbell (B4)
- $Y(s)$ = system function (when the performance equation terms are written as Laplace transforms); Gardner and Barnes (G1)
- $Y(p)$ = transfer function (when the terms of the performance equation are written as Laplace transforms); James, Nichols and Phillips (J1)
- Y_T = transfer admittance, adpedance, or immitance; Bode (B3)

b) Names and symbols used by various authors for steady-state sinusoidal performance

Definition Summary 28-9. Various conventions for describing steady-state sinusoidal performance of operating components.

Division, ASME, published in Mechanical Engineering for June, 1952.[A5] Both the AIEE and ASME reports suggest patterns of diagrams and terminology for combining operating components into operating systems. These patterns are substantially identical, and they appear to represent compromises between the "process branch" and the "servomechanisms branch" of the measurement and control field. In both patterns, the operation of a controlled system is to be forced into some desired pattern by a combination of feedback elements and control elements. The controlled system may be a plant or a process, where, by definition, "a process

The following list of definitions is reproduced from reference (A3) by permission of the American Institute of Electrical Engineers.

1. A *Feedback Control System* is a control system which tends to maintain a prescribed relationship of one system variable to another by comparing functions of these variables and using the difference as a means of control.

2. The *Controlled Variable* is that quantity or condition of the controlled system which is directly measured and controlled.

3. The *Indirectly Controlled Variable* is that quantity or condition which is controlled by virtue of its relation to the controlled variable and which is not directly measured for control.

4. The *Command* is the input which is established or varied by some means external to and independent of the feedback control system under consideration.

5. The *Ideal Value* is the value of the ultimately controlled variable that would result from an idealized system operating from the same command as the actual system under consideration. (The expression *Ultimately Controlled Variable* which is used here is a general term which refers to item 3 or, in the absence of a quantity corresponding to item 3, to item 2.)

6. The *Reference Input* is a signal established as a standard of comparison for a feedback control system by virtue of its relation to the command. (The term *Signal* emphasizes that the quantity under consideration conveys information.)

7. *Primary Feedback* is a signal which is a function of the controlled variable and which is compared with the reference input to obtain the actuating signal. (This designation is intended to avoid ambiguity in multiloop systems.)

8. The *Actuating Signal* is the reference input minus the primary feedback.

9. The *Manipulated Variable* is that quantity or condition which the controller applies to the controlled system.

10. A *Disturbance* is a signal (other than the reference input) which tends to affect the value of the controlled variable.

11. A *Parametric Variation* is a change in system properties which may affect the performance or operation of the feedback control system.

12. The *System Error* is the ideal value minus the value of the ultimately controlled variable. (See note under *Ideal Value*.)

13. The *System Deviation* is the value of the ultimately controlled variable minus the ideal value. The system deviation is the negative of the system error. (See note under *Ideal Value*.)

14. The *Idealized System* is one whose performance is agreed upon to define the relationship between the ideal value and the command.

15. The *Controlled System* is the body, process, or machine, a particular quantity or condition of which is to be controlled.

16. The *Indirectly Controlled System* is the body, process, or machine which determines the relationship between the indirectly controlled variable and the controlled variable.

17. The *Feedback Controller* is a mechanism which measures the value of the controlled variable, accepts the value of the command, and, as the result of a comparison, manipulates the controlled system in order to maintain an established relationship between the controlled variable and the command.

18. The *Control Elements* comprise the portion of the feedback control system which is required to produce the manipulated variable from the actuating signal.

19. The *Reference Input Elements* comprise the portion of the feedback control system which establishes the relationship between the reference input and the command.

Definition Summary 28-10. Definitions, symbols, and terms for feedback control systems.
(Page 1 of 2)

20. The *Feedback Elements* comprise the portion of the feedback control system which establishes the relationship between the primary feedback and the controlled variable.

21. The *Summing Point* is a descriptive symbol used in block diagrams to denote the algebraic summation of two or more signals. The direction of information flow is indicated by arrows and the algebraic nature of the summation by plus and minus signs.

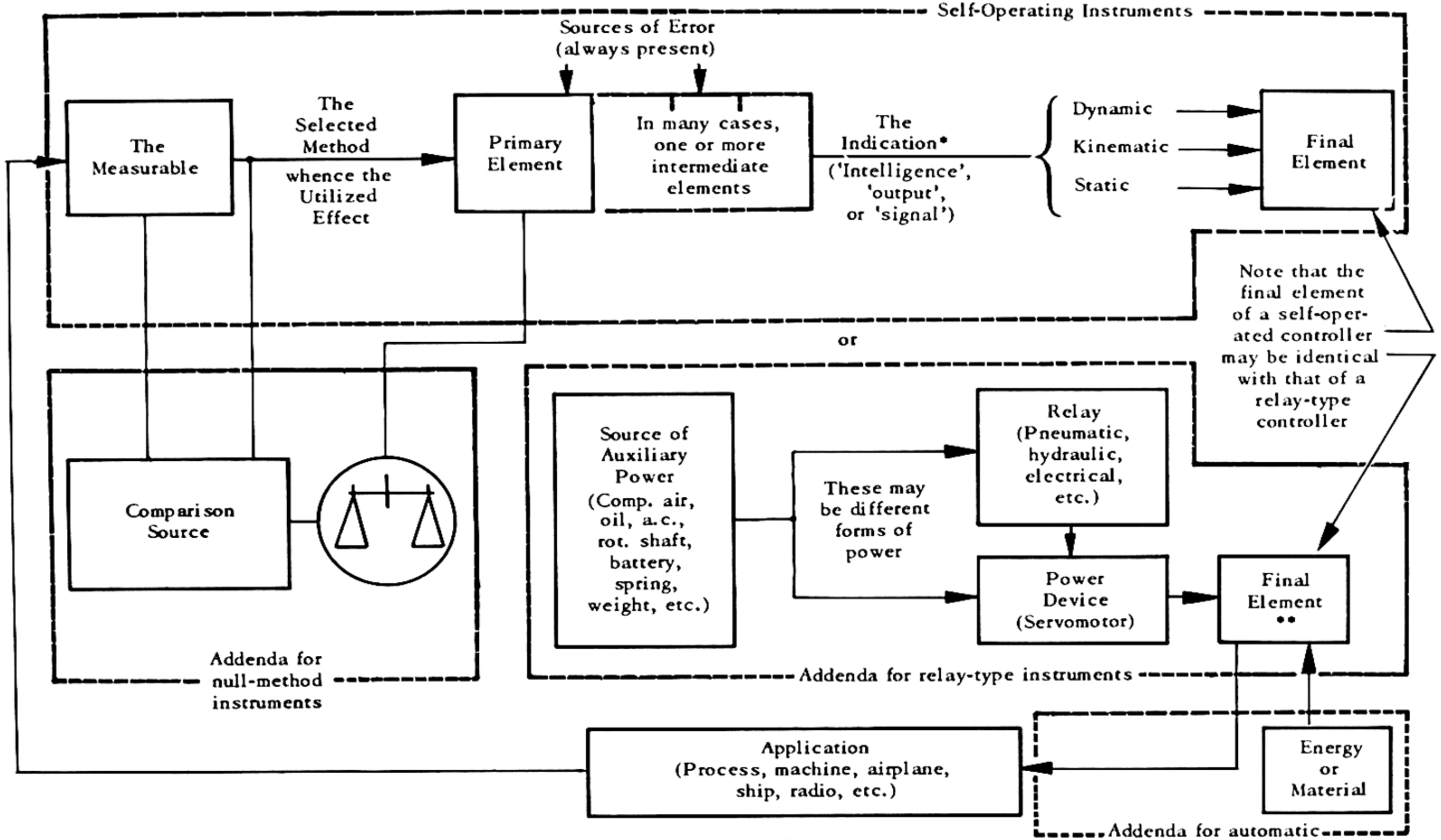
22. A *Servomechanism* is a feedback control system in which the controlled variable is mechanical position.

a) *Proposed definitions of basic feedback control system terms*

Proposed Term and Symbol	Other Terms and Symbols Used
Command, v	Input : desired value : set point : control point. θ_i, d, θ, i as subscript
Reference Input Elements, a	Conversion elements : primary element : sensing elements
Reference Input, r	Input : reference standard : desired value : set point. θ, v, θ_i, d, i
Actuating Signal, e	Error : unbalance : actuating error correction : deviation. ϵ, θ, θ_e, u
Control Elements, g_1	Amplifier : controller : servo amplifier : relay : error corrector. y, kg, h, μ, a
Manipulated Variable, m	. . . . .
Disturbance, u	Load disturbance : upset : noise : drift. l, d, n
Controlled System, g_2	Process : plant : load. y, kg, h, μ, a
Controlled Variable, c	Output : regulated variable : measured variable. θ_o, O, r, o as subscript
Indirectly Controlled System, z	Process : plant : load
Indirectly Controlled Variable, q	Output : regulated variable. O_o, O, r, o as subscript
Feedback Elements, h	Feedback transfer function. y, kg, g, β
Primary Feedback, b	Monitoring feedback : feedback. θ_f
Summing Point	Error detector : error measuring means : discriminator
Idealized System, g_i	Ideal system : desired system : preferred system : reference system
Ideal Value, i	Desired value
System Error, y_e	Error : deviation
System Deviation, y_d	Error : deviation

b) *A glossary of terms and symbols.* [Reproduced by permission from "Proposed Symbols and Terms for Feedback Control Systems," *Electrical Engineering*, Vol. 70, No. 10, October, 1951 (A3).]

Definition Summary 28-10. Definitions, symbols, and terms for feedback control systems.
(Page 2 of 2)



* The indication may also be classified as continuous or discontinuous, null-balance or deflection.

** To avoid showing more than two final-element 'boxes', this one is functionally a valve, rheostat, or other final control element, but the final element of a relay-type measuring instrument may be a pen, a printing device, or even an indicating pointer, operated by the auxiliary power.

Fig. 28-3. Features of the generalized control problem.

[Redrawn by permission from M. F. Behar et al, *The Handbook of Measurement and Control*, 1951, The Instruments Publishing Company, Inc. (B2).]

comprises the collective functions performed in and by the equipment in which a variable is to be controlled."* The controlled system may also be a ship, an airplane, a gun, or any other operating system to which control may be applied. The terms listed in Definition Summary 28-10 generally have backgrounds that are too extensive to be considered here. However, many of the terms and their associated concepts will appear in discussions of various measurement and control systems.

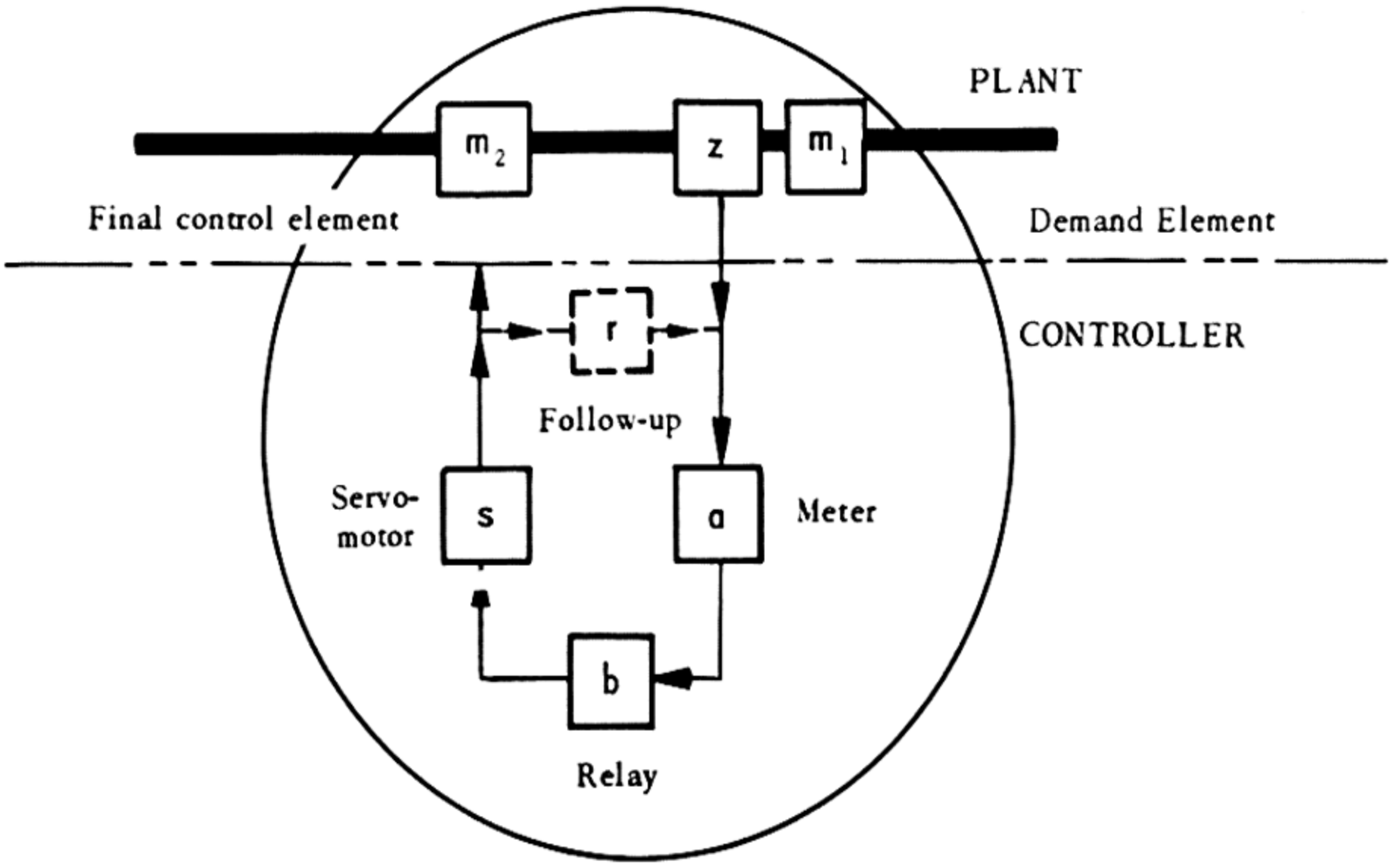


Fig. 28-4. Diagram of the control loop.

[Redrawn by permission from R. C. Oldenbourg and H. Sartorius, *The Dynamics of Automatic Controls*, 1948, The American Society of Mechanical Engineers (O1).]

28.28. Figure 28-3, drawn after an illustration in Behar's The Handbook of Measurement and Control,[B2] suggests a number of the basic features that appear in the generalized control problem. Figures 28-4, 28-5 and 28-6, adapted respectively from Oldenbourg and Sartorius,[O1] Eckman,[E2] and Ahrendt and Taplin,[A1] illustrate the types of diagrams that have been commonly drawn by engineers concerned with the control of plants and processes. Figure 28-7 is a diagram after Brown and Campbell,[B4] showing the features that often appear in diagrams used to represent servomechanism systems. Figure 28-8 shows the features recommended in reference[A3] to represent the basic pattern for feedback control systems. The corresponding diagram recommended by the Terminology Committee, Industrial Instruments and Regulators Division, ASME[A5][A6] is given in Fig. 28-9. It is apparent by inspection that the diagrams of Figs. 28-8 and 28-9 are identical except for small differences in terminology and for the omission of the "idealized system" and the "indirectly controlled system" from the ASME diagram.

28.29. The diagrams of Figs. 28-3 through 28-9 are generally similar. However, for use in representing systems of arbitrary complexity, the schemes of

---

* See ASME (A6), page 8.

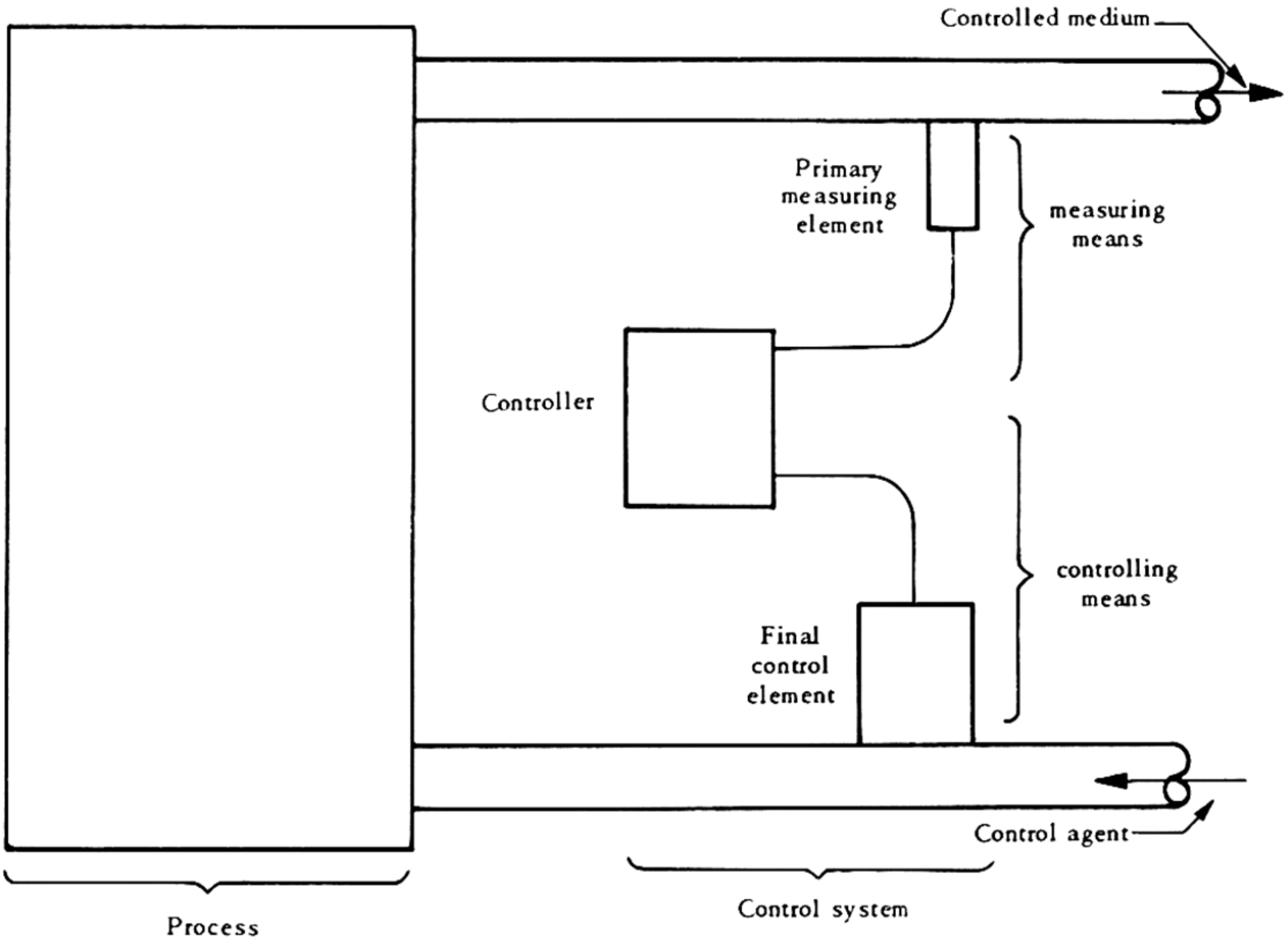


Fig. 28-5. Analysis diagram for a controlled system.

[Redrawn by permission from D. P. Eckman, *Principles of Industrial Process Control*, 1945, John Wiley & Sons, Inc. (E2).]

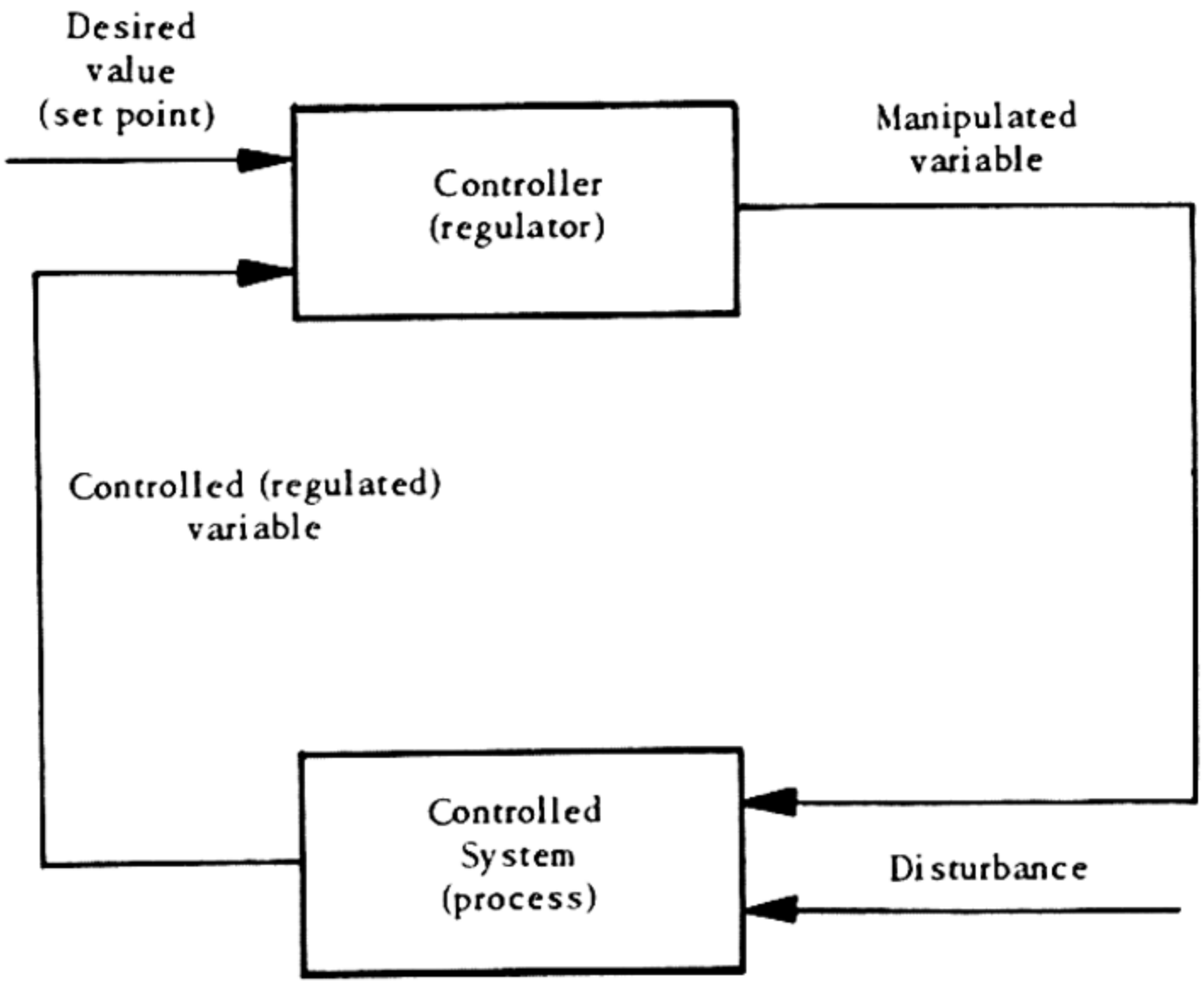


Fig. 28-6. Controlled system diagram.

[Redrawn by permission from *Automatic Feedback Control* by W. R. Ahrendt and J. F. Taplin. Copyright, 1951. McGraw-Hill Book Company, Inc. (A1).]

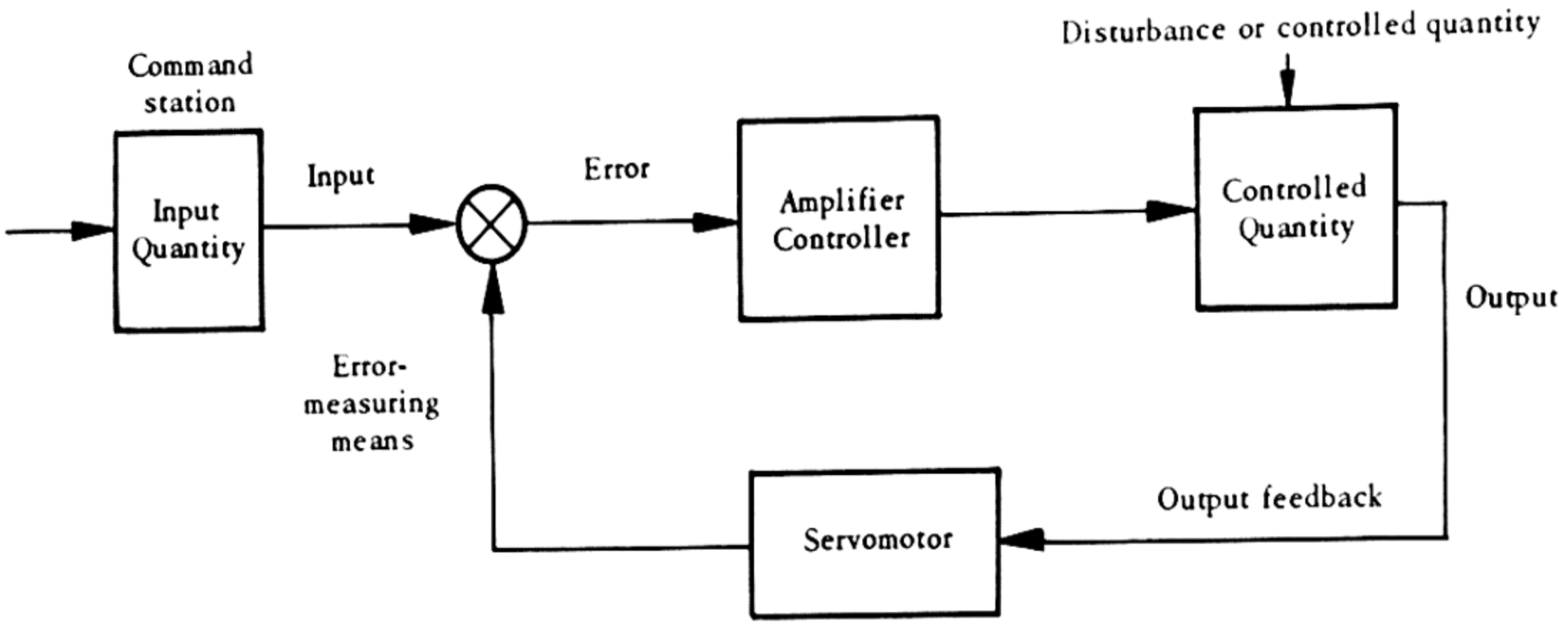


Fig. 28-7. Closed-loop control system.
[Redrawn by permission from G. S. Brown and D. P. Campbell, *Principles of Servomechanisms*, 1948, John Wiley & Sons, Inc. (B4).]

Figs. 28-4, 28-5 and 28-6 offer one feature of superiority over the patterns of Figs. 28-7, 28-8 and 28-9. This feature is the segregation of the representation for the plant, the process, or the controlled system from the control system. In general, it is desirable to make this division because the entity to be controlled is usually much more cumbersome and difficult to change than any arrangement associated with it for control purposes. Another strong reason for showing the controlled system as a well-defined and separate branch in the functional diagram is that a number of more or less independent control systems are often connected to the same controlled system.

28.30. Figure 28-10 is a functional diagram for the combination of a controlled system and a single feedback control system with the arrangement of components suggested above. The necessary connections from the controlled system to the control system are usually receivers of some type, such as thermometer bulbs, acidity (pH) electrodes, and flow meters, that by design are made to have relatively small effects on controlled system operation. The connections from the control system to the controlled system carry the nth input flow adjustor control power, which is the essential output of the feedback system. In practice, the flow adjustor may be a valve if the input is a liquid, a rheostat or generator if the input is an electrical quantity, or the speed control for a conveyor belt if the input is a solid of some kind. The system in which the various inputs are brought together under the proper conditions may be called the converter. The output from this component is the converter output, which is carried out of the controlled system by the output coupler. The flow of this output is adjusted by the output coupler in accordance with the output demand setting, which may be made to affect the coupler either by an open-chain system or a feedback control system.

28.31. An internal combustion engine may be considered as an illustrative controlled system: the air and fuel flow valves serve as input flow adjustors, the cylinder and piston combination act as the converter, and a clutch attached to the

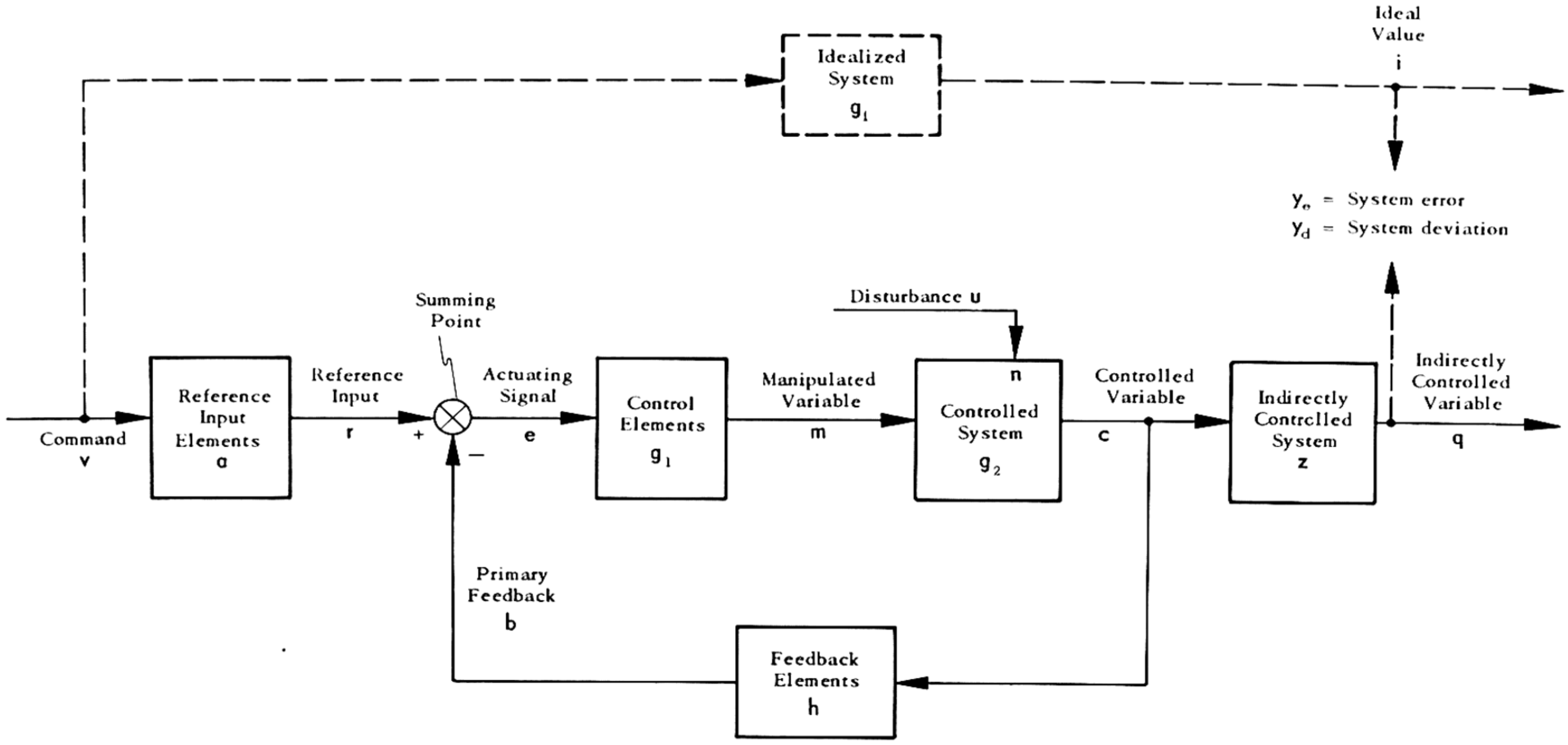


Fig. 28-8. Block diagram for a feedback control system containing all basic elements.

[Redrawn by permission from "Proposed Symbols and Terms for Feedback Control Systems," *Electrical Engineering*, Vol. 70 No. 10, October, 1951.(A3).]

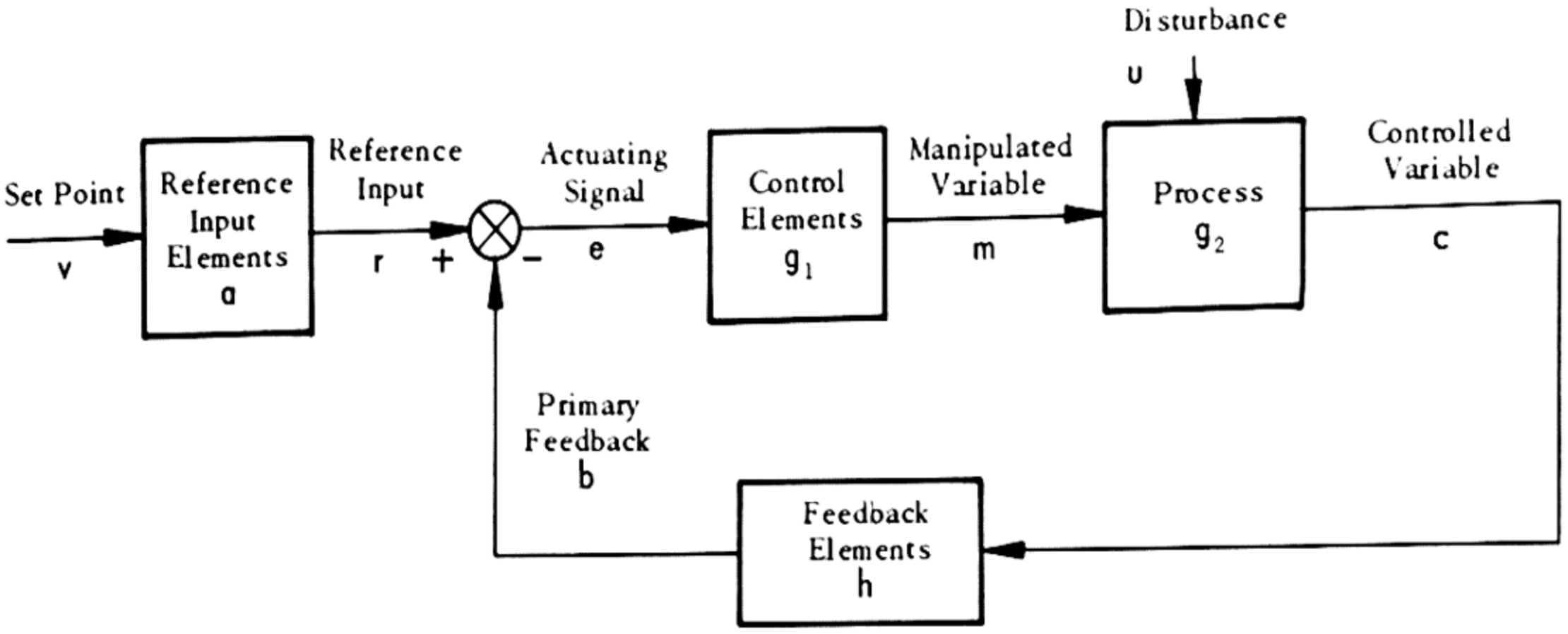


Fig. 28-9. Diagram for a feedback control system.
[Redrawn by permission from "Automatic Control Terminology," *Mechanical Engineering*, Vol. 74, No. 6, June, 1952 (A5).]

crankshaft assumes the output coupler function for power from the system. When a steam-supplied liquid heater is taken as the controlled system, the steam supply valve acts as the input flow adjustor, the heater itself as the converter, and the output flow valve serves as the output coupler.

28.32. Figure 28-11 is a symbol diagram for a controlled system with several feedback control systems acting on various inputs. To simplify this diagram, written names are omitted, leaving only identifying symbols similar to those of Fig. 28-10 to represent the various operating components and subsystems. Each control system is identified by the number of the input with which it is associated. Short lines with identifying numbers in parentheses show connections between the controlled system and the control systems. Simple parentheses are used to indicate connections with the converter; parentheses with a prime after the symbol show connections to the output coupler; primes before the parenthesis identify connections to the flow adjustors. The conventions described may be applied to more complicated situations in which interconnections exist between input adjustors and control systems. A number of examples using the pattern illustrated in Fig. 28-11 appear later in this volume. The reader is referred to the report of the Terminology Committee, Industrial Instruments and Regulators Division, ASME[(A5)] for diagrams illustrating various automatic control combinations.

ILLUSTRATIVE SCHEMATIC AND FUNCTIONAL DIAGRAMS FOR A LIQUID HEATER

28.33. Differences between the diagrams of Figs. 28-8 and 28-9, which are recommended by the committees of the AIEE[(A3)] and ASME,[(A5)(A6)] and diagrams formed under the conventions of Figs. 28-10 and 28-11 are actually not so great as a casual comparison seems to indicate. A diagram of the first type becomes a diagram of the second type when details are changed slightly and components rearranged to separate parts that reasonably belong to the plant from parts that reasonably belong to the control system. To demonstrate the equivalence of the two types of

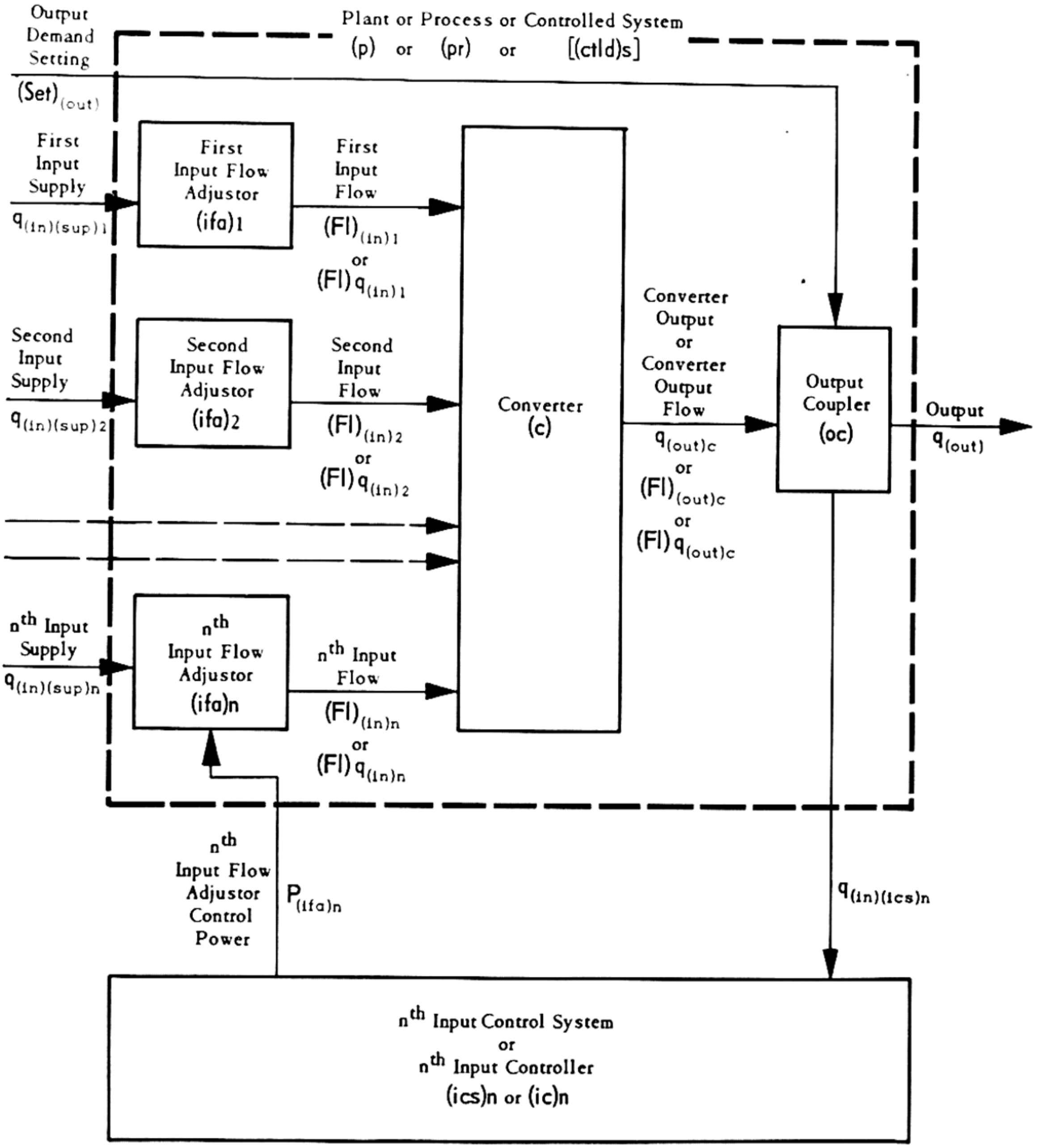
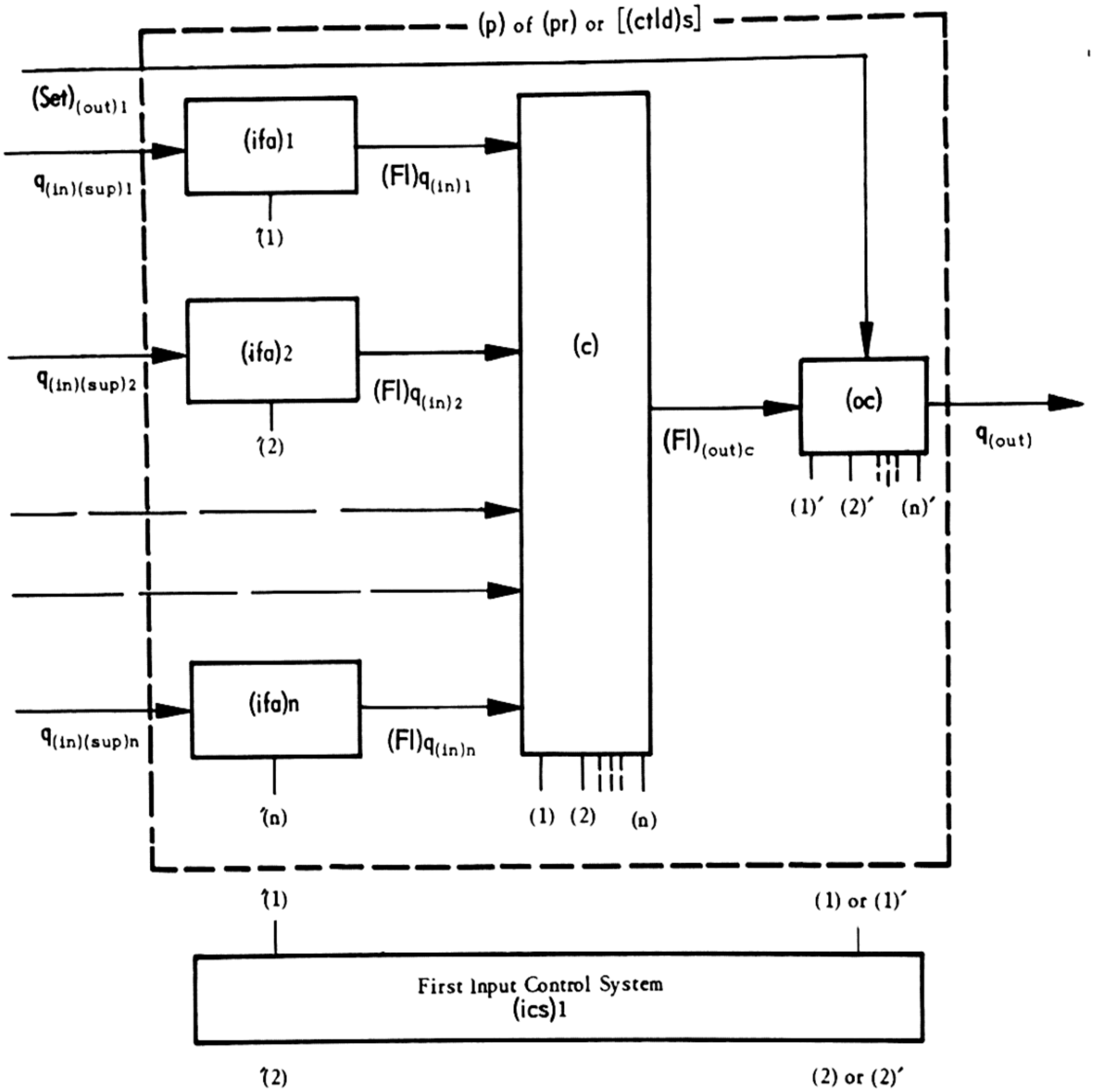


Fig. 28-10. Functional diagram for a controlled system and a single feedback control system.

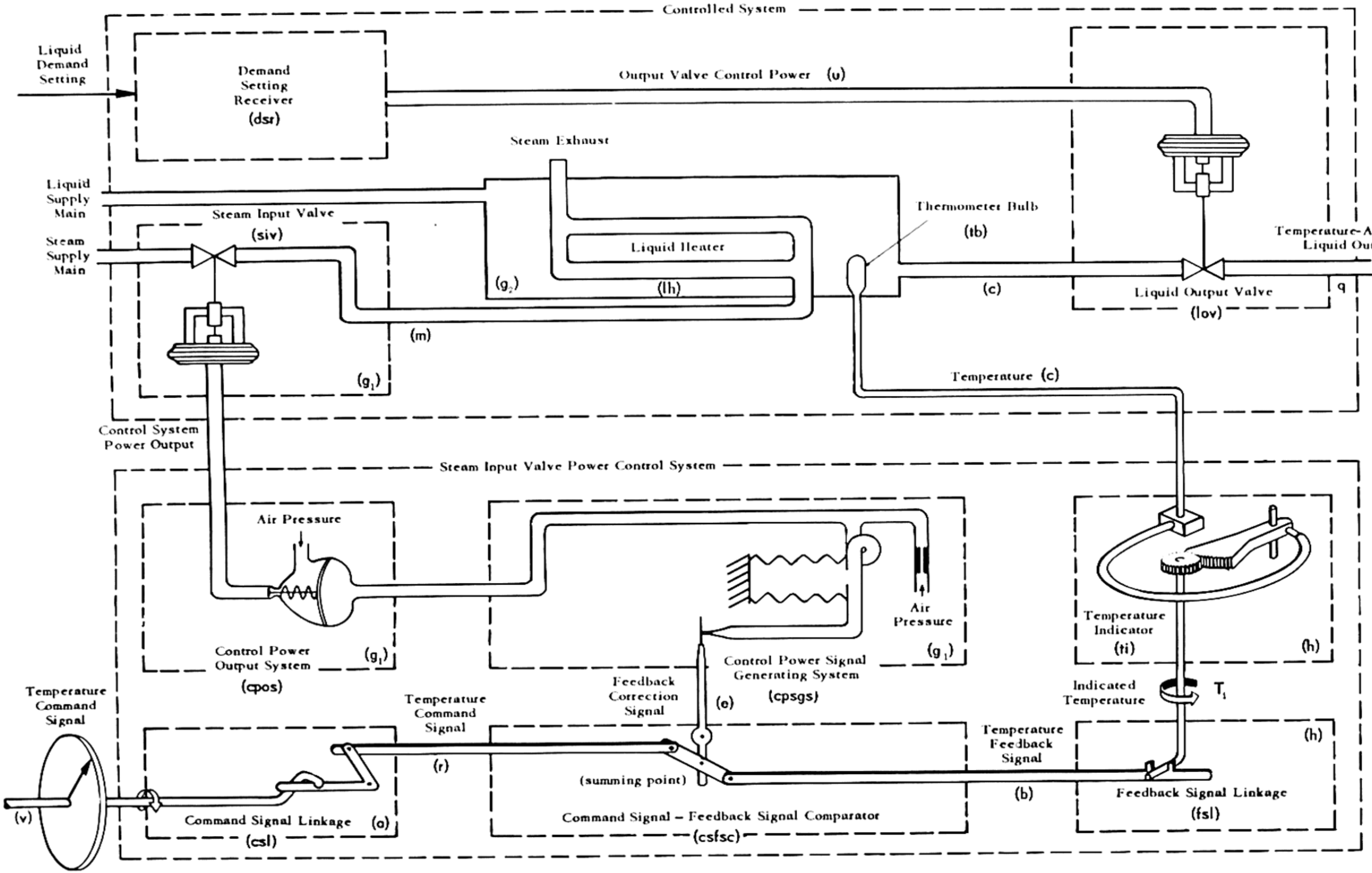
diagrams for a specific system, Figs. 28-12 and 28-13 are provided. Figure 28-12 is a functional-schematic diagram for a steam-supplied heater system that takes liquid from a supply main and adjusts its temperature within certain tolerance limits about a constant setting; this adjustment of temperature is accomplished by means of a feedback control system. Figure 28-13 is a functional diagram showing that the system of Fig. 28-12 falls directly into the pattern of Fig. 28-10 and that this pattern contains the essential concepts of Figs. 28-8 and 28-9.

28.34. Comparison of Figs. 28-12 and 28-13 shows that the first input supply is the liquid supply main, and the second input supply is the steam supply main.



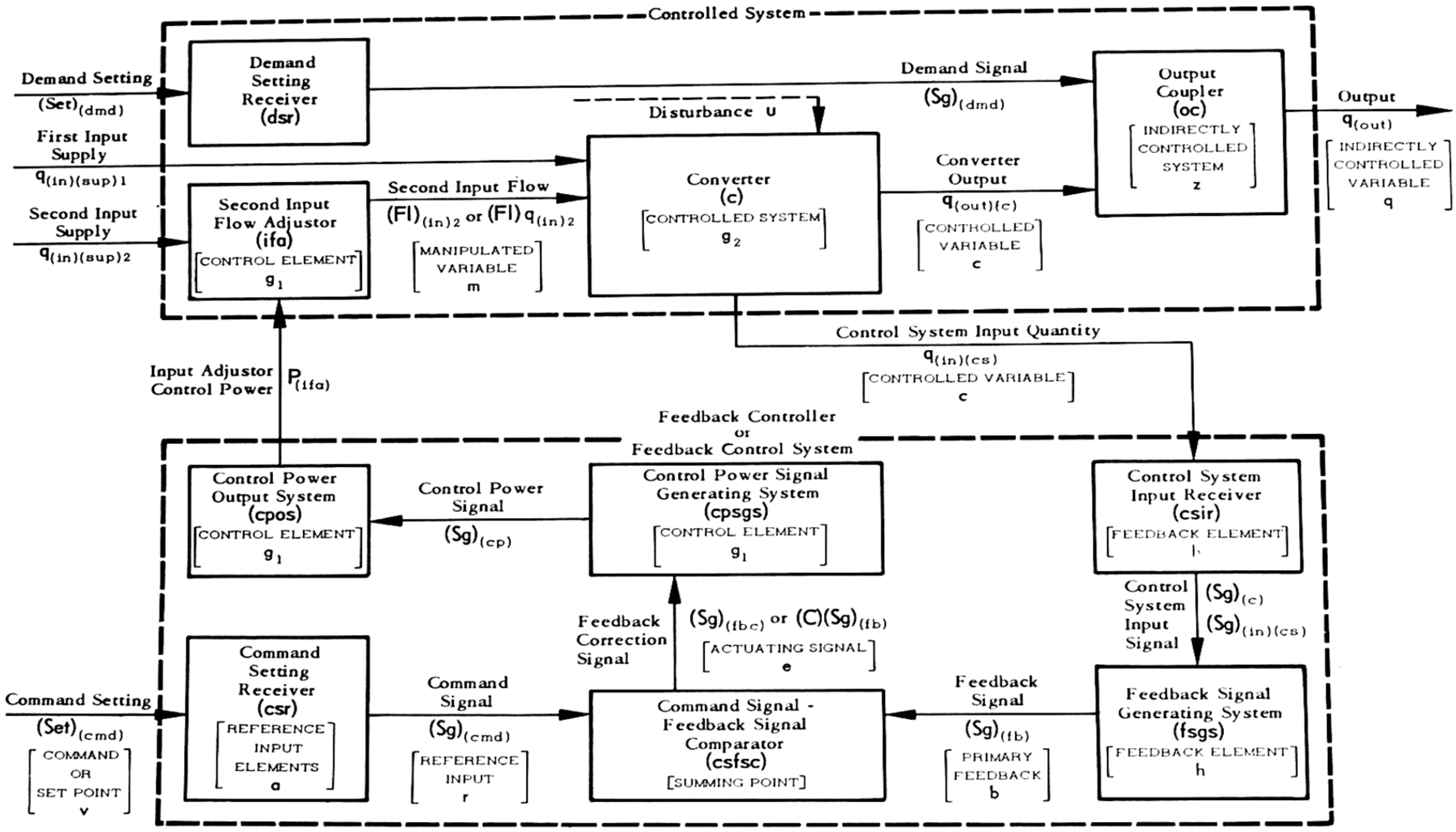
Note: The symbols of this diagram are associated with names by the conventions illustrated in Fig. 28-10. Interconnections between control systems may be shown as required. In practice, each component or subsystem is described by a diagram showing internal details.

Fig. 28-11. Generalized functional diagram for a controlled system with multiple feedback control systems.



Note: Symbols appearing on the diagram identify the quantities that are defined in Figs. 28-8 and 28-9.

Fig. 28-12. Functional-schematic diagram for a liquid heater with proper names for operating components.



Note: Symbols and names from the proposed standard feedback control system diagram of Fig. 28-8 that correspond to symbols and names used in the conventions of Instrument Engineering are shown in square brackets.

Fig. 28-13. Functional diagram for the liquid heater of Fig. 28-12 with functional names for operating components.

No flow adjustor appears in the liquid supply line, since the liquid flow is adjusted by the valve that serves as the output coupler in accordance with the demand setting for temperature-adjusted liquid. A powered steam valve acts as the second input flow adjustor. The liquid heater, with its shell and steam coils, acts as the converter. A thermometer bulb placed inside the heater supplies a temperature-dependent pressure to the Bourdon-tube type temperature indicator, which acts as the control system input receiver. This receiver produces indicated temperature as the control system input signal, a specific angular position of the temperature indicator output shaft. This angular position is received by the feedback signal linkage, which acts as the feedback signal generating system to produce the temperature feedback signal. This feedback signal is one of the inputs to the command signal – feedback signal comparator, which also accepts the temperature command signal from the command signal linkage that acts as the command setting receiver. The output from the comparator is the feedback correction signal, which is the difference between the command signal and the feedback signal. This correction signal is the input for the control power signal generating system, which in Fig. 28-12 is a conventional pneumatic control vane arrangement* that may be associated with various integration and differentiation functions as required for the type of control** to be used, and produces the control power signal as its output. This pneumatic signal is the input for the control power output system, which supplies pneumatic pressure as the control system power output to the steam input valve. The net result of the system operation depicted in Figs. 28-12 and 28-13 is that the feedback control system changes the steam flow so that the temperature of the output liquid is maintained near the temperature command setting for all liquid flows within the operating limits of the system.

28.35. The relationships between the operating components, names and symbols used in the diagrams of Fig. 28-13 and the corresponding components, names and symbols used in the diagrams of Figs. 28-8 and 28-9 are illustrated by placing symbols and names from the latter diagrams on the former diagram. The corresponding quantities and components are listed in Table 28-1.

28.36. In practice, each new physical situation is likely to present special features that must be described by concepts and represented by symbols that are unambiguous, understandable, and easily remembered. When attention is restricted to a narrow range of problem types, any properly descriptive system of terminology will be satisfactory. On the other hand, if a wide variety of problems with many interrelationships must be simultaneously considered, the system of self-defining notation and the diagram patterns illustrated in Figs. 28-10, 28-11, 28-12 and 28-13 offers considerable advantages over other systems in common use. It is not to be

---

* See Ahrendt and Taplin (A1), Behar (B2), and Eckman (E2).

** See AIEE (A3) and ASME (A5).

Table 28-1. Corresponding components, names, and symbols used in Figs. 28-13, 28-9 and 28-8.

In Fig. 28-13	In Fig. 28-9	In Fig. 28-8
Command Setting, $(Set)_{(cmd)}$	Set Point, v	Command, v
Command Setting Receiver, (csr)	Reference Input Elements, a	Reference Input Elements, a
Command Signal, $(Sg)_{(cmd)}$	Reference Input, r	Reference Input, r
Command Signal - Feedback Signal Comparator, (csfsc)	- - - - - -	Summing Point
Feedback Correction Signal, $(Sg)_{(fbc)}$ or Feedback Signal Correction, $(C)(Sg)_{(fb)}$	Actuating Signal, e	Actuating Signal, e
Control Power Signal Generating System, (cpsgs) Control Power Output System, (cpos) (second) Input Flow Adjustor, $(ifa)_2$	Control Elements, g_1	Control Elements, g_1
(second) Input Flow, $(Fl)_{(in)2}$ or $(Fl)q_{(in)2}$	Manipulated Variable, m	Manipulated Variable, m
Converter, (c)	Process, g_2	Controlled System, g_2
Disturbance, u	Disturbance, u	Disturbance, u
Converter Output, $q_{(out)c}$	Controlled Variable, c	Controlled Variable, c
Output Coupler, (oc)	- - - - - -	Indirectly Controlled System, z
Output, $q_{(out)}$	- - - - - -	Indirectly Controlled Variable, q
Control System Input Receiver, (csir) Feedback Signal Generating System, (fbsgs)	Feedback Elements, h	Feedback Elements, h
Feedback Signal, $(Sg)_{(fb)}$	Primary Feedback, b	Primary Feedback, b

expected that an instrument engineer, who must deal with situations and collaborators from various fields of engineering, will be able to restrict himself to the use of any one system and set of conventions. He should be so familiar with various patterns for describing physical situations that he is able to work in the terms that, for any one of many reasons, appear to be most effective in any given case. The discussions of later chapters are presented in the notation commonly used for the particular problems considered and, in addition, are drawn into a common pattern by use of the conventions described in this chapter.

CHAPTER 29

INDICATION AND MEASUREMENT

INTRODUCTION

29.1. Measurement is a term applied to the process of associating numbers with physical quantities. Chapter 8 describes this process and discusses the basic requirements that must be fulfilled by the measure of any actual quantity. Devices designed to meet these requirements by associating numbers with physical quantities are measuring instruments. For example, the pressure gage described in Chapter 2 is a pressure-measuring instrument made up of a pressure-indicating mechanism and a scale. The mechanism is an operating system that receives* pressure as its input and produces a corresponding indication. In this case, the indication is the index position in terms of the index angle measured from the index reference position. The scale is a disk concentrically placed with respect to the axis of rotation of the index and marked with divisions that represent levels of the input pressure. The index position, read in terms of the scale divisions, gives a measure of the input pressure as the pressure scale reading. This reading may also be called the indicated pressure or the pressure reading.

29.2. All measuring instruments include an indicating mechanism and scale combination similar to that illustrated by the pressure gage example. This fact makes it possible to develop certain useful generalizations for measuring instruments. These principles are especially simple and convenient for ideal instruments, which are formed of operating components that behave exactly in accordance with theoretical descriptions of their performance. Actual instruments, whose components only approximate ideal behavior, are more difficult to describe in theoretical terms because corrections and uncertainties must be taken into account.

29.3. Various systems of terminology and notation are described by writers in the field of measurement and control.** The names and symbols used in these systems differ among themselves, but the same basic concepts appear in all discussions. This chapter is devoted to a summary of concepts, methods, definitions, and symbols for the description of measuring instrument operation and performance. The scheme of concepts, definitions, and symbols used in Instrument

* It is also common practice to use the word senses as a synonym for receives in situations of this kind.

** See ASME (A5), (A6), Behar (B2), British Standards Institution (B7), Eckman (E1), National Research Council (N1), Rhodes (R1), Trimmer (T1), and Zimmerman and Lavine (Z1).

Engineering has certain conflicts with proposed standard systems,* but it is also more complete than any system described in the literature. For this reason, it is not possible to make a comparison of each of the concepts developed for the purposes of this book with a corresponding definition in the literature. However, in many instances direct parallels do exist and are mentioned in this chapter.

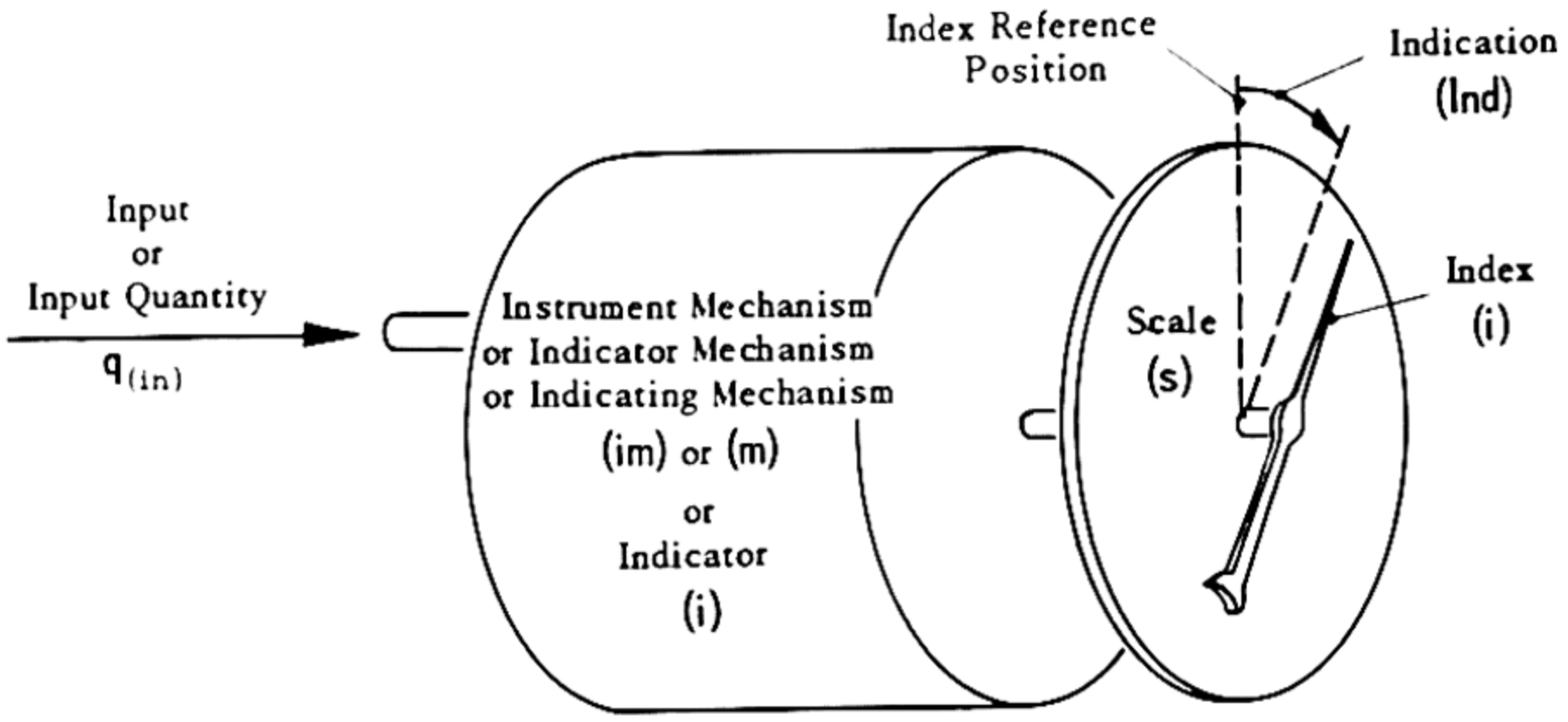
INDICATING INSTRUMENTS

29.4. Indicating instruments, or indicators, are operating systems that associate indications with the levels of an input quantity. Indicators do not carry markings in terms of the input quantity and for this reason do not qualify as measuring instruments. Indications have the form of some directly observable quantity, such as the linear or angular position of a mechanical index or a spot of light. Components or systems that generate output signals to represent the input quantity are receivers, not indicators, unless an indicating system is added to produce some directly observable output that may be classed as an indication. The indicating instrument mechanism produces an indication that varies with changes of the input quantity, but no provision is made for directly associating measures of this quantity with the indication. Sections a and b of Definition Summary 29-1 illustrate schematic and functional diagrams for representing the indicating instrument.

29.5. Section c of Definition Summary 29-1 gives a functional diagram for the indicator mechanism (identical with the indicating instrument mechanism) resolved into three operating components that very often appear as natural components of devices for generating indications. These components are the input receiver, (also called the receiver or sensor), which receives the input quantity and produces the input receiver output; the coupler, which receives the input receiver output and produces the coupler output; and the indicating system, which receives the coupler output and produces the indication.

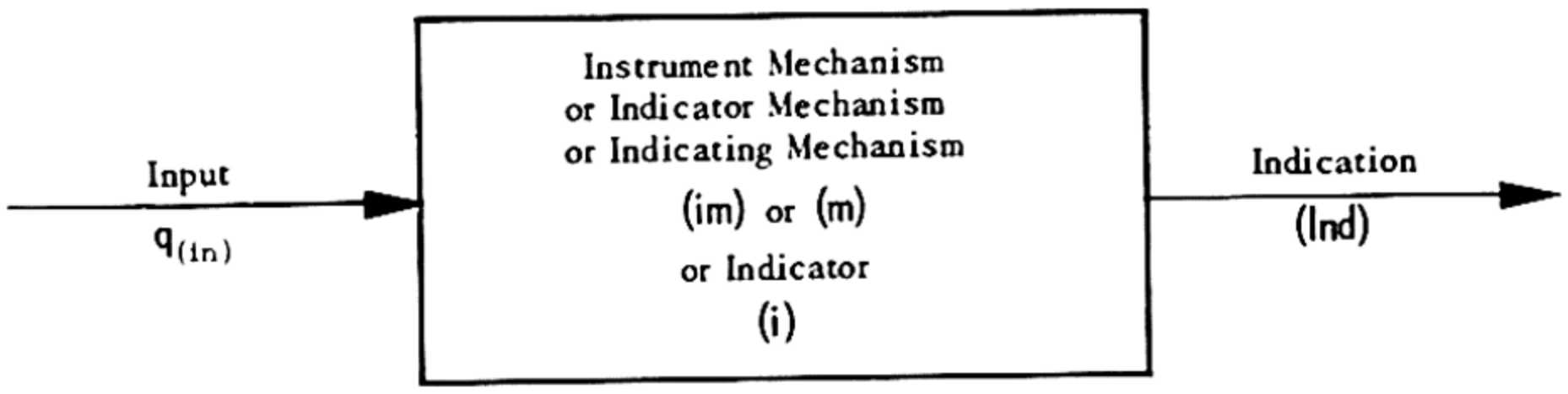
29.6. The static performance and the generalized performance (i.e., combined static and dynamic performance) for the indicator mechanism and its components are listed in section d of Definition Summary 29-1 in terms of static sensitivities and performance functions with identifying subscripts formed by the conventions described in Fig. 4-1 of Chapter 4, Fig. 10-3 of Chapter 10, and Definition Summary 28-6. Section d of Definition Summary 29-1 also gives products of sensitivities and of performance functions, formed in accord with the principles illustrated in Figs. 3-3 and 3-4 of Chapter 3 and used to describe the over-all performance of the indicator mechanism in terms of the input quantity – indication static sensitivity of the indicator and the input quantity – indication performance function of the indicator. Equations (2), (4), (6), (8), (10) and (12) of Definition Summary 29-1

* See AIEE (A3) and ASME (A5), (A6).



Indicating instruments include an indicating mechanism and a scale. Scales for indicating instruments may have no markings and in any case *are not marked in terms of the input quantity*. Indicating instruments may also be called indicators.

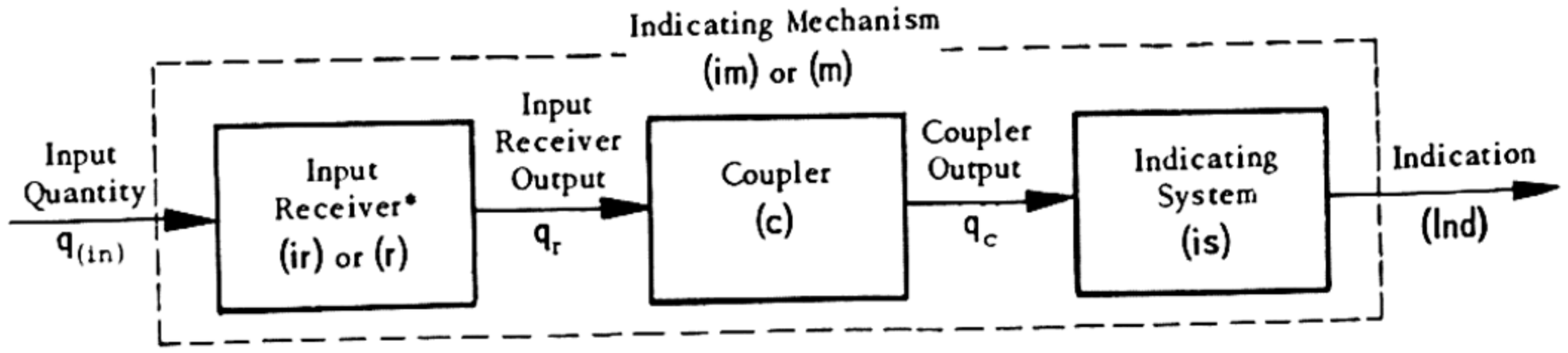
a) Schematic diagram for a typical indicating instrument



The indication may be any observable physical quantity; e.g., the linear or angular position of a mechanical index or light spot.

b) Single-block functional diagram for an indicating instrument

The indicating mechanism may be considered as made up of the three operating components shown below.



* The input receiver may also be called the input sensor or merely the sensor.

c) Functional diagram for an indicating mechanism

Definition Summary 29-1. Representation and performance description for an indicating instrument mechanism. (Page 1 of 3)

Using the notational conventions of Figs. 4-1 and 10-3 and Definition Summary 28-6, the performance of the components and system of section c may be written as follows:

Component or System	Static Performance	Generalized Performance
Input Receiver (ir)	$q_r = S_{(ir)[q_{(in)};q_r](st)} q_{(in)}$	$q_r = [PF]_{(ir)[q_{(in)};q_r]} q_{(in)}$ (1)
	or	or
	$q_r = S_{(ir)(st)} q_{(in)}$	$q_r = [PF]_{(ir)} q_{(in)}$ (2)
Coupler (c)	$q_c = S_{(c)[q_r;q_c](st)} q_r$	$q_c = [PF]_{(c)[q_r;q_c]} q_r$ (3)
	or	or
	$q_c = S_{(c)(st)} q_r$	$q_c = [PF]_c q_r$ (4)
Indicating System (is)	$(Ind) = S_{(is)[q_c;(Ind)](st)} q_c$	$(Ind) = [PF]_{(is)[q_c;(Ind)]} q_c$ (5)
	or	or
	$(Ind) = S_{(is)(st)} q_c$	$(Ind) = [PF]_{(is)} q_c$ (6)
Indicating Mechanism (im)	$(Ind) = S_{(im)[q_{(in)};(Ind)](st)} q_{(in)}$	$(Ind) = [PF]_{(im)[q_{(in)};(Ind)]} q_{(in)}$ (7)
	or	or
	$(Ind) = S_{(m)(st)} q_{(in)}$	$(Ind) = [PF]_m q_{(in)}$ (8)

where

$$S_{(im)[q_{(in)};(Ind)](st)} = S_{(ir)[q_{(in)};q_r](st)} S_{(c)[q_r;q_c](st)} S_{(is)[q_c;(Ind)](st)} \quad (9)$$

or

$$S_{(m)(st)} = S_{(ir)(st)} S_{(c)(st)} S_{(is)(st)} \quad (10)$$

and

$$[PF]_{(im)[q_{(in)};(Ind)]} = [PF]_{(ir)[q_{(in)};q_r]} [PF]_{(c)[q_r;q_c]} [PF]_{(is)[q_c;(Ind)]} \quad (11)$$

or

$$[PF]_m = [PF]_{(ir)} [PF]_c [PF]_{(is)} \quad (12)$$

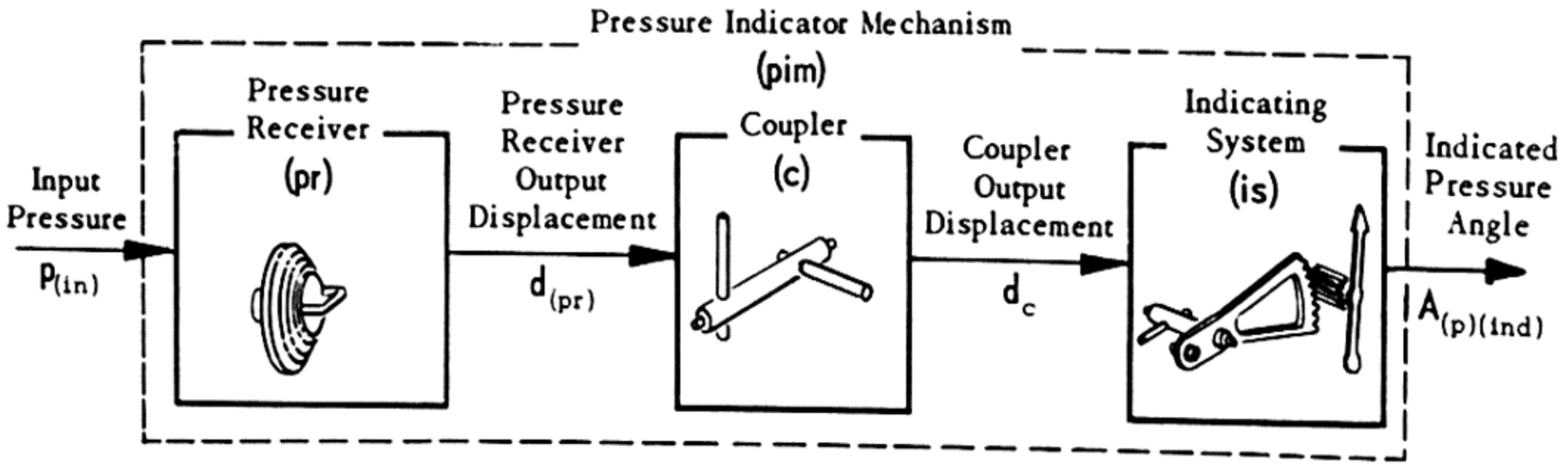
Definitions and names for the symbols of Eqs. (1) through (8) follow the conventions described in Figs. 4-1 and 10-3. For example:

$S_{(im)[q_{(in)};(Ind)](st)}$ = input quantity – indication static sensitivity of the indicating mechanism

$[PF]_{(im)[q_{(in)};(Ind)]}$ = input quantity – indication performance function of the indicating mechanism

d) Description of indicating mechanism performance

As a special example, consider the pressure indicating mechanism of the pressure gage described in Chapter 2:



Definition Summary 29-1. Representation and performance description for an indicating instrument mechanism. (Page 2 of 3)

Component or System	Static Performance	Generalized Performance	
Pressure Receiver (pr)	$d_{(pr)} = S_{(pr)[p;d](st)} p_{(in)}$	$d_{(pr)} = [PF]_{(pr)[p;d]} p_{(in)}$	(13)
	or	or	
	$d_{(pr)} = S_{(pr)} p_{(in)}$	$d_{(pr)} = [PF]_{(pr)} p_{(in)}$	(14)
Coupler (c)	$d_c = S_{(c)[d;d](st)} d_{(pr)}$	$d_c = [PF]_{(c)[d;d]} d_{(pr)}$	(15)
	or	or	
	$d_c = S_{(c)(st)} d_{(pr)}$	$d_c = [PF]_c d_{(pr)}$	(16)
Indicating System (is)	$A_{(p)(ind)} = S_{(is)[d;A](st)} d_c$	$A_{(p)(ind)} = [PF]_{(is)[d;A]} d_c$	(17)
	or	or	
	$A_{(p)(ind)} = S_{(is)(st)} d_c$	$A_{(p)(ind)} = [PF]_{(is)} d_c$	(18)
	or	or	
	$(Ind)_p = S_{(is)(st)} d_c$	$(Ind)_p = [PF]_{(is)} d_c$	(19)
Pressure Indicating Mechanism (pim)	$A_{(p)(ind)} = S_{(pim)[p;A](st)} p_{(in)}$	$A_{(p)(ind)} = [PF]_{(pim)[p;A]} p_{(in)}$	(20)
	or	or	
	$A_{(p)(ind)} = S_{(pim)(st)} p_{(in)}$	$A_{(p)(ind)} = [PF]_{(pim)} p_{(in)}$	(21)
	or	or	
	$(Ind)_p = S_{(m)(st)} p_{(in)}$	$(Ind)_p = [PF]_m p_{(in)}$	(22)

where

$$S_{(pim)[p;A](st)} = S_{(pr)[p;d](st)} S_{(c)[d;d](st)} S_{(is)[d;A](st)}$$

= pressure-angle static sensitivity of the pressure indicating mechanism

$$= S_{(pim)(st)} \longrightarrow S_{(m)(st)} \quad (23)$$

$$[PF]_{(pim)[p;A]} = [PF]_{(pr)[p;d]} [PF]_{(c)[d;d]} [PF]_{(is)[d;A]} \quad (24)$$

or

$$[PF]_{(pim)} = [PF]_{(pr)} [PF]_c [PF]_{(is)} \quad (25)$$

= pressure-angle performance function of the pressure indicating mechanism

and

$$[PF]_{(pim)} \longrightarrow [PF]_m \quad (26)$$

e) *Representation of performance for an illustrative pressure indicator mechanism*

Definition Summary 29-1. Representation and performance description for an indicating instrument mechanism. (Page 3 of 3)

illustrate a simplification of symbols obtained by the omission of input-output bracket subscripts. This modification becomes possible for situations in which the background is so obvious that misunderstanding of symbol meanings is very unlikely. Section e of Definition Summary 29-1 illustrates an application of the generalized pattern of sections c and d to the specific case of the pressure gage mechanism represented in Fig. 2-3 of Chapter 2 and in Definition Summary 28-5.

MEASURING INSTRUMENTS

29.7. Measuring instruments are indicators with scales marked in terms of measures of the input variable. An indicator must have a mechanism and may have scale markings, but it does not become a measuring instrument until input quantity levels in numerical terms are associated with the scale divisions. For

example, a pressure gage might have a mechanism sensitivity of ten degrees per pound per square inch. The scale might actually be marked off in degrees, but the device remains an indicator until numbers in terms of pressure are placed on the scale. Pressure readings may also be found with the aid of tabulations or charts giving pressure readings in terms of indications expressed in degrees, but the devices that provide the indications are not measuring instruments.

29.8. In general, indicator scale markings may be arbitrarily placed without regard to degrees, inches, or any other measure of position. Any indicator whose scale markings are placed so that input quantity measures are given by products of the indications associated with the markings and a numerical factor, falls into the class of measuring instruments when the factor is marked on the instrument itself. The number by which indications must be multiplied in order to obtain input quantity scale readings is the scale factor. It should be noted that the term "scale factor" is also applied by some writers* to a concept identical with that defined in Figs. 4-1 and 4-2 of Chapter 4 as static sensitivity. This usage of "scale factor" will not appear in Instrument Engineering except for comparison purposes.

CALIBRATION

29.9. The calibration** of a measuring instrument is the process of associating indications with input quantity levels and the corresponding scale readings with the indications. Under this definition, an indicator becomes a measuring instrument when it is calibrated in terms of its input quantity. This transition is illustrated in sections a and b of Definition Summary 29-2, where the measuring instrument is shown as made up of an indicator and a scale calibrated in terms of the input quantity.

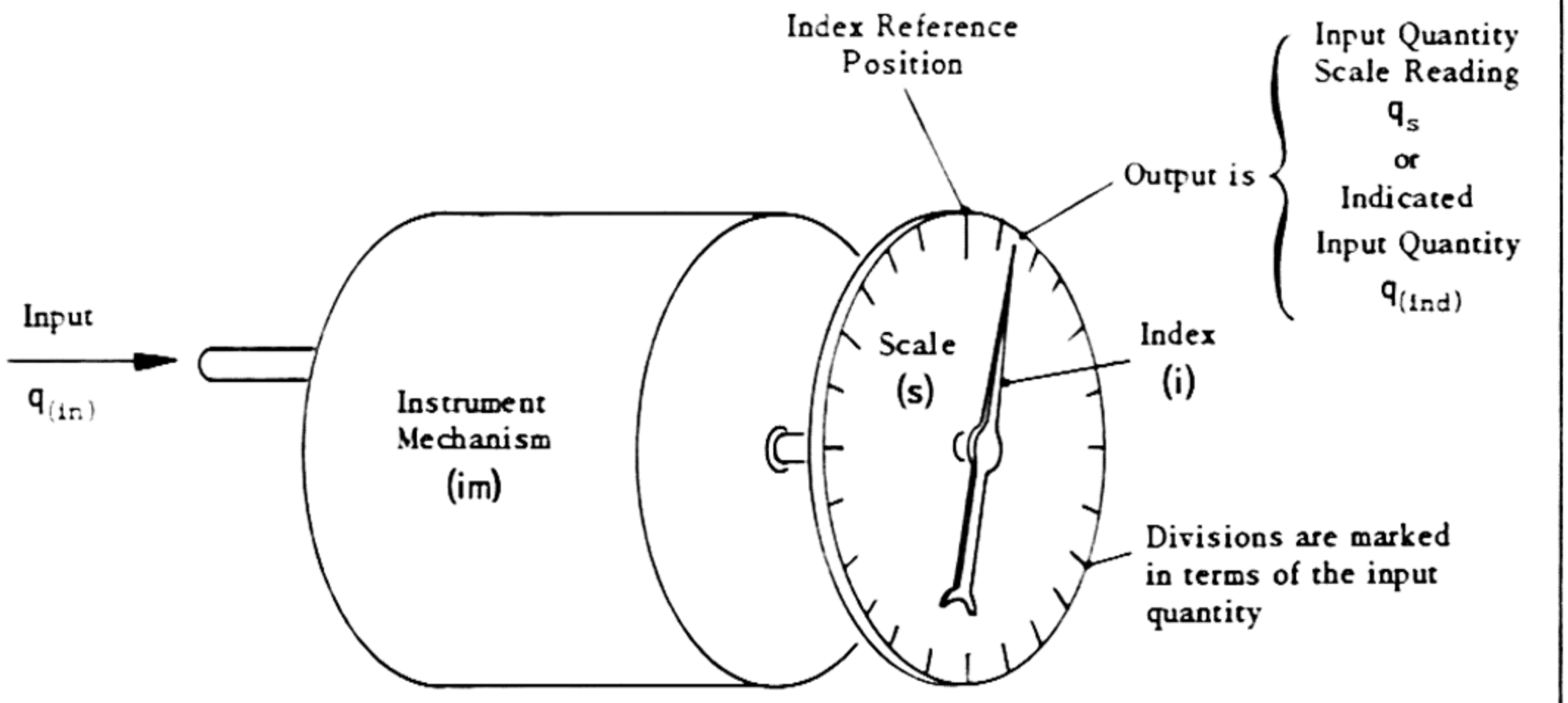
29.10. Equations (1) through (8) of Definition Summary 29-2 describe the performance of a measuring instrument in terms of the performance of its mechanism and the performance of its scale. The scale is usually a series of marks on a piece of solid material, so that, except for special cases, its performance is satisfactorily described by a static sensitivity with the indication as its input and the scale reading as its output.

PERFECT, IDEAL, AND ACTUAL MEASURING INSTRUMENTS

29.11. A measuring instrument is a perfect measuring instrument when its scale readings, which are associated with indications by the scale, are always exactly equal to the true measures of the corresponding input quantity levels. A measuring instrument is an ideal measuring instrument when perfect observation (i.e., observation that gives scale readings exactly matched to indications) produces scale readings that are equal to the true measures of input quantity levels,

* See Frost (F3).

** The calibration of an indicator is the process of associating indications with input quantity levels.



The scale is calibrated in terms of the input quantity, i.e., the scale is given markings and associated numbers that represent indications for levels of the input quantity.

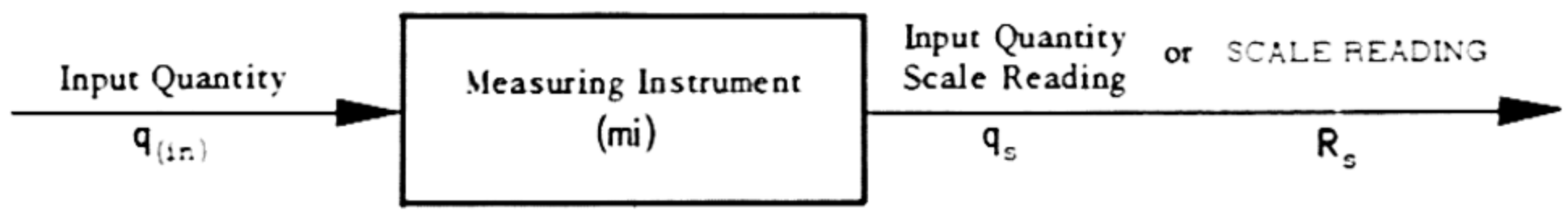
The output of a measuring instrument is the scale reading in terms of a measure of the input quantity.

(See Chapter 8 for definitions associated with measurement.)

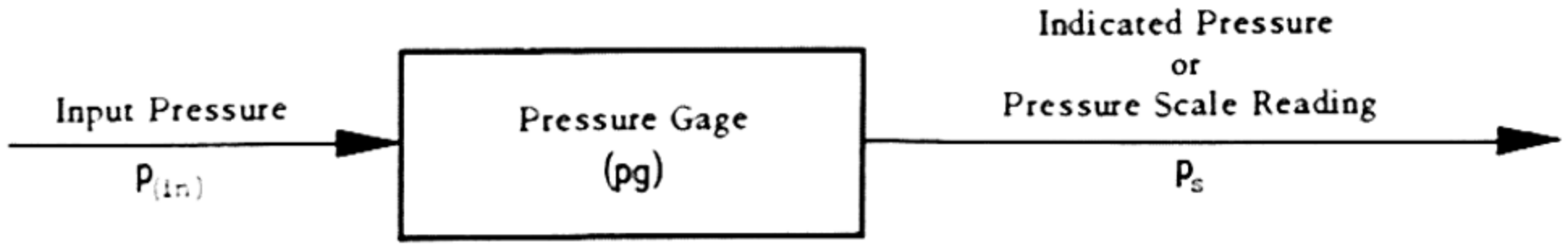
For example, the scale of a pressure gage is given markings and numbers that represent the positions the index will have when the input pressure levels have measures that correspond to the scale readings.

a) Schematic diagram for a measuring instrument

The functional diagram for a measuring instrument is



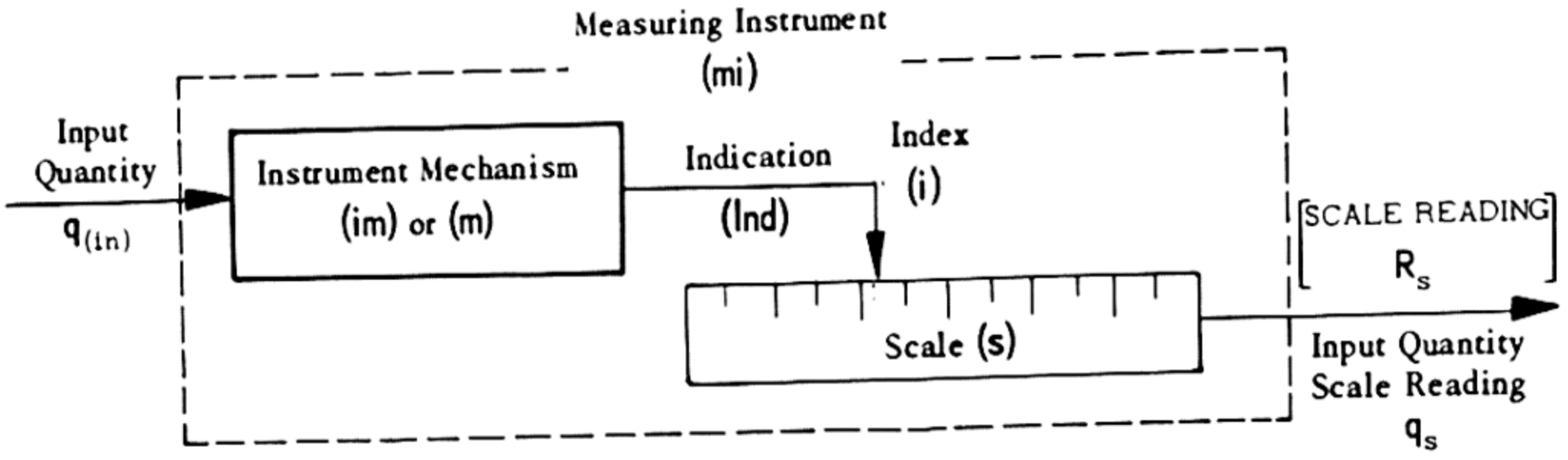
For example, the functional diagram for the pressure gage is



b) Single-block functional diagram for a measuring instrument

Definition Summary 29-2. Functional diagram and performance description for measuring instruments. (Page 1 of 3)

Measuring instruments are combinations of instrument mechanisms (indicators) and scales. A generalized functional diagram for instruments of this kind is



Performance for the measuring instrument and its components may be described in the terms defined in Chapters 3, 4, 5 and 6. A performance description of this kind for the measuring instrument is as follows:

Component or System	Static Performance	Generalized Performance
Indicating Mechanism (im)	$(Ind) = S_{(im)[q_{(in)};(Ind)](st)}q_{(in)}$	$(Ind) = [PF]_{(im)[q_{(in)};(Ind)]}q_{(in)}$ (1)
	or	or
	$(Ind) = S_{(m)(st)}q_{(in)}$	$(Ind) = [PF]_{m}q_{(in)}$ (2)
Scale (s)	$q_s = S_{(s)[(Ind);q]}(Ind)$	$q_s = S_{(s)[(Ind);q]}(Ind)$ (3)
	or	or
	$q_s = S_s(Ind)$	$q_s = S_s(Ind)$ (4)
Measuring Instrument (mi)	$q_s = S_{(im)[q;(Ind)](st)}S_{(s)[(Ind);q]}q_{(in)}$	$q_s = [PF]_{(im)[q;(Ind)]}S_{s[(Ind);q]}q_{(in)}$ (6)
	or	or
	$q_s = S_{(mi)[q;q](st)}q_{(in)}$ (7)	$q_s = [PF]_{(mi)[q;q]}q_{(in)}$ (7)
	or	or
	$q_s = S_{(mi)(st)}q_{(in)}$ (8)	$q_s = [PF]_{(mi)}q_{(in)}$ (8)

Note: The scale division markings are generally not subject to dynamic effects. This means that

$$[PF]_{(s)[(Ind);q]} = S_{(s)[(Ind);q]} = S_{(s)[(Ind);q](st)} \quad (5)$$

In any situation for which this is not true, scale performance is given by a performance function $[PF]_{(s)[(Ind);q]}$ instead of the static scale sensitivity $S_{(s)[(Ind);q](st)}$.

c) Measuring instrument performance in terms of mechanism performance and scale sensitivity

Under static conditions, any given scale reading of an ideal measuring instrument is (except for errors accepted in the calibration) identical with the measure of the input quantity level that produces the index position (indication) corresponding to the given scale reading. As a consequence of this condition, an ideal instrument under static conditions always gives

$$[q_s]_{(ideal)} = q_{(in)} \quad (9)$$

It follows that

$$S_{(mi)[q;q](st)(ideal)} = 1 \quad (10)$$

and

$$S_{(s)[(Ind);q](ideal)} = \frac{1}{S_{(im)[q;(Ind)](st)(ideal)}} \quad (11)$$

= indication – indicated quantity ideal scale sensitivity

Definition Summary 29-2. Functional diagram and performance description for measuring instruments. (Page 2 of 3)

Equation (11) gives the basic calibration condition that represents the static performance goal for all measuring instruments.

When the background of the situation defines the input quantity and the scale reading, Eq. (11) may be written in the form:

$$S_{(s)(ideal)} = \frac{1}{S_{(m)(st)(ideal)}} \tag{12}$$

When it is understood that Eq. (12) is a static performance goal for actual instruments,

$$S_s = \frac{1}{S_m} \tag{13}$$

d) Ideal measuring instrument static performance in terms of mechanism performance and scale sensitivity

Definition Summary 29-2. Functional diagram and performance description for measuring instruments. (Page 3 of 3)

except for discrepancies that are known and accepted in the specified calibration. An actual measuring instrument has the accepted performance discrepancies of the ideal measuring instrument and, in addition, produces scale readings that have other differences from true measures of the input quantity. These additional difference components are not exactly determinable, but they may be estimated within more or less uncertain limits by the use of probability theory, or some other method.

RELATIONSHIP BETWEEN SCALE SENSITIVITY AND MECHANISM SENSITIVITY FOR IDEAL MEASURING INSTRUMENTS

29.12. Perfect observations from any ideal measuring instrument with negligibly small static performance discrepancies give static scale readings equal to the corresponding true levels of the input quantity. This fact means that for an ideal instrument under static conditions the input quantity scale reading, q_s, is equal to the input quantity, $q_{(in)}$ (the input quantity is considered as meaning the measure of the input quantity). The corresponding condition on the mechanism and scale static sensitivities is given by Eqs. (10) and (11) of Definition Summary 29-2. These equations show that the input quantity - scale reading static sensitivity for the instrument must be equal to unity and that the indication - scale reading sensitivity must be equal to the reciprocal of the input quantity - indication static sensitivity. This relationship is the basic rule of measuring instrument static performance and is repeated with simplified notation in Eqs. (12) and (13) of Definition Summary 29-2. A case in which the relationship between mechanism sensitivity and scale sensitivity is an especially important feature of an instrument is described in Design Performance Summary 5-1 and Derivation Summary 5-1 of Chapter 5.

PERFORMANCE-QUALITY-DESCRIBING CONCEPTS FOR ACTUAL MEASURING INSTRUMENTS; INACCURACY, UNCERTAINTY, AND ERROR

29.13. From the standpoint of performance quality, actual measuring instruments differ from perfect measuring instruments because actual scale readings are not identical with the true measures for the corresponding input quantity levels. A system of concepts, definitions, and symbols is developed in this chapter for describing the features that determine performance quality.

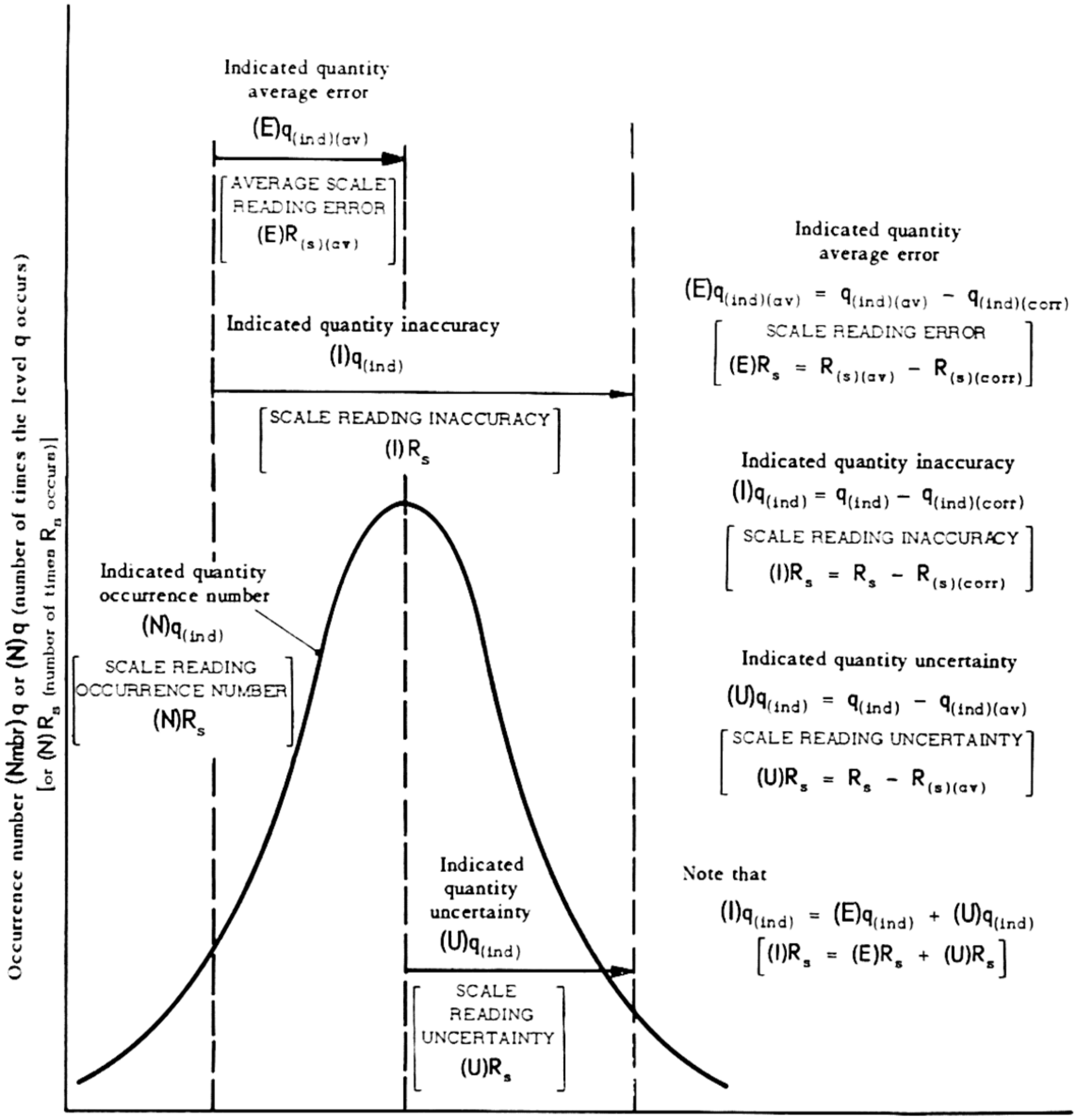
29.14. By definition, the algebraic difference between the actual scale reading (also called the indicated scale reading or simply the scale reading) and the correct scale reading, which is equal to the true measure of the input quantity level, is the indicated quantity inaccuracy or the scale reading inaccuracy. The discussion of Chapter 9 shows that this inaccuracy is a special case of the indicated quantity deviation that for the present situation may be defined as the algebraic difference between the indicated scale reading and a reference scale reading equal to the true scale reading.

29.15. In general, indicated quantity inaccuracy may be resolved into two components. Of these components, indicated quantity uncertainty is not exactly determinable except in special cases and must be treated by a statistical procedure or estimated within limits by some other method. Statistical methods similar to those discussed in Chapter 11 may be applied to the determination of measures for uncertainty when it is possible to take a series of scale readings for the same input quantity level. When the input quantity varies with time in a way that makes repeated observations for the same input level impossible, the methods developed for static quantities must be extended and supplemented by more powerful procedures.

29.16. When a series of scale readings of reasonable length is available for the same input quantity level, uncertainty effects may be theoretically reduced by averaging the readings and treating the resulting average indicated quantity (which may also be called the average scale reading) as effectively free from uncertainty. The remaining component of inaccuracy is the indicated quantity error. Figure 29-1, which is similar to Fig. 9-9, illustrates the definitions of inaccuracy and its components, uncertainty and error, in terms of the normal probability distribution* for static observation. In Fig. 29-1, parallel names and symbols show that scale reading (symbol R_s) may be considered as an equivalent generalization of indicated quantity (symbol $q_{(ind)}$).

29.17. The inherent nature of uncertainty precludes the complete removal of its effect from any particular scale reading. The best that can be done in practice is to provide an estimate of the uncertainty magnitude on the basis of a statistical study of performance for the components involved or from some source that

* A discussion of the normal probability distribution is given in Chapter 11.



Indicated quantity average error

$$(E)q_{(ind)(av)} = q_{(ind)(av)} - q_{(ind)(corr)}$$

$$\left[\text{SCALE READING ERROR}\quad (E)R_s = R_{(s)(av)} - R_{(s)(corr)}\right]$$

Indicated quantity inaccuracy

$$(I)q_{(ind)} = q_{(ind)} - q_{(ind)(corr)}$$

$$\left[\text{SCALE READING INACCURACY}\quad (I)R_s = R_s - R_{(s)(corr)}\right]$$

Indicated quantity uncertainty

$$(U)q_{(ind)} = q_{(ind)} - q_{(ind)(av)}$$

$$\left[\text{SCALE READING UNCERTAINTY}\quad (U)R_s = R_s - R_{(s)(av)}\right]$$

Note that

$$(I)q_{(ind)} = (E)q_{(ind)} + (U)q_{(ind)}$$

$$\left[(I)R_s = (E)R_s + (U)R_s\right]$$

Note: When no likelihood of misunderstanding exists, the indicated quantity average error $(E)q_{(ind)(av)}$ may be replaced by the indicated quantity error, i.e.,

$$(E)q_{(ind)(av)} \longrightarrow (E)q_{(ind)}$$

$$\left[(E)R_{(s)(av)} \longrightarrow (E)R_s\right]$$

(Refer to Fig. 9-9)

Fig. 29-1. Definitions for inaccuracy, uncertainty, and error of indicated quantity and scale reading when repeated observations are possible.

provides an estimate of maximum uncertainty. Scale reading error is unlike scale reading uncertainty because it is systematic in the sense that it is identical for all the readings from a particular measuring instrument each time a given input level is applied. This fact makes it theoretically possible to determine the error associated with any given scale reading and to account for errors by means of scale reading corrections. In the ideal case, these corrections may be used to find correct scale readings by the elimination of error effects. On the other hand, practical situations do not often provide ideal scale reading corrections, so that the actual scale reading corrections that are available produce corrected scale readings, which differ to some extent from the correct scale readings.

29.18. For any given case, the correction is defined as the corresponding error with its sign reversed. When this convention is accepted, all the essential conventions for error and correction are summarized by two rules:

1) Add positive corrections to actual scale readings to find corrected scale readings.
2) Corrections are equal to errors with signs reversed.

Deviation corrections may be defined for indicated scale reading deviations by a relationship identical with that used for scale reading corrections.

29.19. All the foregoing definitions represent special cases of the quantity comparison concepts defined in Chapter 9. The relationships involved are illustrated graphically in Fig. 29-2, which is generally similar to Fig. 9-11. Self-defining symbols formed by use of the conventions described in Chapter 9 are given for each of the quantities illustrated in Fig. 29-2. Parallel names and symbols are used for scale readings and indicated quantities.

29.20. When input quantities and the corresponding scale readings are varying with time, it is impossible to make repeated observations at any given instant, but the erratic component in any given continuous record may be reduced by smoothing. Smoothing may be of many types and may be introduced either by operation of the instrument mechanism or by some mathematical treatment of the data from scale reading records. In any case, the smoothed scale reading under nonstatic conditions corresponds to the average scale reading for static conditions. With a substitution of the smoothed scale reading for the average scale reading, error and deviation for continuous variations are similar to the corresponding concepts defined in Fig. 29-2 for static conditions. Inaccuracy at any given instant may be defined in the same way for varying conditions as for static conditions. On the other hand, simple statistical treatments of inaccuracies are not directly useful when repeated scale readings for the same input quantity level are unavailable. For this reason, it is convenient to define roughness as basically similar to the concept of uncertainty for static conditions. Under this definition, scale reading roughness at any given instant is the difference between the scale reading and the smoothed scale reading. Figure 29-3, which is similar to Fig. 9-10, illustrates

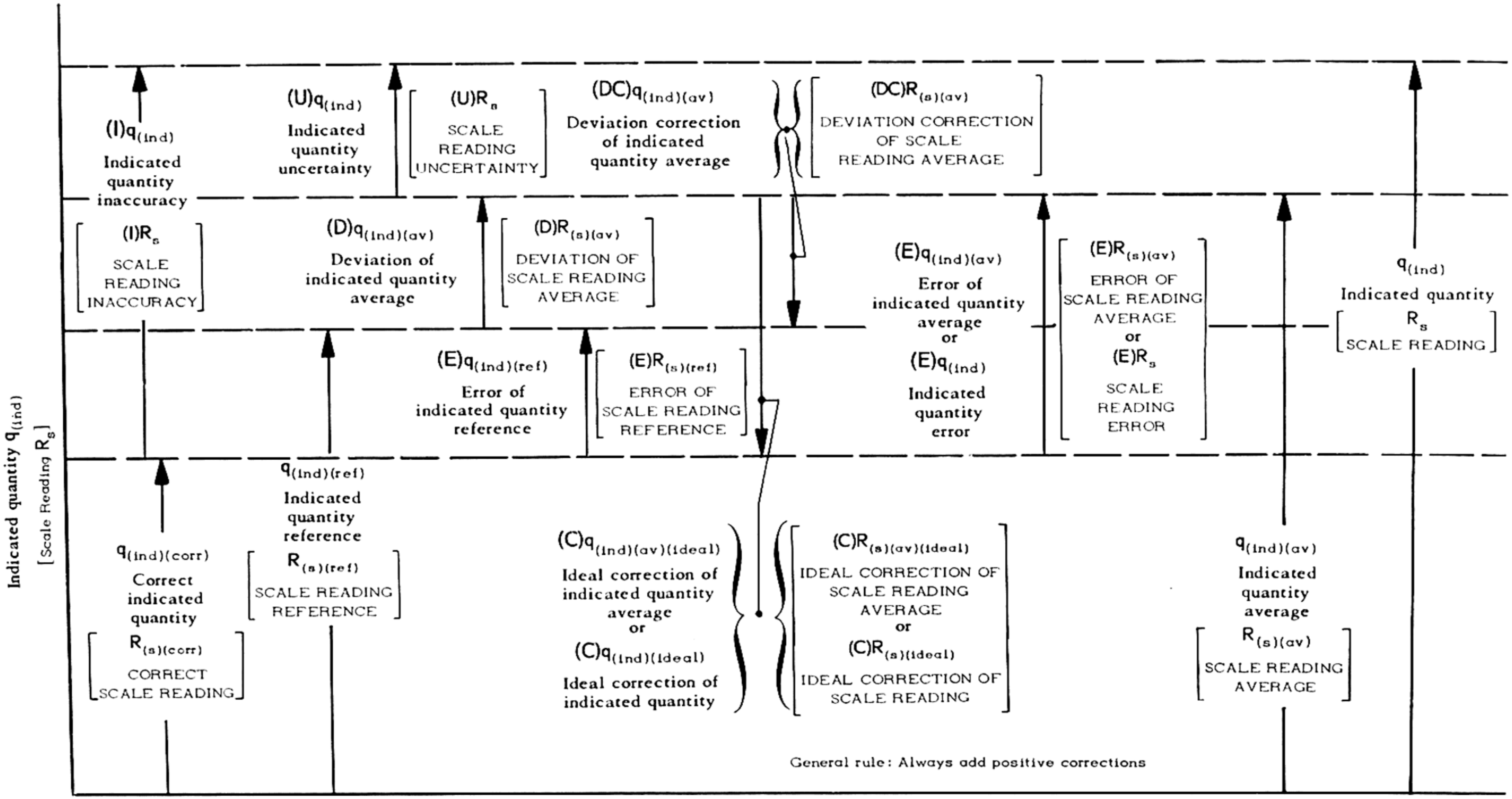


Fig. 29-2. Summary of definitions and symbols for concepts associated with the description of measuring instrument static performance quality.
(Page 1 of 2)

$$(I)\,q_{(ind)} = q_{(ind)} - q_{(ind)(corr)}$$

$$[(I)\,R_s = R_s - R_{(s)(corr)}]$$

$$(U)\,q_{(ind)} = q_{(ind)} - q_{(ind)(av)}$$

$$[(U)\,R_s = R_s - R_{(s)(av)}]$$

$$(E)\,q_{(ind)(av)} \text{ or } (E)\,q_{(ind)} = q_{(ind)(av)} - q_{(ind)(corr)}$$

$$[(E)\,R_{(s)(av)} \text{ or } (E)\,R_s = R_{(s)(av)} - R_{(s)(corr)}]$$

$$(C)\,q_{(ind)(av)} \text{ or } (C)\,q_{(ind)} = q_{(ind)(corr)} - q_{(ind)(av)} = -(E)\,q_{(ind)(av)} \text{ or } -(E)\,q_{(ind)}$$

$$[(C)\,R_{(s)(av)} \text{ or } (C)\,R_s = R_{(s)(corr)} - R_{(s)(av)} = -(E)\,R_{(s)(av)} \text{ or } -(E)\,R_s]$$

$$(D)\,q_{(ind)(av)} = q_{(ind)(av)} - q_{(ind)(ref)}$$

$$[(D)\,R_{(s)(av)} = R_{(s)(av)} - R_{(s)(ref)}]$$

$$(DC)\,q_{(ind)(av)} = q_{(ind)(ref)} - q_{(ind)(av)} = -(D)\,q_{(ind)(av)}$$

$$[(DC)\,R_{(s)(av)} = R_{(s)(ref)} - R_{(s)(av)} = -(D)\,R_{(s)(av)}]$$

When quantities are varying with time, the average quantity level has no application; it must then be replaced by the smoothed quantity; i.e., $q_{(ind)(av)} \approx q_{(ind)(sm)}$. Then

$$(E)\,q_{(ind)(sm)} = q_{(ind)(sm)} - q_{(ind)(corr)}$$

$$[(E)\,R_{(s)(sm)} = R_{(s)(sm)} - R_{(s)(corr)}]$$

$$(C)\,q_{(ind)(sm)} = q_{(ind)(corr)} - q_{(ind)(sm)} = -(E)\,q_{(ind)(sm)}$$

$$[(C)\,R_{(s)(sm)} = R_{(s)(corr)} - R_{(s)(sm)} = -(E)\,R_{(s)(sm)}]$$

$$(D)\,q_{(ind)(sm)} = q_{(ind)(sm)} - q_{(ind)(ref)}$$

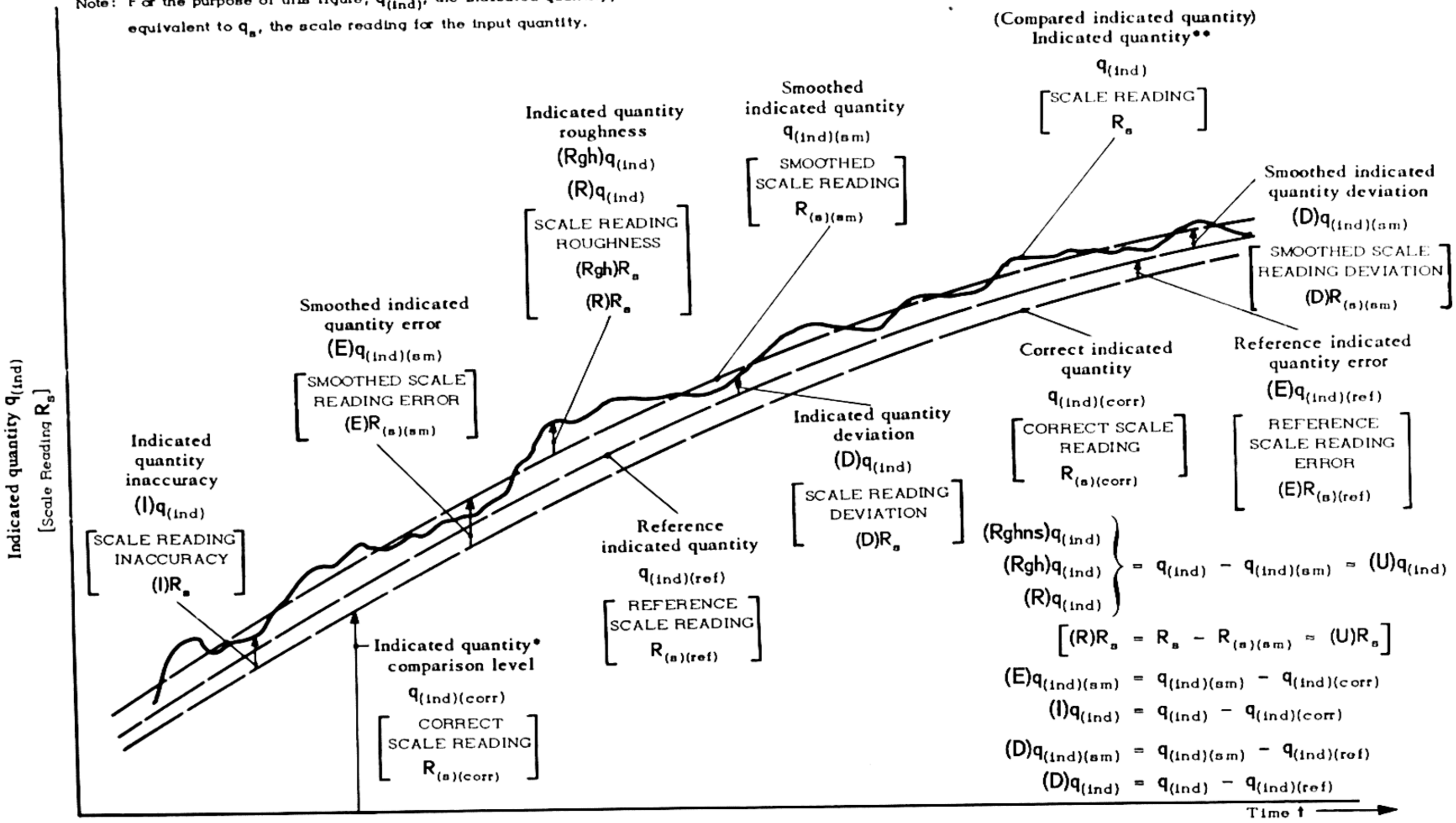
$$[(D)\,R_{(s)(sm)} = R_{(s)(sm)} - R_{(s)(ref)}]$$

$$(DC)\,q_{(ind)(sm)} = q_{(ind)(ref)} - q_{(ind)(sm)} = -(D)\,q_{(ind)(sm)}$$

$$[(DC)\,R_{(s)(sm)} = R_{(s)(ref)} - R_{(s)(sm)} = -(D)\,R_{(s)(sm)}]$$

Fig. 29-2. Summary of definitions and symbols for concepts associated with the description of measuring instrument static performance quality. (Page 2 of 2)

Note: For the purpose of this figure, $q_{(ind)}$, the indicated quantity, is equivalent to q_s, the scale reading for the input quantity.



* The quantity comparison level may be any arbitrary level or the correct level.

** This quantity may in general be any compared quantity or any indication.

Fig. 29-3. Summary of definitions and symbols for concepts associated with the description of measuring instrument performance quality when the input quantity and scale readings vary with time.

the concepts just defined and gives the corresponding self-defining symbols for indicated quantity and scale reading based on the conventions of Chapter 9.

TERMINOLOGY FOR DESCRIBING THE QUALITY OF MEASURING INSTRUMENT PERFORMANCE

29.21. Imperfections in scale readings determine the quality of measuring instrument performance. Thus, an instrument of this class with small scale reading imperfections has performance of high quality, while another instrument with larger scale reading imperfections has lower quality performance. Performance quality is a matter of primary concern in describing measuring instrument characteristics, not only to engineers but also to users and others who are interested only in results. For this reason, it is important to define a complete system of concepts and terms associated with this aspect of instrument operation. In order to facilitate discussions of measuring instrument problems, it is desirable to select commonly used names for essential concepts and to assign meanings that fit into the context patterns generally associated with the names. The concepts and terminology described in this chapter are the result of an effort to develop a system with these characteristics. It is the purpose of this section to outline the background reasons for selecting the definitions summarized in Figs. 29-1, 29-2 and 29-3.

29.22. Writers who discuss terms for describing the quality of measuring instrument performance generally agree that three concepts have fundamental importance:

1) The first concept is associated with the difference between the actual scale reading and the corresponding correct scale reading.

It is a commonly recognized fact that this difference may be resolved into two components, one nonsystematic and the other systematic:

2) The second concept is associated with the component of the difference between the actual scale reading and the corresponding correct scale reading that must be described by a statistical measure of reliability or localized within a maximum limit by some other method.

3) The third concept is associated with the component of the difference between the actual scale reading and the corresponding correct scale reading that is systematic and can be represented reasonably well in exact numerical terms.

29.23. Definition Summary 29-3 lists the definitions given by Webster's New Collegiate Dictionary* for a group of words that might be associated with the three basic concepts of measuring instrument performance quality. The words accuracy, inaccuracy, deviation, variation, variance, and error, which are listed in section a of the summary, might be associated with the first concept, since all appear to have meanings that fit in with a description of differences between actual scale readings and correct scale readings. By definition, the term accurate means "... in exact or careful conformity to truth, or to some standard, esp. as the result

* All definitions reproduced by permission from Webster's New Collegiate Dictionary, copyright, 1949, 1951, by G.&C. Merriam Co.

accurate – *adj.* In exact or careful conformity to truth, or to some standard, esp. as the result of care; exact. – Syn. See CORRECT. . . .

accuracy – *n.* State or quality of being accurate; freedom from mistake or error; precision; exactness.

inaccurate – *adj.* Not accurate; hence, incorrect; erroneous.

inaccuracy – *n.* Quality or fact of being inaccurate; also, a mistake; an error.

deviate – *v.i.* To turn aside from a course; to stray, as from a standard, a topic. . . .

deviation – *n.* Act or instance of deviating; a turning aside.

variation – *n.* 1. Act or an instance of varying; change in the form, position, state, or qualities of a thing; modification, mutation, or deviation, or an instance or example thereof. 2. Extent to which a thing varies; amount or rate of change.

variance – *n.* 1. The fact, quality, or state of being variable or variant; variation or a degree of it; difference; deviation; discrepancy. 2. Dissension; discord; a dispute; quarrel. 3. *Law.* A disagreement between two parts of the same legal proceeding, which, to be effectual, ought to agree, as the writ and the declaration, or the allegation and the proof.

error – *n.* 1. Belief in what is untrue, the state of holding such belief, or an instance of it. 2. A moral offense; sin. 3. An act involving a departure from truth or accuracy; a mistake. . . . 6. *Math.* The difference between an observed or calculated value, generally of a physical quantity, and the true value. Syn. Error, mistake, blunder, slip, lapse mean a departure from what is true, right, or proper. **Error** is the most comprehensive term: it may imply carelessness or intention but it may suggest an inaccuracy where accuracy is impossible; **mistake** implies misconception, misunderstanding, inadvertence, or the like, and is seldom a harsh term; **blunder** commonly implies ignorance or stupidity and, usually, blameworthiness; **slip** carries a stronger implication of inadvertence or accident especially in a trivial mistake; **lapse** implies forgetfulness, weakness, or inattention.

a) Terms that may be associated with differences between indicated quantity readings and correct indicated quantity readings

certain – *adj.* 1. Fixed; settled. 2. One or more specific (things or persons not further described); as, a *certain* town; *certain* persons. 3. Sure or dependable; reliable; as, a *certain* remedy. 4. Assured in mind; sure. . . . 6. Not to be doubted or denied; indubitable. 7. Destined; sure; – followed by an infinitive; as, it is *certain* to happen. . . .

certainty – *n.* 1. Quality, state or fact of being certain; certitude. 2. A fact unquestionably established. Syn. Certainty, certitude, assurance, conviction mean a state of being free from doubt. **Certainty** and **certitude** are distinguished only in very precise use, the former implying the existence of objective, unquestionable proofs, the latter, a faith or belief so strong that it resists all attack; **assurance** stresses sureness or confidence rather than certainty; **conviction**, though it may or may not imply previous doubt, usually implies that one is or has been convinced and is assured of the truth of something.

uncertain – *adj.* 1. Indeterminate. 2. Not certain to occur; indefinite; problematical. 3. Not reliable; untrustworthy. 4.a Not known beyond doubt; dubious. b Not having certain knowledge; doubtful. c Not clearly identified or defined. 5. Not constant; variable; fitful. . . .

uncertainty – *n.* 1. Lack of certainty; doubt. 2. That which is uncertain. Syn. Uncertainty, doubt, dubiety, dubiosity, skepticism, suspicion, mistrust mean lack of sureness about someone or something. **Uncertainty** may imply a falling short of certainty or so far a remove from it that one can only guess or surmise; **doubt** suggests not only uncertainty but an inability to make a decision; **dubiety** and **dubiosity** suggest uncertainty, the former implying wavering and the latter, vagueness or mental confusion; **skepticism** suggests incredulity while any plausible evidence to the contrary exists; **suspicion**, a lack of faith in the truth, reality, fairness, etc., of someone or something; **mistrust**, genuine doubt based upon suspicion.

precise – *adj.* 1. Exactly or sharply defined or stated; not vague or equivocal; as, *precise* directions. 2. Minutely exact; not varying in the slightest degree from truth, accuracy, standard, etc.; as, a *precise* balance. 3. Strictly conforming to rule or usage; punctilious, scrupulous; sometimes, overnice; very strict. – Syn. See CORRECT.

precision – *n.* Quality or state of being precise; accuracy; definiteness. . . .

variation –
variance –
deviation –
error – } see a

b) Terms that may be associated with the components of differences between indicated quantity readings and correct indicated quantity readings that must be represented by statistical measures of difference

By permission. From Webster's New Collegiate Dictionary, copyright, 1949, 1951, by G.&C. Merriam Co.

Definition Summary 29-3. Summary of dictionary definitions for terms associated with descriptions of the quality of measuring instrument performance. (Page 1 of 2)

deviate –
deviation –
variation –
variance –
error – } see a

c) Terms that may be associated with systematic components of differences between indicated quantity readings and correct indicated quantity readings

correct – ... *adj.* 1. Conforming to an approved or conventional standard; proper; as, *correct* manners, costume, grammar. 2. Conforming to fact or truth; of reasoning, in accordance with logical principles; of statements or opinions, according with known facts; of a copy, free from errors. Syn. Correct, accurate, exact, precise, nice, right mean conforming to fact, standard, or truth. **Correct** usually implies freedom from fault or error as judged by some standard; **accurate** implies, more positively, fidelity to fact or truth attained by the exercise of care; **exact** stresses strict accordance with fact, standard, or truth; **precise** stresses sharpness of definition or delimitation; **nice**, as here compared, stresses great precision and delicacy, as in adjustment, discrimination, etc.; **right** comes close to *correct* but throws more emphasis upon conformity to fact, truth, or a standard than on freedom from error or fault.

correction – *n.* 1. Act of correcting; amendment; rectification; also, reproof; punishment; chastisement. ... 3. That which is substituted in the place of what is wrong; an emendation. 4. A quantity applied by way of correcting; as, the index *correction* of a sextant.

compensate – *v.t.* 1. To be equivalent to; to make up for. 2. To make equal return to; to remunerate; to requite suitably. ... Syn. *(1)* Compensate, countervail, balance, offset mean to make up for that which is excessive, deficient, harmful, helpful, etc., in another. **Compensate** implies a making amends for or supplying a recompense for whatever has been suffered or lost through another; **countervail** suggests the counteraction of a bad or harmful influence or of damage suffered through it; **balance** implies the harmonious adjustment of two or more things that are contrary or opposed so that no one outweighs the other or others or can exert a harmful influence; **offset** implies the neutralization of one thing's good or evil effect by something that exerts a contrary effect. ...

compensation – *n.* 1. Act or principle of compensating; also, an instance of this. 2. That which compensates for loss or privation; recompense. ...

d) Terms that may be associated with the reduction of effects due to the systematic component of differences between indicated quantity readings and correct indicated quantity readings

By permission. From Webster's New Collegiate Dictionary, copyright, 1949, 1951, by G.&C. Merriam Co.

Definition Summary 29-3. Summary of dictionary definitions for terms associated with descriptions of the quality of measuring instrument performance. (Page 2 of 2)

of care," and inaccurate means "not accurate." By definition, deviate means ". . . to turn aside from a course; to stray, as from a standard," and deviation is "a turning aside." Variation is the" . . . act or an instance of varying," and variance means" . . . the fact, quality, or state of being variable." Error means" . . . An act involving a departure from truth or accuracy." The definition for correct is ". . . conforming to fact or truth."

29.24. When the correct scale reading is identified with the "true" scale reading, the ideas of deviation and error both have connotations that are wrong for describing the difference between the actual and correct scale readings as they both imply a "turning aside from truth" rather than a difference that contains an element of uncertainty. At the same time, variation and variance are both associated with "change" rather than "difference." These shades of meaning tend to disqualify "deviation," "error," "variation," and "variance" as names to represent the difference between the actual and the correct scale readings. With these terms eliminated, the remaining possibility for the actual-to-correct scale reading difference is inaccuracy. This term is used for the purposes of Instrument Engineering.

29.25. In the "basic terms" recommended by the Terminology Committee, Industrial Instruments and Regulators Division, ASME,[A5][A6] the concept of inaccuracy as defined above is called "error in measurement." In connection with this term, the correct scale reading is called the "true" value of a measured quantity that". . . refers to accepted engineering standards, such as the standard meter, gram, etc. It is assumed that a true value always exists even though it may be impossible to determine."[A6]

29.26. Section b of Definition Summary 29-3 lists uncertainty, precision, variance, deviation, and error as dictionary-defined terms that might reasonably be used to describe the nonsystematic component of inaccuracy (with which the second concept is associated). The definition for uncertainty is ". . . lack of certainty; doubt." The definition for precise is ". . . not varying in the slightest degree from truth, accuracy," and precision is ". . .Quality or state of being precise." The definitions for variance, deviation and error have already been noted. Variance does not appear to be the proper term to describe a statistical concept or a quantity that is known only within limits because it primarily implies change and fails to suggest lack of definite knowledge. Deviation is a term that is often used to represent statistical differences. For example, in the "basic terms" of reference (A6), one of the definitions states that "deviation in measurement is a statistical number representing the randomness among independent measurements of the same true value." Deviation also commonly appears in the literature of probability to describe differences between individual cases and average values. The term is used with this meaning in the discussion of probability that appears in Chapter 11. Error is often identifed with the statistically treated component of inaccuracy. In particular, Trimmer[T1] uses the term random error to describe this inaccuracy component. It has already been noted that the ideas of deviation and error imply a "turning aside" from some reference without any specific connotation of erratic behavior in the process. On the other hand, the accepted definition of uncertainty implies a "lack of certainty or doubt," and carries with it a context that is reasonably associated with the nonsystematic component of inaccuracy. It is true that this component is generally known to remain within certain limits and that, within these limits, the use of probability theory is able to reduce but never to eliminate an associated element of uncertainty. It is for this reason that the term "uncertainty" is used in Instrument Engineering to represent the nonsystematic component of inaccuracy.

29.27. The terms random error and erratic error have connotations that fit in naturally with the concept of uncertainty. It is not likely that the use of these terms to suggest the uncertainty concept will introduce any confusion in practice. On the other hand, deviation might be used for the same purpose but as a term it fits in so nicely for the description of "turning aside" from a reference value* that it is used with this meaning throughout this book. In Chapter 11, devia-

* This definition is illustrated in Figs. 29-2 and 29-3.

tion is given a special meaning to represent the difference between a typical value of a random variable, x, and a reference value that, for theoretical purposes, is the average of an infinite number of x values. The discussion of Chapter 11 considers theoretical situations in which the element of "uncertainty" is eliminated by the use of functions that are definitely specified and in themselves not at all uncertain. It may be considered that the variable x of Chapter 11 is in effect a working variable symbol for the scale reading uncertainty defined in this chapter.

29.28. Precision, the "quality or state of being precise," does not lend itself directly to a description of the uncertainty concept. However, it is natural to consider that an instrument having high precision is an instrument with a low uncertainty. The relationship is discussed further and given a mathematical definition in a later section of this chapter.

29.29. Section c of Definition Summary 29-3 shows that the terms available for describing the systematic component of inaccuracy (with which the third concept is associated) have already been noted as deviation, variation, variance and error. Of these terms, deviation is reserved to describe the difference between a typical value and an arbitrary reference. Variation and variance are rejected as suggesting changes rather than differences. The remaining term that may be associated with the systematic component of inaccuracy is error, which carries the connotation of describing a ". . . departure from truth or accuracy; . . ." This is a proper sense for the present application, if the departure is associated with an average and the reference value is taken as the truth or accurate value of the variable for which the error is defined. Under this definition, error is identical with the concept that is called determinate error by Trimmer.(T1) This concept is not mentioned in the terminology recommendations of references (A3), (A5) and (A6).

29.30. Section d of Definition Summary 29-3 lists dictionary definitions for correction and compensation. Correction means ". . . 3. That which is substituted in the place of what is wrong; an emendation. 4. A quantity applied by way of correcting; as, the index correction of a sextant." Compensate is defined as: "1. To be equivalent to; to make up for . . . 4. Mech. To provide with means of counteracting variation." Compensation means" 1. Act or principle of compensating; also an instance of this." These definitions make it reasonable to assign the term "correction" to a value equal to error with its sign reversed. This means that error is "eliminated" if the corresponding correction is applied. When this result is accomplished within the instrument mechanism instead of by algebraically adding numbers to scale readings, the process of eliminating error effects is called compensation. When correction and compensation are defined in this way, all problems of algebraic sign are resolved by the rule:

Add a positive correction.

29.31. In practice, the concepts and definitions discussed in this section are seldom sufficient to describe the performance quality of any given measuring instrument. Many additional concepts are often needed to fit the requirements of particular situations. It is not feasible to compile a list of all possible terms and symbols. However, the principles illustrated in this section and other sections of this chapter are effective in suggesting the concepts necessary for describing the performance quality of any given instrument.

ACTUAL MEASURING INSTRUMENTS; ACTUATING INPUTS, INTERFERING INPUTS, AND MODIFYING INPUTS

29.32. The discussion of Chapter 10 recognizes the fact that the inputs for any operating system may be resolved into three classes. In terms of measuring instrument operation, the three classes are:

1) Actuating inputs – those quantities that the instrument is designed to receive and measure in terms of scale readings.
2) Interfering inputs – those quantities that produce undesirable scale reading components not directly distinguishable from scale reading components due to actuating inputs. Scales are not ordinarly calibrated in terms of interfering inputs.
3) Modifying inputs – those inputs that change the relationships among actuating inputs, interfering inputs and scale readings.

Figure 29-4 is a functional diagram for a measuring instrument with an indefinite number of inputs of each class. In any given situation, the indication is determined by the resultant effect of all the inputs. The scale reading (symbol R_s) corresponds to this indication.

29.33. The pressure indicator of Figs. 2-1 through 2-8 of Chapter 2 is an example of a measuring instrument with pressure as its actuating input and linear acceleration as an interfering input. In general, temperature will be an interfering input, and possibly a modifying input also, for a pressure gage of the type illustrated. This means that if the temperature of the gage mechanism is changed, the reading will show a corresponding change when the input pressure is held constant. In addition, changes in scale reading will have different relationships to changes of input pressure for various levels of the gage mechanism temperature, which for this reason is a modifying input.

29.34. Measuring instruments may be designed to receive several actuating inputs and to produce readings that represent measures of some quantity that is not any one of the inputs directly, but is some function of all the actuating inputs. For example, a true air speed meter for aircraft must receive barometric pressure, atmospheric temperature and stagnation pressure, as this quantity is defined in Fig. 5-3 of Chapter 5. The readings of this instrument will be in terms of

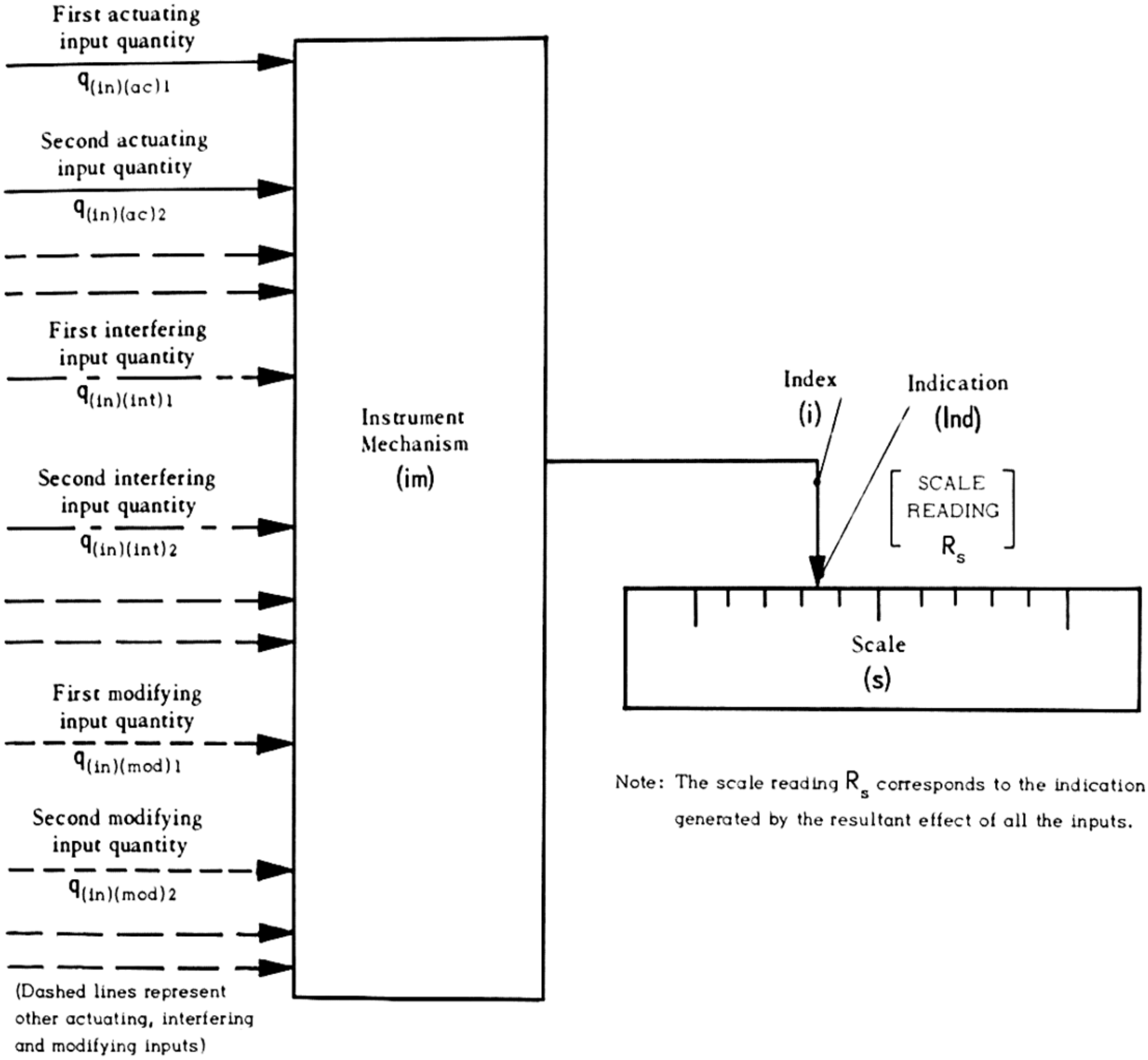


Fig. 29-4. Functional diagram for an actual measuring instrument with multiple inputs.

true air speed generated as a function of the three input quantities that serve as actuating inputs. *

29.35. It is convenient to separate the quantities that affect the indications from any given instrument mechanism into operating inputs, to which the mechanism is designed to respond, and the environment, which is made up of all quantities that produce output changes but are not considered as operating inputs.

CALIBRATION CONDITIONS

29.36. Calibration is defined in an earlier section of this chapter as the process of adjusting instrument mechanism performance and placing scale markings in positions to give scale readings that are properly related to measures of the corresponding actuating quantity levels. Because scale readings are affected by changes in the quantities that make up the environment, calibrations must be carried out under calibration conditions in order that unique positions may be fixed for scale markings. In any given case, calibration conditions are

* The use of temperature as an actuating input is one of the distinctions between a true air speed meter and a pitot-static airspeed meter.

established by the specification of calibration levels for each of the important environmental conditions. For example, calibration conditions for a voltmeter may be established by a specification of the meter temperature under which calibration is to be carried out.

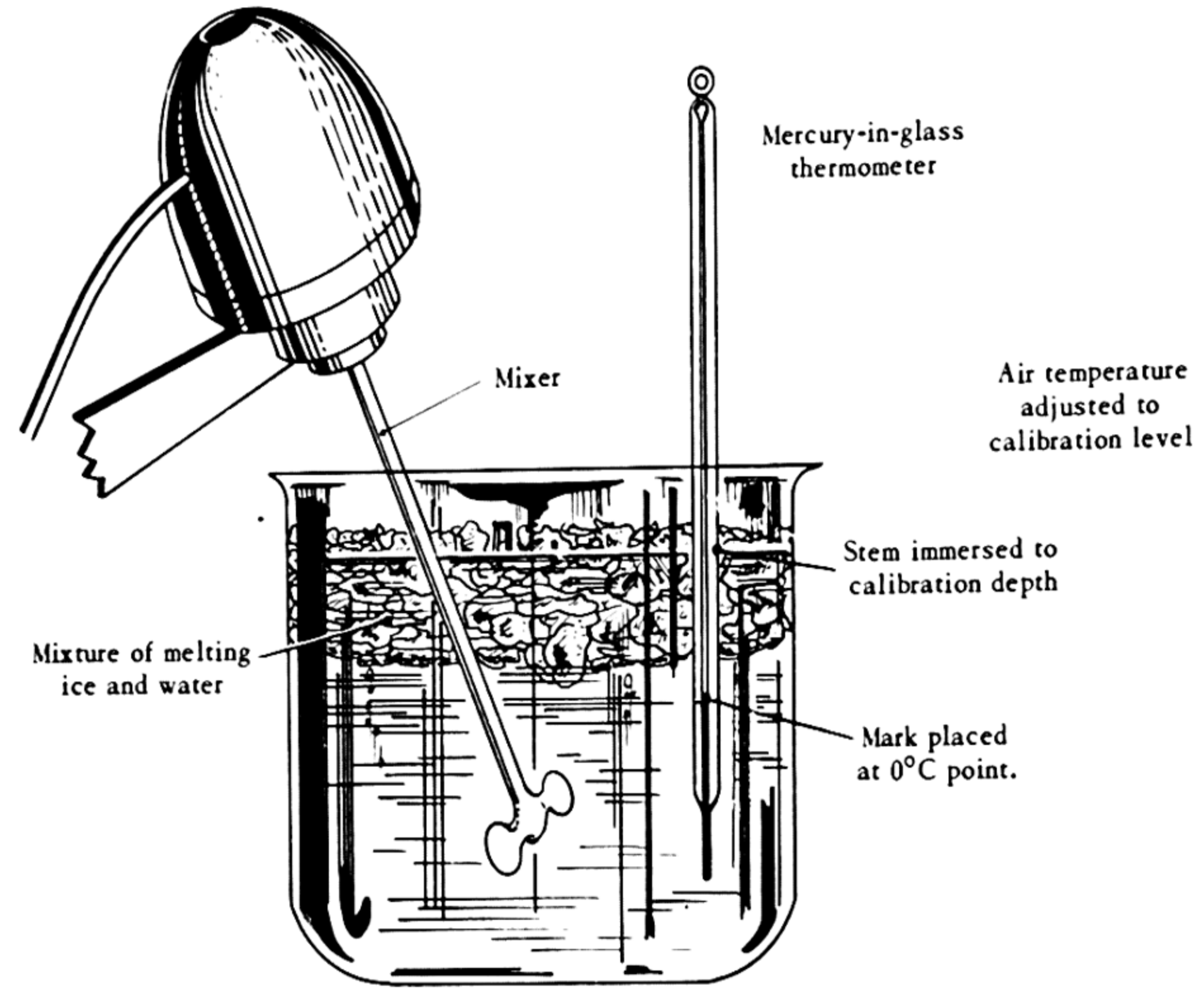
29.37. Calibration levels are the particular levels of the environmental quantities that combine to establish calibration conditions. The instrument mechanism – scale combination is adjusted to give correct readings with these quantities at calibration levels. These levels may also be used to provide known input conditions for determinations of scale reading error and scale reading uncertainty. Calibration levels are fixed by primary calibration standards or by secondary calibration standards. Primary calibration standards are established by specified physical systems under particular circumstances. For example, the primary calibration standard temperature for the zero-degree centigrade point on a thermometer is defined as the temperature of a mixture of melting ice and water. Calibration conditions for this point on a mercury-in-glass thermometer may be established by immersing the thermometer stem in the water to a specified depth with the projecting part of the stem in air at the specified calibration temperature. A typical arrangement for a thermometer calibration at the zero-degree point with a vessel filled with ice and water as the primary standard is illustrated in Fig. 29-5a. In practice, a number of primary standard points are usually required for a complete calibration. For example, water boiling under standard barometric pressure supplies a thermometer calibration level at the 100-degree centigrade point. Intermediate points are placed between the primary standard points by using a specified number of equal spaces or some other specified rule of division.

29.38. Figure 29-5b illustrates the use of a secondary standard for calibration purposes. In this figure, calibration levels are established by scale readings of the secondary-standard ammeter, which has itself been calibrated by means of primary-standard levels. The secondary-standard meter is connected in series with the meter to be calibrated. With proper calibration conditions established by adjusting meter temperatures,* the process of calibration is to place scale marks on the meter under calibration so that the scale readings on this meter are identical with the scale readings of the secondary-standard meter for a selected set of calibration current levels.

SCALES

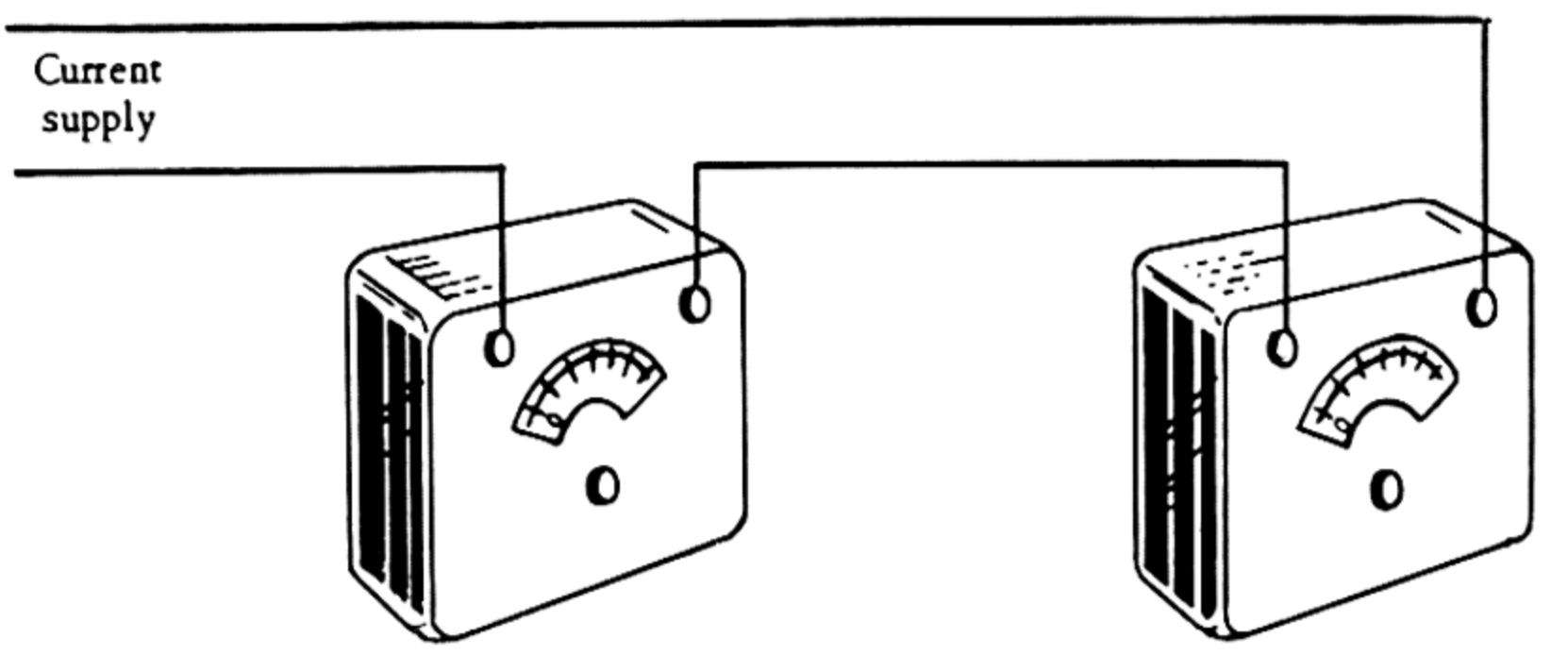
29.39. Measuring instrument scales may be classified in terms of the maximum scale reading, the minimum scale reading, the scale reading range and the location of the zero. By definition, the scale reading range is the algebraic difference between the maximum scale reading and the minimum scale reading.

* Calibration temperatures may be different for the standard meter and the meter under calibration.



Note: Calibration conditions are established by adjusting stem immersion depth and air temperature.

a) Calibration of 0° Centigrade point on thermometer by primary-standard level of actuating quantity



Note: Meter temperatures are at calibration levels to give calibration conditions.

b) Calibration of ammeter by use of a secondary-standard meter

Fig. 29-5. Calibration by means of a primary standard and by means of a secondary standard.

R_s = scale reading (position of index in terms of scale divisions)

$R_{(s)(max)}$ = maximum scale reading

$R_{(s)(min)}$ = minimum scale reading

$[RR]_s$ = scale reading range

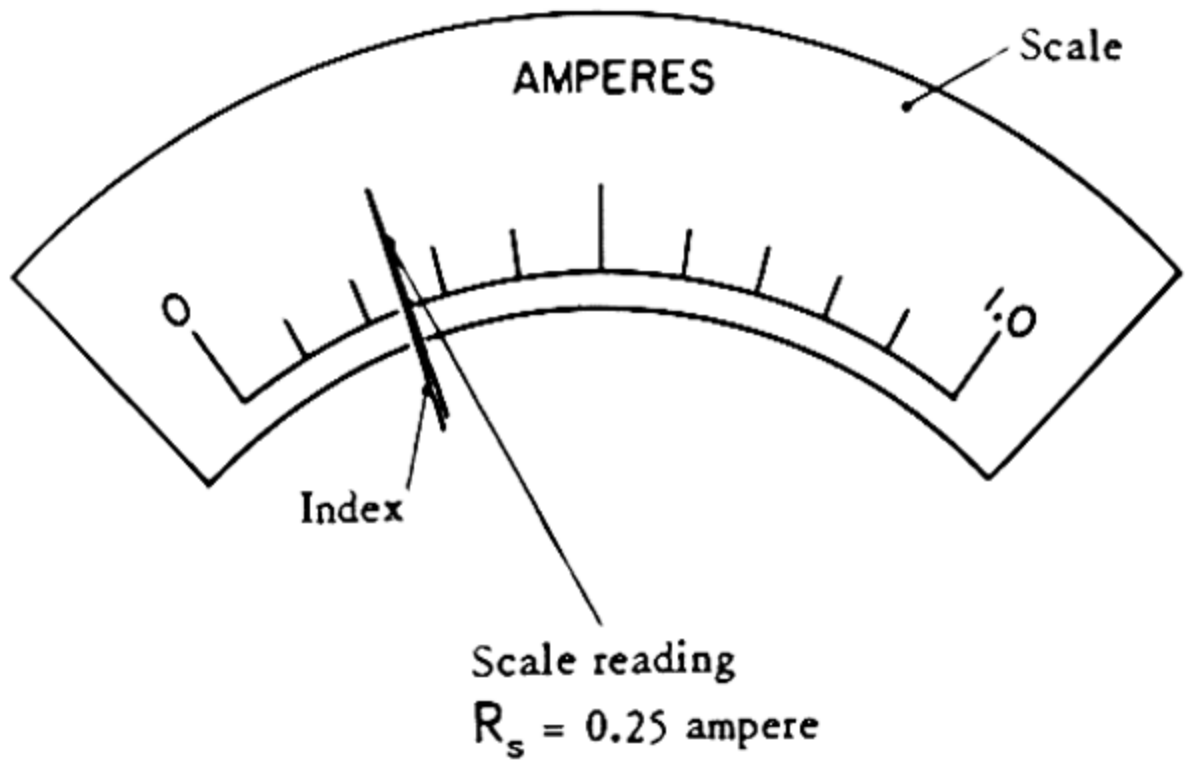
$= R_{(s)(max)} - R_{(s)(min)}$

$R_{(s)(min)} = 0$

$R_{(s)(max)}$ = 1.0 ampere

$[RR]_s = 1.0 - 0 = 1.0$ ampere

A normal-zero scale has $R_{(s)(min)} = 0$



a) Normal-zero scale

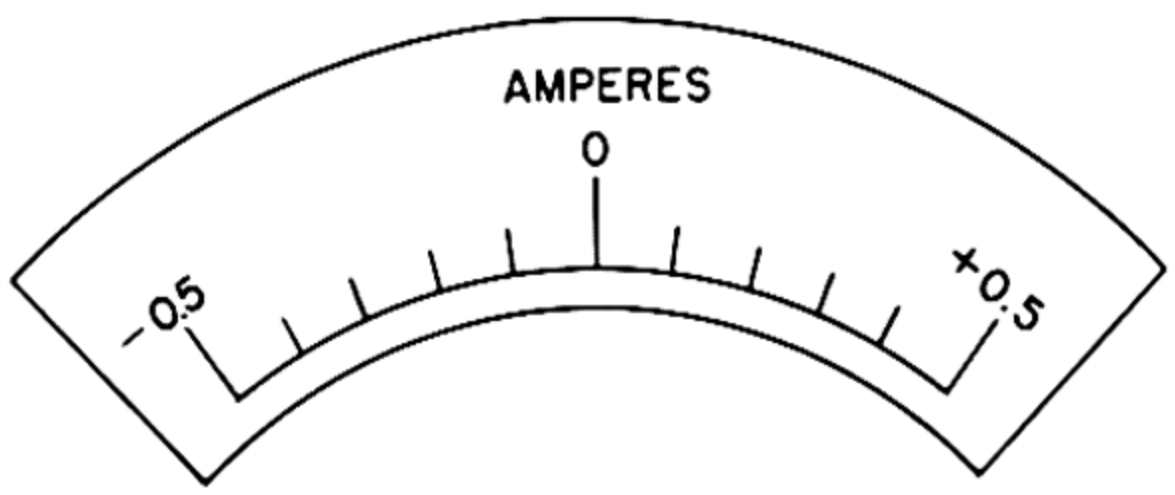
$R_{(s)(min)}$ = –0.5 ampere

$R_{(s)(max)}$ = +0.5 ampere

$[RR]_s = 0.5 - (-0.5) = 1.0$ ampere

A displaced-zero scale has

$R_{(s)(min)} < (R_s = 0) < R_{(s)(max)}$



b) Displaced-zero scale

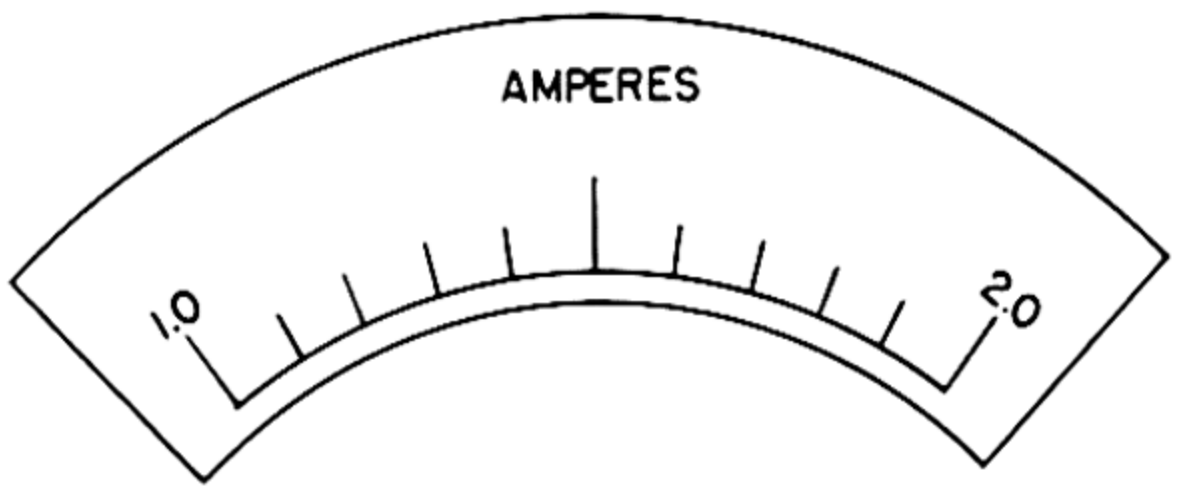
$R_{(s)(min)}$ = 1.0 ampere

$R_{(s)(max)}$ = 2.0 amperes

$[RR]_s = 2.0 - 1.0 = 1.0$ ampere

A suppressed-zero scale has either

$(R_s = 0) < R_{(s)(min)}$ or $R_{(s)(max)} < (R_s = 0)$



c) Suppressed-zero scale

Fig. 29-6. Scale characteristics.

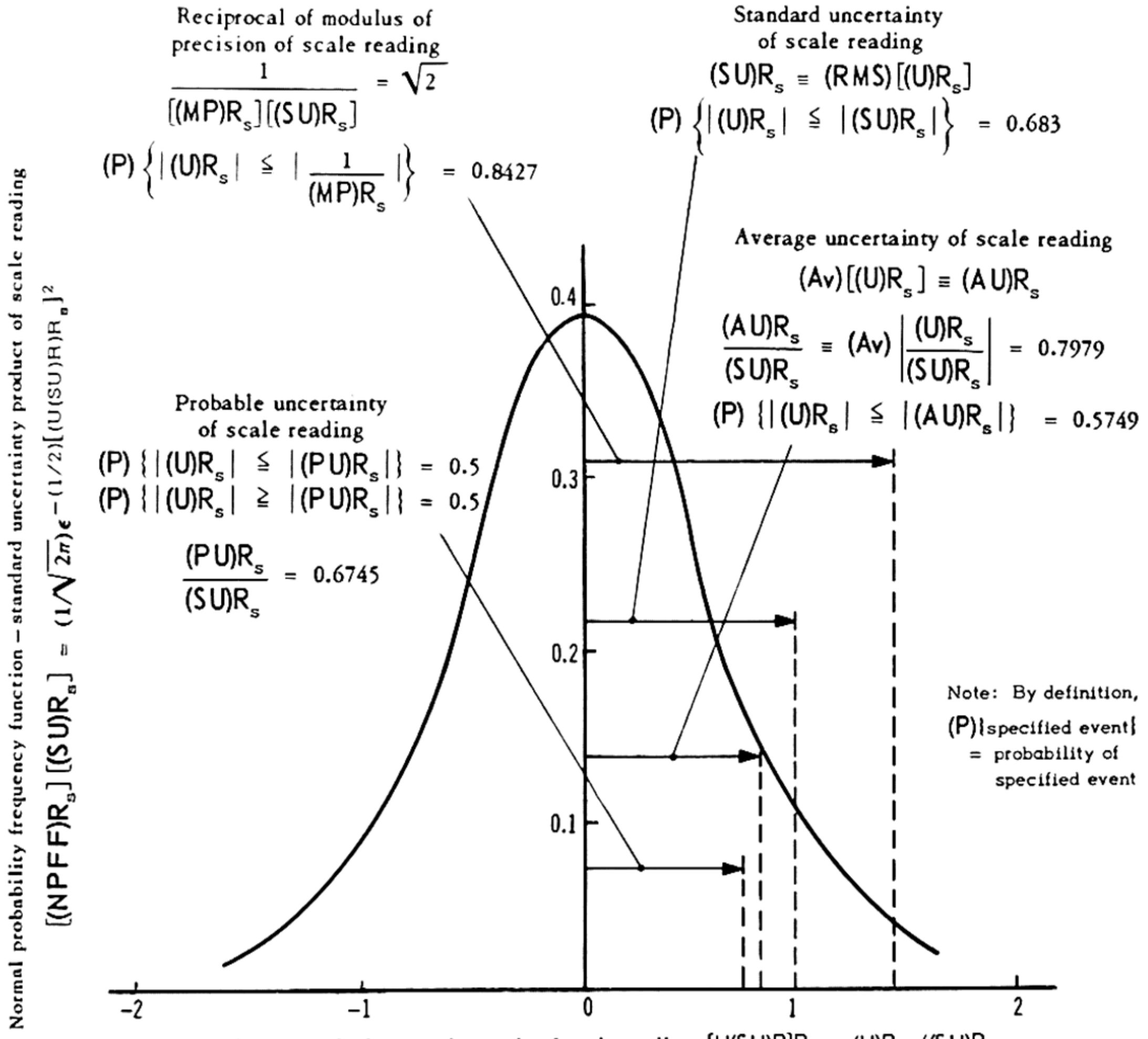
29.40. Normal-zero scales have zero as the minimum scale reading. A normal-zero scale is illustrated in Fig. 29-6a. Figure 29-6b shows a displaced-zero scale, on which the zero is not at the minimum scale reading, but is located between the minimum scale reading and the maximum scale reading. Figure 29-6c illustrates a suppressed-zero scale, on which the zero does not coincide with either the maximum scale reading or the minimum scale reading and does not occur between these two readings.

29.41. Uncertainty, as the term is applied in this book, describes a component of scale reading inaccuracy that cannot be exactly represented by a single number. In some cases, it is possible to specify a maximum magnitude for uncertainty components, but no method is known for predicting the exact value associated with any given scale reading. When repeated observations are possible that would all give the same reading from an ideal instrument under ideal circumstances, the actual readings may be processed by the methods described in Chapter 11 to generate measures for the magnitude of the uncertainty component. To use this procedure in its simplest form, it is necessary to assume that uncertainty is a random variable in the sense that the individual uncertainties of a set follow a normal probability law* curve like that represented in Fig. 29-7. This curve is drawn to represent the idealized situation in which the uncertainties associated with an infinite number of scale readings for the actuating input level are available for plotting purposes. A dimensionless ratio proportional to scale reading uncertainty is used for the abscissae, and the ordinates are values of a dimensionless ratio that is proportional to the relative number of times that a given uncertainty occurs. This normal probability frequency function curve is bell shaped, with its highest point occurring at the zero uncertainty point. This fact, in combination with the relationship given by Eq. (1) of Definition Summary 29-4, means that the most frequently occurring scale readings are near the average scale reading.

29.42. It is noted in Chapter 11 that the area enclosed between the frequency function curve and any two lines drawn parallel to the axis of ordinates is proportional to the probability that any single scale reading will have an uncertainty corresponding to some abscissa within the limits represented by the two parallel lines. Thus, if the two lines are drawn at plus infinity and minus infinity, the area under the curve will be unity, representing the fact that the uncertainty will always fall between these limits. On the other hand, there is zero probability that an uncertainty corresponding to any particular line of zero width will ever occur.

29.43. The normal probability frequency function curve is useful because it may easily be applied in making estimates of the probability that the uncertainty associated with a given scale reading will be less than or greater than certain limits. Various measures of scale reading uncertainty appear when a particular limit is specified and the probability information is transformed into the fraction of a set of readings that is expected to be less than the limit. For example, the probable uncertainty of scale reading has a magnitude so chosen that the uncertainty associated with any new reading has an equal chance of being either less than or greater than the probable uncertainty. This fact means that half of the

* See Cramér (C2), Fry (F4), Hoel (H1), and Whittaker and Robinson (W1).



Note: All relationships of this figure apply directly to indications when the symbol R_s (for scale reading) is replaced by (Ind) (for indication). (Refer to Fig. 11-1 of Chapter 11.)

Fig. 29-7. The normal probability frequency function for scale reading in terms of various uncertainty-describing concepts.

scale readings in any new set of readings will have uncertainties with magnitudes less than the probable uncertainty.

29.44. Section b of Definition Summary 29-4 gives defining equations and symbols for the standard uncertainty of scale reading, the probable uncertainty of scale reading, the average uncertainty of scale reading, and the modulus of precision of scale reading, which are commonly used as uncertainty measures. Section b also defines dimensionless ratios formed when scale reading uncertainties are divided by the various uncertainty measures. For example, the uncertainty - standard uncertainty ratio of scale reading (symbol $[U(SU)R]R_s$) is the scale reading uncertainty divided by the standard uncertainty of the scale reading. The curve of

Scale reading uncertainty, as this concept is defined in Fig. 29-1, is the algebraic difference between the scale reading, R_s, and the average scale reading, $R_{(s)(av)}$; i.e.,

$$(U)R_s = R_s - R_{(s)(av)} \tag{1}$$

where

$(U)R_s$ = scale reading uncertainty

R_s = actual scale reading, or scale reading

$R_{(s)(av)}$ = average scale reading (from a series of readings for the same actuating quantity level)

Comparison of Eq. (1) for scale reading uncertainty with the defining equation for deviation from Fig. 29-2 shows that uncertainty is a special case of deviation with the average scale reading taken as the reference level. The theory of deviations of this type is considered in Chapter 11. The expressions developed in Chapter 11 may be immediately applied to the treatment of instrument mechanism indication uncertainties when the variable, x, is replaced by the indication, (Ind), and the deviation symbol, (D), is replaced by the uncertainty symbol, (U). The results of Chapter 11 may similarly be applied to scale reading uncertainties when x is replaced by R_s and (D) is replaced by (U).

a) Indication uncertainties and scale reading uncertainties

The definitions and results given in Chapter 11 may be used to set up the basic framework for treating scale reading uncertainty in terms of normal probability theory. The fundamental information is summarized in a set of expressions based on Eqs. (11-1) through (11-15) to introduce scale reading and uncertainty instead of x and deviation.

The defining equations and the corresponding concept names are:

$$(Av)R_s = \frac{1}{n}\sum_{i=1}^{i=n}(R_s)_i \tag{2}$$

= average value of scale reading for n readings

$$[(U)R_s]_i = (R_s)_i - (Av)R_s \tag{3}$$

= typical value of scale reading uncertainty (for i^{th} scale reading)

$$(SU)R_s = (RMS)[(U)R_s] = \sqrt{(Av)[(U)R_s]^2} = \sqrt{\frac{1}{n}\sum_{i=1}^{i=n}[(U)R_s]_i^2} \tag{4}$$

= standard uncertainty of scale reading (identical with root mean square of scale reading uncertainty)

$$(AU)R_s = (Av)[(U)R_s] = \frac{1}{n}\sum_{i=1}^{i=n}[(U)R_s]_i \tag{5}$$

= average uncertainty of scale reading (for n readings)

$$[U(SU)R]R_s = \frac{(U)R_s}{(SU)R_s} \tag{6}$$

= uncertainty – standard uncertainty ratio of scale reading

$$[U(AU)R]R_s = \frac{(U)R_s}{(AU)R_s} \tag{7}$$

= uncertainty – average uncertainty ratio of scale reading

The probability of any specified event is defined as a number between zero (i.e., impossibility) and unity (i.e., certainty) that expresses the expectation that this event will occur. In symbols, the probability of a specified event is

$$(P)\{\text{Specified event}\} \tag{8}$$

Definition Summary 29-4. Concepts, definitions and symbols for uncertainty measures associated with measuring instrument operation. (Page 1 of 4)

For example,

$$(P)\{[(U)R_s]_1 < (U)R_s < [(U)R_s]_2\} \tag{9}$$

is the probability that the scale reading uncertainty $(U)R_s$ will be greater than $[(U)R_s]_1$ and less than $[(U)R_s]_2$.

By definition, the probable uncertainty of the scale reading, $(PU)R_s$, is that scale reading uncertainty magnitude for which the probability of a typical reading having a smaller uncertainty magnitude is equal to one half; i.e.,

$$(P)\{|(U)R_s| < |(PU)R_s|\} = \frac{1}{2} \tag{10}$$

In other words, $(PU)R_s$ has a magnitude such that one half of the individual uncertainties can be expected to be smaller, and the other half larger, than $(PU)R_s$. When R_s obeys the normal probability law (described in Chapter 11), it can be shown that $(PU)R_s = 0.6745\,(SU)R_s$; i.e.,

$$(PU)R_s = 0.6745\sqrt{(Av)\,[(U)R_s]^2} \tag{11}$$

By definition,

$$[(U)(PU)R]R_s = \frac{(U)R_s}{(PU)R_s} \tag{12}$$

= uncertainty – probable uncertainty ratio of scale reading

Also, by definition,

$$(MP)R_s = \frac{1}{(SU)R_s\sqrt{2}} \tag{13}$$

= modulus of precision of scale reading

A generally useful expression that describes the relative frequency of occurrence of scale reading uncertainty magnitudes when the normal probability law (see Chapter 11) holds is

$$(NPFF)R_s = \frac{1}{(SU)R_s\sqrt{2\pi}}\,\epsilon^{-(1/2)[(U(SU)R)R_s]^2} \tag{14}$$

= normal probability frequency function

A curve showing the form of the normal probability frequency function in nondimensional terms and the relationship of this curve to the concepts just defined is given in Fig. 29-7, which is generally similar to Fig. 11-1.

b) Uncertainty measures for single scale readings based on a set of n readings

In practice, scale reading uncertainty information must be based on a finite number of readings. It is important to have expressions available for relating results from n readings to the theoretical results that would be obtained from an infinite number of readings and to expected results for a single scale reading. The following summary of information is taken from Chapter 11.

Define

$[(Av)R_s]_n$ = average of n scale readings

$[(Av)R_s]_\infty$ = average of an infinite number of scale readings

When scale reading information is based on the average of a considerable number of scale reading averages, each of which is taken from a set of n scale readings, the resultant average is substantially equal to the average of an infinite number of readings; i.e.,

$$(Av)\,[(Av)R_s]_n = [(Av)R_s]_\infty \tag{15}$$

The theory of probability shows that:

In general, the uncertainty measures associated with the average from a set of n readings are equal to the corresponding uncertainty measures for individual readings of the set multiplied by the reciprocal of the square root of the number of readings.

Definition Summary 29-4. Concepts, definitions and symbols for uncertainty measures associated with measuring instrument operation. (Page 2 of 4)

It is to be noted that the factor used by some authorities is $\sqrt{n-1}$ instead of $\sqrt{n}$. From the standpoint of practice, this difference is generally unimportant.

In equation form, the uncertainty measures for the average of n readings are:

$$(AU)\,[(Av)R_s]_n = \frac{(AU)R_s}{\sqrt{n}} \tag{16}$$

where

$(AU)R_s$ = average uncertainty for a single reading (one reading in a set of n readings)

and

$(AU)\,[(Av)R_s]_n$ = average uncertainty of the average of n readings

Also

$$(SU)\,[(Av)R_s]_n = \frac{(SU)R_s}{\sqrt{n}} \tag{17}$$

where

$(SU)R_s$ = standard uncertainty for a single reading (one reading in a set of n readings)

and

$(SU)\,[(Av)R_s]_n$ = standard uncertainty of the average of n readings

and

$$(PU)\,[(Av)R_s]_n = \frac{(PU)R_s}{\sqrt{n}} \tag{18}$$

where

$(PU)R_s$ = probable uncertainty for a single reading of n readings (one reading in a set of n readings)

$(PU)\,[(Av)R_s]_n$ = probable uncertainty of the average of n readings

The modulus of precision follows the general pattern except that $\sqrt{n}$ appears in the numerator instead of the denominator; i.e.,

$$(MP)\,[(Av)R_s]_n = \frac{\sqrt{n}}{(SU)R_s\sqrt{2}} = \sqrt{n}\,[(MP)R_s] \tag{19}$$

where

$(MP)R_s$ = modulus of precision for a single reading (one reading in a set of n readings)

$(MP)\,[(Av)R_s]_n$ = modulus of precision of the average of n readings

c) Uncertainty measures for the average of n scale readings

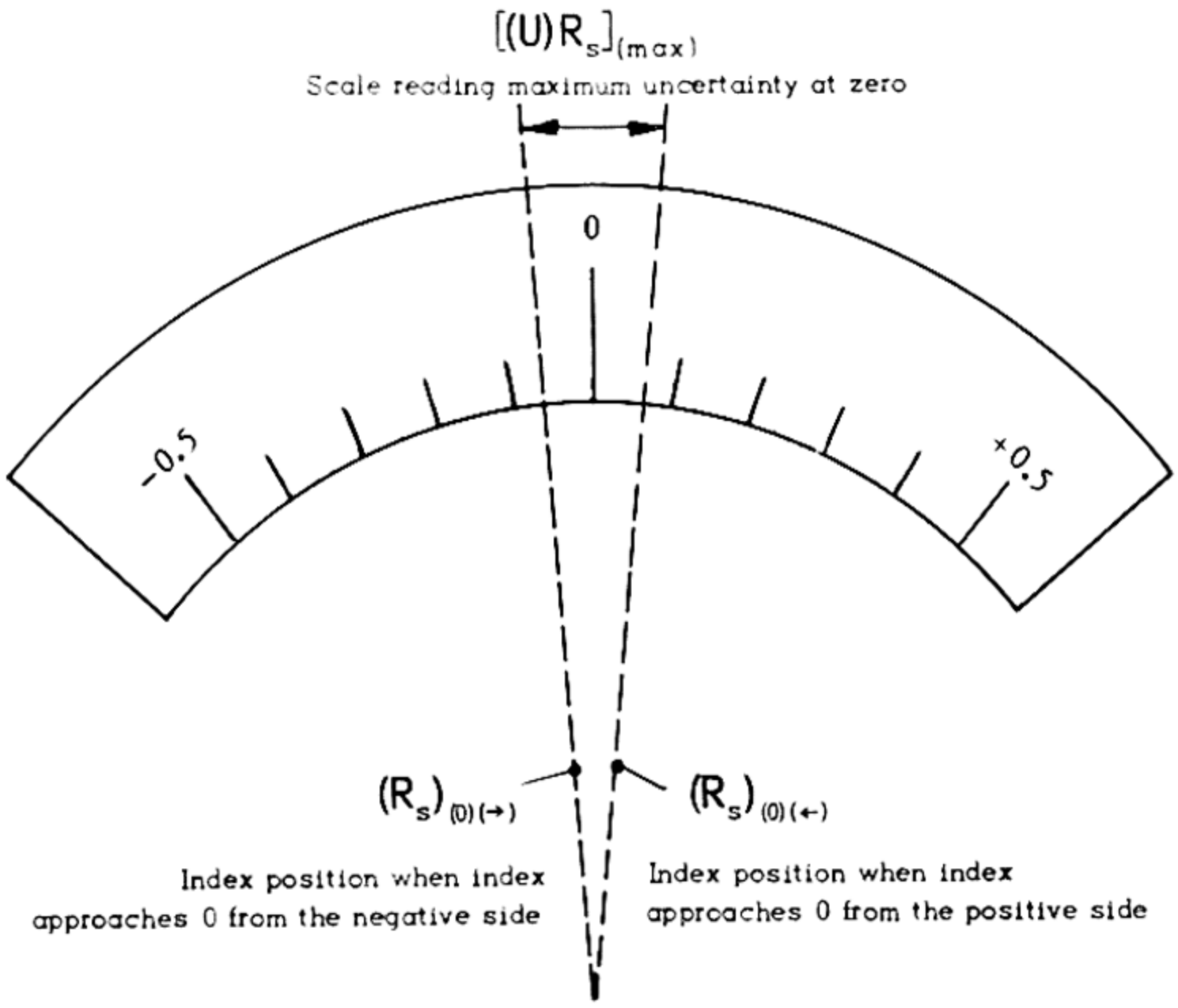
In practice, situations often exist that make it impossible, or not feasible, to take the number of repeated scale readings required for properly determining the uncertainty measures defined in sections a, b and c. Under these circumstances the scale reading maximum uncertainty may be used as a measure of performance quality. In symbols,

$[(U)R_s]_{(max)} = (MU)R_s$ = scale reading maximum uncertainty

This quantity may be defined in various ways, but it is suggested that it be associated with the maximum difference that appears between readings taken when R_s is allowed to increase slowly and when R_s is allowed to decrease slowly. To be most reliable, the readings should be taken under circumstances that represent somewhat unfavorable operating conditions. For example, if a meter is used under conditions of some mechanical vibration, the maximum uncertainty should be determined with less favorable vibration conditions than those found in practice.

The accompanying diagram illustrates the determination of maximum uncertainty for an electrical meter.

Definition Summary 29-4. Concepts, definitions and symbols for uncertainty measures associated with measuring instrument operation. (Page 3 of 4)



$$[(U)R_s]_{(max)} = |(R_s)_{(0)(\leftarrow)} - (R_s)_{(0)(\rightarrow)}| \qquad (20)$$

d) Scale reading maximum uncertainty

Definition Summary 29-4. Concepts, definitions and symbols for uncertainty measures associated with measuring instrument operation. (Page 4 of 4)

Fig. 29-7 is plotted with this ratio as the abscissa and the normal probability frequency function - standard uncertainty product of scale reading, based on Eq. (14) of Definition Summary 29-4, as the ordinate. Four of the dimensionless uncertainty measures given in Definition Summary 29-4 are identified on Fig. 29-7. The probabilites that the uncertainty associated with an additional single scale reading will be equal to or less than each of the uncertainty measure ratios are also given on Fig. 29-7. For example, the probability that the uncertainty associated with a single reading will be equal to or less than the average uncertainty is 0.5749.

29.45. Theoretically, the uncertainty associated with the average of an infinite number of scale readings is zero. This means that when a very large number of readings is available, uncertainty effects may be completely eliminated. In practice, it is seldom feasible to take the required "very large number" of readings. For this reason, it becomes important to estimate uncertainty measures for the average of a limited number of readings. Section c of Definition Summary 29-4 gives the expressions for relating the uncertainty measures associated with the average of n readings to the uncertainty measures for single readings. In general, this relationship is a simple multiplication or division by the square root of the number of readings used in forming the average.

29.46. From the standpoint of practice, normal probability theory is particularly useful when a reasonably large number of readings can be taken under static conditions. It is obvious that the information brought together in Chapter 11 and outlined in this section may be applied in many situations that do not involve instrument scale readings. For example, scale reading as the quantity with which uncertainty is associated may be replaced by some measurement of a factory part with the problem of determining scale reading uncertainty replaced by the problems of estimating the fraction of the total output that will fall within given tolerance limits. However, results of this kind do not apply in situations like that illustrated by Fig. 29-3, in which it is necessary to interpret scale readings that vary continuously with time in a way that effectively prevents repeated observations of any given reading. Procedures that depend on extensions* of normal probability theory are available for the interpretation of data on varying scale readings. These procedures are generally more complex than the calculation of simple averages and deal with roughness, as this term is defined in Fig. 29-3, rather than with uncertainty. Roughness is usually the result of so many factors that it is difficult in any given case to identify effects due to instrument mechanism operation.

29.47. Frequently, the most feasible approach to the problem of describing instrument uncertainty is the use of maximum scale reading uncertainty as a criterion of measuring instrument performance quality. This concept is defined in section d of Definition Summary 29-4 as the maximum difference between scale readings that appears when the indication is caused to approach a constant level from opposite directions. In order to give realistic results, this difference should be determined under conditions that are somewhat less favorable for instrument mechanism operation than the condition expected in normal operation. It is obvious that any satisfactory measuring instrument must have a maximum scale reading uncertainty of negligible magnitude in comparison with the scale reading inaccuracy that is required. When this condition is fulfilled, it is reasonable to disregard uncertainty effects on results from the instrument.

29.48. The list of "basic terms" recommended in the ASME report "Automatic Control Terminology"(A5)(A6) includes three terms defining concepts that correspond to scale reading uncertainty:

"Resolution Sensitivity is the minimum change in the measured variable which produces an effective response of the instrument or automatic controller. Resolution Sensitivity may be expressed in units of the measured variable or as a fraction or percent of the full scale value or the actual value.

"Threshold Sensitivity is the lowest level of the measured variable which produces effective response of the instrument or automatic controller.

"Dead Band is the range of values through which the measured variable can be varied without initiating effective response."

* See, for example, Bode and Shannon (B5), Booton (B6), and Laning and Root (L3).

29.49. It appears that the definition of dead band is similar to that given for maximum uncertainty in the previous discussion. The use of the word "sensitivity" in the terms "resolution sensitivity" and "threshold sensitivity" is in direct conflict with definitions of sensitivity as an output-input ratio (see Chapter 4) and is certainly to be avoided so far as possible. The definition of resolution sensitivity is equivalent to that of maximum uncertainty without a specification of the scale reading considered. Threshold sensitivity is a similar concept with the added condition that the resolution sensitivity is considered at the zero level of the measured variable. If it is assumed that the starting point for the indicating mechanism corresponds exactly to the zero level of the input, it appears that threshold sensitivity is equivalent to half of the maximum uncertainty for zero scale reading.

ERROR AND CORRECTION COMPONENTS OF SCALE READING

29.50. When the maximum scale reading uncertainty is so small that uncertainty effects may be disregarded, scale reading inaccuracy reduces to scale reading error. From the standpoint of theoretical treatment, situations of this type are particularly easy to handle, because error may be described in theoretical terms without regard to uncertainty limits or the use of relatively cumbersome probability theory. All the situations considered in the present section are assumed to be describable in terms of error represented by simple numerical values, without associated uncertainty measures.

29.51. Scale readings from any instrument include an error component that may or may not be important, depending on the inaccuracy magnitudes that are tolerable. In any case, this error is the resultant of error components that are due to various imperfections in the indicating mechanism and its scale. The error components that must be considered in the use of any given measuring instrument are determined by the nature of the instrument mechanism, the scale and the conditions of operation. It is not feasible to give a fixed set of terms and symbols that may be rigidly applied in all cases. On the other hand, it is possible to develop a plan for the description of error that may be used as a pattern for specifying the performance quality of any measuring instrument whose scale readings either have a negligibly small maximum uncertainty or contain uncertainty components with known measures so that uncertainty may be disregarded in analyzing error effects. The error-describing pattern that is outlined in this section is powerful enough to be effective in any practical situation. The essential features of this plan are illustrated at the end of this chapter by an application to a typical measuring instrument.

29.52. In order to demonstrate the error-describing pattern, it is assumed that the measuring instrument considered has performance imperfections of eight types. It is unlikely that all of these effects will be important in any instrument

used for ordinary measurements, but it is also probable that the list will need to be extended for situations where especially small resultant scale reading errors are required. For the sake of generality, the physical arrangement used for illustrating the principles of error analysis is assumed to include a mechanism and a scale that are given independent calibrations and are then brought together to form a complete measuring instrument. This means that the scale reading error may be resolved into one component due to mechanism imperfections and another component due to scale imperfections. With the instrument operating in an environment different from calibration conditions, each of these error components is made up of a calibration condition error component that exists under calibration conditions and an environmental error component due to environmental effects. Definition Summary 29-5 outlines a pattern of concepts, terms and symbols that may be used to describe a group of error components that affect measuring instrument performance quality.

29.53. When scale reading error is known, it is a simple matter to write down the scale reading correction as equal to the error with its sign reversed. When the scale reading correction is perfect, it may be added to the actual scale reading (symbol R_s) to give the correct scale reading (symbol $R_{(s)(corr)}$), which is equal to the correct (or true) measure of the actuating input. In practice, the actual scale reading correction will usually fall short of perfection, so that its application to the actual scale reading does not give the correct scale reading. Under these circumstances, the result of applying an actual scale reading correction is the corrected scale reading, which is given the symbol $R_{(s)(ctd)}$.

ERROR ANALYSIS EXAMPLE

29.54. In the example of Definition Summary 29-5, the maximum uncertainty is assumed to be negligibly small. The scale reading error is made up of eight types of components. The scale reading error due to mechanism imperfections is resolved into three components, as is also the scale reading error due to scale imperfections. A seventh type of error component is assumed to exist because of improper location of the scale with respect to the mechanism. Environmental effects cause the eighth type of error. Thus, each of the mechanism and scale error types is made up of calibration condition components and environmental components.

29.55. The object of the error analysis outlined in Definition Summary 29-5 is to describe a pattern that is easily remembered and is capable not only of describing the illustrative example but also of being easily applied to situations with all degrees of complexity.

INDICATION ERRORS AND INDICATION CORRECTIONS

29.56. Mechanism indication error causes the actual indication (symbol (Ind)) to differ from the correct indication (symbol $(Ind)_{(corr)}$), which by definition is the

indication that would be produced by a perfect indicating mechanism for a given level of the actuating input. Mechanism indication error may be resolved into three components:

1) Mechanism operating error of indication (symbol (MOE)(Ind)); due to imperfect operation of the mechanism.
2) Mechanism calibration matching error of indication (symbol (MCME)(Ind)); due to imperfect matching of the actual calibration of a given mechanism to the specified calibration for ideal mechanisms of its class.
3) Mechanism calibration error of indication (symbol (MCE)(Ind)); due to engineering compromises accepted in the specified calibration for the mechanism. For example, the specified calibration might give equal indication increments between two calibration points when the corresponding actuating input level changes are not actually equal. Situations of this type may appear in calibrations for vapor-pressure thermometer mechanisms.

29.57. These three indication error components are illustrated and defined in section a of Definition Summary 29-5. The figure of this section shows the four indications that correspond to these error components, including the actual indication (symbol (Ind)); the correct indication (symbol $(Ind)_{(corr)}$); the indication with perfect mechanism operation (symbol $(Ind)_{[(MOE)\to 0]}$); and the indication with perfect mechanism operation and perfect mechanism calibration matching (symbol $(Ind)_{[(MOE)\to 0][(MCME)\to 0]}$). This last indication is the indication that would be given by a perfectly operating mechanism with an actual calibration exactly matched to the specified calibration, and for this reason it is also called the calibration indication (symbol $(Ind)_{(cal)}$).

29.58. Section a of Definition Summary 29-5 gives defining equations for each of the indication error components. This section also includes definitions and equations for the indication correction (symbol (C)(Ind)) and its components, which correspond to the error components already defined. In general, names for the correction components are identical with the error component names except that the word "correction" replaces "error" wherever the latter occurs. The indication correction symbols are identical with the indication error symbols except that the letter E, wherever it represents "error," is replaced by C, for "correction." In general, each of the correction components is equal to its corresponding error component with a negative sign.

SCALE READING ERROR AND SCALE READING CORRECTION

29.59. Section b of Definition Summary 29-5 gives definitions and equations for scale reading error and scale reading correction and the components of these quantities. Scale reading error may be resolved into components of four kinds:

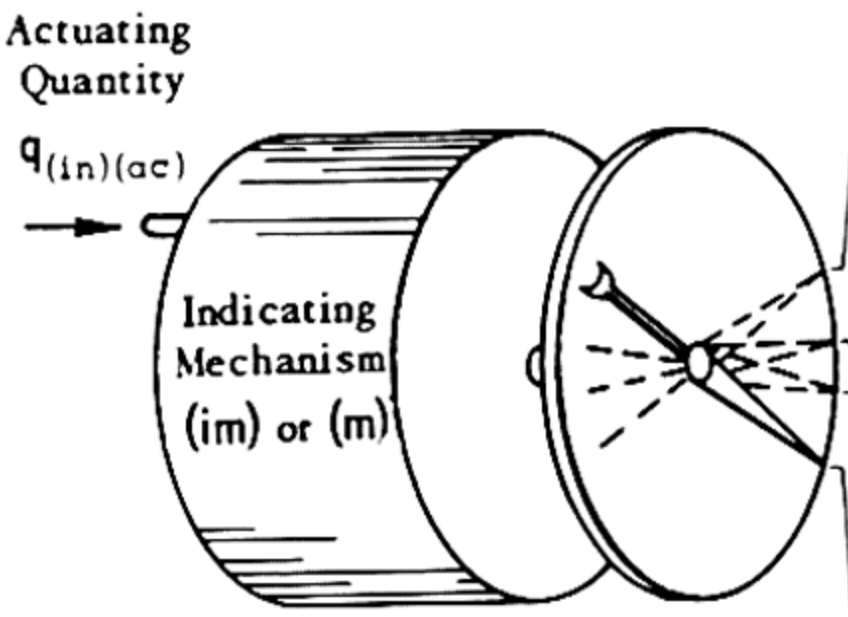
1) The error component due to indication errors.
2) The error component due to imperfect zero setting. This error appears when the position of the index with respect to the scale gives a scale reading error for some definitely known level of the actuating quantity. This error component is called the zero setting error because the zero level for the actuating input is generally used as the definitely known level. It is common practice to include a zero setting adjustment in meters and gages of all types.
3) The error component due to imperfect observation of the index position with respect to the scale. An error of this type appears when an index located somewhat above the scale is observed at an angle that allows parallax effects to influence the readings.
4) The error component due to scale imperfections. This component has two subcomponents, one due to the use of an imperfect specified calibration and the other due to an imperfect matching of the actual scale calibration to the specified scale calibration.

29.60. Section b of Definition Summary 29-5 gives the defining equations and names for the components of scale reading error and scale reading correction. In the final summarizing equations, indication error components are reduced to scale reading error components by using the correct scale sensitivity as a multiplying factor. Names and symbols for the correction components are formed by use of the conventions already described in section a of the summary.

29.61. Section c of Definition Summary 29-5 illustrates the resolution of the mechanism component of scale reading error and the scale reading error due to scale imperfections into calibration condition error components (denoted by (cc) as an identifying subscript) and environmental error components (denoted by (en) as an identifying subscript). The conventions for names, symbols, and definitions illustrated for these error components may be applied to all the error and correction components defined in sections a and b of Definition Summary 29-5. The example of this summary illustrates a pattern of error description that may be applied to systems of all kinds. In practice, the scale and mechanism of a high-quality measuring instrument are usually combined and calibrated as a single entity. When this calibration is carefully done, the zero setting error, the observational error and the environmental error are the only components that remain to be cared for by proper zero adjustment and the use of proper care in observing scale readings.

29.62. The procedure outlined in section b of Definition Summary 29-5 for applying the correct scale sensitivity to transform indication errors into scale reading errors is a special example of a generally useful method. This method may be applied to indefinitely long and complex chains of operating components

Assume that maximum indication uncertainty, $[(U)(Ind)]_{(max)}$, is negligibly small.



Indication with perfect mechanism operation, $[(MOE) \longrightarrow 0]$, perfect mechanism calibration matching, $[(MCME) \longrightarrow 0]$, and perfect mechanism calibration, $[(MCE) \longrightarrow 0]$

$(Ind)_{[(MOE)\to 0][(MCME)\to 0][(MCE)\to 0]}$

or

Correct indication

$(Ind)_{(corr)}$

Indication with perfect mechanism operation, $[(MOE) \longrightarrow 0]$ and perfect mechanism calibration matching, $[(MCME) \longrightarrow 0]$

$(Ind)_{[(MOE)\to 0][(MCME)\to 0]}$

or

Calibration indication

$(Ind)_{(cal)}$

Indication with perfect mechanism operation, $[(MOE) \longrightarrow 0]$

$(Ind)_{[(MOE)\to 0]}$

Actual indication

(Ind)

or

Indication

By definition,

$$(MOE)(Ind) = (Ind) - (Ind)_{[(MOE)\to 0]} = \text{mechanism operating error of indication} \quad (1)$$

$$(MCME)(Ind) = (Ind)_{[(MOE)\to 0]} - (Ind)_{[(MOE)\to 0][(MCME)\to 0]}$$

$$= (Ind)_{[(MOE)\to 0]} - (Ind)_{(cal)} = \text{mechanism calibration matching error of indication} \quad (2)$$

$$(MCE)(Ind) = (Ind)_{[(MOE)\to 0][(MCME)\to 0]} - (Ind)_{[(MOE)\to 0][(MCME)\to 0][(MCE)\to 0]}$$

$$= (Ind)_{[(MOE)\to 0][(MCME)\to 0]} - (Ind)_{(corr)}$$

$$= (Ind)_{(cal)} - (Ind)_{(corr)} = \text{mechanism calibration error of indication} \quad (3)$$

and

$$(Ind) = (MOE)(Ind) + (Ind)_{[(MOE)\to 0]} \quad (4)$$

$$= (MOE)(Ind) + (MCME)(Ind) + (Ind)_{[(MOE)\to 0][(MCME)\to 0]} \quad (5)$$

$$= (MOE)(Ind) + (MCME)(Ind) + (MCE)(Ind) + (Ind)_{(corr)} \quad (6)$$

Also, by definition,

$$(E)(Ind) = (Ind) - (Ind)_{(corr)} = (MOE)(Ind) + (MCME)(Ind) + (MCE)(Ind) \quad (7)$$

$$= \text{indication error (under assumption that } [(U)(Ind)]_{(max)} \longrightarrow 0)$$

The indication correction components corresponding to the indication error components of Eq. (7) are, by definition,

$$(C)(Ind) = -(E)(Ind) = \text{indication correction} \quad (8)$$

and

$$(C)(Ind) = (MOC)(Ind) + (MCMC)(Ind) + (MCC)(Ind) \quad (9)$$

Definition Summary 29-5. Error and correction components associated with indications and scale readings from measuring instruments. (Page 1 of 4)

where

$$(MOC)(Ind) = -(MOE)(Ind) = (Ind)_{[(MOE)\to 0]} - (Ind) \tag{10}$$

= mechanism operation correction for indication

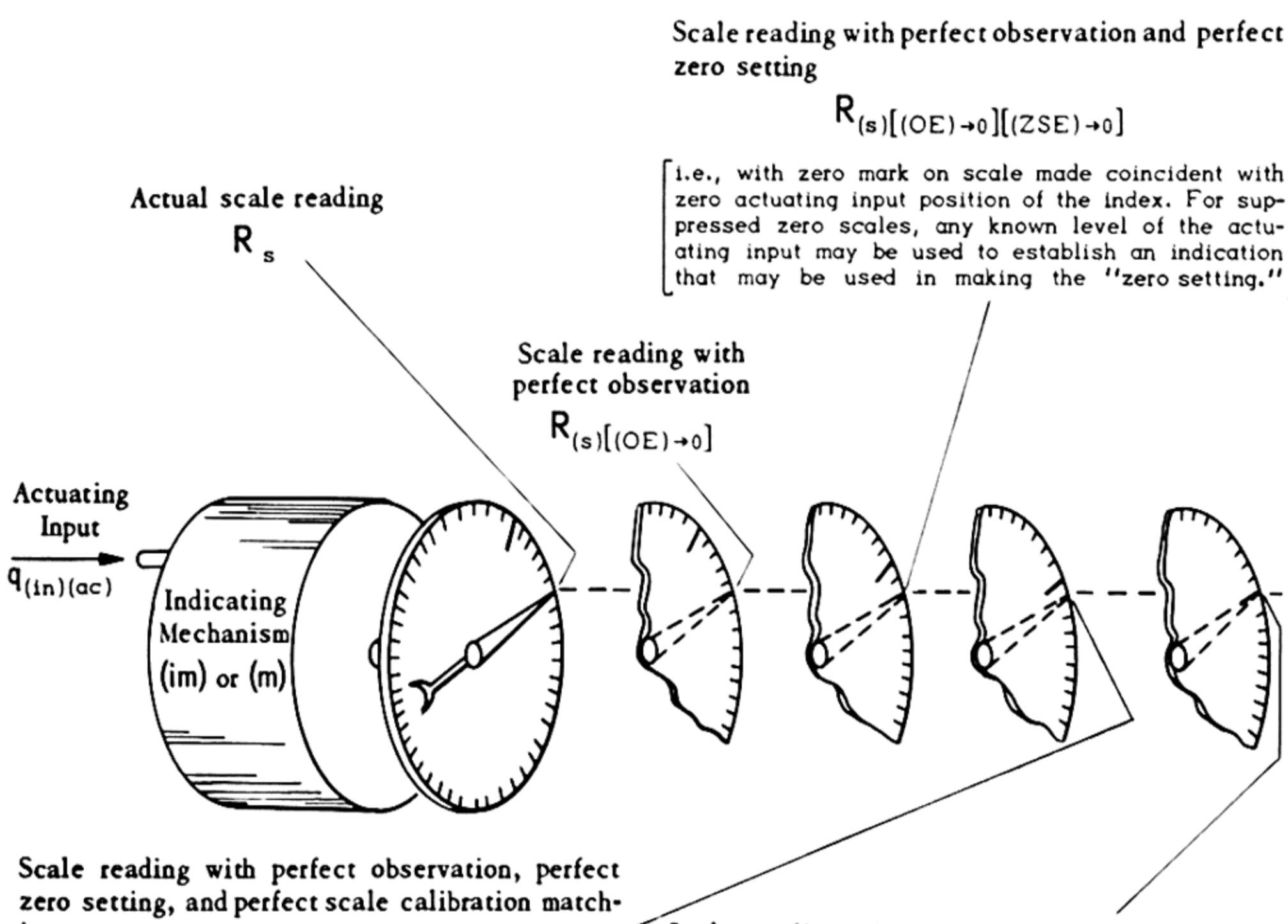
$$(MCMC)(Ind) = -(MCME)(Ind) = (Ind)_{[(MOE)\to 0][(MCME)\to 0]} - (Ind)_{[(MOE)\to 0]} \tag{11}$$

= mechanism calibration matching correction for indication

$$(MCC)(Ind) = -(MCE)(Ind) = (Ind)_{(corr)} - (Ind)_{[(MOE)\to 0][(MCME)\to 0]} \tag{12}$$

= mechanism calibration correction for indication

a) Indication error and indication correction components for an indicating instrument mechanism



Scale reading with perfect observation and perfect zero setting

$$R_{(s)[(OE)\to 0][(ZSE)\to 0]}$$

[i.e., with zero mark on scale made coincident with zero actuating input position of the index. For suppressed zero scales, any known level of the actuating input may be used to establish an indication that may be used in making the "zero setting."]

Scale reading with perfect observation, perfect zero setting, and perfect scale calibration matching

$$R_{(s)[(OE)\to 0][(ZSE)\to 0][(SCME)\to 0]}$$

or

Calibration scale reading

$$R_{(s)(cal)}$$

Note:

The heavy bold line shown on each of the above scales represents the scale reading that would be made if the error-producing effects associated with the scale were eliminated.

Scale reading with perfect observation, perfect zero setting, perfect scale calibration matching, and perfect scale calibration

$$R_{(s)[(OE)\to 0][(ZSE)\to 0][(SCME)\to 0][(SCE)\to 0]}$$

or

Indication correct scale reading

$$R_{(s)(Ind)(corr)} = S_{(s)(corr)}(Ind)$$

[where the correct value of scale sensitivity appears because all error-producing effects associated with the scale have been eliminated]

(13)

where

$$S_{(s)(corr)} = S_{(s)[(Ind);R](corr)} = \frac{R_{(s)(Ind)(corr)}}{(Ind)}$$

= correct scale sensitivity

(14)

Definition Summary 29-5. Error and correction components associated with indications and scale readings from measuring instruments. (Page 2 of 4)

By definition,

$$(OE)R_s = R_s - R_{(s)[(OE)\to 0]} \tag{15}$$

= scale reading observational error

$$(ZSE)R_s = R_{(s)[(OE)\to 0]} - R_{(s)[(OE)\to 0][(ZSE)\to 0]} \tag{16}$$

= scale reading zero setting error

$$(SCME)R_s = R_{(s)[(OE)\to 0][(ZSE)\to 0]} - R_{(s)[(OE)\to 0][(ZSE)\to 0][(SCME)\to 0]}$$

$$= R_{(s)[(OE)\to 0][(ZSE)\to 0]} - R_{(s)(cal)} \tag{17}$$

= scale reading scale calibration matching error

$$(SCE)R_s = R_{(s)[(OE)\to 0][(ZSE)\to 0][(SCME)\to 0]} - R_{(s)[(OE)\to 0][(ZSE)\to 0][(SCME)\to 0][(SCE)\to 0]}$$

$$= R_{(s)(cal)} - R_{(s)(cal)[(SCE)\to 0]}$$

$$= R_{(s)[(OE)\to 0][(ZSE)\to 0][(SCME)\to 0]} - R_{(s)(Ind)(corr)} \tag{18}$$

= scale reading scale calibration error

and

$$R_s = (OE)R_s + R_{(s)[(OE)\to 0]} \tag{19}$$

$$= (OE)R_s + (ZSE)R_s + R_{(s)[(OE)\to 0][(ZSE)\to 0]} \tag{20}$$

$$= (OE)R_s + (ZSE)R_s + (SCME)R_s + R_{(s)[(OE)\to 0][(ZSE)\to 0][(SCME)\to 0]} \tag{21}$$

$$= (OE)R_s + (ZSE)R_s + (SCME)R_s + (SCE)R_s + R_{(s)(Ind)(corr)} \tag{22}$$

Also, by definition,

$$[(E)R_s]_s = R_s - R_{(s)(Ind)(corr)} = (OE)R_s + (ZSE)R_s + (SCME)R_s + (SCE)R_s \tag{23}$$

= scale reading error due to scale imperfections

From Eqs. (7), (13) and (23),

$$R_s = [(E)R_s]_s + S_{(s)(corr)}[(E)(Ind)] + S_{(s)(corr)}(Ind)_{(corr)} \tag{24}$$

Define

$$R_{(s)(corr)} = S_{(s)(corr)}(Ind)_{(corr)} \tag{25}$$

= correct scale reading
(this scale reading is, by definition, equal to the correct (i.e., "true") measure of the actuating quantity that produces the scale reading)

and

$$[(E)R_s]_m = S_{(s)(corr)}[(E)(Ind)] \tag{26}$$

= mechanism component of scale reading error

From Eqs. (7) and (26)

$$[(E)R_s]_m = (MOE)R_s + (MCME)R_s + (MCE)R_s \tag{27}$$

where

$$(MOE)R_s = S_{(s)(corr)}[(MOE)(Ind)] \tag{28}$$

= mechanism operation component of scale reading error

$$(MCME)R_\varepsilon = S_{(s)(corr)}[(MCME)(Ind)] \tag{29}$$

= mechanism calibration matching component of scale reading error

$$(MCE)R_s = S_{(s)(corr)}[(MCE)(Ind)] \tag{30}$$

= mechanism calibration component of scale reading error

From Eqs. (23) through (30)

$$(E)R_s = R_s - R_{(s)(corr)} = [(E)R_s]_s + [(E)R_s]_m \tag{31}$$

$$= (OE)R_s + (ZSE)R_s + (SCME)R_s + (SCE)R_s + (MOE)R_s + (MCME)R_s + (MCE)R_s \tag{32}$$

Definition Summary 29-5. Error and correction components associated with indications and scale readings from measuring instruments. (Page 3 of 4)

The scale reading correction corresponding to Eqs. (31) and (32) is, by definition,

$$(C)R_s = -(E)R_s = R_{(s)(corr)} - R_s = [(C)R_s]_s + [(C)R_s]_m \tag{33}$$

$$= (OC)R_s + (ZSC)R_s + (SCMC)R_s + (SCC)R_s + (MOC)R_s + (MCMC)R_s + (MCC)R_s \tag{34}$$

where

$$(OC)R_s = -(OE)R_s = \text{scale reading observational correction} \tag{35}$$

$$(ZSC)R_s = -(ZSE)R_s = \text{scale reading zero setting correction} \tag{36}$$

$$(SCMC)R_s = -(SCME)R_s = \text{scale calibration matching correction to scale reading} \tag{37}$$

$$(SCC)R_s = -(SCE)R_s = \text{scale calibration correction to scale reading} \tag{38}$$

$$(MOC)R_s = -(MOE)R_s = \text{mechanism operation correction to scale reading} \tag{39}$$

$$(MCMC)R_s = -(MCME)R_s = \text{mechanism calibration matching correction to scale reading} \tag{40}$$

$$(MCC)R_s = -(MCE)R_s = \text{mechanism calibration correction to scale reading} \tag{41}$$

b) Scale reading error and correction components for a measuring instrument

When operating conditions differ from calibration conditions, scale reading error components may be resolved into subcomponents that fall into two classes. One of these classes includes error subcomponents that exist under calibration conditions and for this reason are called calibration condition error components. The other class includes subcomponents that appear when the environment differs from calibration conditions. For this reason, error components in this class are called environmental error components.

In terms of the classes defined above, the scale reading error expression of Eq. (31) may be written in the form

$$(E)R_s = [(E)R_s]_{(cc)} + [(E)R_s]_{(en)}$$

$$= [(E)R_s]_{(s)(cc)} + [(E)R_s]_{(m)(cc)} + [(E)R_s]_{(s)(en)} + [(E)R_s]_{(m)(en)} \tag{42}$$

where

$[(E)R_s]_{(cc)}$ = calibration condition scale reading error

$[(E)R_s]_{(en)}$ = environmental scale reading error

$[(E)R_s]_{(s)(cc)}$ = calibration condition scale reading error due to scale imperfections

$[(E)R_s]_{(m)(cc)}$ = calibration condition mechanism scale reading error

$[(E)R_s]_{(s)(en)}$ = environmental scale reading error due to scale imperfections

$[(E)R_s]_{(m)(en)}$ = environmental mechanism scale reading error

The terminology and notation patterns herein defined may be extended to each of the seven error components that appear on the right-hand side of Eq. (32). The details of this extension are obvious and will not be given here.

Corrections for calibration condition and environmental error components may be defined by the conventions applied in Eqs. (33) through (41).

c) Calibration condition and environmental components of scale reading error for a measuring instrument

Definition Summary 29-5. Error and correction components associated with indications and scale readings from measuring instruments. (Page 4 of 4)

for reducing the effects of errors from various components to a resultant in terms of a single quantity that appears at some point in the system.

NONDIMENSIONAL MEASURES OF PERFORMANCE QUALITY

29.63. The inaccuracy, uncertainty and error measures discussed in earlier sections have all been defined in terms of an illustrative quantity, namely, scale reading, and for this reason carry the dimensions of this quantity. In practice, it is always desirable to state performance-describing concepts in nondimensional terms. This result is achieved when each inaccuracy component measure is divided by some value of the quantity with which the measure is associated. For example, scale reading inaccuracy is nondimensionalized when it is divided by some scale reading value. When scale reading inaccuracy components are considered, three scale reading magnitudes are particularly useful for nondimensionalizing purposes:

1) The maximum scale reading (symbol $R_{(s)(max)}$ or (MSR))
2) The actual scale reading, or scale reading (symbol R_s)
3) The scale reading range (symbol $(RR)_s$ or (SRR))

29.64. Various nondimensional forms for scale reading inaccuracy components are listed as items 49 through 63 of Table 29-1. To show that these inaccuracy measures are nondimensional, the word "fractional" is included in each of the names and the letter F is placed before the symbol that identifies the measure that is represented. A word is placed in each name to describe the function of the basic measure that is being identified, and corresponding symbols are added to the symbol. For example, the reading range reference average fractional uncertainty of scale reading is given the symbol $[(AFU)R_s]_{(RR)}$ and is defined as the average scale reading uncertainty divided by the scale reading range. In the symbol for this quantity, (AFU) represents average fractional uncertainty, and the subscript (RR) shows that the scale reading range, $(RR)_s$, is used as the reference for forming the fraction. The reading reference average fractional uncertainty is similar to the one just described except that the subscript is changed to R in order to show that the reference quantity is the scale reading, R_s, instead of the scale reading range, $(RR)_s$. The maximum reading reference average fractional uncertainty is identical with the other two fractional uncertainty measures except that the maximum scale reading is used as the denominator in forming the dimensionless ratio. This fact is recognized in the corresponding symbol by using $R_{(max)}$ as the identifying subscript. Table 29-1 gives fractional measures for a number of the inaccuracy components listed in Definition Summary 29-5. In addition, maximum fractional uncertainty measures are listed, with uncertainty replaced by maximum uncertainty.

29.65. For practical purposes, fractional inaccuracy component measures may be expressed as fractions, decimal fractions, or percents. No distinction is made in the definitions or symbols among these methods of presenting information: the units employed in any given case are recognized by specifications placed on particular numerical values of the measures.

ACCURACY AND PRECISION

29.66. Accuracy, under its dictionary definition, connotes correctness or agreement with truth. This also implies that a high accuracy is equivalent to a low inaccuracy and vice versa. In quantitative terms, this fact is represented if accuracy is defined as unity minus the absolute magnitude of the fractional inaccuracy. When this magnitude is expressed as a decimal fraction, the measure of accuracy is also a decimal fraction. In percentage terms, accuracy is equal to one hundred minus the fractional inaccuracy expressed as a percentage.

29.67. It is common practice to use the word accuracy to describe measuring instrument performance. For example, the ASME[(A5)(A6)] list of "basic terms" includes the statement that ". . . Accuracy in Measurement is the degree of correctness with which a measuring means yields the 'true' value of a measured quantity." Accuracy is also sometimes used to mean "inaccuracy" as this term is defined in item 19 of Table 29-1. That is, the statement that "the accuracy of this instrument is one part in ten thousand" actually means that the fractional inaccuracy is one ten-thousandth. Little difficulty is introduced by this interchange of the accuracy and inaccuracy definitions because, in any situation of practical interest, inaccuracy is always small compared to unity, while accuracy as defined in item 64 of Table 29-1 is near unity. This natural distinction between accuracy and inaccuracy values makes it possible to use a word that certainly has the proper connotation for specifying instrument performance quality without continually repeating its definition.

29.68. Precision is a word that is related to uncertainty in the same way that accuracy is related to inaccuracy. In the ASME[(A5)(A6)] basic terms, ". . . Precision in Measurement is the degree of reproducibility among several independent measurements of the same true value under specified conditions. . . It is usually expressed in terms of deviation in measurement." Names, symbols and defining equations for various types of precision (symbol (P_r)) are given in items 70 through 75 of Table 29-1. The pattern for each definition is the same; the magnitude of one of the fractional uncertainties defined in items 49 through 54 of Table 29-1 is substracted from unity to give the corresponding precision in fractional terms or as a percentage when the fractional form is multiplied by one hundred.

29.69. The term precision is commonly used to mean a concept that is identical with maximum uncertainty. For example, the statement that a certain

Item	Name	Symbol	Defining Relationship
	BASIC CONCEPTS		
1	Actuating Input or Actuating Input Quantity or Actuating Quantity	$q_{(in)(ac)}$	
2	Interfering Input or Interfering Input Quantity or Interfering Quantity	$q_{(in)(int)}$	
3	Modifying Input or Modifying Input Quantity or Modifying Quantity	$q_{(in)(mod)}$	
4	Output or Output Quantity	$q_{(out)}$	
5	Indication or Index Position (for an indicator or instrument mechanism)	(Ind)	
6	Actuating Input Quantity Scale Reading or Indicated Input or Scale Reading	$q_{(in)s}$ $q_{(ind)}$ R_s	Note: Scale Reading always has the dimensions associated with the actuating input, or a combination of actuating inputs when the measuring instrument is actuated by a combination of inputs
7	Maximum Scale Reading	$R_{(s)(max)}$	
8	Minimum Scale Reading	$R_{(s)(min)}$	
9	Scale Reading Range	$(RR)_s$	$R_{(s)(max)} - R_{(s)(min)}$
10	Maximum Indication	$(Ind)_{(max)}$	
11	Minimum Indication	$(Ind)_{(min)}$	
12	Indication Range	(IR)	$(Ind)_{(max)} - (Ind)_{(min)}$
	COMPONENT PERFORMANCE-DESCRIBING CONCEPTS		
13	Indicating Mechanism Static Sensitivity or Indicator Static Sensitivity	$S_{(im)[q;(Ind)](st)}$ or $S_{(i)[q;(Ind)](st)}$ or $S_{(i)(st)}$ or S_i	$\left[\frac{d(Ind)}{dq_{(in)}}\right]_{(st)}$ Note: The subscript (st) shows that the defining ratio is taken under static conditions
14	Indicating Mechanism Performance Function or Indicator Performance Function	$[PF]_{(im)[q;(Ind)]}$ or $[PF]_{(i)[q;(Ind)]}$ or $[PF]_i$	$\frac{(Ind)}{q_{(in)}}$ Note: $q_{(in)}$ may be $q_{(in)(ac)}$ or $q_{(in)(int)}$
15	Scale Static Sensitivity or Scale Sensitivity (Ordinarily, scales have only static properties so that the scale sensitivity is identical with the static scale sensitivity)	$S_{(s)[(Ind);R](st)}$ or $S_{(s)[(Ind);R]}$ or S_s	$\left[\frac{d(R_s)}{d(Ind)}\right]_{(st)}$ or, in the special case of linear variations with $R_s = 0$ when $(Ind) = 0$ $\left[\frac{R_s}{(Ind)}\right]_{(st)}$

Table 29-1. Names, symbols and defining equations for description of measuring instrument operation.
(Page 1 of 5)

Item	Name	Symbol	Defining Relationship
16	**Indicating Mechanism Calibration Performance Function** **or** **Indicator Calibration Performance Function** (This performance function standard is established by design considerations as the performance goal for the ideal indicating mechanism)	$[PF]_{(im)[q;(Ind)](cal)}$ or $[PF]_{(i)[q;(Ind)](cal)}$ or $[PF]_{(i)(cal)}$	$\left[\frac{(Ind)}{q_{(in)}}\right]_{(cal)}$ Note: The subscript (cal) shows that the identified relationship is the calibration standard for an ideal mechanism under calibration conditions.
17	**Indicating Mechanism Calibration Static Sensitivity**	$S_{(im)[q;(Ind)](cal)}$ or $S_{(m)[q;(Ind)](cal)}$ or $S_{(m)(cal)}$	$\left[\frac{d(Ind)}{dq_{(in)}}\right]_{(st)(cal)}$
18	**Scale Calibration Sensitivity** (This is the standard sensitivity established by design for an ideal scale)	$S_{(s)[(Ind);R](cal)}$ or $S_{(s)(cal)}$	$\left[\frac{d(R_s)}{d(Ind)}\right]_{(cal)}$ Note: The subscript (cal) identifies the calibration function established by design for an ideal scale.
	SCALE READING QUALITY-DESCRIBING CONCEPTS		
19	**Scale Reading Inaccuracy**	$(I)R_s$	$R_s - R_{(s)(corr)}$ where R_s = actual scale reading $R_{(s)(corr)}$ = correct scale reading
20	**Average Scale Reading**	$(Av)R_s$ or $R_{(s)(av)}$	$(Av)R_s = \frac{1}{n}\sum_{i=1}^{i=n}(R_s)_i$ Refer to Eq. (2) of Definition Summary 29-4
21	**Scale Reading Uncertainty**	$(U)R_s$	$R_s - (Av)R_s$ or $R_s - R_{(s)(av)}$
22	**Scale Reading Error**	$(E)R_s$	$(Av)R_s - R_{(s)(corr)}$ or $R_{(s)(av)} - R_{(s)(corr)}$
23	**Scale Reading Inaccuracy** *(Repeated)*	$(I)R_s$	$(E)R_s + (U)R_s$
24	**Scale Reading Ideal Correction**	$[(C)R_s]_{(ideal)}$	$-(E)R_s$ or $R_{(s)(corr)} - R_{(s)(av)}$ Note that $R_{(s)(corr)} = R_{(s)(av)} + [(C)R_s]_{(ideal)}$
25	**Corrected Scale Reading**	$R_{(s)(ctd)}$	(See below)
26	**Scale Reading Correction** (The correction actually applied to the scale reading; this correction is not necessarily the ideal scale reading correction)	$(C)R_s$	$R_{(s)(ctd)} - R_s$ Note that $R_{(s)(ctd)} = R_s + (C)R_s$ $R_{(s)(av)(ctd)} = R_{(s)(av)} + (C)R_s$
27	**Corrected Scale Reading Inaccuracy**	$(I)R_{(s)(ctd)}$	$R_{(s)(ctd)} - R_{(s)(corr)}$
28	**Corrected Scale Reading Uncertainty**	$(U)R_{(s)(ctd)}$	$(U)R_s$ Note: Addition of a correction to the average reading does not affect the uncertainty.
29	**Corrected Scale Reading Error** (This is the residual error that exists after $(C)R_s$ is applied to $R_{(s)(av)}$)	$(E)R_{(s)(ctd)}$	$R_{(s)(av)(ctd)} - R_{(s)(corr)}$
30	**Scale Reading Observational Error**	$(OE)R_s$	$R_s - R_{(s)[(OE)\to 0]}$ where $R_{(s)[(OE)\to 0]}$ = scale reading with perfect observation

Note: See Definition Summary 29-5 for detailed definitions of scale reading error and correction components.

Table 29-1. Names, symbols and defining equations for description of measuring instrument operation.
(Page 2 of 5)

Item	Name	Symbol	Defining Relationship
31	Scale Reading Zero Setting Error	$(ZSE)R_s$	$R_{(s)[(OE)\to 0]} - R_{(s)[(OE)\to 0][(ZSE)\to 0]}$ where $R_{(s)[(OE)\to 0][(ZSE)\to 0]}$ = scale reading with perfect observation and perfect zero setting
32	Scale Reading Scale Calibration Matching Error	$(SCME)R_s$	$R_{(s)[(OE)\to 0][(ZSE)\to 0]} - R_{(s)(cal)}$ where $R_{(s)(cal)}$ = calibration scale reading
33	Scale Reading Scale Calibration Error	$(SCE)R_s$	$R_{(s)(cal)} - R_{(s)(Ind)(corr)}$ where $R_{(s)(Ind)(corr)}$ = indication correct scale reading
34	Scale Reading Error Due to Scale Imperfections	$[(E)R_s]_s$	$R_s - R_{(s)(Ind)(corr)}$
35	Scale Reading Error Due to Mechanism Imperfections	$[(E)R_s]_m$	
36	Calibration Condition Scale Reading Error Due to Mechanism Imperfections	$[(E)R_s]_{(m)(cc)}$	
37	Environmental Scale Reading Error Due to Mechanism Imperfections	$[(E)R_s]_{(m)(en)}$	
38	Scale Reading Error *(Repeated)*	$(E)R_s$	$(OE)R_s + (ZSE)R_s + (SCME)R_s + (SCE)R_s + (MOE)R_s + (MCME)R_s + (MCE)R_s$ Note: See Eqs. (31) and (32) of Definition Summary 29-5. Equation (42) of that summary shows environmental and calibration condition error components.
39	Scale Reading Average Uncertainty or Average Scale Reading Uncertainty or Average Uncertainty of Scale Reading (Associated with any typical single scale reading of a set of n scale readings)	$(AU)R_s$ or $(Av)[(U)R_s]$	$\frac{1}{n}\sum_{i=1}^{i=n}[(U)R_s]_i$
40	Scale Reading Standard Uncertainty or Standard Uncertainty of Scale Reading (Associated with any typical single scale reading of a set of n scale readings)	$(SU)R_s$	$(RMS)[(U)R_s]$
41	Scale Reading Root Mean Square Uncertainty or Root Mean Square Uncertainty of Scale Reading (Associated with any typical single scale reading of a set of n scale readings)	$(RMS)[(U)R_s]$	$\sqrt{(Av)[(U)R_s]^2}$ or $\sqrt{\frac{1}{n}\sum_{i=1}^{i=n}[(U)R_s]_i^2}$
42	Scale Reading Probable Uncertainty or Probable Uncertainty of Scale Reading (Associated with any typical single scale reading of a set of n scale readings)	$(PU)R_s$	$0.6745\ (SU)R_s$ or $0.6745\ \sqrt{(Av)[(U)R_s]^2}$
43	Scale Reading Modulus of Precision or Modulus of Precision of Scale Reading (Associated with any typical reading of a set of n readings)	$(MP)R_s$	$\frac{1}{(SU)R_s\sqrt{2}}$
UNCERTAINTY MEASURES ASSOCIATED WITH THE AVERAGE OF A SET OF SCALE READINGS			
44	Average Uncertainty of the Average of n Scale Readings	$(AU)[(Av)R_s]_n$	$\frac{(AU)R_s}{\sqrt{n}}$
45	Standard Uncertainty of the Average of n Scale Readings	$(SU)[(Av)R_s]_n$	$\frac{(SU)R_s}{\sqrt{n}}$
46	Probable Uncertainty of the Average of n Scale Readings	$(PU)[(Av)R_s]_n$	$\frac{(PU)R_s}{\sqrt{n}}$

Table 29-1. Names, symbols and defining equations for description of measuring instrument operation.
(Page 3 of 5)

Item	Name	Symbol	Defining Relationship
47	Modulus of Precision of the Average of n Scale Readings	$(MP)\,[(Av)R_s]_n$	$\sqrt{n}\,[(MP)R_s]$
48	Maximum Uncertainty of Scale Reading or Scale Reading Maximum Uncertainty	$[(U)R_s]_{(max)}$	Note: This quantity may often be taken as the difference between scale readings corresponding to the maximum spread of indications for the same actuating input level. This difference is due to imperfections in the mechanism.
	NONDIMENSIONAL MEASURES OF SCALE READING QUALITY Note: All quantities may be expressed either as fractions or as percentages.		
49	Reading Range Reference Average Fractional Uncertainty of Scale Reading or Scale Reading Average Fractional Uncertainty with Reading Range Reference	$[(AFU)R_s]_{(RR)}$	$\dfrac{(Av)\,[(U)R_s]}{[RR]_s}$
50	Reading Reference Average Fractional Uncertainty of Scale Reading or Scale Reading Average Fractional Uncertainty	$[(AFU)R_s]_R$ or $(AFU)R_s$	$\dfrac{(Av)\,[(U)R_s]}{R_s}$
51	Maximum Reading Reference Average Fractional Uncertainty of Scale Reading	$[(AFU)R_s]_{R_{(max)}}$	$\dfrac{(Av)\,[(U)R_s]}{R_{(s)(max)}}$
52	Reading Range Reference Maximum Fractional Uncertainty of Scale Reading	$[(MFU)R_s]_{(RR)}$	$\dfrac{[(U)R_s]_{(max)}}{(RR)_s}$
53	Reading Reference Maximum Fractional Uncertainty of Scale Reading or Scale Reading Maximum Fractional Uncertainty	$[(MFU)R_s]_R$ or $(MFU)R_s$	$\dfrac{[(U)R_s]_{(max)}}{R_s}$
54	Maximum Reading Reference Maximum Fractional Uncertainty of Scale Reading	$[(MFU)R_s]_{R_{(max)}}$	$\dfrac{[(U)R_s]_{(max)}}{R_{(s)(max)}}$
55	Reading Range Reference Fractional Error of Scale Reading	$[(FE)R_s]_{(RR)}$	$\dfrac{(E)R_s}{(RR)_s}$
56	Reading Reference Fractional Error of Scale Reading or Scale Reading Fractional Error	$[(FE)R_s]_R$ or $(FE)R_s$	$\dfrac{(E)R_s}{R_s}$
57	Maximum Reading Reference Fractional Error of Scale Reading	$[(FE)R_s]_{R_{(max)}}$	$\dfrac{(E)R_s}{R_{(s)(max)}}$
58	Reading Range Reference Fractional Inaccuracy of Scale Reading	$[(FI)R_s]_{(RR)}$	$\dfrac{(I)R_s}{(RR)_s}$
59	Reading Reference Fractional Inaccuracy of Scale Reading or Scale Reading Fractional Inaccuracy	$[(FI)R_s]_R$ or $(FI)R_s$	$\dfrac{(I)R_s}{R_s}$
60	Maximum Reading Reference Fractional Inaccuracy of Scale Reading	$[(FI)R_s]_{R_{(max)}}$	$\dfrac{(I)R_s}{R_{(s)(max)}}$
61	Reading Range Reference Maximum Fractional Inaccuracy of Scale Reading	$[(MFI)R_s]_{(RR)}$	$\dfrac{[(I)R_s]_{(max)}}{(RR)_s}$
62	Reading Reference Maximum Fractional Inaccuracy of Scale Reading or Scale Reading Maximum Fractional Inaccuracy	$[(MFI)R_s]_R$ or $(MFI)R_s$	$\dfrac{[(I)R_s]_{(max)}}{R_s}$
63	Maximum Reading Reference Maximum Fractional Inaccuracy of Scale Reading	$[(MFI)R_s]_{R_{(max)}}$	$\dfrac{[(I)R_s]_{(max)}}{R_{(s)(max)}}$

Table 29-1. Names, symbols and defining equations for description of measuring instrument operation.
(Page 4 of 5)

Item	Name	Symbol	Defining Relationship
	ACCURACY AND PRECISION MEASURES		
64	Reading Range Reference Accuracy of Scale Reading	$[(A)R_s]_{(RR)}$	$1 - \left\| \frac{(I)R_s}{(RR)_s} \right\|$
65	Reading Reference Accuracy of Scale Reading or Scale Reading Accuracy	$[(A)R_s]_R$ or $(A)R_s$	$1 - \left\| \frac{(I)R_s}{R_s} \right\|$
66	Maximum Reading Reference Accuracy of Scale Reading	$[(A)R_s]_{R_{(max)}}$	$1 - \left\| \frac{(I)R_s}{R_{(s)(max)}} \right\|$
67	Reading Range Reference Minimum Accuracy of Scale Reading	$[(MA)R_s]_{(RR)}$	$1 - \left\| \frac{[(I)R_s]_{(max)}}{(RR)_s} \right\|$
68	Reading Reference Minimum Accuracy of Scale Reading or Scale Reading Minimum Accuracy	$[(MA)R_s]_R$ or $(MA)R_s$	$1 - \left\| \frac{[(I)R_s]_{(max)}}{R_s} \right\|$
69	Maximum Reading Reference Minimum Accuracy of Scale Reading	$[(MA)R_s]_{R_{(max)}}$	$1 - \left\| \frac{[(I)R_s]_{(max)}}{R_{(s)(max)}} \right\|$
70	Reading Range Reference Precision of Scale Reading	$[(Pr)R_s]_{(RR)}$	$1 - \left\| \frac{(U)R_s}{(RR)_s} \right\|$
71	Reading Reference Precision of Scale Reading or Scale Reading Precision	$[(Pr)R_s]_{(R)}$ or $(Pr)R_s$	$1 - \left\| \frac{(U)R_s}{R_s} \right\|$
72	Maximum Reading Reference Precision of Scale Reading	$[(Pr)R_s]_{R_{(max)}}$	$1 - \left\| \frac{(U)R_s}{R_{(s)(max)}} \right\|$
73	Reading Range Reference Minimum Precision of Scale Reading	$[(MPr)R_s]_{(RR)}$	$1 - \left\| \frac{[(U)R_s]_{(max)}}{(RR)_s} \right\|$
74	Reading Reference Minimum Precision of Scale Reading or Scale Reading Minimum Precision	$[(MPr)R_s]_R$ or $(MPr)R_s$	$1 - \left\| \frac{[(U)R_s]_{(max)}}{R_s} \right\|$
75	Maximum Reading Reference Minimum Precision of Scale Reading	$[(MPr)R_s]_{R_{(max)}}$	$1 - \left\| \frac{[(U)R_s]_{(max)}}{R_{(s)(max)}} \right\|$
76	Scale Factor or Calibration Coefficient	(SF)	$\frac{R_s}{(Ind)_{R_s}}$ i.e., $R_s = (SF)[(Ind)_{R_s}]$ where $(Ind)_{R_s}$ = indication in terms of scale reading units
77	Scale Reading Correction Coefficient	$(CC)R_s$	$\frac{R_{(s)(ctd)}}{R_s}$ or $1 + \frac{(C)R_s}{R_s}$

Note: The terms, symbols and defining equations given in this table illustrate a pattern that may easily be extended to cover performance quality-describing concepts not listed. The whole pattern of the table may be immediately applied to any quantity that has an actual value (corresponding to R_s) and a correct value (corresponding to $R_{(s)(corr)}$). For example, all the names and symbols describe the output of an indicating mechanism when "scale reading" is changed to "indication" and R_s is changed to (Ind).

Table 29-1. Names, symbols and defining equations for description of measuring instrument operation.
(Page 5 of 5)

instrument has a precision of one part in five thousand may be taken to mean that the maximum scale reading uncertainty is one five-thousandth of the maximum scale reading (or scale reading or scale reading range). Because, in practice, uncertainty is generally a small fraction while precision is approximately equal to unity, the intended meaning in any given case is usually clear from context without an explicit definition.

SUMMARY OF PERFORMANCE-DESCRIBING CONCEPTS

29.70. Table 29-1 is a summary of names, symbols and defining equations for a number of the concepts associated with the performance of measuring instruments. Each of the concepts in the table (with the exceptions noted below) is either discussed in earlier sections of this chapter or is related in an obvious way to one or more of the concepts that are explained. The two exceptions to this rule are the scale factor (symbol (SF)), or calibration coefficient, and the scale reading correction coefficient (symbol (CC)R_s).

29.71. The scale factor is exactly equivalent to the scale sensitivity as this concept is defined in item 15. It is the number by which the indication must be multiplied to find the proper scale reading in actuating input units. The scale reading correction coefficient is the factor by which the scale reading (actual scale reading) must be multiplied to obtain the corrected scale reading. The correction coefficient is equal to unity plus the scale reading correction divided by the scale reading.

29.72. The concepts listed in Table 29-1 form a system adapted to describing measuring instrument performance. This system is not complete, because other concepts are possible and may be required for special situations. On the other hand, the list contains many concepts that are essentially duplicates in the sense that both concepts would not be used at the same time. In any given situation, Table 29-1 may be used for reference purposes to supply specific information and to suggest the additional concepts and symbols that may be required for a special case.

SPECIFICATION OF MEASURING INSTRUMENTS

29.73. Specifications* describe the physical and functional characteristics of operating systems. In practice, these descriptions vary from the simplest possible statements of shape, size, and function to detailed descriptions of physical dimensions and extensive summaries of theoretical performance information. The number and completeness of the items included in any given situation depend on the equipment being described and the purpose for which the specification is to

* Webster's New Collegiate Dictionary defines specification as "... 2. A specifying, or designation of particulars. 3. A statement containing a minute description or enumeration of particulars, as of the terms of a contract, details of construction not shown in an architect's drawings, etc.; also, any item of such a statement." (By permission. From Webster's New Collegiate Dictionary, copyright, 1949, 1951, by G.&C. Merriam Co.)

SPECIFICATION

I IDENTIFICATION INFORMATION

Name; designation of type; catalog number; information file identification; etc.

II MECHANICAL FEATURES

Weight; geometrical form; linear dimensions; mounting provisions; mounting dimensions; service connections; input connections; output connections; etc.

III SERVICE SUPPLY REQUIREMENTS

Water, steam, gas, electricity, etc., supplies required for operation

IV OPERATING CONDITIONS

Allowable environmental range; input impedance; output impedance; etc.

V STATIC REFERENCE CHARACTERISTICS

Scale reading range; minimum scale reading; maximum scale reading; zero location; maximum uncertainty; maximum error; error curve; etc.

VI DYNAMIC REFERENCE CHARACTERISTICS

Performance equation; performance equation type; performance parameter values; dynamic performance curves; etc.

VII STATIC CORRECTIONS

Calibration condition corrections; environmental corrections; etc.

VIII DYNAMIC ERRORS, DEVIATIONS, AND CORRECTIONS

Deviation functions; dynamic error functions; deviation curves; dynamic error curves; dynamic corrections

IX DESCRIPTIVE DIAGRAMS

Pictorial diagrams; schematic diagrams; functional diagrams; electrical circuit diagrams; etc., with names and symbols

X COMPONENT PERFORMANCE CHARACTERISTICS

Performance equations; performance functions; static sensitivities; static reference sensitivities; performance parameters; etc., for the identified operating components of Item IX.

Specification Form 29-1. Illustrative specification form for measuring instruments.

be used. For example, a mechanical designer may only need a description of the form and the dimensions of the mounting provisions required for a given instrument, while a systems engineer may need complete data on the internal electrical circuits and the functional characteristics of operating components.

29.74. Specification Form 29-1 is a suggested list of items for the specification of measuring instruments. This list starts with basic identification and information on mechanical features, includes service supply requirements and operating conditions, and ends with descriptions of performance characteristics for the complete instrument and its operating components. The ten items of Specification Form 29-1 include the subjects that will usually be of interest for the complete specification of a measuring instrument. Items may be added to or removed from the form as necessary to meet the requirements of any given situation.

29.75. Specification 29-1 illustrates an application of Specification Form 29-1 to the presentation of essential information on a special voltmeter.

29.76. Item I identifies the instrument as a special high-damping voltmeter with the designation X-1.

29.77. Item II gives the weight and physical dimensions of the meter.

29.78. Item III shows that no supplies of water, steam, electricity, etc. are required for operation.

29.79. Item IV notes that the calibration temperature is 25 degrees centigrade.

29.80. Item V gives the essential static characteristics in terms of voltage scale reading range (2 volts), minimum and maximum voltage readings (± 1 volt), and the location of zero (at the middle of the scale). The voltage scale sensitivity is specified as constant and equal to 0.1 volt per division, but the inclusion of Item VII, Static Correction, implies that the specified scale sensitivity is an ideal value and that inaccuracies of various kinds may actually be present in any given reading. The maximum voltage reading uncertainty is given as 0.006 volt, which corresponds to a reading range reference voltage maximum fractional uncertainty of 0.3 percent. This means that repeated readings of the same applied voltage will give the same results within 0.3 percent of the reading range of 2 volts. The reading range reference voltage maximum fractional error is 0.5 percent, so that any reading of the meter taken with uncertainty effects determined and eliminated may be in error by not more than $0.005 \times 2 = 0.01$ volt. The correction for an error of this type might be determined and applied to remove the error; however, so long as the correction is either not known or is not used, it is possible only to set a maximum level for the error at any scale reading. The internal resistance of the meter is an important static characteristic and is given as 2088 ohms at the calibration temperature.

29.81. Item VI shows that for specification purposes the steady-state sinusoidal response performance of the meter is represented by a first-order differential equation with a zero-order independent variable term. This equation is discussed in Derivation Summary 18-10 as the (0; 0,1) equation, and its associated characteristics are plotted in Figs. 18-7, 18-8 and 18-9. The equations and text of Item VI in the specification have been made much more detailed than would be necessary in a normal specification, in order to demonstrate clearly the application of formal results from Volume II and the concepts summarized in Definition Summary 13-6 of Volume I to an illustrative practical situation. The nondimensional plots of Fig. 18-9 are repeated to give the curves of Fig. 1 in the specification.

29.82. In the case of special voltmeter X-1, ideal performance requires that sensitivity be independent of frequency. For this reason, the voltmeter specification reference sensitivity is taken as unity. This choice means that the nondimensional sensitivity - reference sensitivity ratio of Definition Summaries 13-5 and

13-6 is formally identical with the dynamic amplitude ratio - reference dynamic amplitude ratio ratio of Fig. 18-9, which in turn is equivalent to the voltmeter specification sensitivity. This sensitivity appears on the left-hand ordinate of Fig. 1 of Specification 29-1. The abscissa of Fig. 1 is the nondimensional characteristic time - forcing frequency product. This coordinate is changed to forcing frequency when it is divided by the characteristic time (given in Item VI as 3.16 seconds). The plot of Fig. 1 that gives the voltmeter specification dynamic response angle is identical with the (0; 0,1) equation dynamic response angle given in Fig. 18-9.

29.83. In any practical specification, much of the detail given herein would be omitted, leaving only characteristic curves and equations with required numerical data. When theoretical expressions are not available, experimental plots for specification characteristics may be used to describe performance.

29.84. Figure 1 of Specification 29-1 shows that the phase shift as measured by the dynamic response angle becomes -10 degrees at a frequency of about one-hundredth of a cycle per second and decreases rapidly to a value of almost -90 degrees at a frequency of about one cycle per second. The sensitivity is essentially unity at 0.01 cycle per second and has dropped to less than 0.1 at one cycle per second. These characteristics show that voltmeter X-1 will give highly accurate indications of amplitude only when the forcing frequency is less than 0.01 cycle per second.

29.85. Item VII gives the expression for the environmental correction due to variations of voltmeter temperature from the calibration level of 25 degrees centigrade.

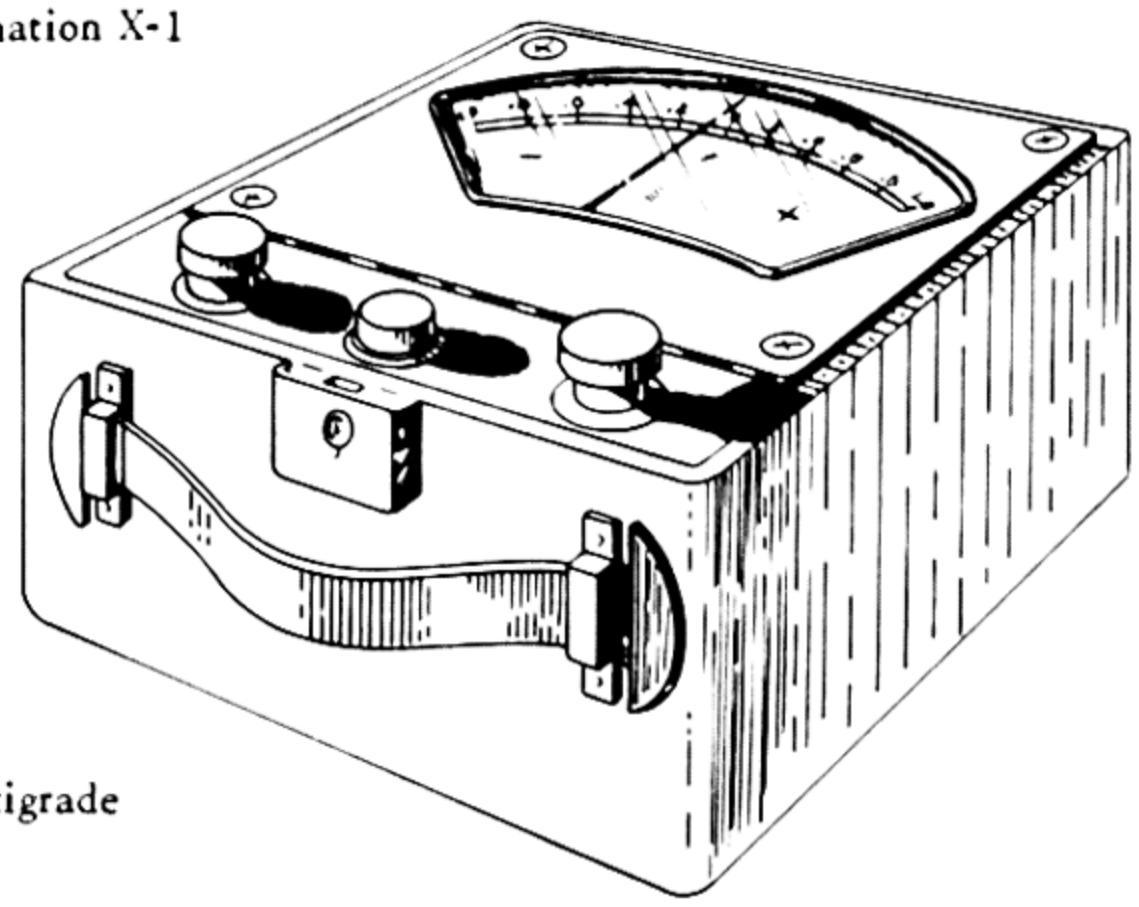
29.86. Item VIII summarizes the deviations and errors of specification dynamic performance as functions of frequency. An unusally long discussion of the background for these quantites is given in order to demonstrate the use of Volume I and Volume II material for describing instrument performance. In order to show in one example a number of the typical situations that may appear in practice, it is assumed that the specification dynamic characteristics based on the (0; 0,1) equation represent approximations that are accepted in order to simplify the associated equations and curves. To present a specific case for discussion, the second-order differential equation with a zero-order independent variable term (the (0; 0,1,2) equation of Derivation Summary 19-10 and Figs. 19-28, 19-29, 19-30, 19-34 and 19-35) is taken as the "correct" performance equation form for the voltmeter.

29.87. In the situation just outlined, the voltmeter specification reading errors with respect to a reference specification sensitivity equal to unity and a reference specification dynamic response angle equal to zero contain components of two types. First, the specification sensitivity and specification phase shift (identical with the dynamic response angle) have deviations with respect to the corresponding reference values; second, the specification sensitivity and specification

SPECIFICATION

I IDENTIFICATION

Special High-Damping Voltmeter, Designation X-1



II MECHANICAL FEATURES

Weight = $W = 4\frac{3}{4}$ pounds

Height = $h = 2\frac{1}{2}$ inches

Width = $w = 7\frac{1}{4}$ inches

Depth = $d = 6\frac{1}{2}$ inches

III SERVICE SUPPLY REQUIREMENTS

None

IV OPERATING CONDITIONS

Calibration conditions = 25 degrees centigrade

V STATIC CHARACTERISTICS

Voltage scale reading range = $[VRR]_s = 2$ volts

Minimum voltage reading = $e_{(s)(min)} = -1$ volt

Maximum voltage reading = $e_{(s)(max)} = +1$ volt

Zero symmetrically placed on scale; i.e.,

$$|e_{(s)(min)} - 0| = |0 - e_{(s)(max)}|$$

Voltage scale sensitivity = $S_{(s)[(Ind);e]}$ = constant = 0.1 volt/division

Maximum voltage reading uncertainty = $[(U)e_s]_{(max)} = 0.006$ volt

Reading range reference voltage maximum fractional uncertainty = $[(MFU)e_s]_{(RR)} = 0.3$ percent

Reading range reference voltage maximum fractional error = $[(MFE)e_s]_{(RR)} = 0.5$ percent

Internal resistance of meter = 2088 ohms at 25 degrees centigrade

VI DYNAMIC CHARACTERISTICS

Specification dynamic performance characteristics correspond to those of the zero-order forcing term – first-order differential equation (the (0;0,1) equation of Chapter 18). This means that the sinusoidal performance function for the meter has the form of the relating function found in Derivation Summary 18-10; i.e.,*

$$\eta = \eta_{(0;0,1)} = \frac{\sigma}{1 + j2\pi a} \tag{1}$$

The corresponding dimensionless dynamic amplitude ratio is

$$\mu = \mu_{(0;0,1)} = \frac{1}{\sqrt{1 + (2\pi a)^2}} \tag{2}$$

---

* Ordinarily, the required mathematical forms would be written down without comment from working variable results. Because this specification is the first concrete example in Volume III where use is made of generalized equation form, the relationships involved are shown with abnormally great detail.

Specification 29-1. Illustrative specification for special voltmeter X-1. (Page 1 of 11)

and the corresponding dynamic response angle is

$$\phi = \phi_{(0;0,1)} = \tan^{-1}(2\pi a) \tag{3}$$

In terms of the generalized self-defining symbols of Eqs. (2) and (20) of Definition Summary 13-6, Chapter 13, Eqs. (1), (2) and (3) are

$$\eta \approx [PF]_{(0;0,1)} = [PF]_{(vm)[e;e]} = \frac{(DAR)_{(vm)[e;e](ref)}}{1 + j2\pi[(CT)(FF)P]} \tag{4}$$

$$\mu \approx [(DAR)(RAR)R]_{(0;0,1)} = [(DAR)(RAR)R]_{(vm)(e;e)} = \frac{1}{\sqrt{1 + \{2\pi[(CT)(FF)P]\}^2}} \tag{5}$$

$$\phi \approx (DRA)_{(0;0,1)} = (DRA)_{(vm)(e;e)} = \tan^{-1}\{-2\pi[(CT)(FF)P]\} \tag{6}$$

Note that, from Fig. 18-6,

$a \approx (CT)(FF)P = (CT)n_f$ = characteristic time – forcing frequency product

$\approx (CT)(FP)R = (CT)/T_f$ = characteristic time – forcing period ratio

where

n_f = forcing frequency

T_f = forcing period

CT = characteristic time

When the corresponding expressions of Eqs. (19) and (20) of Definition Summary 13-6 are matched to express the generalized forms in terms of voltmeter sensitivity,

$(DAR)_{(vm)[e;e](ref)} \approx S_{(vm)[e;e](ref)}$ = voltage – voltage voltmeter reference sensitivity (7)

$[(DAR)(RAR)R]_{(vm)(e;e)} \approx [S(RS)R]_{(vm)(e;e)}$ = voltage – voltage voltmeter sensitivity – reference sensitivity ratio (8)

$$[PF]_{(vm)[e;e]} = \frac{S_{(vm)[e;e](ref)}}{1 + j2\pi[(CT)(FF)P]} \tag{9}$$

$$[S(RS)R]_{(vm)(e;e)} = \frac{1}{\sqrt{1 + \{2\pi[(CT)(FF)P]\}^2}} \tag{10}$$

$$(DRA)_{(vm)(e;e)} = \tan^{-1}\{-2\pi[(CT)(FF)P]\} \tag{11}$$

where, in accord with Definition Summary 13-4,

$(DAR)_{(vm)[e;e](ref)}$ = voltage – voltage voltmeter reference dynamic amplitude ratio

$$[(DAR)(RAR)R]_{(vm)(e;e)} = \frac{(DAR)_{(vm)[e;e]}}{(DAR)_{(vm)[e;e](ref)}} \tag{12}$$

$(DAR)_{(vm)[e;e]}$ = voltage – voltage voltmeter dynamic amplitude ratio

Note that, from Eqs. (16) and (17) of Definition Summary 13-6,

$(DAR)_{(vm)[e;e]} \approx S_{(vm)[e;e]}$ = voltage – voltage voltmeter sensitivity

In terms of the forms of Eqs. (9), (10) and (11), the steady-state sinusoidal specification response for the voltmeter is given by the equations

$$e_s = [PF]_{(vm)(spec)} e_{(in)} \tag{13}$$

$$e_s = S_{(vm)(ref)(spec)} [S(RS)R]_{(vm)(spec)} \epsilon^{j(DRA)_{(vm)(spec)}} e_{(in)} \tag{14}$$

(Refer to Eqs. (1) and (19) of Definition Summary 13-6.)

Note: The input-output subscript brackets, [e;e], are omitted from Eqs. (13) and (14) because in the present situation it is obvious that the input and output for the voltmeter must both have the dimensions of voltage.

The voltmeter specification reference sensitivity is

$$S_{(vm)(ref)(spec)} = 1 \text{ volt per volt} \tag{15}$$

The specification dynamic characteristics for the voltmeter are

$$[PF]_{(vm)(spec)} = \frac{1}{1 + j2\pi [(CT)(FF)P]} \tag{16}$$

= voltmeter specification performance function

$$[S(RS)R]_{(vm)(spec)} = \frac{1}{\sqrt{1 + \{2\pi [(CT)(FF)P]\}^2}} \tag{17}$$

= voltmeter specification sensitivity – reference sensitivity ratio

$$(DRA)_{(vm)(spec)} = \tan^{-1} \{- 2\pi [(CT)(FF)P]\} \tag{18}$$

where = voltmeter specification dynamic response angle

$$(CT) \approx (CT)_{(vm)} = 3.16 \text{ seconds} \tag{19}$$

= voltmeter specification characteristic time

Because $S_{(vm)(ref)(spec)} = 1$,

$$S_{(vm)(spec)} = [S(RS)R]_{(vm)(spec)} S_{(vm)(ref)(spec)} = \frac{1}{\sqrt{1 + \{2\pi [(CT)(FF)P]\}^2}} \tag{20}$$

See Fig. 1 of this specification for logarithmic scale plots of $(DRA)_{(vm)(spec)}$ and $S_{(vm)(spec)}$, taken from Fig. 18-9.

VII STATIC CORRECTION

Voltage reading environmental temperature correction factor = $[(C) e_s]_{(en)} = 1 + 0.0007 (T_{(en)} - 25)$ (21)

where

$T_{(en)}$ = environmental temperature in degrees centigrade

VIII DYNAMIC DEVIATIONS AND DYNAMIC ERRORS

By definition:

Deviations of specification dynamic characteristics

$$(D)[S(RS)R]_{(vm)(spec)} = [S(RS)R]_{(vm)(spec)} - [S(RS)R]_{(vm)(spec)(ref)} \tag{22}$$

= specification sensitivity – reference sensitivity ratio deviation

or, since $S_{(vm)(ref)(spec)} = 1$,

$$(D) S_{(vm)(spec)} = S_{(vm)(spec)} - S_{(vm)(spec)(ref)} \tag{23}$$

= specification sensitivity deviation

and

$$(D)(DRA)_{(vm)(spec)} = (DRA)_{(vm)(spec)} - (DRA)_{(vm)(spec)(ref)} \tag{24}$$

By specification,

$$[S(RS)R]_{(vm)(spec)(ref)} = 1 \tag{25}$$

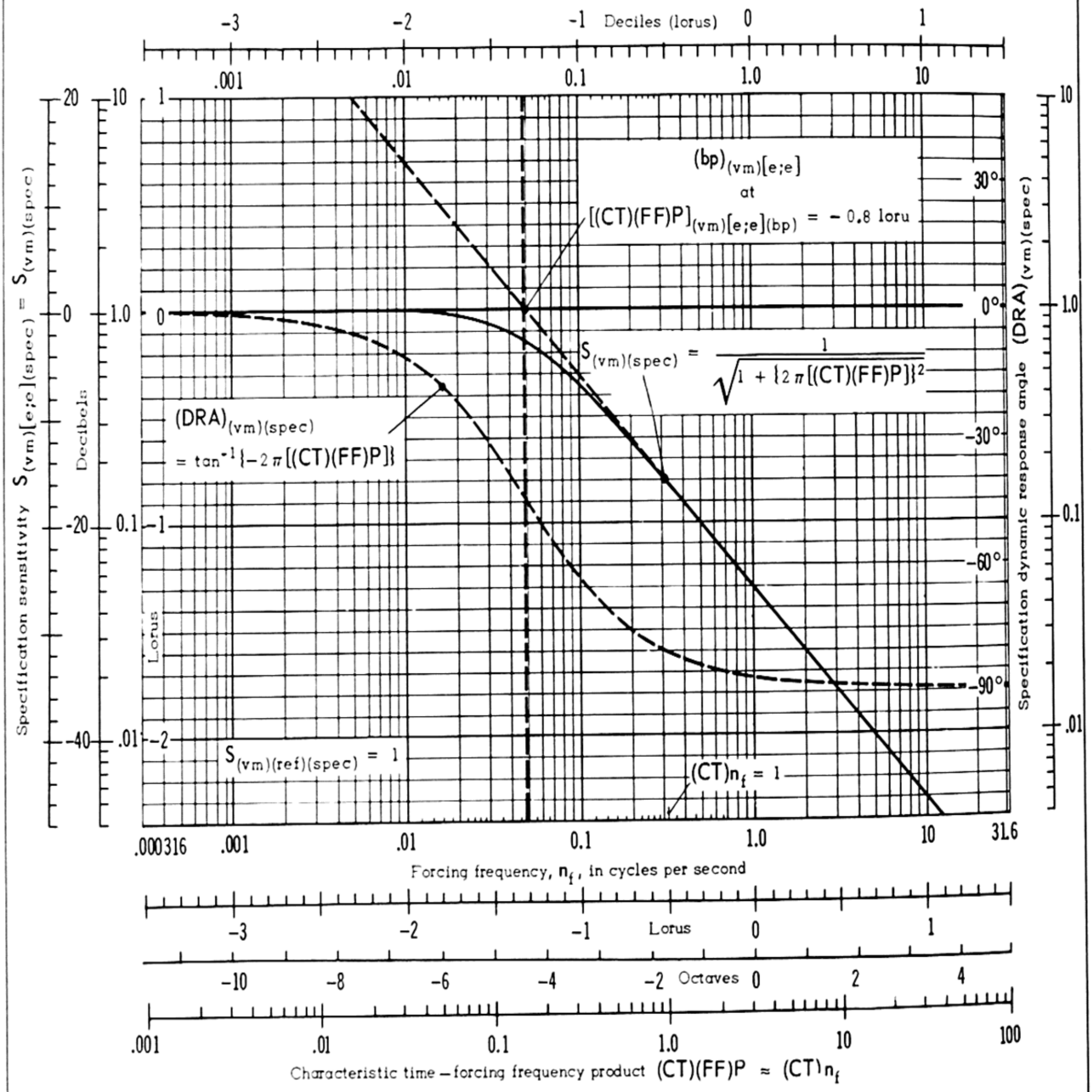
and

$$(DRA)_{(vm)(spec)(ref)} = 0 \tag{26}$$

Combining Eqs. (17), (22) and (25) gives

$$(D)[S(RS)R]_{(vm)(spec)} = \frac{1}{\sqrt{1 + \{2\pi [(CT)(FF)P]\}^2}} - 1 \tag{27}$$

Specification 29-1. Illustrative specification for special voltmeter X-1. (Page 3 of 11)



(see Fig. 18-9)

$S_{(vm)(ref)(spec)} = (RS)_{(vm)[e;e](spec)} = 1$ = voltmeter specification reference sensitivity

$S_{(vm)(spec)} = [S(RS)R]_{(vm)(e;e)(spec)} S_{(vm)(ref)(spec)}$

$(CT)(FP)R = (CT)/T_f = (CT)(FF)P$

$n_f = [(CT)(FP)R]/(CT)$; $CT = 3.16$ seconds

$[S(RS)R]_{(vm)(spec)}$ = voltmeter specification sensitivity – reference sensitivity ratio

(Refer to Fig. 18-9, Eqs. (19) and (20) of Definition Summary 13-6, and Derivation Summary 18-10)

Note: Quantities used for logarithmic coordinate scales must be dimensionless. This means that the cycles-per-second scale is actually made with the ratio of forcing frequency to unit forcing frequency as the variable.

Fig. 1. Specification sinusoidal response characteristics of special voltmeter X-1.

Specification 29-1. Illustrative specification for special voltmeter X-1. (Page 4 of 11)

Combining Eqs. (18), (24) and (26) gives

$$(D)(DRA)_{(vm)(spec)} = \tan^{-1}\{-2\pi[(CT)(FF)P]\} \tag{28}$$

The right-hand side of Eq. (27) is identical with the expression plotted in Fig. 18-15 as $\Delta\mu$ for the (0;0,1) equation. This plot is repeated in Fig. 2 of this specification with $(D)S_{(vm)(spec)}$ as the ordinate and $[(CT)(FF)P]$ as the abscissa. The right-hand side of Eq. (28) is identical with the expression plotted in Fig. 18-15 as $\Delta\phi$ for the (0;0,1) equation. This plot is likewise repeated in Fig. 2.

Errors of Specification Dynamic Characteristics

The first-order performance equation for the voltmeter is actually an approximation. The correct performance equation is a zero-order independent variable – second-order differential equation (i.e., the (0;0,1,2) equation solved for steady-state sinusoidal conditions in Derivation Summary 19-10 and with curves as plotted in Figs. 19-28, 19-29, 19-30, 19-34 and 19-35).

The errors in specification dynamic response characteristics are given by the equations

$$(E)[S(RS)R]_{(vm)(spec)} = [S(RS)R]_{(vm)(spec)} - [S(RS)R]_{(vm)(corr)} \tag{29}$$

= voltmeter specification sensitivity – reference sensitivity ratio error

$$(E)(DRA)_{(vm)(spec)} = (DRA)_{(vm)(spec)} - (DRA)_{(vm)(corr)} \tag{30}$$

= voltmeter specification dynamic response angle error

For the particular voltmeter in question,

$$(E)[S(RS)R]_{(vm)(spec)} = [S(RS)R]_{(0;0,1)} - [S(RS)R]_{(0;0,1,2)} \tag{31}$$

$$(E)(DRA)_{(vm)(spec)} = (DRA)_{(0;0,1)} - (DRA)_{(0;0,1,2)} \tag{32}$$

From the results of Derivation Summaries 18-10 and 19-10 and relationships taken from Table 19-1,

$$(E)[S(RS)R]_{(vm)(spec)} = \frac{1}{\sqrt{1 + \{2\pi[(CT)(FF)P]\}^2}}$$

$$- \frac{1}{\sqrt{\left[1 - \left\{\frac{\pi}{DR}[(CT)(FF)P]\right\}^2\right]^2 + \{2\pi[(CT)(FF)P]\}^2}} \tag{33}$$

$$(E)(DRA)_{(vm)(spec)} = \tan^{-1}\{-2\pi[(CT)(FF)P]\} - \tan^{-1}\left\{\frac{-2\pi[(CT)(FF)P]}{1 - \frac{\pi^2}{(DR)^2}[(CT)(FF)P]^2}\right\} \tag{34}$$

where (CT) in Eqs. (33) and (34) is identical with $(CT)_{(hdr)(sum)}$, the high damping ratio characteristic time sum, defined in Table 19-1, and the basic relationship between the independent variable for first- and second-order forms (taken from Table 19-1) is

$$(FR) = \frac{n_f}{n_n} = \text{frequency ratio} = \frac{\pi}{DR}[(CT)(FF)P] \tag{35}$$

in which

n_n = undamped natural frequency associated with second-order forms

DR = damping ratio associated with second-order forms

For the X-1 voltmeter,

n_n = 0.3 cycle per second

DR = 3.00

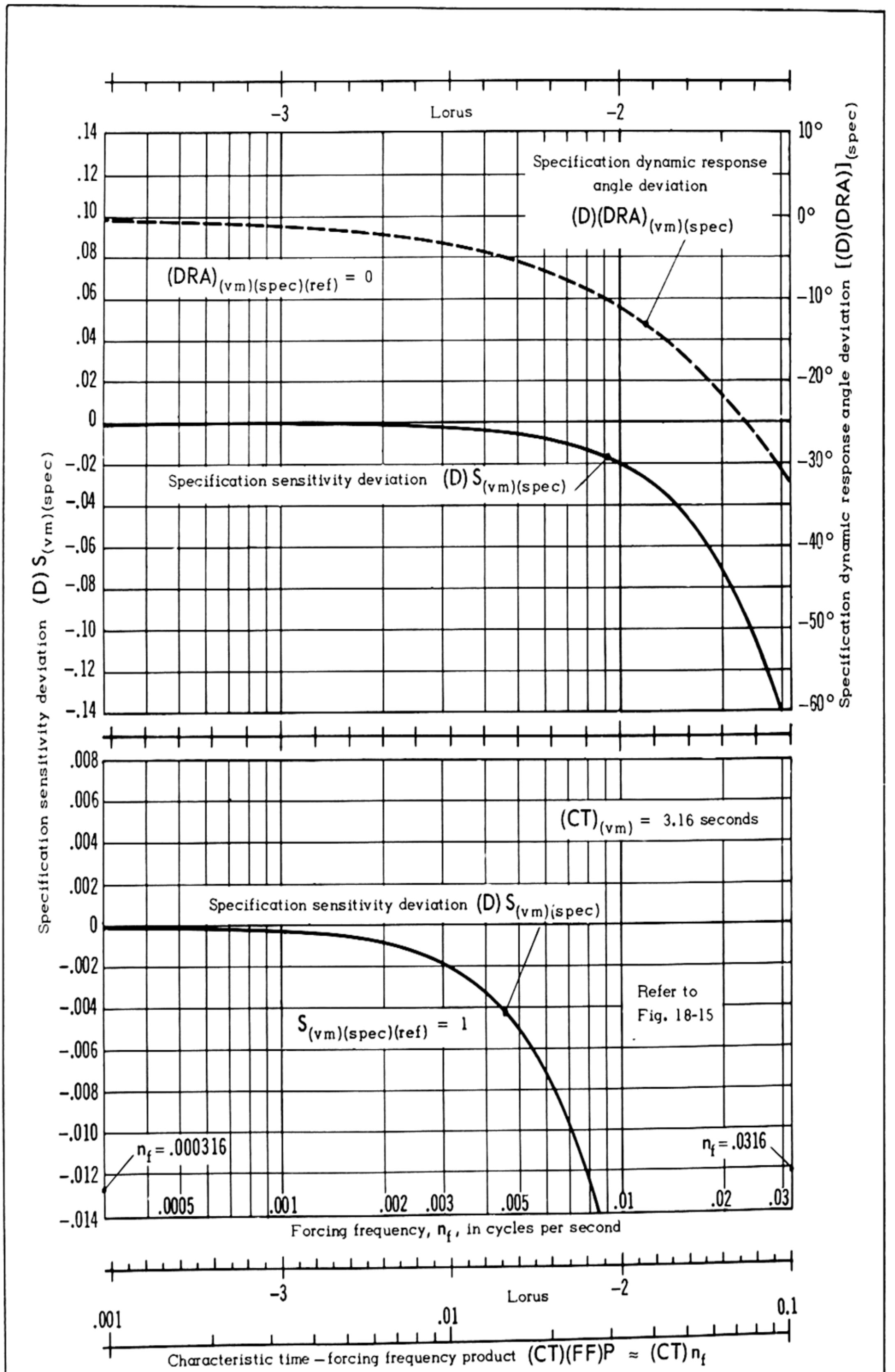


Fig. 2. Deviations of sinusoidal response characteristics of special voltmeter X-1.

Specification 29-1. Illustrative specification for special voltmeter X-1. (Page 6 of 11)

Figure 3 of this specification gives logarithmic scale plots for voltmeter specification sensitivity and voltmeter correct sensitivity as functions of forcing frequency. Figure 4 gives semilogarithmic scale plots for voltmeter specification dynamic response angle and voltmeter correct dynamic response angle as functions of forcing frequency. Figures 5a and 5b give plots of specification sensitivity error and specification dynamic response angle error, respectively, as functions of forcing frequency.

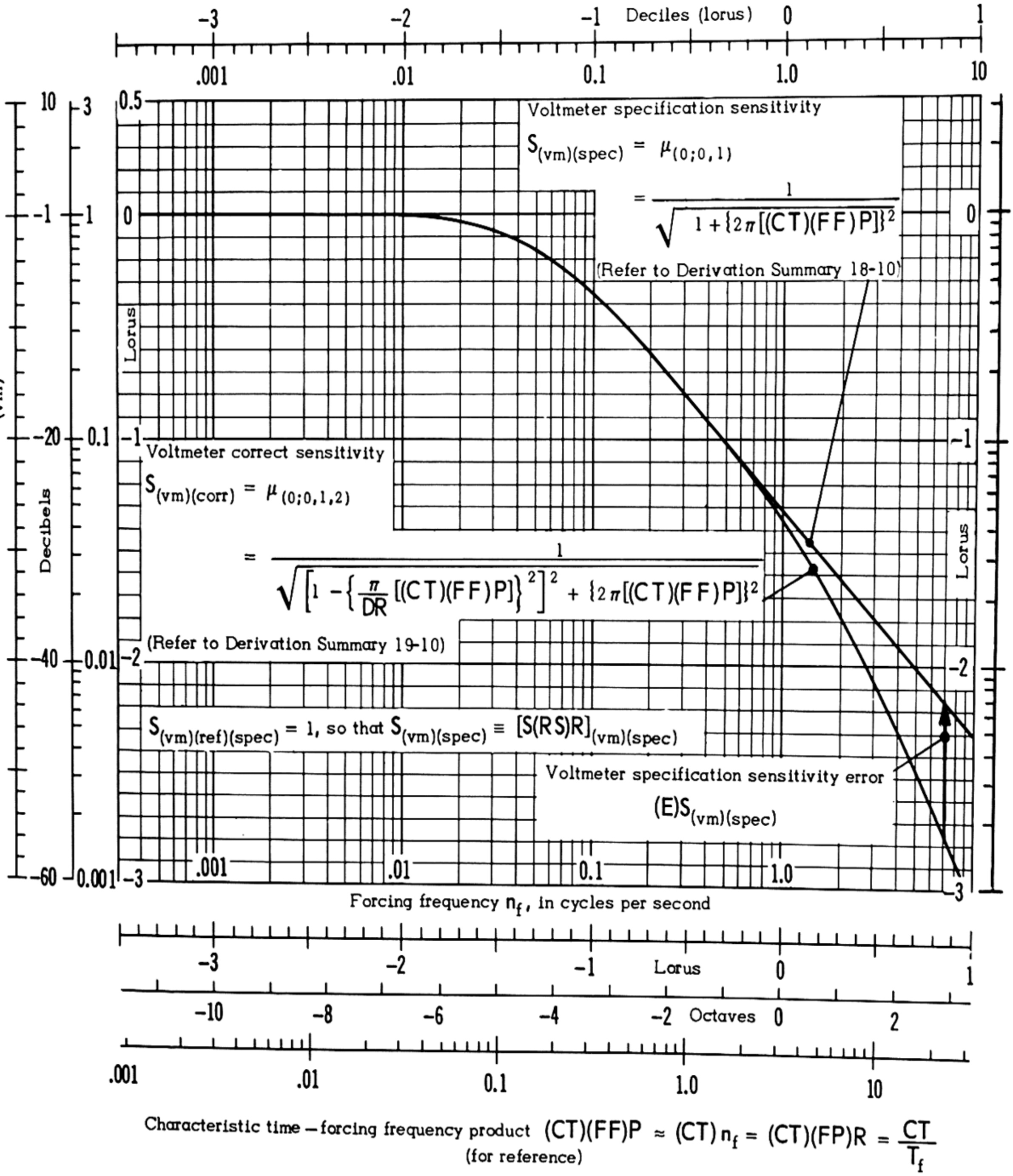
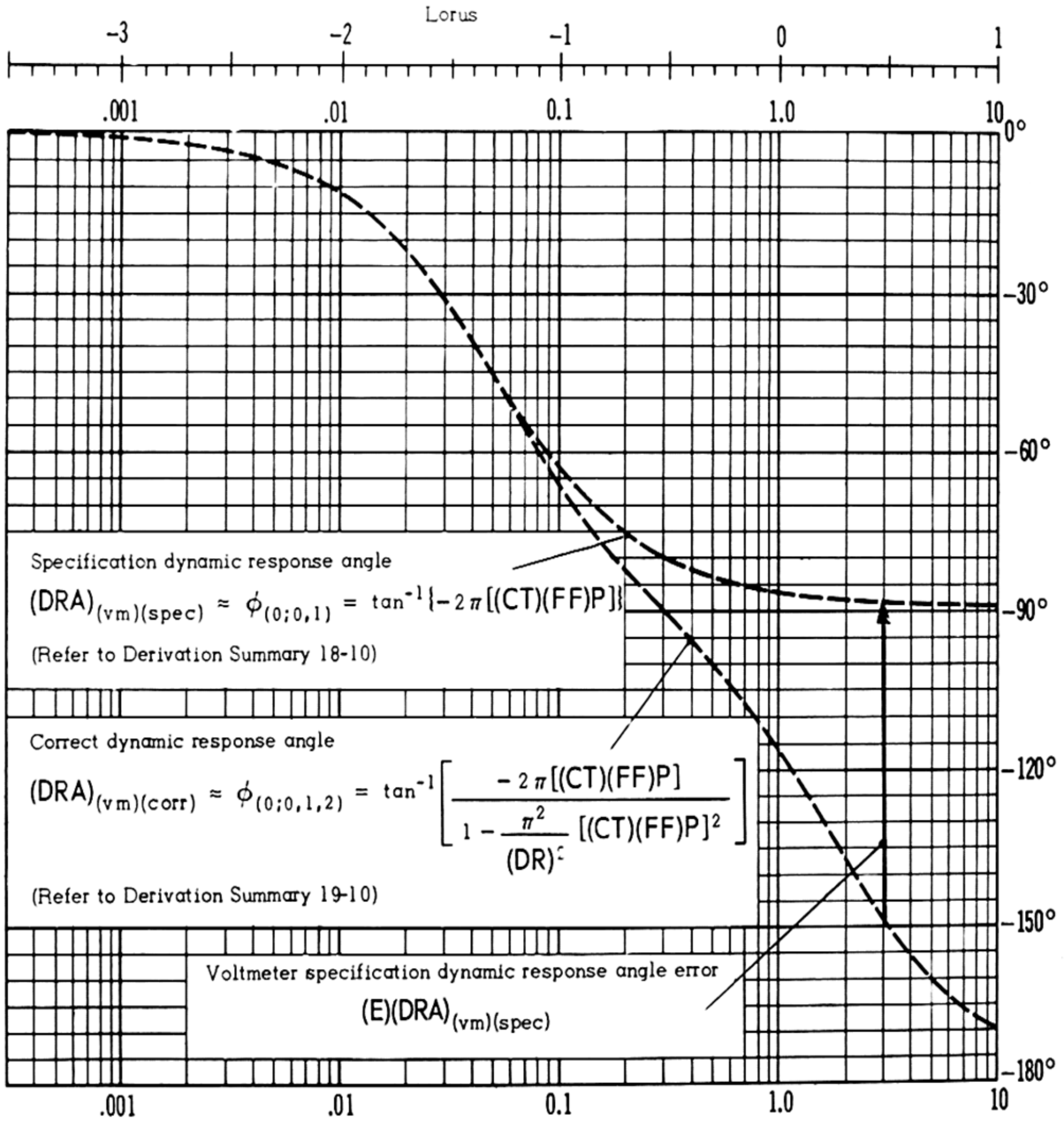


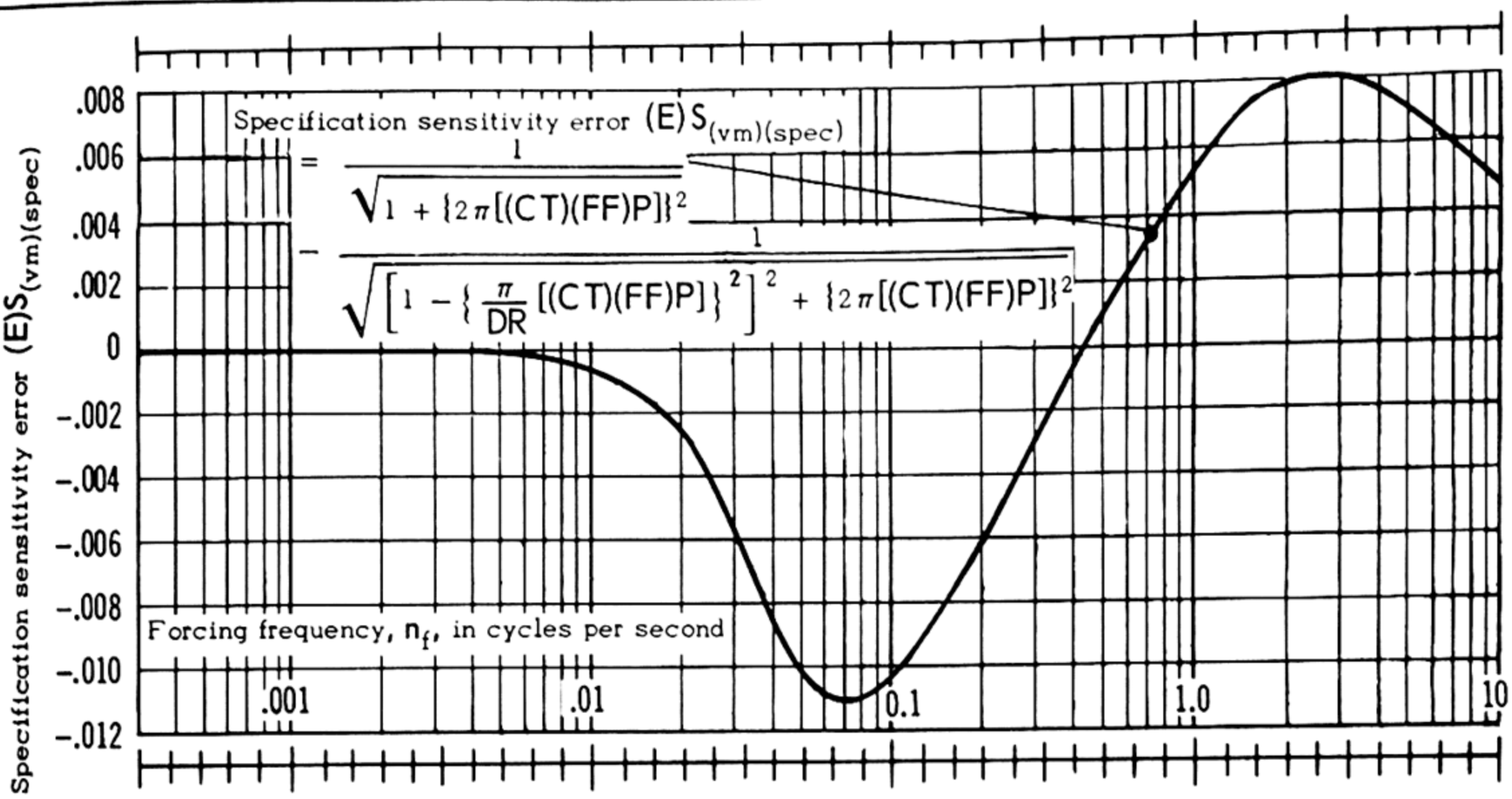
Fig. 3. Plots of specification sensitivity and correct sensitivity for special voltmeter X-1.



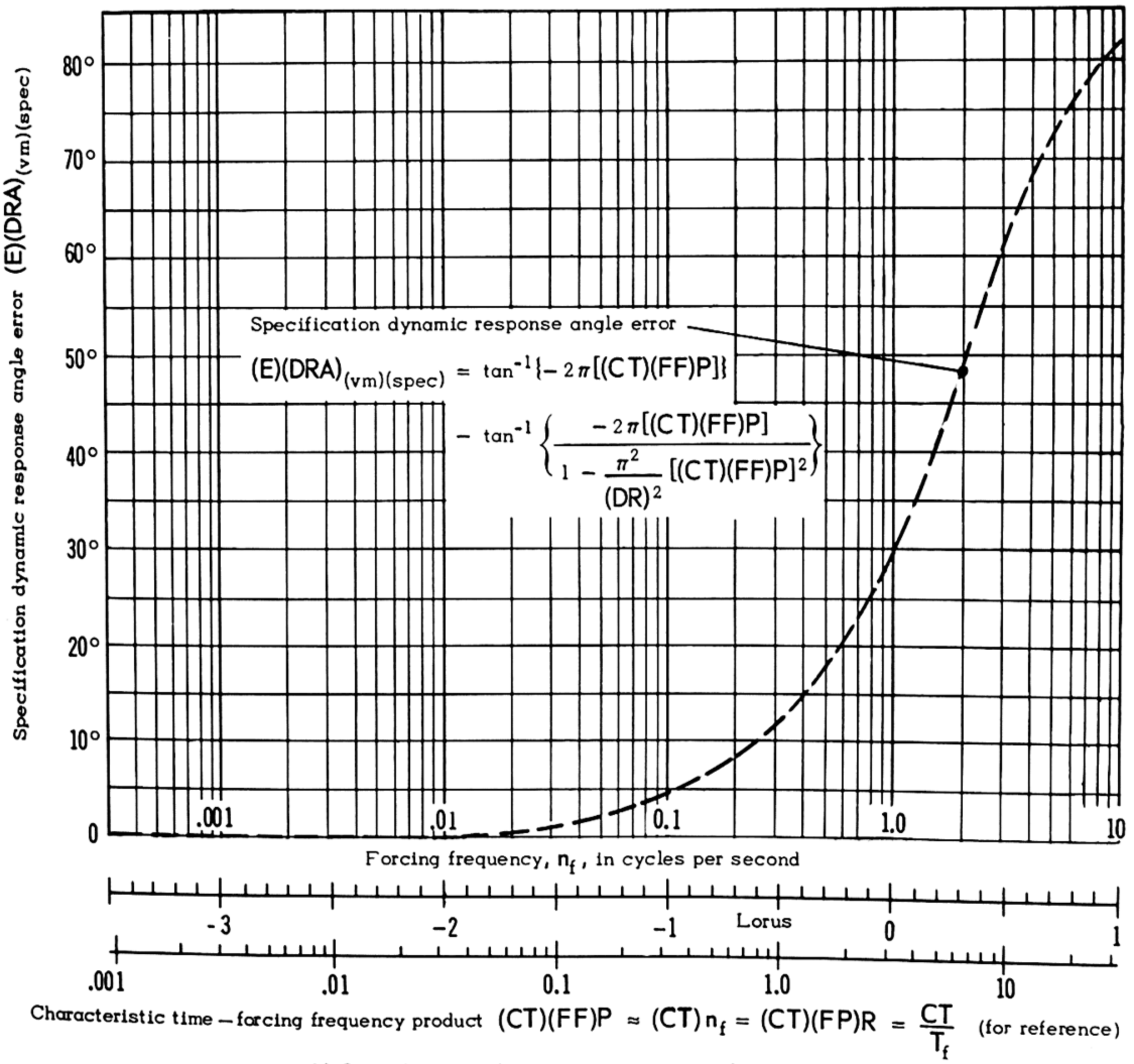
Characteristic time – forcing frequency product $(CT)(FF)P \approx (CT)\,n_f = (CT)(FP)R = \frac{CT}{T_f}$

(for reference)

Fig. 4. Plots of specification dynamic response angle and correct dynamic response angle for special voltmeter X-1.



a) Specification sensitivity error



b) Specification dynamic response angle error

Fig. 5. Plots of specification sensitivity error and specification dynamic response angle error for special voltmeter X-1.

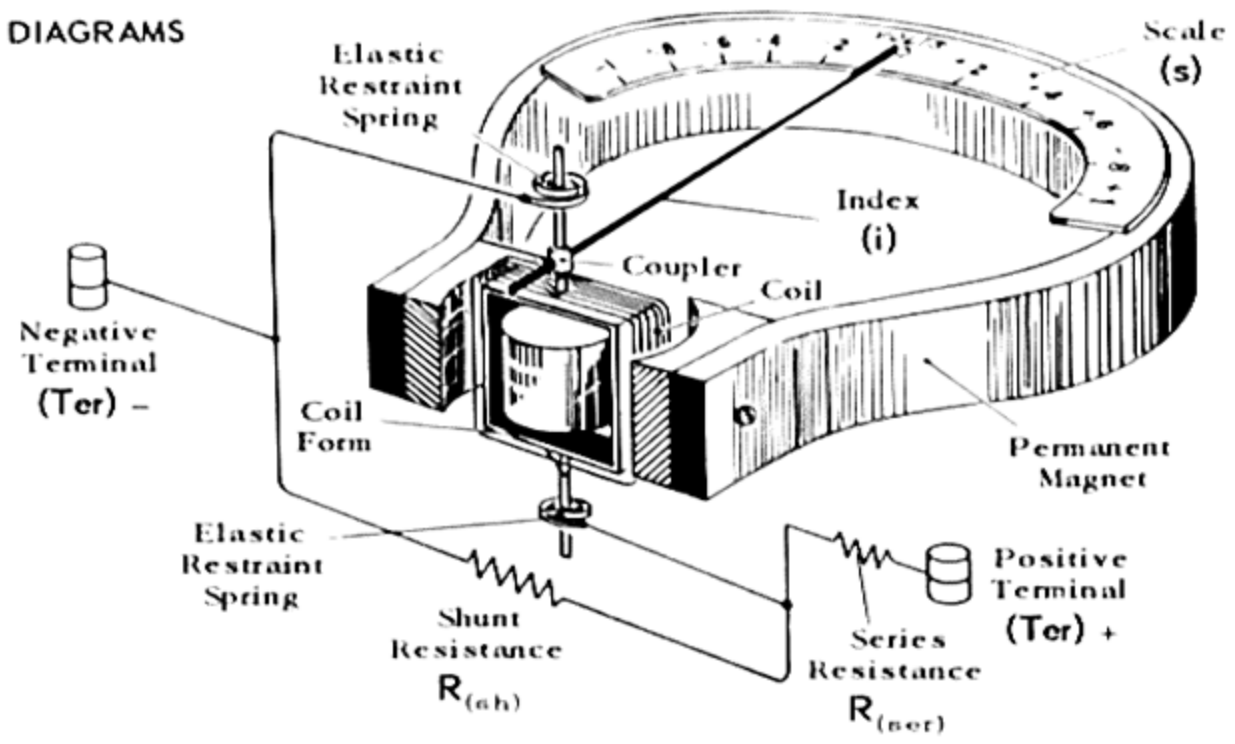


Fig. 6. Pictorial-schematic diagram for special voltmeter X-1.

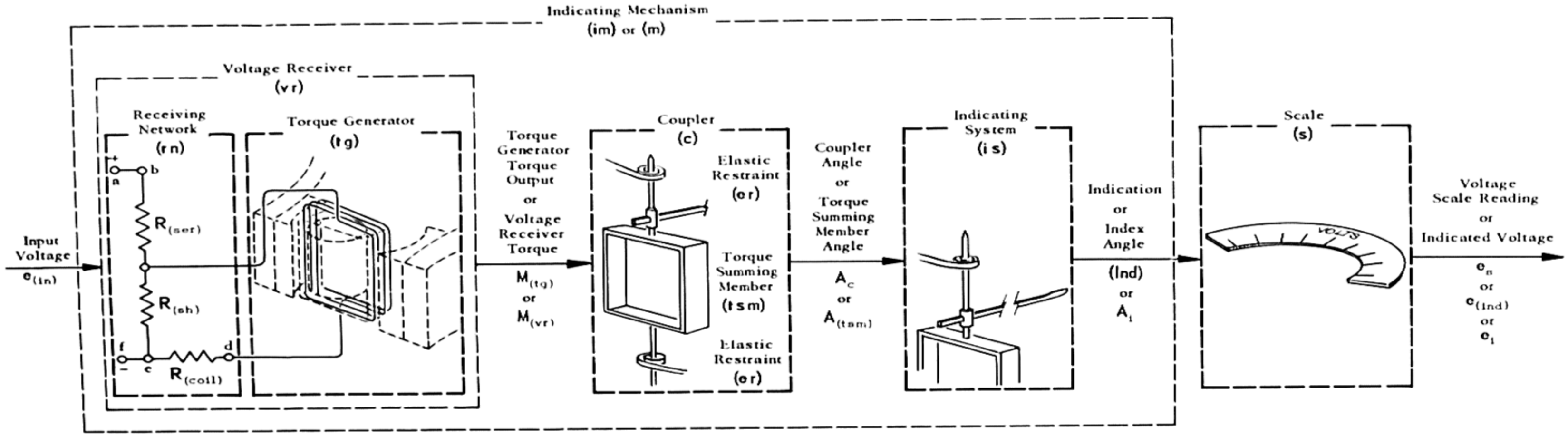


Fig. 7. Pictorial-functional diagram for special voltmeter X-1.

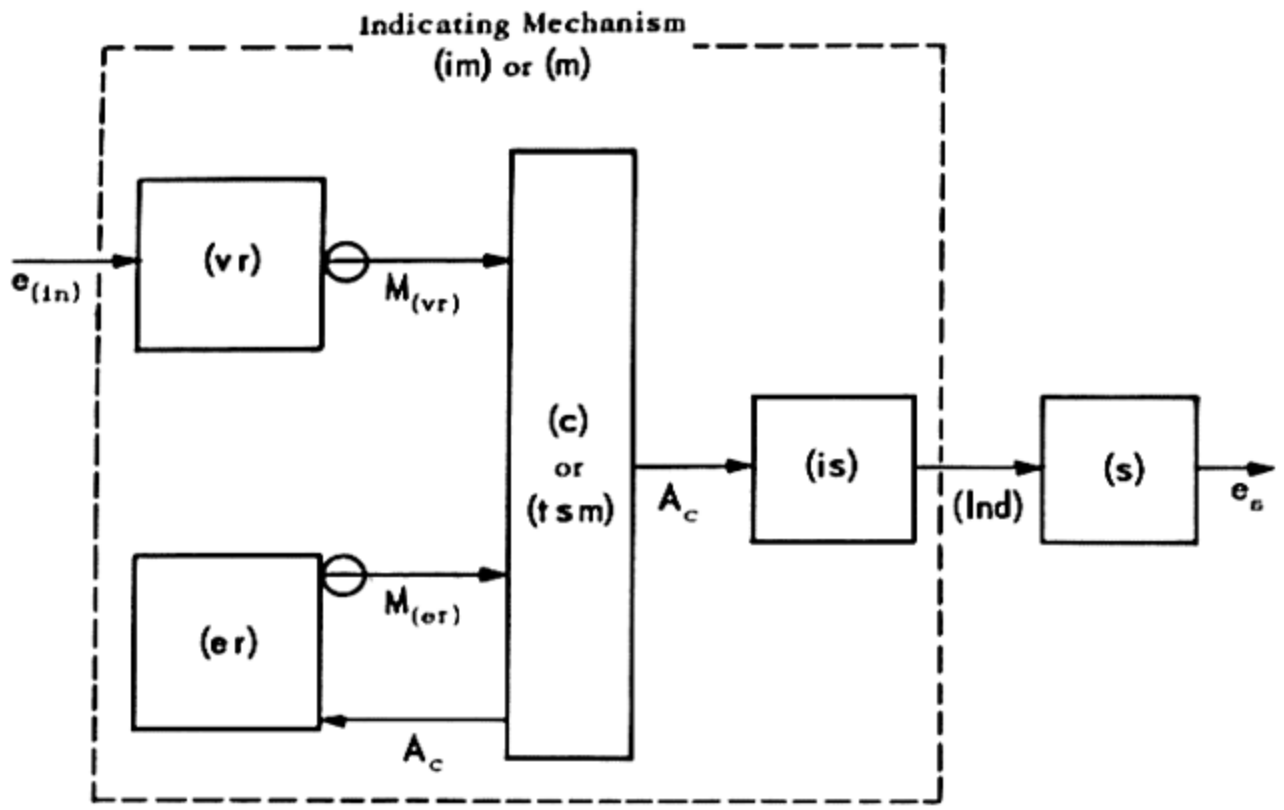


Fig. 8. Functional diagram for special voltmeter X-1.

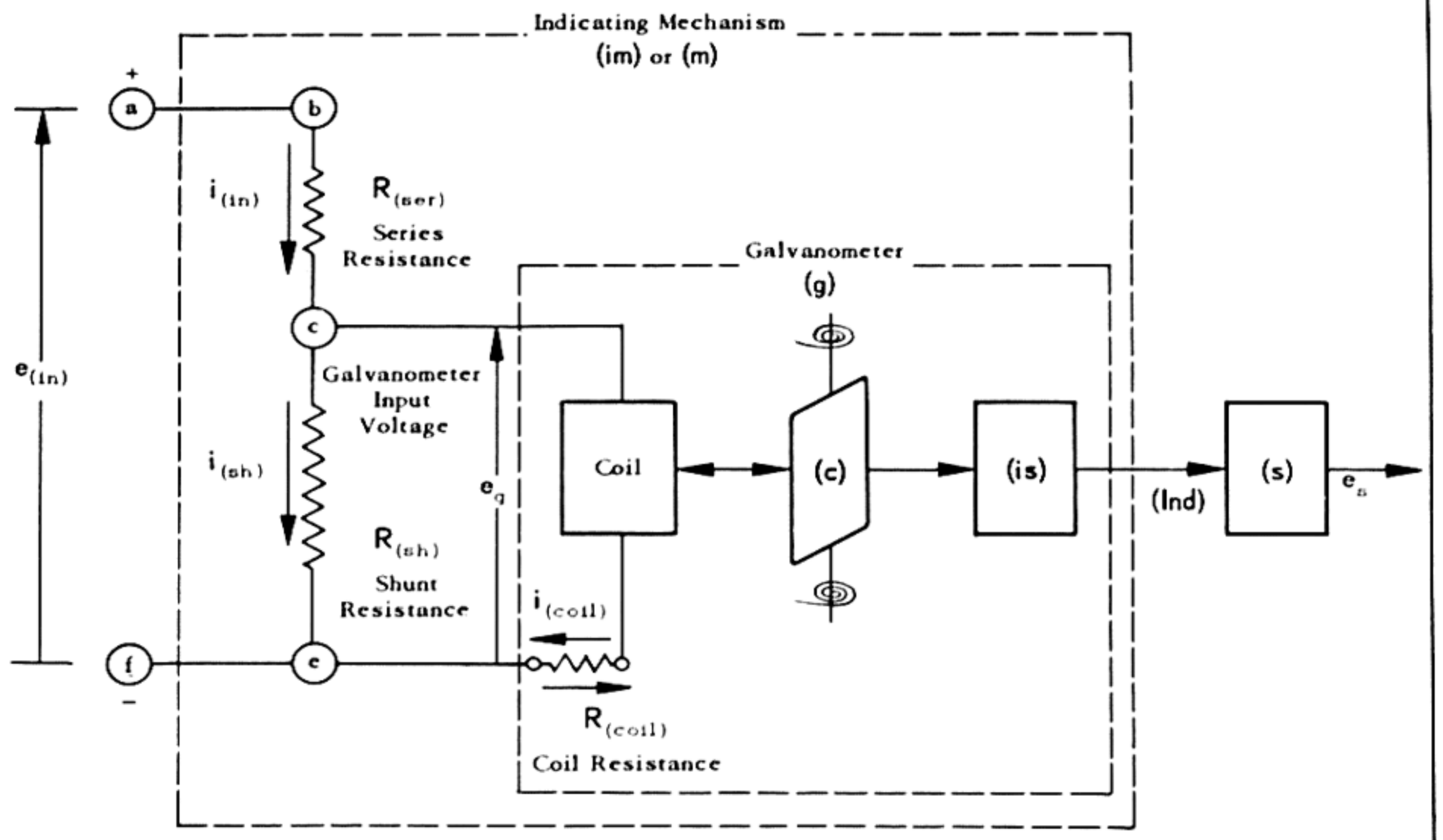


Fig. 9. Electromechanical circuit diagram for special voltmeter X-1.

X COMPONENT PERFORMANCE CHARACTERISTICS

$R_{(coil)} = 99.5$ ohms ; $R_{(sh)} = 5.920$ ohms ; $R_{(ser)} = 2082$ ohms

$S_{(g)[e_g;(Ind)](at)} = 3.76 \times 10^3$ divisions per volt = galvanometer voltage – indication static sensitivity

$$S_{(im)[e_{(in)};(Ind)]} = \frac{1}{1 + R_{(ser)}\dfrac{R_{(coil)} + R_{(sh)}}{R_{(coil)}R_{(sh)}}} S_{(g)[e_g;(Ind)]}$$

= indicating mechanism voltage – indication static sensitivity
= 10 divisions per volt

$$R_{(a\text{-}f)} = R_{(ser)} + \frac{R_{(coil)}R_{(sh)}}{R_{(coil)} + R_{(sh)}} \quad ; \quad \frac{e_g}{e_{(in)}} = \frac{1}{1 + R_{(ser)}\cdot\dfrac{R_{(coil)} + R_{(sh)}}{R_{(coil)}\ R_{(sh)}}}$$

Specification 29-1. Illustrative specification for special voltmeter X-1. (Page 11 of 11)

phase shift both have errors with respect to the "correct" sensitivity and "correct" dynamic response angle.

29.88. In the example of Specification 29-1, the specification sensitivity and the specification dynamic response angle are represented by the plots of Fig. 1. With the specification reference sensitivity taken as unity and the specification reference dynamic response angle taken as zero, the dynamic performance deviation curves are identical with the (0; 0,1) equation nondimensional amplitude ratio deviation and dynamic response angle deviation curves of Fig. 18-15. These curves are repeated as Fig. 2 of the specification, with the coordinates relabeled to describe voltmeter performance. The corresponding mathematical expressions are given as Eqs. (27) and (28) of Item VIII.

29.89. The specification sensitivity error is shown in Eq. (31) of Item VIII as the difference between the sensitivity – reference sensitivity ratios for the (0; 0,1) equation and the (0; 0,1,2) equation. The specification phase shift error is given in Eq. (32) as the difference between the (0; 0,1) equation dynamic response angle and the (0; 0,1,2) dynamic response angle. The corresponding mathematical forms, as taken from Derivation Summaries 18-10 and 19-10, are given in Eqs. (33) and (34). In these equations, the variable that takes forcing frequency changes into account is made identical for the first-order form and the second-order form by using the relationship of Eq. (35).

29.90. Figure 3 of Specification 29-1 shows the specification sensitivity and the correct sensitivity plotted on the same logarithmic coordinates. The specification sensitivity error is represented as an arrow drawn from the correct sensitivity curve to the specification sensitivity curve. Figure 4 gives similar curves for the specification dynamic response angle and the correct dynamic response angle, with the specification dynamic response angle error represented by an arrow.

29.91. Figure 5a is a plot of the specification sensitivity error as a function of forcing frequency. Figure 5b is a similar plot for the specification dynamic response angle error. The sensitivity error curve shows that this error is less than $|0.001|$ for all frequencies less than 0.01 cycle per second. The maximum error is less than $|0.012|$ and occurs at about 0.07 cycle per second. The dynamic response angle error is less than 5 degrees at 0.1 cycle per second but increases at higher frequencies. The rate of increase of this error reaches a maximum at about 2 cycles per second. Comparison of the error curves of Fig. 5 with the deviation curves of Fig. 2 shows that for frequencies less than about 0.1 cycle per second, the deviations are so much larger than the errors that no practical penalty in accuracy of performance specification is incurred by use of the (0;0,1) equation instead of the more complicated, correct (0;0,1,2) equation.

29.92. Correction curves are unnecessary in Item VIII when deviation and error curves are available. In this situation, the corrections for any specific case

are equal to the corresponding deviations or errors with their signs reversed.

29.93. Item IX, Fig. 6, gives a pictorial-schematic diagram that shows the essential features of the experimental voltmeter. Pictorial-functional and functional diagrams are given in Figs. 7 and 8. Figure 9 is an electrical circuit diagram for the voltmeter, with the essential parts of the instrument mechanism grouped together as the galvanometer.

29.94. Item X gives expressions for the static sensitivity of the indicating mechanism in terms of electrical network constants and galvanometer sensitivity. These expressions are related to the specified scale sensitivity by equations that are useful for making design changes in the meter performance.

29.95. In the interests of limiting the material included in an illustrative example, a discussion of the interaction of the shunt resistance and the torque generator in providing damping for the galvanometer is omitted from Item X. This phase of electrical meter operation is discussed in Chapter 32.

29.96. Specification 29-1 is given here to illustrate the data that may be included in the description of a measuring instrument. The example given supplies more information than would ordinarily be used to specify a conventional voltmeter. However, the data provided are all pertinent if the instrument is to be applied in making high-accuracy measurements under circumstances that vary considerably from static calibration conditions.

29.97. The purpose of the present discussion is to illustrate an approach to the problem of specifying measuring instruments, not to examine all details of their performance. For this reason, the present section is ended here, leaving the operational details of particular instruments and systems to be discussed in later chapters, where the pattern of Specification 29-1 is used as required. It is to be noted that both static and dynamic characteristics may be described in nonmathematical terms on the basis of experimental results. For practical purposes, sensitivity and dynamic response angle data may be plotted on suitable coordinates, whether the information presented is calculated or measured. In many situations, it is convenient to use some relatively simple and well-known mathematical form as the reference for describing performance and to plot the error curves for this reference from the actually measured "correct" performance characteristics. This procedure is illustrated in Item VIII of Specification 29-1, in which the first-order equation representation is used as a convenient reference to replace the "correct" second-order representation. A number of situations of this kind appear in later chapters.

CHAPTER 30

ELEMENTS AND COMPONENTS ASSOCIATED WITH INSTRUMENT SYSTEMS

H. B. Brainerd

INTRODUCTION

30.1. The purpose of any instrument system is to receive as input one or more physical quantities and to produce as output one or more physical quantities that are in more useful forms than the inputs. The outputs may represent measures of the input quantities, as in a measuring system, or they may represent controls on the operation of some equipment or process. Many physical laws and phenomena come into play in the operation of instrument systems. The study of these laws and phenomena in connection with their practical applications comprises the fundamental background of instrument engineering. The use of creative imagination in selecting and combining these fundamentals into useful forms constitutes the art of instrument engineering.

30.2. The purpose of this chapter is to summarize in readily available form some of the physical laws, processes and devices that are useful in the synthesis, operation and analysis of instrument systems. The treatment is intended to recall to the reader the more commonly used relations and characteristics of devices, and to serve as a guide to more comprehensive references for each of the topics covered. The material that is of principal interest occurs naturally in several basic fields, including mechanics, electricity, magnetism, pneumatics, hydraulics and heat. In studying a system in a less familiar field, there may be a temptation to replace it by an equivalent system having a more familiar form. However, the use of analogs is limited by the fact that comparable quantities are seldom, if ever, fully equivalent, and in some cases there is no quantity in one system that corresponds to an important quantity in a comparable system. Further, the practical limitations on the performance of various kinds of system components arise from different causes and the use of analogs tends to obscure the differences between ideal and actual systems. For these reasons, it is more desirable to study the dynamic characteristics of a system in terms of the governing differential equation rather than in terms of the performance of an analogous physical system. Accordingly, in this chapter, the way in which the various physical phenomena are represented mathematically is used as the basis for presentation.

30.3. The material of this chapter is presented under two main headings: Elements and Components. The section entitled Elements deals with the physical laws and quantities associated with the basic elements used in instrument systems. The section entitled Components includes specific devices that employ these elements to perform desired operations. Many of these operations may be characterized by the functions that are performed. For example:

Comparison, which is frequently the basis of measurement, includes:

1) Comparison of an index displacement with a numbered scale.
2) Balancing or nulling between two quantities of the same physical nature.
3) Comparison by substitution of a readily measured quantity for one not so readily measured.

Magnitude Conversion is an operation in which a physical quantity is altered in size, but not in form, by either amplification or attenuation. This is the mathematical equivalent of multiplication by a constant.

Physical Conversion is an operation in which the character, as well as the magnitude, of a physical quantity is altered by the action of the device in question. This includes a vast array of principles and devices.

Computation involves the operations encountered in arithmetic, algebra, trigonometry and calculus, as well as the generation of other functions, sometimes empirical ones.

Selection implies the presence of interfering inputs that are to be rejected, and uses for this purpose techniques such as amplitude or frequency discrimination, compensation, averaging, gating or time selection, and other methods.

ELEMENTS

30.4. Mechanical Elements (see Information Summaries 30-1 and 30-2*). Equations of motion involving translational and rotational motion are obtained by applying Newton's third law to the elements of the system. Quantities such as force, torque, linear and angular displacements, velocities and accelerations are involved. These are vector quantities in that they have directional properties as well as magnitudes. Such vector quantities are designated by placing bars over the quantity symbols. Nonvectors lack directional properties and are called scalar quantities. Certain scalars such as elastic coefficients, damping coefficients and moments of inertia are directional in that their magnitudes depend on the direction in which they are taken; but in the mathematical sense, they are scalar quantities. For information on mathematical operations involving vector quantities, see Chapters 7 and 9.

* Summaries for Elements are located at the end of this section.

30.5. Although angular displacements have magnitude and direction, they do not obey the law of commutative vector addition unless the angles are coplanar or infinitesimal. However, in many practical situations where the individual angles are small, they may be approximated as vectors with adequate accuracy. The advantage gained by treating angles as vectors is that much analytical work involving angular orientation is greatly simplified. A rigorous treatment of this problem is given by Laning.*

30.6. Newton's law states that applied force or torque is equal to the time rate of change of linear or angular momentum, respectively, this rate of change being referred to an inertial system.** For a constant mass, this reduces in the translational case to the familiar relationship that force is equal to mass times acceleration with respect to any inertial space. When the acceleration is taken with respect to a space that has either linear acceleration or angular velocity with respect to a reference inertial space, account must be taken of the motion of this moving space with respect to the reference inertial space. This is readily accomplished by application of the theorem of Coriolis, which relates the rate of change of a vector with respect to inertial space to the rate of change of the same vector with respect to a moving space. This relationship is derived in Fig. 9-5 of Chapter 9.

30.7. The elastic and damping forces and torques shown in Information Summaries 30-1 and 30-2 are of linear form if the elastic restraint coefficients and the damping coefficients are presumed to be constant. This condition, if desired, can be realized in practical devices by careful design. Inertia reaction forces and torques are inherently linear by virtue of Newton's law. In some situations, linearity may not be achievable, nor may it be desired. Often nonlinearities may be exploited to practical advantage even though the simplicity of the analysis is lost. Coulomb friction is nonlinear since its magnitude is independent of the motion and only its sense is established by the sign of the velocity.

30.8. Elements of Electric Circuits (see Information Summary 30-3). Differential equations involving electric circuits are obtained by applying Kirchoff's laws to the circuits of interest. Voltages and currents are the pertinent quantities, and the relations between them are given in terms of resistances, capacitances and inductances. When these quantities are taken to be constant lumped parameters, independent of voltage or current, the resulting differential equations are linear. In the case of inductances involving ferrous cores, the condition of linearity is not fulfilled if the magnetization curve of the core is nonlinear. Under these circumstances, linear equations are applicable only over the range of

---

* See Laning (L5).

** This topic is discussed at length in Part 2 of Vol. III. For further explanation of what constitutes an inertial system, see Chapter III of Einstein and Infeld (E3) and Chapter IV of Richtmyer and Kennard (R5).

current for which the corresponding portion of the magnetization curve can be approximated by a straight line. Within this limitation, for normal service, resistances, capacitances and inductances behave as constant lumped parameters within very close limits. On the other hand, inductors and capacitors are never entirely devoid of resistance, and resistors exhibit inductive and capacitive properties. These limitations become important under extreme conditions, but their effects can be minimized by appropriate design techniques if required.

30.9. Inductive and capacitive reactance and impedance do not enter directly into the original differential equations. They appear when the currents and voltages are sinusoidal with respect to time, as is the case in a very great proportion of practical circuits. In fact, frequency analysis techniques were devised for this very purpose and it is common practice to handle nonsinusoidal as well as sinusoidal circuit problems by Fourier or Laplace transforms.

30.10. Elements of Magnetic Circuits (see Information Summary 30-4). Practical magnetic circuit relationships are characterized by the nonlinearities introduced by ferrous-core materials. Linear laws are valid over only small incremental values of flux. Accordingly, energy concepts are useful in associating mechanical forces and torques with magnetic fields. Thus, the rate of change of magnetic energy with respect to linear or angular displacement is the corresponding mechanical force or torque.

30.11. Magnetic flux and magnetomotive force are often considered to be analogous respectively to electric current and voltage. This is a good example of a supposed physical analogy that actually hides pertinent information. Flux is associated with energy; current with power, which is one derivative order higher. Flux permeates its surroundings, while current is confined to well-defined paths; hence, magnetic circuit parameters must be determined experimentally, while electric circuit parameters are readily computed. What is truly analogous is the similarity of mathematical form between expressions relating energy, flux, magnetomotive force and reluctance and expressions relating power, current, voltage and resistance.

30.12. Permanent magnets or electromagnets are sources of magnetomotive force. The design of efficient magnetic circuits utilizing permanent magnets involves the selection of permanent magnet material and its geometrical shape, taken together with the remainder of the magnetic circuit so as to make magnetic energy a maximum.

30.13. Current-carrying conductors in a magnetic field are of great importance since these form the basis for many practical applications. These include string and D'Arsonval galvanometers, direct-current motors and generators, electromagnetic shakers and loudspeakers, and many more. There are two aspects of this situation, both of which are important:

1) The current-carrying conductor has a lateral force exerted on it.

2) A voltage is induced in the moving conductor.

30.14. Elements of Heat Flow (see Information Summary 30-5). Newton's law of cooling governs in many heat-flow situations. This law states that the rate of heat transfer between a body and its surroundings is proportional to the temperature difference between the body and its fluid or solid surroundings, and to the thermal conductivity of the surroundings. Since rate of change of body temperature is proportional to heat-flow rate, the governing differential equation becomes one of first order, with body temperature as the dependent variable. Convective or conductive heat flow is presumed responsible for the transfer of heat. Also, it is assumed that heat transfer throughout the body is sufficiently rapid to enable characterization of the body temperature by a single value.

30.15. When heat transfer is effected by radiation, the Stefan-Boltzmann fourth-power law applies and the first-order differential equation no longer holds true. If the difference in the fourth powers of the temperatures of two bodies involved may be adequately approximated by the difference of the first powers, then a first-order differential equation will represent the process in the same way as is true for the conductive and convective cases. A detailed analysis of this situation is given in Derivation Summary 31-2.

30.16. When heat transfer takes place by a combination of convection and conduction successively through several bodies, each of which may be represented by its heat capacity, its thermal conductivity and its temperature, the corresponding differential equations become a set of coupled equations, the number of equations being equal to the number of separate heat transfer processes that must be considered. When the number of bodies is increased without limit, a partial differential equation must be employed to describe the temperature gradients that prevail. This corresponds to the case of a single body in which the flow of heat is relatively slow; the temperature is then no longer uniform throughout the body.

30.17. In the transfer of heat between fluids and solids, most of the fluid is usually in turbulent motion, so that convection, that is, mixing, keeps the fluid at nearly uniform temperature. At the surface of the solid, however, a thin layer of the fluid has laminar flow, that is, it moves only parallel to the surface. Between the laminar and the turbulent regions there is a buffer layer where turbulence occurs intermittently. In the laminar layer, heat transfer is largely by conduction. There is also radiant heat transfer between all parts of the fluid and the surface of the solid. The component of heat transfer due to convection and conduction is dependent mainly on the conductivity of the fluid and the thickness of the laminar flow layer. The thickness of this layer is in turn dependent on many variables including the shape and roughness of the solid surface, the effective velocity of the fluid, and all the factors that influence this effective velocity.

30.18. Elements of Fluid Mechanics (see Information Summary 30-6). A fluid is defined as a substance that cannot support a static shear force. Thus, liquids and gases are fluids. A liquid is characterized by its definite volume and slight compressibility. A gas, on the other hand, is highly compressible, and its volume is established only by the container that encloses it.

30.19. Forces normal to the surface of any body in contact with a fluid are transmitted through the fluid as pressures that act equally in all directions. The component of fluid pressure caused by external forces acting on the fluid is uniform throughout the fluid. The pressure associated with dynamic and gravitational forces varies from place to place in the fluid, as for example the variation of pressure with height. If a body is immersed in the fluid, the action of this gravitational pressure gradient is to produce an upward force on the body equal to the weight of the displaced fluid. This buoyant force may develop a buoyant torque on the immersed body, determined by the location of the center of buoyancy of the immersed body relative to the selected support axis. In the case of a gas, the variation of pressure with height is governed by the compressibility of the gas. Typical relationships that are applicable to the Earth's atmosphere are given in Information Summary 30-6.

30.20. Viscosity is a parameter of a fluid that relates shear stress to rate of shear strain. It is not applicable to a static situation because by definition no static shear force can exist in a fluid. The physical phenomenon of fluid flow with shear forces is referred to as viscous flow or as fluid friction. Viscous forces are proportional to surface area and velocity gradient. In any situation where fluid flows past a solid body, compressive and inertial forces can act only normally to the surface of the body. Hence, any component of force parallel to the surface of the body must be due to fluid friction.

30.21. Problems involving fluid motion lead to partial differential equations with respect to time and three spatial dimensions; these are known as the Navier-Stokes equations. These equations embody Newton's law for a fluid element, the requirement of continuity, and thermodynamic effects. The usual engineering approach is to use an integrated form of these equations, known as Bernoulli's theorem, which expresses the principle of conservation of energy in a system containing a flowing fluid. This theorem is broadly applicable in many practical cases. Frequently, one or more of the terms appearing in the energy equation may be neglected, thus yielding a simpler expression. The relations governing the pitot tube, impact pressure, and flow through a constriction are cases in point. Many other examples can be found in the reference literature.

30.22. The Reynolds number is a dimensionless parameter relating viscosity, density, flow velocity, and a characteristic linear dimension of the geometrical situation. For any given geometrical situation, the Reynolds number expresses

the ratio of inertial to viscous forces. For example, in a long circular pipe, where the characteristic dimension is the diameter, conditions are related to the Reynolds number as follows:

1) When the Reynolds number is less than 2100, viscous forces predominate and flow is laminar.
2) When the Reynolds number is greater than 3100, inertial forces predominate and flow is turbulent.
3) When the Reynolds number is between 2100 and 3100, the two forces are of the same order and the character of flow is determined by entrance conditions.

The principle of dynamic similitude states that if the Reynolds number is the same in two similar geometrical situations, the flow will also be geometrically similar. Thus, for any geometrical situation, any property of the flow can be expressed by a function of the Reynolds number. In a few cases, such as laminar flow in a pipe, this function of the Reynolds number is analytic, but more often it is empirical.

30.23. The Mach number is the ratio of flow velocity to the velocity of propagation of a small pressure disturbance, that is, the velocity of sound. In a perfect gas, sonic velocity is a function of temperature only. Physically, the Mach number represents the ratio of inertial force to the elastic force associated with the compressibility of the gas. For this reason, the Mach number is the governing parameter in establishing aerodynamic forces on bodies at high speeds.

30.24. Dimensions and Units (see Table 30-1). The dimensions of the physical quantities mentioned in Information Summaries 30-1 through 30-6, and the units in which they can be expressed, have been brought together in Table 30-1. Some writers state that only three primary quantities are needed, but this applies only to a dimensional system for mechanical quantities. One more primary quantity is needed to bring electromagnetic quantities into the dimensional system, and still another to bring in thermal quantities. In Table 30-1, the accepted set of mass, length, and time is used for the three primary mechanical quantities. Force, length, and time are given as an alternate set, since they express many quantities more simply.

30.25. The additional primary quantity used in Table 30-1 for expressing dimensions of electromagnetic quantities is electric charge. Other choices (not used in Table 30-1) could be electromagnetic permeability or electrostatic permittivity. Alternate sets given in Table 30-1 are voltage, charge, length, and time for electrical quantities and force, charge, length, and time for magnetic quantities; these sets eliminate the dimension of mass where it is foreign to the physical concept.

30.26. The additional primary quantity for dimensions of thermal quantities is temperature. It would be possible to use specific heat or thermal conductivity

instead, but there is no advantage to be gained by doing so. Alternate dimensions are given to include heat, that is, energy in thermal form. This eliminates a dimension of mass where it is foreign to the physical concept, but keeps mass in the one case of specific heat, where the concept involves heat energy per unit mass.

30.27. Units for the physical quantities shown are given in three systems, each consistent within itself. These are the rationalized m.k.s. system, the unrationalized c.g.s. system, and the English system using the slug, the foot, the second, and the degree Fahrenheit.

30.28. The distinction between a rationalized and an unrationalized system is confined to a few magnetic quantities for which the two sets of units are related by a factor of 4π. The m.k.s. system is comparatively new and is becoming widely used. It has the advantage of including the practical electrical units of volt, ampere, watt, joule, coulomb, ohm, henry, and farad. The c.g.s. system is older and well-established, but is now becoming less popular. The c.g.s. electrical units given here belong to the electromagnetic system. There is also a c.g.s. electrostatic system, which is of little use to the engineer.

30.29. The English system of units has widespread acceptance and usage as its only advantage. As given here, it is consistent within itself and is based on the foot, the slug, and the second. No attempt is made to include the many alternative units based on inches or other units of length, minutes or hours, pounds mass and poundals force.

30.30. Since angles are dimensionless, they are not given in Table 30-1. Two units of angular measurement are commonly used: radian measure (ratio of arc to radius) is the basis of all calculus formulae; measurement in degrees is used in almost all practical geometry involving angles, such as navigation, surveying, and shop layouts. The military mil is a less common unit, sometimes used in fire control. The following conversion relationships may be used:

angle in radians × 57.2957795 = angle in degrees

angle in degrees × 0.01745329 = angle in radians

1 minute angle = 0.0002909 radian

1 second angle = 0.0000048 radian

1 radian = 57° 17' 44".8 = 1018.591634 military mils

1 milliradian = 3'.4377 = 3'26".26 = 1.01859 military mils

circle = 360° = 2π radians = 6.28318531 radians = 6400 military mils

right angle = 90° = $\pi/2$ radians = 1.57079633 radians = 1600 military mils

Note: Table 30-1 and Information Summaries 30-1 through 30-6 follow immediately. These are followed in turn by the discussion on Components on page 125.

Table 30-1. Dimensions and units.*

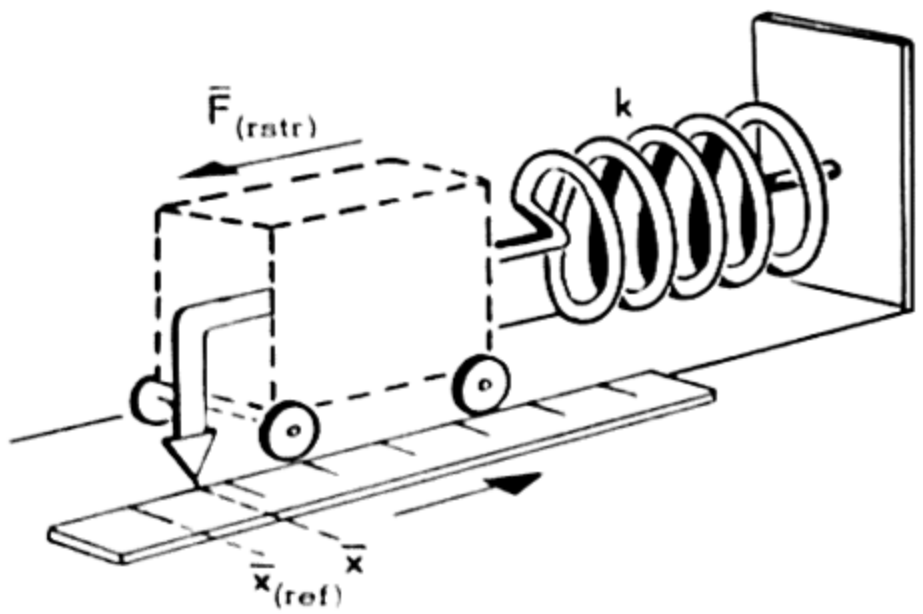
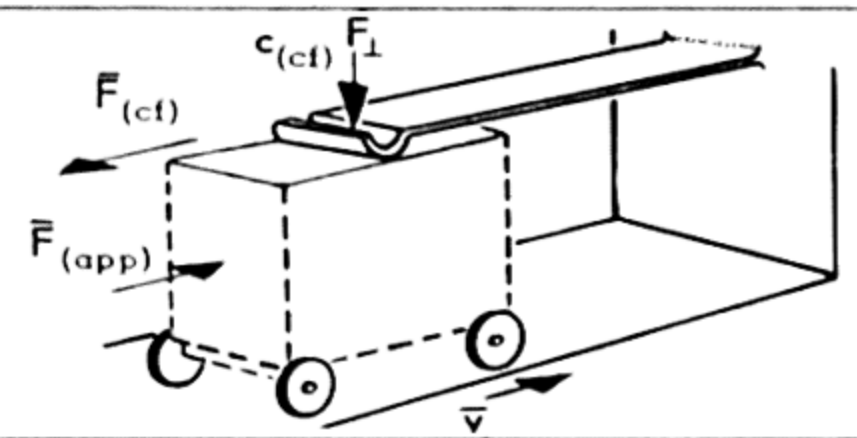
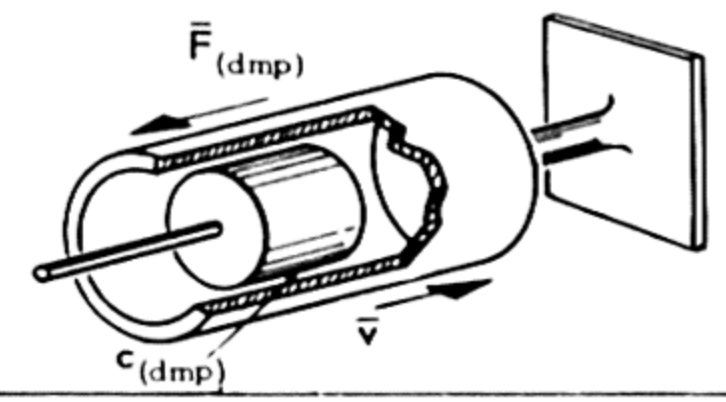
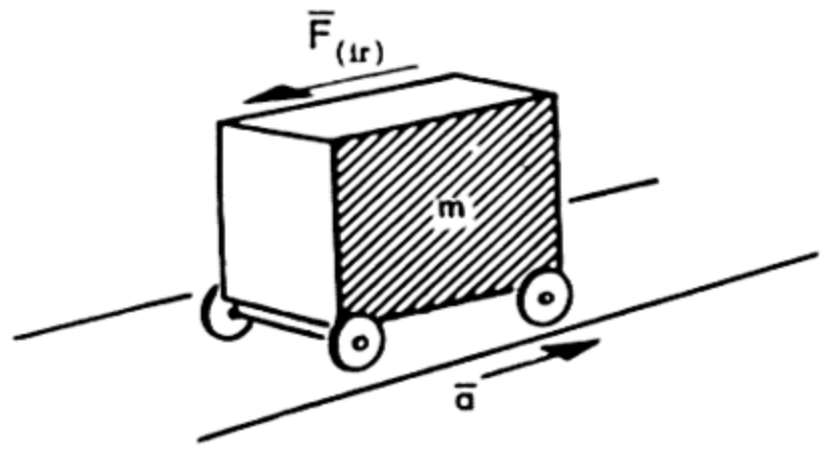
Symbol	Quantity	Primary dimensions	Other dimensions
	Primary quantities		
m	Mass		——
l	Length	l	——
t	Time	t	——
Q	Electric charge	Q	——
T	Temperature	T	——
	Mechanical quantities		
F	Force	mlt^{-2}	F
M	Torque	ml^2t^{-2}	Fl
E	Energy	ml^2t^{-2}	Fl, (volt)Q
P	Power	ml^2t^{-3}	Flt^{-1}, (volt)Qt^{-1}
k	Elastic restraint coefficient	mt^{-2}	Fl^{-1}
$k_{(rot)}$	Rotational elastic restraint coefficient	ml^2t^{-2}	Fl
$c_{(dmp)}$	Damping coefficient	mt^{-1}	$Fl^{-1}t$
$c_{(rot)}$	Rotational damping coefficient	ml^2t^{-1}	Flt
I	Moment of inertia	ml^2	Flt^2
v	Velocity	lt^{-1}	——
W	Angular velocity	t^{-1}	——
a	Acceleration	lt^{-2}	——
α	Angular acceleration	t^{-2}	——
A	Area	l^2	——
V	Volume	l^3	——
ρ	Density	ml^{-3}	——
LM	Linear momentum	mlt^{-1}	Ft
H	Angular momentum	ml^2t^{-1}	Flt
μ	Viscosity	$ml^{-1}t^{-1}$	$Fl^{-2}t$
	Electric and magnetic quantities		
i	Current	Qt^{-1}	——
e	Voltage	$Q^{-1}ml^2t^{-2}$	volt
C	Capacitance	$Q^2m^{-1}l^{-2}t^2$	$(volt)^{-1}Q$
R	Resistance	$Q^{-2}ml^2t^{-1}$	(volt) $Q^{-1}t$
L	Inductance	$Q^{-2}ml^2$	(volt)$Q^{-1}t^2$
ϕ	Flux	$Q^{-1}ml^2t^{-1}$	$FQ^{-1}lt$
B	Flux density	$Q^{-1}mt^{-1}$	$FQ^{-1}l^{-1}t$
$\mathcal{F}$	Magnetomotive force	Qt^{-1}	——
H	Magnetic field strength	$Ql^{-1}t^{-1}$	——
G	Conductance	$Q^2m^{-1}l^{-2}t$	$(volt)^{-1}Qt^{-1}$
ρ	Resistivity	$Q^{-2}m^{-1}l^3t^{-1}$	(volt)$Q^{-1}lt$
$\mathcal{R}$	Reluctance	$Q^2m^{-1}l^{-2}$	$F^{-1}Q^2l^{-1}t^{-2}$
μ	Permeability	$Q^{-2}ml$	$FQ^{-2}t^2$
	Thermal quantities		
Q	Quantity of heat	ml^2t^{-2}	heat
HC	Heat capacity	$ml^2t^{-2}T^{-1}$	(heat) T^{-1}
SH	Specific heat	$l^2t^{-2}T^{-1}$	(heat) $m^{-1}T^{-1}$
k	Thermal conductivity	$mlt^{-3}T^{-1}$	(heat)$l^{-1}t^{-1}T^{-1}$

* See Langsdorf, Principles of Direct-Current Machines (L4), M.I.T., Staff, E. E. Dep't, Electric Circuits (M7), Moon and Spencer, "Utilizing the M. K. S. System" (M13) and Zimmerman and Lavine, Conversion Factors and Tables (Z2).

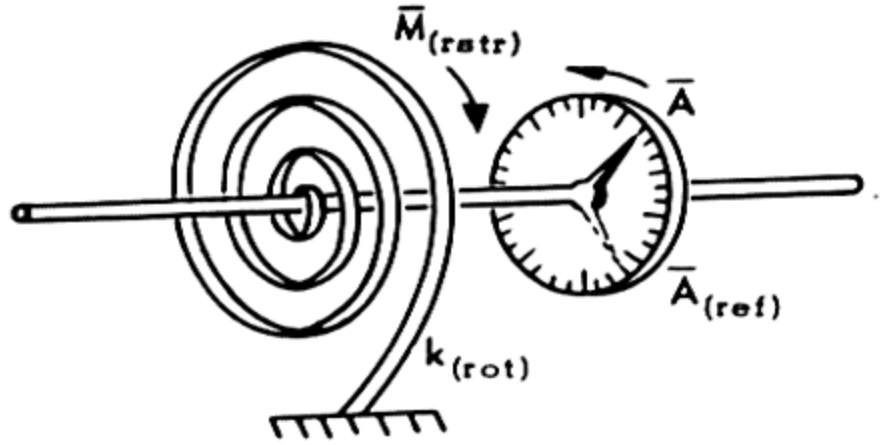
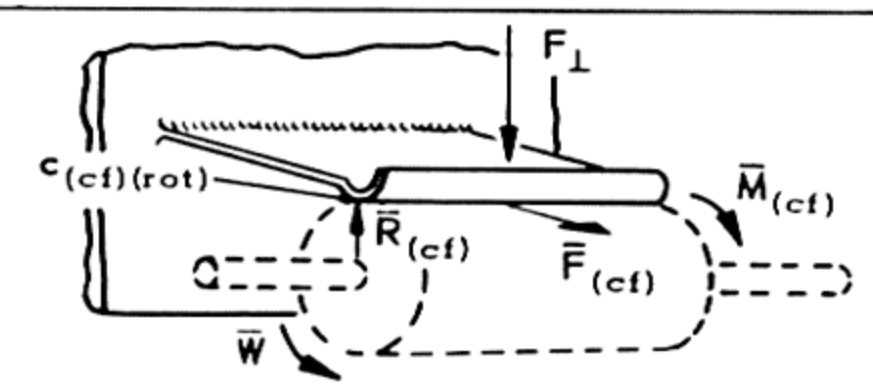
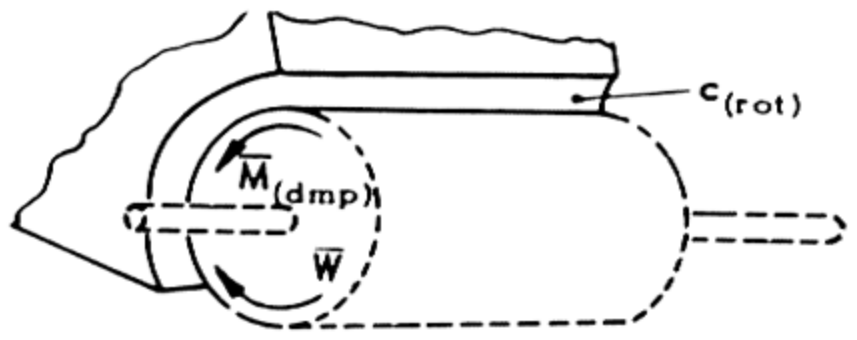
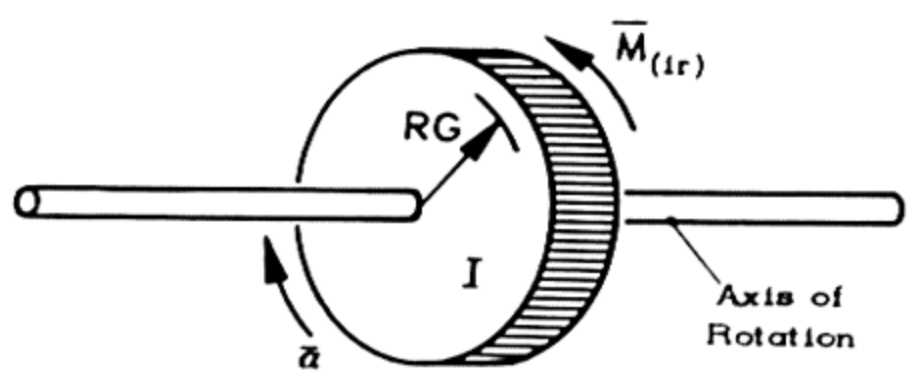
Table 30-1. Dimensions and units. (cont.)

Symbol	Rationalized m.k.s. unit	× Conversion factor	= Unrationalized c.g.s. unit	× Conversion factor	= English unit**
m	kilogram	10^3	gram	6.852×10^{-5}	slug
l	meter	10^2	centimeter (cm)	3.281×10^{-2}	foot (ft)
t	second (sec)	1	second (sec)	1	second (sec)
Q	coulomb	10^{-1}	abcoulomb	———	———
T	degree (Centigrade or Kelvin) 0°C=32°F=273°K=460°R	1	degree (Centigrade or Kelvin)	1.80	degree (Fahrenheit or Rankine)
F	newton	10^5	dyne	2.248×10^{-6}	pound (lb)
M	newton-meter	10^7	dyne-cm	7.376×10^{-8}	lb-ft
E	joule	10^7	erg or dyne-cm	7.376×10^{-8}	ft-lb
P	watt	10^7	erg/sec	1.341×10^{-10} 7.376×10^{-8}	horsepower lb-ft/sec
k	newton/meter	10^3	dyne/cm	6.852×10^{-5}	lb/ft
$k_{(rot)}$	newton-meter/unit angle	10^7	dyne-cm/unit angle	7.376×10^{-8}	lb-ft/unit angle
$c_{(dmp)}$	newton-sec/meter	10^3	dyne-sec/cm	6.852×10^{-5}	lb-sec/ft
$c_{(rot)}$	newton-meter-sec	10^7	dyne-cm-sec	7.376×10^{-8}	lb-ft-sec
I	kilogram-meter^2	10^7	gram-cm^2	7.376×10^{-8}	slug-ft^2
v	meter/sec	10^2	cm/sec	3.281×10^{-2}	ft/sec
W	unit angle/sec	1	unit angle/sec	1	unit angle/sec
a	meter/sec^2	10^2	cm/sec^2	3.281×10^{-2}	ft/sec^2
α	unit angle/sec^2	1	unit angle/sec^2	1	unit angle/sec^2
A	meter^2	10^4	cm^2	1.076×10^{-3}	ft^2
V	meter^3	10^6	cm^3	3.531×10^{-5}	ft^3
ρ	kilogram/meter^3	10^{-3}	gram/cm^3	1.941	slug/ft^3
LM	kilogram-meter/sec newton-sec	10^5	gram-cm/sec dyne-sec	2.248×10^{-6}	lb-sec
H	kilogram-meter^2/sec newton-meter-sec	10^7	gram-cm^2/sec dyne-cm-sec	7.376×10^{-8}	lb-ft-sec
μ	———	—	poise (gram/cm-sec)	2.089×10^{-3}	slug/ft-sec
i	ampere	10^{-1}	abampere	———	———
e	volt	10^8	abvolt	———	———
C	farad	10^{-9}	abfarad	———	———
R	ohm	10^9	abohm	———	———
L	henry	10^9	abhenry	———	———
ϕ	weber	10^8	maxwell (line)	———	———
B	weber/meter^2	10^4	gauss (line/cm^2)	———	———
$\mathcal{F}$	ampere turn	$4\pi \times 10^{-1}$	gilbert (oersted-cm)	———	———
H	ampere turn/meter	$4\pi \times 10^{-3}$	oersted	———	———
G	mho	10^{-9}	abmho	———	———
ρ	ohm-meter	10^{11}	abohm-cm	———	———
$\mathcal{R}$	$\frac{\text{ampere turns}}{\text{weber}}$	$4\pi \times 10^{-9}$	gilbert/maxwell	———	———
μ	$\frac{\text{weber}}{\text{ampere turns-meter}}$	$\frac{1}{4\pi} \times 10^7$	gauss/oersted	———	———
Q	joule	2.389×10^{-1}	calorie (cal)	3.97×10^{-3}	British thermal unit (Btu)
HC	joule/°C	2.389×10^{-1}	cal/°C	2.20×10^{-3}	Btu/°F
SH	joule/kg°C	2.389×10^{-4}	cal/gm-°C	1	Btu/lb-°F
k	watt/cm°C	2.389×10^{-1}	cal/sec-cm-°C	241.9	Btu/hr-ft-°F

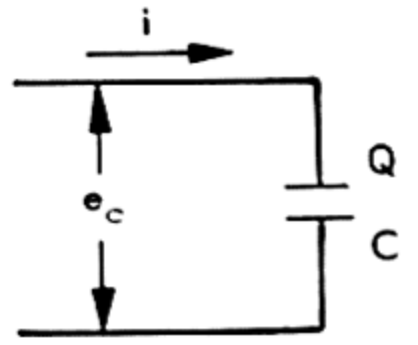
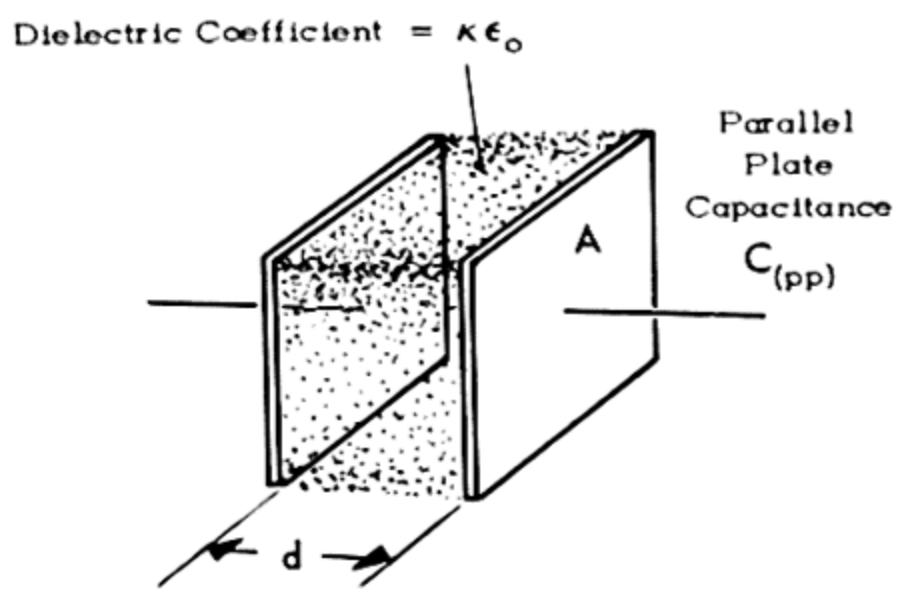
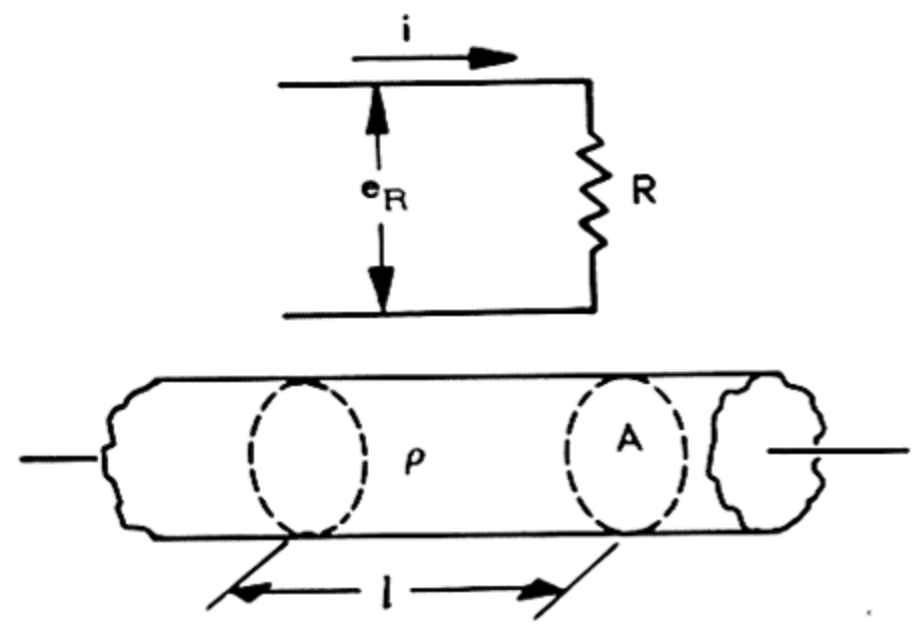
** Multiply quantity in m.k.s. units by conversion factor to obtain same quantity in c.g.s. units.
Multiply quantity in c.g.s. units by conversion factor to obtain same quantity in English units.

Figure	Concept and Symbol		Performance Relation	
	*a) Elastic restraint (zero order in $\bar{x}$)**			
	Displacement or position	$\bar{x}$		
	Elastic restraint coefficient	k		
	Reference position (position where restraining force is zero)	$\bar{x}_{(ref)}$		
	Restraining force	$\bar{F}_{(rstr)}$	$\bar{F}_{(rstr)} = -k(\bar{x}-\bar{x}_{(ref)})$	(1)
	Potential energy	PE	$PE = \frac{1}{2}k\lvert\bar{x}-\bar{x}_{(ref)}\rvert^2$	(2)
	Hooke's Law. See Timoshenko and Lessels, Applied Elasticity (T5), and spring design manuals, such as Associated Spring Corporation, "Handbook of Mechanical Spring Design" (A9), Instrument Specialties Company, Inc., catalog on miniature springs (I3), and American Steel & Wire Company, "Manual of Spring Engineering" (A8).			
	*b) Coulomb friction (independent of $\bar{x}$)*			
	Force perpendicular to direction of motion	$F_{\perp}$		
	Coefficient of Coulomb friction	$c_{(cf)}$	When $\bar{v}=0$, $F_{(app)} < F_{\perp}\, c_{(cf)}$ and $\bar{F}_{(cf)} = -\bar{F}_{(app)}$	(3)
	Coulomb friction force	$\bar{F}_{(cf)}$	When $\bar{v}\neq 0$, $\bar{F}_{(cf)} = -\frac{\bar{v}}{v}F_{\perp}\, c_{(cf)}$	(4)
	Applied force	$\bar{F}_{(app)}$		
	See Bowden and Tabor, The Friction and Lubrication of Solids (B14), Den Hartog, Mechanics (D6) and Mechanical Vibrations (D5).			
	*c) Linear damping (first order in $\bar{x}$)*			
	Velocity	$\bar{v}$	$\bar{v} = \dot{\bar{x}}$	(5)
	Damping coefficient	$c_{(dmp)}$		
	Damping force	$\bar{F}_{(dmp)}$	$\bar{F}_{(dmp)} = -c_{(dmp)}\bar{v}$	(6)
	Dissipated power	$P_{(dmp)}$	$P_{(dmp)} = c_{(dmp)}v^2$	(7)
	See Den Hartog, Mechanical Vibrations (D5) and Lees, "Integration by the Viscous Shear Process" (L10).			
	*d) Mass or inertia (second order in $\bar{x}$)*			
	Acceleration	$\bar{a}$	$\bar{a} = \dot{\bar{v}} = \ddot{\bar{x}}$	(8)
	Mass	m		
	Inertia reaction force	$\bar{F}_{(ir)}$	$\bar{F}_{(ir)} = -m\bar{a}$	(9)
	Acceleration due to gravity	$\bar{g}$	Note that mass = weight/g	
	Linear momentum	$\bar{LM}$	$\bar{LM} = m\bar{v}$	(10)
	Kinetic energy	KE	$KE = \frac{1}{2}mv^2$	(11)
	See Sears, Principles of Physics (S3), Vol. I, and Den Hartog, Mechanics (D6).			
* Bars over symbols indicate vector quantities.				
Combining Law: $\Sigma\bar{F} = 0$ where $\Sigma\bar{F}$ includes all external and internal forces. Newton's third law.				

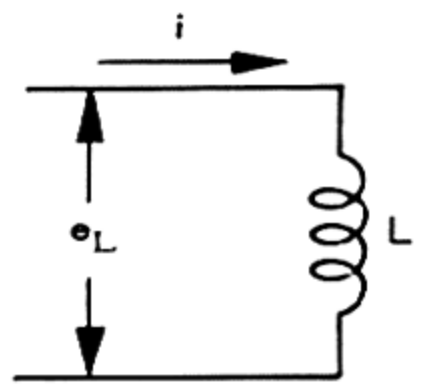
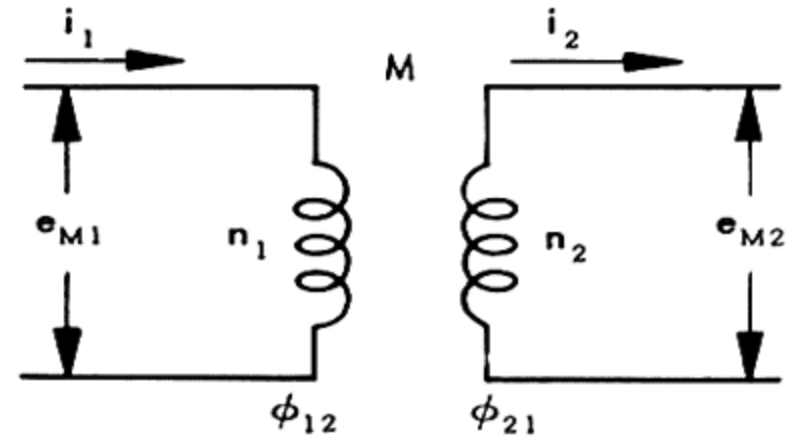
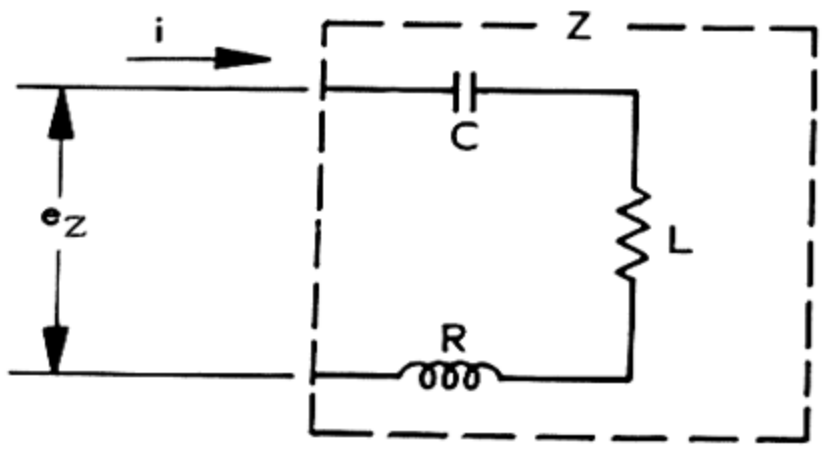
Information Summary 30-1. Elements of translational mechanics.

Figure	Concept and Symbol		Performance Relation
	*a) Elastic restraint (zero order in $\bar{A}$)* Angular displacement or position Rotational elastic restraint coefficient Reference position (where restraining torque is zero) Restraining torque Potential energy Hooke's Law. See Timoshenko and Lessels, Applied Elasticity (T5), and spring design manuals such as American Steel & Wire Company, "Manual of Spring Engineering" (A8); springs: see Marks, Mechanical Engineers' Handbook (M4), and Wallace Barnes Company, "Mechanical Springs: their engineering and design" (B8).	$\bar{A}$ $k_{(rot)}$ $\bar{A}_{(ref)}$ $\bar{M}_{(rstr)}$ PE	For more than one degree of freedom, angles must be small if they are to be treated as vectors. See Laning, The Vector Analysis of Finite Rotations and Angles. $\bar{M}_{(rstr)} = -k_{(rot)}(\bar{A} - \bar{A}_{(ref)})$ (1) $PE = \frac{1}{2}k_{(rot)}\lvert\bar{A} - \bar{A}_{(ref)}\rvert^2$ (2)
	*b) Coulomb friction (independent of $\bar{A}$)* Coulomb friction force Radius at which force acts Coulomb friction torque Rotational Coulomb friction coefficient See Bowden and Tabor, The Friction and Lubrication of Solids (B14), Den Hartog, Mechanics (D6) and Mechanical Vibrations (D5).	$\bar{F}_{(cf)}$ $\bar{R}_{(cf)}$ $\bar{M}_{(cf)}$ $c_{(cf)(rot)}$	See Information Summary 30-1 $\bar{M}_{(cf)} = \bar{R}_{(cf)} \times \bar{F}_{(cf)}$ (3) $c_{(cf)(rot)} = c_{(cf)} R_{(cf)}$ (4)
	*c) Linear damping (first order in $\bar{A}$)* Angular velocity Rotational damping coefficient Damping torque Dissipated power See Lees, "Integration by the Viscous Shear Process" (L10).	$\bar{W}$ $c_{(rot)}$ $\bar{M}_{(dmp)}$ $P_{(dmp)}$	$\bar{W} = \dot{\bar{A}}$ (5) $\bar{M}_{(dmp)} = -c_{(rot)}\bar{W}$ (6) $P_{(dmp)} = c_{(rot)}W^2$ (7)
	*d) Inertia (second order in $\bar{A}$)* Angular acceleration Moment of inertia Inertia reaction torque Radius of gyration Angular momentum Kinetic energy Moment of inertia: see Marks, Mechanical Engineers' Handbook (M4) and Eshbach, Handbook of Engineering Fundamentals (E5).	$\bar{\alpha}$ I $\bar{M}_{(ir)}$ RG $\bar{H}$ KE	$\bar{\alpha} = \dot{\bar{W}} = \ddot{\bar{A}}$ (8) $I = \int r^2 dm$ taken over entire body; dm is element of mass; r is distance from axis to dm (9) $\bar{M}_{(ir)} = -I\bar{\alpha}$ (10) $RG = \sqrt{I/m}$ (11) $\bar{H} = I\bar{W}$ (12) $KE = \frac{1}{2}IW^2$ (13)
Combining Law: $\Sigma\bar{M} = 0$ where $\Sigma\bar{M}$ includes all external and internal torques. Newton's third law applied to rotation.			

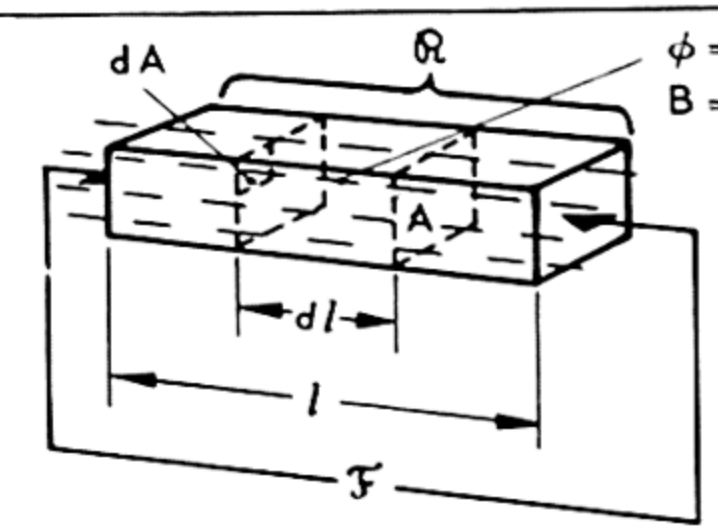
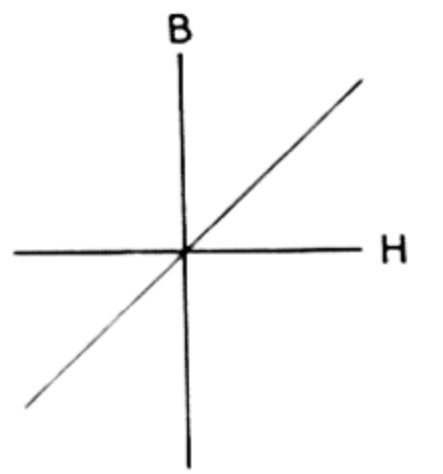
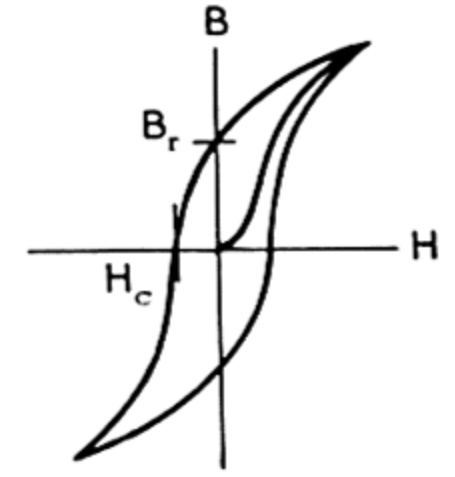
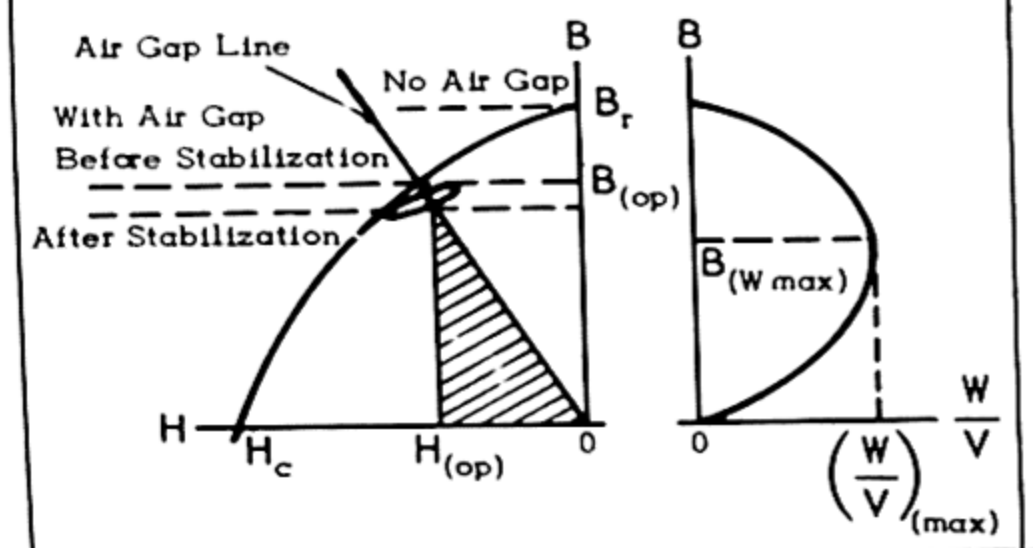
Information Summary 30-2. Elements of rotational mechanics.

Figure	Concept and Symbol		Performance Relation	
	*a) Capacitance (zero order in charge, integral order in current)*			
	Charge	Q		
	Capacitive reactance voltage	e_c	$e_c = -\frac{Q}{C} = -\frac{1}{C}\int i\,dt$	(1)
	Capacitance	C		
	Current	i	$i = \frac{dQ}{dt}$	(2)
	Potential energy	PE	$PE = \left\lvert \frac{1}{2}\frac{Q^2}{C} \right\rvert = \left\lvert \frac{1}{2} Q e_c \right\rvert$	(3)
	Capacitance of parallel plates	$C_{(pp)}$	$C_{(pp)} = \kappa\epsilon_o\frac{A}{d}$	(4)
	Dielectric coefficient of free space	ϵ_o		
	Relating coefficient of a substance (commonly called "dielectric constant")	κ		
	Plate area	A		
	Distance between plates	d		
	Capacitive reactance for sinusoidal voltage of angular frequency w_f	X_c	$X_c = 1/j\,w_f C$	(5)
	Capacitances in series	C_s	$\frac{1}{C_s} = \frac{1}{C_1} + \frac{1}{C_2} + \frac{1}{C_3} + \cdots$	(6)
	Capacitances in parallel	C_p	$C_p = C_1 + C_2 + C_3 + \cdots$	(7)
	*b) Resistance (first order in charge, zero order in current)*			
	Resistance	R		
	Resistive voltage	e_R	$e_R = -iR$	(8)
	Dissipated power	P	$P = i^2R$	(9)
	Resistivity	ρ	$\rho = RA/l$	(10)
	Conductance	G	$G = \frac{1}{R}$	(11)
	Resistances in series	R_s	$R_s = R_1 + R_2 + R_3 + \cdots$	(12)
	Resistances in parallel	R_p	$\frac{1}{R_p} = \frac{1}{R_1} + \frac{1}{R_2} + \frac{1}{R_3} + \cdots$	(13)

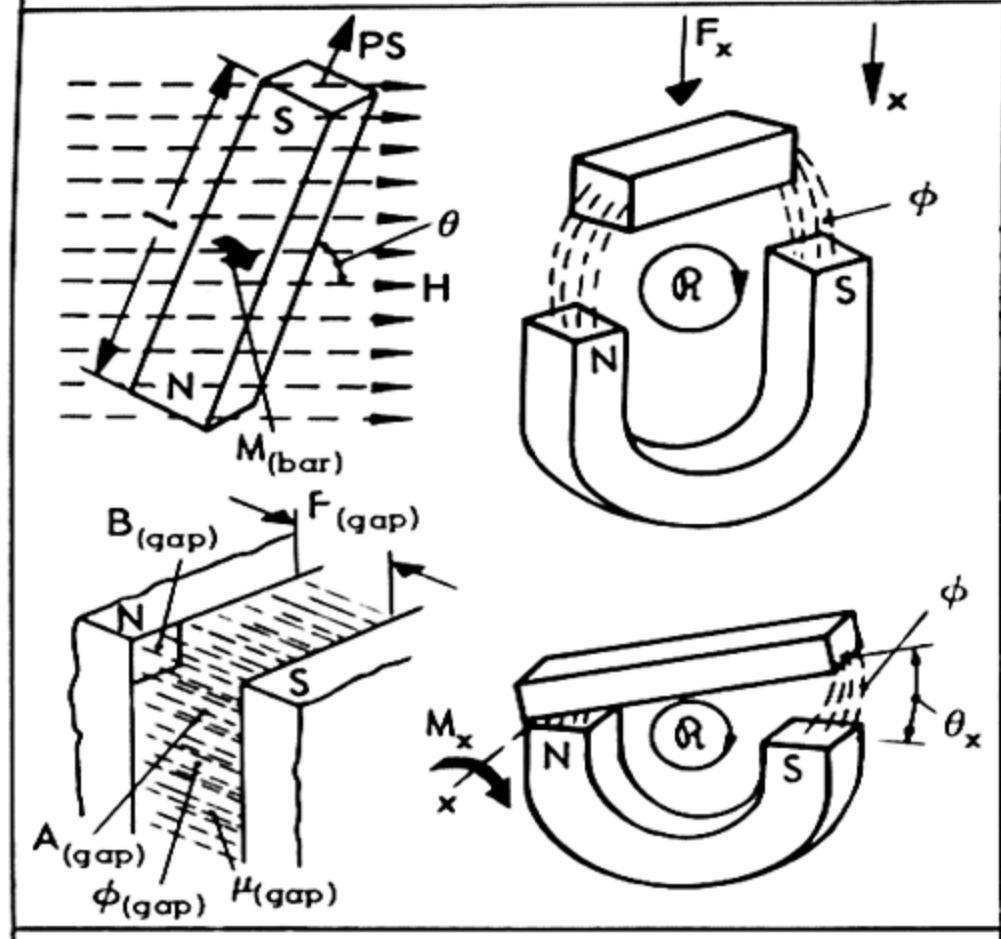
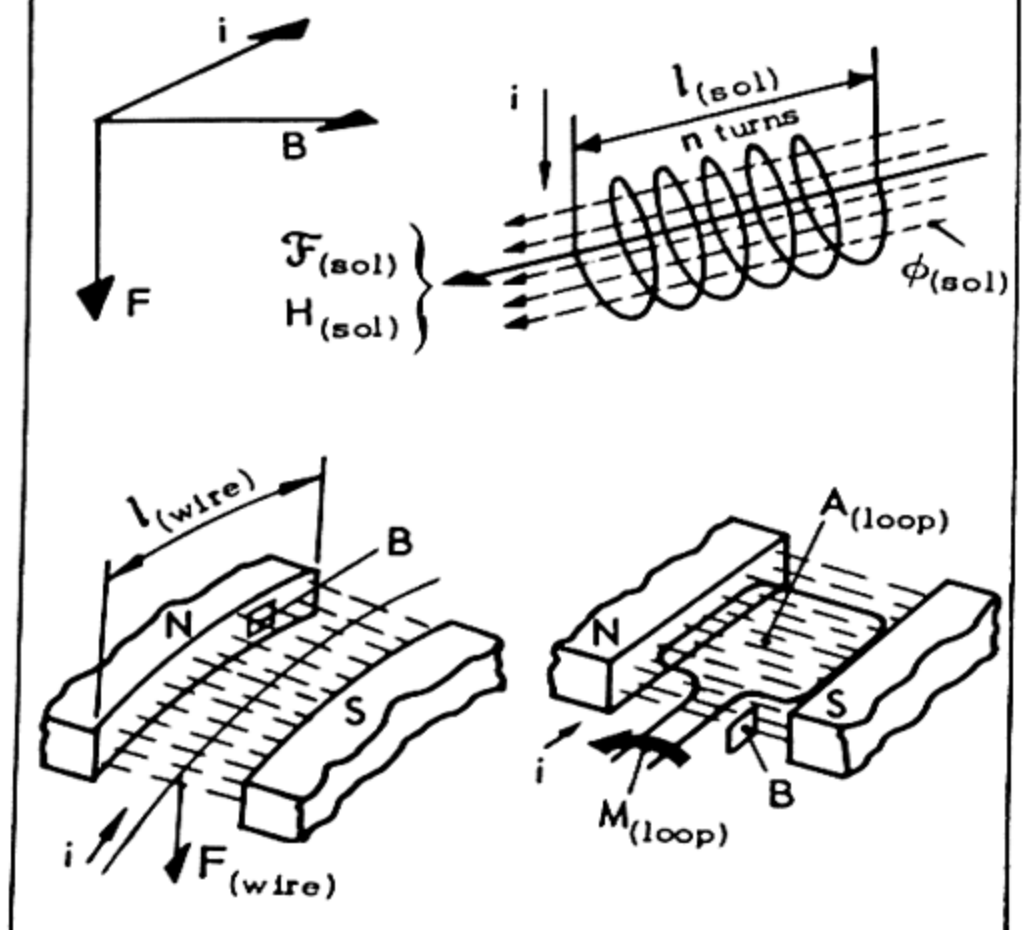
Information Summary 30-3. Elements of electric circuits. (Page 1 of 2)

Figure	Concept and Symbol		Performance Relation
	*c) Inductance (second order in charge, first order in current)*		
	Self inductance	L	$L = \frac{n\phi}{i}$ (flux linkages per unit current) (14)
	Magnetic flux	ϕ	
	Number of turns linked by flux	n	
	Inductive reactance voltage (for self-inductance)	e_L	$e_L = -L\frac{di}{dt}$ (15)
	Potential energy	PE	$PE = \frac{1}{2}Li^2$ (16)
	Inductive reactance for sinusoidal voltage of angular frequency w_f	X_L	$X_L = j w_f L$ (17)
	Inductances in series	L_s	$L_s = L_1 + L_2 + L_3 + \ldots$ (18)
	Inductances in parallel	L_p	$\frac{1}{L_p} = \frac{1}{L_1} + \frac{1}{L_2} + \frac{1}{L_3} + \ldots$ (19)
	Mutual inductance (between coil 1 and coil 2)	M_{12}	$M_{12} = \frac{n_2\phi_{21}}{i_1} = \frac{n_1\phi_{12}}{i_2} = M_{21}$ (20) (flux linkages in either coil per unit current in the other coil)
	Magnetic flux established by coil 1 and linking coil 2	ϕ_{21}	
	Energy stored in M_{12}	W_{12}	$W_{12} = W_{21} = M_{12} i_1 i_2$ (21)
	Inductive reactance voltage (in coil 1 due to current in coil 2)	e_{M1}	$e_{M1} = -M_{12}(di_2/dt)$; $e_{M2} = -M_{12}(di_1/dt)$ (22)
	*d) Impedance*		
	Impedance	Z	
	Voltage across impedance	e_Z	$e_Z = -iZ$ (23)
	Admittance	Y	$Y = \frac{1}{Z}$ (24)
	Impedance of RLC series circuit	Z_{RLC}	$Z_{RLC} = R + j w_f L + 1/j w_f C$ (25)
	Impedances in series	Z_s	$Z_s = Z_1 + Z_2 + Z_3 + \ldots$ (26)
	Impedances in parallel	Z_p	$\frac{1}{Z_p} = \frac{1}{Z_1} + \frac{1}{Z_2} + \frac{1}{Z_3} + \ldots$ (27)
	See Sears, Principles of Physics (S3), Vol. II; M.I.T., Department of Electrical Engineering, Electric Circuits (M7); and Blackburn, Components Handbook (B13).		
Kirchoff's laws: The instantaneous algebraic sum of voltages around any closed path is zero. The instantaneous algebraic sum of currents at any junction is zero.			

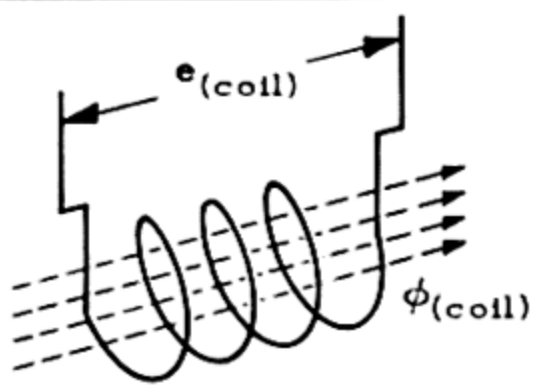
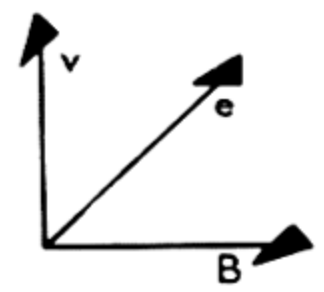
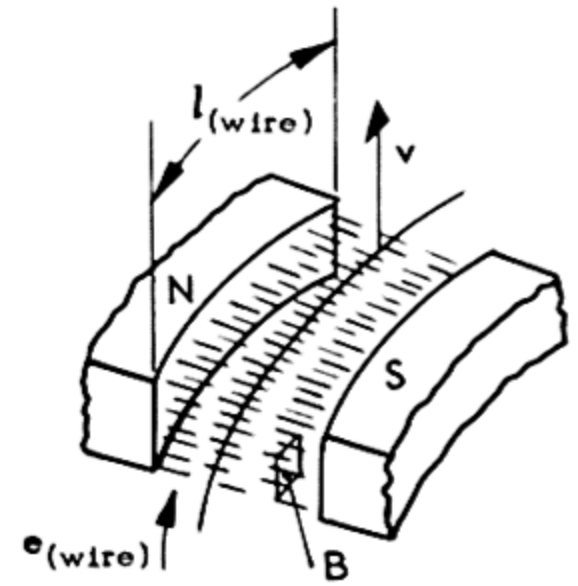
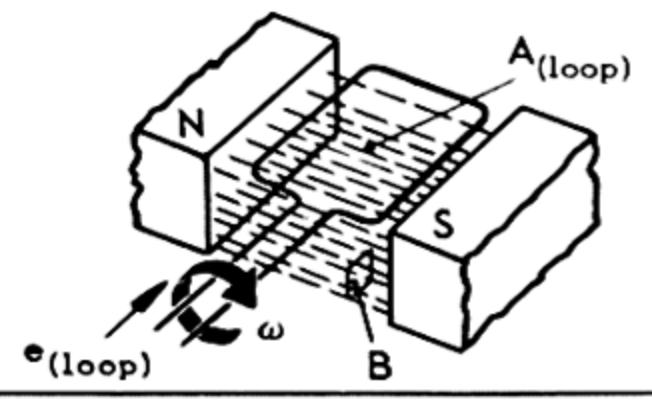
Information Summary 30-3. Elements of electric circuits. (Page 2 of 2)

Figure	Concept and Symbol		Performance Relation
	*a) Magnetic elements (zero order)*		
	Magnetic field of force	H	
	Magnetomotive force	ℱ	$\mathcal{F} = \oint H dl = \mathcal{R}\phi$ (1)
	Length of path	l	
	Reluctance	ℜ	$\mathcal{R} = l/\mu A$ (2)
	Permeance	𝒫	$\mathcal{P} = 1/\mathcal{R}$ (3)
	Magnetic flux	ϕ	$\phi = \int B dA$ (4)
	Magnetic flux density	B	
	Area of cross section	A	
	Permeability	μ	$\mu = B/H$ (5)
	Magnetic energy per unit volume	$\frac{W}{V}$	$\frac{W}{V} = \begin{cases} \int H dB = \frac{\mathcal{F}^2}{2\mathcal{R}V} = \frac{\mathcal{R}\phi^2}{2V} & (6) \\ \frac{1}{2}BH = \frac{B^2}{2\mu} \text{ if } \mu \text{ is a constant} & (7) \end{cases}$
	Volume	V	
	Retentivity	B_r	
	Coercive force	H_c	
	Magnetic flux density in stabilized magnetic circuit with air gap	$B_{(op)}$	
	Magnetic field of force when flux density is $B_{(op)}$	$H_{(op)}$	
			
			
			
	See references on page 3 of this summary.		

Information Summary 30-4. Elements of magnetic circuits. (Page 1 of 3)

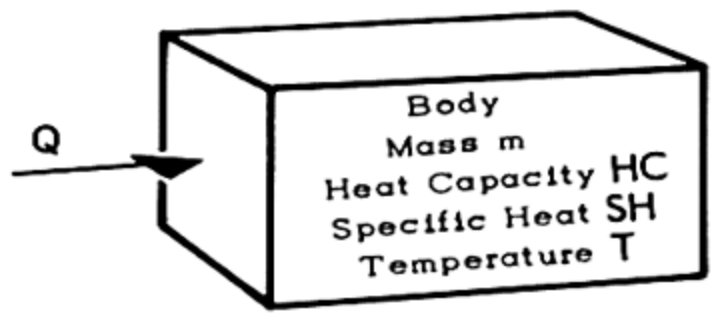
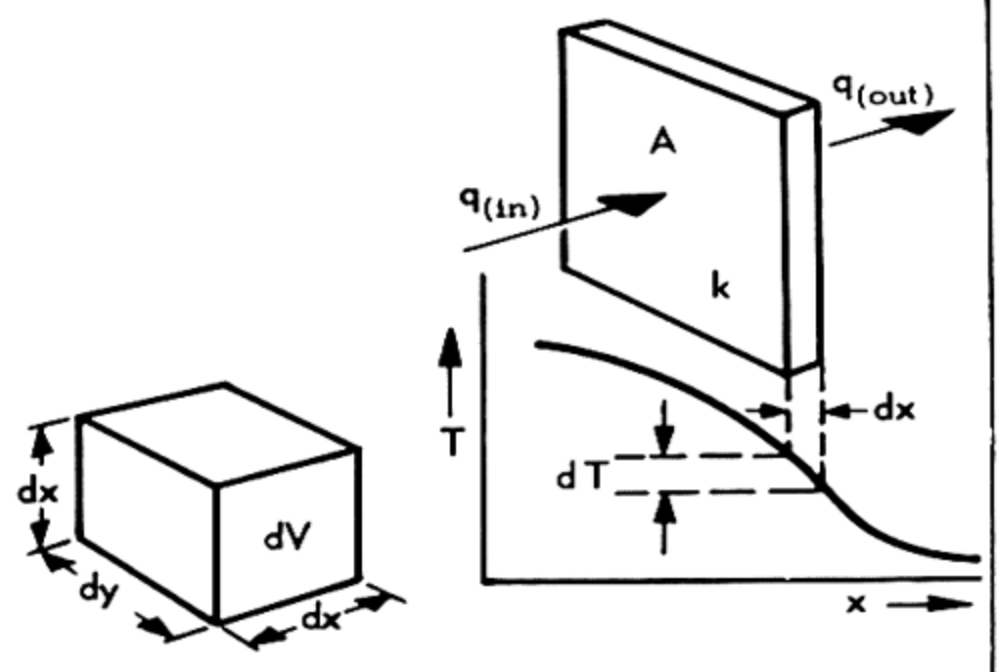
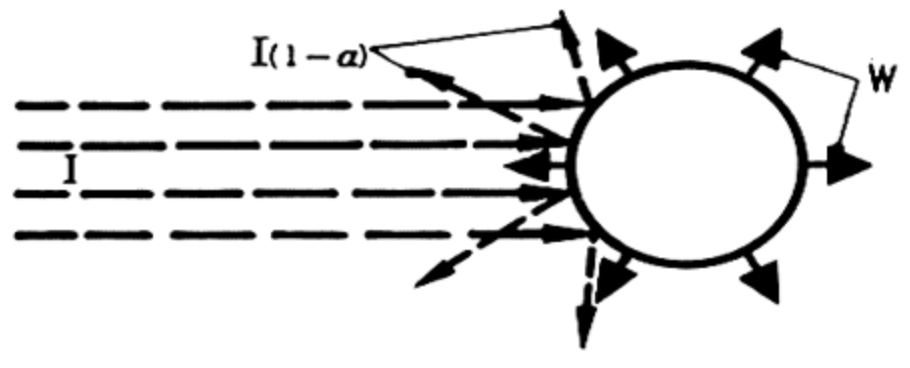
Figure	Concept and Symbol		Performance Relation	
	Magnetic pole strength	PS	$PS = \phi_{(op)} = B_{(op)} A$	(8)
	Magnetic moment of bar magnet of length l and cross-sectional area A	$M_{(mag)}$	$M_{(mag)} = (PS)\,l$ $= B_{(op)}\,l\,A$	(9) (10)
	Torque on bar magnet in uniform field H	$M_{(bar)}$	$M_{(bar)} = M_{(mag)} H \sin\theta \quad ; \quad B_{(op)} >> H$	(11)
	Angle between bar magnet and direction of field	θ		
	Force in x direction	F_x	$F_x = -\frac{\phi^2}{2}\frac{d\mathcal{R}}{dx}$	(12)
	Force across small gap	$F_{(gap)}$	$F_{(gap)} = \frac{B^2_{(gap)} A_{(gap)}}{2\mu_{(gap)}} = \frac{\phi^2_{(gap)}}{2\mu_{(gap)} A_{(gap)}}$	(13)
	Torque about x axis	M_x		(14)
	Angular displacement about x axis			
	*b) Electromagnetic elements (zero order)*			
	Magnetic field of solenoid	$H_{(sol)}$	$H_{(sol)} = ni/l_{(sol)}$	(15)
	Number of turns (or parallel conductors)	n		
	Electric current	i		
	Length of solenoid	$l_{(sol)}$		
	Magnetomotive force of solenoid	$\mathcal{F}_{(sol)}$	$\mathcal{F}_{(sol)} = ni$	(16)
	Force acting on a wire lying perpendicular to flux direction	$F_{(wire)}$	$F_{(wire)} = B l_{(wire)} i$	(17)
	For a circular turn of radius r	$F_{(turn)}$	$F_{(turn)} = 2\pi r B i$	(18)
	Length of wire	$l_{(wire)}$		
	Torque on loop (plane parallel to flux)	$M_{(loop)}$	$M_{(loop)} = B A_{(loop)} i$	(19)
	Area of loop	$A_{(loop)}$		
	See references on page 3 of this summary.			

Information Summary 30-4. Elements of magnetic circuits. (Page 2 of 3)

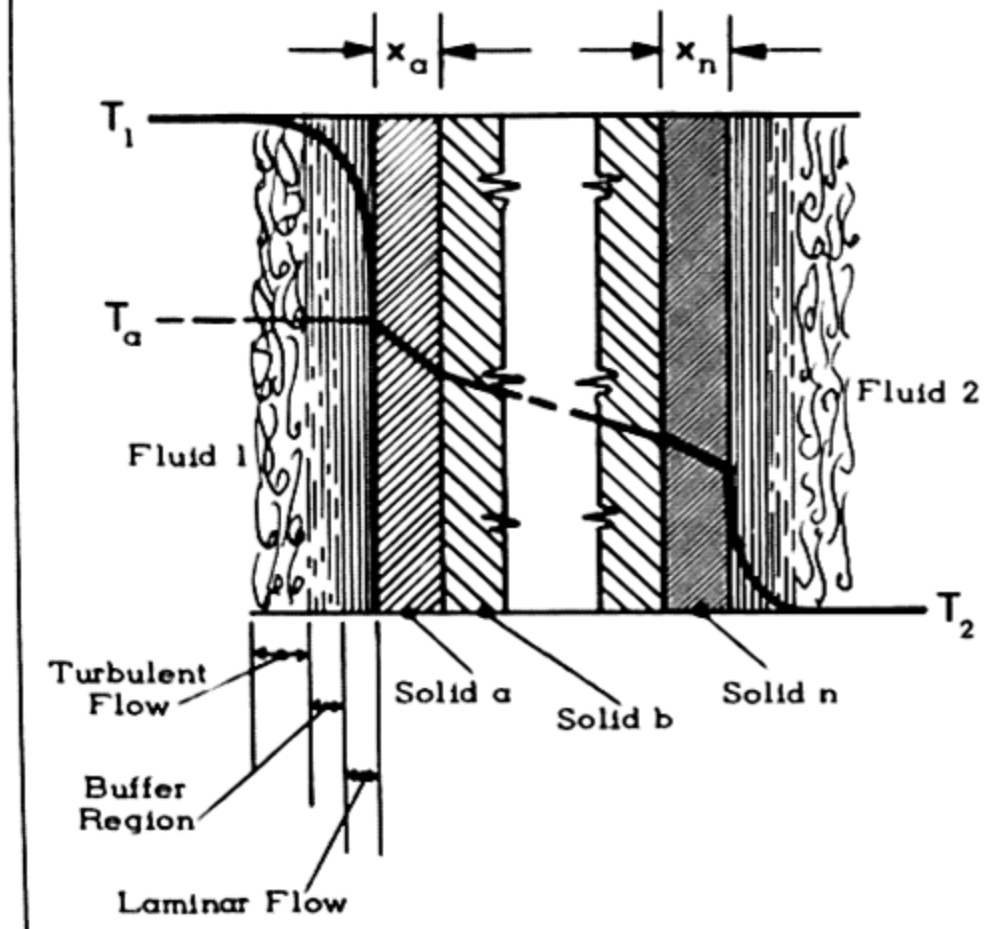
Figure	Concept and Symbol		Performance Relation	
	*c) Electromagnetic elements (first order)*			
	Voltage induced in a coil	$e_{(coil)}$	$e_{(coil)} = -\frac{n d\phi_{(coil)}}{dt}$	(20)
	Voltage induced in a wire lying perpendicular to flux plane	$e_{(wire)}$	$e_{(wire)} = -Bl_{(wire)}v$	(21)
	For a circular wire of radius r	$e_{(turn)}$	$e_{(turn)} = -2\pi rBV$	(22)
	Linear velocity perpendicular to wire and flux	v		
	Voltage induced in a loop perpendicular to flux and flux plane	$e_{(loop)}$	$e_{(loop)} = -BA_{(loop)}\omega$	(23)
	Angular velocity of loop relative to flux	ω		
				
				

See Frank, Introduction to Electricity and Optics (F11); M.I.T., Department of Electrical Engineering, Magnet Circuits and Transformers (M8); Roters, Electromagnetic Devices (R7); and Sears, Principles of Physics (S3), Vol. II.

Information Summary 30-4. Elements of magnetic circuits. (Page 3 of 3)

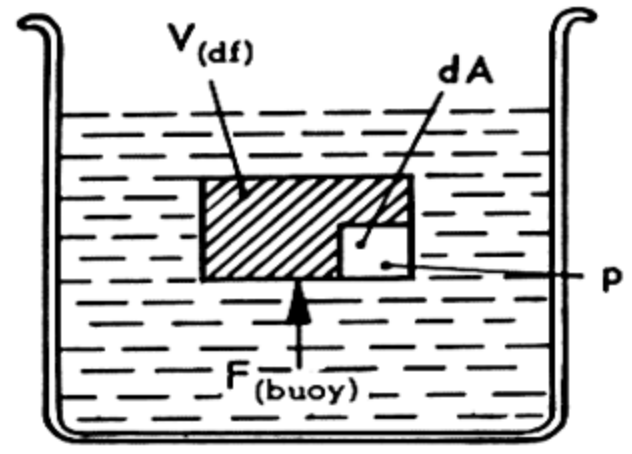
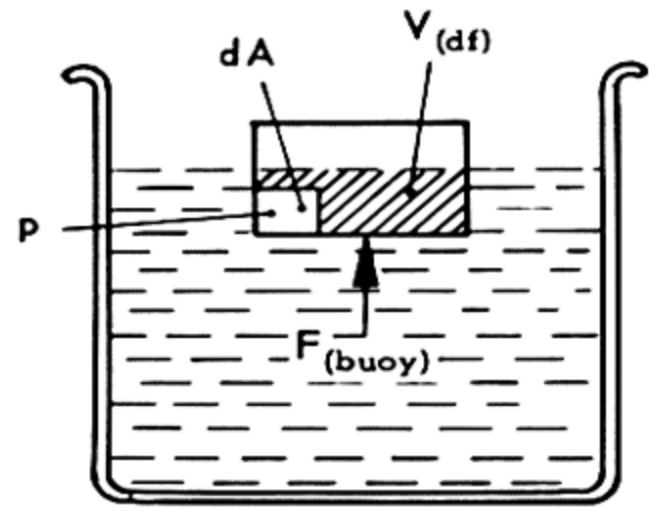
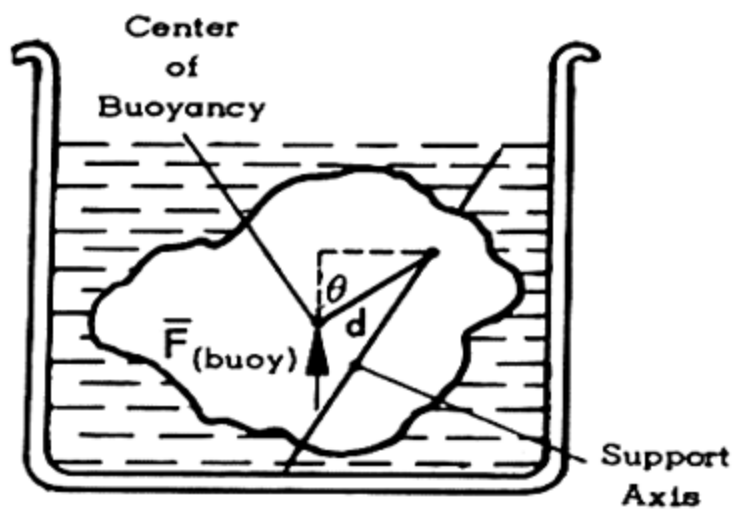
Figure	Concept and Symbol		Performance Relation
	*a) Heat capacity of a body*	HC	$HC = Q/\Delta T = m(SH)$ (1)
	Transferred heat energy	Q	$Q = m(SH)(\Delta T) = (HC)(\Delta T)$ (2)
	Temperature	T	
	Increment of temperature	ΔT	
	Body mass	m	
	Body specific heat	SH	
	*b) Heat conduction*		
	Rate of change of heat energy	q	$q = \frac{dQ}{dt}$ (3)
	Temperature gradient in direction x of heat flow	$\frac{dT}{dx}$	$q = -kA\frac{dT}{dx}$ (4)
	Heat conductivity	k	
	Cross-section area of heat flow	A	
	Thermal power transferred to body	$q_{(in)} - q_{(out)}$	$q_{(in)} - q_{(out)} = (HC)\frac{dT}{dt}$ (5)
			(If $dT/dt = 0$, T = constant and $q_{(in)} = q_{(out)}$)
	Increment of volume dV having dimensions "Fourier law of conduction"	dx, dy, dz	$dq_{(in)} - dq_{(out)} = \rho\,dx\,dy\,dz\,(SH)\frac{\partial T}{\partial t}$ (6a) $= k\,dx\,dy\,dz\left[\frac{\partial^2 T}{\partial x^2} + \frac{\partial^2 T}{\partial y^2} + \frac{\partial^2 T}{\partial z^2}\right]$ (6b)
	*c) Heat radiation*		
	Incident energy per unit time	I	$q = I\alpha - W$ (7)
	Absorptivity	α	$\alpha = 1$ for "black body" $\alpha < 1$ for "gray body"
	Reflectivity	$1 - \alpha$	
	Radiated energy per unit time	W	$W = \sigma \epsilon T^4$ (to free space) (8)
	See references on page 2 of this summary.		

Information Summary 30-5. Elements of heat flow. (Page 1 of 2)

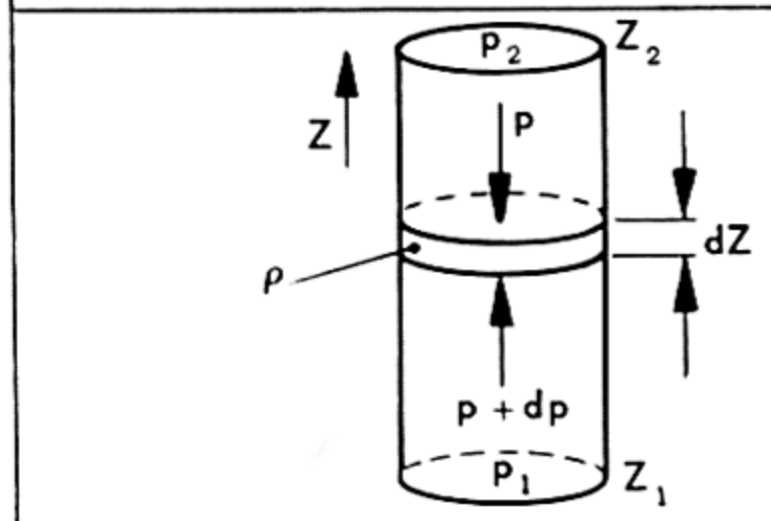
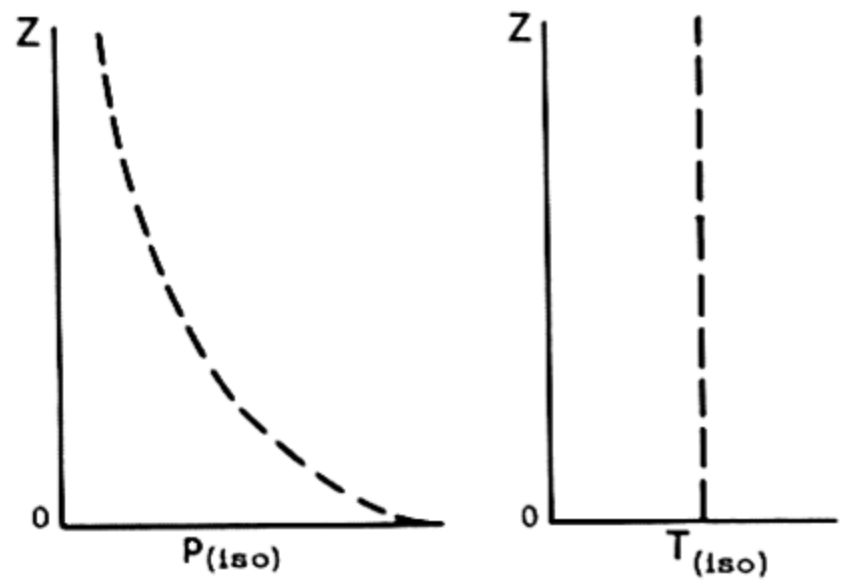
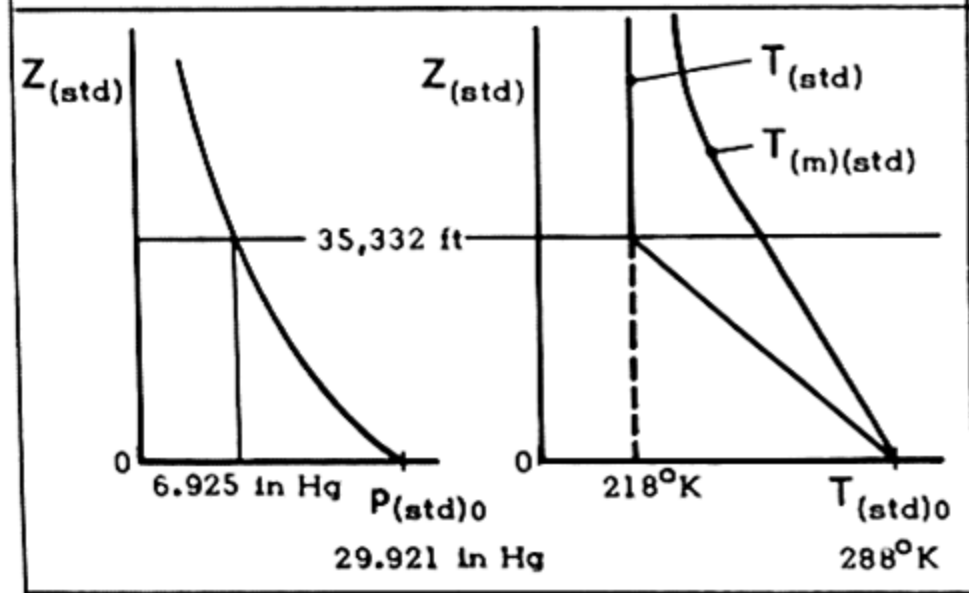
Figure	Concept and Symbol	Performance Relation
	Heat radiation (cont.)	
	Emissivity ϵ	$\begin{cases}\epsilon = 1 \text{ for "black body"} \\ \epsilon < 1 \text{ for "gray body"}\end{cases}$
	Dimensional factor σ	$\sigma = \begin{cases} 0.173 \times 10^{-8} \text{ Btu/ft}^2 \text{ hr } ^\circ\text{R}^4 \\ 4.92 \times 10^{-8} \text{ kg cal/m}^2 \text{ hr } ^\circ\text{K}^4 \end{cases}$
	Energy radiated per unit time from body at T_1 to surroundings at T_2 $q_{(T_1, T_2)}$	$q_{(T_1, T_2)} = \sigma \epsilon (T_1^4 - T_2^4)$ (9)
	*d) Heat transfer from fluids to solids (for steady-state flow)*	
	Coefficient of heat transfer from fluid 1 at temperature T_1 to surface of solid a at temperature T_a h_1	$q = Ah_1(T_1 - T_a)$ (10)
	Coefficient of heat transfer for layer of solid a, of thickness x_a, heat conductivity k_a, temperature T_a at one surface and T_b at other surface h_a	$h_a = \frac{k_a}{x_a}$ (11)
	Coefficient of heat transfer from fluid 1 at temperature T_1 through layers of solids a, b . . . n, to fluid 2 at temperature T_2 h	$\frac{1}{h} = \frac{1}{h_1} + \frac{x_a}{k_a} + \frac{x_b}{k_b} + \cdots + \frac{x_n}{k_n} + \frac{1}{h_2}$ (12) $q = Ah(T_1 - T_2)$ (13)

See Sears, Principles of Physics (S3), Vol. I, McAdams, Heat Transmission (M10), and Franklin, Differential Equations for Electrical Engineers (F12).

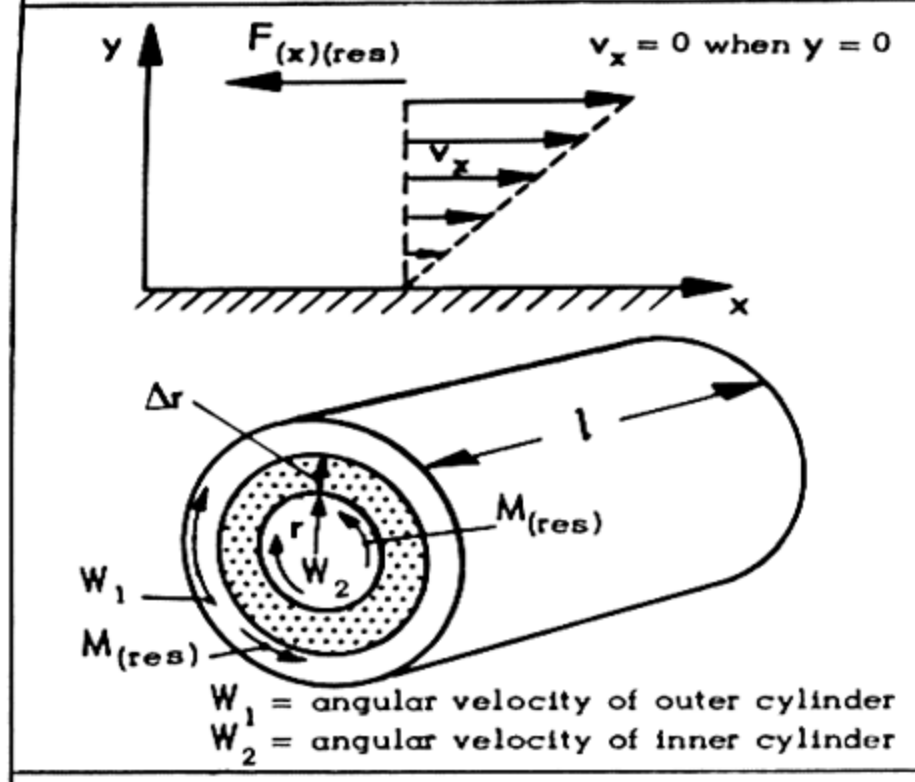
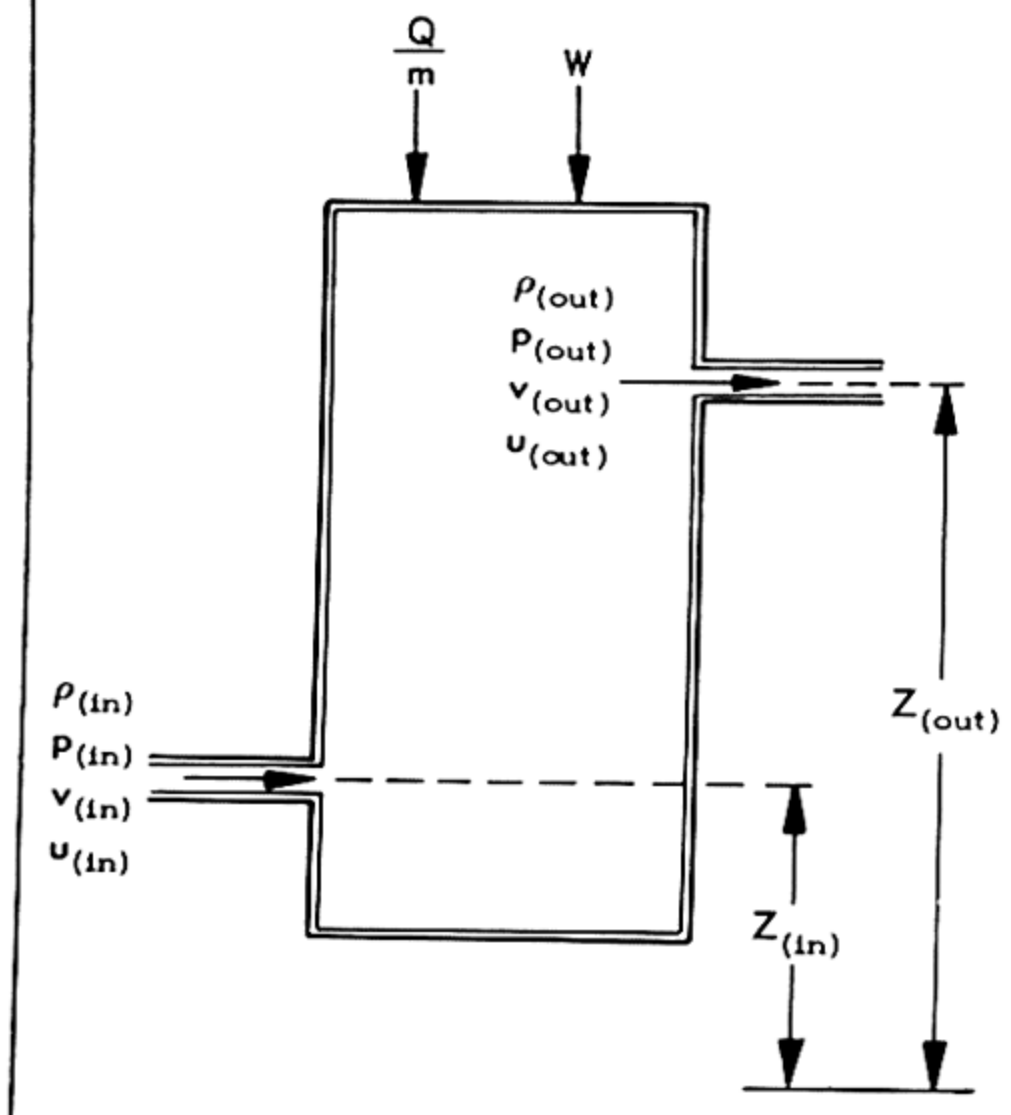
Information Summary 30-5. Elements of heat flow. (Page 2 of 2)

Figure	Concept and Symbol		Performance Relation
	*a) Hydrostatics (zero-order)*		
	Volume	V	
	Pressure	p	$p = \frac{F_{(area)}}{A}$ $\qquad dp = -\rho g dZ$ (1)
	Force acting on an area	$F_{(area)}$	
	Area	A	
	Density	ρ	
	Acceleration due to gravity	g	
	Height (altitude)	Z	
	Buoyant force (on an immersed body) "Archimedes' principle"	$F_{(buoy)}$	$F_{(buoy)} = \int \rho dV_{(df)} = \rho V_{(df)}$ for ρ = constant (2)
	Volume of displaced fluid	$V_{(df)}$	$= \int_{(body)} p dA_{(body)}$ (3)
	Area of displacing body	$A_{(body)}$	
	Location vectors from any reference point: to center of buoyancy	$r_{(cb)}$	$r_{(cb)} = \frac{\int r dV}{\int dV}$ (4)
	to an element of volume	r	
	Buoyant torque	$\bar{M}_{(buoy)}$	$\bar{M}_{(buoy)} = \bar{F}_{(buoy)} d \sin\theta$ (5)
	Compressibility	β	$\beta = -\frac{1}{V}\frac{dV}{dp}$ (6)
	Bulk modulus	$k_{(bulk)}$	$k_{(bulk)} = \frac{1}{\beta} = -V\frac{dp}{dV}$ (7)
	Absolute temperature	T	$p = \rho\frac{TR}{(MW)}$ or $\rho = p\frac{(MW)}{TR}$ for a perfect gas (8)
	Universal gas constant	R	
	Molecular weight	MW	$R = 8.32 \times 10^7$ (ergs/° Centigrade)/mole
	Specific heat of gas at constant volume	$(SH)_V$	
	Specific heat of gas at constant pressure	$(SH)_p$	
	Specific heat of liquid or solid	SH	
	Specific heat ratio	γ	$\gamma = \frac{(SH)_p}{(SH)_V}$ (9)
	For adiabatic compression (no heat exchange with surroundings)		pv^γ = constant ; γ = 1.4 for perfect gases (10)
	For isothermal compression (no change in temperature)		pv = constant (11)

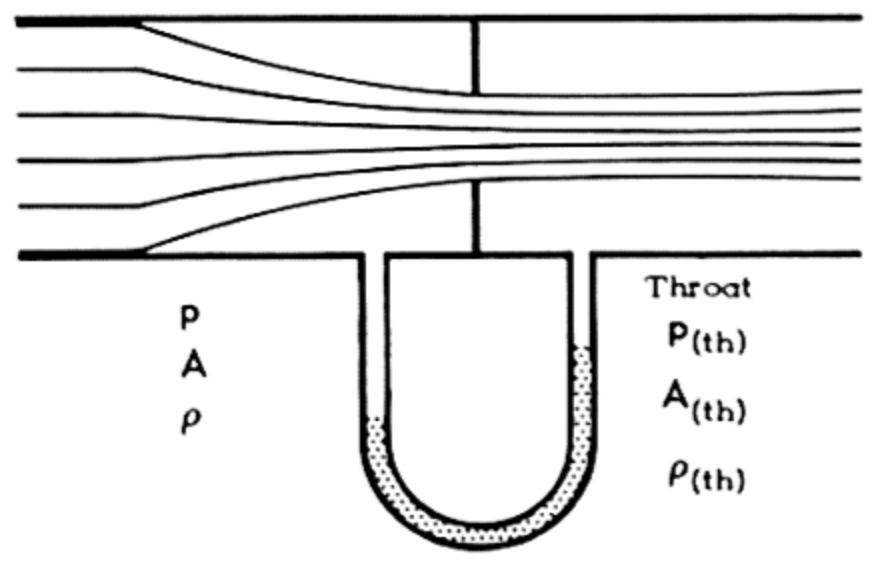
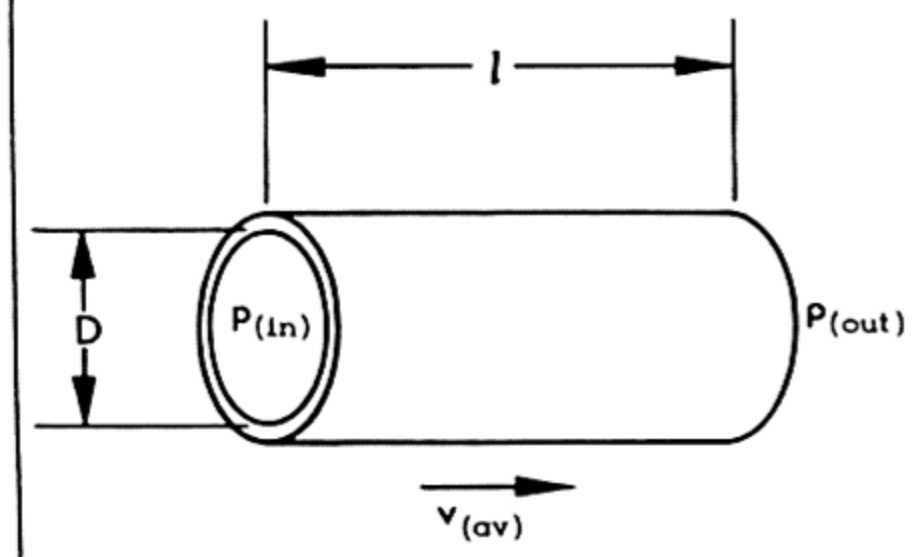
Information Summary 30-6. Elements of fluid mechanics. (Page 1 of 4)

Figure	Concept and Symbol	Performance Relation
	*Special cases:* Pressure in an incompressible fluid	$(p_2 - p_1) = -\rho g(Z_2 - Z_1)$ (12)
	Pressure in a perfect gas under isothermal (constant temperature) conditions $p_{(iso)}$ Isothermal temperature $T_{(iso)}$	$\ln\left(\frac{p_{(iso)1}}{p_{(iso)2}}\right) = \frac{Z_2 - Z_1}{T_{(iso)}} \frac{(MW)}{R} g$ (13)
	Pressure in a perfect gas where temperature varies with height	$\ln\left(\frac{p_1}{p_2}\right) = +g \frac{(MW)}{R} \int_{Z_1}^{Z_2} \frac{dZ}{T}$ (14) $= +g \frac{(Z_2 - Z_1)}{T_m} \frac{(MW)}{R}$ (15)
	Mean temperature T_m	where $T_m \equiv \frac{Z_2 - Z_1}{\int_{Z_1}^{Z_2} dZ/T}$ (16)
	See Binder, Fluid Mechanics (B12), Marks, Mechanical Engineers' Handbook (M4), Sears, Principles of Physics (S3), Vol. I, and M.I.T., M. E. Dep't., "Fluid Power Control" (M9).	
	*b) Pressure-altitude-temperature relations in the "Standard Atmosphere"*	
	Altitude $Z_{(std)}$	$Z_{(std)} = K \frac{T_{(m)(std)}}{T_{(std)0}} \log_{10}\left(\frac{p_{(std)0}}{p_{(std)}}\right)$ (17)
	Dimensional factor K	$K = 63{,}691.8$ ft (18)
	See Brombacher, "Altitude-Pressure Tables Based on the United States Standard Atmosphere" (B15).	

Information Summary 30-6. Elements of fluid mechanics. (Page 2 of 4)

Figure	Concept and Symbol		Performance Relation	
 W_1 = angular velocity of outer cylinder W_2 = angular velocity of inner cylinder	*c) Viscous flow (first-order)* Coordinate parallel to surface Coordinate perpendicular to surface Resistive force in x direction Viscosity (dynamic) Area of surface Velocity in x direction Kinematic viscosity Resistive torque between rotating cylinders	x y $F_{(x)(res)}$ μ $A_{(sfc)}$ v_x ν $M_{(res)}$	$F_{(x)(res)} = -\mu A_{(sfc)} \frac{dv_x}{dy}$ $= -\mu A_{(sfc)} \frac{v_x}{y}$ for a constant velocity gradient $\nu = \mu/\rho$ $M_{(res)} = -2\pi\mu r^3 l \frac{(W_1 - W_2)}{\Delta r}$	(19) (20) (21) (22)
	*d) Laws of fluid flow (including second-order effects)* Energy equation for steady-state flow (energy per unit mass) "Bernoulli's theorem" Mechanical equivalent of heat Heat transferred to unit mass of fluid Mechanical work transferred to unit mass of fluid Velocity Internal thermal energy per unit mass of fluid Reynolds number Characteristic linear dimension Velocity of sound Mach number	 J $\frac{Q}{m}$ W v u RN $l_{(char)}$ v_c MN	$J\left(\frac{Q}{m}\right) + W + \left(\frac{P_{(in)}}{\rho_{(in)} g} - \frac{P_{(out)}}{\rho_{(out)} g}\right) + \left(\frac{v^2_{(in)}}{2g} - \frac{v^2_{(out)}}{2g}\right) + J(u_{(in)} - u_{(out)}) + (Z_{(in)} - Z_{(out)}) = 0$ $J = 778.2$ ft-lb/Btu $= 4.187$ joules/cal $u_{(in)} - u_{(out)} = (SH)(T_{(in)} - T_{(out)})$ for a liquid $u_{(in)} - u_{(out)} = (SH)_V (T_{(in)} - T_{(out)})$ for a perfect gas $RN = \frac{\rho l_{(char)} v}{\mu}$ $v_c = \sqrt{\frac{dp}{d\rho}} = \sqrt{\frac{\gamma p}{\rho}}$ (adiabatic) $= \sqrt{\gamma g \frac{R}{(MW)} T}$ (perfect gas) $MN = \frac{v}{v_c}$	(23) (24) (25) (26) (27) (28) (29)

Information Summary 30-6. Elements of fluid mechanics. (Page 3 of 4)

Figure	Concept and Symbol		Performance Function
	*General flow through constrictions* Mass flow rate	MFR.	$MFR = F \rho A_{(th)} \sqrt{\frac{2g}{\rho}(p - p_{(th)})}$ (30) where $F = f\left(\frac{A_{(th)}}{A}, RN, \gamma, \frac{p_{(th)}}{p}\right)$ (31)
	Throat area	$A_{(th)}$	
	*Viscous, incompressible fluid flow through a circular pipe, "Hagen-Poiseuille law"* Velocity (averaged over entire cross section)	$V_{(av)}$	$(RN)_{(pipe)} = \frac{\rho D V_{(av)}}{\mu}$ (32) $p_{(in)} - p_{(out)} = \frac{f l \rho V^2_{(av)}}{2D}$ for all values of $(RN)_{(pipe)}$ (33)
	Friction factor	f	$p_{(in)} - p_{(out)} = \frac{32 \mu l V_{(av)}}{D^2}$ for $(RN)_{(pipe)} < 2100$ (34) or $f = \frac{64}{(RN)_{(pipe)}}$ (i.e., viscous forces predominate) (35) When $(RN)_{(pipe)} > 2100$, f must be evaluated experimentally or empirically

See references at end of section a, page 2 of this summary; see also Rauscher, Introduction to Aeronautical Dynamics (R3).

Information Summary 30-6. Elements of fluid mechanics. (Page 4 of 4)

COMPONENTS

30.31. Components (see paragraph 30.3) are treated in the following information summaries (located at the end of this section):

Information Summary 30-7. Mechanism Components
Information Summary 30-8. Electromagnetic Components
Information Summary 30-9. Electronic Components
Information Summary 30-10. Thermometric Components
Information Summary 30-11. Fluid Components

The treatment of components in these summaries parallels the treatment of elements in the preceding summaries; that is, only the most useful components are shown, and these are defined broadly. Also, performance relationships are simplified by omitting deviations from the ideal, such as those resulting from friction; components that are simple embodiments of elements previously stated are omitted; and references are made as complete as possible.

30.32. Mechanism Components (see Information Summary 30-7). The basic purpose of the common mechanism components is magnitude conversion or computation of motion, force, or torque. In general, the actual relationship between input and output motion closely approximates the ideal relationship shown in the summary. The ideal relationship for force or torque is always inversely proportional to that of motion, but, in the actual case, the output is decreased by friction losses. In one group of components, which includes gears (except differential gears), screws, and levers (for small motions), motion is limited to a single degree of freedom, the ideal relationships are linear, and the components are generally used for transmitting force, torque, or motion. Friction, however, is not negligible for this group. For example, with a worm and wheel, or a screw and nut, the friction is so great that it makes the component performance effectively irreversible. That is, if force or torque is applied at the output (axial force applied to the screw or torque to the wheel), there is no resulting motion at the input (rotation of the worm or the screw).

30.33. Another group of mechanism components are those that are used primarily for types of computation such as summing and function generating. In this group are cams and followers, crank and connecting rod combinations, differential gears, summing linkages, and generalized linkage computers. Here, the input and output forces, and hence the effects of friction, are of only secondary importance since motion is the variable used in computation.

30.34. The principal use made of the single-degree-of-freedom gyroscope (see page 4 of Information Summary 30-7) is as a means of developing a torque proportional to angular velocity. If this torque is opposed by a linear elastic restraint device, such as a spring, then the gimbal angular position becomes a measure of the input angular velocity. The two-degree-of-freedom gyroscope is normally

used as an angular position reference. One example is the gyroscopic vertical indicator, in which the position of the spin axis of a gyroscope is controlled by auxiliary pendulums* that cause it to remain, on the average, along the vertical. The pendulum serves to indicate the resultant of gravitational and accelerational forces acting on its center of mass. If the dynamic response of the pendulum is slowed by lengthening its natural period, the indication tends to approach the average position of this resultant.

30.35. The seismic element (see page 5 of Information Summary 30-7) is particularly useful in the measurement of vibratory motion; more complete details are set forth in Chapter 35. The centrifugal tachometer is used as a device for measuring angular velocities. When used with a suitable feedback mechanism that actuates a throttle, it forms a speed regulator for engines and is known as a flyball governor.

30.36. Electromagnetic Components (see Information Summary 30-8). Electromagnetic components occupy many places in instrument systems, particularly in sensing inputs, transmitting information, and driving mechanical components.

30.37. All d-c rotating machines (see pages 1 and 2 of Information Summary 30-8) have a wound armature with commutator and brushes, and a stationary field. Their differing characteristics are based principally on different types of field excitation. Each type of field excitation can be used in either a motor or a generator. A field winding in series with the armature carries the same current as the armature, and hence the excitation is dependent on all variables that influence armature current. Other forms of excitation are independent of armature current, but (except for a permanent magnet) they are dependent on the voltage across the field winding. Since armature voltage is proportional to the speed of the armature times the field strength, a series field winding makes generator voltage dependent on load current. In a motor, this same effect of a series field cancels the speed regulation that is inherent when field strength is constant. Certain particular applications of d-c machines should be noted. A permanent-magnet generator puts out a voltage proportional to speed and hence acts as a tachometer. A separately excited generator acts as an amplifier with field current as its input and mechanical drive as its power source. The amplidyne is a further extension of this principle, incorporating two stages of gain in a single machine. The separately excited motor combines external control of speed, by varying the ratio of armature to field voltage, with self regulation to hold this speed against load changes.

30.38. Most a-c motors and generators (see pages 2 and 3 of Information Summary 30-8) have stator windings connected to the line, and a rotor inductively coupled to the stator. The one exception is the series motor, often called a

* The pendulum and the gyroscope are treated in much greater detail in separate chapters of Part 2, Vol. III.

"universal" motor, which operates with practically the same characteristics on a-c power as on d-c. The rotor of an a-c motor may have a winding of insulated wire (wound rotor), a set of parallel conducting bars connected to a ring at each end (squirrel cage rotor), or a disc or cup of conducting material (eddy-current rotor). An induction motor uses two- or three-phase excitation on the stator to form a rotating magnetic field that cuts the conductors of the rotor, induces currents, and thereby creates a torque. This action requires a difference in speed between the rotating field and the rotor, called "slip." At synchronous speed (where the rotor is at the same speed as the rotating field), there is no "slip," no induced current, and no torque. If the rotor is driven beyond synchronous speed, an opposing torque appears and energy is returned to the line. Wound, squirrel cage, or eddy-current rotor construction may be used. The pulsating field excited by a single-phase voltage produces a similar effect on a moving wound rotor, but no starting torque with the rotor stationary. The effect of a multi-phase excitation can be obtained on single phase by using a stator with two windings and introducing a phase shift in one of these windings by an additional inductance (split-phase motor) or by a series capacitance (capacitor motor). Still another single-phase arrangement is the repulsion motor, which has a single winding on the stator, and a rotor with a winding and commutator similar to a d-c machine. The brushes on the commutator are placed at an angle to the effective pole axis of the stator and are short-circuited. The combination of the transformer action of the stator on the rotor and the current path determined by the position of the brushes produces a large starting torque. A motor arranged to start by repulsion and run by induction is called a repulsion-induction motor. One special form of two-phase machine that is useful in instrument work has an eddy-current rotor, and one winding continually energized by the "reference voltage." The other winding is energized by the variable "control voltage" at ± 90 degrees phase angle from the reference. The output torque is nearly linear with control voltage, and reverses when the phase is reversed. Damping can be achieved by applying a d-c voltage to the control winding. This same type of machine can serve as an a-c tachometer. When one winding is energized, a voltage proportional to the rotor speed is generated in the second winding. This voltage has a phase angle of 90 degrees that reverses from plus to minus when the direction of rotation changes.

30.39. Synchronous machines (see page 4 of Information Summary 30-8) have stator windings similar to an induction motor, but the rotor is a permanent magnet (or an electromagnet excited by d-c current). As generators, they supply almost all a-c power. As motors, they are used wherever exact speed regulation is required, as in clocks, gyroscopes, and sound recorders. A synchronous motor in its fundamental form produces an output torque only when the rotor is turning at synchronous speed, that is, exactly in step with the a-c power source. The rotor

must be brought up to this speed by some other means than synchronous action. In the hysteresis motor, the rotor is a ring of permanent magnet material, which is magnetized by the rotating field of the stator. The magnetization of the ring rotates with the stator field, lagging behind it because of the large hysteresis of the ring, and thus produces an accelerating torque on the rotor. When the rotor reaches synchronous speed, the retained magnetism is stationary with respect to the ring, and the motor operates like any other synchronous machine.

30.40. Meters (see page 5 of Information Summary 30-8) differ from motors in that they are arranged to move only a fraction of a turn, usually working against elastic restraint. They are also typically much smaller and lighter, with only a pointer, a pen, or contacts as a load. The D'Arsonval type is equivalent to a d-c motor with a permanent-magnet field. It can be made responsive to a-c inputs by means of a rectifier, or responsive to the heating effect of currents up to radio frequencies by use of a thermocouple. It can be made very nearly linear in its response to d-c inputs. The wattmeter is equivalent to a d-c motor with separately excited field. It will respond to either a-c or d-c inputs, and is very nearly linear with wattage. The same type of device with rotor and stator windings connected in series is known as an electro-dynamometer. It responds to either a-c or d-c inputs in proportion to the square of the input current, and can be built to a high degree of accuracy. The solenoid or "moving iron" meter is a much simpler device than the electro-dynamometer. It also has a square-law response, and is accurate enough for many applications. Other types of meters are described in detail in manuals published by the principal meter manufacturers.

30.41. A transformer (see page 6 of Information Summary 30-8) is a practical application of mutual inductance. Deviations from the ideal relationships result from ohmic resistance losses in the windings, eddy-currents, and hysteresis losses in the core. High-frequency performance is limited by the distributed capacitance of the windings and by leakage inductance that occurs because flux from one winding does not entirely link the turns of the other winding. Low-frequency performance is limited as a result of the self-inductive impedance of the primary winding decreasing with frequency until it shunts out the secondary load. A magnetic amplifier (see page 3 of Information Summary 30-8), which is also called a saturable reactor, is a practical application of incremental inductance. A d-c current in the control winding saturates the core and reduces the impedance of the a-c power windings. The latter windings are arranged to oppose each other, thereby increasing their mutual impedance and at the same time cancelling their effect on the control winding. Feedback can be introduced by rectifying the output and applying it to an added control winding.

30.42. A translational transducer (see page 6 of Information Summary 30-8) is the counterpart (for a small range of translational excursions) of the permanent-

magnet d-c motor and generator, and of the D'Arsonval meter. It serves as a loud-speaker, microphone, vibration pickup, and string galvanometer, and is used in many similar applications where the amplitude seldom exceeds 0.01 inch and the frequency is less than 20 kilocycles per second.

30.43. An eddy-current damper (see page 6 of Information Summary 30-8) applies the same basic laws as a motor with an eddy-current rotor, except that it uses a stationary magnetic field to exert a torque opposing motion of the rotor.

30.44. Synchros, Microsyns, and the differential transformer are all devices whose primary purpose is to transmit positional information electrically. The basic synchro (see pages 7 and 8 of Information Summary 30-8) is a unit that has a rotor with slip rings and a single winding, and a stator with a triple winding like a three-phase motor. The rotor is energized by single-phase a-c voltage that induces in the stator windings voltages whose ratios are functions of the angular position of the rotor. If two such units energized from the same power source have their stators connected electrically, and one rotor (arbitrarily designated as the transmitter) is driven to a given position, the second rotor (designated as the receiver) is subject to a torque tending to bring it to the corresponding position. The control transformer is a similar unit, but, instead of its rotor being excited from an a-c source, it acts as a comparator to produce a signal that passes through zero when its position corresponds to that of the transmitter. The differential synchro has triple windings on both rotor and stator. As a differential transmitter, it can receive a signal from a transmitter on one set of windings and transmit with the other set a signal that represents the original transmitter position plus or minus its own angular position. As a receiver or motor, the differential synchro can receive signals from two transmitters and develop a torque tending to drive it to the position representing the sum or difference of the two transmitter angles. An angle resolver is an auxiliary computing device. It is included with synchros because of its similar construction.

30.45. The differential transformer (see page 6 of Information Summary 30-8) consists of a primary, two secondaries connected in opposition, and a core that can be displaced longitudinally. The output, which is the difference between the two secondary voltages, is proportional to the displacement of the core from zero position.

30.46. Microsyns (see page 9 of Information Summary 30-8) are specialized components for shafts that rotate no more than ±10 degrees from a reference position. Each has four stator poles with windings and an iron rotor with two quadrants cut away. In the reference position, the quadrant edges are aligned with the centers of the poles. The three forms of Microsyns differ in purpose. The signal generator is excited by an a-c input and puts out a signal proportional to the angular displacement of its rotor from a reference position, without applying torque.

The torque generator is usually energized by two d-c currents. Its output is a torque proportional to the product of these currents and independent of angular position. The elastic restraint generator is energized by a single d-c current. Its output is a restoring torque proportional to the square of the input current and to the angular displacement of the rotor from a reference position.

30.47. The magnetostriction transducer (see page 9 of Information Summary 30-8) utilizes the property of certain materials to change in length with magnetization (and vice versa). It is useful principally at ultrasonic frequencies.

30.48. Electronic Components (see Information Summary 30-9). Vacuum tubes (diode, triode, and multi-electrode) are widely used, and are thoroughly covered in many texts and handbooks. They are essentially nonlinear devices, but may be treated as approximately linear for reasonably large increments of voltage and current. The diode is a rectifier with current flow approximately proportional to the square of positive plate voltage. The addition of a control grid makes the tube a triode with a voltage gain of μ; that is, applying an incremental voltage e_g to the negatively biased grid has the same effect as an incremental voltage $-\mu e_g$ at the positively biased plate. This voltage reaches the output circuit through a source impedance of r_p. This is an incremental impedance relating increments of voltage and current. Adding a second grid with positive bias makes the tube a tetrode. This second grid or screen shields the plate from the grid capacitatively. It also increases current gain (mutual conductance, g_m) and incremental source impedance so that the output is essentially a current source of $-e_g g_m$. Adding a third grid or suppressor at ground potential makes the tube a pentode. The tube characteristics of a pentode and a tetrode are similar; the main function of the suppressor is to repel secondary electrons so that they return to the plate instead of being attracted to the screen. Still more grids may be added to create a converter or mixer, with two control grids shielded from each other and from the plate.

30.49. Gas diodes and gas triodes (thyratrons) are almost as widely used and described as vacuum tubes. They have two states: conducting, with a voltage drop independent of current; and nonconducting. The voltage relationships that start and stop conduction are the characteristics of interest. A gas diode starts conducting at a plate voltage somewhat higher than its operating voltage, and stops when the voltage drops below this operating value. The operating voltage depends on the pressure and chemical nature of the gas in the tube, and is independent of the spacing between electrodes. In a gas triode, a ratio of negative grid voltage to positive plate voltage in excess of a critical value also prevents conduction. After conduction starts, performance is the same as for a gas diode. Gas tubes can handle larger currents than vacuum tubes, and at smaller voltage drops. That is, they handle larger power at higher efficiency, but control of output current is stepwise rather than continuous.

30.50. Solid rectifiers consist of a semiconducting material such as germanium, silicon, copper oxide, or selenium, in combination with some form of contact or junction at which charges move more easily in one direction than in the reverse direction.

30.51. Transistors ("crystal triodes") consist of two rectifying regions close enough together for mutual interrelations to take place. In the point-contact type of transistor, the rectifier is a metal point held mechanically against a crystal surface; in the junction type, the rectifier is the boundary between "p" and "n" impurities in the crystal. The emitter (input rectifier) is biased for conduction, while the collector (output rectifier) is biased against conduction. The interaction between the rectifiers is such that an input signal current through a low impedance causes an output signal current to flow through a much higher impedance. The point-contact transistor also has a gain in output current up to five times input current; the junction type has output current always somewhat less than input current, but it can operate at higher power levels. As compared with vacuum tubes, transistors are somewhat more nonlinear and have more random variation between individual units. The requirements for space, energy supply, and heat dissipation, however, are very much less.

30.52. The photocell (phototube) consists basically of a photo-emissive cathode that emits electrons in response to incident light, and a positively biased anode to attract these electrons. The electron flow is a function of wavelength, and at any wavelength the flow is proportional to light energy rate. The sensitivity of the cell can be increased by introducing a gas that is ionized by the photoelectrons, or by adding a chain of electron multipliers in the same envelope with the photo-emissive cathode. Other photosensitive components are the photovoltaic cell, in which photoelectrons cross a rectifying barrier and accumulate to create a voltage; and the photoconductive cell, in which photoelectrons act as free electrons to increase the electrical conductivity of the cell.

30.53. The applications of the cathode ray tube in oscilloscopes and television are too widely known to need comment. However, attention should be drawn to its use in multiplying, function generating, and axis conversion, in which either the light output or the electrostatic charge at the face of the tube are detected by suitable sensing devices.

30.54. An amplifier is an assembly of coducers,* each of which introduces a net gain. These coducers must be interconnected by means of coupling devices in order to achieve a usable amplifier. In most cases the coupling devices, rather than the coducers, determine the frequency function of the amplifier.

30.55. The distinction between a negative feedback amplifier and an oscillator is not sharply drawn. Every physical possible feedback loop in an amplifier

* See first sections of Chapter 28 for a discussion of coducers.

includes phase shifts that at some frequency total 180 degrees and thus convert negative feedback to positive feedback. If there is not enough attenuation around the loop at this frequency to make the net gain less than unity, the amplifier will oscillate. When a circuit oscillates, the amplitude increases exponentially with time until some condition limits it. This limitation is necessarily a nonlinearity that must be taken into account if unwanted distortion in an oscillator is to be avoided.

30.56. The processes of amplitude modulation and demodulation are well known. It should be pointed out that they are inherently nonlinear, even though the end result is effectively linear. An amplitude-modulated carrier necessarily includes "sidebands" that are the sum and difference of carrier and signal frequency.

30.57. The bridge is widely useful, since it can be made selectively responsive to a minute desired input while cancelling out the effect of interfering inputs. For example, a strain gage contains two windings of resistance wire so oriented that the resistance of one increases and the other decreases when the gage is under strain, but the thermal effects on the two windings are identical. When the windings form two arms of a bridge, the output responds to the strain while thermal interference cancels itself.

30.58. Bridges containing rectifiers are useful as modulators or demodulators, particularly for signals that pass through zero, where reversal of d-c polarity or carrier phase denotes reversal of algebraic sign. In such a demodulator, a reference voltage of carrier frequency is required to detect phase reversal of the carrier. Components such as the Microsyn signal generator, the differential transformer, and the a-c tachometer generate signals that reverse phase when passing through zero. The two-phase motor requires this type of input for its control phase.

30.59. The piezoelectric effect is found in crystals of quartz, rochelle salt, and certain other materials. A similar effect designated by the name electrostriction is found in barium titanate ceramics that have been heat treated in an electrostatic field. Piezoelectric devices serve as electromechanical transducers over a frequency range from audio to more than ten megacycles. However, they are noted for nonlinear distortion in the audio region, as compared with other transducers. Another application is as electric circuit components for frequency determination or selection when mounted so as to have negligible mechanical load. In this application, a crystal is equivalent to an almost pure reactive network (very small energy dissipation) having a frequency of resonance ("series" or minimum impedance) and a slightly higher frequency of antiresonance ("parallel" or maximum impedance).

30.60. The filters shown in Information Summary 30-9 are the fundamental components of most of the more elaborate filters, compensators, and networks found in practice. Almost all desired frequency functions can be realized or at

least approximated. The low-pass R-C filter serves as an integrator for frequencies where $w > RC$ ($w = 2\pi n$), and the high-pass R-C filter functions as a differentiator for frequencies where $w < RC$.

30.61. Thermometric Components (see Information Summary 30-10). Temperature is commonly measured in terms of thermal expansion of a working substance, or alternatively it may be measured by thermal effects on electric circuit components.

30.62. The two liquid-filled types of thermometers shown in Information Summary 30-10 differ only in their indicating means. In the liquid-in-glass type, the thermal increment of the volume of the liquid is visible as an increase of column length in a small-bore transparent tube. In the completely filled liquid type, this increment of volume actuates a pressure type of gage, overcoming whatever elastic restraint the gage imposes.

30.63. The gas pressure thermometer (see page 1 of Information Summary 30-10) is a true thermal pressure device; that is, the principal effect is change in pressure, and change in volume is negligible. This is not the form of gas thermometer that is used as the primary standard for defining a temperature scale. In that form, pressure of an ideal gas is kept constant by varying volume, and temperature is defined as being proportional to volume.

30.64. The vapor pressure thermometer (see page 2 of Information Summary 30-10) contains a volatile liquid in equilibrium with its own vapor. The vapor pressure increases approximately exponentially with an increase of temperature, resulting in a nonlinear temperature scale unless the sensitivity of the associated pressure gage is varied to compensate for this nonlinearity.

30.65. A bimetal utilizes the differential expansion of two dissimilar metals. Because of its simplicity and ruggedness, the bimetal is often used in thermostatic controls.

30.66. A resistance thermometer is simply a utilization of the temperature coefficient of resistivity of an electrical resistor, under conditions where the heating caused by an electric current can be neglected. A platinum resistance thermometer is used to extend reference scales of temperature beyond the practicable upper limit of a constant-pressure gas thermometer.

30.67. A thermocouple utilizes the thermoelectric effect. Two dissimilar metals are connected to form an electric circuit. When the two junctions are at different temperatures, a voltage proportional to this temperature difference is generated. The thermocouple is adaptable to a large range of temperatures, and it can be made to have a very small heat capacity, with a resulting small characteristic time. If the actual temperature at the input junction is the quantity to be measured, then the temperature at the reference junction must be known by other means.

30.68. All the foregoing components are approximately linear except the vapor pressure thermometer. Deviations from linearity are small enough to be neglected except for very precise work or for large ranges of temperature.

30.69. Pyrometers have been omitted from Information Summary 30-10 because they are applicable only to a small and highly specialized portion of the instrument engineering field, and because they involve performance relations that are not readily stated in such a summary. Basically, a pyrometer involves measuring radiation from a high-temperature source and applying the Stefan-Boltzmann law and Planck's radiation laws to compute the temperature of the source. Either total spectrum energy or energy in a narrow band of wavelengths may be used as the basis of measurement and computation. Pyrometers are described and references given in Chapter 31 (see paragraphs 31.20 through 31.23 and Description Summary 31-1).

30.70. The dynamic performance of temperature-measuring devices is treated at length in Chapter 31.

30.71. Fluid Components (see Information Summary 30-11). According to their application, fluid components can be classified as pressure-measuring devices, signal generators, flow-measuring devices, valves, and pumps and motors.

30.72. Pressure-measuring devices operate in response to the difference in forces exerted by two sources of pressure. In a manometer, these forces act on the ends of a column of relatively dense liquid in a U-shaped tube, and cause a displacement of the liquid toward the lesser pressure until the difference in gravitational pressure between the two ends of the column balances the input pressure difference. The difference in height between the two ends of the column is the observable output quantity, and is linearly proportional to the applied pressure difference. In the other devices shown in Information Summary 30-11, the difference in forces acts against either elastic walls or a separate spring, and linearity in each device depends on the particular construction used. For an analysis of the dynamic performance of the pressure-measuring components shown in Information Summary 30-11, together with descriptions of numerous other pressure-measuring components, see Chapter 33.

30.73. A nozzle flapper is a positional signal generator in which the distance of the flapper from the nozzle is the input. The change in flow pattern as the flapper is brought toward the nozzle causes a change in flow rate and pressure drop through the nozzle. Since the nozzle is fed through a fixed constriction, the pressure in the pipe between the constriction and the nozzle is an output signal representing the position of the flapper. This input-output relationship is roughly exponential.

30.74. Flow-measuring devices operate by virtue of Bernoulli's theorem (see Eq. (23) of Information Summary 30-6) to measure flow velocity in terms of an increment of pressure. In a pitot tube, this increment is the increase in pressure that results from decelerating the small portion of the flow that impinges on the end

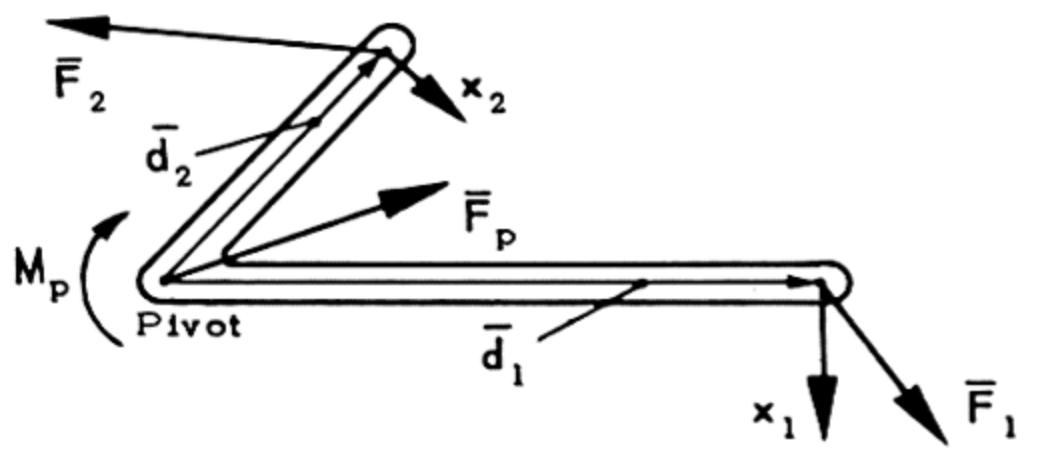
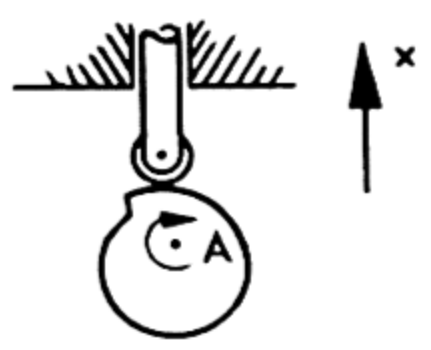
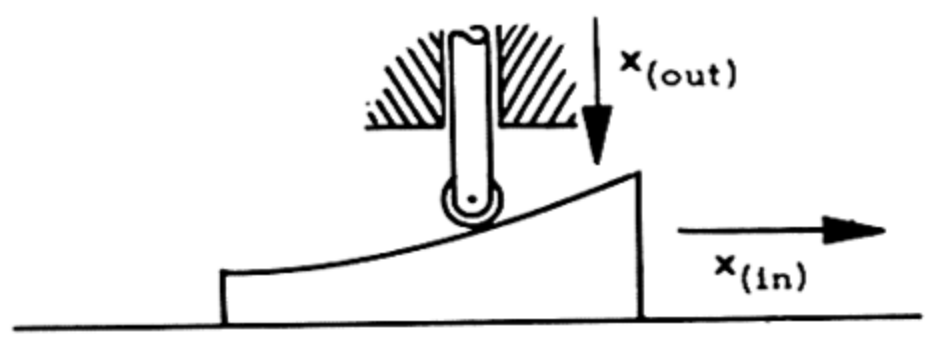
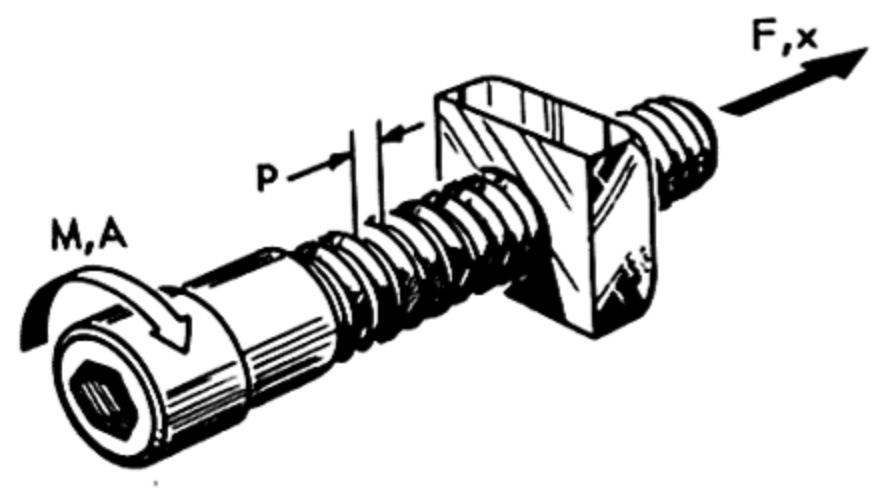
of the tube. In a venturi tube, this increment is the decrease in pressure that results from the increased flow velocity through the throat of the tube. In both of these devices, the flow velocity is proportional to the square root of the pressure difference, with a compressibility correction required for gases flowing at high speed. A frictionless fluid would theoretically recover its full initial pressure where the expanding outlet of a venturi tube reaches the same diameter as the entrance. Actually, viscous fluids can recover only about three quarters of the pressure drop. The same square-root relationship of velocity to pressure holds when other forms of constriction are used in place of a venturi tube, but an empirical calibration coefficient must be included. A flow nozzle introduces more turbulence and friction, thus allowing less pressure recovery than the venturi tube; an orifice plate introduces still more turbulence, and allows practically no pressure recovery.

30.75. Valves perform a variety of functions that include directing flow (routing, commutating, or reversing), controlling flow rate, controlling pressure, generating a positional signal, and amplifying. The relationship of flow rate proportional to the square root of pressure drop holds in pressure and flow control. Valves can be designed for any desired relationship, including linearity, between valve position and flow area. By using empirical knowledge of flow through valve openings, the relationship between valve position and flow rate can be made to approximate any desired function. Most valves are externally controlled; the principal exceptions are those controlled by direction of flow (check valve), by pressure (relief valve), or by liquid level (float valve). Some of the more elaborate configurations of valves combine several functions. The balanced-pressure spool valve, for example, combines position detection, reversal, and approximately linear control of flow rate.

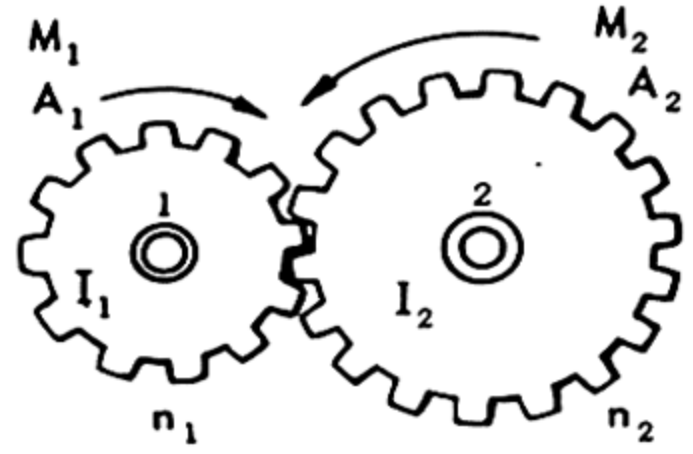
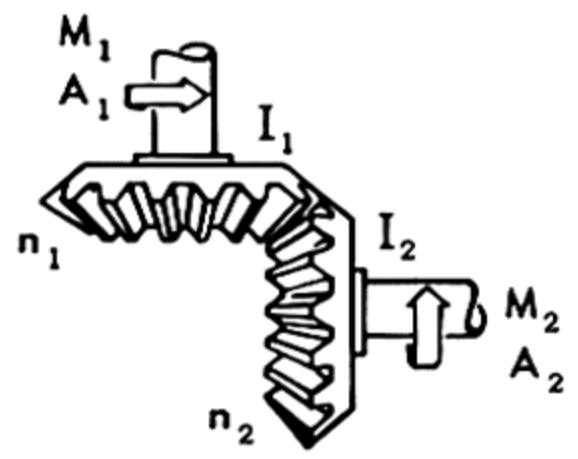
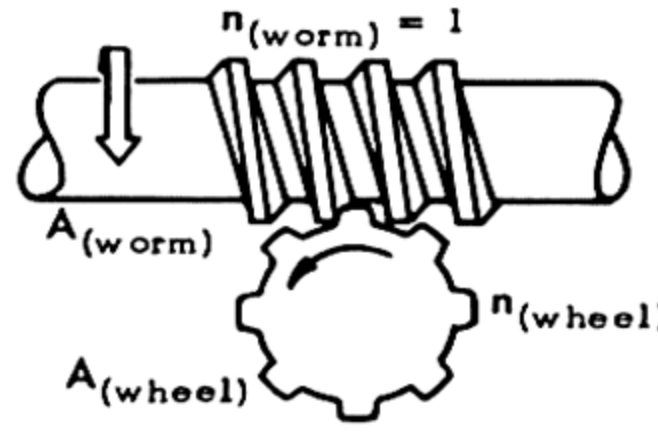
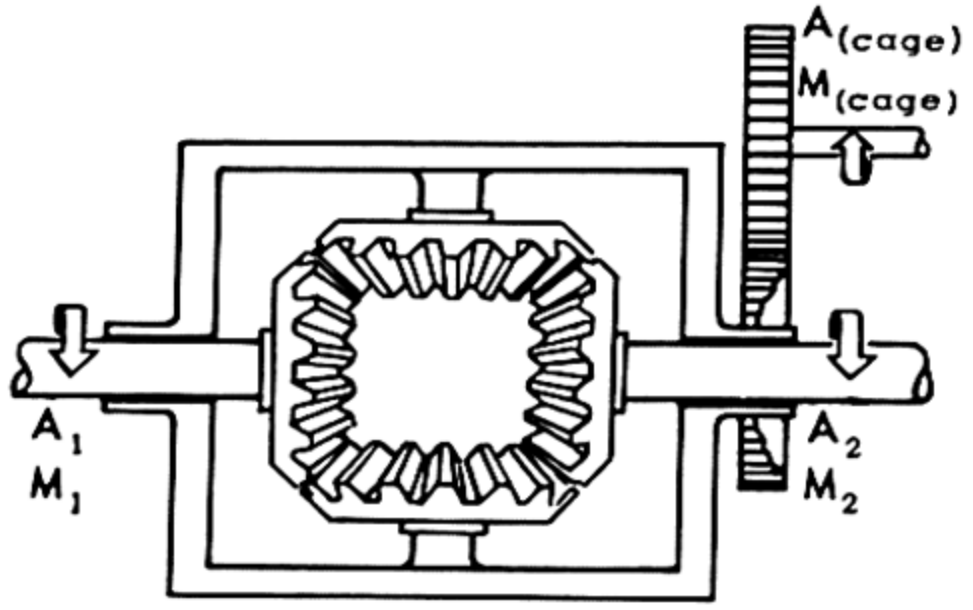
30.76. Pumps and motors can be called displacement devices or fluid-mechanical transducers. This class of fluid components also serves as a volume meter or flow integrator.

30.77. A diaphragm and a piston are examples of devices having limited translational motion. With suitable check or commutating valves, a diaphragm or a piston can deliver, or be driven by, a unidirectional flow. Bellows and other flexible enclosures may also be used. A gear pump is an example of a continuous-flow rotating device. Various forms of eccentric and follower, nutating disc, and movable-fin eccentric also belong to this class.

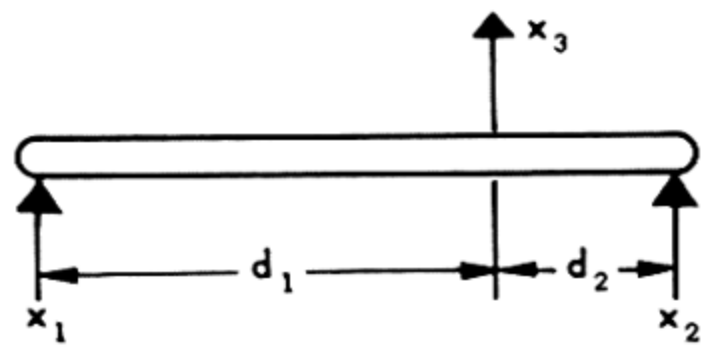
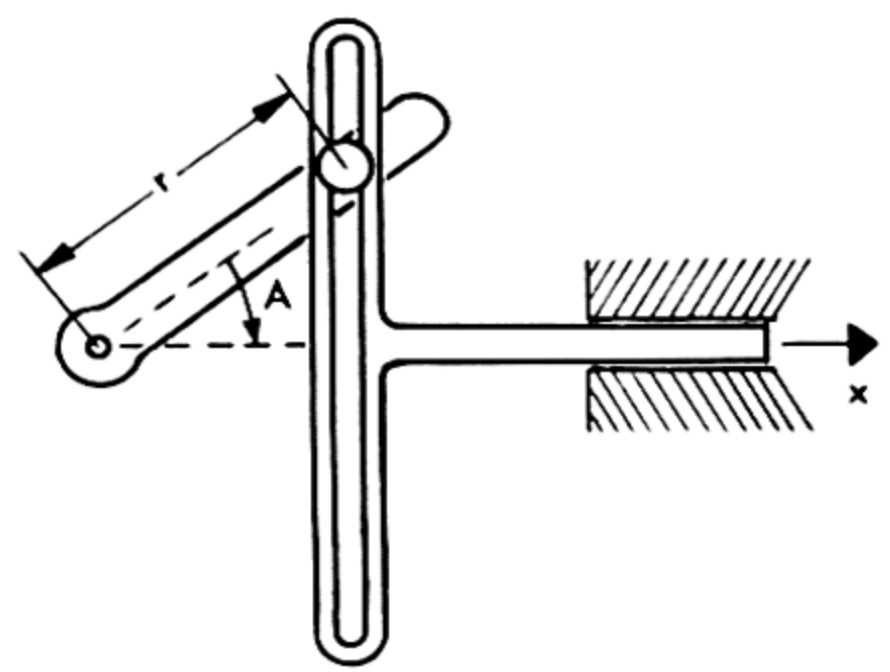
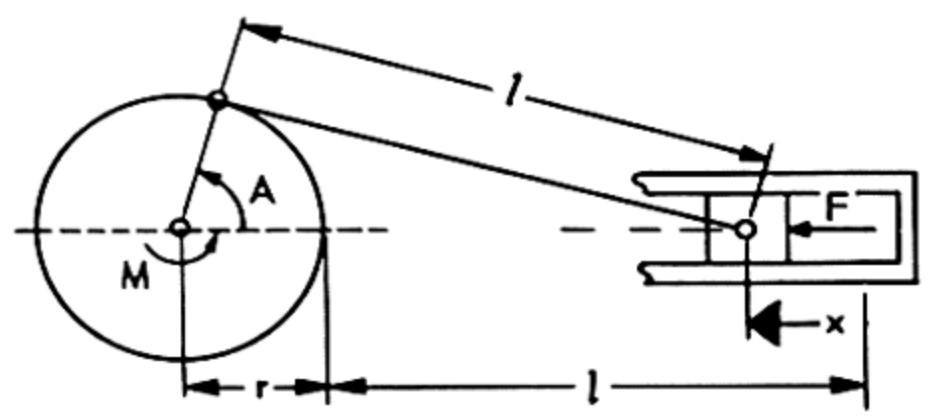
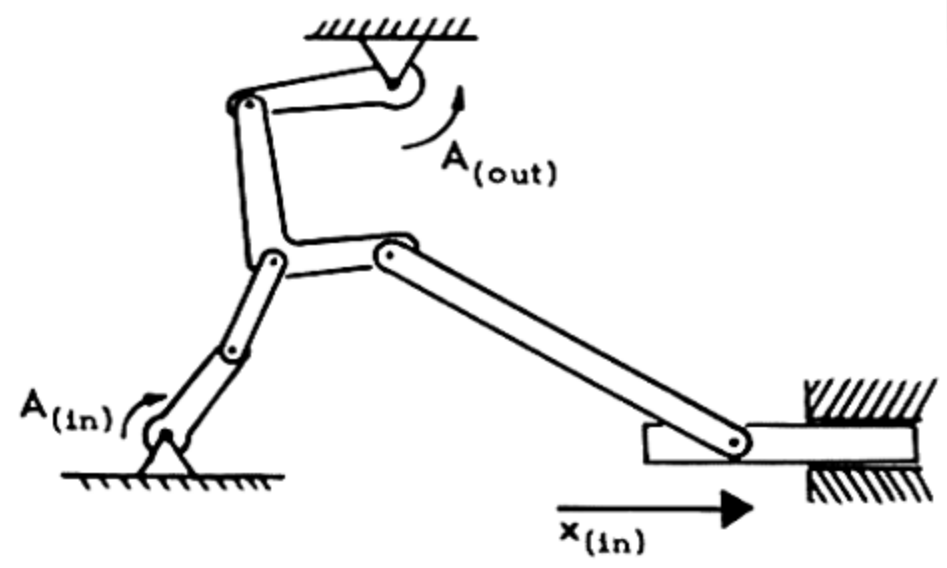
30.78. A radial pump or motor uses a rotating assembly of several pistons and a commutating valve. The flow can be varied or reversed by shifting the center of the rotor and thereby changing the stroke of the pistons. The same effect can also be obtained with pistons parallel to the axis and a drive with variable tilt. A pump with variable stroke and a motor connected to form a closed hydraulic circuit constitute an effective variable-speed transmission with a very small rotational inertia.

Figure	Component and Performance Relation	Reference
	*a) Levers* $\Sigma\bar{F} = \bar{F}_1 + \bar{F}_2 + \bar{F}_p = 0$ (1) $\Sigma\bar{M}_p = \bar{d}_1 \times \bar{F}_1 + \bar{d}_2 \times \bar{F}_2 = 0$ (2) $\frac{x_1}{x_2} = \frac{d_1}{d_2}$ (3)	Jones, Ingenious Mechanisms for Designers and Inventors (J2), Vols. I and II. Maleev, Machine Design (M3). Pearce, Principles of Mechanism (P3). Sloane, Engineering Kinematics (S8). Spotts, Design of Machine Elements (S12).
 	*b) Cams* *Rotating:* $x = f(A)$ (4) *Translating:* $x_{(out)} = f(x_{(in)})$ (5)	
	*c) Screws* $M = \frac{Fp}{2\pi}$ (6) $x = p\frac{A}{2\pi}$ (7)	

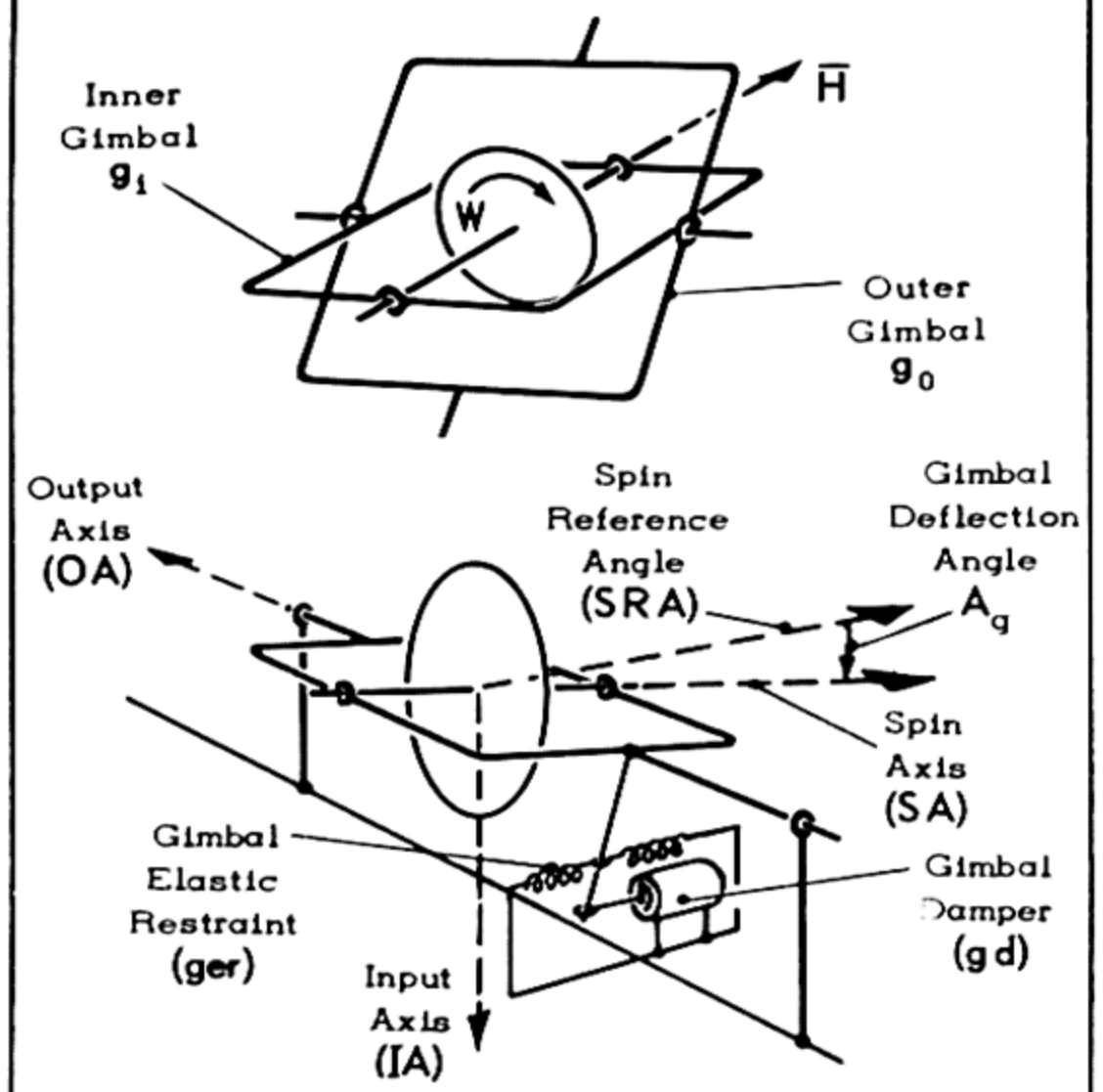
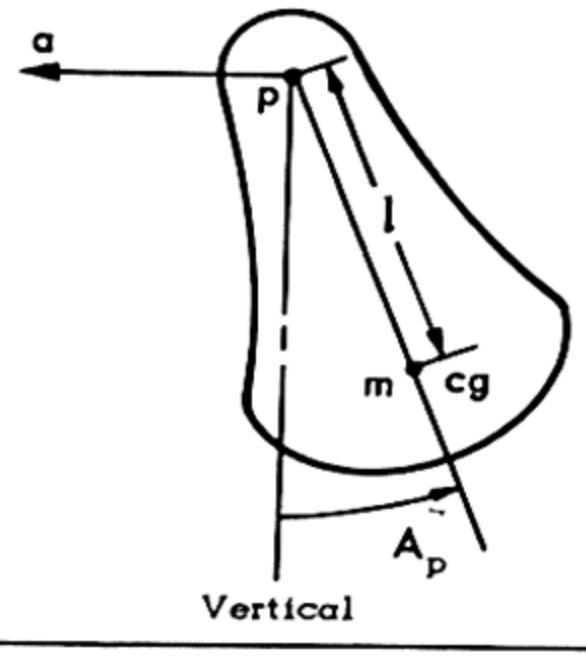
Information Summary 30-7. Mechanism components. (Page 1 of 5)

Figure	Component and Performance Relation	Reference
	*d) Gears* *Spur or bevel:* $\frac{A_1}{A_2} = \frac{n_2}{n_1} = \frac{M_2}{M_1}$ (8) Referred to shaft 1 Total $I = I_1 + I_2\left(\frac{n_1}{n_2}\right)^2$ (9) Referred to shaft 2 Total $I = I_2 + I_1\left(\frac{n_2}{n_1}\right)^2$ (10)	Buckingham, Analytical Mechanics of Gears (B16). Kuntny, "Gear Standards and Design" (K2). Martin, "Designing Instrument Gearing" (M5). Spotts, Design of Machine Elements (S12).
		
	*Single-pitch worm and wheel:* $n_{(worm)} = 1$; i.e., worm advances one tooth per revolution (11) $\frac{A_{(worm)}}{A_{(wheel)}} = n_{(wheel)}$ (12)	
	*Differential:* $A_{(cage)} = \frac{1}{2}(A_1 + A_2)$ (13) $M_1 = M_2 = -\frac{1}{2} M_{(cage)}$ (14)	

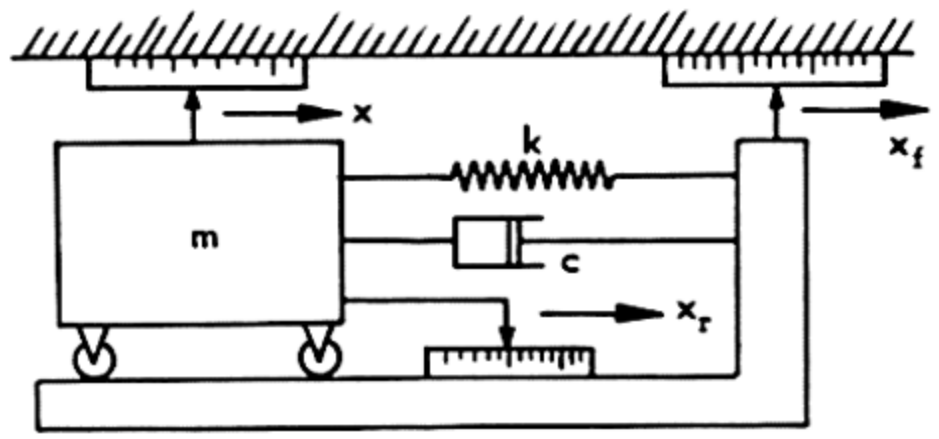
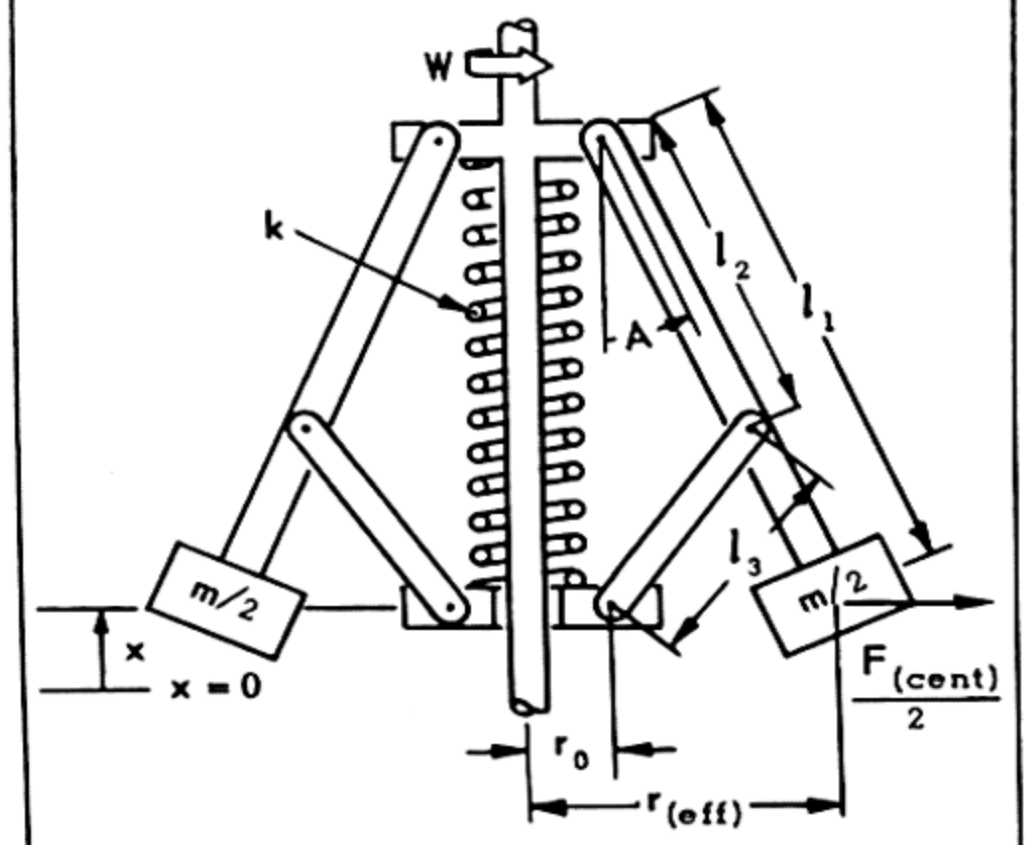
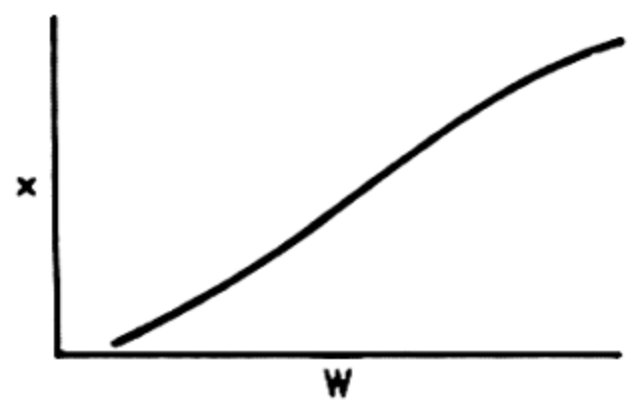
Information Summary 30-7. Mechanism components. (Page 2 of 5)

Figure	Component and Performance Relation	Reference
	**e) *Linkages*** *Summing:* $x_3\left(\frac{d_1 + d_2}{d_1 d_2}\right) = \frac{x_1}{d_1} + \frac{x_2}{d_2}$ (15)	Hrones and Nelson, Analysis of the Four-bar Linkage (H5). Pearce, Principles of Mechanism (P3). Sloane, Engineering Kinematics (S8). Svoboda, Computing Mechanisms and Linkages (S14).
	*Sinusoidal:* $x = r \cos A$ (16)	
	*Crank and connecting rod:* $\frac{x}{r} = 1 - \cos A + \frac{l}{r} - \sqrt{\left(\frac{l}{r}\right)^2 - \sin^2 A}$ (17) $M = Fr\left(\sin A + \frac{\frac{1}{2}\frac{r}{l}\sin 2A}{\sqrt{1 - \left(\frac{r}{l}\sin A\right)^2}}\right)$ (18)	
	*General linkage:* $A_{(out)} = f(A_{(in)}, x_{(in)})$ (19)	

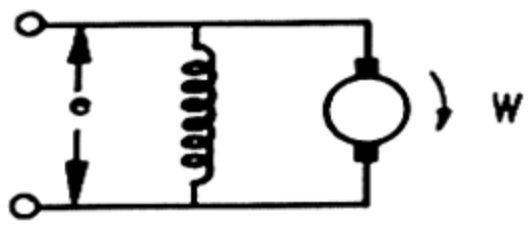
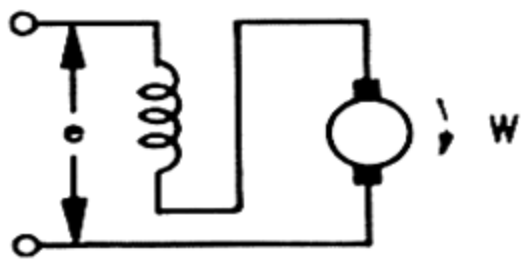
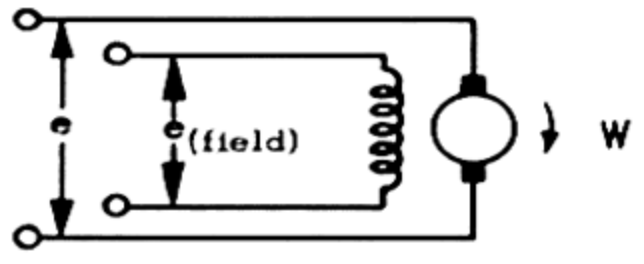
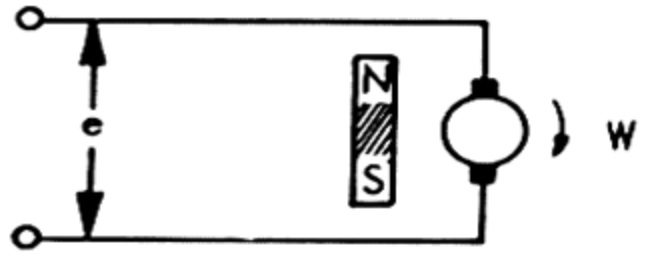
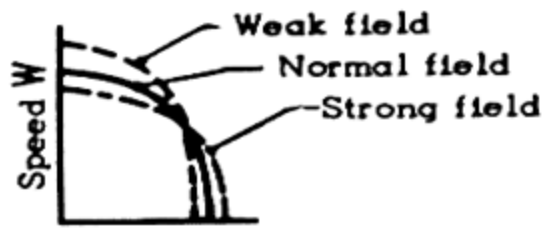
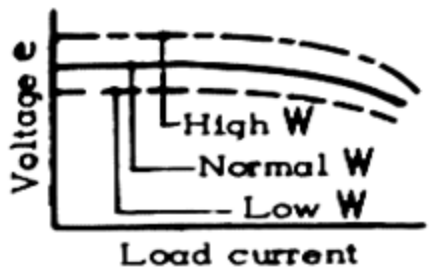
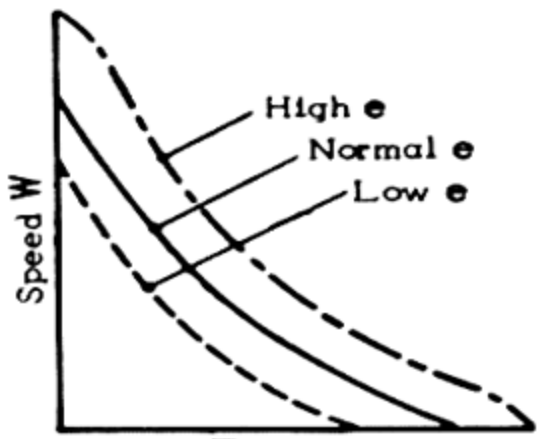
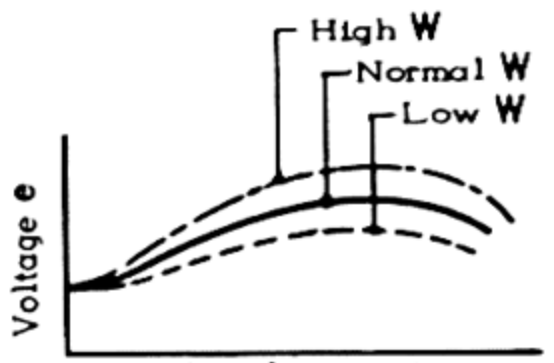
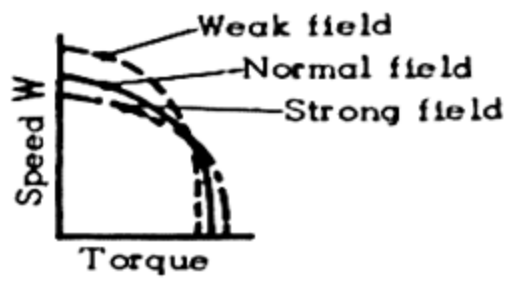
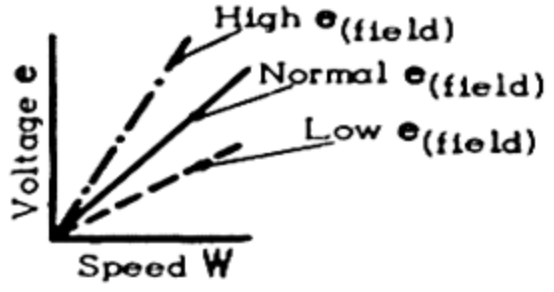
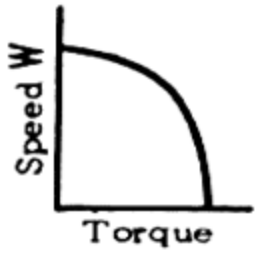
Information Summary 30-7. Mechanism components. (Page 3 of 5)

Figure	Component and Performance Relation	Reference
	*f) Gyroscopes* *General:* $\bar{M} = \left(\frac{d\bar{H}}{dt}\right)_I = \bar{W}_{I(g_i)} \times \bar{H}$ (20) I = inertial reference *Single degree of freedom:* Neglecting the angular acceleration of the case with respect to I, and considering A_g as a small angle. $-I_{(OA)}\ddot{A}_g - c_{(gd)}\dot{A}_g - k_{(ger)}A_g + HW_{(IA)} = 0$ (21) For the static case, $A_g = \frac{H}{k_{(ger)}} W_{(IA)}$ (22) If $k_{(ger)} = 0$, then statically $A_g = \frac{H}{c_{(gd)}} \int W_{(IA)}\, dt$ (23)	Crabtree, An Elementary Treatment of the Theory of Spinning Tops and Gyroscopic Motion (C5). Davidson, The Gyroscope and its Applications (D2). Deimel, Mechanics of the Gyroscope (D4). Draper, McKay, Lees, Instrument Engineering Vol. I, Chapter 7, and Vol. III, Chapter 40. Ferry, Applied Gyrodynamics (F6). Grammel, Der Kreisel, seine Theorie und seine Anwendungen (G5). Weems, An Introduction to the Study of Gyroscopic Instruments (W3). Whitman, Wales and Andersen, "The Type H Gyro, Computing and Accelerometer Units" (W2).
	*g) Pendulums* $I_p\ddot{A}_p + mglA_p = -I_p \frac{a}{R_E} + mal$ (24) A_p is a small angle a is the horizontal acceleration of the pivot point with respect to the earth R_E = the radius of the earth Period $= 2\pi \sqrt{\frac{I_p}{mgl}}$ (25)	Sears, Principles of Physics (S3), Vol. I. Whitman, Wales and Andersen, "The Type H Gyro, Computing and Accelerometer Units" (W2). Wrigley, "An Investigation of Methods Available for Indicating the Direction of the Vertical from Moving Bases" (W7). Wrigley, "Schuler Tuning Characteristics in Navigational Instruments" (W8).

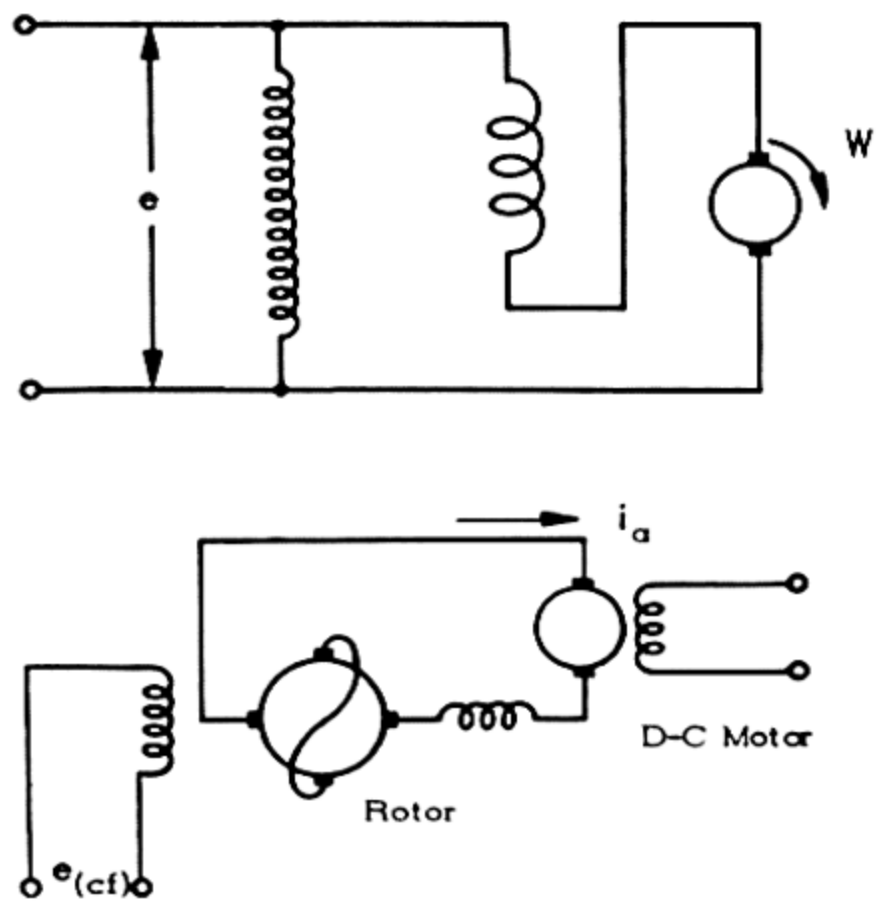
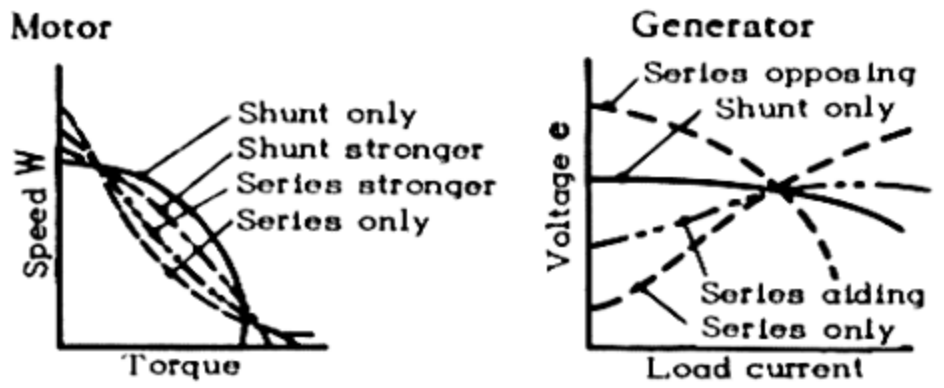
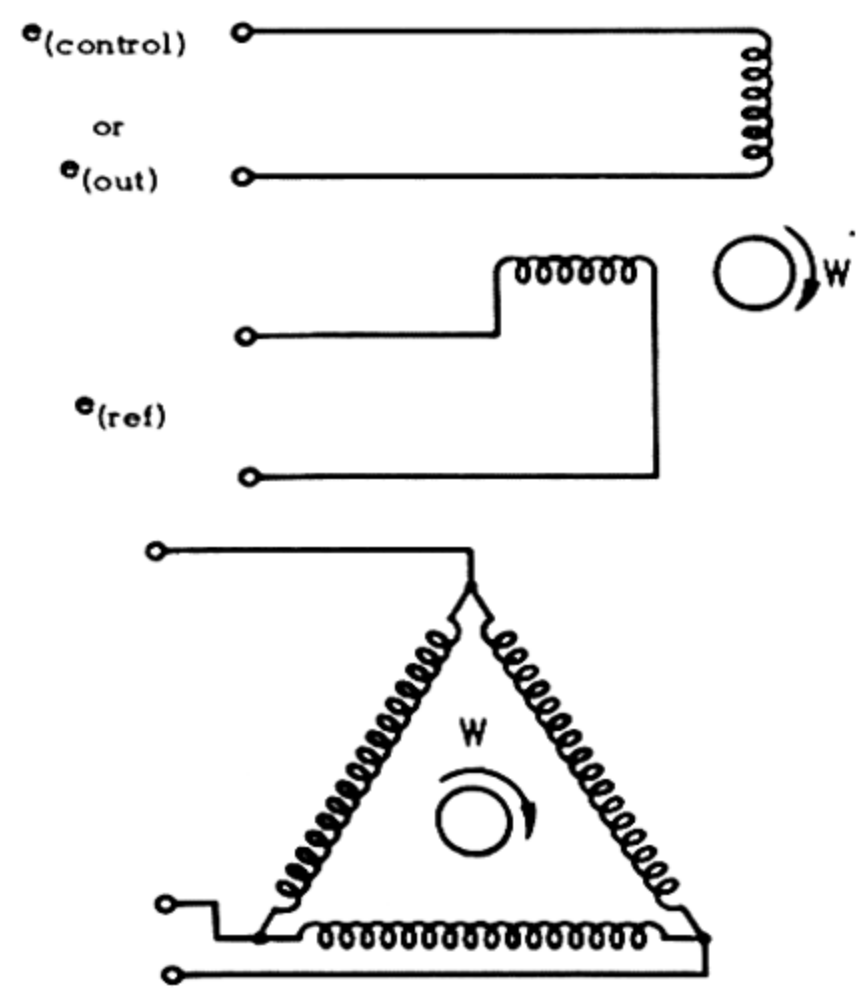
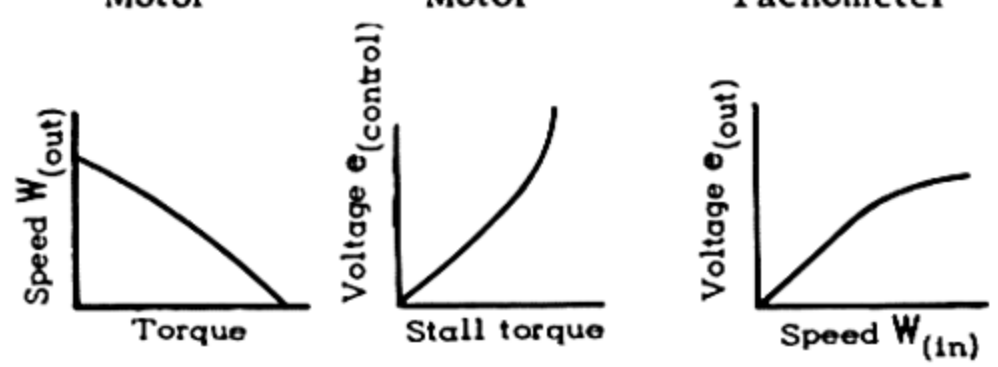
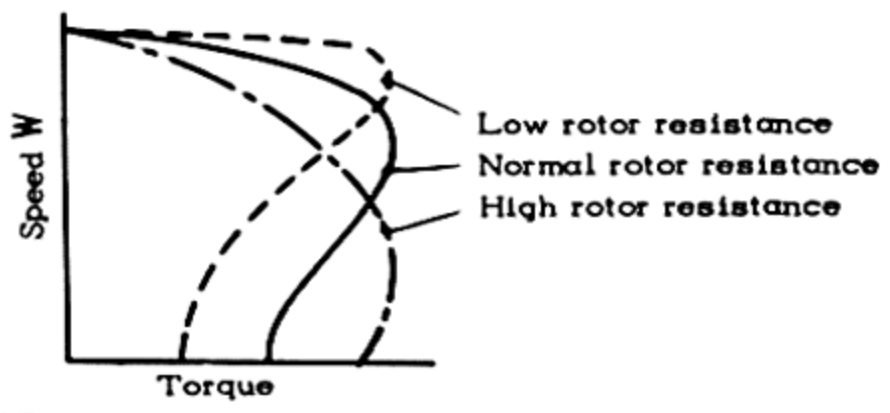
Information Summary 30-7. Mechanism components. (Page 4 of 5)

Figure	Component and Performance Relation	Reference
	*h) Seismic elements* $x = x_r + x_f$ (26) $-m\ddot{x} - c\dot{x}_r - kx_r = 0$ (27) $m\ddot{x} + c\dot{x} + kx = c\dot{x}_f + kx_f$ (28) $m\ddot{x}_r + c\dot{x}_r + kx_r = -m\ddot{x}_f$ (29)	Bernhard, Mechanical Vibrations (B11). Den Hartog, Mechanical Vibrations (D5). Draper and Wrigley, "An Instrument for Measuring Low Frequency Accelerations in Flight" (D8). Draper, McKay and Lees, Instrument Engineering, Vol. III, Chapter 35. Timoshenko, Vibration Problems in Engineering (T4).
	*i) Centrifugal tachometers* $F_{(cent)} = mW^2 (r_0 + l_1 \sin A)$ (30) $x = \frac{W^2}{k/m} f(r_0, l_1, l_2, l_3, x)$ (31) 	Sontag and Brombacher, Aircraft Power-Plant Instruments (S11).

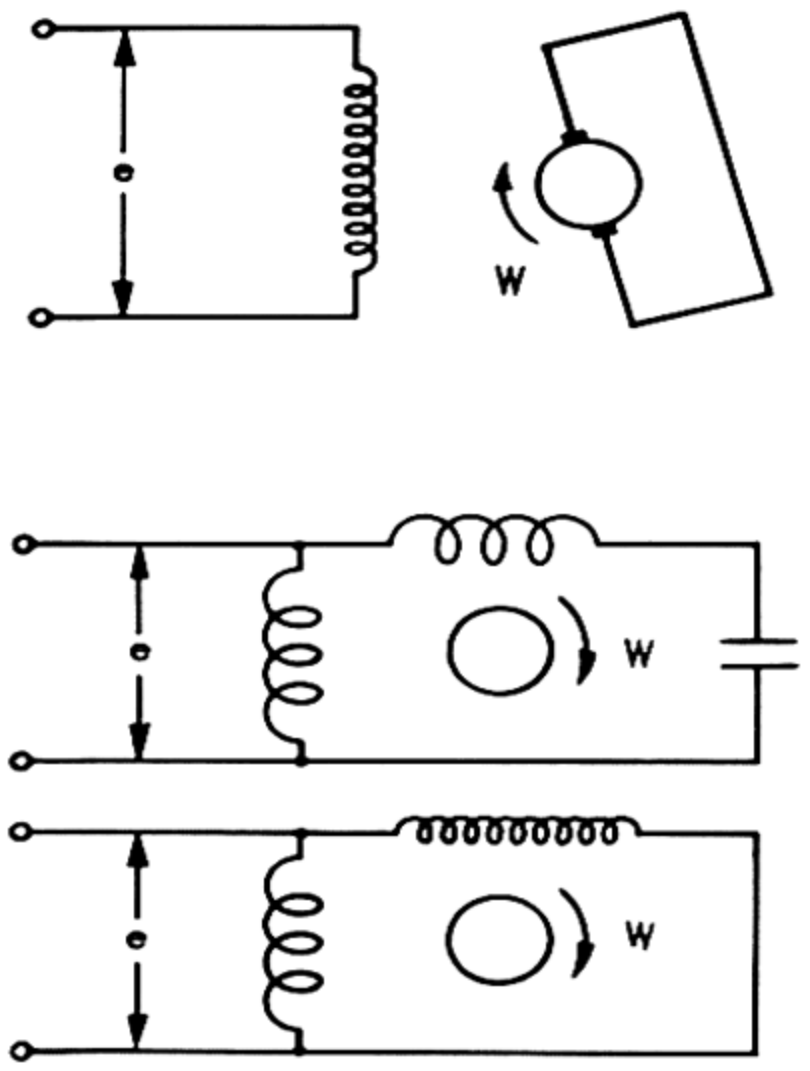
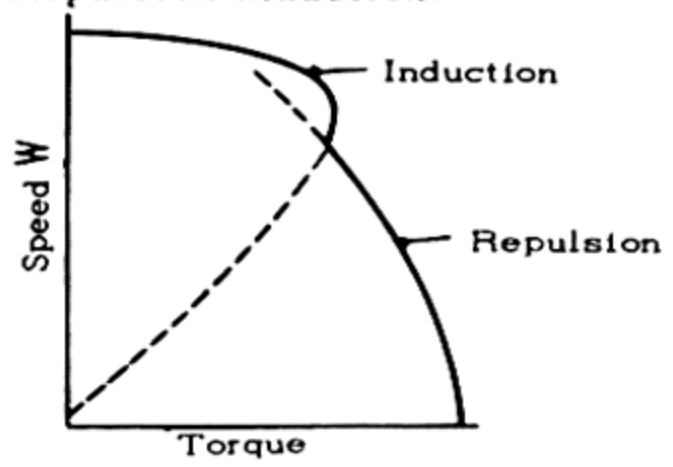
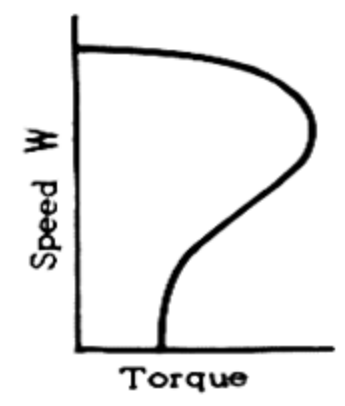
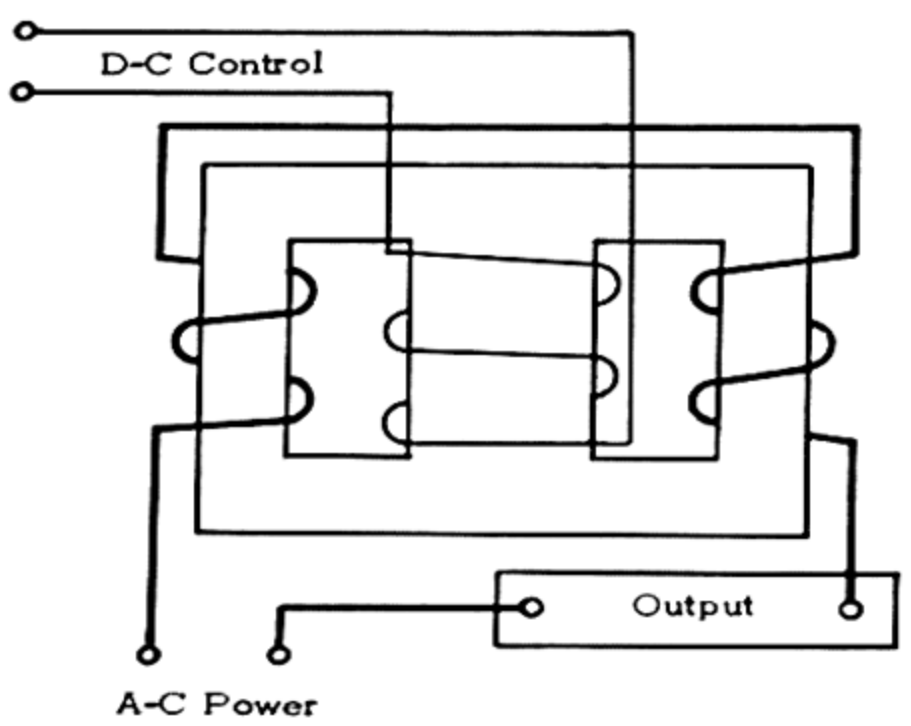
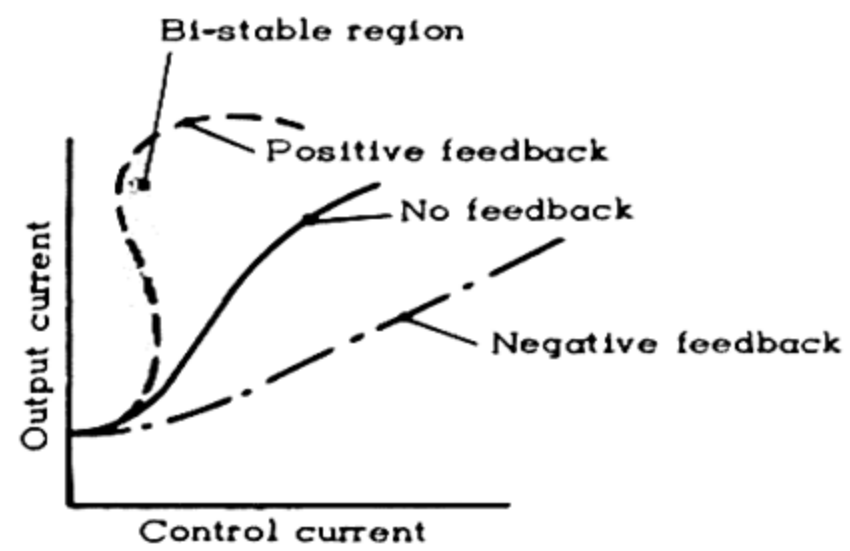
Information Summary 30-7. Mechanism components. (Page 5 of 5)

Figure	Component and Performance Relation	Reference
   	*a) D-C motors and generators* *Shunt:* Motor  Generator  e = constant *Series:* Motor (a-c or d-c)  Generator  *Separately excited:* Motor  Generator  *Permanent magnet:* Motor  Generator  	Batcher and Moulic, The Electronic Control Handbook (B1). Blackburn, Components Handbook (B13). Fitzgerald, Basic Electrical Engineering (F8). Fitzgerald and Kingsley, Electric Machinery (F10). Jones, Electric Control Systems (J3). M.I.T., Staff, E. E. Dep't, Magnetic Circuits and Transformers (M8). Pender and Del Mar, Electrical Engineers' Handbook (P4). Roters, Electromagnetic Devices (R7). Thaler and Brown, Servomechanism Analysis (T3). Veinott, Fractional Horsepower Electric Motors (V3).

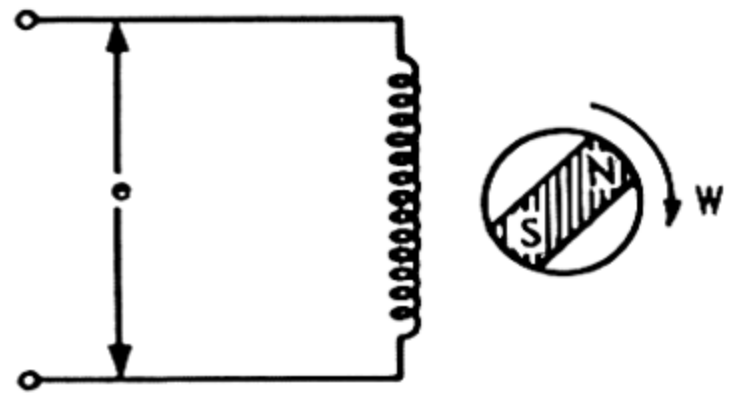
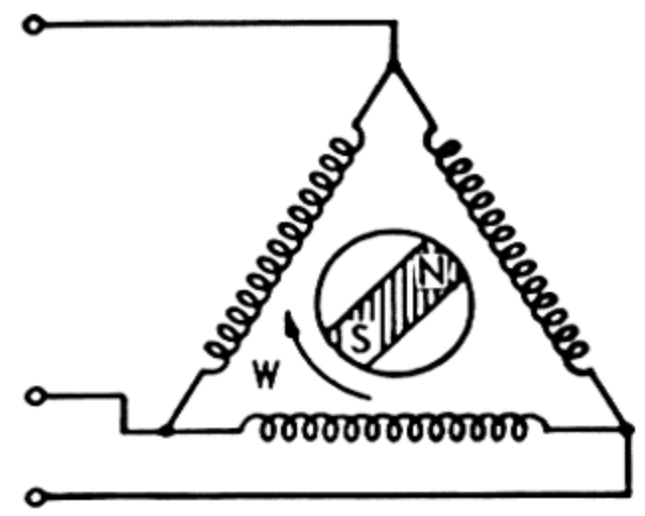
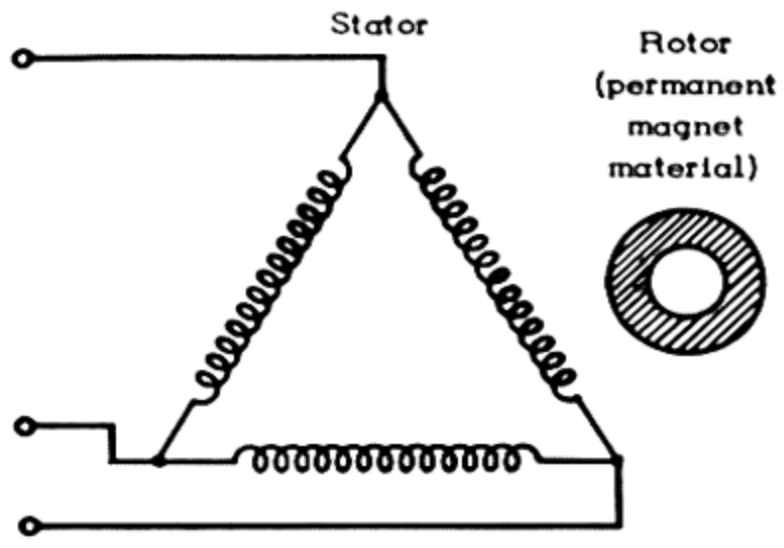
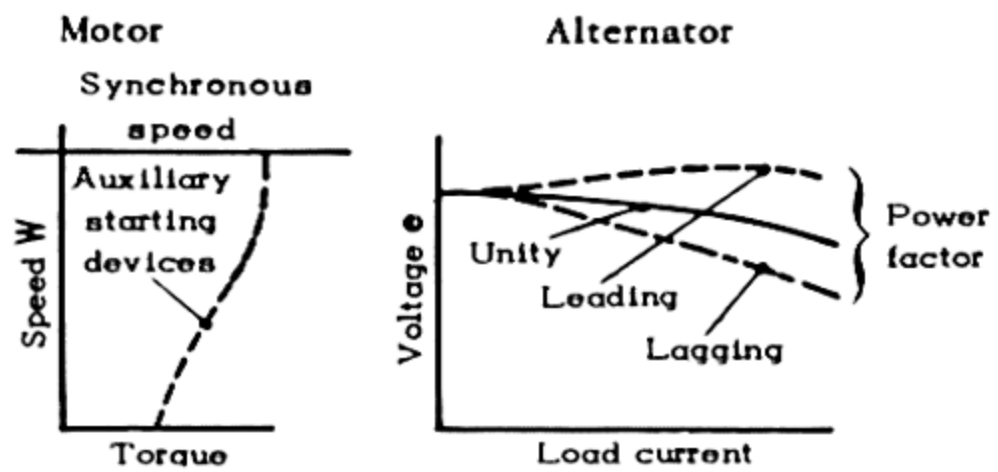
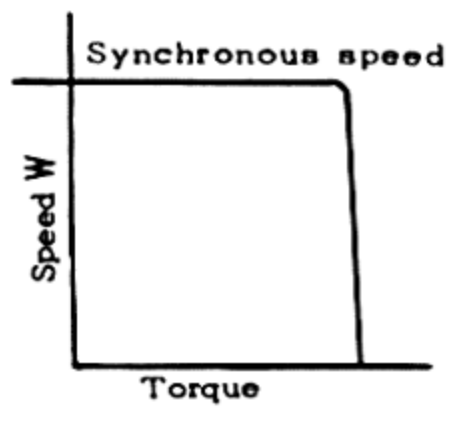
Information Summary 30-8. Electromagnetic components. (Page 1 of 9)

Figure	Component and Performance Relation	Reference
	*D-C motors and generators (continued)* *Compound:*  *Amplidyne:* $i_a \sim S_{[e_{(cf)};\, i_a]}\, e_{(cf)}$ (1)	Fitzgerald and Kingsley, Electric Machinery (F10). Greenwood, Holdam, and MacRae, Electronic Instruments (G3). James, Nichols, and Phillips, Theory of Servomechanisms (J1).
	*b) A-C induction motors and generators* *Two-phase:*  *Three-phase:* 	Lawrence, Principles of Alternating Current Machinery (L6). Frazier, "Analysis of Drag Cup A-C Tachometer" (F13). Moore, "Eddy Currents in Disks: Driving and Damping Forces on Torques" (M14). Smythe, "On Eddy Currents in a Rotating Disk" (S10).

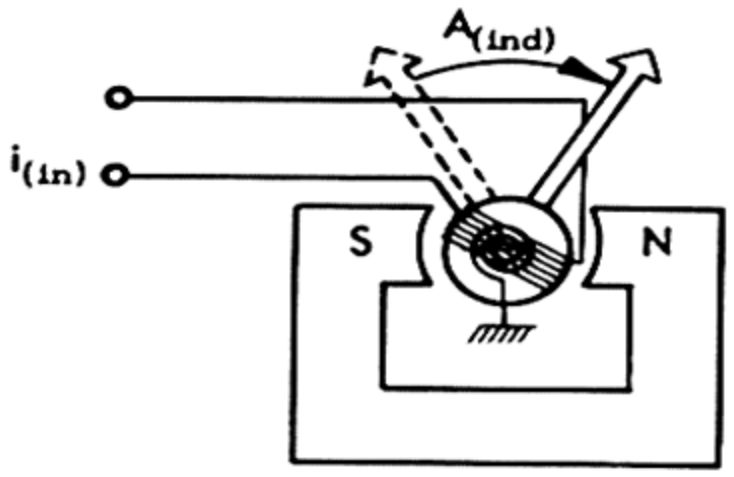
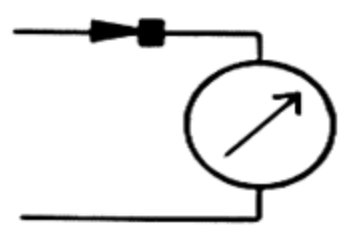
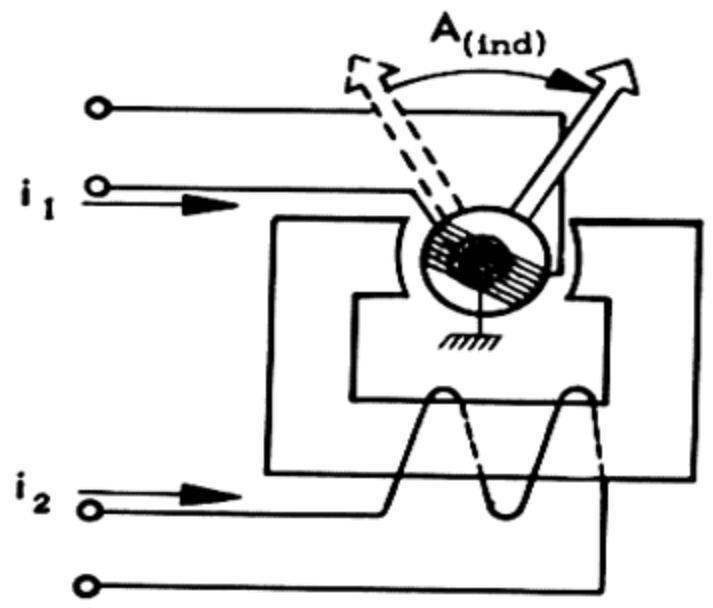
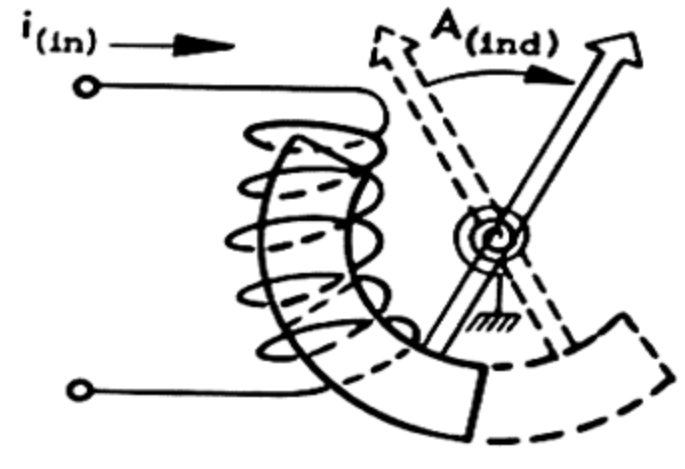
Information Summary 30-8. Electromagnetic components. (Page 2 of 9)

Figure	Component and Performance Relation	Reference
	***A-C induction motors and generators (continued)*** *Repulsion-induction:*  *Capacitor and Split-phase:* 	Lawrence, Principles of Alternating Current Machinery (L6).
	*c) Magnetic amplifier* 	Crow, Saturating Core Devices (C6). Finzi and Beaumarriage, "Magnetic Amplifier Characteristics" (F7). Fitzgerald, "Magnetic Amplifier Characteristics" (F9). Geyger, "A New Type of Magnetic Servo Amplifier" (G4). Lufcy, Schmid, and Barnhart, "An Improved Magnetic Servo Amplifier" (L11). Miles, "Bibliography of Magnetic Amplifier Devices and the Saturable Reactor Art" (M12). Smith, "A Transient Analyzer for Magnetic Amplifiers" (S9).

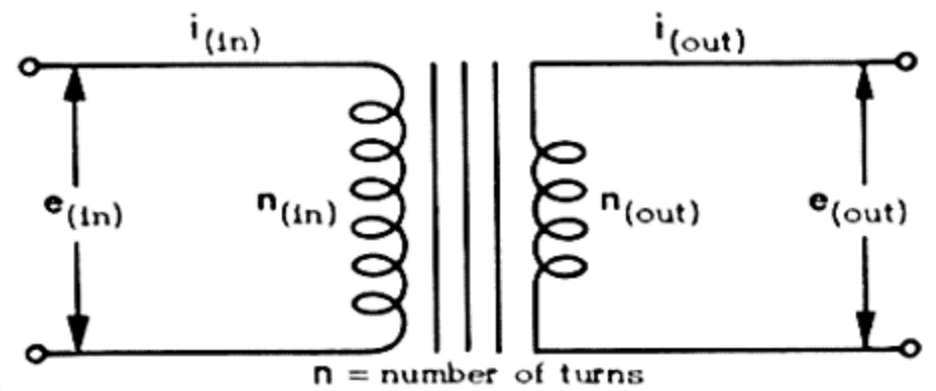
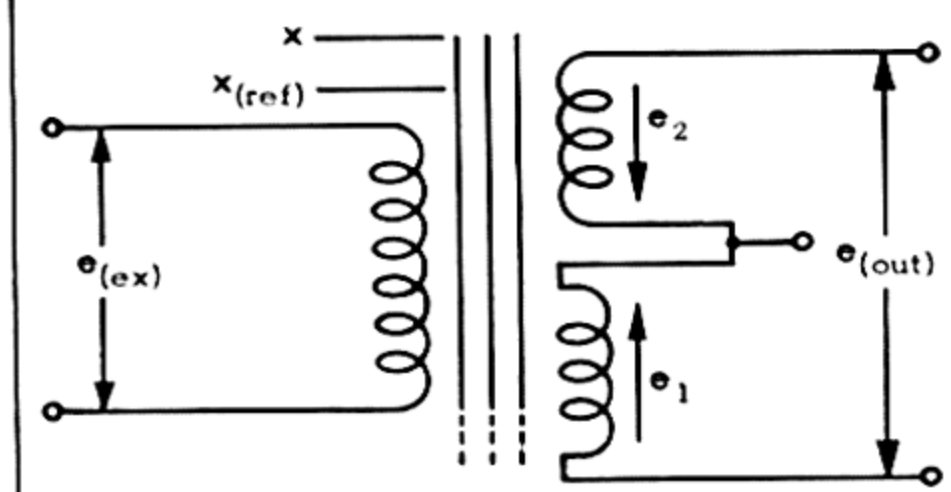
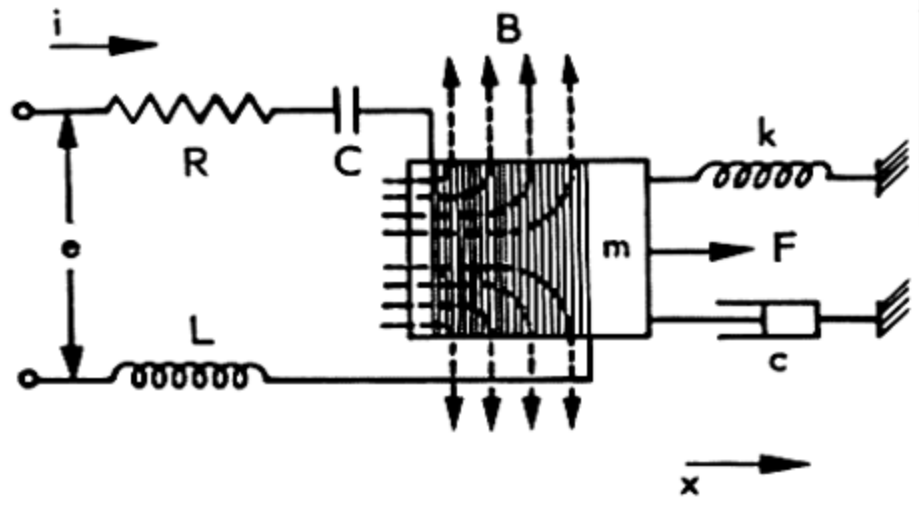
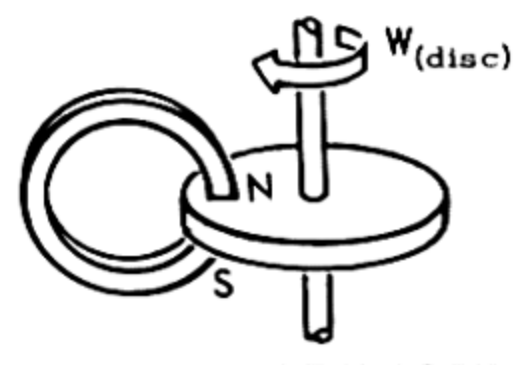
Information Summary 30-8. Electromagnetic components. (Page 3 of 9)

Figure	Component and Performance Relation	Reference
  	*d) A-C synchronous motors and generators* *Synchronous (also serves as a generator)* *Single-phase and three-phase:*  *Hysteresis:* 	Roters, "The Hysteresis Motor" (R8).

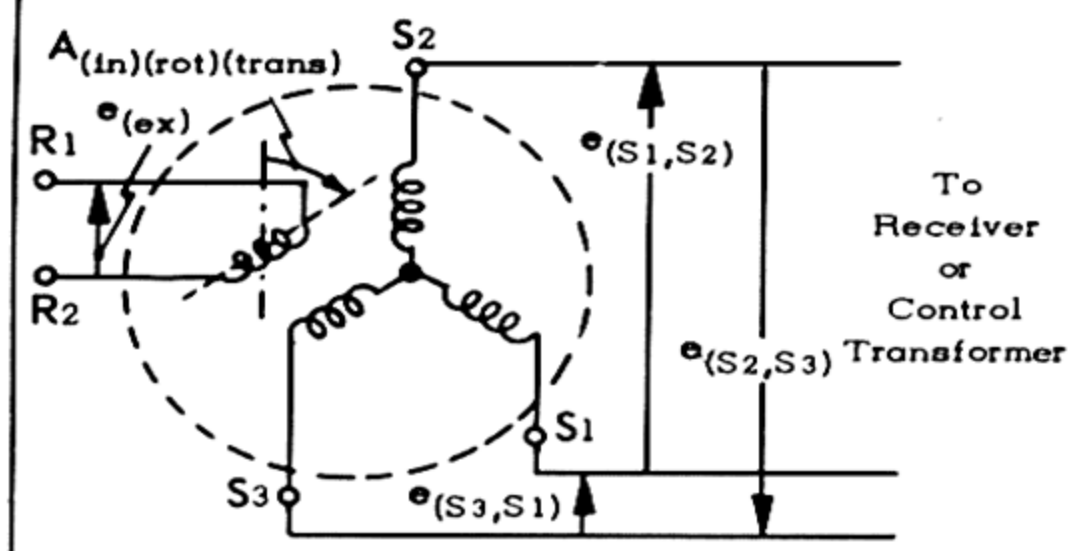
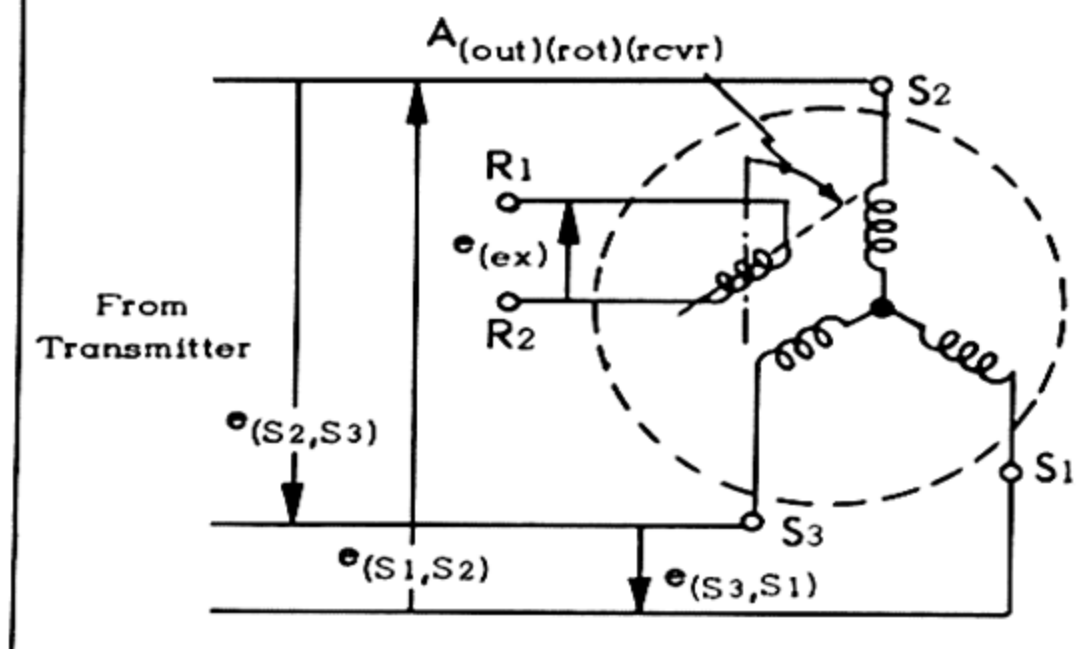
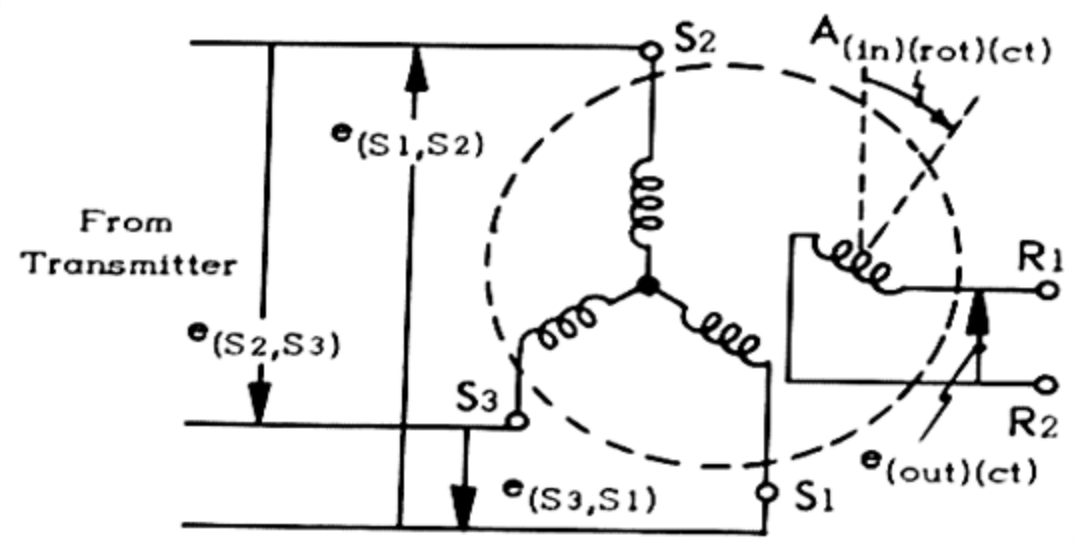
Information Summary 30-8. Electromagnetic components. (Page 4 of 9)

Figure	Component and Performance Relation	Reference
	*e) Meters* *D'Arsonval (d-c):* $A_{(ind)} = S_{[i;A]} i_{(in)}$ (2)	Drysdale and Jolley, Electrical Measuring Instruments (D9). Laws, Electrical Measurements (L7). Weston Electrical Instrument Corporation, The Instrument Sketch Book (W4).
(with rectifier for a-c) 		
(with thermocouple for r.f.) 		
	*Wattmeter (a-c or d-c):* $A_{(ind)} = S_{[i,i;A]} i_1 i_2$ (3)	
	*Moving iron (a-c or d-c):* $A_{(ind)} = S_{[i^2;A]} i^2_{(in)}$ (4)	

Information Summary 30-8. Electromagnetic components. (Page 5 of 9)

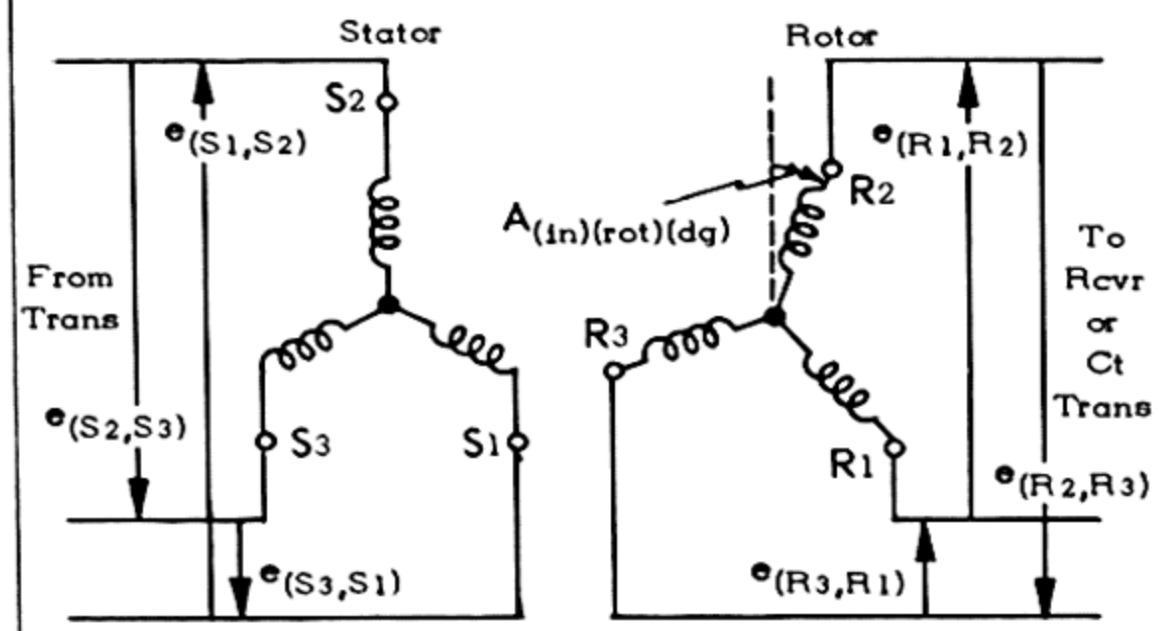
Figure	Component and Performance Relation	Reference
	*f) Transformers* *Ideal relationship:* $\frac{e_{(out)}}{e_{(in)}} = \frac{n_{(out)}}{n_{(in)}} = \frac{i_{(in)}}{i_{(out)}}$ (5) $\frac{e_{(out)}}{i_{(out)}} = \left(\frac{n_{(out)}}{n_{(in)}}\right)^2 \frac{e_{(in)}}{i_{(in)}}$ (6)	M.I.T., Staff, E. E. Dep't, Magnetic Circuits and Transformers (M8).
	*Differential transformer (positional signal generator):* At $x = x_{(ref)}$, $e_2 = e_1$, $e_{(out)} = 0$ (7) $e_{(out)} = S_{[e,x;e]} e_{(ex)} (x - x_{(ref)})$ (8)	Roberts, Mechanical Measurements by Electrical Methods (R6). Schaevitz, "The Linear Variable Differential Transformer" (S2).
	*g) Transducer (translational or linear)* $\begin{cases} m\ddot{x} + c\dot{x} + kx + nBli = F_{(out)} \text{ or } -F_{(app)} \\ L\frac{di}{dt} + Ri + \frac{1}{C}\int i\,dt + nBl\dot{x} = -e_{(app)} \text{ or } e_{(out)} \end{cases}$ (9) (10)	Beranek, Acoustics (B9). Olson, Elements of Acoustical Engineering (O2).
	*h) Eddy current damper* $M_{(disc)} = -S_{(dmp)[W;M]} W_{(disc)}$ (11)	Moore, "Eddy Currents in Disks: Driving and Damping Forces and Torques" (M14). Smythe, "On Eddy Currents in a Rotating Disk" (S10).

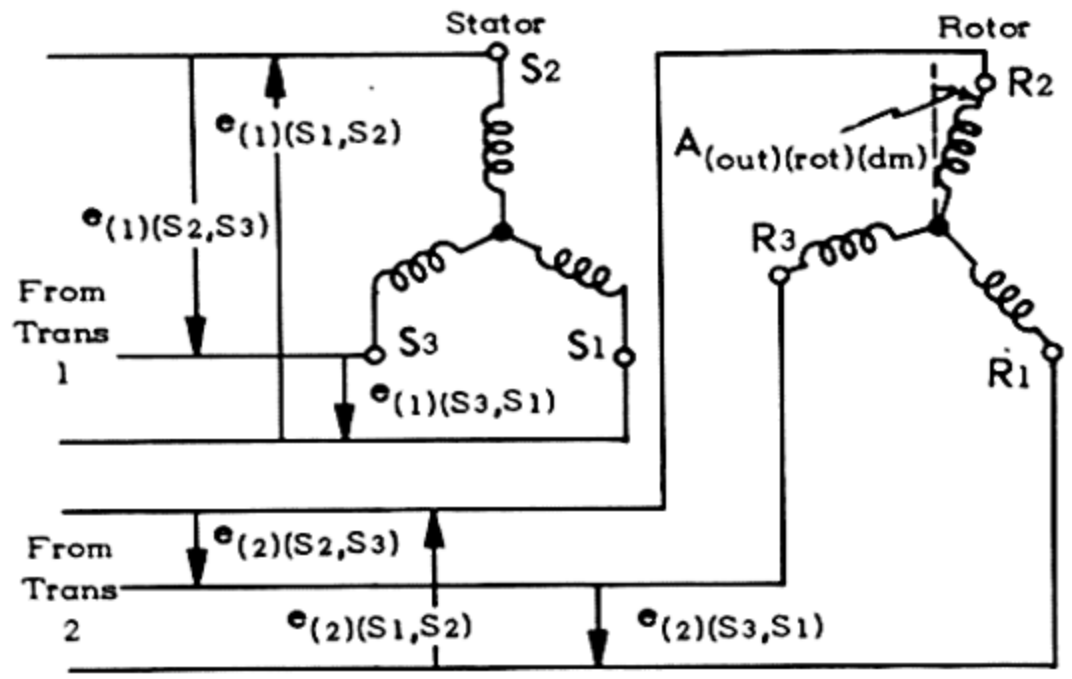
Information Summary 30-8. Electromagnetic components. (Page 6 of 9)

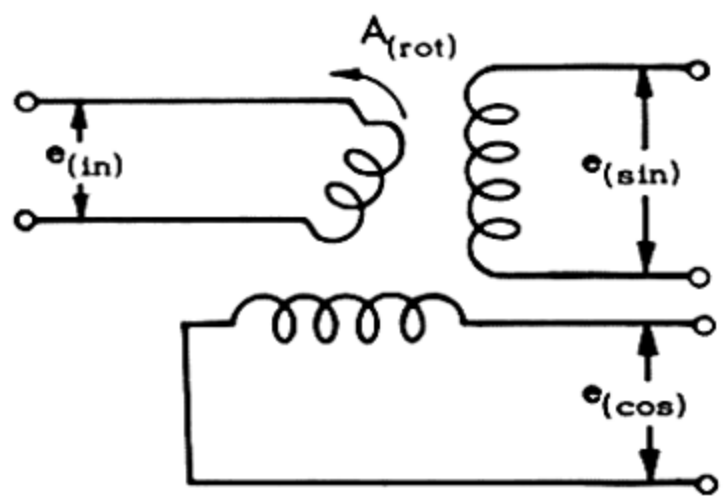
Figure	Component and Performance Relation	Reference
	*i) Synchros (selsyns, autosyns, teletorques, diehlsyns)(a-c)* *Transmitter (generator):* $e_{(S3,S1)} \sim e_{(ex)} \sin A_{(in)(rot)(trans)}$ (12) $e_{(S1,S2)} \sim e_{(ex)} \sin (A_{(in)(rot)(trans)} - 120°)$ (13) $e_{(S2,S3)} \sim e_{(ex)} \sin (A_{(in)(rot)(trans)} - 240°)$ (14) Note: The positive sense of the input angle is clockwise when rotation is viewed from the electrical-connection end of the synchro unit.	Blackburn, Components Handbook (B13). Greenwood, Holdam, and MacRae, Electronic Instruments (G3). James, Nichols, and Phillips, Theory of Servomechanisms (J1). Navy Department, BuOrd-BuShips, "United States Navy Synchros, Description and Operations" (N2).
	*Receiver (motor):* $M_{(rot)(rcvr)} \sim e_{(ex)} \sin (A_{(in)(rot)(trans)} - A_{(out)(rot)(rcvr)})$ (15) Note: The positive sense for each of these two angles is clockwise when rotation is viewed from the electrical-connection end of the synchro unit.	
	*Control transformer:* $e_{(out)(ct)} \sim \sin (A_{(in)(rot)(trans)} - A_{(in)(rot)(ct)})$ (16) Note: The positive sense for each of these two angles is clockwise when rotation is viewed from the electrical-connection end of the synchro unit. The winding of a control transformer rotor in its zero position is 90 degrees from the winding of a transmitter rotor in its zero position.	

Information Summary 30-8. Electromagnetic components. (Page 7 of 9)

Figure	Component and Performance Relation	Reference







Synchros (continued)

Differential generator:

$$e_{(R3,R1)} \sim \sin\left(A_{(in)(rot)(trans)} - A_{(in)(rot)(dg)}\right) \qquad (17)$$

Note: The positive sense for each of these two angles is clockwise when rotation is viewed from the electrical-connection end of the synchro unit.

$e_{(R1,R2)}$ lags $e_{(R3,R1)}$ by 120°

$e_{(R2,R3)}$ lags $e_{(R3,R1)}$ by 240°

Differential motor:

$$M_{(rot)(dm)} \sim \sin\left(A_{(in)(rot)(trans)1} - A_{(in)(rot)(trans)2} - A_{(out)(rot)(dm)}\right) \qquad (18)$$

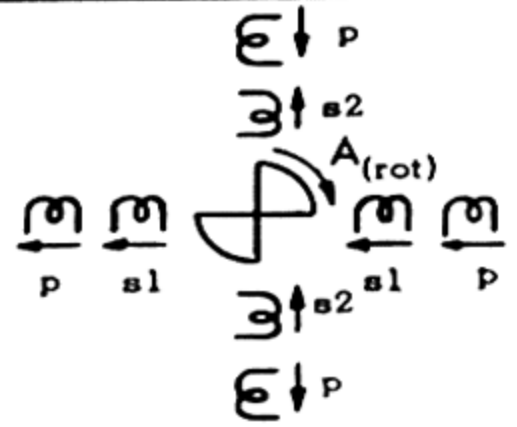
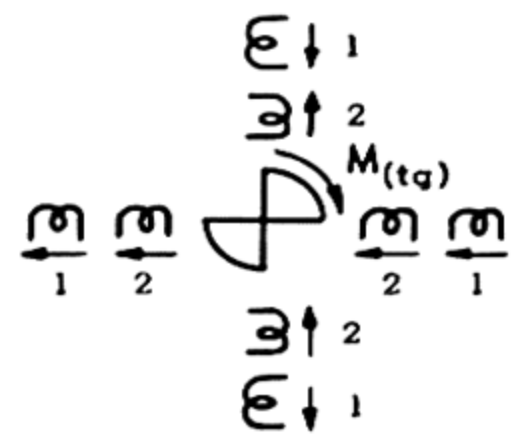
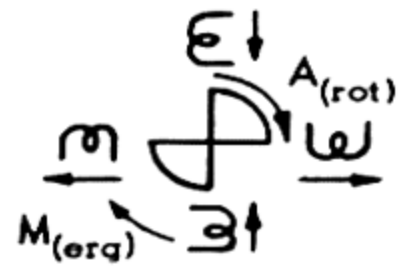
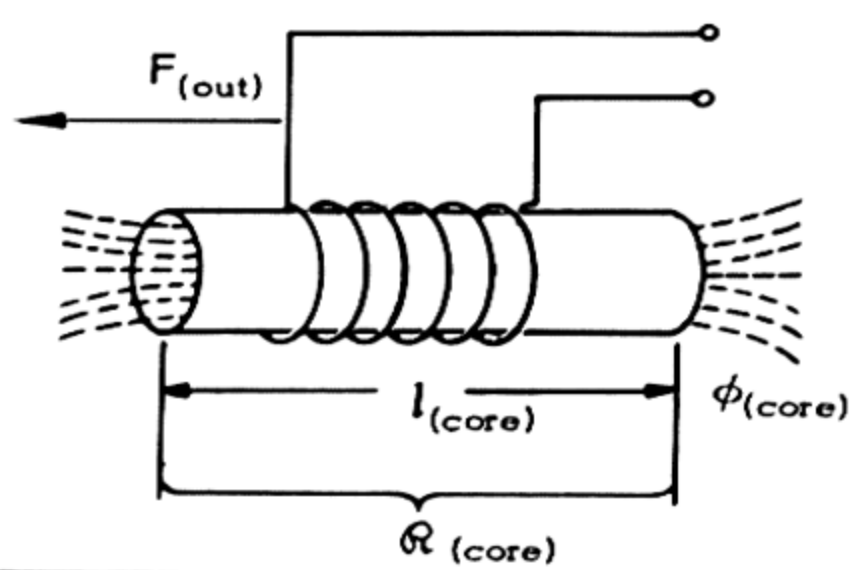
Note: The positive sense for each of these three angles is clockwise when rotation is viewed from the electrical-connection end of the synchro unit.

Angle resolver:

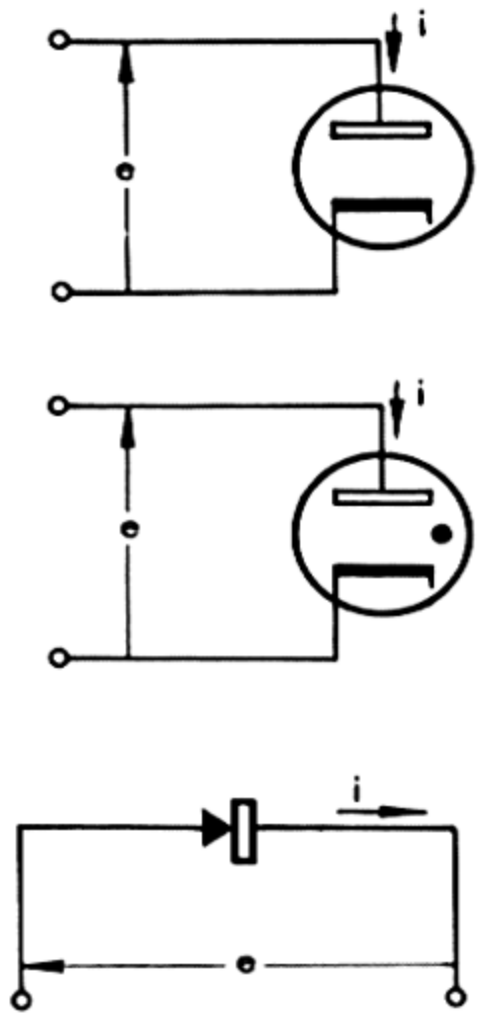
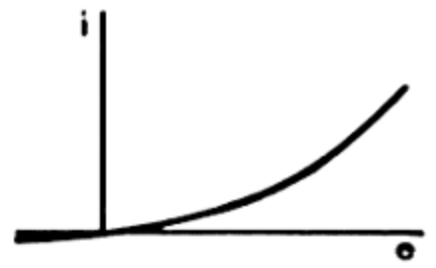
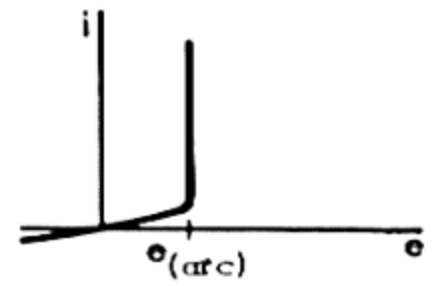
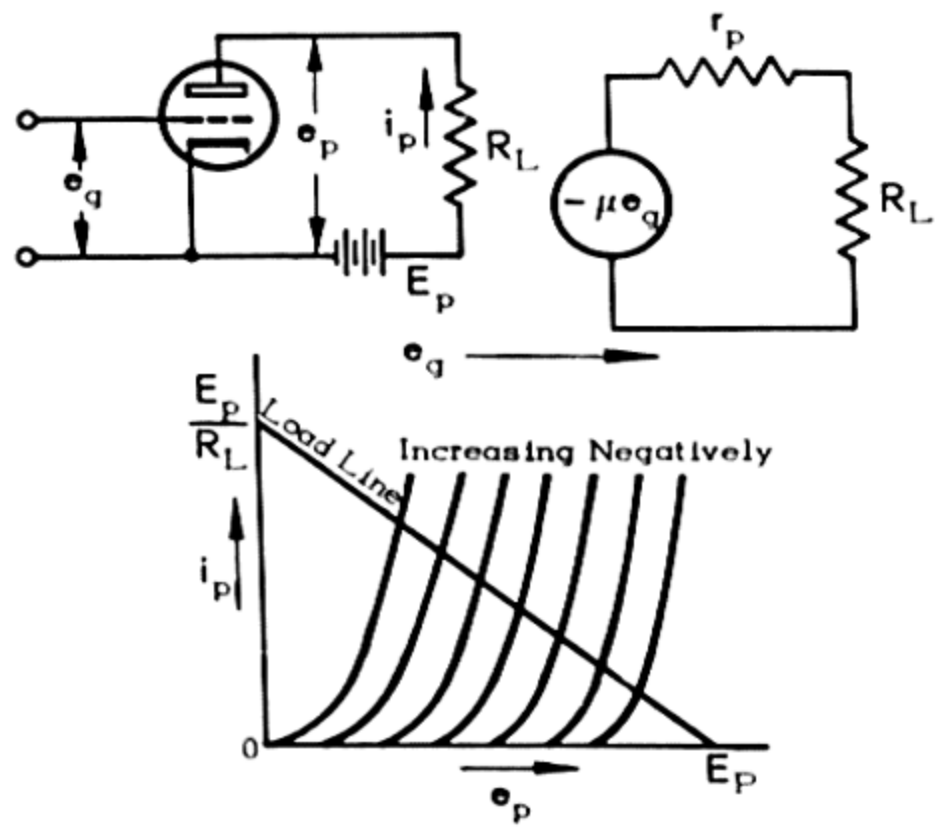
$$e_{(sin)} \sim e_{(in)} \sin A_{(rot)} \qquad (19)$$

$$e_{(cos)} \sim e_{(in)} \cos A_{(rot)} \qquad (20)$$

Information Summary 30-8. Electromagnetic components. (Page 8 of 9)

Figure	Component and Performance Relation	Reference
	*j) Microsyns* *Signal generator (a-c):* $e_{(sg)} = e_{s1} + e_{s2}$ (21) $= S_{(sg)[1,A;e]} i_p A_{(rot)}$ (22) p = primary winding s = secondary winding	Haltmaier, "Coupled Circuit Analysis of Microsyn Signal Generators" (H3). Mueller, "Microsyn Electromagnetic Components" (M15).
	*Torque generator (d-c or a-c):* $M_{(tg)} = S_{(tg)[1,1;M]} i_1 i_2$ (23)	
	*Elastic restraint generator (d-c):* $M_{(erg)} = -S_{(erg)[i^2,A;M]} i^2 A_{(rot)}$ (24)	
	*k) Magnetostriction transducer* $F_{(out)} = -\frac{1}{2} \phi^2_{(core)} \frac{d\mathcal{R}_{(core)}}{dl_{(core)}}$ (25)	Bergman, Ultrasonics (B10).

Information Summary 30-8. Electromagnetic components. (Page 9 of 9)

Figure	Component and Performance Relation	Reference
	*a) Rectifiers* *Vacuum diode:*  *Gas diode:*  *Crystal diode, copper oxide or selenium:* 	Aronson, Electronic Circuitry for Instruments (A10). Batcher and Moulic, The Electronic Control Handbook (B1). Bode, Network Analysis and Feedback Design (B3). Dumont Laboratories, A Compilation of Analog Transducers (D1). Electronics Magazine Everitt, Communication Engineering (E6). Federal Telephone and Radio Corporation, Reference Data for Radio Engineers (F5). Fitzgerald, Basic Electrical Engineering (F8). Greenwood, Holdam and MacRae, Electronic Instruments (G3). Guillemin, Communication Networks (G7). Harvard University, Cruft Electronics Staff, Electronic Circuits and Tubes (H4). Kloeffler and Horrell, Basic Electronics (K1). M.I.T., Staff, E. E. Dep't., Applied Electronics (M6). M.I.T., Staff, E. E. Dep't., Electric Circuits (M7). Radio Corporation of America, Tube Handbook H-B-3 (R2). Reich, Theory and Application of Electron Tubes (R4). Sylvania Tube Handbook (S15). Terman, Radio Engineers' Handbook (T2). Valley and Wallman, Vacuum Tube Amplifiers (V1). Westinghouse Electric Corporation, Industrial Electronics Reference Book (W5).
	*b) Vacuum tube (triode)* Amplification factor $\mu = \left(\frac{\Delta e_p}{\Delta e_g}\right)_{i_p = \text{constant}}$ (1) Transconductance $g_m = \left(\frac{\Delta i_p}{\Delta e_g}\right)_{e_p = \text{constant}}$ (2) Plate resistance $r_p = \left(\frac{\Delta e_p}{\Delta i_p}\right)_{e_g = \text{constant}}$ (3) $= \frac{\mu}{g_m}$ (4) Plate current $i_p = \frac{-\mu e_g}{r_p + R_L}$ (5)	

Information Summary 30-9. Electronic components. (Page 1 of 5)

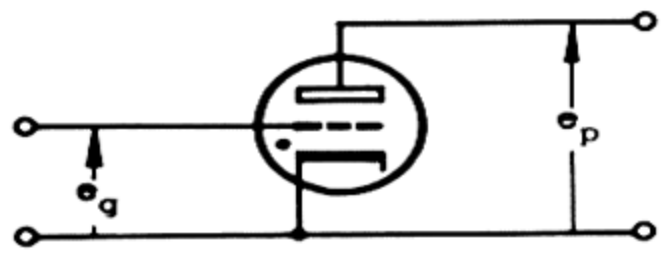
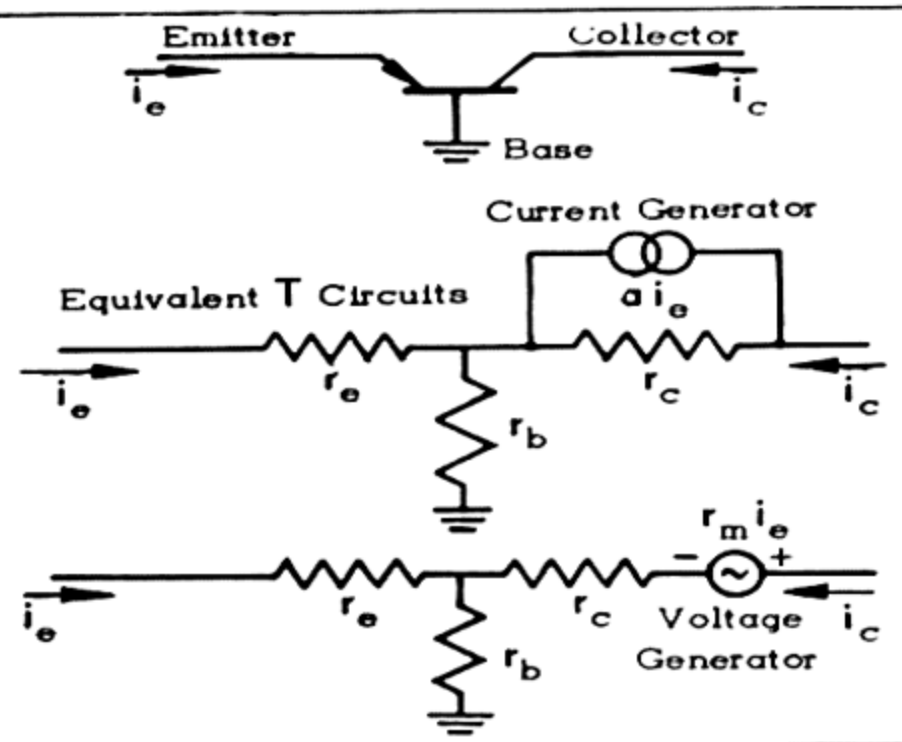
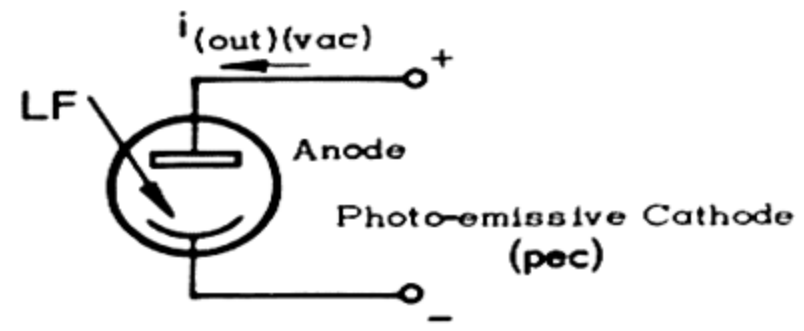
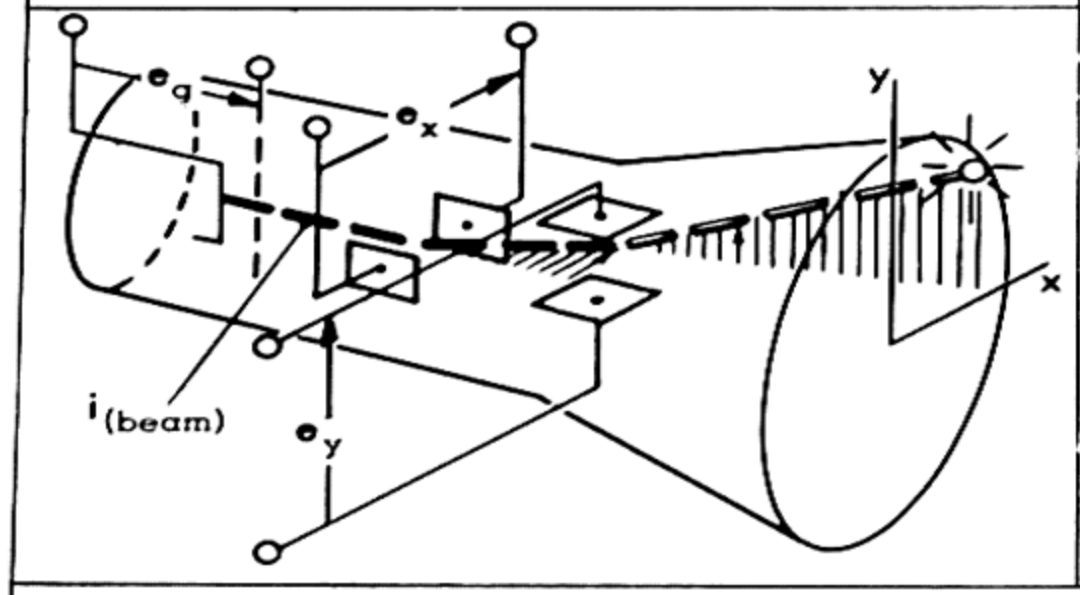
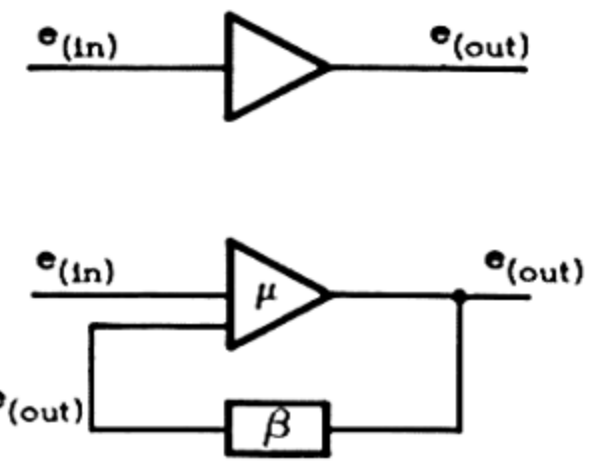
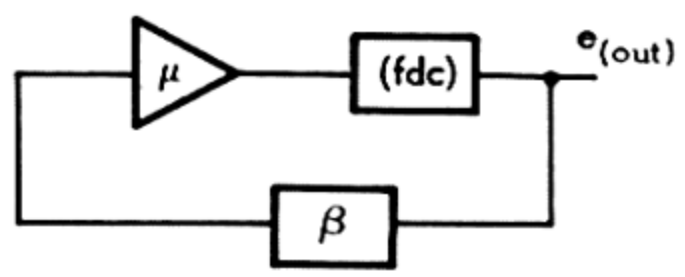
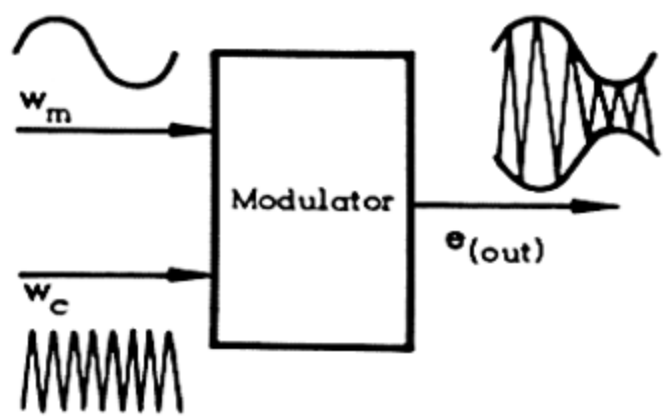
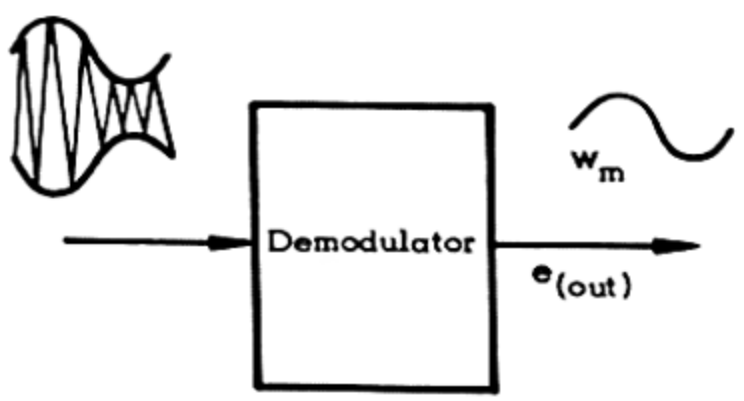
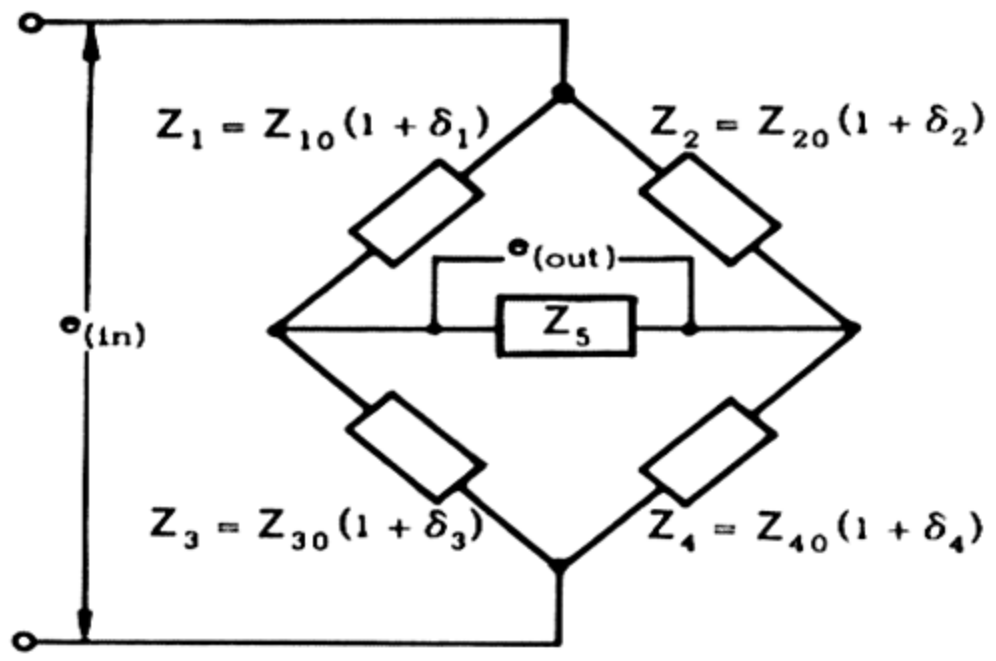
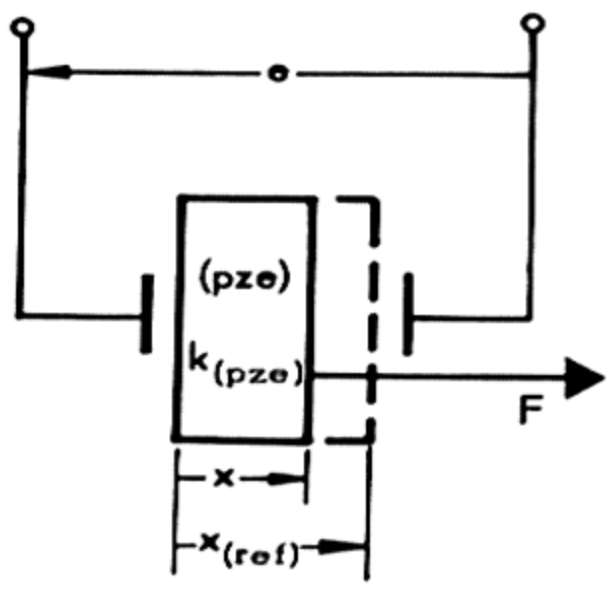
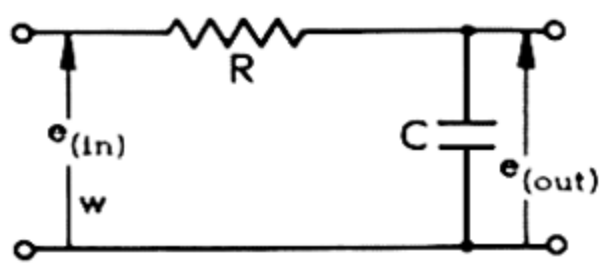
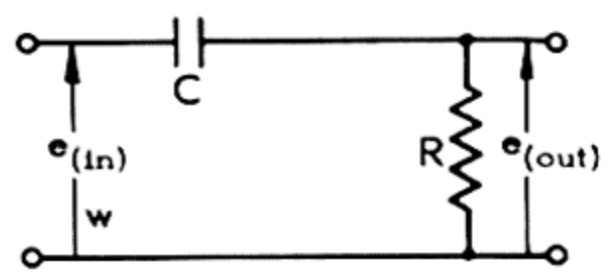
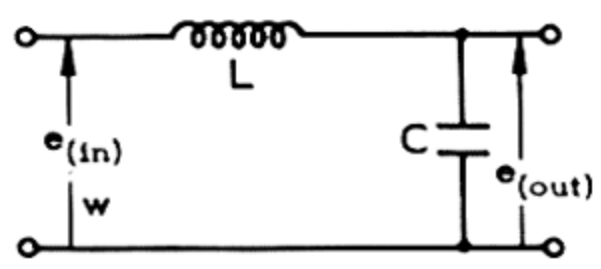
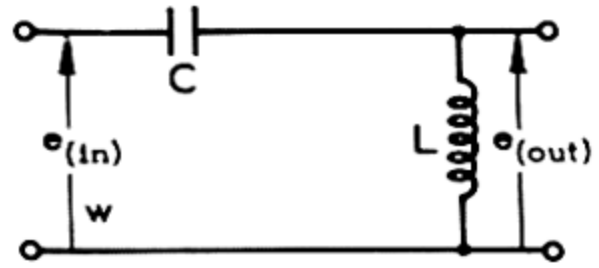
Figure	Component and Performance Relation	Reference
	*c) Thyratron (grid glow tube, gas triode)* When $\left(\frac{e_p}{-e_g}\right) < \left(\frac{e_p}{-e_g}\right)_{(critical)}$, tube does not start to conduct (6) $\left(\frac{e_p}{-e_g}\right) \geq \left(\frac{e_p}{-e_g}\right)_{(critical)}$, tube starts to conduct (7) $e_p < e_{(minimum)}$, tube stops conducting (8)	See references on page 1 of this summary.
	*d) Transistor* $\alpha = a + \frac{r_b}{r_c}(a-1)$ (9) $a = \left[-\frac{\partial i_c}{\partial i_e}\right]_{e_c}$ for point contact transistor: $1 < a < 5$; for junction transistor: $a < 1$ (10) $r_b = \left[\frac{\partial e_e}{\partial i_c}\right]_{i_e}$ $r_c + r_b = \left[\frac{\partial e_c}{\partial i_c}\right]_{i_e}$ (11),(12) $r_m + r_b = \left[\frac{\partial e_c}{\partial i_e}\right]_{i_c}$ $r_e + r_b = \left[\frac{\partial e_e}{\partial i_e}\right]_{i_c}$ (13),(14)	Proceedings of I. R. E., Transistor issue (P5). Shea, Principles of Transistor Circuits (S4). Shockley, Electrons and Holes in Semi-Conductors (S6). Shockley, The Transistor (S7).
	*e) Phototube* $i_{(out)(vac)} = S_{(pec)[LF;1]}(LF)$ (15) LF = luminous flux = time rate of luminous energy	See references on page 1 of this summary.
	*f) Cathode-ray tube* Intensity $i_{(beam)} = S_{[e;1]}(e_g - e_{g(cut\ off)})$ (16) Deflection $x = S_{[e;x]}e_x$ (17) $y = S_{[e;y]}e_y$ (18)	

Figure	Component and Performance Relation	Reference
	*g) Amplifiers* $e_{(out)} = -(\text{Gain})\, e_{(in)}$ (19) *Amplifier with negative feedback:* $\text{Gain} = \frac{\mu}{1 + \mu\beta}$ (20)	See references on page 1 of this summary.
	*h) Oscillators* $e_{(out)} = e_{(max)} \sin w_{(fdc)} t$ (21) (fdc) = frequency determining component	
	*i) Modulators (amplitude)* $e_{(out)} = e_0 (1 + m \sin w_m t) \sin w_c t$ (22) e_0 = average amplitude m = degree of modulation	
	*j) Demodulators* $e_{(out)} = e_{(out)(amp)} \sin w_m t$ (23)	

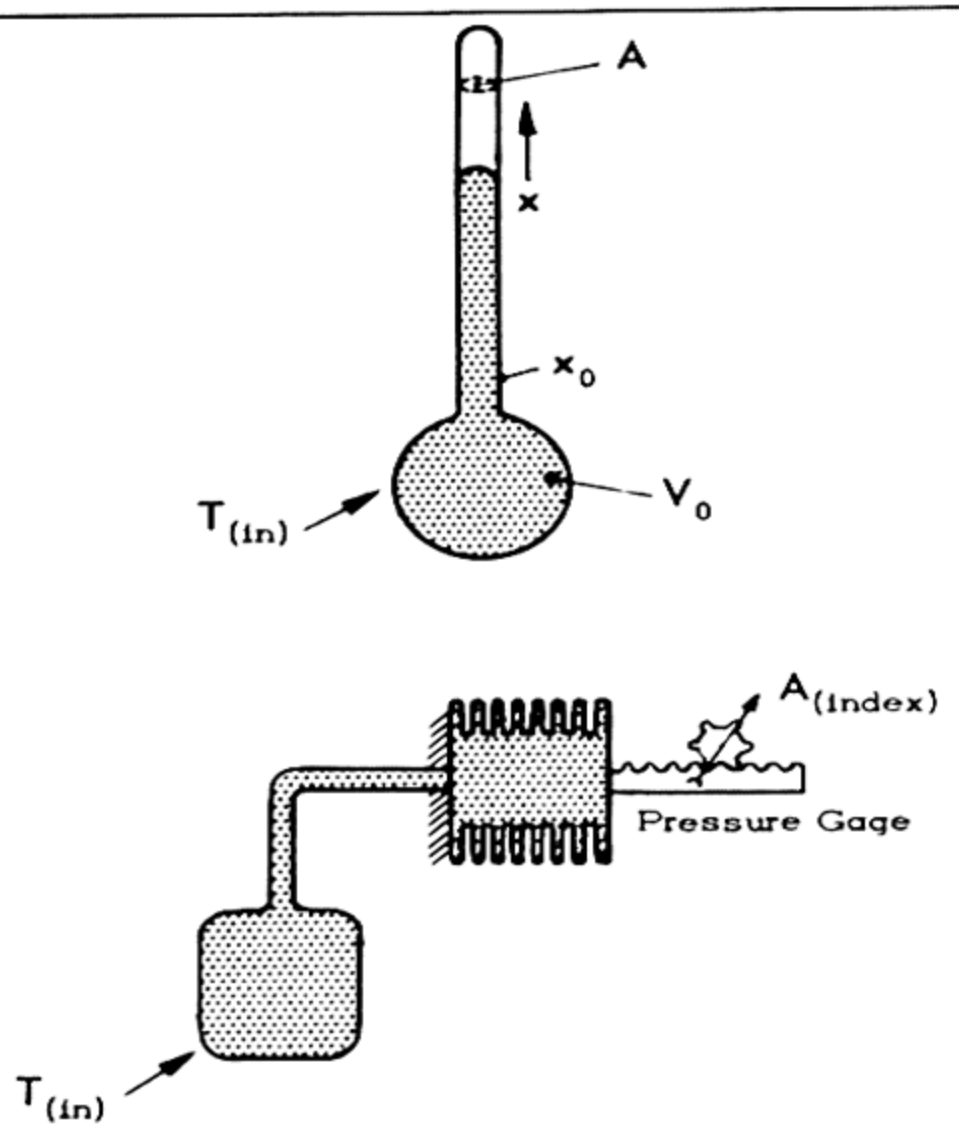
Information Summary 30-9. Electronic components. (Page 3 of 5)

Figure	Component and Performance Relation	Reference
	*k) Bridge* $e_{(out)} = 0$ when $Z_1 Z_4 = Z_2 Z_3$ (24) $\delta_1, \delta_2, \delta_3, \delta_4 << 1$ and are complex (25) $Z_5 >> Z_{10}, Z_{20}, Z_{30}, Z_{40}$ (26) $Z_{10} Z_{40} = Z_{20} Z_{30}$ (27) *Equal arms:* $Z_{10} = Z_{20} = Z_{30} = Z_{40}$ (28) $\frac{e_{(out)}}{e_{(in)}} = \frac{\delta_1 + \delta_3 - \delta_2 - \delta_4}{4}$ (29)	Draper and Wrigley, "An Instrument for Measuring Low Frequency Accelerations in Flight" (D8). Hague, Alternating Current Bridge Methods (H2).
	*l) Piezoelectric or electrostriction transducer* $e = S_{[x;e]}(x - x_{(ref)})$ (30) $F = -k_{(pze)}(x - x_{(ref)})$ (31) (operates reversibly)	

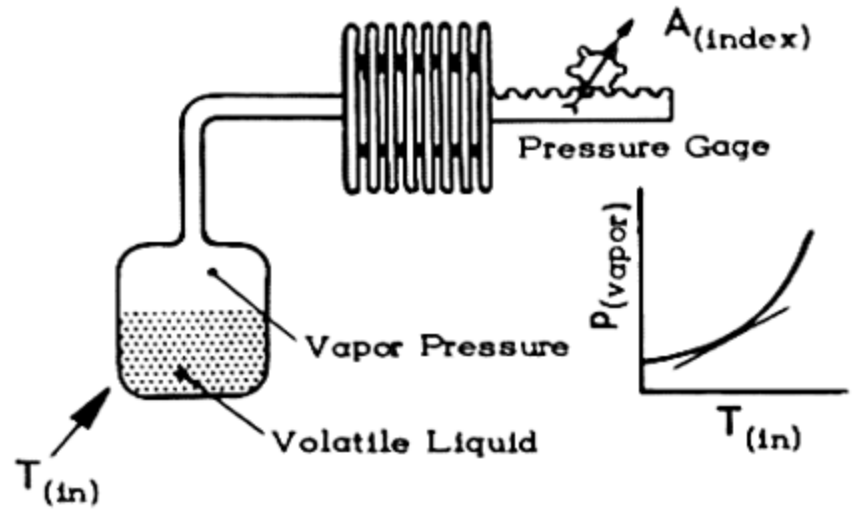
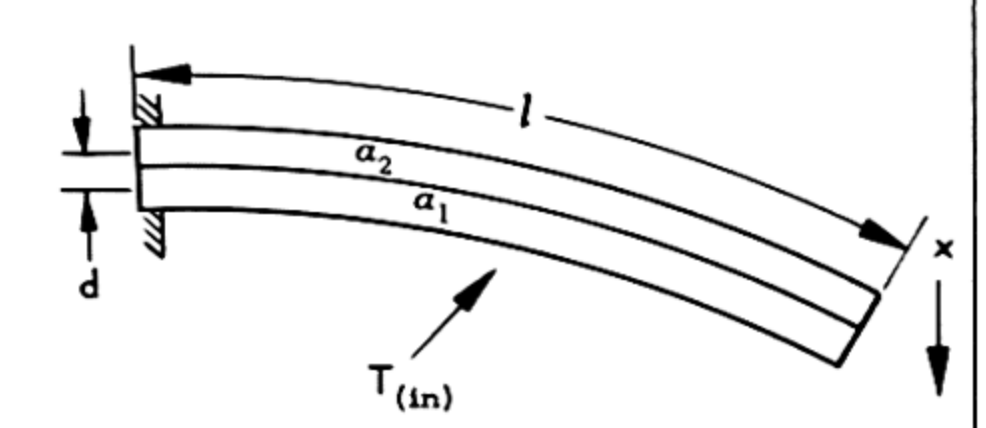
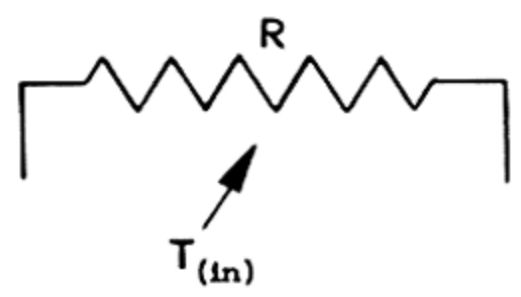
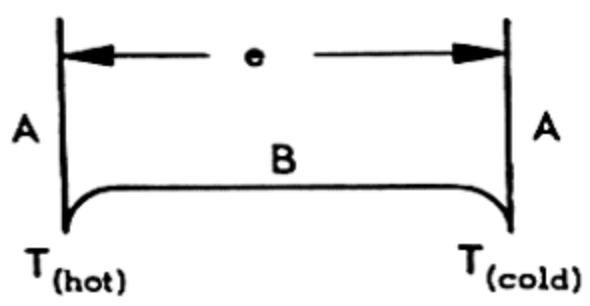
Information Summary 30-9. Electronic components. (Page 4 of 5)

Figure	Component and Performance Relation	Reference
	*m) Simple filters* *Low-pass R-C:* $\frac{e_{(out)}}{e_{(in)}} = \frac{1}{1 + jw(RC)}$ (32) Characteristic time $(CT) = RC$ (33)	See references on page 1 of this summary, especially Everitt (E6) and Guillemin (G7).
	*High-pass R-C:* $\frac{e_{(out)}}{e_{(in)}} = \frac{jw(RC)}{1 + jw(RC)}$ (34) Characteristic time $(CT) = RC$ (35)	
	*Low-pass L-C:* $\frac{e_{(out)}}{e_{(in)}} = \frac{1}{1 - w^2(LC)}$ (36) Resonant frequency $w_{(res)} = \frac{1}{\sqrt{LC}}$ (37)	
	*High-pass L-C:* $\frac{e_{(out)}}{e_{(in)}} = \frac{1}{1 - \frac{1}{w^2(LC)}}$ (38) Resonant frequency $w_{(res)} = \frac{1}{\sqrt{LC}}$ (39)	

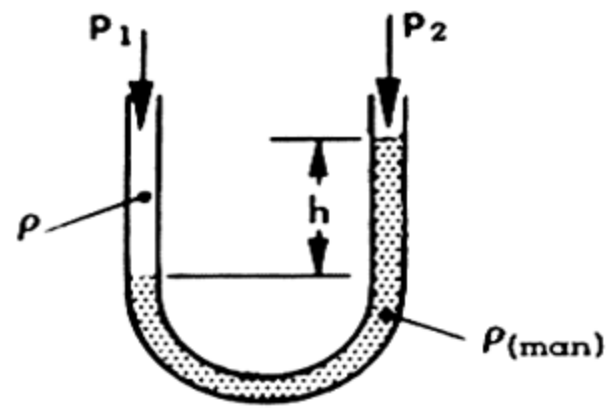
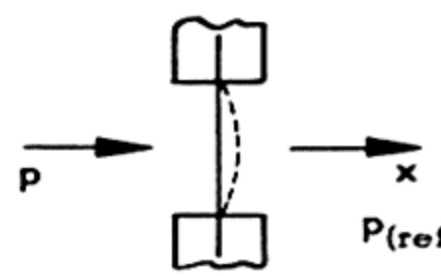
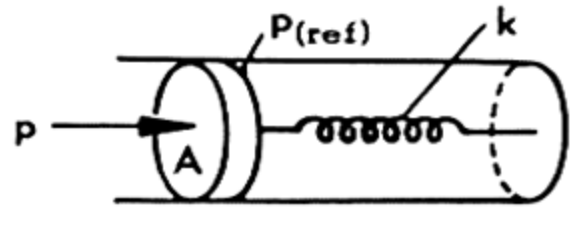
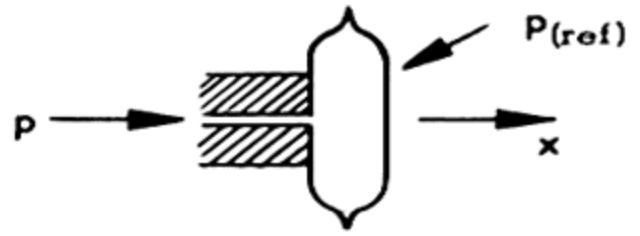
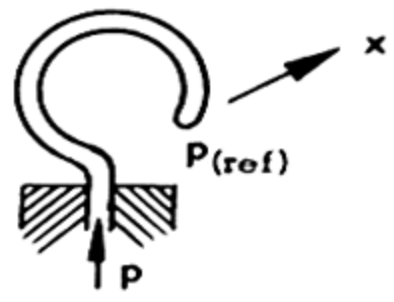
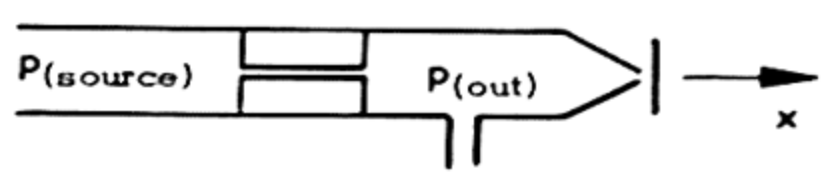
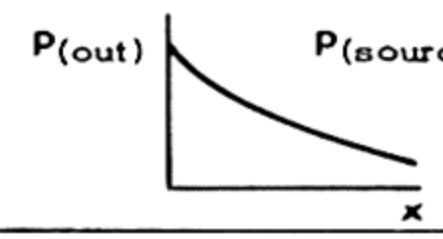
Information Summary 30-9. Electronic components. (Page 5 of 5)

Figure	Concept and Performance Relation	Reference
	*a) Thermometers* *Liquid in glass:* $S_{[T_{(in)};x]} = \frac{V_0 \beta}{A}$ (1) V_0 = liquid volume when x = 0 β = differential volumetric coefficient of expansion between liquid and container A = area of bore *Completely filled liquid:* $S_{[T_{(in)};A_{(index)}]} = \frac{S_{[p;A_{(index)}]}\beta}{S_{[p;\frac{\Delta V}{V}]}}$ (2) $S_{[p;A_{(index)}]}$ = sensitivity of pressure gage $S_{[p;\frac{\Delta V}{V}]}$ = fractional volume change of container per unit pressure *Gas pressure:* $S_{[T_{(in)};A_{(index)}]} = S_{[p;A_{(index)}]} \frac{\rho R}{(MW)}$; for perfect gas ρ = gas density (3)	American Institute of Physics, Temperature, Its Measurement and Control in Science and Industry (A7). Batcher and Moulic, The Electronic Control Handbook (B1). Behar, The Handbook of Measurement and Control (B2). Chemical Rubber Publishing Company Handbook of Chemistry and Physics (C3). Clifford Manufacturing Company, "A Chart of Vapor Pressure vs Temperature for Various Fluids" (C4). Diederichs and Andrae, Experimental Mechanical Engineering (D7). Eckman, Industrial Instrumentation (E1). Irvin, Aircraft Instruments (I1). Leeds and Northrup Company, "Standard Conversion Tables for Leeds and Northrup Thermocouples" (L9). Middleton, Meteorological Instruments (M11). Rhodes, Industrial Instruments for Measurement and Control (R1).

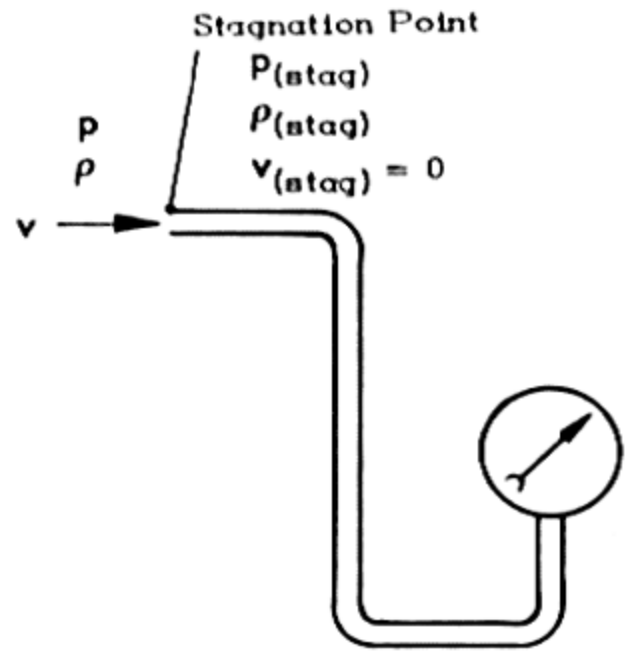
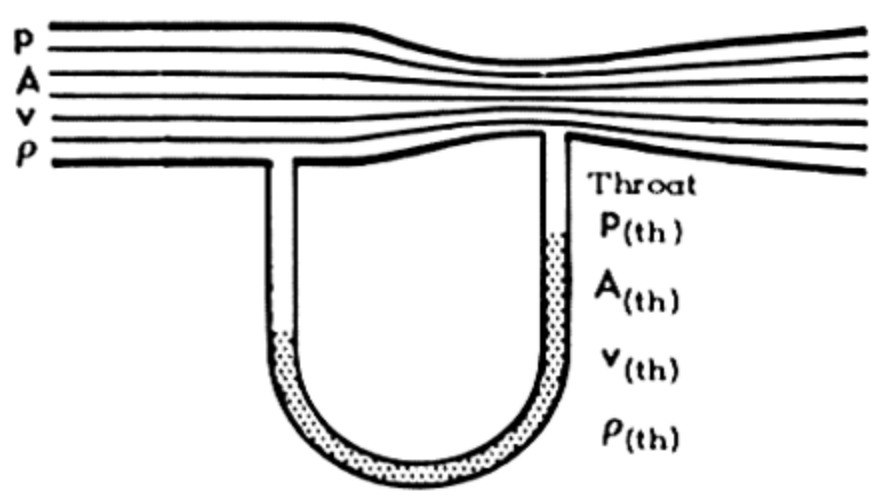
Information Summary 30-10. Thermometric components. (Page 1 of 2)

Figure	Concept and Performance Relation	Reference
	*Thermometers (continued)* *Vapor pressure:* $S_{[T_{(in)};A_{(index)}]} = S_{[p;A_{(index)}]} \frac{dp_{(vapor)}}{dT_{(in)}}$ (4)	
	*Bimetal:* $S_{[T_{(in)};x]} \cong \frac{(a_2 - a_1) l^2 \Delta T}{2d}$ (5) a = temperature coefficient of linear expansion	H. A. Wilson Company, The Blue Book of Thermometals and Electrical Contacts (W6).
	*Resistance:* $S_{[T_{(in)};R]} = R_0$ (temperature coefficient of resistivity) (6)	
	*Thermocouple:* $S_{[T_{(hot)} - T_{(cold)};e]} \cong$ constant (7) The constant depends on metals A and B	Federal Telephone and Radio Corporation, Reference Data for Radio Engineers (F5).

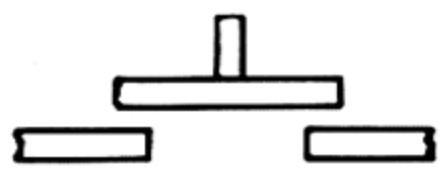
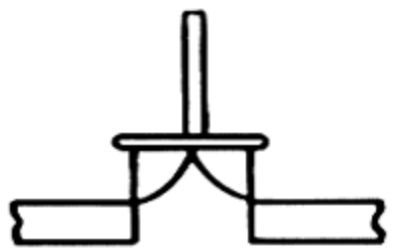
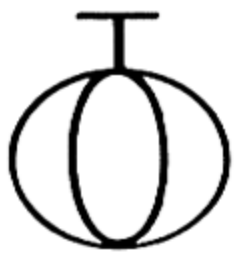
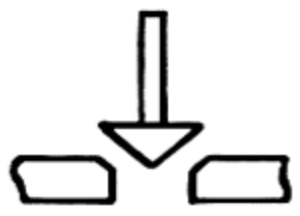
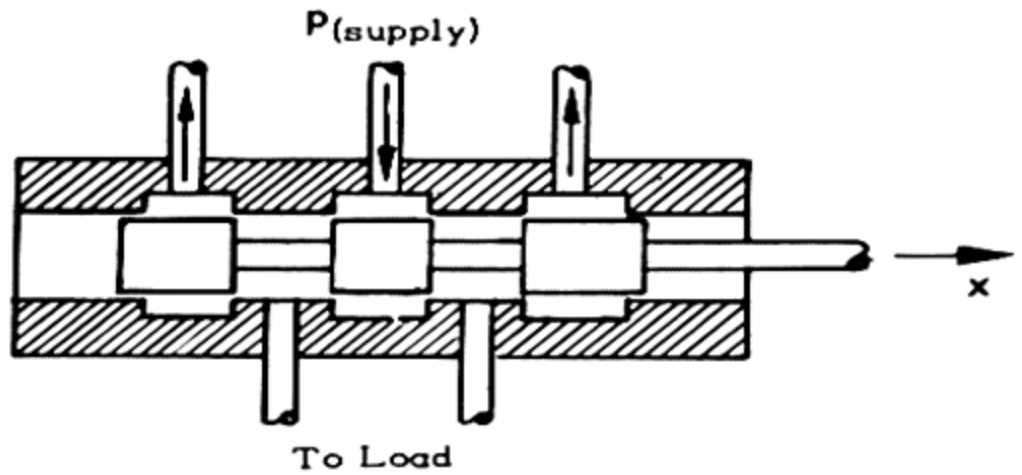
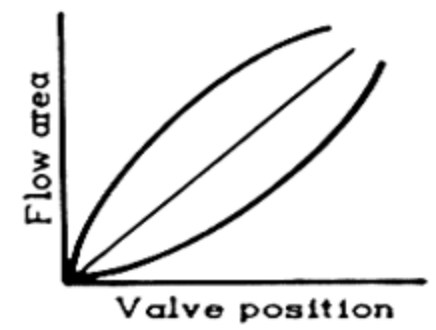
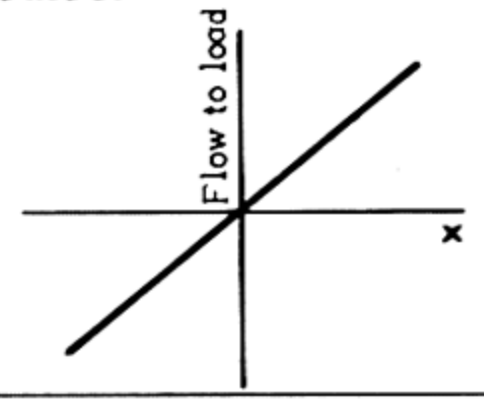
Information Summary 30-10. Thermometric components. (Page 2 of 2)

Figure	Component and Performance Relation	Reference
	***a) Pressure-measuring components*** *Manometer:* $P_1 - P_2 = (\rho_{(man)} - \rho)gh$ (1) $\rho_{(man)}$ = density of manometer fluid ρ = density of fluid	Diederichs and Andrae, Experimental Mechanical Engineering (D7). Eckman, Industrial Instrumentation (E1). Gould and Smith, "Dynamic Behavior of Pneumatic Devices" (G6).
 Diaphragm  Spring and Piston  Capsule  Bellows  Bourdon Tube	*Area-elastic restraint combinations:* $x = S_{(pr)}(p - P_{(ref)})$ (2) $S_{(pr)} = \frac{A_{(eff)}}{k_{(eff)}}$ (3)	Van der Pyl, "ASME Paper No. 53-IRD-1" (V2).
	***b) Nozzle flapper*** 	Gould and Smith, "Dynamic Behavior of Pneumatic Devices" (G6). New York State Vocational and Practical Arts Association, Instruments and Process Control (N3).

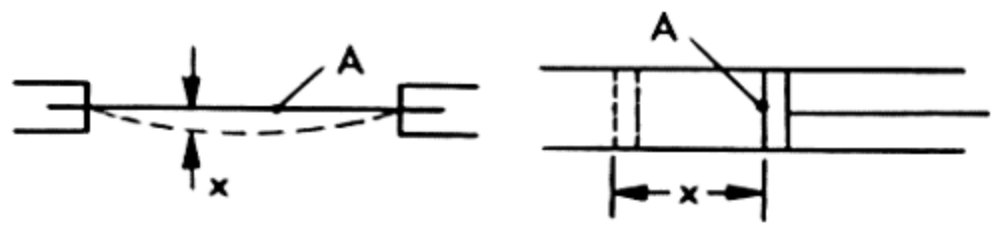
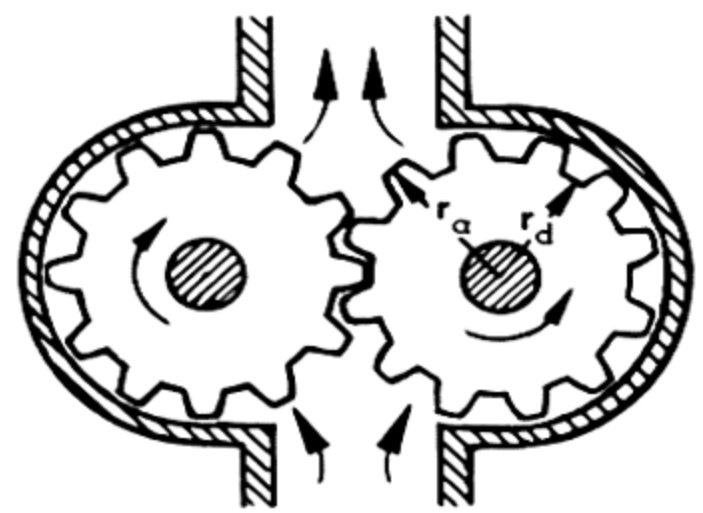
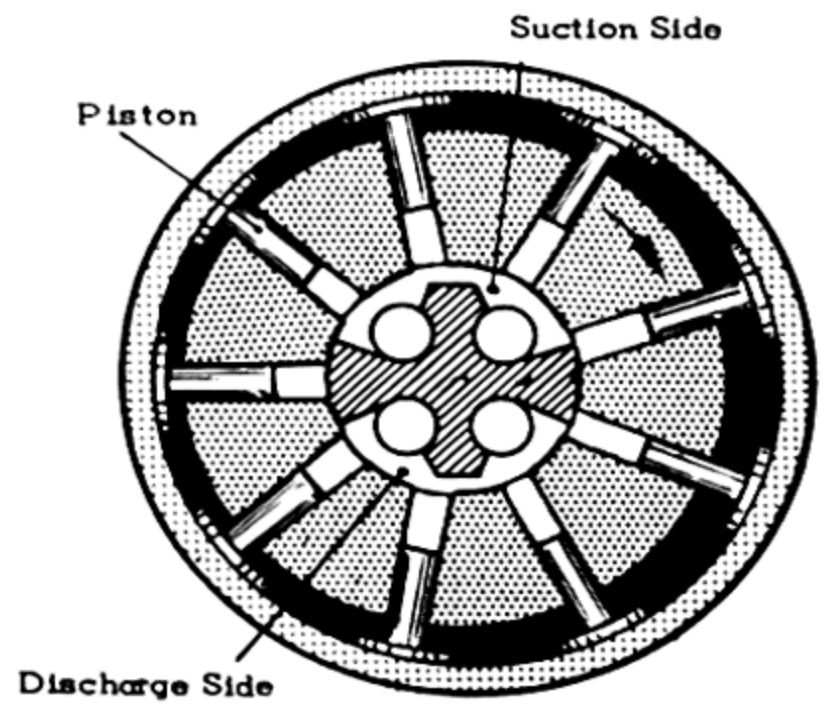
Information Summary 30-11. Fluid components. (Page 1 of 4)

Figure	Component and Performance Relation	Reference
	c) *Flow-measuring components* *Pitot tube:* Incompressible case $\rho = \rho_{(stag)}$ (4) $P_{(stag)} - p = \frac{1}{2}\rho v^2$ (5) Compressible adiabatic case $\frac{p}{\rho^\gamma} = \frac{P_{(stag)}}{\rho^\gamma_{(stag)}}$ (6) $\frac{P_{(stag)}}{p} = \left[1 + \frac{\gamma-1}{2}(MN)^2\right]^{\gamma/\gamma-1}$ or, (7) if $\frac{\gamma-1}{2}(MN)^2 < 1$, (8) $P_{(stag)} - p = \frac{1}{2}\rho v^2\left[1 + \frac{1}{4}(MN)^2 + \frac{2-\gamma}{24}(MN)^4 + \ldots\right]$ (9) *Venturi tube:* Incompressible case $\rho = \rho_{(th)}$ (10) $v_{(th)} = C\sqrt{\frac{2g(p - P_{(th)})}{\rho\left[1 - \left(\frac{A_{(th)}}{A}\right)^2\right]}}$ (11) C = discharge coefficient = $f(RN)$ (12) Compressible adiabatic case $\frac{p}{\rho^\gamma} = \frac{P_{(th)}}{\rho^\gamma_{(th)}}$ (13) $v_{(th)} = C\sqrt{\frac{\frac{2g\gamma}{\gamma-1}\frac{p}{\rho}\left[1 - \left(\frac{A_{(th)}}{A}\right)^{\gamma-1/\gamma}\right]}{1 - \left(\frac{A_{(th)}}{A}\right)^2\left(\frac{P_{(th)}}{p}\right)^{2/\gamma}}}$ (14) $\frac{P_{(th)}}{p} > \left(\frac{2}{\gamma+1}\right)^{\gamma/\gamma-1}$; 0.53 for air (15)	Dean, "Aerodynamic Measurements" (D3).
		

Information Summary 30-11. Fluid components. (Page 2 of 4)

Figure	Component and Performance Relation	Reference
 Plug  V-port  Butterfly  Parabolic plug  Needle 	*d) Flow-controlling components* *General valves:*  *Balanced pressure spool valve:* 	Eckman, Industrial Instrumentation (E1). Ernst, Oil Hydraulic Power and Its Industrial Applications (E4). Lee and Blackburn, "Contributions to Hydraulic Control" (L8). St. George, "List of Theses and Reports on Hydraulic Control" (S13).

Information Summary 30-11. Fluid components. (Page 3 of 4)

Figure	Component and Performance Relation	Reference
	e) *Pumps and motors* *Diaphragm-piston:* $FR = Axn$ (16) FR = flow rate n = number of cycles per unit time	Ernst, Oil Hydraulic Power and Its Industrial Applications (E4). MacMillan, An Introduction to the Theory of Control in Mechanical Engineering (M2). Shearer, "Proportional Control of Rate-Type Servomotors" (S5) and "Dynamic Characteristics of Valve-Controlled Hydraulic Servomotors" (S5).
	*Gear:* $FR = \pi(r_a^2 - r_d^2)bn$ (17) b = axial length of gears	
	*Radial:* $FR = 2eA_{(piston)}Nn$ (18) e = eccentricity 2e = stroke N = number of pistons	

Information Summary 30-11. Fluid components. (Page 4 of 4)

CHAPTER 31

TEMPERATURE-MEASURING INSTRUMENTS

INTRODUCTION

31.1. Temperature measurement is one of the basic problems of instrument engineering. In practice, this field includes situations of many types that range from simple weather observations to very accurate scientific measurements requiring complex laboratory equipment. Methods for the measurement of temperature have been discussed as an integral part of classical physics* from the very beginnings of written material on this subject. In addition, an extensive literature** dealing with the engineering problems of temperature instruments is available. For example, the dynamic errors of temperature instruments*** have received considerable attention in recent years.

31.2. The details of theory and design for temperature indicating and measuring devices are so well known and exhaustively discussed in the literature that there is little justification for a complete review here. However, the performance of temperature-actuated devices is so important in practice, and the associated theory illustrates the analysis of an instrument problem so well, that the basic principles involved are taken as the subject matter for the present chapter. The discussion is simplified by the fact that the available couplers, indicating systems, and scales for temperature-measuring instruments have dynamic response characteristics that are fast in comparison with those of the commonly used temperature receivers. This means that one of the primary temperature-instrument problems is that of designing receivers to follow input temperature changes with acceptable rapidity. It is possible to write formal expressions for the essential physical process involved, but it is so difficult to make accurate theoretical predictions that accurate determinations of the performance of actual instruments must usually be found by experimental methods. The theoretical background for the measurement of instrument characteristics is developed in this chapter. In order to reduce the problems involved to definite terms, the discussion is started with a brief description of various temperature-instrument types.

---

* See Preston (P8), Chapters II and III, and Roberts (R9), Chapter I.

** See Batcher and Moulic (B1), Behar (B2), Harper (H7), Rhodes (R1), and Wood and Cork (W9).

*** See Hendrickson and Brombacker (H8), Hendrickson (H9), and Timoshenko (T6).

ESSENTIAL FEATURES OF TEMPERATURE-MEASURING INSTRUMENTS

31.3. The essential operating components of a temperature-measuring instrument are shown in the generalized functional diagram of section a of Description Summary 31-1. The temperature receiver has the temperature to be measured (i.e., the input temperature) as its input and generates the receiver temperature as its output. The coupler takes the receiver temperature as its input and produces an output suitable for the indicating system input. The indicating system receives this input and produces the indication as its output. The receiver, the coupler, and the indicating system combine to form the temperature indicator. When the scale is added to the indicator to receive indications and produce temperature scale readings as its output, the complete system becomes a temperature-measuring instrument.

31.4. In the operating chain of a temperature-measuring instrument, the receiver has the function of transferring the temperature to be measured from the fluid or material with which it is associated to some component from which it may be taken by the coupler. Perfect performance exists when the receiver temperature is always exactly equal to the input temperature. This fact means that the perfect performance function for the temperature receiver is unity. In practice, this behavior is not achievable because the material of the receiver always has a finite heat capacity, and a temperature difference must always exist in order for heat to flow in or out of the receiver as its temperature follows the input temperature. Under ordinary conditions, the input temperature is the average temperature over some range of variation rather than a sharply defined single level. Similarly, the receiver temperature is usually an effective average over some mass of material, not the level at some particular point. Departure from perfect performance resulting from these factors is minimized by receiver design and, in any case, may be taken into account by proper static and dynamic calibration procedures.

LIQUID-IN-GLASS THERMOMETERS

31.5. Section b of Description Summary 31-1 is a pictorial diagram showing the essential parts of a typical liquid-in-glass thermometer. A bulb is filled with some liquid that expands into a glass tube as the bulb temperature increases. The top of the liquid column serves as the index, and a temperature-calibrated scale is marked on the stem, which contains the tube and the liquid column index.

31.6. Section c of Description Summary 31-1 is an illustrative pictorial-functional diagram for a liquid-in-glass thermometer. The bulb and the contained liquid act as the temperature receiver. The liquid within the bulb and in the column below the index supplies the coupling function of transforming the receiver temperature into the indication, which is the index position. It is to be noted that the

essential action of the coupler is determined by the expansion of the liquid with respect to the glass of the bulb and the tube rather than by the expansion of the liquid alone. The indicating system of the liquid-in-glass thermometer is simply the meniscus top of the coupler column. The markings on the stem act as the scale to give temperature scale readings.

31.7. The design and application problems associated with liquid-in-glass thermometers are documented so extensively in the literature* that no further discussion of this topic is required here.

BIMETAL THERMOMETERS

31.8. Many thermometer designs depend on the use of strips made up of metals with different coefficients of thermal expansion. These bimetal strips have the property of producing considerable bending moments when they are subjected to changes of temperature. A typical bimetal thermometer is illustrated in section d of Description Summary 31-1. A bulb, which is continuous with the stem, is designed for location in the region of the temperature to be measured. The indicating head, which contains the index and the scale, is attached to the stem. The bulb contains a bimetal spiral that causes a shaft passing through the stem to vary its angular position with changes in temperature so that the index is rotated with respect to the scale.

31.9. Section e of Description Summary 31-1 is a pictorial-functional diagram for the thermometer of section d. The temperature receiver includes the bulb attached to the end of the stem and the parts of the bimetal component** whose average temperature determines the angular position of the shaft to which the spiral element is attached. The coupler consists of the bimetal spiral and the shaft that passes from the bulb to the indicating head. The indicating system is the mechanism that receives the coupler output angle and produces the indication as the index angle. The scale is a calibrated disk mounted just behind the plane of motion of the index.

31.10. The theory of bimetal strip action is discussed by Timoshenko and Kleinschmidt.*** At the present time, this theory is of academic interest only, as specific design information in terms suitable for engineering use is available in reference books and manufacturers' catalogs.†

FLUID-PRESSURE-COUPLED THERMOMETERS

31.11. A very large class of temperature-measuring instruments is represented

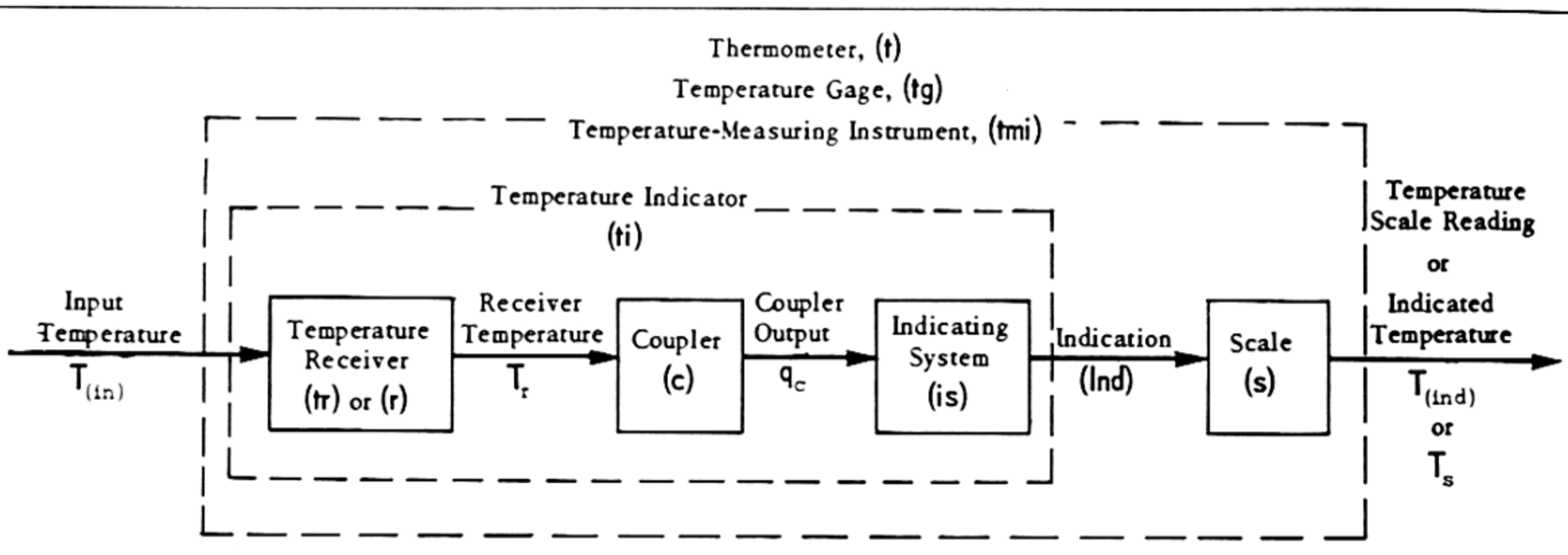
---

* See American Institute of Physics (A7), Behar (B2), Lyle (L2), Preston (P8), Chapters II and III, Rhodes (R1), and Roberts (R9), Chapter I.

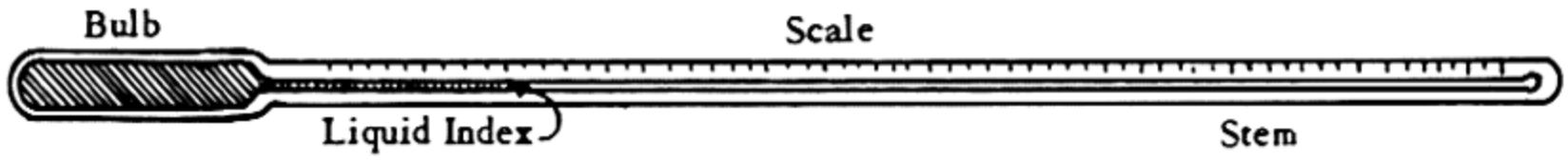
** Bimetal parts are included in the receiver because their heat capacity is a factor in determining receiver performance.

*** See Timoshenko (T6) and Kleinschmidt (K4).

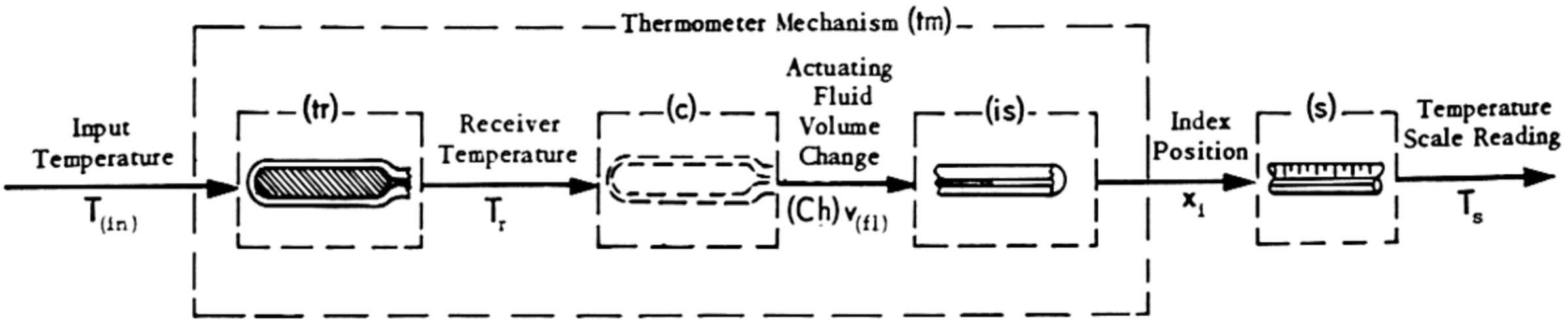
† See H. A. Wilson Company (W6).



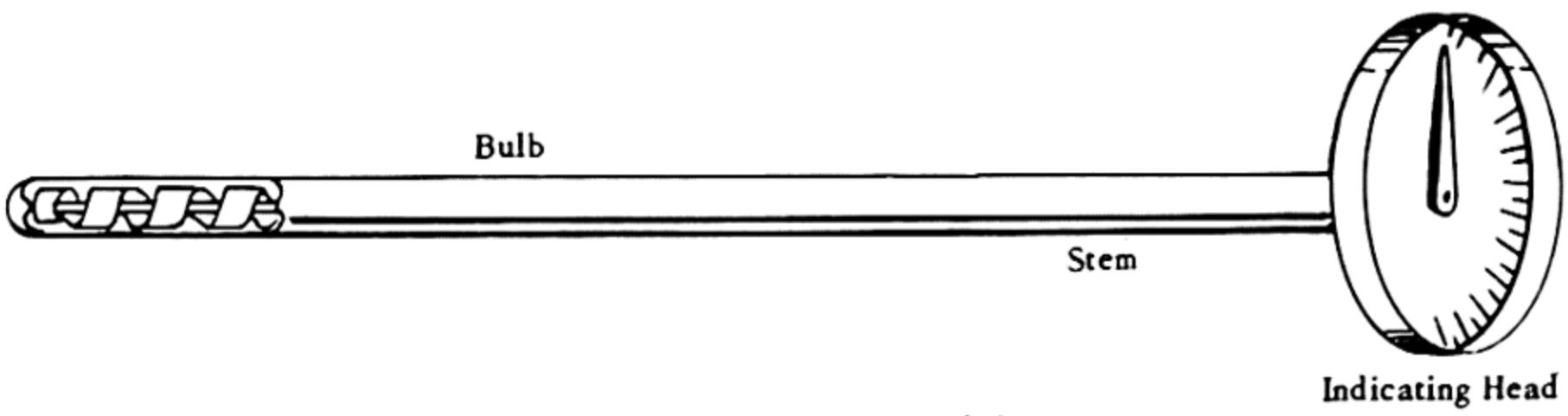
a) Functional diagram for a generalized temperature-measuring instrument



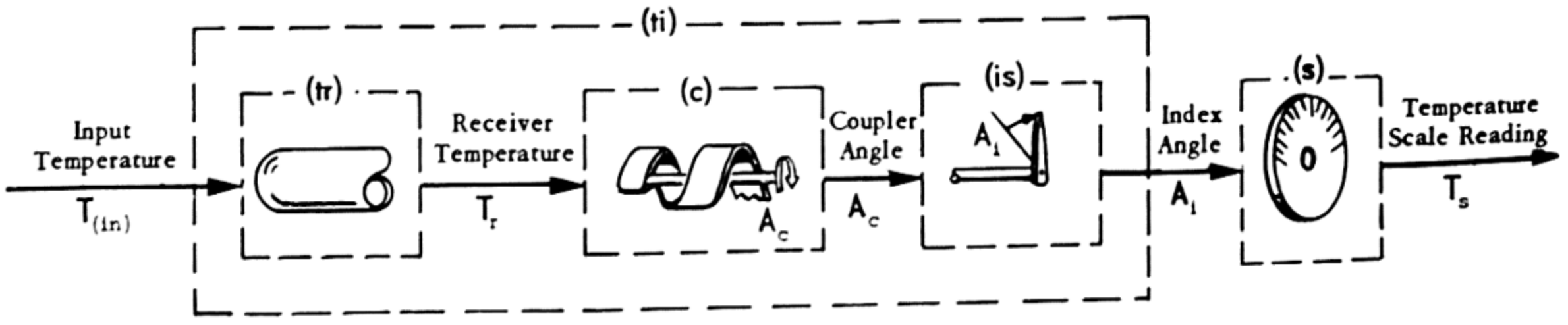
b) Pictorial diagram for a liquid-in-glass thermometer



c) Illustrative pictorial-functional diagram for a liquid-in-glass thermometer

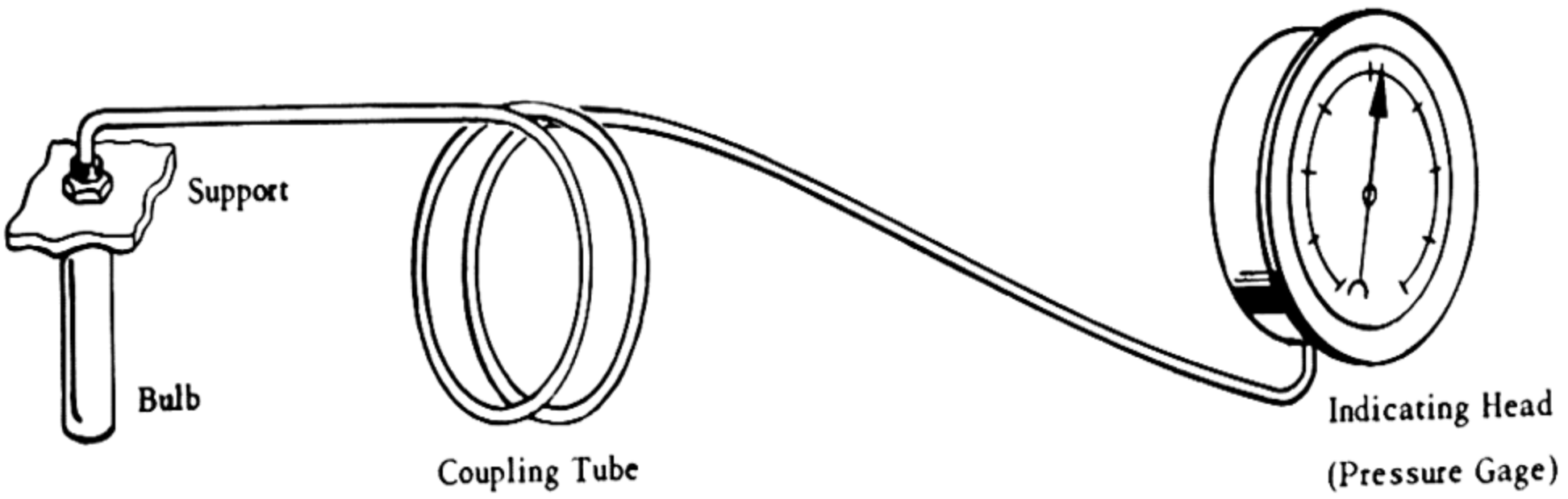


d) Pictorial diagram for a bimetal thermometer

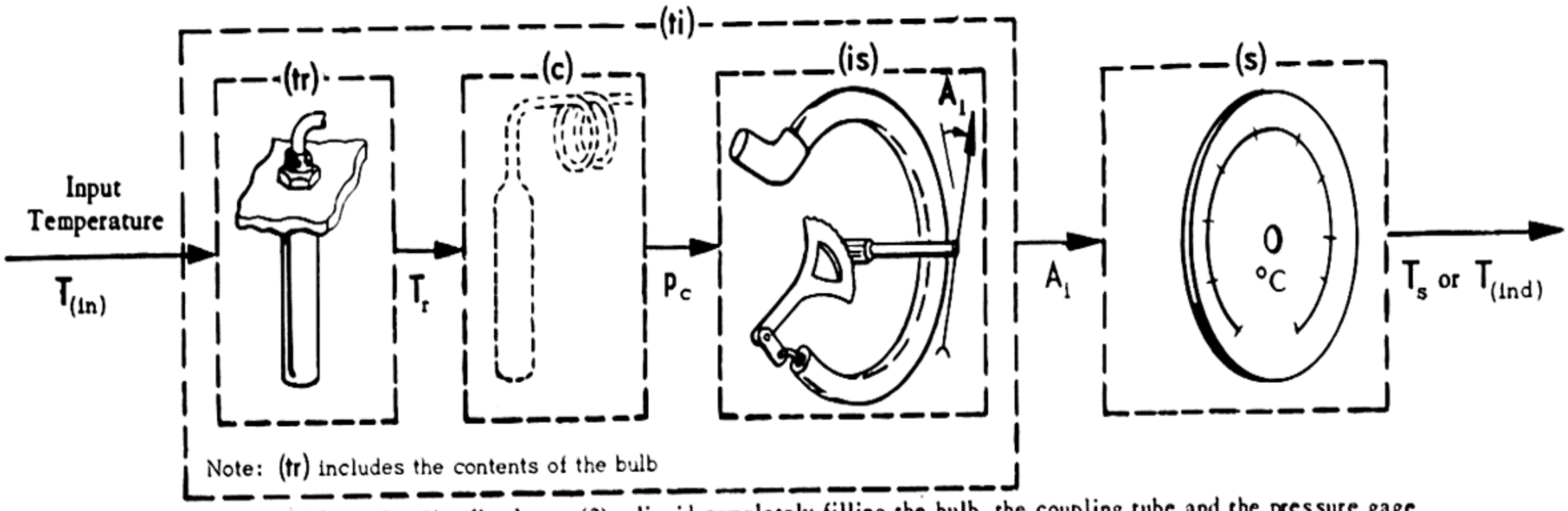


e) Illustrative pictorial-functional diagram for a bimetal thermometer

Description Summary 31-1. Illustrative pictorial-functional and pictorial diagrams for common temperature-measuring instruments. (Page 1 of 4)

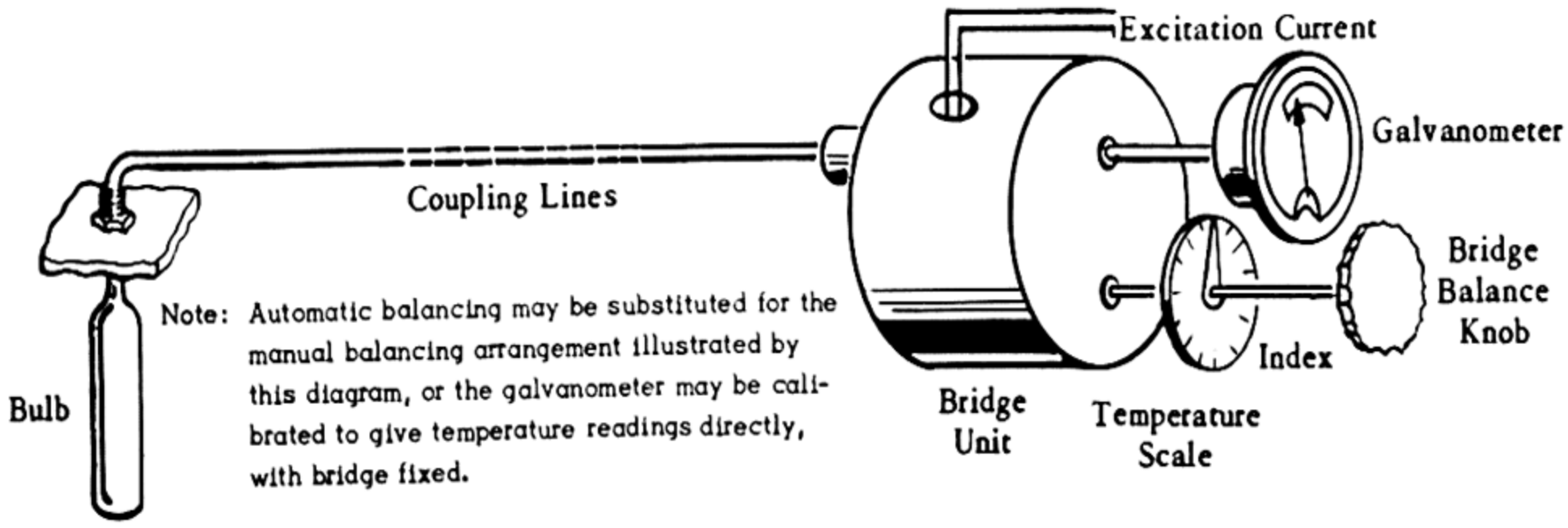


f) Pictorial diagram for a fluid-pressure-coupled temperature gage

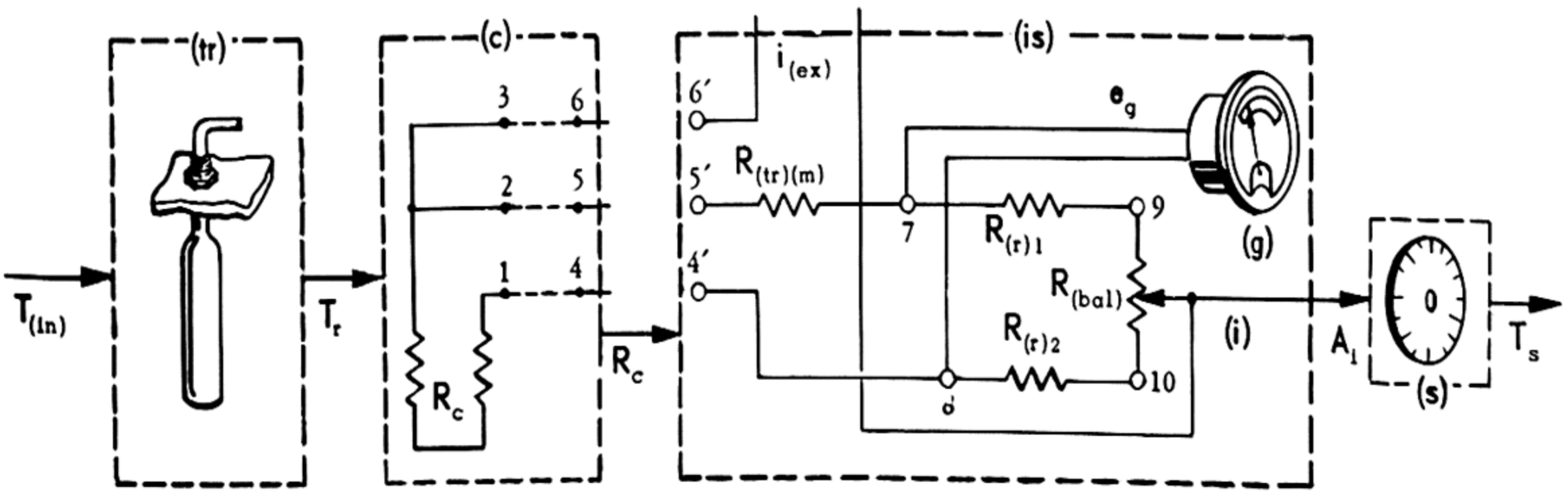


The coupling fluid may be (1) a fixed gas; (2) a liquid completely filling the bulb, the coupling tube and the pressure gage receiver; (3) a vapor in contact with a free liquid surface in the temperature receiver.

g) Illustrative pictorial-functional diagram for a fluid-pressure-coupled temperature gage

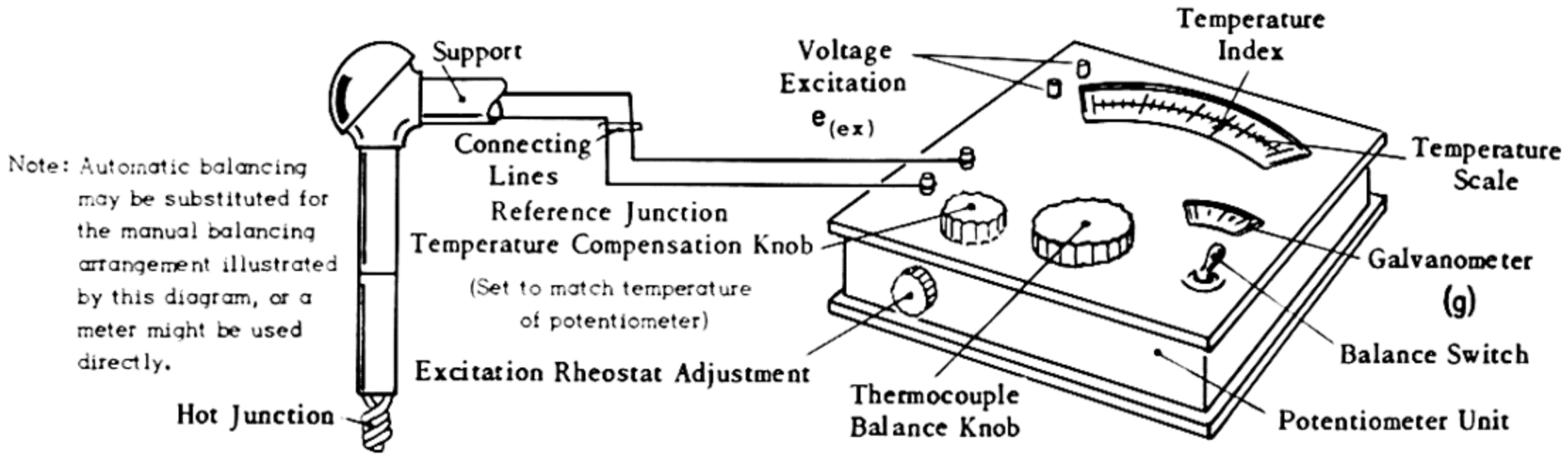


h) Pictorial diagram for an electrical resistance temperature gage

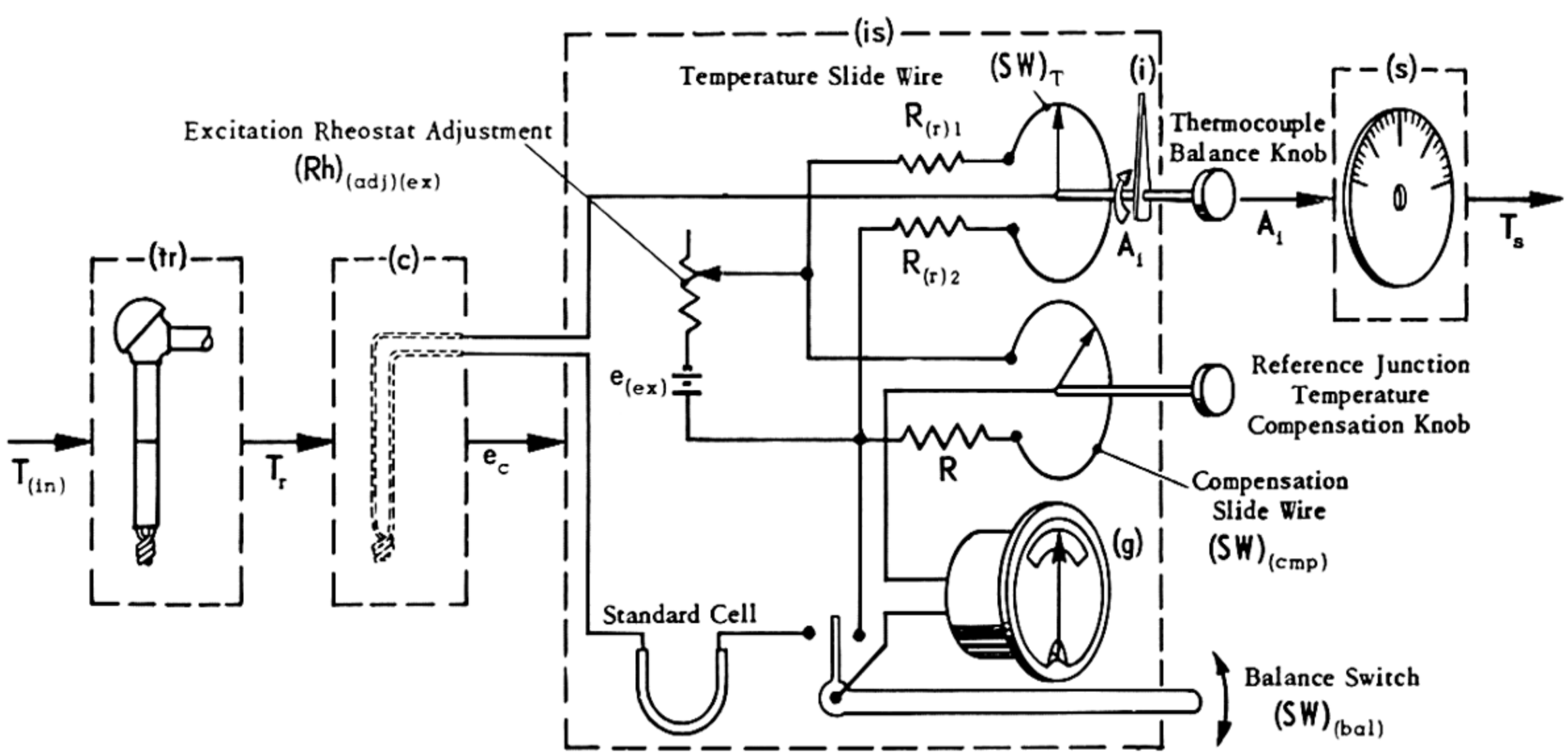


i) Illustrative functional-electrical circuit diagram for an electrical resistance temperature gage

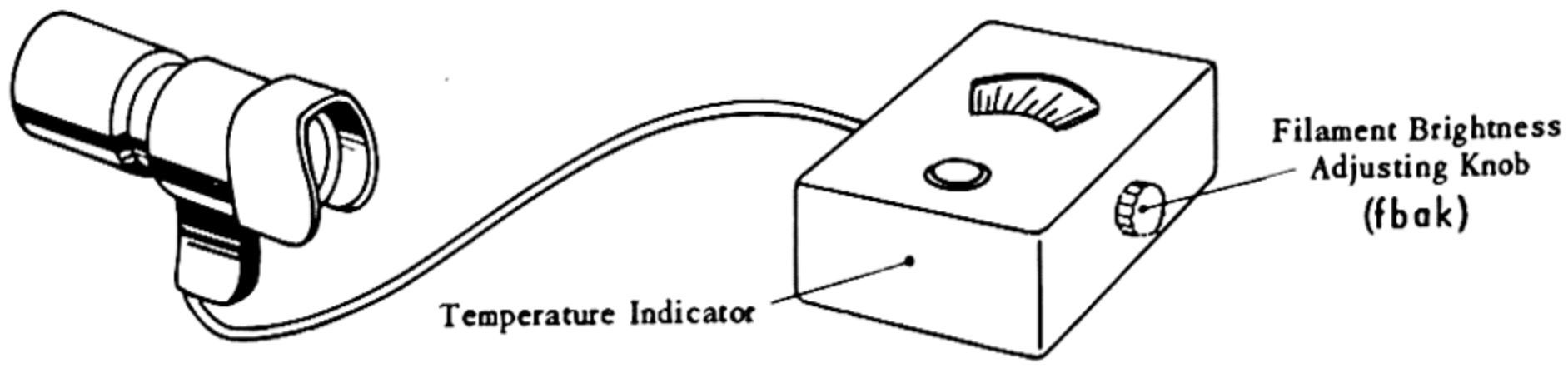
Description Summary 31-1. Illustrative pictorial-functional and pictorial diagrams for common temperature-measuring instruments. (Page 2 of 4)



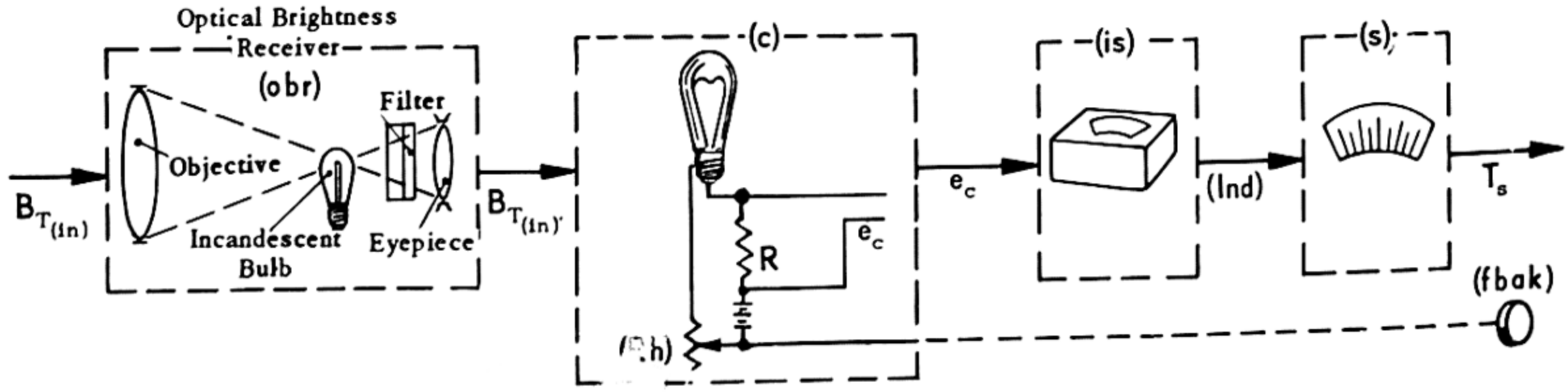
j) Pictorial diagram for a thermocouple temperature gage



k) Illustrative functional-electrical circuit diagram for a thermocouple temperature gage

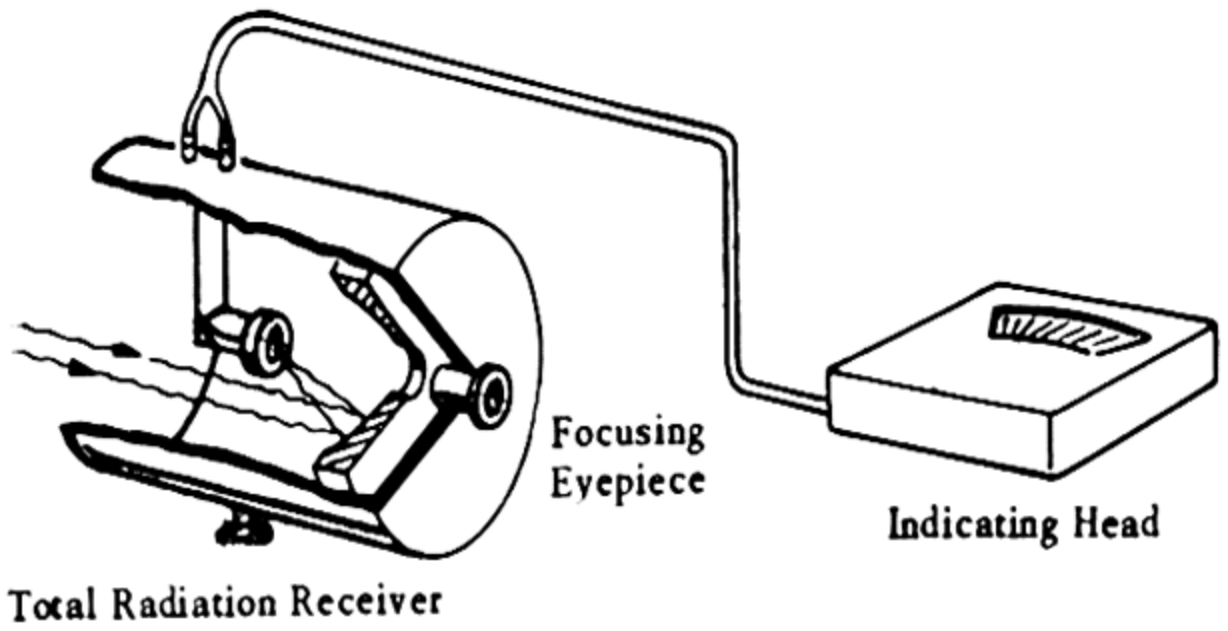


l) Pictorial diagram for an optical pyrometer

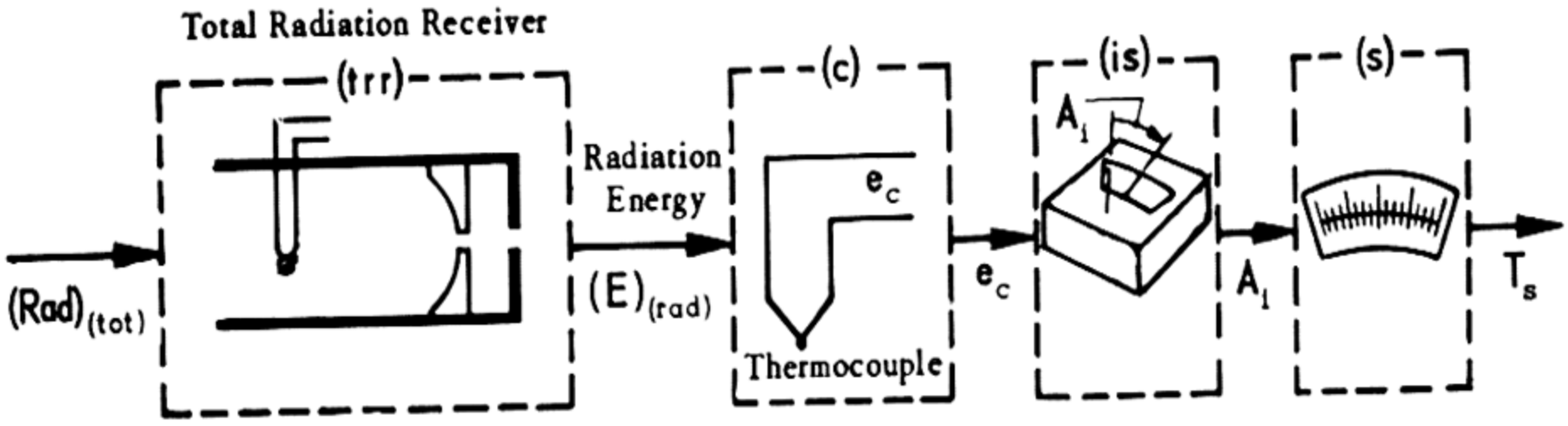


m) Illustrative pictorial-functional diagram for an optical pyrometer

Description Summary 31-1. Illustrative pictorial-functional and pictorial diagrams for common temperature-measuring instruments. (Page 3 of 4)



n) Pictorial diagram for a total radiation pyrometer



o) Illustrative pictorial-functional diagram for a total radiation pyrometer

Description Summary 31-1. Illustrative pictorial-functional and pictorial diagrams for common temperature-measuring instruments. (Page 4 of 4)

by the pictorial diagram of section f of Description Summary 31-1. These instruments include a bulb that is connected to an indicating head by means of a relatively long tube of small diameter. The indicating head is basically a pressure indicator with a rotating pointer as its index.

31.12. The diagram of section g of Description Summary 31-1 shows the bulb of section f as the temperature receiver. The coupling function is carried out by fluid sealed in the bulb, in the tubing, and in the indicating head. The input to the coupling medium is an average temperature, which is effectively the receiver output. The output from the coupling medium is a pressure that acts as the input to the indicating head. The coupler is made up of the coupling medium, the bulb, and the tubing. It is apparent that the fluid within the bulb acts as part of the receiver so far as its heat capacity is concerned and as part of the coupler so far as its action in generating a temperature-dependent pressure is concerned. The calibration of the pressure indicator in terms of input temperature depends on the temperature-pressure relationship established by the coupling medium.

31.13. Coupling media of three types are in common use:

1) Fixed gases
2) Liquids
3) Vapor in contact with liquid

The ordinary gas law relationship may be applied in the design of fixed-gas thermometers. Liquid-filled thermometers may be considered as dependent on the coefficient of volume expansion for the liquid used, with the indicating head acting to measure the changes in volume that accompany receiver temperature variations. Vapor-pressure instruments are designed to operate with some liquid always remaining in the receiver. As long as this condition exists, the vapor pressure is a function of temperature only and is independent of the amount of liquid in the bulb. The effective temperature-vapor pressure relationship depends upon the liquid considered and the range of operating temperatures. In general, this relationship is nonlinear, so that the indicating-head scale must show a corresponding nonlinearity if the pressure indicator is to have a constant pressure-index deflection sensitivity.

31.14. Rhodes* gives a comprehensive treatment of design considerations for fluid-pressure-coupled thermometers. It would be out of place here to either repeat or attempt to expand Rhodes' treatment.

RESISTANCE-COUPLED THERMOMETERS

31.15. Sections h and i of Description Summary 31-1 show the arrangement of components in an illustrative electrical resistance thermometer. In instruments of this class, the bulb, which acts as the temperature receiver, is a protective shell that contains a winding of resistance wire. This winding and a Wheatstone bridge arrangement for transforming resistance variations into voltage changes act as the coupler and indicating system. In the example of sections h and i, the bridge is shown as a manually balanced arrangement in which an operator rotates a knob until the galvanometer reading is zero and then reads the indicated temperature from the position of an index coupled to the knob. Actual resistance thermometers may have the manual operating feature replaced by an automatic balancing arrangement or, in special cases, the galvanometer index may be allowed to deflect over a scale calibrated in terms of temperature.

31.16. The theory of the effect of temperature on electrical resistance is discussed in texts on physics and electricity.** The principles of electrical bridge systems are treated in books on physics, electrical measurement, and instruments.***

THERMOCOUPLE THERMOMETERS

31.17. The coupling function for temperature-measuring instruments may be carried out by thermoelectric action. The use of this principle is illustrated in

* See Rhodes (R1).

** Physics: see Preston (P8), Chapters II and III. Electricity: see Page and Adams (P7), pages 189-192, 218-228 and Sears (S3), Vol. II, Chapters 4, 5 and 6.

*** Physics: see Preston (P8), Chapters II and III, and Sears (S3), Vol. II, Chapters 4, 5 and 6. Electrical measurement: see Hague (H2) and Laws (L7). Instruments: see Rhodes (R1).

sections j and k of Description Summary 31-1. The hot junction of the couple is either part of the temperature receiver or is actually the receiver itself. The coupler is complemented by an indicating system with a potentiometer unit that includes the cold junction and a cell for standardization purposes. In operation, an excitation adjustment rheostat is used to manually set the slide-wire current at the calibration value, as shown by the galvanometer with the balance switch in the balance position. The reference junction temperature compensation knob is set to account for the cold junction temperature, which is effectively identical with the temperature of the potentiometer unit. With the balance switch in the temperature-measuring position, the thermocouple balance knob is rotated to bring the galvanometer reading to zero. The indicated temperature is read from the position of the temperature index with respect to the temperature scale.

31.18. Thermocouple temperature-measuring instruments may be made automatic by the use of a servo drive for balancing purposes and self-compensating networks to eliminate excitation errors and cold-junction temperature errors.

31.19. The theory of thermoelectric action and its use for temperature measurement is discussed in texts on physics and electricity and in books on instruments.* This information is readily available for use in the design and application of thermoelectrically coupled temperature-measuring instruments and will not be repeated here.

OPTICAL PYROMETERS

31.20. High temperatures are difficult to measure directly by means of any of the thermometer types described in the previous sections. This limitation does not apply to optical pyrometers, which depend on the variation in color of radiation emitted by a hot body as its temperature changes. The basic relationships involved are described by the Stefan-Boltzmann law and Planck's radiation laws. These laws are discussed in texts on theoretical physics and optics** and show that under proper conditions the color and intensity of radiation from a hot body are uniquely related to the temperature of the body. Various types of optical pyrometers*** are designed to apply this fact in the measurement of temperature.

31.21. A typical instrument of this class is illustrated in sections l and m of Description Summary 31-1. A brightness receiver consisting of an objective and an eyepiece includes a filter that limits the transmitted radiation to a narrow band in the red region of the spectrum. The coupler consists of the filament of an

---

* Physics: see Preston (P8), Chapters II and III, and Roberts (R9), Chapter I. Electricity: see Laws (L7) and Sears (S3), Vol. II, Chapters 4, 5 and 6. Instruments: see Behar (B2), Eckman (E1), and Rhodes (R1).

** Theoretical physics: see Schaefer (S16), Vol. III, Chapter 30. Optics: see Hardy and Perrin (H6).

*** See Rhodes (R1).

incandescent bulb placed at the focal point of the eyepiece, a battery for heating the filament, and a rheostat and knob for adjusting the filament temperature. The indicating system is a meter for indicating the current through the filament. The scale may be calibrated directly in terms of the temperature of the body whose brightness is received by the objective. To use an optical pyrometer, the observer looks at the hot body* and adjusts the filament temperature until the filament brightness just matches the brightness of the hot body, so that the image of the filament seems to disappear against the background of the hot body. The theory and practice of optical pyrometry is discussed by many authorities.**

RADIATION PYROMETERS

31.22. Radiation pyrometers depend on the functional relationship that exists*** between the total radiation from a hot body and its temperature. Sections n and o of Description Summary 31-1 illustrate a typical radiation pyrometer. Radiation from the hot body is brought to a focus by an optical system that is the principal component of the total radiation receiver. The input to the coupler is the energy falling on the hot junction of a thermocouple placed at the focal point. The output from the coupler is a voltage that acts as the input to the indicating system. The indicating system is an electrical meter that produces an index position with respect to a scale. The scale is calibrated in terms of the temperature of the hot body from which radiation is received.

31.23. The features of radiation pyrometer design and use are discussed in many references** and are not given further attention here.

TEMPERATURE INDICATORS FOR RECORDING AND CONTROL

31.24. Temperature-measuring instruments that differ from those illustrated in Description Summary 31-1 are described in the literature on the subject,† but the fundamental principles applied in systems of practical importance are fairly well illustrated in the summary. Many variants of the basic types exist that may be easily identified from a description of the design features used in any given case. For example, the replacement of the human operator by a photocell and servomechanism system for adjusting the filament brightness for an optical pyrometer is an obvious step in the design of an automatic device for measuring high temperatures.

31.25. All classes of temperature-measuring instruments may be made to function as recorders by proper modifications of the coupler and indicating system to produce lines on a photographic print or marks on chart paper. The

---

* Proper results from optical pyrometers depend on making observations under black-body conditions for the hot body. The practical requirements of black-body conditions are discussed by Rhodes (R1).

** See American Institute of Physics (A7), Behar (B2), Preston (P8), Chapters II and III, Rhodes (R1), Roberts (R9), Chapter I, and Wood and Cork (W9).

*** See Hardy and Perrin (H6), Rhodes (R1), and Schaefer (S16), Vol. III, Chapter 30.

† See American Institute of Physics (A7), Behar (B2), Rhodes (R1), and Wood and Cork (W9).

modifications usually include some provision for moving the paper, and means for moving the index with relatively great force that may be either an exceptionally powerful indicating system of some conventional type or a servomechanism designed to operate from the coupler output.

31.26. With instruments for measuring temperature available, it is an obvious step to use these devices for control purposes by introducing indications as controller inputs. Examples of temperature control are discussed in later chapters.

RELATIONSHIP OF TEMPERATURE RECEIVER PERFORMANCE TO TEMPERATURE-MEASURING INSTRUMENT PERFORMANCE

31.27. Perfect performance of any of the temperature-measuring instruments of Description Summary 31-1 produces indicated temperature readings that are identical with the corresponding input temperatures.* Ideal performance differs from perfect performance because indicated temperature readings from ideal instruments have accepted differences from the corresponding correct indicated temperature readings. Under the circumstances that usually exist, static inaccuracies may be maintained at tolerable levels by calibration, but dynamic errors are very often so great that they have a serious effect on performance. From the standpoint of practice, it is ordinarily possible to produce couplers, indicating systems, and scales with negligibly small time delays. On the other hand, it is difficult to design temperature receivers free from troublesome dynamic effects. The physical problem involved is to balance the heat interchange between the receiver and its surroundings against the heat capacity of the receiver so that the receiver temperature remains substantially equal to the input temperature at all times. Receivers that depend on this principle are so generally used that they may be considered typical for all temperature-measuring instruments.

31.28. The discussion of the following sections is restricted to typical instruments with the following characteristics:

1) Over-all instrument static sensitivity is unity.

2) Receiver static sensitivity is unity.

3) Over-all instrument dynamics are determined by receiver dynamics.

Derivation Summary 31-1 outlines the theoretical consequences of these assumptions and shows that the temperature input – indicated temperature output performance function for the typical temperature-measuring instrument reduces to the frequency function of the receiver.

PERFORMANCE EQUATION FOR A TYPICAL TEMPERATURE RECEIVER

31.29. The function of the typical temperature receiver is to generate a

---

* As the term "input temperatures" is used here, it means measures of the input temperature. This is common usage in discussions of measurement and is followed in this book.

The operation of a generalized temperature-measuring instrument with the features shown in section a of Description Summary 31-1 may be described in terms of performance functions for the individual operating components. These performance functions are listed below, in terms of the identifying symbols given on the diagram.

(tr) or (r): $[PF]_{(r)[T;T]}$ (c): $[PF]_{(c)[T;q]}$

(is): $[PF]_{(is)[q;(Ind)]}$ (s): $[PF]_{(s)[(Ind);T]}$

(ti): $$[PF]_{(ti)[T;(Ind)]} = [PF]_{(r)[T;T]}\,[PF]_{(c)[T;q]}\,[PF]_{(is)[q;(Ind)]} \tag{1}$$

(tmi): $$[PF]_{(tmi)[T;T]} = [PF]_{(ti)[T;(Ind)]}\,[PF]_{(s)[(Ind);T]} \tag{2}$$

Under static conditions, the performance functions reduce to static sensitivities, so that

$$[PF]_{(tmi)[T;T](st)} \longrightarrow S_{(tmi)[T;T](st)} = S_{(ti)[T;(Ind)](st)}\,S_{(s)[(Ind);T](st)} \tag{3}$$

For static calibration conditions, an instrument with ideal performance gives indicated temperatures that are equal to the corresponding input temperatures; i.e.,

$$T_{(s)(st)} = T_{(in)} \tag{4}$$

This means that

$$S_{(tmi)[T;T](st)} = 1 \tag{5}$$

In each of the temperature-measuring instrument types illustrated in Description Summary 31-1, the coupler, the indicating system and the scale may be designed to operate so rapidly that their performance functions reduce to static sensitivities. For the purposes of generalized discussion, this situation may be considered as typical, with other circumstances taken as special cases.

The performance function of the complete ideal instrument has the form

$$[PF]_{(tmi)[T;T]} = [PF]_{(r)[T;T]}\,S_{(c+(is)+s)[T;T](st)} \tag{6}$$

where

$$S_{(c+(is)+s)[T;T](st)} = S_{(c)[T;q](st)}\,S_{(is)[q;(Ind)](st)}\,S_{(s)[(Ind);T]} \tag{7}$$

When attention is restricted to designs in which the receiver temperature becomes equal to the input temperature under static conditions,

$$S_{(r)[T;T](st)} = 1 \tag{8}$$

By Eqs. (3) and (5),

$$S_{(tmi)[T;T](st)} = S_{(r)[T;T](st)}\,S_{(c+(is)+s)[T;T](st)} = 1 \tag{9}$$

From Eqs. (8) and (9),

$$S_{(c+(is)+s)[T;T](st)} = 1 = [PF]_{(c+(is)+s)[T;T]} \tag{10}$$

It follows that the generalized performance of typical temperature-measuring instruments may be described by a performance function of the form

$$[PF]_{(tmi)[T;T]} = [PF]_{(r)[T;T]} \tag{11}$$

The form of Eq. (10) of Definition Summary 13-6 may be used to express the receiver performance function in terms of a reference sensitivity and a frequency function; i.e.,

$$[PF]_{(tmi)[T;T]} = S_{(r)[T;T](ref)}\,(FF)_{(r)[T;T]} \tag{12}$$

where

$S_{(r)[T;T](ref)}$ = receiver reference sensitivity

$(FF)_{(r)[T;T]}$ = receiver frequency function

Under static conditions, both the frequency function and the performance function are equal to unity. It follows that

$$S_{(r)[T;T](ref)} = 1 \tag{13}$$

Derivation Summary 31-1. Performance functions for the generalized temperature-measuring instrument. (Page 1 of 2)

From Eqs. (12) and (13),

$$[PF]_{(tm1)[T;T]} = (FF)_{(r)[T;T]} \qquad (14)$$

Equation (14) shows that

for typical temperature-measuring instruments the performance function of the instrument is identical with the frequency function of the receiver.

Derivation Summary 31-1. Performance functions for the generalized temperature-measuring instrument. (Page 2 of 2)

temperature input for the coupler that is as nearly equal to the input temperature as possible. Temperature-measuring instruments may be designed to have receiver output temperatures different from the corresponding input temperatures, but these will be classed as special cases and omitted from the present discussion. All other receivers operate by absorbing or rejecting heat whenever the receiver temperature is different from the input temperature until, under static conditions, a condition of temperature equality is reached. When the input temperature is varying with time, the instantaneous heat flow to the receiver is a function of the instantaneous difference between the receiver temperature and the input temperature. The corresponding variation in receiver temperature is determined by the balance between the heat flow and the heat capacity of the receiver. In practice, the receiver temperature will usually be an average of some kind for the various parts of the receiver mass that may be considered as the effective input for the coupler. Under static conditions, the fact that temperature may not be constant throughout the receiver is usually of little importance, but it may be a determining factor in dynamic performance when the receiver is so large that considerable temperature gradients may accompany rapid input temperature changes. One of the goals of instrument design is to minimize the effect of thermal gradients. In the discussion of this section, the implicit assumption is made that the effects of gradients are so small that the thermal condition of the receiver may be represented by a single temperature under both static and dynamic conditions. The degree to which this assumption represents any given situation may sometimes be found by theoretical analysis based on the theory of heat conduction* or by experimental studies, but a proper combination of both approaches is ordinarily required to produce satisfactory results. Under practical conditions, the difficulties introduced by the use of a single temperature to represent the receiver output are not usually serious, because of the freedom that may be applied in specification and design. Extraordinary requirements placed on measuring-instrument performance may make special design procedures necessary, but the available physical principles will generally be those illustrated by the examples of Description Summary 31-1.

* See Carslaw (C7), McAdams (M10), and Schaefer (S16), Vol. II, Chapter 1.

31.30. Section a of Derivation Summary 31-2 represents a typical situation in which a receiver is attached to the wall of a duct that carries a fluid whose temperature is to be measured. In order to set up a definite problem, it is assumed that the duct wall temperature is effectively identical with the fluid temperature. Symbols and definitions for quantities that determine receiver performance are listed. Fluid temperature is the essential receiver input, and receiver temperature is the corresponding output. The receiver performance equation is the differential equation that describes the relationship between the output temperature and the input temperature. This relationship depends on the heat balance for the receiver, which is a statement of the fact that the flow of heat into the receiver is equal to the rate of increase of heat inside the receiver. When the material of the receiver remains in the same physical state,* so that latent heat effects may be neglected, the heat balance equates the heat flowing into the receiver to the heat capacity of the receiver per degree of temperature change (specific heat capacity) multiplied by the time rate of change of the receiver temperature. With latent heat effects negligible, the specific heat capacity of the receiver is equal to the average density of the receiver multiplied by the volume of the receiver and the average specific heat of the receiver. Equation (2) of Derivation Summary 31-2 is a formal expression for the receiver heat balance in terms of this product.

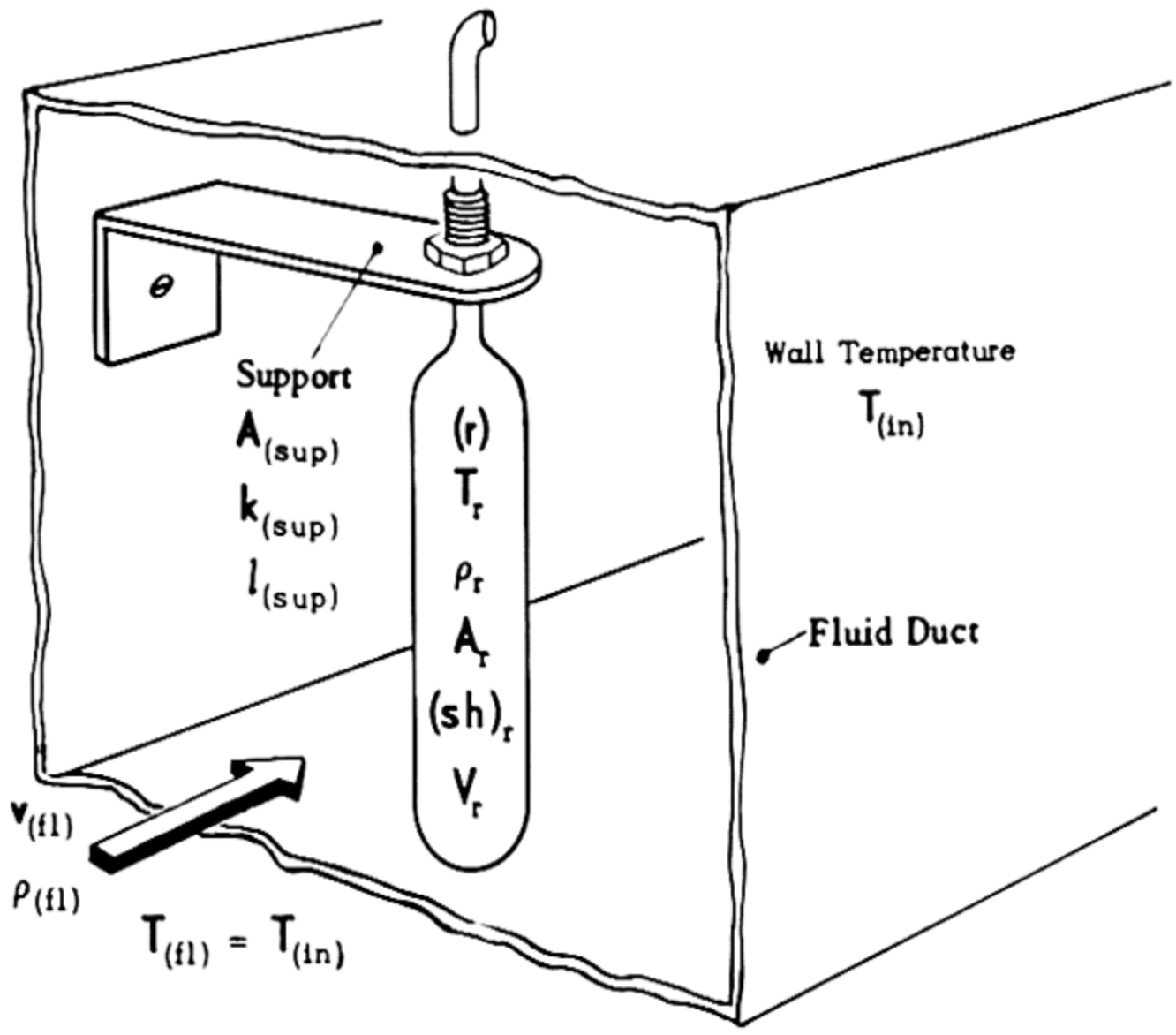
31.31. Equations (3) and (4) of Derivation Summary 31-2 are formal statements of the heat balance for a typical temperature receiver. In general, the inward heat flow for a temperature receiver has three components. These components are shown in section b of Derivation Summary 31-2 to be:

1) Convective heat flow, the flow across the fluid film on the surface of the receiver (first term on the right-hand side of Eq. (4)).
2) Radiation heat flow, the flow due to radiation exchange between receiver surface and surroundings (second term on the right-hand side of Eq. (4)).
3) Solid conduction heat flow, the flow through the solid parts that support the receiver (third term on the right-hand side of Eq. (4)).

31.32. In practice, the temperature receiver for any given instrument is designed to depend predominantly on one of these three types of heat flow. When the essential heat flow component is convective, the receiver temperature is determined by fluid temperature, and the instrument of which the receiver is a component acts as a fluid thermometer. When convective heat flow and conductive heat flow are both small in comparison with radiation heat flow, the receiver is part of a radiation meter. If heat flow through the solid material path corresponding

---

* This assumption means that the heat required to evaporate coupling fluid in the receiver of a vapor-pressure thermometer is a negligibly small fraction of the total heat flow involved in the operation of the receiver.



$T_{(in)}$ = input temperature = $T_{(fl)}$ = fluid temperature

$v_{(fl)}$ = velocity of the fluid past the temperature receiver

$\rho_{(fl)}$ = fluid density

T_r = receiver temperature = average temperature of the receiver mass that acts as the input to the coupler

ρ_r = average density of the receiver

A_r = surface area of the receiver for convective heat flow and radiation heat flow

$(sh)_r$ = average specific heat of the receiver

V_r = volume of the receiver

$A_{(sup)}$ = cross-section area of the support

$k_{(sup)}$ = thermal conductivity of the support

$l_{(sup)}$ = length of the support

a) *Illustrative arrangement of a receiver for the temperature of a moving fluid*

A heat balance for the temperature receiver shows that

$$\begin{pmatrix}\text{heat flow } \textit{into}\\ \text{the receiver}\end{pmatrix} = \begin{pmatrix}\text{rate of increase of}\\ \text{heat } \textit{within} \text{ the receiver}\end{pmatrix} \tag{1}$$

When the amount of heat involved in changes of physical state is negligibly small, increases in heat within the receiver cause the receiver temperature to change in accordance with an expression of the form:

$$\frac{dQ}{dt} = \rho_r V_r (sh)_r \frac{dT_r}{dt} \tag{2}$$

where

$\frac{dQ}{dt}$ = heat flow into the receiver

and

$\rho_r V_r (sh)_r$ = heat capacity of the receiver

Derivation Summary 31-2. Temperature receiver performance equation under idealized conditions.
(Page 1 of 3)

The heat flow into the receiver has three components; i.e.,

$$\begin{pmatrix}\text{heat flow}\\ \text{into receiver}\end{pmatrix} = \begin{pmatrix}\text{inward convective}\\ \text{heat flow across}\\ \text{fluid film on sur-}\\ \text{face of receiver}\end{pmatrix} + \begin{pmatrix}\text{inward heat flow due}\\ \text{to radiation exchange}\\ \text{between receiver sur-}\\ \text{face and surroundings}\end{pmatrix} + \begin{pmatrix}\text{inward heat flow}\\ \text{through support}\end{pmatrix} \tag{3}$$

In symbols, Eq. (3) is

$$\frac{dQ}{dt} = \frac{dQ_{(cnv)}}{dt} + \frac{dQ_{(rad)}}{dt} + \frac{dQ_{(cnd)}}{dt} \tag{4}$$

b) Heat balance for a temperature receiver

The convective heat flow to the receiver may be described by an equation of the form:

$$\frac{dQ_{(cnv)}}{dt} = h_{(cnv)} A_r [T_{(in)} - T_r] \tag{5}$$

where

$h_{(cnv)}$ = film conductivity coefficient of the receiver for heat flow

From Information Summary 30-5, the value of this coefficient depends on many factors; i.e.,

$h_{(cnv)} = f$ [(fluid), $\rho_{(fl)}$, $\nu_{(fl)}$, T_r, $(T_{(fl)} - T_r)$, (fluid viscosity), (fluid compressibility), (receiver shape), (receiver size), (receiver surface), (orientation of receiver with respect to fluid velocity) . . .] (6)

In any given situation, accurate data on $h_{(cnv)}$ must be based on experimental results. See Information Summary 30-5 for a further discussion of heat transfer from solids to fluids.

c) Convective heat transfer across the fluid film on a receiver surface

The Stefan-Boltzmann law (see section c of Information Summary 30-5) shows that the energy radiated from a body is proportional to the fourth power of the absolute temperature. When the situation illustrated by the figure of section a exists with the receiver as a radiating body surrounded by radiating walls, the net heat gain of the receiver is given by an equation of the form:

$$\frac{dQ_{(rad)}}{dt} = A_r p c_{(rad)} (T_{(in)}^4 - T_r^4) \tag{7}$$

where

p = surface emissivity (a function of material and surface)

$c_{(rad)}$ = black-body radiation coefficient

$= 0.172 \times 10^{-8}$ BTU/hr/sq ft/$(^\circ F_{(abs)}/100)^4$

$= 0.000137 \times 10^{-8}$ g-cal/sec/sq cm/$(^\circ C_{(abs)}/100)^4$

It is possible to write the fourth-power difference of Eq. (7) with $(T_{(in)} - T_r)$ and T_r^3 taken out as factors; i.e.,

$$T_{(in)}^4 - T_r^4 = (T_{(in)} - T_r)(T_{(in)}^3 + T_{(in)}^2 T_r + T_{(in)} T_r^2 + T_r^3)$$

$$= T_r^3 (T_{(in)} - T_r)\left(1 + \frac{T_{(in)}}{T_r} + \frac{T_{(in)}^2}{T_r^2} + \frac{T_{(in)}^3}{T_r^3}\right) \tag{8}$$

When the receiver temperature T_r is so near $T_{(in)}$ that $T_{(in)}/T_r \approx 1$, Eq. (8) becomes

$$T_{(in)}^4 - T_r^4 = 4 T_r^3 (T_{(in)} - T_r) \tag{9}$$

Define

$h_{(rad)}$ = equivalent radiation heat flow coefficient of the receiver

Derivation Summary 31-2. Temperature receiver performance equation under idealized conditions.
(Page 2 of 3)

where

$$h_{(rad)} = 4\rho c_{(rad)} T_r^3 \tag{10}$$

Substituting Eqs. (9) and (10) in Eq. (7) gives

$$\frac{dQ_{(rad)}}{dt} = h_{(rad)} A_r (T_{(in)} - T_r) \tag{11}$$

d) Linear approximation for radiation heat transfer for a receiver surrounded by walls at the input temperature

For the constant cross-section support of section a, and with the outer end of the support attached to a wall at the input temperature $T_{(in)}$, the law of heat conduction in solids (see section b of Information Summary 30-5) shows that

$$\frac{dQ_{(cnd)}}{dt} = \frac{k_{(sup)} A_{(sup)}}{l_{(sup)}} (T_{(in)} - T_r) \tag{12}$$

or

$$\frac{dQ_{(cnd)}}{dt} = h_{(cnd)} A_{(sup)} (T_{(in)} - T_r) \tag{13}$$

where

$h_{(cnd)} = \dfrac{k_{(sup)}}{l_{(sup)}}$ = heat conductivity coefficient for the support

e) Heat flow into a receiver through its support

Combining Eqs. (2), (4), (5), (11) and (13) gives

$$\rho_r V_r (sh)_r \frac{dT_r}{dt} = (h_{(cnv)} A_r + h_{(rad)} A_r + h_{(cnd)} A_{(sup)}) (T_{(in)} - T_r) \tag{14}$$

A rearrangement of terms in Eq. (14) gives the performance equation for the temperature receiver as

$$(CT)_r \frac{dT_r}{dt} + T_r = T_{(in)} \tag{15}$$

where

$$(CT)_r = \frac{\rho_r V_r (sh)_r}{h_{(cnv)} A_r + h_{(rad)} A_r + h_{(cnd)} A_{(sup)}} \tag{16}$$

Any consistent system of units may be used for the terms of Eq. (16). In either English or metric units, for example, the following tabulation would apply.

Quantity	English Units	Metric Units
T	°F	°C
ρ_r	lb/(ft)^3	gm/(cm)^3
V_r	(ft)^3	(cm)^3
$(sh)_r$	BTU/lb/°F	g-cal/gm/°C

Quantity	English Units	Metric Units
A_r $A_{(sup)}$	(ft)^2	(cm)^2
$h_{(cnv)}$ $h_{(rad)}$ $h_{(cnd)}$	BTU/hr/(ft)^2/°F	g-cal/sec/(cm)^2/°C

f) Performance equation for a temperature receiver

Derivation Summary 31-2. Temperature receiver performance equation under idealized conditions.
(Page 3 of 3)

to the support of section a of Derivation Summary 31-2 determines the receiver temperature, the instrument that includes the receiver is a thermometer for solids.

31.33. The heat balance of a fluid temperature receiver usually represents the generalized situation in which heat flow components of all three types are important. For this reason, the analysis of Derivation Summary 31-2 is carried out in terms of an illustrative fluid temperature receiver. The results of this analysis are typical for the fluid thermometer, and may also be directly applied to temperature-measuring instruments of other kinds.

CONVECTIVE HEAT FLOW INTO A RECEIVER

31.34. Section c of Derivation Summary 31-2 gives the formal expression for convective heat flow into a temperature receiver. The actual mechanism of this heat flow is too complicated for exact description in mathematical terms, but for practical purposes it is possible to use an equivalent film coefficient of heat conductivity to represent the effects associated with heat transfer to a solid from a fluid. The background theory of film coefficients and typical values for many situations are given by McAdams.* Equation (5) of Derivation Summary 31-2 has the form used by McAdams to describe heat flow between a fluid and a solid. This equation shows that the heat flow is proportional to the area of the exposed surface multiplied by a heat conductivity coefficient and a temperature difference. For the temperature receiver, the area involved is the receiver area (symbol A_r); the coefficient is the film heat transfer coefficient (symbol $h_{(cnv)}$); and the temperature difference is the difference between the fluid temperature (symbol $T_{(fl)}$ or $T_{(in)}$ for input temperature in the present case) and the receiver temperature (symbol T_r).

31.35. McAdams shows that the film heat transfer coefficient is a function of several factors, including fluid properties, receiver geometry, and the film temperature (see Eq. (6) of Derivation Summary 31-2). Except for certain generalities that may be based on dimensional analysis and physical principles, the heat transfer characteristics of fluid films for particular receiver shapes and operating conditions must be found by experiment. This phase of temperature receiver performance is discussed later.

RADIATION HEAT FLOW INTO A RECEIVER

31.36. The Stefan-Boltzmann law for radiant energy** shows that the total heat radiated by a body is proportional to the active area, the surface emissivity (which depends on the material and the type of surface), the black-body radiation coefficient, and the fourth power of the absolute temperature. When a body at one

---

* See McAdams (M10).

** See McAdams (M10), Preston (P8), Chapters II and III, and Schaefer (S16), Vol. II, Chapter 1.

temperature is completely surrounded by an environment at a second temperature, the fourth-power law applies to the body and its surroundings. The net interchange of radiant heat is proportional to the difference of the fourth power of the body temperature and the fourth power of the environmental temperature. The formal expression for this law as it applies to temperature receivers is written as Eq. (7) of Derivation Summary 31-2.

31.37. In practice, a difference of fourth powers is troublesome for many applications of analysis. This difficulty may be eliminated by taking advantage of two special conditions that exist when good temperature measurement practice is followed. The first of these conditions is that fluid temperature receivers are generally either completely or substantially surrounded by a surface at the fluid temperature to be measured. The illustrative diagram of section a of Derivation Summary 31-2 shows a situation in which the receiver is completely enveloped by a radiating surface at the input temperature. In other circumstances, the duct walls may be absent, but a radiation shield of some type placed around the receiver is a necessity if fluid temperatures are to be measured accurately. The second of the two conditions that makes it possible to simplify the fourth-power difference term of Eq. (7) in Derivation Summary 31-2 is that, when tolerable temperature measurement performance exists, the difference between the input temperature and the receiver temperature is small. This means that the ratio of input temperature to receiver temperature will be nearly equal to unity.

31.38. Equation (8) of Derivation Summary 31-2 gives the result of factoring out the cube of the receiver temperature and the difference between the input temperature and the receiver temperature from the fourth-power difference of Eq. (7). With these two factors removed, the fourth-power difference expression reduces to the sum of unity and the first, second and third powers of the ratio of input temperature to receiver temperature. When it is assumed that this ratio is substantially equal to unity under the normal operating conditions for a temperature receiver, the fourth-power difference expression may be written as four times the cube of the receiver temperature multiplied by the difference between the input temperature and the receiver temperature (see Eq. (9) of Derivation Summary 32-1).

31.39. When an equivalent radiation heat flow coefficient is defined in terms of emissivity, black-body radiation coefficient and receiver temperature in the form of Eq. (10) of Derivation Summary 31-2, the radiation heat flow into a typical temperature receiver may be written as Eq. (11). This equation is based on assumptions that are not exactly fulfilled, but it does show that radiation heat may be described to a reasonable degree of approximation by a temperature difference equation similar to that of Eq. (5) for convective heat flow. It is true that the equivalent radiation heat flow coefficient depends on receiver temperature; however, for reasonably small ranges of temperature, the effect of this dependence

will usually be smaller than the effect of film heat conductivity coefficient changes. As a matter of practical necessity, temperature receiver performance is usually determined by experimental procedures, so that it is not required of heat-flow expressions like those of Eqs. (5) and (11) to do more than to suggest forms for the expressions involved and to provide first-approximation values for design purposes.

CONDUCTION HEAT FLOW INTO A RECEIVER

31.40. Heat flow through a solid bar of constant cross section is proportional to the area of the bar and the thermal conductivity of the bar divided by the length of the bar and multiplied by the temperature difference between the ends of the bar. This expression is given as Eq. (12) of Derivation Summary 31-2. When the ratio of thermal conductivity to length is defined as a conductivity coefficient, the heat flow into the receiver illustrated in section a of Derivation Summary 31-2 is given by Eq. (13), which is an expression identical in form with Eqs. (5) and (11) for convective and radiation heat flow, respectively.

TEMPERATURE RECEIVER PERFORMANCE EQUATION

31.41. When the heat-flow expressions of Eqs. (5), (11) and (13) are combined with Eqs. (4) and (2) of Derivation Summary 31-2, the result is Eq. (14). Under circumstances that make it possible to consider as constants the coefficients of the terms that contain temperatures, Eq. (14) reduces to a first-order differential equation with constant coefficients. This equation is given by Eq. (15), with the coefficient of the time-derivative term written as the receiver characteristic time. The defining expression for this characteristic time is given in Eq. (16). English and metric units that give consistent results for characteristic time calculations are listed below Eq. (16).

RESPONSE CHARACTERISTICS FOR IDEAL THERMOMETERS

31.42. The discussion of Derivation Summary 31-1 notes that actual thermometers ordinarily have couplers, indicating systems, and scales with characteristics that cause the indicated temperature to be substantially identical with the receiver temperature under all operating conditions of practical interest.* This means that thermometer performance may be effectively discussed in terms of ideal receiver characteristics, with the combined performance function of all other operating components outside the receiver equal to unity. When this condition is accepted, the ideal performance equation for a complete temperature-

---

* Certain thermometer types may be designed so that the coupler – indicating system – scale combination will introduce inaccuracies of appreciable size. However, it should always be possible to eliminate inaccuracies of this kind by a redesign of the components involved.

measuring instrument is identical with Eq. (15) of Derivation Summary 31-2 except that the subscript r (for receiver) on the temperature symbol, T, is replaced by the subscript s (for scale). The resulting expression is

$$(CT)_{(th)}\dot{T}_s + T_s = T_{(in)} \tag{31-1}$$

where

T_s = temperature scale reading

$(CT)_{(th)}$ = thermometric characteristic time (identical with the receiver characteristic time defined by Eq. (16) of Derivation Summary 31-2)

31.43. The thermometer performance expression of Eq. (31-1) is a typical example of the zero-order independent variable first-order differential equation. This equation is one of the working variable forms discussed in Chapter 18. All of the pertinent results of that chapter may be directly applied to the description of thermometer performance if:

1) The working variable, u (for the independent variable), is identified with $(T_{(in)} - T_{(ref)})$, the difference between the input temperature and an arbitrary reference temperature.
2) The working variable, v (for the dependent variable), is identified with $(T_s - T_{(ref)})$, the difference between the temperature scale reading and the reference temperature.
3) The working variable characteristic time, τ, is identified with $(CT)_{(th)}$.
4) The working variable dimensional similarity factor, σ, becomes unity.

With these changes in notation, the (0; 0,1) working variable equation

$$\tau\dot{v} + v = \sigma u \tag{31-2}$$

of Figs. 18-1 through 18-9 corresponds to the thermometer performance equation written in the form

$$(CT)_{(th)}\dot{T}_s + (T_s - T_{(ref)}) = (T_{(in)} - T_{(ref)}) \tag{31-3}$$

31.44. For situations in which the thermometric characteristic time, $(CT)_{(th)}$, is substantially constant, the temperature readings corresponding to various typical changes of the input temperature may be taken directly from the nondimensional response curves of Figs. 18-1 through 18-9. Representative examples of these plots, with coordinate axes labeled in terms of temperature difference ratios, are repeated as Figs. 31-1 through 31-6.

STEP FUNCTION RESPONSE OF A THERMOMETER

31.45. When the input temperature is constant both before and after the instant $t = 0$, but has a step change at this instant, the corresponding solution of Eq. (31-3) gives the step function response for ideal thermometers with first-order characteristics. This solution has a form identical with the real exponential solution found in Derivation Summary 18-2 for the (0; 0,1) equation. The specific equation appears when:

1) The dependent variable is taken as the difference between the indicated temperature and the input temperature level that exists before the instant of the step.
2) The reference dependent variable is taken as the difference between the constant input temperature level existing after the step and the constant input temperature level before the step.

The input temperature before the step is considered as remaining constant for a period long enough to give a constant temperature reading equal to the constant input.

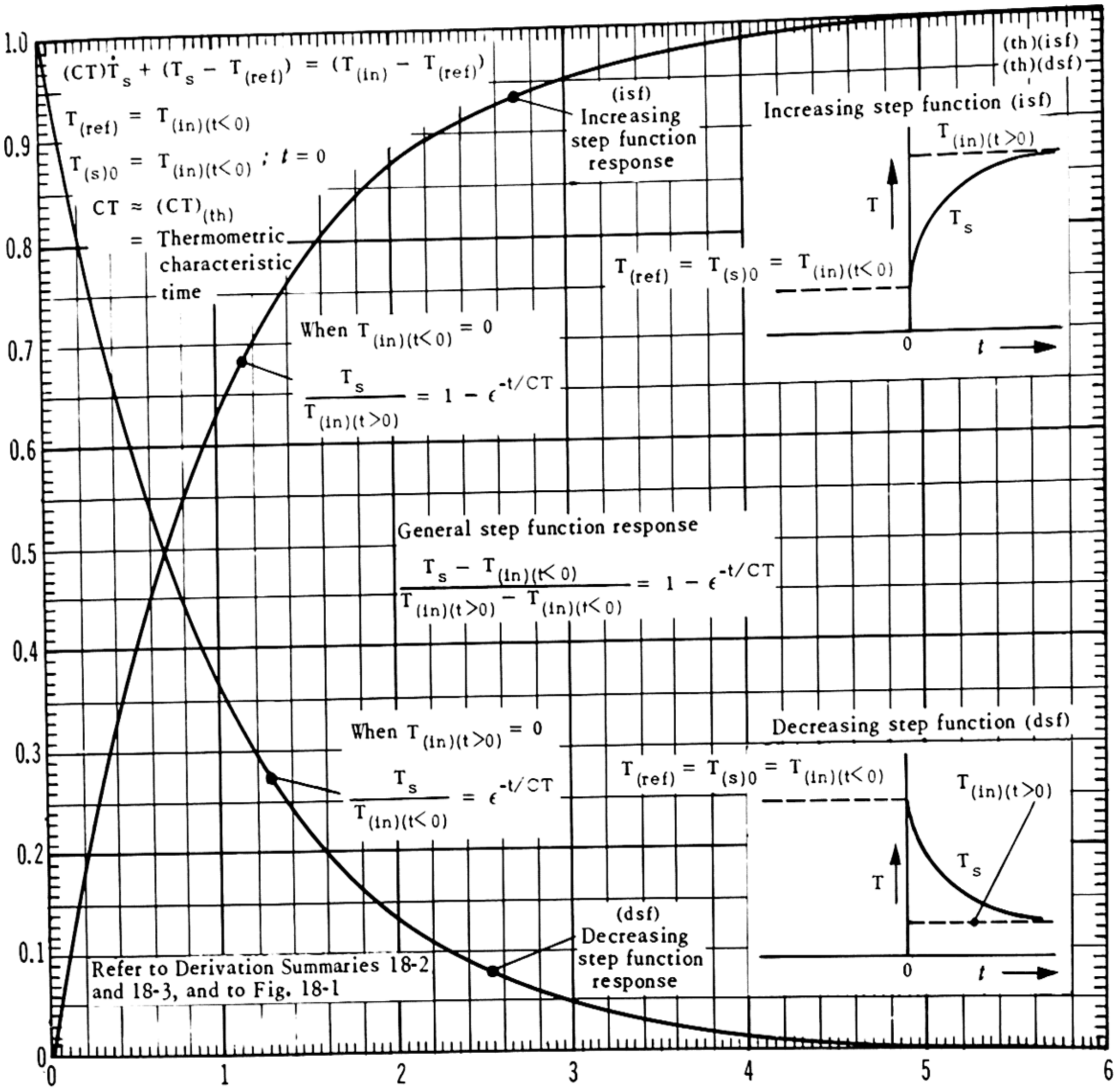
31.46. The choice of variables described above specifies a step of arbitrary magnitude and direction starting from any given level. The small illustrative diagrams in Fig. 31-1 show an increasing step function and a decreasing step function, with the reference level in each case taken as the input temperature before the step. The curves of Fig. 31-1 are taken directly from the (0; 0,1) step function plots of Fig. 18-1 and give quantitative information on the step response for thermometers with first-order characteristics. The ordinate is the ratio of the difference between the instantaneous reading and the input temperature before the step to the temperature difference equal to the complete step. The abscissa is the time - characteristic time ratio, which is equal to the elapsed time after the step divided by the thermometric characteristic time.

31.47. The ratio chosen for the ordinate scale of Fig. 31-1 in effect takes the height of any arbitrary step as unity and takes the input temperature after the step as either zero or unity, depending on the direction of the step. The increasing step function curve may thus be interpreted as the thermometer response when the temperature step is between the levels of zero and unity. Similarly, the decreasing step function gives the response when the step is between levels of unity and zero.

31.48. The equations and curves given in Fig. 31-1 show that the temperature reading is asymptotic to the final constant level of the input temperature. Intermediate temperatures follow the real exponential law. A series of these intermediate levels for integral values of the time - characteristic time ratio is listed in Fig. 31-1.

31.49. It is of fundamental importance to note that the curves of Fig. 31-1 describe the step function response for all thermometers that have first-order characteristics. When the thermometric characteristic time is known for any given instrument with these characteristics, its response to any step forcing function is completely determined. Changes in the characteristic time will cause the numbers on the abscissa scale to be different only when the generalized plots of Fig. 31-1 are to be associated with a specific situation.

31.50. When the thermometric characteristic time is not constant but varies



t/CT	1	2	3	4	5
$\frac{T_s - T_{(in)(t<0)}}{T_{(in)(t>0)} - T_{(in)(t<0)}}$	0.6321	0.8647	0.9502	0.9817	0.9933

Fig. 31-1. Step function response of an ideal thermometer with first-order performance characteristics and a constant characteristic time.

during the course of a step function response, the response-describing curve will not be a simple exponential. Methods for treating experimental data from situations of this kind are considered in the discussion of Derivation Summary 31-3.

RAMP FUNCTION RESPONSE OF A THERMOMETER

31.51. Figure 31-2 is a plot taken from the generalized curves of Fig. 18-2, and shows the response of a first-order thermometer to a ramp-function input temperature variation starting at any arbitrary reference temperature level with the temperature reading at the initial input temperature. The ordinate is the

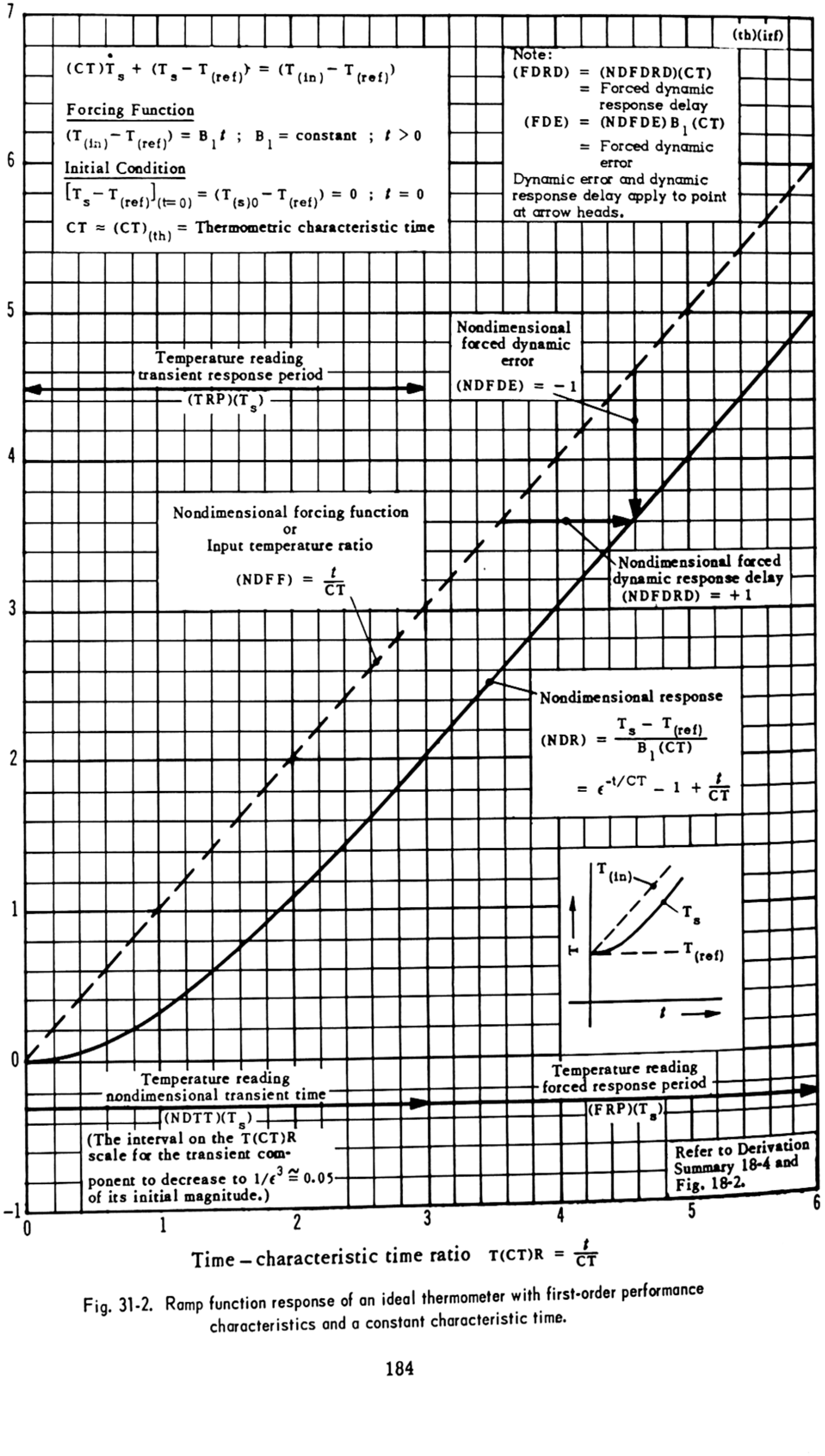


Fig. 31-2. Ramp function response of an ideal thermometer with first-order performance characteristics and a constant characteristic time.

indicated temperature – reference temperature difference ratio, which is the difference between the indicated temperature and the reference temperature divided by the change in the input temperature that occurs during one characteristic time. The abscissa is the time – characteristic time ratio. On this plot, the input temperature starts from zero (which corresponds to the reference temperature on a plot with indicated temperature as the ordinate) and has an upward slope of plus one, shown by a heavy dotted line. A similar line with a forty-five degree downward slope would represent a decreasing-ramp-function change of input temperature.

31.52. The temperature reading response function is shown by the full line in Fig. 31-2. Starting at the zero point as required by the assumed initial condition, the response "lags behind" the straight line that represents the input temperature variation until it finally reaches and holds parallelism with the forcing function. The interval on the dimensionless time scale (the time – characteristic time ratio scale) required for the response curve to reach this condition of parallelism is substantially equal to the temperature reading nondimensional transient time shown in Fig. 31-2 as three units on the abscissa scale. This definition is chosen so that it corresponds to the time period required for the magnitude of the transient component in the response to decrease to about five percent* (the approximate magnitude of the reciprocal of the cube of the natural logarithm base) of its initial value.

31.53. After the end of the temperature reading transient response period, which corresponds to the nondimensional transient time, the transient response component effects are substantially gone, and the forced response period starts and continues as long as the forcing function remains unchanged. During the forced response period, the dynamic error and the response delay, as these quantities are defined in Chapter 6, remain constant because the response curve holds parallel to the forcing function line. In the nondimensional coordinates of Fig. 31-2, the forced dynamic error is minus one unit, and the forced dynamic response delay is plus one unit. The forced dynamic error of one negative unit means that in any actual situation in which a linear temperature variation occurs, the forced dynamic error will cause the temperature reading to lag the input temperature (i.e., be lower when the input temperature is increasing and higher when the input temperature is decreasing) by an amount equal to the change of input temperature during one characteristic time. The corresponding forced dynamic response delay of one positive unit means that during the forced response period the temperature

---

* Other values of this "remaining transient component" percentage are frequently used. Five percent is chosen here because it corresponds to an integral value in nondimensionalized time units and has a value that is large enough for reliable measurements with ordinarily available equipment. Values of the remaining transient component smaller than five percent are difficult to measure with reasonable accuracy, while values that are substantially greater than five percent do not satisfactorily represent the end of the transient period. When the criterion of five percent is not sufficiently small, two "transient times" may be allowed, in which case the transient component will decay to less than three-tenths of one percent of its initial magnitude. A remaining transient component of this size would be very difficult to measure in practice.

reading does not reach a given level until one characteristic time has elapsed after the input temperature has passed through the given level.

31.54. All of the characteristics noted here for the plots of Fig. 31-2 hold for any system whose behavior may be described by a first-order differential equation with a constant characteristic time and a zero-order forcing function term (i.e., a (0; 0,1) equation). The curve of Fig. 31-2 will apply equally well to a situation where the change in one characteristic time is one unit and the characteristic time is one microsecond, and to a situation with a characteristic time change of one hundred units and a characteristic time of one hour. The response has the same shape, and it is only necessary to change the numbers on the coordinate scales for values to be read off directly for either case.

THERMOMETER RESPONSE TO A PARABOLIC INPUT TEMPERATURE CHANGE

31.55. The response of a first-order thermometer with a constant characteristic time is shown by the curves of Fig. 31-3, which are taken directly from the plots of Fig. 18-3. The nondimensional ordinate is the ratio of the difference between the indicated temperature and the reference temperature at which the input variation starts to the input change that occurs during the time interval from zero to one characteristic time. The abscissa is the time - characteristic time ratio. A dashed curve, which is a simple parabola, is used to represent the forcing function, and a full-line curve indicates the response.

31.56. The curves of Fig. 31-3 do not actually extend into the forced response period because of space limitations, but equations given on the figure show that the forced dynamic error and the forced dynamic response delay both become larger as the time - characteristic time ratio increases. This is a different type of behavior from that shown by the ramp function response curve of Fig. 31-2. A review of the discussion of first-order equation response characteristics given in Chapter 18 leads to the conclusion that forcing function variations corresponding to cubic and higher order forcing functions lead to response curves with forced dynamic errors and forced dynamic response delays that vary more strongly with time than the corresponding quantities for the parabolic input variation. The equations required to express responses to higher order forcing functions become so cumbersome that, as a matter of practice, it is better to describe complex forcing functions by means of the Fourier series or Fourier integral representations discussed in Chapter 12 or the impulse function representation of Chapter 17 than it is to use a power series that includes high-order terms. The general usefulness of sinusoidal terms and impulse terms for reducing physical variations to mathematical forms makes it important to summarize information on responses to these forms by means of nondimensional curves. Curves of this kind are discussed in the following two sections.

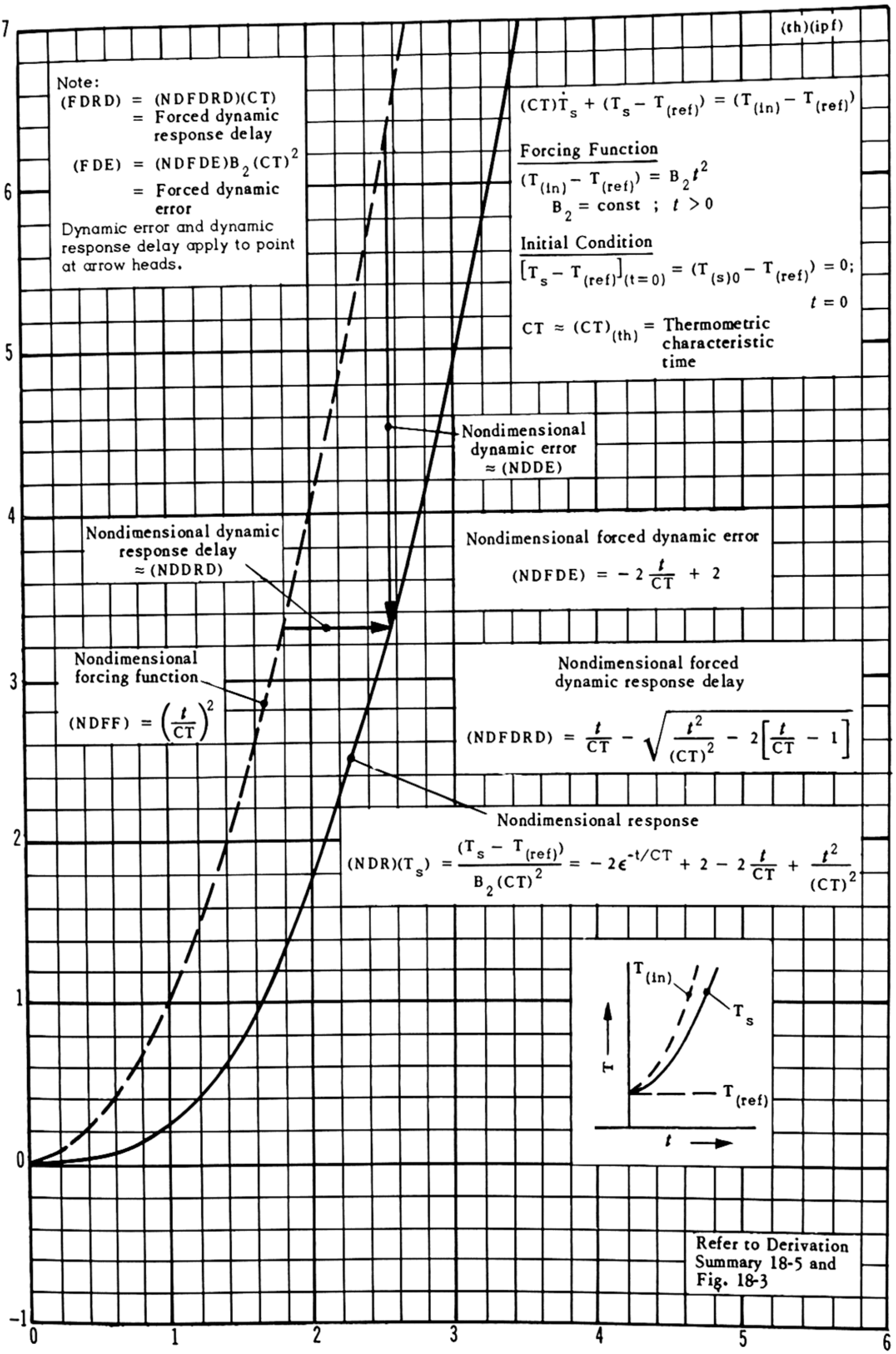


Fig. 31-3. Parabolic function response of an ideal thermometer with first-order performance characteristics and constant characteristic time.

STEADY-STATE RESPONSE TO SINUSOIDAL INPUT TEMPERATURE CHANGE

31.57. The steady-state response of the first-order thermometer with a constant characteristic time to a sinusoidal forcing function is represented by the curves of Figs. 31-4, 31-5 and 31-6. These curves are taken respectively from Figs. 18-7, 18-8 and 18-9, which represent the results of the analysis outlined in Derivation Summary 18-10. The terminolgy and notation used are based on the conventions described in Definition Summaries 13-3, 13-4, 13-5 and 13-6.

31.58. The forcing function to which the curves of Fig. 31-4 apply is a sinusoidal input temperature variation about a constant reference temperature level, as shown by the small diagram on the figure. The analysis of Derivation Summary 18-10 shows that the steady-state response corresponding to this forcing function is equal to the product of a reference amplitude ratio multiplied by a dynamic amplitude ratio – reference amplitude ratio ratio as a scalar factor for the forcing function and an imaginary exponential with the dynamic response angle in the exponent. The graphical interpretation of the forcing function and the steady-state response in these terms is illustrated in Figs. 13-2 and 13-3, using the concepts and notation described in Definition Summaries 13-4 and 13-5. For the case of an instrument, sensitivity may be identified with the dynamic amplitude ratio, and a reference sensitivity may be taken as equivalent to the reference amplitude ratio, so that the dynamic amplitude ratio – reference amplitude ratio ratio reduces to the sensitivity – reference sensitivity ratio. The formal relationships involved are specifically described in Definition Summary 13-5 and applied in Eqs. (16) through (21) of Definition Summary 13-6.

31.59. For the performance-describing purpose of Figs. 31-4, 31-5 and 31-6, it is convenient to take the static sensitivity of the typical ideal thermometer as the reference sensitivity. It is shown in Derivation Summary 31-1 that the ideal thermometer static sensitivity is unity. With this value for the reference sensitivity, the left-hand ordinate for Figs. 31-4, 31-5 and 31-6 may be taken directly from the ordinate of Figs. 18-7, 18-8 and 18-9 and labeled as the thermometric sensitivity.* The right-hand ordinate is the dynamic response angle plotted on a scale identical with that used in Figs. 18-7, 18-8 and 18-9. The abscissa of Figs. 31-4, 31-5 and 31-6 is a nondimensional frequency scale in terms of the characteristic time – forcing frequency product.** This choice of abscissa is convenient in practice because the nondimensional frequency may be transformed to the forcing frequency by a simple application of characteristic time as a dividing factor.

---

* It should be noted that the present situation is a special case. In general, the corresponding ordinate would be the sensitivity – reference sensitivity ratio, with a reference sensitivity not equal to unity.

** The characteristic time – forcing frequency product is identical with the characteristic time – forcing period ratio.

31.60. Figure 31-4 shows that the thermometric sensitivity starts from unity at zero frequency, decreases by a curved path for intermediate frequencies, and then becomes asymptotic to zero for high frequencies. The mathematical expression for sensitivity shows that the high-frequency asymptotic approach to zero is actually linear. The dynamic response angle is zero at zero frequency, decreases along a curved path for intermediate frequencies, and is asymptotic to minus 90 degrees for high frequencies.

31.61. Figure 31-5 is similar to Fig. 31-4, except that the distance on the nondimensional frequency scale that corresponds to ten units in Fig. 31-4 is used for one unit in Fig. 31-5.

31.62. The logarithmic scale curves of Fig. 31-6 supply steady-state sinusoidal performance information on the first-order thermometer with a constant characteristic time that is identical with the sensitivity and dynamic response angle data given in the linear scale plots of Figs. 31-4 and 31-5. In Fig. 31-6, the left-hand ordinate scale is marked in loru units (which are simply logarithms to the base 10 of the sensitivity), in direct numerical sensitivity units, and in decibels, which are equal to loru values multiplied by 20. The abscissa scale is marked in direct numerical characteristic time - forcing frequency units, in lorus (or deciles, which are identical with lorus), and in octaves, which are logarithms with 2 as their base. The dynamic response angle scale, on the right-hand side, is linear, with 50 degrees of this scale covering the same scale length as one loru (twenty decibels) on the left-hand ordinate scale.

31.63. The curves of Figs. 31-4, 31-5 and 31-6 correspond to the sinusoidal response characteristic representations of Figs. 13-1b and 13-1c discussed in Chapter 13. Figure 13-1a illustrates a complex plane representation for sinusoidal response characteristics that is not included in the plots of Figs. 31-4, 31-5 and 31-6. This representation of thermometer response is given directly by the polar plot of Fig. 18-6 when the nondimensional amplitude ratio is made identical with the thermometric sensitivity. It is important to note that in Fig. 18-6 only the lower half-circle, which corresponds to positive values of the characteristic time - forcing frequency product, has a physical meaning. The upper half-circle is mathematically present, but has no physical significance because it is associated with nonexistent negative frequencies.

31.64. The logarithmic-scale plots of Fig. 31-6 have shapes that are simpler than the curved forms of the corresponding linear scale plots of Figs. 31-4 and 31-5. For the low-frequency range, the sensitivity plot is asymptotic to the zero loru level (the unity sensitivity level) and in the high-frequency range is asymptotic to a straight line with a geometrical slope of minus one. The point of intersection of the high-frequency asymptote with the low-frequency asymptote is the break point, which is also sometimes called the corner point. The actual sensitivity

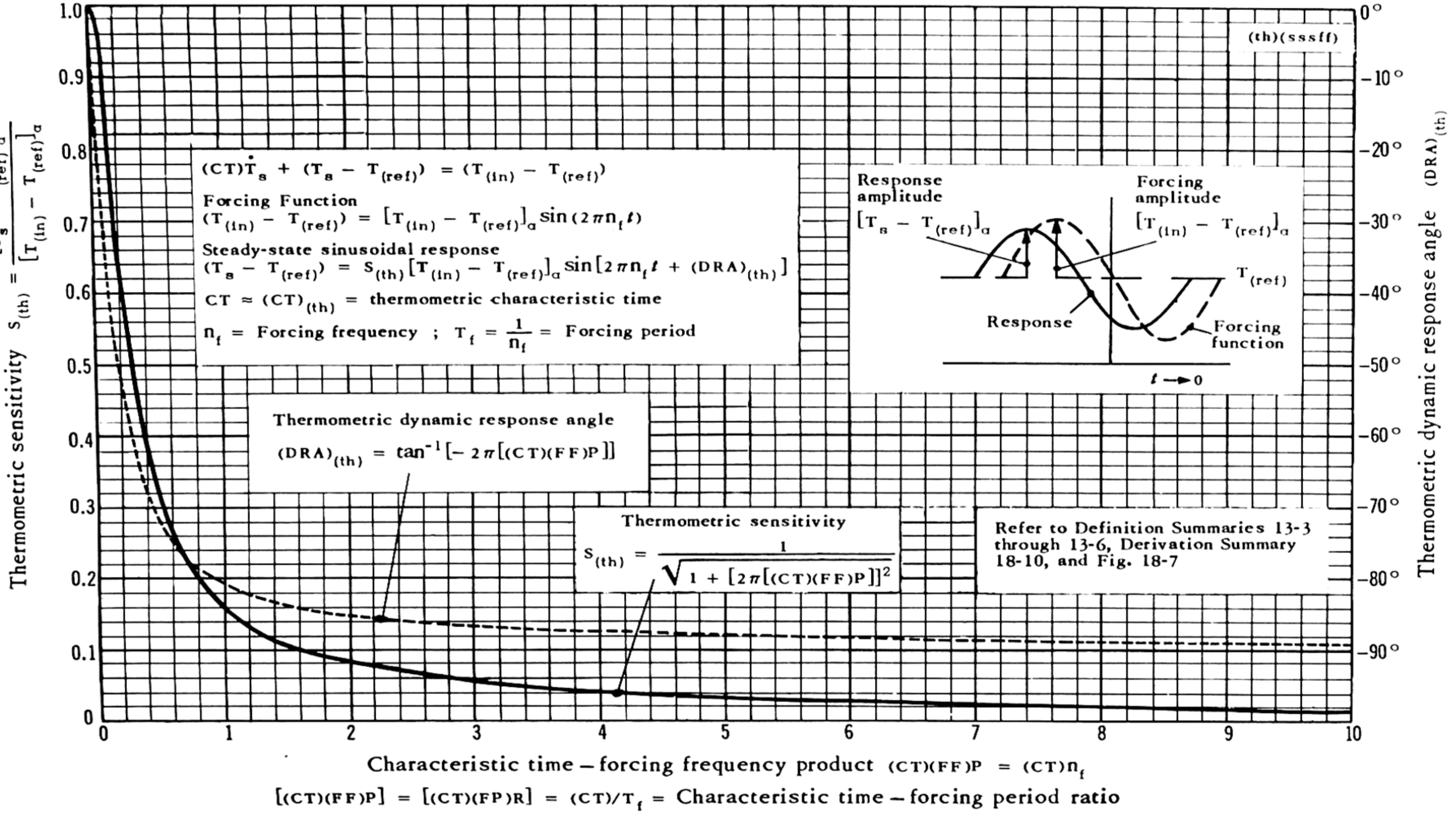


Fig. 31-4. Steady-state sinusoidal response of an ideal thermometer with first-order performance characteristics and constant characteristic time – linear scale plots.

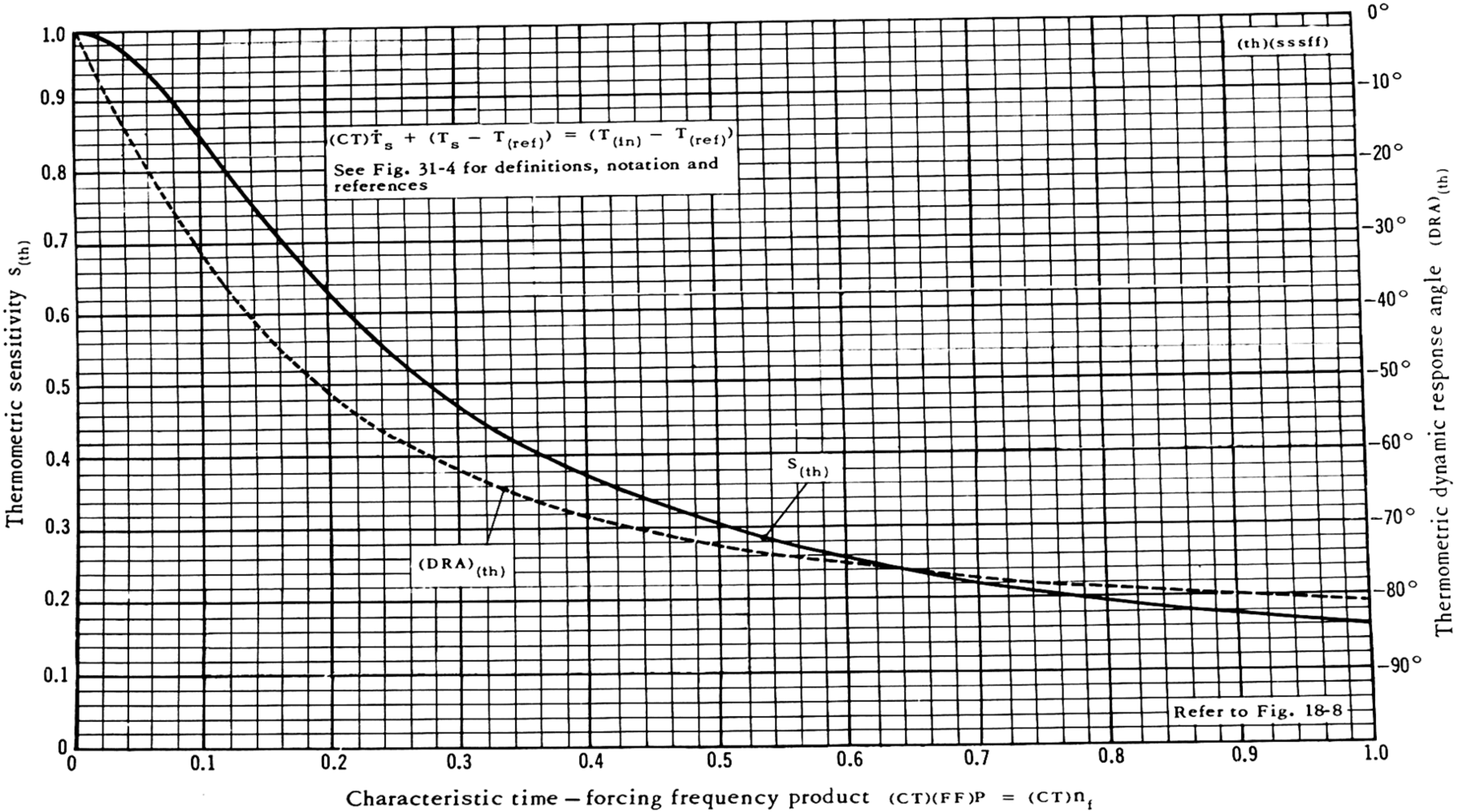


Fig. 31-5. Steady-state sinusoidal response of an ideal thermometer with first-order performance characteristics and constant characteristic time – linear scale plots – low frequency range.

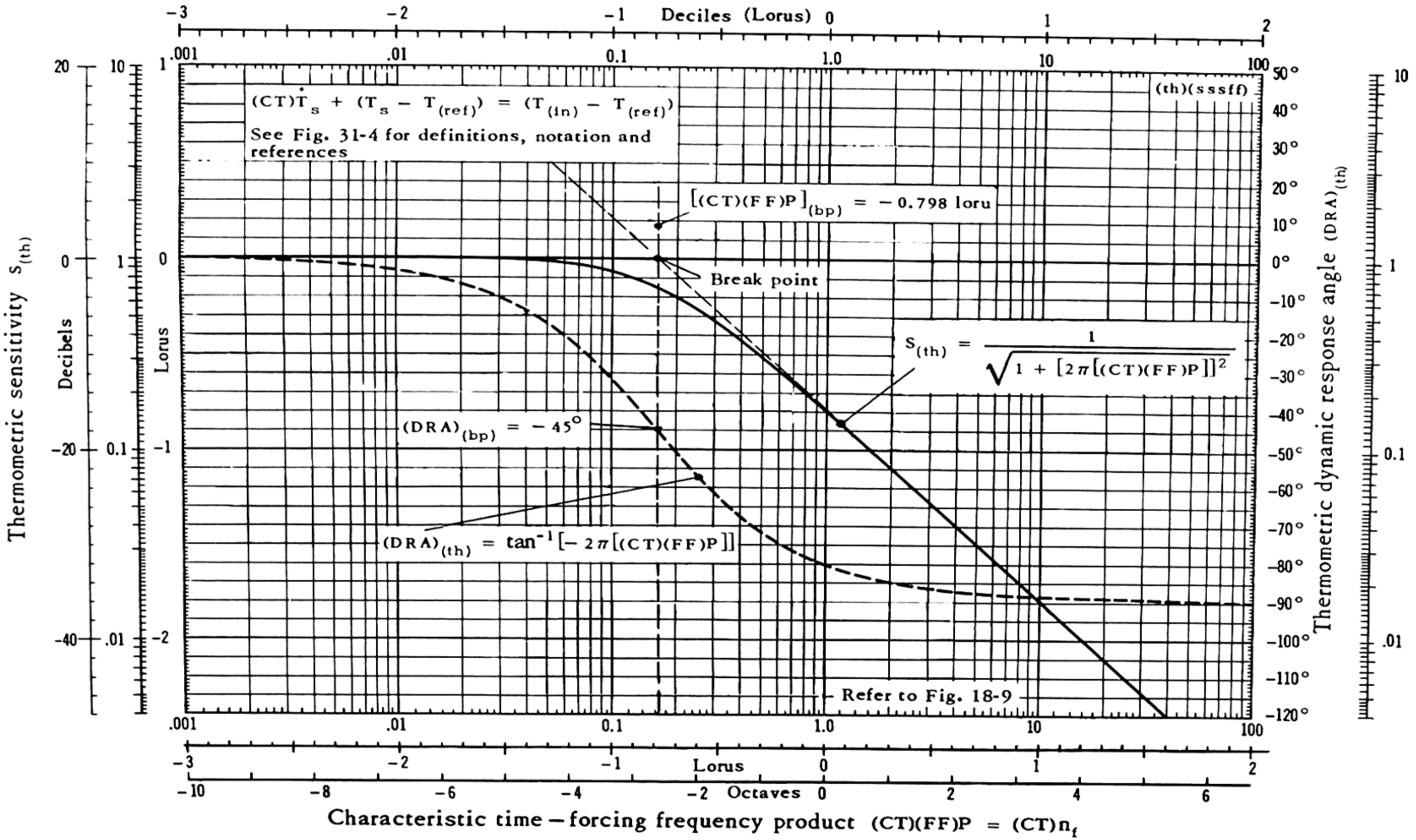


Fig. 31-6. Steady-state sinusoidal response of an ideal thermometer with first-order performance characteristics and constant characteristic time — logarithmic scale plots.

follows a simple curve that joins the two asymptote lines and falls below the break point. The dynamic response angle for the breakpoint abscissa (this abscissa is -0.798 loru in Fig. 31-6) is minus 45 degrees. The response angle curve is asymptotic to zero for abscissae below the break point and is asymptotic to minus 90 degrees for abscissae above the break point. It reverses curvature at the intersection of the breakpoint ordinate and the minus 45-degree line, with segments of similar shape on either side.

31.65. In addition to advantages in terms of curve simplicity, the logarithmic abscissa scale of Fig. 31-6 has the advantage over the linear scales of Figs. 31-4 and 31-5 in that it covers a forcing frequency range of five orders of magnitude, as compared with one order of magnitude for Fig. 31-4 and one-tenth order of magnitude for Fig. 31-5.

IMPULSE FUNCTION RESPONSE OF A FIRST-ORDER THERMOMETER

31.66. Forcing functions of arbitrary shape may be formed of impulse functions combined under the conventions illustrated in Derivation Summary 17-1. When an input temperature forcing function for a first-order thermometer with a constant characteristic time is expressed in terms of impulses, the corresponding response function is the resultant of the responses to the individual impulses summed in the way illustrated in Derivation Summary 17-2. The impulse function response that is fundamental in building up the response to an arbitrary forcing function is developed in Derivation Summaries 18-8 and 18-13. This response has the form of the simple exponential plotted as the decreasing step function response of Fig. 31-1, with the reference temperature difference taken as the strength of the impulse* divided by the characteristic time. In any specific case of thermometer response, the exponential responses to the individual impulses may be summed up graphically to give the resultant by a procedure similar to that illustrated in Derivation Summary 17-2; or the convolution integral forms of Eqs. (17) and (18) of that summary may be used to set up a mathematical expression for the response.

SEMILOGARITHMIC PLOTS OF THERMOMETER RESPONSE TO STEP CHANGES OF INPUT TEMPERATURE

31.67. The linear-scale step function response plots of Fig. 31-1 become straight lines when the ordinate scale is changed from linear to logarithmic. When the natural logarithm of the temperature difference ratio is used for the ordinate, and the time - characteristic time ratio is taken for the abscissa, the decreasing step function response is a straight line starting at the zero ordinate level for the

---

* Refer to the discussion of Definition Summary 18-8, Volume II, for the definition of impulse function strength.

initial instant and sloping downward at 45 degrees. A plot of this type is illustrated in Fig. a of Derivation Summary 31-3. When natural logarithms are replaced by logarithms to the base of 10, the semilogarithmic step function response plot remains a straight line starting at the zero ordinate, but the minus one slope is replaced by a negative slope with a magnitude equal to the reciprocal of the natural logarithm of 10.* As shown by Fig. b of Derivation Summary 31-3, a single plot of the logarithm to the base 10 of the temperature difference ratio as ordinate against the time – characteristic time ratio as abscissa represents all possible decreasing step function responses.

31.68. When time instead of the time – characteristic time ratio is used as the abscissa for semilogarithmic representations of step function response, all possible plots start from zero at the initial instant, but have slopes that are inversely proportional to the characteristic time. An illustrative semilogarithmic plot for step function response with time as the abscissa is shown in Fig. c of Derivation Summary 31-3.

DETERMINATION OF CHARACTERISTIC TIME FROM SEMILOGARITHMIC PLOTS OF STEP FUNCTION RESPONSE

31.69. In practice, the factors that control the dynamic characteristics of temperature-measuring instruments can be only approximately estimated as individual quantities. This fact means that the theory outlined in Derivation Summary 31-2 may be helpful for preliminary study purposes, but must be supplemented by experiments on completed instruments in order to determine accurately the dynamic characteristics of any given thermometer design. When the experimental information has the form of step function response data, semilogarithmic plots will immediately show whether or not the thermometer under test acts as a first-order system. If a straight line can be drawn through the experimental points from an input temperature step, the thermometer involved acts as a first-order system under the test conditions. In many actual situations, the test points do not fall exactly on a straight line, but may still be represented reasonably well by a linear approximation. When time is used for the abscissa of semilogarithmic plots of this kind, the effective characteristic time of the thermometer tested may be found from the slope of the response line. The relationships involved in finding this slope and formulae for determining characteristic times from two response-line points are developed in Derivation Summary 31-3.

DIMENSIONAL ANALYSIS OF FACTORS CONTROLLING THERMOMETRIC CHARACTERISTIC TIME

31.70. The principles of dimensional analysis discussed in Chapter 8 can be applied to the problem of temperature-measuring instrument performance. The

* The natural logarithm of 10 is the factor required to transform logarithms to the base of 10 to natural logarithms as required by the defining equations for logarithms. If $\log_b N = x$, then $b^x = N$, b = base of logarithm, $\log_b N = \log_a N / \log_a b$, and $\log_a N$ = logarithm of N to base a.

The working variable results of Derivation Summaries 18-2 and 18-3, specialized to describe the step function response of an ideal thermometer with first-order characteristics and constant characteristic time, may be written in the form:

$$\frac{T_s - T_{(in)(t>0)}}{T_{(in)(t<0)} - T_{(in)(t>0)}} = \epsilon^{-t/(CT)} \tag{1}$$

Linear scale representations of Eq. (1) are given in Fig. 31-1.

When natural logarithms are taken of both sides, Eq. (1) becomes

$$\ln\left[\frac{T_s - T_{(in)(t>0)}}{T_{(in)(t<0)} - T_{(in)(t>0)}}\right] = -\frac{t}{(CT)} \tag{2}$$

Applying the relationship

$$\ln N = [\ln(10)]\log N \tag{3}$$

where

$$\ln N = \text{natural logarithm of } N$$
$$\log N = \text{logarithm of } N \text{ to base } 10$$
$$\ln(10) = 2.3026 \tag{4}$$

to Eq. (2) gives

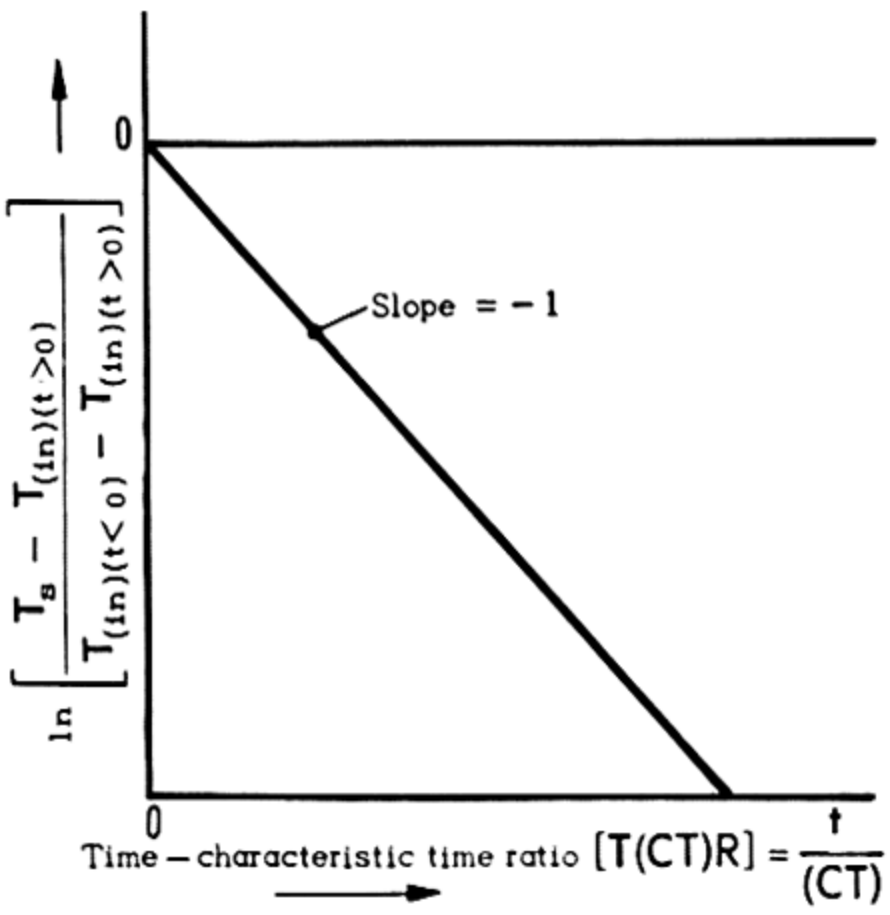
$$\log \frac{T_s - T_{(in)(t>0)}}{T_{(in)(t<0)} - T_{(in)(t>0)}} = -\frac{1}{2.3026}\frac{t}{(CT)} \tag{5}$$

Using the point designations of Fig. c of this summary, expressions for (CT) may be written in the forms

$$(CT) = -0.4343\frac{t_1 - t_2}{\log\left[\frac{T_s - T_{(in)(t>0)}}{T_{(in)(t<0)} - T_{(in)(t>0)}}\right]_1 - \log\left[\frac{T_s - T_{(in)(t>0)}}{T_{(in)(t<0)} - T_{(in)(t>0)}}\right]_2} \tag{6}$$

$$(CT) = -0.4343\frac{t_1 - t_2}{\log\left\{\left[\frac{T_s - T_{(in)(t>0)}}{T_{(in)(t<0)} - T_{(in)(t>0)}}\right]_1 \Big/ \left[\frac{T_s - T_{(in)(t>0)}}{T_{(in)(t<0)} - T_{(in)(t>0)}}\right]_2\right\}} \tag{7}$$

$$(CT) = -0.4343\frac{t_1 - t_2}{\log\left[\frac{[T_s - T_{(in)(t>0)}]_1}{[T_s - T_{(in)(t>0)}]_2}\right]} \tag{8}$$



Figures a, b, and c give semilogarithmic plots for the first-order thermometer step function responses that correspond respectively to the forms of Eqs. (2), (5), and (6). Note that the plots are straight lines.

Fig. a. Semilogarithmic plot of step function response with natural-logarithm ordinate and dimensionless abscissa.

Derivation Summary 31-3. Semilogarithmic plot representations for the step function response of an ideal thermometer with first-order performance characteristics and a constant characteristic time. (Page 1 of 2)

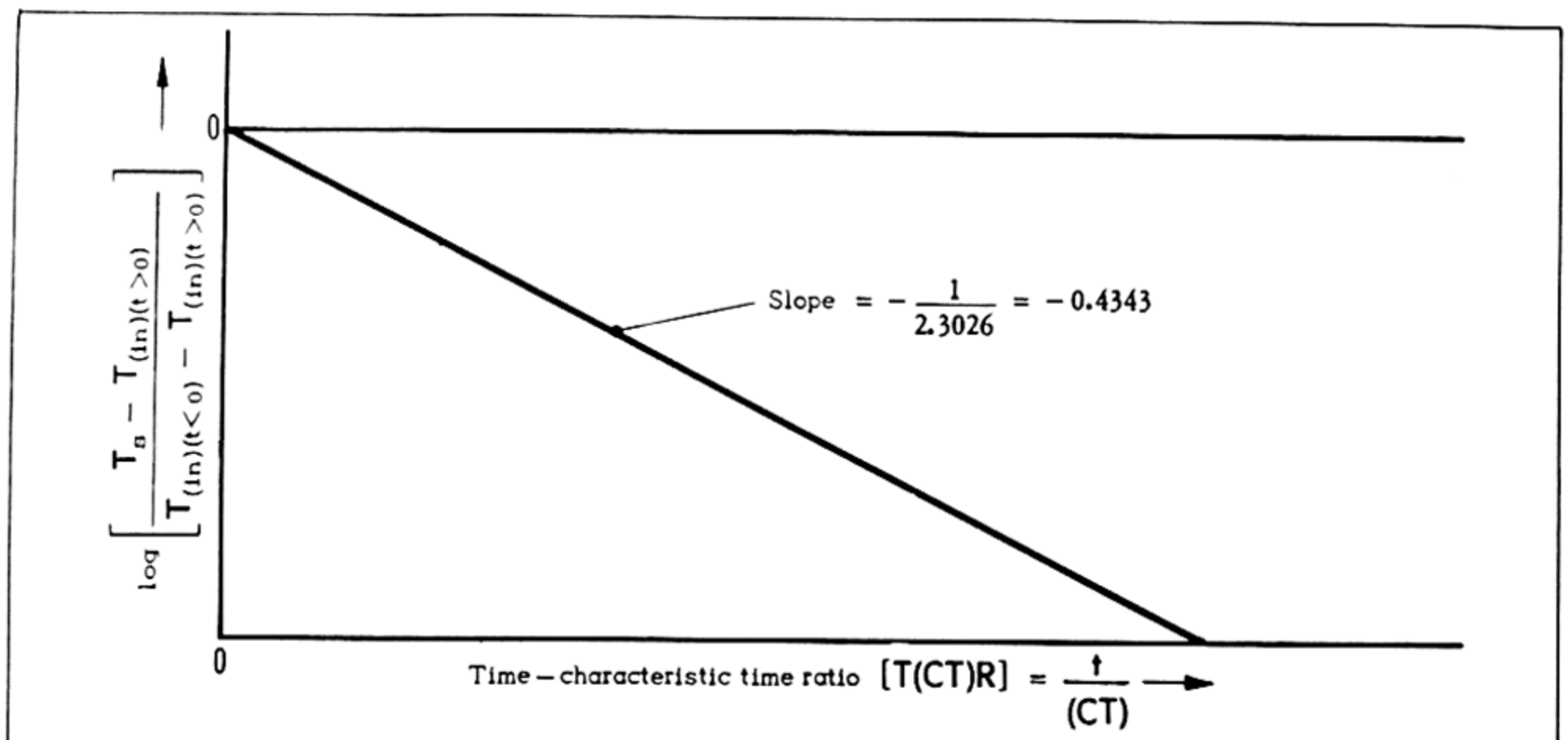


Fig. b. Semilogarithmic plot of step function response with base-ten-logarithm ordinate and dimensionless abscissa

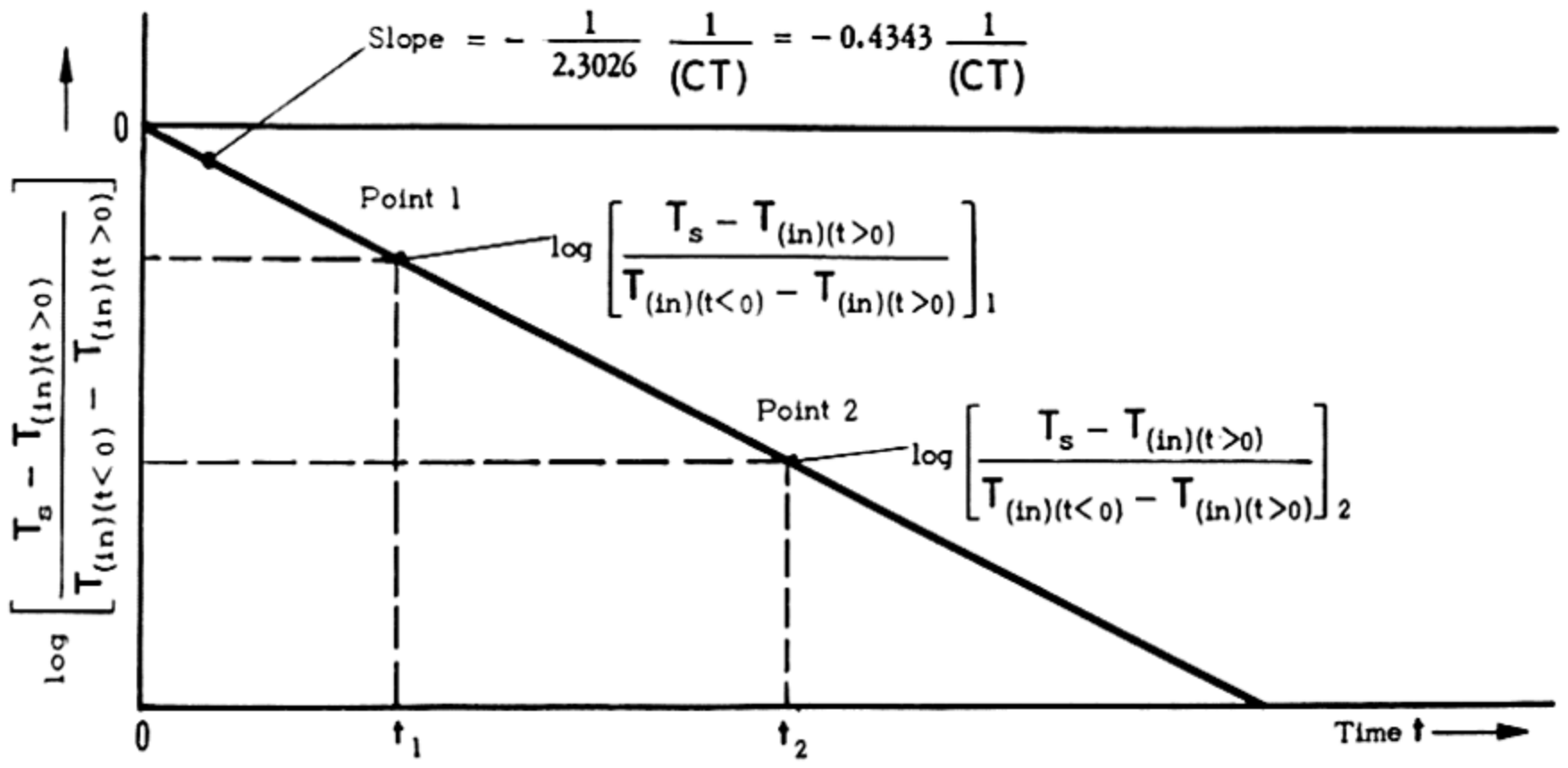


Fig. c. Semilogarithmic plot of step function response with base-ten-logarithm ordinate and time abscissa

Derivation Summary 31-3. Semilogarithmic plot representations for the step function response of an ideal thermometer with first-order performance characteristics and a constant characteristic time. (Page 2 of 2)

procedure for using dimensional analysis is to list all the physical quantities that affect performance with their dimensional formulae and then to form a number of dimensionless variables from these quantities. The Π Theorem shows that the number of independent variables of this kind is equal to the difference between the number of physical quantities involved and the number of primary units that appear in these quantities.

31.71. With a thermometer having the properties set forth in Derivation Summary 31-1, the quantities that control performance are those that determine the way receiver temperature follows input temperature changes. Under the conditions assumed in Derivation Summary 31-2, the behavior of the receiver is

described by a first-order differential equation. The performance associated with such an equation is completely determined when the characteristic time appearing in the equation is known and can be considered as constant over the operating range considered. This means that the basic problem of describing first-order thermometer performance is that of finding characteristic time as a function of the variables by which it is determined. Equation (16) of Derivation Summary 31-2 gives a formula for characteristic time that depends on the receiver heat balance expressed by Eqs. (4) and (14). This relationship contains the product of receiver density, volume, and specific heat in the numerator, and a sum of heat transfer coefficients and receiver area products in the denominator. These heat transfer coefficients represent the effects of fluid convection and radiation, and of conduction through the support. In any practical case, the receiver characteristic time depends on the relative effects of heat flow associated with these three processes. Convection heat flow involves transfer across a film on the receiver surface, whose properties are determined by the complex interactions of many factors. On the other hand, conduction through the receiver support and radiation may be described by relatively simple analysis. For this reason, the convection type of heat flow offers the best example for illustrating an application of dimensional analysis to temperature-measuring instruments.

31.72. For the purposes of discussion, it is assumed that receiver temperature is determined by a heat balance in which all heat flow effects except convection are negligibly small. Items 1 through 5 of Derivation Summary 31-4 list the characteristic time and the quantities that control its magnitude as given by Eq. (16) of Derivation Summary 31-2. Item 5 is the average surface film thermal conductivity coefficient, which depends on several other factors. These factors and the typical heat flow problem with which they are usually associated are discussed by Bridgman, who reports work by Lord Rayleigh, and by Johnson.* It is generally accepted that for operating regions in which fluid compressibility is not important, the film coefficient depends on fluid density, fluid viscosity, the heat conductivity of the fluid, and the velocity of the fluid past the body involved in the heat flow. These four quantities are listed as items 6 through 9 in the table of Derivation Summary 31-4. The dimensional formulae in the fourth column of this table show that five primary quantities – mass, length, time, heat, and temperature – occur in the nine quantities involved. This means that, by the Π Theorem, these nine variables may be combined into four dimensionless ratios.

31.73. The four Π's given in Derivation Summary 31-4 are formed by the principles discussed in Chapter 8. The first Π is simply the characteristic time multiplied by the factors that remain in Eq. (16) of Derivation Summary 31-2 when the radiation and conduction coefficients are zero. In this Π, the ratio of

* See Bridgman (B18) and Johnson (J5).

FACTORS AFFECTING THERMOMETRIC CHARACTERISTIC TIME

Item No.	Name	Symbol	Dimensional Formula
1	Characteristic Time	(CT)	T
2	$\frac{\text{Receiver Volume}}{\text{Receiver Area}}$ } Receiver Volume – Area Ratio	$\frac{V_r}{A_r} = (VAR)_r$	$\frac{L^3}{L^2} \approx L$
3	Receiver Average Density	ρ_r	ML^{-3}
4	Receiver Average Specific Heat	$(sh)_r$	$QM^{-1}(Tmp)^{-1}$
5	Receiver Average Surface Film Thermal Conductivity Coefficient	h_r	$QT^{-1}L^{-2}(Tmp)^{-1}$
6	Fluid Density	$\rho_{(fl)}$	ML^{-3}
7	Fluid Viscosity	$\mu_{(fl)}$	$ML^{-1}T^{-1}$
8	Fluid Heat Conductivity	$k_{(fl)}$	$QT^{-1}L^{-1}(Tmp)^{-1}$
9	Fluid Velocity	$v_{(fl)}$	LT^{-1}

Primary quantities: $M \approx$ mass; $L \approx$ length; $T \approx$ time; $Q \approx$ heat; $(Tmp) \approx$ temperature

Arguments involved = 9 ; Primary quantities = 5

Number of dimensionless ratios = 9 – 5 = 4

$$\Pi_1 = \frac{(CT)(sh)_r \rho_r}{h_r}\left(\frac{V_r}{A_r}\right) \quad ; \quad \Pi_2 = \frac{h_r}{k_{(fl)}}\left(\frac{V_r}{A_r}\right)$$

$$\Pi_3 = \frac{\rho_{(fl)}}{\rho_r} \quad ; \quad \Pi_4 = \frac{\rho_{(fl)} v_{(fl)}}{\mu_{(fl)}}\left(\frac{V_r}{A_r}\right)$$

(Note that Π_4 has the form of Reynolds number.)

Therefore,

$$(CT) = \frac{h_r}{(sh)_r \rho_r}\left(\frac{A_r}{V_r}\right) f\left[\frac{h_r}{k_{(fl)}}\left(\frac{V_r}{A_r}\right) , \frac{\rho_{(fl)}}{\rho_r} , \frac{\rho_{(fl)} v_{(fl)}}{\mu_{(fl)}}\left(\frac{V_r}{A_r}\right)\right] \qquad (1)$$

Note: The list of factors given in Eq. (1) applies only to situations in which fluid compressibility effects are negligibly small.

Derivation Summary 31-4. Application of dimensional analysis to the development of a generalized functional expression for thermometric characteristic time.

receiver volume to receiver area is indicated as a single quantity with the dimension of length to match item 2 of the table in Derivation Summary 31-4. The second Π is the ratio of the film coefficient to the fluid conductivity multiplied by the volume – area ratio. The third Π is the ratio of fluid density to receiver density. The fourth Π is the product of fluid density, fluid velocity, and the volume – area ratio divided by fluid viscosity. This ratio often appears in fluid flow problems when compressibility effects are negligible and is known as the Reynolds number. *

* Reynolds number is commonly used as a basic variable in aerodynamics, hydrodynamics, and related subjects. Any text on these subjects may be consulted for detailed information on Reynolds number effects.

31.74. Equation (1) of Derivation Summary 31-4 shows the result of solving the first Π for the characteristic time and gives the other Π's as arguments of an unspecified function. It is generally impossible to write down the form of this function from theoretical considerations, but it may be found by a properly designed series of experiments. The determination of the relationship between Reynolds number and characteristic time illustrates a typical experimental procedure for supplementing the results of dimensional analysis. The required changes in Reynolds number might be made by changing the ratio of fluid density to fluid viscosity, the volume-area ratio of the receiver, or the fluid velocity. In practice, volume-area ratio variations would require mechanical features in the receiver that would generally be difficult to realize. Modifications in the density-viscosity ratio would require either a change in the fluid used or in the fluid temperature. Any change in either of these factors would be accompanied by changes in the second and third Π's of Derivation Summary 31-4, so that Reynolds number effects on characteristic time would be difficult to isolate. On the other hand, variations in fluid velocity will affect only Reynolds number. For this reason, fluid velocity is selected as the independent variable in the experimental determination of the relationship between Reynolds number and characteristic time.

TEST ARRANGEMENT FOR PRODUCING STEP FUNCTION CHANGES OF THERMOMETER INPUT

31.75. The diagram of Fig. 31-7 shows the essential features of an arrangement for subjecting an air-temperature thermometer of the vapor-pressure type to a step function change of the input temperature. Air is forced by a centrifugal blower through a duct fitted with a thermometer to measure the steady-state temperature of the air stream. A pitot-static tube and a manometer are used to measure the air velocity. The inlet to the blower is fitted with a control valve to adjust the air velocity in the duct. A trigger arrangement is provided to support the bulb of a vapor-pressure thermometer within a cylindrical electric oven mounted above the duct. When the bulb reaches oven temperature the trigger is tripped, and the bulb immediately drops into the air stream. At the instant the bulb support hits the stop, temperature scale readings on the indicating head are started and timed as the reading changes from the oven temperature to the airstream temperature. The temperature and time data may be collected either by a human observer or by a photographic arrangement.

31.76. The effect of air velocity on step function response may be studied with the arrangement of Fig. 31-7 by applying the same temperature step with different air control valve settings. A proper choice of the range for these settings provides the data required for a survey of thermometer performance.

TEST PROCEDURE

1) Start blower.
2) Adjust damper to give desired air speed as measured by the pitot-static tube and airspeed manometer.
3) Read airstream temperature from air temperature thermometer.
4) Adjust current through heating coil of tubular oven to bring oven temperature to desired level T_0.
5) Bring bulb of thermometer under test to the raised position and lock it in this position by means of trigger.
6) Leave bulb in raised position until thermometer under test reaches steady temperature T_0.
7) Trip trigger so that bulb suddenly falls into lowered position.
8) Record temperature readings from thermometer under test at measured time intervals until the reading reaches the airstream temperature.
9) Adjust damper setting to give changed air velocity and repeat steps 1 through 8 as required to survey the velocity range under study.

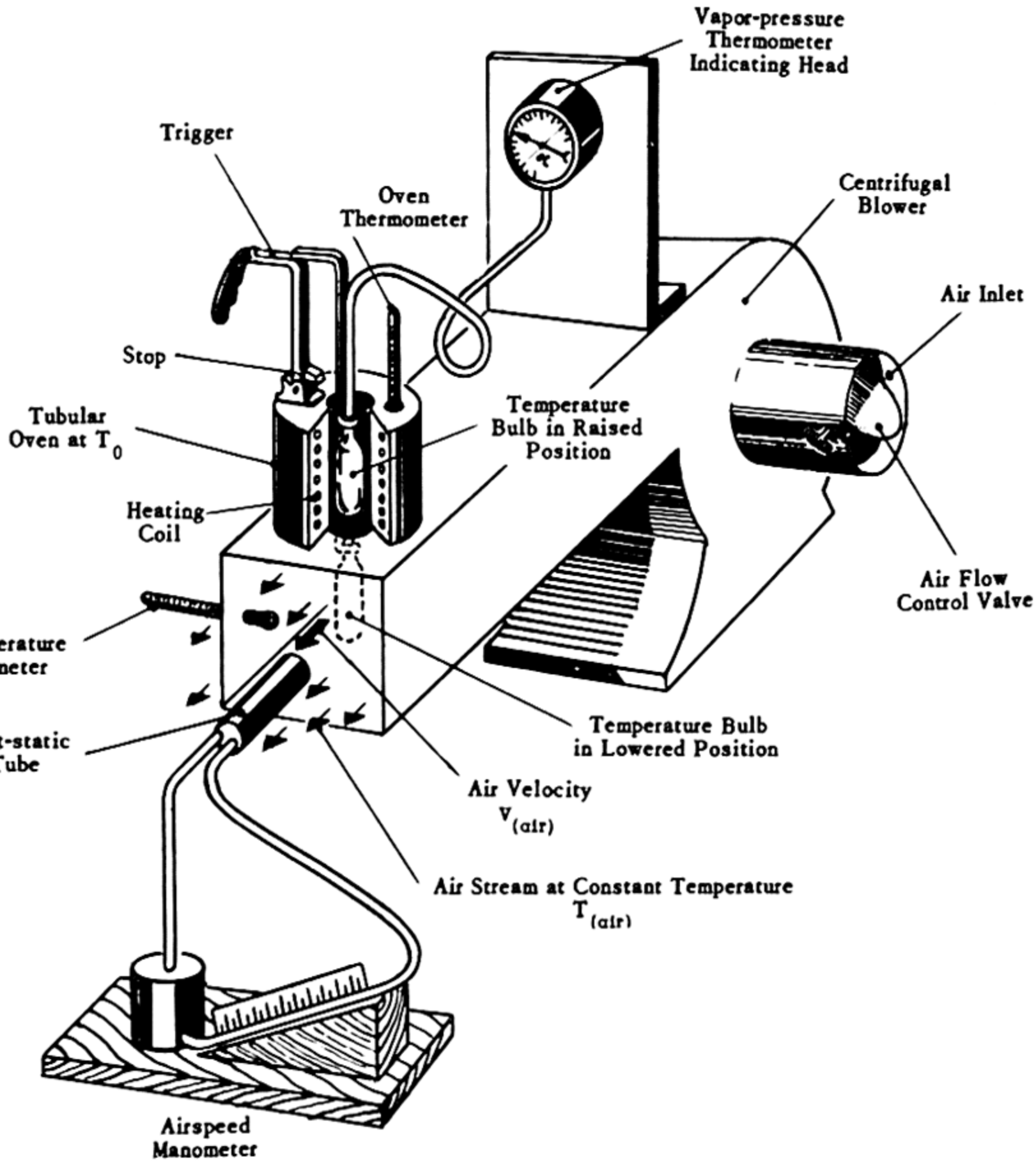


Fig. 31-7. Test apparatus for step function response of air temperature thermometer.

ILLUSTRATIVE RESULTS FROM A STEP FUNCTION SURVEY OF THERMOMETER PERFORMANCE

31.77. Table 31-1 gives a summary of step function response data* for a vapor-pressure thermometer with a receiver volume of 20 cubic centimeters and a receiver area of 55 square centimeters. The tests were run with an oven temperature of 100 degrees centigrade and an airstream temperature of about 25 degrees centigrade, and covered an air-velocity range from about 5 feet per second to 75 feet per second. The left-hand column of Table 31-1 gives the air velocity and the corresponding Reynolds number for each trial. The second column gives the accurately measured stream temperature. The third column is the temperature reading difference ratio as this ratio appears in the equation of Derivation Summary 31-3. The fourth column is the logarithm (to the base 10) of the temperature difference ratio. The fifth column shows the elapsed time corresponding to each difference ratio. The last column gives the characteristic time, calculated by use of Eq. (8) of Derivation Summary 31-3 for a typical observation of each step function response.

31.78. Semilogarithmic plots of temperature reading difference ratio versus time, like the typical plot of Fig. c of Derivation Summary 31-3, are given in Fig. 31-8 for the data of Table 31-1. It is possible to fit a straight line to the points from each set of the experimental step function response data. A comparison of this result with typical plots of the logarithmic forms of Derivation Summary 31-3 shows that the measured step function response for the thermometer must have followed the pattern of first-order response represented by the curves of Fig. 31-1. This means that the dynamic behavior of the thermometer under test is describable by first-order differential equations with characteristic times that are constant for any constant air speed, but which change with air velocity past the bulb.

31.79. The simple exponential form of the thermometer step function response means that after a time interval equal to the characteristic time the temperature reading ratio reaches a magnitude equal to the reciprocal of the base of natural logarithms. This means that if a line is drawn along the $1/\epsilon$ ordinate of Fig. 31-8, characteristic times may be read off directly at the intersections of the step function response lines with the $1/\epsilon$ line. Characteristic time values determined in this way are given in Fig. 31-8. The values determined graphically in this way agree closely with the corresponding calculated values given in Table 31-1.

31.80. The nature of the functional relationship between Reynolds number and characteristic time may be found by plotting characteristic times from Fig. 31-8

* The data summarized in Table 31-1 are based on tests made by Theodore Kaslow of the Instrument and Control Laboratory, Aeronautical Engineering Department, Massachusetts Institute of Technology.

Table 31-1. Step function response data for a vapor-pressure thermometer at various air speeds.*
(Page 1 of 2)

Air velocity $v_{(air)}$ (ft/sec)	Air temperature $T_{(in)(t>0)}$ (°C)	Temperature reading difference ratio $\frac{T_s - T_{(in)(t>0)}}{T_{(in)(t<0)} - T_{(in)(t>0)}}$	Logarithm of temperature reading difference ratio	Elapsed time t (sec)	Characteristic time (CT) (sec)
5.5	25.1	1.00	0	0	
		0.866	−0.062	16.3	
RN		0.734	−0.135	38.0	
$= 0.37 \times 10^3$		0.600	−0.222	65.7	139
		0.466	−0.331	107.8	
		0.323	−0.491	157.6	
		0.199	−0.701	233.5	
8.8	25.0	1.00	0	0	
		0.866	−0.062	14.0	
RN		0.734	−0.135	32.5	
$= 0.59 \times 10^3$		0.600	−0.222	55.7	113
		0.466	−0.331	87.0	
		0.323	−0.491	128.7	
		0.199	−0.701	196.4	
23.2	23.5	1.00	0	0	
		0.870	−0.062	8.0	
RN		0.739	−0.135	19.0	
$= 1.55 \times 10^3$		0.608	−0.222	32.8	71.0
		0.476	−0.331	51.0	
		0.346	−0.461	75.5	
		0.216	−0.701	114.0	
30.8	24	1.00	0	0	
		0.869	−0.061	7.2	
RN		0.737	−0.132	16.0	
$= 2.05 \times 10^3$		0.605	−0.218	28.6	59.8
		0.474	−0.325	43.7	
		0.342	−0.466	64.4	
		0.210	−0.678	96.4	
41.1	24	1.00	0	0	
		0.869	−0.061	6.3	
RN		0.737	−0.132	14.4	
$= 2.74 \times 10^3$		0.605	−0.218	25.0	52.3
		0.474	−0.325	38.2	
		0.342	−0.466	56.2	
		0.210	−0.678	83.7	

* Based on tests made by Theodore Kaslow of the Instrument and Control Laboratory, Aeronautical Engineering Department, Massachusetts Institute of Technology.

Table 31-1. Step function response data for a vapor-pressure thermometer at various air speeds.*
(Page 2 of 2)

Air velocity $v_{(air)}$ (ft/sec)	Air temperature $T_{(in)(t>0)}$ (°C)	Temperature reading difference ratio $\frac{T_s - T_{(in)(t>0)}}{T_{(in)(t<0)} - T_{(in)(t>0)}}$	Logarithm of temperature reading difference ratio	Elapsed time t (sec)	Characteristic time (CT) (sec)
51.3 RN $= 3.42 \times 10^3$	24	1.00 0.869 0.737 0.605 0.474 0.342 0.210	0 −0.061 −0.132 −0.218 −0.325 −0.466 −0.678	0 5.7 13.1 22.5 35.0 50.8 75.8	47.1
74.9 RN $= 4.98 \times 10^3$	24	1.00 0.869 0.737 0.605 0.474 0.342 0.210	0 −0.061 −0.132 −0.218 −0.325 −0.466 −0.678	0 5.0 11.2 19.0 29.6 42.8 63.9	39.6

Receiver volume = $V_r = 20\ cm^3$; Receiver area = $A = 55\ cm^2$

At 25°C:

Air density = $\rho_{(air)} = 1122 \times 10^{-6}\ gm/cm^3$

Air viscosity = $\mu_{(air)} = 187 \times 10^{-6} \frac{dyne\text{-}cm}{cm^2}$ (poise)

$v_{(air)(cm/sec)} = 30.5\, v_{(air)(ft/sec)}$

Reynolds number = $RN = \frac{\rho_{(air)}}{\mu_{(air)}} \frac{V_r}{A_r} v_{(air)} = 66.6\, v_{(air)(ft/sec)}$

$T_{(in)(t<0)} = 100°C$

as ordinates against Reynolds number as abscissae. A plot of this kind on linear coordinates is given in Fig. 31-9a, and the same data are replotted on logarithmic coordinates in Fig. 31-9b. On linear coordinates, characteristic time decreases along a curved path as Reynolds number increases. On logarithmic coordinates, the points for this curve can be approximated by a straight line with a slope of minus one half. This means that for the range considered the particular thermometer used in the tests has a characteristic time that varies with the inverse square root of air velocity.

31.81. The test result noted in the previous paragraph does not necessarily apply in the particular case of any thermometer, but it illustrates the type of performance variation to be expected with changing air speeds in the low-velocity range. Other factors must be included in the list of variables when air speeds

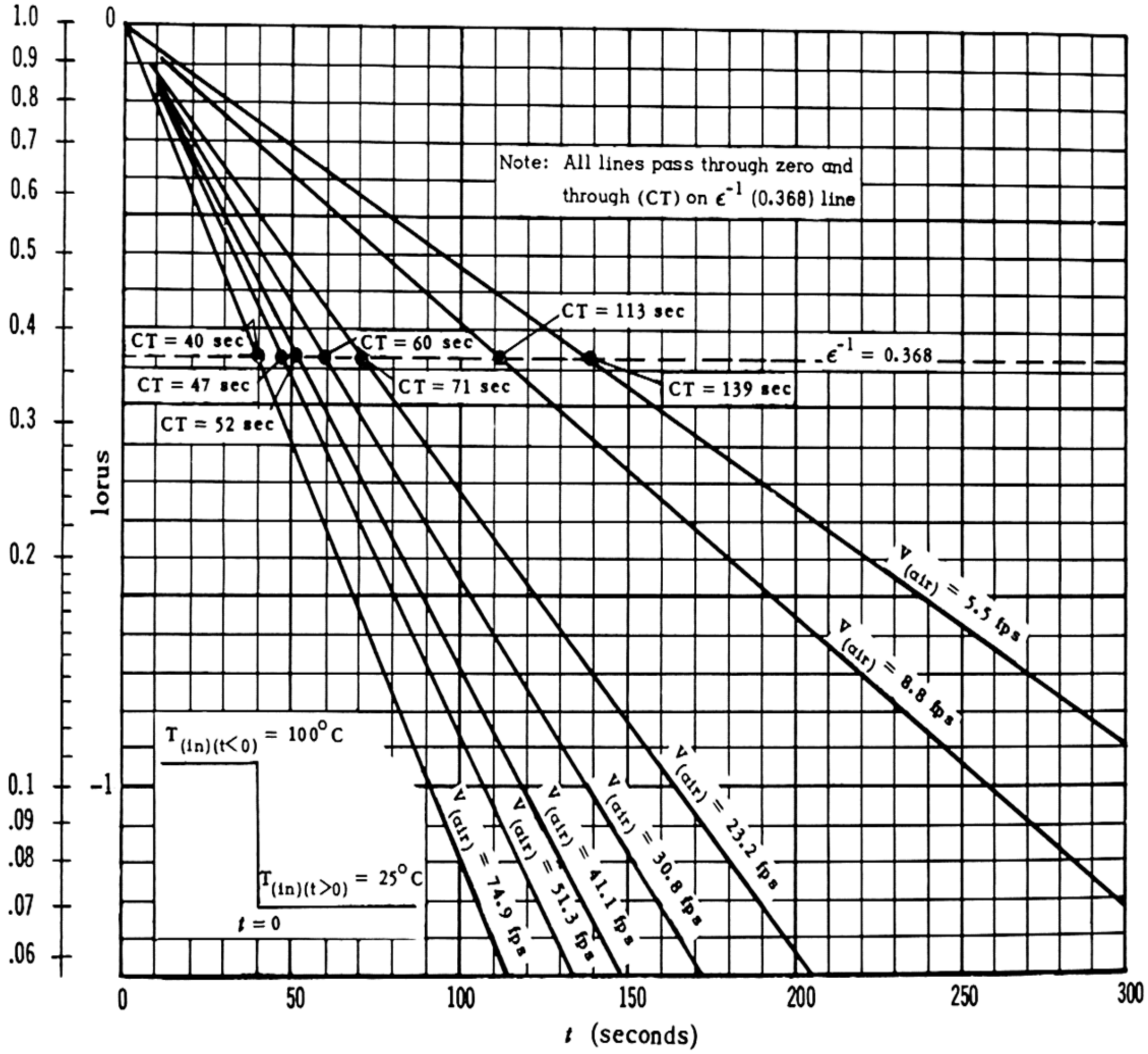


Fig. 31-8. Semilog plots of step function response of vapor-pressure thermometer with various air speeds.

are so high that compressibility and thermodynamic heating must be considered in addition to the quantities listed in Derivation Summary 31-4. The new list may be processed to obtain a corresponding set of dimensionless variables. When the functional relationship between any one of these variables and characteristic time is not known from theoretical considerations, a series of tests generally similar to that just described may be devised to supply the missing information.

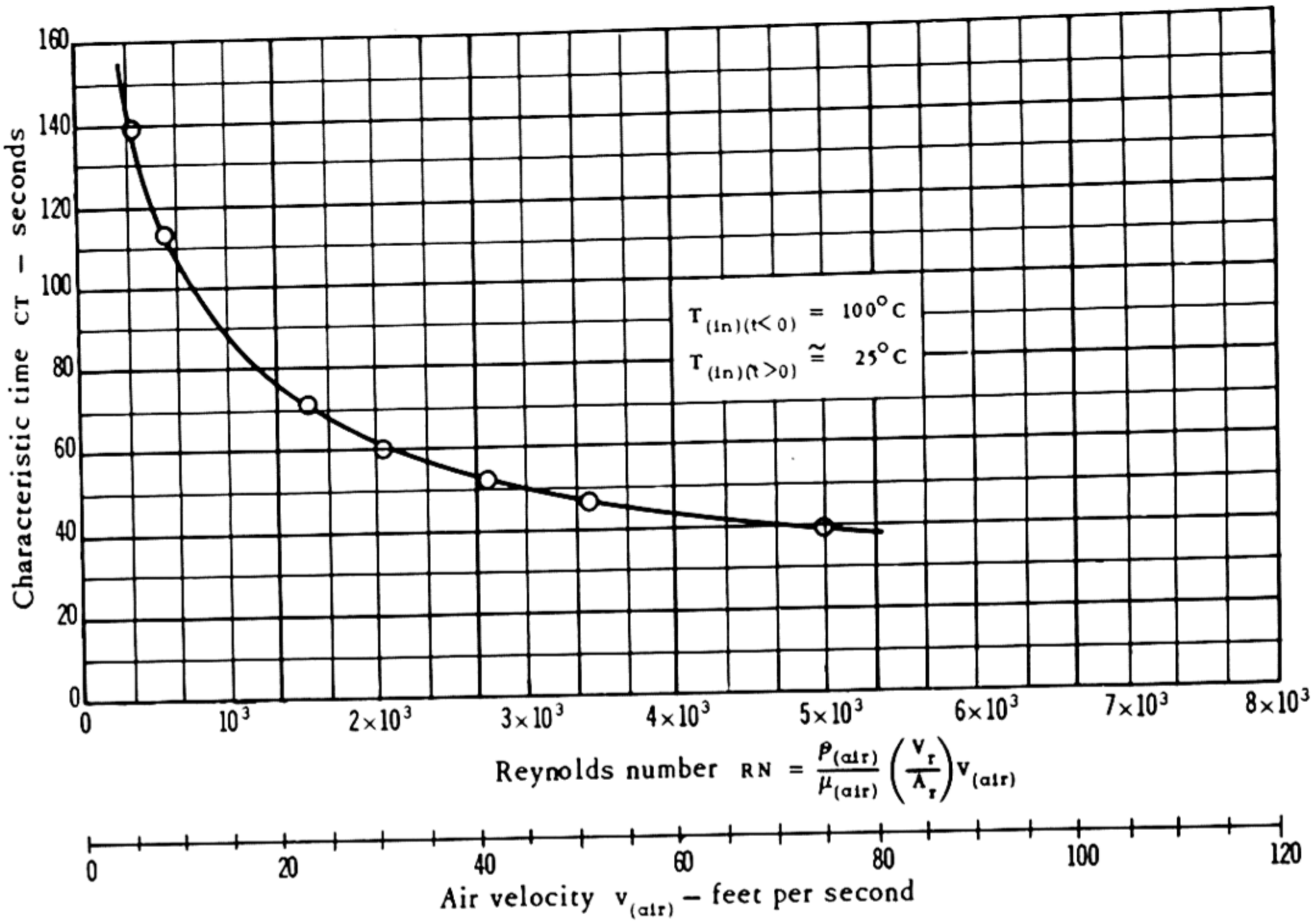
TEMPERATURE MEASUREMENT IN HIGH-SPEED FLOW*

31.82. The instruments and techniques described earlier in this chapter can be applied also to the measurement of temperature in high-speed fluid flow.**

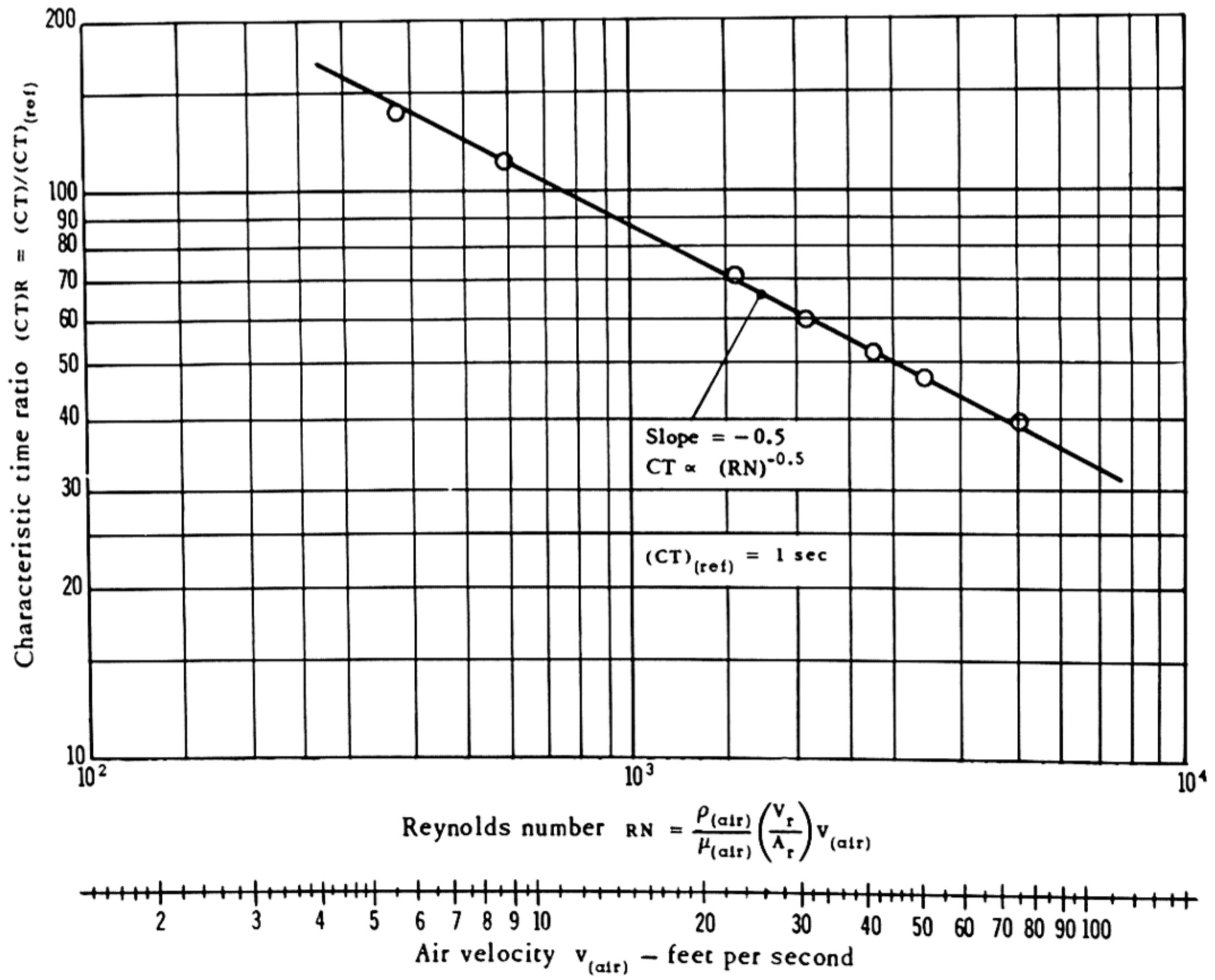
---

* This section has been prepared by Morton Finston, Assistant Professor of Aeronautical Engineering, Massachusetts Institute of Technology.

** For the purposes of this discussion, fluid flow that lies in the region of high subsonic flow or higher is considered to be high-speed flow.



a) Linear scale plot of characteristic time as a function of Reynolds number



b) Log-log plot of characteristic time as a function of Reynolds number

Fig. 31-9. Linear and log-log plots of air temperature characteristic time as a function of air velocity at bulb.

There are, however, certain difficulties inherent in this type of application that make it worth while to discuss the matter in some detail. As already shown in the discussion starting with paragraph 31.27, the values of the input temperature, $T_{(in)}$, and the receiver temperature, T_r, are not necessarily the same, even for low values of flow speed. The discrepancy becomes progressively more exaggerated as the flow speed increases. The following paragraphs discuss the source of this difference between $T_{(in)}$ and T_r as related to high-speed flow and describe current techniques employed to relate one to the other.

31.83. As a preliminary, it is necessary to introduce some ideas from the so-called boundary layer theory.* In most cases in which there is relative motion between a gas or liquid and a solid body, there are two more or less distinct regions in the fluid: the free stream and the boundary layer. Near the body, there is a thin boundary layer in which the velocity changes from that of the body to that of the free stream, away from the body. In the boundary layer, the viscosity of the fluid affects the flow pattern; in the free stream, the effect of the viscosity is almost negligible. Figures 31-10a and 31-10b respectively show typical velocity profiles when (a) a body moves through a fluid at rest, and (b) a fluid moves past a body at rest. It is important to note that imposing a uniform velocity equal to $-v_{(af)}$ on the body and fluid in Fig. 31-10a yields the situation shown in Fig. 31-10b. This characteristic relative motion property means, for example, that the discussion of temperature measurements obtained in a wind tunnel is also valid for the analogous temperature measurements in flight.

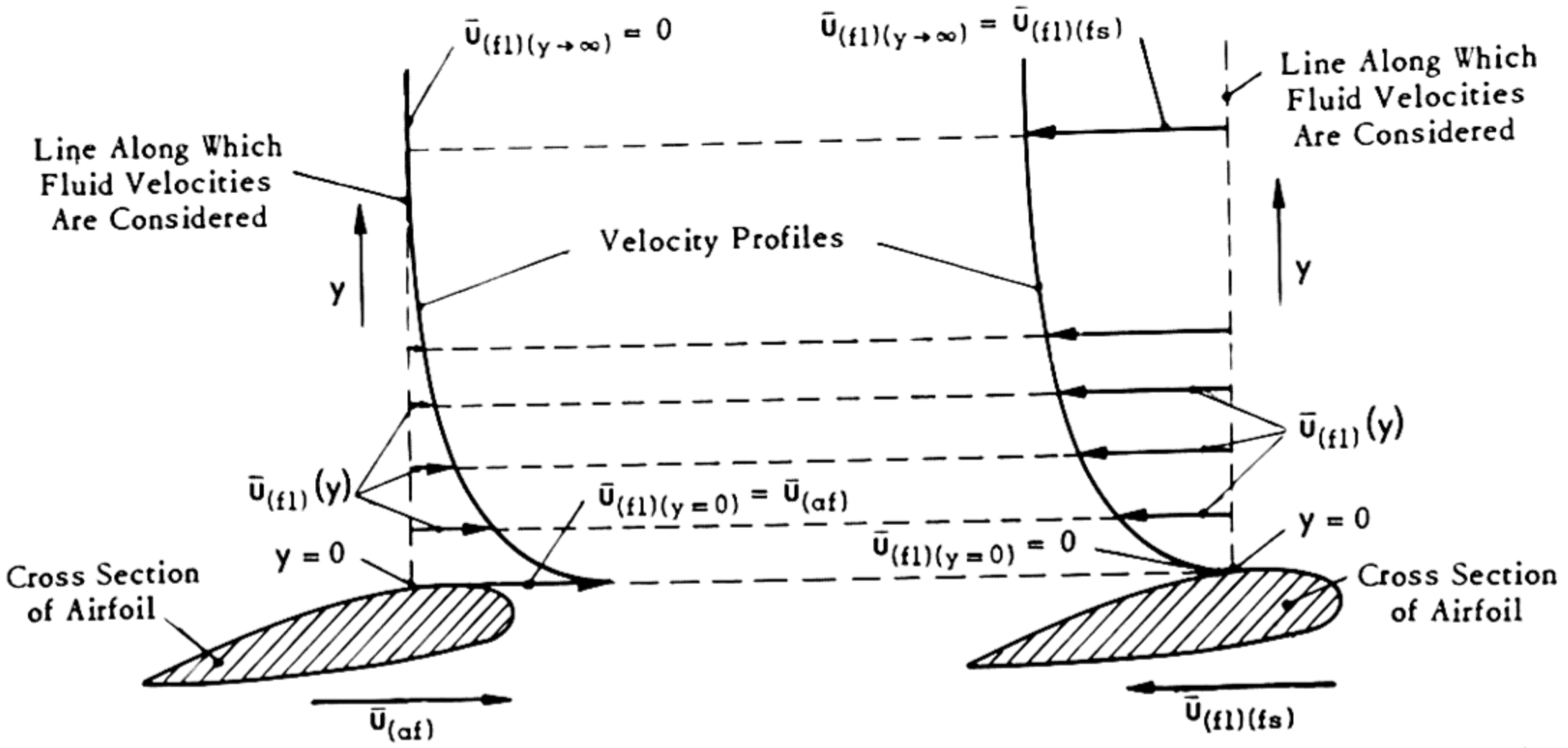
31.84. In the boundary layer around any body, the viscous action, which increases rapidly with the speed of flow, dissipates mechanical energy into heat energy. Thus, in the boundary-layer region, the energy balance depends on dissipation as well as on convection, conduction, and radiation. The relative importance of each varies along the body, as well as with the speed of flow. In particular, when the body is a temperature probe, the temperature along the surface, which determines receiver temperature, T_r, is dependent not only on the free-stream input temperature, $T_{(in)}$, but also on the energy balance in the boundary layer on the probe. This dependency has received much attention recently, and a great deal of the available information is presented by Young and by Squire.** The relationship between T_r and $T_{(in)}$ is, then, complicated in the static case, as well as in the dynamic case, when high-speed flow is involved.

31.85. A typical form of the boundary-layer energy equation is given by Eq. (1) of Derivation Summary 31-5. This equation applies to the case of incompressible fluid flow past a semi-infinite flat plate. Its solution will not be discussed here,

---

* See Goldstein (G9).

** See Howarth (H10), Vol. I, Chapter X, "Boundary Layers," by A. D. Young; Vol. II, Chapter XIV, "Heat Transfer," by H. B. Squire.



a) Airfoil moving in fluid at rest ($u_{(fl)(fs)} = 0$)

b) Airfoil at rest in moving fluid ($u_{(af)} = 0$)

Note: The velocity profiles of (a) and (b) are identical in shape, as shown, when $\bar{U}_{(af)} = -\bar{U}_{(fl)(fs)}$. When this condition holds, imposing a uniform velocity equal to $-\bar{U}_{(af)}$ on both the fluid and airfoil of (a) yields the situation shown in (b).

Definitions of Symbols

$\bar{U}_{(af)}$ = velocity of airfoil

$\bar{U}_{(fl)}(y)$ = velocity of fluid at y

$\bar{U}_{(fl)(fs)}$ = free-stream velocity of fluid $\equiv \bar{U}_{(fl)(y\to\infty)}$

y = distance from surface of airfoil on line along which fluid velocities are considered

Fig. 31-10. Typical velocity profiles, greatly enlarged in the vertical direction.

other than to point out that mathematical difficulties result because:

1) The fluid properties $(sh)_{(fl)}$, $k_{(fl)}$, and $\mu_{(fl)}$ are themselves temperature-dependent.

2) A knowledge of the velocity components u and v is required.

Because of these difficulties, only limited success has been achieved to date in solving the mathematical problem. *

31.86. When the fluid concerned is compressible, additional terms are required in the energy equation, to take into account the resulting changes of mechanical energy to heat energy, or vice versa; for example, as work is done on a gas in compression. This is true for air and most other gases, except at very low speeds of flow. Compression effects, like dissipation effects, increase rapidly with the Mach number of free stream, ** and thereby further complicate the relationship between T_r and $T_{(in)}$ during high-speed flow.

31.87. In the region of flow where the influence of viscosity is negligible, that is, in the free stream, there is a very simple relationship between the stagnation temperature, $T_{(stag)}$, and the free-stream static temperature, $T_{(stat)(fs)}$. This relationship, given by Eq. (2) of Derivation Summary 31-5, says that if a

* See Howarth (H10), Vol. I, Chapter X, "Boundary Layers," by A. D. Young.

** The Mach number of flow at any point is the ratio of the speed of flow to the speed of sound at that point.

flow at a Mach number M and a free-stream static temperature $T_{(stat)(fs)}$ is decelerated to rest isentropically,* converting all the mechanical energy into kinetic energy of the molecules, the temperature reached will be $T_{(stag)}$ (both temperatures in Eq. (2) are in degrees absolute). For air, for which $\gamma = 1.4$, the ratio of $T_{(stag)}$, to $T_{(stat)(fs)}$ is then $1 + 0.2\,M^2$. Conversely, if $T_{(stag)}$ and M are known, the value of $T_{(stat)(fs)}$ for an isentropic expansion is given by the same expression. This fact is important in instrument calibration, as shown in the next paragraph in connection with the so-called recovery factor.

31.88. When a gas is brought to rest at the surface of a body, the temperature attained by the gas is generally not $T_{(stag)}$, since the process is not isentropic because of the boundary-layer effect already discussed. In fact, the temperature is near to, but usually less than, $T_{(stag)}$ when equilibrium is reached. That is, in the static case, a probe in a flowing stream usually has a receiver temperature, T_r, such that T_r is greater than $T_{(stat)(fs)}$ but less than, although close to, $T_{(stag)}$. From this result, it is easy to see the effect of Mach number on measurements of the free-stream static temperature. As M decreases to zero, $T_{(in)}$ (that is, $T_{(stat)(fs)}$) becomes approximately equal to $T_{(stag)}$, and therefore T_r becomes approximately equal to $T_{(in)}$. At a Mach number of 0.2, Eq. (2) of Derivation Summary 31-5 shows that for air ($\gamma = 1.4$) the ratio of $T_{(stag)}$ to $T_{(in)}$ is 1.008, so that T_r will be within 0.8 percent of $T_{(in)}$. As M increases, this situation changes rapidly, as can be seen from the curve family of Fig. 31-11 for the case when $r = 1$ (the curve for $r = 1$ is a plot of Eq. (2) of Derivation Summary 31-5). Available theoretical and experimental** work indicates that T_r, in fact, is given by Eq. (3) of Derivation Summary 31-5, where the recovery factor, r, depends on probe geometry and the dimensionless parameters Mach number, M, Reynolds number, RN, and Prandtl number, PN (see Eq. (9) of Derivation Summary 31-5). This functional dependence can be established by following the dimensionless analysis procedure given in Chapter 8. The results are given in Eqs. (5) through (11) of Derivation Summary 31-5. Although r is usually less than one for air, and generally between 0.85 and 0.95,*** it can be found only by experiment, that is, by calibration. Figure 31-11 gives a family of plots of the ratio $T_r / T_{(stat)(fs)}$ as a function of Mach number for three values of the recovery factor, r.

31.89. With one exception, which is described later in this section, instruments used in high-speed-flow temperature measurements are similar to those discussed earlier in this chapter. The instrument most frequently used is the shielded-thermocouple probe, shown schematically in Fig. 31-12. The advantage of this instrument is that the shield is the major component of the probe environment.

---

* That is, with no heat loss to the surroundings.

** See Johnson and Rubesin (J4).

*** See Kaye (K3).

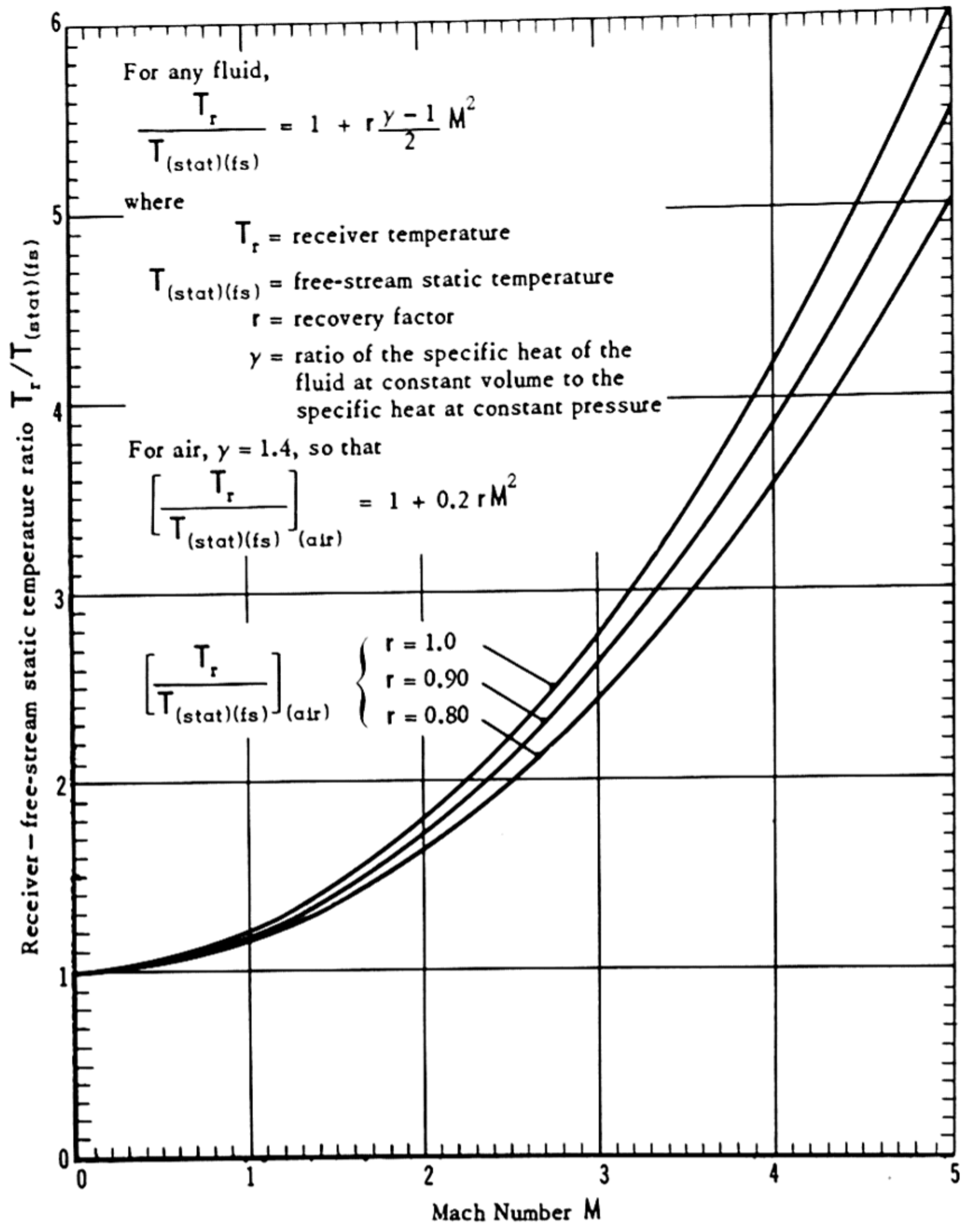
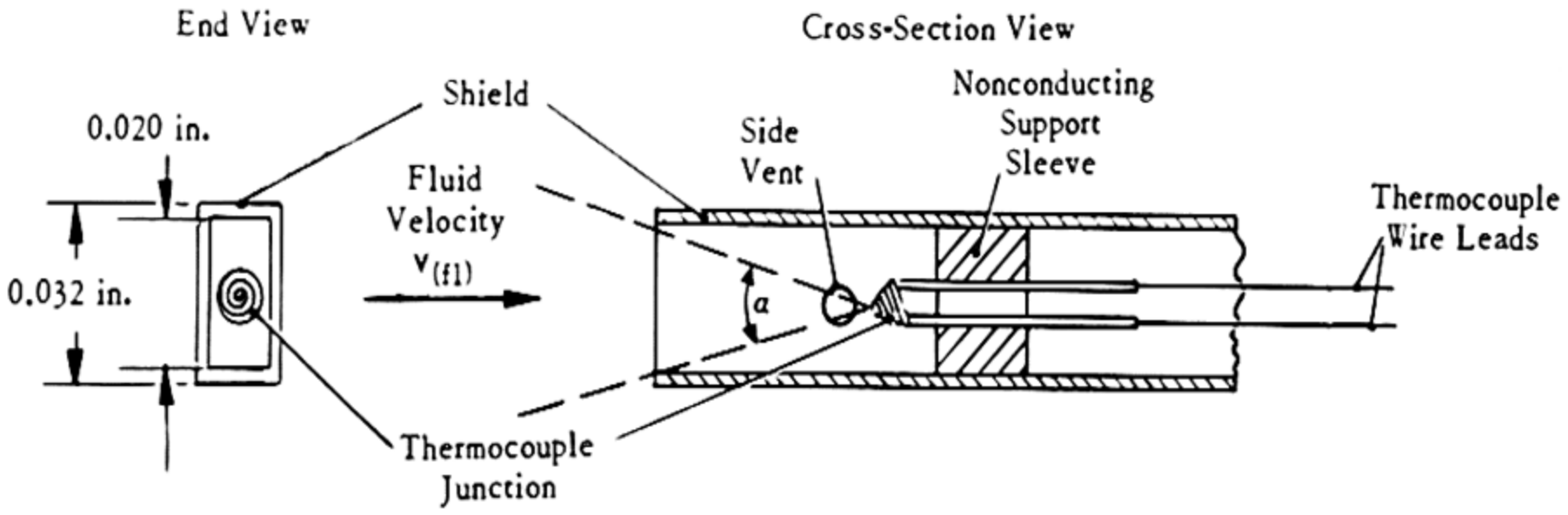


Fig. 31-11. Receiver – free-stream static temperature ratio as a function of Mach number and recovery factor for the case of air flow.

Thus, the radiation heat transfer between the thermocouple and the total environment is largely determined by the transfer between the thermocouple and the shield. That is, most of what the probe "sees" is its shield, so that the effect of changes in the geometry of the over-all configuration (such as would result from a change in location of the probe in a wind tunnel, for example) is minimized. The selected instrument is calibrated in the following way: The flow in a wind tunnel, except in the boundary layers on the walls, is essentially isentropic. Therefore, Eq. (2) of Derivation Summary 31-5 is applicable. Thus, measurement of the temperature in the stilling section of the wind tunnel, which is essentially the stagnation temperature, and a knowledge of the Mach number at the point where the probe is to be inserted, means that the free-stream static input temperature can be calculated. Then, measuring T_r in the free stream and using Eq. (3) of



α is the angle through which the thermocouple junction "sees" an environment other than the shield. The dimensions are typical of probes used in high-speed-flow temperature measurement. Except for the tip details, sections j and k of Description Summary 31-1 apply.

Fig. 31-12. Views showing tip of shielded thermocouple probe.

Derivation Summary 31-5 provides the required calibration for r as a function of M, RN and PN, as indicated in Eq. (9) of Derivation Summary 31-5. Figure 31-13 gives typical data for an instrument of the type shown in Fig. 31-12. Since T_r is usually near $T_{(stag)}$, it is customary to try to adjust the probe geometry so that r is approximately equal to unity (see Eq. (4) of Derivation Summary 31-5) and independent of M and RN.* Ordinarily the probe is calibrated in regions of uniform flow and can be used for measurements under similar circumstances. Elsewhere, such as in determining temperature profiles in boundary layers, where the flow velocity and static temperature vary in a direction transverse to the flow direction, the situation is still somewhat unsettled with regard to the use of probes.** This results from the distortion of the velocity profile by the presence of the probe (see Fig. 31-14). The probe, having a finite height, responds to a weighted average temperature over some distance. Because of the distortion of the flow by the presence of the probe, the probe averages over differently weighted distributions as the velocity and temperature profiles change or the probe position changes. Optical methods, such as schlieren and interferometer systems,*** are sometimes used for measurement in these regions. In any case, for a given fluid, the probe calibration relates T_r to $T_{(in)}$ as a function of M and RN, RN being based on the inlet diameter of the probe shield and free-stream characteristics. Another characteristic of high-speed-flow temperature measurements should be noted here: Once calibration is completed, one additional measurement, such as that of M, is always required to find $T_{(in)}$ from T_r.

31.90. The preceding remarks pertain to the static case. For the dynamic response, which has been very little studied at this writing,† techniques parallel to those described earlier in this chapter may be utilized.

---

* See Goldstein and Scherrer (G8).

** See Blue and Low (B17).

*** See Liepmann and Puckett (L12).

† See Dahl and Freeze (D10).

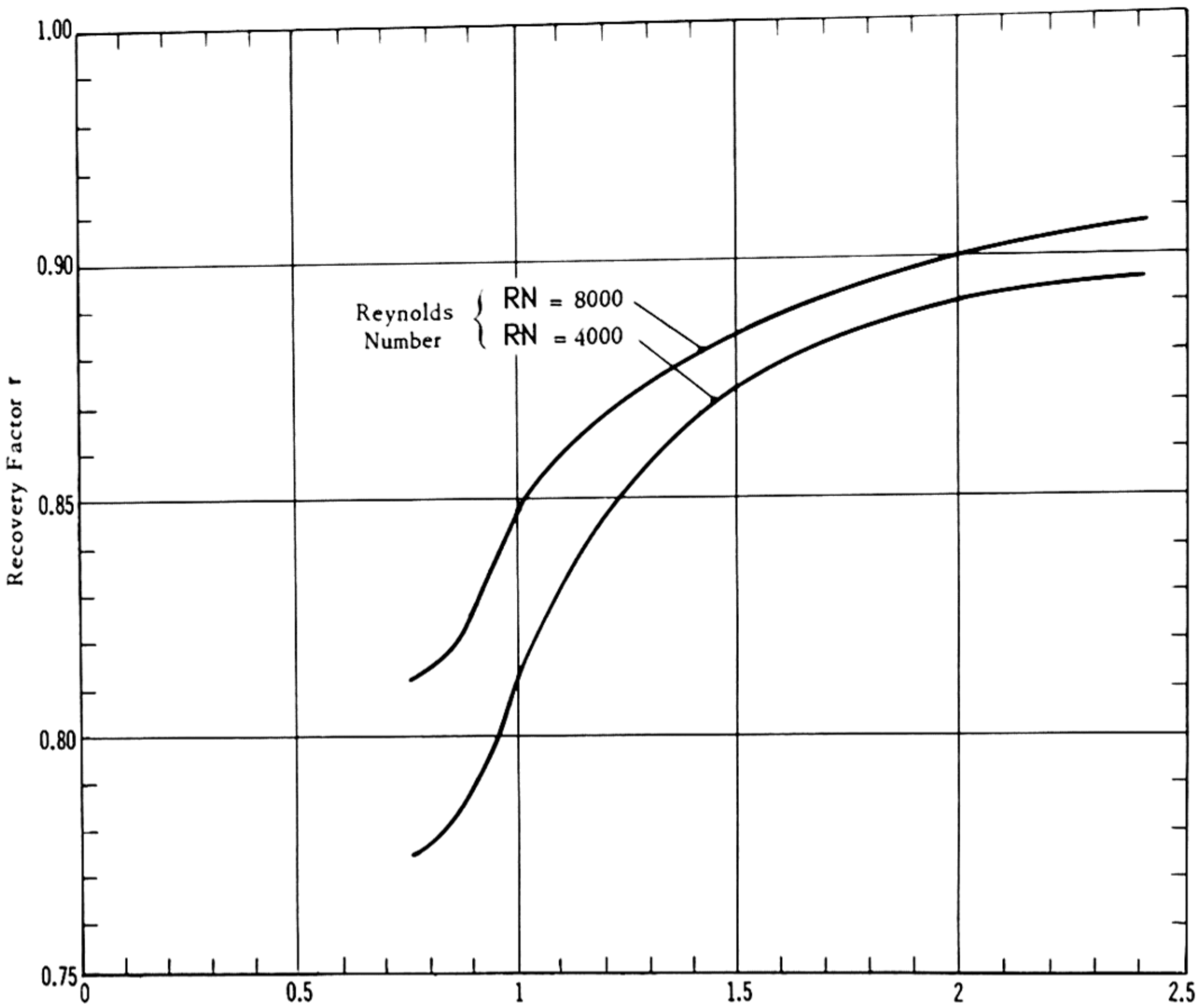


Fig. 31-13. Typical illustrative temperature probe calibration of recovery factor as a function of Mach number and Reynolds number.

31.91. For some situations, it is convenient to measure free-stream temperatures by means other than the use of probes. One method is to measure the surface temperature at some point of a body in motion relative to the surrounding fluid. For example, in flight, a temperature receiver somewhere in the surface of the aircraft could be used. Again $T_{(in)}$ would be given by Eq.(3) of Derivation Summary 31-5 after r is determined. For the probe just discussed, the effect of RN would be accounted for in the calibration, as would be that of PN, if the instrument were used in the temperature range and fluid for which it was calibrated. In the present case, a new element enters. The Reynolds number of interest is that of the body where the temperature receiver is situated (for example, the airfoil), not that of the sensing element. As is well known, there are three types of boundary-layer flow: laminar, transition, and turbulent.* For a given configuration and Mach number, the value of RN determines which type is present at any point on the airfoil. As the flow regime changes, the value of r does also. The calibration of the temperature receiver now involves the configuration of the carrying body, and may be determined by the procedure used for the probe. A

* See Goldstein (G9).

For the simple case of the flow of an incompressible fluid past a semi-infinite flat plate, the temperature in the boundary layer is governed by the energy equation

$$\rho_{(fl)}(sh)_{(fl)}\left(\frac{\partial T}{\partial t} + u\frac{\partial T}{\partial x} + v\frac{\partial T}{\partial y}\right) = \frac{\partial}{\partial y}\left(k_{(fl)}\frac{\partial T}{\partial y}\right) + \mu_{(fl)}\left(\frac{\partial u}{\partial y}\right)^2 \qquad (1)$$

where

$\rho_{(fl)}$ = fluid density

$(sh)_{(fl)}$ = specific heat of the fluid at constant pressure

T = temperature

t = time

u, v = velocities parallel and perpendicular to the plate, respectively

x, y = coordinates parallel and perpendicular to the plate, respectively

$k_{(fl)}$ = thermal conductivity of the fluid

$\mu_{(fl)}$ = fluid viscosity

At high velocities, it is essential to consider $\rho_{(fl)}$, $(sh)_{(fl)}$, $k_{(fl)}$, and $\mu_{(fl)}$ as functions of T, which results in a very complicated equation. When there is a pressure gradient, as in the case of flow past an airfoil, further terms must be added to Eq. (1).

a) A typical form of the boundary-layer energy equation

For isentropic flow,

$$\frac{T_{(stag)}}{T_{(stat)(fs)}} = 1 + \left(\frac{\gamma - 1}{2}\right)M^2 \qquad (2)$$

where

$T_{(stag)}$ = stagnation temperature (degrees absolute); i.e., the temperature reached by isentropic deceleration to rest

$T_{(stat)(fs)}$ = free-stream static temperature (degrees absolute); i.e., the temperature recorded by an observer moving with the stream

γ = ratio of the specific heat of the fluid at constant volume to the specific heat at constant pressure

For the case in which a thermometer is being used to measure the steady-state temperature of a flowing gas, the receiver temperature differs from the stagnation temperature, even though the fluid is at rest at the thermometer surface. Therefore, Eq. (2) cannot be used to relate T_r to $T_{(stat)(fs)}$. Experiments and theoretical work indicate that the actual relationship between T_r and $T_{(stat)(fs)}$ is

$$\frac{T_r}{T_{(stat)(fs)}} = 1 + r\left(\frac{\gamma - 1}{2}\right)M^2 \qquad (3)$$

where

T_r = receiver temperature

$$r = \frac{T_r - T_{(stat)(fs)}}{T_{(stag)} - T_{(stat)(fs)}} \qquad (4)$$

= recovery factor

Note that r is a dimensionless ratio.

b) Temperature ratios arising in measurements in a flowing fluid

Derivation Summary 31-5. Relationships associated with high-speed-flow temperature measurement. (Page 1 of 2)

Either by an application of the Π Theorem, as detailed in Chapter 8 and elsewhere,* or by putting the partial differential equations of heat transfer at high-speed flow into dimensionless form,** the important dimensionless parameters can be identified. They are

1) The Reynolds number, RN.

$$RN = \frac{\rho_{(fl)} v_{(fl)} l}{\mu_{(fl)}} \tag{5}$$

2) The Prandtl number, PN.

$$PN = \frac{\mu_{(fl)} (sh)_{(fl)}}{k_{(fl)}} \tag{6}$$

3) The Mach number, M.

$$M = \frac{v_{(fs)}}{v_{(sound)}} \tag{7}$$

where

$v_{(fl)}$ = fluid velocity

$v_{(fs)}$ = free-stream velocity

$v_{(sound)}$ = velocity of sound

l = a typical length (for example, the probe height)

and the other quantities are as defined in section a of this summary.

The dimensionless temperature ratio can then be shown to be

$$\frac{T_r}{T_{(stat)(fs)}} = F_1 (RN, PN, M) \tag{8}$$

Thus, from Eq. (3), it appears that

$$r = F_2 (RN, PN, M) \tag{9}$$

The best available information*** indicates that r is independent of M over fairly wide ranges of fluid velocity and that its dependence on RN is of a limited type. That is, in the laminar-flow range, as RN varies, r remains approximately constant if PN does; at transition, r increases, and then attains a nearly constant value in the turbulent-flow range (see Fig. 31-15).

Although a calibration for r is required of each instrument used for making high-speed-flow temperature measurements, fairly good accuracy is found by setting r equal to $\sqrt{PN}$ for laminar flow, so that

$$\frac{T_r}{T_{(stat)(fs)}} = 1 + \sqrt{PN}\left(\frac{\gamma - 1}{2}\right) M^2 \tag{10}$$

and equal to $\sqrt[3]{PN}$ for turbulent flow, so that

$$\frac{T_r}{T_{(stat)(fs)}} = 1 + \sqrt[3]{PN}\left(\frac{\gamma - 1}{2}\right) M^2 \tag{11}$$

These relationships are used in the following way. If temperature is to be measured by a thermocouple in the surface of a wing, for example, the procedure would be to compute RN and measure T_r and M. For values of RN less than the transition value, Eq. (10) would be used to find $T_{(stat)(fs)}$; for values of RN greater than the transition value, Eq. (11) would be used. In other words, the measurements obtained by means of a thermocouple in an airfoil surface depend on its chordwise location.

A probe, such as that shown in Fig. 31-12, has its Reynolds number dependency determined at calibration.

c) *Dimensional analysis of heat transfer at high-speed flow*

---

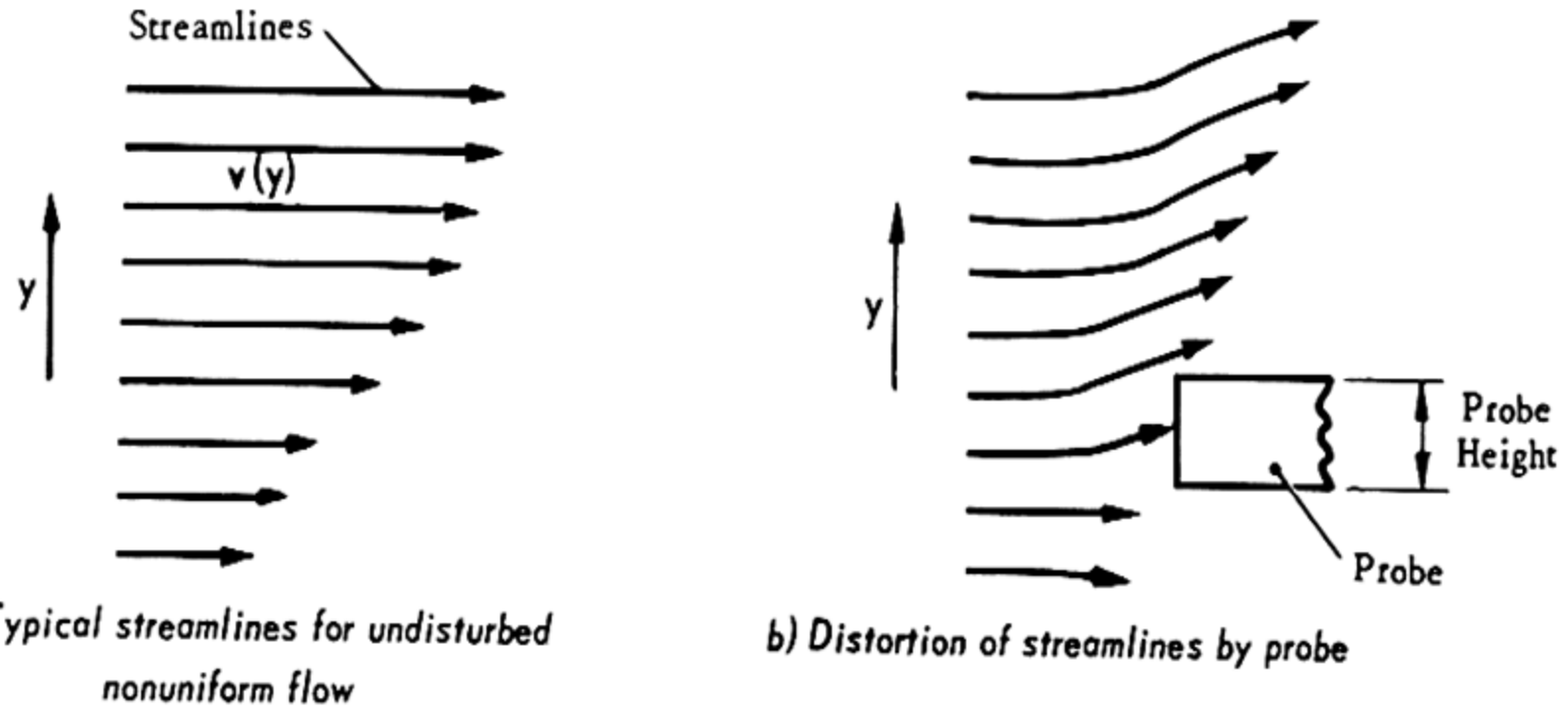
* See Durand (D11), Vol. VI, Division T, "Aerodynamics of Cooling," by H. L. Dryden.

** See Schlichting (S17).

*** See Kaye (K3), and Johnson and Rubesin (J4).

Derivation Summary 31-5. Relationships associated with high-speed-flow temperature measurement. (Page 2 of 2)

y = direction perpendicular to fluid flow



a) Typical streamlines for undisturbed nonuniform flow

b) Distortion of streamlines by probe

Fig. 31-14. Distortion of a velocity profile by the presence of a probe.

typical curve of r as a function of RN, for the case of a flat surface aligned with the free stream, is shown in Fig. 31-15.

31.92. A more detailed account of these problems may be found in articles by Young, Squire,* and others. There is one currently promising development that should be mentioned. It utilizes the results embodied in Eqs. (2) and (3) of Derivation Summary 31-5 in a different way than discussed heretofore. So far, discussion has been concerned with an instrument more or less directly exposed to the flowing fluid whose temperature is to be measured. Measurements are made to find the relationship of T_r to $T_{(in)}$. Suppose, instead, that the input temperature be designated as $T_{(in)1}$. Then it can be asked if it is possible to devise an instrument that will produce a temperature $T_{(in)2}$ around a second instrument, the temperature receiver, such that the relations between $T_{(in)1}$ and $T_{(in)2}$ and between $T_{(in)2}$ and T_r cause T_r to equal $T_{(in)1}$. Reference to Eq. (3) of Derivation Summary 31-5, shows that $T_{(in)2}$ must be less than $T_{(in)1}$ for high-speed flow. Recent developments** indicate that this can be done, at least up to high subsonic speeds, by use of the vortex free-air thermometer. This device is based on the possibility of balancing the heating of a probe in a flowing fluid against the cooling known to exist in a so-called "vortex tube." This instrument is shown schematically in Fig. 31-16. Although the theory of the tube's operation is still incomplete, certain important facts have been established experimentally: By adjusting the geometry of the tube, the extent and temperature of the cold-air core shown in Fig. 31-16 can be varied. If a probe, thermocouple or otherwise, is inserted in the cold-air core, its input temperature, which corresponds to $T_{(in)2}$, is that of the cold-air core. If the opening of the tube, through which compressed air enters,

---

* See Howarth (H10), Vol. I, Chapter X, "Boundary Layers," by A. D. Young; Vol. II, Chapter XIV, "Heat Transfer," by H. B. Squire.

** See Packer and Box (P6).

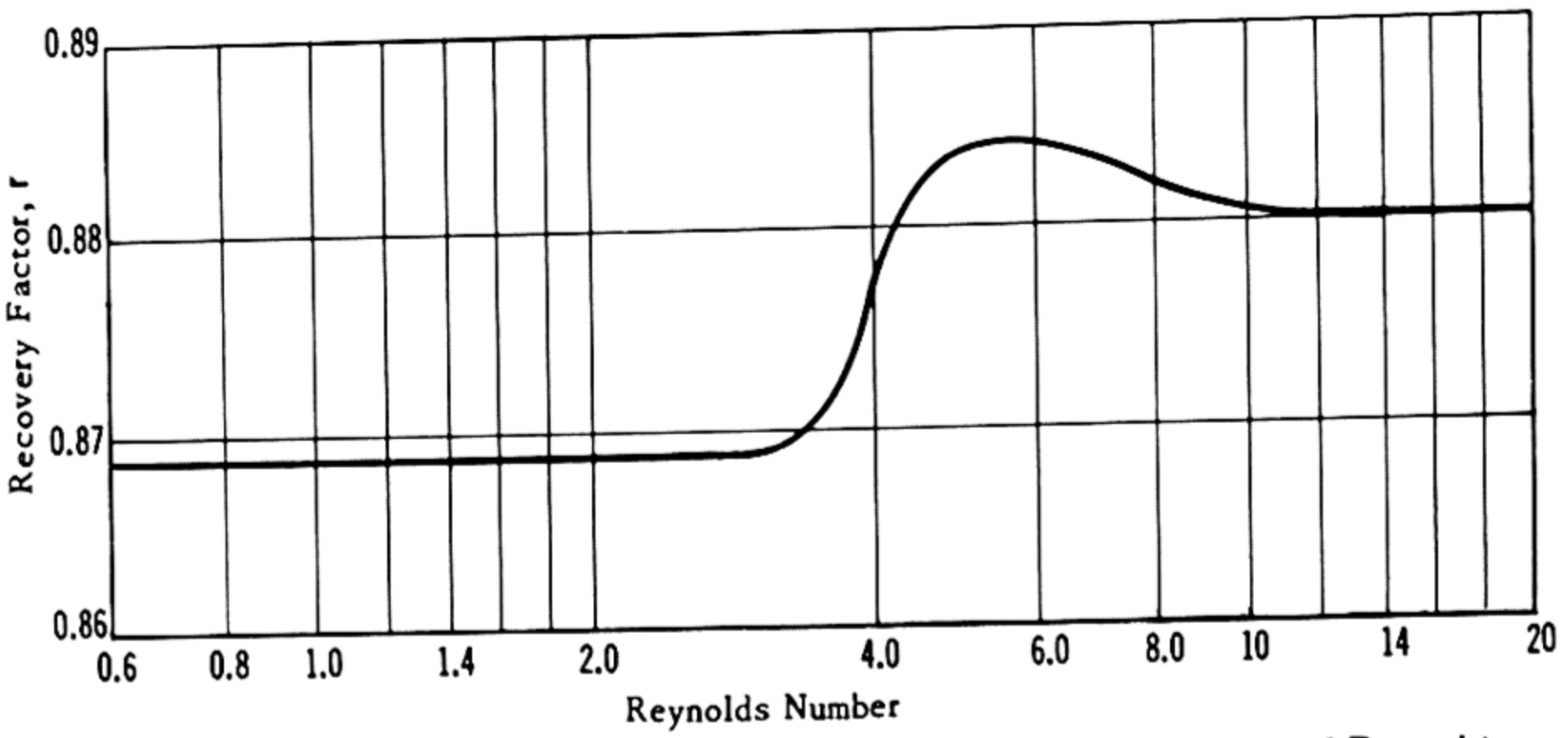


Fig. 31-15. Illustrative plot showing recovery factor as a function of Reynolds number at a nominal Mach number of 2.0.

is aligned with the free stream whose temperature is to be measured, the temperature of the cold-air core will depend on the free-stream temperature, which corresponds to $T_{(in)1}$, and the speed of flow. Results of preliminary work are shown in Fig. 31-17, and indicate considerable promise.

31.93. In summary, the measurement of free-stream static temperature (the temperature recorded by an ideal temperature receiver moving with the fluid) becomes increasingly difficult as the speed of flow increases. The value of T_r depends on r, which, in turn, depends on probe geometry, M, PN, and RN, so that even the static case presents serious difficulties. Analytical evaluations of these relationships are almost impossible, but a given instrument may be calibrated for use in uniform flows without excessive effort. For nonuniform flows, calibration procedures are somewhat unsettled. At high speeds of flow, the heating resulting from compression and viscous dissipation raises the value of T_r far above $T_{(in)}$. This may be countered by placing the probe in the cold-air core of a vortex tube, although this development is still in its earlier phases.

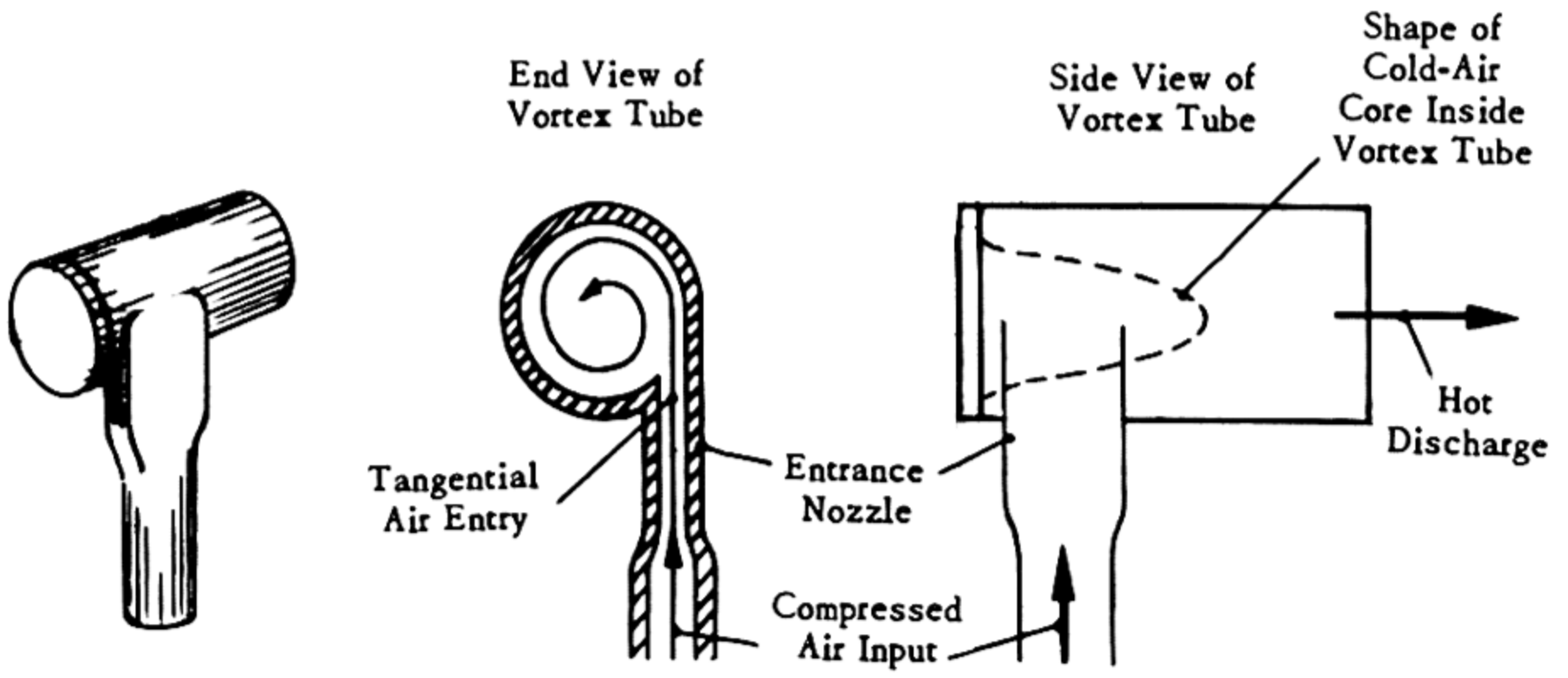


Fig. 31-16. Vortex tube.

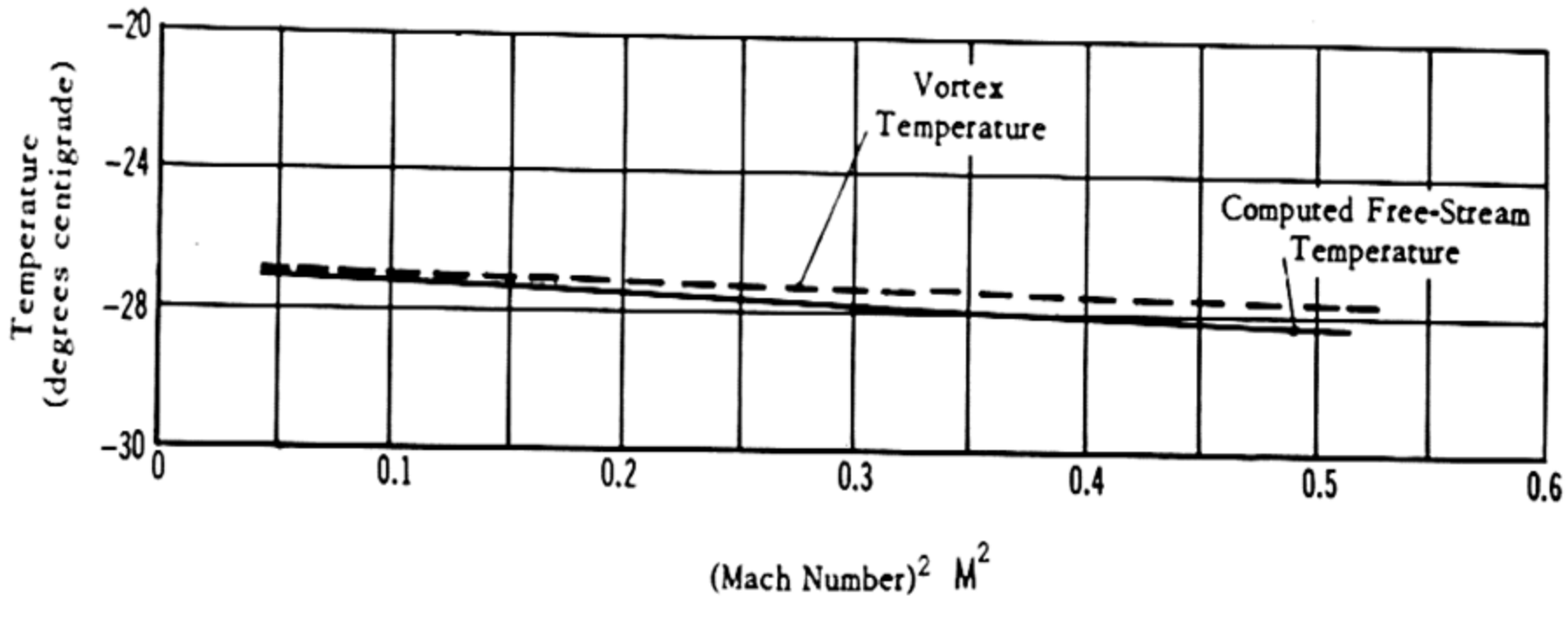


Fig. 31-17. Results of flight tests of a vortex thermometer.
[*From Fig. 25 of Packer and Box (P6).*]

CONCLUSION

31.94. The performance of temperature-measuring instruments is discussed in the previous sections from the standpoint of the basic physical processes involved when heat flow effects associated with the receiver determine the dynamic characteristics. When this condition is fulfilled, thermometers for measuring fluid temperatures often behave as first-order systems with characteristic times that depend on fluid velocity. Such a thermometer is chosen as an example to illustrate principles and procedures for theoretical analysis and experimental tests. The characteristic time varies with air speed, but it is effectively constant at a given air speed for a temperature step of at least 75 degrees centigrade. This is generally typical of devices for measuring air temperature. For example, Harper, Hendrickson and Brombacher, and Hendrickson* report conclusions from tests made on a group of twenty-two air thermometers of various types. At an air speed of 17 miles per hour, the tests showed that step function responses all followed the exponential response law closely enough to indicate constant characteristic times. These characteristic times were distributed in groups that roughly corresponded to the type of thermometer under test. The results are summarized in Table 31-2.

Table 31-2. Characteristic times of temperature-measuring instruments.

Thermometer Type	Characteristic Time Range (seconds)
Vapor pressure or liquid-filled bulb with Bourdon tube	30 to 75
Laboratory liquid-in-glass	20 to 30
Bimetal	10 to 20
Electric resistance	3 to 10

---

* See Harper (H7), Hendrickson and Brombacher (H8), and Hendrickson (H9).

31.95. Under the definition of response time given in Fig. 6-8 of Chapter 6, three characteristic times* must elapse before the response has completed 95 per-
cent of the magnitude of the forcing step. For the particular case of measuring in-
struments, it is reasonable to define indication time as identical with the more
general concept of response time. When measurement situations require indica-
tion times that do not fall within the range established by three times the upper
and lower limits given in Table 31-2, it will usually be necessary to construct
special equipment. Each problem will have its peculiar difficulties, but the prin-
ciples discussed in this chapter may always be applied in the design of instruments
to meet the required specifications.

---

* This statement is true because the response time limit is taken as 0.05 of the step height from the forced response, which is the final constant level for a step function, and 0.05 is substantially equal to $1/\epsilon^3$.

CHAPTER 32

ELECTROMECHANICAL MEASURING INSTRUMENTS

INTRODUCTION

32.1. Electromechanical measuring instruments are devices in which the quantities to be measured are represented by voltage or current inputs that act through force- or torque-generating components and a mechanical coupler to position the index of an indicating system. In practice, the components that convert electrical quantities to mechanical quantities are usually designed to produce torque as the basic output quantity. For example, the input current to the conventional ammeter generates a torque that under static conditions is balanced by the elastic reaction of a spring, which determines the deflection of an index with respect to a scale calibrated in terms of the input quantity. Electromechanical instrument theory and practice are discussed in physics texts, in books on electrical measurements, and in manufacturers' publications.*

32.2. Ammeters, voltmeters, and wattmeters are generally familiar to scientists and engineers as instruments for measuring quantities that vary slowly. Oscillographs with mechanical or optical indicating systems are indispensable for recording quantities that vary rapidly with time. Wide variations in design and construction** exist among individual examples, but as a general rule the operating components of any electromechanical instrument will fit into the pattern described by the generalized functional diagram in section a of Information Summary 32-1.

32.3. In the generalized functional diagram, the current or voltage input is applied to an input receiving network that reduces the input to a form and magnitude adapted for operation of the torque generator. For the purposes of a functional diagram, the properties of the torque generator that affect the output of the input receiving network are considered as part of this network. This means that the resistance of a galvanometer coil is functionally associated with a branch of the input receiving network. This resistance is therefore represented by a dotted line

---

* Physics: see Page and Adams (P7) and Sears (S3); electrical measurements: see Laws (L7) and Hague (H2); manufacturer's publications: see Weston Electrical Instrument Corp. (W4) and General Electric Company (G2).

** See Weston Electrical Instrument Corp. (W4) and General Electric Company (G2).

in the pictorial-functional diagram of section b, Information Summary 32-1, to show that its physical presence in the network is only one of its important properties. Any coil connected to the input receiving network is an essential part of the torque generator, which is designed so that its input current interacts with magnetic flux lines to produce the output torque. The element on which the output torque acts directly is attached to the coupler. The coupler produces the coupler output angle, which is mechanically transferred to the indicating system. The indicating system output is the indication or the index angle. This angle is the input to the scale, from which the input quantity reading is taken as the essential output of the measuring instrument.

32.4. Many different designs using the fundamental principles of electricity and magnetism have been developed for receiving networks and torque generators. The details of construction vary with the quantities to be measured and the accuracy required, but the essential function of producing a torque output from an electrical input quantity is always preserved. So far as the static-functional diagram in section a of Information Summary 32-1 is concerned, the coupler merely receives a torque and produces an output angle that is completely determined by the input torque. Because of mechanical effects of the type illustrated in the examples of Chapters 4 and 8, torque components not accounted for in the generalized static-functional diagram will appear when dynamic conditions exist. The sources of these torque components* and the components themselves are represented in the functional diagram of Derivation Summary 32-1.

32.5. The static-functional diagrams of sections b through e of Information Summary 32-1 illustrate the essential features that are characteristic of four commonly used types of electromechanical measuring instruments. The actual construction of these and many other types is shown so well in readily available manufacturers' catalogs and special pamphlets** that no detailed description of design features is required here. However, it is worth while to show how physical principles are applied in the operation of a group of typical electromechanical measuring instruments and to develop performance equations for the individual members of the group.

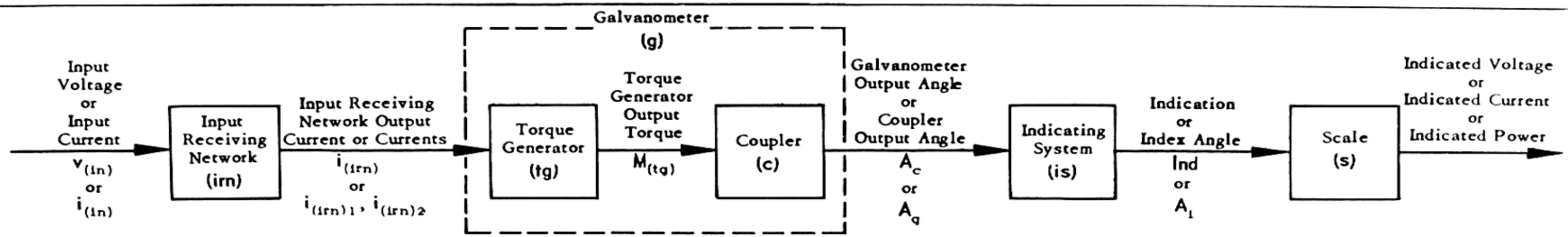
32.6. The four instrument types illustrated in sections b through e of Information Summary 32-1 are classified on the basis of the principle applied in the torque generator. Moving-coil instruments*** (represented in section b) are designed around a coil and a magnetic circuit structure (usually including a permanent

---

* Inertia reaction torque components do not appear explicitly in the functional diagrams of this book. In accordance with the convention established in Chapter 7, any mechanical component that is accelerated in operation is assumed to have inertia reaction effects.

** See Oscillograph manufacturers (O3).

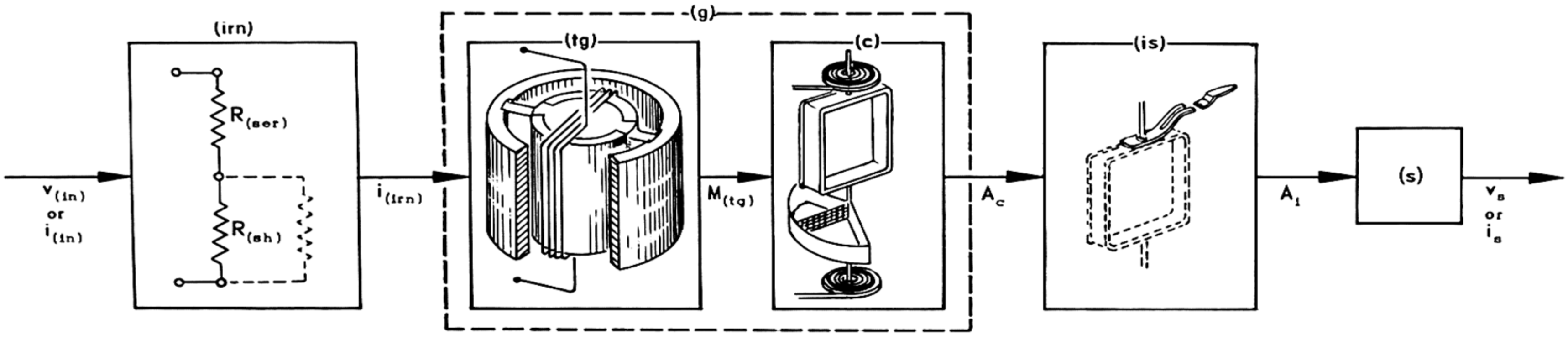
*** Meters using the moving-coil principle are commonly called D'Arsonval instruments.



Note: Both $v_{(in)}$ and $i_{(in)}$ are inputs for power measurements

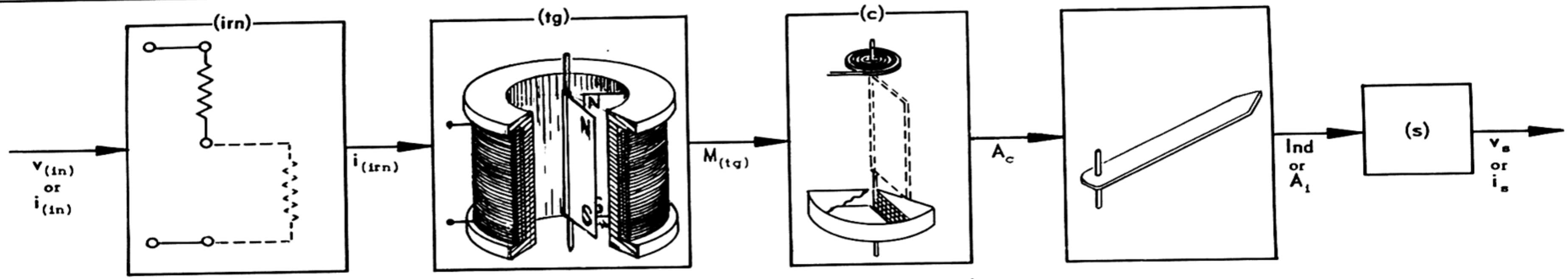
Note: Static-functional diagrams include only components with effects that are important under static conditions.

a) Generalized static-functional diagram for electromechanical measuring instruments

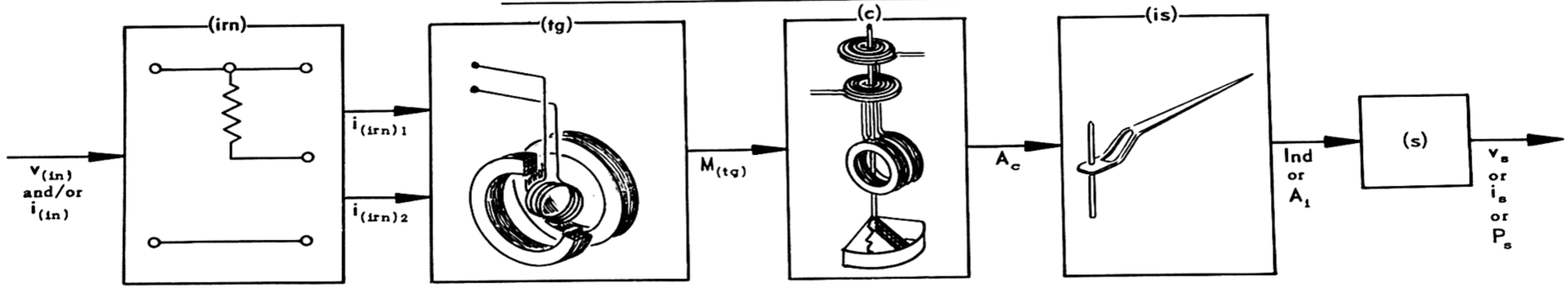


b) Pictorial-functional diagram for permanent magnet moving-coil electrical instruments

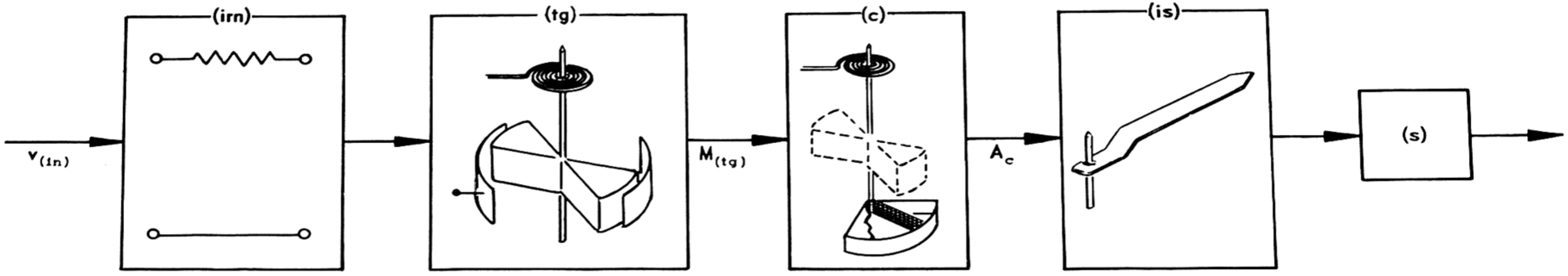
Information Summary 32-1. Static-functional diagram and pictorial-functional diagrams for electromechanical measuring instruments. (Page 1 of 2)



c) Pictorial-functional diagram for moving iron electrical instruments



d) Pictorial-functional diagram for electrodynamometer measuring instruments



e) Pictorial-functional diagram for electrostatic measuring instruments

Information Summary 32-1. Static-functional diagram and pictorial-functional diagrams for electromechanical measuring instruments. (Page 2 of 2)

magnet) that establishes an effectively uniform field at right angles to the wires in the torque-producing parts of the coil. The input receiving network is a combination of resistors connected in series and in parallel with the torque generator coil, and is designed to produce a current suitable for the torque generator coil, with a known relationship to the meter input voltage or current. The typical coupler shown in section b includes a rigid coil form attached to pivots that allow rotation of the form with respect to the instrument case about the axis established by the pivots. The output angle of the coupler is determined by the balance of torque components from the elastic restraint springs, the damper, the torque generator, and inertia reaction effects associated with the angular acceleration of parts that move with the coil form.* The coupler output angle is received by an indicating system consisting of a simple mechanical index that moves with respect to a scale calibrated to give readings of the input voltage or current.

32.7. Section c of Information Summary 32-1 illustrates one of many types** of moving-iron instruments. The torque generators used in these instruments have a stationary coil (or coils) that set up a magnetic field in a region containing a configuration of elements with good magnetic permeabilities. One of these elements is designed to receive a torque depending on the magnetic field set up by the coil structure. This field varies with the coil current, which in turn depends on the meter input. The coupler of a moving-iron instrument is a mechanical structure with the operating characteristics just described for the couplers of moving-coil instruments. The indicating system – scale combination for moving-iron instruments is functionally identical with the corresponding combination of moving-coil meter components.

32.8. Section d of Information Summary 32-1 shows the elements of the electrodynamometer instrument type. In devices of this kind, the torque generator consists of two coil systems whose magnetic fields interact to produce the operating torque for the coupler. The input receiving network is effectively divided into two sections, thereby producing a separate current input for each of the torque generator coil systems. When these two currents are associated with independent input quantities, the torque generator output represents the product of these quantities. This characteristic makes instruments of the electrodynamometer type particularly suitable for measurements associated with power in alternating-current circuits. Couplers, indicating systems, and scales are functionally identical with the corresponding components for moving-coil and moving-iron instruments.

32.9. Section e of Information Summary 32-1 illustrates the essential features of electrostatic instruments. In devices of this class, the torque generator action

---

* In practice, coil forms may be separate structural members, or they may be effectively replaced by the insulation varnish and cement that hold the torque generator coil wires together.

** See General Electric Company (G2) and Weston Electrical Instrument Corp. (W4).

is designed to use the electrostatic forces between conducting surfaces charged to potentials that correspond to the input voltage difference. The function of the input receiving network is to reduce the input voltage to a level suitable for driving the torque generator and to provide a high-resistance path for limiting current flow in the event of insulation failure. Except for the input receiving network and the torque generator, the components for electrostatic instruments are similar to those of other electromechanical instrument types. In practice, electrostatic instruments are particularly suitable for measuring voltages with a minimum of current drain on the system from which the input is taken.

32.10. The static-functional diagrams of Information Summary 32-1 are illustrative only and do not properly suggest the great range of individual instruments that have been developed for the purposes of science and industry. An introduction to the descriptive material in this field can be found in references (G2) and (W4). The theoretical aspects of electromechanical instrument performance are discussed in the following section.

GENERALIZED FUNCTIONAL DIAGRAM FOR ELECTROMECHANICAL MEASURING INSTRUMENTS

32.11. The static-functional diagrams of Information Summary 32-1 represent the operating components that are combined to make up typical electromechanical measuring instruments with no direct suggestion of the interactions that occur under dynamic conditions. These interactions are represented by the functional diagram in section a of Derivation Summary 32-1, which follows the pattern established by the rate-of-turn indicator and pressure indicator examples of Chapters 7 and 8. The same functional diagram applies to all electromechanical instruments, including the conventional meter type described in Specification 29-1 and the oscillograph to be discussed later. In all cases, an input receiving network takes the input or inputs to the instrument and supplies a corresponding input or inputs to a torque generator of some type. The output from this generator is one of the inputs to the torque summing member, which is one of the essential parts of the coupler.* The torque summing member also receives torque components from the elastic restraint and the damper. The coupler output is the coupler angle, which acts as the input to the indicating system. In conventional meters, the indicating system output is the indication or the index angle, which is equal to the coupler angle. On the other hand, when optical indicating systems are used in galvanometers or oscillographs, the indicating system output usually differs from the corresponding input by some factor. The combination of an input receiving

---

* For convenience, the coupler (symbol c) is often considered as identical with the torque summing member (symbol tsm), although the coupler properly includes the elastic restraint and the damper in addition to the torque summing member.

network, a torque generator, and a coupler is often considered as a single unit and called the galvanometer.* Any instrument with a proper calibration will have indicating system and scale characteristics adjusted to give an over-all sensitivity under calibration conditions (usually defined as static conditions) equal to unity, so that scale readings will be equal to input levels.

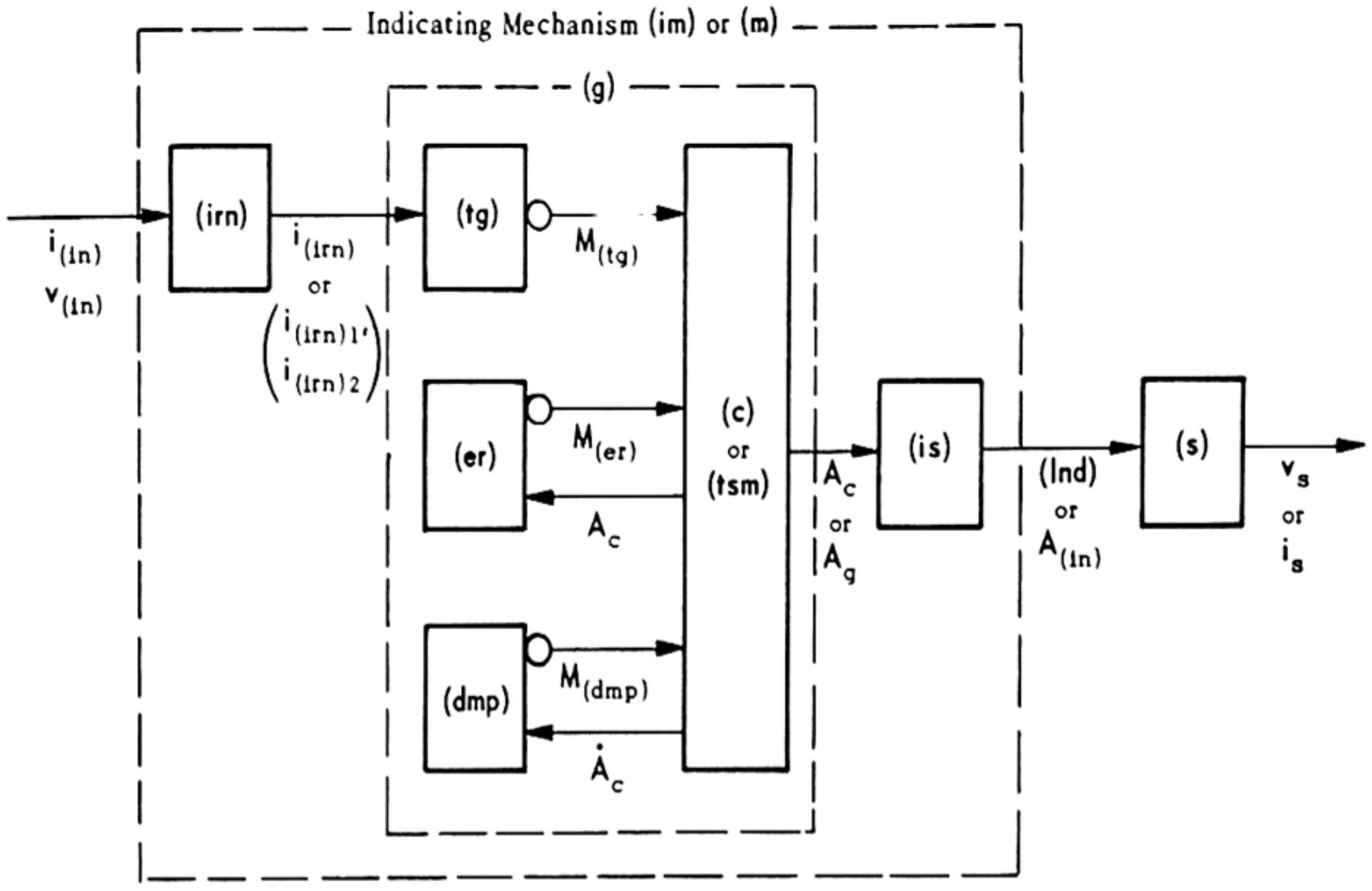
32.12. Section b of Derivation Summary 32-1 lists symbols that describe the performance of the operating components and subsystems shown in the functional diagram of section a in terms of performance functions, sensitivities, and equations. As written, the performance equations are based on the assumptions that dynamic actions have negligibly small effects on the behavior of input receiving networks and torque generators. In formal terms, the differences between various instrument types are completely taken into account by modifications in performance function and sensitivity subscripts. The pattern followed in developing performance equations is the same for all the instrument types and leads to a form that is identical for all the cases considered. In working variable terms, this form is identical with the (0; 0,1,2) differential equation discussed and solved for a number of forcing functions in Chapter 19. This means that quantitative information on many situations of practical importance in the use of electromechanical measuring instruments is immediately available from the solution-describing nondimensional equations and curves of Chapter 19.

32.13. To apply the generalized information of Chapter 19 to any particular situation, it is necessary to determine the sensitivities associated with each operating component and then to calculate the damping ratio, undamped natural frequency, or other equivalent parameters. In practice, it is seldom possible to estimate performance-describing coefficients with the required accuracy. This means that theory is primarily useful for preliminary design purposes and to suggest effective test procedures for refining performance information. In applying experimental methods for this purpose, it is generally better to measure performance functions and sensitivities and record data on these quantities directly than it is to interpret results in terms of individual design factors. For example, it is convenient to study torque generator performance by applying various input levels and measuring the corresponding output torque so that the corresponding sensitivity may be found by a direct comparison as one of the quantities of primary interest. Once sensitivity is known for a proper range of different designs, the influence of any given factor may be found by proper studies of the results.

32.14. The performance equation forms given by Eqs. (3) and (4) of Derivation

---

* The components considered as included in a galvanometer may be changed for convenience in any special case. For example, a complete electromechanical instrument of the wall-mounted type, including the input receiving network, may be called a galvanometer. On the other hand, the mechanical assembly, excluding the magnetic system, for an oscillograph is also often referred to as a galvanometer.



Note: The conventions used in this diagram are defined in Chapter 7.

a) Functional diagram for electromechanical measuring instruments

Performance information on each component and subsystem of the diagram of section a follows, identified by the symbols defined by the diagram.

Note: The performance functions (main symbol PF) and sensitivities (main symbol S) that follow are represented by symbols formed under the conventions described in Chapter 10.

(im) Input Receiving Network

When voltage is considered as the input,

$$[PF]_{(irn)} \approx \begin{cases} S_{(irn)[v;i](st)} \\ \text{or} \\ S_{(irn)[v;v](st)} \end{cases}$$

When current is considered as the input,

$$[PF]_{(irn)} \approx S_{(irn)[i;i](st)}$$

When power is considered as the input,

$$[PF]_{(irn)} \approx S_{(irn)[P;i_1,i_2](st)}$$

(tg) Torque Generator

$$[PF]_{(tg)} \approx \begin{cases} S_{(tg)[i;M](st)} \\ S_{(tg)[i_1,i_2;M](st)} \end{cases}$$

(dmp) Damper

$$[PF]_{(dmp)} \approx S_{(dmp)[\dot{A};M](st)} = -c_{(dmp)}$$

where

$c_{(dmp)}$ = damping coefficient

Derivation Summary 32-1. Functional diagram and performance equations for electromechanical measuring instruments. (Page 1 of 7)

(er) Elastic Restraint

$$[PF]_{(er)} \approx S_{(er)[A;M]_{(st)}} = -k_{(er)}$$

where

$k_{(er)}$ = elastic restraint coefficient

(is) Indicating System

$$[PF]_{(is)} \approx S_{(is)[A;A]_{(st)}}$$

(s) Scale

$$[PF]_{(s)} \approx \begin{cases} S_{(s)[A;v]_{(st)}} \\ \text{or} \\ S_{(s)[A;i]_{(st)}} \\ \text{or} \\ S_{(s)[A;P]_{(st)}} \end{cases}$$

(g) Galvanometer

$$-I_{(tsm)(eq)}\ddot{A}_g - c_{(dmp)}\dot{A}_g - k_{(er)}A_g + \begin{cases} S_{(tg)[i;M]}\, i_{(irn)} \\ S_{(tg)[i_1,i_2;M]}\, i_{(irn)1}\, i_{(irn)2} \end{cases} = 0 \qquad (1)$$

where

$I_{(tsm)(eq)}$ = equivalent moment of inertia of mechanical parts rotating with the torque summing member

Rearranging the terms of Eq. (1) and changing signs gives

$$I_{(tsm)(eq)}\ddot{A}_g + c_{(dmp)}\dot{A}_g + k_{(er)}A_g = \begin{cases} S_{(tg)[i;M]}\, i_{(irn)} \\ S_{(tg)[i_1,i_2;M]}\, i_{(irn)1}\, i_{(irn)2} \end{cases} \qquad (2)$$

(irn) + (g) Input Receiving Network and Galvanometer

$$I_{(tsm)(eq)}\ddot{A}_g + c_{(dmp)}\dot{A}_g + k_{(er)}A_g = \begin{cases} S_{(irn)[v;i]}\, S_{(tg)[i;M]}\, v_{(in)} \\ \text{or} \\ S_{(irn)[i;i]}\, S_{(tg)[i;M]}\, i_{(in)} \\ \text{or} \\ S_{(irn)[v;i]}\, S_{(irn)[i;i]}\, S_{(tg)[i_1,i_2;M]}\, v_{(in)}\, i_{(in)} \end{cases} \qquad (3)$$

Note: The symbols $v_{(in)}$ and $i_{(in)}$ represent instantaneous values of voltage and current, respectively. Conventional alternating-current forms may be used for steady-state sinusoidal input variations.

(irn) + (g) + (is) Input Receiving Network, Galvanometer and Indicating System

$$I_{(tsm)(eq)}\ddot{A}_1 + c_{(dmp)}\dot{A}_1 + k_{(er)}A_1 = \begin{cases} S_{(irn)[v;i]}\, S_{(tg)[i;M]}\, S_{(is)[A;A]}\, v_{(in)} \\ \text{or} \\ S_{(irn)[i;i]}\, S_{(tg)[i;M]}\, S_{(is)[A;A]}\, i_{(in)} \\ \text{or} \\ S_{(irn)[v;i]}\, S_{(irn)[i;i]}\, S_{(tg)[i_1;i_2;M]}\, S_{(is)[A;A]}\, v_{(in)}\, i_{(in)} \end{cases} \qquad (4)$$

(irn) + (g) + (is) + (s) Input Receiving Network, Galvanometer, Indicating System and Scale; or (vm) Voltmeter; or (am) Ammeter; or (wm) Wattmeter

Derivation Summary 32-1. Functional diagram and performance equations for electromechanical measuring instruments. (Page 2 of 7)

$$\left.\begin{matrix}\ddot{v}_s\\ \ddot{i}_s\\ \ddot{P}_s\end{matrix}\right\} + \frac{c_{(dmp)}}{I_{(tsm)(eq)}}\left\{\begin{matrix}\dot{v}_s\\ \dot{i}_s\\ \dot{P}_s\end{matrix}\right\} + \frac{k_{(er)}}{I_{(tsm)(eq)}}\left\{\begin{matrix}v_s\\ i_s\\ P_s\end{matrix}\right\}$$

$$= \begin{cases} \dfrac{S_{(irn)[v;i]}S_{(tg)[i;M]}S_{(is)[A;A]}S_{(s)[A;v]}}{I_{(tsm)(eq)}}\, v_{(in)} \\ \text{or} \\ \dfrac{S_{(irn)[i;i]}S_{(tg)[i;M]}S_{(is)[A;A]}S_{(s)[A;i]}}{I_{(tsm)(eq)}}\, i_{(in)} \\ \text{or} \\ \dfrac{S_{(irn)[v;i]}S_{(irn)[i;i]}S_{(tg)[i_1,i_2;M]}S_{(is)[A;A]}S_{(s)[A;P]}}{I_{(tsm)(eq)}}\, v_{(in)}\, i_{(in)} \end{cases} \tag{5}$$

Rewriting Eq. (5) gives

$$\left.\begin{matrix}\ddot{v}_s\\ \ddot{i}_s\\ \ddot{P}_s\end{matrix}\right\} + 2(DR)w_n\left\{\begin{matrix}\dot{v}_s\\ \dot{i}_s\\ \dot{P}_s\end{matrix}\right\} + w_n^2\left\{\begin{matrix}v_s\\ i_s\\ P_s\end{matrix}\right\} = \left\{\begin{matrix}w_n^2 S_{(vm)[v;v]}v_{(in)}\\ w_n^2 S_{(am)[i;i]}i_{(in)}\\ w_n^2 S_{(wm)[P;P]}P_{(in)}\end{matrix}\right. \tag{6}$$

where

$P_{(in)} = v_{(in)}\, i_{(in)}$ = input power

P_s = power scale reading

DR = damping ratio

$$w_n = \sqrt{\frac{k_{(er)}}{I_{(tsm)(eq)}}} = \text{undamped angular natural frequency} \tag{7}$$

(Refer to Definition Summary 19-1 and Table 19-1 for additional relationships.)

$$S_{(vm)[v;v](st)} = \frac{S_{(irn)[v;i]}S_{(tg)[i;M]}S_{(is)[A;A]}S_{(s)[A;v]}}{k_{(er)}} = \text{voltmeter over-all static sensitivity} \tag{8}$$

Note that

$$S_{(c)[M;A](st)} = -k_{(er)}$$

$$S_{(am)[i;i](st)} = \frac{S_{(irn)[i;i]}S_{(tg)[i;M]}S_{(is)[A;A]}S_{(s)[A;v]}}{k_{(er)}} = \text{ammeter over-all static sensitivity} \tag{9}$$

$$S_{(wm)[P;P](st)} = \frac{S_{(irn)[v;i]}S_{(irn)[i;i]}S_{(tg)[i_1,i_2;M]}S_{(is)[A;A]}S_{(s)[A;P]}}{k_{(er)}}$$

$$= \text{wattmeter over-all static sensitivity} \tag{10}$$

Note: The electrostatic instrument illustrated in section e of Information Summary 32-1 is not specifically included in the development just summarized. The electrostatic instrument performance equation may be derived by use of an identical pattern to show that

$$\ddot{v}_s + 2(DR)w_n\dot{v}_s + w_n^2 v_s = w_n^2 S_{(esvm)[v;v]}v_{(in)} \tag{11}$$

Derivation Summary 32-1. Functional diagram and performance equations for electromechanical measuring instruments. (Page 3 of 7)

where DR and w_n are as already defined and

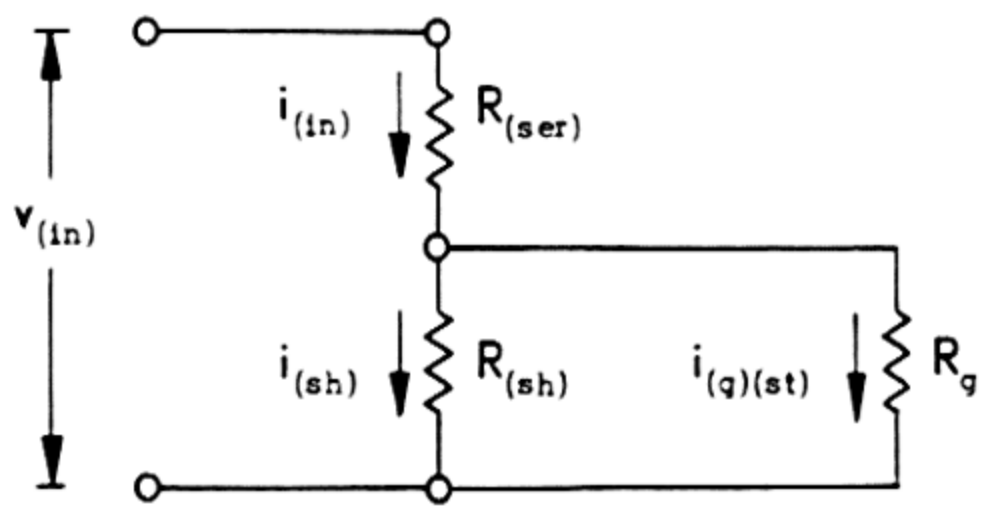
$$S_{(esvm)[v;v](st)} = \frac{S_{(irn)[v;v]} S_{(tq)[v;M]} S_{(ts)[A;A]} S_{(s)[A;v]}}{k_{(er)}}$$

$$= \text{electrostatic voltmeter over-all static sensitivity} \tag{12}$$

Note: In general, for properly calibrated instruments, each of the over-all static sensitivities has a magnitude of unity.

b) Generalized performance equations for electromechanical measuring instruments

(irn) Input Receiver Network (Static Conditions)



$R_{(ser)}$ = series resistance
$R_{(sh)}$ = shunt resistance
R_q = galvanometer resistance

$$v_{(in)} = i_{(in)} R_{(ser)} + i_{(sh)} R_{(sh)} \tag{13}$$

$$i_{(in)} = i_{(sh)} + i_{(q)(st)} \tag{14}$$

$$i_{(sh)} R_{(sh)} = i_{(q)(st)} R_q \tag{15}$$

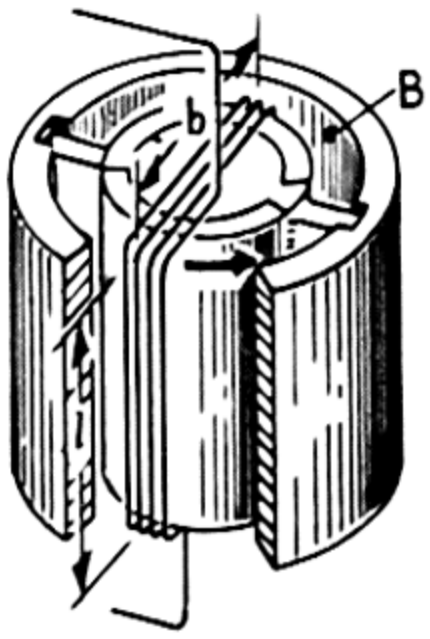
Solving Eqs. (13), (14) and (15) for $i_{(q)(st)}$ in terms of $v_{(in)}$ and the three resistances shows that

$$i_{(q)(st)} = \frac{1}{R_q \left[1 + \dfrac{R_{(ser)}(R_q + R_{(sh)})}{R_q R_{(sh)}} \right]} v_{(in)} \tag{16}$$

so that

$$S_{(irn)[v;i](st)} = \frac{1}{R_q \left[1 + \dfrac{R_{(ser)}(R_q + R_{(sh)})}{R_q R_{(sh)}} \right]} \tag{17}$$

(irn) Input Receiver Network (Dynamic Conditions)



B = effective flux density in air gap
b = effective width of coil
l = effective length of coil
N = number of active turns
$\frac{dA_c}{dt}$ = angular velocity of coil
ϕ = magnetic flux

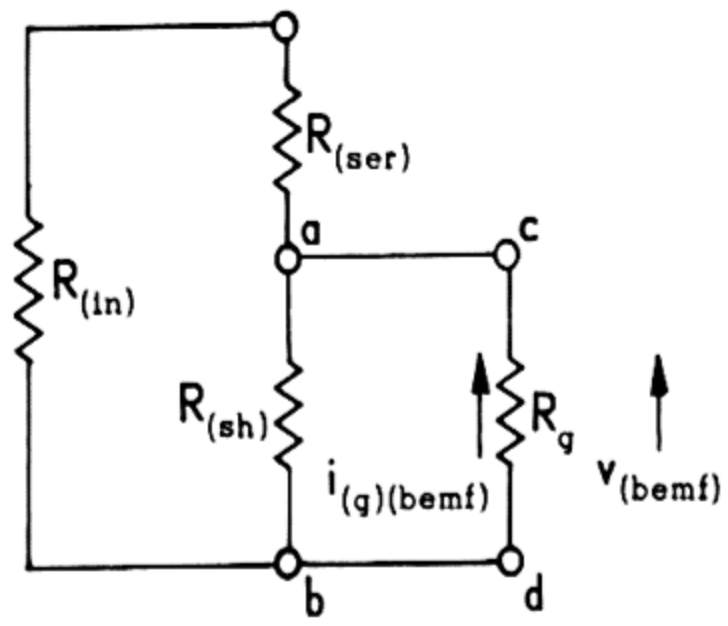
The generated back electromotive force is proportional to the rate of change of flux linkages; i.e.,

$$v_{(bemf)} = -N \frac{d\phi}{dt} = -2NBl \left(\frac{b}{2}\right) \frac{dA_c}{dt} \tag{18}$$

so that

$$S_{q[\dot{A};v]} = -NBlb \tag{19}$$

Derivation Summary 32-1. Functional diagram and performance equations for electromechanical measuring instruments. (Page 4 of 7)



$R_{(in)}$ = internal resistance of input circuit

$i_{(g)(bemf)}$ = component of galvanometer current due to back electromotive force

$v_{(bemf)}$ = back electromotive force

When viewed from points a and b, the parallel circuits $R_{(ser)} + R_{(in)}$ and $R_{(sh)}$ have the reciprocal resistance $1/R_{(ab)}$, where

$$\frac{1}{R_{(ab)}} = \frac{1}{R_{(sh)}} + \frac{1}{R_{(ser)} + R_{(in)}} \tag{20}$$

so that

$$R_{(ab)} = \frac{R_{(sh)}(R_{(ser)} + R_{(in)})}{R_{(sh)} + R_{(ser)} + R_{(in)}} \tag{21}$$

To a voltage applied from d to c, $R_{(ab)}$ is in series with R_g, so that

$$i_{(g)(bemf)} = \frac{v_{(bemf)}}{R_g + \dfrac{R_{(sh)}(R_{(ser)} + R_{(in)})}{R_{(sh)} + R_{(ser)} + R_{(in)}}} \tag{22}$$

Using Eqs. (18) and (19) to express $v_{(bemf)}$, and rearranging terms gives

$$i_{(g)(bemf)} = \frac{S_{(g)[\dot{A};v]}\dot{A}_c}{R_g\left[1 + \dfrac{R_{(sh)}(R_{(ser)} + R_{(in)})}{R_g(R_{(sh)} + R_{(ser)} + R_{(in)})}\right]} \tag{23}$$

or

$$i_{(g)(bemf)} = S_{(g)[\dot{A};i]}\dot{A}_c \tag{24}$$

where

$$S_{(g)[\dot{A};i]} = S_{(g)[\dot{A};v]} \frac{1}{R_g\left[1 + \dfrac{R_{(sh)}(R_{(ser)} + R_{(in)})}{R_g(R_{(sh)} + R_{(ser)} + R_{(in)})}\right]} \tag{25}$$

(tg) Moving-Coil Torque Generator



Derivation Summary 32-1. Functional diagram and performance equations for electromechanical measuring instruments. (Page 5 of 7)

The law of current – magnetic field interaction shows that

$$M_{(tg)} = \frac{2BblN}{2} \frac{i_g}{10} \tag{26}$$

or

$$M_{(tg)} = S_{(tg)[i;M]} i_g \tag{27}$$

where

$$S_{(tg)[i;M]} = \frac{NBbl}{10} \tag{28}$$

where

B = magnetic flux density, in lines per square centimeter
b = width of coil, in centimeters
l = length of coil sides in magnetic field, in centimeters
i_g = galvanometer current, in amperes
$M_{(tg)}$ = torque generator output torque, in dyne centimeters

Note: In general, B, b, and l will be effective values.

(dmp) Damper

The damping torque due to the back electromotive force generated in the galvanometer coil is due to the back electromotive force current acting through the torque-producing action of the torque generator; i.e.,

$$M_{(dmp)(bemf)} = S_{(tg)[i;M]} S_{(g)[\dot{A};i]} \dot{A}_c = S_{(tg)[\dot{A};M](bemf)} \dot{A}_c \tag{29}$$

where

$$S_{(tg)[\dot{A};M](bemf)} = -\frac{N^2B^2b^2l^2}{10} \frac{1}{R_g\left[1 + \frac{R_{(sh)}(R_{(ser)} + R_{(in)})}{R_g(R_{(sh)} + R_{(ser)} + R_{(in)})}\right]} \tag{30}$$

By definition,

$$S_{(tg)[\dot{A};M](bemf)} = -c_{(dmp)(bemf)} \tag{31}$$

where

$c_{(dmp)(bemf)}$ = back electromotive force damping coefficient

Therefore,

$$c_{(dmp)(bemf)} = \frac{N^2B^2b^2l^2}{10R_g} \frac{1}{1 + \frac{R_{(sh)}(R_{(ser)} + R_{(in)})}{R_g(R_{(sh)} + R_{(ser)} + R_{(in)})}} \tag{32}$$

Eddy currents in a conducting coil form or a part of conducting material moving in the field of a permanent magnet will give a damping torque component; i.e.,

$$M_{(g)(dmp)(ec)} = S_{(tg)[\dot{A};M](ec)} \dot{A}_c \tag{33}$$

By definition,

$$S_{(tg)[\dot{A};M](ec)} = -c_{(dmp)(ec)} \tag{34}$$

where

$c_{(dmp)(ec)}$ = eddy current damping coefficient

Drag effects generated by viscous action in a fluid (either gaseous or liquid) will produce a damping torque component of the form

$$M_{(tg)(dmp)(vis)} = S_{(tg)[\dot{A};M](vis)} \dot{A}_c \tag{35}$$

Derivation Summary 32-1. Functional diagram and performance equations for electromechanical measuring instruments. (Page 6 of 7)

By definition,

$$S_{(g)[\dot{A};M](vis)} = -C_{(dmp)(vis)} \tag{36}$$

where

$C_{(dmp)(vis)}$ = viscous damping coefficient

The resultant damping torque has the form

$$M_{(dmp)} = -C_{(dmp)}\dot{A}_c \tag{37}$$

where

$$C_{(dmp)} = C_{(dmp)(bemf)} + C_{(dmp)(ec)} + C_{(dmp)(vis)} \tag{38}$$

The elastic restraint coefficient $k_{(er)}$ (or $S_{(er)[A;M]}$, which is equal to $-k_{(er)}$) for moving-coil instruments depends on design in any particular case and usually must be determined and adjusted by experimentation.

With the performance-controlling coefficients related to design features by Eqs. (13) through (38), the typical performance equation (6) for instruments of the moving-coil type may be written in the working variable form as

$$a_2\ddot{v} + a_1\dot{v} + a_0 v = b_0 u \tag{39}$$

where

$$a_2 \approx I_{(tsm)(eq)} \quad ; \quad a_1 \approx C_{(dmp)} \quad ; \quad a_0 \approx k_{(er)} \tag{40}$$

and

$$b_0 \approx S_{(irn)[v;i]}S_{(tg)[i;M]}S_{(is)[A;A]}S_{(s)[A;v]} \tag{41}$$

or

$$b_0 \approx S_{(irn)[i;i]}S_{(tg)[i;M]}S_{(is)[A;A]}S_{(s)[A;i]} \tag{42}$$

Equation (39) is a typical (0;0,1,2) equation, which in practice usually has coefficients that are effectively constant.

Solutions for the (0;0,1,2) equation are developed and summarized in Chapter 19.

c) Performance equation for moving-coil voltmeters and ammeters

Derivation Summary 32-1. Functional diagram and performance equations for electromechanical measuring instruments. (Page 7 of 7)

Summary 32-1 are based on the assumption that the inertia reaction effects associated with operation of the coupler may be represented by masses attached to the torque summing member to form a single rigid body. This assumption leads to the second-order performance-describing form of Eq. (6). In practice, conclusions based on this form may fail to describe actual performance because the mechanical parts of the indicating system may not behave as a single rigid structure, but show flexibility in a way that must be represented either as a continuous cantilever beam or as an equivalent system that approximates the action of such a beam. Even a first approximation, when the indicating system is represented by a single mass attached to the torque summing member by a simple elastic element and a small damper, changes the second-order performance equation to a fourth-order equation with solutions that are more complex than those given in Chapter 19. It is entirely feasible to derive engineering results from performance equations of any order, but the mathematical approaches discussed in Chapters 20 through 27 are required instead of the direct differential equation solution procedure of Chapter 19.

DERIVATION OF PERFORMANCE COEFFICIENTS AND PARAMETERS IN TERMS OF DESIGN FACTORS FOR MOVING-COIL INSTRUMENTS

32.15. From the standpoint of operation, all electromechanical instruments whose components follow the performance equations assumed in section b of Derivation Summary 32-1 follow the same performance pattern. The essential differences between instrument types depend on the mechanization used to achieve the behavior described by the performance equations. Differences between individual instruments of a given type lie in the magnitudes chosen for the design factors that determine performance coefficients and parameters. A development of these coefficients and parameters for moving-coil instruments is outlined in section c of Derivation Summary 32-1. This example is chosen not only because of the great practical importance of moving-coil instruments, but also because it clearly illustrates a pattern of analysis that may be applied to the design of any electromechanical instrument. The background information on physical principles required for performance equation derivations is available in texts on physics and electricity and in books dealing with the special field of electrical measurements.*

32.16. The general procedure for deriving the performance equation for any instrument is to write an equation for the operation of each component and then to combine these separate equations into a single over-all equation. In the case of the moving-coil instrument, the first component is the input receiving network, which consists of a resistance in series with a parallel circuit consisting of the torque generator coil and a shunt resistance. When the input quantity is considered as a voltage, the essential action of the network is to establish a relationship between this voltage and the galvanometer coil current. When attention is restricted to operating conditions that are not accompanied by dynamic effects, the input receiver performance is described by a voltage – current sensitivity that may be derived by a simple application of direct-current circuit theory. The expression for this sensitivity in terms of network resistance is given by Eq. (17) of Derivation Summary 32-1.

32.17. When static conditions no longer exist, but the galvanometer coil is rotating so that its active wires are cutting magnetic flux lines, a back electromotive force is generated in the coil. The direction of this generated voltage is such that, if it actually causes current to flow, the flux from this current always causes a torque that tends to retard the coil motion. The magnitude of the back electromotive force is proportional to the effective strength of the magnetic field in which the active sides of the coil move, the length of these sides, the number of effective turns on the coil, the effective radius of the active sides, and the angular velocity of the coil with respect to the structure that supports the magnet. As indicated by Eqs. (18) and (19) of Derivation Summary 32-1, this product is a

* Physics and electricity: see Page and Adams (P7) and Sears (S3); electrical measurements: see Laws (L7) and Hague (H2).

simplified expression for the rate at which flux linkages are cut by the coil as it rotates about its axis. The angular velocity – voltage sensitivity of the torque generator is given by Eq. (19) as the ratio of the back electromotive force to the angular velocity of the coil.

32.18. The current component due to the back electromotive force can be found by considering the action of this voltage on the circuit shown in section c of Derivation Summary 32-1. This circuit consists of the galvanometer resistance, R_g , in series with the shunt resistance, $R_{(sh)}$, which, in turn, is in parallel with two further resistances in series: the internal resistance, $R_{(in)}$, and the series resistance, $R_{(ser)}$, both of the input circuit. The expression for the back electromotive force current is given by Eq. (22) of Derivation Summary 32-1.

32.19. The result of combining the expression for the back electromotive force current with the angular velocity – voltage sensitivity of the torque generator is the angular velocity – current sensitivity of the input receiving network – torque generator combination. This sensitivity is given by Eq. (25) of Derivation Summary 32-1.

32.20. The force acting on each side of the torque generator coil is proportional to the flux density in the air gap, the active length of each conductor in the coil, the number of active turns, and the current flowing in each turn. The corresponding torque output is given by the product of the force on each of the two active coil sides and the radii of these sides from the axis of rotation. The resulting torque generator performance is described by Eq. (26) of Derivation Summary 32-1. The corresponding current – torque sensitivity of the torque generator is given by Eq. (28).

32.21. The damping action that occurs within the coupler is the resultant of the torque component produced by the back electromotive force current, the torque component due to eddy currents induced in conducting parts that move in magnetic field regions, and the torque component caused by fluid shearing actions that accompany rotation of the torque summing member. The back electromotive force damping torque is equal to the product of the current – torque sensitivity of the torque generator, the angular velocity – current sensitivity of the galvanometer, and the coupler angular velocity. The form of the expression for the corresponding angular velocity – torque back electromotive force sensitivity of the torque generator is given by Eq. (31) of Derivation Summary 32-1. As shown by Eqs. (31) and (32), this sensitivity has the same magnitude as the back electromotive force damping coefficient, which by convention has a negative sign.

32.22. Eddy current and viscous damping effects may be described by the forms of Eqs. (33) through (36). The values of the sensitivities and damping coefficients involved depend on the designs used for eddy current and fluid damper systems. The principles applied in damper designs* are well known, but the details

* See Lamb (L13) and Bingham (B19).

vary considerably among instrument types and are not usually easy to analyze accurately in general terms. For this reason, eddy current and viscous damper performances are described in Derivation Summary 32-1 by sensitivities and coefficients without equations giving relationships to design features. The resultant damping coefficient is given in Eq. (38) as the sum of the back electromotive force damping coefficient, the eddy current damping coefficient, and the viscous damping coefficient.

32.23. The elastic restraint coefficient of the coupler is determined by the mechanical features used in any particular instrument. The relationships among design details and elastic restraint coefficients are determined by the principles of the theory of elasticity. These relationships are summarized for engineering use by handbooks on spring design.* For the purposes of instrument performance analysis, it is sufficient to represent elastic restraint effects in terms of the coefficient associated with the first-order term on the left-hand side of Eq. (4) of Derivation Summary 32-1.

32.24. Equations (39) through (42) of Derivation Summary 32-1 give the definitions and the working variable form associated with Eq. (6), which describes the performance of any electromechanical measuring instrument with the features shown in Information Summary 32-1. As noted, Eq. (6) has the (0;0,1,2) working variable equation form, for which solutions are developed in Chapter 19. It is obvious that these results may be immediately applied to any system whose behavior can be described by the (0;0,1,2) equation.

PERFORMANCE CHARACTERISTICS OF ELECTROMECHANICAL MEASURING INSTRUMENTS

32.25. Variations in the readings from electromechanical measuring instruments with the features described in Information Summary 32-1 are given by the nondimensional curves** of Chapter 19 for a number of typical forcing functions. In order to apply these curves, which are given in working variable terms, to any particular measuring instrument, it is convenient to note that the voltage, current, and power variables of Eq. (6) of Derivation Summary 32-1 may be represented by R_s for scale reading and $R_{(s)(corr)}$ for the correct scale reading that corresponds to the actual level of the input quantity. In these terms, the performance equation takes the form

$$\ddot{R}_s + 2(DR)\,w_n \dot{R}_s + w_n^2 R_s = w_n^2 S_{(mi)[R_{(s)(corr)};R_s](ref)} R_{(s)(corr)} \qquad (32\text{-}1)$$

---

* Theory of elasticity: see Love (L14) and Timoshenko (T7); spring design: see American Steel & Wire Company (A8), Wallace Barnes Company (B8), and Wickwire Spenser Steel (W10).

** These curves also apply directly to responses from systems of any kind with (0;0,1,2) performance equations.

where

$R_s \equiv$ scale reading, corresponding to $\begin{cases} v_s - \text{voltage scale reading} \\ i_s - \text{current scale reading} \\ P_s - \text{power scale reading} \end{cases}$

$R_{(s)(corr)} \equiv$ correct scale reading, corresponding to $\begin{cases} v_{(in)} - \text{voltage input} \\ i_{(in)} - \text{current input} \\ v_{(in)} i_{(in)} = \\ P_{(in)} - \text{power input} \end{cases}$

$S_{(mi)[R_{(s)(corr)};R_s](ref)}$ = correct scale reading − scale reading
reference sensitivity of measuring instrument

DR = damping ratio

w_n = undamped angular natural frequency

32.26. The reference sensitivity for any properly calibrated measuring instrument is unity. This means that Eq. (32-1) reduces to

$$\ddot{R}_s + 2(DR) w_n \dot{R}_s + w_n^2 R_s = w_n^2 R_{(s)(corr)} \qquad (32\text{-}2)$$

32.27. In the working variable terms used in the developments of Chapter 19, Eq. (32-2) corresponds to the form

$$\ddot{v} + 2\zeta w_n \dot{v} + w_n^2 v = w_n^2 \sigma u \qquad (32\text{-}3)$$

where

$v \equiv$ dependent variable

$u \equiv$ independent variable

$\zeta \equiv$ damping ratio

w_n = undamped angular natural frequency

σ = dimensional similarity factor

32.28. Equation (32-3) is derived from a basic working variable equation corresponding to a generalized performance equation similar to Eq. (4) of Derivation Summary 32-1. The basic working variable equation is

$$a_2 \ddot{v} + a_1 \dot{v} + a_0 v = b_0 u \qquad (32\text{-}4)$$

where a_2, a_1, a_0, and b_0 are differential equation coefficients.

32.29. Table 32-1, which is taken from Table 19-1, summarizes definitions and relationships among the parameters and coefficients of second-order performance equations. These relationships are based on the second-order equation forms described in Definition Summary 19-1 and used for developments of transient solutions and complete solutions in Derivation Summaries 19-1 through 19-8. The discussion that follows outlines the general nature of these solutions and gives typical response curves for measuring instruments with (0;0,1,2) performance equations. The curves are specialized from the second-order nondimensional solution plots of Chapter 19.

IMPULSE FUNCTION RESPONSE

32.30. Figure 32-1 gives a family of curves that describes the response of measuring instruments with (0;0,1,2) performance equations to impulse forcing functions. Functions of this type are discussed in Chapter 17 as being formed from a sudden rise in the forcing quantity followed by a sudden drop to the original level after a short time interval. By definition, the impulse function strength is the product of the impulse height multiplied by the duration of the impulse. This means that the impulse function strength is proportional to the area enclosed by the lines representing the impulse and the level from which the change starts. In Fig. 32-1, the ordinate is the scale reading ratio, which is the ratio of the scale reading to a reference scale reading. The reference scale reading is taken as the product of the correct scale reading impulse strength multiplied by the undamped angular natural frequency. The running variable taken for the abscissa is the time - undamped natural frequency product. The impulse function response curves are damped oscillations that start from zero at the instant of the impulse and have the nature of damped oscillations for damping ratios less than unity and smooth curves with single peaks for higher damping ratios.

32.31. The family of curves given in Fig. 32-2 is like the impulse response family of Fig. 32-1, except that the abscissa is the time - high damping ratio characteristic time sum ratio. The high damping ratio characteristic time sum is defined in Table 32-1 as the ratio of the first-order differential equation coefficient to the zero-order differential equation coefficient. Equation (10) of Definition Summary 18-1 shows that the first-order characteristic time (given the symbol (CT) with the subscript (-;0,1)) has this same definition in terms of differential equation coefficients. This identity in definitions suggests the use of the characteristic time sum as the nondimensionalizing factor for the time variable. In Fig. 32-2, the impulse function curves approach, and finally become substantially identical to, a simple exponential as the damping ratio is made larger. This approach is very nearly complete when the damping ratio has reached a value of 5, so that the same response curve applies for all higher damping ratios.

32.32. Figure 32-3 is a family of deviation curves that shows in quantitative terms the differences between the impulse function response of a second-order system and the impulse function response of a first-order system that has the same first- and zero-order coefficients as those that occur in the second-order system. The deviation curves show that, except for a very short interval immediately after the impulse, the second-order response has a maximum difference less than 0.01 when the second-order response has a damping ratio of 5 or more. This means that satisfactory results may be achieved, so far as impulse function responses are concerned, by substituting a first-order performance equation for a second-order performance equation associated with a high damping ratio.

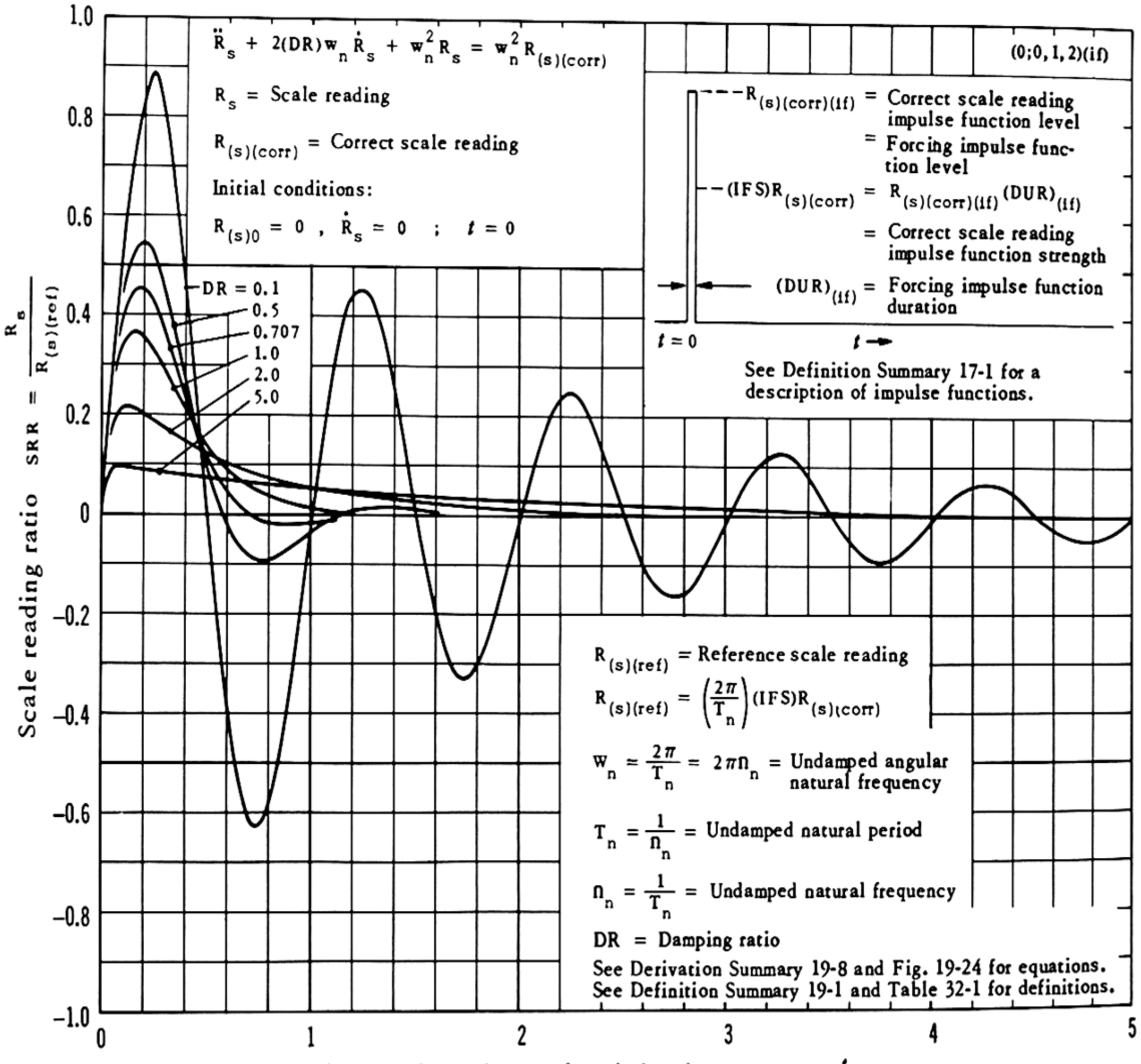


Fig. 32-1. Impulse function response curves for measuring instruments with (0;0,1,2) performance equations when the time – undamped natural frequency product is the running variable.

This simplification is often very useful in describing the behavior of measuring instruments that actually have (0;0,1,2) performance equations.

STEP FUNCTION RESPONSE

32.33. Figures 32-4, 32-5 and 32-6 are curve families that describe the step function response of measuring instruments with (0;0,1,2) performance equations.

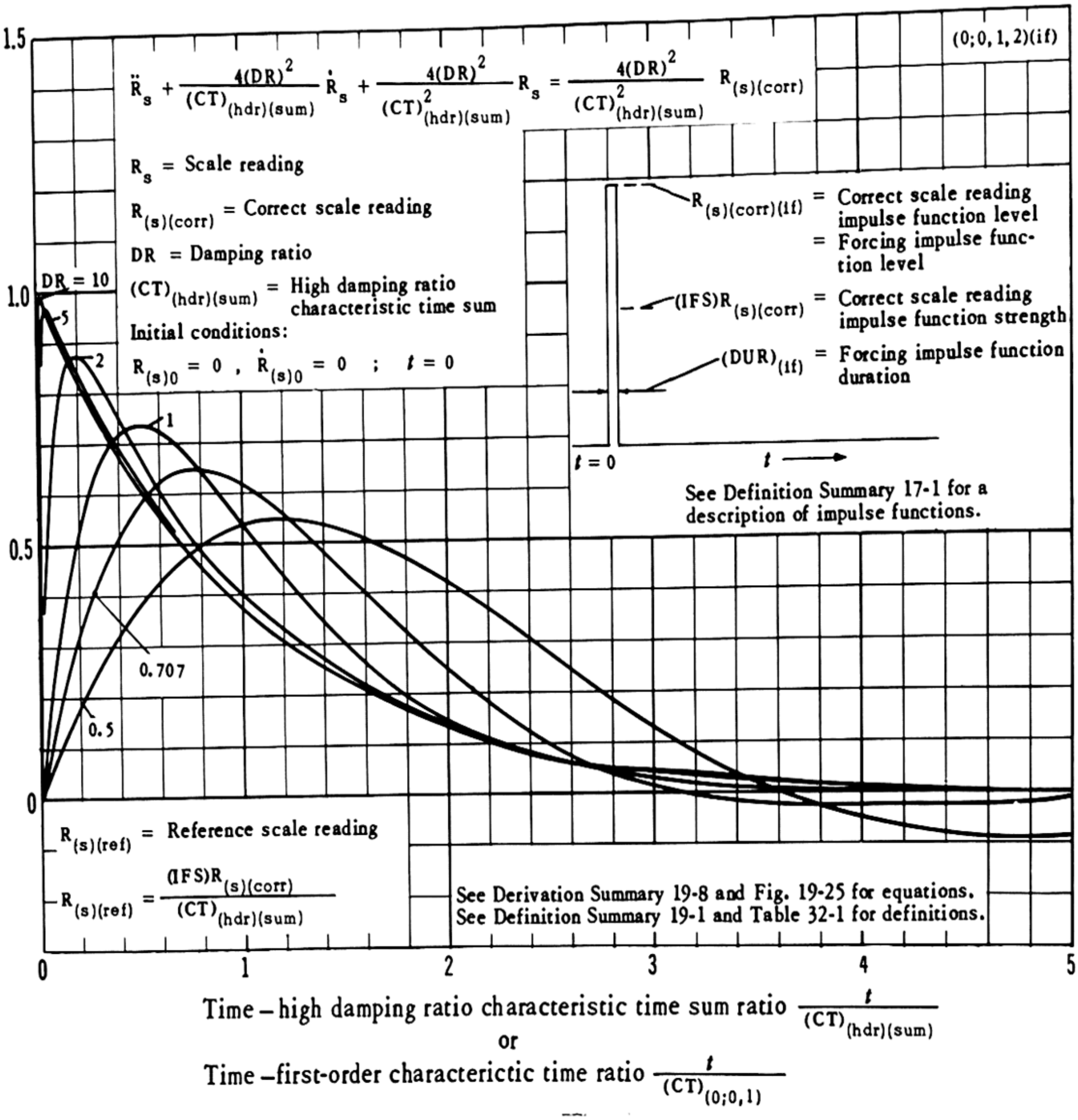


Fig. 32-2. Impulse function response curves for measuring instruments with (0;0,1,2) performance equations when the time – high damping ratio characteristic time sum ratio is the running variable.

In each of these three families, the nondimensional ordinate is the scale reading difference ratio, which is the difference between the scale reading and an arbitrarily chosen constant reference scale reading divided by the difference between the correct scale reading that exists just after the step function occurs and the reference scale reading. The difference between the families is in the quantity used to nondimensionalize time for the running variable. In Fig. 32-4, the nondimensionalizing term is the undamped natural period; in Fig. 32-5, this term is the low damping ratio characteristic time; and in Fig. 32-6, the high damping ratio characteristic time sum is used in forming the nondimensional running variable. The curve families show that the step function response is oscillatory for damping

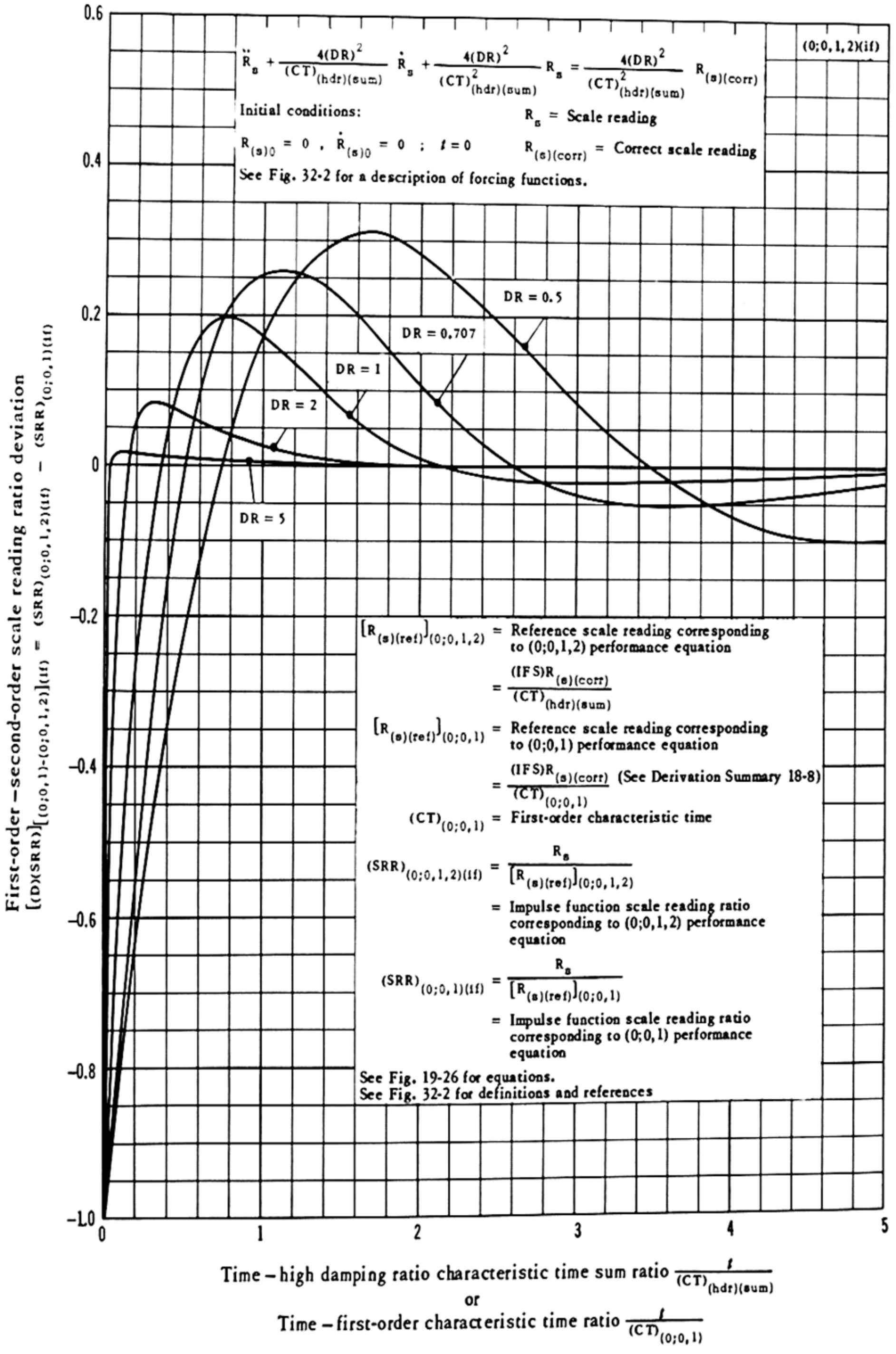


Fig. 32-3. Measuring instrument performance deviation curves for second-order impulse function response with respect to first-order impulse function response.

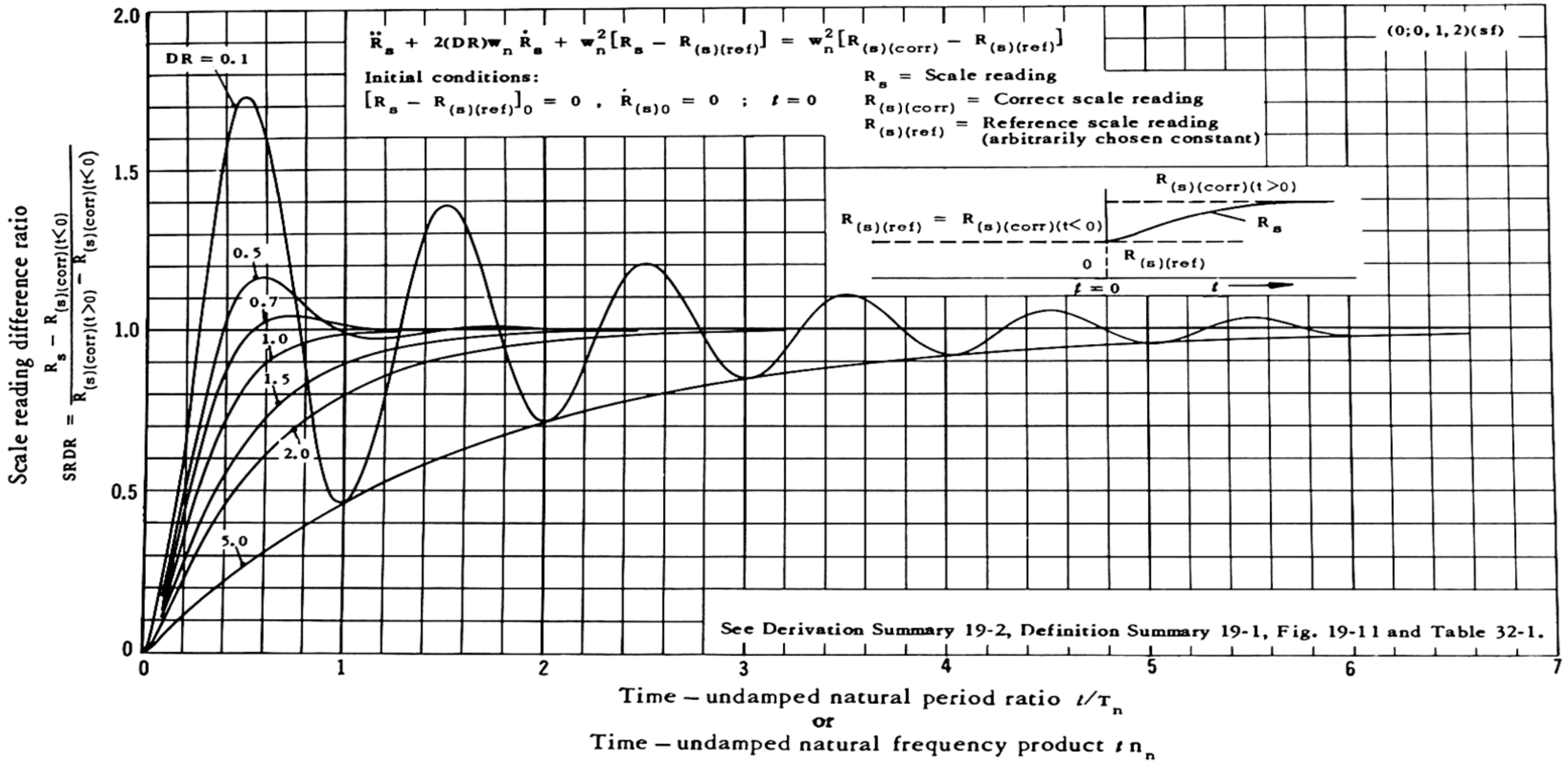


Fig. 32-4. Step function response of measuring instruments with (0;0,1,2) performance equations when the time – undamped natural frequency product is the running variable.

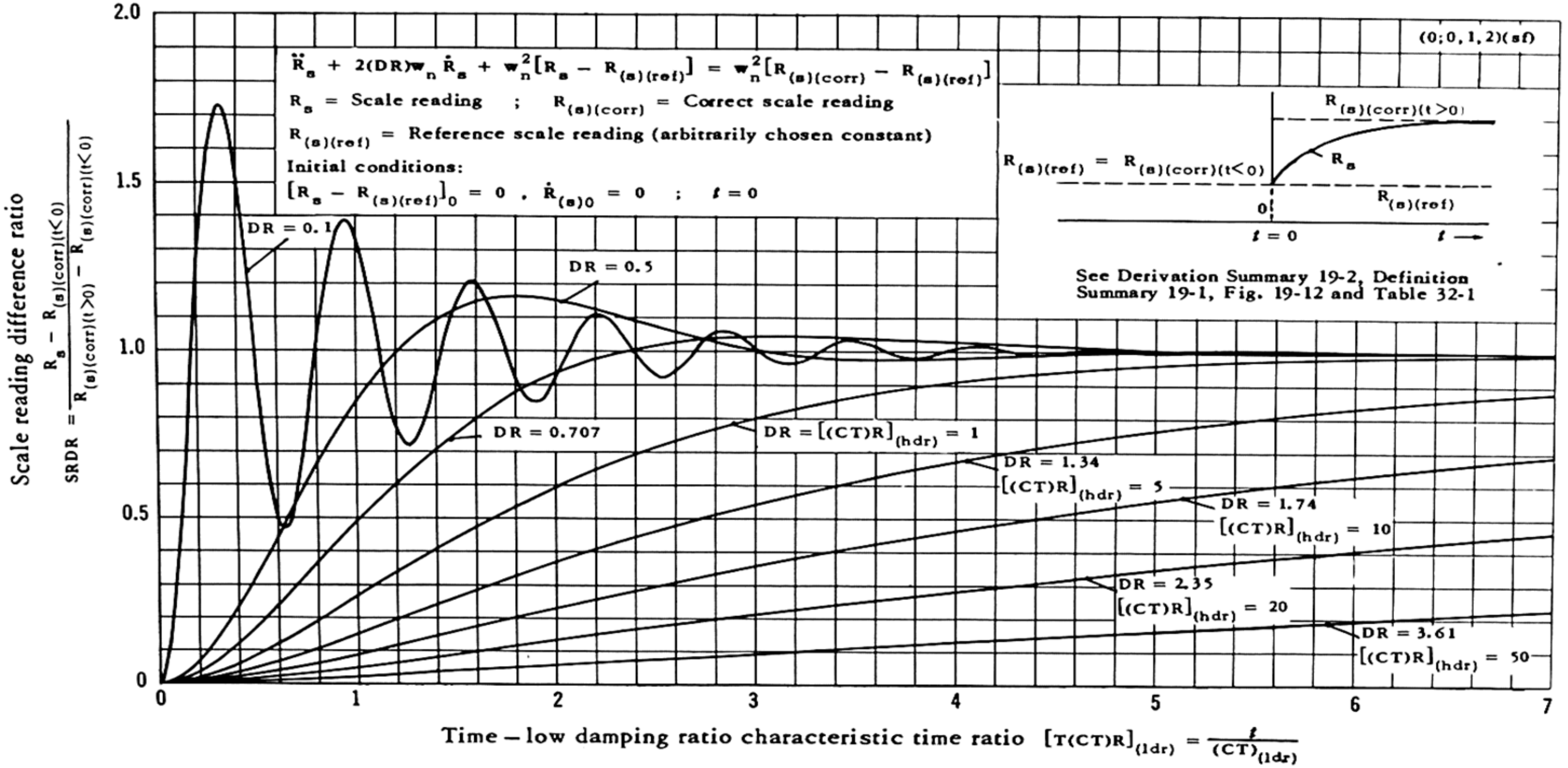
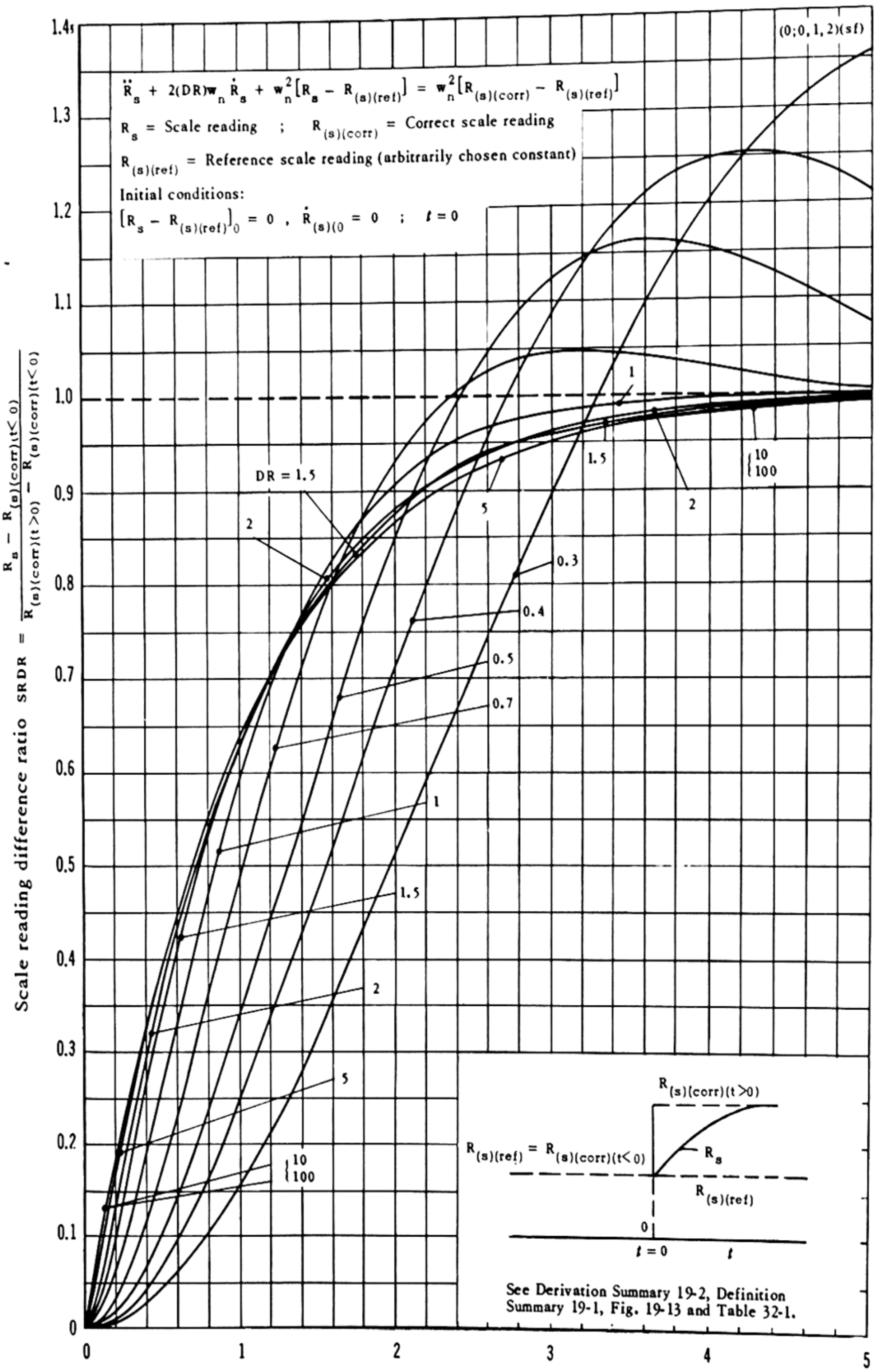


Fig. 32-5. Step function response of measuring instruments with (0;0,1,2) performance equations when the time – low damping ratio characteristic time ratio is the running variable.



Time – high damping ratio characteristic time sum ratio $\frac{t}{(CT)_{(hdr)(sum)}}$

or

Time – first-order characteristic time ratio $\frac{t}{(CT)_{(0;0,1)}}$

Fig. 32-6. Step function response of measuring instruments with (0;0,1,2) performance equations when the time – high damping ratio characteristic time sum ratio and time – first-order characteristic time ratio are running variables.

ratios less than unity and nonoscillatory for damping ratios greater than unity. In Fig. 32-4, the low damping ratio oscillation period increases as the damping ratio increases. Even for high damping ratios, the response is a considerable part of the forcing step at the end of one undamped period (i.e., at unity on the running variable scale). In contrast with this behavior, the high damping ratio curves show very little response at the end of one low damping ratio characteristic time (see Fig. 32-5). In Fig. 32-6, the second-order step function response becomes identical with the corresponding first-order response when high damping ratios are considered. Figure 32-7 is a family of deviation curves that gives quantitative information on the differences between second-order step function response and first-order step function response as these differences change with damping ratio. It appears that the deviation of second-order response from first-order response is less than a maximum of 1 percent for all damping ratios greater than 5.

32.34. For practical applications, it is useful to define indication time as the length of time required for a transient to be reduced to 0.05 of its initial value. The factor of 0.05 is chosen because it is nearly equal to the base of natural logarithms raised to the minus-third power. This means that the indication time for a measuring instrument having a simple exponential transient form is equal to three characteristic times. Indication time often has a more complicated relationship to the running variable than the simple exponential. For example, the plot of Fig. 32-8 gives the indication time – undamped natural period ratio as a function of damping ratio for systems with (–;0,1,2) performance equations. The derivation of this indication time curve is outlined in Chapter 19 as part of a discussion of Figs. 19-9 and 19-10. Figure 32-8 shows that the indication time – undamped natural period ratio has high values for both small and large damping ratios. The minimum point is about 0.48, and occurs at a damping ratio of about 0.7.

32.35. In Fig. 32-8, the high indication time – undamped natural period ratio for low values of the damping ratio is due to the considerable number of oscillations required for the response to pass within the 0.05 limit and then to remain within the 0.05 limit. The step-like discontinuities in the left-hand branch of the curve are due to oscillation effects. The upward-sloping right-hand branch of the curve is due to the increasing slowness with which response curves complete the forcing step as the damping ratio is increased beyond unity.

RAMP FUNCTION RESPONSE

32.36. Figures 32-9, 32-10 and 32-11 represent the ramp function response, with respect to an arbitrarily chosen scale reading reference, of measuring instruments with (0;0,1,2) performance equations when the scale reading is constant at the reference level at the time the ramp function starts. Figure 32-9 is an illustrative ramp function response curve for a damping ratio of unity. The ordinate is a scale

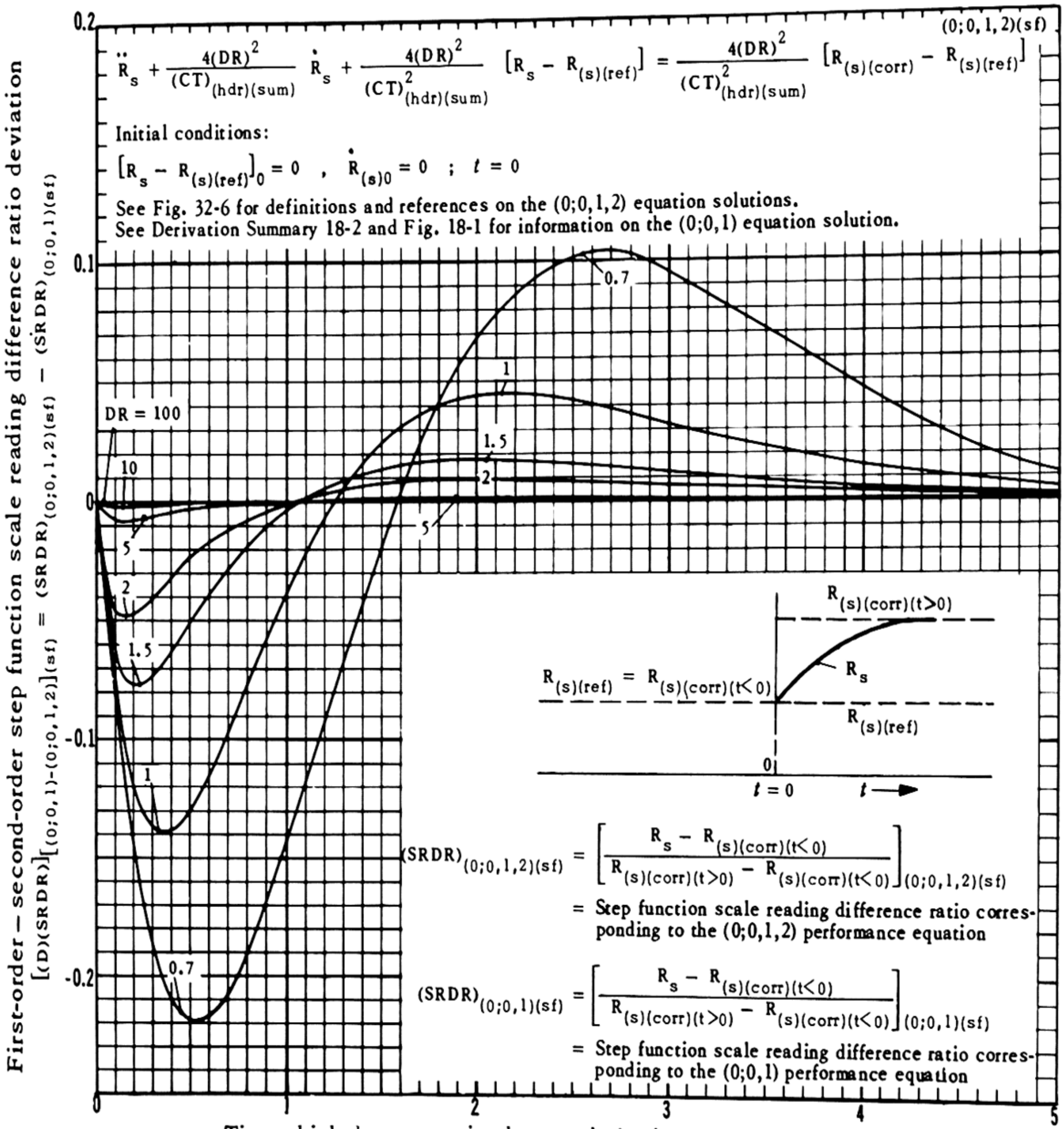


Fig. 32-7. Measuring instrument performance deviation curves for second-order step function response with respect to first-order step function response.

reading difference ratio in which the numerator is the difference between the scale reading and the reference scale reading, and the denominator is the amount the correct scale reading changes in one low damping ratio characteristic time. The abscissa is the time – low damping ratio characteristic time ratio. The correct scale reading difference ratio, equal to the time – characteristic time ratio, is shown

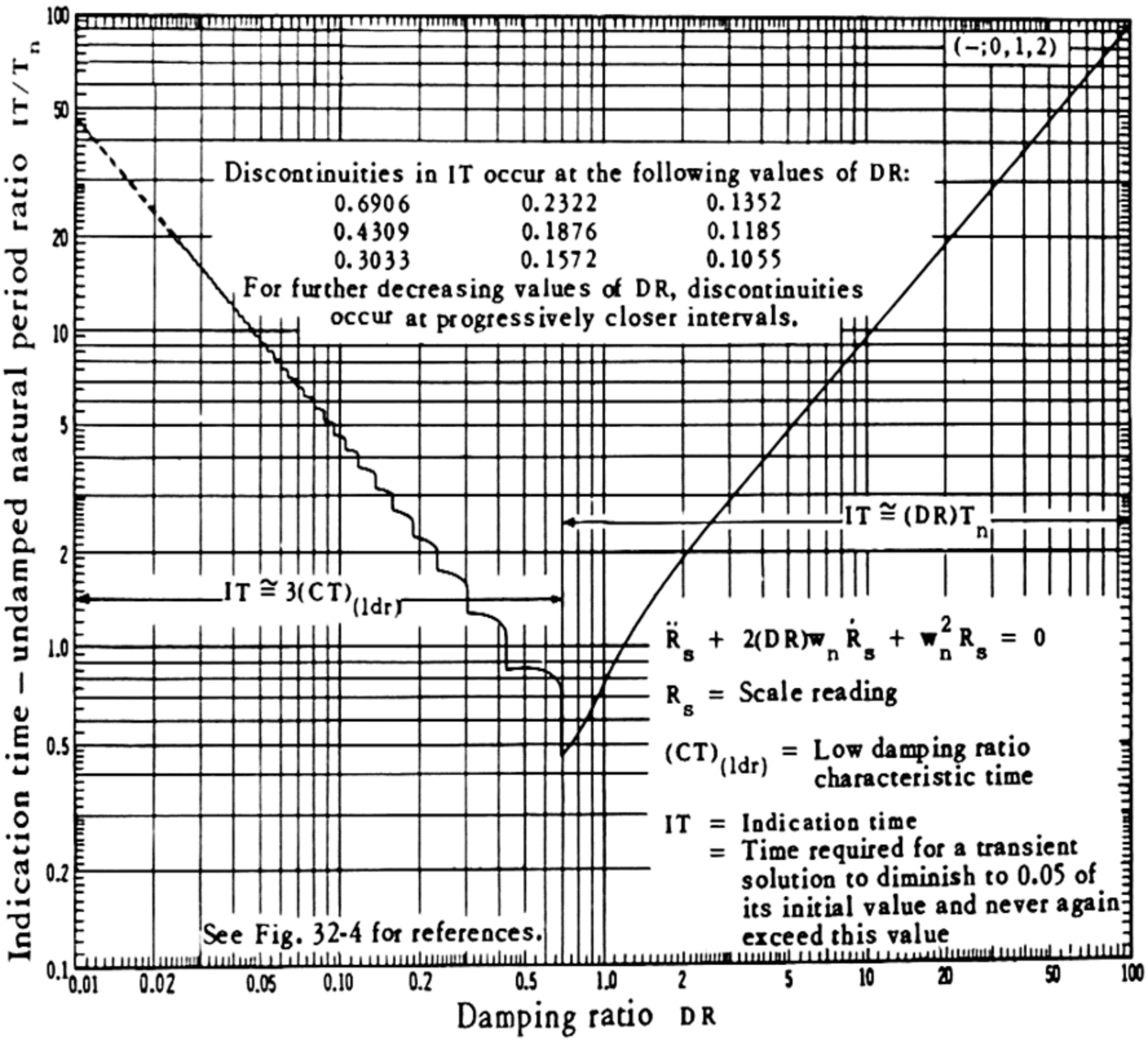


Fig. 32-8. Indication time – undamped natural period ratio as a function of damping ratio for measuring instruments with (–;0,1,2) performance equations.

by a heavy dashed line as the forcing function. The scale reading difference ratio is shown by a heavy full line representing the response. The forced response is shown by a light dashed line parallel to the forcing function line. The scale reading transient response period is the period from the start of the ramp function to the point at which the difference between the response and the forced response reaches a level equal to 0.05 of its initial value. The period that starts after the end of the transient response period is the forced response period, which continues indefinitely so long as the ramp forcing function continues. In Fig. 32-9, this occurs at a time – low damping ratio characteristic time ratio of about 4. The scale reading difference ratio forced dynamic error and the scale reading difference ratio forced dynamic response delay are shown in Fig. 32-9 as special cases of the generalized definitions illustrated in Fig. 6-1.

32.37. Figures 32-10 and 32-11 give curve families for the ramp function response of measuring instruments with (0;0,1,2) performance equations. The individual curves of these families are each generally similar to the illustrative response curve of Fig. 32-9. In Fig. 32-10, the time – low damping ratio characteristic time ratio is used for the running variable. In Fig. 32-11, the second-order

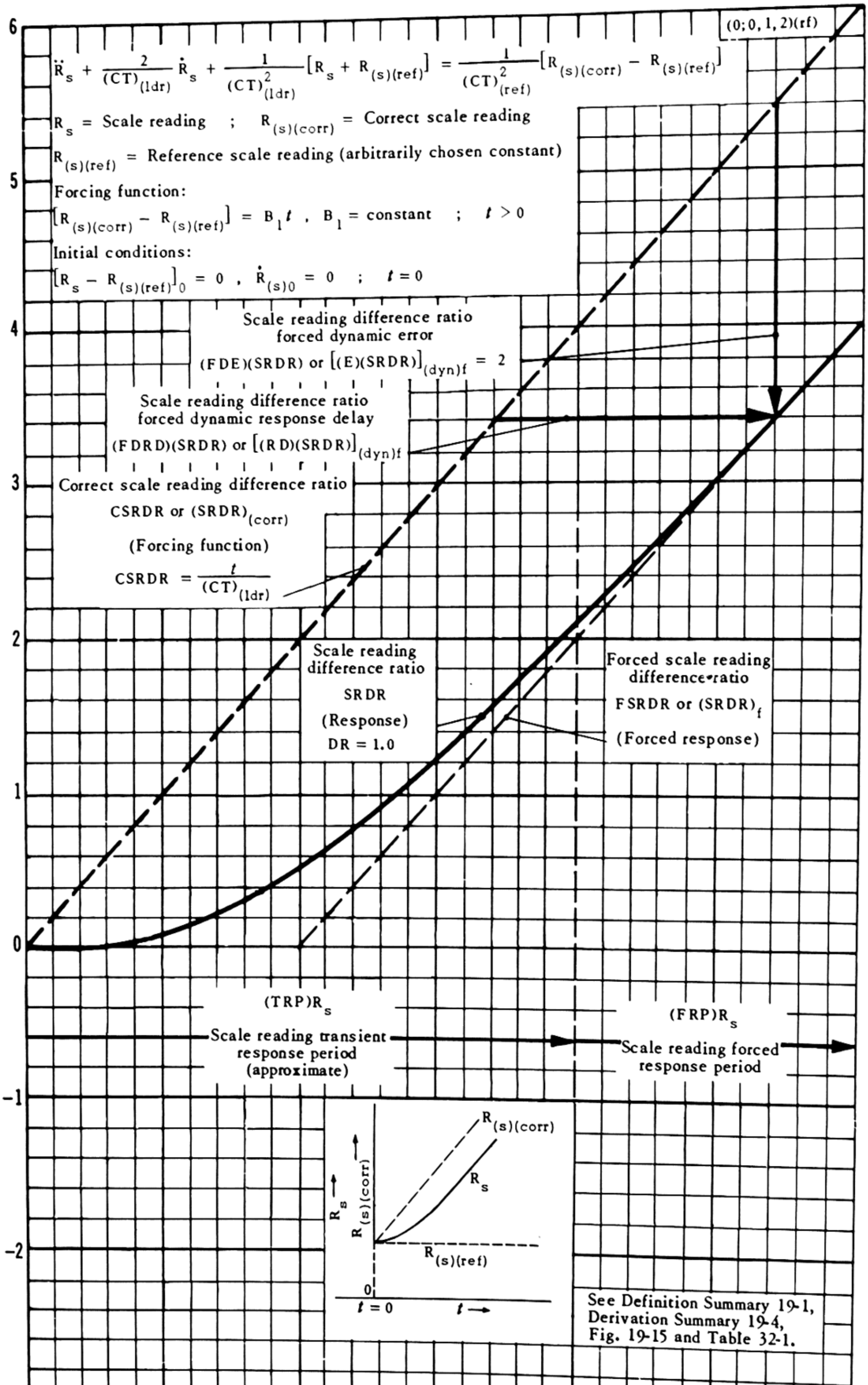


Fig. 32-9. Illustrative critically damped ramp function response curve for measuring instruments with (0;0,1,2) performance equations when the time – low damping ratio characteristic time ratio is the running variable.

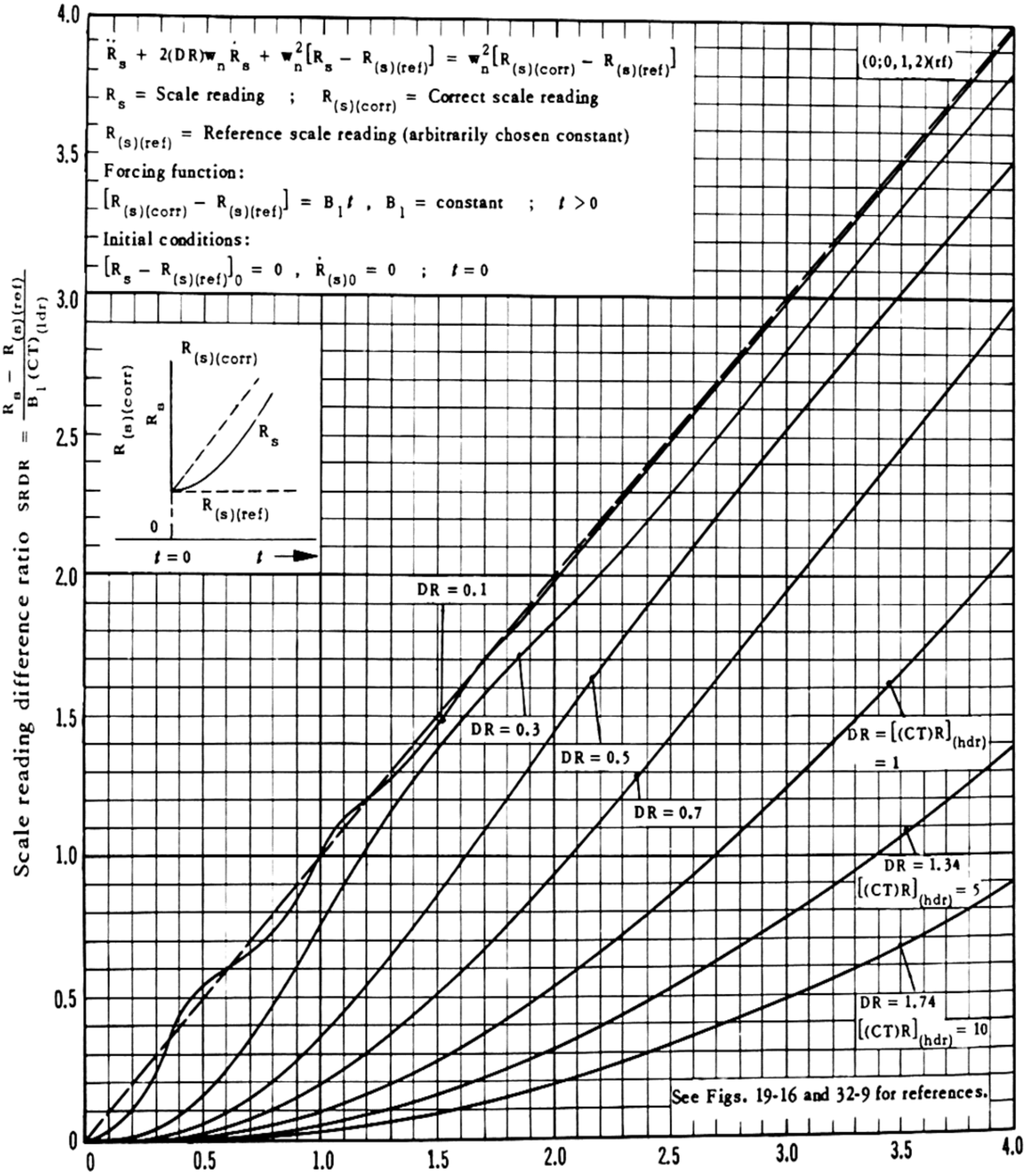
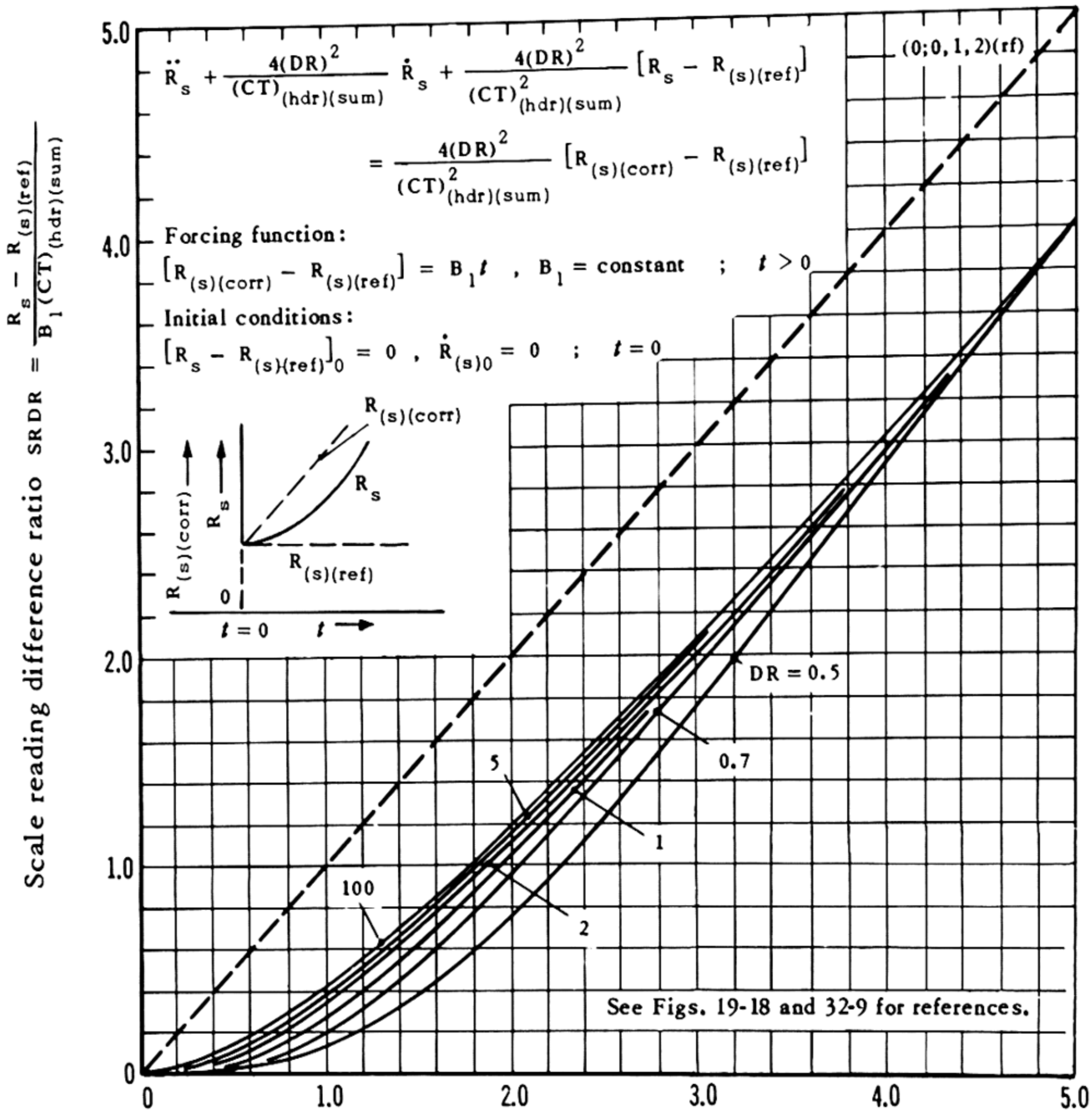


Fig. 32-10. Ramp function response for measuring instruments with (0;0,1,2) performance equations when the time – low damping ratio characteristic time ratio is the running variable.

response curves are made to merge into the corresponding first-order response curve by using the time – high damping ratio characteristic time sum ratio as the running variable. Figure 32-12 is a curve family showing deviations of second-order ramp function response from first-order ramp function response. It is apparent that first- and second-order ramp function responses are substantially identical for damping ratios greater than 5.

32.38. Figure 32-13 gives a family of curves showing the ramp function



Time – high damping ratio characteristic time sum ratio $\frac{t}{(CT)_{(hdr)(sum)}}$

or

Time – first-order characteristic time ratio $\frac{t}{(CT)_{(0;0,1)}}$

Fig. 32-11. Ramp function response for measuring instruments with (0;0,1,2) performance equations when the time – high damping ratio characteristic time sum ratio and time – first-order characteristic time ratio are running variables.

response – forcing function ratio as a function of the time – low damping ratio characteristic time ratio. This ratio is asymptotic to unity for all damping ratios as the running variable increases indefinitely. The low damping ratio curves rise rapidly after the initial instant and have oscillations for a period that decreases as the damping ratio increases. High damping ratios produce smooth ratio curves that rise more slowly as the damping ratio increases.

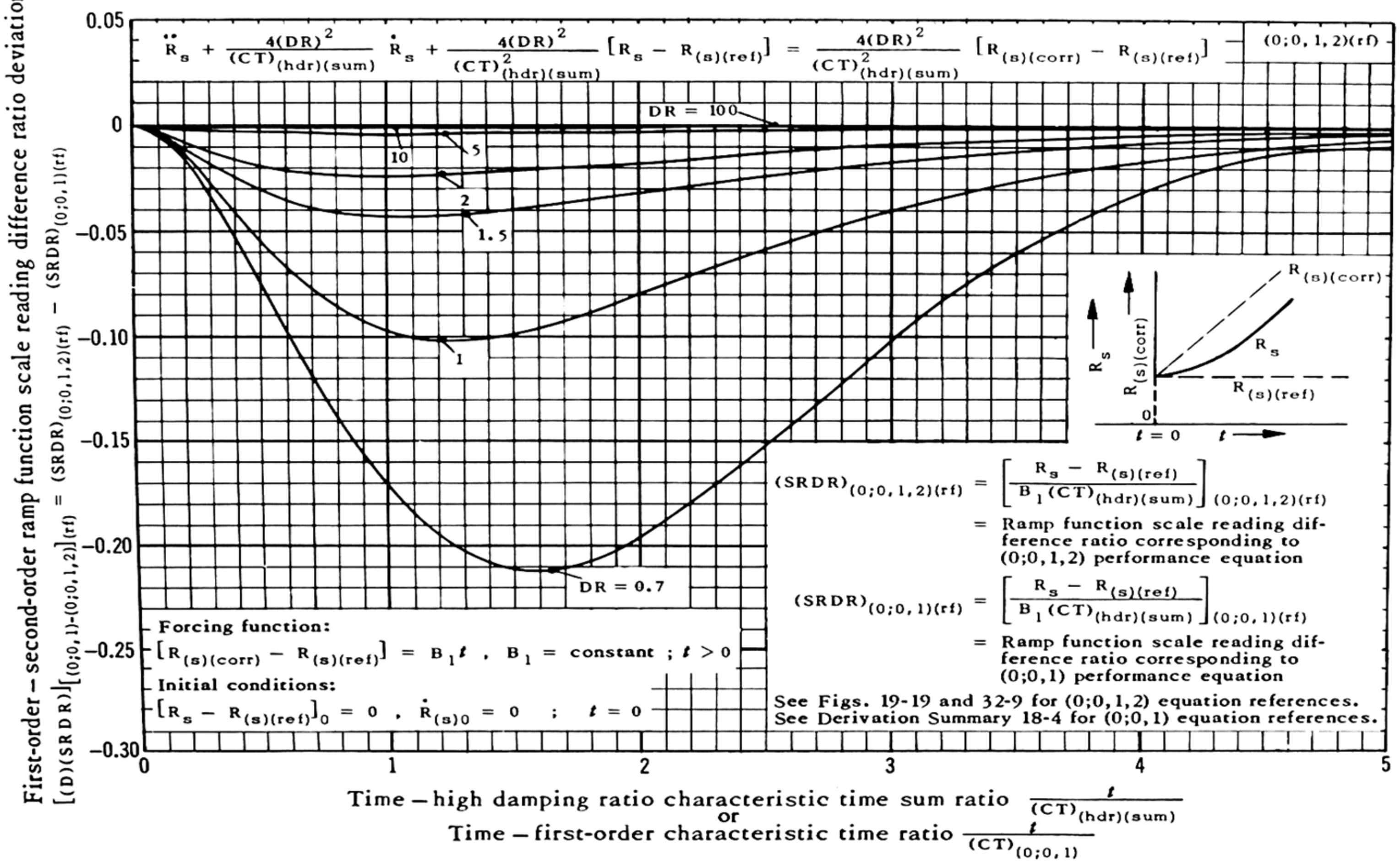


Fig. 32-12. Measuring instrument performance deviation curves for second-order ramp function response with respect to first-order ramp function response.

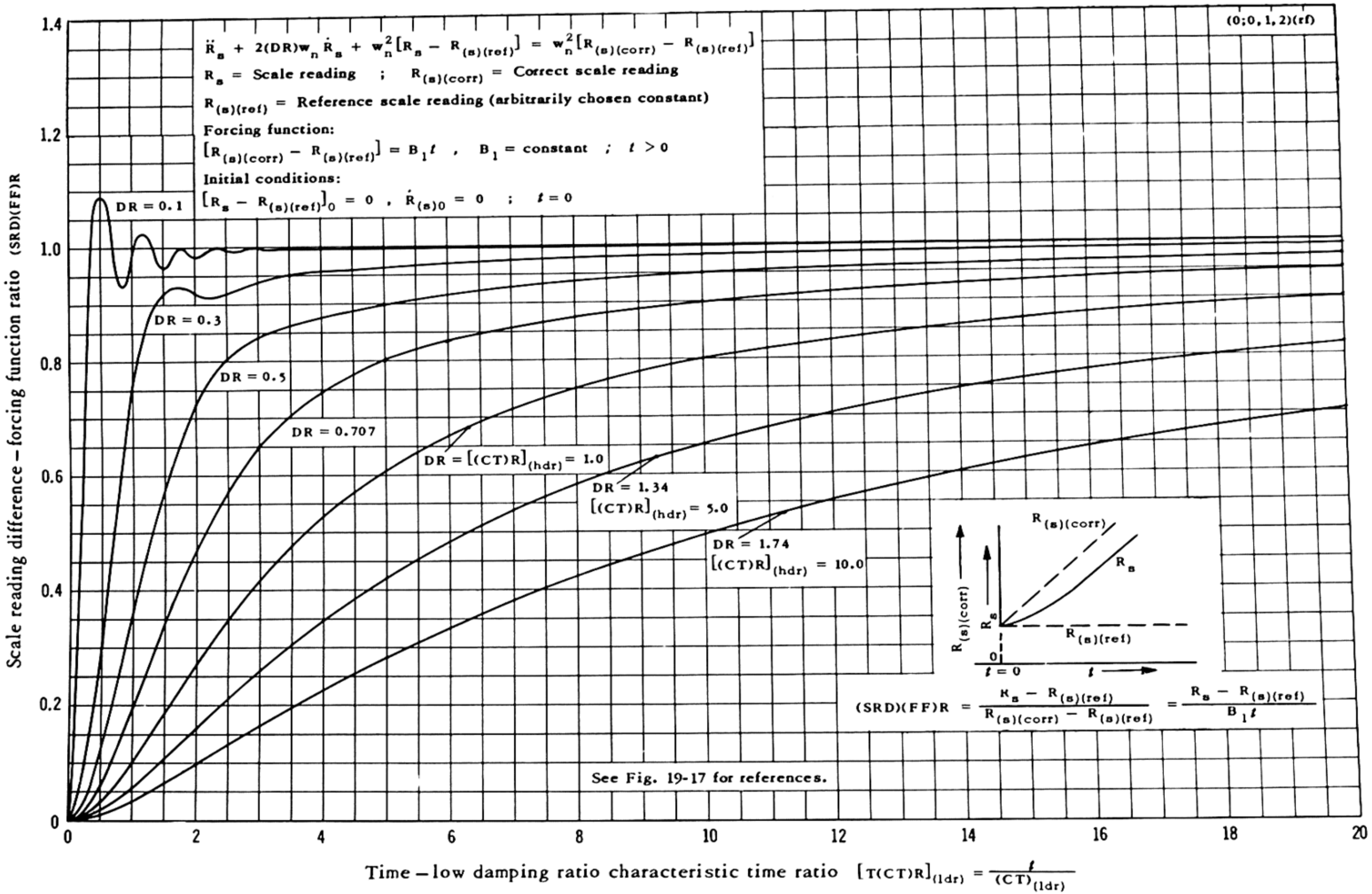


Fig. 32-13. Ramp function response – forcing function ratio for measuring instruments with (0;0,1,2) performance equations when the time – low damping ratio characteristic time ratio is the running variable.

PARABOLIC RESPONSE

32.39. Figure 32-14 is a family of second-order response curves for a parabolic forcing function based on the results of Derivation Summary 19-5 and Fig. 19-21. The ordinate is the ratio of the scale reading difference to the change in the square-law forcing function that occurs during one low damping ratio characteristic time. The forcing function is shown as a heavy dashed curve, with the responses represented by full lines. It is apparent that the response curves "open up" with respect to the forcing function as the running variable increases. This means that the forced dynamic error and forced dynamic response delay are both variables that increase with time. These opening-up effects are larger for high damping ratios than for small damping ratios.

RAMP-FOLLOWED-BY-STEP RESPONSE

32.40. Figure 32-15, which is based on Fig. 19-23, gives a family of response curves for a ramp followed by a constant level. The ordinate for this family is the ratio of the difference between the scale reading and the reference scale reading to the forcing ramp function that occurs in one low damping ratio characteristic time. The abscissa is the time – low damping ratio characteristic time ratio. The particular forcing function used in Fig. 32-15 represents a situation in which the ramp function is suddenly replaced by a constant correct scale reading after the lapse of two low damping ratio characteristic times. It is obvious that a new response curve family will be required when the transition point for the forcing functions is shifted along the abscissa scale. However, the family of Fig. 32-15 is sufficient to show the principles involved. The lower damping ratio curves in this figure differ considerably among themselves, while, during the ramp function period, the higher damping ratio curves all tend toward the axis of abscissae as a limit. This means that for a sufficiently high damping ratio, very little response has occurred and a low response rate exists when the ramp forcing function reaches a constant level. For the damping ratio range in which this situation exists, the constant level starts while the response is effectively at the reference level, so that the forcing condition is effectively identical with that associated with a step function. The result is a curve like a step function response for the step between the reference level and the constant level. The generalization to be drawn from this fact is that any forcing change of arbitrary shape that is completed before an appreciable response occurs may be replaced by a simple step between the initial and final forcing levels.

STEADY-STATE SINUSOIDAL RESPONSE: PERFORMANCE FUNCTIONS

32.41. The steady-state response of a measuring instrument to a sinusoidal forcing function of arbitrary amplitude and frequency is a very important operating

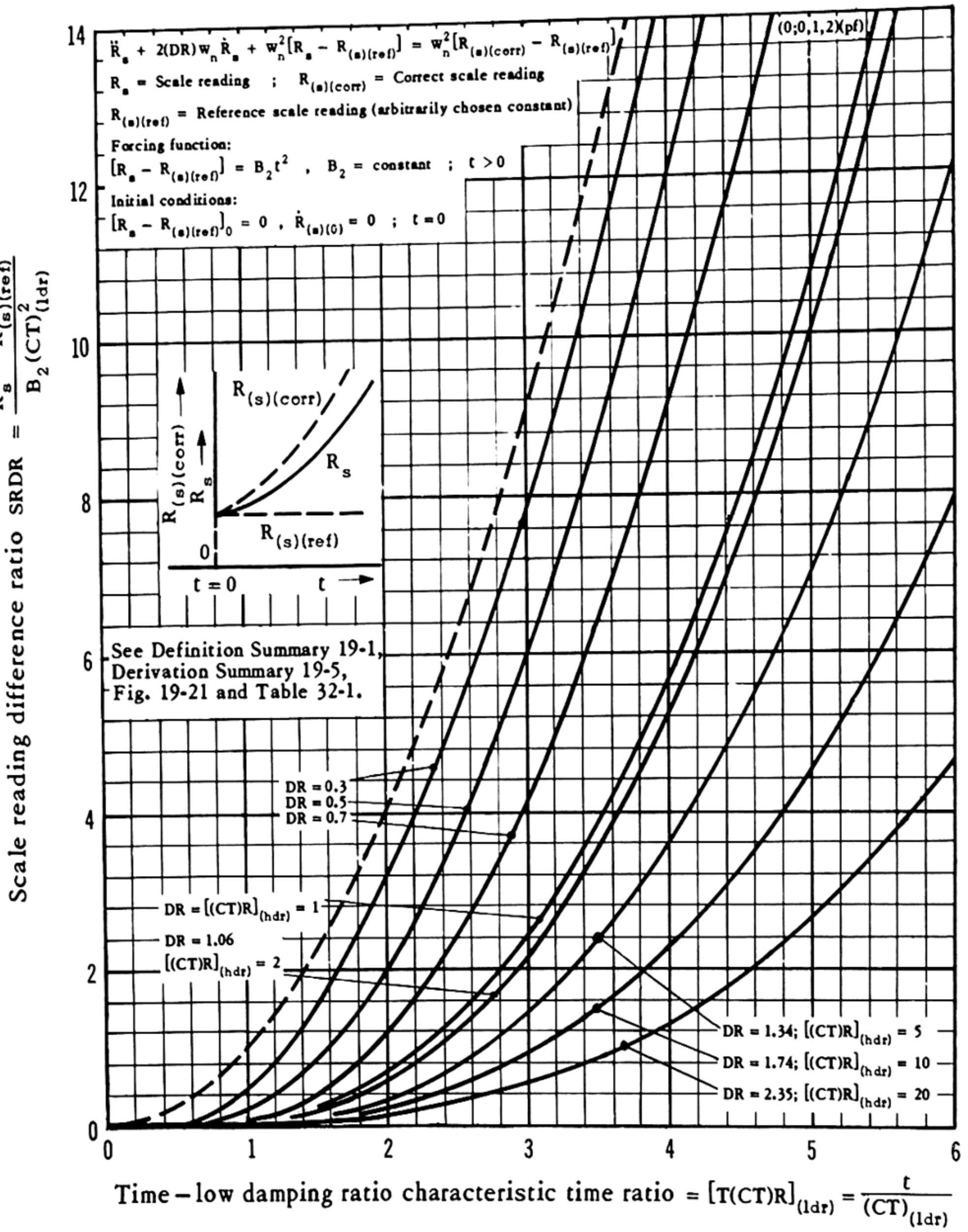


Fig. 32-14. Parabolic response for measuring instruments with (0;0,1,2) performance equations when the time – low damping ratio characteristic time ratio is the running variable.

characteristic. This is true, first, because it is very often convenient to represent forcing function shapes by means of Fourier series or Fourier integrals in which the basic forms are sinusoidal and, second, because the solutions corresponding to terms of this type are especially simple to write down and manipulate. Various applications of sinusoidal forms to the description of physical situations and

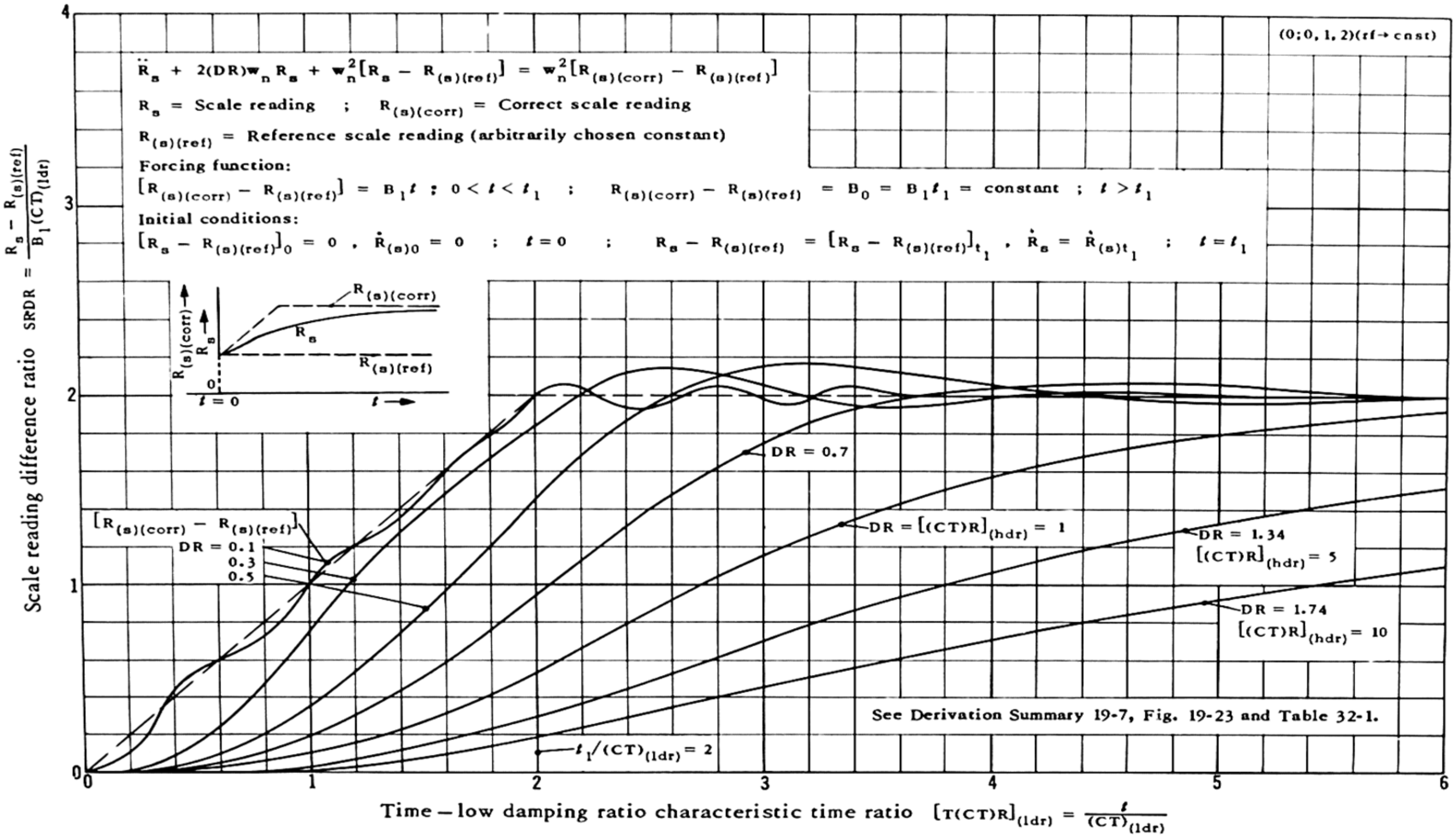


Fig. 32-15. Ramp-followed-by-constant response for measuring instruments with (0;0,1,2) performance equations when the time – low damping ratio characteristic time ratio is the running variable.

graphical meanings of the expressions involved are discussed in Chapter 12. The general nature of the steady-state response of an operating system to a sinusoidal forcing function and various methods for expressing and representing this response are described in Chapter 13.

32.42. It is shown in Chapter 17 that a considerable practical advantage is gained in finding solutions for differential equations when the initial conditions are zero. This situation exists when the forcing function is represented as the sum of sinusoidal terms, and the response is formed as the sum of the corresponding steady-state solution terms. Under these conditions, it is possible to express the action of an operating system having a linear performance equation with constant coefficients by means of a performance function that is determined by the differential equation. When attention is restricted to forcing functions represented by terms of the proper type, the corresponding response function is given by an equation of the form

$$\begin{pmatrix}\text{RESPONSE}\\ \text{FUNCTION}\end{pmatrix} = \begin{bmatrix}\text{PERFORMANCE}\\ \text{FUNCTION}\end{bmatrix} \begin{pmatrix}\text{FORCING}\\ \text{FUNCTION}\end{pmatrix} \tag{32-5}$$

The relationship in Chapter 17 that corresponds to Eq. (32-5) is

$$\begin{pmatrix}\text{RESPONSE}\\ \text{FUNCTION}\end{pmatrix} = \begin{bmatrix}\text{RELATING}\\ \text{FUNCTION}\end{bmatrix} \begin{pmatrix}\text{FORCING}\\ \text{FUNCTION}\end{pmatrix} \tag{17-1}$$

This means that all the discussions, derivations, and results of Volume II that are associated with the relating function as an abstract concept may be immediately applied to the performance of actual operating systems by noting that the relating function, which is not directly associated with any physical situation, is equivalent to the performance function expressed in mathematical terms.

32.43. From the standpoint of engineering applications, expressions describing steady-state sinusoidal behavior provide very useful performance function forms. Derivation Summary 17-3 outlines a development of sinusoidal relating function expressions to represent the effects associated with linear integro-differential equations of arbitrary order with constant coefficients. The particular forms taken by the sinusoidal performance function for first-order integro-differential equations are developed in Derivation Summaries 18-9, 18-10 and 18-11. Similar developments for second-order integro-differential equations are given in Derivation Summaries 19-9 through 19-13.

32.44. Information Summary 32-2 brings together the background of concepts, definitions, notation, and procedure leading to the description of second-order measuring instrument behavior in sinusoidal performance function* terms. Section a

* When the term "performance function" is used in practical applications, it is usually obvious from context whether sinusoidal forcing functions or forcing functions of some other type are considered.

of Information Summary 32-2 gives the basic performance equation for an ideal second-order measuring instrument and identifies the terms of this equation with the terms of the (0; 0,1,2) working variable equation from Derivation Summary 19-10. The dependent working variable is identified with the difference between the actual scale reading and an arbitrarily selected constant reference scale reading. The independent working variable is identified with the difference between the correct scale reading and the reference scale reading. The dimensional similarity factor of the working variable equation is identified with the correct scale reading - scale reading sensitivity, which may also be called the measuring instrument over-all sensitivity or simply the over-all sensitivity. Except for the replacement of Greek-letter working variable symbols by self-defining symbols, damping ratio and undamped angular natural frequency appear unchanged in both working variable equations and performance equations.

32.45. Section b of Information Summary 32-2 defines the concepts and symbols for describing a sinusoidal forcing variation in the correct scale reading - reference scale reading difference, and the corresponding steady-state response of an operating system in terms of a sinusoidal variation and a dynamic response angle.

32.46. Section c of Information Summary 32-2 gives various forms for expressing the correct scale reading difference - scale reading difference performance function, which describes the relationship between a sinusoidal forcing function and the corresponding steady-state response. The basic performance function relationship is given by Eq. (7). Equation (8) shows the performance function resolved into a reference sensitivity and a frequency function. In Eq. (9), the performance function is written as the product of an over-all sensitivity and an imaginary exponential, with a dynamic response angle as the coefficient of the imaginary unit in the exponent. Equation (10) is similar to Eq. (9), except that the sensitivity has been multiplied and divided by the reference sensitivity, so that performance function is a product of the reference sensitivity, the sensitivity - reference sensitivity ratio, and the imaginary exponential of Eq. (9).

32.47. Equation (12) of Information Summary 32-1 identifies the over-all sensitivity with the dynamic amplitude ratio (symbol (DAR)), which is the ratio of the response amplitude to the forcing function amplitude. Because of the unity value for the reference sensitivity of any ideal measuring instrument, performance functions are identical with frequency functions, and over-all sensitivities are identical with sensitivity - reference sensitivity ratios. These facts are recognized in Eqs. (13) and (14) of Information Summary 32-2.

32.48. Equations (15), (16), (17) and (18) of Information Summary 32-2 give the particular frequency function, sensitivity, and dynamic response angle expressions that describe the steady-state sinusoidal characteristics of ideal measuring instruments with (0;0,1,2) performance equations. In effect, Eq. (15) completely

The performance equation developed as Eq. (6) of Derivation Summary 32-1 for electromechanical measuring instruments may be generalized to Eq. (1) below, which represents the behavior of any instrument with second-order characteristics. When the scale reading, R_s, and the correct scale reading, $R_{(s)(corr)}$, are replaced by differences from an arbitrarily chosen constant reference scale reading, $R_{(s)(ref)}$, the performance equation becomes

$$\ddot{R}_s + 2(DR)w_n\dot{R}_s + w_n^2[R_s - R_{(s)(ref)}] = w_n^2 S_{(mi)[R;R]}[R_{(s)(corr)} - R_{(s)(ref)}] \qquad (1)$$

Equation (1) is similar to the (0;0,1,2) working variable form of Eq. (3) of Derivation Summary 19-10, which in time-derivative form (i.e., with $v'' \longrightarrow \ddot{v}$, $v' \longrightarrow \dot{v}$ as noted in section f of Definition Summary 19-1) is

$$\ddot{v} + 2\zeta\omega_n\dot{v} + \omega_n^2 v = \sigma\omega_n^2 u \qquad (2)$$

The correspondence between symbols in Eqs. (1) and (2) means that all the (0;0,1,2) solution results of Chapter 19 may be immediately applied to the response of measuring instruments with (0;0,1,2) performance equations when

$\zeta \approx DR$ = damping ratio

$\omega_n \approx w_n$ = undamped angular natural frequency

$v \approx [R_s - R_{(s)(ref)}]$ = scale reading difference
or
scale reading difference response

$u \approx [R_{(s)(corr)} - R_{(s)(ref)}]$ = correct scale reading difference
or
scale reading difference forcing function

$\sigma \approx S_{(mi)[R_{(s)(corr)};R_s]}$ = correct scale reading – scale reading sensitivity

For convenience this sensitivity may be written in simpler forms; i.e.,

$$S_{(mi)[R_{(s)(corr)};R_s]} \longrightarrow S_{(mi)[R;R]} \longrightarrow S_{(mi)(ref)}$$

and may be called the measuring instrument over-all sensitivity, the measuring instrument sensitivity, or, when no misunderstanding is possible, merely the reference sensitivity.

Note that for an ideal measuring instrument the reference sensitivity is unity.

a) Generalized and working variable forms of (0;0,1,2) measuring instrument performance equation

When the forcing function is a sinusoidal variation with respect to the reference scale reading, i.e., when

$$[R_{(s)(corr)} - R_{(s)(ref)}] = [R_{(s)(corr)} - R_{(s)(ref)}]_a \sin w_f t \qquad (3)$$

which, under the relationships illustrated in Fig. 12-3 and section a of Definition Summary 13-2, may be written in the equivalent form

$$[R_{(s)(corr)} - R_{(s)(ref)}] = [R_{(s)(corr)} - R_{(s)(ref)}]_a \epsilon^{jw_f t} \qquad (4)$$

then the corresponding steady-state solution is given by the expression

$$[R_s - R_{(s)(ref)}] = [R_s - R_{(s)(ref)}]_a \sin[w_f t + (DRA)_{(mi)(R;R)}] \qquad (5)$$

or the equivalent form

$$[R_s - R_{(s)(ref)}] = [R_s - R_{(s)(ref)}]_a \epsilon^{j(DRA)_{(mi)(R;R)}} \epsilon^{jw_f t} \qquad (6)$$

where

$[R_{(s)(corr)} - R_{(s)(ref)}]_a$ = correct scale reading forcing function amplitude
or
correct scale reading difference amplitude

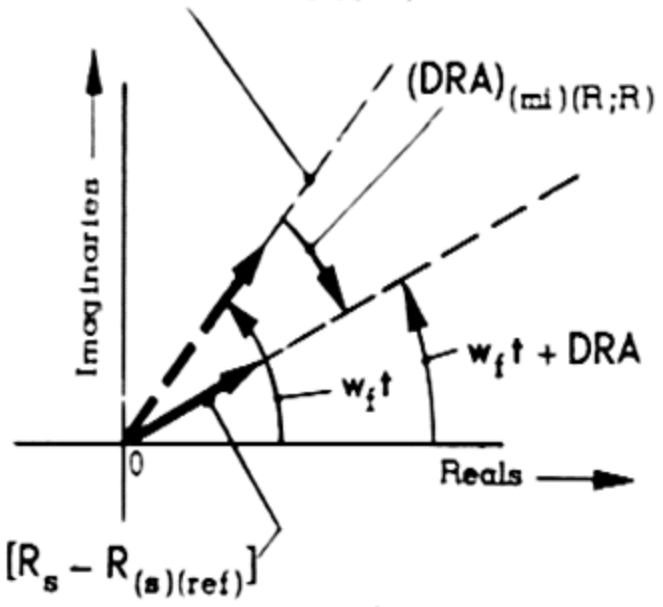
$[R_s - R_{(s)(ref)}]_a$ = scale reading response amplitude
or
scale reading difference amplitude

Information Summary 32-2. Description of steady-state sinusoidal response forms for measuring instruments with (0;0,1,2) performance equations. (Page 1 of 3)

$(DRA)_{(mi)(R_{(s)(corr)};R_s)}$ or $(DRA)_{(mi)(R;R)}$ = correct scale reading – scale reading dynamic response angle for a (0;0,1,2) measuring instrument

The following figure, which is similar to the figure of section c of Definition Summary 13-3, gives the graphical interpretation of Eqs. (3) through (6).

$$[R_{(s)(corr)} - R_{(s)(ref)}] = [R_{(s)(corr)} - R_{(s)(ref)}]_a \epsilon^{jw_f t}$$

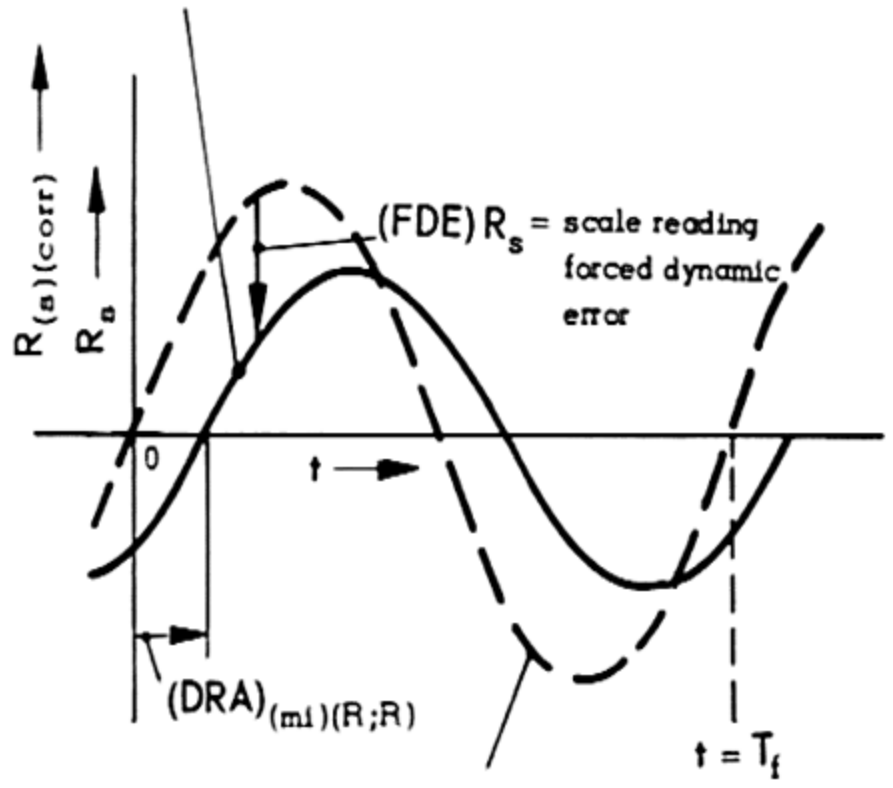


$$= [R_s - R_{(s)(ref)}]_a \epsilon^{j(DRA)_{(mi)(R;R)}} \epsilon^{jw_f t}$$

$(FDRD)R_s$ = scale reading forced dynamic response delay

$$= -\left[\frac{DRA}{w_f}\right]$$

$$[R_s - R_{(s)(ref)}] = [R_s - R_{(s)(ref)}]_a \sin [w_f t + (DRA)_{(mi)(R:R)}]$$



$$[R_{(s)(corr)} - R_{(s)(ref)}] = [R_{(s)(corr)} - R_{(s)(ref)}]_a \sin w_f t$$

Note: $(DRA)_{(mi)(R;R)}$ is shown negative, which corresponds to a lag and a positive forced dynamic response delay.

b) Steady-state response of measuring instruments to sinusoidal forcing functions

Definition Summaries 13-3, 13-4, 13-5 and 13-6 show that the relationship of steady-state response to a sinusoidal forcing function may be described in many ways. For example, when the input quantity, $q_{(in)}$, and the output quantity, $q_{(out)}$, of Definition Summary 13-6 are taken as corresponding to the correct scale reading difference and the scale reading difference, respectively, Eqs. (1), (10), (16) and (19) of that summary may be rewritten in the forms

$$[R_s - R_{(s)(ref)}] = [PF]_{(mi)[R;R]} [R_{(s)(corr)} - R_{(s)(ref)}] \quad (7)$$

$$[R_s - R_{(s)(ref)}] = S_{(mi)[R;R](ref)} (FF)_{(mi)(R;R)} [R_{(s)(corr)} - R_{(s)(ref)}] \quad (8)$$

$$[R_s - R_{(s)(ref)}] = S_{(mi)[R;R]} \epsilon^{j(DRA)_{(mi)(R;R)}} [R_{(s)(corr)} - R_{(s)(ref)}] \quad (9)$$

$$[R_s - R_{(s)(ref)}] = S_{(mi)[R;R](ref)} [S(RS)R]_{(mi)(R;R)} \epsilon^{j(DRA)_{(mi)(R;R)}} [R_{(s)(corr)} - R_{(s)(ref)}] \quad (10)$$

where, in addition to the definitions already given,

$[PF]_{(mi)[R;R]} = [PF]_{(mi)[R_{(s)(corr)};R_s]}$ = correct scale reading – scale reading sinusoidal performance function for measuring instruments

$(FF)_{(mi)(R;R)} = (FF)_{(mi)(R_{(s)(corr)};R_s)}$ = correct scale reading – scale reading frequency function for measuring instruments

$S_{(mi)[R;R]} = S_{(mi)[R_{(s)(corr)};R_s]}$ = correct scale reading – scale reading sensitivity for measuring instruments
or
measuring instrument over-all sensitivity
or
measuring instrument sensitivity

Information Summary 32-2. Description of steady-state sinusoidal response forms for measuring instruments with (0;0,1,2) performance equations. (Page 2 of 3)

$[S(RS)R]_{(m1)(R;R)} = [S(RS)R]_{(m1)(R_{(s)(corr)};R_s)}$ = measuring instrument over-all sensitivity ratio

$$= \frac{S_{(m1)[R;R]}}{S_{(m1)[R;R](ref)}} \tag{11}$$

Comparison of Eqs. (16) and (17) of Definition Summary 13-6 shows that

$$S_{(m1)[R;R]} = (DAR)_{(m1)[R;R]} = \frac{[R_s - R_{(s)(ref)}]_a}{[R_{(s)(corr)} - R_{(s)(ref)}]_a} = \begin{array}{l}\text{scale reading difference – correct}\\ \text{scale reading difference dynamic}\\ \text{amplitude ratio}\end{array} \tag{12}$$

For any properly calibrated measuring instrument $S_{(m1)[R;R](ref)} = 1$, so that the corresponding sinusoidal response may be written in the forms

$$[R_s - R_{(s)(ref)}] = (FF)_{(m1)(R;R)}\,[R_{(s)(corr)} - R_{(s)(ref)}] \tag{13}$$

$$[R_s - R_{(s)(ref)}] = S_{(m1)[R;R]}\,\epsilon^{\,j(DRA)_{(m1)(R;R)}}\,[R_{(s)(corr)} - R_{(s)(ref)}] \tag{14}$$

The steady-state sinusoidal response characteristics of any given measuring instrument are completely described by numerical or graphical representations of $(FF)_{(m1)(R;R)}$ or $S_{(m1)[R;R]}$ and $(DRA)_{(m1)(R;R)}$. Section a of Fig. 13-1 illustrates a complex plane plot similar to that for a typical frequency function. Sections b and c of Fig. 13-1 illustrate linear scale and logarithmic scale plots similar to those for a typical sensitivity and a dynamic response angle.

In the plots of Fig. 13-1 and the equations of Definition Summary 13-6, the following relationships exist between measuring instrument performance symbols and working variable symbols:

$FF \approx \eta_f = \acute{\eta} = \acute{}[RF]$ = dimensionless relating function

$[S(RS)R] \approx \mu$ = dimensionless amplitude ratio

$DRA \approx \phi$ = dynamic response angle

$FR \approx \beta$ = frequency ratio

Note that when properly calibrated measuring instruments are considered, i.e., when $S_{(m1)[R;R](ref)} = 1$,

$$S_{(m1)[R;R]} = [S(RS)R]_{(m1)(R;R)} \approx \mu$$

c) Generalized representations for the steady-state sinusoidal response of measuring instruments

The particular expressions that describe steady-state sinusoidal response for measuring instruments with (0;0,1,2) performance equations are developed in Derivation Summaries 19-9 and 19-10. These expressions are given by Eqs. (6), (7) and (8) of Derivation Summary 19-10 as

$$\acute{\eta} \approx [PF]_{(m1)[R;R]} = (FF)_{(m1)(R;R)} = \frac{1}{1 - (FR)^2 + j\,2(DR)(FR)} \tag{15}$$

$$= S_{(m1)[R;R]}\,\epsilon^{\,j(DRA)_{(m1)(R;R)}} \tag{16}$$

$$\mu \approx S_{(m1)[R;R]} = \frac{1}{\sqrt{[1 - (FR)^2]^2 + [2(DR)(FR)]^2}} \tag{17}$$

$$(DRA)_{(m1)(R;R)} = \tan^{-1}\left[\frac{-2(DR)(FR)}{1 - (FR)^2}\right] \tag{18}$$

d) Steady-state sinusoidal response characteristic equations for measuring instruments with (0;0,1,2) performance equations

Information Summary 32-2. Description of steady-state sinusoidal response forms for measuring instruments with (0;0,1,2) performance equations. (Page 3 of 3)

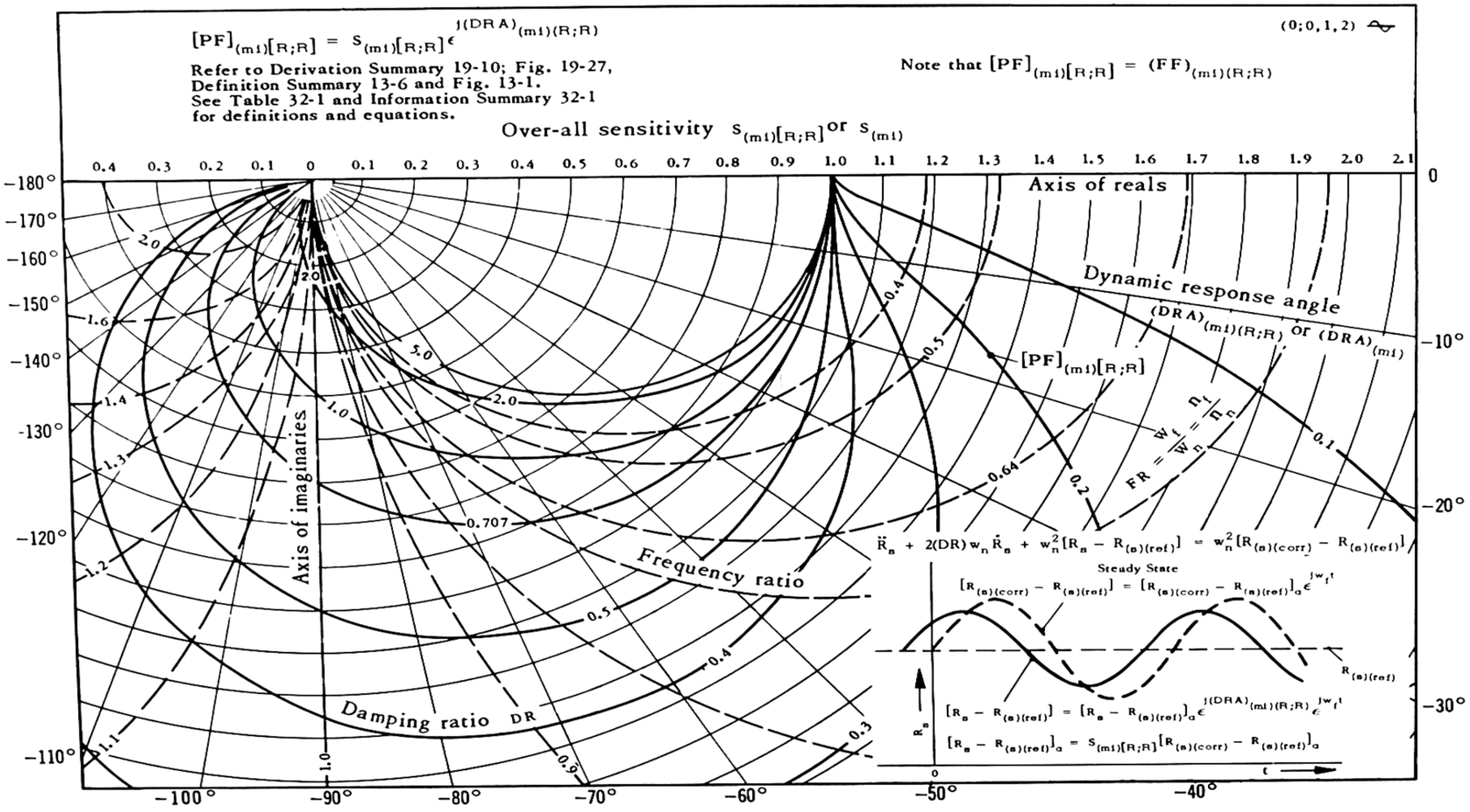


Fig. 32-16. Linear-scale complex plane performance function plots for measuring instruments with (0;0,1,2) performance equations.

describes the performance function and provides in a single expression the information given by the sensitivity and dynamic response angle expressions of Eqs. (17) and (18). In each case, the variables that determine the performance function and its components are the frequency ratio and the damping ratio. The relationships involved are developed in Derivation Summaries 19-9 and 19-10 and are plotted in nondimensional working variable terms in Figs. 19-27, 19-28, 19-29, 19-30, 19-34 and 19-35. The curve families of these figures, which are expressed in general terms, are specialized to describe the performance functions of ideal second-order measuring instruments in Figs. 32-16 through 32-21. Each of these figures lists references containing essential information on the concepts, definitions, symbols, and derivations that are used in plotting the curve families.

LINEAR COMPLEX PLANE PERFORMANCE FUNCTION PLOTS

32.49. Figure 32-16 shows a family of performance function plots on linear complex plane coordinates based on Eq. (15) of Information Summary 32-2. The axis of ordinates is used for imaginaries, and the axis of abscissae is used for reals, in accordance with the conventions shown in Figs. 12-1 and 13-1. With this choice of coordinates, the relationships of Eqs. (16), (17) and (18) mean that distance from the origin along radial lines represents sensitivity, and angles measured from the axis of reals to radial lines represent dynamic response angle. Each of the full-line curves passing through the origin, and also the +1 point on the axis of reals, represents the performance function for a constant damping ratio. The dashed half-circles, all of which pass through the origin at the point of tangency to the axis of imaginaries and have their centers on the axis of reals, are lines of constant frequency ratio. The +1 point on all the performance function curves corresponds to zero frequency ratio, while the origin of coordinates corresponds to a frequency ratio of infinity. The performance function curves approach a semicircle of unit diameter lying below the axis of reals and passing through the origin and the +1 point. Reference to Fig. 18-10 shows that this semicircle is identical with the performance function plot for the (0;0,1) differential equation. As the damping ratio is decreased, the performance function curves become more and more distorted from the semicircular shape, so that a maximum occurs in the value of the sensitivity. This maximum first appears in the lower right-hand section of the plot with a value slightly greater than unity and moves downward and toward the negative side of the axis of imaginaries, which is part of the unity frequency ratio "circle," until it reaches a value of minus infinity when the damping ratio is made equal to zero.

32.50. All the performance function curves start with a dynamic response angle equal to zero for zero frequency ratio and all approach the origin from the negative direction of the axis of reals. This latter characteristic is easily apparent

Refer to Derivation Summary 19-10, Fig. 19-28, Definition Summary 13-6, and Fig. 13-1.
See Table 32-1 and Information Summary 32-1 for definitions and equations.

(0;0,1,2)

$$\ddot{R}_n + 2(DR)\,w_n \dot{R}_n + w_n^2[R_n - R_{(n)(ref)}] = w_n^2[R_{(n)(corr)} - R_{(n)(ref)}]$$

Steady State

$$[R_{(n)(corr)} - R_{(n)(ref)}] = [R_{(n)(corr)} - R_{(n)(ref)}]_a e^{jw_f t}$$

$$[R_n - R_{(n)(ref)}] = [R_n - R_{(n)(ref)}]_a e^{j(DRA)_{(m1)(R;R)}} e^{jw_f t}$$

$$[R_n - R_{(n)(ref)}]_a = S_{(m1)[R;R]}[R_{(n)(corr)} - R_{(n)(ref)}]_a$$

$R_{(n)(ref)}$, R_n, 0, t

$(DRA)_{(m1)(R;R)}$

$S_{(m1)[R;R]}$

Over-all sensitivity $S_{(m1)[R;R]}$ or $S_{(m1)}$

Dynamic response angle DRA = ϕ

DR = 0.1, 0.2, 0.3, 0.4, 0.5, 0.707, 1.0, 2.0, 5.0

ζ = 0.1, 0.2, 0.3, 0.4, 0.5, 0.707, 1.0, 2.0, 5.0

0, 0.5, 1.0, 1.5, 2.0, 2.5, 3.0, 3.5, 4.0

0, 1, 2, 3, 4, 5, 6

60°, 30°, 0, −30°, −60°, −90°, −120°, −150°, −180°

Frequency ratio $FR = \frac{w_f}{w_n} = \frac{n_f}{n_n}$

Fig. 32-17. Linear-scale over-all sensitivity and dynamic response angle curves for the steady-state sinusoidal response of measuring instruments with (0;0,1,2) performance equations.

for low damping ratios, but for high damping ratios it occurs at such high frequency ratios and small sensitivities that it is concealed in the curve family of Fig. 32-16.

LINEAR SCALE SENSITIVITY AND DYNAMIC RESPONSE ANGLE PLOTS

32.51. Figure 32-17 includes two linear scale curve families plotted with frequency ratio as the abscissa. The left-hand ordinate scale is marked in terms of over-all sensitivity. The ordinate scale on the right is marked in dynamic response angle degrees. Each curve of the full-line family represents the variation of sensitivity with frequency ratio for a constant damping ratio. The dashed-line curves show the changes in dynamic response angle with frequency ratio. At zero frequency ratio, all the sensitivity curves start at unity and finally become asymptotic to zero for very high frequency ratios. For damping ratios larger than the reciprocal of $\sqrt{2}$, a maximum sensitivity occurs for some frequency ratio between zero and unity. This maximum is slightly over unity and near zero frequency ratio for damping ratios that just allow a peak, and moves toward infinity at unity frequency ratio as the damping ratio approaches zero.

32.52. The dynamic response angle curves of Fig. 32-17 all start at zero degrees for zero frequency ratio, all pass through -90° at unity frequency ratio, and are all asymptotic to -180° at very large frequency ratios. The change from zero to -180° occurs sharply at unity frequency ratio for zero damping ratio. As the damping ratio is made larger, the angle increases in magnitude from zero more rapidly at low frequency ratios and slopes more gently toward zero for high values of the frequency ratio.

32.53. Figure 32-18 is an expanded-ordinate linear scale plot of dynamic response angle as a function of frequency ratio.

32.54. Figure 32-19 gives the families of sensitivity and dynamic response angle with ordinate scales similar to those of Fig. 32-17, and the frequency ratio scale expanded for the region from zero to unity.

LOGARITHMIC SCALE SENSITIVITY AND DYNAMIC RESPONSE ANGLE PLOTS

32.55. In Fig. 32-20, the family of sensitivity curves given in Fig. 32-17 are plotted with logarithmic scales for both coordinates. The features noted in the discussion of Fig. 32-17 are all present in the curves of Fig. 32-20, but the curved regions for low damping ratios and high damping ratios have both been replaced by straight lines. The slope in the low-frequency-ratio region is zero for all damping ratios. The slope in the high-frequency-ratio region is -2. For low damping ratios, the sensitivity curves show maxima in the region of zero on the abscissa loru scale (zero on this loru scale corresponds to unity frequency ratio) and have straight-line portions in this same region for high damping ratios.

32.56. The coordinate scales of Fig. 32-20 have uniform divisions representing

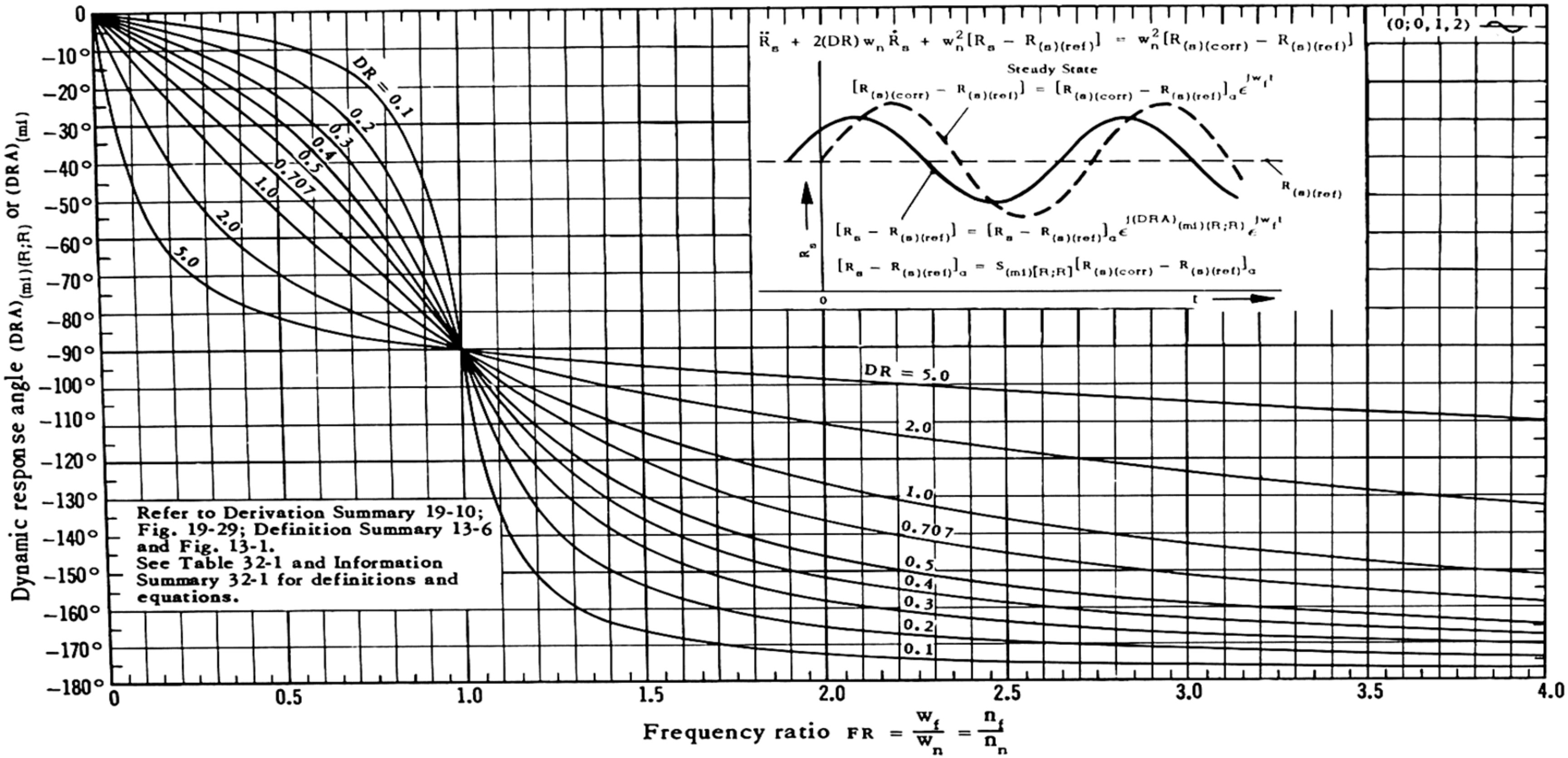


Fig. 35-18. Logarithmic-scale curves of forcing velocity input – relative displacement output dimensionless sensitivity ratio for the seismographic system with viscous damping only.

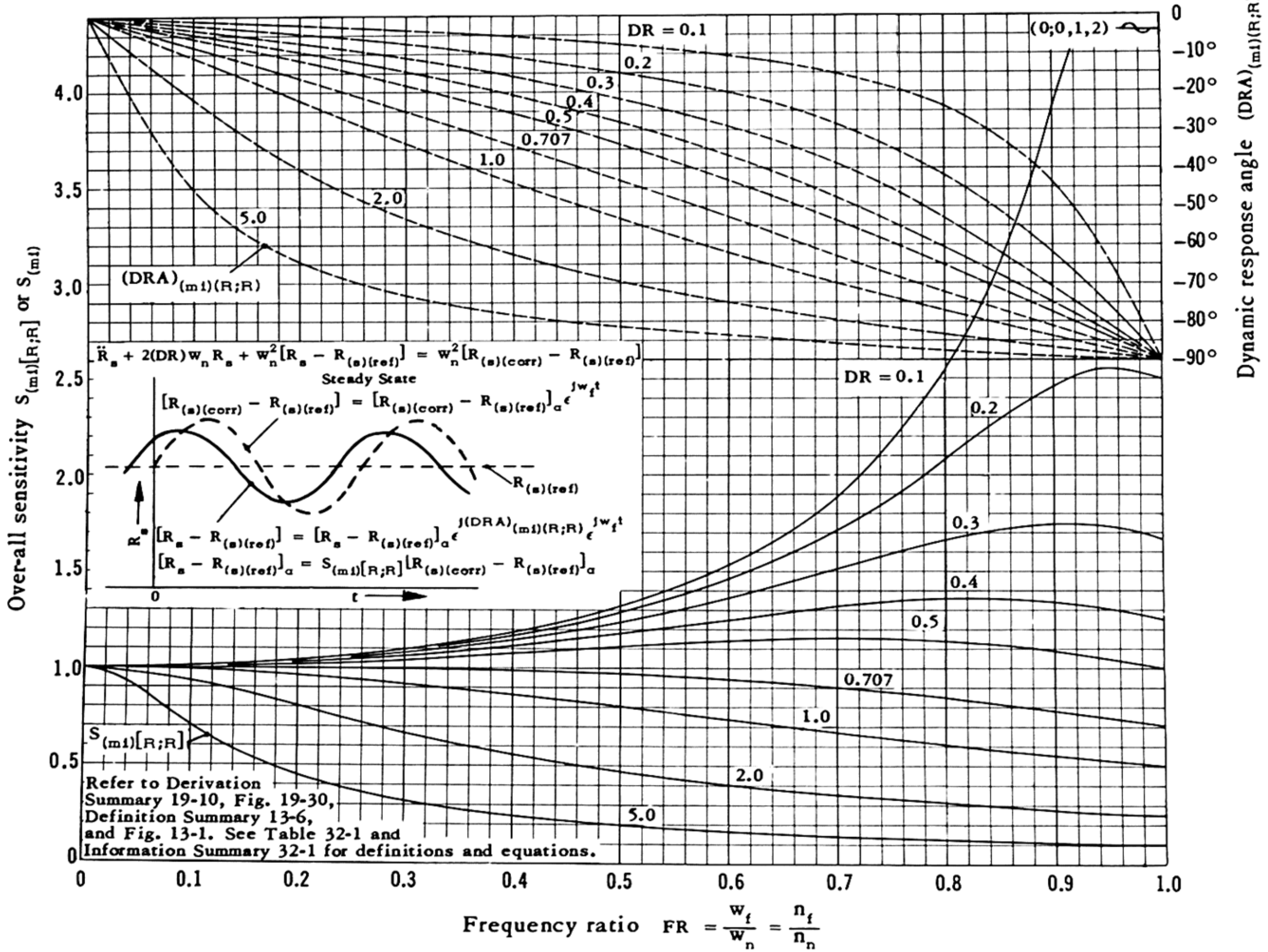


Fig. 32-19. Expanded linear-scale over-all sensitivity and dynamic response angle curves for the steady-state sinusoidal response of measuring instruments with (0;0,1,2) performance equations.

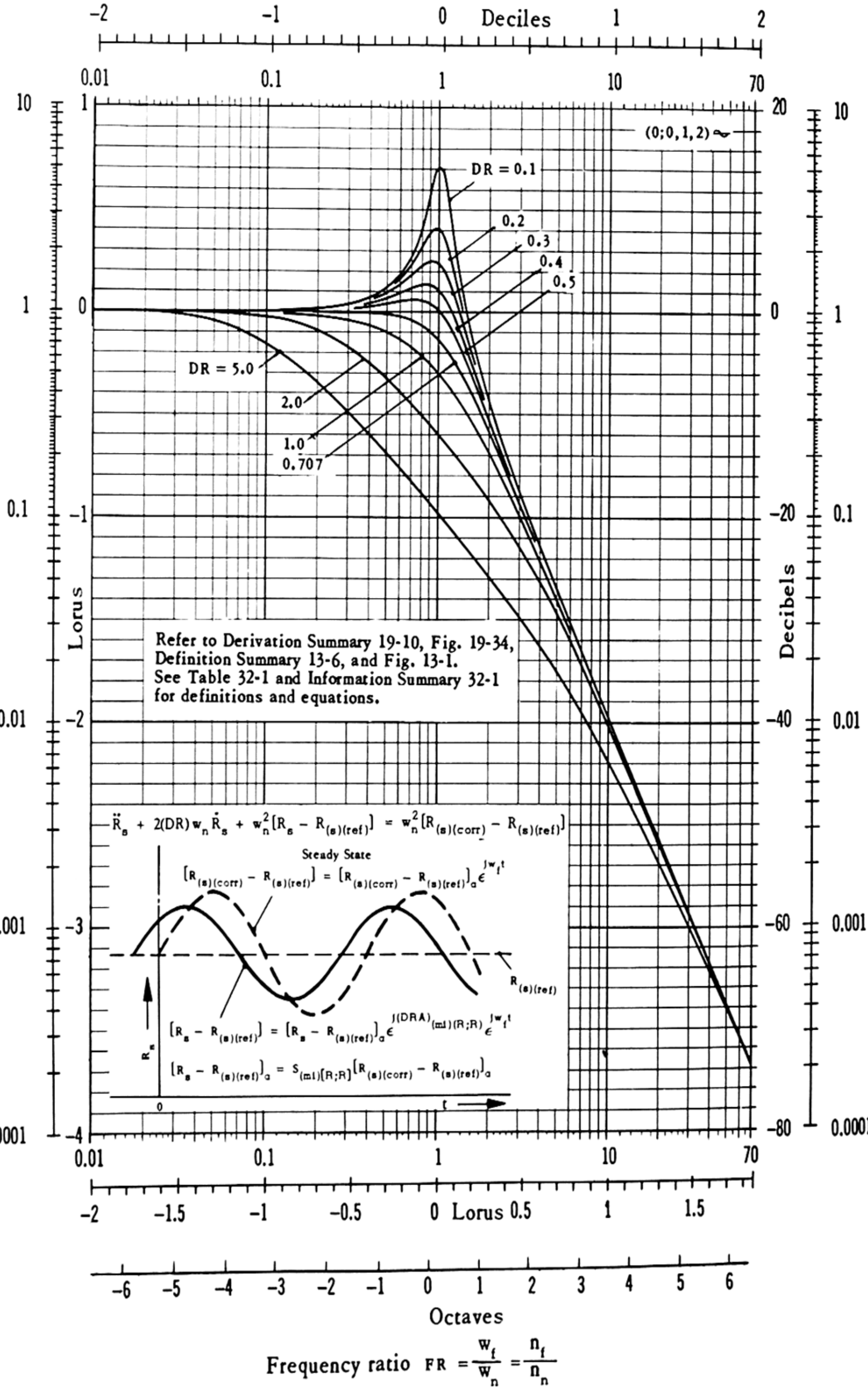


Fig. 32-20. Logarithmic-scale over-all sensitivity curves for the steady-state sinusoidal response of measuring instruments with (0;0,1,2) performance equations.

the three logarithmic systems illustrated in Fig. 5-4. Numerical values of the variables are given on logarithmically divided scales. The logarithmic scales used are:

1) Lorus – logarithmic ratio units, which are logarithms to the base ten. Lorus are also called deciles.
2) Decibels – 20 times logarithms to the base ten.
3) Octaves – logarithms with the base two.

Logarithmic spacing is used in Fig. 32-20 for the grid lines parallel to the axis of ordinates. Uniform spacing with ten subdivisions for each loru is used for the grid lines parallel to the abscissa axis. This arrangement is convenient for lorus and also for decibels, which have two units for each 0.1 loru. Intermediate divisions on the coordinate scales are provided to assist in reading numerical values from the curves in terms of lorus, decibels, or direct numbers. An abscissa scale in octaves is provided for comparison purposes.

32.57. Figure 32-21 gives the family of dynamic response angle curves plotted with a uniform ordinate scale for angles and logarithmic abscissa scales for frequency ratio. The features of this family are identical with those of the dynamic response angle plots of Fig. 32-17, but the curves have the same general shapes right and left of the zero loru line.

SENSITIVITY AND DYNAMIC RESPONSE ANGLE DEVIATION CURVES

32.58. The curve families of Figs. 32-16 through 32-21 show the general characteristics of the performance function associated with the (0;0,1,2) performance equation, but the requirement of reasonable size for the plots prevents their use for reading accurate numerical values. This situation is greatly improved by the deviation curve families of Figs. 32-22 and 32-23.

32.59. In practical applications of measuring instruments, it is generally desirable to have over-all sensitivities independent of the input frequency over the operating range. For this reason, a value of unity is taken as the reference sensitivity for the curves of Fig. 32-22. The frequency ratio scale is logarithmic and covers the range from just less than -2 lorus up to 0 lorus (the frequency ratio number range from 0.005 to 1). A linear ordinate scale is used in Fig. 32-22, covering the range between -0.14 and +0.14 in the upper family of curves and -0.014 to +0.014 in the lower curve family. Both families are drawn for a series of damping ratio values between 0.1. and 10. The values are chosen to give curves with fairly even spacing over the region covered. The scales used in Fig. 32-22 are expanded in comparison to those of Fig. 32-17, so that sensitivity data accurate to better than 0.1 percent may be read directly from the curves.

32.60. Figure 32-23 is a semilogarithmic plot of dynamic response angle deviations covering the frequency ratio range from -3 lorus to 0 lorus (the frequency ratio number range from 0.001 to 1), and the damping ratio range from 0.1 to 100.

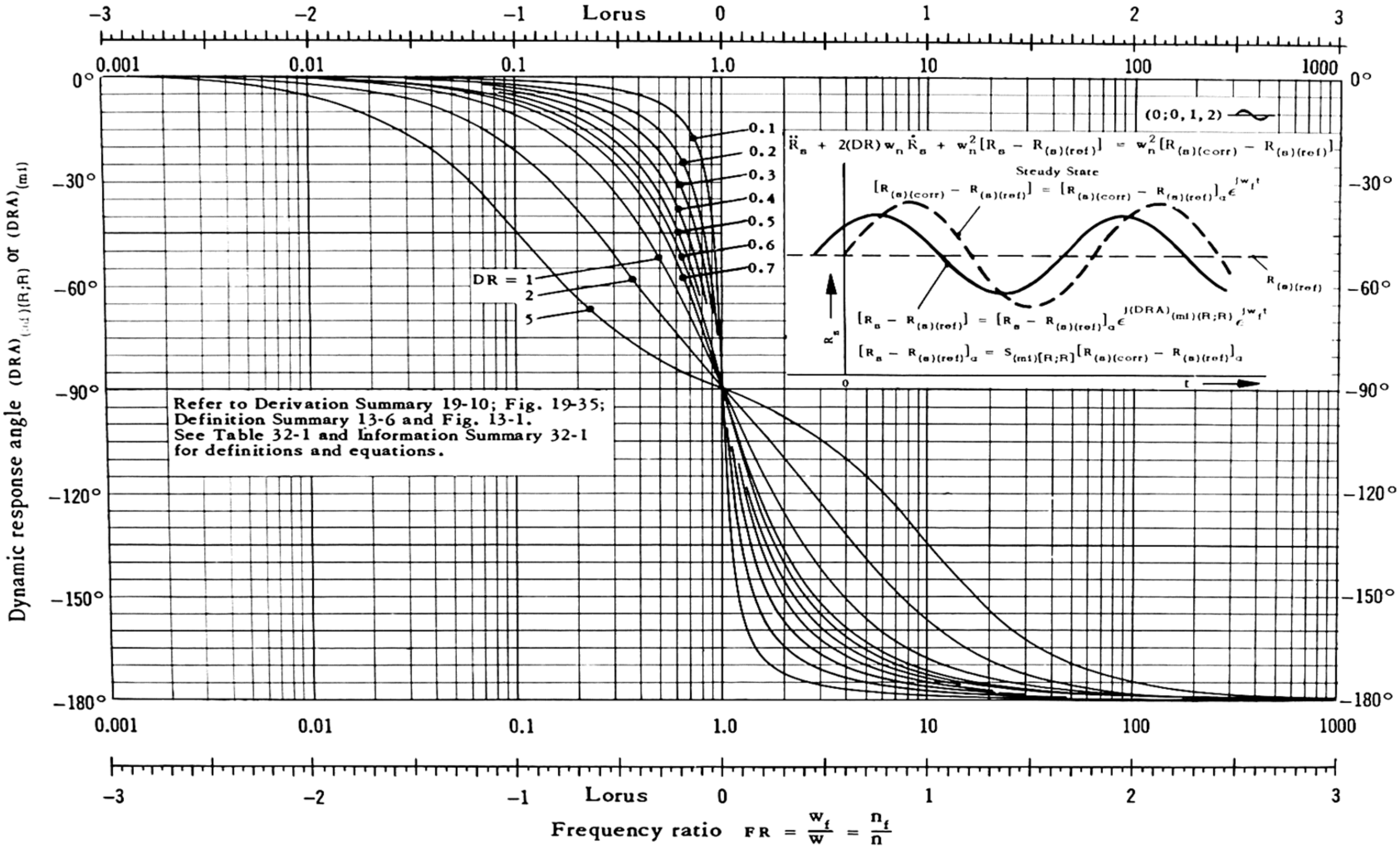


Fig. 32-21. Semilogarithmic-scale dynamic response angle curves for the steady-state sinusoidal response of measuring instruments with (0;0,1,2) performance equations.

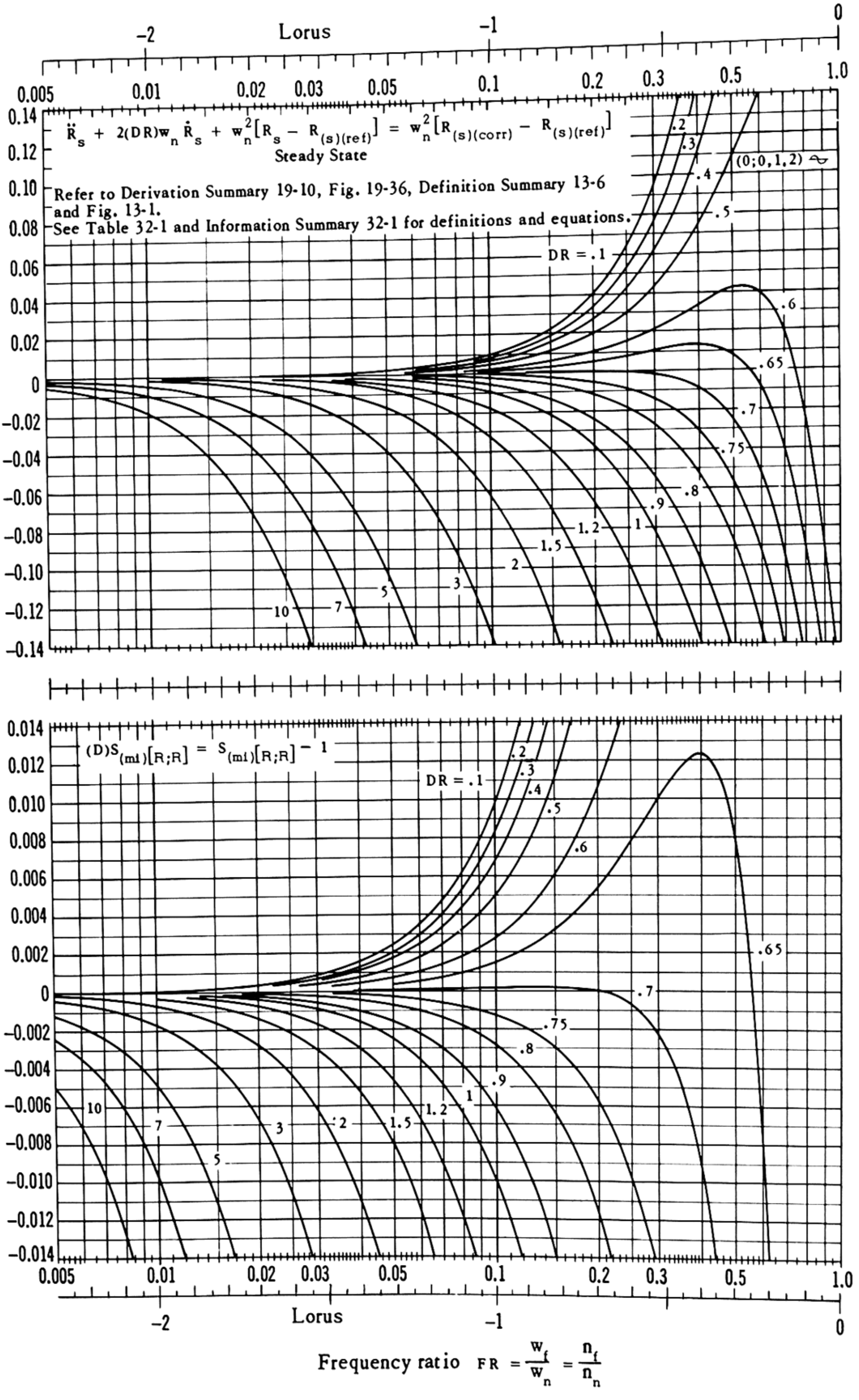


Fig. 32-22. Semilogarithmic-scale over-all sensitivity deviation curves for the steady-state sinusoidal response of measuring instruments with (0;0,1,2) performance equations.

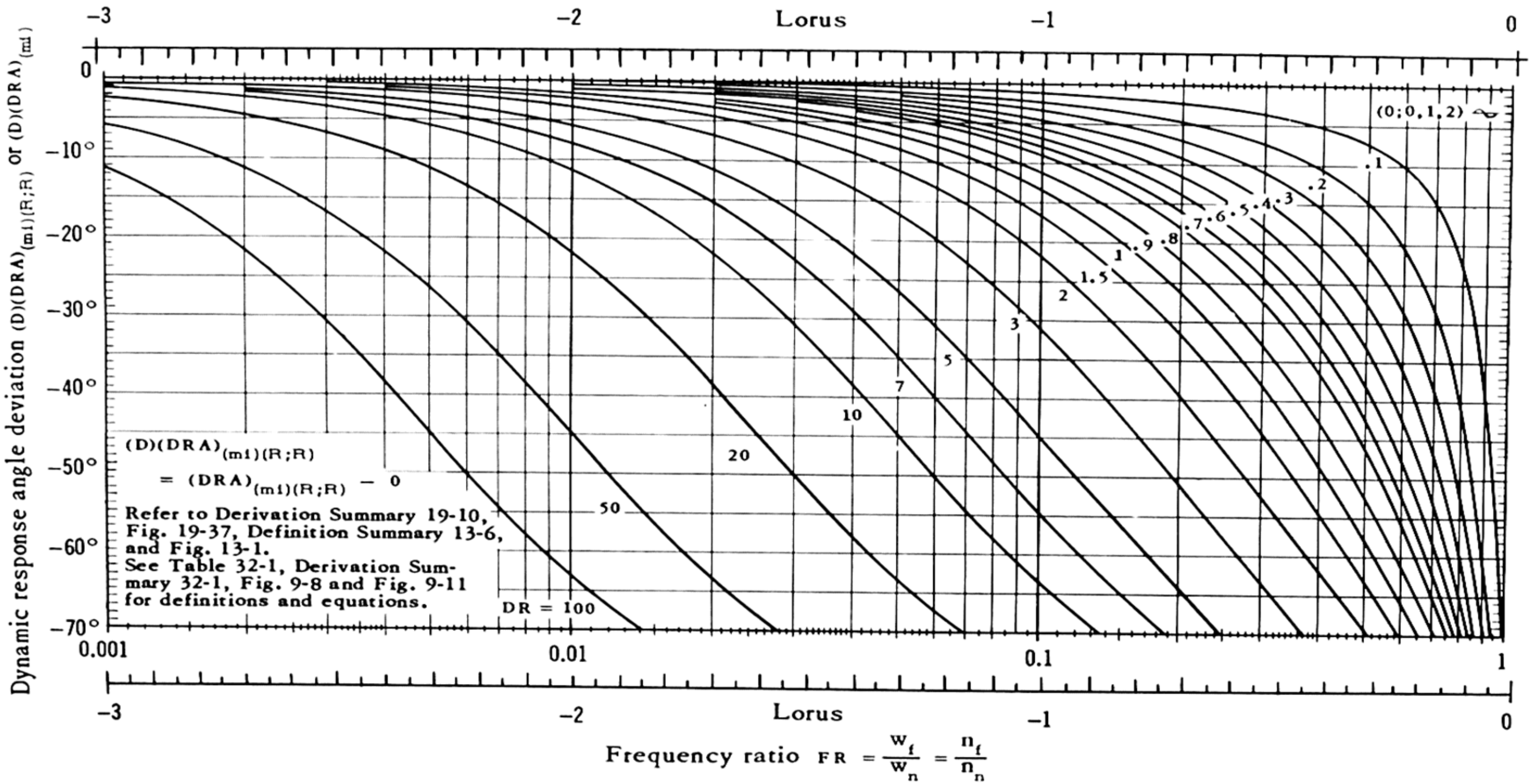


Fig. 32-23. Semilogarithmic-scale dynamic response angle deviation curves for the steady-state sinusoidal response of measuring instruments with (0;0,1,2) performance equations.

Because it is very often desired to have scale readings follow correct scale readings as closely as possible, zero is chosen as the dynamic response angle reference. The scales chosen for Fig. 32-23 make it possible to estimate angle deviations to 1 degree or better.

APPLICATIONS OF PERFORMANCE-DESCRIBING EQUATIONS AND CURVES TO ENGINEERING PROBLEMS ASSOCIATED WITH MEASURING INSTRUMENTS

32.61. The engineering problems associated with measuring instruments occur in many forms, ranging from preliminary design work through detailed design, manufacture, adjustment, test, inspection, installation and maintenance. In addition to these phases of instrument engineering practice, which are directly concerned with equipment and its unit behavior, the engineering of systems in which instruments serve as operating components is a field of great and increasing importance.

32.62. The theoretical aspects of measuring-instrument engineering involve problems of three types:

1) Direct performance analysis, in which performance equations (or equivalent performance functions), forcing functions, and initial conditions are known, and the corresponding responses are to be found.
2) Performance function design, in which it is required to determine the performance function necessary for a system to have specified response characteristics when it is subjected to specified forcing functions.
3) Inverse performance analysis, in which specific quantitative information on the responses of a given system to known forcing functions with known initial conditions is available, and the performance equation (or performance function) of the given system is to be found.

32.63. The combination of Derivation Summary 32-1, Derivation Summary 19-4, and the calculations required for plotting the ramp function curve of Fig. 32-9 is an example of direct performance analysis. The performance equation is the (0;0,1,2) equation; the forcing function is the ramp function; and the initial conditions are zero scale reading difference and zero rate of change of scale reading.

32.64. The curve families of Figs. 32-16 to 32-23 are typical of the information required for performance function design. For example, when limits are specified on sensitivity and dynamic response angle changes within a given frequency ratio range, the curve families of Fig. 32-17 may be used to determine by inspection whether or not a (0;0,1,2) system is capable of providing the required characteristics. If the (0;0,1,2) system characteristics are found to be suitable, the necessary damping ratio may also be estimated directly from one of the plotted curves or by interpolation between two of these curves. In practice, performance function design problems are frequently too complex for solution by any commonly

available family of performance function curves. It is not possible to give any simple, universally effective procedure for performance function design, but a number of mathematical approaches to this problem are described in Chapters 15 through 27. In any particular situation, the method to be used must be selected on the basis of the theoretical knowledge, practical experience, and judgment of the engineers concerned. The examples discussed in the following chapters of this book are intended to help in building up the background required to find effective solutions for performance function design problems.

32.65. In any given situation, inverse performance analysis starts with recordings or numerical data on the response of the measuring instrument under study to a known forcing function when known initial conditions exist. It is theoretically possible to "work backward" from this information to find the performance characteristics of the instrument producing the response. When the instrument is a functionally complex system, the problem of identifying the form of the performance equation involved and finding reasonably accurate numerical values for the necessary parameters may be an involved procedure requiring applications of several of the techniques described in Volume II. It is always reasonable to start the testing process by applying a step forcing function. When the response does not exhibit any oscillation, a semilogarithmic plot will show whether the instrument is a first-order system or has a higher-order performance equation. The discussion of Derivation Summary 31-3 shows that when the semilogarithmic plot is a straight line, the system concerned is a first-order system with a characteristic time that may be determined from the slope of this line. When the semilogarithmic plot of step function response is not a straight line, it immediately follows that the operating system involved has a performance equation of second or higher order. Applications of the general theory developed in Chapter 19 make it possible to identify second-order systems from semilogarithmic plots of step function response. When any given step function response record does not show either (-;0,1) or (-;0,1,2) characteristics (i.e., does not correspond to linear first- or second-order differential equations with constant coefficients), it must have been produced by a linear system of higher order with constant coefficients or by a nonlinear system of some type. If this situation exists, it is still possible to associate a performance equation with the available information, but the procedure of analysis must be worked out for each case using the physical principles and mathematical relationships involved.

32.66. Performance functions may be derived from the response produced by a forcing function of any type. For example, transients following impulse or pulse inputs of known characteristics may be used to establish performance equations. Steady-state responses to known forcing functions may also be used for this purpose. For example, the first-order ramp function response function of Fig. 31-2

shows a constant forced dynamic error equal to the characteristic time. From the standpoint of usefulness for engineering purposes, the steady-state sinusoidal response that directly represents the performance function of a system is of primary importance. For linear first- and second-order systems with constant coefficients, the relationship between steady-state sinusoidal response and impulse or step transient responses is known and expressible in convenient form. Similar relationships are more complex for linear systems of higher than second order and for nonlinear systems, but they follow such well-defined general principles that pulse, step, ramp, sinusoidal, or other forcing function forms can always be applied to an operating system to produce response curves from which performance equation forms and parameter values may be deduced. The linear second-order differential equation with constant coefficients has solutions that are completely known. They can be concisely described in terms of equations and represented by relatively simple curve families that illustrate all the basic features that appear in responses from operating systems having performance equations of arbitrary complexity. Because of these facts, it is worth while to examine typical response patterns associated with the (0; 0,1,2) equation. These patterns illustrate oscillatory transients and steady-state sinusoidal response characteristics that pass through points of maximum magnitude as frequency changes. In addition, the general procedure for finding performance equations and parameters from experimental data is demonstrated and specific methods applying to second-order systems are described.

32.67. Figure 32-24 shows the frequency ratio at which the maximum values of over-all sensitivity occur on the full-line curves of Fig. 32-17 as a function of damping ratio. For zero damping ratio, the peak occurs at unity on the frequency ratio scale. The peak location moves back toward zero frequency ratio as the damping ratio increases, until the damping ratio reaches 0.707 (the reciprocal of the square root of 2) when the peak value is unity. No peak exists for damping ratios higher than 0.707. Figure 32-25 shows the peak height as a function of damping ratio. The peak height remains between 1 and 2 for damping ratios higher than about 0.25. For lower damping ratios, it increases very sharply to a theoretical value of infinity when the damping ratio is zero. The information given by Figs. 32-24 and 32-25, which is taken from Figs. 19-31 and 19-32, makes it possible to estimate damping ratio at a glance from frequency response data on any system that is known to have a (0; 0,1,2) performance equation.

32.68. Table 32-2 summarizes the procedures for determining quantitative information on the performance parameters of (0; 0,1,2) systems from step function response data. The definitions and notation used in this table are listed in Table 32-1. The mathematical equations applied in Table 32-2 are developed in Derivation Summary 19-2 and plotted in the curve families of Figs. 32-4, 32-5, 32-6 and 32-7. The column on the left-hand side of Table 32-2 gives the damping

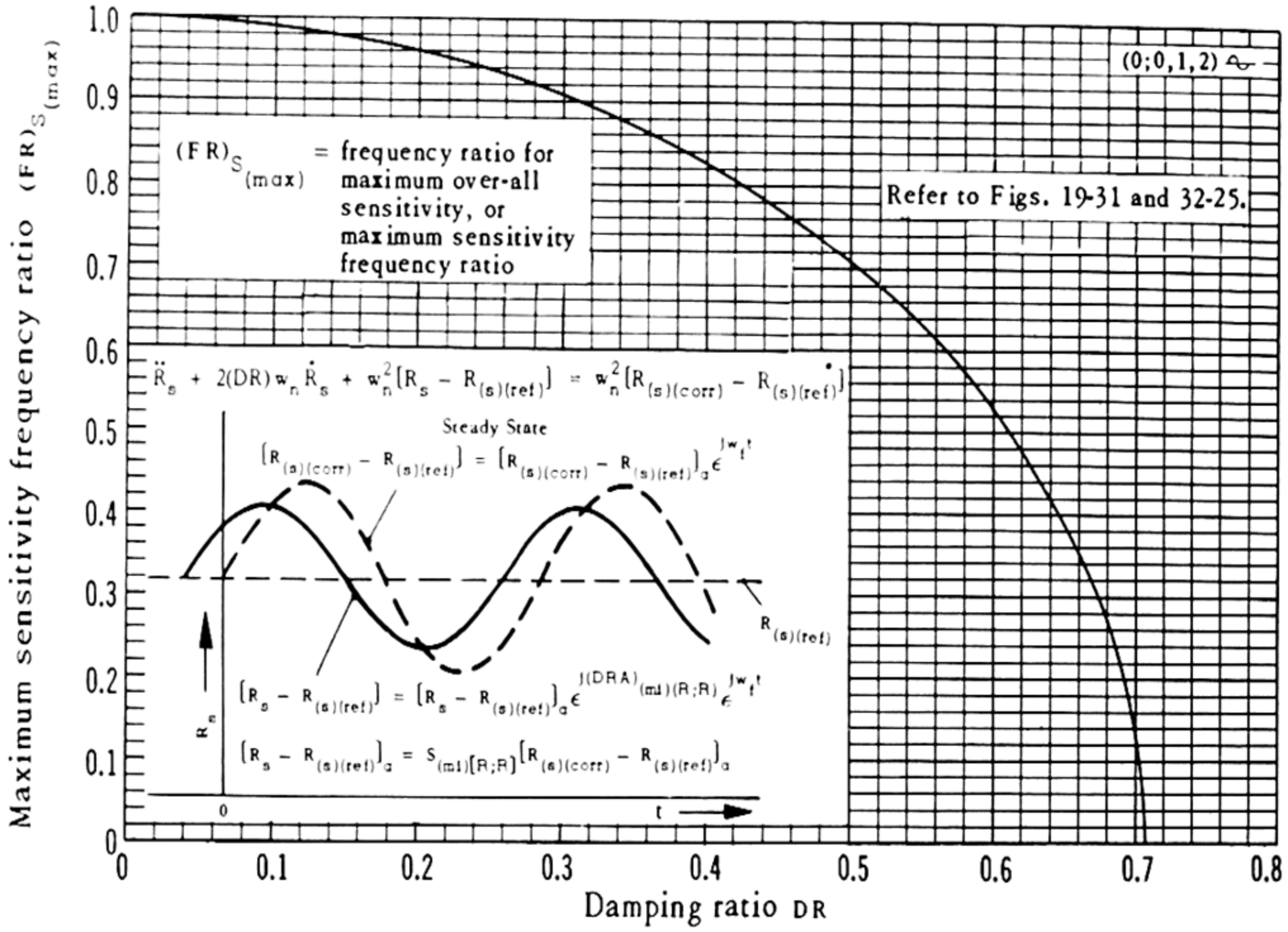


Fig. 32-24. Frequency ratio for maximum steady-state sinusoidal over-all sensitivity as a function of damping ratio.

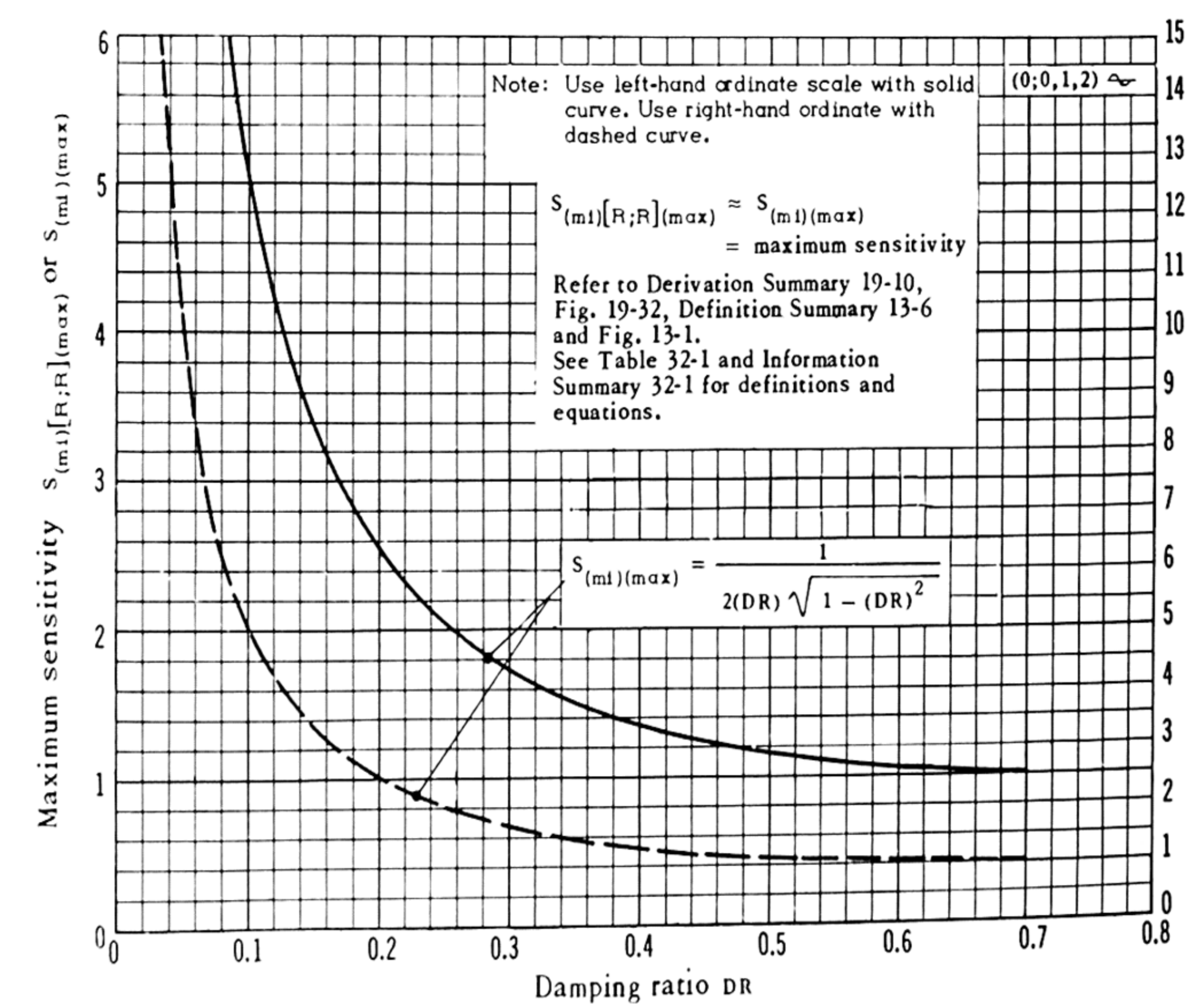


Fig. 32-25. Maximum steady-state sinusoidal over-all sensitivity as a function of damping ratio.

ratio ranges for which step function transients from a (0;0,1,2) system will have the general features shown in the next column to the right. The third column lists the most convenient performance parameters to use in the damping ratio ranges for each row. The fourth column summarizes briefly a procedure that may be used in finding performance parameters for each type of response curve. The last column lists equations from Table 32-1 that describe the relationships of the first- and second-order term performance equation coefficients to the performance parameters and the zero-order term equation coefficient. A procedure for finding the zero-order coefficient is omitted from Table 32-2 because this coefficient may be found from static tests that are independent of the way input changes are made.

32.69. When step function response data are available, the first step is to identify the damping ratio region involved by inspection. When the response shows damped oscillation at a single, well-defined frequency,* it is immediately obvious that the system has a damping ratio less than 0.5. In this situation, the procedure outlined in the top row of Table 32-2 will provide performance parameter information. If the step function response curve is not clearly oscillatory, but starts from the initial instant with a slope that steepens before the final asymptotic shape begins, the damping ratio will probably lie in the region between 0.5 and 2.0. This hypothesis can be checked and the parameters determined by the procedure described in the middle row of Table 32-2. When a nonoscillatory transient curve slopes downward sharply near the initial instant after a short low-slope region, the damping ratio will lie in the region of 1.5. In this region, the procedure given in the bottom row can be applied to find the performance parameters. When nonoscillatory response curves are encountered, confusion may arise as to which of the nonoscillatory curve procedures is to be applied. This question may be resolved by applying the method of the middle row and then that of the bottom row if the first method does not give satisfactory results.

DETERMINATION OF (–;0,1,2) SYSTEM PERFORMANCE PARAMETERS FROM OSCILLATORY STEP FUNCTION TRANSIENTS

32.70. When the step function transient given by a measuring instrument is oscillatory, the procedure of the top row of Table 32-2 is to measure the scale reading ratios at peaks in the curve and also the time intervals between points at which the curve crosses the zero ordinate line. The peak heights are considered as magnitudes only and may be measured either in actual scale units or in length units of any kind. The units are immaterial, since the peak magnitudes are used to form nondimensional ratios. The abscissa scale, on the other hand, must be

---

* The existence of a single frequency shows that the operating system producing the transient has a second-order performance equation. When more than one frequency appears, the system is obviously at least fourth order, for reasons discussed in Chapters 21 and 22.

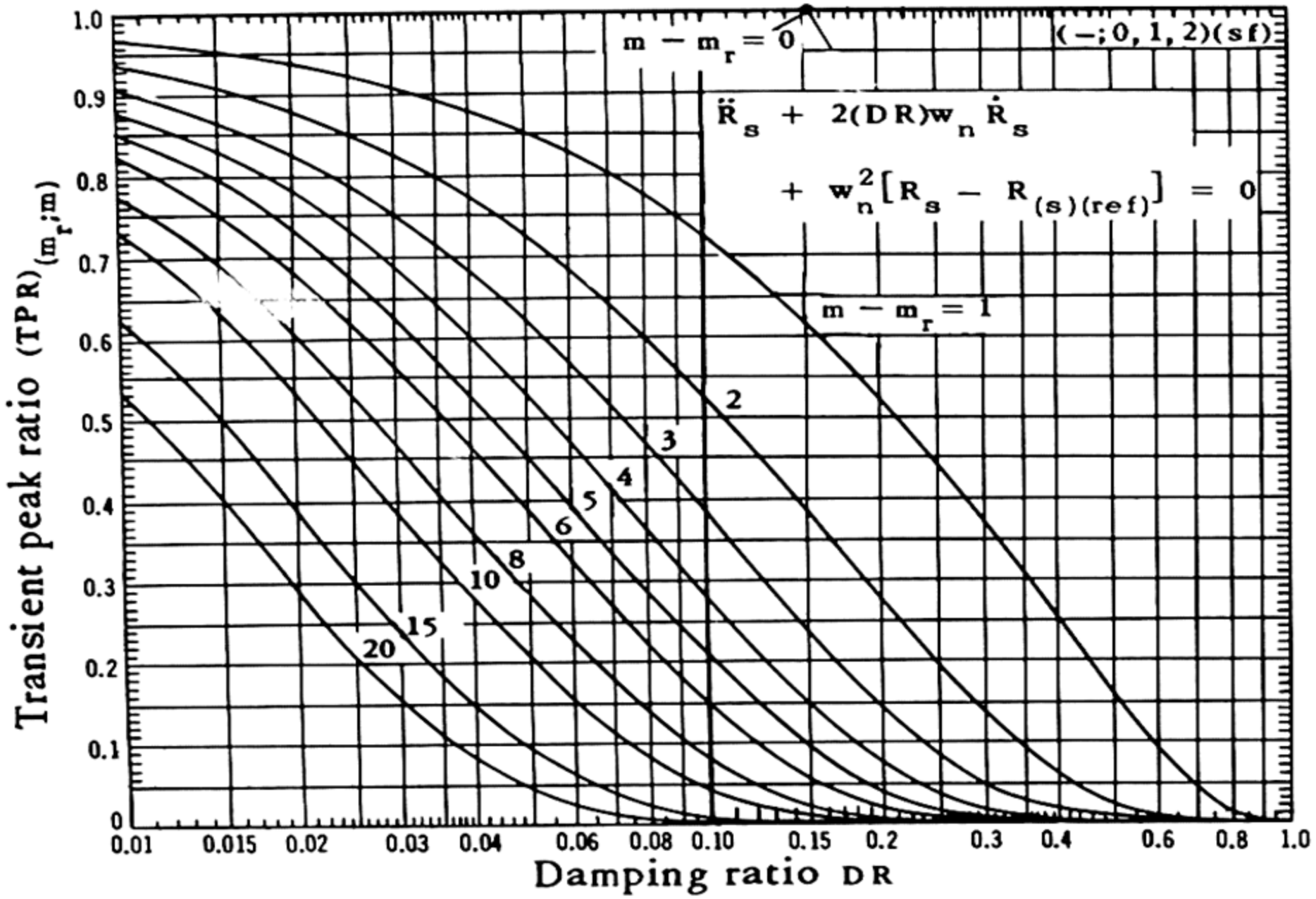
calibrated in time units in order to translate distance between crossing points into the damped natural period.

32.71. In measuring the natural period, it is important to locate the zero scale reading axis accurately, either by information from recording equipment or by trial and error, until the distances between crossing points for various half cycles are equal. When this axis is located properly, ratio comparisons of various pairs of peaks will correspond to a single damping ratio. On the other hand, when the zero ordinate axis is either displaced or tilted, inconsistencies may appear in damping ratio values based on different pairs of transient peaks. When transient peaks in scale reading have been identified and measured, transient peak ratios for various peaks, with the initial peak taken as the reference, are formed. These ratios are used to enter the curve families of Fig. 32-26, in which transient peak ratio is the ordinate and damping ratio is the abscissa. Each curve is plotted for the difference between the identifying numbers for the peaks, with later peak height divided by the earlier peak height. For example, the identification of 1 for the upper curve in Fig. 32-26 means that the transient peak ratio is computed for the next peak after the reference peak. The family of Fig. 32-26a is plotted on semilogarithmic coordinates, and the family of Fig. 32-26b is plotted on completely logarithmic coordinates. The former plot is well suited for accurate readings in the low damping ratio range but gives poor results for high damping ratios, while the regions of poor and good accuracy are reversed for the latter family.

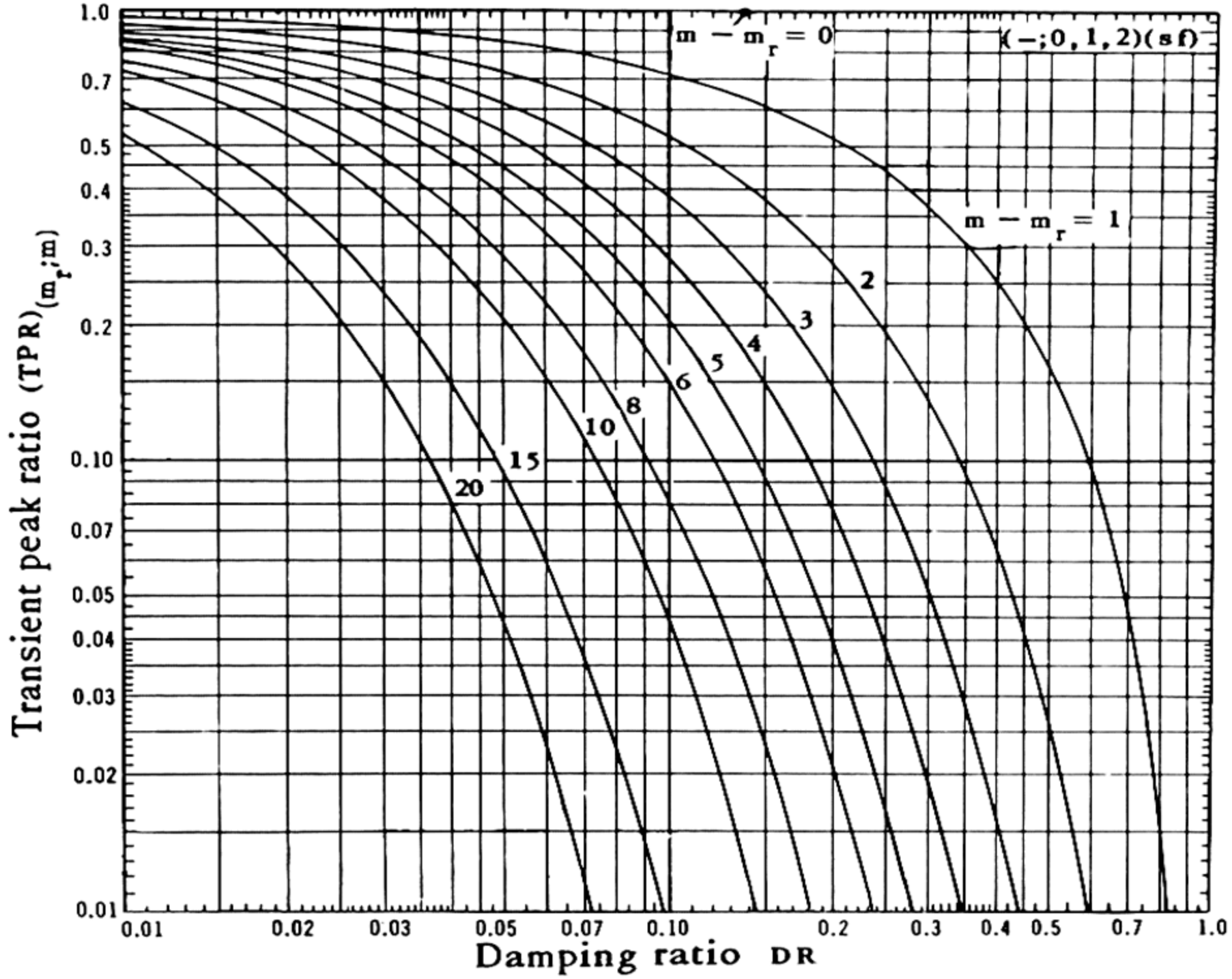
32.72. In practice, the relationship between step function response and steady-state sinusoidal response is important, because it often happens that data on only one type of forcing function are available, while information on the other type of response is of primary interest. It is always possible to determine the performance relationships by finding the parameters from tests of one type and then using these parameters to enter the curve families describing performance of the other type. This procedure, however, is made unnecessary by the curve family of Fig. 32-27, in which maximum over-all sensitivity is plotted on a logarithmic ordinate scale against transient peak ratio on a uniform abscissa scale. Damping ratio ordinate scales are placed outside the coordinate field for reference purposes.

DETERMINATION OF (–;0,1,2) SYSTEM PERFORMANCE PARAMETERS FROM NON-OSCILLATORY TRANSIENTS IN THE CRITICALLY APERIODIC DAMPING RATIO REGION

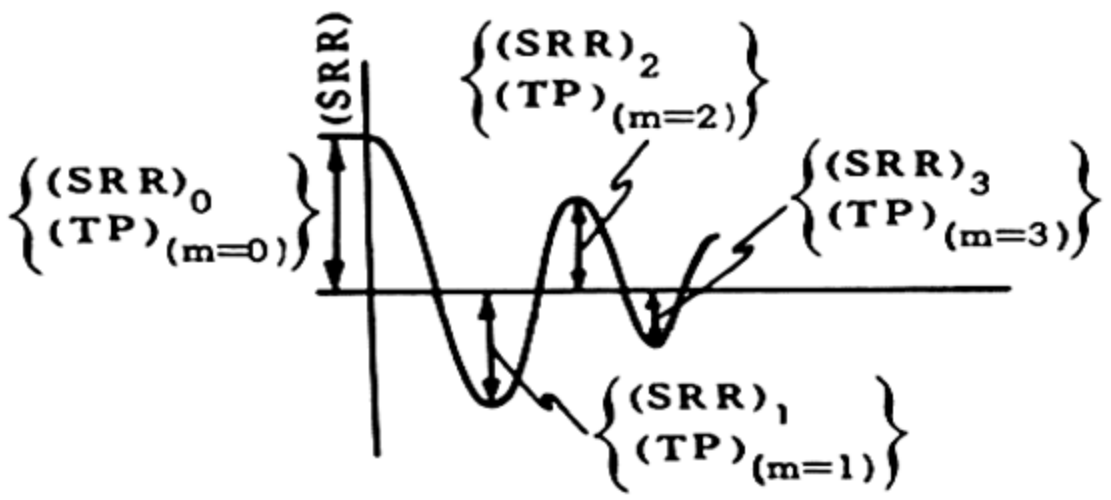
32.73. When the step function response curve is nonoscillatory, with a well-defined region of low slope near the initial instant, the procedure outlined in the middle row of Table 32-2 may be used. Starting from the initial scale reading ratio as unity, three levels below unity are marked off on a linear ordinate scale. These levels (0.736, 0.406 and 0.199) are the theoretical points reached by a (-;0,1,2) system with critical damping (i.e., with unity damping ratio) after the



a) Logarithmic scale abscissa – linear scale ordinate plot



b) Logarithmic scale plot

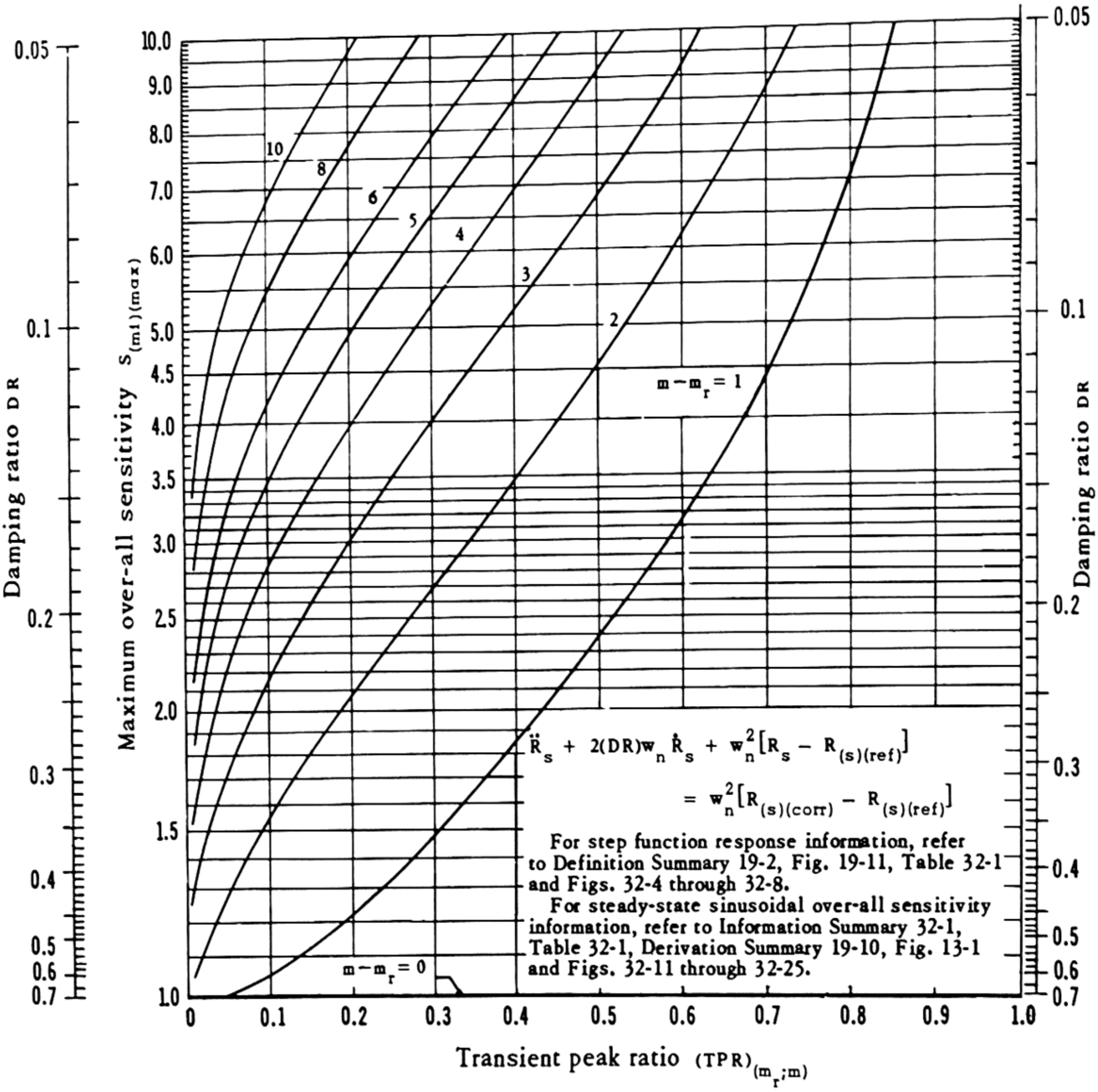


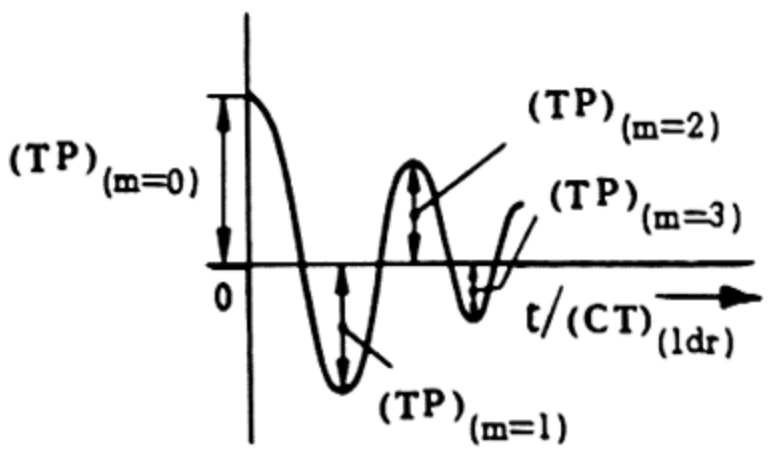
$$(TPR)_{(m_r;m)} = \frac{(SRR)_m}{(SRR)_{m_r}} = \frac{(TP)_m}{(TP)_{m_r}}$$

$$= m^{th} \text{ reference peak ratio}$$

Refer to Definition Summary 19-1, Derivation Summary 19-2, Fig. 19-4, Table 32-1 and Figs. 32-4 through 32-8.

Fig. 32-26. Transient peak ratio as a function of damping ratio for step function oscillatory response of measuring instruments with (0;0,1,2) performance equations.





$$(TP)_{(m_r;m)} = \frac{(TP)_m}{(TP)_{m_r}}$$

where
m and m_r are order integers of transient peaks. The reference peak m_r may be chosen as any peak.

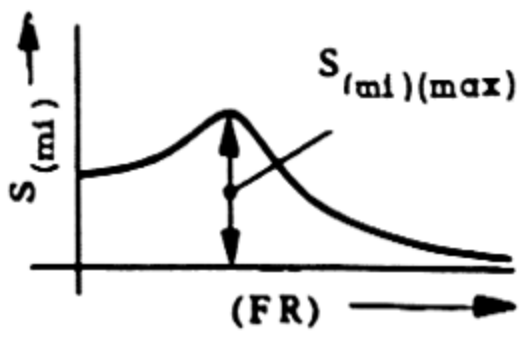


Fig. 32-27. Logarithmic-scale curves of maximum over-all sensitivity as a function of step function transient peak ratio for instruments with (0;0,1,2) performance equations.

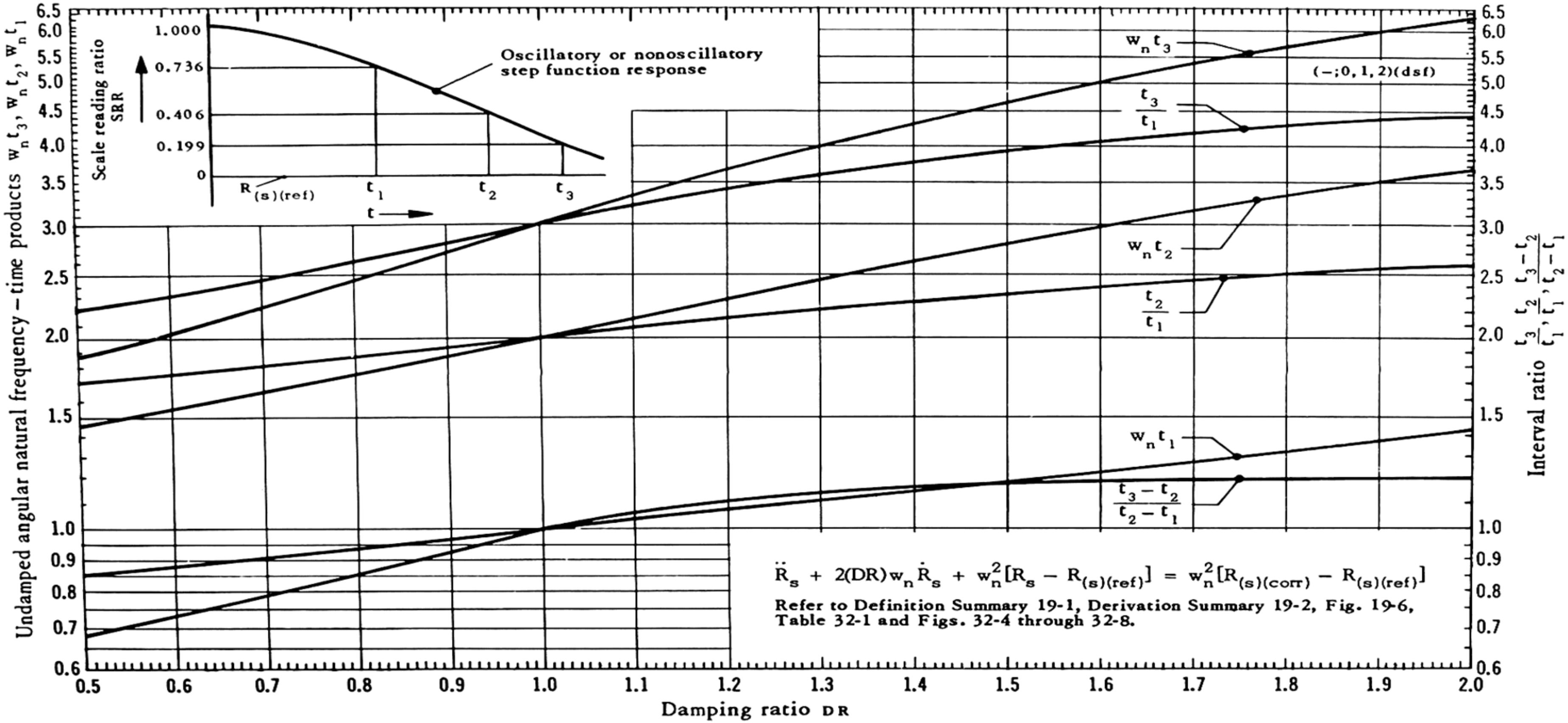


Fig. 32-28. Time ratio and undamped angular natural frequency – time product as a function of damping ratio for the step function response of measuring instruments with (0;0,1,2) performance equations.

lapse of 1, 2 and 3 characteristic times, respectively. When, in any specific case, the abscissa intervals corresponding to the three marked ordinates are all equal, it follows immediately that the system giving the response has critical damping, with a low damping ratio characteristic time corresponding to the common length of the abscissa intervals.

32.74. When the abscissa intervals corresponding to the 0.736, 0.406 and 0.199 ordinate levels are different in length, the abscissa interval ratios defined in the fourth column of the second row in Table 32-2 are formed. It is to be noted that under the definitions, the abscissa intervals do not have to be in time units, but may be expressed in any convenient units of length. The abscissa interval ratios may be used to enter the interval ratio curve family of Fig. 32-28 so that the corresponding damping ratios may be taken from the abscissa scale. If the system producing the response curve under analysis actually behaves as an ideal second-order system and the response data values are accurate, the three interval ratios will give a single damping ratio. In practice, the three damping ratio values are usually not in perfect agreement, and it becomes a matter of judgment and experience as to the degree of confidence to be placed on the derived damping ratio. In particular, if the interval ratios correspond to a damping ratio above about 1.3, the curves of Fig. 32-28 are too flat to permit accurate estimates of damping ratio values. When this occurs, the procedure of the bottom row of Table 32-2 should be applied.

DETERMINATION OF (–;0,1,2) SYSTEM PARAMETERS FROM NONOSCILLATORY RESPONSE TRANSIENTS IN THE HIGH DAMPING RATIO REGION

32.75. The procedure described in the bottom row of Table 32-2 is to plot scale reading ratio* as taken from a given response curve in which the logarithmic scale ordinate is plotted against time as the linear scale abscissa. The fact, shown in Derivation Summary 19-2, that high damping ratio step function response is represented by an equation made up of two real exponential terms, means that the semilogarithmic plot just described reduces to a straight line when one of the exponential terms becomes negligibly small. In the region for which this condition exists, the response curve plot is essentially similar to the first-order step function response on semilogarithmic coordinates that is discussed in Derivation Summary 31-3. By extending the straight portion of the semilogarithmic plot to the zero time line (i.e., the axis of ordinates), the second-order step function response plot is reduced to the representation of a single real exponential whose slope is determined by the larger high damping ratio characteristic time. This characteristic time may be determined from the slope of the extended straight line by the procedure described in Derivation Summary 31-3.

* Because ratios are used, any length units may be used for the original plots, so long as the initial level is taken as unity.

32.76. The high damping ratio characteristic time ratio defined in Table 32-1 is often useful to supplement damping ratio as a performance parameter for the high damping ratio region. The high damping ratio characteristic time ratio determines the relative importance of the two real exponentials that make up the step function response immediately after the initial instant and may be found by taking the ratio of the extended straight line response component ordinate point to the difference between this point and the actual initial ordinate point. Once the high damping ratio characteristic time ratio is known, the corresponding damping ratio may be found either by using the proper relationship from Table 32-1 or by means of Fig. 32-29, which shows damping ratio on a linear ordinate scale against high damping ratio characteristic time ratio on a logarithmic abscissa scale.

DETERMINATION OF (0;0,1,2) SYSTEM PERFORMANCE PARAMETERS FROM STEADY-STATE SINUSOIDAL RESPONSE INFORMATION

32.77. Performance parameters for operating systems may be determined by means of frequency response tests in which steady-state responses to sinusoidal input variations of known amplitude and frequency are measured in terms of dynamic amplitude ratio and dynamic response angle. By using a series of properly selected frequencies, it is possible to cover the operating range that is of interest for any given measuring-instrument problem.

32.78. In taking frequency response data, the first step is to select a range of input amplitudes that are compatible with the capabilities of the equipment to be tested and the situations in which it is to be applied. The second step is to experimentally determine the frequency at which the steady-state response has a lagging (i.e., negative) dynamic response angle of -90 degrees with respect to the sinusoidal input. The frequency at which this 90-degree angle occurs corresponds to the frequency ratio value of unity (refer to Derivation Summary 19-10 and Figs. 32-17 and 32-18). With the unity frequency ratio frequency determined, a schedule of frequency ratios is laid out with close spacing in the vicinity of unity, and with progressively wider spacing for high and low frequency ratios. Dynamic amplitude ratio and dynamic response angle readings are taken for each of the frequency ratio settings and compared with the theoretical values found by computation from Eqs. (17) and (18) of Information Summary 32-2, taken from second-order data tables, or read from curves like those of Figs. 32-16 through 32-21. This comparison shows the shape of the experimental frequency response curves as compared to the theoretical frequency response curves for various damping ratios, so that the damping ratio of the system under test may be estimated.

32.79. The procedure outlined in the preceding paragraph shows whether or not the tested system behaves as a second-order system. When the experimental frequency response data indicate that the system is actually a second-order system,

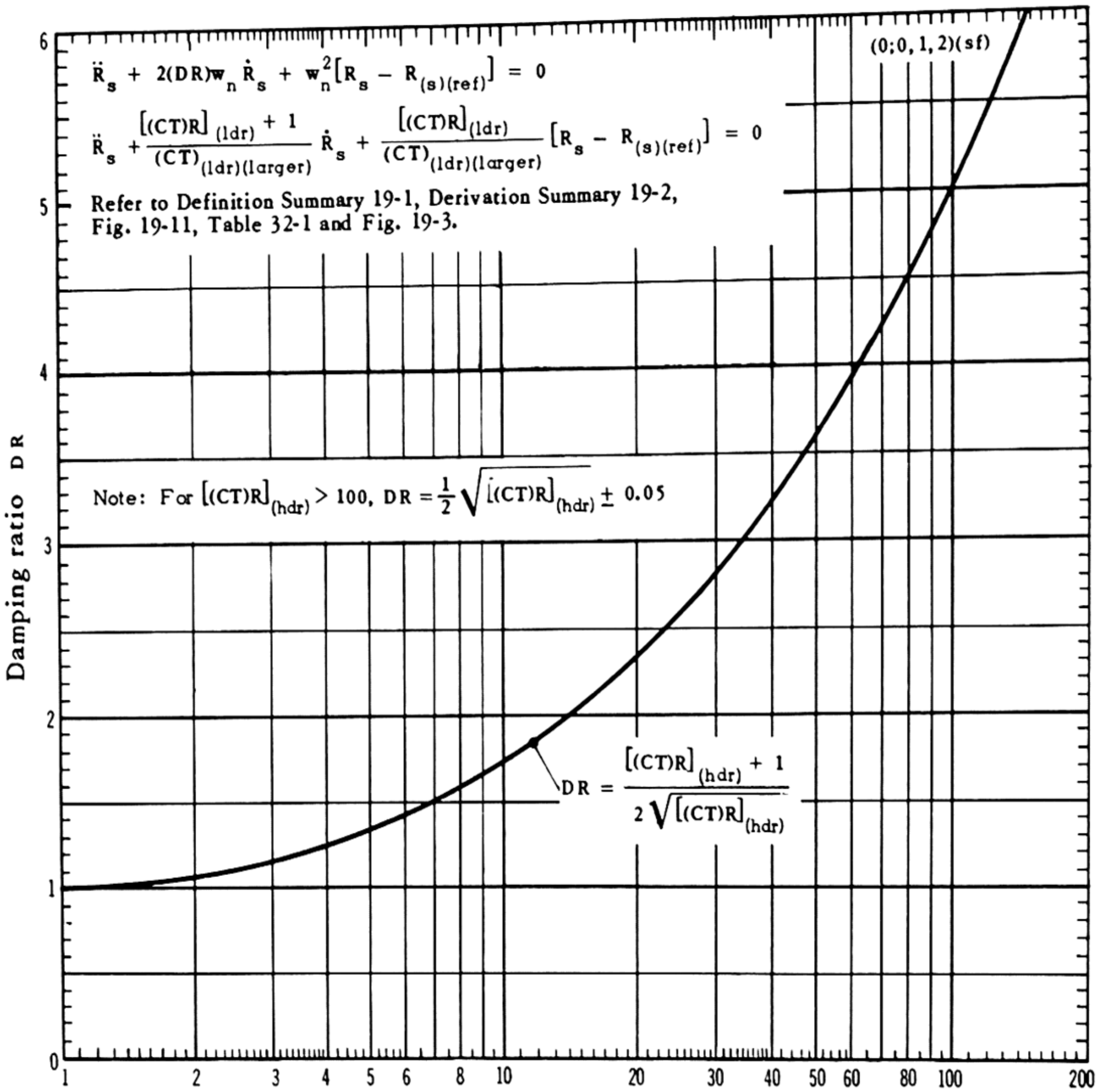


Fig. 32-29. Damping ratio as a function of high damping ratio characteristic time ratio for measuring instruments with (0;0,1,2) performance equations.

the damping ratio may be found directly from an observation of the maximum over-all sensitivity (identical with the dynamic amplitude ratio) and the frequency at which it occurs. With the maximum sensitivity known, the corresponding damping ratio may be read directly from one of the curves of Fig. 32-25 or computed from the equation given on that figure. The corresponding frequency ratio for maximum sensitivity may be read from the curve of Fig. 32-24. With this information and a knowledge of the actual frequency at which the maximum takes place, the undamped natural frequency for the tested system may be found from the proper relationships given in Table 32-1.

INTERPRETATION OF RESPONSE INFORMATION NOT COMPATIBLE WITH THE THEORETICAL RESPONSE OF (0;0,1,2) SYSTEMS

32.80. When the experimentally determined step function response, steady-state sinusoidal response, or response to any other known forcing function from any given operating system do not match one of the first- or second-order response patterns described in the figures of this chapter and those of Chapter 31, the performance equation for the system is either nonlinear or is linear but has an order higher than the second order. In situations of this kind, the available data and the accuracy requirements of the applications considered should be studied to determine whether or not the errors introduced by the use of first- or second-order approximations are intolerably large. When the discrepancies associated with simplifying assumptions of this kind are not acceptable, one or more of the methods discussed in Chapters 23, 24, 25 and 27 may be applied to the determination and description of performance characteristics. This will usually involve plots and tables in addition to numerical values for a number of parameters that may have various values for different ranges of operation. The choice of method and parameters for describing performance in any specific case must be based on the experience and judgment of the engineer concerned. A number of typical examples appear in the later chapters of this book.

MOVING-COIL OSCILLOGRAPHS

32.81. Oscillographs are electrical indicators designed to follow rapidly changing inputs. Instruments of this kind are ordinarily either of the cathode-ray type or the electromechanical type. Under usual conditions cathode-ray oscillograph behavior depends primarily on the electrical circuits involved and will not be discussed here. On the other hand, electromechanical oscillographs fit directly into the pattern of Information Summary 32-1. These instruments have relatively small torque generators and are combined with either optical or stiff, light-weight mechanical indicating systems to make records by photography, inking pens, or other means. The performance equations developed in Derivation Summary 32-1 may be applied without modification to electromechanical oscillographs.

32.82. Figure 32-30 is a pictorial schematic diagram showing the essential features of the photographic recording oscillograph using the moving-coil galvanometer. The galvanometer consists of a small moving coil located between the pole pieces of a permanent magnet and carried by an elastic suspension. A mirror is rigidly attached to the coil assembly. The combination of a spherical lens over the mirror and a cylindrical lens placed before the sensitive side of the photographic paper or film used for recording brings light from a special incandescent lamp into focus as a sharply defined spot. Rotation of the coil assembly about its suspension axis causes the spot to shift in a direction at right angles to the motion of

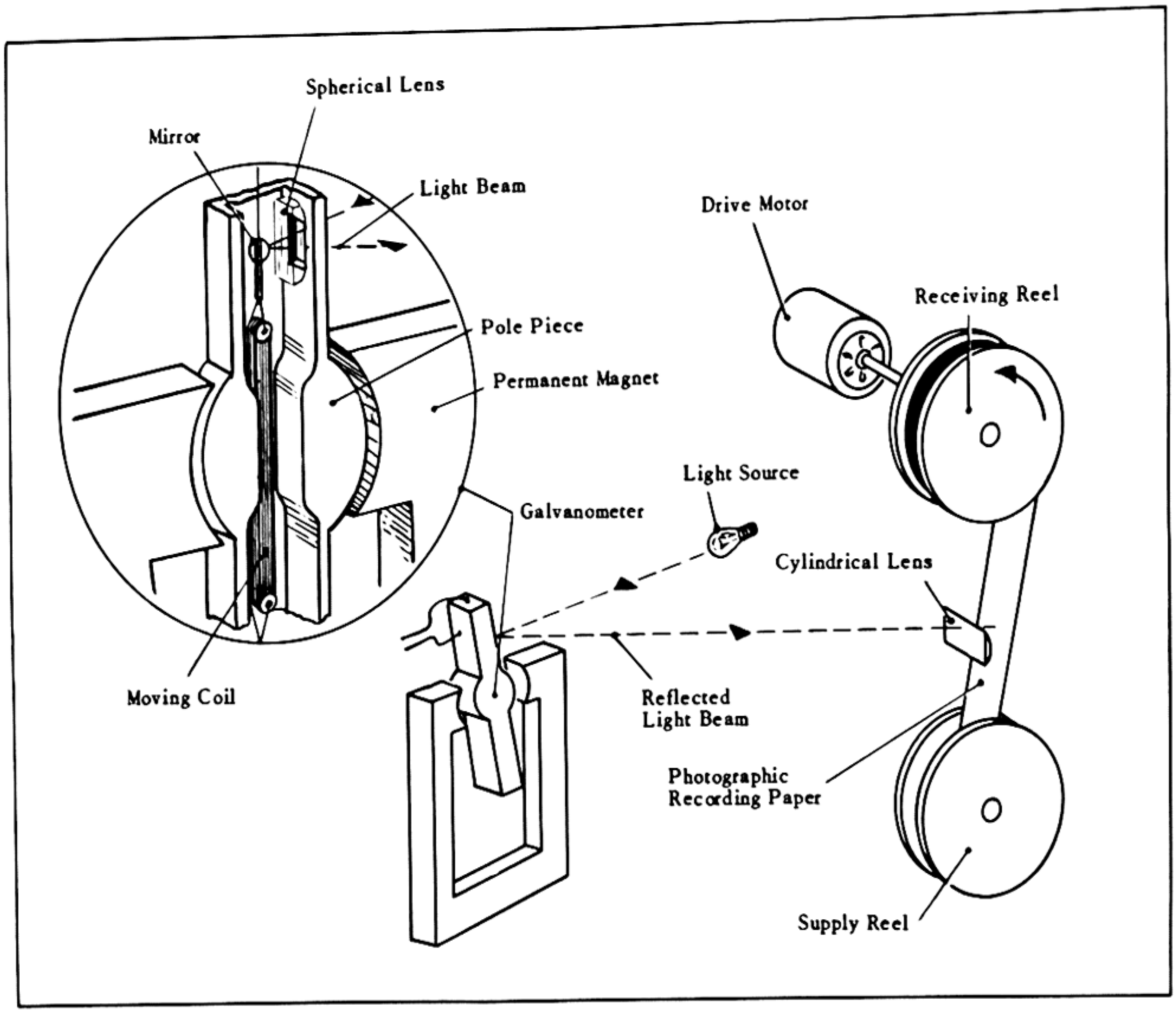


Fig. 32-30. Pictorial schematic diagram for a photographic recording oscillograph with a moving-coil galvanometer.

the recording surface as the film or paper is moved by a drive motor. Moving-coil oscillographs with optical recording systems are available from many electrical equipment and instrument manufacturers.* Other moving-coil oscillographs use mechanical inking pens or hot wires to melt line traces on paraffined paper.** Optical recording systems impose such light mechanical loads on the moving-coil system that they do not introduce serious dynamic errors, but mechanical recording systems often show resonance effects at high forcing frequencies. This means that oscillographs with optical recording systems ordinarily have second-order performance equations, but that oscillographs with mechanical indicating systems often require higher order equations to describe their performance.

DETERMINATION OF OPTICAL OSCILLOGRAPH PERFORMANCE CHARACTERISTICS FROM OSCILLATORY STEP FUNCTION RESPONSE

32.83. The procedures summarized in Table 32-2 may be applied to determine

---

* See General Electric Company, Westinghouse Electric Corporation, Consolidated Engineering Corporation, William Miller Corporation and Heiland Research Corporation (03).

** Inking pens: see Hathaway Instrument Company; hot wires: see Century Geophysical Corporation (03).

oscillograph performance characteristics from step function response records. A record of this type from an oscillograph with oscillatory response characteristics is shown in Fig. 32-31. Distances proportional to transient peaks and time are marked on the figure. The processing of these data by the procedure given in the top row of Table 32-2 to determine performance parameters is outlined in Data Analysis Summary 32-1. This summary shows that with the damping shunt resistance of 1000 ohms that was used in taking the record of Fig. 32-31, the oscillograph behaved nearly enough like a (0;0,1,2) system to give a close check between the damping ratio values for successive pairs of peaks. The damping ratio for a third pair of peaks differs somewhat from these values, but should be given relatively less weight because of the relatively small magnitude of the third peak. The damping ratios read from Fig. 32-27 for the zero-to-first and the zero-to-second transient peaks have an average value of 0.157, which can be reasonably approximated by a damping ratio of 0.16 for the oscillograph used in taking the record of Fig. 32-31.

32.84. The half-cycle distance taken from successive crossing points of the Fig. 32-31 record is 3.07 centimeters. When the known film speed of 100 inches per second is applied to the distance, the natural frequency appears as 41.4 cycles per second. Correction of this frequency for the effect of damping gives 42 cycles per second as the undamped natural frequency of the oscillograph.

OSCILLOGRAPH PERFORMANCE CHARACTERISTICS FROM APERIODIC STEP FUNCTION RESPONSE

32.85. Figure 32-32 is a step function response record for the oscillograph used for Fig. 32-31, with the damping shunt resistance changed from 1000 ohms to 120 ohms. Inspection shows that the record is nonoscillatory, with a definite region of increasing slope near the start of the transient. These characteristics mean that if the oscillograph acts as a second-order system, the damping ratio is nearly equal to unity. Under these circumstances, the procedure given in the middle row of Table 32-2 is properly applied to the record. Data Analysis Summary 32-2 outlines the application of this procedure to the record of Fig. 32-32. In that summary, it appears that the interval ratios corresponding to indication ratios of 0.736, 0.406 and 0.199 give damping ratio values of 0.99, 0.99 and 1.01, respectively, from the curves of Fig. 32-28. This agreement indicates that the oscillograph behaves as a (0;0,1,2) system with a damping ratio of unity.

32.86. The 0.92-centimeter distance for the first time interval in Fig. 32-32, with the known 97 inches per second film speed, corresponds to 0.0037 second. Entering the undamped natural frequency – interval product curves of Fig. 32-28 gives an undamped natural frequency of 42.6 cycles per second. This value is in good agreement with the analysis of the record of Fig. 32-31, which gives the response for the same oscillograph with a different damping shunt resistance.

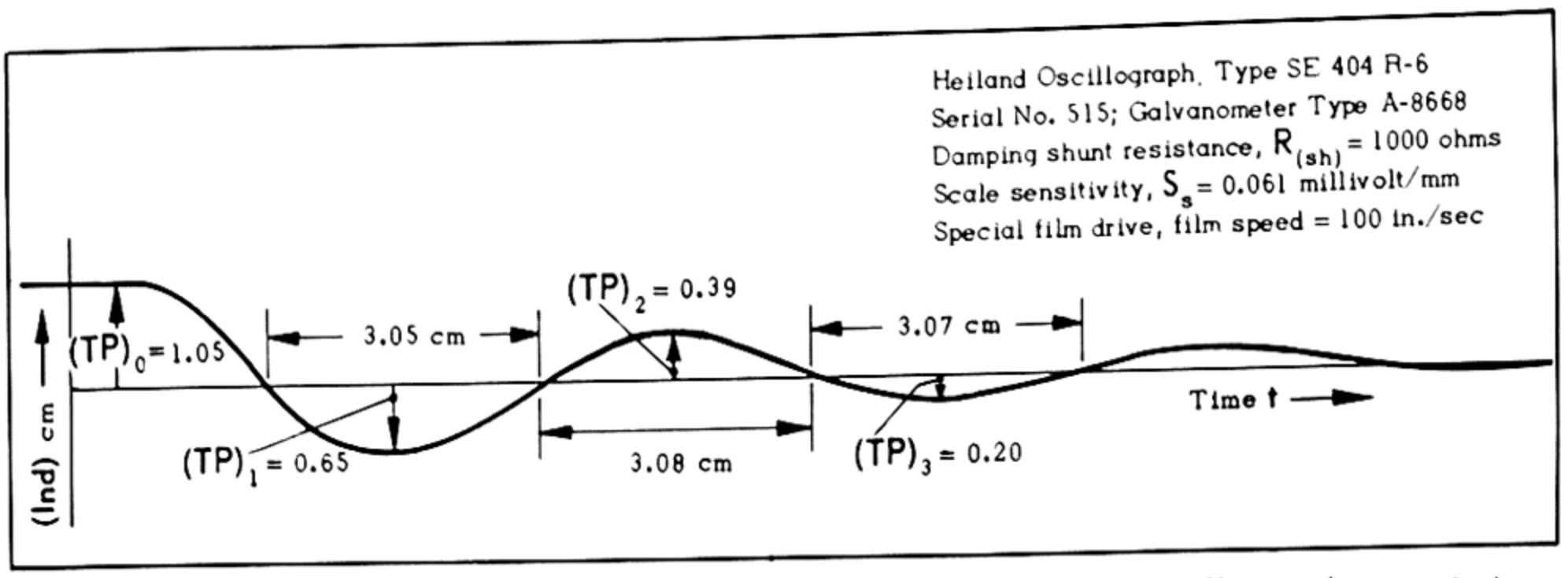
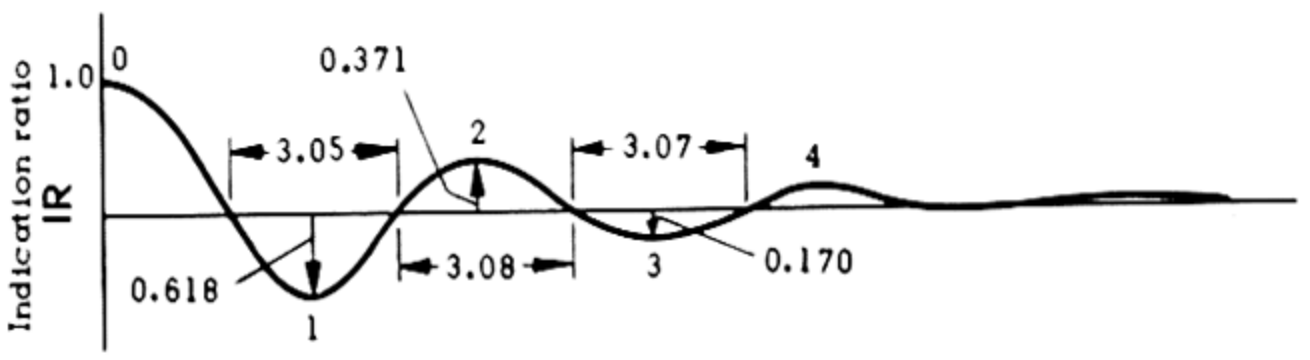


Fig. 32-31. Step function response record from moving-coil oscillograph with oscillatory characteristics.



Heiland Oscillograph
Type SE 404 R-6
Serial No. 515
Galvanometer Type A-8668
Damping shunt resistance
$R_{(sh)}$ = 1000 ohms
Scale sensitivity
S_s = 0.061 millivolt/mm
Special film drive (See Fig. 32-31.)

$$\text{Indication ratio} = IR = \frac{Ind}{(Ind)_{(ref)}} \quad ; \quad \text{Reference indication} = (Ind)_{(ref)}$$

From Fig. 32-31, $(Ind)_{(ref)} = 1.05 = (Ind)_0$

Film speed = 100 inches per second

Inches per cycle = 2(3.07/2.54) = 2.42

Natural frequency = n = 100/2.42 = 41.4 cycles per second

Undamped natural frequency = $n_n = \dfrac{41.4}{\sqrt{1-(0.16)^2}}$ = 42 cycles per second

(See Table 32-1 for formula $n = n_n\sqrt{1-(DR)^2}$)

Peak Number m	Indication at Peak m $(Ind)_m$ [Transient Peak m $(TP)_m$]	$0^{th}-m^{th}$ Peak Indication Ratio $(IR)_{(0-m)}$	Damping Ratio from Fig. 32-27
0	1.05	1.00	—
1	0.65	0.618	0.155
2	0.39	0.371	0.158
3	0.20	0.190	0.170

The agreement of damping ratio values for $(IR)_{(0-1)}$ and $(IR)_{(0-2)}$ shows that the oscillograph may be considered as a second-order (–;0,1,2) system with a damping ratio of 0.157.

It is reasonable to discount the $(IR)_{(0-3)}$ point because of the low $(TP)_3$ value.

(Refer to Table 32-2 for analysis procedure.)

Analyzed 9/25/52
By C. S. Draper

Data Analysis Summary 32-1. Analysis of step function data for an optical oscillograph with oscillatory response.

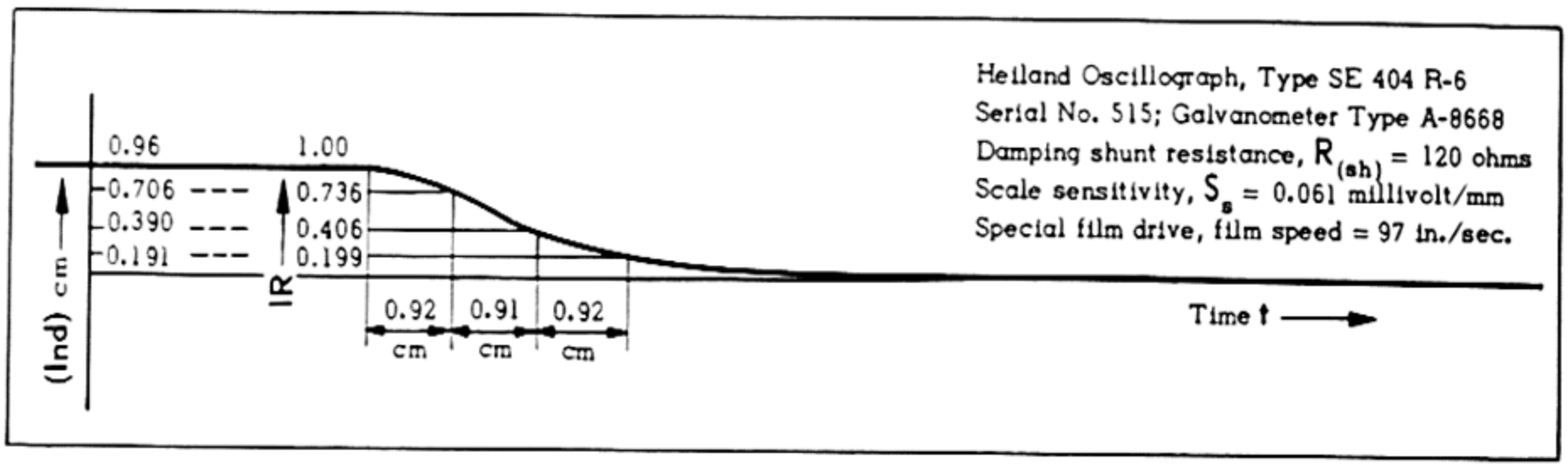
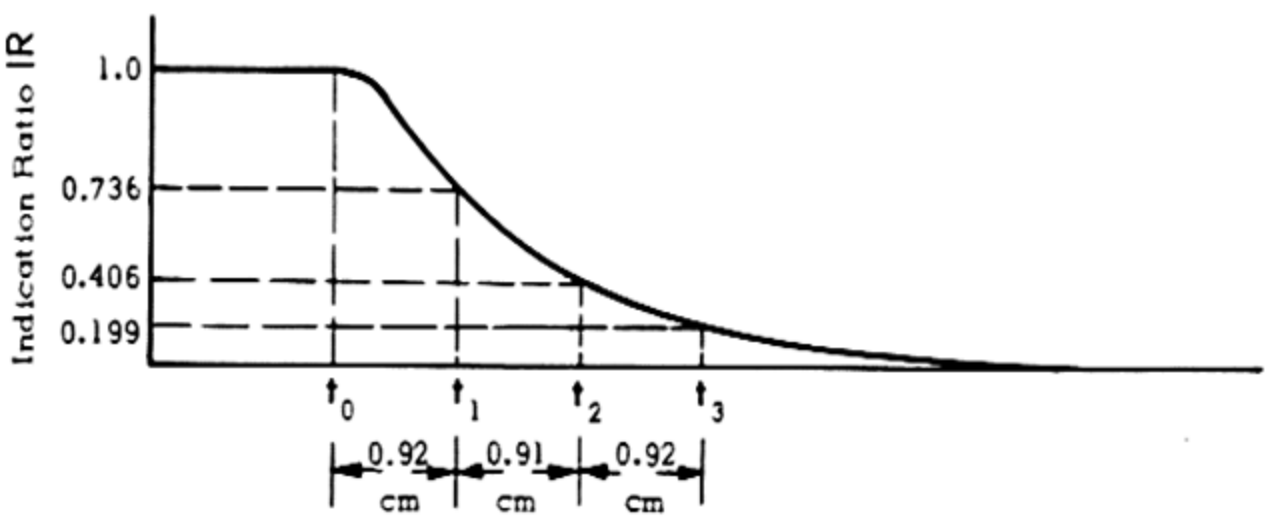


Fig. 32-32. Step function response record from moving-coil oscillograph with nonoscillatory characteristics.



Heiland Oscillograph
Type SE 404 R-6
Serial No. 515
Galvanometer Type A-8668
Damping shunt resistance
$R_{(sh)}$ = 120 ohms
Scale sensitivity
S_s = 0.061 millivolt/mm
Special film drive (See Fig. 32-32.)

$$\text{Indication ratio} = IR = \frac{Ind}{(Ind)_{(ref)}} \quad ; \quad \text{Reference indication} = (Ind)_{(ref)}$$

From Fig. 32-32, $(Ind)_{(ref)} = 0.96 \text{ cm} = (Ind)_0$

Film speed = 97 inches per second

Using procedure of Table 32-2:

$$\frac{t_2}{t_1} = \frac{1.83}{0.92} = 1.99 \quad ; \quad \frac{t_3}{t_1} = \frac{2.75}{0.92} = 2.99$$

$$\frac{t_3 - t_2}{t_2 - t_1} = \frac{0.92}{0.91} = 1.01$$

From the Interval Ratio Curves of Fig. 32-28

$$\frac{t_2}{t_1} = 1.99 \text{ gives } DR = 0.99 \quad ; \quad \frac{t_3}{t_1} = 2.99 \text{ gives } DR = 0.99$$

$$\frac{t_3 - t_2}{t_2 - t_1} = 1.01 \text{ gives } DR = 1.01$$

Take $DR = 1.0$ as the average value from the three experimental values. From Fig. 32-28, $w_n t_1 = 1$ for $DR = 1$.

$$t_1 = \frac{0.92}{2.54 \times 97} = 0.373 \times 10^{-2} \text{ second}$$

$$n_n = \frac{1}{2\pi\, 0.373 \times 10^{-2}} = 42.6 \text{ cycles per second}$$

Analyzed 9/25/52
By C. S. Draper

Data Analysis Summary 32-2. Analysis of step function data for an optical oscillograph with aperiodic response.

OSCILLOGRAPH PERFORMANCE CHARACTERISTICS FROM STEADY-STATE SINUSOIDAL RESPONSE

32.87. Figure 32-33 shows an effective arrangement for taking data on the steady-state sinusoidal response of instruments with optical indicating systems. For optical oscillographs with the features illustrated in Fig. 32-30, a narrow slit with its opening at right angles to the recording light spot motion is placed in the position normally occupied by the film. A photocell is located behind the slit so that it receives a pulse of light when the light spot passes across the slit. The output from this photocell is passed through a pulse-sharpening amplifier and applied to the spot intensity terminals of a cathode-ray oscillograph.

32.88. A special electronic oscillator, giving two signals of the same frequency but with a 90-degree relative phase displacement, is connected to the cathode-ray oscillograph. One of the signals is connected to the horizontal deflection terminals. The other signal is connected to the vertical deflection plates. With proper adjustment, a circle of low intensity appears on the face of the cathode-ray tube.

32.89. Momentary actuation of the angle reference switch of the oscillator changes the circular trace to a line. Due to the use of a long-persistence screen, however, the circle remains visible long enough for its two points of intersection with the line to be observed. These points correspond to the zero-voltage instants for the signal connected to the vertical deflection plates.

32.90. When an optical oscillograph is to be tested, the galvanometer is connected to the oscillator output signal that has its zero points synchronized with the angle reference line. A rough setting of the photocell slit is made by positioning the slit along the length of the light spot path to give a maximum output signal with no input to the oscillograph.

32.91. An observation of dynamic response angle is made by depressing the angle reference switch long enough for a given applied sinusoidal input to impress the angle reference line on the cathode-ray screen and then releasing the switch. When the switch is released, the circle appears with bright spots at positions corresponding to the instants when the photocell slit is illuminated by the passage of the oscillograph light spot. Zero dynamic response angle is indicated by the coincidence of the two bright spots on the input signal circle with the two ends of the angle reference line. When the slit adjustment for this condition is completed, the apparatus is ready for taking dynamic response angle data.

32.92. The procedure for measuring the dynamic response angle at a given frequency involves the following steps:

1) Set the frequency adjustment knob to the given frequency.
2) Depress the angle reference switch to place the angle reference line on the cathode-ray tube.
3) Release the angle reference switch.

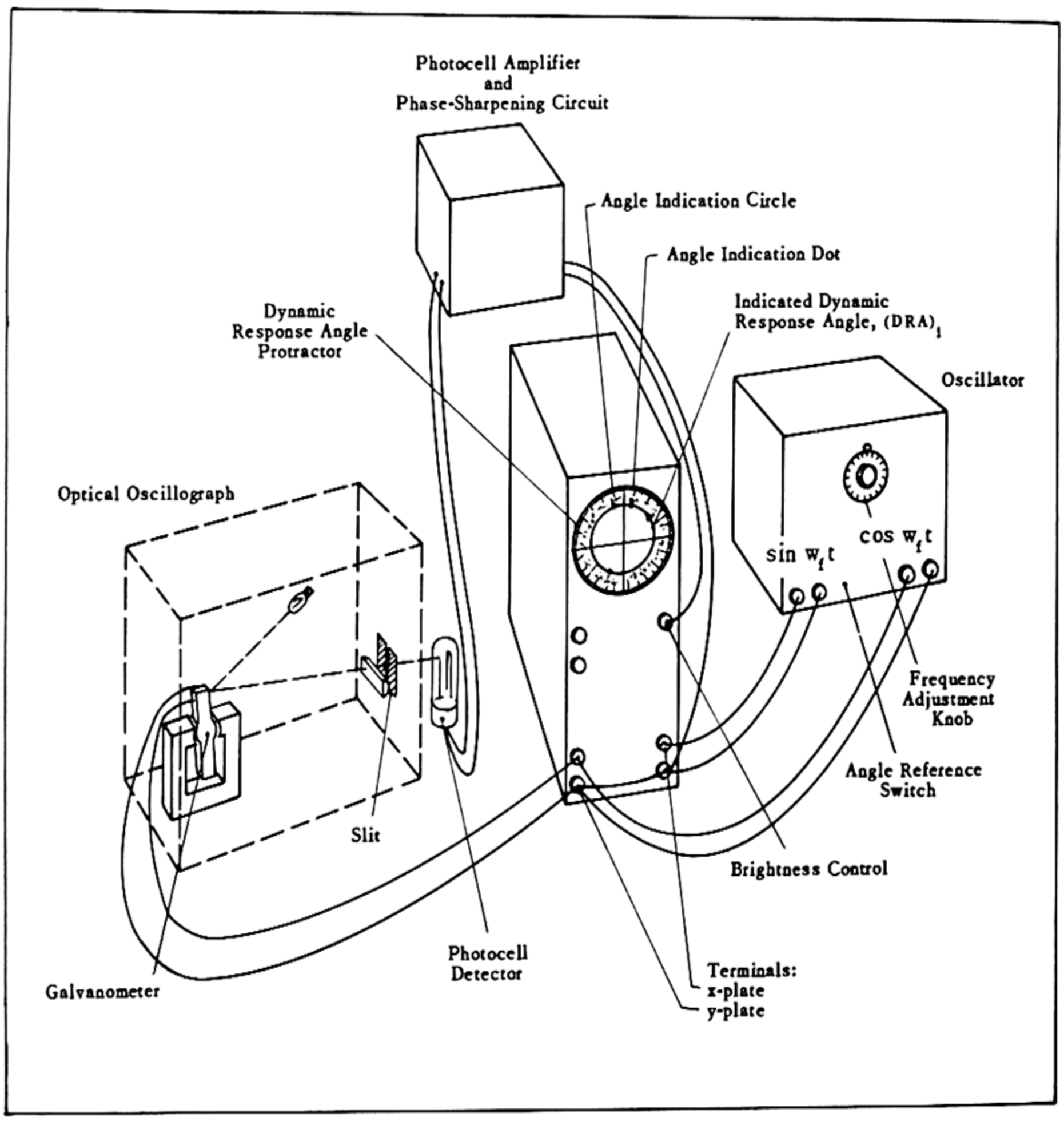


Fig. 32-33. Arrangement for determining dynamic response angle of oscillograph.
(Photocell detects null position of light beam.)

4) Use the dynamic response angle protractor to measure the angle between the ends of the angle reference line and the bright spots corresponding to the instants of zero oscillograph light spot deflection.
5) Record the angle measured in step 4 as the dynamic response angle for the frequency setting of step 1.

32.93. The dynamic response angle curves of Figs. 32-17, 32-18 and 32-21 show that the dynamic response angle associated with the steady-state sinusoidal response of systems having (0;0,1,2) performance equations is -90 degrees when the applied frequency is identical with the undamped natural frequency of the system (i.e., when the frequency ratio is unity). This fact makes it simple to determine the reference frequency for the frequency ratio as the first step in measuring the performance characteristics for an operating system by the steady-state

sinusoidal response method. The procedure is to vary the input frequency and observe the corresponding dynamic response angle until this angle becomes -90 degrees. The frequency at which this angle occurs corresponds to unity frequency ratio and is the undamped natural frequency if the instrument under test behaves as a (0;0,1,2) system.

32.94. Data Summary 32-1 lists the dynamic response angle results of a steady-state sinusoidal input test of the indicating performance for an optical oscillograph. This test was carried out with the arrangement of Fig. 32-33. The frequency giving -90 degrees as the dynamic response angle was 42 cycles per second. The corresponding frequency ratio was taken as unity, and tests were run at frequencies corresponding to frequency ratio values from 0.1 to 2.0, with intervals at the one-tenth points. Beyond the frequency ratio of 2.0, points were taken at 2.5, 3.0 and 3.5. To illustrate the effect of damping, one frequency analysis run was made with a damping shunt resistance identical with that used in making the step function record of Fig. 32-31 (i.e., $R_{(sh)}$ = 1000 ohms), and a second run was made with the damping shunt resistance used in taking the step function record of Fig. 32-32 (i.e., $R_{(sh)}$ = 120 ohms).

32.95. The data listed in Data Summary 32-1 are plotted as identified points in Fig. 32-34. Theoretical curves for the sinusoidal response of (0;0,1,2) systems with damping ratios of 0.155 and 1.0 are given in Fig. 32-34 for comparison purposes. The experimental dynamic response angle points do not fall perfectly on the theoretical curves, but the agreement is generally close enough to show that the oscillograph under test behaved as a (0;0,1,2) system with both values of the shunt damping resistance. The points taken with the higher damping shunt resistance are close enough to the 0.155 damping ratio curve to show that the frequency analysis result is in substantial agreement with the step-function-determined damping ratio value of Data Analysis Summary 32-1. Similarly, the points for the lower damping shunt frequency analysis run are effectively identical with the theoretical unity damping ratio curve and thus give a result identical with that of Data Analysis Summary 32-2 for the step function test record of Fig. 32-32.

32.96. In addition to the variation of dynamic response angle with frequency, the over-all sensitivity of any measuring instrument also changes with the forcing frequency. Because the quasi-static sensitivity of any properly calibrated measuring instrument is unity, it follows that the ratio of actual sensitivity at any frequency to the quasi-static frequency sensitivity as the reference sensitivity is just the actual sensitivity itself. In taking frequency analysis data, either scale readings or indications in any convenient units will give identical results. This follows from the sensitivity definitions, i.e.,

$$\text{Over-all sensitivity of measuring instrument} = S_{(mi)[q_{(in)};q_s]} = \frac{q_{(s)a}}{q_{(in)a}} \qquad (32\text{-}6)$$

Frequency Ratio FR or $n_f/n_{(ref)}$ $\left[n_{(ref)} = n_{(DRA=90°)} = 42 \text{ cps}\right]$	Forcing Frequency n_f (cycles per second)	Dynamic Response Angle for $R_{(sh)} = 1000$ ohms $(DRA)_{(R_{(sh)}=1000)}$ (degrees)	Dynamic Response Angle for $R_{(sh)} = 120$ ohms $(DRA)_{(R_{(sh)}=120)}$ (degrees)
0.1	4.2	−3.0	−11.0
0.2	8.4	−5.0	−24.0
0.3	12.6	−9.0	−34.0
0.4	16.8	−10.0	−43.0
0.5	21.0	−14.0	−55.0
0.6	25.2	−16.0	−60.0
0.7	29.4	−24.0	−71.0
0.8	33.6	−31.0	−76.0
0.9	37.8	−55.0	−85.0
1.0	42.0	−90.0	−90.0
1.1	46.1	−121	−96.0
1.2	50.4	−141	−100
1.3	54.6	−150	−106
1.4	58.8	−156	−108
1.5	63.0	−161	−111
1.6	67.1	−164	−115
1.7	71.5	−166	−120
1.8	75.6	−167	−121
1.9	79.8	−168	−122
2.0	84.0	−169	−127
2.5	105	−172	−135
3.0	126	−174	−141
3.5	147	−177	−145

Heiland Optical Oscillograph, Type SE 404R-6, Serial No. 515; Galvanometer Type A-8668. Data taken 12/2/52 by S. Lees and G. Masters

Data Summary 32-1. Steady-state sinusoidal dynamic response angle for an optical oscillograph with two damping shunt resistances.

Quasi-static over-all sensitivity of measuring instrument $= S_{(mi)[q_{(in)};q_s](qs)} = 1$ (32-7)

so that

$$\frac{S_{(mi)[q_{(in)};q_s]}}{S_{(mi)[q_{(in)};q_s](qs)} = \frac{S_{(mi)[q_{(in)};q_s]}}{1}} \tag{32-8}$$

32.97. In general, the over-all sensitivity is the product of the indicator sensitivity and the scale sensitivity, i.e.,

$$\frac{S_{(mi)[q_{(in)};q_s]}}{S_{(mi)[q_{(in)};q_s](qs)}} = \frac{S_{(i)[q_{(in)};(Ind)]}S_{(s)[(Ind);q_s]}}{S_{(i)[q_{(in)};(Ind)](qs)}S_{(s)[(Ind);q_s]}} \tag{32-9}$$

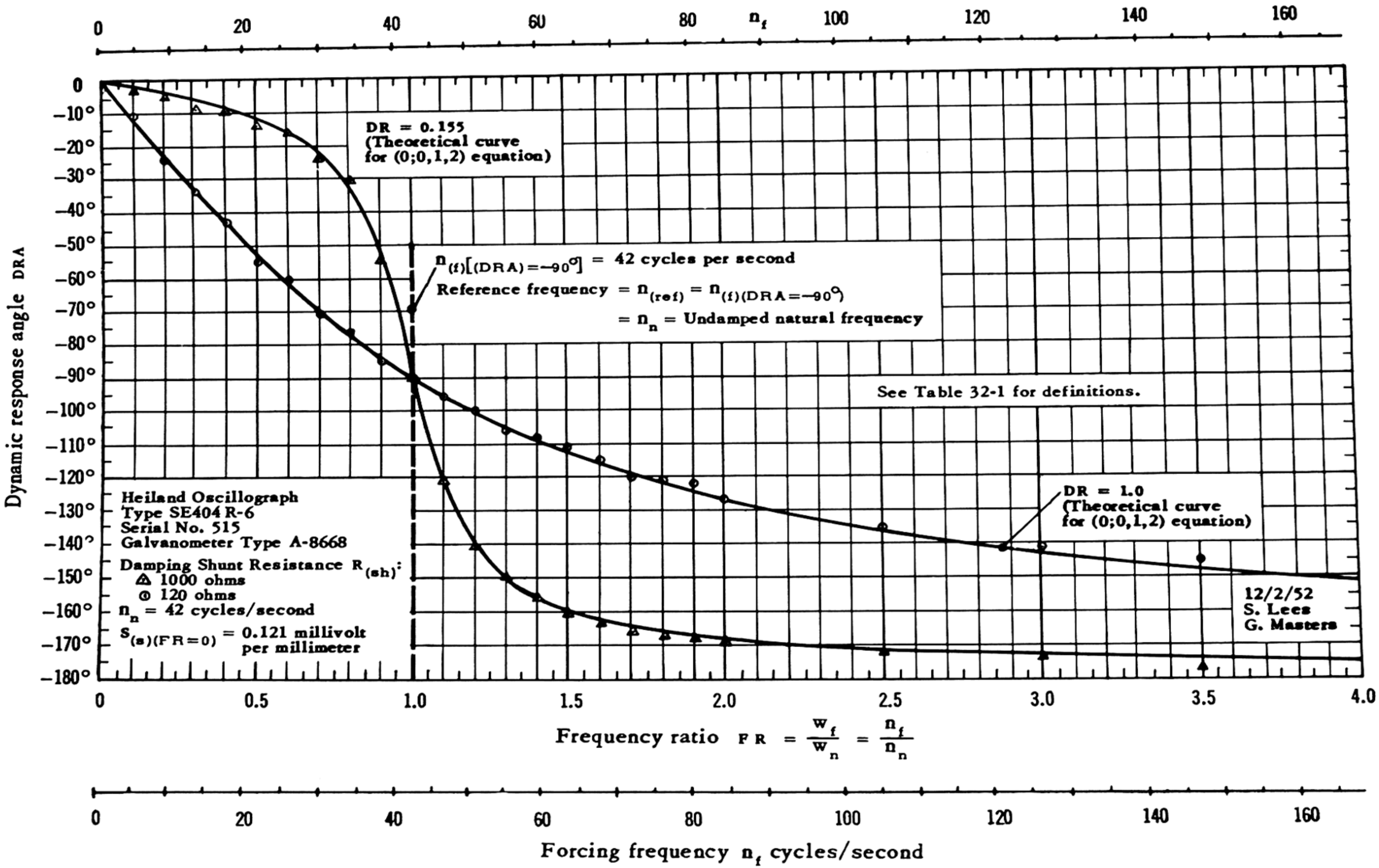


Fig. 32-34. Linear-scale experimental data plots of dynamic response angle as a function of frequency and frequency ratio for an optical oscillograph.

32.98. The scale sensitivity is not affected by dynamic actions, so that Eq. (32-9) may be combined with Eqs. (32-6) and (32-8) and written as

$$S_{(mi)[q_{(in)};q_s]} = \frac{S_{(i)[q_{(in)};(Ind)]}}{S_{(i)[q_{(in)};(Ind)](qs)}} = \frac{(Ind)_a \, q_{(in)(qs)a}}{q_{(in)a} \, (Ind)_{(qs)a}} \qquad (32\text{-}10)$$

where

$(Ind)_a$ = indication amplitude

$(Ind)_{(qs)a}$ = quasi-static indication amplitude

32.99. From Eq. (32-10), it follows that if in the experimental procedure the input amplitude, $q_{(in)a}$, for all forcing frequencies is held constant at the quasi-static level, i.e.,

$$q_{(in)a} = q_{(in)(qs)a} \qquad (32\text{-}11)$$

then

$$S_{(mi)[q_{(in)};q_s]} = \left[\frac{(Ind)_a}{(Ind)_{(qs)a}} \right]_{(q_{(in)a} = const)} \qquad (32\text{-}12)$$

32.100. Equation (32-12) is a generalized result that holds for any measuring instrument. When an optical oscillograph is considered with voltage as the scale reading,

$$S_{(mi)[q_{(in)};q_s]} \approx S_{(oo)[v;v]} \longrightarrow S_{(oo)} \qquad (32\text{-}13)$$

where

$S_{(oo)[v;v]}$ = over-all sensitivity for voltage-reading optical oscillograph

32.101. The frequency analysis data on sensitivity for an optical oscillograph like that illustrated in Fig. 32-30 may be taken by applying a constant input voltage amplitude and making an exposure with the film stationary at a new place for each test frequency. After development, the indication amplitude may be read from the photographic records as half of the line lengths of the individual records. Any convenient length unit may be used in making these measurements. The quasi-static indication amplitude required by Eq. (32-12) is found by making at least two records at the lowest possible frequencies. The quasi-static nature of the response is identified by the substantial equality of amplitudes for two frequencies, one of which is at least twice the other.

32.102. Sensitivity data for frequency analysis runs on the optical oscillograph used in the tests of Figs. 32-31, 32-32 and 32-34 are given in Data Summary 32-2 for frequency ratio points identical with those used for the dynamic response angle plots of Fig. 32-34. The quasi-static response amplitude is based on a frequency ratio of 0.024.

32.103. The over-all sensitivity values of Data Summary 32-2 are located as points in Fig. 32-35. Theoretical curves with damping ratios of 0.155 and 1.0 for (0;0,1,2) systems are also plotted. Inspection shows that the frequency response

Frequency Ratio FR or $n_f/n_{(ref)}$ $\left[n_{(ref)} = n_{(DRA=90^\circ)} = 42 \text{ cps}\right]$	Forcing Frequency n_f (cycles per second)	Damping Shunt Resistance $= R_{(sh)} = 1000$ ohms		Damping Shunt Resistance $= R_{(sh)} = 120$ ohms	
		Indication (inches)	Over-all Sensitivity $S_{(\infty)[v;v]}$ or $S_{(\infty)}$	Indication (inches)	Over-all Sensitivity $S_{(\infty)[v;v]}$ or $S_{(\infty)}$
0.024	1.0	1.15	1.00	0.44	1.00
0.10	4.2	1.13	0.98	0.44	1.00
0.20	8.4	1.10	0.96	0.48	1.09
0.30	12.6	1.05	0.91	0.51	1.16
0.40	16.8	0.95	0.83	0.52	1.18
0.50	21.0	0.90	0.78	0.58	1.32
0.60	25.2	0.82	0.71	0.65	1.48
0.70	29.4	0.75	0.65	0.81	1.84
0.80	33.6	0.68	0.59	1.03	2.34
0.90	37.8	0.62	0.54	1.32	3.00
1.00	42.0	0.57	0.50	1.40	3.18
1.10	46.2	0.51	0.44	1.04	2.36
1.20	50.4	0.46	0.40	0.74	1.68
1.30	54.6	0.42	0.36	0.53	1.20
1.40	58.8	0.38	0.33	0.41	0.93
1.50	63.0	0.35	0.30	0.33	0.75
1.60	67.1	0.32	0.28	0.27	0.61
1.70	71.5	0.29	0.25	0.22	0.50
1.80	75.6	0.27	0.23	0.19	0.43
1.90	79.8	0.25	0.22	0.16	0.36
2.00	84.0	0.23	0.20	0.15	0.34
2.50	105	0.16	0.14	0.08	0.18
3.00	126	0.11	0.10	0.06	0.14
3.50	147	0.09	0.08	0.04	0.09

Heiland Optical Oscillograph, Type SE 404R-6, Serial No. 515; Galvanometer Type A-8668. Data taken 12/2/52 by S. Lees and G. Masters

Data Summary 32-2. Steady-state sinusoidal indication sensitivity for an optical oscillograph with two damping shunt resistances.

sensitivity points are consistent with the step function and dynamic response angle results and show that the high and low shunt damping resistors gave damping ratios of about 0.16 and 1.0, respectively.

32.104. The procedure of taking data for a range of frequency ratios like those illustrated in Figs. 32-34 and 32-35 may be reduced to a single frequency adjustment and a single sensitivity measurment when it is known that the instrument under test behaves as a (0;0,1,2) system and when either the quasi-static over-all

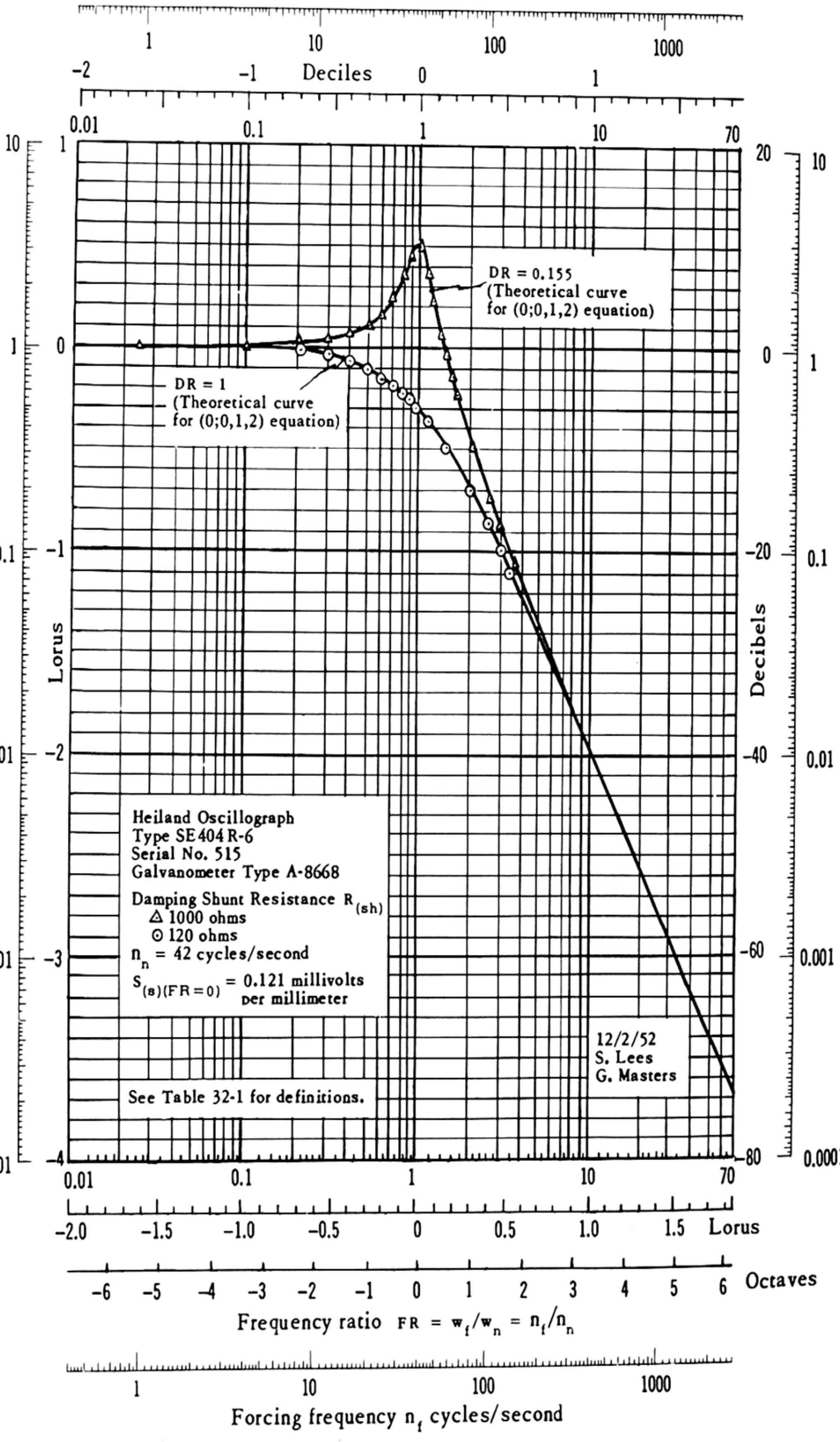


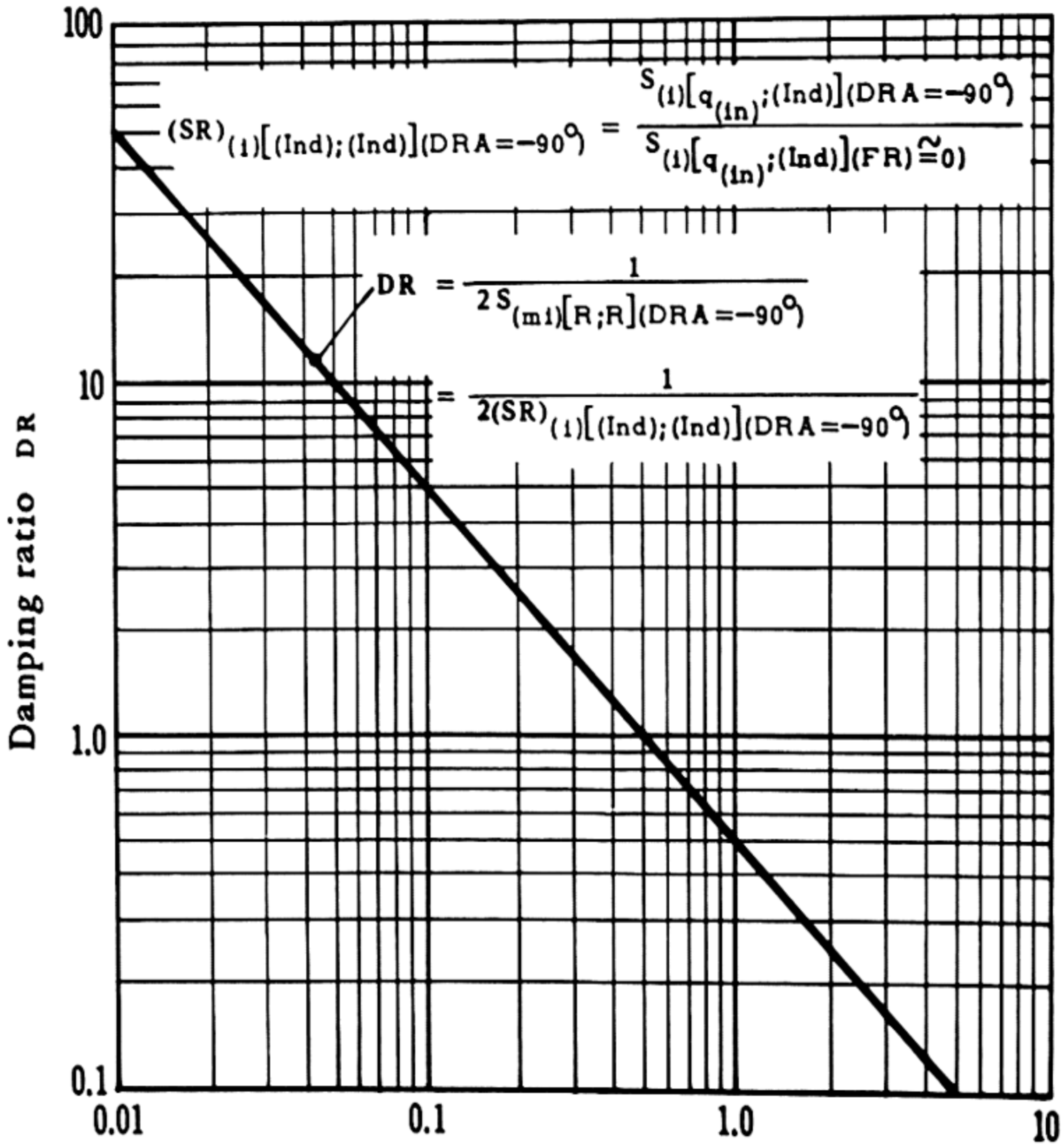
Fig. 32-35. Logarithmic-scale plots of experimental data on variation of an optical oscillograph indicator sensitivity with frequency for steady-state sinusoidal input variation.

sensitivity or indication sensitivity is available. Under these circumstances, the damping ratio may be determined by the following procedure:

1) Vary the forcing frequency to find the point at which the dynamic response angle becomes equal to -90 degrees. This determines the undamped natural frequency of the instrument under test and establishes the point at which the frequency ratio is equal to unity.
2) Measure the indication or scale reading amplitude for the frequency of step 1 and compute the corresponding sensitivity.* The damping ratio is given by the relationship (refer to Table 32-1)

$$\text{Damping ratio} = DR = \frac{1}{2S_{(m1)[R;R](DRA=-90^\circ)}} = \frac{1}{2S_{(1)[q_{(in)};(Ind)](DRA=-90^\circ)}} \qquad (32\text{-}14)$$

For convenience, this relationship is plotted in Fig. 32-36.



Over-all sensitivity at $DRA = -90^\circ$ $S_{(m1)[R;R](DRA=-90^\circ)}$
or
Indication sensitivity ratio at $DRA = -90^\circ$

Fig. 32-36. Relationship between damping ratio and sensitivity at dynamic response angle $= -90^\circ$ for instruments with (0;0,1,2) performance equations.

---

* It is worth while to note that the procedure for determining performance parameters may be applied to (0;0,1,2) systems of any type when sensitivity is replaced by dynamic amplitude ratio.

MEASUREMENT OF INSTRUMENT PERFORMANCE PARAMETERS BY STROBOSCOPIC OBSERVATIONS

32.105. Photographic methods must be used to take response data on instruments designed for visual observations when rapid changes must be recorded. Response variations may be photographed by a motion-picture camera supplemented by a system to give timing information on the film. It is also possible to use a light flashing at accurately-timed intervals to make stroboscopic exposures for a conventional still camera. In general, the choice between the motion-picture method and the stroboscopic-light method depends on the availability of equipment and the nature of the variations to be recorded rather than on any basic limitation of either method.

32.106. Figure 32-37 illustrates the essential components of an arrangement to make stroboscopic records* of the response of a conventional voltmeter. A commercial high-intensity stroboscopic light illuminates the meter, which is photographed by a still camera with open shutter. A sine-function potentiometer, mounted on the output shaft of a variable-speed motor is used to produce a sinusoidal voltage input for the meter. The motor is also fitted with a cam-actuated microswitch to synchronize the light flashes with the step function input change.

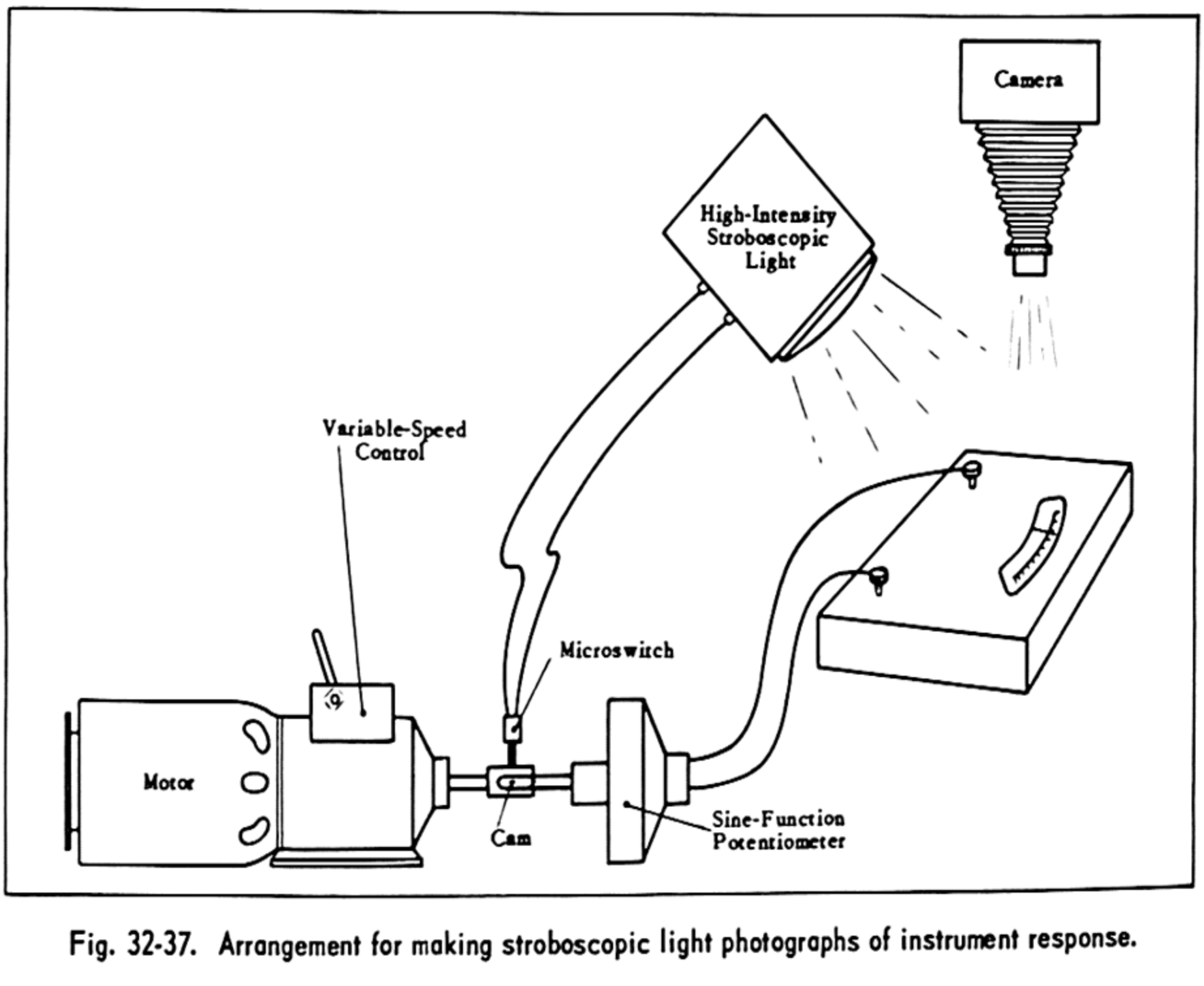
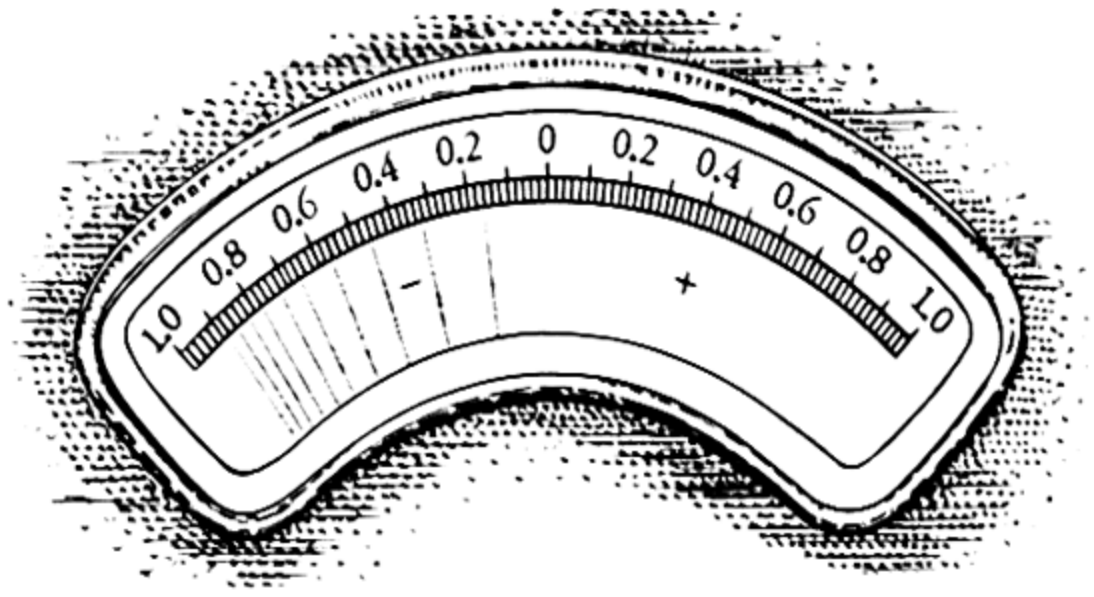


Fig. 32-37. Arrangement for making stroboscopic light photographs of instrument response.

---

* The arrangement shown in the figure was developed by Asst. Prof. J. E. Forbes of the Massachusetts Institute of Technology.



Time t (seconds)	Scale Reading R_s Voltage Reading VR (volts)	Voltage Reading Difference (D)VR = VRD $= VR - (VR)_{(t=\infty)}$ (volts)	Voltage Reading Difference Ratio VRDR $= \frac{VR - (VR)_{(t=\infty)}}{(VR)_{(t=0)} - (VR)_{(t=\infty)}}$
0	0	1.000	1.0
0.625	−0.162	0.838	0.83
1.250	−0.325	0.675	0.675
1.875	−0.457	0.543	0.543
2.500	−0.565	0.430	0.430
3.125	−0.655	0.345	0.345
3.750	−0.722	0.278	0.278
4.375	−0.779	0.221	0.221
5.000	−0.821	0.179	0.179
5.625	−0.858	0.142	0.142
6.250	−0.883	0.117	0.117
.	.	.	.
.	.	.	.
.	.	.	.
∞	−1.000	0	0
Data taken 8/11/52 by J. E. Forbes			

Fig. 32-38. Drawing of a stroboscopic light photograph and data summary for step function response of special heavily damped voltmeter X-1.

32.107. Figure 32-38 gives a typical stroboscopic-light photograph showing the index positions at successive equal time intervals of 0.625 second after the occurrence of the step function, and includes a summary of data read from the photograph. At the initial instant, the scale reading was zero, and a voltage input step of -1.0 volt was applied. The data summary of Fig. 32-38 lists the voltage difference for each instant corresponding to one of the stroboscopically recorded index positions. This difference is found by subtracting the final reading of -1.0 volt from the actual reading. The voltage reading difference ratio is the ratio of the voltage reading difference to the difference between the initial and final voltage readings.

32.108. The data of Fig. 32-38 are plotted on semilogarithmic coordinates in Fig. 32-39. This plot shows that the step function response data fall close to a straight line except for the initial point. This result is characteristic of a heavily damped aperiodic transient from a (0; 0,1,2) system that may be interpreted by the procedure described in the bottom row of Table 32-2. The slope of the straight-line portion of the response record of Fig. 32-39 is determined by the larger high damping ratio characteristic time. This characteristic time is determined by the time interval required for the straight line to fall from its intercept on the ordinate scale to a level equal to 1/e of the intercept value. In Fig. 32-39, the larger high damping ratio characteristic time found by this procedure is 2.83 seconds. The high damping ratio characteristic time ratio found from the proper equation in the bottom row of Table 32-2 for the plot of Fig. 32-39 is 26. The smaller high damping ratio characteristic time is found by dividing the larger characteristic time by the characteristic time ratio. The value found by this procedure is 0.109 second.

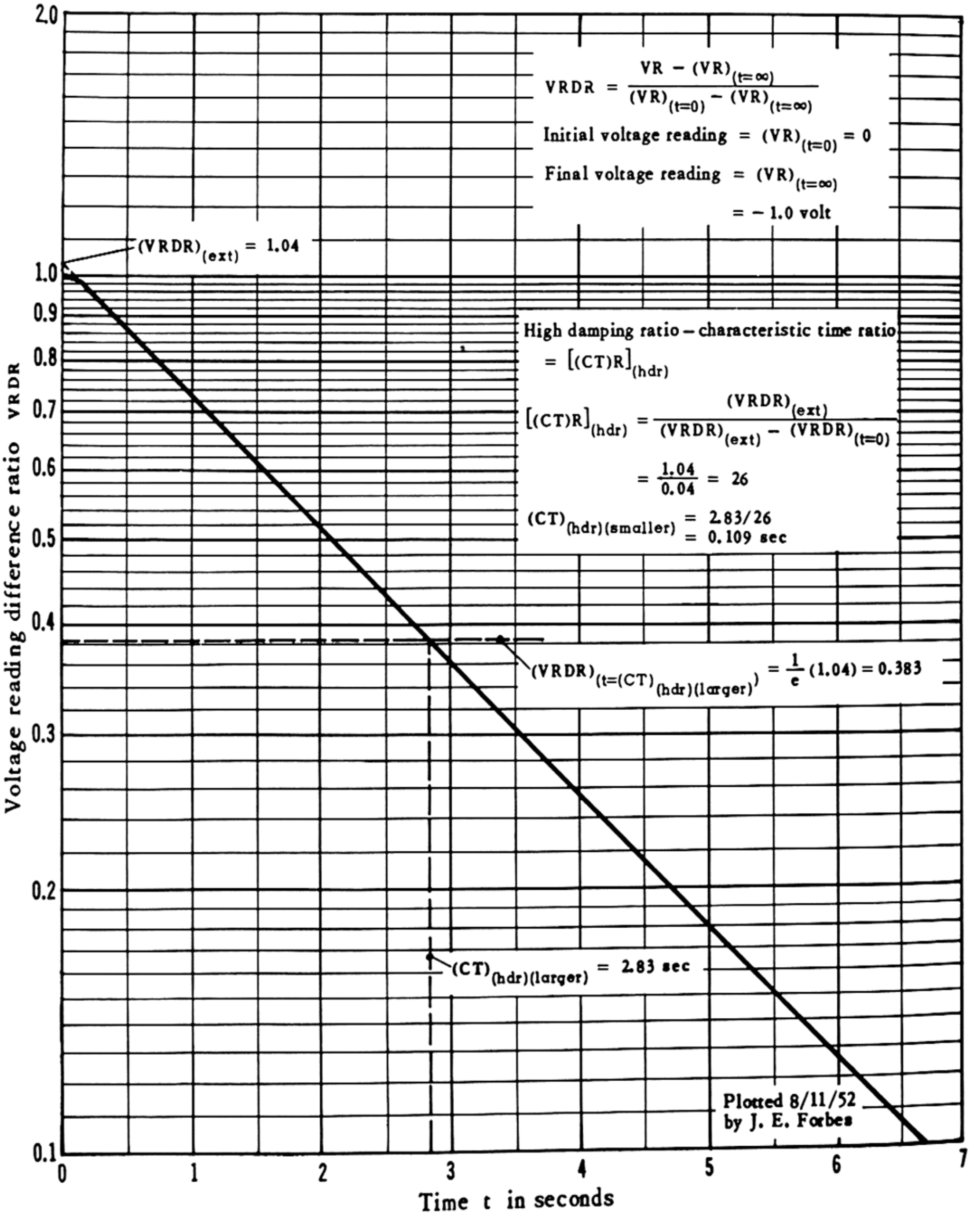


Fig. 32-39. Semilogarithmic plot of step function response of special heavily damped voltmeter X-1.

PULSE TESTING

32.109. Another method for evaluating the performance parameters of an operating system may be described as pulse testing. In this method, the input quantity to the system is disturbed from a stationary reference value and then restored to this value after going through a defined variation. The response of the system to this input is then examined for information concerning the performance parameters.

32.110. An introductory description of pulse functions as well as impulse functions is given in Definition Summary 12-7 of Chapter 12. Chapter 17 shows how to relate the response of a system to an arbitrary input with zero initial conditions by means of the known response of the system to a unit impulse function input. In Chapter 25, a general method is presented by which the performance function of a given system may be determined from its response to a known pulse function. The method of Chapter 25 is to convert the input and output time histories into equivalent frequency distributions by means of numerical Fourier transformations. The performance function is found as the ratio of the output frequency distribution to the input frequency distribution.

32.111. Generally, pulse functions have been associated with the rectangular shape defined in previous chapters as the rectangular pulse function. As indicated in Chapter 25, other pulse shapes are frequently employed. The theoretical advantages of rectangular pulse functions are the ease of mathematical treatment and the simplicity of generating such forcing functions. In practice, however, it is not a simple matter to generate a true rectangular pulse function since discontinuous changes of the manipulated quantity are required. Furthermore, the system performance for discontinuous inputs large enough to produce a usable output is often quite different from the performance for continuous inputs. For example, limit conditions are often reached if the input changes too rapidly. When electrical components reach such limits, they are said to saturate.

32.112. It is suggested in Chapter 25 that the input pulse have the shape described as the displaced cosine pulse. Such pulses are generated by a function that is equal to one minus the cosine for the duration of the pulse and zero elsewhere. The argument of the cosine is 2π multiplied by the ratio of time to pulse duration. Displaced cosine pulse functions and their first time derivatives are continuous. Discontinuities exist in the second and higher time derivatives.

RECTANGULAR PULSE FUNCTIONS

32.113. Rectangular pulse functions are introduced in Derivation Summary 12-7. Additional properties and applications of these functions are given in Chapters 12, 16, 17 and 25. A rectangular pulse function is one that changes discontinuously from one value to another at the beginning of the pulse. For the

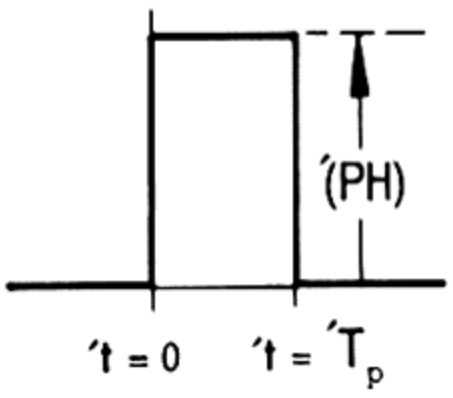
duration of the pulse, the function is constant until it discontinuously returns to its initial value. Figure 16-1 shows how a rectangular pulse function may be constructed from an increasing step function beginning at time t_1 followed by a decreasing step function at time t_2. A typical rectangular pulse function is shown in the figure of Derivation Summary 32-2. It is important to recognize that the pulse function defined by Eq. (1) of the summary begins at zero time. This property affects the expression for the Fourier transform of rectangular pulse functions that is developed in the summary. Rectangular pulse functions may be defined that begin at a different instant from zero time. However, when a rectangular pulse function input is applied to a system, and the system response is to be related to the specified input, it is convenient from practical considerations to have the input begin at the initial instant. An additional property of pulse functions is the pulse strength, which is defined as the area of the pulse. The strength of a rectangular pulse function is equal to the pulse height times the pulse duration.

32.114. With these considerations taken into account, the Fourier transform for rectangular pulse functions is developed in Derivation Summary 32-2. The expressions of Eqs. (5), (6), (8) and (9) show how to represent this type of function in terms of a continuous frequency distribution. A useful form of the frequency function is given by Eq. (6). It is seen to be the product of three quantities. The first factor is the pulse height. The second is the sine function divided by its argument. The third factor is an imaginary exponential function with its exponent equal to the negative argument of the second factor. The argument of the second and third factors is π times the frequency ratio multiplied by the nondimensional pulse duration.

32.115. From the definitions given in Derivation Summary 12-1, the continuous frequency distribution may be represented by an amplitude ratio distribution and a phase angle distribution. The amplitude ratio distribution is equal to the magnitude of Eq. (6) of Derivation Summary 32-2 divided by a reference amplitude. For convenience, this reference amplitude is taken as the nondimensional pulse height. Since the sine function divided by its argument appears frequently in Fourier transformations, it has been given numerically in Table 25-1 of Chapter 25. The function is plotted in Fig. 25-1, where it is seen to be alternately positive and negative. The amplitude ratio function associated with rectangular pulse functions is equal to the magnitude of the sine function divided by its argument as given by Eq. (8) of Derivation Summary 32-2. A plot of the magnitude function is shown in Fig. 32-40.

32.116. The phase angle distribution is equal to the sum of two quantities according to Eq. (6) of Derivation Summary 32-2. The first quantity is the phase angle of the sine function divided by its argument. The second is the exponent of the imaginary exponential factor. The expression for the phase angle function is given by

Rectangular pulse functions are defined in Derivation Summary 25-4 of Chapter 25. Let $q_{(in)}(\acute{t})$ be a nondimensional rectangular pulse function, $\acute{}$(rpf).



$$\left.\begin{aligned} q_{(in)} &= 0 \quad ; \quad \acute{t} < 0 \\ q_{(in)} &= \acute{}(PH) \quad ; \quad 0 \leqq \acute{t} \leqq \acute{T}_p \\ q_{(in)} &= 0 \quad ; \quad \acute{T}_p < \acute{t} \end{aligned}\right\} \qquad (1)$$

where

$\acute{}(PH)$ = nondimensional pulse height

$\acute{T}_p = \dfrac{T_p}{T_{(ref)}}$ = nondimensional pulse duration

$\acute{t} = \dfrac{t}{T_{(ref)}}$ = nondimensional time

$T_{(ref)}$ = reference period

The strength of the pulse is equal to the pulse height times the pulse duration; i.e.,

$$RPFS = \acute{}(PH)\,\acute{T}_p = \text{rectangular pulse function strength} \qquad (2)$$

From Eq. (1) of Derivation Summary 25-1, the nondimensional Fourier transform for the expression of Eq. (1) above is given by an integral relationship. This may be written as

$$[FT]\,q_{(in)}(\acute{t}) = q_{(in)}(\beta) = \int_{-\infty}^{\infty} q_{(in)}\,\epsilon^{-j2\pi\beta(\acute{t})}\,d(\acute{t}) = \int_{0}^{\acute{T}_p} \acute{}(PH)\,\epsilon^{-j2\pi\beta(\acute{t})}\,d(\acute{t}) \qquad (3),(4)$$

$$= \frac{\acute{}(PH)}{j2\pi\beta}\left[1 - \epsilon^{-j2\pi\beta\,\acute{T}_p}\right] = \acute{}(PH)\frac{\sin \pi\beta\,\acute{T}_p}{\pi\beta\,\acute{T}_p}\,\epsilon^{-j\pi\beta\,\acute{T}_p} \qquad (5),(6)$$

where

$$\beta = \frac{n_f}{n_{(ref)}} = \frac{T_{(ref)}}{T_f} \qquad (7)$$

Define the reference amplitude as the pulse height, $\acute{}(PH)$. From Derivation Summary 12-1, the amplitude ratio function is

$$(AR)_{(rpf)} = \left|\frac{\sin \pi\beta\,\acute{T}_p}{\pi\beta\,\acute{T}_p}\right| \quad \text{when } A_{(rpf)(ref)} = \acute{}(PH) \qquad (8)$$

The phase angle function is

$$(PA)_{(rpf)} = -\pi\beta\,\acute{T}_p + n\pi \quad \text{for } n < \beta\,\acute{T}_p < n + 1 \quad ; \quad :n = 0, 1, 2, \ldots \qquad (9)$$

The phase angle is discontinuous for integral values of the argument, $\beta\,\acute{T}_p$.

Derivation Summary 32-2. Fourier transform for rectangular pulse functions.

Eq. (9). It is plotted as the dashed line curve in Fig. 32-40. The phase angle function is discontinuous for integral values of the frequency ratio – pulse duration product because of the alternations in the sense of the sine function. The phase angle function is different from zero because the rectangular pulse function is not symmetrical with respect to zero time.

DISPLACED COSINE PULSE FUNCTIONS

32.117. Displaced cosine pulse functions represent a type of input that, unlike rectangular pulse functions, are continuous and have continuous first derivatives. A discussion of these functions is given in Chapter 25. The definition of a typical displaced cosine pulse function in nondimensional terms is given by Eq. (1) of Derivation Summary 32-3, and is illustrated in the accompanying figure. The

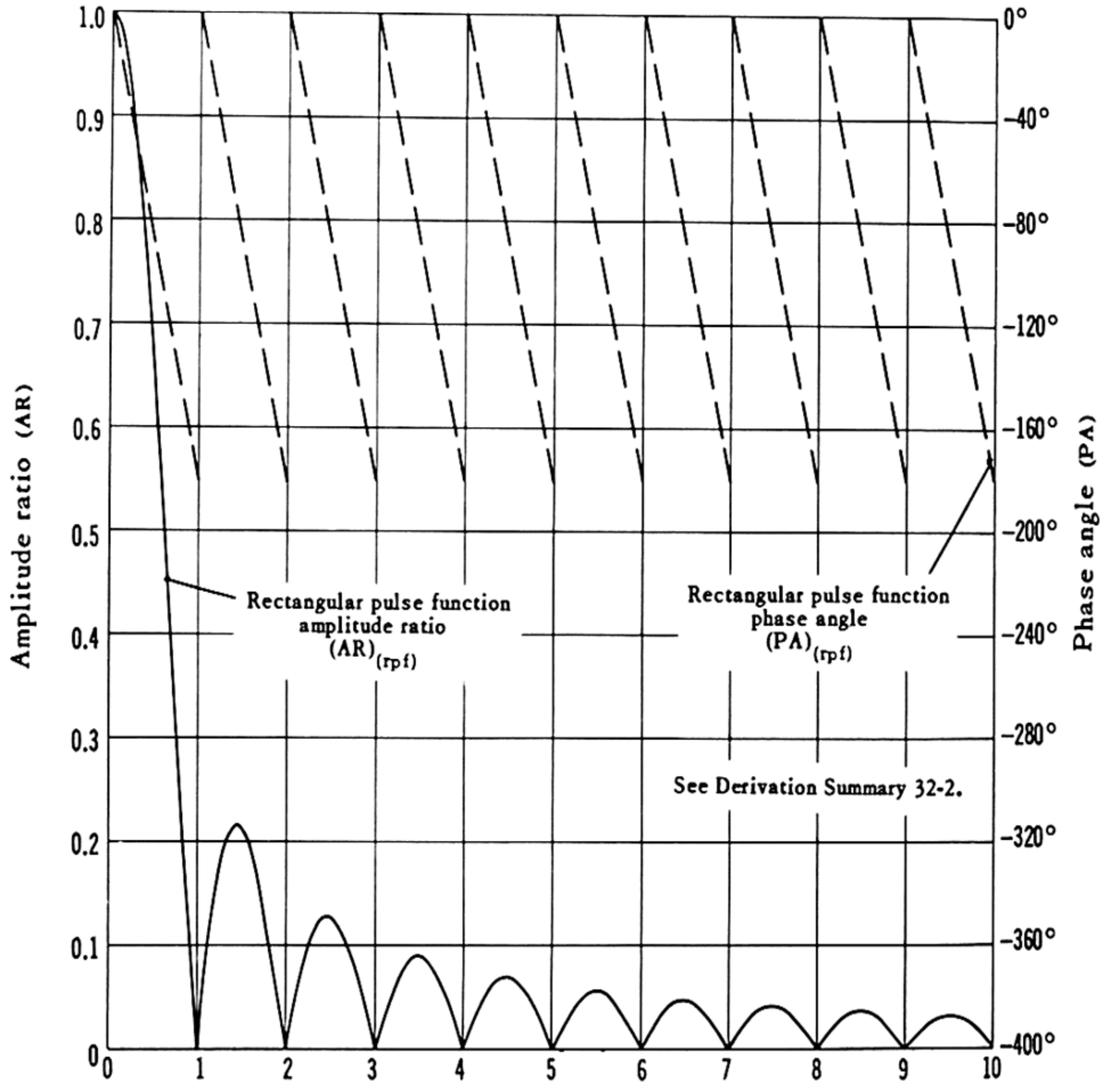
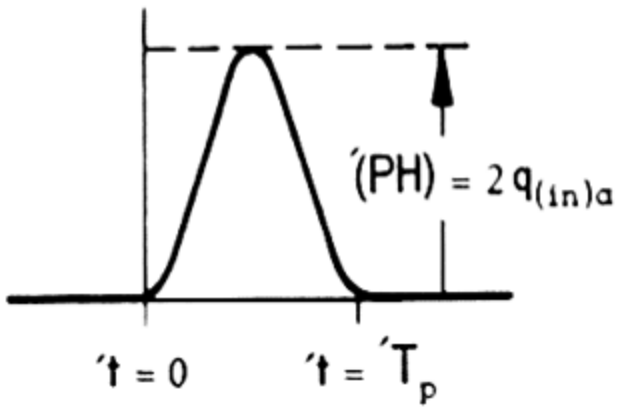


Fig. 32-40. Fourier transform of a rectangular pulse function.

pulse is different from zero only during a finite interval defined as the pulse duration. During this interval, it takes the form of an amplitude multiplied by one minus a cosine function. Again, as for the rectangular pulse function just discussed, the displaced cosine pulse function defined in Derivation Summary 32-3 begins at zero time. This affects the phase angle function of its Fourier transform. The pulse strength is equal to one-half of the pulse height multipled by the pulse duration.

32.118. The continuous frequency distribution associated with the displaced cosine pulse function is found from the Fourier transformation carried out in Derivation Summary 32-3. An appropriate form for this expression is shown as Eq. (7). It may be seen that this is one-half the product of the Fourier transform for the rectangular pulse function and a (0;0,1,2) frequency function with damping

Displaced cosine pulse functions are defined in Derivation Summary 25-5 of Chapter 25. Let $q_{(in)}(\acute{t})$ be a nondimensional displaced cosine pulse function, $\acute{}$(dcpf).



$$\left.\begin{aligned} q_{(in)} &= 0 \quad ; \quad \acute{t} < 0 \\ q_{(in)} &= \frac{\acute{}(PH)}{2}\left(1 - \cos 2\pi \frac{\acute{t}}{\acute{T}_p}\right) ; \quad 0 \leqq \acute{t} \leqq \acute{T}_p \\ q_{(in)} &= 0 \quad ; \quad \acute{T}_p < \acute{t} \end{aligned}\right\} \quad (1)$$

where

$\acute{}(PH)$ = nondimensional pulse height

$q_{(in)(a)}$ = pulse amplitude

$\acute{T}_p = \dfrac{T_p}{T_{(ref)}}$ = nondimensional pulse duration

$\acute{t} = \dfrac{t}{T_{(ref)}}$ = nondimensional time

$T_{(ref)}$ = reference period

The strength of the pulse is equal to one-half the pulse height times the pulse duration; i.e.,

$$DCPFS = \frac{1}{2}\,\acute{}(PH)\,\acute{T}_p = \text{displaced cosine pulse function strength} \quad (2)$$

From Eq. (1) of Derivation Summary 25-1, the nondimensional Fourier transform of the displaced cosine pulse function is obtained from the following integral:

$$[FT]\,q_{(in)}(\acute{t}) = q_{(in)}(\beta) = \int_{-\infty}^{\infty} q_{(in)} \epsilon^{-j2\pi\beta(\acute{t})}\, d(\acute{t}) = \int_{0}^{\acute{T}_p} \frac{\acute{}(PH)}{2}\left(1 - \cos 2\pi \frac{\acute{t}}{\acute{T}_p}\right)\epsilon^{-j2\pi\beta(\acute{t})}\, d(\acute{t}) \quad (3),(4)$$

$$= \frac{\acute{}(PH)}{2}\left[1 - \epsilon^{-j2\pi\beta\,\acute{T}_p}\right]\left[\frac{1}{j2\pi\beta} - \frac{j2\pi\beta}{\left(\frac{2\pi}{\acute{T}_p}\right)^2 - (2\pi\beta)^2}\right] \quad (5)$$

$$= \frac{1}{2}\,\frac{\acute{}(PH)}{j2\pi\beta}\left[1 - \epsilon^{-j2\pi\beta\,\acute{T}_p}\right]\,\frac{\frac{1}{\acute{T}_p^2}}{\left(\frac{1}{\acute{T}_p}\right)^2 - \beta^2} \quad (6)$$

$$= \frac{\acute{}(PH)}{2}\,\frac{\sin \pi\beta\,\acute{T}_p}{\pi\beta\,\acute{T}_p}\,\epsilon^{-j\pi\beta\,\acute{T}_p}\,\frac{1}{1 + (j\beta\,\acute{T}_p)^2} \quad (7)$$

where

$$\beta = \frac{n_f}{n_{(ref)}} = \frac{T_{(ref)}}{T_f} \quad (8)$$

Define the reference amplitude as $\acute{}(PH)/2$. From Derivation Summary 12-1, the amplitude ratio function is

$$(AR)_{(dcpf)} = \left|\frac{\sin \pi\beta\,\acute{T}_p}{\pi\beta\,\acute{T}_p}\right|\left|\frac{1}{1 - (\beta\,\acute{T}_p)^2}\right| = \left|\frac{1}{1 - (\beta\,\acute{T}_p)^2}\right|(AR)_{(rpf)} \quad (9)$$

where $(AR)_{(rpf)}$ is given by Eq. (8) of Derivation Summary 32-2. The phase angle function is

$$(PA)_{(dcpf)} = -\pi\beta\,\acute{T}_p \quad \text{for } 0 < \beta\,\acute{T}_p < 2$$

$$= -\pi\beta\,\acute{T}_p + (n+1)\pi \quad \text{for } n < \beta\,\acute{T}_p < n+1 \quad \text{for } n > 2 \quad ; \quad n = 2, 3, 4, \ldots \quad (10)$$

The phase angle function is discontinuous for integral values of the argument, $\beta\,\acute{T}_p$, greater than 2.

Derivation Summary 32-3. Fourier transform for displaced cosine pulse functions.

ratio equal to zero. By defining the reference amplitude as equal to one-half the pulse height, the amplitude ratio function is given by Eq. (9) of the summary. This function is equal to the product of the rectangular pulse function amplitude ratio and the magnitude of zero-damping-ratio (0;0, 1, 2) frequency function. A plot of the amplitude ratio function is given by the solid-line curve of Fig. 32-41. A comparison with the corresponding curve of Fig. 32-40 is helpful. The major difference is that the displaced cosine pulse function amplitude ratio goes to zero more quickly than the rectangular pulse function amplitude ratio. For $\beta' T_p$ equal to 9.5, the rectangular pulse function amplitude ratio is still 3 percent of the initial amplitude ratio. The displaced cosine pulse function amplitude ratio is essentially zero for all values of the running variable greater than 4. Almost all of the displaced cosine pulse function harmonic content occurs for values of the running variable less than 2. Another detail is that the rectangular pulse function amplitude ratio is zero for $\beta' T_p$ equal to unity, but the displaced cosine pulse function is 0.5. The displaced cosine pulse function emphasizes the effect of the lower frequencies more than the rectangular pulse function does.

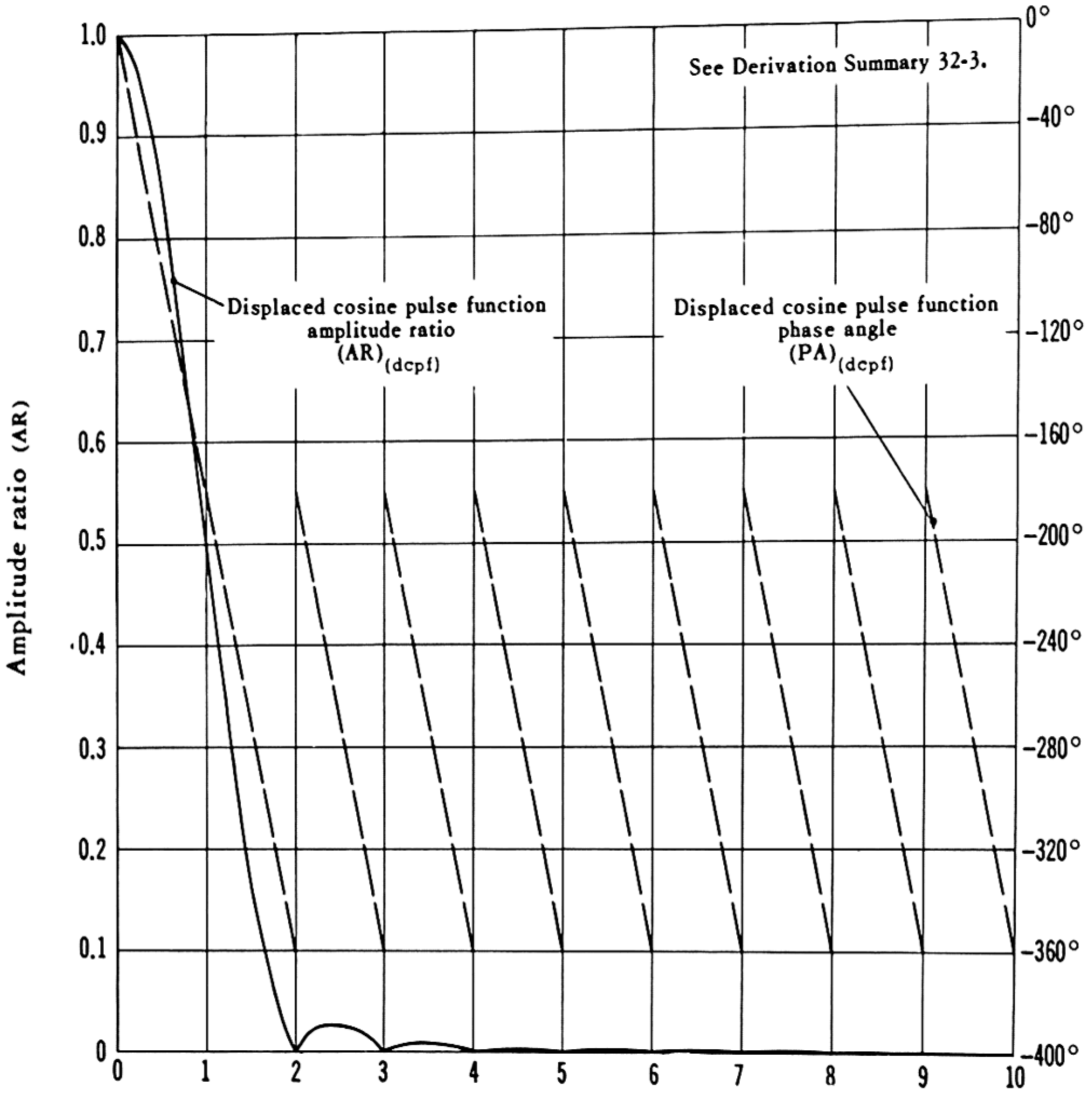
32.119. The phase angle function is given by the expression of Eq. (10) of Derivation Summary 32-3. This is a discontinuous function because of the change in the sense of the sine function in Eq. (7) for integral values of π. The dashed-line plot representing the phase angle function in Fig. 32-41 is seen to be a straight line with negative slope as $\beta' T_p$ goes from 0 to 2. It attains a minimum value of −360 degrees before it returns to −180 degrees. Thereafter it varies cyclically from −180 to −360 degrees between integral values of the running variable. The difference between phase angle functions of the two types of pulse functions may be noted by comparing Figs. 32-40 and 32-41.

EVALUATION OF PERFORMANCE FUNCTIONS FROM PULSE FUNCTION RESPONSES

32.120. A general method is presented in Chapter 25 for determining the performance function of a system from its response to a known pulse forcing function. The basis for the method may be derived from Eq. (32-5), given earlier in this chapter. By rearranging the terms of that equation, it is found that

$$[\text{PERFORMANCE FUNCTION}] = \frac{(\text{RESPONSE FUNCTION})}{(\text{FORCING FUNCTION})} \qquad (32\text{-}15)$$

32.121. A practical procedure for using Eq. (32-15) is to apply a displaced cosine pulse forcing function input to a system and record the response time history. When both the forcing function and the response function are reduced to continuous frequency distributions, the performance function may be deduced from Eq. (32-15). The displaced cosine pulse function frequency distribution is obtained from Derivation Summary 32-3 and Fig. 32-41. The response function frequency distribution is obtained by numerical Fourier transformation, using the methods



Frequency ratio – pulse duration product $(FR)(PD) \approx \beta' T_p$

Fig. 32-41. Fourier transform of a displaced cosine pulse function.

of Chapter 25. A linear differential equation with constant coefficients may be approximated by use of the profile templates described in Chapter 24.

RESPONSE FUNCTIONS OF (0;0,1,2) MEASURING INSTRUMENTS

32.122. When the performance of a particular measuring instrument may be associated with a (0;0, 1, 2) performance equation, it is possible to dispense with Fourier transformations in evaluating performance parameters from pulse function inputs. The background theory for this procedure is developed at the end of Chapter 25. The method makes use of simultaneous measurements of the input forcing function and the response.

32.123. A subfigure in each of Figs. 32-42, 32-43 and 32-44 shows a typical displaced cosine pulse forcing function as a dashed-line curve. A typical response

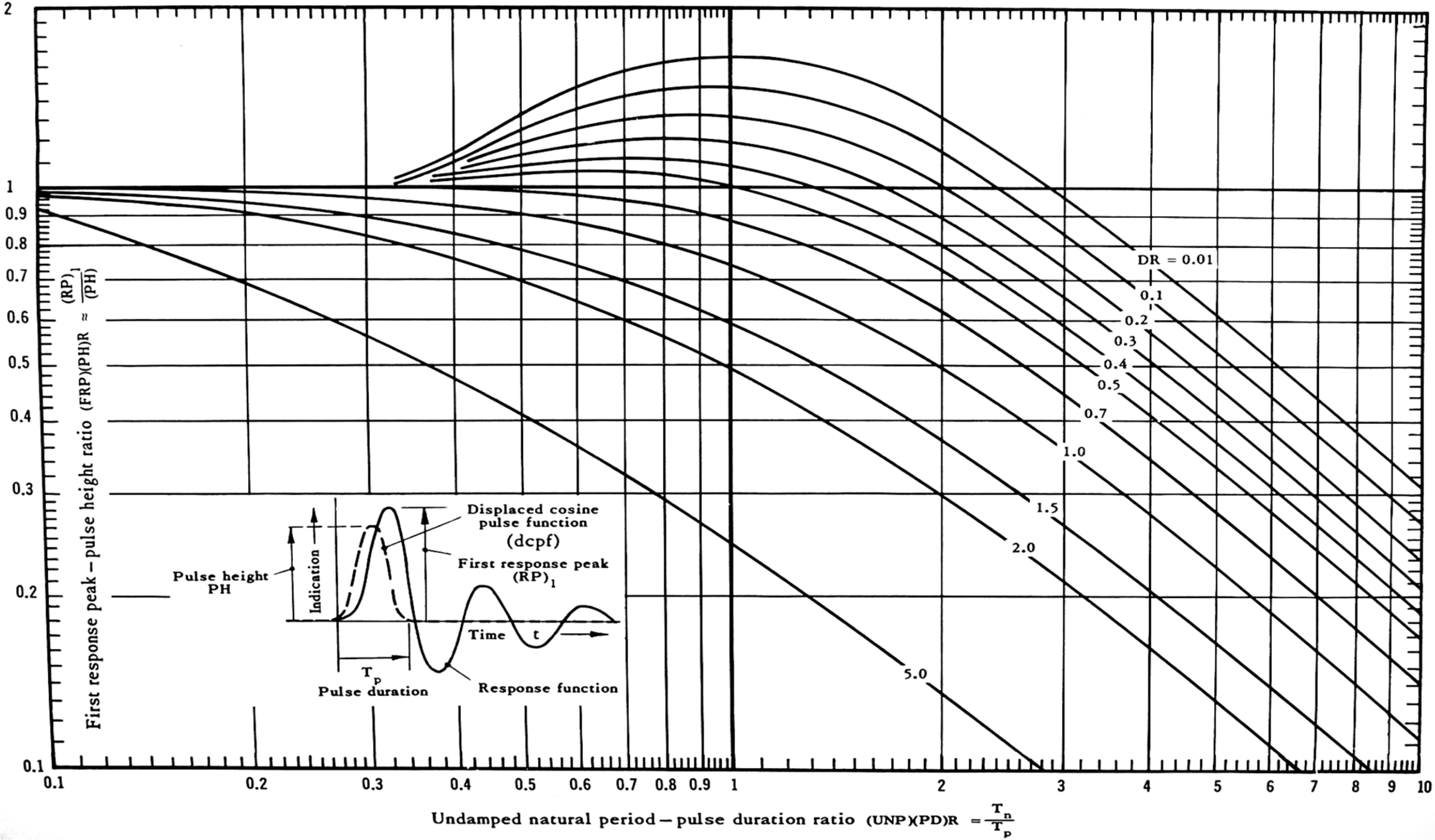


Fig. 32-42. First response peak – pulse height ratio for the displaced cosine pulse function response of (0;0,1,2) measuring instruments.

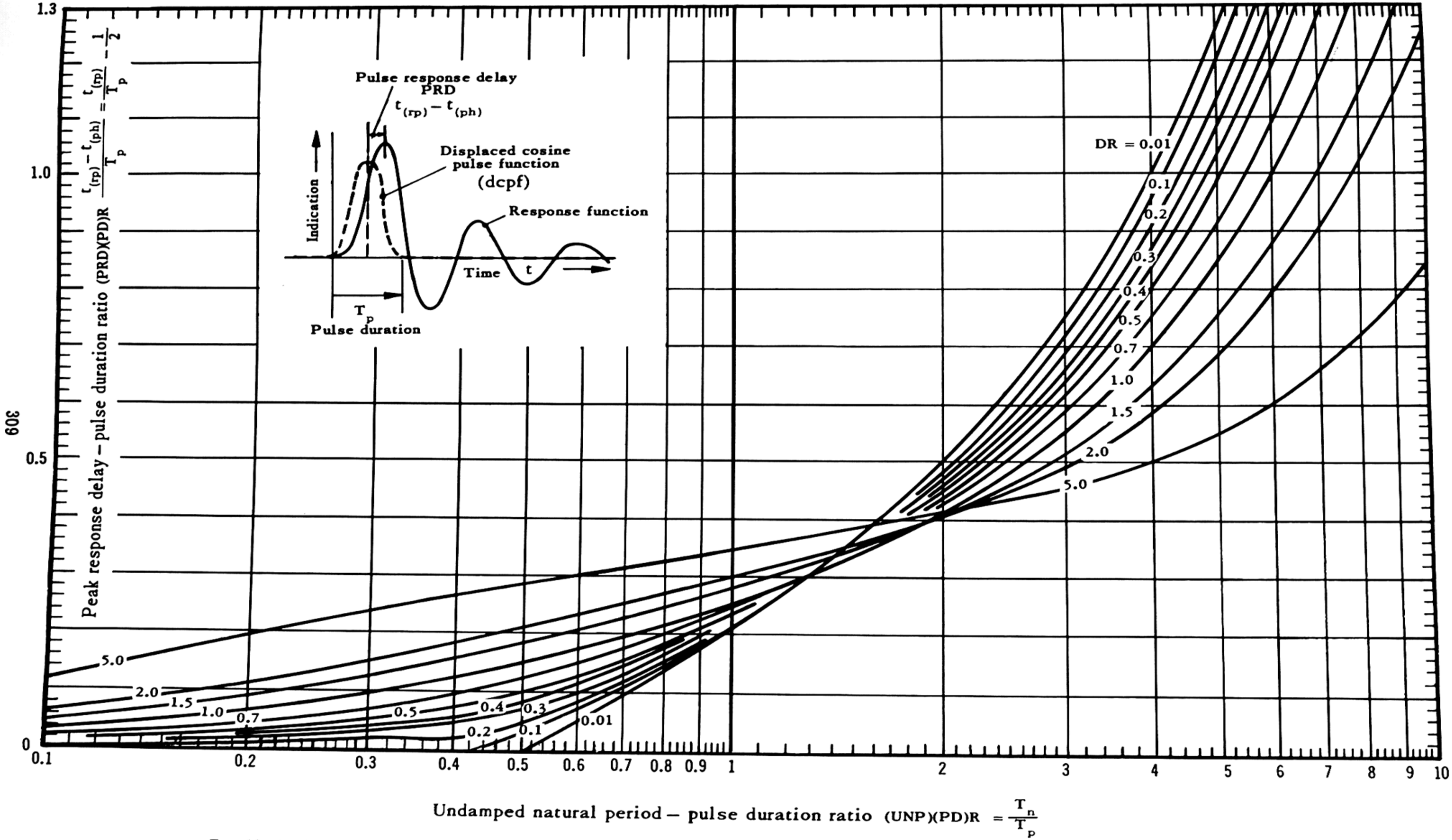


Fig. 32-43. Peak response delay – pulse duration ratio for the displaced cosine pulse function response of (0;0,1,2) measuring instruments.

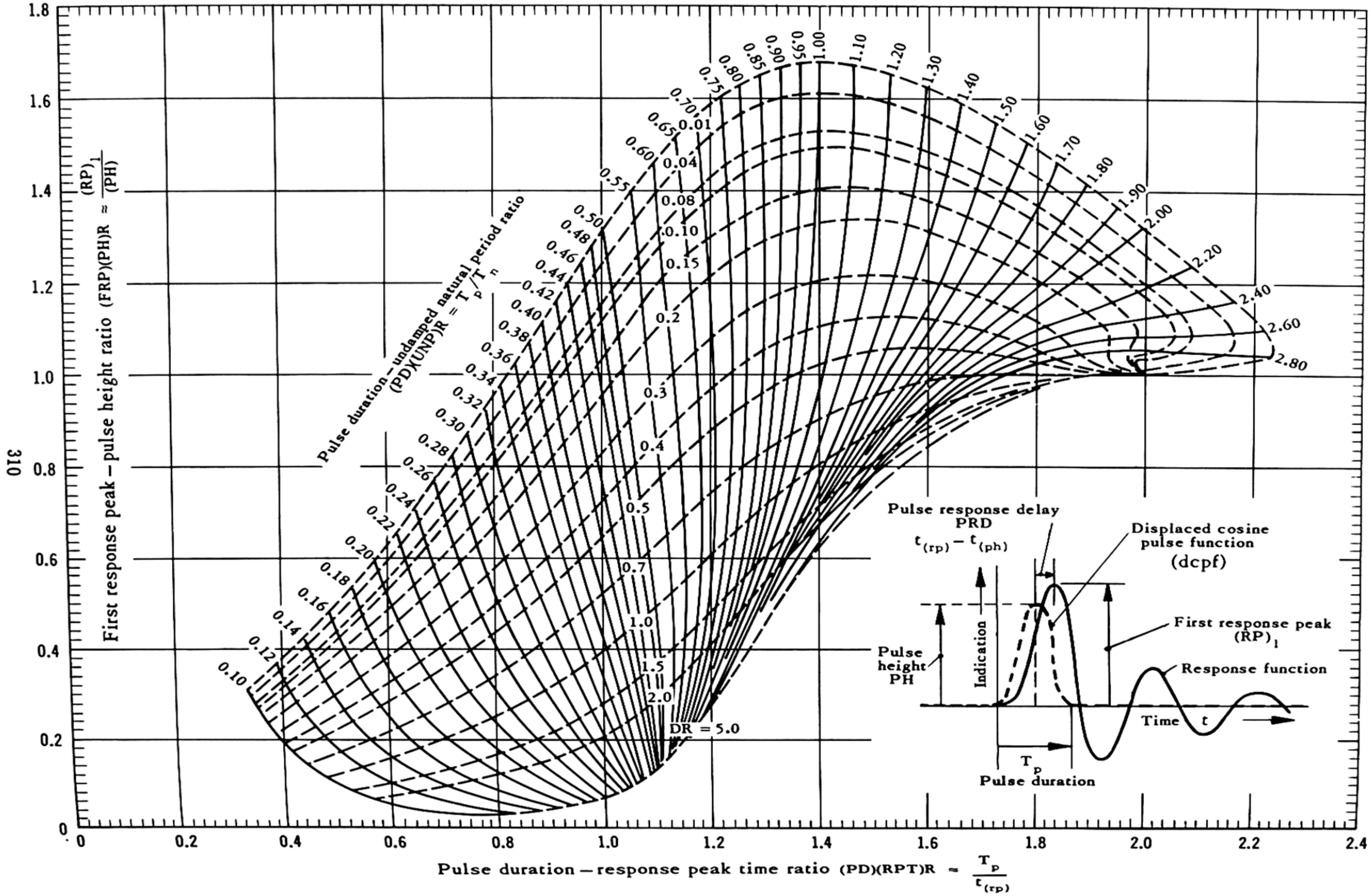


Fig. 22-44. Nondimensional first response peak characteristics associated with (0:0.1:2) measuring instruments

function of a (0;0,1,2) measuring instrument is given by the solid-line curve. Since the input forcing function has a peak, the response must also show at least one peak. In order to use the method that follows, it is necessary to determine the pulse height, the first response peak height, the pulse duration and the time at which the first response peak occurs. In some instances, it is convenient to measure the time of the first response peak by referring to the initial instant of the pulse. In other situations, it is more practical to determine the delay between the displaced cosine pulse peak and the first response peak. These two durations are uniquely related since

$$(\text{PRD}) = t_{(rp)} - t_{(ph)} = t_{(rp)} - \frac{T_p}{2} \approx \text{pulse response delay} \qquad (32\text{-}16)$$

where

$t_{(rp)}$ = time of response peak; $t_{(ph)}$ = time of pulse height; T_p = pulse duration

32.124. From the measured data, the first response peak – pulse height ratio and the peak response delay – pulse duration ratio are computed. Alternatively, the pulse duration – peak response time ratio may be found for the nondimensional time quantity. Figures 32-42, 32-43 and 32-44 show how these nondimensional ratios vary as a function of damping ratio and pulse duration – undamped natural period ratio. By plotting the appropriate forms of the computed data as indicated on each of these figures, the damping ratio and undamped natural period of a (0;0, 1, 2) measuring instrument may be determined.

32.125. In Fig. 32-42, the ratio of the height of the first response peak to the pulse height is plotted as a function of the undamped natural period – pulse duration ratio. Curves for constant damping ratio are plotted on a log-log scale, with one loru equal to 5 inches. The abscissa is comparable to a frequency ratio employed in steady-state sinusoidal response curves. The ordinate may be likened to a dynamic amplitude ratio. The plotted curves bear a resemblance to the steady-state sinusoidal response curves shown in Fig. 32-20. The curves are asymptotic to unity at the left-hand side for small values of the abscissa. They are all asymptotic to straight lines with a slope of –1 for large values of the abscissa, rather than a slope of –2 as in Fig. 32-20. The maximum value of the first response peak – pulse height ratio never exceeds 2. While the curves are asymptotic to parallel lines of slope –1 for large values of the abscissa, there does not seem to be a common break point as for the steady-state sinusoidal responses.

32.126. By plotting the ratio of the first response peak delay to the pulse duration as a function of the undamped natural period – pulse duration ratio, the curves shown in Fig. 32-43 are obtained. Curves for constant damping ratios are given, with the ordinate plotted to a uniform scale and the abscissa to a logarithmic scale for which one loru is equal to 5 inches. Figure 32-43 corresponds to the dynamic response angle curves shown in Fig. 32-21. The peak response delay – pulse

duration ratio tends to zero for small values of the abscissa, but increases indefinitely as the pulse duration decreases compared with the undamped natural period. There does not seem to be a limit value as for steady-state sinusoidal responses. The curves cross over for values of the abscissa between 1 and 3, rather than at a unique point as in Fig. 32-21. Lightly damped measuring instruments suffer less response delay than more heavily damped ones when the pulse duration is long compared with the undamped natural period, while the reverse condition holds for short-duration pulses.

32.127. The curve families of Figs. 32-42 and 32-43 may be combined to produce a curvilinear grid. One way to do this is shown in Fig. 32-44, which is an extended plot of Fig. 25-16 of Chapter 25. The coordinates are plotted to a uniform scale. The ordinate is the same as for Fig. 32-42, namely the first response peak – pulse height ratio. The abscissa corresponds to the ordinate of Fig. 32-43, but in Fig. 32-44 it is taken as the pulse duration – response peak time ratio. The solid lines represent curves of constant pulse duration – undamped natural period ratio, the inverse of the abscissa for Figs. 32-42 and 32-43. The dashed lines correspond to constant damping ratio curves.

32.128. The limiting situation as the displaced cosine pulse duration increases is for the response to be identical with the forcing function. In the limit, the first response peak – pulse height ratio becomes unity, while the pulse duration – response peak time ratio becomes equal to two. The curves show that for sufficiently large damping ratios, the response function approaches the limit uniformly. However, for lightly damped measuring instruments, the situation is more complicated. Four response curves are shown in Fig. 32-45 for a measuring instrument with a damping ratio of 0.01. The ratio of the pulse duration to the undamped natural period increases from 1.5 to 3. When this ratio is 1.5, the first response peak occurs after the forcing function peak, and a well-defined oscillatory transient exists after the termination of the pulse. The first response peak is sharp enough to define the time at which the maximum occurs. For a pulse duration – undamped natural period ratio equal to 2, the transient has effectively vanished at the end of the forcing function pulse. When this time ratio is 2.6, an oscillatory transient reappears. The first response peak is somewhat misshapen and the maximum occurs prior to the forcing function peak. When the time ratio is 3, the oscillatory transient has again been suppressed. The first response peak is so broad that it is difficult to locate the maximum precisely.

32.129. This condition occurs because to the measuring instrument the forcing function for large pulse durations resembles an increasing ramp followed by a constant value followed by a decreasing ramp. When the damping ratio is small enough, the measuring instrument response follows the input closely during the first increasing portion. At the crest of the displaced cosine pulse, the measuring

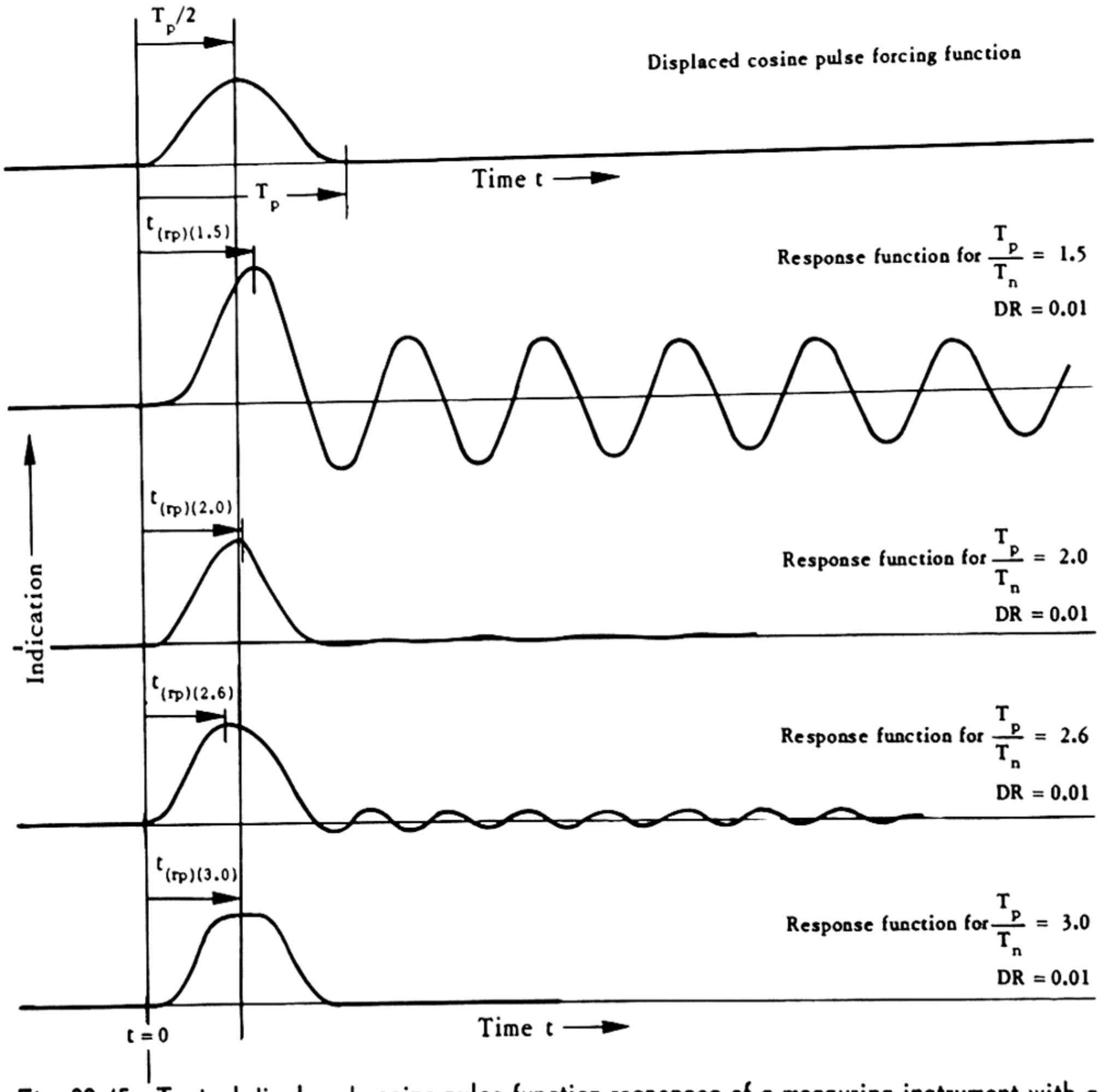


Fig. 32-45. Typical displaced cosine pulse function responses of a measuring instrument with a very low damping ratio (0;0,1,2) performance equation. Pulse duration is long compared with undamped natural period.

instrument response transient becomes dominant. The location of the response maximum depends upon the transient excitation and the position of the first oscillatory peak during the pulse.

32.130. When imperfections due to uncertainties are present in the response, the location of the peak for responses like the bottom curve in Fig. 32-45 may be rather imprecise. For this reason, it is not recommended that the curves in Fig. 32-44 be used when the abscissa is greater than two.

DISPLACED COSINE PULSE FUNCTION TEST OF A RECORDING OSCILLOGRAPH

32.131. An example of displaced cosine pulse function test procedures is illustrated in Fig. 32-46. The measuring instrument being tested is the recording oscillograph shown previously in Fig. 32-30. A special film drive is used to replace the one supplied with the instrument in order to provide a higher film speed. As demonstrated earlier in this chapter, optical recording oscillographs may be

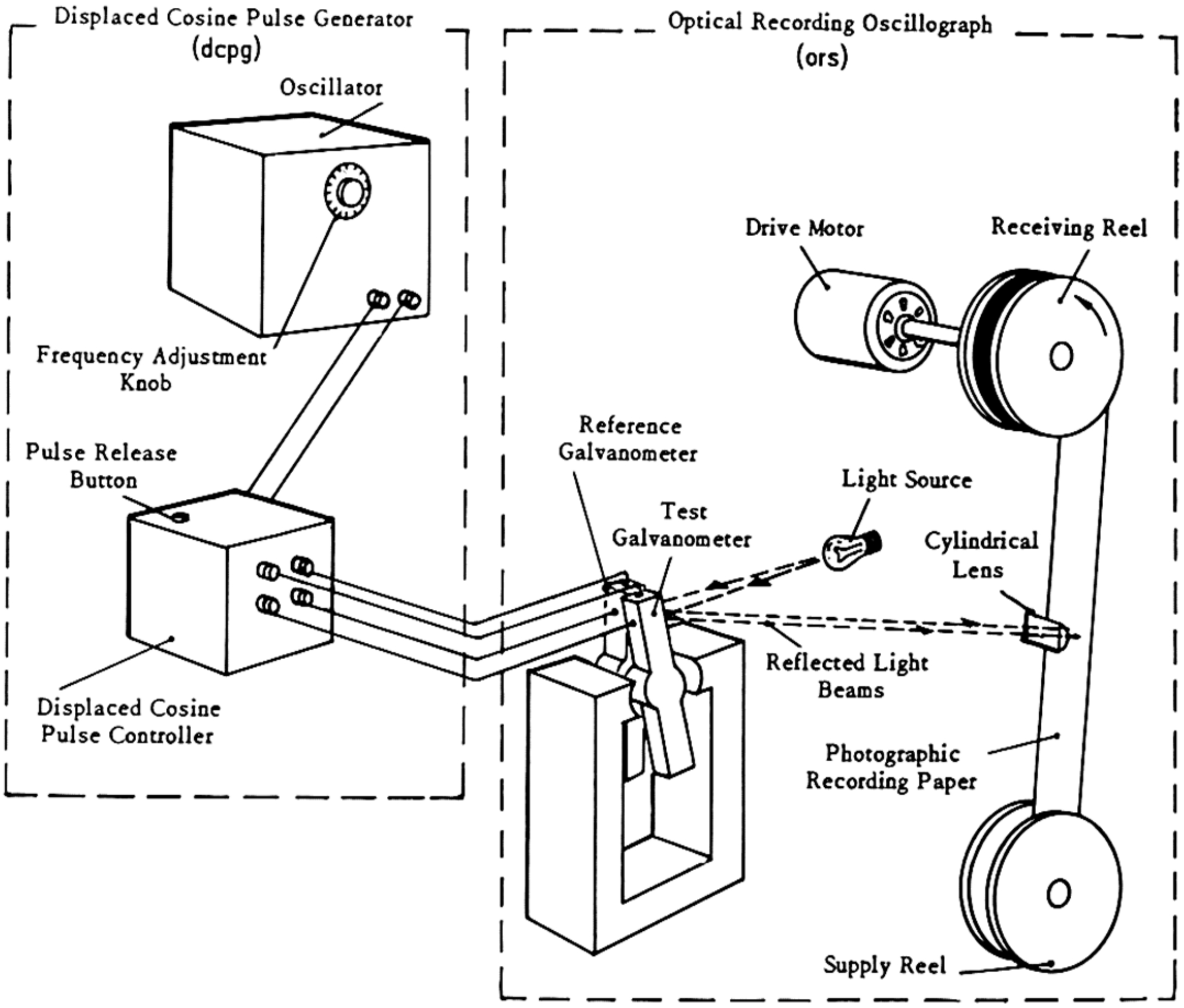


Fig. 32-46. Pictorial schematic diagram showing setup for making displaced cosine pulse tests on an optical recording oscillograph with a moving-coil galvanometer.

associated with (0;0, 1, 2) performance equations. The input forcing function is generated from the output of an oscillator with an electrical output, as shown in Fig. 32-46. The displaced cosine pulse controller allows one cycle of the oscillator output to be applied to the galvanometer when the pulse release button is depressed. After the passage of the displaced cosine pulse, the controller is restored to its original condition and it is necessary to depress the pulse release button to pass another pulse. The pulse duration is adjusted by changing the frequency of the oscillator output. The pulse height is controlled by attenuating the oscillator output.

32.132. For the purposes of the test, it is necessary to use a second galvanometer to provide an output forcing function trace. The reference galvanometer is chosen to have an undamped natural frequency much greater than the one being tested.

32.133. The sensitivity of the galvanometer is determined from d-c inputs and is found to be 0.061 millivolt per millimeter. Four pulses are applied, with durations of 0.2, 0.1, 0.05 and 0.02 second. The resulting traces are shown in Fig. 32-47, along with the reference trace for each pulse. The height of each input

Fig. 32-47. Displaced cosine pulse function response records from an optical recording oscillograph.

pulse as well as the corresponding first response peak height are measured from the records. Each peak response delay is determined by comparison with the pulse duration as a reference period. It is helpful to provide marks indicating the beginning and end of the displaced cosine pulse.

32.134. The information derived from the traces shown in Fig. 32-47 is presented in Data Analysis Summary 32-3 with derived quantities suitable for use on the prepared curve families. The first three columns and the fifth are measured data. The other three are derived nondimensional ratios. By taking the height of the response to the longest pulse as a reference, the values of the nondimensional response peak – pulse height ratio shown in the fourth column are computed from the second and third columns. The two types of time ratios given in the last two columns are self-explanatory.

32.135. The data from the fourth column of Data Analysis Summary 32-3 is plotted as the ordinate of Fig. 32-48, while the abscissa comes from the extreme right-hand column of the summary. The points fall on the curve for which the damping ratio is unity. Two values of the pulse duration – undamped natural period ratio have been determined. From the pulse duration corresponding to each point, it is found that the undamped natural frequency is a little greater than 41 cycles per second.

32.136. Figures 32-49 and 32-50 have been constructed by plotting the data from the fourth and sixth columns of Data Analysis Summary 32-3 to the indicated

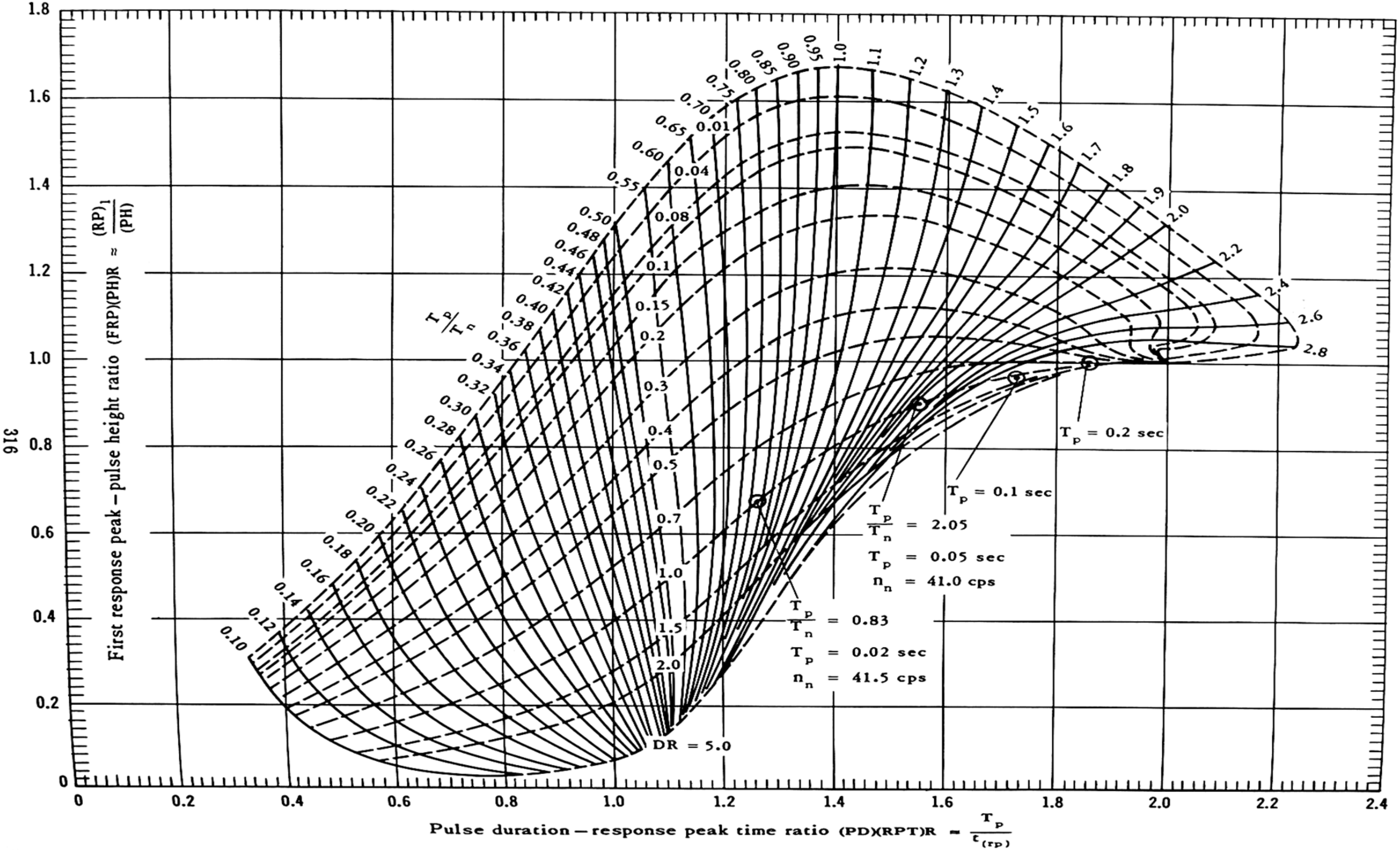


Fig. 32-48. Plot of first response peak characteristics from displaced cosine pulse tests of an optical recording oscillograph.

Pulse Duration $PD \approx T_p$ (seconds)	Pulse Height PH (mv)	First Response Peak FRP (centimeters)	Nondimensional First Response Peak – Pulse Height Ratio $\frac{FRP}{PH}$	Peak Response Delay $t_{(rp)} - t_{(ph)} = PRD$ (seconds)	Peak Response Delay – Pulse Duration Ratio $\frac{t_{(rp)} - t_{(ph)}}{T_p} = \frac{PRD}{PD}$	Pulse Duration – Response Peak Time Ratio $\frac{T_p}{t_{(rp)}} \approx \frac{PD}{RPT}$
0.2	1.0	1.64	1.00	0.0081	0.0405	1.85
0.1	1.0	1.575	0.96	0.0080	0.080	1.725
0.05	1.0	1.48	0.904	0.00725	0.145	1.55
0.02	1.0	1.10	0.672	0.0059	0.295	1.26

Heiland Oscillograph, Type SE 404 R-6, Serial No. 515; Galvanometer Type A-8668
Damping shunt resistance, $R_{(sh)}$ = 120 ohms; Scale sensitivity, S_s = 0.061 millivolt/mm; Special film drive

Data Analysis Summary 32-3. Analysis of displaced cosine pulse function response data for an optical recording oscillograph.

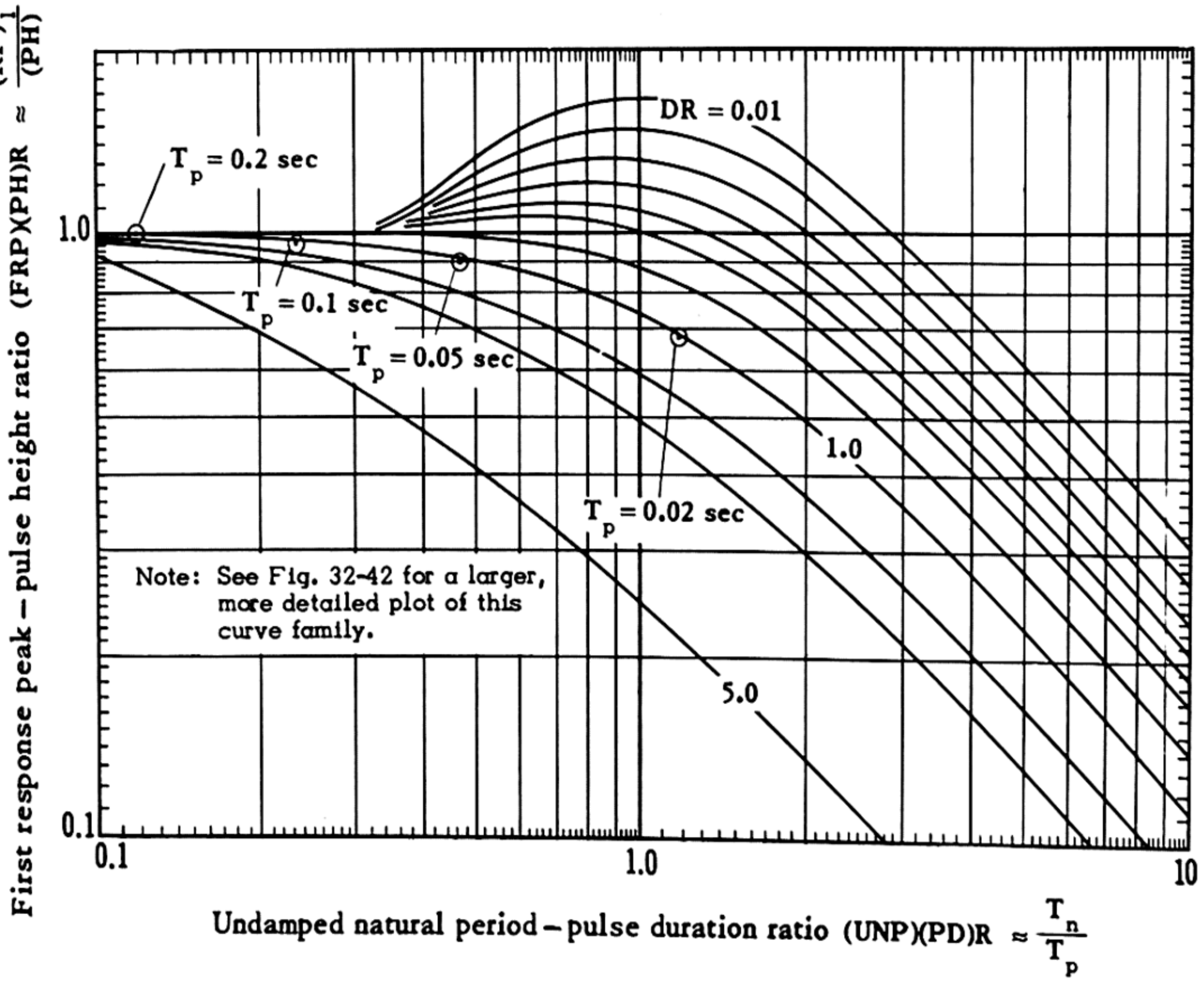


Fig. 32-49. Plot of first response peak – pulse height ratios from displaced cosine pulse tests of an optical recording oscillograph.

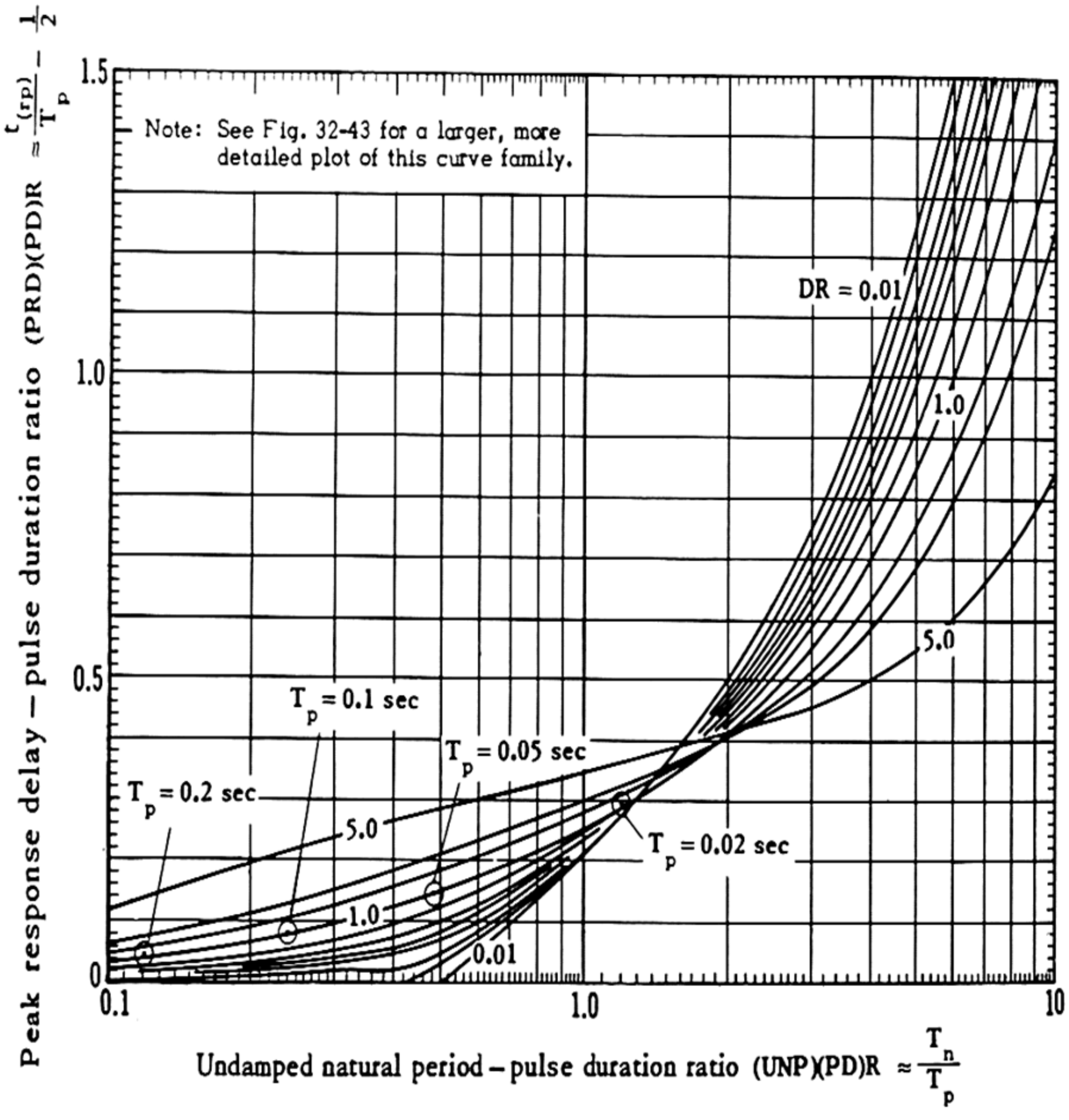


Fig. 32-50. Plot of peak response delay – pulse duration ratios from displaced cosine pulse tests of an optical recording oscillograph.

ordinates and adjusting the abscissa values for the best fit. The plotted points in each case fall on the unity damping ratio curve. From the abscissa values of these points, the undamped natural frequency is found to be between 41 and 42 cycles per second. These frequency values compare favorably with the information in Data Analysis Summary 32-2, obtained by an analysis of step function response.

CHAPTER 33

PRESSURE-MEASURING SYSTEMS

Y. T. Li

INTRODUCTION

33.1. Pressure measurements in gases, fluids and solids are of primary importance not only for science and industry but also for military applications and the commonplace activities of everyday living. Science is often interested in accurate measurements over a wide range of pressures; industry is generally concerned with pressure data for either automatic or manual control of processes. Modern military equipment such as jet aircraft could not operate without pressure-actuated instruments, while systems such as home heating plants and automobiles provide pressure gages as normal equipment to be used in routine operations.

PRESSURE-MEASURING UNITS

33.2. Many physical principles are applied in pressure-measuring devices, which vary in complexity from the simple Bourdon tubes or bellows devices used for automobile oil-pressure indications to the complex electrical systems required to record the cylinder pressures of modern high-performance internal combustion engines.* When a single unit receives the pressure input and also provides the pressure scale readings, the situation is often generally similar to that described in Chapter 2 for the diaphragm-type pressure gage. Chapters 2 through 8 outline a procedure that may be applied to describe the physical features and set up the performance equation of any pressure-measuring unit.

33.3. When performance equations are available for specified units, the methods developed in the chapters of Volume II may be applied to find the pressure readings for given input variations and other performance information. A typical pattern for presenting these data is given in Specification 29-1. The problem of writing specifications is especially simple when the unit can be described by first- or second-order differential equations, because it is possible to apply the procedure developed in Chapters 31 and 32. In any case, the generalized concepts discussed in Chapter 29 for describing indicating and measuring instruments may be used to meet the requirements of special situations.

* Bourdon tubes: see Van der Pyl (V2); automobile oil-pressure gage: see Blanchard (B20); engine indicators: see Draper and Li (D13) and Grinstead, Frawley, Chapman and Schultz (G11).

PRESSURE-MEASURING SYSTEMS

33.4. In practice, it is often impossible to carry out satisfactory pressure measurements over a wide range of application with any single unit. This is understandable because access to the source of input pressure is frequently limited to a small space with such unfavorable environmental conditions that it is impossible to mount and use any satisfactory single pressure-recording unit. In addition to problems of this kind, it is very often completely out of the question to combine all the necessary mechanical and electrical functions in one package of feasible size. For example, high-speed piston-engine pressure indicators must have small receivers capable of withstanding severe shock and vibration while generating interference-free signals for use with amplifying and recording equipment of considerable weight and size. This means that a pressure-measuring unit must often be replaced by a pressure-measuring system that comprises a group of components, each selected to provide one of the functions that must be combined to produce satisfactory over-all performance.

33.5. The discussion of this chapter is largely concerned with procedures for using the methods of Volumes I and II in the development and specification of performance characteristics of pressure-measuring systems. From the standpoint of the measurement problem discussed in Chapters 8 and 29, the components required are arranged so that they fall into the class of open-chain systems under the definition of Fig. 3-3 of Chapter 3. In the present chapter, attention is confined to systems of this type. Units that appear as parts of measuring-system chains may contain feedback loops, however. The theory of such loops is considered in Chapters 36 and 37, but is disregarded in this chapter as being a detail of internal design in units whose properties of concern here are externally measurable performance characteristics only.

METHODS OF PERFORMANCE ANALYSIS

33.6. Performance characteristics for complete pressure-measuring systems can be derived from the differential equations associated with the performance of individual components by combining the component equations into a single equation. The required information can then be derived from the solutions of the single equation, carried out by the methods described in Chapters 14 through 19. A generally useful alternative procedure is to transform the differential equations for individual components into relating functions of the type discussed in Chapter 17. This change in form has the effect of replacing problems in differential equations by much less difficult problems in algebra. Definition Summaries 28-6, 28-7 and 28-8, which outline concepts and notation developed in Volumes I and II, show that the relating function, which is basically an abstract mathematical concept, corresponds to the performance function when a specific physical situation is considered.

33.7. Performance characteristics for operating systems are particularly easy to describe when attention is concentrated on physical quantity changes represented in terms of sinusoidal forms by one or more of the methods described in Chapter 12. When the physical systems involved are made up of operating components with characteristics that may be described by first- or second-order differential equations, steady-state sinusoidal performance information is immediately available from the curve families developed in Chapters 18 and 19 and applied to measurement problems in Chapters 31 and 32. When a number of open-chain connected components have either first- and second-order characteristics or sinusoidal performance that must be represented by plots for more complicated relationships, it is convenient to derive results by use of the complex plane procedures of Chapter 23 or the graphical techniques described in Chapter 24. In many situations, it may also be advantageous to handle performance function problems in terms of the forcing-pulse method of attack described in Chapter 25.

33.8. The units involved in the discussion of this chapter are all assumed to be functionally stable under the definitions of stability given in Chapter 20. When components of this kind are combined to form open-chain systems, amplitude ratio and dynamic response angle curves are convenient for building up over-all performance information. The procedure in any given situation is some special case of the generalized frequency response technique discussed in Chapter 24. Applications of this technique are given primary importance in this chapter.

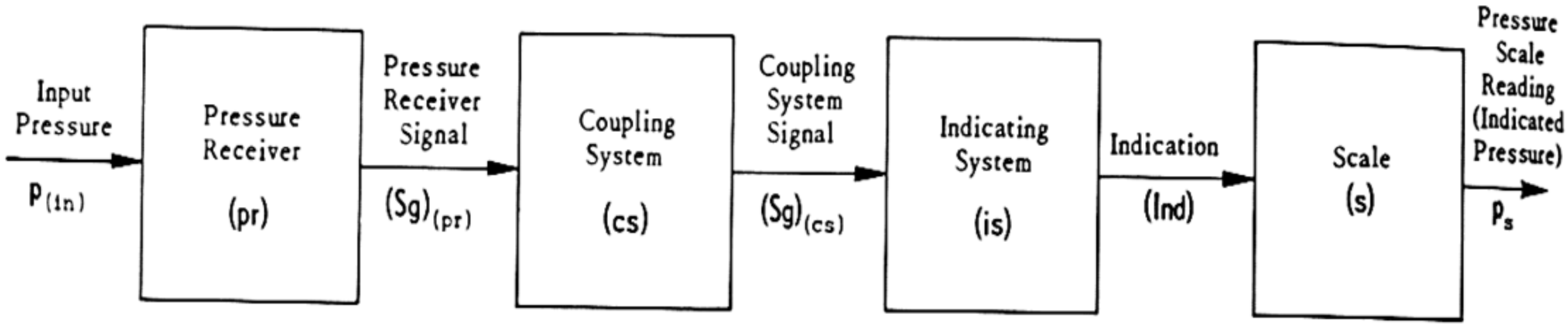
STATIC-FUNCTIONAL DIAGRAMS FOR PRESSURE-MEASURING UNITS AND SYSTEMS

33.9. Figure 33-1a is a static functional diagram, based on the pattern established in Definition Summaries 29-1 and 29-2, for representing the essential features of all pressure-measuring instruments* or pressure-measuring systems. A pressure receiver of some kind is acted on by the input pressure and produces a corresponding pressure receiver signal. This signal is applied to a coupling system, which generates a signal suitable for operation of the indicating system. The output of this system is the indication,** which gives the indicated pressure reading when it is properly interpreted with the aid of the scale. Figure 33-1a differs from Fig. 2-6 of Chapter 2 by the replacement of the "coupler" by a coupling system, and by the omission of the linear acceleration interfering input. The components of the diaphragm-type pressure gage described in Chapter 2 fit immediately into the pattern of Fig. 33-1a.

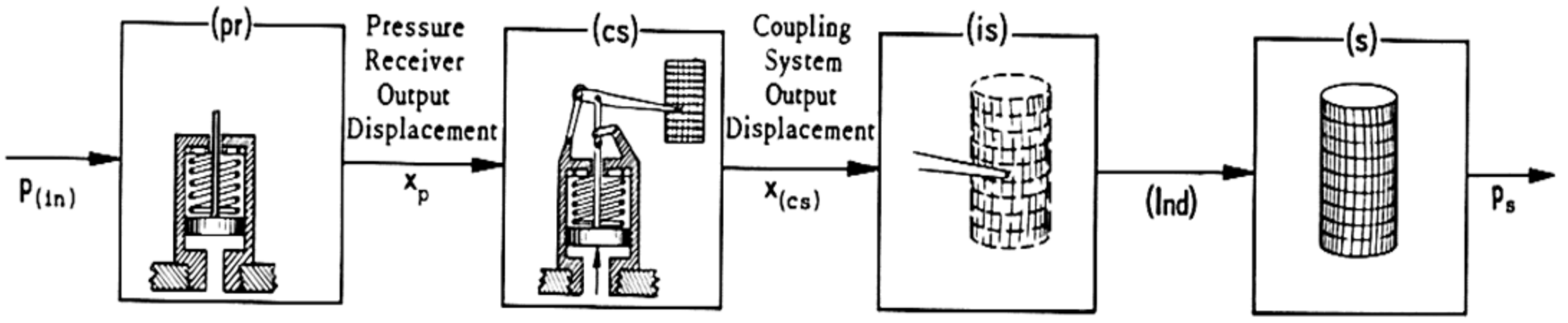
33.10. Figure 33-1b illustrates a breakdown of the spring-and-piston-type engine indicator described in Figs. 8-1 and 8-2 of Chapter 8 into the operating

* As a matter of convenience, the terms pressure-measuring instrument and pressure-measuring unit are used interchangeably to mean any arrangement of devices that operates to produce pressure measurements.

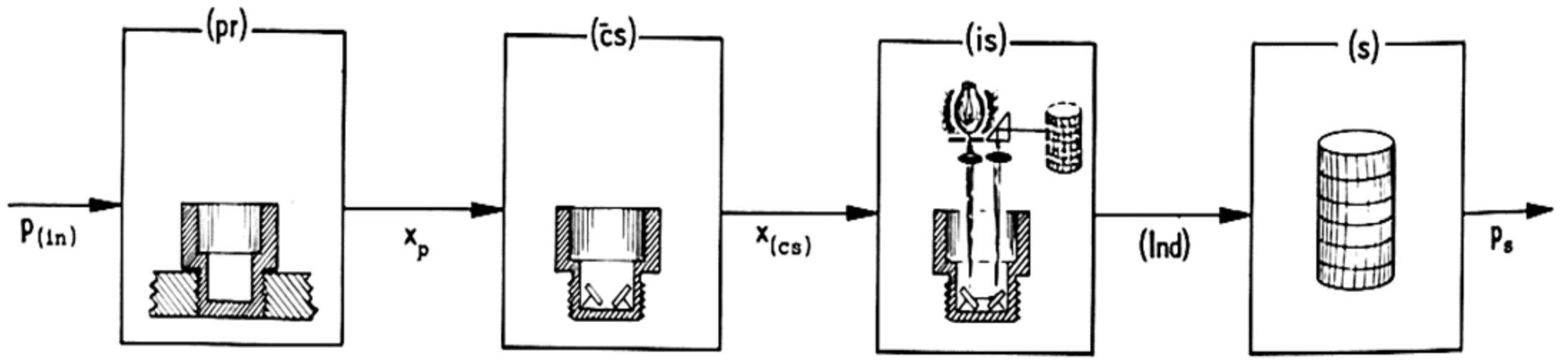
** See Chapter 29.



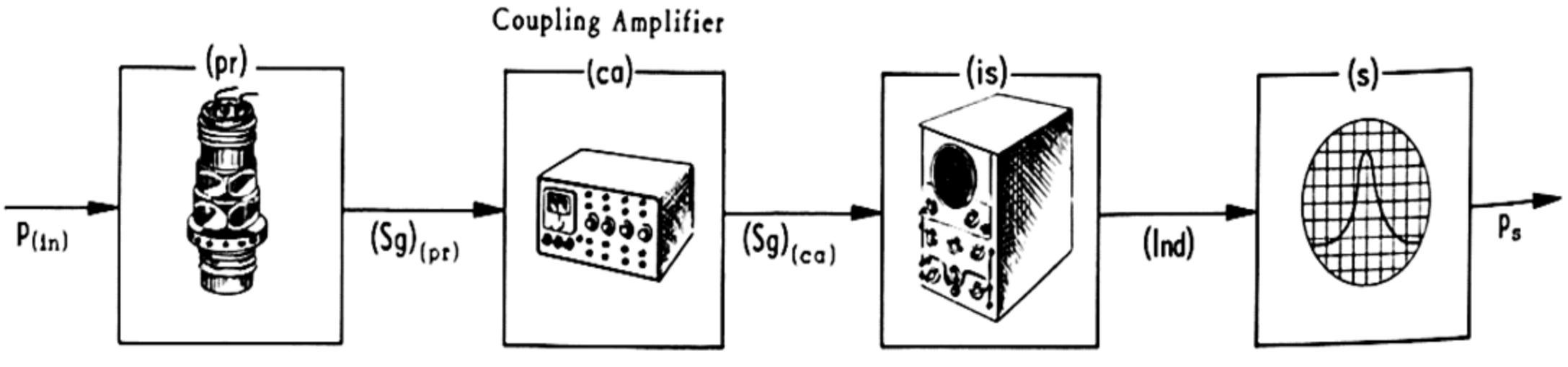
a) Static-functional diagram for pressure-measuring instruments and systems



b) Static-functional diagram for a spring-and-piston-type engine indicator



c) Static-functional diagram for a diaphragm-type optical engine indicator



Note: The pressure receiver* may be any device designed to receive pressure and produce a suitable electrical signal. Several examples of such pressure receivers are shown in Fig. 33-4.

Note: A cathode-ray-oscilloscope indicating system is shown in the diagram. In practice, the indicating system may be an oscillograph of any type.

* The pressure receiver is often called the "pressure pickup."

d) Static-functional diagram for an electrical pressure-measuring system

Fig. 33-1. Illustrative static-functional diagrams of pressure-measuring instruments and systems.

component pattern of Fig. 33-1a. Figure 33-1c shows a similar diagram for a diaphragm-type optical engine indicator.* The receiver is a simple diaphragm that subjects a system of mirrors in the coupling system to rotations when the diaphragm bends under a pressure input. The indicating system is made up of a light source, lenses and a prism that combine to deflect a light beam when the coupling system mirrors are moved by diaphragm bending. The scale is associated with photographic paper** mounted on a rotating drum that is effectively part of the indicating system.

33.11. Spring-and-piston-type engine indicators and optical engine indicators are typical pressure-measuring units capable of handling changing pressures. In practice, the many existing examples of these instruments*** are not satisfactory for use with modern high-speed piston engines, because they are so large that they can not be fitted into the space available near operating cylinders. They are also unsuitable for making records that are free from the interfering effects of temperature changes, shock, and vibration. In addition to these troubles, it is also practically impossible for spring-and-piston-type instruments to meet the dynamic performance specifications that are required in modern practice.

33.12. The difficulties outlined in the previous paragraph may be reduced to tolerable levels by means of systems based on electronic amplifying and recording techniques. The general features of a typical electrical pressure-measuring system**** are illustrated in Fig. 33-1d. The receiver is a small, rugged pressure pickup, designed to be screwed into an engine cylinder opening, that produces an electrical signal corresponding to the pressure input. This signal acts as the input for an electronic amplifier that provides the coupling function. The indicating system is a cathode-ray oscillograph that receives the coupling amplifier output and produces deflections of a light spot as the indication. The scale is a grid superposed on the face of the cathode-ray tube. In practice, any oscillograph with proper performance characteristics may be used instead of the cathode-ray instrument shown in the illustrative diagram of Fig. 33-1d.

33.13. Many physical principles have been applied in receivers for pressure-measuring systems, but the commonly available units usually generate electrical signals, so that it is possible to use electronic amplifiers for coupling purposes. In practice, the indicating system unit is usually a cathode-ray oscillograph or an electromechanical recording oscillograph with a D'Arsonval galvanometer of

---

* See Heldt (H12) and Nakanishi, Ito and Kitamura (N4).

** The scale might be printed on the paper, but it is more often associated with a separate ruler or template to be applied when finished records are available for study.

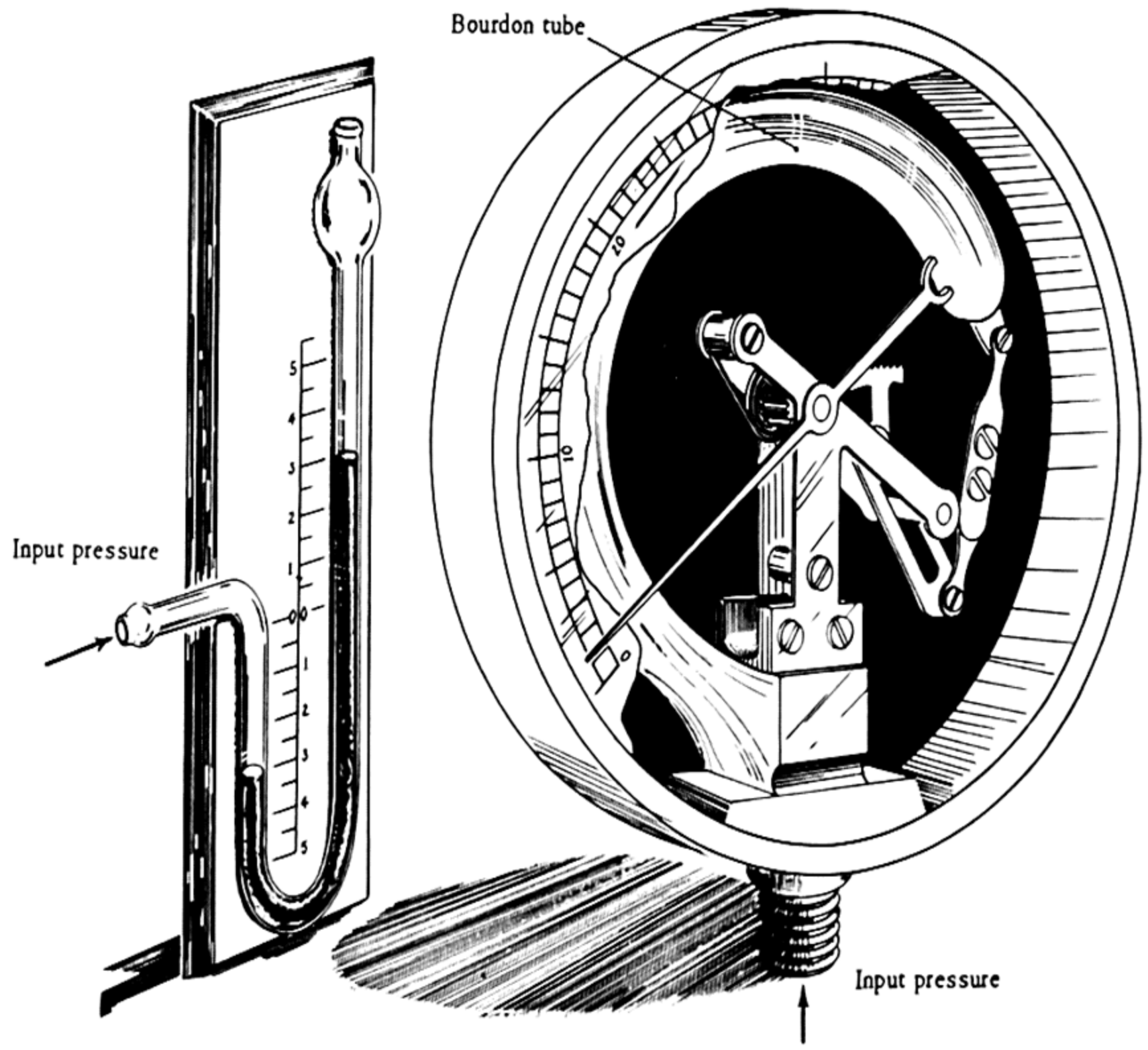
*** See DeJuhasz (D12).

**** See Draper and Li (D13), Grinstead, Frawley, Chapman and Schultz (G11), Li (L15), and Taylor and Draper (T8).

the type discussed in Chapter 32. Magnetic tape recorders or punch-card-type recorders are also used in limited applications.

TYPICAL PRESSURE-MEASURING INSTRUMENTS

33.14. Figure 33-2 illustrates two pressure-measuring-unit types that are commonly used as gages for static or slowly varying pressures. The fluid manometer of Fig. 33-2a balances the pressure of a liquid column against the input pressure. The height of the supported liquid column is a direct measure of the pressure. Bourdon-tube gages with the features of Fig. 33-2b are the staple instruments of the pressure-measuring field. In operation, pressure is applied to a blind, curved elastic tube of oval cross section. The forces generated by this pressure tend to move the closed end of the tube by straightening out the curve. A mechanical linkage transforms this motion into rotation of a shaft that carries the index. The indication is the angle of the index from its zero-pressure position. For any given indication within the operating range of the gage, pressure readings may be taken directly from the scale.



a) Liquid manometer

b) Bourdon-tube pressure gage

Note: For further details of construction, see texts on engineering instruments; e.g., Diederichs and Andrae (D7).

Fig. 33-2. Essential features of two commonly used pressure-measuring instruments.

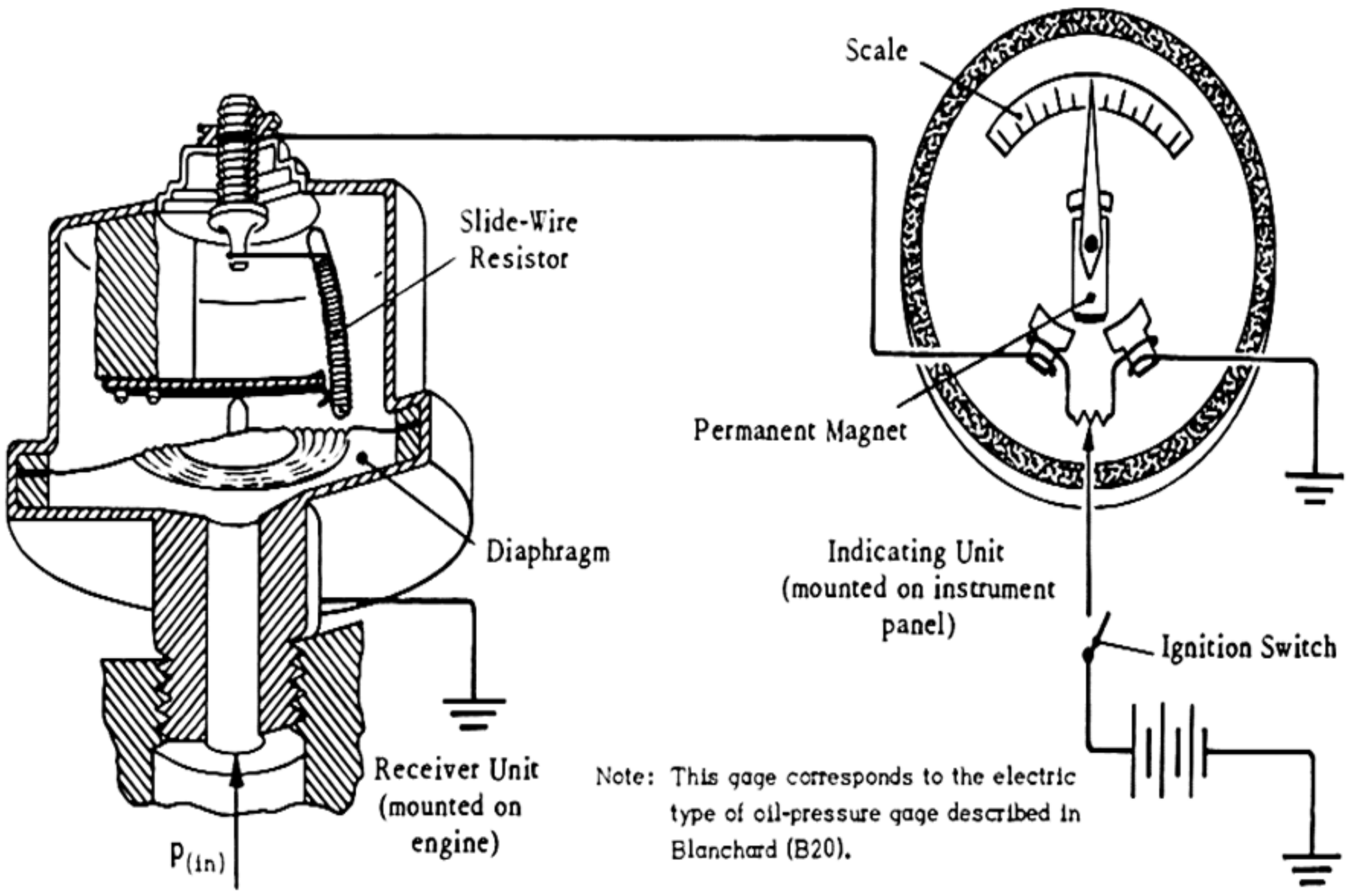
33.15. Mechanical pressure gages of the Bourdon-tube type or the diaphragm type described in Chapter 2 must be calibrated against known inputs in order to insure satisfactory readings. On the other hand, fluid manometers are primary-standard instruments* when the density of the liquid and the acceleration of gravity are given.

33.16. In many cases, the characteristics of pressure gages like those illustrated in Fig. 33-2 are essentially those of first- or second-order systems. This means that it is often possible to use the curve families of Chapters 31 and 32 as sources of performance data in any specific situation. The detailed working out of an illustrative pressure-gage example is omitted at this point because it would not add any new feature to the general principles already developed.

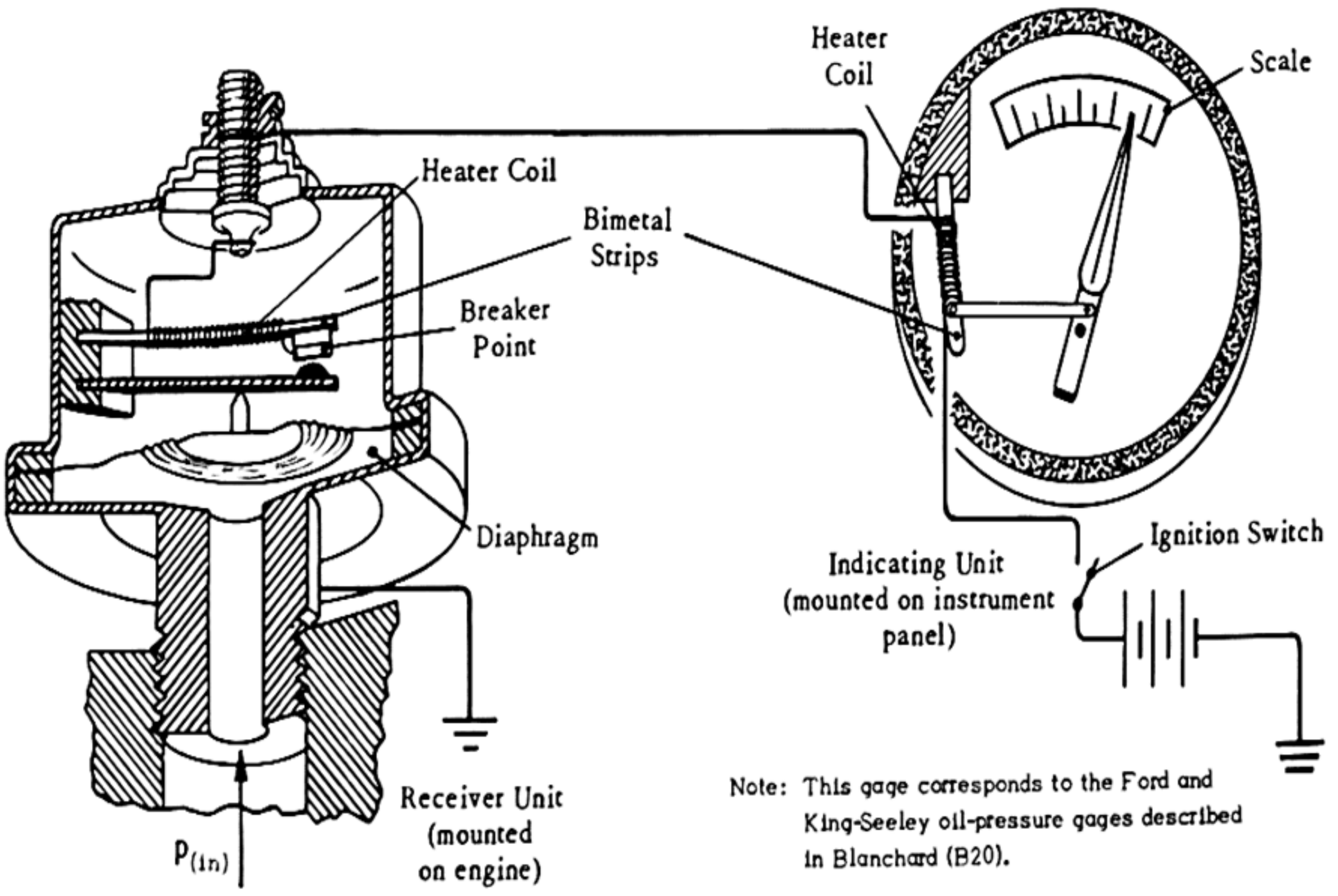
33.17. Figure 33-3 shows the features of two typical automobile oil-pressure gages. Each of these instruments consists of a receiver unit, exposed to the input pressure, and an indicating unit, mounted on the instrument panel, with an electrical circuit interconnection. The pressure receiving element of the gage shown in Fig. 33-3a is a diaphragm that deflects under pressure to move the slider on a wire-wound coil and reduce the resistance of a circuit energized by the automobile battery. The indicator unit is a moving-magnet galvanometer with two field coils and three pole pieces. The pole pieces are magnetically coupled through the case of the indicating unit. The current in one of the coils is controlled by the resistance of the receiver unit circuit and causes the magnetomotive force of this coil to vary as a function of input pressure. The winding of the second coil is connected directly between the battery supply terminal and ground and produces a constant magnetomotive force. The direction of the resultant magnetic field depends on the relative strengths of the two field coils. The permanent magnet of the galvanometer is pivoted so that it is free to rotate, and in operation it aligns itself with the direction of the resultant flux field produced by the two coils. The index is rigidly attached to the magnet. The two coil circuits, both supplied by the same battery, produce a compensating action as far as battery voltage is concerned.

33.18. Figure 33-3b shows a pressure-gage system utilizing a thermal follow-up system for driving the indicating pointer. The pressure receiver consists of a diaphragm similar to that shown in Fig. 33-3a. The deflection of the diaphragm closes a pair of electrical contacts, one of which is mounted on the tip of a bimetal strip, while the other is at the end of a cantilever mechanically driven by the diaphragm. When the contacts are closed, current from the automobile battery flows in a resistance coil wound around the bimetal strip. This strip is mounted so that it moves its contact away from the cantilever point when it is heated. This means that in operation the intermittent current causes the strip deflection to match the pressure-determined position of the diaphragm contact. The indicating unit contains a bimetal strip and resistance-winding combination similar to that

* See discussion of Fig. 29-5.



a) Magnetic-type oil-pressure gage



b) Bimetal-strip-type oil-pressure gage

Fig. 33-3. Typical automobile-engine oil-pressure gages.

used in the receiver. This winding is connected in series with the receiver winding so that the deflection of the indicating-head cantilever tends to match the movement of the bimetal in the receiver. This deflection is changed to a rotation of the index by a mechanical coupling link. Index positions are associated with pressure readings by means of the scale, which usually carries a coarse graduation.

33.19. The performance characteristics of the pressure-indicating systems shown in Fig. 33-3 are somewhat more complicated than those of the gages shown

in Fig. 33-2. However, the primary object of the ordinary oil-pressure gage is to give reliable readings of relatively low accuracy under conditions in which dynamic performance characteristics are not important. Because of constructional features that are dictated by reliability, price, and production considerations, performance analysis of gages like those of Fig. 33-3 present problems that are not considered here because of their specialized nature.

33.20. Dynamic performance characteristics are relatively unimportant for pressure gages like those of Fig. 33-2, in which high static accuracy is of primary interest, or the gage types of Fig. 33-3, in which reliability and cost are primary considerations. On the other hand, high-quality dynamic performance in units with low sensitivity to interfering inputs is an essential characteristic for receivers to be used in pressure-measuring systems of the type illustrated in Fig. 33-1d. Figure 33-4 gives illustrative pictorial diagrams and functional diagrams for seven electrical signal generating receivers that have such high-quality performance.

33.21. Diaphragms are used as pressure receiving elements for all the receiver types of Fig. 33-4 except that shown in section f. In each case, the diaphragm is exposed to the input pressure on the outer side and to some reference pressure on the other side, which is internal to the unit. The unit shown in section f uses a flexible metal bellows as the receiving element. The output of each receiving-element type is, in general, a mechanical displacement that is applied as the input to the pressure receiver signal generating system to produce the pressure receiver signal as the output.

33.22. In Fig. 33-4, each type of pressure receiver is represented in a separate row according to a common pattern. A pictorial diagram of the unit appears at the left-hand side; a static-functional diagram is shown next; and the corresponding basic electrical circuit diagram is given at the right-hand side of each row.

33.23. Figure 33-4a shows the essential features of a carbon-disc-stack resistance bridge receiver.* The carbon-disc stacks are mounted under an adjustable pressure on either side of a steel cantilever beam that is connected to the pressure-receiving diaphragm by means of a steel rod. Each stack is one of the adjacent arms in a Wheatstone bridge, with wire resistors as the opposite pair of arms. These wire resistors are located in the pressure receiver unit so that the interfering effects of temperature can be minimized by maintaining all bridge arms under the same environmental conditions. The bridge is excited with either alternating-current voltage or direct-current voltage applied across one pair of arm connection points. The voltage taken from the other pair of arm connection points is the pressure receiver output signal. This signal is made a

* See Martin and Caris (M16).

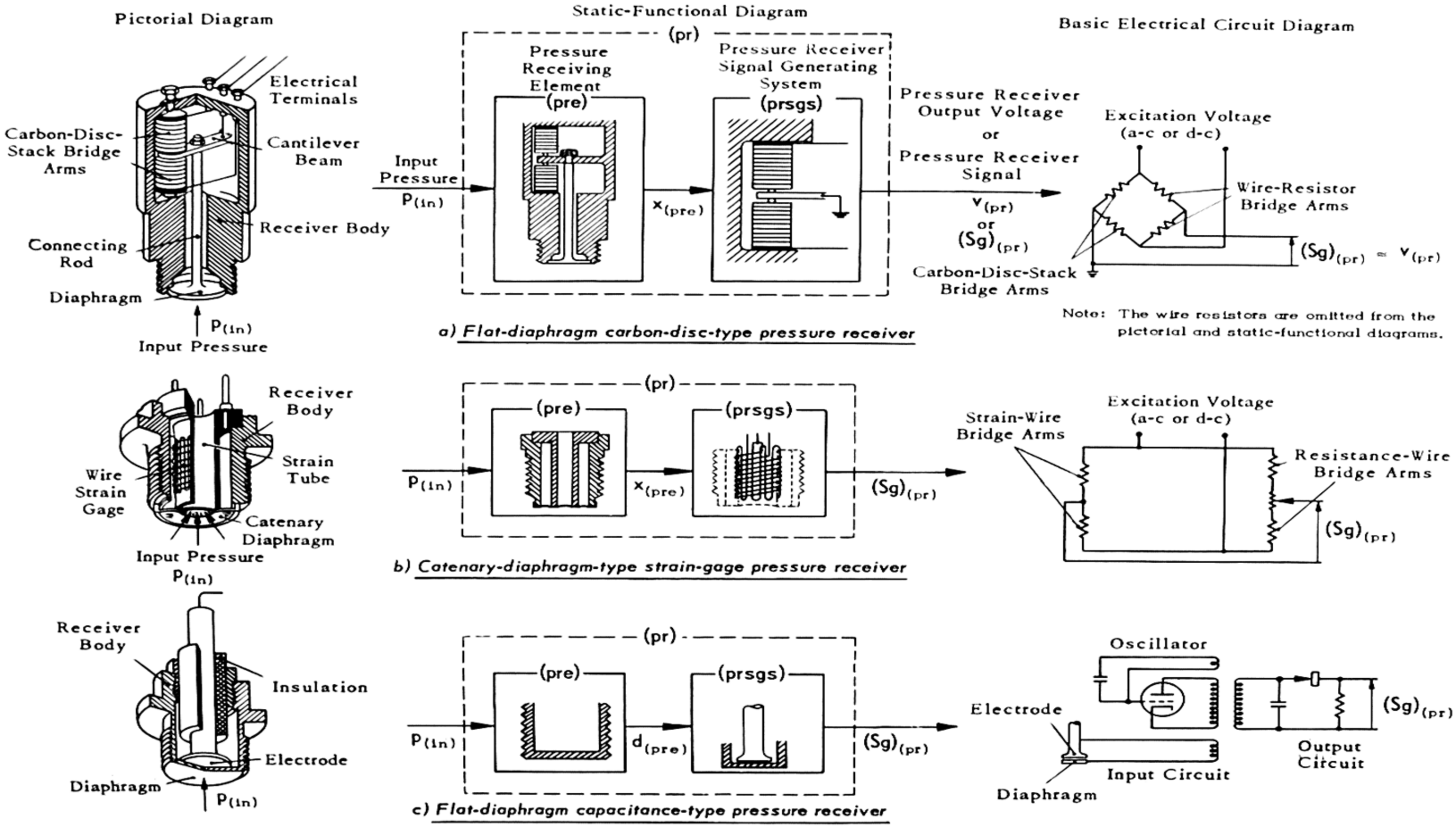
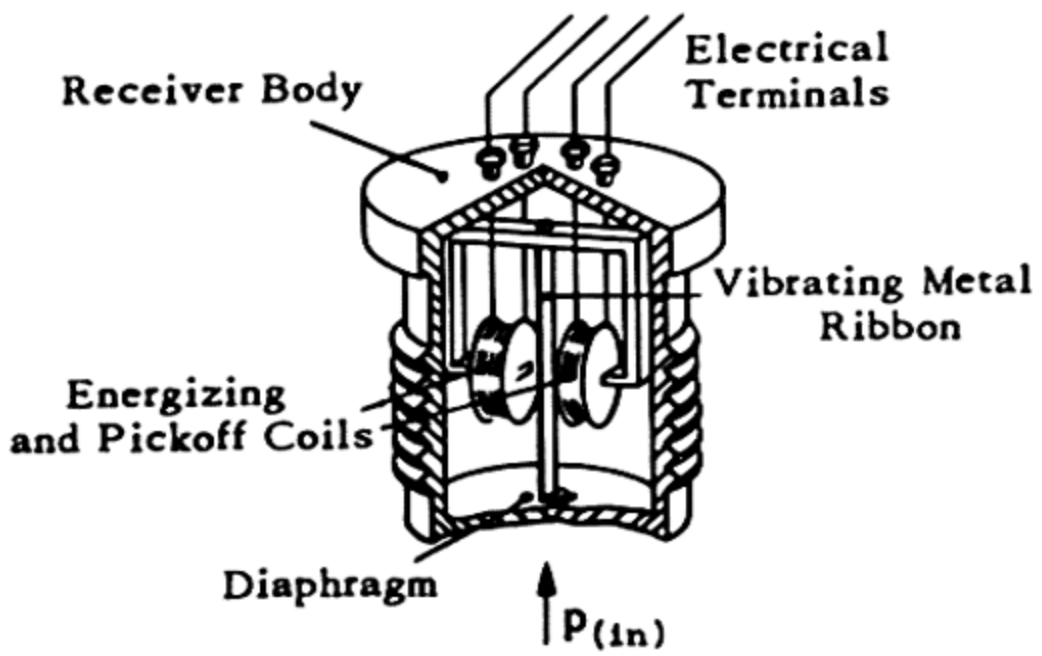
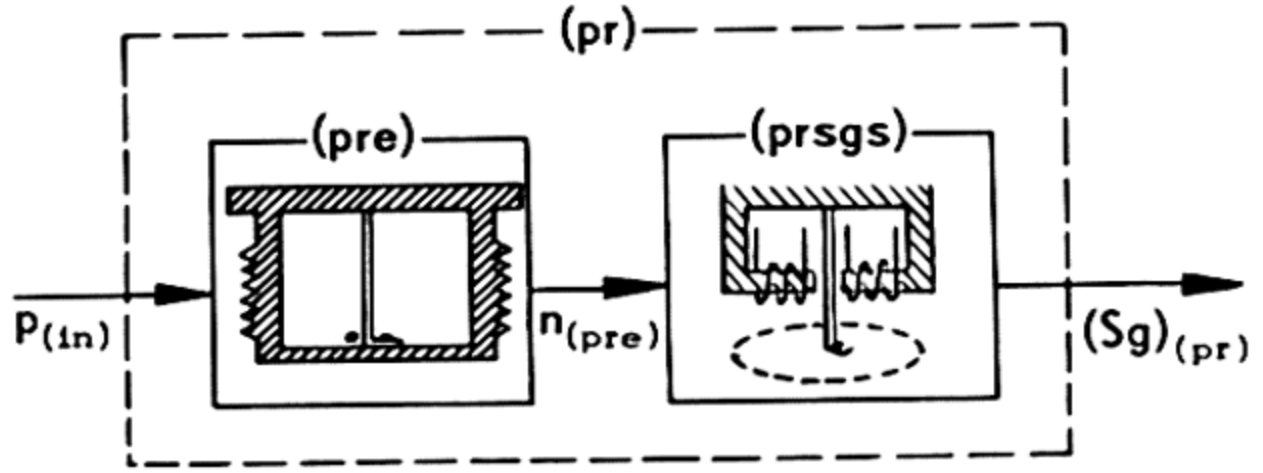


Fig. 33-4. Illustrative pictorial, static-functional, and basic electrical circuit diagrams for seven typical pressure receivers. (Page 1 of 3)

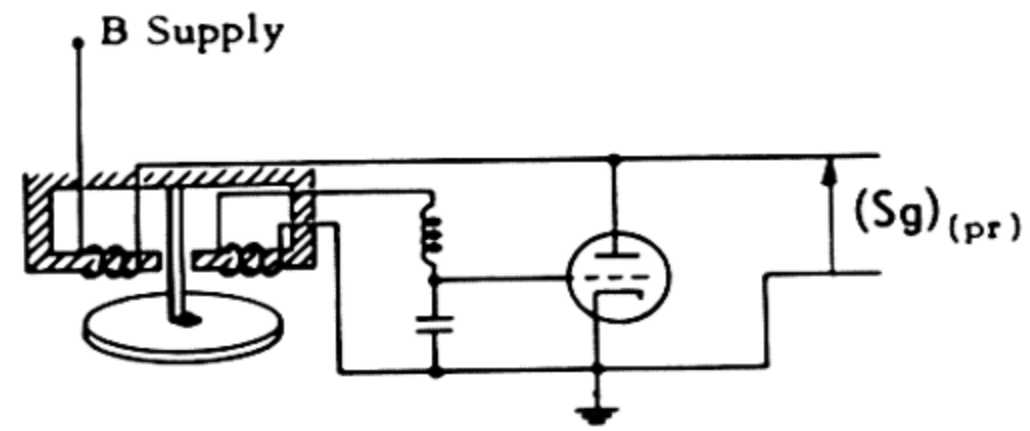
Pictorial Diagram



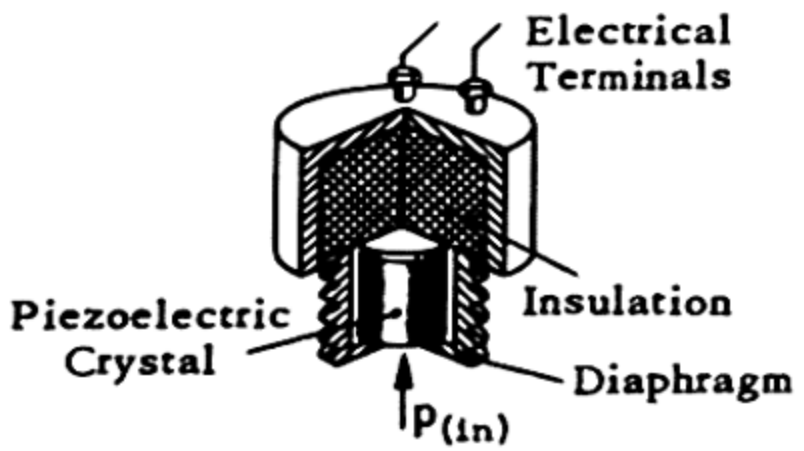
Static-Functional Diagram

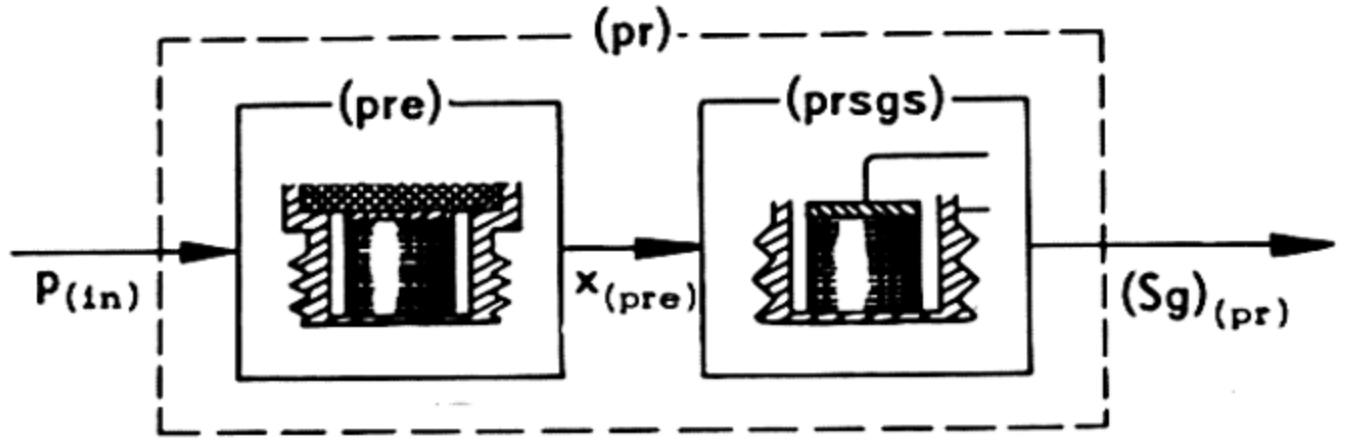


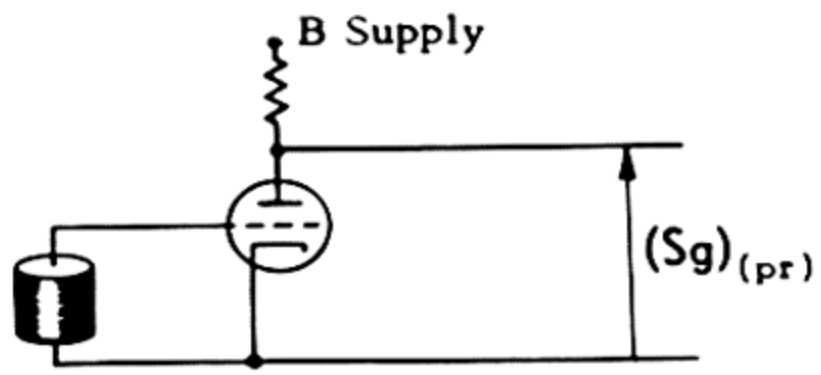
Basic Electrical Circuit Diagram



d) Tuned-ribbon-type pressure receiver

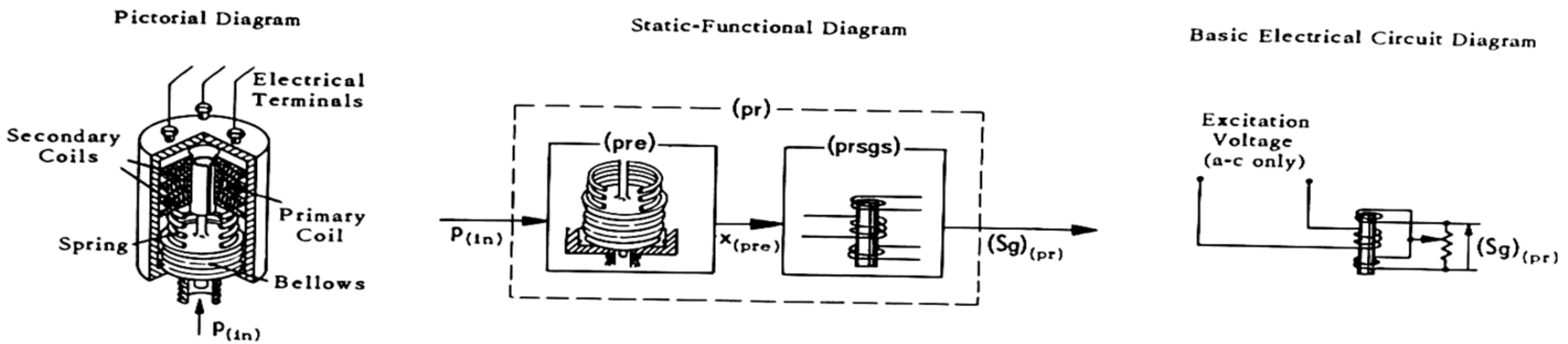




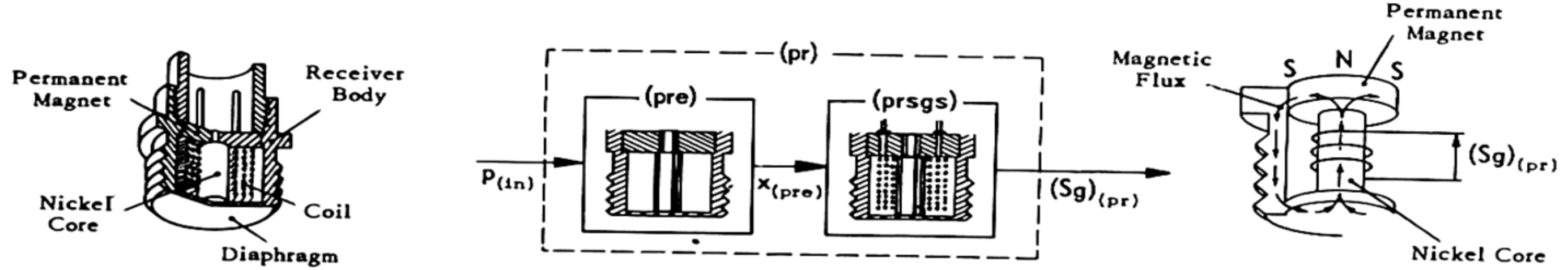


e) Diaphragm-piezoelectric-type pressure receiver

Fig. 33-4. Illustrative pictorial, static-functional, and basic electrical circuit diagrams for seven typical pressure receivers. (Page 2 of 3)



f) Bellows-inductance-type pressure receiver



g) Magnetostriction-type rate-of-change-of-pressure receiver.

Fig. 33-4. Illustrative pictorial, static-functional, and basic electrical circuit diagrams for seven typical pressure receivers. (Page 3 of 3)

function of the input pressure by the action of the connecting rod, which bends the cantilever and unbalances the bridge by changing the resistances in the carbon-stack arms through variations in compression between the discs.

33.24. Figure 33-4b illustrates the essential features of a strain-gage pressure receiver of the catenary-diaphragm type.* The pressure receiving element is a diaphragm designed with a double catenary shape to have maximum load-carrying capacity with minimum bending stiffness. The outer radius of the diaphragm is fixed to a shell (the receiver body) that screws into the vessel containing the pressure to be measured. At the inner boundary of the catenary annulus, the diaphragm is supported by the end of a strain tube whose radius is approximately equal to the shell radius. The diaphragm itself is so thin that the strain tube carries substantially all of the load corresponding to the input pressure. This means that strain in the tube is effectively proportional to the input pressure.

33.25. The pressure receiver signal generating system consists of the strain tube and two electrical-bridge arms of strain-sensitive wires bonded to the tube with high-temperature-resisting cement. Because the two arms occupy effectively the same space, they are subjected equally to all temperature variations, which thus have compensating effects as far as the output signal is concerned. One strain-gage winding has its wires looped parallel to the axis of the strain tube, while the other arm is looped circumferentially around the tube. With this arrangement, a given compressive strain in the tube produces a maximum net resistance unbalance between the two strain-wire bridge arms.

33.26. Two resistance-wire bridge arms, connected together through a potentiometer for balancing purposes, complete the resistance bridge as shown by the circuit diagram of Fig. 33-4b. Excitation, which may be either a-c or d-c, is supplied to the bridge across one pair of interconnection points for the arms. The voltage change appearing across the opposite pair of bridge connection points is the pressure receiver signal.

33.27. Figure 33-4c illustrates the essential features of a capacitance-type pressure receiver** whose pressure receiving element is a flat diaphragm. The deflection of this diaphragm under pressure changes the capacity of the condenser formed by the air gap, the inner surface of the diaphragm, and a fixed electrode parallel to the low-pressure surface of the diaphragm. The circuit diagram shows this condenser as an element of a tuned circuit in a rectifier detector system. The circuit is designed so that a variation in the condenser air gap causes a capacity change, which in turn modifies the resonant frequency of the tuned circuit. When this frequency changes with respect to the fixed-frequency oscillation of the excitation supply, the associated electrical circuits produce a voltage change that is

* See Draper and Li (D13).

** See Grinstead, Frawley, Chapman and Schultz (G11).

picked up by an inductively coupled winding and then rectified. This rectified voltage is the output signal of the pressure receiver.

33.28. Figure 33-4d shows the elements of a tuned-ribbon-type pressure receiver.* The pressure receiving element consists of a diaphragm and a thin strip of metal ribbon stretched between the diaphragm and the receiver body. The natural frequency of the ribbon in its lateral mode of vibration is a function of the tension of the ribbon. Since the tension of the ribbon is determined by diaphragm deflections, a change in the pressure applied to the diaphragm causes a change in the natural frequency of the ribbon. The ribbon motion is linked through the coils and magnetic circuit shown to an electronic unit that supplies power to the coils. The complete electromechanical system acts as an oscillator whose frequency is determined by the ribbon tension. The frequency of this oscillator is the output of the pressure receiver.

33.29. Figure 33-4e shows the essential elements of a piezoelectric-type pressure receiver.** The pressure receiving element consists of a diaphragm supported by a piezoelectric material, such as an X-cut quartz crystal. In principle, the elastic portion of the receiving element is composed of the combined structure of the diaphragm and the crystal, although the crystal is also used to produce the electrical signal. When pressure is applied to the diaphragm, a certain amount of strain is placed on the crystal, and an electrical charge is produced on the crystal faces due to the piezoelectric action. A voltage is determined by the charge, the capacity of the condenser formed by the crystal, and the leakage in the electrical connections to its surfaces. This voltage is the output signal of the pressure receiver.

33.30. Figure 33-4f shows the arrangement of the components in a typical bellows-inductance-type pressure receiver. The pressure receiving element of this receiver is a bellows supported by a coil spring to increase its mechanical stiffness. The deflection of the bellows under pressure produces axial motion of an iron sleeve inside a series of three coils. These coils are used as a transformer, with the center coil serving as the primary and the outer two coils as the secondary. The two secondary coils are connected in series opposition, so that with the cylindrical iron armature sleeve in its magnetically centralized position the net voltage output is zero. The armature is mechanically connected to the free end of the bellows and adjusted so that zero electrical signal occurs for zero input pressure. A constant frequency excitation is supplied to the primary of the signal generating system. The terminals of the series-connected secondaries join the ends of a potentiometer, with the common point connected to the slider for

---

* See Ohman (O4).

** See Head (H11).

balancing purposes. The pressure receiver output signal is taken from the potentiometer terminals.

33.31. Figure 33-4g shows the arrangement of a magnetostriction-type pressure receiver. The pressure receiving element of this unit consists of a diaphragm supported by a column made of some magnetostriction material such as nickel. A ring-shaped magnet is placed on top of the column. The case of the receiver and the diaphragm complete the magnetic flux circuit. A coil is placed outside the column to sense a change in flux. In operation, a change of pressure applied to the diaphragm causes a change of strain in the column and so produces a change in magnetic flux, which in turn produces a voltage across the coil. Because the coil can produce a voltage signal only in proportion to a change of flux, a device like this is virtually a rate-of-change-of-pressure pickup. An integration unit must be used if a pressure signal is desired.

PRESSURE-MEASURING SYSTEMS AS OPEN-CHAIN SYSTEMS

33.32. Pressure-measuring devices of various kinds are represented by illustrative diagrams in Figs. 33-1, 33-2, 33-3 and 33-4 from the standpoint of physical features. By judicious applications of the method illustrated in Chapters 2, 3, 7, 8, 31 and 32 it is possible to set up a more or less exact performance equation for each of the instruments described. When pressure-measuring units are considered, the technique in any given case is substantially identical with that demonstrated in the chapters noted. On the other hand, when systems are made up by the combination of several components, the procedure used for single units must be generalized to provide satisfactory solutions for the engineering problems of measurement. The illustrative diagrams of sections a and d of Fig. 33-1 show that measuring systems may be represented as open-chain combinations of operating components. This means that, from the standpoint of theory, the problem of developing performance equations for measuring systems is a special case of the problem of deriving the performance equation for the generalized open-chain system illustrated by Fig. 3-3 of Chapter 3.

33.33. Open-chain system performance equations depend on the performance equations for the operating components that make up the chain. For the purposes of the present discussion, it is assumed that performance equations or effectively equivalent information is known for each operating component before any attempt is made to derive the performance equation for a complete system. It is immaterial whether or not the internal organization of the components involved follows an open-chain pattern or some closed-chain pattern so long as proper information on the over-all performance that may be measured externally is available. For example, when a self-balancing bridge recorder has certain response

characteristics for indicating-system application, it is unimportant whether or not these characteristics depend on servomechanism actions within the recorder.

33.34. In the developing pattern of this book, the discussions of Chapters 31 and 32 have concerned themselves with typical measurement devices having performance characteristics describable by first- and second-order differential equations, respectively. The next step in complexity is the open-chain system made up of components with known characteristics. The pressure-measuring system is actually only one of many examples that fall into the open-chain category, but because of its place in a logical sequence of instruments with increasing complexity, it will be used in this chapter to illustrate methods suitable for treating generalized open-chain systems.

PERFORMANCE PROBLEMS ASSOCIATED WITH PRESSURE-MEASURING SYSTEMS

33.35. Performance information on pressure-measuring systems should make it possible to predict the response in terms of indicated pressure to any given input variation, or to determine the input change that must have occurred to produce a record of indicated pressure. In practice, the problems associated with description of performance occur in two ways:

1) Performance data are known for each component of the pressure-measuring system, and it is required to find the resultant performance characteristics of the complete system.
2) The measuring system is available in operational form, and it is necessary to determine performance characteristics from the response records produced by known input variations.

A third variant of the performance problem is associated with design. In this form, the problem is to select the performance characteristics of each one of a number of components so that they may actually be realized in practice and at the same time may be put together in an open-chain combination with specified over-all performance properties.

33.36. A very effective and widely used method of attack for all three aspects of the pressure-measuring-system performance problem is based on the steady-state response to a combination of sinusoidal input variations. This approach is generally useful because steady-state sinusoidal response is particularly simple to handle. The principles discussed in Chapter 12 make it possible to resolve many arbitrary pressure variations into the discrete sinusoidal components of a Fourier series. When the Fourier series representation is not satisfactory, it may be supplemented or replaced by Fourier integrals based on a continuous frequency spectrum of sinusoidal components.

33.37. When the representation of any given physical input is reduced to sinusoidal forms, the essential operational characteristics of any measuring unit

or system that receives the input may be based on steady-state performance equation solutions.* The discussion of Chapter 17 shows that, under these circumstances, differential equations may be replaced by easily derived relating functions that depend on forcing frequency and the equation coefficients. When the relating function is given, the response corresponding to a given sinusoidal forcing function component is found by taking the operational product of the relating function and the expression for the input variation. Generalized procedures and techniques for applying relating functions to solutions of problems in terms of steady-state sinusoidal components are described in Chapter 24. The corresponding information for open-chain systems is outlined in Procedure Summary 33-1, and the theoretical background for first- and second-order systems is given in Derivation Summaries 33-1 and 33-2, respectively.

33.38. The relating function is a concept derived from an extensive background of mathematical reasoning. However, this background is not required for ordinary engineering applications of the relating function and, in fact, it is usually an advantage to stress the physical significance of the concept rather than the mathematical implications involved. For this reason, it is practically useful to make the term performance function, defined in Chapter 3 on the basis of physical considerations, mathematically equivalent to the relating function of Chapter 17. Under the meaning of Chapter 3, the performance function for an operating component describes the performance of the component to the extent that the component produces output variations corresponding to given input changes. A number of mathematical forms and graphical representation methods for sinusoidal response characteristics in performance function terms are defined in Chapter 13.

PERFORMANCE FUNCTIONS FOR OPEN-CHAIN SYSTEMS

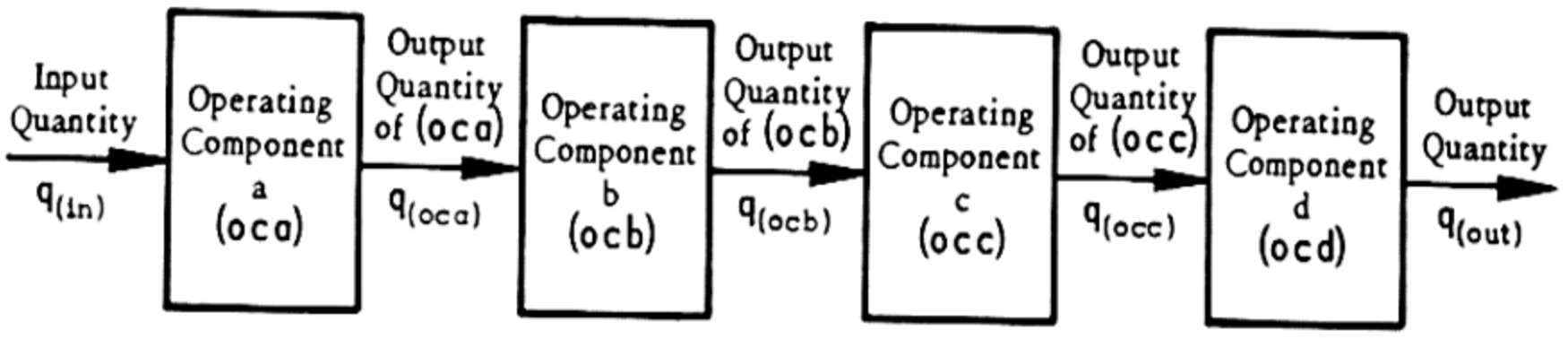
33.39. Measurement and control systems and their subsystems that are organized as open-chain configurations fit into the pattern that appears in Fig. 33-1. When open chains are to be analyzed, the frequency-response procedure of Chapter 24 is particularly effective. This technique may be applied by carrying out, in order, the steps detailed in Procedure Summary 33-1. Through this procedure, beginning with descriptive functional diagrams accompanied by component performance functions, performance function information for the complete system may be obtained.

33.40. From the standpoint of mathematical theory, the performance function forms of Definition Summary 13-6 have the properties of the relating function as this concept is defined and discussed in Chapter 17. The essential fact is that, as far as steady-state sinusoidal input components are concerned, the performance

---

* If equations are not available, frequency response plots may be used to describe performance characteristics.

1) Draw a functional diagram for the system under consideration, with names and symbols for all essential components and physical quantities. (Refer to Chapters 1, 2 and 3 of Volume I.)



2) List the operating characteristics for each of the components in terms of performance functions. These functions may be (a) given as special equations, (b) identified with standard equation forms, and (c) given as graphical plots based on experimental data. (Refer to Chapters 3, 4, 5, 6, 7, 10 and 13 of Volume I.) For the system represented by the functional diagram:

(oca) Operating component a

$$[PF]_{(oca)[q_{(in)};q_{(oca)}]} = f[(FR)_{(ref)}, P_1, P_2 \ldots] \qquad (1)$$

where

$$(FR)_{(ref)} = \frac{n_f}{n_{(ref)}} \qquad (2)$$

n_f = forcing frequency

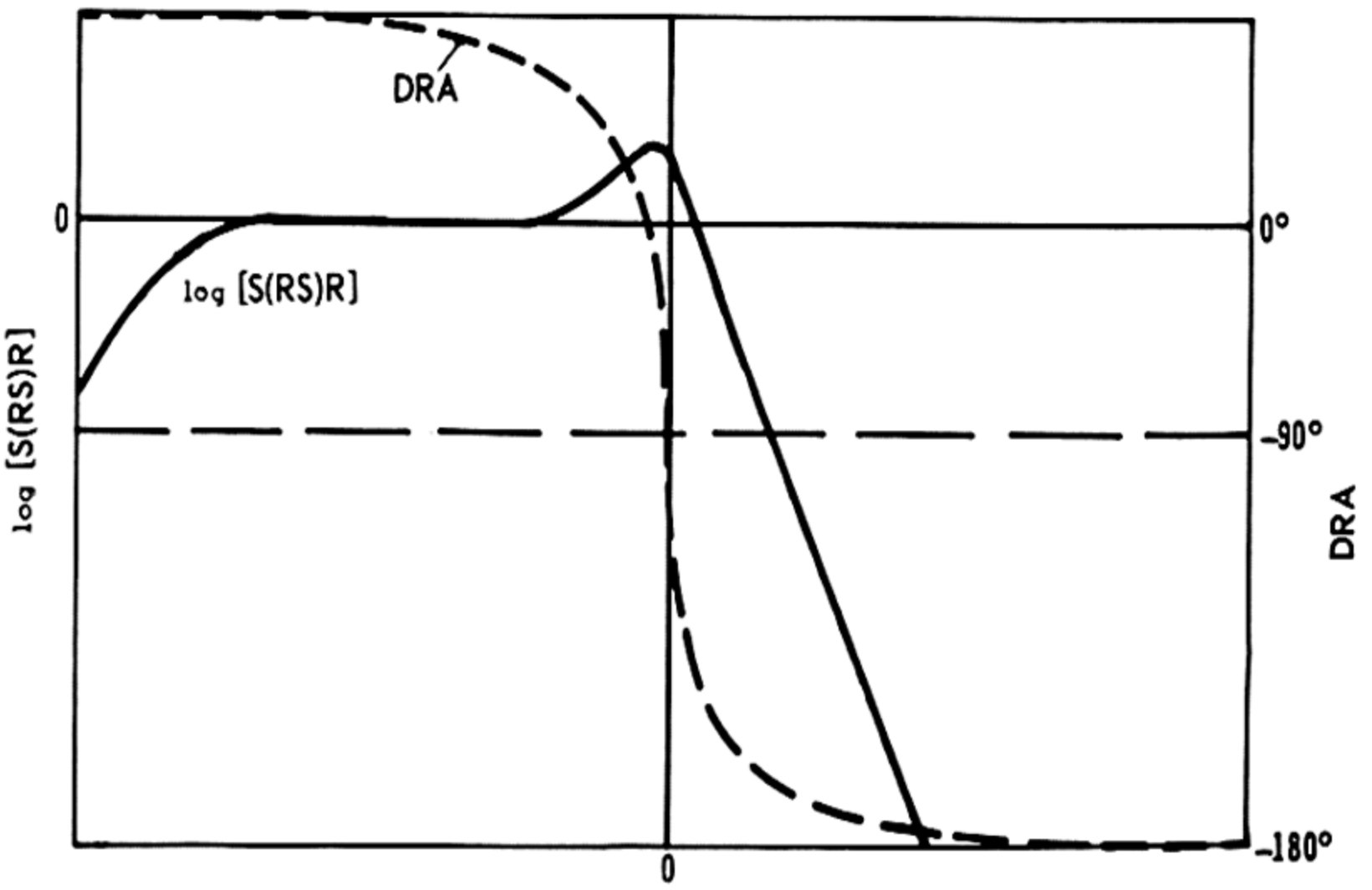
$n_{(ref)}$ = arbitrary reference frequency

= ____ cps. $n_{(ref)}$ is chosen at a value that reduces the $(FR)_{(ref)}$ numbers to simple values. It is usually convenient to take $n_{(ref)}$ as the multiple of ten nearest in value to the important undamped natural frequencies or reciprocal characteristic times of the components involved.

$P_1, P_2 \ldots$ = special parameters for Eq. (1)

(ocb) Operating component b

$[PF]_{(ocb)[q_{(oca)};q_{(ocb)}]}$ is given by plots:



(Refer to Chapter 13.)

$\log (FR)_{(ref)} = \log [n_f / n_{(ref)}]$ $\qquad n_{(ref)} =$ _____ cps

Procedure Summary 33-1. Logarithmic-scale-plot graphical method for finding open-chain performance functions from the performance functions of the operating components in the chains. (Page 1 of 3)

(occ) Operating component c

$$[PF]_{(occ)[q_{(ocb)};q_{(occ)}]} = [RF]_{(0;0,1)} \approx \eta_{(0;0,1)} \tag{3}$$

(Refer to Derivation Summary 18-10 and Figs. 18-6 through 18-9.)

$$S_{(occ)[q_{(ocb)};q_{(occ)}](ref)} = ____ \; ; \quad (CT)_{(occ)} = ____ \text{ seconds}$$

$$T_{(ref)} = \frac{1}{n_{(ref)}} = ____ \text{ seconds} \; ; \quad (bp)_{(occ)} = \frac{T_{(ref)}}{(CT)_{(occ)}} \frac{1}{2\pi} = ____ \tag{4),(5)}$$

(Refer to Derivation Summary 33-1.)

(ocd) Operating component d

$$[PF]_{(ocd)[q_{(occ)};q_{(out)}]} = [RF]_{(0;0,1,2)} \approx \eta_{(0;0,1,2)} \tag{6}$$

(Refer to Derivation Summary 19-10 and Figs. 19-27 through 19-37.)

$$n_n = ____ \text{ cps} \; ; \quad (DR) = ____$$

$$S_{(ocd)[q_{(occ)};q_{(out)}](ref)} = ____$$

$$n_{(ref)} = ____ \text{ cps} \; ; \quad (bp)_{(ocd)} = \frac{n_n}{n_{(ref)}} = ____$$

(Refer to Derivation Summary 33-2.)

3) Reduce all performance functions to reference sensitivities and curves of the logarithm of sensitivity – reference sensitivity ratio and the dynamic response angle plotted against the logarithm of reference frequency ratio based on a common reference frequency. Use identical scales for all component functions.

   Note: Profiles may be used to draw first- and second-order performance function curves. These profiles are located by break points and the low-frequency ratio asymptote (refer to Figs. 24-5, 24-11 and 24-12). For convenience, each curve should be labeled with the identifying letters of the operating component with which it is associated. To avoid confusion when several components are involved, it is desirable to make the plots of the sensitivity – reference sensitivity ratio separate from the plots of the dynamic response angle.

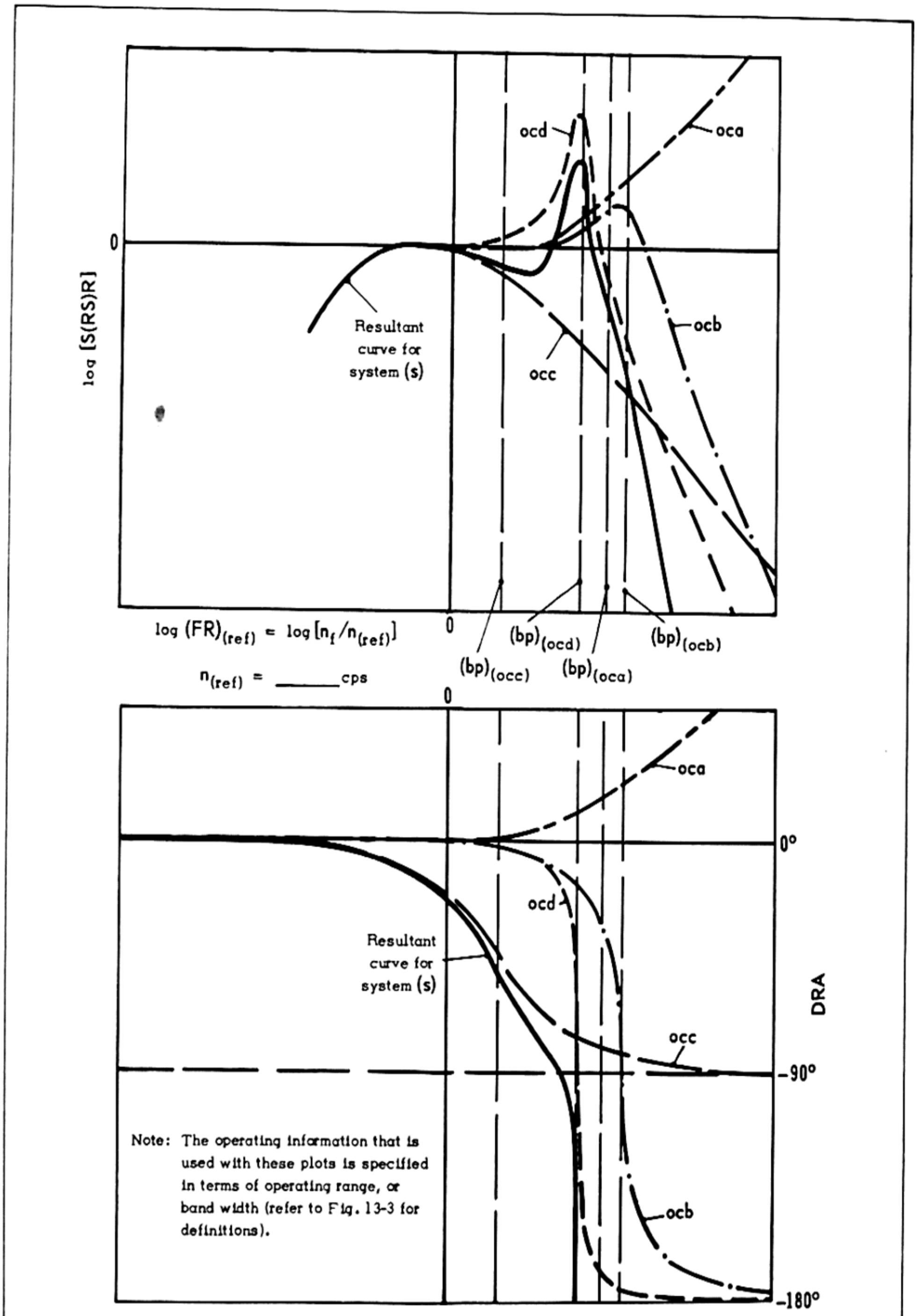
4) Sum the component curves graphically to generate plots of the sensitivity – reference sensitivity ratio and the dynamic response angle for the performance function of the complete system corresponding to the functional diagram of step 1. A technique for carrying out this summation is described in Procedure Summary 24-1.

5) Change the reference frequency ratio scale to a forcing frequency scale by marking the zero point on the reference frequency scale with the reference frequency and continuing the logarithmic frequency scale on either side of this point. (Note that for logarithms to be used, the frequency labels on the plot must actually be nondimensional with the reference frequency in this special case taken as unity.)

6) Find the reference sensitivity for the complete system as the product of reference sensitivities of the components; i.e.,

$$S_{(s)[q_{(in)};q_{(out)}](ref)} = S_{(oca)[q_{(in)};q_{(oca)}](ref)} S_{(ocb)[q_{(oca)};q_{(ocb)}](ref)} S_{(occ)[q_{(ocb)};q_{(occ)}](ref)} S_{(ocd)[q_{(occ)};q_{(out)}](ref)} \tag{7}$$

Procedure Summary 33-1. Logarithmic-scale-plot graphical method for finding open-chain performance functions from the performance functions of the operating components in the chains. (Page 2 of 3)



Graphical construction of sensitivity – reference sensitivity and dynamic response angle curves for system (s) described in step 4.

Procedure Summary 33-1. Logarithmic-scale-plot graphical method for finding open-chain performance functions from the performance functions of the operating components in the chains. (Page 3 of 3)

function for an open-chain system is the product of the performance functions for the components of the chain. This product may be

a) generated by conventional mathematical processes when the performance functions are expressed by equation forms,
b) found by numerical operations, or
c) generated by graphical procedures when the performance function information is available in the form of curves plotted in one of the typical forms that are illustrated by Fig. 13-1 and the figures of Chapter 24.

GRAPHICAL MANIPULATION OF COMPONENT PERFORMANCE FUNCTIONS TO PRODUCE OPEN-CHAIN SYSTEM PERFORMANCE FUNCTIONS

33.41. The representation illustrated by the curves of Fig. 13-1c is particularly effective for handling performance function problems with all degrees of complexity. Logarithms of frequency ratio are used for the abscissae, with dynamic response angle and the logarithms of the nondimensional amplitude ratio as the ordinates. Because multiplication corresponds to the addition of logarithms, the logarithm of the nondimensional amplitude ratio for the resultant performance function may be plotted by a simple addition of ordinates for the nondimensional amplitude ratio curves that are associated with the performance functions of the components. In a similar way, the resultant dynamic response angle curve is formed by addition of the corresponding curves for the component performance functions.

FIRST- AND SECOND-ORDER LOGARITHMIC-SCALE PERFORMANCE FUNCTION PROFILES

33.42. The background theory associated with the use of logarithmic-scale plots for the combination of component performance functions to form resultant performance functions is developed in generalized terms by discussions given in Chapter 24. Specialized derivations for first- and second-order performance functions are outlined respectively in Derivation Summaries 33-1 and 33-2. These summaries also provide complete information for computing all the necessary parameters from performance equations. Graphical techniques based on the use of templates with properly shaped profiles for quickly drawing logarithmic-scale plots of first- and second-order performance functions are discussed in Chapter 24. Profiles of these two types may actually be combined to produce any arbitrary performance function. In addition to the profile method, component performance functions may be described by mathematical equations of any order, or may be based on plots made from experimental measurements of amplitude ratios and dynamic response angles.

33.43. Plotting problems are simplified when equations are available for which standard-form profiles either may be purchased or made up as required. The generalized discussion of Derivation Summary 24-2 shows that it is always possible to make up a performance function for any arbitrary linear integro-

differential equation with constant coefficients from first- and second-order steady-state sinusoidal relating functions. In logarithmic coordinates, a wide range of situations may be covered by a relatively small number of profiles giving nondimensional amplitude ratios and dynamic response angles. These profiles have forms that are not affected by position on the abscissa scale and may be easily located on this scale by means of the break points defined in generalized terms in section a of Derivation Summary 24-2.

33.44. The essential features of the generalized performance function development in Derivation Summary 24-2 are repeated in simplified forms in Derivation Summary 33-1 for the first-order differential equation and in Derivation Summary 33-2 for the second-order differential equation. These summaries express results in terms of an arbitrarily selected reference frequency and break points. These break points depend only on the coefficients of the differential equations associated with the performance functions. In practice, the numbers representing the frequency ratios that are used for the logarithmic abscissa scale are simplified by choosing the reference frequency as the multiple of ten nearest in value to the important undamped natural frequencies or reciprocal characteristic times that are involved in any given problem. Profiles based on the final performance equation forms of Derivation Summaries 33-1 and 33-2 are used in finding solutions for many of the problems discussed in this volume.

DYNAMIC ERROR EFFECTS IN TERMS OF SINUSOIDAL RESPONSE CHARACTERISTICS

33.45. Dynamic error, as this term is defined in Chapter 6, appears in the scale readings of any measuring unit or measuring system when input variations become too rapid for the indicating mechanisms to follow accurately. The use of performance functions in the frequency response method provides an easily handled systematic pattern for reducing dynamic error information to quantitative terms. The basic features of this pattern are illustrated in Chapters 31 and 32, respectively, for units with first- and second-order characteristics. In this chapter, the pattern is extended to include open-chain combinations with an arbitrary number of components. Typical pressure-measuring systems are used as the illustrative examples for this development.

33.46. When a sinusoidal input variation is applied to a measuring unit or system, the corresponding readings are subject to dynamic errors of two types:

1) The over-all instrument sensitivity* is, in general, a function of the forcing frequency, so that it varies from the sensitivity for ideal performance.
2) The dynamic response angle is a function of forcing frequency, so that, in general, it differs from the value for ideal performance.

* This term is identical with the input quantity – scale reading sensitivity for a measuring instrument.

The (0;0,1) differential equation has the form (refer to Definition Summary 18-1)

$$a_1 \dot{v} + a_0 v = b_0 u \tag{1}$$

where

$$\dot{v} = \frac{dv}{dt}$$

a) Generalized (0;0,1) differential equation

Dividing the terms of Eq. (1) by a_0 gives

$$\frac{a_1}{a_0} \dot{v} + v = \frac{b_0}{a_0} u \tag{2}$$

In accordance with the notation of Eq. (2), Definition Summary 18-1, define

$$\sigma = \frac{b_0}{a_0} = \text{dimensional similarity factor} \tag{3}$$

$$r = (CT) = \frac{a_1}{a_0} = \text{characteristic time} \tag{4}$$

Note: Greek letters represent working variables. The symbol ≈ is used to mean "corresponds to."

In the symbols of Eqs. (3) and (4), Eq. (2) becomes

$$r \dot{v} + v = \sigma u \tag{5}$$

or

$$(CT) \dot{v} + v = \sigma u \tag{6}$$

b) (0;0,1) differential equation in special notation form

Consider the case of steady-state response to a sinusoidal forcing function (refer to Derivation Summaries 18-9 and 18-10).

Take (refer to Definition Summary 13-2)

$$u = u_a \epsilon^{j\omega_f t} \tag{7}$$

$$\omega_f = 2\pi n_f = \frac{2\pi}{T_f} = \text{angular forcing frequency} \tag{8}$$

$$n_f = \text{forcing frequency} \quad ; \quad T_f = \frac{1}{n_f} = \text{forcing period} \tag{9}$$

With the form of Eq. (7) substituted in Eq. (5)

$$r \dot{v} + v = \sigma u_a \epsilon^{j\omega_f t} \tag{10}$$

Assume a solution of the form

$$v = \eta u \tag{11}$$

where

$\eta \approx [RF]$ = relating function (refer to Chapter 17)

Equation (11) will give the steady-state solution of Eq. (10) when ω_f is constant and the proper form is used for η.

Differentiating Eq. (11) gives

$$\dot{v} = \eta \dot{u} = \eta j\omega_f u_a \epsilon^{j\omega_f t} = \eta j\omega_f u \tag{12}$$

Substituting the expressions of Eqs. (11) and (12) in Eq. (10) gives

$$\eta(j r\omega_f + 1) u = \sigma u \tag{13}$$

Derivation Summary 33-1. (0;0,1) equation performance function as the steady-state sinusoidal response for operating components with (0;0,1) characteristics: expressed in terms of reference frequency ratio and break point. (Page 1 of 5)

Equation (13) is always true when ω_f is constant if

$$\eta = \frac{\sigma}{1 + j2\pi a} \tag{14a}$$

Note that in common operational notation, with $p \longrightarrow d/dt$,

$$\eta = \frac{\sigma}{1 + p\,\tau} \tag{14b}$$

Identifying the results with the (0;0,1) equation by means of the subscript (0;0,1), and using the notation of Eqs. (3) through (14) of Derivation Summary 18-10 gives:

$$a = \frac{\tau}{T_f} = n_f \tau \approx [(CT)(FP)R] = \text{characteristic time – forcing period ratio} \tag{15}$$

$$\eta_{(0;0,1)} = \frac{\sigma}{1 + j2\pi a} \tag{16}$$

$$\eta_{(0;0,1)} = \rho_{(r)(0;0,1)}\,\mu_{(0;0,1)}\,\epsilon^{j\phi_{(0;0,1)}} \approx [RF]_{(0;0,1)} = \text{(0;0,1) equation relating function} \tag{17}$$

$$\rho_{(r)(0;0,1)} \approx (RAR)_{(0;0,1)} = \sigma = \text{(0;0,1) equation reference amplitude ratio} \tag{18}$$

$$\mu_{(0;0,1)} \approx [(DAR)(RAR)R]_{(0;0,1)} = \frac{1}{\sqrt{1 + (2\pi a)^2}} \tag{19}$$

= (0;0,1) equation dynamic amplitude ratio – reference amplitude ratio ratio (or (0;0,1) dimensionless amplitude ratio)

$$\phi_{(0;0,1)} \approx (DRA)_{(0;0,1)} = \tan^{-1}(-2\pi a) \tag{20}$$

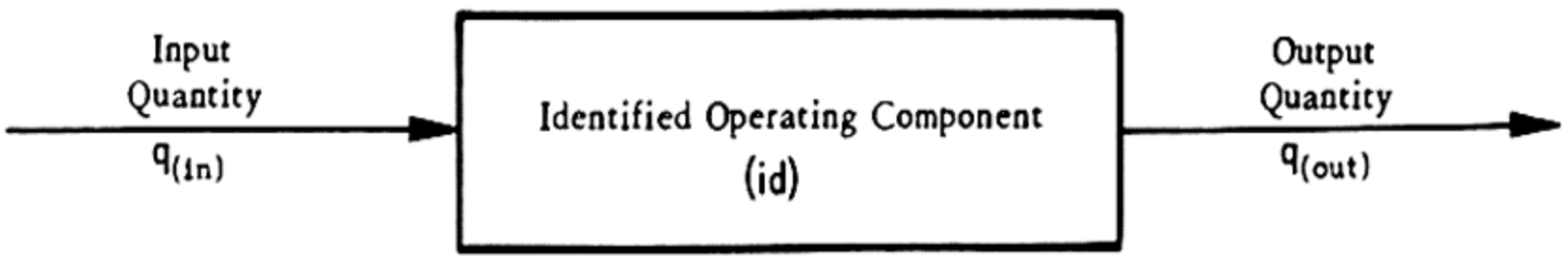
= (0;0,1) equation dynamic response angle (or (0;0,1) phase angle)

(See Figs. 18-6, 18-7, 18-8 and 18-9 for plots of $\mu_{(0;0,1)}$ and $\phi_{(0;0,1)}$.)

c) *Forms of the (0;0,1) equation relating function*

The relating function forms of Eqs. (16), (17), (19) and (20) may be used to describe the behavior of any operating component with a single input and a single output and having performance characteristics that are describable by a (0;0,1) linear differential equation with constant coefficients.

The typical functional diagram is



Let

$$U \approx q_{(in)} \quad ; \quad V \approx q_{(out)}$$

In the notation of Eqs. (1), (3), (19), (20) and (21) of Definition Summary 13-6, and Definition Summaries 28-6, 28-7 and 28-8,

$\eta \approx [RF] \longrightarrow [PF]_{(id)[q_{(in)};q_{(out)}]}$ = input quantity – output quantity performance function of (id) identified operating component

$\rho_r \approx (RAR)_{(id)[q_{(in)};q_{(out)}]}$ = input quantity – output quantity reference amplitude ratio for (id) identified operating component

Also

$\rho_r \approx (RAR)_{(id)[q_{(in)};q_{(out)}]} \approx S_{(id)[q_{(in)};q_{(out)}](ref)}$ = input quantity – output quantity reference sensitivity for (id) identified operating component

$\mu \approx [(DAR)(RAR)R]_{(id)(q_{(in)};q_{(out)})}$ = input quantity – output quantity dynamic amplitude ratio – reference amplitude ratio ratio for (id) identified operating component

* See Hildebrand (H13).

Derivation Summary 33-1. (0;0,1) equation performance function as the steady-state sinusoidal response for operating components with (0;0,1) characteristics: expressed in terms of reference frequency ratio and break point. (Page 2 of 5)

Also

$\mu \simeq [(DAR)(RAR)R]_{(id)(q_{(in)};q_{(out)})} \simeq [S(RS)R]_{(id)(q_{(in)};q_{(out)})}$ = input quantity – output quantity sensitivity – reference sensitivity ratio for (id) identified operating component

$\phi \simeq (DRA)_{(id)(q_{(in)};q_{(out)})}$ = input quantity – output quantity dynamic response angle for (id) identified operating component

Note: Square brackets, i.e., [ ], on the input-output subscript mean that dimensions and algebraic signs are required to completely define the symbol carrying the subscript. Rounded brackets, i.e., ( ), mean that the subscript quantities are for identification purposes only. (Refer to section b of Definition Summary 10-1.)

Also define:

$$n_f r = \frac{r}{T_f} \simeq \frac{(CT)}{T_f} = [(CT)(FP)R] = \text{characteristic time – forcing period ratio (repeated from Eq. (15))} \quad (21)$$

$$n_f r = \frac{r}{T_f} \simeq (CT)n_f = [(CT)(FF)P] = \text{characteristic time – forcing frequency product} \quad (22)$$

$T_{(ref)}$ = arbitrarily selected reference period

$n_{(ref)} = \frac{1}{T_{(ref)}}$ = reference frequency

$$\beta_r \simeq (FR)_{(ref)} = \frac{n_f}{n_{(ref)}} = \frac{T_{(ref)}}{T_f} = \text{reference frequency ratio} \quad (23)$$

$$[(RP)(CT)R] = \frac{T_{(ref)}}{(CT)} = \frac{T_{(ref)}}{a_1/a_0} = \text{reference period – characteristic time ratio} \quad (24)$$

Combining Eqs. (21), (23) and (24) shows that

$$\frac{(CT)}{T_f} = [(CT)(FP)R] = \frac{(CT)}{T_{(ref)}} \frac{T_{(ref)}}{T_f} = \frac{n_f}{n_{(ref)}} \frac{1}{\frac{T_{(ref)}}{(CT)}} = (FR)_{(ref)} \frac{1}{[(RP)(CT)R]} \quad (25)$$

d) Summary of performance function definitions and notation for the special case of an operating component with (0;0,1) characteristics

From Eqs. (15), (16), (19), (20), (21), (23), (24) and (25), the definitions of performance function and reference sensitivity given in section d are

$$\eta_{(0;0,1)} \simeq [PF]_{(id)[q_{(in)};q_{(out)}]} = \frac{S_{(id)[q_{(in)};q_{(out)}](ref)}}{1 + j2\pi \frac{(FR)_{(ref)}}{[(RP)(CT)R]}} \quad (26)$$

where

$$\sigma \simeq S_{(id)[q_{(in)};q_{(out)}](ref)} = \frac{b_0}{a_0} \quad (27)$$

and also

$$\mu_{(0;0,1)} \simeq [S(RS)R]_{(id)(q_{(in)};q_{(out)})} = \frac{1}{\sqrt{1 + \left(2\pi \frac{(FR)_{(ref)}}{[(RP)(CT)R]}\right)^2}} \quad (28)$$

Derivation Summary 33-1. (0;0,1) equation performance function as the steady-state sinusoidal response for operating components with (0;0,1) characteristics: expressed in terms of reference frequency ratio and break point. (Page 3 of 5)

$$\phi_{(0;0,1)} \approx (DRA)_{(id)(q_{(in)};q_{(out)})} = \tan^{-1}\left[-2\pi \frac{(FR)_{(ref)}}{[(RP)(CT)R]}\right] \tag{29}$$

e) *Performance function forms for operating components with (0;0,1) characteristics in terms of the reference frequency ratio and the reference period – characteristic time ratio*

Define

$$(bp)_{(0;0,1)} = \frac{[(RP)(CT)R]_{(0;0,1)}}{2\pi} = \frac{1}{2\pi}\frac{T_{(ref)}}{a_1/a_0} \tag{30}$$

$$= (0;0,1) \text{ equation break point}$$

Note: $(bp)_{(0;0,1)} \approx (FR)_{(ref)(bp)(0;0,1)} = (0;0,1)$ equation breakpoint reference frequency ratio. (Break points are also called corner points.)

Combining Eq. (30) with Eqs. (26), (28) and (29) gives

$$\eta_{(0;0,1)} \approx [PF]_{(id)[q_{(in)};q_{(out)}]} = \frac{S_{(id)[q_{(in)};q_{(out)}](ref)}}{1 + j\dfrac{(FR)_{(ref)}}{(bp)_{(0;0,1)}}} \tag{31}$$

$$\mu_{(0;0,1)} \approx [S(RS)R]_{(id)(q_{(in)};q_{(out)})} = \frac{1}{\sqrt{1 + \left(\dfrac{(FR)_{(ref)}}{(bp)_{(0;0,1)}}\right)^2}} \tag{32}$$

$$\phi_{(0;0,1)} \approx (DRA)_{(id)(q_{(in)};q_{(out)})} = \tan^{-1}\left[-\frac{(FR)_{(ref)}}{(bp)_{(0;0,1)}}\right] \tag{33}$$

Also

$$\sigma \approx S_{(id)[q_{(in)};q_{(out)}](ref)} = \frac{b_0}{a_0} \tag{27 (repeated)}$$

For reference purposes, the basic (0;0,1) equation is

$$a_1\dot{v} + a_0 v = b_0 u \tag{1 (repeated)}$$

f) *Performance function forms for operating components with (0;0,1) characteristics in terms of the reference frequency ratio and the break point*

Taking logarithms of both sides of Eq. (32) gives

$$\log [S(RS)R] = \log\left[1 + \frac{(FR)^2_{(ref)}}{(bp)^2_{(0;0,1)}}\right]^{-1/2} \tag{34}$$

When

$$\frac{(FR)^2_{(ref)}}{(bp)^2_{(0;0,1)}} << 1 \tag{35}$$

then

$$\log [S(RS)R]_{(FR/bp<<1)} = \log(1) = 0 \tag{36}$$

which is the equation for the low frequency ratio asymptote.

Derivation Summary 33-1. (0;0,1) equation performance function as the steady-state sinusoidal response for operating components with (0;0,1) characteristics: expressed in terms of reference frequency ratio and break point. (Page 4 of 5)

When

$$\frac{(FR)^2_{(ref)}}{(bp)^2_{(0;0,1)}} >> 1 \tag{37}$$

then

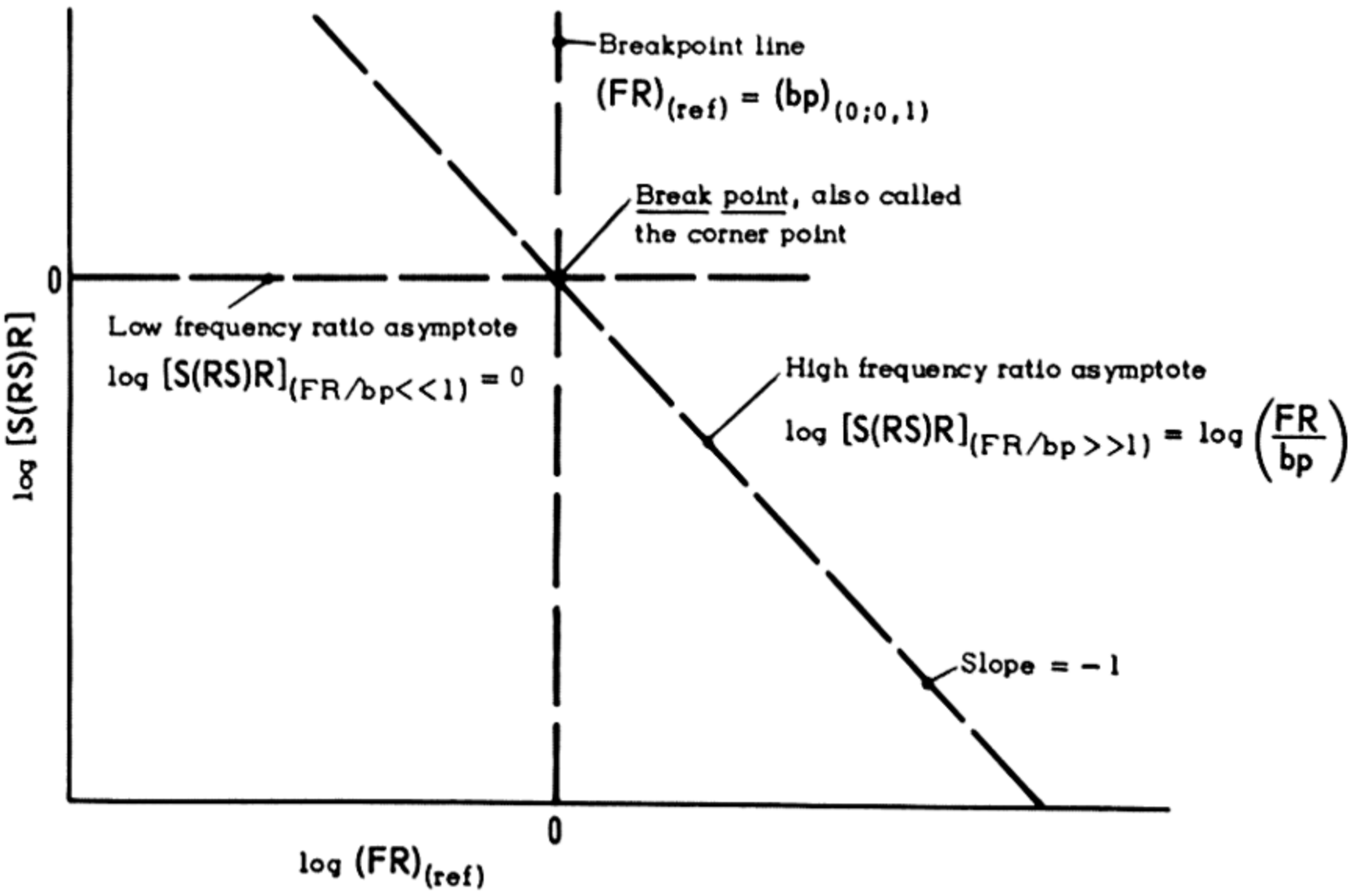
$$\log [S(RS)R]_{(FR/bp>>1)} = \log \left[\frac{(FR)_{(ref)}}{(bp)_{(0;0,1)}} \right]^{-1} \tag{38}$$

which is the equation for the high frequency ratio asymptote.

The high frequency asymptote intersects the low frequency asymptote at the break point, also called the corner point, which occurs when

$$\frac{(FR)_{(ref)(bp)}}{(bp)_{(0;0,1)}} = 1 \quad \text{so that} \quad (FR)_{(ref)(bp)} = (bp)_{(0;0,1)} \tag{39}$$

Note that $(DRA)_{(0;0,1)} = \tan^{-1}(-1) = -45°$ at the break point.



g) Logarithmic plot representation of the (0;0,1) performance function

Derivation Summary 33-1. (0;0,1) equation performance function as the steady-state sinusoidal response for operating components with (0;0,1) characteristics: expressed in terms of reference frequency ratio and break point. (Page 5 of 5)

The first effect causes actual reading magnitudes to differ from the corresponding correct reading magnitudes. The second effect causes a given point on a curve of indicated values to occur at an instant different from the correct instant. This difference in time is a special case of the response delay defined in Figs. 6-1 and 6-2 of Chapter 6 and corresponds to a phase shift between the correct curve of measured values and the actual curve of measured values.

33.47. When measurements are to be made of an input variation that may be represented by a single sinusoidal curve, or when attention is concentrated on

one frequency component of a complex wave form, a knowledge of instrument sensitivity for the given forcing frequency is sufficient information for obtaining accurate measurement information. On the other hand, when an instrument is required to supply records of input variations so complex that many sinusoidal components are required for satisfactory representations, variations in sensitivity and dynamic response angle with forcing frequency must be considered. The ideal situation for measurement purposes exists when the over-all instrument sensitivity is unity for all important forcing frequencies and the dynamic response angle remains constant over the same frequency range.

33.48. When the sensitivity and the dynamic response angle are not constant over the range of frequencies required to represent input variations, dynamic effects cause discrepancies between instrumental records and true input wave shapes. It generally is not possible to estimate the exact nature of these distortions for any given case without working through a detailed analysis. The procedure for determining the record shape that will be produced by an instrument with specified performance characteristics for a given input wave shape can be illustrated by typical examples. The examples discussed in this chapter are based on the cylinder pressure variation for a piston-type internal combustion engine and the corresponding records produced by measurement equipment with various types of performance defects.

33.49. The internal combustion engine cylinder indicator card shown in Figs. 12-8 and 12-10 of Chapter 12 is taken as one form of a complex input pressure variation. A spring-and-piston indicator of the type described in Figs. 8-1 and 8-2 of Chapter 8, with performance that may be represented by the second-order equation developed in Derivation Summary 8-1, is chosen as one of the instruments for recording the engine cylinder pressure. To illustrate the effect of changes in the range of frequencies required to describe the input variations, record shapes are calculated for engine speeds of 2400 rpm and 800 rmp. A system of the type illustrated in Fig. 33-1d, with a high-performance pressure receiver and a typical cathode-ray oscillograph indicating system, is chosen as a second instrument for recording the internal combustion engine cylinder pressure.

33.50. Pressure waves within turbojet engine turbine nozzle chambers (see Fig. 33-13) are taken as a second type of input pressure variation to be recorded by a measuring system similar to that of Fig. 33-1d. The measuring system is assumed to be made up of a bellows-actuated strain-gage pressure receiver, a carrier-frequency coupling amplifier, and a D'Arsonval galvanometer recording oscillograph. A pressure receiver coupler is used to transmit the input pressure from the nozzle chamber to the diaphragm of the receiver. This coupler consists of a fitting threaded for the pressure receiver and a small-diameter tube projecting through the chamber wall. In effect, this coupler is a

The (0;0,1,2) differential equation has the form (refer to Definition Summary 19-1)

$$a_2 \ddot{v} + a_1 \dot{v} + a_0 v = b_0 u \tag{1}$$

where

$$\dot{v} = \frac{dv}{dt} \quad ; \quad \ddot{v} = \frac{d^2 v}{dt^2}$$

a) Generalized (0;0,1,2) differential equation

Dividing the terms of Eq. (1) by a_0 gives

$$\frac{a_2}{a_0} \ddot{v} + \frac{a_1}{a_0} \dot{v} + v = \frac{b_0}{a_0} u \tag{2}$$

In accordance with the notation of Definition Summary 19-1, define

$$\sigma = \frac{b_0}{a_0} = \text{dimensional similarity factor} \tag{3}$$

$$\omega_n = w_n = \sqrt{\frac{a_0}{a_2}} = 2\pi n_n = \frac{2\pi}{T_n} = \text{undamped angular natural frequency} \tag{4}$$

n_n = undamped natural frequency

$$T_n = \frac{1}{n_n} = \text{undamped natural period} \tag{5}$$

$$\zeta \approx DR = \frac{a_1}{2\sqrt{a_0 a_2}} = \text{damping ratio} \tag{6}$$

Note: Greek letters represent working variables. The symbol ≈ is used to mean "corresponds to."

Using these definitions in Eq. (2) produces the forms

$$\frac{1}{\omega_n^2} \ddot{v} + \frac{2\zeta}{\omega_n} \dot{v} + v = \sigma u \tag{7}$$

or

$$\ddot{v} + 2\zeta\omega_n \dot{v} + \omega_n^2 v = \sigma \omega_n^2 u \tag{8}$$

Refer to Eq. (36) of Definition Summary 19-1.

b) (0;0,1,2) differential equation in special notation form

Consider the case of the steady-state response to a sinusoidal forcing function (refer to Derivation Summaries 19-9 and 19-10).

Take (refer to Definition Summary 13-2)

$$u = u_a \epsilon^{j\omega_f t} \tag{9}$$

where

$$\omega_f = 2\pi n_f = \frac{2\pi}{T_f} = \text{angular forcing frequency} \tag{10}$$

n_f = forcing frequency ; $T_f = \frac{1}{n_f}$ = forcing period

It remains to find the forced solution for the equation form

$$\ddot{v} + 2\zeta\omega_n \dot{v} + \omega_n^2 v = \sigma \omega_n^2 u_a \epsilon^{j\omega_f t} \tag{11}$$

Derivation Summary 33-2. (0;0,1,2) equation performance function as the steady-state sinusoidal response for operating components with (0;0,1,2) characteristics: expressed in terms of reference frequency ratio and break point. (Page 1 of 6)

Assume a solution of the form

$$V = \eta U = \eta U_a \epsilon^{j\omega_f t} \tag{12}$$

where

$\eta \approx [RF]$ = relating function (refer to Chapter 17)

Equation (12) will be true for ω_f = constant when the proper form is used for η

$$\dot{V} = \eta \dot{U} = \eta j\omega_f U_a \epsilon^{j\omega_f t} = \eta j\omega_f U \tag{13}$$

$$\ddot{V} = \eta \ddot{U} = \eta (j\omega_f)^2 U_a \epsilon^{j\omega_f t} = -\eta \omega_f^2 U \tag{14}$$

Substituting the expressions of Eqs. (12), (13) and (14) in Eq. (11) gives

$$\eta(-\omega_f^2 + j2\zeta\omega_n\omega_f + \omega_n^2) U = \sigma\omega_n^2 U \tag{15}$$

Dividing both sides of Eq. (15) by ω_n^2 and solving for η with

$$\beta \approx FR = \frac{\omega_f}{\omega_n} = \frac{n_f}{n_n} = \frac{T_n}{T_f} = \text{frequency ratio} \tag{16}$$

shows that

$$\eta = \frac{\sigma}{1 - \beta^2 + j2\zeta\beta} \tag{17a}$$

Note that in common operational notation, with $p \longrightarrow \frac{d}{dt}$,

$$\eta = \frac{\sigma}{\left(\frac{p}{w_n}\right)^2 + 2\zeta\frac{p}{w_n} + 1} \tag{17b}$$

When the transformations of section d, Derivation Summary 19-9, are used, Eq. (17) becomes identified with Eq. (6) of Derivation Summary 19-10; i.e.,

$$\eta_{(0;0,1,2)} = \sigma\mu_{(0;0,1,2)}\epsilon^{j\phi_{(0;0,1,2)}} \tag{18}$$

= (0;0,1,2) equation relating function

where

$$\mu_{(0;0,1,2)} \approx [(DAR)(RAR)R]_{(0;0,1,2)} = \frac{1}{\sqrt{(1-\beta^2)^2 + (2\zeta\beta)^2}} \tag{19}$$

= (0;0,1,2) equation dynamic amplitude ratio – reference amplitude ratio ratio (or (0;0,1,2) dimensionless amplitude ratio)

$$\phi_{(0;0,1,2)} \approx (DRA)_{(0;0,1,2)} = \tan^{-1}\frac{-2\zeta\beta}{1-\beta^2} \tag{20}$$

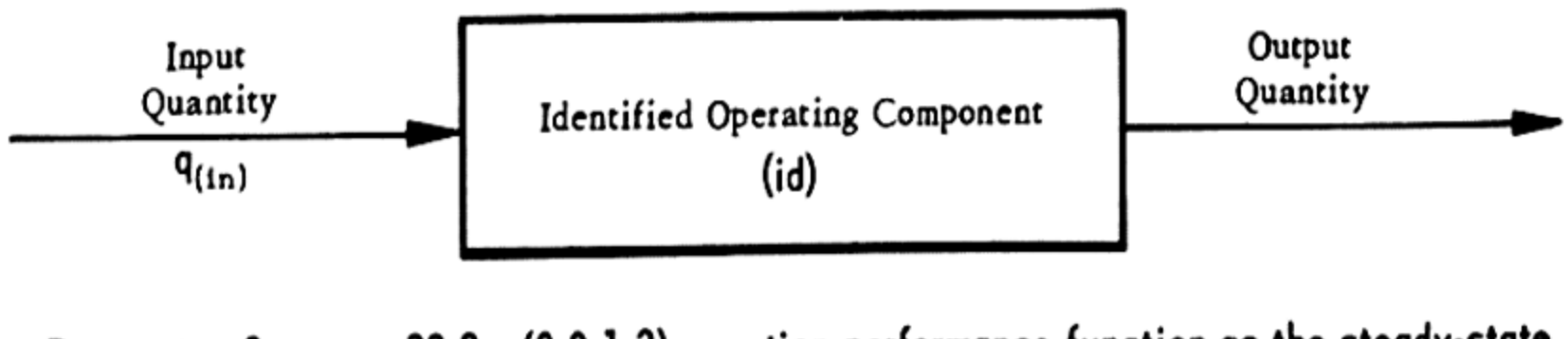
= (0;0,1,2) equation dynamic response angle (or (0;0,1,2) phase angle)

See curve families of Figs. 19-27 through 19-37 for plots of Eqs. (17), (19) and (20).

c) Forms of the (0;0,1,2) equation relating function

The forms of Eqs. (17), (18), (19) and (20) may be used to describe the behavior of any operating component with a single input and a single output, and with performance characteristics that are describable by a (0;0,1,2) linear equation with constant coefficients.

The typical functional diagram is



Derivation Summary 33-2. (0;0,1,2) equation performance function as the steady-state sinusoidal response for operating components with (0;0,1,2) characteristics: expressed in terms of reference frequency ratio and break point. (Page 2 of 6)

Let

$$u \simeq q_{(in)} \quad ; \quad v \simeq q_{(out)}$$

In the notation of Eqs. (1) and (3) of Definition Summary 13-6,

$\eta \simeq [PF]_{(id)[q_{(in)};q_{(out)}]}$ = input quantity – output quantity performance function of (id) identified operating component

See Definition Summaries 28-6, 28-7 and 28-8, and also section d of Derivation Summary 33-1 for additional definitions, symbols and references.

For the special case of an operating component with (0;0,1,2) characteristics,

$$\eta_{(0;0,1,2)} \simeq [PF]_{(id)[q_{(in)};q_{(out)}]} = \frac{S_{(id)[q_{(in)};q_{(out)}](ref)}}{1-(FR)^2 + j2(DR)(FR)} \tag{21}$$

$$\rho_r = \sigma \simeq S_{(id)[q_{(in)};q_{(out)}](ref)} = \frac{b_0}{a_0} \tag{22}$$

$$\mu_{(0;0,1,2)} \simeq [S(RS)R]_{(id)(q_{(in)};q_{(out)})} = \frac{1}{\sqrt{[1-(FR)^2]^2 + [2(DR)(FR)]^2}} \tag{23}$$

$$\phi_{(0;0,1,2)} \simeq (DRA)_{(id)(q_{(in)};q_{(out)})} = \tan^{-1}\left[\frac{-2(DR)(FR)}{1-(FR)^2}\right] \tag{24}$$

d) Performance function for an operating component with (0;0,1,2) characteristics in terms of damping ratio and frequency ratio

The frequency ratio variable of Eqs. (21), (23) and (24) may be reduced to the reference frequency ratio – breakpoint ratio form corresponding to the results of Derivation Summary 24-2 and Derivation Summary 33-1 by the following steps:

1. Choose $T_{(ref)}$, an arbitrarily selected reference period of convenient size.
2. Define

$$[(NF)(RF)R] = \frac{n_n}{n_{(ref)}} = \text{undamped natural frequency – reference frequency ratio} \tag{25}$$

When misunderstanding is unlikely, $[(NF)(RF)R]$ may be reduced to $(NFR) \equiv$ natural frequency ratio

3. Define

$$\beta_r \simeq (FR)_{(ref)} = \frac{n_f}{n_{(ref)}} = \text{reference frequency ratio} \tag{26}$$

Note that

$$FR = \frac{n_f}{n_n} = \frac{n_f}{n_{(ref)}} \frac{1}{n_n/n_{(ref)}} = \frac{(FR)_{(ref)}}{(NFR)} \tag{27}$$

In terms of the relationships of Eq. (27), Eqs. (21), (23) and (24) may be written in the forms

$$\eta_{(0;0,1,2)} \simeq [PF]_{(id)[q_{(in)};q_{(out)}]} = \frac{S_{(id)[q_{(in)};q_{(out)}](ref)}}{1 - \frac{(FR)^2_{(ref)}}{(NFR)^2} + j2(DR)\frac{(FR)_{(ref)}}{(NFR)}} \tag{28}$$

$$\mu_{(0;0,1,2)} \simeq [S(RS)R]_{(id)(q_{(in)};q_{(out)})} = \frac{1}{\sqrt{\left[1 - \frac{(FR)^2_{(ref)}}{(NFR)^2}\right]^2 + \left[2(DR)\frac{(FR)_{(ref)}}{(NFR)}\right]^2}} \tag{29}$$

Derivation Summary 33-2. (0;0,1,2) equation performance function as the steady-state sinusoidal response for operating components with (0;0,1,2) characteristics: expressed in terms of reference frequency ratio and break point. (Page 3 of 6)

$$\phi_{(0;0,1,2)} \approx (DRA)_{(1d)(q_{(in)};q_{(out)})} = \tan^{-1}\left[\frac{-2(DR)\dfrac{(FR)_{(ref)}}{(NFR)}}{1-\dfrac{(FR)^2_{(ref)}}{(NFR)^2}}\right] \tag{30}$$

e) *Performance function for an operating component with (0;0,1,2) characteristics in terms of damping ratio, reference frequency ratio, and natural frequency ratio*

Define

$(bp)_{(0;0,1,2)} = (NFR)$ = (0;0,1,2) equation break point

In terms of the break point, Eqs. (28), (29) and (30) become

$$\eta_{(0;0,1,2)} \approx [PF]_{(1d)[q_{(in)};q_{(out)}]} = \frac{S_{(1d)[q_{(in)};q_{(out)}](ref)}}{1-\dfrac{(FR)^2_{(ref)}}{(bp)^2_{(0;0,1,2)}} + j2(DR)\dfrac{(FR)_{(ref)}}{(bp)_{(0;0,1,2)}}} \tag{31}$$

$$\mu_{(0;0,1,2)} \approx [S(RS)R]_{(1d)(q_{(in)};q_{(out)})} = \frac{1}{\sqrt{\left[1-\dfrac{(FR)^2_{(ref)}}{(bp)^2_{(0;0,1,2)}}\right]^2 + \left[2(DR)\dfrac{(FR)_{(ref)}}{(bp)_{(0;0,1,2)}}\right]^2}} \tag{32}$$

$$\phi_{(0;0,1,2)} \approx (DRA)_{(1d)(q_{(in)};q_{(out)})} = \tan^{-1}\left[\frac{-2(DR)\dfrac{(FR)_{(ref)}}{(bp)_{(0;0,1,2)}}}{1-\dfrac{(FR)^2_{(ref)}}{(bp)^2_{(0;0,1,2)}}}\right] \tag{33}$$

(Refer to Derivation Summary 24-2.)

For convenience, definitions of the symbols of Eqs. (31), (32) and (33) are summarized below in terms of the coefficients of Eq. (1):

$$a_2\ddot{v} + a_1\dot{v} + a_0 v = b_0 u \qquad (1)\ \text{(repeated)}$$

$$\rho_r = \sigma \approx S_{(1d)[q_{(in)};q_{(out)}](ref)} = \frac{b_0}{a_0} \qquad (22)\ \text{(repeated)}$$

$$\omega_n \approx w_n = \sqrt{\frac{a_0}{a_2}} = 2\pi n_n = \frac{2\pi}{T_n} \qquad (4)\ \text{(repeated)}$$

$$\zeta \approx DR = \frac{a_1}{2\sqrt{a_0 a_2}} \qquad (6)\ \text{(repeated)}$$

$$\omega_f = 2\pi n_f = \frac{2\pi}{T_f} \qquad (10)\ \text{(repeated)}$$

$$\beta \approx FR = \frac{\omega_f}{\omega_n} = \frac{n_f}{n_n} = \frac{T_n}{T_f} \qquad (16)\ \text{(repeated)}$$

Derivation Summary 33-2. (0;0,1,2) equation performance function as the steady-state sinusoidal response for operating components with (0;0,1,2) characteristics: expressed in terms of reference frequency ratio and break point. (Page 4 of 6)

$$\beta_r \simeq (FR)_{(ref)} = \frac{\omega_f}{\omega_{(ref)}} = \frac{n_f}{n_{(ref)}} = \frac{T_{(ref)}}{T_f} \qquad (26)$$
(repeated with additions)

where

$T_{(ref)}$ = arbitrarily chosen reference period

$$(NFR) \simeq [(NF)(RF)R] = \frac{n_n}{n_{(ref)}} = \frac{T_{(ref)}}{T_n} = \frac{\omega_n}{\omega_{(ref)}} \qquad (25)$$
(repeated with additions)

$$(bp)_{(0;0,1,2)} = (NFR) = \frac{2\pi n_n}{2\pi n_{(ref)}} = \frac{1}{2\pi n_{(ref)}} \sqrt{\frac{a_0}{a_2}} \qquad (34)$$

f) Performance function for an operating component with (0;0,1,2) characteristics in terms of damping ratio, reference frequency ratio, and break point

In logarithmic coordinate terms,

$$\log \mu_{(0;0,1,2)} \simeq \log [S(RS)R]_{(id)(q_{(in)};q_{(out)})} = \log \left[\left(1 - \frac{(FR)^2_{(ref)}}{(bp)^2_{(0;0,1,2)}} \right)^2 + \left(2(DR) \frac{(FR)_{(ref)}}{(bp)_{(0;0,1,2)}} \right)^2 \right]^{-1/2} \qquad (35)$$

When

$$\frac{(FR)^2_{(ref)}}{(bp)^2_{(0;0,1,2)}} << 1 \qquad (36)$$

then

$$\log \mu_{(0;0,1,2)(FR/bp<<1)} \simeq \log [S(RS)R]_{(id)(q_{(in)};q_{(out)})(FR/bp<<1)} = \log (1)^{-1/2} = 0 \qquad (37)$$

which is the equation for the low frequency ratio asymptote.

When

$$\frac{(FR)^2_{(ref)}}{(bp)^2_{(0;0,1,2)}} >> 1 \qquad (38)$$

then

$$\log \mu_{(0;0,1,2)(FR/bp>>1)} \simeq \log [S(RS)R]_{(id)(q_{(in)};q_{(out)})(FR/bp>>1)} = \log \left[\frac{(FR)_{(ref)}}{(bp)_{(0;0,1,2)}} \right]^{-2} \qquad (39)$$

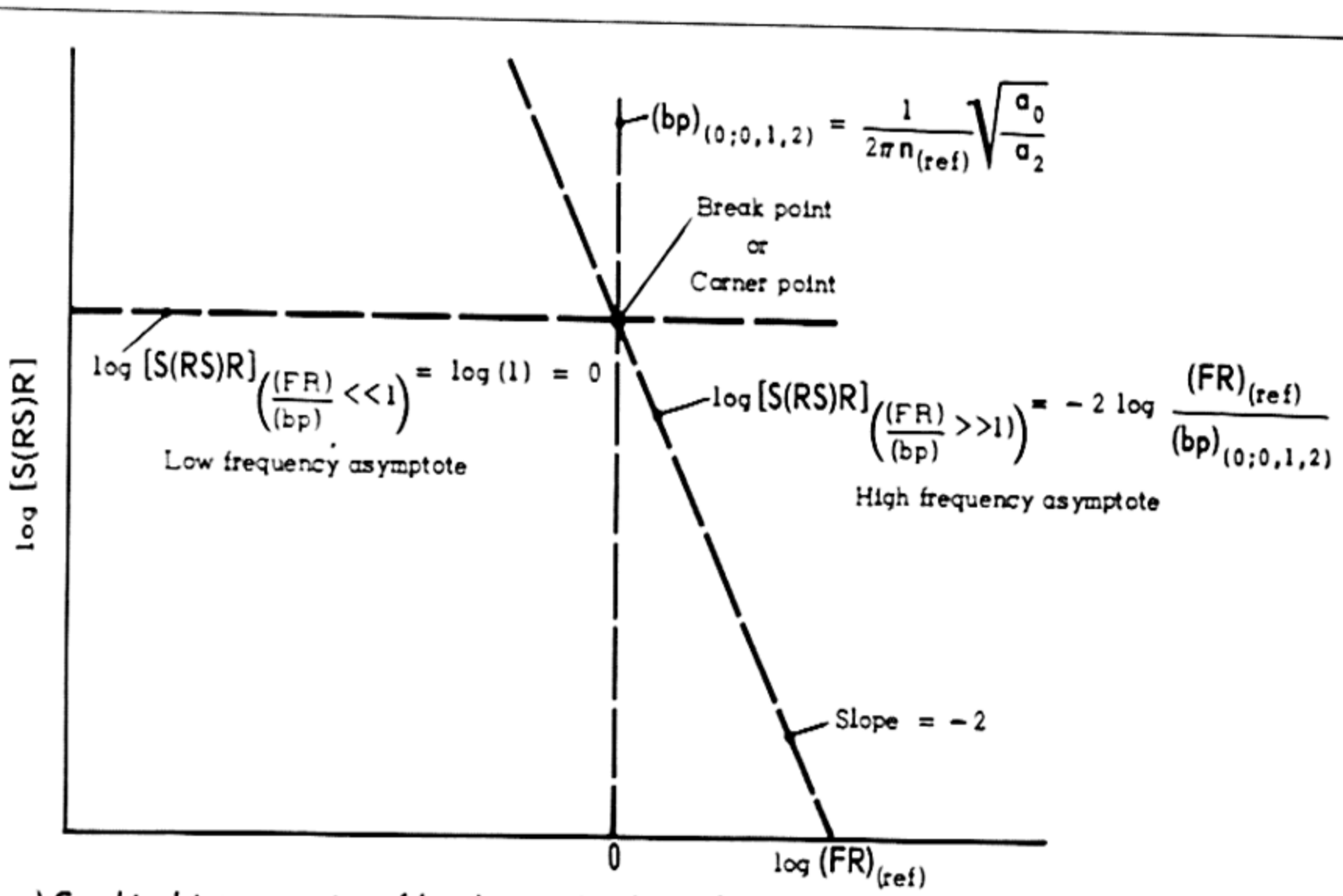
which is the equation for the high frequency ratio asymptote.

The high frequency ratio asymptote intersects the low frequency ratio asymptote at the break point (also called the corner point), which occurs when

$$\frac{(FR)_{(ref)(bp)}}{(bp)_{(0;0,1,2)}} = 1 \quad \text{so that} \quad (FR)_{(ref)(bp)} = (bp)_{(0;0,1,2)} \qquad (40)$$

Note that $(DRA)_{(0;0,1,2)} = \tan^{-1}(-\infty) = -90°$ at the break point.

Derivation Summary 33-2. (0;0,1,2) equation performance function as the steady-state sinusoidal response for operating components with (0;0,1,2) characteristics: expressed in terms of reference frequency ratio and break point. (Page 5 of 6)



g) Graphical interpretation of break point for the performance function of an operating component with (0;0,1,2) characteristics

Derivation Summary 33-2. (0;0,1,2) equation performance function as the steady-state sinusoidal response for operating components with (0;0,1,2) characteristics: expressed in terms of reference frequency ratio and break point. (Page 6 of 6)

narrow restriction that terminates in a cavity formed by the fitting and the bellows (see Fig. 33-13). To be satisfactory, the pressure-measuring system, including the receiver coupler, must record a specified range of input frequencies with tolerable accuracy.

33.51. The measuring-system examples are designed to include operating components with first- and second-order performance characteristics and also components with performance characteristics represented by plots not described by equations. In each example, the frequency response method is applied for finding the resultant performance of the complete system. This performance is derived from dimensionless sensitivity ratio and dynamic response angle curves for the components of the measuring systems. These curves are located by means of the break points defined in Derivation Summaries 33-1 and 33-2. The profiles described in Chapter 24 are used to introduce the effects of components having first- and second-order characteristics. With the over-all system performance characteristics determined, pressure-time records are plotted for comparison with the assumed input pressure variation.

INDICATOR CARDS FROM A SPRING-AND-PISTON-TYPE INDICATOR

33.52. Spring-and-piston-type indicators with the features illustrated in Fig. 8-1 generally have second-order performance equations. The development

of Fig. 8-2 and Derivation Summary 8-1 shows that, in particular, spring-and-piston-type indicator performance is described by the (0;0,1,2) differential equation.* The results of Derivation Summary 33-2 show that the performance function for a system with characteristics of this type is completely specified when the damping ratio (symbol DR $\approx \zeta$) and the undamped natural frequency (symbol n_n) are known (the reference sensitivity is taken as unity). For the purposes of the present discussion, the instrument for recording engine cylinder pressure variations, with the shape given by the heavy dashed-line curve of Fig. 12-8, is assumed to be a spring-and-piston-type indicator with a damping ratio of 0.1 and an undamped natural frequency of 154 cycles per second. The tabulation of Fig. 12-8 gives the amplitude ratios and phase angles for the components that combine in a Fourier series to give the input pressure wave as a function of time. The amplitude ratios are based on average cylinder pressure. The phase angles are based on bottom dead center of the compression stroke as the crankshaft angle reference and are expressed in terms of degrees for each individual order. The time scale depends on the engine speed, which effectively determines the frequency of the fundamental component in the series.

33.53. The technique described in Procedure Summary 33-1 is applied to find the amplitude ratios and phase angles for the Fourier components that combine to make up the record that would be obtained from the spring-and-piston indicator. The procedure is carried out graphically, with the second-order profile for 0.1 damping ratio used to introduce instrument characteristics. For convenience, the undamped natural frequency of the indicator is taken as the reference frequency defined in Derivation Summary 33-2. With this reference, the break point** of the indicator performance function is zero on the logarithmic reference frequency ratio scale. This point is unity on the corresponding linear reference frequency ratio scale.

33.54. Actual frequencies may be read directly with respect to a frequency ratio scale by changing the reference frequency to unity. When this transformation is made, unity on the ratio scale with the undamped natural frequency as the reference coincides with a frequency scale point numerically equal to the undamped natural frequency.

33.55. The frequency response method for finding indicator-card shapes in the problem under discussion is especially effective when the amplitude ratios of

---

* This fact is completely specified by writing $[PF]_{(ind)[p;p]} \approx \eta_{(0;0,1,2)} \approx [RF]_{(0;0,1,2)}$. In words, these symbols mean that the pressure input – pressure reading performance function (the over-all performance function) has the form of the relating function associated with the (0;0,1,2) differential equation, that is, the differential equation of the form $a_2\ddot{v} + a_1\dot{v} + a_0 v = b_0 u$. (See Definition Summary 28-8 for generalized symbols.)

** The break point for a second-order equation is defined in Derivation Summary 33-2.

the input wave shape are plotted on log-log coordinates using scales identical with those used for the second-order profiles.* When a plot of this kind is available, the first step is to shift the 0.1 damping ratio, second-order profile, which represents the performance of the indicator, along the frequency ratio scale so that its break point coincides with the indicator breakpoint frequency – engine cycle frequency ratio.** With the break point of the profile for the indicator over-all sensitivity*** properly located with respect to the log-log amplitude ratio plot for the input pressure variation, amplitude ratios for each sinusoidal component of the record may be formed by graphical addition of ordinates at the Fourier series component frequencies. This procedure is equivalent to multiplying Fourier series component amplitude ratios by the over-all indicator sensitivity for each frequency at which an input component occurs. Under the reasonable assumption that the amplitude ratios for the input wave components are not substantially changed by engine speed, results for any speed may be found by graphical additions when the profile break point is properly shifted with respect to the frequency ratio scale for the corresponding input amplitude ratio plot.

33.56. Figure 33-5 gives amplitude ratio and phase angle plots for the data of Fig. 12-8, with the logarithm of the rth component – first-order component frequency ratio taken as abscissa. Because only frequency ratios are involved, these two plots are valid for all engine speeds.

33.57. When the engine speed is 2400 rpm, there are 20 pressure cycles per second. This frequency is one-half the engine cycle frequency in revolutions per second.† For these conditions and the assumed spring-and-piston indicator, the breakpoint frequency – input series fundamental frequency ratio is 7.7, which is equal to 154 (the undamped natural frequency of the indicator) divided by 20. Figure 33-6a presents the indicator sensitivity curve (with its break point located at 7.7 on the input series component frequency ratio scale, that is, the rth-to-first-order frequency ratio scale), the input amplitude ratio curve and the resulting

---

* The profile scales use 2.5 inches for each logarithmic ratio unit, that is, each loru. This means that on a decibel scale, 1 decibel is represented by 0.125 inch.

** This ratio is, by definition, equal to

$$\frac{\text{Indicator breakpoint frequency}}{\left[\frac{\text{Engine revolution frequency}}{2}\right]}$$

where

indicator breakpoint frequency = indicator undamped natural frequency.

*** Definition Summary 29-2 shows that the ideal over-all sensitivity for any measuring instrument is unity. In the present case, the reference sensitivity is taken as unity, so that [S(RS)R], the sensitivity – reference sensitivity ratio, reduces to the over-all instrument sensitivity defined in Information Summary 32-2, and all the plots of Fig. 32-16 through Fig. 32-25 may be directly applied to calibrated pressure indicators.

† The data of Fig. 12-8 are based on a four-cycle engine, which requires two crankshaft revolutions to complete one indicator-card cycle.

indicator record amplitude ratio curve. The input amplitude ratio curve (solid dots) is drawn with short dashes; the indicator sensitivity curve has long dashes; and the indicator record amplitude ratio curve (hollow dots) is a full line. The ordinates of this full-line curve are the logarithms of the amplitude ratios of the Fourier series components that combine to represent the record produced by the indicator. Figure 33-6b gives the input phase angles, the indicator dynamic response angles, and the phase angles of the indicator record frequency components that correspond to the amplitude ratio and sensitivity plots of Fig. 33-6a.

33.58. Figure 33-7 gives a dashed-line curve showing the correct pressure ratio* and a full-line curve showing the indicated pressure ratio record for the 2400-rpm engine speed. The record is formed by combining the amplitude ratio and phase angle data from the full-line plots of Fig. 33-6. Each amplitude ratio and phase angle determines one sinusoidal component in the record, and the summation of all these components gives the indicated pressure as a function of time. The additions necessary for finding the resultant of many sinusoidal components is tedious if it is done either numerically or by graphical methods.

33.59. The indicated pressure ratio of Fig. 33-7 was found by use of a harmonic synthesizer developed in the Instrumentation Laboratory, Massachusetts Institute of Technology.** This device consists of synchros*** geared to a common drive in such a way that the relative rotational speeds correspond to the ratios of the sinusoidal component frequencies. One synchro is required for each sinusoidal component in the function to be synthesized. The phase angles among sinusoidal components are introduced by adjusting angular positions of the synchro stators with respect to the zero fundamental phase angle positions of the rotors. Amplitude ratios are introduced by potentiometers that control the fractional part of each synchro output to be added to the resultant sum that represents the synthesized function.

33.60. It is necessary to keep in mind the fact that the amplitude ratio and phase angle data given in Fig. 12-8 do not represent the complete information for the Fourier expression of the true cylinder pressure – average cylinder pressure curve. However, since the breakpoint frequency of the spring-and-piston indicator is relatively low, the twenty sinusoidal components available provide sufficient information to show the general features of the record that would be obtained from a spring-and-piston indicator with the assumed characteristics.

33.61. In Fig. 33-7, the deviations of the indicator record from the correct record include errors in magnitude, delays in response, and sinusoidal oscillations

---

* By definition, the pressure ratio is the ratio of a given instantaneous pressure level to the average cylinder pressure.

** This synthesizer is described in Seamans, Blasingame and Clementson (S18).

*** Synchros are used as sine wave generators.

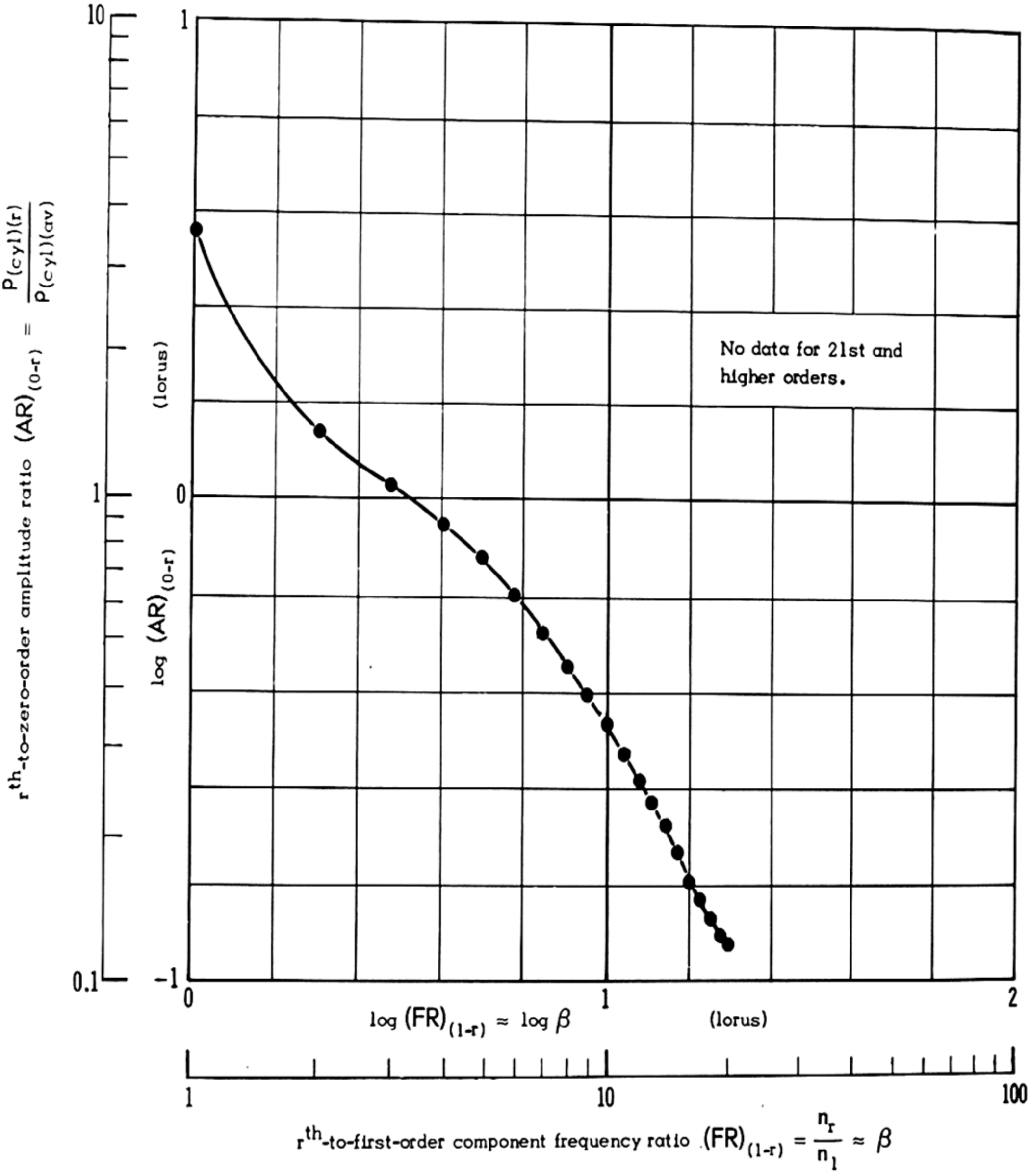
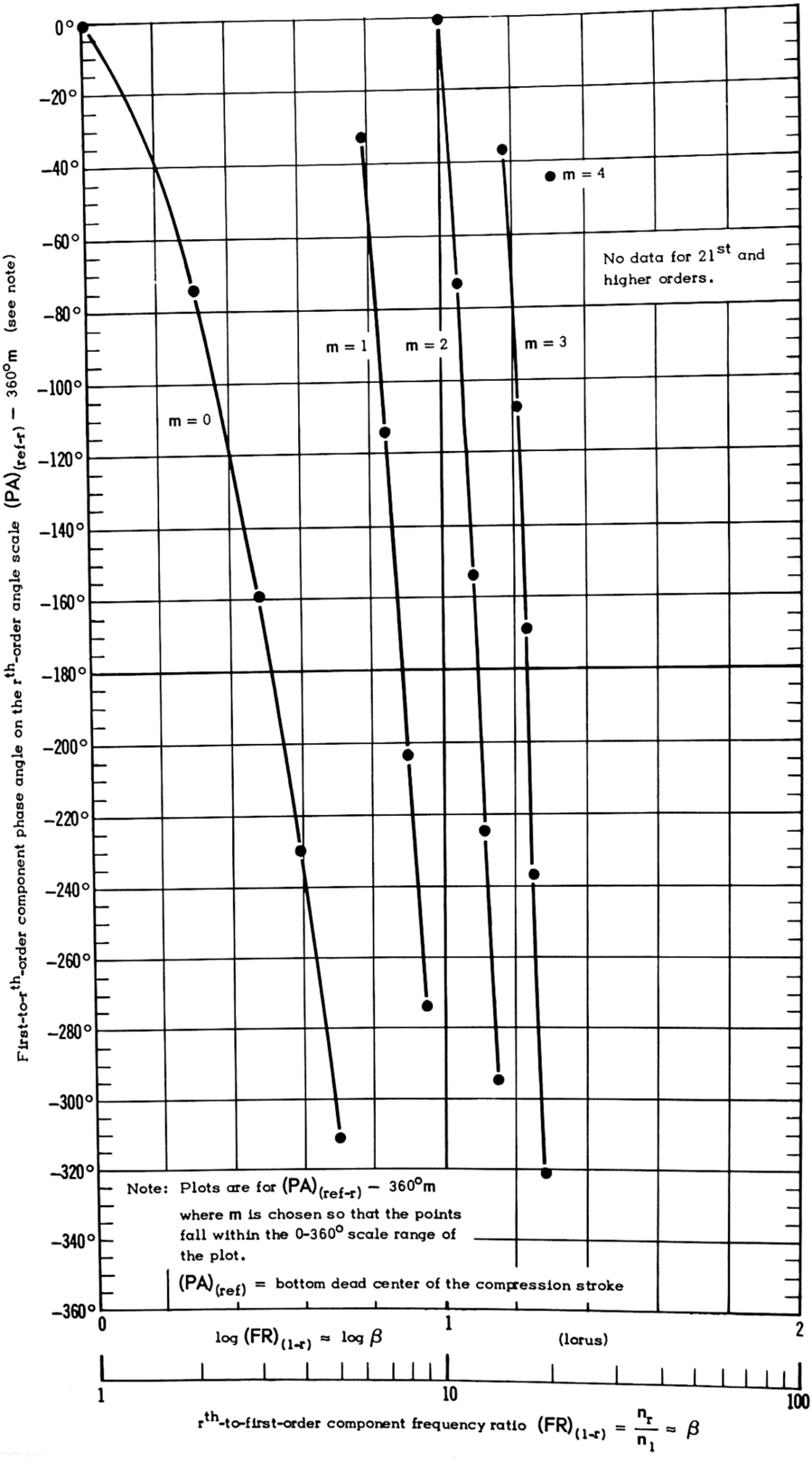


Fig. 33-5a. Illustrative logarithmic-scale plot of the Fourier-series amplitude ratios for the cylinder pressure record from an internal combustion engine given in Figs. 12-8 and 12-10.

Fig. 33-5b. Illustrative semilogarithmic-scale plot of the Fourier-series component phase angles for the cylinder pressure record from an internal combustion engine given in Figs. 12-8 and 12-10.


0°
−20°
−40°
−60°
−80°
−100°
−120°
−140°
−160°
−180°
−200°
−220°
−240°
−260°
−280°
−300°
−320°
−340°
−360°
m = 0
m = 1
m = 2
m = 3
m = 4
No data for 21st and higher orders.
Note: Plots are for (PA)(ref-r) − 360°m where m is chosen so that the points fall within the 0-360° scale range of the plot.
(PA)(ref) = bottom dead center of the compression stroke
First-to-rth-order component phase angle on the rth-order angle scale (PA)(ref-r) − 360°m (see note)
0
1
2
log (FR)(1-r) ≈ log β
(lorus)
1
10
100
rth-to-first-order component frequency ratio (FR)(1-r) = nr/n1 ≈ β

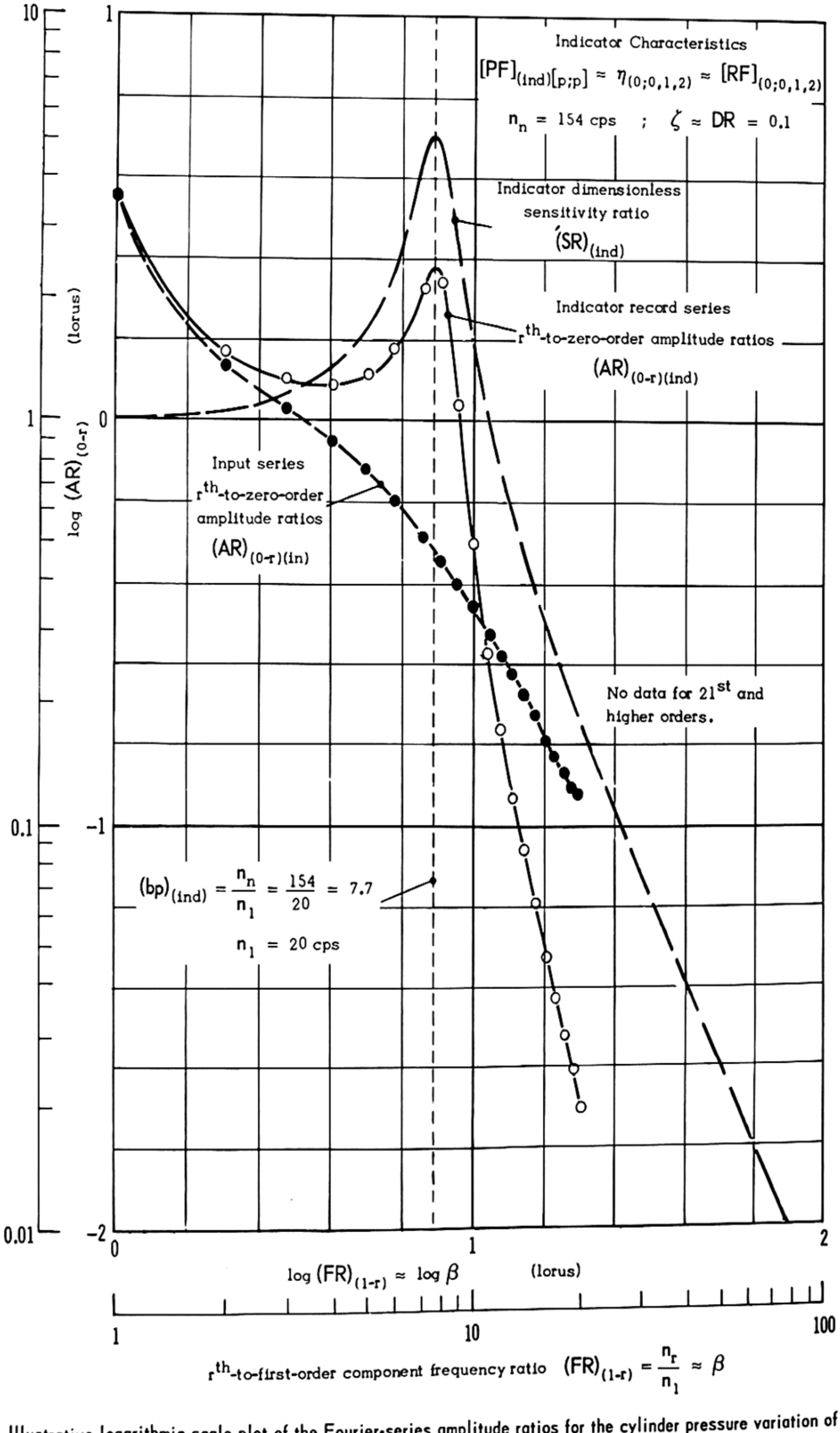


Fig. 33-6a. Illustrative logarithmic-scale plot of the Fourier-series amplitude ratios for the cylinder pressure variation of an internal combustion engine at 2400 rpm, and the corresponding amplitude ratios for the pressure record from a spring-and-piston indicator.

Fig. 33-6b. Illustrative semilogarithmic-scale plot of the Fourier-series component phase angles for the cylinder pressure variation of an internal combustion engine at 2400 rpm, and the corresponding phase angles for the pressure record from a spring-and-piston indicator.

Indicator Characteristics

$[PF]_{(ind)[p;p]} \approx \eta_{(0;0,1,2)} \approx [RF]_{(0;0,1,2)}$

n_n = 154 cps ; $\zeta \approx DR \approx 0.1$

Indicator dynamic response angle $(DRA)_{(ind)}$

Input series first-to-r^{th}-order phase angles $(PA)_{(1-r)(in)}$

Indicator record series first-to-r^{th}-order phase angles $(PA)_{(1-r)(ind)}$

m = 0

m = 1

m = 2

m = 3

m = 4

No data for 21st and higher orders

$(bp)_{(ind)} = \frac{n_n}{n_1} = \frac{154}{20} = 7.7$

n_1 = 20 cps

Note: Plots are for $(PA)_{(ref-r)} - 360°m$ where m is chosen so that the points fall within the 0-360° scale range of the plot.

$(PA)_{(ref)}$ = bottom dead center of the compression stroke

0°, −20°, −40°, −60°, −80°, −100°, −120°, −140°, −160°, −180°, −200°, −220°, −240°, −260°, −280°, −300°, −320°, −340°, −360°

First-to-r^{th}-order component phase angle on the rth-order angle scale $(PA)_{(ref-r)} - 360°m$ (see note)

0 1 2

$\log (FR)_{(1-r)} \approx \log \beta$

10 100

r^{th}-to-first-order component frequency ratio $(FR)_{(1-r)} = \frac{n_r}{n_1} \approx \beta$

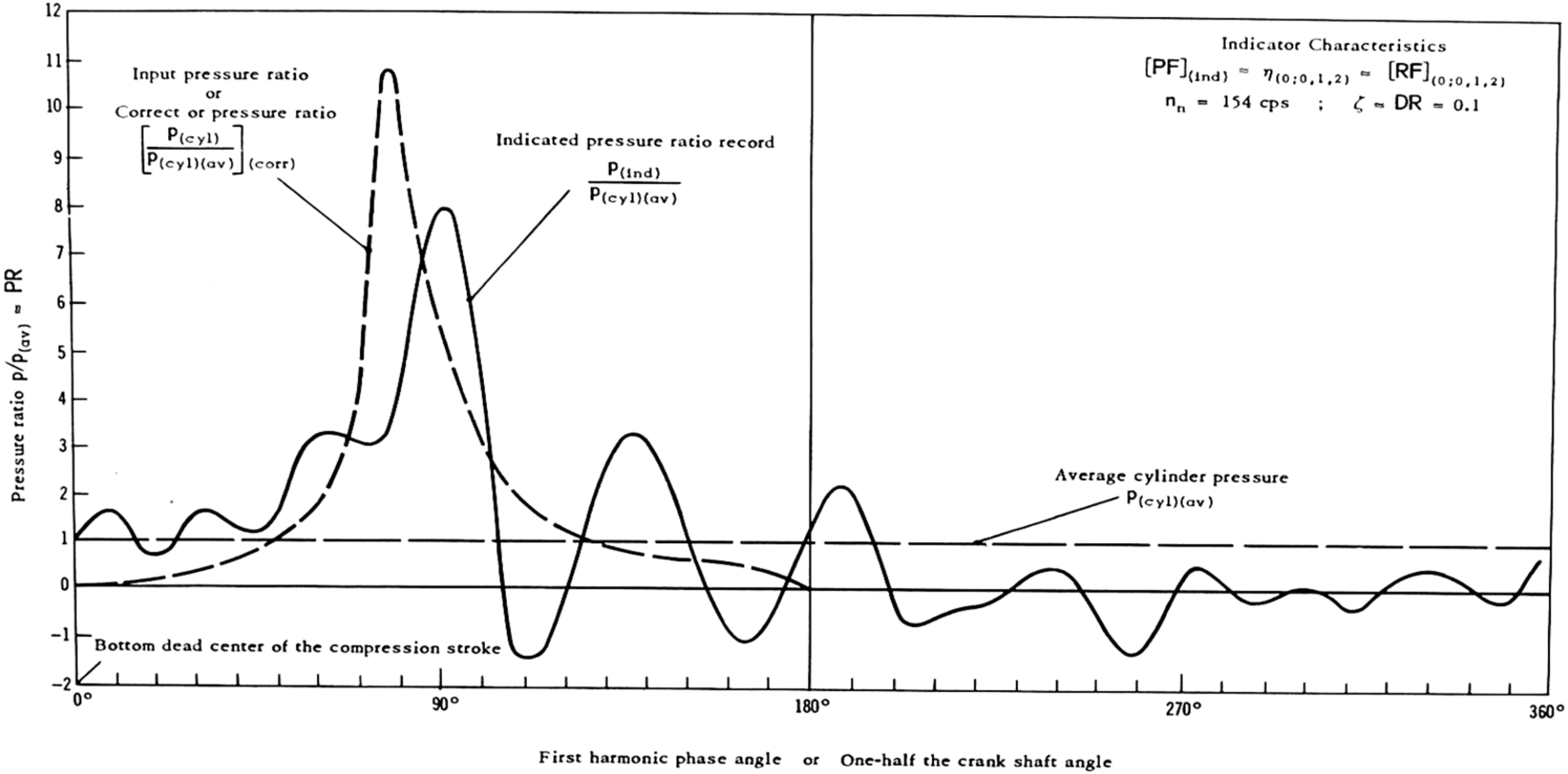


Fig. 33-7. Illustrative theoretical plot for the cylinder pressure variation of an internal combustion engine at 2400 rpm and the corresponding pressure record from a spring-and-piston indicator.

not present in the forcing pressure. The peak of the indicator record lags the true peak by 30 crankshaft degrees and has a magnitude equal to about 0.7 times the magnitude of the true peak. The oscillations introduced by the indicator have a frequency approximately equal to the undamped natural frequency of the indicator and a maximum amplitude equal to about 0.3 times the magnitude of the indicator record peak. The curves of Fig. 33-7 show at a glance that the assumed spring-and-piston indicator is unable to give satisfactory internal combustion engine cylinder pressure records at 2400 rpm. However, it is reasonable to expect that a reduction in engine speed would allow the indicator performance to improve since the input frequency components of large magnitude would be moved away from the undamped natural frequency of the indicator.

33.62. To illustrate the effect of reduced engine speed on the records that would be obtained from the assumed spring-and-piston indicator, the indicated pressure record is determined for an engine speed of 800 rpm. The log-log amplitude ratio plots of Fig. 33-8a for this engine speed correspond to the amplitude ratio plots of Fig. 33-6a for 2400 rpm. Similarly, the phase angle plots of Fig. 33-8b for 800 rpm correspond to the plots of Fig. 33-6b for 2400 rpm.

33.63. Figure 33-9 gives plots of correct pressure ratio and indicated pressure ratio for 800 rpm that correspond to the curves of Fig. 33-7. The procedure used in deriving the 800-rpm indicated pressure ratio curves is identical with that already described in finding the 2400-rpm indicated pressure ratio plots. The derived indicator record of Fig. 33-9 is a better approximation to the correct record than the record of Fig. 33-7, but the dynamic errors still have magnitudes that are intolerably great. The indicated peak has a magnitude about 0.9 times the magnitude of the correct peak and is delayed from the correct peak by about 12 degrees of crankshaft travel. The indicator natural frequency oscillations that appear on the record have a maximum amplitude approximately 0.2 times the amplitude of the record peak.

ELECTRICAL PRESSURE-RECORDING SYSTEM

33.64. Pressure records of a given complex wave form, as taken from a given indicator that is subject to dynamic errors, will improve as the pressure variation is restricted to relatively slow rates. A comparison of Figs. 33-7 and 33-9 illustrates this effect. The essential factor is the magnitude of the undamped natural frequency of the indicator with respect to the important frequency components in the forcing pressure variation. When the input wave contains sudden changes, the Fourier series representation must include strong high-frequency components. The sudden rise in the internal combustion engine pressure corresponding to combustion is a pressure variation of this type. Even if the engine speed were made very low, the steep combustion rise would mean the presence of

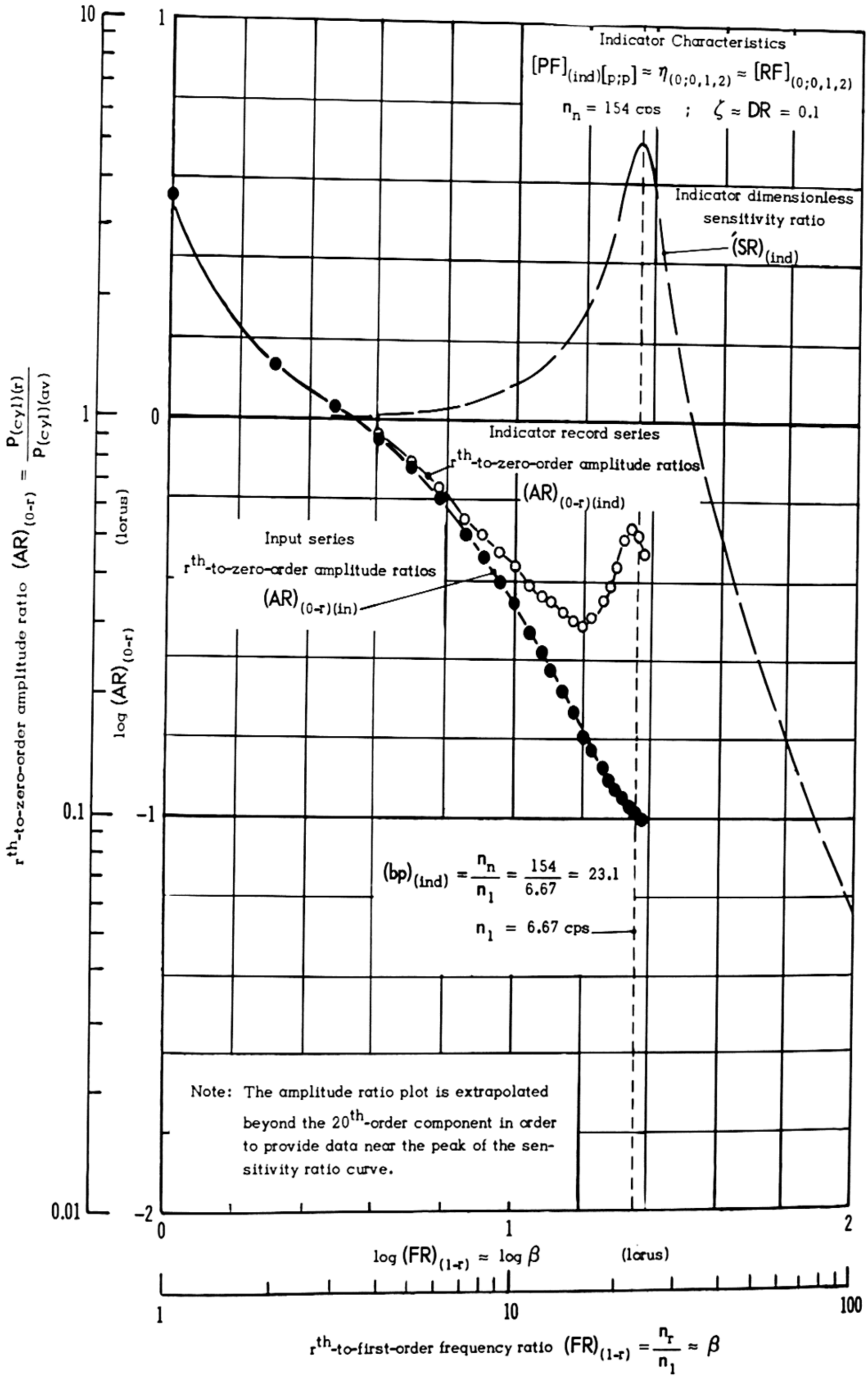
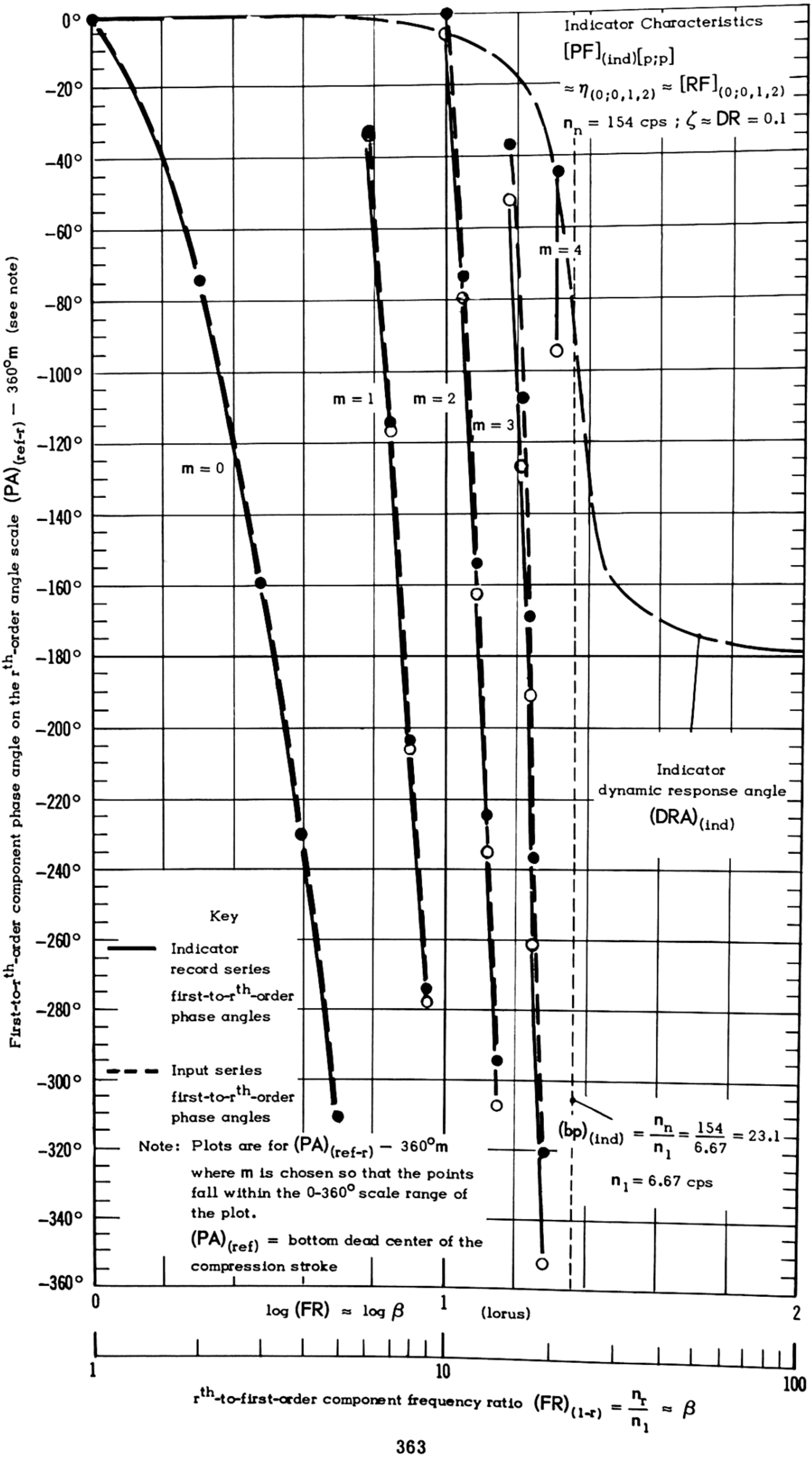


Fig. 33-8a. Illustrative semilogarithmic-scale plot of the Fourier-series amplitude ratios for the cylinder pressure variation of an internal combustion engine at 800 rpm, and the corresponding amplitude ratios for the pressure record from a spring-and-piston indicator.

Fig. 33-8b. Illustrative semilogarithmic-scale plot of the Fourier-series component phase angles for the cylinder pressure variation of an internal combustion engine at 800 rpm, and the corresponding phase angles for the pressure record from a spring-and-piston indicator.


Indicator Characteristics
[PF](ind)[p;p]
≈ η(0;0,1,2) ≈ [RF](0;0,1,2)
nn = 154 cps ; ζ ≈ DR = 0.1
m = 0
m = 1
m = 2
m = 3
m = 4
0°
-20°
-40°
-60°
-80°
-100°
-120°
-140°
-160°
-180°
-200°
-220°
-240°
-260°
-280°
-300°
-320°
-340°
-360°
First-to-rth-order component phase angle on the rth-order angle scale (PA)(ref-r) − 360°m (see note)
Indicator dynamic response angle (DRA)(ind)
Key
Indicator record series first-to-rth-order phase angles
Input series first-to-rth-order phase angles
Note: Plots are for (PA)(ref-r) − 360°m where m is chosen so that the points fall within the 0-360° scale range of the plot.
(PA)(ref) = bottom dead center of the compression stroke
(bp)(ind) = nn/n1 = 154/6.67 = 23.1
n1 = 6.67 cps
0
log (FR) ≈ log β
1
(lorus)
2
1
10
100
rth-to-first-order component frequency ratio (FR)(1-r) = nr/n1 ≈ β

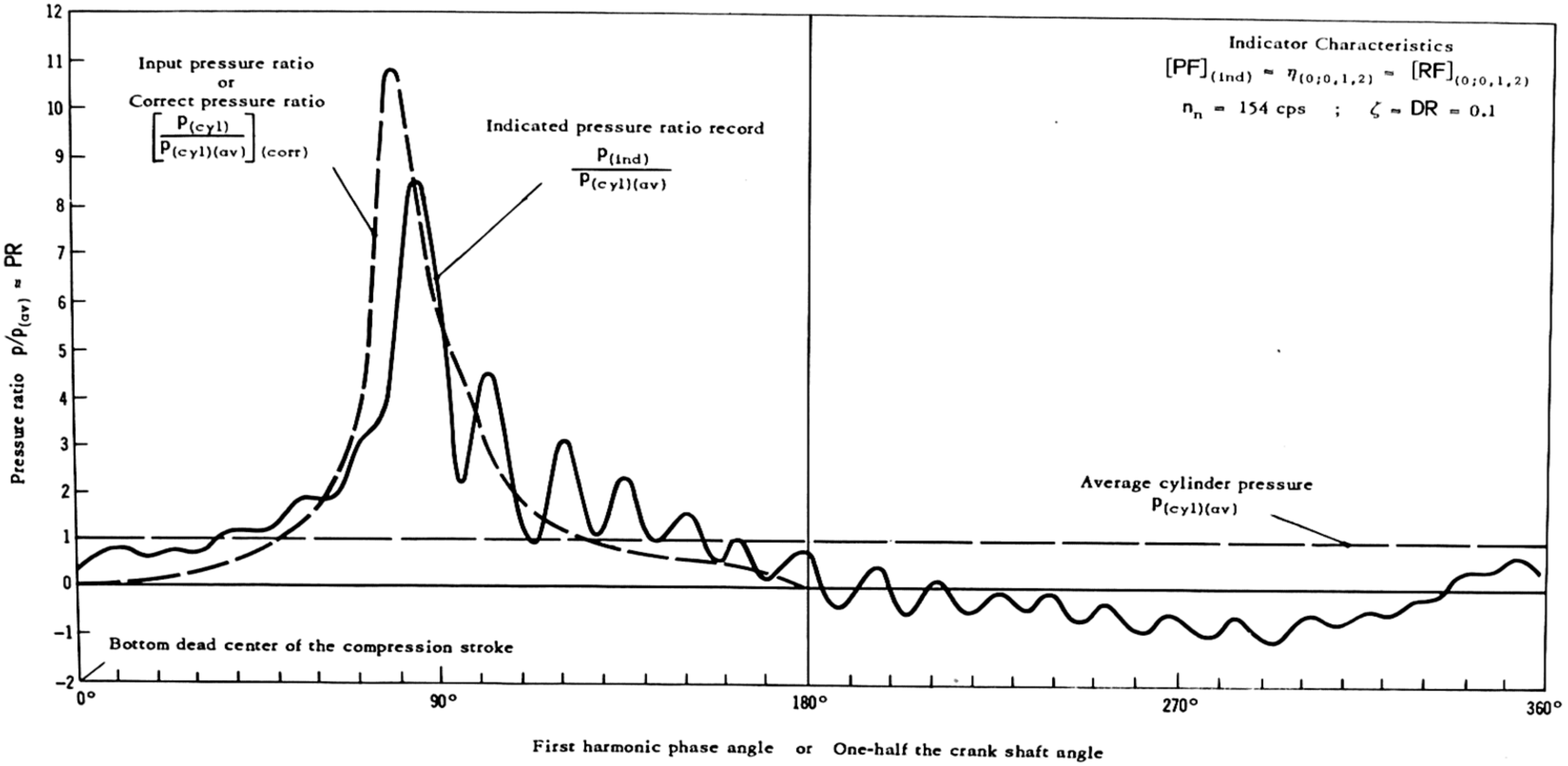


Fig. 33-9. Illustrative theoretical plot for the cylinder pressure variation of an internal combustion engine at 800 rpm and the corresponding pressure record from a spring-and-piston indicator.

high-frequency components in any accurate Fourier series representation. Because of this fact, satisfactory records should not be expected from any indicator with a low undamped natural frequency, even when the engine speed is restricted to low values.

33.65. It might appear that increasing the damping without altering the undamped natural frequency would present a solution to the problem of improving pressure records at high engine speeds. The increased damping would certainly cause the high-frequency oscillations excited by the sharp pressure rise to be less prominent on the record. On the other hand, the downward-sloping sensitivity characteristic for frequencies higher than the undamped natural frequency, as shown by the long-dashed-line curves of Figs. 33-6a and 33-8a, effectively prevents high frequencies from being truly represented in the record. Because high-frequency components are required to describe sharp changes in any curve, the improper representation of these frequencies means that any indicator with low undamped natural frequency will give distorted records of sharp pressure changes. As a consequence of this fact, it is necessary to look for pressure-measuring systems with undamped natural frequencies well above the 154 cycles per second of the spring-and-piston indicator used for illustrative purposes in the previous section. It is possible to design and produce pressure receivers with undamped natural frequencies more than two orders of magnitude above those found in conventional spring-and-piston indicators. Several of the principles illustrated in Fig. 33-4 have been successfully applied in units of this type. Figure 33-10 illustrates a typical pressure-measuring system using a high-performance pressure pickup,* an electronic coupling amplifier, a cathode-ray oscillograph indicating system, and a special camera for making photographic records.

33.66. The technique presented in Procedure Summary 33-1 outlines a generalized approach to the problem of associating over-all measuring-system performance with the characteristics of the operating components that are combined to form an open-chain system. However, it is desirable to develop certain general aspects of the situation in more detail before specific results are worked out for a given system applied to a particular problem.

OVER-ALL MEASURING-SYSTEM PERFORMANCE WHEN COMPONENT PERFORMANCE FUNCTIONS ARE EXPRESSED AS EQUATIONS

33.67. Procedure Summary 33-1 shows that the amplitude ratio for a complete system may be found graphically by summing the ordinates of log-log plots of component amplitude ratio versus frequency ratio. A similar summation process

---

* For discussion purposes, the terms pressure receiver, pressure receiver unit, and pressure pickup may all be considered to have the same meaning.

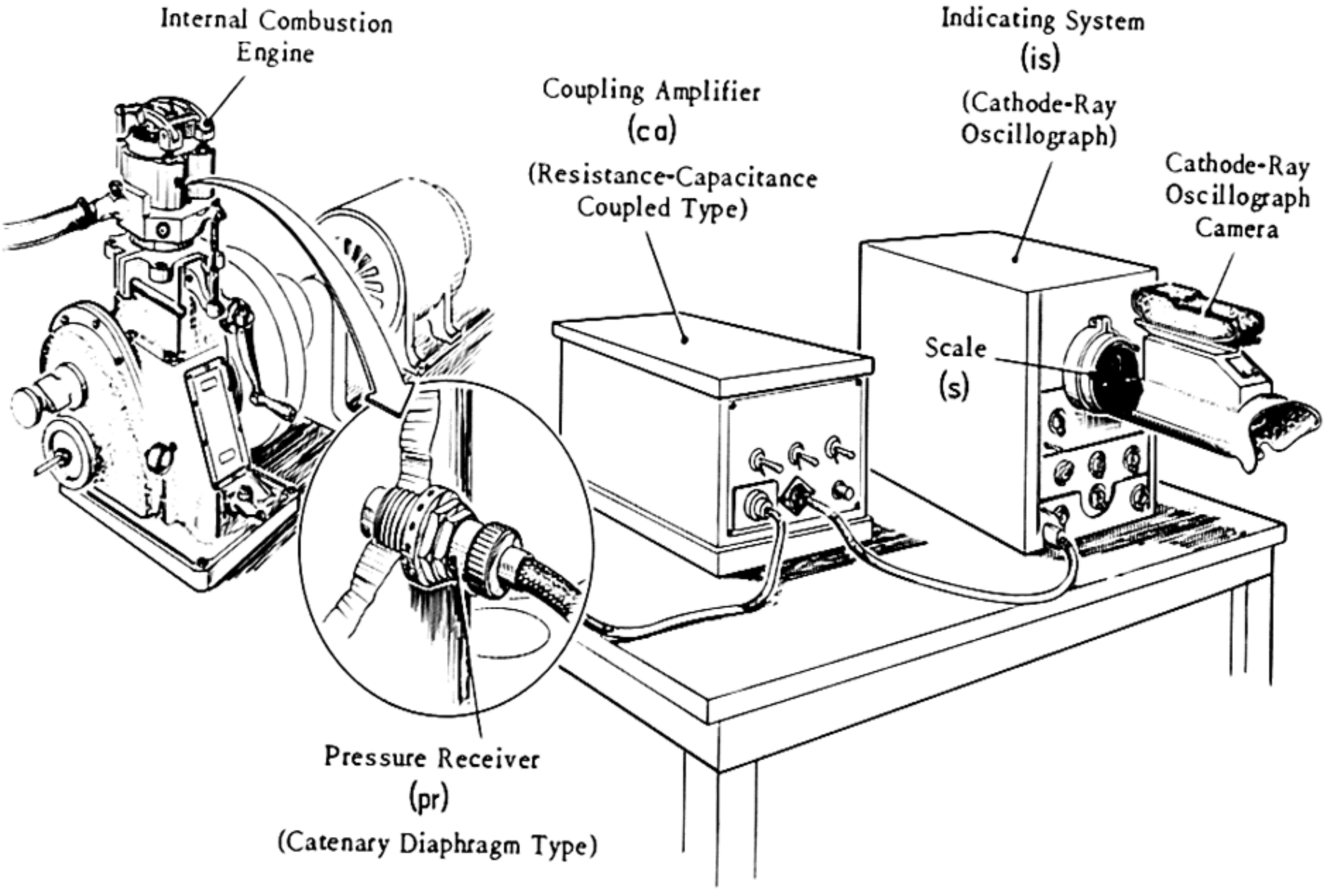


Fig. 33-10. Pictorial diagram for a typical pressure-measuring system with electrical components.

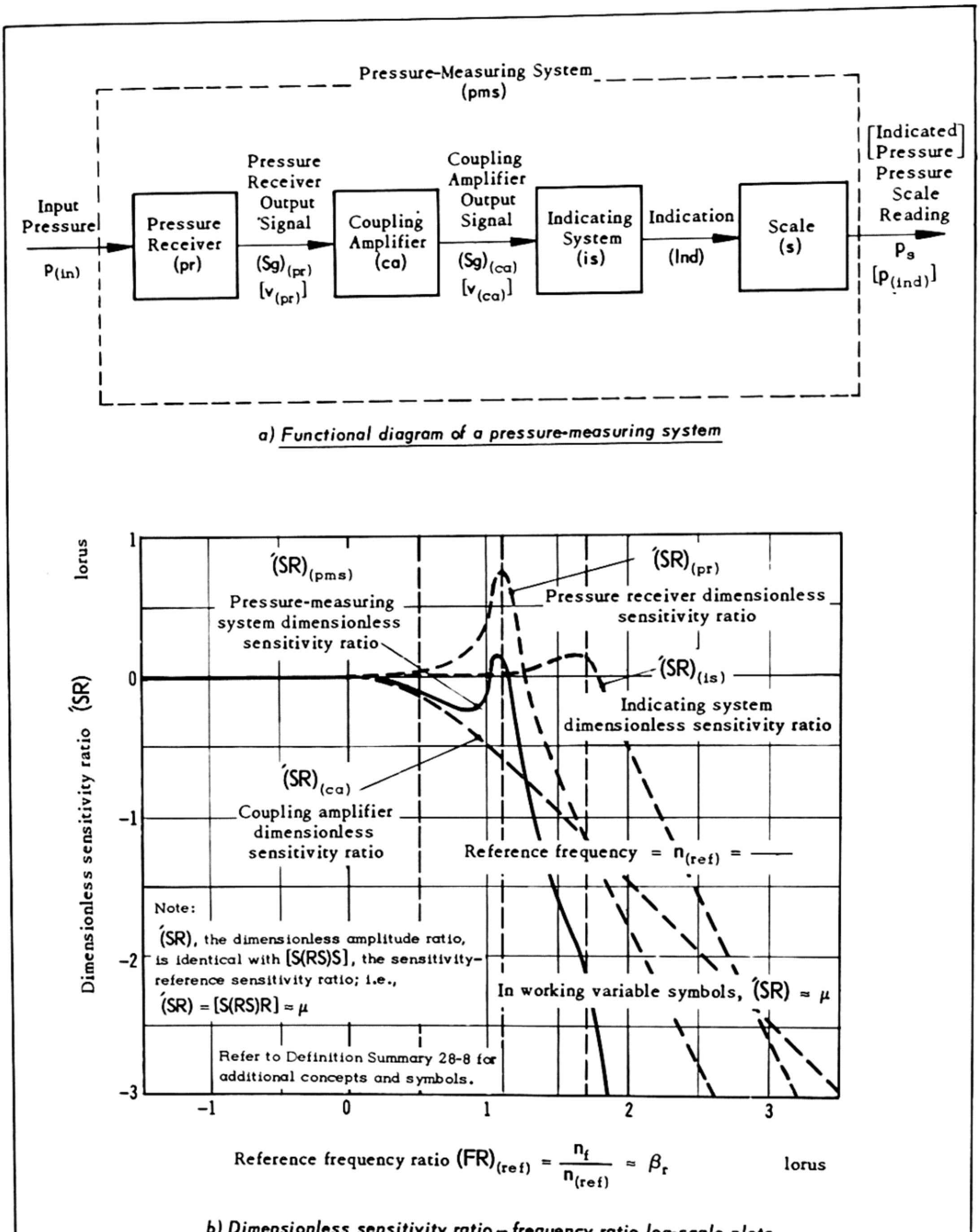
gives the resultant dynamic response angle. The figures of sections b and c of Derivation Summary 33-3 illustrate the graphical method for finding the over-all sensitivity ratio and dynamic response angle that represent the performance function for a pressure-measuring system similar to that described by Fig. 33-10 and section a of Derivation Summary 33-3.

33.68. Section d of Derivation Summary 33-3 contains expressions for the over-all reference sensitivity, the over-all dimensionless sensitivity ratio, and the resultant dynamic response angle when the performance function for an individual operating component is given as the product of a reference sensitivity, a dimensionless sensitivity ratio, and an imaginary exponential with the dynamic response angle in the exponent.

33.69. The over-all reference sensitivity is the product of all the component reference sensitivities. It is shown in Definition Summary 29-2 that the ideal over-all reference sensitivity for any properly calibrated measuring instrument is unity. This condition is so nearly fulfilled in all practical systems that it may be adopted as an engineering rule.*

---

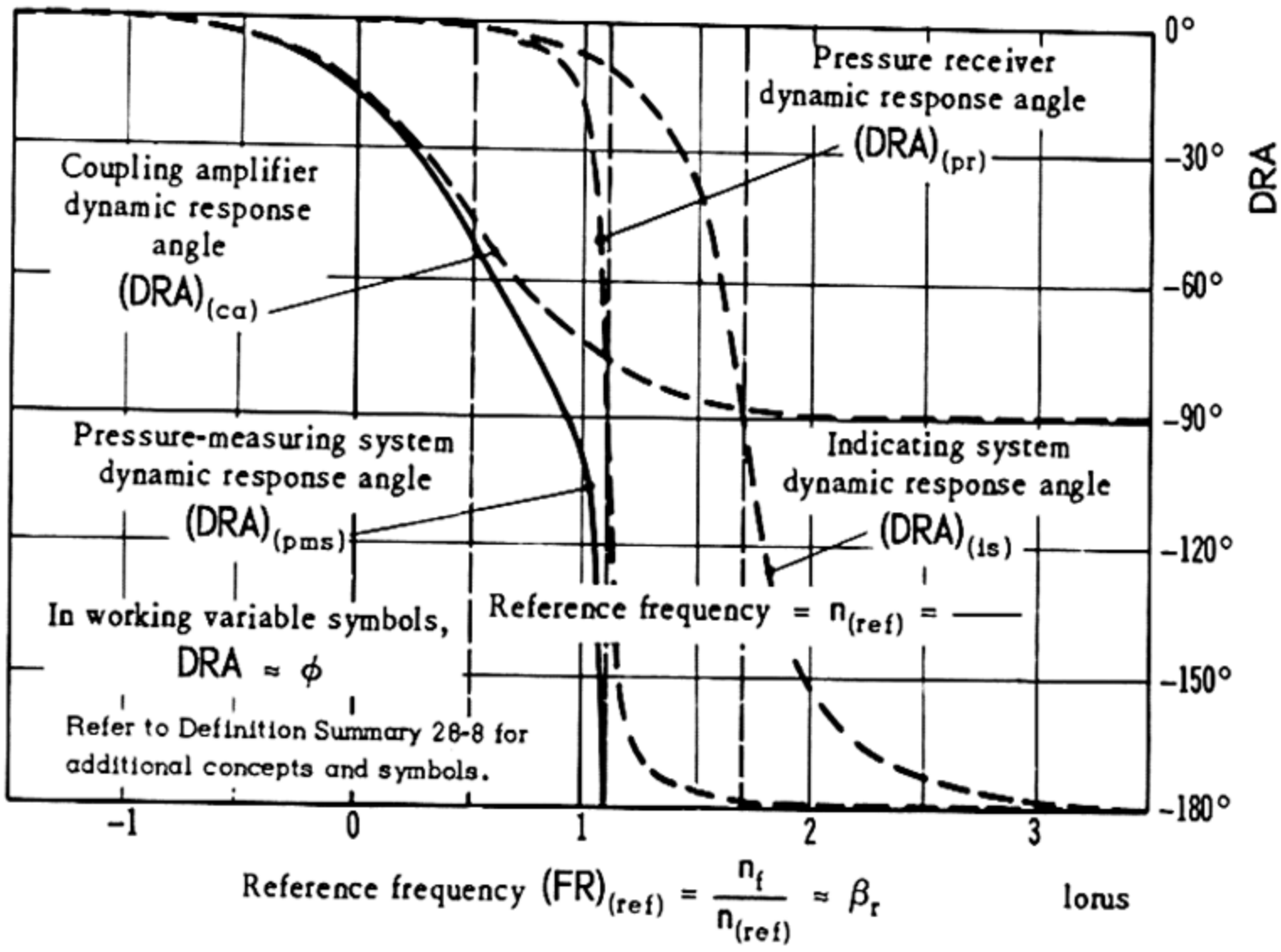
* Discrepancies between actual values of measuring-system reference sensitivity and unity are generally so small that they fall into the class of inaccuracies and may be treated by the technique described in Chapter 29.



a) *Functional diagram of a pressure-measuring system*

b) *Dimensionless sensitivity ratio – frequency ratio log-scale plots*

Derivation Summary 33-3. Functional diagram, frequency response information in performance function form, and indicated pressure record of a pressure-measuring system when the input pressure is described in Fourier series terms. (Page 1 of 3)



c) *Dynamic response angle – reference frequency ratio semilogarithmic plots*

When the steady-state sinusoidal performance characteristics of any operating component or system are described by a performance function, the essential information may be expressed in any of the forms given in Definition Summary 28-8 or listed in Definition Summary 13-6. Of the various forms available, the reference sensitivity – dimensionless sensitivity ratio – dynamic response angle form is generally useful for engineering purposes. In this form,

$$[PF]_{(id)} = S_{(id)(ref)} [S(RS)R]_{(id)} \epsilon^{j(DRA)_{(id)}} \tag{1}$$

or

$$[PF]_{(id)} = S_{(id)(ref)} (SR)_{(id)} \epsilon^{j(DRA)_{(id)}} \tag{2}$$

The working variable form of Eq. (2) is

$$\eta_{(\ \ )} = \rho_{(r)(\ \ )} \mu_{(\ \ )} \epsilon^{j\phi_{(\ \ )}} \tag{3}$$

The open-parenthesis subscripts may contain the identification of some operating component or operating system, but more often they have the identification of a differential equation form.

When a number of operating components are combined in an open-chain system, the performance function for the system has the form

$$[PF]_{(sys)} \equiv \prod_{i=0}^{i=n} S_{(c)(ref)i} \prod_{i=0}^{i=n} (SR)_{(c)i} \epsilon^{j \sum_{i=0}^{i=n} (DRA)_{(c)i}} \tag{4}$$

where

$[PF]_{(sys)}$ = performance function of the system

$S_{(c)(ref)i}$ = reference sensitivity for the ith operating component

$(SR)_{(c)i}$ = dimensionless sensitivity ratio for the ith operating component

$(DRA)_{(c)i}$ = dynamic response angle for the ith operating component

In Eq. (4), the symbols are simplified by omitting the input-output subscript brackets. It is understood that these brackets are added when input-output information is desirable.

Derivation Summary 33-3. Functional diagram, frequency response information in performance function form, and indicated pressure record of a pressure-measuring system when the input pressure is described in Fourier series terms. (Page 2 of 3)

The products and the summation appearing in Eq. (4) have special significance with respect to the system performance function.

$$S_{(sys)(ref)} = \prod_{i=0}^{i=n} S_{(c)(ref)i} = \text{reference sensitivity for the system} \tag{5}$$

$$\hat{(SR)}_{(sys)} = \prod_{i=0}^{i=n} \hat{(SR)}_{(c)i} = \text{dimensionless sensitivity ratio for the system} \tag{6}$$

Note that

$$\hat{(SR)}_{(sys)} \equiv [S(RS)R]_{(sys)} = \text{sensitivity} - \text{reference sensitivity ratio for the system}$$

$$(DRA)_{(sys)} = \sum_{i=0}^{i=n} (DRA)_{(c)i} = \text{dynamic response angle for the system} \tag{7}$$

For the special case of measuring systems (refer to Definition Summary 29-2),

$$S_{(sys)[q_{(in)};q_s](ref)} = 1 \tag{8}$$

Also the ideal value for $\hat{(SR)}_{(sys)}$ is unity; i.e.,

$$\hat{(SR)}_{(sys)(ideal)} = 1 \tag{9}$$

d) Generalized performance function form for open-chain measuring systems

For the special case of the pressure-measuring system represented by the functional diagram of section a,

$$S_{(pms)[p_{(in)};p_s](ref)} = S_{(pr)[p;v](ref)} S_{(ca)[v;v](ref)} S_{(is)[v;(Ind)](ref)} S_{(s)[(Ind);p](ref)} = 1 \tag{10}$$

$$\hat{(SR)}_{(pms)(p;p)} = \hat{(SR)}_{(pr)(p;v)} \hat{(SR)}_{(ca)(v;v)} \hat{(SR)}_{(is)(v;(Ind))} \hat{(SR)}_{(s)((Ind);p)} \tag{11}$$

$$(DRA)_{(pms)(p;p)} = (DRA)_{(pr)(p;v)} + (DRA)_{(ca)(v;v)} + (DRA)_{(is)(v;(Ind))} + (DRA)_{(s)((Ind);p)} \tag{12}$$

e) Performance function forms for the pressure-measuring system of section a

Applying the performance function forms of sections d and e to an input variation given by a specific Fourier series of the form (refer to Chapter 12)

$$P_{(in)} = P_{(av)} \left[1 + \sum_{r=1}^{r=m} (AR)_{(p)(0-r)(in)} \epsilon^{j(PA)_{(p)(1-r)(in)}} \right] \tag{13}$$

gives a corresponding Fourier series for the indicated pressure as follows:

$$P_{(Ind)} = P_s = P_{(av)} \left[S_{(pms)[p;p](st)} + \sum_{r=1}^{r=m} (AR)_{(p)(0-r)(s)} \epsilon^{j(PA)_{(p)(1-r)(s)}} \right] \tag{14}$$

where

$$(AR)_{(p)(0-r)(s)} = \hat{(SR)}_{(pms)(p;p)((FR)=(FR)_{(in)1})} (AR)_{(p)(0-r)(in)} \tag{15}$$

$$(PA)_{(p)(1-r)(s)} = (PA)_{(p)(1-r)(in)} + (DRA)_{(pms)(1-r)((FR)=(FR)_{(in)1})} \tag{16}$$

Equations (13) through (16) are formal expressions of the operations already carried out in Figs. 33-5 through 33-9 with the indicator card of Fig. 12-8 as the input pressure variation and a specified spring-and-piston-type indicator as the pressure-measuring system.

f) Indicated pressure record from a pressure-measuring system with a given performance function when the input function is given by a Fourier series

Derivation Summary 33-3. Functional diagram, frequency response information in performance function form, and indicated pressure record of a pressure-measuring system when the input pressure is described in Fourier series terms. (Page 3 of 3)

33.70. Under the conventions described in Chapter 28 for forming dimensionless sensitivity ratios, the dimensionless sensitivity ratio for a measuring instrument has an asymptote that represents ideal performance for the component or system under consideration. A similar condition exists for the dynamic response angle of the over-all system. For any particular measuring system, Eq. (6) of Derivation Summary 33-3 shows that the system dimensionless sensitivity ratio is equal to the product of the dimensionless sensitivity ratios of the system components. The corresponding relationship for the system dynamic response angle is the summation given by Eq. (7) of Derivation Summary 33-3. Section e of the summary gives the equations that describe the reference sensitivity, the dimensionless sensitivity ratio, and the dynamic response angle for the pressure-measuring system described by the functional diagram of section a.

33.71. Section f of Derivation Summary 33-3 lists the equations that represent an input pressure variation in terms of a Fourier series (see Eq. (13)), and the corresponding series for the indicated pressure record (see Eq. (14)) with the expressions for component amplitude ratios and phase angles given respectively by Eqs. (15) and (16). Equation (15) shows that the amplitude ratio for a given component of indicated pressure is equal to the corresponding input pressure component amplitude ratio multiplied by the dimensionless amplitude ratio of the indicator for the frequency of the given component. Equation (16) gives the phase angle for a given output component as the sum of the phase angle of the corresponding input component and the dynamic response angle of the indicator for the frequency of the given component.

CUTOFF FREQUENCIES AND BAND WIDTHS

33.72. Dimensionless sensitivity ratio and dynamic response angle plots contain the essential data on the performance of any operating system. So far as the frequency response method is concerned, this information is complete, but its form of presentation is unnecessarily cumbersome for many purposes. This difficulty is remedied by introducing the concepts of cutoff frequency and operating frequency range (also called band width), which depend on the principles illustrated in Fig. 13-3 of Chapter 13. The single basic idea involved is that of defining tolerance limits for deviations from ideal values of dimensionless sensitivity ratio and dynamic response angle and then identifying the reference frequency ratios* at which the performance-describing curves cross the tolerance limits. Definition Summary 33-1 illustrates the concepts involved and establishes generalized conventions for names and symbols to describe any given situation.

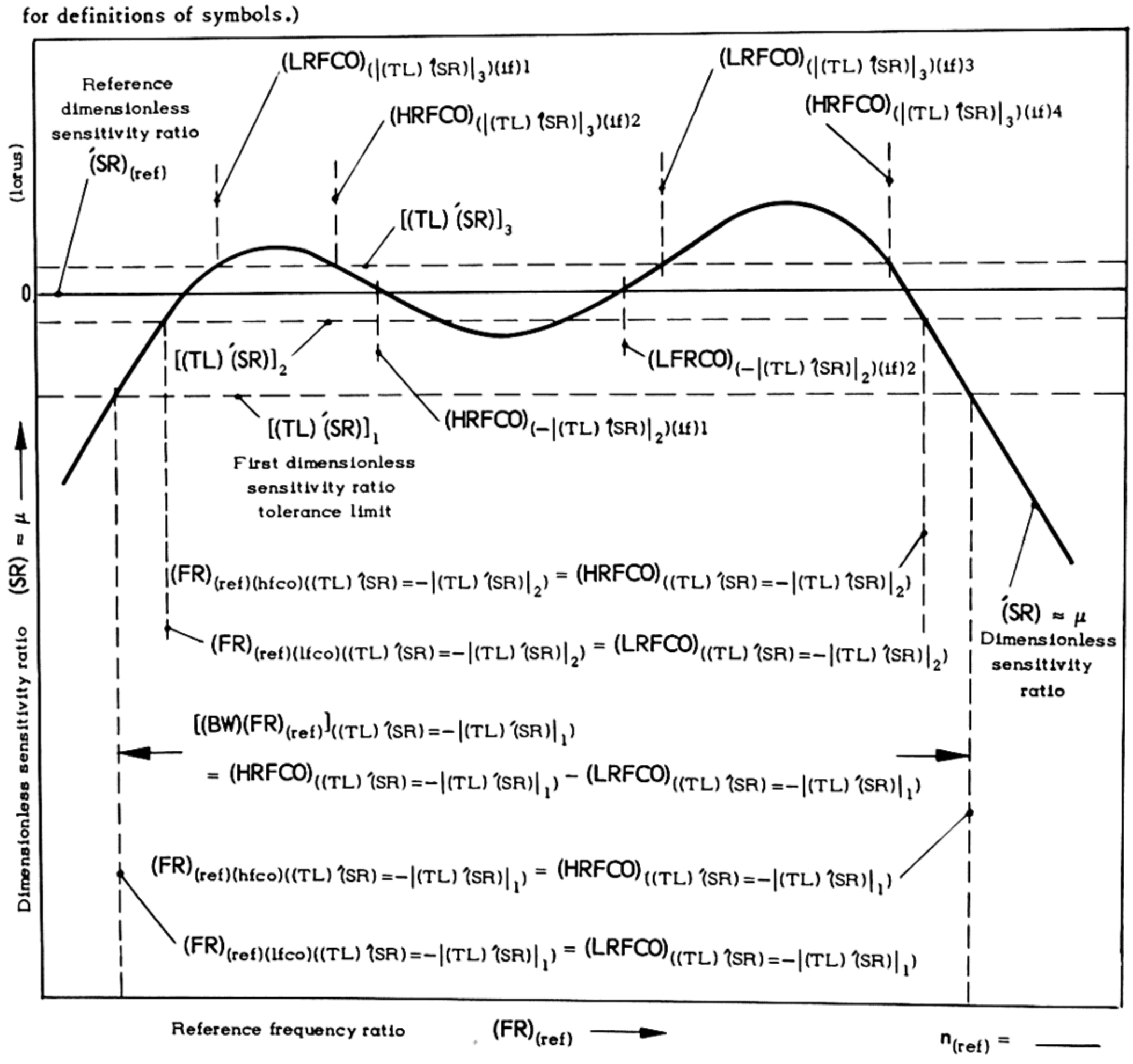
---

* In practice, either the reference frequency ratio or the forcing frequency, which is the reference frequency ratio multiplied by the reference frequency, may be used to represent the frequency variable.

When the frequency response method is applied to engineering problems associated with operating components and operating systems, the essential information on performance may be summarized in plots of dimensionless amplitude ratio and dynamic response angle as functions of reference frequency ratio. It is convenient to summarize the important features of these plots in concise numerical terms. The terms in common use are cutoff frequency, band width, pass band and operating range. The essential quantities used in defining these terms are summarized in Fig. 13-3. In each case, the concept involved is the frequency ratio or ratios at which the performance-describing plot involved deviates more than some given tolerance limit from a specified reference value.

a) Cutoff frequency, band width, and associated concepts

The dimensionless amplitude ratio plot illustrates the graphical meaning of several typical terms and establishes a pattern for the definition of additional concepts as they become useful. (See section c for definitions of symbols.)



b) Cutoff frequency ratios and band widths based on dimensionless sensitivity ratio tolerance limits

Definition Summary 33-1. Definitions, symbols and names for concepts used in describing essential features of dimensionless sensitivity ratio and dynamic response angle plots: cutoff frequency and band width. (Page 1 of 4)

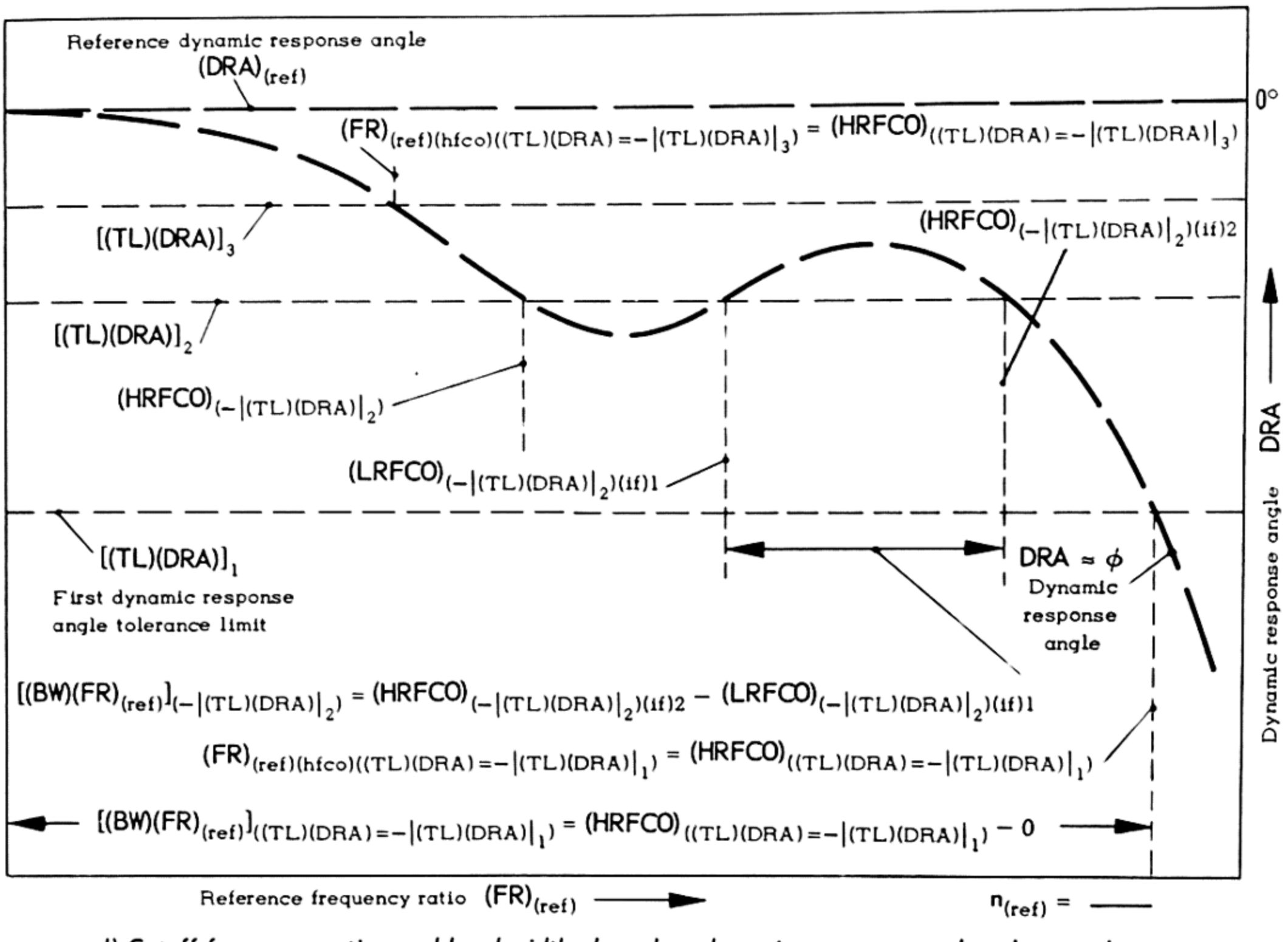
Concept Symbols (Self-defining symbols are listed above working variable symbols)	Concept Names
$(FR)_{(ref)(lfco)((TL)\uparrow SR)=-\lvert(TL)\uparrow SR)\rvert_1)}$ $= (LRFCO)_{((TL)\uparrow SR)=-\lvert(TL)\uparrow SR)\rvert_1)}$ $\beta_{(r)(lfco)((TL)\mu)1} \approx (LRFCO)_{((TL)\mu)1}$	first dimensionless sensitivity ratio tolerance limit low reference frequency ratio cutoff
$(FR)_{(ref)(hfco)((TL)\uparrow SR)=-\lvert(TL)\uparrow SR)\rvert_1)}$ $= (HRFCO)_{((TL)\uparrow SR)=-\lvert(TL)\uparrow SR)\rvert_1)}$ $\beta_{(r)(hfco)((TL)\mu)1} \approx (HRFCO)_{((TL)\mu)1}$	first dimensionless sensitivity ratio tolerance limit high reference frequency ratio cutoff
$[(BW)(FR)_{(ref)}]_{((TL)\uparrow SR)=-\lvert(TL)\uparrow SR)\rvert_1)}$ $= (HRFCO)_{((TL)\uparrow SR)=-\lvert(TL)\uparrow SR)\rvert_1)}$ $- (LRFCO)_{((TL)\uparrow SR)=-\lvert(TL)\uparrow SR)\rvert_1)}$ $[(BW)\beta_r]_{((TL)\mu)1} \approx (HRFCO)_{((TL)\mu)1} - (LRFCO)_{((TL)\mu)1}$	first dimensionless sensitivity ratio tolerance limit reference frequency ratio band width
$(FR)_{(ref)(hfco)((TL)\uparrow SR)=-\lvert(TL)\uparrow SR)\rvert_2)(lf)1}$ $= (HRFCO)_{((TL)\uparrow SR)=-\lvert(TL)\uparrow SR)\rvert_2)(lf)1}$ $= (HRFCO)_{(-\lvert(TL)\uparrow SR)\rvert_2)(lf)1}$ $\beta_{(r)(hfco)((TL)\mu)(2)(lf)1} \approx (HRFCO)_{((TL)\mu)(2)(lf)1}$	second dimensionless sensitivity ratio tolerance limit first intermediate frequency high reference frequency ratio cutoff
$(FR)_{(ref)(lfco)((TL)\uparrow SR)=-\lvert(TL)\uparrow SR)\rvert_2)}$ $= (LRFCO)_{((TL)\uparrow SR)=-\lvert(TL)\ (SR)\rvert_2)}$ $\beta_{(r)(lfco)((TL)\mu)2} \approx (LRFCO)_{((TL)\mu)2}$	second dimensionless sensitivity ratio tolerance limit low reference frequency ratio cutoff
$[(BW)(FR)_{(ref)}]_{((TL)\uparrow SR)=-\lvert(TL)\uparrow SR)\rvert_2)((lf)_1-(lfco))}$ $= (HRFCO)_{((TL)\uparrow SR)=-\lvert(TL)\uparrow SR)\rvert_2)(lf)1}$ $- (LRFCO)_{((TL)\uparrow SR)=-\lvert(TL)\uparrow SR)\rvert_2)}$ $[(BW)\beta_r]_{((TL)\mu)2} \approx (HRFCO)_{((TL)\mu)(2)(lf)1} - (LRFCO)_{((TL)\mu)2}$	second dimensionless sensitivity ratio tolerance limit first intermediate reference frequency ratio cutoff – low reference frequency ratio cutoff band width

These conventions may be used to form symbols and names for the cutoff frequency ratios and associated band widths illustrated in section b, but without the corresponding tabulated definitions.

c) Symbols and names for the concepts defined graphically in section b

Definition Summary 33-1. Definitions, symbols and names for concepts used in describing essential features of dimensionless sensitivity ratio and dynamic response angle plots: cutoff frequency and band width. (Page 2 of 4)

The dynamic response angle plot illustrates graphic meanings for concepts corresponding to those defined in section b. (See section e for definitions of symbols.)



d) Cutoff frequency ratios and band widths based on dynamic response angle tolerance limits

Concept Symbols (Self-defining symbols are listed above working variable symbols)	Concept Names
$(FR)_{(ref)(hfco)((TL)(DRA)=-\|(TL)(DRA)\|_1)}$ $= (HRFCO)_{((TL)(DRA)=-\|(TL)(DRA)\|_1)}$ $\beta_{(r)(hfco)((TL)\phi)1} \approx (HRFCO)_{((TL)\phi)1}$	first dynamic response angle tolerance limit high reference frequency ratio cutoff
$[(BW)(FR)_{(ref)}]_{((TL)(DRA)=-\|(TL)(DRA)\|_1)}$ $= (HRFCO)_{((TL)(DRA)=-\|(TL)(DRA)\|_1)} - 0$ $(BW)(\beta_r)_{((TL)\phi)1} \approx (HRFCO)_{((TL)\phi)1} - 0$	first dynamic response angle tolerance limit reference frequency ratio band width

These conventions may be used to form symbols and names for the cutoff frequency ratios and associated band widths illustrated in section c, but without the corresponding tabulated definitions.

e) Symbols and names for the concepts defined graphically in section d

Definition Summary 33-1. Definitions, symbols and names for concepts used in describing essential features of dimensionless sensitivity ratio and dynamic response angle plots: cutoff frequency and band width. (Page 3 of 4)

When no misunderstanding is possible, identifying subscripts may be omitted from the complete symbols listed in the tables. Similarly descriptive words may be omitted from the corresponding names.

For example, when it is understood that a certain dimensionless sensitivity ratio tolerance limit is to be applied and that frequency (not frequency ratio) is the variable considered, then

$(FR)_{(ref)(lfco)((TL)\,\hat{}SR)=-|(TL)\,\hat{}SR)|_1)}$ = first dimensionless sensitivity ratio tolerance limit low reference frequency ratio cutoff

may become

$n_{(f)(lco)}$ = (LFCO) = low-frequency cutoff

and

$[(BW)(FR)_{(ref)}]_{((TL)\,\hat{}SR)=-|(TL)\,\hat{}SR)|_1)}$ = first dimensionless sensitivity ratio tolerance limit reference frequency ratio band width

may become

(BW) = band width

Note: In practice, the terms

(operating frequency range) = (OFR) ; (operating frequency band) = (OFB)

(operating range) = (OR) ; (operating frequency band width) = (OFBW)

are equivalent to (BW) = band width.

f) Simplification of symbols

Cutoffs and band widths expressed in terms of reference frequency ratios are transformed into terms of frequency when they are multiplied by the reference frequency. For example,

$$(FR)_{(ref)(hfco)((TL)\,\hat{}SR)=-|(TL)\,\hat{}SR)|_1)} = \left[\frac{n_f}{n_{(ref)}}\right]_{(hfco)((TL)\,\hat{}SR)=-|(TL)\,\hat{}SR)|_1)} \quad (1)$$

so that

$$(FF)_{(hfco)((TL)\,\hat{}SR)=-|(TL)\,\hat{}SR)|_1)} = (FR)_{(ref)(hfco)((TL)\,\hat{}SR)=-|(TL)\,\hat{}SR)|_1)} n_{(ref)}$$

$$= n_{(f)(hfco)((TL)\,\hat{}SR)=-|(TL)\,\hat{}SR)|_1)} \quad (2)$$

= first dimensionless sensitivity ratio tolerance limit high-frequency cutoff

In working variable terms,

$$n_{(f)(hfco)((TL)\,\hat{}SR))1} = (HFCO)_{((TL)\,\hat{}SR))1} \approx (HFCO)_{((TL)\mu)1} = n_{(f)(hfco)((TL)\mu)1} \quad (3)$$

$$[(BW)(FR)_{(ref)}]_{((TL)\,\hat{}SR)=-|(TL)\,\hat{}SR)|_1)} n_{(ref)} = \left[(BW)\frac{n_f}{n_{(ref)}}\right]_{((TL)\,\hat{}SR)=-(TL)\,\hat{}SR)_1)} n_{(ref)}$$

$$= [(BW)\,n_f]_{((TL)\,\hat{}SR)=-(TL)\,\hat{}SR)_1)}$$

= first dimensionless sensitivity ratio frequency band width

g) Cutoffs and band widths expressed in terms of frequency

Definition Summary 33-1. Definitions, symbols and names for concepts used in describing essential features of dimensionless sensitivity ratio and dynamic response angle plots: cutoff frequency and band width. (Page 4 of 4)

33.73. In the figure of section a of Definition Summary 33-1, the first dimensionless sensitivity ratio tolerance limit is shown by the lowest dashed line parallel to the axis of abscissae. The symbol for this tolerance limit is $(TL)_1$ followed by $\hat{}(SR)$ to show that the tolerance limit is in the dimensionless sensitivity ratio. The subscript 1 is used to designate the particular limit involved. In order for

this symbol to have a definite meaning, it is necessary to define a reference dimensionless sensitivity ratio that is actually arbitrary, but is usually made coincident with the ideal performance level for the dimensionless sensitivity ratio.* In the illustration of section a of Definition Summary 33-1, the reference dimensionless sensitivity ratio level is taken to be at zero on the logarithmic ordinate scale (this is equivalent to unity on the dimensionless sensitivity ratio scale).

33.74. The lowest reference frequency ratio at which the dimensionless sensitivity ratio curve crosses the first tolerance limit is the first dimensionless sensitivity ratio tolerance limit low reference frequency ratio cutoff and is represented by (FR) as the main symbol; with (ref), for reference, as the first subscript; (lfco) for low-frequency cutoff, as the second subscript; and $(TL)'(SR) = -|(TL)'(SR)|_1$ inside the third subscript parenthesis to show that the cutoff is associated with a negative tolerance limit on the dimensionless sensitivity ratio equal to the magnitude of the first tolerance limit as shown on the figure in section b of Definition Summary 33-1. The symbol just described may also be written as (LRFCO), for low reference frequency cutoff, with a subscript to identify the tolerance limit and the quantity in which the tolerance limit is taken.

33.75. The right-hand intersection of the dimensionless sensitivity curve with the first tolerance limit establishes the first dimensionless sensitivity ratio tolerance limit high reference frequency ratio cutoff in the same way that the low-frequency intersection establishes the low reference frequency cutoff. The symbols and names associated with the high-frequency cutoff are identical with the symbols and names for the low-frequency ratio cutoff except for the use of (hfco) as an identifying subscript. The high-frequency cutoff symbols and names are listed in the table of section c, Definition Summary 33-1.

33.76. The dimensionless sensitivity ratio tolerance limit band width is the difference between the high reference frequency cutoff and the low reference frequency cutoff. The corresponding symbol is (BW), for band width, followed by $(FR)_{(ref)}$ to show that the band width is expressed in reference frequency ratio terms. A subscript identifying the dimensionless sensitivity ratio tolerance limit is added to complete the symbol.

33.77. When the dimensionless sensitivity ratio curve has a shape that causes a given tolerance limit line to have more than two intersections, cutoffs may be defined for each intersection. The cutoffs that are located between the lowest frequency cutoff and the highest frequency cutoff are intermediate frequency cutoffs. Two intermediate frequency cutoffs are shown in the illustrative diagram of section b of Definition Summary 33-1. Band widths based on intermediate frequency

---

* As illustrated in the figure of section b of Definition Summary 33-1, the reference dimensionless sensitivity ratio is constant. In practice, this level is not necessarily a constant or even a straight line, but may be chosen according to the purpose for which the system is designed.

cutoffs may be established by use of the conventions already described for naming and writing symbols for band widths between the highest and lowest frequency ratio cutoffs. To identify bandwidth symbols with particular intermediate frequency cutoffs, subscript (if), for intermediate frequency, followed by designating numbers is added to the bandwidth symbol and the cutoffs from which it is derived. Section c of Definition Summary 33-1 gives symbols and names associated with several of the cutoffs and band widths illustrated in the diagram of section b of Definition Summary 33-1. This list is not complete, but it serves to illustrate the conventions and symbols associated with the concepts of cutoff frequency and band width.

33.78. The illustration in section d of Definition Summary 33-1 illustrates a dynamic response angle variation and shows several tolerance limits in terms of this variable. Symbols and names for various cutoffs and band widths established by the curve and tolerance limits are placed on the figure and listed in the table of section e of the summary. These symbols and names are similar to those associated with the dimensionless sensitivity ratio except for the replacement of dimensionless sensitivity ratio symbols by dynamic response angle symbols.

33.79. One new feature appears in the first dynamic response angle tolerance limit. Because the low reference frequency ratio side of the dynamic response angle curve coincides with the reference dynamic response angle level of zero degrees, no low reference frequency cutoff exists. This means that the low-dynamic-response-angle-tolerance-limit-determined band widths that extend to the low reference frequency ratio limit are numerically equal to the high reference frequency cutoff.

33.80. All the cutoff frequency ratio and bandwidth symbols of Definition Summary 33-1 may be written in working variable symbols instead of self-defining symbols. In the tabulations of sections c and e, working variable symbol forms are placed below the equivalent self-defining symbol forms.

33.81. Under circumstances that make the chances of misunderstanding small, the terms and symbols given in Definition Summary 33-1 may be simplified. For example (see section f), a low reference frequency cutoff symbol may be reduced to (LFCO) , with a specification of the tolerance limit as an implied condition. Similarly, the bandwidth symbol may become (BW) , with tolerance limit and the location of the associated cutoffs as implied conditions. Various terms with the same meaning as band width are given in section f of Definition Summary 33-1. These terms may be used to offer an alternative to the continual repetition of the same term in problems involving band width.

33.82. Cutoffs and band widths expressed in terms of reference frequency ratios can be transformed into terms of frequency by multiplying them by the reference frequency. Examples of this procedure are given in section g of Derivation Summary 33-1.

MEASURING-SYSTEM PERFORMANCE REQUIREMENTS FOR SATISFACTORY INTERNAL COMBUSTION ENGINE CYLINDER-PRESSURE RECORDS

33.83. Spring-and-piston indicator records like those of Figs. 33-7 and 33-9 owe their imperfections to poor high-frequency performance. The low-frequency performance is ideal in the sense that near zero frequency the dimensionless sensitivity ratio is unity, and the dynamic response angle is zero. On the other hand, the plots of Figs. 33-6 and 33-8 show that well within the range of input pressure variation frequency components the dimensionless sensitivity ratio rises away from unity to a peak and then falls rapidly away from unity. Within the same range, the dynamic response angle drops well away from the ideal value of zero. This means that, for any reasonable tolerance limits in dimensionless sensitivity ratio and dynamic response angle, the spring-and-piston indicator has a band width that is too small. An equivalent statement is that the high-frequency cutoff is too low.

33.84. By use of a cathode-ray oscillograph, the high-frequency cutoff for the indicating system may be placed above 50,000 cycles per second. Pressure receiver units with undamped natural frequencies of the same magnitude are also available.* By proper design, it is possible to extend the operating range down to zero frequency for both the indicating system and the pressure receiver. This means that the performance of a pressure-measuring system like that illustrated in Fig. 33-10 should not be limited by either the pressure receiver or the indicating system.

33.85. Electronic amplifiers are suitable for the coupling function in pressure-measuring systems. It is easily possible to place the high-frequency cutoff in the 50,000-cycles-per-second region. On the other hand, it is difficult to achieve good low-frequency performance while maintaining this high-frequency cutoff. In other words, the basic amplifier problem is that of designing for a sufficiently wide band width rather than that of reaching a proper high-frequency cutoff.

33.86. The conventional R-C amplifier is characterized by good high-frequency performance, but poor low-frequency performance. For this reason, an R-C amplifier is not a good choice for a system to be used for recording internal combustion engine cylinder pressures. However, to illustrate the indicated pressure errors that accompany the use of a coupling amplifier with poor low-frequency response, a typical R-C amplifier will be assumed for the example that follows in the next section.

33.87. Carrier-frequency amplifiers that operate on modulated a-c signals of constant frequency have substantially ideal low-frequency performance, but have high-frequency performance that is limited by the magnitude of the carrier frequency. Filtering is required to eliminate carrier-frequency effects in the output, so that a high-frequency cutoff is introduced at a frequency somewhat below the

---

* See Draper and Li (D13).

carrier frequency. The final example is based on a pressure-measuring system using a carrier-frequency amplifier for the coupling function.

INTERNAL COMBUSTION ENGINE CYLINDER-PRESSURE RECORD FROM AN ELECTRICAL MEASURING SYSTEM

33.88. Performance Data Summary 33-1 gives the functional diagram, and component performance information on the operating components, of the pressure-measuring system shown in Fig. 33-10. The pattern followed in this summary is similar to that illustrated in Procedure Summary 33-1. In order to insure that meanings for the symbols are clearly understood, the pressure receiver (p_r) performance section is provided with full notes and references. This detail is omitted in the sections for the other operating components as being unnecessary once the general plan of attack and the symbols are understood.

33.89. The pressure receiver behaves as a second-order system with a reference sensitivity of 0.030 millivolt per pound per square inch with an excitation of 45 volts.* The damping ratio is 0.05, and the undamped natural frequency is 45,000 cycles per second. The coupling amplifier has a reference sensitivity of 33.3 volts per volt and has a frequency function** that is defined by the dimensionless sensitivity ratio and dynamic response angle curves of Fig. 33-11.

33.90. The indicating system has a reference sensitivity of 0.01 inch per millivolt and has a frequency function of unity. This latter characteristic is shown by a listed dimensionless amplitude ratio of unity and a dynamic response angle of zero. The scale sensitivity, which in this case is taken as identical with the static scale sensitivity, is 100 pounds per square inch per inch.

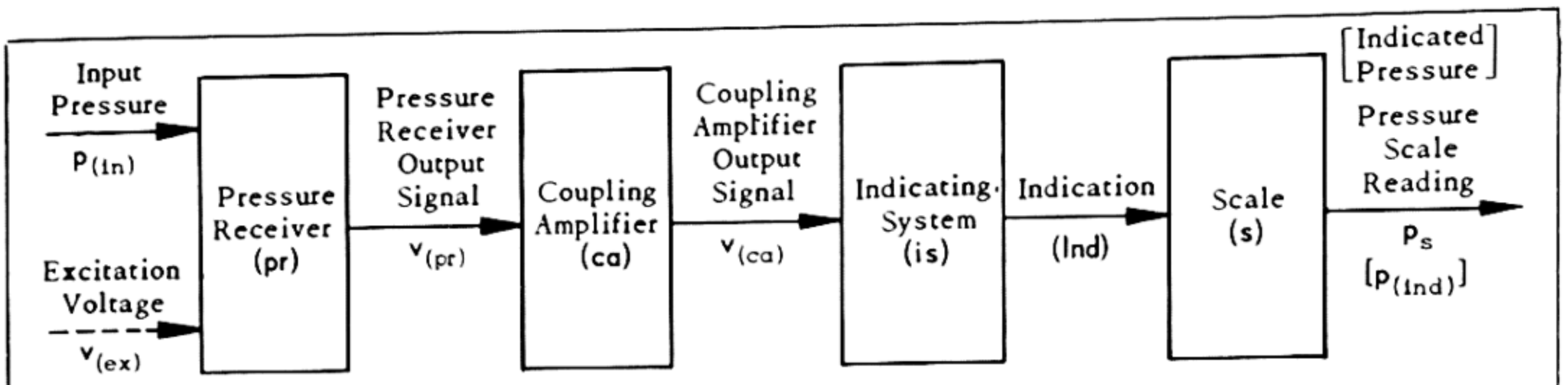
33.91. In describing performance for situations where the frequency function is unity (that is, where the dimensionless amplitude ratio is unity and the dynamic response angle is zero), it is convenient to list the static sensitivity as the only necessary performance-describing concept. By implication, the omission of symbols means that the concepts they represent remain in their reference condition throughout the operating range considered.

33.92. Figure 33-11a is a log-log plot with the pressure cycle frequency for an engine speed of 800 rpm as the reference frequency. With this reference frequency, the break point for the pressure receiver dimensionless sensitivity ratio is located at 3.829 lorus (that is, the undamped natural frequency of the pressure receiver is 6.75×10^3 times the fundamental frequency of the input pressure variation). The dimensionless sensitivity ratio for the coupling amplifier falls away

---

* See Draper and Li (D13).

** The term frequency function is defined in Definition Summary 13-4 of Chapter 13 and is applied in Eqs. (10), (11), (13) and (14) of Definition Summary 13-6.



a) Functional diagram

(pr) Pressure receiver

$$[PF]_{(pr)[p;v]} \approx \eta_{(0;0,1,2)} = [RF]_{(0;0,1,2)} \qquad (1)$$

This expression means that the pressure input – voltage output performance function of the pressure receiver has the form of the relating function for the (0;0,1,2) differential equation form.

Refer to Definition Summary 13-6 for various performance function forms.

Refer to Chapter 19 and Figs. 19-27 through 19-47 for information on the (0;0,1,2) relating function.

Refer to Information Summary 32-2 and Figs. 32-16 through 32-25 for data on the performance function associated with the (0;0,1,2) relating function.

$$\hat{'}(SR)_{(pr)(p;v)} \approx \mu_{(0;0,1,2)} \qquad (DRA)_{(pr)(p;v)} \approx \phi_{(0;0,1,2)}$$

Note that $\hat{'}(SR)$, the nondimensional sensitivity ratio is identical with $[S(RS)R]$, the sensitivity – reference sensitivity ratio, which corresponds to $\hat{'}(DAR)$, the dimensionless dynamic amplitude ratio, where $\hat{'}(DAR) \equiv [(DAR)(RAR)R]$, the dynamic amplitude ratio – reference amplitude ratio ratio, as this term is used in the derivation summaries and curves of Volume II of Instrument Engineering.

$$S_{(pr)[p;v](ref)} \approx \rho_{(r)(0;0,1,2)}$$

For the particular catenary-diaphragm strain-gage pressure receiver used in the system of section a (refer to section b of Fig. 33-4),

$S_{(pr)[p;v](ref)} = 0.030 \dfrac{\text{millivolt}}{\text{pounds per square inch}}$ with a direct-current excitation of 45 volts

$n_n = 45{,}000$ cycles per second

$\zeta \approx DR = 0.05$ = damping ratio

$(bp)_{(pr)} = \dfrac{45{,}000}{6.67} = 6.75 \times 10^3 = 3.829$ lorus

$n_{(ref)} = n_1 = 6.67$ cps = fundamental engine pressure cycle frequency

(ca) Coupling amplifier

$$S_{(ca)[v;v](ref)} = 33.3 \frac{\text{millivolts}}{\text{millivolt}}$$

This reference sensitivity is commonly called amplifier gain with the symbol G.

$\hat{'}(SR)_{(ca)(v;v)}$ is given as one of the plots in Fig. 33-11a.

$(DRA)_{(ca)(v;v)}$ is given as one of the plots in Fig. 33-11b.

(is) Indicating system

$$S_{(is)[v;(Ind)](ref)} = 0.01 \frac{\text{inch}}{\text{millivolt}}$$

$$\hat{'}(SR)_{(is)(v;(Ind))} = 1 \qquad (DRA)_{(is)(v;(Ind))} = 0$$

(s) Scale

$$S_{(s)[(Ind);p](st)} = S_{(s)[(Ind);p](ref)} = 100 \frac{\text{pounds per square inch}}{\text{inch}}$$

$$\hat{'}(SR)_{(s)} = 1 \qquad (DRA)_{(s)} = 0$$

b) Component performance data

Performance Data Summary 33-1. Performance of the components of the pressure-measuring system shown in Fig. 33-10.

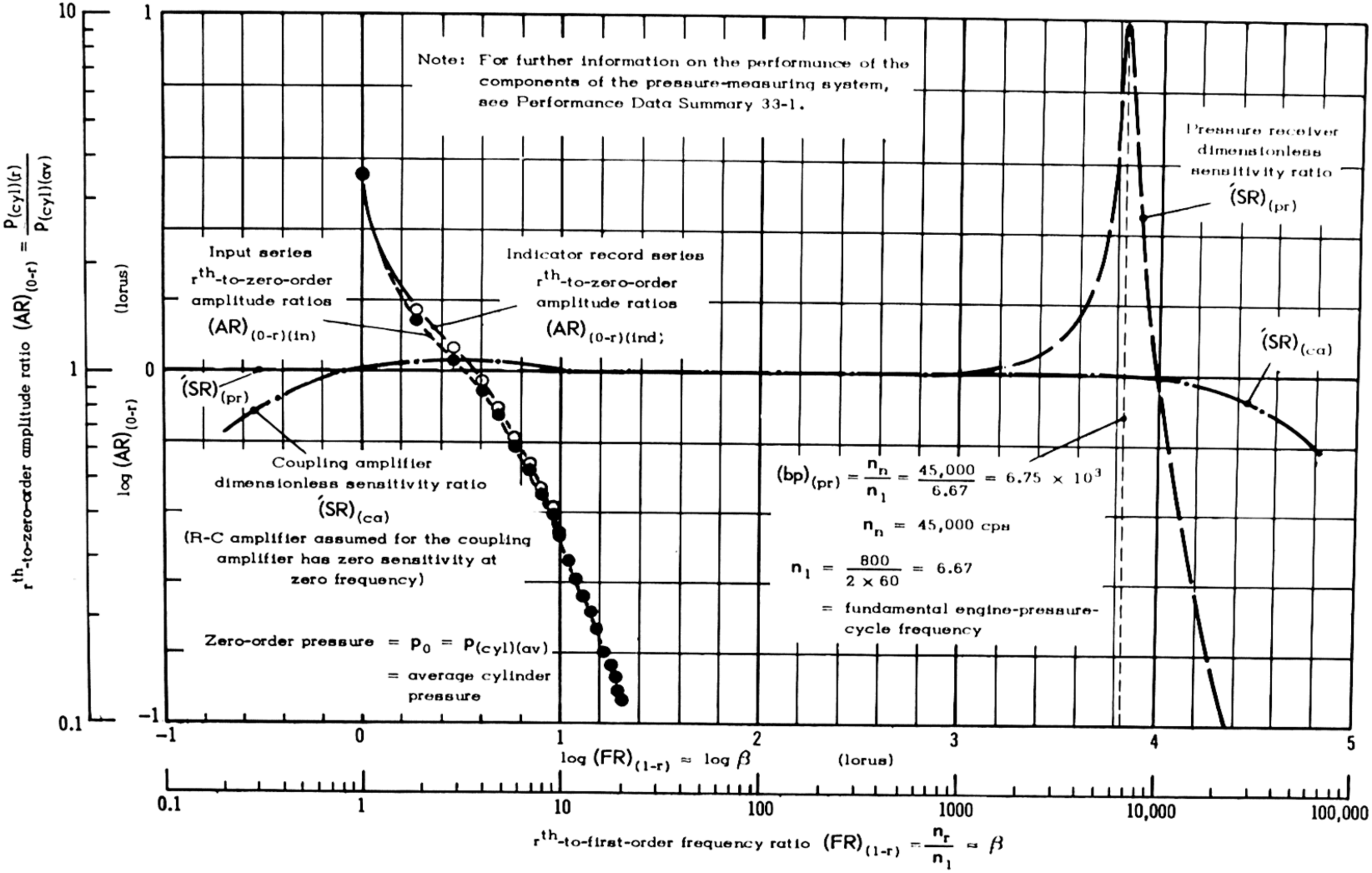
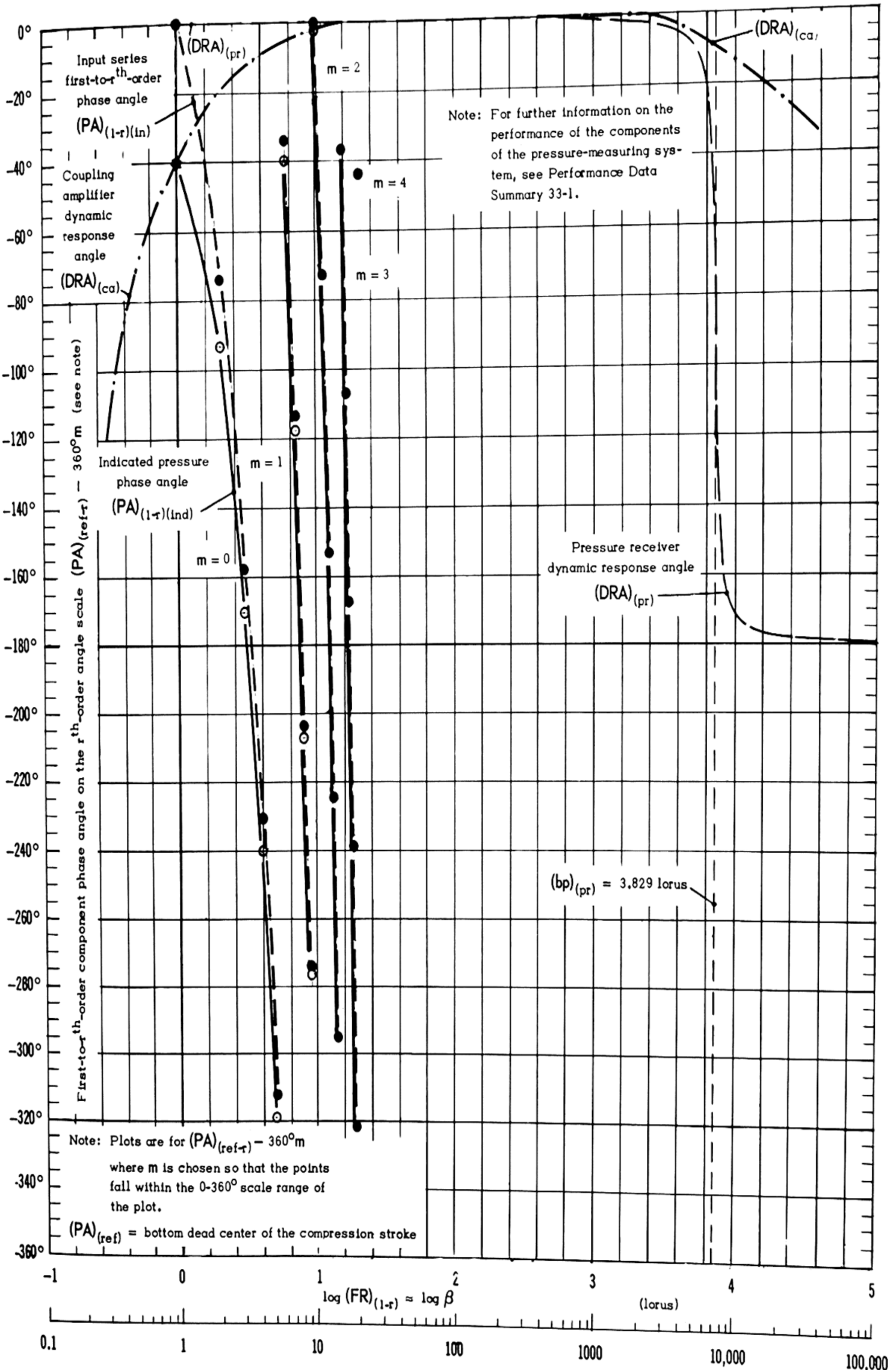


Fig. 33-11a. Illustrative logarithmic-scale plot of the Fourier-series amplitude ratios for the cylinder pressure variation of an internal combustion engine at 800 rpm, and the corresponding amplitude ratios for the pressure record from a pressure-measuring system using electrical components.

Fig. 33-11b. Illustrative semilogarithmic-scale plot of the Fourier-series component phase angles for the cylinder pressure variation of an internal combustion engine at 800 rpm, and the corresponding phase angles for the pressure record from a pressure-measuring system using electrical components.


0°
-20°
-40°
-60°
-80°
-100°
-120°
-140°
-160°
-180°
-200°
-220°
-240°
-260°
-280°
-300°
-320°
-340°
-360°
First-to-rth-order angle scale (PA)(ref-τ) − 360°m (see note)
Input series first-to-rth-order phase angle (PA)(1-r)(in)
Coupling amplifier dynamic response angle (DRA)(ca)
(DRA)(pr)
(DRA)(ca)
m = 2
m = 4
m = 3
m = 1
m = 0
Indicated pressure phase angle (PA)(1-r)(ind)
Pressure receiver dynamic response angle (DRA)(pr)
(bp)(pr) = 3.829 lorus
Note: For further information on the performance of the components of the pressure-measuring system, see Performance Data Summary 33-1.
Note: Plots are for (PA)(ref-τ) − 360°m where m is chosen so that the points fall within the 0-360° scale range of the plot.
(PA)(ref) = bottom dead center of the compression stroke
-1
0
1
2
3
4
5
log (FR)(1-r) ≈ log β
(lorus)
0.1
1
10
100
1000
10,000
100,000
rth-to-first-order frequency ratio (FR)(1-r) = nr/n1 ≈ β

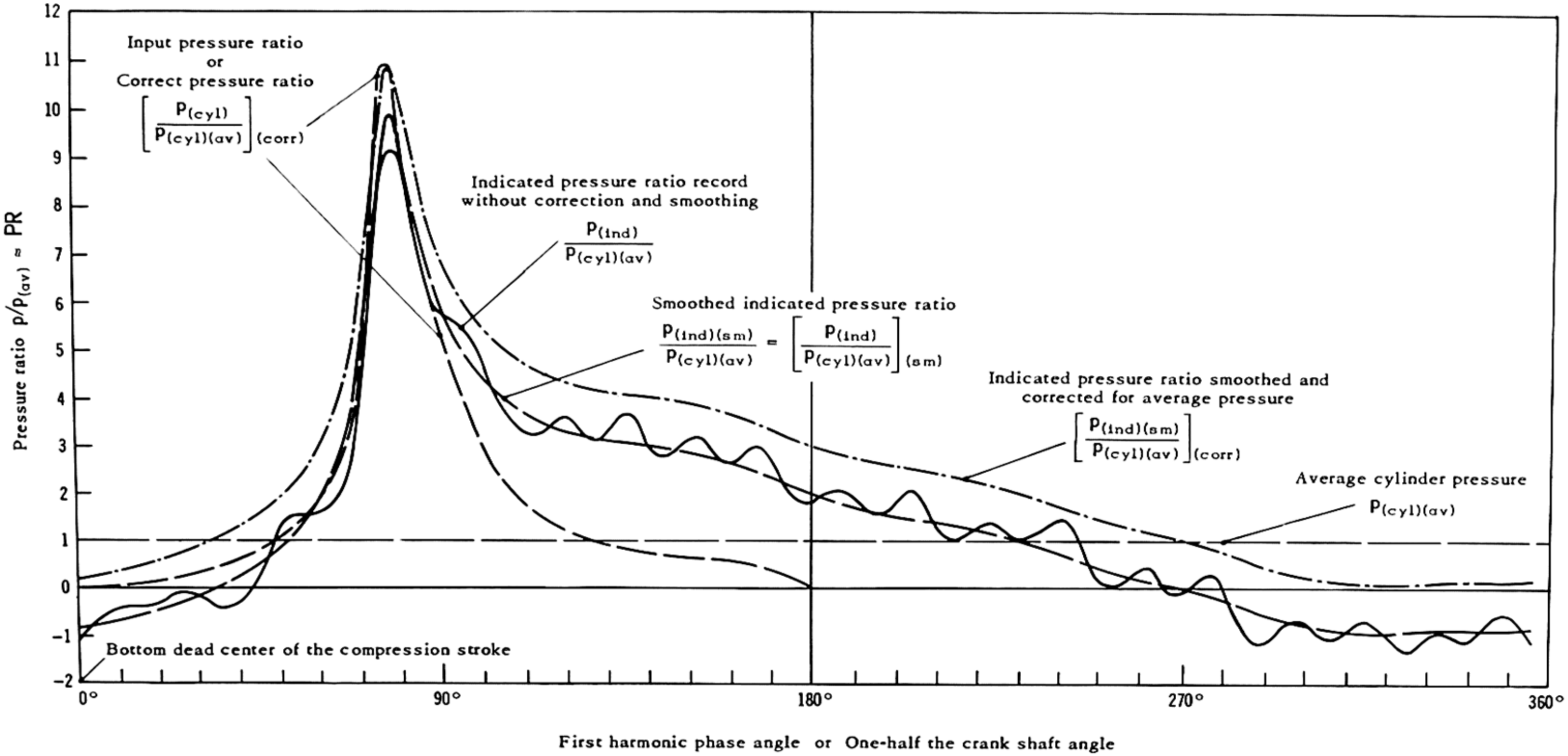


Fig. 33-12. Illustrative theoretical plot for the cylinder pressure variation of an internal combustion engine at 800 rpm and the corresponding pressure record from a pressure-measuring system with inadequate low-frequency performance.

from the reference level of unity (0 on the loru scale) at high-frequency ratios and also at low frequencies. Because an R-C amplifier is chosen for the coupling function, the static sensitivity (that is, the zero-frequency sensitivity) is zero. The reference sensitivity ratio corresponds to the value that exists at intermediate frequencies. This situation is shown by the dimensionless sensitivity ratio curve for the coupling amplifier in Fig. 33-11a.

33.93. The frequency of the first-order input component* is taken as the reference frequency for the plots of Fig. 33-11. This means that unity on the reference frequency ratio scale corresponds to 6.67 cycles per second. The same point is zero on the loru scale. The input pressure variation amplitude ratio points taken from Fig. 33-5 are plotted in Fig. 33-11a as solid dots connected by a short-dashed line and start with the fundamental at unity on the reference frequency ratio scale. The corresponding amplitude ratio points for the pressure record found by graphical addition are represented by hollow dots connected by the full line. Similarly, phase angles for the indicated pressure record components are found by a summation of the points on the dashed-line phase-angle-plot curves given in Fig. 33-11b. The phase angles for the pressure record components are connected by the full line.

33.94. In Fig. 33-11a, the amplitude ratio points for the indicated pressure are substantially identical with the corresponding points for the input pressure. In particular, no perceptible deviation exists for the high-order components. On the other hand, Fig. 33-11b shows that the coupling amplifier dynamic response angle introduces considerable phase angle differences between the input components and the corresponding output components. These differences are significant for the lower frequency components, but effectively disappear for orders higher than the tenth.

33.95. The dimensionless sensitivity ratio and phase angle information given in Fig. 33-11 for the components of the indicated pressure are combined by means of a harmonic synthesizer to give the full-line curve of Fig. 33-12. This curve deviates in three ways from the correct indicated pressure ratio curve (short heavy dashes), which is identical with the input pressure ratio:

1) It contains irregular oscillations not present in the correct curve.
2) During the first part of the cycle, its average position is below the correct curve.
3) In the region of decreasing pressure ratio, it is considerably above the correct curve.

33.96. The first type of deviation is present because of the limited number of terms used in the Fourier series for the input pressure. The tabulation of Fig. 12-8

---

* At an engine speed of 800 rpm, the fundamental frequency of the pressure variation is $800/2 \times 60 = 6.67$ cycles per second.

shows that the amplitude ratio for the 20th order is approximately 1/8 and shows a relatively small decrease between orders. This means that many more terms will probably be required for the synthesizer to show a truly smooth curve. If the hypothesis that the roughness of the indicated pressure ratio curve is due to terms that are missing from the Fourier series representation is accepted, it is reasonable to approximate the proper curve by drawing a smoothed curve through the irregular curve. The long-thin-dash-line curve of Fig. 33-12 is a smoothed curve of this kind.

33.97. The second type of deviation occurs because the sensitivity of the coupling amplifier is zero for a constant pressure component. This means that the sinusoidal response components will be effectively centered about the zero pressure level rather than the average pressure level. The net effect on the indicated pressure record is to produce a constant lowering equal in magnitude to the average pressure. A correction for this effect is introduced by raising the smoothed curve of indicated pressure ratio by an amount equal to the average cylinder pressure. The resulting curve is shown by the dash-and-dot line in Fig. 33-12. The smoothed and corrected indicated pressure ratio curve agrees very closely with the correct curve during the period of rapid pressure rise. This is to be expected from the dimensionless sensitivity ratio and dynamic response angle plots of Fig. 33-11, which show small errors for both quantities over the range of high-order components that determine steep portions of the indicated curve.

33.98. The third type of deviation stems from phase angle differences between corresponding input and output phase angle components. Figure 33-11b shows phase angle differences ranging from about 40 degrees for the fundamental to less than 2 degrees for the 10th-order component. These phase angle differences mean that large amplitude ratio terms with relatively broad peaks are shifted toward the right-hand side of the record. The result is that the indicated pressure is generally too high after the peak value has passed. This effect is very apparent in Fig. 33-12.

33.99. It is obvious that the electrical pressure-measuring system assumed for the illustrative example is unsatisfactory for making internal combustion engine indicator cards. The pressure receiver and the indicating system both give excellent performance, but the poor low-frequency performance of the R-C coupling amplifier causes the over-all system performance to be unacceptable. It is technically feasible to design and build amplifiers with substantially ideal low-frequency performance and an operating range of sufficient width to permit excellent pressure records from electrical pressure-measuring systems. The example discussed here was deliberately formulated to give defective performance in order to illustrate the importance of proper coupling amplifier characteristics on the operation of electrical pressure-measuring systems.

TURBINE-NOZZLE-CHAMBER PRESSURE MEASUREMENT IN A TURBOJET ENGINE

33.100. In the examples discussed in the previous sections, a spring-and-piston indicator was used to illustrate the effect of inadequate high-frequency performance on pressure records from internal combustion engine cylinders. In the same way, an electrical pressure-measuring system with an R-C coupling amplifier was used to show the effect of poor low-frequency performance on engine cylinder records. In both of the examples, the performance of a single operating component dominates the performance characteristics of the instrument under discussion. In the turbine-nozzle-chamber pressure-measurement example illustrated in Fig. 33-13 and discussed in the following sections, the performance characteristics of all the components that make up the open chain are assumed to have break points within a small frequency range. For this reason, the performance of the system formed by the components must be found by combining performance information from each one of the components. Of the four components involved, three are assumed to have second-order performance equations, while the fourth is a first-order system. Under these circumstances, the over-all system performance may be found graphically by use of first- and second-order profiles located by computed break points on a suitably chosen reference frequency ratio scale.

33.101. The pressure-measuring system must be able to record the static pressure that is closely associated with the turbojet engine thrust and must also handle pressure waves up to a maximum frequency of 100 cycles per second. The accuracy requirements are less stringent for high frequencies than for low frequencies. A dimensionless sensitivity ratio tolerance limit of ±0.10 is placed on the high-frequency cutoff at 50 cycles per second. A tolerance limit of ±0.01 is specified for the zero-frequency limit. The high-frequency cutoff at 100 cycles per second is given a dimensionless sensitivity ratio tolerance limit of ±0.25.

33.102. The specified characteristic of accurate measurement at low frequencies and under static conditions may be met by use of a carrier-frequency amplifier for coupling purposes. A D'Arsonval galvanometer oscillograph is used for the indicating system. For the components chosen, the tolerance limits for low-frequency performance are determined by interference effects. Effects of this type are discussed later in the chapter. It is sufficient for present purposes to assume that interference effects in the operating components chosen for use are small enough for the over-all system to meet the ±0.01 dimensionless sensitivity ratio tolerance limits under quasi-static conditions.

33.103. Turbojet-turbine-nozzle-chamber pressure measurements can not be carried out by means of a pressure receiver without special cooling means, because high environmental temperature would not only introduce temperature errors in the records but also cause intolerable damage to the receiver unit itself.*

* See Li (L15) and (L16).

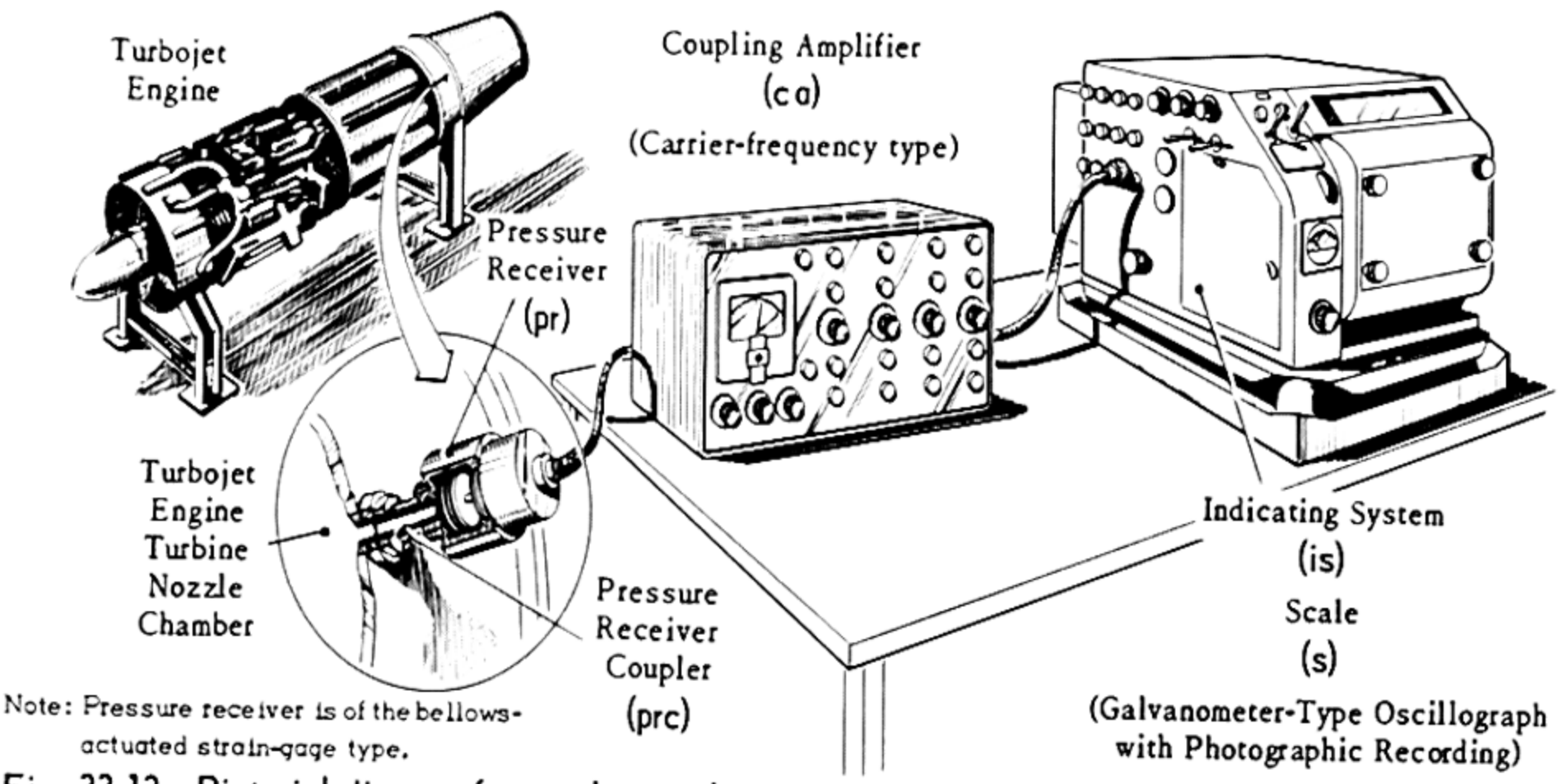


Fig. 33-13. Pictorial diagram for an electrical pressure-measuring system applied to the turbine nozzle chamber of a jet engine.

For these reasons, a pressure receiver coupler with the features illustrated in Fig. 33-13 is used to bring nozzle chamber pressures into contact with the receiving element. This coupler is effectively a cavity connected to the source of input pressure by a tube. As shown in Fig. 33-13, the tube is attached to the nozzle chamber by a special fitting and leads to the cavity formed by the inside of the bellows in a receiver unit similar to that illustrated in Fig. 33-4f.

33.104. An accurate mathematical description of the dynamic effects associated with pressure receiver couplers of the tube-and-cavity type is very difficult to formulate in generalized terms.* Under quasi-static conditions, the pressure inside the cavity becomes identical with the input pressure, so that the natural choice for reference sensitivity is unity. When the tube is long and has a small diameter compared with the linear dimensions of the cavity, the dynamic performance of the coupler is effectively described by a first-order (0;0,1) form. On the other hand, when a large-diameter tube is connected to a cavity whose volume is small compared with that of the tube, the coupler behaves as an organ pipe excited in its lowest frequency mode. This action is well described by a second-order (0;0,1,2) performance equation with an undamped natural frequency equal to the organ pipe fundamental frequency and with a relatively low damping ratio that must be determined by experimental methods.

33.105. Between the "small-tube-diameter" and "large-tube-diameter" ranges, tube-and-cavity couplers have performance characteristics that are complicated by the nonlinear behavior of gases under high temperatures and pressures and by the nonlinear effects caused by high velocity gradients in gas flow through tubes and constrictions. These nonlinear actions are especially serious because they invalidate the law of superposition, which must hold true if results based on the frequency response method are to be accurate.

* See Iberall (I4).

33.106. With these noted limitations in mind, it is assumed that the performance of the pressure receiver coupler of Fig. 33-13 may be satisfactorily represented by the (0;0,1,2) second-order equation. The undamped natural frequency is taken to be 150 cycles per second, and a damping ratio of 0.5 is used.

33.107. The pressure receiver and the indicating system for the pressure indicator of Fig. 33-13 are second-order systems. The coupling amplifier has an R-C first-order filter in the demodulation stage to remove the carrier frequency. This means that the amplifier behaves as a (0;0,1) system.

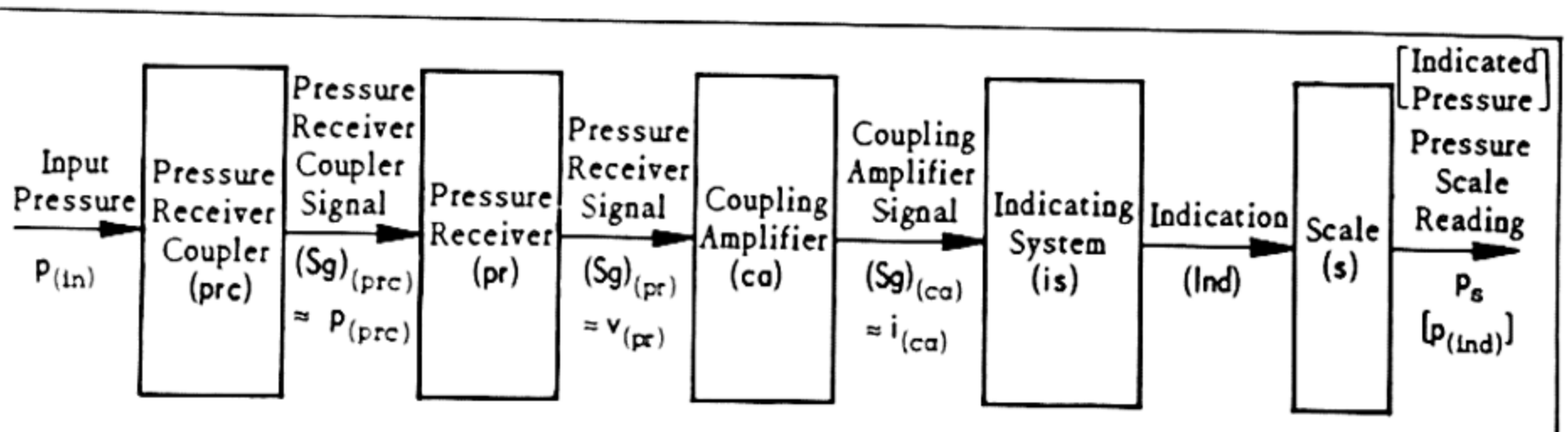
33.108. Performance function forms and numerical information on the characteristics for the operating components of the pressure-measuring system shown in Fig. 33-13 are given in Performance Data Summary 33-2. Break points are calculated and listed on a reference frequency ratio scale with an assumed reference frequency of 100 cycles per second. The reference frequency is chosen to be 100 cyles per second because this is the largest integral power of 10 that yields positive values for the logarithms of the break points that are of primary importance in the problem under discussion.

33.109. Figure 33-14a shows log-log dimensionless sensitivity ratio plots for each of the four operating components. These component performance plots are made by use of the first- and second-order profile templates described in Chapter 24, with the break points located from the information given in Performance Data Summary 33-2.

33.110. In Fig. 33-14a, the component performance curves are shown as thin dashed lines. The over-all performance curve for the system is found by the ordinate-addition process described in Procedure Summary 33-1 and is shown as a heavy solid line. In order to give the results directly on a frequency scale instead of the reference frequency ratio scale, the reference frequency of 100 cycles per second is written in square brackets directly under the reference frequency ratio of unity. Other frequencies may now be read directly from the numerical scale by placing the proper multiples of 10 under the end point of each decile on either side of the 100-cycles-per-second point. The square brackets show that these values are alternates to the reference frequency ratio values associated with the logarithmic scale.

33.111. Tolerance-limit lines drawn at ±0.10 and ±0.25 levels on Fig. 33-14a show that the 0.25 limit cutoff is 130 cycles per second and the 0.10 high-frequency cutoff is at 75 cycles per second. These results show that the 0.25 tolerance limit high-frequency cutoff has a safety margin of 30 cycles per second over its specification value, while the 0.10 tolerance limit has a safety margin of 25 cycles per second over the specification.

33.112. Figure 33-14b shows the dynamic response angle curves that correspond to the dimensionless sensitivity ratio plots of Fig. 33-14a. In the original



a) Functional diagram

Assume $n_{(ref)} = 100$ cycles per second.

(prc) Pressure Receiver Coupler: Tube from combustion chamber to chamber with pressure receiver

$$[PF]_{(prc)[p;p]} \approx \eta_{(0;0,1,2)} \quad ; \quad S_{(prc)[p;p](ref)} = 1$$

(Refer to Derivation Summary 33-2.)

$$n_n = 150 \text{ cps} \quad ; \quad DR = 0.5$$

From Eq. (35) of Derivation Summary 33-2

$$(bp)_{(prc)} = (NFR)_{(prc)} = \frac{150}{100} = 1.5 \quad ; \quad \log (bp)_{(prc)} = 0.1761$$

(pr) Pressure Receiver: Bellows actuated strain gage type

$$[PF]_{(pr)[p;v]} \approx \eta_{(0;0,1,2)} \quad ; \quad S_{(pr)[p;v](ref)} = 0.04 \text{ mv/psi}$$

$$n_n = 200 \text{ cps} \quad ; \quad DR = 0.1 \quad ; \quad (bp)_{(pr)} = 2.00 \quad ; \quad \log (bp)_{(pr)} = 0.3010$$

(ca) Coupling Amplifier: Carrier frequency type – 3000 cps carrier

$$[PF]_{(ca)[v;i]} \approx \eta_{(0;0,1)} \quad ; \quad S_{(ca)[v;i](ref)} = 0.385 \text{ ma/mv}$$

$$(CT)_{(ca)} = 0.53 \times 10^{-3} \text{ second} \quad ; \quad (bp)_{(ca)} = \frac{T_{(ref)}}{(CT)_{(ca)}} \frac{1}{2\pi} = \frac{1}{(CT)_{(ca)} n_{(ref)} 2\pi} = 3.0$$

$$\log (bp)_{(ca)} = 0.477$$

(is) Indicating System: D'Arsonval galvanometer type with photographic recording

$$[PF]_{(is)[i;d]} \approx \eta_{(0;0,1,2)} \quad ; \quad S_{(is)[i;d](ref)} = 1.3 \text{ inches/ma}$$

$$n_n = 450 \text{ cps} \quad ; \quad DR = 0.4 \quad ; \quad (bp)_{(is)} = 4.5 \quad ; \quad \log (bp)_{(is)} = 0.6532$$

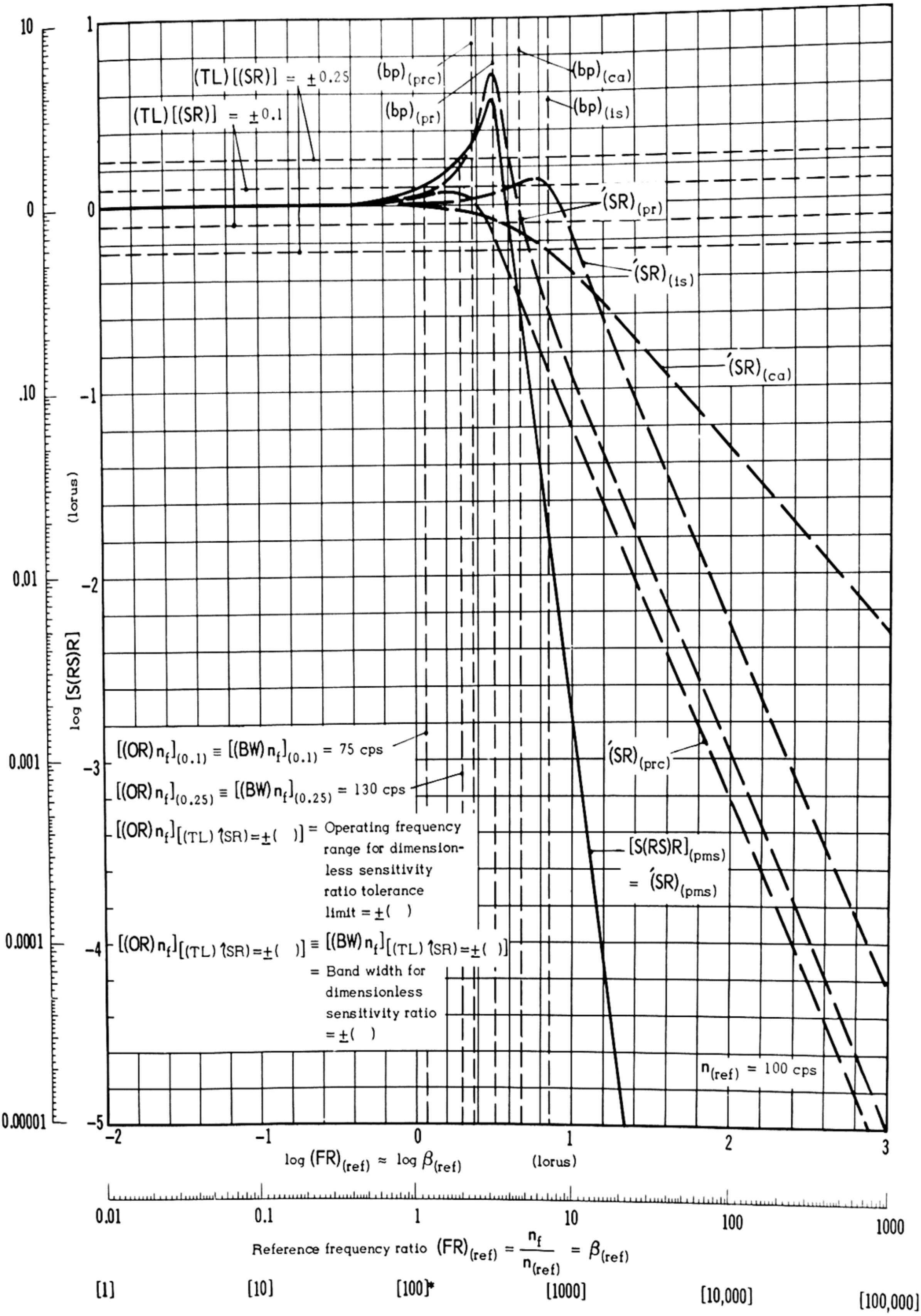
(s) Scale: Separate ruler (timing marks only on record)

$$[PF]_{(s)[d;p]} = S_{(s)[d;p]} = \frac{1}{S_{(prc)[p;p](ref)} \times S_{(pr)[p;v](ref)} \times S_{(ca)[v;i](ref)} \times S_{(is)[i;d](ref)}}$$
$$= 50 \text{ psi/inch}$$

(Refer to Eqs. (9), (10), (11), (12) and (13) of Definition Summary 29-2.)

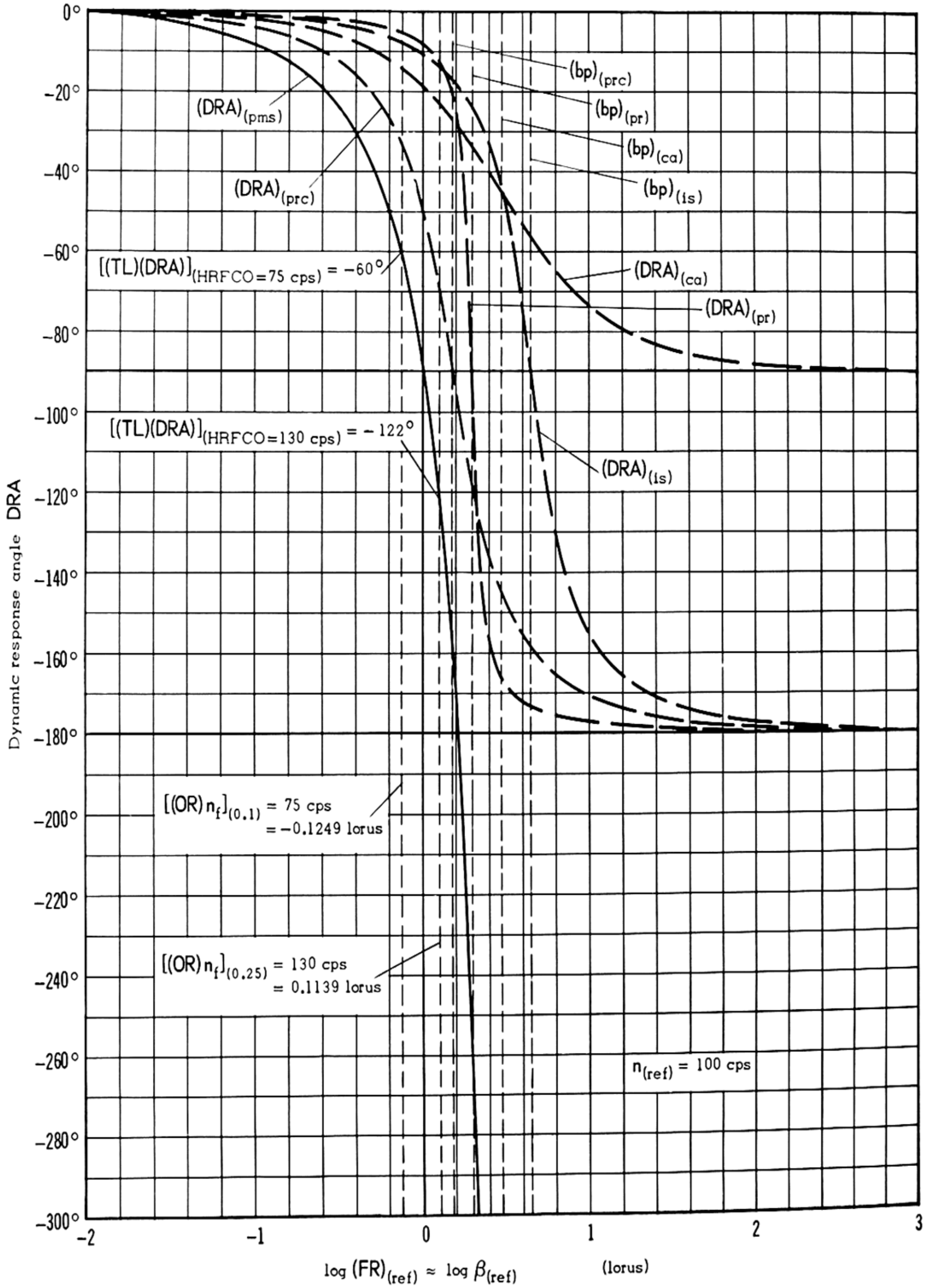
b) Component performance data

Performance Data Summary 33-2. Performance of the components of the pressure-measuring system of Fig. 33-13.



* Numbers in brackets = $(FR)_{[n_{(ref)}=1]}$

Fig. 33-14a. Dimensionless sensitivity ratio performance characteristic for pressure-measuring system of Fig. 33-13.



* Numbers in brackets = $(FR)_{[n_{(ref)}=1]}$

Fig. 33-14b. Dynamic response angle performance characteristic for pressure-measuring system of Fig. 33-13.

specifications, dynamic response angle tolerance limits were not mentioned. However, it is of some interest to note that the dynamic response angle tolerance limits corresponding to the 0.10 and 0.25 tolerance limits of Fig. 33-14a are −60 degrees and −122 degrees, respectively.

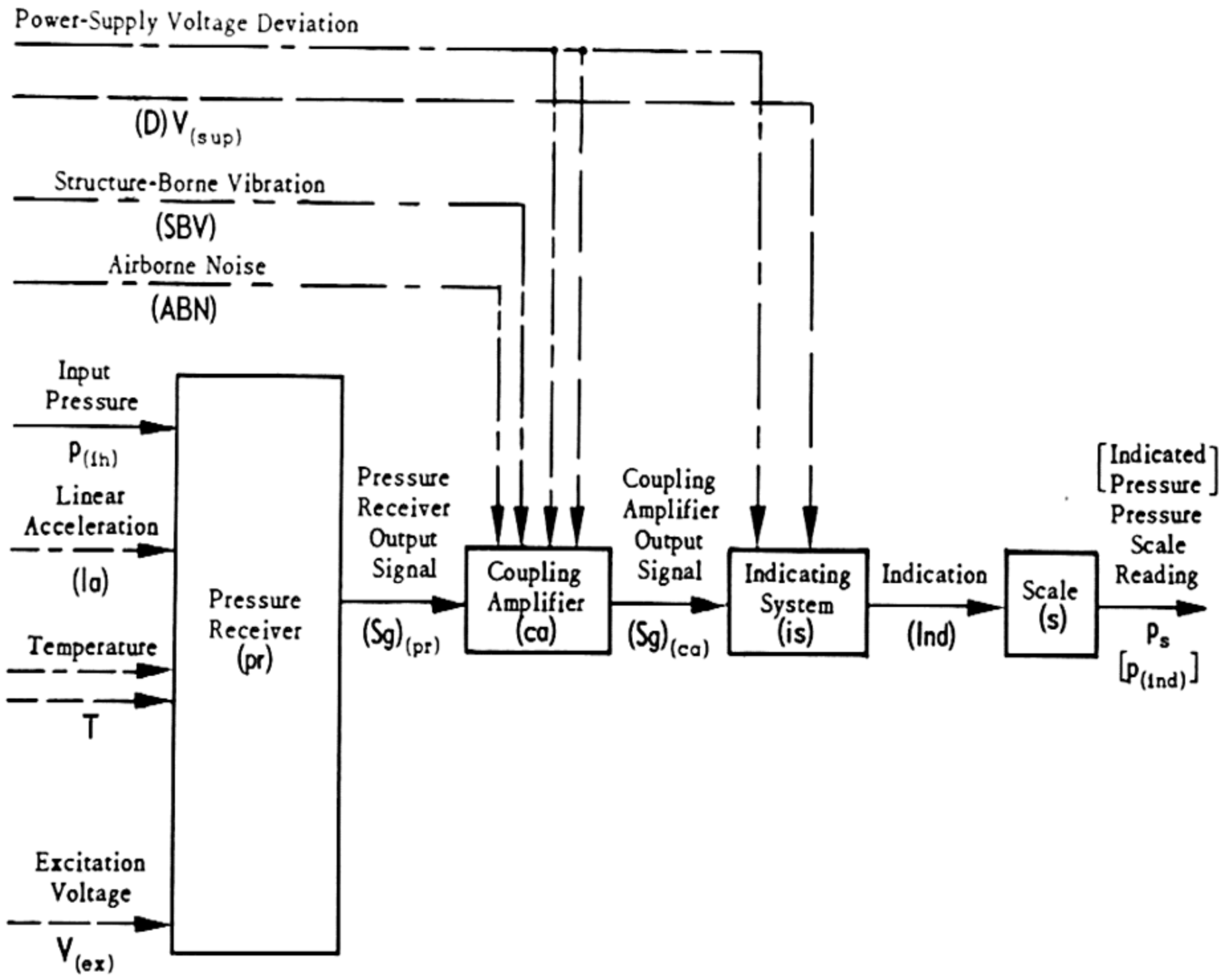
33.113. The system whose performance is represented by the plots of Fig. 33-14 is made up of well-balanced components in the sense that each individual dimensionless sensitivity ratio curve is near unity over the specified operating range and drops off sharply only after the specified high-frequency cutoffs are exceeded. If the cutoffs were to be materially increased, the characteristics of each component would have to be improved. It is not possible to draw all the problems that may appear in particular situations into a single neat package. A detailed study in each case is the only sure way of achieving satisfactory results.

33.114. Interference effects are of fundamental importance in determining the performance possible with any given set of operating components. The details of these effects were not considered in the discussion of pressure-measuring systems. Completely generalized conclusions with regard to interference effects are not possible, but certain principles are available to guide performance studies. These principles are discussed in the following sections.

INTERFERING AND MODIFYING EFFECTS IN PRESSURE-MEASURING SYSTEMS

33.115. Pressure is shown as the only input for the pressure-measuring system represented by the static-functional diagram of section d of Fig. 33-1. This diagram illustrates the idealized situation of a single actuating input and no interfering or modifying inputs. In practice, the environment usually includes several interfering inputs that produce false components of scale reading. Modifying inputs are also present in many instances. Some modifying inputs are often necessary for normal system operation, but other modifying inputs produce interfering effects by changing the relationships between the output and various actuating inputs. The generalized theory of systems with multiple inputs is discussed in Chapter 10.

33.116. Figure 33-15 is a static-functional diagram for a typical pressure-measuring system. In addition to responding to the pressure actuating input, the receiver is sensitive to linear acceleration and temperature. The receiver is directly sensitive to temperature as an interfering input, to excitation voltage as a modifying input, and to temperature as a modifying input also. Airborne noise, structure-borne vibration, and power-supply voltage variations all act as interfering inputs for the coupling amplifier. Supply-voltage change may also affect the amplifier gain and for this reason falls into the class of modifying inputs. The indicating system is sensitive to power-supply voltage fluctuation both as a direct interfering input and as a modifying input that affects the indicating system sensitivity.



This diagram represents the pressure-measuring system of Fig. 33-1d.

Note: In accordance with the conventions defined in Figs. 10-1 and 29-4:

Actuating Inputs are represented by full lines ——————————→

Interfering Inputs are represented by dash-dot lines —— – —— – —— – —— – →

Modifying Inputs are represented by dashed lines — — — — — — — — — →

From paragraph 29.32:

Actuating Inputs include those quantities the instrument is designed to receive and measure in terms of scale readings.

Interfering Inputs include those quantities that produce undesirable scale reading components not directly distinguishable from scale reading components due to actuating inputs.

Modifying Inputs include those quantities that change the relationships among actuating inputs, interfering inputs and scale readings.

Fig. 33-15. Static-functional diagram for a typical pressure-measuring system showing interfering inputs and modifying inputs.

33.117. Mechanical isolation may be used to minimize the interfering effects of noise and vibration, while filtering and stabilization of power supplies may be used to reduce the undesirable effects of voltage variations. On the other hand, it is difficult to reduce interference effects in the pressure receiver to tolerable levels.

33.118. Figure 33-16 is a static-functional diagram for the pressure receiving element of the pressure receiver shown in Fig. 33-15. For the purposes of this diagram, the diaphragm is considered as the pressure receiving element, and both diaphragm temperature and body temperature are represented as having interfering and modifying properties. Receiver excitation voltage is not shown as a

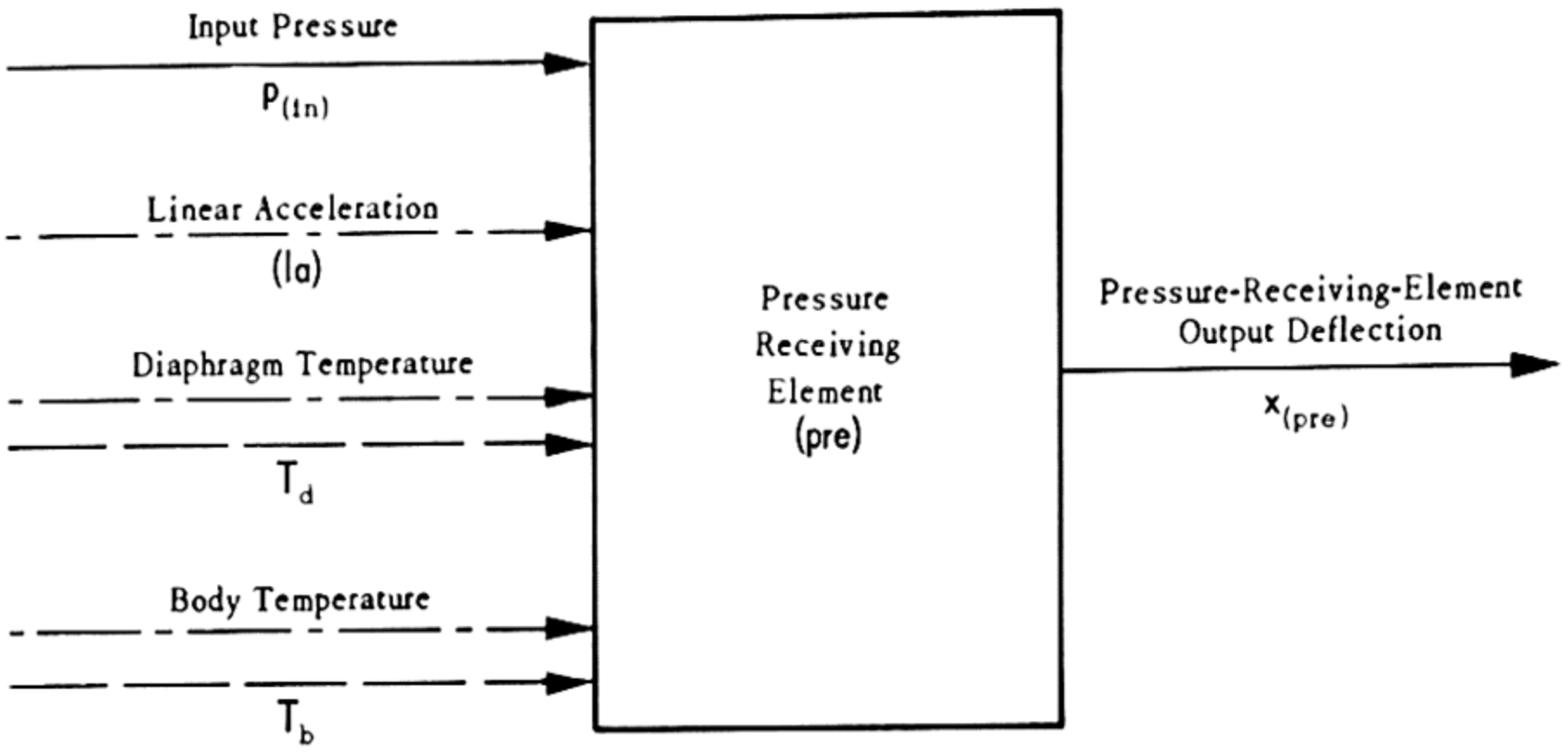


Fig. 33-16. Static-functional diagram for the pressure receiving element of the pressure receiver of Fig. 33-15, showing interfering inputs.

modifying input for the pressure receiving element because it actually affects the pressure receiver output signal by acting as a modifying input for the pressure receiver signal generating system without influencing the deflection that is the output of the pressure receiving element.

PRESSURE-RECEIVING-ELEMENT PERFORMANCE EQUATIONS

33.119. Equations describing the performance of the pressure receiving element of Fig. 33-16 are developed in Derivation Summary 33-4. These equations give a specific example of the generalized performance-describing pattern discussed in Chapter 10. This pattern starts with a single output quantity, $x_{(pre)}$, the pressure-receiving-element output deflection in the example under discussion, expressed as a sum of terms (see Eq. (1) of Derivation Summary 33-4). Each of these terms is the product of a performance function and one of the input quantities, and represents the output component corresponding to this input quantity. The first term on the right-hand side of Eq. (1) gives the deflection component due to pressure as the actuating input. The second term is the deflection component due to linear acceleration as an interfering input. The third and fourth terms represent respectively the interfering effects of diaphragm temperature and body temperature. The variable actually used in each of these terms is the deviation of the temperature concerned (symbol (D)T) from its value when its effect on the output deflection is assumed to be zero.

33.120. In addition to direct interfering effects, diaphragm temperature and body temperature introduce modifying actions that change the sensitivity of the pressure receiving element. The existence of this change is recognized by placing

A pattern of concepts, notation and conventions for representing a single output in terms of the combined effects of many inputs is described in Definition Summaries 10-1 through 10-7 of Chapter 10.

In terms of this pattern, the output of the pressure receiving element of Fig. 33-16 is given by a performance equation of the form

$$x_{(pre)} = [PF]_{(pre)[p;T;x]}p_{(in)} + [PF]_{(pre)[(la);T;x]}(la) + [PF]_{(pre)[T_d;T_d;x]}(D)T_d + [PF]_{(pre)[T_b;T_b;x]}(D)T_b \quad (1)$$

where

$[PF]_{(pre)[p;T;x]}$ ≡ pressure actuating input – temperature modifying input – deflection output of pressure receiving element

$[PF]_{(pre)[(la);T;x]}$ ≡ linear acceleration input – temperature modifying input – deflection output of pressure receiving element

$[PF]_{(pre)[T_d;T_d;x]}$ ≡ diaphragm temperature input – diaphragm temperature modifying input – deflection output of pressure receiving element

$[PF]_{(pre)[T_b;T_b;x]}$ ≡ body temperature input – body temperature modifying input – deflection output of pressure receiving element

$(D)T_d = T_d - T_{(d)(ref)}$ = pressure receiver diaphragm temperature deviation

$(D)T_b = T_b - T_{(b)(ref)}$ = pressure receiver body temperature deviation

$T_{(d)(ref)}$ = diaphragm reference temperature (temperature at which diaphragm temperature effect on $x_{(pre)}$ is negligibly small)

$T_{(b)(ref)}$ = body reference temperature (temperature at which body temperature effect on $x_{(pre)}$ is negligibly small)

a) Performance function form

Equation (1) may be expressed in a second form when the performance functions are expressed in terms of reference sensitivities and frequency functions (see Definition Summaries 13-5 and 13-6), that is, for example, when

$$[PF]_{(pre)[p;T;x]} = S_{(pre)[p;T;x](ref)}(FF)_{(pre)(p;T;x)} \quad (2)$$

where

$S_{(pre)[p;T;x](ref)}$ = pressure actuating input – temperature modifying input – deflection output reference sensitivity of pressure receiving element

$(FF)_{(pre)(p;T;x)}$ = pressure actuating input – temperature modifying input – deflection output frequency function of pressure receiving element

In terms of reference sensitivities and frequency functions, Eq. (1) becomes

$$x_{(pre)} = S_{(pre)[p;T;x](ref)}(FF)_{(pre)(p;T;x)}p_{(in)} + S_{(pre)[(la);T;x](ref)}(FF)_{(pre)((la);T;x)}(la) + S_{(pre)[T_d;T_d;x](ref)}(FF)_{(pre)(T_d;T_d;x)}(D)T_d + S_{(pre)[T_b;T_b;x]}(FF)_{(pre)(T_b;T_b;x)}(D)T_b \quad (3)$$

where

$S_{(pre)[(la);T;x](ref)}$ = linear acceleration input – temperature modifying input – deflection output reference sensitivity of pressure receiving element

$(FF)_{(pre)((la);T;x)}$ = linear acceleration input – temperature modifying input – deflection output frequency function of pressure receiving element

$S_{(pre)[T_d;T_d;x](ref)}$ = diaphragm temperature input – diaphragm temperature modifying input – deflection output reference sensitivity of pressure receiving element

$(FF)_{(pre)(T_d;T_d;x)}$ = diaphragm temperature input – diaphragm temperature modifying input – deflection output frequency function of pressure receiving element

Derivation Summary 33-4. Pressure-receiving-element performance equation forms with the effects of interfering inputs and modifying inputs included. (Page 1 of 4)

$S_{(pre)[T_b;T_b;x](ref)}$ = body temperature input – body temperature modifying input – deflection output reference sensitivity of pressure receiving element

$(FF)_{(pre)(T_b;T_b;x)}$ = body temperature input – body temperature modifying input – deflection output frequency function of pressure receiving element

b) Reference sensitivity – frequency function form

When each term of Eq. (3) is divided by the reference sensitivity of the first term and the input pressure, this equation may be written in the form

$$x_{(pre)} = S_{(pre)[p;T;x](ref)} p_{(in)} \left[(FF)_{(pre)(p;T;x)} + (SR)_{(pre)[(la);p]} (FF)_{(pre)((la);T;x)} \frac{(la)}{p_{(in)}} + (SR)_{(pre)[T_d;p]} (FF)_{(pre)(T_d;T_d;x)} \frac{(D)T_d}{p_{(in)}} + (SR)_{(pre)[T_b;p]} (FF)_{(pre)(T_b;T_b;x)} \frac{(D)T_b}{p_{(in)}} \right] \quad (4)$$

where

$$(SR)_{(pre)[(la);p]} = \frac{S_{(pre)[(la);T;x](ref)}}{S_{(pre)[p;T;x](ref)}} \equiv \text{linear acceleration – pressure sensitivity ratio of pressure receiving element} \quad (5)$$

$$(SR)_{(pre)[T_d;p]} = \frac{S_{(pre)[T_d;T_d;x](ref)}}{S_{(pre)[p;T;x](ref)}} \equiv \text{diaphragm temperature – pressure sensitivity ratio of pressure receiving element} \quad (6)$$

$$(SR)_{(pre)[T_b;p]} = \frac{S_{(pre)[T_b;T_b;x](ref)}}{S_{(pre)[p;T;x](ref)}} \equiv \text{body temperature – pressure sensitivity ratio of pressure receiving element} \quad (7)$$

c) Sensitivity ratio – frequency function form

When the frequency functions of Eq. (4) are written in the conventional form of Eq. (4) of Definition Summary 28-8 as products of a dimensionless sensitivity ratio and an imaginary exponential; that is, for example, when

$$(FF)_{(pre)(p;T;x)} = \hat{(SR)}_{(pre)(p;T;x)} \epsilon^{J(DRA)_{(pre)(p;T;x)}} \quad (8)$$

the result is

$$x_{(pre)} = S_{(pre)[p;T;x](ref)} p_{(in)} \left[\hat{(SR)}_{(pre)(p;T;x)} \epsilon^{J(DRA)_{(pre)(p;T;x)}} + (SR)_{(pre)[(la);p]} \hat{(SR)}_{(pre)((la);T;x)} \epsilon^{J(DRA)_{(pre)((la);T;x)}} \frac{(la)}{p_{(in)}} + (SR)_{(pre)[T_d;p]} \hat{(SR)}_{(pre)(T_d;T_d;x)} \epsilon^{J(DRA)_{(pre)(T_d;T_d;x)}} \frac{(D)T_d}{p_{(in)}} + (SR)_{(pre)[T_b;p]} \hat{(SR)}_{(pre)(T_b;T_b;x)} \epsilon^{J(DRA)_{(pre)(T_b;T_b;x)}} \frac{(D)T_b}{p_{(in)}} \right] \quad (9)$$

d) Sensitivity ratio – imaginary exponential form

The ideal value for $\hat{(SR)}_{(pre)(p;T;x)}$ is unity. The ideal values for the $(SR)_{(\ )}$ $\hat{(SR)}_{(\ )}$ coefficients of the last three terms of Eq. (9) (which represent interference effects) are all zero.

Using these ideal values as references, define

$$[(FD)x_{(pre)}]_{(dyn)(p_{(in)})} = \hat{(SR)}_{(pre)(p;T;x)} - 1 \quad (10)$$

≡ input pressure dynamic fractional deviation of the pressure-receiving-element deflection

Derivation Summary 33-4. Pressure-receiving-element performance equation forms with the effects of interfering inputs and modifying inputs included. (Page 2 of 4)

$$[(FD)x_{(pre)}]_{(int)(la)} = (SR)_{(pre)[(la);p]}\hat{(SR)}_{(pre)((la);T;x)}\frac{(la)}{p_{(in)}} - 0 \quad (11)$$

≡ linear acceleration interference fractional deviation of the pressure-receiving-element deflection

$$[(FD)x_{(pre)}]_{(int)(T_d)} = (SR)_{(pre)[T_d;p]}\hat{(SR)}_{(pre)(T_d;T_d;x)}\frac{(D)T_d}{p_{(in)}} - 0 \quad (12)$$

≡ diaphragm temperature interference fractional deviation of the pressure-receiving-element deflection

$$[(FD)x_{(pre)}]_{(int)(T_b)} = (SR)_{(pre)[T_b;p]}\hat{(SR)}_{(pre)(T_b;T_b;x)}\frac{(D)T_b}{p_{(in)}} - 0 \quad (13)$$

≡ body temperature interference fractional deviation of the pressure-receiving-element deflection

Using the definitions of Eqs. (10), (11), (12) and (13) gives for Eq. (9):

$$x_{(pre)} = S_{(pre)[p;T;x](ref)}p_{(in)}\left\{[1 + [(FD)x_{(pre)}]_{(dyn)(p_{(in)})}]\epsilon^{j(DRA)_{(pre)(p;T;x)}}\right.$$
$$+ [(FD)x_{(pre)}]_{(int)(la)}\epsilon^{j(DRA)_{(pre)((la);T;x)}} + [(FD)x_{(pre)}]_{(int)(T_d)}\epsilon^{j(DRA)_{(pre)(T_d;T_d;x)}}$$
$$\left. + [(FD)x_{(pre)}]_{(int)(T_b)}\epsilon^{j(DRA)_{(pre)(T_b;T_b;x)}}\right\} \quad (14)$$

e) *Fractional deviation form*

In addition to the fractional deviation form of Eq. (14), it is useful to derive a frequency function ratio function form by dividing each term in the bracket of Eq. (4) by $(FF)_{(pre)(p;T;x)}$. The resulting equation is

$$x_{(pre)} = S_{(pre)[p;T;x](ref)}(FF)_{(pre)(p;T;x)}p_{(in)}\left[1 + (SR)_{(pre)[(la);p]}(FFRF)_{(pre)((la);p)}\left(\frac{(la)}{p_{(in)}}\right)\right.$$
$$\left. + (SR)_{(pre)[T_d;p]}(FFRF)_{(pre)(T_d;p)}\left(\frac{(D)T_d}{p_{(in)}}\right) + (SR)_{(pre)[T_b;p]}(FFRF)_{(pre)(T_b;p)}\left(\frac{(D)T_b}{p_{(in)}}\right)\right] \quad (15)$$

where

$$(FFRF)_{(pre)((la);p)} = \frac{(FF)_{(pre)((la);T;x)}}{(FF)_{(pre)(p;T;x)}} \equiv \text{linear acceleration – pressure frequency function ratio function of pressure receiving element} \quad (16)$$

$$(FFRF)_{(pre)(T_d;p)} = \frac{(FF)_{(pre)(T_d;T_d;x)}}{(FF)_{(pre)(p;T;x)}} \equiv \text{diaphragm temperature – pressure frequency function ratio function of pressure receiving element} \quad (17)$$

$$(FFRF)_{(pre)(T_b;p)} = \frac{(FF)_{(pre)(T_b;T_b;x)}}{(FF)_{(pre)(p;T;x)}} \equiv \text{body temperature – pressure frequency function ratio function of pressure receiving element} \quad (18)$$

When the frequency functions of Eqs. (16), (17) and (18) are expressed in dimensionless sensitivity ratio – imaginary exponential product forms, Eqs. (16), (17) and (18) become

$$(FFRF)_{(pre)((la);p)} = \frac{\hat{(SR)}_{(pre)((la);T;x)}}{\hat{(SR)}_{(pre)(p;T;x)}}\epsilon^{j[(DRA)_{(pre)((la);T;x)} - (DRA)_{(pre)(p;T;x)}]} \quad (19)$$

Derivation Summary 33-4. Pressure-receiving-element performance equation forms with the effects of interfering inputs and modifying inputs included. (Page 3 of 4)

$$(FFRF)_{(pre)(T_d;p)} = \frac{(SR)_{(pre)(T_d;T_d;x)}}{(SR)_{(pre)(p;T;x)}} \epsilon^{j[(DRA)_{(pre)(T_d;T_d;x)} - (DRA)_{(pre)(p;T;x)}]} \tag{20}$$

$$(FFRF)_{(pre)(T_b;p)} = \frac{(SR)_{(pre)(T_b;T_b;x)}}{(SR)_{(pre)(p;T;x)}} \epsilon^{j[(DRA)_{(pre)(T_b;T_b;x)} - (DRA)_{(pre)(p;T;x)}]} \tag{21}$$

Note: The frequency function ratio function as a concept is similar to the concept of performance function ratio function of Definition Summary 10-4 and the time response function ratio function of Definition Summary 10-6.

f) Frequency function ratio function form

Derivation Summary 33-4. Pressure-receiving-element performance equation forms with the effects of interfering inputs and modifying inputs included. (Page 4 of 4)

temperature symbols in the modifying input positions of the input-output subscript brackets of the performance-describing concept symbols used in Derivation Summary 33-4. When this modifying input symbol is omitted, it is assumed that the modifying input effect is either constant and known or is negligibly small.

33.121. When each of the performance functions in Eq. (1) of Derivation Summary 33-4 is resolved into a reference sensitivity and a frequency function according to the convention of Eq. (2) of Definition Summary 28-8, the resulting performance equation form is given by Eq. (3) of Derivation Summary 33-4. When each term of this equation is divided by the product of the pressure – deflection reference sensitivity and the input pressure, the sensitivity ratio – frequency function form of the performance equation appears. This form is given as Eq. (4) of Derivation Summary 33-4. Each frequency function in this equation may be resolved into a dimensionless sensitivity ratio and an imaginary exponential. The resulting performance equation form is given as Eq. (9) of Derivation Summary 33-4.

33.122. For the purposes of discussing imperfections in performance, it is useful to change each of the output deflection components so that they include deviation terms based on references equal to ideal forms. For example, the ideal value for the pressure-input-term dimensionless sensitivity ratio is unity. The corresponding ideal values for the other terms are all zero. Because each term is dimensionless, the deviations are all dimensionless and for this reason are called fractional deviations. The fractional deviation form of the performance equation is given as Eq. (14) of Derivation Summary 33-4.

33.123. In addition to the fractional deviation form of the performance equation, it is useful to define a frequency function ratio function form in which each term of Eq. (4) is divided by the frequency function of the actuating input. The resulting performance equation form and the associated definitions are given in section f of Derivation Summary 33-4.

MODIFYING INPUT EFFECTS

33.124. As far as performance equation forms are concerned, modifying input effects are more obscure than actuating input effects and interfering input effects. This difference depends on the fact that modifying inputs occur in the performance equation only as symbols in subscript brackets while inputs of the other types occur explicitly in terms giving output components. Modifying inputs that are not classed as interfering inputs determine the numerical values associated with performance functions and in certain cases may even affect performance function forms. On the other hand, one of the primary objectives of measuring-instrument design is to reduce to the lowest possible levels the effects of modifying inputs that produce only interference. This means that the corresponding performance functions should be made to approach zero as the ideal value.

33.125. In terms of the fractional deviation performance equation form of Eq. (14) of Derivation Summary 33-4, the effect of temperature as a modifying input is to change the value of the pressure-deflection reference sensitivity and to affect the fractional deviation levels. Because in any practical situation fractional deviations must all have small magnitudes as compared with unity, temperature modifying actions or interference effects will generally be of second order and may be disregarded.

REDUCTION OF PRESSURE-RECEIVING-ELEMENT INTERFERENCE EFFECTS DUE TO MODIFYING INPUTS

33.126. Three methods are commonly used to minimize interference effects due to modifying inputs:

1) By design and, in particular, by proper selection of materials. A typical example is the use of "isoelastic"* metal to replace ordinary steel for spring applications.
2) By isolating component parts from the interference-producing modifying input. This scheme is applied in the pressure-measuring system shown in Fig. 33-13, where a tube is used to couple the pressure receiver to the nozzle chamber. In this way, the pressure receiver is protected from injury due to the high environmental temperature.
3) By use of compensation. Typical examples are the brass rod and mercury combination for clock pendulums and the bimetallic balance wheel for watches. In the catenary diaphragm – strain gage pressure receiver, temperature compensation is introduced by two strain-sensitive windings, one placed so that it receives compressive strain and the other located so that it reacts to tensile strain. The tensile strain is equal to the product of Poisson's Ratio and the compressive

* The word "isoelastic" implies that the material described has elastic properties that are not affected by environmental conditions.

strain. Compensation action occurs because compressive strain depends on Young's Modulus, which increases with temperature, while Poisson's Ratio decreases with temperature.

33.127. Another method for compensating strain-gage indicators for temperature is to place a high-temperature-coefficient resistance-wire coil where it will be subjected to the pressure-receiver body temperature. This compensating resistance is connected in series with the receiver excitation source and the strain-receiving bridge. When the receiver body temperature increases, the compensating resistance becomes larger and reduces the effective excitation voltage applied to the strain-gage bridge. This means that the sensitivity of the pressure receiver signal generating system decreases as body temperature increases. The sensitivity of the pressure receiving element increases with temperature, so that the net effect of the compensating resistance is to reduce the effect of temperature on the pressure-signal sensitivity of the pressure receiver.

COMPONENT PERFORMANCE FUNCTIONS FOR PRESSURE RECEIVING ELEMENTS

33.128. Figure a of Derivation Summary 33-5 represents a flat-diaphragm pressure receiving element with an equivalent spring-restrained piston-and-mass system shown by dotted lines. A complete analysis on the basis of elastic theory shows that an elastic diaphragm has many modes of vibration, with the lowest mode having a frequency considerably lower than the frequency of the next higher mode. The actual behavior of the diaphragm in its lowest mode may be approximated by using equivalent mass, damping, elastic restraint and area values combined in the form of Eq. (1) of Derivation Summary 33-5. It is to be understood that while theoretical values of the equivalent coefficients may be calculated from considerations of the lowest-frequency diaphragm mode, specific values for any given pressure receiving element will depend upon experimental tests.

33.129. The pressure-receiving-element performance equation for a pressure input is set up by a force summation procedure identical with that described in Figs. 8-1 and 8-2 and in Derivation Summary 8-1 of Chapter 8. The definitions and symbols required to express and define the performance function associated with the resulting second-order equation are given in Eqs. (2) through (11) of Derivation Summary 33-5.

33.130. Section b of Derivation Summary 33-5 derives the linear-acceleration-input performance function for the flat-diaphragm pressure receiving element. This derivation is similar to that described for the pressure-input performance function except that the forcing action is produced by an inertia reaction force acting on the equivalent mass instead of a pressure acting over the exposed area of the diaphragm. Equation (14) of Derivation Summary 33-5 shows that the resulting second-order form is identical with the pressure-input performance

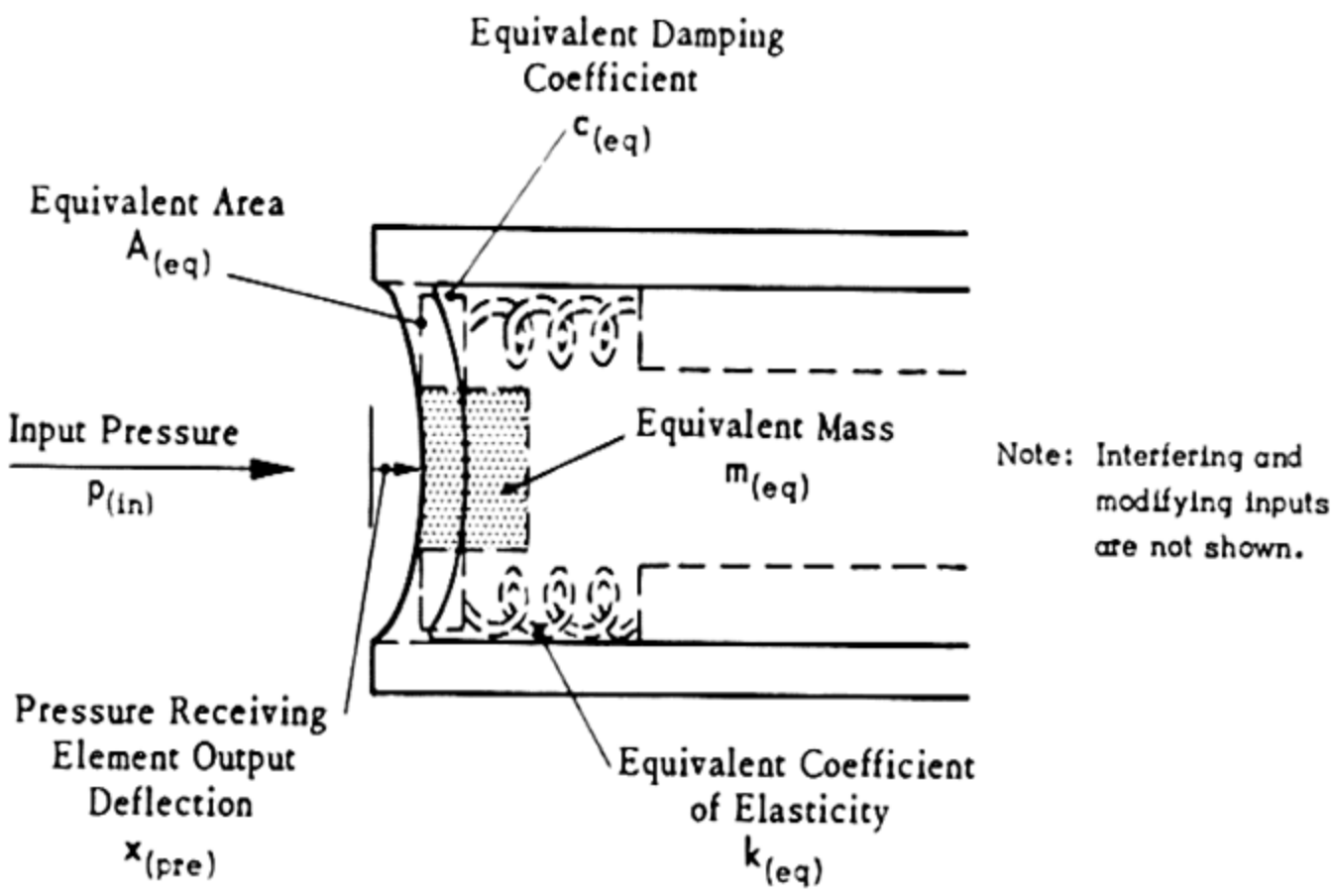


Fig. a. Flat-diaphragm pressure receiving element and equivalent spring-restrained piston-and-mass pressure receiving element, with pressure as the actuating input.

The performance equation for the equivalent spring-restrained piston-and-mass pressure receiving element of Fig. a may be derived by applying the pattern of Fig. 8-2 and Derivation Summary 8-1. The resulting equation is

$$- m_{(eq)}\ddot{x}_{(pre)} - c_{(eq)}\dot{x}_{(pre)} - k_{(eq)}x_{(pre)} + A_{(eq)}p_{(in)} = 0 \tag{1}$$

Equation (1) is a typical (0;0,1,2) equation for which the standard form is

$$\ddot{v} + 2\zeta w_n \dot{v} + w_n^2 v = \sigma w_n^2 u \tag{2}$$

Solutions for Eq. (2) are discussed in Chapters 19 and 32.

For present purposes, it is convenient to write Eq. (2) as

$$\ddot{x}_{(pre)} + 2(DR)w_n \dot{x}_{(pre)} + w_n^2 x_{(pre)} = S_{(pre)[p;x](ref)} w_n^2 p_{(in)} \tag{3}$$

where

$$w_n = \sqrt{\frac{k_{(eq)}}{m_{(eq)}}} = \text{undamped angular natural frequency of the pressure receiving element} \tag{4}$$

$$DR = \frac{c_{(eq)}}{2\sqrt{k_{(eq)} m_{(eq)}}} = \text{damping ratio of the pressure receiving element} \tag{5}$$

$$S_{(pre)[p;x](ref)} = \frac{A_{(eq)}}{k_{(eq)}} = \text{pressure – deflection reference sensitivity of the pressure receiving element} \tag{6}$$

For steady-state sinusoidal forcing variations, the (0;0,1,2) relating function gives the form of the performance function associated with Eq. (3); i.e.,

$$[PF]_{(pre)[p;x]} = [RF]_{(0;0,1,2)} \tag{7}$$

where, from Derivation Summary 33-3 and Derivation Summary 19-10 or Information Summary 32-2,

$$[PF]_{(pre)[p;x]} = S_{(pre)[p;x](ref)} (SR)'_{(pre)(p;x)} \epsilon^{J(DRA)_{(pre)(p;x)}} \tag{8}$$

$$\mu_{(0;0,1,2)} \approx (SR)'_{(pre)(p;x)} = [S(RS)R]_{(pre)(p;x)} = \frac{1}{\sqrt{[1 - (FR)_p^2]^2 + [2(DR)(FR)_p]^2}} \tag{9}$$

Derivation Summary 33-5. Performance functions of a flat-diaphragm pressure receiving element for a pressure input and for a linear acceleration input. (Page 1 of 3)

$$\phi_{(0;0,1,2)} \approx (DRA)_{(pre)(p;x)} = \tan^{-1}\left(\frac{-2(DR)(FR)_p}{1-(FR)_p^2}\right) \tag{10}$$

where

$$(FR)_p = \frac{n_{(f)p}}{n_n} \tag{11}$$

$n_{(f)p}$ = input pressure forcing frequency

$$n_n = \frac{w_n}{2\pi} = \text{undamped natural frequency of the pressure receiving element} \tag{12}$$

a) Performance function of a flat-diaphragm pressure receiving element for a pressure input

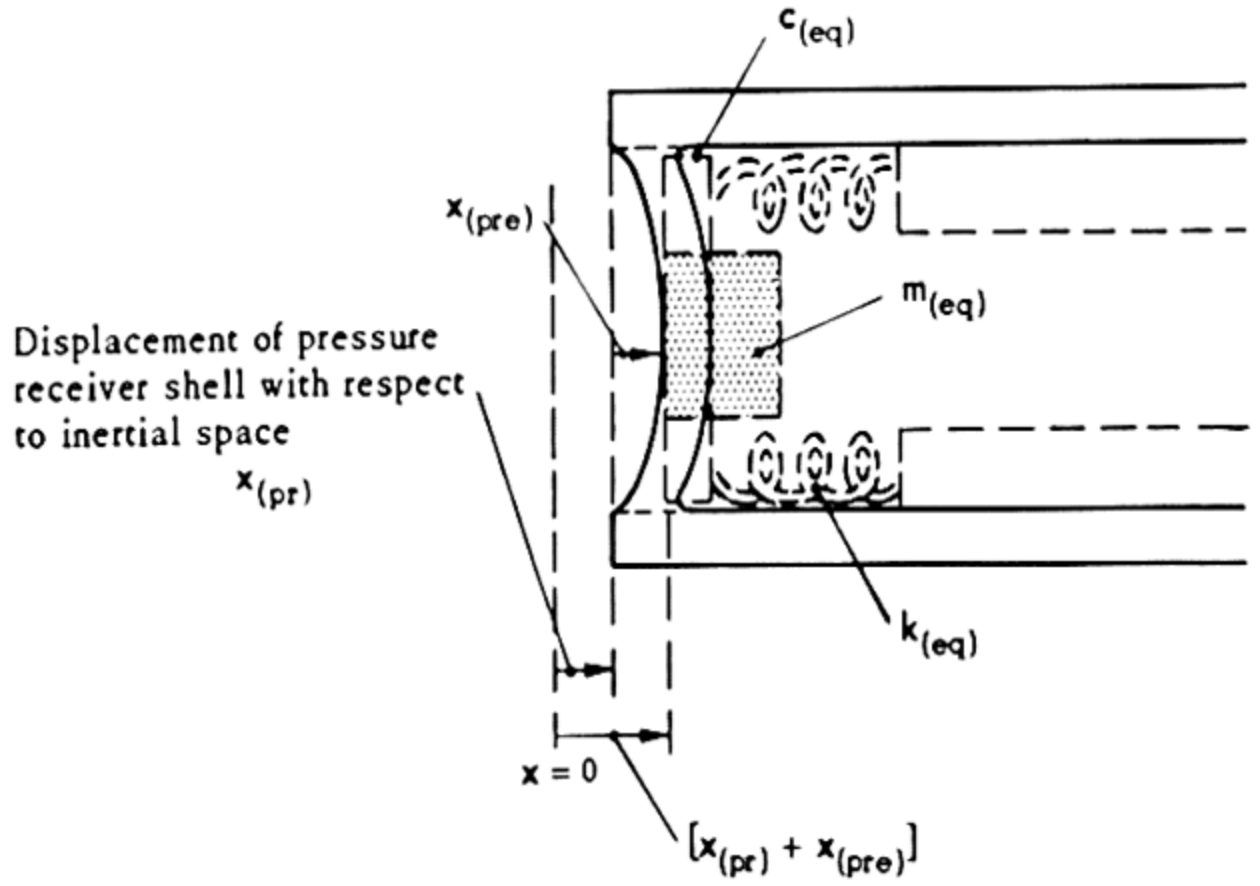


Fig. b. Flat-diaphragm pressure receiving element and equivalent spring-restrained piston-and-mass pressure receiving element, with linear acceleration as the actuating input.

For the pressure receiving element of Fig. b, the inertia reaction force on the equivalent piston and mass is

$$F_{(IR)(pre)(eqv)} = -m_{(eq)}(\ddot{x}_{(pr)} + \ddot{x}_{(pre)}) \tag{13}$$

Summing the forces on the equivalent piston and mass gives

$$-m_{(eq)}(\ddot{x}_{(pr)} + \ddot{x}_{(pre)}) - c_{(eq)}\dot{x}_{(pre)} - k_{(eq)}x_{(pre)} = 0 \tag{14}$$

Rearranging terms and dividing by $m_{(eq)}$ shows that Eq. (14) has the standard (2;0,1,2) form discussed in Derivation Summary 19-12; i.e., Eq. (14) becomes

$$\ddot{x}_{(pre)} + 2(DR)w_n\dot{x}_{(pre)} + w_n^2 x_{(pre)} = -\ddot{x}_{(pr)} \tag{15}$$

where

$$w_n = \sqrt{\frac{k_{(eq)}}{m_{(eq)}}} \quad \text{(identical with Eq. (4))} \tag{16}$$

$$DR = \frac{c_{(eq)}}{2\sqrt{k_{(eq)}m_{(eq)}}} \quad \text{(identical with Eq. (5))} \tag{17}$$

Equation (15) may be written in the form

$$\frac{1}{w_n^2}\ddot{x}_{(pre)} + \frac{2(DR)}{w_n}\dot{x}_{(pre)} + x_{(pre)} = S_{(pre)[\ddot{x};x](ref)}\ddot{x}_{(pr)} \tag{18}$$

Derivation Summary 33-5. Performance functions of a flat-diaphragm pressure receiving element for a pressure input and for a linear acceleration input. (Page 2 of 3)

where

$$S_{(pre)[\ddot{x};x](ref)} = -\frac{1}{w_n^2} = \text{acceleration – displacement reference sensitivity of the pressure receiving element} \tag{19}$$

When both sides of Eq. (18) are multiplied by w_n^2 and the pressure receiver input $\ddot{x}_{(pr)}$ is considered as the input, the result is

$$\ddot{x}_{(pre)} + 2(DR)w_n\dot{x}_{(pre)} + w_n^2 x_{(pre)} = S_{(pre)[\ddot{x};x](ref)}\, w_n^2 \ddot{x}_{(pr)} \tag{20}$$

Except for differences in reference sensitivities, Eqs. (20) and (3) are identical. This means that

$$\mu_{(0;0,1,2)} \approx (SR)_{(pre)(\ddot{x};x)} = (SR)_{(pre)(p;x)} \tag{21}$$

$$\phi_{(0;0,1,2)} \approx (DRA)_{(pre)(\ddot{x};x)} = (DRA)_{(pre)(p;x)} \tag{22}$$

where it is understood that the linear acceleration frequency ratio symbol $(FR)_{(la)}$ is to be used in place of the pressure frequency ratio symbol $(FR)_p$ in the relationships corresponding to Eqs. (9) and (10). The expression for the linear acceleration frequency ratio, corresponding to Eq. (11), is

$$(FR)_{(la)} = \frac{n_{(f)(la)}}{n_n} \tag{23}$$

where

$n_{(f)(la)}$ = linear acceleration forcing frequency

Note that $\ddot{x}_{(pr)}$ is identical with (la), the linear acceleration symbol used in Derivation Summary 33-4, so that

$$(SR)_{(pre)(\ddot{x};x)} \equiv (SR)_{(pre)((la);x)} \tag{24}$$

$$(DRA)_{(pre)(\ddot{x};x)} \equiv (DRA)_{(pre)((la);x)} \tag{25}$$

b) Performance function of a flat-diaphragm pressure receiving element for a linear acceleration input

Derivation Summary 33-5. Performance functions of a flat-diaphragm pressure receiving element for a pressure input and for a linear acceleration input. (Page 3 of 3)

equation except that the negative of the linear acceleration appears as the forcing function instead of the product of the diaphragm area and the input pressure. When the linear acceleration input – deflection output sensitivity of the pressure receiving element is defined as the negative of the reciprocal of the undamped natural frequency squared, Eq. (20) for the linear acceleration input has a form that is identical with Eq. (3) for the pressure input. This means that the acceleration-input performance function is identical with the pressure-input performance function except for different reference sensitivities and the requirement for using frequency ratios associated with the proper input quantity. The relationships involved are given in Eqs. (21) through (25) of Derivation Summary 33-5.

33.131. Derivations of performance functions to represent temperature interference effects are more difficult than the corresponding derivations for linear acceleration interference. For this reason no development of temperature-input performance functions is attempted here. As a practical matter, it is probable that temperature-input performance functions will be first-order forms with characteristic times that may be determined by proper test procedures.

EXPRESSIONS FOR DYNAMIC DEVIATION EFFECTS AND INTERFERENCE EFFECTS IN PRESSURE RECEIVING ELEMENTS

33.132. The results of Derivation Summary 33-5 may be used to develop specific expressions for the fractional deviation terms that appear in the pressure-receiving-element performance-describing form of Eq. (14) of Derivation Summary 33-4. This development is carried out in Derivation Summary 33-6. Equations (5) and (6) of this summary show that the linear acceleration – pressure sensitivity ratio, which is a direct measure of the amount of input pressure required to give the same effect on the pressure-receiving-element output deflection as a unit amount of linear acceleration, is equal in magnitude to the ratio of the equivalent mass of the diaphragm to the equivalent diaphragm area. The sensitivity ratio is actually equal to the negative of this equivalent mass-area ratio. The negative sign is not important for the sensitivity ratio; it merely shows that a negative acceleration has the same effect on the diaphragm as a positive pressure.

33.133. The fractional deviation for the pressure input describes the dynamic error associated with various pressure-input frequencies. It has the form of the (0;0,1,2) dimensionless relating function minus unity. This deviation is described by the curve families of Fig. 32-22. The corresponding family of dynamic response angles is given by Fig. 32-23.

33.134. The linear-acceleration-input performance function has a form that is identical with the form of the pressure-input performance function. This means that the numerator and denominator of the frequency function ratio function given by Eq. (15) of Derivation Summary 33-6 have identical forms and that the dynamic response angles also have the same forms. The only differences that exist are in the frequency ratios. The frequency ratio appearing in the denominator is associated with the linear-acceleration-input forcing frequency while the frequency ratio in the numerator is associated with the pressure-input forcing frequency. A similar situation exists in the dynamic response angle expressions. Because of this situation, the frequency function ratio function reduces to unity when the linear-acceleration-interference forcing frequency is equal to the input-pressure forcing frequency.

33.135. Section b of Derivation Summary 33-6 gives the expression for the diaphragm-temperature-interference fractional deviation when the interference performance function is assumed to have the form of the (0;0,1) relating function. In order to apply this fractional deviation expression to any specific case, it is necessary to have an experimentally determined value for the diaphragm thermal characteristic time.

33.136. Body-temperature interference effects may be described by equations identical in form with those for diaphragm-temperature interference effects. The

Equation (5) of Derivation Summary 33-4 has the form

$$(SR)_{(pre)[(1a);p]} = \frac{S_{(pre)[(1a);T;x](ref)}}{S_{(pre)[p;T;x](ref)}} \tag{1}$$

When temperature is considered as having the same modifying effect on both of the sensitivities of Eq. (1), the symbol T may be removed from the subscript brackets of the sensitivity symbols.

The symbol $\ddot{x}$ for linear acceleration used in Derivation Summary 33-5 is identical with the symbol (la) of Derivation Summary 33-4.

Taken together the statements of the previous two paragraphs mean that Eq. (1) is equivalent to

$$(SR)_{(pre)[(1a);p]} = \frac{S_{(pre)[\ddot{x};x](ref)}}{S_{(pre)[p;x](ref)}} \tag{2}$$

Substituting the reference sensitivity expressions of Eqs. (6) and (18) of Derivation Summary 33-5 in Eq. (2) gives

$$(SR)_{(pre)[(1a);p]} = \left(-\frac{1}{w_n^2}\right)\frac{k_{(eq)}}{A_{(eq)}} \tag{3}$$

From Eq. (4) of Derivation Summary 33-5,

$$w_n^2 = \frac{k_{(eq)}}{m_{(eq)}} \tag{4}$$

so that

$$(SR)_{(pre)[(1a);p]} = -\left(\frac{m_{(eq)}}{A_{(eq)}}\right)_{(pre)} \tag{5}$$

$$= -(MAR)_{(eq)(pre)} \tag{6}$$

where

$(MAR)_{(eq)(pre)}$ = equivalent mass-area ratio of the pressure receiving element

From Eqs. (9), (10) and (11) of Derivation Summary 33-5

$$\hat{(SR)}_{(pre)(p;x)} = \frac{1}{\sqrt{[1-(FR)_p^2]^2 + [2(DR)(FR)_p]^2}} \tag{7}$$

$$(DRA)_{(pre)(p;x)} = \tan^{-1}\left(\frac{-2(DR)(FR)_p}{1-(FR)_p^2}\right) \tag{8}$$

where

$$(FR)_p = \frac{n_{(f)p}}{n_n} = \text{pressure frequency ratio} \tag{9}$$

and

$n_{(f)p}$ = input pressure forcing frequency

From Eqs. (9), (10), (20), (21) and (22) of Derivation Summary 33-5

$$\hat{(SR)}_{(pre)((1a);x)} = \frac{1}{\sqrt{[1-(FR)_{(1a)}^2]^2 + [2(DR)(FR)_{(1a)}]^2}} \tag{10}$$

$$(DRA)_{(pre)((1a);x)} = \tan^{-1}\left(\frac{-2(DR)(FR)_{(1a)}}{1-(FR)_{(1a)}}\right) \tag{11}$$

where

$$(FR)_{(1a)} = \frac{n_{(f)(1a)}}{n_n} = \text{linear acceleration frequency ratio} \tag{12}$$

Derivation Summary 33-6. Equations for dynamic deviation effects and interference effects in pressure receiving elements. (Page 1 of 3)

and

$n_{(f)(la)}$ = linear acceleration forcing frequency

Using the expressions of Eqs. (7), (8), (10) and (11) in the fractional deviation equation of Eqs. (10) and (11) of Derivation Summary 33-4 gives

$$[(FD)x_{(pre)}]_{(dyn)(p_{(in)})} = \frac{1}{\sqrt{[1-(FR)_p^2]^2 + [2(DR)(FR)_p]^2}} - 1 \tag{13}$$

and

$$[(FD)x_{(pre)}]_{(int)(la)} = \frac{(SR)_{(pre)[(la);p]}}{\sqrt{[1-(FD)_{(la)}^2]^2 + [2(DR)(FR)_{(la)}]^2}} \frac{(la)}{p_{(in)}} \tag{14}$$

Note that Fig. 32-22 gives two families of curves showing the function of Eq. (13) for frequency ratios within the range of 0.1 to 10. Figure 32-19 gives a family of curves for the function of Eq. (14) for frequency ratios between 0.1 and 5.0. Figure 32-23 gives the corresponding family of dynamic response angle deviation curves.

The frequency function ratio function of Eq. (19) of Derivation Summary 33-4 combined with Eqs. (7), (8), (10) and (11) becomes

$$(FFRF)_{(pre)((la);p)} = \sqrt{\frac{[1-(FR)_p^2]^2 + [2(DR)(FR)_p]^2}{[1-(FR)_{(la)}^2]^2 + [2(DR)(FR)_{(la)}]^2}} \times \epsilon^{j\left[\tan^{-1}\left(\frac{-2(DR)(FR)_{(la)}}{1-(FR)_{(la)}^2}\right) - \tan^{-1}\left(\frac{-2(DR)(FR)_p}{1-(FR)_p^2}\right)\right]} \tag{15}$$

Note that when the linear acceleration frequency is identical with the pressure input frequency so that

$$(FR)_{(la)} = (FR)_p \tag{16}$$

then

$$(FFRF)_{(pre)((la);p)} = 1 \tag{17}$$

a) Linear acceleration interference effects and dynamic error effects in pressure receiving elements

Generally speaking, the effects of interfering temperatures are describable by performance functions with forms like the (0;0,1) relating function form developed in Derivation Summary 18-10. This means that from Eq. (12) of Derivation Summary 33-4

$$[(FD)x_{(pre)}]_{(int)(T_d)} = \frac{(SR)_{(pre)[T_d;p]}}{\sqrt{1+2\pi[(CT)(FF)P]_{T_d}}} \frac{(D)T_p}{p_{(in)}} \tag{18}$$

where

$$\frac{1}{\sqrt{1+[2\pi[(CT)(FF)P]_{T_d}]^2}} = (SR)_{(pre)(T_d;x)} \tag{19}$$

and

$$[(CT)(FF)P]_{T_d} = (CT)_{(pre)(d)}(FF)_{(pre)T_d}$$

= diaphragm characteristic time – diaphragm temperature forcing frequency product for the pressure receiving element (20)

$(CT)_{(pre)d}$ = diaphragm thermal characteristic time for pressure receiving element

$(FF)_{(pre)T_d} = n_{(f)T_d}$ = diaphragm temperature forcing frequency

Derivation Summary 33-6. Equations for dynamic deviation effects and interference effects in pressure receiving elements. (Page 2 of 3)

The dynamic response angle corresponding to $(SR)_{(pre)(T_d;x)}$ is

$$(DRA)_{(pre)(T_d;x)} = \tan^{-1}(-2\pi\,[(CT)(FF)P]_{T_d}) \tag{21}$$

The frequency function ratio function for diaphragm temperature interference is

$$(FFRF)_{(pre)(T_d;p)} = \sqrt{\frac{[1-(FR)_p^2]^2 + [2(DR)(FR)_p]^2}{[1+[2\pi\,[(CT)(FF)P]_{(T_d)}]^2}}$$

$$\times \epsilon^{j\left[\tan^{-1}(-2\pi[(CT)(FF)_p]_{T_d}) - \tan^{-1}\left(\frac{-2(DR)(FR)_p}{1-(FR)_p^2}\right)\right]} \tag{22}$$

The expressions associated with body temperature that correspond to Eqs. (19), (20), (21) and (22) have forms identical with those of these equations except that the subscript T_d is replaced by the subscript T_b.

b) Equations for temperature interference effects in pressure receiving elements

Derivation Summary 33-6. Equations for dynamic deviation effects and interference effects in pressure receiving elements. (Page 3 of 3)

only essential difference is that the diaphragm thermal characteristic time must be replaced by an experimentally determined body thermal characteristic time.

REDUCTION OF PRESSURE-RECEIVING-ELEMENT INTERFERENCE EFFECTS DUE TO INTERFERING INPUTS

33.137. Environmental quantities that produce output changes cause interference effects. Figures 33-15 and 33-16 show that linear acceleration and temperature are interfering inputs for pressure receiving elements. In designing pressure-measuring equipment, a primary objective is to reduce effects due to interfering inputs while maintaining satisfactory response to actuating inputs. Solutions for this problem are often made difficult by the fact that design features that improve sensitivity to the actuating input often increase the sensitivity to interfering inputs at the same time. For example, any changes in the pressure receiver signal generating system reference sensitivity, coupling amplifier reference sensitivity, or indicating system reference sensitivity for the pressure-measuring system of Fig. 33-15 will have equal effects on interfering inputs and actuating inputs. Therefore, the only hope for reducing the relative importance of interference effects due to interfering inputs is to modify pressure receiver characteristics. Methods for reducing the response of a measuring system to interfering inputs are generally similar to those already discussed in connection with modifying input effects.

33.138. In rough outline, the procedure for holding interference effects within acceptable limits involves applications of the following lines of attack:

1) Selection of design features and materials.
2) Application of mechanical and electrical filtering techniques.
3) Isolation of system components from interfering inputs.
4) Use of compensation.

33.139. General specifications are given for a pressure-measuring system in terms of size, maximum scale reading, uncertainty tolerance limits, range of interfering inputs, the frequency spectrum of the actuating input, the frequency spectrum of interfering inputs, dynamic error tolerances, and other pertinent data. When this information is available, design studies may be started. The interference control phase of these studies may logically begin with a selection of the general design features and materials to be used.

SELECTION OF DESIGN FEATURES AND MATERIALS

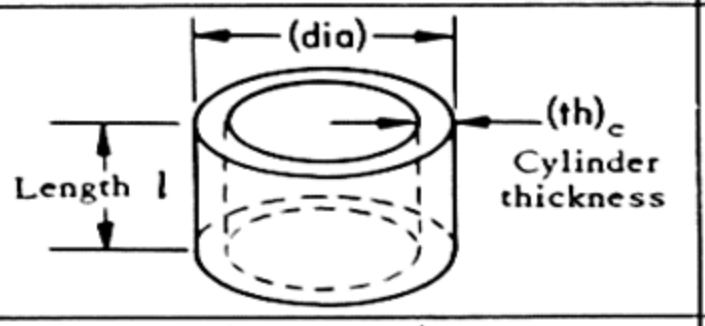
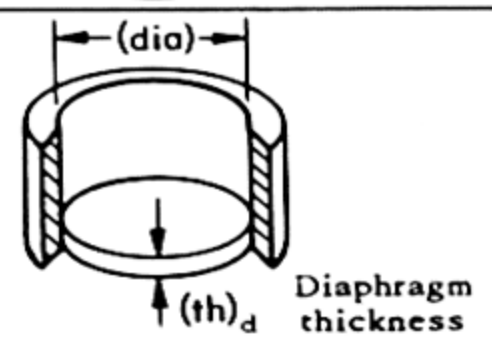
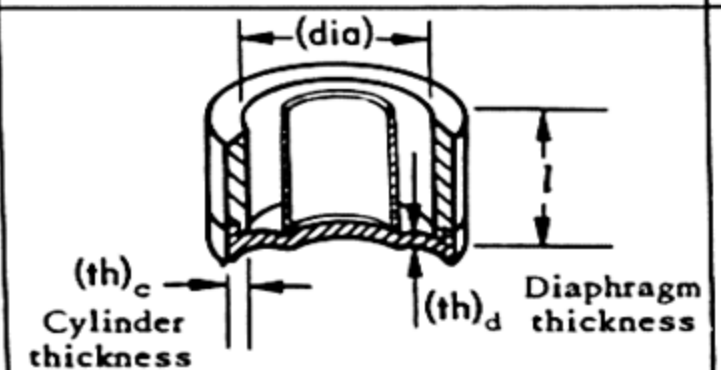
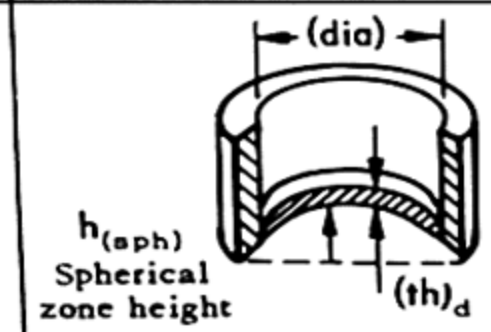
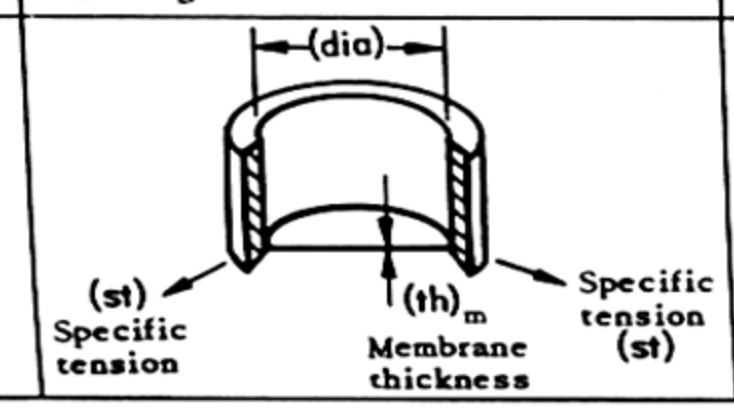
33.140. Table 33-1 lists generally useful relationships among the parameters of several pressure-receiving-element types. In order to give the tabulated information the widest possible usefulness, all quantities are reduced to nondimensional terms. The reference quantities are chosen so that, for any given pressure-receiving-element type, they depend upon the material of the element and the permissible size of the element. For the purposes of design, the diameter of the element may be taken as a measure of size. Density, stress at the elastic limit, sound velocity, and Young's Modulus are used to represent material properties.*

33.141. Column 1 of Table 33-1 lists the pressure-receiving-element types considered. Column 2 gives simplified diagrams of the various types. Column 3 lists the allowed pressure – elastic limit stress ratio for each type. In this ratio, the allowed pressure is the input pressure for which the maximum stress in the element becomes equal to the stress at the elastic limit for the material. Column 4 is the ratio of the effective mass of the element to the total mass of the element. For the purposes of this ratio, the effective mass is the moving mass of a second-order system that has the dynamic behavior of the actual system vibrating in its lowest mode. Column 5 gives the ratio of the mass-area ratio defined in Derivation Summary 33-6 to the characteristic mass-area ratio, which depends on the allowed input pressure – elastic limit stress ratio, the material density, and the receiving-element diameter. Column 6 is the ratio of the pressure-deflection sensitivity to the characteristic pressure-deflection sensitivity. This characteristic sensitivity is the ratio of receiving element diameter to Young's Modulus for the

* A complete performance study of any given pressure receiving element involves the hysteresis properties of the critical material in the element. However, for the sake of simplicity, hysteresis effects are disregarded in the present discussion.

Table 33-1. Characteristics of several pressure-receiving-element types.*

This table is based on the assumption that the receiving element acts as an equivalent second-order system with performance characteristics like those of the actual system in its lowest frequency.

Type	2 Diagram	3 Allowed pressure – elastic limit stress ratio $\frac{P_{(in)(allwd)(el)}}{(str)_{(el)}}$	4 Effective mass – total mass ratio** $\frac{m_{(eff)}}{m_{(tot)}}$	5 Effective mass-area ratio – characteristic mass-area ratio ratio*** $\frac{(MAR)_{(eff)}}{(MAR)_{(char)}}$	6 Pressure-deflection sensitivity – characteristic pressure-deflection ratio $\frac{S_{(pre)[p;x]}}{S_{(pre)[p;x](char)}}$	7 Undamped natural frequency – characteristic frequency ratio $\frac{n_n}{n_{(char)}}$
Cylindrical		$2\frac{(th)_c}{(dia)}$	1	$\frac{1}{2}$	$0.25\frac{(dia)}{(th)_c}$	2
Flat Diaphragm		$\frac{16}{3}\frac{(th)_d^2}{(dia)^2}$	0.6	$\frac{1.8}{16}\frac{(dia)}{(th)}$ $= 0.6\sqrt{\frac{3}{16}\frac{(str)_{(el)}}{P_{(allwd)}}}$	$0.011\frac{(dia)^3}{(th)_d^3}$	$12.2\frac{(th)_d}{(dia)}$
Catenary Diaphragm		$2.82\frac{(th)_d}{(dia)}$ for $l \approx (dia)$	1.60 effective mass includes mass of column and diaphragm total mass based on diaphragm only	$\frac{1.6}{2.82} = 0.567$	$0.202\frac{l}{(th)_d}$	$1.76\frac{(dia)}{l}$ for $l \approx (dia)$
Spherical Cap Diaphragm		$16\frac{h_{(aph)}}{(dia)}\frac{(th)_d}{(dia)}$ for $\frac{h_{(aph)}}{(dia)} < 0.1$	0.6	$\frac{0.6}{16}\frac{1}{\frac{h_{(aph)}}{(dia)}}$	$0.0058\frac{(dia)}{(th)}\frac{(dia)^2}{h_{(aph)}^2}$	$16\frac{h_{(aph)}}{(dia)}$
Stretched Membrane		$8.8\frac{(th)_m}{(dia)}\sqrt{\frac{(str)_{(el)}-\frac{(st)}{(th)_m}}{E}}$	0.6	$\frac{0.6}{8.8}\sqrt{\frac{E}{(str)_{(el)}-\frac{(st)}{(th)_m}}}$	$0.13\frac{E}{(st)}\frac{(dia)}{(th)_m}$	$4.8\sqrt{\frac{(st)}{E}}$

$(str)_{(el)}$
- = elastic limit stress
- = stress in the critical pressure-receiver material at the working elastic limit of the material (force/area)

$P_{(in)(allwd)}$
- = allowed input pressure
- = input pressure applied to the pressure receiving element when the critical stress is equal to the elastic limit stress (force/area)

$(MAR)_{(char)}$
- $= \frac{P_{(in)(allwd)}}{(str)_{(el)}}(den)(dia)$
- = characteristic mass-area ratio (mass/area)

(den)
- = density of the critical pressure-receiver material (mass/volume)

(sv)
- = sound velocity
- = velocity of sound in the critical pressure-receiver material (distance/second)

$\frac{(sv)}{(dia)}$
- = characteristic frequency of the pressure receiving element
- = $n_{(char)}$ (cycles/second)

$S_{(pre)[p;x](char)}$
- $= \frac{(dia)}{E}$
- = pressure-deflection characteristic sensitivity (distance/force/unit area)

E
- = Young's Modulus for the critical receiver material (force/unit area)

(st)
- = specific tension
- = tension divided by the distance over which the tension acts (force/distance)

* For further information, see Timoshenko (T9), Den Hartog (D5), and Kármán and Biot (K5).

** Corresponds to constant thickness of diaphragm.
*** Corresponds to a constant pressure-stress ratio.

material. Column 7 is the ratio of the undamped natural frequency for the receiving element to the characteristic frequency for the given material with the specified element diameter. By definition, the characteristic frequency is the ratio of sound velocity in the element material to the diameter of the element.

33.142. With a single exception, the items listed in Table 33-1 are functions of receiving-element dimensions or some combination of material properties and element dimensions. The exception is the effective mass – total mass ratio (see column 4), which has a range between 1/6 and 1.60 over the range of design types considered.

33.143. With the receiving-element diameter and the maximum input pressure specified, column 3 of Table 33-1 makes it possible to set up a requirement on the elastic limit stress for the material to be used in the receiver.

33.144. With the frequency spectra of the actuating input and the interfering inputs specified, and the reasonable assumption that the equivalent second-order system of any practical pressure receiving element will have a low damping ratio, a limiting value for undamped natural frequency may be established. Column 7 of Table 33-1 relates the undamped natural frequency of the receiving element to the characteristic frequency of the material considered and to the element diameter. The criterion of column 7 eliminates receiver type and material combinations with which it is impossible to meet dynamic performance specifications.

33.145. When a list of materials has been selected that will meet the size specifications, maximum input pressure, and undamped natural frequency criteria of columns 3 and 7 of Table 33-1, column 6 gives the pressure-deflection sensitivity for each receiving-element type in terms of the characteristic sensitivity for each material. For reference purposes, column 4 gives the effective mass – total mass ratio for each receiver type.

33.146. In addition to the immediately available information of Table 33-1, pressure receiver design must take into account heat conductivities and thermal coefficients of possible materials. For example, invar steel has good mechanical properties, but relatively poor heat conductivity, while aluminum has good thermal conductivity, but poor mechanical properties. In certain cases, a proper combination of these materials might produce a more satisfactory result than any one material alone.

33.147. The development of Derivation Summary 33-6 shows that the mass-area ratio of a flat-diaphragm pressure receiving element determines the pressure – linear acceleration sensitivity ratio. This means that linear acceleration interference effects are reduced by reducing the mass-area ratio. Column 5 of Table 33-1 gives values of the effective mass-area ratio in terms of the characteristic mass-area ratio for each receiving-element type. Other things being equal, the ratio

of column 5 should have the lowest possible value in order to minimize linear acceleration interference.

33.148. The many interlocking requirements associated with good actuating input sensitivity and low interfering input sensitivities make it impossible to set up a hard-and-fast design procedure. The approach just outlined may be used as a starting point, and supplemented with a cut-and-try procedure. When any trial design fails to meet specifications, more or less extensive changes are introduced and a new trial design is carried through. This process is continued until a unit with satisfactory performance is produced.

MECHANICAL AND ELECTRICAL FILTERING TECHNIQUES

33.149. When the essential frequencies appearing in the actuating input are well-separated from the frequencies that occur in the spectra of the interfering inputs, it is possible to use filtering actions for reducing interference effects to tolerable levels. Mechanical filtering in the pressure receiver is possible when interference frequencies are well above actuating input frequencies. Filtering in this instance is introduced by placing the undamped natural frequency of the receiver below the interference frequencies. In the usual situation, the pressure receiver picks up both actuating and interfering inputs. In this case, the output signal from the receiver is subjected to low-pass, band-pass, or high-pass electrical filtering as required to minimize interference components in scale readings. The required filters may be incorporated in the coupling amplifier, the indicating system, or both of these systems.

33.150. When interference frequencies are high and have low amplitudes with respect to actuating input variations, pressure receiver signals may be recorded without filtering. A smoothing process similar to that discussed in Chapter 6 may be applied to the record in order to substantially eliminate interference components.

ISOLATION OF SYSTEM COMPONENTS

33.151. Interference effects may be reduced by isolating measuring-system components from the interfering inputs. For example, microphonic signal components may be eliminated by isolating the coupling amplifier in a sound-proof enclosure. In addition, the pressure receiver itself may be placed in a shock mounting to minimize mechanical disturbances. The isolation of the strain-receiving tube from temperature effects in the catenary-diaphragm pressure receiver has already been mentioned in connection with the discussion of temperature as a modifying input.

COMPENSATION

33.152. The use of compensation to reduce interference effects due to interfering inputs is identical in principle and execution with the use of compensation

to control interference effects due to modifying inputs. The compensation effect is introduced by some operating component or components that receive the interfering inputs and produce outputs that are used to balance out undesirable components in the actuating input receiver.

PRACTICAL FACTORS OF PRESSURE-RECEIVING-ELEMENT DESIGN

33.153. Equation (5) of Derivation Summary 33-6 shows that the linear acceleration – pressure sensitivity ratio of a flat-diaphragm pressure receiving element is proportional to the mass-area ratio. A similar relationship exists for the dynamic error of pressure receiving elements of all types. For situations in which linear acceleration is present as a serious interfering input, it is always desirable to design for the lowest feasible mass-area ratio. Values in Column 5 of Table 33-1 give the effective mass-area ratio – characteristic mass-area ratio ratio for the five types of receiver under equal pressure-stress ratio. Column 5 shows that the catenary-diaphragm pressure receiver has a relatively small mass-area ratio. This result is achieved by the use of a high-efficiency structural design in which every part of the critical element carries a uniform stress.

33.154. The catenary-diaphragm pressure receiver provides some isolation to the strain-receiving tube from temperature effects. It is difficult to estimate temperature response from theory alone, but experimental tests have shown that temperature interference in the catenary-diaphragm element is reduced to about 1/30 of that for a flat-diaphragm receiver with similar specifications when both receiving elements are subjected to the same inputs under the same environmental conditions.

33.155. A spherical cap diaphragm that has a relatively large diameter-depth ratio gives the lowest value in Column 5, and represents the best choice when dynamic performance is the only criterion. The cylindrical type has a constant low value, and gives a better dynamic performance than a spherical cap diaphragm that has a small diameter-depth ratio. But since the spherical cap diaphragm element has no appreciable cavity as compared with the cavity of the cylindrical type, the spherical cap type is to be preferred for the high-frequency measurement of gas pressure.

33.156. Next in the value of its mass-area ratio to the spherical cap and cylindrical receivers is the catenary-diaphragm receiver. For these three types, the mass-area ratios are constant numbers. In contrast, the nondimensionalized mass-area ratio of the flat diaphragm is a function of stress-pressure ratio. For a typical 1000-psi receiving element of steel stressed to 20,000 psi, the nondimensional mass-area ratio is more than double that of a cylinder.

33.157. The nondimensional mass-area ratio of the stretched membrane is a function of its circumferential tension. In this type of receiving element, specific

tension is the essential parameter. The natural frequency is proportional to the square root of the specific tension. On the other hand, both the sensitivity and the nondimensional mass-area ratio decrease as the specific tension increases. Even with moderate tension, however, it can be shown from the expressions of column 5 that the stretched membrane has a higher nondimensional mass-area ratio than any of the other pressure-receiving-element types in Table 33-1. For this reason, the stretched-membrane type of pressure receiving element is not desirable for use when high-frequency characteristics are important. It is to be noted that the expressions in column 5 are based upon a characteristic mass-area ratio that corresponds to a constant pressure-stress ratio. A high value in this column, such as for a membrane, means a poor structure member for carrying pressure.

33.158. Pressure-carrying capacity is often not the limiting factor in design. The actual limitation in this situation is in the thickness of the diaphragm that can be produced in practice. This condition usually exists for low-pressure-range receivers. When a minimum diaphragm thickness is established, the effective mass – total mass ratio of the receiver is constant for each of the receiver types listed in Table 33-1. The mass-area ratio for different types of receivers is therefore proportional to the effective mass – total mass ratio given in column 4. From this column, the spherical diaphragm has the lowest mass-area ratio, but the flat diaphragm and the membrane also have quite favorable values. For low-pressure applications, and in particular when temperature interference is low, a stretched-diaphragm receiving element is usually the best choice when moderately-high-frequency input variations are to be recorded.

DETERMINATION OF PERFORMANCE CHARACTERISTICS FOR PRESSURE-MEASURING INSTRUMENTS

33.159. The performance information on any pressure-measuring unit or system is complete when the data provided make it possible to predict the indicated pressure record corresponding to a given input pressure variation. The required information includes numerical values for the pressure input – indication output static sensitivity of the instrument mechanism and for a complete set of dynamic-performance-describing parameters.* The problems of determining these parameters and the static sensitivity may be solved by procedures that are identical with those described in Chapters 31 and 32 for first- and second-order systems, respectively.

33.160. The pressure-indication static sensitivity may always be found by noting the pressure readings that correspond to a series of known constant input-pressure levels. This sensitivity is background rather than essential information

* In practice, graphical representations of various types (for example, dimensionless sensitivity ratio curves and dynamic response angle curves) are often substituted for numerical parameters.

for any properly calibrated pressure-measuring instrument, which always has an input pressure – scale reading sensitivity of unity.

DETERMINATION OF DYNAMIC PERFORMANCE PARAMETERS

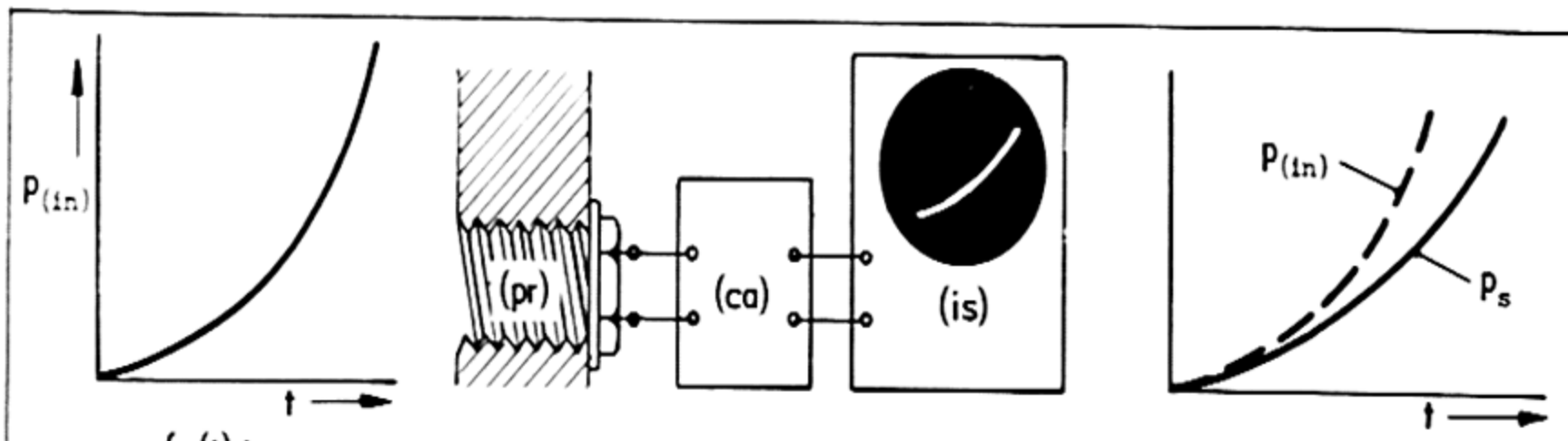
33.161. The number of parameters required to specify the dynamic performance of any given system depends on the order of the performance equation for the system. One parameter with the dimension of time is sufficient for a first-order system. One parameter with the dimension of time and one dimensionless parameter are required to specify the dynamic performance of a second-order system. The discussion of Chapter 22 shows that, as a general rule, one more dimensionless parameter is required for each additional order of the equation under consideration.

33.162. From known design features of any given unit or system, it is always possible to estimate the order of the performance equation involved and a set of values for the parameters involved. In practice, it is often necessary to make assumptions in setting up performance equations that make calculated parameters somewhat inaccurate. In any case, it is very desirable to make experimental tests both to check the validity of the performance equation* and to find exact values for the performance parameters.

33.163. The general procedure for checking performance-equation validity and determining parameters for any measuring unit or system is to observe responses to input changes. From the standpoint of theory, the comparison of any scale-reading record with the corresponding input change supplies all the information necessary to check performance-equation form and parameter values. In practice, there is a considerable difference in convenience and complexity of equipment required for satisfactory results, depending on the nature of the forcing function used for the tests. For the purposes of discussion, several typical functions are illustrated in Information Summary 33-1, which also lists references to detailed information on each function.

33.164. Section a of Information Summary 33-1 represents the most general situation, in which a forcing function of precisely known mathematical form is used. Comparison of the record corresponding to this input with the input itself supplies data on dynamic errors and dynamic response delays. The data contain all the information necessary for determining whether or not a given performance equation is valid and, in addition, provide numerical values for the essential parameters. The situation is particularly simple for certain forcing functions when

* In many instances, experimental results show that a simplified performance equation will serve within the tolerance limits involved. The use of experimentally determined parameters in simplified equations very often gives completely satisfactory results over an adequate range of operation. The use of a first-order equation to represent the behavior of the heavily damped meter (which is actually a second-order system) discussed at the end of Chapter 29 is an example of performance-equation simplification. The Chapter 29 example also describes a pattern for representing the error associated with the use of a simplified performance equation.

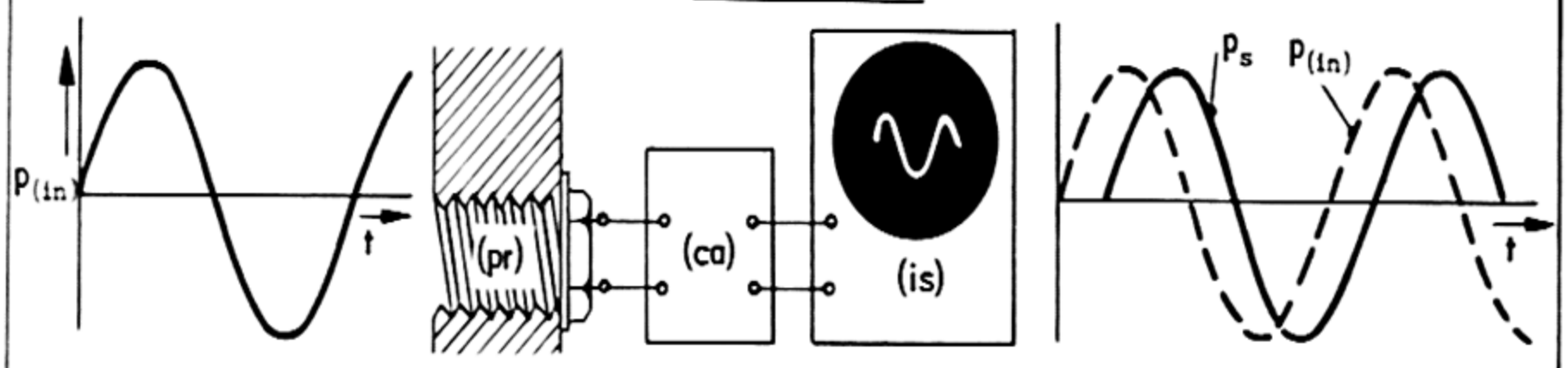


$p_{(in)} = f_1(t)$ known

$p_s = f_2(t)$ recorded

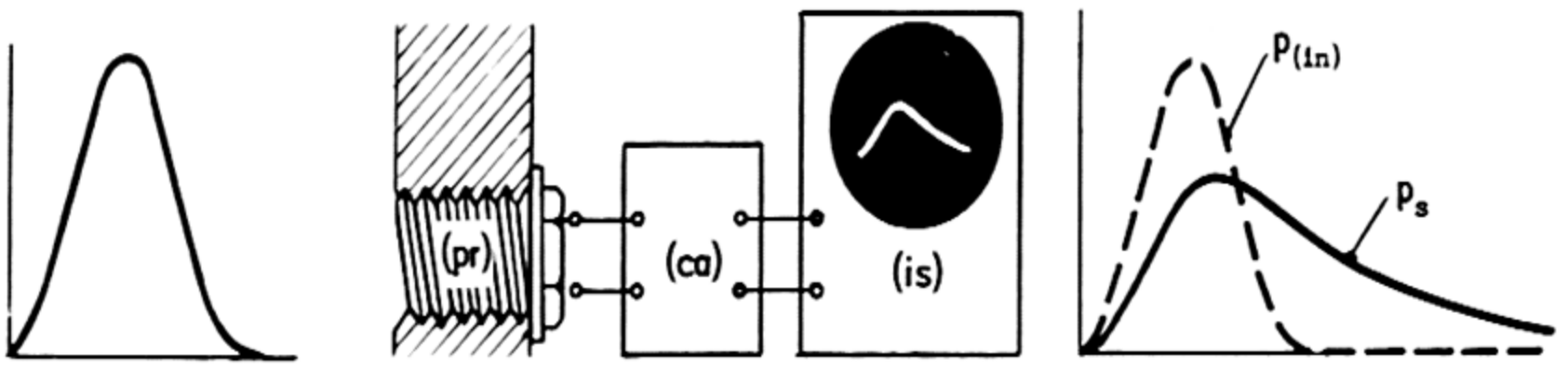
Refer to Chapter 15 for general theory when $p_{(in)}$ is expressed in equation form, and to Chapters 18 and 19 for the special theory of first- and second-order response.

a) Forced response



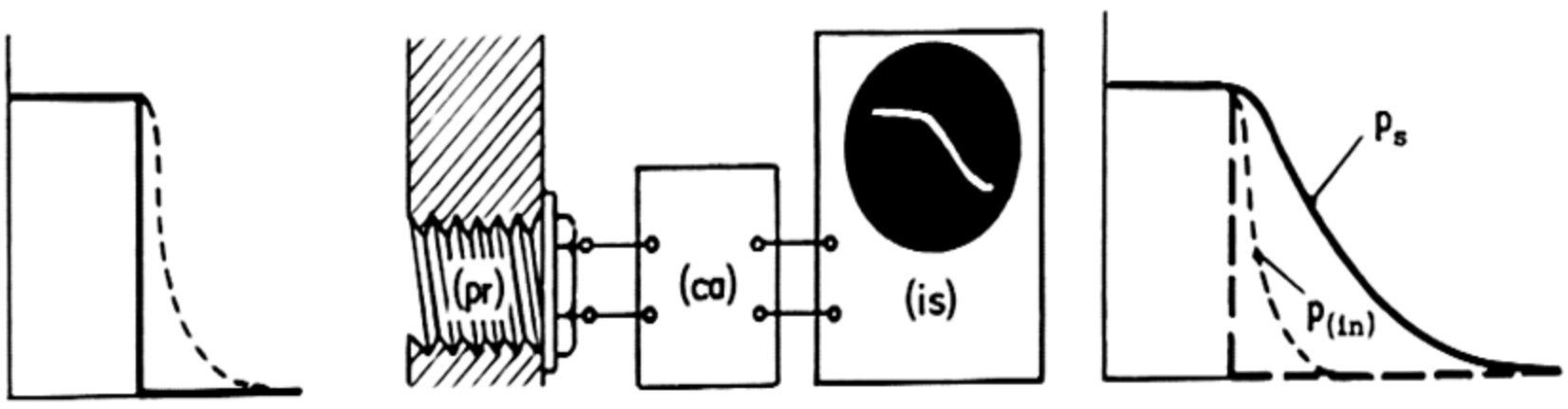
Refer to Chapter 17 for general theory, to Chapters 18 and 31 for the special theory of first-order response, and to Chapters 19 and 32 for the special theory of second-order response.

b) Steady-state sinusoidal response



Refer to Chapter 25 for generalized pulse-function theory, and particularly to Figs. 25-9 through 25-16 for first- and second-order responses to rectangular and displaced cosine pulse functions.

c) Pulse function response



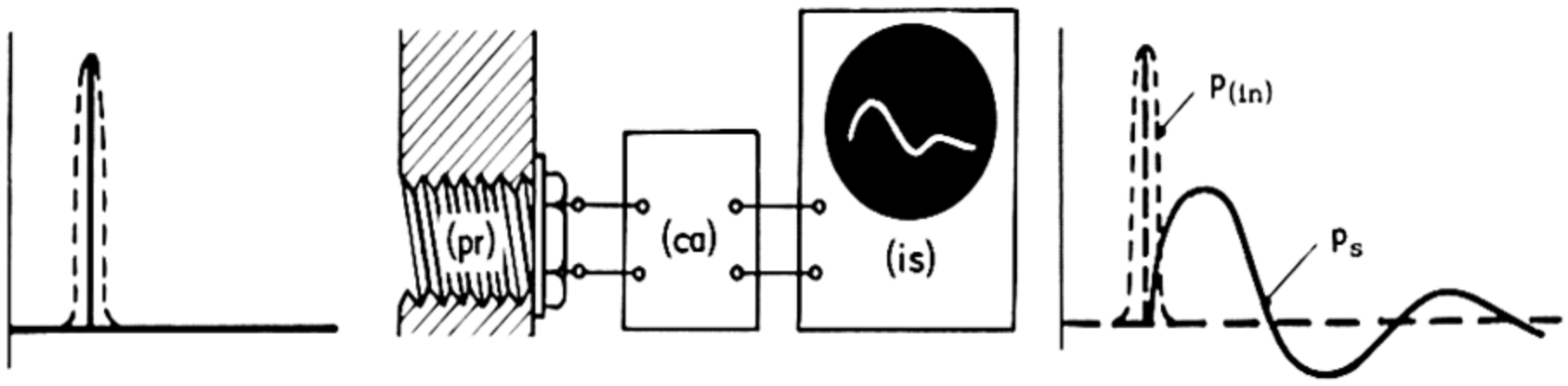
Refer to Chapter 15 for general theory, to Derivation Summaries 18-1, 18-2 and 18-3 and Fig. 31-1 for the theory of first-order response, and to Derivation Summaries 19-1, 19-2 and 19-3 and Figs. 32-4, 32-5 and 32-6 for the theory of second-order response.

Note: In practice, it is immaterial whether the input change is a decrease or an increase.

Note: Any change of input pressure is effectively a step function when the change is completed before any appreciable change in the response has occurred.

d) Effective step function response

Information Summary 33-1. Typical forcing functions for experimental determination of the performance parameters of pressure-measuring systems. (Page 1 of 2)



Refer to Chapter 17 for impulse theory, to Derivation Summary 18-8 for the theory of first-order response to an impulse function and to Derivation Summary 19-8 for the theory of second-order response to an impulse function.

e) *Effective impulse function response*

Information Summary 33-1. Typical forcing functions for experimental determination of the performance parameters of pressure-measuring systems. (Page 2 of 2)

the response records cover such a long time interval that transient effects are negligible. This means that only the forced response remains, which is described by the forced solution of the performance equation. Forced responses for first- and second-order systems with linear input variations are given in Figs. 31-2 and 32-9 through 32-13. These figures show that a particularly simple relationship exists between the forced dynamic response delay and the time parameter for the system under test.

33.165. It is obviously possible to use the forced response of any system to check performance-function validity and to determine parameters. However, the forcing function must be accurately known and controlled. This control is easy enough when the measuring-instrument response is not too rapid. On the other hand, when high natural frequencies and light damping are involved, transient responses are usually so simple to excite and interpret that, for test purposes, they are to be preferred to forced responses.

33.166. Section b of Information Summary 33-1 illustrates the use of steady-state sinusoidal response for the determination of performance characteristics by the frequency response method. This method is particularly advantageous for the electrical instrument applications discussed in Chapter 32. The advantage stems from the general availability of equipment to generate sinusoidal test voltages. When accurately known sinusoidal input variations are difficult to produce over a wide range of frequencies, the steady-state response method is not useful. This statement is particularly true for high-pressure-range measuring equipment capable of responding to rapid pressure changes.

33.167. Section c of Information Summary 33-1 illustrates the use of an input pulse for determining response characteristics. When the pulse shape is accurately controlled, and the pulse duration is adjusted so that a considerable portion of the total response occurs before the pulse disappears, all the required information may be taken from a single record. For high-natural-frequency

instruments with inputs difficult to pulse accurately, the pulse method suffers from the handicaps of the forced response method and the frequency response method.

33.168. Transient response methods are generally easier to apply than the methods just discussed. This advantage is based on the fact that as long as a transient-producing disturbance of sufficient power is applied, and the input is returned to some constant level while a considerable transient effect is still present in the response, the shape of the input change is not important. That is, so long as a transient is set up and the input is then immediately reduced to a condition with a simple forced response, the input change may have any unknown form. Sections d and e of Information Summary 33-1 illustrate transients excited by effective step functions and effective impulse functions, respectively. The transient analysis is particularly simple if the effective step or effective impulse is completed before the instrument response has changed more than a negligible amount from its pre-disturbance level.

SHOCK TUBE FOR DETERMINING CHARACTERISTICS OF HIGH-NATURAL-FREQUENCY PRESSURE-MEASURING INSTRUMENTS*

33.169. Figure 33-17 illustrates the essential features of a small shock tube constructed at Massachusetts Institute of Technology for testing high-natural-frequency pressure-measuring instruments. A steel pipe two inches in diameter is divided into two sections by a gas-tight partition made of thin plastic. A gage pressure of two or three atmospheres is built up in a two-foot length of the tube behind the plastic sheet, which is selected so that it is near the point of failure under stress. The pressure receiver of the equipment to be tested is mounted in the end of a tube section four feet long that is mechanically connected to the diaphragm-sealed end of the pressure-containing section of the tube.

33.170. When the diaphragm of Fig. 33-17 is punctured by a pin driven into its center by a rod actuated from outside the tube, the gas pressure is suddenly released and rushes as a pressure wave into the longer section of the tube. At the end of the tube, the wave is reflected as illustrated by the typical instantaneous pressure distribution diagrams shown in Fig. 33-17. At the start of the reflection, the pressure receiver is subjected to a sharp pressure step of twice the original gas pressure behind the diaphragm seal. After this instant and until the following rarefaction strikes the end of the tube, the pressure receiver is subjected to a constant pressure. This means that the instrument receives a sharp step disturbance followed by a steady-state condition.

TYPICAL PRESSURE RECORD FROM SHOCK-TUBE TEST

33.171. The photographic record of the figure given in section a of Data Analysis Summary 33-1 shows the response of a flat-diaphragm pressure receiver in

* See Geiger, Mantz and Laporte (G10).

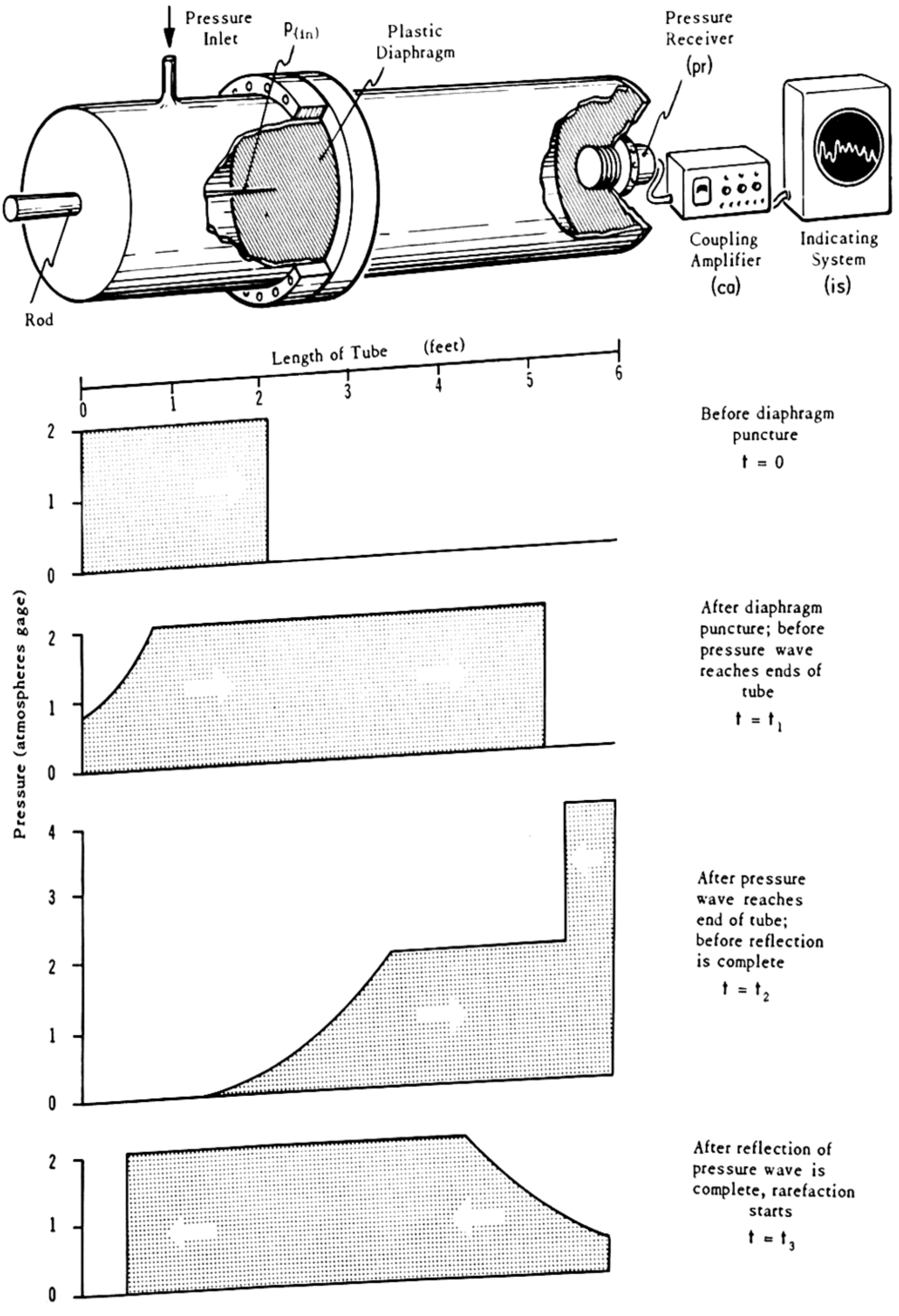
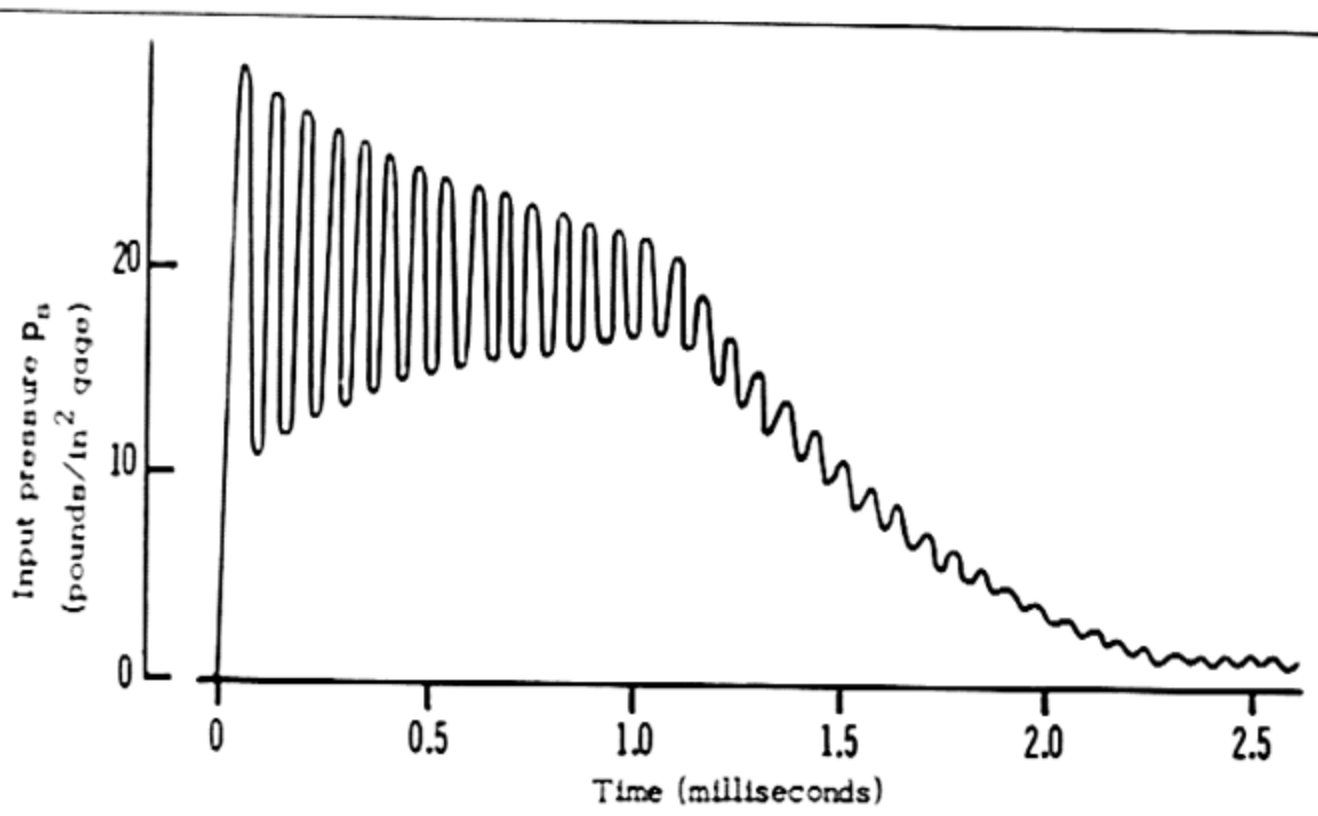


Fig. 33-17. Shock tube for exciting transients in high-natural-frequency pressure-measuring instruments.



a) Record of the transient response of the pressure-measuring system

See Fig. 33-17 for a pictorial diagram of the pressure-measuring system.

(pr) Pressure receiver

Pressure receiving element: flat-diaphragm type
Signal generating system: electrostatic type
Diaphragm material: steel
Diaphragm diameter: 0.500 inch
Diaphragm thickness: 0.010 inch
Undamped natural frequency (computed*): 15,700 cycles per second

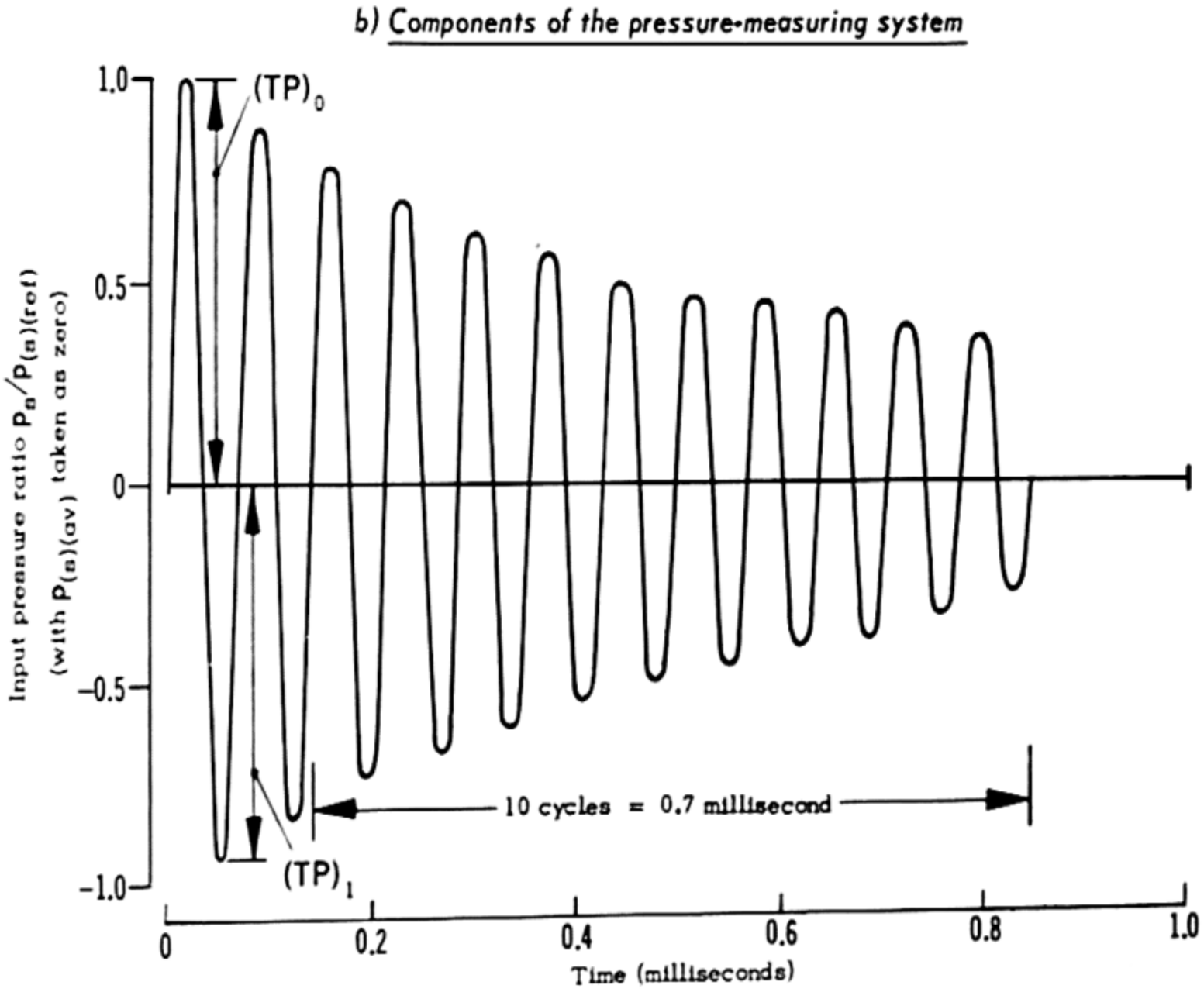
(ca) Coupling amplifier

Negligible dynamic error

(is) Indicating system

Cathode-ray oscilloscope, negligible dynamic error

b) Components of the pressure-measuring system



c) Replot of the transient record

* See Draper and Li (D13) for the method of computing the pressure receiver natural frequency from its physical characteristics.

Data Analysis Summary 33-1. Experimental determination of the damping ratio and undamped natural frequency of a pressure receiver from a transient response record. (Page 1 of 3)

Transient Peak Number	Transient Peak*	m^{th} to n^{th} Transient Peak Ratio			Damping Ratio** (DR)	Deviation of Damping Ratio $\lvert(DR)_{(av)} - (DR)\rvert$
		n	m	$(TPR)_{(n-m)}$		
0	1.66	0	2	0.874	0.020	0.0057
1	1.53	1	3	0.883	0.019	0.0047
2	1.45	2	4	0.897	0.017	0.0027
3	1.35	3	5	0.888	0.0175	0.0032
4	1.30	4	6	0.885	0.0175	0.0032
5	1.20	5	7	0.901	0.016	0.0017
6	1.15	6	8	0.913	0.014	0.0003
7	1.08	7	9	0.908	0.015	0.0007
8	1.05	8	10	0.904	0.015	0.0007
9	0.98	9	11	0.898	0.017	0.0027
10	0.95	10	12	0.925	0.013	0.0013
11	0.88	11	13	0.950	0.009	0.0053
12	0.88	12	14	0.931	0.010	0.0043
13	0.84	13	15	0.928	0.010	0.0043
14	0.83	14	16	0.915	0.014	0.0003
15	0.78	15	17	0.948	0.009	0.0053
16	0.76	16	18	0.908	0.015	0.0007
17	0.74	17	19	0.932	0.010	0.0043
18	0.69					
19	0.69	0	5	0.722	0.022	0.0064
20	0.63	5	10	0.792	0.016	0.0004
25	0.55	10	15	0.821	0.013	0.0026
		15	20	0.808	0.014	0.0016
		20	25	0.874	0.013	0.0026
		0	10	0.573	0.018	0.002
		10	20	0.664	0.014	0.002

* Transient peaks measured in millimeters from original record.

** Damping ratios are obtained from plots of transient peak ratio versus damping ratios given in Vol. II, Fig. 19-14.

From the sets of experimentally determined damping ratios, it is possible to calculate the standard deviation* and the probable deviation of the damping ratio. These calculations can be made with different values of $m - n$.

$(SD)(DR)$ = standard deviation of the damping ratio

$$= \frac{(AD)(DR)}{0.7979}$$

where

$(AD)(DR)$ = average deviation of the damping ratio

$$= \frac{1}{r} \sum_{i=1}^{r} \lvert(DR)_{(av)} - (DR)_i\rvert$$

$(PD)(DR)$ = probable deviation of the damping ratio

$$= 0.6745\ (SD)(DR)$$

$m - n$	2	5	10
$(DR)_{(av)}$	0.0143	0.0156	0.016
$(AD)(DR)$	0.00285	0.00272	0.002
$(SD)(DR)$	0.00356	0.00340	0.0025
$(PD)(DR)$	0.0024	0.0023	0.0017
$\frac{(PD)(DR)}{(DR)_{(av)}}$	0.17 or 17 %	0.15 or 15 %	0.11 or 11 %

d) Determination of the damping ratio of the pressure receiver

* See Vol. I, Chapter 11, for definitions.

Data Analysis Summary 33-1. Experimental determination of the damping ratio and undamped natural frequency of a pressure receiver from a transient response record. (Page 2 of 3)

From the replot of the transient response, it is seen that the indicated pressure goes through 10 cycles in 0.7 millisecond.

T = damped period

$= \frac{0.7 \times 10^{-3}}{10} = 7 \times 10^{-5}$ seconds

n = damped natural frequency

$= \frac{1}{T}$

$= \frac{1}{7 \times 10^{-5}} = 14{,}300$ cycles per second

From Table 32-1

n_n = undamped natural frequency

$= \frac{n}{\sqrt{1 - (DR)^2}}$

With $(DR) << 1$,

$n_n \approx n = 14{,}300$ cycles per second

Note: The value for the undamped natural frequency given in section b, which was computed from the physical characteristics of the pressure receiver, was 15,700 cycles per second.

e) *Determination of the undamped natural frequency of the pressure receiver*

Data Analysis Summary 33-1. Experimental determination of the damping ratio and undamped natural frequency of a pressure receiver from a transient response record. (Page 3 of 3)

combination with a cathode-ray oscilloscope and coupling amplifier, giving substantially ideal response over the frequency range involved. The first part of the record is an upward pressure step producing an oscillatory transient about a substantially constant raised pressure level. After about one millisecond, the oscillation continues with an exponentially decreasing axis. These record features correspond to the doubled pressure regime during the first shock-wave reflection, which is followed by the decreasing pressure as the first rarefaction moves to the end of the shock tube.

33.172. Section c of Data Analysis Summary 33-1 is a replot of the first part of the record of section a with the average taken as zero. Definitions and typical numerical values are marked on the replot in accordance with the pattern used in Data Analysis Summary 32-1. Section d of Data Analysis Summary 33-1 gives a tabulation of pressure peaks from the curve of section c. The table also includes transient peak ratios based on separations of 2, 5, and 10 peak numbers, and the corresponding damping ratios for a second-order system, taken from Fig. 32-26. These damping ratios are averaged, and probable deviations* are computed for each average. The 2-peak separation gives an average damping ratio of 0.0143, with a probable deviation – average damping ratio ratio of 17 percent; the 5-peak separation gives an average damping ratio of 0.0156, with a probable deviation – average damping ratio ratio of 15 percent; and the 10-peak separation gives an average damping ratio of 0.016, with a probable deviation – average damping ratio ratio of 10.5 percent. When the uncertainties in reading values from the record are considered, and the possible deviations from theoretical conditions in the pressure receiver are considered, the damping ratio results show that, to a satisfactory degree of approximation, the unit under test behaves as a second-order system with a damping ratio of about 0.015.

* Probable deviation is defined in Chapter 11.

33.173. Measurements along the time axis of the record of section a of Data Analysis Summary 33-1 show that the measured undamped natural frequency of the pressure receiver is 14,300 cycles per second. This experimental result agrees reasonably well with the theoretical value of 15,700 cycles per second for an ideal flat diaphragm. The difference between experimental and measured values probably lies in details of the fillets at the diaphragm edges, machining imperfections, and deviations of the material properties from assumed values.

CONCLUSION

33.174. The discussion of this chapter has centered about the pressure-measuring system, but it is obvious that the conventions and procedure patterns may be immediately applied to open-chain systems of any type having any degree of complexity. Accordingly, free use of the material developed in this chapter will be made whenever necessary in the remainder of this book.

CHAPTER 34

INTEGRATORS AND DIFFERENTIATORS

INTRODUCTION

34.1. Integration and its inverse, differentiation, are mathematical concepts* of primary importance for the purposes of instrument engineering. Integration corresponds to the summation of physical quantity increments. Differentiation is a process that gives the rate of change of one physical quantity with respect to a second physical quantity as the ratio of infinitesimally small increments. A number of devices that act as integrators or differentiators appear as operating components in the systems that are discussed in later chapters of this book.

34.2. The generalized theory of integrators and differentiators is the primary subject matter of this chapter. In order to reduce the discussion to specific terms, the essential features of various devices that are commonly used to provide the functions of integration and differentiation are described,** and the corresponding performance equations are derived. A basic pattern for specifying the performance of actual equipment in terms of deviations from ideal performance is developed, and is applied in a number of typical examples. The chapter ends with a discussion of the analog computers that are formed by combinations of integrating components.

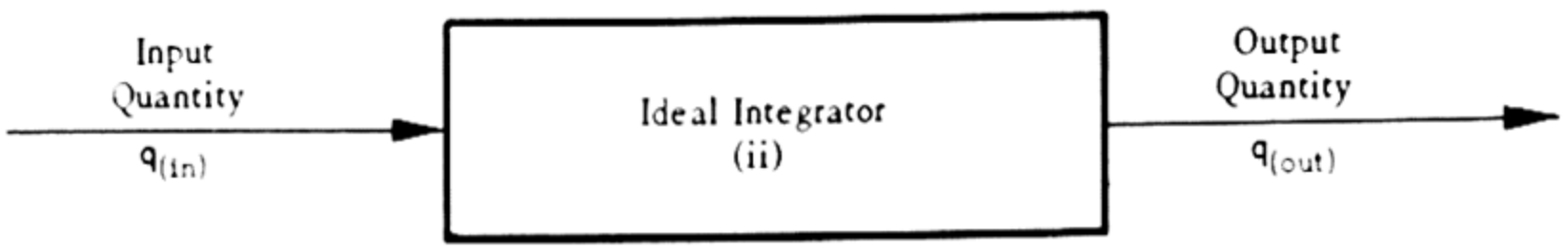
IDEAL INTEGRATORS

34.3. Ideal integration is produced by any device that causes the rate of change of its output to be accurately proportional to its input. Section a of Derivation Summary 34-1 is the functional diagram for the ideal integrator. The corresponding performance equation in integral form is given by Eq. (1) of the summary. Differentiation of Eq. (1) shows that when the input quantity – output quantity rate sensitivity is constant, the time rate of change of the output quantity is accurately proportional to the input quantity. This fact is shown by Eq. (2), which has the form of a conventional (0;1) differential equation.

34.4. Integrator performance may be conveniently described in terms of the steady-state sinusoidal performance function derived in section c of Derivation Summary 34-1. The development of this section follows the general pattern described

* See texts on calculus; for example, Bacon (B21), Courant (C8), Franklin (F13), and Phillips (P9).

** See also Ahrendt (A1) and (A12), Brown and Campbell (B4), Chestnut and Mayer (C1), Greenwood, Holdam and Macrae (G3), James, Nichols and Phillips (J1), Korn and Korn (K6), Lauer, Lesnick and Matson (L1), Laws (L7), MacColl (M1), Navy Department (N5) and (N6), and Porter (P2).



Refer to Definition Summary 28-8 for conventions.

a) Functional diagram for the ideal integrator

The performance equation for the ideal integrator is

$$q_{(out)} = \int S_{(ii)[q_{(in)};\dot{q}_{(out)}]}\, q_{(in)}\, dt \tag{1}$$

or, differentiating Eq. (1),

$$\frac{dq_{(out)}}{dt} = S_{(ii)[q_{(in)};\dot{q}_{(out)}]}\, q_{(in)} \tag{2}$$

where

$S_{(ii)[q_{(in)};\dot{q}_{(out)}]}$ = input quantity – output quantity rate sensitivity of the ideal integrator

This sensitivity is constant for the ideal integrator.

Note that Eq. (2) has the form of the typical (0;1) differential equation. In working variable terms, this equation is

$$a_1 \dot{v} = b_o u \tag{3}$$

b) Generalized performance equations for the ideal integrator

When the input variation has the form of a simple sinusoid, that is, when

$$q_{(in)} = q_{(in)a}\, \epsilon^{jw_f t} \tag{4}$$

where

$$w_f = 2\pi n_f = \frac{2\pi}{T_f} = \text{angular forcing frequency} \tag{5}$$

$$n_f = \frac{1}{T_f} = \text{forcing frequency} \tag{6}$$

T_f = forcing period

and when attention is restricted to steady-state conditions, the integrator output is

$$q_{(out)} = S_{(ii)[q_{(in)};\dot{q}_{(out)}]} \int q_{(in)a}\, \epsilon^{jw_f t}\, dt \tag{7}$$

or, in operational form,

$$q_{(out)} = S_{(ii)[q_{(in)};\dot{q}_{(out)}]}\, \frac{1}{p}\, q_{(in)} \tag{8}$$

where

$$p = \frac{d}{dt} \tag{9}$$

(See Derivation Summary 17-5 of Chapter 17.)

Derivation Summary 34-1. Performance equation and performance function for the ideal integrator.
(Page 1 of 4)

Define

$$T_{(ref)} = \text{reference period (arbitrarily chosen)} \tag{10}$$

$$n_{(ref)} = \frac{1}{T_{(ref)}} = \text{reference frequency} \tag{11}$$

Then

$$q_{(out)} = S_{(11)[q_{(in)};\dot{q}_{(out)}]} T_{(ref)} \frac{1}{j w_f T_{(ref)}} q_{(in)} \tag{12}$$

From Eq. (12), the performance function for the ideal integrator has the form

$$[FF]_{(11)[q_{(in)};q_{(out)}]} = S_{(11)[q_{(in)};q_{(out)}](ref)} \frac{1}{j2\pi (FR)_{(ref)}} \tag{13}$$

where

$$S_{(11)[q_{(in)};q_{(out)}](ref)} = S_{(11)[q_{(in)};\dot{q}_{(out)}]} T_{(ref)} \tag{14}$$

= input quantity – output quantity reference sensitivity for the ideal integrator

$$(FR)_{(ref)} = \frac{n_f}{n_{(ref)}} = \frac{T_{(ref)}}{T_f} = \text{reference frequency ratio} \tag{15}$$

Define

$$(FR)_{(ref)(bp)} = (bp)_{(11)} = \frac{1}{2\pi} = \text{ideal integrator breakpoint reference frequency ratio or ideal integrator break point} \tag{16}$$

so that

$$[PF]_{(11)[q_{(in)};q_{(out)}]} = S_{(11)[q_{(in)};q_{(out)}](ref)} \frac{1}{\frac{j(FR)_{(ref)}}{(bp)_{(11)}}} \tag{17}$$

or

$$[PF]_{(11)[q_{(in)};q_{(out)}]} = S_{(11)[q_{(in)};q_{(out)}](ref)} \frac{1}{j(FR)_{(bpr)(11)}} \tag{18}$$

where

$$(FR)_{(bpr)(11)} = \frac{(FR)_{(ref)}}{(bp)_{(11)}} = \text{breakpoint-reference frequency ratio for the ideal integrator} \tag{19}$$

Refer to Definition Summary 28-8 and Chapters 13, 17, 18, 19 and 24, for background theory, definitions, and conventions of notation.

c) Complex variable forms for the ideal integrator performance function

In terms of the reference sensitivity, dimensionless sensitivity ratio and dynamic response angle concepts tabulated in Definition Summary 28-8 and developed in the references cited in that summary, Eq. (17) becomes

$$\eta_{(11)} = \rho_{(r)(11)} \mu_{(11)} \epsilon^{j\phi_{(11)}} = [PF]_{(11)[q_{(in)};q_{(out)}]} \tag{20}$$

where

$$[PF]_{(11)[q_{(in)};q_{(out)}]} = S_{(11)[q_{(in)};q_{(out)}](ref)} [S(RS)R]_{(11)(q_{(in)};q_{(out)})} \epsilon^{j(DRA)_{(11)(q_{(in)};q_{(out)})}} \tag{21}$$

$$= S_{(11)[q_{(in)};q_{(out)}](ref)} (SR)'_{(11)(q_{(in)};q_{(out)})} \epsilon^{j(DRA)_{(11)(q_{(in)};q_{(out)})}} \tag{22}$$

Derivation Summary 34-1. Performance equation and performance function for the ideal integrator. (Page 2 of 4)

$\rho_{(r)(11)} \approx S_{(11)[q_{(1n)};q_{(out)}](ref)}$ (defined in Eq. (14))

$\mu_{(11)} \approx [S(RS)R]_{(11)(q_{(1n)};q_{(out)})}$ = input quantity – output quantity sensitivity – reference sensitivity ratio for the ideal integrator

$[S(RS)R]_{(11)(q_{(1n)};q_{(out)})} = {}'(SR)_{(11)(q_{(1n)};q_{(out)})}$ = input quantity – output quantity dimensionless sensitivity ratio for the ideal integrator

$\phi_{(11)} \approx (DRA)_{(1d)(q_{(1n)};q_{(out)})}$ = input quantity – output quantity dynamic response angle for the ideal integrator

From Eqs. (14), (17), (19) and (22),

$$\rho_{(r)(11)} \approx S_{(11)[q_{(1n)};q_{(out)}](ref)} = S_{(11)[q_{(1n)};\dot{q}_{(out)}]T_{(ref)}} \tag{23}$$

$$\mu_{(11)} \approx [S(RS)R]_{(11)(q_{(1n)};q_{(out)})} = {}'(SR)_{(11)(q_{(1n)};q_{(out)})} \approx \frac{1}{\frac{(FR)_{(ref)}}{(bp)_{(11)}}} = \frac{1}{(FR)_{(bpr)(11)}}$$

$$\approx \frac{1}{\frac{\beta_r}{(bp)_{(11)}}} = \frac{1}{\beta_{(bpr)(11)}} \tag{24}$$

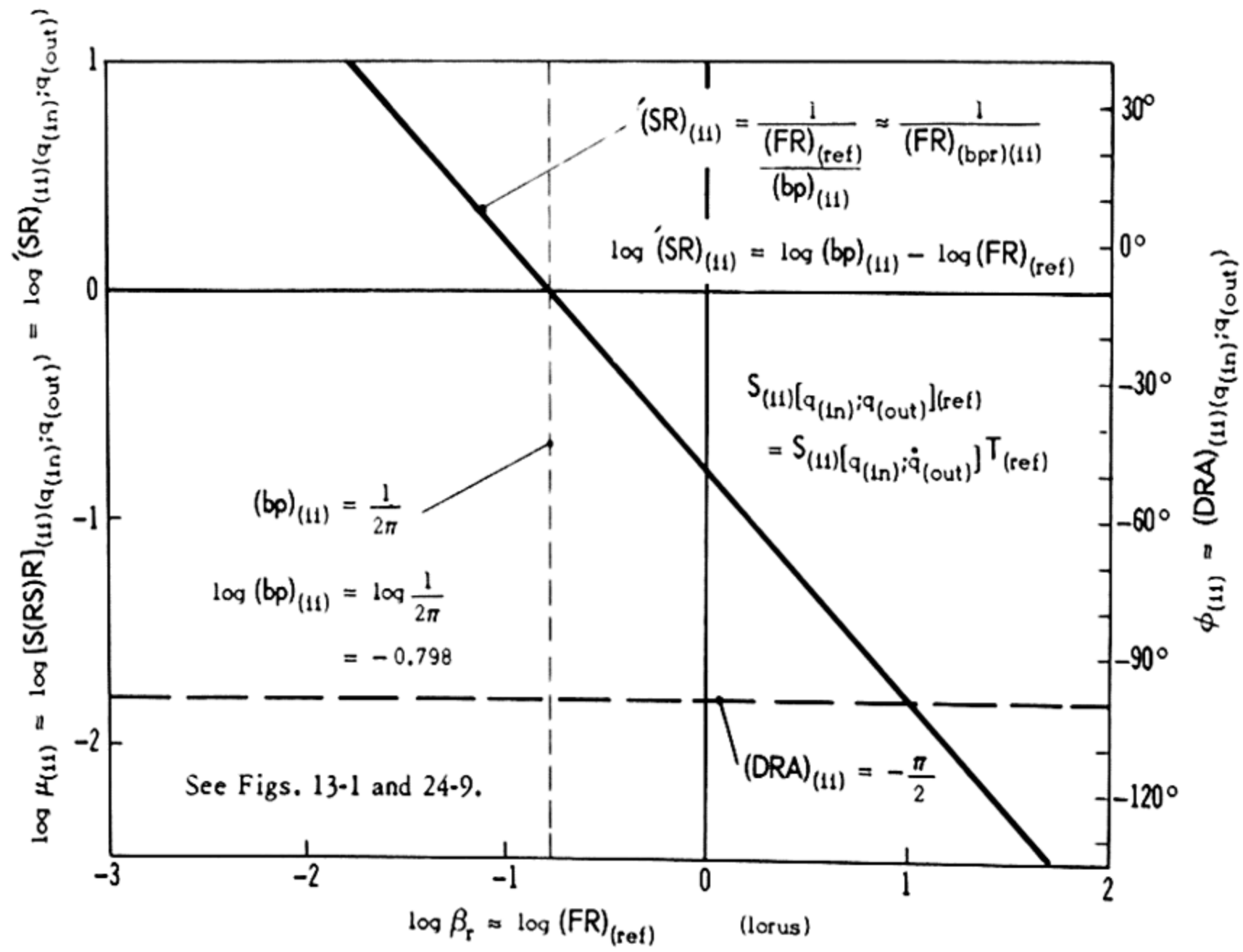
$$\phi_{(11)} \approx (DRA)_{(11)(q_{(1n)};q_{(out)})} = -\frac{\pi}{2} \tag{25}$$

where

$$\beta_r \approx (FR)_{(ref)} \tag{26}$$

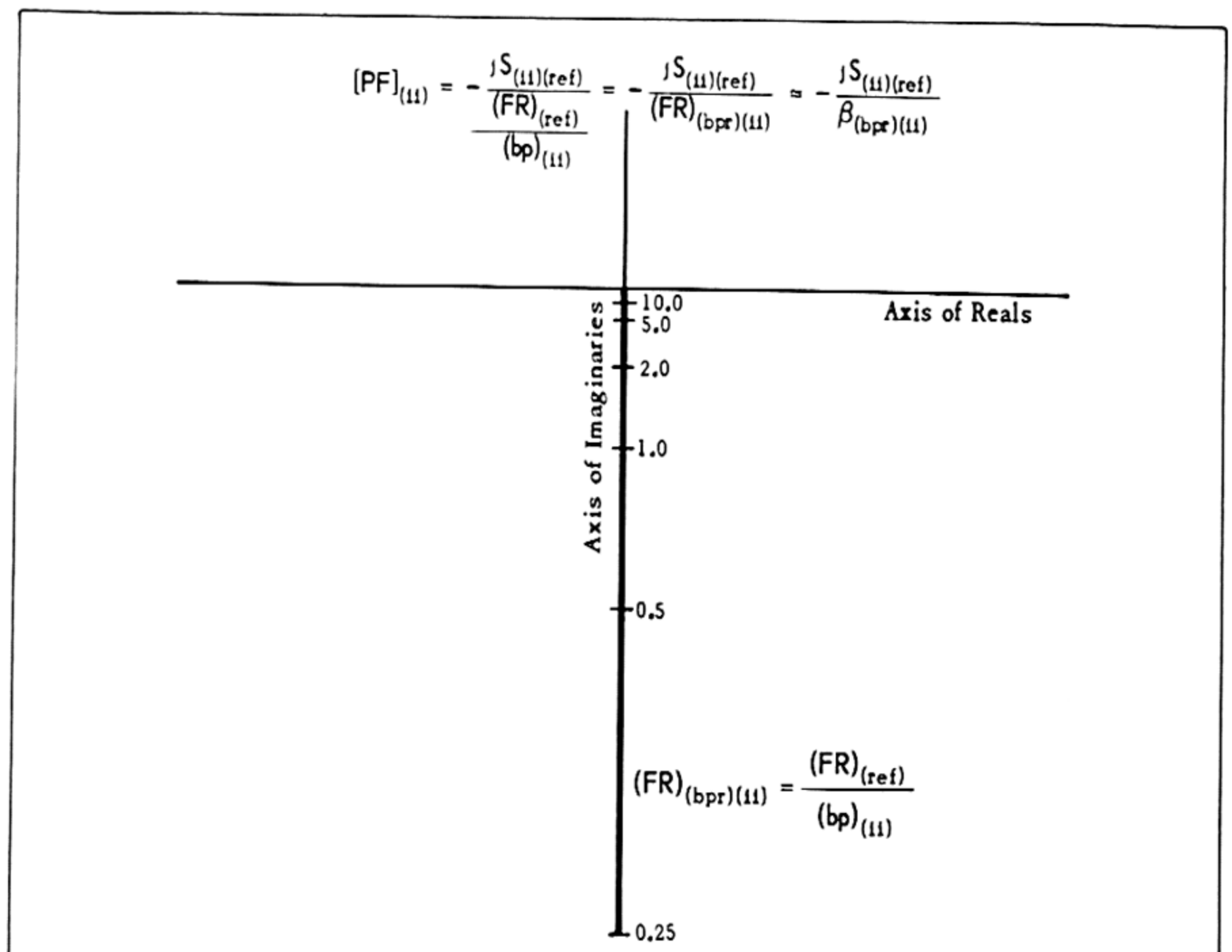
$$\beta_{(bpr)} \approx (FR)_{(bpr)(11)} \tag{27}$$

d) Dimensionless sensitivity ratio and dynamic response angle forms for the ideal integrator performance function



e) Logarithmic-scale plots of the dimensionless sensitivity ratio and the dynamic response angle for the ideal integrator

Derivation Summary 34-1. Performance equation and performance function for the ideal integrator. (Page 3 of 4)



f) Uniform-scale complex plane plot of the performance function for the ideal integrator

Derivation Summary 34-1. Performance equation and performance function for the ideal integrator. (Page 4 of 4)

in Derivation Summary 18-9, which leads to expressions for sinusoidal relating functions that are mathematically equivalent to the performance functions for operating components. The conventions for describing performance functions and their relationships to relating function forms are described in Definition Summaries 28-6, 28-7 and 28-8.

34.5. In Derivation Summary 34-1, an arbitrarily chosen reference period, $T_{(ref)}$, is introduced as a factor in Eq. (12), and in Eq. (14) the input quantity – output quantity reference sensitivity for the ideal integrator is defined as the product of this reference period and the input quantity – output quantity rate sensitivity of the ideal integrator. In Eq. (15), the reference frequency ratio is defined as the ratio of the forcing frequency to the reference frequency, which is the reciprocal of the reference period. The ideal integrator breakpoint reference frequency ratio, or ideal integrator break point, is the value of the reference frequency ratio for which the magnitude of the fractional factor in Eq. (13) becomes unity. The ideal integrator break point is defined in Eq. (16) as the reciprocal of 2π. Equation (17) is an expression for the input quantity – output quantity performance function for the ideal integrator expressed as a function of the reference frequency ratio – break point ratio. Equation (18) is identical with Eq. (17) except that the ratio appearing in

the denominator of Eq. (17) is replaced by a single symbol, the breakpoint-reference frequency ratio.

34.6. Section d of Derivation Summary 34-1 outlines the concepts and symbols for expressing the performance function of section c in terms of the dimensionless sensitivity ratio and the dynamic response angle. Section e gives an illustrative log-log plot for the dimensionless sensitivity ratio as a function of reference frequency ratio. This function is a straight line that slopes downward with increasing values of reference frequency ratio and crosses the zero-ordinate line at the logarithm of the break point, log $(1/2\pi)$. The corresponding dynamic response angle is constant at $-\pi/2$ radians. Section f shows the ideal integrator performance function plotted on uniform-scale complex-plane coordinates. In this representation, the performance function is identical with the negative imaginary axis, with the zero reference frequency ratio at minus infinity, and the high reference frequency ratio range compressed near the zero-point of the coordinates.

IDEAL DIFFERENTIATORS

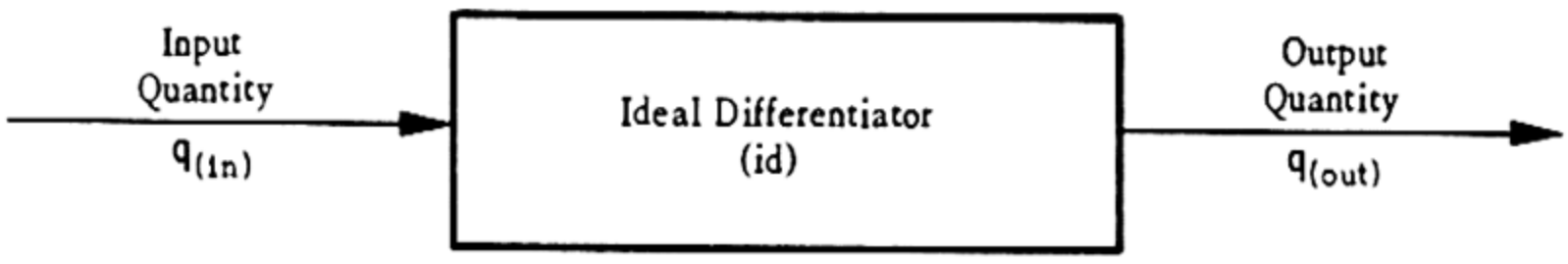
34.7. Derivation Summary 34-2 outlines a development of the performance equation and performance function forms for the ideal differentiator. The results of this development are expressed in terms of the concepts and notation already defined for the ideal integrator. The pattern of Derivation Summary 34-2 is essentially similar to that of Derivation Summary 34-1.

34.8. The basic functional differences between the ideal differentiator and the ideal integrator are brought out by a comparison of the plots of section e of Derivation Summary 34-2 with the corresponding plots given in section e of Derivation Summary 34-1. Both dimensionless sensitivity ratios cross the zero-ordinate line at a break point of $1/2\pi$. For the integrator, the sensitivity ratio line has a slope of 45 degrees downward toward high reference frequency ratios. For the differentiator, the sensitivity ratio line has a slope of 45 degrees upward toward high reference frequency ratios. The dynamic response angle for the ideal integrator is minus $\pi/2$ radians. The corresponding angle for the ideal differentiator is plus $\pi/2$ radians.

34.9. On the uniform-scale complex plane, the differentiator performance function is identical with the positive imaginary axis. Low reference frequency ratios are near the origin of coordinates and approach infinity as the magnitude of the imaginary-axis coordinate approaches infinity.

TYPICAL INTEGRATORS AND DIFFERENTIATORS

34.10. In practice, the devices available for use as integrators and differentiators do not have ideal characteristics. The deviations from ideal performance that exist when a given input quantity variation is considered depend upon the



Refer to Definition Summary 28-8 for conventions.

a) Functional diagram for the ideal differentiator

The performance equation for the ideal differentiator is

$$q_{(out)} = S_{(id)[\dot{q}_{(in)};q_{(out)}]} \frac{dq_{(in)}}{dt} \tag{1}$$

where

$S_{(id)[\dot{q}_{(in)};q_{(out)}]}$ = input quantity rate – output quantity sensitivity of the ideal differentiator

This sensitivity is constant for the ideal differentiator.

Note that Eq. (1) has the form of the typical (1;0) differential equation. In working variable terms, this equation is

$$a_0 v = b_1 \dot{u} \tag{2}$$

b) Generalized performance equations for the ideal differentiator

When the input variation has the form of a simple sinusoid, that is, when

$$q_{(in)} = q_{(in)a} \epsilon^{jw_f t} \tag{3}$$

so that

$$\frac{dq_{(in)}}{dt} = jw_f q_{(in)a} \epsilon^{jw_f t} = jw_f q_{(in)} \tag{4}$$

the differentiator output is given by substituting the expression of Eq. (4) in Eq. (1); i.e.,

$$q_{(out)} = S_{(id)[\dot{q}_{(in)};q_{(out)}]} jw_f q_{(in)} \tag{5}$$

or, in operational form,

$$q_{(out)} = S_{(id)[\dot{q}_{(in)};q_{(out)}]} p\, q_{(in)} \tag{6}$$

Introducing the reference period $T_{(ref)}$ makes it possible to write Eq. (5) in the forms

$$q_{(out)} = S_{(id)[q_{(in)};q_{(out)}](ref)} jw_f T_{(ref)} q_{(in)} \tag{7}$$

$$= S_{(id)[q_{(in)};q_{(out)}](ref)} j2\pi (FR)_{(ref)} q_{(in)} \tag{8}$$

$$= S_{(id)[q_{(in)};q_{(out)}](ref)} j \frac{(FR)_{(ref)}}{(bp)_{(id)}} q_{(in)} \tag{9}$$

$$= S_{(id)[q_{(in)};q_{(out)}](ref)} j (FR)_{(bpr)(id)} q_{(in)} \tag{10}$$

where

$$S_{(id)[q_{(in)};q_{(out)}](ref)} = \frac{S_{(id)[\dot{q}_{(in)};q_{(out)}]}}{T_{(ref)}} \tag{11}$$

= input quantity – output quantity reference sensitivity for the ideal differentiator

Derivation Summary 34-2. Performance equation and performance function for the ideal differentiator. (Page 1 of 3)

and

$$(bp)_{(id)} = \frac{1}{2\pi} = \text{ideal differentiator break point} \tag{12}$$

The performance function forms corresponding to the performance equations (7), (8), (9) and (10) are

$$[PF]_{(id)[q_{(in)};q_{(out)}]} = S_{(id)[q_{(in)};q_{(out)}](ref)}\, jw_f T_{(ref)} \tag{13}$$

$$= S_{(id)[q_{(in)};q_{(out)}](ref)}\, j2\pi (FR)_{(ref)} \tag{14}$$

$$= S_{(id)[q_{(in)};q_{(out)}](ref)}\, j \frac{(FR)_{(ref)}}{(bp)_{(id)}} \tag{15}$$

$$= S_{(id)[q_{(in)};q_{(out)}](ref)}\, j (FR)_{(bpr)(id)} \tag{16}$$

See Derivation Summary 34-1 for definitions of the concepts and symbols appearing in the equations of this section. Refer to Definition Summary 28-8 and Chapters 13, 17, 18, 19 and 24 for background theory, definitions and conventions of notation.

c) Complex variable forms for the ideal differentiator performance function

In terms of the reference sensitivity, dimensionless sensitivity ratio and dynamic response angle concepts tabulated in Definition Summary 28-8 and developed in the cited references, Eqs. (15) and (16) become

$$\eta_{(id)} = \rho_{(r)(id)}\, \mu_{(id)} \epsilon^{j\phi_{(id)}} \simeq [PF]_{(id)[q_{(in)};q_{(out)}]} \tag{17}$$

where

$$[PF]_{(id)[q_{(in)};q_{(out)}]} = S_{(id)[q_{(in)};q_{(out)}](ref)}\, [S(RS)R]_{(id)(q_{(in)};q_{(out)})}\, \epsilon^{j(DRA)_{(id)(q_{(in)};q_{(out)})}} \tag{18}$$

$$= S_{(id)[q_{(in)};q_{(out)}](ref)}\, {}'(SR)_{(id)(q_{(in)};q_{(out)})}\, \epsilon^{j(DRA)_{(id)(q_{(in)};q_{(out)})}} \tag{19}$$

and

$\rho_{(r)(id)} \simeq S_{(id)[q_{(in)};q_{(out)}](ref)}$ (defined by Eq. (11))

$\mu_{(id)} \simeq [S(RS)R]_{(id)(q_{(in)};q_{(out)})}$ = input quantity – output quantity sensitivity – reference sensitivity ratio for the ideal differentiator

$[S(RS)R]_{(id)(q_{(in)};q_{(out)})} = {}'(SR)_{(id)(q_{(in)};q_{(out)})}$

= input quantity – output quantity dimensionless sensitivity ratio for the ideal differentiator

$\phi_{(id)} \simeq (DRA)_{(id)(q_{(in)};q_{(out)})}$ = input quantity – output quantity dynamic response angle for the ideal differentiator

From Eqs. (11), (13), (14), (15) and (16),

$$\rho_{(r)(id)} \simeq S_{(id)[q_{(in)};q_{(out)}](ref)} = -\frac{S_{(id)[\dot{q}_{(in)};q_{(out)}]}}{T_{(ref)}} \tag{20}$$

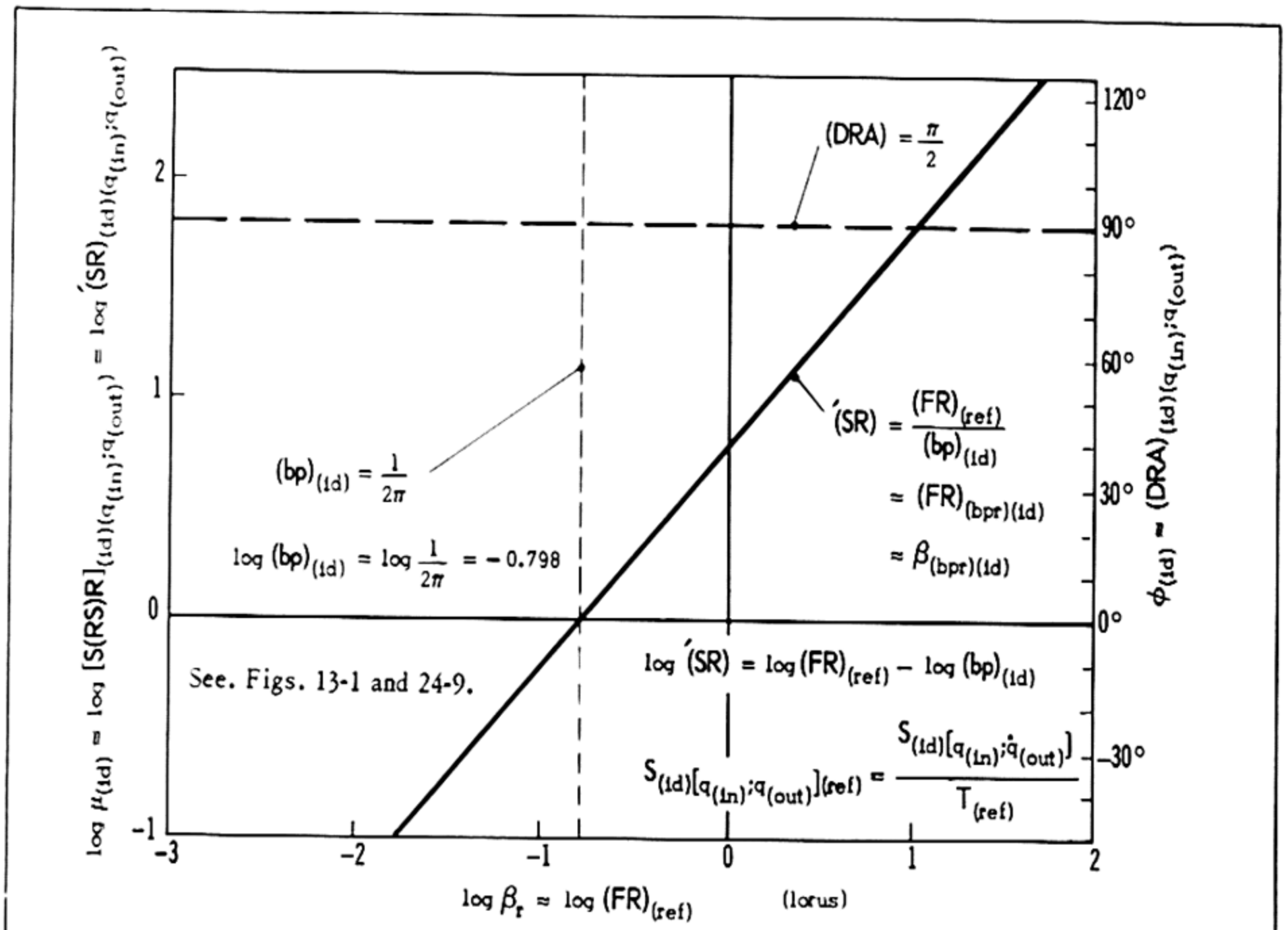
$$\mu_{(id)} \simeq [S(RS)R]_{(id)(q_{(in)};q_{(out)})} = {}'(SR)_{(id)(q_{(in)};q_{(out)})} = w_f T_{(ref)} = 2\pi (FR)_{(ref)}$$

$$= \frac{(FR)_{(ref)}}{(bp)_{(id)}} = (FR)_{(bpr)(id)} \simeq \frac{\beta_r}{(bp)_{(id)}} = \beta_{(bpr)(id)} \tag{21}$$

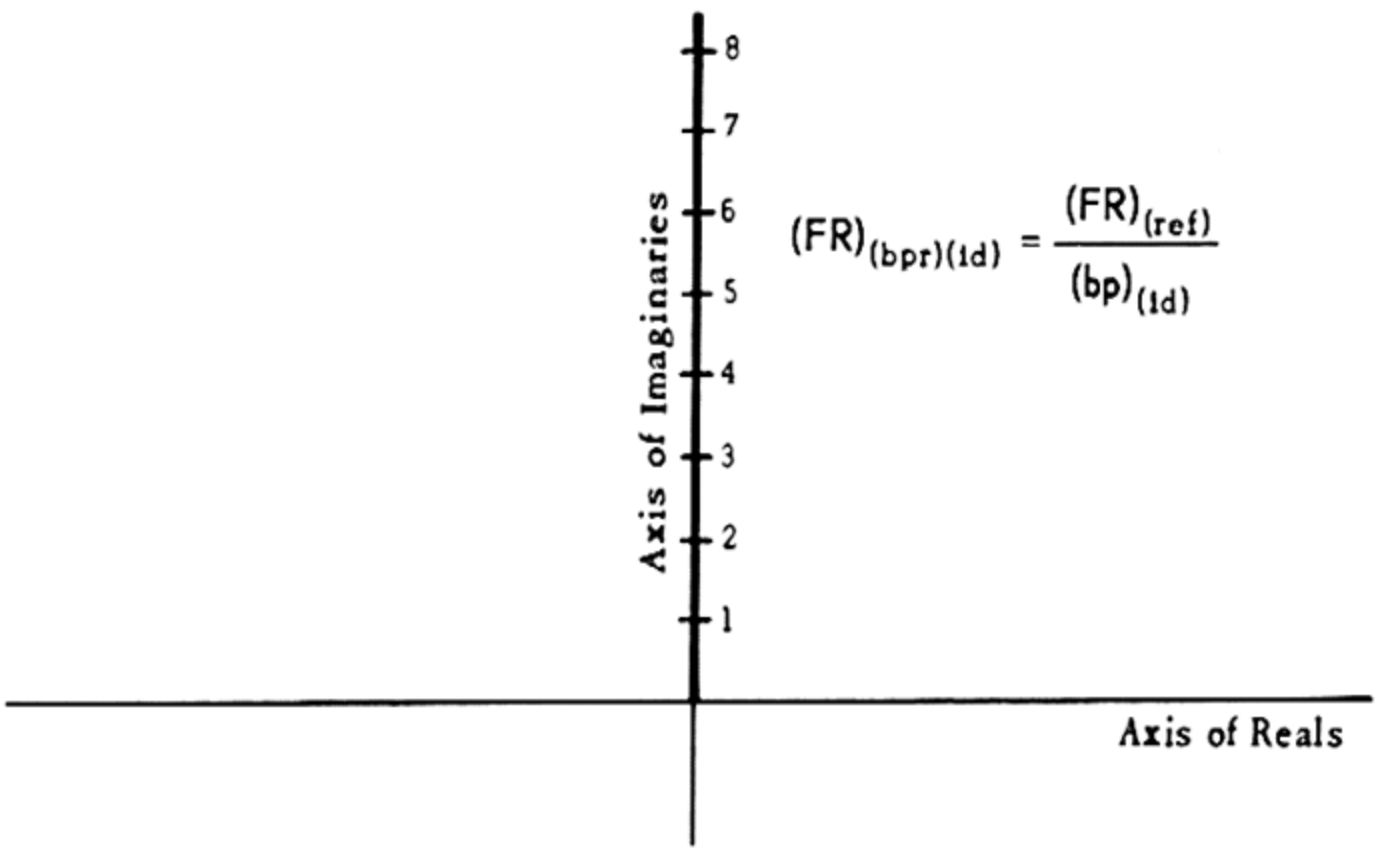
$$\phi_{(id)} \simeq (DRA)_{(id)(q_{(in)};q_{(out)})} = \pi/2 \tag{22}$$

d) Dimensionless amplitude ratio and dynamic response angle forms for the ideal differentiator performance function

Derivation Summary 34-2. Performance equation and performance function for the ideal differentiator. (Page 2 of 3)



e) *Logarithmic-scale plots of the dimensionless sensitivity ratio and the dynamic response angle for the ideal differentiator*



$$[PF]_{(1d)} \approx jS_{(1d)(ref)} \frac{(FR)_{(ref)}}{(bp)_{(1d)}} = jS_{(1d)(ref)}(FR)_{(bpr)(1d)} \approx jS_{(1d)(ref)}\beta_{(bpr)(1d)}$$

f) *Uniform-scale complex plane plot of the performance function for the ideal differentiator*

Derivation Summary 34-2. Performance equation and performance function for the ideal differentiator. (Page 3 of 3)

design of the integrating or differentiating equipment employed. In this chapter, the deviation characteristics of typical integrators and differentiators are derived and tabulated in generalized nondimensional terms.

34.11. Integrators and differentiators may have any possible input-output combination. The natures of the input and output quantities are unimportant; only the functional relationship established by the operating component involved is essential. For example, both the input and the output may be mechanical. They may equally well both be electrical, or the input may be mechanical while the output is electrical.

34.12. The integrator and differentiator examples chosen for discussion are not meant to cover all types of these devices completely, but rather are intended to illustrate the principles that are commonly applied in practical designs and to establish a pattern of analysis powerful enough to serve the purposes of any special situation that may appear. The integrating and differentiating devices considered are as follows:

INTEGRATING DEVICES	DIFFERENTIATING DEVICES
1) Ball-and-disc mechanical integrator.	1) Ball-and-disc mechanical differentiator.
2) Eddy-current-drag-disc watt-hour-meter-type integrator.	2) Centrifugal tachometer.
3) Viscous-shear-drag-generator-type integrator.	3) Rotating-magnet drag-cup tachometer.
4) Liquid-flow integrator.	4) Direct-current electrical tachometer.
5) Thermal integrator.	5) Alternating-current drag-cup electrical tachometer.
6) Pneumatic pressure integrator.	6) Resistance-inductance electrical differentiator.
7) Resistance-capacitance electrical integrator.	7) Resistance – amplifier – feedback-inductance differentiator.
8) Resistance – amplifier – feedback-capacitance integrator.	8) Resistance-capacitance electrical differentiator.
9) Motor – amplifier – feedback-tachometer integrator.	9) Capacitance – amplifier – feedback-resistance differentiator.

34.13. The general plan of presentation is to give a pictorial diagram of each device, showing the essential features of construction, and to follow this with a static-functional diagram and a derivation summary, in which performance equations and performance functions are developed from generalized information on operating components. The performance equations from the derivation summaries associated with individual integrators and differentiators are classified and tabulated as typical working variable forms. Performance functions for each typical form are developed and tabulated in terms of expressions for dimensionless amplitude

ratios and dynamic response angles as functions of reference frequency ratios. Equations for deviations of the typical integrator and differentiator performance equations with respect to the ideal integrator and ideal differentiator performance equations, respectively, are derived and tabulated. Curves for these deviation functions are plotted against reference frequency ratio as the independent variable. Cutoff frequencies and operating ranges (band widths) in terms of reference frequency ratio for typical tolerance limits are indicated on the deviation plots and are tabulated in terms of generalized system parameters.

34.14. To illustrate the pattern for applying the generalized information on integrators and differentiators to specific situations, several typical problems are worked out in numerical terms. A viscous-shear integrator is taken as the first illustrative problem. The second illustrative problem concerns a motor-tachometer feedback-amplifier integrator. A final group of problems deals with combinations of resistance-capacitance feedback-amplifier integrators and other components to form electronic computing systems.

BALL-AND-DISC MECHANICAL INTEGRATOR

34.15. Figure 34-1 is a pictorial diagram illustrating the essential features of a ball-and-disc mechanical integrator. A disc with a carefully finished flat surface is driven by a constant-speed motor through a gear train. The motor speed is adjusted* by a speed-setting knob. The accurately finished, circular-cross-section output cylinder has its axis carefully aligned so that it intersects, and is perpendicular to, the axis of rotation of the disc. The cylinder axis is located above the disc surface at the distance required to keep a proper load on two balls placed between the disc surface and the cylinder surface. In practice, this load is maintained by springs not shown in Fig. 34-1. A ball cage holds the balls so that the points of contact between the disc, the two balls, and the cylinder are all on a line perpendicular to the disc surface and passing through both ball centers and the axis of rotation of the cylinder. Within the range of operation for which no slipping occurs between any of the contacting surfaces, the cylinder is driven from the disc with an angular velocity that causes the surface velocity of the cylinder to be equal to the surface velocity of the disc at the point of ball contact. The velocity at this contact point depends on the position of the ball cage slide, which is controlled by the input drive shaft acting through the ball cage slide gear train and the ball cage rack. The output cylinder angular velocity is effectively integrated with respect to time to build up the output cylinder angle. This angle is transferred to the output index by the output gear train to give the output angle, which is shown by the output scale.

* When the disc angular velocity is not held constant, but is varied so that it represents an actuating input, the arrangement of Fig. 34-1 serves no longer as an integrator, but instead functions as a multiplier.

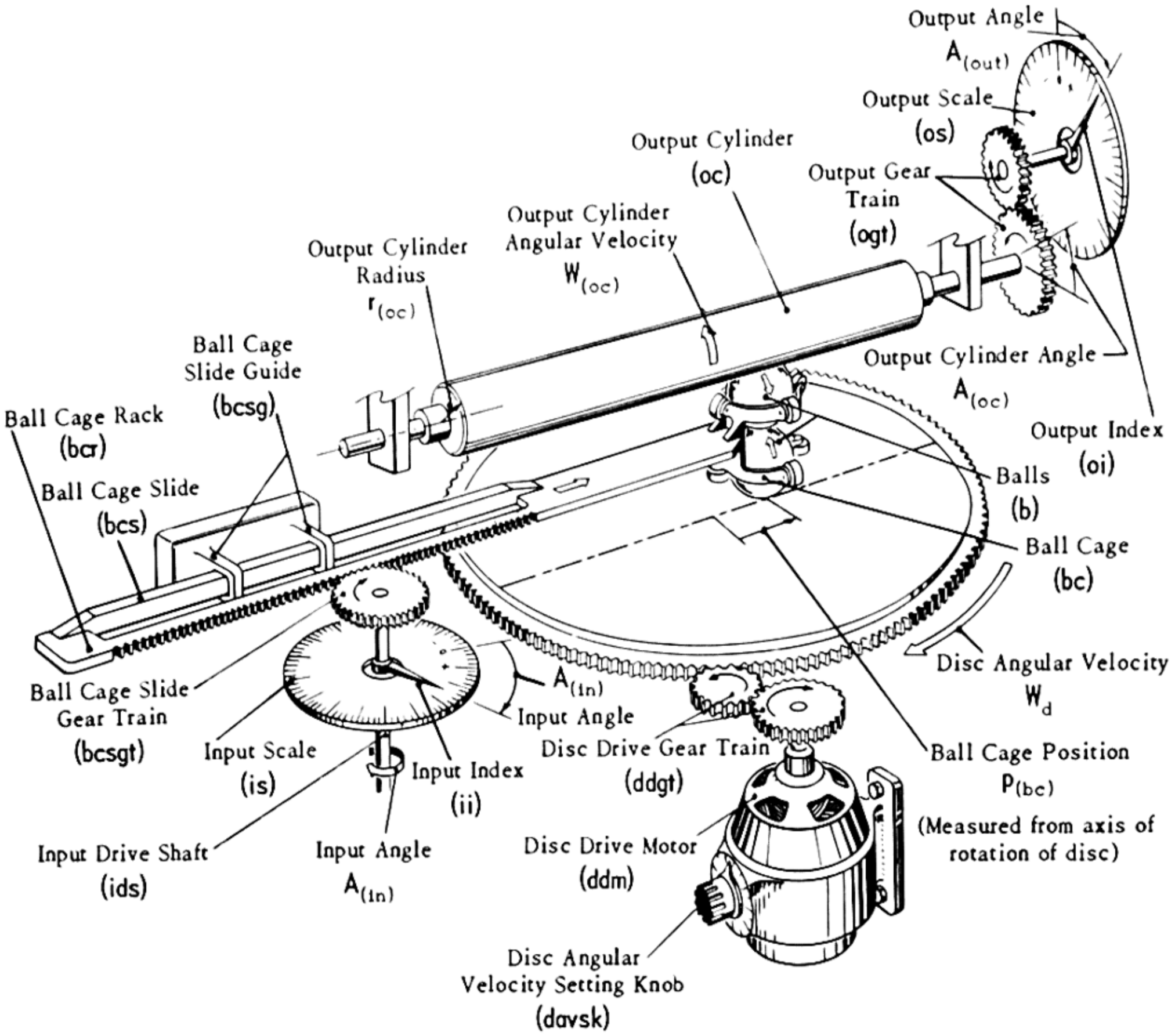


Fig. 34-1. Illustrative pictorial diagram of a ball-and-disc mechanical integrator.

34.16. The pictorial-functional diagram of Fig. 34-2 shows the component systems of the ball-and-disc integrator, starting with the input receiving system and ending with the output system. The input receiving system produces the ball cage position, corresponding to the input angle, as its output quantity. The disc drive system of Fig. 34-2 receives the disc angular velocity setting, which acts as a modifying input for the complete integrator, and supplies the disc angular velocity. The ball-and-disc system of Fig. 34-2 receives the ball cage position as an actuating input and the disc angular velocity as a modifying input, and produces the output cylinder angle as its output. The output system receives this angle and produces the output angle as the output for the complete ball-and-disc integrator.

34.17. Section a of Derivation Summary 34-3 gives a functional diagram for the ball-and-disc integrator of Figs. 34-1 and 34-2. Section b of Derivation Summary 34-3 gives a development of the performance equation for the ball-and-disc integrator under the assumption of perfect transmission of surface velocity from the disc to the output cylinder. This assumption will obviously not be valid when

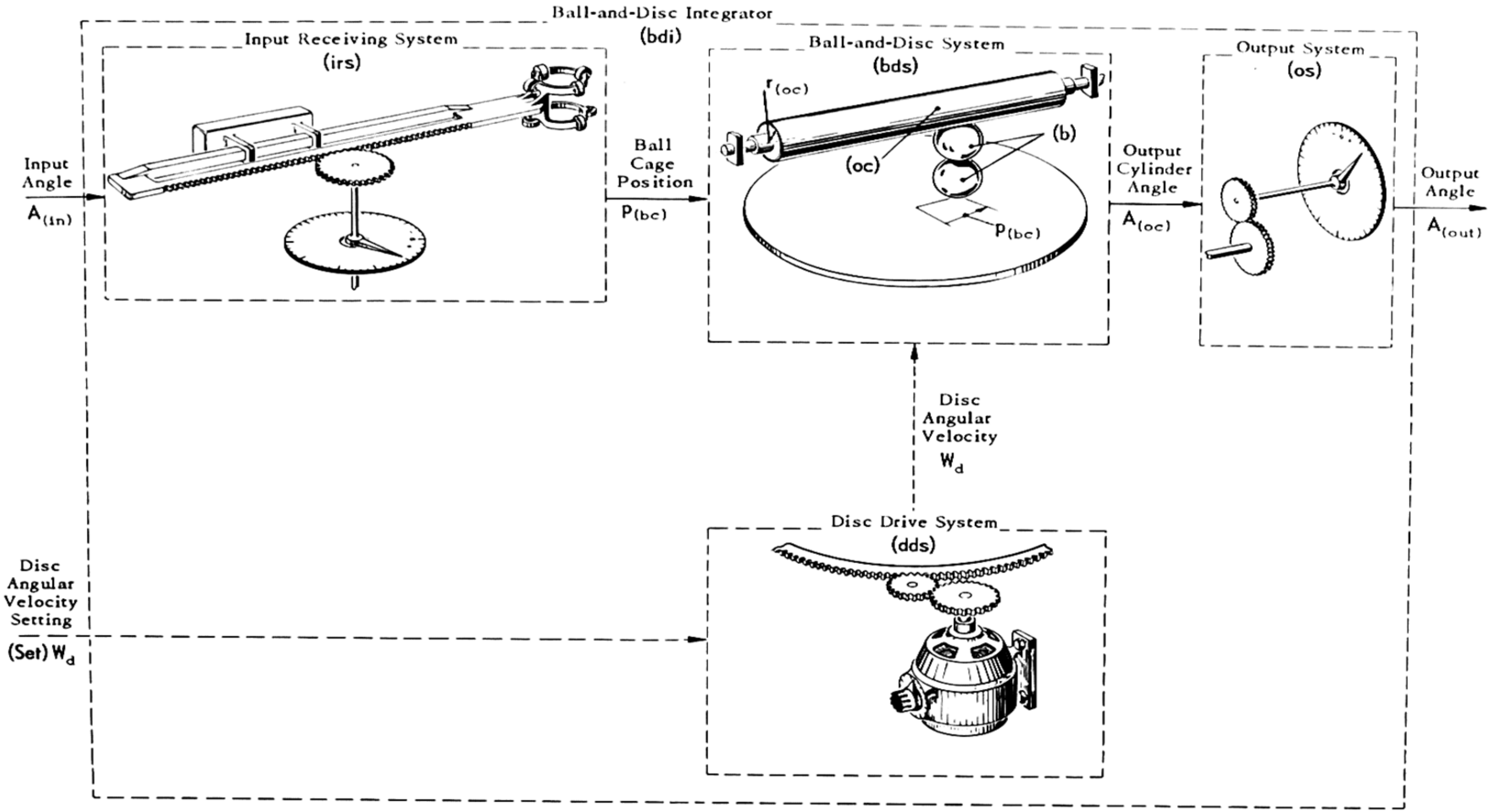
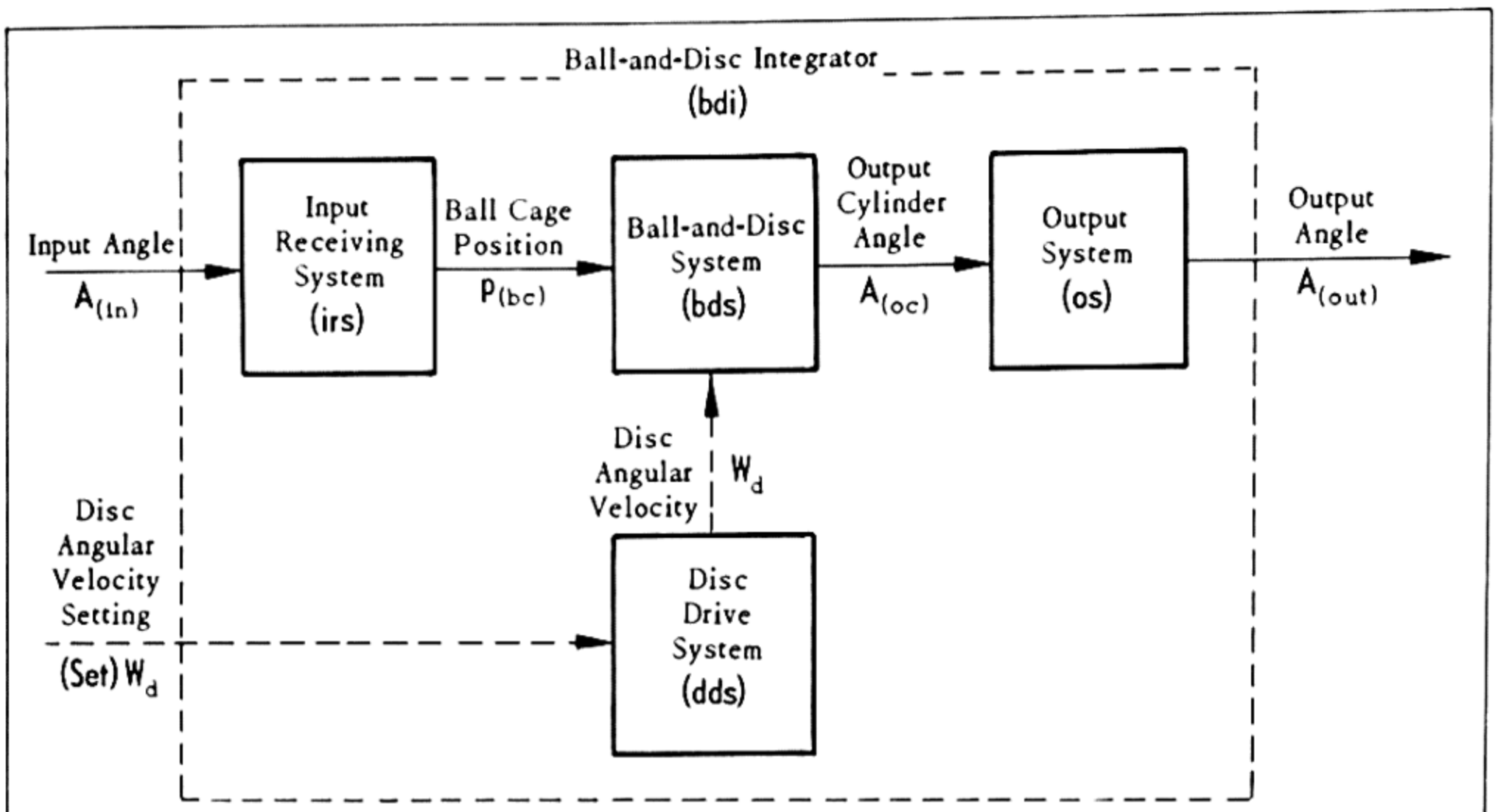


Fig. 34-2. Illustrative pictorial-functional diagram of a ball-and-disc mechanical integrator.



a) Functional diagram

(irs) Input receiving system

$$P_{(bc)} = S_{(irs)[A_{(in)};P_{(bc)}]} A_{(in)} \tag{1}$$

$S_{(irs)[A_{(in)};P_{(bc)}]}$ = angle input – position output sensitivity of input receiving system

(dds) Disc drive system

$$W_d = S_{(ddm)[(Set);W_{(ddm)}]} S_{(ddgt)[W_{(ddm)};W_d]} (Set) W_d = S_{(dds)[(Set);W_d]} (Set) W_d \tag{2}$$

$S_{(ddm)[(Set);W_{(ddm)}]}$ = angular velocity setting – drive motor angular velocity sensitivity of disc drive motor

$$S_{(ddgt)[W_{(ddm)};W_d]} = S_{(ddgt)[A_{(gt)(in)};A_{(gt)(out)}]} \tag{3}$$

= angular velocity input – angular velocity output sensitivity of disc drive gear train

$S_{(ddgt)[A_{(gt)(in)};A_{(gt)(out)}]}$ = angle input – angle output sensitivity of disc drive gear train

$S_{(dds)[(Set);W_d]}$ = angular velocity setting input – disc angular velocity output of disc drive system

(bds) Ball-and-disc system

$$\frac{dA_{(oc)}}{dt} = \frac{W_d}{r_{(oc)}} P_{(bc)} \tag{4}$$

(os) Output system

$$A_{(out)} = S_{(os)[A_{(oc)};A_{(out)}]} A_{(oc)} \tag{5}$$

$$S_{(os)[A_{(oc)};A_{(out)}]} = S_{(ogt)[A_{(oc)};A_{(out)}]} \tag{6}$$

$$S_{(ogt)[A_{(oc)};A_{(out)}]} \approx S_{(ogt)[A;A]} = \text{angle input – angle output sensitivity of output gear train} \tag{7}$$

(bdi) Ball-and-disc integrator

$$\frac{dA_{(out)}}{dt} = S_{(os)[A;\dot{A}]} \frac{S_{(dds)[(Set);W_d]}}{r_{(oc)}} S_{(irs)[A;p]} (Set) W_d \, A_{(in)} \tag{8}$$

Derivation Summary 34-3. Performance equation for a ball-and-disc mechanical integrator.
(Page 1 of 2)

With the disc angular velocity setting constant, Eq. (8) may be written in the form

$$\frac{dA_{(out)}}{dt} = S_{(bdi)[A;\dot{A}]} A_{(in)} \tag{9}$$

where

$$S_{(bdi)[A;\dot{A}]} = S_{(os)[A;A]} \frac{S_{(dds)[(Set);W_d]}}{r_{(oc)}} S_{(irs)[A;p]}(Set)\, W_d \tag{10}$$

= angle input – angular velocity output sensitivity of ball-and-disc integrator

Equation (9) is the performance equation for the ball-and-disc integrator. This equation has the typical (0;1) differential equation form. It is shown in Derivation Summary 34-1 that the (0;1) equation is the performance equation for the ideal integrator. In practice, ball-and-disc integrators will have performance that deviates from Eq. (9) as a result of mechanical imperfections, ball slippage, etc.

b) Performance equation

Derivation Summary 34-3. Performance equation for a ball-and-disc mechanical integrator. (Page 2 of 2)

the ball cage is moved so rapidly that the frictional forces at the points of ball contact are insufficient to accelerate the output cylinder and the parts that move with it. When slippage occurs, the performance equation derived in Derivation Summary 34-3 is no longer valid for describing the ensuing action. This means that more than a minute amount of slippage removes the ball-and-disc system from the class of ideal integrators.

34.18. The performance equation development of section b of Derivation Summary 34-3 follows the pattern established in earlier summaries. Performance equations are written for each operating component and subsystem of the ball-and-disc integrator. In each case, the form of the equation is taken as completely specifying the assumptions that are made, without additional statements of conditions. For illustrative purposes, performance parameters are given complete names in section b. Except for special cases, the practice of writing names for performance parameters is not followed in later summaries. It is assumed, for these later summaries, that the conventions for forming self-defining symbols are so well-known, and illustrated by so many examples, that word definitions are unnecessary.

34.19. As shown in section b of Derivation Summary 34-3, the input receiving system causes the ball cage position, measured in terms of the radius from the disc center to the point of ball contact, to be proportional to the input angle. The constant of proportionality is the angle input – position output sensitivity of the input receiving system. The disc drive system causes the disc to rotate with an angular velocity that is determined by the disc angular velocity setting. The ball-and-disc system receives the ball cage position and the disc angular velocity and produces the angular velocity of the output cylinder (that is, the time rate of change of the output cylinder angle) as the product of the disc angular velocity and the ball

cage position divided by the radius of the output cylinder. When the angle input – angle output sensitivity of the output system is taken into account, the performance of the ball-and-disc integrator is given by Eqs. (9) and (10) of Derivation Summary 34-3. Equation (9) is the performance equation for the ball-and-disc integrator. Equation (10) relates the over-all sensitivity of the integrator to the component sensitivities and the disc angular velocity setting.

34.20. The essential fact about the ball-and-disc integrator performance equation is that it has the form of the (0;1) differential equation. Since the ideal integrator performance equation developed in Derivation Summary 34-1 has the (0;1) form, it follows that, under proper operating conditions, the ball-and-disc arrangement gives ideal integration.

EDDY-CURRENT-DRAG-DISC WATT-HOUR-METER-TYPE INTEGRATOR

34.21. Integration by the ball-and-disc arrangement of Fig. 33-1 is based completely on kinematic effects in the sense that it involves linear displacements and rotations of rigid parts under the assumption that inertial reactions and other dynamic effects may be neglected. In addition to the class of kinematic integrators to which the ball-and-disc integrator belongs, there is a class of integrators that depend on dynamic interactions among mechanical parts. For this type of integrator, electrical operating components may be used to receive inputs, produce torques, and provide output signals, but the essential integration process is associated with a balance of mechanical forces or torques.

34.22. Dynamic integration depends on the simultaneous application of a driving torque and a drag torque to a substantially rigid body that acts as a torque summing member.* When the drag torque is made to resist motion with a magnitude proportional to the angular velocity of the torque summing member with respect to the supporting case, the application of an input torque will cause the angular velocity output of the torque summing member to be proportional to the input torque. This proportionality of the rate of change of the output to the applied input is shown in Derivation Summary 34-1 to be the condition for ideal integration.

34.23. When the input torque acting on the torque summing member of a dynamic integrator is changing with time, the member will experience an angular acceleration. This acceleration is always accompanied by an inertia reaction torque that tends to prevent changes in the angular velocity. The inertia reaction torque, which is equal to the product of the acceleration and the effective moment of inertia of the torque summing member, causes the integrating action of a dynamic integrator to deviate from ideal performance. The deviation decreases as the effective moment of inertia of the torque summing member is made smaller with respect to the torque output of the drag-generating component for a given angular velocity input.

* It is usually convenient to use rotational effects for dynamic integration, but linear motion effects may be applied in the same way to the integration problem.

34.24. Figure 34-3 is a pictorial schematic diagram showing the essential features of the dynamic integrator used in conventional watt-hour meters. An electrodynamometer-type torque generator consisting of a system of field coils and a spherical armature receives a voltage input and a current input from an input receiving circuit. The illustrative arrangement is shown as a direct-current motor.

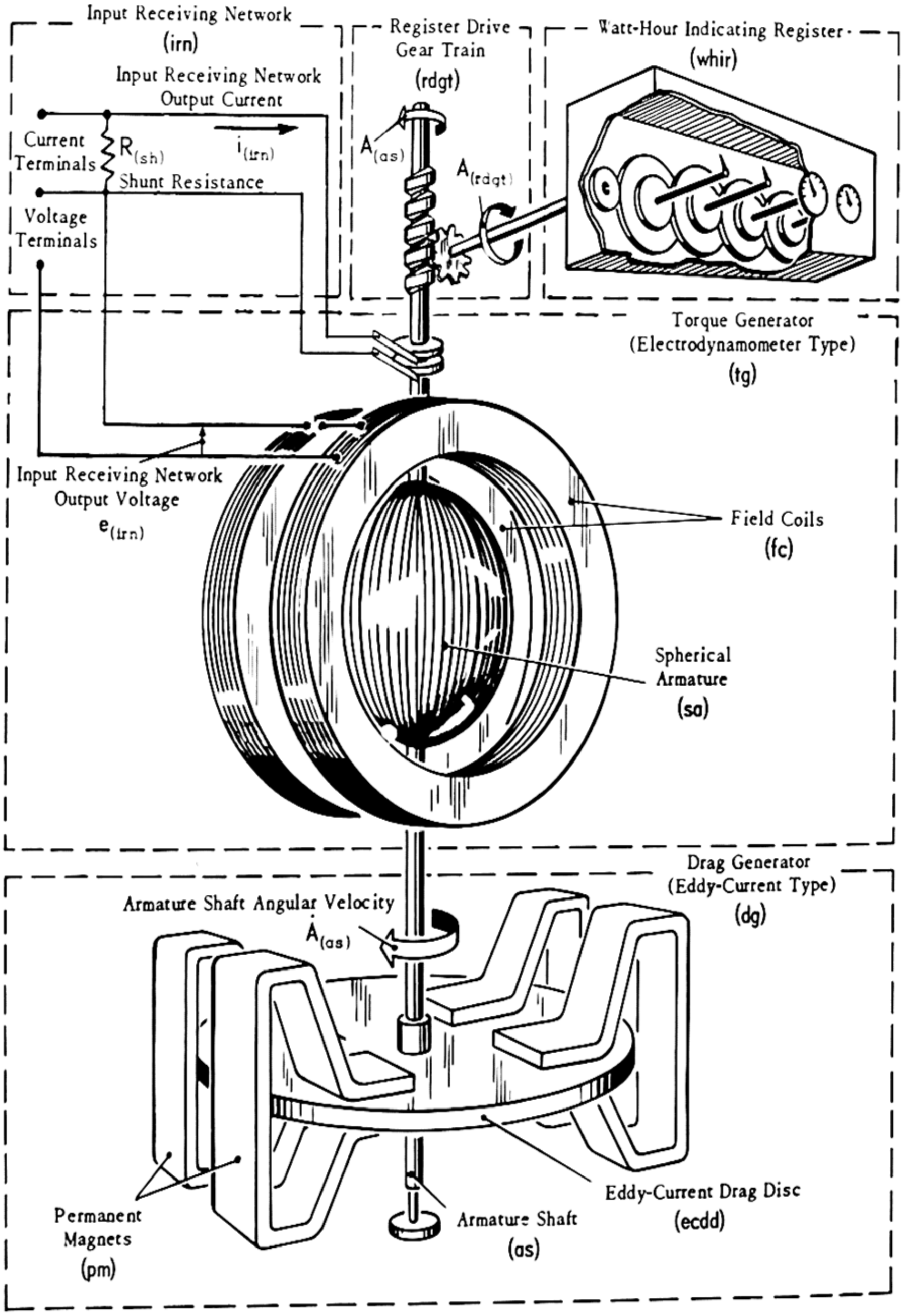


Fig. 34-3. Illustrative pictorial diagram of an eddy-current-drag-disc watt-hour-meter integrator.

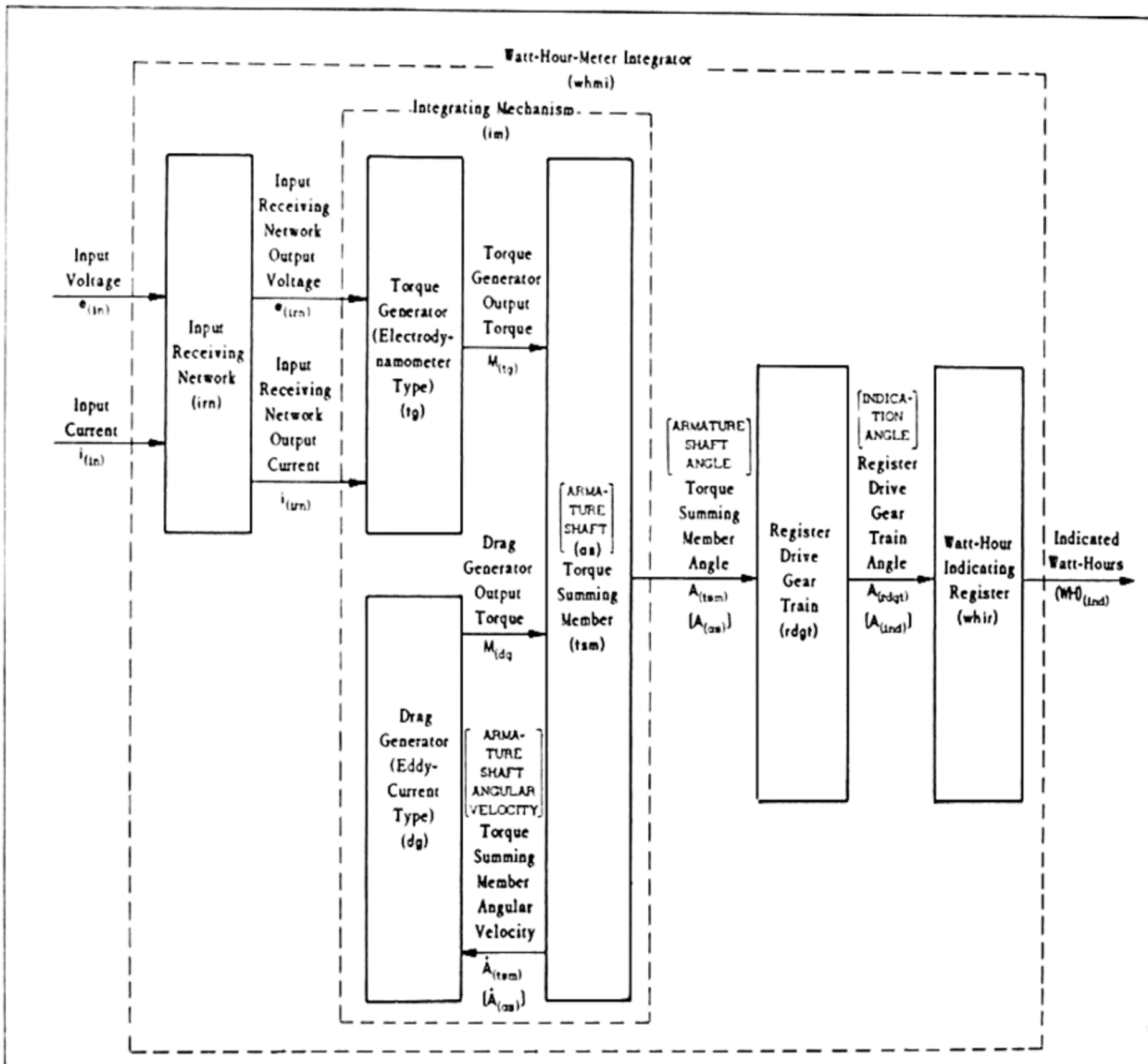
This motor choice was made to simplify the description of operation; an alternating-current motor would be equally satisfactory as an input torque generator.

34.25. The torque generator armature of Fig. 34-3 is mounted on an armature shaft that also carries an eddy-current drag disc. This disc rotates between the poles of four permanent magnets that in an actual instrument are radially adjustable with respect to the disc. The armature shaft is free to rotate on low-friction bearings that maintain the position of the armature with respect to the field coils and the position of the eddy-current disc with respect to the permanent magnets. In operation, the armature shaft provides the functions of a torque summing member. In addition, the armature shaft carries the worm gear member of the register drive gear train, which positions the indices of the watt-hour indicating register.

34.26. The diagram of section a of Derivation Summary 34-4 shows the functional relationships among the operating components and subsystems of the eddy-current-drag-disc watt-hour-meter integrator of Fig. 34-3. The input receiving network receives a voltage and a current as actuating inputs and delivers a voltage and a current to the torque generator. The torque generator produces an output torque proportional to the product of the two inputs and applies it to the torque summing member. The drag generator receives the angular velocity of the torque summing member as its input and delivers a drag torque proportional to this input to the torque summing member. The torque summing member output is its angular displacement with respect to the meter case. The torque summing member angle is received by the register drive gear train and serves to drive the watt-hour indicating register.

34.27. Section b of Derivation Summary 34-4 gives the development of the performance equations for the eddy-current-drag-disc watt-hour-meter integrator. The pattern used for this development is similar to that applied in previous derivations and does not require description here. Equation (7) of Derivation Summary 34-4 is the indication performance equation for the eddy-current-drag-generator integrating mechanism. Equation (10) is the corresponding performance equation for the complete watt-hour-meter integrator. Both of these equations have the (0;1,2) differential equation form with two performance parameters. For the integrating mechanism equation, these parameters are the integrating mechanism characteristic time and the voltage-current product input – angular velocity output indication sensitivity of the watt-hour-meter integrator.

34.28. Inspection of the performance equation of the eddy-current-drag-disc watt-hour-meter integrator (Eq. (10) of Derivation Summary 34-4) shows that it reduces to the (0;1) ideal integrator performance equation when the second-derivative term is negligibly small compared with the first-derivative term. Equations (12), (13) and (14) of Derivation Summary 34-4 illustrate the conditions that must exist for ideal integration.



a) Functional diagram

(irn) Input receiving network

$$e_{(irn)} = S_{(irn)[e;e]}\, e_{(in)} \tag{1}$$

$$i_{(irn)} = S_{(irn)[i;i]}\, i_{(in)} \tag{2}$$

(tg) Torque generator

$$M_{(tg)} = S_{(tg)[e,i;M]}\, e_{(irn)}\, i_{(irn)} \tag{3}$$

(dg) Drag generator

$$M_{(dg)} = S_{(dg)[\dot{A};M]}\, \dot{A}_{(tsm)} = -\,|S_{(dg)[\dot{A};M]}|\, \dot{A}_{(tsm)} = -\,S_{(dg)|\dot{A};M|} \cdot \dot{A}_{(tsm)} \tag{4}$$

(im) Integrating mechanism

The torque summation equation is formed by following the pattern described in Chapter 7. In words, this equation is

$$\begin{pmatrix}\text{Inertia}\\ \text{Reaction}\\ \text{Torque}\end{pmatrix} + \begin{pmatrix}\text{Drag}\\ \text{Generator}\\ \text{Torque}\end{pmatrix} + \begin{pmatrix}\text{Torque}\\ \text{Generator}\\ \text{Torque}\end{pmatrix} = 0 \tag{5}$$

In symbols, Eq. (5) becomes

$$-I_{(tsm)}\ddot{A}_{(tsm)} - S_{(dg)|\dot{A};M|}\dot{A}_{(tsm)} + S_{(tg)[e,i;M]}\, e_{(irn)}\, i_{(irn)} = 0 \tag{6}$$

---

* Under the convention of Note 2 in section b of Definition Summary 10-1, Chapter 10, straight vertical lines on either side of the input-output subscript mean that only the magnitude of the sensitivity is considered.

Derivation Summary 34-4. Functional diagram and generalized performance equations for an eddy-current-drag-disc watt-hour-meter integrator. (Page 1 of 2)

where

$I_{(tsm)}$ = effective moment of inertia of the torque summing member
= equivalent moment of inertia about the axis of rotation of all parts rotating with the torque generator armature

(whmi) Watt-hour-meter integrator

Transforming $A_{(tsm)}$ to $A_{(ind)}$ and combining factors gives

$$(CT)_{(im)}\ddot{A}_{(ind)} + \dot{A}_{(ind)} = S_{(whmi)[e,i;\dot{A}](ind)}\, e_{(in)}\, i_{(in)} \tag{7}$$

where

$$(CT)_{(im)} = \frac{I_{(tsm)}}{S_{(dg)|\dot{A};M|}} = \text{indicating mechanism characteristic time} \tag{8}$$

$$S_{(whmi)[e,i;\dot{A}](ind)} = \frac{S_{(tg)[e,i;M]}}{S_{(dg)|\dot{A};M|}} S_{(irn)[e;e]} S_{(irn)[i;i]} S_{(rdgt)[A;A]} \tag{9}$$

= voltage-current product input – angular velocity output indication sensitivity of the watt-hour-meter integrator

Equation (7) is the indication performance equation for the eddy-current-drag-generator integrating mechanism.

When the action of the watt-hour integrating register is introduced, Eq. (7) becomes

$$(CT)_{(im)} \frac{d^2(WH)_{(ind)}}{dt^2} + \frac{d(WH)_{(ind)}}{dt} = S_{(whmi)[e,i;(\dot{WH})]}\, e_{(in)}\, i_{(in)} \tag{10}$$

where

$$S_{(whmi)[e,i;(\dot{WH})]} = S_{(whmi)[e,i;\dot{A}](ind)} S_{(whir)[A;(WH)]} \tag{11}$$

= voltage-current product input – watt-hour-reading rate output sensitivity of the watt-hour meter

The integrator performance equation (10) has the form of the standard (0;1,2) differential equation.

Under static conditions, that is, when

$$(CT)_{(im)}(\dot{\dot{WH}})_{(ind)} << (\dot{WH})_{(ind)} \tag{12}$$

Eq. (10) reduces to

$$\frac{d(WH)_{(ind)}}{dt} = (\dot{WH})_{(ind)} = S_{(whmi)[e,i;(\dot{WH})]}\, e_{(in)}\, i_{(in)} \tag{13}$$

When $S_{(whmi)[e,i;(\dot{WH})]}$ is constant, integration of Eq. (13) shows that

$$(WH)_{(ind)2} - (WH)_{(ind)1} = \int_{(WH)_{(ind)1}}^{(WH)_{(ind)2}} d(WH)_{(ind)} = S_{(whmi)[e,i;(\dot{WH})]} \int_{t_1}^{t_2} e_{(in)}\, i_{(in)}\, dt \tag{14}$$

b) Performance equations

Derivation Summary 34-4. Functional diagram and generalized performance equations for an eddy-current-drag-disc watt-hour-meter integrator. (Page 2 of 2)

VISCOUS-SHEAR-DRAG-GENERATOR-TYPE INTEGRATOR

34.29. Other integrators may be constructed that use the drag-generator principle of the watt-hour-meter-type integrator described in the preceding section. Any drag generator will be satisfactory if the force or torque output is proportional respectively to the linear or angular velocity of some part of the unit with respect to another part. Performance of this type may be based on the resistance to motion set up across a gap filled with viscous fluid when a shearing action exists in the fluid.

34.30. One of the many possible arrangements of parts to utilize viscous shear for drag generation* is illustrated by the drag generator shown in Fig. 34-4.

* See Lees (L10) for a complete discussion of integration by means of the viscous shear process; see also Information Summaries 30-2 and 30-6.

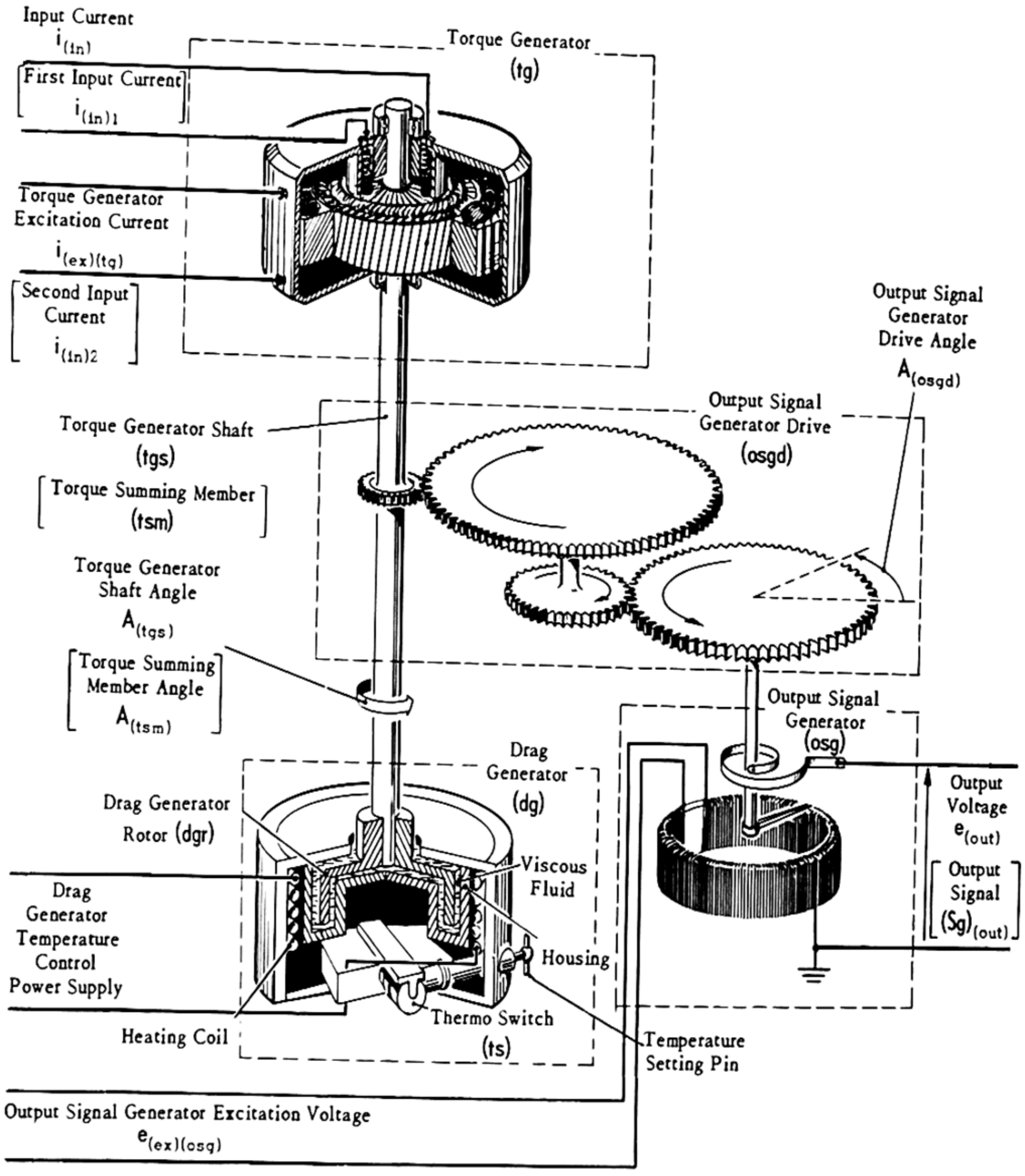


Fig. 34-4. Illustrative pictorial diagram for a viscous-shear-drag-generator-type integrator.

A cup-shaped rotor is rigidly attached to the shaft of a torque generator. Bearings not shown in Fig. 34-4 are used to maintain accurate alignment of the rotor with respect to the structural parts of the unit. The drag generator housing is shaped to surround the rotor except for an opening through which the shaft enters. A viscous fluid* fills the relatively small clearances between the rotor and the housing. For ideal operation, the viscosity of the fluid must be maintained constant by control of the housing and rotor temperatures. In the drag generator of Fig. 34-4, the thermal control is achieved by using an electrical resistance coil and thermoswitch

* In order for this fluid to give ideal operation, it must have Newtonian properties. That is, the shearing force between any two parallel surfaces completely immersed in the fluid must be proportional to the relative velocity of the surfaces.

arrangement that keeps the entire drag generator at a specified temperature above the environmental temperature. With this arrangement, it is possible to make accurate adjustments of the drag generator performance by changing the set point of the thermoswitch.

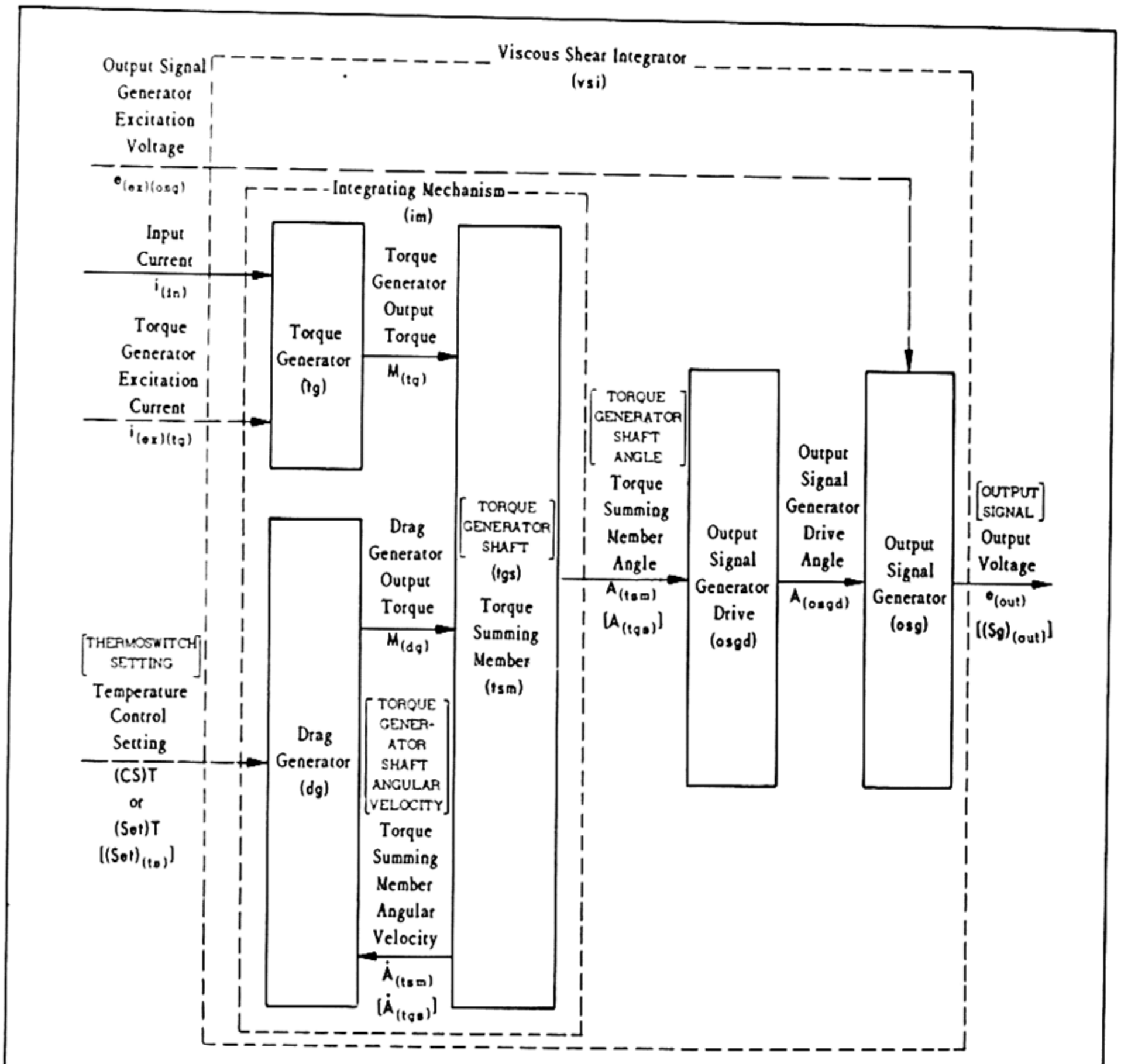
34.31. In the viscous-shear-drag-generator-type integrator of Fig. 34-4, the torque generator is a separately-excited direct-current motor with the field current as excitation and the armature current as the actuating input. In practice, the torque generator may be a two-phase alternating-current motor or a torque-producing device of any other kind. The armature shaft acts as the torque summing member and carries the input pinion for the output signal generator drive. This gear train drives the rotating contact of the output signal generator, which consists of a potentiometer winding with its center tap grounded and its ends connected to a source of excitation voltage. The output signal is the voltage between the rotating-slider contact and ground.

34.32. Section a of Derivation Summary 34-5 gives a functional diagram for the viscous shear integrator of Fig. 34-4. Except for differences in the names of the operating components and the replacement of the watt-hour indicating register by the output signal generator, this functional diagram is essentially identical with the functional diagram for the watt-hour-meter integrator given in section a of Derivation Summary 34-4.

34.33. Section b of Derivation Summary 34-5 gives a development of the performance equation for the viscous shear integrator. This equation has the standard (0;1,2) differential equation form, which is identical with that of the performance equation for the eddy-current-drag-disc watt-hour-meter-type integrator. In practice, the magnitudes of the parameters involved may differ considerably between the two integrator types, but it is possible to design for equivalent performance in each case. The viscous shear integrator has torque generator excitation, drag generator temperature setting, and output signal generator excitation voltage as modifying inputs. These inputs give the viscous shear integrator great flexibility as an operating component for computing systems. On the other hand, for the watt-hour-meter integrator, both electrical inputs are actuating inputs; no modifying inputs are present, and temperature is considered as an interference. This viewpoint of temperature effects is taken because the watt-hour-meter integrator must function as an accurate measuring instrument in the presence of environmental changes.

LIQUID-FLOW INTEGRATOR

34.34. Integration based on kinematic and dynamic interactions of mechanical components is discussed in the preceding sections. In this section, a widely used integrator type is described that depends on the reversible flow of some fluid



a) Functional diagram

(tg) Torque generator

$$M_{(tg)} = S_{(tg)[i_{(in)};i_{(ex)(tg)};M]}\, i_{(ex)(tg)}\, i_{(in)}\,^{*} \tag{1}$$

$$= S_{(tg)[i_{(in)};M]}\, i_{(in)} \tag{2}$$

$$i_{(ex)(tg)} = \text{——}$$

where

$$S_{(tg)[i_{(in)};M]} = S_{(tg)[i_{(in)};i_{(ex)(tg)};M]}\, i_{(ex)(tg)} \tag{3}$$

(dg) Drag generator

$$M_{(dg)} = -S_{(dg)|\dot{A}_{(tsm)};M|}\, \dot{A}_{(tsm)} \tag{4}$$

$$(CS)T = \text{——}$$

(im) Integrating mechanism

$$\begin{pmatrix}\text{Inertia}\\ \text{Reaction}\\ \text{Torque}\end{pmatrix} + \begin{pmatrix}\text{Drag}\\ \text{Generator}\\ \text{Torque}\end{pmatrix} + \begin{pmatrix}\text{Torque}\\ \text{Generator}\\ \text{Torque}\end{pmatrix} = 0 \tag{5}$$

---

* Note that $i_{(ex)(tg)}$, the torque generator excitation current, is a modifying input. Under the conventions of Fig. 10-3 and Definition Summary 10-1, modifying inputs are separated from actuating inputs and outputs by semicolons in the input-output subscript brackets.

Derivation Summary 34-5. Functional diagram and generalized performance equations for a viscous-shear-drag-generator-type integrator. (Page 1 of 3)

$$-I_{(tsm)}\ddot{A}_{(tsm)} - S_{(dq)|\dot{A}_{(tsm)};M|}\dot{A}_{(tsm)} + S_{(tg)[i_{(in)};i_{(ex)(tg)};M]}i_{(ex)(tg)}i_{(in)} = 0 \qquad (6)$$

$$(CS)T = ____$$

Introducing definitions and rearranging terms gives

$$(CT)_{(im)}\ddot{A}_{(tsm)} + \dot{A}_{(tsm)} = S_{(im)[i_{(in)};i_{(ex)(tg)};\dot{A}_{(tsm)}]}i_{(ex)(tg)}i_{(in)} \qquad (7)$$

$$(CS)T = ____$$

or

$$(CT)_{(im)}\ddot{A}_{(tsm)} + \dot{A}_{(tsm)} = S_{(im)[i_{(in)};\dot{A}_{(tsm)}]}i_{(in)} \qquad (8)$$

$$i_{(ex)(tg)} = ____ \quad ; \quad (CS)T = ____$$

where

$I_{(tsm)}$ = effective moment of inertia of parts rotating with the torque summing member (the torque generator shaft)

$$(CT)_{(im)} = \frac{I_{(tsm)}}{S_{(dq)|\dot{A}_{(tsm)};M|}} = \text{characteristic time of the integrating mechanism} \qquad (9)$$

$$S_{(im)[i_{(in)};i_{(ex)(tg)};\dot{A}_{(tsm)}]} = \frac{S_{(tg)[i_{(in)};i_{(ex)(tg)};M]}}{S_{(dq)|\dot{A};M|}} \qquad (10)$$

$$(CS)T = ____$$

$$S_{(im)[i_{(in)};\dot{A}_{(tsm)}]} = S_{(im)[i_{(in)};i_{(ex)(tg)};\dot{A}_{(tsm)}]}i_{(ex)(tg)} \qquad (11)$$

$$(CS)T = ____ \quad ; \quad i_{(ex)(tg)} = ____$$

(osgd) Output signal generator drive

$$A_{(osgd)} = S_{(osgd)[A;A]}A_{(tsm)} \qquad (12)$$

(osg) Output signal generator

$$(Sg)_{(out)} \approx e_{(out)} = S_{(osg)[A;e_{(ex)(osg)};e]}e_{(ex)(osg)}A_{(osgd)} \qquad (13)$$

(vsi) Viscous shear integrator

$$(CT)_{(vsi)}\ddot{e}_{(out)} + \dot{e}_{(out)} = S_{(vsi)[i_{(in)};i_{(ex)(tg)},e_{(ex)(osg)};\dot{e}]}i_{(ex)(tg)}e_{(ex)(osg)}i_{(in)} \qquad (14)$$

$$(CS)T = ____$$

$$(CT)_{(vsi)}\ddot{e}_{(out)} + \dot{e}_{(out)} = S_{(vsi)[i_{(in)};\dot{e}]}i_{(in)} \qquad (15)$$

$$(CS)T = ____ \quad ; \quad i_{(ex)(tg)} = ____ \quad ; \quad e_{(ex)(osg)} = ____$$

where

$$(CT)_{(vsi)} = (CT)_{(im)} = \text{characteristic time of the viscous shear integrator} \qquad (16)$$

$$S_{(vsi)[i_{(in)};i_{(ex)(tg)},e_{(ex)(osg)};\dot{e}]} = S_{(im)[i_{(in)};i_{(ex)(tg)};\dot{A}_{(tsm)}]}S_{(osgd)[A;A]}S_{(osg)[A;e_{(ex)(osg)};e]} \qquad (17)$$

$$S_{(vsi)[i_{(in)};\dot{e}]} = S_{(vsi)[i_{(in)};i_{(ex)(tg)},e_{(ex)(osg)};\dot{e}]}i_{(ex)(tg)}e_{(ex)(osg)} \qquad (18)$$

= current – voltage rate sensitivity of the viscous shear integrator

$$(CS)T = ____ \quad ; \quad i_{(ex)(tg)} = ____ \quad ; \quad e_{(ex)(osg)} = ____$$

Note that the (vsi) performance equation of Eqs. (14) and (15) has the form of a (0;1,2) differential equation.

When

$$(CT)_{(vsi)}\ddot{e}_{(out)} << \dot{e}_{(out)} \qquad (19)$$

Derivation Summary 34-5. Functional diagram and generalized performance equations for a viscous-shear-drag-generator-type integrator. (Page 2 of 3)

then Eq. (15) reduces to

$$\frac{de_{(out)}}{dt} = \dot{e}_{(out)} = S_{(vsd)[i_{(in)};\dot{e}]}\, i_{(in)} \tag{20}$$

When $S_{(vsd)[i_{(in)};\dot{e}]}$ is constant, integration of Eq. (20) shows that

$$e_{(out)2} - e_{(out)1} = \int_{e_{(out)1}}^{e_{(out)2}} de_{(out)} = S_{(vsd)[i_{(in)};\dot{e}]} \int_{t_1}^{t_2} i_{(in)}\, dt \tag{21}$$

b) Performance equations

Derivation Summary 34-5. Functional diagram and generalized performance equations for a viscous-shear-drag-generator-type integrator. (Page 3 of 3)

(or some fluid-like quantity) through a resistive element* into a second element capable of receiving and storing the fluid. Ideal performance depends on the rate of flow through the resistive element being proportional to the pressure difference across the element (or the difference in levels of some other quantity corresponding to pressure). Scale readings are generated by an indicating system operated by the quantity of fluid present in the storage element.

34.35. Figure 34-5 is an illustrative pictorial diagram of a resistive element – storage element integrator designed to operate with liquid as the working fluid. The input quantity is pressure applied to the surface of the fluid in the liquid supply reservoir. A capillary tube, or capillary, is located with its opening just beneath the liquid level in the reservoir. The capillary leads into the integrating tube, which is fitted with a scale to measure the liquid level in the integrating tube above the capillary outlet. The reservoir area is made very large compared with the area of the integrating tube so that the liquid level in the reservoir does not vary appreciably over the complete range of operation of the device. In order to provide a means of adjusting the pressure level for integration, a reference pressure is applied to the inside of the integrating tube above the liquid level.

34.36. Section a of Derivation Summary 34-6 gives a functional diagram for the liquid-flow integrator of Fig. 34-5. The names and symbols appearing in the functional diagram are identical with those of the figure. Pressure levels are shown by labelled dots in the operating-component boxes near the input or output indicating arrows that correspond to the positions at which the pressures exist.

34.37. Section b of Derivation Summary 34-6 gives a development of the performance equation for the liquid-flow integrator of section a. It is assumed that the height of liquid over the inlet to the capillary is so small that the capillary inlet pressure is effectively identical with the input pressure to the liquid supply reservoir, which is also the input for the integrator. The flow of liquid mass through the capillary is equal to the liquid density multiplied by the average velocity of the liquid through the capillary. From Eq. (34) of Information Summary 30-6, the average fluid velocity through a capillary for a Reynolds number

* See Eq. (34) of Information Summary 30-6 for the relationship governing viscous flow through a capillary.

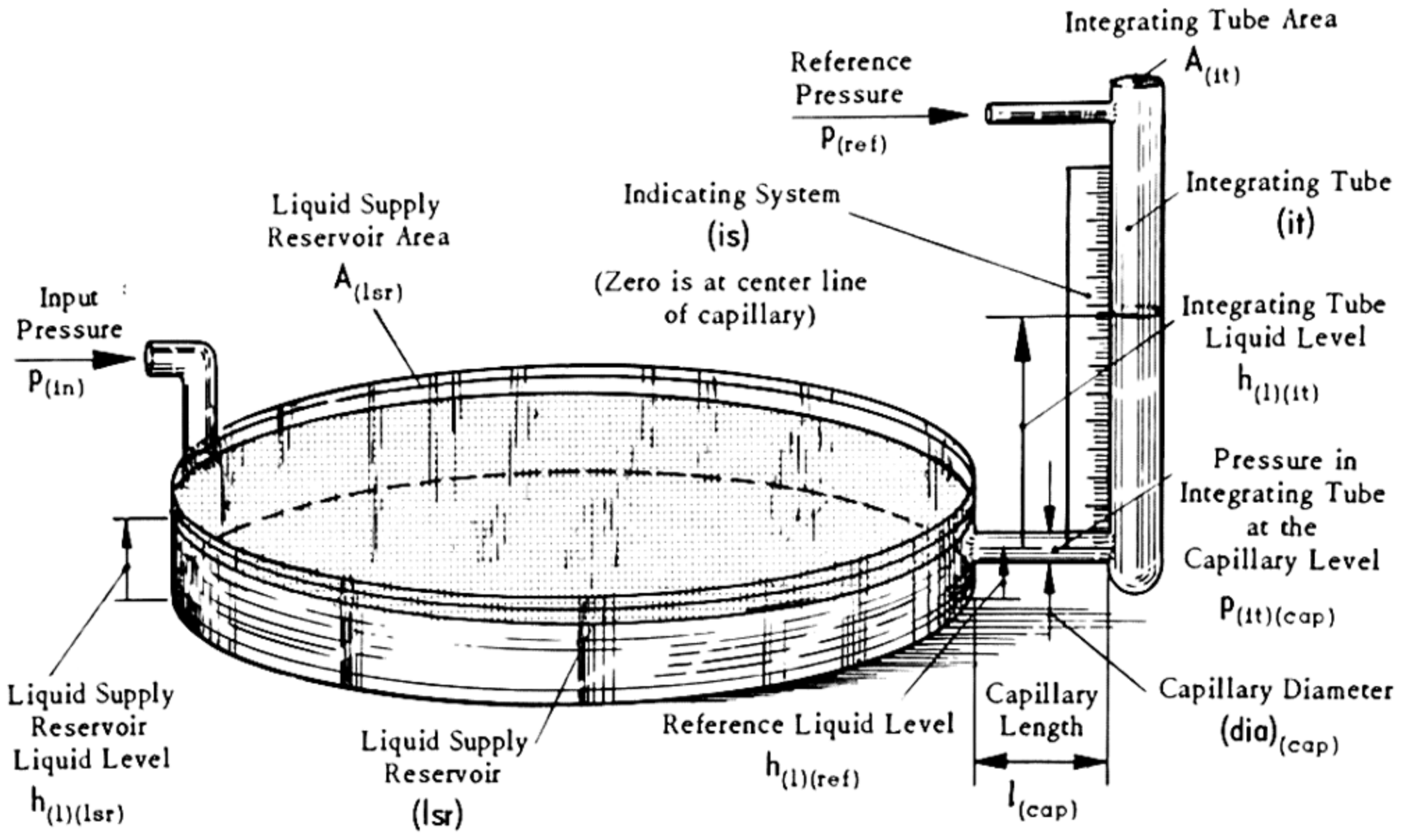


Fig. 34-5. Illustrative pictorial diagram for a liquid-flow integrator.

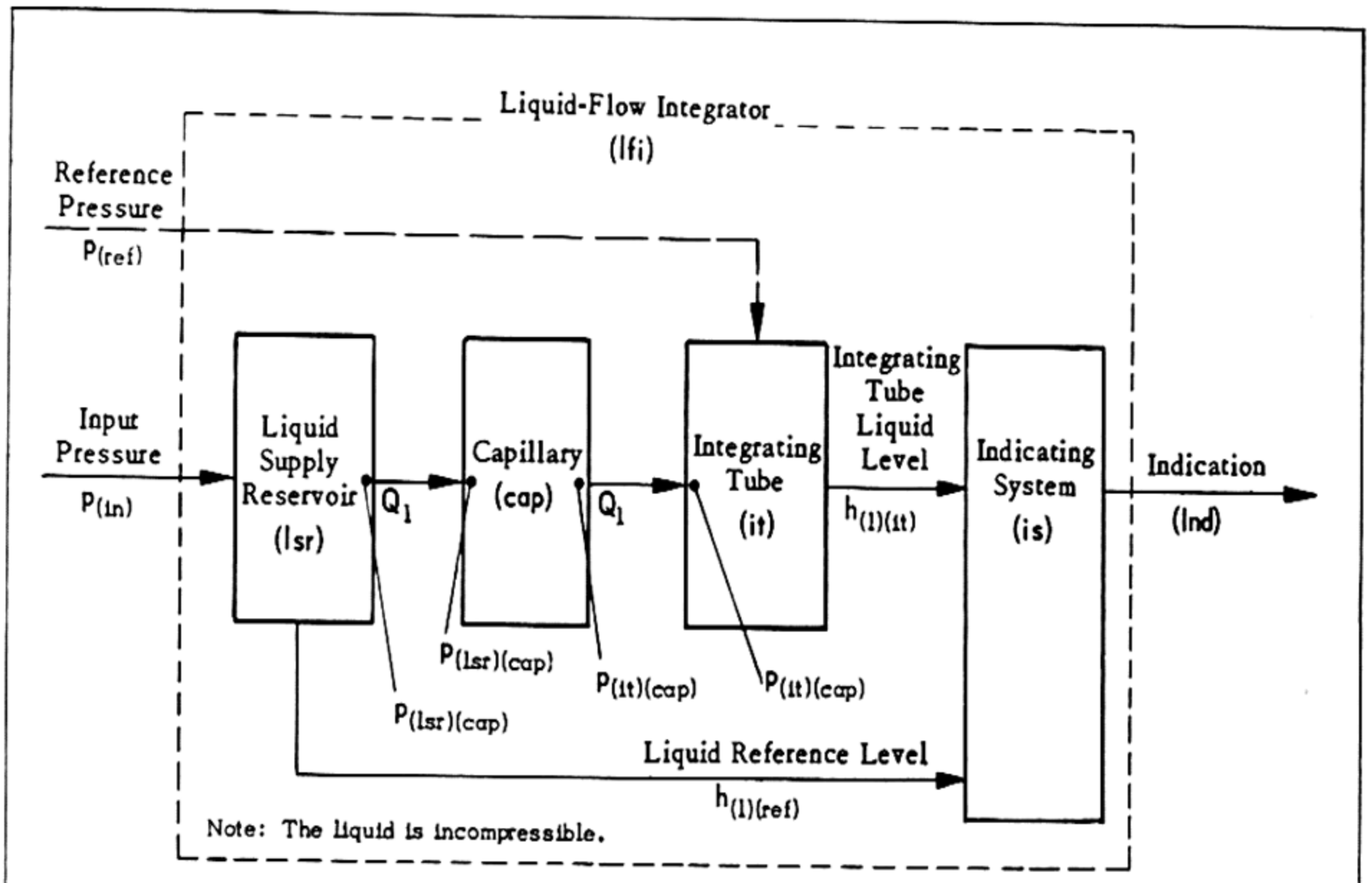
range of 0 to 2100 is proportional to the pressure difference across the capillary and the diameter of the capillary, and is inversely proportional to the length of the capillary and the fluid viscosity. Equation (5) of Derivation Summary 34-6 is an expression for the mass flow of liquid from the capillary into the integrating tube. The liquid pressure at the integrating-tube end of the capillary is the sum of the reference pressure and the product of liquid density and the height of the liquid above the capillary-tube level in the integrating tube. The mass of liquid above the capillary level is equal to the liquid density multiplied by the height of liquid above the capillary opening in the integrating tube and the integrating tube area.

34.38. The liquid-flow integrator performance equation is formed by equating the rate of mass flow through the capillary to the time rate of change of liquid mass in the integrating tube. Rearranging terms in this equation of continuity gives Eq. (10) of Derivation Summary 34-6, which is the performance equation for the liquid-flow integrator. This equation has the form of the (0;0,1) differential equation.

34.39. Equations (17) and (18) of Derivation Summary 34-6 show that the liquid-flow integrator gives ideal integration when the time rate of change of the indication multiplied by the integrator characteristic time is very large compared with the indication itself. When this condition exists, the change in indication is proportional to the time integral of input pressure changes.

THERMAL INTEGRATOR

34.40. Figure 34-6 is an illustrative pictorial diagram for a form of the resistive element – storage element integrator in which heat is the working fluid.



a) Functional diagram

(lsr) Liquid supply reservoir

$$P_{(lsr)(cap)} = P_{(in)} + (den)_l (h_{(l)(lsr)} - h_{(l)(ref)}) \tag{1}$$

where

$P_{(lsr)(cap)}$ = pressure in liquid supply reservoir at capillary inlet

By design,

$$A_{(lsr)} >> A_{(it)}$$

so that

$$h_{(l)(lsr)} - h_{(l)(ref)} \longrightarrow 0$$

Therefore,

$$P_{(lsr)(cap)} = P_{(in)} \tag{2}$$

(cap) Capillary

$$\left(\frac{dQ_l}{dt}\right)_{(cap)} = (den)_l v_{(av)(cap)} \tag{3}$$

= mass flow rate of liquid through the capillary

From Chapter 30, for a Reynolds number range of 0 to 2100,

$$v_{(av)(cap)} = \frac{2(dia)_{(cap)}}{32\,\mu_l l_{(cap)}} (p_{(lsr)(cap)} - P_{(it)(cap)}) \tag{4}$$

= average velocity of liquid flowing through the capillary

where

$(den)_l$ = density of liquid

$(dia)_{(cap)}$ = capillary diameter

$l_{(cap)}$ = capillary length

μ_l = viscosity of liquid

$P_{(it)(cap)}$ = pressure inside integrating tube at capillary level

Derivation Summary 34-6. Functional diagram and performance equation for a liquid-flow integrator. (Page 1 of 3)

From Eqs. (2), (3) and (4),

$$\left(\frac{dQ_1}{dt}\right)_{(cap)} = \frac{(den)_1 (dia)_{(cap)}}{16\,\mu_1 l_{(cap)}} (p_{(in)} - p_{(it)(cap)}) \tag{5}$$

(it) Integrating tube

$$p_{(it)(cap)} = p_{(ref)} + (den)_1 h_{(l)(it)} \tag{6}$$

where

$h_{(l)(it)}$ = liquid height above capillary opening inside integrating tube

$$Q_{(l)(it)} = (den)_1 A_{(it)} h_{(l)(it)} \tag{7}$$

= mass of liquid inside integrating tube above capillary opening

$$\left(\frac{dQ_1}{dt}\right)_{(it)} = \left(\frac{dQ_1}{dt}\right)_{(cap)} \tag{8}$$

or

$$\begin{pmatrix}\text{Rate of liquid mass flow}\\ \text{into integrating tube}\end{pmatrix} = \begin{pmatrix}\text{Rate of liquid mass flow}\\ \text{through capillary}\end{pmatrix}$$

From Eqs. (5), (7) and (8)

$$(den)_1 A_{(it)} \frac{dh_{(l)(it)}}{dt} = (den)_1 \frac{(dia)_{(cap)}}{l_{(cap)}} \frac{1}{16\,\mu_1} (p_{(in)} - p_{(it)(cap)}) \tag{9}$$

Using Eq. (6) and rearranging terms gives

$$A_{(it)} \frac{l_{(cap)}}{(dia)_{(cap)}} \frac{16\,\mu_1}{(den)_1} \frac{dh_{(l)(it)}}{dt} + h_{(l)(it)} = \frac{1}{(den)_1} (p_{(in)} - p_{(ref)}) \tag{10}$$

or

$$(CT)_{(lfi)} \frac{dh_{(l)(it)}}{dt} + h_{(l)(it)} = S_{(lfi)[p;h]} (p_{(in)} - p_{(ref)}) \tag{11}$$

where

$$(CT)_{(lfi)} = A_{(it)} \frac{l_{(cap)}}{(dia)_{(cap)}} \frac{16\,\mu_1}{(den)_1} \tag{12}$$

= characteristic time of the liquid-flow integrator

$$S_{(lfi)[p;h]} = \frac{1}{(den)_1} \tag{13}$$

= pressure input – integrating tube liquid level output sensitivity of liquid-flow integrator

Note that Eq. (11) has the typical form of the (0;0,1) differential equation.

(is) Indicating system

$$(Ind) = S_{(is)[h;(Ind)]} h_{(l)(it)} \tag{14}$$

When the sensitivity of the indicating system is introduced into Eq. (11), the performance equation of the liquid-flow integrator becomes

$$(CT)_{(lfi)} (\dot{Ind}) + (Ind) = S_{(lfi)[p;(Ind)]} (p_{(in)} - p_{(ref)}) \tag{15}$$

where

$$S_{(lfi)[p;(Ind)]} = S_{(lfi)[p;h]} S_{(is)[h;(Ind)]} \tag{16}$$

Ideal integration exists within operating ranges for which

$$(Ind) << (CT)_{(lfi)} (Ind) \tag{17}$$

Derivation Summary 34-6. Functional diagram and performance equation for a liquid-flow integrator. (Page 2 of 3)

Under these conditions, Eq. (15) reduces to the (0;1) equation and integration gives

$$(\mathrm{Ind})_2 - (\mathrm{Ind})_1 = \int_{(\mathrm{Ind})_1}^{(\mathrm{Ind})_2} d(\mathrm{Ind}) = \frac{S_{(\mathrm{lf1})[p;(\mathrm{Ind})]}}{(CT)_{(\mathrm{lf1})}} \int_{t_1}^{t_2} (p_{(\mathrm{in})} - p_{(\mathrm{ref})})\, dt \qquad (18)$$

b) Performance equation

Derivation Summary 34-6. Functional diagram and performance equation for a liquid-flow integrator. (Page 3 of 3)

The input temperature acts on the temperature receiver, which has good thermal contact with one end of the thermal coupling rod. The other end of the rod is thermally connected to a temperature-integrating mass of high conductivity. Except for the exposed surfaces of the temperature receiver, the thermal coupling rod and the integrating mass are enclosed in a shell of thermal insulation to minimize heat losses. The indicating system has the integrating-mass temperature as its input and an index position as its output.

34.41. Section a of Derivation Summary 34-7 is a functional diagram for the thermal integrator of Fig. 34-6. The performance equation for the integrator is developed in section b of the summary. This development follows the general pattern used in Chapter 31 for deriving the performance equations of temperature-measuring instruments. The essential step is based on a balance between heat flowing through the thermal coupling rod and the quantity of heat inside the integrating mass.

34.42. The temperature integrator output is an indication produced by an indicating system operated by the temperature of the integrating mass. The performance equation has the form of the (0;0,1) differential equation. When the first derivative term, which is the product of the thermal integrator characteristic time and the time rate of change of the indication, is very large compared with the indication itself, the (0;0,1) performance equation reduces to the (0;1) equation of the ideal integrator.

PNEUMATIC PRESSURE INTEGRATOR

34.43. Figure 34-7 is an illustrative pictorial diagram for a resistive element – storage element integrator in which the working fluid is compressible and, in particular, has the properties of a perfect gas. The input pressure is applied directly to one end of a capillary tube whose other end is connected to a fixed volume that acts as the integrating chamber. Interference effects due to temperature changes are minimized by enclosing the capillary and the integrating chamber in an envelope of thermal insulation. Indications are provided by a pressure gage connected to the integrating chamber.

34.44. Section a of Derivation Summary 34-8 is a functional diagram for the pneumatic pressure integrator. Section b gives a development of the pneumatic

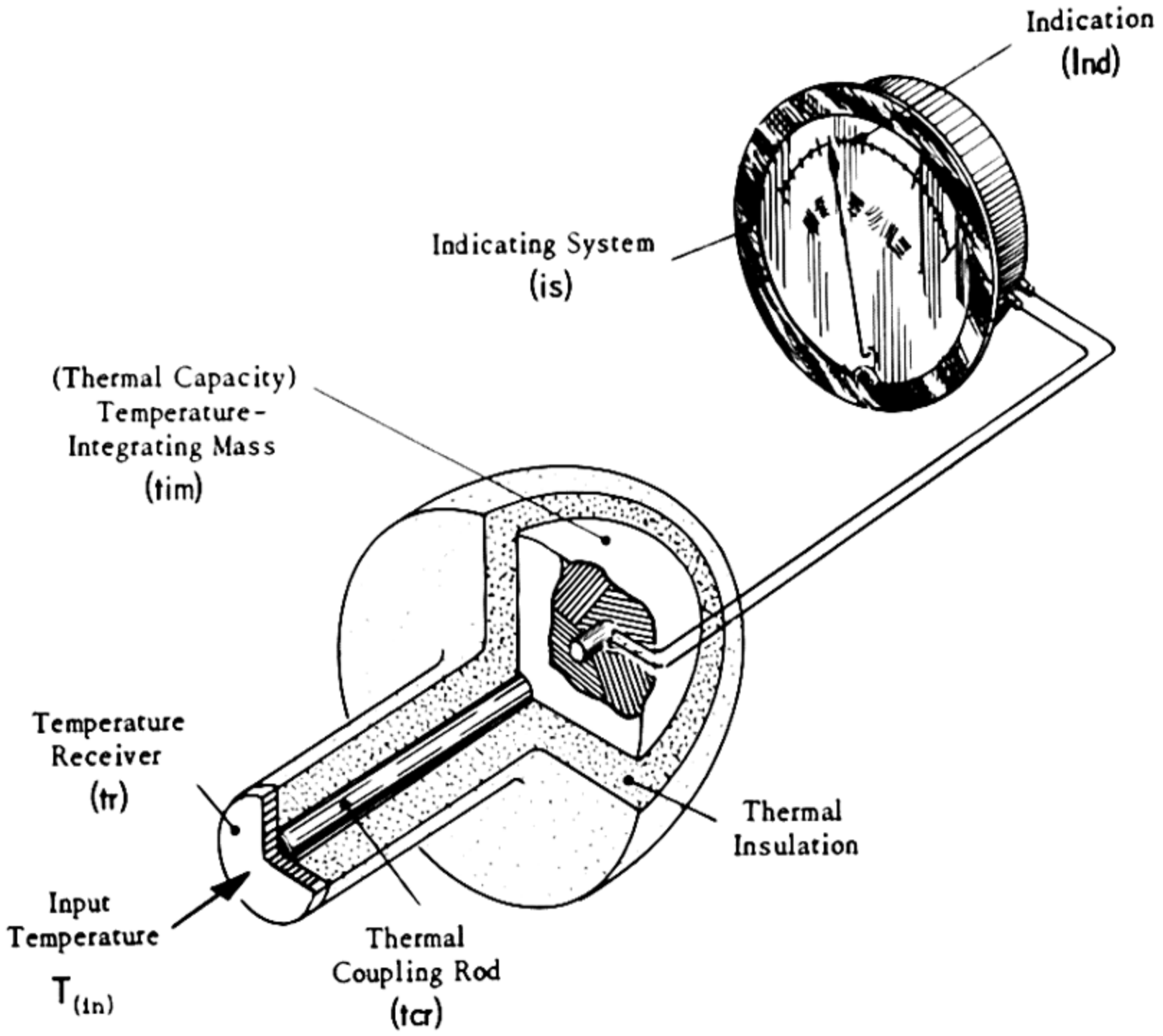


Fig. 34-6. Illustrative pictorial diagram for a thermal integrator.

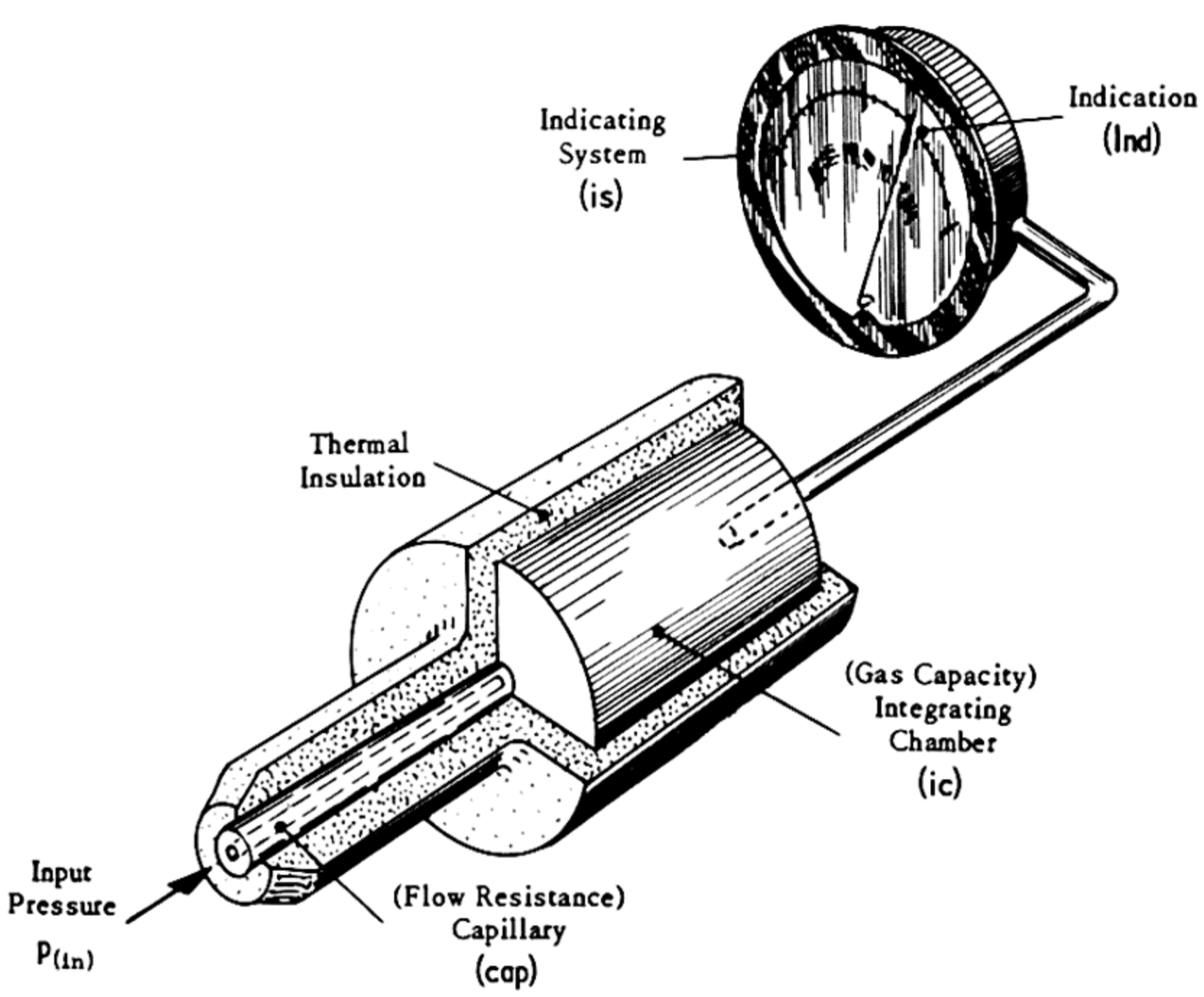
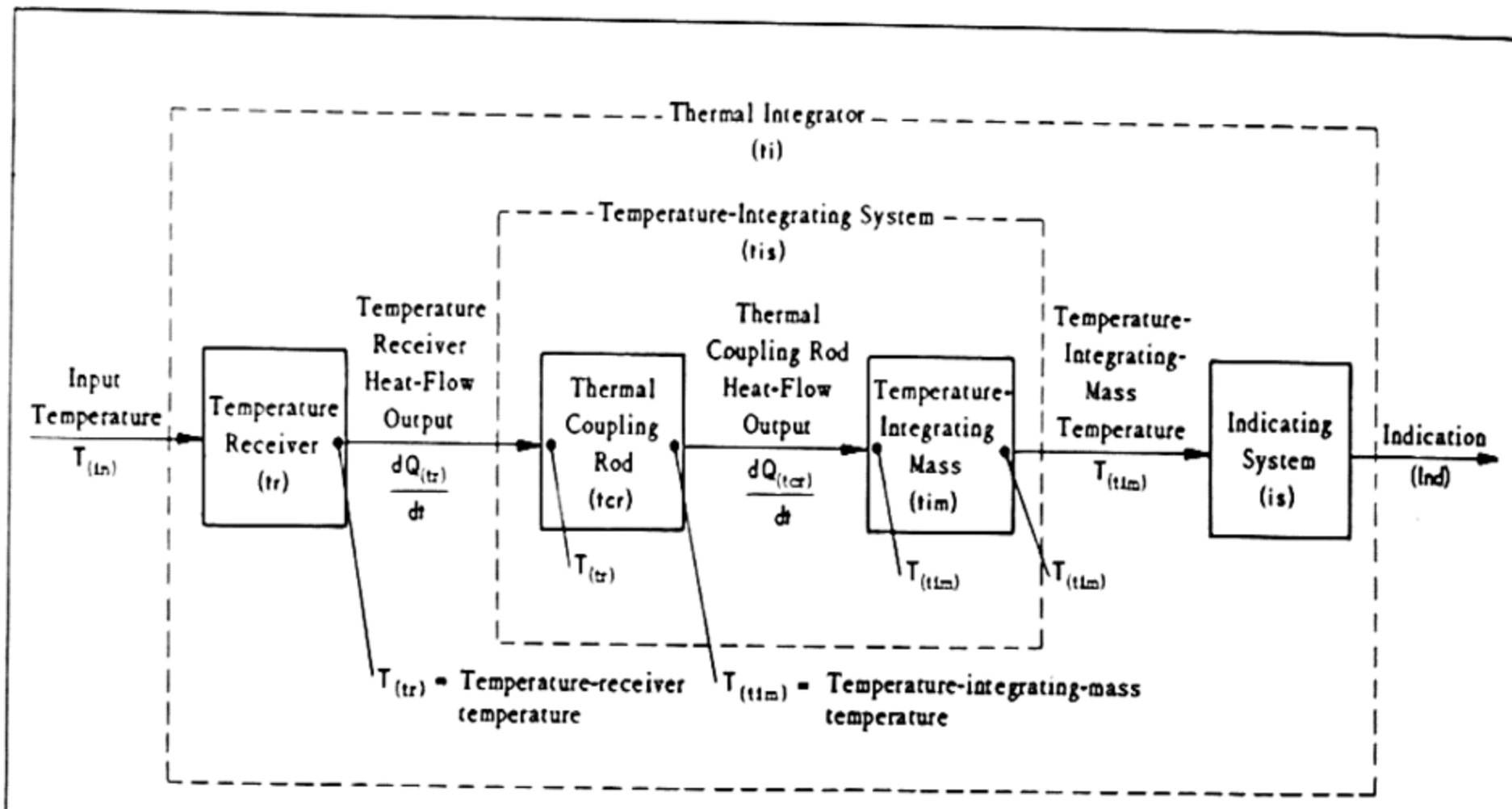


Fig. 34-7. Illustrative pictorial diagram for a pneumatic integrator.



a) Functional diagram

(tr) Temperature receiver

$$T_{(tr)} = T_{(in)} \tag{1}$$

(tcr) Thermal coupling rod

$$\frac{dQ_{(tcr)}}{dt} = \frac{k_{(tcr)} A_{(tcr)}}{l_{(tcr)}} [T_{(tr)} - T_{(tim)}] \tag{2}$$

where

$\frac{dQ_{(tcr)}}{dt}$ = heat flow through thermal coupling rod

$k_{(tcr)}$ = thermal conductivity of thermal coupling rod

$A_{(tcr)}$ = cross-sectional area of thermal coupling rod (either constant or an effective area)

$l_{(tcr)}$ = length of thermal coupling rod

(tim) Temperature-integrating mass

$$\left(\frac{dQ_{(tim)}}{dt}\right)_{(in)} = V_{(tim)} (den)_{(tim)} (sh)_{(tim)} \frac{dT_{(tim)}}{dt} \tag{3}$$

where

$\left(\frac{dQ_{(tim)}}{dt}\right)_{(in)}$ = time rate of change of heat inside temperature-integrating mass

$V_{(tim)}$ = volume of temperature-integrating mass

$(den)_{(tim)}$ = density (effective) of temperature-integrating mass

$(sh)_{(tim)}$ = specific heat (effective) of temperature-integrating mass

(tis) Temperature-integrating system

$$\begin{pmatrix}\text{Heat flow through} \\ \text{thermal coupling rod}\end{pmatrix} = \begin{pmatrix}\text{Time rate of change of heat} \\ \text{within temperature-integrating mass}\end{pmatrix} \tag{4}$$

$$\frac{dQ_{(tcr)}}{dt} = \left(\frac{dQ_{(tim)}}{dt}\right)_{(in)} \tag{5}$$

Derivation Summary 34-7. Functional diagram and performance equations for a thermal integrator. (Page 1 of 2)

$$\frac{k_{(tcr)}A_{(tcr)}}{l_{(tcr)}}\left[T_{(tr)} - T_{(tim)}\right] = V_{(tim)}(den)_{(tim)}(sh)_{(tim)}\frac{dT_{(tim)}}{dt} \tag{6}$$

Rearranging terms in Eq. (6) and defining $(CT)_{(tis)}$ as the temperature-integrating-system characteristic time gives

$$(CT)_{(tis)}\frac{dT_{(tim)}}{dt} + T_{(tim)} = T_{(tr)} \tag{7}$$

where

$$(CT)_{(tis)} = \frac{V_{(tim)}(den)_{(tim)}(sh)_{(tim)}l_{(tcr)}}{k_{(tcr)}A_{(tcr)}} \tag{8}$$

(ti) Thermal integrator

If attention is restricted to situations for which the performance characteristics of the temperature receiver (tr) and the indicating system (is) make $T_{(tr)} = T_{(in)}$ and $(Ind) = S_{(is)[T;(Ind)]}T_{(tim)}$ then Eq. (7) becomes

$$(CT)_{(ti)}\frac{d(Ind)}{dt} + (Ind) = S_{(is)[T;(Ind)]}T_{(in)} \tag{9}$$

where

$(CT)_{(ti)}$ = thermal integrator characteristic time = $(CT)_{(tis)}$

Equation (9) is the performance equation for the thermal integrator. This performance equation has the form of the (0;0,1) differential equation. Within the operating range for which

$$(CT)_{(ti)}\frac{d(Ind)}{dt} >> (Ind) \tag{10}$$

Eq. (9) may be integrated to give

$$(Ind)_2 - (Ind)_1 = \int_{(Ind)_1}^{(Ind)_2} d(Ind) = \frac{S_{(is)[T;(Ind)]}}{(CT)_{(ti)}}\int_{t_1}^{t_2} T_{(in)}\,dt \tag{11}$$

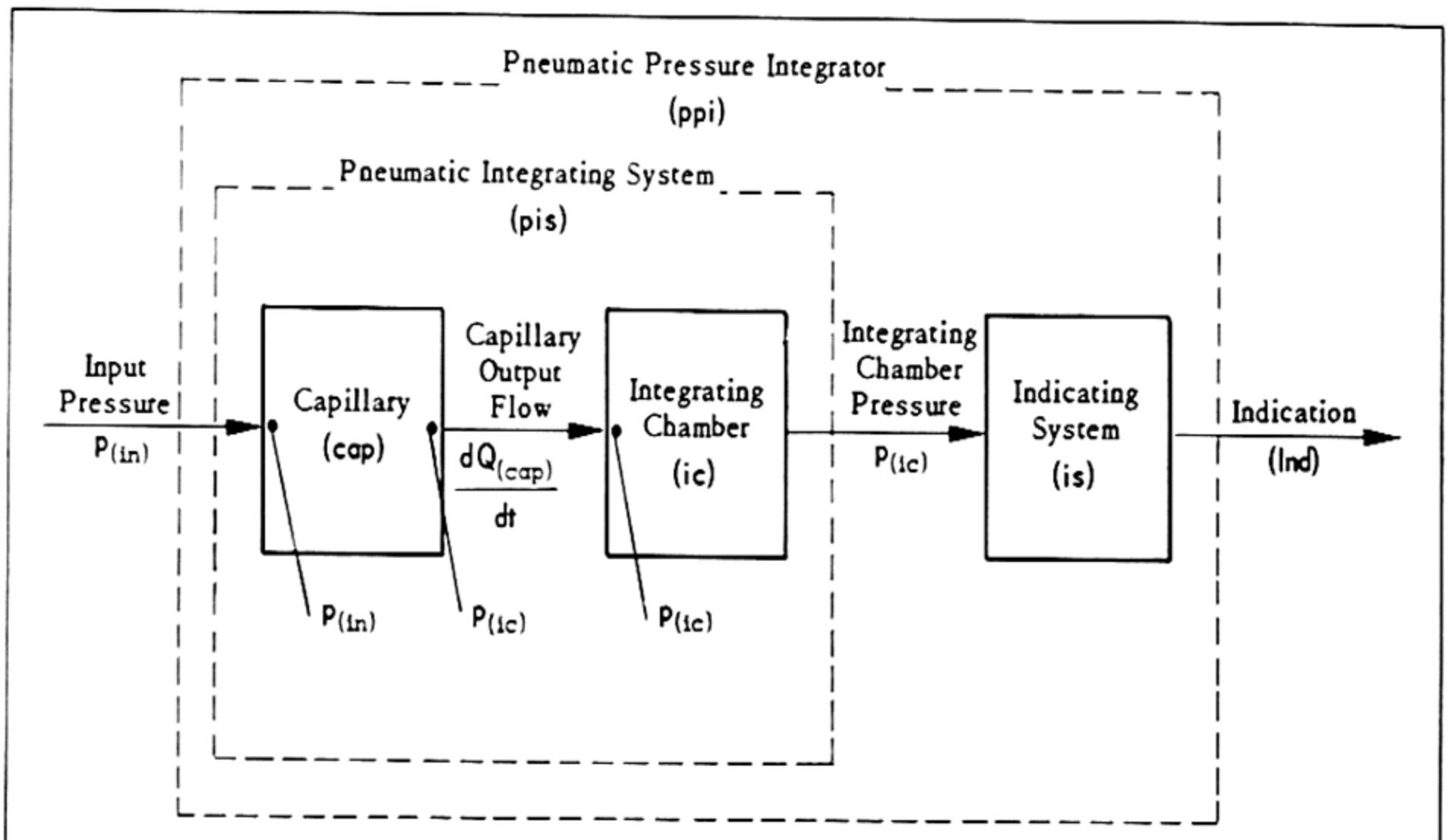
b) Performance equations for subsystems and components of the thermal integrator

Derivation Summary 34-7. Functional diagram and performance equations for a thermal integrator. (Page 2 of 2)

pressure integrator performance equation, which depends on the equality of mass flow through the capillary and the rate of change of mass inside the integrating chamber. Attention is restricted to the range of Reynolds number for which the average fluid velocity in the capillary is proportional to the pressure drop across the capillary. The fluid is assumed to be a perfect gas of known molecular weight. The pneumatic pressure integrator performance equation is formed by combining the mass balance equation with the perfect gas law and the pressure-indication sensitivity of a pressure-gage indicating system. The resulting performance equation, which has the (0;0,1) equation form, reduces to the (0;1) form of the ideal integrator over the operating range for which the indication term is negligible in comparison with the rate of change of indication term.

RESISTANCE-CAPACITANCE ELECTRICAL INTEGRATOR

34.45. Electrical integrators using the resistive element – storage element combination may be made in various forms. The principles involved are identical with those applied in liquid-flow integrators, thermal integrators, and pneumatic



a) Functional diagram

(cap) Capillary

Equation (34) of Information Summary 30-6 shows that for a Reynolds number range of 0 to 2100,

$$v_{(av)(cap)} = \frac{1}{16} \frac{(dia)_{(cap)}}{\mu_{(f)(cap)} l_{(cap)}} (p_{(in)} - p_{(ic)}) \tag{1}$$

where

$v_{(av)(cap)}$ = average fluid velocity in capillary

$(dia)_{(cap)}$ = capillary diameter (effective)

$l_{(cap)}$ = capillary length (effective)

$\mu_{(f)(cap)}$ = fluid viscosity (effective) in capillary

$$\frac{dQ_{(cap)}}{dt} = (den)_{(f)(cap)} v_{(av)(cap)} \tag{2}$$

where

$(den)_{(f)(cap)}$ = fluid density (effective) in capillary

Therefore,

$$\frac{dQ_{(cap)}}{dt} = \frac{1}{16} \frac{(den)_{(f)(cap)}(dia)_{(cap)}}{\mu_{(f)(cap)} l_{(cap)}} (p_{(in)} - p_{(ic)}) \tag{3}$$

(ic) Integrating chamber

$$m_{(ic)} = v_{(ic)}(den)_{(f)(ic)} \tag{4}$$

= mass of fluid inside integrating chamber

where

$v_{(ic)}$ = volume of integrating chamber

$(den)_{(f)(ic)}$ = density of fluid in integrating chamber

When the fluid is a perfect gas, the perfect gas law shows that

$$(den)_{(f)(ic)} = \frac{P_{(ic)}}{T_{(ic)}} \frac{(MW)_f}{R} \tag{5}$$

Derivation Summary 34-8. Functional diagram and performance equations for a pneumatic pressure integrator. (Page 1 of 2)

$T_{(1c)}$ = temperature (effective) of fluid inside integrating chamber

$(MW)_f$ = molecular weight of fluid

R = gas constant

When $v_{(1c)}$ = constant, $T_{(1c)}$ = constant (effective), and $(MW)_f$ = constant, then

$$\frac{dm_{(1c)}}{dt} = \frac{v_{(1c)}(MW)_f}{R}\frac{1}{T_{(1c)}}\frac{dp_{(1c)}}{dt} \tag{6}$$

(pis) Pneumatic integrating system

$$\begin{pmatrix}\text{Mass flow}\\ \text{through capillary}\end{pmatrix} = \begin{pmatrix}\text{Rate of increase of mass}\\ \text{inside integrating chamber}\end{pmatrix}$$

$$\frac{1}{16}\frac{(den)_{(f)(cap)}(dia)_{(cap)}}{\mu_{(f)(cap)}l_{(cap)}}(p_{(1n)} - p_{(1c)}) = \frac{v_{(1c)}(MW)_f}{RT_{(1c)}}\frac{dp_{(1c)}}{dt} \tag{7}$$

In terms of capillary temperature and average capillary pressure, $(den)_{(f)(cap)}$ can be expressed as

$$(den)_{(f)(cap)} = \frac{(p_{(1n)} + p_{(1c)})}{2}\frac{1}{T_{(cap)}}\frac{(MW)_f}{R} \tag{8}$$

Assume that the construction used causes $T_{(cap)}$ to be effectively identical with $T_{(1c)}$. Under this condition, the proper substitutions and rearrangement of terms in Eq. (7) gives

$$(CT)_{(pis)}\frac{dp_{(1c)}}{dt} + p_{(1c)} = p_{(1n)} \tag{9}$$

where

$$(CT)_{(pis)} = \frac{32\,\mu_{(f)(cap)}l_{(cap)}v_{(1c)}}{(p_{(1n)} + p_{(1c)})(dia)_{(cap)}} = \text{characteristic time of pneumatic integrating system} \tag{10}$$

(is) Indicating system

$$(Ind) = S_{(1s)[p;(Ind)]}p_{(1c)} \tag{11}$$

$$S_{(1s)[p;(Ind)]} = \text{constant} \tag{12}$$

(ppi) Pneumatic pressure integrator

Using Eq. (11), Eq. (9) can be written

$$(CT)_{(ppi)}\frac{d(Ind)}{dt} + (Ind) = S_{(ppi)[p;(Ind)]}p_{(1n)} \tag{13}$$

where

$$S_{(ppi)[p;(Ind)]} = S_{(1s)[p;(Ind)]} = \text{pressure-indication sensitivity of pneumatic pressure integrator} \tag{14}$$

$$(CT)_{(ppi)} = (CT)_{(pis)} = \text{pneumatic pressure integrator characteristic time} \tag{15}$$

Equation (13) is the performance equation for the pneumatic pressure integrator. It has the form of the (0;0,1) differential equation.

Within the operating range for which

$$(CT)_{(ppi)}\frac{d(Ind)}{dt} >> (Ind) \tag{16}$$

Eq. (13) may be integrated to give

$$(Ind)_2 - (Ind)_1 = \int_{(Ind)_1}^{(Ind)_2} d(Ind) = \frac{S_{(ppi)[p;(Ind)]}}{(CT)_{(ppi)}}\int_{t_1}^{t_2} p_{(1n)}\,dt \tag{17}$$

b) Performance equations for components and subsystems of the pneumatic pressure integrator

Derivation Summary 34-8. Functional diagram and performance equations for a pneumatic pressure integrator. (Page 2 of 2)

pressure integrators. The capillaries and heat-conducting rod are replaced by electrical resistance, and electrostatic capacity provides the storage function for electrical charge, which is the working fluid.

34.46. Figure 34-8a is a pictorial diagram for a resistance-capacitance electrical integrator. Figure 34-8b gives the corresponding electrical circuit diagram. Section a of Derivation Summary 34-9 is a functional diagram for the integrator of Fig. 34-8. Section b of the summary gives a development of the performance equation for the resistance-capacitance electrical integrator. The procedure used is based on straightforward applications of the voltage and current equations of conventional electrical circuit analysis.*

34.47. Equation (1) of Derivation Summary 34-9 is an expression for the potential drop across the resistor of Fig. 34-8 in terms of current and of voltage differences from the reference voltage. Equation (2) shows that the output voltage is identical with the voltage across the condenser, which is equal to the product of the reciprocal of the capacitance and the time integral of the current into the condenser. Equations (3), (4) and (5) are formed by combining Eqs. (1) and (2) and differentiating the resulting expression with respect to time. Equations (6) and (7) are based on a solution of Eq. (4) for current and a differentiation with respect to time. Equations (8) and (9) give the performance equation for the resistance-capacitance eletrical integrator. The performance equation has the (0;0,1) differential equation form. This equation is identical in form with the performance equations for the other resistive element – storage element integrators.

34.48. When the product of the characteristic time and the rate of change of the output-reference voltage difference is so large that the output-reference voltage difference itself is negligible by comparison, the electrical integrator performance equation reduces to the (0;1) form of the ideal integrator. It follows that, for any given input conditions, the operating range depends on the characteristic time, which is equal to the resistance-capacitance product, RC, for the electrical integrator of Fig. 34-8.

RESISTANCE – AMPLIFIER – FEEDBACK-CAPACITANCE INTEGRATOR

34.49. Deviations of the resistance-capacitance electrical integrator from perfect performance are due to increases in magnitude of the zero-order output-reference voltage-difference term on the left-hand side of the performance equation given by Eq. (9), Derivation Summary 34-9, as compared with the corresponding voltage-difference rate term. Physically, this effect corresponds to the building up of the output voltage to a level where it is no longer negligible in comparison with the voltage drop across the resistor. This situation may be improved by providing means for effectively isolating the resistor of Fig. 34-8 from voltage

* Refer to Information Summary 30-3.

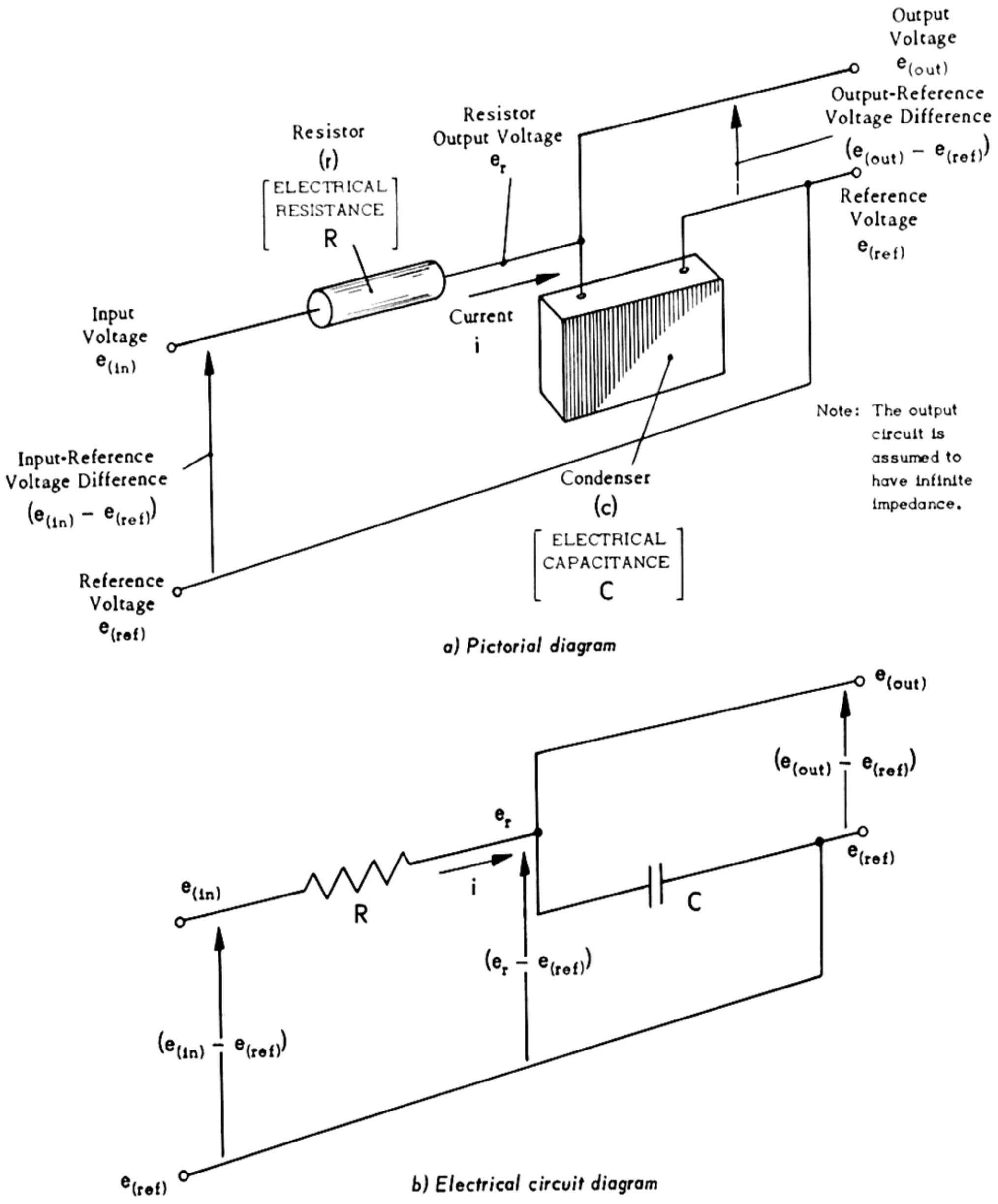
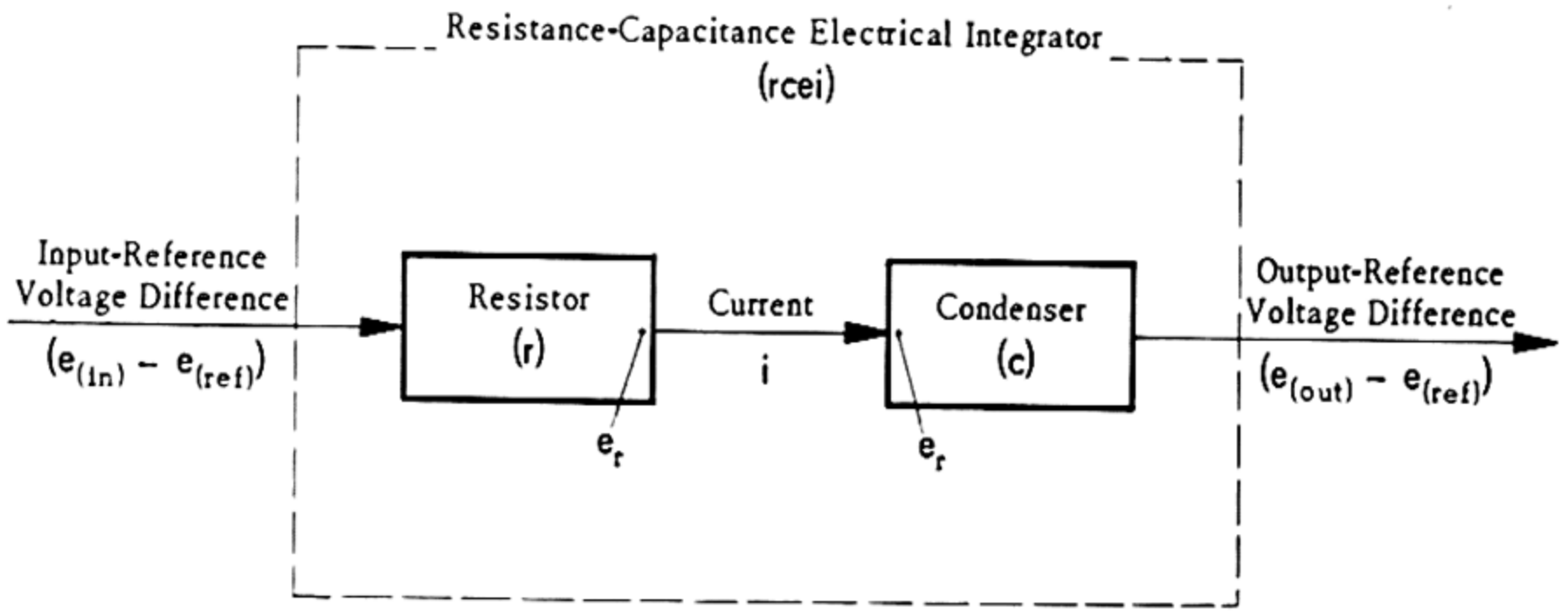


Fig. 34-8. Illustrative pictorial and circuit diagrams for a resistance-capacitance electrical integrator.

changes across the condenser. When this isolation is complete, so that the voltage e_r is constant for a constant input voltage, the resistance is an ideal device for transforming the input voltage into a current proportional to the voltage. Integration occurs when this current is made to flow into a condenser. The voltage across the condenser is then proportional to the time integral of the current.

34.50. The isolation of the resistance voltage drop from the voltage drop across the condenser may be achieved by connecting the condenser as a feedback element between the input and output terminals of an amplifier as shown in Fig. 34-9.



a) Functional diagram

(r) Resistor

$$(e_{(in)} - e_{(ref)}) - (e_r - e_{(ref)}) = iR \tag{1}$$

(c) Condenser

$$(e_r - e_{(ref)}) = (e_{(out)} - e_{(ref)}) = \frac{1}{C}\int i\,dt \tag{2}$$

(rcei) Resistance-capacitance electrical integrator

$$iR + \frac{1}{C}\int i\,dt = (e_{(in)} - e_{(ref)}) \tag{3}$$

or

$$iR + (e_{(out)} - e_{(ref)}) = (e_{(in)} - e_{(ref)}) \tag{4}$$

Differentiating Eq. (3) gives

$$R\frac{di}{dt} + \frac{i}{C} = \frac{d(e_{(in)} - e_{(ref)})}{dt} \tag{5}$$

Solving Eq. (4) for i yields

$$i = \frac{(e_{(in)} - e_{(ref)}) - (e_{(out)} - e_{(ref)})}{R} \tag{6}$$

Differentiating Eq. (6) gives

$$\frac{di}{dt} = \frac{(\dot{e}_{(in)} - \dot{e}_{(ref)}) - (\dot{e}_{(out)} - \dot{e}_{(ref)})}{R} \tag{7}$$

Substitution of the expressions of Eqs. (6) and (7) in Eq. (5) shows that

$$(\dot{e}_{(in)} - \dot{e}_{(ref)}) - (\dot{e}_{(out)} - \dot{e}_{(ref)}) + \frac{(e_{(in)} - e_{(ref)}) - (e_{(out)} - e_{(ref)})}{RC} = (\dot{e}_{(in)} - \dot{e}_{(ref)}) \tag{8}$$

or, simplifying Eq. (8),

$$(CT)_{(rcei)}(\dot{e}_{(out)} - \dot{e}_{(ref)}) + (e_{(out)} - e_{(ref)}) = (e_{(in)} - e_{(ref)}) \tag{9}$$

where

$$(CT)_{(rcei)} = RC = \text{characteristic time of the resistance-capacitance electrical integrator} \tag{10}$$

Equation (9) is the performance equation for the resistance-capacitance electrical integrator. This equation has the form of the (0;0,1) differential equation.

Within the operating range for which

$$(CT)_{(rcei)}\frac{d(e_{(out)} - e_{(ref)})}{dt} >> (e_{(out)} - e_{(ref)})$$

Derivation Summary 34-9. Functional diagram and performance equation for a resistance-capacitance electrical integrator. (Page 1 of 2)

Eq. (9) may be integrated to give

$$(e_{(out)} - e_{(ref)})_2 - (e_{(out)} - e_{(ref)})_1 = \int_{(e_{(out)}-e_{(ref)})_1}^{(e_{(out)}-e_{(ref)})_2} d(e_{(out)} - e_{(ref)})$$

$$= \frac{1}{(CT)_{(rcel)}} \int_{t_1}^{t_2} (e_{(in)} - e_{(ref)})\, dt \qquad (11)$$

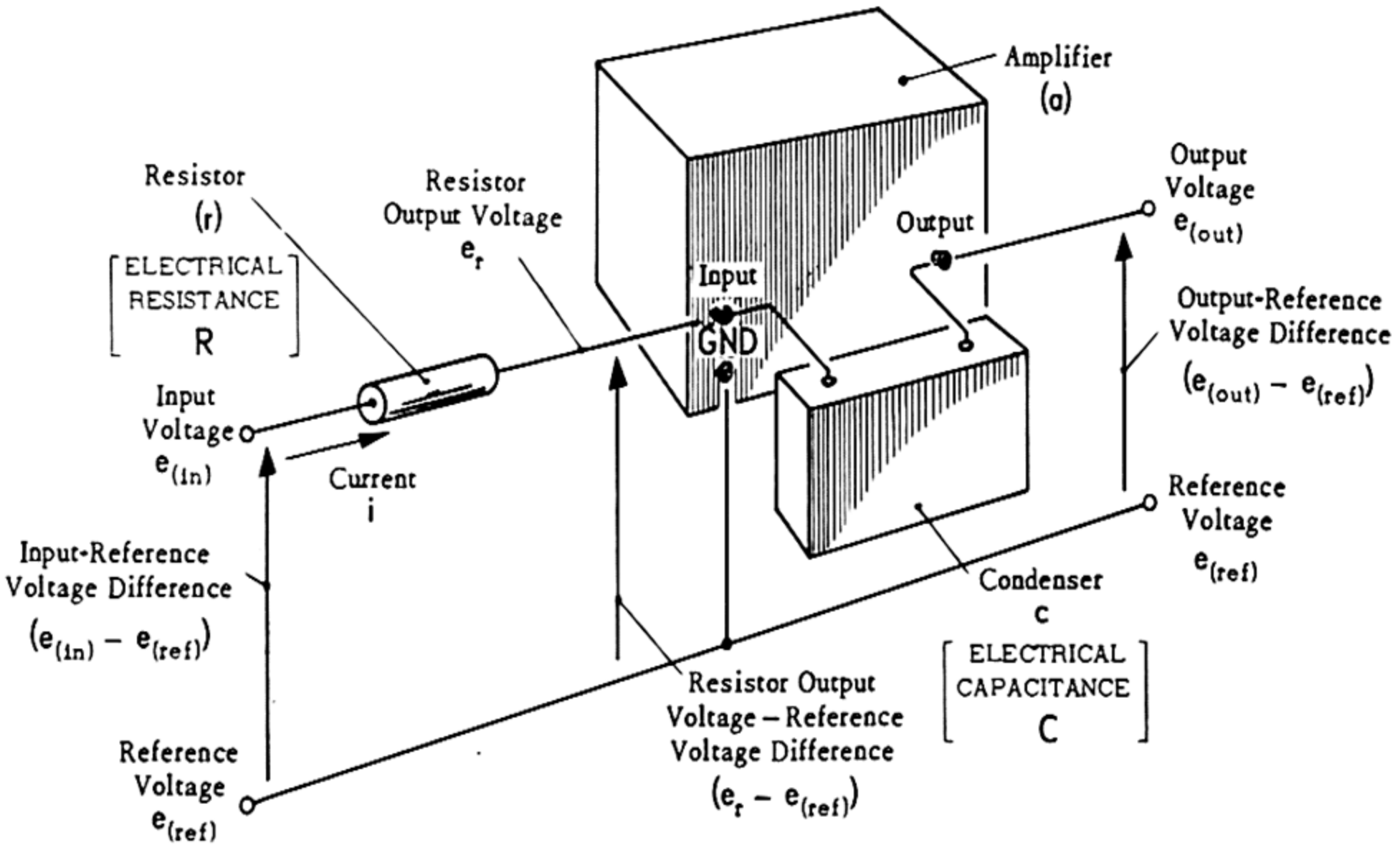
b) Performance equations for the resistance-capacitance electrical integrator

Derivation Summary 34-9. Functional diagram and performance equation for a resistance-capacitance electrical integrator. (Page 2 of 2)

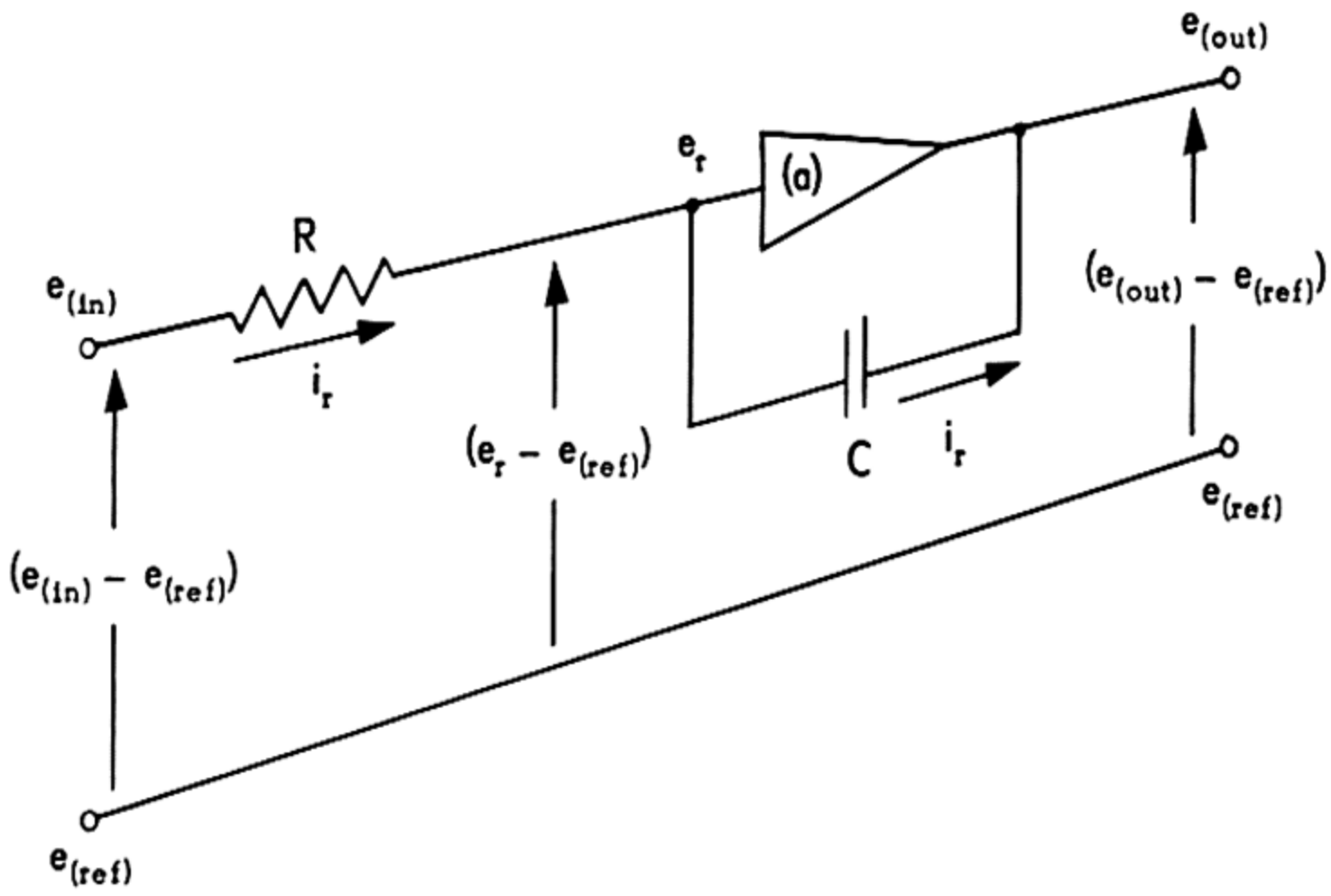
In order to be effective, the amplifier must draw no more than a negligibly small input current, must have high gain (that is, its voltage input – voltage output sensitivity must be high), and must invert, in the sense that an increase of input voltage causes a decrease in output voltage. When an amplifier with these characteristics is used, any small increase in the resistor output voltage (symbol e_r in Fig. 34-9) will cause a much larger decrease in amplifier output voltage. This means that a voltage drop is set up across the condenser that forces the condenser current to increase. Because the amplifier draws a negligibly small input current from the resistance, the amplifier input voltage must change until the amplifier output voltage has the proper value to cause the condenser current to be identical with the current through the resistance. When the amplifier has an infinite gain, so that the required amplifier output voltage changes are produced by substantially zero changes of the amplifier input voltage, the amplifier in effect holds the resistor output voltage constant while causing a current equal to the current through the resistance to pass into the condenser. Under these circumstances, the amplifier output voltage is accurately equal to the time integral of the input voltage. In practice, the amplifier gain is never infinite, so that these ideal actions are never realized. A better approximation to the real situation may be worked out in equation form by an electrical circuit analysis similar to the development of Derivation Summary 34-9 except for the introduction of an equation giving the amplifier output voltage in terms of the amplifier input voltage.

34.51. Section a of Derivation Summary 34-10 is a functional diagram for the resistance – amplifier – feedback-capacitance integrator of Fig. 34-9 with all potential levels specified in terms of voltage above a reference level. Section b of Derivation Summary 34-10 gives a development of the performance equation for this integrator. Equations (1) and (2) describe the voltage drops across the resistance and condenser in terms of the current passing through them. Because the amplifier draws a negligibly small input current, the same current passes through both the circuit elements. Equation (3) gives the output-reference voltage difference in terms of the voltage input – voltage output sensitivity magnitude* of

* This sensitivity magnitude is identical with the voltage gain (symbol $G_{(a)|e;e|}$) of the amplifier.



a) Pictorial diagram



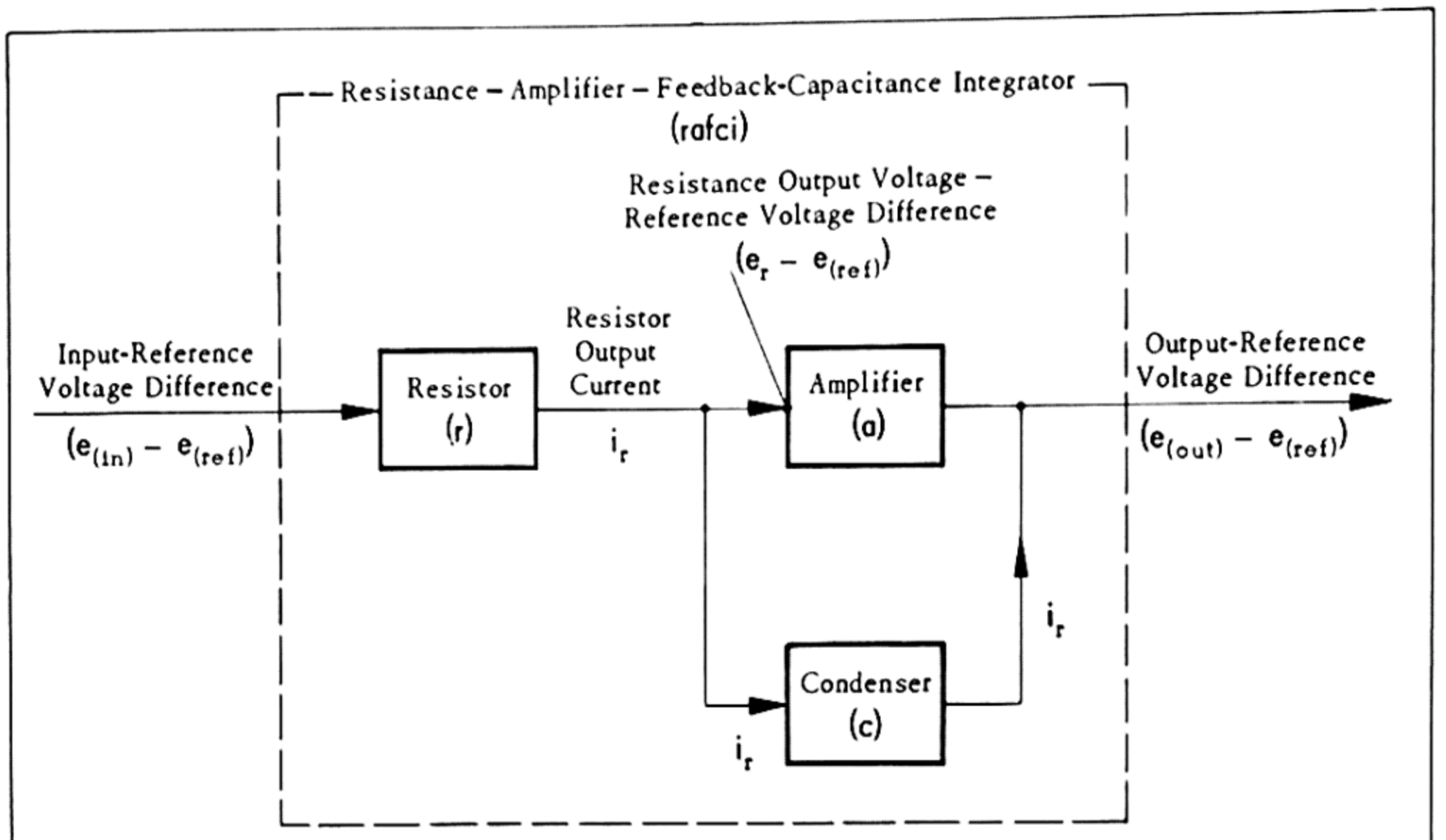
b) Electrical circuit diagram

Fig. 34-9. Illustrative pictorial and electrical circuit diagrams for a resistance – amplifier – feedback-capacitance integrator.

the amplifier. In writing this relationship, the magnitude of the sensitivity is used, with a minus sign shown explicitly, in order to stress the fact that the amplifier inverts in the sense that an increase of input voltage produces a decrease in output voltage.*

34.52. The combination of Eqs. (1) through (4) of Derivation Summary 34-10 to produce the performance equation of Eqs. (10) and (11) is described by Eqs. (5)

• The fact that the sensitivity magnitude is to be used is designated by using the convention of Note 2 of Definition Summary 10-1, Chapter 10. In this convention, straight lines instead of brackets are used to enclose the input-output subscript.



a) Functional diagram

(r) Resistor

$$(e_{(in)} - e_{(ref)}) - (e_r - e_{(ref)}) = i_r R \tag{1}$$

(c) Condenser

When the amplifier input current is negligibly small

$$(e_r - e_{(ref)}) - (e_{(out)} - e_{(ref)}) = \frac{1}{C} \int i_r \, dt \tag{2}$$

(a) Amplifier

$$(e_{(out)} - e_{(ref)}) = -S_{(a)|e;e|}(e_r - e_{(ref)}) \tag{3}$$

Note: $S_{(a)|e;e|}$, the voltage input – voltage output sensitivity magnitude of the amplifier, is identical with $G_{(a)|e;e|}$, the voltage input – voltage output gain magnitude of the amplifier.

From Eq. (3),

$$(e_r - e_{(ref)}) = -\frac{1}{S_{(a)|e;e|}} (e_{(out)} - e_{(ref)}) \tag{4}$$

(rafci) Resistance – amplifier – feedback-capacitance integrator

Substituting the expression of Eq. (4) for $(e_r - e_{(ref)})$ in Eq. (2) gives

$$-\frac{1}{S_{(a)|e;e|}} (e_{(out)} - e_{(ref)}) - (e_{(out)} - e_{(ref)}) = \frac{1}{C} \int i_r \, dt \tag{5}$$

or

$$(e_{(out)} - e_{(ref)}) \frac{S_{(a)|e;e|} + 1}{S_{(a)|e;e|}} = -\frac{1}{C} \int i_r \, dt \tag{6}$$

Differentiating Eq. (6) with respect to time shows that

$$\frac{S_{(a)|e;e|} + 1}{S_{(a)|e;e|}} (\dot{e}_{(out)} - \dot{e}_{(ref)}) = -\frac{i_r}{C} \tag{7}$$

Derivation Summary 34-10. Functional diagram and performance equation for a resistance – amplifier – feedback-capacitance integrator. (Page 1 of 2)

Substitution of the expression of Eq. (4) in Eq. (1) shows that

$$(e_{(in)} - e_{(ref)}) + \frac{1}{S_{(a)|e;e|}}(e_{(out)} - e_{(ref)}) = i_r R \tag{8}$$

Solving Eq. (8) for i_r gives

$$i_r = \frac{(e_{(in)} - e_{(ref)})}{R} + \frac{1}{RS_{(a)|e;e|}}(e_{(out)} - e_{(ref)}) \tag{9}$$

Substituting the expression of Eq. (9) for i_r in Eq. (7) and rearranging terms shows that

$$(S_{(a)|e;e|} + 1)\,RC\,(\dot{e}_{(out)} - \dot{e}_{(ref)}) + (e_{(out)} - e_{(ref)}) = -S_{(a)|e;e|}(e_{(in)} - e_{(ref)}) \tag{10}$$

or

$$(CT)_{(rafc1)}(\dot{e}_{(out)} - \dot{e}_{(ref)}) + (e_{(out)} - e_{(ref)}) = -S_{(a)|e;e|}(e_{(in)} - e_{(ref)}) \tag{11}$$

where

$$\left.\begin{aligned}(CT)_{(rafc1)} &= (S_{(a)|e;e|} + 1)RC \\ &\text{or} \\ &= (G_{(a)|e;e|} + 1)RC\end{aligned}\right\} = \text{characteristic time of resistance – amplifier – feedback-capacitance integrator} \tag{12}$$

Equation (11) is the performance equation for the resistance – amplifier – feedback-capacitance integrator. This equation has the form of the (0;0,1) differential equation.

Within the operating range for which

$$(CT)_{(rafc1)}\frac{d(e_{(out)} - e_{(ref)})}{dt} >> (e_{(out)} - e_{(ref)}) \tag{13}$$

Eq. (11) may be integrated to give

$$(e_{(out)} - e_{(ref)})_2 - (e_{(out)} - e_{(ref)})_1 = \int_{(e_{(out)}-e_{(ref)})_1}^{(e_{(out)}-e_{(ref)})_2} d(e_{(out)} - e_{(ref)})$$

$$= \frac{S_{(a)|e;e|}}{(CT)_{(rafc1)}}\int_{t_1}^{t_2}(e_{(in)} - e_{(ref)})\,dt \tag{14}$$

b) Performance equation for the resistance – amplifier – feedback-capacitance integrator

Derivation Summary 34-10. Functional diagram and performance equation for a resistance – amplifier – feedback-capacitance integrator. (Page 2 of 2)

through (9). The performance equation has the same (0;0,1) differential equation form as the performance equation for the simple resistance-capacitance electrical integrator. The essential difference between the simple RC integrator and the resistance – amplifier – feedback-capacitance integrator is shown by comparison of Eq. (10) of Derivation Summary 34-9 with Eq. (12) of Derivation Summary 34-10. The characteristic time of the feedback-capacitance integrator is larger than the characteristic time of the simple RC integrator by a factor of the amplifier sensitivity plus one. In practice, this sensitivity may be very large, so that from the standpoint of operating range, the feedback-capacitance arrangement offers a considerable advantage over the simple RC-circuit integrator. Equations (13) and (14) show that the resistance – amplifier – feedback-capacitance integrator has ideal performance as long as the voltage-difference term is negligible in comparison with the rate of change of voltage-difference term.

MOTOR – AMPLIFIER – FEEDBACK-TACHOMETER INTEGRATOR

34.53. Integration is provided by any device that has an output whose rate of change is proportional to the input. An obvious way to build a device with this performance characteristic is to use an electric motor designed to have armature speeds accurately proportional to the input voltage. In practice, it is difficult to produce motors with this kind of behavior. On the other hand, instruments are available that produce output signals accurately representing angular velocity inputs. These instruments function as angular velocity signal generators, and are commonly called tachometers. By connecting the input shaft of a tachometer to the armature shaft of a motor, a signal representing the motor speed may be generated. This signal may be used as the feedback input to a signal comparator that also receives the integrator input signal. The output from the comparator is zero if the motor is running at a speed that causes the tachometer output to be equal to the integrator input signal. When the motor is running slower than the speed required to generate a feedback signal that will match the integrator input signal, the comparator generates an angular velocity correction signal. This correction signal becomes an input to the motor with the proper sense to cause an increase in armature speed. When the motor speed is initially higher than that required to produce a tachometer feedback signal that will match the integrator input signal, the angular velocity correction signal causes the motor speed to decrease.

34.54. The interaction between the integrator input signal and the tachometer feedback signal is in effect a continuous balancing process that forces the armature speed to follow slow changes in the integrator input signal with an accuracy that depends on the operating components used to handle signal-level power. As long as the torque generator is able to overcome armature-shaft bearing friction and inertia reaction effects satisfactorily, the proportionality between integrator input and output angular velocity is not affected by nonlinearities or changes in the motor characteristics.

34.55. Figure 34-10 is an illustrative pictorial diagram showing the essential parts of a motor – amplifier – feedback-tachometer integrator. The motor includes a two-phase alternating-current torque generator that has a drag-cup rotor. The rotor shaft carries the disc of a viscous shear damper and the drag-cup rotor of the alternating-current tachometer. This rotor shaft, which acts as a torque summing member, is mechanically connected to deliver the angular output of the torque summing member to the output signal generator drive gear train. The output rotation from this gear train moves the sliding brush of a potentiometer,* which acts as the electrical circuit component of the output signal generator. Excitation voltage is supplied to the ends of the potentiometer winding, which has its

* In Fig. 34-10, the representation is simplified by showing a single-turn potentiometer. In practice, spiral potentiometers designed for many turns are commonly used.

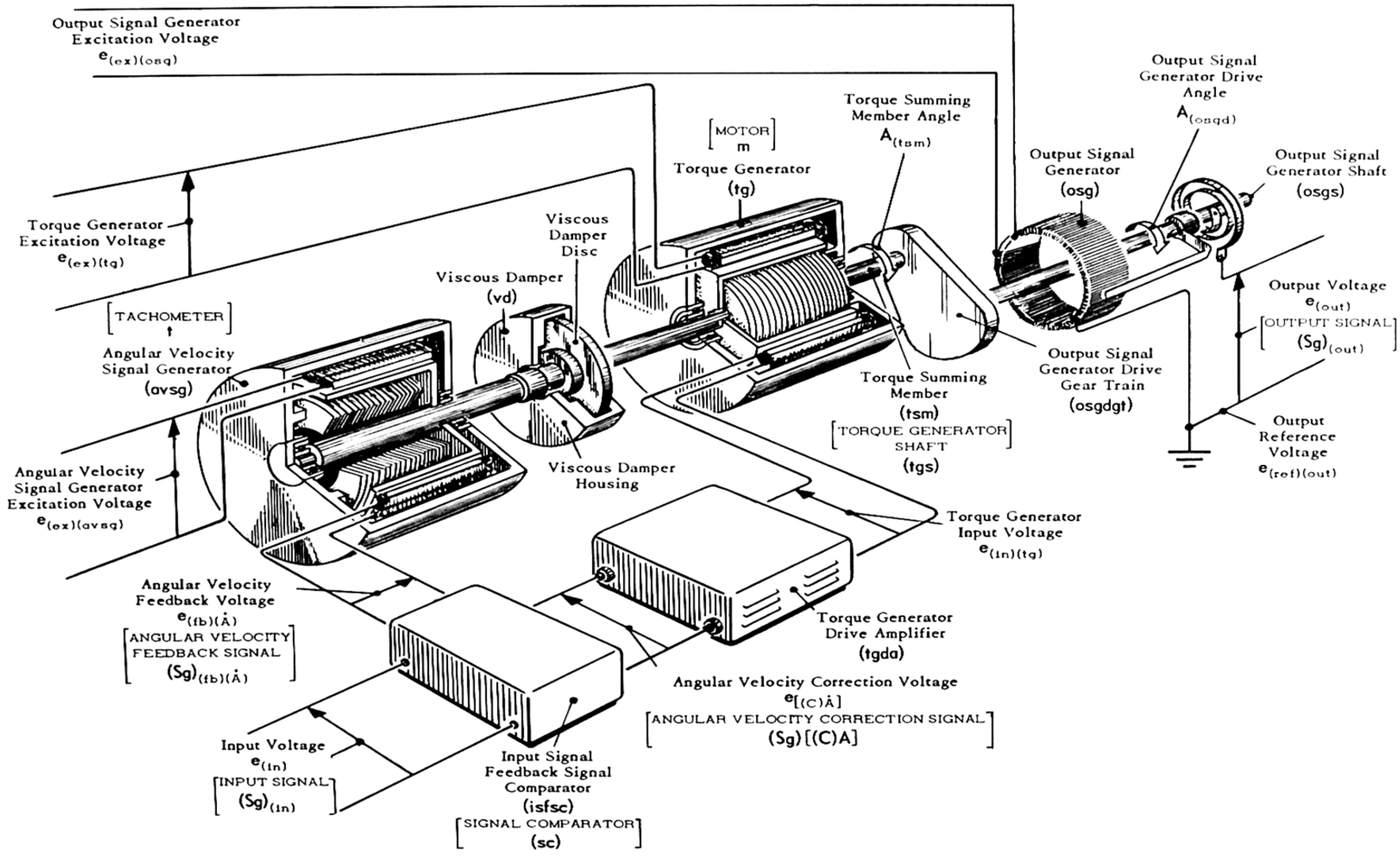


Fig. 34-10. Illustrative pictorial diagram for a motor – amplifier – feedback-tachometer integrator

center grounded to permit positive and negative sensing of the output voltage with respect to a reference voltage.

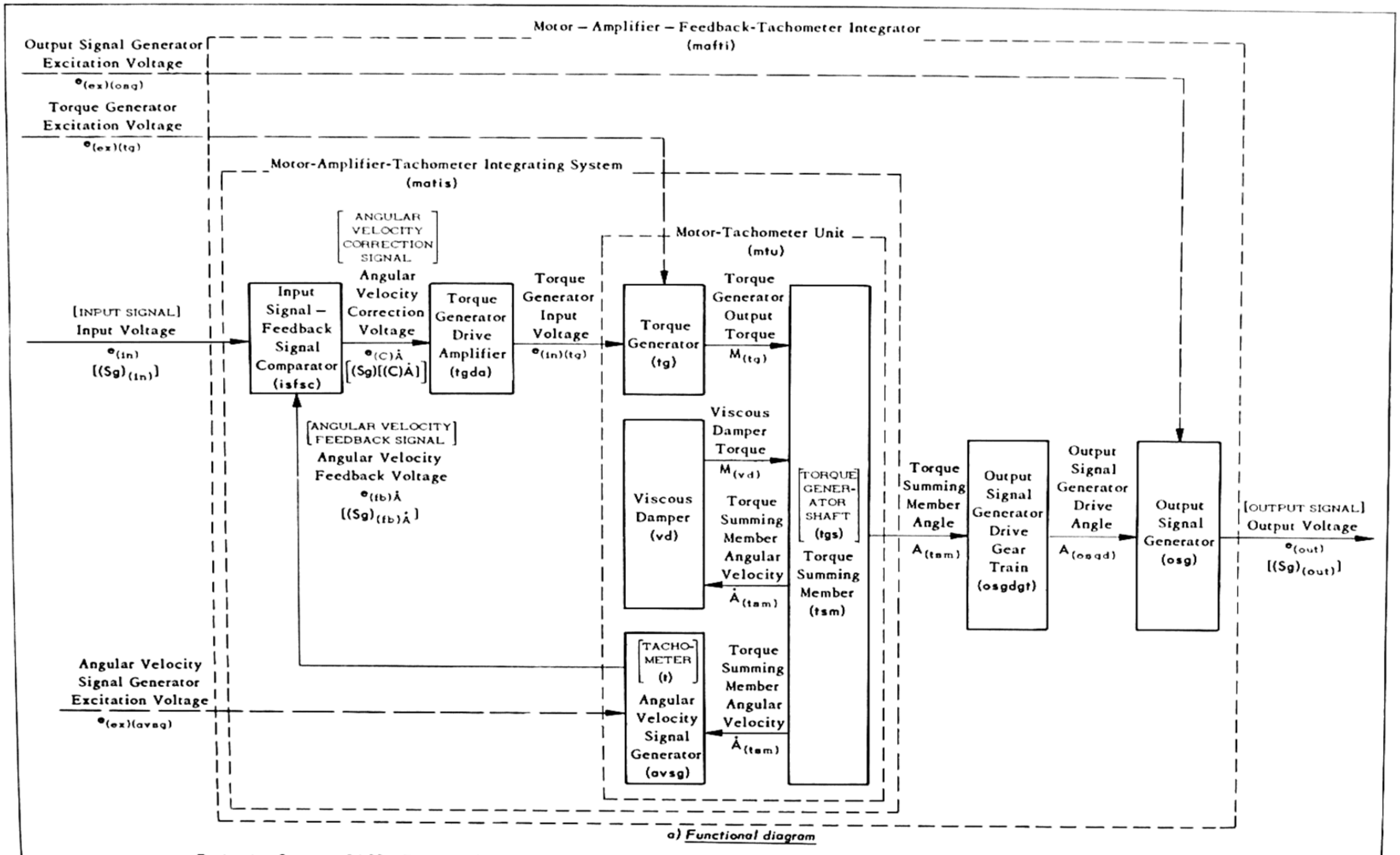
34.56. The torque-generator stator has a two-phase alternating-current winding. One winding is supplied with an excitation voltage of constant magnitude and frequency that acts as one of the modifying inputs for the complete integrator. The other winding receives the input voltage, which is the actuating input for the complete integrating system. The angular velocity signal generator has a two-phase alternating-current winding similar to that of the torque generator. In operation, one winding is supplied with an excitation voltage of constant magnitude and frequency. The other winding produces the angular velocity feedback voltage, which is an accurate representation of the speed of the armature shaft.

34.57. The angular-velocity-signal-generator output is used as the feedback-signal input to the input signal – feedback signal comparator. The input signal for the complete integrator is used as the other input to the signal comparator. The output signal from the comparator is the angular velocity correction voltage. The magnitude of this correction voltage is a function of the magnitude of the change in armature shaft speed required for perfect matching with the commanded speed corresponding to the input signal. The torque generator drive amplifier receives the angular velocity correction voltage and supplies the torque generator actuating input voltage. This voltage is phased so that the torque generator output torque tends to speed up or slow down the armature shaft in the proper way to reduce the angular velocity correction voltage.

34.58. In practice, the signal comparator may be a simple voltage summing circuit or it may include rectifying components that change the alternating-current feedback signal into a direct-current signal with the proper magnitude and polarity for combination with a direct-current input signal. The correction signal may have the form of a direct-current voltage or, if a direct-current signal is actually formed, it may be remodulated in the comparator to give an alternating-current correction signal for the drive amplifier input, with the proper magnitude and relative phase for satisfactory operation of the integrator.

34.59. Section a of Derivation Summary 34-11 is a functional diagram for the motor – amplifier – feedback-tachometer integrator of Fig. 34-10. The names and symbols of the functional diagram are those defined in the figure.

34.60. Section b of Derivation Summary 34-11 gives a development of the performance equation for the integrator of Fig. 34-10. Equation (1) is the defining equation for the angular velocity correction signal as this signal is produced by the input signal – feedback signal comparator. The correction signal is the difference between the integrator input signal multiplied by the input voltage – output voltage direct sensitivity magnitude of the comparator and the angular velocity feedback signal multiplied by the feedback voltage – output voltage feedback sensitivity



a) Functional diagram

Derivation Summary 34-11. Functional diagram and performance equations for a motor – amplifier – feedback-tachometer integrator. (Page 1 of 4)

(isfsc) Input signal – feedback signal comparator

$$(Sg)[(C)\dot{A}] = e_{(C)\dot{A}} = S_{(isfsc)|e;e|(dir)} e_{(in)} - S_{(isfsc)|e;e|(fb)} e_{(fb)\dot{A}} \quad (1)$$

where

$S_{(isfsc)|e;e|(dir)}$ = input voltage – output voltage direct sensitivity magnitude of signal comparator

$S_{(isfsc)|e;e|(fb)}$ = feedback voltage – output voltage feedback sensitivity magnitude of signal comparator

(tgda) Torque generator drive amplifier

$$e_{(in)(tq)} = S_{(tgda)|e;e|} e_{(C)\dot{A}} \quad (2)$$

(vd) Viscous damper

$$M_{(vd)} = -S_{(vd)|\dot{A};M|} \dot{A}_{(tsm)} \quad (3)$$

(tg) Torque generator

$$M_{(tg)} = M_{(tg)(in)} + M_{(tg)(dmp)} \quad (4)$$

$$M_{(tg)} = S_{(tg)[e;e;M]} e_{(ex)(tg)} e_{(in)(tg)} - S_{(tg)|\dot{A};M|} \dot{A}_{(tsm)} \quad (5)$$

$$= S_{(tg)[e;M]} e_{(in)(tg)} - S_{(tg)|\dot{A};M|} \dot{A}_{(tsm)} \quad (6)$$

where $e_{(ex)(tg)} = ____$

$$S_{(tg)[e;M]} = S_{(tg)[e;e;M]} e_{(ex)(tg)} \quad (7)$$

(mtu) Motor-tachometer unit

The torque summation equation for the torque summing member is

$$\begin{pmatrix}\text{Inertia}\\ \text{Reaction}\\ \text{Torque}\end{pmatrix} + \begin{pmatrix}\text{Torque Generator}\\ \text{Effective Internal}\\ \text{Damping Torque}\end{pmatrix} + \begin{pmatrix}\text{Viscous}\\ \text{Damper}\\ \text{Torque}\end{pmatrix} + \begin{pmatrix}\text{Uncertainty}\\ \text{Torque}\end{pmatrix} + \begin{pmatrix}\text{Torque}\\ \text{Generator}\\ \text{Input Torque}\end{pmatrix} = 0 \quad (8)$$

or

$$M_{(lr)} + M_{(tg)(dmp)} + M_{(vd)} + (U)M_{(tsm)} + M_{(tg)(in)} = 0 \quad (9)$$

$$-I_{(tsm)} \ddot{A}_{(tsm)} - S_{(tg)|\dot{A};M|} \dot{A}_{(tsm)} - S_{(vd)|\dot{A};M|} \dot{A}_{(tsm)} \pm (U)M_{(tsm)} + S_{(tg)[e;M]} e_{(in)(tg)} = 0 \quad (10)$$

$$e_{(ex)(tg)} = ____$$

Changing signs and rearranging terms gives

$$I_{(tsm)} \ddot{A}_{(tsm)} + (S_{(tg)|\dot{A};M|} + S_{(vd)|\dot{A};M|}) \dot{A}_{(tsm)} = S_{(tg)[e;M]} e_{(in)(tg)} \pm (U)M_{(tsm)} \quad (11)$$

$$e_{(ex)(tg)} = ____$$

(avsg) Angular velocity signal generator

$$e_{(fb)\dot{A}} = S_{(avsg)[\dot{A};e;e]} e_{(ex)(avsg)} \dot{A}_{(tsm)} \quad (12)$$

$$= S_{(avsg)[\dot{A};e]} \dot{A}_{(tsm)} \quad (13)$$

where $e_{(ex)(avsg)} = ____$

$$S_{(avsg)[\dot{A};e]} = S_{(avsg)[\dot{A};e;e]} e_{(ex)(avsg)} \quad (14)$$

(matis) Motor-amplifier-tachometer integrating system

From Eqs. (1), (2) and (13),

$$e_{(in)(tg)} = S_{(tgda)|e;e|} S_{(isfsc)|e;e|(dir)} e_{(in)} - S_{(tgda)|e;e|} S_{(isfsc)|e;e|(fb)} S_{(avsg)[\dot{A};e]} \dot{A}_{(tsm)} \quad (15)$$

$$e_{(ex)(avsg)} = ____$$

Derivation Summary 34-11. Functional diagram and performance equations for a motor – amplifier – feedback-tachometer integrator. (Page 2 of 4)

Combining Eq. (15) with Eq. (11) gives

$$I_{(tsm)}\ddot{A}_{(tsm)} + (S_{(tg)|\dot{A};M|} + S_{(vd)|\dot{A};M|})\dot{A}_{(tsm)}$$
$$= S_{(tg)[e;M]}S_{(tgda)|e;e|}S_{(isfsc)|e;e|(dir)}e_{(in)} - S_{(tg)[e;M]}S_{(tgda)|e;e|}S_{(isfsc)|e;e|(fb)}S_{(avsg)[\dot{A};e]}\dot{A}_{(tsm)} \pm (U)M_{(tsm)} \quad (16)$$

$$e_{(ex)(avsg)} = ____ \quad ; \quad e_{(ex)(tg)} = ____$$

Defining $(CT)_{(matis)}$, $S_{(matis)[e;\dot{A}]}$ and $S_{(matis)[M;\dot{A}]}$, and rearranging the terms of Eq. (16) gives

$$(CT)_{(matis)}\ddot{A}_{(tsm)} + \dot{A}_{(tsm)} = S_{(matis)[e;\dot{A}]}e_{(in)} \pm S_{(matis)[M;\dot{A}]}(U)M_{(tsm)} \quad (17)$$

$$e_{(ex)(avsg)} = ____ \quad ; \quad e_{(ex)(tg)} = ____$$

where

$$(CT)_{(matis)} = \frac{I_{(tsm)}}{S_{(tg)|\dot{A};M|} + S_{(vd)|\dot{A};M|} + S_{(isfsc)|e;e|(fb)}S_{(tgda)|e;e|}S_{(tg)[e;M]}S_{(avsg)[\dot{A};e]}} \quad (18)$$

= motor-amplifier-tachometer integrating system characteristic time

$$S_{(matis)[e;\dot{A}]} = \frac{S_{(isfsc)|e;e|(dir)}S_{(tgda)|e;e|}S_{(tg)[e;M]}}{S_{(tg)|\dot{A};M|} + S_{(vd)|\dot{A};M|} + S_{(isfsc)|e;e|(fb)}S_{(tgda)|e;e|}S_{(tg)[e;M]}S_{(avsg)[\dot{A};e]}} \quad (19)$$

= motor-amplifier-tachometer integrating system voltage input – angular velocity output sensitivity

$$S_{(matis)[M;\dot{A}]} = \frac{1}{S_{(tg)|\dot{A};M|} + S_{(vd)|\dot{A};M|} + S_{(isfsc)|e;e|(fb)}S_{(tgda)|e;e|}S_{(tg)[e;M]}S_{(avsg)[\dot{A};e]}} \quad (20)$$

= motor-amplifier-tachometer integrating system torque input – angular velocity output sensitivity

(osgdgt) Output signal generator drive gear train

$$A_{(osgd)} = S_{(osgdgt)[A;A]}A_{(tsm)} \quad (21)$$

(osg) Output signal generator

$$(Sg)_{(out)} = e_{(out)} = S_{(osg)[A;e;e]}e_{(ex)(osg)}A_{(osgd)} \quad (22)$$

$$= S_{(osg)[A;e]}A_{(osgd)} \quad (23)$$

where $e_{(ex)(osg)} = ____$

$$S_{(osg)[A;e]} = S_{(osg)[A;e;e]}e_{(ex)(osg)} \quad (24)$$

(mafti) Motor – amplifier – feedback-tachometer integrator

Introducing the relationships of Eqs. (21) and (23) in Eq. (17) gives the performance equation for the motor – amplifier – feedback-tachometer integrator as

$$(CT)_{(mafti)}\ddot{e}_{(out)} + \dot{e}_{(out)} = S_{(mafti)[e;\dot{e}]}e_{(in)} \pm S_{(mafti)[M;\dot{e}]}(U)M_{(tsm)} \quad (25)$$

where $e_{(ex)(tg)} = ____ \quad ; \quad e_{(ex)(avsg)} = ____ \quad ; \quad e_{(ex)(osg)} = ____$

$$(CT)_{(mafti)} = (CT)_{(matis)} \quad (26)$$

= motor – amplifier – feedback-tachometer integrator characteristic time

$$S_{(mafti)[e;\dot{e}]} = S_{(matis)[e;\dot{A}]}S_{(osgdgt)[A;A]}S_{(osg)[A;e]} \quad (27)$$

= motor – amplifier – feedback-tachometer integrator voltage input – voltage rate output sensitivity

Derivation Summary 34-11. Functional diagram and performance equations for a motor – amplifier – feedback-tachometer integrator. (Page 3 of 4)

$$S_{(maftl)[M;\dot{e}]} = S_{(matls)[M;\dot{A}]} S_{(osgdgt)[A;A]} S_{(osg)[A;e]} \tag{28}$$

= motor – amplifier – feedback-tachometer integrator torque input – voltage rate output sensitivity

The performance equation (25) has the (0;1,2) differential equation form.

Within the range of operating conditions for which

$$(CT)_{(maftl)} \frac{d^2 e_{(out)}}{dt^2} << \frac{de_{(out)}}{dt} \tag{29}$$

and when the uncertainty torque, $\pm (U) M_{(tsm)}$, is zero, then

$$e_{(out)2} - e_{(out)1} = \int_{e_{(out)1}}^{e_{(out)2}} de_{(out)} = S_{(maftl)[e;\dot{e}]} \int_{t_1}^{t_2} e_{(in)}\, dt \tag{30}$$

Derivation Summary 34-11. Functional diagram and performance equations for a motor – amplifier – feedback-tachometer integrator. (Page 4 of 4)

magnitude of the signal comparator.* Equation (2) shows that the performance of the torque generator drive amplifier is assumed to be representable by a sensitivity (that is, a simple gain). When the amplifier actually introduces nonlinearities and dynamic effects, the sensitivity must be replaced by the proper performance function.

34.61. Equation (3) of Derivation Summary 34-11 gives for the viscous damper a performance that produces an output torque proportional in magnitude and opposite in sign to the angular velocity of the rotor.** Equations (4) through (7) describe the performance of the torque generator by means of two terms. The first term is the product of the voltage actuating input – voltage modifying input – torque output sensitivity, the excitation voltage, and the input voltage. The second term describes the fact that the torque generator output decreases as the rotor speed increases.*** This effect is usually so small that it may be described with satisfactory accuracy by a constant angular velocity input – torque output sensitivity of the torque generator. In practice, numerical values for this sensitivity are usually taken from experimental data.

34.62. The torque summation equation for the motor-tachometer unit is given by Eqs. (8) through (11) of Derivation Summary 34-11. The terms of this equation include the inertia reaction torque, the torque generator effective internal

---

* In practice, the comparator may perform other operations than a simple multiplication on the input signal. When this is true, the sensitivity concerned is replaced by the proper performance operator or performance function.

** In practice, some viscous damping action will usually be present due to lubricated bearings and other mechanical parts, even though the mechanical system does not include a viscous damper as a separate operating component. Refer to Information Summary 30-6 for a brief summary of the principles of viscous damping action.

*** This falling off of output torque with increasing speed produces a net effect similar to that produced by a viscous damper. For this reason, it may be called inherent torque generator damping. Refer to section b of Information Summary 30-8 for a typical speed-torque characteristic curve.

damping torque, the viscous damper torque, the uncertainty torque, and the torque generator input torque. In this list, all the terms are expressible as simple functions of specific variables except the uncertainty torque, which depends on bearing friction and other effects that are not describable by definitely known equations. It will appear later that the quality of performance obtainable from devices that include mechanical operating components very often depends on uncertainty torque components. In practice, these components are usually determined by experimental methods and represented by plots similar to the performance ratio curves discussed in Chapter 5.

34.63. Equations (12), (13) and (14) of Derivation Summary 34-11 show that the voltage output of the angular velocity signal generator is proportional to the product of the torque summing member angular velocity and an excitation voltage. When the angular velocity signal generator output is subject to dynamic effects because of actions within the generator itself, the sensitivities of Eqs. (12) and (13) must be replaced by proper performance functions.

34.64. Equations (15) through (20) of Derivation Summary 34-11 draw operating component performance equations together into the performance equation for the motor-amplifier-tachometer integrating system with voltage as the input and the angular position of the torque summing member as the output. Except for the uncertainty torque term, the integrating system performance equation (17) has the (0;1,2) differential equation form. As shown by Eq. (18), the characteristic time appearing in the performance equation is the ratio of the effective moment of inertia of the torque summing member to a sum of two sensitivities and a product of sensitivities. The single sensitivity terms represent the effects of the viscous damper action and the inherent damping of the torque generator. The sensitivity product represents the action of the feedback system, the amplifier, and the torque generator in determining the resultant damping that acts on the torque summing member. Equation (19) gives the voltage input - angular velocity output sensitivity of the integrating system. This sensitivity is the ratio of the product of sensitivities of the operating components in the direct branch of the integrator to a sum of three sensitivity terms that are identical with those appearing in the expression for the characteristic time.

34.65. Equations (21) through (24) give the relationships necessary to write the integrator performance equation with voltage as the output quantity. The complete performance equation including uncertainty effects is given as Eq. (25). In order to complete the information required to specify the performance equation, the torque generator excitation, the angular velocity signal generator excitation, and the output signal generator excitation must be given. The performance equation itself has the (0;1,2) differential equation form. Equations (29) and (30) show that the motor – amplifier – feedback-tachometer integrator has the characteristics

of an ideal integrator when the uncertainty torque is zero and the rate of change of output voltage is so large that the characteristic time – voltage-second-derivative product is negligibly small by comparison.

BALL-AND-DISC MECHANICAL DIFFERENTIATOR

34.66. Differentiation may be carried out in terms of kinematic displacements by a modification of the ball-and-disc integrator illustrated in Fig. 34-1. The first part of the required modification is the addition of a mechanical differential and gear train arrangement for comparing the angular velocity of the ball-driven cylinder with the rate of change of the input angle. The second part of the modification is the addition of a rack-and-pinion drive system to receive the differential output angular velocity and automatically change the ball cage position in the proper direction to cause an increase or decrease in the cylinder angular velocity as required to match this angular velocity with the rate of change of the input angle. With the disc driven at a constant angular velocity, the ball cage position is a measure of the time derivative of the input angle.

34.67. Figure 34-11 is an illustrative pictorial diagram showing the essential features* of the ball-and-disc differentiator. The input angle is introduced as a shaft rotation that turns one side of a mechanical differential through a gear train. The other side of the differential is driven by the output cylinder of the ball-and-disc unit.** The differential acts as the input angular velocity – feedback angular velocity comparator and delivers an output that is proportional to the angular velocity correction. In magnitude and direction, this correction is the change in cylinder angular velocity required for an exact match with the rate of change of the input angle. The angular velocity correction acts through the ball cage drive and the ball cage input slide and introduces a rate of change of ball change position that tends to correct the cylinder angular velocity. The cylinder angular velocity is determined by the ball cage position and the disc angular velocity, which is controlled by the disc drive motor angular velocity acting through the disc drive gear train. The drive motor angular velocity is adjustable and is controlled by means of the speed-setting knob. With the disc angular velocity fixed, the cylinder angular velocity depends only on the ball cage position. Readings giving the indicated angular velocity of the input shaft are supplied by the ball cage output slide, indicating system and scale, which, in effect, transform ball cage position into an angular indication.

---

* Only those features that contribute to the basic kinematic relationships are shown. Details of spring loading devices, servo drives and like items (ref. Navy Department (N5)) are omitted, since they do not affect the basic theory of operation, even though they are necessary functional details.

** In Fig. 34-11, the output cylinder is directly connected to the differential. This arrangement is used only to simplify the diagram. A gear train connection may be used if a speed change is desirable.

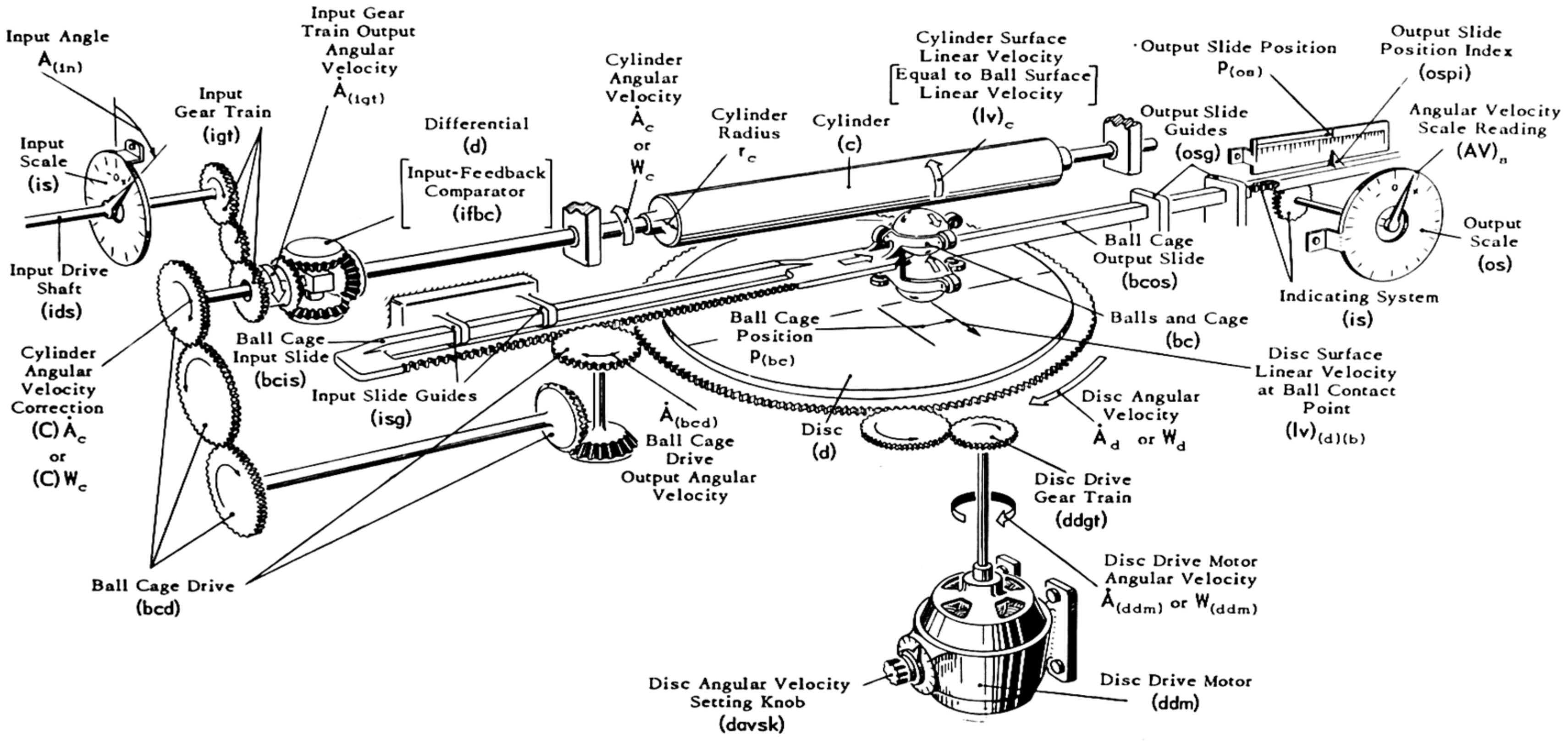


Fig. 34-11. Illustrative pictorial diagram for a ball-and-disc differentiator.

34.68. Figure 34-12 is an illustrative pictorial-functional diagram for the ball-and-disc differentiator of Fig. 34-11. The labels and symbols on the two diagrams are identical.

34.69. Section a of Derivation Summary 34-12 is a functional diagram for the illustrative ball-and-disc differentiator of Figs. 34-11 and 34-12. The subsystems, operating components, names and symbols in the functional diagram are identical with those of Fig. 34-12.

34.70. A development of the ball-and-disc differentiator performance equation, under the assumption of no slippage between surfaces in rolling contact, is given in section b of Derivation Summary 34-12. The procedure applied in this development follows the general pattern used in Derivation Summaries 34-3 through 34-11 for the various integrator types. Equation (2) of Derivation Summary 34-12 gives the output angular velocity of the input gear train in terms of the input angle – output angle sensitivity and the rate of change of the input angle. Equation (3) shows that the cylinder angular velocity correction, which is the output of the differential that acts as the input-feedback comparator, is the difference between the input gear train output angular velocity and the cylinder angular velocity. Equations (4) and (5) relate the rate of change of the ball cage position to the cylinder angular velocity correction. Equations (6) through (10) give cylinder angular velocity in terms of disc angular velocity and ball position. Equations (11) through (16) combine the preceding equations into the performance equation for the ball-and-disc differentiating unit. Equations (17), (18) and (19) relate the angular velocity scale reading to the ball cage position. These expressions are combined with Eq. (14) to give Eq. (20), the performance equation for the ball-and-disc differentiator. This equation has the form of the (1;0,1) differential equation.

34.71. Equations (23) and (24) of Derivation Summary 34-12 show that the ball-and-disc differentiator has the performance of an ideal differentiator for operating ranges within which the product of the characteristic time and the rate of change of the angular velocity reading is negligibly small in comparison with the angular velocity reading itself.

TACHOMETERS AS DIFFERENTIATORS

34.72. Differentiation of the angular position of a mechanical member is a very common function of certain instrument units. Functionally, these units belong to the class of angular velocity signal generators and are generally called tachometers. Many physical principles may be applied in the design of tachometers, which usually operate as indicators or measuring instruments. The procedure for deriving tachometer performance equations follows the pattern established in Chapters 31 and 32 for first- and second-order measuring instruments, respectively. Details of the derivation for any given instrument depend on the physical

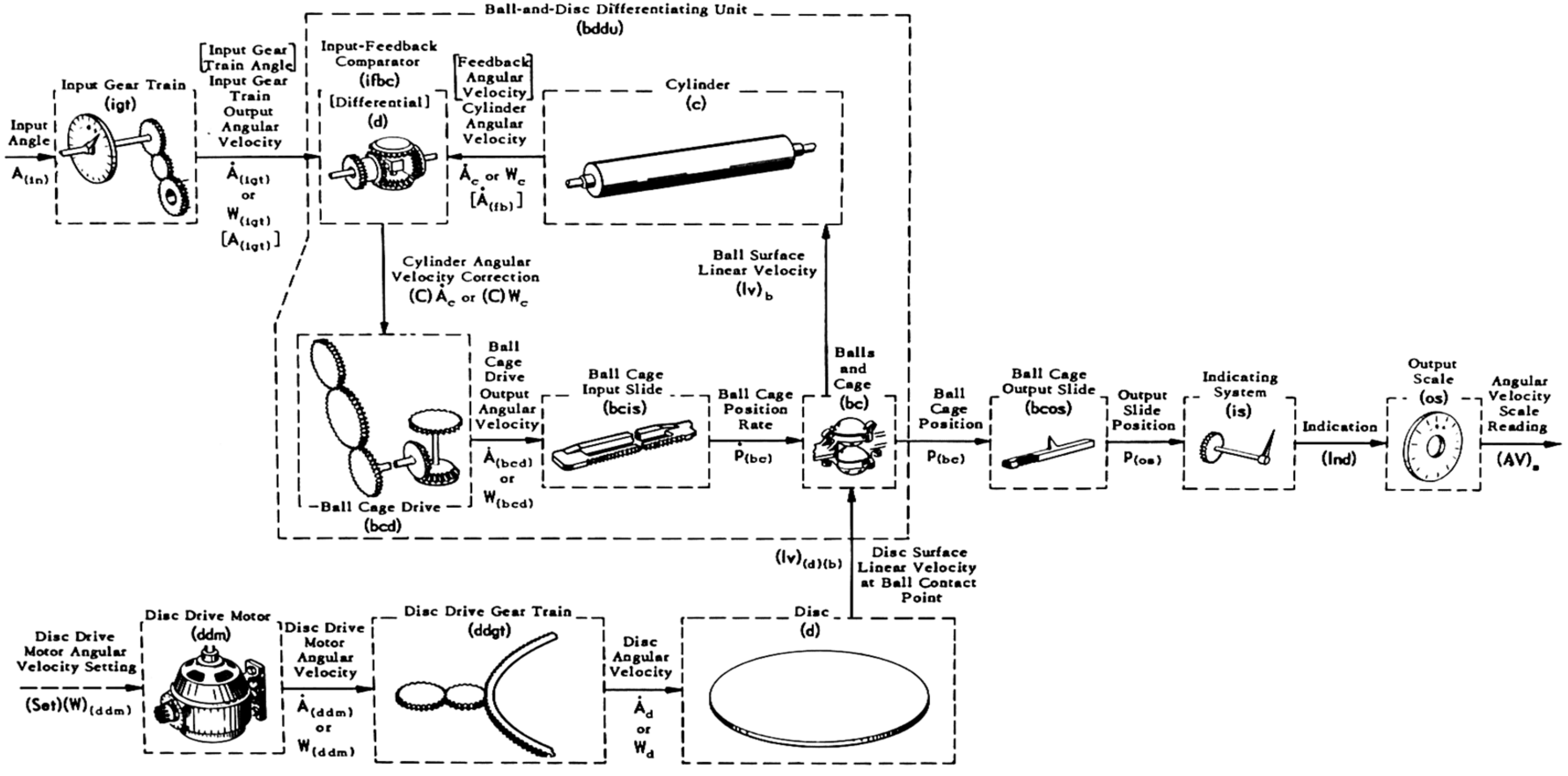
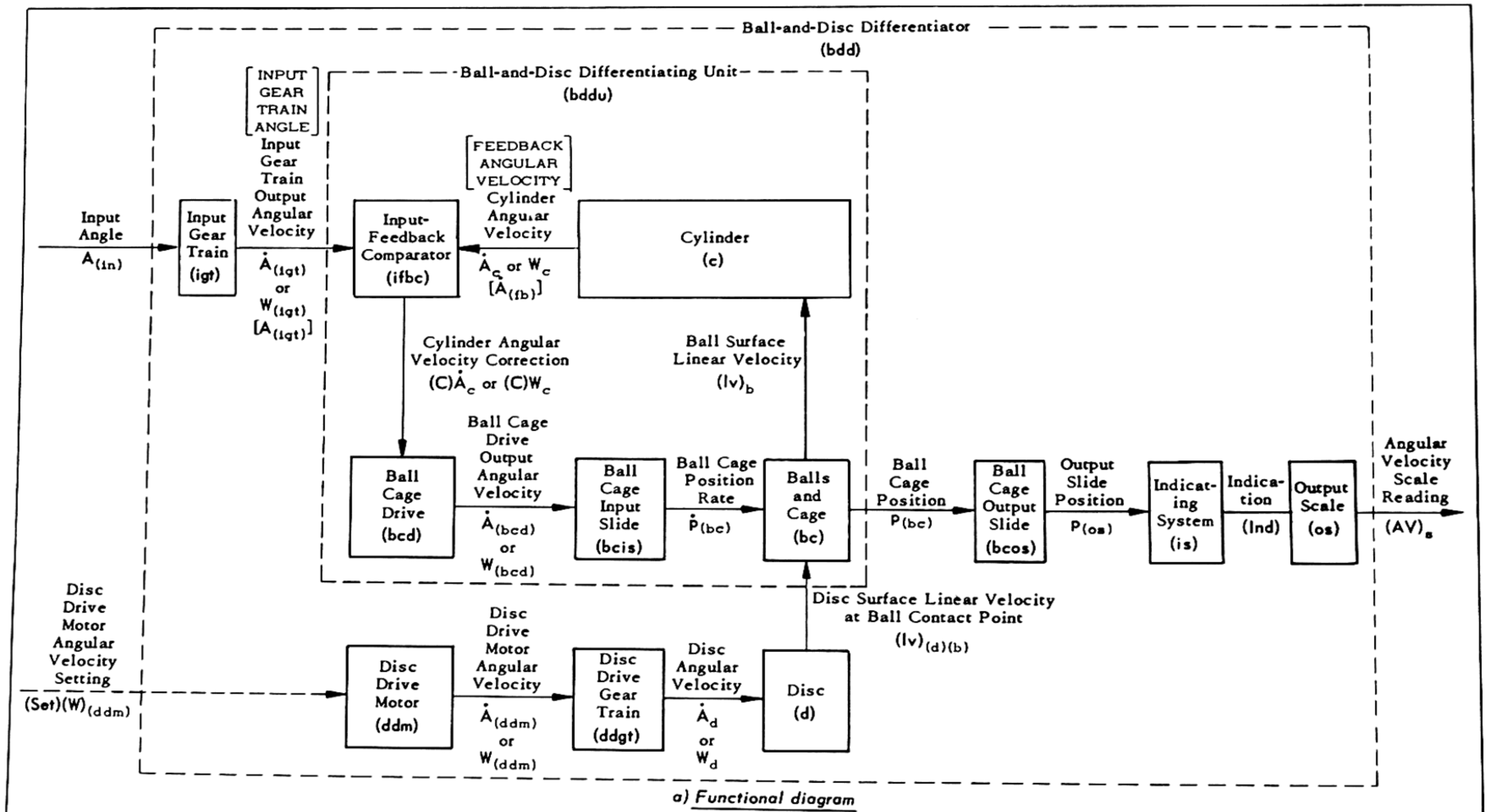


Fig. 34-12. Illustrative pictorial-functional diagram for a ball-and-disc differentiator.



a) Functional diagram

Derivation Summary 34-12. Functional diagram and performance equations for a ball-and-disc differentiator. (Page 1 of 3)

(igt) Input gear train

$$A_{(igt)} = S_{(igt)[A;A]} A_{(in)} \tag{1}$$

$$\dot{A}_{(igt)} = S_{(igt)[A;A]} \dot{A}_{(in)} \tag{2}$$

(ifbc) Input-feedback comparator

$$(C)\dot{A}_c = \dot{A}_{(igt)} - \dot{A}_c \tag{3}$$

(bcd) Ball cage drive

$$\dot{A}_{(bcd)} = S_{(bcd)[A;A]} (C)\dot{A}_c \tag{4}$$

(bcis) Ball cage input slide

$$\dot{p}_{(bc)} = S_{(bcis)[A;p]} \dot{A}_{(bcd)} \tag{5}$$

(bc) Balls and cage

Under the assumption of no slippage between surfaces in rolling contact,

$$(lv)_b = S_{(bc)[p;(lv)]} p_{(bc)} \tag{6}$$

where

$$S_{(bc)[p;(lv)]} = W_d \tag{7}$$

(c) Cylinder

$$\dot{A}_c = S_{(c)[(lv);\dot{A}]} (lv)_b \tag{8}$$

where

$$S_{(c)[(lv);\dot{A}]} = \frac{1}{r_c} \tag{9}$$

r_c = cylinder radius

(bddu) Ball-and-disc differentiating unit

From Eqs. (8) and (6),

$$\dot{A}_c = S_{(c)[(lv);\dot{A}]} S_{(bc)[p;(lv)]} p_{(bc)} \tag{10}$$

From Eqs. (5) and (4),

$$\dot{p}_{(bc)} = S_{(bcis)[A;p]} S_{(bcd)[A;A]} (C)\dot{A}_c \tag{11}$$

or

$$(C)\dot{A}_c = \frac{1}{S_{(bcis)[A;p]} S_{(bcd)[A;A]}} \dot{p}_{(bc)} \tag{12}$$

Combining the expressions of Eqs. (3), (10) and (12) shows that

$$\frac{1}{S_{(bcis)[A;p]} S_{(bcd)[A;A]}} \dot{p}_{(bc)} = \dot{A}_{(igt)} - S_{(c)[(lv);\dot{A}]} S_{(bc)[p;(lv)]} p_{(bc)} \tag{13}$$

Rearranging the terms of Eq. (13) and defining $(CT)_{(bddu)}$ and $S_{(bddu)[\dot{A};p]}$ gives

$$(CT)_{(bddu)} \dot{p}_{(bc)} + p_{(bc)} = S_{(bddu)[\dot{A};p]} \dot{A}_{(igt)} \tag{14}$$

where

$$(CT)_{(bddu)} = \frac{1}{S_{(c)[(lv);\dot{A}]} S_{(bc)[p;(lv)]} S_{(bcis)[A;p]} S_{(bcd)[A;A]}} \tag{15}$$

= characteristic time of the ball-and-disc differentiating unit

$$S_{(bddu)[\dot{A};p]} = \frac{1}{S_{(c)[(lv);\dot{A}]} S_{(bc)[p;(lv)]}} \tag{16}$$

= angular velocity input – slide position output of the ball-and-disc differentiating unit

Derivation Summary 34-12. Functional diagram and performance equations for a ball-and-disc differentiator. (Page 2 of 3)

(bcos) Ball cage output slide

$$P_{(os)} = S_{(bcos)[p;p]} P_{(bc)} \tag{17}$$

(is) Indicating system

$$(Ind) = S_{(is)[p;(Ind)]} P_{(os)} \tag{18}$$

(os) Output scale

$$(AV)_s = S_{(os)[(Ind);(AV)]} (Ind) \tag{19}$$

(bdd) Ball-and-disc differentiator

Using Eqs. (1), (17), (18) and (19) to replace $P_{(bc)}$ by $(AV)_s$ and $A_{(igt)}$ by $A_{(in)}$ in Eq. (14) shows that the ball-and-disc differentiator performance equation is

$$(CT)_{(bdd)} (\dot{AV})_s + (AV)_s = S_{(bdd)[\dot{A};(AV)]} \dot{A}_{(in)} \tag{20}$$

where

$$(CT)_{(bdd)} = (CT)_{(bbdu)} \tag{21}$$

= characteristic time of ball-and-disc differentiator

$$S_{(bdd)[\dot{A};(AV)]} = S_{(igt)[A;A]} S_{(bddu)[\dot{A};p]} S_{(bcos)[p;p]} S_{(is)[p;(Ind)]} S_{(os)[(Ind);(AV)]} \tag{22}$$

= input angular velocity – angular velocity reading sensitivity of the ball-and-disc differentiator

Equation (20), the performance equation for the ball-and-disc differentiator, has the (1;0,1) differential equation form.

Within the operating range for which

$$(CT)_{(bdd)} (\dot{AV})_s << (AV)_s \tag{23}$$

the performance equation reduces to a (1;0) differential equation; i.e.,

$$(AV)_s = S_{(bdd)[\dot{A};(AV)]} \dot{A}_{(in)} \tag{24}$$

Derivation Summary 34-2 shows this to be the equation form for the ideal differentiator.

b) Performance equations for components and subsystems of the ball-and-disc differentiator

Derivation Summary 34-12. Functional diagram and performance equations for a ball-and-disc differentiator. (Page 3 of 3)

details involved; no new principles or processes are required. For this reason, the illustrative tachometer diagrams that follow in this chapter are not accompanied by performance equation derivations.

34.73. Four widely used tachometer types are illustrated. These types do not in any way exhaust the design possibilities, but they do comprise instruments that are often applied as components of control systems. The tachometer types described are:

1) Centrifugal tachometer.
2) Rotating-magnet drag-cup tachometer.
3) Direct-current electrical tachometer.
4) Alternating-current drag-cup electrical tachometer.

Types 1 and 2 have angular velocity receivers that provide mechanical inputs for their indicating systems. The angular velocity signal generators of types 3 and 4 give direct-current and alternating-current electrical signal outputs, respectively.

CENTRIFUGAL TACHOMETER

34.74. Figure 34-13 is an illustrative pictorial diagram for the centrifugal tachometer. The input angle is introduced by the input shaft, which drives the input gear train. The input gear train output angular velocity is the essential input to the angular velocity receiver, which consists of a four-link arrangement carrying two flyweights. Two of the links are pivoted at one end on a collar fixed to the top of the angular velocity receiver spindle. The other ends of these two links are pivoted on the flyweights. Two lower links that match the upper links are pivot-connected between the flyweights and the angular velocity receiver output collar. A spiral spring located on the spindle between the fixed collar and output collar tends to force the output collar downward and pull the flyweights toward their equilibrium positions. When the spindle is rotated by the input gear train, centrifugal force tends to move the flyweights away from the spindle. The pivoted links convert this outward force into the compression of the spiral spring required to prevent further radial motion of the flyweights. The corresponding deflection of the output collar is the essential input to the indicating system. The indicating system output is the indication in the form of the angular deflection of the index. The scale associates angular velocity readings with indications. These readings represent the time derivative of the input angle, and thus justify the classification of the centrifugal tachometer as a differentiator.

34.75. Figure 34-14 is an illustrative pictorial-functional diagram for the centrifugal tachometer. The resolution of the mechanism into subsystems is intended to suggest a functional diagram form for use in a performance equation derivation.

ROTATING-MAGNET DRAG-CUP TACHOMETER

34.76. Figure 34-15 is an illustrative pictorial diagram for the rotating-magnet drag-cup tachometer. Figure 34-16 is the corresponding illustrative pictorial-functional diagram. The permanent magnet rotor is driven by the input shaft through the input gear train. Interaction between the permanent magnet field and the eddy currents induced in the drag cup produces a torque tending to rotate the cup. This torque is the input to the indicating system, which consists of a torsional hair-spring-restrained shaft connected to the index. The indications associated with index positions are translated into angular velocity scale readings by the scale.

DIRECT-CURRENT ELECTRICAL TACHOMETER

34.77. Figures 34-17 and 34-18 are illustrative pictorial and pictorial-functional diagrams, respectively, for the direct-current electrical tachometer. This instrument is based on a permanent-magnet-field direct-current generator driven from the input shaft through the input gear train. The generator acts as the angular velocity signal generator, which produces an angular velocity signal

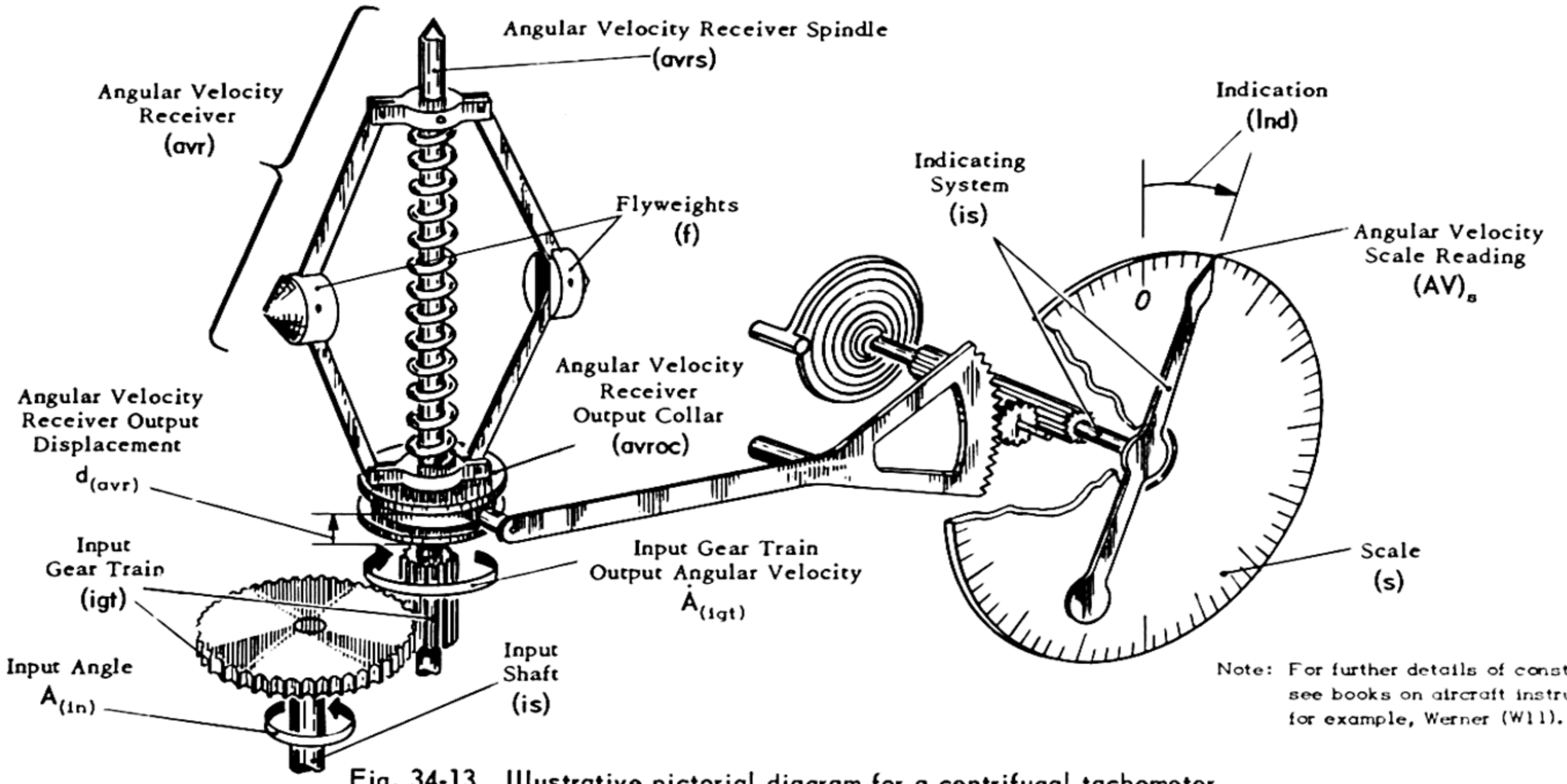


Fig. 34-13. Illustrative pictorial diagram for a centrifugal tachometer.

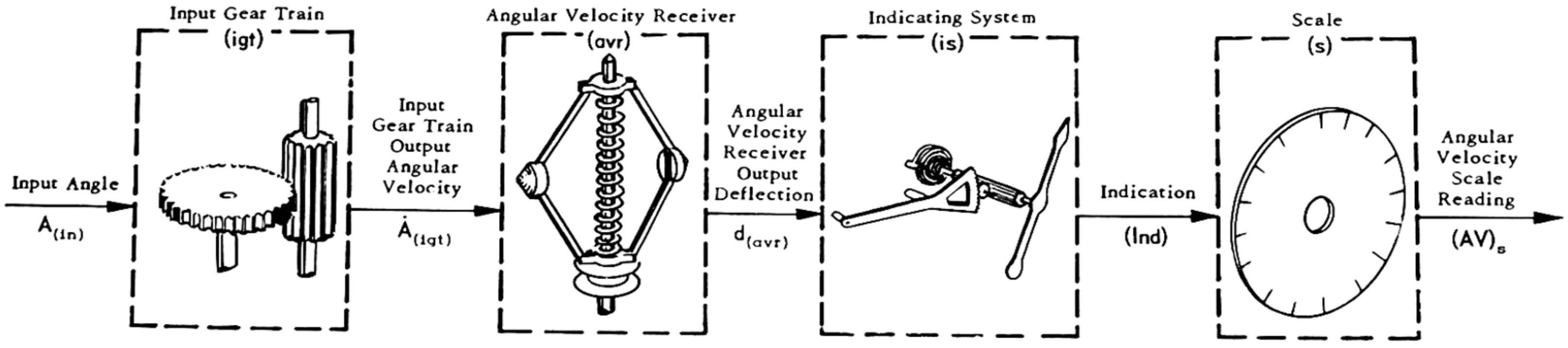
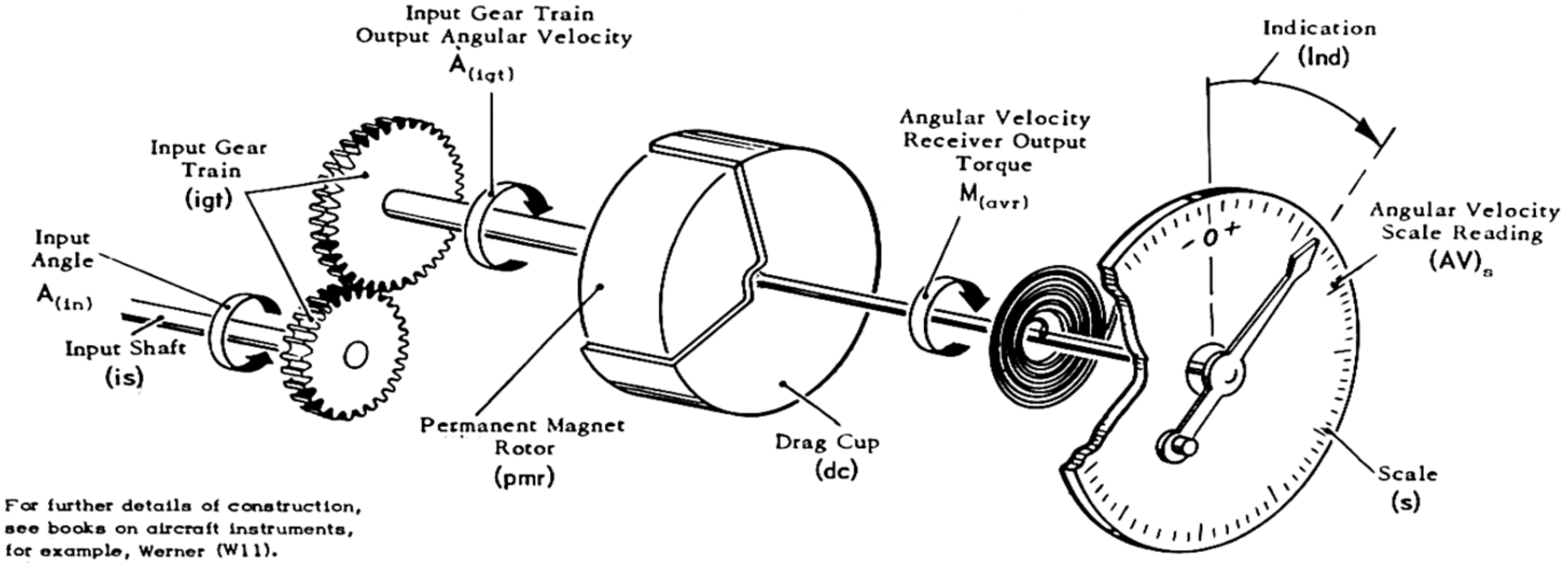


Fig. 34-14. Illustrative pictorial-functional diagram for a centrifugal tachometer.



Note: For further details of construction, see books on aircraft instruments, for example, Werner (W11).

Fig. 34-15. Illustrative pictorial diagram for a rotating-magnet drag-cup tachometer.

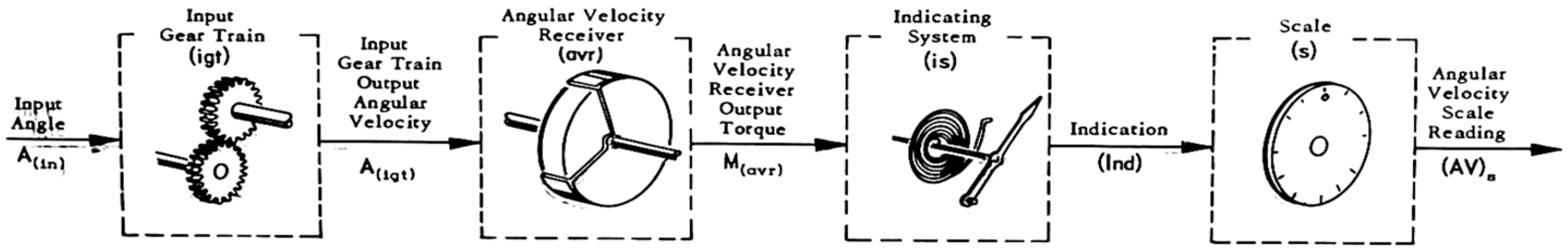
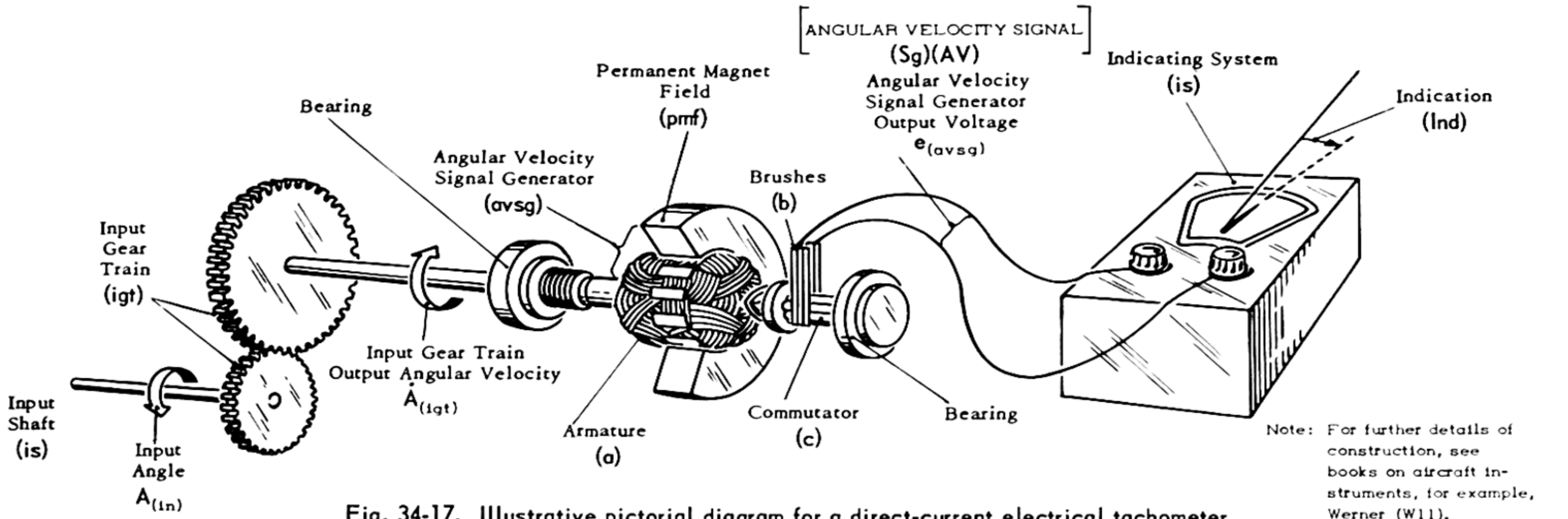


Fig. 34-16. Illustrative pictorial-functional diagram for a rotating-magnet drag-cup tachometer.



Note: For further details of construction, see books on aircraft instruments, for example, Werner (W11).

Fig. 34-17. Illustrative pictorial diagram for a direct-current electrical tachometer.

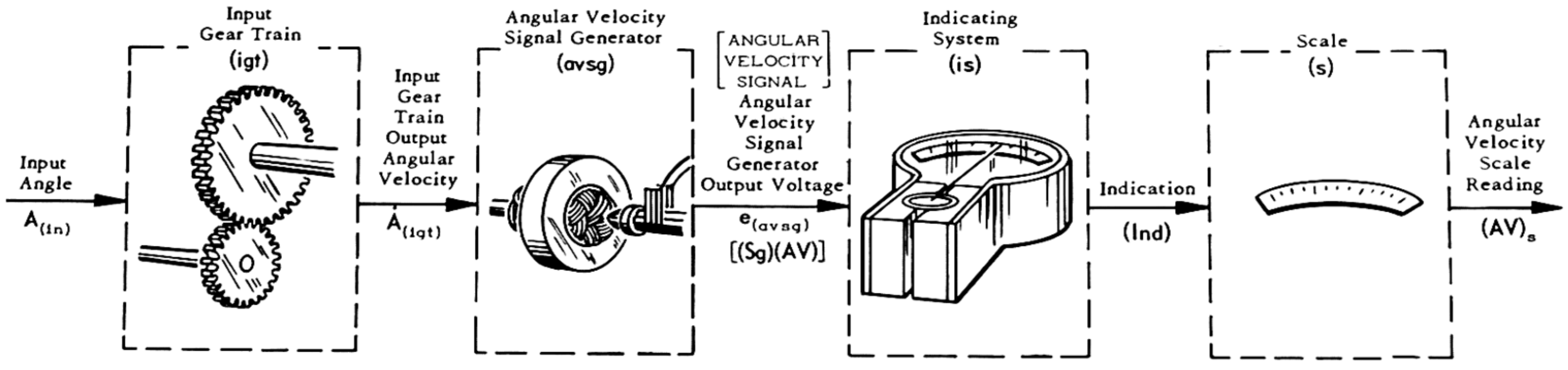


Fig. 34-18. Illustrative pictorial-functional diagram for a direct-current electrical tachometer.

in the form of a direct-current voltage. The indicating system is a direct-current meter that produces index deflection as the indication. Angular velocity scale readings that represent the time derivative of the input angle are associated with indications by means of the scale.

ALTERNATING-CURRENT DRAG-CUP ELECTRICAL TACHOMETER

34.78. Figure 34-19 is an illustrative pictorial diagram for the alternating-current electrical tachometer. Figure 34-20 is the corresponding illustrative pictorial-functional diagram. The angular velocity signal generator includes the drag-cup rotor, which is driven from the input shaft through the input gear train. The drag cup rotates outside a stationary cylinder of magnetic material and inside a stator that carries two-phase alternating-current windings. One of these windings receives the constant-frequency, constant-magnitude voltage excitation. The angular velocity signal is taken from the terminals of the other winding. The angular velocity signal is transformed into an angular indication by an alternating-current voltmeter. The angular velocity scale reading is provided by the scale of this meter.

RESISTANCE-INDUCTANCE ELECTRICAL DIFFERENTIATOR

34.79. Differentiation may be provided by combinations of electrical circuit elements. For example, if the condenser in the resistance-capacitance integrating circuit of Fig. 34-8b is replaced by an inductor, the output voltage becomes proportional to the time derivative of the input. Figure 34-21 shows the details of the resistance-inductance differentiator. A resistor is connected in series with an inductor. The input voltage is applied across the series combination. The voltage appearing across the inductance is considered as the output voltage.

34.80. Derivation Summary 34-13 gives the development of the performance equation for the resistance-inductance electrical differentiator of Fig. 34-21. Equation (1) expresses the drop across the resistance in terms of the input-reference voltage difference and the output-reference voltage difference. Equation (2) expresses the output-reference voltage difference in terms of the inductance and the current flowing through it. Equations (3) through (7) show the steps by which the combination of Eqs. (1) and (2) leads to Eq. (5), which is the desired performance equation. This equation has the (1;0,1) differential equation form. Equations (8) and (9) show that the resistance-inductance differentiator gives ideal performance under operating conditions for which the product of the characteristic time and the output-reference voltage difference rate is negligibly small compared with the output-reference voltage difference itself.

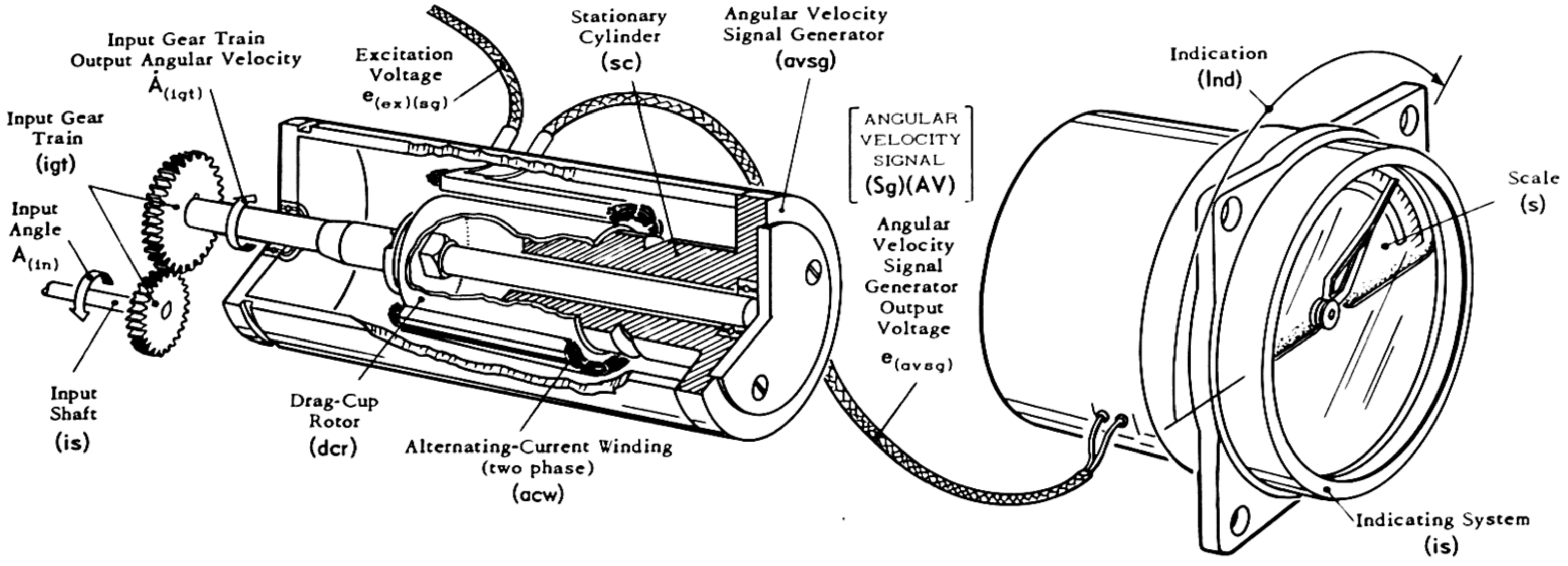


Fig. 34-19. Illustrative pictorial diagram for an alternating-current drag-cup electrical tachometer.

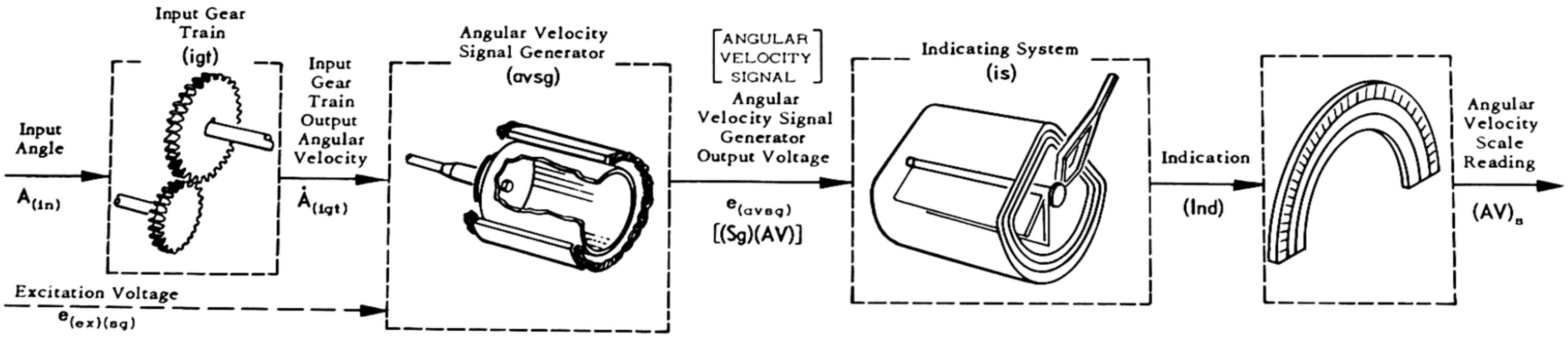


Fig. 34-20. Illustrative pictorial-functional diagram for an alternating-current drag-cup electrical tachometer.

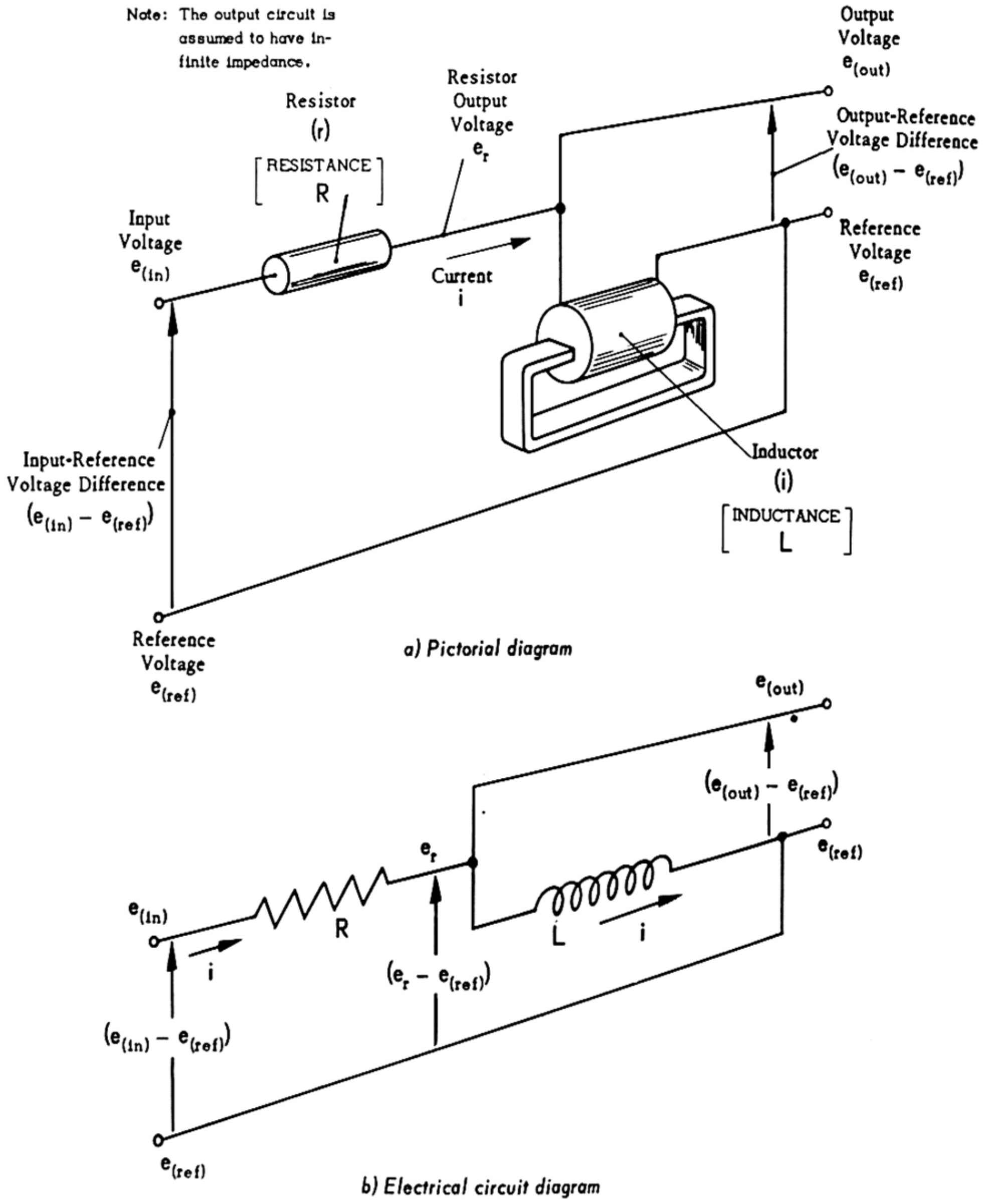


Fig. 34-21. Illustrative pictorial and circuit diagrams for a resistance – inductance electrical differentiator.

RESISTANCE – AMPLIFIER – FEEDBACK-INDUCTANCE DIFFERENTIATOR

34.81. Improved differentiator performance will be produced by the resistance-inductance electrical differentiator if a high-gain direct-current amplifier is connected with its ground side at the reference-voltage level, its input terminal at the resistor-output-voltage level, and its output terminal at the output-voltage level of the differentiator. This arrangement is illustrated in the diagrams of Fig. 34-22. The reasons for improved differentiating performance from the addition of a high-gain amplifier to the resistance-inductance circuit of Fig. 34-21

From Fig. 34-21,

$$(e_{(in)} - e_{(ref)}) - (e_{(out)} - e_{(ref)}) = iR \tag{1}$$

$$e_{(out)} - e_{(ref)} = L\frac{di}{dt} \tag{2}$$

Differentiating Eq. (1) gives

$$(\dot{e}_{(in)} - \dot{e}_{(ref)}) - (\dot{e}_{(out)} - \dot{e}_{(ref)}) = R\frac{di}{dt} \tag{3}$$

Combining Eq. (2) with Eq. (3) shows that

$$(\dot{e}_{(in)} - \dot{e}_{(ref)}) - (\dot{e}_{(out)} - \dot{e}_{(ref)}) = (e_{(out)} - e_{(ref)})\frac{R}{L} \tag{4}$$

Defining $(CT)_{(rid)}$ and rearranging the terms of Eq. (4) yields the equation

$$(CT)_{(rid)}(\dot{e}_{(out)} - \dot{e}_{(ref)}) + (e_{(out)} - e_{(ref)}) = S_{(rid)[\dot{e};e]}(\dot{e}_{(in)} - \dot{e}_{(ref)}) \tag{5}$$

where

$$(CT)_{(rid)} = \frac{L}{R} = \text{characteristic time of the resistance-inductance differentiator} \tag{6}$$

$$S_{(rid)[\dot{e};e]} = (CT)_{(rid)} = \text{input rate – output voltage sensitivity of the resistance-inductance differentiator} \tag{7}$$

Equation (5) is the performance equation for the resistance-inductance differentiator. It has the form of the (1;0,1) differential equation.

Within the range of operating conditions for which

$$(CT)_{(rid)}(\dot{e}_{(out)} - \dot{e}_{(ref)}) << (e_{(out)} - e_{(ref)}) \tag{8}$$

the performance equation becomes

$$(e_{(out)} - e_{(ref)}) = S_{(rid)[\dot{e};e]}(\dot{e}_{(in)} - \dot{e}_{(ref)}) \tag{9}$$

Equation (9) has the (1;0) form that is shown in Derivation Summary 34-2 to be associated with ideal differentiation.

Derivation Summary 34-13. Performance equations for a resistance-inductance electrical differentiator.

are similar to those already given in the discussion of the resistance – amplifier – feedback-capacitance integrator and therefore are not repeated here.

34.82. Derivation Summary 34-14 gives a development of the performance equation for the resistance – amplifier – feedback-inductance differentiator of Fig. 34-22. Equation (1) is an expression relating voltage differences to the drop across the resistor. Equation (2) gives the voltage drop across the inductor in terms of the inductance and the rate of change of current through the inductor. For the purposes of the present discussion, the amplifier input may be considered as drawing no more than a negligibly small current, so that the current through the resistor is effectively identical with the current through the inductor. Equation (3) shows that the amplifier output voltage changes are proportional in magnitude but opposite in sign to amplifier input voltage changes. Equations (4) through (10) show a series of steps that combine the basic circuit equations to give the resistance – amplifier – feedback-inductance performance equation in the (1;0,1) differential equation form. Equations (11) and (12) show that ideal

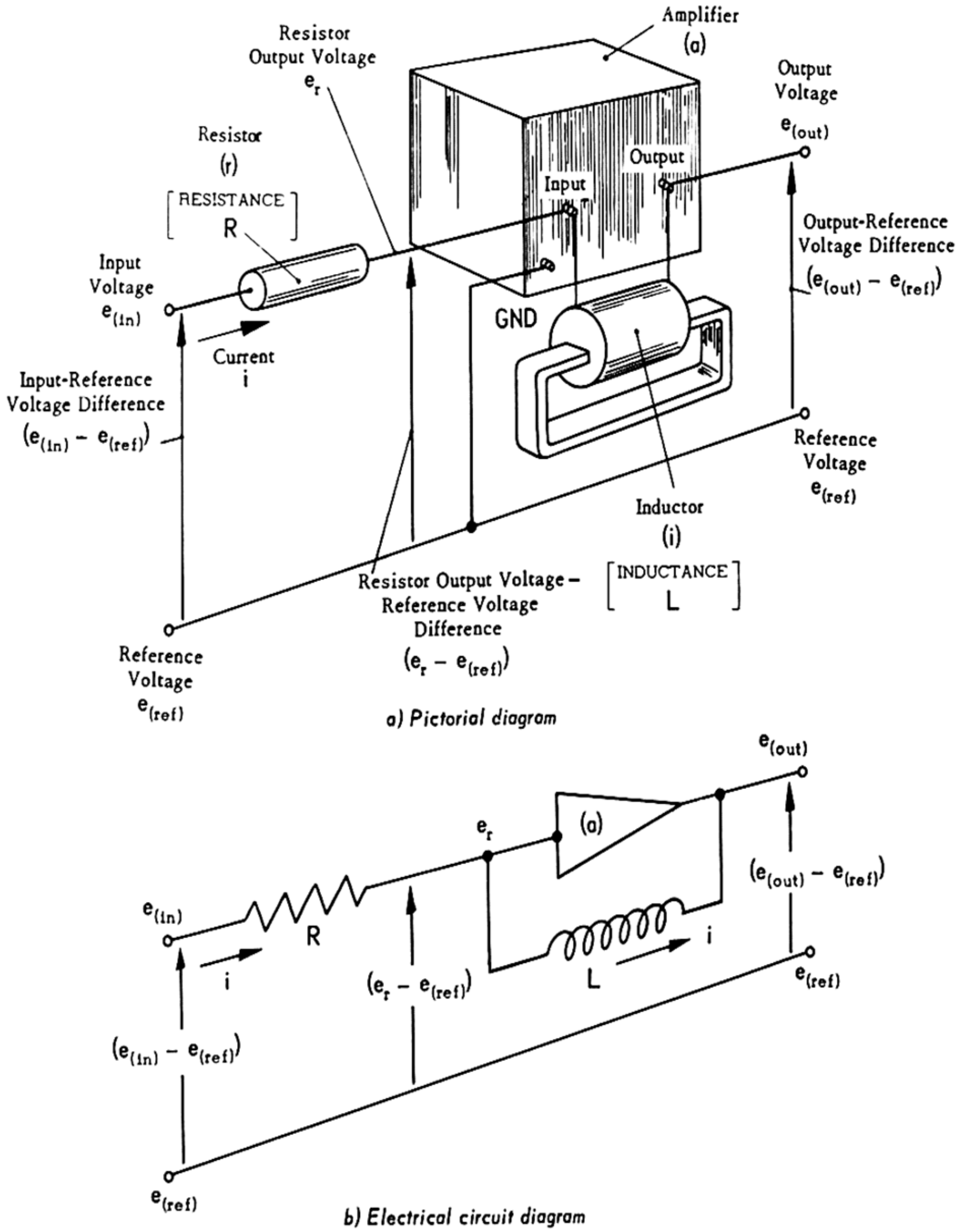


Fig. 34-22. Illustrative pictorial and circuit diagrams for a resistance–amplifier–feedback-inductance differentiator

differentiator performance is given by Eq. (8) when the product of the characteristic time and the output-reference voltage difference rate is negligibly small compared with the output-reference voltage difference itself.

RESISTANCE-CAPACITANCE ELECTRICAL DIFFERENTIATOR

34.83. Differentiator action may be achieved by an interchange of positions of the resistor and condenser in the resistance-capacitance integrator of Fig. 34-8. Figure 34-23 shows an arrangement of this kind. The condenser and resistor are

From Fig. 34-22,

$$(e_{(in)} - e_{(ref)}) - (e_r - e_{(ref)}) = iR \tag{1}$$

Under the assumption that the amplifier draws a negligibly small input current,

$$(e_r - e_{(ref)}) - (e_{(out)} - e_{(ref)}) = L\frac{di}{dt} \tag{2}$$

Also,

$$(e_{(out)} - e_{(ref)}) = -S_{(a)|e;e|}(e_r - e_{(ref)}) \tag{3}$$

where

$S_{(a)|e;e|}$ = voltage input – voltage output sensitivity magnitude of the amplifier

From Eq. (3),

$$(e_r - e_{(ref)}) = -\frac{1}{S_{(a)|e;e|}}(e_{(out)} - e_{(ref)}) \tag{4}$$

Combining Eqs. (2) and (4) gives

$$-\frac{S_{(a)|e;e|} + 1}{S_{(a)|e;e|}}(e_{(out)} - e_{(ref)}) = L\frac{di}{dt} \tag{5}$$

From Eqs. (1) and (4),

$$(e_{(in)} - e_{(ref)}) + \frac{(e_{(out)} - e_{(ref)})}{S_{(a)|e;e|}} = iR \tag{6}$$

Differentiating Eq. (6) yields

$$(\dot{e}_{(in)} - \dot{e}_{(ref)}) + \frac{(\dot{e}_{(out)} - \dot{e}_{(ref)})}{S_{(a)|e;e|}} = R\frac{di}{dt} \tag{7}$$

Combining Eqs. (5) and (7) and rearranging terms gives

$$(CT)_{(rafid)}(\dot{e}_{(out)} - \dot{e}_{(ref)}) + (e_{(out)} - e_{(ref)}) = S_{(rafid)[\dot{e};e]}(\dot{e}_{(in)} - \dot{e}_{(ref)}) \tag{8}$$

where

$$(CT)_{(rafid)} = \frac{L}{R}\frac{1}{S_{(a)|e;e|} + 1} \tag{9}$$

= characteristic time of the resistance – amplifier – feedback-inductance differentiator

$$S_{(rafid)[\dot{e};e]} = -(CT)_{(rafid)}S_{(a)|e;e|} \tag{10}$$

= input rate – output voltage sensitivity of the resistance – amplifier – feedback-inductance differentiator

Equation (8) is the performance equation for the resistance – amplifier – feedback-inductance differentiator. It has the form of the (1;0,1) differential equation.

Within the operating range for which

$$(CT)_{(rafid)}(\dot{e}_{(out)} - \dot{e}_{(ref)}) << (e_{(out)} - e_{(ref)}) \tag{11}$$

the performance equation reduces to

$$(e_{(out)} - e_{(ref)}) = S_{(rafid)[\dot{e};e]}(\dot{e}_{(in)} - \dot{e}_{(ref)}) \tag{12}$$

which has the (1;0) form associated with ideal differentiation.

Derivation Summary 34-14. Performance equations for a resistance – amplifier – feedback-inductance differentiator.

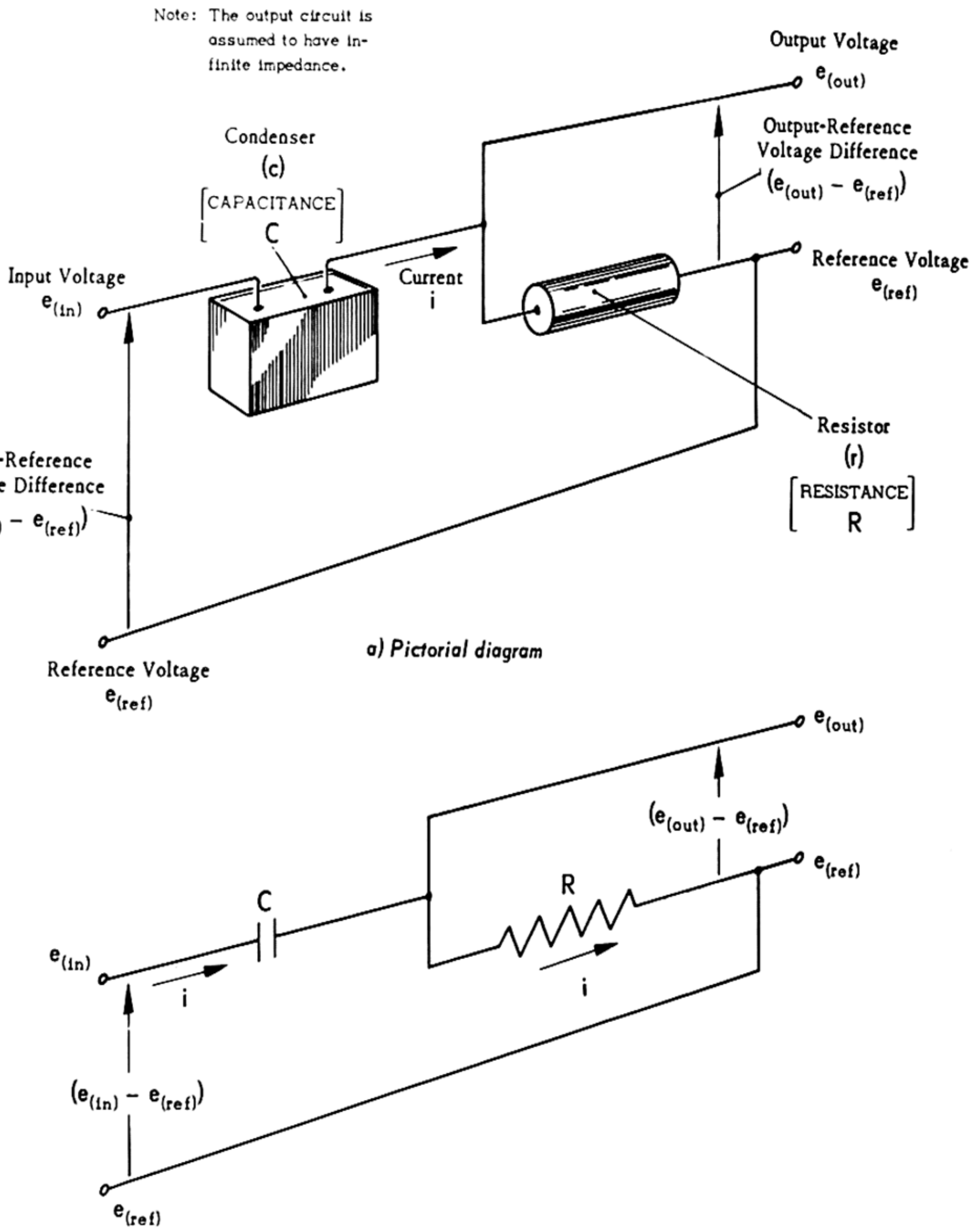


Fig. 34-23. Illustrative pictorial and circuit diagrams for a resistance-capacitance electrical differentiator.

connected in series with the input voltage applied across the combination. The output voltage is measured across the resistor.

34.84. The performance equation for the capacitance-resistance electrical differentiator is developed in Derivation Summary 34-15. This equation, Eq.(3), has the (1;0,1) differential equation form, which gives ideal differentiation when the output-reference voltage rate term is negligibly small compared with the output-reference voltage difference itself.

From Fig. 34-23,

$$(\dot{e}_{(in)} - \dot{e}_{(ref)}) - (\dot{e}_{(out)} - \dot{e}_{(ref)}) = \frac{i}{C} \tag{1}$$

$$(e_{(out)} - e_{(ref)}) = iR \tag{2}$$

Combining Eqs. (1) and (2) gives

$$(CT)_{(rcd)}(\dot{e}_{(out)} - \dot{e}_{(ref)}) + (e_{(out)} - e_{(ref)}) = S_{(rcd)[\dot{e};e]}(\dot{e}_{(in)} - \dot{e}_{(ref)}) \tag{3}$$

$(CT)_{(rcd)} = RC$ = characteristic time of the resistance-capacitance differentiator (4)

$S_{(rcd)[\dot{e};e]} = (CT)_{(rcd)}$ = input rate – output voltage sensitivity of the resistance-capacitance differentiator (5)

Equation (3) is the performance equation for the resistance-capacitance differentiator. It has the form of the (1;0,1) differential equation.

Within the operating range for which

$$(CT)_{(rcd)}(\dot{e}_{(out)} - \dot{e}_{(ref)}) << (e_{(out)} - e_{(ref)}) \tag{6}$$

the performance equation reduces to

$$(e_{(out)} - e_{(ref)}) = S_{(rcd)[\dot{e};e]}(\dot{e}_{(in)} - \dot{e}_{(ref)}) \tag{7}$$

which has the (1;0) form associated with the ideal differentiator.

Derivation Summary 34-15. Performance equations for a resistance-capacitance electrical differentiator.

CAPACITANCE – AMPLIFIER – FEEDBACK-RESISTANCE DIFFERENTIATOR

34.85. Figure 34-24 shows the resistance-capacitance differentiator with the addition of an amplifier across the resistor. The performance equation for this capacitance – amplifier – feedback-resistance differentiator is developed in Derivation Summary 34-16. This equation, Eq. (7), has the (1;0,1) differential equation form. Ideal differentiation is provided over the range of operating conditions for which the term containing the time derivative of the output-reference voltage difference is negligibly small compared with the output-reference voltage difference itself.

INTEGRATOR AND DIFFERENTIATOR PERFORMANCE EQUATION FORMS

34.86. When the ball-and-disc integrator and the tachometers are excluded from consideration, all of the illustrative integrators and differentiators described in the preceding sections have performance equations that fall into four differential equation forms:

1) The (0;1,2) form.
2) The (1;1,2) form.
3) The (0;0,1) form.
4) The (1;0,1) form.

The developments of Derivation Summaries 34-1 and 34-2 show that the ideal integrator has a performance equation with the (0;1) differential equation form and that the ideal differentiator has a performance equation with the (1;0) differential equation form.

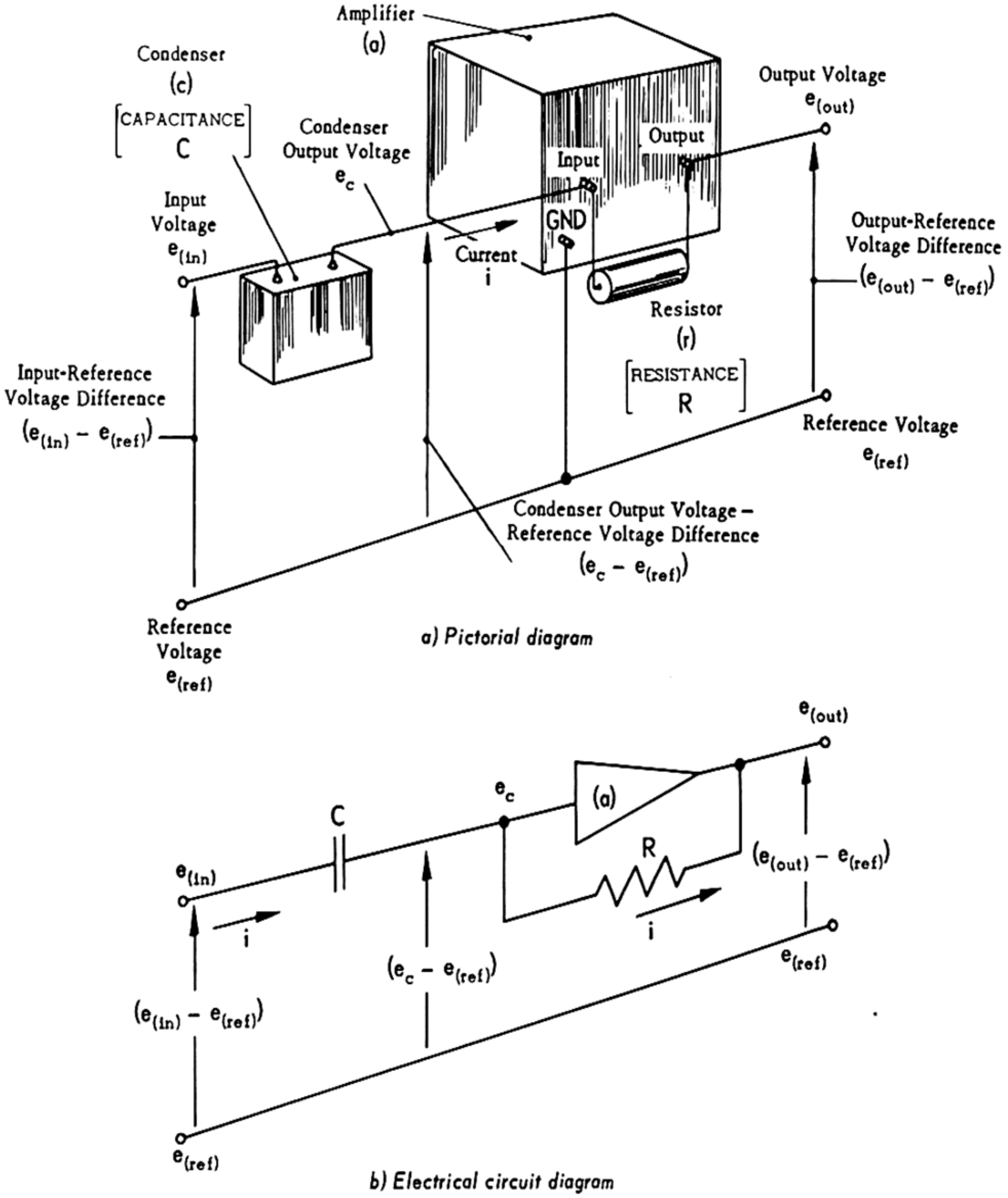


Fig. 34-24. Illustrative pictorial and electrical circuit diagrams for a capacitance – amplifier – feedback-resistance differentiator.

RELATING FUNCTION DEVIATIONS

34.87. In practice, it is useful to describe the performance of actual integrators and differentiators in terms of deviations of their performance equations from the performance equations for ideal integrators and differentiators. A generally satisfactory method for specifying the characteristics of any given differential equation is to use the relating function associated with the equation.* With relating functions expressed in terms of dimensionless dynamic amplitude

* The general theory of relating functions is discussed in Chapter 17.

From Fig. 34-24,

$$(\dot{e}_{(in)} - \dot{e}_{(ref)}) - (\dot{e}_c - \dot{e}_{(ref)}) = \frac{i}{C} \tag{1}$$

Under the assumption that the amplifier draws a negligibly small input current,

$$(e_c - e_{(ref)}) - (e_{(out)} - e_{(ref)}) = iR \tag{2}$$

Also,

$$(e_{(out)} - e_{(ref)}) = -S_{(a)|e;e|}(e_c - e_{(ref)}) \tag{3}$$

From Eq. (3)

$$(e_c - e_{(ref)}) = -\frac{1}{S_{(a)|e;e|}}(e_{(out)} - e_{(ref)}) \tag{4}$$

Combining Eq. (2) and Eq. (4) gives

$$-\left[\frac{S_{(a)|e;e|} + 1}{S_{(a)|e;e|}}\right](e_{(out)} - e_{(ref)}) = iR \tag{5}$$

From Eqs. (1) and (4),

$$(\dot{e}_{(in)} - \dot{e}_{(ref)}) + \frac{(\dot{e}_{(out)} - \dot{e}_{(ref)})}{S_{(a)|e;e|}} = \frac{i}{C} \tag{6}$$

Combining Eqs. (5) and (6) and rearranging terms gives

$$(CT)_{(cafrd)}(\dot{e}_{(out)} - \dot{e}_{(ref)}) + (e_{(out)} - e_{(ref)}) = S_{(cafrd)[\dot{e};e]}(\dot{e}_{(in)} - \dot{e}_{(ref)}) \tag{7}$$

where

$$(CT)_{(cafrd)} = \frac{RC}{S_{(a)|e;e|} + 1} \tag{8}$$

= characteristic time of the capacitance – amplifier – feedback-resistance differentiator

$$S_{(cafrd)[\dot{e};e]} = -(CT)_{(cafrd)} S_{(a)|e;e|} \tag{9}$$

= input rate – output voltage sensitivity of the capacitance – amplifier – feedback-resistance differentiator

Equation (7) is the performance equation of the capacitance – amplifier – feedback-resistance differentiator. It has the form of the (1;0,1) differential equation.

Within the operating range for which

$$(CT)_{(cafrd)}(\dot{e}_{(out)} - \dot{e}_{(ref)}) << (e_{(out)} - e_{(ref)}) \tag{10}$$

the performance equation reduces to

$$(e_{(out)} - e_{(ref)}) = S_{(cafrd)[\dot{e};e]}(\dot{e}_{(in)} - \dot{e}_{(ref)}) \tag{11}$$

which has the (1;0) form associated with ideal differentiation.

Derivation Summary 34-16. Performance equations for a capacitance – amplifier – feedback-resistance differentiator.

ratios and dynamic response angles, differences between equations may be expressed in terms of deviations. Concepts and notation for expressing these deviations are given in Definition Summary 34-1.

34.88. Equations (1) through (4) of Definition Summary 34-1 and the associated definitions give the basic reference and compared relating function forms required in deviation equations. The reference-compared dimensionless dynamic amplitude ratio deviation is defined by Eqs. (5) and (6) as the compared dimensionless dynamic amplitude ratio minus the reference dimensionless dynamic amplitude ratio. The

Given two differential equations to be compared:

1) A reference differential equation with its relating function expressed in working variable terms as

$$\eta_{(ref)} = \rho_{(r)(ref)} \mu_{(ref)} \epsilon^{j\phi_{(ref)}} \tag{1}$$

or, in self-defining terms, as

$$\eta_{(ref)} \approx [RF]_{(ref)} = (RAR)_{(ref)} \hat{'}(DAR)_{(ref)} \epsilon^{j(DRA)_{(ref)}} \tag{2}$$

2) A compared differential equation with its relating function expressed in working variable terms as

$$\eta_{(cmprd)} = \rho_{(r)(cmprd)} \mu_{(cmprd)} \epsilon^{j\phi_{(cmprd)}} \tag{3}$$

or, in self-defining terms, as

$$\eta_{(cmprd)} \approx [RF]_{(cmprd)} = (RAR)_{(cmprd)} \hat{'}(DAR)_{(cmprd)} \epsilon^{j(DRA)_{(cmprd)}} \tag{4}$$

where, in terms of the notation of Definition Summaries 13-3, 13-4 and 13-6 of Chapter 13 and Definition Summary 28-8 of Chapter 28,

$\rho_{(r)(ref)} \approx (RAR)_{(ref)}$ = reference reference amplitude ratio

$\mu_{(ref)} = \hat{'}(DAR)_{(ref)}$ = reference dimensionless dynamic amplitude ratio

$\phi_{(ref)} \approx (DRA)_{(ref)}$ = reference dynamic response angle

$\rho_{(r)(cmprd)} \approx (RAR)_{(cmprd)}$ = compared reference amplitude ratio

$\mu_{(cmprd)} \approx \hat{'}(DAR)_{(cmprd)}$ = compared dimensionless dynamic amplitude ratio

$\phi_{(cmprd)} \approx (DRA)_{(cmprd)}$ = compared dynamic response angle

Note: $\hat{'}(DAR)$, the dimensionless dynamic amplitude ratio, is identical with $[(DAR)(RAR)R]$, the dynamic amplitude ratio—reference amplitude ratio ratio of Definition Summary 13-4 and Eq. (20) of Definition Summary 13-6.

Using conventions similar to those established in Figs. 9-6, 9-7 and 9-8 of Chapter 9 for the comparison of physical quantities, dimensionless dynamic amplitude ratio deviation and dynamic response angle deviation may be defined by the expressions

$$[(D)\mu]_{[(ref)-(cmprd)]} = \mu_{(cmprd)} - \mu_{(ref)} \tag{5}$$

$$\mu_{(ref)} = \text{——}$$

$$[(D)\mu]_{[(ref)-(cmprd)]} \approx [(D)\hat{'}(DAR)]_{[(ref)-(cmprd)]} = \hat{'}(DAR)_{(cmprd)} - \hat{'}(DAR)_{(ref)} \tag{6}$$

$$\hat{'}(DAR)_{(ref)} = \text{——}$$

= reference-compared dimensionless dynamic amplitude ratio deviation

$$[\Delta\mu]_{[(ref)-(cmprd)]} = \frac{[(D)\mu]_{[(ref)-(cmprd)]}}{\mu_{(ref)}} = \frac{\mu_{(cmprd)}}{\mu_{(ref)}} - 1 \tag{7}$$

$$[\Delta\mu]_{[(ref)-(cmprd)]} = [(FD)\hat{'}(DAR)]_{[(ref)-(cmprd)]} = \frac{\hat{'}(DAR)_{(cmprd)}}{\hat{'}(DAR)_{(ref)}} - 1 \tag{8}$$

= reference-compared dimensionless dynamic amplitude ratio fractional deviation

$$[(D)\phi]_{[(ref)-(cmprd)]} = \phi_{(cmprd)} - \phi_{(ref)} \tag{9}$$

$$\phi_{(ref)} = \text{——}$$

Definition Summary 34-1. Concepts and notation for describing differences between relating functions in terms of dynamic amplitude ratio and dynamic response angle deviations.
(Page 1 of 2)

$$[(D)\phi]_{[(ref)-(cmprd)]} \equiv [(D)(DRA)]_{[(ref)-(cmprd)]} = (DRA)_{(cmprd)} - (DRA)_{(ref)} \tag{10}$$

$$(DRA)_{(ref)} = \text{———}$$

= reference-compared dynamic response angle deviation

and

$$[\Delta\phi]_{[(ref)-(cmprd)]} \equiv [(D)\phi]_{[(ref)-(cmprd)]} \tag{11}$$

Definition Summary 34-1. Concepts and notation for describing differences between relating functions in terms of dynamic amplitude ratio and dynamic response angle deviations.
(Page 2 of 2)

reference-compared dimensionless dynamic amplitude ratio fractional deviation is defined by Eqs. (7) and (8) as the reference-compared dimensionless dynamic amplitude ratio deviation divided by the reference dimensionless dynamic amplitude ratio. The reference-compared dynamic response angle deviation is defined by Eqs. (9) and (10) as the compared dynamic response angle minus the reference dynamic response angle.

RELATING FUNCTIONS FOR INTEGRATOR AND DIFFERENTIATOR PERFORMANCE EQUATION FORMS

34.89. The relating function for the (0;0,1) form is developed in Derivation Summaries 18-10 and 33-1. The relating function for the (1;0,1) equation is developed in Derivation Summary 18-11. The relating function for the (0;1,2) equation is developed in Derivation Summary 34-17, and the relating function for the (1;1,2) equation is developed in Derivation Summary 34-18.

34.90. Table 34-1 summarizes relating function information for the differential equation forms associated with integration and differentiation. In this table, column 1 gives the identification symbol for the equation considered, while column 2 gives the differential equation form itself. Column 3 defines the characteristic time for the individual equations, and column 4 gives the reference amplitude ratios for these equations. Subscripts identifying the equations with which these concepts are associated are added to the characteristic time and reference amplitude ratio symbols. Column 5 defines and gives the break points in terms of the reference frequency ratio based on an arbitrarily chosen reference frequency. Column 6 gives relating functions in various complex variable forms including the conventional operational form with the symbol p used to represent differentiation with respect to time. Column 7 gives dimensionless dynamic amplitude ratios, and column 8 gives the corresponding dynamic response angles.

Given the (0;1,2) differential equation form

$$a_2\ddot{v} + a_1\dot{v} = b_0 u \tag{1}$$

(Refer to Chapter 19 for a discussion of more general second-order forms.)

Define

$$\tau_{(0;1,2)} \approx (CT)_{(0;1,2)} = \frac{a_2}{a_1} \equiv \text{(0;1,2) characteristic time} \tag{2}$$

$$\sigma_{(0;1,2)} \approx S_{(0;1,2)} = \frac{b_0}{a_1}(CT)_{(0;1,2)} \equiv \text{(0;1,2) dimensional similarity factor} \tag{3}$$

Using the definitions of Eqs. (2) and (3) in Eq. (1) gives the working variable equation

$$\tau_{(0;1,2)}\ddot{v} + \dot{v} = \frac{\sigma_{(0;1,2)}}{\tau_{(0;1,2)}} u \tag{4}$$

and the self-defining symbol equation

$$(CT)_{(0;1,2)}\ddot{v} + \dot{v} = \frac{S_{(0;1,2)}}{(CT)_{(0;1,2)}} u \tag{5}$$

a) Generalized (0;1,2) equation

Consider the steady-state solution associated with Eq. (4) for a sinusoidal forcing function; i.e., take

$$u = u_a \epsilon^{j\omega_f t} \tag{6}$$

and assume

$$v = \eta u = \eta u_a \epsilon^{j\omega_f t} \tag{7}$$

so that

$$\dot{v} = \eta\dot{u} = \eta j\omega_f u \tag{8}$$

and

$$\ddot{v} = \eta\ddot{u} = \eta(-\omega_f^2)u \tag{9}$$

Substituting the expressions of Eqs. (8) and (9) in Eq. (4) gives

$$\eta(-\omega_f^2\tau_{(0;1,2)} + j\omega_f)u = \frac{\sigma_{(0;1,2)}}{\tau_{(0;1,2)}} u \tag{10}$$

Multiplying both sides of Eq. (10) by $\tau_{(0;1,2)}$ and solving for the relating function $\eta(\approx [RF])$ shows that

$$[RF]_{(0;1,2)} \approx \eta_{(0;1,2)} = \frac{\sigma_{(0;1,2)}}{j\omega_f\tau_{(0;1,2)}(1 + j\omega_f\tau_{(0;1,2)})} \tag{11}$$

Define

$$T_{(ref)} = \frac{1}{n_{(ref)}} = \text{reference period (arbitrarily chosen)} \tag{12}$$

$$\beta_r \approx (FR)_{(ref)} = \frac{T_{(ref)}}{T_f} = \frac{n_f}{n_{(ref)}} = \text{reference frequency ratio} \tag{13}$$

$$[(RP)(CT)R]_{(0;1,2)} = \frac{T_{(ref)}}{(CT)_{(0;1,2)}} = \text{(0;1,2) reference period – characteristic time ratio} \tag{14}$$

and

$$\beta_{(r)(bp)(0;1,2)} \approx (FR)_{(ref)(bp)(0;1,2)} = (bp)_{(0;1,2)} = \frac{[(RP)(CT)R]_{(0;1,2)}}{2\pi} \tag{15}$$

$$= \text{(0;1,2) breakpoint reference frequency ratio}$$

Derivation Summary 34-17. Relating function for the (0;1,2) linear differential equation with constant coefficients. (Page 1 of 2)

so that

$$\omega_f \tau_{(0;1,2)} \approx 2\pi \frac{T_{(ref)}}{T_f} \frac{(CT)_{(0;1,2)}}{T_{(ref)}} = \frac{(FR)_{(ref)}}{(bp)_{(0;1,2)}} \tag{16}$$

and Eq. (11) may be written in the form

$$\eta_{(0;1,2)} \approx [RF]_{(0;1,2)} = \frac{\sigma_{(0;1,2)}}{j \dfrac{(FR)_{(ref)}}{(bp)_{(0;1,2)}} \left(1 + j \dfrac{(FR)_{(ref)}}{(bp)_{(0;1,2)}}\right)} \tag{17}$$

Take

$$\rho_{(r)(0;1,2)} = \sigma_{(0;1,2)} \approx (RAR)_{(0;1,2)} = \left(\frac{b_0}{a_1}\right)(CT)_{(0;1,2)} = (0;1,2) \text{ reference amplitude ratio} \tag{18}$$

Then

$$\mu_{(0;1,2)} \approx \hat{(}DAR)_{(0;1,2)} = \frac{1}{\dfrac{(FR)_{(ref)}}{(bp)_{(0;1,2)}} \sqrt{1 + \left[\dfrac{(FR)_{(ref)}}{(bp)_{(0;1,2)}}\right]^2}} \tag{19}$$

$$= (0;1,2) \text{ dimensionless amplitude ratio}$$

and

$$\phi_{(0;1,2)} \approx (DRA)_{(0;1,2)} = \tan^{-1}\left[-\frac{(FR)_{(ref)}}{(bp)_{(0;1,2)}}\right] - \frac{\pi}{2} \tag{20}$$

$$= (0;1,2) \text{ dynamic response angle}$$

b) (0;1,2) steady-state sinusoidal relating function

Derivation Summary 34-17. Relating function for the (0;1,2) linear differential equation with constant coefficients. (Page 2 of 2)

STEP FUNCTION RESPONSE DEVIATIONS FROM IDEAL INTEGRATION

34.91. In addition to the steady-state sinusoidal relating function approach to the description of integrator performance, it is useful to express differences between actual and ideal integrator performance in terms of step function response curves. In practice, this criterion may be extended to include the forms associated with integrators and differentiators of all types. In the present discussion, however, a single example will be used for illustration purposes. This example is a comparison of the step function response of an actual integrator whose performance is given by the (0;0,1) equation with the step function response of the ideal integrator.

34.92. The expressions for the step function response associated with the (0;0,1) differential equation are developed in Derivation Summaries 18-2 and 18-3 of Chapter 18. The corresponding response curves in nondimensional terms are given in Fig. 34-25. These curves are exponentials that start at zero on the time – characteristic time ratio scale, and have an initial slope identical with the slope of the associated response curve for an ideal integrator. As shown in Fig. 34-25, the response for the ideal integrator continues as a straight line with increasing time while the slope of the response of the (0;0,1) equation decreases.

Given the (1;1,2) differential equation form

$$a_2\ddot{v} + a_1\dot{v} = b_1\dot{u} \tag{1}$$

(Refer to Chapter 19 for a discussion of more general second-order forms.)

Define

$$\tau_{(1;1,2)} \approx (CT)_{(1;1,2)} = \frac{a_2}{a_1} \equiv \text{(1;1,2) characteristic time} \tag{2}$$

$$\sigma_{(1;1,2)} \approx S_{(1;1,2)} \approx \frac{b_1}{a_1} \equiv \text{(1;1,2) dimensional similarity factor} \tag{3}$$

Using the definitions of Eqs. (2) (3) in Eq. (1) gives the working variable equation

$$\tau_{(1;1,2)}\ddot{v} + \dot{v} = \sigma_{(1;1,2)}\dot{u} \tag{4}$$

and the self-defining symbol equation

$$(CT)_{(1;1,2)}\ddot{v} + \dot{v} = S_{(1;1,2)}\dot{u} \tag{5}$$

a) Generalized (1;1,2) equation forms

Consider the steady-state solution associated with Eq. (4) for a sinusoidal forcing function; i.e., take

$$u = u_a \epsilon^{j\omega_f t} \tag{6}$$

and assume

$$v = \eta u = \eta u_a \epsilon^{j\omega_f t} \tag{7}$$

so that

$$\dot{v} = \eta\dot{u} = \eta j\omega_f u \tag{8}$$

and

$$\ddot{v} = \eta\dot{u} = \eta(-\omega_f^2)u \tag{9}$$

Substituting the expressions of Eqs. (8) and (9) in Eq. (4) gives

$$\eta(-\omega_f^2\tau_{(1;1,2)} + j\omega_f)u = \sigma_{(1;1,2)}j\omega_f u \tag{10}$$

Dividing both sides of Eq. (10) by $j\omega_f$ and solving for the relating function $\eta (\approx [RF])$ shows that

$$[RF]_{(1;1,2)} \approx \eta_{(1;1,2)} = \frac{\sigma_{(1;1,2)}}{1 + j\omega_f\tau_{(1;1,2)}} \tag{11}$$

Define

$$T_{(ref)} = \frac{1}{n_{(ref)}} \equiv \text{reference period (arbitrarily chosen)} \tag{12}$$

$$\beta_r \approx (FR)_{(ref)} = \frac{T_{(ref)}}{T_f} = \frac{n_f}{n_{(ref)}} = \text{reference frequency ratio} \tag{13}$$

$$[(RP)(CT)R]_{(1;1,2)} = \frac{T_{(ref)}}{(CT)_{(1;1,2)}} \equiv \text{(1;1,2) reference period – characteristic time ratio} \tag{14}$$

and

$$\beta_{(r)(bp)(1;1,2)} \approx (FR)_{(ref)(bp)(1;1,2)} = (bp)_{(1;1,2)} = \frac{[(RP)(CT)R]_{(1;1,2)}}{2\pi}$$
$$= \text{(1;1,2) breakpoint reference frequency ratio} \tag{15}$$

so that

$$\omega_f\tau_{(1;1,2)} \approx 2\pi\,\frac{T_{(ref)}}{T_f}\,\frac{(CT)_{(1;1,2)}}{T_{(ref)}} = \frac{(FR)_{(ref)}}{(bp)_{(1;1,2)}} \tag{16}$$

Derivation Summary 34-18. Relating function for the (1;1,2) linear differential equation with constant coefficients. (Page 1 of 2)

and Eq. (11) may be written in the form

$$\eta_{(1;1,2)} \simeq [RF]_{(1;1,2)} = \frac{\sigma_{(1;1,2)}}{1 + j \dfrac{(FR)_{(ref)}}{(bp)_{(1;1,2)}}} \tag{17}$$

Take

$$\rho_{(r)(1;1,2)} = \sigma_{(1;1,2)} \simeq (RAR)_{(1;1,2)} = \frac{b_1}{a_1} = (1;1,2) \text{ reference amplitude ratio}$$

Then

$$\mu_{(1;1,2)} \simeq (DAR)_{(1;1,2)} = \frac{1}{\sqrt{1 + \left[\dfrac{(FR)_{(ref)}}{(bp)_{(1;1,2)}}\right]^2}} \tag{18}$$

and

$$\phi_{(1;1,2)} \simeq (DRA)_{(1;1,2)} = \tan^{-1}\left[-\frac{(FR)_{(ref)}}{(bp)_{(1;1,2)}}\right] \tag{19}$$

b) (1;1,2) steady-state sinusoidal relating function

Derivation Summary 34-18. Relating function for the (1;1,2) linear differential equation with constant coefficients. (Page 2 of 2)

By definition, the deviation of the dependent variable ratio that represents the imperfection in actual integrator operation is the difference between points on the exponential response curve and the corresponding points on the ideal integrator curve. At any given time – characteristic time ratio, the magnitude of this deviation is the same for the increasing step function and the decreasing step function. The deviation for the increasing step function case is plotted in Fig. 34-26. The upper plot covers a deviation range from zero to about -0.4. The lower plot covers a range from zero to about -0.02.

NONDIMENSIONAL DYNAMIC AMPLITUDE RATIO AND DYNAMIC RESPONSE ANGLE DEVIATIONS

34.93. Figures 34-27 and 34-28 illustrate the various concepts associated with dimensionless dynamic amplitude ratio deviations. In Fig. 34-27, the (0;1) amplitude ratio is taken as the reference, and the (0;0,1) amplitude ratio is taken as the compared quantity. On the basis of data from Table 34-1, the (0;1) amplitude ratio has a downward slope of minus unity toward the right on a log-log plot with the reference frequency ratio as the independent variable. This straight line crosses the zero-ordinate line at the break point for the (0;0,1) amplitude ratio. The (0;0,1) amplitude ratio is unity for small reference frequency ratios and is asymptotic to the (0;1) amplitude ratio line for large values of the reference frequency ratio. The amplitude ratio deviation is shown in Fig. 34-27 by an arrow drawn from the (0;1) line to the (0;0,1) curve. The deviation for any particular reference frequency ratio is calculated by reading the corresponding values for the two dimensionless dynamic amplitude ratios from the direct-number ordinate scale outside of the loru scale and subtracting these values as indicated. Figure 34-28 is similar to Fig. 34-27 except that the (1;0) amplitude ratio is taken as the reference and the (1;0,1) amplitude ratio is taken as the compared amplitude ratio.

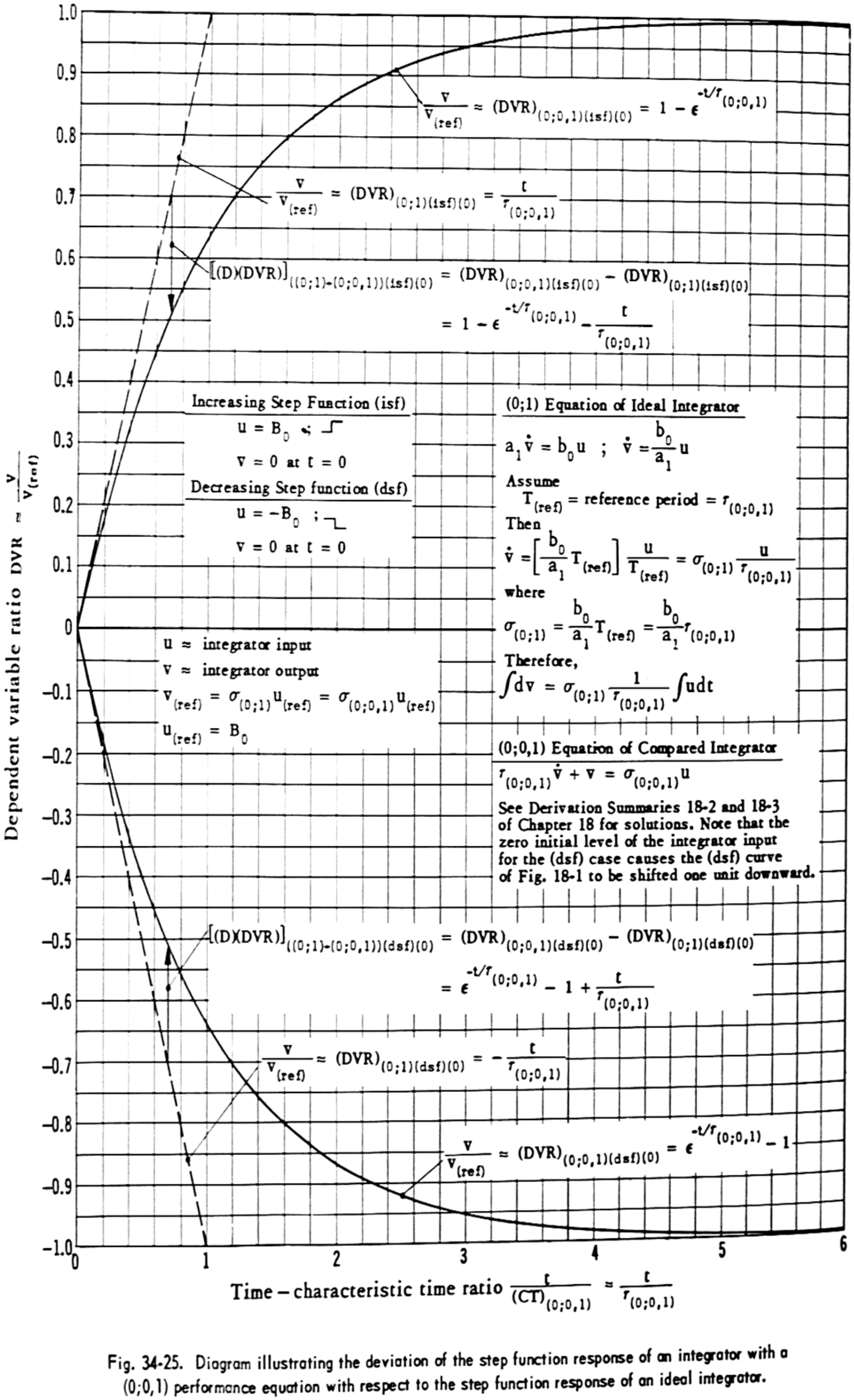
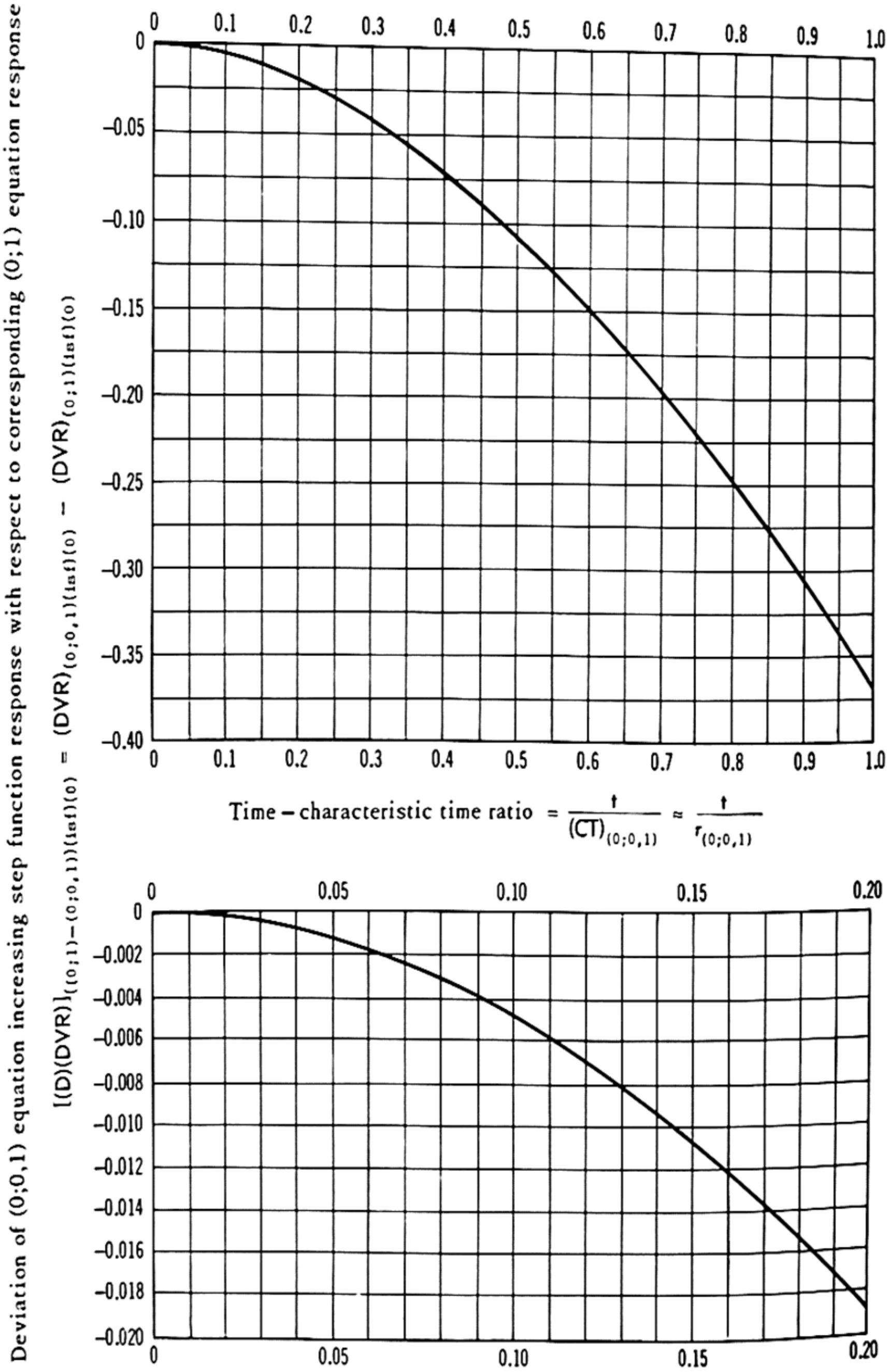
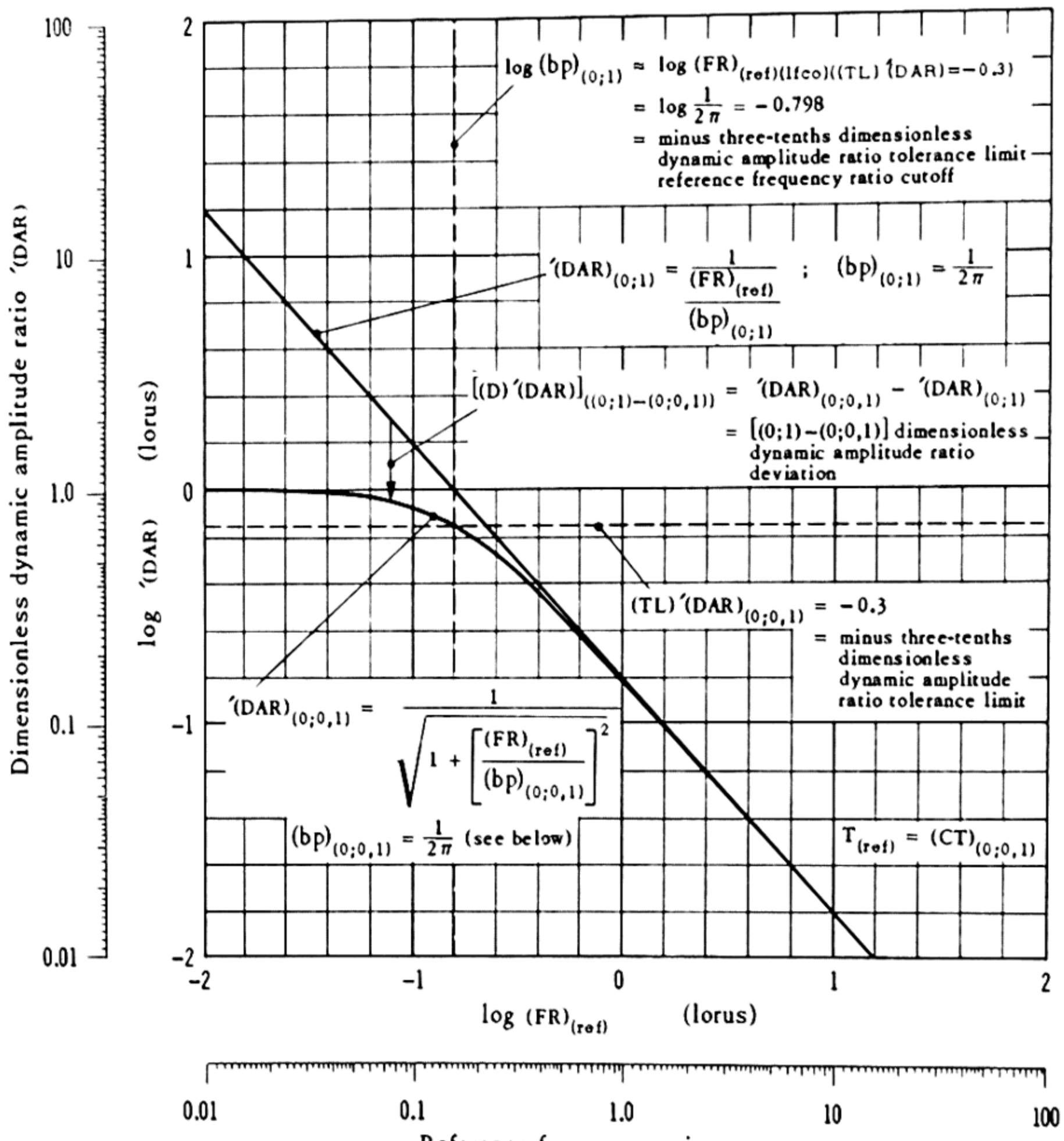


Fig. 34-25. Diagram illustrating the deviation of the step function response of an integrator with a (0;0,1) performance equation with respect to the step function response of an ideal integrator.



Note: The corresponding deviation curves for decreasing step function response are identical with the plots of this figure except for a reversal in the sign of the deviation.

Fig. 34-26. Deviation of the (0;0,1) equation increasing step function response with respect to the corresponding (0;1) equation response.



$$(FR)_{(ref)} = \frac{n_f}{n_{(ref)}} = n_f T_{(ref)} \quad ; \quad n_{(ref)} = \text{reference frequency}$$

$$n_f = \text{forcing frequency} \quad ; \quad T_{(ref)} = \text{reference period}$$

For the (0;1) equation:

$\log {}'(DAR)_{(0;1)} = \log (bp)_{(0;1)} - \log (FR)_{(ref)}$

At the break point,

$$(FR)_{(ref)(bp)} = (bp)_{(0;1)}$$

so that

$$\log {}'(DAR) = 0$$

at

$(FR)_{(ref)(bp)} = (bp)_{(0;1)} = \frac{1}{2\pi} = 0.159 = -0.798$ loru

(see Derivation Summary 34-1)

For the (0;0,1) equation:

At the break point,

$$(FR)_{(ref)(bp)} = (bp)_{(0;0,1)} = \frac{1}{2\pi}\,\frac{T_{(ref)}}{(CT)_{(0;0,1)}}$$

(see Derivation Summary 33-1)

For the $'(DAR)_{(0;0,1)}$ plot,

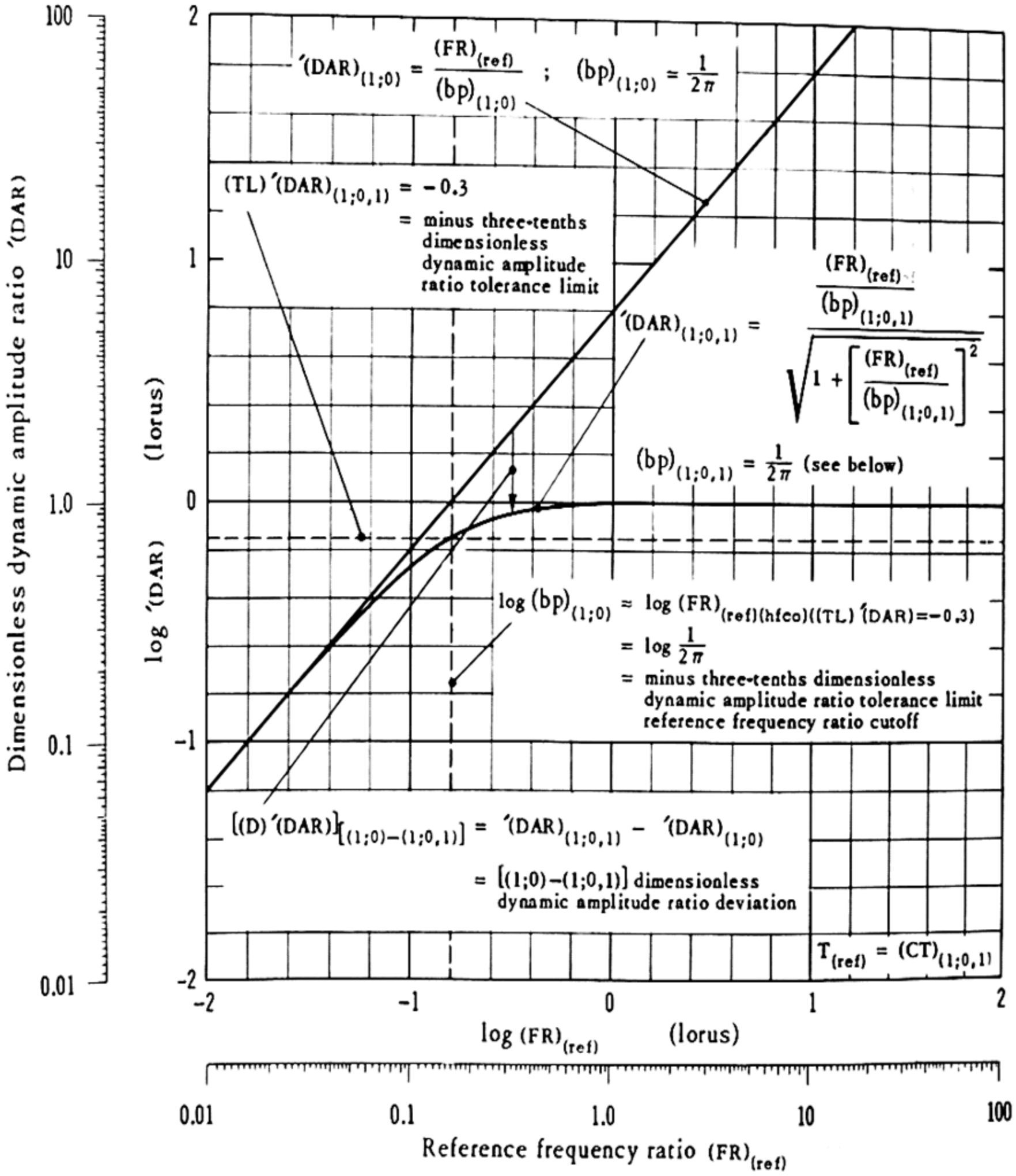
$$T_{(ref)} = (CT)_{(0;0,1)}$$

so that

$$(bp)_{(0;0,1)} = \frac{1}{2\pi}$$

Note: The deviation, (D)'(DAR), for any particular reference frequency ratio, $(FR)_{(ref)}$, is calculated by reading the corresponding values for the two dimensionless dynamic amplitude ratios from the direct-number ordinate scale outside of the loru scale and subtracting these values as indicated.

Fig. 34-27. Diagram illustrating the definition of the [(0;1)−(0;0,1)] dimensionless dynamic amplitude ratio deviation.



$$(FR)_{(ref)} = \frac{n_f}{n_{(ref)}} = n_f T_{(ref)} \quad ; \quad n_{(ref)} = \text{reference frequency}$$

n_f = forcing frequency ; $T_{(ref)}$ = reference period

<u>For the (1;0) equation:</u>

$$\log {}'(DAR)_{(1;0)} = \log (FR)_{(ref)} - \log (bp)_{(1;0)}$$

At the break point,

$$(FR)_{(ref)(bp)} = (bp)_{(1;0)}$$

so that

$$\log {}'(DAR) = 0$$

at

$(FR)_{(ref)(bp)} = (bp)_{(1;0)} = \frac{1}{2\pi} = 0.159 = -0.798$ loru

(see Derivation Summary 34-2)

<u>For the (1;0,1) equation:</u>

At the break point,

$$(FR)_{(ref)(bp)} = (bp)_{(1;0,1)} = \frac{1}{2\pi}\,\frac{T_{(ref)}}{(CT)_{(1;0,1)}}$$

as in the case of the (0;0,1) equation. For the $'(DAR)_{(1;0,1)}$ plot,

$$T_{(ref)} = (CT)_{(1;0,1)}$$

so that

$$(bp)_{(1;0,1)} = \frac{1}{2\pi}$$

Note: The deviation, $(D)\,'(DAR)$, for any particular reference frequency ratio, $(FR)_{(ref)}$, is calculated by reading the corresponding values for the two dimensionless dynamic amplitude ratios from the direct-number ordinate scale outside of the loru scale and subtracting these values as indicated.

Fig. 34-28. Diagram illustrating the definition of the [(1;0)–(1;0,1)] dimensionless dynamic amplitude ratio deviation.

34.94. Tolerance limit lines at -0.3 on the antilog scale are drawn on both Fig. 34-27 and Fig. 34-28. The corresponding reference frequency ratio cutoff (as this concept is defined in Definition Summary 33-1) falls at the break points of the (0;0, 1) and the (1;0, 1) equations.

34.95. Table 34-2 lists expressions for the dimensionless dynamic amplitude ratio fractional deviations and dynamic response angle deviations for the four relating function forms that are associated with the performance equations for actual integrators and differentiators. Each equation is considered as the compared equation, with the (0;1) equation and the (1;0) equation, in turn, considered as the reference equations.

34.96. The deviation expressions of Table 34-2 that have applications for describing the performance of practical integrators and differentiators are represented by the plots of Figs. 34-29 and 34-30. The dashed-line curve in the upper section of Fig. 34-29 gives the dynamic response angle deviation of the (0;1,2) relating function with respect to the (0;1) relating function. This curve also represents the dynamic response angle deviation for the (1;0,1) relating function with respect to the (1;0) relating function. The common abscissa for the deviation curves is the reference frequency ratio, with the characteristic times of the equations associated with the compared relating function taken as the reference period. Dynamic response angle tolerance limits of -2 degrees, -5 degrees, -10 degrees, and -25 degrees are represented in Fig. 34-29 by dotted lines parallel to the axis of abscissas. The high frequency cutoff limits corresponding to these tolerance limits are shown by dotted lines parallel to the axis of ordinates.

34.97. The full-line curve in the upper section of Fig. 34-29 is the dimensionless dynamic amplitude ratio deviation corresponding to the dashed-line dynamic response angle deviation curve. In this upper section, the maximum amplitude ratio deviation plotted is -0.14. The lower section of Fig. 34-29 is a replot of the amplitude ratio deviation with the ordinate scale expanded by a factor of 10. Dimensionless dynamic amplitude ratio fractional deviation tolerance limits at −0.001, −0.01, −0.05, and −0.10 are represented in Fig. 19-29 by dotted lines parallel to the axis of abscissas. The corresponding high frequency cutoff limits are shown by dotted lines parallel to the ordinate axis.

34.98. The curves of Fig. 34-30 give deviations of the (0;0, 1) and the (1;1, 2) relating functions with respect to the (0;1) relating function. The coordinates used in Fig. 34-30 are similar to the coordinates of Fig. 34-29. Tolerance limits for the values used in Fig. 34-29 and the corresponding low frequency cutoff limits are marked on Fig. 34-30.

34.99. The performance information associated with the tolerance limit and cutoff frequency lines of Figs. 34-29 and 34-30 is summarized by Tables 34-3 and 34-4 in terms of cutoff frequencies and band widths. In Table 34-3, the top row

Table 34-2. Dimensionless dynamic amplitude ratio and dynamic response angle deviations for first- and second-order differential equation forms associated with integration and differentiation. (Page 1 of 2)

REFERENCE EQUATION SYMBOL	COMPARED EQUATION SYMBOL	DIMENSIONLESS DYNAMIC AMPLITUDE RATIO FRACTIONAL DEVIATION $[\Delta\mu]_{(\text{ref})\text{-}(\text{cmprd})} = [(\text{FD})\,\hat{}(\text{DAR})]_{(\text{ref})\text{-}(\text{cmprd})}$ (Refer to Definition Summary 34-1.)	DYNAMIC RESPONSE ANGLE DEVIATION $[\Delta\phi]_{(\text{ref})\text{-}(\text{cmprd})} = [(\text{D})(\text{DRA})]_{(\text{ref})\text{-}(\text{cmprd})}$ (Refer to Definition Summary 34-1.)
(0;1)	(0;1,2)	$[\Delta\mu]_{(0;1)\text{-}(0;1,2)} = \dfrac{\mu_{(0;1,2)}}{\mu_{(0;1)}} - 1$ $[\Delta\mu]_{(0;1)\text{-}(0;1,2)} = \dfrac{\beta_{(\text{bpr})(0;1)}}{\beta_{(\text{bpr})(0;1,2)}\sqrt{1+\beta^2_{(\text{bpr})(0;1,2)}}} - 1$ $[(\text{FD})\,\hat{}(\text{DAR})]_{(0;1)\text{-}(0;1,2)} = \dfrac{(\text{FR})_{(\text{bpr})(0;1)}}{(\text{FR})_{(\text{bpr})(0;1,2)}\sqrt{1+(\text{FR})^2_{(\text{bpr})(0;1,2)}}} - 1$ (see Table 34-1) Assume $T_{(\text{ref})} = (\text{CT})_{(0;1,2)}$ so that $[(\text{FD})\,\hat{}(\text{DAR})]_{(0;1)\text{-}(0;1,2)} = \dfrac{1}{\sqrt{1+(\text{FR})^2_{(\text{bpr})(0;1,2)}}} - 1$ Reference to Table 34-1 shows that this fractional deviation expression is equivalent to $[\Delta\mu]_{(0;0,1)} = \mu_{(0;0,1)} - 1 \quad ; \quad \mu_{(\text{ref})} = 1$ Taking $T_{(\text{ref})} = (\text{CT})_{(0;0,1)}$, this deviation is plotted in Fig. 34-29. The plot is taken from Fig. 18-15.	$[\Delta\phi]_{(0;1)\text{-}(0;1,2)} = \phi_{(0;1,2)} - \phi_{(0;1)}$ $[\Delta\phi]_{(0;1)\text{-}(0;1,2)} = [(\text{D})(\text{DRA})]_{(0;1)\text{-}(0;1,2)}$ $= \tan^{-1}[-\beta_{(\text{bpr})(0;1,2)}] - \frac{\pi}{2} + \frac{\pi}{2}$ $= \tan^{-1}[-(\text{FR})_{(\text{bpr})(0;1,2)}] - \frac{\pi}{2} + \frac{\pi}{2}$ (see Table 34-1) Assume $T_{(\text{ref})} = (\text{CT})_{(0;1,2)} \longrightarrow (\text{CT})_{(0;0,1)}$ for plotting purposes, so that, from Table 34-1, $[(\text{D})(\text{DRA})]_{(0;1)\text{-}(0;1,2)} = (\text{DRA})_{(0;0,1)}$ and $[(\text{D})(\text{DRA})]_{(0;1)\text{-}(0;1,2)} = \Delta\phi_{(0;0,1)} = \phi_{(0;0,1)}$; $\phi_{(\text{ref})} = 0$ This deviation is plotted in Fig. 34-29 and is taken from Fig. 18-15.
(0;1)	(1;1,2)	$[\Delta\mu]_{(0;1)\text{-}(1;1,2)} = \dfrac{\mu_{(1;1,2)}}{\mu_{(0;1)}} - 1$ Using $\mu_{(1;1,2)}$ and $\mu_{(0;1)}$ from Table 34-1 gives $[\Delta\mu]_{(0;1)\text{-}(1;1,2)} = \dfrac{\beta_{(\text{bpr})(0;1)}}{\sqrt{1+\beta^2_{(\text{bpr})(1;1,2)}}} - 1$ $[(\text{FD})\,\hat{}(\text{DAR})]_{(0;1)\text{-}(1;1,2)} = \dfrac{(\text{FR})_{(\text{bpr})(0;1)}}{\sqrt{1+(\text{FR})^2_{(\text{bpr})(1;1,2)}}} - 1$ Taking $T_{(\text{ref})} = (\text{CT})_{(1;1,2)}$, this deviation is plotted in Fig. 34-30 This plot is taken from Fig. 18-16 with $\beta_{(\text{bpr})(0;1)} = 2\pi n$.	$[\Delta\phi]_{(0;1)\text{-}(1;1,2)} = \phi_{(1;1,2)} - \phi_{(0;1)}$ From Table 34-1, $[\Delta\phi]_{(0;1)\text{-}(1;1,2)} = [(\text{D})(\text{DRA})]_{(0;1)\text{-}(1;1,2)}$ $= \tan^{-1}[-\beta_{(\text{bpr})(1;1,2)}] + \frac{\pi}{2}$ $= \tan^{-1}[-(\text{FR})_{(\text{bpr})(1;1,2)}] + \frac{\pi}{2}$ Taking $T_{(\text{ref})} = (\text{CT})_{(1;1,2)}$, this deviation is plotted in Fig. 34-30 and is taken from Fig. 18-16.
(0;1)	(0;0,1)	$[\Delta\mu]_{(0;1)\text{-}(0;0,1)} = \dfrac{\mu_{(0;0,1)}}{\mu_{(0;1)}} - 1$ Using $\mu_{(0;0,1)}$ and $\mu_{(0;1)}$ from Table 34-1 gives $[\Delta\mu]_{(0;1)\text{-}(0;0,1)} = \dfrac{\beta_{(\text{bpr})(0;1)}}{\sqrt{1+\beta^2_{(\text{bpr})(0;0,1)}}} - 1$ $[(\text{FD})\,\hat{}(\text{DAR})]_{(0;1)\text{-}(0;0,1)} = \dfrac{(\text{FR})_{(\text{bpr})(0;1)}}{\sqrt{1+(\text{FR})^2_{(\text{bpr})(0;0,1)}}} - 1$ Taking $T_{(\text{ref})} = (\text{CT})_{(0;0,1)}$, this expression is identical with that for $[\Delta\mu]_{(0;1)\text{-}(1;1,2)}$, so that the curves of Fig. 34-30 represent $[\Delta\mu]_{(0;1)\text{-}(0;0,1)}$.	$[\Delta\phi]_{(0;1)\text{-}(0;0,1)} = \phi_{(0;0,1)} - \phi_{(0;1)}$ From Table 34-1, $[\Delta\phi]_{(0;1)\text{-}(0;0,1)} = [(\text{D})(\text{DRA})]_{(0;1)\text{-}(0;0,1)}$ $= \tan^{-1}[-\beta_{(\text{bpr})(0;0,1)}] + \frac{\pi}{2}$ $= \tan^{-1}[-(\text{FR})_{(\text{bpr})(0;0,1)}] + \frac{\pi}{2}$ Taking $T_{(\text{ref})} = (\text{CT})_{(0;0,1)}$, this deviation equation becomes identical with that for $[\Delta\phi]_{(0;1)\text{-}(1;1,2)}$, so that the curve of Fig. 34-30 represents $[\Delta\phi]_{(0;1)\text{-}(0;0,1)}$.
(0;1)	(1;0,1)	$[\Delta\mu]_{(0;1)\text{-}(1;0,1)} = \dfrac{\mu_{(1;0,1)}}{\mu_{(0;1)}} - 1$ Using $\mu_{(1;0,1)}$ and $\mu_{(0;1)}$ from Table 34-1 gives $[\Delta\mu]_{(0;1)\text{-}(1;0,1)} = \dfrac{\beta_{(\text{bpr})(0;1)}\beta_{(\text{bpr})(1;0,1)}}{\sqrt{1+\beta^2_{(\text{bpr})(1;0,1)}}} - 1$ $[(\text{FD})\,\hat{}(\text{DAR})]_{(0;1)\text{-}(1;0,1)} = \dfrac{(\text{FR})_{(\text{bpr})(0;1)}(\text{FR})_{(\text{bpr})(1;0,1)}}{\sqrt{1+(\text{FR})^2_{(\text{bpr})(1;0,1)}}} - 1$ Taking $T_{(\text{ref})} = (\text{CT})_{(1;0,1)}$, $[\Delta\mu]_{(0;1)\text{-}(1;0,1)} = \dfrac{\beta^2_{(\text{bpr})(1;0,1)}}{\sqrt{1+\beta^2_{(\text{bpr})(1;0,1)}}} - 1$ This deviation equation shows that $[\Delta\mu]_{(0;1)\text{-}(1;0,1)}$ does not have a region of $\beta_{(\text{bpr})}$ values for which it is substantially zero. This means that the (1;0,1) equation never approximates the action of the (0;1) equation as far as steady-state sinusoidal solutions are concerned. For this reason the (1;0,1) equation is of no interest here.	$[\Delta\phi]_{(0;1)\text{-}(1;0,1)} = \phi_{(1;0,1)} - \phi_{(0;1)}$ From Table 34-1, $[\Delta\phi]_{(0;1)\text{-}(1;0,1)} = \tan^{-1}[-\beta_{(\text{bpr})(1;0,1)}] + \frac{\pi}{2} + \frac{\pi}{2}$ This expression shows that $[\Delta\phi]_{(0;1)\text{-}(1;0,1)}$ will not be substantially zero for any frequency range.

Table 34-2. Dimensionless dynamic amplitude ratio and dynamic response angle deviations for first- and second-order differential equation forms associated with integration and differentiation. (Page 2 of 2)

REFERENCE EQUATION SYMBOL	COMPARED EQUATION SYMBOL	DIMENSIONLESS DYNAMIC AMPLITUDE RATIO FRACTIONAL DEVIATION $[\Delta\mu]_{(\text{ref})\text{-}(\text{cmprd})} = [(\text{FD})(\text{DAR})]_{(\text{ref})\text{-}(\text{cmprd})}$ (Refer to Definition Summary 34-1.)	DYNAMIC RESPONSE ANGLE DEVIATION $[\Delta\phi]_{(\text{ref})\text{-}(\text{cmprd})} = [(\text{D})(\text{DRA})]_{(\text{ref})\text{-}(\text{cmprd})}$ (Refer to Definition Summary 34-1.)
(1;0)	(0;1,2)	$[\Delta\mu]_{(1;0)\text{-}(0;1,2)} = \dfrac{\mu_{(0;1,2)}}{\mu_{(1;0)}} - 1$ From Table 34-1, $[\Delta\mu]_{(1;0)\text{-}(0;1,2)} = \dfrac{1}{\beta_{(\text{bpr})(1;0)}\beta_{(\text{bpr})(0;1,2)}\sqrt{1+\beta^2_{(\text{bpr})(0;1,2)}}} - 1$ $[(\text{FD})(\text{DAR})]_{(1;0)\text{-}(0;1,2)}$ $= \dfrac{1}{(\text{FR})_{(\text{bpr})(1;0)}(\text{FR})_{(\text{bpr})(0;1,2)}\sqrt{1+(\text{FR})^2_{(\text{bpr})(0;1,2)}}} - 1$ When $T_{(\text{ref})} \longrightarrow (\text{CT})_{(0;1,2)}$, $\beta_{(\text{bpr})(1;0)} \longrightarrow \beta_{(\text{bpr})(0;1,2)}$, so that $[\Delta\mu]_{(1;0)\text{-}(0;1,2)](T_{(\text{ref})}=(\text{CT})_{(0;1,2)})}$ $= \dfrac{1}{\beta^2_{(\text{bpr})(0;1,2)}\sqrt{1+\beta^2_{(\text{bpr})(0;1,2)}}} - 1$ No region of frequency ratio values exists within which this fractional deviation is substantially zero. For this reason, $\mu_{(0;1,2)}$ is not of interest as a form for approximating $\mu_{(1;0)}$.	$\phi_{(0;1,2)}$ is of no interest as an approximation to $\phi_{(1;0)}$ because $\mu_{(0;1,2)}$ never approaches $\mu_{(1;0)}$. $\left[[(\text{FD})(\text{DAR})]_{(1;0)\text{-}(0;1,2)} = \dfrac{1}{(\text{FR})_{(\text{bpr})(1;0)}(\text{FR})_{(\text{bpr})(0;1,2)}\sqrt{1+(\text{FR})^2_{(\text{bpr})(0;1,2)}}} - 1\right]$
(1;0)	(1;1,2)	$[\Delta\mu]_{(1;0)\text{-}(1;1,2)} = \dfrac{\mu_{(1;1,2)}}{\mu_{(1;0)}} - 1$ From Table 34-1, $[\Delta\mu]_{(1;0)\text{-}(1;1,2)} = \dfrac{1}{\beta_{(\text{bpr})(1;0)}\sqrt{1+\beta^2_{(\text{bpr})(1;1,2)}}} - 1$ $[(\text{FD})(\text{DAR})]_{(1;0)\text{-}(1;1,2)} = \dfrac{1}{(\text{FR})_{(\text{bpr})(1;0)}\sqrt{1+(\text{FR})^2_{(\text{bpr})(1;1,2)}}} - 1$ When $T_{(\text{ref})} \longrightarrow (\text{CT})_{(1;1,2)}$, $\beta_{(\text{bpr})(1;0)} \longrightarrow \beta_{(\text{bpe})(1;1,2)}$, so that $[\Delta\mu]_{(1;0)\text{-}(1;1,2)](T_{(\text{ref})}=(\text{CT})_{(1;1,2)})}$ $= \dfrac{1}{\beta_{(\text{bpe})(1;1,2)}\sqrt{1+\beta^2_{(\text{bpe})(1;1,2)}}} - 1$ No region of frequency ratio value exists within which this fractional deviation is substantially zero. For this reason $\mu_{(1;1,2)}$ is not of interest as a form for approximating $\mu_{(1;0)}$.	$\phi_{(1;1,2)}$ is of no interest as an approximation to $\phi_{(1;0)}$ because $\mu_{(1;1,2)}$ never approaches $\mu_{(1;0)}$.
(1;0)	(0;0,1)	From Table 34-1, $\mu_{(0;0,1)}$ has the same form as $\mu_{(1;1,2)}$. It is of no interest for the reason cited above.	$\phi_{(0;0,1)}$ is of no interest for the reason cited above.
(1;0)	(1;0,1)	$[\Delta\mu]_{(1;0)\text{-}(1;0,1)} = \dfrac{\mu_{(1;0,1)}}{\mu_{(1;0)}} - 1$ From Table 34-1, $[\Delta\mu]_{(1;0)\text{-}(1;0,1)} = \dfrac{\beta_{(\text{bpe})(1;0,1)}}{\beta_{(\text{bpr})(1;0)}\sqrt{1+\beta^2_{(\text{bpr})(1;0,1)}}} - 1$ $[(\text{FD})(\text{DAR})]_{(1;0)\text{-}(1;0,1)} = \dfrac{(\text{FR})_{(\text{bpr})(1;0,1)}}{(\text{FR})_{(\text{bpr})(1;0)}\sqrt{1+(\text{FR})_{(\text{bpr})(1;0,1)}}} - 1$ Taking $T_{(\text{ref})} = (\text{CT})_{(1;0,1)}$, $[\Delta\mu]_{(1;0)\text{-}(1;0,1)} = \dfrac{1}{\sqrt{1+\beta^2_{(\text{bpr})(1;0,1)}}} - 1$ Reference to Table 34-1 shows that $[\Delta\mu]_{(1;0)\text{-}(1;0,1)} = \mu_{(0;0,1)(T_{(\text{ref})}=(\text{CT})_{(1;0,1)})} - 1$ This deviation is plotted in Fig. 34-29 and is taken from Fig. 18-15.	$[\Delta\phi]_{(1;0)\text{-}(1;0,1)} = \phi_{(1;0,1)} - \phi_{(1;0)}$ From Table 34-1, $[\Delta\phi]_{(1;0)\text{-}(1;0,1)} = \tan^{-1}[-\beta_{(\text{bpr})(1;0,1)}] + \frac{\pi}{2} - \frac{\pi}{2}$ $= \tan^{-1}[-\beta_{(\text{bpe})(1;0,1)}]$ From Table 34-1, this deviation may be written as $[\Delta\phi]_{(1;0)\text{-}(1;0,1)} = \phi_{(0;0,1)(T_{(\text{ref})}=(\text{CT})_{(1;0,1)})}$ This deviation is plotted in Fig. 34-29 and is taken from Fig. 18-15.

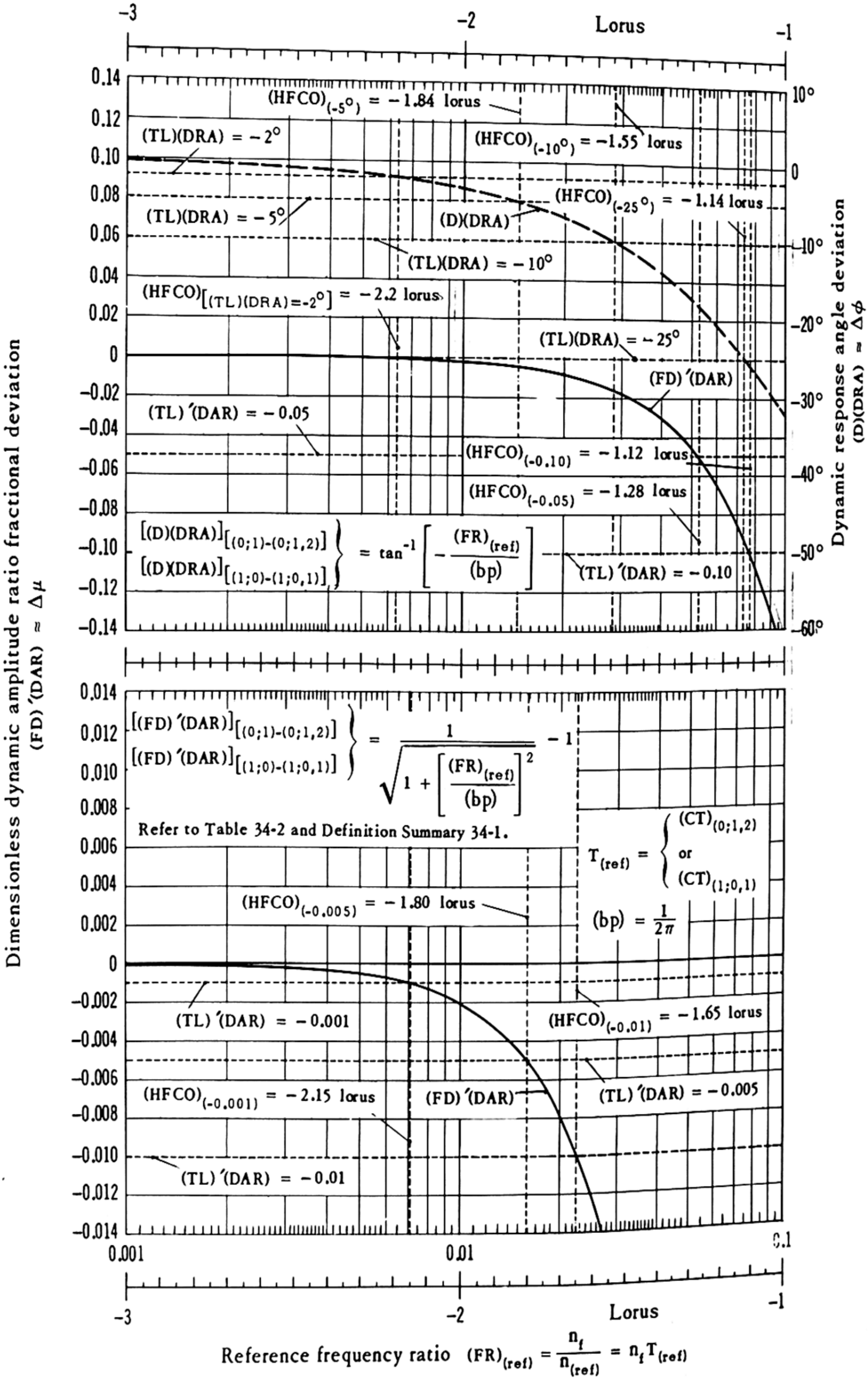


Fig. 34-29. Dimensionless dynamic amplitude ratio and dynamic response angle deviation plots for the (0;1,2) and (1;0,1) differential equations with respect to the (0;1) and (1;0) differential equations, respectively.

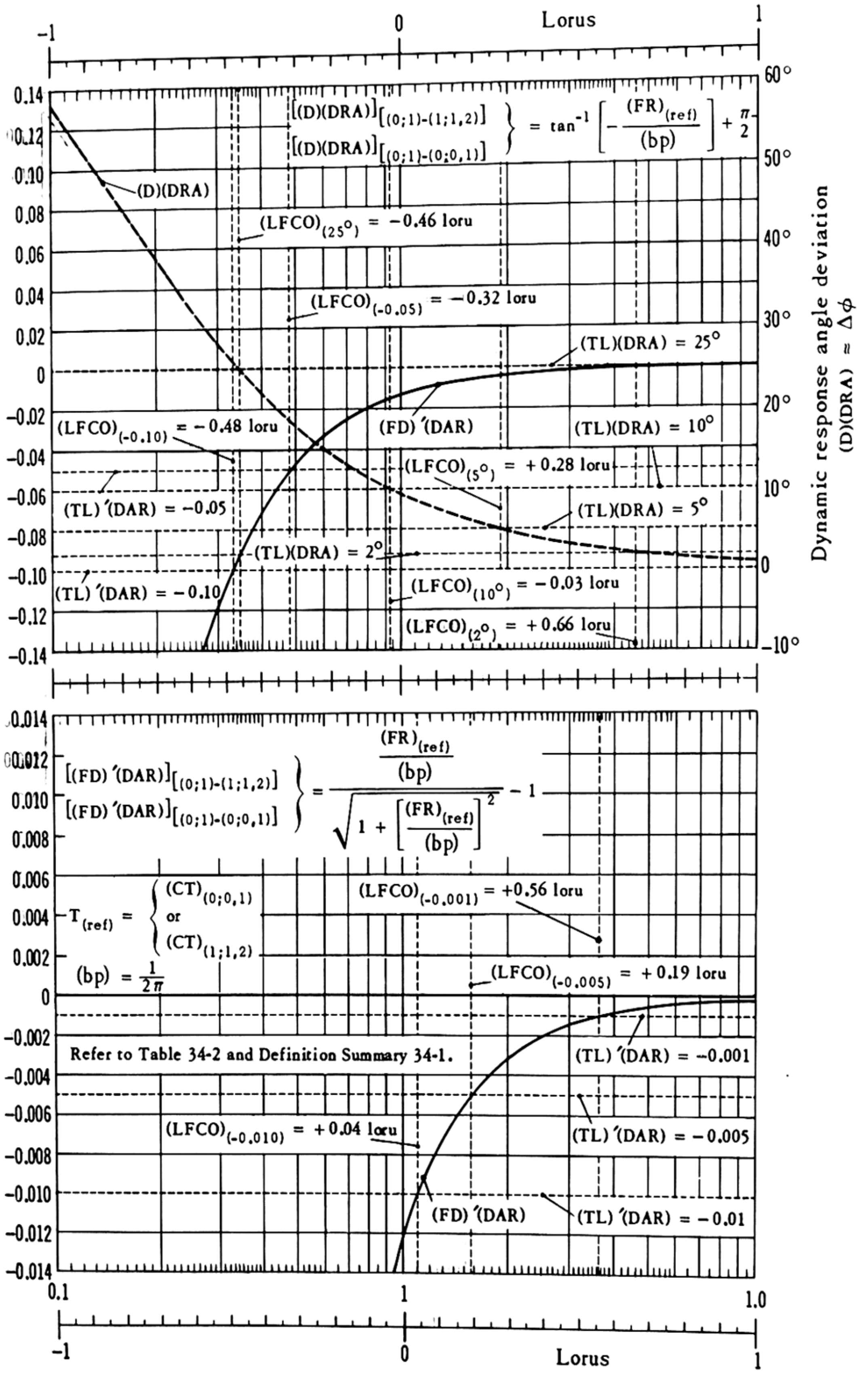


Fig. 34-30. Dimensionless dynamic amplitude ratio and dynamic response angle deviation plots for the (0;0,1) and (1;1,2) differential equations with respect to the (0;1) differential equation.

identifies the equations corresponding to the reference relating function and the compared relating function. The second and third rows give deviation tolerance limits for the dynamic response angle and the dimensionless dynamic amplitude ratio, respectively. The fourth and fifth rows give the high reference frequency ratio cutoff values corresponding to the various specified dynamic response angle deviation tolerance limits and dimensionless dynamic amplitude ratio fractional deviation tolerance limits. The cutoff frequency ratios are given both in lorus and in numerical values. The sixth and seventh rows are the high frequency cutoffs, which are obtained by dividing the numerical frequency ratio values by the characteristic times used for the reference period. The eighth and ninth rows give the band widths corresponding to the high frequency cutoffs of the sixth and seventh rows. Because all the deviation curves approach zero asymptotically for low frequency ratios, the band widths are identical with the high frequency cutoffs.

34.100. Table 34-4 summarizes the cutoff frequency and bandwidth information from Fig. 34-30 in the same way that Table 34-3 summarizes information from Fig. 34-29.

34.101. When the form of the performance equation and the characteristic time for any given integrator or differentiator are known, the cutoff frequency and the band width for any tolerance limit listed in Tables 34-3 and 34-4 may be read directly from the proper row and column. For example, if the integration performance of a system with a performance equation of the (0;0,1) form and a characteristic time of 0.01 second is to be judged on a dynamic amplitude ratio fractional deviation tolerance limit of −0.1, Table 34-4 shows that the low frequency cutoff occurs at 0.331 divided by 0.01, or 33.1 cycles per second. Cutoff frequencies and band widths for the other tolerance limits listed in the table may be read directly. The same information for tolerance limits not listed in the table is available by inspection of Fig. 34-30.

VISCOUS SHEAR INTEGRATOR EXAMPLE

34.102. To illustrate the pattern for the application of the generalized information summarized in the earlier parts of this chapter to specific problems, a preliminary engineering analysis of the performance to be expected from a viscous shear integrator made up of operating components with specified characteristics is carried out in Derivation Summary 34-19. Refer to Derivation Summary 34-5 for a generalized analysis of the viscous shear integrator.

34.103. Section a of Derivation Summary 34-19 repeats the pictorial diagram for the typical viscous shear integrator given in Fig. 34-4. Section b is the corresponding functional diagram, repeated from Derivation Summary 34-5. Section c outlines the development of performance information on a typical direct-current torque generator, which has the excitation current supplied to the field and the input current supplied to the armature. Figure a gives plots of output torque

as a function of input current for three levels of the excitation current under blocked-rotor* conditions. All the curves start at zero torque for zero input current and increase linearly until the input current exceeds about 60 milliamperes. For higher currents, the curves break from the initial linear portion and tend asymptotically toward constant torque levels. This effect is due to saturation in the magnetic circuit parts of the torque generator. For the purposes of performance specification, slopes of the linear portions of the input current – torque output curves are taken to determine the input current – excitation current – torque output reference sensitivity of the torque generator given by Eq. (1) of Derivation Summary 34-19. When a constant excitation current is specified, this sensitivity becomes the current-torque reference sensitivity as given by Eq. (3) of the summary.

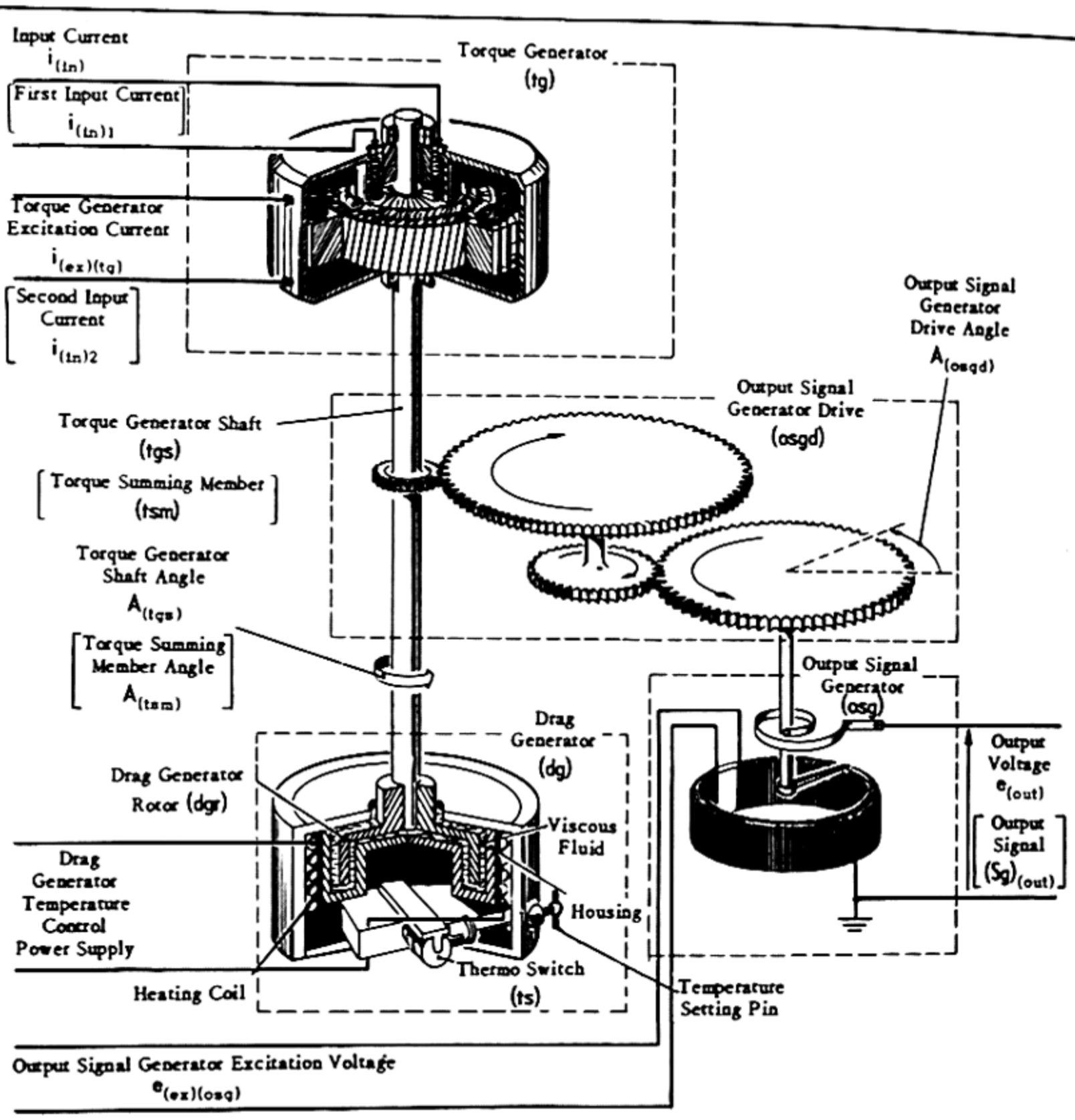
34.104. The current-torque sensitivity performance ratio of the torque generator for any input current and a specified excitation current is formed by dividing the current-torque sensitivity for the input current by the current-torque reference sensitivity, which is based on the linear portion of the torque generator performance characteristic curve. Figure b shows the performance ratio curve, based on data from Fig. a, for the case when the excitation current is 400 milliamperes. The performance ratio is substantially constant at unity for input currents less than 60 milliamperes and falls off rapidly for larger input currents. In order to magnify small departures of the performance ratio from the ideal performance ratio value of unity, the performance ratio deviation is defined as the performance ratio minus unity. This deviation is plotted as a dashed-line curve in Fig. b on an expanded ordinate scale. This curve shows, for example, that saturation causes a negative deviation of approximately one percent when the input current becomes 65 milliamperes.

34.105. Section d of Derivation Summary 34-19 outlines a calculation of the damping coefficient for the drag generator based on the use of a fluid with a viscosity of 20 poises at 160 degrees Fahrenheit. For the small fluid-layer thicknesses used in the drag generator, the shearing force acting on any small area exposed to the fluid is proportional to the viscosity, the velocity of the moving area with respect to the corresponding stationary area, and the area involved, and is inversely proportional to the thickness of the fluid layer. In the damping coefficient calculations, the resultant coefficient is found by summing effects due to the various parts of the drag motor.

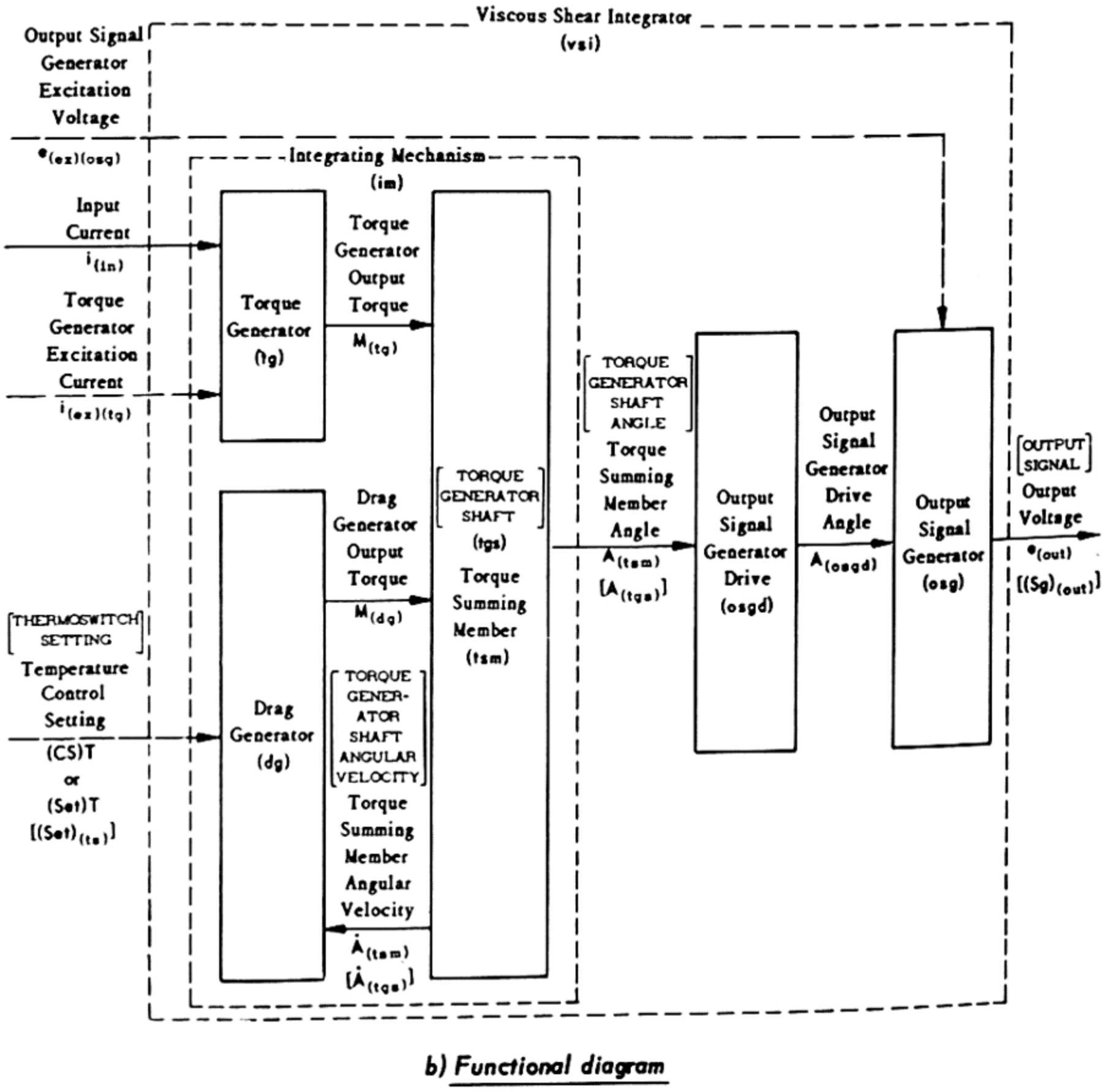
34.106. Section e of Derivation Summary 34-19 gives the performance characteristics of the output signal generating system, which consists of a gear train and a potentiometer.

---

* In general, it is reasonable to assume that, in practical operation of the viscous shear integrator, the rotor angular velocity will be limited to values so small that the output torque is effectively identical with the blocked-rotor torque.



a) Pictorial diagram



b) Functional diagram

Derivation Summary 34-19. Illustrative performance analysis for a viscous shear integrator.
(Page 1 of 12)

(tg) Torque generator

The characteristics shown in Fig. a were determined from experimental tests on the direct-current torque generator with the rotor blocked ($\dot{A}_{(tsm)} = 0$). (In the viscous shear integrator, the rotor speed is limited to the low range in which the output torque is substantially independent of speed.)

Based on slopes taken from the linear portions of the characteristic curves (input currents less than 60 milliamperes), the reference sensitivity of the torque generator is

$$S_{(tg)[i_{(in)},i_{(ex)};M](ref)} = 191 \frac{\text{dyne-centimeters}}{(\text{milliampere})^2} \tag{1}$$

For the special case when

$$i_{(ex)(tg)} = 400 \text{ milliamperes} \tag{2}$$

the reference sensitivity (slope of the current-torque curve for $i_{(ex)(tg)} = 400$ ma) becomes

$$S_{(tg)[i_{(in)};M](ref)} = (191)(400) = 7.64 \times 10^4 \frac{\text{dyne-centimeters}}{\text{milliampere}} \tag{3}$$

For this special case, the performance of the torque generator in terms of deviation from the reference sensitivity is summarized in the performance ratio plot of Fig. b.

The moment of inertia of the torque generator rotor is

$$I_{(tg)} = 9000 \text{ gram-(centimeters)}^2 \tag{4}$$

In addition,

$$\text{Winding resistance of armature} = 30 \text{ ohms} \tag{5}$$

$$\text{Winding resistance of field} = 240 \text{ ohms} \tag{6}$$

c) Torque generator

(dg) Drag generator

A cross-sectional view of the drag generator is given in Fig. c.

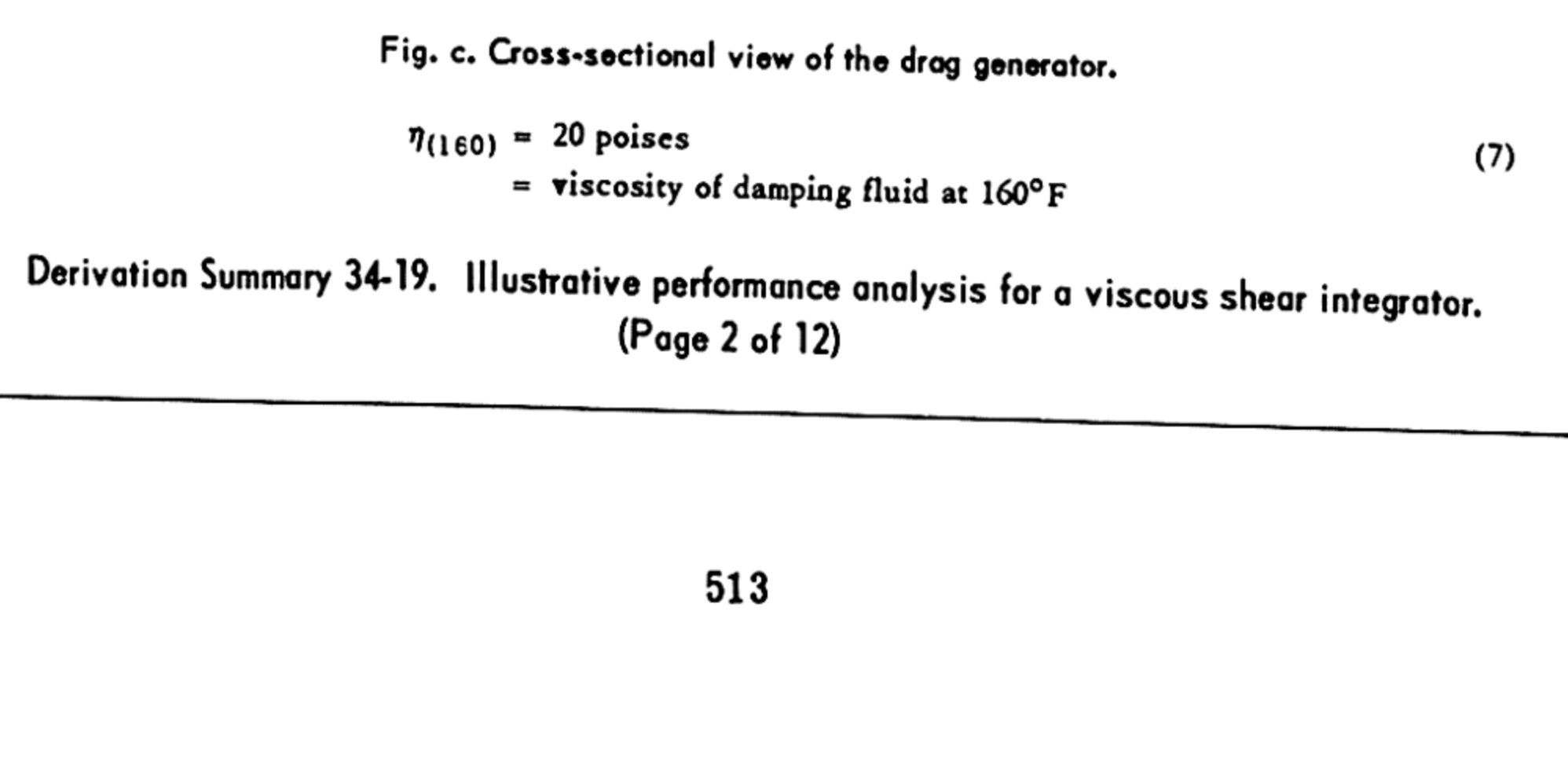


Fig. c. Cross-sectional view of the drag generator.

$$\eta_{(160)} = 20 \text{ poises} = \text{viscosity of damping fluid at } 160^\circ\text{F} \tag{7}$$

Derivation Summary 34-19. Illustrative performance analysis for a viscous shear integrator.
(Page 2 of 12)

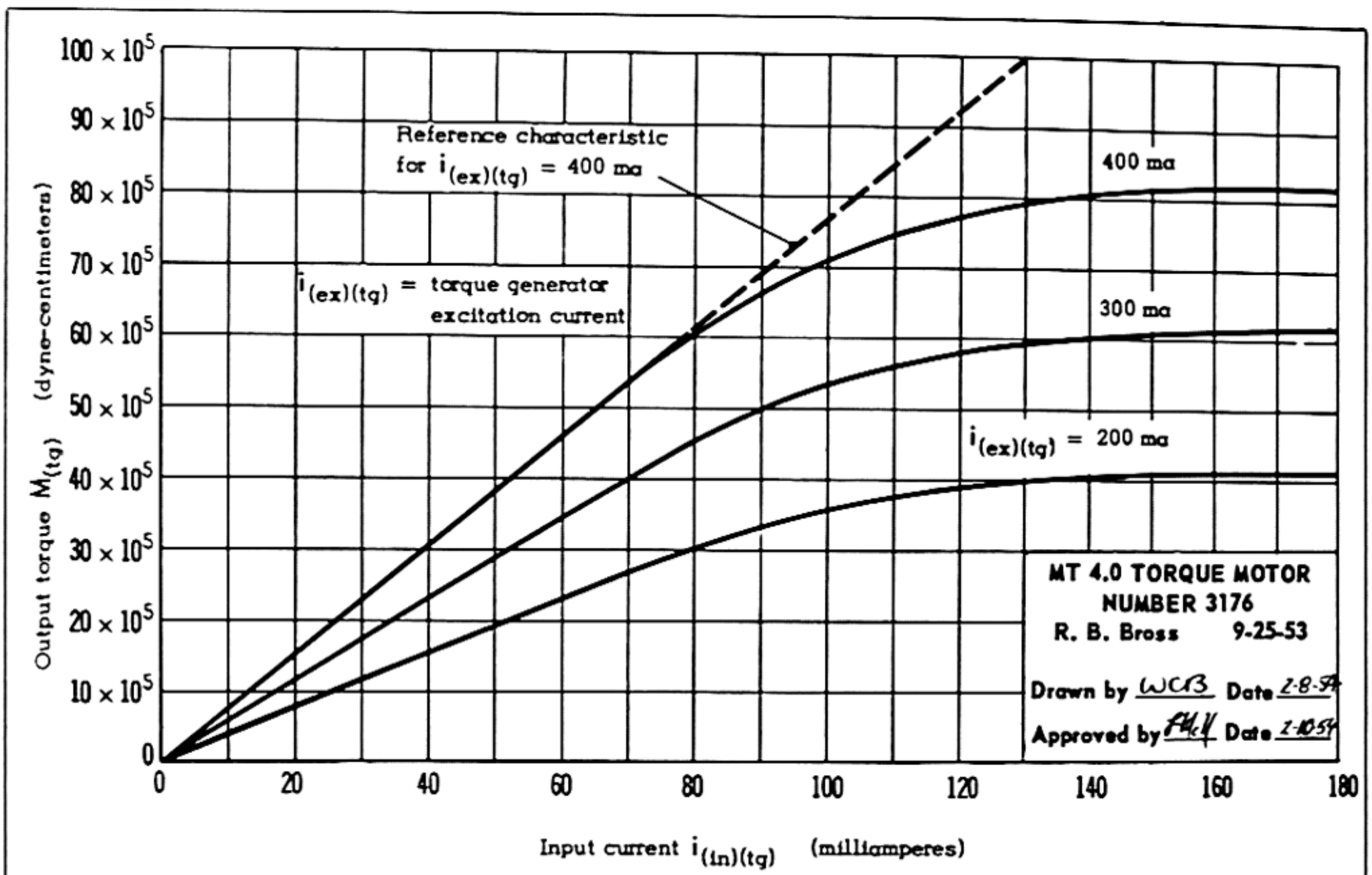


Fig. a. Typical performance characteristic curves for a direct-current torque generator.

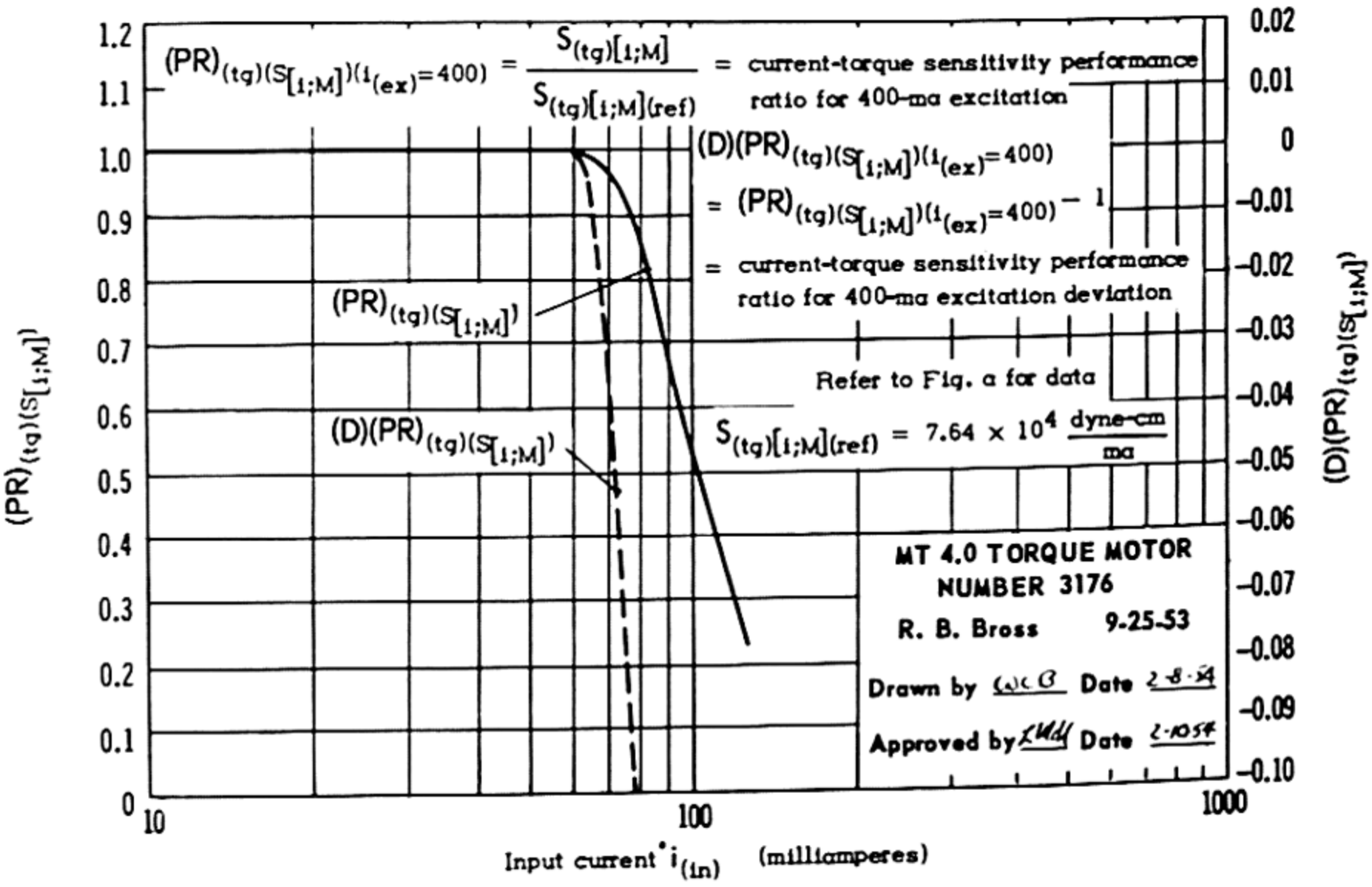


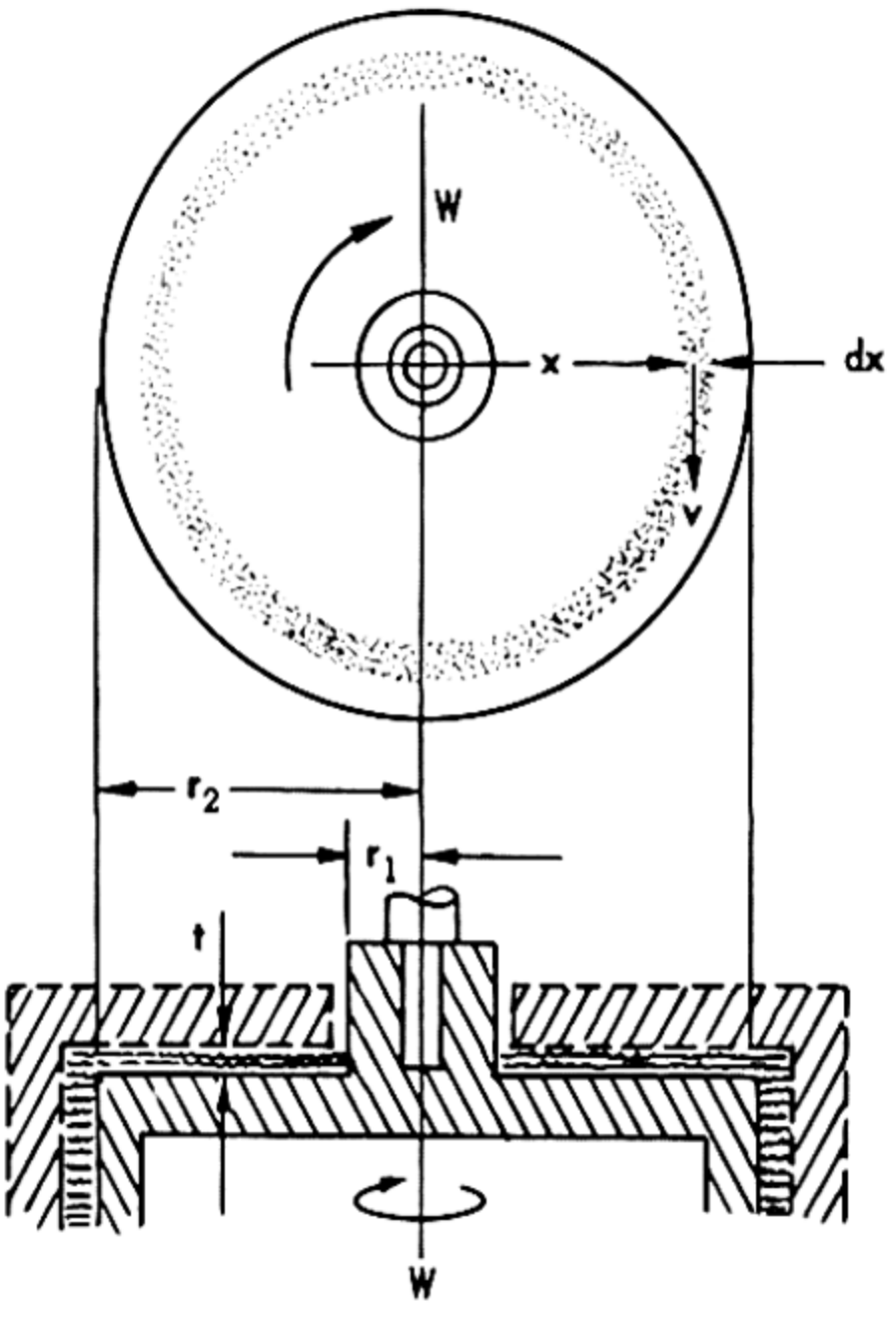
Fig. b. Typical performance ratio and performance ratio deviation curves for a direct-current torque generator.

Derivation Summary 34-19. Illustrative performance analysis for a viscous shear integrator.
(Page 3 of 12)

$$\text{Temperature coefficient of viscosity} = -3 \frac{\text{percent}}{\text{degree Fahrenheit}} \tag{8}$$

The sensitivity of the drag generator may be calculated by considering the viscous shear torque components produced by various sections of the rotor.

The contribution of the top surface of the rotor (tsr) can be calculated as follows.



The incremental moment applied to the rotor due to the fluid forces acting in the shaded area is

$$dM = x\,dF \tag{9}$$

where

$$dF = -\eta \frac{v\,d(\text{Area})}{t} \; ; \quad d(\text{Area}) = \text{differential area} \tag{10}$$

Since

$$d(\text{Area}) = 2\pi x\,dx \tag{11}$$

and

$$v = Wx \tag{12}$$

then

$$dM = -x\,\eta \frac{2\pi x\,dx}{t} Wx \tag{13}$$

and the total moment exerted on the top surface of of the rotor is

$$M_{(tsr)} = -\frac{2\pi W\eta}{t} \int_{r_1}^{r_2} x^3\,dx$$

$$= -\frac{\pi W\eta}{2t}(r_2^4 - r_1^4) \tag{14}$$

$W = \dot{A}$ = angular velocity of the rotor with respect to the case

t = thickness of the fluid layer

From the cross-sectional diagram of the rotor given in Fig. c,

$$r_2 = 5.398 \text{ cm} \; ; \; r_1 = 0.794 \text{ cm} \; ; \; t = 0.254 \text{ cm} \tag{15}$$

which gives

$$\left[\frac{M}{W}\right]_{(tsr)} = -1.06 \times 10^5 \frac{\text{dyne-cm}}{\text{rad/sec}} \tag{16}$$

= torque – angular velocity ratio for the top surface of the rotor with damping fluid at 160°F

Equation (14) can be used to calculate the contribution of the bottom surface of the rotor (bsr) with

$$r_2 = 5.398 \text{ cm} \quad ; \quad r_1 = 0 \quad ; \quad t = 0.254 \text{ cm} \tag{17}$$

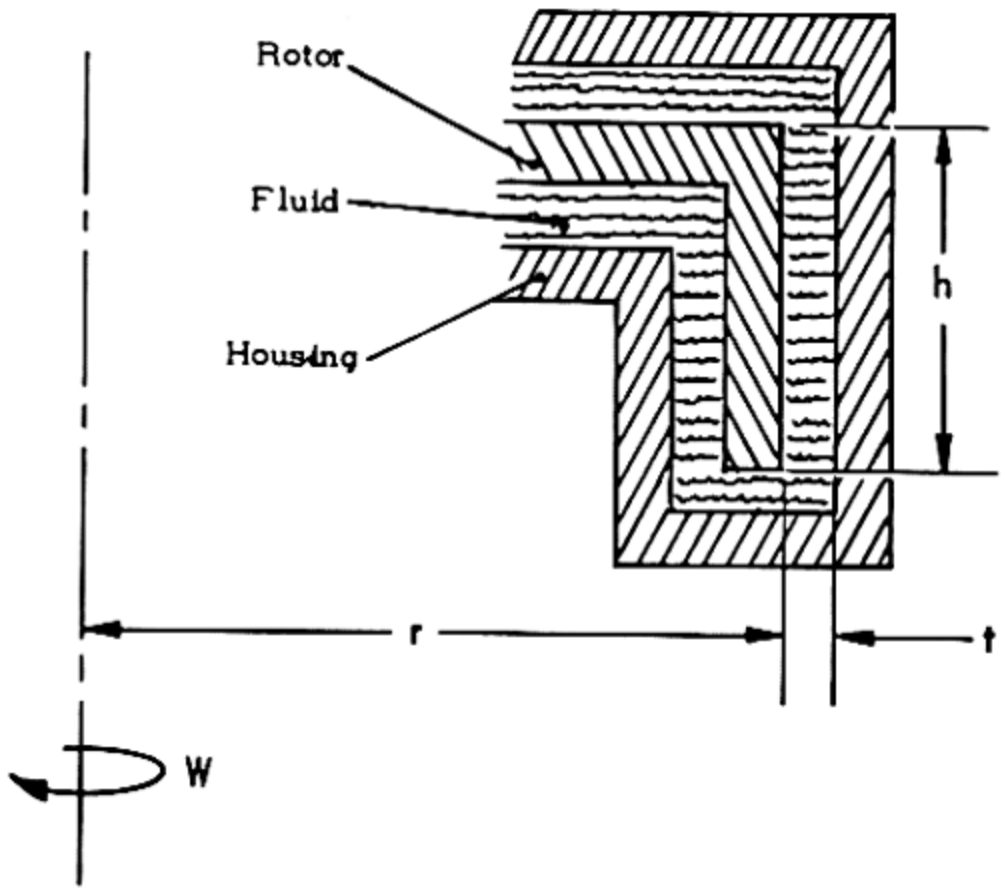
These values give

$$\left[\frac{M}{W}\right]_{(bsr)} = -1.06 \times 10^5 \frac{\text{dyne-cm}}{\text{rad/sec}} \tag{18}$$

= torque – angular velocity ratio for the bottom surface of the rotor with damping fluid at 160°F

The contribution of the side walls of the rotor (swr) can be calculated in a similar way.

Derivation Summary 34-19. Illustrative performance analysis for a viscous shear integrator.
(Page 4 of 12)



For either the inner or outer surface, the moment exerted by the side walls of the rotor is given by the expression

$$M_{(swr)} = -r\eta \frac{2\pi r h}{t} Wr \qquad (19)$$

For the inner surface of the rotor (isr)

$r = 5.08$ cm ; $h = 2.064$ cm ; $t = 0.0254$ cm (20)

which gives

$$\left[\frac{M}{W}\right]_{(isr)} = -1.34 \times 10^6 \frac{\text{dyne-cm}}{\text{rad/sec}} \qquad (21)$$

= torque – angular velocity ratio for the inner surface of the rotor with damping fluid at 160°F

For the outer surface of the rotor (osr),

$r = 5.398$ cm ; $h = 2.54$ cm ; $t = 0.0254$ cm (22)

so that

$$\left[\frac{M}{W}\right]_{(osr)} = -1.98 \times 10^6 \frac{\text{dyne-cm}}{\text{rad/sec}} \qquad (23)$$

= torque – angular velocity ratio for the outer surface of the rotor with damping fluid at 160°F

The resultant angular velocity input – torque output sensitivity of the drag generator is

$$\left[\frac{M}{W}\right]_{(dg)} = \left[\frac{M}{W}\right]_{(tsr)} + \left[\frac{M}{W}\right]_{(bsr)} + \left[\frac{M}{W}\right]_{(isr)} + \left[\frac{M}{W}\right]_{(osr)} = -3.53 \times 10^6 \frac{\text{dyne-cm}}{\text{rad/sec}} \qquad (24)$$

$$\left[\frac{M}{W}\right]_{(dg)} = C_{(damp)(dg)} = S_{(dg)|\dot{A};M|} = 3.53 \times 10^6 \frac{\text{dyne-cm}}{\text{rad/sec}} \qquad (25)$$

The moment of inertia of the drag generator rotor is

$$I_{(dg)} = 3400 \text{ gm-cm}^2 \qquad (26)$$

d) Drag generator

(osgd) Output signal generator drive

$$S_{(osgd)[A_{(tg)};A_{(osgd)}]} = 0.1 \qquad (27)$$

$$I_{(osgd)} = 500 \text{ gm-cm}^2 \qquad (28)$$

= moment of inertia of the moving parts of the output signal generator drive referred to the torque summing member

(osg) Output signal generator

$$S_{(osg)[A;e_{(ex)(osg)};e]} = 0.159 \text{ rad}^{-1} \qquad (29)$$

$$e_{(ex)(osg)} = 150 \text{ volts} \qquad (30)$$

$$S_{(osg)[A;e]} = 23.9 \frac{\text{volts}}{\text{rad}} \qquad (31)$$

e) Output signal generating system

(vsi) Viscous shear integrator

The development of Derivation Summary 34-5 shows that the viscous shear integrator performance equation has the form

$$(CT)_{(vsi)}\ddot{e}_{(out)} + \dot{e}_{(out)} = S_{(vsi)[i_{(in)};\dot{e}](ref)} i_{(in)} \qquad (32)$$

Derivation Summary 34-19. Illustrative performance analysis for a viscous shear integrator.
(Page 5 of 12)

where the sensitivity on the right-hand side of the equation is to be taken as the constant value associated with a specified set of operating conditions.

Assume the following operating conditions:

$$(CS)T = 160^{\circ} = \text{temperature control setting}$$

$$i_{(in)} < 60 \text{ milliamperes} \quad ; \quad i_{(ex)(tq)} = 400 \text{ milliamperes} \quad ; \quad e_{(ex)(osq)} = 150 \text{ volts} \tag{33}$$

$$(U)M_{(tsm)} = 0 = \text{torque summing member uncertainty torque}$$

From the definitions of Derivation Summary 34-5,

$$(CT)_{(vsi)} = \frac{I_{(tsm)}}{S_{(dq)|\dot{A};M|}} \tag{34}$$

and

$$I_{(tsm)} = I_{(tq)} + I_{(dq)} + I_{(osqd)} = 12{,}900 \text{ gm-cm}^2 \tag{35}$$

Therefore,

$$(CT)_{(vsi)} = \frac{12{,}900}{3.53 \times 10^6} = 3.66 \times 10^{-3} \text{ sec} \tag{36}$$

In addition,

$$S_{(vsi)[i_{(in)};\dot{e}](ref)} = \frac{S_{(tq)[i_{(in)};M](ref)} S_{(osqd)[A;A]} S_{(osq)[A;e]}}{S_{(dq)|\dot{A};M|}} = 51.7 \frac{\text{mv/sec}}{\text{ma}} \tag{37}$$

The viscous shear integrator performance equation has the (0;1,2) differential equation form. The performance function for the viscous shear integrator has the form of the (0;1,2) relating function, which is developed in Derivation Summary 34-17; i.e.,

$$[RF]_{(0;1,2)} \approx [PF]_{(vsi)[i_{(in)};e]} = \frac{S_{(vsi)[i_{(in)};e](ref)}}{j\dfrac{(FR)_{(ref)}}{(bp)_{(vsi)}}\left(1 + j\dfrac{(FR)_{(ref)}}{(bp)_{(vsi)}}\right)} \tag{38}$$

where

$$S_{(vsi)[i_{(in)};e](ref)} = S_{(vsi)[i_{(in)};\dot{e}](ref)}(CT)_{(vsi)} = 0.189 \text{ mv/ma} \tag{39}$$

$$(FR)_{(ref)} = \frac{T_{(ref)}}{T_f} \tag{40}$$

Assume

$$T_{(ref)} = (CT)_{(vsi)} = 3.66 \times 10^{-3} \text{ sec} \tag{41}$$

Then, from Eq. (15) of Derivation Summary 34-17,

$$(bp)_{(vsi)} = \frac{1}{2\pi} \tag{42}$$

From Eqs. (19) and (20) of Derivation Summary 34-17,

$$\angle(DAR)_{(0;1,2)} \approx \angle(SR)_{(vsi)(i;e)} = \frac{1}{\dfrac{(FR)_{(ref)}}{(bp)_{(vsi)}}\sqrt{1 + \left[\dfrac{(FR)_{(ref)}}{(bp)_{(vsi)}}\right]^2}} \tag{43}$$

$$(DRA)_{(0;1,2)} \approx (DRA)_{(vsi)(i;e)} = -\frac{\pi}{2} + \tan^{-1}\left[\frac{-(FR)_{(ref)}}{(bp)_{(vsi)}}\right] \tag{44}$$

The development of Derivation Summary 34-1 shows that the ideal integrator performance function has the form of the (0;1) relating function; i.e.,

$$[PF]_{(vsi)[i;e](ideal)} = \frac{S_{(vsi)[i;e](ref)(ideal)}}{j\dfrac{(FR)_{(ref)}}{(bp)_{(vsi)}}} \tag{45}$$

Derivation Summary 34-19. Illustrative performance analysis for a viscous shear integrator.
(Page 6 of 12)

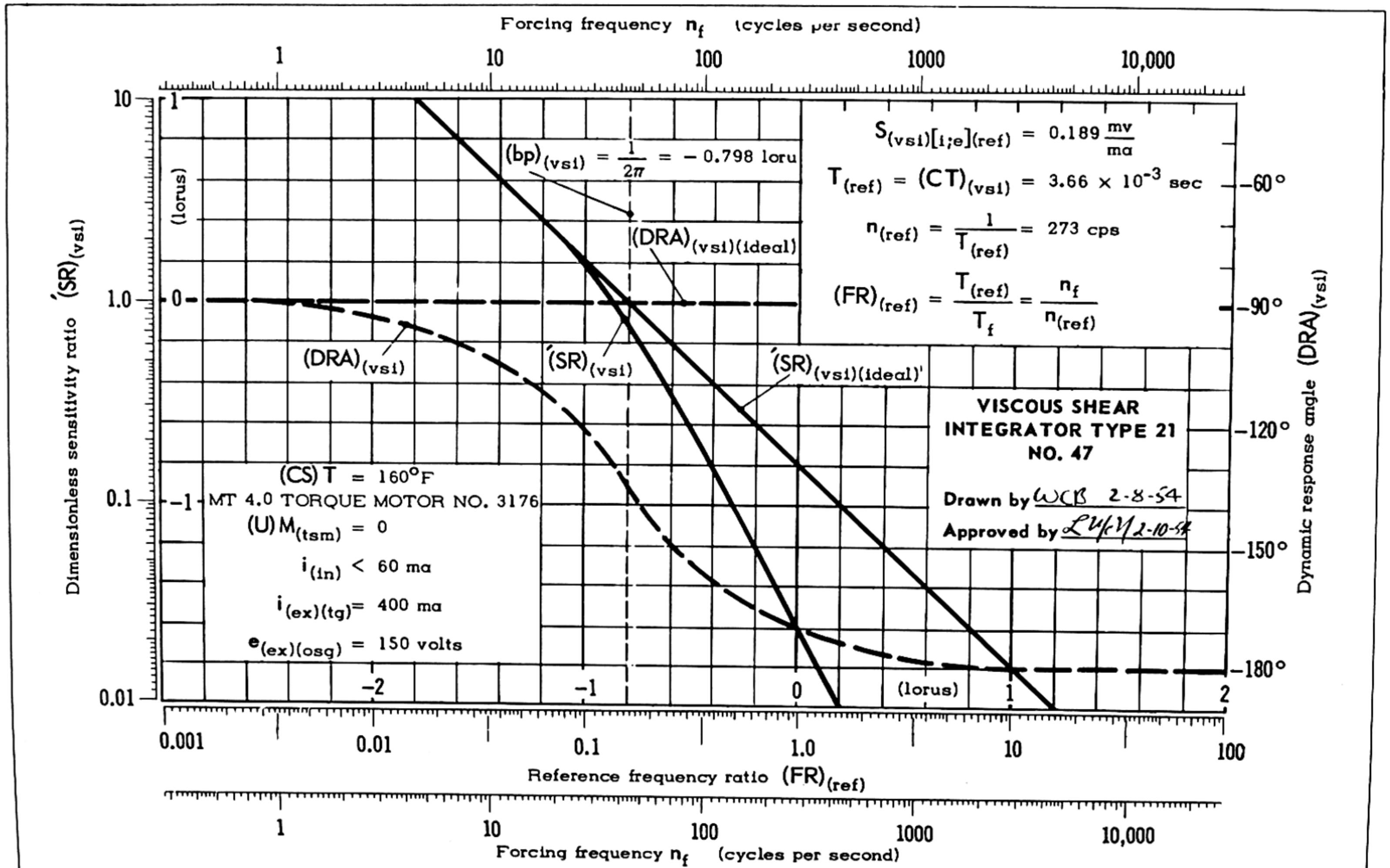


Fig. d. Dimensionless sensitivity ratio and dynamic response angle for the viscous shear integrator.

Derivation Summary 34-19. Illustrative performance analysis for a viscous shear integrator. (Page 7 of 12)

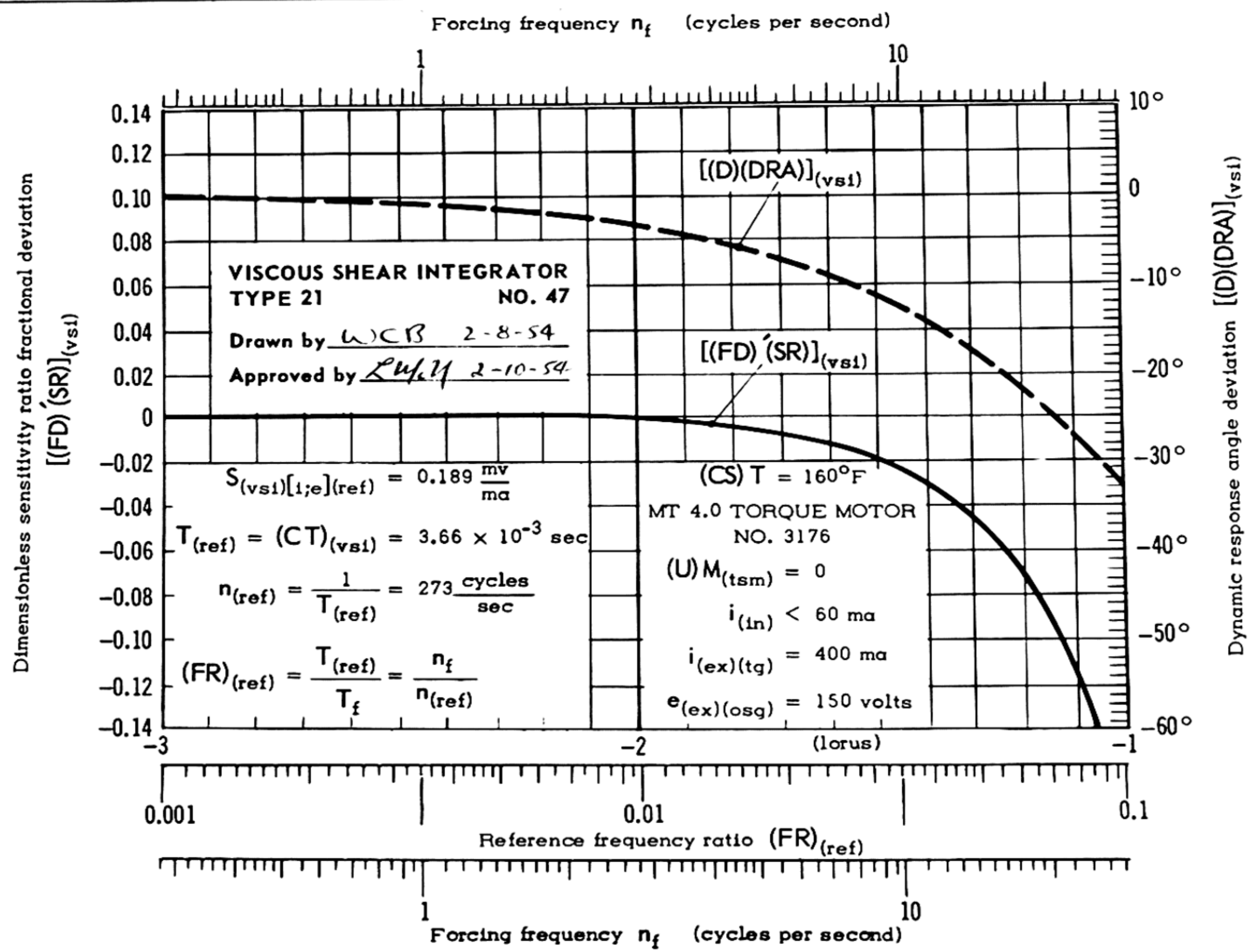


Fig. e. Dimensionless sensitivity ratio fractional deviation and dynamic response angle deviation for the viscous shear integrator.

Derivation Summary 34-19. Illustrative performance analysis for a viscous shear integrator. (Page 8 of 12)

where

$$S_{(vsi)[i;e](ref)(ideal)} = S_{(vsi)[i;\dot{e}](ref)}(CT)_{(vsi)} = S_{(vsi)[i;e](ref)} \quad (46)$$

$$'(SR)_{(vsi)(i;e)(ideal)} = \frac{1}{\frac{(FR)_{(ref)}}{(bp)_{(vsi)}}} \quad ; \quad (DRA)_{(vsi)(i;e)(ideal)} = -\frac{\pi}{2} \quad (47),(48)$$

When the ideal performance function for an integrator is taken as the reference function in Eq. (8) of Definition Summary 34-1, the fractional deviation of the dimensionless sensitivity ratio of the viscous shear integrator becomes

$$[(FD)'(SR)]_{(vsi)} = \frac{1}{\sqrt{1 + \left[\frac{(FR)_{(ref)}}{(bp)_{(vsi)}}\right]^2}} - 1 \quad (49)$$

The corresponding dynamic response angle deviation is

$$[(D)(DRA)]_{(vsi)} = \tan^{-1}\left[\frac{-(FR)_{(ref)}}{(bp)_{(vsi)}}\right] \quad (50)$$

The dimensionless sensitivity ratio and the dynamic response angle of the viscous shear integrator are plotted in Fig. d. The fractional deviation of the dimensionless sensitivity ratio and the deviation of the dynamic response angle are plotted in Fig. e.

f) Performance function and performance plots for the viscous shear integrator with zero uncertainty torque and reference torque generator characteristics

Cutoff frequencies and band widths for the viscous shear integrator are given in Table a. The tolerance limits are specified values of the derivation of the actual integrator performance from the ideal integrator performance. (See Derivation Summaries 34-1 and 34-17, Definition Summary 34-1, Fig. 34-29 and Table 34-3.)

Table a. Cutoff frequencies and band widths for the viscous shear integrator for zero uncertainty torque and reference torque generator characteristics.

(TL)(DRA)	$-2°$	$-5°$	$-10°$
$(FR)_{(ref)(hfco)((TL)(DRA))}$	-2.2 lorus ≈ 0.0063	-1.84 lorus ≈ 0.0145	-1.55 lorus ≈ 0.0282
$n_{(hfco)((TL)(DRA))}$ cycles per second (cps)	$\frac{0.0063}{(CT)_{(vsi)}} \approx 1.72$	$\frac{0.0145}{(CT)_{(vsi)}} \approx 3.96$	$\frac{0.0282}{(CT)_{(vsi)}} \approx 7.71$
$(BW)_{((TL)(DRA))}$ (cps)	1.72 – 0	3.96 – 0	7.71 – 0

(TL)'(DAR)	-0.001	-0.005	-0.01	-0.05
$(FR)_{(ref)(hfco)((TL)'(DAR))}$	-2.15 lorus ≈ 0.0071	-1.80 lorus ≈ 0.0159	-1.65 lorus ≈ 0.0224	-1.28 lorus ≈ 0.0525
$n_{(hfco)((TL)'(DAR))}$ (cps)	$\frac{0.0071}{(CT)_{(vis)}} \approx 1.94$	$\frac{0.0159}{(CT)_{(vsi)}} \approx 4.35$	$\frac{0.0224}{(CT)_{(vsi)}} \approx 6.12$	$\frac{0.0525}{(CT)_{(vsi)}} \approx 14.34$
$(BW)_{((TL)'(DAR))}$ (cps)	1.94 – 0	4.35 – 0	6.12 – 0	14.34 – 0

$(CS)T = 160°F$; $e_{(ex)(osg)} = 150$ v ; $(CT)_{(vsi)} = 3.66 \times 10^{-3}$ sec ; $i_{(in)} < 60$ ma

MT 4.0 Torque Motor No. 3176 $i_{(ex)(tg)} = 400$ ma $(U)M_{(tsm)} = 0$

g) Cutoff frequencies and band widths

Derivation Summary 34-19. Illustrative performance analysis for a viscous shear integrator.
(Page 9 of 12)

When uncertainty torque components act on the torque summing member of the viscous shear integrator, additional deviations from ideal performance appear when the torque generator output is reduced to a level comparable with the maximum value of the uncertainty torque. Further deviations from ideal performance result when the torque generator operates in the region where saturation effects occur ($i_{(in)} > 60$ ma; see Figs. a and b). From Derivation Summary 34-5 and the equation in Fig. b of this summary, the performance equation for a viscous shear integrator whose torque generator operates in the region of saturation effects and whose torque summing member is subjected to uncertainty torque may be written as

$$(CT)_{(vsi)}\ddot{e}_{(out)} + \dot{e}_{(out)} = \frac{S_{(tg)[i;M](ref)}S_{(osgd)[A;A]}S_{(osg)[A;e]}}{S_{(dg)|\dot{A};M|}}(PR)_{(tg)(S_{[i;M]})}i_{(in)}$$

$$\pm \frac{S_{(osgd)[A;A]}S_{(osg)[A;e]}}{S_{(dg)|\dot{A};M|}}|(U)M_{(tsm)}| \qquad (51)$$

where

$|(U)M_{(tsm)}|$ = uncertainty torque magnitude, which, by its inherent nature, is never exactly known. For the purposes of this discussion, in order to arrive at conservative results, $|(U)M_{(tsm)}|$ will be considered as representing $|(U)M_{(tsm)}|_{(max)}$ the maximum value of the uncertainty torque

$$(PR)_{(tg)(S_{[i;M]})} = \frac{S_{(tg)[i;M]}}{S_{(tg)[i;M](ref)}} \qquad (52)$$

= current input – torque output sensitivity performance ratio of the torque generator

By using the reference sensitivity for the torque generator, the uncertainty torque magnitude may be reduced to an equivalent current-input uncertainty magnitude. From Eq. (37), Eq. (51) may be written in the form

$$(CT)_{(vsi)}\ddot{e}_{(out)} + \dot{e}_{(out)} = \left[(PR)_{(tg)(S_{[i;M]})} \pm \frac{|(U)i_{(in)}|}{i_{(in)}}\right]S_{(vsi)[i;\dot{e}](ref)}i_{(in)} \qquad (53)$$

where, by definition,

$$|(U)i_{(in)}| = \frac{|(U)M_{(tsm)}|}{S_{(tg)[i;M](ref)}} \qquad (54)$$

Note that Eq. (54) is strictly valid only when the input current to the torque generator is less than 60 milliamperes, that is, when $(D)(PR)_{(tg)(S_{[i;M]})} = 0$.

From Eq. (53),

$$S_{(vsi)[i;\dot{e}]} = \left[(PR)_{(tg)(S_{[i;M]})} \pm \frac{|(U)i_{(in)}|}{i_{(in)}}\right]S_{(vsi)[i;\dot{e}](ref)} \qquad (55)$$

By definition,

$$(PR)_{(vsi)(S_{[i;\dot{e}]})} = \frac{S_{(vsi)[i;\dot{e}]}}{S_{(vsi)[i;\dot{e}](ref)}} \qquad (56)$$

Therefore, from Eqs. (55) and (56),

$$(PR)_{(vsi)(S_{[i;\dot{e}]})} = (PR)_{(tg)(S_{[i;M]})} \pm \frac{|(U)i_{(in)}|}{i_{(in)}}* \qquad (57)$$

= current input – voltage rate output sensitivity performance ratio of the viscous shear integrator

* For convenience, the negative sign is generally used for drawing performance ratio plots. It is understood that a second branch of the performance ratio curve exists corresponding to the plus sign for the $|(U)i_{(in)}|/i_{(in)}$ term. In any case, the actual performance ratio curve will lie between the $-|(U)i_{(in)}|/i_{(in)}$ and the $+|(U)i_{(in)}|/i_{(in)}$ curves.

Derivation Summary 34-19. Illustrative performance analysis for a viscous shear integrator.
(Page 10 of 12)

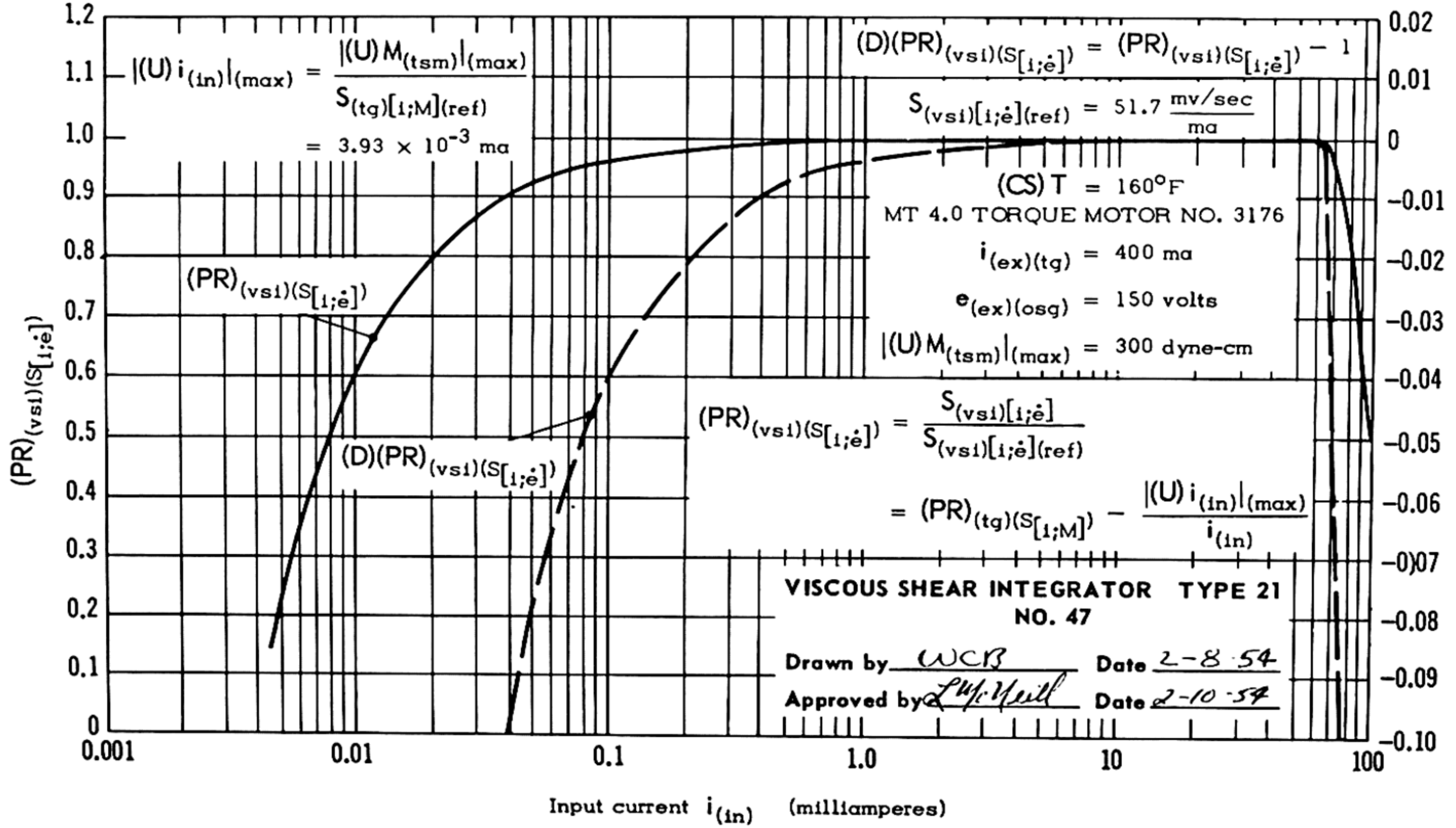


Fig. f. Typical input current – voltage rate output sensitivity performance ratio and performance ratio deviation curves for the viscous shear integrator with constant uncertainty torque and torque generator saturation effects.

Derivation Summary 34-19. Illustrative performance analysis for a viscous shear integrator. (Page 11 of 12)

Measurement shows a maximum uncertainty torque of about 300 dyne-centimeters. Therefore, from Eq. (54),

$$|(U)\,i_{(in)}|_{(max)} = 3.93 \times 10^{-3} \text{ milliamperes} \tag{58}$$

The corresponding sensitivity performance ratio and performance ratio deviation are plotted in Fig. f as functions of input current.

h) Performance ratio for an integrator with uncertainty torque and torque generator saturation effects

Derivation Summary 34-19. Illustrative performance analysis for a viscous shear integrator.
(Page 12 of 12)

34.107. Section f summarizes the performance information of the complete viscous shear integrator when there is zero uncertainty torque and operation of the torque generator occurs in the linear region of the performance characteristic curve. This information is based on the (0;1, 2) performance equation and associated definitions developed in Derivation Summary 34-5. The assumed operating conditions are as follows:

1) Control temperature setting is 160°F.
2) Torque generator input current is less than 60 milliamperes.
3) Torque generator excitation current is 400 milliamperes.
4) Output signal generator excitation voltage = 150 volts.
5) Torque summing member uncertainty torque is zero.

Equation (36) of the summary shows that

$$(CT)_{(vsi)} = 3.66 \times 10^{-3} \text{ seconds}$$
$$= \text{characteristic time of the viscous shear integrator}$$

and that

$$S_{(vsi)[i_{(in)};\dot{e}](ref)} = 51.7 \frac{\text{millivolts/second}}{\text{milliampere}}$$
$$= \text{current input – voltage rate output reference sensitivity of the viscous shear integrator.}$$

34.108. Equations (38) through (44) of Derivation Summary 34-19 give the particular expressions for the viscous shear integrator performance functions that are based on the (0;1,2) relating function forms developed in Derivation Summary 34-17. The corresponding ideal viscous shear integrator performance function and the performance function deviation expressions based on the (0;1) relating function developed in Derivation Summary 34-1 are given by Eqs. (45) through (50) of the summary. The full-line curves shown in Fig. d of the summary are log-log dimensionless sensitivity ratio plots for the actual viscous shear integrator and the ideal viscous shear integrator. The abscissa scale is marked off in loru units of the reference frequency ratio, directly in reference frequency ratio, and also directly in frequency with the reference frequency taken as 273 cycles per second, which is numerically equal to the reciprocal of 3.66×10^{-3} second, the characteristic time

of the actual viscous shear integrator. The dashed-line curves of Fig. d are the corresponding dynamic response angle plots for the actual viscous shear integrator and the ideal viscous shear integrator.

34.109. Figure e of Derivation Summary 34-19 gives the fractional deviation of the dimensionless sensitivity ratio for the viscous shear integrator with the dimensionless sensitivity ratio of the ideal integrator as the reference. This curve is shown as a full line and is related to the left-hand, loru and direct-number ordinate scales. The dashed-line curve of Fig. e represents the dynamic response angle deviation for the viscous shear integrator with the ideal value of minus $\pi/2$ as the reference. The abscissa scales give reference frequency ratio directly and in lorus, and give the forcing frequency in cycles per second.

34.110. The deviation curves of Fig. e show a minus one percent fractional deviation in the dimensionless sensitivity ratio and a dynamic response angle deviation of minus eight degrees at a forcing frequency of about six cycles per second. The frequency limits corresponding to other sensitivity ratio and dynamic response angle tolerances may be read directly from Fig. e. Table a of the summary lists cutoff frequencies and band widths for a number of dimensionless sensitivity ratio fractional deviation and dynamic response angle deviation tolerance limits.

34.111. It is important to note that the curves of Figs. d and e and the data of Table a are based on the assumption of linear behavior of the viscous shear integrator as a system. This means that 1) the torque generator input current must not exceed the 60-milliampere level that the performance ratio deviation curve of Fig. b shows as the limit of linearity (that is, constant current-torque sensitivity) for the torque generator, and 2) there must be no uncertainty torques present.

VISCOUS SHEAR INTEGRATOR WITH UNCERTAINTY TORQUE

34.112. The viscous shear integrator performance equation developed in section h of Derivation Summary 34-19 includes a term that represents the effect of uncertainty torque acting on the torque summing member. No commitment as to the exact nature of this term is made beyond the implicit assumption that it is not linearly related to displacement, velocity, or acceleration of the torque summing member.

34.113. Uncertainty torques are due to actions that are too inconsistent for their effects to be estimated in quantitative terms.* For example, rubbing friction between solid parts causes friction that usually has a behavior intermediate between the constant-magnitude characteristic of coulomb friction and the linear dependence

* Torque components that could actually be taken into account by the inclusion of design features not present in a given design must be considered as uncertainty components.

on velocity of viscous shear. Ball bearings are even more erratic sources of uncertainty torque because of the "lockup" and "release" action that accompanies rotation of ball-and-race combinations, particularly at low angular velocities. Gear trains adjusted for low backlash usually have "tight" and "loose" positions as they transmit rotation. Side shake in rotor bearings causes electromagnetic components to have eccentricity effects that cause output torque changes due to variations in flux-carrying gaps. Any systems in which gravity and acceleration can act on mechanically unbalanced units to apply torque to the rotor will be subject to uncertainty effects when physical distortion of the parts involved is caused by thermal gradients. A similar uncertainty torque is produced by dimensional changes due to "creep" in the material used for solid parts. In addition to the effects mentioned above, the particular features of any given design will often contribute uncertainty torque components that must be considered as special cases. For example, the slider of the output signal generator potentiometer in the viscous shear integrator of Derivation Summary 34-19 will require a driving torque that may be expected to vary with time and environmental conditions.

34.114. The inherent nature of uncertainty torque makes it impossible to apply exact theoretical methods for determining the corresponding effects on overall performance of any given system. It is true, however, that statistical methods are available for estimating average and root-mean-square values of uncertainty effects, and these methods are often useful for predicting the performance of a specified system. On the other hand, for engineering purposes, it is generally more useful in theoretical treatments to assume that the uncertainty torque has a constant magnitude and that it follows the coulomb friction law of changing signs so that it always acts against motion in the system with which it is associated. The use of the constant-magnitude assumption at the maximum value for the uncertainty torque existing in a given case will always result in the prediction of conservative performance characteristics. By reducing the performance-describing forms to nondimensional terms, results for a given system may be easily applied to situations with any given maximum value of uncertainty torque magnitude.

34.115. To illustrate a procedure for including uncertainty torque effects, a derivation for the performance of the viscous shear integrator* of sections a and b is given in section h of Derivation Summary 34-19 for the case when uncertainty torque components act on the torque summing member. A typical performance ratio curve covering the entire operating range for the input current is also provided.

34.116. Equation (51) of Derivation Summary 34-19 gives the viscous shear integrator performance equation with uncertainty torque included. This equation

* The viscous shear integrator is a typical electromechanical system. The method for taking uncertainty torque effects into account for this case may be directly applied to any similar situation.

is also written to include the effect of deviations of the torque motor sensitivity from its reference value. By reducing the uncertainty torque to an equivalent current-input uncertainty, the right-hand side of the performance equation can be written as the product of the current input – voltage rate output reference sensitivity, the input current, and the sum or difference of two terms. This form of the performance equation is given in Eq. (53) and shows that the first term is the current input – torque output sensitivity performance ratio of the torque generator. The second term is the ratio of the equivalent current-input uncertainty to the input current. By definition, this equivalent uncertainty current is the input current that would be required to produce a torque generator output equal to the uncertainty torque. In order to improve the usefulness of the uncertainty current definition, it is based on the current input – torque output reference sensitivity of the torque generator. This means that the uncertainty current is equal to the uncertainty torque divided by the current-torque reference sensitivity of the torque generator. For the reasons discussed in paragraph 34.114, the uncertainty torque is assumed to have a constant value equal to the actually existing maximum value.

34.117. By definition, the current input – voltage rate output sensitivity of the viscous shear integrator is the coefficient of the input-current term on the right-hand side of Eq. (53) of Derivation Summary 34-19, as indicated by Eq. (55). The corresponding definition of the current input – voltage rate output sensitivity performance ratio of the viscous shear integrator is given by Eq. (56) as the ratio of the current input – voltage rate output sensitivity to the current input – voltage rate output reference sensitivity. Equation (57) shows that this performance ratio is equal to the sum or difference of the two terms described in the previous paragraph.

34.118. Figure f of Derivation Summary 34-19 shows the current input – voltage rate output sensitivity performance ratio curve and the corresponding performance ratio deviation curve for the viscous shear integrator when the maximum uncertainty torque is 300 dyne-centimeters. The low-input-current portions of these curves are drawn for the negative sign of the uncertainty current. The high-input-current portions of the performance ratio curves are identical with the high-input-current performance ratio curves for the torque generator.

34.119. The viscous shear integrator performance ratio curve of Fig. f of Derivation Summary 34-19 is a special example of the typical semilogarithmic performance ratio curve of Fig. 5-2, which is discussed in generalized terms in Chapter 5. The falling off of the curve at low input levels is due to the interfering effects of uncertainty torque. The falling off at high input levels is due to saturation of electromagnetic circuits in the torque generator.

34.120. The performance deviation curve for the viscous shear integrator operating under the specified conditions shows that, for a deviation of not more

than one percent, the input current should never be less than 0.4 milliampere nor more than 67 milliamperes.

MOTOR – AMPLIFIER – FEEDBACK-TACHOMETER INTEGRATOR WITH ZERO UNCERTAINTY

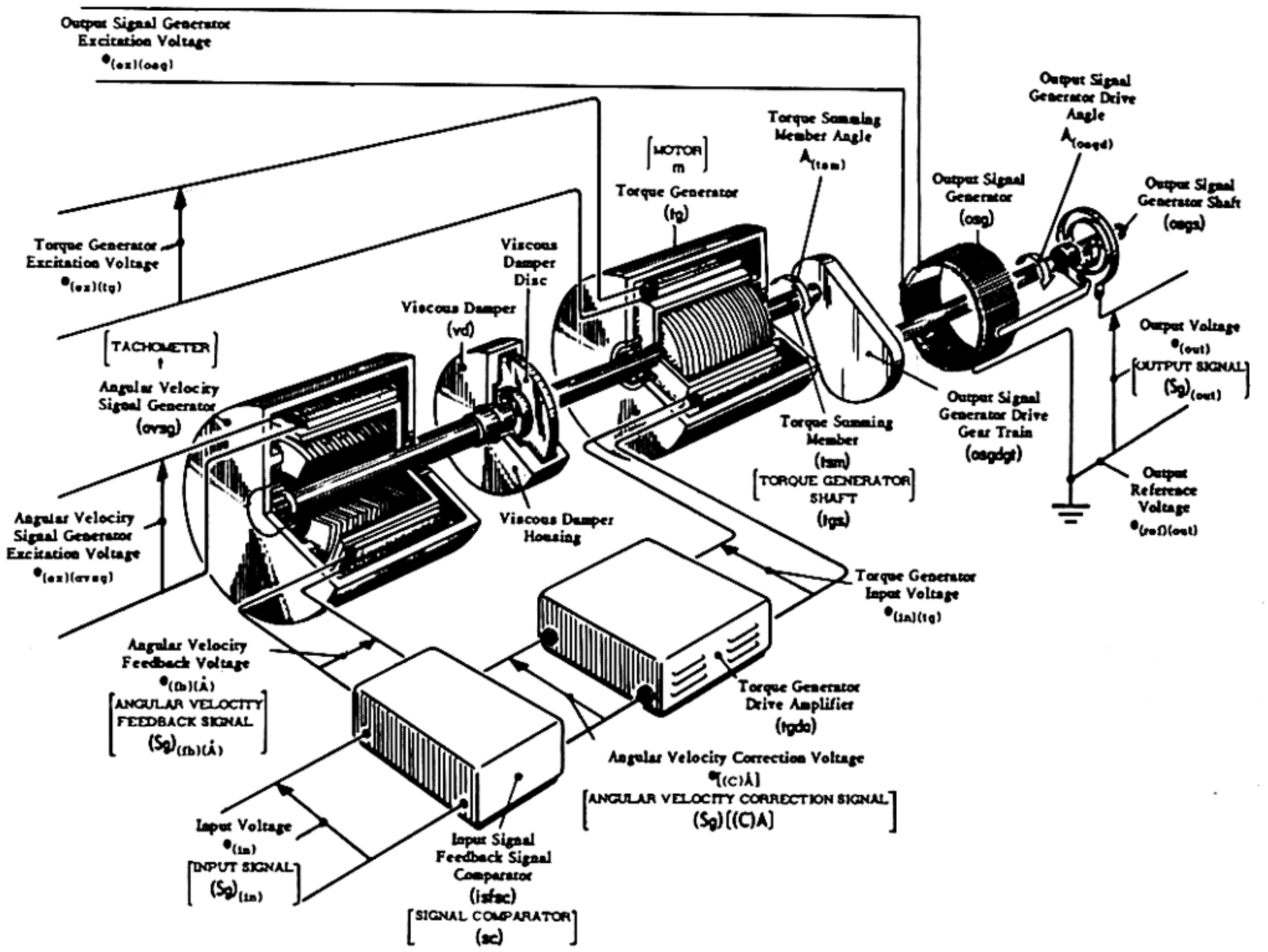
34.121. The pictorial diagram of section a and the functional diagram of section b of Derivation Summary 34-20 show the essential features of a typical motor – amplifier – feedback-tachometer integrator. Section c gives the direct and feedback sensitivities of the signal comparator. The use of simple sensitivities shows that the signal comparator performance is not affected by either magnitude or frequency of the input and feedback signals. Section d shows that the torque generator drive amplifier has a constant gain, independent of the frequency and magnitude of the input signal over the operating range required by integrator operation.

34.122. Section e of Derivation Summary 34-20 gives the performance characteristics of the two-phase alternating-current torque generator. Figure a shows the blocked-rotor input voltage – output torque characteristic curves for three levels of voltage excitation. These characteristics are all straight lines within the range of input voltage used for the plots and lead to an input voltage – excitation voltage – torque output sensitivity of 9.60 dyne-centimeters per volt-squared. When an excitation of 115 volts at a frequency of 400 cycles per second is applied, the voltage-torque sensitivity is 1104 dyne-centimeters per volt. The running speed-torque characteristics for 115-volts excitation at 400 cycles per second are given by Fig. b for the three constant levels of input voltage. The downward slopes of these characteristics show that the angular velocity – torque sensitivity magnitude of the torque generator is 119 dyne-centimeters per radian-per-second.

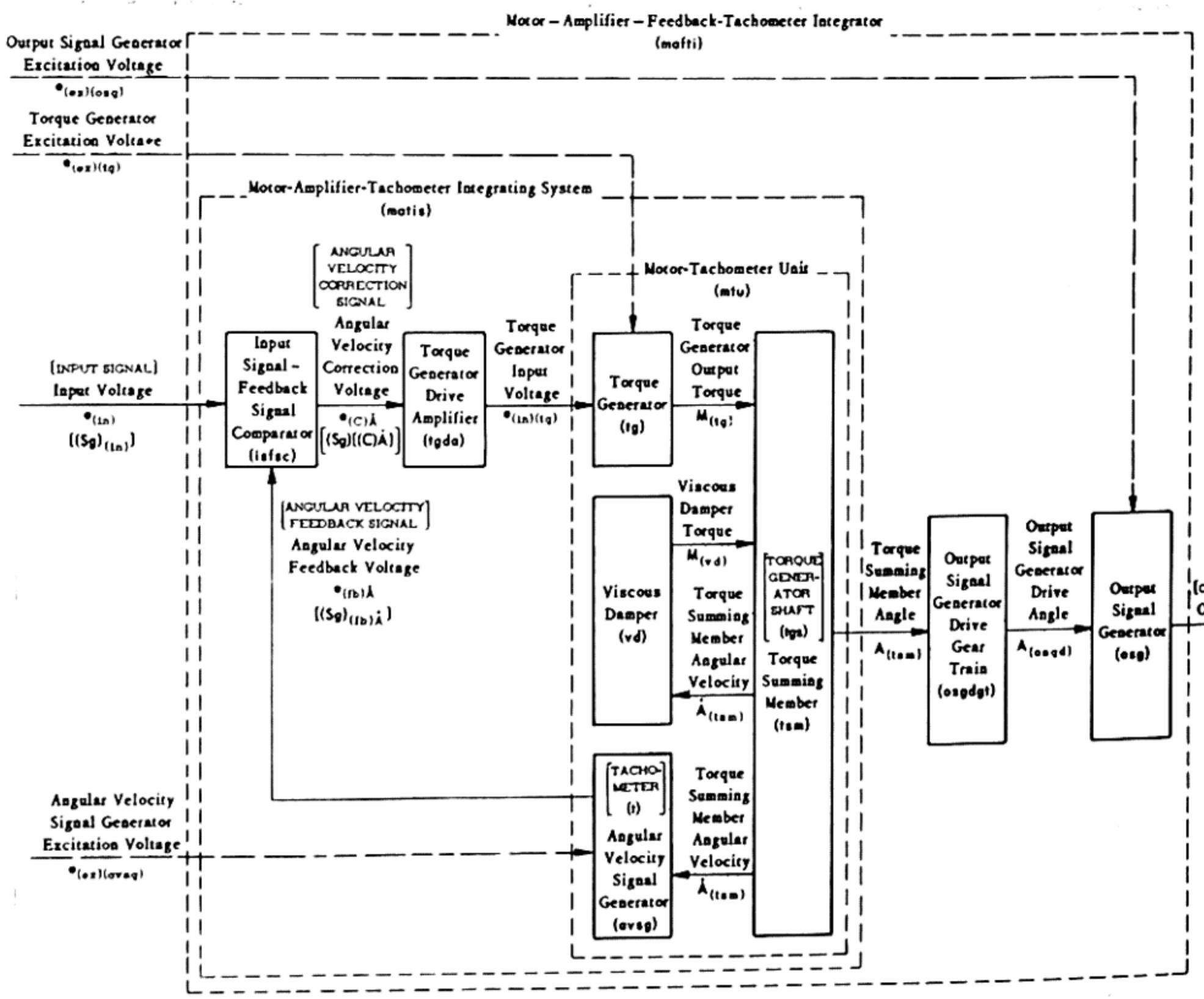
34.123. Section f of Derivation Summary 34-20 gives the angular velocity – torque sensitivity of the viscous damper and the moment of inertia of the torque summing member. The calculations for finding these quantities are identical in nature with those described for similar quantities in Derivation Summary 34-19. In the interest of brevity, only the results are given in section f.

34.124. Section g of Derivation Summary 34-20 gives the performance data on the angular velocity signal generator. Section h gives the corresponding information on the output signal generating system.

34.125. Section i of Derivation Summary 34-20 gives the performance equation developed in Derivation Summary 34-11 for the motor – amplifier – feedback-tachometer integrator and summarizes the defining equations for the characteristic time and sensitivity that completely specify the operation of the integrator when no uncertainties are present. Equations (22) and (24) shows that the characteristic time is 4.22×10^{-3} second, and that the voltage input – voltage rate output sensitivity is 0.0355 volt-per-second per volt.



a) Pictorial diagram



b) Functional diagram

Derivation Summary 34-20. Illustrative performance analysis for a motor – amplifier – feedback-tachometer integrator. (Page 1 of 9)

(isfsc) Input signal – feedback signal comparator

$$S_{(isfsc)|e;e|(dir)} = 0.175 \frac{\text{volt}}{\text{volt}} \quad (1)$$

$$S_{(isfsc)|e;e|(fb)} = 0.65 \frac{\text{volt}}{\text{volt}} \quad (2)$$

c) Input signal – feedback signal comparator

(tgda) Torque generator drive amplifier

$$S_{(tgda)|e;e|} = 4550 \frac{\text{volts}}{\text{volt}} \quad (3)$$

d) Torque generator drive amplifier

(tg) Torque generator

The blocked-rotor ($\dot{A}_{(tsm)} = 0$) characteristics of the two-phase alternating-current torque generator are given in Fig. a.

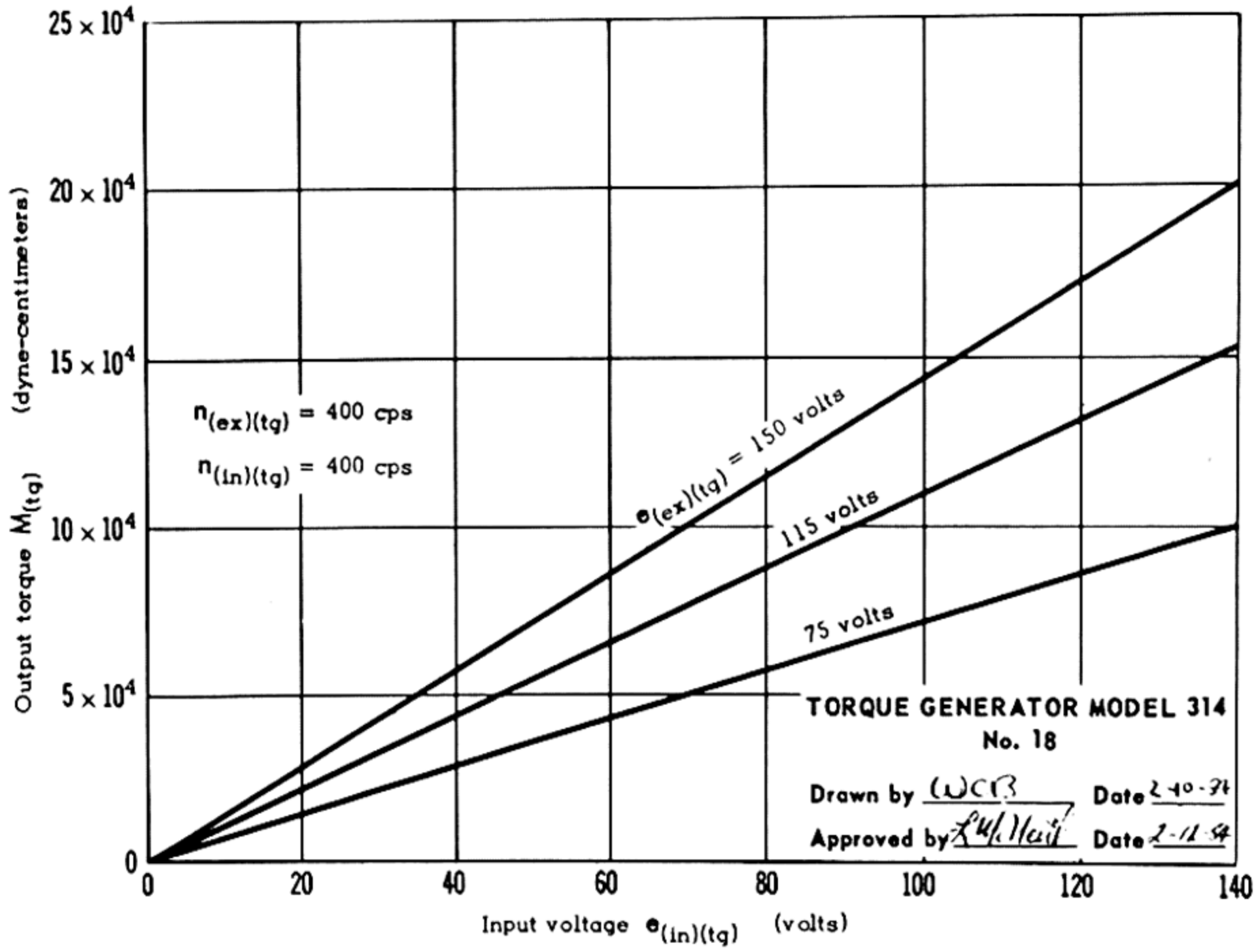


Fig. a. Typical blocked-rotor performance characteristic curves for a two-phase alternating-current torque generator.

On the basis of slopes taken from the characteristic lines of Fig. a,

$$S_{(tg)[e;e;M](\dot{A}_{(tsm)=0})} = 9.60 \frac{\text{dyne-cm}}{(\text{volt})^2} \quad (4)$$

When

$$e_{(ex)(tg)} = 115 \text{ volts} \quad ; \quad n_{(ex)(tg)} = 400 \text{ cycles/second} \quad (5)$$

then

$$S_{(tg)|e;M|} = (9.60)(115) = 1104 \frac{\text{dyne-centimeters}}{\text{volt}} \quad (6)$$

Derivation Summary 34-20. Illustrative performance analysis for a motor – amplifier – feedback-tachometer integrator. (Page 2 of 9)

The running ($\dot{A}_{(tsm)} \neq 0$) characteristics of the torque generator are given in Fig. b.

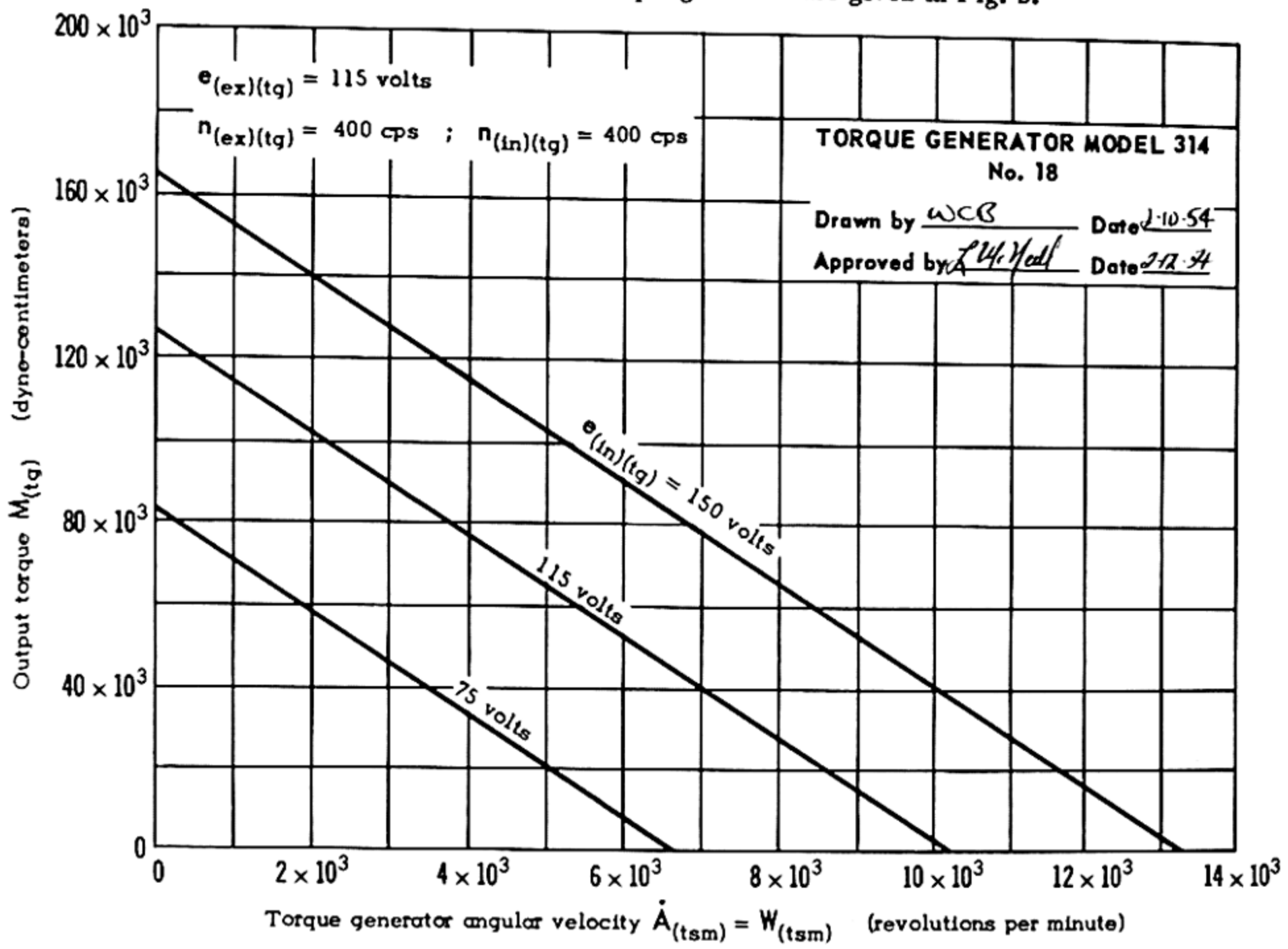


Fig. b. Typical running performance characteristic curves for a two-phase alternating-current torque generator.

On the basis of slopes taken from Fig. b,

$$S_{(tg)|A;M|} = \frac{dM}{d\dot{A}} = 12.5 \frac{\text{dyne-cm}}{\text{rpm}} = 119 \frac{\text{dyne-cm}}{\text{rad/sec}} \tag{7}$$

for $n_{(ex)}$ = 400 cycles/second; $e_{(ex)}$ = 115 volts

e) Torque generator

(vd) Viscous damper

From experimental data,

$$S_{(vd)|\dot{A};M|} = 1200 \frac{\text{dyne-cm}}{\text{rad/sec}} \tag{8}$$

Note: This sensitivity is assumed to be independent of environmental temperature (a thermo-static system is used).

By calculation, the moment of inertia of the torque summing member is

$$I_{(tsm)} = 137 \text{ gm-cm}^2 \tag{9}$$

f) Viscous damper

(avsg) Angular velocity signal generator

From experimental data,

$$S_{(avsg)[\dot{A};e;e]} = 8.3 \times 10^{-5} \frac{\text{volt}}{\text{volt-rad/sec}} \tag{10}$$

When

$$e_{(ex)(avsg)} = 115 \text{ volts} \quad ; \quad n_{(ex)(avsg)} = 400 \text{ cps} \tag{11}$$

then

$$S_{(avsg)[\dot{A};e]} = (8.3 \times 10^{-5})(115) = 9.55 \times 10^{-3} \frac{\text{volt}}{\text{rad/sec}} \tag{12}$$

g) Angular velocity signal generator

Derivation Summary 34-20. Illustrative performance analysis for a motor – amplifier – feedback-tachometer integrator. (Page 3 of 9)

(osgdgt) Output signal generator drive gear train

$$S_{(osgdgt)[A_{(tsm)};A_{(osgd)}]} = \frac{1}{2295} \tag{13}$$

(osg) Output signal generator

$$S_{(osg)[A;e;e]} = 1 \frac{\text{volt}}{\text{volt-rev}} \tag{14}$$

When

$$e_{(ex)(osg)} = 19 \text{ volts} \tag{15}$$

then

$$S_{(osg)[A;e]} = (19)(1) = 19 \frac{\text{volts}}{\text{rev}} = 3.02 \frac{\text{volts}}{\text{rad}} \tag{16}$$

h) Output signal generating system

(mafti) Motor – amplifier – feedback-tachometer integrator

The development of Derivation Summary 34-11 shows that the performance equation of the motor – amplifier – feedback-tachometer integrator with zero uncertainty torque has the form

$$(CT)_{(mafti)} \ddot{e}_{(out)} + \dot{e}_{(out)} = S_{(mafti)[e;\dot{e}]} e_{(in)} \tag{17}$$

where

$$(CT)_{(mafti)} = \frac{I_{(tsm)}}{S_{(tg)|\dot{A};M|} + S_{(vd)|\dot{A};M|} + S_{(isfsc)|e;e|(fb)} S_{(tgda)|e;e|} S_{(tg)[e;M]} S_{(avsg)[\dot{A};e]}} \tag{18}$$

$$S_{(mafti)[e;\dot{e}]} = S_{(matts)[e;\dot{A}]} S_{(osgdgt)[A;A]} S_{(osg)[A;e]} \tag{19}$$

$$S_{(matts)[e;\dot{A}]} = \frac{S_{(isfsc)|e;e|(dir)} S_{(tgda)|e;e|} S_{(tg)[e;M]}}{S_{(tg)|\dot{A};M|} + S_{(vd)|\dot{A};M|} + S_{(isfsc)|e;e|(fb)} S_{(tgda)|e;e|} S_{(tg)[e;M]} S_{(avsg)[\dot{A};e]}} \tag{20}$$

When the modifying inputs have the values

$$e_{(ex)(tg)} = 115 \text{ volts} \quad ; \quad e_{(ex)(avsg)} = 115 \text{ volts} \quad ; \quad e_{(ex)(osg)} = 19 \text{ volts} \tag{21}$$

then

$$(CT)_{(mafti)} = 4.22 \times 10^{-3} \text{ sec} \tag{22}$$

$$S_{(matts)[e;\dot{A}]} = 27.0 \frac{\text{rad/sec}}{\text{volt}} \tag{23}$$

and

$$S_{(mafti)[e;\dot{e}]} = 0.0355 \frac{\text{volt/sec}}{\text{volt}} \tag{24}$$

i) Integrator component performance information

The performance equation of the motor – amplifier – feedback-tachometer integrator has the (0;1,2) differential equation form. Therefore, the performance function of the motor – amplifier – feedback-tachometer integrator for voltage in and voltage out has the form of the (0;1,2) relating function developed in Derivation Summary 34-17; i.e.,

$$[RF]_{(0;1,2)} = [PF]_{(mafti)[e;e]} = \frac{S_{(mafti)[e;e](ref)}}{j \frac{(FR)_{(ref)}}{(bp)_{(mafti)}} \left(1 + j \frac{(FR)_{(ref)}}{(bp)_{(mafti)}}\right)} \tag{25}$$

Derivation Summary 34-20. Illustrative performance analysis for a motor – amplifier – feedback-tachometer integrator. (Page 4 of 9)

where

$$S_{(mafti)[e;e](ref)} = S_{(mafti)[e;\dot{e}]}(CT)_{(mafti)} = 1.495 \times 10^{-4} \text{ volt/volt} \tag{26}$$

$$(FR)_{(ref)} = \frac{T_{(ref)}}{T_f} \tag{27}$$

Assume

$$T_{(ref)} = (CT)_{(mafti)} = 4.22 \times 10^{-3} \text{ sec} \tag{28}$$

Then, from Eqs. (14) and (15) of Derivation Summary 34-17,

$$(bp)_{(mafti)} = \frac{1}{2\pi} \tag{29}$$

From Eq. (25),

$$'(DAR)_{(0;1,2)} \approx '(SR)_{(mafti)(e;e)} = \frac{1}{\frac{(FR)_{(ref)}}{(bp)_{(mafti)}} \sqrt{1 + \left(\frac{(FR)_{(ref)}}{(bp)_{(mafti)}}\right)^2}} \tag{30}$$

and

$$(DRA)_{(0;1,2)} \approx (DRA)_{(mafti)(e;e)} = -\frac{\pi}{2} + \tan^{-1}\left[\frac{-(FR)_{(ref)}}{(bp)_{(mafti)}}\right] \tag{31}$$

From Derivation Summary 34-1, the performance function of an ideal integrator has the form

$$[PF]_{(mafti)[e;e](ideal)} = \frac{S_{(mafti)[e;e](ref)(ideal)}}{j\,\frac{(FR)_{(ref)}}{(bp)_{(mafti)}}} \tag{32}$$

where

$$S_{(mafti)[e;e](ref)(ideal)} = S_{(mafti)[e;\dot{e}]}(CT)_{(mafti)} = S_{(mafti)[e;e](ref)} \tag{33}$$

From Eq. (32),

$$'(SR)_{(mafti)(e;e)(ideal)} = \frac{1}{\frac{(FR)_{(ref)}}{(bp)_{(mafti)}}} \tag{34}$$

$$(DRA)_{(mafti)(e;e)(ideal)} = -\frac{\pi}{2} \tag{35}$$

With the ideal performance function as a reference, the fractional deviation of the dimensionless sensitivity ratio of the actual integrator is

$$[(FD)'(SR)]_{(mafti)} = \frac{1}{\sqrt{1 + \left(\frac{(FR)_{(ref)}}{(bp)_{(mafti)}}\right)^2}} - 1 \tag{36}$$

and the corresponding dynamic response angle deviation is

$$[(D)(DRA)]_{(mafti)} = \tan^{-1}\left[\frac{-(FR)_{(ref)}}{(bp)_{(mafti)}}\right] \tag{37}$$

The dimensionless sensitivity ratio and the dynamic response angle of the motor – amplifier – feedback-tachometer integrator are plotted in Fig. c. The fractional deviation of the dimensionless sensitivity ratio and the deviation of the dynamic response angle are plotted in Fig. d.

i) Performance function and performance plots for the motor – amplifier – feedback-tachometer integrator with zero uncertainty torque

Derivation Summary 34-20. Illustrative performance analysis for a motor – amplifier – feedback-tachometer integrator. (Page 5 of 9)

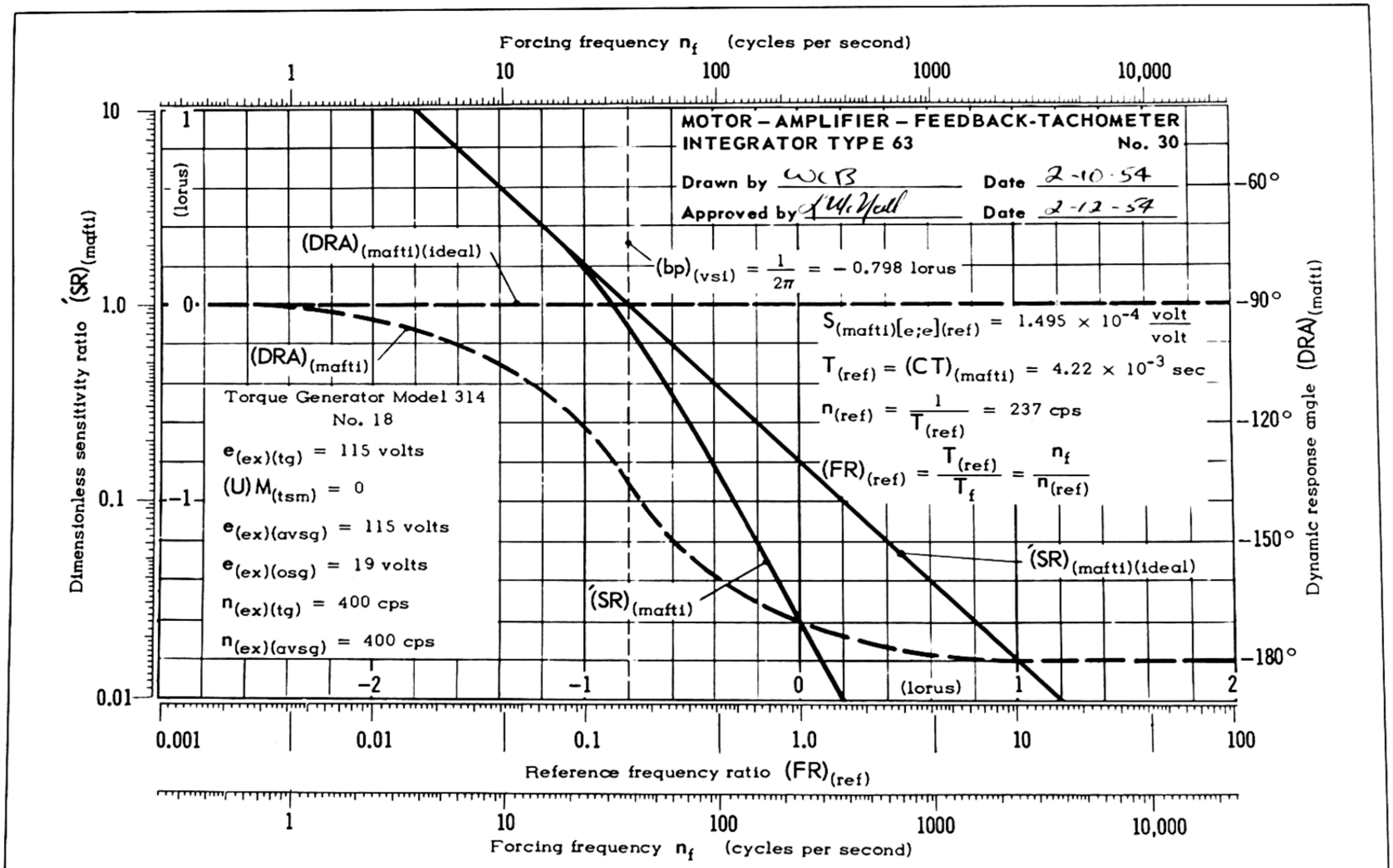


Fig. c. Dimensionless sensitivity ratio and dynamic response angle for the motor – amplifier – feedback-tachometer integrator.

Derivation Summary 34-20. Illustrative performance analysis for a motor – amplifier – feedback-tachometer integrator. (Page 6 of 9)

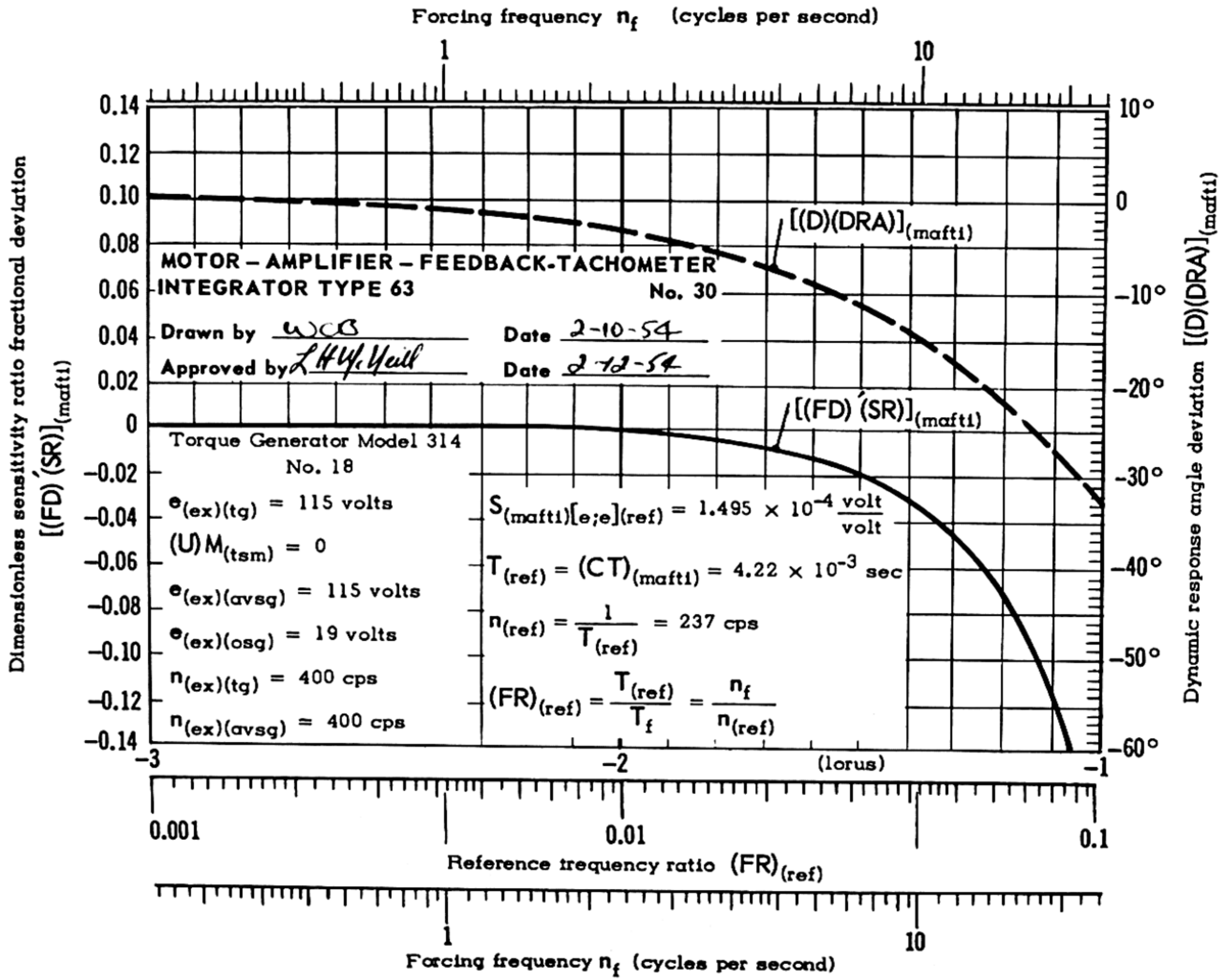


Fig. d. Dimensionless sensitivity ratio fractional deviation and dynamic response angle deviation for the motor – amplifier – feedback-tachometer integrator.

Derivation Summary 34-20. Illustrative performance analysis for a motor – amplifier – feedback-tachometer integrator. (Page 7 of 9)

The cutoff frequencies and band widths for the motor tachometer integrator are given in the following table. The tolerance limits are specified values of the deviation of the actual integrator performance from the ideal integrator performance. (See Derivation Summaries 34-1 and 34-17, Definition Summary 34-1, Fig. 34-29 and Table 34-3.)

Table a. Cutoff frequencies and band widths for the motor – amplifier – feedback-tachometer integrator with zero uncertainty torque.

$(TL)(DRA)$	$-2°$	$-5°$	$-10°$
$(FR)_{(ref)(hfco)((TL)(DRA))}$	-2.2 lorus ≈ 0.0063	-1.84 lorus ≈ 0.0145	-1.55 lorus ≈ 0.0282
$n_{(hfco)((TL)(DRA))}$ cycles per second (cps)	$\frac{0.0063}{(CT)_{(maft1)}} \approx 1.49$	$\frac{0.0145}{(CT)_{(maft1)}} \approx 3.44$	$\frac{0.0282}{(CT)_{(maft1)}} \approx 6.69$
$(BW)_{((TL)(DRA))}$ (cps)	$1.49 - 0$	$3.44 - 0$	$6.69 - 0$

$(TL)'(DAR)$	-0.001	-0.005	-0.01	-0.05
$(FR)_{(ref)(hfco)((TL)'(DAR))}$	-2.15 lorus ≈ 0.0071	-1.80 lorus ≈ 0.0159	-1.65 lorus ≈ 0.0224	-1.28 lorus ≈ 0.0525
$n_{(hfco)((TL)'(DAR))}$ (cps)	$\frac{0.0071}{(CT)_{(maft1)}} \approx 1.68$	$\frac{0.0159}{(CT)_{(maft1)}} \approx 3.77$	$\frac{0.0224}{(CT)_{(maft1)}} \approx 5.31$	$\frac{0.0525}{(CT)_{(maft1)}} \approx 12.43$
$(BW)_{((TL)'(DAR))}$ (cps)	$1.68 - 0$	$3.77 - 0$	$5.31 - 0$	$12.43 - 0$

$e_{(ex)(tg)} = 115$ v ; $e_{(ex)(avsg)} = 115$ v ; $e_{(ex)(osg)} = 19$ v ; $(CT)_{(maft1)} = 4.22 \times 10^{-3}$ sec

$n_{(ex)(tg)} = 400$ cps ; $n_{(ex)(avsg)} = 400$ cps Torque Generator Model 314, No. 18 $(U)M_{(tsm)} = 0$

k) Cutoff frequencies and band widths

The effects of uncertainty torques considered in Derivation Summary 34-11 may be converted to an equivalent voltage-input uncertainty. From Eq. (25) of Derivation Summary 34-11,

$$(CT)_{(maft1)}\ddot{e}_{(out)} + \dot{e}_{(out)} = S_{(maft1)[e;\dot{e}](ref)}e_{(in)} \pm S_{(maft1)[(U)e;\dot{e}]}|(U)e_{(in)}| \tag{38}$$

where

$$S_{(maft1)[(U)e;\dot{e}]} = S_{(maft1)[M;\dot{e}]}S_{(isfsc)|e;e|(dir)}S_{(tqda)|e;e|}S_{(tg)[e;M]} = S_{(maft1)[e;\dot{e}](ref)} \tag{39}$$

and

$$|(U)e_{(in)}| = \frac{|(U)M_{(tsm)}|}{S_{(isfsc)|e;e|(dir)}S_{(tqda)|e;e|}S_{(tg)[e;M]}} \tag{40}$$

= equivalent voltage-input uncertainty magnitude

Equation (38) can be rewritten in the form

$$(CT)_{(maft1)}\ddot{e}_{(out)} + \dot{e}_{(out)} = \left(1 \pm \frac{|(U)e_{(in)}|}{e_{(in)}}\right) S_{(maft1)[e;\dot{e}](ref)}e_{(in)} = S_{(maft1)[e;\dot{e}]}e_{(in)} \tag{41}$$

By definition,

$$(PR)_{(maft1)(S_{[e;\dot{e}]})} = \frac{S_{(maft1)[e;\dot{e}]}}{S_{(maft1)[e;\dot{e}](ref)}} \tag{42}$$

From Eqs. (41) and (42),

$$(PR)_{(maft1)(S_{[e;\dot{e}]})} = 1 \pm \frac{|(U)e_{(in)}|}{e_{(in)}} = \text{voltage input – voltage rate output sensitivity performance ratio of the integrator} \tag{43}$$

Derivation Summary 34-20. Illustrative performance analysis for a motor – amplifier – feedback-tachometer integrator. (Page 8 of 9)

In the preceding expressions, $S_{(mafti)[e;\dot{e}](ref)}$ is given by Eq. (19). By experiment, the uncertainty in torque applied to the torque summing member due to friction is no greater than the torque corresponding to the application of 2.8 volts to the control field of the torque generator with the main field excited at 115 volts. It follows that

$$|(U)e_{(in)}|_{(max)} = \frac{2.8 \text{ volts}}{S_{(isfsc)|e;e|(dir)}S_{(tgda)|e;e|}} = 3.52 \times 10^{-3} \text{ volt} \quad (44)$$

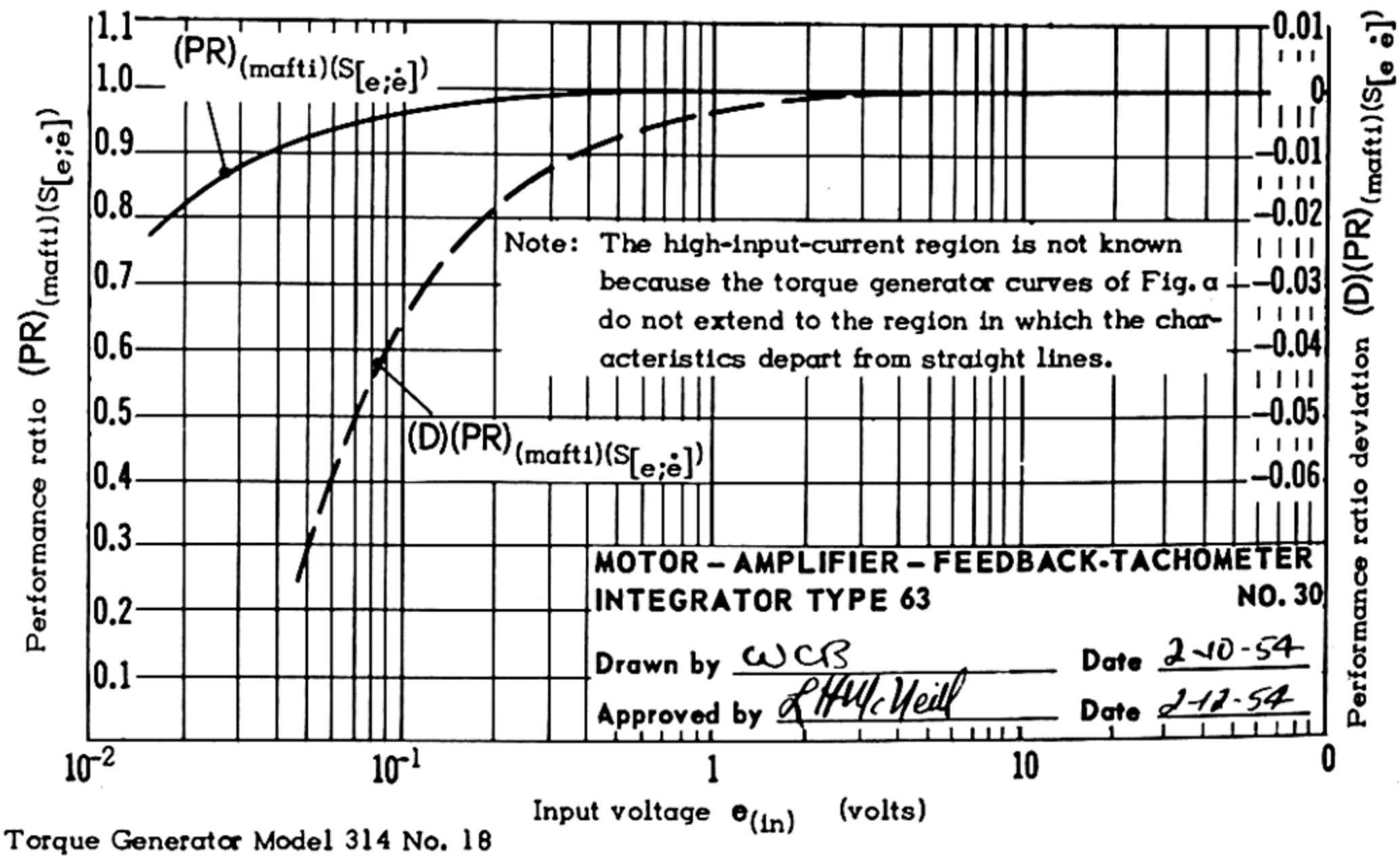
From Eqs. (43) and (44),

$$(PR)_{(mafti)(S_{[e;\dot{e}]})} = 1 \pm \frac{3.52 \times 10^{-3}}{e_{(in)}} \quad (45)$$

and

$$[(D)(PR)]_{(mafti)(S_{[e;e]})} = (PR)_{(mafti)(S_{[e;\dot{e}]})} - 1 = \pm \frac{3.52 \times 10^{-3}}{e_{(in)}} \quad (46)$$

The performance ratio and performance ratio deviation curves for the minus signs in Eqs. (45) and (46) are plotted in semilogarithmic coordinates in Fig. e.



Torque Generator Model 314 No. 18

$e_{(ex)(tg)} = 115$ volts

$n_{(ex)(tg)} = 400$ cps

$e_{(ex)(avsg)} = 115$ volts

$n_{(ex)(avsg)} = 400$ cps

$e_{(ex)(osg)} = 19$ volts

$|(U)M_{(tsm)}|_{(max)} = 3090$ dyne-cm

$|(U)e_{(in)}|_{(max)} = 3.52 \times 10^{-3}$

$$(PR)_{(mafti)(S_{[e;\dot{e}]})} = \frac{S_{(mafti)[e;\dot{e}]}}{S_{(mafti)[e;\dot{e}](ref)}}$$

$$(D)(PR)_{(mafti)(S_{[e;\dot{e}]})} = (PR)_{(mafti)(S_{[e;\dot{e}]})} - 1$$

$$S_{(mafti)[e;\dot{e}](ref)} = 35.5 \frac{\text{mv/sec}}{\text{volt}}$$

Fig. e. Performance ratio and performance ratio deviation of the sensitivity of the motor – amplifier – feedback-tachometer integrator with constant uncertainty torque.

l) Performance ratio and performance ratio deviation

Derivation Summary 34-20. Illustrative performance analysis for a motor – amplifier – feedback-tachometer integrator. (Page 9 of 9)

34.126. Section j of Derivation Summary 34-20 summarizes the performance function forms and numerical data for the motor – amplifier – feedback-tachometer integrator and gives dimensionless sensitivity ratio and dynamic response angle curves in Fig. c. Figure d gives the corresponding deviation curves. Table a of the summary lists cutoff frequency and bandwidth information for several sensitivity ratio and dynamic response angle deviation tolerance limits.

34.127. Section l of Derivation Summary 19-20 outlines a procedure for describing the influence of uncertainty torques on the operation of the motor – amplifier – feedback-tachometer integrator. In the integrator performance equation given by Eq. (38), which is based on the development of Derivation Summary 34-11, uncertainty effects are lumped together in a resultant equivalent voltage-input uncertainty. Reasoning similar to that used to find the viscous shear integrator performance equation in Derivation Summary 34-19 is applied in section l to show that the performance ratio for the motor – amplifier – feedback-tachometer integrator may be written as the sum of unity plus or minus the ratio of the equivalent voltage-input uncertainty magnitude to the input voltage. Figure e gives the voltage input – voltage rate output sensitivity performance ratio and the corresponding performance ratio deviation for the operating conditions listed on the figure and a maximum input voltage uncertainty of 3.52×10^{-3} volt.

34.128. The performance equation for the motor – amplifier – feedback-tachometer integrator has the (0;1,2) differential equation form, which is identical with the (0;1,2) form for the viscous shear integrator. This means that, except for the design coefficients that determine the characteristic time and reference sensitivity, the two integrator types give similar results. The performance-describing curves of Figs. d and e of Derivation Summary 34-19 and Figs. c and d of Derivation Summary 34-20 show that both integrator types give performance that, except for uncertainty effects at low input currents and saturation effects at high input currents, is theoretically perfect in the low-frequency range and drops off in the high-frequency range. This high-frequency characteristic is basically due to inertia reaction effects associated with mechanical parts. The high-frequency cutoff depends on the deviation tolerance limits specified for the dynamic amplitude ratio and the dynamic response angle.

34.129. At low input levels, both of the integrator types considered show strong negative performance ratio deviations due to uncertainty effects. This falling off of the performance ratio at low input levels is characteristic of many electromechanical devices. It is important to note that the frequency range for satisfactory operation may always be increased by reducing the effective uncertainties.

34.130. At high input levels, the performance deteriorates because of saturation in electromagnetic components. This effect is shown by the viscous shear integrator performance ratio deviation curve of Derivation Summary 34-19, but

is absent from the corresponding performance ratio deviation curve of Derivation Summary 34-20 for the motor – amplifier – feedback-tachometer integrator because the blocked-rotor characteristic curves were not carried to sufficiently high input voltages for saturation effects to reach appreciable magnitudes.

34.131. The curves of Figs. d and e of Derivation Summary 34-19 and Figs. c and d of Derivation Summary 34-20 are identical from the standpoint of shape and the coordinates used. This means that these curves may be applied to any particular case of an integrator that has a performance equation of the (0;1, 2) form by listing the essential numerical data and placing a logarithmically divided numerical scale parallel to the abscissa axis with the reference frequency aligned with zero on the loru scale and 1.0 on the reference frequency ratio scale. When this scale adjustment is completed, the operation of any system with a (0;1, 2) performance equation and with no uncertainty or saturation effects present is adequately described by plots identical with Figs. d and e of Derivation Summary 34-19.

34.132. When uncertainties are not negligibly small and saturation effects are present, performance ratio curves plotted with input level as the independent variable will have the general shape of the full-line curve of Fig. f of Derivation Summary 34-19. Because of special circumstances that are likely to appear in particular cases, it is impossible to draw a generalized input level – performance ratio curve that may be applied to any situation. Curves of this type must be developed for any given device by a special consideration of the design features involved.

34.133. The preceding discussions of a typical viscous shear integrator and a typical motor – amplifier – feedback-tachometer integrator are intended to be illustrative rather than exhaustive. While many of the characteristics associated with the components of the two integrator types have been described, some of the possible problems of designing and testing electromechanical integrators have not even been mentioned. However, a pattern has been described for specifying component performance, deriving performance equations and performance functions, computing numerical data, and summarizing results by means of graphical representations. This pattern is useful in solving the engineering problems associated with integrators of any kind.

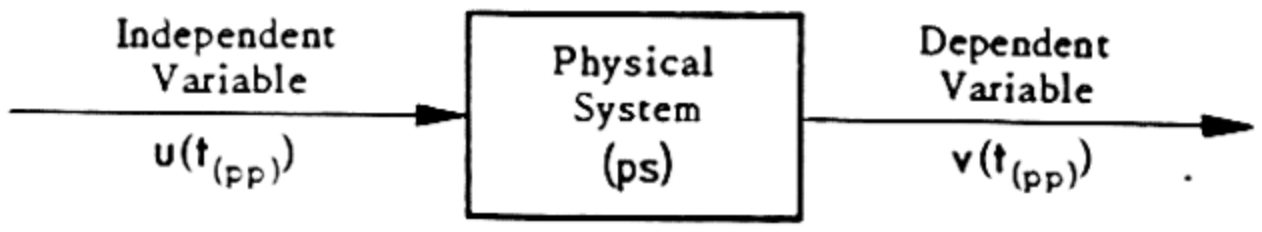
ANALOG COMPUTERS

34.134. Analog computers are devices that solve differential equations. Alternatively, and more important in practice, analog computers are counterparts of the physical systems they are set up to represent, and thus provide convenient means for obtaining the dynamic responses of such systems. Such computers as used for the study of linear systems consist basically of arrays of integrators, coefficient multipliers and summers or adders, capable of being interconnected in any desired manner in accordance with the problem under study. Theoretically,

differentiators might be employed in place of integrators, but in practice they are never used because of difficulties experienced in handling rapidly varying signals. In addition to the basic elements just mentioned, a variety of additional analog-computer components are used for performing other operations, such as the multiplication of two variables and nonlinear function generation in many forms. The use of these components makes it possible for an analog computer to solve many physical problems that could otherwise be solved only by numerical methods.

34.135. If the physical system is available and may be readily subjected to test inputs, then tests on the system itself will generally be preferable to analogous tests on a computer. This is because in practice there is never exact correspondence between components of the physical system and the corresponding computer components; the excellence of this correspondence is the index to the accuracy of the computer solutions. Usually, however, the system under study will not be available for test. In fact, the purpose of an analog-computer study will most often be to aid in the initial design of such a system. Here, the analog computer can reduce greatly the time required for analytical studies. Its convenience in use and low cost per solution will frequently mean that solutions will be obtained where none would have been attempted had the computer not been available. Because of these advantages, analog-computer solutions may sometimes be preferable even when the physical system is available. And, of course, by a reconnection of the computer components, the computer may be changed from one problem to another and hence may be utilized efficiently in an organization in which a number of problems are under simultaneous study.

34.136. Generally speaking, an analog computer will solve a problem in a time different from that taken by the physical system to complete the corresponding response (presuming, of course, that the same type of input disturbance is used in both cases). A time transformation is thus involved, and it is necessary to think very clearly to avoid confusion between two kinds of time: physical problem time and analog computer time. Both are physical times in the sense that they represent the running variable in a physical situation, the first in the physical system under study and the second in the analog computer. One may think of the time transformation in terms of a) the ratio of elapsed time in the analog-computer solution to elapsed time at the same point in the actual physical-problem situation or b) to its equivalent, the ratio of the rate at which the physical system generates a solution to the rate at which the analog computer obtains a corresponding solution. These ratios are shown by Eqs. (3) and (4) of Derivation Summary 34-21 to be equal to the solution time ratio, STR, which is an important quantity in the scaling of a problem for analog-computer solution. Figure 34-31 illustrates the various concepts associated with physical problem time, analog computer time, and the solution time ratio.

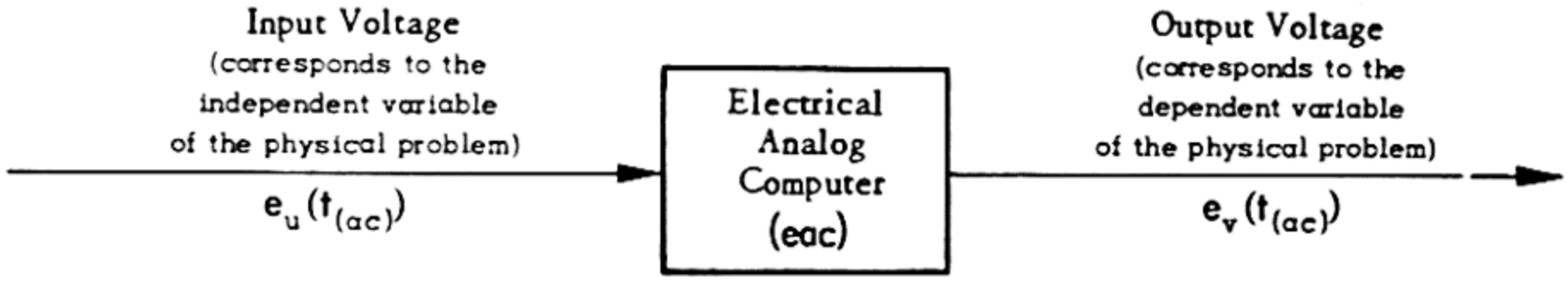


As indicated, both the independent variable, u, and the dependent variable, v, vary with $t_{(pp)}$, where

$t_{(pp)}$ = physical problem time; time associated with the actual physical problem

≈ running variable associated with the physical situation

a) Functional diagram associated with the physical problem



As indicated, both the input voltage, e_u, and the output voltage, e_v, vary with $t_{(ac)}$, where

$t_{(ac)}$ = analog computer time; time associated with the analog-computer representation of the physical problem

≈ running variable associated with the analog-computer representation

b) Functional diagram associated with the analog-computer representation of the physical problem

From a comparison of sections a and b, the following quantities can be defined:

$$(SF)_{(u;e)} = \frac{e_u(t_{(ac)})}{u(t_{(pp)})} = \frac{e_u}{u}^{*} = \text{independent variable} - \text{input voltage scale factor} \quad (1)$$

$$(SF)_{(v;e)} = \frac{e_v(t_{(ac)})}{v(t_{(pp)})} = \frac{e_v}{v}^{*} = \text{dependent variable} - \text{output voltage scale factor} \quad (2)$$

As shown in Fig. 34-31, the solution time ratio relates the analog computer time and the physical problem time as follows:

$$STR = \frac{(ST)_{(ac)}}{(ST)_{(pp)}} = \frac{t_{(ac)}}{t_{(pp)}} = \frac{dt_{(ac)}}{dt_{(pp)}} = \text{solution time ratio} \quad (3)$$

where

$(ST)_{(ac)}$ = analog-computer solution time ; $(ST)_{(pp)}$ = physical-problem solution time

A simple rearrangement of terms in Eq. (3) shows that the solution time ratio, and hence the time transformation between the actual physical situation and the corresponding computer solution, can be thought of in terms of rates of solution generation as well as in terms of elapsed time; i.e.,

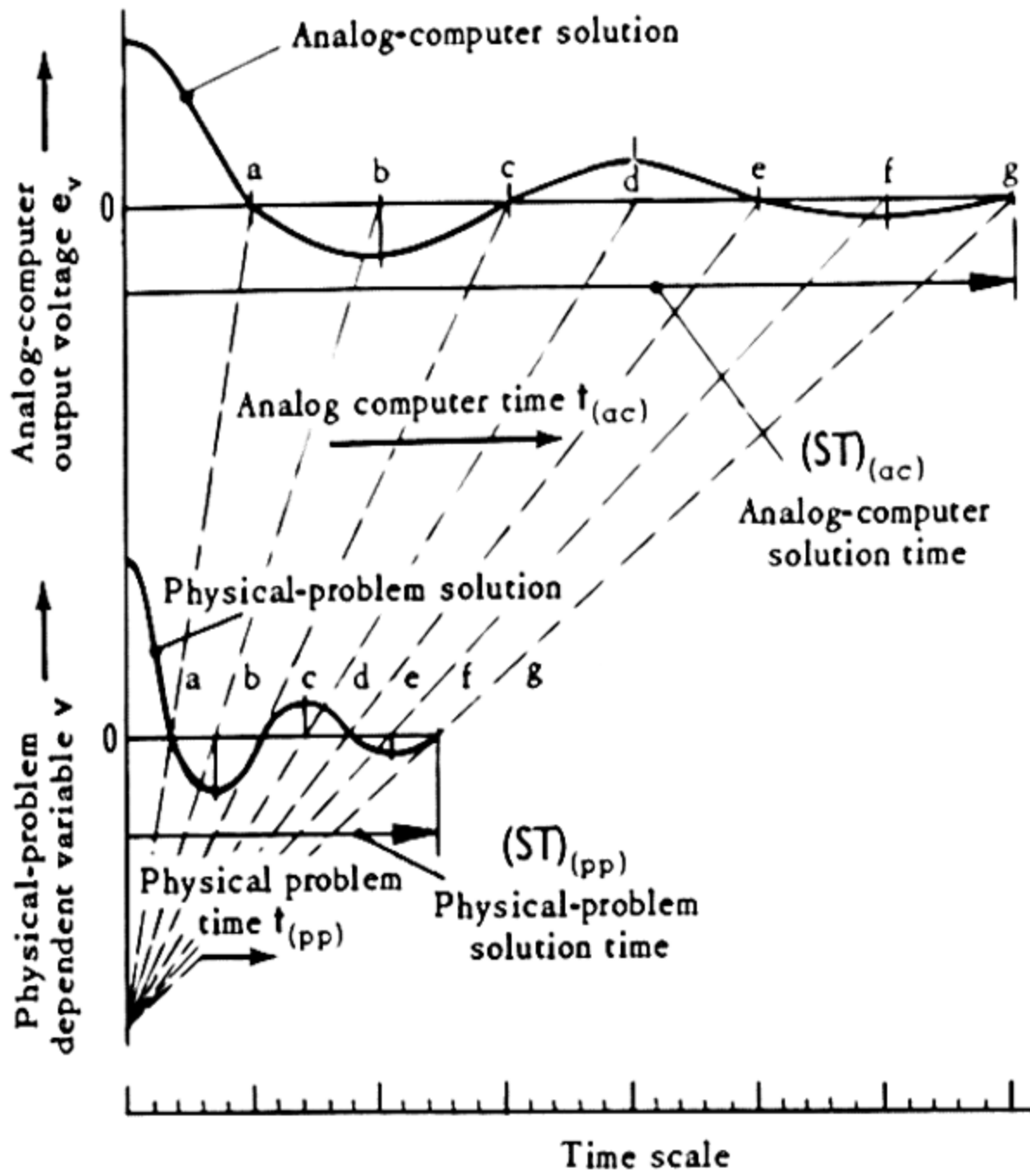
$$STR = \frac{\frac{100}{(ST)_{(pp)}}}{\frac{100}{(ST)_{(ac)}}} = \frac{\left[\begin{array}{c}\text{percent of physical-problem}\\ \text{solution developed per unit}\\ \text{of time}\end{array}\right]}{\left[\begin{array}{c}\text{percent of analog-computer}\\ \text{solution developed per unit}\\ \text{of time}\end{array}\right]} = \left\{\begin{array}{l}\text{ratio of the rate at which the actual}\\ \text{physical problem progresses to the}\\ \text{rate at which the analog computer}\\ \text{solves the physical problem}\end{array}\right\} \quad (4)$$

c) Basic relationships between the variables of the physical problem and those of the corresponding analog-computer representation

---

* The running variable may be omitted when no confusion will result from this omission.

Derivation Summary 34-21. Basic concepts and relationships associated with an electrical analog computer in which voltages represent the dependent and independent variables of a physical problem.



Note: The same time units are used for physical problem time and analog computer time.

By definition,

$$STR = \frac{(ST)_{(ac)}}{(ST)_{(pp)}} = \text{solution time ratio}$$

where

$(ST)_{(pp)}$ = physical-problem solution time; time required for the actual physical system to reach a solution in response to a given input

$(ST)_{(ac)}$ = analog-computer solution time; time required for the analog computer to generate the corresponding solution for the same given input

From the diagram,

$$\frac{(ST)_{(ac)}}{(ST)_{(pp)}} = \frac{t_{(ac)a}}{t_{(pp)a}} = \frac{t_{(ac)b}}{t_{(pp)b}} = \cdots = \frac{t_{(ac)}}{t_{(pp)}}$$

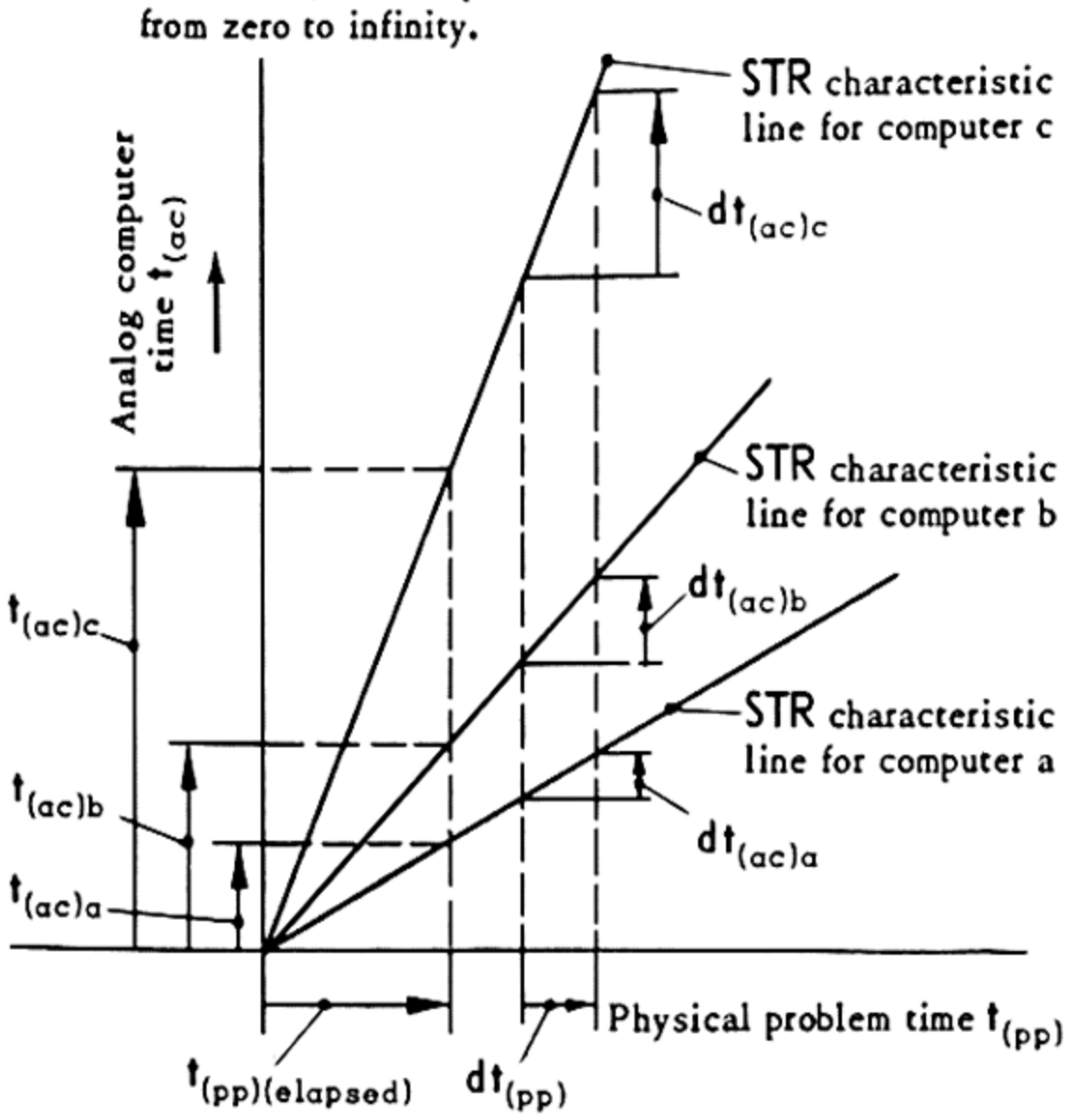
where

$$\frac{t_{(ac)a}}{t_{(pp)a}} = \frac{t_{(ac)b}}{t_{(pp)b}} = \cdots = \frac{t_{(ac)}}{t_{(pp)}}$$ = ratio of elapsed time in the analog-computer solution to the elapsed time in the actual physical-problem solution at corresponding points in the two solutions

a) Relationships between physical problem time and analog computer time for the case of a "slow" computer

$$((ST)_{(ac)} > (ST)_{(pp)})$$

Although the presentation shown in Fig. a above adequately represents the relationship between $t_{(ac)}$ and $t_{(pp)}$, it has the limitation that the relationship applies for only one value of STR. The following presentation, on the other hand, is less pictorial in nature but shows the relationship between $t_{(ac)}$ and $t_{(pp)}$ for any value of STR, from zero to infinity.



Note: The time scales for both coordinate axes are identical.

For computer a (a "fast" computer),

$$(STR)_a = \frac{t_{(ac)a}}{t_{(pp)(elapsed)}} = \frac{dt_{(ac)a}}{dt_{(pp)}} < 1$$

For computer b (a real time computer),

$$(STR)_b = \frac{t_{(ac)b}}{t_{(pp)(elapsed)}} = \frac{dt_{(ac)b}}{dt_{(pp)}} = 1$$

For computer c (a "slow" computer),

$$(STR)_c = \frac{t_{(ac)c}}{t_{(pp)(elapsed)}} = \frac{dt_{(ac)c}}{dt_{(pp)}} > 1$$

Definitions:

$(STR)_{a,b,c}$ = solution time ratios for computers a, b, and c, respectively

$t_{(ac)a,b,c}$ = elapsed time in solutions generated by analog computers a, b, and c, respectively, at points corresponding to a given elapsed time in the physical-problem solution

$dt_{(ac)a,b,c}$ = differential change in analog computer time corresponding to a differential change in physical problem time for computers a, b, and c, respectively

b) Relationship between physical problem time and analog computer time for any value of the solution time ratio

Fig. 34-31. Pictorial representation of the relationship between physical problem time and analog computer time in terms of the solution time ratio.

34.137. When the solution time ratio is unity, the solution rate in both the physical system and the analog computer are the same. Under these circumstances, the computer is said to be a real time computer. With such a computer, it becomes possible to arrange a composite system consisting in part of physical system components and with the remainder made up of analog-computer components. At the interconnection points it is necessary to change the physical quantity in the physical system to the voltage required by the computer or vice versa. This technique is valuable where only part of a complete physical system is available and where this part contains effects difficult to represent on the analog computer. When the solution time ratio differs from unity, the computer may be characterized as "slow" or "fast," depending on whether the computer solves the problem at a slower or faster rate than the physical situation that the computer represents. It should be noted that the terms "slow" and "fast" refer to rates relative to the physical problem rather than to any absolute rates.

OPERATION OF ANALOG-COMPUTER COMPONENTS

34.138. Commercially available analog computers utilize electrical voltages as the computer variables. Computers based on angular shaft position and on pneumatic pressure have also been constructed, but these types are quite rare. As shown in Derivation Summary 34-21, the physical system input, u, is related to the analog-computer input voltage, e_u, by a scale factor $(SF)_{(u;e)}$, which is the ratio of e_u to u. Similarly, another scale factor $(SF)_{(v;e)}$ relates the physical system output, v, to the analog-computer output voltage, e_v. These scale factors are used to transform the system equations in terms of u and v to equations in terms of e_u and e_v for purposes of analog-computer scaling.

34.139. Simple techniques for performing computing operations may be used when the computer variables are voltages. For example, addition may be achieved by simple series connections, although in practice the more sophisticated method of current addition is used. Likewise, multiplication by a constant coefficient may be carried out by means of a voltage divider, or potentiometer if the coefficient is less than unity. More versatile is the variable gain amplifier, which can handle coefficients greater than, as well as less than, unity. As for integration, the devices already studied in this chapter for integrating voltages are applicable. The most extensively used is the resistance – amplifer – feedback-capacitance integrator shown in Fig. 34-9 and analyzed in Derivation Summary 34-10.

34.140. When voltages are used to represent the input and output quantities of an integrator, it is evident that if the output is to represent the time integral of the input a proportionality constant that has the dimension of time must exist between the input and output voltages. Section c of Derivation Summary 34-22 develops this relationship for the resistance – amplifier – feedback-capacitance integrator

The generalized form of the linear differential equation with constant coefficients applicable to the generalized physical problem represented in section a of Derivation Summary 34-21 is given by

$$\sum_{i=0}^{i=n} a_i \frac{d^i v}{dt_{(pp)}^i} = \sum_{j=0}^{j=m} b_j \frac{d^j u}{dt_{(pp)}^i} \tag{1}$$

where

$t_{(pp)}$ = physical problem time

$\approx$ running variable of the physical problem

v = dependent variable of the physical problem

u = independent variable of the physical problem

$\frac{d^i v}{dt_{(pp)}^i}$ = i^{th} dependent variable derivative with respect to the running variable

$\frac{d^j u}{dt_{(pp)}^j}$ = j^{th} independent variable derivative with respect to the running variable

a_i = i^{th} dependent variable differential equation coefficient

b_j = j^{th} independent variable differential equation coefficient

The notation of Eq. (1) is identical with that used in Chapter 14 in the discussion of the general linear integro-differential equation with constant coefficients. The purely differential equation form of Eq. (1) is used in the present discussion since it is the more generally encountered situation. No loss in generality is incurred by this procedure, however, since, if integral terms should arise, they may be removed by successive differentiation.

As can be seen from Eq. (1), the mathematical operations needed to solve this equation are:

1) Integration of the dependent and independent variables v and u.
2) Multiplication of the integrated quantities by the constant differential equation coefficients a_i and b_j.
3) Summation of terms between the limits imposed by the summation notation.

a) Generalized linear differential equation with constant coefficients applicable to a physical problem, and the mathematical operations required to solve it

The discussion of section a shows that electrical analog computers used to solve physical problems that can be represented by differential equations of the form given by Eq. (1) must comprise three basic types of components, as follows:

(i) Integrators

While any integrator that receives an electrical input signal and produces an electrical output signal could function in an electrical analog computer, practical requirements usually demand that an integrator of the type represented in Fig. 34-9 and described in Derivation Summary 34-10 be used. Section c of the present summary derives the relationships associated with the application of such resistance – amplifier – feedback-capacitance integrators to the integrator requirements of an electrical analog computer.

(cm) Coefficient multipliers

As in the case of the integrator, a basic requirement for a coefficient multiplier* used in an electrical analog computer is that it receive an electrical input signal and produce an electrical output signal. Two

* Since the function of each multiplier used in an electrical analog computer is to produce an output proportional to the product of a differential equation coefficient and an input quantity, such multipliers are called coefficient multipliers.

Derivation Summary 34-22. Performance relationships associated with the components of a linear-system electrical analog computer. (Page 1 of 8)

possible types of coefficient multipliers are described in section d of this summary. One coefficient multiplier is based on the use of a variable-gain amplifier, while the other depends on voltage-divider action.

(s) Summers

As in the case of the coefficient multiplier, there are two common types of components used for summation in analog computers, one based on the use of an amplifier (fixed gain in this application) and the other independent of any such element.

b) *Basic computer components for linear-system electrical analog computers*

An analysis of the resistance – amplifier – feedback-capacitance integrator is given in Derivation Summary 34-10. As shown in that summary, within the operating range for which the output voltage-difference term of Eq. (11) is negligible in comparison with the rate of change of the output voltage-difference term,* the performance relationship for the resistance – amplifier – feedback-capacitance integrator is

$$e_{(out)} - e_{(ref)} = -\frac{S_{(a)|e;e|}}{(S_{(a)|e;e|} + 1)RC} \int (e_{(in)} - e_{(ref)})\, dt_{(ac)} \tag{2}$$

Assume

$$S_{(a)|e;e|} >> 1 \quad ; \quad e_{(ref)} = 0 \tag{3}$$

Then, differentiating Eq. (2) with respect to analog computer time shows that

$$\frac{de_{(out)}}{dt_{(ac)}} = -\frac{1}{RC} e_{(in)} = -\frac{1}{(CT)_{(RC)}} e_{(in)} \tag{4}$$

where

$(CT)_{(RC)}$ = ratio of the integrator input voltage to the rate of change of the integrator output voltage

As shown by Eq. (12) of Derivation Summary 34-10, $(CT)_{(RC)}$ is related to the dynamic performance governing the characteristic time of the resistance – amplifier – feedback-capacitance integrator, $(CT)_{(rafc1)}$, by the expression

$$(CT)_{(RC)} = \frac{(CT)_{(rafc1)}}{S_{(a)|e;e|} + 1} \tag{5}$$

By means of Eq. (3) of Derivation Summary 34-21, the running variable $t_{(ac)}$ of Eqs. (2) and (3), which is associated with the analog computer, may be replaced by the running variable $t_{(pp)}$, which is associated with the actual physical problem being represented by the analog computer, to yield

$$e_{(out)} = -\frac{STR}{(CT)_{(RC)}} \int e_{(in)}\, dt_{(pp)} \tag{6}$$

where

STR = solution time ratio

Define

$$T_{(ref)} = \frac{(CT)_{(RC)}}{STR} \tag{7}$$

= reference time

Then

$$e_{(out)} = -\frac{1}{T_{(ref)}} \int e_{(in)}\, dt_{(pp)} = -\int e_{(in)}\, d't_{(pp)} \tag{8}$$

---

* This can be accomplished in practice by making the gain of the amplifier high, as indicated by Eq. (12) of Derivation Summary 34-10.

Derivation Summary 34-22. Performance relationships associated with the components of a linear-system electrical analog computer. (Page 2 of 8)

where

$$'t_{(pp)} = \frac{t_{(pp)}}{T_{(ref)}} \tag{9}$$

= nondimensional physical problem time

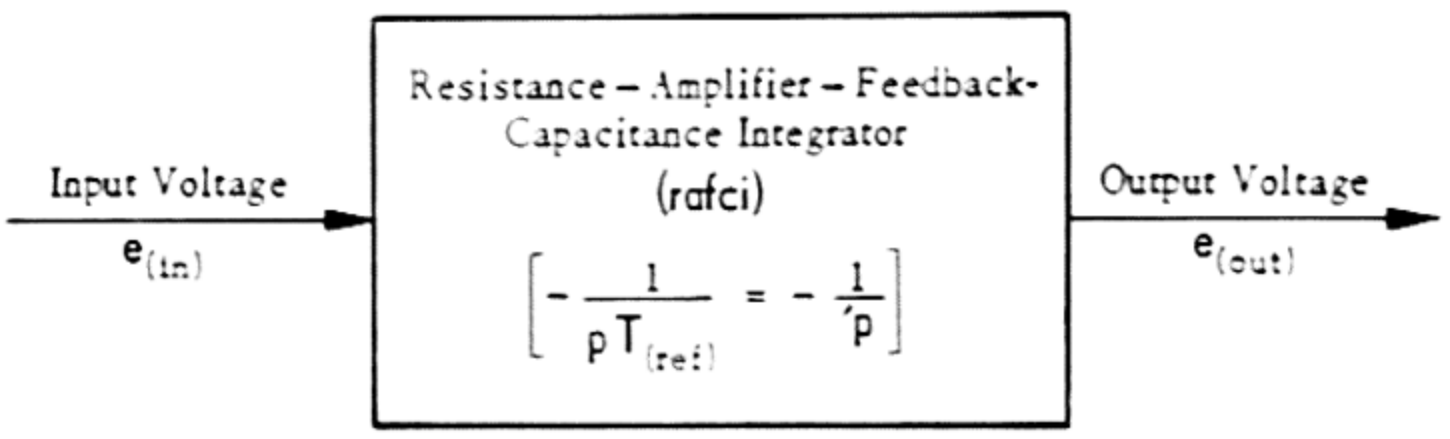
In operational form, Eq. (8) can be written

$$e_{(out)} = -\frac{1}{pT_{(ref)}} e_{(in)} = -\frac{1}{'p} e_{(in)} \tag{10}$$

where

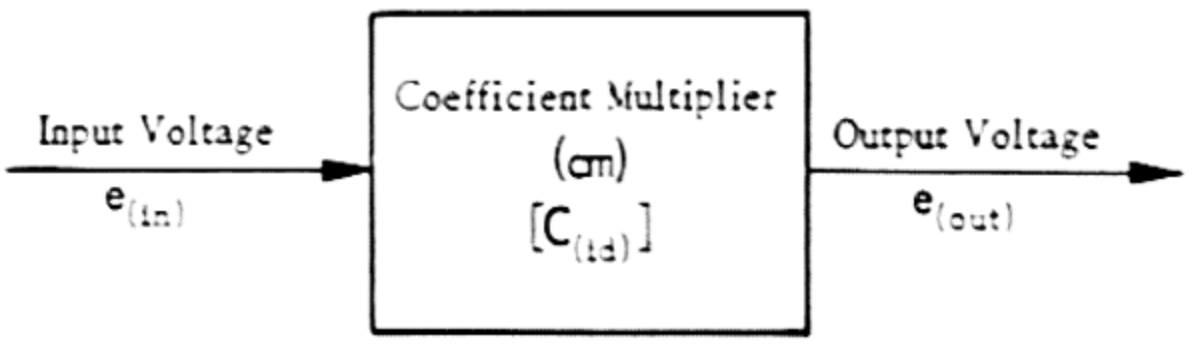
$$p = \frac{d}{dt_{(pp)}} \quad ; \quad 'p = \frac{d}{d\,'t_{(pp)}} = \frac{d}{d\left(\frac{t_{(pp)}}{T_{(ref)}}\right)} = pT_{(ref)} \tag{11}$$

Equation (10) can be represented by the following mathematical-functional diagram, which represents ideal integrator operation. The minus sign present in Eq. (10) presents no problem in practical application since, if a sign inversion is required, this may be accomplished by means of a coefficient multiplier of the feedback-amplifier type described in the following section.



c) Performance relationships associated with the resistance – amplifier – feedback-capacitance integrator when used as a component of an electrical analog computer

An ideal coefficient multiplier can be represented by the following mathematical-functional diagram.



The performance equation corresponding to this diagram is

$$e_{(out)} = C_{(id)} e_{(in)} \tag{12}$$

where

$$C_{(id)} = \frac{e_{(out)}}{e_{(in)}}$$

= identified coefficient

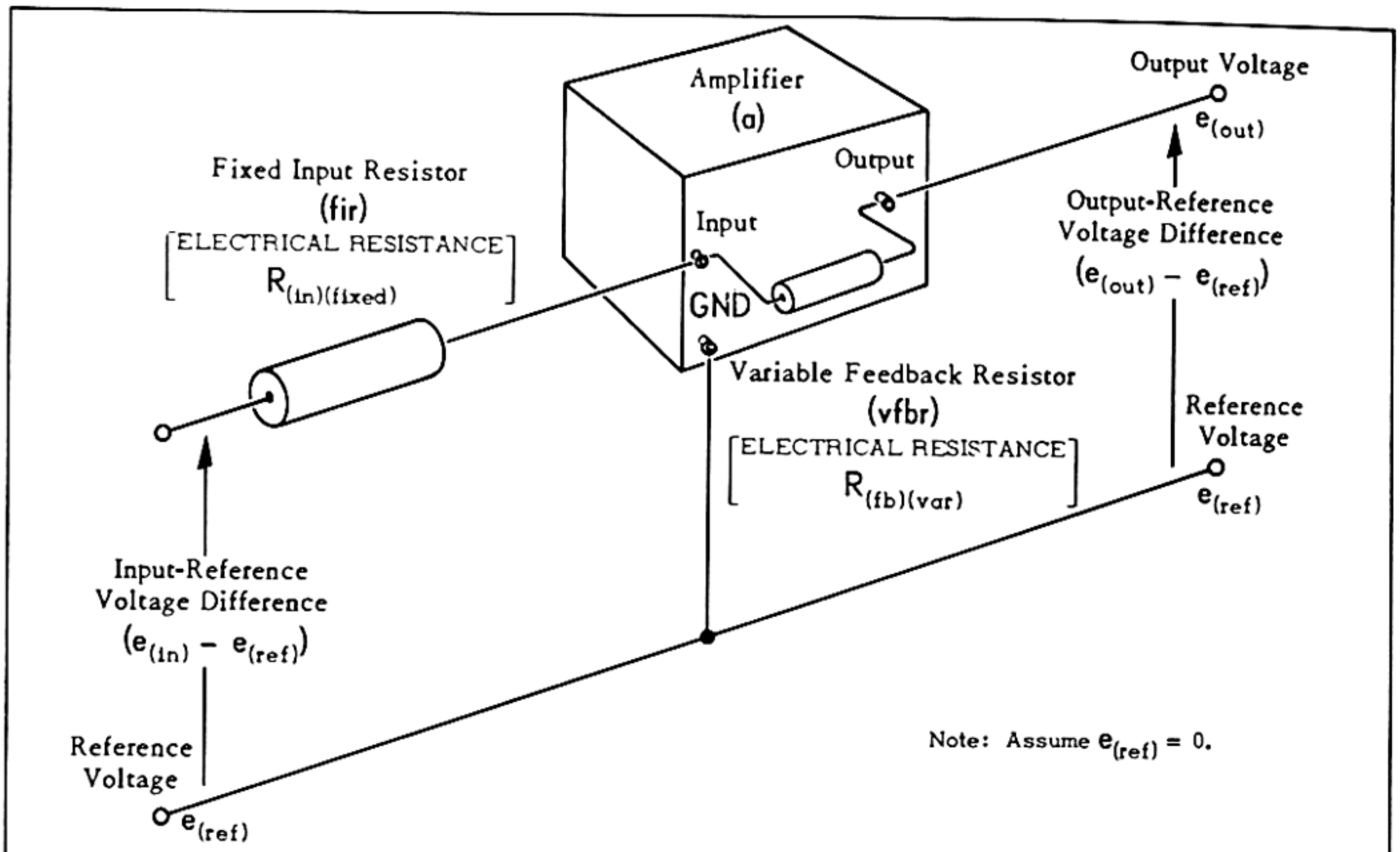
Note: For the case of a particular coefficient, the subscript (id) is replaced by proper identifying subscripts.

Specific performance relationships for the two coefficient multipliers noted in section b are given in the remainder of this section.

(vgacm) Variable-gain-amplifier coefficient multiplier

The following functional diagram represents the components of the variable-gain-amplifier coefficient multiplier.

Derivation Summary 34-22. Performance relationships associated with the components of a linear-system electrical analog computer. (Page 3 of 8)



The performance relationship of the variable-gain-amplifier coefficient multiplier is*

$$e_{(out)} = -\frac{S_{(a)|e;e|}\, R_{(fb)(var)}}{R_{(in)(fixed)}\,(S_{(a)|e;e|} + 1) + R_{(fb)(var)}}\, e_{(in)} \tag{13}$$

where

$R_{(in)(fixed)}$ = fixed input resistance

$R_{(fb)(var)}$ = variable feedback resistance

Assume

$$S_{(a)|e;e|} >> 1 \quad ; \quad S_{(a)|e;e|} >> \frac{R_{(fb)(var)}}{R_{(in)(fixed)}} \tag{14}$$

and define

$$C_{(id)} = \frac{R_{(fb)(var)}}{R_{(in)(fixed)}} \tag{15}$$

Then Eq. (13) reduces to

$$e_{(out)} = -C_{(id)}\, e_{(in)}\ ** \tag{16}$$

Comparison of Eq. (16) with Eq. (12) shows that ideal operation is obtained from the variable-gain-amplifier coefficient multiplier as long as the conditions of Eq. (14) are met.

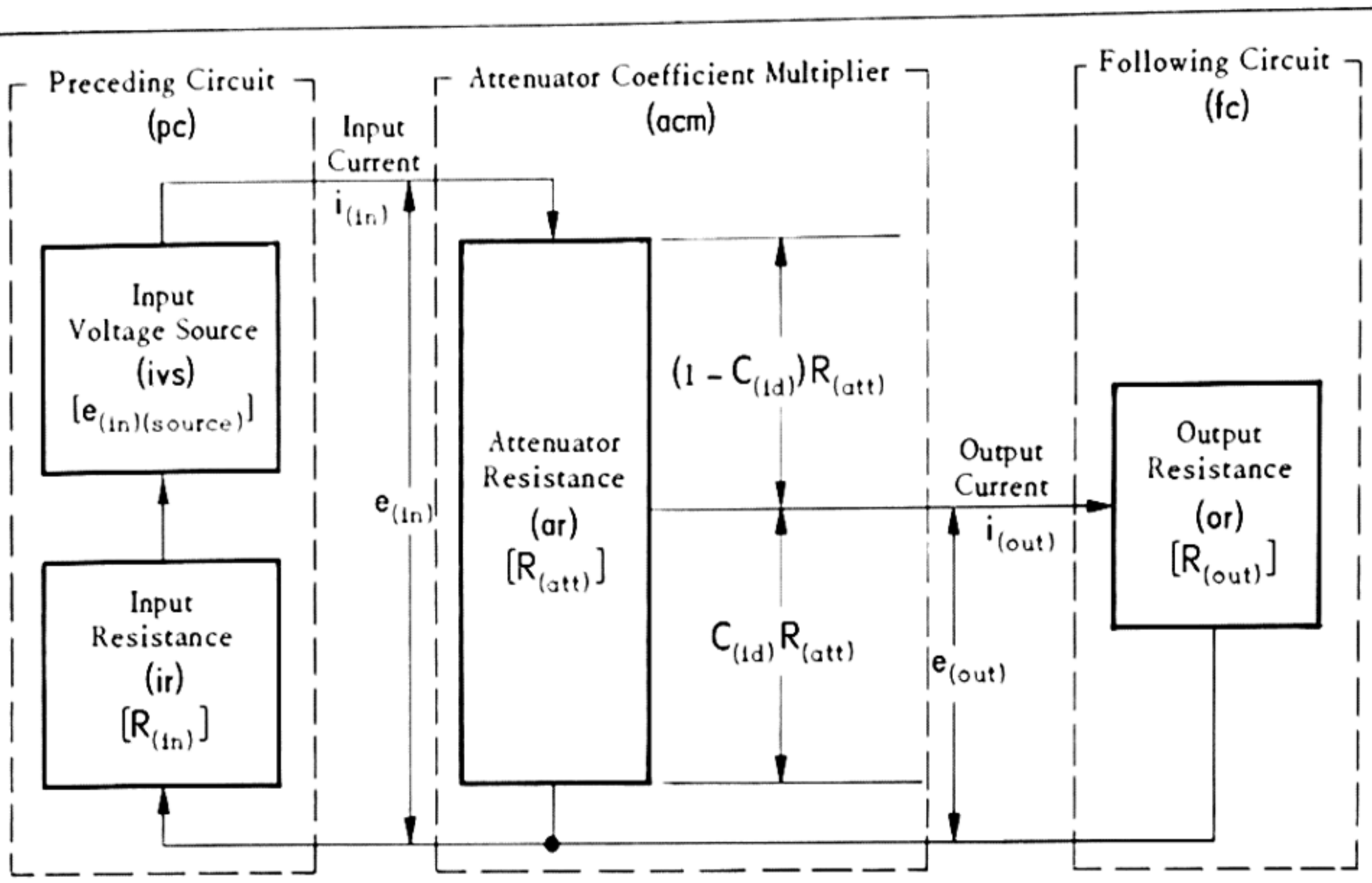
(acm) Attenuator coefficient multiplier

The following functional circuit diagram represents the attenuator coefficient multiplier and its tie-in with the preceding circuit and the following circuit. These outside circuits must be considered because their presence will in general cause the actual coefficient obtained to differ from the attenuator setting. Here $e_{(out)}$ and $e_{(in)}$ represent the voltages that would be measured at the output and input of the attenuator.

* Since the derivation of this performance relationship is identical with that of Derivation Summary 34-10 when the voltage drop across the feedback condenser of the integrator $(1/C)\int i_r dt$, is replaced by the voltage drop across the feedback resistor of the multiplier, $i_r R$, this derivation is omitted.

** If a sign inversion is required, this may be accomplished by means of an amplifier similar to that of the multiplier but having an over-all gain of unity.

Derivation Summary 34-22. Performance relationships associated with the components of a linear-system electrical analog computer. (Page 4 of 8)



Application of Kirchoff's laws to this functional diagram yields the following expressions for $e_{(out)}$ and $e_{(in)}$ in terms of the input voltage source level $e_{(in)(source)}$.

$$\frac{e_{(out)}}{e_{(in)(source)}} = \frac{C_{(id)}}{1 + \frac{R_{(in)}}{R_{(att)}} + C_{(id)}\left(\frac{R_{(in)} + R_{(att)}}{R_{(out)}}\right) - C_{(id)}^2 \frac{R_{(att)}}{R_{(out)}}} \tag{17}$$

and

$$\frac{e_{(in)}}{e_{(in)(source)}} = \frac{\left(\frac{R_{(out)}}{R_{(att)}} + C_{(id)}\right)}{\left(1 + \frac{R_{(in)}}{R_{(att)}}\right)\frac{R_{(out)}}{R_{(att)}} + \left(1 + \frac{R_{(in)}}{R_{(att)}}\right)C_{(id)} - C_{(id)}^2} \tag{18}$$

Equation (17), which gives the output voltage – input source voltage relationship for the coefficient multiplier, and Eq. (18), which gives the relationship between the input voltage applied to the coefficient multiplier and the actual source voltage, show that special conditions must be imposed on the resistances if the ideal relationship given by Eq. (12) is to be obtained.

Impose the special condition that

$$R_{(out)} >> R_{(in)} + R_{(att)} \tag{19}$$

Then, Eqs. (17) and (18) reduce to the form

$$\frac{e_{(out)}}{e_{(in)(source)}} = \frac{C_{(id)}}{1 + \frac{R_{(in)}}{R_{(att)}}} \tag{20}$$

and

$$\frac{e_{(in)}}{e_{(in)(source)}} = \frac{1}{1 + \frac{R_{(in)}}{R_{(att)}}} \tag{21}$$

Derivation Summary 34-22. Performance relationships associated with the components of a linear-system electrical analog computer. (Page 5 of 8)

Next, separately impose the special condition that

$$R_{(att)} >> R_{(in)} \tag{22}$$

Under this condition, Eqs. (17) and (18) become

$$\frac{e_{(out)}}{e_{(in)(source)}} = \frac{C_{(id)}}{1 + C_{(id)}(1 - C_{(id)})\dfrac{R_{(att)}}{R_{(out)}}} \tag{23}$$

$$\frac{e_{(in)}}{e_{(in)(source)}} = \frac{1}{1 - \dfrac{C^2_{(id)}}{\dfrac{R_{(out)}}{R_{(att)}} + C_{(id)}}} \tag{24}$$

If both of the conditions given by Eqs. (19) and (20) are simultaneously imposed, then

$$\frac{e_{(out)}}{e_{(in)(source)}} = C_{(id)} \tag{25}$$

and

$$\frac{e_{(in)}}{e_{(in)(source)}} = 1 \tag{26}$$

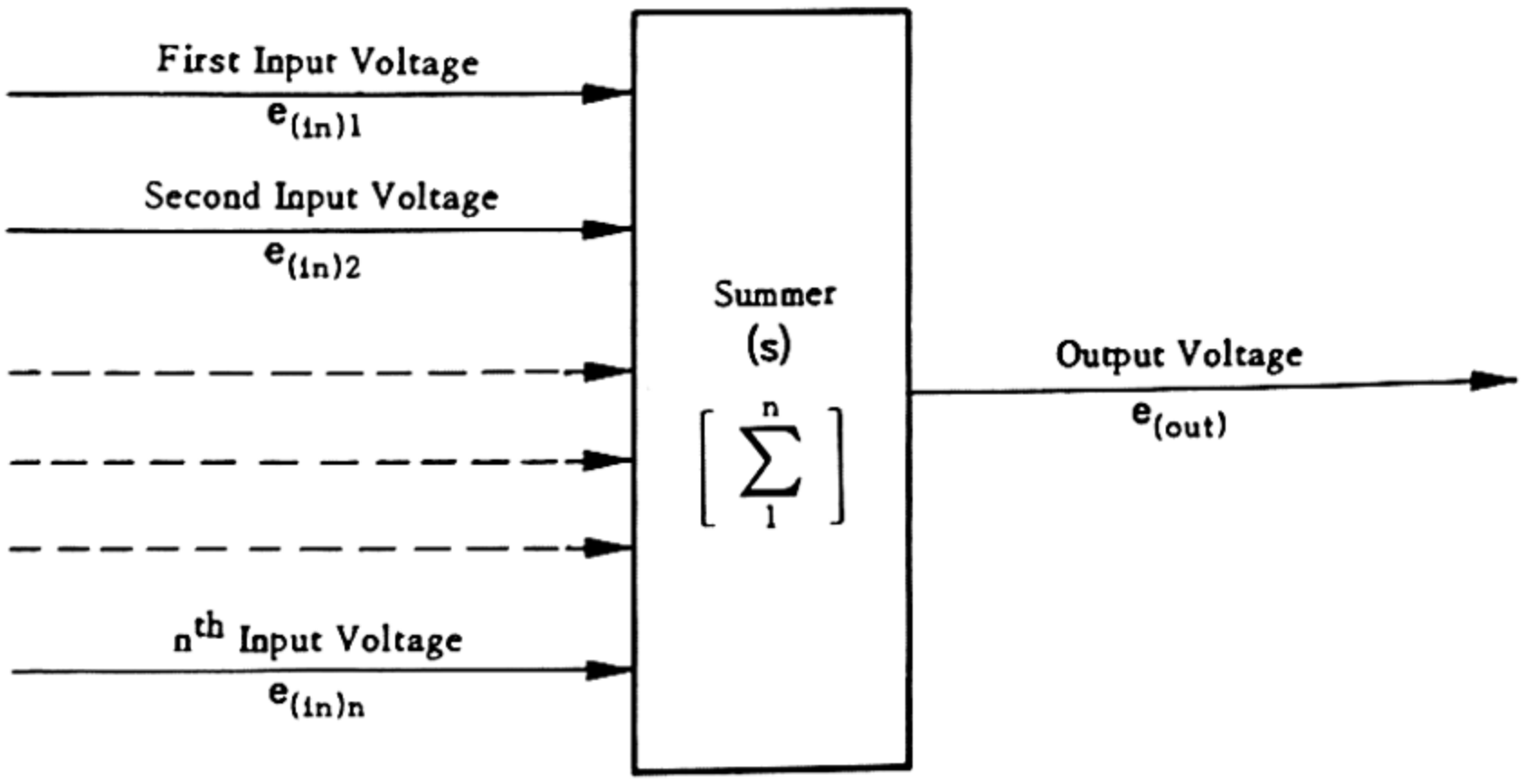
Equation (26) shows that when both special conditions are imposed, Eq. (25) reduces to the form

$$\frac{e_{(out)}}{e_{(in)}} = C_{(id)} \tag{27}$$

which is identical with the ideal form given by Eq. (12).

d) Performance relationships associated with a variable-gain-amplifier coefficient multiplier and an attenuator coefficient multiplier when either is used as a component of an electrical analog computer

An ideal summer can be represented by the following mathematical-functional diagram.



The performance equation corresponding to this functional diagram is

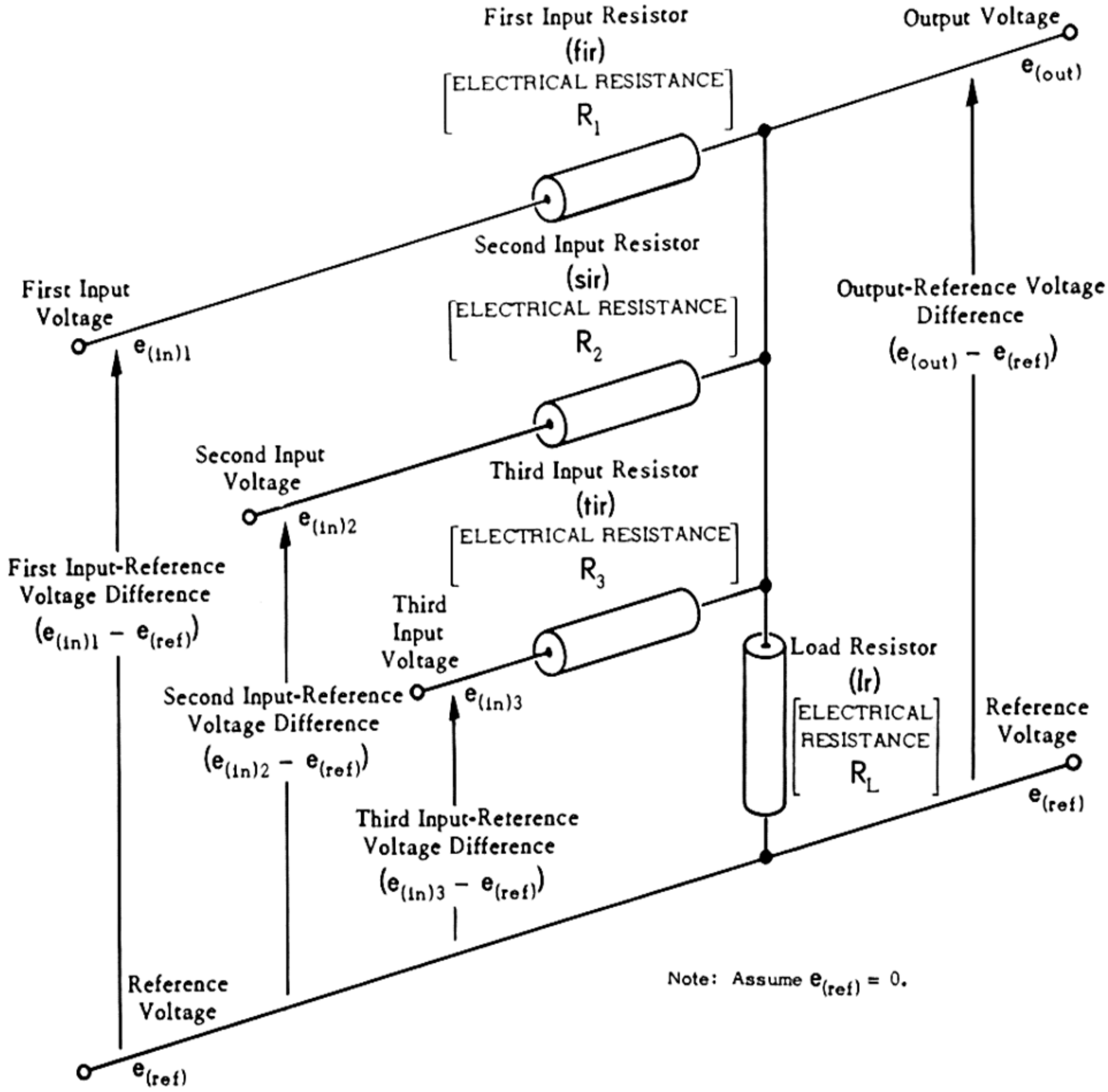
$$e_{(out)} = \sum_{i=1}^{i=n} e_{(in)i} \tag{28}$$

Derivation Summary 34-22. Performance relationships associated with the components of a linear-system electrical analog computer. (Page 6 of 8)

Specific performance relationships for the two summers noted in section b are given in the remainder of this section.

(rns) Resistance network summer

The following pictorial circuit diagram represents the components of a resistance network summer for the case of three input voltages.



Note: Assume $e_{(ref)} = 0$.

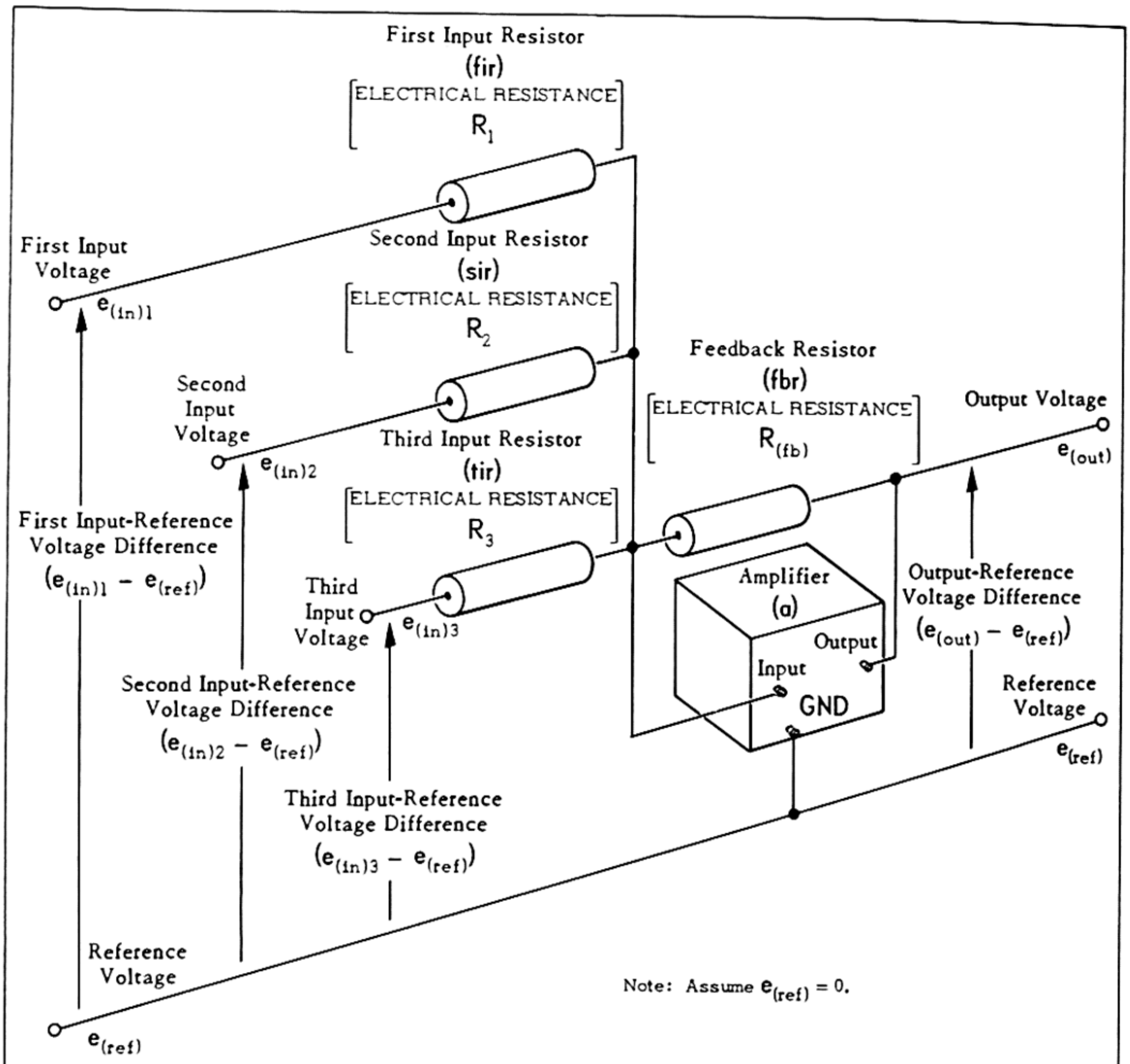
Application of Kirchoff's laws to this pictorial circuit diagram shows that the performance relationship of the resistance network summer, with $e_{(ref)}$ equal to zero as in the previous cases, is

$$e_{(out)} = \frac{\frac{e_{(in)1}}{R_1} + \frac{e_{(in)2}}{R_2} + \frac{e_{(in)3}}{R_3}}{\frac{1}{R_1} + \frac{1}{R_2} + \frac{1}{R_3} + \frac{1}{R_L}} \tag{29}$$

(rafrs) Resistance – amplifier – feedback-resistance summer

The following pictorial circuit diagram represents the components of a resistance – amplifier – feedback-resistance summer for the case of three input voltages.

Derivation Summary 34-22. Performance relationships associated with the components of a linear-system electrical analog computer. (Page 7 of 8)



Note: Assume $e_{(ref)} = 0$.

A derivation procedure similar to those already used in the summary shows that the performance relationship of a resistance – amplifier – feedback-resistance summer is

$$(e_{(out)} - e_{(ref)}) = S_{(a)|e;e|} \frac{\frac{(e_{(in)1} - e_{(ref)})}{R_1} + \frac{(e_{(in)2} - e_{(ref)})}{R_2} + \frac{(e_{(in)3} - e_{(ref)})}{R_3}}{\frac{1 - S_{(a)|e;e|}}{R_{(fb)}} + \frac{1}{R_1} + \frac{1}{R_2} + \frac{1}{R_3}} \tag{30}$$

Assume

$$S_{(a)|e;e|} >> 1 \quad ; \quad e_{(ref)} = 0 \tag{31}$$

Then Eq. (30) reduces to

$$e_{(out)} = -\left[\left(\frac{R_{(fb)}}{R_1}\right)e_{(in)1} + \left(\frac{R_{(fb)}}{R_2}\right)e_{(in)2} + \left(\frac{R_{(fb)}}{R_3}\right)e_{(in)3}\right] \tag{32}$$

e) *Performance relationships associated with a resistance network summer and a resistance – amplifier – feedback-resistance summer when either is used as a component of an electrical analog computer*

Derivation Summary 34-22. Performance relationships associated with the components of a linear-system electrical analog computer. (Page 8 of 8)

in terms of physical problem time as the running variable. The proportionality constant so found is denoted as the reference time, $T_{(ref)}$, and depends upon the values of the resistance and feedback capacitance used in the integrator, as well as upon the solution time ratio. Thus, the value of $T_{(ref)}$ governs the rate with respect to physical problem time at which integrator output voltage increases for, say, a step in input voltage. Or, what amounts to the same thing, it is the ratio of input voltage to rate of change of output voltage taken with respect to physical problem time. Accordingly, the value of $T_{(ref)}$ that is employed will be seen to be of significance in governing the relative voltage levels that exist in different parts of the computer.

34.141. Nondimensionalization is advantageous in representing the process of integration. In operational form, the ratio of output to input for an integrator is $1/p\,T_{(ref)}$, where p is the differential operator taken with respect to physical problem time. If time in this operator is nondimensionalized by means of $T_{(ref)}$ and the dimensionless operator denoted by $'p$, the performance function for an integrator becomes simply $1/'p$, as represented by the functional block at the end of section c, Derivation Summary 34-22. This may also be thought of as replacing the dimensionless product $p\,T_{(ref)}$ by the dimensionless operator $'p$, which means that the dimensional operator p appearing in the system equation may be replaced by $'p/T_{(ref)}$. The computer integrators are considered to provide the operation $1/'p$, as already noted. The quantity $T_{(ref)}$ that remains is lumped together with the coefficients of the differential equation, along with the scale factors transforming input and output quantities to voltages, to yield the coefficients that will be set on the analog-computer coefficient multipliers. This is the essence of scaling a problem for solution by an analog computer.

34.142. Derivation Summary 34-22 also gives relations for the common forms of coefficient multipliers and summers used with electrical analog computers. Taken together with integrators, these units will solve any linear-system problem, if they are available in adequate numbers. This is evident on inspection of Eq. (1) of Derivation Summary 34-22 in which the operations of integration (preferred over differentiation), coefficient multiplication and addition are implicit.

SOLUTION OF THE GENERAL LINEAR DIFFERENTIAL EQUATION WITH CONSTANT COEFFICIENTS BY AN ANALOG COMPUTER

34.143. In Derivation Summary 34-23, the general linear differential equation with constant coefficients that represents the physical problem is converted to a form directly applicable for analog-computer solution. The steps involve the introduction of the input and output scale factors and $T_{(ref)}$. General expressions for the values of the analog-computer coefficient settings are written down, and are seen in each case to involve the system coefficients, the scale factors and the reference time, $T_{(ref)}$.

As noted in section a of Derivation Summary 34-22, the physical problem may be represented mathematically by the linear differential equation with constant coefficients

$$\sum_{i=0}^{i=n} a_i \frac{d^i v}{dt_{(pp)}^i} = \sum_{j=0}^{j=m} b_j \frac{d^j u}{dt_{(pp)}^j} \tag{1}$$

The running variable $t_{(pp)}$ can be nondimensionalized by the procedure used in Eq. (9) of Derivation Summary 34-22; i.e.,

$$'t_{(pp)} = \frac{t_{(pp)}}{T_{(ref)}} = \text{nondimensional physical problem time} \tag{2}$$

where, as defined by Derivation Summaries 34-21 and 34-22,

$$T_{(ref)} = \frac{(CT)_{(RC)}}{STR} = \text{reference time} \tag{3}$$

$$(CT)_{(RC)} = RC = \text{ratio of integrator input voltage to the rate of change of integrator output voltage} \tag{4}$$

$$STR = \frac{(ST)_{(ac)}}{(ST)_{(pp)}} = \frac{t_{(ac)}}{t_{(pp)}} = \frac{dt_{(ac)}}{dt_{(pp)}} = \text{solution time ratio} \tag{5}$$

In terms of $'t_{(pp)}$, Eq. (1) becomes

$$\sum_{i=0}^{i=n} \frac{a_i}{T_{(ref)}^i} \frac{d^i v}{d('t_{(pp)})^i} = \sum_{j=0}^{j=m} \frac{b_j}{T_{(ref)}^j} \frac{d^j u}{d('t_{(pp)})^j} \tag{6}$$

The independent and dependent variables u and v can now be replaced by their analogous voltages e_u and e_v by means of the following relationships, which are derived in Derivation Summary 34-21:

$$u = \frac{e_u}{(SF)_{(u;e)}} \quad ; \quad v = \frac{e_v}{(SF)_{(v;e)}} \tag{7),(8}$$

Application of the scale-factor relationships to the physical-problem differential equation given by Eq. (6) yields the corresponding analog-computer differential equation; i.e.,

$$\sum_{i=0}^{i=n} \frac{a_i}{T_{(ref)}^i (SF)_{(v;e)}} \frac{d^i e_v}{d('t_{(pp)})^i} = \sum_{j=0}^{j=m} \frac{b_j}{T_{(ref)}^j (SF)_{(u;e)}} \frac{d^j e_u}{d('t_{(pp)})^j} \tag{9}$$

If the coefficients of Eq. (9) are denoted by $C_{(a_i)}$ and $C_{(b_j)}$, this equation becomes

$$\sum_{i=0}^{i=n} C_{(a_i)} \frac{d^i e_v}{d('t_{(pp)})^i} = \sum_{j=0}^{j=m} C_{(b_j)} \frac{d^j e_u}{d('t_{(pp)})^j} \tag{10}$$

where

$$C_{(a_i)} = \frac{a_i}{T_{(ref)}^i (SF)_{(v;e)}} = \text{coefficient associated with the } i^{th} \text{ output-voltage term of the analog-computer differential equation} \tag{11}$$

and

$$C_{(b_j)} = \frac{b_j}{T_{(ref)}^j (SF)_{(u;e)}} = \text{coefficient associated with the } j^{th} \text{ input-voltage term of the analog-computer differential equation} \tag{12}$$

As is shown in the next summary, generalized coefficients such as $C_{(a_i)}$ and $C_{(b_j)}$ determine the numerical values of the coefficient settings of the various coefficient multipliers used in the analog computer.

Since from Eq. (11) of Derivation Summary 34-22,

$$'p = \frac{d}{d('t_{(pp)})} \tag{13}$$

Derivation Summary 34-23. Transformation of an nth-order linear differential equation with constant coefficients to a form suitable for solution by an electrical analog computer.
(Page 1 of 3)

Eq. (9) can be further modified to the operational-notation form

$$\sum_{i=0}^{i=n} C_{(a_i)}\, {}'p^i e_v = \sum_{j=0}^{j=m} C_{(b_j)}\, {}'p^j e_u \tag{14}$$

The subscripts a_i and b_j of Eqs. (10) through (14) indicate that the generalized coefficients $C_{(a_i)}$ and $C_{(b_j)}$ are respectively directly proportional to the a_i^{th} and the b_j^{th} coefficients of the physical-problem differential equation and independent of each of the other physical-problem differential equation coefficients.

The analog-computer differential equation may be multiplied by a constant in order to increase or decrease the magnitude of all the generalized coefficients as desired. For example, if Eq. (14) is multiplied by the constant $1/C_{(a_k)}$ in order to make the coefficient of the kth output-voltage term equal to unity, that equation can be written

$$\sum_{i=0}^{i=n} C_{(a_i/a_k)}\, {}'p^i e_v = \sum_{j=0}^{j=m} C_{(b_j/a_k)}\, {}'p^j e_u \tag{15}$$

where

$$C_{(a_i/a_k)} = \frac{C_{(a_i)}}{C_{(a_k)}} = \text{coefficient associated with the } i^{th} \text{ output-voltage term of the analog-computer differential equation modified by multiplying all terms by } 1/C_{(a_k)} \tag{16}$$

and

$$C_{(b_j/a_k)} = \frac{C_{(b_j)}}{C_{(a_k)}} = \text{coefficient associated with the } j^{th} \text{ input-voltage term of the analog-computer differential equation modified by multiplying all terms by } 1/C_{(a_k)} \tag{17}$$

In this case, the subscript ratio a_i/a_k indicates that the generalized coefficient $C_{(a_i/a_k)}$ is directly proportional to the a_i^{th} coefficient of the physical-problem differential equation, inversely proportional to the a_k^{th} coefficient, and independent of each of the other coefficients. Similar information is conveyed by the subscript of the generalized coefficient $C_{(b_j/a_k)}$. The coefficient of the kth output-voltage term is of course unity, as shown by the relationship

$$C_{(a_k/a_k)} = \frac{C_{(a_k)}}{C_{(a_k)}} = 1 \tag{18}$$

There is no restriction on the choice of constant factors that could be applied to increase or decrease the magnitude of the coefficients of Eq. (14). For example, Eq. (14) could be multiplied by the constant $1/C_{(b_l)}$ in order to make the coefficient of the lth input-voltage term equal to unity. In the general case, where it is desirable to multiply all terms of the analog-computer differential equation by a constant factor but without necessarily reducing any term coefficient to unity, the following equation applies

$$\sum_{i=0}^{i=n} C_{[a_i/(CF)]}\, {}'p^i e_v = \sum_{j=0}^{j=m} C_{[b_j/(CF)]}\, {}'p^j e_u \tag{19}$$

where

$$C_{[a_i/(CF)]} = \frac{C_{(a_i)}}{(CF)} = \text{coefficient associated with the } i^{th} \text{ output-voltage term of the analog-computer differential equation modified by multiplying all terms by the reciprocal of a constant factor } (CF) \tag{20}$$

$$C_{[b_j/(CF)]} = \frac{C_{(b_j)}}{(CF)} = \text{coefficient setting associated with the } j^{th} \text{ input-voltage term of the analog-computer differential equation modified by multiplying all terms by the reciprocal of a constant factor } (CF) \tag{21}$$

and

(CF) = constant factor

Derivation Summary 34-23. Transformation of an nth-order linear differential equation with constant coefficients to a form suitable for solution by an electrical analog computer.
(Page 2 of 3)

In this case, the subscript ratio $a_i/(CF)$ indicates that the generalized coefficient $C_{[a_i/(CF)]}$ is directly proportional to the a_i^{th} coefficient of the physical-problem differential equation, is independent of each of the other coefficients, and is associated with an analog-computer differential equation modified by multiplying all terms by $1/(CF)$.

Either of the analog-computer differential equation forms given by Eqs. (14), (15), and (19) are suitable for direct handling by an electrical analog computer that uses the integrators, coefficient multipliers and summers already described in Derivation Summary 34-22.

Derivation Summary 34-23. Transformation of an nth-order linear differential equation with constant coefficients to a form suitable for solution by an electrical analog computer.
(Page 3 of 3)

34.144. A computer block diagram for solving the converted linear differential equation with constant coefficients may have various possible forms. For example, insofar as the right-hand side of the equation is concerned (Eqs. (10), (15) and (19) of Derivation Summary 34-23 are all applicable here), one might at first visualize the input voltage e_u successively differentiated m times, each derivative multiplied by the appropriate coefficient, and then the sum taken. However, as has been already mentioned, the use of differentiation would introduce difficulties. For example, if e_u were taken as a step function, the values of the derivatives of e_u would become unmanageable at the instant the step occurs. As a consequence, this approach is not used. One might next conceive an arrangement in which the highest derivative of e_u is the input voltage to the computer and m integrators are used to produce all the needed lower derivatives. This eliminates the difficulty with differentiators but introduces an equally formidable problem whenever m is greater than zero; namely, that of producing the input signal if e_u itself is to be some simple function, such as a step. In this instance, if m were equal to unity, so that only one integration would be required, the input signal would have to be an idealized impulse, which is a quantity incapable of physical realization. For larger values of m, such difficulties would multiply. As for the left-hand side of the equation, if the highest derivative of e_v is presumed to exist as a voltage, it may be successively integrated n times to produce all lower derivatives of e_v including the zero-order term. Each of these may be multiplied by its proper coefficient and the sum taken together with the terms on the right-hand side of the equation. The result of this summation is then the highest derivative in e_v multiplied by its coefficient. Thus, such a feedback connection could serve to develop the signal that was initially presumed to be available. It is apparent, then, that the left-hand side of the equation offers no problem if the right-hand side can be managed.

34.145. The connection of computer elements shown in Derivation Summary 34-24* serves to solve this general problem and will herein be called the

* This connection was proposed by Mr. Loebe Julie while at Columbia University in 1943 and later independently, it is understood, in England by Mr. J. G. L. Michel, then of Manchester University. No published reference disclosing this idea is known to the authors.

"least number of components" connection since, for a linear system, this connection requires the fewest computer elements. An auxiliary variable, z, defined for the physical problem, represents physically the response of the system to a unit impulse. The array of computer elements used in the "least number of components" connection makes available voltages proportional to z and its derivatives at points between n integrators, which are arranged in a series chain. When these voltages are multipled by coefficients representing those on the right-hand side of the differential equation and the resulting voltages are added together, the output voltage, e_v, is obtained. This technique is a direct manifestation of the principle of superposition, since the output voltage is seen to be the sum of m + 1 voltages, each of which represents the response of the system to one term on the right-hand side of the equation. This connection of computer elements is also most economical of computer components since n integrators are sufficient to solve the problem. Derivation Summary 34-24 shows this analog-computer connection and develops the performance relations that govern the operation of the computer.

SOLUTION OF THE (0;0,1) DIFFERENTIAL EQUATION BY AN ANALOG COMPUTER

34.146. The simplest dynamical system is the first-order (0;0, 1) system studied in Chapter 18. Derivation Summary 34-25 shows how such a system is set up on an analog computer. Scaling of the problem or calculation of the computer coefficient setting involves selection of the reference time, $T_{(ref)}$, input and output scale factors, and the coefficients of the governing differential equation. Three such coefficient settings are needed, proportional respectively to a_1, a_0 and b_0, the differential equation coefficients. The block diagram in section a of Derivation Summary 34-25 shows the computer arrangement for handling this system.

34.147. It is evident that the original differential equation may be multiplied through by a constant. If this is done, the numerical values of the computer coefficient setting will be modified in either direct or inverse proportion to the value of the constant. This makes it possible to further adjust the values of the computer coefficient settings so as to fall within desired numerical ranges appropriate to the capabilities of the computer. Special cases of this occur when the multiplying constant is so chosen as to make one of the coefficient settings equal to unity. There will be three such possibilities for a (0;0, 1) system, depending on which of the three coefficient settings is made equal to unity. Each of these possible choices is shown by the block diagrams of sections b, c and d, respectively. For example, in the block diagram of section c, the analog-computer equation is divided through by $a_0/(SF)_{(v;e)}$ to make the feedback coefficient setting equal to unity. This makes the elimination of one coefficient multiplier possible. More significantly, it makes the coefficient setting of the multiplier that receives the summer output voltage inversely proportional to the reciprocal of the first-order system time

An arrangement that provides for the most economical use of components in an analog computer designed for handling linear systems is called the "least number of components" connection.* Under this scheme, the minimum number of integrators required is n, the order of the system. The minimum number of coefficient multipliers is n + m + 2, the number of coefficients present in the differential equation transformed for analog-computer solution, unless the equation is multiplied by a constant such that one of the coefficients becomes unity,** in which case n + m + 1 coefficient multipliers are needed. Two summers are needed if $m \geq 1$, but if only the zero-order term in u is present (that is, if m = 0) one summer is sufficient, provided it has provision for handling the needed number of inputs.

Inherent in this scheme is the presence of a voltage proportional to a valuable auxiliary variable of the problem, which is represented by the symbol z. The significance of this auxiliary variable can be seen from the following analysis. Based on the operational form of Eq. (1) of Derivation Summary 34-23; i.e.,

$$\sum_{i=0}^{i=n} a_i p^i v = \sum_{j=0}^{j=m} b_j p^j u \tag{1}$$

the auxiliary variable, z, can be defined as

$$z = \frac{u}{\sum_{i=0}^{i=n} a_i p^i} = \frac{v}{\sum_{j=0}^{j=m} b_j p^j} \tag{2}$$

This definition of z has a useful interpretation. If the input u is taken equal to unity, then z is seen to be equal to v/b_o. This quantity, except for the constant, b_o, is the response of the physical system to an impulse input of unit magnitude, otherwise called the weighting function. In general, v is the sum of successive derivatives of z, each multiplied by its appropriate coefficient, b_j. This sum is a direct manifestation of the principle of superposition.

The auxiliary variable voltage, e_z, can be related to the auxiliary variable, z, by a procedure analogous to that of Derivation Summary 34-21; i.e., define

$$(SF)_{(z;e)} = \frac{e_z}{z} = \text{auxiliary variable} - \text{auxiliary variable voltage scale factor} \tag{3}$$

A study of the voltage relationships of Michel's computer arrangement reveals that

$$e_z = (SF)_{(u;e)}(SF)_{(v;e)} z \text{ ***} \tag{4}$$

so that

$$(SF)_{(z;e)} = (SF)_{(u;e)}(SF)_{(v;e)} \text{ ***} \tag{5}$$

Section b gives a functional diagram showing the computer arrangement for solving a general n^{th}-order linear differential equation. The voltage e_z occurs naturally as a measure of the auxiliary variable z. Implicit in this diagram is the assumption that, initially, voltages at all points in the circuit are at the correct level, which may be zero. The input to the computer is the voltage e_u and the output, corresponding to the solution of the physical problem, is the voltage e_v. As noted on the diagram, this scheme requires that the order of the dependent variable side of the equation, n, be greater than the order of the independent variable side of the equation, m.

The integrators, coefficient multipliers and summers are units of the types discussed in Derivation Summary 34-22. The coefficient settings of the coefficient multipliers have numerical values equal to the corresponding generalized coefficients $C_{(a_i)}$ and $C_{(b_j)}$ given by Eqs. (11) and (12) of Derivation Summary 34-23,

* See footnote for paragraph 34.145.

** See Derivation Summary 34-23 for this procedure.

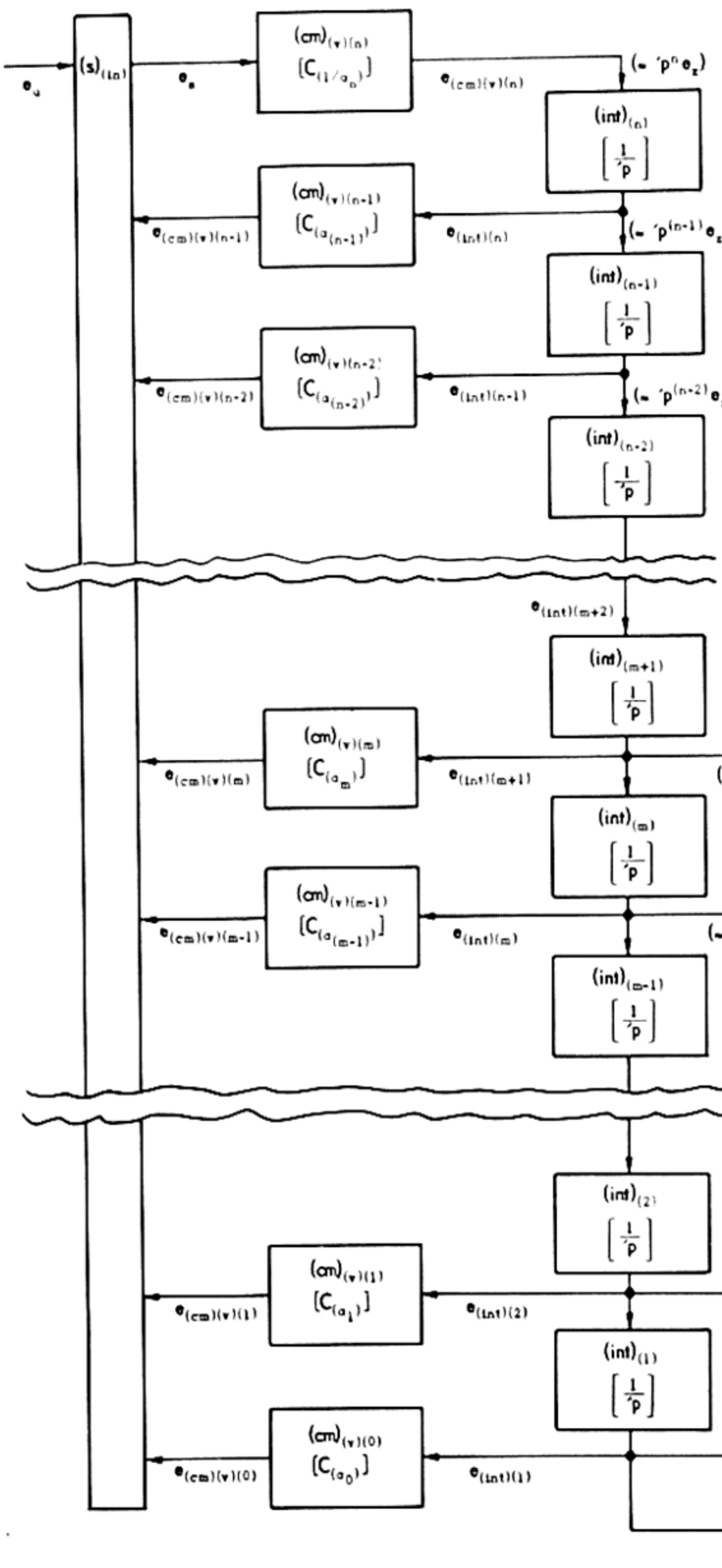
*** These relationships are derived in section d of this summary.

Derivation Summary 34-24. Functional diagram and performance equations of an analog-computer arrangement based on the "least number of components" connection and representing a general n^{th}-order linear system. (Page 1 of 5)

with the exception of the coefficient setting of the nth-order dependent variable coefficient multiplier, $(cm)_{(v)(n)}$, which is related to the corresponding generalized coefficient $C_{(a_n)}$ as follows:

$$C_{(1/a_n)} = 1/C_{(a_n)} \tag{6}$$

a) "Least number of components" connection of basic analog-computer components



$(cm)_{(v)(n)}$ = n^{th}-order dependent variable coefficient multiplier;

$$C_{(1/a_n)} = \frac{T^n_{(ref)}(SF)_{(v;e)}}{a_n}$$

$(cm)_{(v)(i)}$ = Zero-order through $(n-1)^{st}$-order dependent variable coefficient multipliers;

$$C_{(a_i)} = \frac{a_i}{T^i_{(ref)}(SF)_{(v;e)}}; \quad i = 0, 1, 2 \ldots (n-1)$$

$(cm)_{(u)(j)}$ = Zero-order through m^{th}-order independent variable coefficient multipliers;

$$C_{(b_j)} = \frac{b_j}{T^j_{(ref)}(SF)_{(u;e)}}; \quad j = 0, 1, 2 \ldots m$$

$(int)_{(i)}$ = i^{th}-order integrator; $i = 1, 2, \ldots n$

$$T_{(ref)} = \frac{(CT)_{(RC)}}{STR}$$

$$STR = \frac{t_{(ac)}}{t_{(pp)}} = \frac{dt_{(ac)}}{dt_{(pp)}}$$

$$'p = \frac{d}{d\,'t_{(pp)}} = pT_{(ref)}$$

$$'t_{(pp)} = \frac{t_{(pp)}}{T_{(ref)}}$$

Note: This computer arrangement is based on the assumption that $n > m$.

b) Generalized functional diagram of an analog-computer arrangement based on the "least number of components" connection

Derivation Summary 34-24. Functional diagram and performance equations of an analog-computer arrangement based on the "least number of components" connection and representing a general n^{th}-order linear system. (Page 2 of 5)

Assuming ideal operation, the performance equations for the components shown in the functional diagram of section b can be written as follows from inspection and the ideal relationships developed in Derivation Summary 34-22.

$(s)_{(in)}$ Input summer

$$e_s = e_u - \sum_{i=0}^{i=n-1} e_{(cm)(v)(i)} \tag{7}$$

$(cm)_{(v)(n)}$ n^{th}-order dependent variable coefficient multiplier

$$e_{(cm)(v)(n)} = C_{(1/a_n)} e_s \tag{8}$$

$(cm)_{(v)(i)}$ $(i = 0, 1, \ldots n-1)$ Zero-order through $(n-1)^{st}$-order dependent variable coefficient multipliers

$$e_{(cm)(v)(i)} = C_{(a_i)} e_{(int)(i+1)} \quad ; \quad i = 0, 1, \ldots n-1 \tag{9}$$

$(int)_{(i)}$ $(i = 1, 2, \ldots n)$ First-order through n^{th}-order integrators

$$e_{(int)(i)} = \int_{n-i+1} \cdots \int e_{(cm)(v)(n)} \, d't_{(pp)}^{(n-i+1)} = \frac{1}{'p^{(n-i+1)}} e_{(cm)(v)(n)} \quad ; \quad i = 1, 2, \ldots n \tag{10}$$

$$= \frac{d}{d't_{(pp)}^{(i-1)}} e_z = 'p^{(i-1)} e_z \tag{11}$$

$(cm)_{(u)(j)}$ $(j = 0, 1, \ldots m)$ Zero-order through m^{th}-order independent variable coefficient multipliers

$$e_{(cm)(u)(j)} = C_{(b_j)} e_{(int)(j+1)} = C_{(b_j)} 'p^j e_z \quad ; \quad j = 0, 1, \ldots m \tag{12}$$

$(s)_{(out)}$ Output summer

$$e_v = \sum_{j=0}^{j=m} e_{(cm)(u)(j)} \tag{13}$$

As shown by the diagram of section b, the output voltages of the n integrators are fed back to the input summer through the zero-order through $(n-1)^{st}$-order dependent variable coefficient multipliers in which each voltage is modified by a particular multiplying coefficient. The output voltage of the summer, which is the sum of the input voltage and the zero-order through $(n-1)^{st}$-order feedback voltages, is modified by the nth-order dependent variable coefficient and is applied to the nth-order integrator. The output voltage of this integrator is successively integrated $n-1$ times by the computer integrators as indicated on the functional diagram of section b. As indicated by the functional diagram of section b, the auxiliary variable voltage, e_z, is the output voltage, $e_{(int)(1)}$, of the first-order integrator.

The relationship between the auxiliary variable voltage, e_z, and the input voltage, e_u, may be found by eliminating e_s from Eqs. (7) and (9) and substituting Eqs. (9), (10), and (11) in the result.

$$\sum_{i=0}^{i=n} C_{(a_i)} 'p^i e_z = e_u \tag{14}$$

The voltage $e_{(int)(m+1)}$ produced by the $(m+1)^{st}$-order integrator, is not only fed back to the input summer through the mth-order dependent variable coefficient multiplier $(cm)_{(v)(m)}$, and fed forward to the mth-order integrator, but is also applied to the mth-order independent variable coefficient multiplier, $(cm)_{(u)(m)}$. The integrator output voltages $e_{(int)(m)}$ to $e_{(int)(1)}$ inclusive are applied to the remaining independent variable coefficient multipliers $(cm)_{(u)(0)}$ through $(cm)_{(u)(m-1)}$, in addition to being fed back to the dependent variable coefficient multipliers $(cm)_{(v)(0)}$ through $(cm)_{(v)(m-1)}$, as already noted.

The output voltages of the m independent variable coefficient multipliers $(cm)_{(u)(0)}$ through $(cm)_{(u)(m)}$ are related to the corresponding integrator voltages by Eq. (12) in terms of the auxiliary variable voltage, e_z, which, as already noted, is the output voltage of the first-order integrator $(int)_{(1)}$.

Derivation Summary 34-24. Functional diagram and performance equations of an analog-computer arrangement based on the "least number of components" connection and representing a general n^{th}-order linear system. (Page 3 of 5)

Substituting the relationship of Eq. (12) in Eq. (13) shows that the auxiliary variable voltage, e_z, and output voltage, e_v, of the summer, which is also the output voltage of the analog computer, are related as follows:

$$e_v = \sum_{j=0}^{j=m} C_{(b_j)}\, {}'p^j e_z \tag{15}$$

Solving Eqs. (14) and (15), both of which are in operational-notation form, for e_z and equating the two relationships shows that

$$\frac{e_u}{\sum_{i=0}^{i=n} C_{(a_i)}\, {}'p^i} = \frac{e_v}{\sum_{j=0}^{j=m} C_{(b_j)}\, {}'p^j} \tag{16}$$

or

$$\sum_{i=0}^{i=n} C_{(a_i)}\, {}'p^i e_v = \sum_{j=0}^{j=m} C_{(b_j)}\, {}'p^j e_u \tag{17}$$

The relationship between e_u and e_v represented by Eq. (17) is identical with Eq. (12) of Derivation Summary 34-23, which is the transformation of an nth-order linear differential equation with constant coefficients to a form suitable for solution by an electrical analog computer. This means that the analog computer provides the required performance, such that the output voltage, e_v, is at all times related to the physical-problem dependent variable, v, by the scale-factor relationship

$$e_v = (SF)_{(v;e)} v \tag{18}$$

c) *Performance equations of an analog-computer arrangement based on the "least number of components" connection and representing a general n^{th}-order linear system*

The performance-equation development made in the previous section provides the basis for deriving the scale-factor relationship given in section a. From Eq. (15), the auxiliary variable voltage, e_z, and the output voltage, e_v, of the analog computer are related as follows:

$$e_v = \sum_{j=0}^{j=m} C_{(b_j)}\, {}'p^j e_z \tag{19}$$

A substitution for the generalized independent variable coefficient, $C_{(b_j)}$, of Eq. (19), using Eq. (12) of Derivation Summary 34-23, i.e.,

$$C_{(b_j)} = \frac{b_j}{T^j_{(ref)}(SF)_{(u;e)}} \tag{20}$$

yields

$$e_v = \sum_{j=0}^{j=m} \frac{b_j}{T^j_{(ref)}(SF)_{(u;e)}}\, {}'p^j e_z \tag{21}$$

If the nondimensional operator, ${}'p^j$, is replaced by $p^j T^j_{(ref)}$, Eq. (21) can be written as

$$e_v = \sum_{j=0}^{j=m} \frac{b_j}{(SF)_{(u;e)}} p^j e_z \tag{22}$$

The output voltage, e_v, of the analog computer is related to the dependent variable, v, of the differential equation representation of the physical problem by the scale-factor relationship

$$e_v = (SF)_{(v;e)} v \tag{23}$$

Derivation Summary 34-24. Functional diagram and performance equations of an analog-computer arrangement based on the "least number of components" connection and representing a general n^{th}-order linear system. (Page 4 of 5)

Substitution of this relationship for e_v in Eq. (22) yields

$$(SF)_{(v;e)}v = \sum_{j=0}^{j=m} \frac{b_j}{(SF)_{(u;e)}} p^j e_z \tag{24}$$

Or, rearranging the terms of Eq. (24),

$$e_z = (SF)_{(u;e)}(SF)_{(v;e)} \frac{v}{\sum_{j=0}^{j=m} b_j p^j} \tag{25}$$

Equation (2) of this summary shows that the ratio on the right-hand side of Eq. (25) is equal to the auxiliary variable, z, so that Eq. (25) can be rewritten in the form

$$e_z = (SF)_{(u;e)}(SF)_{(v;e)}z = (SF)_{(z;e)}z \tag{26}$$

so that

$$(SF)_{(z;e)} = (SF)_{(u;e)}(SF)_{(v;e)} \tag{27}$$

d) Auxiliary variable-independent variable-dependent variable relationships

Derivation Summary 34-24. Functional diagram and performance equations of an analog-computer arrangement based on the "least number of components" connection and representing a general n^{th}-order linear system. (Page 5 of 5)

constant τ. Since the time constant in such a system is the one and only dynamic parameter, it is desirable to have a coefficient multiplier that varies this quantity. All variations in system dynamics are thus included in a single coefficient setting. In this same arrangement, the other coefficient multiplier varies the quantity σ, which is the sensitivity, or ratio of output to input under static conditions. This kind of parameter-setting dependence is often more directly useful in system studies than the ability to vary all three system coefficients independently, so this connection is of great practical importance.

34.148. The computer connections shown in the block diagrams of sections b and d are less useful. In both of these arrangements, the system characteristic time is involved in both of the coefficient settings. In order to vary this parameter alone, then, it is necessary to change by properly related amounts two coefficient multiplier settings. This is, of course, a more complicated procedure and usually is to be avoided.

SOLUTION OF THE (0;0,1,2) DIFFERENTIAL EQUATION BY AN ANALOG COMPUTER

34.149. In Derivation Summary 34-26, the same approach is applied to the second-order (0;0,1,2) linear system, which is treated extensively in Chapter 19. The same generalities as those just stated for the first-order system also apply here. This time, however, there are two dynamic parameters, the undamped angular natural frequency, w_n, and the damping ratio, DR, in addition to the static parameter σ. Here, the computer connection shown in the block diagram of Fig. d, in which the coefficient setting in the zero-order feedback path is made equal to unity, yields the arrangement in which the system parameters are most nearly

The generalized form of the (0;0,1) first-order differential equation that represents a linear-system physical problem is

$$a_1 \frac{dv}{dt_{(pp)}} + a_0 v = b_0 u \qquad (1)$$

Following the pattern of Derivation Summary 34-23, Eq. (1) can be written in terms of the nondimensional running variable, $'t_{(pp)}$, as

$$\frac{a_1}{T_{(ref)}} \frac{dv}{d\,'t_{(pp)}} + a_0 v = b_0 u \qquad (2)$$

where

$$'t_{(pp)} = \frac{t_{(pp)}}{T_{(ref)}} \qquad (3)$$

The independent and dependent variables u and v can now be replaced by their analogous voltages e_u and e_v by means of the following relationships, which are derived in Derivation Summary 34-21:

$$u = \frac{e_u}{(SF)_{(u;e)}} \quad ; \quad v = \frac{e_v}{(SF)_{(v;e)}} \qquad (4),(5)$$

With these relationships, Eq. (2) becomes

$$\frac{a_1}{T_{(ref)}(SF)_{(v;e)}} \frac{de_v}{d\,'t_{(pp)}} + \frac{a_0}{(SF)_{(v;e)}} e_v = \frac{b_0}{(SF)_{(u;e)}} e_u \qquad (6)$$

A comparison of Eq. (6) with Eqs. (10), (11), and (12) of Derivation Summary 34-23 shows that, in terms of the generalized coefficients discussed in that summary, the physical-problem differential equation given by Eq. (1), as transformed for computer operation, can be written

$$C_{(a_1)} \frac{de_v}{d\,'t_{(pp)}} + C_{(a_0)} e_v = C_{(b_0)} e_u \qquad (7)$$

where

$$C_{(a_1)} = \frac{a_1}{T_{(ref)}(SF)_{(v;e)}} \quad ; \quad C_{(a_0)} = \frac{a_0}{(SF)_{(v;e)}} \quad ; \quad C_{(b_0)} = \frac{b_0}{(SF)_{(u;e)}} \qquad (8),(9),(10)$$

In the operational notation form of Eq. (14) of Derivation Summary 34-23, Eq. (7) becomes

$$C_{(a_1)}\, 'p e_v + C_{(a_0)} e_v = C_{(b_0)} e_u \qquad (11)$$

where, from Eq. (11) of Derivation Summary 34-22,

$$'p = \frac{d}{d\,'t_{(pp)}} = p T_{(ref)} \qquad (12)$$

The discussion given in section a of Derivation Summary 34-24 shows that an analog-computer arrangement of the type discussed in that summary must include the following components if it is to solve the physical problem represented by Eqs. (7) and (11):

1) The number of integrators required is one, since Eqs. (7) and (11) represent a first-order system; i.e., n = 1.
2) The minimum number of coefficient multipliers is three, since three coefficients are involved; i.e., m + n + 2 = 3.
3) One summer is sufficient, since only the zero-order term of the independent variable is present; i.e., m = 0.

Application of these requirements to the generalized computer functional diagram of Derivation Summary 34-23 yields the following computer arrangement for the first-order situation represented by Eqs. (7) and (11) of the present summary. In this arrangement, the coefficient settings of the three coefficient multipliers are separately adjustable in terms of a_1, a_0, and b_0, respectively. The numerical values of these settings,

Derivation Summary 34-25. Analog-computer arrangements for solving a first-order linear differential equation with constant coefficients. (Page 1 of 7)

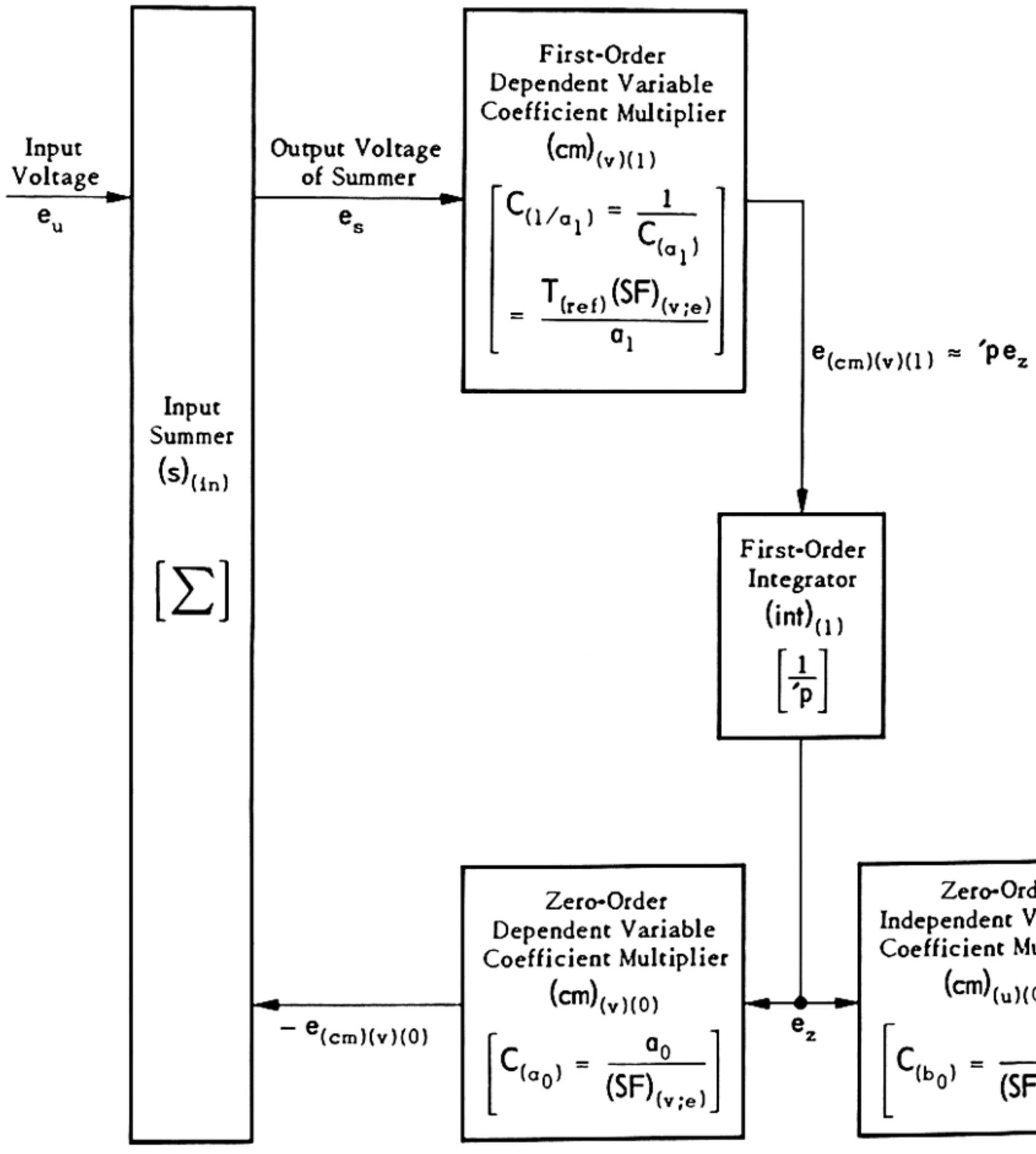
which are given by the quantities within brackets on each of the coefficient-multiplier blocks, are determined in accordance with the discussion of section a, Derivation Summary 34-24; namely,

1) The numerical value of the coefficient setting of the first-order dependent variable coefficient multiplier is equal to the reciprocal of the generalized first-order dependent variable coefficient $C_{(a_1)}$; i.e.,

$$C_{(1/a_1)} = 1/C_{(a_1)} = \frac{T_{(ref)}(SF)_{(v;e)}}{a_1} \tag{13}$$

2) The numerical values of the other two coefficient settings are equal to the corresponding generalized coefficients; i.e.,

$$C_{(a_0)} = \frac{a_0}{(SF)_{(v;e)}} \quad ; \quad C_{(b_0)} = \frac{b_0}{(SF)_{(u;e)}} \tag{14),(15}$$



a) Analog-computer arrangement for solving the (0;0,1) first-order differential equation when all the generalized analog-computer differential equation coefficients are different from unity

As noted in Derivation Summary 34-23, the number of coefficient multipliers may be reduced by one when the analog-computer differential equation is multiplied by a constant so that one of the generalized

Derivation Summary 34-25. Analog-computer arrangements for solving a first-order linear differential equation with constant coefficients. (Page 2 of 7)

coefficients becomes unity. For example, if Eq. (7) is multiplied by $1/C_{(a_1)}$, the reciprocal of the first-order output-voltage term coefficient, the following relationship is obtained.

$$\frac{de_v}{dt_{(pp)}} + \frac{C_{(a_0)}}{C_{(a_1)}} e_v = \frac{C_{(b_0)}}{C_{(a_1)}} \frac{(SF)_{(v;e)}}{(SF)_{(u;e)}} e_u \tag{16}$$

For the modified form of the analog-computer differential equation represented by Eq. (16),

$$\frac{C_{(a_0)}}{C_{(a_1)}} = C_{(a_0/a_1)} = \frac{a_0 T_{(ref)}}{a_1} = \frac{T_{(ref)}}{r} \approx C_{(1/r)} \tag{17}$$

$$\frac{C_{(b_0)}}{C_{(a_1)}} = C_{(b_0/a_1)} = \frac{b_0 T_{(ref)}}{a_1} \frac{(SF)_{(v;e)}}{(SF)_{(u;e)}} = \frac{\sigma T_{(ref)}}{r} \frac{(SF)_{(v;e)}}{(SF)_{(u;e)}} \approx C_{(\sigma/r)} \tag{18}$$

where the quantities, σ and r, associated with first-order differential equations solutions, are defined as*

$$\sigma = \frac{b_0}{a_0} = \text{dimensional similarity factor} \tag{19}$$

$$r = \frac{a_1}{a_0} = \text{first-order characteristic time} \tag{20}$$

In accordance with the discussion of Derivation Summary 34-23, the subscript a_0/a_1 means that the generalized coefficient $C_{(a_0/a_1)}$ is directly proportional to the coefficient a_0 of the physical-problem differential equation, is inversely proportional to the coefficient a_1, and is independent of all the other coefficients. The subscripts b_0/a_1, $1/r$, and σ/r have a similar significance.

The following functional diagram represents the computer arrangement associated with Eq. (16). Here, the first-order dependent variable coefficient multiplier, which is associated with the first-order output-voltage term of the analog-computer differential equation and is present in the functional diagram of section a, has been eliminated. The numerical values of the coefficient settings in the other two coefficient multipliers have been changed as indicated by the quantities within the brackets in the blocks. With the modified computer arrangement, the settings of the coefficient multipliers are no longer separately adjustable in terms of a_1, a_0, and b_0, but must be set in terms of $1/r$ and σ/r.

These changes result from application of the discussion of section a of Derivation Summary 34-24 as follows:

1) Since, from Eq. (16) of the present summary, the numerical value of the coefficient setting of the first-order dependent variable coefficient multiplier would be equal to unity, it is evident that this coefficient multiplier can be eliminated from the computer arrangement of section a, so that the output voltage of the summer, e_s, will now be applied directly to the integrator.
2) The numerical values of the coefficient settings for the two coefficient multipliers that remain are equal to the corresponding generalized coefficients associated with the analog-computer equation modified by multiplying all terms by $1/C_{(a_1)}$; i.e.,

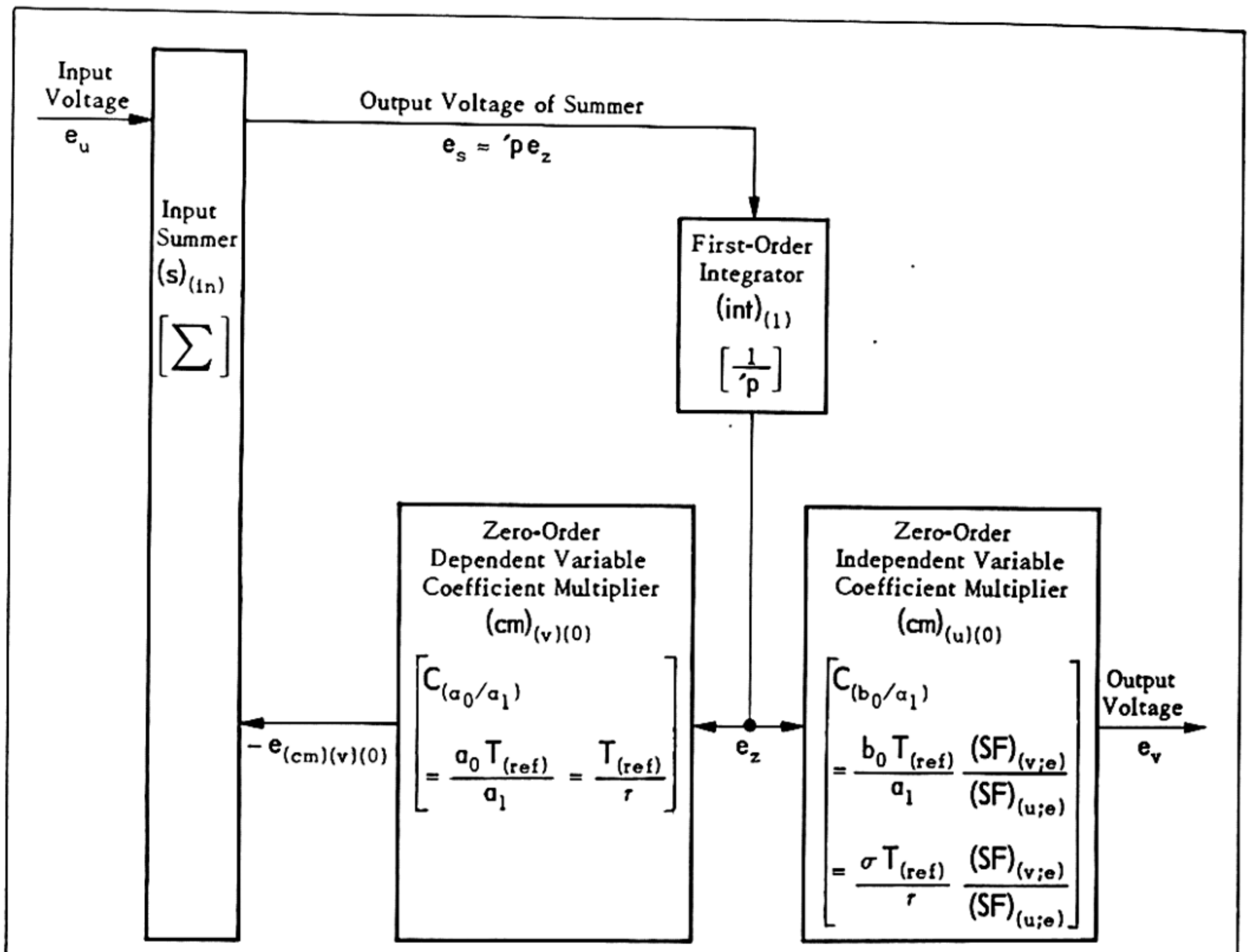
$$C_{(a_0/a_1)} = \frac{C_{(a_0)}}{C_{(a_1)}} = \frac{a_0 T_{(ref)}}{a_1} = \frac{T_{(ref)}}{r} \approx C_{(1/r)} \tag{21}$$

$$C_{(b_0/a_1)} = \frac{C_{(b_0)}}{C_{(a_1)}} = \frac{b_0 T_{(ref)}}{a_1} \frac{(SF)_{(v;e)}}{(SF)_{(u;e)}} = \frac{\sigma T_{(ref)}}{r} \frac{(SF)_{(v;e)}}{(SF)_{(u;e)}} \approx C_{(\sigma/r)} \tag{22}$$

---

* See Definition Summary 18-1 of Chapter 18. Note that Eq. (19) is obtained by setting $b_{(0)(ref)}$ in Eq. (2) of Definition Summary 18-1 equal to b_0.

Derivation Summary 34-25. Analog-computer arrangements for solving a first-order linear differential equation with constant coefficients. (Page 3 of 7)



b) Analog-computer arrangement for solving the (0;0,1) first-order differential equation when the analog-computer differential equation is modified by multiplying each term by the reciprocal of the generalized coefficient $C_{(a_1)}$

The zero-order dependent variable coefficient multiplier, which is associated with the zero-order output-voltage term of the analog-computer differential equation, may be eliminated from the functional diagram of section a by multiplying Eq. (7) by $1/C_{(a_0)}$; i.e.,

$$\frac{C_{(a_1)}}{C_{(a_0)}} \frac{de_v}{d\,{}'t_{(pp)}} + e_v = \frac{C_{(b_0)}}{C_{(a_0)}} e_u \tag{23}$$

For the modified form of the analog-computer differential equation represented by Eq. (23),

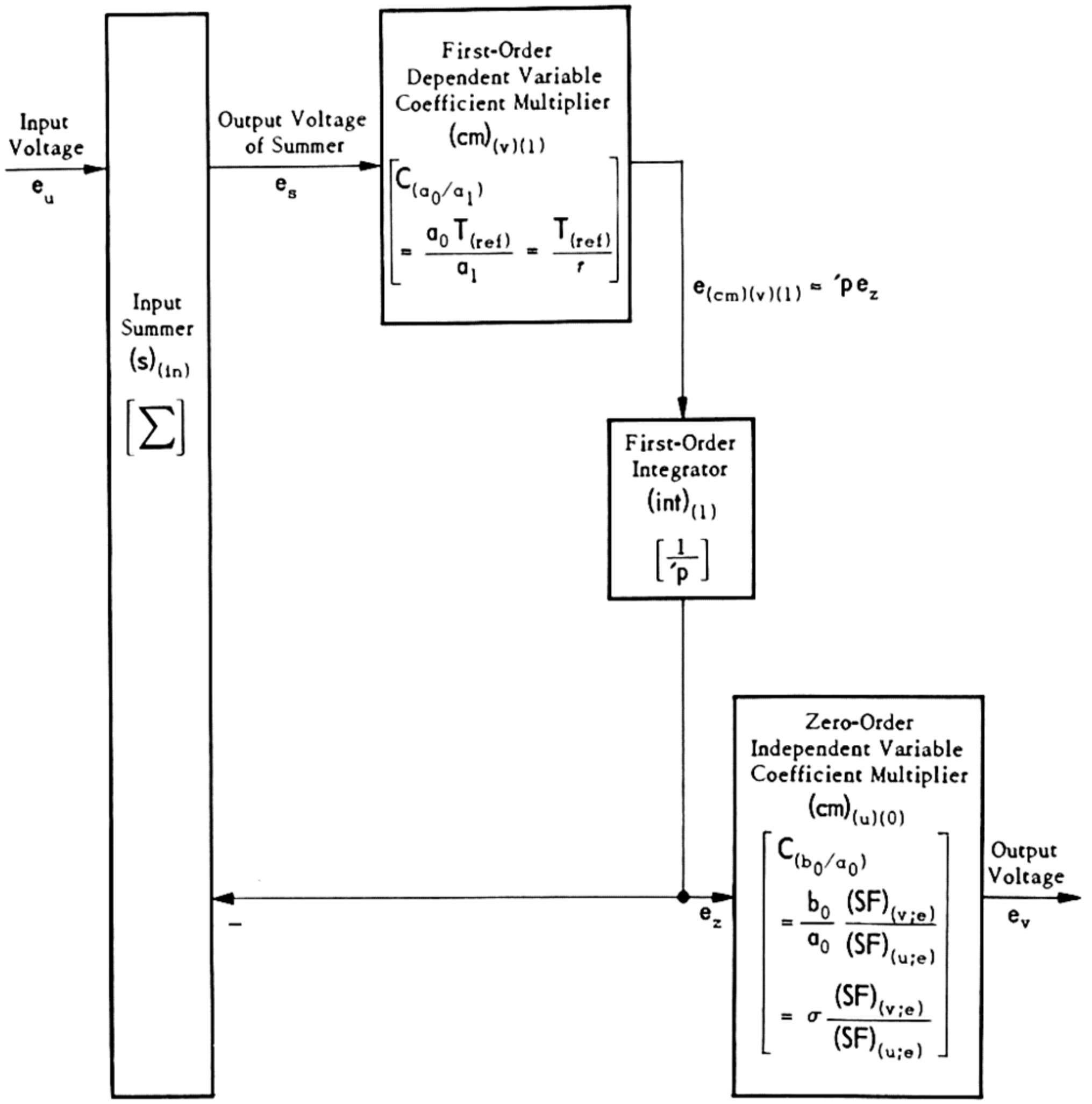
$$\frac{C_{(a_1)}}{C_{(a_0)}} = C_{(a_1/a_0)} = \frac{a_1}{a_0 T_{(ref)}} = \frac{r}{T_{(ref)}} \approx C_{(r)} \tag{24}$$

$$\frac{C_{(b_0)}}{C_{(a_0)}} = C_{(b_0/a_0)} = \frac{b_0}{a_0} \frac{(SF)_{(v;e)}}{(SF)_{(u;e)}} = \sigma \frac{(SF)_{(v;e)}}{(SF)_{(u;e)}} \approx C_{(\sigma)} \tag{25}$$

In the corresponding analog-computer arrangement, shown by the accompanying functional diagram, the zero-order dependent variable coefficient multiplier has been eliminated from the functional diagram of section a because its coefficient setting has been made unity by multiplying Eq. (7) by $1/C_{(a_0)}$. The

Derivation Summary 34-25. Analog-computer arrangements for solving a first-order linear differential equation with constant coefficients. (Page 4 of 7)

numerical values of the coefficient settings in the other two coefficient multipliers have been changed as indicated by the quantities within the brackets in the blocks. These changes are made in accordance with the procedure already described in the previous section.



c) Analog-computer arrangement for solving the (0;0,1) first-order differential equation when the analog-computer differential equation is modified by multiplying each term by the reciprocal of the generalized coefficient $C_{(a_0)}$

By a procedure similar to that used in sections b and c of this summary, the zero-order independent variable coefficient multiplier may be eliminated from the functional diagram of section a by multiplying Eq. (7) by $1/C_{(b_0)}$; i.e.,

$$\frac{C_{(a_1)}}{C_{(b_0)}} \frac{de_v}{d\,'t_{(pp)}} + \frac{C_{(a_0)}}{C_{(b_0)}} e_v = e_u \tag{26}$$

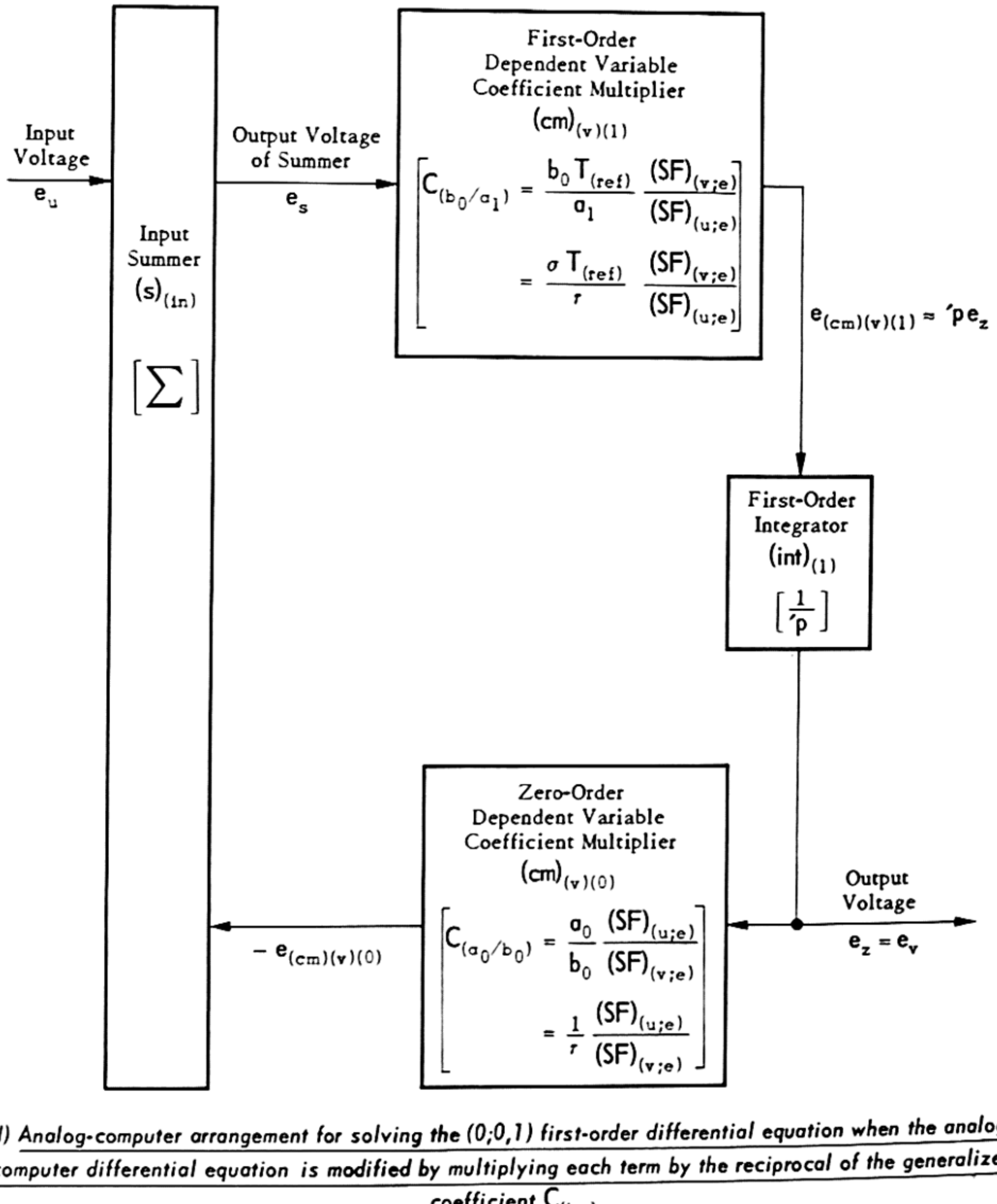
Derivation Summary 34-25. Analog-computer arrangements for solving a first-order linear differential equation with constant coefficients. (Page 5 of 7)

For the modified form of the analog-computer differential equation represented by Eq. (26),

$$\frac{C_{(a_1)}}{C_{(b_0)}} = C_{(a_1/b_0)} = \frac{a_1}{b_0 T_{(ref)}} \frac{(SF)_{(u;e)}}{(SF)_{(v;e)}} = \frac{\tau}{\sigma T_{(ref)}} \frac{(SF)_{(u;e)}}{(SF)_{(v;e)}} \approx C_{(\tau/\sigma)} \qquad (27)$$

$$\frac{C_{(a_0)}}{C_{(b_0)}} = C_{(a_0/b_0)} = \frac{a_0}{b_0} \frac{(SF)_{(u;e)}}{(SF)_{(v;e)}} = \frac{1}{\tau} \frac{(SF)_{(u;e)}}{(SF)_{(v;e)}} \approx C_{(1/\tau)} \qquad (28)$$

The following functional diagram is the corresponding simplified form of the analog-computer arrangement given in section a.



d) Analog-computer arrangement for solving the (0;0,1) first-order differential equation when the analog-computer differential equation is modified by multiplying each term by the reciprocal of the generalized coefficient $C_{(b_0)}$

Derivation Summary 34-25. Analog-computer arrangements for solving a first-order linear differential equation with constant coefficients. (Page 6 of 7)

	First-Order Dependent Variable Coefficient Multiplier Setting	Zero-Order Dependent Variable Coefficient Multiplier Setting	Zero-Order Independent Variable Coefficient Multiplier Setting
All analog-computer differential equation coefficients different from unity	$C_{(1/a_1)} = \frac{(SF)_{(v;e)}\, T_{(ref)}}{a_1}$	$C_{(a_0)} = \frac{a_0}{(SF)_{(v;e)}}$	$C_{(b_0)} = \frac{b_0}{(SF)_{(u;e)}}$
First-order output-voltage term coefficient equal to unity	1	$C_{(a_0/a_1)} = \frac{a_0\, T_{(ref)}}{a_1} = \frac{T_{(ref)}}{\tau}$	$C_{(b_0/a_1)} = \frac{b_0\, T_{(ref)}}{a_1}\,\frac{(SF)_{(v;e)}}{(SF)_{(u;e)}} = \frac{\sigma\, T_{(ref)}}{\tau}\,\frac{(SF)_{(v;e)}}{(SF)_{(u;e)}}$
Zero-order output-voltage term coefficient equal to unity	$C_{(a_0/a_1)} = \frac{a_0\, T_{(ref)}}{a_1} = \frac{T_{(ref)}}{\tau}$	1	$C_{(b_0/a_0)} = \frac{b_0}{a_0}\,\frac{(SF)_{(v;e)}}{(SF)_{(u;e)}} = \sigma\,\frac{(SF)_{(v;e)}}{(SF)_{(u;e)}}$
Zero-order input-voltage term coefficient equal to unity	$C_{(b_0/a_1)} = \frac{b_0\, T_{(ref)}}{a_1}\,\frac{(SF)_{(v;e)}}{(SF)_{(u;e)}} = \frac{\sigma\, T_{(ref)}}{\tau}\,\frac{(SF)_{(v;e)}}{(SF)_{(u;e)}}$	$C_{(a_0/b_0)} = \frac{a_0}{b_0}\,\frac{(SF)_{(u;e)}}{(SF)_{(v;e)}} = \frac{1}{\sigma}\,\frac{(SF)_{(u;e)}}{(SF)_{(v;e)}}$	1

e) Summary of coefficient settings associated with the analog-computer solution of the (0;0,1) first-order differential equation

Derivation Summary 34-25. Analog-computer arrangements for solving a first-order linear differential equation with constant coefficients. (Page 7 of 7)

separated. The block diagrams for the other possible arrays are presented in Figs. b, c and e and the results are presented in tabular form in section f.

NUMERICAL EXAMPLE OF SCALING A PROBLEM FOR ANALOG-COMPUTER SOLUTION

34.150. In the foregoing derivation summaries, a general approach for handling linear systems is given. In Derivation Summary 34-27, a specific example of a second-order system is studied from the viewpoint of scaling it for analog-computer solution. A positional servo with tachometric feedback is chosen for this purpose.

34.151. A description of the system and its block diagram is given in section a of Derivation Summary 34-27. The governing relationships for each of the operating components are written in section b. These are combined to yield Eq. (13), the equation of motion for the positional servo system. This is seen to

Certain physical problems may be represented by a second-order differential equation. The generalized form of the (0;0,1,2) equation is

$$a_2 \frac{d^2 v}{dt^2_{(pp)}} + a_1 \frac{dv}{dt_{(pp)}} + a_0 v = b_0 u \tag{1}$$

By nondimensionalizing the running variable ($'t_{(pp)} = t_{(pp)}/T_{(ref)}$) and by replacing the independent and dependent variables u and v by their analogous voltages e_u and e_v, Eq. (1) can be written as

$$\frac{a_2}{T^2_{(ref)}(SF)_{(v;e)}} \frac{d^2 e_v}{d\,'t^2_{(pp)}} + \frac{a_1}{T_{(ref)}(SF)_{(v;e)}} \frac{de_v}{d\,'t_{(pp)}} + \frac{a_0}{(SF)_{(v;e)}} e_v = \frac{b_0}{(SF)_{(u;e)}} e_u \tag{2}$$

In terms of the generalized coefficients $C_{(a_i)}$ and $C_{(b_j)}$, Eq. (2) becomes

$$C_{(a_2)} \frac{d^2 e_v}{d\,'t^2_{(pp)}} + C_{(a_1)} \frac{de_v}{d\,'t_{(pp)}} + C_{(a_0)} e_v = C_{(b_0)} e_u \tag{3}$$

where

$$C_{(a_i)} = \frac{a_i}{T^i_{(ref)}(SF)_{(v;e)}} \quad ; \quad i = 0,\ 1,\ 2 \tag{4}$$

and

$$C_{(b_j)} = \frac{b_j}{T^j_{(ref)}(SF)_{(u;e)}} \quad ; \quad j = 0 \tag{5}$$

Equation (3) is now in a form suitable for direct handling by an electrical analog computer. The functional diagram of Fig. a shows the analog-computer component arrangement for the solution of the (0;0,1,2) physical-problem differential equation. The numerical value of each coefficient multiplier setting is given within the brackets on each block.

a) *Analog-computer solution of the (0;0,1,2) second-order differential equation when all the generalized analog-computer differential equation coefficients are different from unity*

If a particular coefficient of the analog-computer differential equation is made equal to unity, the corresponding coefficient multiplier can be eliminated from the functional diagram of Fig. a. Hence, if the second-order analog-computer differential equation represented by Eq. (3) is multiplied by a constant, $1/C_{(a_2)}$, the following relationship is obtained.

$$\frac{d^2 e_v}{d\,'t^2_{(pp)}} + \frac{C_{(a_1)}}{C_{(a_2)}} \frac{de_v}{d\,'t_{(pp)}} + \frac{C_{(a_0)}}{C_{(a_2)}} e_v = \frac{C_{(b_0)}}{C_{(a_2)}} e_u \tag{6}$$

For the modified form of the analog-computer differential equation represented by Eq. (6),

$$\frac{C_{(a_1)}}{C_{(a_2)}} = C_{(a_1/a_2)} = \frac{a_1}{a_2} T_{(ref)} = 2\zeta\omega_n T_{(ref)} \tag{7}$$

$$\frac{C_{(a_0)}}{C_{(a_2)}} = C_{(a_0/a_2)} = \frac{a_0}{a_2} T^2_{(ref)} = \omega_n^2 T^2_{(ref)} \tag{8}$$

$$\frac{C_{(b_0)}}{C_{(a_2)}} = C_{(b_0/a_2)} = \frac{b_0 T^2_{(ref)}}{a_2} \frac{(SF)_{(v;e)}}{(SF)_{(u;e)}} = \sigma\omega_n^2 T^2_{(ref)} \frac{(SF)_{(v;e)}}{(SF)_{(u;e)}} \tag{9}$$

Derivation Summary 34-26. Analog-computer arrangements for solving a second-order linear differential equation with constant coefficients. (Page 1 of 9)

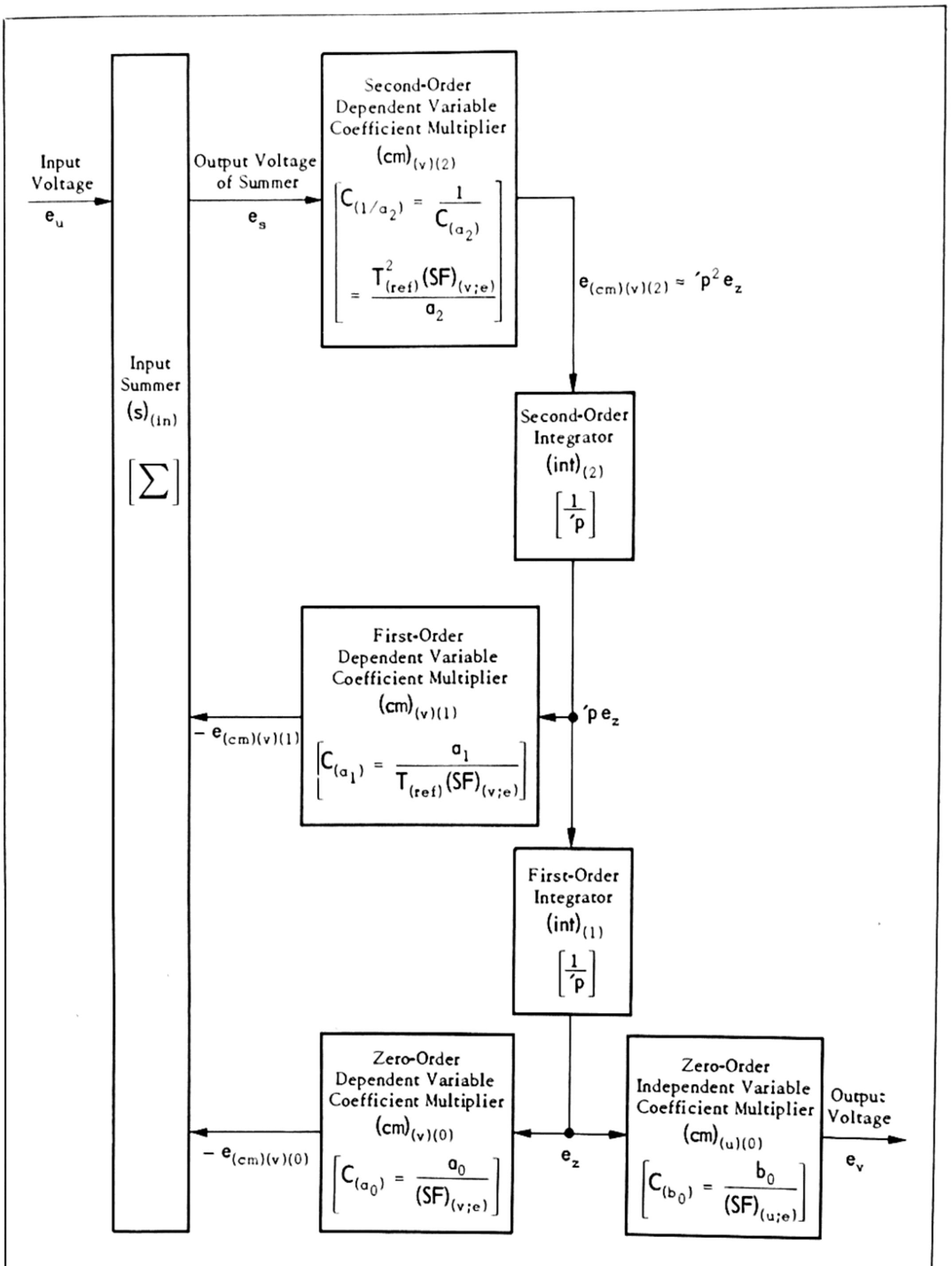


Fig. a. Analog-computer arrangement for solving the (0;0,1,2) second-order differential equation when all the generalized analog-computer differential equation coefficients are different from unity.

Derivation Summary 34-26. Analog-computer arrangements for solving a second-order linear differential equation with constant coefficients. (Page 2 of 9)

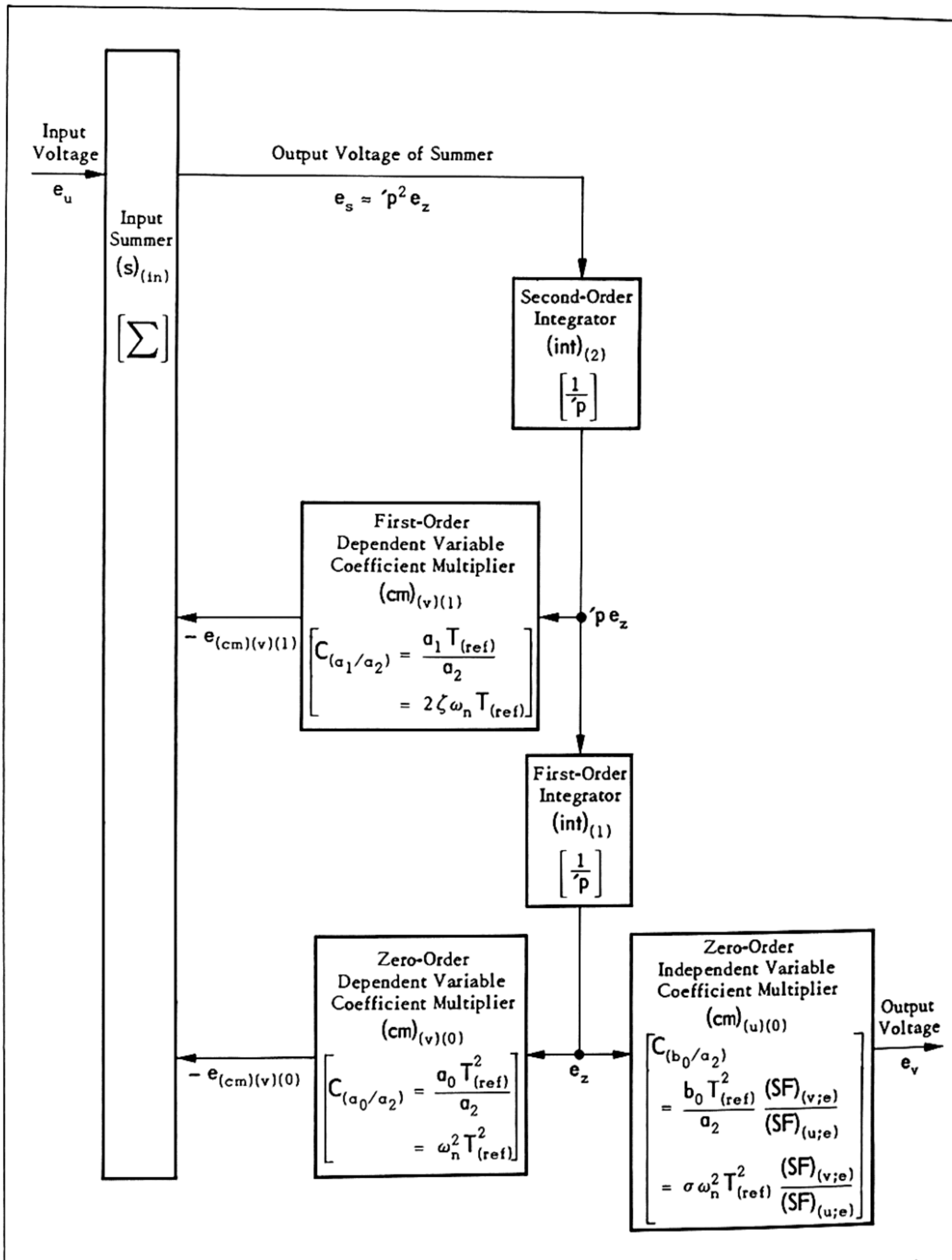


Fig. b. Analog-computer arrangement for solving the (0;0,1,2) second-order differential equation when the analog-computer differential equation is modified by multiplying each term by the reciprocal of the generalized coefficient $C_{(a_2)}$.

Derivation Summary 34-26. Analog-computer arrangements for solving a second-order linear differential equation with constant coefficients. (Page 3 of 9)

where the quantities, ζ and ω, associated with the second-order differential equation solution, are defined according to Definition Summary 19-1 as

$$\zeta \approx DR = \frac{a_1}{2\sqrt{a_0 a_2}} = \text{damping ratio} \tag{10}$$

$$\omega_n = \sqrt{\frac{a_0}{a_2}} = \text{undamped angular natural frequency} \tag{11}$$

and the quantity σ, used in Derivation Summary 34-25, is

$$\sigma = \frac{b_0}{a_0} = \text{dimensional similarity factor} \tag{12}$$

The functional diagram of Fig. b represents the analog-computer arrangement associated with Eq. (6). Here, the second-order dependent variable coefficient multiplier, which is associated with the second-order output-voltage term of the analog-computer differential equation and is present in the functional diagram of Fig. a, has been eliminated because the coefficient of the second-order output-voltage term of Eq. (6) was made equal to unity.

b) Analog-computer solution of the (0;0,1,2) second-order differential equation when the analog-computer differential equation is modified by multiplying each term by the reciprocal of the generalized coefficient $C_{(a_2)}$

The first-order dependent variable coefficient multiplier, which is associated with the first-order output-voltage term of the analog-computer differential equation, may be eliminated from the functional diagram of Fig. a by multiplying Eq. (3) by $1/C_{(a_1)}$; i.e.,

$$\frac{C_{(a_2)}}{C_{(a_1)}} \frac{d^2 e_v}{d't^2_{(pp)}} + \frac{de_v}{d't_{(pp)}} + \frac{C_{(a_0)}}{C_{(a_1)}} e_v = \frac{C_{(b_0)}}{C_{(a_1)}} e_u \tag{13}$$

where

$$\frac{C_{(a_2)}}{C_{(a_1)}} = C_{(a_2/a_1)} = \frac{a_2}{a_1 T_{(ref)}} = \frac{1}{2\zeta\omega_n T_{(ref)}} \tag{14}$$

$$\frac{C_{(a_0)}}{C_{(a_1)}} = C_{(a_0/a_1)} = \frac{a_0 T_{(ref)}}{a_1} = \frac{\omega_n}{2\zeta} T_{(ref)} \tag{15}$$

$$\frac{C_{(b_0)}}{C_{(a_1)}} = C_{(b_0/a_1)} = \frac{b_0 T_{(ref)}}{a_1} \frac{(SF)_{(v;e)}}{(SF)_{(u;e)}} = \frac{\sigma\omega_n T_{(ref)}}{2\zeta} \frac{(SF)_{(v;e)}}{(SF)_{(u;e)}} \tag{16}$$

The functional diagram of Fig. c represents the analog-computer arrangement corresponding to Eq. (13). The first-order dependent variable coefficient multiplier has been eliminated from the functional diagram of Fig. a because the coefficient of the first-order output-voltage term of Eq. (13) has been made equal to unity, which corresponds to a coefficient setting of unity.

c) Analog-computer solution of the (0;0,1,2) second-order differential equation when the analog-computer differential equation is modified by multiplying each term by the reciprocal of the generalized coefficient $C_{(a_1)}$

If Eq. (3) is multiplied by the constant $1/C_{(a_0)}$, the coefficient of the zero-order output-voltage term is made equal to unity, which means that the zero-order dependent variable coefficient multiplier can be eliminated from the functional diagram of Fig. a.

Derivation Summary 34-26. Analog-computer arrangements for solving a second-order linear differential equation with constant coefficients. (Page 4 of 9)

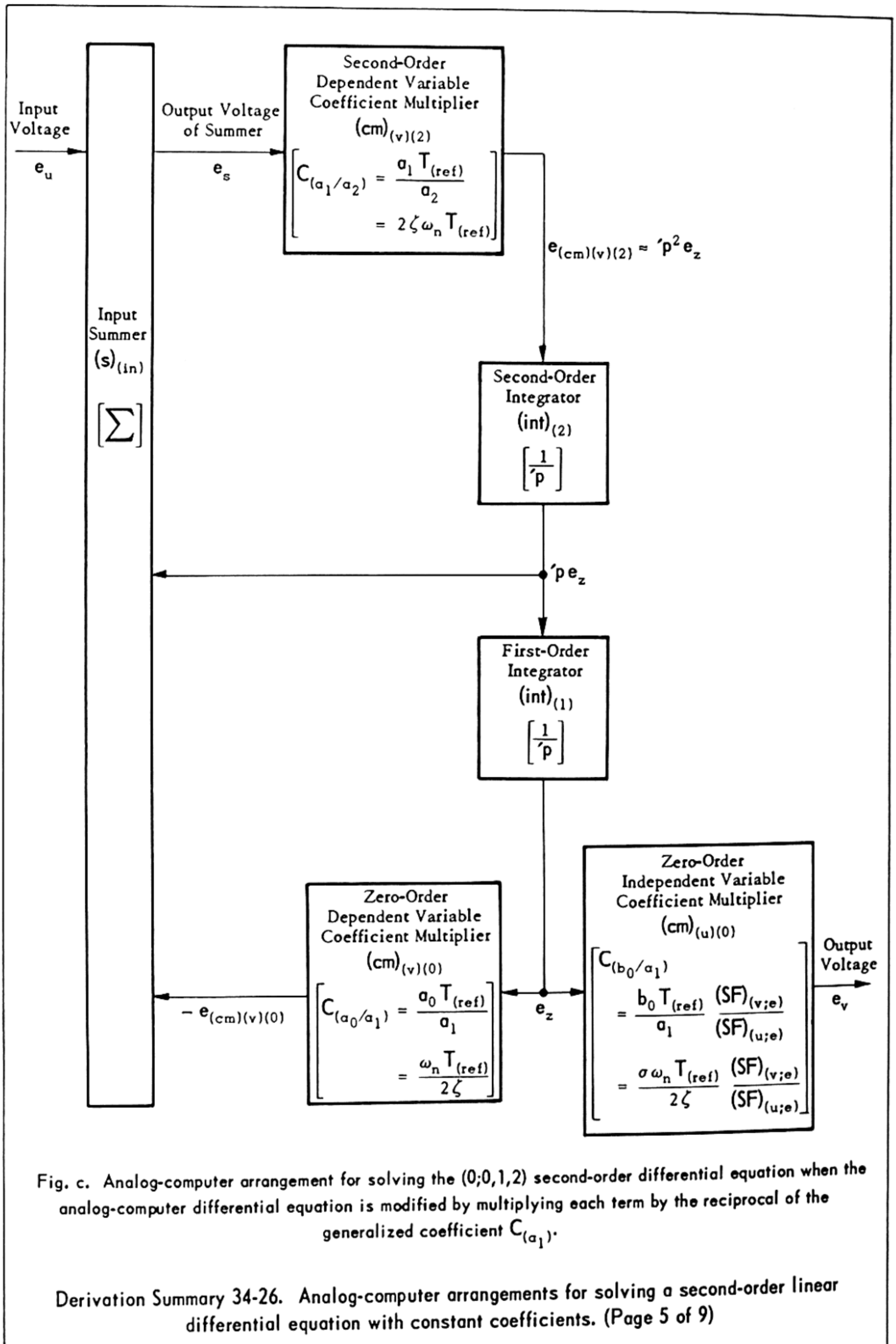


Fig. c. Analog-computer arrangement for solving the (0;0,1,2) second-order differential equation when the analog-computer differential equation is modified by multiplying each term by the reciprocal of the generalized coefficient $C_{(a_1)}$.

Derivation Summary 34-26. Analog-computer arrangements for solving a second-order linear differential equation with constant coefficients. (Page 5 of 9)

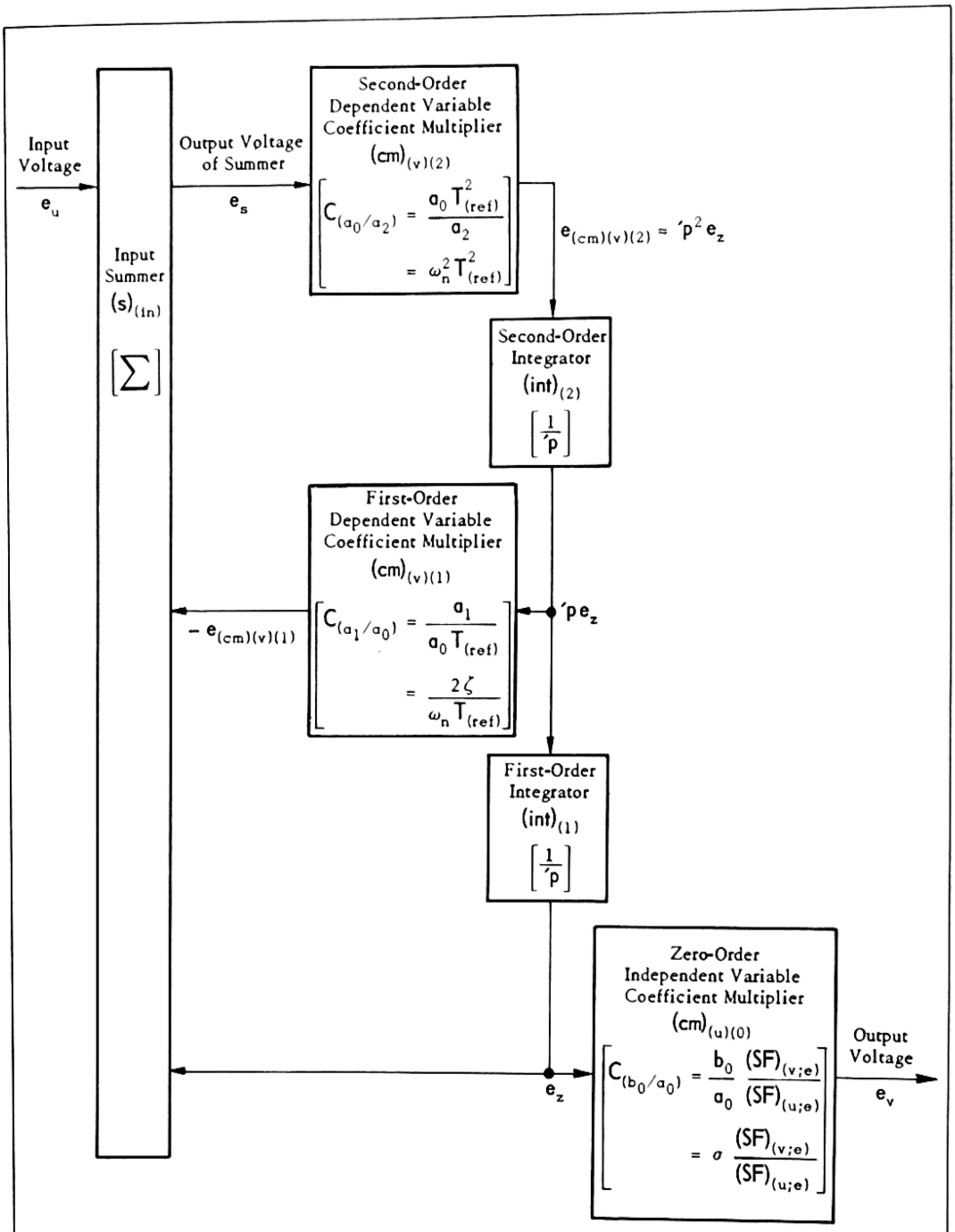


Fig. d. Analog-computer arrangement for solving the (0;0,1,2) second-order differential equation when the analog-computer differential equation is modified by multiplying each term by the reciprocal of the generalized coefficient $C_{(a_0)}$.

Derivation Summary 34-26. Analog-computer arrangements for solving a second-order linear differential equation with constant coefficients. (Page 6 of 9)

The analog-computer differential equation with the coefficient of the zero-order voltage term equal to unity can be represented by the equation

$$\frac{C_{(a_2)}}{C_{(a_0)}} \frac{d^2 e_v}{d' t^2_{(pp)}} + \frac{C_{(a_1)}}{C_{(a_0)}} \frac{de_v}{d' t_{(pp)}} + e_v = \frac{C_{(b_0)}}{C_{(a_0)}} e_u \tag{17}$$

where

$$\frac{C_{(a_2)}}{C_{(a_0)}} = C_{(a_2/a_0)} = \frac{a_2}{a_0 T^2_{(ref)}} = \frac{1}{\omega_n^2 T^2_{(ref)}} \tag{18}$$

$$\frac{C_{(a_1)}}{C_{(a_0)}} = C_{(a_1/a_0)} = \frac{a_1}{a_0 T_{(ref)}} = \frac{2\zeta}{\omega_n T_{(ref)}} \tag{19}$$

$$\frac{C_{(b_0)}}{C_{(a_0)}} = C_{(b_0/a_0)} = \frac{b_0}{a_0} \frac{(SF)_{(v;e)}}{(SF)_{(u;e)}} = \sigma \frac{(SF)_{(v;e)}}{(SF)_{(u;e)}} \tag{20}$$

The analog-computer arrangement corresponding to Eq. (17) is given in the functional diagram of Fig. d. Here, the zero-order dependent variable coefficient multiplier has been eliminated from the functional diagram of Fig. a because its coefficient setting is unity. The settings of the other coefficient multipliers are given within the brackets on each block.

d) Analog-computer solution of the (0;0,1,2) second-order differential equation when the analog-computer differential equation is modified by multiplying each term by the reciprocal of the generalized coefficient $C_{(a_0)}$

The zero-order independent variable coefficient multiplier, which is associated with the zero-order input-voltage term of the analog-computer differential equation, may be eliminated from the functional diagram of Fig. a by multiplying Eq. (3) by $1/C_{(b_0)}$; i.e.,

$$\frac{C_{(a_2)}}{C_{(b_0)}} \frac{d^2 e_v}{d' t^2_{(pp)}} + \frac{C_{(a_1)}}{C_{(b_0)}} \frac{de_v}{d' t_{(pp)}} + \frac{C_{(a_0)}}{C_{(b_0)}} e_v = e_u \tag{21}$$

For the modified form of the analog-computer differential equation represented by Eq. (21)

$$\frac{C_{(a_2)}}{C_{(b_0)}} = C_{(a_2/b_0)} = \frac{a_2}{b_0 T^2_{(ref)}} \frac{(SF)_{(u;e)}}{(SF)_{(v;e)}} = \frac{1}{\sigma \omega_n^2 T^2_{(ref)}} \frac{(SF)_{(u;e)}}{(SF)_{(v;e)}} \tag{22}$$

$$\frac{C_{(a_1)}}{C_{(b_0)}} = C_{(a_1/b_0)} = \frac{a_1}{b_0 T_{(ref)}} \frac{(SF)_{(u;e)}}{(SF)_{(v;e)}} = \frac{2\zeta}{\sigma \omega_n T_{(ref)}} \frac{(SF)_{(u;e)}}{(SF)_{(v;e)}} \tag{23}$$

$$\frac{C_{(a_0)}}{C_{(b_0)}} = C_{(a_0/b_0)} = \frac{a_0}{b_0} \frac{(SF)_{(u;e)}}{(SF)_{(v;e)}} = \frac{1}{\sigma} \frac{(SF)_{(u;e)}}{(SF)_{(v;e)}} \tag{24}$$

Elimination of the zero-order independent variable coefficient from the functional diagram of Fig. a results in the following analog-computer arrangement. The coefficient setting of the zero-order independent variable coefficient multiplier is unity; all other settings are given within the brackets on each block.

e) Analog-computer solution of the (0;0,1,2) second-order differential equation when the analog-computer differential equation is modified by multiplying each term by the reciprocal of the generalized coefficient $C_{(b_0)}$

Derivation Summary 34-26. Analog-computer arrangements for solving a second-order linear differential equation with constant coefficients. (Page 7 of 9)

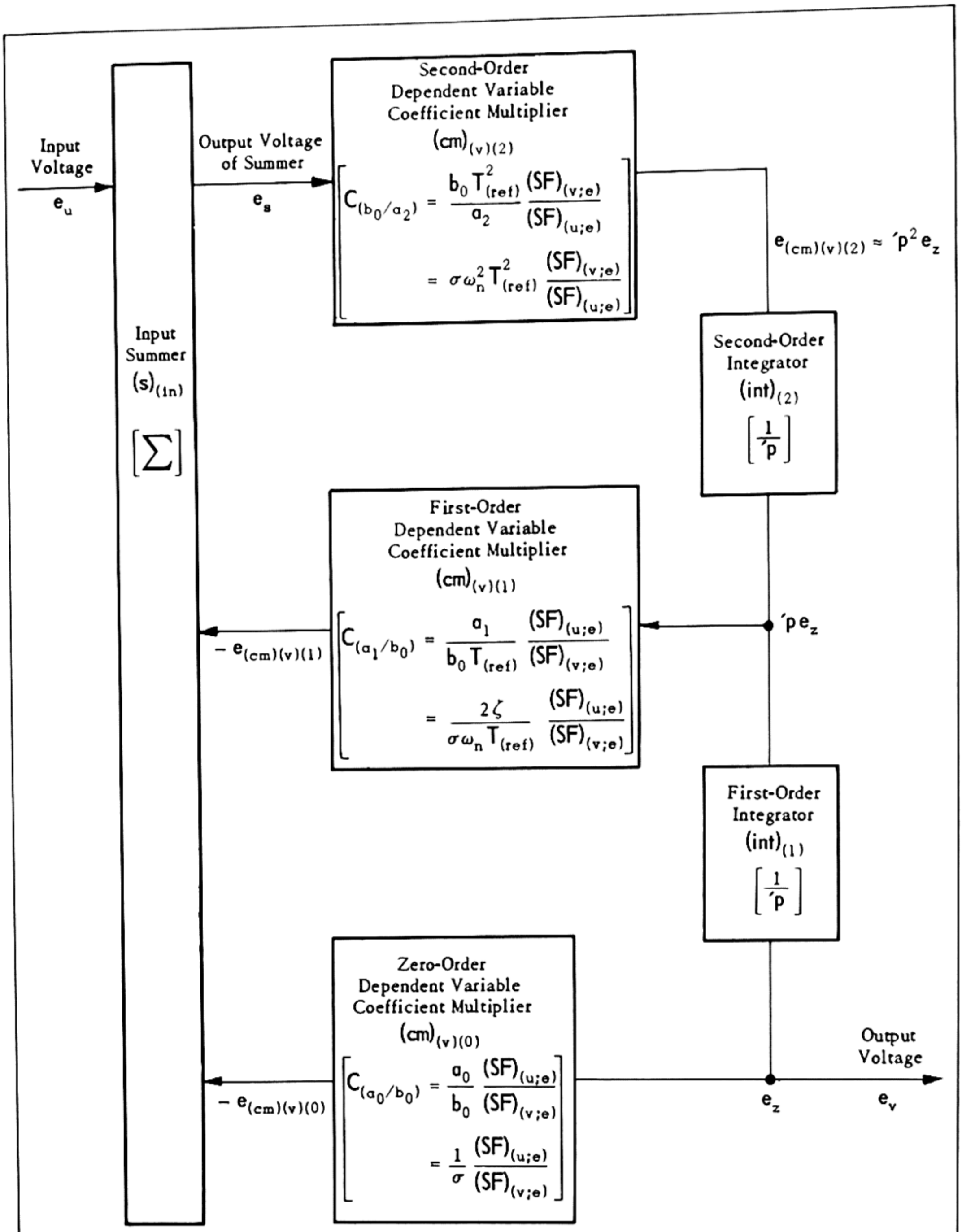


Fig. e. Analog-computer arrangement for solving the (0;0,1,2) second-order differential equation when the analog-computer differential equation is modified by multiplying each term by the reciprocal of the generalized coefficient $C_{(b_0)}$.

Derivation Summary 34-26. Analog-computer arrangements for solving a second-order linear differential equation with constant coefficients. (Page 8 of 9)

	Second-Order Dependent Variable Coefficient Multiplier Setting	First-Order Dependent Variable Coefficient Multiplier Setting	Zero-Order Dependent Variable Coefficient Multiplier Setting	Zero-Order Independent Variable Coefficient Multiplier Setting
All analog-computer differential equation coefficients different from unity	$C_{(1/a_2)} = \frac{T^2_{(ref)}(SF)_{(v;e)}}{a_2}$	$C_{(a_1)} = \frac{a_1}{T_{(ref)}(SF)_{(v;e)}}$	$C_{(a_0)} = \frac{a_0}{(SF)_{(v;e)}}$	$C_{(b_0)} = \frac{b_0}{(SF)_{(u;e)}}$
Second-order output-voltage term coefficient equal to unity	1	$C_{(a_1/a_2)} = \frac{a_1 T_{(ref)}}{a_2} = 2\zeta\omega_n T_{(ref)}$	$C_{(a_0/a_2)} = \frac{a_0 T^2_{(ref)}}{a_2} = \omega_n^2 T^2_{(ref)}$	$C_{(b_0/a_2)} = \frac{b_0 T^2_{(ref)}}{a_2}\frac{(SF)_{(v;e)}}{(SF)_{(u;e)}} = \sigma\omega_n^2 T^2_{(ref)}\frac{(SF)_{(v;e)}}{(SF)_{(u;e)}}$
First-order output-voltage term coefficient equal to unity	$C_{(a_1/a_2)} = \frac{a_1 T_{(ref)}}{a_2} = 2\zeta\omega_n T_{(ref)}$	1	$C_{(a_0/a_1)} = \frac{a_0 T_{(ref)}}{a_1} = \frac{\omega_n T_{(ref)}}{2\zeta}$	$C_{(b_0/a_1)} = \frac{b_0 T_{(ref)}}{a_1}\frac{(SF)_{(v;e)}}{(SF)_{(u;e)}} = \frac{\sigma\omega_n T_{(ref)}}{2\zeta}\frac{(SF)_{(v;e)}}{(SF)_{(u;e)}}$
Zero-order output-voltage term coefficient equal to unity	$C_{(a_0/a_2)} = \frac{a_0 T^2_{(ref)}}{a_2} = \omega_n^2 T^2_{(ref)}$	$C_{(a_1/a_0)} = \frac{a_1}{a_0 T_{(ref)}} = \frac{2\zeta}{\omega_n T_{(ref)}}$	1	$C_{(b_0/a_0)} = \frac{b_0}{a_0}\frac{(SF)_{(v;e)}}{(SF)_{(u;e)}} = \sigma\frac{(SF)_{(v;e)}}{(SF)_{(u;e)}}$
Zero-order input-voltage term coefficient equal to unity	$C_{(b_0/a_2)} = \frac{b_0 T^2_{(ref)}}{a_2}\frac{(SF)_{(v;e)}}{(SF)_{(u;e)}} = \sigma\omega_n^2 T^2_{(ref)}\frac{(SF)_{(v;e)}}{(SF)_{(u;e)}}$	$C_{(a_1/b_0)} = \frac{a_1}{b_0 T_{(ref)}}\frac{(SF)_{(u;e)}}{(SF)_{(v;e)}} = \frac{2\zeta}{\sigma\omega_n T_{(ref)}}\frac{(SF)_{(u;e)}}{(SF)_{(v;e)}}$	$C_{(a_0/b_0)} = \frac{a_0}{b_0}\frac{(SF)_{(u;e)}}{(SF)_{(v;e)}} = \frac{1}{\sigma}\frac{(SF)_{(u;e)}}{(SF)_{(v;e)}}$	1

f) Summary of coefficient settings associated with the analog-computer solution of the (0;0,1,2) second-order differential equation

Derivation Summary 34-26. Analog-computer arrangements for solving a second-order linear differential equation with constant coefficients. (Page 9 of 9)

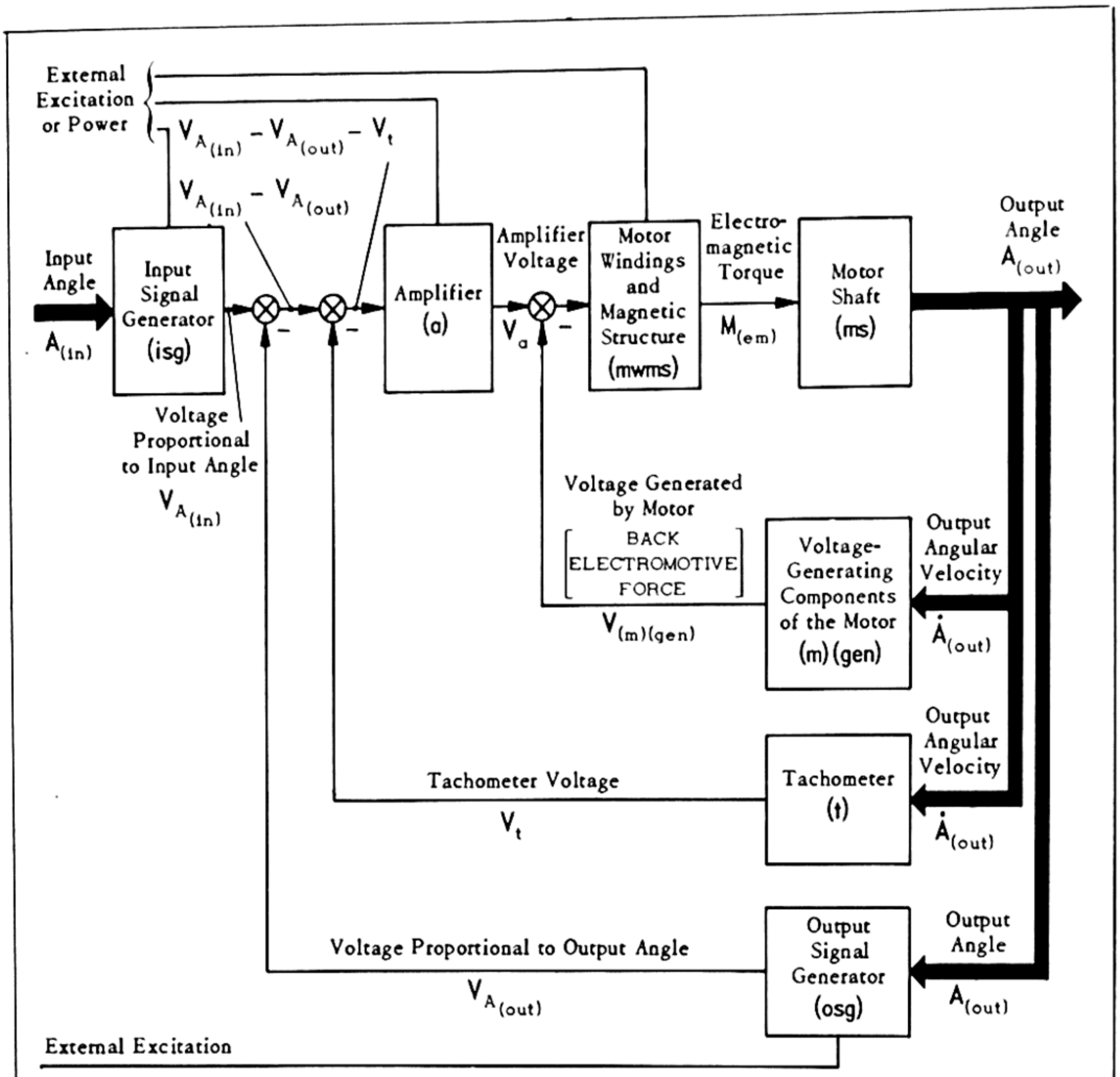


Fig. a. Functional diagram showing the components and interconnections of a typical positional servo system.

The positional servo system discussed in the present summary and represented in the functional diagram of Fig. a causes the angular motion of an output shaft to follow the angular motion of an input shaft, without any mechanical connection between the shafts. This action is accomplished by means of an electrical system that develops an electrical signal proportional to the difference in the angular positions of the two shafts, and uses this signal to drive a motor connected to the output shaft in a direction such as to reduce the difference in the angular positions of the two shafts. As shown by Fig. a, the electrical system comprises two signal generators, a motor, an amplifier, and a tachometer.

Derivation Summary 34-27. Component analysis and performance equation of a typical positional servo system; derivation of the corresponding analog-computer equation and the equivalent analog-computer arrangement; determination of the coefficient settings. (Page 1 of 20)

The two signal generators, which are identical, are coupled to the input and output shafts, respectively, and are connected electrically so as to produce a voltage proportional to the difference in the angular positions of the two shafts. Synchros are typical signal generators used in this kind of application. These devices require electrical excitation that must be provided by external means not considered here. The error signal that results from such a pair of signal generators is generally of low power level, and hence requires amplification if it is to operate an electric motor. Either an electronic or a magnetic amplifier may be employed for this purpose. External power is needed for such a device, of course.

The amplifier output is supplied to the motor in a manner suitable to control the output torque of the motor. Typically, the motor might be a two-phase induction motor with one of the phases supplied from an external power source and the other phase connected to the amplifier. If the motor shaft is held stationary, the electromagnetic torque developed is proportional to the amplifier voltage as long as the magnetic material of the motor remains unsaturated. This torque accelerates the motor shaft in a direction such as to reduce the error voltage obtained from the signal generators. The control loop as thus far described would behave like a second-order undamped system. The second-order aspect arises at the motor shaft since the angular acceleration of the output shaft, which determines the inertia reaction torque, is proportional to the second derivative of the angular position of the output shaft, to which the driving torque is proportional if the input shaft is at rest.

The undamped system described in the preceding paragraphs would be of no practical interest since it would be inherently unstable. In such a system, however, a certain amount of damping is contributed by the tendency of the motor to act as a generator when it is rotating. A back electromotive force is developed, which is proportional to the angular velocity of the output shaft. This voltage acts in opposition to the voltage supplied by the amplifier and reduces the net voltage that is effective at the motor terminals, and hence reduces the motor current, also. The electromagnetic torque is correspondingly modified by the addition of a damping-torque component that acts in opposition to the output angular velocity. However, the amount of damping thus developed is often insufficient to prevent excessive oscillation. In such cases, it is not practical to increase the amount of damping by amplifying the back electromotive force since this voltage is not available at the motor terminals. Rather, an independently generated electrical signal proportional to the output-shaft angular velocity is developed, either by appropriate electrical circuitry or, as in this example, by means of a tachometer that is mechanically connected to the output shaft. If the size of such a tachometer is held to a minimum, the power level of its output signal is insufficient to have any appreciable effect directly on the motor. Amplification is therefore required in the same manner as for the signal-generator error signal. Hence, it is appropriate to add the tachometer signal to the signal-generator error signal at the amplifier input.

It may be possible to reduce the size of the motor required by providing step-down gearing between the motor shaft and the output shaft. This would also serve to increase the torsional stiffness at the output shaft and hence render the system less sensitive to load disturbances, which are not considered here. Such gearing down is not considered in this summary since it adds nothing to the generality of the problem insofar as scaling values for the analog computer is concerned.

a) Functional diagram and description of a typical positional servo system

The performance relationships for the components shown in the functional diagram of Fig. a can be written as follows, assuming ideal operation:

(isg) Input signal generator

$$V_{A_{(in)}} = S_{(isg)[A;V]} A_{(in)} \tag{1}$$

Derivation Summary 34-27. Component analysis and performance equation of a typical positional servo system; derivation of the corresponding analog-computer equation and the equivalent analog-computer arrangement; determination of the coefficient settings. (Page 2 of 20)

(osg) Output signal generator

$$V_{A_{(out)}} = S_{(osg)[A;V]} A_{(out)} \tag{2}$$

Note: Since the input signal generator and the output signal generator are assumed to be identical, $S_{(sg)[A;V]}$ is used in the remainder of this summary in place of $S_{(isg)[A;V]}$ and $S_{(osg)[A;V]}$.

(t) Tachometer

$$V_t = S_{(t)[\dot{A};V]} \dot{A}_{(out)} \tag{3}$$

(a) Amplifier

$$V_a = S_{(a)[V;V]} [V_{A_{(in)}} - V_{A_{(out)}} - V_t] \tag{4}$$

(m)(gen) Voltage-generating components of the motor

$$V_{(m)(gen)} = S_{(m)(gen)[\dot{A};V]} \dot{A}_{(out)} = \text{back electromotive force} \tag{5}$$

(mwms) Motor windings and magnetic structure

$$M_{(em)} = S_{(m)[V;M]} [V_a - V_{(m)(gen)}] \tag{6}$$

where

$M_{(em)}$ = electromagnetic torque produced by the motor

$S_{(m)[V;M]}$ = voltage input – torque output sensitivity of the motor

Substituting Eq. (5) in Eq. (6) gives

$$M_{(em)} = S_{(m)[V;M]} [V_a - S_{(m)(gen)[\dot{A};V]} \dot{A}_{(out)}] \tag{7}$$

$$= S_{(m)[V;M]} V_a - S_{(m)(gen)[\dot{A};V]} S_{(m)[V;M]} \dot{A}_{(out)} \tag{8}$$

The second term on the right-hand side of Eq. (8) represents the damping-torque component noted in section a. This torque results from the generation of a back electromotive force and acts in opposition to the output angular velocity. The angle rate input – torque output sensitivity of the motor that is associated with the generation of this damping torque is equal to the ratio of the torque generated to the angular velocity of the output shaft; i.e.,

$$S_{(m)[\dot{A};M]} = \frac{S_{(m)(gen)[\dot{A};V]} S_{(m)[V;M]} \dot{A}_{(out)}}{\dot{A}_{(out)}} = S_{(m)(gen)[\dot{A};V]} S_{(m)[V;M]} \tag{9}$$

= angle rate – torque sensitivity associated with the damping-torque component generated by the motor

or, solving Eq. (9) for $S_{(m)(gen)[\dot{A};V]}$,

$$S_{(m)(gen)[\dot{A};V]} = \frac{S_{(m)[\dot{A};M]}}{S_{(m)[V;M]}} \tag{10}$$

The sensitivities $S_{(m)[\dot{A};M]}$ and $S_{(m)[V;M]}$ are determined from motor characteristic curves of the type shown in Fig. b. The left-hand plot represents the torque developed by the motor when the output shaft is allowed to rotate, and shows the reduction in torque produced by the back electromotive force. The initial value of each characteristic line, which corresponds to a value of $\dot{A}_{(out)}$ equal to zero, is determined by the characteristic line of the right-hand plot. As indicated in Fig. b:

1) The sensitivity $S_{(m)[\dot{A};M]}$ is equal to the magnitude of the slope of the characteristic lines that represent the relationships between $M_{(em)}$ and $\dot{A}_{(out)}$ for constant values of the input voltage from the amplifier.
2) The sensitivity $S_{(m)[V;M]}$ is equal to the slope of the characteristic line that represents the relationship between $M_{(em)}$ and V_a when the motor shaft is held stationary, so that $\dot{A}_{(out)} = 0$.

Derivation Summary 34-27. Component analysis and performance equation of a typical positional servo system; derivation of the corresponding analog-computer equation and the equivalent analog-computer arrangement; determination of the coefficient settings. (Page 3 of 20)

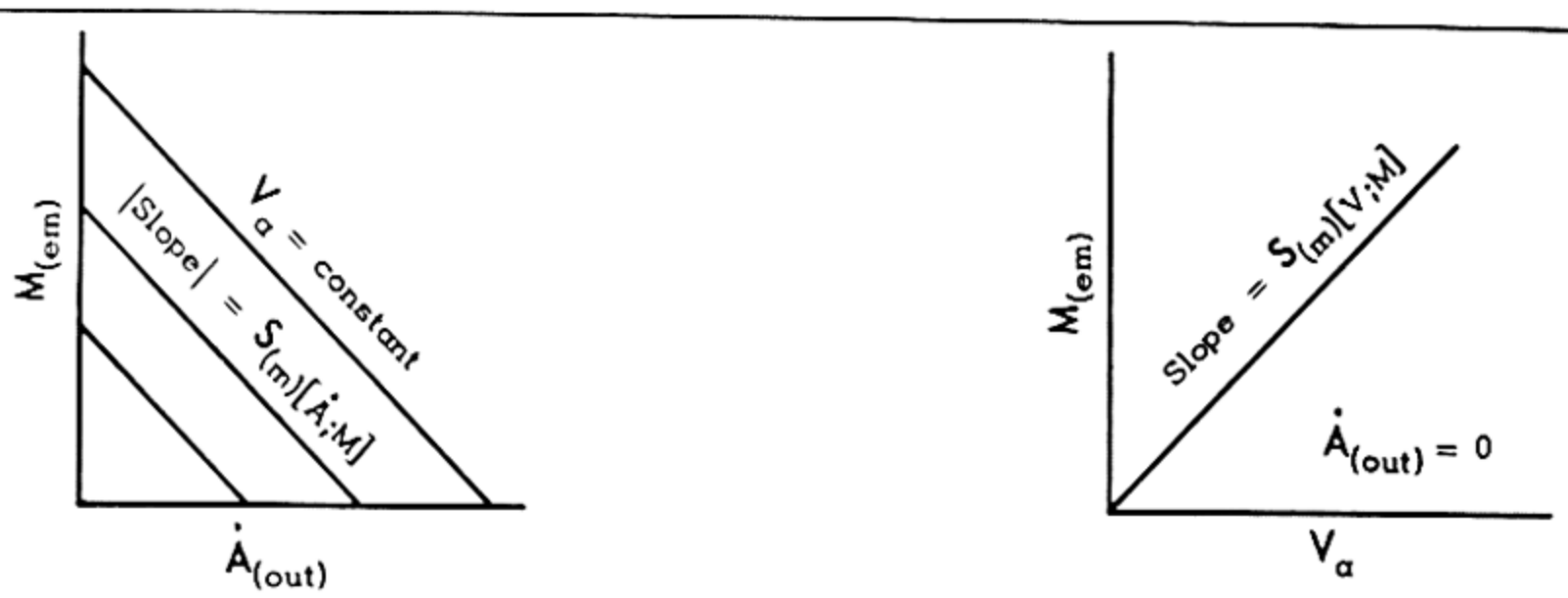


Fig. b. Motor characteristic curves.

(ms) Motor shaft

A summation of the torques acting on the motor shaft shows that

$$M_{(em)} + M_{(ir)} = 0 \tag{11}$$

where

$$M_{(ir)} = -I_m \ddot{A}_{(out)} \tag{12}$$

$M_{(ir)}$ = inertia reaction torque acting on the motor shaft

I_m = moment of inertia of the motor shaft and the connected mechanical load

Substitution of the relationships for $M_{(em)}$ and $M_{(ir)}$ given respectively by Eqs. (8) and (12) in Eq. (11), and subsequent use of Eqs. (1), (2), (3), (4) and (10) shows that the performance equation of the positional servo system shown in Fig. a is

$$I_m \ddot{A}_{(out)} + (S_{(m)[\dot{A};M]} + S_{(t)[\dot{A};V]} S_{(a)[V;V]} S_{(m)[V;M]}) \dot{A}_{(out)} + S_{(sg)[A;V]} S_{(a)[V;V]} S_{(m)[V;M]} A_{(out)}$$

$$= S_{(sg)[A;V]} S_{(a)[V;V]} S_{(m)[V;M]} A_{(in)} \tag{13}$$

b) Component analysis and derivation of the over-all performance equation of the positional servo system shown in Fig. a

An alternative procedure to that of section b for arriving at the performance equation of the positional servo system of Fig. a is to use loop relationships instead of component relationships. Starting with the innermost loop, each of the three feedback loops is consolidated into a single operating component. These three loops, in order of consolidation, are:

1) The back-electromotive-force feedback loop.
2) The tachometer feedback loop.
3) The output-signal-generator feedback loop.

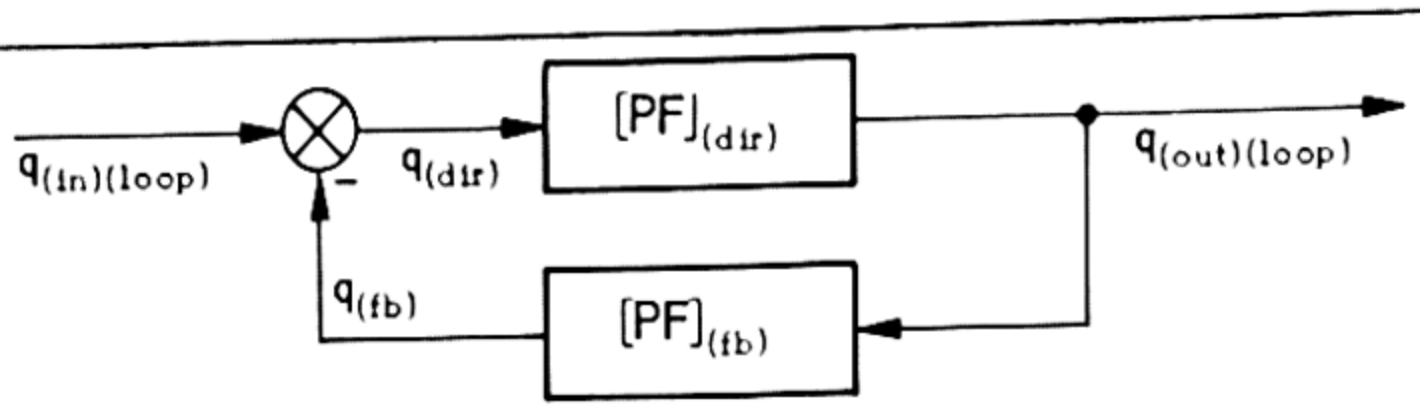
This procedure results in a reduction of the loops in the functional diagram by successive steps until the entire diagram is consolidated into a single block whose performance equation is identical with that derived in section b. The procedure also serves to delineate the mathematical form of progressively more complete parts of the positional servo system.

The consolidation of each loop of Fig. a is based on the generalized procedure already described in Fig. 3-4 of Chapter 3. This consolidation procedure is reduced to direct applicability to the present situation in Fig. c. As shown in that figure, any feedback loop can be reduced to a single equivalent component whose performance function is expressed in terms of the direct and feedback performance functions of the loop as follows:

$$[PF]_{(loop)} = \frac{[PF]_{(dir)}}{1 + [PF]_{(dir)} [PF]_{(fb)}} \tag{14}$$

This relationship is used in turn for each of the three loops of Fig. a.

Derivation Summary 34-27. Component analysis and performance equation of a typical positional servo system; derivation of the corresponding analog-computer equation and the equivalent analog-computer arrangement; determination of the coefficient settings. (Page 4 of 20)



$[PF]_{(dir)}$ = performance function associated with the direct path of the feedback loop

$[PF]_{(fb)}$ = performance function associated with the feedback path of the feedback loop

$q_{(in)(loop)}$ = input quantity to the feedback loop

$q_{(out)(loop)}$ = output quantity of the feedback loop

$q_{(dir)}$ = input quantity to the direct path of the feedback loop

$q_{(fb)}$ = output quantity of the feedback path of the feedback loop

The output obtained from the feedback path of the feedback loop is

$$q_{(fb)} = [PF]_{(fb)}\, q_{(out)(loop)}$$

Hence, the input to the direct path of the feedback loop is

$$q_{(dir)} = q_{(in)(loop)} - [PF]_{(fb)}\, q_{(out)(loop)}$$

The output of the direct path is identical with the output of the loop and is related to the input to the direct path as follows:

$$q_{(out)(loop)} = [PF]_{(dir)}\, q_{(dir)} = [PF]_{(dir)}\, [q_{(in)(loop)} - [PF]_{(fb)}\, q_{(out)(loop)}]$$

The foregoing means that any feedback loop can be replaced by a single operating component



whose performance function is

$$[PF]_{(loop)} = \frac{q_{(out)(loop)}}{q_{(in)(loop)}} = \frac{[PF]_{(dir)}}{1 + [PF]_{(dir)}\, [PF]_{(fb)}}$$

Fig. c. Feedback loop reduced to a single operating component.

Figure d is the mathematical-functional diagram of the positional servo system that corresponds to the functional diagram of Fig. a. The performance function of each operating component, assuming ideal operation, appears inside brackets in the appropriate block of the diagram. These performance functions, obtained from the component equations given in section b, are written in the operational-notation form for ease in algebraic manipulation. As a result, the input to the voltage-generating components of the motor and the tachometer is shown as $A_{(out)}$, rather than $\dot{A}_{(out)}$ as in Fig. a. That is, the process of differentiation is represented as taking place inside the block, as shown by the presence of the operator p.

Since the over-all performance function of an open chain of operating components is equal to the product of the performance functions of the individual components,* consideration of the back-electromotive-force feedback loop shows that

$$[PF]_{(dir)(bemf)} = S_{(m)[V;M]} \frac{1}{I_m p^2} \qquad (15)$$

= performance function associated with the direct path of the back-electromotive-force feedback loop

* See the discussion of Chapter 3.

Derivation Summary 34-27. Component analysis and performance equation of a typical positional servo system; derivation of the corresponding analog-computer equation and the equivalent analog-computer arrangement; determination of the coefficient settings. (Page 5 of 20)

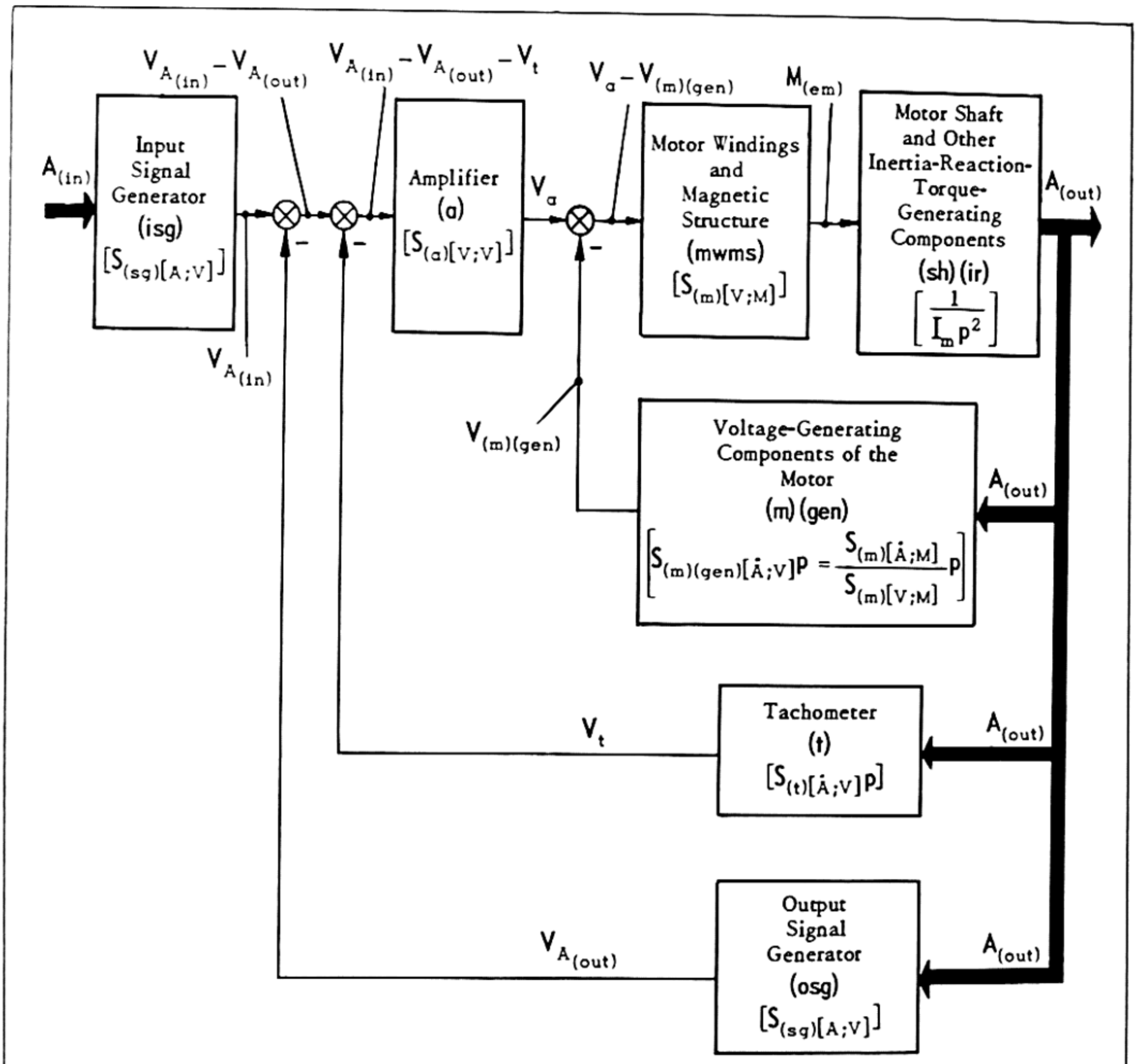


Fig. d. Mathematical-functional diagram for a positional servo system corresponding to the functional diagram of Fig. a.

$$[PF]_{(fb)(bemf)} = \frac{S_{(m)[\dot{A};M]}}{S_{(m)[V;M]}}\,p \tag{16}$$

= performance function associated with the feedback path of the back-electromotive-force feedback loop

From Eq. (14),

$$[PF]_{(loop)(bemf)} = \frac{S_{(m)[V;M]}\dfrac{1}{I_m p^2}}{1 + \left[S_{(m)[V;M]}\dfrac{1}{I_m p^2}\right]\left[\dfrac{S_{(m)[\dot{A};M]}}{S_{(m)[V;M]}}\,p\right]} = \frac{\dfrac{S_{(m)[V;M]}}{S_{(m)[\dot{A};M]}}}{p\left(\dfrac{I_m}{S_{(m)[\dot{A};M]}}\,p + 1\right)} \tag{17}$$

= performance function of the back-electromotive-force feedback loop

Derivation Summary 34-27. Component analysis and performance equation of a typical positional servo system; derivation of the corresponding analog-computer equation and the equivalent analog-computer arrangement; determination of the coefficient settings. (Page 6 of 20)

The consolidation of Fig. d obtained by considering the back-electromotive-force feedback loop as a single operating component is represented in Fig. e. The performance function of this component is identical with that of the loop it replaces and is given by Eq. (17).

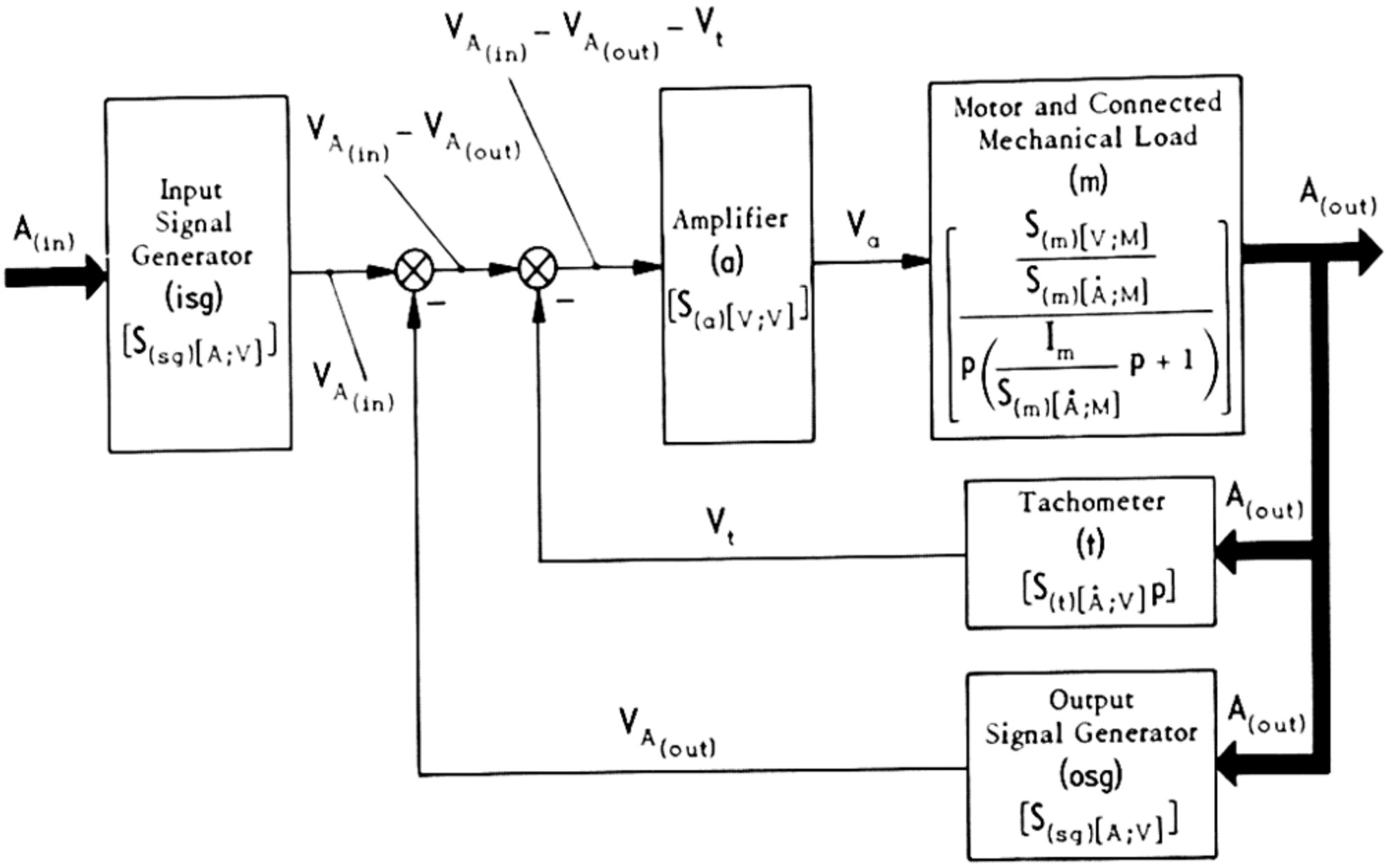


Fig. e. Mathematical-functional diagram for a positional servo system with the back-electromotive-force feedback loop of Fig. d consolidated into a single operating component.

Figure f represents the consolidation obtained when the tachometer feedback loop of Fig. e is replaced by an equivalent operating component whose performance function is identical with that of the loop. This

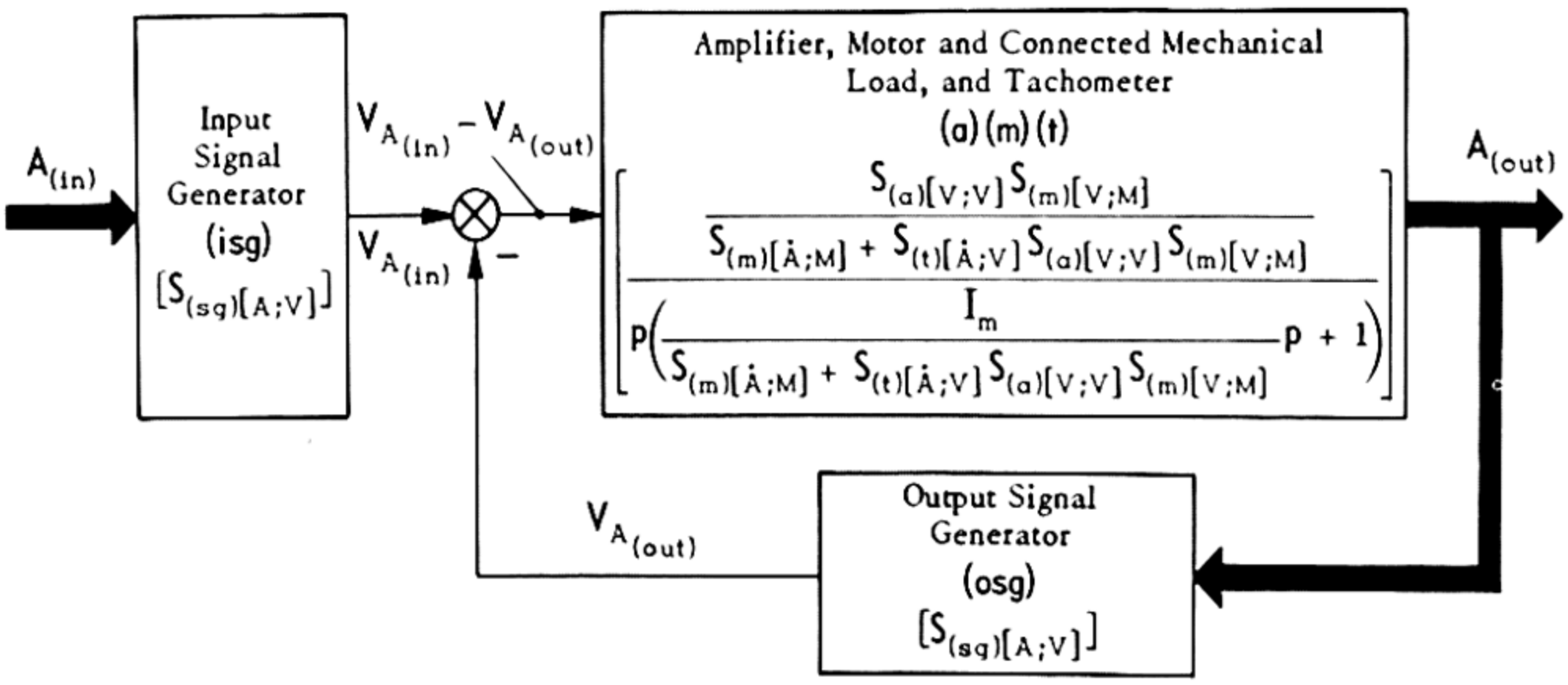


Fig. f. Mathematical-functional diagram for a positional servo system with the back-electromotive-force feedback loop and the tachometer feedback loop of Fig. d consolidated into a single pseudo operating component.

Derivation Summary 34-27. Component analysis and performance equation of a typical positional servo system; derivation of the corresponding analog-computer equation and the equivalent analog-computer arrangement; determination of the coefficient settings. (Page 7 of 20)

performance function is given by the expression inside brackets in the large block of Fig. f, and is obtained by the same procedure used in the consolidation of the back-electromotive-force feedback loop. The algebraic combination of the direct and feedback performance functions to form the loop performance function is omitted here since no new principles or procedures are involved.

Consolidation of the final loop, the output-signal-generator feedback loop of Fig. f, is accomplished by the same procedure used for the other two loops. The performance function of the complete positional servo system is then obtained by multiplying the performance function of the output-signal-generator feedback loop of Fig. f by the performance function of the input signal generator. This latter performance function is simply the signal-generator sensitivity $S_{(sg)[A;V]}$. The resulting performance function of the positional servo system appears inside brackets in the block of Fig. g. This figure represents the functional diagram of Fig. d with all feedback paths eliminated.

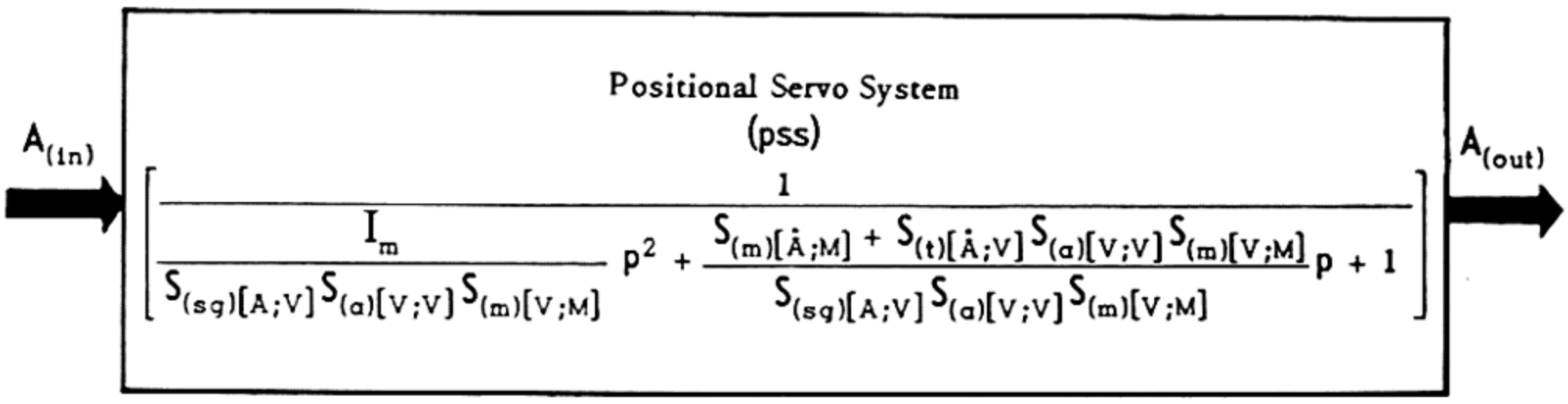


Fig. g. Mathematical-functional diagram for a positional servo system with all components of Fig. d consolidated into a single pseudo operating component.

Multiplication of the performance function shown in Fig. g by the input angle, $A_{(in)}$, gives the expression for the output angle, $A_{(out)}$, of the positional servo system. Except for the fact that the resulting performance relationship is in operational notation, it is identical with the performance equation derived in section b and given by Eq. (13).

c) Determination of the over-all performance equation of the positional servo system of Fig. a by using loop relationships

The (0;0,1,2) second-order performance equation for the positional servo system written in operational-notation form is

$$[I_m p^2 + (S_{(m)[\dot{A};M]} + S_{(t)[\dot{A};V]}S_{(a)[V;V]}S_{(m)[V;M]})p + S_{(sg)[A;V]}S_{(a)[V;V]}S_{(m)[V;M]}]A_{(out)} = S_{(sg)[A;V]}S_{(a)[V;V]}S_{(m)[V;M]}A_{(in)} \quad (18)$$

From Eqs. (1) and (2) of Derivation Summary 34-21, the scale-factor relationships may be written directly as

$$e_{A_{(in)}} = (SF)_{(A_{(in)};e)}A_{(in)}\text{*} \quad (19)$$

$$e_{A_{(out)}} = (SF)_{(A_{(out)};e)}A_{(out)}\text{*} \quad (20)$$

---

* As an aid in readily distinguishing a voltage associated with the positional servo system from a voltage associated with the analog computer, the main symbol V is used for a servo system voltage while the main symbol e is used for an analog computer voltage.

The use of the nondimensional operator ($'p^1 = p^1 T^1_{(ref)}$) and Eqs. (19) and (20) shows that Eqs. (18) can be transformed for analog-computer application as follows:

$$\left[\frac{I_m}{T^2_{(ref)}(SF)_{(A_{(out)};e)}} \, 'p^2 + \frac{S_{(m)[\dot{A};M]} + S_{(t)[\dot{A};V]} S_{(a)[V;V]} S_{(m)[V;M]}}{T_{(ref)}(SF)_{(A_{(out)};e)}} \, 'p \right.$$

$$\left. + \frac{S_{(sg)[A;V]} S_{(a)[V;V]} S_{(m)[V;M]}}{(SF)_{(A_{(out)};e)}} \right] e_{A_{(out)}} = \frac{S_{(sg)[A;V]} S_{(a)[V;V]} S_{(m)[V;M]}}{(SF)_{(A_{(in)};e)}} \, e_{A_{(in)}} \qquad (21)$$

Following the pattern of Derivation Summary 34-26, the coefficient settings can be written from Eq. (21) as:

$$C_{(a_2)} = \frac{I_m}{T^2_{(ref)}(SF)_{(A_{(out)};e)}} \qquad (22)$$

$$C_{(1/a_2)} = \frac{T^2_{(ref)}(SF)_{(A_{(out)};e)}}{I_m} \qquad (23)$$

$$C_{(a_1)} = \frac{S_{(m)[\dot{A};M]} + S_{(t)[\dot{A};V]} S_{(a)[V;V]} S_{(m)[V;M]}}{T_{(ref)}(SF)_{(A_{(out)};e)}} \qquad (24)$$

$$C_{(a_0)} = \frac{S_{(sg)[A;V]} S_{(a)[V;V]} S_{(m)[V;M]}}{(SF)_{(A_{(out)};e)}} \qquad (25)$$

$$C_{(b_0)} = \frac{S_{(sg)[A;V]} S_{(a)[V;V]} S_{(m)[V;M]}}{(SF)_{(A_{(in)};e)}} \qquad (26)$$

The accompanying analog-computer functional diagram of Fig. h corresponds to the system functional diagram of Fig. a, and is identical in form with the (0;0,1,2) analog-computer functional diagram given by

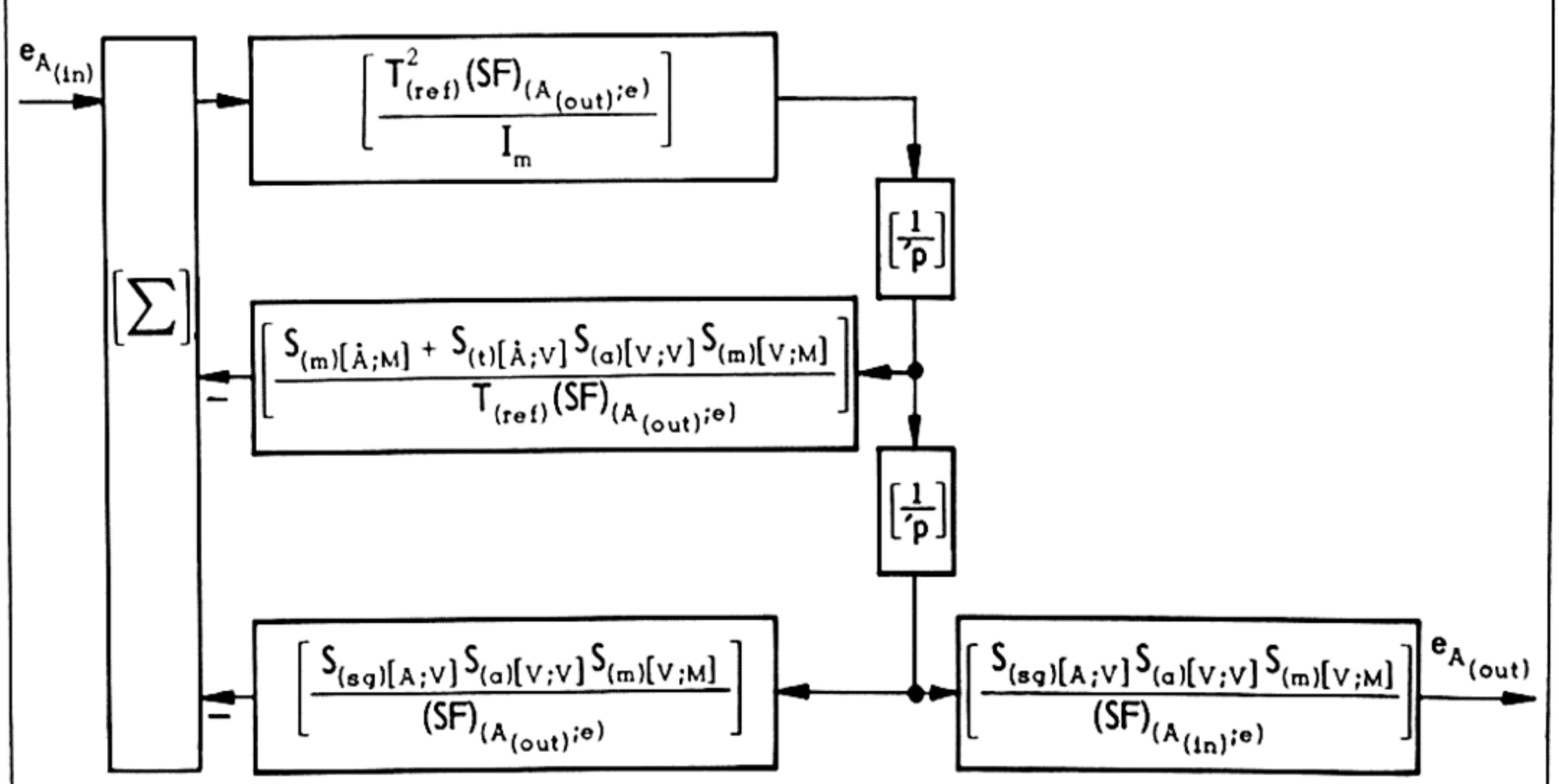


Fig. h. Analog-computer functional diagram for the positional servo system.

Derivation Summary 34-27. Component analysis and performance equation of a typical positional servo system; derivation of the corresponding analog-computer equation and the equivalent analog-computer arrangement; determination of the coefficient settings. (Page 9 of 20)

Fig. a of Derivation Summary 34-26. The values within the brackets on the blocks are the coefficient settings given by Eqs. (23) through (26), and have the dimensions of torque units per volt.

As can be seen from the functional diagram of Fig. h, the parameters of the system (that is, the component sensitivities) are lumped together in each coefficient-multiplier block. This means that any adjustment of the coefficient settings cannot be associated with a change in value of a particular system parameter. Although the functional diagram of Fig. h could be simplified by the procedure of Derivation Summary 34-26 to the extent that any one of the four coefficient multipliers shown could be eliminated, the coefficient settings would still have no individual relationships with the system parameters. Fortunately, the parameters can be separated by modifying the analog-computer functional diagram in a step-by-step procedure. The end result is an analog-computer diagram that resembles the positional servo system of Fig. a. The various steps involved are described in the following paragraphs.

Step 1

If Eq. (21) is multiplied by $1/S_{(a)[V;V]}S_{(m)[V;M]}$, the resulting analog-computer differential equation has the form

$$\left[\frac{I_m}{S_{(a)[V;V]}S_{(m)[V;M]}T^2_{(ref)}(SF)_{(A_{(out)};e)}}\,'p^2 + \frac{S_{(m)[\dot{A};M]} + S_{(t)[\dot{A};V]}S_{(a)[V;V]}S_{(m)[V;M]}}{S_{(a)[V;V]}S_{(m)[V;M]}T_{(ref)}(SF)_{(A_{(out)};e)}}\,'p + \frac{S_{(sg)[A;V]}}{(SF)_{(A_{(out)};e)}}\right]e_{A_{(out)}} = \frac{S_{(sg)[A;V]}}{(SF)_{(A_{(in)};e)}}\,e_{A_{(in)}} \tag{27}$$

For this form of the analog-computer differential equation:

a) Each coefficient setting is a dimensionless quantity.

b) The coefficient setting of the zero-order dependent variable coefficient multiplier is determined by only one system parameter; namely, the signal-generator sensitivity.

c) The associated functional diagram is modified to the form given by the accompanying Fig. i.

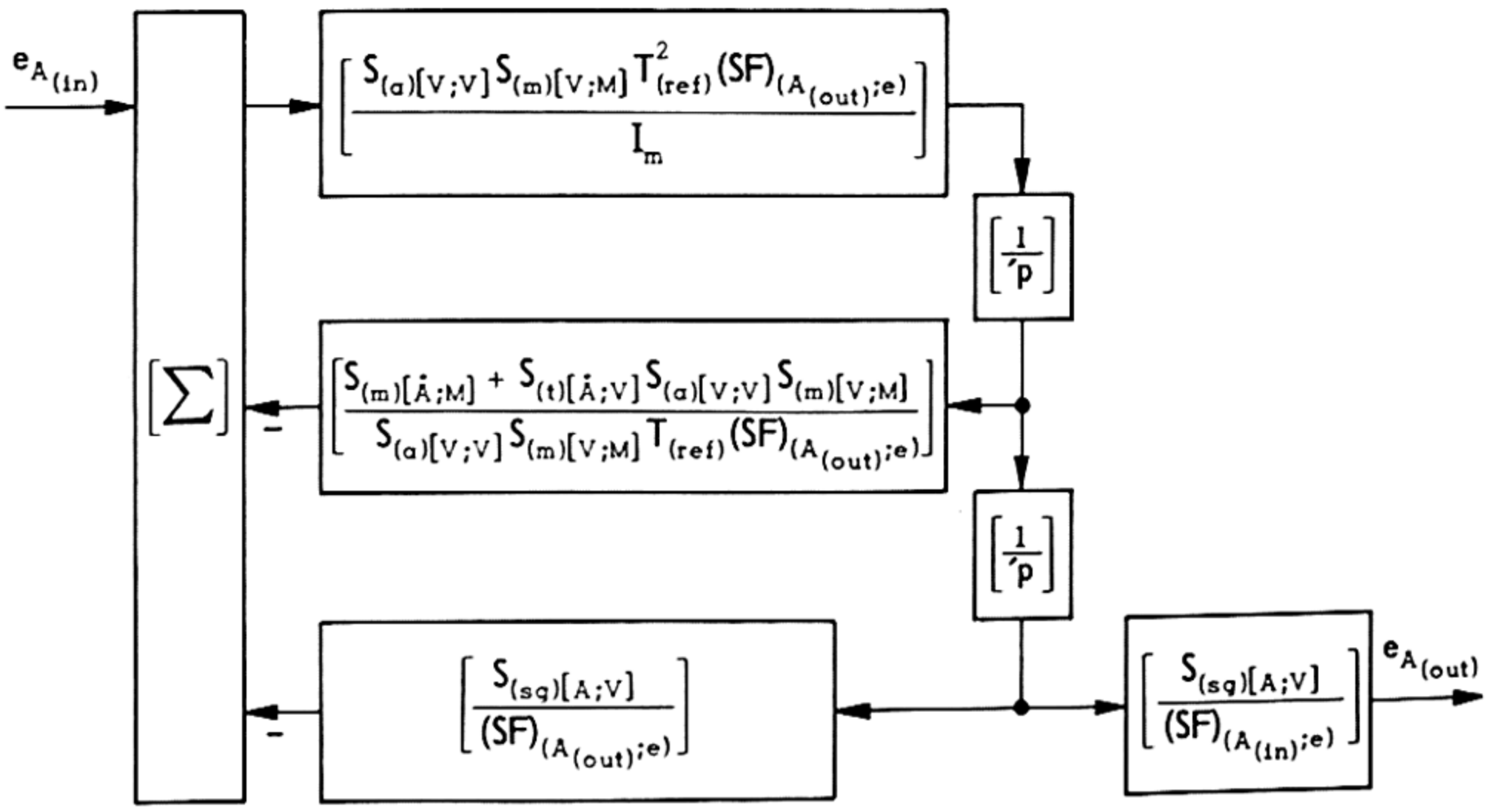


Fig. i. Analog-computer functional diagram for the positional servo system when the analog-computer differential equation is multiplied by $1/S_{(a)[V;V]}S_{(m)[V;M]}$.

Derivation Summary 34-27. Component analysis and performance equation of a typical positional servo system; derivation of the corresponding analog-computer equation and the equivalent analog-computer arrangement; determination of the coefficient settings. (Page 10 of 20)

Step 2

The next step in transforming the analog-computer diagram into one that resembles the positional servo system functional diagram of Fig. a is to move the zero-order independent variable coefficient-multiplier block from the output side of the analog-computer diagram to the input side. When this is done, the analog-computer differential equation remains the same, but the voltage levels in the analog computer undergo change. The functional diagram of Fig. j represents the results of this step.

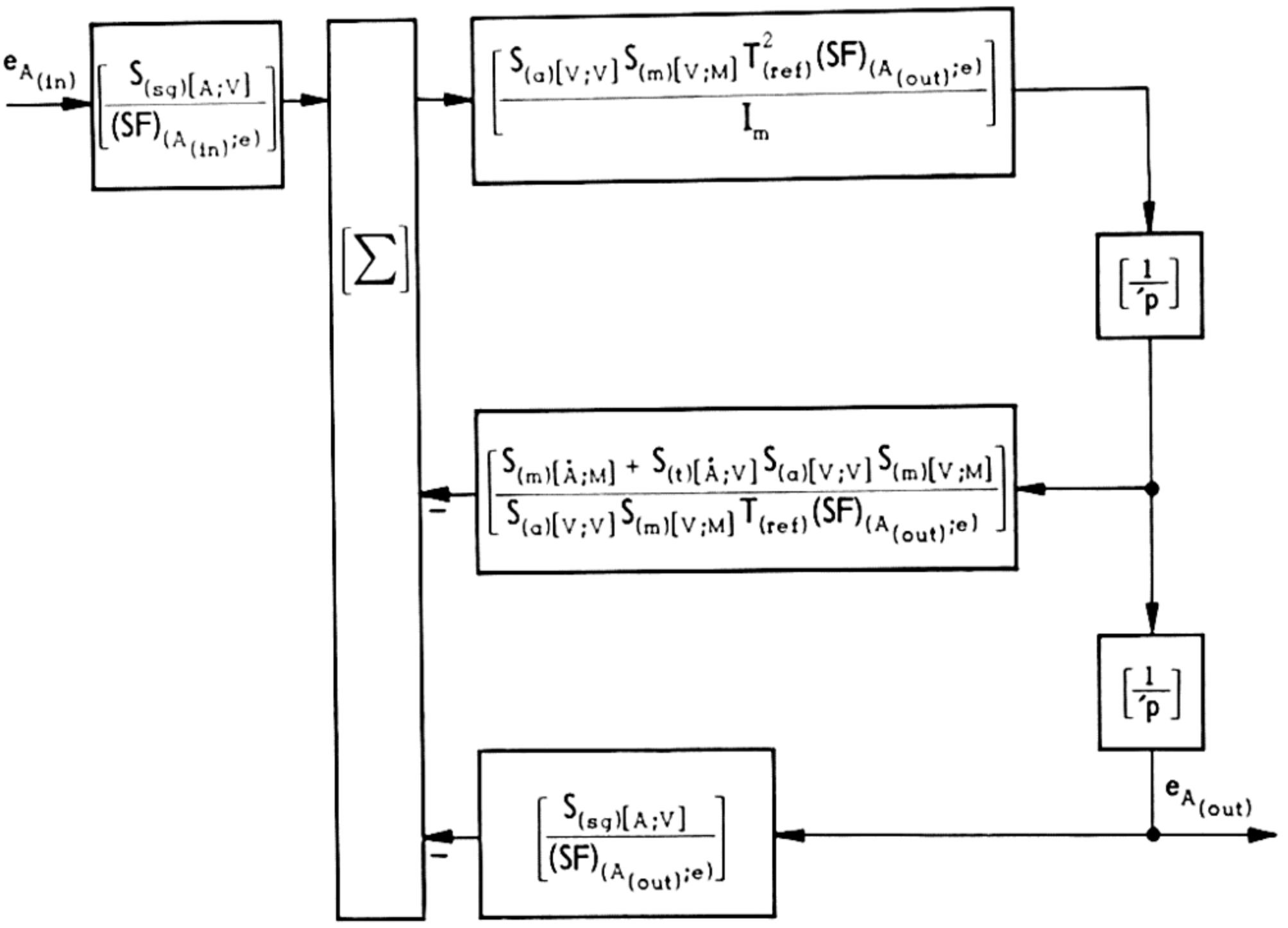


Fig. j. Modified analog-computer functional diagram for the positional servo system corresponding to a shift of the zero-order independent variable coefficient-multiplier block from the output side of the diagram to the input side.

Step 3

The tachometer sensitivity can be separated from the first-order dependent variable coefficient setting by rewriting the expression as the sum of two fractions; i.e.,

$$\frac{S_{(m)[\dot{A};M]} + S_{(t)[\dot{A};V]}\,S_{(m)[V;V]}\,S_{(m)[V;M]}}{S_{(a)[V;V]}\,S_{(m)[V;M]}\,T_{(ref)}\,(SF)_{(A_{(out)};e)}} = \frac{S_{(m)[\dot{A};M]}}{S_{(a)[V;V]}\,S_{(m)[V;M]}\,T_{(ref)}\,(SF)_{(A_{(out)};e)}} + \frac{S_{(t)[\dot{A};V]}}{T_{(ref)}\,(SF)_{(A_{(out)};e)}} \qquad (28)$$

Figure k shows the corresponding addition of a coefficient multiplier and a summer to the analog-computer functional diagram of Fig. j. The dashed line in Fig. k that surrounds some of the blocks groups the coefficient settings that are associated with only the amplifier and the motor.

Derivation Summary 34-27. Component analysis and performance equation of a typical positional servo system; derivation of the corresponding analog-computer equation and the equivalent analog-computer arrangement; determination of the coefficient settings. (Page 11 of 20)

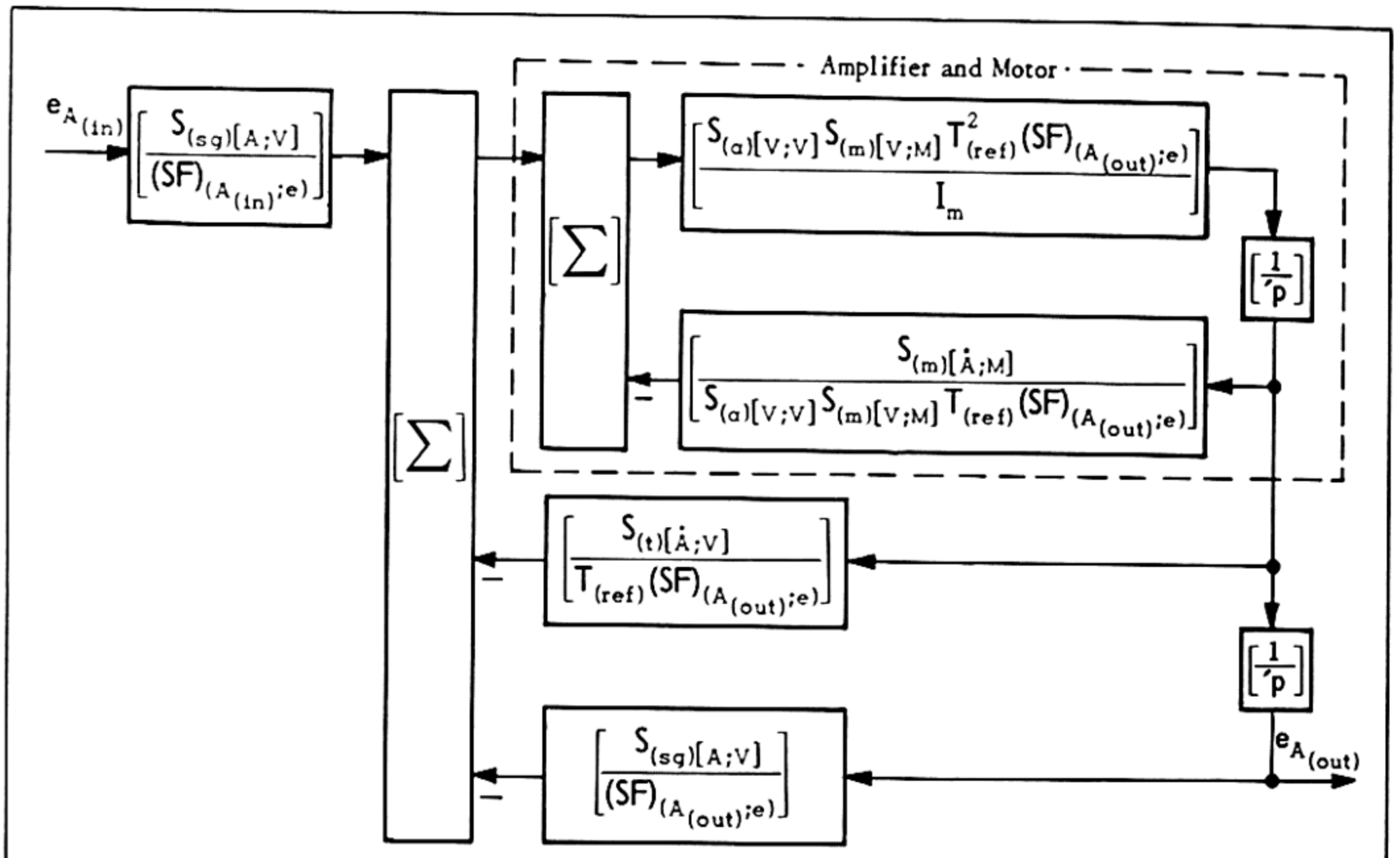


Fig. k. Modified analog-computer functional diagram for the positional servo system with only the amplifier and motor parameters not separated.

Step 4

The next step is to separate the amplifier and motor parameters from each other. This is done in two substeps:

a) Introduce a coefficient multiplier to handle $S_{(a)[V;V]}$ as shown in Fig. l.

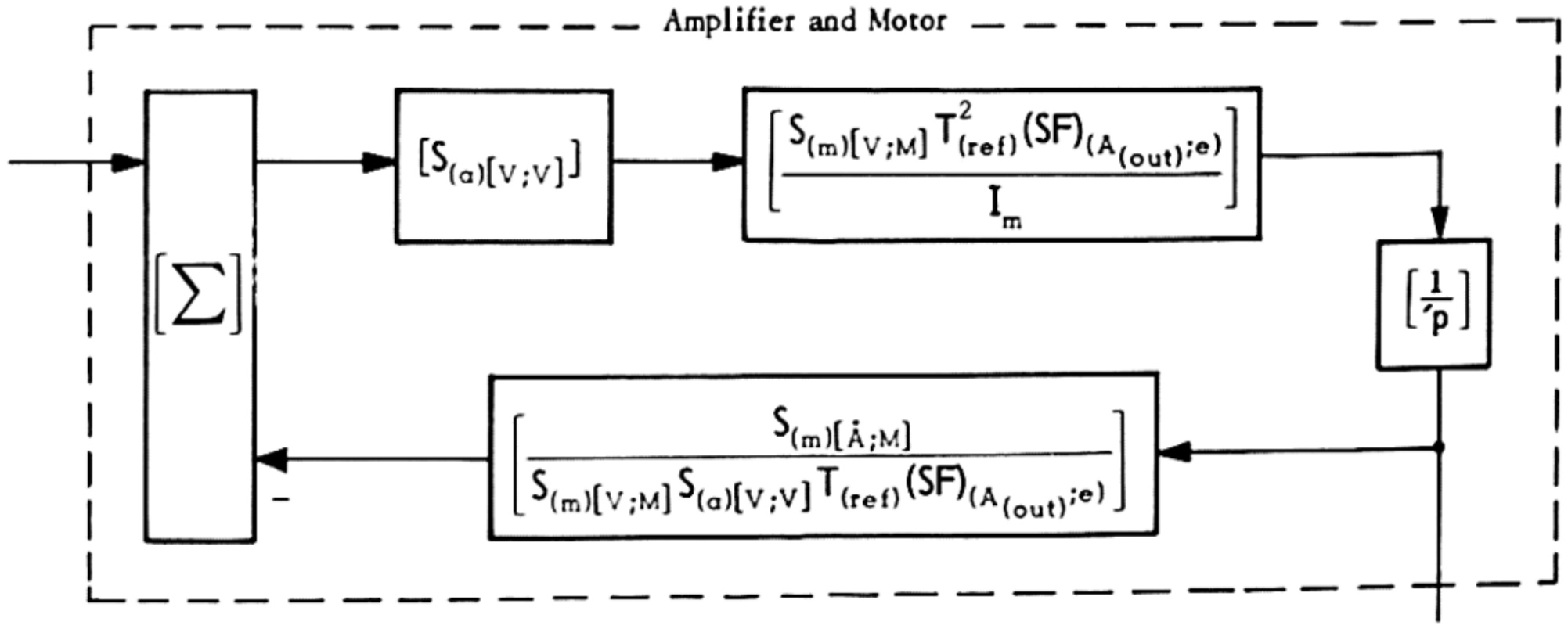


Fig. l. Coefficient multiplier added to handle the amplifier sensitivity.

b) Move the coefficient-multiplier block representing $S_{(a)[V;V]}$ to the input side of the summer shown in Fig. l. This allows the amplifier sensitivity to be removed from the coefficient-multiplier block in the feedback path, as shown in Fig. m, which means that each coefficient setting is now in terms of either a motor sensitivity or the amplifier sensitivity, but not of both.

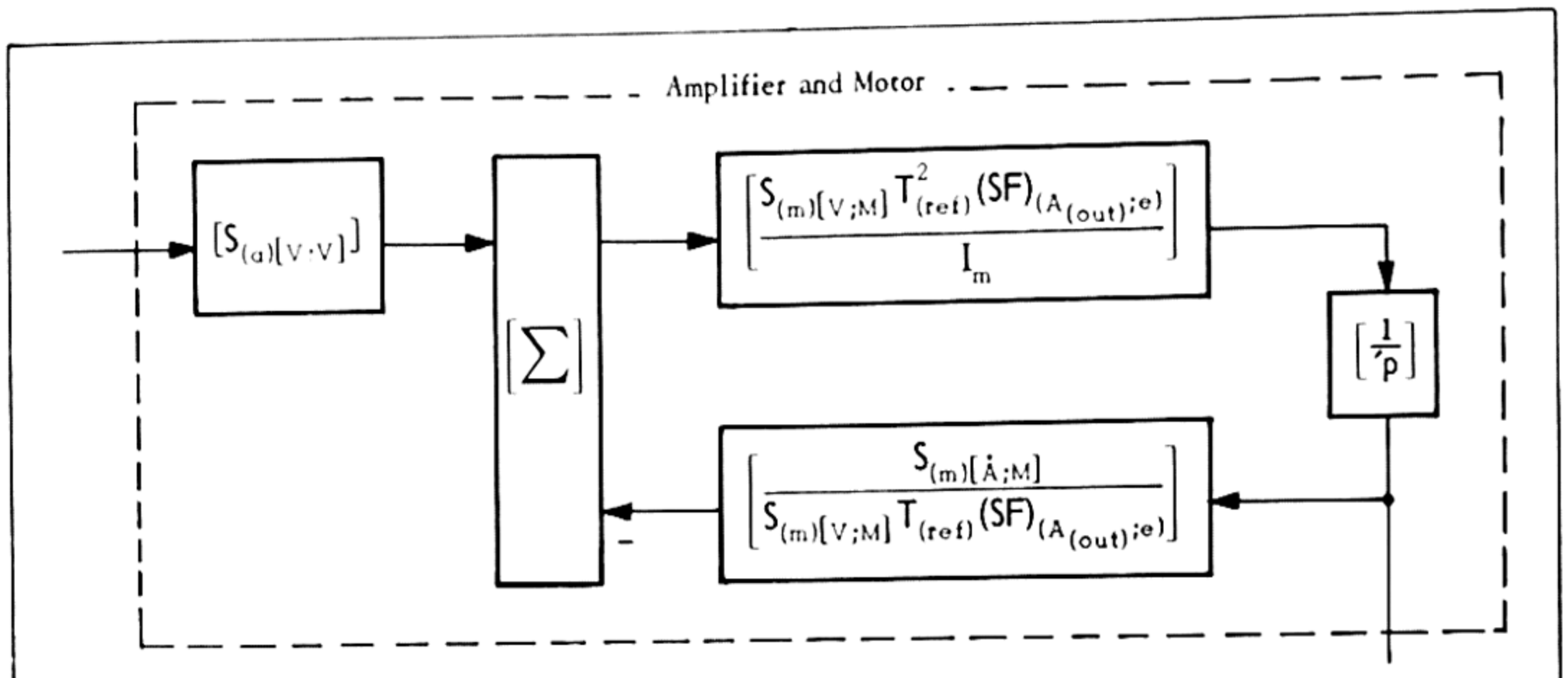


Fig. m. Modified motor and amplifier functional diagram with amplifier and motor parameters separated.

Step 5

The tachometer feedback signal and the output-signal-generator feedback signal are introduced at different points in the positional servo system. In order to show this in the analog-computer functional diagram, one more summer is introduced in the manner shown in Fig. n. This diagram corresponds completely to the positional servo system functional diagram given in Fig. a. Two coefficient multipliers and two summers have been introduced in addition to those in the original analog-computer functional diagram of Fig. h, but the direct correspondence to the physical situation makes the additional complication desirable in practice.

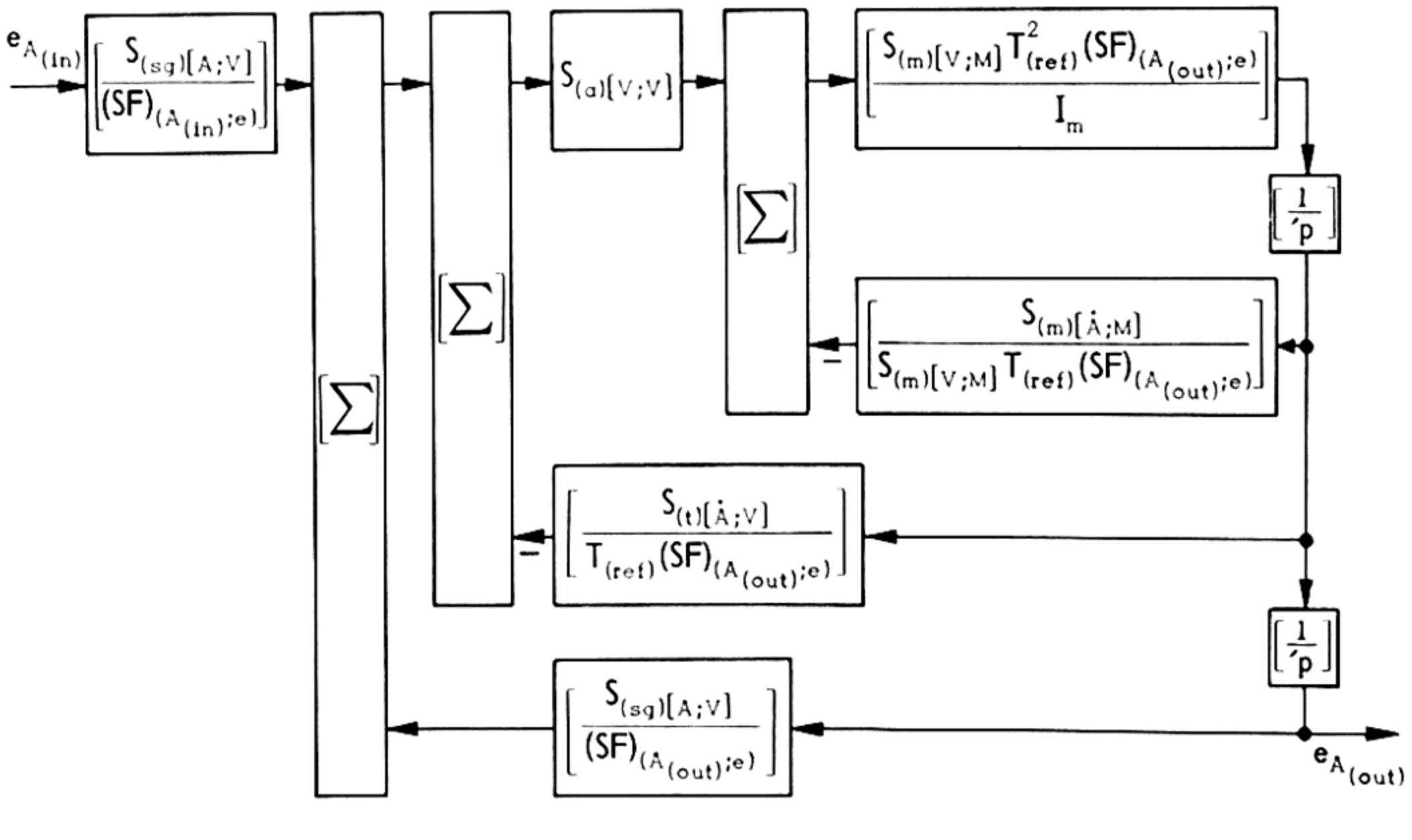


Fig. n. Analog-computer functional diagram with all parameters separated and with complete correspondence to the actual positional servo system functional diagram.

Derivation Summary 34-27. Component analysis and performance equation of a typical positional servo system; derivation of the corresponding analog-computer equation and the equivalent analog-computer arrangement; determination of the coefficient settings. (Page 13 of 20)

Except for the multiplication of each coefficient setting by a constant factor, the analog-computer functional diagram of Fig. n is in a form that is best adapted for the study of the positional servo system. All parameters have been separated and each is associated with a particular coefficient multiplier.

All the coefficient settings in any one of the three feedback loops may be modified by a constant factor without altering the input to and the output from this particular loop. Thus, insofar as the input and the output signals are concerned, the two following loop diagrams are equivalent.* Figure p shows the constant factor (CF) introduced into the input coefficient setting C_1. In order to maintain the same output signal as in Fig. o, the direct coefficient setting in the loop, C_2, must be multiplied by $1/(CF)$ and the feedback coefficient C_3 multiplied by (CF), as shown. The presence of an integrator has no effect on the constant factor in the loop. The constant-factor technique is a means of modifying the values of the signals combined at the summer in order to bring them into the useful working voltage range of the analog computer.

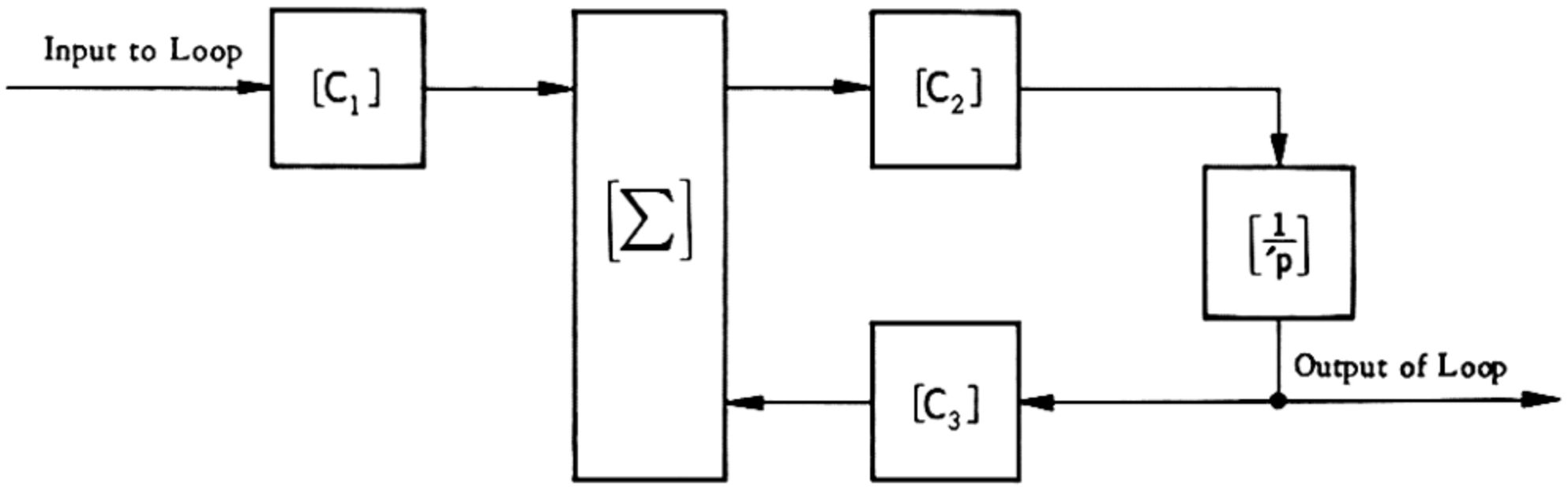


Fig. o. Loop diagram with coefficient settings C_1, C_2 and C_3.

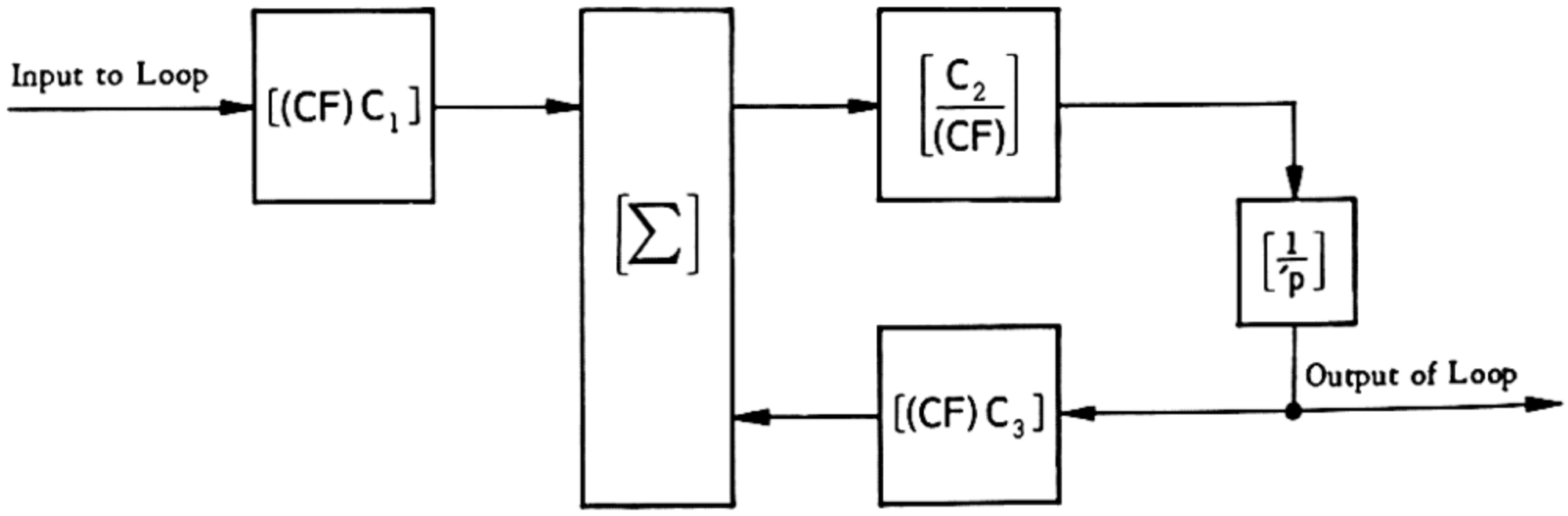


Fig. p. Loop diagram of Fig. o with the coefficient settings modified by a constant factor (CF) without altering the input to or output from the loop.

A different constant factor may be employed for each loop. In the system under consideration, there are three such loops, so that three constant factors, designated as $(CF)_1$, $(CF)_2$ and $(CF)_3$, can be utilized. When this is done, the analog-computer functional diagram for the system under study becomes as shown in Fig. q.

---

* Note that, as used in the present application, the term "loop" includes the simple loop considered in section c plus the operating component preceding the loop.

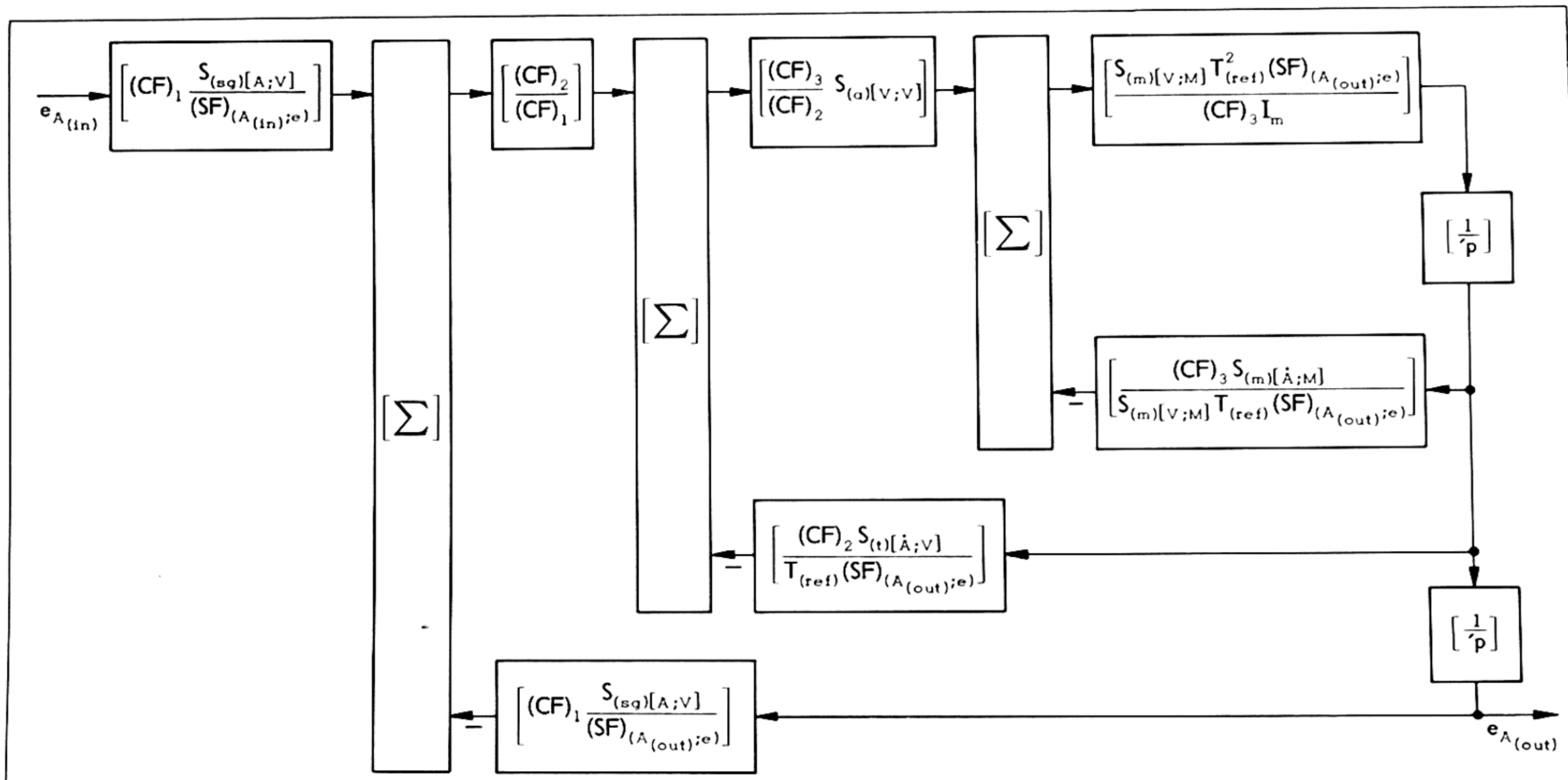


Fig. q. Analog-computer functional diagram with three constant factors utilized.

d) Derivation of the analog-computer differential equation for the positional servo system and the equivalent analog-computer arrangement

Derivation Summary 34-27. Component analysis and performance equation of a typical positional servo system; derivation of the corresponding analog-computer equation and the equivalent analog-computer arrangement; determination of the coefficient settings. (Page 15 of 20)

If the values of the positional servo system parameters are given, the problem may now be scaled for analog-computer solution. Typical values of these parameters for a positional servo system utilizing a 10-watt, two-phase motor are listed.*

$$\left.\begin{aligned} S_{(sg)[A;V]} &= 10 \text{ volts/rad} \\ S_{(m)[V;M]} &= 0.027 \text{ oz-in/volt} \\ S_{(m)[\dot{A};M]} &= 0.020 \text{ oz-in/rad/sec} \\ S_{(t)[\dot{A};V]} &= 0.060 \text{ volt/rad/sec} \\ S_{(a)[V;V]} &= 50 \text{ volts/volt} \\ I_m &= 0.00050 \text{ oz-in sec}^2/\text{rad} \end{aligned}\right\} \quad (29)$$

The torsional stiffness of the positional system servo is then

$$k_{(\text{torsional})} = S_{(sg)[A;V]} S_{(a)[V;V]} S_{(m)[V;M]}^{**} = 13.5 \text{ oz-in/rad} \quad (30)$$

and the undamped angular natural frequency is

$$w_n = \sqrt{\frac{S_{(sg)[A;V]} S_{(a)[V;V]} S_{(m)[V;M]}}{I_m}}^{**} = 164 \text{ rad/sec} \quad (31)$$

The damping ratio provided by the back electromotive force effect of the motor is

$$(DR)_{(\text{bemf})} = \frac{S_{(m)[\dot{A};M]}}{2\sqrt{I_m S_{(sg)[A;V]} S_{(a)[V;V]} S_{(m)[V;M]}}}^{**} = 0.12 \quad (32)$$

The damping ratio provided by the tachometer feedback is

$$(DR)_t = \frac{S_{(t)[\dot{A};V]} S_{(a)[V;V]} S_{(m)[V;M]}}{2\sqrt{I_m S_{(sg)[A;V]} S_{(a)[V;V]} S_{(m)[V;M]}}}^{**} = 0.49 \quad (33)$$

The total damping ratio is thus

$$(DR)_{(\text{total})} = (DR)_{(\text{bemf})} + (DR)_t = 0.61 \quad (34)$$

The characteristic time of the positional servo system corresponding to these values is

$$(CT)_{(pss)} = \frac{1}{(DR)\, w_n}^{**} \cong 0.01 \text{ second} \quad (35)$$

In accordance with this characteristic time, a step-function response time of 0.03 second is indicated,*** or say 0.04 second to provide a safe margin. Thus, the time duration associated with the response of the system to the step function, which is generally used in analog computers, will be taken to be 0.04 second. This interval, considered together with the time in which the analog computer solves the problem, determines the solution time ratio, STR, which in turn determines $T_{(ref)}$, the reference time applicable to the analog computer – physical problem combination.

The information of the preceding paragraphs is now applied to the problem of scaling two different representative types of computers, which will be referred to as Computer No. 1 and Computer No. 2.

---

* As noted in section a of this summary, it is assumed that there is no gearing between the motor shaft and the output shaft. Normally, high torque output per unit difference between input and output shaft positions will be needed and this can be provided by such gearing at the expense of the dynamic response of the output shaft. As treated here, it is presumed that a high-powered motor is used to produce rapid response without gearing.

** These equations are obtained by applying the relationships of Table 19-1 of Chapter 19 to Eq. (18), the performance equation of the positional servo system.

*** See Fig. 19-9 of Chapter 19.

Derivation Summary 34-27. Component analysis and performance equation of a typical positional servo system; derivation of the corresponding analog-computer equations and the equivalent analog-computer arrangement; determination of the coefficient settings. (Page 16 of 20)

COMPUTER NO. 1

For this computer, the proportionality constant RC between integrator input and rate of change of integrator output is

$$RC = 1 \text{ second} \tag{36}$$

A computer solution time of 4 seconds will be assumed since this choice will be seen to give coefficient settings and voltage levels that lie well within the capability of the computer and associated recording equipment.* This gives for the solution time ratio (see Eq. (3) of Derivation Summary 34-21):

$$STR = \frac{\text{computer solution time}}{\text{physical-problem solution time}} = \frac{4}{0.04} = 100 \tag{37}$$

The corresponding value of $T_{(ref)}$ (see section c of Derivation Summary 34-22) is

$$T_{(ref)} = \frac{RC}{STR} = 0.01 \text{ second} \tag{38}$$

Take as output- and input-quantity scale factors

$$(SF)_{(A_{(out)};e)} = (SF)_{(A_{(in)};e)} = 100 \text{ volts/rad} \tag{39}$$

This enables computation of the coefficient settings in terms of the constant factors $(CF)_1$, $(CF)_2$ and $(CF)_3$. The result of this procedure is shown in the functional diagram of Fig. r.

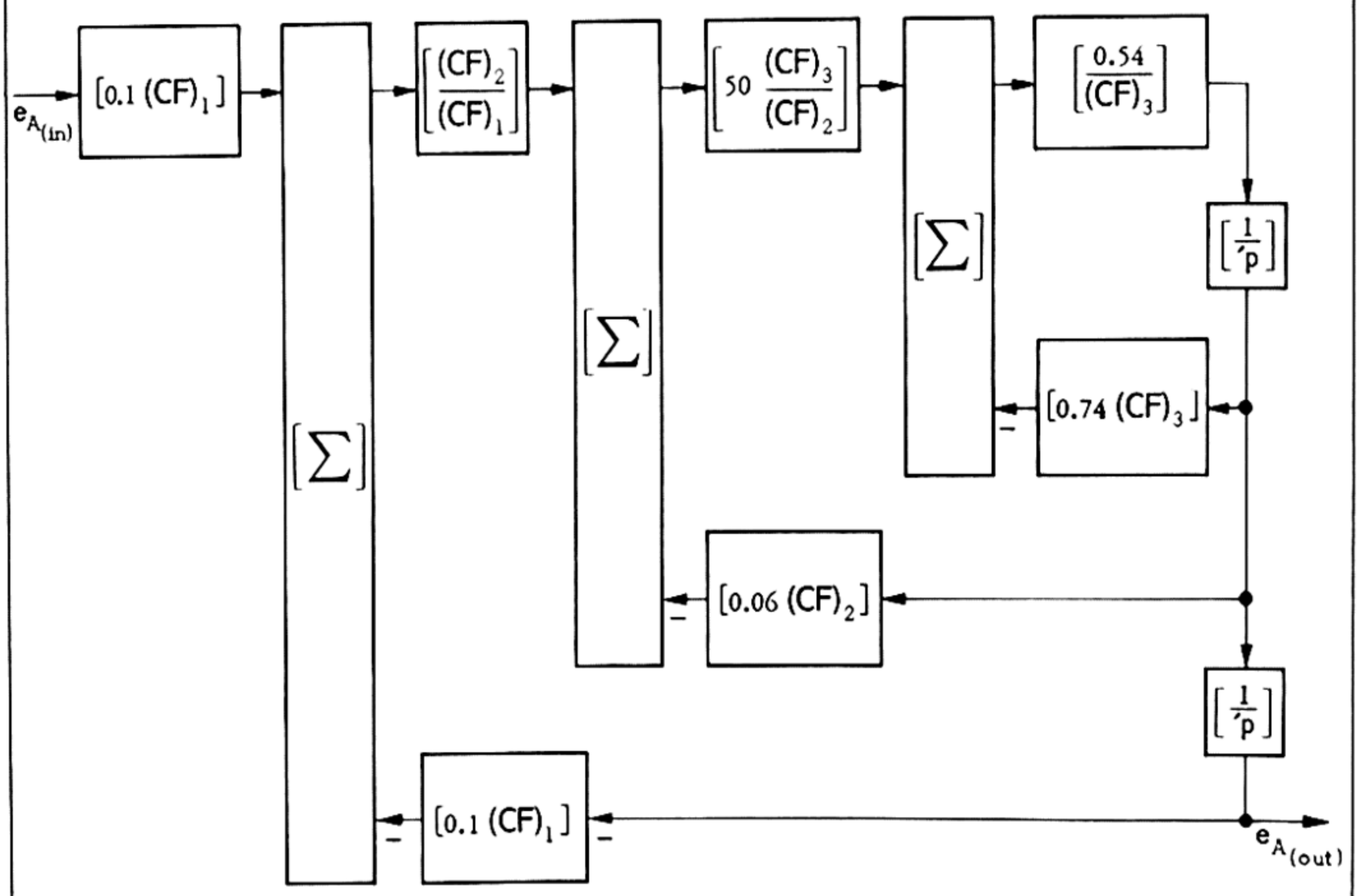


Fig. r. Analog-computer functional diagram for Computer No. 1 with constant factors $(CF)_1$, $(CF)_2$ and $(CF)_3$ undetermined.

* Knowledge of the limitations of the particular analog computer as regards range of coefficient settings and computer solution time is essential in order to scale a problem intelligently.

The values of the constant factors may be chosen by considering each loop in turn, using as a guide the magnitude of the coefficients so that they will become neither excessively large nor small. This may best be accomplished by making the direct-path coefficient setting numerically equal to the corresponding feedback-path coefficient setting. As applied to the motor loop, this means making

$$\frac{0.54}{(CF)_3} = 0.74\,(CF)_3 \tag{40}$$

whence

$$(CF)_3 = 0.853 \ldots \text{say } 1.0 \tag{41}$$

For the next outer loop, the same procedure shows that

$$\frac{50}{(CF)_2} = 0.06\,(CF)_2 \tag{42}$$

whence

$$(CF)_2 = 28.9 \ldots \text{say } 30 \tag{43}$$

Similarly, for the outer loop,

$$\frac{30}{(CF)_1} = 0.1\,(CF)_1 \tag{44}$$

whence

$$(CF)_1 = 17.3 \ldots \text{say } 20 \tag{45}$$

In terms of these values, the coefficient settings become those shown in the functional diagram of Fig. s. These values are reasonable and hence the scaling is satisfactory insofar as coefficient values are concerned.

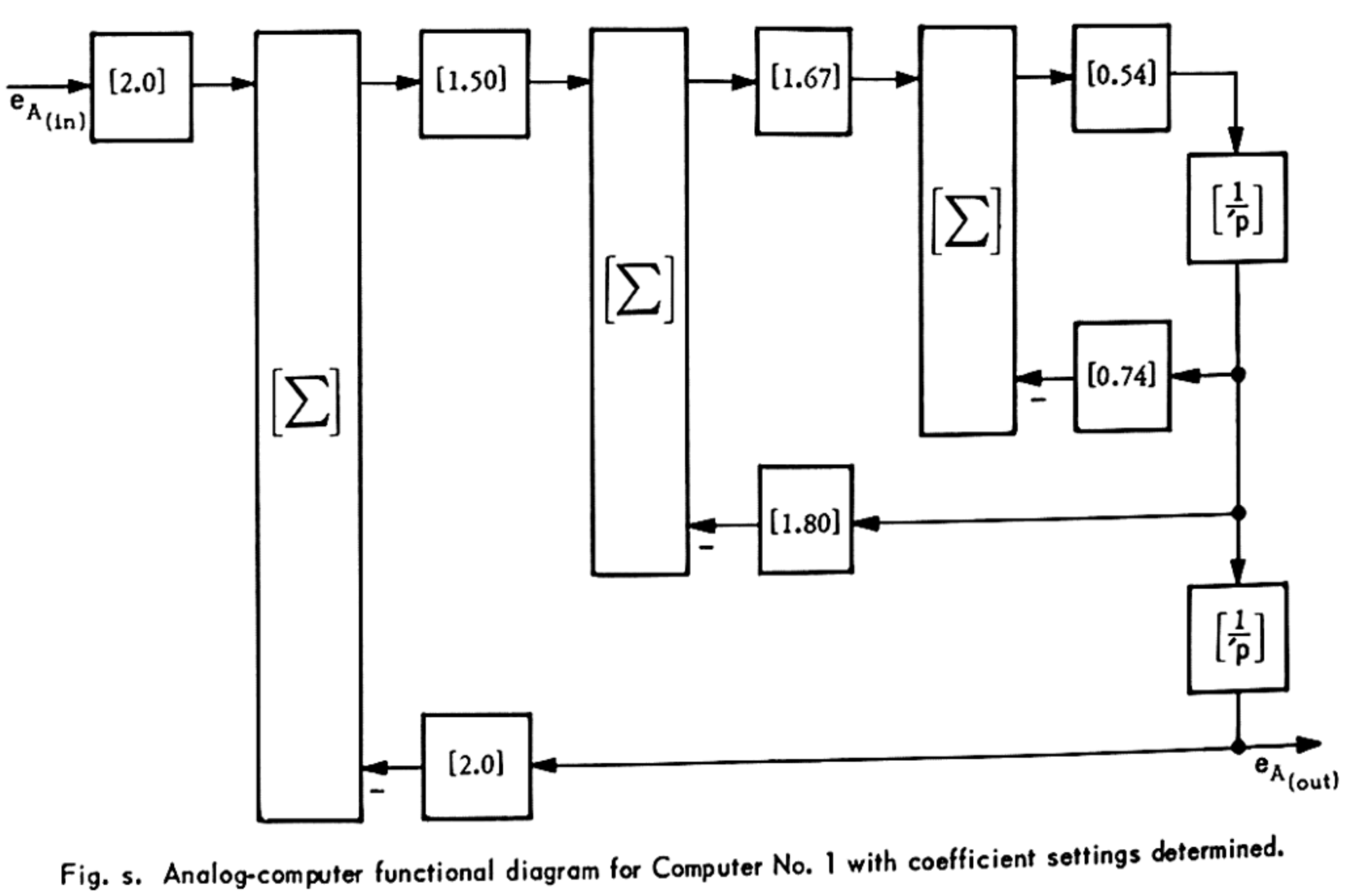


Fig. s. Analog-computer functional diagram for Computer No. 1 with coefficient settings determined.

Derivation Summary 34-27. Component analysis and performance equation of a typical positional servo system; derivation of the corresponding analog-computer equation and the equivalent analog-computer arrangement; determination of the coefficient settings. (Page 18 of 20)

COMPUTER NO. 2

For Computer No. 2,

$$RC = 0.0004 \text{ second} \tag{46}$$

Following the same procedure as for Computer No. 1, assume a solution time of 0.004 second. Then

$$STR = \frac{0.004}{0.04} = 0.1 \tag{47}$$

and

$$T_{(ref)} = 0.004 \text{ second} \tag{48}$$

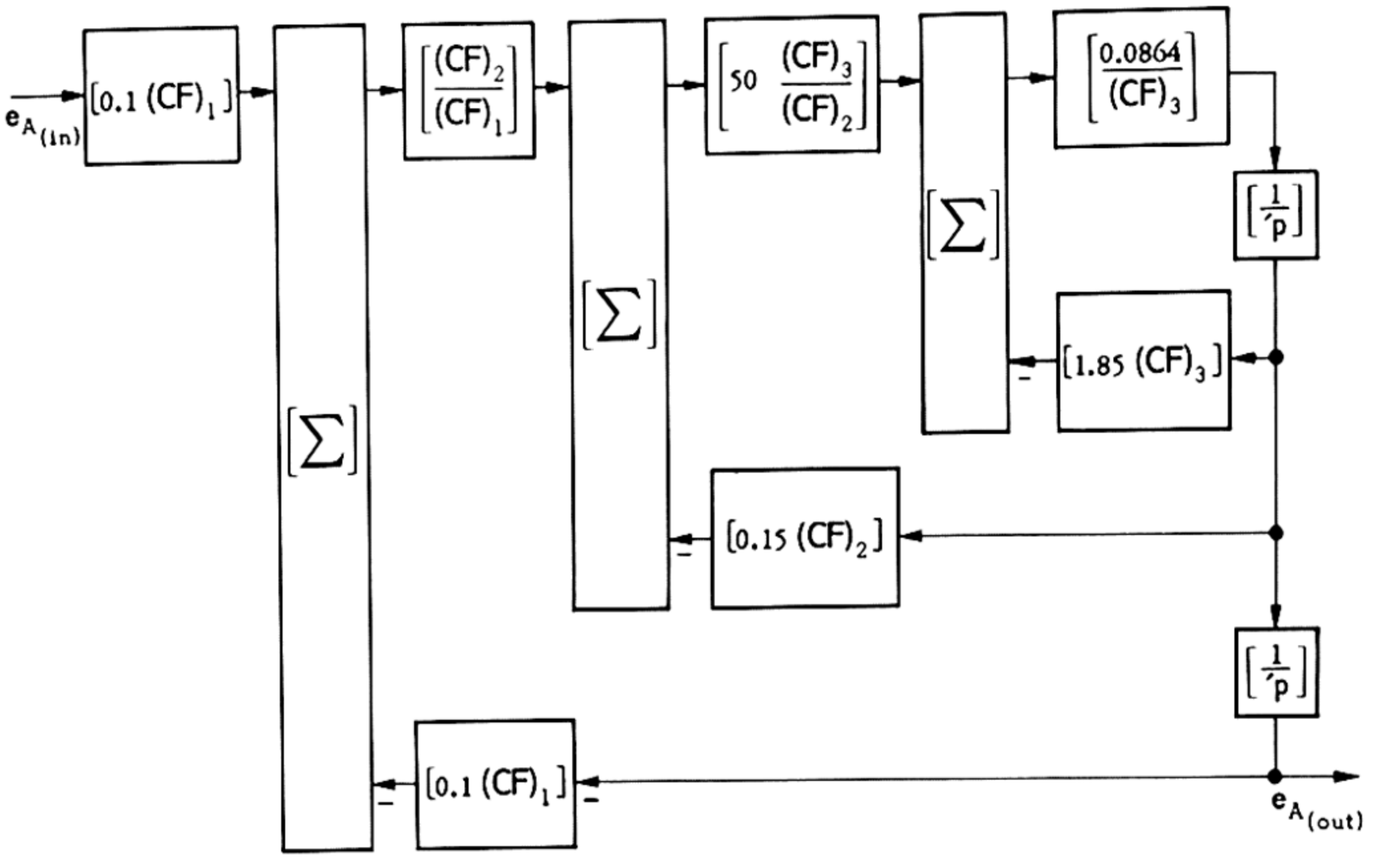


Fig. t. Analog-computer functional diagram for Computer No. 2 with constant factors $(CF)_1$, $(CF)_2$ and $(CF)_3$ undetermined.

$$\frac{0.0864}{(CF)_3} = 1.85\ (CF)_3 \tag{49}$$

$$(CF)_3 = 0.216 \ldots \text{ say } 0.2 \tag{50}$$

$$\frac{50 \times 0.2}{(CF)_2} = 0.15\ (CF)_2 \tag{51}$$

$$(CF)_2 = 8.16 \ldots \text{ say } 10 \tag{52}$$

$$\frac{10}{(CF)_1} = 0.1\ (CF)_1 \tag{53}$$

$$(CF)_1 = 10 \tag{54}$$

Derivation Summary 34-27. Component analysis and performance equation of a typical positional servo system; derivation of the corresponding analog-computer equation and the equivalent analog-computer arrangement; determination of the coefficient settings. (Page 19 of 20)

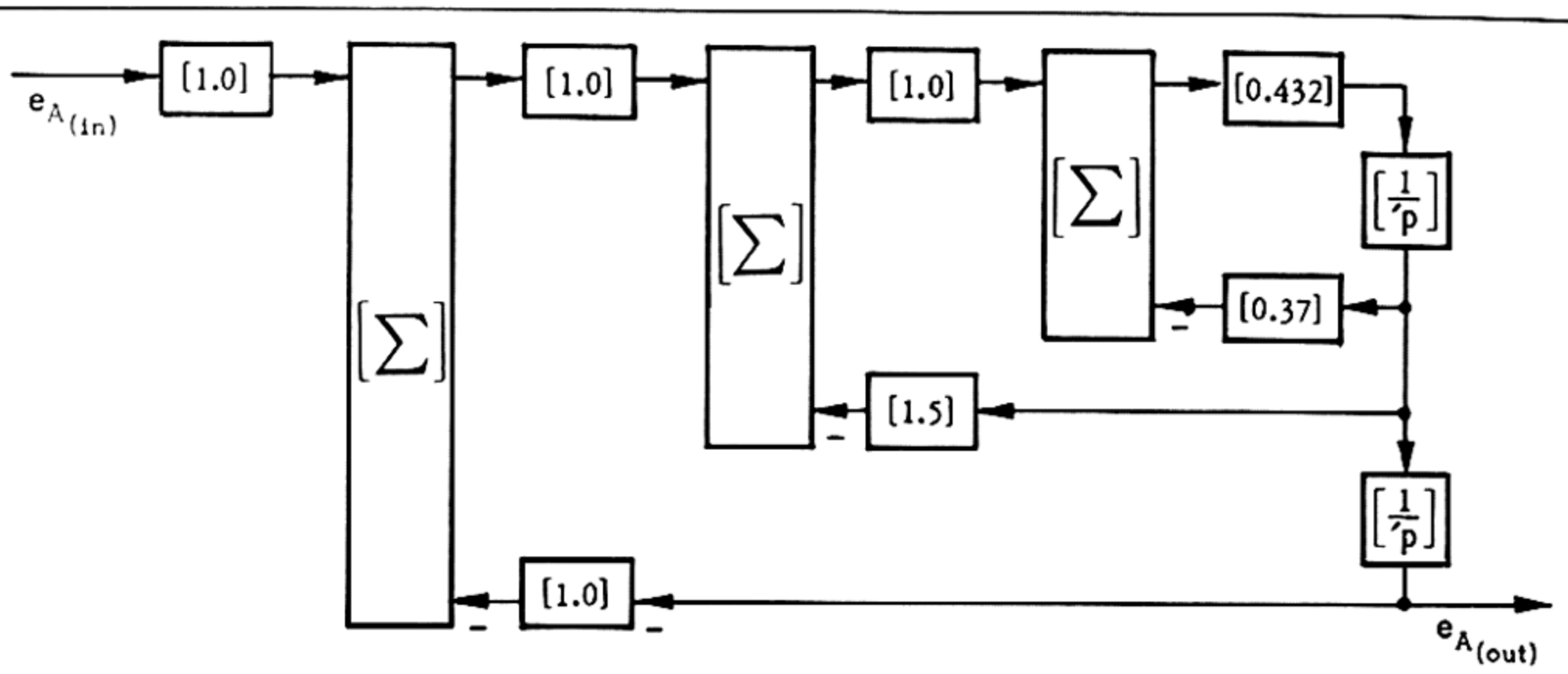


Fig. u. Analog-computer functional diagram for Computer No. 2 with coefficient settings determined.

Here again the coefficients are well within reasonable values, and hence the scaling can be considered to be satisfactory.

Had the coefficient values obtained for Computers No. 1 and No. 2 turned out to be more widely spaced numerically, there would be two possible reasons for this:

1) The value for $T_{(ref)}$ was not favorably chosen. This involves both the characteristics of the computer and the solution time of the physical problem under study.
2) If the coefficient settings cannot be brought within working range by employing the full capabilities of the computer, then the part of the block diagram having the numerically small coefficient setting probably represents an unimportant part of the system and may be safely neglected.

e) *Determination of coefficient settings for two different types of analog computers used to represent the positional servo system*

Derivation Summary 34-27. Component analysis and performance equation of a typical positional servo system; derivation of the corresponding analog-computer equation and the equivalent analog-computer arrangement; determination of the coefficient settings. (Page 20 of 20)

be a second-order equation of the (0;0,1,2) type, the solutions of which are worked out in Chapter 19. The second-order-term coefficient stems from the inertia of the output shaft. The first-order, or damping, terms come from two separate sources. One is due to the back electromotive force generated by the motor; the other results from the action of the tachometer coupled to the motor shaft. The zero-order, or restoring torque, term originates in the development of a torque proportional to the difference in angular positions of input and output shaft positions and involves the signal generators, amplifier and stall-torque-per-volt characteristics of the motor.

34.152. Given the system block diagram, the equation of motion may also be arrived at from the standpoint of feedback-loop algebra. In Figs. d through g, the three feedback paths are successively eliminated by the repeated process of replacing the innermost loop by its equivalent single block. This leads to consolidation of the system into a single block, the performance function of which represents in operational form the ratio of system output to system input.

34.153. However obtained, the differential equation is next transformed for computer scaling by introducing input and output scale factors and the dimensionless integrating operator, together with the computer-system time parameter $T_{(ref)}$. Following the pattern of section a, Derivation Summary 34-26, the computer block diagram given in Fig. h is obtained. This diagram might be modified to eliminate one of the coefficient multipliers after the fashion of Derivation Summary 34-26. Whether or not this is done, it is apparent that each of the coefficient settings is dependent on more than one of the system coefficients and, further, each system coefficient appears in more than one coefficient-multiplier setting. This means that a computer study in which it is desired to determine the effect of changing one system variable is more complicated than it need be. A better arrangement for this purpose would be one in which each coefficient multiplier controls only one system coefficient. This suggests a computer arrangement like the system block diagram itself. In Figs. i through n, the minimum-component second-order block diagram of Fig. h is expanded step-by-step with the object of leaving only one system parameter within any coefficient-multiplier setting. This procedure is guided by making the various diagram changes in a manner such as to collect into separate parts of the diagram the individual physical elements of the system. Inevitably, additional coefficient multipliers and summers are required in order to achieve this conformance of computer arrangement to system arrangement. It is a worthwhile complication, however, since the expanded arrangement focuses principal attention on the physical system and its components rather than on the defining differential equation.

34.154. The coefficient multipliers in any loop can be modified by multiplication or division of the coefficient settings by a constant factor in such a way that there will be no change in loop input and output. This is shown in Figs. o and p. Such a procedure is useful to modify the numerical values of the coefficient settings. In the positional servo system under examination, three such constant factors may be used, one for each loop. Mathematically, this corresponds to multiplying each of three simultaneous equations by a different constant factor. This adds the last possible freedom of choice in scaling the problem for analog-computer solution. Recapitulating, then, the factors that govern the coefficient-multiplier settings for a physical problem are the values of the physical constants of the system, the input and output scale factors, the reference time, $T_{(ref)}$, and the constant factors. It should be unnecessary to note that the units chosen in assigning numerical values to the physical system coefficients must be dimensionally consistent, unless the problem is so set up that every coefficient multiplier has associated with it a dimensionless quantity, in which case only the dimensions of the quantities comprising each unit need be consistent.

34.155. With this background, the problem at hand can now be scaled. This

is done in section e of Derivation Summary 34-27 for two different computers, referred to as Computer No. 1 and Computer No. 2, whose solution times differ by a factor of a thousand. For each computer it is necessary to select scale factors and $T_{(ref)}$ with regard to the voltage levels that are developed in various parts of the computer and the rate at which the solution is generated.

34.156. The choice of $T_{(ref)}$ may be made by examining the definition of this quantity; namely,

$$T_{(ref)} = \frac{RC}{STR} = (RC)\frac{(ST)_{(pp)}}{(ST)_{(ac)}}$$

In some computers, the value of RC is fixed in the design of the computer; if this is so, there will be no latitude available in its choice. An estimate can usually be made as to the magnitude of the system response time, that is, the physical-problem solution time, $(ST)_{(pp)}$. For instance, if the characteristic time of the slowest natural mode of the positional servo system can be approximated, then $(ST)_{(pp)}$ can be estimated to be say four times this interval. As for the analog-computer solution time, $(ST)_{(ac)}$, the value chosen will be governed by the drift of the integrator and by auxiliary considerations, such as the nature of the available input and how the output is to be displayed or recorded.

34.157. For Computer No. 1, RC is 1 second and $(ST)_{(ac)}$ will range from the order of a second to the order of a minute if best results are to be obtained. For the example of Derivation Summary 34-27, a value of $(ST)_{(ac)}$ equal to 4 seconds is chosen, which gives a value of $T_{(ref)}$ equal to 0.25 $(ST)_{(pp)}$. The minimum solution-time limit for a computer arrangement employing only integrators, coefficient multipliers and adders is established by the dynamic limitations of the direct-writing recorder used to record the output voltage. The dynamic capabilities of servo units used as multipliers of two variables or as function generators also limit the minimum time that may be used for a solution. For many problems, the type of computer represented by Computer No. 1 can be used as a real time computer for which, with an RC value of 1 second, $T_{(ref)}$ will be one second. The general arrangement of one computer of this type is shown in Fig. 34-32.

34.158. Computer No. 2 is normally used as a repetitive type of computer. This means that the computer solution time is made small, so as to permit a number of identical solutions to be repeated sufficiently rapidly to enable use of a continuous-appearing display on a cathode-ray oscilloscope, with the scope swept at the solution repetition rate. For such a computer, a typical value of RC is 0.0004 second and an associated value of $(ST)_{(ac)}$ of 0.004 second gives good results. This combination gives a value of $T_{(ref)}$ equal to 0.1 $(ST)_{(pp)}$. If $T_{(ref)}$ were to have this same value for Computer No. 1, this would mean a computer solution time of 10 seconds. The general arrangement of a computer of the repetitive type is shown in Fig. 34-33.

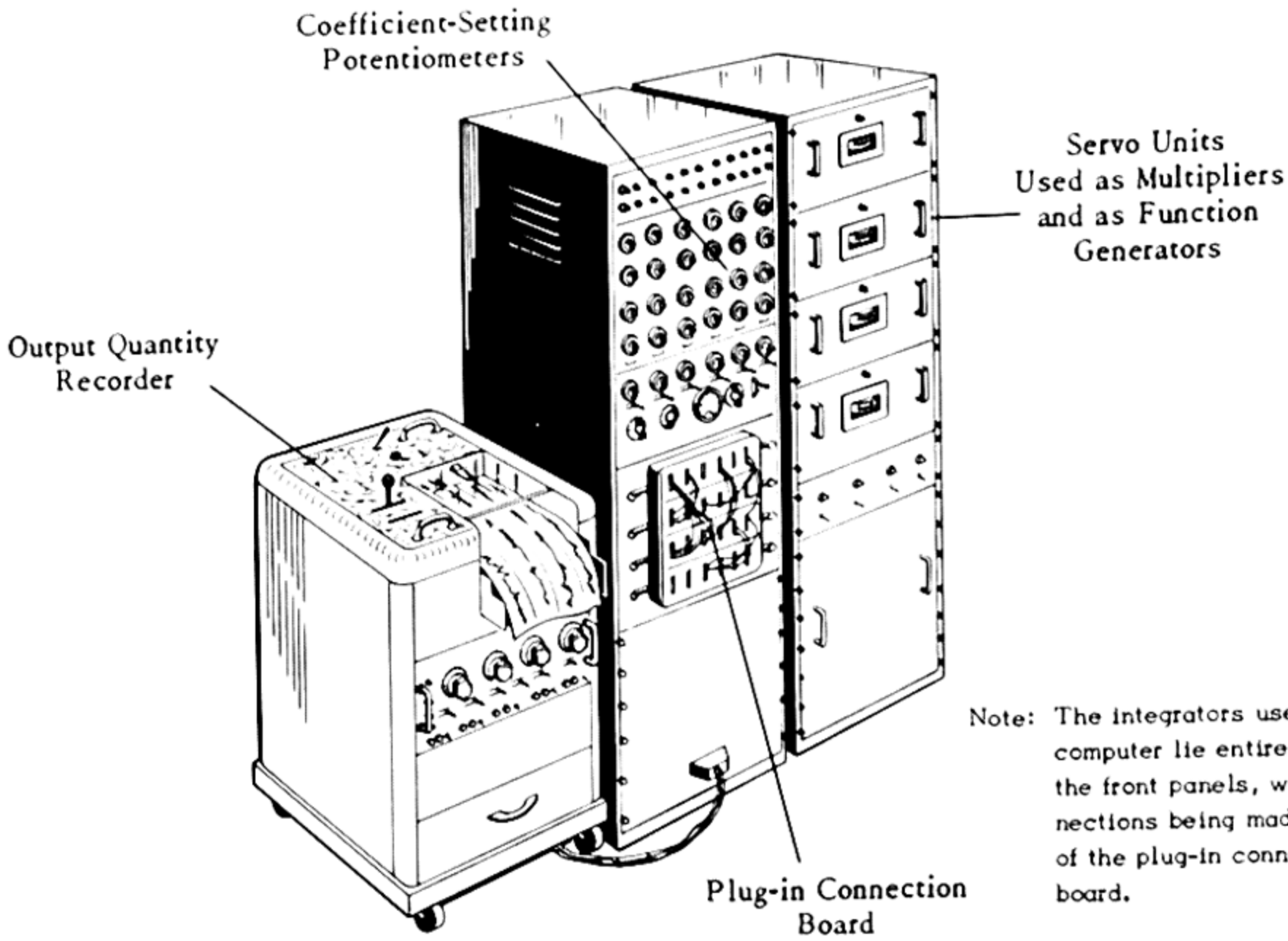


Fig. 34-32. General arrangement of Computer No. 1.

34.159. The determination of input and output scale factors is based on estimates of the maximum desired value of input and corresponding expected maximum output, taken together with the maximum voltage levels for which the computer is designed. In a system such as the positional servo system considered in Derivation Summary 34-27, the change in output shaft angular position must be of the same order as the change in the input shaft position, so that making input and output scale factors equal is logical in this instance. The choice of values for these scale factors should also be reconciled with the desirability of having the input signal be of a voltage level adequate to submerge unwanted responses to random noise.

34.160. Constant factors are chosen with a view to bringing the numerical values of the coefficient-multiplier settings into the desired ranges. This may be required for the entire computer arrangement or to just a part thereof. The constant factors may be selected in the manner shown in the numerical examples worked out in Derivation Summary 34-27. There, the constants are chosen such that the numerical values of the coefficient settings occurring in the summer output are approximately equal to the numerical values of the coefficient settings in the feedback paths to the same summers. This guarantees the best compromise between two coefficient settings widely divergent in magnitude.

34.161. Even though the procedure outlined in the preceding paragraphs and illustrated in section e of Derivation Summary 34-27 is followed, extreme values

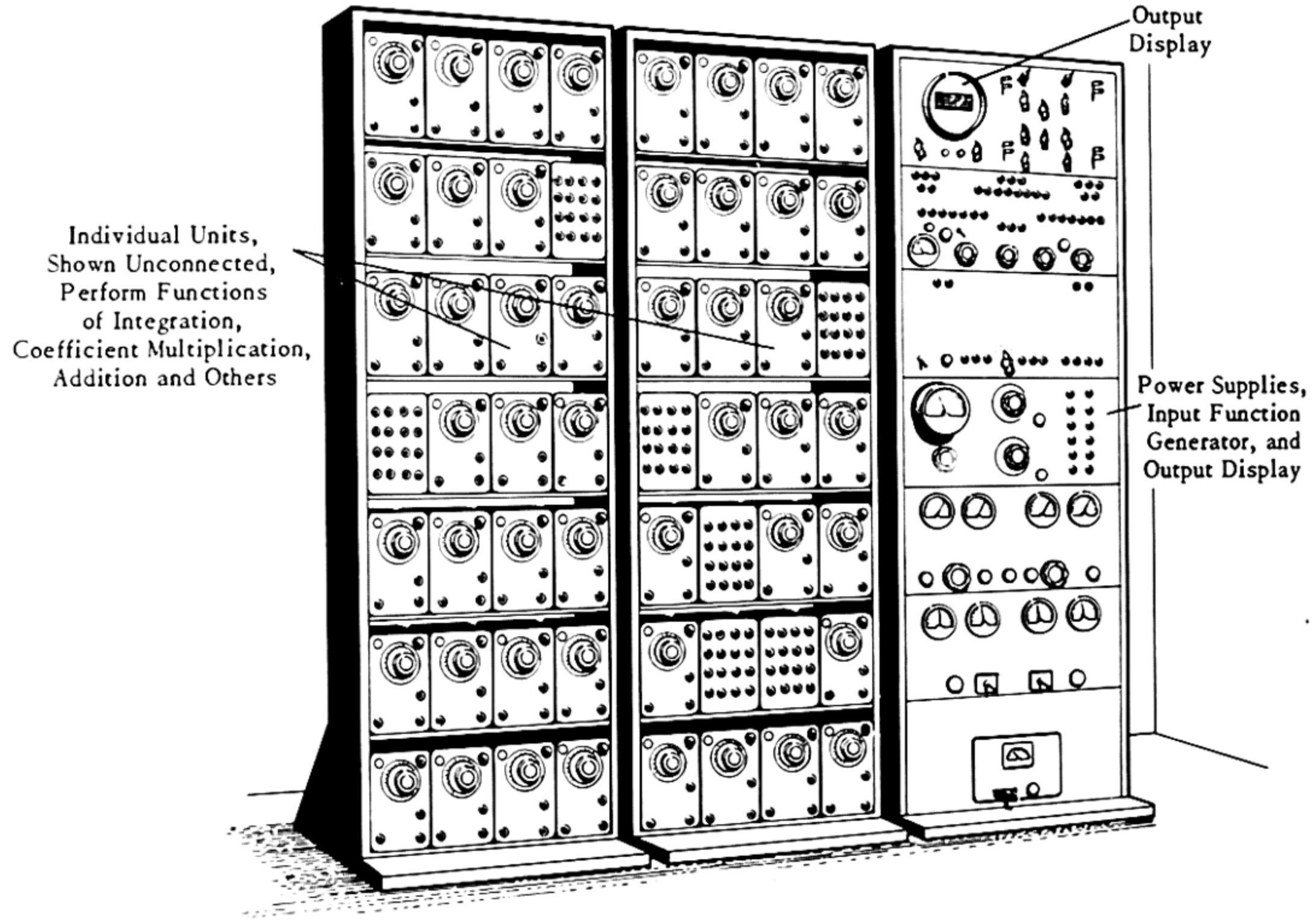


Fig. 34-33. General arrangement of Computer No. 2.

of coefficient settings may still be encountered. This is to be expected in high-gain loops where there is a wide variation in signal levels, and in systems having among its components dynamic elements that, relatively speaking, do not contribute significantly to the dynamic response and may in consequence be neglected.

34.162. The effect of $T_{(ref)}$ on the settings of the coefficient multipliers may be seen by comparing the setting values determined for Computer No. 1 and Computer No. 2. These values appear in the blocks of Figs. s and u of Derivation Summary 34-27. The only difference between the two sets of values stems from the difference in $T_{(ref)}$.

34.163. It should be noted that there are other ways of attacking the scaling problem than that presented here.* For example, if maximum values of the problem derivatives are known, this will serve to fix the value of $T_{(ref)}$.**

---

* A paper by Reswick (R10) presents an excellent treatment of the problem of analog-computer scaling.

** See Korn and Korn (K6) and MIT Servomechanisms Laboratory (M17) for information on this method.

CHAPTER 35

VIBRATION MEASUREMENT AND VIBRATION ISOLATION

Y. T. Li

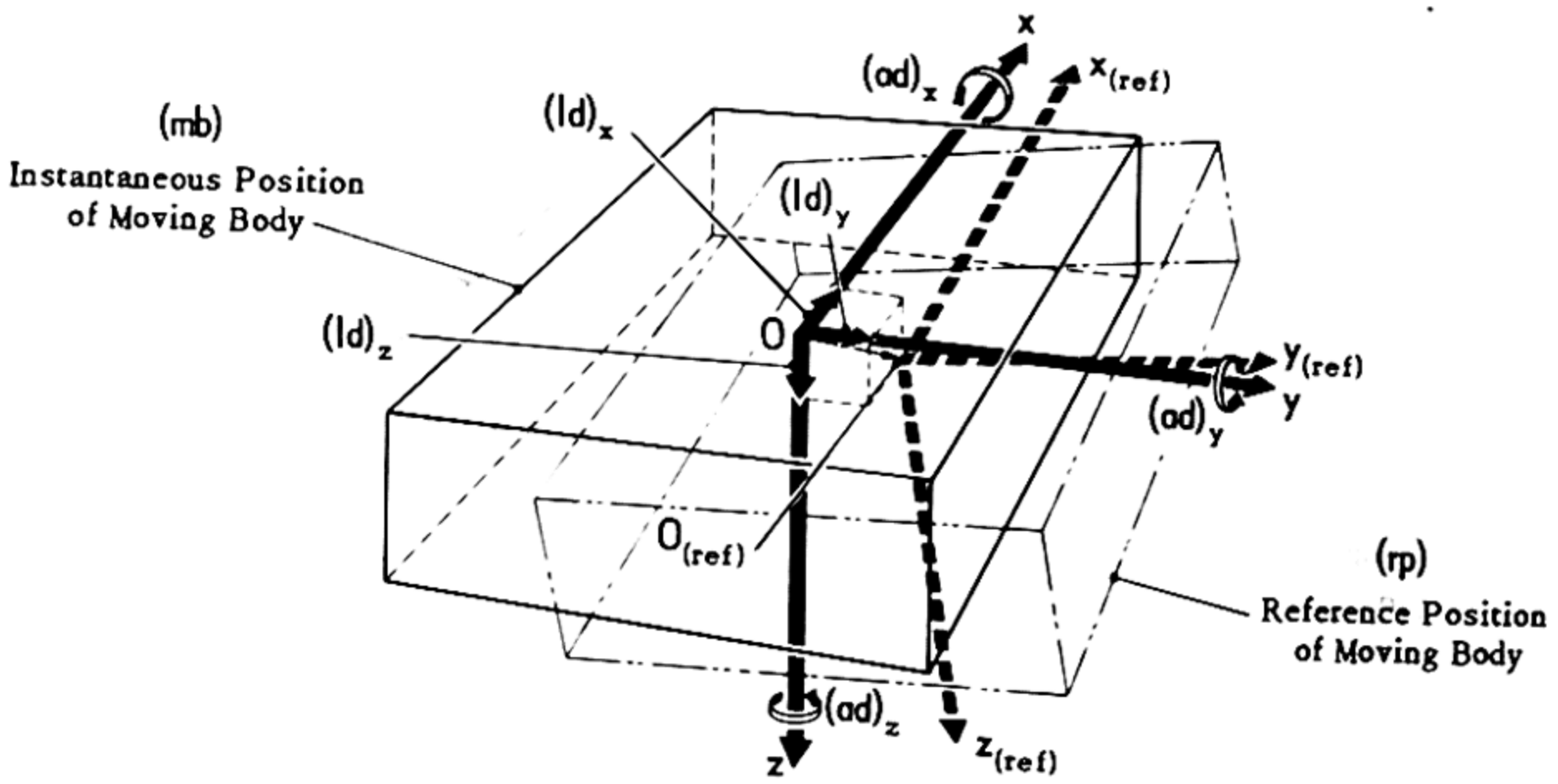
INTRODUCTION

35.1. Vibration is a term associated with cyclic changes of physical quantities with respect to specified reference conditions. The problem of vibration measurement is that of producing records or scale readings to represent the deviations that correspond to these cyclic changes. In particular, mechanical vibration is the cyclic displacement of a moving body with respect to some reference position. Measurements in this instance may be made by any device, or system of devices, capable of indicating instantaneous positions of the vibrating body with respect to some reference position of the body.

35.2. The most general problem of mechanical vibration involves six degrees of freedom – three translational components and three rotational components. An illustrative example of the generalized vibration problem is shown in Fig. 35-1, which represents a simple three-dimensional body that has been given a generalized displacement with respect to a reference position shown by dashed lines. In order to describe the displacement of the body from its reference position, a set of three mutually perpendicular axes is fixed to the body. Any arbitrary position of the body may be described in terms of coordinates along these axes, and a reference position of the axes that corresponds to their position when the body is in its reference position, with no vibratory motion present.

35.3. In terms of the coordinate system of Fig. 35-1, any mechanical vibration may be resolved into six components. Three of these components are linear and correspond to the displacement of the moving origin with respect to the reference origin, taken as projections along the x, y, and z axes, respectively. The remaining three vibration components are angular displacements of the moving axis system with respect to the reference axis system, taken as rotations about the x, y, and z axes. At any instant, six independent numbers would be required to specify the position of the moving axes with respect to the reference axes. For this reason, the moving body shown in Fig. 35-1 is said to have six vibratory-motion degrees of freedom.

35.4. A body that is constrained so that its only motion with respect to a reference position is translation along a single axis or rotation about a single axis



x, y, z – axes fixed in moving body

$x_{(ref)}$, $y_{(ref)}$, $z_{(ref)}$ – reference axes; identical with x, y, z axes when moving body is in reference position

O – origin of x, y, z axes

$O_{(ref)}$ – reference origin; position of O when moving body is in the reference position

$(ld)_x$, $(ld)_y$, $(ld)_z$ – linear displacements of O with respect to $O_{(ref)}$, measured along x, y, z axes, respectively

$(od)_x$, $(od)_y$, $(od)_z$ – angular displacements of x, y, z axes with respect to $x_{(ref)}$, $y_{(ref)}$, $z_{(ref)}$ axes, measured about the x, y, z axes, respectively

Fig. 35-1. Generalized six-degree-of-freedom displacement of a moving body with respect to a reference position of the body.

is said to have a single degree of freedom. In practical engineering problems, vibrating bodies often have several degrees of freedom, while the instruments used to indicate or measure the motion usually operate as single-degree-of freedom devices. This means that the vibration-receiving element responds to linear motion along a single axis or rotation about a single axis, but disregards all other vibration components. Vibration-measuring equipment is almost universally based on combinations of subsystems, each made up of a single-degree-of-freedom receiver associated with suitable coupling and recording units that are generally similar to those used in pressure-measuring systems. From the standpoint of engineering practice, a clear understanding of the theory of single-degree-of-freedom instruments is generally sufficient for handling vibration measurement problems of all types. This theory is developed in the following sections, and the generalized results are summarized in nondimensional terms.

THE GENERALIZED PROBLEM OF SINGLE-DEGREE-OF-FREEDOM VIBRATION MEASUREMENTS

35.5. The situations associated with vibration measurements always involve three elements:

1) A vibrating member.
2) A reference member.
3) A device for measuring the motion of the vibrating member with respect to the reference member.

When single-degree-of-freedom measurements are made, it is sufficient for the reference member to be nonvibrating along a single axis or nonrotating about a single axis. The measuring device operates to produce records or scale readings proportional to the linear or angular motion of the vibrating member with respect to the reference member.

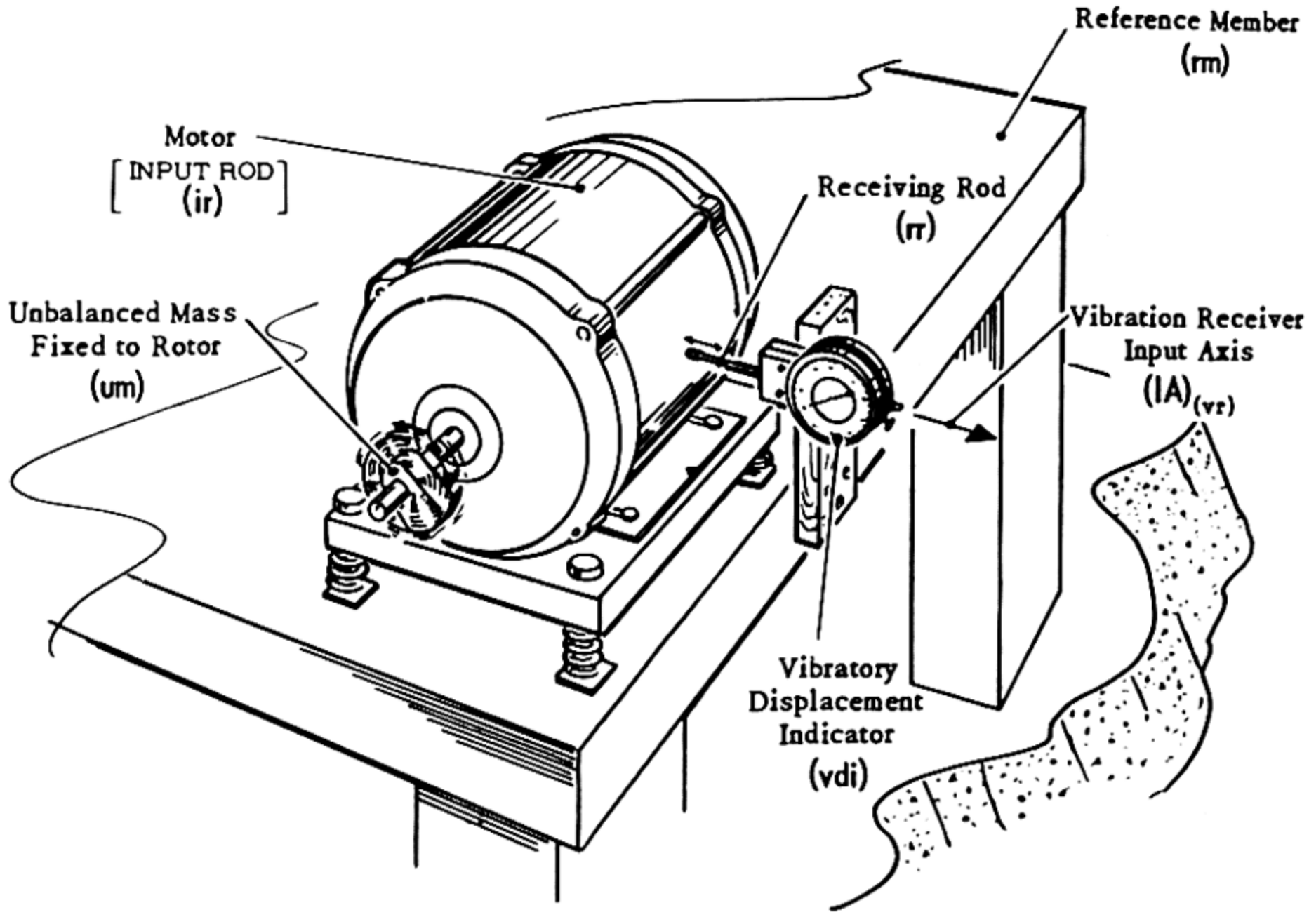
35.6. From the standpoint of instrument design, two typical situations exist:

1) A nonvibrating member suitable for use as the reference is available in the vicinity of the vibrating member.
2) No nonvibrating member suitable for reference purposes is available, so that a reference must be included within the vibration-measuring equipment itself.

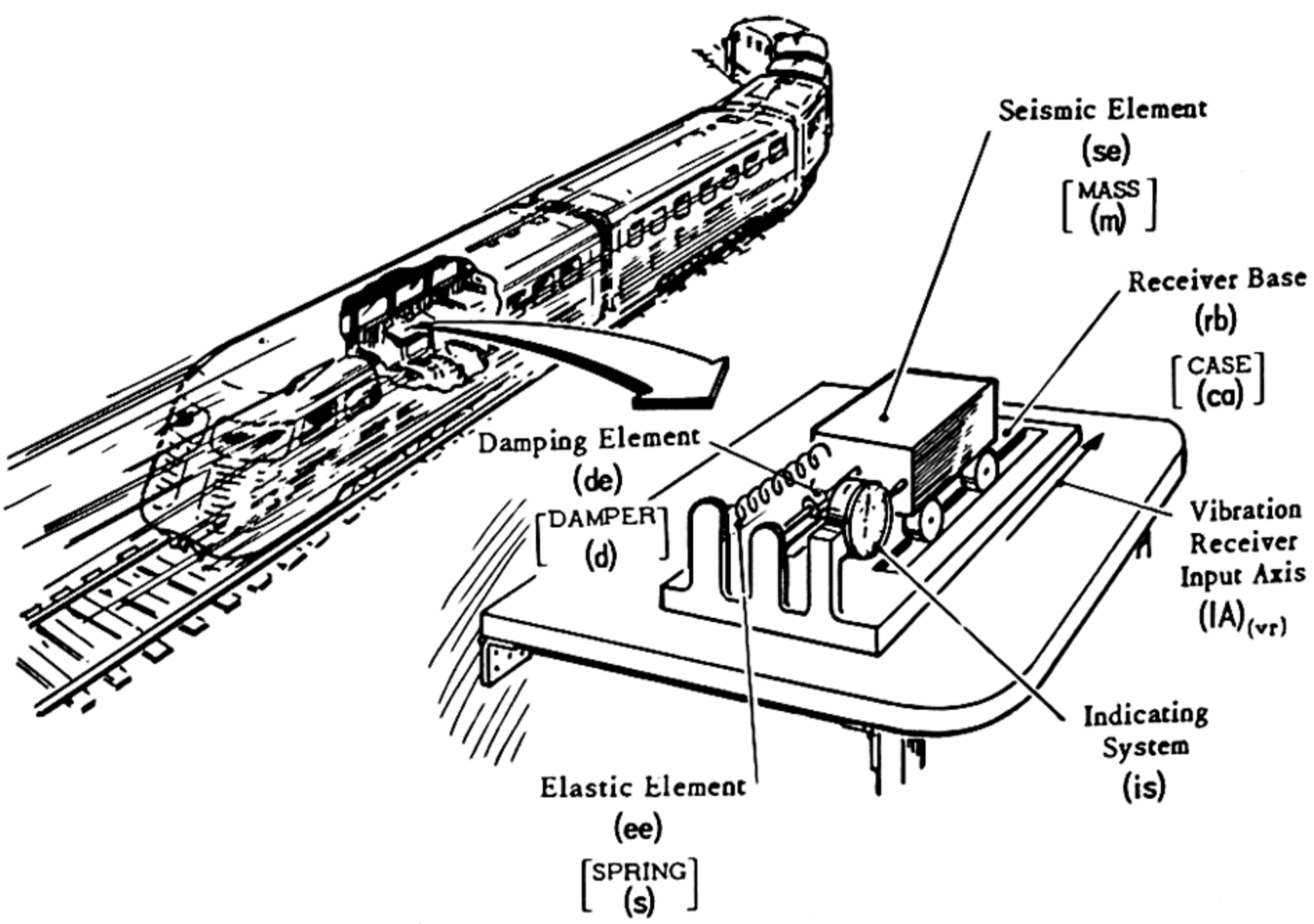
35.7. The first situation is illustrated in Fig. 35-2a, which represents an electric motor mounted on a heavy table by means of coil springs. An unbalanced mass attached to one end of the rotating motor shaft causes the motor frame to vibrate with respect to the table. A conventional dial gage rigidly fixed to the table has its receiving rod in contact with the side of the motor frame. This contact is maintained by using initial compression in the antibacklash spring within the dial gage. The movement of the dial gage index gives an indication of the component of linear vibration along the vibration receiver input axis, which is determined by the direction of dial gage operation.

35.8. Except for very slow vibratory motion, the dial gage arrangement of Fig. 35-2a is capable of indicating only the limits of displacement. A high-speed motion-picture camera might be used to photograph instantaneous dial-gage-index positions to provide pictures for plotting vibration displacement as a function of time. However, the common practice is to use an electrical signal-generating system and an oscillographic recording system to replace the dial gage.

35.9. When vibration is to be measured in environments that do not include available nonvibrating members, some internal component of the vibration receiver must provide the reference. A typical situation of this kind is illustrated by Fig. 35-2b, in which the fore-and-aft vibration of a parlor-car table on a moving train is to be indicated. Because no vibration-free member is available, the vibration receiver is shown as a self-contained "breadboard" unit with its base, which corresponds to the case of any practical unit, placed on the table. The reference is provided by a mass mounted on low-friction rollers that move along straight grooves cut into the base. In addition to this support, the mass is connected to the base by a spring and a damper. The spring and damper used are so weak that they are unable to force the mass to follow the vibratory motion of the base. At the same time, the spring is strong enough to keep the mass moving with the train, so that it remains near its centered position on the base. Under these circumstances, a dial gage indicator rigidly mounted on the base with its receiving rod in



a) Vibratory displacement measurement when an external reference member is available



b) Vibratory displacement measurement when an external reference member is not available

Fig. 35-2. Essential features of the vibration measurement problem.

contact with the mass as the reference member will indicate vibratory displacements of the base along the input axis. With the base on the table and with the input axis parallel to the longitudinal centerline of the car, the dial gage indications will show vibration of the table in this direction.

THE SEISMOGRAPHIC SYSTEM

35.10. Arrangements similar to that shown in Fig. 35-2b are commonly used to indicate disturbances in the Earth's crust, and for this reason are called seismographs.* The essential function in devices of this kind is provided by the combination of a mass free to move in a straight line with respect to a support, except for the restraining effects of an elastic element and a damping element. This combination of elements is called a seismographic system. Seismographic systems are universally used in vibration receivers for situations in which nonvibrating references are not available and, for the purposes of convenience, are often applied even when references that might be used are actually present.

35.11. The three illustrative pictorial diagrams of Fig. 35-3 show the essential features of seismographic systems designed to give direct indications of vibratory acceleration, vibratory velocity, and vibratory displacement, respectively. In each of the diagrams, the seismic element (the mass of the seismographic system) is free to move in a straight line with respect to a base that is shown as serving the function of the case** in an actual vibration receiver. The base is carried by rollers that permit it to move with a single degree of freedom over a platform that is assumed to be unaccelerated with respect to inertial space.

35.12. In seismographic system operation, three linear displacement components are important. Scale and index combinations marked with plus and minus conventions are shown in Fig. 35-3 to illustrate the relationships among these displacements and the parts of the seismographic system. The displacements are:

1) The displacement of the case with respect to inertial space, which is the input motion or the forcing motion for the seismographic system. Under the conventions of Fig. 9-1a of Chapter 9, the symbol for the displacement has x (for displacement) as its main letter, with I (for inertial space) in the reference-space subscript position, and ca (for case) in the located-point position.
2) The displacement of the seismic element with respect to inertial space. The symbol for this displacement is similar to that for the case displacement except that se (for seismic element) is substituted for ca in the located-point subscript position.

---

* The combining form *seismo* comes from the Greek *seismos*, meaning earthquake.

** The case of any instrument or instrument component encloses the mechanism more or less completely and, in addition, serves as the structure supporting the instrument during operation.

3) The displacement of the seismic element with respect to the case, which is the quantity available as the output of the seismographic system and for this reason is called the response motion or the relative motion. The symbol for this displacement has x for its main letter and a subscript with ca (for case) in the reference position and se (for seismic element) in the located-point position.

SEISMOGRAPHIC SYSTEM OPERATION IN THE ACCELEROMETER RANGE

35.13. Figure 35-3a shows a relatively heavy spring connecting the seismic element to the case. This spring is so strong that the seismic element follows movements of the case along the seismographic system input axis very closely. From the standpoint of relating this physical action with the theoretical background given in Volume II, this means that the seismographic system has a high undamped natural frequency.* The small but essential relative motion is a measure of the spring deflection necessary to provide the force for accelerating the seismic element so that it "stays with" the case. Under these conditions, displacements of the seismic element index with respect to the relative motion scale give instantaneous indications of the case acceleration. For this reason, a seismographic system with a "heavy spring" is said to be operating in the accelerometer range.

35.14. In practice, any seismographic system must include some damping in order to reduce transient effects that may be excited by sudden changes in the motion of the case. However, the essential performance feature of a seismographic system working in the accelerometer range is that displacements of the seismic element with respect to the case are proportional to the acceleration of the case with respect to inertial space.

SEISMOGRAPHIC SYSTEM OPERATION IN THE VELOCIMETER RANGE

35.15. When the force acting on the seismic element to make it move with the case of a seismographic system is proportional to the relative velocity, the relative displacement is proportional to the velocity of the case with respect to inertial space. Figure 35-3b illustrates a system of this kind, with the force on the seismic element provided by a strong viscous damper in which a fluid is forced from one side of a piston to the other side of the piston through a properly designed constriction. The position of the seismic element index with respect to the relative motion scale indicates the instantaneous vibratory velocity of the case. The seismographic system with this characteristic is said to be operating in the velocimeter range.

---

* See Definition Summary 19-1 and Table 19-1 of Chapter 19 for definitions of the undamped natural frequency in terms of differential equation coefficients and parameters associated with the linear second-order differential equation with constant coefficients.

SEISMOGRAPHIC SYSTEM OPERATION IN THE VIBROMETER RANGE

35.16. When the elastic element of a seismographic system is made weak enough, it is only able to keep the seismic element near the average position of the case without forcing it to have any vibratory motion with respect to inertial space. This means that the seismic element becomes a substantially ideal vibration-free reference, and index positions on the relative motion scale are direct indications of vibratory displacements of the case with respect to inertial space. A seismographic system with this performance characteristic is said to be operating in the displacement meter range. This operating range is also called the vibrometer range. Figure 35-3c shows the essential features of a seismographic system operating in the displacement meter range. As in the case of operation in the accelerometer range, some damping must be included in order to reduce transient effects.

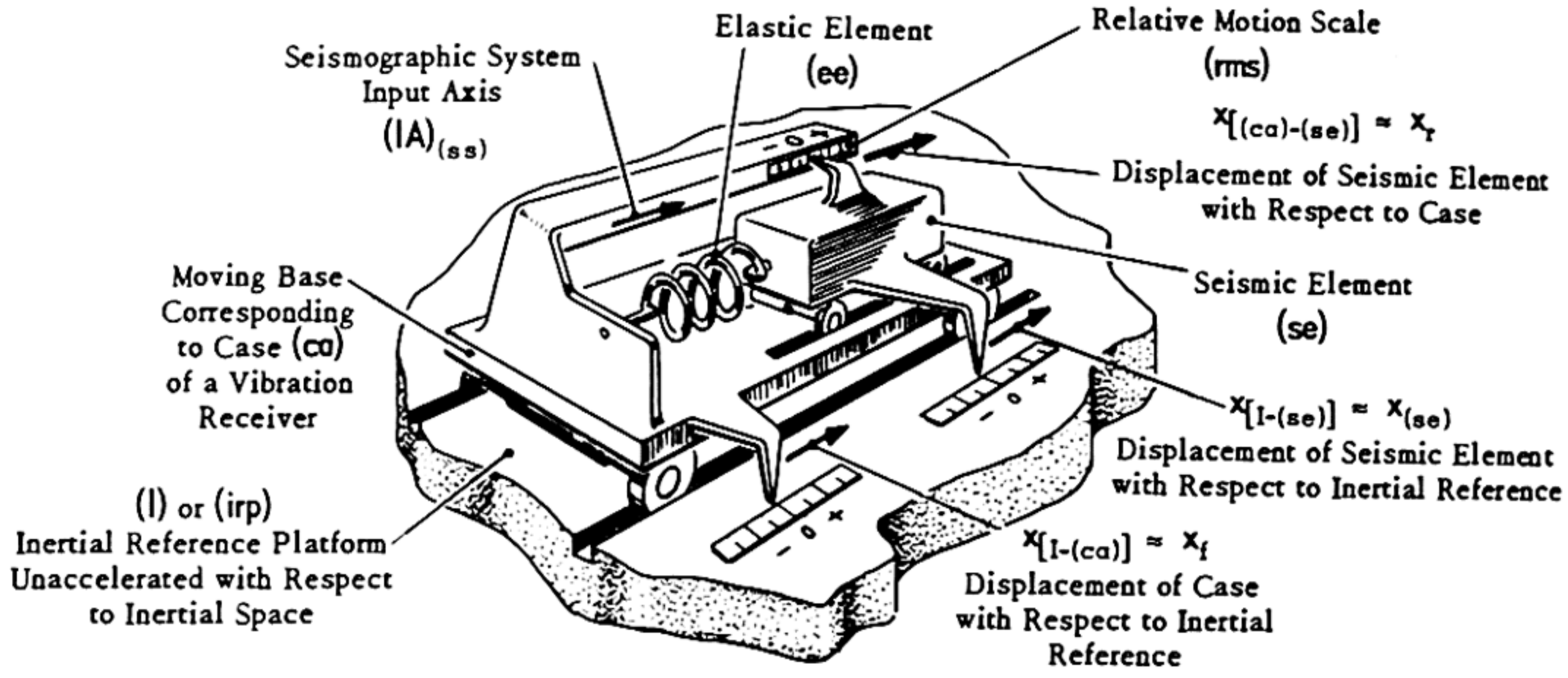
VIBRATION RECEIVERS

35.17. Vibration receivers are devices that respond to vibration inputs and produce outputs that represent these inputs. Output quantities are chosen for their suitability for transferring vibration signals to coupling components or indicating systems. The output quantities are usually mechanical or electrical, but may be optical, hydraulic or pneumatic, or may take any other form required for special purposes.

35.18. Vibration receivers or vibration pickups, as they are often called, may be divided into two classes, depending on whether a nonvibrating reference external to the receiver is used or a seismographic system is incorporated as part of the receiver. Figures 35-4a, b, c and d illustrate the essential features of receivers that belong to the first class. Figures 35-4e, f and g show examples of the arrangements used for receivers of the second class. Since the vibration-receiving function of receivers in the first class depends on the relative motion between the vibrating member and some external reference member, such receivers are called external-reference vibration receivers. Receivers of the second class, which are independent of an external reference member, are called self-contained vibration receivers.

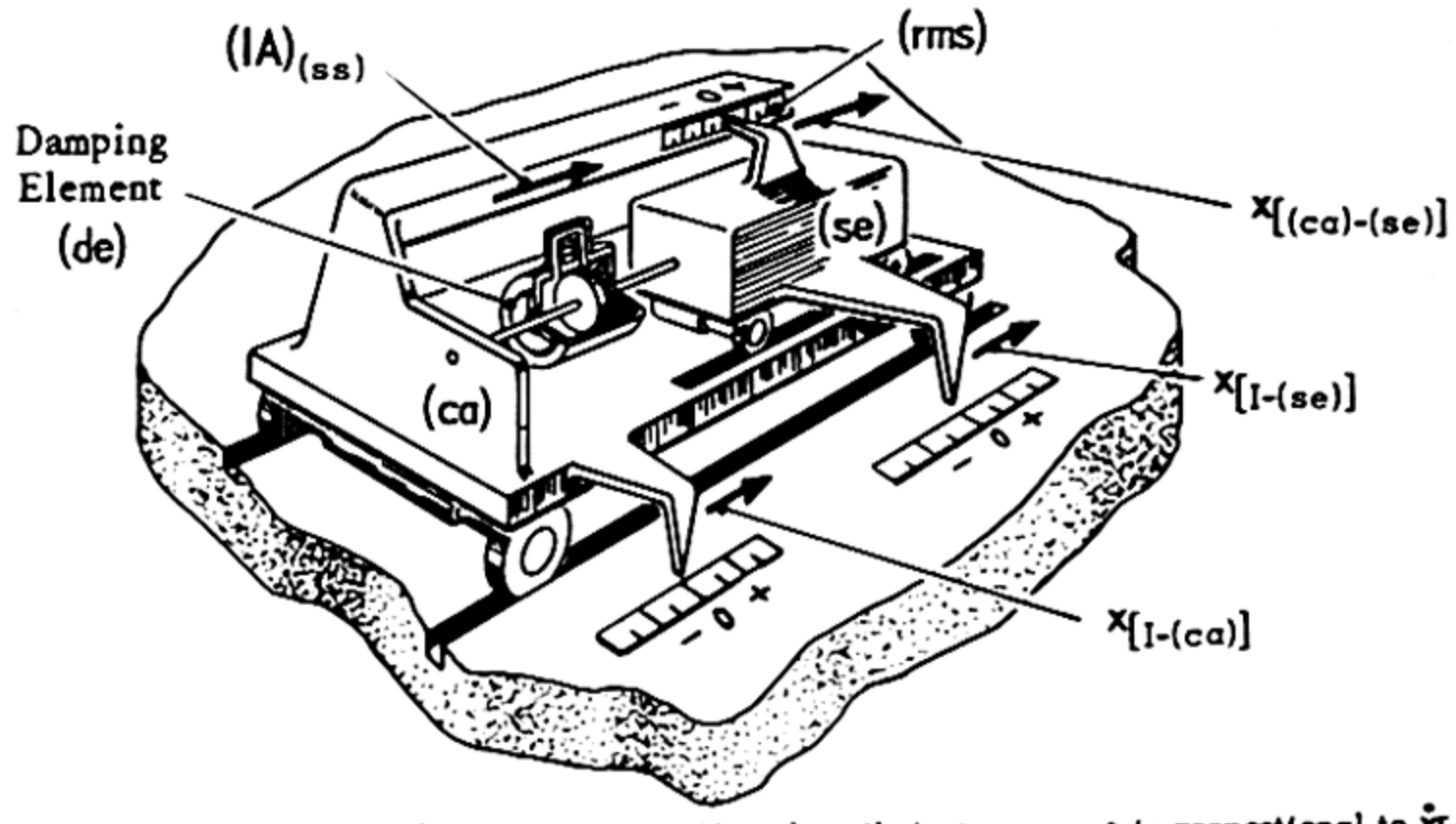
EXTERNAL-REFERENCE VIBRATION RECEIVERS

35.19. The simplest type of external-reference vibration receiver is a scale-and-index combination, such as that shown in Fig. 35-4a, with the scale on the reference and the index on the vibrating member. If the scale is calibrated in terms of the input displacement, that is, if appropriate numbers are associated with the scale markings (see Definition Summary 29-2), a simple vibration-measuring instrument is obtained. When the vibratory motion is very slow, it is possible for a human observer to determine both the amplitude of vibration and



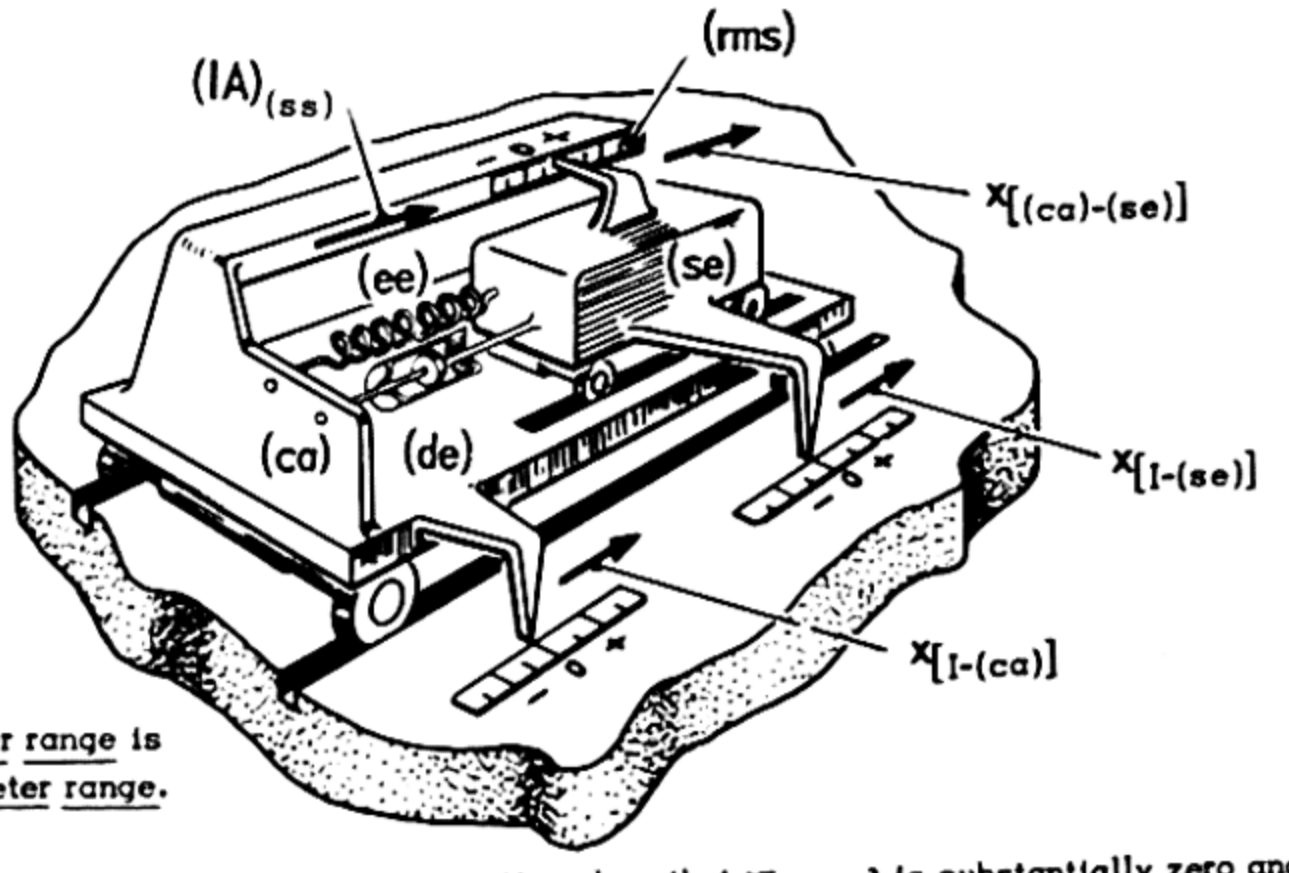
Note: The elastic element is so strong that $x_{[(ca)-(se)]}$ is proportional to $\ddot{x}_{[I-(ca)]}$ within the operating range of the instrument.

a) Essential features of a seismographic system operating in the accelerometer range



Note: The viscous damper and the seismic element are proportioned so that $x_{[(ca)-(se)]}$ is proportional to $\dot{x}_{[I-(ca)]}$ within the operating range of the instrument.

b) Essential features of a seismographic system operating in the velocimeter range



Note: The displacement meter range is also called the vibrometer range.

Note: The elastic element and the seismic element are proportioned so that $x_{[I-(se)]}$ is substantially zero and $x_{[(ca)-(se)]}$ is substantially equal to $-x_{[I-(ca)]}$ within the operating range of the instrument.

c) Essential features of a seismographic system operating in the displacement meter range

Fig. 35-3. Essential features of single-degree-of-freedom seismographic systems for receiving vibration.

the instant at which any given displacement occurs. As the vibration frequency increases, human senses are no longer able to spot instantaneous index positions, and can only estimate the displacement limits by means of the blur caused by the pointer oscillation. The combination of a stroboscopic light source with the scale and pointer of Fig. 35-4a is shown in Fig. 35-4b. The short-duration flashes of the stroboscopic light on the index may be controlled to occur at a definite point in each vibration cycle, so that the persistence of human vision causes the index to appear as stationary at these points. When the vibratory motion is truly a steady-state condition, the flashes may be independently timed to the cycle frequency. Slow variations of the flashing frequency from the vibration frequency cause the index image to move over the range of vibratory displacement. When the vibration is not a steady-state condition, the index position observations may be associated with the vibration by means of a timing arrangement actuated by the vibrating member. This arrangement makes it possible to study the details of complex vibratory motion by the use of relatively simple equipment.

35.20. When the vibratory displacements to be examined have such small magnitudes that acceptable accuracy by direct observation is impractical, mechanical magnification by some device such as the dial gage shown in Fig. 35-4c may be used. The only advantage gained from an arrangement of this type is expanded indication. Total displacement limits will appear as the boundaries of a blur when ordinary illumination is used. Stroboscopic light may be used to study displacement-time relationships, but a high-frequency limit will certainly be imposed by the action of the dial gage mechanism. This limitation may be made less severe by replacing the mechanical system by an optical system. However, when continuous records of vibratory motion are desired, the methods suggested in Figs. 35-4a, b and c will often be unsatisfactory.

35.21. When continuous records of vibration are required, it is desirable to design the receiver so that it will produce an electrical signal suitable for operating the various types of commonly available electrical recording equipment. Figure 35-4d, which shows a spring-loaded cord attached to the vibrating member and wrapped around a drum fixed to the input shaft of a potentiometer, represents a simple approach to this problem. The ends of the potentiometer winding, which has its mid-point grounded, are electrically connected to a source of excitation voltage. The output voltage is taken between ground and the slider of the potentiometer, which rotates over the winding as the vibrating member moves back and forth along the input axis. The output voltage may be used as the input for any electrical recording system with the proper performance characteristics.

35.22. The electrical signal generating system of Fig. 35-4d will cease to work properly when the vibratory motion becomes so rapid that the spring can no longer maintain tension in the cord. This means that the arrangement shown has

limited usefulness and must be replaced by other devices in high-performance vibration receivers. A number of these devices are illustrated in later figures of this chapter.

SELF-CONTAINED VIBRATION RECEIVERS

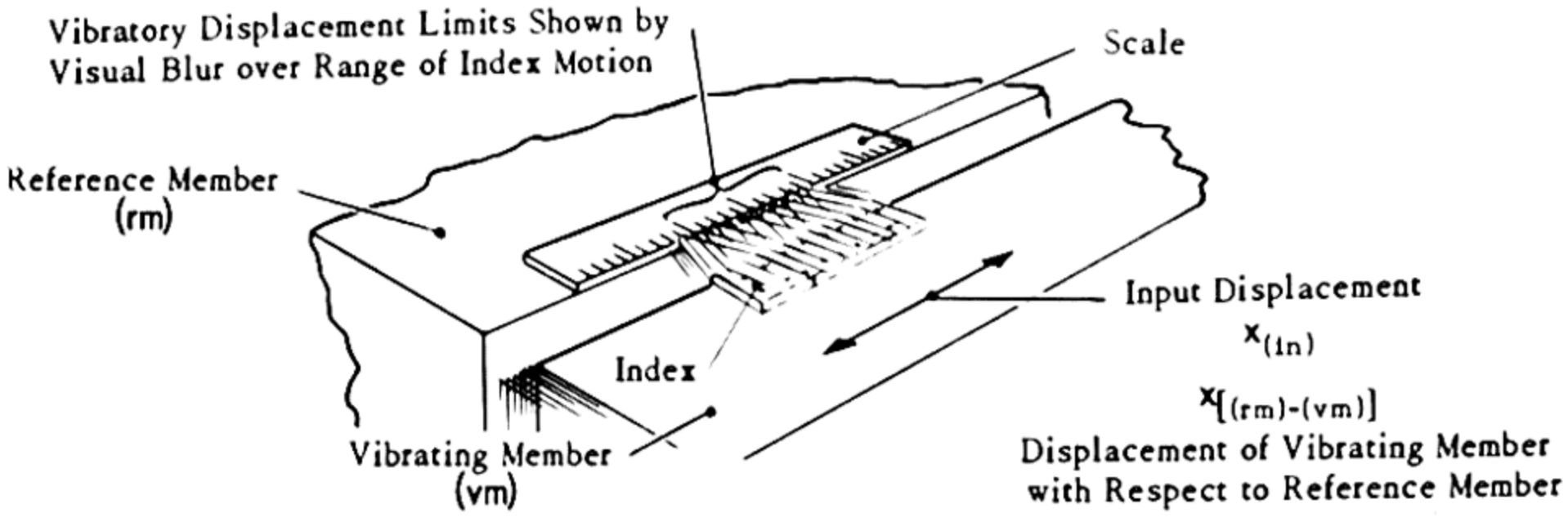
35.23. Self-contained vibration receivers have the vibration-indicating features illustrated in Figs. 35-4a, b, c and d and, in addition, include seismographic systems that provide the necessary references. Figure 35-4e illustrates a lightly damped vibration receiver with a direct-reading visual indicating system. The seismic element is a mass mounted on the free end of a cantilever spring whose other end is fixed to the case. The direction of freedom is parallel to the input axis of the receiver. When the vibrating member oscillates along the input axis with a frequency near the natural frequency of the spring-and-mass combination, the index attached to the mass moves with respect to the scale on the case. The limits of relative motion are indicated by the visual blur resulting from index motion.

35.24. Vibration receivers of the type illustrated in Fig. 35-4e are principally useful for identifying a given frequency component in the motion of a vibrating member. Instruments made up of a number of vibrating systems covering a range of natural frequencies will indicate the simultaneous presence of frequency components that match any of the individual natural frequencies. Another method for extending the range of frequencies covered by a given lightly damped vibration receiver is to provide means for varying the effective length of the cantilever spring. In operation, this length is changed until index displacement reaches a maximum. When this occurs, the corresponding frequency may be read from a calibrated scale associated with the spring length adjustment. Instruments of this type may be used to give approximate measurements of vibration amplitudes, but they are more generally useful for making surveys of the frequency components present in the motions of vibrating members.

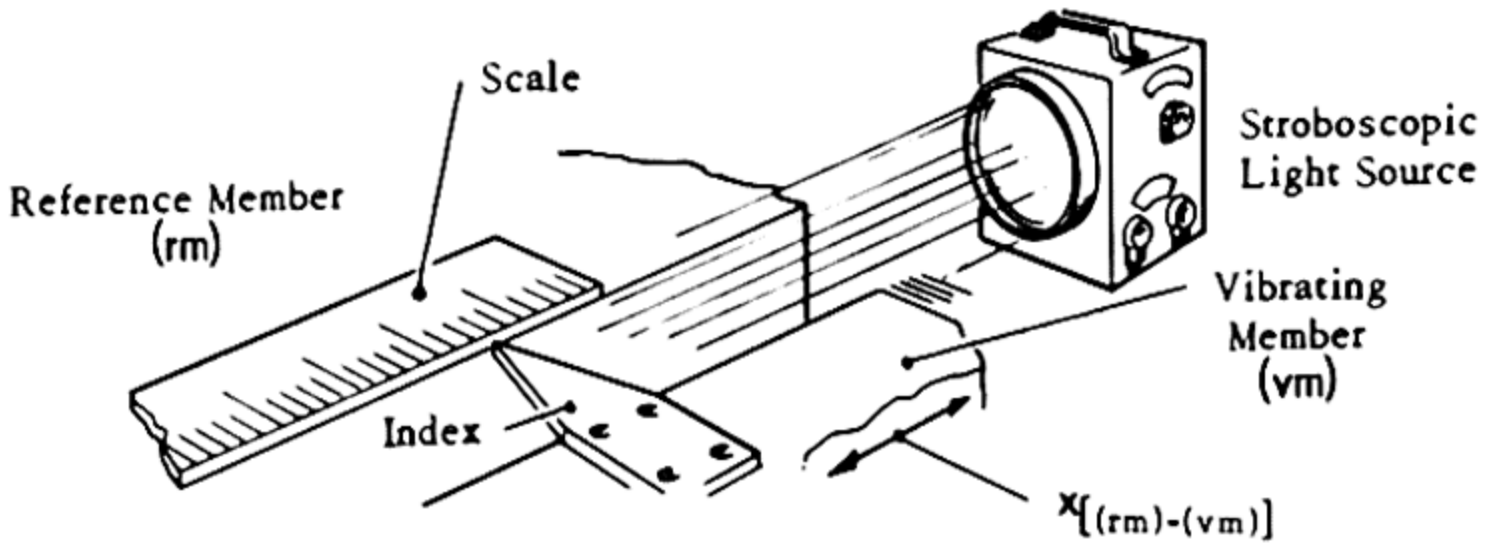
35.25. The illustrative pictorial diagram of Fig. 35-4f shows the essential elements of a self-contained vibration receiver with a mechanical pen that records on paper carried by a rotating drum. This arrangement is basically the seismographic system shown in Fig. 35-3, with the relative motion scale replaced by a recording drum and the index attached to the seismic element replaced by a pen or pencil.

ELECTRICAL-SIGNAL-GENERATING VIBRATION RECEIVERS

35.26. Practical limitations on weight, size, and ruggedness imposed on vibration receivers by operating conditions require self-contained units designed to produce electrical output signals suitable for operating conventional recording

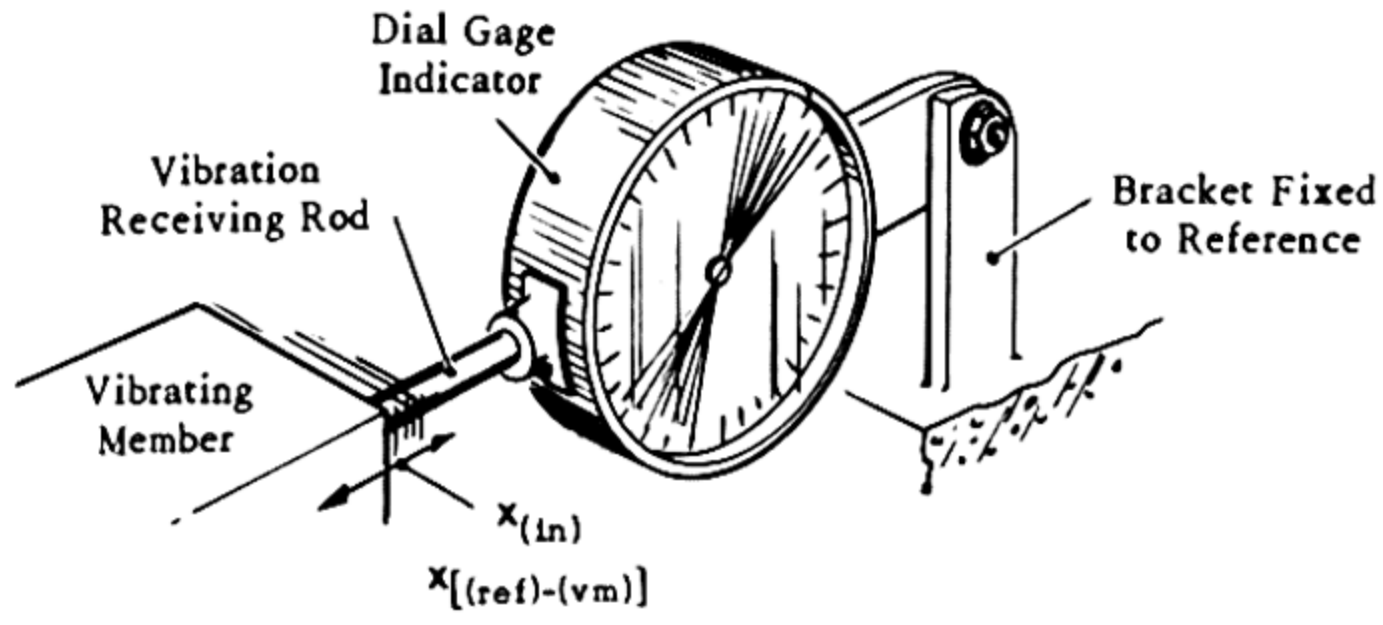


a) Scale-and-index relative-motion vibration receiver

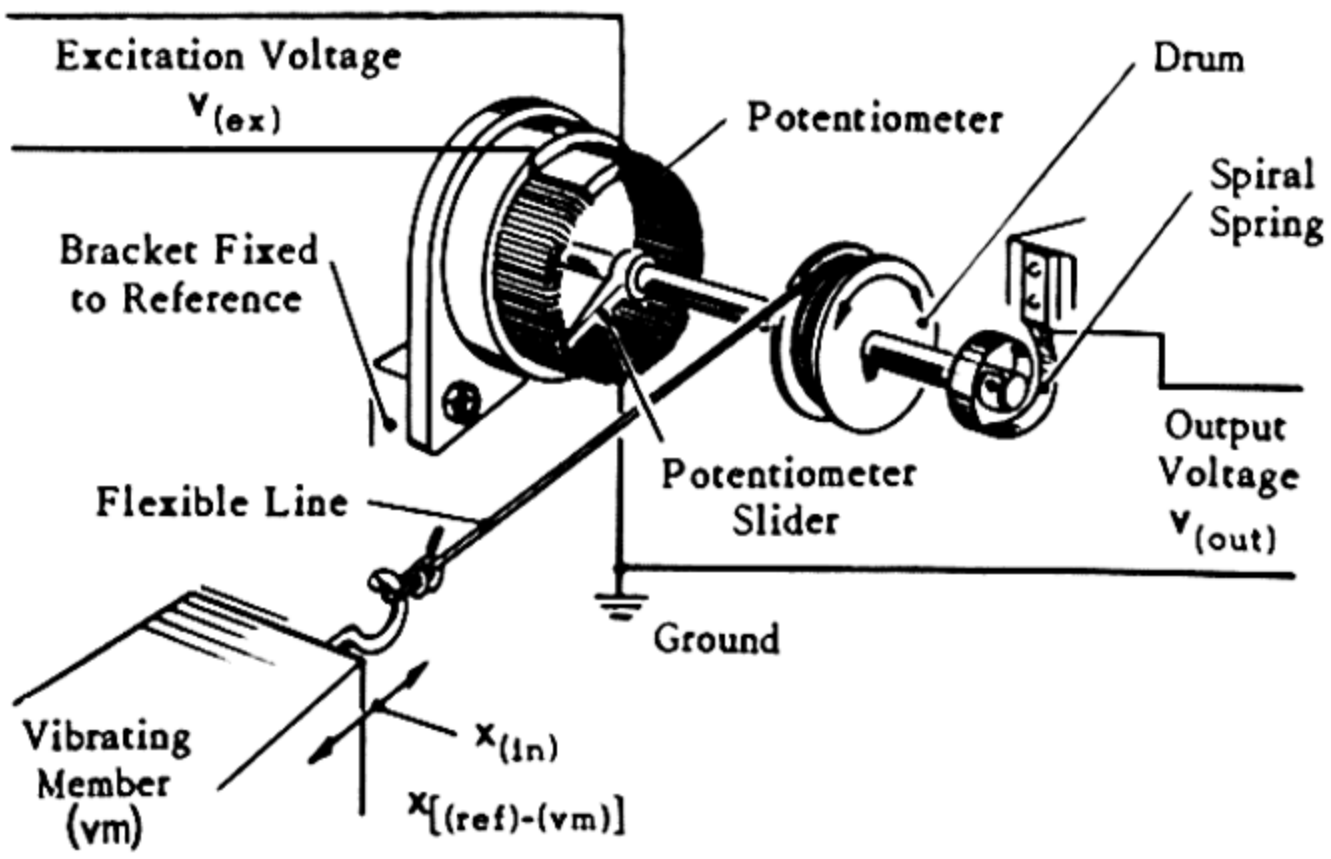


Note: The index appears stationary when stroboscopic light is flashing with a frequency equal to the frequency of vibration. The index appears to move between the limits of vibratory displacement when the stroboscopic light frequency is varied slowly away from the vibration frequency.

b) Scale-index-and-stroboscopic-light-source relative-motion vibration receiver

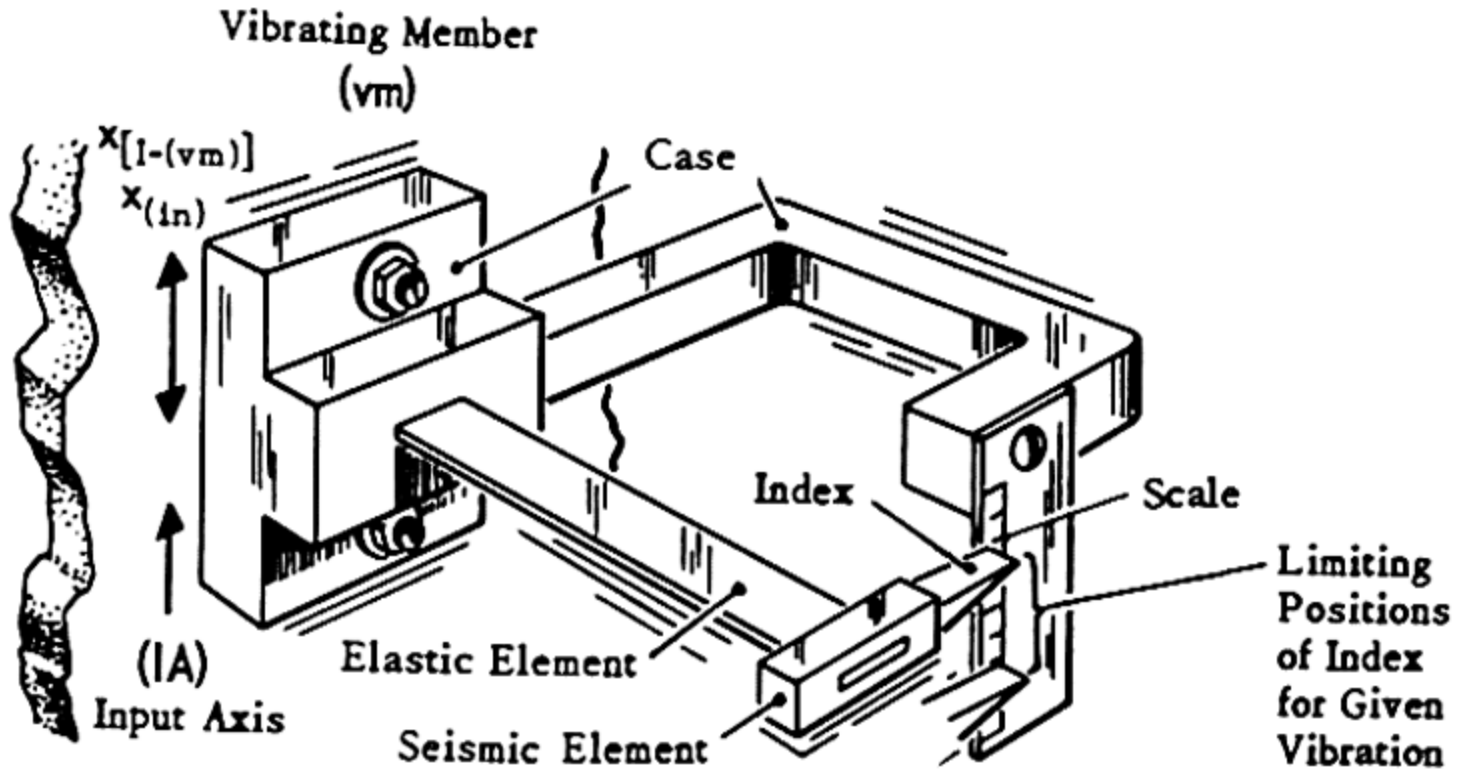


c) Mechanical relative-motion vibration receiver



d) Electrical-potentiometer-type relative-motion vibration receiver

Fig. 35-4. Diagrams illustrating the essential features of external-reference vibration receivers and self-contained vibration receivers. (Page 1 of 2)

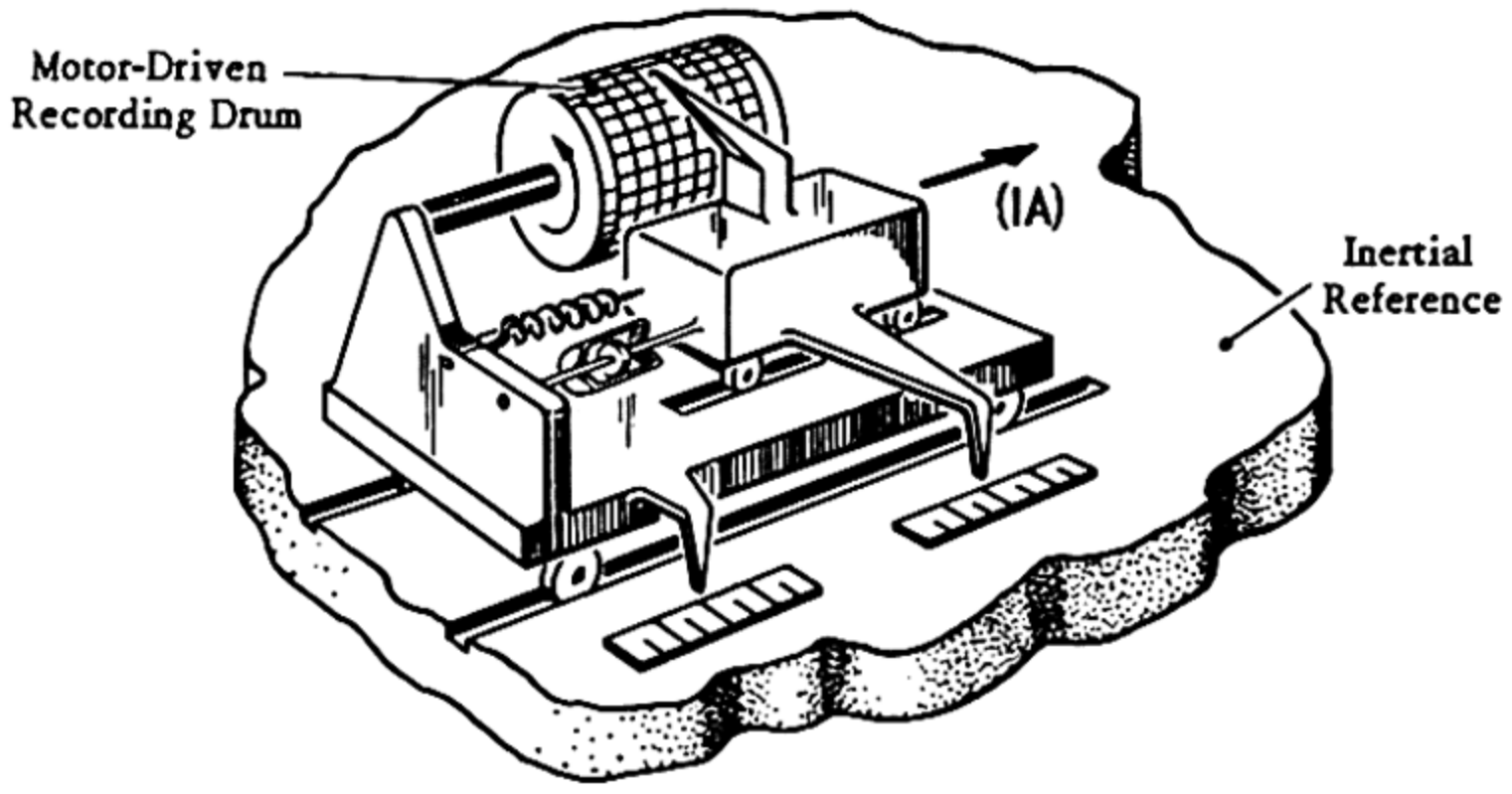


Note: The single lightly damped seismographic system illustrated here gives a strong response from a vibration input frequency near its own undamped natural frequency. Its response to other input frequencies is much less. In practice, the frequency response range may be extended by the use of a number of similar systems with different known undamped natural frequencies.

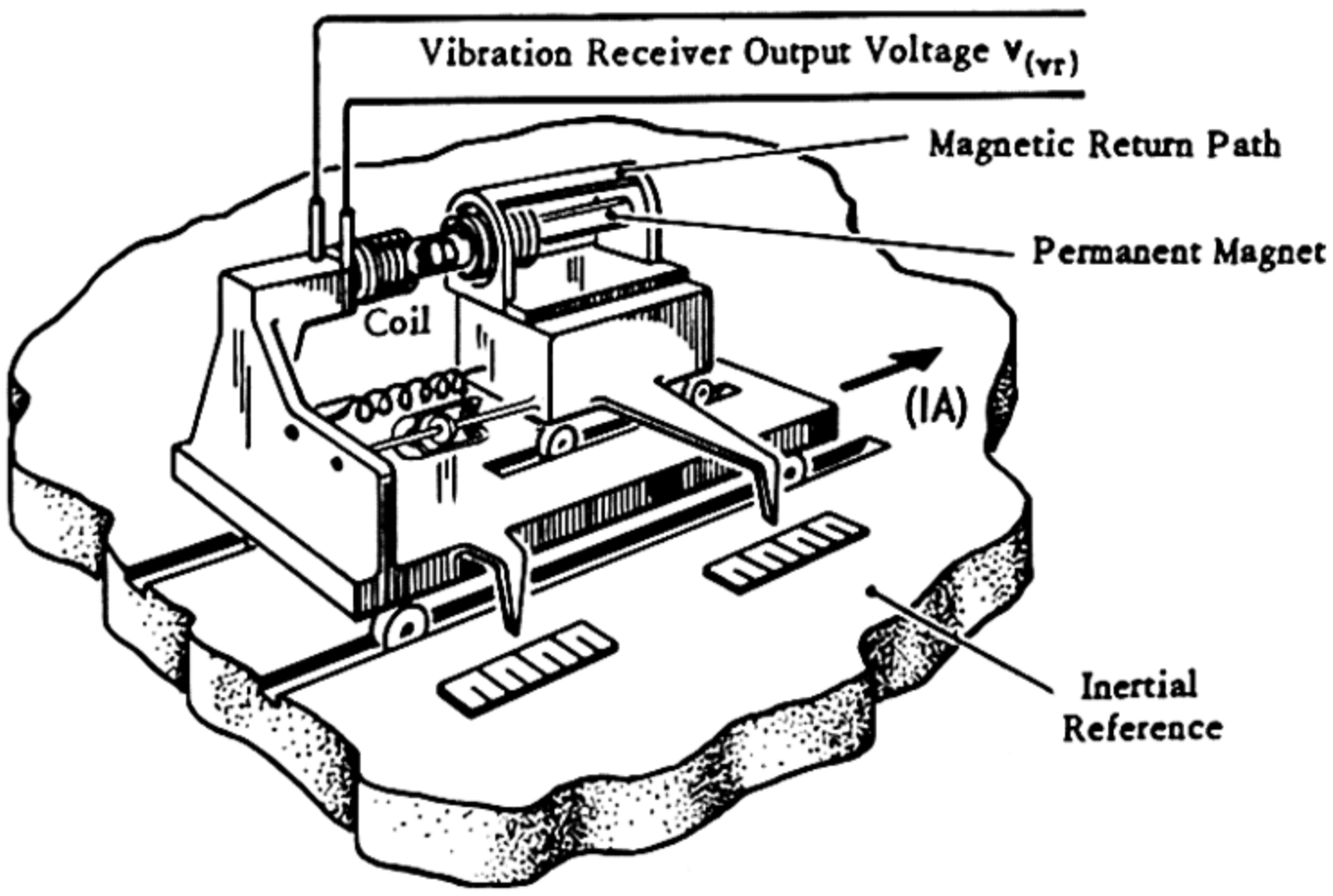
The frequency range may also be extended by incorporating means for continuously changing the length of the cantilever beam, with a scale for indicating the frequency corresponding to each beam length.

Devices using the features illustrated in this figure are most useful for indicating the frequency components in a given vibration input.

e) Lightly damped self-contained vibration receiver with visual indicating system



f) Vibration receiver with mechanical recording system



g) Vibration receiver with electromagnetic signal generating system

Fig. 35-4. Diagrams illustrating the essential features of external-reference vibration receivers and self-contained vibration receivers. (Page 2 of 2)

equipment. The essential features of such an electrical-signal-generating vibration receiver are illustrated in Fig. 35-4g. The receiver is basically a seismographic system with the relative motion scale and index replaced by an electromagnetic signal generating system. The illustrative pictorial diagram shows that this system is made up of a coil attached to the case of the receiver, a permanent magnet, and a magnetic circuit arranged to sweep flux lines across the winding when relative motion exists. A system of this type produces an output voltage proportional to the relative velocity. This means that a vibration receiver with its seismographic system operating in the displacement meter range would generate an output signal proportional to the vibratory velocity input to the receiver case.

35.27. The essential function of the signal generating system and associated parts is to accept the relative motion between a base and a moving member as an input and to produce an output signal that represents this motion. The arrangement that fulfills this function is called a relative motion receiver. All self-contained vibration receivers are made up of a seismographic system, which provides the reference, and a relative motion receiver, which takes the motion between the seismic element and the base of the seismographic system and provides the corresponding output signal. All external-reference vibration receivers are only relative motion receivers whose input is the motion of the vibrating member with respect to a reference member to which the receiver base is fixed. Various types of relative motion receivers are described in the following sections.

RELATIVE MOTION RECEIVERS AND INDICATORS

35.28. Relative motion receivers are devices designed to accept displacement, velocity, acceleration, or some higher derivative of the movement between a receiving element and a base, which serves as the geometrical reference, and to produce an output signal that depends on this input. Relative motion indicators are complete instruments in that an indicating system is associated with a receiver to give a readable index position as the essential output. In practice, these indicators have a comparatively small field of application because of space and reading difficulties and the greater usefulness of small and rugged devices that generate output signals suitable for operating high-speed recording equipment. Figures 35-5a through 35-5t illustrate the features that are commonly found in typical relative motion receivers and indicators.

DIAL GAGE DISPLACEMENT INDICATOR

35.29. Figure 35-5a shows the essential features of a dial gage displacement indicator. The receiving element is a rod constrained to move along the input axis by bushings and forced into contact with any moving member under study by

means of a linear spring. Rack teeth cut into the receiving element mesh with the input pinion of the indicating system gear train. The output of this gear train is the angular position of the index with respect to a scale carried by the receiver case, which is attached to the base. Backlash in the train is removed by a torsion spring that maintains loading toward the input rack.

35.30. The operation of any instrument of the dial-gage type is subject to an upper acceleration limit for the receiving element that occurs when the spring force available is not sufficient to keep the element in contact with the moving member as it recedes from the case. This limit may be improved by placing the indicator case closer to the moving member so that the tension of the contact spring is increased.* When this tension is not sufficient, the index indicates correctly the closest-approach position of the moving member, but gives erratic readings for the other extreme of motion. A similar effect occurs when the torque exerted on the gear train by the torsion spring is too small, so that the index motion exhibits a "jump" as the backlash shifts from one side to the other of the output pinion.

35.31. High-quality dial gage indicators may have input displacement – index tip displacement sensitivities up to 500, with uncertainty levels in the region of 0.0001 inch. Because of this performance possibility, and because they are simple, self-contained, and direct reading, dial gage indicators have many applications. On the other hand, they are not suitable for situations that involve high accelerations or require continuous records of relative motion. Subject to the acceleration limitation noted in the previous paragraph, the use of stroboscopic illumination and photographic recording improves performance in these situations, but high-quality performance in the high-acceleration region cannot be expected from dial gage indicators.

35.32. Dial gage indicators may fail to meet the relative motion requirements associated with many situations for two other reasons:

1) Because of the comparatively great force required to operate the receiving element of a dial gage indicator, the moving member whose displacement is being measured must be fairly heavy and strongly driven if the indicator is to be effective.
2) Because of internal inertia reaction effects associated with moving parts, the gage mechanism itself sets a high-frequency limit that varies with the amplitude of the input displacement. Although the high-frequency limit becomes greater as the input amplitude becomes smaller, there is an upper high-frequency limit in the neighborhood of 100 cycles per second,** no matter how small the input displacements may become.

---

* While this requires changing the zero-displacement position of the scale, no difficulty arises since such scales are designed to be movable.

** This assumes that amplitude readings made from the blurred index image would be acceptable.

OPTICAL DISPLACEMENT INDICATOR

35.33. As noted in the preceding paragraph, displacement indicators with mechanical indicating systems always have high-frequency limits that are imposed by inertia reaction effects associated with moving parts. Since it is a basic fact that inertia reactions increase with approximately the second power of the indicating system sensitivity, * the acceleration errors of any completely mechanical instrument must become worse as its sensitivity is increased. One way out of this difficulty is to replace mechanical parts by optical elements. Because parts used to move light beams have very low effective inertias, it is possible to design optical displacement indicators with the optimum dynamic characteristics for a given sensitivity. In practice, good design makes it possible at the same time to achieve an input displacement – index deflection sensitivity approximately the same as that provided by the best dial gage indicators.

35.34. Figure 35-5b illustrates the essential features of an optical displacement indicator. The receiving element is supported with respect to the base by means of a system of flexible hinges. These support flexures constrain the receiving element to move parallel to the input axis, which is fixed with respect to the base. The linear displacement of the receiving element with respect to the base is transformed into rotation of a mirror by means of two linkage flexures. The indicating system is made up of these flexures, the attached mirror, a light source, and the additional parts required to form an index spot that moves along the scale as the relative motion input varies.

35.35. In addition to the good dynamic performance characteristics associated with low indicating-system inertia, optical indicators are especially adapted to making continuous photographic records. This becomes possible when the scale is replaced by a moving strip of film. The principal disadvantage of the optical indicator is its relatively large size and weight. It is possible to improve this situation somewhat by the use of multiple reflectors and miniaturized light sources, but the design compromises required to construct practical instruments considerably reduce the usefulness of these instruments, except for special purposes.

ELECTRICAL-SIGNAL-GENERATING RELATIVE MOTION RECEIVERS

35.36. Practical solutions for the size, weight, and dynamic performance problems associated with instruments for measuring relative motion are almost universally based on some combination of a receiving element with an electrical signal generating system. Designs based on this approach lead to small, lightweight receiver units capable of driving any type of oscillographic indicating system. Because physical separation of units is possible, the indicating system may

* In the case of a simple gear train, this fact is merely another way of stating that the effective moment of inertia of a driven member at one end of the train is equal to the actual moment of inertia at the other end multiplied by the square of the ratio of the train.

generally be selected on the basis of performance characteristics, without serious limitations on the bulk or weight of the equipment. The receiver units, on the other hand, may be made acceptably small and light, with connecting wires that do not impose serious loads on the member to which the receiver is attached.

35.37. The physical effects that have been commonly applied in signal generators for receiving relative motion inputs and producing electrical signal outputs are listed below with references to the pertinent illustrative diagrams in Fig. 35-5.

1) Resistance change (Figs. 35-5c and 35-5d).
2) Electrostatic field change (Figs. 35-5e, 35-5f, 35-5g and 35-5h).
3) Electromagnetic field linkage change:
    a) Generator action (Figs. 35-5i, 35-5j, 35-5k, 35-5 l and 35-5m).
    b) Transformer action (Figs. 35-5n, 35-5o, 35-5p, 35-5q and 35-5r).
4) Piezo-electric change (Figs. 35-5s and 35-5t).

The diagrams of Fig. 35-5 show typical applications of these effects in electrical-signal-generating relative motion receivers, but are not meant to represent an exhaustive survey of designs that have been reduced to practice.

UNBONDED RESISTANCE WIRE DISPLACEMENT RECEIVER

35.38. The electrical resistance of any given piece of metal wire varies with the state of strain of the wire. This makes it possible to use Wheatstone bridge arrangements in which one arm or more than one arm is stressed by the displacement of the receiving element with respect to the base. By placing the active pair, or pairs, of bridge arms in the same environment, it is possible to compensate for temperature effects.

35.39. In Fig. 35-5c, four windings of unbonded strain-sensitive wire are each stretched between pairs of insulating pins. One pin of each pair is attached to the base of the receiver. The second pin of each pair is fixed to a rigid member attached to the receiving element. This member is constrained to move parallel to the input axis by flexures or other means not shown in the diagram. With the receiving element in its zero-relative-displacement position, each winding is stretched to approximately half of the stress corresponding to its elastic limit. With the arrangement shown in Fig. 35-5c, an input displacement in the positive direction of the input axis increases the strain in the arms between terminals 1 and 2 and between terminals 3 and 4. Since the strain-gage wire in ordinary use has greater resistance for larger strains, a positive input displacement of the receiving element is accompanied by a positive change in the resistance of the 1-2 and 3-4 windings. Similarly, the windings between terminals 5 and 6 and between terminals 7 and 8 have their strain level reduced by a positive displacement of the receiving element. Consequently, these windings have negative changes in resistance for positive input displacements.

35.40. The electrical circuit diagram on the right-hand side of Fig. 35-5c shows that the two windings with positive displacement – positive resistance change arms may be connected as a pair of opposite arms in a Wheatstone bridge. The remaining two windings are used to complete the bridge. The excitation applied to the bridge between one pair of the opposite junction points may be either direct-current voltage or alternating-current voltage. The output signal from the bridge appears as a voltage between the other two bridge junctions. The slider of a balancing potentiometer connected across the source of excitation provides a means for adjusting the output signal to its null level when the receiving element is in its zero-relative-displacement position.

35.41. In the arrangement of Fig. 35-5c, all four active bridge windings are subjected to the same environmental temperature. This means that resistance effects due to temperature variations are the same in all of the arms and are consequently balanced out within the bridge, so that temperature errors do not appear in the output signal.

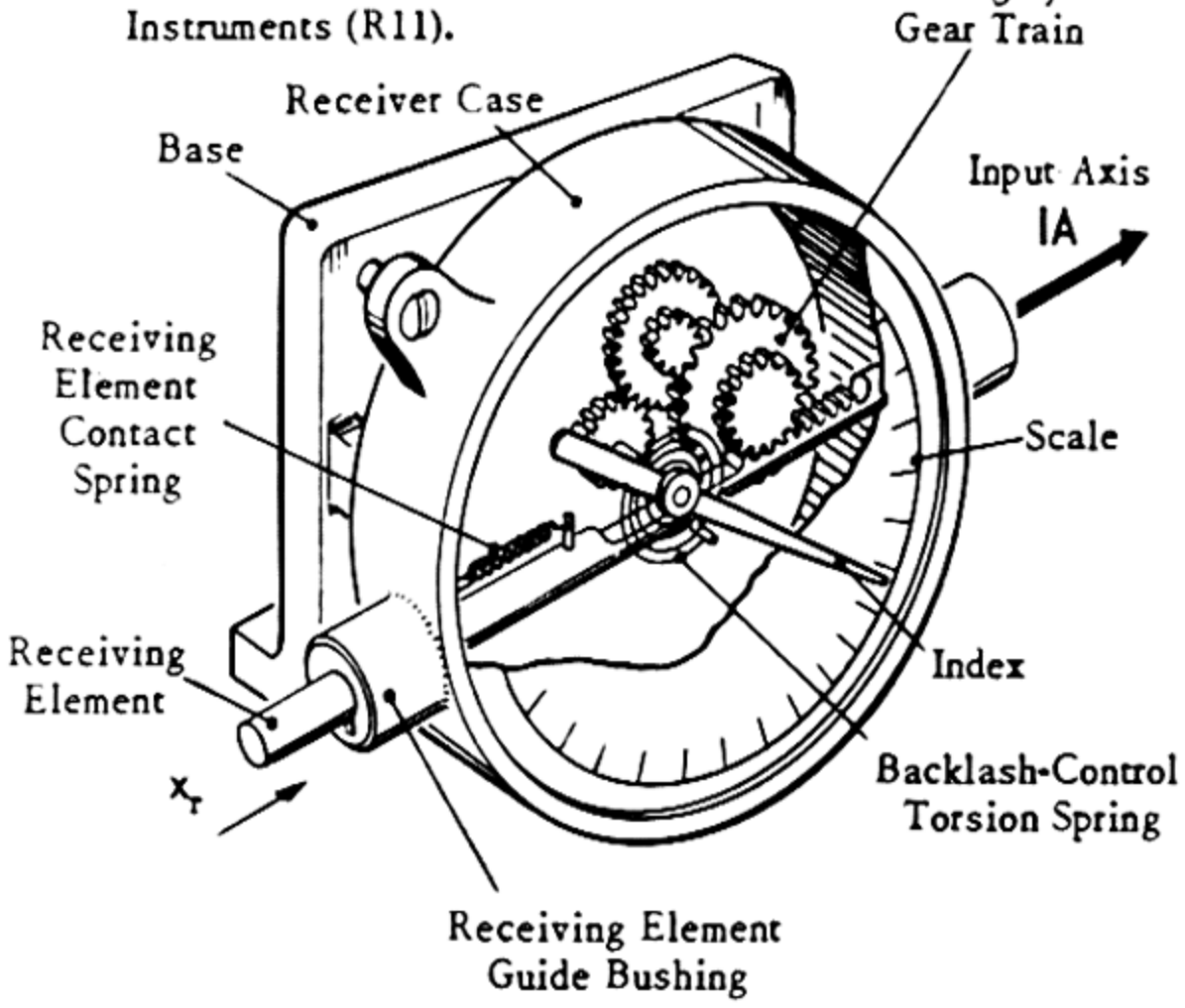
35.42. The resistance between output terminals of typical unbonded resistance wire displacement receivers is between 80 and 1500 ohms. The maximum input displacement amplitude is ordinarily between 0.0005 and 0.004 inch. Within an excitation voltage range of 6 to 30 volts, the maximum open-circuit output voltage is in the region of 2 to 4 millivolts per volt of excitation, depending upon the resistance and the heat-dissipating conditions. Units with these characteristics may be contained in about 1 cubic inch and do not weigh more than about 1 ounce. For the recording of frequencies less than about 100 cycles per second, an unbonded resistance wire displacement receiver may be coupled directly into a matched-impedance D'Arsonval-type recording oscillograph.

BONDED RESISTANCE WIRE DISPLACEMENT RECEIVER

35.43. Figure 35-5d shows the essential features of a bonded resistance wire displacement receiver. In this device, the receiving element is the tip of an elastic cantilever fixed to the base. In the form shown in the diagram, two resistance-wire windings are cemented to one side of the cantilever. One of these windings is located with its wires positioned at right angles to the top of the base, except for end connections, so that bending strains in the cantilever are transferred through the cement to the wires themselves. The other winding is located so that its wires, except for end connections, are positioned parallel to the top of the base. With this arrangement, the first winding is affected by bending strains in the cantilever, while the second winding is not appreciably affected by these strains.

35.44. The electrical circuit diagram in Fig. 35-5d shows the two bonded windings connected as opposite arms of a Wheatstone bridge, and a balancing

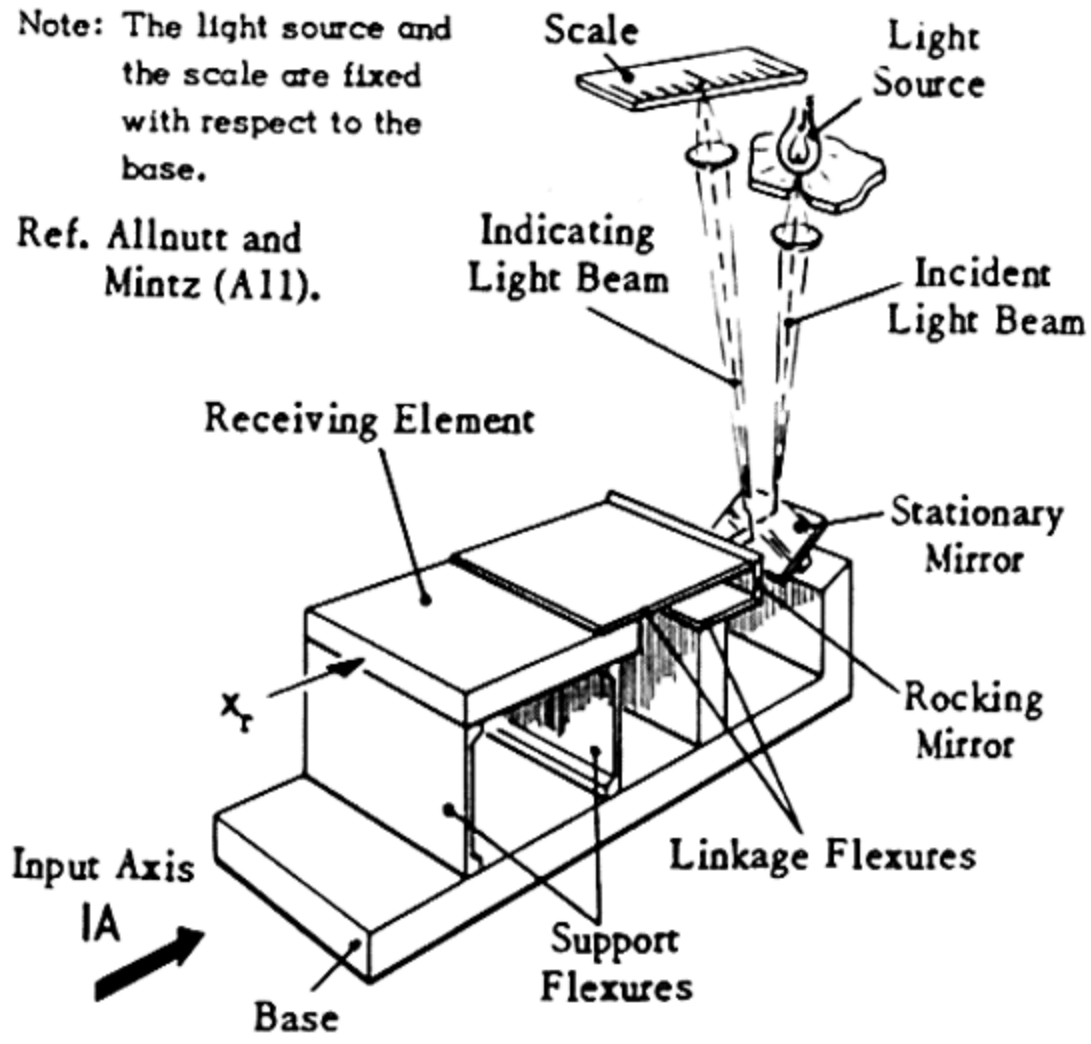
Ref. Review of Scientific Instruments (R11).



a) Dial gage displacement indicator

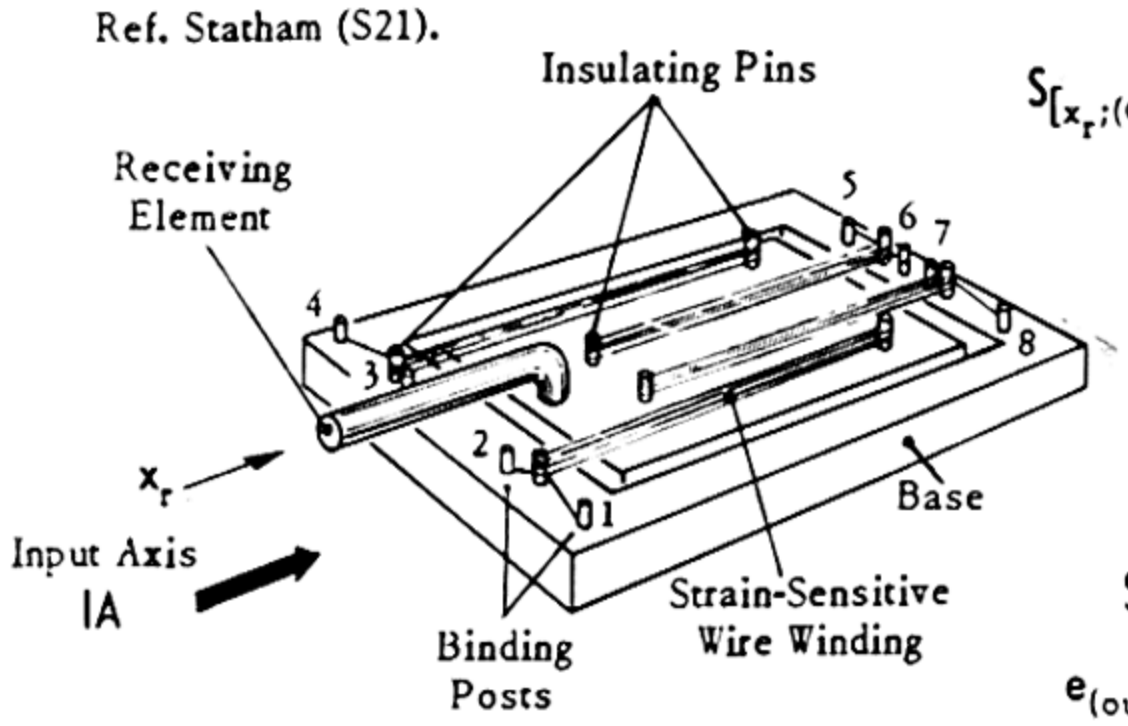
Note: The light source and the scale are fixed with respect to the base.

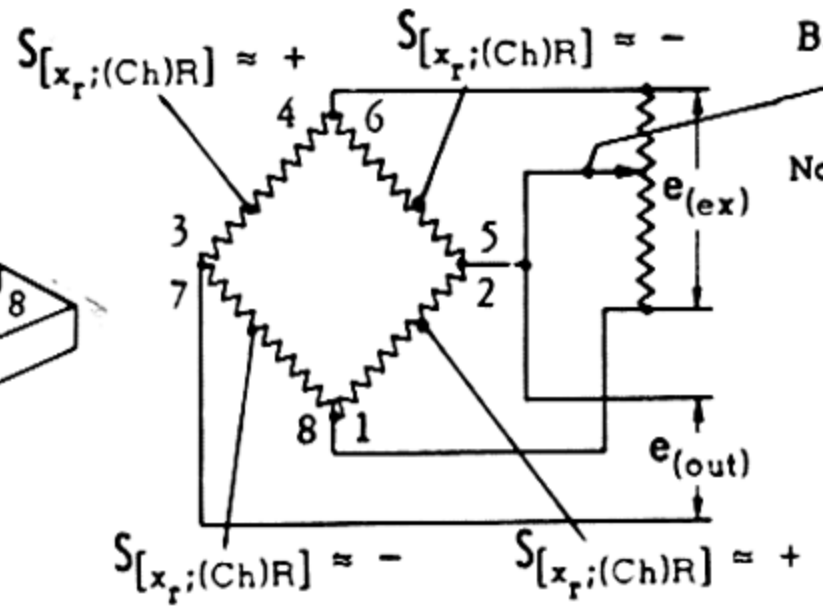
Ref. Allnutt and Mintz (A11).



b) Optical displacement indicator

Ref. Statham (S21).



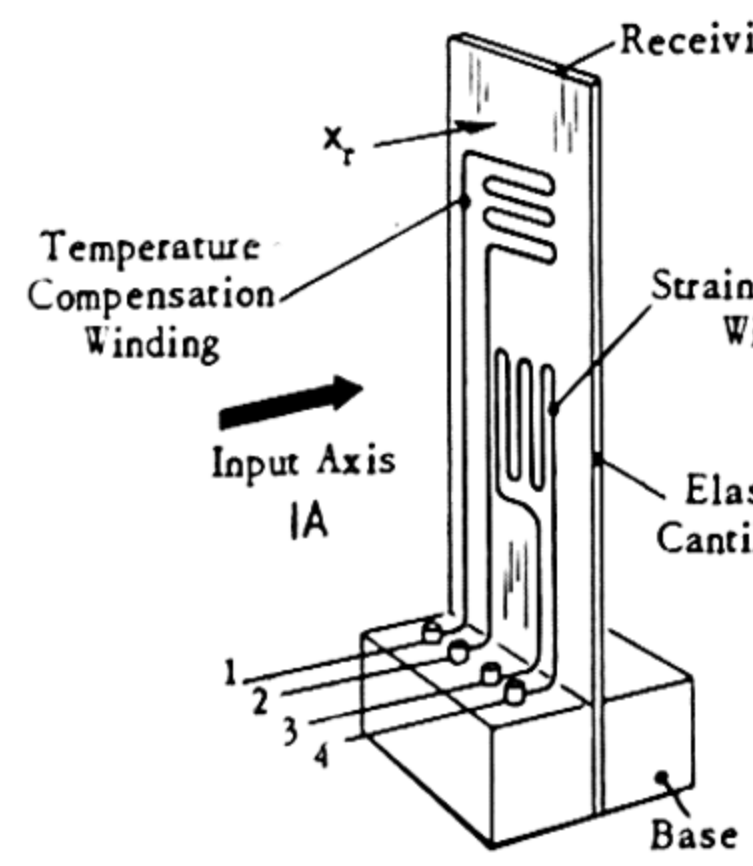


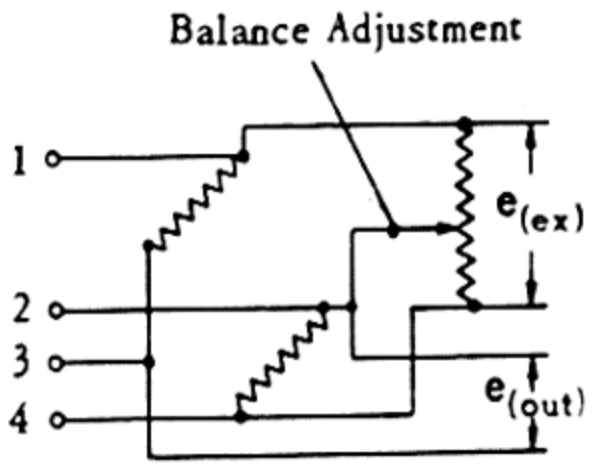
$$e_{(out)} = S_{[x_r;e_{(ex)};e_{(out)}]} e_{(ex)} x_r$$

where $e_{(ex)}$ may be either alternating-current or direct-current voltage

Note: The strain-sensitive wire winding is placed under tension approximately one-half the maximum allowable stress when the receiving element is in the zero-input-displacement position. The receiving element is constrained to move parallel to the input axis by means not shown in the diagram.

c) Unbonded resistance wire displacement receiver





$$e_{(out)} = S_{[x_r;e_{(ex)};e_{(out)}]} e_{(ex)} |x_r|$$

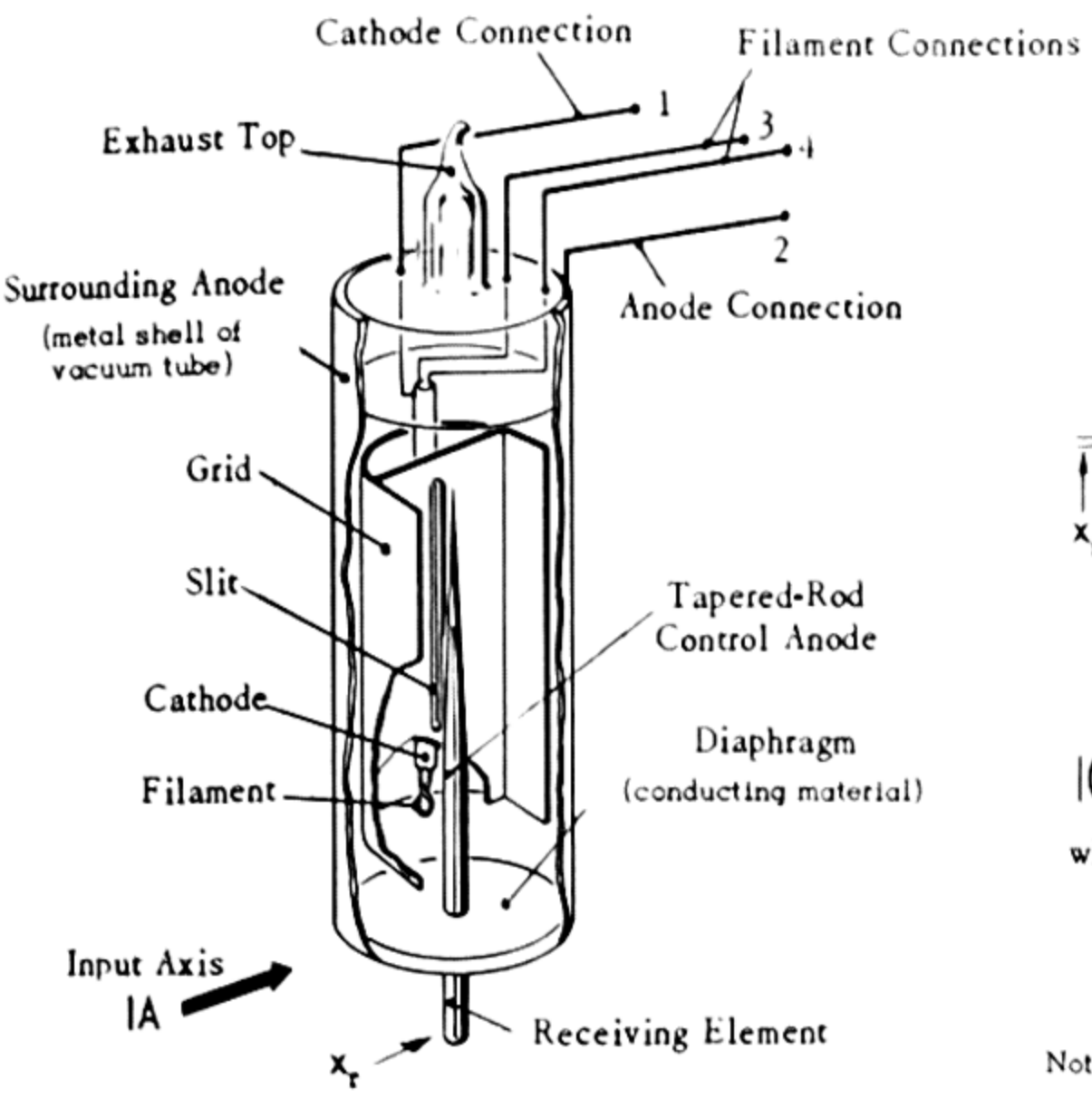
where $e_{(ex)}$ may be either alternating-current or direct-current voltage

Note: The strain-sensitive winding and temperature compensation winding are cemented to the surface of the cantilever. A single strain-sensitive arm arrangement like that shown in the diagram gives signals that represent input magnitudes only. Algebraic sign information must be generated by some other means. The use of a second strain-sensitive arm on the opposite side of the cantilever, along with the matching nonstrain-sensitive arm, provides algebraic sign information, in addition to improved sensitivity.

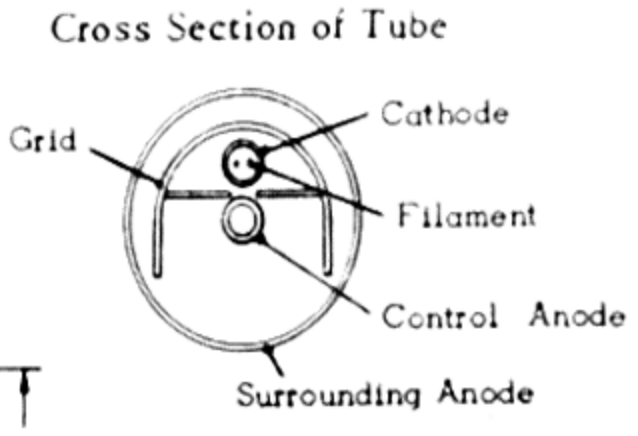
Ref. Ball (B22), Hetényi (H14) and Mason (M18).

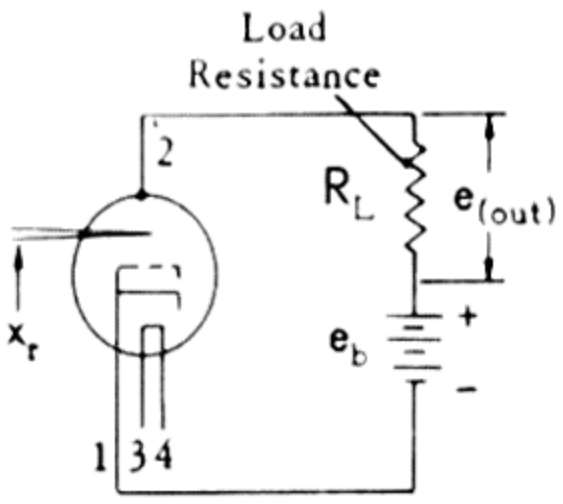
d) Bonded resistance wire displacement receiver

Fig. 35-5. Illustrative diagrams of typical relative motion receivers and indicators. (Page 1 of 6)



Ref. Lewis (L17).





$$|(Ch)\,e_{(out)}| = S_{|x_r;(Ch)R_p|}\, S_{|(Ch)R_p;e_b;(Ch)e_{(out)}|}\, e_b\, |x_r|$$

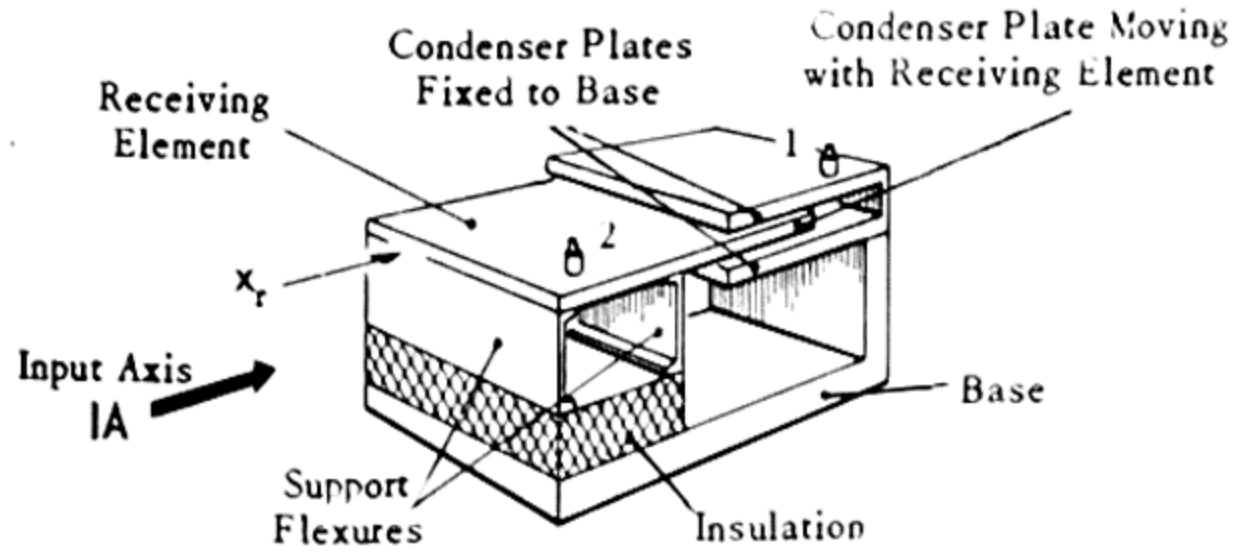
where

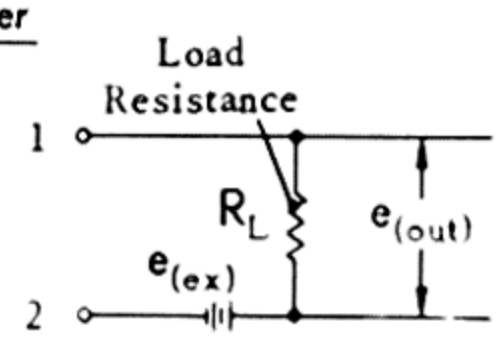
$(Ch)\,e_{(out)}$ = change in output voltage

$(Ch)\,R_p$ = change in plate resistance of tube

Note: The input axis is parallel to the grid surface that contains the slit. The output voltage magnitude depends on the input deflection. Algebraic signs must be introduced by fixing a zero-input position by means external to the receiver.

e) *Electronic tube displacement receiver*





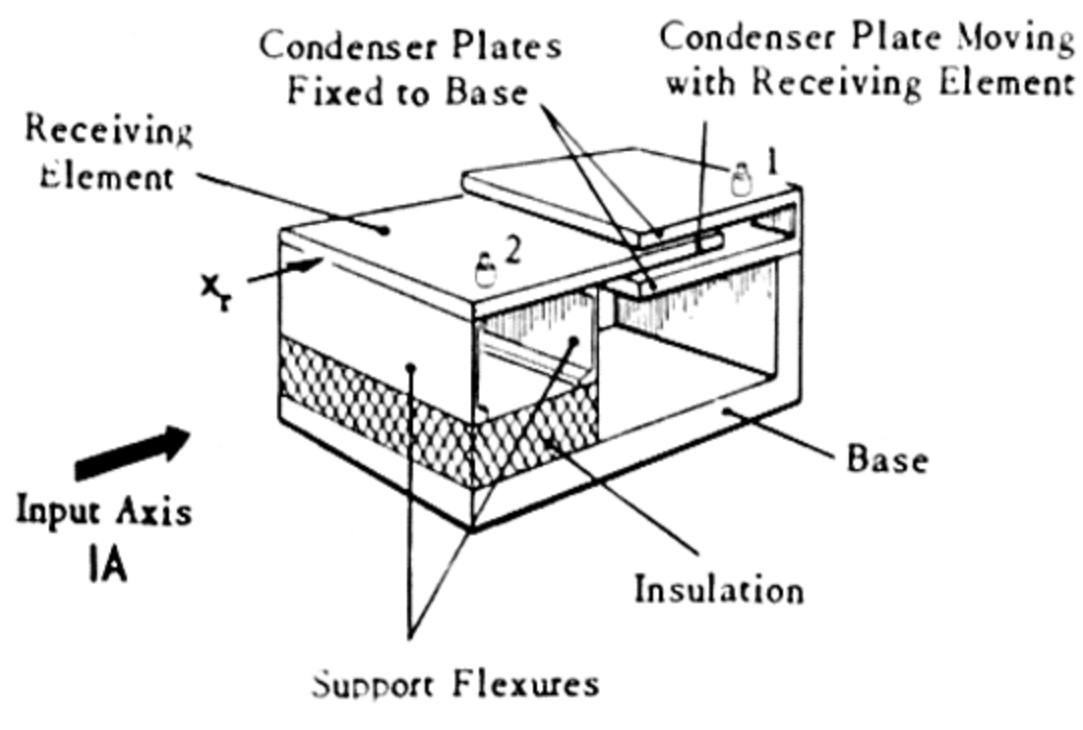
$e_{(ex)}$ = direct-current excitation voltage

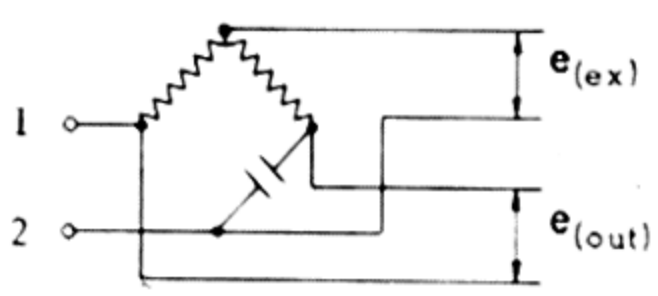
$$e_{(out)} = S_{[\dot{x}_r;e_{(ex)};e_{(out)}]}\, e_{(ex)}\, \dot{x}_r$$

Note: In practice, the variable-condenser element may have design features differing from the illustrative arrangement shown.

Ref. Hetényi (H14) and Mason (M18).

f) *Electrostatic capacity linear velocity receiver*





$$e_{(out)} = S_{[x_r;e_{(ex)},n_{(ex)};e_{(out)}]}\, e_{(ex)}\, n_{(ex)}\, x_r$$

where

$e_{(ex)}$ = alternating-current excitation voltage

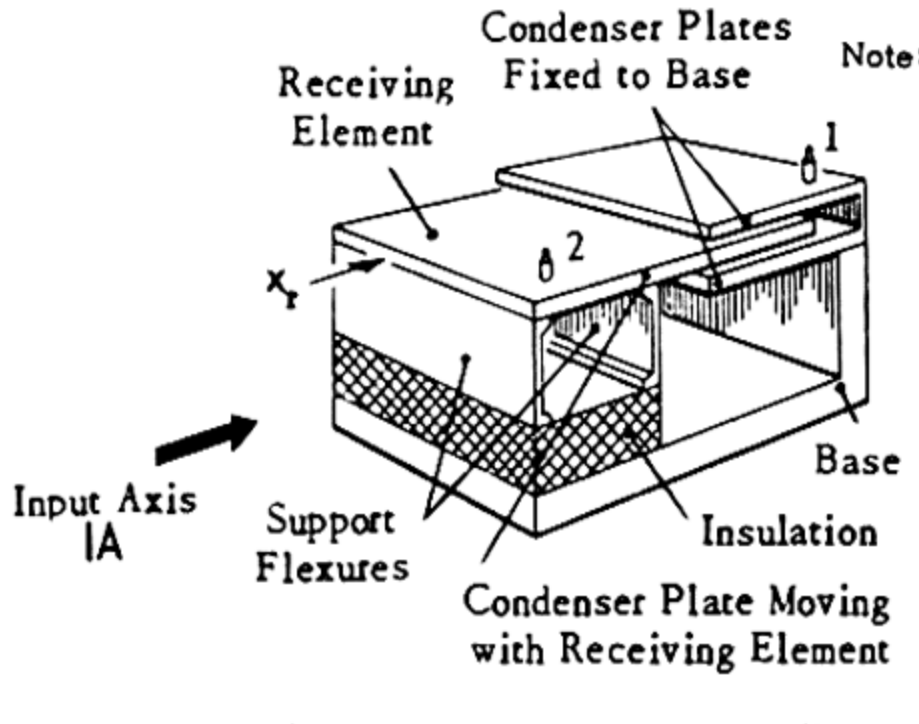
$n_{(ex)}$ = excitation frequency

Note: In practice, the variable-condenser element may have design features differing from the illustrative arrangement shown.

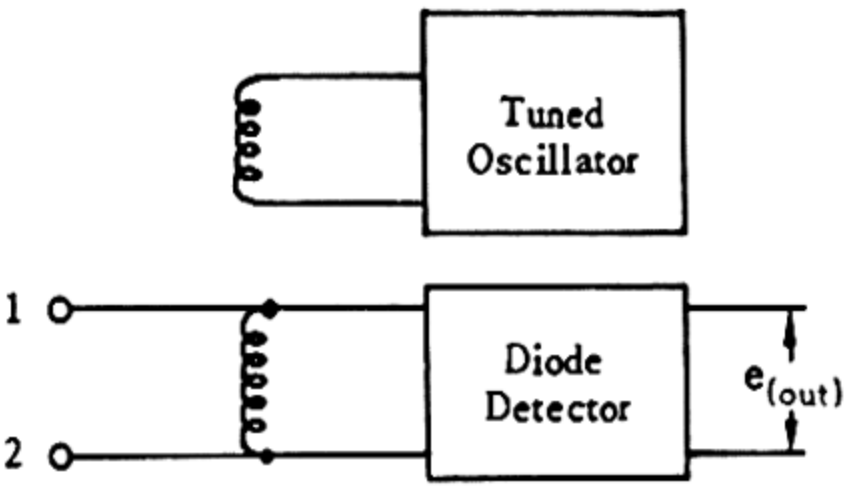
Ref. Hetényi (H14) and Mason (M18).

g) *Electrostatic capacity bridge displacement receiver*

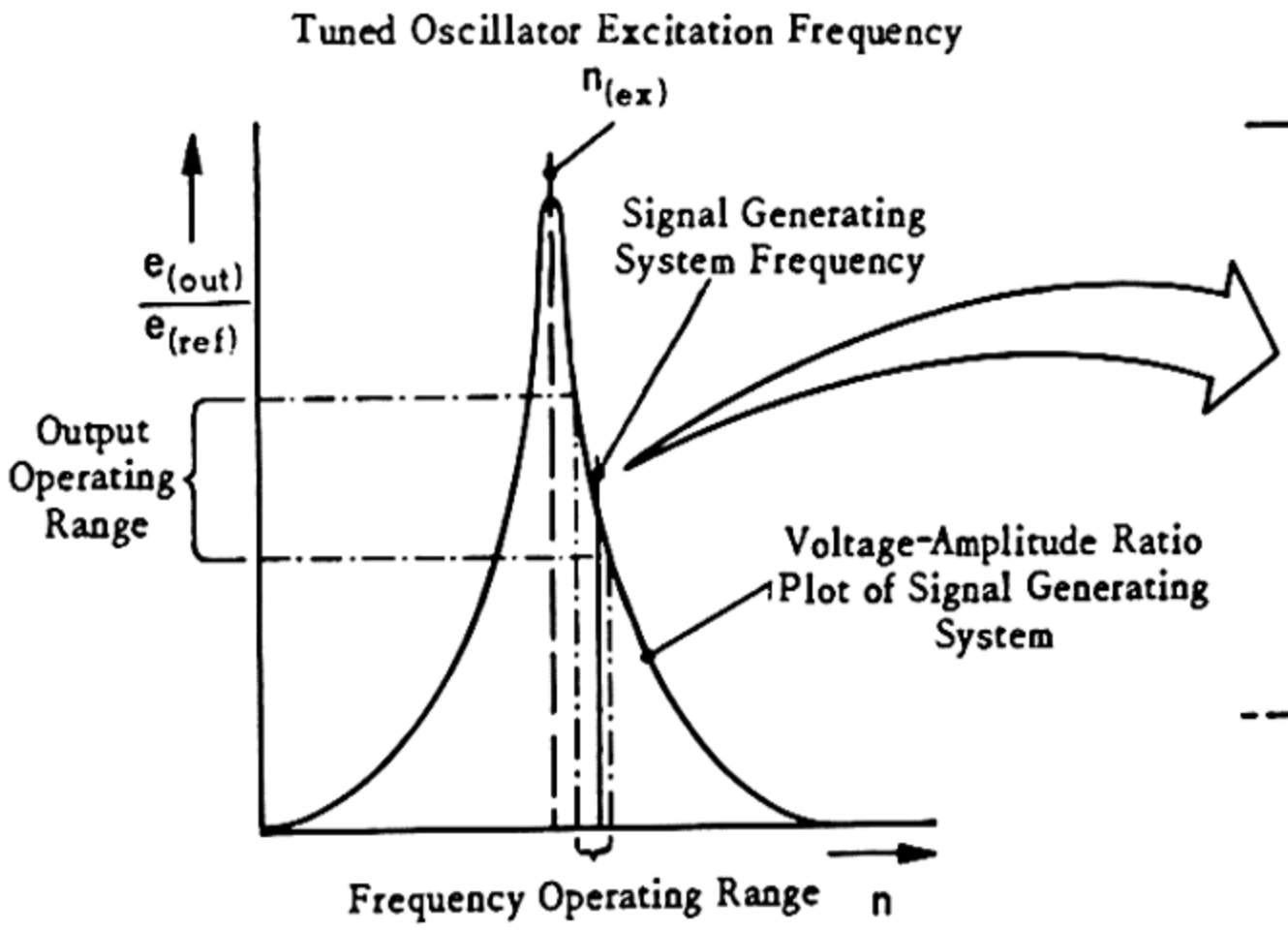
Fig. 35-5. Illustrative diagrams of typical relative motion receivers and indicators. (Page 2 of 6)

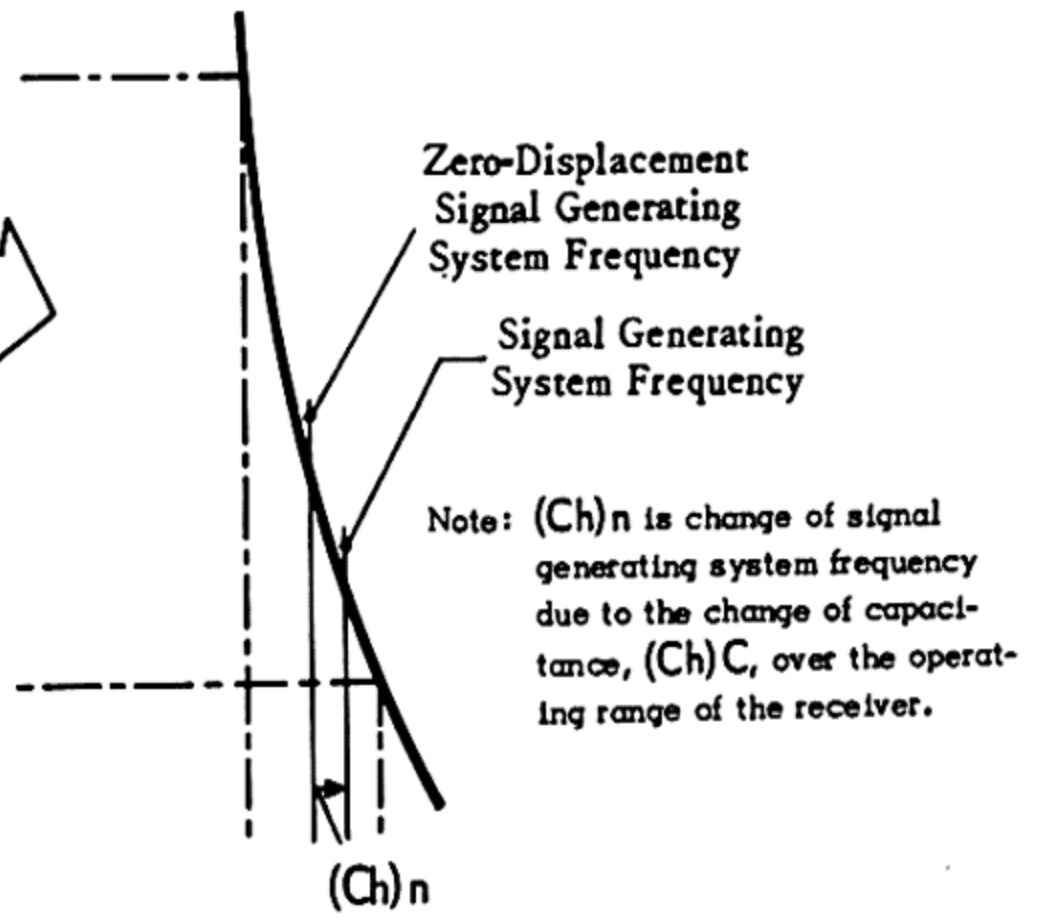


Note: In practice, the variable-condenser element may have design features differing from the illustrative arrangement shown.



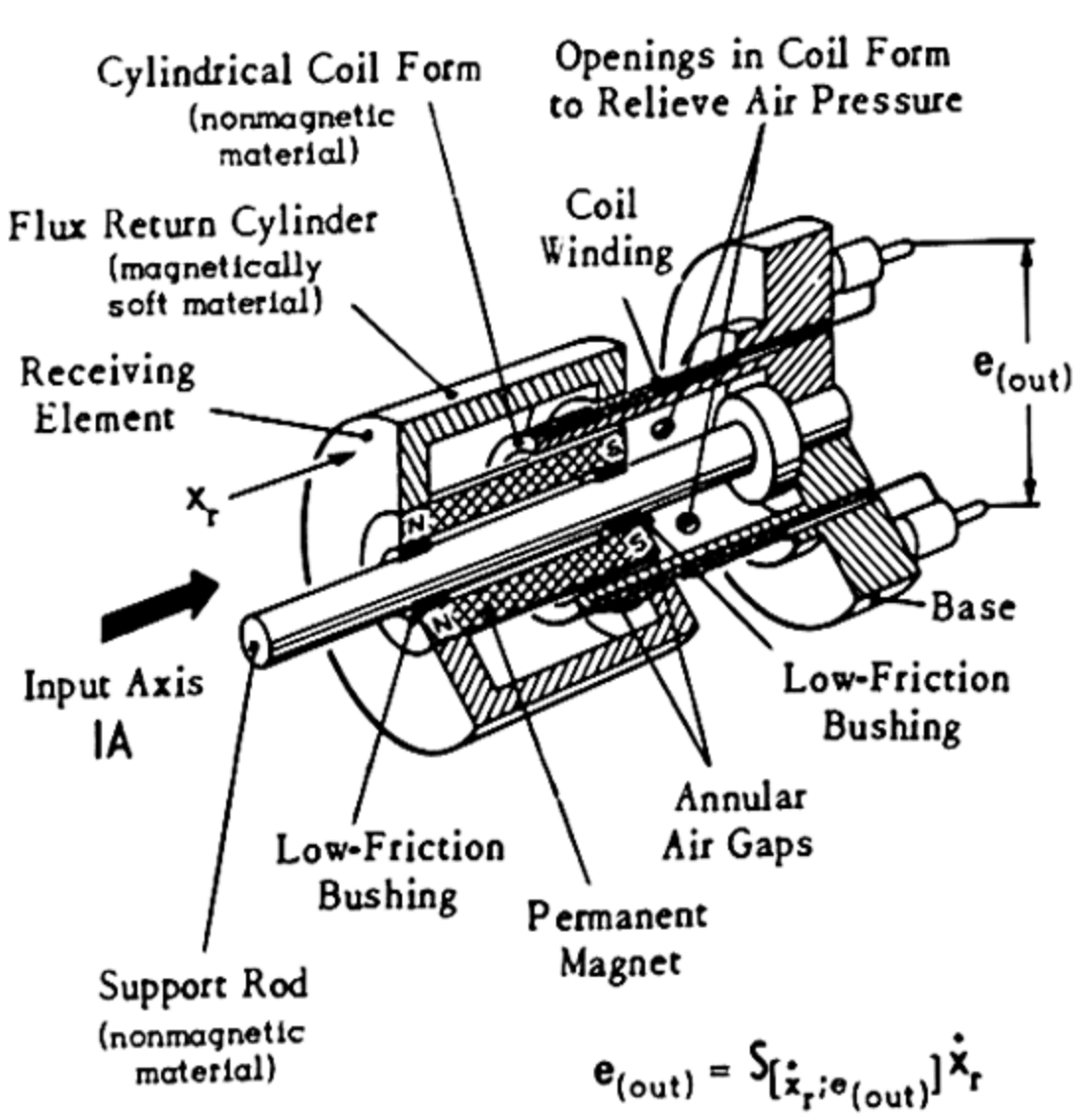
$$e_{(out)} = e_{(out)(x_r=0)} + S_{[x_r;(Ch)C]} S_{[(Ch)C;(Ch)n]} S_{[(Ch)n;(Ch)e_{(out)}]} x_r$$



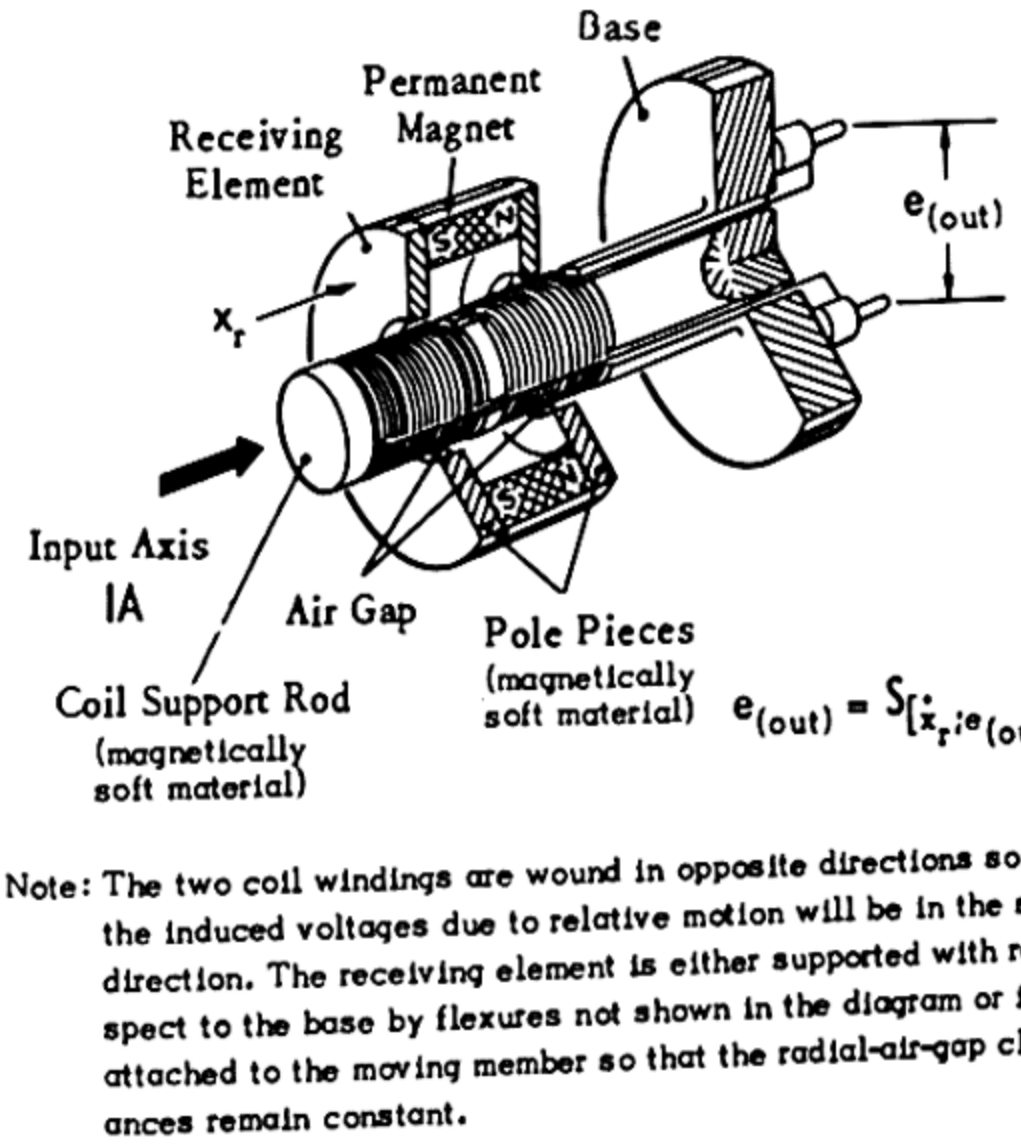


Note: (Ch)n is change of signal generating system frequency due to the change of capacitance, (Ch)C, over the operating range of the receiver.

h) Electrostatic-capacity-controlled oscillator displacement receiver



$$e_{(out)} = S_{[\dot{x}_r;e_{(out)}]} \dot{x}_r$$



$$e_{(out)} = S_{[\dot{x}_r;e_{(out)}]} \dot{x}_r$$

Note: The two coil windings are wound in opposite directions so that the induced voltages due to relative motion will be in the same direction. The receiving element is either supported with respect to the base by flexures not shown in the diagram or is attached to the moving member so that the radial-air-gap clearances remain constant.

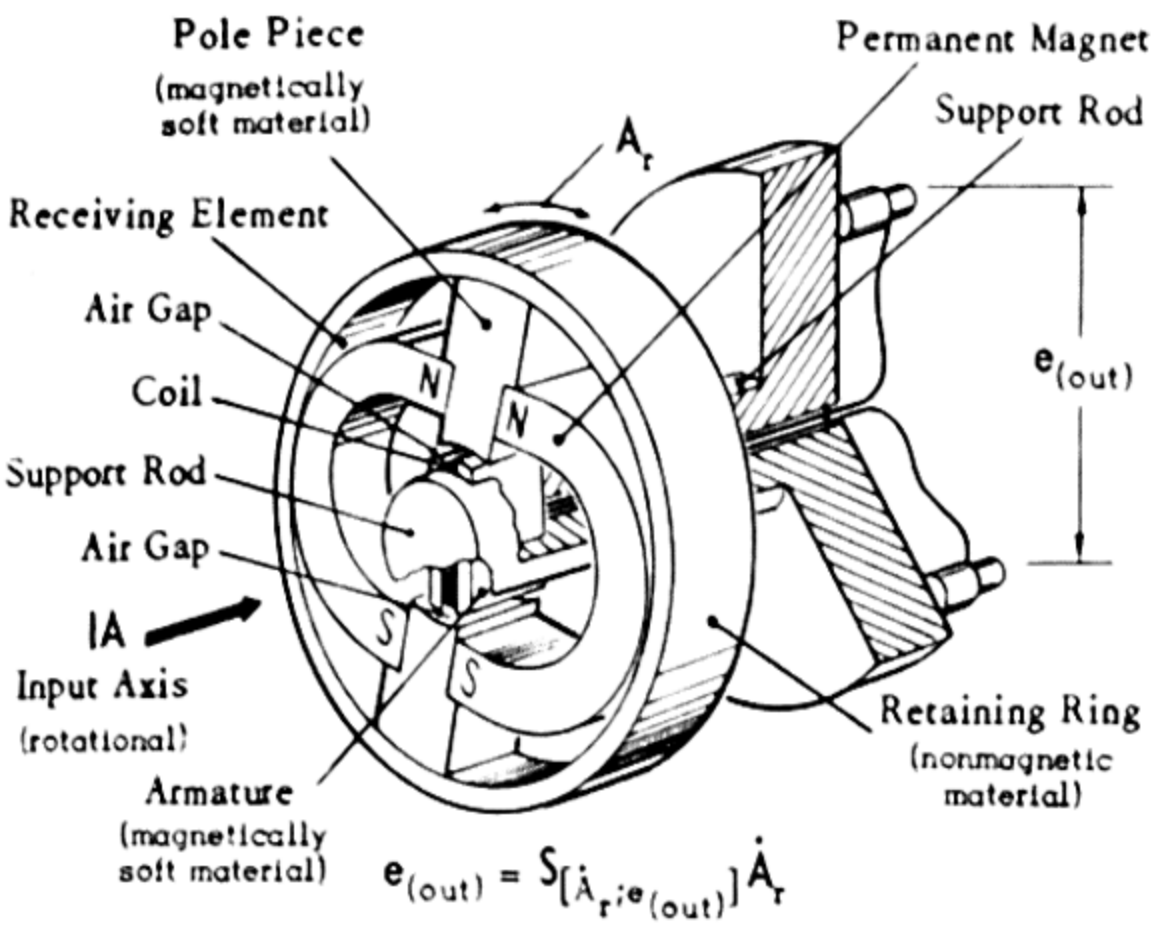
Ref. Draper, Bentley and Willis (D14) and Grinstead (G11).

Ref. Consolidated Engineering Corp. (C11).

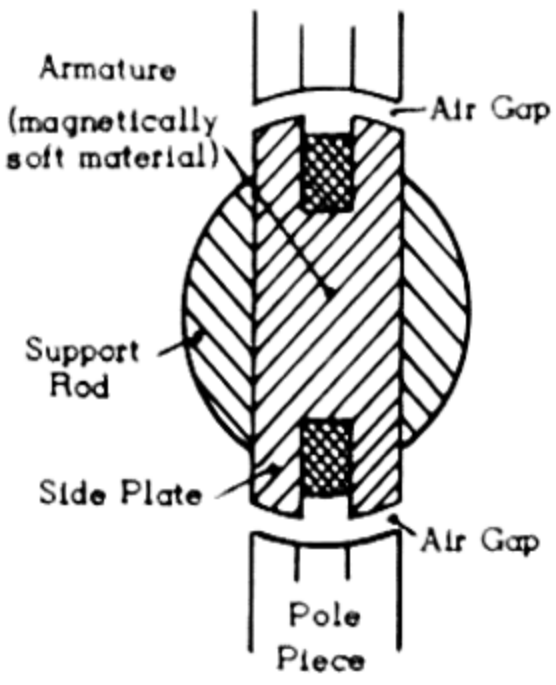
i) Single-coil-type electromagnetic generator linear velocity receiver

j) Double-coil-type electromagnetic generator linear velocity receiver

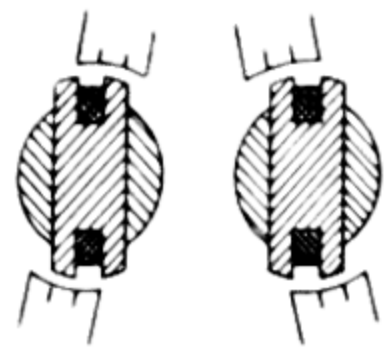
Fig. 35-5. Illustrative diagrams of typical relative motion receivers and indicators. (Page 3 of 6)



$$e_{(out)} = S_{[\dot{A}_r;e_{(out)}]}\dot{A}_r$$



Zero Displacement Position

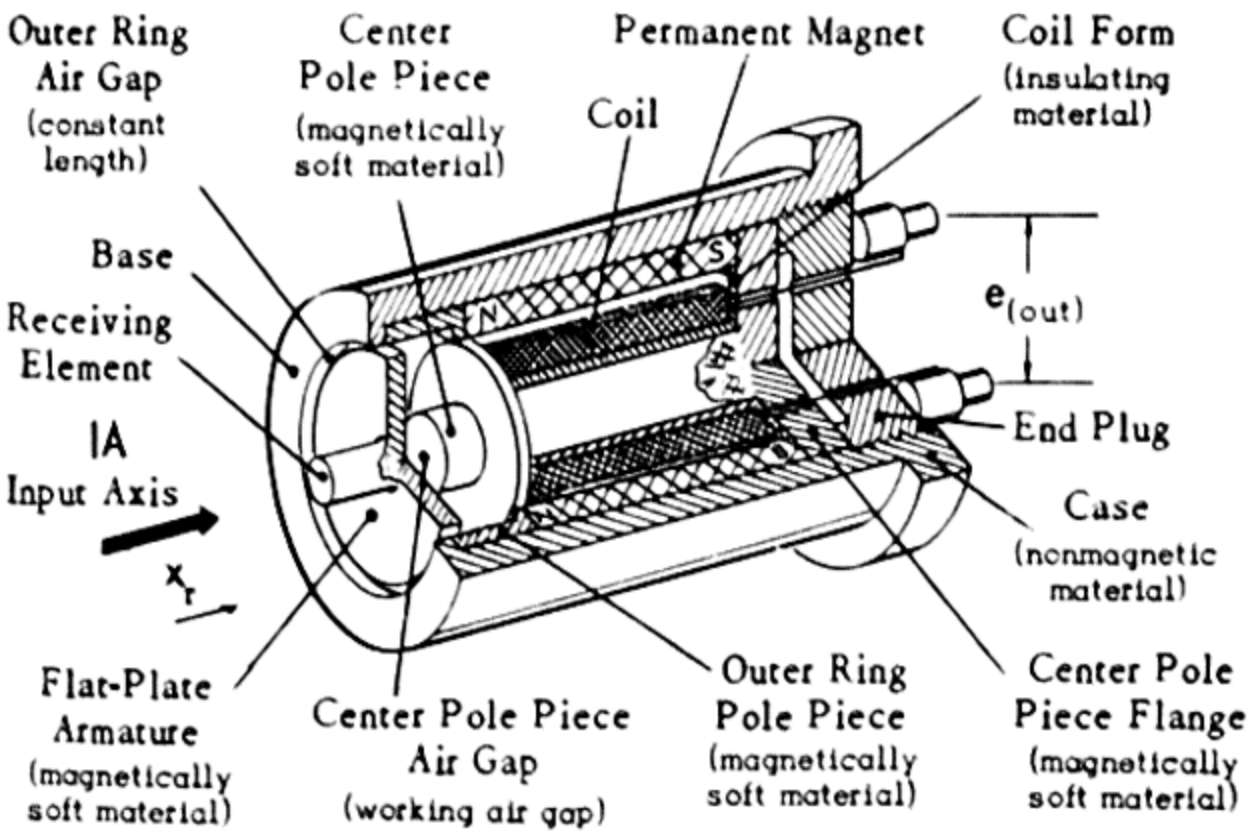


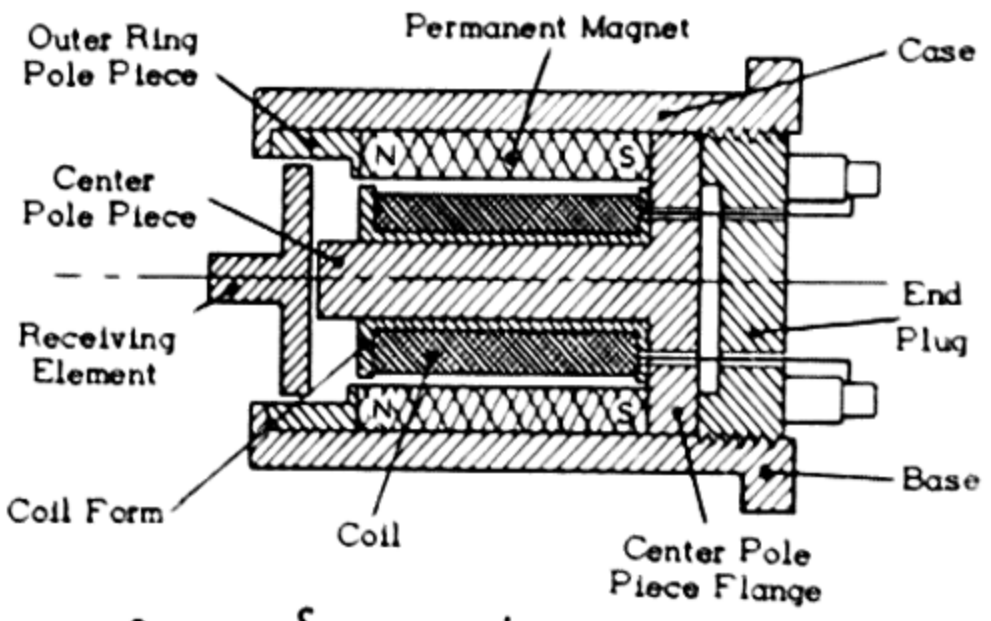
Extreme Displacement to Either Side

Ref. Consolidated Engineering Corp. (C10) and Draper, Bentley and Willis (D14).

Note: The receiving element is either located concentrically with respect to the support rod by means of bearings or flexures or is carried by the moving member.

k) Electromagnetic generator angular velocity receiver



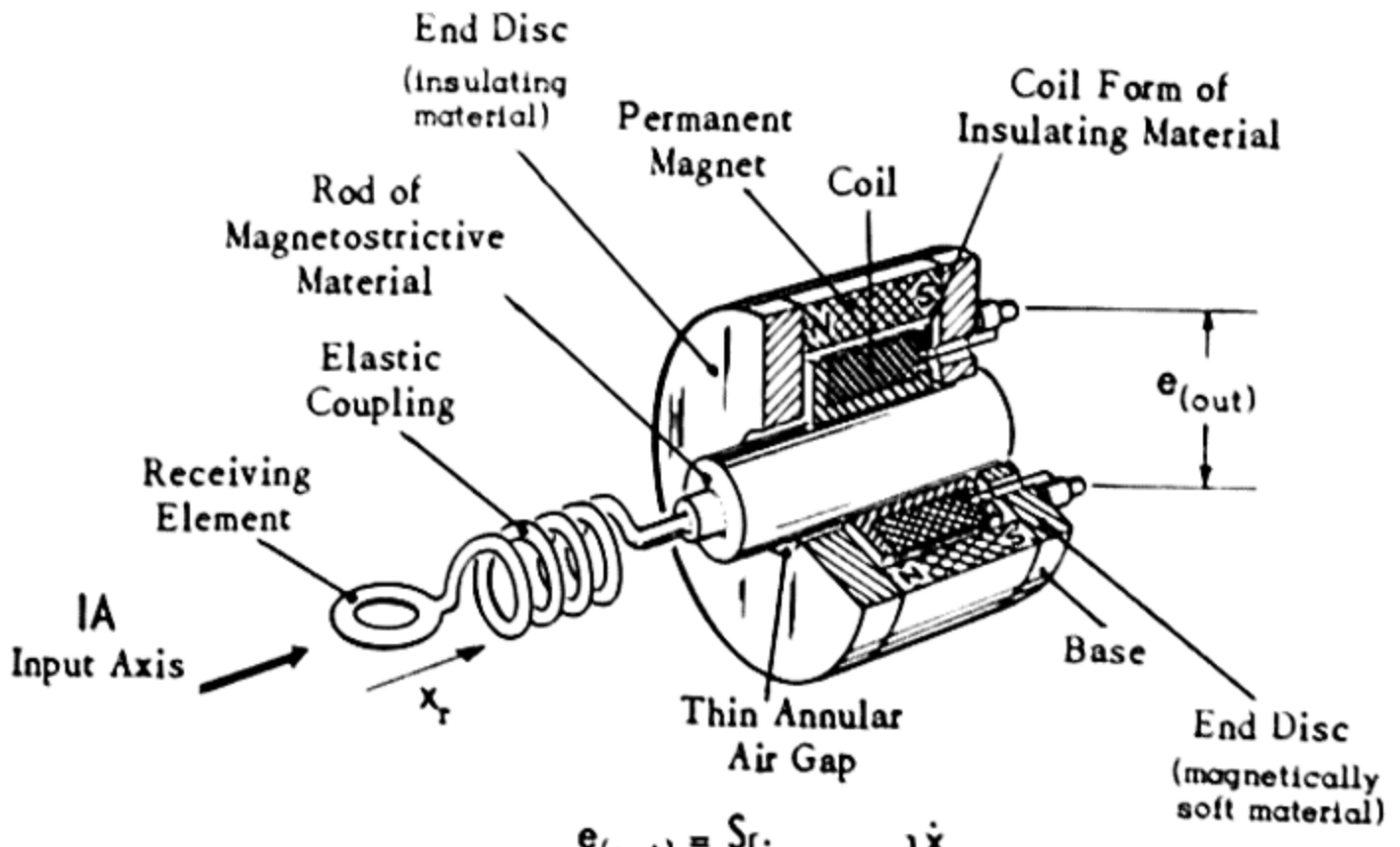


$$e_{(out)} = S_{[\dot{x}_r;e_{(out)}]}\dot{x}_r$$

Note: In practice, the armature may be formed as a diaphragm with the outer air gap replaced by the clamping ring. In other applications, the armature may be held in alignment by support from the moving input member.

Ref. Draper, Taylor, Lancor and Coffey (D15).

l) Variable-air-gap linear velocity receiver

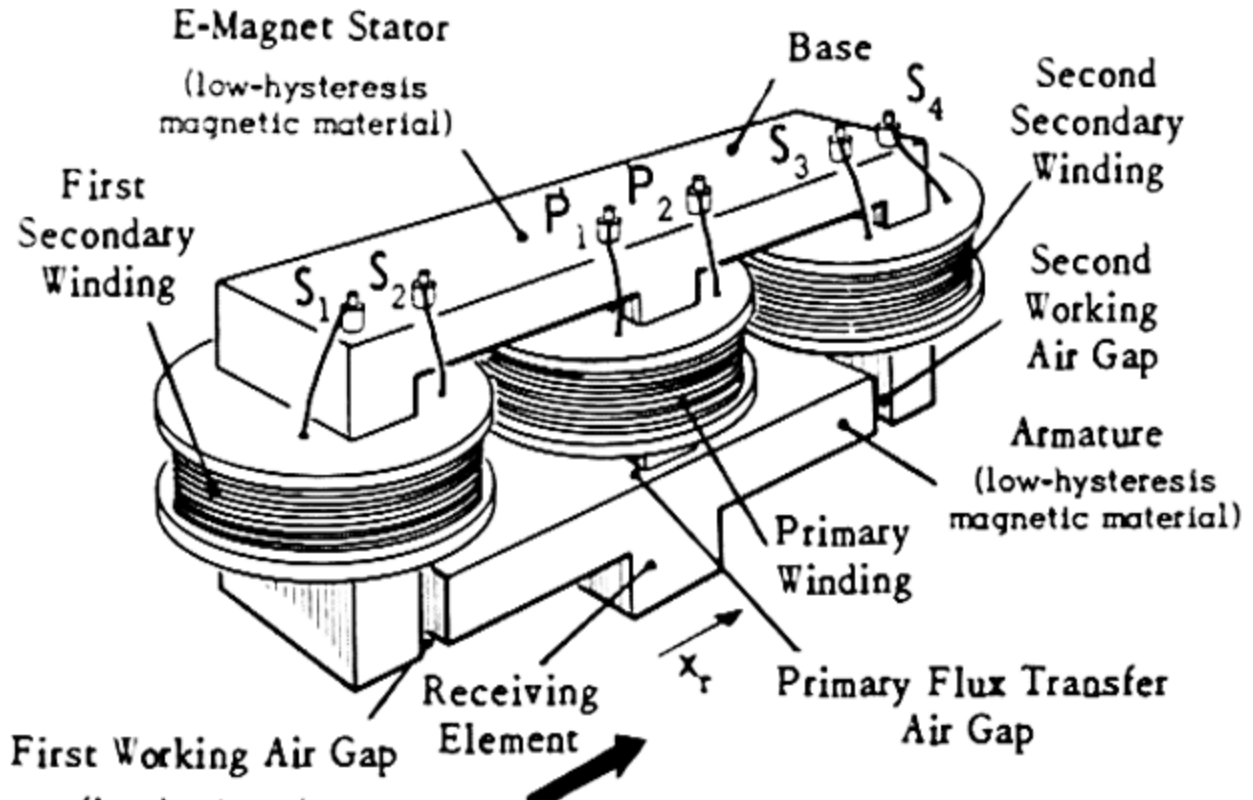


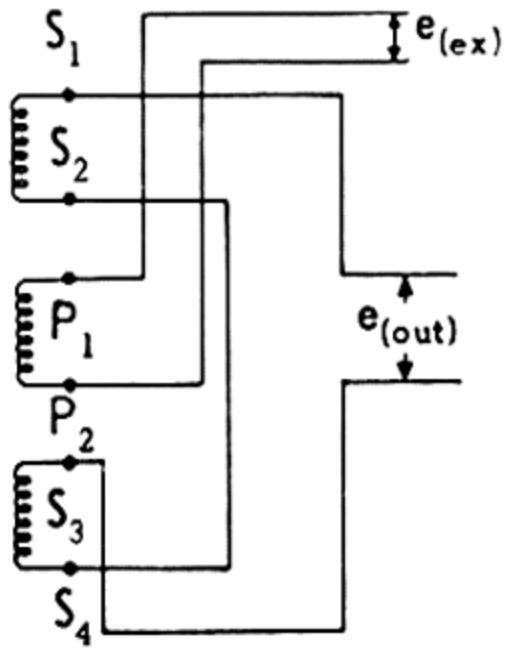
$$e_{(out)} = S_{[\dot{x}_r;e_{(out)}]}\dot{x}_r$$

Ref. Smith and Luxford (S19).

m) Magnetostrictive linear velocity receiver

Fig. 35-5. Illustrative diagrams of typical relative motion receivers and indicators. (Page 4 of 6)





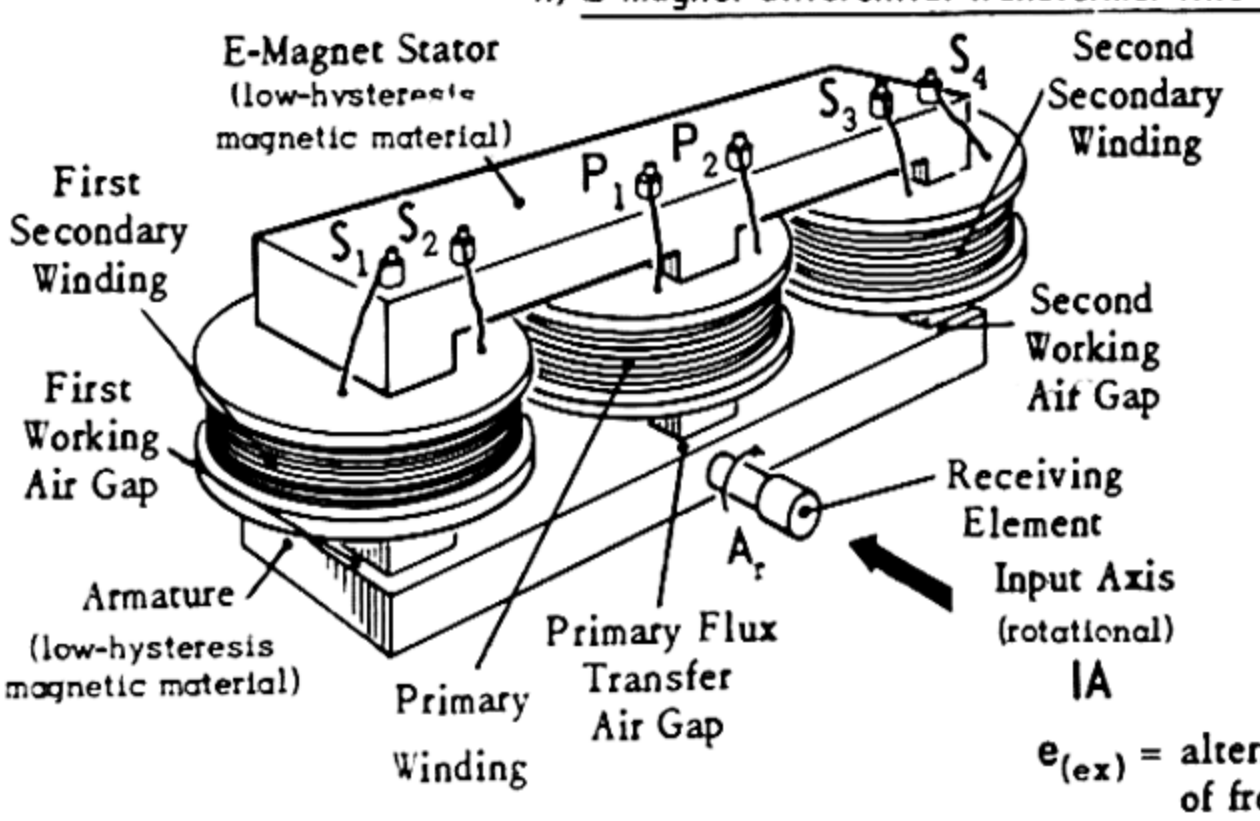
Note: Excitation current, $i_{(ex)}$, rather than excitation voltage, $e_{(ex)}$, appears in the input-output relationship since current is more closely associated with flux than voltage is, and in most practical situations it is easier to measure the excitation current than the excitation voltage.

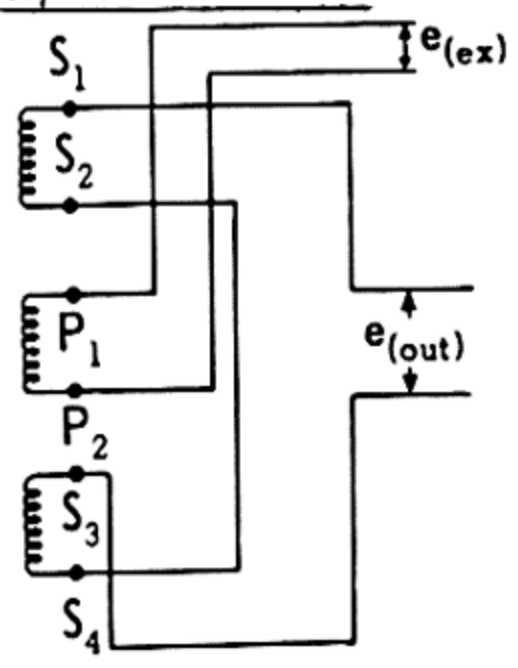
Ref. Hetényi (H14) and Mason (M18).

$e_{(ex)}$ = alternating-current voltage of frequency $n_{(ex)}$ and current $i_{(ex)}$

$e_{(out)} = S_{[x_r; n_{(ex)}, i_{(ex)}; e_{(out)}]} n_{(ex)} i_{(ex)} x_r$

n) E-magnet differential transformer linear displacement receiver





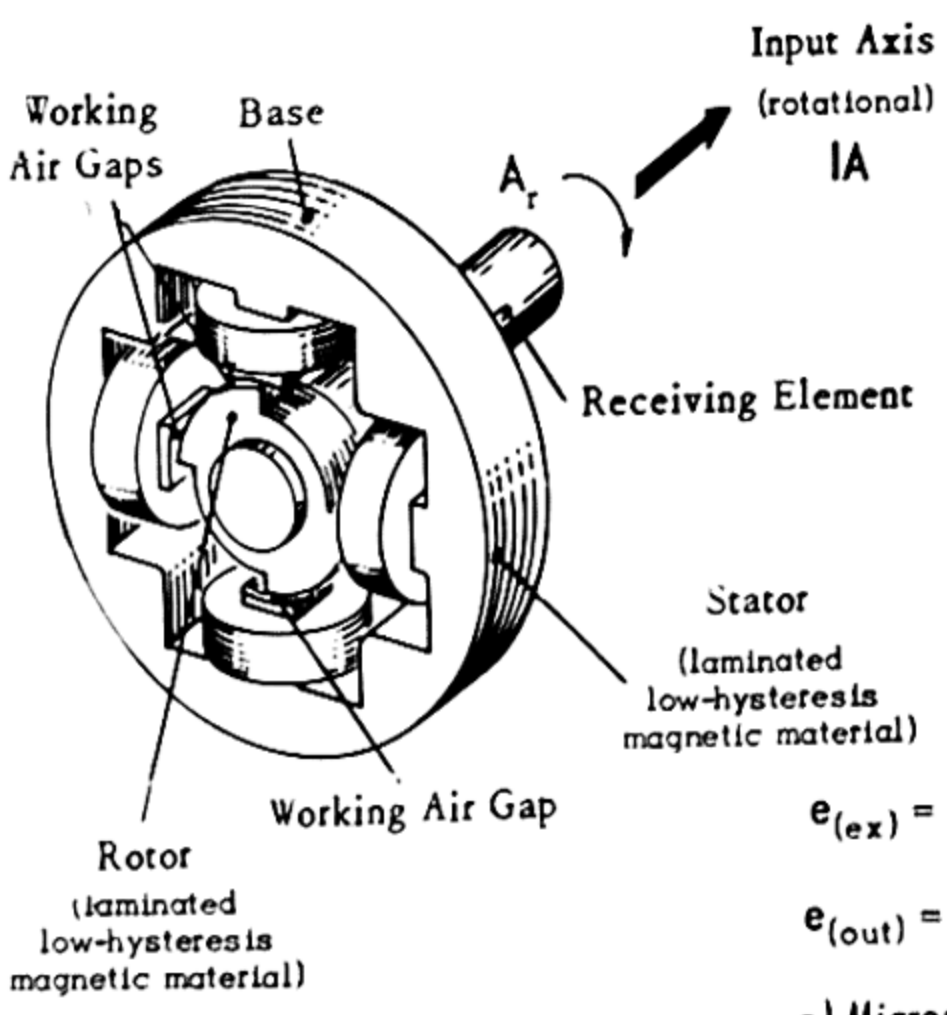
Ref. Hetényi (H14) and Mason (M18).

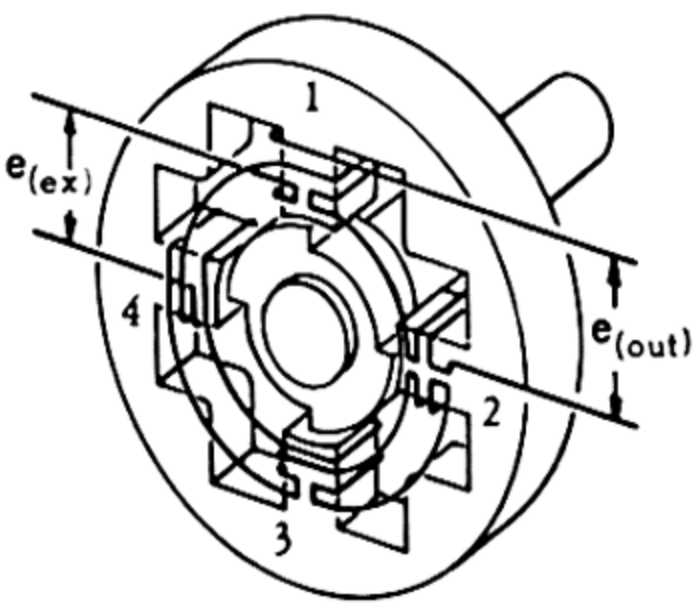
$e_{(ex)}$ = alternating-current voltage of frequency $n_{(ex)}$ and current $i_{(ex)}$

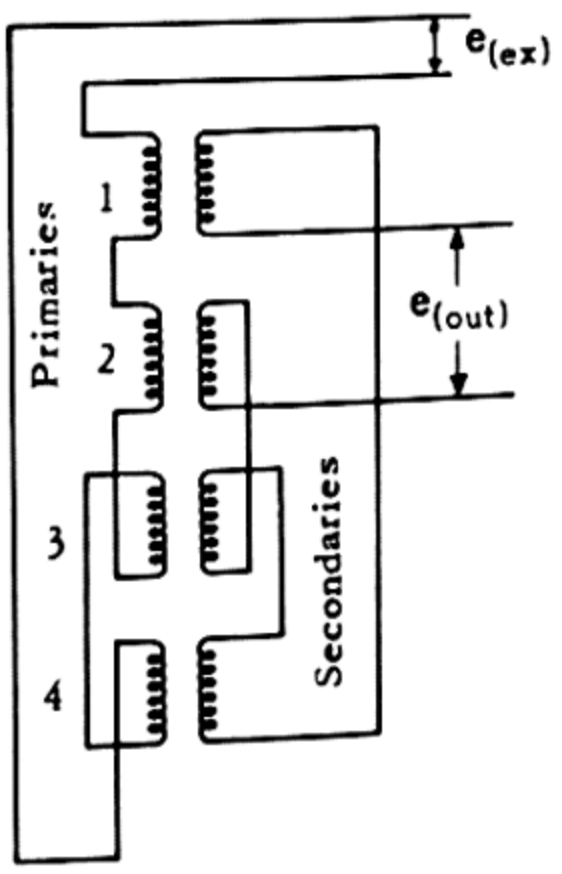
$e_{(out)} = S_{[A_r; n_{(ex)}, i_{(ex)}; e_{(out)}]} n_{(ex)} i_{(ex)} A_r$

o) E-magnet differential transformer angular displacement receiver

Note: In practice, the rotor is centralized with respect to the stator by means of bearings or flexures not shown in the diagram.







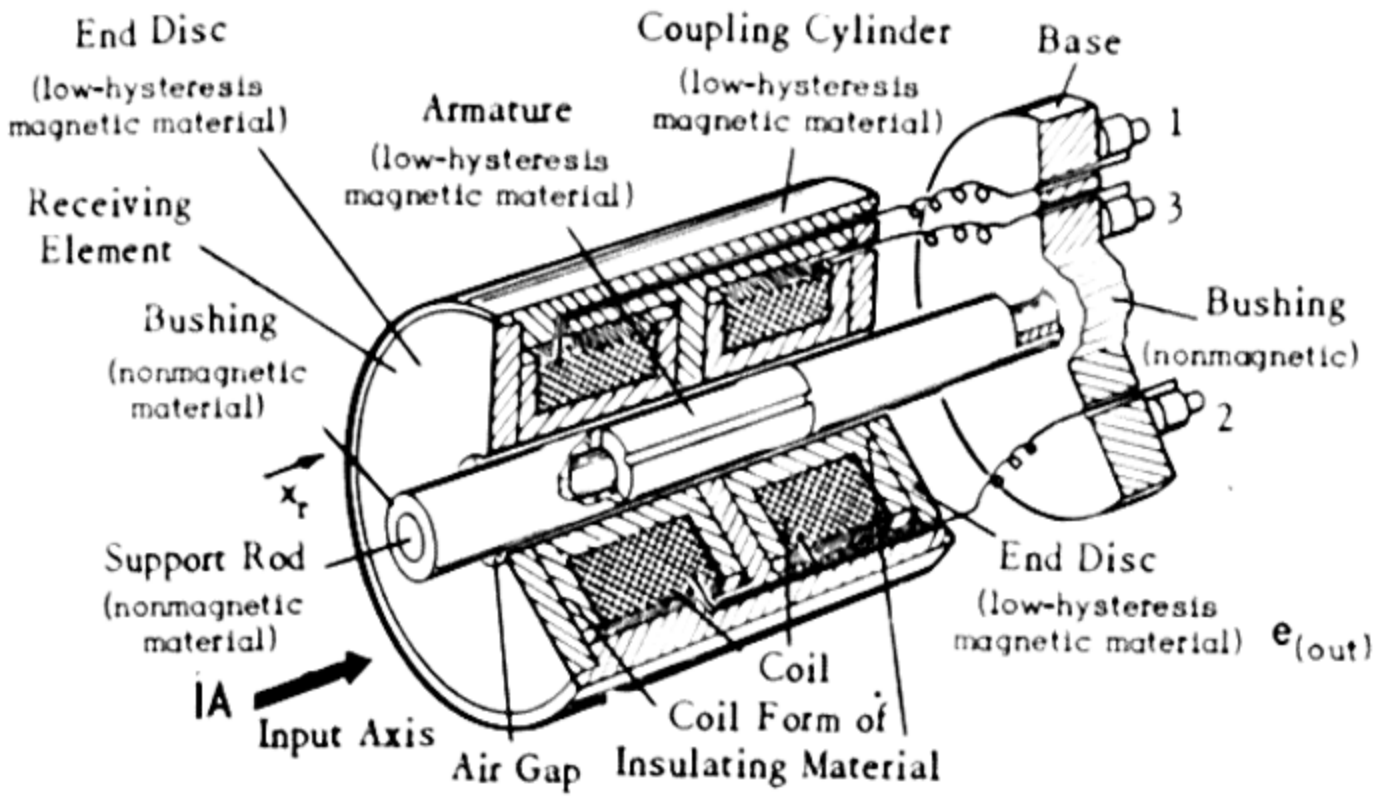
$e_{(ex)}$ = alternating-current voltage of frequency $n_{(ex)}$ and current $i_{(ex)}$

$e_{(out)} = S_{[A_r, i_{(ex)}, n_{(ex)}; e_{(out)}]} i_{(ex)} n_{(ex)} A_r$

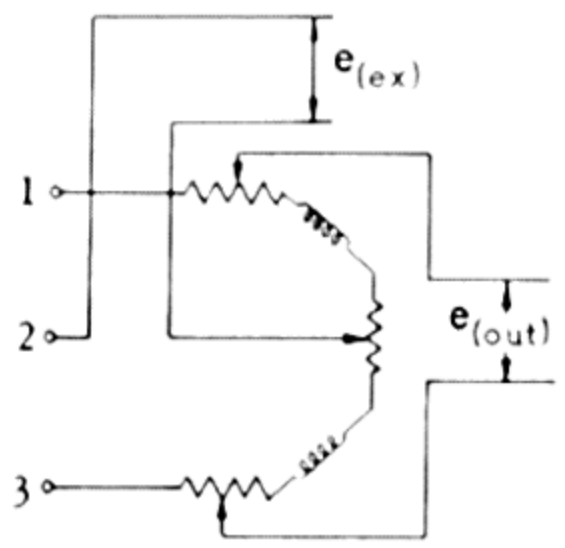
Ref. Mueller (M15).

p) Microsyn angular displacement receiver

Fig. 35-5. Illustrative diagrams of typical relative motion receivers and indicators. (Page 5 of 6)



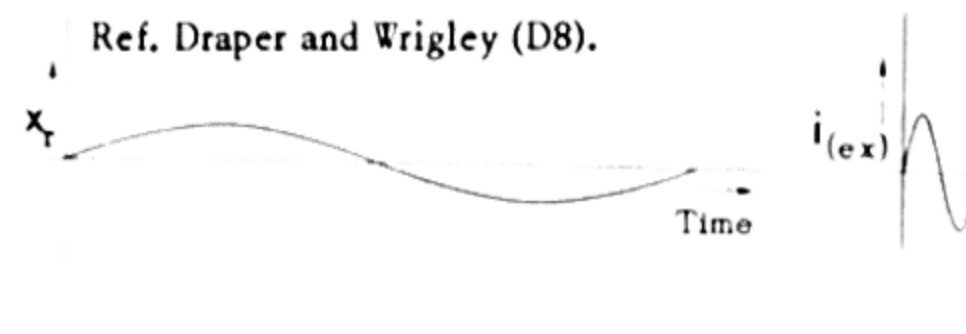
Ref. Draper and Wrigley (D8).



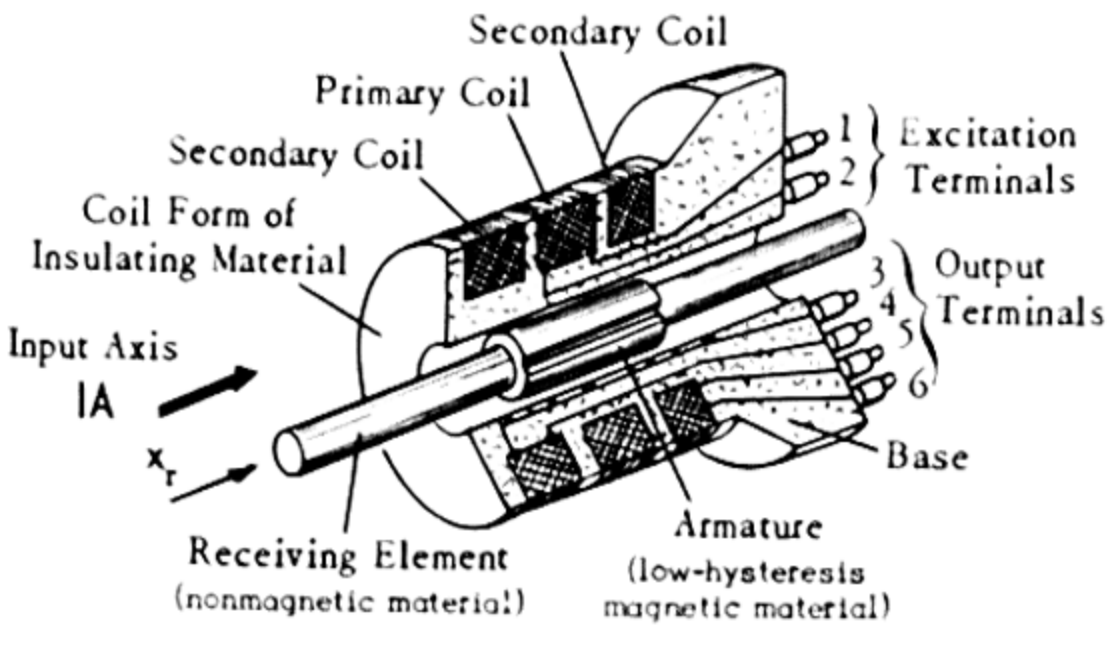
Note: The receiving element is aligned concentrically with respect to the support rod either by flexures or bearings or by attachment to the moving member. These means of alignment are not shown in the diagram.

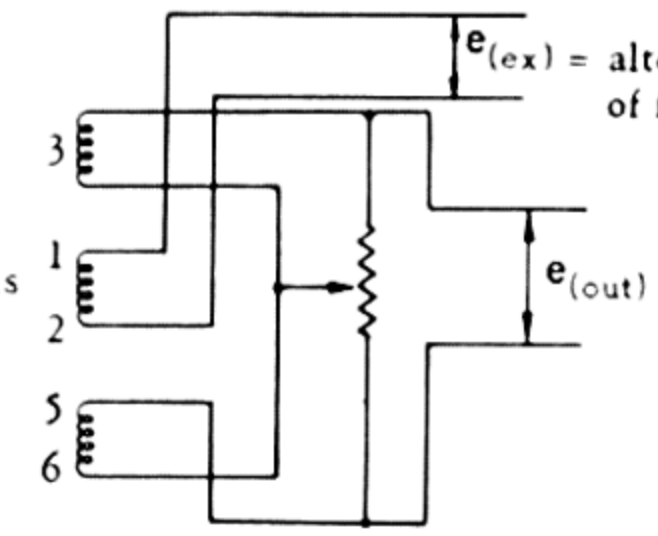
$$e_{(out)} = e_{(out)(x_r=0)} + S_{[x_r;e_{(ex)},n_{(ex)};e_{(out)}]} e_{(ex)} n_{(ex)} x_r$$

$e_{(ex)}$ = alternating-current voltage of frequency $n_{(ex)}$ and current $i_{(ex)}$



q) Concentric-coil inductance-bridge linear displacement receiver





$e_{(ex)}$ = alternating-current voltage of frequency $n_{(ex)}$ and current $i_{(ex)}$

Note: The receiving member alignment with respect to the base is maintained either by flexure supports from the base or by attachment to the moving member.

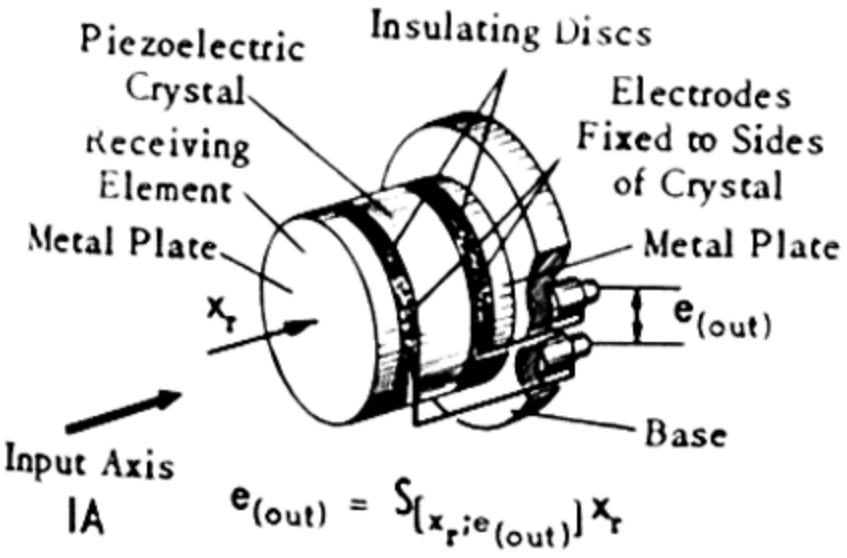
$$e_{(out)} = S_{[x_r;i_{(ex)},n_{(ex)};e_{(out)}]} i_{(ex)} n_{(ex)} x_r$$

Ref. Boggis (B23).

r) Concentric-coil differential coupling transformer linear displacement receiver

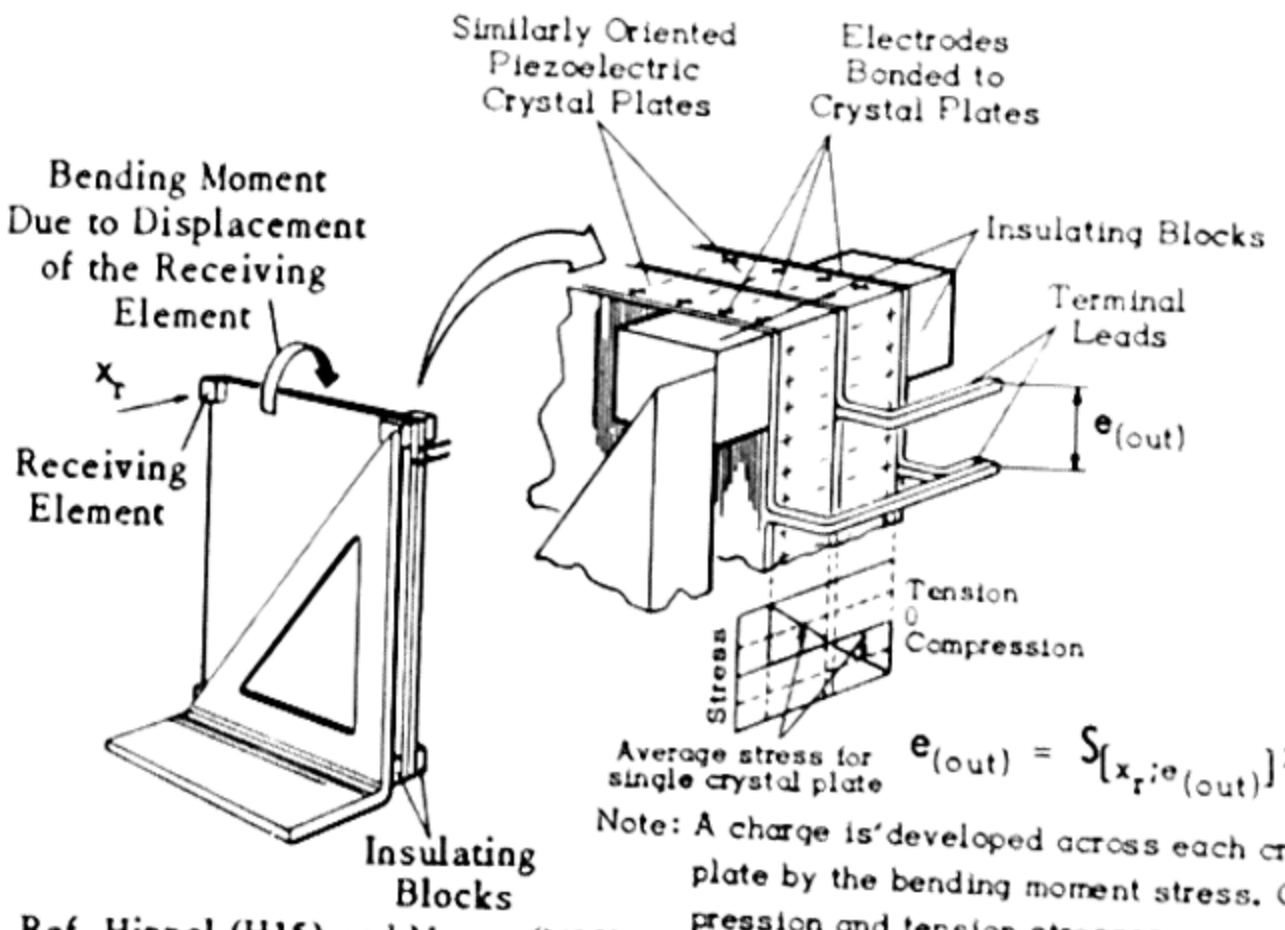
Note: Piezoelectric material may be obtained in the form of properly cut natural crystals, such as quartz and Rochelle salt, or in the form of ferroelectric ceramics, such as barium titanate, which can be polarized to give piezoelectric properties by the application of electric potential.

Ref. Hippel (H15) and Mason (M18).



$$e_{(out)} = S_{[x_r;e_{(out)}]} x_r$$

s) Normal-stress piezoelectric linear displacement receiver



$$e_{(out)} = S_{[x_r;e_{(out)}]} x_r$$

Note: A charge is developed across each crystal plate by the bending moment stress. Compression and tension stresses cause charges of opposite polarity.

Ref. Hippel (H15) and Mason (M18).

t) Bending-moment-stress piezoelectric linear displacement receiver

Fig. 35-5. Illustrative diagrams of typical relative motion receivers and indicators. (Page 6 of 6)

potentiometer connected across the source of excitation, which may be either direct-current voltage or alternating-current voltage. Changes of temperature of the cantilever affect the bonded arms of the bridge equally, so that the output voltage contains no component due to temperature variations. On the other hand, a displacement of the receiving element parallel to the input axis causes a shift in the state of strain of the cantilever that changes the resistance of the longitudinal winding without affecting the transverse winding. The result is an unbalance of the bridge, which produces the output signal.

35.45. Bonded resistance wire displacement receivers are simple and rugged, but the energy input is larger than that required by an unbonded resistance wire receiver because of the greater amount of elastic material that must be stressed. A typical bonded wire receiver may have a cantilever several inches long and be capable of accepting input displacements up to 1 inch. With an excitation of 60 volts applied to a bridge with arms of 2000 ohms, the open-circuit-output displacement-voltage sensitivity may be 100 millivolts per inch.

ELECTRONIC TUBE DISPLACEMENT RECEIVER

35.46. Figure 35-5e illustrates the essential features of an electronic tube displacement receiver based on the control of an electron stream by interacting electrostatic fields. Except for a narrow slit, a hot cathode is completely enclosed by a solid metal grid. The slit is parallel to the length of the cylinder that forms the cathode. A tapered cylindrical rod is positioned with its length parallel to the slit. This rod passes through the center of a metal diaphragm that seals the end of the metal shell enclosure for the tube. The exposed end of the rod that projects through the diaphragm serves as the receiving element for displacements that rotate the rod in a plane parallel to the grid surface containing the slit.

35.47. The electrical circuit diagram of Fig. 35-5e shows the grid connected to the cathode, and the receiving element rod connected to the tube shell so that both act as anodes. This anode system is made positive with respect to the cathode by a voltage source acting through a load resistor. The output signal that represents the input displacement is taken across the load resistor.

35.48. With the receiving element positioned so that it is completely clear of the path from the cathode to the outer shell anode, electrons build up on the grid to produce an electrostatic field that substantially cuts off current flow through the slit. When an input displacement tilts the control anode so that it is partially in front of the slit, the electron-retarding negative electrostatic field of the grid is neutralized to some extent by the positively charged rod close to the grid surface. This action allows more electrons to be drawn to the anode surfaces, so that the effective resistance of the tube is decreased, and a change occurs in the output voltage taken from the load resistor. When the tapered rod is tilted away

from the slit in the other direction, the action just described is reversed, and the current through the output resistor is decreased.

35.49. Interactions of the kind described in the previous paragraph cause the output voltage of the electronic tube receiving system to follow variations of the input displacement. The output circuit may be modified as required for operation of any desired indicating system. Typical electronic tube displacement receivers occupy about 0.5 cubic inch and have a weight in the region of 0.25 ounce. With a load resistor of about 50,000 ohms and a plate supply of 20 volts, the displacement-voltage sensitivity of the system is in the region of 5000 volts per inch over an input displacement range of ±0.001 inch.

ELECTROSTATIC CAPACITY RELATIVE MOTION RECEIVERS

35.50. Signal generating systems for relative displacement receivers may be based on changes in electrostatic capacity due to motion between the conducting surfaces of a condenser. The diagrams of Figs. 35-5f, 35-5g and 35-5h illustrate the essential mechanical features of relative motion receivers designed to use electrostatic capacity variations for producing output signals. The receiving element is a metal plate with flexure supports that allow motion with respect to the base in the direction parallel to the input axis. These flexure supports are insulated from the base so that the connected plate acts as one side of an air-insulated condenser. The other side of the condenser is a rigid U-shaped structure of two plates mounted on the base and positioned with their faces parallel to the plane of the receiving element. A positive relative displacement causes the receiving element to move toward the closed end of the U-shaped structure so that the overlapping area of the plates in the small-air-gap region is made greater, and the electrostatic capacity increases. In a similar way, a negative relative displacement causes a decrease in capacity.

35.51. The electrical circuit diagram of Fig. 35-5f shows the condenser of the relative motion receiver connected in series with a source of direct-current excitation and a load resistance. The output is voltage taken from the ends of the load resistance. In an arrangement of this kind, current flows through the resistor only when the capacity is changing. This current is substantially proportional to the rate of change of capacity and consequently depends on the relative velocity input. Since the open-circuit output signal, which is the voltage drop across the resistance, depends on the relative velocity input, the system acts as a linear velocity receiver.

35.52. Typical condenser-type relative velocity receivers occupy approximately 1 cubic inch, may weigh 1 ounce, and operate over an input displacement range of ±0.1 inch. With a zero-deflection capacity of 100 microfarads, a load resistance of 10,000 ohms, and an excitation of 100 volts, the linear velocity - voltage sensitivity may be in the region of 0.04 millivolt per centimeter-per-second.

35.53. The electrical circuit diagram of Fig. 35-5g shows the plates of a condenser-type displacement receiver connected as one arm of an alternating-current-excited resistance-capacitance bridge. The output signal is taken from the pair of bridge-arm connection points opposite to those at which the excitation is applied. A receiver unit with characteristics similar to those noted in the previous paragraph, a fixed-value bridge-arm condenser whose capacity is equal to the zero-input-deflection capacity of the receiver unit, equal resistance arms of 300,000 ohms, and an excitation of 10 volts at 5000 cycles per second has a displacement – voltage amplitude sensitivity of approximately 2 volts amplitude per centimeter.

35.54. The circuit diagram of Fig. 35-5h illustrates a method for improving the sensitivity of a relative motion receiver of the electrostatic type. The receiver unit output terminals are connected so that the internal capacity acts as the condenser in a resonant circuit with low damping. This means that the resonant frequency of this tuned circuit changes as the input displacement varies. The tuned circuit is excited with a frequency very close to the region of resonant frequencies determined by the input displacements. Under these conditions, the output voltage taken from the resonant circuit by a detector circuit varies with frequency along a curve similar to that illustrated by the voltage amplitude ratio plot of Fig. 35-5h. By proper selection of the range of operation, the displacement – voltage amplitude sensitivity may be maintained at a high and substantially constant value. With a receiver having a variable-condenser element like that of Figs. 35-5f and 35-5g, and reasonable circuit constants, it is possible to achieve a displacement – voltage amplitude sensitivity of 10 volts amplitude per centimeter.

ELECTROMAGNETIC GENERATOR RELATIVE VELOCITY RECEIVERS

35.55. Electromagnetic generators are often applied in signal generating systems for relative motion receivers. Many different designs have been developed, but all have the common feature of depending on variations of magnetic flux linkages with a coil or a system of coils. The essential feature of such arrangements is that the source of the magnetic field (either a permanent magnet or an electromagnet) must have its motion controlled by either the receiving element or the base while the coil winding is carried by the other member of this pair. Under the law of electromagnetic induction, the open-circuit voltage at the terminals of the coil or coil system is proportional to the rate of change of magnetic flux linkages. This rate of change varies with the velocity of the receiving element with respect to the base. The net result of operation of the electromagnetic system described is that the terminal voltage has the properties of the output signal from a relative velocity receiver.

35.56. Figure 35-5i shows a linear velocity receiver in which a single coil winding from which the output is taken is wound on a hollow, cylindrical coil form

fixed to the base. The receiving element is a composite structure with a cylindrical permanent magnet fitted with internal low-friction bushings that is free to slide on a straight support rod mounted on the base. The center line of this rod is concentric with the center line of the coil form and is parallel to the input axis of the receiver. The receiving element is completed by a cylinder of magnetically soft material with end pieces. One of these end pieces is a press fit to the magnet. The other end piece has a circular hole with an internal diameter sufficient to permit free passage of the coil as the receiving element moves with respect to the base. Any velocity of the receiving element with respect to the base along the input axis causes the turns of the coil to be swept through the radial magnetic flux in the air gaps between the coil end of the magnet and the end piece with the cylindrical hole. The induced voltage in the coil that results from this cutting of flux lines is the output signal of the linear velocity receiver.

35.57. Electromagnetic signal generating systems of the type shown in Fig. 35-5i have been designed in various sizes. For example, a unit occupying a volume of 2 cubic inches might weigh 4 ounces and have a velocity-voltage sensitivity of 0.03 volt per centimeter-per-second.

35.58. Figure 35-5j illustrates the features of a modified form of the linear velocity receiver of Fig. 35-5i. In this receiver, in which the slide-rod support of the receiving element is eliminated, two coils wound in opposite directions are carried on a rod of magnetically soft material fixed to the base, and the receiving element includes a hollow-cylinder permanent magnet and two end discs of magnetically soft material with cylindrical holes. With this arrangement, two annular air gaps are formed between the end discs and the coil windings. In actual units, the receiving element is either supported and constrained to move along the input axis by means of a flexure system or attached to the moving member so that it remains in proper alignment, with the radial-air-gap clearances maintained constant. For comparable sizes, a unit with the double-air-gap, double-coil configuration of Fig. 35-5j has a velocity-voltage sensitivity approximately one and a half times the sensitivity of a single-coil unit of the type shown in Fig. 35-5i.

35.59. Figure 35-5k illustrates the features of an electromagnetic generator angular velocity receiver. The cylindrical support rod and the base are made from the same piece of nonmagnetic material, with the center line of the rod along the input axis for the unit. This rod carries a soft-iron armature consisting of a coil space enclosed on both sides by soft-iron end plates. The total thickness of the armature is divided into three equal parts, two for the end plates and one for the coil itself. The armature is fitted tightly into a slot cut through the support rod, with the axis of the coil intersecting the input axis at right angles, and the plane of symmetry for the flat surfaces of the armature sides passing through the

input axis. The exposed end surfaces of the armature side pieces are shaped as cylindrical segments, with the input axis as the common center. Leads from a coil wound on insulating material cemented in the space between the armature side plates are carried through a hole in the support rod to terminals mounted on the base.

35.60. The receiving element for the unit of Fig. 35-5k is made up of a tightly fitting retaining ring that holds two horseshoe magnets with their ends forced into contact with two pole pieces of magnetically soft material. The inner surfaces of these pole pieces are cylindrical segments with their common center coincident with the input axis of the unit. The diameter and circumferential extent of the inner surfaces of the pole pieces match the outer surfaces of the armature to form four radial air gaps, with the outer surfaces of the armature side plates completely covered when the receiving element is in its zero-input-deflection position. In practice, the receiving element is either carried by bearings or flexures mounted on the support rod or is kept in proper alignment and position with respect to the rod by attachment to the member from which the input is taken. The working angular input range of the receiver is between the two extreme positions in which the inner face of one side plate is in radial alignment with the outer edges of the pole pieces. When the receiving element is in its zero-input-deflection position, each side of the armature carries half of the total flux that passes across the four air gaps. When the receiving element rotates with respect to the base so that it moves away from this position, magnetic flux shifts from the air gaps of one side plate to the air gaps of the other side plate. In making this shift, the flux cuts across the turns of the coil wound on the magnetic section of the armature that holds the two side plates together. The voltage induced by this action is proportional to the rate of change of the flux, which in turn is determined by the angular velocity of the receiving element with respect to the base.

35.61. An example of an electromagnetic generator relative angular velocity receiver occupying 6 cubic inches, weighing 10 ounces, and operating over an input range of ±10 degrees has an angular velocity – voltage sensitivity of 1.04 millivolts per degree-per-second.

VARIABLE-AIR-GAP LINEAR VELOCITY RECEIVER

35.62. Signal generating systems for linear motion receivers may be based on any principle available for changing the reluctances associated with magnetic circuits so that motion of the receiving element causes flux lines to cut the turns of a coil system as they shift from one magnetic path to another path. This mode of operation is generally similar to that applied in the rotational motion receiver of Fig. 35-5k. The essential features of a signal generating system using changes in axial air gap length to produce signals is shown in Fig. 35-5l. A permanent magnet with the shape of an annular cylinder is closed at one end by the flange of a center pole piece of magnetically soft material. The other end of the permanent

magnet is in contact with the outer ring pole piece, an annular ring of magnetically soft material that serves as the outer surface for the outer air gap of an armature of magnetically soft material. The flange and the annular ring are clamped to the ends of the permanent magnet by an enclosing case of nonmagnetic material and a threaded end plug that carries the output terminals. A flange on the case acts as the base. The armature, to which the receiving element is directly attached, is a thin circular plate that fits inside the outer ring pole piece with a small-clearance constant-length air gap. The center pole piece air gap, which is the working air gap, is formed between the central area of the armature and the end of the center pole piece. This gap has a length equal to a small fraction of the pole diameter when the receiving element is in its zero-input-deflection position. The pole piece is located by its flange and clamped by the case so that its center line is identical with the center line of the cylindrical permanent magnet and is parallel to the input axis of the unit. The coil in which the output voltage is generated is wound on an insulating form that is firmly cemented to the center pole piece.

35.63. In the receiver arrangement of Fig. 35-51, a positive input deflection of the receiving element causes the armature to approach the center pole piece so that the center air gap is shortened and the reluctance of the path through the pole decreases and the flux in this part of the circuit increases. The voltage induced in the coil as this flux change occurs is the open-circuit output voltage of the unit. The output voltage is proportional to the rate of change of flux linkages and consequently depends on the velocity of the receiving element. When the input velocity is in the negative direction, the gap length increases, the flux linkages decrease, and the induced voltage is in the direction opposite to that produced by a positive input velocity. Except for changes in magnetic flux fringing that accompany changes in the ratio of gap length to gap diameter, the output voltage from a unit with the features shown in Fig. 35-51 is proportional to the rate of change of the input displacement. These fringing effects are of secondary importance as long as input deflections remain small in comparison with the center pole diameter.

35.64. In practical receivers, the outer air gap is often eliminated by using a diaphragm as the armature. When a diaphragm is used, the air gap surface opposite the center pole face is not a plane, but is a surface of revolution determined by the thickness and elastic properties of the metal used for the disc. For small air gap – pole diameter ratios and small displacement – air gap ratios, differences of the diaphragm surface from a perfect plane do not seriously affect the performance of the unit as a linear velocity receiver.

35.65. The gap-length variation principle may be applied in many ways in addition to that illustrated in Fig. 35-51. For example, two variable gaps may be designed to vary differentially to improve linearity and to increase output.

35.66. In practice, a variable-air-gap-length velocity receiver of the type shown in Fig. 35-51 may have a volume of 1 cubic inch, weigh 4 ounces, and operate with substantially constant sensitivity over an input displacement variation in the region of ±0.001 inch. The open-circuit velocity-voltage sensitivity of a unit of this type is in the range of 15 millivolts per centimeter-per-second.

MAGNETOSTRICTIVE LINEAR VELOCITY RECEIVER

35.67. Magnetostrictive effects that accompany strains in certain metals may be used to transform mechanical displacements into variations of magnetic reluctance. This makes it possible to design signal generating systems for relative motion receivers with variable-reluctance air gaps replaced by continuous paths of metal. Figure 35-5m illustrates a linear velocity receiver that includes an outer cylindrical permanent magnet with a soft-iron disc acting as the base on one end and a similar soft-iron disc with a central hole closing the other end. A cylindrical rod of magnetostrictive material is tightly pressed into the base and passes through the disc on the other end with a very small annular air gap that does not change its reluctance with input displacements. A spiral spring is fixed to the magnetostrictive rod. The free end of the spring serves as the receiving element. When this element is subjected to linear displacements, the other end of the spring applies corresponding force variations to the rod of magnetostrictive material.

35.68. The consequent strain effects in the magnetostrictive rod are accompanied by reluctance variations in the magnetic circuit that encloses the turns of the coil, and cause changes in the flux linkages. The resulting induced voltage is the open-circuit output voltage from the coil. Within the operating range of a given receiver, this signal is proportional to the input velocity.

35.69. A typical magnetostrictive linear velocity receiver has a volume of 1.5 cubic inches, a weight of 4 ounces, and operates over an input region of ±0.00025 centimeter. The open-circuit velocity-voltage sensitivity is approximately 0.002 volt per centimeter-per-second.

35.70. The magnetostrictive receiver structure of Fig. 35-5m may be adapted for use as a linear displacement receiver by substituting a soft-iron cylinder for the permanent magnet and using the coil as one arm of an alternating-current bridge. Compensating actions for temperature and nonlinearities may be introduced by properly arranging two air-gap-and-coil combinations to form differential transformer units.

E-MAGNET DIFFERENTIAL TRANSFORMER LINEAR DISPLACEMENT RECEIVER

35.71. The variable-length-air-gap principle is applied in differential transformer units that are commonly called "E-magnet pickoffs." Figure 35-5n illustrates the features of a linear displacement receiver of this type. A stator

of low-hysteresis magnetic material acts as the base of the receiver and has three open-end cores in an E configuration. Each of the two outer legs, which are longer than the middle leg, carries a secondary winding. The middle leg carries the primary winding. A rectangular bar-shaped armature of low-hysteresis material is located with its flat end surfaces adjacent to the inner surfaces of the outer legs of the stator. The length of the armature is chosen so that working air gaps somewhat greater than the desired maximum input displacement for the unit exist between the ends of the armature and the stator pole faces when the armature is in its zero-input-displacement position. The armature is constrained to move parallel to its length and, at the same time, to have a small constant-length primary flux transfer air gap opposite the end of the middle pole of the stator. A projection from the armature acts as the receiving member for displacements along the input axis, which is parallel to the longitudinal center line of the armature.

35.72. The electrical circuit diagram of Fig. 35-5n shows the connections of the E-magnet linear displacement receiver. The primary is connected to a source of alternating current of substantially constant frequency and magnitude. The two secondaries are connected in series opposition, with the output signal taken from the terminals of the combined secondaries. This signal has its null* level when the armature is positioned with the working air gaps effectively equal in reluctance so that the same amount of alternating-current excitation flux from the primary is coupled into each one of the identical coil secondaries. When the receiving element is moved away from the zero-input-displacement position, one working air gap increases in reluctance while the other working gap decreases in reluctance, so that the flux coupled with one secondary increases while the flux coupled with the other secondary decreases. In this situation, the output voltage changes from the null condition to a greater amplitude at the excitation frequency. Depending on the directions of the windings and the connections used, the output voltage is either in phase or 180 degrees out of phase with respect to the phase of the excitation current in the primary. Over the range of linear operation, the amplitude of the excitation-frequency component of the output signal increases as the input displacement is made greater in the same direction, while the phase with respect to the excitation remains unchanged. Input displacements in the opposite direction from the zero position cause a similar increase in output signal amplitude, but with a phase shift of 180 degrees with respect to the excitation.

35.73. One practical E-magnet linear displacement receiver unit has a volume of 2 cubic inches, a weight of 6 ounces, and operates over an input displacement range of ±0.01 centimeter. With an excitation current of 50 amperes

* When used in connection with electrical bridge circuits, the term "null" refers to the condition in which the output signal is adjusted as closely as possible to its zero level.

at a frequency of 60 cycles per second, this unit has a displacement – voltage amplitude sensitivity of 50 millivolts per 0.001 inch.

E-MAGNET DIFFERENTIAL TRANSFORMER ANGULAR DISPLACEMENT RECEIVER

35.74. The E-magnet receiver may be used to receive angular displacements by arranging for the input to rotate the armature so that one working air gap increases in length and the other working air gap decreases in length, while the primary air gap remains effectively unchanged. The essential features of an angular displacement receiver of this type are shown in Fig. 35-5o. Except for shortening the two secondary pole pieces and pivoting the armature about its midpoint, the features of the angular displacement receiver are similar to the corresponding features of the linear displacement receiver of Fig. 35-5n.

35.75. A typical E-magnet angular displacement receiver has a volume of 2 cubic inches, a weight of 6 ounces, and operates over a range of input angles of ± 0.1 radian. With an excitation current of 50 milliamperes at a frequency of 60 cycles per second, this unit has an open-circuit angle-voltage sensitivity of 300 millivolts per milliradian.

MICROSYN ANGULAR DISPLACEMENT RECEIVER*

35.76. The Microsyn angular displacement receiver is based on the symmetrical four-pole stator structure shown in Fig. 35-5p. Each of the two wide pole faces of the symmetrical rotor has a circumferential spread equal to one quarter of the circle corresponding to the inner faces of the stator poles. The shaft that carries the rotor is the receiving element. In practice, this shaft locates the rotor (by means not shown in Fig. 35-5p) so that equal-length radial air gaps exist between the rotor and stator pole faces. With the receiving element in the zero-angular-input-deflection position, the rotor pole faces cover the adjacent halves of poles 4 and 1 and also 2 and 3.

35.77. Figure 35-5p shows that each stator pole carries two windings. One winding of each pair is used as a primary that receives an alternating-current excitation current. The other winding of each pair is used as a secondary to supply an output voltage component determined by the flux coupled with the turns of its winding. In operation, the four primaries are connected in series, and the secondaries are connected in series, as shown in the electrical circuit diagram of Fig. 35-5p. This circuit diagram and the associated wiring schematic diagram indicate the relative effects of the primary coils in forcing flux into the rotor

---

* This section has been prepared by Dr. Robert K. Mueller, Associate Professor of Aeronautical Engineering and General Staff Consultant for the Instrumentation Laboratory of the Massachusetts Institute of Technology. Dr. Mueller has credit for the original concept of the Microsyn and is responsible for many advanced developments and refinements of the Microsyn principles.

when the same current is flowing in all coils. These diagrams also show the aiding or opposing senses of the voltages induced in the individual secondary coils when the primary coil system is excited with alternating current.

35.78. In the Microsyn angular displacement receiver, poles 1 and 2 combine to direct exciting flux into the armature through the action of those windings around them that form part of the exciting circuit. This flux is removed by the corresponding windings on poles 3 and 4, which act in a similar joint manner. The differential-coupling effect is applied to the windings in the output circuit, which are adjacent to the exciting windings, as follows. From pole 1 to pole 2, the output windings change their coupling aspect with respect to the excitation windings so that for the centered position of the rotor (zero-angular-displacement position) the net coupling is zero. The same applies to poles 3 and 4 for the centered position of the rotor. When an angular displacement input is applied to the receiving element, the flux linkage becomes predominant in poles 1 and 3 or in poles 2 and 4, depending upon the sign of the angular displacement, and an output voltage is produced. Because of the opposite polarity of the output windings with respect to the excitation windings, one pole pair to the other, respectively, the output voltage changes in phase by 180 degrees when the rotor passes through its zero-displacement position.

35.79. In practice, Microsyn angular displacement receivers are found in a variety of sizes, with the outer diameter only rarely exceeding 2 inches, however. For certain applications where space requirements are critical, Microsyn units are designed to have an outer diameter of about 0.75 inch. A typical Microsyn angular displacement receiver that has an outer diameter of approximately 1.5 inches occupies about 1 cubic inch and weighs about 2 ounces. With an excitation current of 50 milliamperes at a frequency of 400 cycles per second, the angular displacement – voltage amplitude sensitivity for this Microsyn unit is in the region of 12 millivolts per milliradian over an input angle range of ±10 degrees.

CONCENTRIC-COIL INDUCTANCE-BRIDGE DISPLACEMENT RECEIVER

35.80. Inductance variations produced by the changing configuration of a system of magnetic circuits may be applied in relative displacement receivers. Figure 35-5q illustrates the essential features of a concentric-coil inductance-bridge displacement receiver. A nonmagnetic support rod fixed to the base along the input axis carries a hollow cylindrical armature between two nonmagnetic bushings. The receiving element structure is a composite structure that includes an outer cylinder of low-hysteresis material. A disc, machined as an integral part halfway between the ends of the cylinder, has a center hole that is slightly larger than the outer diameter of the armature. The ends of the cylinder are

closed by discs of low-hysteresis material with holes of the same diameter as the hole in the disc at the middle of the cylinder. The radial air gaps between these holes and the bushings on the support rod are maintained by means not shown in Fig. 35-5q. These means may include bearings, flexures, or attachment of the receiving element to the moving member from which the input motion is taken.

35.81. The two cylindrical spaces inside the receiving element cylinder between the middle disc and the end discs contain two coils wound on forms of insulating material. These coils are connected as adjacent arms of an inductance bridge, as shown by the electrical circuit diagram of Fig. 35-5q. The other two bridge arms contain equal fixed-value inductances. Potentiometers are connected at each one of the bridge junctions that are external to the receiver unit. For operation, the bridge is supplied with an alternating-current excitation voltage. When the receiving element is in its zero-input-displacement position, the bridge is brought into inductive and resistive phase and magnitude balance by adjustments of the potentiometers. This balance is complete when the output signal is reduced to its minimum level as an alternating-current voltage amplitude.

35.82. When the input displacement changes from zero, the corresponding movement of the receiving element causes the length of the armature in one coil to decrease, while the armature length in the other coil increases. Because of the reduced reluctance in the magnetic circuit, the inductance of the coil with the greater length of armature increases, while the inductance of the other coil decreases. These changes of inductance unbalance the bridge, so that the amplitude of the alternating-current voltage output from the bridge increases above the null level. A typical situation is illustrated by Fig. 35-5q, in which a constant-amplitude excitation frequency is modulated by the bridge when it receives a sinusoidal input displacement. The corresponding output voltage is a sequence of variable-amplitude sinusoids of the excitation frequency, with a sinusoidal envelope corresponding to the input motion. If the input displacement is symmetrical about zero, and both sides of this envelope are considered, the output signal is a double sinusoid filled in with cycles of excitation frequency. So far as the envelope is concerned, the envelope of these excitation cycles is the same for either direction of the input displacement from the zero position of the input. However, when the phase of individual excitation cycles in the output is considered with respect to the corresponding cycles of the excitation supply, it appears that this phase angle is zero when the input displacement is positive (that is, has the direction from zero that is assigned the positive sense) and is 180 degrees when the input displacement is negative.* This change of relative phase in the output signal occurs

---

* This choice of phase angles for positive and negative inputs is obviously arbitrary. The essential thing is the 180-degree shift of phase in the output voltage with respect to the excitation supply when the input displacement passes through the zero position.

sharply at the zero-input displacement, which corresponds to the balanced bridge condition and makes it possible to apply phase-sensitive detectors* in reducing output signals to continuous curves that represent input displacements.

35.83. A typical inductance-bridge linear displacement receiver occupies a volume of 2 cubic inches and weighs 3 ounces. With an excitation of 10 volts at 3000 cycles per second, it has an input displacement – output signal sensitivity of 1.6 volts per centimeter.

CONCENTRIC-COIL DIFFERENTIAL COUPLING TRANSFORMER DISPLACEMENT RECEIVER

35.84. Inductance-bridge circuits are subject to difficulties in adjustment because it is necessary to establish balance for the arm resistances and at the same time to balance the arm inductances for the zero-displacement condition of the receiving element. The necessity for resistance balance is eliminated when the inductance bridge is replaced by a differential coupling transformer with a single primary and two secondaries. The operating principles of differential transformer arrangements have already been outlined in the discussion of Fig. 35-5n.

35.85. Figure 35-5r illustrates the essential features of a concentric-coil differential coupling transformer linear displacement receiver. A coil-form structure mounted on a base carries three coaxial coils located in adjacent positions along the input axis of the receiver. The middle coil is used as the primary, with its connections brought out to the excitation terminals. Connections to the output terminals are brought out from the other two coils, which act as the opposed secondaries. In operation, the alternating-current excitation is supplied to the primary, and the secondaries are used to generate the output signal, as shown by the circuit diagram in Fig. 35-5r.

35.86. The receiving element for the differential transformer is a rod of nonmagnetic metal with an armature of low-hysteresis material that extends halfway into the secondary coils for the null-output-signal condition. In an actual unit, the receiving element alignment is maintained either by flexure supports from the base or by attachment to the moving member.

35.87. A typical concentric-coil differential coupling transformer displacement receiver occupies about 1 cubic inch and weighs 1 ounce. With an excitation of 6 volts at a frequency of 60 cycles per second, the displacement – voltage amplitude sensitivity is in the region of 2 volts amplitude per centimeter over an input displacement range of ±0.25 centimeter.

PIEZOELECTRIC DISPLACEMENT RECEIVER

35.88. Electrical potential difference is generated between the surfaces of a crystal with piezoelectric properties when it is stressed in the proper way. Figure 35-5s illustrates a method for applying piezoelectric crystals for the generation of output signals for relative displacement receivers. A wafer of

* See Greenwood, Holdam and Macrae (G3) for a discussion of phase-sensitive detectors.

piezoelectric material that has two parallel surfaces covered with thin metal electrodes is mounted between two insulating discs. These discs are in contact with metal plates. The various parts are arranged so that one of these plates acts as the receiving element for relative motion, while the other plate is attached to the base.

35.89. When the receiving element of Fig. 35-5s is given a displacement with respect to the base, the resulting strain set up in the crystal produces a potential difference between the electrodes. This potential difference is received by the electrodes on the surfaces of the crystal and is transferred to terminals by proper connections. Although the potential difference may be of considerable magnitude, the amount of current available is small. This means that very effective insulation must be used in piezoelectric displacement receivers, and that any indicating or recording device to be used with receivers of this type must have high-impedance input circuits. Aside from this special requirement, indicating systems of all kinds may be used with piezoelectric receivers.

35.90. When relative motion is directly used to generate compressive strains in crystals, the allowable motion is small and the input force must be large. This means that piezoelectric crystals effectively act as force receivers. For applications that require large input displacements, an elastic element or a mechanical linkage may be added to the basic arrangement of Fig. 35-5s to convert motion into force. One arrangement for making this conversion is illustrated by the magnetostrictive receiver shown in Fig. 35-5m.

35.91. One example of the piezoelectric displacement receiver of the type shown in Fig. 35-5s occupies about 0.25 cubic inch, weighs 1 ounce, and operates over an input displacement range of ±0.0001 inch. This unit has an internal impedance of 1000 megohms and has an open-circuit displacement-voltage sensitivity of about 5000 volts per inch.

35.92. Figure 35-5t illustrates a form of the piezoelectric linear displacement receiver in which bending strain in a rectangular crystal plate assembly supported at three corners is substituted for the compressive strain used in the arrangement of Fig. 35-5s. The application of bending strain makes it possible to use relatively large plates that allow larger input deflections of the unsupported corner for smaller forces than those realized when compressive strain is applied. In addition to the satisfactory input characteristics, receivers using bending strain may be designed to use larger crystals than crystals available for the compression type of unit and consequently produce more available output.

35.93. A typical piezoelectric displacement receiver with the features of Fig. 35-5t occupies 0.5 cubic inch, weighs 2 ounces, and accepts a relative displacement up to ±0.002 inch. The open-circuit displacement-voltage sensitivity is about 250 volts per inch.

FACTORS DETERMINING SELECTION OF RELATIVE MOTION RECEIVERS

35.94. The diagrams of Fig. 35-5 are intended to illustrate the principles commonly used in relative motion receivers rather than to cover exhaustively the details of all the units that actually may be used. The success of any particular design depends largely upon the quality of the engineering applied and the amount of effort expended in its development. Because of a considerable background of experience with equipment of some particular design, it may often be better practice to use available devices of that design rather than to originate special apparatus for a given purpose. The choice of the receiver type to be used in a particular situation must depend on the judgment of the responsible engineers rather than on the exclusive use of any single set of physical principles.

35.95. The selection of a relative motion receiver for any given application often depends on factors that do not provide sufficient basis for making a clear-cut decision that some particular design is superior to all others. The more usual situation is for a consideration of the factors to provide a number of possible technical compromises that may give nonideal performance within acceptable tolerance limits. These compromises generally do not depend upon the characteristics of a relative motion receiver alone but rather on the over-all performance of the motion-measuring system that includes the receiver and the particular indicating systems with which it is used. It is not feasible to do more than to suggest a list of factors to be studied in selecting the relative motion receiver to be used for meeting the requirements of a specific problem. Such a list follows:

1) Type of Input. It is obvious that a relative motion receiver accepting the desired input must be used. For example, if the input is linear displacement, an angular displacement receiver is not acceptable.
2) Input Range. The receiver must operate over the range of input variations to be handled.
3) Maximum Uncertainty in the Low-Input-Magnitude Range. With the smallest input magnitude to be reliably indicated or recorded specified, it is necessary for the relative motion receiver to be inherently capable of giving reliable output changes for the minimum input change. For example, a receiver based on a wire-wound potentiometer unit must use a wire size small enough to give output "jumps" between adjacent turns that are less than the smallest input displacements to be measured. When these jumps are too great, the relationship between the output signal and input changes in the small-magnitude region will not be accurate, but will have an uncertainty with an intolerably large maximum magnitude.
4) Maximum Uncertainty in the High-Input-Magnitude Range. This property of a relative motion receiver is like the concept of (3) except that the maximum uncertainty associated with high input magnitudes is considered.

When the maximum uncertainty magnitude is identical for large and small input levels, the percentage effect on the output signal is less for high levels and may therefore be acceptable for high inputs but not for low inputs.

5) Average or Root Mean Square Uncertainty over the Input Range. For many relative motion receiver applications, the simple but pessimistic maximum uncertainty may be replaced by a statistical measure. This measure may be selected as the average, the root mean square, or any other concept to fit the requirements of particular situations.

6) Dynamic Characteristics. To be satisfactory for a given application, a relative motion receiver must have tolerably low dynamic errors. For example, an alternating-current bridge or differential transformer arrangement must be capable of using excitation frequencies well above any input frequency components to be handled.

7) Adaptability for Operation with Available Indicating and Recording Equipment. When relative motion receivers are to be used by a facility in which indicating and recording units are already available, it is an economy to select designs that may be used with the existing equipment. For example, when coupling units and oscillographs are designed to handle carrier wave signals from signal generating systems of the low-impedance inductance bridge or differential transformer type, it would be unnecessarily expensive to use a high-impedance electrostatic capacity relative motion receiver when units of the low-impedance type would be equally satisfactory.

8) Availability. When no unacceptable penalty in reduced performance must be paid, it is always better to use designs that may be built from commercially available parts and ordinary materials rather than to design special units requiring rare materials for proper operation.

9) Size and Shape of Space Occupied. In order to provide a solution for any given problem, the relative motion receiver selected must fit into the space limitations determined by the components with which it is to be associated.

10) Weight. Relative motion receiver weight must be compatible with the requirements of the system in which it is to be incorporated.

11) Useful Life and Reliability. Reliability over a reasonably long useful life is a primary requirement of any satisfactory relative motion receiver.

12) Maintenance. The characteristics of (11) should be achievable without an excessively great maintenance effort.

13) Cost. When two or more relative motion receiver types have similar characteristics on the basis of the previously listed factors, units of lowest cost would normally be selected.

14) Proprietary Rights. When a choice of relative motion receivers giving acceptable performance is possible, the use of one particular type may be dictated by proprietary rights held by some organization. Thus a company holding patent rights to piezoelectric devices would naturally use crystals rather than inductance bridges in the signal generating systems of their products.

35.96. The foregoing list of factors is primarily concerned with relative motion receivers as individual units, rather than with the over-all systems in which the receivers are used. In practice, it is always necessary to base final choices of relative motion receiver types on over-all system performance rather than unit characteristics. This performance is partly determined by the receiver and partly depends on the indicating or recording systems to which the receiver is connected. A list of the over-all system performance-determining factors follows:

1) Sensitivity to Mechanical Interference (Shock and Vibration). The environment under which motion receivers must operate often includes mechanical interference made up of varying degrees of shock and vibration. Ideal equipment would be completely insensitive to these effects, so that indications or records would not contain any corresponding components. In practice, it is very difficult to achieve this result, and considerable attention may be required to produce even marginally satisfactory performance. For example, a pressure-indicating system may be sensitive to shock and vibration because the pressure-receiving element and the associated relative displacement receiver of which it is a part may both respond to some extent, and, in addition, the amplifiers required for the indicating system may be microphonic for airborne noise. Any judgment on the type of relative motion receiver to be chosen in this case must depend on the possibility of a satisfactorily low sensitivity to mechanical interference for the complete pressure-measuring system.
2) Sensitivity to Temperature Interference. Temperature may be a difficult environmental input to handle from the standpoint of interference with scale readings. Any satisfactory equipment must be able to give continued operation under the specified environmental temperatures. In addition to this condition, the effects of temperature variations in changing sensitivity or producing indication components directly due to temperature as an input must not exceed specified tolerance limits.
3) Sensitivity to Electrical Interference. Relative motion receivers are often required to operate in the presence of varying electromagnetic fields, power supply units with extraneous voltage variations, grounds with erratic current flows, and other sources of electrical interference. To be satisfactory, a relative motion receiver must be suitable for operation

with indicating systems of a type that gives sufficiently low sensitivity of the over-all system to electrical interference. In general, this sensitivity is lower for systems based on relative motion receivers that have low internal impedance. Receivers with high internal impedance are not excluded from use in any given situation, but usually must have more careful shielding and electrical circuit design than is required for applications of low-impedance units. Impedance is only one of many factors that may be important from the standpoint of sensitivity to electrical interference in any given case. The choice of a receiver type to meet the specifications for a particular situation must depend on a study of characteristics for a number of units combined with various indicating systems.

4) Sensitivity to Other Environmental Interference. To be acceptable for a specified purpose, a relative motion receiver must have satisfactorily low sensitivity to interference from all the environmental quantities not already listed. For example, a receiver that is required to operate under large changes in pressure must not be affected beyond specified tolerance limits.

5) Services Required for Operation. Relative motion receivers that require a minimum of services are preferable to receivers that must be supplied a greater number of auxiliary supplies and devices. For example, receivers that are capable of operating oscillographic recording systems directly are preferred to receivers that require amplifiers in the system. For the same reason, units with magnetic fields provided by permanent magnets are superior to units with electromagnetic excitation that must be supplied by an external direct-current supply. Similarly, systems capable of operating with a single source of standard alternating-current power have obvious advantages over systems that may require both alternating- and direct-current power.

6) Ease of Operation. Relative motion receivers that fit into systems with simple operating procedures are to be preferred to units and systems requiring more complicated procedures. For example, a system requiring no special adjustment or balancing procedures is more practical than any system that must be continually checked and rebalanced.

7) Size and Weight. Size and weight of the complete system may be controlling factors in the choice of the relative motion receiver type and its associated indicating system. For example, equipment to be used for flight measurements in small aircraft must be compact enough and light enough to fit into limited space and keep within a small weight allowance.

8) Reliability. Other factors being equal in the performance of a group of possible relative motion receivers, the type that provides the highest degree of reliability in operation is beyond question to be preferred over

other types. It is important to note that reliability often depends on care and refinement in design and construction rather than on the physical principles involved.

9) Maintenance Characteristics. Maintenance is a factor closely associated with reliability. As a general rule, equipment requiring the least maintenance for satisfactory reliability is selected in any given situation.

10) Cost. When acceptable compromises have been worked out among the factors mentioned above, final decisions on choices of relative motion receiver types will be based on the relative cost of competing equipments. In some cases, small differences may be accepted for special reasons, but these reasons must become more powerful as the cost margin increases.

35.97. The list of factors that assist in forming decisions on relative motion receiver types will usually be modified by the circumstances associated with the engineering problems to be solved in any particular situation. Almost always, certain factors will be dictated by nontechnical facts beyond the control of the instrument engineer. For example, some company policy may limit the funds available for capital equipment so severly that unsatisfactory makeshift relative motion receivers must be applied as better than nothing until a change occurs in the financial situation.

VIBRATORY MOTION RECEIVERS AND INDICATORS

35.98. As already indicated in paragraph 35.27, the distinction between the relative motion receiver and the vibration receiver as operating units is not important when suitable external nonvibrating references are available. In order for the motion receiver output to serve as a vibration signal, it is necessary only to connect the receiving element of the motion receiver to the moving member, and the base of the motion receiver to the nonvibrating reference.* This signal may represent displacement, velocity, or acceleration, or any other function of the relative motion, depending on the characteristics of the receiver used. Since, as noted in paragraph 35.28, relative motion indicators are units in which an indicating system is associated with a relative motion receiver to give a readable index postion as the essential output, the distinction between a relative motion indicator and the corresponding vibration indicator as operating units is likewise unimportant when suitable external nonvibrating references are available.

35.99. The self-contained vibration receiver or indicator is formed by adding a relative motion receiver or indicator to a seismographic system.** The

---

* From the standpoint of practice, it is immaterial whether the base of the motion receiver is connected to the nonvibrating reference member or to the moving member.

** The seismographic system is defined in the discussion of paragraph 35.10.

receiving element and the base of the receiver or indicator are attached to the seismic element and the case of the seismographic system so that the movement of the seismic element with respect to the case is the input for the receiver or indicator. The output of the relative motion receiver or indicator is the output signal or the indication for the vibration receiver or indicator. The functional relationships involved are represented in Fig. 35-6. Vibratory motion is the input to the seismographic system;* the relative motion between the seismic element and the case of the system is the corresponding output. This motion is the input for the relative motion receiver or indicator, which produces a signal or an indication that corresponds to the vibratory motion input.

TYPICAL VIBRATORY MOTION RECEIVERS AND INDICATORS

35.100. It is common practice to use the name vibration pickup when referring to either vibration indicators or vibration receivers. Vibration receivers, which are distinguished from vibration indicators by the fact that they produce output signals instead of directly observable indications, are also known as vibration transducers. Figures 35-7a through 35-7m illustrate the essential features of several typical vibration receivers and indicators.**

SELF-CONTAINED VIBRATORY MOTION INDICATORS

35.101. Figure 35-7a shows a hand-held linear vibration indicator in which the seismic mass (the case of the unit) is isolated from the input vibration by the body of the operator.*** The receiving element is a plate maintained in contact with the vibrating member by means of a relatively weak spring. The indicating system is a dial gage indicator with features similar to those shown in Fig. 35-5a. In practice, the hand-supported seismic mass is part of a seismographic system with an undamped natural frequency so low† that dial gage pickup units effectively operate in the vibrometer range to indicate displacements of the vibrating member with respect to inertial space. For a limited range of situations, these indications give information on input amplitudes, but in general are not useful so far as response delays or phase angles are concerned.

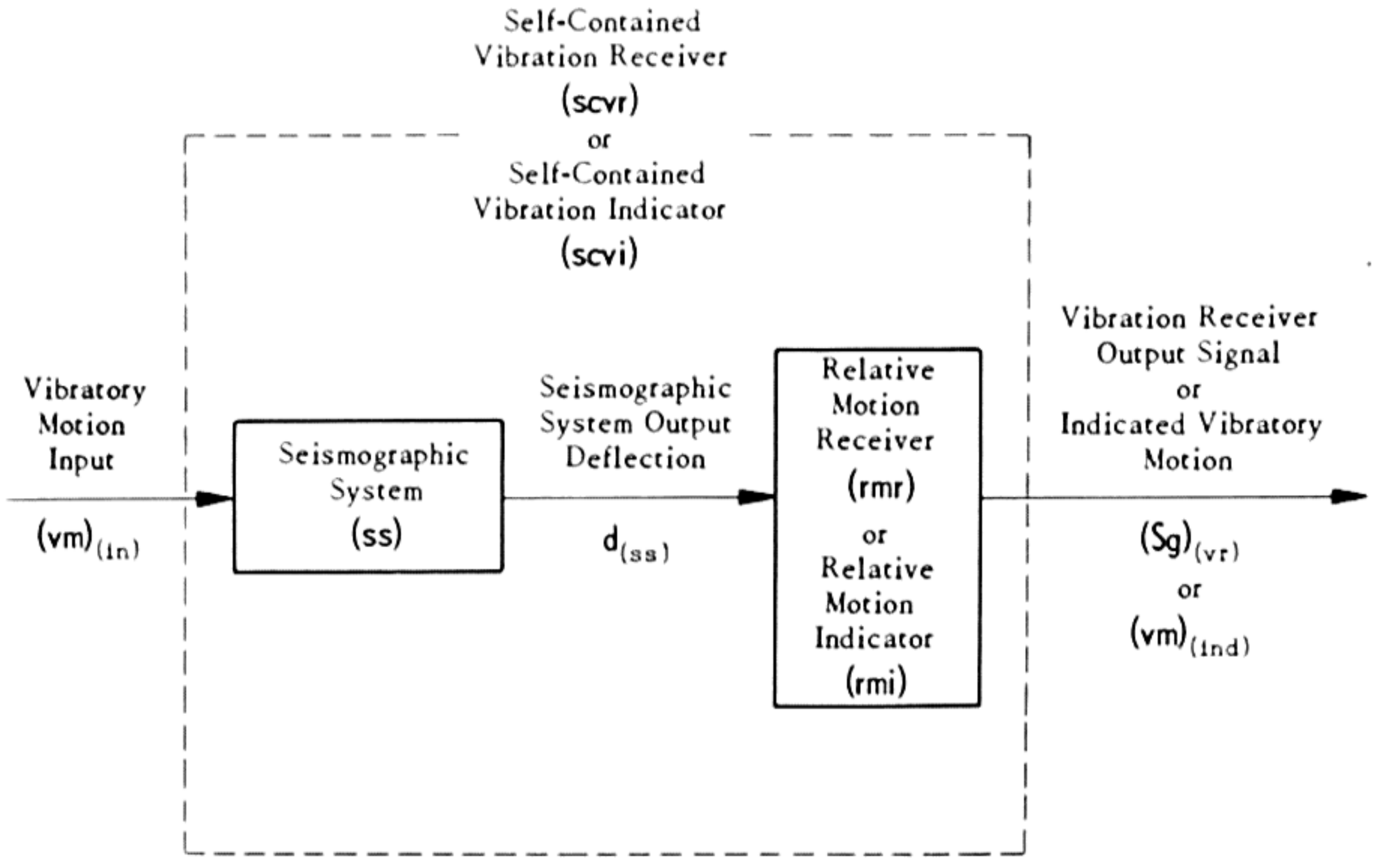
---

* This input may be treated as displacement, velocity or acceleration, or any other function of the vibratory motion input, depending on the characteristics chosen for the vibration receiver.

** In this series of illustrations, the input axis is usually taken to be horizontal so that the effect of gravity on the operation of the vibration receivers need not be taken into account. In general, both gravitational forces and linear acceleration forces act on the seismic element, but, since gravity is constant, consideration of the effect of gravitational forces is not pertinent to the present discussion of vibration receivers.

*** Because of the inertia of the seismic mass, the operator's arm is incapable of responding to the input vibration.

† See footnote for paragraph 35.13 and also Derivation Summary 35-1 for a discussion of the factors that determine the undamped natural frequency.



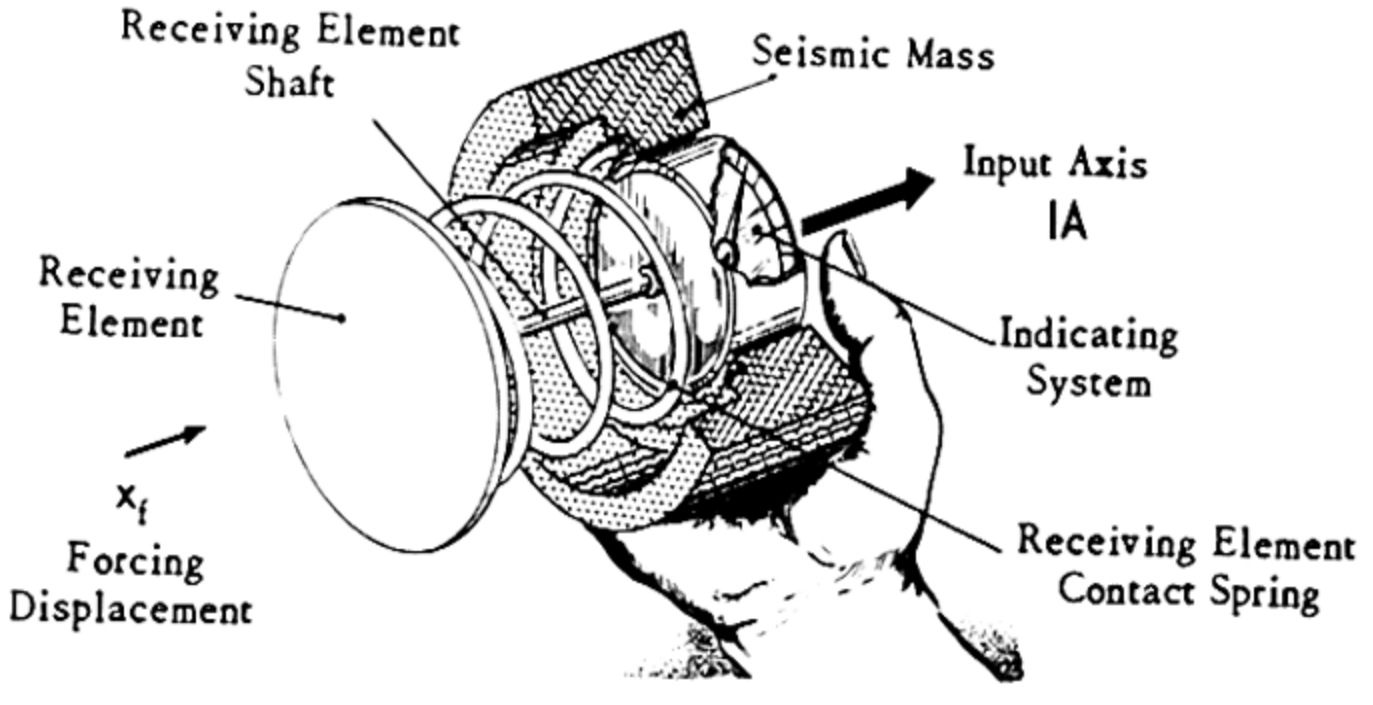
Note: The vibratory motion input, $(vm)_{(in)}$, may be displacement, velocity, acceleration or any other function of the vibratory motion input. Relative motion indicators are units in which an indicating system is associated with a relative motion receiver to give a directly observable indication as the output, based on the output of the relative motion receiver.

Fig. 35-6. Functional diagram showing the self-contained vibration receiver or indicator formed by combining a seismographic system and a relative motion receiver or indicator.

35.102. A typical dial gage vibrometer has a volume of 20 cubic inches, a weight of 4 pounds, and operates over an input amplitude range of ± 1/32 inch at frequencies from 1 to approximately 10 cycles per second.

35.103. Figure 35-7b illustrates the essential features of a self-contained optical accelerometer. This device consists of a seismographic system used in conjunction with an optical indicating system similar to that shown in Fig. 35-5b. The seismic element is a cylinder attached to the case by means of flexures that effectively restrict motion to linear displacement parallel to the input axis and serve as the elastic coupling of the seismographic system. Damping is provided by an annular film of viscous fluid between the inside of the seismic element cylinder and the outside of a cylindrical inner core fixed with respect to the base. Additional flexures are used to supply the seismic element motion with respect to the base as the input to the optical indicating system. Indications corresponding to the vibratory input acceleration are given by the position of the light-spot index on a transparent scale attached to the case, when the instrument is used at a frequency below its natural frequency.

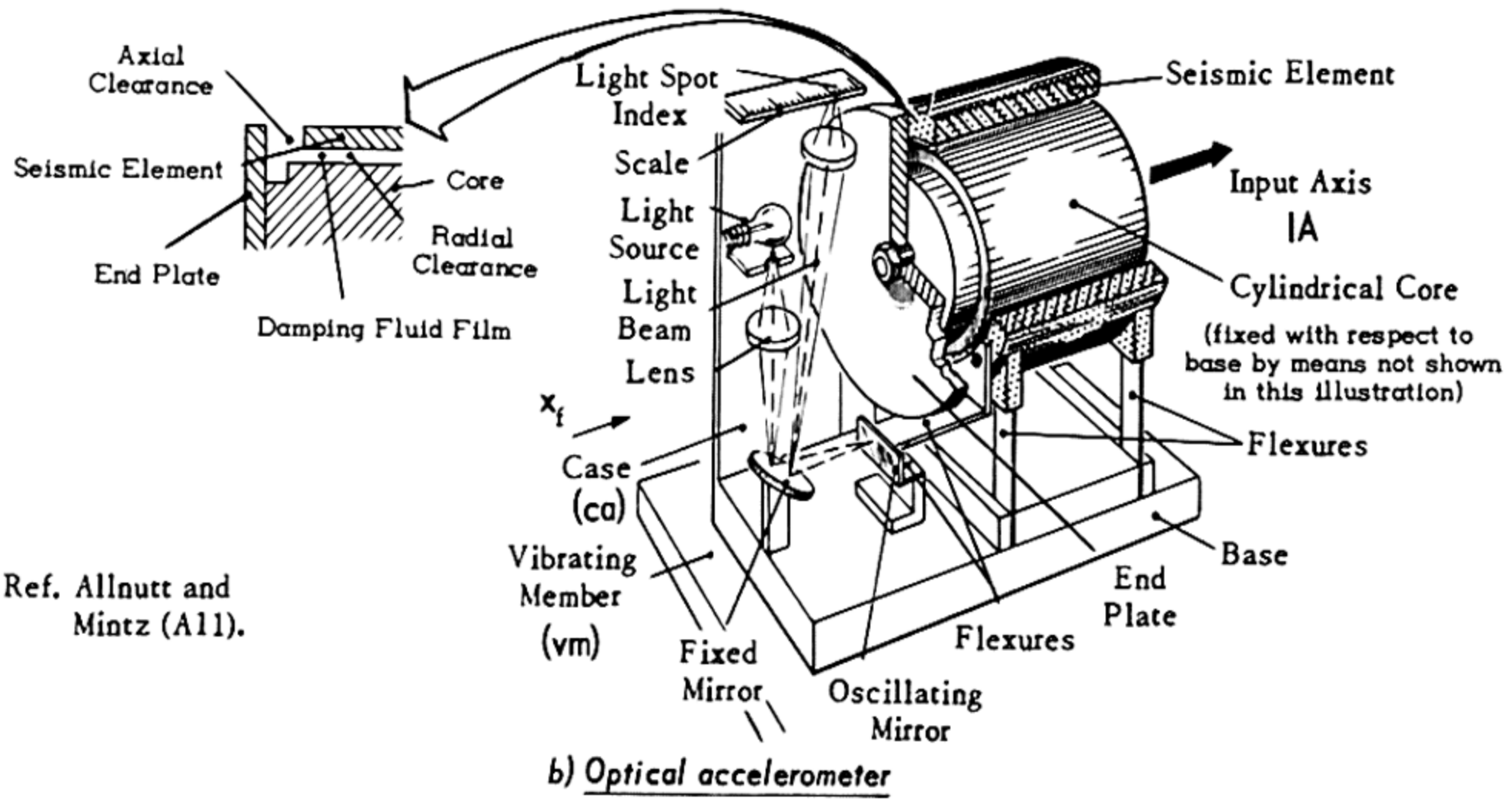
35.104. A typical optical accelerometer (without recording system) has a volume of about 4 cubic inches, weighs about 0.5 pound, and operates over an acceleration range of 0.01 to 2 gravities, and a frequency range from 0 to about 100 cycles per second.



Note: Linear motion of the receiving element shaft is converted into angular motion of the indicating-system index by means not depicted in the illustration.

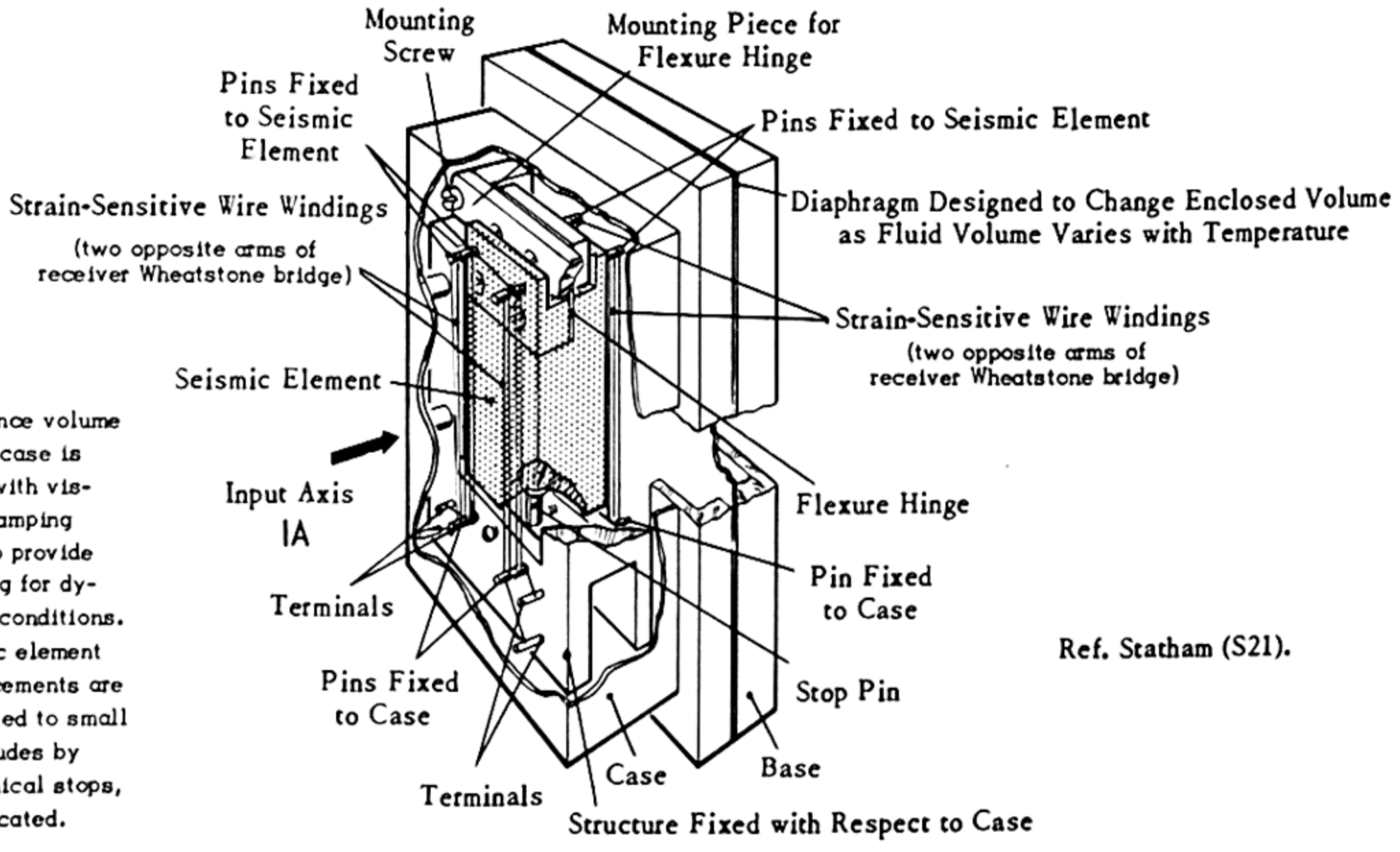
Ref. Review of Scientific Instruments (R11).

a) Hand-held mechanical vibrometer



Ref. Allnutt and Mintz (A11).

b) Optical accelerometer



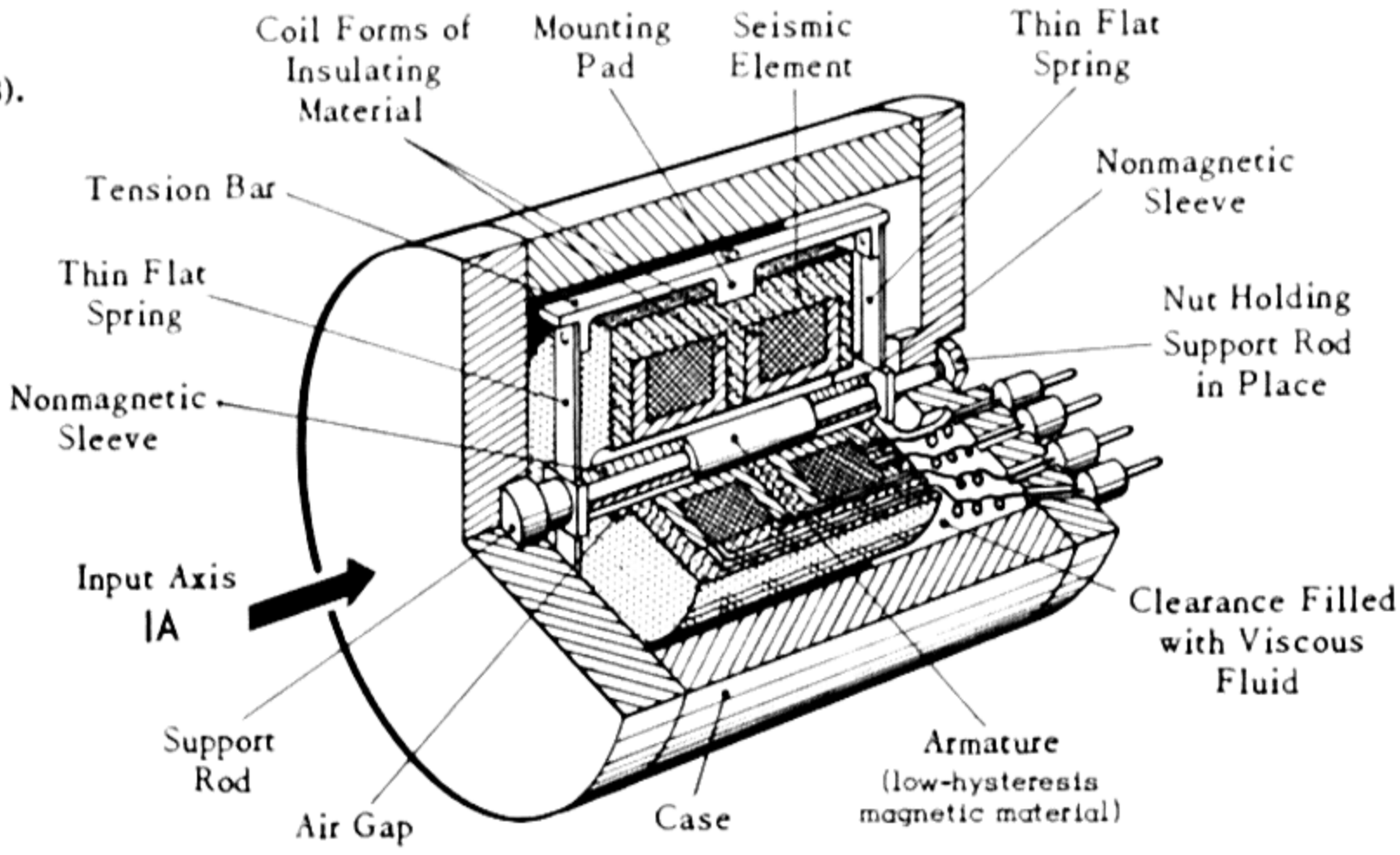
Note: Clearance volume inside case is filled with viscous damping fluid to provide damping for dynamic conditions. Seismic element displacements are restricted to small magnitudes by mechanical stops, as indicated.

Ref. Statham (S21).

c) Unbonded resistance wire linear vibration receiver

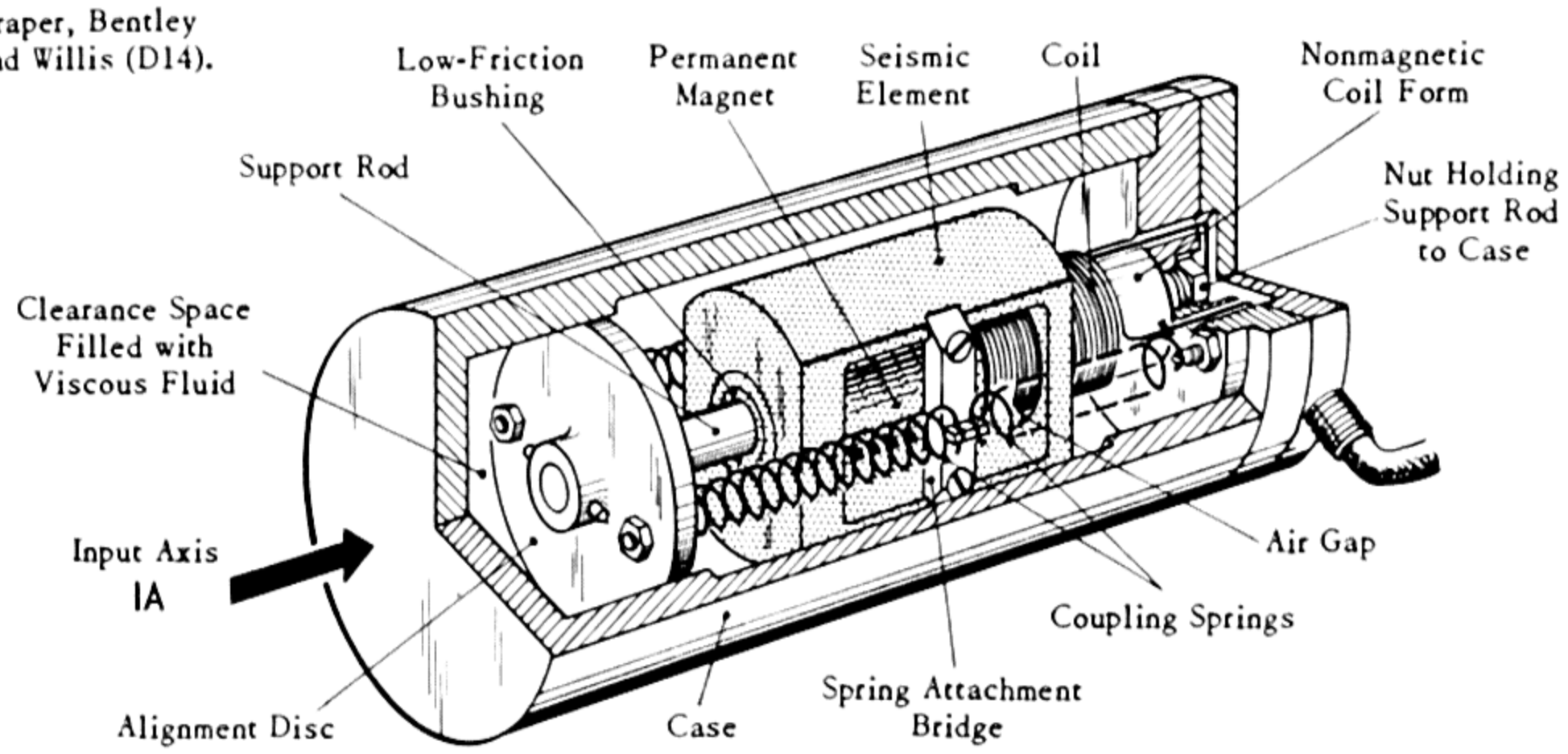
Fig. 35-7. Typical single-degree-of-freedom vibration-measuring systems. (Page 1 of 5)

Ref. Draper and Wrigley (D8).



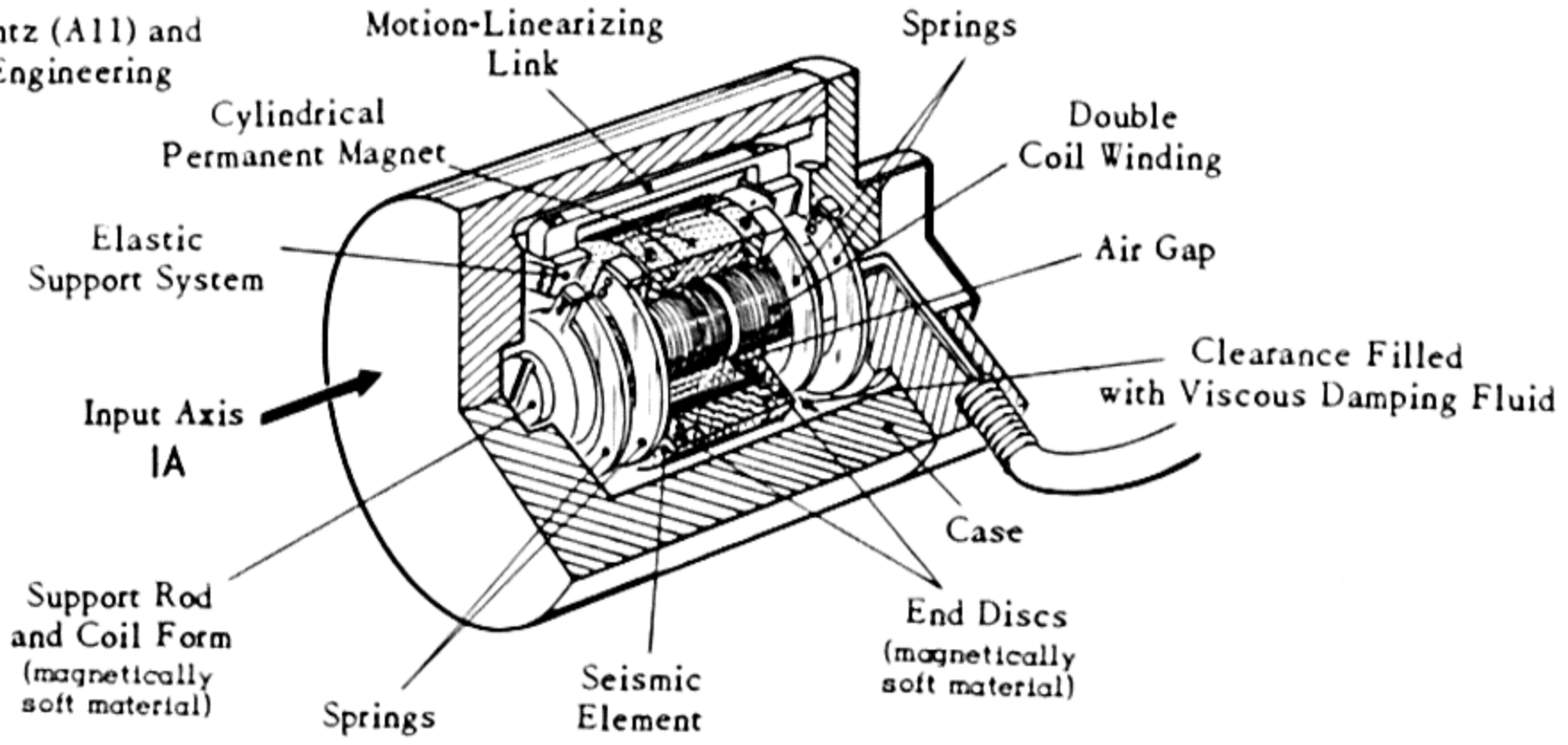
d) Inductance-bridge linear acceleration receiver

Ref. Draper, Bentley and Willis (D14).



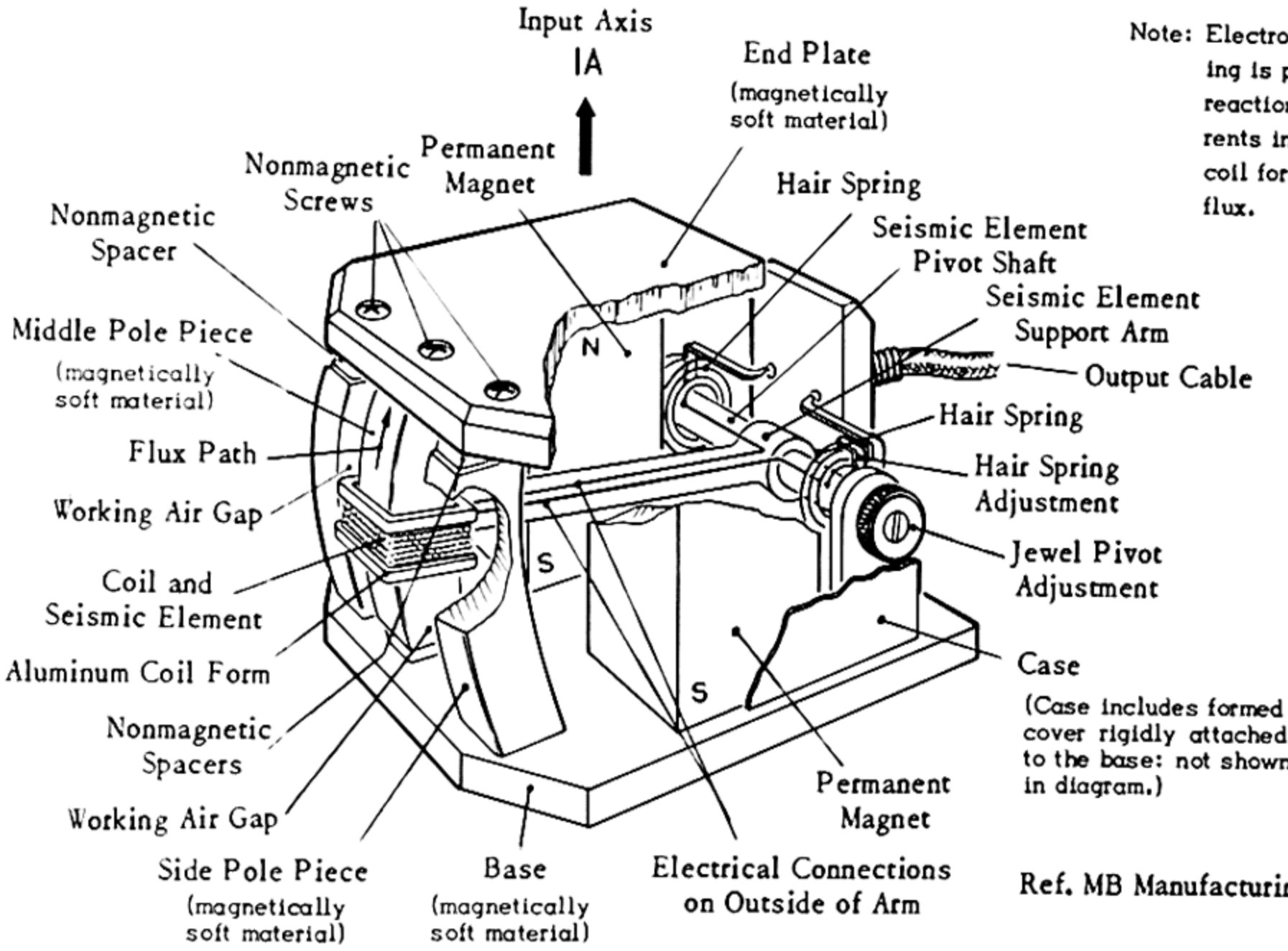
e) Single-coil electromagnetic generator linear vibration receiver with sliding-contact support for the seismic element

Ref. Allnutt and Mintz (A11) and Consolidated Engineering Corp. (C11).



f) Double-coil electromagnetic generator linear vibration receiver with elastic coupling support for the seismic element

Fig. 35-7. Typical single-degree-of-freedom vibration-measuring systems. (Page 2 of 5)

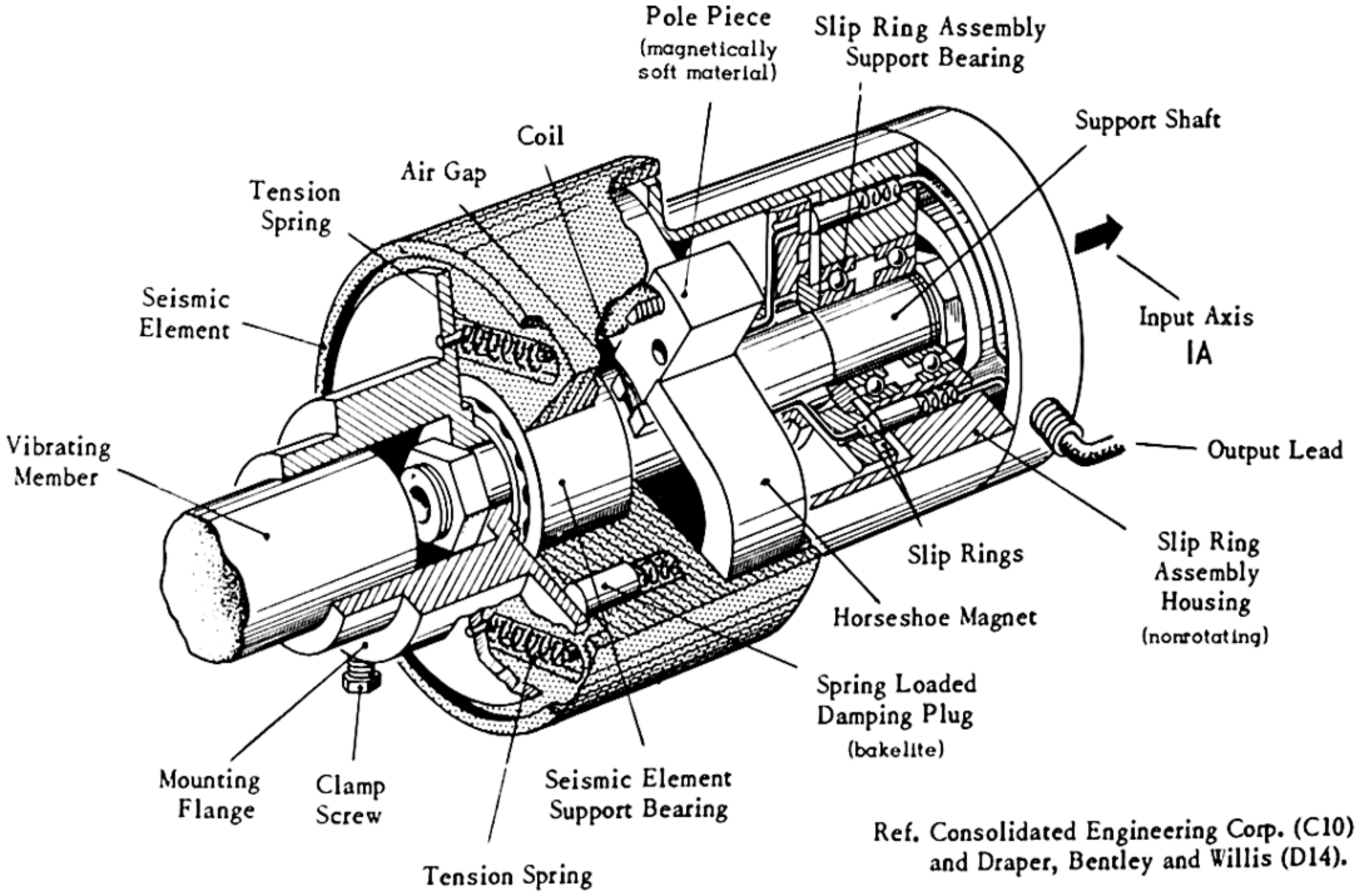


Note: Electromagnetic damping is provided by reaction of eddy currents induced in the coil form with air-gap flux.

(Case includes formed cover rigidly attached to the base: not shown in diagram.)

Ref. MB Manufacturing Co. (M19).

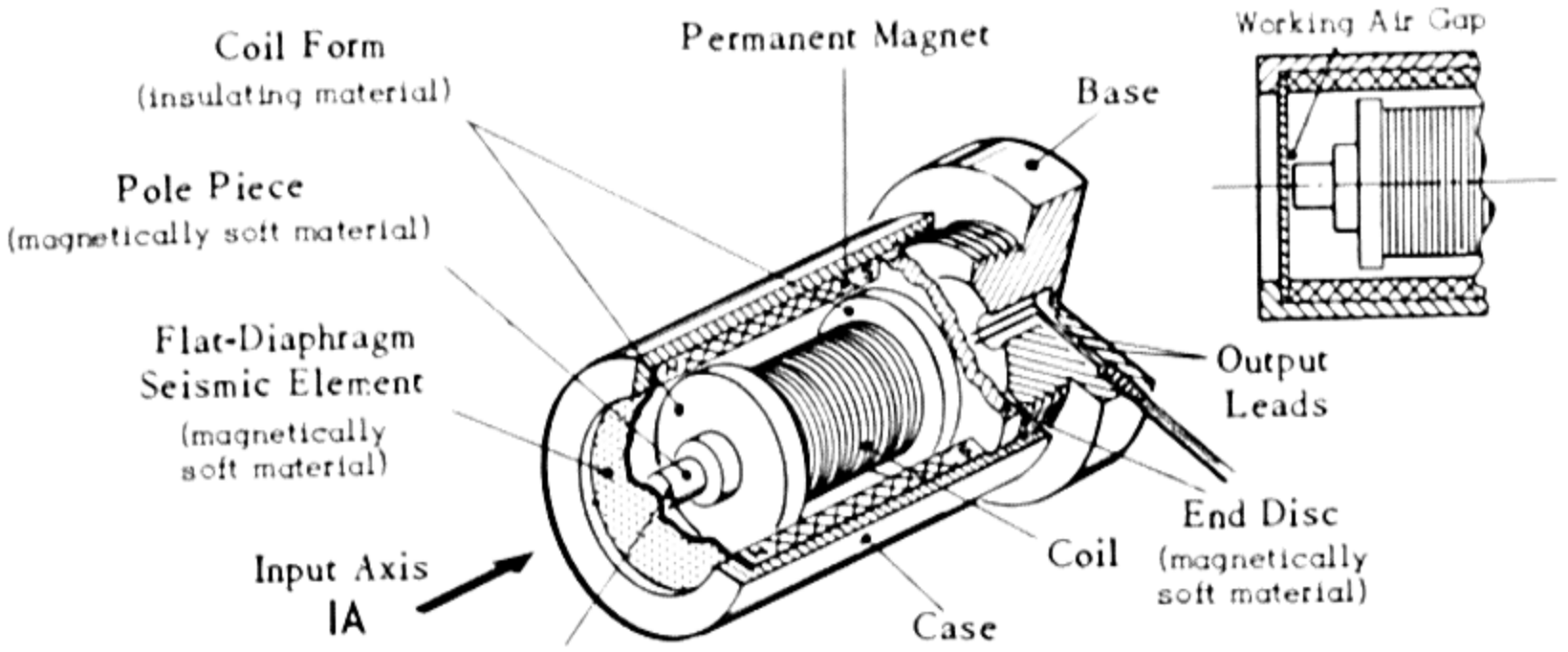
g) Moving-coil electromagnetic generator linear vibration receiver with jewel-pivot support for the seismic element and electromagnetic damping



Ref. Consolidated Engineering Corp. (C10) and Draper, Bentley and Willis (D14).

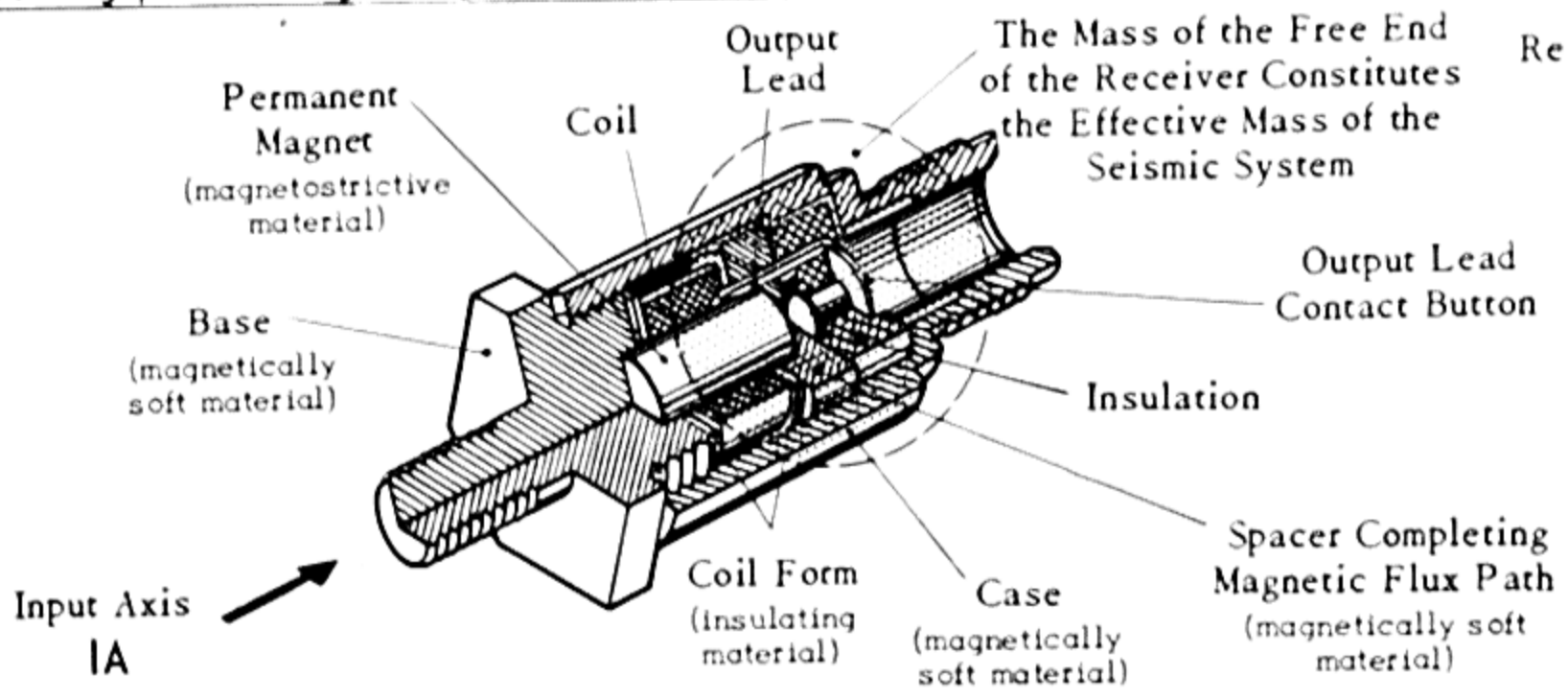
h) Electromagnetic generator torsional vibration receiver with Coulomb friction damping

Fig. 35-7. Typical single-degree-of-freedom vibration-measuring systems. (Page 3 of 5)



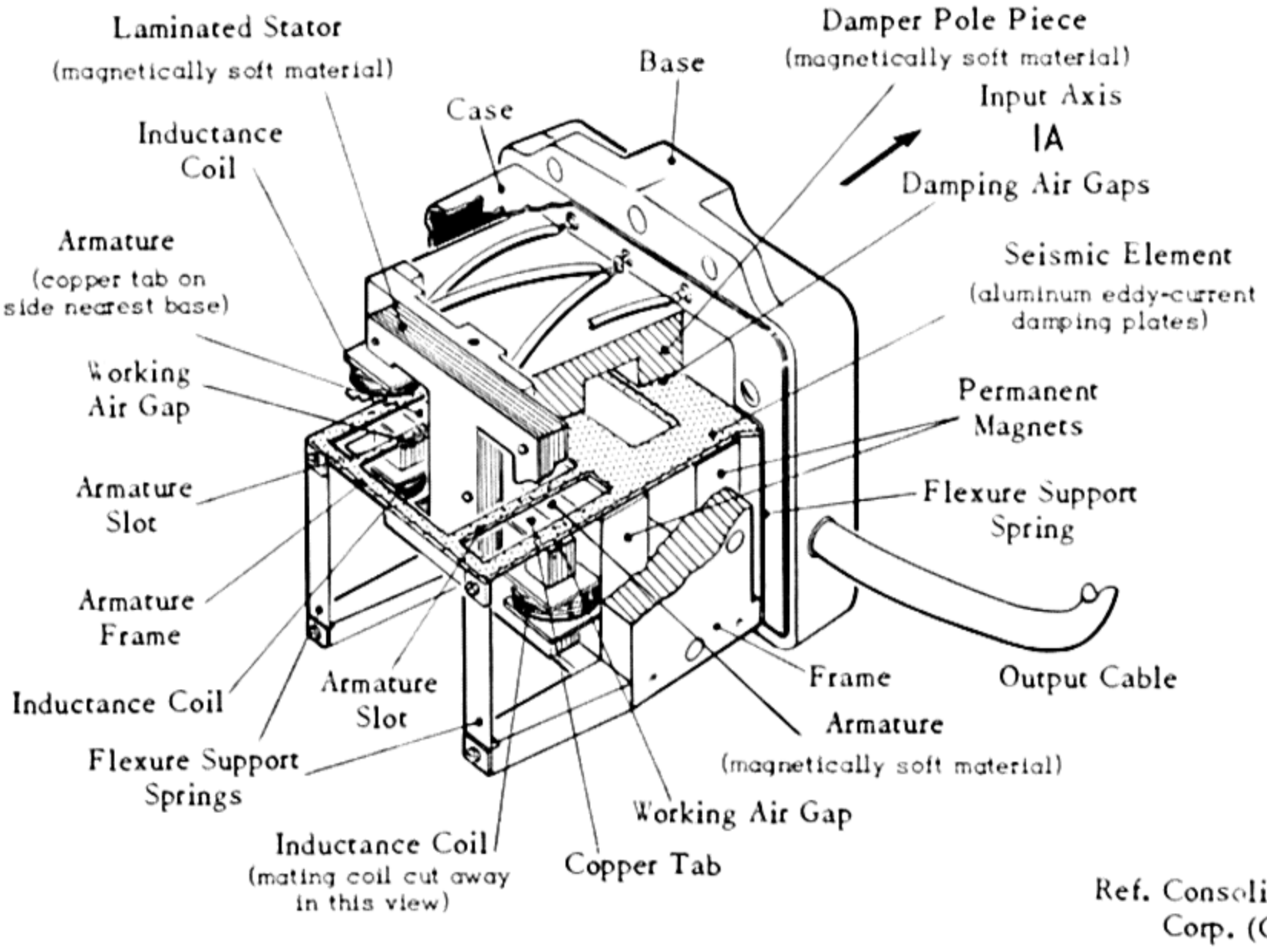
Ref. Draper, Taylor, Lancor and Coffey (D15).

i) Variable-air-gap electromagnetic generator linear vibration receiver with flat-diaphragm seismic element



Ref. Sperry Gyroscope Company (S20).

j) Magnetostriction electromagnetic generator linear vibration receiver

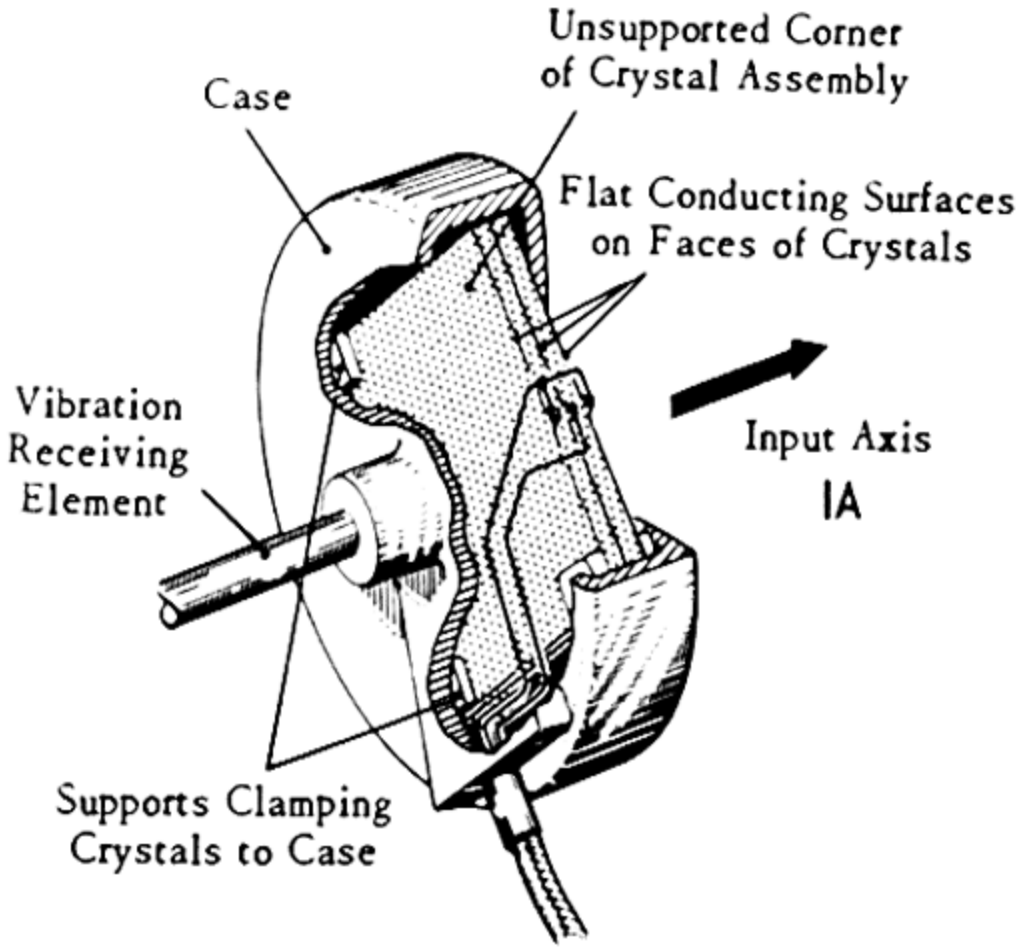


Ref. Consolidated Engineering Corp. (C10).

k) Inductance-bridge linear vibration receiver with electromagnetic damping and with flexure spring support for the seismic element

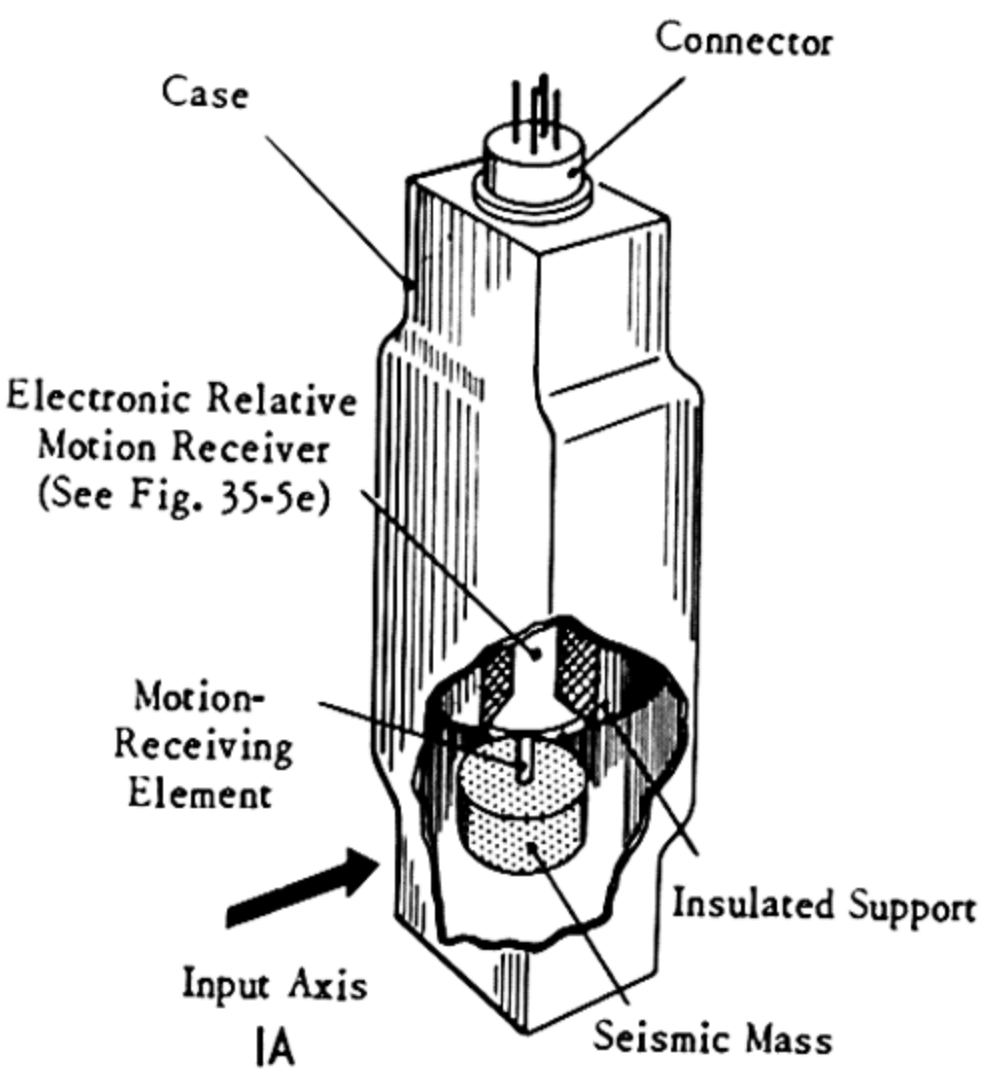
Fig. 35-7. Typical single-degree-of-freedom vibration-measuring systems. (Page 4 of 5)

Ref. Hetényi (H14) and Mason (M18).



l) Piezoelectric crystal linear vibration receiver

Ref. Calidyne Instrument Co. (C9) and Lewis (L17).



m) Electronic tube linear vibration receiver

Fig. 35-7. Typical single-degree-of-freedom vibration-measuring systems. (Page 5 of 5)

SELF-CONTAINED VIBRATORY MOTION RECEIVERS WITH ELECTRICAL OUTPUTS

35.105. Vibratory motion receivers with electrical outputs may be based on combinations of seismographic systems and electrical signal generating relative motion receivers of various types, including those illustrated in Fig. 35-5.

35.106. Figure 35-7c shows the features of a linear vibration receiver based on the combination of a seismographic system and an unbonded resistance wire relative motion receiver. The seismic element is a rectangular block attached to the case structure by means of a flexure hinge that allows relative-motion rotation about an axis at right angles to the input axis of the receiver. Four unbonded resistance wire windings provide an elastic restraint that establishes a position of equilibrium of the seismic element with respect to the case. The elastic action is provided by drawing each winding tight over a pair of pins. As shown in Fig. 35-7c, one pin of each pair is fixed with respect to the case, and the other pin is attached to the seismic element in such a position that rotation of the seismic element with respect to the case changes the condition of strain in the wires of the winding. The windings are arranged in two matching pairs. The two windings of each pair exert opposing torque components on the seismic element. In the elastic equilibrium position of the seismic element, these components are equal and opposite when the tension in the wires of all their windings corresponds to about half of the greatest strain to be expected under operating conditions. When the seismic element is rotated away from the position of elastic equilibrium in the windings, strain is increased in one pair of windings and decreased in the other pair of windings. The corresponding changes in tension introduce a net restoring torque. In addition to this strain

effect, the electrical resistances of the windings undergo corresponding changes. This means that the unbonded resistance windings may be connected to form the Wheatstone bridge of a motion receiver similar to that described in Fig. 35-5c. When proper excitation is applied, this bridge provides the output signal for the unbonded resistance wire linear vibration receiver.

35.107. When a unit with the features shown in Fig. 35-7c is given a vibratory motion along the input axis, the center of gravity of the seismic element is subjected to an inertia reaction force. Because the flexure hinge is at some distance from the center of gravity, the inertia reaction force causes a torque to act on the seismic element. If the acceleration is constant, equilibrium is reached when this input torque is balanced by the elastic torque set up by the wire windings as the seismic element is rotated about the flexure hinge. Damping for dynamic conditions is provided by filling the clearance volume within the case with a viscous fluid.

35.108. Wire windings like those used in the unbonded resistance wire linear vibration receiver of Fig. 35-7c are only linear for small deflections. This means that seismic element displacements must be restricted by mechanical stops to such small magnitudes that vibrometers based on the features illustrated in the diagram would not be generally useful. On the other hand, when the seismographic system is designed to have a high undamped natural frequency with a low damping ratio, the unbonded resistance wire vibration receiver is particularly suitable for acceleration measurements.

35.109. A typical unbonded resistance wire accelerometer occupies a volume of 1 cubic inch, weighs 2 ounces, has an undamped natural frequency of 100 cycles per second, and is limited to an acceleration magnitude of ± 10 gravities. This unit has a sensitivity of 1.2 millivolts per gravity when an excitation of 6 volts is used.

35.110. Figure 35-7d shows the essential features of a vibration receiver based on the combination of a seismographic system and an inductance bridge. The seismic element is a cylinder of low-hysteresis magnetic material supported from the case by a spring system consisting of two thin flat springs and two relatively thick tension bars. The thin springs have holes at their midpoints and are clamped between washers located on the support rod by spacers. These springs are parallel to each other and at right angles to the input axis of the unit. The separation of the thin springs is just equal to the distance between the ends of two tension bars that are attached to the seismic element, with their long dimensions parallel to the input axis. Pads machined at the midpoints of the tension bars are clamped to mating depressions in the outer surface of the seismic element. The bars are thinned out except at the pads so that both ends are free to bend toward the center line of the seismic element. The distances between the

attachment holes in the outer ends of the thin springs are somewhat less than the distances between the corresponding holes in the ends of the tension bars when these bars are mounted on the seismic element and are free from bending stress. This means that when the seismographic system is assembled with the thin springs clamped to the tension bars, the bars will be bent inward enough to maintain tension in the thin springs.

35.111. The arrangement of spring components shown in Fig. 35-7d maintains annular air gaps between the outside diameter of the sleeve spacers on the support rod and the inside diameters of discs that form parts of the seismic element. In addition, when any force deflects the seismic element from its zero-force equilibrium position with respect to the case, tension and bending in the thin flat springs and bending in the tension bars combine to cause an elastic restoring force to act on the seismic element. The practical magnitudes of the elastic coefficient and the seismic element mass combine to give relatively high undamped natural frequencies for systems made up of tension bars and thin end springs. Damping is provided by filling the clearance within the case with a viscous fluid. The combinations of damping and undamped natural frequency possible with the features in Fig. 35-7d largely restrict units of this type to operation in the accelerometer range.

35.112. The relative motion receiver used with the seismographic system of Fig. 35-7d is based on the inductance-bridge principle illustrated in Fig. 35-5q. Two coils wound on forms of insulating material are placed on either side of a low-hysteresis disc midway between the ends of the seismic element cylinder. The ends of the cylinder are closed by similar discs. All three discs have center holes that provide annular air gaps between the discs and sleeve spacers on the support rod. The armature is a hollow cylindrical sleeve of low-hysteresis magnetic material and has a length equal to the distance between the midpoints of each coil form. This armature is located by means of nonmagnetic sleeve spacers so that it projects halfway into each coil form when the elastic support system is in its position of elastic equilibrium when no external force is acting. The external bridge connections, which are identical with those shown in Fig. 35-5q, are adjusted so that the output signal has its null level when the seismic element is in this position.

35.113. When the inductance bridge associated with the unit of Fig. 35-7d is excited with an alternating-current excitation voltage and an acceleration is applied along the input axis, the seismic element moves away from its position of elastic equilibrium under the combined inertia reaction force, elastic restoring force, and damping force produced by the fluid in the clearance volume. The bridge output voltage corresponding to this displacement is the signal output from the inductance-bridge linear acceleration receiver.

35.114. One example of the acceleration receiver of Fig. 35-7d occupies a volume of 3 cubic inches, weighs 7 ounces, has an operating range up to 10 gravities, and has a sensitivity of 0.1 volt amplitude per gravity with an excitation of 10 volts at 400 cycles per second.

35.115. Figure 35-7e shows the essential features of a seismographic system combined with a single-coil electromagnetic generator relative motion receiver to form a linear vibration receiver. The seismic element is a composite metal structure fitted with low-friction bushings that are aligned with the center line of the structure. These bushings slide over the support rod so that the seismic element is constrained to move parallel to the input axis of the unit. At one end, the support rod is clamped to the case, and at the other end it is located by an alignment disc that fits closely within the cylindrical bore of the case. The elastic element of the seismographic system is provided by four tension springs that couple the seismic element to the case. As shown in Fig. 35-7e, one spring is connected between the spring attachment bridge and the case. A matching spring connected between the bridge and the alignment disc exerts a tension that is equal and opposite to the tension of the first spring when the seismic element is in the position of elastic equilibrium. The remaining two springs are connected in corresponding positions on the side of the seismic element that is not visible in the figure. Damping is provided for the seismographic system by viscous fluid that fills the clearance volume inside the case.

35.116. The electromagnetic signal generating system for the vibration receiver of Fig. 35-7e is similar to the linear velocity receiver of Fig. 35-5i. A hollow permanent magnet carries the seismic element support bushings and is press-fitted into the yoke of cold rolled steel that forms the outer part of the seismic element. The free end of the magnet slides within the coil form of nonmagnetic material with a small air-gap separation. The end of the seismic element yoke overlaps the coil form and provides the outer cylindrical surface for the annular air gap outside the coil. With this arrangement, motion of the seismic element with respect to the case causes the air-gap flux to cut the wires of the coil. This movement of flux lines across the coil generates a voltage that is proportional to the linear velocity of the gap along the coil. The corresponding voltage gives an output signal that depends on the linear velocity input to the case.

35.117. Seismographic systems with the features shown in Fig. 35-7e usually have relatively low undamped natural frequencies and for this reason are particularly well adapted for operation in the vibrometer range. The electromagnetic signal generating system in effect differentiates the relative displacement output of the seismographic system to produce an output signal that in the operating range is proportional to the input as a vibratory velocity.

35.118. A typical single-coil electromagnetic generator vibration receiver

occupies a volume of 6 cubic inches, weighs 16 ounces, has an undamped natural frequency of 10 cycles per second, and a damping ratio of 0.7 at 70 degrees Fahrenheit, with a decrease of 15 percent for each 10-degree increase in temperature. This unit has an open-circuit input velocity – output voltage sensitivity of 0.03 volt per centimeter-per-second in the range of operating frequencies. This range is limited at the low-frequency end by the undamped natural frequency of the seismographic system* and by Coulomb friction effects due to imperfect lubrication of the seismic element bushings with respect to the support rod. The unit will operate properly within a range of input displacements of ±0.5 centimeter.

35.119. Figure 35-7f shows the essential features of a vibration receiver that is generally similar to the unit of Fig. 35-7e except that the slide-rod support is replaced by an elastic coupling support and the single-coil electromagnetic generator is replaced by a double-coil electromagnetic generator.

35.120. The seismic element consists of a hollow cylindrical permanent magnet with its ends closed by discs of magnetically soft material. These discs act as pole pieces to provide the outer surfaces for annular air gaps outside of coils wound on the support rod. The elastic coupling support consists of two identical assemblies of split spring washers, placed at opposite ends of the seismic element. Each assembly has one end of one split washer attached to the support rod by means of a fitting. The other end of this washer is riveted to one end of the motion-linearizing link. A second split washer of each assembly has one end attached to the seismic element, while the other end is riveted to the end of the motion-linearizing link that is attached to the other washer of the pair. The action of the complete elastic coupling support system is to limit seismic element motion to the direction of the input axis and at the same time to maintain the air-gap clearances with respect to the coil surfaces. The support system also acts as the elastic element between the case and the seismic element. Damping for the seismic element is provided by filling the clearance volume within the case with a viscous fluid.

35.121. The action of the double-coil electromagnetic signal generating system of Fig. 35-7f is identical with that of the linear velocity receiver illustrated in Fig. 35-5j. The two coils are wound on thin insulating material cemented in shallow grooves on the magnetic support rod. These grooves are located so that they are each centralized under one of the air gaps when the seismic element is in its position of elastic equilibrium and extend along the support a distance that is somewhat greater than the maximum relative displacement of the seismic element.

35.122. A typical double-coil electromagnetic generator vibration receiver with elastic coupling support for the seismic element occupies 5 cubic inches and

* The mathematical background for this statement is developed in Derivation Summary 35-3.

weighs 13 ounces. With the mass of the damping fluid included in the effective mass of the seismic element, the seismographic system has an undamped natural frequency of 9 cycles per second and, at a temperature of 70 degrees Fahrenheit, has a damping ratio of 0.64. This unit has an open-circuit input velocity – voltage sensitivity of 45 millivolts per centimeter-per-second. The range of input displacements for which the unit will operate properly is ± 0.5 centimeter.

35.123. The vibration receiver of Fig. 35-7f has the same general characteristics as the unit of Fig. 35-7e except that the use of an elastic support coupling instead of the sliding contact support removes Coulomb friction as a limiting factor in performance at low frequencies.

35.124. Figure 35-7g shows the essential features of a linear vibration receiver with a jewel-pivot support for the seismic element and a moving-coil electromagnetic generator. The seismic element is a coil wound on an aluminum form attached to a support arm. The support arm is carried by a pivot shaft that rotates freely in two jewel bearings fixed in the case. Two hair springs acting between the case and the pivot shaft provide elastic restraint for the seismic element, with the position of equilibrium halfway between the base and the end plate. The input axis of the unit is the direction, fixed with respect to the case, that is at right angles to the pivot shaft and the seismic element support arm when this arm is in the position of elastic equilibrium. When the unit is given a linear acceleration along the input axis, the resulting inertia reaction forces cause the seismic element to move against the elastic restraint. Damping is provided by electromagnetic reactions explained in the next paragraph.

35.125. The electromagnetic signal generating system of the unit shown in Fig. 35-7g includes three curved pole pieces of magnetically soft material that are mounted between the base and the end plate. The radius of curvature is made equal to the radius of the seismic element support arm. The middle pole piece is placed so that it is enclosed by the seismic element coil form with sufficient clearance to permit free motion of the coil. The two side pole pieces are located parallel to the middle pole piece with sufficient spacing to provide working air gaps for the two sides of the coil form that lie between the pole pieces. The middle pole piece is in good magnetic-circuit contact with the end plate and is magnetically isolated from the base by means of a spacer of nonmagnetic material. The side pole pieces are in good magnetic-circuit contact with the base and are separated from the end plate by nonmagnetic spacers. Two permanent magnets of large cross section are mounted with good magnetic-circuit contact between the base and the end plate. Flux from these magnets passes through the pole pieces and across the working air gaps. When the seismic element moves with respect to the case, lines of air-gap flux are cut by the turns of the coil. The voltage generated in the coil by this action is transferred from the output leads of the coil, which are fixed to the support

arm, to the output cable by means of the two hair springs. This voltage is the output signal of the vibration receiver. Eddy currents induced in the aluminum coil form react with the air-gap flux to provide electromagnetic damping for the seismographic system.

35.126. Seismographic systems with the features illustrated in Fig. 35-7g are best adapted for low undamped natural frequencies and consequently usually operate in the vibrometer range. With the electromagnetic signal generating system shown, the output voltage is proportional to the linear velocity input over the operating range of the unit.

35.127. A typical linear vibration receiver of the type shown in Fig. 35-7g occupies a volume of 6 cubic inches, weighs 10 ounces, has an undamped natural frequency of 5 cycles per second and a damping ratio of 0.65, and operates over a range of ± 0.5 centimeter input displacement. This unit has an open-circuit velocity input – voltage output sensitivity of 35 millivolts per centimeter-per-second.

35.128. Figure 35-7h shows the essential features of an electromagnetic-generator torsional vibration receiver with Coulomb friction damping. The seismic element is a cylindrical structure mounted on the support shaft by means of a double-row ball bearing. The support shaft is rigidly attached to the mounting flange, which is provided with a cylindrical hole and a clamping screw, designed to be used for attaching the vibration receiver unit tightly on the vibrating member whose motion is to be studied. A pair of opposed tension springs placed on opposite sides of the support shaft provide the elastic coupling for the seismographic system. Each spring is connected between a pin fixed to the seismic element and another pin fixed to the mounting flange in such a way that the opposing tension forces establish a position of elastic equilbrium for the seismic element. Coulomb friction damping for the system is introduced by a plug of bakelite constrained to slide in a tight-fitting hole in the seismic element and rub on the mounting flange at some distance from the axis under the pressure of a spiral spring acting parallel to the support shaft.

35.129. The input axis for the torsional vibration receiver is parallel to the support shaft. Any forced oscillation of the mounting flange transmitted from the vibrating member tends to produce a corresponding rotation of the seismic element due to the elastic torque and the friction of the bakelite plug. The inertia reaction torque acting on the seismic element tends to prevent changes in angular velocity of the seismic element. With reasonable values of elastic coupling and bakelite plug friction within the operating range of the unit, this inertia reaction effect predominates for vibration components of the input motion. This means that the seismic element will rotate at the average speed of the mounting flange without following any vibratory component of input rotation, so that the unit of Fig. 35-7h performs within the vibrometer range so far as the seismographic

system operation is concerned. For operation of this type to exist, the input acceleration must be high enough to break the seismic element away from the Coulomb friction of the bakelite plug. Also, the input vibration must lie in the frequency range well above the undamped natural frequency of the seismographic system. *

35.130. The signal generating system used in the vibration receiver of Fig. 35-7h is identical with the reluctance-change type of angular velocity receiver shown in Fig. 35-5k. An armature of magnetically soft material is set into the support shaft. This armature consists of two side plates and a coil form machined from a single piece of stock. The ends of the side plates are cylindrical arcs coaxial with the axis of the support shaft. These arcs are the inner surfaces of annular air gaps between the armature and two magnetically soft pole pieces mounted in the seismic element. Magnetic flux is forced across the air gaps by a pair of horseshoe magnets clamped in the seismic element with their ends in close contact with the pole pieces. With this arrangement, relative angular displacements of the seismic element from the flange cause the effective air-gap area to shift from one side of the armature to the other. The corresponding movement of flux cuts across the turns of the coil wound on the middle portion of the armature and generates a voltage proportional to the rate of change of relative angular displacement. This voltage is connected to the output leads through slip rings mounted in a nonrotating housing.

35.131. Except for special effects due to Coulomb friction, ** the performance characteristics of the torsional vibration receiver illustrated in Fig. 35-7h are generally similar to the characteristics of the linear vibration receivers of Figs. 35-7e, 35-7f, and 35-7g.

35.132. A particular torsional vibration receiver unit with the features shown in Fig. 35-7h occupies 16 cubic inches, weighs 4 pounds, 3 ounces, has an undamped natural frequency of 5 cycles per second, operates over an angular displacement input range of ± 10 degrees, and breaks away from the Coulomb friction plug at an input amplitude of approximately 0.5 degree and a frequency of 15 cycles per second. The open-circuit angular velocity – voltage sensitivity of the unit is 1.04 millivolt per degree-per-second.

35.133. Figure 35-7i illustrates the essential features of a vibration receiver in which the seismographic system is a simple flat diaphragm, and the signal generating system is a variable air gap, permanent magnet, and coil arrangement similar to the variable-reluctance relative velocity receiver of Fig. 35-5 l. The effective mass of the diaphragm acts as the seismic element, and the material of the diaphragm supplies the functions of the elastic element and the damper. As a general rule, seismographic systems of this type have very high undamped

* The mathematical background for this statement is developed in Derivation Summary 35-3.

** A theoretical discussion of the effects of Coulomb friction on seismographic system operation is given in Derivation Summary 35-6.

natural frequencies and very low damping ratios for very small relative displacements. For these reasons, vibration receiver units with diaphragm-type seismic elements are usually adapted for operation in the accelerometer range. The variable-air-gap electromagnetic generator produces a signal that depends on the velocity of seismic element motion with respect to the case, so that the output signal from a vibration receiver of the type shown in Fig. 35-7i is proportional to the rate of change of acceleration.

35.134. A typical unit of the flat-diaphragm seismic element, variable-air-gap electromagnetic generator type occupies 1.5 cubic inches, weighs 2 ounces, and has an undamped natural frequency of 40,000 cycles per second with a damping ratio of about 0.005. The unit operates over a range of acceleration inputs from 100 to 20,000 gravities. The open-circuit acceleration rate – voltage sensitivity is 5×10^{-10} volt per gravity-per-second.

35.135. Figure 35-7j shows a vibration receiver utilizing the magnetostriction effect. The operation of this unit is similar to that of the magnetostrictive relative motion receiver of Fig. 35-5m except that the permanent magnet is used both as the source of the magnetic flux and as the magnetostriction-sensitive element.

35.136. A typical vibration receiver using the magnetostrictive principle has about the same dimensions and operating range as the variable-air-gap unit just described. The undamped natural frequency is approximately 50,000 cycles per second with a damping ratio of about 0.005. The open-circuit sensitivity is 100 millivolts per gravity-per-second.

35.137. Figure 35-7k illustrates the essential features of a vibration receiver with a flexure spring suspension for the seismic element, eddy-current damping, and an inductance-bridge relative motion receiving system based on the principle described in Fig. 35-5q. As shown in Fig. 35-7k, the seismic element is an aluminum plate with cutouts as required for operation. The seismic element is attached to the base by means of four flexure support springs that allow relative motion along the input axis, but prevent displacements in other directions. The flexure springs also act as the elastic coupling for the seismographic system. Damping is provided by the two sections of the aluminum plate that move across the flux lines in the air gaps between two permanent magnets and a U-shaped pole piece of magnetically soft material. Seismographic systems of this type are easily designed to have high undamped natural frequencies, and are therefore suited for operation in the accelerometer range.

35.138. The inductance-bridge-element parts of the vibration receiver of Fig. 35-7k include a laminated stator structure, four coils, two air gaps, and two plates of magnetically soft material and two plates of copper. The coils are connected in pairs, with each pair forming one arm of an inductance bridge similar to that described in Fig. 35-5q. The coils of each pair are mounted on the

stator poles that are opposite each other across one of the working air gaps. Rectangular pieces of magnetically soft material mounted in the seismic element slots act as armatures to vary the inductance of the two coil pairs by changing the areas of high-permeability material in the working air gaps. One side of each armature is located so that one half of each working air gap is covered when the seismic element is in its position of elastic equilibrium. One armature extends from the gap center line toward the base, while the other armature extends away from the base. This means that a relative displacement of the seismic element increases the inductance of one pair of coils, and decreases the inductance of the other pair of coils. A copper-plate tab, similar in shape and size to the armature, covers the half of the air gap not occupied by the armature. Eddy currents in the copper tabs tend to reduce the air-gap flux and so have the opposite effect to that of the armatures in changing the inductance of the coil pairs. This action accentuates the inductance-unbalancing action of relative displacements of the seismic element.

35.139. A vibration receiver of the type illustrated in Fig. 35-7k occupies 12 cubic inches, weighs 16 ounces, and has an undamped natural frequency of 60 cycles per second with a damping ratio of 0.64 and a range of acceleration input of 15 gravities. With proper auxiliary bridge components and an excitation of 10 volts at 1000 cycles per second, this unit has an acceleration-voltage sensitivity of 16.6 millivolts per gravity in the accelerometer operation region.

35.140. Figure 35-7l illustrates the essential features of a piezoelectric crystal linear vibration receiver. In units of this type, the crystal acts as the seismographic system and also as the signal generating system. The crystal is clamped to the case at three clamping points in such a way that one corner is unsupported. The input axis is normal to the plane of the undistorted crystal, so that the effective mass of the unsupported corner acts as the seismic element, with the crystal material itself serving as the elastic coupling and also providing relatively small amounts of damping. The undamped natural frequency of piezoelectric crystals as seismographic systems is relatively high, so that vibration receivers in which they are applied usually operate in the accelerometer range. The action of the crystal in generating output signals from deflections of the unsupported corner is identical with that described in Fig. 35-5t for the bending-strain piezoelectric crystal relative motion receiver.

35.141. A typical piezoelectric crystal vibration receiver occupies a volume of 8 cubic inches with a weight of 7 ounces and has an undamped natural frequency of approximately 2000 cycles per second with a damping ratio of about 0.005. The open-circuit sensitivity is 0.5 volt per gravity.

35.142. Figure 35-7m shows the features of a linear vibration receiver based on the electronic tube relative motion receiver of Fig. 35-5e. The vibration receiver

is identical with the motion receiver except that a seismic mass of proper size is rigidly fixed to the motion receiving element. The elastic restraint and damping functions are provided by the end diaphragm and moving grid rod of the tube structure. The undamped natural frequency of the seismographic system of an electronic tube linear vibration receiver is usually designed to be relatively high, so that these vibration receivers generally operate as accelerometers.

35.143. A typical electronic tube accelerometer occupies 3 cubic inches, weighs 2 ounces, and has an undamped natural frequency of 200 cycles per second with a damping ratio of 0.65. With an excitation of 270 volts, the sensitivity is 3 volts per gravity.

SELECTION OF VIBRATION RECEIVERS

35.144. Selection of vibration receivers to be used in any particular situation must be based on the judgment of experienced engineers who balance a list of factors, including those already discussed, that are deemed important in choosing design features for relative motion receivers. In addition to these factors, which enter because a relative motion receiver is an integral subsystem of any vibration receiver, the characteristics of the seismographic system must be considered. In practice, it is usually possible to design the relative motion receiver so that its operation is substantially ideal for the purposes of the unit in which it is used. This means that the performance of any given vibration receiver is effectively determined by the characteristics of the seismographic system with which it is associated.

35.145. For any particular application, it is obvious that the vibration receiver chosen must operate from the input it is desired to measure and that it must be capable of handling the proper magnitudes over the required range of frequencies with errors less than specified tolerance limits. Because many receivers are sensitive to vibratory motion not only along the input axis but also to motion along the direction at right angles to this axis, it is often important to be sure that coupling effects of this kind do not exceed acceptable limits. For example, the relative displacement in a receiver with a flexure-suspended seismic element is actually a rotation and the unit will therefore be increasingly sensitive to motion along a direction parallel to the elastic-equilibrium position of the arm as the relative deflection angle becomes larger.

35.146. Vibration receiver performance as it is determined by seismographic-system operation depends on well-established theory. This theory is worked out and reduced to engineering terms in the series of derivation summaries that follow this section.

GENERALIZED THEORY OF THE SINGLE-DEGREE-OF-FREEDOM SEISMOGRAPHIC SYSTEM

35.147. All vibration receivers designed as self-contained units include

elements with the properties of mass, elasticity and damping, combined to provide the seismographic-system functions illustrated in Fig. 35-3. For example, each of the typical vibration receivers represented in Fig. 35-7 contains some form of the single-degree-of-freedom seismographic system. From the standpoint of theory, it is possible to reduce such systems to a basic arrangement whose essential behavior may be described by a common performance equation. A pictorial diagram illustrating the essential features of the generalized single-degree-of-freedom vibration receiver and showing definitions for the forcing displacement, the relative displacement, and the seismic element displacement is given in section a of Derivation Summary 35-1. The corresponding functional diagram appears in section b of Derivation Summary 35-1. Section c of the summary lists the performance characteristics for each operating component of the seismographic system and develops the corresponding performance equation.

35.148. From the figure of section a of Derivation Summary 35-1, the displacement with respect to the inertial reference of the seismic element along the vibration receiver input axis* is equal to the sum, along the input axis, of the case displacement with respect to the inertial reference and the relative displacement of the seismic element with respect to the case. In terms of the abbreviated notation of section a, this means that the relative displacement, x_r, is equal to the seismic element displacement, $x_{(se)}$, minus the forcing displacement, x_f (the displacement of the case with respect to the inertial reference).

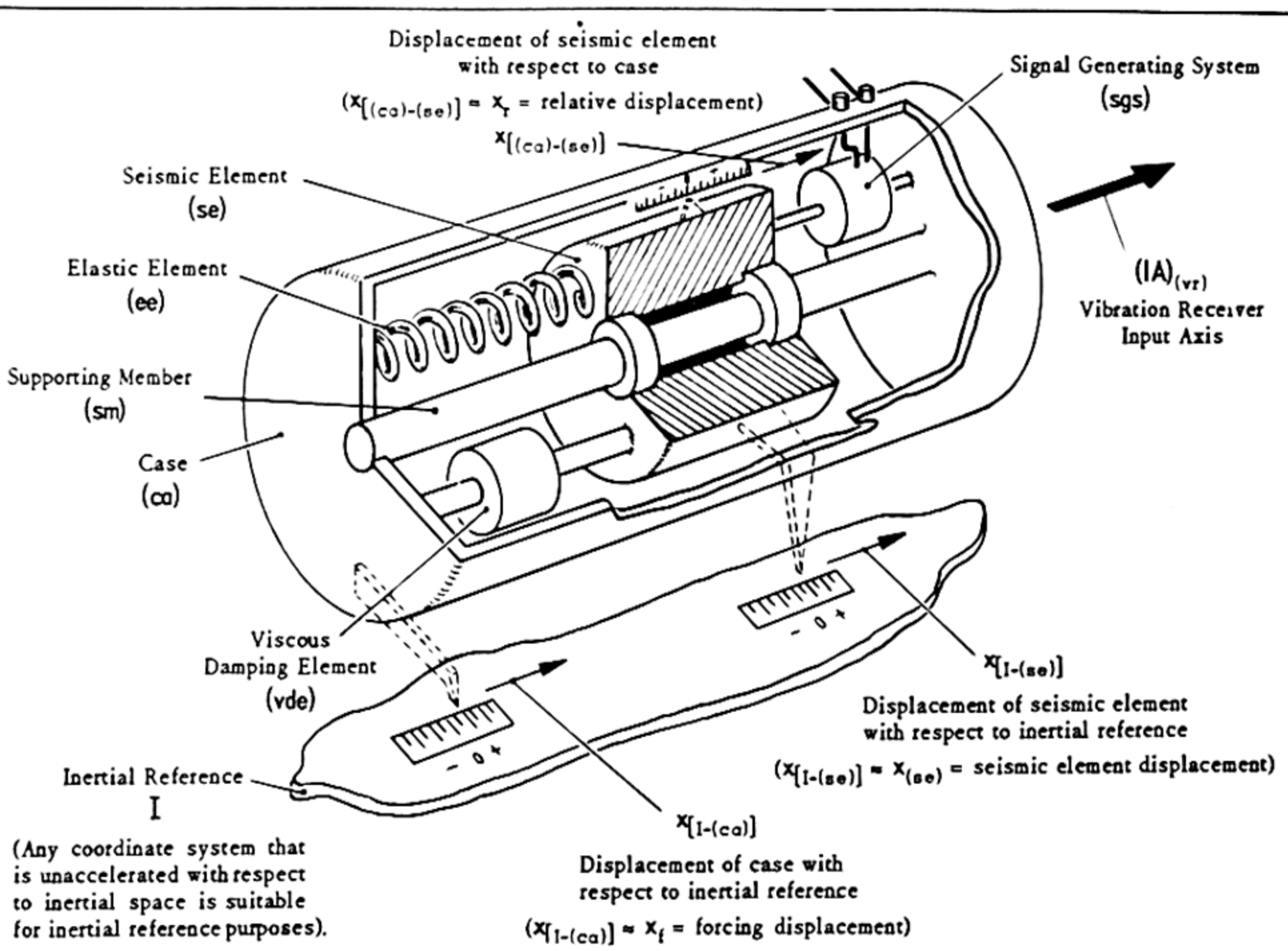
35.149. The force along the input axis that is applied to the seismic element by the elastic element is equal to the product of the relative displacement and the relative displacement – force sensitivity of the elastic element. The magnitude of this sensitivity is identical with the elastic coefficient of the elastic element. The minus sign in Eq. (3) of Derivation Summary 35-1 shows that the elastic element force always acts to reduce the relative displacement.

35.150. The force along the input axis that is applied to the seismic element by the viscous damping element is equal to the product of the relative velocity and the relative velocity – force sensitivity of the viscous damping element. The magnitude of this sensitivity is identical with the viscous damping coefficient of the viscous damping element. The negative sign in the viscous damping force equation of Derivation Summary 35-1 corresponds to the physical fact that the viscous damping element always acts to reduce the relative velocity.

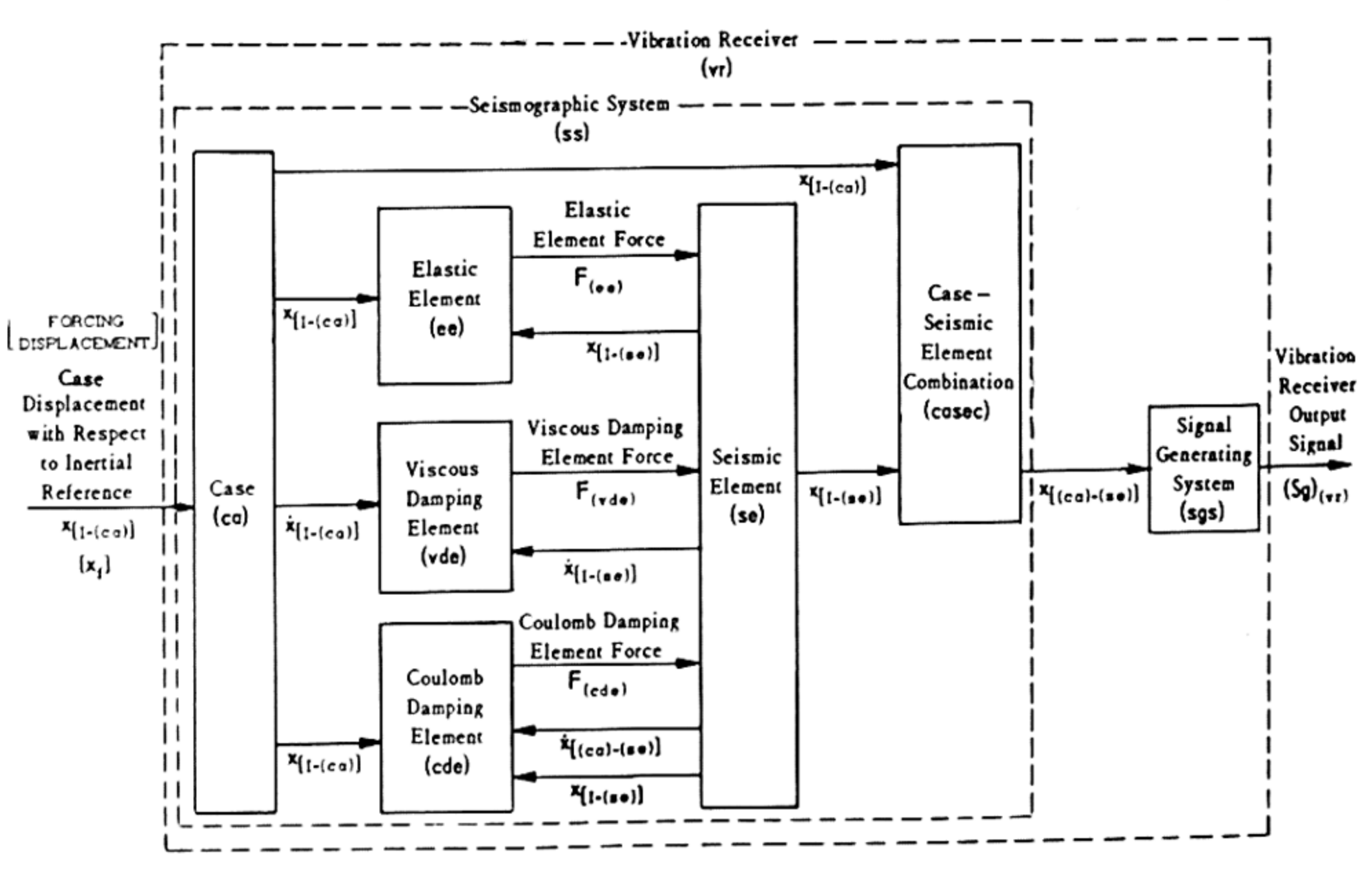
35.151. The force along the input axis that is applied to the seismic element by the Coulomb damping element stems from the presence of Coulomb friction in the seismographic system. Coulomb friction is due to rubbing between solid parts.

---

* The vibration receiver input axis is a direction fixed with respect to the case and parallel to the direction in which the seismic element is free to move with respect to the case.



a) Illustrative pictorial diagram showing the essential features of the generalized single-degree-of-freedom vibration receiver



b) Functional diagram for the generalized single-degree-of-freedom vibration receiver

Derivation Summary 35-1. Pictorial diagram, functional diagram, and performance equation for the single-degree-of-freedom seismographic system that has combined viscous damping and Coulomb damping. (Page 1 of 3)

Geometrical relationships:

$$x_{[I-(se)]} = x_{[I-(ca)]} + x_{[(ca)-(se)]} \quad ; \quad x_{[(ca)-(se)]} = x_{[I-(se)]} - x_{[I-(ca)]} \tag{1),(2}$$

(ee) Elastic element

$$F_{(ee)} = -S_{(ee)|x_{[(ca)-(se)}];F|}\, x_{[(ca)-(se)]} = -k_{(ee)}\, x_{[(ca)-(se)]} \tag{3}$$

where

$S_{(ee)|x_{[(ca)-(se)}];F|}$ = relative displacement – force sensitivity magnitude of the elastic element

$\equiv k_{(ee)}$ = elastic coefficient of the elastic element

(vde) Viscous damping element

$$F_{(vde)} = -S_{(vde)|\dot{x}_{[(ca)-(se)}];F|}\, \dot{x}_{[(ca)-(se)]} = -c_{(vde)}\, \dot{x}_{[(ca)-(se)]} \tag{4}$$

where

$S_{(vde)|\dot{x}_{[(ca)-(se)}];F|}$ = relative velocity – force sensitivity magnitude of the viscous damping element

$\equiv c_{(vde)}$ = viscous damping coefficient of the viscous damping element

(cde) Coulomb damping element (combination of the seismic-element bearing rings and the supporting member surfaces with which they are in sliding contact)

$$F_{(cde)} \approx F_{(cf)} = \pm |F_{(cf)}| \tag{5}$$

where

$F_{(cf)}$ = Coulomb friction force

Note: The Coulomb friction force is constant in magnitude when relative motion exists and always acts to resist relative motion. This constant value, which is the largest possible Coulomb friction force, is called the maximum Coulomb friction force and is given the symbol $F_{(cf)(max)}$. Throughout the rest of this chapter, this symbol is abbreviated to $F_{(cf)m}$ for convenience.

(ss) Seismographic system

The sum of the forces acting on the seismic element along the input axis is

$$\begin{pmatrix}\text{Inertia}\\ \text{Reaction}\\ \text{Force}\end{pmatrix} + \begin{pmatrix}\text{Viscous}\\ \text{Damping}\\ \text{Force}\end{pmatrix} + \begin{pmatrix}\text{Elastic}\\ \text{Element}\\ \text{Force}\end{pmatrix} + \begin{pmatrix}\text{Coulomb}\\ \text{Friction}\\ \text{Force}\end{pmatrix} = 0 \tag{6}$$

That is,

$$-m_{(se)}\, \ddot{x}_{[I-(se)]} - c_{(vde)}\, \dot{x}_{[(ca)-(se)]} - k_{(ee)}\, x_{[(ca)-(se)]} \mp |F_{(cf)}| = 0 \tag{7}$$

where

$m_{(se)}$ = mass of the seismic element

Note: $F_{(cf)}$ is negative when $\dot{x}_{[(ca)-(se)]}$ is positive and vice versa.

Equation (7) holds true whether there is relative motion present or not since $|F_{(cf)}|$ adjusts itself as required to just balance the resultant of the other applied forces whenever there is no relative motion. For the situation where relative motion exists, the Coulomb friction force magnitude, $|F_{(cf)}|$, in Eq. (7) can be replaced by the maximum Coulomb friction force magnitude, $|F_{(cf)m}|$. Combining Eq. (1) with Eq. (7), substituting $|F_{(cf)m}|$ for $|F_{(cf)}|$, rearranging terms, dividing by $m_{(se)}$, and writing j^2 for -1 gives

$$\ddot{x}_{[(ca)-(se)]} + \frac{c_{(vde)}}{m_{(se)}}\, \dot{x}_{[(ca)-(se)]} + \frac{k_{(ee)}}{m_{(se)}}\, x_{[(ca)-(se)]} = j^2 \ddot{x}_{[I-(ca)]} \mp \frac{k_{(ee)}}{m_{(se)}} \frac{|F_{(cf)m}|}{k_{(ee)}} \tag{8}$$

Except for the Coulomb friction term, Eq. (8) has the form of the (2;0,1,2) differential equation, which is a special case of the (2,1,0;0,1,2) equation considered in Chapter 19 (see Definition Summary 19-1 and Derivation Summary 19-12). The Coulomb friction term is a typical rate-determined step term of the type discussed in Chapter 26.

Derivation Summary 35-1. Pictorial diagram, functional diagram, and performance equation for the single-degree-of-freedom seismographic system that has combined viscous damping and Coulomb damping. (Page 2 of 3)

When the definitions of Table 19-1 and section f of Definition Summary 19-1 are used, Eq. (8) becomes

$$\ddot{x}_r + 2(DR)_{(ss)} w_{(n)(ss)} \dot{x}_r + w^2_{(n)(ss)} x_r = j^2 \ddot{x}_f \mp w^2_{(n)(ss)} |x_{(cf)m}| \tag{9}$$

where

$$x_r \approx x_{[(ca)-(se)]} = \text{relative displacement} \tag{10}$$

$$x_f \approx x_{[I-(ca)]} = \text{forcing displacement} \tag{11}$$

$$|x_{(cf)m}| = \frac{|F_{(cf)m}|}{k_{(ee)}} = \text{magnitude of maximum relative displacement due to Coulomb friction in the seismographic system or maximum Coulomb friction displacement magnitude} \tag{12}$$

$$w_{(n)(ss)} = \sqrt{\frac{k_{(ee)}}{m_{(se)}}} = \text{undamped angular natural frequency of the seismographic system} \tag{13}$$

$$(DR)_{(ss)} = \frac{c_{(vde)}}{2\sqrt{k_{(ee)} m_{(se)}}} = \text{damping ratio of the seismographic system} \tag{14}$$

In working variable terms, Eq. (9) may be written in the form

$$\ddot{v} + 2\zeta\omega_n \dot{v} + \omega_n^2 v = \left(\frac{1}{\omega_n^2}\right) j^2 \omega_n^2 \ddot{u} \mp \omega_n^2 u_{(rs)} \tag{15}$$

where

$$x_r \approx v = \text{dependent variable} \tag{16}$$

$$x_f \approx u = \text{independent variable} \tag{17}$$

$$|x_{(cf)m}| \approx u_{(rs)} = \text{rate-determined step term} \tag{18}$$

$$(DR)_{(ss)} \approx \zeta \quad ; \quad w_{(n)(ss)} \approx \omega_n \tag{19),(20}$$

Note: The first term on the right-hand side of Eq. (15) is multiplied and divided by $w^2_{(n)(ss)}$ in order to match the standard form of Eq. (36) of Definition Summary 19-1 in Chapter 19.

c) Performance equation

Derivation Summary 35-1. Pictorial diagram, functional diagram, and performance equation for the single-degree-of-freedom seismographic system that has combined viscous damping and Coulomb damping. (Page 3 of 3)

The effect of this physical action may be represented by a force of constant magnitude that always acts to oppose the relative motion and consequently reverses its sign each time the relative velocity changes direction. When this Coulomb friction force is sufficient to "lock" two surfaces together, so that the relative velocity is zero, the friction force magnitude adjusts itself to just balance the resultant of other applied forces. In the seismographic system, when the combination of elastic element force and inertia reaction force acting on the seismic element exceeds the maximum possible Coulomb friction force, "breakaway" occurs and the seismic element starts to move with respect to the vibration receiver case. When the resultant of all the other forces remains enough greater in magnitude than the maximum Coulomb friction force, the form of the relative displacement is substantially sinusoidal under steady-state conditions with a sinusoidal forcing motion input. The relationships that determine this response are derived later in this chapter.

35.152. The seismographic system performance equation represents a summation of the forces acting on the seismic element along the input axes. The inertia reaction force along the input axis is equal to the product of the seismic element effective mass and the seismic element acceleration with respect to inertial space. This term includes a minus sign to show that the reaction force acts in the direction opposite to that of the acceleration. Because inertia reaction effects are always associated with any material body, blocks representing inertia reaction effects are omitted from functional diagrams. When mass is present, it is understood without explicit statement that inertia reaction terms must be included in writing performance equations.

35.153. Equation (7) of Derivation Summary 35-1 is the basic form of the seismographic system performance equation. This equation is a summation of the following terms, which represent the forces applied to the seismic element:

1) The inertia reaction force term.
2) The viscous damping force term.
3) The elastic element force term.
4) The Coulomb friction force term.

35.154. When the geometrical relationship between seismic element displacement and case displacement is used to replace the seismic element acceleration term of Eq. (7) by a relative acceleration term and a forcing acceleration term, and the Coulomb friction magnitude is replaced by the maximum Coulomb friction magnitude, with the restriction that the new equation applies only when relative motion is present, the result is Eq. (8) of Derivation Summary 35-1. In this equation, each term is divided by the mass of the seismic element, and the Coulomb friction term is multiplied and divided by the elastic element coefficient. Reference to Table 19-1 of Chapter 19 shows that the coefficient of the first derivative term may be written as twice the product of the damping ratio and the undamped angular natural frequency. Similarly, the coefficient of the zero-order term is the square of the undamped angular natural frequency. The ratio of the maximum Coulomb friction force (that is, the constant force that occurs when relative motion exists) to the elastic coefficient is defined as the maximum Coulomb friction displacement. The coefficient of this Coulomb friction displacement is the square of the undamped angular natural frequency.

35.155. With the transformations noted in the preceding paragraph, the seismographic system performance equation has the form given by Eq. (9) of Derivation Summary 35-1. Except for the Coulomb friction term, the seismographic system performance equation has the (2;0, 1, 2) differential equation form, which is a special case of the (2, 1, 0;0, 1, 2) equation considered in Chapter 19. The Coulomb friction term, with its constant magnitude and its relative-velocity-determined sign, has mathematical properties that are identical with those of the

nonlinear, rate-determined step term that is considered in Chapter 26. Equation (15) of Derivation Summary 35-1 is the working variable form of the seismographic system performance equation. This form is one of those studied in detail in Chapter 26.

GENERALIZED PERFORMANCE FUNCTION FOR THE SINGLE-DEGREE-OF-FREEDOM SEISMOGRAPHIC SYSTEM WITH VISCOUS DAMPING ONLY

35.156. The seismographic system performance equation with viscous damping but no Coulomb damping has the (2;0, 1, 2) differential equation form. The relating function for this equation is developed in Derivation Summaries 19-9 and 19-12 of Chapter 19. In order to review the mathematical procedures involved, a simplified development of the (2;0, 1, 2) relating function is given in Derivation Summary 35-2. The results of this development are expressed in working variable symbols and the corresponding generalized, self-defining symbols,* with corresponding symbols written out in words.

PERFORMANCE CHARACTERISTICS OF THE SEISMOGRAPHIC SYSTEM AS AN OPERATING COMPONENT FOR RECEIVING VIBRATION

35.157. Section a of Derivation Summary 35-3 gives a line schematic diagram representing the seismographic system with viscous damping but no Coulomb damping. The functional diagram for the seismographic system, with forcing displacement as the input and the displacement of the seismic element with respect to the case (relative displacement) as the output, is shown in section b of Derivation Summary 35-3. When the seismographic system is considered as an operating component with this combination of input and output quantities, it falls into the class of vibratory displacement receivers. In practice, devices of this class are also called vibrometers.

35.158. The region of operation within which a given device gives a relative displacement output that is an acceptably close representation of the forcing displacement input is the vibratory displacement receiving range, or the vibrometer range, for the given device. This range depends upon the tolerance limits specified as determining acceptable operation and upon the basic performance characteristics of the seismographic system itself. These characteristics may be described by a pattern of nondimensional equations and curve families that provide

* Generalized self-defining symbols describe the behavior of any physical configuration that may be associated with the differential equation from which the performance function represented by the symbols is derived. The middle row of each section of Definition Summary 13-6 of Chapter 13 is made up of generalized self-defining symbol forms; for example,

$$[PF]_{(id)[q_{(ref)};q_{(dep)}]} = (RAR)_{(id)[q_{(ref)};q_{(dep)}]}\,[(DAR)(RAR)R]_{(id)(q_{(ref)};q_{(dep)})}\,\epsilon^{j(DRA)_{(id)(q_{(ref)};q_{(dep)})}}$$

In Derivation Summary 35-2, $q_{(ref)} \approx x_f$, $q_{(dep)} \approx x_r$, and (id) ≈ (ss) = seismographic system identification. The names given in Derivation Summary 35-2 apply directly when the indicated substitutions are made in the subscript symbols.

immediately available quantitative information on seismographic system performance in any specific situation. The mathematical steps required to generate the performance-describing equations and curves for the seismographic system are largely available in Chapter 19. It is the purpose of the following discussion to associate the generalized results of Chapter 19 with the specific characteristics of the seismographic system as an operating component for receiving vibratory motion. In order to achieve this objective, some derivations and curves not available in Chapter 19 are worked out and fitted into the pattern in which all symbols and definitions are adapted for application to the analysis of the seismographic system as a component of a self-contained vibration receiver or indicator.

35.159. Section b of Derivation Summary 35-3 gives two forms for the seismographic system performance equation. Equation (1) is written with the forcing function as the forcing acceleration. In Eq. (5), the forcing displacement appears as the forcing function.

35.160. Section c of Derivation Summary 35-3 summarizes the performance function forms for the seismographic system, expressed in operating-component self-defining notation.* In this notation, the sensitivity, the reference sensitivity, the dimensionless sensitivity ratio, and the dynamic response angle for the seismographic system, with forcing displacement as the input and relative displacement as the output, are respectively identical with the dynamic amplitude ratio, the

---

* Self-defining symbols adapted for direct use to describe operating component performance are given in the upper row of each section of Definition Summary 13-6. In operating component notation,

a) Sensitivity corresponds to the dynamic amplitude ratio of the generalized notation; i.e.,

$$S_{(oc)[q_{(in)};q_{(out)}]} \approx (DAR)_{(id)[q_{(ref)};q_{(dep)}]} \approx \rho$$

b) Dynamic response angle is identical with the dynamic response angle of the generalized notation; i.e.,

$$(DRA)_{(oc)(q_{(in)};q_{(out)})} \approx (DRA)_{(id)(q_{(ref)};q_{(dep)})} \approx \phi$$

c) Reference sensitivity corresponds to the reference amplitude ratio of the generalized notation; i.e.,

$$S_{(oc)[q_{(in)};q_{(out)}](ref)} \approx (RAR)_{(id)[q_{(ref)};q_{(dep)}]} \approx \rho_r$$

d) Sensitivity – reference sensitivity ratio corresponds to the dynamic amplitude ratio – reference amplitude ratio ratio of the generalized notation; i.e.,

$$[S(RS)R]_{(oc)(q_{(in)};q_{(out)})} \approx [(DAR)(RAR)R]_{(id)(q_{(ref)};q_{(dep)})} \approx \mu$$

The sensitivity – reference sensitivity ratio is also called the dimensionless sensitivity ratio, and the dynamic amplitude ratio – reference amplitude ratio ratio is also called the dimensionless amplitude ratio; i.e.,

$$[S(RS)R]_{(oc)(q_{(in)};q_{(out)})} \equiv \acute{(}SR)_{(oc)(q_{(in)};q_{(out)})}$$

$$[(DAR)(RAR)R]_{(id)(q_{(ref)};q_{(dep)})} \equiv \acute{(}DAR)_{(id)(q_{(ref)};q_{(dep)})}$$

From the relationships given in Definition Summary 13-6,

$$[PF]_{(oc)[q_{(in)};q_{(out)}]} \approx S_{(oc)[q_{(in)};q_{(out)}]}\, \epsilon^{j(DRA)_{(oc)(q_{(in)};q_{(out)})}}$$

$$= S_{(oc)[q_{(in)};q_{(out)}](ref)}\, \acute{(}SR)_{(oc)(q_{(in)};q_{(out)})}\, \epsilon^{j(DRA)_{(oc)(q_{(in)};q_{(out)})}}$$

From Derivation Summary 35-1, the performance equation for the seismographic system with combined viscous damping and Coulomb damping may be written in the form

$$\ddot{x}_r + 2(DR)_{(ss)} w_{(n)(ss)} \dot{x}_r + w^2_{(n)(ss)} x_r = \frac{1}{w^2_{(n)(ss)}} j^2 w^2_{(n)(ss)} \ddot{x}_f \mp w^2_{(n)(ss)} |x_{(cf)m}| \qquad (1)$$

where the first term on the right-hand side of Eq. (1) is multiplied and divided by $w^2_{(n)(ss)}$ in order to match the standard form of Eq. (36) of Definition Summary 19-1 in Chapter 19.

When no Coulomb friction is present, Eq. (1) becomes

$$\ddot{x}_r + 2(DR)_{(ss)} w_{(n)(ss)} \dot{x}_r + w^2_{(n)(ss)} x_r = \frac{1}{w^2_{(n)(ss)}} j^2 w^2_{(n)(ss)} \ddot{x}_f \qquad (2)$$

When no viscous damping is present, Eq. (1) becomes

$$\ddot{x}_r + w^2_{(n)(ss)} x_r = \frac{1}{w^2_{(n)(ss)}} j^2 w^2_{(n)(ss)} \ddot{x}_f \mp w^2_{(n)(ss)} |x_{(cf)m}| \qquad (3)$$

Equation (2) has the (2;0,1,2) equation form, which is a special case of the (2,1,0;0,1,2) equation form discussed in Derivation Summaries 19-1 and 19-9. The steady-state sinusoidal relating function for the (2;0,1,2) differential equation form is developed in Derivation Summary 19-12.

Steady-state sinusoidal relating functions for the (2,1,0;0,1,2) form,including a rate-determined step term which is a mathematical term representing the effect of Coulomb friction, are developed in Derivation Summaries 26-3, 26-4, and 26-5 of Chapter 26. An approximate but generally useful form of the steady-state sinusoidal relating function for the (2;0,1,2) form with the rate-determined step term is given in section d of Derivation Summary 26-5.

In order to illustrate the general nature of the mathematical procedure involved, a derivation of the (2;0,1,2) sinusoidal relating function for the case of viscous damping only is given in section b.

a) Seismographic system performance equations

In working variable terms, the seismographic system performance equation for the case of viscous damping only is

$$\ddot{v} + 2\zeta\omega_n \dot{v} + \omega_n^2 v = \frac{1}{\omega_n^2} j^2 \omega_n^2 \ddot{u} \qquad (4)$$

where

$v \approx x_r$ = relative displacement

$u \approx x_f$ = forcing displacement

$\zeta \approx DR$ = damping ratio

$\omega_n \approx w_n$ = undamped angular natural frequency

When the forcing function, u, is sinusoidal, it may be expressed in the imaginary exponential form described in Definition Summary 12-3 and Figs. 12-1 through 12-4 of Chapter 12; i.e.,

$$u = u_a \epsilon^{j\omega_f t} \qquad (5)$$

where

u_a = forcing function amplitude

$\omega_f = 2\pi n_f$ = angular forcing frequency

n_f = forcing frequency

Differentiating Eq. (5) with respect to time shows that

$$\dot{u} = j\omega_f (u_a \epsilon^{j\omega_f t}) = j\omega_f u \qquad (6)$$

Derivation Summary 35-2. The (2;0,1,2) relating function and the performance function for the single-degree-of-freedom seismographic system that has viscous damping only. (Page 1 of 4)

and

$$\ddot{u} = (j\omega_f)^2 (u_a \epsilon^{j\omega_f t}) = j^2 \omega_f^2 u \tag{7}$$

Substituting the expression of Eq. (7) in Eq. (4) shows that

$$\ddot{v} + 2\zeta\omega_n \dot{v} + \omega_n^2 v = \frac{1}{\omega_n^2} \omega_n^2 \omega_f^2 u \tag{8}$$

The steady-state solution of Eq. (8) may be written in the form

$$v = \eta u \tag{9}$$

where

$\eta \approx \eta_{(2;0,1,2)} \approx [RF]_{(2;0,1,2)}$ = (2;0,1,2) relating function

is to be determined.

From Eq. (9),

$$\dot{v} = \eta \dot{u} = \eta j\omega_f u \tag{10}$$

$$\ddot{v} = \eta \ddot{u} = \eta j^2 \omega_f^2 u \tag{11}$$

Substituting the expressions of Eqs. (9), (10) and (11) in Eq. (8) gives

$$\eta(-\omega_f^2 + j2\zeta\omega_n\omega_f + \omega_n^2) u = \omega_f^2 u \tag{12}$$

Equation (12) will be true and Eq. (9) will be the solution of Eq. (4) when

$$\eta = \frac{\omega_f^2}{\omega_n^2 - \omega_f^2 + j2\zeta\omega_n\omega_f} \tag{13}$$

Dividing the numerator and denominator of Eq. (13) by ω_n^2 gives the form

$$\eta = \frac{\beta^2}{1 - \beta^2 + j2\zeta\beta} \tag{14}$$

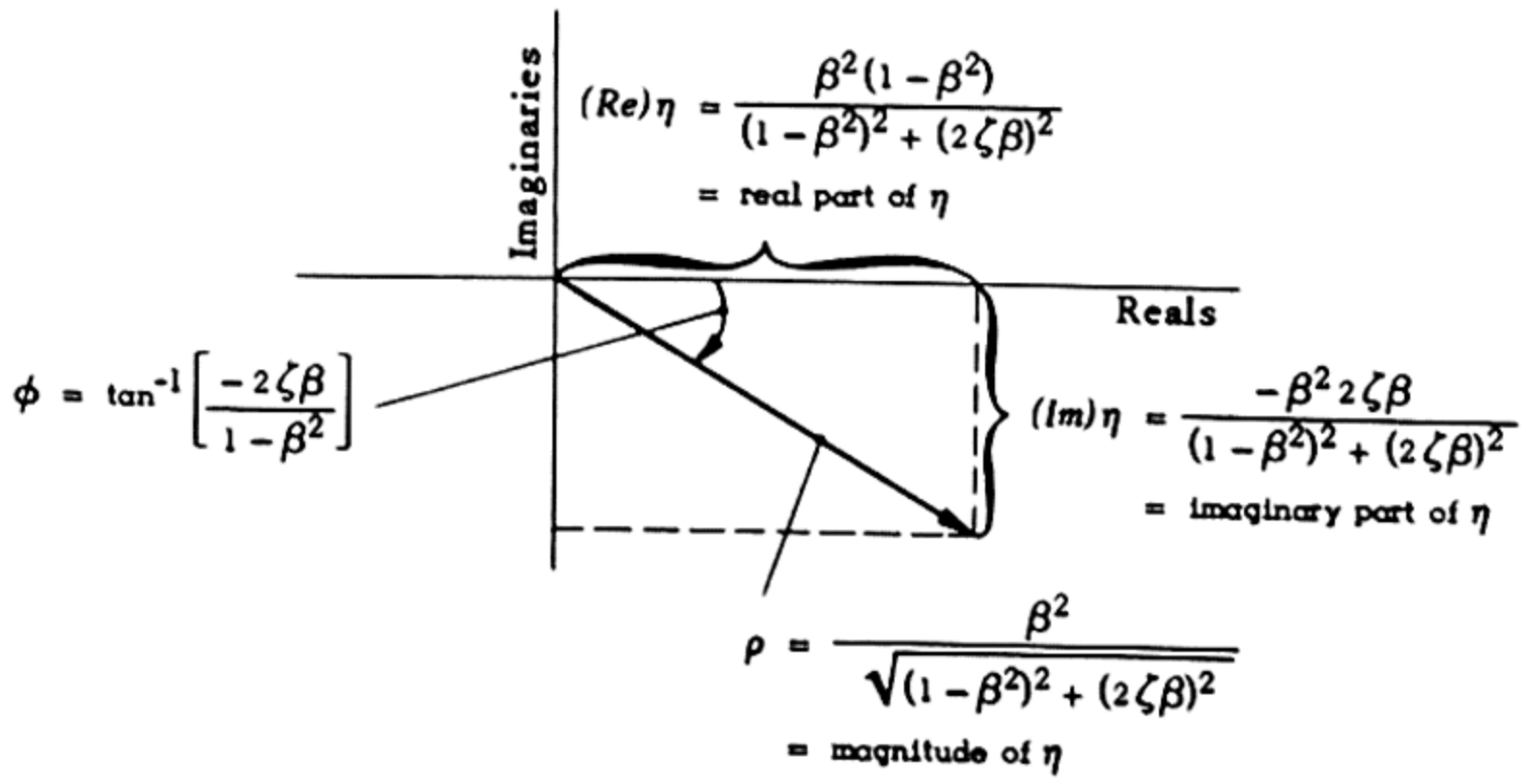
where

$$\beta = \frac{\omega_f}{\omega_n} = \frac{n_f}{n_n} = \frac{T_n}{T_f} \approx FR = \text{frequency ratio} \tag{15}$$

Equation (14) may be changed to a form suitable for the graphical representation described in Fig. 12-1 by multiplication of the numerator and the denominator by the complex conjugate of the denominator. The result of this transformation is

$$\eta = \frac{\beta^2(1-\beta^2)}{(1-\beta^2)^2 + (2\zeta\beta)^2} - j\frac{\beta^2 2\zeta\beta}{(1-\beta^2)^2 + (2\zeta\beta)^2} \tag{16}$$

The vector diagram corresponding to Eq. (16) is



Derivation Summary 35-2. The (2;0,1,2) relating function and the performance function for the single-degree-of-freedom seismographic system that has viscous damping only. (Page 2 of 4)

From the figure,

$$\eta_{(2;0,1,2)} = \rho_{(2;0,1,2)} \epsilon^{j\phi_{(2;0,1,2)}} \tag{17}$$

where

$$\rho_{(2;0,1,2)} = \frac{\beta^2}{\sqrt{(1-\beta^2)^2 + (2\zeta\beta)^2}} \tag{18}$$

= (2;0,1,2) dynamic amplitude ratio

$$\phi_{(2;0,1,2)} = \tan^{-1}\left[\frac{-2\zeta\beta}{1-\beta^2}\right]^{*} \tag{19}$$

= (2;0,1,2) dynamic response angle

Taking ρ_r, the reference dynamic amplitude ratio, equal to unity gives

$$\eta_{(2;0,1,2)} = \rho_r \mu_{(2;0,1,2)} \epsilon^{j\phi_{(2;0,1,2)}} \tag{20}$$

where

$$\mu_{(2;0,1,2)} = \frac{\rho_{(2;0,1,2)}}{\rho_r} = \frac{\beta^2}{\sqrt{(1-\beta^2)^2 + (2\zeta\beta)^2}} \tag{21}$$

= (2;0,1,2) dimensionless amplitude ratio

b) Sinusoidal relating function for the (2;0,1,2) differential equation form for the case of viscous damping only

In the self-defining symbols developed in Chapter 13, with special application to the seismographic system as an operating component, and with x_f as the input quantity and x_r as the output quantity,

$\eta_{(2;0,1,2)} \approx [RF]_{(2;0,1,2)} \approx [PF]_{(ss)[x_f;x_r]}$ = forcing displacement input – relative displacement output performance function of the seismographic system

$$[PF]_{(ss)[x_f;x_r]} = (DAR)_{(ss)[x_f;x_r]} \epsilon^{j(DRA)_{(ss)(x_f;x_r)}}$$

$$= (RAR)_{(ss)[x_f;x_r]} [(DAR)(RAR)R]_{(ss)(x_f;x_r)} \epsilon^{j(DRA)_{(ss)(x_f;x_r)}} \tag{22}$$

where, from Eqs. (17) through (21),

$$\rho_{(2;0,1,2)} \approx (DAR)_{(ss)[x_f;x_r]} = \frac{(FR)^2}{\sqrt{[1-(FR)^2]^2 + [2(DR)(FR)]^2}} \tag{23}$$

= forcing displacement input – relative displacement output dynamic amplitude ratio of the seismographic system

$$\rho_r \approx (RAR)_{(ss)[x_f;x_r]} = 1 \tag{24}$$

= forcing displacement input – relative displacement output reference amplitude ratio of the seismographic system

$$\mu_{(2;0,1,2)} \approx [(DAR)(RAR)R]_{(ss)(x_f;x_r)} = \frac{(FR)^2}{\sqrt{[1-(FR)^2]^2 + [2(DR)(FR)]^2}} \tag{25}$$

= forcing displacement input – relative displacement output dynamic amplitude ratio – reference amplitude ratio ratio of the seismographic system

---

* The phase angle $\phi_{(2;0,1,2)}$ developed here is 180° out of phase with the phase angle $\phi_{(2;0,1,2)}$ developed in Derivation Summary 19-12 since in that summary it was assumed that $\nu_{(2-2)} > 0$, whereas for the case of the seismographic system $\nu_{(2-2)} < 0$.

Derivation Summary 35-2. The (2;0,1,2) relating function and the performance function for the single-degree-of-freedom seismographic system that has viscous damping only. (Page 3 of 4)

$$\phi_{(2;0,1,2)} = (DRA)_{(ss)(x_i;x_r)} = \tan^{-1}\left[\frac{-2(DR)(FR)}{1-(FR)^2}\right] \qquad (26)$$

= forcing displacement input – relative displacement output dynamic response angle of the seismographic system

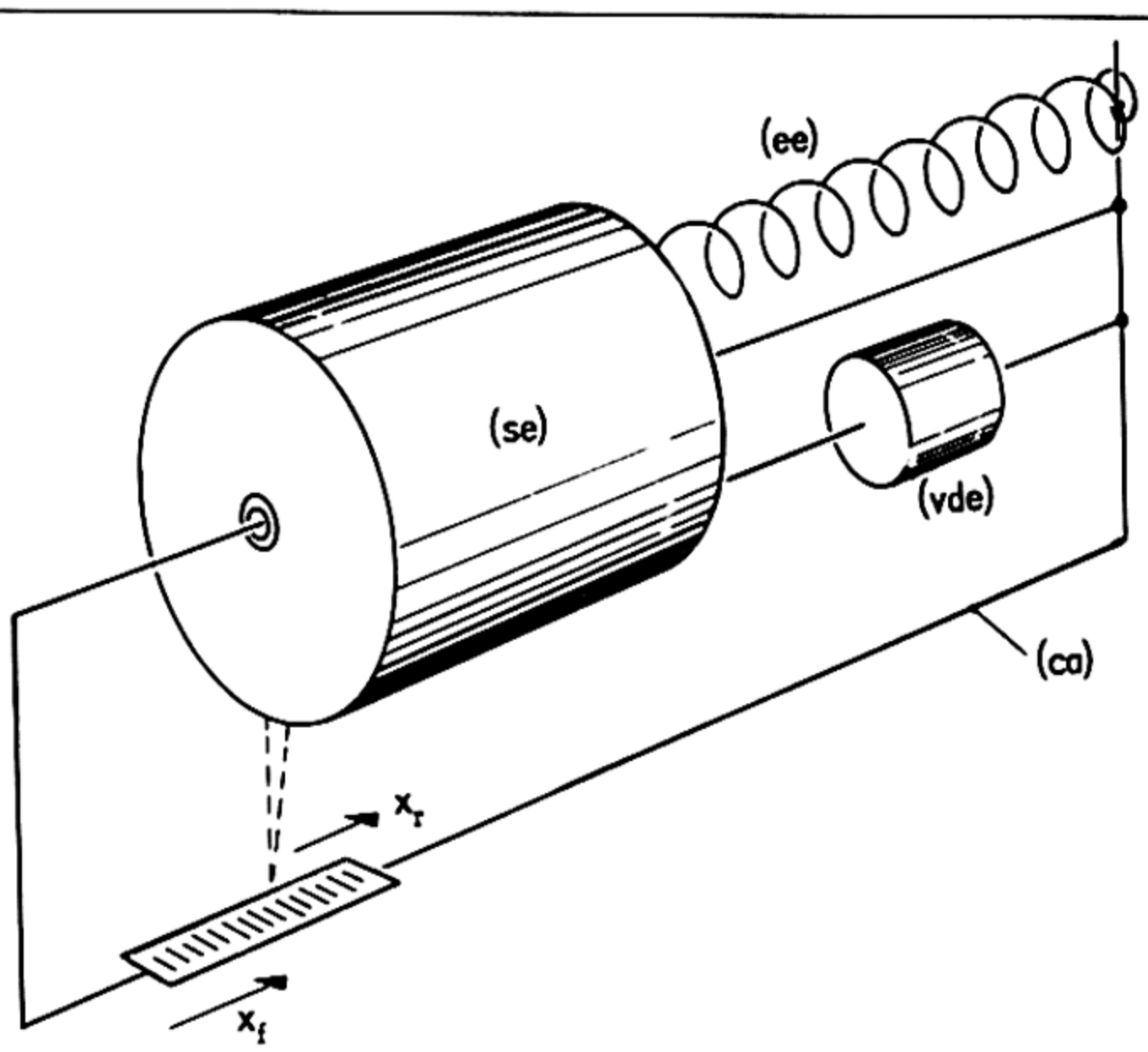
c) Seismographic system performance function for the case of viscous damping only

Derivation Summary 35-2. The (2;0,1,2) relating function and the performance function for the single-degree-of-freedom seismographic system that has viscous damping only. (Page 4 of 4)

reference amplitude ratio, the dynamic amplitude ratio – reference amplitude ratio ratio, and the dynamic response angle developed in generalized notation in Derivation Summary 35-2. These performance-describing concepts are identical with the corresponding concepts associated with the relating function for the (2;0, 1, 2) differential equation. The specific relationships, with frequency ratio and damping ratio as independent variables, are given in Eqs. (6) through (11) of Derivation Summary 35-3. The physical interpretation of these equations in terms of the vibration-receiving performance of the seismographic system with viscous damping only is summarized in the curve families of Figs. 35-8 through 35-11.

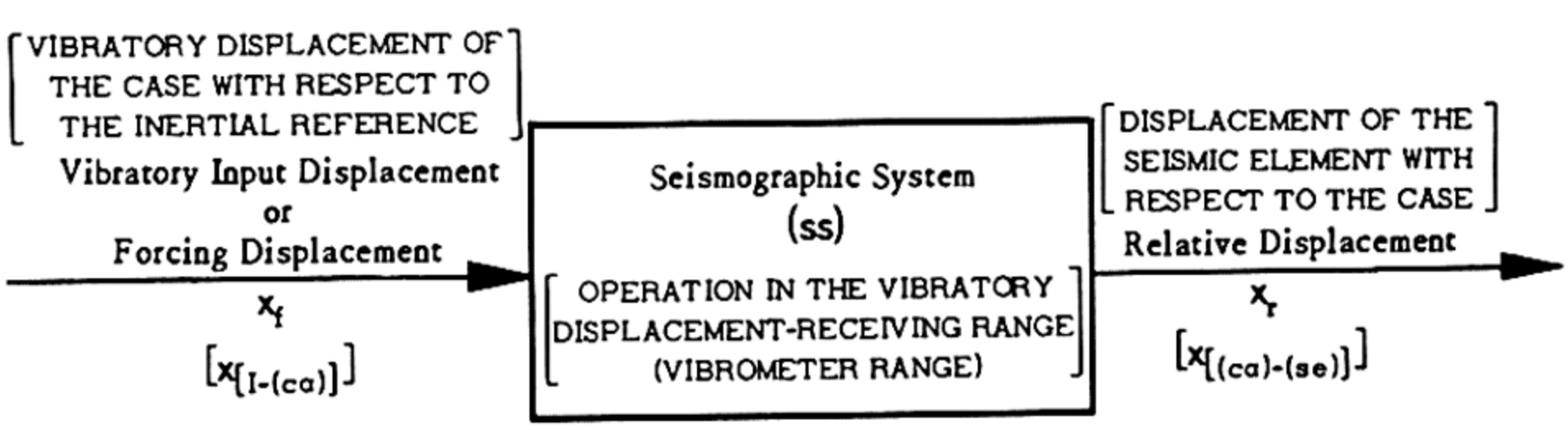
35.161. Figure 35-8 is a linear-scale curve family with frequency ratio as the abscissa, with dimensionless sensitivity ratio as the ordinate, and with each individual curve drawn for a particular value of the damping ratio. Every curve of the family starts from zero at zero frequency ratio. This characteristic corresponds to the physical fact that the inertia reaction force produced by very low forcing frequencies is too small to produce any appreciable relative displacement of the seismic element against the restoring force of the spring. All the curves are asymptotic to unity at very high frequency ratios. This result is due to the inertia reaction force effectively preventing motion of the seismic element with respect to inertial space during the short half-cycle periods between reversals of the elastic and damping forces acting on the seismic element. In other words, the forcing periods are so short that inertia "holds the seismic element still," so that the relative motion amplitude is effectively equal to the forcing amplitude for the high frequency-ratio range. Because of this fact, the high frequency-ratio range is called the displacement-receiving range or the vibrometer range of the seismographic system.

35.162. In the low frequency-ratio range, the forcing acceleration of the case is so low that the elastic element causes the seismic element to follow the case very closely. The small relative displacement of the spring is proportional to the acceleration of the case, which, for sinusoidal motion, has an amplitude equal to the square of the forcing frequency multiplied by the forcing displacement amplitude. This means that in the low frequency-ratio region, where the spring



a) Line schematic diagram of the single-degree-of-freedom seismographic system

When forcing displacement is considered as the input and relative displacement is taken as the output, the functional diagram for the seismographic system is



When Coulomb friction effects are negligible, the single-degree-of-freedom seismographic system performance equation has the form of Eq. (2) of Derivation Summary 35-2; i.e.,

$$\ddot{x}_r + 2(DR)\,w_n \dot{x}_r + w_n^2 x_r = \frac{1}{w_n^2}\, j^2 w_n^2 \ddot{x}_f \tag{1}$$

In Eq. (1), the subscripts (ss) that appear in Eq. (2) of Derivation Summary 35-2 are omitted because, for present purposes, no misunderstanding of the operating component associated with the symbols is possible.

When the forcing displacement is sinusoidal, that is, when

$$x_f = x_{(f)a} \epsilon^{j w_f t} \tag{2}$$

then

$$\dot{x}_f = j w_f x_f \tag{3}$$

$$\ddot{x}_f = j^2 w_f^2 x_f \tag{4}$$

Derivation Summary 35-3. Line schematic diagram, functional diagram, performance equation, performance function and performance deviation equations for the seismographic system that has viscous damping only and operates in the displacement-receiving range. (Page 1 of 4)

Substituting the relationship of Eq. (4) in Eq. (1) shows that

$$\ddot{x}_r + 2(DR)\,w_n \dot{x}_r + w_n^2 x_r = (FR)^2 w_n^2 x_f \tag{5}$$

b) Functional diagram and performance equation for the seismographic system operating in the displacement-receiving range

Equation (1) has the (2;0,1,2) differential equation form, for which the forcing displacement input – relative displacement output performance function is developed in section c of Derivation Summary 35-2.

When the seismographic system is considered as a measuring system component with forcing displacement as the input and relative displacement as the output, the performance equation may be expressed in terms of reference sensitivity, sensitivity – reference sensitivity ratio, and dynamic response angle, as these quantities are defined in Chapter 13, listed in Definition Summary 13-6 and reviewed in Definition Summary 28-8. Reference to these summaries and to sections b and c of Derivation Summary 35-2 shows that

$$\eta_{(2;0,1,2)} = [PF]_{(ss)[x_f;x_r]} = \frac{(FR)^2}{1 - (FR)^2 + j\,2(DR)(FR)} \tag{6}$$

and

$$[PF]_{(ss)[x_f;x_r]} = S_{(ss)[x_f;x_r]}\,\epsilon^{\,j(DRA)_{(ss)(x_f;x_r)}} = S_{(ss)[x_f;x_r](ref)}\,\hat{}(SR)_{(ss)(x_f;x_r)}\,\epsilon^{\,j(DRA)_{(ss)(x_f;x_r)}} \tag{7}$$

where

$$\rho_{(2;0,1,2)} = (DAR)_{(ss)[x_f;x_r]} = S_{(ss)[x_f;x_r]} = \frac{(FR)^2}{\sqrt{[1 - (FR)^2]^2 + [2(DR)(FR)]^2}} \tag{8}$$

$$\rho_r = (RAR)_{(ss)[x_f;x_r]} = S_{(ss)[x_f;x_r](ref)} = 1 \tag{9}$$

$$\mu_{(2;0,1,2)} = [(DAR)(RAR)R]_{(ss)(x_f;x_r)} = [S(RS)R]_{(ss)(x_f;x_r)} = \hat{}(SR)_{(ss)(x_f;x_r)}$$

$$= \frac{(FR)^2}{\sqrt{[1 - (FR)^2]^2 + [2(DR)(FR)]^2}} \tag{10}$$

$$\phi_{(2;0,1,2)} = (DRA)_{(ss)(x_f;x_r)} = \tan^{-1}\left[\frac{-2(DR)(FR)}{1 - (FR)^2}\right] \tag{11}$$

and where

$[PF]_{(ss)[x_f;x_r]}$ = forcing displacement – relative displacement performance function of the seismographic system

$S_{(ss)[x_f;x_r]}$ = forcing displacement – relative displacement sensitivity of the seismographic system

$S_{(ss)[x_f;x_r](ref)}$ = forcing displacement – relative displacement reference sensitivity of the seismographic system

$\hat{}(SR)_{(ss)(x_f;x_r)}$ = forcing displacement – relative displacement dimensionless sensitivity ratio of the seismographic system

$(DRA)_{(ss)(x_f;x_r)}$ = forcing displacement – relative displacement dynamic response angle of the seismographic system

c) Forcing displacement – relative displacement performance function for the seismographic system

From the standpoint of vibratory displacement receiving performance, ideal operation exists when the seismic element has no vibratory displacement with respect to inertial space. Under this condition,

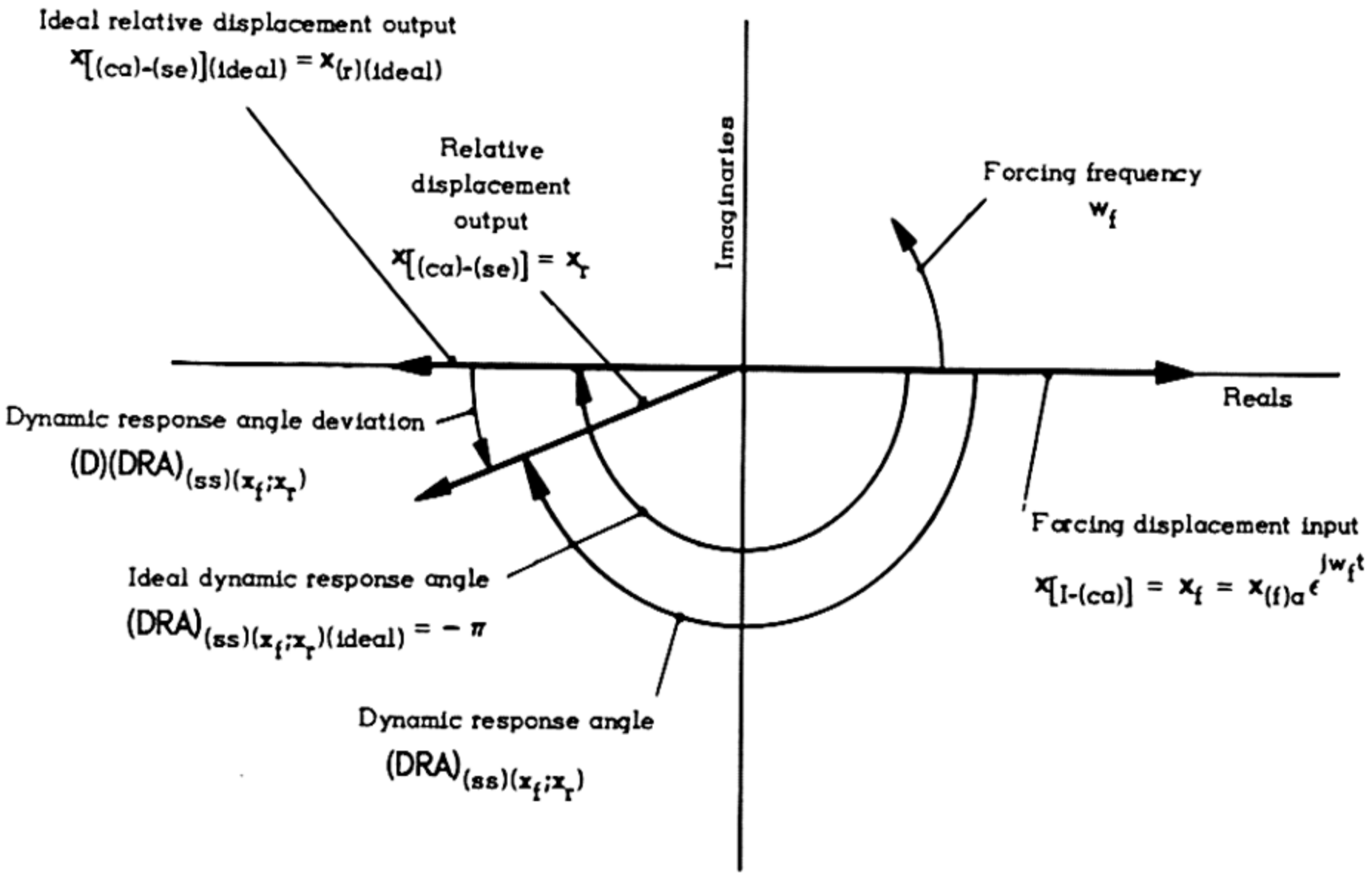
$$|x_{[(ca)-(se)](ideal)}| = |x_r| = |x_{[I-(ca)]}| = |x_f| \tag{12}$$

Derivation Summary 35-3. Line schematic diagram, functional diagram, performance equation, performance function and performance deviation equations for the seismographic system that has viscous damping only and operates in the displacement-receiving range. (Page 2 of 4)

Reference to the pictorial diagram of section a shows that, with the seismic element standing still with respect to inertial space so far as vibratory motion is concemed, a positive x_f displacement will produce a negative x_r displacement. This reversal in sign between x_f and x_r occurs because of the conventions used for convenience in setting up the performance equation.

The required sign reversal for ideal operation corresponds to an ideal dynamic response angle of π. From the standpoint of ideal operation only, the sign of this angle may be either positive or negative. Because the dynamic response angle of the seismographic system approaches the ideal value through negative values, the ideal dynamic response angle is taken as $-\pi$.

The rotating vector diagram (drawn under the conventions described in Definition Summary 13-2) when forcing displacement – relative displacement relationships are considered is



Define

$$(D)(DRA)_{(ss)(x_f;x_r)} = (DRA)_{(ss)(x_f;x_r)} - (DRA)_{(ss)(x_f;x_r)(ideal)} \tag{13}$$

$$= (DRA)_{(ss)(x_f;x_r)} + \pi \tag{14}$$

= dynamic response angle deviation of the seismographic system in the displacement-receiving range

In order that the seismographic system may give ideal operation in the displacement-receiving range, the dimensionless sensitivity ratio must be unity; that is, since, from Eq. (12),

$$x_{(r)(ideal)a} = x_{(f)a} \tag{15}$$

and, from Eq. (9),

$$S_{(ss)[x_f;x_r](ref)} = 1 \tag{16}$$

then

$$(SR)_{(ss)(x_f;x_r)(ideal)} = 1 \tag{17}$$

d) Conditions for ideal operation in the displacement-receiving range

Derivation Summary 35-3. Line schematic diagram, functional diagram, performance equation, performance function and performance deviation equations for the seismographic system that has viscous damping only and operates in the displacement-receiving range. (Page 3 of 4)

Define

$$(PR)_{(ss)(S_{[x_f;x_r]})} = \frac{S_{(ss)[x_f;x_r]}}{S_{(ss)[x_f;x_r](ideal)}} = \frac{S_{(ss)[x_f;x_r](ref)}\,'(SR)_{(ss)(x_f;x_r)}}{S_{(ss)[x_f;x_r](ref)}} = {}'(SR)_{(ss)(x_f;x_r)} \tag{18}$$

= sensitivity performance ratio of the seismographic system operating in the displacement-receiving range

From Eq. (10),

$$(PR)_{(ss)(S_{[x_f;x_r]})} = {}'(SR)_{(ss)(x_f;x_r)} = \frac{(FR)^2}{\sqrt{[1-(FR)^2]^2 + [2(DR)(FR)]^2}} \tag{19}$$

By definition

$$(D)(PR)_{(ss)(S_{[x_f;x_r]})} = (PR)_{(ss)(S_{[x_f;x_r]})} - 1 \tag{20}$$

= sensitivity performance ratio deviation of the seismographic system operating in the displacement-receiving range

and

$$(D)(DRA)_{(ss)(x_f;x_r)} = (DRA)_{(ss)(x_f;x_r)} - (DRA)_{(ss)(x_f;x_r)(ref)}$$

$$= (DRA)_{(ss)(x_f;x_r)} - (DRA)_{(ss)(x_f;x_r)(ideal)} \tag{21}$$

From Eqs. (11), (13) and (14),

$$(D)(DRA)_{(ss)(x_f;x_r)} = \tan^{-1}\left[\frac{-2(DR)(FR)}{1-(FR)^2}\right] + \pi \tag{22}$$

e) Performance deviation equations for the seismographic system operating in the displacement-receiving range

Derivation Summary 35-3. Line schematic diagram, functional diagram, performance equation, performance function and performance deviation equations for the seismographic system that has viscous damping only and operates in the displacement-receiving range. (Page 4 of 4)

displacements are proportional to inertia reaction effects, the curve of dimensionless sensitivity ratio increases as the square of the frequency ratio. The range within which any given dimensionless sensitivity ratio curve is acceptably close to the parabolic shape is called the accelerometer range for the given curve.

35.163. Within a range of comparatively great viscous damping, the relative displacement of the seismic element is substantially proportional to the vibratory velocity, which, for sinusoidal motion, has an amplitude equal to the product of the forcing frequency and the forcing displacement amplitude. This means that a curve for a given high damping ratio will decrease from parabolic for low frequency ratios through linear for intermediate frequency ratios to zero slope for high frequency ratios. By making the damping ratio sufficiently great, the intermediate-frequency region of linear dimensionless sensitivity ratio variation may be extended to useful proportions. This intermediate-frequency region is called the velocimeter range.

35.164. The accelerometer range, the velocimeter range, and the vibrometer range are indicated on the curve family of Fig. 35-8. Because the limits of each range depend upon the damping ratios used and the tolerance limits specified, the boundaries between the three regions are not sharp lines, but rather are indefinite regions that depend on the special circumstances of any particular situation.

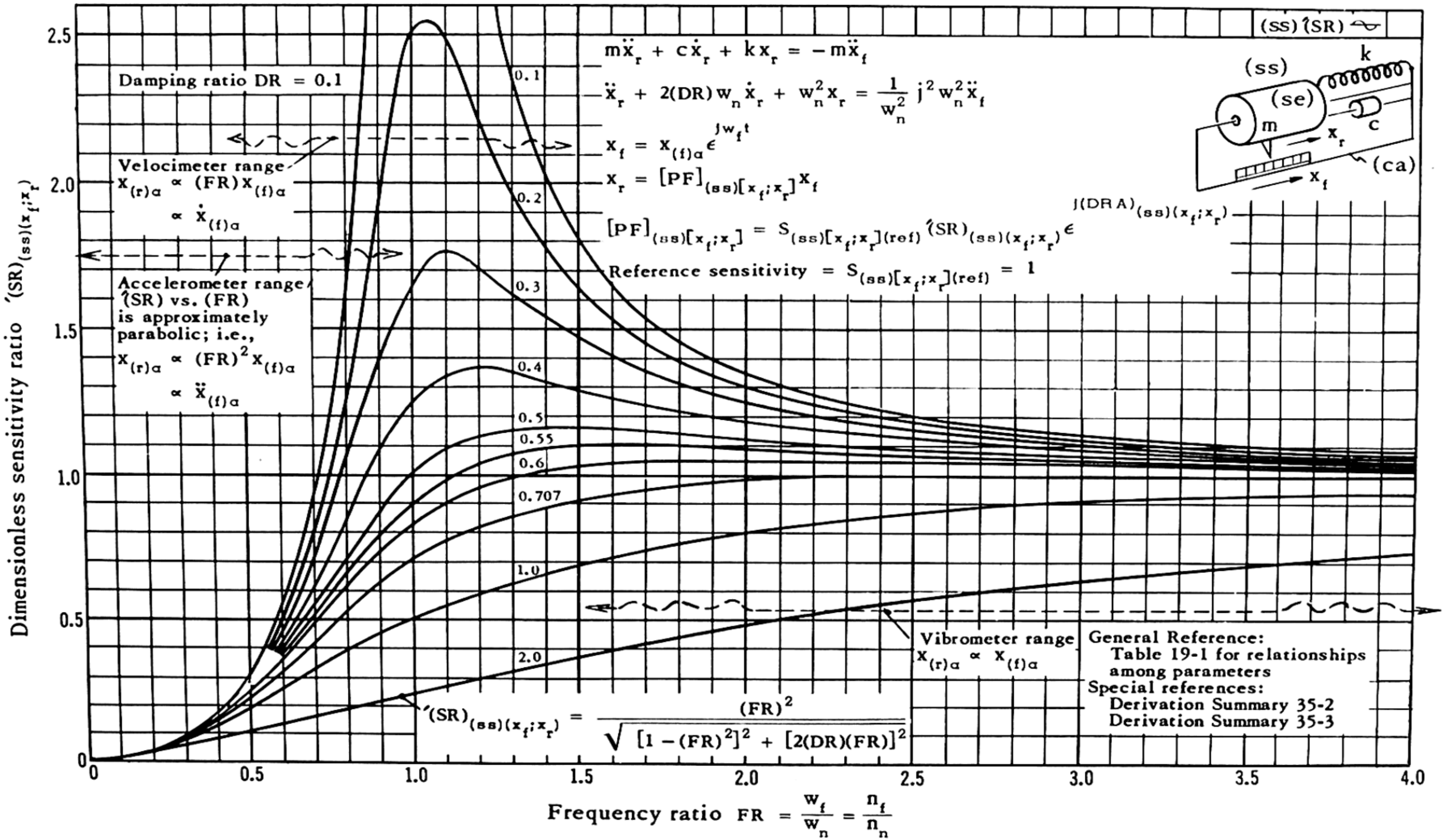


Fig. 35-8. Linear-scale plots of the forcing displacement input – relative displacement output dimensionless sensitivity ratio for the seismographic system with viscous damping only.

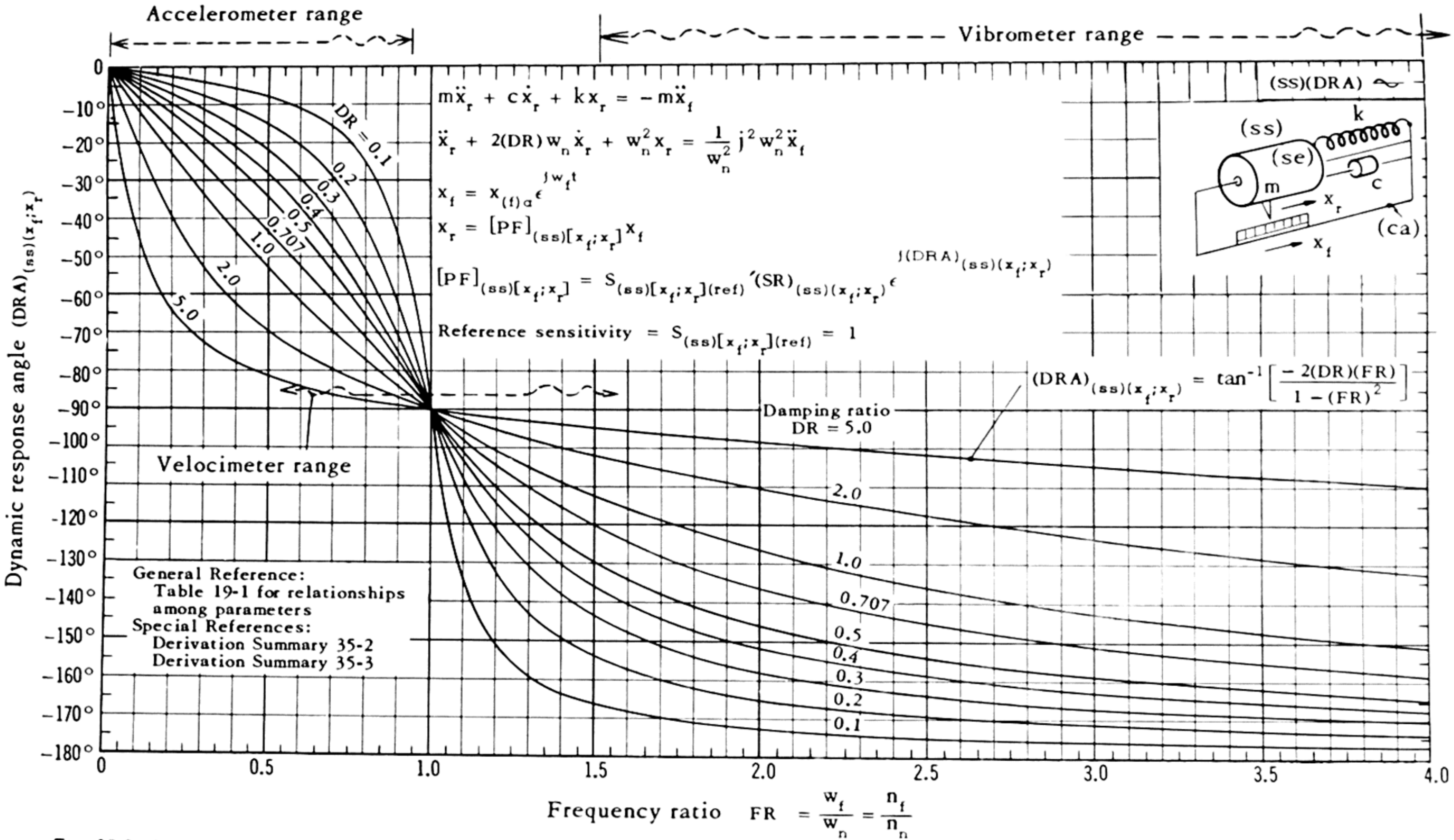
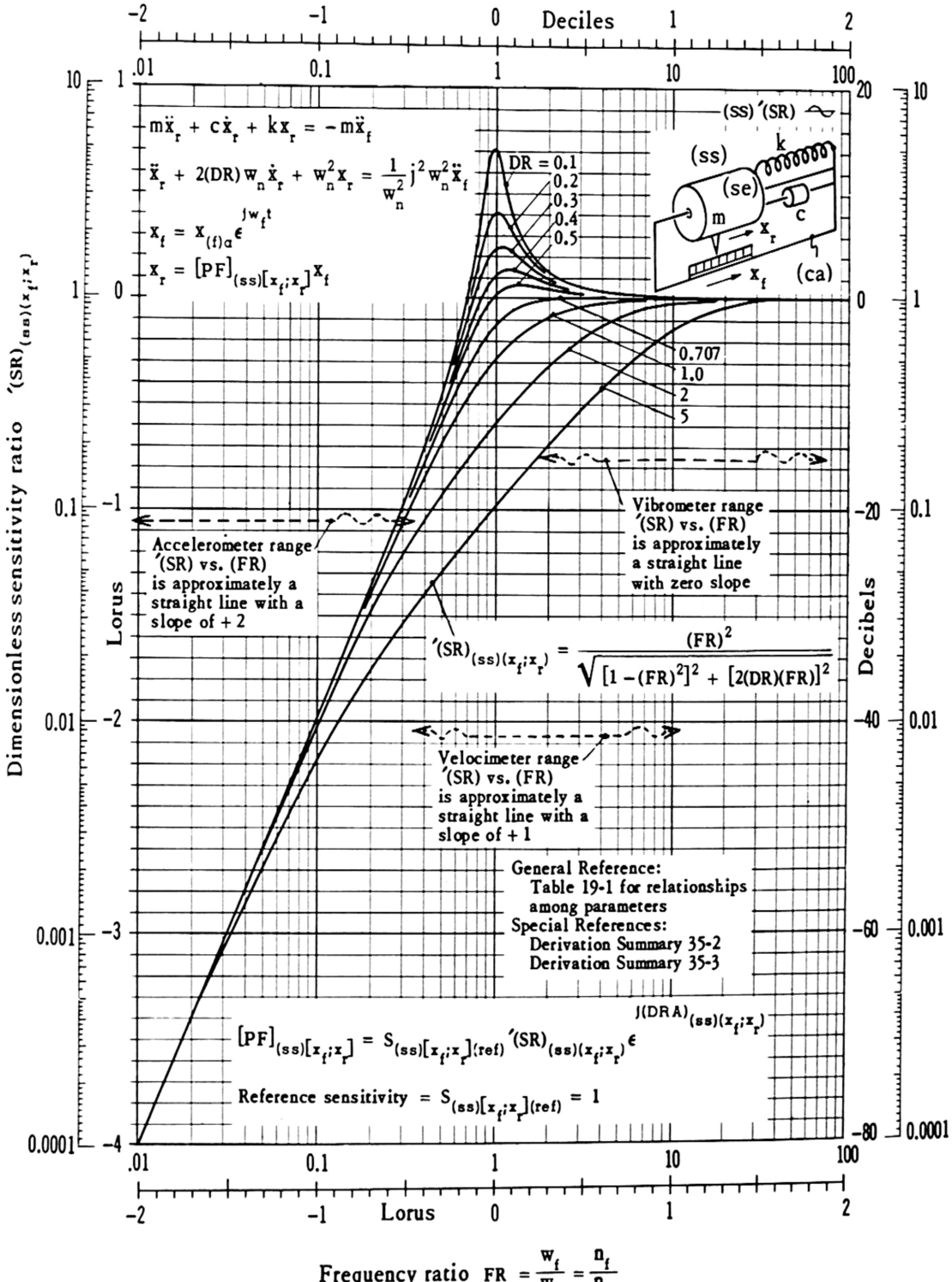


Fig. 35-9. Linear-scale plots of the forcing displacement input – relative displacement output dynamic response angle for the seismographic system with viscous damping only.



Frequency ratio $FR = \frac{w_f}{w_n} = \frac{n_f}{n_n}$

Fig. 35-10. Logarithmic-scale plots of the forcing displacement input – relative displacement output dimensionless sensitivity ratio for the seismographic system with viscous damping only.

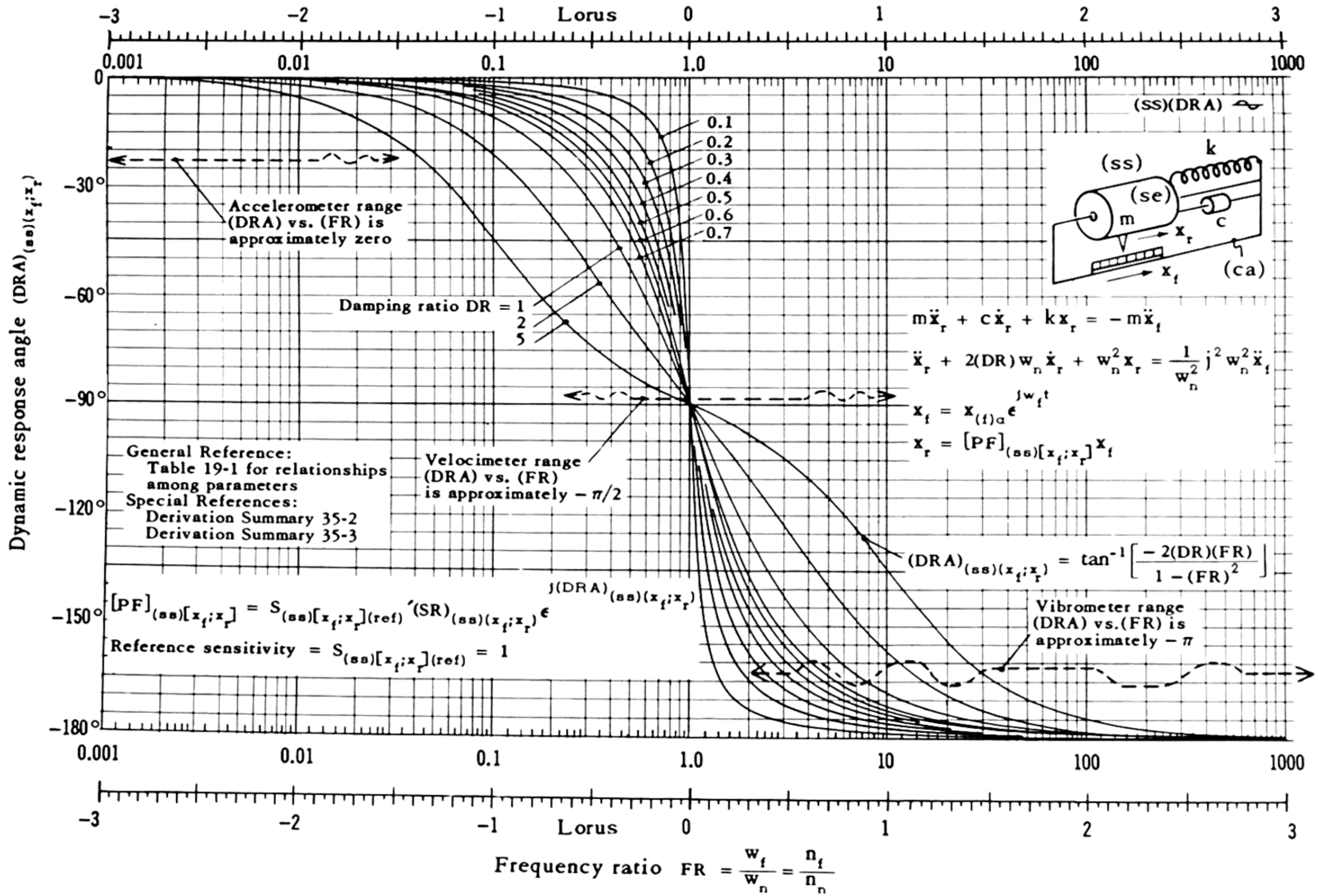


Fig. 35-11. Logarithmic-scale abscissa – linear-scale ordinate plots of the forcing displacement input – relative displacement output dynamic response angle for the seismographic system with viscous damping only.

35.165. Figure 35-9 gives the corresponding linear-scale family of dynamic response angle curves plotted against frequency ratio for a range of damping ratios. This curve family shows that:

a) The accelerometer range is characterized by dynamic response angles in the vicinity of zero.
b) The velocimeter range is characterized by dynamic response angles in the vicinity of -90 degrees.
c) The vibrometer range is characterized by dynamic response angles in the vicinity of -180 degrees.

35.166. Figure 35-10 gives a logarithmic-scale curve family of dimensionless sensitivity ratio plotted against frequency ratio for various damping ratios. With the logarithmic coordinates, the accelerometer range corresponds to a straight line with a slope of +2. The velocimeter range corresponds to a straight line with a slope of +1, and the vibrometer range corresponds to a straight line with a slope of zero. The curve family of Fig. 35-10 illustrates the effect of changing damping ratio on the three types of vibration-receiving performance of the seismographic system. From the standpoint of accelerometer range, it appears that the best performance is achieved with a damping ratio of about 0.7. This same damping ratio value gives the greatest vibrometer range, which extends from a frequency ratio of approximately 2 to infinity. The velocimeter range does not become appreciable until the damping ratio is made 2, and increases as this ratio is made greater and greater. The logarithmic scales chosen for Fig. 35-10 make it possible to cover a frequency ratio range of 10,000 on a page of the same size as that used for a range of 4.0 in Fig. 35-8. The wider range of the logarithmic-scale plot is especially adapted for showing all aspects of the vibration-receiving performance of the seismographic system.

35.167. Figure 35-11 gives a curve family with dynamic response angle as a linear ordinate and frequency ratio as a logarithmic abscissa. A range of one million in frequency ratio makes it possible to show the zero-angle-region of the accelerometer range, the -90-degree-angle region of the velocimeter range, and the -180-degree-angle region of the vibrometer range more clearly than is possible by means of the linear-scale family of Fig. 35-9.

SEISMOGRAPHIC SYSTEM PERFORMANCE IN THE DISPLACEMENT-RECEIVING (VIBROMETER) RANGE

35.168. The curve families of Figs. 35-8 and 35-10 show that the forcing displacment input – relative displacement output dimensionless sensitivity ratio for the seismographic system is asymptotic to unity as the frequency ratio approaches infinity in the vibrometer range. This means that the relative motion amplitude is equal to the forcing motion amplitude when the seismographic system

is acting as an ideal vibratory displacement receiver. It does not follow that the relative displacement is identical with the forcing displacement. As a matter of fact, the curve families of Figs. 35-9 and 35-11 show that the dynamic response angle associated with seismographic system operation approaches -180 degrees as the frequency ratio approaches large values. In terms of physical behavior, this angle is equivalent to the reversal in sign of the relative displacement as compared with the forcing displacement that results from the choice of conventions for the displacements associated with the seismographic system. Reference to the figure of section a of Derivation Summary 35-3 shows that the conventions used cause a positive forcing displacement to produce a negative relative displacement when the seismic element is stationary with respect to inertial space. This simple physical fact is described mathematically by the -180-degree dynamic response angle that is the ideal value in the vibrometer range.

35.169. The rotating vector diagram of section d of Derivation Summary 35-3 illustrates dynamic response angles for ideal and nonideal seismographic system operation in the vibrometer range. The forcing displacement vector is shown when it is instantaneously coincident with the axis of reals. When ideal operation exists, the corresponding instantaneous position of the relative displacement vector is 180 degrees behind (that is, away in the negative direction) from the forcing displacement vector. This means that the ideal relative displacement vector is in line with the forcing displacement vector and has its arrowhead pointed away from the forcing displacement vector.

35.170. The curve families of Figs. 35-9 and 35-11 show that, for nonideal operation in the vibrometer range, the dynamic response angle is negative and has a magnitude somewhat less than 180 degrees. A typical relative displacement vector corresponding to this condition is shown in the figure of section d of Derivation Summary 35-3.

35.171. By definition, the dynamic response angle deviation of the seismographic system in the vibrometer range is equal to the dynamic response angle given by Eq. (11) of Derivation Summary 35-3 minus $(-\pi)$ radians.* This deviation is illustrated in the figure of section d of Derivation Summary 35-3. Because the magnitude of the actual dynamic response angle is always less than π, the subtraction of $(-\pi)$ gives a positive sign to the dynamic response angle deviation. This means that in the vibrometer range the dynamic response angle deviation is always positive, as shown in the rotating vector diagram of Derivation Summary 35-3.

35.172. In the vibrometer range, the ideal value of the dimensionless sensitivity ratio is unity. With the reference sensitivity chosen as unity, this means

* Note that the definition of deviation applied here is consistent with the conventions established in Chapter 9 for the comparison of physical quantities.

that the ideal forcing displacement input – relative displacement output sensitivity is unity.

35.173. Equation (18) of Derivation Summary 35-3 defines the performance ratio of the seismographic system operating in the vibrometer range as the ratio of the forcing displacement input – relative displacement output sensitivity to the ideal value of this same sensitivity.* In the present situation, the ideal sensitivity value is identical with the reference sensitivity. When the sensitivity is written as the product of the reference sensitivity and the dimensionless sensitivity ratio, the performance ratio reduces to identity with the dimensionless sensitivity ratio. The corresponding expression for the performance ratio is given in Eq. (19) of Derivation Summary 35-3. Because of the form of this equation, the curve families of Figs. 35-8 and 35-10 are direct representations of the vibratory displacement-receiving performance ratio of the seismographic system.

35.174. The scales used in Figs. 35-8 and 35-10 do not permit direct readings with the accuracies required for many engineering purposes. This situation may be remedied by using curve families of the performance ratio deviation defined by Eq. (20) of Derivation Summary 35-3. This expression is a special case of the generalized definition of performance ratio deviation under which the deviation of any given performance ratio is equal to the performance ratio minus the ideal value of the performance ratio.** Because the reference value of the sensitivity used in forming the performance ratio is taken as the ideal sensitivity, the ideal performance ratio is unity. This means that the performance ratio deviation is equal to the performance ratio minus unity.

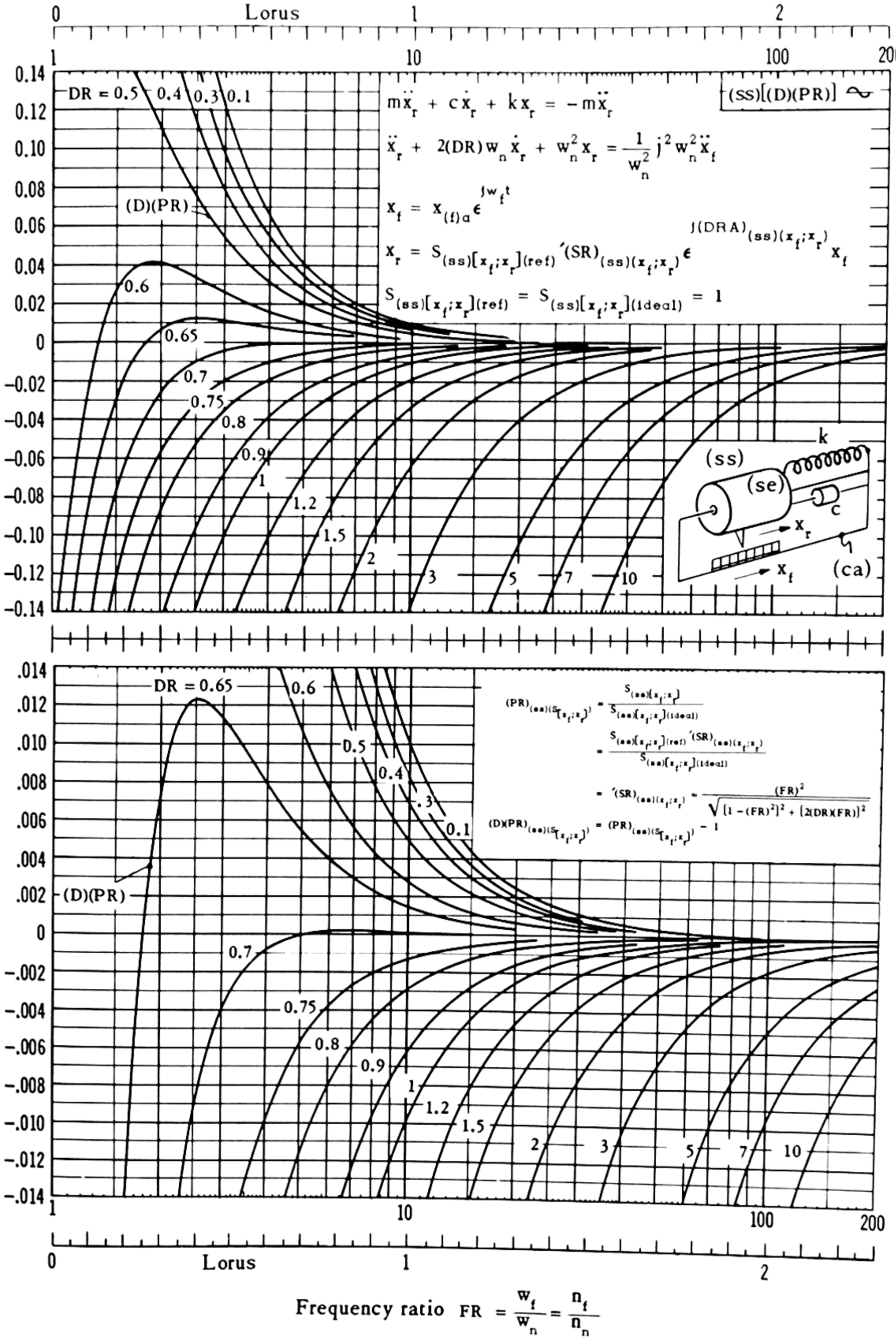
35.175. Curve families of the performance ratio deviation are plotted in Fig. 35-12 for damping ratio values ranging from 0.1 to 10. In the upper curve family of this figure, frequency ratios from 1 to 200 are plotted on a logarithmic abscissa scale, with performance ratio deviations from -0.14 to +0.14 plotted on a linear ordinate scale. The lower curve family of Fig. 35-12 is similar to the upper curve family, with the ordinate scale expanded to cover a range of -0.014 to +0.014.

35.176. The deviation curves of Fig. 35-12, in effect, give the fractional inaccuracy in relative displacement magnitude associated with the operation of a seismographic system in the vibrometer range as a function of frequency ratio. For example, a seismographic system with a damping ratio of 0.7 would have a sensitivity inaccuracy of -0.01 (that is, 1 percent) at a frequency ratio of 2.4 (that is, at a forcing frequency equal to 2.4 times the undamped natural frequency of the system). In other words, with a relative displacement magnitude tolerance

---

* The definition of performance ratio applied here is a special case of the generalized conventions established in Chapter 5.

** The background conventions for the performance ratio deviation are discussed in Chapter 5.



Frequency ratio $FR = \frac{w_f}{w_n} = \frac{n_f}{n_n}$

General reference: Table 19-1
Special references: Derivation Summaries 35-2 and 35-3

Fig. 35-12. Forcing displacement input – relative displacement output sensitivity performance ratio deviation for the seismographic system with viscous damping only.

limit of minus 1 percent, the lower frequency-ratio limit of the operating band width would be 2.4.

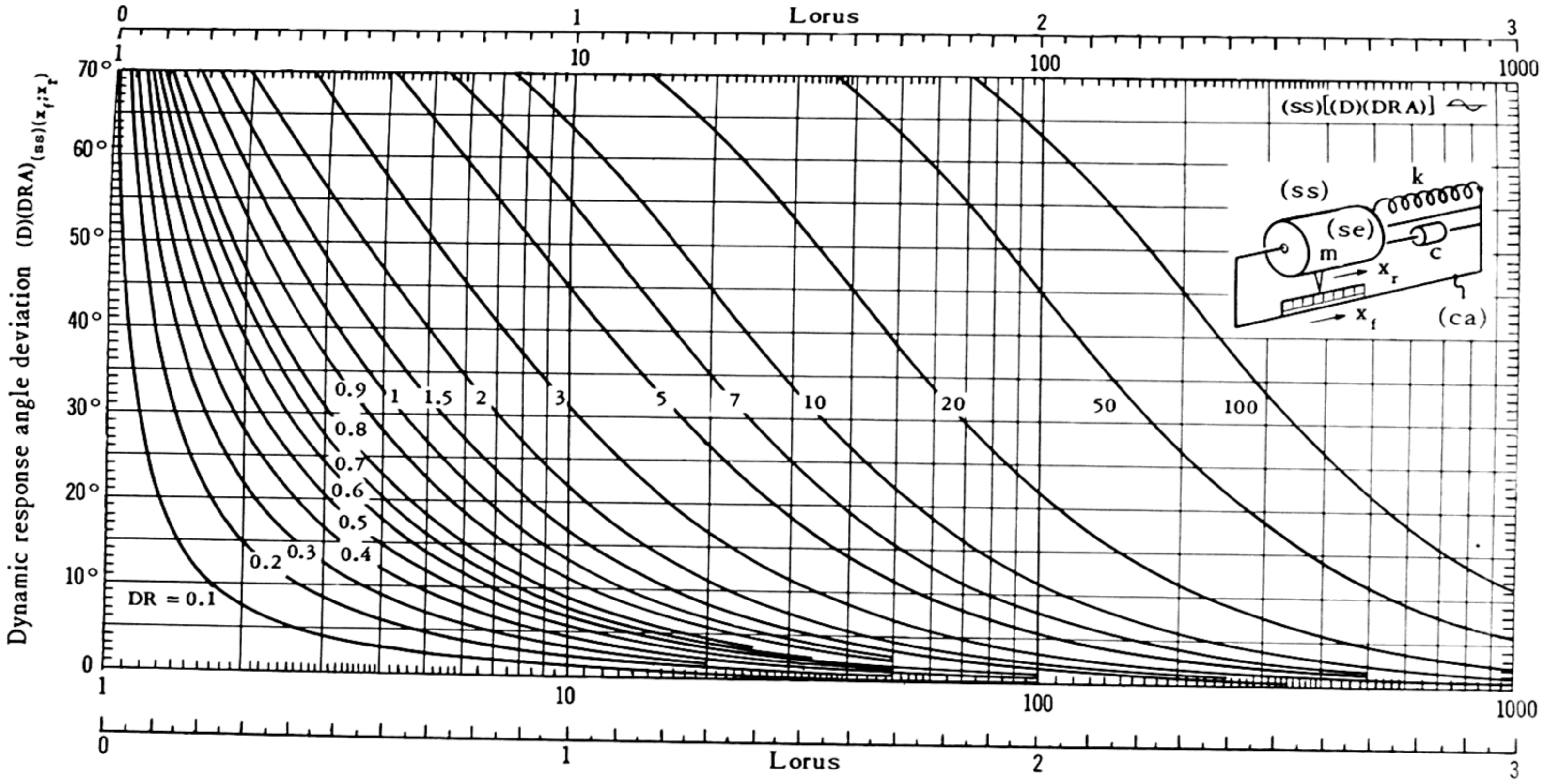
35.177. The performance ratio deviation curve families of Fig. 35-12 make it possible to estimate to small fractions of 1 percent, and without the use of large-area plots, the relative displacement magnitude inaccuracies of the seismographic system that has viscous damping only and operates in the vibratory displacement-receiving range. This technique is useful for engineering purposes and is applied many times in this book.

35.178. The curve family of Fig. 35-13, which is plotted from Eq. (22) of Derivation Summary 35-3, gives the dynamic response angle deviation plotted on a linear ordinate scale as a function of frequency ratio plotted on a logarithmic abscissa scale, for damping ratio values ranging from 0.1 to 100. In practice, this curve family is applied in determining the frequency ratios associated with dynamic response angle inaccuracy tolerance limits in the same way that the curves of Fig. 35-12 are used to determine the frequency ratio limits for various sensitivity tolerance limits.

VIBRATORY FREQUENCY-RECEIVING CHARACTERISTICS OF THE LIGHTLY DAMPED SEISMOGRAPHIC SYSTEM

35.179. A lightly damped seismographic system gives a strong relative displacement response for forcing frequencies near the undamped natural frequency of the system. This means that combinations of spring-and-mass systems of this type, like that illustrated in Fig. 35-4e, with each system tuned to one of a closely spaced sequency of natural frequencies, may be used to indicate the frequency of an unknown forcing vibration. From the standpoint of performance, the important characteristic of the individual spring-and-mass systems is the height and sharpness of the resonance peak near the undamped natural frequency. When this peak is very sharp for each individual system, forcing frequencies may be determined with good accuracy, but many units would be required for substantially continuous coverage over a reasonably wide frequency range.

35.180. The seismographic system performance function developed in Derivation Summary 35-2 provides a means for determining the characteristics of the lightly damped seismographic system. For the purposes of frequency indication by devices of this type, the relative displacement amplitude provides the desired information on the forcing input, while the dynamic response angle is unimportant. With the reference sensitivity taken as unity, the low damping ratio dimensionless sensitivity ratio curves in the region of unity frequency ratio in the plots of Figs. 35-8 and 35-10 illustrate the behavior of the relative displacement amplitude in the region that is of interest for frequency indication purposes. However, the curve families of these figures are compressed into areas that are too small



$$m\ddot{x}_r + c\dot{x}_r + kx_r = -m\ddot{x}_f \quad ; \quad \ddot{x}_r + 2(DR)w_n\dot{x}_r + w_n^2 x_r = \frac{1}{w_n^2} j^2 w_n^2 \ddot{x}_f$$

$$x_f = x_{(f)a}\epsilon^{jw_f t} \quad ; \quad x_r = S_{(ss)[x_f;x_r](ref)}(SR)_{(ss)(x_f;x_r)}\epsilon^{j(DRA)_{(ss)(x_f;x_r)}} x_f$$

$$S_{(ss)[x_f;x_r](ref)} = S_{(ss)[x_f;x_r](ideal)} = 1$$

$$(D)(DRA)_{(ss)(x_f;x_r)} = (DRA)_{(ss)(x_f;x_r)} - (DRA)_{(ss)(x_f;x_r)(ref)}$$

$$(DRA)_{(ss)(x_f;x_r)(ref)} = -\pi$$

$$(D)(DRA)_{(ss)(x_f;x_r)} = \tan^{-1}\left[\frac{-2(DR)(FR)}{1-(FR)^2}\right] + \pi$$

$$(DRA)_{(ss)(x_f;x_r)} = \tan^{-1}\left[\frac{-2(DR)(FR)}{1-(FR)^2}\right]$$

Fig. 35-13. Forcing displacement input – relative displacement output dynamic response angle deviation for the seismographic system with viscous damping only.

to provide quantitative information on the performance of the lightly damped seismographic system. This difficulty is eliminated by using the plots of Figs. 35-14, 35-15, 35-16, and 35-17.

35.181. The linear-scale curve of Fig. 35-14 gives the frequency ratio at which the maximum value of the dimensionless frequency ratio occurs as a function of the damping ratio. This plot shows that for damping ratios less than 0.1 the maximum dimensionless sensitivity ratio occurs at a frequency ratio very nearly equal to unity. The highest damping ratio for which a maximum occurs is 0.707. The frequency ratio at which this maximum is located approaches infinity as the damping ratio approaches the value of 0.707.

35.182. Figure 35-15 gives two linear-scale curves of the maximum value of the dimensionless sensitivity ratio as a function of damping ratio. The left-hand ordinate scale (for the full-line curve) runs from 0 to 6, while the right-hand ordinate scale (for the dashed-line curve) runs from 0 to 15. These curves show that sensitivity ratio peak heights are relatively unaffected by damping ratio variations until the damping ratio is made less than 0.2. The peak heights rise rapidly for lower damping ratios and, in particular, undergo a very steep change for damping ratios less than about 0.05. Figure 35-16 gives a logarithmic-scale plot of maximum dinensionless sensitivity ratio as a function of damping ratio. In this plot, the curve is substantially a straight line, with a slight curvature near a damping ratio value of 0.707. The logarithmic scales make it possible for the single curve to cover a damping ratio range from 0.0001 to 1.0 and a maximum dimensionless sensitivity ratio range from 1.0 to 5000.

35.183. The linear-scale curve family of Fig. 35-17 gives the ratio of the dimensionless sensitivity ratio to the maximum value of this sensitivity ratio as a function of the deviation of the frequency ratio from the frequency ratio at which the maximum sensitivity ratio occurs. Individual curves are plotted for damping ratio values from 0.10 to 0.002. The frequency ratio deviation range is from -0.20 to +0.20.

35.184. For any given seismographic system subjected to a constant forcing amplitude, the proper damping ratio curve from the family of Fig. 35-17 has a shape similar to the shape of the variation of the relative displacement amplitude as the frequency ratio is changed slightly with respect to the frequency ratio at which the maximum amplitude of the relative displacement occurs. Once it is specified that a certain fractional change in relative displacement amplitude is required for the positive identification of the desired minimum change in forcing frequency, the necessary damping ratio may be estimated from the curve family of Fig. 35-17. For example, if it is assumed that a fractional frequency change of 0.002 from the frequency giving peak amplitude must be indicated by at least a 20-percent reduction in output amplitude, the lowest curve in the family of

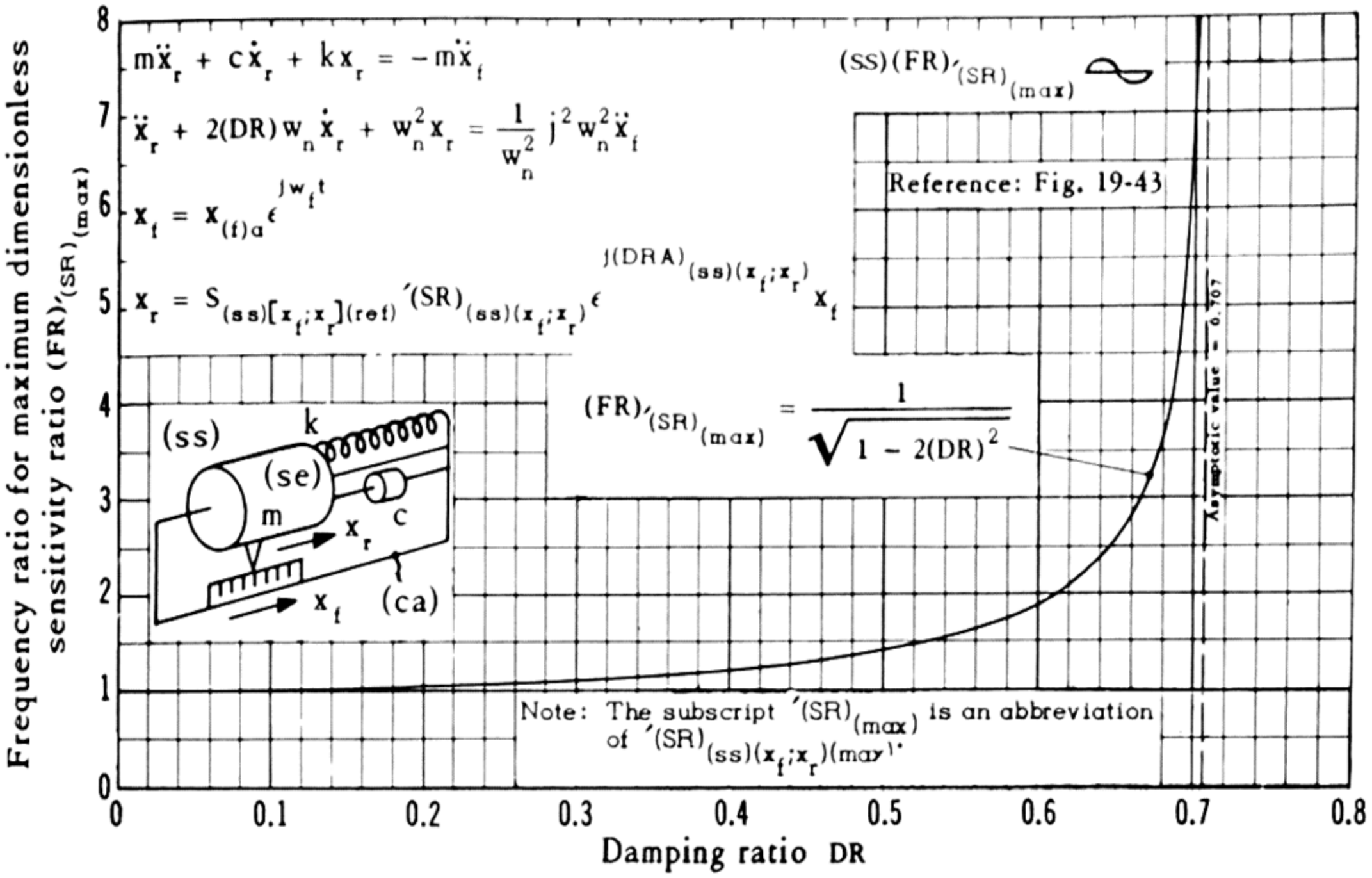


Fig. 35-14. Frequency ratio for maximum forcing displacement input – relative displacement output dimensionless sensitivity ratio as a function of damping ratio for the seismographic system with viscous damping only.

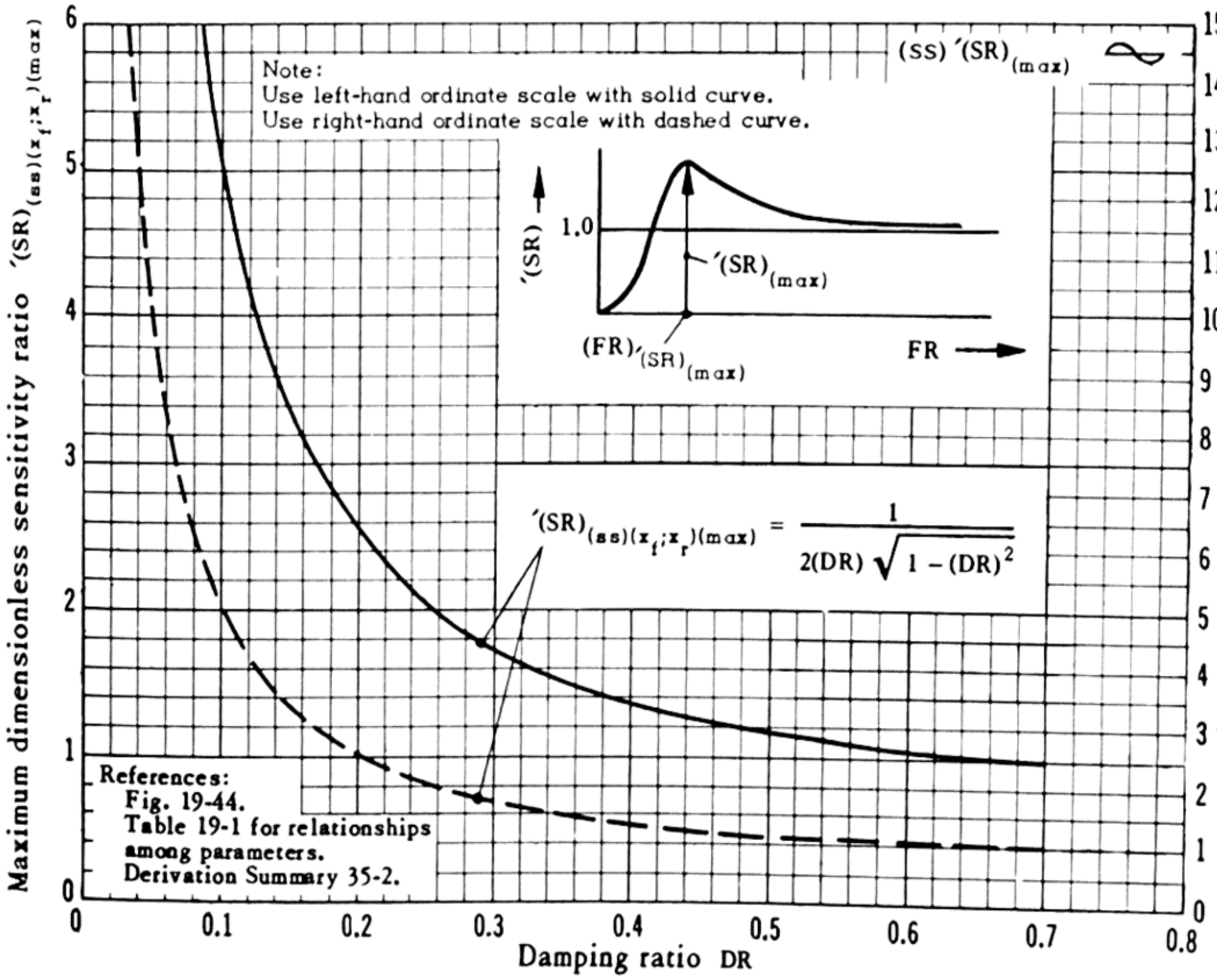


Fig. 35-15. Maximum forcing displacement input – relative displacement output dimensionless sensitivity ratio as a function of damping ratio for the seismographic system with viscous damping only.

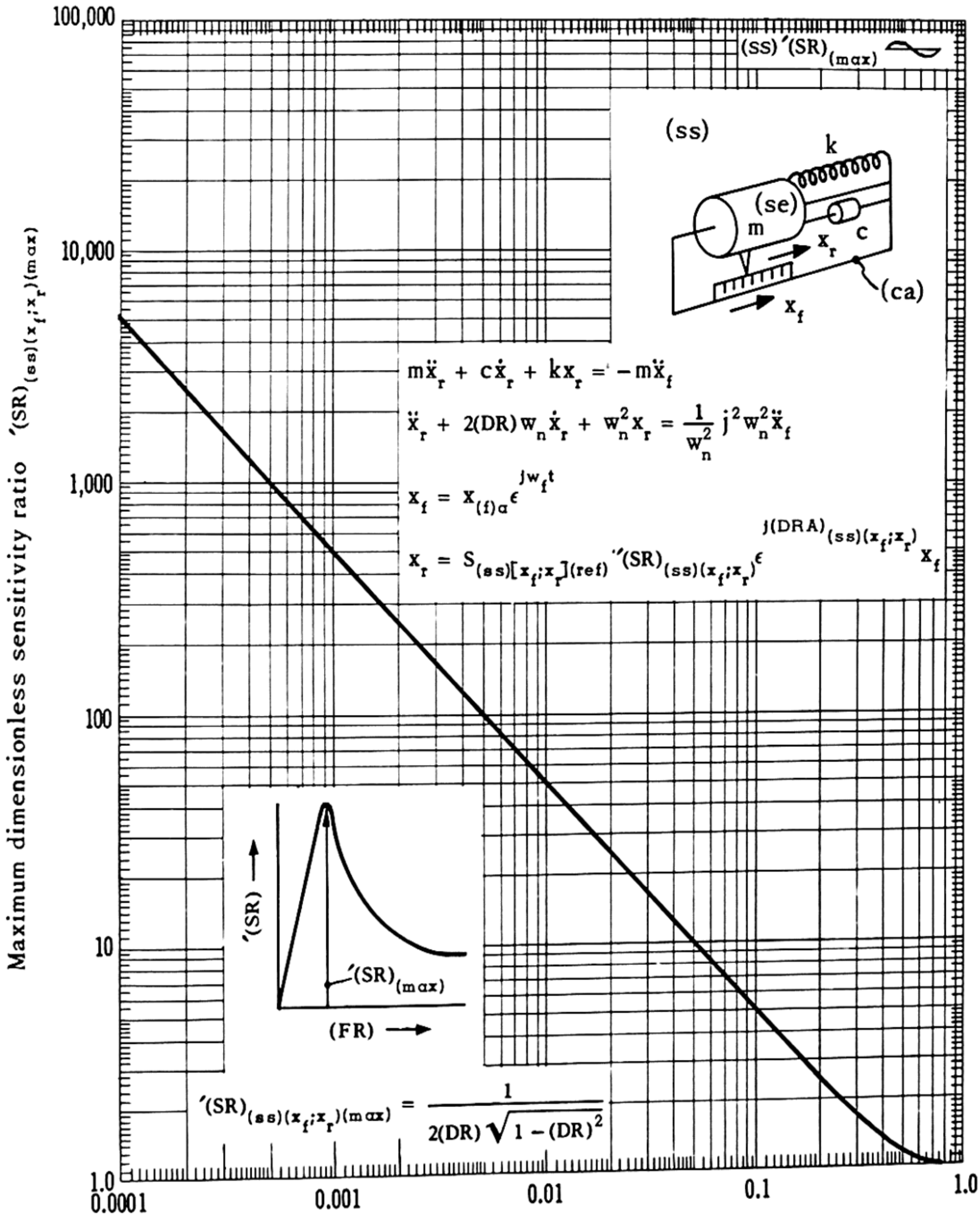


Fig. 35-16. Logarithmic-scale plot of maximum forcing displacement input – relative displacement output dimensionless sensitivity ratio as a function of damping ratio for the seismographic system with viscous damping only.

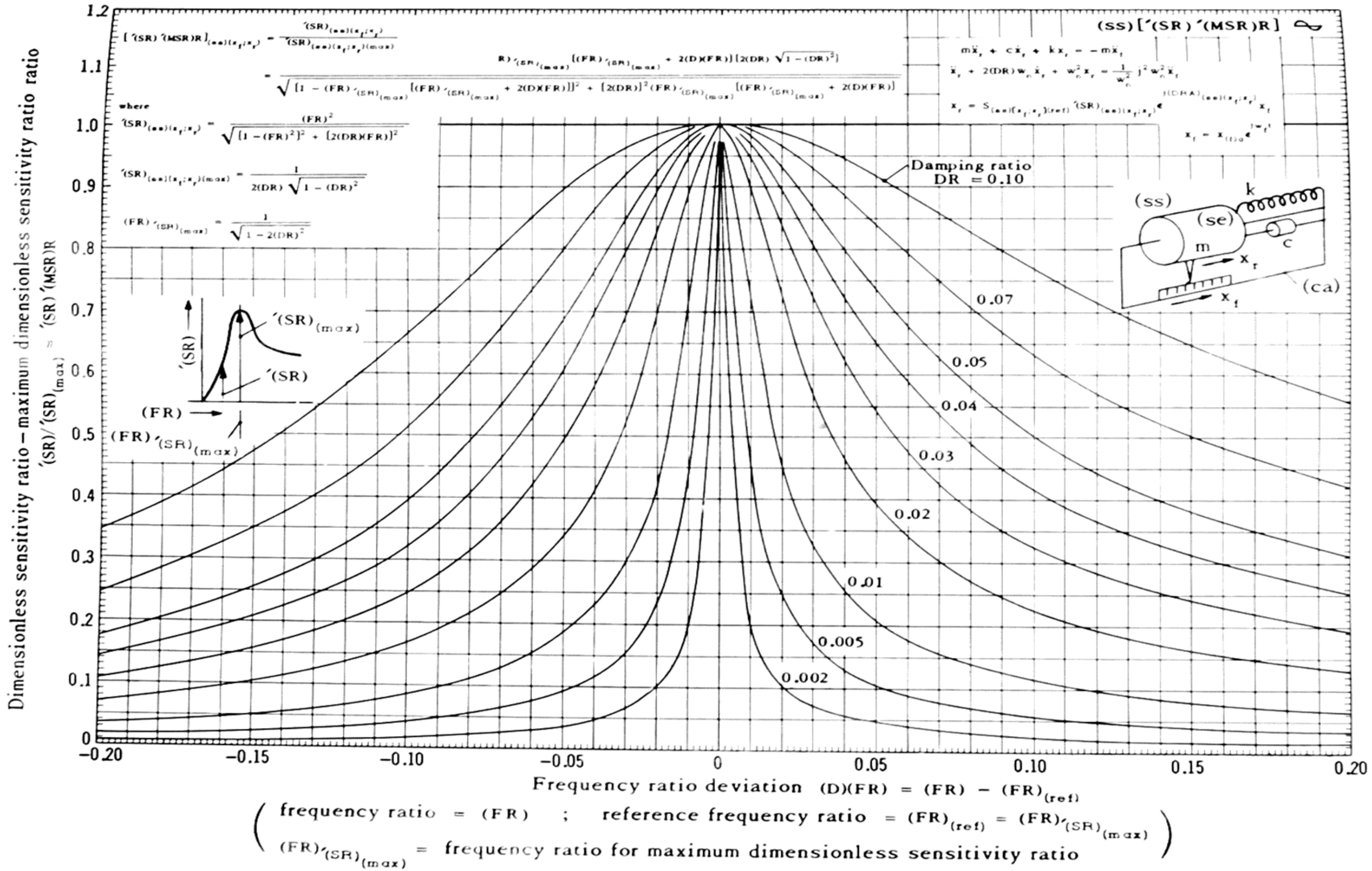


Fig. 35-17. Dimensionless sensitivity ratio – maximum dimensionless sensitivity ratio ratio as a function of frequency ratio deviation for the seismographic system with viscous damping only.

Fig. 35-17 shows that a damping ratio of 0.002 would be required. If practical considerations show that it is impossible to realize a damping ratio of this magnitude, the curve family makes it possible to estimate immediately the frequency ratio deviation that could be identified by equipment using a damping ratio that is feasible for actual equipment. For example, if the lowest feasible damping ratio is 0.01 and a 20-percent reduction from peak amplitude is required, the smallest identifiable change in frequency ratio would also be approximately 0.01.

SEISMOGRAPHIC SYSTEM PERFORMANCE IN THE VELOCITY-RECEIVING (VELOCIMETER) RANGE

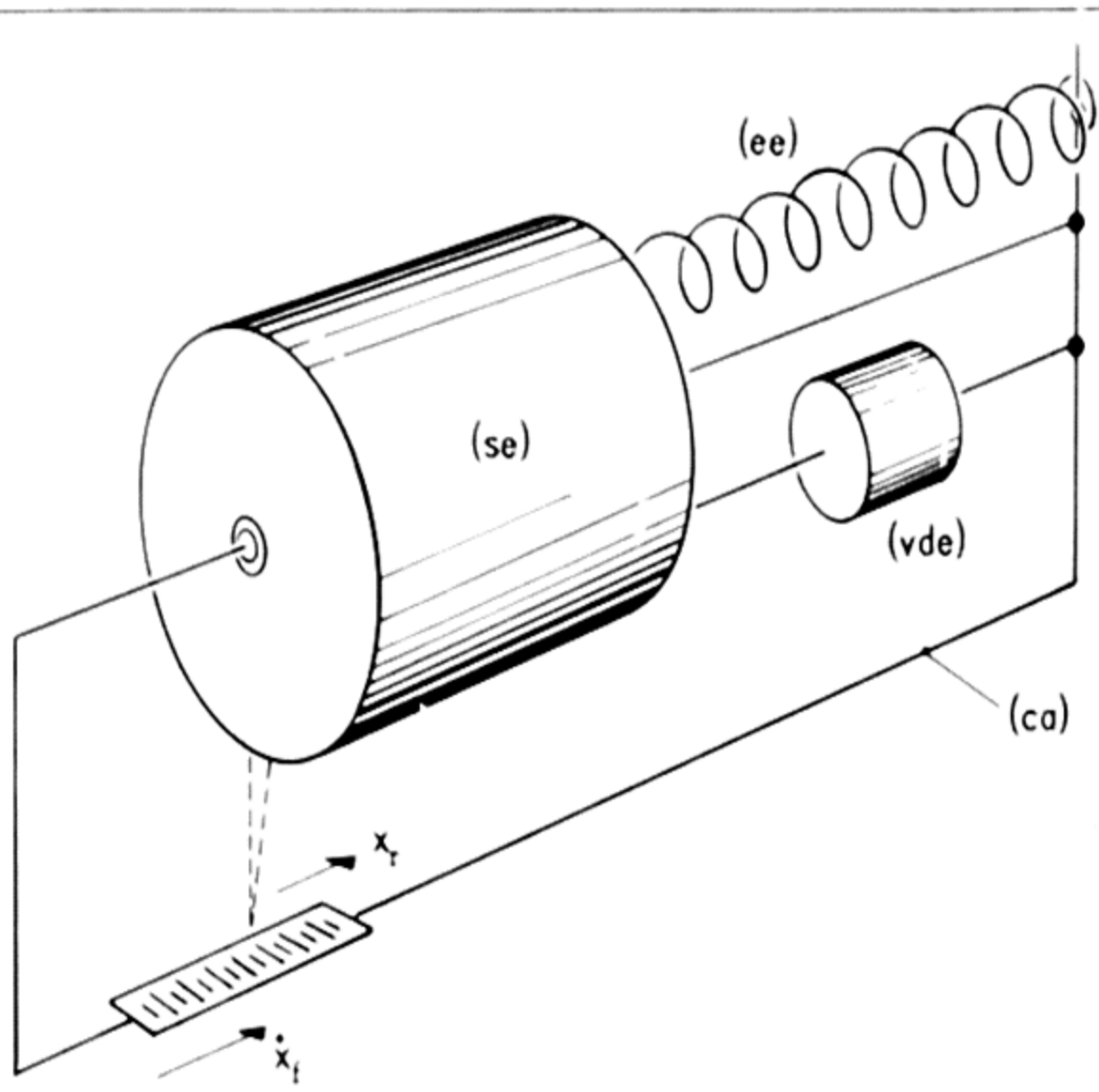
35.185. Satisfactory operation of the seismographic system when used for receiving vibratory velocity requires that the relative displacement output amplitude have an effectively constant ratio to the forcing velocity amplitude and an effectively negligible response delay. These performance characteristics are achieved when:

1) With the forcing velocity – relative displacement reference sensitivity chosen so that ideal performance corresponds to a dimensionless sensitivity ratio value of unity, the corresponding dimensionless sensitivity ratio value differs from unity (the ideal value) by less than specified tolerance limits over the operating frequency ratio range (the operating band width for the specified tolerance limits).

2) The forcing velocity – relative displacement dynamic response angle deviates from the ideal value of $-\pi$ by less than specified tolerance limits over the operating band width.

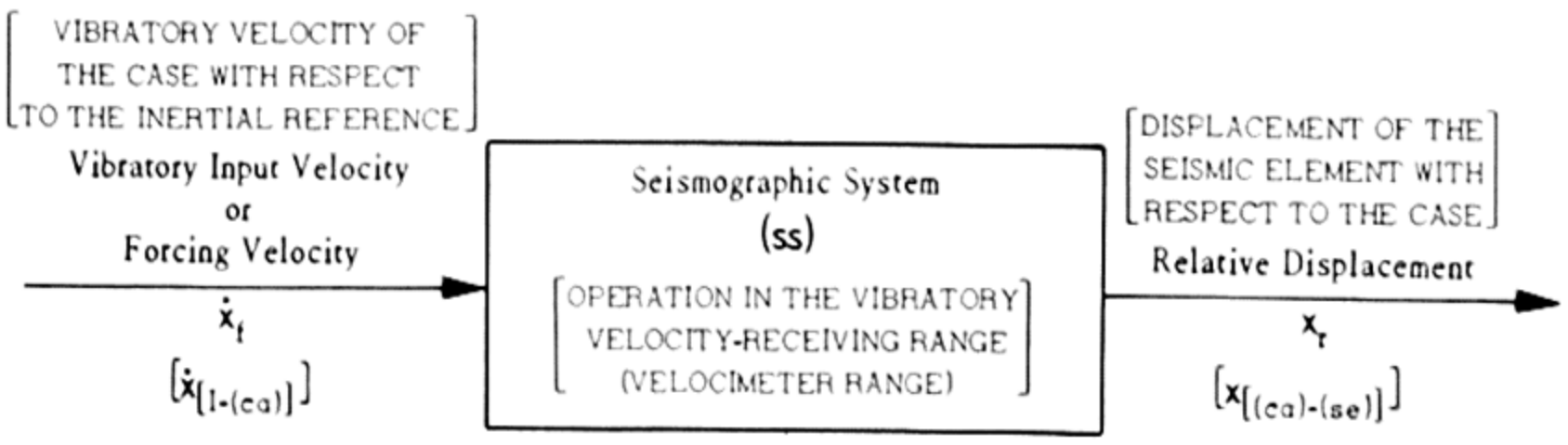
35.186. The special forms of the seismographic system performance function for operation in the velocity-receiving range (velocimeter range) are developed in Derivation Summary 35-4. Section a of this summary shows a line schematic diagram, and section b shows a functional diagram, for the single-degree-of-freedom seismographic system when the vibratory forcing velocity is considered as the input and the relative displacement is taken as the output. With the forcing acceleration of Eq. (1) of Derivation Summary 35-4 replaced by forcing velocity on the basis of Eq. (3), the (2;0, 1, 2) form of the performance equation becomes the (1;0, 1, 2) form of Eq. (5). Equations (6), (7), (8) and (9) are based on the (1;0, 1, 2) relating function developed in Derivation Summary 19-11 and summarize the information for describing the velocity-receiving-range performance characteristics of the seismographic system with viscous damping only. These characteristics are described in quantitative terms by the curve families of Figs. 35-18, 35-19, 35-20 and 35-21.

35.187. The forcing velocity – relative displacement dimensionless sensitivity ratio curve family based on Eq. (8) of Derivation Summary 35-4 is plotted in



a) *Line schematic diagram of the single-degree-of-freedom seismographic system*

When forcing velocity is considered as the input and relative displacement is taken as the output, the functional diagram for the seismographic system is



When Coulomb friction effects are negligible, the single-degree-of-freedom seismographic system performance equation has the form of Eq. (2) of Derivation Summary 35-2; i.e.,

$$\ddot{x}_r + 2(DR)w_n\dot{x}_r + w_n^2 x_r = \frac{1}{w_n^2} j^2 w_n^2 \ddot{x}_f \tag{1}$$

When x_f is sinusoidal, that is, when

$$x_f = x_{(f)a}\epsilon^{jw_f t} \tag{2}$$

then

$$\dot{x}_f = j w_f x_f \tag{3}$$

and

$$\ddot{x}_f = j w_f (j w_f x_f) = j w_f \dot{x}_f \tag{4}$$

Derivation Summary 35-4. Line schematic diagram, functional diagram, performance equation, performance function and performance deviation equations for the seismographic system that has viscous damping only and operates in the velocity-receiving range. (Page 1 of 3)

Substituting the expression of Eq. (4) in Eq. (1), dividing out w_n^2 in the right-hand-side term, and multiplying and dividing the right-hand-side term by $2(DR)w_n$ gives

$$\ddot{x}_r + 2(DR)w_n\dot{x}_r + w_n^2 x_r = \frac{1}{2(DR)w_n} j^2 j\, 2(DR)w_n w_f \dot{x}_f \tag{5}$$

b) Functional diagram and performance equation for the seismographic system operating in the velocity-receiving range

Equation (5) has the (1;0,1,2) differential equation form discussed in Derivation Summary 19-11. Use of the relating function form developed in that summary shows that

$$\eta_{(1;0,1,2)} \approx [RF]_{(1;0,1,2)} = [PF]_{(ss)[\dot{x}_f;x_r]} = \frac{1}{2(DR)w_n} \frac{j^2 j2(DR)(FR)}{1-(FR)^2 + j2(DR)(FR)} \tag{6}$$

Taking

$$\rho_r \approx S_{(ss)[\dot{x}_f;x_r](ref)} = \frac{1}{2(DR)w_n} \tag{7}$$

gives

$$\mu_{(1;0,1,2)} \approx {}'(SR)_{(ss)(\dot{x}_f;x_r)} = \frac{2(DR)(FR)}{\sqrt{[1-(FR)^2]^2 + [2(DR)(FR)]^2}} \tag{8}$$

$$\phi_{(1;0,1,2)} \approx (DRA)_{(ss)(\dot{x}_f;x_r)} = \tan^{-1}\left[\frac{-2(DR)(FR)}{1-(FR)^2}\right] - \frac{\pi}{2} \tag{9}$$

where

$[PF]_{(ss)[\dot{x}_f;x_r]}$ = forcing velocity – relative displacement performance function of the seismographic system

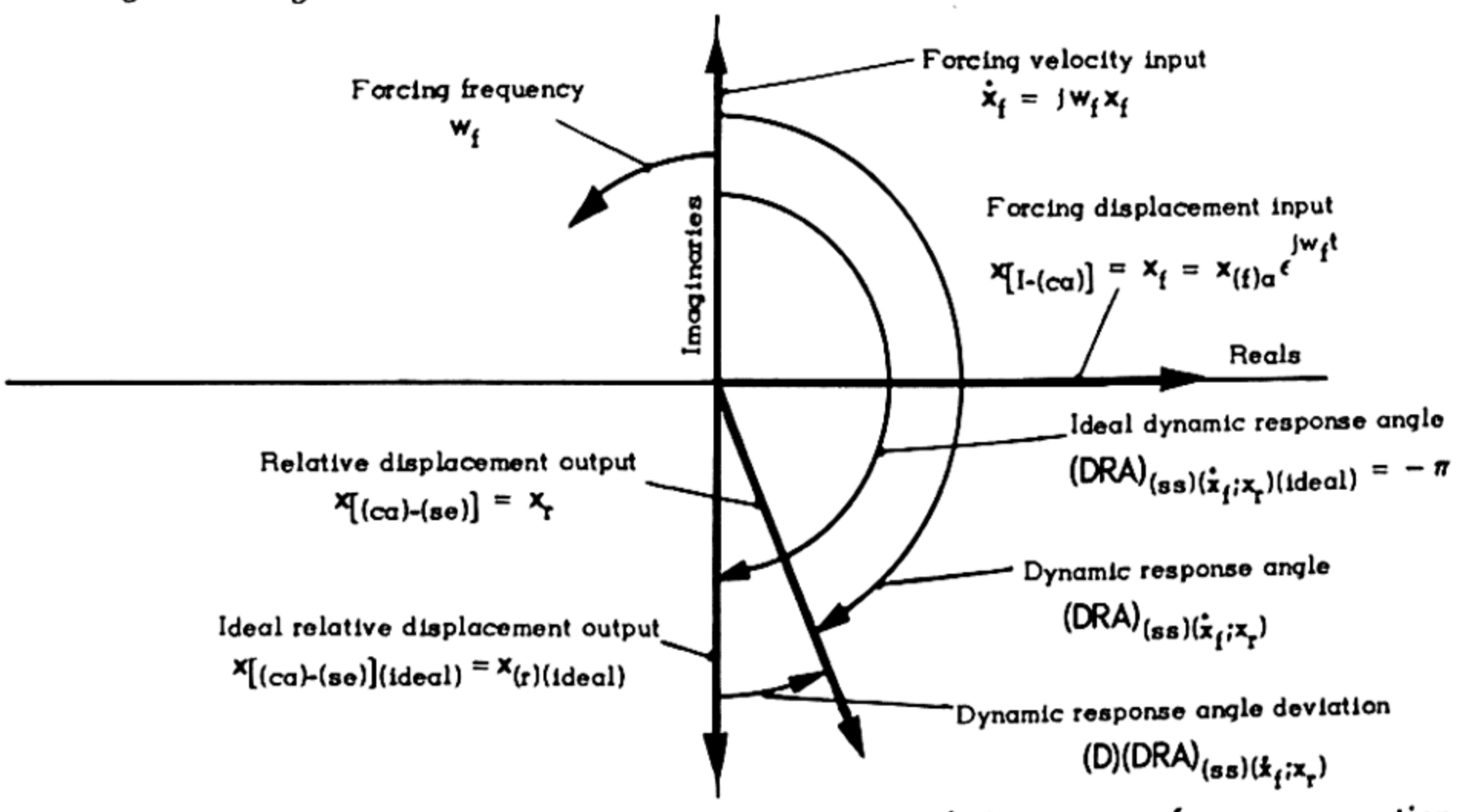
$S_{(ss)[\dot{x}_f;x_r](ref)}$ = forcing velocity – relative displacement reference sensitivity of the seismographic system

${}'(SR)_{(ss)(\dot{x}_f;x_r)}$ = forcing velocity – relative displacement dimensionless sensitivity ratio of the seismographic system

$(DRA)_{(ss)(\dot{x}_f;x_r)}$ = forcing velocity – relative displacement dynamic response angle of the seismographic system

c) Forcing velocity – relative displacement performance function for the seismographic system

The steady-state relationships between forcing velocity and relative displacement may be represented by a rotating vector diagram as follows:



Derivation Summary 35-4. Line schematic diagram, functional diagram, performance equation, performance function and performance deviation equations for the seismographic system that has viscous damping only and operates in the velocity-receiving range. (Page 2 of 3)

For ideal operation in the velocity-receiving range, the forcing velocity – relative displacement sensitivity must be constant and the dynamic response angle must be constant at $-\pi$. When these conditions are fulfilled, the ratio of the relative displacement amplitude to the forcing velocity amplitude is constant and the relative displacement is out of phase with the forcing velocity.

In equation form,

$$S_{(ss)[\dot{x}_f;x_r](ideal)} = S_{(ss)[\dot{x}_f;x_r](ref)}\,{}'(SR)_{(ss)(\dot{x}_f;x_r)} = \text{constant} \tag{10}$$

and

$$(DRA)_{(ss)(\dot{x}_f;x_r)(ideal)} = -\pi \tag{11}$$

The condition of Eq. (10) is fulfilled when

$${}'(SR)_{(ss)(\dot{x}_f;x_r)} = 1 \tag{12}$$

so that, from Eq. (7),

$$S_{(ss)[\dot{x}_f;x_r](ideal)} = S_{(ss)[\dot{x}_f;x_r](ref)} = \frac{1}{2(DR)w_n} \tag{13}$$

By definition,

$$(PR)_{(ss)(S_{[\dot{x}_f;x_r]})} = \frac{S_{(ss)[\dot{x}_f;x_r]}}{S_{(ss)[\dot{x}_f;x_r](ideal)}} = \frac{S_{(ss)[\dot{x}_f;x_r](ref)}\,{}'(SR)_{(ss)(\dot{x}_f;x_r)}}{S_{(ss)[\dot{x}_f;x_r](ref)}} = {}'(SR)_{(ss)(\dot{x}_f;x_r)} \tag{14}$$

= sensitivity performance ratio for the seismographic system operating in the velocity-receiving range

From Eq. (8),

$$(PR)_{(ss)(S_{[\dot{x}_f;x_r]})} = \frac{2(DR)(FR)}{\sqrt{[1-(FR)^2]^2 + [2(DR)(FR)]^2}} \tag{15}$$

For ideal velocity-receiving operation,

$$(PR)_{(ss)(S_{[\dot{x}_f;x_r]})(ideal)} = 1 \tag{16}$$

d) Conditions for ideal operation in the velocity-receiving range

By definition,

$$(D)(PR)_{(ss)(S_{[\dot{x}_f;x_r]})} = (PR)_{(ss)(S_{[\dot{x}_f;x_r]})} - 1 \tag{17}$$

= sensitivity performance ratio deviation for the seismographic system operating in the velocity-receiving range

and

$$(D)(DRA)_{(ss)(\dot{x}_f;x_r)} = (DRA)_{(ss)(\dot{x}_f;x_r)} - (DRA)_{(ss)(\dot{x}_f;x_r)(ref)}$$

$$= (DRA)_{(ss)(\dot{x}_f;x_r)} - (DRA)_{(ss)(\dot{x}_f;x_r)(ideal)} \tag{18}$$

= dynamic response angle deviation for the seismographic system operating in the velocity-receiving range

From Eqs. (9) and (11),

$$(D)(DRA)_{(ss)(\dot{x}_f;x_r)} = \tan^{-1}\left[\frac{-2(DR)(FR)}{1-(FR)^2}\right] + \frac{\pi}{2} \tag{19}$$

e) Performance deviation equations for the seismographic system operating in the velocity-receiving range

Derivation Summary 35-4. Line schematic diagram, functional diagram, performance equation, performance function and performance deviation equations for the seismographic system that has viscous damping only and operates in the velocity-receiving range. (Page 3 of 3)

Fig. 35-18. Equation (14) of the summary shows that the sensitivity performance ratio is identical with the dimensionless sensitivity ratio, so that the curve family of Fig. 35-18 also represents the performance ratio for operation of the seismographic system in the velocimeter range. In order for the forcing velocity – relative displacement sensitivity to be effectively constant at the ideal value, which is equal to the reference value given by Eq. (13) of Derivation Summary 35-4, the performance ratio must have a value of unity within the tolerance limits specified for any particular situation. Since the dimensionless sensitivity ratio is identical with the performance ratio, the curve family of Fig. 35-18 shows that velocimeter operation exists only for a range of frequency ratios centered on unity and, within this range, only for damping ratios considerably greater than unity. For example, if a tolerance limit of –0.1 is specified for the performance ratio, acceptable operation is achieved for frequency ratio range lying between approximately 0.4 and 2.5 when the damping ratio is 2. When the damping ratio is 10 and the same performance ratio tolerance limit is specified, the frequency ratio range for satisfactory results is between 0.1 and 10.

35.188. Figure 35-19 gives the forcing velocity input – relative displacement output dynamic response angle curve family that corresponds to the dimensionless sensitivity ratio curve family of Fig. 35-18. The dynamic response angle plot of Fig. 35-19 is based on Eq. (9) of Derivation Summary 35-4. This curve family shows that, within the velocimeter operating region (in the vicinity of unity frequency ratio), the dynamic response angle is near the ideal value of –180 degrees, but deviates rapidly from this value as the frequency ratio changes from unity when the damping ratio is less than 10. In fact, the damping ratio must be considerably greater than 10 if the response angle tolerance limits are to be specified as reasonably small values.

35.189. The relationship between ideal and actual seismographic system operation in the velocimeter range is represented by the rotating vector diagram of section d of Derivation Summary 35-4. This diagram depicts the forcing displacement vector at the instant it is coincident with the axis of reals, and shows that (a) the forcing velocity vector is 90 degrees ahead of the forcing displacement vector, (b) the ideal relative displacement vector is –180 degrees away from the forcing velocity vector, and (c) the actual response vector differs in angle from the ideal response vector by the dynamic response angle deviation.

35.190. Figure 35-20 is the curve family for the sensitivity performance ratio deviation as this quantity is defined by Eq. (17) of Derivation Summary 35-4. The logarithmic frequency ratio scale covers two lorus on the abscissa coordinate. The linear performance ratio deviation scale has a range of –0.14 to +0.14 for the ordinates of the upper plot and a range of –0.014 to +0.014 for the ordinates of the lower plot. Within the region covered by these curve families, the frequency

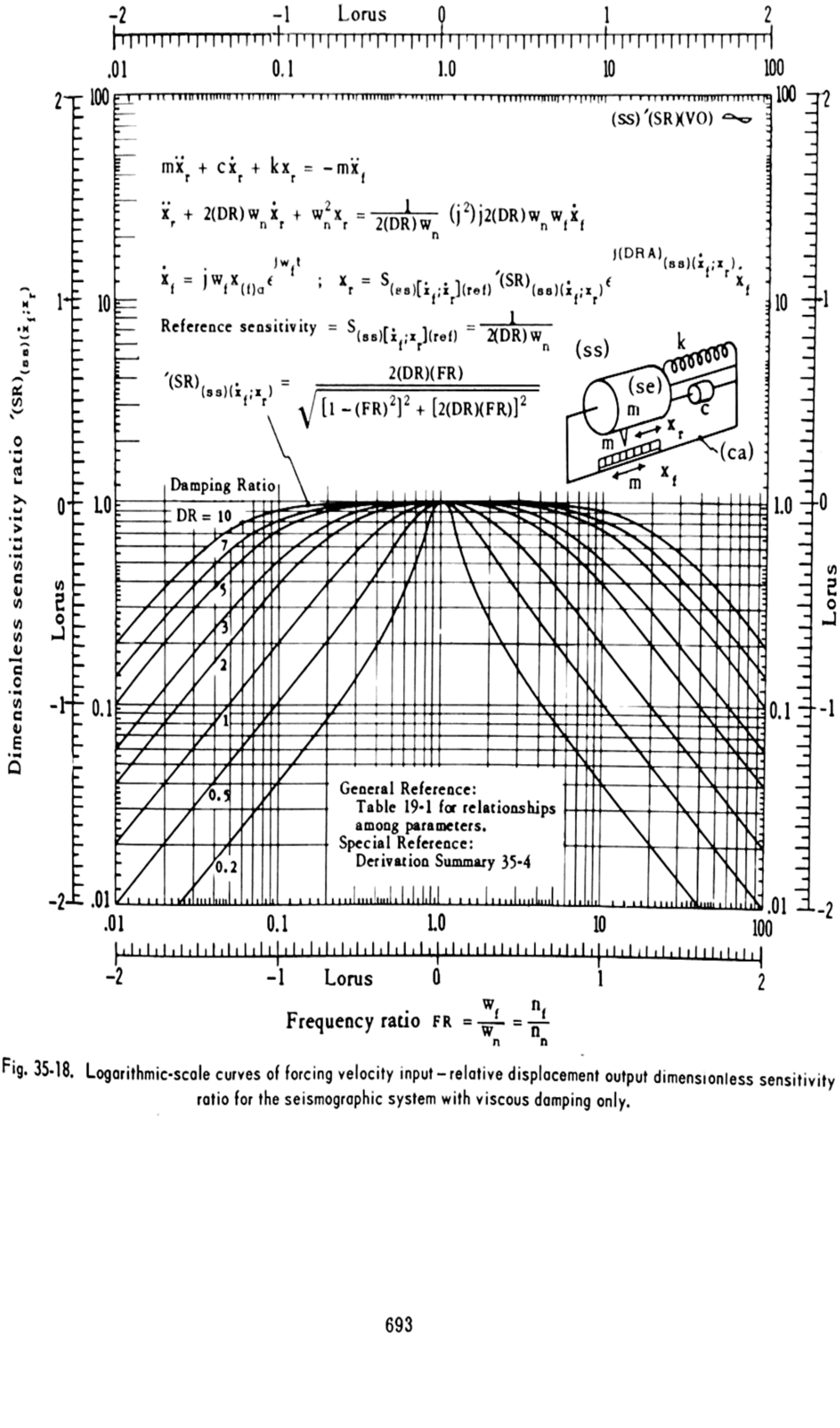


Fig. 35-18. Logarithmic-scale curves of forcing velocity input – relative displacement output dimensionless sensitivity ratio for the seismographic system with viscous damping only.

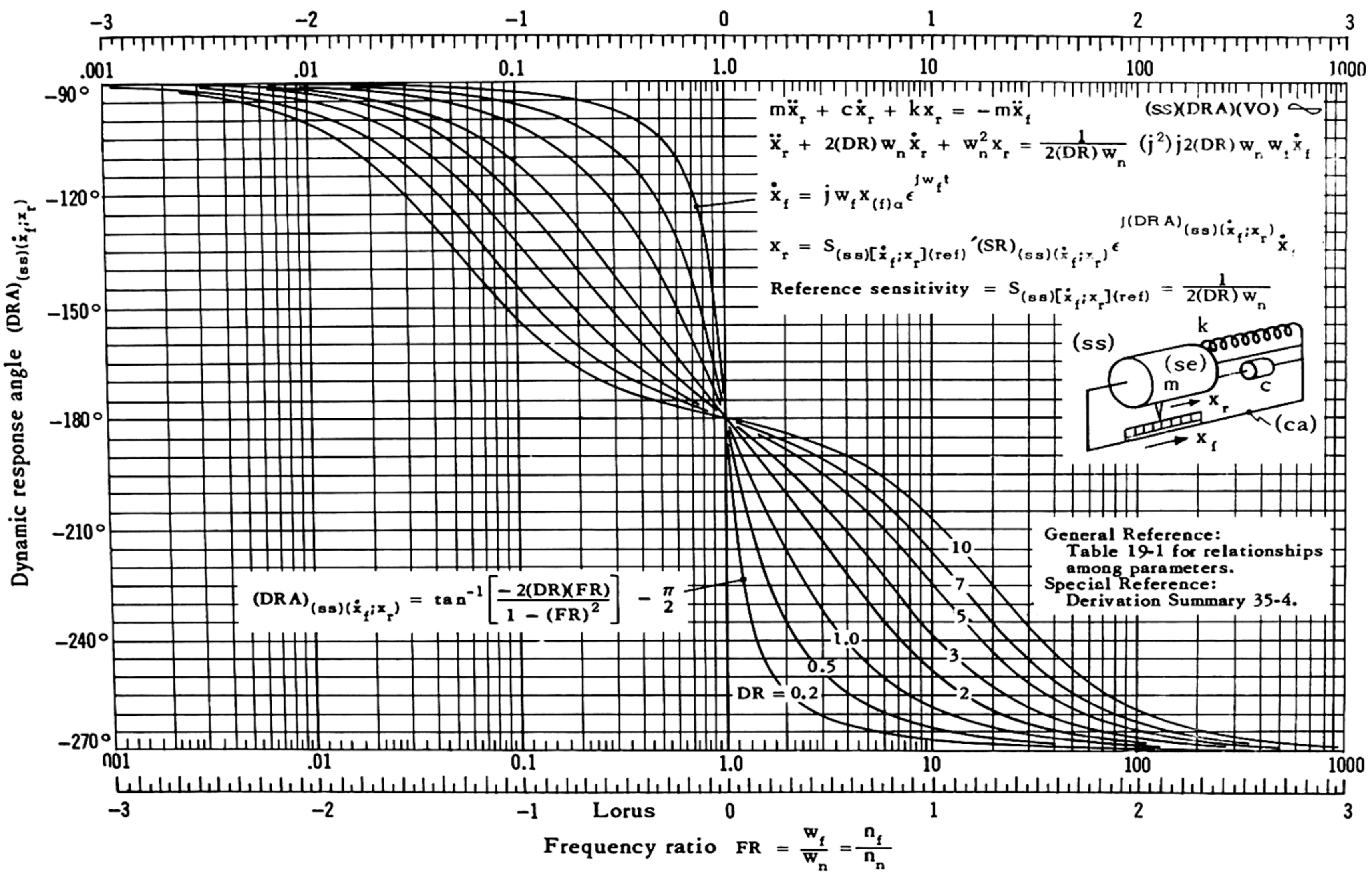


Fig. 35-19. Semilogarithmic-scale curves of forcing velocity input – relative displacement output dynamic response angle for the seismographic system with viscous damping only.

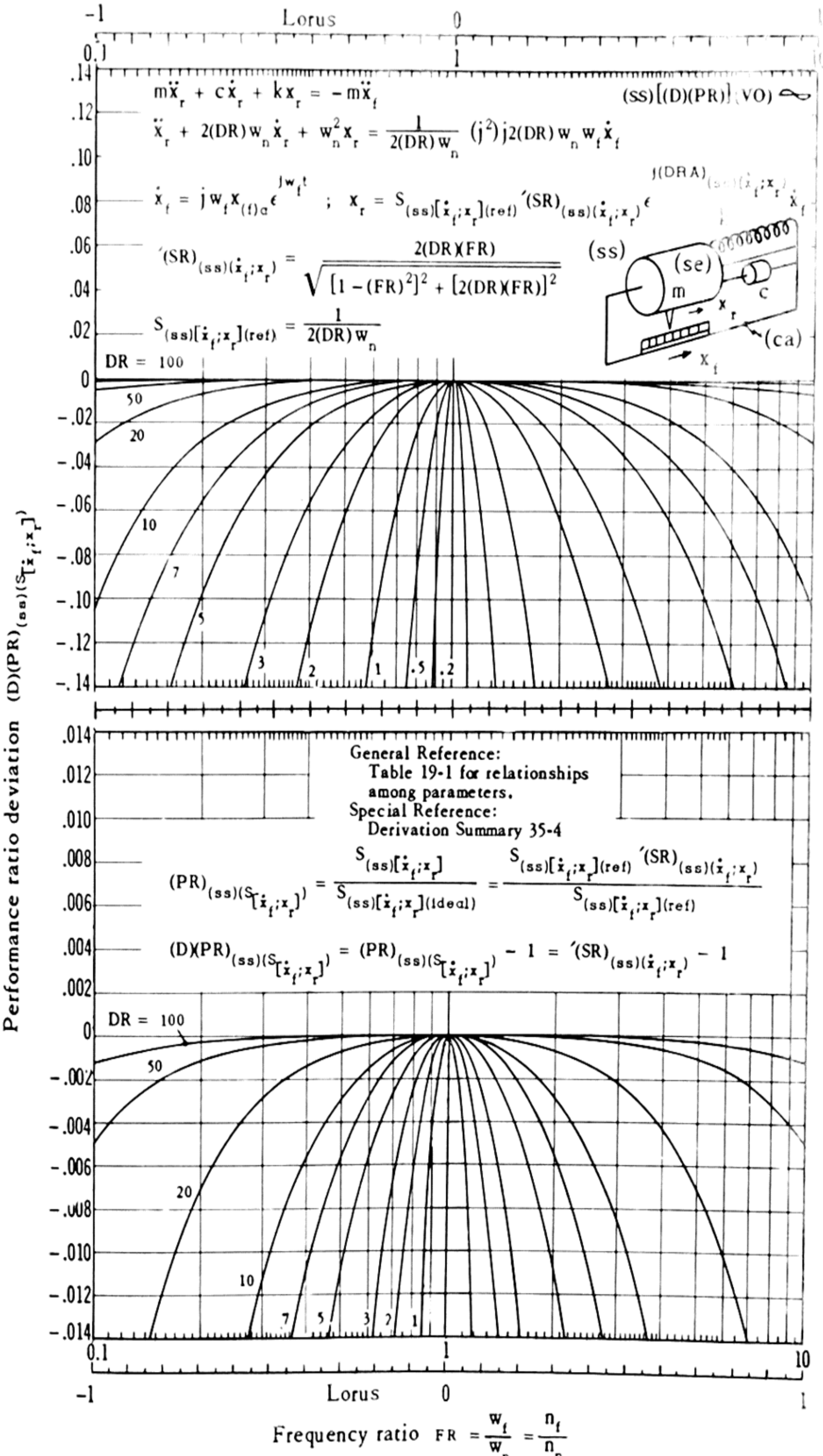


Fig. 35-20. Semilogarithmic-scale curves of forcing velocity input – relative displacement output sensitivity performance ratio deviation for the seismographic system with viscous damping only.

ratio limits corresponding to a given sensitivity ratio tolerance may be read directly from the plots when the damping ratio is specified. For example, the lower curve family shows that with a damping ratio of 100 the dimensionless sensitivity ratio will exceed a negative tolerance limit of 0.1 percent for any frequency ratio that lies outside the range between the values 0.1 and 10.

35.191. Figure 35-21 gives the curve family for the forcing velocity input – relative displacement output dynamic response angle deviation plotted from Eq. (19) of Derivation Summary 35-4. The frequency ratio range for any damping ratio and tolerance specification may be taken from Fig. 35-21 in the same way that the corresponding information is read from the performance ratio deviation curves of Fig. 35-20. For example, if a dynamic response angle deviation tolerance of ±3 degrees is specified, a damping ratio of 100 will permit a frequency ratio range of about 0.1 to 1.0.

35.192. It appears from the deviation curves of Figs. 35-20 and 35-21 that for given tolerance limits the operating frequency ratio range may be extended indefinitely by increasing the damping. It is certainly possible to improve performance in this way, but it must be remembered that, in accordance with Eq. (7) of Derivation Summary 35-4, the reference sensitivity is inversely proportional to the damping ratio. Since the sensitivity of any system is given by the product of the reference sensitivity and the corresponding dimensionless sensitivity ratio, and the dimensionless sensitivity ratio is acceptably close to unity within the frequency-ratio operating range, the sensitivity of the seismographic system in the velocimeter range decreases as the damping ratio increases. For example, the price of a tenfold increase in damping ratio to widen the operating range is a reduction in sensitivity by a factor of one tenth.

35.193. Equation (7) of Derivation Summary 35-4 suggests that with any finite damping ratio the reference sensitivity may be made very great by reducing the undamped natural frequency. From the physical side, with a given seismic mass, this means reducing the spring coupling between the case and the seismic element. A practical limit is reached when the spring is no longer able to keep the seismic element properly located with respect to the case under the nonvibratory motions of the structure to which the case is attached. Under circumstances in which this effect is not important, the undamped natural frequency actually becomes zero, and the (1;0, 1, 2) performance equation of the seismographic system reduces to the (0;1, 2) performance equation of the viscous shear integrator described in Fig. 34-4 and Derivation Summary 34-19.

SEISMOGRAPHIC SYSTEM PERFORMANCE IN THE ACCELERATION-RECEIVING (ACCELEROMETER) RANGE

35.194. When forcing acceleration is considered as the input and relative displacement is taken as the output (that is, operation in the accelerometer range

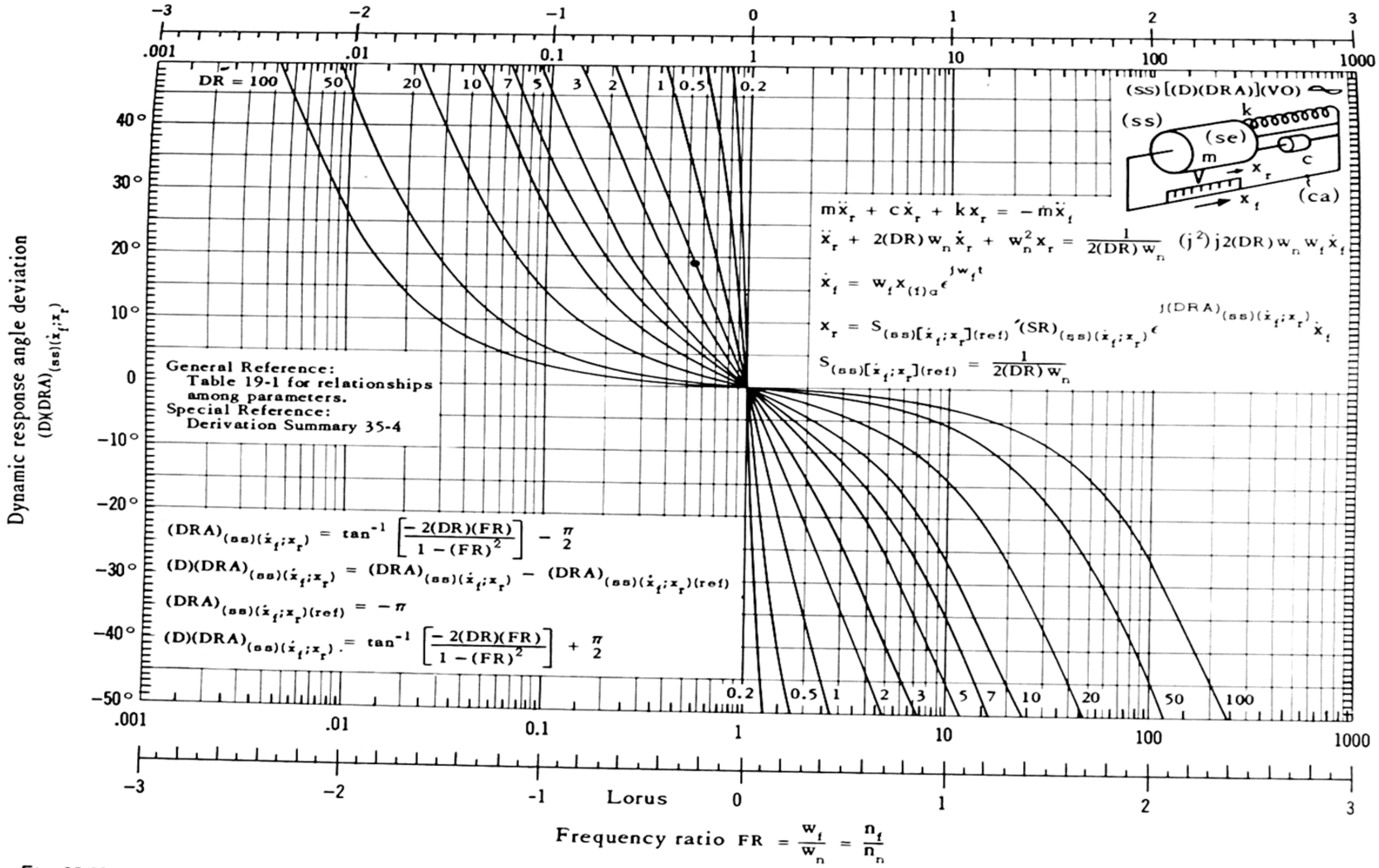
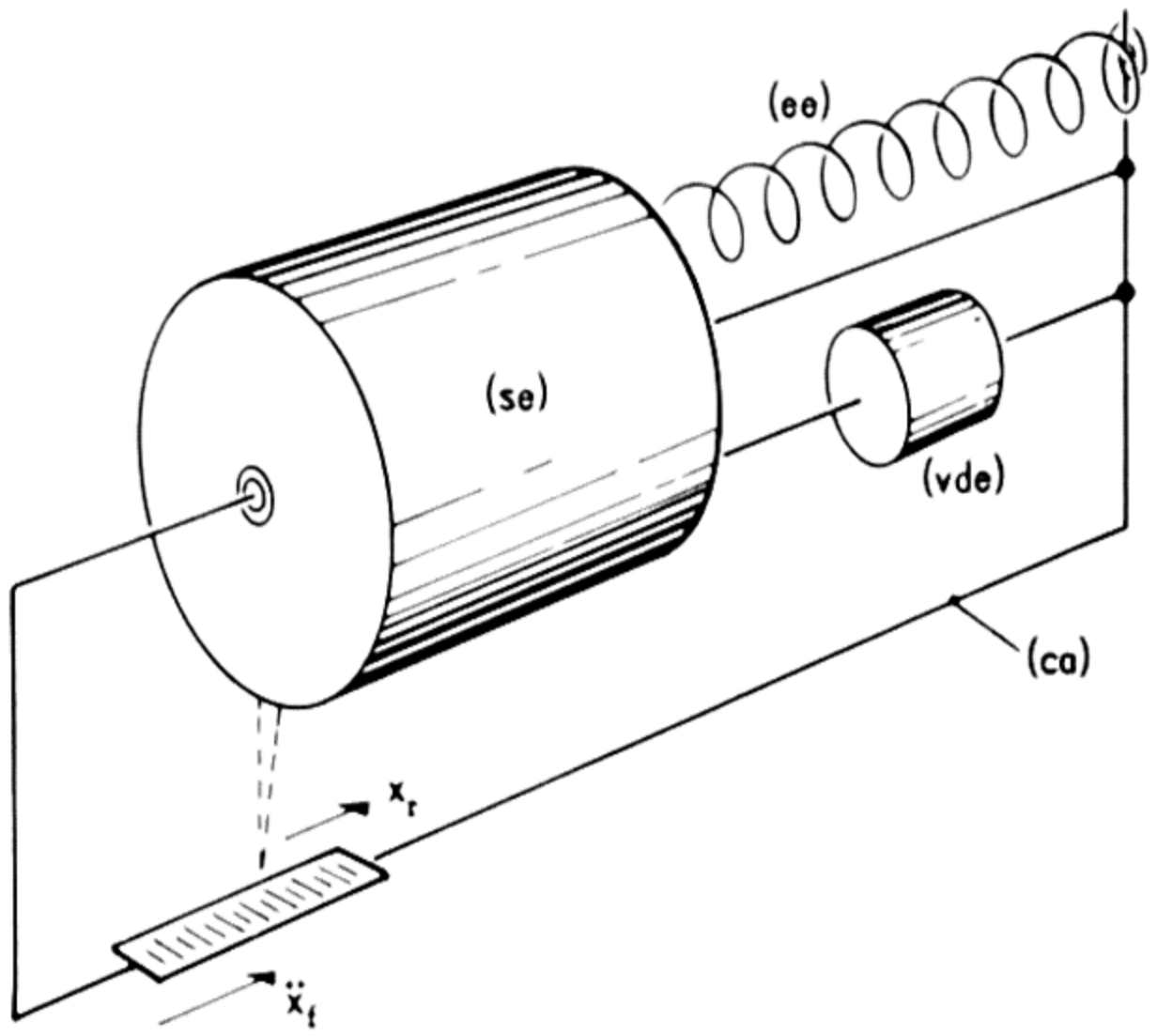


Fig. 35-21. Semilogarithmic-scale curves of forcing velocity input – relative displacement output dynamic response angle deviation for the seismographic system with viscous damping only.

is considered), the line schematic diagram of section a of Derivation Summary 35-5 and the functional diagram of section b of the same summary describe the situation to be considered. The performance equation, written as Eq. (1) of Derivation Summary 35-5, is identical with the generalized seismographic system equation developed in Derivation Summaries 35-1 and 35-2. This equation has the (0;0, 1, 2) form when the forcing acceleration multiplied by the square of the imaginary unit is considered as the forcing function. The performance function associated with Eq. (1) is identical with the (0;0, 1, 2) relating function developed in Derivation Summary 19-10, except for the appearance of j^2 as a multiplying factor. The performance function form is given as Eq. (2). The associated reference sensitivity is the reciprocal of the square of the undamped angular natural frequency; the dimensionless sensitivity ratio is identical with the (0;0, 1, 2) dimensionless dynamic amplitude ratio; and the dynamic response angle differs from the (0;0, 1, 2) dynamic response angle by the addition of $(-\pi)$ to account for the effects of the j^2 factor in the forcing function.

35.195. The upper curve family of Fig. 35-22, which is shown dotted, is made up of linear-scale plots of the forcing acceleration – relative displacement dynamic response angle for the seismographic system. The lower curve family of Fig. 35-22 is a linear-scale representation of the forcing acceleration – relative displacement dimensionless sensitivity ratio for the seismographic system. To fulfill the ideal accelerometer-range-operation requirement of constant sensitivity and constant dynamic response angle, the curve families of Fig. 35-22 show that the frequency ratio region is from zero to some high frequency limit that depends on the tolerances specified and the damping ratio of the system. The ideal dynamic response angle value is –180 degrees, and the ideal dimensionless sensitivity ratio value is unity. This means that in the accelerometer range the forcing acceleration – relative displacement sensitivity must have no more than allowable tolerance differences from the reference sensitivity, which is equal to the reciprocal of the square of the undamped angular natural frequency.

35.196. When the ideal sensitivity is taken as the reciprocal of the square of the undamped angular natural frequency, the forcing acceleration – relative displacement sensitivity performance ratio given by Eq. (13) of Derivation Summary 35-5 reduces to the dimensionless sensitivity ratio defined by Eq. (4). This means that the lower curve family of Fig. 35-22 is a direct representation of the performance ratio of the seismographic system operating in the accelerometer range. The forcing acceleration – relative displacement sensitivity performance ratio deviation defined by Eqs. (13) and (14) of Derivation Summary 35-5 is the actual performance ratio minus the ideal performance ratio value of unity. The upper curve family of Fig. 35-23 gives the performance ratio deviation on a linear ordinate scale against frequency ratio on a logarithmic abscissa scale. The range



a) Line schematic diagram of the single-degree-of-freedom seismographic system

When forcing acceleration is considered as the input and relative displacement is taken as the output, the functional diagram for the seismographic system is

[VIBRATORY ACCELERATION OF THE CASE WITH RESPECT TO THE INERTIAL REFERENCE]
Vibratory Input Acceleration or Forcing Acceleration
$\ddot{x}_f$
$[\ddot{x}_{[1-(ca)]}]$

→ Seismographic System (ss) [OPERATION IN THE VIBRATORY ACCELERATION-RECEIVING RANGE (ACCELEROMETER RANGE)] →

[DISPLACEMENT OF THE SEISMIC ELEMENT WITH RESPECT TO THE CASE]
Relative Displacement
x_r
$[x_{[(ca)-(ee)]}]$

When Coulomb friction effects are negligible, the single-degree-of-freedom seismographic system performance equation has the form of Eq. (2) of Derivation Summary 35-2; i.e.,

$$\ddot{x}_r + 2(DR)\omega_n \dot{x}_r + \omega_n^2 x_r = \frac{1}{\omega_n^2}\omega_n^2 j^2 \ddot{x}_f \tag{1}$$

b) Functional diagram and performance equation for the seismographic system operating in the acceleration-receiving range

When $j^2\ddot{x}_f$ is considered as the independent variable, Eq. (1) has the standard form of the (0;0,1,2) differential equation discussed in Derivation Summary 19-10. Use of the relating function form developed in that summary shows that

$$\eta_{(0;0,1,2)} = [RF]_{(0;0,1,2)} = [PF]_{(ss)[\ddot{x}_f;x_r]} = \frac{1}{\omega_n^2} j^2 \frac{1}{1-(FR)^2 + j2(DR)(FR)} \tag{2}$$

Taking

$$\rho_r = S_{(ss)[\ddot{x}_f;x_r](ref)} = \frac{1}{\omega_n^2} \tag{3}$$

Derivation Summary 35-5. Line schematic diagram, functional diagram, performance function and performance deviation equations for the seismographic system that has viscous damping only and operates in the acceleration-receiving range. (Page 1 of 3)

gives

$$\mu_{(0;0,1,2)} \approx {}'(SR)_{(ss)(\ddot{x}_f;x_r)} = \frac{1}{\sqrt{[1-(FR)^2]^2 + [2(DR)(FR)]^2}} \tag{4}$$

$$\phi_{(0;0,1,2)} - \pi \approx (DRA)_{(ss)(\ddot{x}_f;x_r)} = \tan^{-1}\left[\frac{-2(DR)(FR)}{1-(FR)^2}\right] - \pi \tag{5}$$

In Eq. (5), the angle $-\pi$ is added to $\phi_{(0;0,1,2)}$ to account for the j^2 factor in the forcing function The minus sign is chosen for the angle representing the effect of j^2 because in the acceleration-receiving range it is convenient to describe the physical fact that the sign of the relative displacement is negative when the forcing acceleration is positive by a lagging dynamic response angle with a magnitude of π.

$[PF]_{(ss)[\ddot{x}_f;x_r]}$ = forcing acceleration – relative displacement performance function of the seismographic system

$S_{(ss)[\ddot{x}_f;x_r](ref)}$ = forcing acceleration – relative displacement reference sensitivity of the seismographic system

${}'(SR)_{(ss)(\ddot{x}_f;x_r)}$ = forcing acceleration – relative displacement dimensionless sensitivity ratio of the seismographic system

$(DRA)_{(ss)(\ddot{x}_f;x_r)}$ = forcing acceleration – relative displacement dynamic response angle of the seismographic system

c) Forcing acceleration – relative displacement performance function of the seismographic system

From the standpoint of vibratory acceleration-receiving performance, ideal operation exists when the relative displacement is:

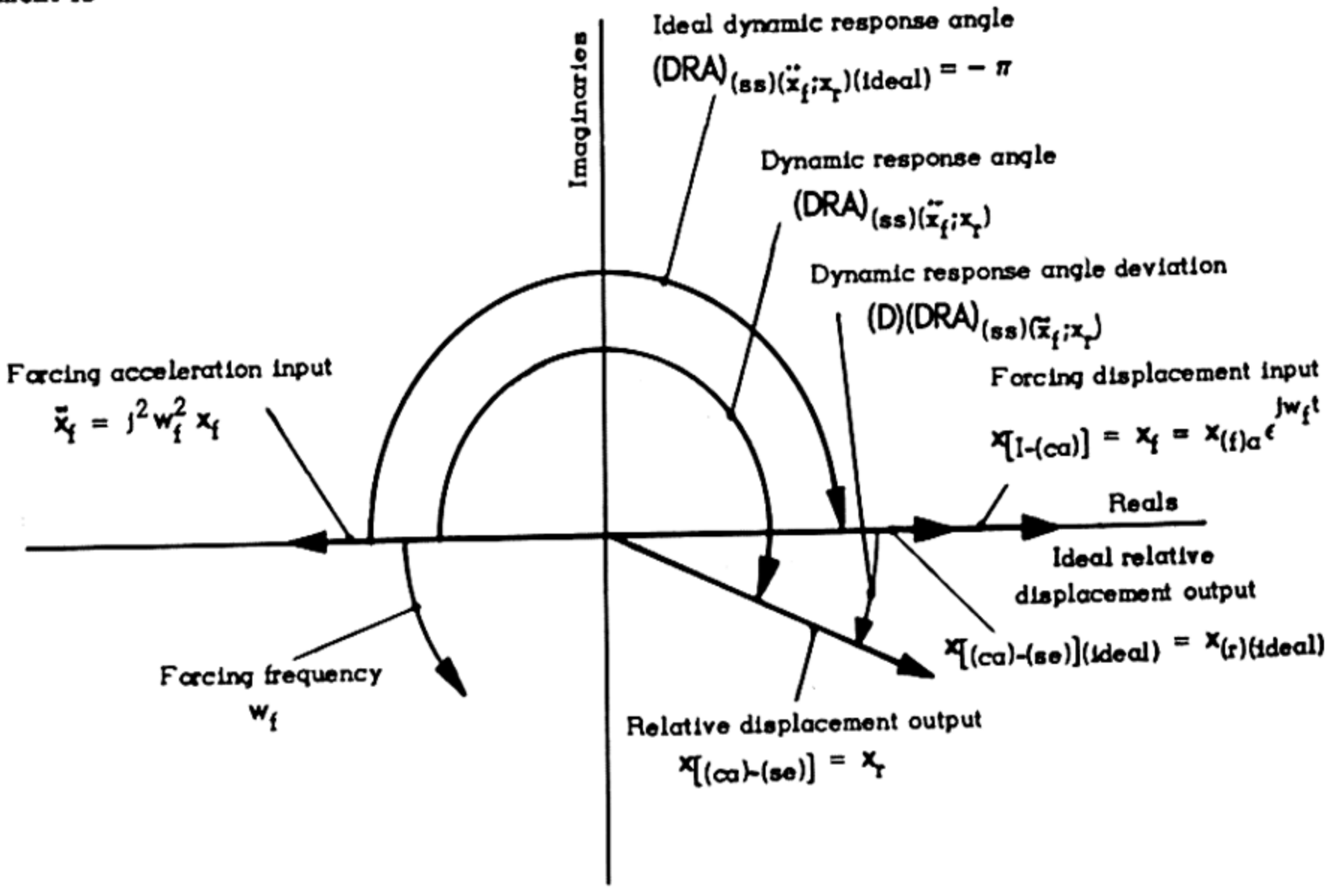
1) Instantaneously proportional in magnitude to the magnitude of the input acceleration; i.e.,

$$|x_r| = (\text{constant})\,|\ddot{x}_f| \tag{6}$$

2) Exactly out of phase with the input acceleration; i.e.,

$$x_r = -(\text{constant})\ddot{x}_f \tag{7}$$

The rotating vector diagram showing the relationships between the forcing acceleration and the relative displacement is



Derivation Summary 35-5. Line schematic diagram, functional diagram, performance function and performance deviation equations for the seismographic system that has viscous damping only and operates in the acceleration-receiving range. (Page 2 of 3)

For ideal operation in the acceleration-receiving range,

$$S_{(ss)[\ddot{x}_f;x_r](ideal)} = S_{(ss)[\ddot{x}_f;x_r](ref)}\,{}'(SR)_{(ss)(\ddot{x}_f;x_r)} = \text{constant} \tag{8}$$

From Eqs. (3) and (4), Eq. (8) is fulfilled when

$${}'(SR)_{(ss)(\ddot{x}_f;x_r)} = 1 \tag{9}$$

so that

$$S_{(ss)[\ddot{x}_f;x_r](ideal)} = S_{(ss)[\ddot{x}_f;x_r](ref)} = \frac{1}{w_n^2} \tag{10}$$

The corresponding ideal dynamic response angle is

$$(DRA)_{(ss)(\ddot{x}_f;x_r)(ideal)} = -\pi \tag{11}$$

d) Conditions for ideal operation in the acceleration-receiving range

By definition,

$$(PR)_{(ss)(S[\ddot{x}_f;x_r])} = \frac{S_{(ss)[\ddot{x}_f;x_r]}}{S_{(ss)[\ddot{x}_f;x_r](ideal)}} = \frac{S_{(ss)[\ddot{x}_f;x_r](ref)}\,{}'(SR)_{(ss)(\ddot{x}_f;x_r)}}{S_{(ss)[\ddot{x}_f;x_r](ref)}} = {}'(SR)_{(ss)(\ddot{x}_f;x_r)} \tag{12}$$

= sensitivity performance ratio of the seismographic system operating in the acceleration-receiving range

From Eq. (4)

$$(PR)_{(ss)(S[\ddot{x}_f;x_r])} = {}'(SR)_{(ss)(\ddot{x}_f;x_r)} = \frac{1}{\sqrt{\left[1-(FR)^2\right]^2 + \left[2(DR)(FR)\right]^2}} \tag{13}$$

By definition,

$$(D)(PR)_{(ss)(S[\ddot{x}_f;x_r])} = (PR)_{(ss)(S[\ddot{x}_f;x_r])} - 1 \tag{14}$$

= sensitivity performance ratio deviation of the seismographic system operating in the acceleration-receiving range

and

$$(D)(DRA)_{(ss)(\ddot{x}_f;x_r)} = (DRA)_{(ss)(\ddot{x}_f;x_r)} - (DRA)_{(ss)(\ddot{x}_f;x_r)(ref)}$$

$$= (DRA)_{(ss)(\ddot{x}_f;x_r)} - (DRA)_{(ss)(\ddot{x}_f;x_r)(ideal)} \tag{15}$$

= dynamic response angle deviation of the seismographic system operating in the acceleration-receiving range

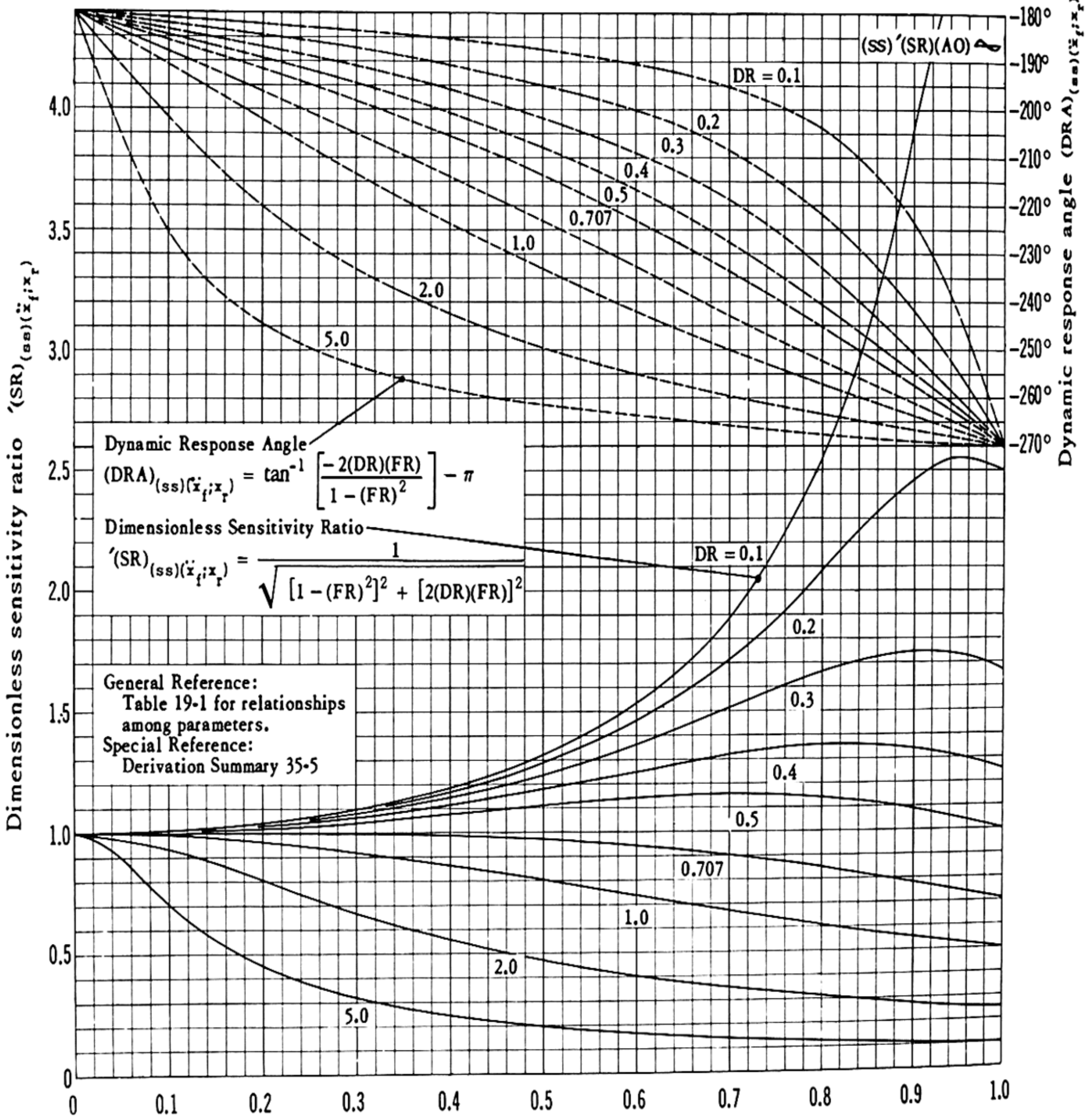
From Eq. (5) and the vector diagram of section d,

$$(D)(DRA)_{(ss)(\ddot{x}_f;x_r)} = \tan^{-1}\left[\frac{-2(DR)(FR)}{1-(FR)^2}\right] - \pi - (-\pi) = \tan^{-1}\left[\frac{-2(DR)(FR)}{1-(FR)^2}\right] \tag{16}$$

e) Performance deviation equations for the seismographic system operating in the acceleration-receiving range

Derivation Summary 35-5. Line schematic diagram, functional diagram, performance function and performance deviation equations for the seismographic system that has viscous damping only and operates in the acceleration-receiving range. (Page 3 of 3)

of the deviation scale is from −0.14 to +0.14, and the frequency ratio scale limits are 0.005 and unity. The lower curve family of Fig. 35-23 is an enlargement of that portion of the upper curve family that lies within the region of ordinate-scale deviations between −0.014 and +0.014. These performance ratio deviation curve families supply information of the type already explained in the discussion of vibrometer and velocimeter operation.



$$m\ddot{x}_r + c\dot{x}_r + kx_r = -m\ddot{x}_f$$

$$\ddot{x}_r + 2(DR)w_n\dot{x}_r + w_n^2 x_r = \frac{1}{w_n^2} j^2 w_n^2 \ddot{x}_f$$

$$\ddot{x}_f = j^2 w_f^2 X_{(f)a} \epsilon^{jw_f t}$$

$$x_r = S_{(ss)[\ddot{x}_f;x_r](ref)}\, {}'(SR)_{(ss)(\ddot{x}_f;x_r)}\, \epsilon^{j(DRA)_{(ss)(\ddot{x}_f;x_r)}} \ddot{x}_f$$

$$\text{Reference Sensitivity} = S_{(ss)[\ddot{x}_f;x_r](ref)} = \frac{1}{w_n^2}$$

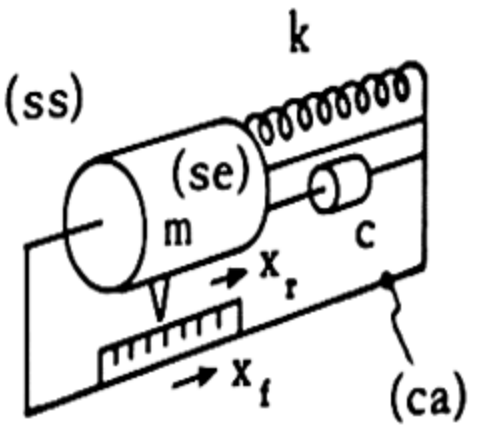


Fig. 35-22. Linear-scale curve families of forcing acceleration input – relative displacement output dimensionless sensitivity ratio and dynamic response angle for the seismographic system with viscous damping only.

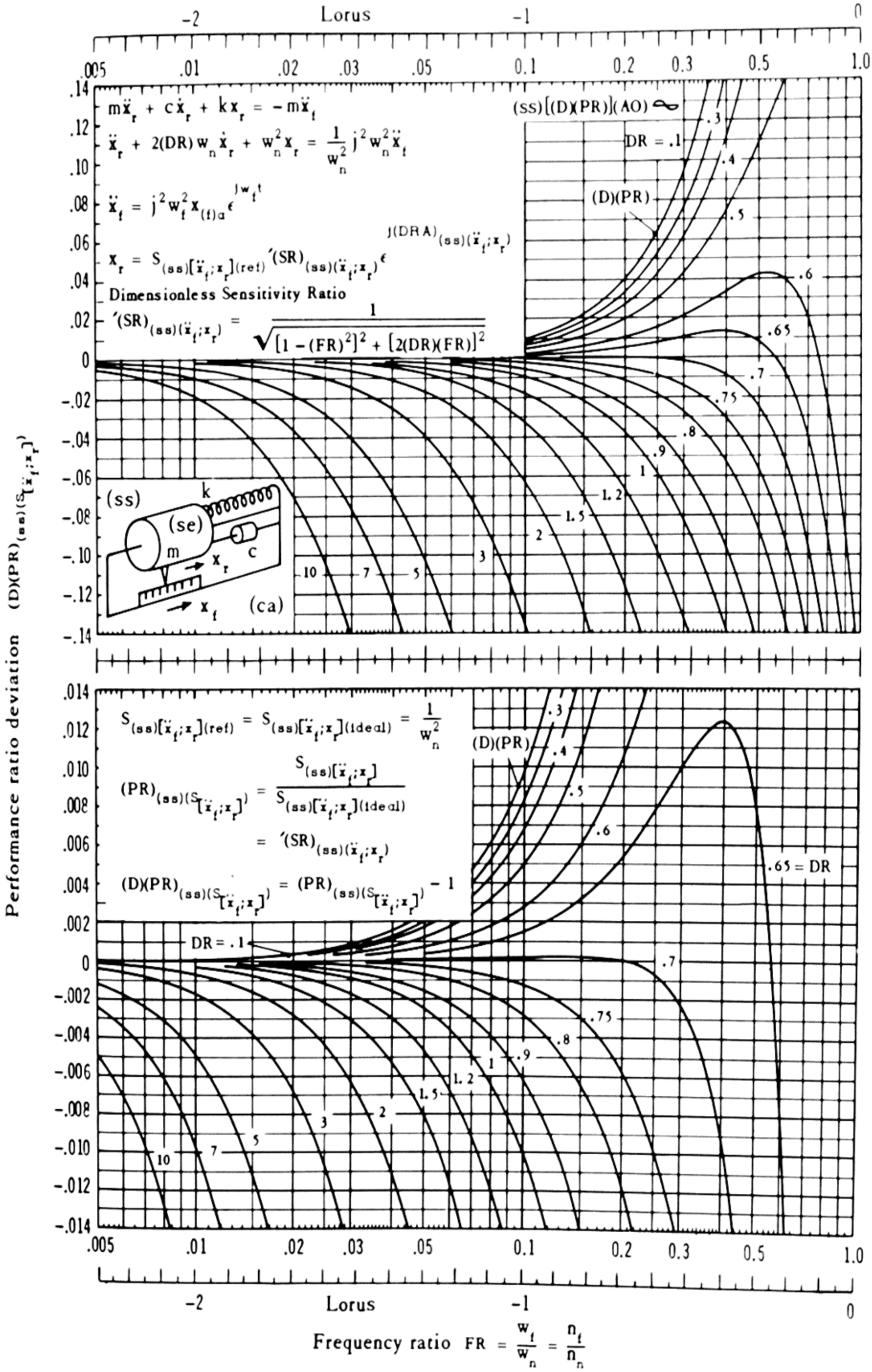


Fig. 35-23. Semilogarithmic-scale curves of forcing acceleration input – relative displacement output sensitivity performance ratio deviation of the seismographic system with viscous damping only.

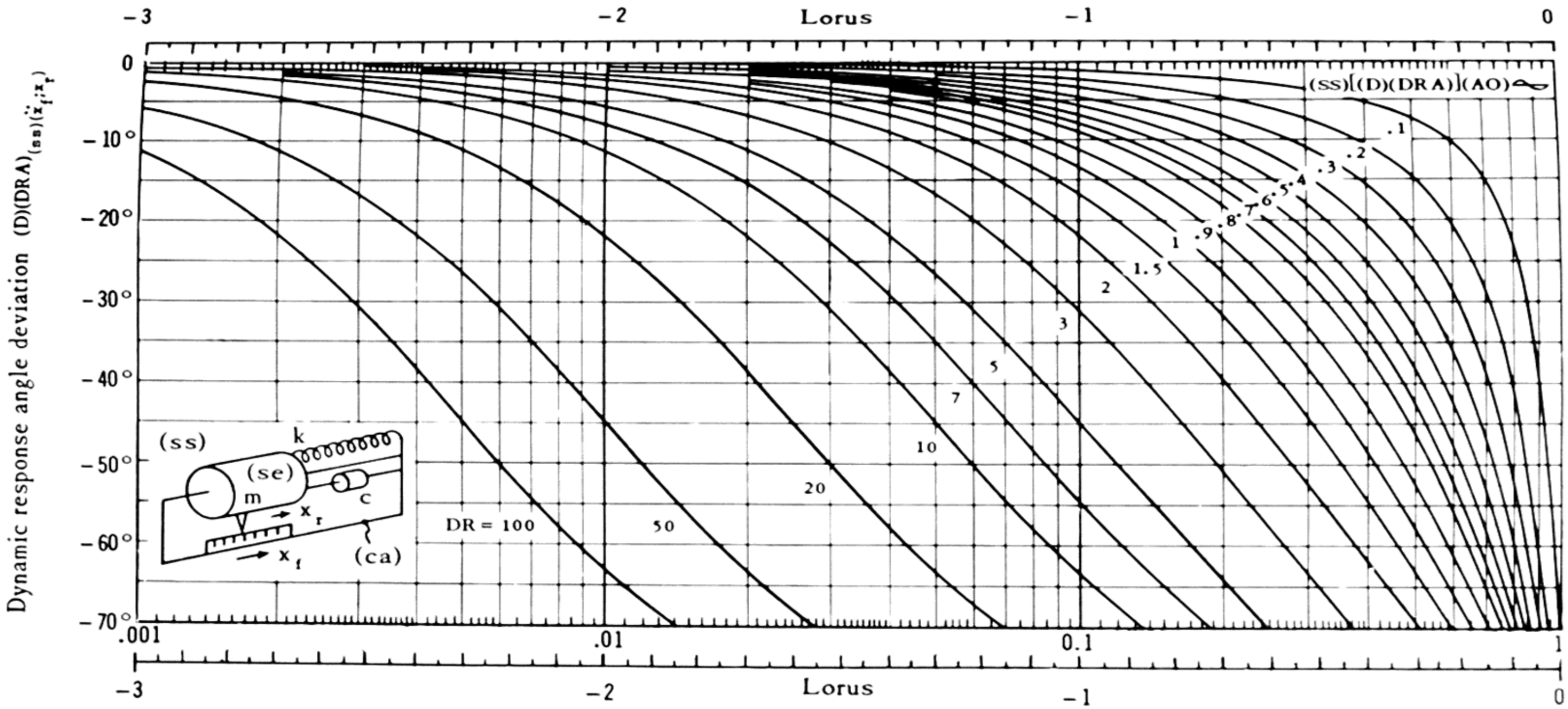
35.197. Figure 35-24 is the dynamic response angle deviation curve family based on Eq. (16) of Derivation Summary 35-5 and the rotating vector diagram of section d of the same summary. With the reference angle chosen as -180 degrees, the deviation is always negative and is given by an equation identical with the equation for the (0;0, 1, 2) dynamic response angle. The curve family shows that for a given tolerance specification the high frequency-ratio limit is improved as the damping ratio is reduced. For example, with a specified tolerance of -5 degrees, the high frequency-ratio limit is approximately 0.21 for a damping ratio of 0.2. When the damping ratio is 2, the high frequency-ratio limit is approximately 0.022, that is, about one order of magnitude less.

SUMMARY OF VIBRATION-RECEIVING CHARACTERISTICS OF THE SEISMOGRAPHIC SYSTEM WITH VISCOUS DAMPING ONLY

35.198. A pattern describing the characteristics of the seismographic system as a vibration-receiving component may be formed from the information developed in the preceding sections. A summary of this kind is given by Table 35-1. In Table 35-1, column 1 names the various characteristics covered by the table. Columns 2, 3 and 4 give specific information on these characteristics for the vibrometer range, the velocimeter range, and the accelerometer range, respectively. Row 1 gives the functional diagram corresponding to each operating range. Row 2 lists the ideal sensitivity for each of the three operating ranges. As noted in the table, the reference sensitivity in each instance is taken as identical with the ideal sensitivity. Row 3 gives the corresponding ideal dynamic response angles, each of which is equal to -180 degrees. As noted, the reference dynamic response angles are taken as identical with the ideal dynamic response angles. Row 4 gives the defining equations for the sensitivity performance ratios for the three operating ranges. Row 5 lists the corresponding performance ratio deviations. Row 6 gives the dynamic response angle deviations. Row 7 lists the conditions on frequency ratio and damping ratio that determine the frequency-ratio operating range limits. These conditions can be determined from the performance ratio relationships of row 4 under the assumption that the performance ratio is reasonably close to unity within the limits of the operating range concerned. In order to extend the usefulness of Table 35-1, references are made to the derivation summaries from which the information in the table is taken and to the figures where the relationships given are plotted.

SEISMOGRAPHIC SYSTEM WITH BOTH VISCOUS DAMPING AND COULOMB DAMPING

35.199. Coulomb friction enters as a factor in seismographic system performance because rubbing between the surfaces of solid parts is unavoidable in certain



$$m\ddot{x}_r + c\dot{x}_r + kx_r = -m\ddot{x}_f \quad ; \quad \ddot{x}_r + 2(DR)w_n\dot{x}_r + w_n^2 x_r = \frac{1}{w_n^2} j^2 w_n^2 \ddot{x}_f$$

$$\ddot{x}_f = j^2 w_f^2 x_{(f)a} \epsilon^{jw_f t} \quad ; \quad x_r = S_{(ss)[\ddot{x}_f;x_r](ref)}(SR)_{(ss)(\ddot{x}_f;x_r)} \epsilon^{j(DRA)_{(ss)(\ddot{x}_f;x_r)}} \ddot{x}_f$$

$$S_{(ss)[\ddot{x}_f;x_r](ref)} = \frac{1}{w_n^2}$$

$$(D)(DRA)_{(ss)(\ddot{x}_f;x_r)} = (DRA)_{(ss)(\ddot{x}_f;x_r)} - (DRA)_{(ss)(\ddot{x}_f;x_r)(ref)}$$

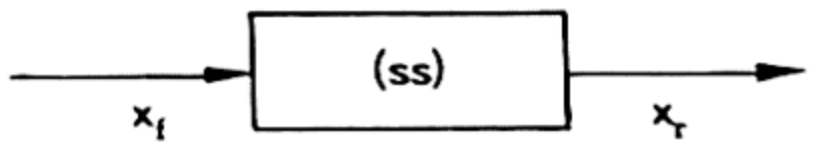
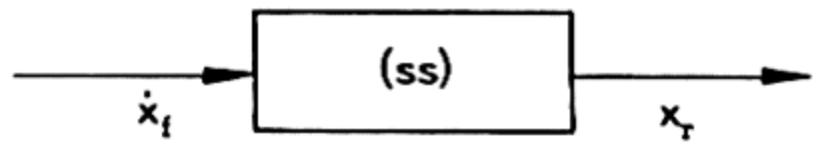
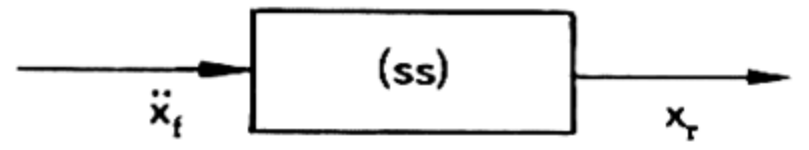
$$(DRA)_{(ss)(\ddot{x}_f;x_r)(ref)} = -\pi$$

$$(D)(DRA)_{(ss)(\ddot{x}_f;x_r)} = \tan^{-1}\left[\frac{-2(DR)(FR)}{1-(FR)^2}\right]$$

$$(DRA)_{(ss)(\ddot{x}_f;x_r)} = \tan^{-1}\left[\frac{-2(DR)(FR)}{1-(FR)^2}\right] - \pi$$

Fig. 35-24. Semilogarithmic-scale curves of forcing acceleration input – relative displacement output dynamic response angle deviation of the seismographic system with viscous damping only.

Table 35-1. Summary of seismographic system performance characteristics in various operating ranges when the system has viscous damping only.

Column I	Column II DISPLACEMENT-RECEIVING RANGE (Vibrometer Range)	Column III VELOCITY-RECEIVING RANGE (Velocimeter Range)	Column IV ACCELERATION-RECEIVING RANGE (Accelerometer Range)
Functional Diagram Row 1			
Ideal Sensitivity Row 2	$S_{(ss)[x_f;x_r](ideal)} = 1$ (See Derivation Summary 35-3.)	$S_{(ss)[\dot{x}_f;x_r](ideal)} = \frac{1}{2(DR)\,w_n}$ (See Derivation Summary 35-4.)	$S_{(ss)[\ddot{x}_f;x_r](ideal)} = \frac{1}{w_n^2}$ (See Derivation Summary 35-5.)
	Note: The reference sensitivity is taken as identical with the ideal sensitivity for each type of operation.		
Ideal Dynamic Response Angle Row 3	$(DRA)_{(ss)(x_f;x_r)(ideal)} = -\pi$ (See Derivation Summary 35-3.)	$(DRA)_{(ss)(\dot{x}_f;x_r)(ideal)} = -\pi$ (See Derivation Summary 35-4.)	$(DRA)_{(ss)(\ddot{x}_f;x_r)(ideal)} = -\pi$ (See Derivation Summary 35-5.)
	Note: The reference dynamic response angle is taken as identical with the ideal dynamic response angle for each type of operation.		
Sensitivity Performance Ratio Row 4	$(PR)_{(ss)(S_{[x_f;x_r]})} = \frac{(FR)^2}{\sqrt{[1-(FR)^2]^2 + [2(DR)(FR)]^2}}$ (See Figs. 35-8 and 35-10.)	$(PR)_{(ss)(S_{[\dot{x}_f;x_r]})} = \frac{2(DR)(FR)}{\sqrt{[1-(FR)^2]^2 + [2(DR)(FR)]^2}}$ (See Fig. 35-18.)	$(PR)_{(ss)(S_{[\ddot{x}_f;x_r]})} = \frac{1}{\sqrt{[1-(FR)^2]^2 + [2(DR)(FR)]^2}}$ (See Fig. 35-22.)
Sensitivity Performance Ratio Deviation Row 5	$(D)(PR)_{(ss)(S_{[x_f;x_r]})} = (PR)_{(ss)(S_{[x_f;x_r]})} - 1$ (See Fig. 35-12.)	$(D)(PR)_{(ss)(S_{[\dot{x}_f;x_r]})} = (PR)_{(ss)(S_{[\dot{x}_f;x_r]})} - 1$ (See Fig. 35-20.)	$(D)(PR)_{(ss)(S_{[\ddot{x}_f;x_r]})} = (PR)_{(ss)(S_{[\ddot{x}_f;x_r]})} - 1$ (See Fig. 35-23.)
Dynamic Response Angle Deviation Row 6	$(D)(DRA)_{(ss)(x_f;x_r)} = \tan^{-1}\left[\frac{-2(DR)(FR)}{1-(FR)^2}\right] + \pi$ (See Fig. 35-13.)	$(D)(DRA)_{(ss)(\dot{x}_f;x_r)} = \tan^{-1}\left[\frac{-2(DR)(FR)}{1-(FR)^2}\right] + \frac{\pi}{2}$ (See Fig. 35-21.)	$(D)(DRA)_{(ss)(\ddot{x}_f;x_r)} = \tan^{-1}\left[\frac{-2(DR)(FR)}{1-(FR)^2}\right]$ (See Fig. 35-24.)
Determining Conditions for Frequency-Ratio Operating Range Limits Row 7	$(FR)^2 >> 1$ $(FR)^2 >> [2(DR)]^2$	$[2(DR)(FR)]^2 >> [1-(FR)^2]^2$	$1 >> (FR)^2$ $1 >> [2(DR)(FR)]^2$
	Note: These conditions are based on the performance ratio relationships of row 4 and the assumption that the performance ratio is reasonably close to unity within the limits of the operating range concerned.		

single-degree-of-freedom vibration receiver designs and because other designs rely upon Coulomb friction for all the required damping. For example, several of the linear vibration receivers illustrated in Fig. 35-7 use rods or slides to restrict the motion of the seismic element to a straight line with respect to the case. Even though the sliding surfaces are immersed in oil, the side-loading due to acceleration and gravity is great enough to introduce a Coulomb friction component that appreciably affects the relative motion. The theoretical analysis for systems of this kind must account for a combination of viscous friction and Coulomb friction. Systems with only Coulomb friction may be treated as a special case of the complete theory in which viscous friction effects and Coulomb friction effects are both taken into account.* The discussion of this section is concerned with this general situation and also with the limiting case in which only Coulomb friction is important.

35.200. The diagram of section a of Derivation Summary 35-6 is a line schematic diagram representing a seismographic system in which both viscous damping and Coulomb damping are present. In this diagram, the Coulomb-friction-producing element is shown as a flat spring rubbing against the supporting member under a normal force tending to move the rubbing surfaces into closer contact. Due to the friction between these surfaces, a force acting to prevent relative motion exists. As long as the resultant force tending to cause relative motion is less than or equal to the maximum value of the Coulomb friction force, the seismic element is effectively locked to the support element and there is no relative velocity. When the resultant force applied to the seismic element exceeds the maximum value of the Coulomb friction force, relative motion starts and continues, with the rubbing friction contributing a force that always opposes the relative velocity. It is a physical fact that the magnitude of the rubbing friction force when relative velocity is present depends on many factors, including surface finish, surface materials, lubrication, and relative velocity. However, when motion exists, the resultant effect may be described for many engineering purposes as a force of constant magnitude. This magnitude is termed the maximum Coulomb friction force magnitude.

35.201. Equation (1) of Derivation Summary 35-6, which is based on the development of Derivation Summary 35-1, includes a positive or negative term with the square of the undamped angular natural frequency multiplied by the magnitude of the maximum Coulomb friction displacement, which is equal to the maximum Coulomb friction force magnitude divided by the elastic restraint coefficient. This term has the same mathematical form as the rate-determined step term that appears on the right-hand side of Eq. (2) of Derivation Summary 26-1 in Chapter 26. A comparison of the last term on the right-hand side of Eq. (1) of Derivation Summary 35-6 with the right-hand side of Eq. (2) of Derivation Summary 26-1 shows that

* See Den Hartog (D5) and (D16).

$$|x_{(cf)_m}| \approx u_{(rs)}$$

or

$$\left(\begin{array}{c}\text{MAGNITUDE OF MAXIMUM}\\ \text{COULOMB FRICTION DISPLACEMENT}\end{array}\right) = \left(\begin{array}{c}\text{RATE-DETERMINED STEP TERM}\\ \text{(a term of constant magnitude)}\end{array}\right)$$

When this equivalence is recognized, all the results developed in Chapter 26 may be immediately applied to the problems of single-degree-of-freedom mechanical systems that have Coulomb friction and a second-order performance equation.

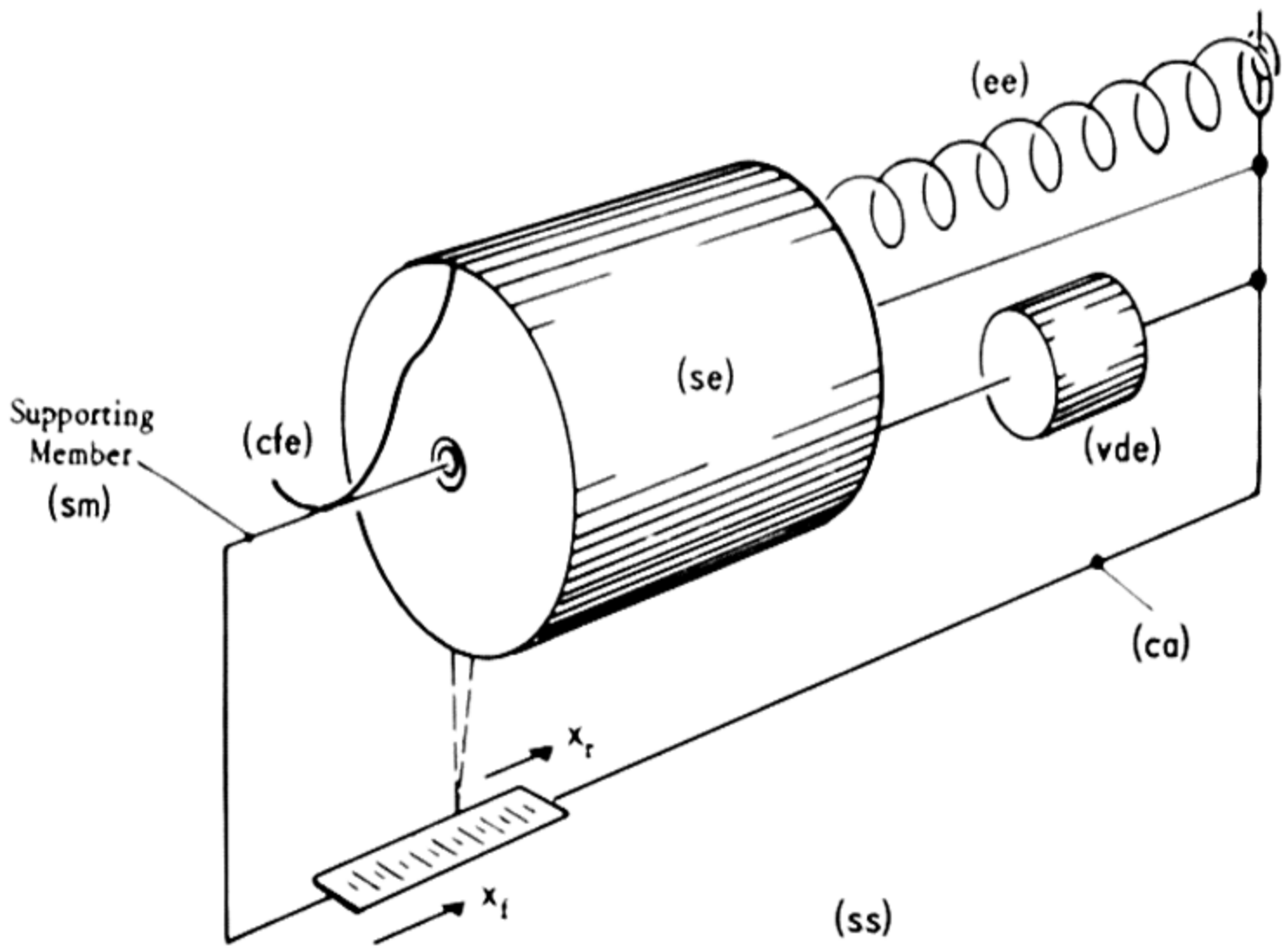
35.202. An application of this kind for the single-degree-of-freedom seismographic system with Coulomb friction is illustrated in Derivation Summary 35-6. This summary develops the dimensionless sensitivity ratio and the dynamic response angle for the (2;0, 1, 2) differential equation with an added Coulomb friction term. In order to represent the effects of Coulomb friction on a physical system, one of the several mathematical procedures used in Chapter 26 for developing performance functions from differential equations with rate-determined step terms is repeated in Derivation Summary 35-6. This procedure is based on replacing the rate-determined step term by a linear damping term that is made to account for Coulomb friction effects by the use of an equivalent damping ratio. For the case of a physical system, this equivalent damping ratio is chosen so that if its magnitude is associated with viscous damping, the energy dissipation obtained is equal to the dissipation actually caused by the Coulomb friction when a steady-state sinusoidal oscillation exists. In the discussions of Chapter 26, all the mathematical steps are carried out in terms of working variables without reference to any physical application. On the other hand, the development of Derivation Summary 35-6 is directly associated with the specific problem of the seismographic system in which both viscous damping and Coulomb damping are present.

35.203. In order to provide a background of information on the behavior of mechanical systems with both viscous damping and Coulomb damping, a series of figures from Chapter 26 showing step function transient responses are repeated at this point before proceeding with the discussion of steady-state sinusoidal performance functions.

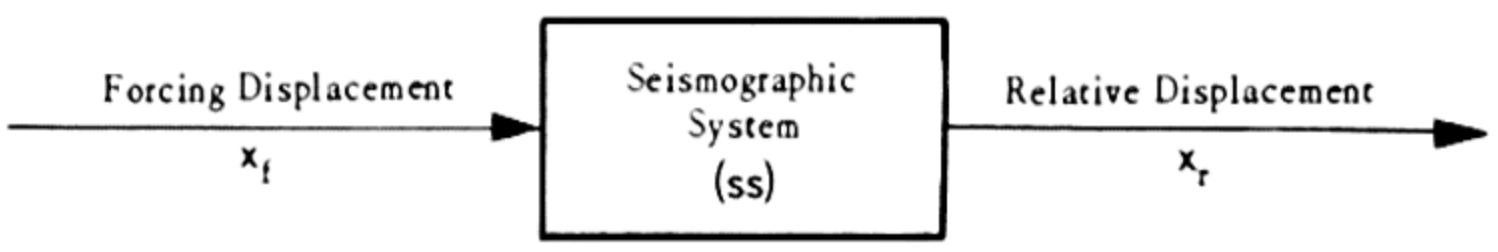
TRANSIENT RESPONSE OF THE SEISMOGRAPHIC SYSTEM WITH COMBINED VISCOUS DAMPING AND COULOMB DAMPING

35.204. Step function transient response equations for the (2;0, 1, 2) equation with a rate-determined step term are developed in Derivation Summary 26-1. The graphical interpretation of these equations is illustrated in working variable symbols by the curves of Figs. 26-2 through 26-5. These figures are repeated in seismographic-system terms by Figs. 35-25 through 35-28.

35.205. Section c of Fig. 35-25 summarizes the relative-motion step function response equations for the seismographic system with combined viscous damping



a) Line schematic diagram for a single-degree-of-freedom seismographic system with both Coulomb damping and viscous damping



Equation (9) of Derivation Summary 35-1 gives the performance equation of the seismographic system with combined viscous damping and Coulomb damping. With minor modifications, this equation is

$$\ddot{x}_r + 2(DR)_{(vde)} w_n \dot{x}_r + w_n^2 x_r = \frac{1}{w_n^2} j^2 w_n^2 \ddot{x}_f \mp w_n^2 |x_{(cf)m}| \qquad (1)$$

where

$(DR)_{(vde)}$ = damping ratio due to the viscous damping element acting with no Coulomb friction present in the seismographic system

$|x_{(cf)m}| = \dfrac{|F_{(cf)m}|}{k_{(ee)}}$ = magnitude of the maximum relative displacement due to Coulomb friction in the seismographic system

The algebraic sign associated with the second term on the right-hand side of Eq. (1) changes as necessary for it to be negative when $\dot{x}_r$ is positive and vice versa.

Equation (1) corresponds to the generalized (2,1,0;0,1,2) differential equation form of Eq. (1) of Derivation Summary 26-5 in Chapter 26 when $\nu_{(1-1)} = 0$; $\nu_{(2-2)} = 0$ and $\nu_{(0-0)} \neq 0$. With these conditions and with time as the running variable, the generalized-working-variable form given by Eq. (1) of Derivation Summary 26-5 becomes

$$\ddot{v} + 2\zeta\omega_n \dot{v} + \omega_n^2 v = \sigma_s \nu_{(0-0)} \omega_n^2 u \mp \omega_n^2 \sigma u_{(rs)} \qquad (2)$$

Derivation Summary 35-6. Performance equation, performance functions and breakaway frequency ratios for seismographic systems with Coulomb damping. (Page 1 of 7)

A comparison of Eqs. (1) and (2) shows that

$$v \approx x_r \quad ; \quad \zeta \approx (DR)_{(vde)} \quad ; \quad \omega_n \approx w_n$$

$$\sigma_s \nu_{(0\text{-}0)} \approx \frac{1}{w_n^2} \quad ; \quad u \approx j^2 \ddot{x}_f \quad ; \quad \sigma = 1 \quad ; \quad u_{(rs)} \approx |x_{(cf)m}| \tag{3}$$

b) Functional diagram and performance equation for the seismographic system with combined viscous damping and Coulomb damping

When the forcing displacement is sinusoidal and the slope of the steady-state displacement response does not become zero except at the points of maximum displacement, the effects of the nonlinear Coulomb friction term may be approximated by adding an equivalent Coulomb friction linear damping term $2(DR)_{(cf)} w_n \dot{x}_r$ to the left-hand side of Eq. (1) and dropping the actual Coulomb friction term on the right-hand side. When this change is made, Eq. (1) becomes

$$\ddot{x}_r + 2[(DR)_{(vde)} + (DR)_{(cf)}] w_n \dot{x}_r + w_n^2 x_r = \frac{1}{w_n^2} j^2 w_n^2 \ddot{x}_f \tag{4}$$

where

$(DR)_{(cf)}$ = Coulomb friction equivalent damping ratio

The value of $(DR)_{(cf)}$ is determined so that the energy dissipation per cycle due to the equivalent Coulomb friction linear damping term is equal to the actual energy dissipation per cycle caused by the Coulomb friction force, $F_{(cf)m}$, acting against the relative velocity. This method for replacing the actual Coulomb friction term by an equivalent viscous damping term corresponds to the procedure described in section a of Derivation Summary 26-5 for replacing a rate-determined step term by an equivalent linear damping term.

In general, the energy dissipation due to damping effects associated with a small relative displacement is

$$dE_{(dis)} = (\text{dissipative force}) |dx_r| \tag{5}$$

The dissipative force due to the action of the viscous damping element is

$$|F_{(vde)}| = \left| c_{(vde)} \frac{dx_r}{dt} \right| \tag{6}$$

where

$F_{(vde)}$ = damping force generated by the viscous damping element

$c_{(vde)}$ = damping coefficient associated with the viscous damping element

When the relative displacement is sinusoidal

$$x_r = x_{(r)a} \sin w_f t \tag{7}$$

and

$$\frac{dx_r}{dt} = x_{(r)a} w_f \cos w_f t \tag{8}$$

Also

$$dx_r = x_{(r)a} \cos(w_f t) d(w_f t) \tag{9}$$

Therefore, when applied to the action of the viscous damping element, Eq. (5) becomes

$$dE_{(dis)(vde)} = c_{(vde)} x_{(r)a}^2 w_f \cos^2(w_f t) d(w_f t) \tag{10}$$

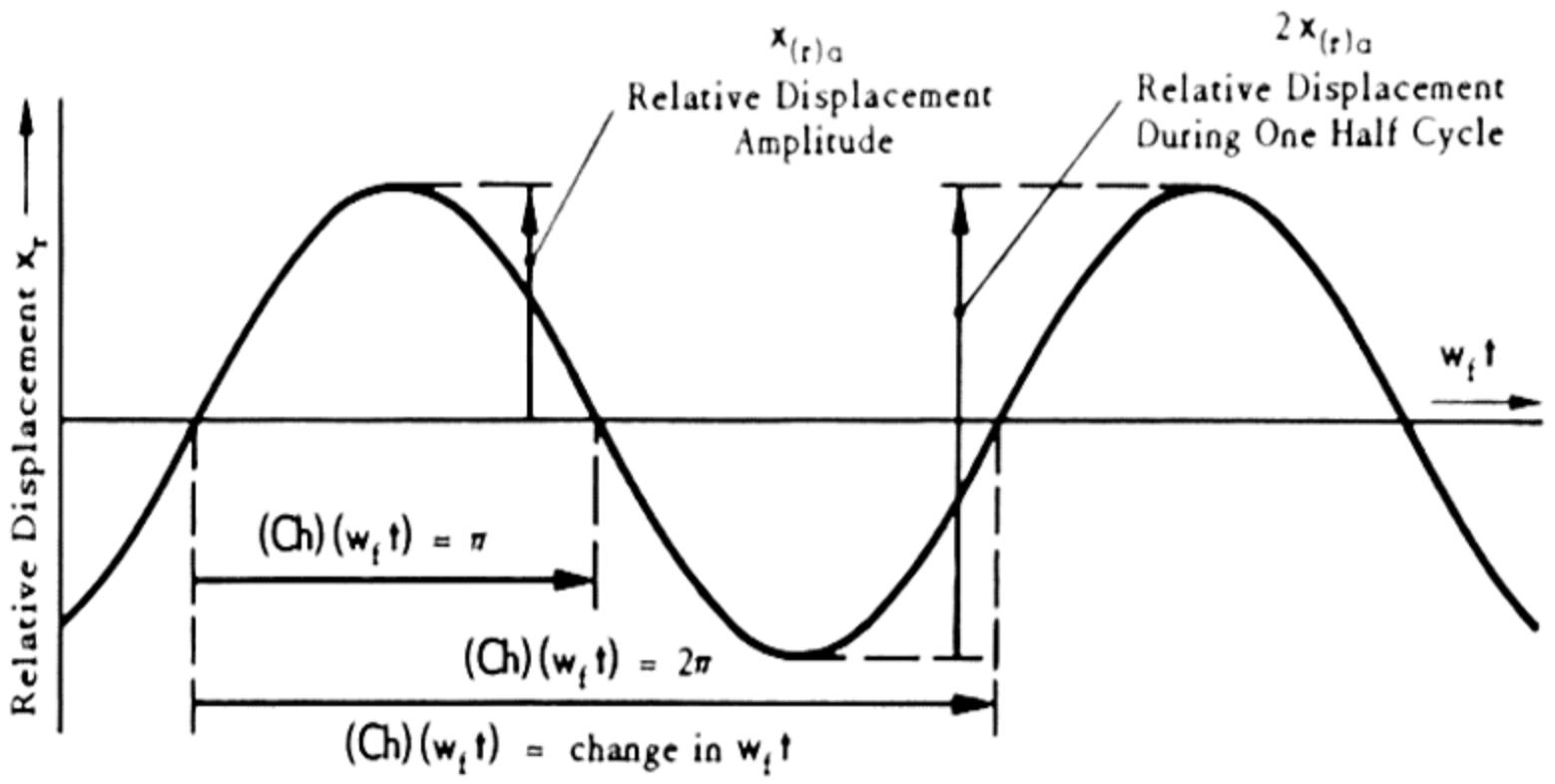
The energy dissipated by viscous damping during one complete cycle is the integral of $dE_{(dis)(vde)}$ as $w_f t$ varies from zero to 2π; i.e.,

Derivation Summary 35-6. Performance equation, performance functions and breakaway frequency ratios for seismographic systems with Coulomb damping. (Page 2 of 7)

$$E_{(dis)(vde)(cycle)} = C_{(vde)} x^2_{(r)a} w_f \int_0^{2\pi} \cos^2(w_f t)\, d(w_f t)$$

$$= C_{(vde)} x^2_{(r)a} w_f \left[\frac{w_f t}{2} \Bigg|_0^{2\pi} + \frac{\sin 2 w_f t}{4} \Bigg|_0^{2\pi} \right] = C_{(vde)} x^2_{(r)a} w_f \pi \qquad (11)$$

The energy dissipated by Coulomb friction during one half of a complete cycle with the seismic element in continuous relative motion is equal to the product of the maximum Coulomb friction force (that is, the constant force magnitude developed when relative motion exists) and the distance moved by the seismic element against this force. The accompanying diagram shows that the relative displacement during one half cycle is twice the relative displacement amplitude.



Using $2x_{(r)a}$ as the distance moved against the constant Coulomb friction force, $F_{(cf)m}$, the dissipation during one half cycle is

$$E_{(dis)(cf)(1/2\ cycle)} = 2|F_{(cf)m}|\, x_{(r)a} \qquad (12)$$

The dissipation per cycle is twice the dissipation during one half cycle; i.e.,

$$E_{(dis)(cf)(cycle)} = 2E_{(dis)(cf)(1/2\ cycle)} = 4|F_{(cf)m}|\, x_{(r)a} \qquad (13)$$

The Coulomb friction equivalent viscous damping coefficient $C_{(vd)(equiv)(cf)}$ corresponding to the viscous damping element coefficient $C_{(vde)}$ has a magnitude that would give the same dissipation per cycle as the Coulomb friction force actually present. From Eqs. (11) and (13), this means that

$$C_{(vd)(equiv)(cf)} x^2_{(r)a} w_f \pi = 4|F_{(cf)m}|\, x_{(r)a} \qquad (14)$$

Solving Eq. (14) for the damping coefficient shows that

$$C_{(vd)(equiv)(cf)} = \frac{4}{\pi} \frac{|F_{(cf)m}|}{x_{(r)a}} \frac{1}{w_f} \qquad (15)$$

Reference to Table 19-1 shows that, for the (−;0,1,2) differential equation,

$$2(DR) w_n = \frac{a_1}{a_2} \qquad (16)$$

or

$$DR = \frac{a_1}{a_2} \frac{1}{2 w_n} \qquad (17)$$

Equations (8) and (9) of Derivation Summary 35-1 show that, for the seismographic system

$$a_1 \approx C_{(vde)} \quad \text{and} \quad a_2 \approx m_{(se)} \qquad (18)$$

Derivation Summary 35-6. Performance equation, performance functions and breakaway frequency ratios for seismographic systems with Coulomb damping. (Page 3 of 7)

so that, defining $(DR)_{(cf)}$ as the Coulomb friction equivalent damping ratio,

$$(DR)_{(cf)} = \frac{c_{(vd)(equiv)(cf)}}{m_{(se)}} \frac{1}{2w_n} \tag{19}$$

Combining Eqs. (15) and (19) gives

$$(DR)_{(cf)} = \frac{4}{\pi} \frac{|F_{(cf)m}|}{x_{(r)a} w_f} \frac{1}{m_{(se)}} \frac{1}{2w_n} \tag{20}$$

Multiplying and dividing the right-hand side of Eq. (20) by $k_{(ee)}$, the elastic coefficient of the seismographic system elastic element, and noting that $w_n^2 = k_{(ee)}/m_{(se)}$ and that $|x_{(cf)m}| = |F_{(cf)m}| / k_{(ee)}$ (see Derivation Summary 35-1) shows that Eq. (20) can be written in the form

$$(DR)_{(cf)} = \frac{2}{\pi} \frac{w_n}{w_f} \frac{|x_{(cf)m}|}{x_{(r)a}} = \frac{4}{\pi} \frac{1}{2(FR)} \frac{|x_{(cf)m}|}{x_{(r)a}} \tag{21}$$

where

$$FR = \frac{w_f}{w_n} = \frac{n_f}{n_n}$$

In working variable terms, Eq. (21) is identical with Eq. (10) of Derivation Summary 26-5, which is

$$\zeta_{(rs)} = \frac{4}{\pi} \frac{1}{2\beta} \frac{\sigma u_{(rs)}}{v_a} \tag{22}$$

c) *The Coulomb friction equivalent damping ratio*

When Coulomb friction effects are represented by the equivalent viscous damping term derived in section c, Eq. (1) may be written in the form

$$\ddot{x}_r + 2(DR)_{[(vf)+(cf)]} w_n \dot{x}_r + w_n^2 x_r = \frac{1}{w_n^2} j^2 w_n^2 \ddot{x}_f \tag{23}$$

for

$$x_f = x_{(f)a} \epsilon^{jw_f t} \tag{24}$$

$$\ddot{x}_f = j^2 w_f^2 x_f \tag{25}$$

where

$$(DR)_{[(vf)+(cf)]} = (DR)_{(vde)} + (DR)_{(cf)} \tag{26}$$

= resultant damping ratio based on combined viscous damping and Coulomb damping

Substituting Eqs. (25) and (26) into Eq. (4) gives

$$\ddot{x}_r + 2(DR)_{[(vf)+(cf)]} w_n \dot{x}_r + w_n^2 x_r = w_n^2 (FR)^2 x_f \tag{27}$$

Equation (27) has the (0;0,1,2) form for which the steady-state sinusoidal performance function corresponds to the product of $(FR)^2$ and the (0;0,1,2) relating function developed in Derivation Summary 19-10. This means that

$$(SR)_{(ss)(x_f;x_r)[(vf)+(cf)]} = \frac{x_{(r)a}}{x_{(f)a}} = \frac{(FR)^2}{\sqrt{[1-(FR)^2]^2 + [2(DR)_{[(vf)+(cf)]}(FR)]^2}} \tag{28}$$

= forcing displacement – relative displacement dimensionless sensitivity ratio for the seismographic system with combined viscous damping and Coulomb damping

The corresponding dynamic response angle, from Derivation Summary 19-10, is

$$(DRA)_{(ss)(x_f;x_r)} = \tan^{-1}\left[\frac{-2(DR)_{[(vf)+(cf)]}(FR)}{1-(FR)^2}\right] \tag{29}$$

d) *Forcing displacement – relative displacement performance function for the seismographic system with combined viscous damping and Coulomb damping*

Derivation Summary 35-6. Performance equation, performance functions and breakaway frequency ratios for seismographic systems with Coulomb damping. (Page 4 of 7)

When viscous damping effects are negligibly small in comparison with Coulomb friction effects, Eqs. (28) and (29) become

$$'(SR)_{(ss)(x_f;x_r)(cf)} = \frac{x_{(r)a}}{x_{(f)a}} = \frac{(FR)^2}{\sqrt{[1-(FR)^2]^2 + [2(DR)_{(cf)}(FR)]^2}} \tag{30}$$

$$(DRA)_{(ss)(x_f;x_r)(cf)} = \tan^{-1}\left[\frac{-2(DR)_{(cf)}(FR)}{1-(FR)^2}\right] \tag{31}$$

From Eq. (21)

$$(DR)_{(cf)} = \frac{4}{\pi}\frac{1}{2(FR)}\frac{|x_{(cf)m}|}{x_{(r)a}} \quad \text{(repeated)} \tag{21}$$

$$= \frac{4}{\pi}\frac{1}{2(FR)}[(MCFD)(RDA)R] \tag{32}$$

where

$[(MCFD)(RDA)R] = \dfrac{|x_{(cf)m}|}{x_{(r)a}}$ = maximum Coulomb friction displacement – relative displacement amplitude ratio

An explicit solution for the dimensionless sensitivity ratio requires a proper algebraic solution for Eq. (30) with $(DR)_{(cf)}$ eliminated by means of Eq. (21). Substituting the expression of Eq. (21) for $(DR)_{(cf)}$ in Eq. (30), squaring both sides, and rearranging terms gives

$$\left(\frac{x_{(r)a}}{x_{(f)a}}\right)^2[1-(FR)^2]^2 + \left(\frac{x_{(r)a}}{x_{(f)a}}\right)^2\left[2\frac{4}{\pi}\frac{1}{2(FR)}\frac{|x_{(cf)m}|}{x_{(f)a}}\frac{x_{(f)a}(FR)}{x_{(r)a}}\right]^2 = (FR)^4 \tag{33}$$

In order to simplify Eq. (33), the second term on the left-hand side has been multiplied and divided by $x^2_{(f)a}$. Solving Eq. (33) for the dimensionless sensitivity ratio gives

$$'(SR)_{(ss)(x_f;x_r)(cf)} = '(SR)_{(ss)(x_f;x_r)((DR)_{(vde)}=0)((DR)_{(cf)}\neq 0)} = \frac{x_{(r)a}}{x_{(f)a}}$$

$$= \sqrt{\frac{(FR)^4 - \left(\frac{4}{\pi}\right)^2\left(\frac{|x_{(cf)m}|}{x_{(f)a}}\right)^2}{[1-(FR)^2]^2}} \tag{34}$$

The dimensionless sensitivity ratio expression of Eq. (34) is equivalent to the working variable form for the (2;0,1,2) equation with the effects of a rate-determined step term, $\sigma u_{(rs)}$, represented by an equivalent damping ratio, $\zeta_{(rs)}$. From Eq. (30) of Derivation Summary 26-5, this working variable form is

$$\mu_{(2;0,1,2)(u_{(rs)}\neq 0)(\zeta_{(u_{(rs)}=0)}=0)} = \frac{1}{1-\beta^2}\sqrt{\beta^4 - \left(\frac{4}{\pi}\right)^2\left(\frac{u_{(rs)}}{u_a}\right)^2} \tag{35}$$

The dynamic response angle for the same equation is

$$\phi_{(2;0,1,2)(u_{(rs)}\neq 0)(\zeta_{(u_{(rs)}=0)}=0)} = \sin^{-1}\left[-\frac{4}{\pi}\frac{u_{(rs)}}{u_a}\frac{1}{\beta^2}\right] \tag{36}$$

The self-defining symbol form corresponding to Eq. (36) is

$$(DRA)_{(ss)(x_f;x_r)(cf)} = (DRA)_{(ss)(x_f;x_r)((DR)_{(vde)}=0)((DR)_{(cf)}\neq 0)} = \sin^{-1}\left[-\frac{4}{\pi}\frac{x_{(cf)m}}{x_{(f)a}}\frac{1}{(FR)^2}\right] \tag{37}$$

e) Performance function for the seismographic system with Coulomb damping only

Derivation Summary 35-6. Performance equation, performance functions and breakaway frequency ratios for seismographic systems with Coulomb damping. (Page 5 of 7)

Equation (34) shows that for frequency ratios less than the critical value required to make the combination of terms under the radical equal to zero the quantity under the radical is negative, so that the dimensionless sensitivity ratio is imaginary. This means that for sufficiently low frequency ratios the dimensionless sensitivity ratio equation has no physical significance, which corresponds to the physical fact that when such frequency ratios exist the maximum Coulomb friction force is great enough to hold the seismic element motionless on the supporting element.

The frequency ratio for which the quantity under the radical of Eq. (34) is equal to zero determines the point at which the dimensionless sensitivity ratio begins to be real and relative motion is on the verge of starting because inertia reaction force is reaching a level at which the Coulomb friction force is no longer able to prevent relative motion. This frequency ratio is called the breakaway frequency ratio and is defined by the equation

$$(FR)_{(b)(edr)} = \sqrt{\frac{4}{\pi}} \sqrt{\frac{|x_{(cf)m}|}{x_{(f)a}}} \tag{38}$$

= equivalent damping ratio breakaway frequency ratio

f) Breakaway frequency ratio based on the Coulomb friction equivalent damping ratio

When in Eq. (1) the forcing acceleration is so low that $F_{(cf)m}$, the maximum value of Coulomb friction force, is sufficient to prevent relative motion so that $\dot{x}_r = 0$ and $\ddot{x}_r = 0$ with $x_r = 0$, the seismographic system is inoperative and is said to be in the sub-breakaway region. When the seismographic system reaches the breakaway point, the relative velocity starts to differ from zero. This occurs when the right-hand side of Eq. (1) is just equal to zero, that is, when

$$|\ddot{x}_f|_m = w_n^2 |x_{(cf)m}| \tag{39}$$

where

$|\ddot{x}_f|_m$ = maximum value of the forcing acceleration

When x_f is sinusoidal,

$$\ddot{x}_f = w_f^2 x_{(f)a} \epsilon^{jw_f t} \tag{40}$$

and

$$|\ddot{x}_f|_m = w_f^2 x_{(f)a} \tag{41}$$

Combining Eqs. (39) and (41) gives

$$w_f^2 x_{(f)a} = w_n^2 |x_{(cf)m}| \tag{42}$$

or

$$\frac{w_f^2}{w_n^2} = (FR)^2_{(b)(ab)} = \frac{|x_{(cf)m}|}{x_{(f)a}} \tag{43}$$

so that

$$(FR)_{(b)(ab)} = \sqrt{\frac{|x_{(cf)m}|}{x_{(f)a}}} \tag{44}$$

= acceleration-balance breakaway frequency ratio

g) Breakaway frequency ratio based on the acceleration reaction force – Coulomb friction force balance

Comparison of Eq. (44) with Eq. (38) shows that $(FR)_{(b)(edr)}$, the breakaway frequency ratio based on the Coulomb friction equivalent damping ratio, is not equal to $(FR)_{(b)(ab)}$, the acceleration-balance breakaway frequency ratio. The reason for this discrepancy is that the equivalent damping ratio method is based on the assumption that there are no stops in the relative displacement (that is, zero slopes in the response curve) except when the amplitude is a maximum. It follows that any breakaway frequency ratios based on equivalent damping ratio expressions will be valid only for motion without stops. The following tabulation summarizes the physical situations that correspond to various ranges and limiting values of the frequency ratio.

Derivation Summary 35-6. Performance equation, performance functions and breakaway frequency ratios for seismographic systems with Coulomb damping. (Page 6 of 7)

Seismic element does not move relative to case $x_r = 0 \quad ; \quad x_{(se)} = x_f$	Seismic element moves relative to case with stops $x_r \cong 0 \quad ; \quad x_{(se)} \cong x_f$	Seismic element moves sinusoidally relative to case $x_r \neq 0 \quad ; \quad x_{(se)} \neq x_f$
$(FR) \leq (FR)_{(b)(ab)}$ Coulomb friction force balances acceleration force at all times for frequency ratios less than $(FR)_{(b)(ab)}$.	$(FR)_{(b)(ab)} < (FR) \leq (FR)_{(b)(edr)}$ Acceleration force exceeds Coulomb friction force during part of each cycle for some frequency ratios less than $(FR)_{(b)(edr)}$.	$(FR)_{(b)(edr)} < (FR)$ No appreciable stops in relative motion.

$(FR)_{(b)(ab)} = \sqrt{\dfrac{|x_{(cf)m}|}{x_{(f)a}}}$ = acceleration-balance breakaway frequency ratio. (Based on balance of Coulomb friction force and inertia reaction force. Refer to section g.)

$(FR)_{(b)(edr)} = \sqrt{\dfrac{4}{\pi}\dfrac{|x_{(cf)m}|}{x_{(f)a}}}$ = equivalent damping ratio breakaway frequency ratio (Based on Coulomb friction equivalent damping ratio. Refer to section f.)

h) *Physical situations corresponding to breakaway frequency ratios based on force balance and on the Coulomb friction equivalent damping ratio*

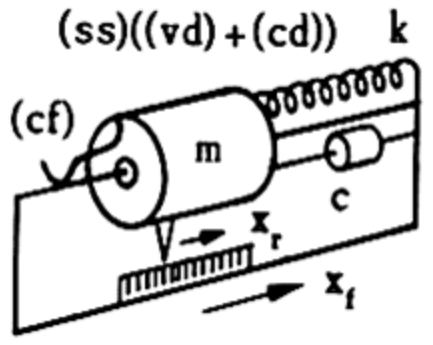
Derivation Summary 35-6. Performance equation, performance functions and breakaway frequency ratios for seismographic systems with Coulomb damping. (Page 7 of 7)

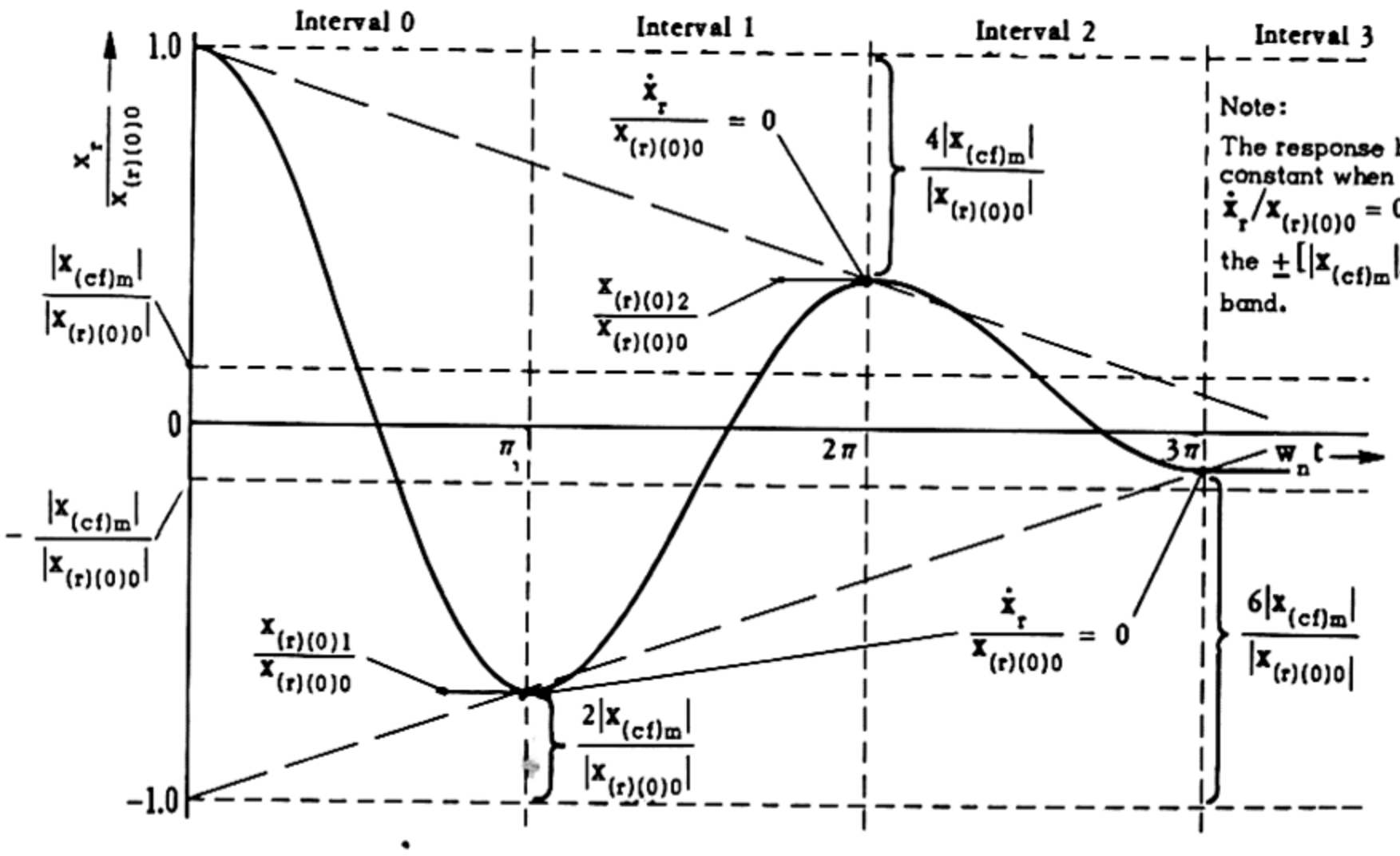
and Coulomb damping, based on zero case displacement with respect to the inertial reference. These equations are identical with working variable equations given in Derivation Summary 26-1, except for the use of symbols that are either defined in Table 19-1 or associated directly with the seismographic system in Derivation Summary 35-1. The quantity σ that appears in the equations of Derivation Summary 26-1 is shown by section b of Derivation Summary 35-6 to be equal to unity. Sections a and b of Fig. 35-25 show illustrative step function response curves for the seismographic system with Coulomb damping only. These curves and the equations of section c suggest that the effect of Coulomb friction is to cause the relative motion to be sinusoidal with respect to an axis displaced upward or downward by an amount proportional to the maximum Coulomb friction displacement magnitude. In the curves of Fig. 35-25, the ordinate is the ratio of relative displacement to the maximum value of the relative displacement, which occurs at the initial instant. * With this coordinate, each half cycle of the oscillation has one of the dotted lines on either side of the abscissa axis as its zero level. These dotted lines are located on the ordinate scale at plus and minus the maximum Coulomb friction displacement - initial peak maximum magnitude ratio. Whenever the slope of the response curve becomes zero within these Coulomb-friction-determined limits, no inertia reaction force exists, and the elastic restraint force is less than that required to overcome the Coulomb friction force, so that the seismic element remains at rest with respect to the case. This means that the transient phase of response always ends

* The maximum is referred to as the initial peak maximum in the ensuing discussion, since it always occurs at the initial peak.

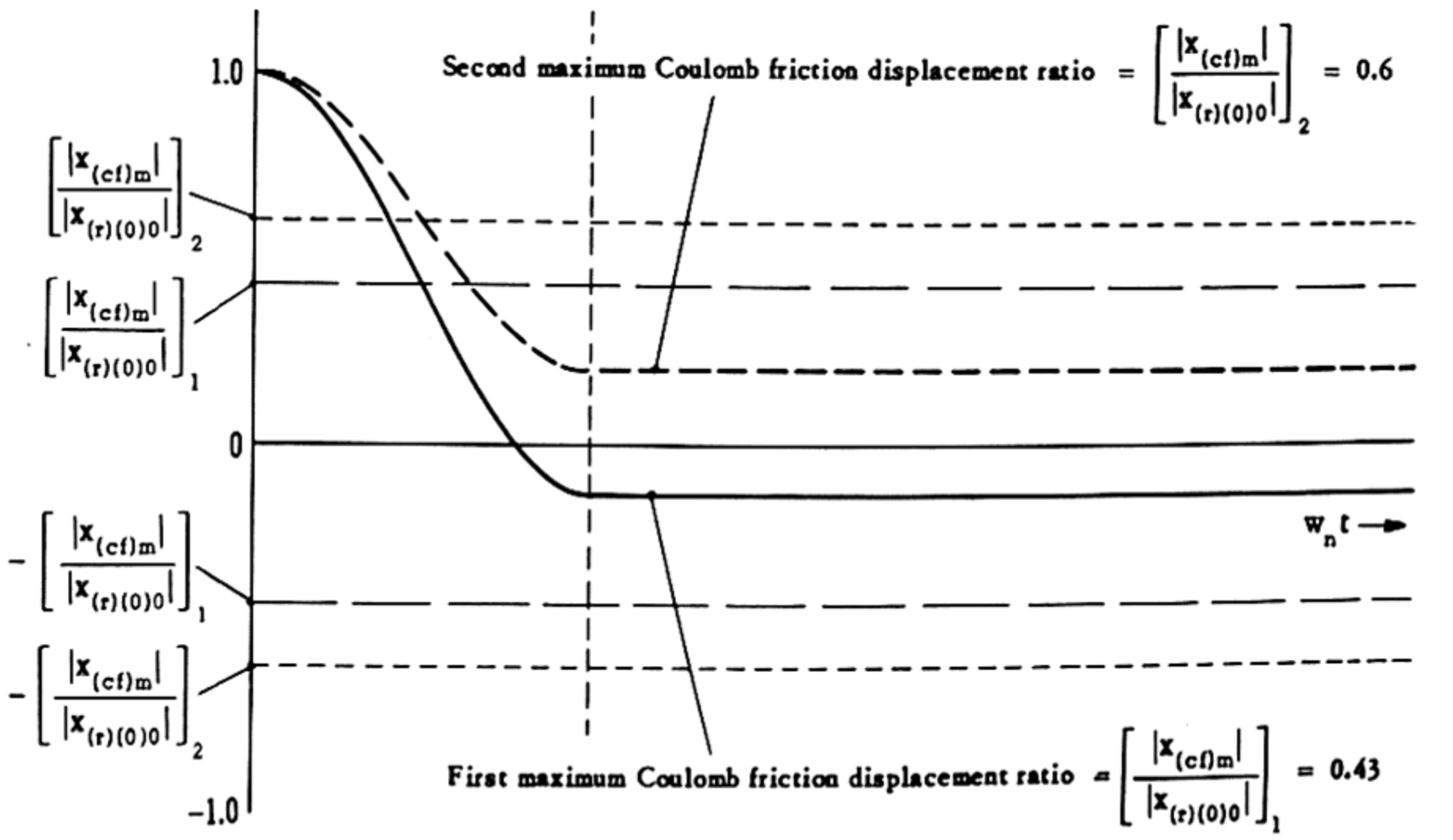
$$m\ddot{x}_r + c\dot{x}_r + kx_r = -m\ddot{x}_f \mp F_{(cf)m}$$

$$\ddot{x}_r + 2(DR)_{(vde)}w_n\dot{x}_r + w_n^2 x_r = \frac{1}{w_n^2} j^2 w_n^2 \ddot{x}_f \mp w_n^2 |x_{(cf)m}| \; ; \; |x_{(cf)m}| = \frac{|F_{(cf)m}|}{k}$$





a) Oscillatory transient response for zero viscous damping



b) Nonoscillatory transient response for zero viscous damping

Fig. 35-25. Illustrative step function transient response curves for the seismographic system with Coulomb damping and no viscous damping; step function transient response equations for the seismographic system with combined viscous damping and Coulomb damping. (Page 1 of 2)

$\underline{(DR)_{(vde)} < 1}$

For Interval 0 only (note that any peak may be taken as the zeroth peak),

$$\left[\frac{x_r}{x_{(r)(0)0}}\right]_0 = \frac{1}{\cos(PA)_{(fc)}}\left(1 - \frac{|x_{(cf)m}|}{|x_{(r)(0)0}|}\right)\epsilon^{-t/(CT)_{(ldr)}}\cos[wt + (PA)_{(fc)}] + \frac{|x_{(cf)m}|}{|x_{(r)(0)0}|}$$

= relative displacement ratio

where

$$(PA)_{(fc)} = \tan^{-1} - \frac{(DR)_{(vde)}}{\sqrt{1 - (DR)^2_{(vde)}}}$$

= fitting constant phase angle

The peak value of the relative displacement ratio for the beginning of the mth interval is

$$\left[\frac{x_r}{x_{(r)(0)0}}\right]_{(t = m\pi/w)} = (-1)^m\left\{\left(1 - \frac{|x_{(cf)m}|}{|x_{(r)(0)0}|}\right)\epsilon^{-m\pi/w(CT)_{(ldr)}} - \frac{|x_{(cf)m}|}{|x_{(r)(0)0}|}\left[1 + 2\left(\epsilon^{-\pi/w(CT)_{(ldr)}} + \epsilon^{-2\pi/w(CT)_{(ldr)}} + \ldots + \epsilon^{-(m-1)\pi/w(CT)_{(ldr)}}\right)\right]\right\}$$

When the viscous damping is zero, this equation reduces to

$$\left[\frac{x_{(r)0}}{x_{(r)(0)0}}\right]_{(m)((DR)_{(vde)}=0)} = (-1)^m\left(1 - 2m\frac{|x_{(cf)m}|}{|x_{(r)(0)0}|}\right)$$

$\underline{(DR)_{(vde)} = 1}$

$$\frac{x_r - |x_{(cf)m}|}{x_{(r)0} - |x_{(cf)m}|} = \epsilon^{-t/(CT)_{(ldr)}} + \frac{t}{(CT)_{(ldr)}}\epsilon^{-t/(CT)_{(ldr)}}$$

$\underline{(DR)_{(vde)} > 1}$

$$\frac{x_r - |x_{(cf)m}|}{x_{(r)0} - |x_{(cf)m}|} = \frac{[(CT)R]_{(hdr)}}{[(CT)R]_{(hdr)} - 1}\left[\epsilon^{-t/(CT)_{(hdr)(larger)}} - \frac{1}{[(CT)R]_{(hdr)}}\epsilon^{-[(CT)R]_{(hdr)}t/(CT)_{(hdr)(larger)}}\right]$$

Notes: 1. See Table 19-1 for definitions and names of symbols.
2. See Derivation Summary 26-1 for the development of these equations in working variable terms.
3. All equations are based on zero case displacement with respect to inertial reference space (i.e., $x_f = 0$).
4. In the symbol $x_{(r)(0)0}$, the first zero of the subscript identifies the represented value of the relative displacement, x_r, as an initial value. The second zero of the subscript identifies the initial value as being associated with the first interval, beginning at $t = 0$.
5. The ratio $|x_{(cf)m}|/|x_{(r)(0)0}|$ is defined as the maximum Coulomb friction displacement – initial peak maximum magnitude ratio, and is represented by the self-defining symbol (MCFD)(IPM)MR, in which
MCFD = $x_{(cf)m}$ = maximum Coulomb friction displacement
IPM = $x_{(r)(0)0}$ = initial peak maximum

c) Step function transient response equations for the seismographic system with combined viscous damping and Coulomb damping

Fig. 35-25. Illustrative step function transient response curves for the seismographic system with Coulomb damping and no viscous damping; step function transient response equations for the seismographic system with combined viscous damping and Coulomb damping. (Page 2 of 2)

with the relative displacement ratio somewhere within the limits set by the maximum Coulomb friction displacement – initial peak maximum magnitude ratio lines.

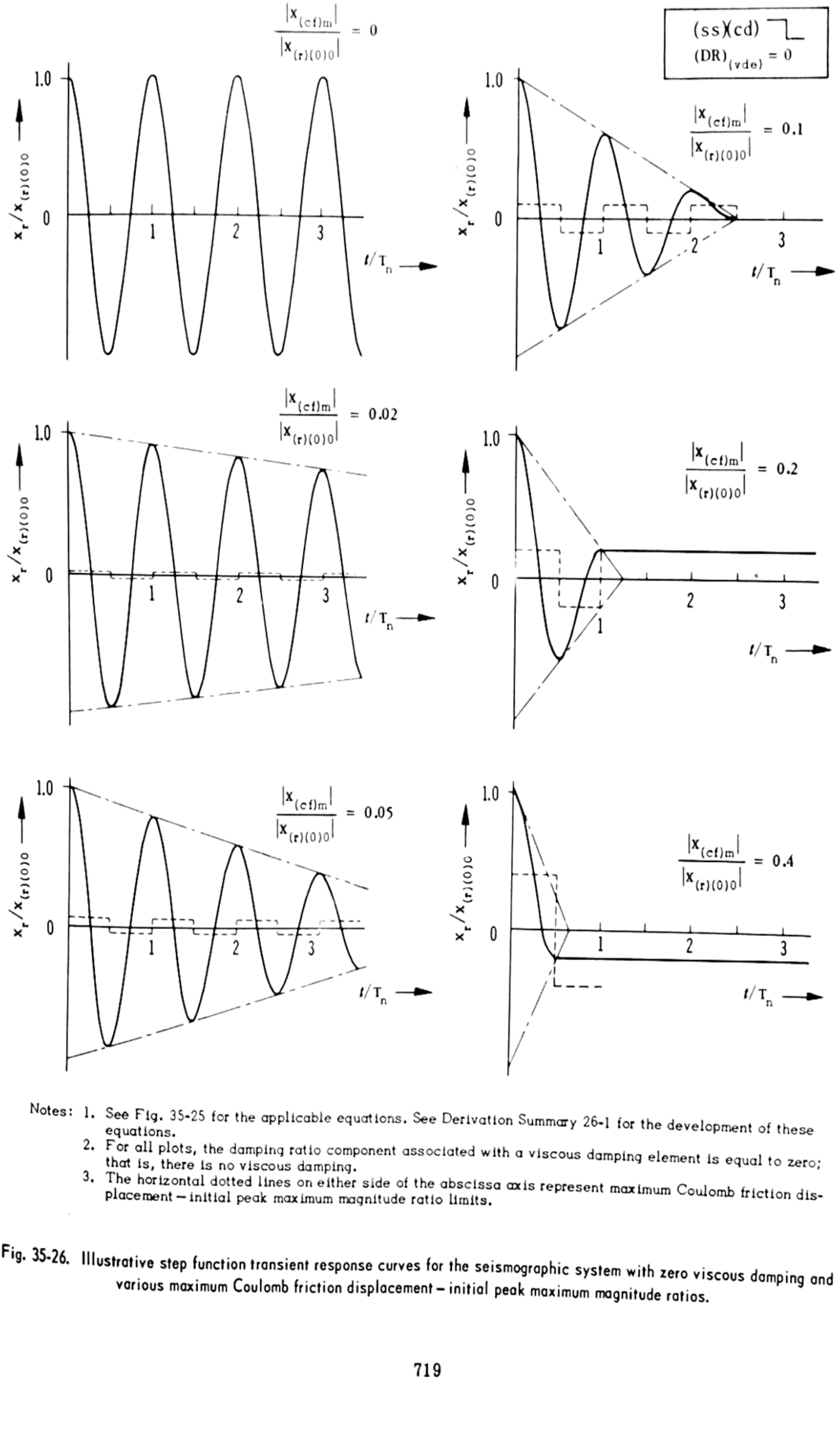
35.206. When no viscous damping is present, the shifting axis of equilibrium for the successive half cycles of transient response corresponds to a reduction of twice the maximum Coulomb friction displacement – initial peak maximum magnitude ratio during each half-cycle interval of the oscillation. This means that for each complete cycle the peak amplitude ratio is reduced by four times the maximum

Coulomb friction displacement – initial peak maximum magnitude ratio. The corresponding envelope of the step function transient curve is made up of two straight lines sloping inward toward the abscissa axis as the time – undamped natural period ratio increases. The amount of this slope per cycle is four times the ordinate equal to the maximum Coulomb friction displacement – initial peak maximum magnitude ratio. Section b of Fig. 35-25 shows two cases in which the kinetic energy associated with the seismic element when it enters the Coulomb friction zone across one limit is not sufficient to carry it outside the other limit. As indicated, the seismic element stops closer to the limit of entry as the maximum Coulomb friction displacement – initial peak maximum magnitude ratio is made larger.

35.207. In practice, seismographic systems often operate with both viscous damping and Coulomb damping. The range of combinations of these two effects is so great that it is not feasible to show a generalized representation of all the possible cases in a simple fashion. However, a reasonable coverage of practical situations is given by the curves of Figs. 35-26, 35-27 and 35-28. Figure 35-26 shows the effect of varying the maximum Coulomb friction displacement – initial peak maximum magnitude ratio from 0 to 0.4 when no viscous damping is present. Values of this ratio less than 0.1 give step function transients similar to those that occur in second-order systems with viscous damping sufficient to produce damping ratios less than 0.1. Values of this ratio greater than 0.2 are very effective in stopping the relative motion of step function transients. In general, some relative displacement remains after the seismic element is brought to rest. That is, the seismic element "sticks off" from the position of zero elastic element force because of Coulomb friction.

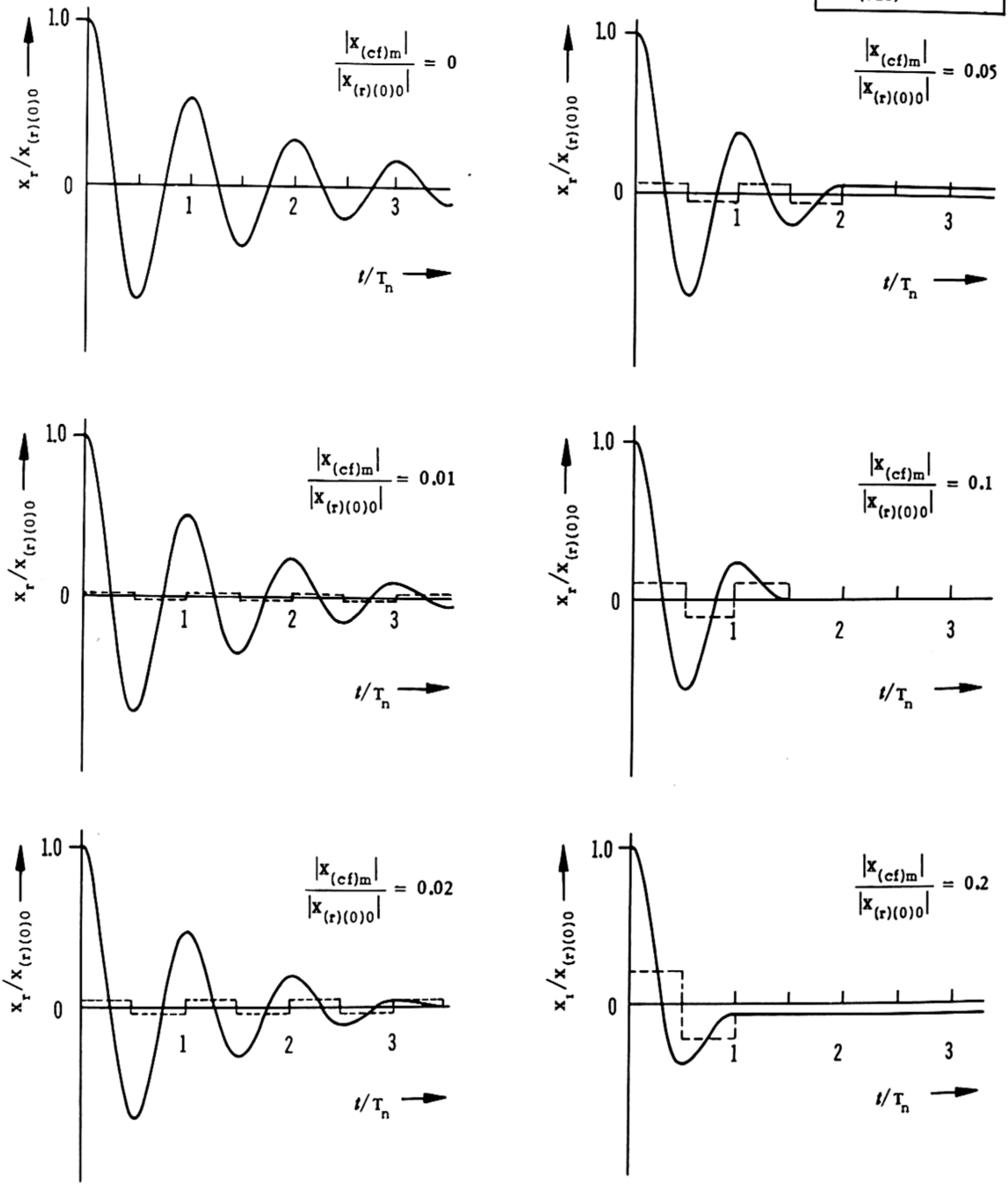
35.208. Figure 35-27 shows the effect of combining various maximum Coulomb friction displacement – initial peak maximum magnitude ratios from zero to 0.2 with the viscous damping that corresponds to a damping ratio component of 0.1. Figure 35-28 gives a similar set of curves for the same range of maximum Coulomb friction displacement – initial peak maximum magnitude ratios combined with the viscous damping that produces a damping ratio component of 0.2. The common pattern shown by each set of curves is a variation from the exponential envelope of viscous damping alone to the steep decay and residual displacement characteristic of second-order systems strongly damped by Coulomb friction.

35.209. Paragraphs 26.12 through 26.18 of Chapter 26 describe procedures for determining the viscous damping and the Coulomb damping components present in a given system by use of a step function transient from the system. These procedures and the equations given in Fig. 35-25 make it possible to handle the Coulomb-friction problems that are ordinarily encountered in applications of seismographic systems to the measurement of vibration.



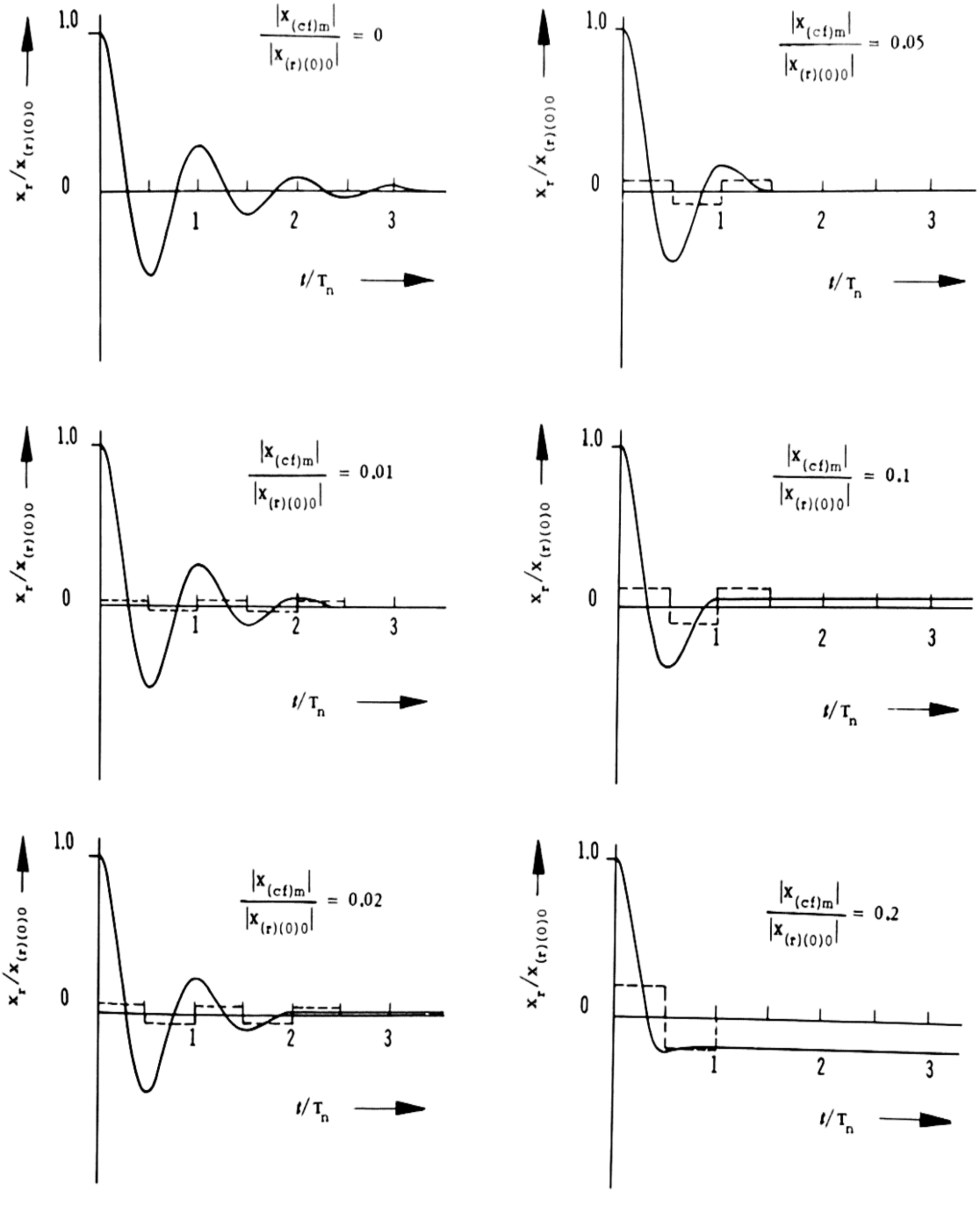
Notes:
1. See Fig. 35-25 for the applicable equations. See Derivation Summary 26-1 for the development of these equations.
2. For all plots, the damping ratio component associated with a viscous damping element is equal to zero; that is, there is no viscous damping.
3. The horizontal dotted lines on either side of the abscissa axis represent maximum Coulomb friction displacement – initial peak maximum magnitude ratio limits.

Fig. 35-26. Illustrative step function transient response curves for the seismographic system with zero viscous damping and various maximum Coulomb friction displacement – initial peak maximum magnitude ratios.



Notes: 1. See Fig. 35-25 for the applicable equations. See Derivation Summary 26-1 for the development of these equations.
2. For all plots, the damping ratio component due to the viscous damping element acting with no Coulomb friction present in the seismographic system is equal to 0.1.
3. The horizontal dotted lines on either side of the abscissa axis represent maximum Coulomb friction displacement – initial peak maximum magnitude ratio limits.

Fig. 35-27. Illustrative step function transient response curves for the seismographic system with the damping ratio component due to viscous damping equal to 0.1 and various maximum Coulomb friction displacement – initial peak maximum magnitude ratios.



Notes:
1. See Fig. 35-25 for the applicable equations. See Derivation Summary 26-1.for the development of these equations.
2. For all plots, the damping ratio component due to the viscous damping element acting with no Coulomb friction in the seismographic system is equal to 0.2.
3. The horizontal dotted lines on either side of the abscissa axis represent maximum Coulomb friction displacement – initial peak maximum magnitude ratio limits.

Fig. 35-28. Illustrative step function transient response curves for the seismographic system with the damping ratio component due to viscous damping equal to 0.2 and various maximum Coulomb friction displacement – initial peak maximum magnitude ratios.

STEADY-STATE RESPONSE OF THE SEISMOGRAPHIC SYSTEM WITH COMBINED VISCOUS DAMPING AND COULOMB DAMPING

35.210. Equations (1) and (2) of Derivation Summary 35-6 describe the performance of the seismographic system in physical terms and in working variable terms, respectively. Equation (4) is a rewritten form of Eq. (1) in which the Coulomb friction term is replaced by a first derivative term containing an equivalent Coulomb friction damping ratio component. The theory for determining this Coulomb friction damping ratio component is outlined in section c of Derivation Summary 35-6. This development is based on a steady-state relative displacement of sustantially sinusoidal form. An expression for the viscous damping energy dissipation per cycle is written as Eq. (11), and the corresponding expression for Coulomb friction damping is given as Eq. (13). These two energy dissipation expressions, with the viscous damping element coefficient, $c_{(vde)}$, of Eq. (11) replaced by the Coulomb friction equivalent viscous damping coefficient, $c_{(vd)(equiv)(cf)}$, are equated in Eq. (14), and a solution for the equivalent viscous damping coefficient that will give an energy dissipation equal to the actual Coulomb friction dissipation is obtained in Eq. (15). The relationships of Table 19-1 are applied in finding the Coulomb friction equivalent damping ratio given by Eqs. (19), (20) and (21) of Derivation Summary 35-6.

35.211. Section d of Derivation Summary 35-6 gives the performance function for the seismographic system with combined viscous and Coulomb damping, based on the resultant damping ratio. In section e of Derivation Summary 35-6, the performance function is developed for the seismographic system with negligible viscous damping, but with Coulomb friction force of appreciable magnitude. The result is summarized by Eqs. (34), (35), (36) and (37), which give the dimensionless dynamic amplitude ratio and the dynamic response angle in terms of the maximum Coulomb friction displacement - relative displacement amplitude ratio and the frequency ratio.

35.212. The dimensionless sensitivity ratio relationship of Eq. (34) has a numerator that becomes imaginary when the square of $4/\pi$ multipled by the square of the maximum Coulomb friction displacement - relative displacement amplitude ratio exceeds the fourth power of the frequency ratio. When this condition exists, the dimensionless sensitivity ratio is imaginary, and corresponds on the physical side to a nonexistent relative motion. When the numerator of the dimensionless sensitivity ratio becomes real, relative motion starts to exist. Because this action corresponds to the seismic element "breaking away" from the supporting element, the frequency ratio at which it occurs is called the breakaway frequency ratio. This quantity is determined by Eq. (34) of Derivation Summary 35-6 and is given as an explicit expression by Eq. (38).

35.213. From the standpoint of physical action, the breakaway point, or

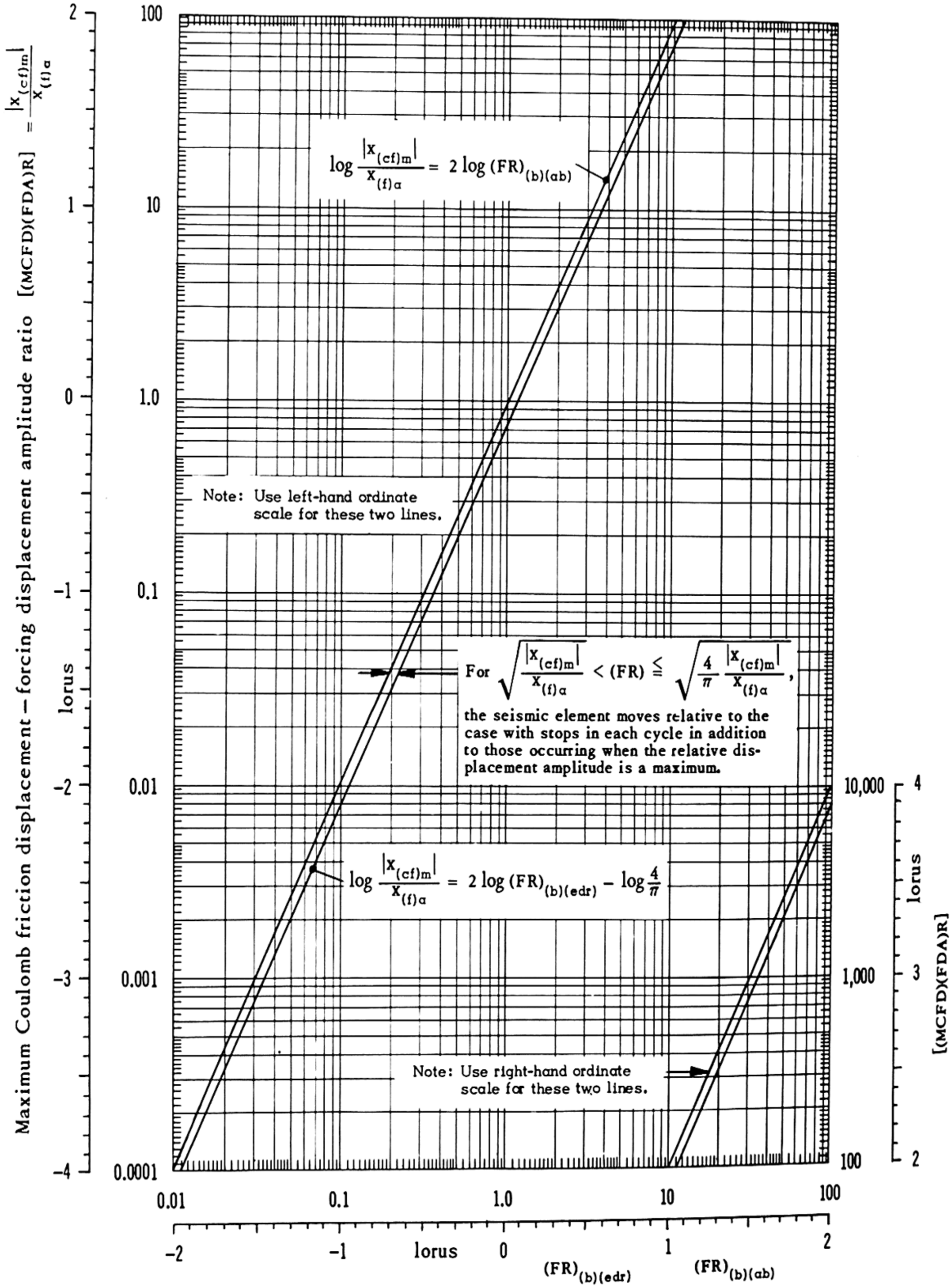
breakaway frequency, that corresponds to the breakaway frequency ratio occurs when the peak acceleration given to the seismic element by the supporting element produces an inertia reaction force just equal to the maximum magnitude of the Coulomb friction force.* The breakaway frequency thus depends on both the forcing frequency and the forcing amplitude. The relationship involved is given by Eq. (39) of Derivation Summary 35-6, which is taken from Eq. (1) when the relative displacement and its first and second derivatives are all zero. The result of solving this equation for the acceleration-balance breakaway frequency ratio is given by Eq. (44). A comparison of this equation with Eq. (38) shows that the two breakaway frequency ratios differ by a multiplying factor with the magnitude of the square root of $4/\pi$. Information on the mathematical relationships that determine the two breakaway frequency ratios is summarized in section h of Derivation Summary 35-6. The corresponding breakaway-point equations are plotted on logarithmic coordinates in Fig. 35-29. Breakaway frequency ratios are plotted as abscissae, and maximum Coulomb friction displacement – forcing amplitude ratios are plotted as ordinates. Both the acceleration-balance and equivalent-damping-ratio values give straight lines. These two lines have a relative displacement parallel to the axis of ordinates equal to the logarithm of $4/\pi$, measured on the loru scale. The lines of Fig. 35-29 may be used to identify immediately the breakaway frequency ratio for any given Coulomb friction effect when the forcing amplitude is known.

35.214. Figure 35-30 gives a linear scale family of dimensionless sensitivity ratio curves plotted from Eq. (34) of Derivation Summary 35-6. This equation describes the action of the seismographic system with Coulomb damping but no viscous damping. When the maximum Coulomb friction force is substantially zero, the dimensionless sensitivity ratio curve is identical with the zero maximum Coulomb friction displacement – forcing displacement amplitude ratio curve of Fig. 35-30. As the maximum Coulomb friction displacement – forcing displacement amplitude ratio increases, the dimensionless sensitivity ratio is zero until the breakaway frequency ratio** given by the plots of Fig. 35-29 is reached. From this point, the dimensionless sensitivity ratio increases, and finally becomes identical with the zero Coulomb damping curve,*** that is, the curve for which the maximum Coulomb friction displacement – forcing displacement amplitude ratio is equal to zero. The transition interval on the frequency ratio scale is small for small values of the maximum Coulomb friction displacement – forcing displacement amplitude ratio and increases as this ratio changes toward larger values.

* This is under the assumption that the seismic element is in its zero-relative-displacement position prior to breaking away.

** The two lines of Fig. 35-29 give the equivalent damping ratio breakaway frequency ratio and the acceleration-balance breakaway frequency ratio. These two breakaway points have values that are substantially identical as far as practical applications are concerned.

*** This curve is also identical with the corresponding zero viscous damping curve.



$(FR)_{(b)(edr)} = \sqrt{\frac{4}{\pi}} \sqrt{\frac{|X_{(cf)m}|}{X_{(f)a}}}$ = equivalent damping ratio breakaway frequency ratio for the seismographic system

$(FR)_{(b)(ab)} = \sqrt{\frac{|X_{(cf)m}|}{X_{(f)a}}}$ = acceleration-balance breakaway frequency ratio for the seismographic system

Fig. 35-29. Maximum Coulomb friction displacement – forcing displacement amplitude ratio as a function of breakaway frequency ratio for the seismographic system.

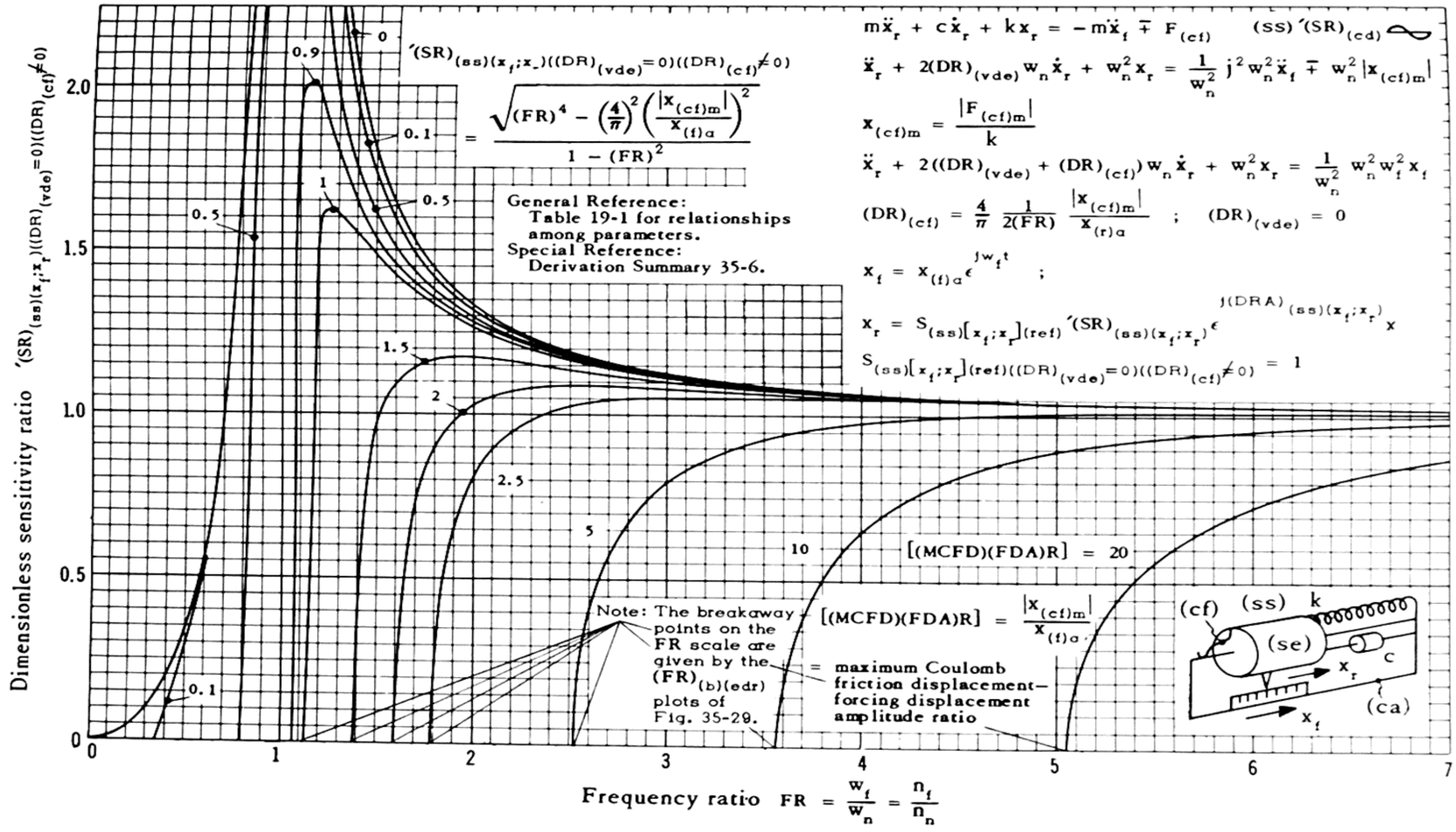


Fig. 35-30. Linear-scale plots of the forcing displacement input – relative displacement output dimensionless sensitivity ratio as a function of frequency ratio for the seismographic system with Coulomb damping only.

35.215. Figure 35-31 is the linear-scale family of dynamic response angle curves that corresponds to the dimensionless sensitivity ratio plots of Fig. 35-30. The dynamic response angle curves of Fig. 35-31 are based on Eq. (37) of Derivation Summary 35-6. The essential feature of this family is that the curves for all values of the maximum Coulomb friction displacement – forcing displacement amplitude ratio approach –180 degrees as the frequency ratio becomes larger. Near the breakaway points on the frequency ratio scale, the dynamic response angle changes sharply from an initial value of –90 degrees. For breakaway points at frequency ratios less than unity, the angle first has a steep increase to smaller negative values until unity frequency ratio is reached; at this point, the angle suddenly decreases to a curve that changes toward the –180-degree asymptote. For breakaway points at frequency ratios greater than unity, the dynamic response angle starts at –90 degrees and then decreases smoothly toward the asymptotic value.

SINGLE-DEGREE-OF-FREEDOM VIBRATION ISOLATION

35.216. Vibration components of considerable magnitude are often present in the motion of structural members from which operating equipment must be suspended. When the connection between the supporting member and the operating equipment is rigid, the vibration may cause malfunctions or even failures of the equipment. For this reason, it is important to develop the theory of vibration isolation, which deals with methods for reducing the vibratory motion of an isolated member carried by a vibrating support. The elements of the vibration isolation problem are shown in the diagram of section a of Derivation Summary 35-7. In order to illustrate the essential features in terms that are amenable to a simple and effective mathematical treatment, the figure shows a single-degree-of-freedom arrangement in which the isolated member is free to slide on four rods that are rigidly attached to the support and act as the supporting members. The isolated member is coupled to the support by means of coil springs that supply the elastic element function and a viscous damping element. Coulomb friction is introduced by bushings in the isolated member that slide over the supporting members.

35.217. A comparison of the single-degree-of-freedom vibration isolation system of section a of Derivation Summary 35-7 with the single-degree-of-freedom seismographic system of section a of Derivation Summary 35-1 shows that the physical elements of the two systems are similar. From the standpoint of theory, the performance equation developed in section c of Derivation Summary 35-1 applies equally to both systems. For practical application of results based on the performance equation, the motion of the seismic element with respect to the case is of primary interest for seismographic systems, while the motion of the isolated member with respect to inertial space* is the important quantity for vibration

* In vibration isolation, the inertia reaction force accompanying acceleration with respect to inertial space is the essential factor. This acceleration is determined by the inertial-space motion of the isolated member.

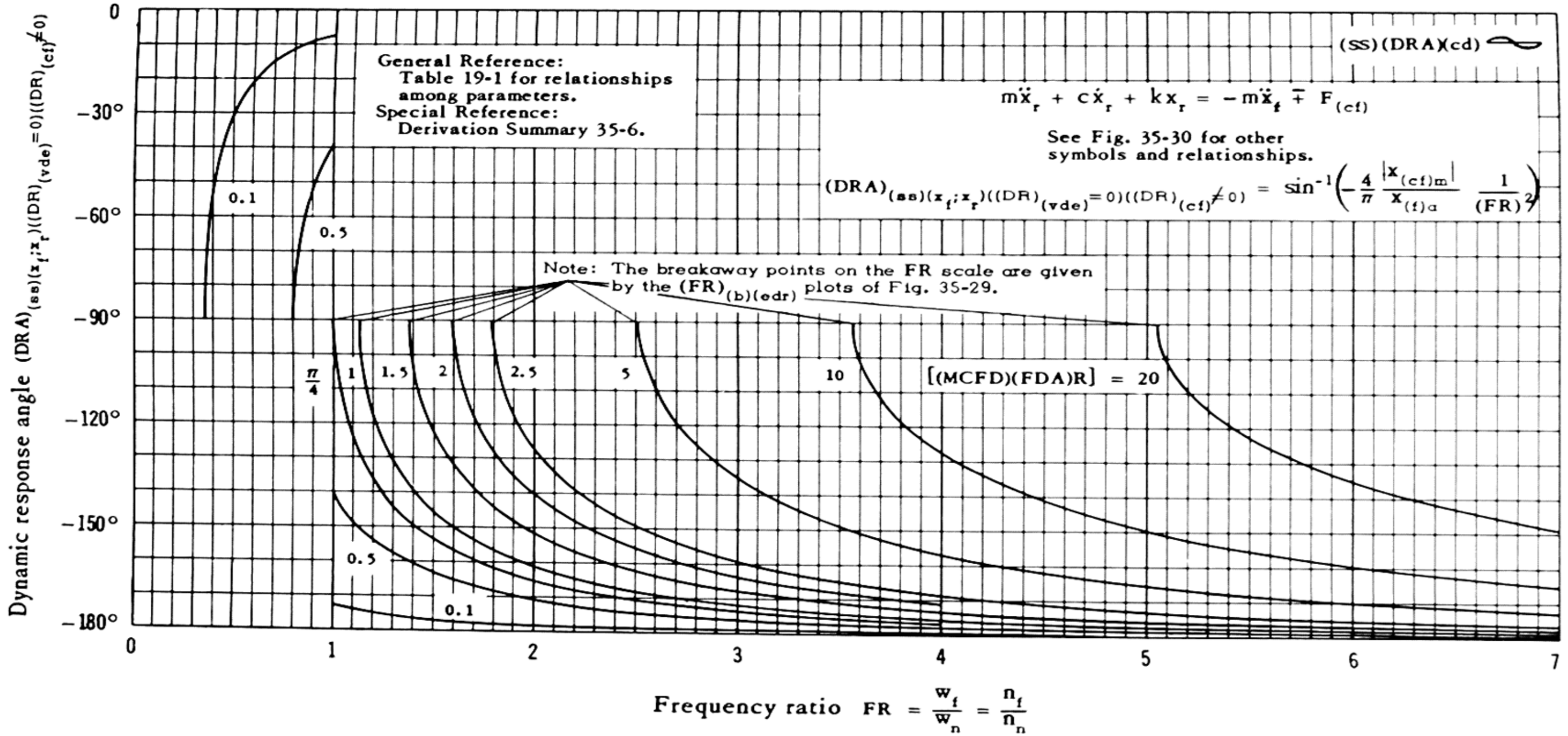
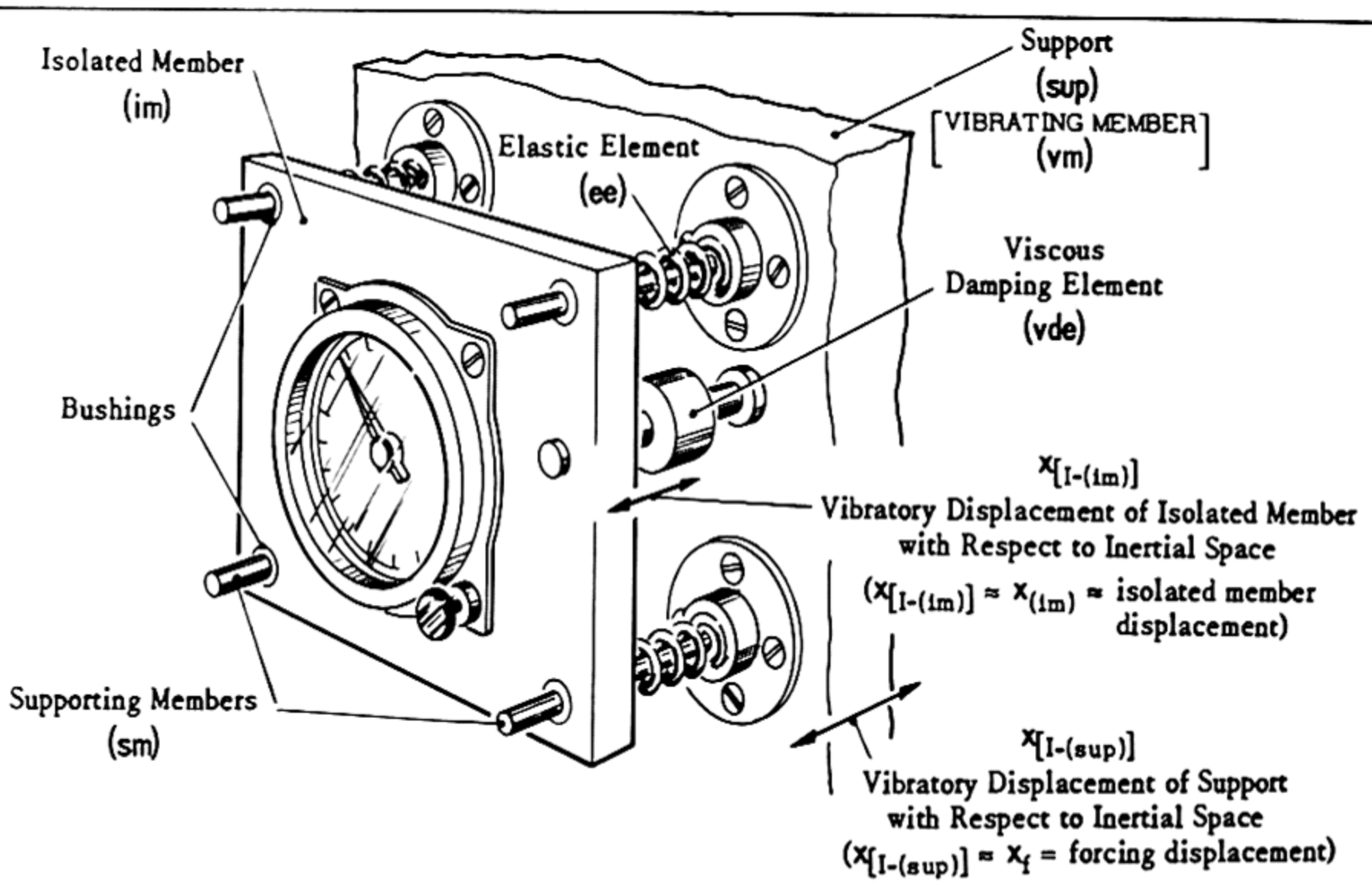


Fig. 35-31. Linear-scale plots of the forcing displacement input – relative displacement output dynamic response angle as a function of frequency ratio for the seismographic system with Coulomb damping only.



a) Illustrative pictorial diagram of the single-degree-of-freedom vibratory motion isolation problem

Geometrical relationships:

$$x_{[I-(im)]} = x_{[I-(sup)]} + x_{[(sup)-(im)]} \quad ; \quad x_{[(sup)-(im)]} = x_{[I-(im)]} - x_{[I-(sup)]} \qquad (1),(2)$$

(ee) Elastic element

$$F_{(ee)} = -S_{(ee)|x_{[(sup)-(im)]};F|}\, x_{[(sup)-(im)]} = -k_{(ee)}\, x_{[(sup)-(im)]} \qquad (3)$$

where

$S_{(ee)|x_{[(sup)-(im)]};F|}$ = relative displacement – force sensitivity of the elastic element

$\equiv k_{(ee)}$ = elastic coefficient of the elastic element

(vde) Viscous damping element

$$F_{(vde)} = -S_{(vde)|\dot{x}_{[(sup)-(im)]};F|}\, \dot{x}_{[(sup)-(im)]} = -c_{(vde)}\, \dot{x}_{[(sup)-(im)]} \qquad (4)$$

where

$S_{(vde)|\dot{x}_{[(sup)-(im)]};F|}$ = relative velocity – force sensitivity of the viscous damping element

$\equiv c_{(vde)}$ = damping coefficient of the viscous damping element

(cfe) Coulomb friction element

$$F_{(cf)} = \pm |F_{(cf)}| \qquad (5)$$

= Coulomb friction force

Note: When $\dot{x}_{[(sup)-(im)]} \neq 0$, $F_{(cf)}$ is constant in magnitude and equal to the maximum Coulomb friction force, $F_{(cf)m}$. When $\dot{x}_{[(sup)-(im)]} = 0$, $F_{(cf)}$ is equal and opposite to the resultant of all the other forces.

(ims) Isolated member system

The equation of motion of the isolated member system for the case when $\dot{x}_{[(sup)-(im)]} \neq 0$ can be written from a summation of forces as follows:

$$-m_{(im)}\ddot{x}_{[I-(im)]} - c_{(vde)}\left[\dot{x}_{[I-(im)]} - \dot{x}_{[I-(sup)]}\right] - k_{(ee)}\left[x_{[I-(im)]} - x_{[I-(sup)]}\right] \mp |F_{(cf)m}| = 0 \qquad (6)$$

where

$m_{(im)}$ = effective mass of the isolated member

Derivation Summary 35-7. The (1,0;0,1,2) relating function and the performance function for the single-degree-of-freedom vibratory motion isolation system with viscous damping only.
(Page 1 of 4)

Changing signs on all terms of Eq. (6) and rearranging terms gives

$$m_{(1m)}\ddot{x}_{[1-(1m)]} + c_{(vde)}\dot{x}_{[1-(1m)]} + k_{(ee)}x_{[1-(1m)]} = k_{(ee)}x_{[1-(sup)]} + c_{(vde)}\dot{x}_{[1-(sup)]} \mp |F_{(cf)m}| \quad (7)$$

When each term of Eq. (7) is divided by $m_{(1m)}$, $x_{[1-(1m)]}$ is replaced by $x_{(1m)}$ and $x_{[1-(sup)]}$ by x_f, and the relationships of Table 19-1 are used, Eq. (7) becomes the equation of single-degree-of-freedom vibration isolation, which is

$$\ddot{x}_{(1m)} + 2(DR)\,w_n\dot{x}_{(1m)} + w_n^2 x_{(1m)} = w_n^2 x_f + 2(DR)\,w_n\dot{x}_f \mp w_n^2 |x_{(cf)m}| \quad (8)$$

where

$|x_{(cf)m}| = \dfrac{F_{(cf)m}}{k_{(ee)}}$ = maximum Coulomb friction displacement magnitude in the isolated member system

b) Single-degree-of-freedom vibration isolation equation

In working variable terms, the vibration isolation equation is

$$\ddot{v} + 2\zeta\omega_n\dot{v} + \omega_n^2 v = \omega_n^2 u + 2\zeta\omega_n\dot{u} \mp \omega_n^2 u_{(rs)} \quad (9)$$

where

$$v = x_{(1m)} \quad ; \quad \zeta = DR \quad ; \quad u = x_f \quad ; \quad u_{(rs)} = x_{(cf)m} \quad ; \quad \omega_n = w_n$$

The symbols ζ, DR, ω_n and w_n are defined in Table 19-1.

When no Coulomb friction is present, Eq. (9) becomes

$$\ddot{v} + 2\zeta\omega_n\dot{v} + \omega_n^2 v = \omega_n^2 u + 2\zeta\omega_n\dot{u} \quad (10)$$

Equation (10) has the (1,0;0,1,2) differential equation form. The sinusoidal relating function for this form is developed in Derivation Summaries 19-9 and 19-13. For reference purposes, a simplified development of this relating function is given here.

Assume

$$u = u_a e^{j\omega_f t} \quad (11)$$

so that

$$\dot{u} = j\omega_f u_a e^{j\omega_f t} = (j\omega_f)u \quad (12)$$

Then Eq. (10) becomes

$$\ddot{v} + 2\zeta\omega_n\dot{v} + \omega_n^2 v = \omega_n^2 u + 2\zeta\omega_n j\omega_f\dot{u} \quad (13)$$

Assume

$$v = \eta u \quad (14)$$

where the relating function η is to be determined. From Eq. (14),

$$\dot{v} = \eta u = \eta j\omega_f u \quad (15)$$

$$\ddot{v} = \eta\ddot{u} = \eta(j\omega_f)^2 u = -\eta\omega_f^2 u \quad (16)$$

Substituting the expressions of Eqs. (14), (15) and (16) in Eq. (13) gives

$$\eta(-\omega_f^2 + j2\zeta\omega_n\omega_f + \omega_n^2)u = (\omega_n^2 + j2\zeta\omega_n\omega_f)u \quad (17)$$

The relating function, η, is determined from Eq. (17) to be

$$\eta_{(1,0;0,1,2)} = \frac{\omega_n^2 + j2\zeta\omega_n\omega_f}{\omega_n^2 - \omega_f^2 + j2\zeta\omega_n\omega_f} \quad (18)$$

Dividing each term of Eq. (18) by ω_n^2 changes this equation to

$$\eta_{(1,0;0,1,2)} = \frac{1 + j2\zeta\beta}{1 - \beta^2 + j2\zeta\beta} \quad (19)$$

Derivation Summary 35-7. The (1,0;0,1,2) relating function and the performance function for the single-degree-of-freedom vibratory motion isolation system with viscous damping only.
(Page 2 of 4)

where

$$\beta = \frac{\omega_f}{\omega_n} = \frac{n_f}{n_n} = \frac{T_n}{T_f} = \text{frequency ratio}$$

The denominator of Eq. (19) is identical with the denominator of the relating function developed in Derivation Summary 35-2, which is similar to the (0;0,1,2) relating function of Derivation Summary 19-10. The dynamic amplitude ratio–dynamic response angle form of the relating function may be taken directly from this latter summary as

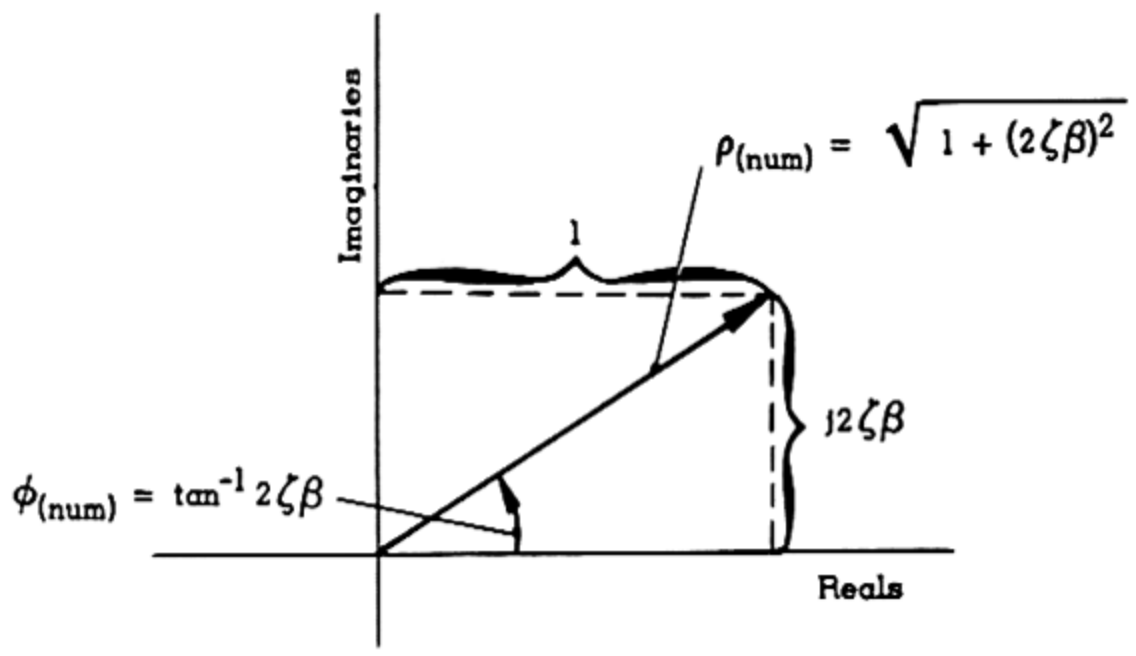
$$\eta_{(0;0,1,2)} = \frac{1}{1 - \beta^2 + j2\zeta\beta} = \rho_{(0;0,1,2)} \epsilon^{j\phi_{(0;0,1,2)}} \tag{20}$$

where

$$\rho_{(0;0,1,2)} = \frac{1}{\sqrt{(1-\beta^2)^2 + (2\zeta\beta)^2}} \tag{21}$$

$$\phi_{(0;0,1,2)} = \tan^{-1}\left[\frac{-2\zeta\beta}{1-\beta^2}\right] \tag{22}$$

The graphical representation for the numerator of Eq. (19) is



so that

$$1 + j2\zeta\beta = \sqrt{1 + (2\zeta\beta)^2}\, \epsilon^{j \tan^{-1} 2\zeta\beta} \tag{23}$$

Combining Eqs. (19) through (23) gives

$$\eta_{(1,0;0,1,2)} = \frac{1 + j2\zeta\beta}{1 - \beta^2 + j2\zeta\beta} = \frac{\sqrt{1 + (2\zeta\beta)^2}}{\sqrt{(1-\beta^2)^2 + (2\zeta\beta)^2}}\, \epsilon^{j[\tan^{-1}(-2\zeta\beta/(1-\beta^2)) + \tan^{-1} 2\zeta\beta]} \tag{24}$$

$$= \rho_{(1,0;0,1,2)} \epsilon^{j\phi_{(1,0;0,1,2)}} = \rho_r \mu_{(1,0;0,1,2)} \epsilon^{j\phi_{(1,0;0,1,2)}} \tag{25),(26}$$

When

$$\rho_r = 1 \tag{27}$$

then

$$\mu_{(1,0;0,1,2)} = \frac{\sqrt{1 + (2\zeta\beta)^2}}{\sqrt{(1-\beta^2)^2 + (2\zeta\beta)^2}} \tag{28}$$

and

$$\phi_{(1,0;0,1,2)} = \tan^{-1}\left[\frac{-2\zeta\beta}{1-\beta^2}\right] + \tan^{-1} 2\zeta\beta \tag{29}$$

Derivation Summary 35-7. The (1,0;0,1,2) relating function and the performance function for the single-degree-of-freedom vibratory motion isolation system with viscous damping only.
(Page 3 of 4)

In self-defining notation,

$$\eta_{(1,0;0,1,2)} = [PF]_{(vmis)[x_f;x_{(im)}]} = (DAR)_{(vmis)[x_f;x_{(im)}]} \epsilon^{j(DRA)_{(vmis)(x_f;x_{(im)})}} \tag{30}$$

$$= (RAR)_{(vmis)[x_f;x_{(im)}]}[(DAR)(RAR)R]_{(vmis)(x_f;x_{(im)})} \epsilon^{j(DRA)_{(vmis)(x_f;x_{(im)})}} \tag{31}$$

= forcing displacement – isolated member displacement performance function of the single-degree-of-freedom vibratory motion isolation system

$$\rho_{(1,0;0,1,2)} = (DAR)_{(vmis)[x_f;x_{(im)}]} = \frac{\sqrt{1 + [2(DR)(FR)]^2}}{\sqrt{[1 - (FR)^2]^2 + [2(DR)(FR)]^2}} \tag{32}$$

= forcing displacement – isolated member displacement dynamic amplitude ratio of the single-degree-of-freedom vibratory motion isolation system

$$\rho_r = (RAR)_{(vmis)[x_f;x_{(im)}]} = 1 \tag{33}$$

= forcing displacement – isolated member displacement reference amplitude ratio of the single-degree-of-freedom vibratory motion isolation system

$$\mu_{(1,0;0,1,2)} = [(DAR)(RAR)R]_{(vmis)(x_f;x_{(im)})} = \acute{(}DAR)_{(vmis)(x_f;x_{(im)})} = \frac{\sqrt{1 + [2(DR)(FR)]^2}}{\sqrt{[1 - (FR)^2]^2 + [2(DR)(FR)]^2}} \tag{34}$$

where

$[(DAR)(RAR)R]_{(vmis)(x_f;x_{(im)})}$ = forcing displacement – isolated member displacement dynamic amplitude ratio – reference amplitude ratio ratio of the single-degree-of-freedom vibratory motion isolation system

$\acute{(}DAR)_{(vmis)(x_f;x_{(im)})}$ = forcing displacement – isolated member displacement dimensionless dynamic amplitude ratio of the single-degree-of-freedom vibratory motion isolation system

$$\phi_{(1,0;0,1,2)} = (DRA)_{(vmis)(x_f;x_{(im)})} = \tan^{-1}\left[\frac{-2(DR)(FR)}{1 - (FR)^2}\right] + \tan^{-1} 2(DR)(FR) \tag{35}$$

= forcing displacement – isolated member displacement dynamic response angle of the single-degree-of-freedom vibratory motion isolation system

c) Performance function for the vibratory motion isolation system with viscous damping only

Derivation Summary 35-7. The (1,0;0,1,2) relating function and the performance function for the single-degree-of-freedom vibratory motion isolation system with viscous damping only. (Page 4 of 4)

isolation problems. The discussion of this section is directed toward developing engineering information on the factors that affect the vibratory motion of the isolated member with respect to inertial space. When the displacement corresponding to this motion is known, vibratory velocity and vibratory acceleration may be found by conventional methods.

35.218. The pattern of procedure used in Derivation Summary 35-1 for developing the performance equation of the seismographic system is repeated in Eqs. (1) through (6) of Derivation Summary 35-7. Equation (7) of this summary

is the form that appears when terms are rearranged to place the displacement of the isolated member with respect to inertial space as the dependent variable and to show the displacement of the support with respect to inertial space as the forcing function. Equation (8) is written from Eq. (7) as a (1,0;0,1,2) differential equation with an additional Coulomb friction term. Section c of Derivation Summary 35-7 outlines a simplified development of the (1, 0;0, 1, 2) relating function in working variable terms and summarizes the results in Eqs. (30) through (35). From the standpoint of physical action, these results apply to the single-degree-of-freedom vibratory motion isolation system with viscous damping, but without an appreciable amount of Coulomb damping. The vibratory motion isolation system does not receive an input and produce an output for instrumental purposes in the same sense that the seismographic system acts as an operating component in a measuring system. This means that the concept of sensitivity would be out of its proper context if it were used to describe the behavior of the vibratory motion isolation system. For this reason, vibratory motion isolation effects are represented in terms of the dynamic amplitude ratio, which may be resolved into the product of a reference amplitude ratio and a dynamic amplitude ratio – reference amplitude ratio ratio. This latter quantity is identical with the dimensionless dynamic amplitude ratio.

35.219. Figure 35-32 gives a family of curves that represents the dimensionless dynamic amplitude ratio as a function of frequency ratio for the vibratory motion isolation system. The curves of this family are based on Eq. (34) of Derivation Summary 35-7. For all values of the damping ratio, the dimensionless dynamic amplitude ratio, which is identical with the ratio of the isolated member displacement amplitude to the forcing displacement amplitude of the support, starts at unity and remains higher than unity for all frequency ratios less than the square root of two. At this frequency ratio point, all curves pass through unity on the ordinate scale. For all higher frequency ratios, the dimensionless dynamic amplitude ratio is always less than unity, with smaller values associated with lower damping ratios for a given frequency ratio. All curves become asymptotic to zero as the frequency ratio approaches very high values.

35.220. The curve family of Fig. 35-33 is based on Eq. (35) of Derivation Summary 35-7 and gives the dynamic response angles corresponding to the dimensionless dynamic amplitude ratios of Fig. 35-32. These curves all start at zero for zero frequency ratio and asymptotically approach –90 degrees for very large frequency ratios. With low damping ratios, intermediate values of the dynamic response angle go below –90 degrees and approach a minimum near –180 degrees for damping ratios less than 0.1.

35.221. Figure 35-34 is a plot giving the frequency ratio at which the maximum dimensionless dynamic amplitude ratio occurs as a function of damping ratio. Figure 35-35 is a semilogarithmic-scale curve showing the maximum value of the

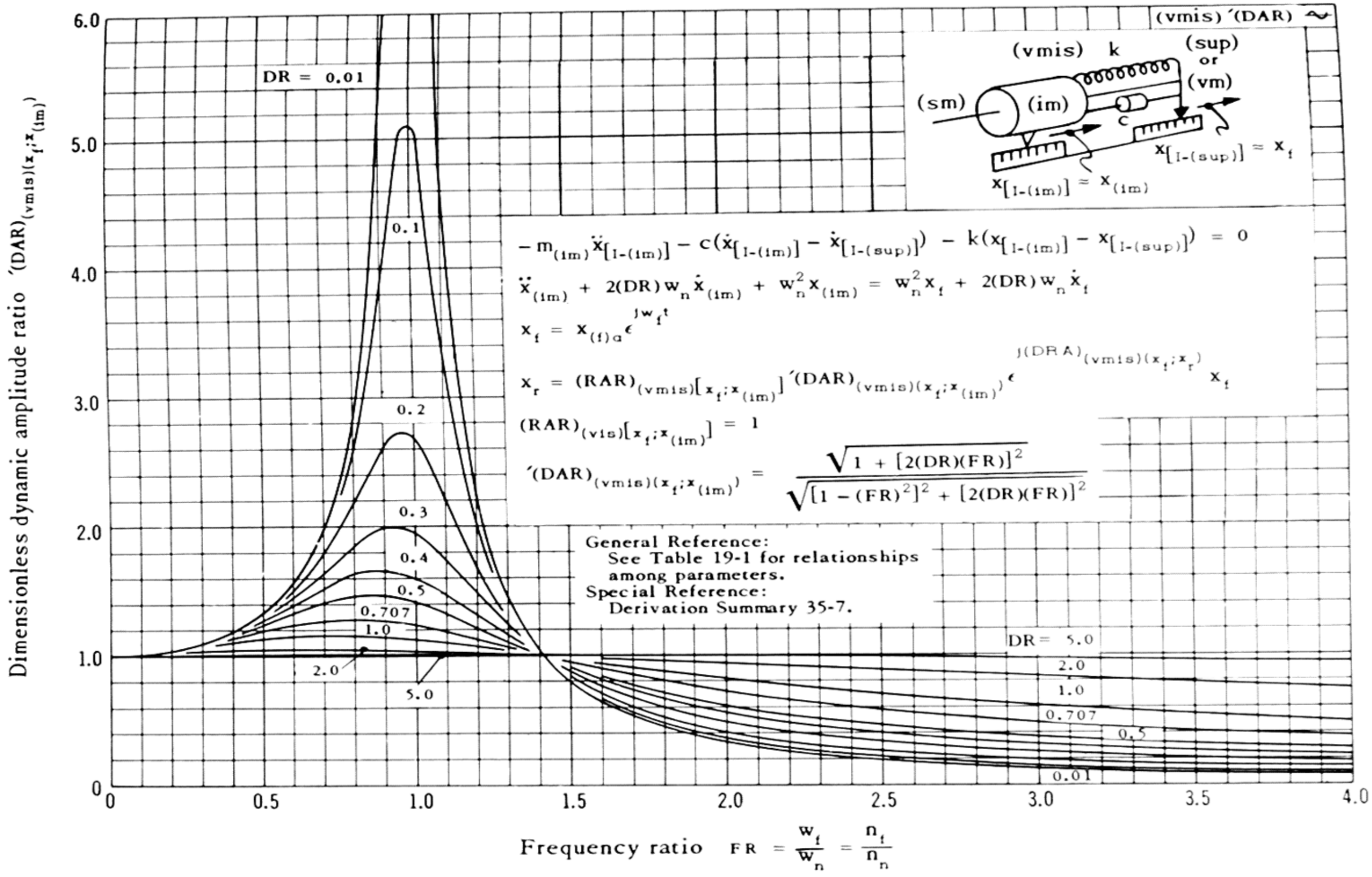


Fig. 35-32. Linear-scale plots of the forcing displacement – isolated member displacement dimensionless dynamic amplitude ratio as a function of frequency ratio for the single-degree-of-freedom vibratory motion isolation system with viscous friction only.

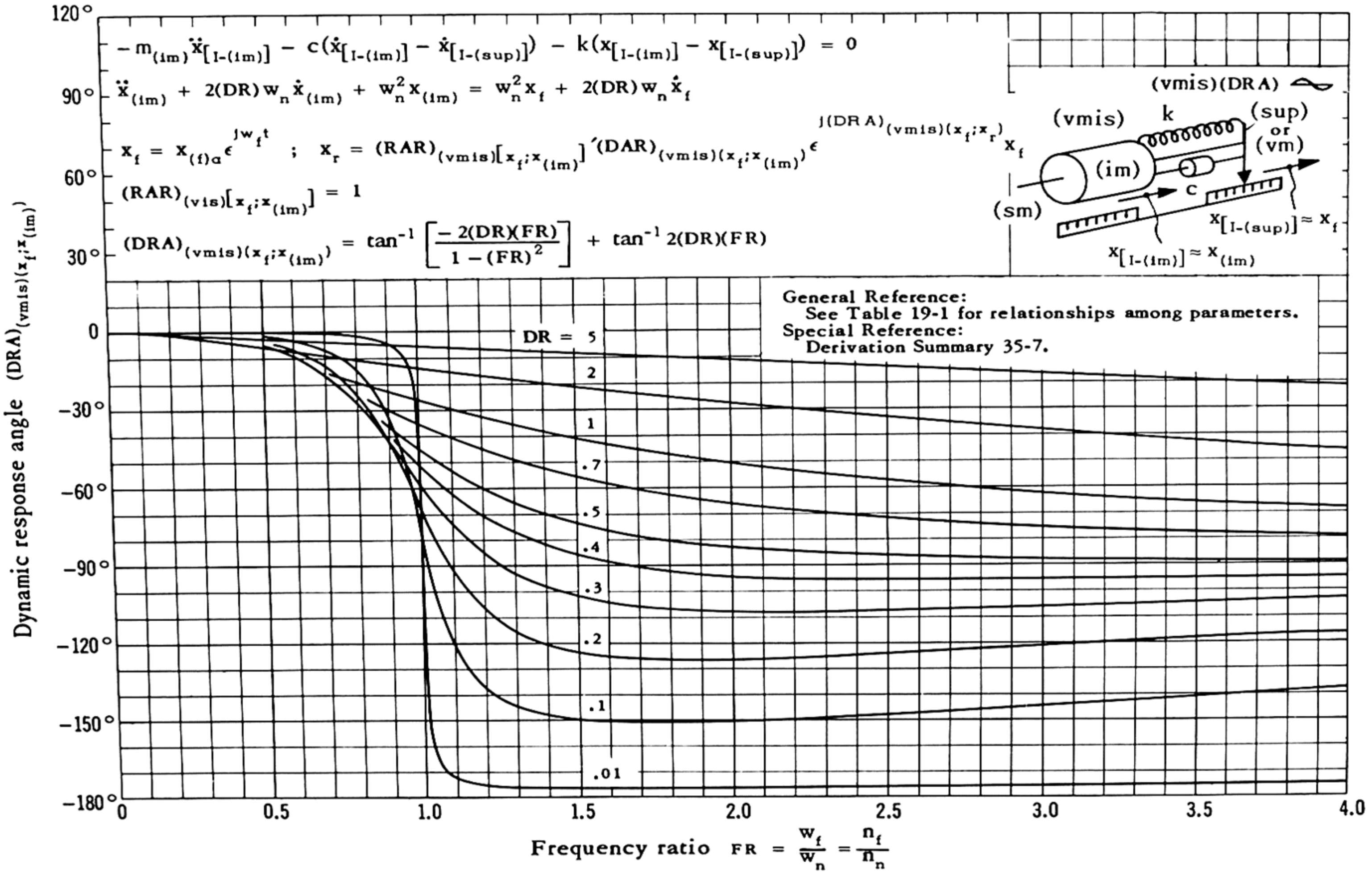


Fig. 35-33. Linear-scale plots of the forcing displacement — isolated member displacement dynamic response angle as a function of frequency ratio for the single-degree-of-freedom vibratory motion isolation system with viscous friction only.

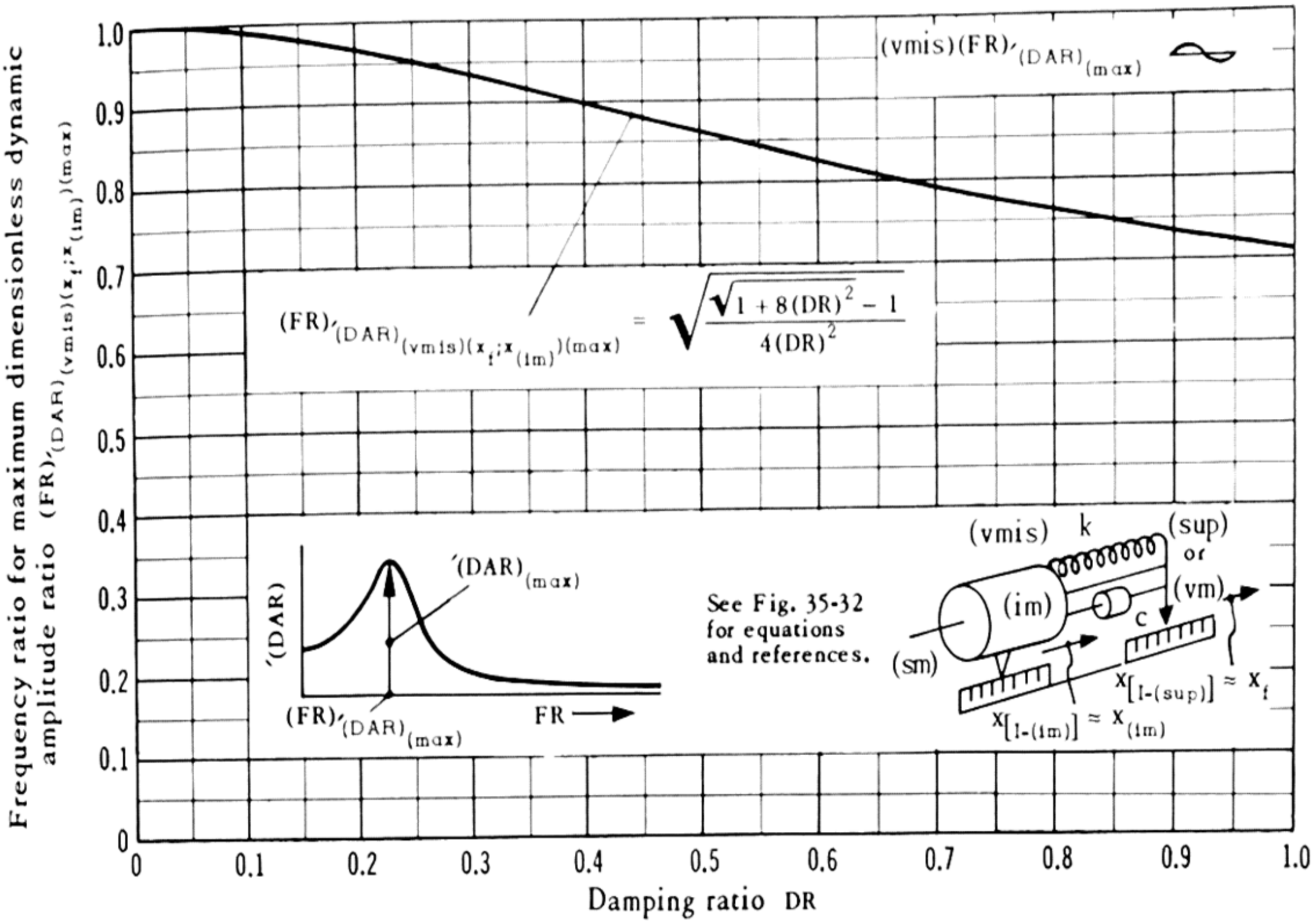


Fig. 35-34. Frequency ratio for maximum dimensionless dynamic amplitude ratio as a function of damping ratio for the single-degree-of-freedom vibratory motion isolation system.

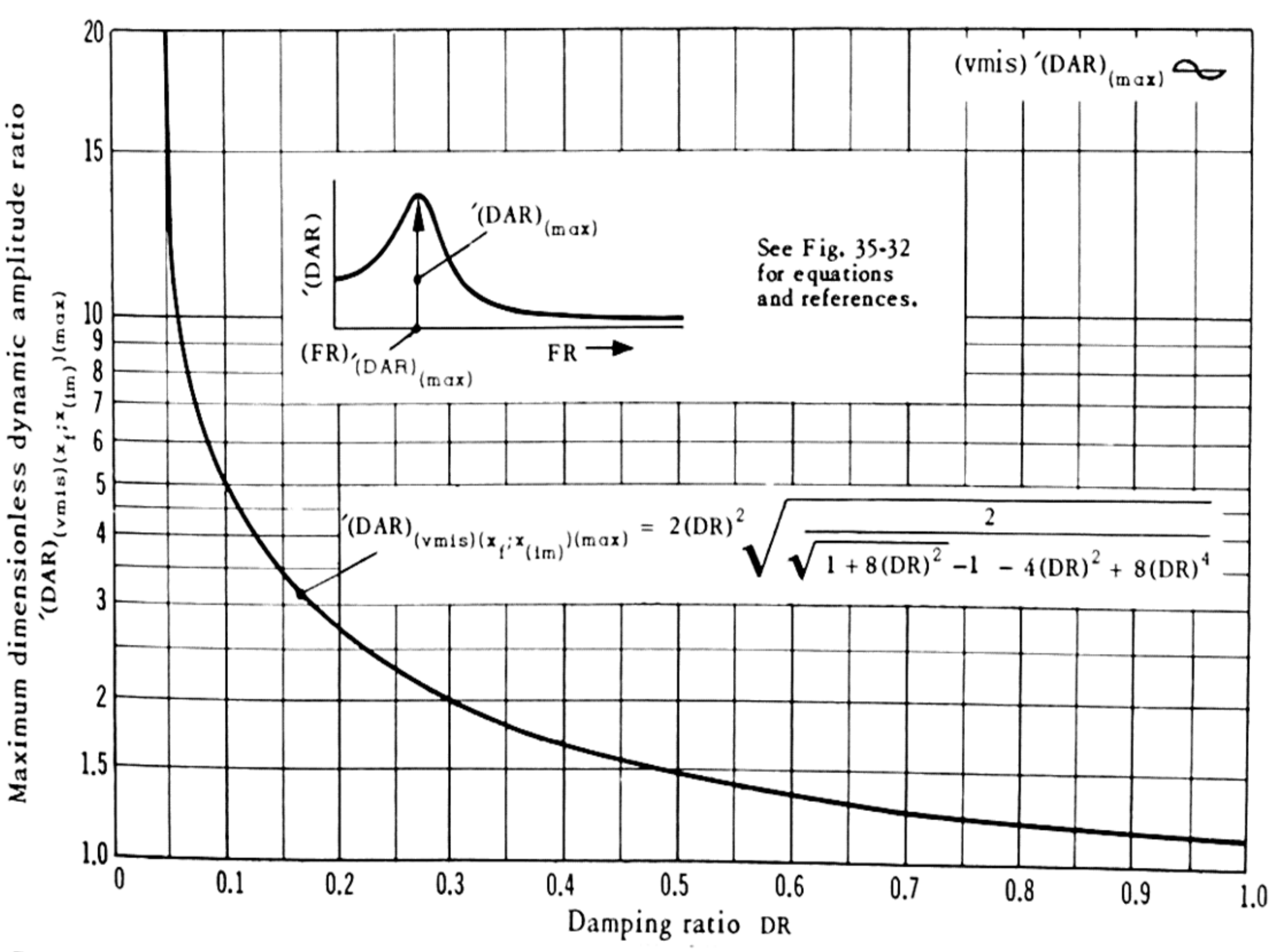


Fig. 35-35. Maximum dimensionless dynamic amplitude ratio as a function of damping ratio for the single-degree-of-freedom vibratory motion isolation system.

dimensionless dynamic amplitude ratio as a function of damping ratio. Figure 35-36 is a logarithmic-scale representation of the dimensionless dynamic amplitude ratio curve family given in Fig. 35-32.

35.222. Derivation Summary 35-8 outlines the theoretical background for a development of the performance function and the breakaway frequency ratio equations associated with the single-degree-of-freedom vibratory motion isolation system with Coulomb damping only. This development follows the general pattern established in Chapter 26 and applied to the seismographic system in Derivation Summary 35-6.

35.223. Figure 35-37 gives logarithmic-scale breakaway plots for the vibratory motion isolation system. Except for necessary changes in symbols, terminology, and titles, Fig. 35-37 is identical with Fig. 35-29. The ordinate is the ratio of the maximum Coulomb friction displacement to the amplitude of the forcing displacement. The abscissae are the frequency ratios at which breakaway occurs. The upper line is based on the limiting equality between the peak acceleration force and the maximum Coulomb friction force. The lower line represents a condition in which relative motion occurs without being continuous between the two maximum relative displacement peaks that normally occur twice in each cycle. For example, when the maximum Coulomb friction displacement is equal to 0.1 of the forcing displacement amplitude, the breakaway point on the basis of acceleration balance occurs at a frequency ratio of about 0.32. The corresponding equivalent damping ratio breakaway point is at a frequency ratio of about 0.36.

35.224. Figure 35-38 is a linear-scale curve family based on the dimensionless dynamic amplitude expression of Eq. (7) of Derivation Summary 35-8. The ordinate of this figure is the dimensionless dynamic amplitude ratio. The abscissa is the frequency ratio, and each curve is drawn for an identified value of the maximum Coulomb friction displacement – forcing displacement amplitude ratio.

35.225. For frequency ratios less than the equivalent damping ratio breakaway point, the dimensionless dynamic amplitude ratio has a value of unity. From the standpoint of the physical situation, this means that the isolated member is "stuck" to the supporting member and has the same motion with respect to inertial space as the support itself. When, for a given system, the frequency ratio increases until it reaches the breakaway point given by the equivalent damping ratio breakaway frequency ratio plot of Fig. 35-37, the isolated member starts to move with respect to the support. If breakaway occurs for some frequency ratio less than $\sqrt{2}$, the dimensionless dynamic amplitude ratio increases and finally reaches coincidence with the zero damping ratio curve either before or at the unity ordinate level. If the breakaway point occurs at a value of frequency ratio greater than $\sqrt{2}$, all curves of the family immediately decrease and finally become asymptotic to the zero damping ratio curve in the high frequency-ratio range.

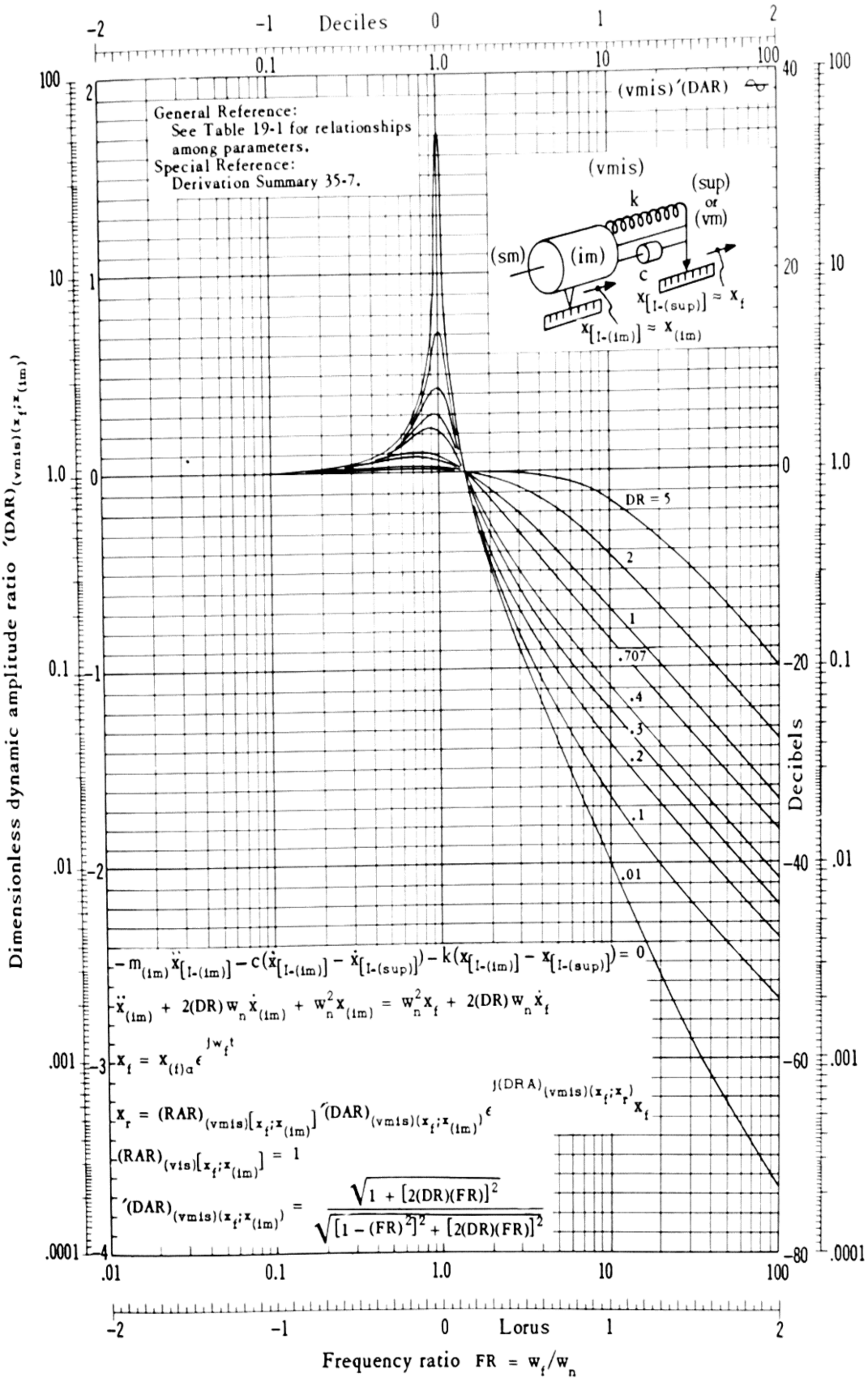
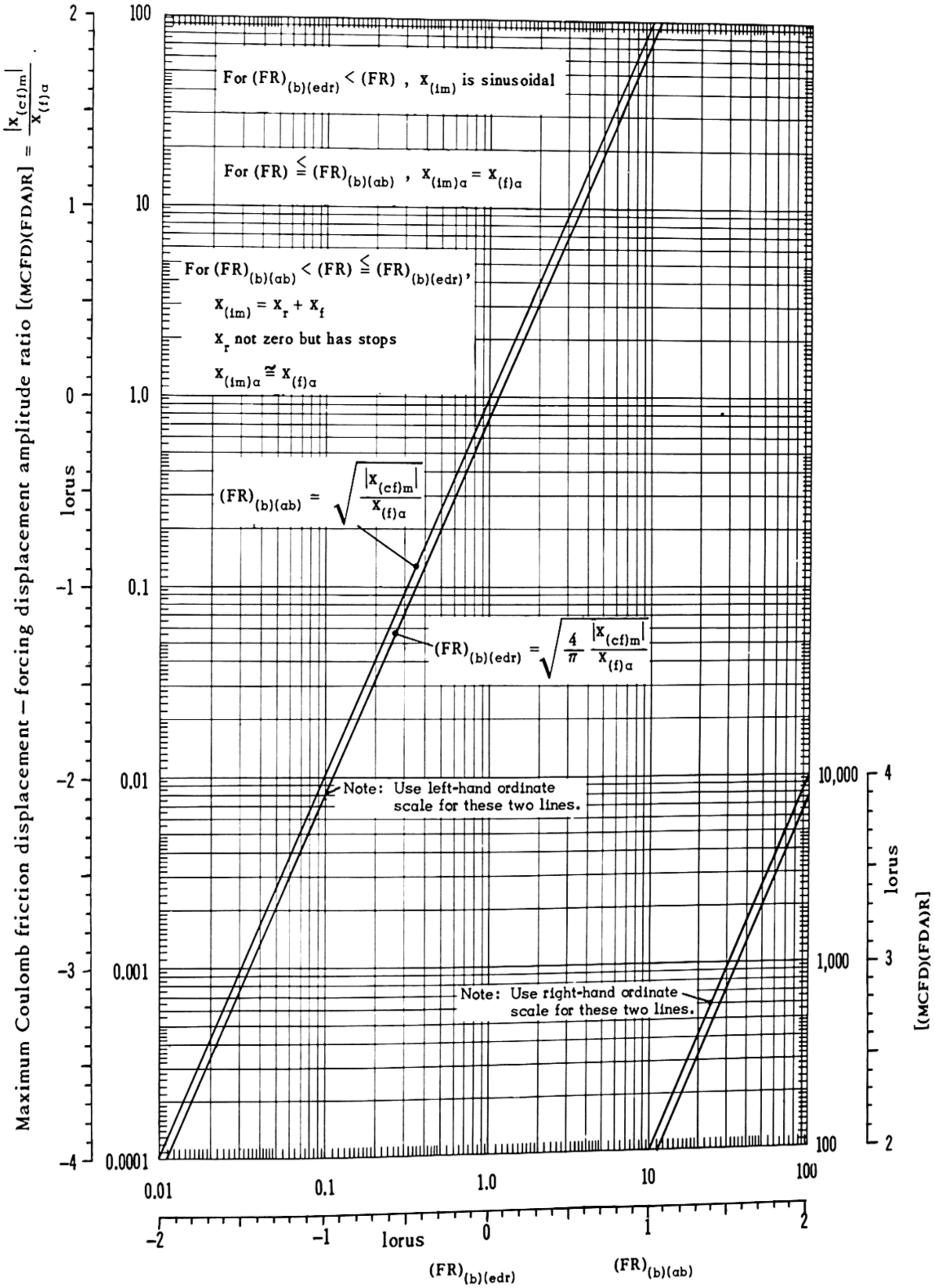


Fig. 35-36. Logarithmic-scale plot of forcing displacement – isolated member displacement dimensionless dynamic amplitude ratio as a function of frequency ratio for the single-degree-of-freedom vibratory motion isolation system.



Breakaway frequency ratios for the vibration isolation system

Fig. 35-37. Maximum Coulomb friction displacement – forcing displacement amplitude ratio as a function of breakaway frequency ratio for the vibratory motion isolation system.

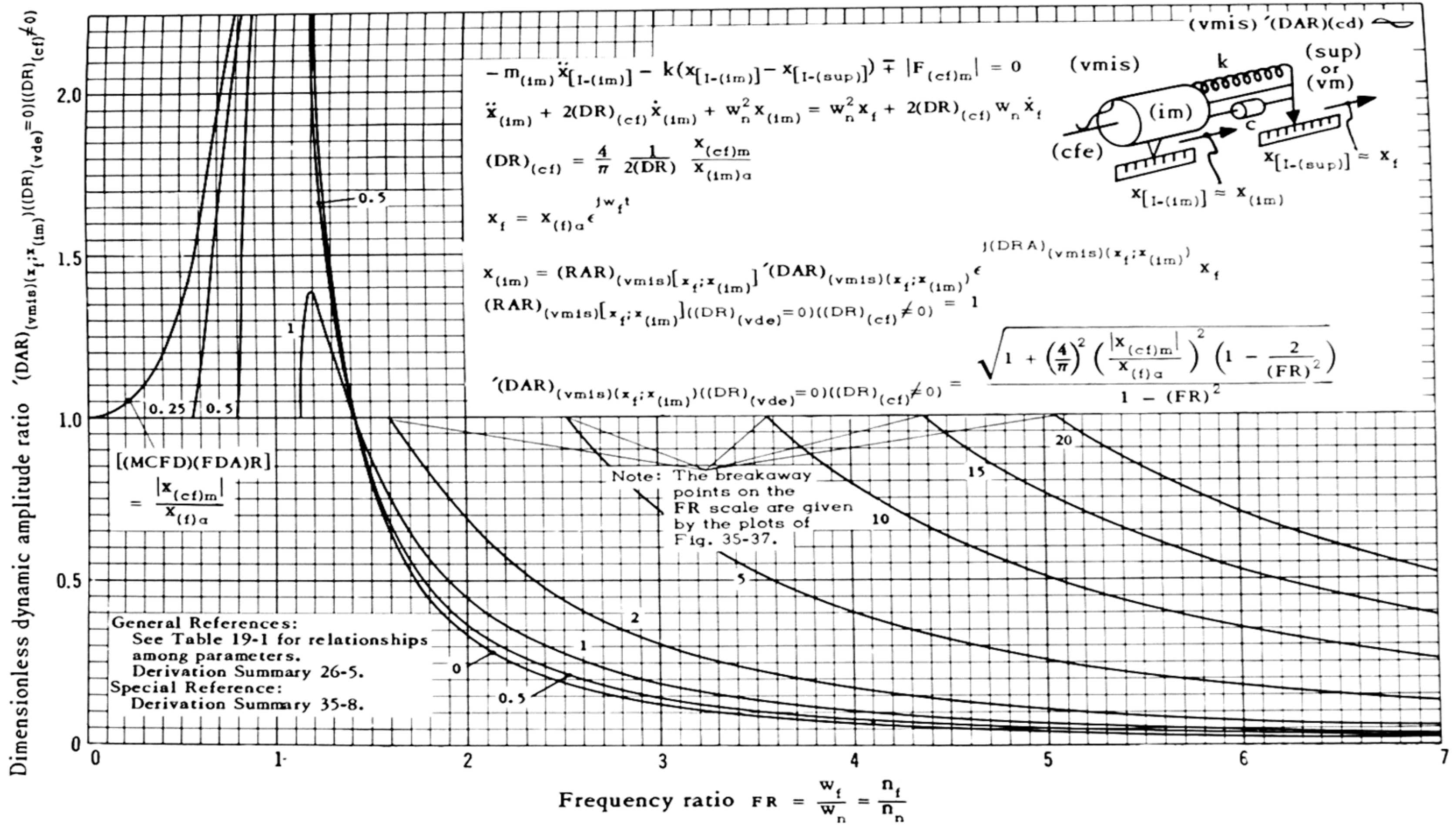
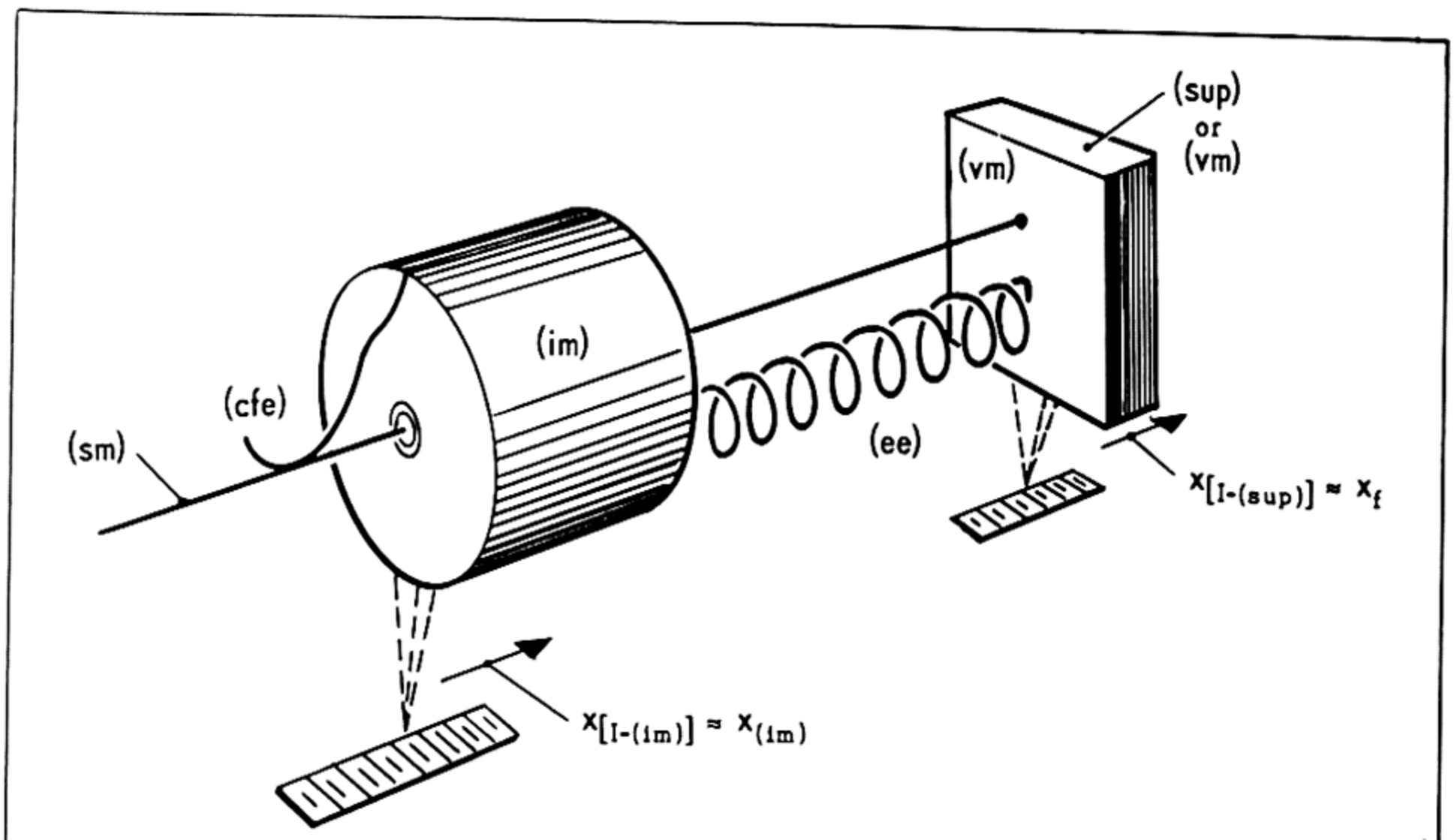
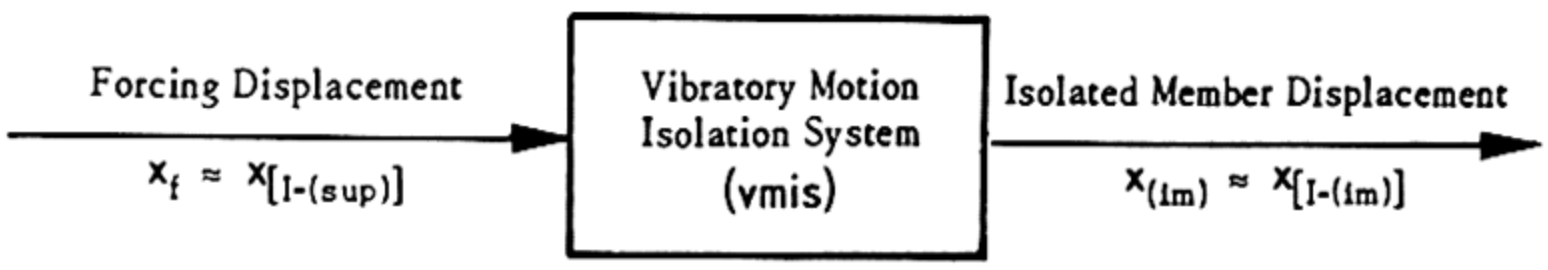


Fig. 35-38. Linear-scale plots of the forcing displacement – isolated member displacement dimensionless dynamic amplitude ratio as a function of frequency ratio for the single-degree-of-freedom vibratory motion isolation system with Coulomb damping only.



a) Line schematic diagram for a single-degree-of-freedom vibratory motion isolation system with Coulomb damping only



Equation (8) of Derivation Summary 35-7 gives the performance equation for the single-degree-of-freedom vibratory motion isolation system in the form

$$\ddot{x}_{(im)} + 2(DR)\,w_n \dot{x}_{(im)} + w_n^2 x_{(im)} = w_n^2 x_f + 2(DR)\,w_n \dot{x}_f \mp w_n^2 |x_{(cf)m}| \qquad (1)$$

b) Functional diagram and performance equation

When the forcing motion is sinusoidal and no relative motion stops occur except those that take place at the relative motion displacement peaks, the Coulomb friction term may be replaced by an equivalent viscous damping term. This equivalent viscous damping term may be based on equal Coulomb friction and equivalent viscous friction energy dissipation per cycle to give the Coulomb friction equivalent damping ratio in the form developed in section c of Derivation Summary 35-6 and given by Eq. (21) of that summary. This expression is

$$(DR)_{(cf)} = \frac{4}{\pi} \frac{1}{2(FR)} \frac{|x_{(cf)m}|}{x_{(r)a}} \qquad (2)$$

When the Coulomb friction term is replaced by an equivalent viscous damping term, Eq. (1) may be written in the form

$$\ddot{x}_{(im)} + 2(DR)_{[(vf)+(cf)]}\,w_n \dot{x}_{(im)} + w_n^2 x_{(im)} = w_n^2 x_f + 2(DR)_{[(vf)+(cf)]}\,w_n \dot{x}_f \qquad (3)$$

where

$$(DR)_{[(vf)+(cf)]} = (DR)_{(vde)} + (DR)_{(cf)} \qquad (4)$$

Derivation Summary 35-8. Performance equation, performance function and breakaway frequency ratio for the single-degree-of-freedom vibratory motion isolation system with Coulomb damping only. (Page 1 of 3)

The performance function corresponding to Eq. (3) may be found. However, because the Coulomb friction equivalent damping ratio, $(DR)_{(cf)}$, includes the amplitude of the relative displacement, $x_{(r)a}$, as a factor, the process of finding the forcing displacement – isolated member displacement dynamic amplitude ratio is difficult and will not be carried through here. This dynamic amplitude ratio is developed in Derivation Summary 26-5 for the case corresponding to Coulomb damping only and is given in working variable terms by Eq. (32) of that summary. This expression has the form

$$\mu_{(1,0;0,1,2)(u_{(rs)}\neq 0)(\zeta_{(u_{(rs)}=0)}=0)} = \sqrt{\frac{1+\left(\frac{4}{\pi}\right)^2\left(\frac{U_{(rs)}}{U_a}\right)^2\left(1-\frac{2}{\beta^2}\right)}{(1-\beta^2)^2}} \tag{5}$$

The corresponding dynamic response angle is

$$\phi_{(1,0;0,1,2)(u_{(rs)}\neq 0)(\zeta_{(u_{(rs)}=0)}=0)} = \tan^{-1}\left[\frac{\sqrt{\beta^4\left(\frac{\pi}{4}\right)^2\left(\frac{U_a}{U_{(rs)}}\right)^2-1}}{\beta^2\left(\frac{\pi}{4}\right)^2\left(\frac{U_a}{U_{(rs)}}\right)^2-1}\right] \tag{6}$$

In self-defining symbols, the expressions of Eqs. (5) and (6) are

$$(DAR)_{(vmis)(x_f;x_{(im)})((DR)_{(vde)}=0)((DR)_{(cf)}\neq 0)} = \frac{\sqrt{1+\left(\frac{4}{\pi}\right)^2\left(\frac{x_{(cf)m}}{x_{(f)a}}\right)^2\left(1-\frac{2}{(FR)^2}\right)}}{1-(FR)^2} \tag{7}$$

$$(DRA)_{(vmis)(x_f;x_{(im)})((DR)_{(vde)}=0)((DR)_{(cf)}\neq 0)} = \tan^{-1}\left[\frac{\sqrt{(FR)^4\left(\frac{\pi}{4}\right)^2\left(\frac{x_{(f)a}}{x_{(cf)m}}\right)^2-1}}{(FR)^2\left(\frac{\pi}{4}\right)^2\left(\frac{x_{(f)a}}{x_{(cf)m}}\right)^2-1}\right] \tag{8}$$

c) Performance function for the vibratory motion isolation system with Coulomb damping only

When the maximum Coulomb friction force is great enough so that it exceeds the inertia reaction force associated with the peak magnitude of the support acceleration with respect to inertial space, no relative motion of the isolated member will occur, and the ratio of isolated member displacement to forcing displacement is always unity. Breakaway occurs when, for a given forcing amplitude, the forcing frequency becomes high enough for the acceleration amplitude to produce an inertia reaction force just equal to the maximum Coulomb friction force.

Breakaway theory is best treated in terms of relative motion between the isolated member and the supporting member. This theory is available in sections c, e, f and g of Derivation Summary 35-6. The generally useful results are listed in the table of section h of that summary. This table, with the minor changes necessary to make it directly applicable to the vibratory motion isolation system, follows.

Derivation Summary 35-8. Performance equation, performance function and breakaway frequency ratio for the single-degree-of-freedom vibratory motion isolation system with Coulomb damping only. (Page 2 of 3)

Motion of isolated member is equal to forcing motion $x_{(im)} = x_f$	Isolated member moves relative to vibratory member $x_r \cong 0 \quad ; \quad x_{(im)} \cong x_f$	Isolated member moves sinusoidally relative to inertial space $x_{(im)} \neq x_f$
$(FR) \leqq (FR)_{(b)(ab)}$ Coulomb friction force balances acceleration force at all times for frequency ratios less than $(FR)_{(b)(ab)}$.	$(FR)_{(b)(ab)} < (FR) \leqq (FR)_{(b)(edr)}$ Acceleration force exceeds Coulomb friction force during part of each cycle for some frequency ratios less than $(FR)_{(b)(edr)}$.	$(FR)_{(b)(edr)} < (FR)$ No appreciable stops in relative motion.

$(FR)_{(b)(ab)} = \sqrt{\dfrac{|x_{(cf)m}|}{x_{(f)a}}}$ = acceleration-balance breakaway frequency ratio
(Based on balance of Coulomb friction force and inertia reaction force. Refer to section g of Derivation Summary 35-6.)

$(FR)_{(b)(edr)} = \sqrt{\dfrac{4}{\pi}\dfrac{|x_{(cf)m}|}{x_{(f)a}}}$ = equivalent damping ratio breakaway frequency ratio
(Based on Coulomb friction equivalent damping ratio. Refer to section f of Derivation Summary 35-6.)

d) Breakaway conditions for the vibratory motion isolation system

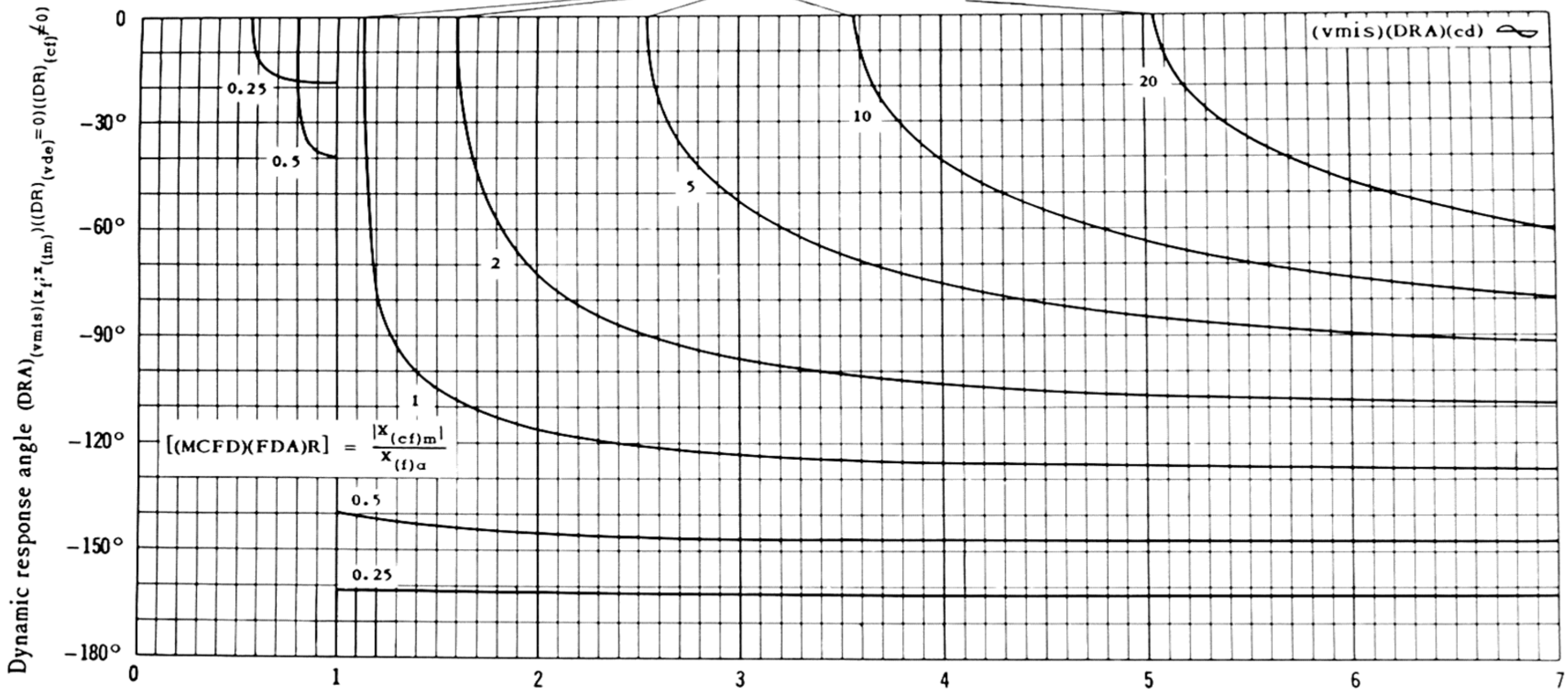
Derivation Summary 35-8. Performance equation, performance function and breakaway frequency ratio for the single-degree-of-freedom vibratory motion isolation system with Coulomb damping only. (Page 3 of 3)

35.226. With the reference amplitude ratio equal to unity, the ordinate of Fig. 35-38 is proportional to the isolated member displacement amplitude for a given forcing displacement amplitude. This means that the curve family of Fig. 35-38 represents the general pattern of frequency ratio and Coulomb damping effects on the vibratory motion isolation system. The curve family of Fig. 35-39 is based on Eq. (8) of Derivation Summary 35-8 and gives the dynamic response angles corresponding to the dimensionless dynamic amplitude ratios of Fig. 35-38.

VIBRATORY FORCE ISOLATION SYSTEM

35.227. Vibratory forces are often generated by the normal operation of mechanical and electrical devices. These forces act on the frame of the device and must ultimately be absorbed by the support that carries the device. When a rigid connection is used between the support and the device on which the vibratory force acts, the structure associated with the support receives the full effect of this force. As a result, shaking motions and noise may be set up that are undesirable at best and may actually be intolerable in terms of broken parts and excessive sound levels. For example, if the motor of an electrical refrigerator unit were bolted directly to the frame, this arrangement would probably be unsatisfactory because of the noise generated and the vibration of the floor and walls of any room in which the refrigerator might be placed. The vibratory force reaching the support may be reduced by replacing rigid mountings by relatively soft elastic connections and a sufficient amount of damping to keep transient effects within

Note: The breakaway points on the FR scale are given by the plots of Fig. 35-37.



See Fig. 35-38 for background equations and references.

$$(DRA)_{(vmis)(x_f;x_{(im)})((DR)_{(vde)}=0)((DR)_{(cf)}\neq 0)} = \tan^{-1}\left(\frac{\sqrt{(FR)^4\left(\frac{\pi}{4}\right)^2\left(\frac{X_{(f)a}}{|X_{(cf)m}|}\right)^2 - 1}}{(FR)^2\left(\frac{\pi}{4}\right)^2\left(\frac{X_{(f)a}}{|X_{(cf)m}|}\right)^2 - 1}\right)$$

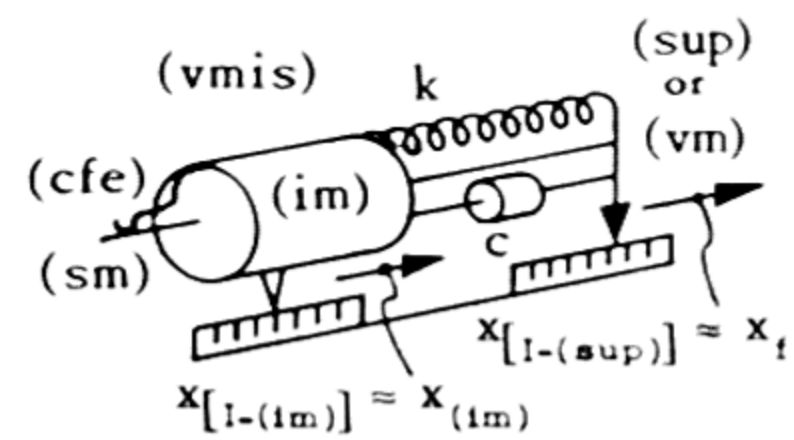


Fig. 35-39. Linear-scale plots of the forcing displacement – isolated member displacement dynamic response angle as a function of frequency ratio for the single-degree-of-freedom vibratory motion isolation system with Coulomb damping only.

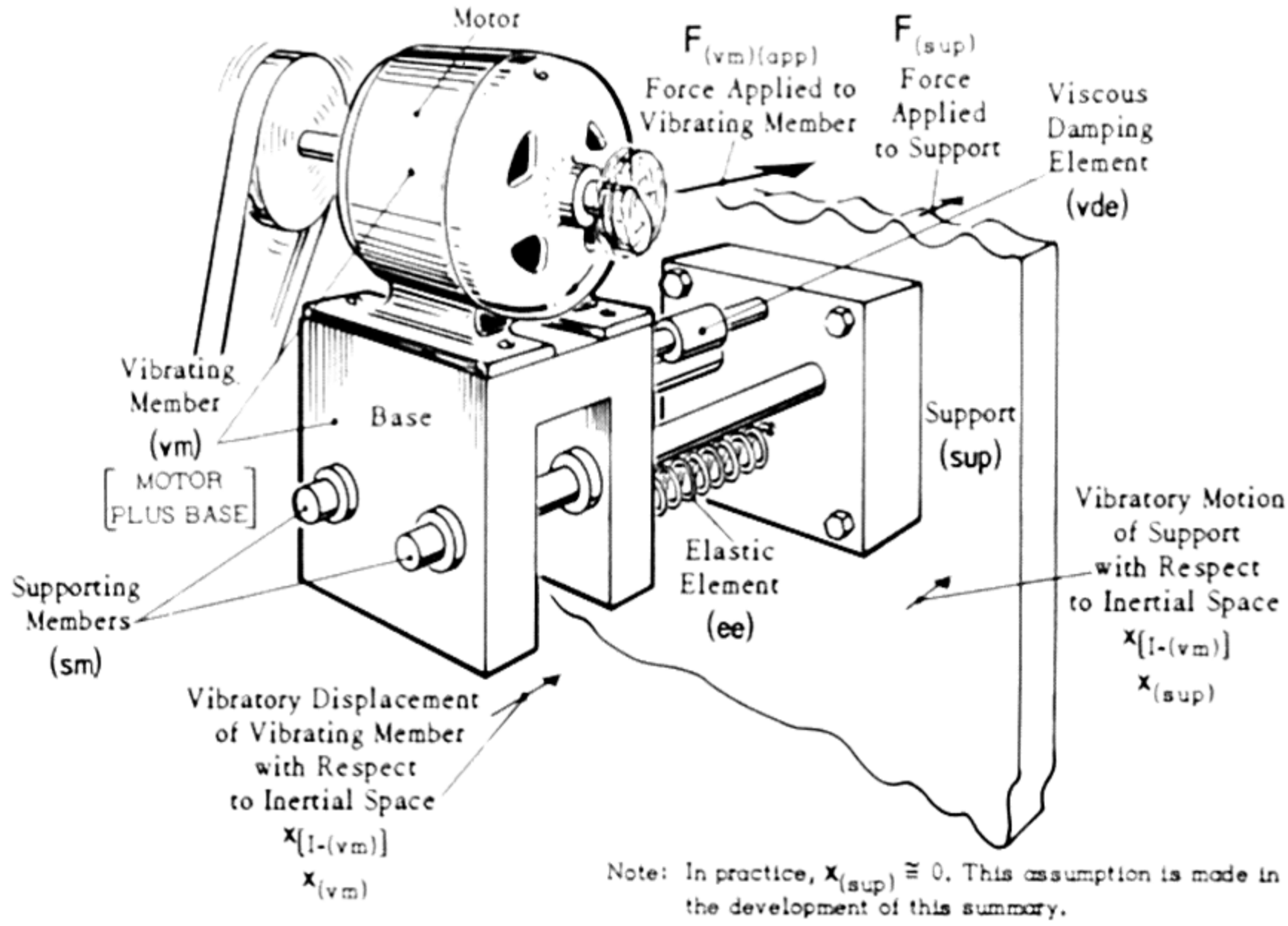
tolerable limits. The action of any system that accomplishes this result is vibratory force isolation, and the components that contribute essential effects form the vibratory force isolation system. The figure of section a of Derivation Summary 35-9 illustrates a typical vibratory force isolation system with one degree of freedom. A motor with an unbalanced mass on its shaft is mounted on a base that is free to slide on a pair of rods that are rigidly attached to the support. In addition to Coulomb friction between the supporting rods and the bushings fixed in the base, a spring and a viscous damper couple the vibrating member (the motor plus the base) to the support.

35.228. The theory of vibratory force isolation has been brought to a high degree of effectiveness by many engineers. In particular, J. P. Den Hartog in his book on mechanical vibrations* provides an exceptionally clear development of the physical principles involved and deserves credit for giving a strong impetus to the development of vibration control as a branch of engineering. A proper treatment of this subject must include material that is not properly part of this chapter, in which consideration is limited to arrangements that are similar to the seismographic system. For example, tuned vibration absorbers with and without damping are widely used in practice. A typical application of the vibration absorber is in piston-type aircraft engines where vibratory torques acting on the crankshaft-propeller combination must be prevented from causing mechanical failures. The theory and methods described in this section may be extended to cover vibration absorber performance or any other problem in vibration control. However, consideration of these applications is beyond the scope of Instrument Engineering.

35.229. Derivation Summary 35-9 outlines the development of performance information on the single-degree-of-freedom vibratory force isolation system. The general plan of attack is to set up an equation for the motion of the vibrating member under the applied force when the vibratory motion of the support is negligibly small and to use solutions of this equation for finding the elastic and damping forces applied to the support. The sum of these forces gives the resultant force acting on the support. Under a definition introduced by Den Hartog, the ratio of the amplitude of the force acting on the support to the amplitude of the force acting on the vibrating member is called transmissibility. This concept is effectively identical with the dimensionless dynamic amplitude ratio for force applied to the support with respect to force applied to the vibrating member.

35.230. Equation (2) of Derivation Summary 35-9 is the generalized performance equation for the single-degree-of-freedom vibratory force isolation system with both viscous damping and Coulomb damping when a steady-state sinusoidal force is applied to the vibrating member. Equation (3) is derived from Eq. (2) by taking the vibratory motion of the support as negligibly small, and making the usual

* See Den Hartog (D5).



a) Pictorial diagram illustrating the single-degree-of-freedom vibratory force isolation system

When the force applied to the vibrating member of the system shown in the diagram of section a may be represented by a steady-state sinusoidal function, that is, when

$$F_{(vm)(app)} = F_{(vm)(app)a} \epsilon^{jw_f t} \tag{1}$$

then the other forces acting on the vibrating member are identical with those that are important for the seismographic system and the vibratory motion isolation system. The performance equations for these systems are developed in Derivation Summaries 35-2 and 35-7. When the terms representing forces in these equations are written down with the force expression of Eq. (1) added, the single-degree-of-freedom equation of motion for the vibrating member of the vibratory force isolation system is shown to be

$$-m_{(vm)}\ddot{x}_{[I-(vm)]} - c_{(vde)}\left[\dot{x}_{[I-(vm)]} - \dot{x}_{[I-(sup)]}\right] - k_{(ee)}\left[x_{[I-(vm)]} - x_{[I-(sup)]}\right] + F_{(vm)(app)a}\epsilon^{jw_f t} \mp |F_{(cf)m}| = 0 \tag{2}$$

When attention is restricted to situations in which the vibratory displacement of the support with respect to inertial space is effectively zero and each term of Eq. (2) is divided by $m_{(vm)}$, the mass of the vibrating member, Eq. (2) may be written in the form

$$\ddot{x}_{[I-(vm)]} + 2(DR)w_n\dot{x}_{[I-(vm)]} + w_n^2 x_{[I-(vm)]} = w_n^2 x_{[I-(vm)](F_{(app)})(qs)a}\epsilon^{jw_f t} \mp w_n^2 |x_{[I-(vm)](cf)m}| \tag{3}$$

where

$$x_{[I-(vm)](F_{(app)})(qs)a} = \frac{F_{(vm)(app)a}}{k_{(ee)}} = \text{quasi-static vibratory amplitude of the vibrating member displacement produced by the applied force} \tag{4}$$

$$x_{[I-(vm)](cf)m} = \frac{|F_{(cf)m}|}{k_{(ee)}} = \text{maximum vibratory displacement of the vibrating member due to Coulomb friction} \tag{5}$$

Derivation Summary 35-9. Pictorial diagram, differential equation, performance functions and transmissibility equations for the single-degree-of-freedom vibratory force isolation system.
(Page 1 of 4)

Under the definition illustrated in Fig. 6-1 and discussed in Chapters 4 and 6, quasi-static conditions exist when inertial and damping forces are negligibly small so that the force associated with the vibrating member displacement is entirely determined by the elastic element.

When Coulomb friction effects are negligibly small, Eq. (3) reduces to

$$\ddot{x}_{[I-(vm)]} + 2(DR)\omega_n \dot{x}_{[I-(vm)]} + \omega_n^2 x_{[I-(vm)]} = \omega_n^2 x_{[I-(vm)](F_{(app)})(qs)} \tag{6}$$

where

$$x_{[I-(vm)](F_{(app)})(qs)} = \frac{F_{(vm)(app)}}{k_{(ee)}} = \frac{F_{(vm)(app)a}}{k_{(ee)}} \epsilon^{j\omega_f t} \tag{7}$$

= quasi-static displacement of the vibrating member with respect to inertial space due to the applied force

Equation (6) has the (0;0,1,2) differential equation form for which solutions are developed in Derivation Summaries 19-1 through 19-10 and in Derivation Summary 33-2.

b) Equation for the displacement of the vibrating member in response to a sinusoidal applied force

In working variable terms, Eq. (6) becomes

$$\ddot{V} + 2\zeta\omega_n V + \omega_n^2 V = \omega_n^2 U \tag{8}$$

When

$$U = U_a \epsilon^{j\omega_f t} \tag{9}$$

the developments of Derivation Summaries 19-10 and 33-2 show that the sinusoidal relating function for Eq. (8) is

$$\eta_{(0;0,1,2)} = \rho_r \mu_{(0;0,1,2)} \epsilon^{j\phi_{(0;0,1,2)}} = \frac{1}{1 - \beta^2 + j2\zeta\beta} \tag{10}$$

where

$$\mu_{(0;0,1,2)} = \frac{1}{\sqrt{(1-\beta^2)^2 + (2\zeta\beta)^2}} \tag{11}$$

$$\phi_{(0;0,1,2)} = \tan^{-1}\left[\frac{-2\zeta\beta}{1-\beta^2}\right] \tag{12}$$

$$\beta = \frac{\omega_f}{\omega_n} = \frac{n_f}{n_n} = \frac{T_n}{T_f} = \text{frequency ratio} \tag{13}$$

$$\rho_r = 1 \tag{14}$$

In self-defining symbols, the steady-state vibratory force applied to the support due to variations in the length of the elastic element is

$$F_{(sup)(app)(ee)} = +k_{(ee)} x_{[I-(vm)]} \tag{15}$$

From Eqs. (6) through (15), in self-defining terms,

$$F_{(sup)(app)(ee)} = +k_{(ee)} \frac{1}{k_{(ee)}} [PF]_{(vfis)[F;F](ee)} F_{(vm)(app)} \tag{16}$$

where

$$[PF]_{(vfis)[F;F](ee)} = (RAR)_{(vfis)[F;F](ee)} {}'(DAR)_{(vfis)(F;F)(ee)} \epsilon^{j(DRA)_{(vfis)(F;F)(ee)}} F_{(vm)(app)} \tag{17}$$

$$\rho_r \approx (RAR)_{(vfis)[F;F](ee)} = 1 \tag{18}$$

$$\mu_{(0;0,1,2)} \approx [(DAR)(RAR)R]_{(vfis)(F;F)(ee)} = {}'(DAR)_{(vfis)(F;F)(ee)} \approx \frac{1}{\sqrt{[1-(FR)^2]^2 + [2(DR)(FR)]^2}} \tag{19}$$

and

$$\phi_{(0;0,1,2)} \approx (DRA)_{(vfis)(F;F)(ee)} = \tan^{-1}\left[\frac{-2(DR)(FR)}{1-(FR)^2}\right] \tag{20}$$

Derivation Summary 35-9. Pictorial diagram, differential equation, performance functions and transmissibility equations for the single-degree-of-freedom vibratory force isolation system.
(Page 2 of 4)

Note that because the support has no vibratory displacement of the quasi-static force on the support always has the same sign as the displacement of the vibrating member.

Reasoning similar to that just outlined shows that the force on the support due to the action of the damping element is

$$F_{(sup)(app)(vde)} = + c_{(vde)} \dot{x}_{[I-(vm)]} \tag{21}$$

$$= c_{(vde)}\, j w_f\, x_{[I-(vm)]} \tag{22}$$

$$= \frac{c_{(vde)}}{k_{(ee)}}\, j w_f\, [PF]_{(vfis)[F;F](ee)} F_{(vm)(app)} \tag{23}$$

From the defining relationships of Table 19-1,

$$\frac{c_{(vde)}}{k_{(ee)}} = \frac{a_1}{a_0} = \frac{2(DR)}{w_n} \tag{24}$$

Therefore,

$$F_{(sup)(vde)} = \frac{2(DR)}{w_n}\, j w_f\, [PF]_{(vfis)[F;F](ee)} F_{(vm)(app)} \tag{25}$$

The total force applied to the support by the vibrating member is the sum of the elastic element force component and the viscous damping element force component; i.e.,

$$F_{(sup)(app)} = F_{(sup)(app)(ee)} + F_{(sup)(app)(vde)}$$

$$= [1 + j2(DR)(FR)]\, [PF]_{(vfis)[F;F](ee)} F_{(vm)(app)} \tag{26}$$

Using the form of Eq. (10),

$$\eta_{(0;0,1,2)} = [PF]_{(vfis)[F;F](ee)} = \frac{1}{1 - (FR)^2 + j2(DR)(FR)} \tag{27}$$

From Eqs. (26) and (27),

$$F_{(sup)(app)} = [PF]_{(vfis)[F;F]} F_{(vm)(app)} \tag{28}$$

where

$$\eta_{(1,0;0,1,2)} = [RF]_{(1,0;0,1,2)} = [PF]_{(vfis)[F;F]} = \frac{1 + j2(DR)(FR)}{1 - (FR)^2 + j2(DR)(FR)} \tag{29}$$

Equation (29) may also be written in the form

$$[PF]_{(vfis)[F;F]} = (RAR)_{(vfis)[F;F]}\, '(DAR)_{(vfis)(F;F)}\, \epsilon^{\,j(DRA)_{(vfis)(F;F)}} \tag{30}$$

where

$$\rho_{(r)(1,0;0,1,2)} = (RAR)_{(vfis)[F;F]} = 1 \tag{31}$$

$$\mu_{(1,0;0,1,2)} = [(DAR)(RAR)R]_{(vfis)(F;F)} = '(DAR)_{(vfis)(F;F)} = \frac{\sqrt{1 + [2(DR)(FR)]^2}}{\sqrt{[1 - (FR)^2]^2 + [2(DR)(FR)]^2}} \tag{32}$$

$$\phi_{(1,0;0,1,2)} = (DRA)_{(vfis)(F;F)} = \tan^{-1}\left[\frac{-2(DR)(FR)}{1 - (FR)^2}\right] + \tan^{-1} 2(DR)(FR) \tag{33}$$

c) Vibratory force isolation system performance equation when only viscous damping is present

By definition,

$$(VFTF)_{(vfis)} = [PF]_{(vfis)[F;F]} = \frac{F_{(sup)(app)}}{F_{(vm)(app)}} \tag{34}$$

= vibratory force transmissibility function for the single-degree-of-freedom vibratory force isolation system

Derivation Summary 35-9. Pictorial diagram, differential equation, performance functions and transmissibility equations for the single-degree-of-freedom vibratory force isolation system. (Page 3 of 4)

Comparison of Eqs. (30), (32) and (33) with Eqs. (31), (34) and (35) of Derivation Summary 35-7 shows that single-degree-of-freedom force transmissibility equation is also identical with the performance function for the single-degree-of-freedom vibratory motion isolation system.

By definition,

$$\mu_{(1,0;0,1,2)} \approx (VFT)_{(vfis)} = [(DAR)(RAR)R]_{(vfis)(F;F)} = {}'(DAR)_{(vfis)(F;F)} = \frac{F_{(sup)(app)a}}{F_{(vm)(app)a}} \quad (35)$$

= vibratory force dimensionless dynamic amplitude ratio for the single-degree-of-freedom vibratory force isolation system

= vibratory force transmissibility for the single-degree-of-freedom vibratory force isolation system

d) Transmissibility function and transmissibility for the vibratory force isolation system

Derivation Summary 35-9. Pictorial diagram, differential equation, performance functions and transmissibility equations for the single-degree-of-freedom vibratory force isolation system.
(Page 4 of 4)

transformations from coefficients to parameters. The relationship obtained is a (0;0, 1, 2) differential equation with the addition of a Coulomb friction term.

35.231. Section c of Derivation Summary 35-9 shows the development of equations for the elastic and viscous damping forces applied to the support and gives the essential results as Eqs. (28) through (33). These equations show that the vibratory force applied to the support is related to the force applied to the vibrating member by the performance function of the (1, 0;0, 1, 2) differential equation, which is identical with the performance function found for the vibratory motion isolation system in Derivation Summary 35-7.

35.232. The curve family of Fig. 35-40 gives the dimensionless dynamic amplitude ratio for the force applied to the support as compared to the force applied to the vibrating member as a function of frequency ratio for various damping ratios when only viscous damping is present in the vibratory force isolation system. This amplitude ratio is identical with the vibratory force transmissibility, which is defined as the ratio of the force amplitude applied to the support to the force amplitude applied to the vibrating member. Except for changes in meaning required by differences in the physical quantities involved, the curve family of Fig. 35-40, based on Eq. (32) of Derivation Summary 35-9, is identical with the curve family of Fig. 35-32, which applies to the vibratory motion isolation system. This identity of form means that the discussion of vibratory motion isolation associated with Fig. 35-32 applies with equal validity to the vibratory force isolation represented by the curves of Fig. 35-40.

35.233. The curve family of Fig. 35-41 is plotted from Eq. (33) of Derivation Summary 35-9 and represents the dynamic response angles associated with the dimensionless dynamic amplitude ratio curves of Fig. 35-40.

35.234. Coulomb damping is effective for the vibratory force isolation system in the same way that friction of this type acts in the vibratory motion isolation

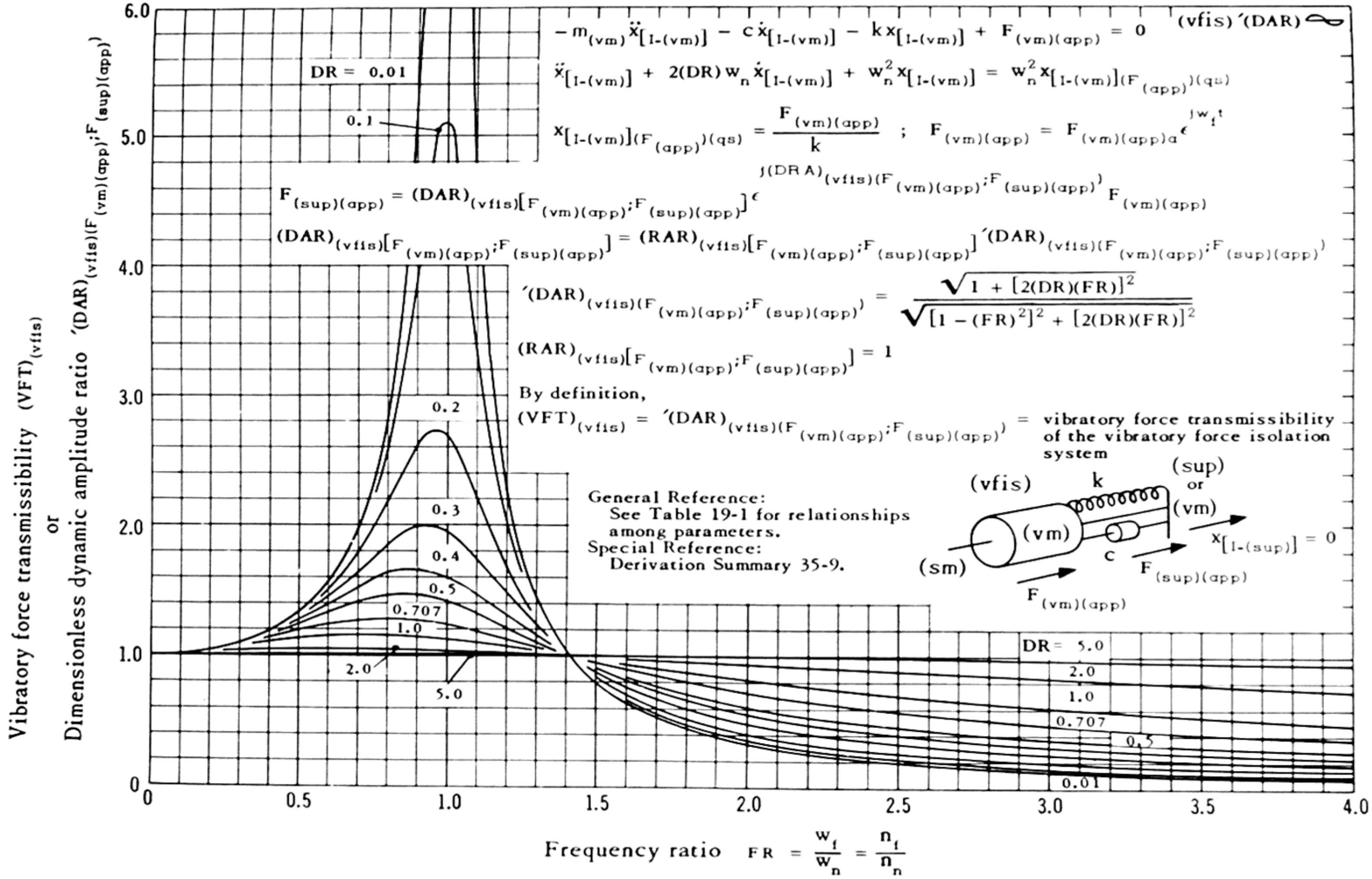


Fig. 35-40. Linear-scale plots of the force-applied-to-vibrating-member – force-applied-to-support dimensionless dynamic amplitude ratio for the single-degree-of-freedom vibratory force isolation system with viscous damping only.

See Fig. 35-40 for background equations and references.

$$(DRA)_{(vfis)(F_{(vm)(app)};F_{(sup)(app)})} = \tan^{-1}\left[\frac{-2(DR)(FR)}{1-(FR)^2}\right] + \tan^{-1} 2(DR)(FR)$$

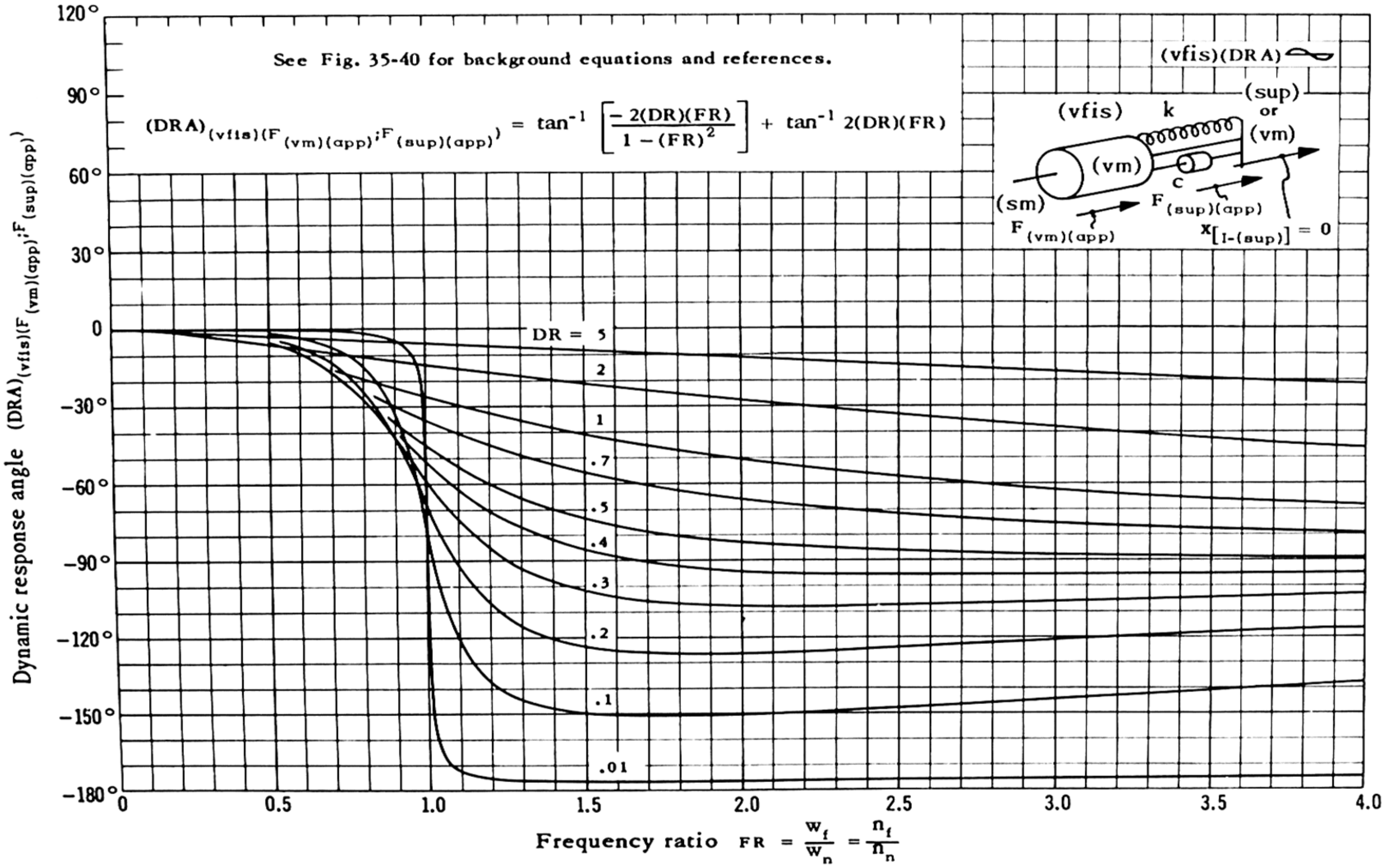


Fig. 35-41. Linear-scale plots of the force-applied-to-vibrating-member – force-applied-to-support dynamic response angle for the single-degree-of-freedom vibratory force isolation system with viscous damping only.

system. The development of a performance function for the vibratory force isolation system with either combined Coulomb damping and viscous damping or Coulomb damping alone would follow the patterns of Derivation Summaries 35-8 and 35-9. This development is omitted here, but the general nature of the results is easily predicted. When the maximum force applied to the vibrating member is less than the maximum Coulomb friction force, the force applied to the support is identical with the force acting on the vibrating member. Breakaway occurs when the maximum force on the vibrating member reaches the maximum Coulomb friction force. For convenience in theoretical descriptions of the physical situation, both of these forces should be divided by the elastic coefficient to permit the computation of the maximum Coulomb friction displacement – quasi-static applied-force displacement amplitude ratio. With this ratio available, the plots of Fig. 35-37 are immediately available for use in estimating breakaway frequency ratios. For frequency ratios appreciably higher than the breakaway point, the displacement of the vibrating member for the case of zero viscous damping would follow the zero-damping-ratio dimensionless dynamic amplitude ratio curve for the (0;0, 1, 2) performance function. The force applied to the support would be proportional to the displacement of the elastic element from its zero-force position with the addition of the maximum Coulomb friction force to always oppose the motion. With small amounts of Coulomb friction, the vibratory force transmissibility should be given reasonably well by the (0;0, 1, 2) dimensionless dynamic amplitude ratio plot for zero damping. When combinations of viscous damping and Coulomb damping are present, special curves should be plotted.

ILLUSTRATIVE TEST REPORT ON THE EXPERIMENTAL CALIBRATION OF A LINEAR VIBRATION RECEIVER

35.235. If vibration-measuring equipment is to be useful in practical applications, it must have performance characteristics that are reasonably free from variation for given operating conditions, and these characteristics must be known. As a general rule, any device should behave well enough to give consistent results within a few percent if it is to warrant classification as a measuring instrument. The accuracy to which the performance characteristics must be known depends on the purposes for which the results are to be used.

35.236. The only reliable method for determining the performance of a given piece of equipment at any particular time is to carry out an experimental calibration. In practice, calibration depends on applying input variations to the unit or system under calibration, recording the corresponding output changes, and using the results as the basis for a quantitative description of performance. When it is possible to fit the experimental results into a well-known theoretical pattern, a relatively small amount of test work may be used to produce a practically complete calibration. For this reason, it is always desirable to reduce calibration data to

dimensionless terms and plots suitable for comparison with corresponding curves based on known differential equations. The equations most likely to be useful for this purpose are generally the performance equations for the operating components of the unit under calibration. Once differential equation forms have been identified that give patterns similar to test results, representations of performance with any desired level of precision may be given by use of deviation plots. Final descriptions of performance may be made in words, using any suitable concepts, or by means of curves and tabulations of essential numerical data.

35.237. To illustrate the calibration process as it may be applied to vibration-measuring equipment, the accompanying Test Report No. 35-1 for a linear vibration receiver is given. In order to demonstrate various approaches to the representation of calibration results, this test report includes more plots than would ordinarily be used. A number of these plots are duplications in the sense that they supply the same information. This duplication is used (in this test report only) to show the characteristics of various types of plots.

35.238. The general objective of processing the data from the experimental phases of any calibration test is to produce an effectively complete quantitative description of performance in concise terms. This general objective may be broken down into four subsidiary objectives or steps:

1) The identification of a differential equation with a relating function very similar to the measured performance function of the unit under test.
2) The comparison of the experimentally determined points with the relating function of the identified differential equation.
3) The comparison of the identified relating function with the ideal performance characteristics for the unit being calibrated.
4) The comparison of the experimental points with the ideal performance characteristics.

The identification of a suitable differential equation depends on a study of the design features of the unit being tested and the general nature of the experimental results obtained from the unit. The comparisons associated with steps 2, 3 and 4 are made in terms of deviation functions and deviations.

35.239. By definition, these deviation functions are quotients formed by dividing values of the experimental results by the corresponding values determined from the theoretical performance-describing equation identified in step 1. The deviations are differences between values of experimental results and the corresponding values of the theoretical performance-describing equation or of the ideal performance characteristics. Deviation functions and deviations are useful for suggesting whether differences between actual and ideal results are due to uncertainties associated with the processes of measurement or whether they represent errors

SUMMARY: Test Form A **TEST REPORT NO.** 35-1 Sheet 1 of 13

Instruments Laboratory · Aeronautical Engineering Department · Massachusetts Institute of Technology · Cambridge · Massachusetts

Title of test LINEAR VIBRATION RECEIVER CALIBRATION; STEADY-STATE SINUSOIDAL INPUT

Date 6/22/54 **In charge of test** J.L. STOCKARD **Assisting with test** J. BARLEY

Equipment tested CONSOLIDATED LINEAR VIBRATION RECEIVER (VR)

Type 4 **Model** 102 **Serial No.** 7510 **Calculations** J.L. STOCKARD

Plots J.L. STOCKARD

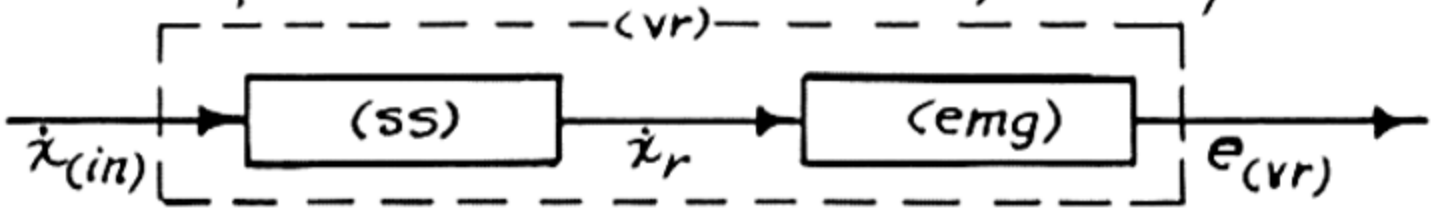
Equipment used for test SPERRY-M.I.T. VIBRATION CALIBRATOR (CONSOLIDATED) SER. NO. C875; DUMONT CATHODE-RAY OSCILLOGRAPH (CRO), TYPE 304H, SER. NO. 1012; BALLANTINE VACUUM TUBE VOLTMETER (VTVM); MODEL 300, SER. NO. 6390

Input quantity LINEAR VELOCITY $\dot{x}_{(in)}$ **Output quantity** VOLTAGE $e_{(vr)}$

Environmental conditions: Temperature 70° F Pressure —

Other —

Summary of results: (when the input is considered to be vibratory velocity)



(ss) = seismographic system (emg) = electromagnetic generator

$$[PF]_{(vr)[\dot{x};e](theo)} \approx [RF]_{(2;0,1,2)} = S_{(vr)[\dot{x};e](ref)} \frac{(FR)^2}{1-(FR)^2+j2(DR)(FR)}$$

$$'(SR)_{(vr)(\dot{x};e)(theo)} \approx '(DAR)_{(2;0,1,2)} = \frac{(FR)^2}{\sqrt{[1-(FR)^2]^2+[2(DR)(FR)]^2}}$$

$$(DRA)_{(vr)(\dot{x};e)(theo)} \approx (DRA)_{(2;0,1,2)} - 180° = \tan^{-1}\left[\frac{-2(DR)(FR)}{1-(FR)^2}\right]$$

Reference frequency = $n_{(ref)}$ = 7 $\frac{cycles}{second}$ Damping ratio = DR = 0.7

Reference sensitivity = $S_{(vr)[\dot{x};e](ref)}$ = 0.11 $\frac{volt}{in/sec}$ Reference dynamic response angle = $(DRA)_{(ref)}$ = −180°

Frequency ratio = FR = $n_f/n_{(ref)}$; Forcing frequency = n_f ; Dynamic response angle = $(DRA)_{(id)(q_{(in)};q_{(out)})}$

Performance function = $[PF]_{(id)[q_{(in)};q_{(out)}]} = \frac{q_{(out)}}{q_{(in)}} = S_{(id)[q_{(in)};q_{(out)}](ref)}\ '(SR)_{(id)(q_{(in)};q_{(out)})}\ \epsilon^{j(DRA)_{(id)(q_{(in)};q_{(out)})}}$

Dimensionless sensitivity ratio = $'(SR)_{(id)(q_{(in)};q_{(out)})} = S_{(id)[q_{(in)};q_{(out)}]}/S_{(id)[q_{(in)};q_{(out)}](ref)}$; Identified component = (id)

Theoretical dimensionless sensitivity ratio = $'(SR)_{(vr)(\dot{x};e)(theo)}$ → Theoretical dynamic amplitude ratio = $'(DAR)_{(theo)} = '(DAR)_{(2;0,1,2)}$

Theoretical dynamic response angle = $(DRA)_{(theo)} = (DRA)_{(2;0,1,2)}$ Theoretical performance function for the unit under test = $[PF]_{(vr)[\dot{x};e](theo)}$

Relating function associated with the (2;0,1,2) differential equation = $[RF]_{(2;0,1,2)}$

Instruments Laboratory · Aeronautical Engineering Department · Massachusetts Institute of Technology · Cambridge · Massachusetts

Title of test LINEAR VIBRATION RECEIVER CALIBRATION; STEADY-STATE SINUSOIDAL INPUT

Date 6/22/54 In charge of test J. L. STOCKARD Assisting with test J. BARLEY

Equipment tested CONSOLIDATED LINEAR VIBRATION RECEIVER (vr)

Type 4 Model 102 Serial No. 7510 Calculations J. L. STOCKARD

Plots J. L. STOCKARD

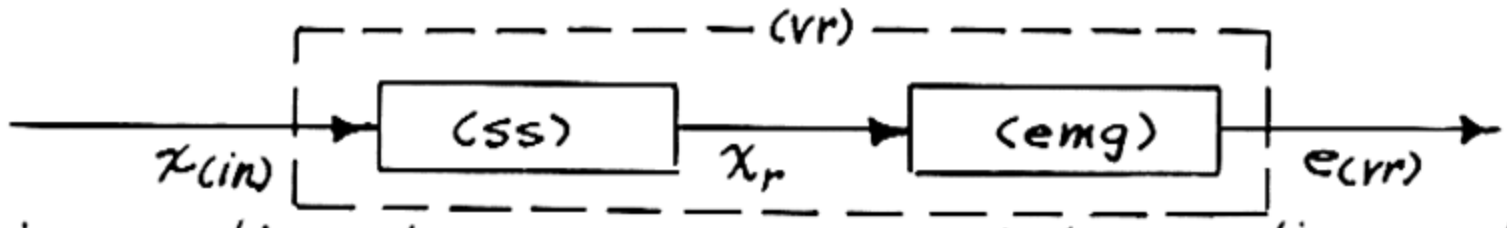
Equipment used for test SPERRY-M.I.T. VIBRATION CALIBRATOR (CONSOLIDATED) SER. NO. C875
DUMONT CATHODE-RAY OSCILLOGRAPH (cro), TYPE 304H, SER. NO. 1012
BALLANTINE VACUUM TUBE VOLTMETER (vtvm); MODEL 300, SER. NO. 6390

Input quantity LINEAR DISPLACEMENT $x_{(in)}$ Output quantity VOLTAGE $e_{(vr)}$

Environmental conditions: Temperature 70° F Pressure —

Other —

Summary of results: (when the input is considered to be vibratory displacement)



(ss) = seismographic system (emg) = electromagnetic generator

$$[PF]_{(vr)[x;e](theo)} \approx [RF]_{(2;0,1.2)x(1;0)} = S_{(vr)[x;e](ref)} \left(\frac{(FR)^2}{1-(FR)^2+j2(DR)(FR)}\right) j(FR)$$

$$[PF]_{(ss)[x;x](theo)} \approx [RF]_{(2;0,1,2)} = S_{(ss)[x;x](ref)} \frac{(FR)^2}{1-(FR)^2+j2(DR)(FR)}$$

$$[PF]_{(emg)[x;e](theo)} \approx [RF]_{(1;0)} = S_{(emg)[x;e](ref)}\, j(FR)$$

$$'(SR)_{(vr)(x;e)(theo)} \approx '(DAR)_{(2;0,1,2)x(1;0)} = \left(\frac{(FR)^2}{[1-(FR)^2]^2+[2(DR)(FR)]^2}\right)(FR)$$

$$(DRA)_{(vr)(x;e)(theo)} \approx (DRA)_{(2;0,1,2)x(1;0)} = \tan^{-1}\left(\frac{-2(DR)(FR)}{1-(FR)^2}\right)+90°$$

Reference frequency = $n_{(ref)}$ = 7 $\frac{\text{cycles}}{\text{second}}$

Damping ratio = DR = 0.7

Reference sensitivity = $S_{(vr)[x;e](ref)}$
$= 2\pi n_{(ref)}\, S_{(vr)[x;e]} = 4.84 \frac{\text{volts}}{\text{inch}}$

Reference dynamic response angle = $(DRA)_{(ref)} = -90°$

$[RF]_{(2;0,1,2)x(1;0)} = [RF]_{(2;0,1,2)} \times [RF]_{(1;0)}$

Frequency ratio = FR = $n_f/n_{(ref)}$; Forcing frequency = n_f ; Dynamic response angle = $(DRA)_{(id)(q_{(in)};q_{(out)})}$

Performance function = $[PF]_{(id)[q_{(in)};q_{(out)}]} = \frac{q_{(out)}}{q_{(in)}} = S_{(id)[q_{(in)};q_{(out)}](ref)}\, '(SR)_{(id)(q_{(in)};q_{(out)})}\, \epsilon^{\,j(DRA)_{(id)(q_{(in)};q_{(out)})}}$

Dimensionless sensitivity ratio = $'(SR)_{(id)(q_{(in)};q_{(out)})} = S_{(id)[q_{(in)};q_{(out)}]}/S_{(id)[q_{(in)};q_{(out)}](ref)}$; Identified component = (id)

Theoretical dimensionless sensitivity ratio = $'(SR)_{(vr)(x;e)(theo)}$ → Theoretical dynamic amplitude ratio = $'(DAR)_{(theo)} = '(DAR)_{(2;0,1,2)(1,0)}$

Theoretical dynamic response angle = $(DRA)_{(theo)} = (DRA)_{(2;0,1,2)(1,0)}$ Theoretical performance function for the unit under test = $[PF]_{(vr)[x;e](theo)}$

Relating function associated with the (2;0,1,2)(1,0) differential equation = $[RF]_{(2;0,1,2)}\,[RF]_{(1;0)}$

Instruments Laboratory · Aeronautical Engineering Department · Massachusetts Institute of Technology · Cambridge · Massachusetts

Title of test LINEAR VIBRATION RECEIVER CALIBRATION ; STEADY-STATE SINUSOIDAL INPUT

Date 6/22/54 **In charge of test** J. L. STOCKARD **Assisting with test** J. BARLEY

Equipment tested CONSOLIDATED LINEAR VIBRATION RECEIVER (vr)

Type 4 **Model** 102 **Serial No.** 7510 **Calculations** J. L. STOCKARD

Plots J. L. STOCKARD

Equipment used for test SPERRY-M.I.T. VIBRATION CALIBRATOR (CONSOLIDATED) SER. NO. C875
DUMONT CATHODE-RAY OSCILLOGRAPH (cro), TYPE 304H, SER. NO. 1012
BALLANTINE VACUUM TUBE VOLTMETER (vtvm); MODEL 300, SER. NO. 6390

Input quantity LINEAR VELOCITY $\dot{X}_{(in)}$ **Output quantity** VOLTAGE $e_{(vr)}$

Environmental conditions: Temperature 70° F **Pressure** —

Other —

Dimensionless sensitivity ratio performance ratio tolerance limit $(TL)_{(PR)'(SR)}$	Performance ratio low frequency limit* $n_{(f)(PR)((TL)=\quad)l}$ cps	Performance ratio high frequency limit* $n_{(f)(PR)((TL)=\quad)h}$ cps	Performance ratio operating frequency range (OFR)$_{(PR)((TL)=\quad)}$** cps	Dynamic response angle tolerance limit $(TL)_{(DRA)}$ degrees	Dynamic response angle low frequency limit* $n_{(f)(DRA)((TL)=\quad)l}$ cps	Dynamic response angle high frequency limit* $n_{(f)(DRA)((TL)=\quad)h}$ cps	Dynamic response angle operating frequency range* (OFR)$_{(DRA)((TL)=\quad)}$** cps					
-0.01	FR=2.4 16.8	∞	17→∞	+1	FR≅100 700	∞	700→∞					
-0.02	FR=2.2 15.4	∞	16→∞	+5	FR=15.5 108	∞	108→∞					
-0.05	FR=1.7 11.9	∞	12→∞	+10	FR=8 56	∞	56→∞					
-0.10	FR=1.35 9.5	∞	9→∞	+20	FR=4 28	∞	28→∞					
-0.30	FR=0.9 6.3	∞	6→∞	+30	FR=2.7 18.9	∞	19→∞					

Frequency ratio = FR = $n_f/n_{(ref)}$; Reference frequency = $n_{(ref)}$ = 7 $\frac{\text{cycles}}{\text{second}}$

Refer to Fig. 35-12 for PR tolerance-limit information. Refer to Fig. 35-13 for DRA tolerance-limit information.

* When used outside a context that defines the tolerance limit concerned, each of these concept names must be completed by the addition of the name of the quantity in which the tolerance limit exists and the numerical value and algebraic sign of this limit. For example, when the performance ratio tolerance limit is −0.1, the complete name for the performance ratio low frequency limit is minus one-tenth performance ratio tolerance limit low frequency limit and the corresponding symbol is $n_{(f)(PR)(-0.1)l}$.

** The operating frequency range is also called the band width. In bandwidth terms,

Performance ratio band width ≡ $(BW)_{(PR)((TL)=\quad)}$ ≈ $(OFR)_{(PR)((TL)=\quad)}$

Dynamic response angle band width ≡ $(BW)_{(DRA)((TL)=\quad)}$ ≈ $(OFR)_{(DRA)((TL)=\quad)}$

(SR) PLOTS: Test Form F **TEST REPORT NO.** 35-1 Sheet 4 of 13

Instruments Laboratory · Aeronautical Engineering Department · Massachusetts Institute of Technology · Cambridge · Massachusetts

Title of test LINEAR VIBRATION RECEIVER CALIBRATION; STEADY-STATE SINUSOIDAL INPUT

Date 6/22/54 In charge of test J.L. STOCKARD Assisting with test J. BARLEY

Equipment tested CONSOLIDATED LINEAR VIBRATION RECEIVER (vr)

Type 4 Model 102 Serial No. 7510 Calculations J.L. STOCKARD

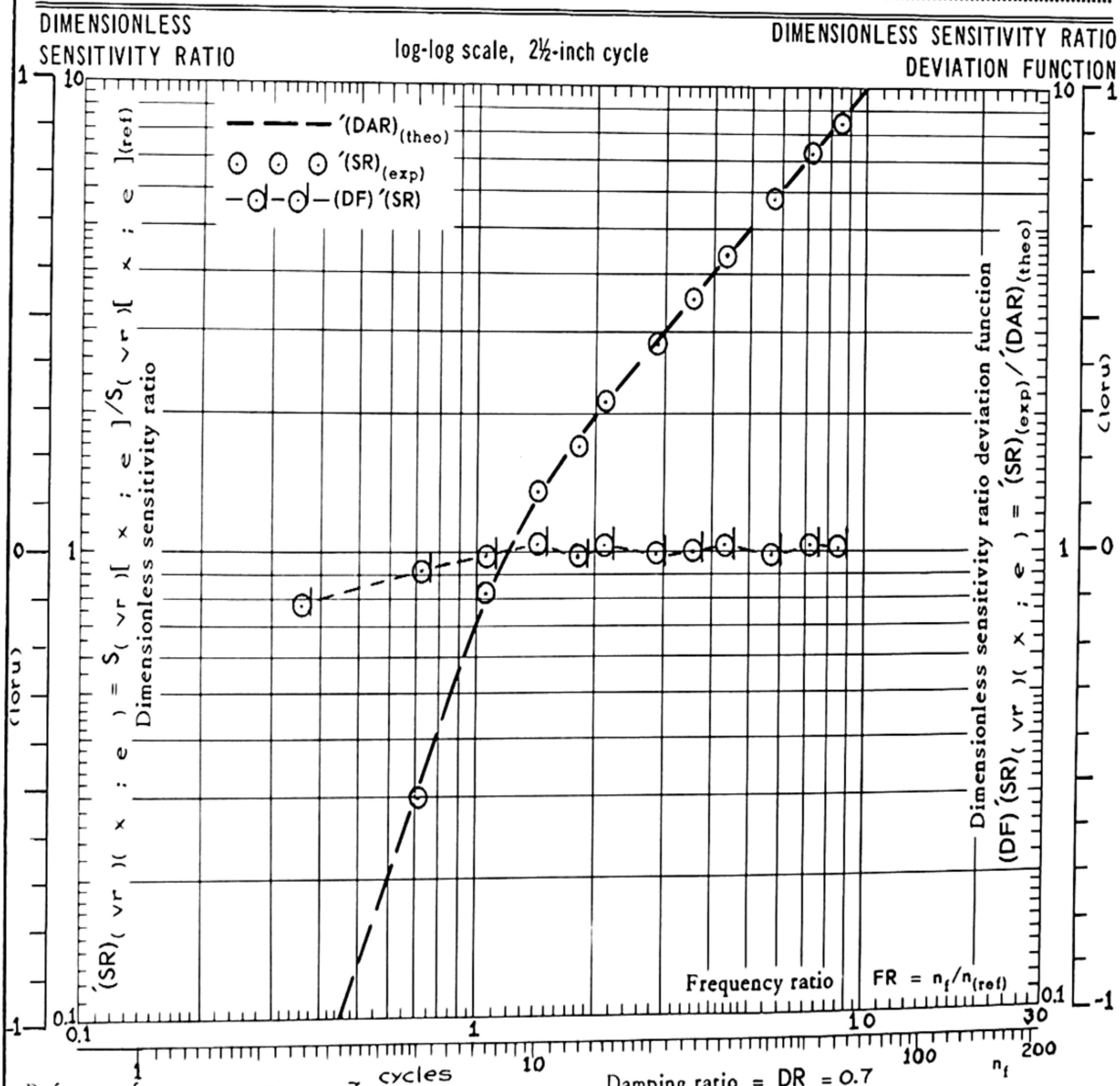
Plots J.L. STOCKARD

Equipment used for test SPERRY-M.I.T. VIBRATION CALIBRATOR (CONSOLIDATED) SER. NO. C875
DUMONT CATHODE-RAY OSCILLOGRAPH (cro), Type 304H, SER. NO. 1012
BALLANTINE VACUUM TUBE VOLTMETER (vtvm); MODEL 300, SER. NO. 6390

Input quantity LINEAR DISPLACEMENT $X_{(in)}$ Output quantity VOLTAGE $e_{(vr)}$

Environmental conditions: Temperature 70° F Pressure —

Other —



Reference frequency = $n_{(ref)} = 7 \frac{\text{cycles}}{\text{second}}$ Damping ratio = DR = 0.7

Reference sensitivity = $S_{(\ vr\ )[\ x\ ;\ e\ ](ref)} = 4.84$ volts/inch

Theoretical dimensionless dynamic amplitude ratio $= {}'(DAR)_{(theo)} \approx {}'(DAR)_{(2;0,1,2)\times(1;0)} = \dfrac{(FR)^2}{\sqrt{[1-(FR)^2]^2 + [2(DR)(FR)]^2}}(FR)$

$'(DAR)_{(theo)}$ is $'(SR)_{(theo)}$, the theoretical dimensionless sensitivity ratio for the unit under test; $'(SR)_{(exp)}$ is the dimensionless sensitivity ratio determined by experiment.

DRA PLOTS: Test Form K

TEST REPORT NO. 35-1

Instruments Laboratory · Aeronautical Engineering Department · Massachusetts Institute of Technology · Cambridge · Massachusetts

Title of test LINEAR VIBRATION RECEIVER CALIBRATION; STEADY-STATE SINUSOIDAL INPUT

Date 6/22/54 **In charge of test** J.L. STOCKARD **Assisting with test** J. BARLEY

Equipment tested CONSOLIDATED LINEAR VIBRATION RECEIVER (vr)

Type 4 **Model** 102 **Serial No.** 7510

Calculations J.L. STOCKARD

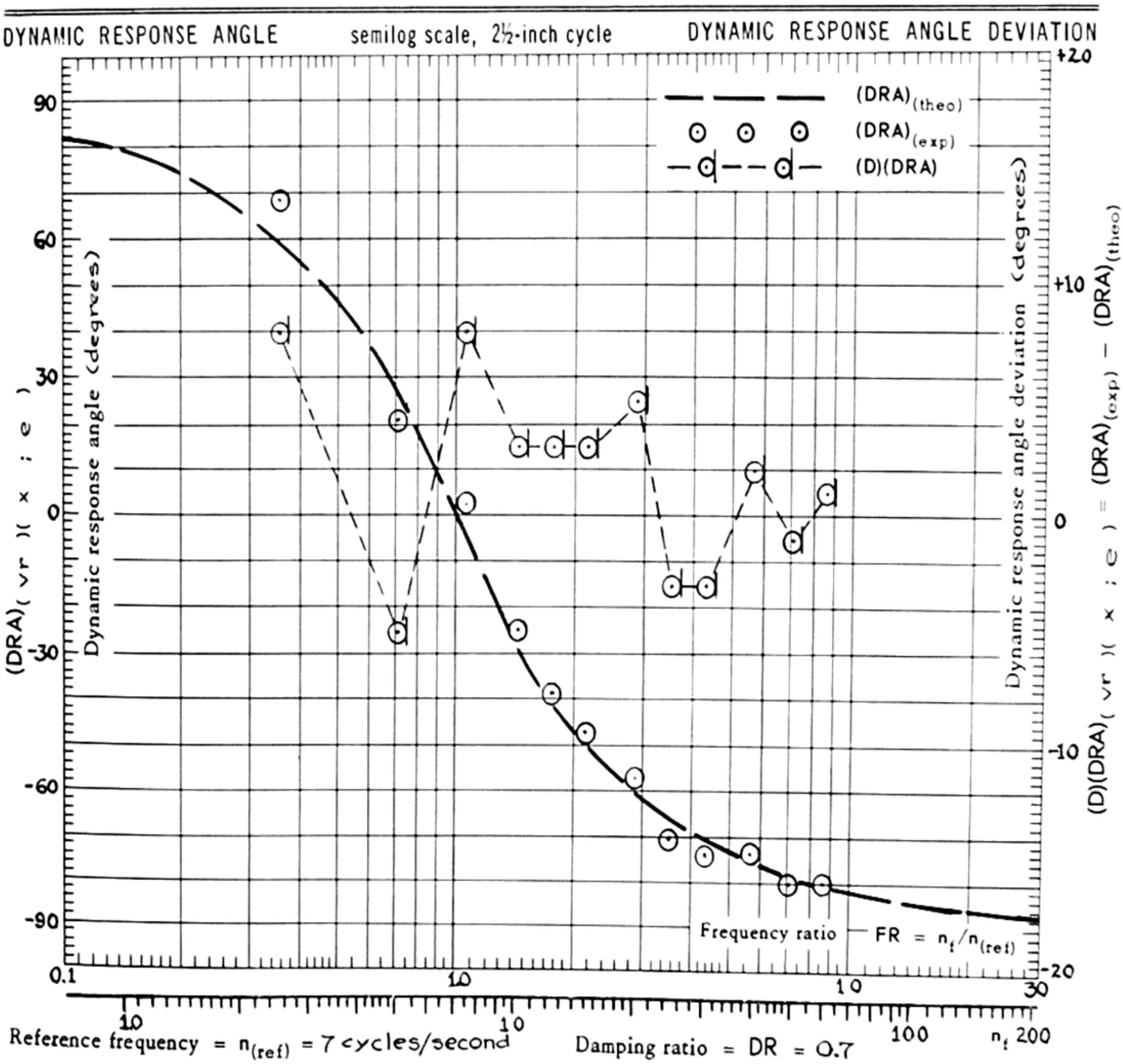
Plots J.L. STOCKARD

Equipment used for test SPERRY-M.I.T. VIBRATION CALIBRATOR (CONSOLIDATED) SER. NO. C875; DUMONT CATHODE-RAY OSCILLOGRAPH (cro), Type 304H, SER. NO. 1012; BALLANTINE VACUUM TUBE VOLTMETER (vtvm): MODEL 300, SER. NO. 6390

Input quantity LINEAR DISPLACEMENT $x_{(in)}$ **Output quantity** VOLTAGE $e_{(vr)}$

Environmental conditions: Temperature 70° F **Pressure** –

Other –



Reference frequency = $n_{(ref)}$ = 7 cycles/second Damping ratio = DR = 0.7

Reference dynamic response angle = $(DRA)_{(ref)} = -90°$

Theoretical dynamic response angle = $(DRA)_{(theo)} = (DRA)_{(2;0,1,2)x(1;0)} = (DRA)_{(2;0,1,2)} + (DRA)_{(1;0)} = \tan^{-1}\left[\frac{-2(DR)(FR)}{1-(FR)^2}\right] + 90°$

$(DRA)_{(theo)}$ is the theoretical dynamic response angle for the unit under test; $(DRA)_{(exp)}$ is the dynamic response angle determined by experiment.

(SR) PLOTS: Test Form F **TEST REPORT NO.** 35-1 Sheet 6 of 13

Instruments Laboratory · Aeronautical Engineering Department · Massachusetts Institute of Technology · Cambridge · Massachusetts

Title of test LINEAR VIBRATION RECEIVER CALIBRATION; STEADY-STATE SINUSOIDAL INPUT

Date 6/22/54 In charge of test J. L. STOCKARD Assisting with test J. BARLEY

Equipment tested CONSOLIDATED LINEAR VIBRATION RECEIVER (vr)

Type 4 Model 102 Serial No. 7510 Calculations J. L. STOCKARD

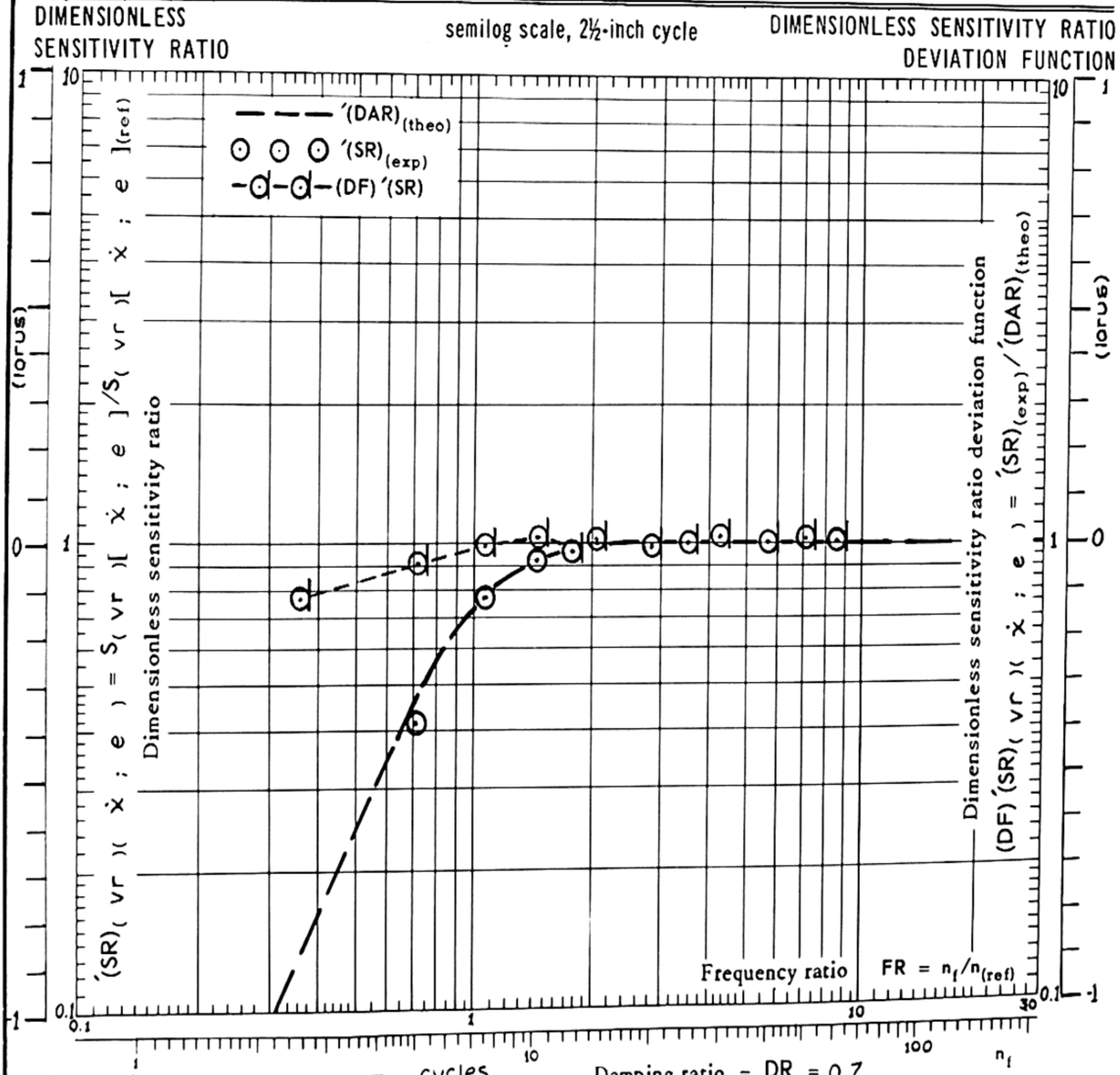
Plots J. L. STOCKARD

Equipment used for test SPERRY-M.I.T. VIBRATION CALIBRATOR (CONSOLIDATED) SER. NO. C875
DUMONT CATHODE-RAY OSCILLOGRAPH (cro), Type 304H, SER. NO. 1012
BALLANTINE VACUUM TUBE VOLTMETER (vtvm); MODEL 300, SER NO. 6390

Input quantity LINEAR VELOCITY $\dot{x}_{(in)}$ Output quantity VOLTAGE $e_{(vr)}$

Environmental conditions: Temperature 70° F Pressure —

Other —



Reference frequency = $n_{(ref)}$ = 7 $\frac{\text{cycles}}{\text{second}}$ Damping ratio = DR = 0.7

Reference sensitivity = $S_{(vr)[\dot{x};e](ref)}$ = 0.11 $\frac{\text{volt}}{\text{inch/second}}$

Theoretical dimensionless dynamic amplitude ratio = $'(DAR)_{(theo)} \approx '(DAR)_{(2;0,1,2)} = \frac{(FR)^2}{\sqrt{[1-(FR)^2]^2 + [2(DR)(FR)]^2}}$

$'(DAR)_{(theo)}$ is $'(SR)_{(theo)}$, the theoretical dimensionless sensitivity ratio for the unit under test; $'(SR)_{(exp)}$ is the dimensionless sensitivity ratio determined by experiment.

DRA PLOTS: Test Form K **TEST REPORT NO.** 35-1 Sheet 7 of 13

Instruments Laboratory · Aeronautical Engineering Department · Massachusetts Institute of Technology · Cambridge · Massachusetts

Title of test LINEAR VIBRATION RECEIVER CALIBRATION ; STEADY-STATE SINUSOIDAL INPUT

Date 6/22/54 **In charge of test** J. L. STOCKARD **Assisting with test** J. BARLEY

Equipment tested CONSOLIDATED LINEAR VIBRATION RECEIVER (vr)

Type 4 **Model** 102 **Serial No.** 7510 **Calculations** J. L. STOCKARD

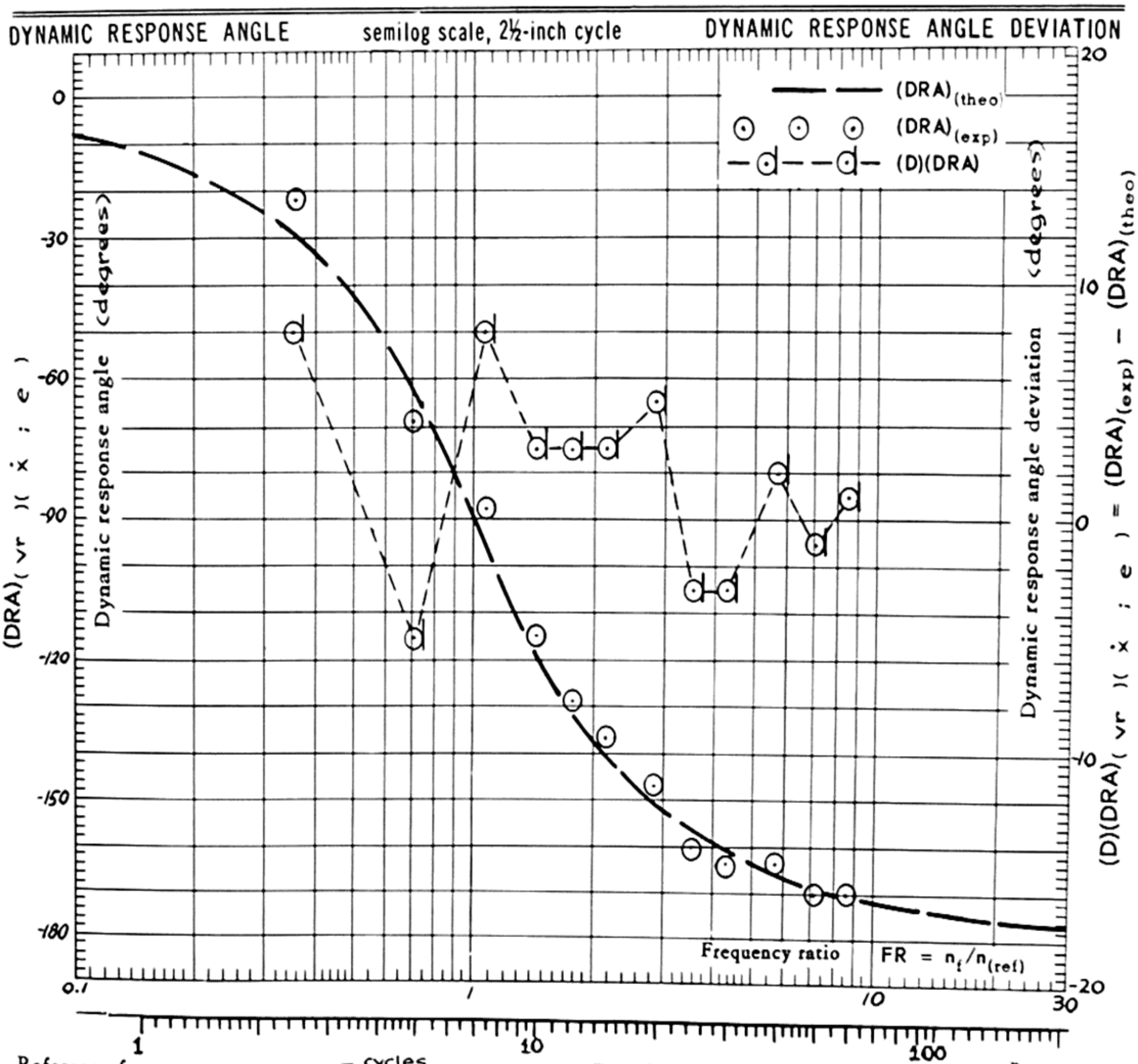
Plots J. L. STOCKARD

Equipment used for test SPERRY - M.I.T. VIBRATION CALIBRATOR (CONSOLIDATED) SER. NO. 0875
DUMONT CATHODE-RAY OSCILLOGRAPH (cro), Type 304H, SER. NO. 1012
BALLANTINE VACUUM TUBE VOLTMETER (vtvm) ; MODEL 300, SER. NO. 6390

Input quantity LINEAR VELOCITY $\dot{x}_{(in)}$ **Output quantity** VOLTAGE $e_{(vr)}$

Environmental conditions: Temperature 70°F **Pressure** —

Other —



Reference frequency = $n_{(ref)} = 7 \frac{\text{cycles}}{\text{second}}$ Damping ratio = DR = 0.7

Reference dynamic response angle = $(DRA)_{(ref)} = -180°$

Theoretical dynamic response angle = $(DRA)_{(theo)} = (DRA)_{(2;0,1,2)} = \tan^{-1}\left[\frac{-2(DR)(FR)}{1-(FR)^2}\right]$

$(DRA)_{(theo)}$ is the theoretical dynamic response angle for the unit under test; $(DRA)_{(exp)}$ is the dynamic response angle determined by experiment.

(SR) PLOTS: Test Form Ia **TEST REPORT NO.** 35-1 Sheet 8 of 13

Instruments Laboratory · Aeronautical Engineering Department · Massachusetts Institute of Technology · Cambridge · Massachusetts

Title of test LINEAR VIBRATION RECEIVER CALIBRATION; STEADY-STATE SINUSOIDAL INPUT

Date 6/22/54 In charge of test J. L. STOCKARD Assisting with test J. BARLEY

Equipment tested CONSOLIDATED LINEAR VIBRATION RECEIVER (vr)

Calculations J. L. STOCKARD

Type 4 Model 102 Serial No. 7510

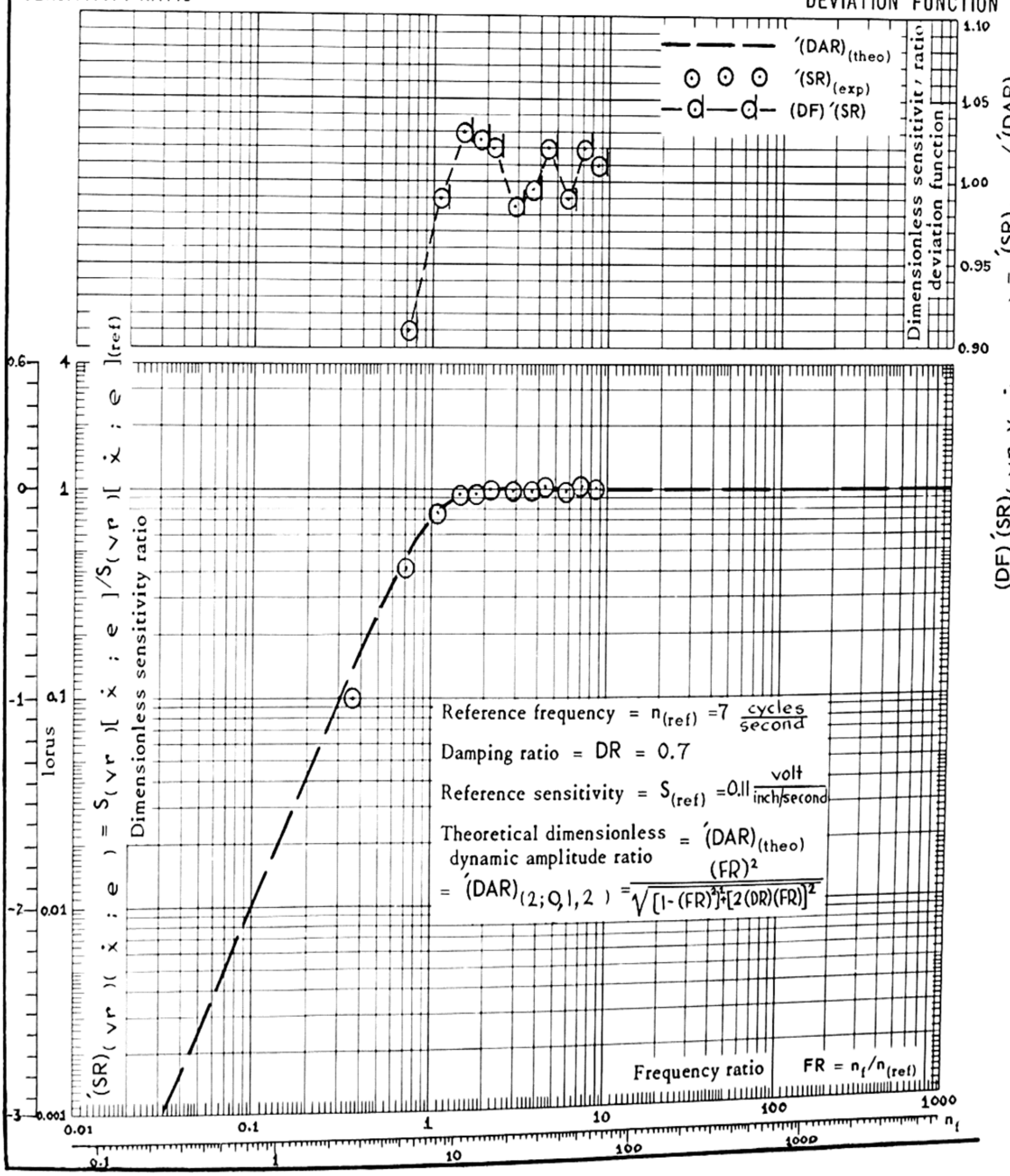
Plots J. L. STOCKARD

Equipment used for test SPERRY-M.I.T. VIBRATION CALIBRATOR (CONSOLIDATED) SER. NO. C875
DUMONT-CATHODE RAY OSCILLOGRAPH (cro), Type 304-H, SER. NO. 1012
BALLANTINE VACUUM TUBE VOLTMETER (vtvm); MODEL 300, SER. NO. 6390

Input quantity LINEAR VELOCITY $\dot{X}_{(in)}$ Output quantity VOLTAGE $e_{(vr)}$

Environmental conditions: Temperature 70° F Pressure —

Other —



DRA PLOTS: Test Form L **TEST REPORT NO.** 35-1 Sheet 9 of 13

Instruments Laboratory · Aeronautical Engineering Department · Massachusetts Institute of Technology · Cambridge · Massachusetts

Title of test LINEAR VIBRATION RECEIVER CALIBRATION ; STEADY-STATE SINUSOIDAL INPUT

Date 6/22/54 In charge of test J. L. STOCKARD Assisting with test J. BARLEY

Equipment tested CONSOLIDATED LINEAR VIBRATION RECEIVER (vr)

Type 4 Model 102 Serial No. 7510 Calculations J. L. STOCKARD

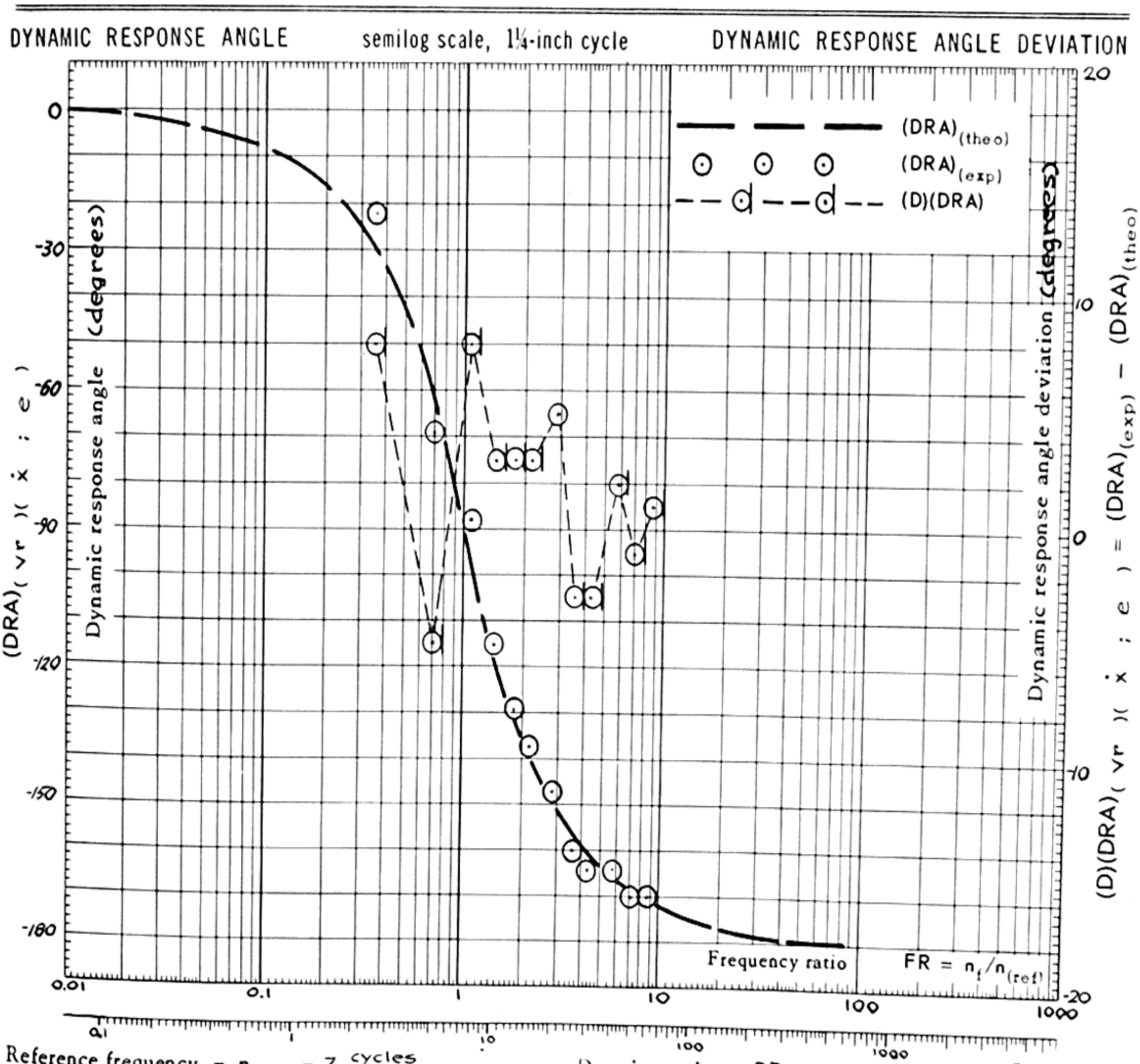
Plots J. L. STOCKARD

Equipment used for test SPERRY-M.I.T. VIBRATION CALIBRATOR (CONSOLIDATED) SER. NO. C875
DUMONT CATHODE-RAY OSCILLOGRAPH (cro), Type 304H, SER. NO. 1012
BALLANTINE VACUUM TUBE VOLTMETER (vtvm); MODEL 300, SER. NO. 6390

Input quantity LINEAR VELOCITY $\dot{x}$ (in) Output quantity VOLTAGE e(vr)

Environmental conditions: Temperature 70° F Pressure —

Other —



Reference frequency = $n_{(ref)} = 7 \frac{\text{cycles}}{\text{second}}$ Damping ratio = DR = 0.7

Reference dynamic response angle = $(DRA)_{(ref)} = -180°$

Theoretical dynamic response angle = $(DRA)_{(theo)} = (DRA)_{(2;0,1,2)} = \tan^{-1}\left[\frac{-2(DR)(FR)}{1-(FR)^2}\right]$

$(DRA)_{(theo)}$ is the theoretical dynamic response angle for the unit under test; $(DRA)_{(exp)}$ is the dynamic response angle determined by experiment.

PR PLOTS: Test Form Ea **TEST REPORT NO.** 35-1 Sheet 10 of 13

Instruments Laboratory · Aeronautical Engineering Department · Massachusetts Institute of Technology · Cambridge · Massachusetts

Title of test LINEAR VIBRATION RECEIVER CALIBRATION ; STEADY-STATE SINUSOIDAL INPUT

Date 6/22/54 In charge of test J. L. STOCKARD Assisting with test J. BARLEY

Equipment tested CONSOLIDATED LINEAR VIBRATION RECEIVER (vr)

Type 4 Model 102 Serial No. 7510 Calculations J. L. STOCKARD

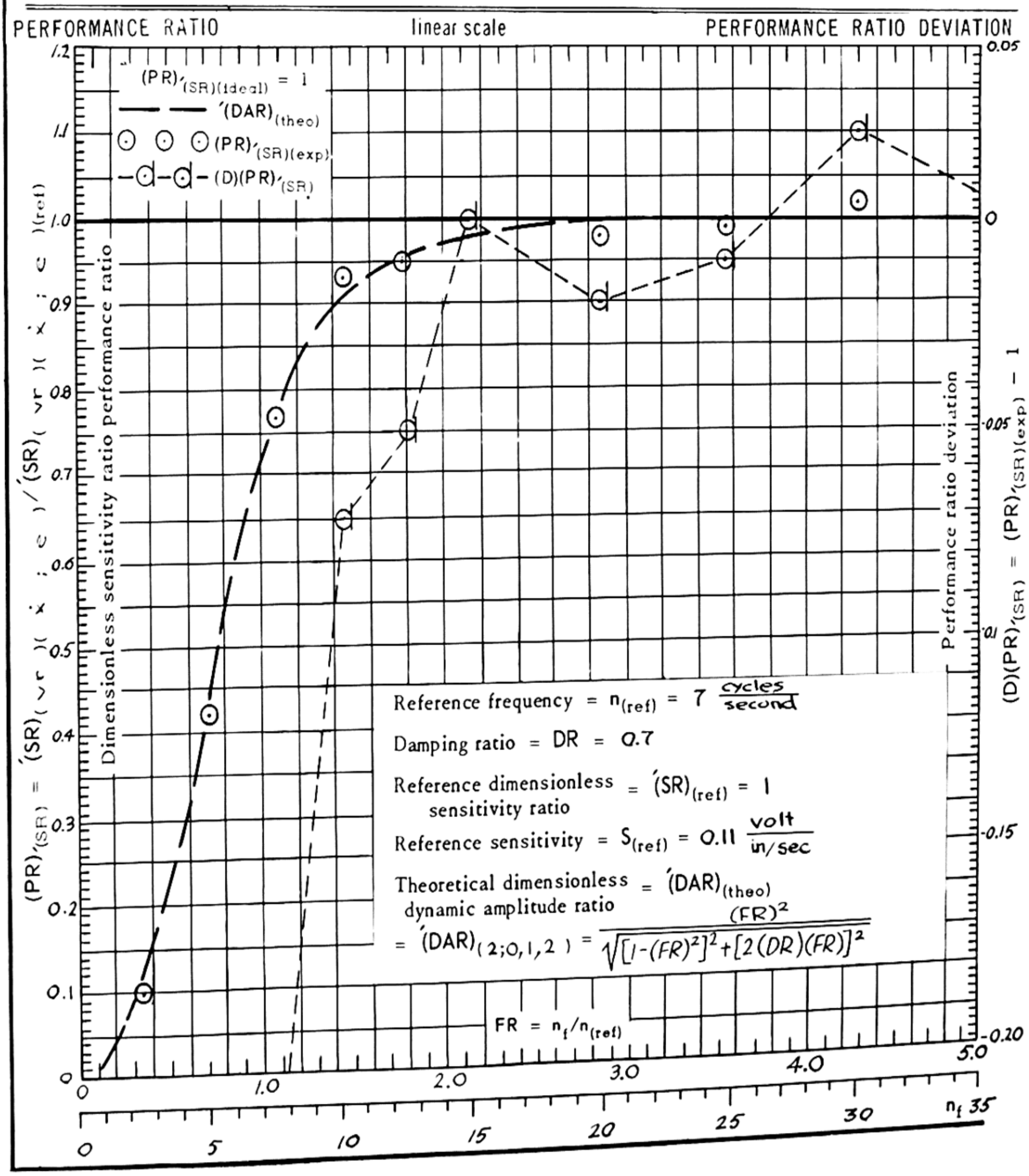
Plots J. L. STOCKARD

Equipment used for test SPERRY-M.I.T. VIBRATION CALIBRATOR (CONSOLIDATED) SER. NO. C875
DUMONT CATHODE-RAY OSCILLOGRAPH (cro), Type 304H, SER. NO. 1012
BALLANTINE VACUUM TUBE VOLTMETER (vtvm); MODEL 300, SER. NO. 6390

Input quantity LINEAR VELOCITY $\dot{x}_{(in)}$ Output quantity VOLTAGE $e_{(vr)}$

Environmental conditions: Temperature 70° F Pressure —

Other —



Instruments Laboratory · Aeronautical Engineering Department · Massachusetts Institute of Technology · Cambridge · Massachusetts

Title of test LINEAR VIBRATION RECEIVER CALIBRATION; STEADY-STATE SINUSOIDAL INPUT

Date 6/22/54 **In charge of test** J. L. STOCKARD **Assisting with test** J. BARLEY

Equipment tested CONSOLIDATED LINEAR VIBRATION RECEIVER (vr)

Type 4 **Model** 102 **Serial No.** 7510

Calculations J. L. STOCKARD

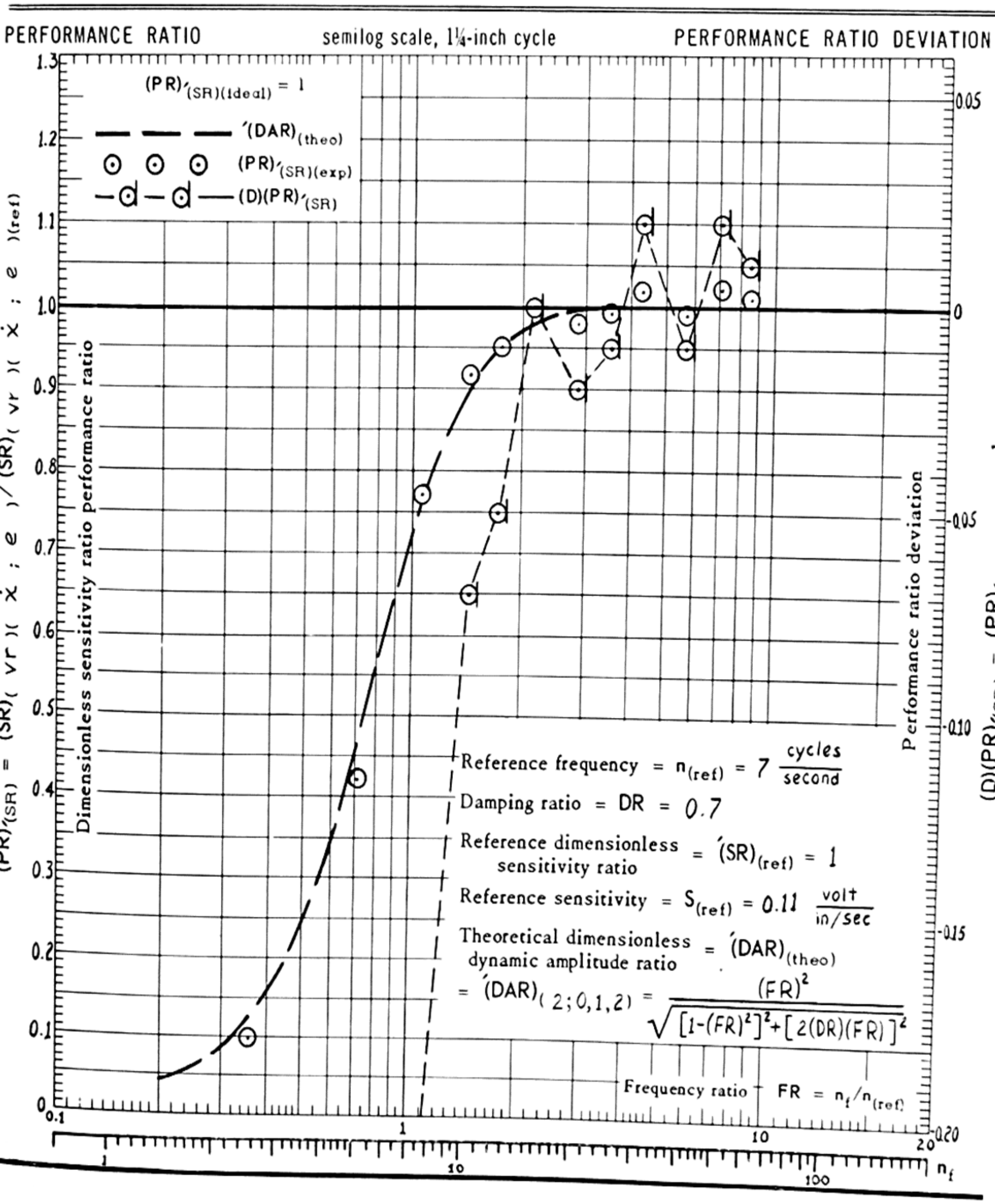
Plots J. L. STOCKARD

Equipment used for test SPERRY-M.I.T. VIBRATION CALIBRATOR (CONSOLIDATED) SER. NO. C875
DUMONT CATHODE-RAY OSCILLOGRAPH (cro), Type 304H, SER. NO. 1012
BALLANTINE VACUUM TUBE VOLTMETER (vtvm); MODEL 300, SER. NO. 6390

Input quantity LINEAR VELOCITY $\dot{x}$(in) **Output quantity** VOLTAGE e(vr)

Environmental conditions: Temperature 70° F **Pressure** –

Other –



TEST DATA: Test Form N **TEST REPORT NO. 35-1** Sheet 12 of 13

Instruments Laboratory · Aeronautical Engineering Department · Massachusetts Institute of Technology · Cambridge · Massachusetts

Title of test LINEAR VIBRATION RECEIVER CALIBRATION; STEADY-STATE SINUSOIDAL INPUT

Date 6/22/54 In charge of test J.L. STOCKARD Assisting with test J. BARLEY

Equipment tested CONSOLIDATED LINEAR VIBRATION RECEIVER (vr)

Type 4 Model 102 Serial No. 7510 Calculations J.L. STOCKARD

Plots J.L. STOCKARD

Equipment used for test SPERRY-M.I.T. VIBRATION CALIBRATOR (CONSOLIDATED) SER. NO. C875
DUMONT CATHODE-RAY OSCILLOGRAPH (cro), Type 304H, SER. NO. 1012
BALLANTINE VACUUM TUBE VOLTMETER (vtvm); MODEL 300, SER. NO. 6390

Input quantity LINEAR VELOCITY $\dot{x}_{(in)}$ Output quantity VOLTAGE $e_{(vr)}$

Environmental conditions: Temperature 70° F Pressure

Other —

Run Number	Forcing Amplitude $\dot{X}$	Forcing Frequency n_f	Output Amplitude $e_{(out)(rms)}$	Output Voltage Amplitude $e_{(out)a}$	Input-Output Sensitivity $S_{(vr)[\dot{x}\ ;\ e]_{(exp)}}$	Dimensionless Sensitivity Ratio $(SR)_{(vr)(\dot{x}\ ;\ e)_{(exp)}}$ *	Theoretical Dimensionless Dynamic Amplitude Ratio $(DAR)_{(theo)} = (DAR)_{(2;0,1,2)}$	Dimensionless Sensitivity Ratio Deviation Function $(DF)(SR) = {}'(SR)_{(exp)}/{}'(DAR)_{(theo)}$	Dynamic Response Angle $(DRA)_{(vr)[\dot{x}\ ;\ e]_{(exp)}}$			Theoretical Dynamic Response Angle $(DRA)_{(theo)} = (DRA)_{(2;0,1,2)}$	Dynamic Response Angle Deviation $(D)(DRA) = (DRA)_{(exp)} - (DRA)_{(theo)}$	Frequency Ratio $FR = n_f/n_{(ref)}$	PERFORMANCE RATIO DEVIATION $(D)(PR) = (PR)(SR) = (PR)(SR) - 1$
Units and References	$X_{(in)a}$ = 0.0255 inch inches/second	cycles/second	$S_{(vtvm)}[e_{rms}] = 1.414$ volts/volt Volts (rms)	volts	$\frac{\text{volts}}{\text{inch/second}}$ $S_{(ref)} = 0.11$ volt/in/sec		Theoretical Dimensionless Dynamic Amplitude Ratio $(DAR)_{(theo)}$	Dimensionless Sensitivity Ratio Deviation Function $(DF)(SR) = {}'(SR)_{(exp)}/{}'(DAR)_{(theo)}$	Dynamic Response Angle $(DRA)_{(vr)[\dot{x}\ ;\ e]_{(exp)}}$			Theoretical Dynamic Response Angle $(DRA)_{(theo)} = (DRA)_{(2;0,1,2)}$	Dynamic Response Angle Deviation $(D)(DRA) = (DRA)_{(exp)} - (DRA)_{(theo)}$	Frequency Ratio $FR = n_f/n_{(ref)}$	PERFORMANCE RATIO DEVIATION $(D)(PR) = (PR)(SR) = (PR)(SR) - 1$
									$(DRA)_{(ref)} = -180°$ degrees					$n_{(ref)} = 7$ $\frac{\text{cycles}}{\text{second}}$	$(PR)(SR)(ideal) = 1$
1	0.4	2.5	0.00315	0.00445	0.0115	0.101	0.127	0.795	-22	-29.8	+8			0.357	-0.899
2	0.8	5	0.0262	0.0370	0.0462	0.420	0.461	0.91	-69	-63.9	-5			0.715	-0.580
3	1.2	7.5	0.0716	0.101	0.0843	0.77	0.759	0.99	-88	-95.6	+8			1.07	-0.230
4	1.6	10	0.113	0.16	0.102	0.93	0.906	1.03	-115	-117.6	+3			1.43	-0.07
5	2	12.5	0.148	0.209	0.1045	0.95	0.955	1.01	-129	-132.0	+3			1.78	-0.05
6	2.4	15	0.186	0.264	0.110	1.0	0.980	1.02	-137	-139.7	+3			2.14	0
7	3.2	20	0.245	0.346	0.108	0.98	0.995	0.985	-147	-151.9	+5			2.86	-0.02
8	4	25	0.308	0.435	0.109	0.99	0.996	0.995	-160	-156.9	-3			3.57	-0.01

* ${}'(SR)_{(exp)} = S_{(exp)}/S_{(ref)}$; Reference sensitivity $= S_{(vr)[\dot{x}\ ;\ e]_{(ref)}} = S_{(ref)}$.

TEST DATA: Test Form 0 — TEST REPORT NO. 35-1 — Sheet 13 of 13

Instruments Laboratory · Aeronautical Engineering Department · Massachusetts Institute of Technology · Cambridge · Massachusetts

Run Number	Forcing Amplitude $\dot{\mathcal{X}}$	Forcing Frequency n_f	Output Amplitude $e_{(out)(rms)}$	Output Voltage Amplitude $e_{(out)a}$	Input-Output Sensitivity $S_{(vr)[\dot{x};e](exp)}$	Dimensionless Sensitivity Ratio $'(SR)_{(vr)(\dot{x};e)(exp)}$*	Theoretical Dimensionless Dynamic Amplitude Ratio $'(DAR)_{(theo)} = {}'(DAR)_{(2;0,1,2)}$	Dimensionless Sensitivity Ratio Deviation Function $(DF)\,'(SR) = {}'(SR)_{(exp)}/{}'(DAR)_{(theo)}$	Dynamic Response Angle $(DRA)_{(vr)(\dot{x};e)(exp)}$	Theoretical Dynamic Response Angle $(DRA)_{(theo)} = (DRA)_{(2;0,1,2)}$	Dynamic Response Angle Deviation $(D)(DRA) = (DRA)_{(exp)} - (DRA)_{(theo)}$	Frequency Ratio $FR = n_f/n_{(ref)}$	PERFORMANCE RATIO DEVIATION $(D)(PR) = (PR)'(SR)^{-1}$
Units and References	$X_{(in)a} = 0.0255$ inch inches/second	cycles/second	$S_{(vtvm)}[e_{rms}/e] = 1.414$ volts/volt volts (rms)	volts	volts / inch/second	$S_{(ref)} = 0.11$ volt/in/sec			$(DRA)_{(ref)} = -180°$ degrees			$n_{(ref)} = 7$ cycles/second	$(PR)'(SR)_{(ideal)} = 1$
9	4.8	30	0.381	0.538	0.112	1.02	1.00	1.02	-164	-161.1	-3	4.3	+0.02
10	6.41	40	0.495	0.70	0.109	0.99	1.00	0.99	-164	-165.6	+2	5.7	-0.01
11	8.02	50	0.64	0.905	0.112	1.02	1.00	1.02	-170	-168.6	-1	7.15	+0.02
12	9.62	60	0.78	1.10	0.111	1.01	1.00	1.01	-170	-170.8	+1	8.6	+0.01

NOTE: THE DATA TABULATION FOR THE DISPLACEMENT INDUT ($\mathcal{X}_{(in)}$) — VOLTAGE OUTPUT PLOTS OF SHEETS 4 AND 5 IS OMITTED.

* $'(SR)_{(exp)} = S_{(exp)}/S_{(ref)}$; Reference sensitivity $= S_{(vr)[\dot{x};e](ref)} = S_{(ref)}$.

produced by mismatches between the actual performance and the theoretical performance equations.

35.240. Test Report No. 35-1 summarizes information on the calibration of a linear vibration receiver with the design features described by Fig. 35-7f. This unit has a Coulomb-friction-free spring suspension for the seismic element with oil damping and an output signal generator of the electromagnetic type. It is generally good practice to include a pictorial diagram and other physical information in the calibration report of any given unit. This physical description is omitted here because of its accessibility in Fig. 35-7f.

35.241. From the standpoint of experimental technique, the performance of a vibration receiver may be studied by means of vibration calibrators, which are designed to apply mechanical input displacements of simple sinusoidal wave shape and accurately known, adjustable amplitude and frequency. By the use of several different amplitudes and a suitable range of frequencies, with proper observations of the corresponding outputs, the performance characteristics of the receiver may be measured in quantitative terms. In many cases, it is not feasible to cover the desired operating range of frequencies completely. When this situation exists, careful observations should be made in critical regions of the frequency spectrum. These regions may be critical because they include the complete range of desired operation or because they involve crucial behavior of the theoretical performance-describing functions. When agreement between experimental and theoretical function points is good in crucial regions, the theoretical function may be used with confidence to give performance characteristics for a range of input frequencies that is much wider than the range covered by experimental data.

35.242. Vibration-measuring equipment may be calibrated by means of input motions of many types other than steady-state sinusoidal oscillations. For example, pulse-function forcing motions may be applied. The problem of finding response characteristics of equipment from pulse-function transient response data is discussed in Chapter 32. The illustrative examples of calibration of vibration-measuring equipment by the sinusoidal-input method are given in the typical test reports that follow.

35.243. Figure 35-42 illustrates the essential features of a mechanical calibrator for vibration-receiving units. The basic element of this device is a heavy flywheel rotating on carefully aligned, preloaded ball bearings. This flywheel is driven by a relatively powerful direct-current motor. Approximate speed measurements are provided by an electrical tachometer. Accurate speed measurements are made by means of a stroboscopic light flashing with a known frequency and three patterns of black and white segments on the flywheel. With this combination, a closely spaced sequence of known forcing frequencies may be determined by adjusting the motor speed to make various combinations of the patterns appear to be stationary under the stroboscopic light.

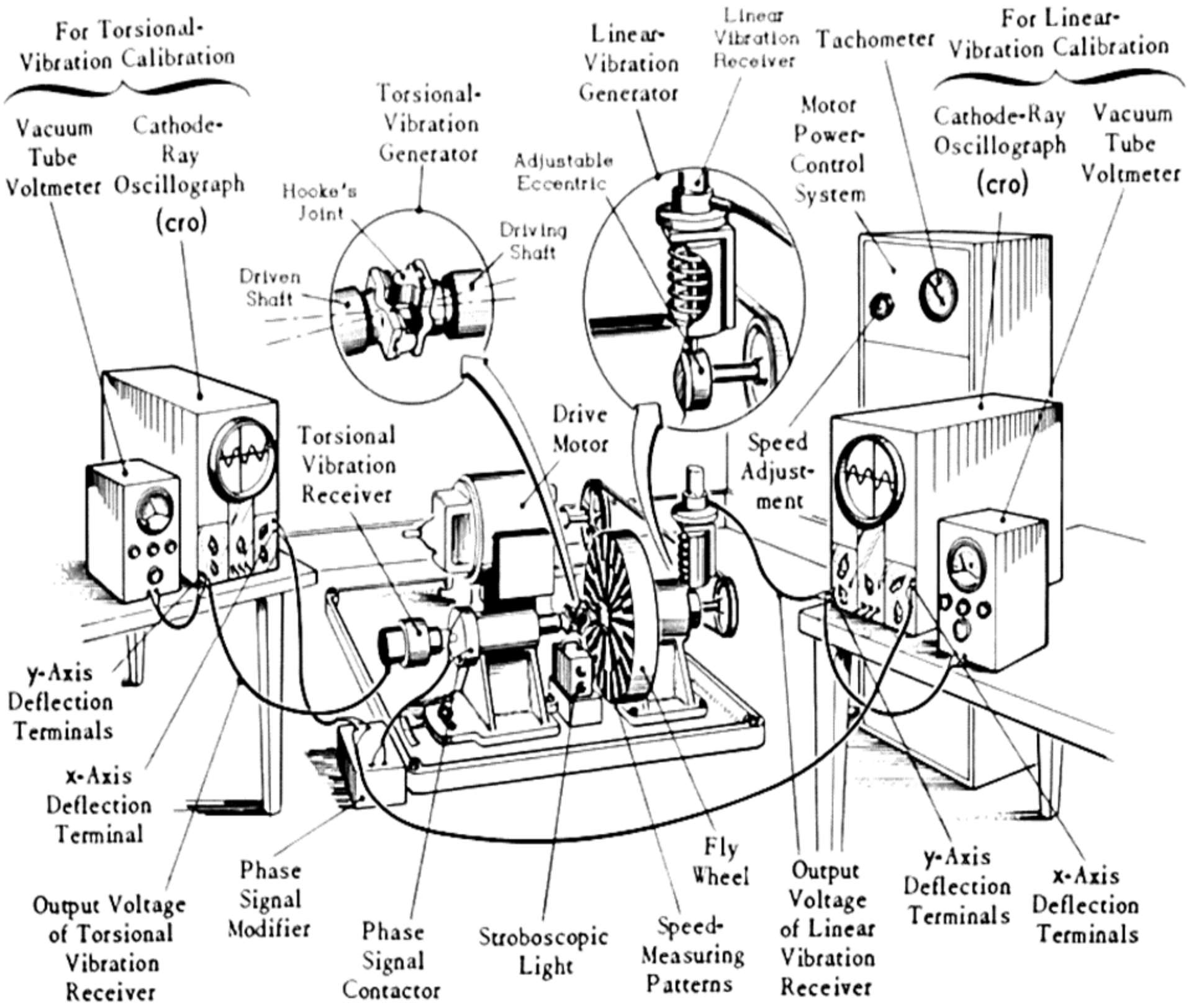


Fig. 35-42. Calibration of linear and torsional vibration receivers.

35.244. Linear vibration receivers are tested on the calibrator of Fig. 35-42 by means of a spring-loaded follower riding on an eccentric fixed to the shaft of the flywheel. The eccentric that drives the follower is fitted outside a second eccentric so that the amplitude of the output displacement may be varied by rotating one eccentric with respect to the other. The unit to be calibrated is fixed to the follower and receives a sinusoidal motion with a forcing frequency equal to the speed of the flywheel. Phase relationships between the forcing motion and the output voltage are determined by a contactor rotating with the flywheel shaft, and an intensifying circuit that causes a bright spot to appear on the output trace of the cathode-ray oscillograph used for indicating the output voltage.

35.245. Sheet 1 of Test Report No. 35-1 gives the essential background information on the calibration of a linear vibration receiver by the use of steady-state sinusoidal inputs applied at a sequence of constant frequencies at a constant amplitude well within the operating limits of the receiver. This sheet identifies the test reported; gives the date the test was made and the names of the personnel involved; identifies the unit tested, the principal pieces of test equipment used, the input quantity and the output quantity; and lists the essential environmental conditions. In practice, it is very important to provide forms, preferably on transparent paper for easy reproduction, with convenient spaces for the descriptive information

just noted. Particular situations will often require items not included on sheet 1, but, in any case, sufficient information should be given to permit the test described to be repeated if this should become necessary.

35.246. The Summary of Results on sheet 1 of Test Report No. 35-1 gives a functional diagram, showing the input as linear velocity and the output as voltage. The performance function for this input quantity – output quantity combination is shown as having the general form of the relating function for the (2;0, 1, 2) differential equation. This function in terms of frequency ratio and damping ratio is given with the linear velocity input – voltage output reference sensitivity as a scalar multiplying factor. This reference sensitivity is given as 0.11 volt per inch-per-second, the damping ratio is listed as 0.7, and the reference frequency is shown as 7 cycles per second. The reference dynamic response angle is taken as -180 degrees.

35.247. Test Report No. 35-1 does not outline the reasoning behind the choice of the (2;0, 1, 2) relating function form as the performance function for the linear vibration receiver under test. The basic reason for this choice is the design of the receiver itself, as illustrated by the diagram of Fig. 35-4g. This diagram shows a seismographic system coupled to an electromagnetic generator. The developments of Derivation Summaries 35-2 and 35-3 lead to the (2;0, 1, 2) relating function as the form for describing steady-state sinusoidal performance. On the basis of the mechanical features used in the receiver, it is reasonable to assume that the undamped natural frequency of the seismographic system is so low that any operating frequency range must be above this frequency. This means that the unit operates in the displacement-receiving range discussed in Derivation Summary 35-3. Within this range, the seismographic system output is a linear displacement proportional in magnitude to the input displacement. The corresponding input to the electromagnetic generator is a motion proportional to the input motion. As indicated in the discussion of Figs. 35-5i and 5j, the electromagnetic generator output is proportional to the linear velocity it receives as its input. The net result of the seismographic system action and the electromagnetic generator action is that linear velocity may be considered as the receiver input with voltage as the corresponding output. When this choice of variables is used, the performance function of the receiver is identical in form with the performance function of the seismographic system.

35.248. The discussion of the preceding paragraph outlines the background reasoning involved in choosing a performance-function form to describe the characteristics of a particular vibration receiver type. Once a tentative choice of a performance function is made, numerical values of the parameters involved and final proof of the suitability of the performance function depend on its agreement with test results. The association of the (2;0,1,2) relating function with the velocity

input – voltage output performance function for the linear vibration receiver implies that experimental results justify the use of the (2;0,1,2) form for representing operational characteristics. The details of this justification are given in various forms by the plots of sheets 4 to 11 of Test Report No. 35-1.

35.249. For the second functional diagram shown on sheet 2 of Test Report No. 35-1, the receiver input is considered to be linear displacement, as is the seismographic system output also. The electromagnetic generator input is considered to be a linear displacement that produces voltage as the output. With this choice of quantities, the performance function for the receiver is the product of the (2;0, 1, 2) relating function form and the (1;0) relating function form. The net result is a performance function similar to the velocity-voltage performance function multiplied by j times the frequency ratio. The reference frequency of 7 cycles per second and the damping ratio of 0.7 remain unchanged. The displacement-voltage reference sensitivity is 4.84 volts/inch, and the reference dynamic response angle is -90 degrees.

35.250. Sheet 3 of Test Report No. 35-1 gives low and high frequency limits and operating frequency ranges for various performance ratio and dynamic response angle tolerance limits. In all cases, the high operating frequency limit is infinity, which corresponds to the basic characteristic of the seismographic system working in the displacement receiving range. The low frequency limits depend on the specified tolerance limits. For example, when the performance ratio tolerance limit is specified at -0.01, the low frequency-ratio limit is 2.4; with a reference frequency of 7 cycles per second, the low frequency limit occurs at about 17 cycles per second. This frequency limit becomes lower as the magnitude of the tolerance increases. With a tolerance of -0.10, the low frequency limit is 9.5 cycles per second and becomes 6.3 cycles per second for a tolerance of -0.30.

35.251. Dynamic response angle tolerance effects are much more restrictive than performance ratio tolerances. For example, a tolerance limit as great as +30 degrees sets the low frequency limit at about 19 cycles per second.

35.252. Various graphical patterns are available for representing test results. In all cases, the representation is used for one or more of three purposes:

1) Comparison of experimental points with the plots representing a possible theoretical performance function.
2) Comparison of experimental points with the plots for ideal performance.
3) Comparison of theoretical performance function plots that satisfactorily represent the experimental results with the plots for ideal performance.

Comparisons of this type are carried out by means of deviation plots that magnify the differences under consideration.

35.253. The heavy-dashed-line plot of sheet 4 of Test Report No. 35-1 presents the combination of the (2;0, 1, 2) theoretical performance equation form with the (1;0) form, which is a straight line with an upward slope of 45 degrees. The points represented by large circles are dimensionless sensitivity ratios taken from the seventh columns of sheets 12 and 13. The relationships used for computing the sensitivity ratios are given in these sheets.

35.254. The theoretical displacement-voltage dimensionless sensitivity ratio plot reduces to the 45-degree-sloping electromagnetic generator characteristics for high frequency ratios. For frequency ratios less than unity, the combination of downward slopes for the (2;0,1,2) function and the (1;0) function gives a very steep downward slope. Deviation function points are computed by dividing the actual dimensionless sensitivity ratio points by corresponding points on the theoretical performance ratio curve. On sheet 4, deviation function points are represented by points placed at the middle of a small letter "d." The deviation plot of sheet 4 shows that, except for a single point that is about 5 percent high, all the experimental data agree with the theoretical performance function within 1 or 2 percent.

35.255. Sheet 5 of Test Report No. 35-1 gives the theoretical dynamic response angle curve corresponding to the dimensionless sensitivity ratio plot of sheet 4. The deviation curve of this sheet shows that the experimental points vary erratically from the theoretical curve with a maximum deviation magnitude of about 8 degrees.

35.256. An over-all survey of the plots of sheets 4 and 5 indicates that the deviations are of a type that may be largely attributed to uncertainties in the process of making observations and to interference effects due to imperfections in the mechanical calibrator. It seems reasonable to conclude, therefore, that the combined (2;0, 1, 2) and (1;0) relating functions, with 7 cycles per second as the reference frequency and 0.7 as the damping ratio, provide a satisfactory theoretical form for describing the displacement-voltage performance function of the linear vibration receiver under calibration. The reference sensitivity for this function is 4.84 volts per inch.

35.257. Sheets 6 and 7 of Test Report No. 35-1 provide essentially the same information as sheets 4 and 5, except that for the plots of sheets 5 and 6 linear velocity is chosen as the receiver input and voltage is chosen as the output. The dimensionless sensitivity ratio plot of sheet 6 is derived from the plot of sheet 4 by subtracting out the 45-degree-slope straight line that represents the FR factor introduced by the electromagnetic generator when linear displacement is considered as its input. The result of taking FR out of the theoretical displacement-voltage sensitivity ratio curve* is to make it similar to the 0.7 damping ratio curve of

* For the purposes of discussion, when no misunderstanding is possible, the word "dimensionless" may be omitted from the term "sensitivity ratio" in referring to dimensionless sensitivity ratios.

Fig. 35-10, which describes the sensitivity ratio performance of the seismographic system operating in the displacement receiver range. From the standpoint of vibratory-displacement-receiving operation, the essential feature of the plot on sheet 6 is that the dimensionless sensitivity ratio is constant for frequency ratios greater than about 2. The deviation-function curve shows good agreement of the experimental points with the theoretical curve for frequency ratios between 2 and 10. The logarithmic scale below the frequency ratio scale is applied in the form of an adhesive-backed strip that makes it possible to supplement the frequency ratio scale with numbers* giving the forcing frequency directly. This result is accomplished by aligning the reference frequency of 7 cycles per second with unity on the frequency ratio scale.

35.258. The heavy-dashed-line curve on sheet 7 gives the theoretical dynamic response angle plot corresponding to the theoretical dimensionless sensitivity ratio curve of sheet 6. The essential difference between the theoretical curve of sheet 7 and the theoretical dynamic response angle curve of sheet 4 is a shift of -90 degrees to compensate for the theoretical removal of the rate-taking action of the electromagnetic generator by considering that this action is transferred to the input quantity. The information provided by sheet 6 on the agreement of experimental points with the (2;0, 1, 2) relating function as the theoretical performance function for the vibration receiver is identical with the information given by the figure of sheet 5.

35.259. Sheets 1, 4, 5, 6 and 7 all give plots with the logarithmic abscissa scale covering a range of 300 to 1 in frequency ratio units, with unity near the midpoint of the coordinate field. This range is suitable for examining the agreement of test points with theoretical performance curves, but does not give a broad picture of the over-all characteristics of the unit under test and the region within this picture that is covered by the test points. The plots of sheet 8 provide such a broad picture of dimensionless sensitivity ratio variations, both theoretical and actual, by halving the length of each decile on the logarithmic scales as compared with the scales of sheets 1, 4, 5, 6 and 7 and using a special deviation function scale with the decile increased in length by 8 times over the previously used decile length. The plot of sheet 9 is similar to the plot of sheet 7 except for the increased range of frequency ratio.

35.260. The information presented by sheets 8 and 9 show that the experimental data covered the crucial frequency ratio range about 1 order of magnitude up and 1 order of magnitude down from unity. Except for a few relatively large deviations where the theoretical performance function is changing rapidly, the test

---

* It is meaningless to consider the logarithm of any dimensional quantity. For this reason, the numbers on the forcing frequency scale are actually frequency ratio numbers with the reference frequency made equal to unity.

information gives good agreement with the plots representing the theoretical performance function. It is probable that these deviations are really due to uncertainty effects, so that the theoretical performance function may be taken as representing actual performance for engineering purposes where an inaccuracy of 1 percent in sensitivity ratio and an inaccuracy of 5 degrees in dynamic response angle are tolerable.

35.261. All the plots of Test Report No. 35-1 that have been considered so far are designed to check the agreement of experimental results with a selected theoretical performance function. This is an important phase in the evaluation of test results because once it is established that actual performance may be satisfactorily represented by some known mathematical form, the essential characteristics of the tested unit are easily available for use in connection with any and all measurement and control applications.

35.262. From the standpoint of practice, the primary interest in performance characteristics of a tested unit centers around the question of how closely the unit follows ideal performance requirements. For example, the linear vibration receiver considered in Test Report No. 35-1 has ideal performance over a frequency region within which its velocity input – voltage output dimensionless sensitivity ratio is unity and its dynamic response angle is -180 degrees. The phase angle information is covered satisfactorily by sheets 7 or 9, but it is convenient to use the concept of performance ratio for describing amplitude ratio performance. By definition, the velocity input – voltage output dimensionless sensitivity ratio performance ratio is the actual dimensionless sensitivity ratio divided by a reference sensitivity ratio that is chosen as identical with the ideal dimensionless sensitivity ratio. For the linear vibration receiver considered in Test Report No. 35-1, the ideal dimensionless sensitivity ratio is unity.

35.263. The linear-scale plots of sheet 10 give the performance ratios of the theoretical dimensionless sensitivity ratio and the experimental results plotted as functions of frequency ratio. The light-dashed-line plot shows the deviations of the test points from the ideal dimensionless sensitivity ratio value of unity. Deviations of the theoretical curve from the ideal dimensionless sensitivity ratio may be read directly from the performance ratio scale.

35.264. The plots of sheet 11 are similar to the plots of sheet 10 except that the linear frequency-ratio scale that covers a range of 5 to 1 is replaced by a logarithmic scale that covers a range of 300 to 1. It is obvious that the frequency-ratio range can be extended by reducing the length chosen for each decile.

35.265. In practice, plots similar to those of sheets 10 and 11 are most generally useful because they give on one plot the ideal performance condition, the theoretical performance curve, and the agreement of experimental points with both of these references. By adding the essential numerical data on reference with sensitivities

and parameters such as damping ratio, a very complete picture of the sensitivity ratio performance of a tested unit may be presented on a single sheet.

ILLUSTRATIVE TEST REPORT ON THE EXPERIMENTAL CALIBRATION OF A TORSIONAL VIBRATION RECEIVER

35.266. Vibratory angular inputs of simple sinusoidal wave form are provided by the Hooke's-joint arrangement of the mechanical vibration calibrator shown in Fig. 35-42. With this arrangement, the center line of the driven shaft is set at a fixed angle with respect to the center line of the driving shaft. As the driving shaft is rotated at constant speed, the motion of the driven shaft may be represented by a constant average angular velocity equal to the speed of the driving shaft, on which is superimposed a substantially sinusoidal* vibratory motion. The vibratory motion completes two cycles for each revolution of the driving shaft. This means that a torsional vibration receiver fixed to the driven shaft is subjected to an input oscillation of known amplitude and frequency that may be used for calibration purposes. The constant-speed rotation that accompanies the angular velocity variation is useful for checking the behavior of slip rings and brushes or other means that may be required for connecting the receiver to recording equipment. The

---

* From Sloane, Engineering Kinematics (S8), page 261, when

ω_t = angular velocity of driven shaft

ω_d = angular velocity of driving shaft

θ = acute angle between shafts

Then

$$\frac{\omega_t}{\omega_d} = \frac{\cos\theta}{1 - \sin^2\theta \sin^2\omega_d t}$$

If

$$0 \leq \theta < \frac{\pi}{2}$$

then

$$\sin^2\theta \sin^2\omega_d t < 1$$

and

$$\frac{1}{1 - \sin^2\theta \sin^2\omega_d t} = 1 + \sin^2\theta \sin^2\omega_d t + \sin^4\theta \sin^4\omega_d t + \sin^6\theta \sin^6\omega_d t + \ldots$$

$$\sin\omega_d t = \frac{\sin 2\omega_d t}{\sqrt{2}\sqrt{1 + \cos 2\omega_d t}}$$

$$\sin^2\omega_d t = \frac{\sin^2 2\omega_d t}{2(1 + \cos 2\omega_d t)} = \frac{1 - \cos^2 2\omega_d t}{2(1 + \cos 2\omega_d t)} = \frac{1 - \cos 2\omega_d t}{2}$$

so that

$$\frac{\omega_t}{\omega_d} = \cos\theta \left[1 + \frac{\sin^2\theta}{2}(1 - \cos 2\omega_d t) + \frac{\sin^4\theta}{4}(1 - \cos 2\omega_d t)^2 + \ldots\right]$$

If θ is small, then terms higher than $(\sin^2\theta)/2$ can be neglected, then

$$\frac{\omega_t}{\omega_d} = \cos\theta \left(1 + \frac{\sin^2\theta}{2}\right) - \frac{\cos\theta \sin^2\theta}{2} \cos 2\omega_d t$$

So that, finally,

$$\omega_t = \cos\theta \left(1 + \frac{\sin^2\theta}{2}\right)\omega_d - \left(\frac{\omega_d \cos\theta \sin^2\theta}{2}\right) \cos 2\omega_d t$$

stroboscopic-light arrangement for accurately measuring input frequencies and the circuits for indicating phase angles between forcing displacements and output voltage waves shown in Fig. 35-42 are applied for torsional-vibration calibrations in the same way that they are used for linear-receiver tests.

35.267. Test Report No. 35-2 summarizes calibration information on a torsional vibration receiver with the features illustrated in Fig. 35-7h. This unit uses Coulomb damping only, and has an electromagnetic generator for producing the output voltage. Leaving out of account the differences in behavior due to the change from viscous damping to Coulomb damping, the torsional vibration receiver study summarized in Test Report No. 35-2 reveals performance characteristics that are similar to those of the linear vibration receiver considered in Test Report No. 35-1. This means that if the input is taken as vibratory angular velocity, the performance function for the torsional vibration receiver is determined by the seismographic system. From Fig. 35-7h, this system includes a seismic element, an elastic element, and a Coulomb damping element, but no viscous damping element. The forms for the dimensionless sensitivity ratio and the dynamic response angle for a seismographic system of this kind are derived in Derivation Summary 35-6 and are given by Eqs. (31) and (34) of that summary. It is reasonable to check the usefulness of these equations for describing the performance characteristics of a torsional vibration receiver damped with Coulomb friction.

35.268. Sheets 6 and 7 of Test Report No. 35-2 give data taken from the torsional vibration receiver identified on sheet 1 when this unit is subjected to steady-state sinusoidal inputs of various frequencies by means of the M.I.T.-Sperry vibration calibrator. The steps for reducing these data to the dimensionless sensitivity ratio as a function of frequency ratio are shown in the tabulations of sheets 6 and 7. In computing these results, the measured* undamped natural frequency of 5 cycles per second for the receiver is taken as the reference frequency in determining frequency ratio values. The breakaway condition was determined by slowly varying the forcing frequency to determine the point at which the output signal changed from zero. With the forcing amplitude of 1 degree used for the tests, breakaway occurred at 20 cycles per second. The plots given on sheet 2 of Test Report No. 35-2 are identical with those on the breakaway graph of Fig. 35-37, except for the numerical data associating the lines with the particular vibration receiver being described. These plots show that the observed breakaway frequency ratio of 4 corresponds to a maximum Coulomb friction displacement – forcing amplitude ratio of 12.6. With the forcing amplitude of 1 degree used in the calibration test, this means that the maximum Coulomb friction displacement angle for the receiver is 12.6 degrees. Special logarithmic scales pasted parallel

* The undamped natural frequency was determined from an oscillograph record of a step function transient taken with the spring pressure removed from the Coulomb friction plug shown in Fig. 35-7h.

SUMMARY: Test Form A **TEST REPORT NO.** 35-2 Sheet 1 of 7

Instruments Laboratory · Aeronautical Engineering Department · Massachusetts Institute of Technology · Cambridge · Massachusetts

Title of test: TORSIONAL VIBRATION RECEIVER CALIBRATION (SINUSOIDAL FORCING MOTION)

Date: 6/28/54 In charge of test: J. L. STOCKARD Assisting with test: C. S. DRAPER

Equipment tested: M.I.T. TORSIONAL VIBRATION RECEIVER (vr) Y. T. LI

Type: A Model: 1 Serial No.: 3 Calculations: J. L. STOCKARD

Plots: J. L. STOCKARD

Equipment used for test: SPERRY-M.I.T. VIBRATION CALIBRATOR (CONSOLIDATED) SER. NO. C875

DUMONT CATHODE-RAY OSCILLOGRAPH (cro), Type 304H, SER. NO. 1012

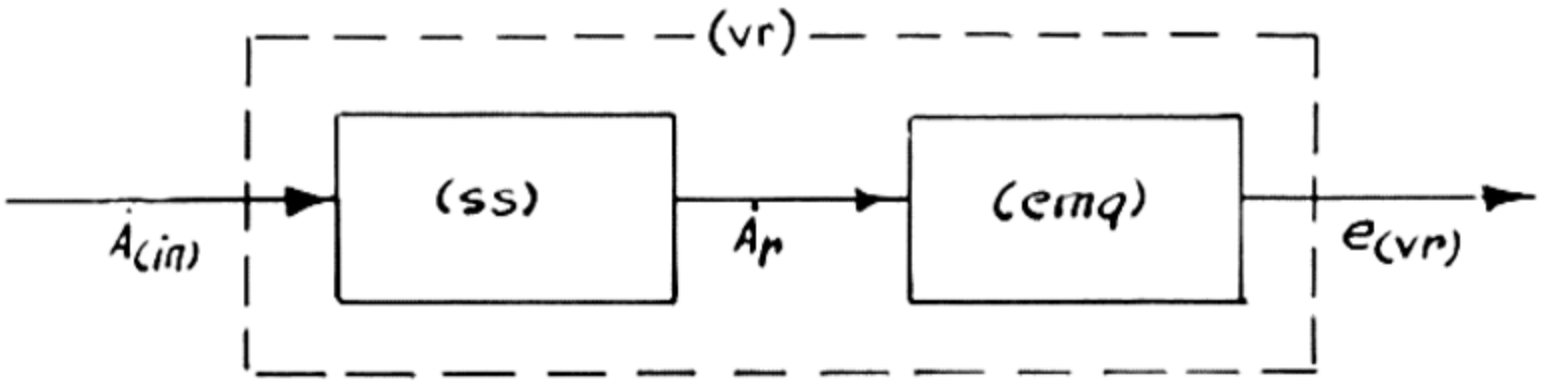
BALLANTINE VACUUM TUBE VOLTMETER (vtvm), MODEL 300, SER. NO. 6390

Input quantity: ANGULAR VELOCITY $\dot{A}_{(in)}$ Output quantity: VOLTAGE $e_{(vr)}$

Environmental conditions: Temperature: 70° F Pressure: —

Other: —

Summary of results:



$$[PF]_{(vr)}[\dot{A} ; e]_{(theo)} \approx [RF]_{(2;9,1,2)(vf=0)(cf\neq 0)}$$

$$(SR)_{(vr)}[\dot{A} ; e]_{(theo)} \approx (DAR)_{(2;0,1,2)(vf=0)(cf\neq 0)} = \frac{\sqrt{(FR)^4 - \left(\frac{4}{\pi}\right)^2 \left[(MCFD)(FDA)R\right]^2}}{\sqrt{\left[1-(FR)^2\right]^2}}$$

$$(DRA)_{(vr)}[\dot{A} ; e]_{(theo)} \approx (DRA)_{(2;0,1,2)(vf=0)(cf\neq 0)} = \sin^{-1}\left[-\frac{4}{\pi}\frac{1}{(FR)^2}\left[(MCFD)(FDA)R\right]\right]$$

Reference frequency = $n_{(ref)} = 5 \frac{cycles}{second}$

Viscous friction Damping ratio = DR = 0

Reference sensitivity = $S_{(vr)}[\dot{A} ; e]_{(ref)} = 1.05 \frac{millivolts}{deg/sec}$

Reference dynamic response angle = $(DRA)_{(ref)} = -180°$

Equivalent damping ratio breakaway frequency ratio = $(FR)_{(b)(edr)} = 4.0$

Equivalent damping ratio breakaway forcing frequency = $n_{(f)b} = 20$ cycles/second

Maximum Coulomb friction displacement angle = $A_{(cf)m} = 12.6$ degrees
= maximum angle that Coulomb friction will hold the seismic element displaced from zero against the restoring torque of the elastic element under conditions of no angular acceleration.

Maximum Coulomb friction displacement – forcing displacement amplitude ratio
$= [(MCFD)(FDA)R] = \frac{A_{(cf)m}}{A_{(f)a}}$

Amplitude of angular forcing displacement = $A_{(f)a} = A_{(in)a}$

For a forcing amplitude of 1 degree, $[(MCFD)(FDA)R]_{(A_{(f)a}=1°)} = 12.6$

Instruments Laboratory · Aeronautical Engineering Department · Massachusetts Institute of Technology · Cambridge · Massachusetts

Title of test TORSIONAL VIBRATION RECEIVER CALIBRATION (SINUSOIDAL FORCING MOTION)

Date 6/28/54 In charge of test J. L. STOCKARD Assisting with test C. S. DRAPER

Equipment tested M.I.T. TORSIONAL VIBRATION RECEIVER (vr) Y. T. LI

Type A Model 1 Serial No. 3 Calculations J. L. STOCKARD

Plots J. L. STOCKARD

Equipment used for test SPERRY-M.I.T. VIBRATION CALIBRATOR (CONSOLIDATED) SER. NO. C785
DUMONT CATHODE-RAY OSCILLOGRAPH (cro), Type 304H, SER. NO. 1012
BALLANTINE VACUUM TUBE VOLTMETER (vtvm), MODEL 300, SER. NO. 6390

Input quantity ANGULAR VELOCITY $\dot{A}_{(in)}$ Output quantity VOLTAGE $e_{(vr)}$

Environmental conditions: Temperature 70° F Pressure —

Other —

MAXIMUM COULOMB FRICTION DISPLACEMENT – FORCING DISPLACEMENT AMPLITUDE RATIO

log-log scale

FORCING DISPLACEMENT AMPLITUDE RECIPROCAL

Reference frequency
= $n_{(ref)}$ = 5 cycles/second

Viscous friction damping ratio
= DR = 0

Maximum Coulomb friction displacement angle
= $A_{(cf)m}$ = 12.6 degrees

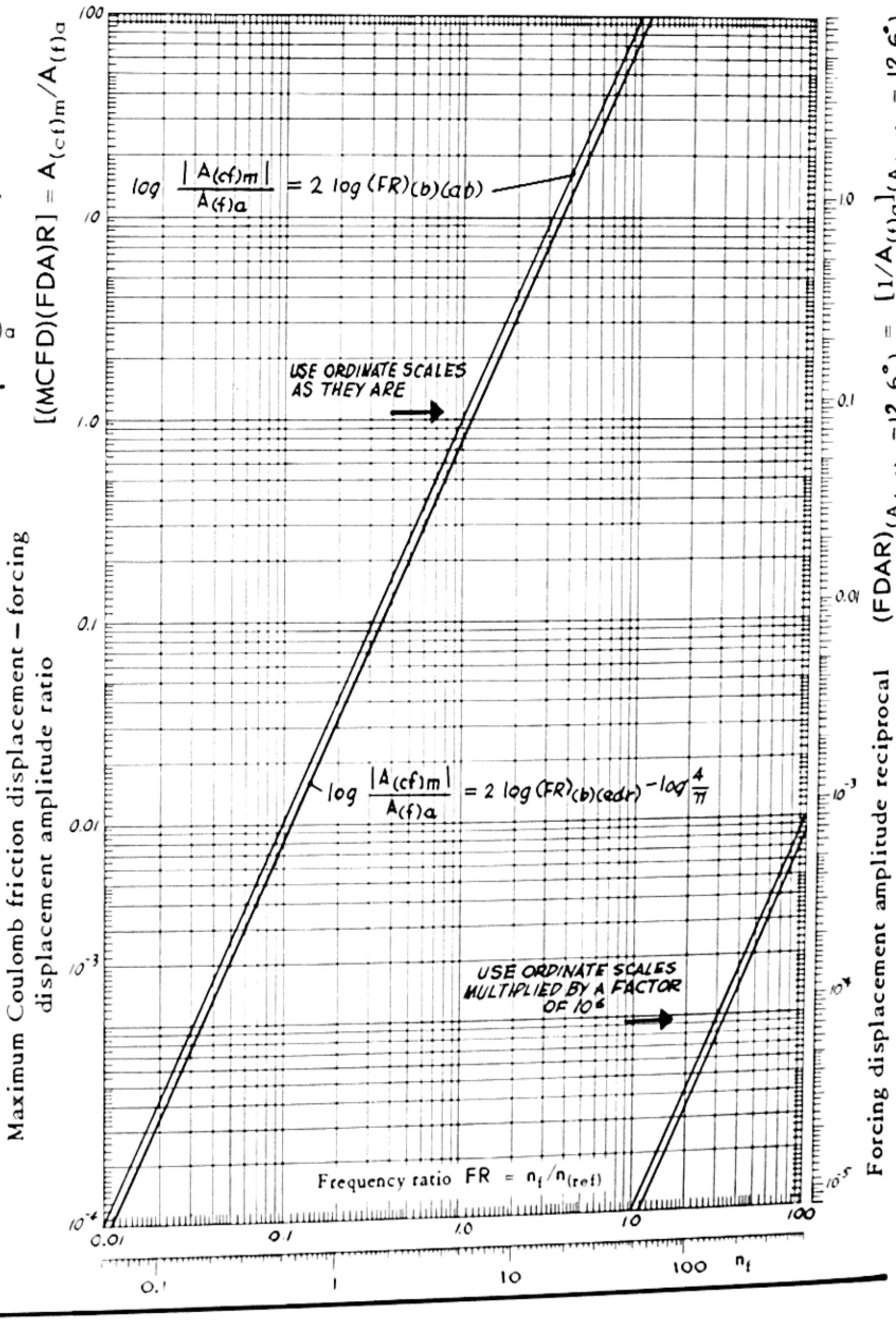
Forcing amplitude angle = $A_{(f)a}$

Dynamic amplitude ratio breakaway frequency ratio
= $(FR)_{(b)(edr)}$

$$= \sqrt{\frac{4}{\pi}}\ \sqrt{\frac{|A_{(cf)m}|}{A_{(f)a}}}$$

Acceleration-balance breakaway frequency ratio
= $(FR)_{(b)(ab)}$

$$= \sqrt{\frac{|A_{(cf)m}|}{A_{(f)a}}}$$



Instruments Laboratory · Aeronautical Engineering Department · Massachusetts Institute of Technology · Cambridge · Massachusetts

Title of test TORSIONAL VIBRATION RECEIVER CALIBRATION (SINUSOIDAL FORCING MOTION)

Date 6/28/54 In charge of test J. L. STOCKARD Assisting with test C. S. DRAPER

Equipment tested M.I.T. TORSIONAL VIBRATION RECEIVER (vr) Y. T. LI

Type A Model 1 Serial No. 3 Calculations J. L. STOCKARD

Plots J. L. STOCKARD

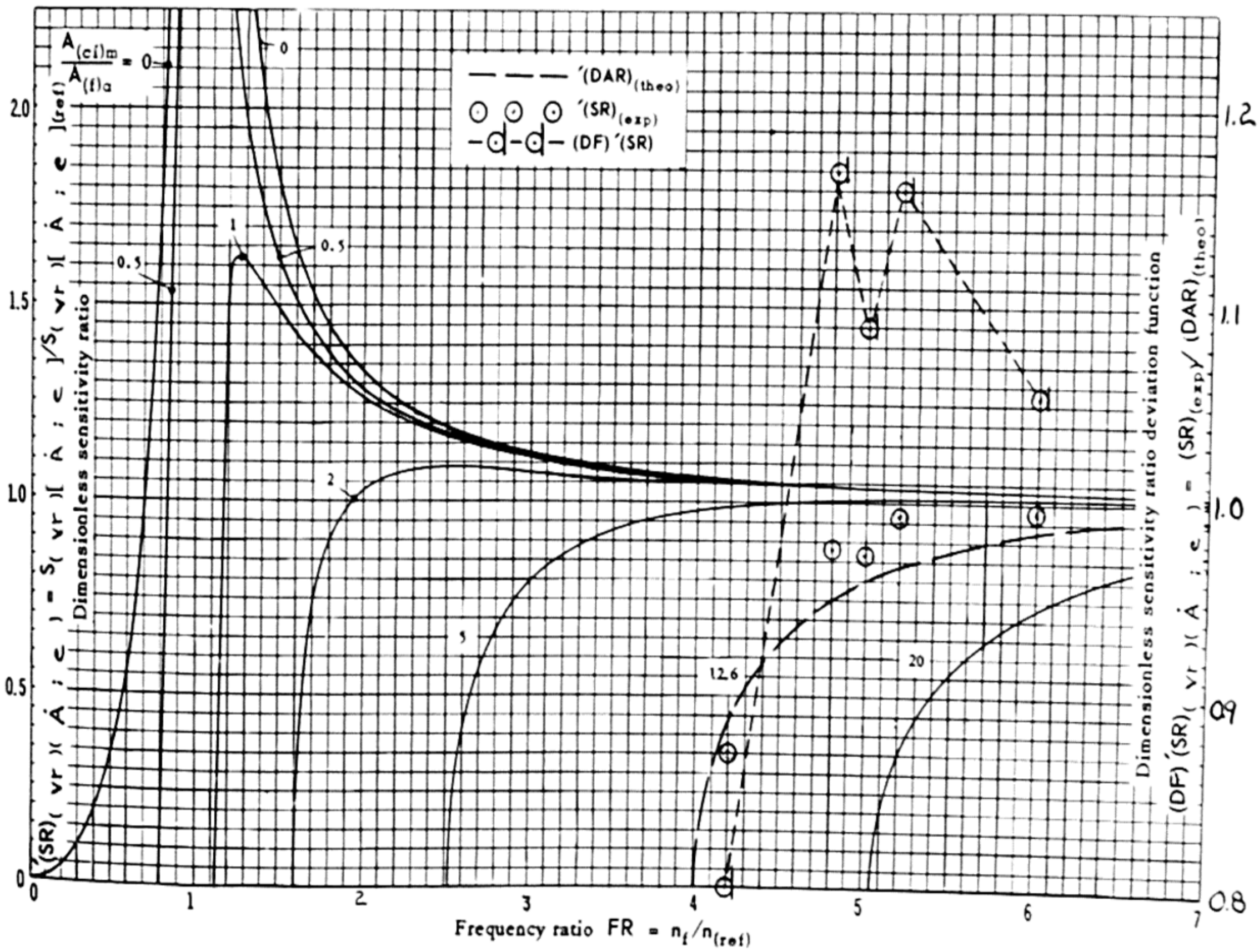
Equipment used for test SPERRY-M.I.T. VIBRATION CALIBRATOR (CONSOLIDATED) SER. NO. C875
DUMONT CATHODE-RAY OSCILLOGRAPH (cro), Type 304H, SER. NO. 1012
BALLANTINE VACUUM TUBE VOLTMETER (vtvm) MODEL 300, SER. NO. 6390

Input quantity ANGULAR VELOCITY $\dot{A}_{(in)}$ Output quantity VOLTAGE $e_{(vr)}$

Environmental conditions: Temperature 70° F Pressure —

Other —

DIMENSIONLESS SENSITIVITY RATIO — linear scale — DIMENSIONLESS SENSITIVITY RATIO DEVIATION FUNCTION



Reference frequency = $n_{(ref)} = 5 \frac{\text{cycles}}{\text{second}}$ Viscous friction Damping ratio = DR = 0

Reference sensitivity = $S_{(vr)}[\dot{A};e]_{(ref)} = 1.05 \frac{\text{volts}}{\text{degree/second}}$

Theoretical dimensionless dynamic amplitude ratio = $'(DAR)_{(theo)} = '(DAR)_{(0;0,1,2)(vf=0)(cf\neq 0)} = \frac{\sqrt{(FR)^4 - \left(\frac{4}{\pi}\right)^2\left[\frac{A_{(cf)m}}{A_{(f)a}}\right]^2}}{\sqrt{[1-(FR)^2]^2}}$

$'(DAR)_{(theo)}$ is $'(SR)_{(theo)}$, the theoretical dimensionless sensitivity ratio for the unit under test; $'(SR)_{(exp)}$ is the dimensionless sensitivity ratio determined by experiment.

Maximum Coulomb friction displacement angle = $A_{(cf)m} = 12.6°$; Forcing angle amplitude = $A_{(f)a}$

Maximum Coulomb friction displacement - forcing displacement amplitude ratio = $[(MCFD)(FDA)R] = \frac{|A_{(cf)m}|}{A_{(f)a}}$

(SR) PLOTS: Test Form Ia **TEST REPORT NO. 35-2** Sheet 4 of 7

Instruments Laboratory · Aeronautical Engineering Department · Massachusetts Institute of Technology · Cambridge · Massachusetts

Title of test TORSIONAL VIBRATION RECEIVER CALIBRATION (SINUSOIDAL FORCING MOTION)

Date 6/28/54 In charge of test J. L. STOCKARD Assisting with test C. S. DRAPER

Equipment tested M.I.T. TORSIONAL VIBRATION RECEIVER (vr) Y. T. LI

Type A Model 1 Serial No. 3 Calculations J. L. STOCKARD

Plots J. L. STOCKARD

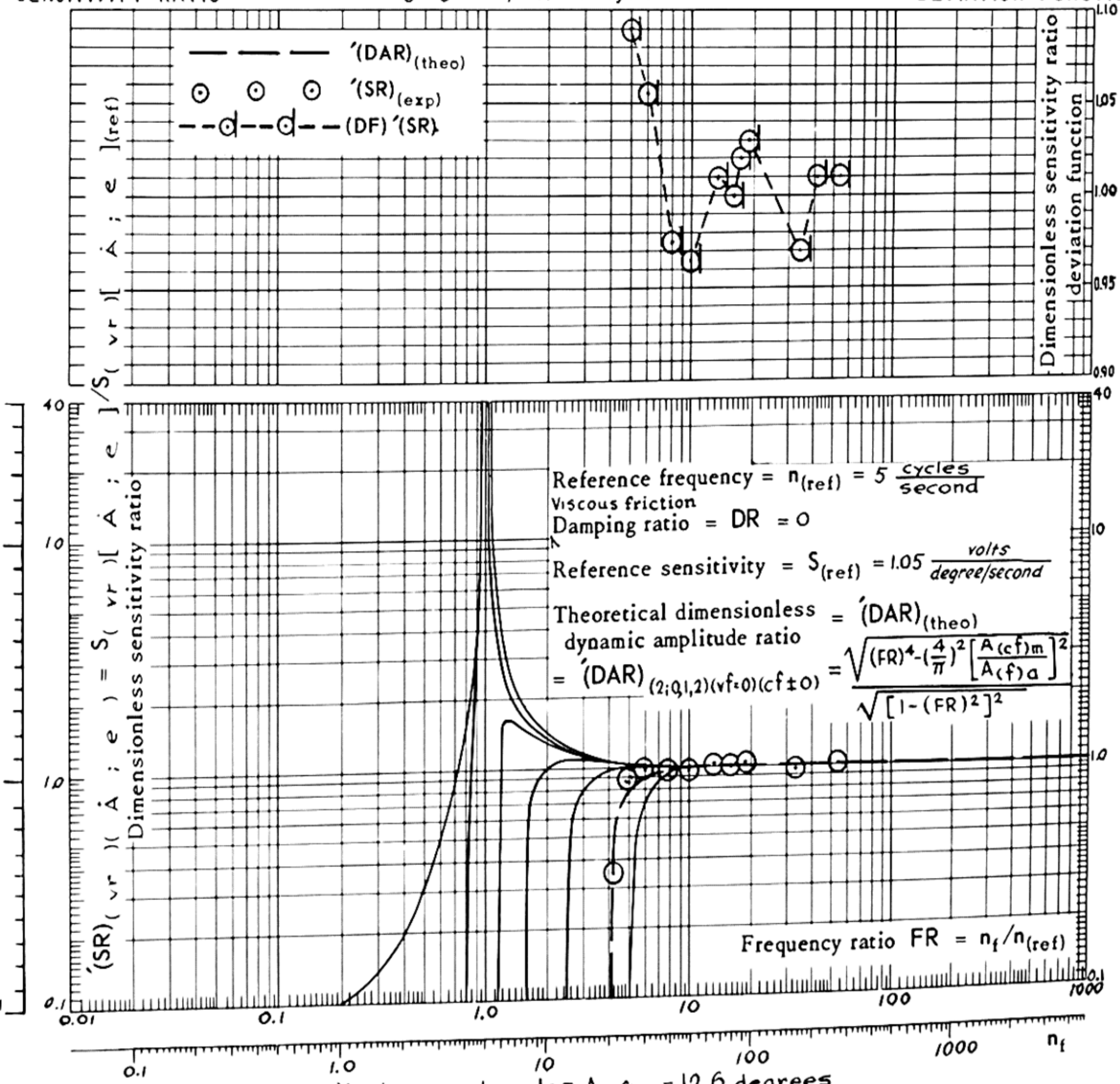
Equipment used for test SPERRY-M.I.T. VIBRATION CALIBRATOR (CONSOLIDATED) SER. NO. C875
DUMONT CATHODE-RAY OSCILLOGRAPH (cro), Type 304H, SER. NO. 1012
BALLANTINE VACUUM TUBE VOLTMETER (vtvm) MODEL 300, SER. NO. 6390

Input quantity ANGULAR VELOCITY $\dot{A}_{(in)}$ Output quantity VOLTAGE $e_{(vr)}$

Environmental conditions: Temperature 70° F Pressure —

Other

DIMENSIONLESS SENSITIVITY RATIO — log-log scale, 1¼-inch cycle — DIMENSIONLESS SENSITIVITY RATIO DEVIATION FUNCTION



(DRA) PLOTS: Test Form M **TEST REPORT NO.** 35-2 Sheet 5 of 7

Instruments Laboratory · Aeronautical Engineering Department · Massachusetts Institute of Technology · Cambridge · Massachusetts

Title of test TORSIONAL VIBRATION RECEIVER CALIBRATION (SINUSOIDAL FORCING MOTION)

Date 6/28/54 In charge of test J. L. STOCKARD Assisting with test C. S. DRAPER

Equipment tested M.I.T. TORSIONAL VIBRATION RECEIVER (vr) Y. T. LI

Type A Model 1 Serial No. 3 Calculations J. L. STOCKARD

Plots J. L. STOCKARD

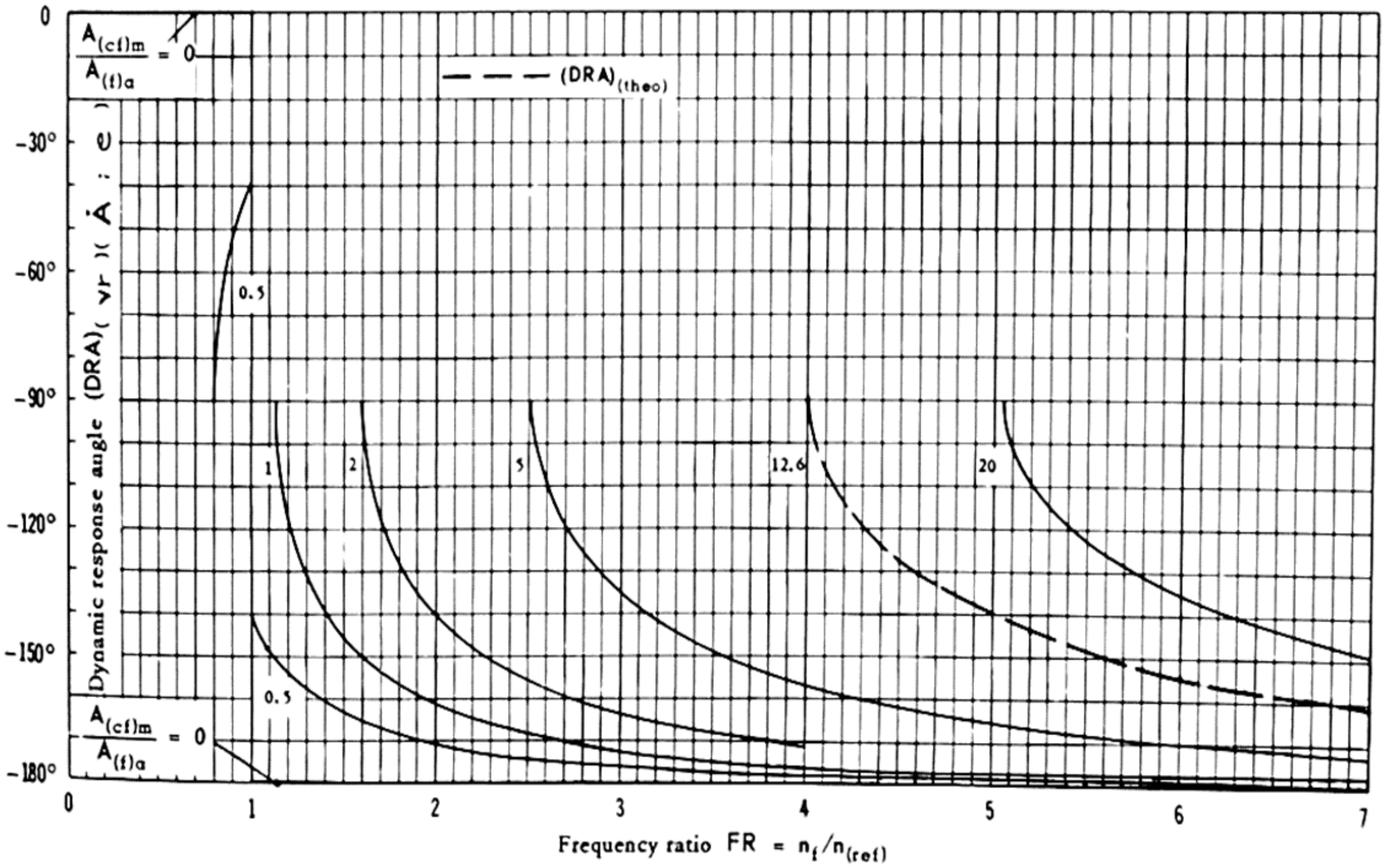
Equipment used for test SPERRY-M.I.T. VIBRATION CALIBRATOR (CONSOLIDATED) SER. NO. C875
DUMONT CATHODE-RAY OSCILLOGRAPH (cro), Type 304H, SER. NO. 1012
BALLANTINE VACUUM TUBE VOLTMETER (vtvm) MODEL 300, SER. NO. 6390

Input quantity ANGULAR VELOCITY A(in) Output quantity VOLTAGE e(vr)

Environmental conditions: Temperature 70° F Pressure –

Other –

DYNAMIC RESPONSE ANGLE linear scale DYNAMIC RESPONSE ANGLE DEVIATION
(no data obtained for this)



Reference frequency = $n_{(ref)}$ = 5 $\frac{cycles}{second}$ Viscous friction Damping ratio = DR = 0

Reference dynamic response angle = $(DRA)_{(ref)}$ = −180 degrees

Theoretical dynamic response angle = $(DRA)_{(theo)} = (DRA)_{(2;0,1,2)(vf=0)(cf\neq 0)} = \sin^{-1}\left[-\frac{4}{\pi}\frac{1}{(FR)^2}[(MCFD)(FDA)R]\right]$

$(DRA)_{(theo)}$ is the theoretical dynamic response angle for the unit under test.

Maximum Coulomb friction displacement angle = $A_{(cf)m}$ = 12.6° ; Forcing angle amplitude = $A_{(f)a}$
Maximum Coulomb friction displacement-forcing displacement amplitude ratio = $[(MCFD)(FDA)R] = \frac{|A_{(cf)m}|}{A_{(f)a}}$

TEST DATA: Test Form N **TEST REPORT NO.** 35-2 Sheet 6 of 7

Instruments Laboratory · Aeronautical Engineering Department · Massachusetts Institute of Technology · Cambridge · Massachusetts

Title of test TORSIONAL VIBRATION RECEIVER CALIBRATION (SINUSOIDAL FORCING MOTION)

Date 6/29/64 **In charge of test** J. L. STOCKARD **Assisting with test** C.S. DRAPER Y.T. Li

Equipment tested M.I.T. TORSIONAL VIBRATION RECEIVER (vr)

Type A Model 1 Serial No. 3 **Calculations** J. L. STOCKARD **Plots** J. L. STOCKARD

Equipment used for test SPERRY-M.I.T. VIBRATION CALIBRATOR (CONSOLIDATED) SER. NO. C875
DUMONT CATHODE-RAY OSCILLOGRAPH (cro), Type 304H, SER. NO. 1012
BALLANTINE VACUUM TUBE VOLTMETER (vtvm), MODEL 300, SER. NO. 6390

Input quantity ANGULAR VELOCITY $\dot{A}_{(in)}$ **Output quantity** VOLTAGE $e_{(vr)}$

Environmental conditions: Temperature 70° F **Pressure** 1

Other 1

Run Number	Forcing Amplitude $A_{(in)a}$	Forcing Frequency n_f	Output Amplitude d_a (of trace on cathode-ray oscillograph)	Output Voltage Amplitude $e_{(out)a}$	Input-Output Sensitivity $S_{(vr)[\dot{A}\ ;\ e]\,(exp)}$	Dimensionless Sensitivity Ratio $'(SR)_{(vr)(\dot{A}\ ;\ e)(exp)}$*	Theoretical Dimensionless Dynamic Amplitude Ratio $(DAR)_{(2;0,1,2)(vf=0)(cf\neq 0)} = (MCFD)(FDA)R = 12.6$	Dimensionless Sensitivity Ratio Deviation Function $(DF)\,'(SR)_{(exp)}/(DAR)_{(theo)}$	Dynamic Response Angle $(DRA)_{(vr)(\dot{A}\ ;\ e)(exp)}$	Theoretical Dynamic Response Angle $(DRA)_{(theo)} = (DRA)_{(2;0,1,2)(cf\neq 0)}^{(vf=0)}$ $(MCFD)(FDA)R = 12.6$	Dynamic Response Angle Deviation $(D)(DRA) = (DRA)_{(exp)} - (DRA)_{(theo)}$	Frequency Ratio $FR = n_f/n_{(ref)}$	
Units and References	$\dot{A}_{(in)a} = 2\pi n_f A_{(in)a}$ $A_{(in)a} = 1^o$ degrees/second	cycles/second	inches	$S_{(cro)[d;e]} = 0.707$ volt/inch volts	millivolts / degree/second	$S_{(ref)} = 1.05$ millivolts / degree/second			$(DRA)_{(ref)} = -180°$ degrees			$n_{(ref)} = 5$ cycles/second	
1	591	94	0.905	0.640	1.08	1.03	1.00	1.03	—	-177.4	—	18.8	
2	535	85	0.810	0.573	1.07	1.02	1.00	1.02	—	177.0	—	17.0	
3	503	80	0.75	0.530	1.06	1.00	1.00	1.00	—	-176.4	—	16.0	
4	427	68	0.64	0.453	1.06	1.01	1.00	1.01	—	-175.1	—	13.6	
5	314	50	0.45	0.318	1.01	0.96	0.993	0.965	—	-170.7	—	10.0	
6	251	40	0.36	0.254	1.01	0.96	0.983	0.975	—	-165.5	—	8.0	
7	251	40	1.6	0.254	1.01	0.96	0.983	0.975	—	-165.5	—	8.0	$S_{(cro)[d;e]}$ changed to
8	189	30	1.22	0.194	1.03	0.98	0.927	1.055	—	-153.6	—	6.0	0.154 volts/inch

* $'(SR)_{(exp)} = S_{(exp)}/S_{(ref)}$; Reference sensitivity $= S_{(vr)[\dot{A}\ ;\ e](ref)} = S_{(ref)}$.

TEST DATA: Test Form 0 TEST REPORT NO. 35-2 Sheet 7 of 7

Instruments Laboratory · Aeronautical Engineering Department · Massachusetts Institute of Technology · Cambridge · Massachusetts

Run Number	Forcing Amplitude $\dot{A}_{(in)a}$	Forcing Frequency n_f	Output Amplitude d_a (of trace on cathode-ray oscillograph)	Output Voltage Amplitude $e_{(out)a}$	Input-Output Sensitivity $S_{(vr)[\dot{A};e]_{(exp)}}$	Dimensionless Sensitivity Ratio $'(SR)_{(vr)(\dot{A};e)_{(exp)}}$ *	Theoretical Dimensionless Dynamic Amplitude Ratio $'(DAR)_{(theo)} = (MCFD)(FDA)R = 12.6$ $'(DAR)_{(0;0,1,2)(r\neq 0)(f\neq 0)}$	Dimensionless Sensitivity Ratio Deviation Function $(DF)'(SR) = '(SR)_{(exp)}/'(DAR)_{(theo)}$	Dynamic Response Angle $(DRA)_{(vr)(\dot{A};e)_{(exp)}}$	Theoretical Dynamic Response Angle $(DRA)_{(theo)} = (DRA)_{(2;0,1,2)}^{(r\neq 0)}{}_{(f\neq 0)}$	Dynamic Response Angle Deviation $(D)(DRA) = (DRA)_{(exp)} - (DRA)_{(theo)}$	Frequency Ratio $FR = n_f/n_{(ref)}$	
Units and References	$\dot{A}_{(in)a} = 2\pi n_f A_{(in)a}$ $A_{(in)a} = 1°$ degrees/second	cycles/second	inches	$S_{(cro)[d;e]} = 0.707$ volts/inch	millivolts/degree/second	$S_{(ref)} = 1.05$ millivolts/degree/second			$(DRA)_{(ref)} = -180°$ degrees			$n_{(ref)} = 5$ cycles/second	
9	164	26	1.05	0.168	1.02	0.97	0.838	1.16	—	-143.5	—	5.2	WAVE FORM IS OK
10	157	25	0.90	0.143	0.91	0.87	0.800	1.09	—	-140.1	—	5.0	
11	157	25	0.90	0.143	0.91	0.87	0.800	1.09	—	-140.1	—	5.0	
12	151	24	0875	0139	0.92	0.88	0.750	1.175	—	-135.8	—	4.8	WAVE FORM STARTS TO DISTORT
13	132	21	0.31	00493	0.37	0.35	0.439	0.80	—	-114.1	—	4.2	
14	126	20	0	0	0	0	0	-	—	-90.0	—	4.0	
15	1070	170	1.54	1.09	1.02	0.97	1.0	0.97	-	-179.2	—	33.0	$S_{(cro)[d;e]} = 0.707$ volt/inch
16	1310	208	1.96	1.39	1.06	1.01	1.0	1.01	—	-179.5	—	44.6	"
17	1700	270	2.54	1.80	1.06	1.01	1.0	1.01	—	-179.7	—	54	"

* $'(SR)_{(exp)} = S_{(exp)}/S_{(ref)}$; Reference sensitivity $= S_{(vr)[\dot{A};e]_{(ref)}} = S_{(ref)}$.

to the abscissa and ordinate axes of sheet 2 are aligned with the dimensionless scales to read directly the forcing frequency and reciprocal of forcing amplitude respectively. They permit the breakaway frequency to be estimated for any given forcing amplitude within the range of the plot.

35.269. Sheet 3 of Test Report No. 35-2 gives linear-scale plots of dimensionless sensitivity ratio as a function of frequency ratio for the torsional vibration receiver. The curve family of sheet 3 is similar to the family of Fig. 35-30, which represents the dimensionless dynamic amplitude ratio for the (2;0,1,2) equation with an equivalent Coulomb damping term, but without a viscous damping term. Points for the measured dimensionless sensitivity ratio show a fair agreement with the curve for a maximum Coulomb friction displacement – forcing amplitude ratio of 12.6. This makes it reasonable to use the dimensionless dynamic amplitude ratio equation for the (2;0,1,2) differential equation with a Coulomb damping term but no viscous damping term as the expression for the theoretical dimensionless sensitivity ratio of the torsional vibration receiver under test.

35.270. Sheet 4 of Test Report No. 35-2 gives logarithmic-scale plots for several of the curves shown on sheet 3. In addition, sheet 4 shows the experimental points and the corresponding deviation function. The logarithmic scales make it possible to extend greatly the range covered on both coordinate axes. Except for the region in which the dimensionless sensitivity ratio is varying rapidly, the agreement of test points with the theoretical dimensionless sensitivity ratio curve is very good. This result certainly justifies the use of the theoretical plots to predict the performance of the torsional vibration receiver for forcing amplitudes and forcing frequencies that differ from those used in the calibration tests.

35.271. Sheet 5 of Test Report No. 35-2 gives a curve family for the dynamic response angle plots corresponding to the dimensionless sensitivity ratio plots of sheets 3 and 4. The curves of sheet 5 are taken directly from Fig. 35-31. These curves are not backed up by test results, but it is reasonable to expect that they provide at least a rough approximation to the angular velocity input – voltage output dynamic response angles associated with operation of the tested torsional vibration receiver.

ILLUSTRATIVE TEST REPORT ON THE CALIBRATION OF AN INTEGRATING AMPLIFIER

35.272. It is demonstrated in Derivation Summary 34-10 that a high-gain amplifier with a feedback condenser has the characteristics of an integrator. A typical circuit for a resistance – amplifier feedback condenser is shown in Fig. 34-9. Common practice is to precede the integrator by stages of electronic amplification and isolation. Very often, similar stages follow the integrator. The entire assembly, called an integrating amplifier, provides an operating component adaptable for accepting outputs from a vibration receiver with an electromagnetic signal

generator, such as the unit described in Test Report No. 35-1. Corresponding integrating amplifier outputs are signals representing vibratory displacement.

35.273. Performance characteristics of integrating amplifiers may be tested by the arrangement shown in Fig. 35-43. Steady-state sinusoidal signals are generated by the beat-frequency oscillator. The magnitude of the oscillator signal is measured by the vacuum tube voltmeter. The oscillator signal is also applied to the x-axis terminals of a cathode-ray oscilloscope for dynamic response angle measurements, as described in the following paragraphs. The integrating amplifier output signal is applied to the same measuring equipment, this signal being connected to the y-axis terminals of the cathode-ray oscilloscope. The vacuum tube voltmeter is connected to the switch blades of the double-pole double-throw switch. The beat-frequency-oscillator output terminals are wired to one side of the switch, while the integrating amplifier output is connected to the other side. This permits both the input and output signal magnitudes to be measured with the same instrument by throwing the switch.

35.274. Dynamic response angles are measured with a cathode-ray oscilloscope by using the method described in Technique Summary 35-1. The wiring connections are shown in section a. Output signals are applied to the y-axis

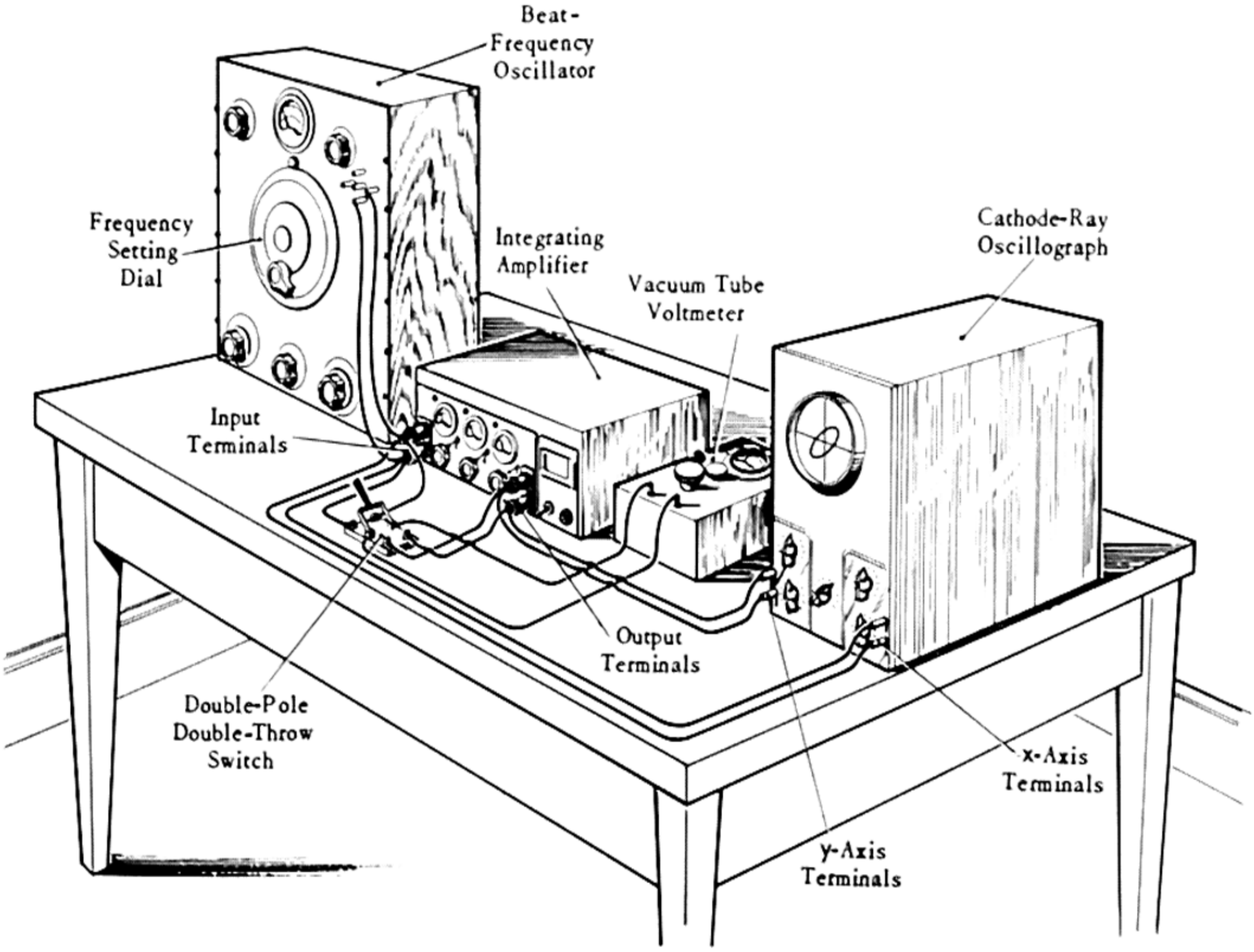
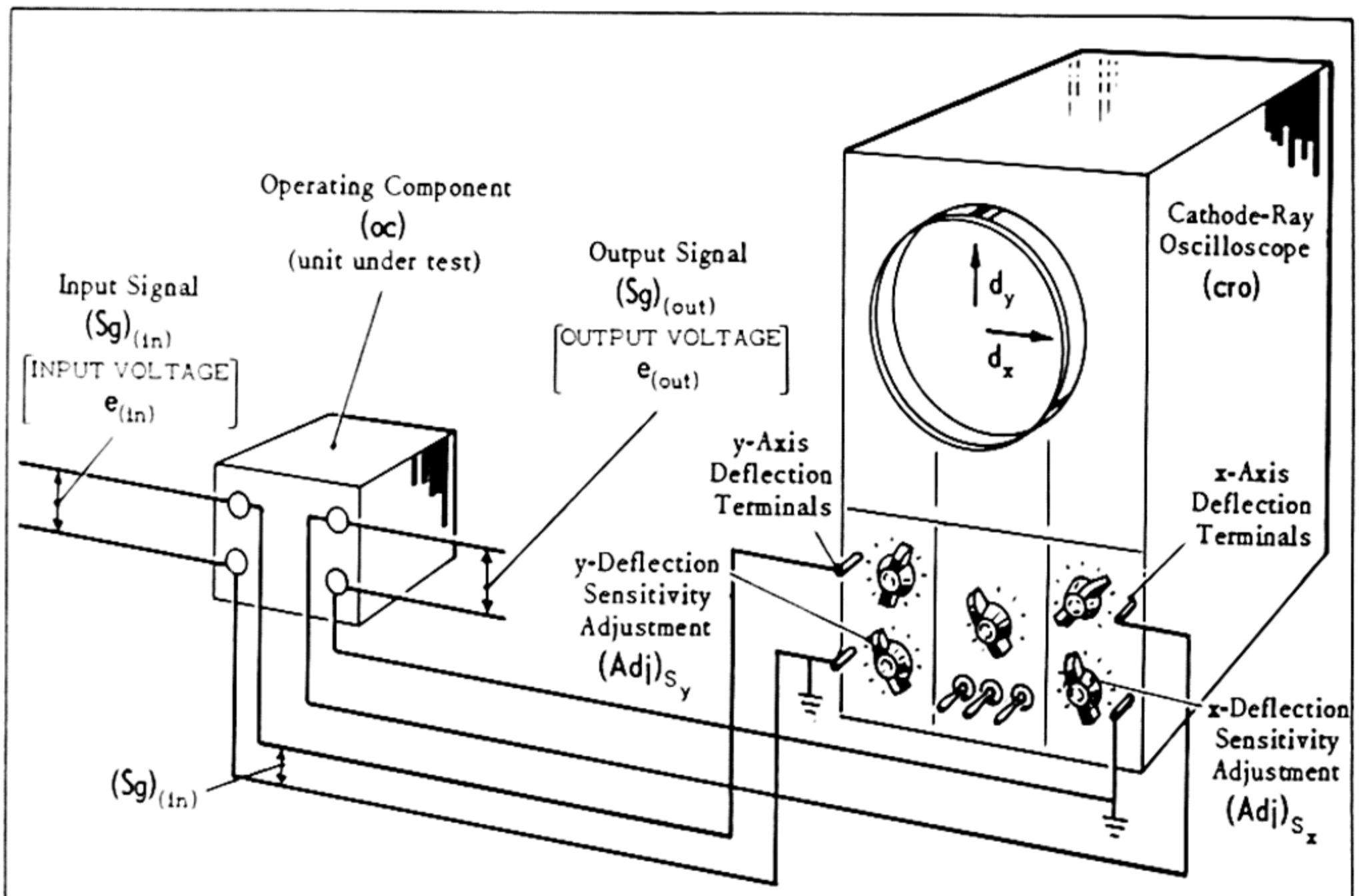


Fig. 35-43. Calibration of an integrating amplifier.



a) Connection diagram for the sinusoidal input test of the operating component

When the input signal to the arrangement shown in section a is sinusoidal,

$$(Sg)_{(in)} = (Sg)_{(in)a} \sin w_f t \tag{1}$$

where

$$w_f = 2\pi n_f \tag{2}$$

n_f = forcing frequency

$(Sg)_{(in)a}$ = input signal amplitude

This signal is often a voltage to start with; if not, it may always be transformed into a voltage. Therefore,

$$(Sg)_{(in)} \approx e_{(in)} = e_{(in)a} \sin w_f t \tag{3}$$

Note: In practice, the input voltage may differ from the input signal by being a different quantity with amplitude and phase angle differences. To simplify the present discussion, $e_{(in)}$ is considered as identical with $(Sg)_{(in)}$.

The corresponding output signal will differ from the input signal in amplitude by the sensitivity of the operating component under test. The output signal will differ in phase from the input signal by the dynamic response angle of the operating component under test. The resulting expression for the output signal may be written in the forms

$$(Sg)_{(out)} = S_{(oc)[(Sg)_{(in)};(Sg)_{(out)}]} (Sg)_{(in)a} \sin\left(w_f t + (DRA)_{(oc)((Sg)_{(in)};(Sg)_{(out)})}\right) \tag{4}$$

and

$$(Sg)_{(out)} = (Sg)_{(out)a} \sin\left(w_f t + (DRA)_{(oc)((Sg)_{(in)};(Sg)_{(out)})}\right) \tag{5}$$

where

$S_{(oc)[(Sg)_{(in)};(Sg)_{(out)}]}$ = input signal – output signal sensitivity of the operating component under test

$(Sg)_{(out)}$ = output signal

$(Sg)_{(out)a}$ = output signal amplitude

Technique Summary 35-1. Use of the cathode-ray oscilloscope to determine operating component dynamic response angles and sensitivities. (Page 1 of 4)

$(DRA)_{(oc)((Sg)_{(in)};(Sg)_{(out)})}$ = input signal – output signal dynamic response angle of the operating component under test

To simplify the present discussion, the output voltage will be taken as identical with the output signal; i.e.,

$$(Sg)_{(out)} = e_{(out)} = e_{(out)a} \sin(w_f t + DRA) \tag{6}$$

where the identifying subscript symbols are omitted from DRA to simplify the symbol, with any possible misunderstanding eliminated by context.

When

$$(Sg)_{(in)} = e_{(in)} \quad \text{and} \quad (Sg)_{(out)} = e_{(out)} \tag{7}$$

then

$$S_{(oc)[(Sg)_{(in)};(Sg)_{(out)}]} = \frac{e_{(out)a}}{e_{(in)a}} \tag{8}$$

b) Input quantity – output quantity relationships for a sinusoidal input quantity variation

The indications appearing on the face of the cathode-ray tube are shown in Fig. a, and are determined by the voltages applied to the x-axis deflection terminals and the y-axis deflection terminals.

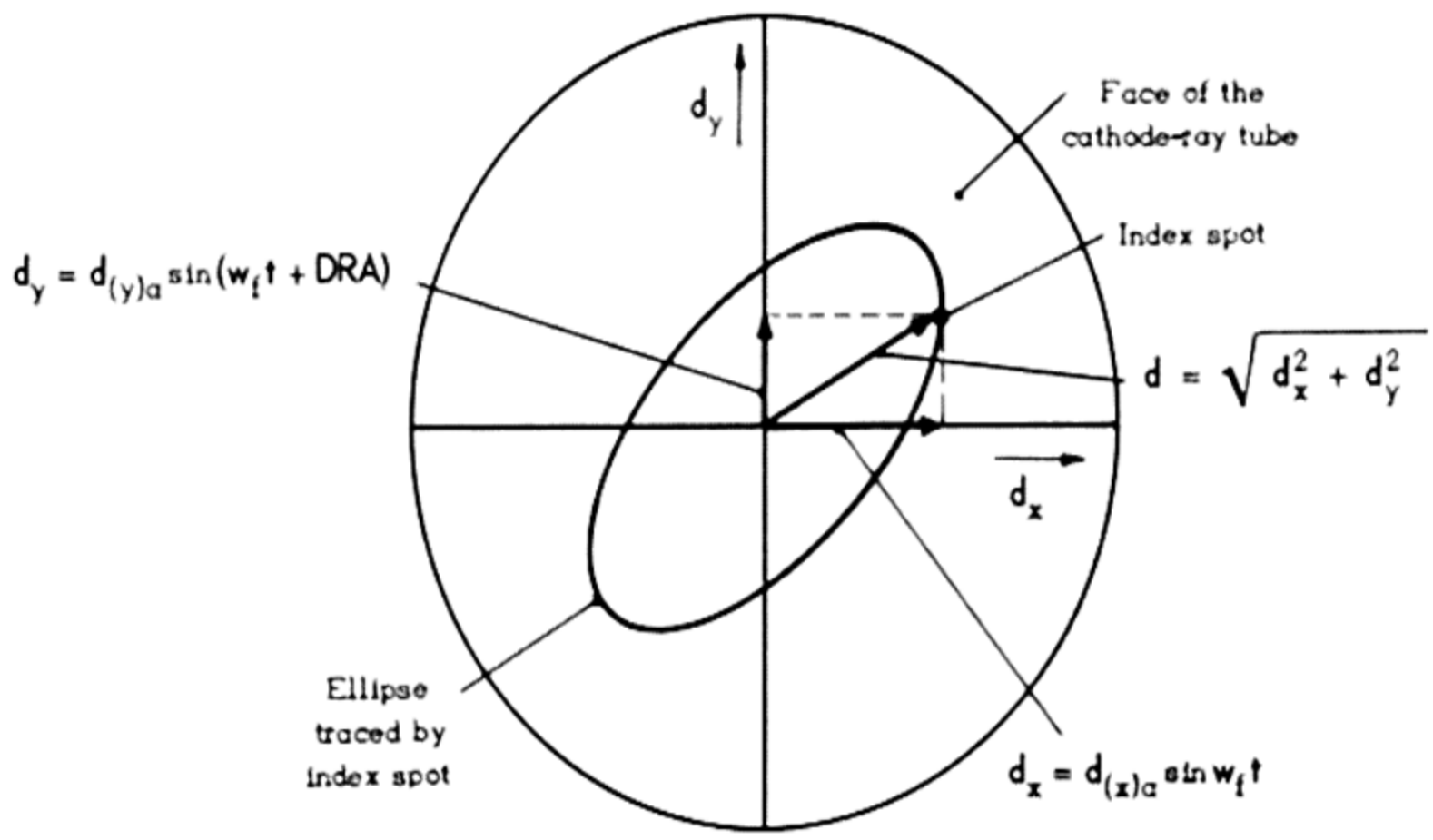


Fig. a. Face of the cathode-ray tube showing a typical figure traced by the index spot.

$$d_x = S_{(cro)[e;d]x} e_{(in)a} \sin w_f t \tag{9}$$

$$= d_{(x)a} \sin w_f t \tag{10}$$

= deflection of the index spot parallel to the x-axis of the cathode-ray oscilloscope tube face

$$d_y = S_{(cro)[e;d]y} e_{(out)a} \sin(w_f t + DRA) \tag{11}$$

$$= d_{(y)a} \sin(w_f t + DRA) \tag{12}$$

= deflection of the index spot parallel to the y-axis of the cathode-ray oscilloscope tube face

$$S_{(cro)[e;d]x} = \frac{d_{(x)a}}{e_{(in)(cro)(x)a}} \tag{13}$$

= voltage-deflection of the x-axis indicating system of the cathode-ray oscilloscope

Technique Summary 35-1. Use of the cathode-ray oscilloscope to determine operating component dynamic response angles and sensitivities. (Page 2 of 4)

$$S_{(cro)[e;d]y} = \frac{d_{(y)a}}{e_{(in)(cro)(y)a}} \tag{14}$$

= voltage-deflection of the y-axis indicating system of the cathode-ray oscilloscope

$e_{(in)(cro)(x)a}$ = amplitude of the input voltage to the x-axis indicating system of the cathode-ray oscilloscope

$e_{(in)(cro)(y)a}$ = amplitude of the input voltage to the y-axis indicating system of the cathode-ray oscilloscope

Note: Equations (13) and (14) imply that the dynamic response angles associated with the indicating systems of the cathode-ray oscilloscope are both negligibly small.

c) *Relationships among inputs and outputs of the cathode-ray oscilloscope*

Elimination of $w_f t$ from Eqs. (10) and (12) yields the equation of the locus traced out by the index spot in terms of x- and y-deflections; i.e.,

$$\left(\frac{d_{(y)a}}{d_{(x)a}}\right)^2 d_x^2 - 2\left(\frac{d_{(y)a}}{d_{(x)a}} \cos (DRA)\right) d_x d_y + d_y^2 - d_{(y)a}^2 \sin^2 (DRA) = 0 \tag{15}$$

If $(DRA) = 0$, Eq. (15) represents a straight line passing through the origin. If $(DRA) \neq 0$, Eq. (15) represents an ellipse with its principal axes rotated with respect to the coordinate axes of the tube face.*

If $w_f t = 0$, the x-deflection of the index is zero and the y-deflection is

$$d_{(y)(w_f t = 0)} = d_{(y)a} \sin (DRA) \tag{16}$$

The maximum y-deflection of the index occurs when $w_f t = \pi/2 - (DRA)$; i.e.,

$$d_{(y)(max)} = d_{(y)(w_f t = \pi/2 - DRA)} = d_{(y)a} \tag{17}$$

When $w_f t = -(DRA)$, the y-deflection of the index is zero and the x-deflection is

$$d_{(x)(w_f t = -DRA)} = d_{(x)a} \sin (-DRA) \tag{18}$$

The maximum x-deflection occurs when $w_f t = \pi/2$; i.e.,

$$d_{(x)(max)} = d_{(x)(w_f t = \pi/2)} = d_{(x)a} \tag{19}$$

The quantities defined in Eqs. (15) through (19) are illustrated in Fig. b.

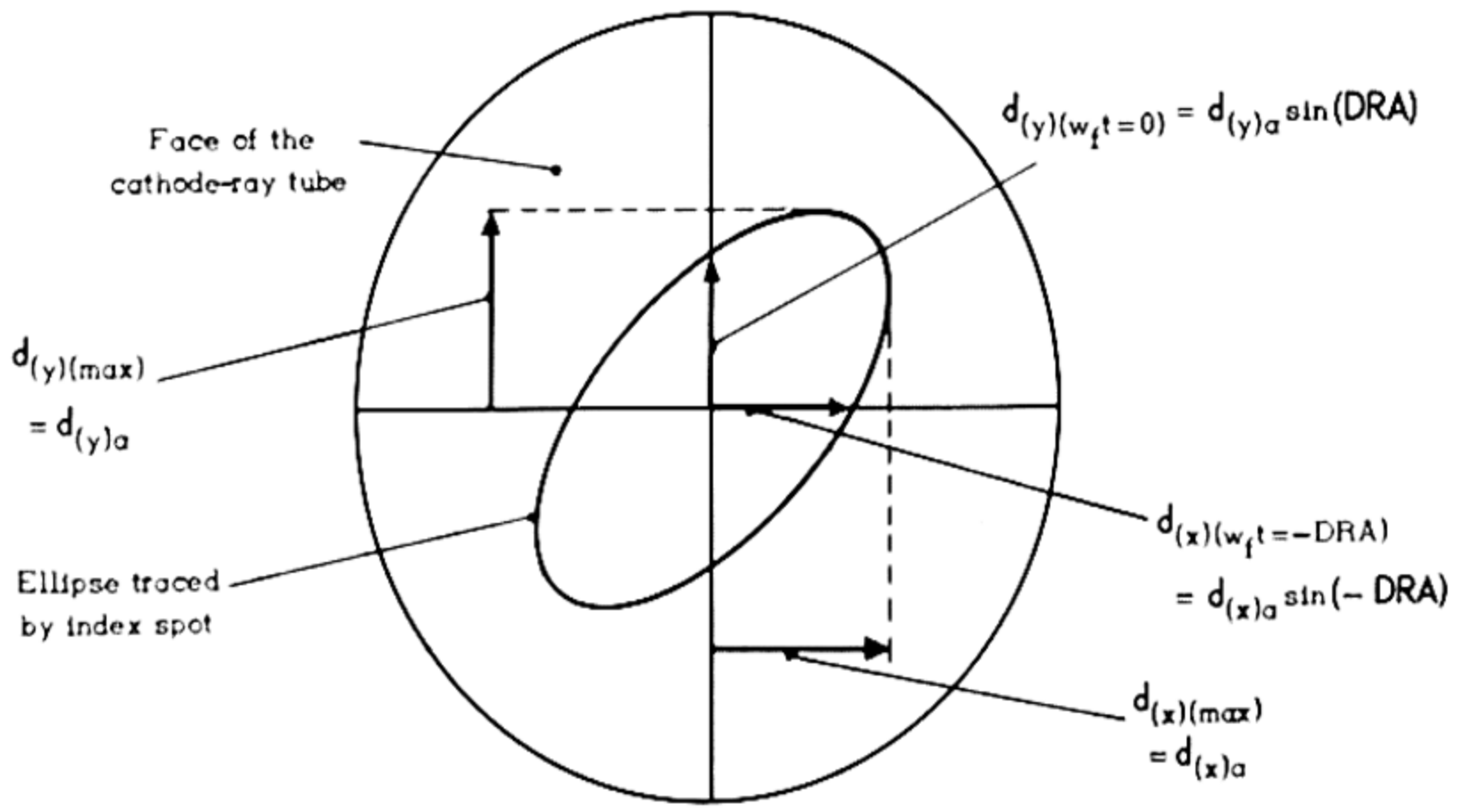


Fig. b. Face of the cathode-ray tube showing the quantities to be measured for the determination of the dynamic response angle and the sensitivity ratio of the operating component.

---

* The locus represented by the general second-degree equation $Ax^2 + Bxy + Cy^2 + F = 0$ depends on the discriminant $B^2 - 4AC$. If $B^2 - 4AC < 0$ and $AF < 0$, the locus is an ellipse. If $B^2 - 4AC = 0$, the equation represents two parallel straight lines. See Osgood and Graustein (OS).

The sine of (DRA) is given by the ratio of $d_{(y)(w_f t=0)}$ to $d_{(y)(max)}$; i.e.,

$$\sin (DRA) = \frac{d_{(y)(w_f t=0)}}{d_{(y)(max)}} \tag{20}$$

$$(DRA) = \sin^{-1}\left[\frac{d_{(y)(w_f t=0)}}{d_{(y)(max)}}\right] \tag{21}$$

From Eqs. (9) through (12),

$$d_{(x)(max)} = S_{(cro)[e;d]x} e_{(in)a} \tag{22}$$

$$d_{(y)(max)} = S_{(cro)[e;d]y} e_{(out)a} \tag{23}$$

Substitution from these equations into Eq. (8), which gives the sensitivity of the operating component, shows that

$$S_{(oc)[e;e]} = \frac{S_{(cro)[e;d]x}}{S_{(cro)[e;d]y}} \frac{d_{(y)(max)}}{d_{(x)(max)}} \tag{24}$$

d) Determination of operating component sensitivity and dynamic response angle from cathode-ray oscilloscope displacements

Technique Summary 35-1. Use of the cathode-ray oscilloscope to determine operating component dynamic response angles and sensitivities. (Page 4 of 4)

deflection terminals. Input signals are applied to the x-axis deflection terminals. The resultant figure appearing on the cathode-ray tube face is given typically by Fig. a of the summary, and may be represented analytically by Eq. (15) of the summary, which shows it to be an ellipse. As shown by section d of the summary, the dynamic response angle is determined from the two y-axis measurements indicated in Fig. b of the summary. These are the y-axis intercept of the ellipse and the maximum y-axis displacement. The dynamic response angle is calculated from Eq. (21). Operating component sensitivities may also be determined from Fig. b, as described in section d of the summary.

35.275. Calibration information for an integrating amplifier is summarized in Test Report No. 35-3. As shown in Chapter 34, the theoretical relating function that may be associated with this operating component is the (0;0, 1) type. The test range of frequencies, shown in sheets 5 and 6, is from 6 to 200 cycles per second. Within this range, the performance of the integrating amplifier may be represented by a (0;1) equation, as the plots show. The data and steps for reduction to dimensionless form are given in the tabulations of sheets 5 and 6. The reference frequency is arbitrarily taken as 10 cycles per second, for convenience. The voltage in – voltage rate out sensitivity is found to be 14.0 volts-per-second per volt. The reference sensitivity for volts in – volts out is taken at the reference frequency. It is equal to 0.224 volt per volt. The theoretical sensitivity ratio is equal to the inverse frequency ratio, as shown on sheet 1 of the test report. The theoretical dynamic response angle is -90 degrees. The ideal performance function is the same as the theoretical.

SUMMARY: Test Form A **TEST REPORT NO.** 35-3 Sheet 1 of 6

Instruments Laboratory · Aeronautical Engineering Department · Massachusetts Institute of Technology · Cambridge · Massachusetts

Title of test INTEGRATING AMPLIFIER CALIBRATION ; STEADY-STATE SINUSOIDAL INPUT

Date 7/30/54 **In charge of test** J. L. STOCKARD **Assisting with test** —

Equipment tested MILLER INTEGRATING AMPLIFIER (ia)

Type A Model AA6 Serial No. 21

Calculations J.L. STOCKARD

Plots J.L. STOCKARD

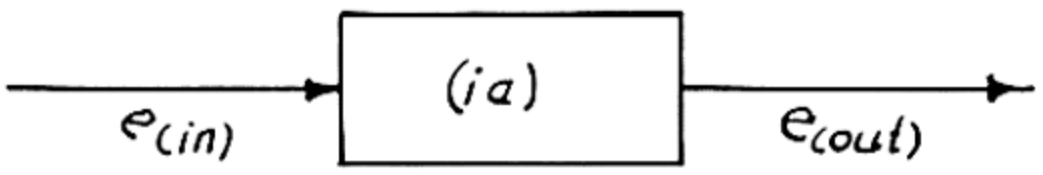
Equipment used for test HEWLETT PACKARD AUDIO OSCILLATOR, SPECIF. 20945 SER. NO. 1378 ; DUMONT CATHODE-RAY OSCILLOGRAPH, Type 279 SER. NO. 112 ; BALLANTINE ELECTRONIC VOLTMETER, MODEL 300, SER. NO. 6390

Input quantity VOLTAGE $e_{(in)}$ Output quantity VOLTAGE $e_{(out)}$

Environmental conditions: Temperature 70° F Pressure —

Other —

Summary of results:



$$[PF]_{(\ ia\ )}[e_{(in)};e_{(out)}](\text{theo}) \approx [RF]_{(\ 0;1\ )} = S_{(ia)[e;e]}\ \frac{1}{j} = S_{(ia)[e;e](ref)}\ \frac{1}{j(FR)}$$

$$S_{(ia)[e;e](ref)} = S_{(ia)[e;\dot{e}](ref)}\ \frac{n_{(ref)}}{2\pi}\ ;\quad S_{(ia)[e;e](ref)} = 14.0\ \frac{\text{volts/second}}{\text{volt}}$$

$$S_{(ia)[e;e]} = \frac{e_{(out)a}}{e_{(in)a}}\ ;\quad S_{(ia)[e;\dot{e}]} = \frac{\dot{e}_{(out)a}}{e_{(in)a}}$$

$$'(SR)_{(\ ia\ )(e_{(in)};e_{(out)})(\text{theo})} \approx '(DAR)_{(\ 0;1\ )} = \frac{1}{FR}$$

$$(DRA)_{(\ ia\ )(e_{(in)};e_{(out)})(\text{theo})} \approx (DRA)_{(\ 0;1\ )} = -90°$$

Reference frequency = $n_{(ref)}$ = 10 cycles/second

Damping ratio = DR = —

Reference sensitivity = $S_{(\ ia\ )[\ e\ ;\ e\ ](ref)}$ = 0.224 volt/volt

Reference dynamic response angle = $(DRA)_{(ref)}$ = −90°

Frequency ratio = FR = $n_f/n_{(ref)}$; Forcing frequency = n_f ; Dynamic response angle = $(DRA)_{(id)(q_{(in)};q_{(out)})}$

Performance function = $[PF]_{(id)[q_{(in)};q_{(out)}]} = \frac{q_{(out)}}{q_{(in)}} = S_{(id)[q_{(in)};q_{(out)}](ref)}\ '(SR)_{(id)(q_{(in)};q_{(out)})}{}^{\epsilon}{}^{)(DRA)_{(id)(q_{(in)};q_{(out)})}}$

Dimensionless sensitivity ratio = $'(SR)_{(id)(q_{(in)};q_{(out)})} = S_{(id)[q_{(in)};q_{(out)}]}/S_{(is)[q_{(in)};q_{(out)}](ref)}$; Identified component = (id)

Theoretical dimensionless sensitivity ratio = $'(SR)_{(\ ia\ )(\ e\ ;\ e\ )(\text{theo})}$ → Theoretical dynamic amplitude ratio = $'(DAR)_{(theo)} = '(DAR)_{(\ 0;1\ )}$

Theoretical dynamic response angle = $(DRA)_{(theo)} = (DRA)_{(\ 0;1\ )}$ Theoretical performance function for the unit under test = $[PF]_{(\ ia\ )[\ e\ ;\ e\ ](theo)}$

Relating function associated with the (0;1) differential equation = $[RF]_{(\ 0;1\ )}$

Instruments Laboratory · Aeronautical Engineering Department · Massachusetts Institute of Technology · Cambridge · Massachusetts

Title of test INTEGRATING AMPLIFIER CALIBRATION; STEADY-STATE SINUSOIDAL INPUT

Date 7/30/54 **In charge of test** J. L. STOCKARD **Assisting with test** —

Equipment tested MILLER INTEGRATING AMPLIFIER (ia) **Calculations** J. L. STOCKARD

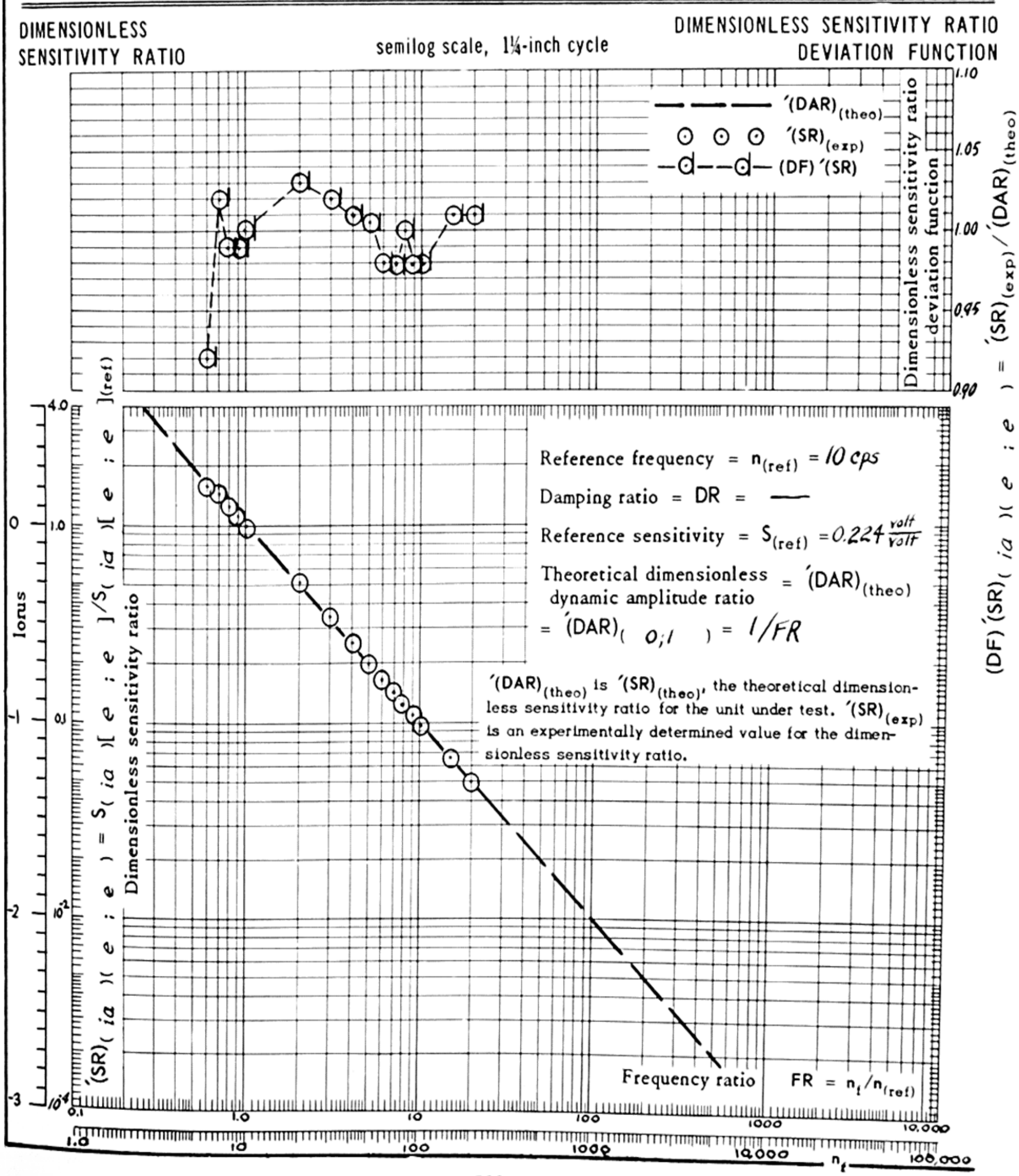
Type A **Model** AA6 **Serial No.** 21 **Plots** J. L. STOCKARD

Equipment used for test HEWLETT PACKARD AUDIO OSCILLATOR, SPECIF. 20945 SER. NO. 1378 ; DUMONT CATHODE-RAY OSCILLOGRAPH, Type 279 SER. NO. 112 ; BALLANTINE ELECTRONIC VOLTMETER, MODEL 300, SER. NO. 6390

Input quantity VOLTAGE $e_{(in)}$ **Output quantity** VOLTAGE $e_{(out)}$

Environmental conditions: Temperature 70° F **Pressure** —

Other —



PR PLOTS: Test Form C **TEST REPORT NO.** 35-3 Sheet 3 of 6

Instruments Laboratory · Aeronautical Engineering Department · Massachusetts Institute of Technology · Cambridge · Massachusetts

Title of test INTEGRATING AMPLIFIER CALIBRATION ; STEADY-STATE SINUSOIDAL INPUT

Date 7/30/54 In charge of test J.L. STOCKARD Assisting with test —

Equipment tested MILLER INTEGRATING AMPLIFIER (ia) Calculations J. L. STOCKARD

Type A Model AA6 Serial No. 21 Plots J.L. STOCKARD

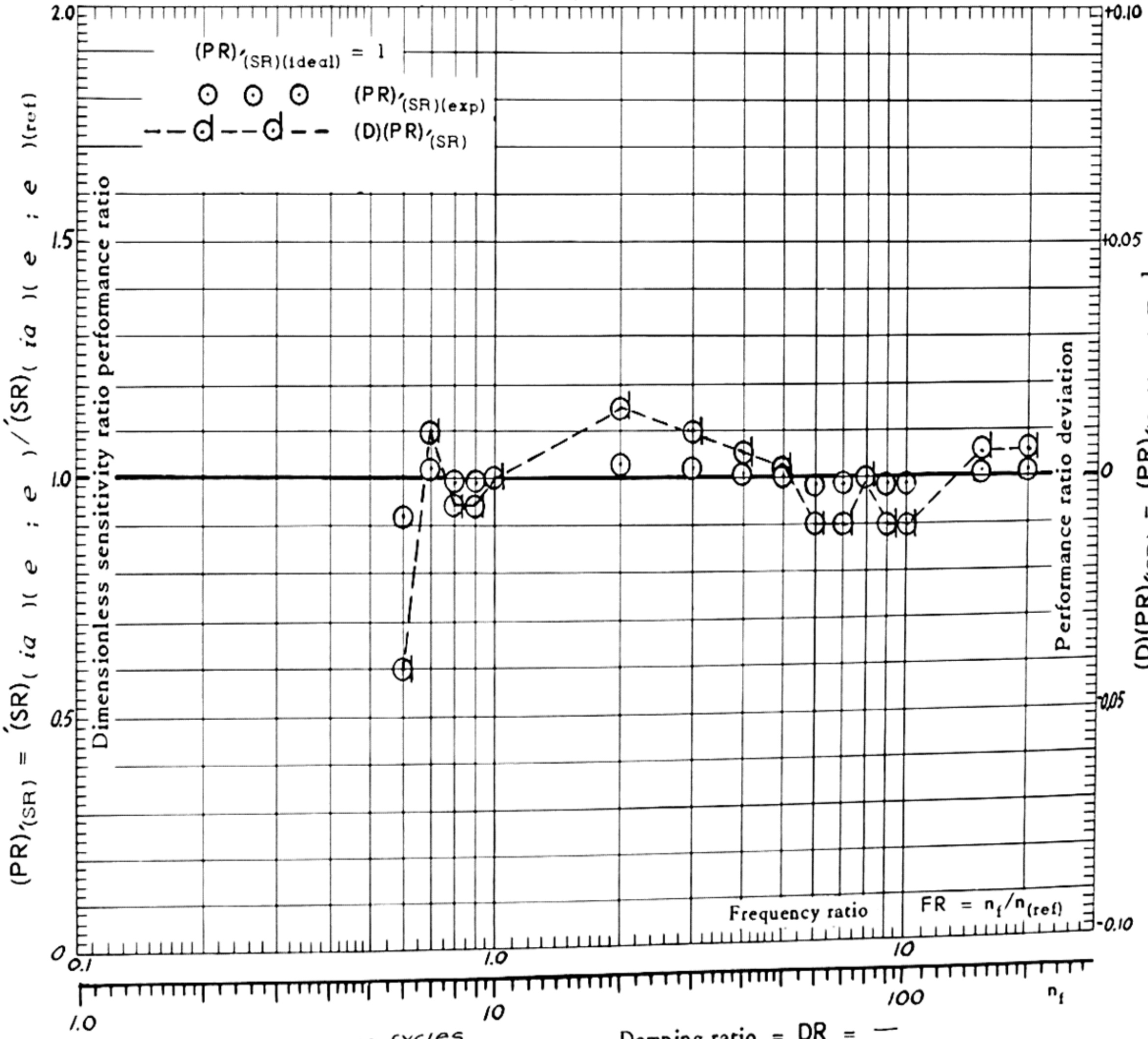
Equipment used for test HEWLETT PACKARD AUDIO OSCILLATOR, SPECIF. 20945 SER. NO. 1378 ; DUMONT CATHODE-RAY OSCILLOGRAPH, TYPE 279 SER. NO. 112 ; BALLANTINE ELECTRONIC VOLTMETER, MODEL 300, SER. NO. 6390

Input quantity VOLTAGE $e_{(in)}$ Output quantity VOLTAGE $e_{(out)}$

Environmental conditions: Temperature 70° F Pressure —

Other —

PERFORMANCE RATIO — semilog scale, 2½-inch cycle — PERFORMANCE RATIO DEVIATION



Reference frequency = $n_{(ref)} = 10 \frac{cycles}{second}$ Damping ratio = DR = —

Reference dimensionless sensitivity ratio = ${}'(SR)_{(\ ia\ )(\ e\ ;\ e\ )(ref)} = 1/FR$

Reference sensitivity = $S_{(\ ia\ )[\ e\ ;\ e\ ](ref)} = 0.244 \frac{volt}{volt}$

Theoretical dimensionless dynamic amplitude ratio = ${}'(DAR)_{(theo)} = {}'(DAR)_{(\ 0;1\ )} = 1/FR$

${}'(SR)_{(\ ia\ )(\ e\ ;\ e\ )} = S_{(\ ia\ )[\ e\ ;\ e\ ]} / S_{(\ ia\ )[\ e\ ;\ e\ ](ref)}$

${}'(DAR)_{(theo)}$ is ${}'(SR)_{(theo)}$, the theoretical dimensionless sensitivity ratio for the unit under test; $(PR)'_{(SR)(exp)}$ is the performance ratio determined from ${}'(SR)_{(exp)}$, the experimental sensitivity ratio.

DRA PLOTS: Test Form K **TEST REPORT NO.** 35-3 Sheet 4 of 6

Instruments Laboratory · Aeronautical Engineering Department · Massachusetts Institute of Technology · Cambridge · Massachusetts

Title of test INTEGRATING AMPLIFIER CALIBRATION; STEADY-STATE SINUSOIDAL INPUT

Date 7/30/54 **In charge of test** J. L. STOCKARD **Assisting with test** —

Equipment tested MILLER INTEGRATING AMPLIFIER (ia)

Type A **Model** AA6 **Serial No.** 21 **Calculations** J. L. STOCKARD

Plots J. L. STOCKARD

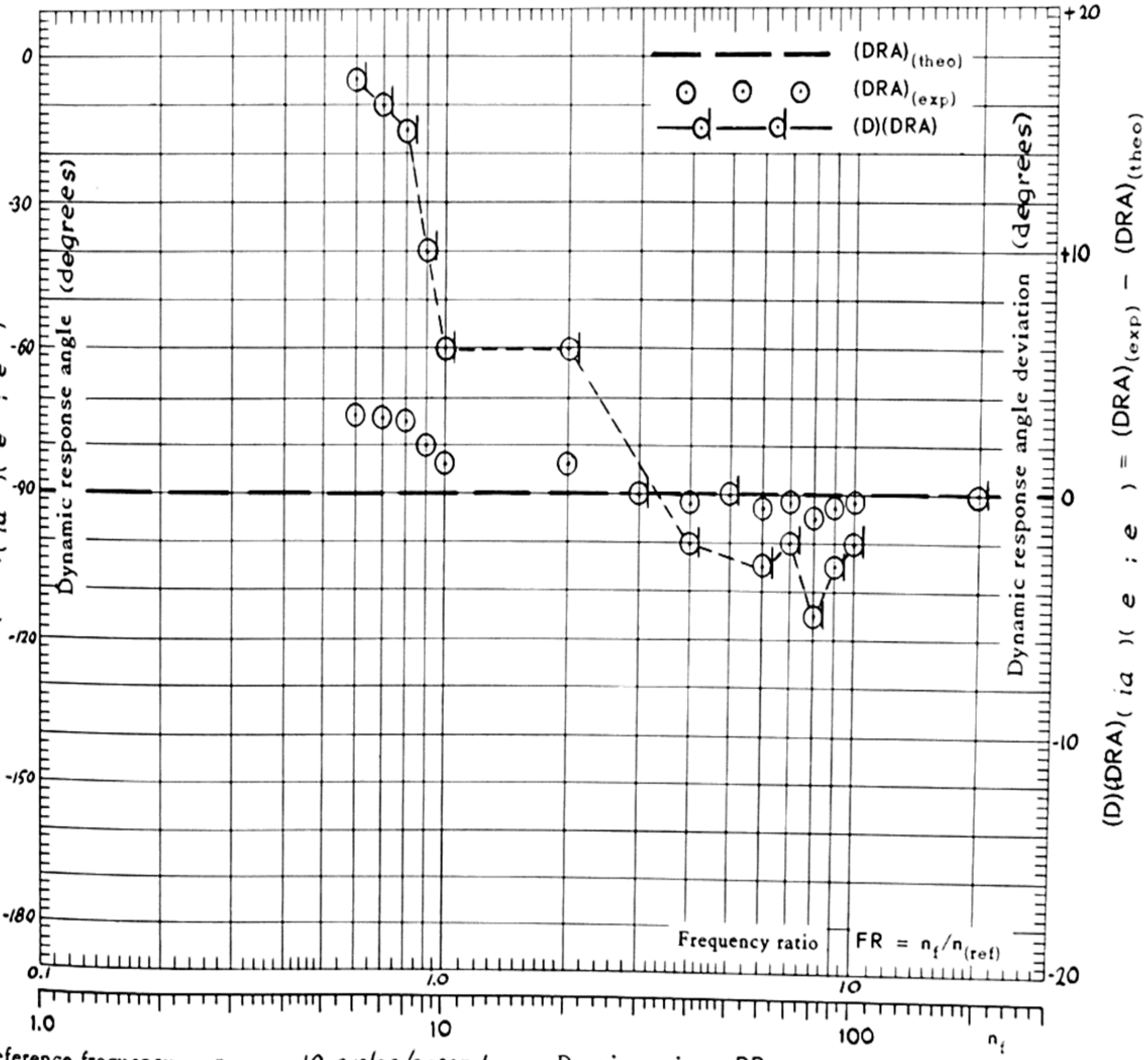
Equipment used for test HEWLETT PACKARD AUDIO OSCILLATOR, SPECIF. 20945 SER. NO. 1378; DUMONT CATHODE-RAY OSCILLOGRAPH, Type 279 SER. NO. 112; BALLANTINE ELECTRONIC VOLTMETER, MODEL 300, SER. NO. 6390

Input quantity VOLTAGE $e_{(in)}$ **Output quantity** VOLTAGE $e_{(out)}$

Environmental conditions: Temperature 70° F **Pressure** —

Other —

DYNAMIC RESPONSE ANGLE — semilog scale, 2½-inch cycle — DYNAMIC RESPONSE ANGLE DEVIATION



Reference frequency = $n_{(ref)}$ = 10 cycles/second Damping ratio = DR = —

Reference dynamic response angle = $(DRA)_{(ref)}$ = −90°

Theoretical dynamic response angle = $(DRA)_{(theo)} = (DRA)_{(0;1)} = -90°$

$(DRA)_{(theo)}$ is the theoretical dynamic response angle for the unit under test; $(DRA)_{(exp)}$ is the dynamic response angle determined by experiment.

TEST DATA: Test Form N **TEST REPORT NO.** 35-3 Sheet 5 of 6

Instruments Laboratory · Aeronautical Engineering Department · Massachusetts Institute of Technology · Cambridge · Massachusetts

Title of test INTEGRATING AMPLIFIER CALIBRATION ; STEADY-STATE SINUSOIDAL INPUT

Date 7/30/54 In charge of test J. L. STOCKARD Assisting with test

Equipment tested MILLER INTEGRATING AMPLIFIER (ia)

Type A Model AA6 Serial No. 21 Calculations J.L. STOCKARD

Plots J.L. STOCKARD

Equipment used for test HEWLETT PACKARD AUDIO OSCILLATOR, SPECIF. 20945 SER. NO. 1378 ; DUMONT CATHODE-RAY OSCILLOGRAPH, Type 279 SER. NO. 112 BALLANTINE ELECTRONIC VOLTMETER, MODEL 300, SER. NO. 6390

Input quantity VOLTAGE $e_{(in)}$ Output quantity VOLTAGE $e_{(out)}$

Environmental conditions: Temperature 70° F Pressure 1

Other —

Run Number	Forcing Amplitude $e_{(in)a}$	Forcing Frequency n_f	Output Amplitude (voltage rate) $\dot{e}_{(out)a}$	Output Voltage Amplitude $e_{(out)a}$	Input-Output Sensitivity $S_{(ia)[e;e](exp)}$	Dimensionless Sensitivity Ratio* $'(SR)_{(ia)(e;e)(exp)}$	Dimensionless Dynamic Amplitude Ratio $'(DAR)_{(o;i)} = 1/FR$	Dimensionless Sensitivity Ratio Deviation Function $'(SR)_{(exp)}/'(DAR)_{(theo)}$	Dynamic Response Angle $(DRA)_{(ia)(e;e)(exp)}$	Theoretical Dynamic Response Angle $(DRA)_{(theo)} = (DRA)_{(o;i)} = -90°$	Dynamic Response Angle Deviation $(DRA)_{(exp)} - (DRA)_{(theo)}$	Frequency Ratio $FR = n_f/n_{(ref)}$	
Units and References	volts	cycles/second	$\frac{\text{volts}}{\text{second}}$	volts	$\frac{e_{(out)a}/e_{(in)a}}{\text{volts/volt}}$	$S_{(ref)} = 0.224 = S_{(ref)(FR=1)}$	Theoretical Dimensionless $'(DAR)_{(theo)} = (DF)'(SR)$	Dimensionless Sensitivity $'(SR) = '(SR)_{(exp)}/'(DAR)_{(theo)}$	Dynamic $(DRA)_{(ia)(e;e)(exp)}$	Theoretical $(DRA)_{(theo)}$	Dynamic $(D)(DRA) = (DRA)_{(exp)} - (DRA)_{(theo)}$	$n_{(ref)} = 10 \frac{\text{cycles}}{\text{second}}$	
									$(DRA)_{(ref)} = -90°$ degrees				
1	2.52	6	32.8	0.870	0.342	1.53	1.67	0.92	-73	-90	+17	0.6	
2	2.42	7	34.8	0.792	0.327	1.46	1.43	1.02	-74	-90	+16	0.7	
3	2.62	8	36.6	0.728	0.278	1.24	1.25	0.99	-75	-90	+15	0.8	
4	2.69	9	37.5	0.663	0.246	1.10	1.11	0.99	-80	-90	+10	0.9	
5	2.69	10	37.8	0.601	0.224	1.00	1.00	1.00	-84	-90	+6	1.0	
6	5.66	20	81.7	0.650	0.115	0.514	0.50	1.03	-84	-90	+6	2.0	
7	5.80	30	83.5	0.443	0.0763	0.340	0.333	1.02	-90	-90	0	3.0	
8	10.00	40	142	5.65	0.0565	0.252	0.25	1.01	-92	-90	-2	4.0	

* $'(SR)_{(exp)} = S_{(exp)}/S_{(ref)}$; Reference sensitivity = $S_{(ia)[e;e](ref)} = S_{(ref)}$.

Run Number	Forcing Amplitude $e_{(in)a}$	Forcing Frequency n_f	Output Amplitude (voltage rate) $\dot{e}_{(out)a}$	Output Voltage Amplitude $e_{(out)a}$	Input-Output Sensitivity $S_{(ia)[e;e]_{(exp)}}$	Dimensionless Sensitivity Ratio $'(SR)_{(ia)(e;e)_{(exp)}}$*	Dimensionless Dynamic Amplitude Ratio $'(DAR)_{(theo)} = {}'(DAR)_{(0;1)} = {}'/FR$	Dimensionless Sensitivity Ratio Deviation Function $(DF)\,{}'(SR) = {}'(SR)_{(exp)}/{}'(DAR)_{(theo)}$	Dynamic Response Angle $(DRA)_{(ia)(e;e)_{(exp)}}$	Theoretical Dynamic Response Angle $(DRA)_{(theo)} = (DRA)_{(0;1)^{=-90^\circ}}$	Dynamic Response Angle Deviation $(D)(DRA) = (DRA)_{(exp)} - (DRA)_{(theo)}$	Frequency Ratio $FR = n_f/n_{(ref)}$	
Units and References	volts	cycles/second	volts/second	volts	$e_{(out)a}/e_{(in)a}$ volts/volt	$S_{(ref)} = 0.224 = S_{(ref)(FR=1)}$	Theoretical Dimensionless Dynamic Amplitude Ratio $(DAR)_{(theo)}$	Dimensionless Sensitivity Ratio $(DF)\,{}'(SR)$	$(DRA)_{(ref)} = -90^\circ$ degrees			$n_{(ref)} = 10\ \frac{cycles}{second}$	
9	1.49	50	21.0	0.067	0.0450	0.201	0.20	1.005	-90	-90	0	5.0	
10	1.77	60	24.6	0.0651	0.0368	0.164	0.167	0.98	-93	-90	-3	6.0	
11	1.98	70	27.3	0.0620	0.0313	0.140	0.143	0.98	-92	-90	-2	7.0	
12	10.00	80	14.1	0.280	0.0280	0.125	0.125	1.00	-95	-90	-5	8.0	
13	2.83	90	39.5	0.069	0.0244	0.109	0.111	0.98	-93	-90	-3	9.0	
14	2.83	100	39.1	0.0621	0.0270	0.0981	0.10	0.98	-92	-90	-2	10.0	
15	2.83	150	40.5	0.043	0.0152	0.0678	0.067	1.01	–	-90	–	15.0	
16	2.83	200	40.1	0.0314	0.0113	0.0505	0.05	1.01	-90	-90	0	20.0	

* $'(SR)_{(exp)} = S_{(exp)}/S_{(ref)}$; Reference sensitivity $= S_{(ia)[e;e]_{(ref)}} = S_{(ref)}$.

35.276. Experimental performance is compared with theoretical performance in sheet 2 of Test Report No. 35-3. The theoretical performance is represented by a straight line with a slope of -1 on the dimensionless sensitivity ratio plot. The circled dots are the experimental values. The dimensionless sensitivity ratio deviation function is calculated by dividing the experimental value of the sensitivity ratio for a given point by the theoretical value of the dynamic amplitude ratio for the point, this reference quantity being equal to the inverse frequency ratio. Sensitivity ratio deviation function values are plotted in the upper half of sheet 2. Performance ratios and performance ratio deviations are plotted on sheet 3 of the test report. The variations in the deviations appear to be random, and hence are attributable to experimental uncertainties rather than to any systematic source.

35.277. The theoretical value as well as the ideal value of the dynamic response angle is -90 degrees. The experimental values of this quantity are plotted on sheet 4.* The light dashed line connects the points representing dynamic response angle deviations. The slight rise at the left-hand side may be due to the dynamic limitation of the integrator, but the experimental uncertainty of phase measurement does not permit a more definite statement.

ILLUSTRATIVE TEST REPORT ON THE CALIBRATION OF A LINEAR ACCELERATION RECORDING SYSTEM

35.278. A second method of generating mechanical sinusoidal input displacements, in addition to that shown in Fig. 35-42, is presented in Fig. 35-44. The main component is the loud-speaker-type electromagnetic linear vibration calibrator. Its field is excited by the passage of direct current. The intensity is regulated by the rheostat control in the lower left-hand corner of the power supply section. Sinusoidal signals are generated by the oscillator, and are increased to power level by the amplifier shown in the figure. The resulting alternating current of adjustable but controlled magnitude and frequency is applied to the armature of the loud-speaker-type electromagnetic linear vibration calibrator. The armature is supported on a pair of cantilever spring flexures, one of which is shown in the figure. The alternating current passing through the armature produces an alternating magnetic field that reacts against the constant magnetic field of the field coil. The resultant alternating mechanical force moves the armature against the cantilever flexures. This results in a mechanical motion that reproduces the electrical input quite faithfully in the operating frequency range. An electromagnetic signal generator, incorporated at the base of the armature, provides a signal for measuring the mechanical input.

35.279. The remainder of Fig. 35-44 shows the operating components of a linear acceleration recording system. The assembly in the figure is arranged for

* These values were determined by the method described in Technique Summary 35-1.

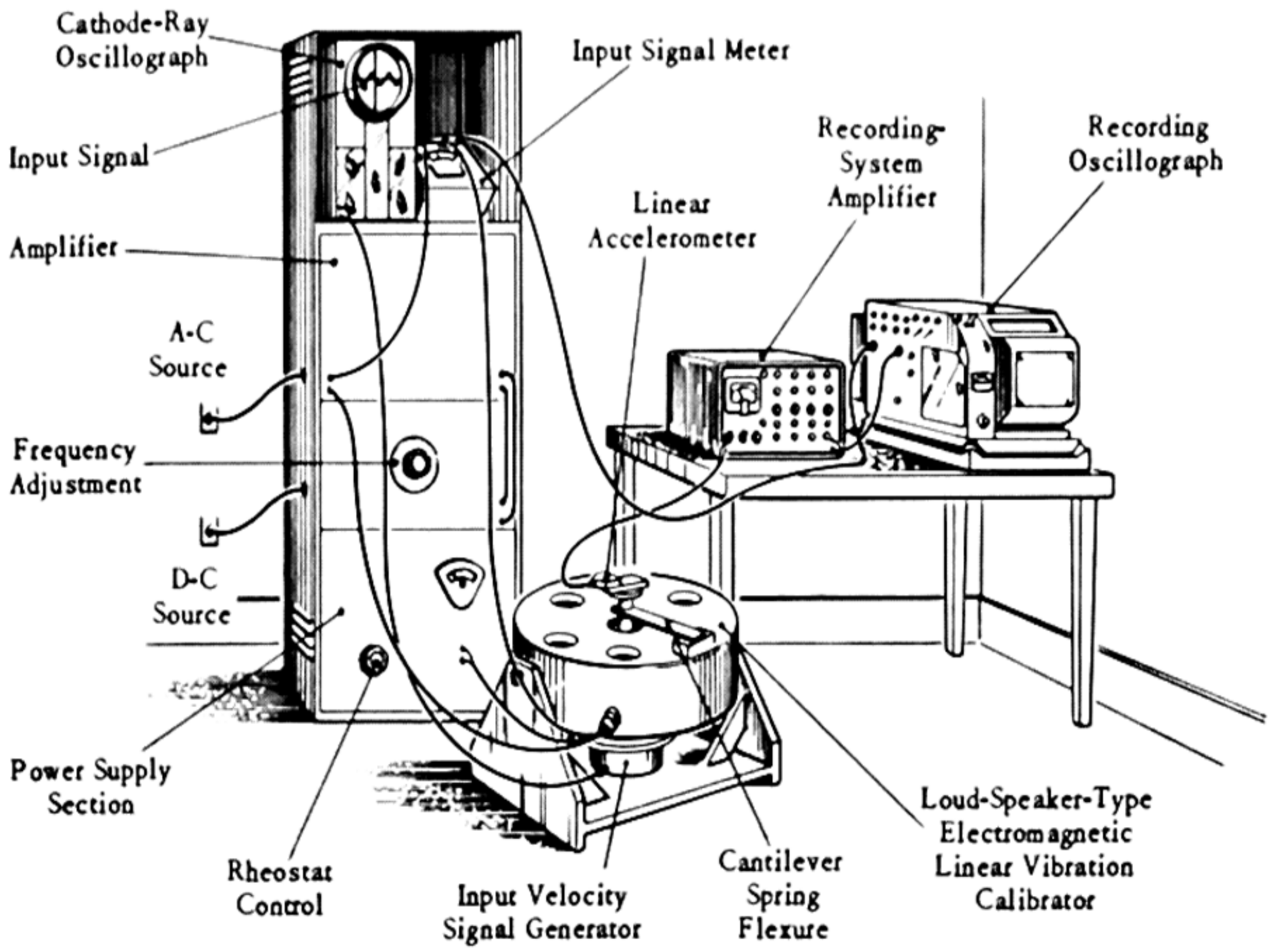


Fig. 35-44. Calibration of a linear acceleration recording system.

calibration purposes. The accelerometer is mounted on the armature of the loud-speaker-type electromagnetic linear vibration calibrator. Accelerometer outputs are applied to the recording-system amplifier, which in turn supplies signals to the recording oscillograph.

35.280. The performance of accelerometers using seismographic systems is described in Derivation Summary 35-5, where it is shown to be associated with the (0;0, 1, 2) differential equation form. The principles of electronic amplifiers are given in Information Summary 30-9, with references to more complete texts. Recording oscillographs using D'Arsonval elements are taken up in Chapter 32. The unit shown in Fig. 35-44 is similar in structure to the component illustrated in Fig. 32-30 of Chapter 32.

35.281. Calibration data, and the steps for reducing this data to dimensionless form, are given in sheets 5 and 6 of Test Report No. 35-4. The reference sensitivity is chosen to be 0.6 inch per gravity. The reference frequency for calculating frequency ratios is taken as 100 cycles per second, for convenience. When the experimental values of the dimensionless sensitivity ratio are plotted on a log-log scale grid, as on sheet 2 of Test Report No. 35-4, they are seen to fall on the curve representing the theoretical response of a (0;0, 1, 2) system with a damping ratio of 0.7 and an undamped natural frequency of 100 cycles per second.

35.282. The logarithmic scale of sheet 2 is 2.5 inches per cycle. A logarithmic scale of 1.25 inches per cycle is used in sheet 3, which shows the performance

SUMMARY: Test Form A **TEST REPORT NO.** 35-4 Sheet 1 of 7

Instruments Laboratory · Aeronautical Engineering Department · Massachusetts Institute of Technoiogy · Cambridge · Massachusetts

Title of test LINEAR ACCELERATION RECORDING SYSTEM (ars) CALIBRATION (STEADY-STATE SINUSOIDAL INPUT)

Date 6/30/54 In charge of test J. L. STOCKARD Assisting with test A. KLAYMAN

Equipment tested STATHAM LINEAR ACCELEROMETER (ar), Type G10-120, SER. NO. 195

CONSOLIDATED CARRIER AMPLIFIER (ca), Type 1-118, SER. NO. 973AP4

CONSOLIDATED RECORDING OSCILLOGRAPH (ro), Type 5-114, SER. NO. 867AV15

Type ..... Model ..... Serial No. ..... Calculations J. L. STOCKARD

Plots J. L. STOCKARD

Equipment used for test MB VIBRATION TEST EQUIPMENT, MODEL P10, SER. NO. 100

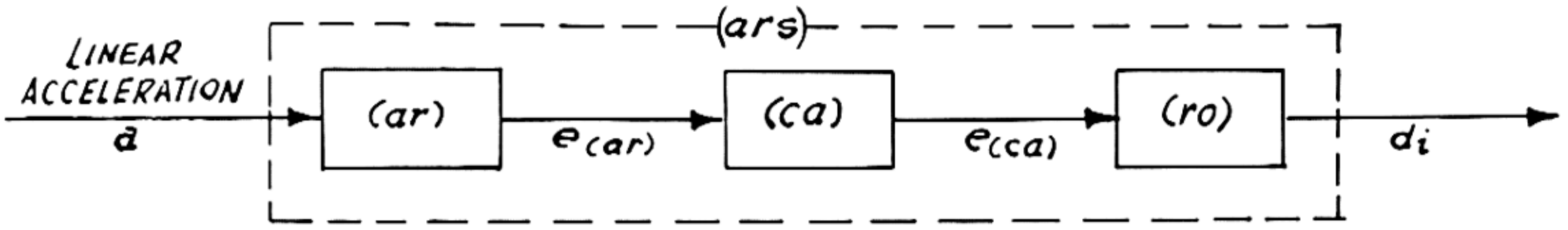
HEWLETT-PACKARD AUDIO OSCILLATOR, MODEL 202D, SER. NO. A15396

Input quantity LINEAR ACCELERATION a Output quantity INDEX DISPLACEMENT d_i

Environmental conditions: Temperature 70° F Pressure —

Other —

Summary of results:



$$[PF]_{(ars)[a\ ;\ d](theo)} = [RF]_{(0;0,1,2)} = S_{(ars)[a;d](ref)} \frac{1}{1-(FR)^2+j\,2(DR)(FR)}$$

$$'(SR)_{(ars)(a\ ;\ d)(theo)} = '(DAR)_{(0;0,1,2)} = \frac{1}{\sqrt{[1-(FR)^2]+[2(DR)(FR)]^2}}$$

$$(DRA)_{(ars)(a\ ;\ d)(theo)} = (DRA)_{(0;0,1,2)} - 180° = \tan^{-1}\left[\frac{-2(DR)(FR)}{1-(FR)^2}\right] - 180°$$

Reference frequency = $n_{(ref)}$ = 100 cycles/second Damping ratio = DR = 0.7

Reference sensitivity = $S_{(ars)[a\ ;\ d](ref)}$ = 0.606 inch/gravity Reference dynamic response angle = $(DRA)_{(ref)}$ = −180 degrees

Frequency ratio = FR = $n_f/n_{(ref)}$; Forcing frequency = n_f ; Dynamic response angle = $(DRA)_{(id)(q_{(in)};q_{(out)})}$

Performance function = $[PF]_{(id)[q_{(in)};q_{(out)}]} = \frac{q_{(out)}}{q_{(in)}} = S_{(id)[q_{(in)};q_{(out)}](ref)}\ '(SR)_{(id)(q_{(in)};q_{(out)})}{}^{\epsilon\,j(DRA)_{(id)(q_{(in)};q_{(out)})}}$

Dimensionless sensitivity ratio = $'(SR)_{(id)(q_{(in)};q_{(out)})} = S_{(id)[q_{(in)};q_{(out)}]}/S_{(id)[q_{(in)};q_{(out)}](ref)}$; Identified component = (id)

Theoretical dimensionless sensitivity ratio = $'(SR)_{(ars)(a\ ;\ d)(theo)}$ → Theoretical dynamic amplitude ratio = $'(DAR)_{(theo)} = '(DAR)_{(0;0,1,2)}$

Theoretical dynamic response angle = $(DRA)_{(theo)} = (DRA)_{(0;0,1,2)} - 180°$ Theoretical performance function for the unit under test = $[PF]_{(ars)[a\ ;\ d](theo)}$

Relating function associated with the (0; 0,1,2) differential equation = $[RF]_{(0;0,1,2)}$

(SR) PLOTS: Test Form F **TEST REPORT NO.** 35-4 Sheet 2 of 7

Instruments Laboratory · Aeronautical Engineering Department · Massachusetts Institute of Technology · Cambridge · Massachusetts

Title of test LINEAR ACCELERATION RECORDING SYSTEM (ars) CALIBRATION (STEADY-STATE SINUSOIDAL INPUT)

Date 6/30/54 **In charge of test** J. L. STOCKARD **Assisting with test** A. KLAYMAN

Equipment tested STATHAM LINEAR ACCELEROMETER (ar), Type G10-120, SER. NO. 195
CONSOLIDATED CARRIER AMPLIFIER (ca), Type 1-118, SER. NO. 973AP4
CONSOLIDATED RECORDING OSCILLOGRAPH (ro), Type 5-114, SER. NO. 867AV15

Type ..... **Model** ..... **Serial No.** ..... **Calculations** J. L. STOCKARD

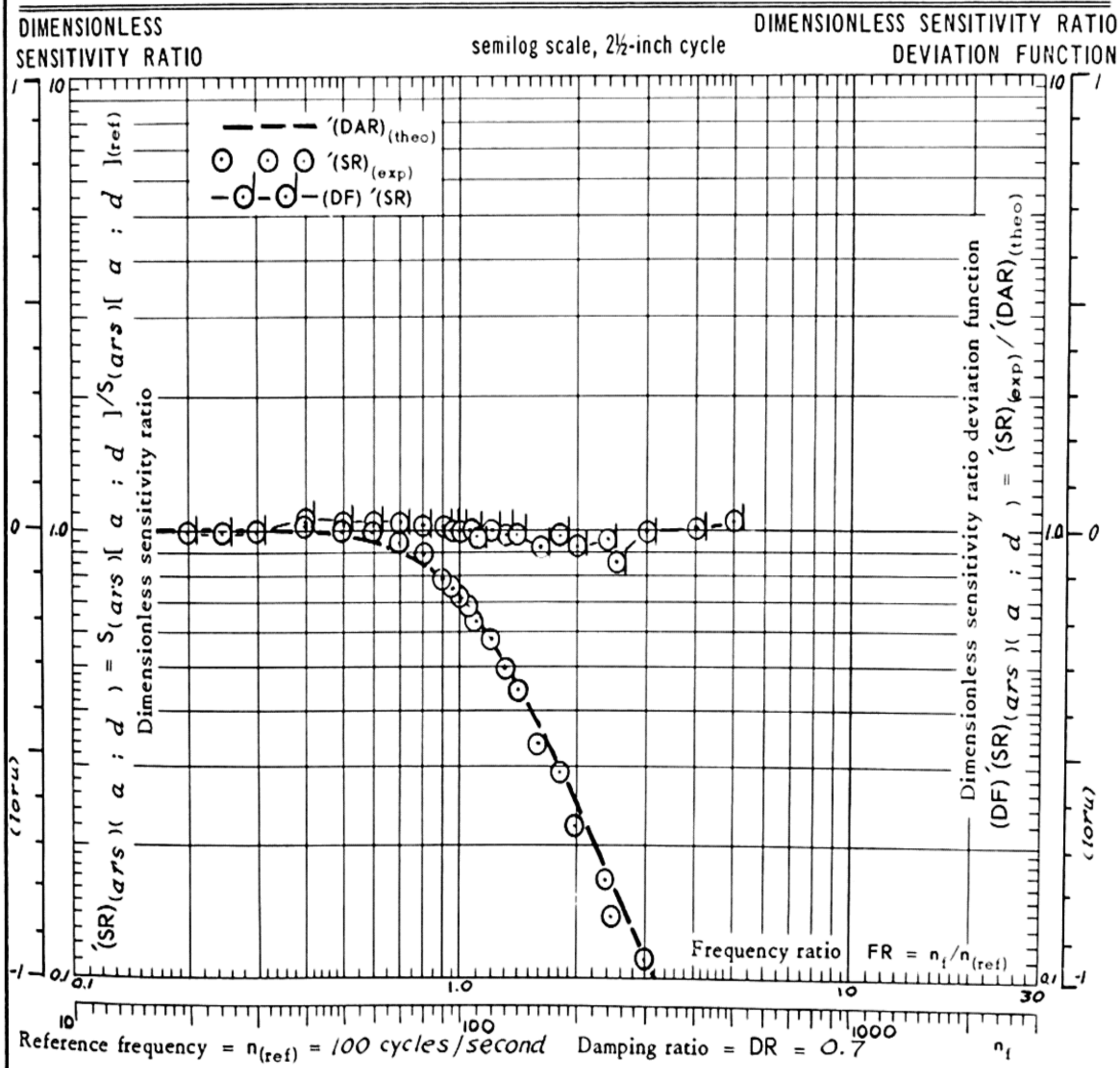
Plots J. L. STOCKARD

Equipment used for test MB VIBRATION TEST EQUIPMENT, MODEL P10, SER. NO. 100
HEWLETT-PACKARD AUDIO OSCILLATOR, MODEL 202D, SER. NO. A15396

Input quantity LINEAR ACCELERATION a **Output quantity** INDEX DISPLACEMENT di

Environmental conditions: Temperature 70° F **Pressure** —

Other —



Reference frequency = $n_{(ref)}$ = 100 cycles/second **Damping ratio** = DR = 0.7

Reference sensitivity = $S_{(ars)}[\ a\ ;\ d\ ]_{(ref)}$ = 0.606 inch/gravity

Theoretical dimensionless dynamic amplitude ratio = $'(DAR)_{(theo)} \approx '(DAR)_{(0;0,1;2)} = \dfrac{1}{\sqrt{[1-(FR)^2]^2 + [2(DR)(FR)]^2}}$

$'(DAR)_{(theo)}$ is $'(SR)_{(theo)}$, the theoretical dimensionless sensitivity ratio for the unit under test; $'(SR)_{(exp)}$ is the dimensionless sensitivity ratio determined by experiment.

(SR) PLOTS: Test Form Ia **TEST REPORT NO.** 35-4 Sheet 3 of 7

Instruments Laboratory · Aeronautical Engineering Department · Massachusetts Institute of Technology · Cambridge · Massachusetts

Title of test LINEAR ACCELERATION RECORDING SYSTEM (ars) CALIBRATION (STEADY-STATE SINUSOIDAL INPUT)

Date 6/30/54 **In charge of test** J. L. STOCKARD **Assisting with test** A. KLAYMAN

Equipment tested STATHAM LINEAR ACCELEROMETER (ar), Type G10-120, SER. NO. 195
CONSOLIDATED CARRIER AMPLIFIER (ca), Type 1-118, SER. NO. 973AP4
CONSOLIDATED RECORDING OSCILLOGRAPH (ro), Type 5-114, SER. NO. 867AV15

Type ..... Model ..... Serial No. .....

Calculations J. L. STOCKARD

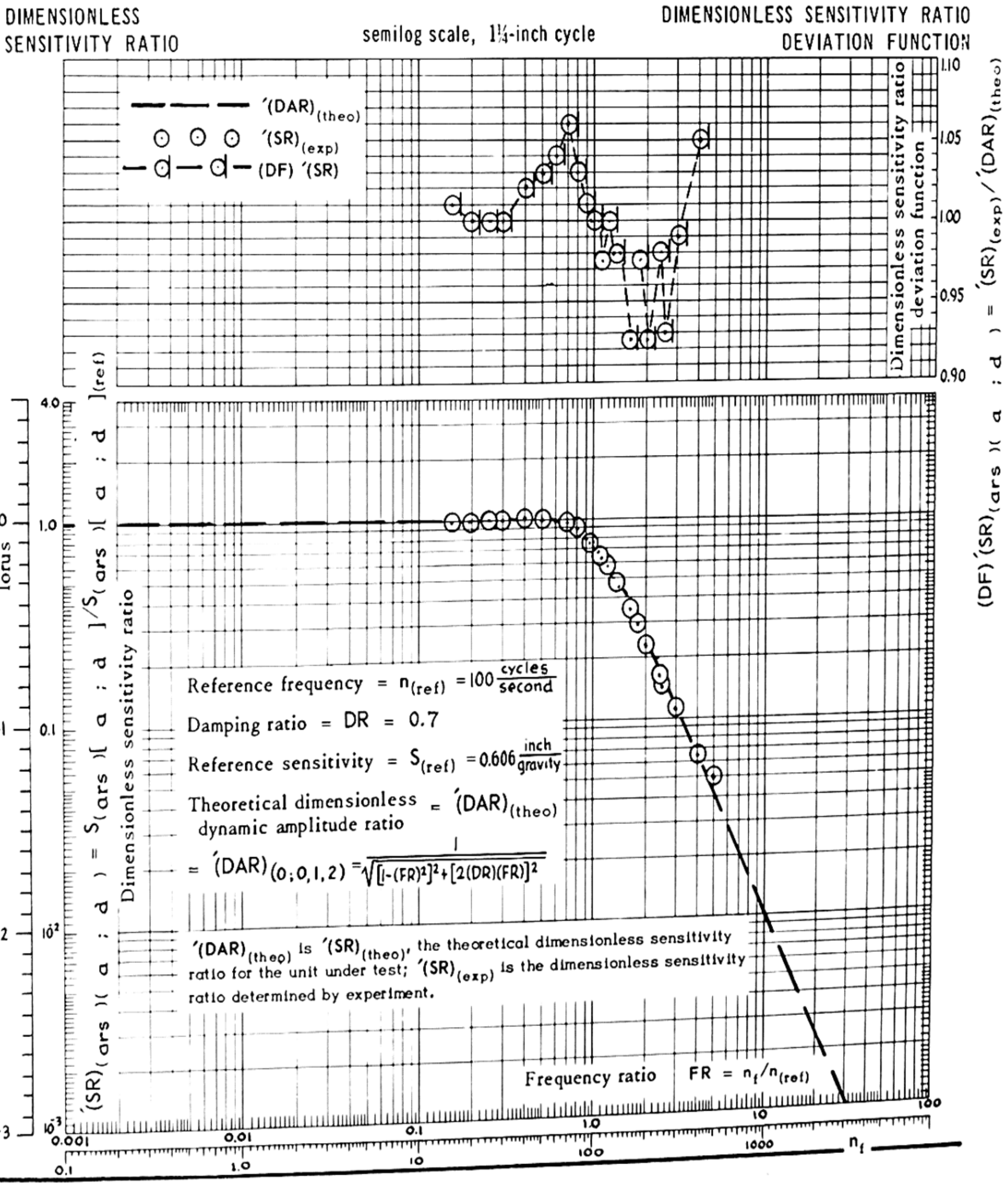
Plots J. L. STOCKARD

Equipment used for test MB VIBRATION TEST EQUIPMENT, MODEL P10, SER NO. 100
HEWLETT-PACKARD AUDIO OSCILLATOR, MODEL 202D, SER. NO. A 15396

Input quantity LINEAR ACCELERATION a **Output quantity** INDEX DISPLACEMENT d_i

Environmental conditions: Temperature 70° F **Pressure** –

Other –



DRA PLOTS: Test Form L **TEST REPORT NO.** 35-4 Sheet 4 of 7

Instruments Laboratory · Aeronautical Engineering Department · Massachusetts Institute of Technology · Cambridge · Massachusetts

Title of test LINEAR ACCELERATION RECORDING SYSTEM (ars) CALIBRATION (STEADY-STATE SINUSOIDAL INPUT)

Date 6/30/54 In charge of test J. L. STOCKARD Assisting with test A. KLAYMAN

Equipment tested STATHAM LINEAR ACCELEROMETER (ar), Type G10-120, SER. NO. 195
CONSOLIDATED CARRIER AMPLIFIER (ca), Type 1-118, SER. NO. 973AP4
CONSOLIDATED RECORDING OSCILLOGRAPH (ro), Type 5-114, SER. NO. 867AV15

Type ..... Model ..... Serial No. .....

Calculations J. L. STOCKARD

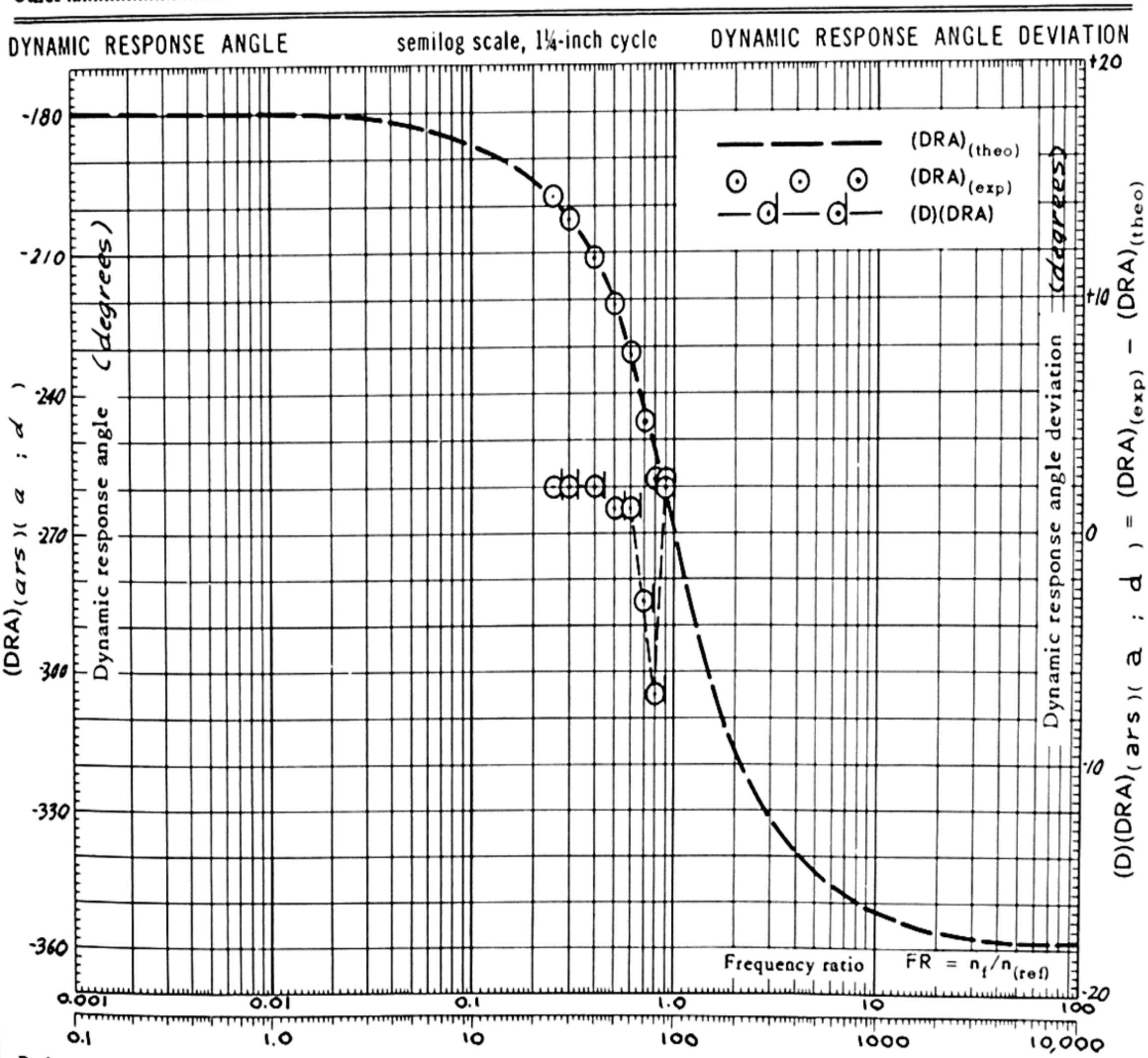
Plots J. L. STOCKARD

Equipment used for test MB VIBRATION TEST EQUIPMENT, MODEL P10, SER. NO. 100
HEWLETT-PACKARD AUDIO OSCILLATOR, MODEL 202D, SER. NO. A15396

Input quantity LINEAR ACCELERATION a Output quantity INDEX DISPLACEMENT d

Environmental conditions: Temperature 70° F Pressure —

Other —



Reference frequency = $n_{(ref)}$ = 100 cycles/second Damping ratio = DR = 0.7

Reference dynamic response angle = $(DRA)_{(ref)}$ = −180°

Theoretical dynamic response angle = $(DRA)_{(theo)} = (DRA)_{(0;0,1,2)} = \tan^{-1}\left[\frac{-2(DR)(FR)}{1-(FR)^2}\right] - 180°$

$(DRA)_{(theo)}$ is the theoretical dynamic response angle for the unit under test; $(DRA)_{(exp)}$ is the dynamic response angle determined by experiment.

TEST DATA: Test Form N **TEST REPORT NO.** 35-4 Sheet 5 of 7

Instruments Laboratory · Aeronautical Engineering Department · Massachusetts Institute of Technology · Cambridge · Massachusetts

Title of test LINEAR ACCELELERATION RECORDING SYSTEM (ars) CALIBRATION (STEADY-STATE SINUSOIDAL INPUT)

Date 6/30/54 In charge of test J. L. STOCKARD Assisting with test A. KLAYMAN

Equipment tested STATHAM LINEAR ACCELEROMETER (ar), Type G10-120, SER. No. 195
CONSOLIDATED CARRIER AMPLIFIER (ca), Type 1-118, SER. No. 973AP4
CONSOLIDATED RECORDING OSCILLOGRAPH (ro), Type 5-114, SER. No. 867AV15

Type ..... Model ..... Serial No. ..... Calculations J. L. STOCKARD

Plots J. L. STOCKARD

Equipment used for test MB VIBRATION TEST EQUIPMENT, MODEL P10, SER. No. 100
HEWLETT-PACKARD AUDIO OSCILLATOR, MODEL 202D, SER. No. A 15396

Input quantity LINEAR ACCELERATION d Output quantity INDEX DISPLACEMENT d_i

Environmental conditions: Temperature 70° F Pressure —

Other —

Run Number	(Forcing Amplitude) x2 $2a_{(in)a}$	Forcing Frequency n_f	(Output Amplitude) x 2 $2d_i$	Output Voltage Amplitude $e_{(out)a}$	Input-Output Sensitivity $S_{(ars)[a\ ;\ d\ ](exp)}$	Dimensionless Sensitivity Ratio $'(SR)_{(ars)(a\ ;\ d\ )(exp)}$*	Dimensionless Dynamic Amplitude Ratio $'(DAR)_{(0;0,1,2)}$	Theoretical Dimensionless Sensitivity Ratio Deviation Function $(DF)'(SR) = {}'(SR)_{(exp)}/{}'(DAR)_{(theo)}$	Dimensionless Sensitivity Ratio Deviation Function $(DF)'(SR) = {}'(SR)_{(exp)}/{}'(DAR)_{(theo)}$	Dynamic Response Angle $(DRA)_{(ars)(a\ ;\ d\ )(exp)}$ degrees	Theoretical Dynamic Response Angle $(DRA)_{(theo)} = (DRA)_{(0;0,1,2)} - 180°$ degrees	Dynamic Response Angle Deviation $(D)(DRA) = (DRA)_{(exp)} - (DRA)_{(theo)}$ degrees	Frequency Ratio $FR = n_f/n_{(ref)}$	
Units and References	gravities g	cycles/second	inches		inches/gravity	$S_{(ref)}$ = 0.606 inch/gravity	Theoretical Dimensionless Dynamic Amplitude Ratio $'(DAR)_{(theo)}$	Dimensionless Sensitivity Ratio Deviation Function $(DF)'(SR) = {}'(SR)_{(exp)}/{}'(DAR)_{(theo)}$		$(DRA)_{(ref)}$ = -180°			$n_{(ref)}$ = 100 cycles/second	
02362	3	25	1.82		0.606	1.00	1.00	1.00	-198	-200	+2	0.25		
02363	3	30	1.83		0.609	1.00	1.00	1.00	-203	-205	+2	0.30		
02364	3	40	1.84		0.613	1.01	0.99	1.02	-212	-214	+2	0.40		
02365	3	50	1.82		0.606	1.00	0.97	1.03	-222	-223	+1	0.50		
02366	3	60	1.8		0.600	0.99	0.95	1.04	-232	-233	+1	0.60		
02367	3	70	1.74		0.580	0.956	0.90	1.06	-246	-243	-3	0.70		
02367	3	80	1.6		0.534	0.88	0.85	1.03	-259	-252	-7	0.80		
02369	3	90	1.4		0.480	0.79	0.78	1.01	-259	-261	+2	0.90		

* $'(SR)_{(exp)} = S_{(exp)}/S_{(ref)}$; Reference sensitivity = $S_{(ars)[a\ ;\ d\ ](ref)} = S_{(ref)}$.

Instruments Laboratory · Aeronautical Engineering Department · Massachusetts Institute of Technology · Cambridge · Massachusetts

Run Number	(Forcing Amplitude) x 2 $2a_{(in)a}$	Forcing Frequency n_f	(Output Amplitude) x 2 $2d_i$	Output Voltage Amplitude $\bullet_{(out)o}$	Input-Output Sensitivity $S_{(ars)[a\ ;\ d\ ](exp)}$	Dimensionless Sensitivity Ratio $'(SR)_{(ars)(a\ ;\ d\ )(exp)}$*	Theoretical Dimensionless Dynamic Amplitude Ratio $'(DAR)_{(theo)} = {}'(DAR)_{(0,0,1,2)}$	Dimensionless Sensitivity Ratio Deviation Function (DF) $'(SR)_{(exp)}/{}'(DAR)_{(theo)}$	Dynamic Response Angle $(DRA)_{(ars)(a\ ;\ d\ )(exp)}$	Theoretical Dynamic Response Angle $(DRA)_{(theo)} = (DRA)_{(0,0,1,2)+180°}$	Dynamic Response Angle Deviation $(D)(DRA) = (DRA)_{(exp)} - (DRA)_{(theo)}$	Frequency Ratio $FR = n_f/n_{(ref)}$	
Units and References	gravities g	cycles/second	inches		$\frac{\text{inches}}{\text{gravity}}$	$S_{(ref)} = 0.606$ inch/gravity			$(DRA)_{(ref)} = -180°$ degrees			$n_{(ref)} = 100$ cycles/second	
02370	3	95	1.37		0.456	0.752	0.750	1.00	-264	-266	+2	0.95	
02371	3	100	1.3		0.433	0.714	0.714	1.00	-270	-270	0	1.00	
02372	3	105	1.23		0.412	0.680	0.680	1.00	-278	-274	-4	1.05	
02373	3	110	1.14		0.38	0.626	0.643	0.975	-280	-278	-2	1.10	
02374	3	120	1.0		0.350	0.575	0.575	1.00	-288	-284	-4	1.20	
02375	3	130	0.88		0.308	0.501	0.514	0.98	–	-291	–	1.30	
02376	3	140	0.79		0.273	0.450	0.458	0.98	-295	-296	+1	1.40	
02377	3	160	0.6		0.206	0.340	0.367	0.925	-305	-305	0	1.60	
02378	3	180	0.5		0.175	0.290	0.297	0.975	–	-312	–	1.80	
02379	3	200	0.4		0.136	0.225	0.243	0.925	-316	-317	+1	2.00	
02380	3	200	0.4		0.136	0.225	0.243	0.925	-316	-317	+1	2.00	
02381	3	240	0.3		0.1	0.165	0.172	0.96	-323	-325	+2	2.40	

* $'(SR)_{(exp)} = S_{(exp)}/S_{(ref)}$; Reference sensitivity = $S_{(ars)[a\ ;\ d\ ](ref)} = S_{(ref)}$.

TEST DATA: Test Form 0 **TEST REPORT NO. 35-4** Sheet 7 of 7

Instruments Laboratory · Aeronautical Engineering Department · Massachusetts Institute of Technology · Cambridge · Massachusetts

Run Number	(Forcing Amplitude) x 2 $2d_{(in)a}$	Forcing Frequency n_f	(Output Amplitude) x 2 $2d_i$	Output Voltage Amplitude $\bullet_{(out)a}$	Input-Output Sensitivity $S_{(ars)[a\ ;\ d\ ](exp)}$	Dimensionless Sensitivity Ratio $'(SR)_{(ars)(a\ ;\ d\ )(exp)}$*	Dimensionless Dynamic Amplitude Ratio $'(DAR)_{(theo)} = {}'(DAR)_{(0;0,1,2)}$	Dimensionless Sensitivity Ratio Deviation Function $(DF)\,{}'(SR) = {}'(SR)_{(exp)}/{}'(DAR)_{(theo)}$	Dynamic Response Angle $(DRA)_{(ars)(a\ ;\ d\ )(exp)}$			Frequency Ratio $FR = n_f/n_{(ref)}$	
Units and References	gravities g	cycles/second	inches		$\frac{\text{inches}}{\text{gravity}}$	$S_{(ref)} = 0.606$ inch / gravity	Theoretical Dimensionless Dynamic Amplitude Ratio $(DAR)_{(0;0,1,2)}$	Dimensionless Sensitivity Ratio Deviation Function $(DF)\,{}'(SR)$	$(DRA)_{(ars)(a\ ;\ d\ )(exp)}$	Theoretical Dynamic Response Angle $(DRA)_{(theo)} = (DRA)_{(0;0,1,2)}{}^{\circ}/180^{\circ}$	Dynamic Response Angle Deviation $(D)(DRA) = (DRA)_{(exp)} - (DRA)_{(theo)}$	$n_{(ref)} = 100$ cycles/second	
									$(DRA)_{(ref)} = -180^{\circ}$ degrees				
02382	3	250	0.25		0.0833	0.137	0.160	0.86	-330	-326	-4	2.5	
02383	3	300	0.2		0.0667	0.110	0.111	0.99	-335	-332	-3	3.0	
02384	3	400	0.12		0.04	0.066	0.0626	1.06	-340	-340	0	4.0	
02385	3	500	0.09		0.03	0.0495	0.042	1.18	-345	-343	-2	5.0	
02386	3	20	1.82		0.607	1.00	1.00	1.00	-193	-196	+3	0.2	
02387	3	15	1.8		0.6	0.99	1.00	1.01	-192	-192	0	0.15	

* $'(SR)_{(exp)} = S_{(exp)}/S_{(ref)}$; Reference sensitivity $= S_{(ars)[a\ ;\ d\ ](ref)} = S_{(ref)}$.

of the system in the useful operating range, lying below 100 cycles per second. The deviation function of the sensitivity ratio shows the performance to be identical with that of the theoretical curve within 6 percent in this operating range. The ragged deviation function curve is due to uncertainties in the calibration.

35.283. Dynamic response angles are measured by recording both the signal representing the mechanical sinusoidal input and the accelerometer output on the same oscillograph chart. The dynamic response angle is determined graphically by the relative displacement of the output sinusoidal curve with respect to the input. Dynamic response angles are plotted on sheet 4 of the test report. The deviations show that the dynamic response angle corresponds to the theoretical (0;0,1,2) form within ± 4 degrees.

35.284. The results of the calibration tests are summarized on sheet 1 of the test report. The performance function of the acceleration recording system shown in the functional diagram may be represented theoretically by a (0;0, 1, 2) function within the operating frequency range. The damping ratio is 0.7 and the undamped natural frequency is 100 cycles per second. The effective operating frequency range is between zero and a frequency no greater than 100 cycles per second. The system reference sensitivity is 0.6 inch displacement of the oscillograph index for each gravity of acceleration. The dynamic response angle has a minimum value of -180 degrees, which is taken as the reference value of this quantity.

THE PERFORMANCE FUNCTION DEVIATION FUNCTION CONCEPT FOR DESCRIBING INSTRUMENT PERFORMANCE

35.285. Several examples have been presented showing how the performance of an instrument may be expressed in terms of deviations from a reference performance function. These examples pertain to experimentally derived information, and the deviations have been taken with respect to a theoretical reference performance function. A similar procedure has been described in Chapter 13 for treating theoretical performance functions.' The concept developed there describes a given performance function as the product of a reference performance function and a performance function deviation function. By employing the concept of deviations, the scale is expanded in the region of interest. For example, measuring instruments should give consistent results within a few percent, as has been indicated earlier in this chapter. In this instance, representing performance in terms of deviations from a known reference provides a useful scale within a reasonable space.

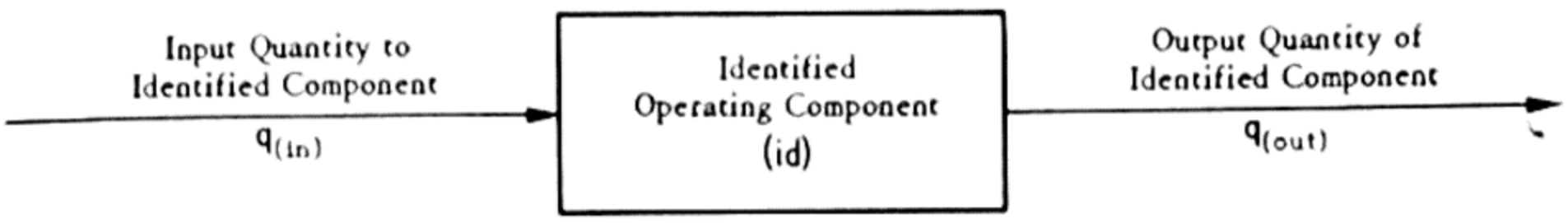
35.286. When a chain of components, each with known performance, makes up an operating system, the system performance may be determined by any of several procedures. For example, steady-state response to a sinusoidal input may be calculated by the graphical method described in Chapter 24. With this

method, component steady-state responses are combined on a logarithmic basis, using the profiles described in the cited chapter. The basis for a variation of the logarithmic technique is developed in Derivation Summary 35-10, using performance function deviation functions.

35.287. Section a of Derivation Summary 35-10 presents the concept of the fractional deviation of an operating component sensitivity ratio. The figure of section a shows a generalized operating component, which is associated with the performance function of Eq. (2). Using the concepts of Definition Summary 13-4 of Chapter 13, the performance function is represented as the product of a reference performance function and a performance function deviation function, as shown in Eq. (3) of Derivation Summary 35-10. The reference performance function is characterized by a reference sensitivity and a reference dynamic response angle. One method of writing generalized performance function deviation functions is given by Eq. (5), where it is shown as the product of a reference sensitivity ratio, a dimensionless sensitivity ratio and an imaginary exponential function whose exponent contains the dynamic response angle deviation. Reference sensitivity ratios are useful when the sensitivity ratio has dimensions. They make it possible to describe deviation function variations in terms of dimensionless quantities only. The dimensionless sensitivity ratio, defined by Eq. (6a), may be taken equal to unity in the operating region by proper choice of the reference sensitivity ratio. The difference between the dimensionless sensitivity ratio and unity is defined as the fractional deviation of the sensitivity ratio by Eq. (7). The performance function deviation function is written in an alternate form in Eq. (8). The performance function itself is shown in terms of the reference quantities, the fractional deviation and the dynamic response angle deviation by the expression of Eq. (9).

35.288. Consider now an open-chain system shown by the figure at the beginning of section b in Derivation Summary 35-10. This system consists of n operating components, each associated with one of the n performance functions of Eq. (10). The performance function of the system is equal to the product of the operating component performance functions as shown in Eq. (11).

35.289. The procedure described previously for developing the fractional deviation and dynamic response angle deviation of an operating component is repeated for the open-chain system formed by the n operating components. It is assumed that there exists an expression like Eq. (9) of Derivation Summary 35-10 associated with each operating component. First, define the reference performance function of the operating system as the product of the component reference performance functions, as in Eq. (12). This permits the system performance function to be expressed as the product of the defined reference performance function and a deviation function. From the way the reference performance function has been defined, the system performance function deviation function must be equal



The performance of the identified component when the input quantity is sinusoidal may be associated with its performance function as follows:

$$q_{(out)} = [PF]_{(id)[q_{(in)};q_{(out)}]}\, q_{(in)} \tag{1}$$

$$[PF]_{(id)[q_{(in)};q_{(out)}]} = S_{(id)[q_{(in)};q_{(out)}]}\, \epsilon^{\,j(DRA)_{(id)(q_{(in)};q_{(out)})}} \tag{2}$$

Since no confusion is possible, the input-output brackets will be omitted in the remainder of this section.

From the discussion in Definition Summary 13-4 of Chapter 13, performance functions may be expressed as the product of a reference performance function and a performance function deviation function; i.e.,

$$[PF]_{(id)} = [PF]_{(id)(ref)}\,(DF)[PF]_{(id)} \tag{3}$$

where

$$[PF]_{(id)(ref)} = S_{(id)(ref)}\, \epsilon^{\,j(DRA)_{(id)(ref)}} \tag{4}$$

$$(DF)[PF]_{(id)} = (SR)_{(id)(ref)}\, '(SR)_{(id)}\, \epsilon^{\,j(D)(DRA)_{(id)}} \tag{5}$$

$$'(SR)_{(id)} = \frac{(SR)_{(id)}}{(SR)_{(id)(ref)}} \quad ; \quad (SR)_{(id)} = \frac{S_{(id)}}{S_{(id)(ref)}} \tag{6a),(6b)}$$

and

$$(D)(DRA)_{(id)} = (DRA)_{(id)} - (DRA)_{(id)(ref)} \tag{6c}$$

Define the fractional deviation of the sensitivity ratio to be the nondimensional sensitivity ratio, $'(SR)$, minus one; i.e.,

$$(FD)'(SR)_{(id)} = '(SR)_{(id)} - 1 \tag{7}$$

where

$(FD)'(SR)_{(id)}$ = fractional deviation of the sensitivity ratio of the identified component

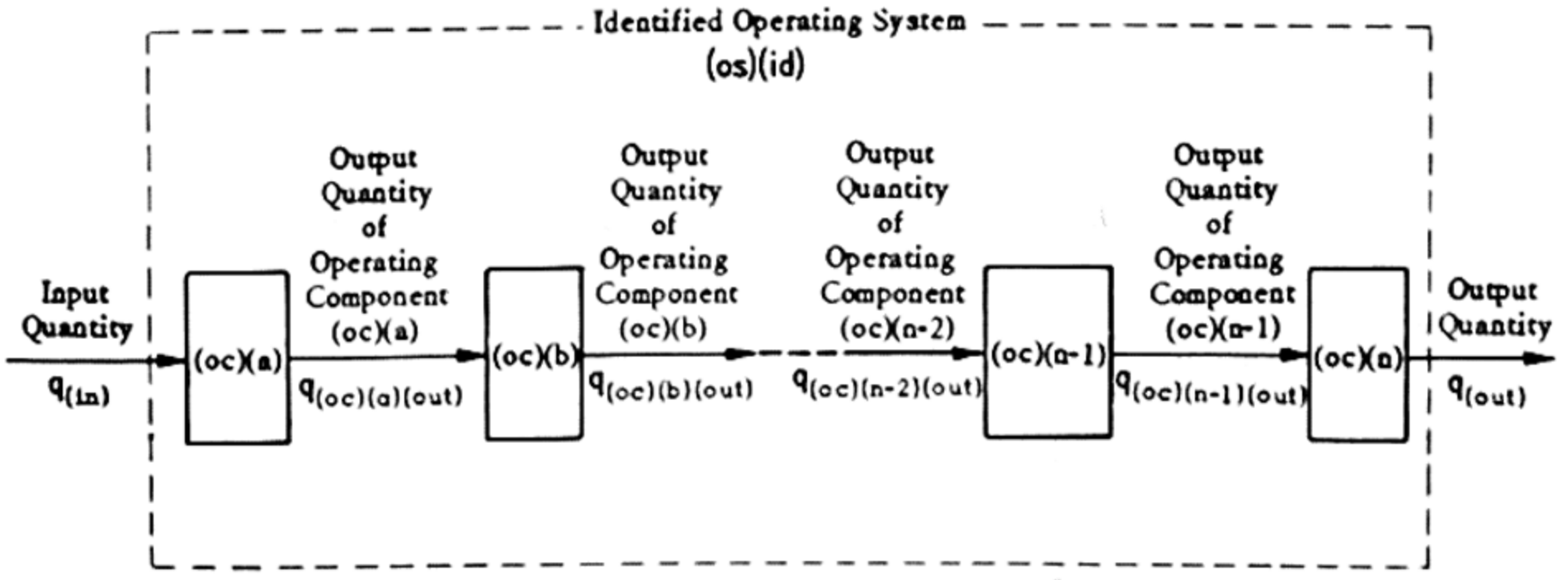
Then, from Eqs. (5) and (7),

$$(DF)[PF]_{(id)} = (SR)_{(id)(ref)}\,[1 + (FD)'(SR)_{(id)}]\,\epsilon^{\,j(D)(DRA)_{(id)}} \tag{8}$$

and, from Eqs. (3), (4) and (8),

$$[PF]_{(id)} = S_{(id)(ref)}\,(SR)_{(id)(ref)}\,[1 + (FD)'(SR)_{(id)}]\,\epsilon^{\,j(DRA)_{(id)(ref)}}\,\epsilon^{\,j(D)(DRA)_{(id)}} \tag{9}$$

a) Fractional deviation of an operating component sensitivity ratio



Derivation Summary 35-10. Sensitivity ratio fractional deviations for an open-chain system.
(Page 1 of 3)

In the identified operating system shown in the preceding diagram, there are n operating components connected in an open chain. A performance function may be associated with each operating component; i.e.,

$$[PF]_{(oc)(a)[q_{(in)};q_{(oc)(a)(out)}]} = \text{performance function associated with operating component a}$$

$$[PF]_{(oc)(b)[q_{(oc)(a)(out)};q_{(oc)(b)(out)}]} = \text{performance function associated with operating component b}$$

$$\vdots \qquad (10)$$

$$[PF]_{(oc)(n-1)[q_{(oc)(n-2)(out)};q_{(oc)(n-1)(out)}]} = \text{performance function associated with operating component (n-1)}$$

$$[PF]_{(oc)(n)[q_{(oc)(n-1)(out)};q_{(out)}]} = \text{performance function associated with operating component n}$$

Each operating component performance function of Eq. (10) may be written in the form of Eq. (3) as the product of a reference performance function and a deviation function.

From Chapter 3, the performance function of the identified operating system is the product of the operating component performance functions; i.e.,

$$[PF]_{(os)(id)[q_{(in)};q_{(out)}]} = [PF]_{(oc)(a)}[PF]_{(oc)(b)} \cdots [PF]_{(oc)(n-1)}[PF]_{(oc)(n)} \qquad (11)$$

Define the reference identified operating system performance function as the product of the n reference operating component performance functions; i.e.,

$$[PF]_{(os)(id)[q_{(in)};q_{(out)}](ref)} = [PF]_{(oc)(a)(ref)}[PF]_{(oc)(b)(ref)} \cdots [PF]_{(oc)(n-1)(ref)}[PF]_{(oc)(n)(ref)} \qquad (12)$$

The identified operating system performance function may now be expressed as the product of a reference performance function and a deviation function, as is done for an individual operating component in Eq. (3); i.e.,

$$[PF]_{(os)(id)[q_{(in)};q_{(out)}]} = [PF]_{(os)(id)[q_{(in)};q_{(out)}](ref)}(DF)[PF]_{(id)[q_{(in)};q_{(out)}]} \qquad (13)$$

From Eqs. (11), (12) and (13), the identified operating system performance function deviation function must be equal to the product of the operating component performance function deviation functions; i.e.,

$$(DF)[PF]_{(os)(id)[q_{(in)};q_{(out)}]} = (DF)[PF]_{(oc)(a)}(DF)[PF]_{(oc)(b)} \cdots (DF)[PF]_{(oc)(n-1)}(DF)[PF]_{(oc)(n)} \qquad (14)$$

Definitions in Eqs. (4) through (9) apply to the identified operating system as well as to all the operating components in the chain. In particular, from Eq. (5), the identified operating system performance function deviation function may be expressed as

$$(DF)[PF]_{(os)(id)[q_{(in)};q_{(out)}]} = (SR)_{(os)(id)[q_{(in)};q_{(out)}](ref)}{}'(SR)_{(os)(id)(q_{(in)};q_{(out)})}{}^{\epsilon^{J(D)(DRA)_{(os)(id)(q_{(in)};q_{(out)})}}} \qquad (15)$$

From Eq. (7), the fractional deviation of the identified operating system sensitivity ratio is

$$(FD)'(SR)_{(os)(id)(q_{(in)};q_{(out)})} = '(SR)_{(os)(id)(q_{(in)};q_{(out)})} - 1 \qquad (16)$$

so that

$$(DF)[PF]_{(os)(id)[q_{(in)};q_{(out)}]} = (SR)_{(os)(id)[q_{(in)};q_{(out)}](ref)}[1 + (FD)'(SR)_{(os)(id)(q_{(in)};q_{(out)})}]\epsilon^{J(D)(DRA)_{(os)(id)(q_{(in)};q_{(out)})}} \qquad (17)$$

Derivation Summary 35-10. Sensitivity ratio fractional deviations for an open-chain system.
(Page 2 of 3)

Since there is an expression like Eq. (8) for each deviation-function factor in Eq. (14), the expression represented by Eq. (17) may be written as

$$(SR)_{(os)(id)[q_{(in)};q_{(out)}](ref)}[1 + (FD)'(SR)_{(os)(id)(q_{(in)};q_{(out)})}]\epsilon^{j(D)(DRA)_{(os)(id)(q_{(in)};q_{(out)})}}$$

$$= [(SR)_{(oc)(a)(ref)}(SR)_{(oc)(b)(ref)} \cdots (SR)_{(oc)(n-1)(ref)}(SR)_{(oc)(n)(ref)}]$$

$$\times [(1 + (FD)'(SR)_{(oc)(a)})(1 + (FD)'(SR)_{(oc)(b)}) \cdots (1 + (FD)'(SR)_{(oc)(n-1)})(1 + (FD)'(SR)_{(oc)(n)})]$$

$$\times \epsilon^{j(D)(DRA)_{(oc)(a)}}\epsilon^{j(D)(DRA)_{(oc)(b)}} \cdots \epsilon^{j(D)(DRA)_{(oc)(n-1)}}\epsilon^{j(D)(DRA)_{(oc)(n)}} \quad (18)$$

Setting similar factors on each side of Eq. (18) equal to one another yields the expressions

$$(SR)_{(os)(id)[q_{(in)};q_{(out)}](ref)} = (SR)_{(oc)(a)(ref)}(SR)_{(oc)(b)(ref)} \cdots (SR)_{(oc)(n-1)(ref)}(SR)_{(oc)(n)(ref)} \quad (19a)$$

$$1 + (FD)'(SR)_{(os)(id)(q_{(in)};q_{(out)})}$$

$$= (1 + (FD)'(SR)_{(oc)(a)})(1 + (FD)'(SR)_{(oc)(b)}) \cdots (1 + (FD)'(SR)_{(oc)(n-1)})(1 + (FD)'(SR)_{(oc)(n)}) \quad (19b)$$

$$(D)(DRA)_{(os)(id)(q_{(in)};q_{(out)})}$$

$$= (D)(DRA)_{(oc)(a)} + (D)(DRA)_{(oc)(b)} + \cdots + (D)(DRA)_{(oc)(n-1)} + (D)(DRA)_{(oc)(n)} \quad (19c)$$

When all of the fractional deviations of the operating components are small enough, the product terms of the expanded form of Eq. (19b) may be neglected. In this situation, the expression may be written approximately as

$$1 + (FD)'(SR)_{(os)(id)(q_{(in)};q_{(out)})}$$

$$\cong 1 + (FD)'(SR)_{(oc)(a)} + (FD)'(SR)_{(oc)(b)} + \cdots + (FD)'(SR)_{(oc)(n-1)} + (FD)'(SR)_{(oc)(n)} \quad (20)$$

To this approximation, the fractional deviation of the identified operating system sensitivity ratio is the sum of the fractional deviations of the operating component sensitivity ratios; i.e.,

$$(FD)'(SR)_{(os)(id)(q_{(in)};q_{(out)})}$$

$$= (FD)'(SR)_{(oc)(a)} + (FD)'(SR)_{(oc)(b)} + \cdots + (FD)'(SR)_{(oc)(n-1)} + (FD)'(SR)_{(oc)(n)} \quad (21)$$

b) Fractional deviation of an open-chain system sensitivity ratio

Derivation Summary 35-10. Sensitivity ratio fractional deviations for an open-chain system.
(Page 3 of 3)

to the product of the component performance function deviation functions. This statement is expressed in symbols by Eq. (14). Following the pattern of section a, the system performance function deviation function is also expressed in general terms as the product of a reference sensitivity ratio, a dimensionless sensitivity ratio and an imaginary exponential function, as shown in Eq. (15). The fractional deviation of the system sensitivity ratio is defined by Eq. (16). A new form of the performance function deviation function for the system can now be written as Eq. (17).

35.290. Replacing all the performance function deviation functions in Eq. (14) by the fractional deviation forms gives Eq. (18). Equating the system reference sensitivity ratio on the left-hand side of Eq. (18) to the product of the component reference sensitivity ratios on the right-hand side gives Eq. (19a). Equating the fractional deviation expression on the left-hand side of Eq. (18) to the product of

the component fractional deviation expressions on the right-hand side produces Eq. (19b). Finally, the exponential function exponents are equated. This step shows (see Eq. (19c)) that the system dynamic response angle deviation is equal to the sum of the component dynamic response angle deviations.

35.291. Since interest exists chiefly in the operating region where the fractional deviations are small, the fractional-deviation product terms may be neglected when the right-hand side of Eq. (19b) is expanded. The expansion is shown in Eq. (20) with the product terms neglected. From this relationship comes Eq. (21), which shows that the system fractional deviation is equal to the sum of the component fractional deviations.

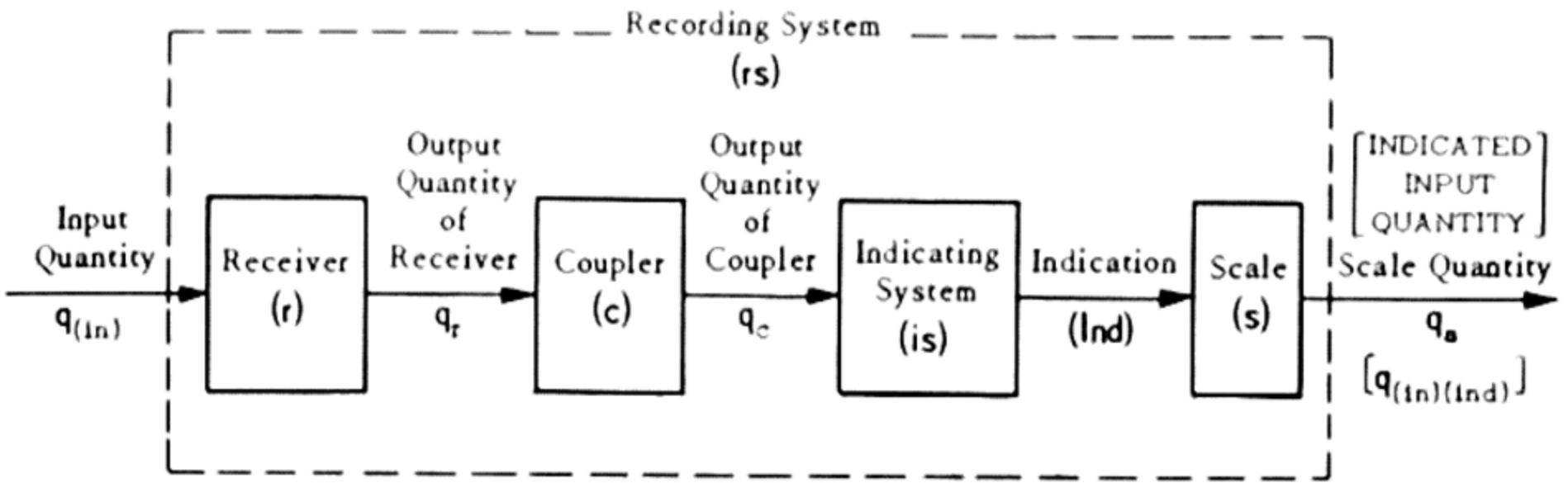
35.292. An alternate development is possible using the logarithmic forms described in Chapter 24. When the magnitudes of the component performance function deviation functions are small, they may each be expanded in series form and the higher order terms neglected. The resultant expression is identical with Eq. (21). This shows that the graphical procedures developed in Chapter 24 for calculating the steady-state response to a sinusoidal input may be applied to the deviation method without further justification.

APPLICATION OF THE DEVIATION METHOD TO THE PERFORMANCE OF A TYPICAL RECORDING SYSTEM

35.293. As an example of the deviation method for calculating the performance of open-chain systems, consider the typical recording system shown in the figure of Derivation Summary 35-11. The input quantity is applied to a receiver. The receiver output is transmitted to the indicating system after passing through a coupler. Indicated values of the input quantity are obtained from the scale. The signal is generally modified as it passes through each operating component. The arrangement is selected to give the recording system the theoretically desired performance.

35.294. A performance function is associated with each component. It is assumed that Eqs. (1), (2), (3) and (4) of Derivation Summary 35-11 represent the component performance functions. Then Eq. (5) gives the recording system performance function as the product of the component performance functions. When the input-output brackets are dropped, the performance function assumes the form of Eq. (6). This expression will now be reformulated in terms of performance function deviation functions. These latter expressions will then be modified into the fractional deviation forms.

35.295. It is assumed that reference performance functions are given for the components. The component performance function deviation functions occur as in Eq. (3) of Derivation Summary 35-10. When the recording system performance function is expressed as the product of a reference performance function and a



A typical recording system is illustrated in the preceding diagram. The performance of each component is specified by its performance function as follows:

$$q_r = [PF]_{(r)[q_{(in)};q_r]}\, q_{(in)} \quad ; \quad q_c = [PF]_{(c)[q_r;q_c]}\, q_r \qquad (1),(2)$$

$$(Ind) = [PF]_{(is)[q_c;(Ind)]}\, q_c \quad ; \quad q_s = [PF]_{(s)[(Ind);q_s]}\, (Ind) \qquad (3),(4)$$

The recording system performance function is equal to the product of the performance functions of the components; i.e.,

$$[PF]_{(rs)[q_{(in)};q_s]} = [PF]_{(r)[q_{(in)};q_r]}\, [PF]_{(c)[q_r;q_c]}\, [PF]_{(is)[q_c;(Ind)]}\, [PF]_{(s)[(Ind);q_{(in)}]} \qquad (5)$$

Since no confusion is possible, the input-output brackets may be eliminated from the performance functions of this equation to give

$$[PF]_{(rs)} = [PF]_r\, [PF]_c\, [PF]_{(is)}\, [PF]_s \qquad (6)$$

As in Eq. (3) of Derivation Summary 35-10, each of the performance functions of Eq. (6) may be expressed as the product of a reference performance function and a performance function deviation function. From Eqs. (12) through (14) of Derivation Summary 35-10, it is seen that

$$[PF]_{(rs)} = [PF]_{(rs)(ref)}\, (DF)\, [PF]_{(rs)} \qquad (7)$$

$$[PF]_{(rs)(ref)} = [PF]_{(r)(ref)}\, [PF]_{(c)(ref)}\, [PF]_{(is)(ref)}\, [PF]_{(s)(ref)} \qquad (8)$$

$$(DF)\, [PF]_{(rs)} = (DF)\, [PF]_r\, (DF)\, [PF]_c\, (DF)\, [PF]_{(is)}\, (DF)\, [PF]_s \qquad (9)$$

a) Typical recording-system performance function

As shown by Eq. (4) of Derivation Summary 35-10, each reference performance function in Eq. (8) of the present summary may be expressed as a product of a reference sensitivity and an imaginary exponential whose exponent is a reference dynamic response angle. From Eq. (8) of Derivation Summary 35-10, each performance function deviation function in Eq. (9) of the present summary may be written in terms of a reference sensitivity ratio, a fractional deviation of the sensitivity ratio, and a dynamic response angle deviation. Thus, Eqs. (8) and (9) can be expressed as follows:

$$[PF]_{(rs)(ref)} = S_{(rs)(ref)}\, \epsilon^{\,j(DRA)_{(rs)(ref)}}$$

$$= S_{(r)(ref)}\, S_{(c)(ref)}\, S_{(is)(ref)}\, S_{(s)(ref)}\, \epsilon^{\,j[(DRA)_{(r)(ref)} + (DRA)_{(c)(ref)} + (DRA)_{(is)(ref)} + (DRA)_{(s)(ref)}]} \qquad (10)$$

$$(DF)\, [PF]_{(rs)} = (SR)_{(rs)(ref)}\, [1 + (FD)\, (SR)_{(rs)}]\, \epsilon^{\,j(D)(DRA)_{(rs)}}$$

$$= (SR)_{(r)(ref)}\, (SR)_{(c)(ref)}\, (SR)_{(is)(ref)}\, (SR)_{(s)(ref)}\, [1 + (FD)\, (SR)_r]\, [1 + (FD)\, (SR)_c]$$

$$\times\, [1 + (FD)\, (SR)_{(is)}]\, [1 + (FD)\, (SR)_s]\, \epsilon^{\,j[(D)(DRA)_r + (D)(DRA)_c + (D)(DRA)_{(is)} + (D)(DRA)_s]} \qquad (11)$$

Derivation Summary 35-11. Performance function of a typical recording system expressed in terms of component deviations. (Page 1 of 2)

From Eq. (10), it is apparent that

$$S_{(rs)(ref)} = S_{(r)(ref)} S_{(c)(ref)} S_{(1s)(ref)} S_{(s)(ref)} \tag{12}$$

$$(DRA)_{(rs)(ref)} = (DRA)_{(r)(ref)} + (DRA)_{(c)(ref)} + (DRA)_{(1s)(ref)} + (DRA)_{(s)(ref)} \tag{13}$$

From Eq. (11), it is found that

$$(SR)_{(rs)(ref)} = (SR)_{(r)(ref)} (SR)_{(c)(ref)} (SR)_{(1s)(ref)} (SR)_{(s)(ref)} \tag{14}$$

$$1 + (FD)'(SR)_{(rs)} = [1 + (FD)'(SR)_r] [1 + (FD)'(SR)_c] [1 + (FD)'(SR)_{(1s)}] [1 + (FD)'(SR)_s] \tag{15}$$

$$(D)(DRA)_{(rs)} = (D)(DRA)_r + (D)(DRA)_c + (D)(DRA)_{(1s)} + (D)(DRA)_s \tag{16}$$

According to Eq. (15), one plus the fractional deviation of the recording system sensitivity ratio is equal to a product of terms, each term being a component sensitivity ratio fractional deviation plus unity. From Eq. (16), the dynamic response angle deviation of the system is equal to the sum of the dynamic response angle deviations of the components.

b) Recording system deviations in terms of deviations of individual components

If the fractional deviations of the components are sufficiently small, then all terms involving products of fractional deviations will be at least an order of magnitude smaller than terms not involving products. Under these circumstances, the expression of Eq. (15) becomes

$$1 + (FD)'(SR)_{(rs)} \cong 1 + (FD)'(SR)_r + (FD)'(SR)_c + (FD)'(SR)_{(1s)} + (FD)'(SR)_s \tag{17}$$

so that

$$(FD)'(SR)_{(rs)} \cong (FD)'(SR)_r + (FD)'(SR)_c + (FD)'(SR)_{(1s)} + (FD)'(SR)_s \tag{18}$$

Equation (18) expresses the result given for the general case by Eq. (21) of Derivation Summary 35-10.

c) Approximation of the recording-system sensitivity ratio fractional deviation

Derivation Summary 35-11 Performance function of a typical recording system expressed in terms of component deviations. (Page 2 of 2)

deviation performance function, it may be written as in Eq. (7) of Derivation Summary 35-11. From the procedure of section b in Derivation Summary 35-10, the recording system reference performance function is given by Eq. (8) and the performance function deviation function by Eq. (9). In terms of the component reference sensitivities and dynamic response angles, the recording system reference performance function takes the form of Eq. (10). The system performance function deviation function is expressed in fractional deviation form in Eq. (11).

35.296. Equating like terms on both sides of Eq. (10) shows that the system reference sensitivity is equal to the product of the component reference sensitivities. The system reference dynamic response angle is equal to the sum of the component references as in Eq. (13). From Eq. (11), a similar process yields the expressions of Eqs. (14), (15) and (16). When the component fractional deviations are small, the product terms in Eq. (15) may be neglected. This leads to the statement given by Eq. (18) that the fractional deviation of the recording system sensitivity ratio is equal to the sum of the component fractional deviations. Recording system dynamic response angle deviations are shown by Eq. (16) to be equal to the sum of the dynamic response angle deviations of the system components.

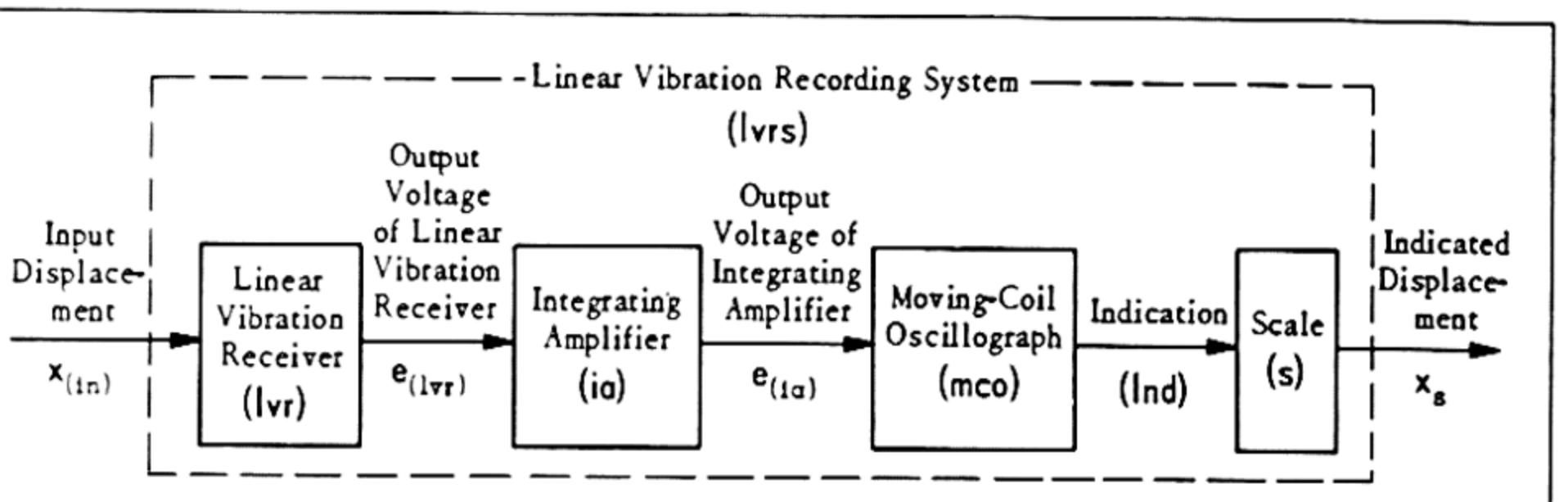
35.297. An illustration of the deviation method for determining the performance of an actual system is given in Performance Data Summary 35-1. The functional diagram in section a represents a linear vibration recording system. The input displacement is converted into an electrical signal by the linear vibration receiver. Since the output of the linear vibration receiver is proportional to the velocity of the input, it is necessary to integrate the voltage signal once before applying it to the moving-coil oscillograph. The indicated vibratory displacement is read from the indicated output on the scale.

35.298. The operating components making up the linear vibration recording system are chosen from the instruments described in this and previous chapters. The linear vibration receiver performance is taken from Test Report No. 35-1. Considered as a component for which the input is a displacement and the output is a voltage, the theoretical performance function is a (2;0, 1, 2) equation multiplied by a (1;0) equation. This means that the sensitivity is proportional to frequency. The performance function variable is a frequency ratio for which the reference is 7 cycles per second, the undamped natural frequency of the component. This is indicated by the subscript (lvr) after the frequency ratio symbol.

35.299. The theoretical performance function for the integrating amplifier is a (0;1) equation. For the component shown in the functional diagram, the characteristics are taken from Test Report No. 35-3. This report shows that within experimental error the amplifier integrates perfectly in the operating range. The performance function variable is a frequency ratio with a reference of 10 cycles per second. The product of the linear vibration receiver and integrating amplifier performance functions yields a (2;0, 1, 2)-type function.

35.300. Moving-coil oscillographs are discussed in Chapter 32. Typical performance characteristics are given by the curves in Fig. 32-35. These may be associated with (0;0, 1, 2) equations. The curves of Fig. 32-35 represent oscillograph performance characteristics obtained with a galvanometer having an undamped natural frequency of 42 cycles per second, which is too low a value for use in the linear vibration recording system. Therefore, that Type A-8668 galvanometer is replaced by the manufacturer's Type C-495 galvanometer, which has an undamped natural frequency of 500 cycles per second. The shunt resistance is adjusted to give the oscillograph a damping ratio of 1.0. The reference frequency in the performance function is the undamped natural frequency of the galvanometer. The scale sensitivity is evaluated after the following procedure is presented.

35.301. While the component performance functions are given in section b of Performance Data Summary 35-1, they must be reduced to a common time base before they can be combined to represent the performance function of the whole system. It is convenient to take the reference period equal to 0.1 second, so that the reference frequency is 10 cycles per second. The system frequency ratio is



a) Functional diagram

(lvr) Linear vibration receiver

(See sheet 1 of Test Report No. 35-1)

$$[PF]_{(lvr)[x;e](theo)} \approx [RF]_{(2;0,1,2)\times(1;0)} = S_{(lvr)[x;e](ref)}\left(\frac{(FR)^2_{(lvr)}}{1-(FR)^2_{(lvr)}+j2(DR)_{(lvr)}(FR)_{(lvr)}}\right) j(FR)_{(lvr)} \tag{1}$$

where

$$(FR)_{(lvr)} = n_f/n_{(n)(lvr)} \quad ; \quad n_{(n)(lvr)} = 7 \text{ cps}$$

$$(DR)_{(lvr)} = 0.7 \quad ; \quad S_{(lvr)[x;e](ref)} = 4.84 \text{ volts/inch} \tag{2}$$

$$'(SR)_{(lvr)(x;e)(theo)} \approx '(DAR)_{(2;0,1,2)\times(1;0)} = \frac{(FR)^2_{(lvr)}}{\sqrt{[1-(FR)^2_{(lvr)}]^2 + [2(DR)_{(lvr)}(FR)_{(lvr)}]^2}}(FR)_{(lvr)} \tag{3}$$

$$(DRA)_{(lvr)(x;e)(theo)} \approx (DRA)_{(2;0,1,2)\times(1;0)} = \tan^{-1}\left[\frac{-2(DR)_{(lvr)}(FR)_{(lvr)}}{1-(FR)^2_{(lvr)}}\right] + 90° \tag{4}$$

$$(DRA)_{(lvr)(x;e)(ref)} = -90° \tag{5}$$

(ia) Integrating amplifier

(See sheet 1 of Test Report No. 35-3)

$$[PF]_{(ia)[e;e](theo)} \approx [RF]_{(0;1)} = S_{(ia)[e;e](ref)}\frac{1}{j(FR)_{(ia)}} \tag{6}$$

where

$$(FR)_{(ia)} = n_f/n_{(ia)(ref)} \quad ; \quad n_{(ia)(ref)} = 10 \text{ cps} \tag{7}$$

$$S_{(ia)[e;\dot{e}](ref)} = 14.0 \text{ (volts/sec)/volt} \quad ; \quad S_{(ia)[e;e](ref)} = \frac{S_{(ia)[e;\dot{e}](ref)}}{2\pi n_{(ia)(ref)}} = 0.224\frac{\text{volt}}{\text{volt}}$$

$$'(SR)_{(ia)(e;e)(theo)} \approx '(DAR)_{(0;1)} = \frac{1}{(FR)_{(ia)}} \tag{8}$$

$$(DRA)_{(ia)(e;e)(theo)} \approx (DRA)_{(0;1)} = -90° \tag{9}$$

(mco) Moving-coil oscillograph

(See Fig. 32-35; Galvanometer Type C-495 replaces Galvanometer Type A-8668 shown in that figure.)

$$[PF]_{(mco)[e;(Ind)](theo)} \approx [RF]_{(0;0,1,2)} = S_{(mco)[e;(Ind)](ref)}\frac{1}{1-(FR)^2_{(mco)}+j2(DR)_{(mco)}(FR)_{(mco)}} \tag{10}$$

Performance Data Summary 35-1. Performance characteristics of a linear vibration recording system. (Page 1 of 4)

where

$$(FR)_{(mco)} = n_f / n_{(n)(mco)} \quad ; \quad n_{(n)(mco)} = 500 \text{ cps}$$

$$(DR)_{(mco)} = 1.0 \quad ; \quad S_{(mco)[e;(Ind)](ref)} = 0.35 \text{ mm/mv} \tag{11}$$

$$\hat{(SR)}_{(mco)(e;(Ind))(theo)} = \hat{(DAR)}_{(0;0,1,2)} = \frac{1}{\sqrt{\left[1 - (FR)^2_{(mco)}\right]^2 + \left[2(DR)_{(mco)}(FR)_{(mco)}\right]^2}} \tag{12}$$

$$(DRA)_{(mco)(e;(Ind))(theo)} = (DRA)_{(0;0,1,2)} = \tan^{-1}\left[\frac{-2(DR)_{(mco)}(FR)_{(mco)}}{1 - (FR)^2_{(mco)}}\right] \tag{13}$$

(s) Scale (numbered divisions of oscillograph chart paper)

$$[PF]_{(s)[(Ind);x]} = S_{(s)[(Ind);x]} \tag{14}$$

b) Component performance data

Choose

$$n_{(lvrs)(ref)} = 10 \text{ cps} \tag{15}$$

and define

$$(FR)_{(lvrs)} = (FR) = \frac{n_f}{n_{(lvrs)(ref)}} \tag{16}$$

Then

$$(FR)_{(lvr)} = \frac{n_{(lvrs)(ref)}}{n_{(n)(lvr)}}(FR) \quad ; \quad \frac{n_{(lvrs)(ref)}}{n_{(n)(lvr)}} = \frac{1}{(bp)_{(lvr)}} \tag{17}$$

where

$(bp)_{(lvr)}$ = linear vibration receiver break point = 0.7 (see Derivation Summary 24-2 for definition and use of break points) (18)

Similarly,

$$(FR)_{(la)} = \frac{n_{(lvrs)(ref)}}{n_{(la)(ref)}}(FR) \quad ; \quad \frac{n_{(lvrs)(ref)}}{n_{(la)(ref)}} = \frac{1}{(bp)_{(la)}} \quad ; \quad (bp)_{(la)} = 1.0 \tag{19}$$

and

$$(FR)_{(mco)} = \frac{n_{(lvrs)(ref)}}{n_{(n)(mco)}}(FR) \quad ; \quad \frac{n_{(lvrs)(ref)}}{n_{(n)(mco)}} = \frac{1}{(bp)_{(mco)}} \quad ; \quad (bp)_{(mco)} = 50 \tag{20}$$

c) Reduction of component frequency ratios to a common time base

In terms of the break points defined in section c, the component performance functions of section b may be written as

$$[PF]_{(lvr)[x;e](theo)} = S_{(lvr)[x;e](ref)} \frac{\left(\frac{(FR)}{(bp)_{(lvr)}}\right)^2}{1 - \left(\frac{(FR)}{(bp)_{(lvr)}}\right)^2 + j2(DR)_{(lvr)}\left(\frac{(FR)}{(bp)_{(lvr)}}\right)} j\left(\frac{(FR)}{(bp)_{(lvr)}}\right) \tag{21}$$

$$[PF]_{(la)[e;e](theo)} = S_{(la)[e;e](ref)} \frac{1}{j(FR)/(bp)_{(la)}} \tag{22}$$

Performance Data Summary 35-1. Performance characteristics of a linear vibration recording system. (Page 2 of 4)

$$[PF]_{(mco)[e;(Ind)](theo)} = S_{(mco)[e;(Ind)](ref)} \frac{1}{1 - \left(\frac{(FR)}{(bp)_{(mco)}}\right)^2 + j2(DR)_{(mco)}\left(\frac{(FR)}{(bp)_{(mco)}}\right)} \tag{23}$$

The performance function of the scale remains unchanged; i.e., $[PF]_{(s)[(Ind);x]} = S_{(s)[(Ind);x]}$.

d) Component performance functions in breakpoint form

The theoretical linear vibration recording system performance function is obtained by multiplying the four performance-function expressions of section d; i.e.,

$$[PF]_{(lvrs)[x;x](theo)} = S_{(lvrs)[x;x](ref)} \frac{\left(\frac{(FR)}{(bp)_{(lvr)}}\right)^2}{1 - \left(\frac{(FR)}{(bp)_{(lvr)}}\right)^2 + j2(DR)_{(lvr)}\left(\frac{(FR)}{(bp)_{(lvr)}}\right)} \times \frac{1}{1 - \left(\frac{(FR)}{(bp)_{(mco)}}\right)^2 + j2(DR)_{(mco)}\left(\frac{(FR)}{(bp)_{(mco)}}\right)} \tag{24}$$

where

$$S_{(lvrs)[x;x](ref)} = S_{(lvr)(ref)} S_{(ia)(ref)} S_{(mco)(ref)} S_{(s)(ref)} \frac{(bp)_{(ia)}}{(bp)_{(lvr)}} \tag{25}$$

Note: The input-output subscripts of the component sensitivities have been dropped since their presence no longer serves any useful purpose.

Define

$$S_{(lvrs)[x;x](ref)} = 1 \tag{26}$$

Then

$$S_{(s)(ref)} = \frac{1}{S_{(lvr)(ref)} S_{(ia)(ref)} S_{(mco)(ref)} \frac{(bp)_{(ia)}}{(bp)_{(lvr)}}} = 1.85 \times 10^{-3} \text{ inch/mm} \tag{27}$$

The dimensionless sensitivity ratio of the linear vibration recording system is equal to the product of the component dimensionless sensitivity ratios; i.e.,

$$'(SR)_{(lvrs)} = '(SR)_{(lvr)}\ '(SR)_{(ia)}\ '(SR)_{(mco)} \tag{28}$$

$$'(SR)_{(lvrs)} = \frac{\left(\frac{(FR)}{(bp)_{(lvr)}}\right)^2}{\sqrt{\left[1 - \left(\frac{(FR)}{(bp)_{(lvr)}}\right)^2\right]^2 + \left[2(DR)_{(lvr)}\left(\frac{(FR)}{(bp)_{(lvr)}}\right)\right]^2}} \times \frac{1}{\sqrt{\left[1 - \left(\frac{(FR)}{(bp)_{(mco)}}\right)^2\right]^2 + \left[2(DR)_{(mco)}\left(\frac{(FR)}{(bp)_{(mco)}}\right)\right]^2}} \tag{29}$$

The dynamic response angle of the linear vibration recording system is equal to the sum of the component dynamic response angles; i.e.,

$$(DRA)_{(lvrs)} = (DRA)_{(lvr)} + (DRA)_{(ia)} + (DRA)_{(mco)} + (DRA)_{(s)} \tag{30}$$

Performance Data Summary 35-1. Performance characteristics of a linear vibration recording system. (Page 3 of 4)

$$(DRA)_{(lvrs)} = \tan^{-1}\left[\frac{-2(DR)_{(lvr)}(FR)_{(lvr)}}{1-(FR)^2_{(lvr)}}\right] + \tan^{-1}\left[\frac{-2(DR)_{(mco)}(FR)_{(mco)}}{1-(FR)^2_{(mco)}}\right] \quad (31)$$

e) Linear vibration recording system performance function

From Eq. (21) of Derivation Summary 35-10, the fractional deviation of the linear vibration recording system sensitivity ratio is the sum of the fractional deviations of the right-hand product factors in Eq. (29); i.e.,

$$(FD)'(SR)_{(lvrs)} = (FD)\{'(SR)_{(lvr)}'(SR)_{(ia)}\}^{\bullet} + (FD)'(SR)_{(mco)} \quad (32)$$

The dynamic response angle deviation is equal to the sum of the component dynamic response angles minus the reference. Define

$$(DRA)_{(lvrs)(ref)} = -180° \quad (33)$$

Then

$$(D)(DRA)_{(lvrs)} = (DRA)_{(lvr)} + (DRA)_{(ia)} + (DRA)_{(mco)} - (DRA)_{(lvrs)(ref)} \quad (34)$$

$$= (D)\{(DRA)_{(lvr)} + (DRA)_{(ia)}\} + (D)(DRA)_{(mco)} \quad (35)$$

where

$$(D)\{(DRA)_{(lvr)}+(DRA)_{(ia)}\} = (DRA)_{(lvr)}+(DRA)_{(ia)}-(DRA)_{(lvrs)(ref)} \; ; \; (D)(DRA)_{(mco)}=(DRA)_{(mco)} - 0° \quad (36)$$

Values for the first fractional deviation on the right-hand side of Eq. (32),

$$(FD)\{'(SR)_{(lvr)}'(SR)_{(ia)}\} = (FD)\left\{\frac{\left(\frac{(FR)}{(bp)_{(lvr)}}\right)^2}{\sqrt{\left[1-\left(\frac{(FR)}{(bp)_{(lvr)}}\right)^2\right]^2 + \left[2(DR)_{(lvr)}\left(\frac{(FR)}{(bp)_{(lvr)}}\right)\right]^2}}\right\} \quad (37)$$

may be obtained from curves given in Fig. 19-46 of Chapter 19 for the (2;0,1,2) equation. Values for the second fractional deviation of Eq. (32),

$$(FD)'(SR)_{(mco)} = (FD)\left\{\frac{1}{\sqrt{\left[1-\left(\frac{(FR)}{(bp)_{(mco)}}\right)^2\right]^2 + \left[2(DR)_{(mco)}\left(\frac{(FR)}{(bp)_{(mco)}}\right)\right]^2}}\right\} \quad (38)$$

are taken from Fig. 19-36 for the (0;0,1,2) equation. The two fractional deviations are combined by the breakpoint method described in Chapter 24 and reviewed in Procedure Summary 33-1 of Chapter 33.

Dynamic response angle deviations are calculated in a similar manner using curves from Fig. 19-47 and Fig. 19-37 of Chapter 19.

Results are shown in Figs. 35-45 and 35-46.

f) Deviation expressions for the linear vibration recording system performance function

---

* This form of the fractional deviation occurs since the first factor on the right-hand side of Eq. (29) is equal to the product of the linear vibration receiver dimensionless sensitivity ratio and the integrating amplifier dimensionless sensitivity ratio.

Performance Data Summary 35-1. Performance characteristics of a linear vibration recording system. (Page 4 of 4)

represented by the symbol FR, and is equal to the ratio of the forcing frequency to the reference frequency. The reduction of the component frequency ratios to a common time base is carried out in section c.

35.302. As shown in section c, each component frequency ratio is equal to a constant multiplied by the system frequency ratio. The constant for each component

is equal to the system reference frequency divided by the component reference frequency. Reference to the discussion in Chapter 33, as well as that in Chapter 24, shows that the constant may be identified as the reciprocal of the component break point. Introduction of the expressions developed in section c into the appropriate component performance functions yields the expressions for the performance functions with a common time base. The breakpoint value occurs at the proper place in each performance function, as shown in section d.

35.303. Multiplication of the component performance functions yields the theoretical linear vibration recording system performance function. The reference sensitivity is equal to the product of the component reference sensitivities and the breakpoint ratio of the integrating amplifier to that of the linear vibration receiver. The reference value for the sensitivity of the linear vibration recording system must be unity. The reference scale sensitivity is found to be 1.85×10^{-3} inch per millimeter scale displacement. The reference dynamic response angle of the recording system is taken equal to -180 degrees. The system dimensionless sensitivity ratio is the product of the sensitivity ratios for a (2;0, 1, 2) and a (0;0, 1, 2) equation. The system dynamic response angle is the sum of the component dynamic response angles.

35.304. Deviation expressions for the linear vibration recording system performance function are developed in section f of the summary. The fractional deviation of the system sensitivity ratio is taken equal to the fractional deviation of the linear vibration receiver sensitivity ratio multiplied by the integrating amplifier sensitivity ratio plus the fractional deviation of the moving-coil oscillograph sensitivity ratio. The dynamic response angle deviation is equal to the sum of the component dynamic response angle deviations less the reference value of -180 degrees.

35.305. The component fractional deviations, as well as component dynamic response angle deviations, are available from the curves in Chapter 19. Performance function deviation functions may be calculated graphically from component deviation functions by employing the breakpoint procedure described in Chapters 24 and 33. The breakpoint line for each component performance function deviation function is located on the graph, as in Figs. 35-45 and 35-46. The component breakpoint line is located on the unity line of the reference deviation and the curve is traced. The system deviation is found by adding the component curves algebraically.

35.306. Figure 35-45 is given in two parts, one for fractional deviations less than about one percent and the other for those greater than this value. Figure 35-46 represents the dynamic response angle deviation of the linear vibration recording system. By establishing tolerance limits on the fractional deviation, low-frequency cutoffs, high-frequency cutoffs, and band widths may be determined. Similar quantities are found by establishing dynamic response angle deviation tolerance limits. Illustrative values are given in Table 35-2.

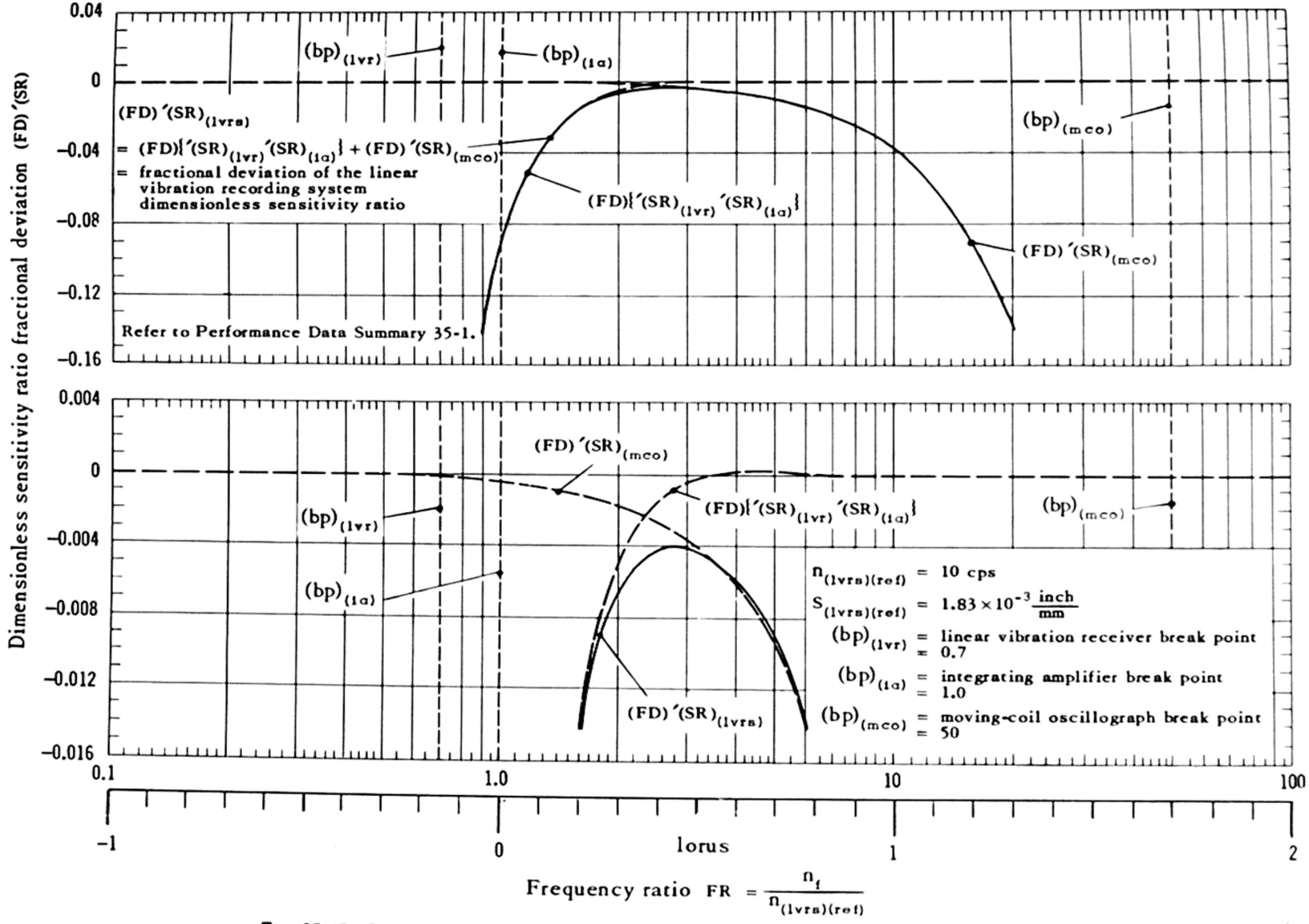


Fig. 35-45. Plot of linear vibration recording system sensitivity ratio fractional deviation.

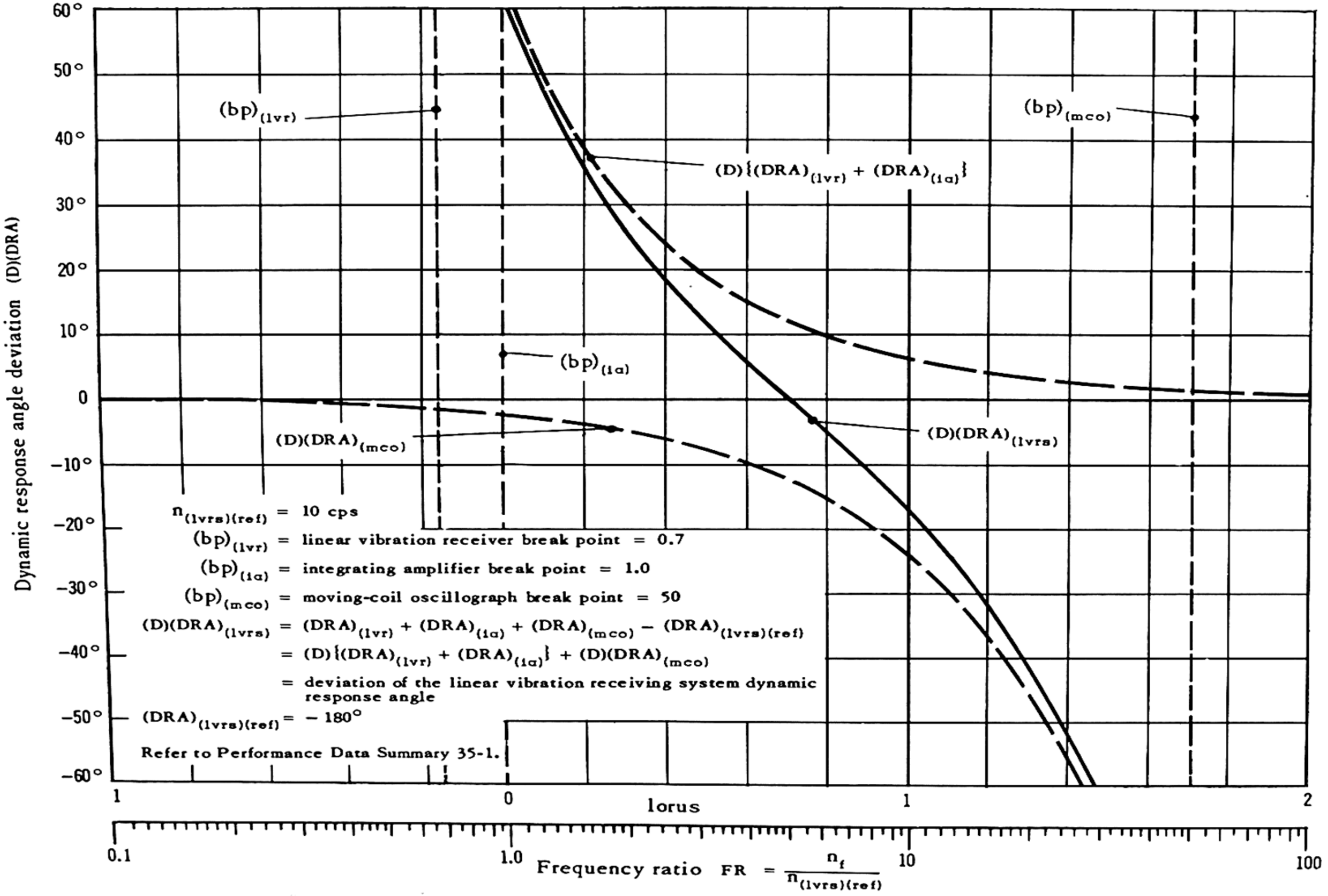


Fig. 35-46. Plot of linear vibration recording system dynamic response angle deviation.

Table 35-2. Cutoff frequencies and bond widths for the linear vibration recording system corresponding to specified values of dimensionless sensitivity ratio fractional deviation tolerance limits and dynamic response angle deviation tolerance limits.
(Refer to Performance Data Summary 35-1 and Figs. 35-45 and 35-46.)

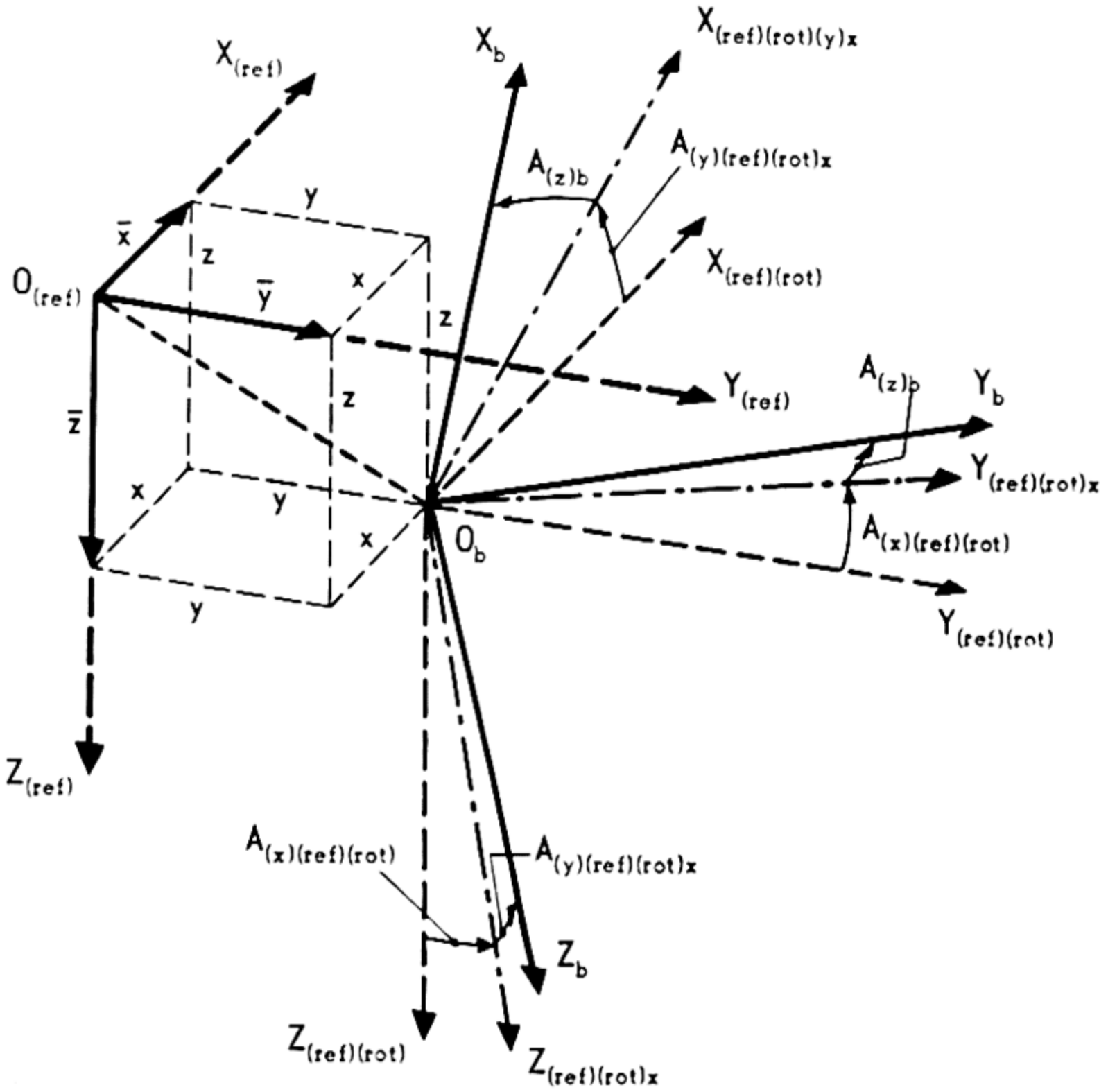
Dimensionless sensitivity ratio fractional deviation tolerance limit $(TL)[(FD)'(SR)_{(1vrs)}]$	Low frequency-ratio cutoff $(FR)_{(1fco)}$	Low forcing-frequency cutoff $n_{(f)(1fco)}$	High frequency-ratio cutoff $(FR)_{(hfco)}$	High forcing-frequency cutoff $n_{(f)(hfco)}$	Frequency-ratio band width $(BW)_{(FR)}$	Forcing-frequency band width $(BW)_{n_f}$		Dynamic response angle deviation tolerance limit $(TL)[(D)(DRA)_{(1vrs)}]$	Low frequency-ratio cutoff $(FR)_{(1fco)}$	Low forcing-frequency cutoff $n_{(f)(1fco)}$	High frequency-ratio cutoff $(FR)_{(hfco)}$	High forcing-frequency cutoff $n_{(f)(hfco)}$	Frequency-ratio band width $(BW)_{(FR)}$	Forcing-frequency band width $(BW)_{n_f}$
-0.01	1.8	18	4.0	40	2.2	22		± 5°	4.2	42	6.5	65	2.3	23
-0.02	1.5	15	7.2	72	5.7	57		± 10°	3.4	34	7.7	77	4.3	43
-0.05	1.2	12	11.6	116	10.4	104		± 20°	2.4	24	11.3	113	8.9	89
-0.10	1.0	10	16.7	167	15.7	157		± 30°	1.8	18	15.1	151	13.3	133

VIBRATION MEASUREMENT FOR A RIGID BODY MOVING IN SPACE

35.307. The motion of a rigid body in space can be conveniently and completely described by the displacement of a coordinate system fixed to the rigid body with respect to a reference coordinate system that is fixed to the inertial reference space. When the motion of the body coordinate system is known, the motion of any particle located on the rigid body can be computed readily from trigonometric relationships. There are an infinite number of possible coordinate systems that may be associated with a rigid body. Quite often, however, a particular coordinate system is most desirable for computing the properties associated with the motion of the particles of the rigid body. A typical example is the use of the principal axes of a homogeneous rigid body as coordinates in the determination of the moment of inertia of the body. In principle, however, any coordinate system inside of or outside of the rigid body may be used as a body coordinate system. Sometimes it may be convenient to first determine the motion of an intermediate coordinate system, and then determine the motion of the coordinate system that is used to compute the motion of the particles.* For the purpose of measurement, it is sufficient to say that the measurement of the motion of a rigid body is the same as the measurement of the motion of a coordinate system fixed to the rigid body.

35.308. The displacement of a body coordinate system with respect to a fixed reference coordinate system may be described as the combination of translational and rotational motion, as shown in Fig. 35-47. In this figure, the fixed

* For details on the manipulation of coordinate systems, see textbooks on kinematics; for example, Rauscher (R3).



Definitions:

$X_{(ref)}$, $Y_{(ref)}$, $Z_{(ref)}$ = axes of the reference coordinate system

X_b, Y_b, Z_b = axes of the body coordinate system

$O_{(ref)}$ = origin of the reference coordinate system

O_b = origin of the body coordinate system

$\bar{x}$, $\bar{y}$, $\bar{z}$ = vector components along the axes of the reference coordinate system representing the translational displacement from $O_{(ref)}$ to O_b

$X_{(ref)(rot)}$, $Y_{(ref)(rot)}$, $Z_{(ref)(rot)}$ = axes of the rotation-reference coordinate system

$Y_{(ref)(rot)x}$, $Z_{(ref)(rot)x}$ = positions of the Y and Z axes of the rotation-reference coordinate system after the system is rotated about the $X_{(ref)(rot)}$ axis through the angle $A_{(x)(ref)(rot)}$

$X_{(ref)(rot)(y)x}$ = position of the X axis of the rotation-reference coordinate system after the system is given an additional rotation about the $Y_{(ref)(rot)x}$ axis through the angle $A_{(y)(ref)(rot)x}$

$A_{(x)(ref)(rot)}$ = angular displacement of the rotation-reference coordinate system about the $X_{(ref)(rot)}$ axis

$A_{(y)(ref)(rot)x}$ = additional angular displacement of the rotation-reference coordinate system, made about the $Y_{(ref)(rot)x}$ axis

$A_{(z)b}$ = final angular displacement of the rotation-reference coordinate system, made about the Z_b axis

Fig. 35-47. Displacement of a body coordinate system X_b, Y_b, Z_b with respect to a fixed reference coordinate system $X_{(ref)}$, $Y_{(ref)}$, $Z_{(ref)}$ by a combination of translational and rotational motion.

reference coordinate system is shown by the heavy dashed lines $X_{(ref)}$, $Y_{(ref)}$ and $Z_{(ref)}$, with their origin at $O_{(ref)}$. The position of the rigid body is defined by the solid-line body coordinate system X_b, Y_b, Z_b, with its origin at O_b. Displacing the reference coordinate system $X_{(ref)}$, $Y_{(ref)}$, $Z_{(ref)}$ until it coincides with the body coordinate system X_b, Y_b, Z_b involves a translation of the origin of the reference coordinate system to O_b following the path $(O_{(ref)} - O_b)$. This translational motion may be represented by the sum of three linear motion vectors, $\bar{x}$, $\bar{y}$, and $\bar{z}$, along the three reference axes. The origin of the reference coordinate system may reach its destination, starting from $O_{(ref)}$, following either of six paths along the sides of the right parallelepiped shown by dotted lines in Fig. 35-47. The six possible paths are x-y-z, y-z-x, z-x-y, x-z-y, y-x-z and z-y-x. This means that the translational motion from $O_{(ref)}$ to O_b is explicitly represented by the three vectors $\bar{x}$, $\bar{y}$ and $\bar{z}$.

35.309. This translational motion moves the origin of the reference coordinate system to its destination, but leaves the three reference coordinate axes parallel to their respective initial directions. The three displaced reference coordinate axes, used as rotation-reference axes, are shown as the light dashed lines $X_{(ref)(rot)}$, $Y_{(ref)(rot)}$ and $Z_{(ref)(rot)}$. Rotating the rotation-reference coordinate system $X_{(ref)(rot)}$, $Y_{(ref)(rot)}$, $Z_{(ref)(rot)}$ to coincidence with the X_b, Y_b and Z_b axes requires three separate rotations, just as translation requires three separate linear motions. In the present instance, Fig. 35-47 shows that the process involves the following steps:

1) Rotate the coordinate system about the $X_{(ref)(rot)}$ axis to bring $Z_{(ref)(rot)}$ to $Z_{(ref)(rot)x}$, so that the Z_b axis will lie in the $X_{(ref)(rot)} - O_b - Z_{(ref)(rot)x}$ plane. As the result of this rotation, $Y_{(ref)(rot)}$ moves to $Y_{(ref)(rot)x}$. These two rotations take place through the angular displacement $A_{(x)(ref)(rot)}$.
2) Rotate the coordinate system about $Y_{(ref)(rot)x}$ through the angle $A_{(y)(ref)(rot)x}$ to bring $Z_{(ref)(rot)x}$ into coincidence with Z_b. In the meantime, $X_{(ref)(rot)}$ rotates to $X_{(ref)(rot)(y)x}$ through the same angle.
3) Rotate the coordinate system about the Z_b axis through the angle $A_{(z)b}$ to bring $Y_{(ref)(rot)x}$ and $X_{(ref)(rot)(y)x}$ into coincidence with Y_b and X_b, respectively.

35.310. The total rotation of the coordinate system in this example is accomplished by a set of three angles of rotation: $A_{(x)(ref)(rot)}$, $A_{(y)(ref)(rot)x}$ and $A_{(z)b}$. Similar processes can be used to rotate the coordinate system following other sequences of angles. A typical order is $A_{(y)(ref)(rot)}$, $A_{(z)(ref)(rot)y}$, $A_{(x)b}$. There are six possible sequences, which make use of a total of twelve angles; that is, four angles for each of the three principal axial directions. For example, the four angles $A_{(x)(ref)(rot)}$, $A_{(x)(ref)(rot)y}$, $A_{(x)(ref)(rot)z}$ and $A_{(x)b}$, are associated with the group of four possible x axes. Each angle is generated by rotation about the axis

designated by the subscript for that angle, and the four angles are all different. For this reason, the rotation of a coordinate system cannot be represented by a unique set of three angles about the three reference axes or the three body axes. However, when the angle of rotation is small, such as is the case in vibration measurement, the four angles $A_{(x)(ref)(rot)}$, $A_{(x)(ref)(rot)y}$, $A_{(x)(ref)(rot)z}$ and $A_{(x)b}$ become substantially equal to each other, and may be considered to be taken about a single axis, the $X_{(ref)(rot)}$ axis. Under this condition, the rotation of a coordinate system may be approximated by a unique set of three rotations about either the three reference axes or the three body axes.

35.311. An angular velocity of finite value is, in effect, the ratio of a small angular displacement to a short time interval, both chosen to be arbitrarily small. For this reason, an angular velocity in space can always be represented by a set of three component angular velocities. This same rule also applies to angular acceleration.

35.312. From the preceding discussion, it appears that, for measuring the vibration of a rigid body in space, three linear vibration receivers and three angular vibration receivers are needed to get the three components of the translational motion and the three components of the rotational motion, respectively. The six vibration receivers may be aligned with the axes of either the reference coordinate system or the body coordinate system.

35.313. Instead of using three linear vibration receivers and three angular vibration receivers to measure the vibration of a rigid body in space, an alternate scheme is to use six linear vibration receivers. The arrangement of the six vibration receivers and the relationship between the six components of motion of the vibrating member (the rigid body) and the linear displacements of the receivers are given in Derivation Summary 35-12. Generally speaking, the scheme described in Derivation Summary 35-12 offers more flexibility in operation than the use of two types of vibration receivers. It allows more freedom in the mounting of the receivers on the body and, because the arm distance between two parallel receivers may be adjusted, it introduces an adjustable sensitivity in the determination of angular motion. Economically, the simplification of using only one type of calibration and the reduction in maintenance and spare-unit allowance also favors the six-linear-receivers scheme. In fact, for ordinary laboratory purposes, three linear receivers are sufficient for a large number of vibration measurements. Three units can be used to measure three-dimensional translational motion in space, or translational motion in a plane plus rotational motion about an axis normal to the plane, or translational motion in a plane plus rotational motion about an axis in that plane.

TYPICAL EXAMPLE OF ANGULAR VIBRATION MEASUREMENT WITH LINEAR VIBRATION RECEIVERS

35.314. A typical example of how two vibration receivers can be used to measure angular motion is illustrated in Fig. 35-48. This figure represents the

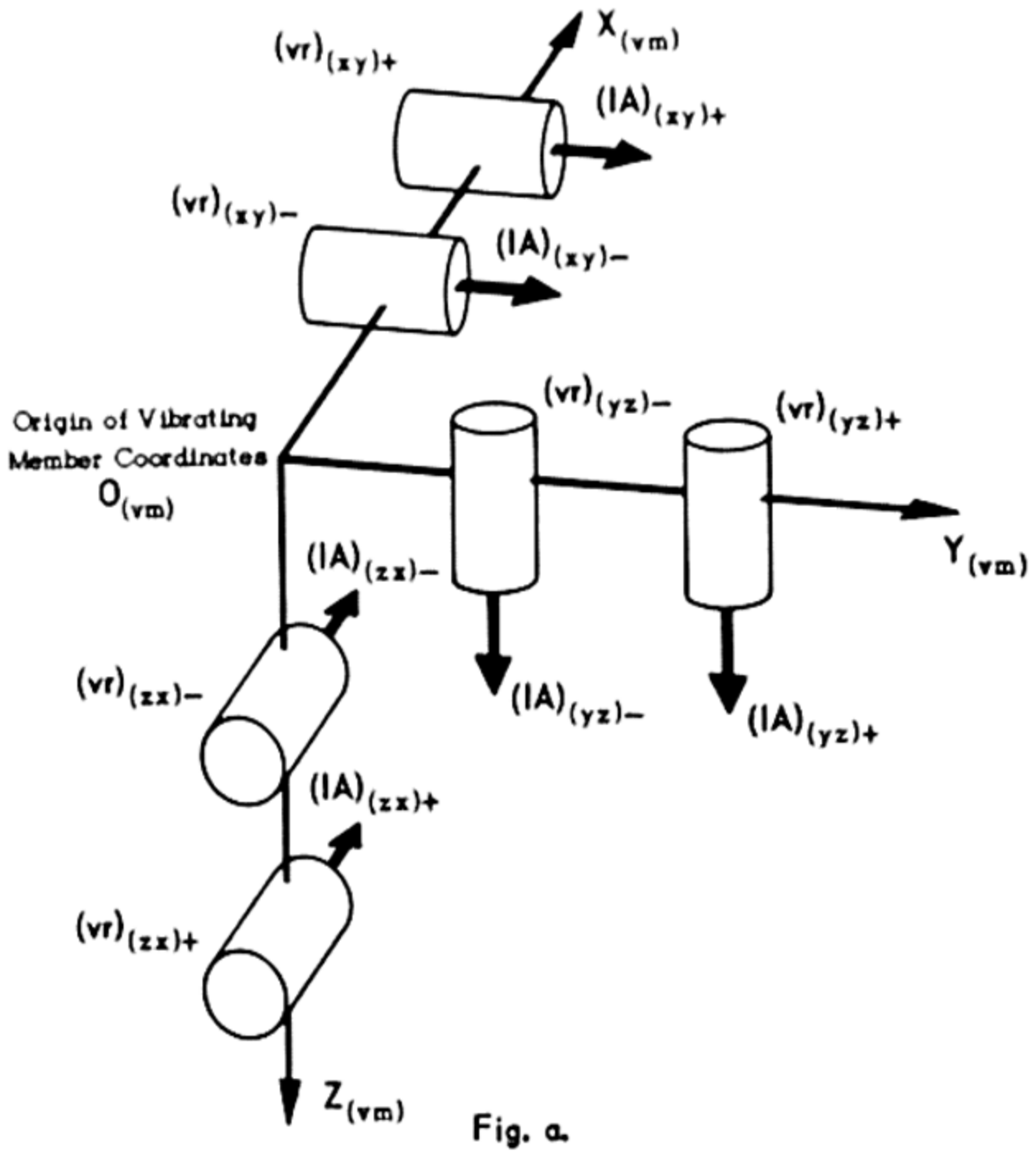


Fig. a.

The coordinate axis system shown in Fig. a is right handed, and the right-handed convention is used in all sequences; that is, x → y → z → x . . . The symbols appearing in Fig. a are defined as follows:

$X_{(vm)}$, $Y_{(vm)}$, $Z_{(vm)}$ = orthogonal axes fixed to vibrating member

$(vr)_{(ab)+}$ = vibration receiver located on the "a" axis, with its input axis parallel to, and in sense agreement with, the "b" axis; the receiver with the more positive position on the "a" axis

Example: $(vr)_{(xy)+}$ is the vibration receiver with the more positive position on the $X_{(vm)}$ axis, and has its input axis parallel to the $Y_{(vm)}$ axis, with the positive sense of the input axis in the direction of the positive $Y_{(vm)}$ axis.

$(vr)_{(ab)-}$ = vibration receiver located on the "a" axis, with its input axis parallel to, and in sense agreement with, the "b" axis; the receiver with the more negative position on the "a" axis

Example: $(vr)_{(yz)-}$ is the vibration receiver with the more negative position on the $Y_{(vm)}$ axis, and has its input axis parallel to the $Z_{(vm)}$ axis, with the positive sense of the input axis in the direction of the positive $Z_{(vm)}$ axis.

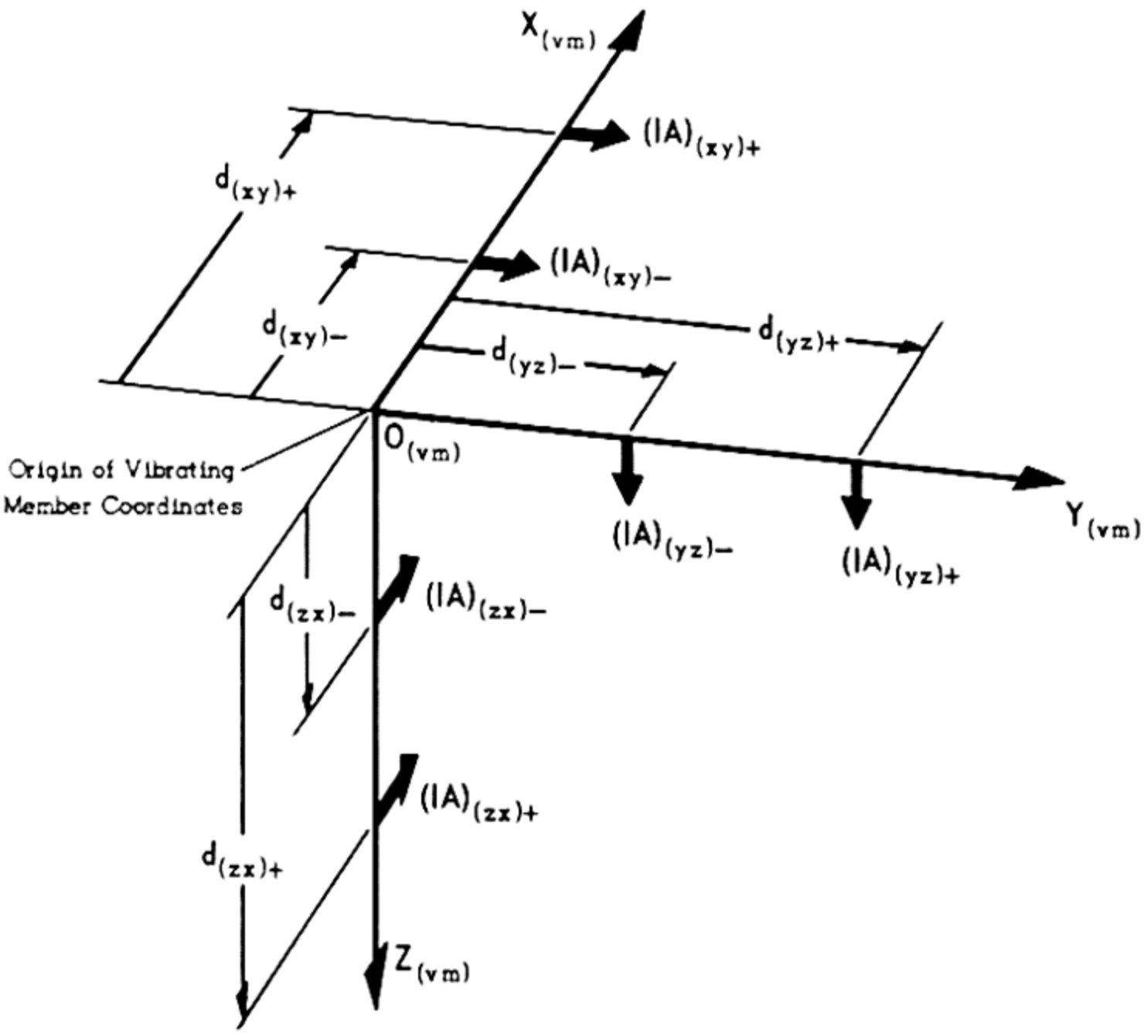
$(IA)_{(ab)+}$ = input axis of $(vr)_{(ab)+}$

$(IA)_{(ab)-}$ = input axis of $(vr)_{(ab)-}$

Example: $(IA)_{(zx)-}$ is the input axis of the vibration receiver located in the more negative position on the $Z_{(vm)}$ axis; the positive sense of this input axis is pointed along the positive direction of the X axis.

a) Schematic diagram showing the arrangement of six single-degree-of-freedom linear vibration receiver units used for receiving the generalized motion of a vibrating member

Derivation Summary 35-12. Schematic diagram showing use of six linear vibration receivers for the generation of signals to determine the generalized motion of a vibrating member; equations for expressing the vibration components in terms of linear displacements of the receivers.
(Page 1 of 6)



$d_{(ab)+}$ = distance of $(IA)_{(ab)+}$ from the origin of coordinates

$d_{(ab)-}$ = distance of $(IA)_{(ab)-}$ from the origin of coordinates

For example, $d_{(xy)+}$ is the distance of $(IA)_{(xy)+}$ from $O_{(vm)}$.

Fig. b.

b) Input-axis position and sense diagram for the six linear vibration receiver units used for receiving the generalized motion of a vibrating member

Definitions:

$X_{(vm)(ref)}$, $Y_{(vm)(ref)}$, $Z_{(vm)(ref)}$ = reference positions of the vibrating member coordinate axes (these axes are free from the vibratory motion under consideration); origin at $O_{(vm)(ref)}$

$X_{(vm)}$, $Y_{(vm)}$, $Z_{(vm)}$ = instantaneous positions of the vibrating member coordinate axes; origin at $O_{(vm)}$

$b_{[I-(vm)](ab)+}$ = displacement with respect to inertial space parallel to the "b" axis of the point of intersection of $(IA)_{(ab)+}$ with the "a" axis at the more positive vibration receiver position*

Examples:

$Y_{[I-(vm)](xy)+}$ = vibratory motion displacement with respect to inertial space and parallel to the $Y_{(vm)}$ axis of the intersection of $(IA)_{(xy)+}$ with the $X_{(vm)}$ axis

$Y_{(ref)[I-(vm)]O}$ = vibratory motion displacement with respect to inertial space and parallel to the $Y_{(vm)(ref)}$ axis of the origin of the vibrating member coordinates, $O_{(vm)}$

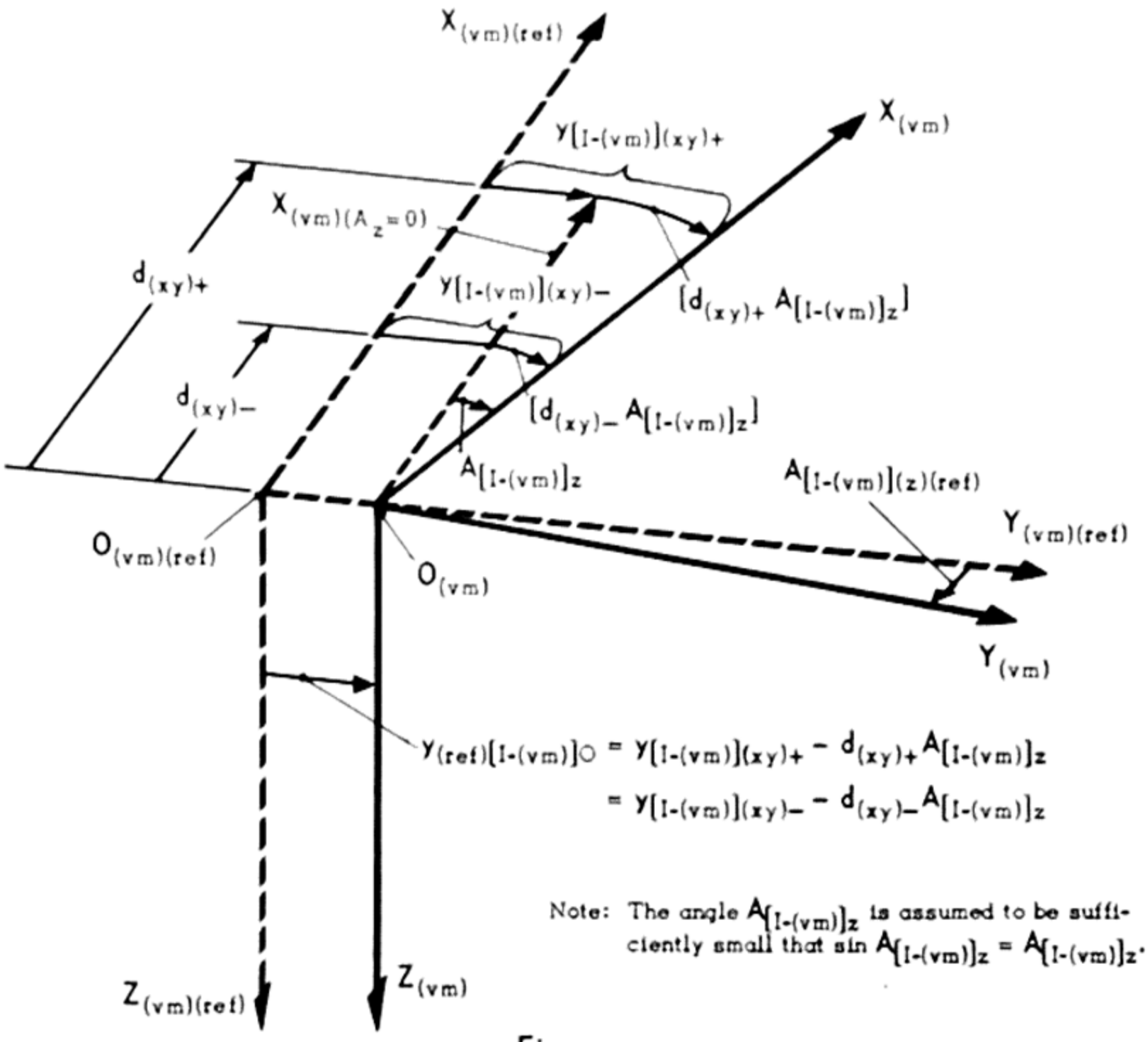
* In accordance with the conventions of Fig. 9-5 of Chapter 9, the subscript [I-(vm)] has "I" in the "reference subscript position" to show that the reference space is inertial space and (vm) in the "located subscript position" to show that the vibrating member is the entity whose position determines the identified geometrical quantity.

Derivation Summary 35-12. Schematic diagram showing use of six linear vibration receivers for the generation of signals to determine the generalized motion of a vibrating member; equations for expressing the vibration components in terms of linear displacements of the receivers.

(Page 2 of 6)

$A_{[I\text{-}(vm)]b}$ = rotation of the vibrating member with respect to inertial space about the "b" axis

Example: $A_{[I\text{-}(vm)]_z}$ is the rotation of the vibrating member with respect to inertial space about the $Z_{(vm)}$ axis, and therefore about the $Z_{(vm)(ref)}$ axis as well.*



Note: The angle $A_{[I\text{-}(vm)]_z}$ is assumed to be sufficiently small that $\sin A_{[I\text{-}(vm)]_z} = A_{[I\text{-}(vm)]_z}$.

Fig. c

Figure c illustrates the situation in which:

1) The $X_{(vm)}$, $Y_{(vm)}$, and $Z_{(vm)}$ coordinate system has a displacement with respect to a reference coordinate position that may be completely represented by a linear displacement of the origin along the direction of $Y_{(vm)(ref)}$.

2) This linear displacement is followed by a rotational displacement about the $Z_{(vm)(ref)}$ axis.

Similar situations may exist for separate linear displacements along $Z_{(vm)(ref)}$ and $X_{(vm)(ref)}$ combined with rotations about $X_{(vm)(ref)}$ and $Y_{(vm)(ref)}$, respectively.

The generalized motion of a vibrating member may be considered as the resultant of three linear displacement components and three rotational components, with each pair of linear and rotational components related by the pattern illustrated by Fig. c. When the individual components are of arbitrarily great size, the relationships among the resultant displacement and the components are given by complex trigonometric expressions involving coupling effects that prevent accurate results from being obtained when the components associated with a single axis are considered separately. This situation does not exist when the linear and angular displacement components all have sufficiently small magnitudes. As a rule, the vibratory

* The rotation of an object with respect to any particular axis is identical with the rotation of the object with respect to any axes parallel to the first axis. In the instance of Fig. c, this means that rotation with respect to the $Z_{(vm)}$ axis and rotation with respect to the $Z_{(vm)(ref)}$ axis are identical.

Derivation Summary 35-12. Schematic diagram showing use of six linear vibration receivers for the generation of signals to determine the generalized motion of a vibrating member; equations for expressing the vibration components in terms of linear displacements of the receivers.

motions for which measurements are required either are made up of components that are all small, or are simple in the sense that either a linear displacement along a single axis or a rotation about a single axis is involved. Geometrical relationships of these types may be developed on the basis of the pattern illustrated by Fig. c, which completely describes the displacement of the vibrating member along the $Y_{(vm)(ref)}$ axis and the rotation of the vibrating member about the $Z_{(vm)(ref)}$ axis.

From Fig. c,

$$y_{[I-(vm)](xy)+} = y_{(ref)[I-(vm)]O} + d_{(xy)+} A_{[I-(vm)]z} \tag{1}$$

$$y_{[I-(vm)](xy)-} = y_{(ref)[I-(vm)]O} + d_{(xy)-} A_{[I-(vm)]z} \tag{2}$$

Subtracting Eq. (2) from Eq. (1) and solving for $A_{[I-(vm)]z}$ gives

$$A_{[I-(vm)]z} = \frac{y_{[I-(vm)](xy)+} - y_{[I-(vm)](xy)-}}{d_{(xy)+} - d_{(xy)-}} \tag{3}$$

Adding Eqs. (1) and (2), and solving for $y_{(ref)[I-(vm)]O}$ gives

$$y_{(ref)[I-(vm)]O} = \frac{y_{[I-(vm)](xy)+} + y_{[I-(vm)](xy)-}}{2} - \frac{d_{(xy)+} + d_{(xy)-}}{2} A_{[I-(vm)]z} \tag{4}$$

Combining Eq. (3) with Eq. (4) shows that

$$y_{(ref)[I-(vm)]O} = \frac{y_{[I-(vm)](xy)+} + y_{[I-(vm)](xy)-}}{2} - \frac{d_{(xy)+} + d_{(xy)-}}{2(d_{(xy)+} - d_{(xy)-})} (y_{[I-(vm)](xy)+} - y_{[I-(vm)](xy)-}) \tag{5}$$

For working purposes, the fact that the displacements are for the vibrating member with respect to inertial space is apparent from context, so that Eqs. (3) and (5) may be written as

$$A_z = \frac{y_{(xy)+} - y_{(xy)-}}{d_{(xy)+} - d_{(xy)-}} \tag{6}$$

and

$$y_O = \frac{y_{(xy)+} + y_{(xy)-}}{2} - \frac{d_{(xy)+} + d_{(xy)-}}{2(d_{(xy)+} - d_{(xy)-})} (y_{(xy)+} - y_{(xy)-}) \tag{7}$$

Equations (6) and (7) become especially simple when $(vr)_{(xy)-}$ is placed on the negative side of the $X_{(vm)}$ axis at a distance equal in magnitude to the coordinate of $(vr)_{(xy)+}$ on the positive side of the $X_{(vm)}$ axis. This situation exists when $d_{(xy)-} = -d_{(xy)+}$. If, under these conditions, d_x is defined so that

$$d_x \equiv |d_{(xy)+}| \tag{8}$$

then Eqs. (6) and (7) become

$$A_z = \frac{y_{(xy)+} - y_{(xy)-}}{2d_x} \tag{9}$$

and

$$y_O = \frac{y_{(xy)+} + y_{(xy)-}}{2} \tag{10}$$

The order of motion shown in Fig. c may be reversed so that a rotational displacement is followed by a linear displacement, as shown in Fig. d.

From Fig. d,

$$y_{[I-(vm)](xy)+} = \frac{y_{(ref)[I-(vm)]O}}{\cos A_{[I-(vm)]z}} + d_{(xy)+} A_{[I-(vm)]z} \tag{11}$$

$$y_{[I-(vm)](xy)-} = \frac{y_{(ref)[I-(vm)]O}}{\cos A_{[I-(vm)]z}} + d_{(xy)+} A_{[I-(vm)]z} \tag{12}$$

When $A_{[I-(vm)]z}$ is a small angle,

$$\cos A_{[I-(vm)]z} = 1$$

Derivation Summary 35-12. Schematic diagram showing use of six linear vibration receivers for the generation of signals to determine the generalized motion of a vibrating member; equations for expressing the vibration components in terms of linear displacements of the receivers.

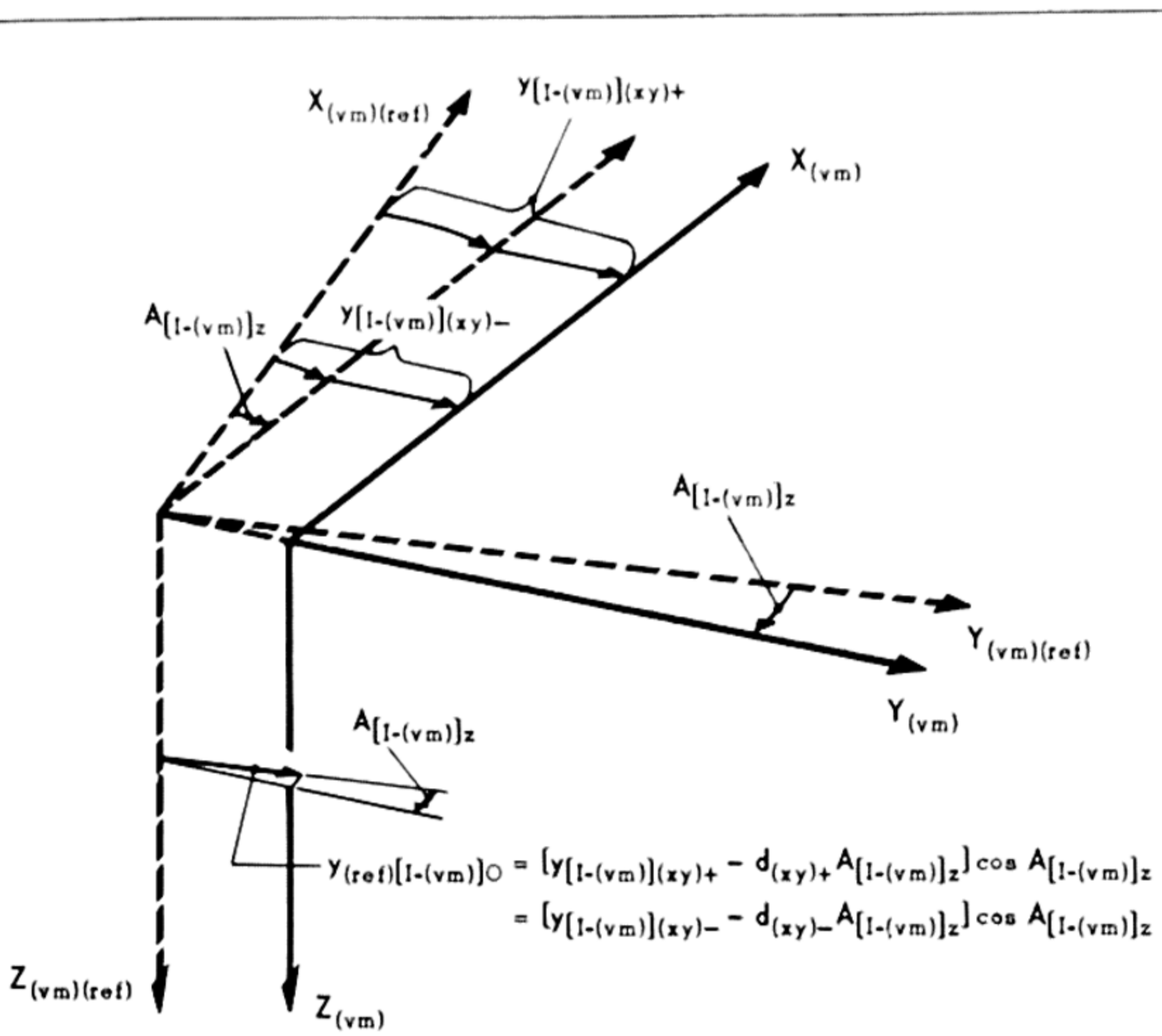


Fig. d.

and Eqs. (11) and (12) reduce to identity with Eqs. (1) and (2). For this reason, Eqs. (9) and (10) are valid for small angular displacements, no matter how the path of motion is prescribed.

c) *Linear displacement of vibrating member parallel to the* $Y_{(vm)(ref)}$ *axis and rotation about the* $Z_{(vm)(ref)}$ *axis in terms of linear displacements of the vibration receivers located on the* $X_{(vm)}$ *axis with their input axes parallel to the* $Y_{(vm)}$ *axis*

When motion of the vibrating member consists of displacements parallel to the $Z_{(vm)(ref)}$ axis and rotations about the $X_{(vm)(ref)}$ axis, the corresponding linear displacement and angular displacement components may be written down in terms of the linear displacements of the receivers located on the $Y_{(vm)}$ axis, from Eqs. (3), (5), (6), (7), (9) and (10), by a cyclic exchange of symbols in which $x \longrightarrow y$, $y \longrightarrow z$ and $z \longrightarrow x$, to give the following series of equations.

$$z_{(ref)[I-(vm)]O} = \frac{z_{[I-(vm)](yz)+} + z_{[I-(vm)](yz)-}}{2} - \frac{d_{(yz)+} + d_{(yz)-}}{2(d_{(yz)+} - d_{(yz)-})} (z_{[I-(vm)](yz)+} - z_{[I-(vm)](yz)-}) \tag{13}$$

$$A_{[I-(vm)]x} = \frac{z_{[I-(vm)](yz)+} - z_{[I-(vm)](yz)-}}{d_{(yz)+} - d_{(yz)-}} \tag{14}$$

In working variable symbols,

$$z_O = \frac{z_{(yz)+} + z_{(yz)-}}{2} - \frac{d_{(yz)+} + d_{(yz)-}}{2(d_{(yz)+} - d_{(yz)-})} (z_{(yz)+} - z_{(yz)-}) \tag{15}$$

Derivation Summary 35-12. Schematic diagram showing use of six linear vibration receivers for the generation of signals to determine the generalized motion of a vibrating member; equations for expressing the vibration components in terms of linear displacements of the receivers.
(Page 5 of 6)

$$A_x = \frac{z_{(yz)+} - z_{(yz)-}}{d_{(yz)+} - d_{(yz)-}} \tag{16}$$

When

$$d_{(yz)-} = -d_{(yz)+} \tag{17}$$

and

$$d_y \equiv |d_{(yz)+}| \tag{18}$$

then

$$z_{\bigcirc} = \frac{z_{(yz)+} + z_{(yz)-}}{2} \tag{19}$$

$$A_x = \frac{z_{(yz)+} - z_{(yz)-}}{2d_y} \tag{20}$$

d) Linear displacement of the vibrating member along the $Z_{(vm)(ref)}$ axis and rotation about the $X_{(vm)(ref)}$ axis in terms of linear displacements of the vibration receivers located on the $Y_{(vm)}$ axis

A cyclic change of symbols in Eqs. (13) through (20) in which z⟶x, y⟶z, and x⟶y gives the corresponding series of equations when motion of the vibrating member consists of displacements parallel to the $X_{(vm)(ref)}$ axis and rotations about the $Y_{(vm)(ref)}$ axis.

$$x_{(ref)[I-(vm)]\bigcirc} = \frac{x_{[I-(vm)](zx)+} + x_{[I-(vm)](zx)-}}{2} - \frac{d_{(zx)+} + d_{(zx)-}}{2(d_{(zx)+} - d_{(zx)-})}(x_{[I-(vm)](zx)+} - x_{[I-(vm)](zx)-}) \tag{21}$$

$$A_{[I-(vm)]y} = \frac{x_{[I-(vm)](zx)+} - x_{[I-(vm)](zx)-}}{d_{(zx)+} - d_{(zx)-}} \tag{22}$$

In working variable symbols,

$$x_{\bigcirc} = \frac{x_{(zx)+} + x_{(zx)-}}{2} - \frac{d_{(zx)+} + d_{(zx)-}}{2(d_{(zx)+} - d_{(zx)-})}(x_{(zx)+} - x_{(zx)-}) \tag{23}$$

$$A_y = \frac{x_{(zx)+} - x_{(zx)-}}{d_{(zx)+} - d_{(zx)-}} \tag{24}$$

When

$$d_{(zx)-} = -d_{(zx)+} \tag{25}$$

and

$$d_z \equiv |d_{(zx)+}| \tag{26}$$

then

$$x_{\bigcirc} = \frac{x_{(zx)+} + x_{(zx)-}}{2} \tag{27}$$

$$A_y = \frac{x_{(zx)+} - x_{(zx)-}}{2d_z} \tag{28}$$

e) Linear displacement of the vibrating member along the $X_{(vm)(ref)}$ axis and rotation about the $Y_{(vm)(ref)}$ axis in terms of linear displacements of the vibration receivers located on the $Z_{(vm)}$ axis

Derivation Summary 35-12. Schematic diagram showing use of six linear vibration receivers for the generation of signals to determine the generalized motion of a vibrating member; equations for expressing the vibration components in terms of linear displacements of the receivers.

(Page 6 of 6)

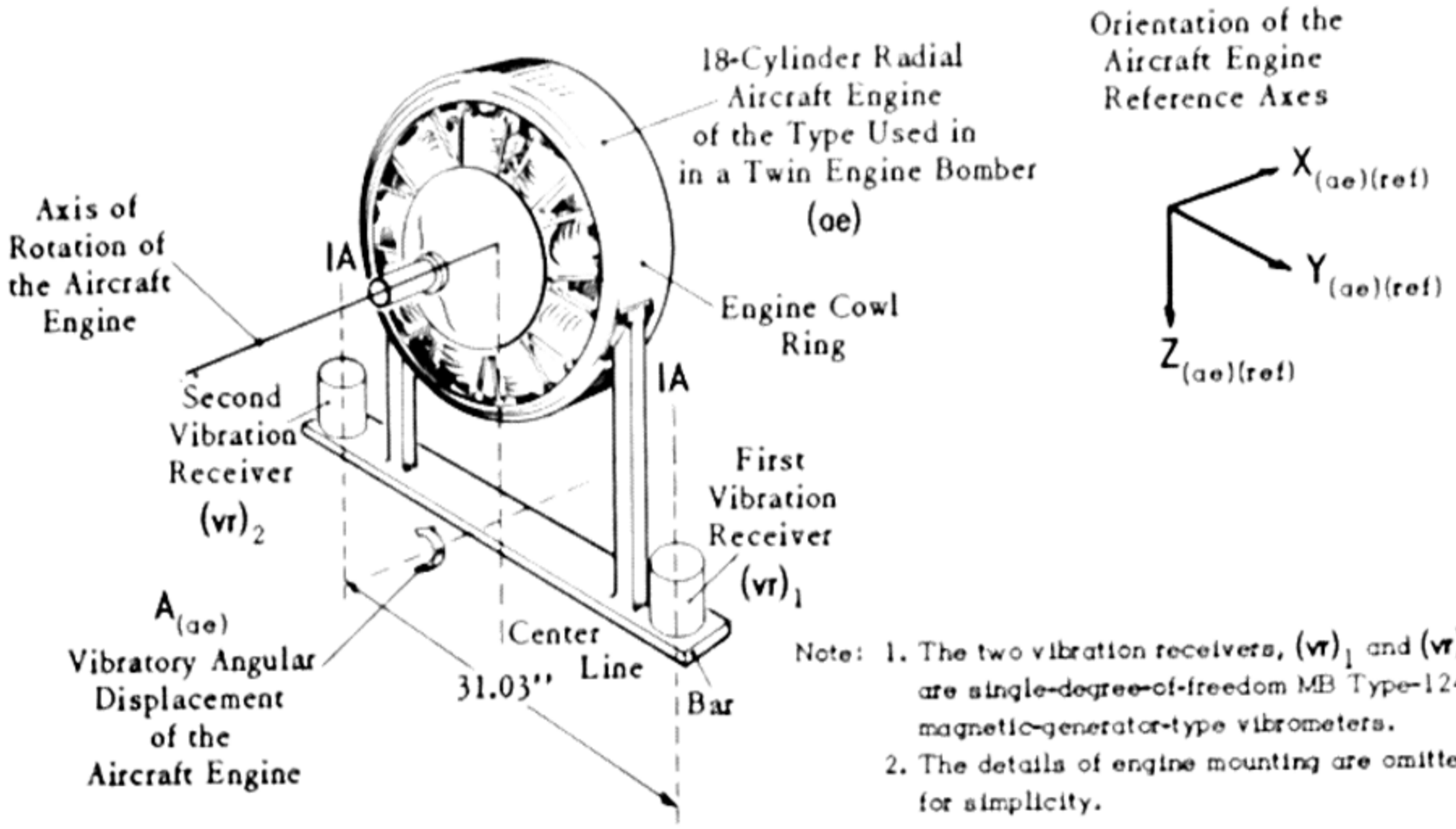


Fig. 35-48. Test setup for determining the angular vibration of an aircraft engine.

test setup for studying the vibratory motion of an 18-cylinder, radial aircraft engine of the type used in a twin-engine bomber. The problem of special interest is the torsional vibration of the engine under a one-spark-misfiring condition during the run-up period before take off. A radial engine has a torsional vibration forcing function whose fundamental frequency is equal to one-half the number of cylinders multiplied by the speed of the engine. When one cylinder misfires, a vibratory component of a lower frequency, equal to one-half the engine speed, becomes prominent. The magnitude of the vibration at this frequency may be used as an indication of the malfunctioning of the engine operation.

35.315. As shown in Fig. 35-48, two single-degree-of-freedom MB Type-124 magnetic-generator-type vibrometers* are mounted on a bar that is rigidly attached to the engine casing. The vibration receivers are placed on opposite sides of the engine at equal distances from the engine center line. The input axes of the vibration receivers are perpendicular to the axis of rotation of the engine, and are set 31.03 inches apart. Equation (16) of Derivation Summary 35-12 shows that, under these conditions, the vibratory angular displacement of the aircraft engine, $A_{(ae)}$, about the axis of rotation (the $X_{(ae)(ref)}$ axis) is given by the difference of the displacements received by the velocity receivers along the $Z_{(ae)(ref)}$ axis divided by the distance between their input axes; that is,

$$A_{(ae)} = \frac{z_{(vr)1} - z_{(vr)2}}{31.03}$$

35.316. A functional diagram showing the tie-in of the vibration recording system used with the test setup of Fig. 35-48 is given in Fig. 35-49. As indicated, the output signals from the two vibration receivers are fed into a signal comparator,

* The construction of this type of linear velocity vibration receiver, whose seismographic system operates in the vibrometer range, is shown in Fig. 35-7g.

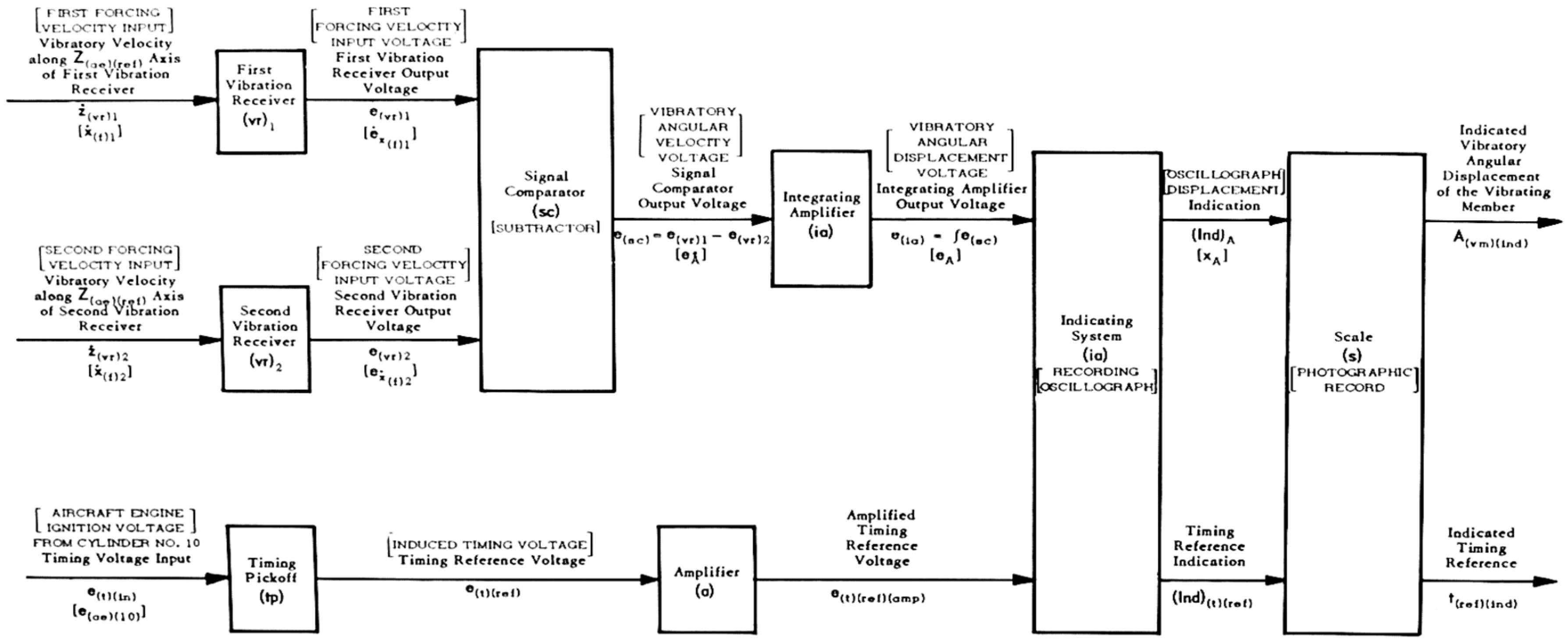


Fig. 35-49. Functional diagram of the aircraft-engine-torsional-vibration recording system.

which produces an output voltage equal to the difference between the vibration receiver voltage signals, and therefore proportional to the vibratory angular velocity of the aircraft engine assembly, $A_{(ae)}$. The output signal from the signal comparator is then integrated to give a signal proportional to the vibratory angular displacement, $A_{(rot)}$. For recording purposes, a Consolidated Type 5-114-P4 oscillograph with a Type 7-219 500-cps galvanometer is used to produce a photographic record.

35.317. When either vibration receiver is used separately with the recording system, the sensitivity of this vibration-measuring system at an amplifier gain setting of -39 decibels is

$$S_{(vms)[x;x]} = \frac{1}{18.4 \times 10^{-3}} \frac{\text{inches of spot deflection}}{\text{inch of vibration}}$$

The sensitivity of the over-all receiver-bar-oscillograph arrangement system used as an angular-vibration-measuring system is equal to this value multiplied by the center-to-center distance of the two linear vibration receivers; that is,

$$S_{(vms)(A;x)} = \frac{31.03}{18.4 \times 10^{-3}} = 1.69 \frac{\text{inches of spot deflection}}{\text{milliradian of angular vibration}} = 29.5 \frac{\text{inches}}{\text{degrees}}$$

35.318. The MB Type-124 magnetic-generator-type vibrometer has an undamped natural frequency of 4.75 cycles per second and a damping ratio of 0.65. The magnetic generator used in this receiver produces a voltage signal proportional to the relative velocity of the seismic mass. For this reason, the dynamic performance of the MB Type-124 vibrometer used in conjunction with an ideal integrator is identical with that of a (2;0, 1, 2) second-order system.* The frequency response curve of the vibrometer – ideal integrator combination is shown in Fig. 35-50a.

35.319. The integrating amplifier actually used has a time constant of about 5 seconds. The ratio of the dynamic performance of the actual integrator to that of an ideal integrator is identical with that of a (1;0,1) system and is shown in Fig. 35-50b. Figure 35-50c shows the performance of the recording oscillograph. The dynamic performance characteristics of the combined receiver-integrator-oscillograph system, shown in Fig. 35-50d, is given by the product of the three curves shown in Figs. 35-50a, b and c. The value of the reference period used to reduce the three curves to a common time base is 0.1 second, so that the reference frequency is 10 cycles per second.

35.320. The engine speed during the run-up period is 2040 revolutions per minute; with 18 cylinders firing, the normal-operation fundamental harmonic is 306 cycles per second. The corresponding single-cylinder-misfire fundamental frequency is 17 cycles per second. This range of operation is marked by shaded lines in Fig. 35-50d. Over practically all of this range, the dynamic error of the vibration-measuring system is less than 1 percent.

* See Derivation Summary 35-3.

35.321. The actual record of the torsional oscillation of the engine on its mount with one cylinder misfiring is reproduced in Fig. 35-51. In this record, the amplitude due to the misfiring is about 0.051 degree while the fundamental harmonic during normal operation has an amplitude of the order of 0.0339 degree.

DISPLACED COSINE PULSE FORCING FUNCTIONS

35.322. The response of systems to displaced cosine pulse function inputs is described at the end of Chapter 32. By reference to the material in Chapter 25, a general method is presented in Chapter 32 for calculating performance functions for systems from pulse function responses. In particular, the performance parameters for operating systems associated with (0;0, 1, 2) performance functions may be determined from displaced cosine pulse responses by employing Figs. 32-42, 32-43 and 32-44. For details of the use of these figures, refer to Chapters 25 and 32.

35.323. Response characteristics to displaced cosine pulse forcing functions are extended in this chapter to operating systems associated with (1, 0;0, 1, 2) performance equations. Examples of such systems are the vibratory motion isolation system of Derivation Summary 35-7 and the vibratory force isolation system of Derivation Summary 35-9. Many other examples occur, particularly in closed-chain components.

35.324. The three accompanying figures correspond to the three similar figures in Chapter 32: Figs. 32-42, 32-43 and 32-44. Figure 35-52 shows the variation of the height of the first response peak as a function of pulse duration when the pulse height is kept constant. Each curve is for a constant damping ratio. It should be noted that the curves fall close together. When the abscissa is unity, that is, when the pulse duration and the undamped natural period of the system are equal, the first response peak is always greater than the pulse height. As the pulse decreases in duration, compared to the system undamped natural period, the first response peaks of lightly damped systems decrease more rapidly than those of systems with larger damping ratios. However, it can be seen that the system with a damping ratio of 0.3 decreases most quickly. As the damping ratio decreases to 0.01, the height of the first response peak increases for a given pulse duration and undamped natural period. These curves are distinctly different from the corresponding curves for a (0;0, 1, 2) system, shown in Fig. 32-42.

35.325. Ratios of peak response delay to pulse duration are shown as a function of damping ratio and undamped natural period – pulse duration ratio in Fig. 35-53. These curves are all separate and distinct for values of the abscissa greater than 0.6. In general, the peak response delay is less for (1, 0;0, 1, 2) systems than for (0;0, 1, 2) systems, as may be seen by comparing Fig. 35-53 with Fig. 32-43.

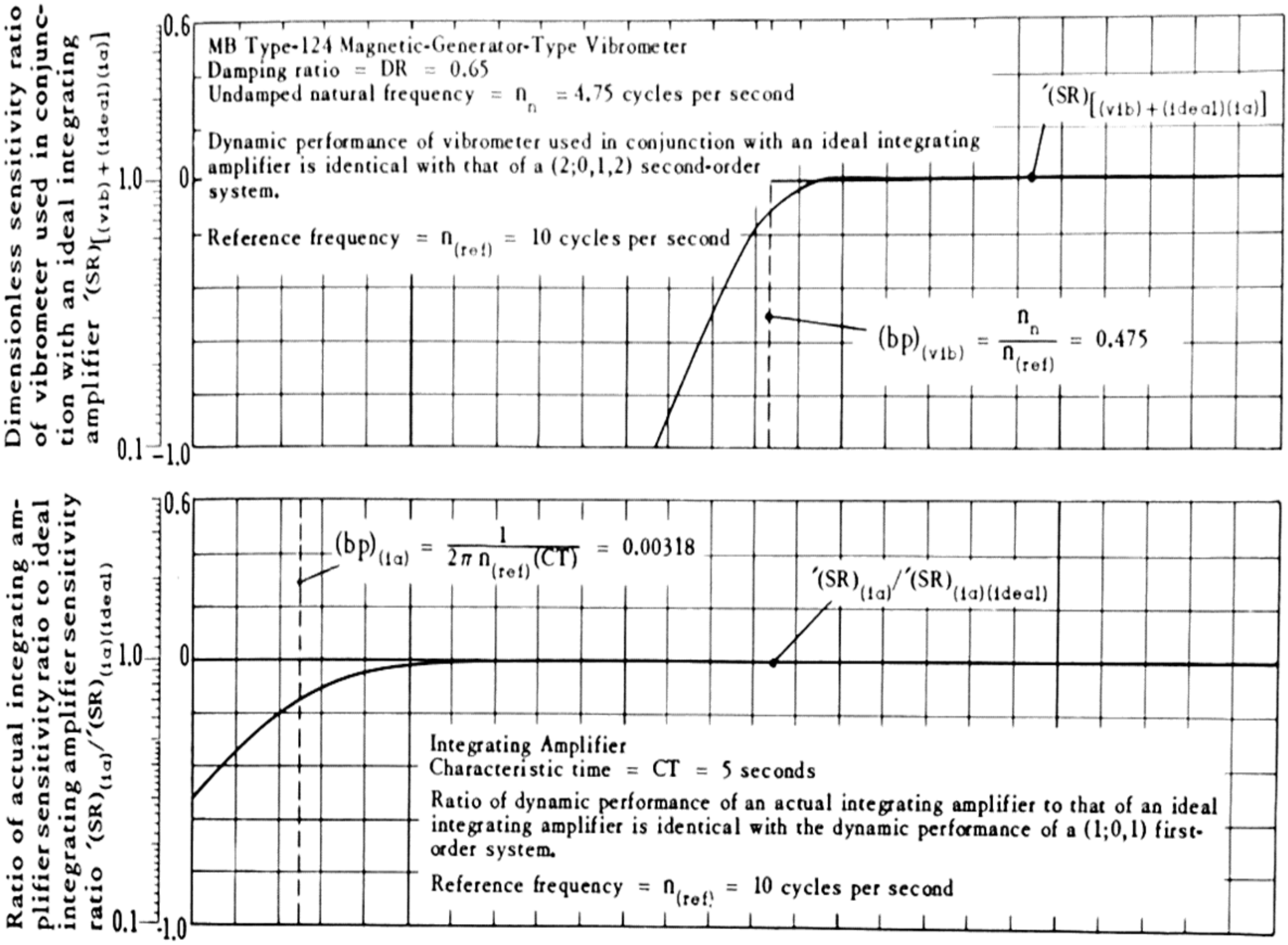


Fig. 35-50. Dynamic response characteristics of the combined receiver-integrator-oscillograph system used to measure the vibratory motion of an 18-cylinder, radial aircraft engine.

Test record for Pratt & Whitney aircraft engine R-2800-79, Serial No. FP-023441; Record No. 1159 Date: May 20, 1953
Engine speed is 2040 rpm; 2 plugs shorted on cylinder No. 6
Propeller ratio is 2:1; blower ratio is 7.6:1

Note: Scale sensitivity = $0.590 \frac{\text{milliradian of angular vibration amplitude}}{\text{inch of record deflection}} = 0.0339 \frac{\text{degree of angular vibration amplitude}}{\text{inch of record deflection}}$

The timing mark is a pip produced by cylinder No. 10. It occurs every two revolutions. Therefore, distance between pips is 1/2040 x 2 minute = 1/1020 minute = 0.0588 second.

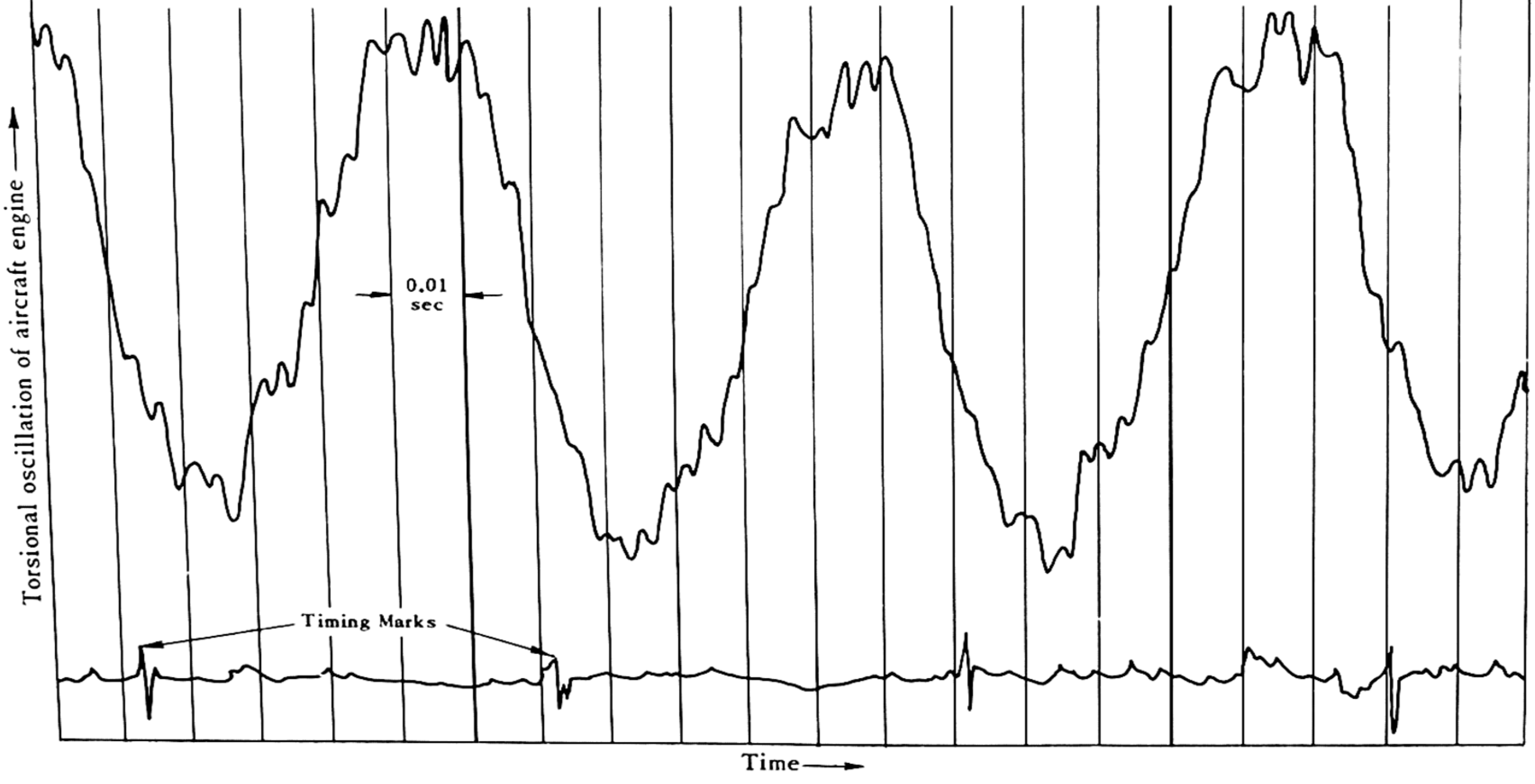


Fig. 35-51. Actual test record of the torsional oscillation of a Pratt & Whitney R-2800-79 aircraft engine on its mount with one cylinder misfiring.

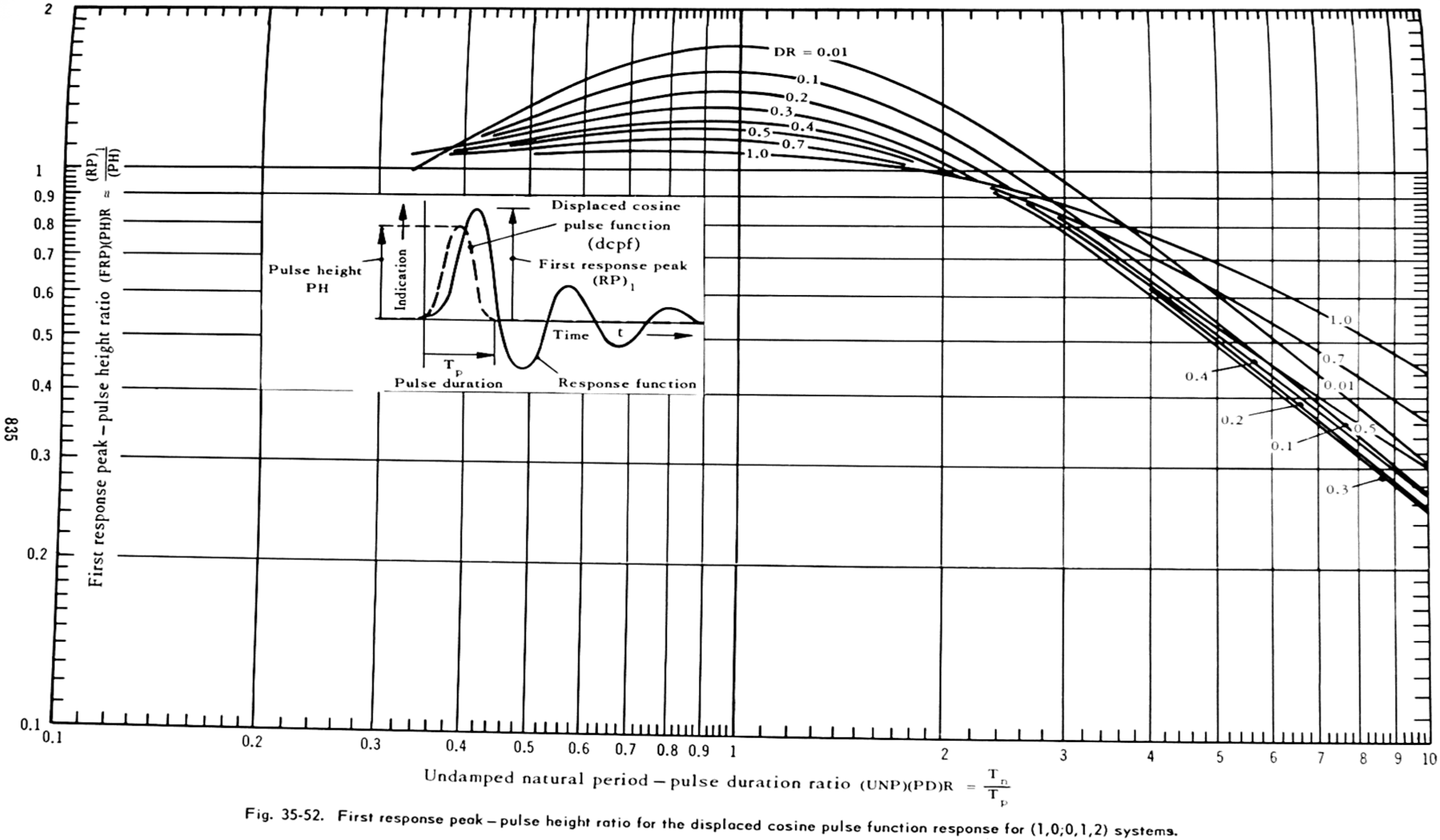


Fig. 35-52. First response peak – pulse height ratio for the displaced cosine pulse function response for (1,0;0,1,2) systems.

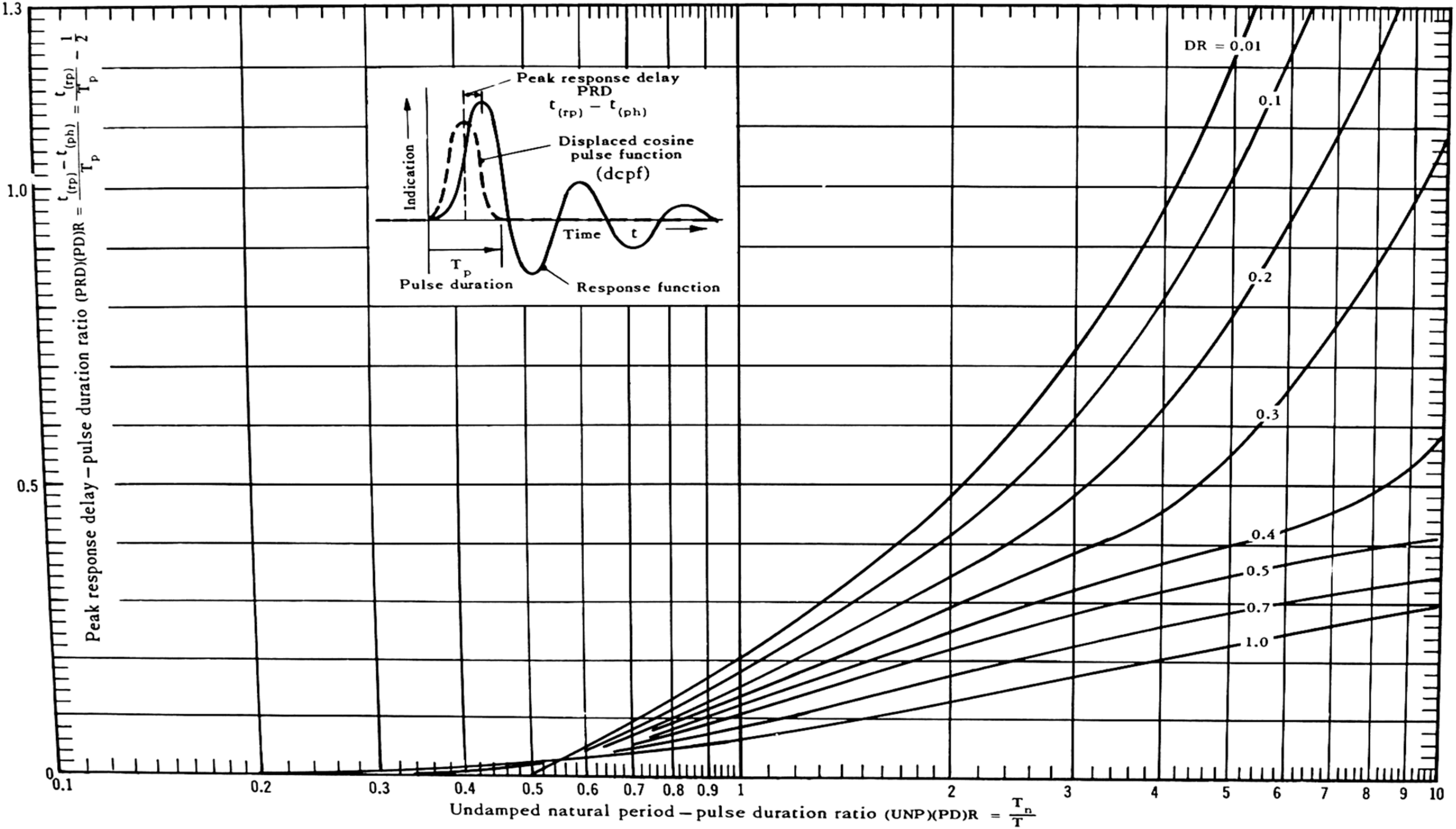


Fig. 35-53. Peak response delay – pulse duration ratio for the displaced cosine pulse function response for (1,0;0,1,2) systems.

35.326. The grid in Fig. 35-54 is obtained by combining the curves of Figs. 35-52 and 35-53. It corresponds to that of Fig. 32-44. When it is known that a particular system may be associated with a (1,0;0,1,2) performance function, the performance parameters can be determined from a single displaced cosine pulse function response. The nondimensional ratios defining the abscissa and ordinate of Fig. 35-54 are computed from the pulse duration, the pulse height, the first response peak height, and the time after the start of the pulse at which the first response peak occurs. Entering the figure with the nondimensional ratios locates a single point on the grid associated with a unique value of damping ratio and pulse duration – undamped natural period ratio. The curves in all three figures cover a damping ratio range of 0.01 to 1.0; higher damping ratios are not useful in vibratory motion or force isolation systems.

ILLUSTRATIVE EXAMPLES OF ISOLATION SYSTEMS ASSOCIATED WITH (1,0;0,1,2) PERFORMANCE EQUATIONS

35.327. Two examples are included that illustrate possible uses of Figs. 35-52, 35-53 and 35-54. The first concerns a typical instrument installation in an aircraft: the recording oscillograph of Fig. 35-55 is to be isolated from vibratory motions of the supporting rack. The effectiveness of a given vibration isolation system is evaluated. The second example is an estimate of the performance of an aircraft engine vibration mount for various engine speeds when the engine misfires.

RECORDING OSCILLOGRAPH VIBRATORY MOTION ISOLATION SYSTEM

35.328. The recording oscillograph shown in Fig. 35-55 is mounted on four vibration isolators. The supporting rack is designed for aircraft installation. Reference to the figure of section a in Derivation Summary 35-7 shows that the recording oscillograph may be identified with the isolated member, the vibration isolators are equivalent to the elastic and viscous damping elements, and the supporting rack corresponds to the support. The assembly shown in Fig. 35-55 represents a vibratory motion isolation system for three translatory degrees of freedom. For vertical motion, considered in the following paragraphs, the system is assumed to be associated with a (1,0;0,1,2) performance equation as developed in Derivation Summary 35-7. Performance parameters of the system are given in Fig. 35-55.

35.329. Under the weight of the recording oscillograph, the vibration isolator cores deflect 0.15 inch, which is almost half their maximum possible axial displacement. If the motion of the recording oscillograph with respect to the supporting rack exceeds half the maximum vibration isolator core axial displacement, the oscillograph strikes limit stops and "bottoms." That is, bottoming occurs if the relative displacement exceeds 0.188 inch.

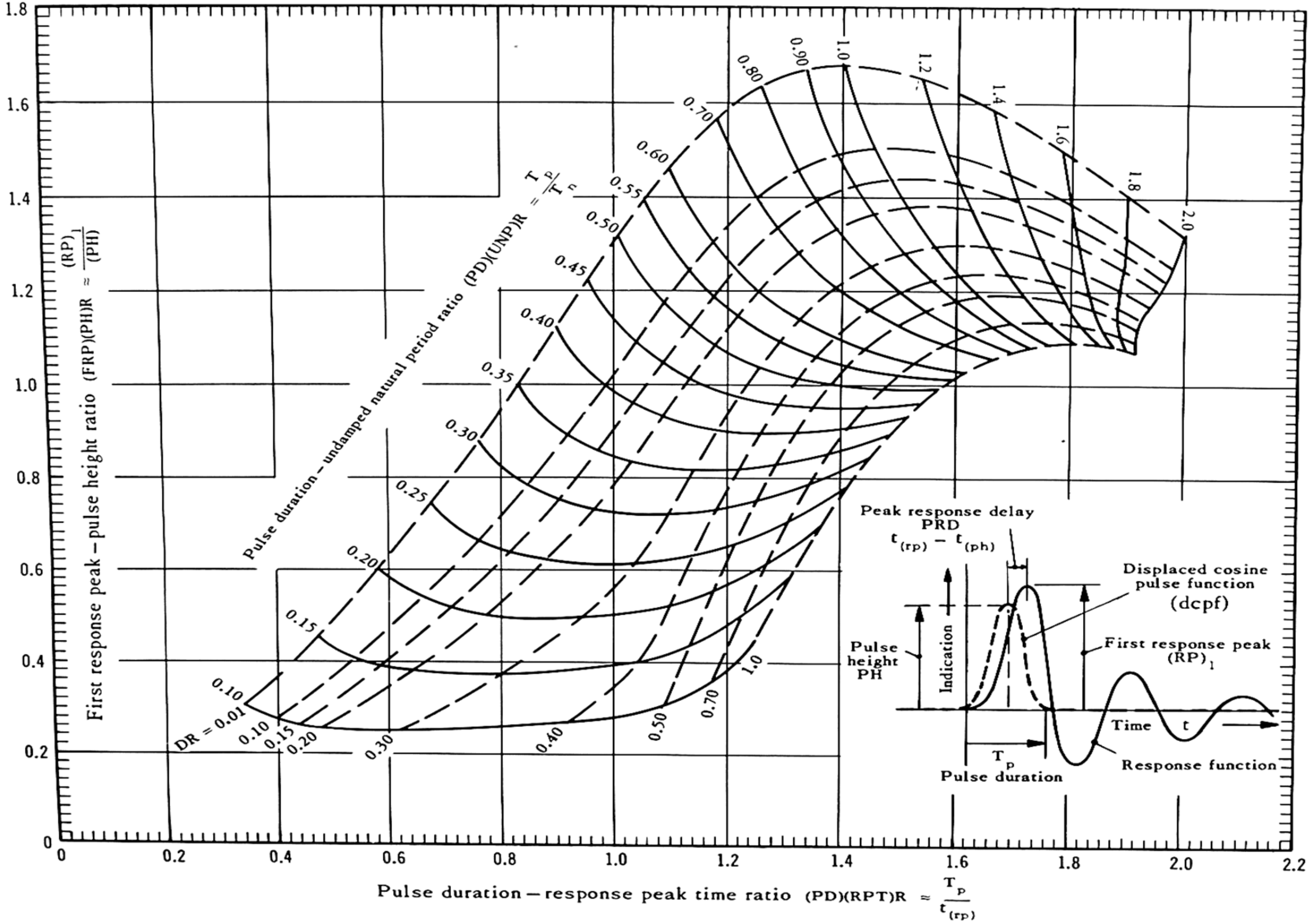
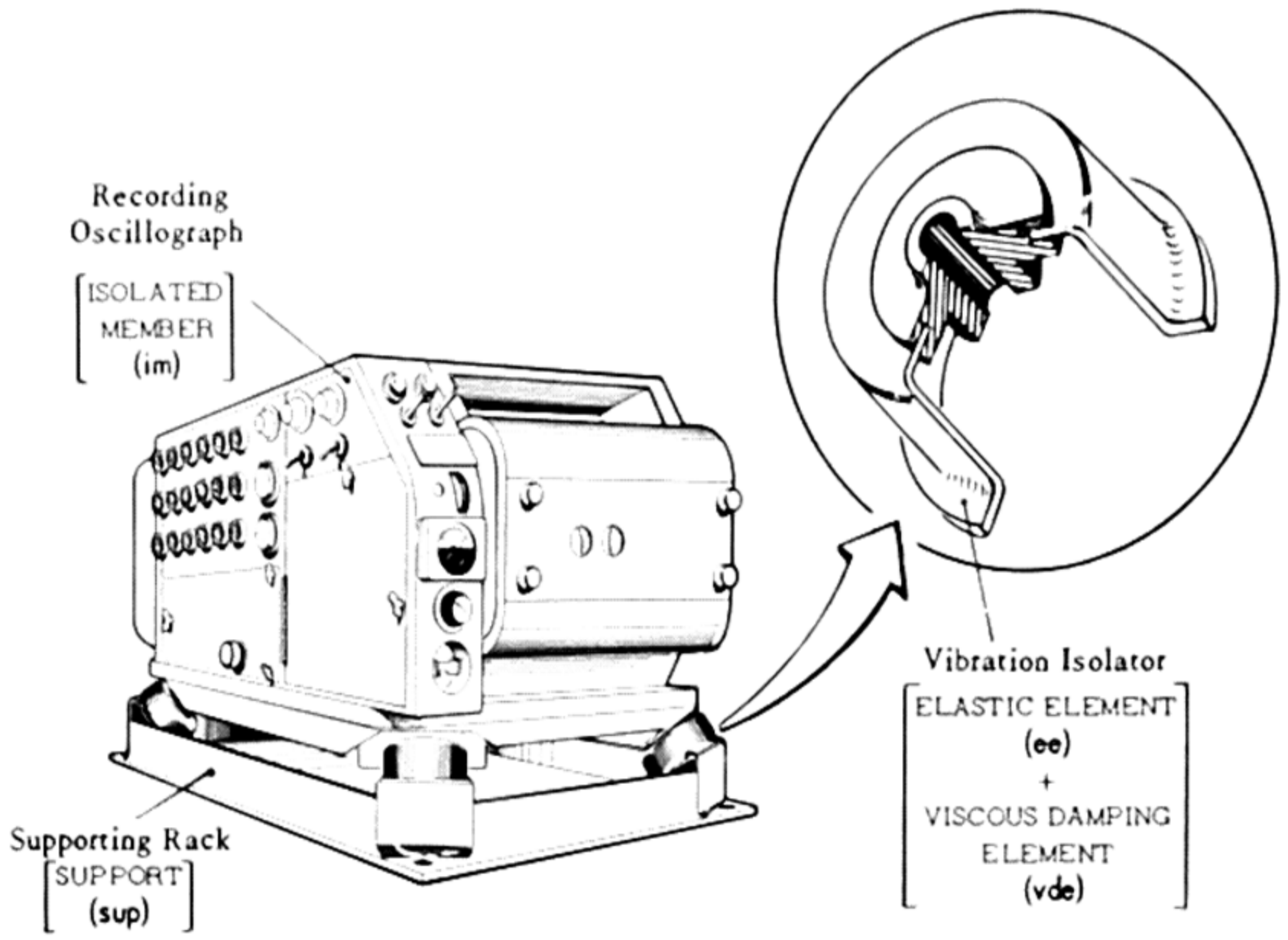


Fig. 35-54. Nondimensional first response peak characteristics associated with (1,0;0,1,2) systems.



Weight of recording oscillograph	65 lbs
Elastic coefficient of vibration isolation assembly	430 lbs/inch
Maximum axial displacement of vibration isolator core	0.375 inch

Specification Values of Vibratory Motion Isolation System Performance Parameters

Undamped natural frequency	8 cps
Damping ratio	0.14

Fig. 35-55. Typical installation of an instrument for vibratory motion isolation.

35.330. It is required of the vibratory motion isolation system that the recording oscillograph follow the major motion of the base while at the same time be free of base motion disturbances. For example, if the recording oscillograph is mounted in an aircraft, it should move with the aircraft without bottoming on the limit stops of the vibration isolators. This requires a certain stiffness of the mounts. On the other hand, to be free of the disturbing motions due to propeller or engine vibration, the undamped natural frequency of the vibratory motion isolation system must be low compared with the disturbance frequency. This follows from the discussion of Derivation Summary 35-7 and the associated figures. A compromise solution is required, which may be obtained by the methods implied in the following two paragraphs.

35.331. First, consider the motion of the recording oscillograph with respect to inertial space. The oscillograph is assumed to be in an aircraft installation where the supporting rack vibrates at a frequency of 1800 cycles per minute due to propeller vibration. The amplitude of the motion is 0.005 inch. The forcing frequency corresponds to 30 cycles per second. When the reference frequency is taken as equal to the undamped natural frequency of the vibratory motion isolation system, 8 cycles per second, the forcing frequency ratio is 3.75. From Fig. 35-36, it is found that for a frequency ratio equal to 3.75 and a damping ratio

equal to 0.14 the dynamic amplitude ratio of a (1,0;0,1,2) system is 0.126. The amplitude of the recording oscillograph displacement with respect to inertial space is 0.00063 inch, an order of magnitude smaller than that of the supporting rack.

35.332. Second, determine how well the instrument follows relatively slow motions of the base. Let the supporting rack motion be a displaced cosine pulse. This may arise, for example, when the aircraft rolls over a bump on the runway. The motion of the supporting rack may be approximated by a displaced cosine pulse with a duration proportional to the ratio of the length of the bump to the speed of the aircraft. Peak responses to displaced cosine pulse forcing functions for (1,0;0,1,2) systems may be determined from Fig. 35-52. When the undamped natural period – pulse duration ratio is less than 0.3, the recording oscillograph displacement for a damping ratio of 0.14 is substantially that of the supporting rack. For a system with an undamped natural period of 0.125 second, the pulse duration should therefore not be less than 0.375 second. The curves of Fig. 35-52 refer to the first peak displacement of the isolated member. After the passage of the pulse, a residual transient oscillation may persist. For pulse durations exceeding 0.375 second, the amplitude of the transient is small and the force on the recording oscillograph due to bottoming is probably slight. The nonlinear character of the vibration isolator performance near the stops will also minimize the acting forces.

AIRCRAFT ENGINE VIBRATORY TORQUE ISOLATION SYSTEM

35.333. The aircraft engine installation shown in Fig. 35-56 represents a Pratt & Whitney R-2800-79 engine supported by vibration isolators in an engine mount. Comparison of Fig. 35-56 with the figure in section a of Derivation Summary 35-9 shows that the engine may be identified with the vibrating member, and the engine mount with the support. For torques generated in the engine, the vibratory torque isolation system consisting of the engine, vibration isolators and engine mount may be associated with a (1,0;0,1,2) performance equation as described in Derivation Summary 35-9. The input quantity is vibratory torque applied to the engine. The output quantity is torque applied to the engine mount. From experimental information, it has been found that the vibratory torque isolation system of Fig. 35-56 has an undamped natural frequency, n_n, of 3 cycles per second and a damping ratio, DR, equal to 0.1.

35.334. The torque developed in a single cylinder due to gas pressure variations during the active half cycle is shown in Fig. 35-57. It occurs for one revolution of the crankshaft. No pressures or torques due to contained gases exist during the next crankshaft revolution. A possible approximation by a displaced cosine pulse function is superimposed upon the cylinder gas torque in the figure. The pulse duration is 0.305 of the time for one crankshaft revolution.

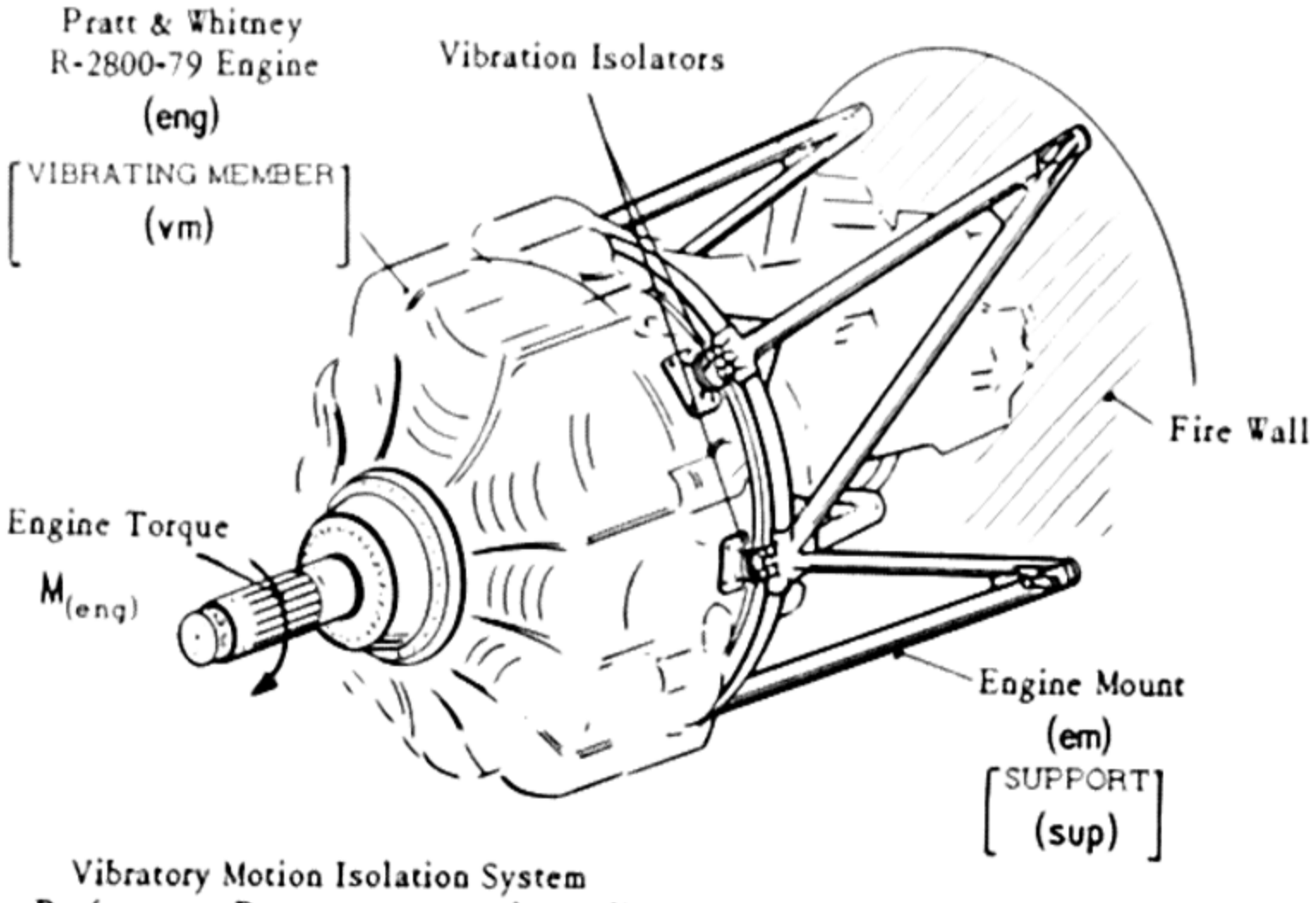


Fig. 35-56. Typical installation of an aircraft engine for vibratory torque isolation.

35.335. When the engine is running, the generated torque vibration is opposed by the stiffness of the vibration isolators on the engine mount. The total range of vibration isolator core motion is 0.25 inch. At cruising speeds, the stiffness is adjusted so that the equilibrium core displacement is 0.125 inch.

35.336. The misfire of a single cylinder is equivalent to imposing a torque variation upon the engine like the cylinder gas torque of Fig. 35-57 in the negative sense. Within the approximation shown in the figure, it may be considered that a displaced cosine pulse in torque is applied to the engine opposing the average engine torque. The torque applied to the engine mount due to a single cylinder misfire therefore resembles the response curve shown in the insert of Figs. 35-52, 35-53 and 35-54.

35.337. For an 18-cylinder engine, each cylinder supplies one-ninth of the average engine torque per crankshaft revolution. From Fig. 35-57, the maximum cylinder gas torque is 5.5 times the average cylinder torque per crankshaft revolution. The displaced cosine pulse peak is 1.1 times the gas torque peak, so that

$$M_{(max)(dcpf)} = \frac{5.5 \times 1.1}{9} M_{(eng)(av)} = 0.67\ M_{(eng)(av)}$$

35.338. In the accompanying tabulation of Data Analysis Summary 35-1, pulse duration is related to engine speed. Pulse duration – undamped natural

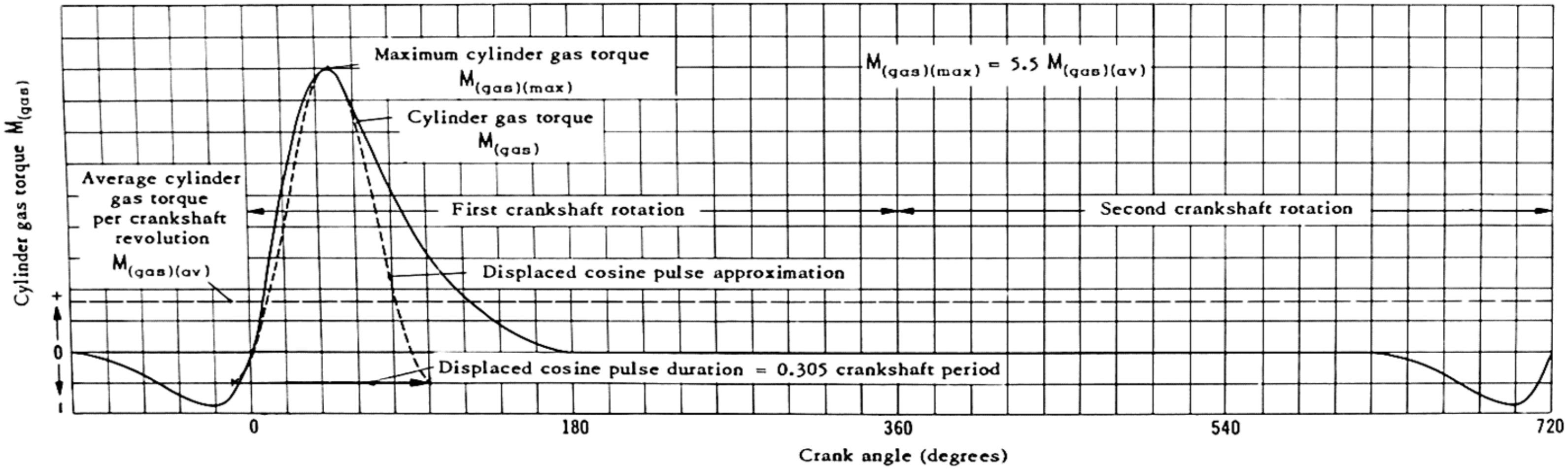


Fig. 35-57. Approximation of a typical internal combustion engine cylinder gas torque by a displaced cosine pulse function.

Engine Speed (rpm)	(rps)	Equivalent Displaced Cosine Pulse Duration T_p (seconds)	Pulse Duration – Undamped Natural Period Ratio $\frac{T_p}{T_n}$	Undamped Natural Period – Pulse Duration Ratio $\frac{T_n}{T_p}$	Maximum Engine Mount Torque – Maximum Cylinder Gas Torque Ratio $\frac{M_{(em)(max)}}{M_{(gas)(max)}}$	Maximum Engine Mount Torque – Average Engine Torque Ratio $\frac{M_{(em)(max)}}{M_{(eng)(av)}}$
2200	36.7	0.0083	0.025	40	0.1 (approx)	0.062 (approx)
500	8.33	0.0366	0.11	9.1	0.3	0.186
180	3.0	0.102	0.305	3.28	0.8	0.496
66	1.1	0.333	1.0	1.0	1.5	0.93

Data Analysis Summary 35-1. Displaced cosine pulse response data for a typical aircraft engine.

period ratios and their reciprocals are calculated by taking the undamped natural period of the vibratory torque isolation system as 0.333 second from experiment. The information in the last two columns is found from Figs. 35-52 and 35-54 by referring to the DR = 0.1 curves. These curves show that the engine can contact the vibration isolator stops for low engine speeds during misfire. At cruising speeds, the engine is rotating so fast that the pulse duration during a single misfire will not impose much torque variation upon the engine mount.

BIBLIOGRAPHY

INTRODUCTION

A1 Ahrendt, W. R., and Taplin, J. F., Automatic Feedback Control, McGraw-Hill Book Company, Inc., New York, 1951.

A2 Ahrendt, W. R., and Taplin, J. F., Automatic Regulation, Vol. I, preliminary edition, published by Ahrendt and Taplin, P. O. Box 4673, Washington 20, D. C., 1947.

A3 AIEE (American Institute of Electrical Engineers), Committee on Feedback Control Systems, "Proposed Symbols and Terms for Feedback Control Systems," Electrical Engineering, Vol. 70, pp. 905-909 (October, 1951).

A4 ASME (American Society of Mechanical Engineers), Committee on Industrial Instruments and Regulators, "Technical Memoranda on Automatic Control," Industrial Instrument Division, Scientific Apparatus Makers of America, Chicago, Ill., 1938.

A5 ASME (American Society of Mechanical Engineers), Terminology Committee of the Industrial Instruments and Regulators Division, "Automatic Control Terminology," Mechanical Engineering, Vol. 74, pp. 486-489 (June, 1952).

A6 ASME (American Society of Mechanical Engineers), Terminology Committee of the Industrial Instruments and Regulators Division, "Automatic Control Terminology," Paper No. 52-SA-29, advance copy of paper presented at the June, 1952, meeting of the American Society of Mechanical Engineers in Cincinnati, Ohio.

A7 American Institute of Physics, Temperature; Its Measurement and Control in Science and Industry. (Symposium held in New York City, November, 1939, under the auspices of the American Institute of Physics with the cooperation of the National Bureau of Standards and the National Research Council.) Reinhold Publishing Corporation, New York, 1941.

B1 Batcher, R. R., and Moulic, William, The Electronic Control Handbook, Caldwell-Clements, Inc., New York, 1946.

B2 Behar, M. F. (with P. R. Ewald and others), The Handbook of Measurement and Control, The Instruments Publishing Company, Inc., Pittsburgh, Pa., 1951.

B3 Bode, H. W., Network Analysis and Feedback Amplifier Design, D. Van Nostrand Company, Inc., New York, 1945.

B4 Brown, G. S., and Campbell, D. P., Principles of Servomechanisms, John Wiley & Sons, Inc., New York, 1948.

C1 Chestnut, Harold, and Mayer, R. W., Servomechanisms and Regulating System Design, Vol. I, John Wiley & Sons, Inc., New York, 1951.

D1 Allen B. DuMont Laboratories, A Compilation of Analog Transducers, Clifton, N. J., 1952.

E1 Eckman, D. P., Industrial Instrumentation, John Wiley & Sons, Inc., New York, 1950.

E2 Eckman, D. P., Principles of Industrial Process Control, John Wiley & Sons, Inc., New York, 1945.

F1 Farrington, G. H., Fundamentals of Automatic Control, John Wiley & Sons, Inc., New York, 1951.

G1 Gardner, M. F., and Barnes, J. L., Transients in Linear Systems (two vols.), John Wiley & Sons, Inc., New York, 1942.

G2 General Electric Company, "Manual of Electric Instruments," Meter and Instrument Division, West Lynn, Mass., 1949.

G3 Greenwood, I. A., Jr., Holdam, J. V., Jr., and Macrae, Duncan, Jr. (editors), Electronic Instruments, Radiation Laboratory Series, 21, McGraw-Hill Book Company, Inc., New York, 1948.

I1 Irvin, G. E., Aircraft Instruments, McGraw-Hill Book Company, Inc., New York, 1941.

I2 Ivanoff, A., "Theoretical Foundations of the Automatic Regulation of Temperature," Journal of the Institute of Fuel (British), Vol. 7, pp. 117-138 (February, 1934).

J1 James, H. M., Nichols, N. B., and Phillips, R. S. (editors), Theory of Servomechanisms, Radiation Laboratory Series, 25, McGraw-Hill Book Company, Inc., New York, 1947.

L1 Lauer, Henri, Lesnick, Robert, and Matson, L. E. (editors), Servomechanism Fundamentals, McGraw-Hill Book Company, Inc., New York, 1947.

L2 Lyle, Oliver, The Efficient Use of Steam, His Majesty's Stationery Office, London, 1947.

M1 MacColl, L. A., Fundamental Theory of Servomechanisms, D. Van Nostrand Company, Inc., New York, 1945.

O1 Oldenbourg, R. C., and Sartorius, H. (translated and edited by H. L. Mason), The Dynamics of Automatic Controls, The American Society of Mechanical Engineers, New York, 1948.

P1 Philbrick, G. A., "Unified Symbolism for Regulatory Controls," Transactions of the American Society of Mechanical Engineers, Vol. 69, p. 47 (January, 1947).

P2 Porter, A., Introduction to Servomechanisms, John Wiley & Sons, Inc., New York, 1950.

R1 Rhodes, T. J., Industrial Instruments for Measurement and Control, McGraw-Hill Book Company, Inc., New York, 1941.

S1 Smith, Ed Sinclair, Automatic Control Engineering, McGraw-Hill Book Company, Inc., New York, 1944.

T1 Trimmer, J. D., Response of Physical Systems, John Wiley & Sons, Inc., New York, 1950.

CHAPTER 28. CONCEPTS, DEFINITIONS, DIAGRAMS, AND NOTATION FOR DESCRIBING OPERATING COMPONENTS AND OPERATING SYSTEMS.

A1 Ahrendt, W. R., and Taplin, J. F., Automatic Feedback Control, McGraw-Hill Book Company, Inc., New York, 1951.

A2 Ahrendt, W. R., and Taplin, J. F., Automatic Regulation, Vol. I, preliminary edition, published by Ahrendt and Taplin, P. O. Box 4673, Washington 20, D. C., 1947.

A3 AIEE (American Institute of Electrical Engineers), Committee on Feedback Control Systems, "Proposed Symbols and Terms for Feedback Control Systems," Electrical Engineering, Vol. 70, pp. 905-909 (October, 1951).

A4 ASME (American Society of Mechanical Engineers), Committee on Industrial Instruments and Regulators, "Technical Memoranda on Automatic Control," Industrial Instrument Division, Scientific Apparatus Makers of America, Chicago, Ill., 1938.

A5 ASME (American Society of Mechanical Engineers), Terminology Committee of the Industrial Instruments and Regulators Division, "Automatic Control Terminology," Mechanical Engineering, Vol. 74, pp. 486-489 (June, 1952).

A6 ASME (American Society of Mechanical Engineers), Terminology Committee of the Industrial Instruments and Regulators Division, "Automatic Control Terminology," Paper No. 52-SA-29, advance copy of paper presented at the June, 1952, meeting of the American Society of Mechanical Engineers in Cincinnati, Ohio.

B2 Behar, M. F., (with P. R. Ewald and others), The Handbook of Measurement and Control, The Instruments Publishing Company, Inc., Pittsburgh, Pa., 1951.

B3 Bode, H. W., Network Analysis and Feedback Amplifier Design, D. Van Nostrand Company, Inc., New York, 1945.

B4 Brown, G. S., and Campbell, D. P., Principles of Servomechanisms, John Wiley & Sons, Inc., New York, 1948.

C1 Chestnut, Harold, and Mayer, R. W., Servomechanisms and Regulating System Design, Vol. I, John Wiley & Sons, Inc., New York, 1951.

E2 Eckman, D. P., Principles of Industrial Process Control, John Wiley & Sons, Inc., New York, 1945.

F2 Franklin, Philip, Methods of Advanced Calculus, McGraw-Hill Book Company, Inc., New York, 1944.

G1 Gardner, M. F., and Barnes, J. L., Transients in Linear Systems (two vols.), John Wiley & Sons, Inc., New York, 1942.

J1 James, H. M., Nichols, N. B., and Phillips, R. S. (editors), Theory of Servomechanisms, Radiation Laboratory Series, 25, McGraw-Hill Book Company, Inc., New York, 1947.

L1 Lauer, Henri, Lesnick, Robert, and Matson, L. E. (editors), Servomechanism Fundamentals, McGraw-Hill Book Company, Inc., New York, 1947.

M1 MacColl, L. A., Fundamental Theory of Servomechanisms, D. Van Nostrand Company, Inc., New York, 1945.

O1 Oldenbourg, R. C., and Sartorius, H. (translated and edited by H. L. Mason), The Dynamics of Automatic Controls, The American Society of Mechanical Engineers, New York, 1948.

P2 Porter, A., Introduction to Servomechanisms, John Wiley & Sons, Inc., New York, 1950.

T1 Trimmer, J. D., Response of Physical Systems, John Wiley & Sons, Inc., New York, 1950.

Z1 Zimmerman, O. T., and Lavine, Irvin, Scientific and Technical Abbreviations, Signs and Symbols, Industrial Research Service, Dover, N. H., 1948.

CHAPTER 29. INDICATION AND MEASUREMENT

A3 AIEE (American Institute of Electrical Engineers), Committee on Feedback Control Systems, "Proposed Symbols and Terms for Feedback Control Systems," Electrical Engineering, Vol. 70, pp. 905-909 (October, 1951).

A5 ASME (American Society of Mechanical Engineers), Terminology Committee of the Industrial Instruments and Regulators Division, "Automatic Control Terminology," Mechanical Engineering, Vol. 74, pp. 486-489 (June, 1952).

A6 ASME (American Society of Mechanical Engineers), Terminology Committee of the Industrial Instruments and Regulators Division, "Automatic Control Terminology," Paper No. 52-SA-29, advance copy of paper presented at the June, 1952, meeting of the American Society of Mechanical Engineers in Cincinnati, Ohio.

B2 Behar, M. F. (with P. R. Ewald and others), The Handbook of Measurement and Control, The Instruments Publishing Company, Inc., Pittsburgh, Pa., 1951.

B5 Bode, H. W., and Shannon, C. E., "A Simplified Derivation of Linear Least Square Smoothing and Prediction Theory," Proceedings of the Institute of Radio Engineers, Vol. 38, No. 4, p. 417 (April, 1950).

B6 Booton, R. C., Jr., "An Optimization Theory for Time-Varying Linear Systems with Nonstationary Statistical Inputs," Proceedings of the Institute of Radio Engineers, Vol. 40, No. 8, p. 977 (August, 1952).

B7 British Standards Institution, "Glossary of Terms Used in Electrical Engineering," British Standard 205, Part 1, Sec. 2, and Part 3, Sec. 4, London, 1943.

C2 Cramér, Harald, Mathematical Methods of Statistics, Princeton University Press, 1946.

E1 Eckman, D. P., Industrial Instrumentation, John Wiley & Sons, Inc., New York, 1950.

F3 Frost, Seymour, "Compact Analogue Computer," Electronics, Vol. 21, p. 116 (July, 1948).

F4 Fry, T. C., Probability and Its Engineering Uses, D. Van Nostrand Company, Inc., New York, 1928.

H1 Hoel, P. G., Introduction to Mathematical Statistics, John Wiley & Sons, Inc., New York, 1947.

L3 Laning, J. H., Jr., and Root, W. L., "Methods of Analysis of Control Systems," Instrument Section, Aeronautical Engineering Department, Massachusetts Institute of Technology, Cambridge, Mass. (Collected course notes for the fall term, 1951. To be issued in revised form as Course 16.37, under the title "Random Processes in Automatic Control," with R. H. Battin contributing.)

N1 National Research Council, Conference on Nuclear Glossary, A Glossary of Terms in Nuclear Science and Technology, Section VII: "Instrumentation," The American Society of Mechanical Engineers, New York, 1951.

R1 Rhodes, T. J., Industrial Instruments for Measurement and Control, McGraw-Hill Book Company, Inc., New York, 1941.

T1 Trimmer, J. D., Response of Physical Systems, John Wiley & Sons, Inc., New York, 1950.

W1 Whittaker, E. T., and Robinson, G., Calculus of Observations, third edition, Blackie & Son, Ltd., London and Glasgow, 1940.

Z1 Zimmerman, O. T., and Lavine, Irvin, Scientific and Technical Abbreviations, Signs and Symbols, Industrial Research Service, Dover, N. H., 1948.

CHAPTER 30. ELEMENTS AND COMPONENTS ASSOCIATED WITH INSTRUMENT SYSTEMS

A7 American Institute of Physics, Temperature; Its Measurement and Control in Science and Industry. (Symposium held in New York City, November, 1939, under the auspices of the American Institute of Physics with the cooperation of the National Bureau of Standards and the National Research Council.) Reinhold Publishing Corporation, New York, 1941.

A8 American Steel & Wire Company, Manual of Spring Engineering, 71 Broadway, New York, 1941.

A9 Associated Spring Corporation, Handbook of Mechanical Spring Design, Bristol, Conn.

A10 Aronson, M. H., Electronic Circuitry for Instruments, The Instruments Publishing Company, Pittsburgh, Pa., 1953.

B1 Batcher, R. R., and Moulic, William, The Electronic Control Handbook, Caldwell-Clements, Inc., New York, 1946.

B2 Behar, M. F. (with P. R. Ewald and others), The Handbook of Measurement and Control, The Instruments Publishing Company, Inc., Pittsburgh, Pa., 1951.

B3 Bode, H. W., Network Analysis and Feedback Amplifier Design, D. Van Nostrand Company, Inc., New York, 1945.

B8 Barnes, Wallace, Company (Division of Associated Spring Corporation), "Mechanical Springs: their engineering and design," 100 Wallace Street, Bristol, Conn., 1944.

B9 Beranek, L. L., Acoustics, McGraw-Hill Book Company, Inc., New York, 1954.

B10 Bergman, Ludwig (translated by H. Stafford Hatfield), Ultrasonics, George Bell & Sons, Ltd., London, 1938.

B11 Bernhard, R. K., Mechanical Vibrations, Pitman Publishing Corporation, New York and Chicago, 1943.

B12 Binder, R. C., Fluid Mechanics, second edition, Prentice-Hall, Inc., New York, 1949.

B13 Blackburn, J. F. (editor), Components Handbook, Radiation Laboratory Series, 17, McGraw-Hill Book Company, Inc., New York, 1949.

B14 Bowden, F. P., and Tabor, D., The Friction and Lubrication of Solids, Oxford at the Clarendon Press, 1950.

B15 Brombacher, W. G., "Altitude-Pressure Tables Based on the United States Standard Atmosphere," Report No. 538, National Advisory Committee for Aeronautics, Washington, D. C., 1935 (reprinted 1948).

B16 Buckingham, Earle, Analytical Mechanics of Gears, McGraw-Hill Book Company, Inc., New York, 1949.

C3 Chemical Rubber Publishing Company, Handbook of Chemistry and Physics (C. D. Hodgman, editor), Cleveland, Ohio.

C4 Clifford Manufacturing Company, "Vapor Pressure – Temperature Curves of Typical Filling Mediums" (fluids) (chart in catalog: Hydron Metallic Bellows), Waltham, Mass., 1941.

C5 Crabtree, Harold, An Elementary Treatment of the Theory of Spinning Tops and Gyroscopic Motion, second edition, Longmans, Green & Company, London, 1914.

C6 Crow, L. R., Saturating Core Devices, Scientific Book Publishing Co., Vincennes, Ind., 1949.

D1 Allen B. DuMont Laboratories, A Compilation of Analog Transducers, Clifton, N. J., 1952.

D2 Davidson, Martin, The Gyroscope and its Applications, Hutchinson's Scientific and Technical Publications, London, 1947.

D3 Dean, R. C., Jr., and others, "Aerodynamic Measurements," Gas Turbine Laboratory, Massachusetts Institute of Technology, Cambridge, Mass., September, 1952.

D4 Deimel, R. F., Mechanics of the Gyroscope, Dover Publications, Inc., New York, 1950.

D5 Den Hartog, J. P., Mechanical Vibrations, third edition, McGraw-Hill Book Company, Inc., New York, 1947.

D6 Den Hartog, J. P., Mechanics, first edition, McGraw-Hill Book Company, Inc., New York, 1948.

D7 Diederichs, Herman, and Andrae, W. C., Engineering Instruments; Vol. 1: Experimental Mechanical Engineering, John Wiley & Sons, Inc., New York, 1930.

D8 Draper, C. S., and Wrigley, W., "An Instrument for Measuring Low Frequency Accelerations in Flight," Journal of the Aeronautical Sciences, Vol. 7, p. 388 (1940).

D9 Drysdale, C. V., and Jolley, A. C., Electrical Measuring Instruments, second edition (revised by G. F. Tagg), Chapman & Hall, Ltd., London, 1952.

E1 Eckman, D. P., Industrial Instrumentation, John Wiley & Sons, Inc., New York, 1950.

E3 Einstein, A., and Infeld, L., The Evolution of Physics, Simon & Schuster, Inc., New York, 1938.

E4 Ernst, Walter, Oil Hydraulic Power and Its Industrial Applications, McGraw-Hill Book Company, Inc., New York, 1949.

E5 Eshbach, O. V. (editor), Handbook of Engineering Fundamentals, second edition, John Wiley & Sons, Inc., New York, 1952.

E6 Everitt, W. L., Communication Engineering, second edition, McGraw-Hill Book Company, Inc., New York, 1932.

F5 Federal Telephone and Radio Corporation, Reference Data for Radio Engineers, third edition, New York, 1949.

F6 Ferry, E. S., Applied Gyrodynamics, John Wiley & Sons, Inc., New York, 1932.

F7 Finzi, L. A., and Beaumarriage, D. C., "Magnetic Amplifier Characteristics," Electrical Engineering, Vol. 69, No. 12 (December, 1950).

F8 FitzGerald, A. E., Basic Electrical Engineering, McGraw-Hill Book Company, Inc., New York, 1945.

F9 FitzGerald, A. E., "Magnetic Amplifier Circuits, Neutral Type," "Some Notes on the Design of Magnetic Amplifiers," "Magnetic Amplifier Characteristics, Neutral Type," Journal of the Franklin Institute, Vol. 244, No. 4, p. 249; No. 5, p. 323; No. 6, p. 415 (October-December, 1947).

F10 FitzGerald, A. E., and Kingsley, Charles, Electric Machinery, McGraw-Hill Book Company, Inc., New York, 1952.

F11 Frank, N. H., Introduction to Electricity and Optics, McGraw-Hill Book Company, Inc., New York, 1940.

F12 Franklin, Philip, Differential Equations for Electrical Engineers, John Wiley & Sons, Inc., New York, 1933.

F13 Frazier, R. H., "Analysis of Drag Cup A-C Tachometer," Transactions of the American Institute of Electrical Engineers, Vol. 70, 1951 (AIEE Paper 51-348).

G3 Greenwood, I. A., Jr., Holdam, J. V., Jr., and Macrae, Duncan, Jr. (editors), Electronic Instruments, Radiation Laboratory Series, 21, McGraw-Hill Book Company, Inc., New York, 1948.

G4 Geyger, W. A., "A New Type of Magnetic Servo Amplifier," Transactions of the American Institute of Electrical Engineers, Part I: Communication and Electronics, Vol. 71, No. 5, pp. 272-280 (September, 1952).

G5 Grammel, R., Der Kreisel, seine Theorie und seine Anwendungen, Braunschweig, Vieweg, 1920.

G6 Gould, L. A., and Smith, P. E., Jr., "Dynamic Behavior of Pneumatic Devices," Journal of the Instrument Society of America, Vol. 9 (bound in Instruments, Vol. 26),(June and July, 1953.)

G7 Guillemin, E. A., Communication Networks, Vols. I and II, John Wiley & Sons, Inc., New York, 1947.

H2 Hague, B., Alternating Current Bridge Methods for the Measurement of Inductance, Capacitance, and Effective Resistance at Low and Telephonic Frequencies, Sir Isaac Pitman & Sons, London, 1946.

H3 Haltmaier, R. G., "Coupled Circuit Analysis of Microsyn Signal Generators," Report E-266, Instrumentation Laboratory, Massachusetts Institute of Technology, Cambridge, Mass., March 23, 1953.

H4 Harvard University, Cruft Electronics Staff, Electronic Circuits and Tubes, McGraw-Hill Book Company, Inc., New York, 1947.

H5 Hrones, J. A., and Nelson, G. L., Analysis of the Four-Bar Linkage, published jointly by the Technology Press of the Massachusetts Institute of Technology and John Wiley & Sons, Inc., New York, 1951.

I1 Irvin, G. E., Aircraft Instruments, McGraw-Hill Book Company, Inc., New York, 1941.

I3 Instrument Specialities Company, Inc., "Micro-Processed Springs of Beryllium Copper," Little Falls, N. J., current catalog.

J1 James, H. M., Nichols, N. B., and Phillips, R. S. (editors), Theory of Servomechanisms, Radiation Laboratory Series, 25, McGraw-Hill Book Company, Inc., New York, 1947.

J2 Jones, Franklin D., Ingenious Mechanisms for Designers and Inventors, The Industrial Press, New York; The Machinery Publishing Company, Ltd., London; Vol. I: 1935, Vol. II: 1936.

J3 Jones, R. W., Electric Control Systems, John Wiley & Sons, Inc., New York, 1953.

K1 Kloeffler, R. G., and Horrell, M. W., Basic Electronics, John Wiley & Sons, Inc., New York, 1949.

K2 Kuntny, G. V., "Gear Standards and Design," Transactions of the American Society of Mechanical Engineers, Vol. 70, Sec. 8 (August 1948).

L4 Langsdorf, A. S., Principles of Direct-Current Machines, Chapter V, "Systems of Electrical Units," fifth edition, McGraw-Hill Book Company, Inc., New York, 1940.

L5 Laning, J. H., Jr., "The Vector Analysis of Finite Rotations and Angles," Report No. 6398-S-3, Instrumentation Laboratory, Massachusetts Institute of Technology, Cambridge, Mass., September, 1949.

L6 Lawrence, R. R., Principles of Alternating Current Machinery, third edition, McGraw-Hill Book Company, Inc., New York, 1940.

L7 Laws, F. A., Electrical Measurements, second edition, McGraw-Hill Book Company, Inc., New York, 1938.

L8 Lee, S.-Y., and Blackburn, J. F., "Contributions to Hydraulic Control," Transactions of the American Society of Mechanical Engineers,

1. "Steady-state axial forces on control-valve pistons," Vol. 74, No. 6, pp. 1005-1011 (1952).
2. "Transient-flow forces and valve instability," Vol. 74, No. 6, pp. 1013-1016 (1952).
3. "Pressure-flow relationships for 4-way valves," Vol. 75, No. 6, pp. 1163-1170 (1953).
4. "Notes on the hydraulic Wheatstone bridge," Vol. 75, No. 6, pp. 1171-1173 (1953).
5. "Lateral forces on hydraulic pistons," Vol. 75, No. 6, pp. 1175-1180 (1953).
6. "New valve configurations for high-performance hydraulic and pneumatic systems," paper presented at the December, 1953, meeting of the American Society of Mechanical Engineers.

L9 Leeds and Northrup Company, "Standard Conversion Tables for Leeds and Northrup Thermocouples."

L10 Lees, Sidney, "Integration by the Viscous Shear Process," D. Sc. Thesis, Department of Aeronautical Engineering, Massachusetts Institute of Technology, 1950. (Published as Report No. 6398-T-10, by Instrumentation Laboratory, Massachusetts Institute of Technology, Cambridge, Mass., September, 1950.)

L11 Lufcy, C. W., Schmid, A. E., and Barnhart, P. W., "An Improved Magnetic Servo Amplifier," Transactions of the American Institute of Electrical Engineers, Part I: Communication and Electronics, Vol. 71, pp. 281-289 (September, 1952).

M2 MacMillan, R. H., An Introduction to the Theory of Control in Mechanical Engineering, Cambridge University Press, Cambridge, England, 1951.

M3 Maleev, V. L., Machine Design, International Textbook Company, Scranton, Pa., 1939.

M4 Marks, L. S., Mechanical Engineers' Handbook, fourth edition, McGraw-Hill Book Company, Inc., New York, 1941.

M5 Martin, L. D., "Designing Instrument Gearing," Machine Design, Vol. 20, pp. 163-168 (April, 1948).

M6 Massachusetts Institute of Technology, Electrical Engineering Staff, Applied Electronics, John Wiley & Sons, Inc., New York, 1948.

M7 Massachusetts Institute of Technology, Electrical Engineering Staff, Electric Circuits, John Wiley & Sons, Inc., New York, 1948.

M8 Massachusetts Institute of Technology, Electrical Engineering Staff, Magnetic Circuits and Transformers, John Wiley & Sons, Inc., New York, 1943.

M9 Massachusetts Institute of Technology, Mechanical Engineering Staff, "Fluid Power Control" (notes for Course 2.789, summer session, 1953), Cambridge, Mass., 1953.

M10 McAdams, W. H., Heat Transmission, second edition, McGraw-Hill Book Company, Inc., New York, 1942.

M11 Middleton, W. E. K., Meteorological Instruments, The University of Toronto Press, Toronto, Canada, 1941.

M12 Miles, J. G., "Bibliography of Magnetic Amplifier Devices and the Saturable Reactor Art," Transactions of the American Institute of Electrical Engineers, Vol. 70 (1951).

M13 Moon, P., and Spencer, D. E., "Utilizing the M. K. S. System," American Journal of Physics, Vol. 16, No. 1, pp. 25-38 (January, 1948).

M14 Moore, A. D., "Eddy Currents in Disks: Driving and Damping Forces and Torques," Transactions of the American Institute of Electrical Engineers, Vol. 66, pp. 1-10 (1947).

M15 Mueller, R. K., "Microsyn Electromagnetic Components," Engineering Memorandum E-224, Instrumentation Laboratory, Massachusetts Institute of Technology, Cambridge, Mass., December, 1952.

N2 Navy Department, "United States Navy Synchros, Description and Operation," Ordnance Pamphlet No. 1303, a joint Bureau of Ordnance and Bureau of Ships publication, Washington, D. C., December 15, 1944.

N3 New York State Vocational and Practical Arts Association, Instruments and Process Control, Delmar Publishers, Incorporated, Albany, N. Y., September, 1945.

O2 Olson, H. F., Elements of Acoustical Engineering, second edition, D. Van Nostrand Company, Inc., New York, 1947.

P3 Pearce, C. E., Principles of Mechanism, John Wiley & Sons, Inc., New York, 1934.

P4 Pender, Harold, and Del Mar, William, Electrical Engineers' Handbook; Vol. I: Electric Power, fourth edition, John Wiley & Sons, Inc., New York, 1950.

P5 Proceedings of the Institute of Radio Engineers, Transistor issue, Vol. 40, No. 11 (November, 1952.)

R1 Rhodes, T. J., Industrial Instruments for Measurement and Control, McGraw-Hill Book Company, Inc., New York, 1941.

R2 Radio Corporation of America, Tube Handbook H-B-3, Camden, N. J.

R3 Rauscher, M., Introduction to Aeronautical Dynamics, John Wiley & Sons, Inc., New York, 1953.

R4 Reich, H. J., Theory and Applications of Electron Tubes, McGraw-Hill Book Company, Inc., New York, 1939.

R5 Richtmyer, F. K., and Kennard, E. H., Introduction to Modern Physics, McGraw-Hill Book Company, Inc., New York, 1947.

R6 Roberts, H. C., Mechanical Measurements by Electrical Methods, second edition, The Instruments Publishing Company, Inc., Pittsburgh, Pa., 1951.

R7 Roters, H. C., Electromagnetic Devices, John Wiley & Sons, Inc., New York, 1944.

R8 Roters, H. C., "The Hysteresis Motor," Electrical Engineering, Vol. 67, No. 3, March, 1948.

S2 Schaevitz, H., "The Linear Variable Differential Transformer," Proceedings of the Society for Experimental Stress Analysis, Vol. IV, No. 2 (1947).

S3 Sears, F. W., Principles of Physics; Vol. I: Mechanics, Heat and Sound, Vol. II: Electricity and Magnetism, second edition, Addison-Wesley Press, Inc., Cambridge, Mass., 1950.

S4 Shea, R. F., Principles of Transistor Circuits, John Wiley & Sons, Inc., New York, 1953.

S5 Shearer, J. L., "Proportional Control of Rate-Type Servomotors," and "Dynamic Characteristics of Valve-Controlled Hydraulic Servomotors" (papers presented at the December, 1953, meeting of the American Society of Mechanical Engineers; to be published in one of the Society's journals).

S6 Shockley, W., Electrons and Holes in Semi-Conductors with Applications to Transistor Electrons, D. Van Nostrand Company, Inc., New York, 1950.

S7 Shockley, W., The Transistor (collection of papers), Bell Telephone Laboratories, New York, 1951.

S8 Sloane, Alvin, Engineering Kinematics, The Macmillan Company, New York, 1941.

S9 Smith, E. J., "A Transient Analyzer for Magnetic Amplifiers," Technical Paper 53-283, American Institute of Electrical Engineers, April, 1953.

S10 Smythe, W. R., "On Eddy Currents in a Rotating Disk," Transactions of the American Institute of Electrical Engineers, Vol. 61, pp. 681-684 (1942).

S11 Sontag, Harcourt, and Brombacher, W. G., Aircraft Power-Plant Instruments, Report No. 466, National Advisory Committee for Aeronautics, U. S. Government Superintendent of Documents, Washington D. C., 1933.

S12 Spotts, M. F., Design of Machine Elements, Prentice-Hall, Inc., New York, 1948.

S13 St. George, E., "List of Theses and Reports on Hydraulic Control," internal memorandum, Dynamic Analysis and Control Laboratory, Massachusetts Institute of Technology, Cambridge, Mass., September, 1953.

S14 Svoboda, Antonin, Computing Mechanisms and Linkages, Radiation Laboratory Series, 27, McGraw-Hill Book Company, Inc., New York, 1948.

S15 Sylvania Electric Products, Inc., Tube Handbook, 500 Fifth Avenue, New York.

T2 Terman, F. E., Radio Engineers' Handbook, McGraw-Hill Book Company, Inc., New York, 1943.

T3 Thaler, G. J., and Brown, R. G., Servomechanism Analysis, McGraw-Hill Book Company, Inc., New York, 1953.

T4 Timoshenko, Stephen, Vibration Problems in Engineering, D. Van Nostrand Company, Inc., New York, 1941.

T5 Timoshenko, Stephen, and Lessells, J. M., Applied Elasticity, East Pittsburgh Westinghouse Technical Night School, 1925.

V1 Valley, G. E., and Wallman, Henry, Vacuum Tube Amplifiers, Radiation Laboratory Series, 18, McGraw-Hill Book Company, Inc., New York, 1948.

V2 Van der Pyl, L. M., "Bibliography on Bourdon Tubes and Bourdon Tube Gages," Paper 53-IRD-1, American Society of Mechanical Engineers, New York, September, 1953.

V3 Veinott, C. G., Fractional Horsepower Electric Motors, McGraw-Hill Book Company, Inc., New York, 1948.

W2 Whitman, H. R., Wales, R. L., and Andersen, J. P., "The Type H Gyro, Computing and Accelerometer Units," Report R-17, Instrumentation Laboratory, Massachusetts Institute of Technology, Cambridge, Mass., September, 1953.

W3 Weems, W. R., "An Introduction to the Study of Gyroscopic Instruments," Department of Aeronautical Engineering, Instrumentation Section, Massachusetts Institute of Technology, Cambridge, Mass., January, 1948.

W4 Weston Electrical Instrument Corporation, The Instrument Sketch Book, Circular E-3-C, Newark, N. J., 1951.

W5 Westinghouse Electric Corporation, Electronic Engineers of the, Industrial Electronics Reference Book, John Wiley & Sons, Inc., New York, 1948.

W6 H. A. Wilson Company, The Blue Book of Thermometals and Electrical Contacts, Newark, N. J., 1939.

W7 Wrigley, Walter, "An Investigation of Methods Available for Indicating the Direction of the Vertical from Moving Bases," D. Sc. Thesis, Department of Physics, Massachusetts Institute of Technology, Cambridge, Mass., 1941.

W8 Wrigley, Walter, "Schuler Tuning Characteristics in Navigational Instruments," Navigation: Journal of the Institute of Navigation, Vol. 2, No. 8 (December, 1950).

Z2 Zimmerman, O. T., and Lavine, Irvin, Conversion Factors and Tables, Industrial Research Service, Dover, N. H., 1944.

CHAPTER 31. TEMPERATURE-MEASURING INSTRUMENTS

A7 American Institute of Physics, Temperature; Its Measurement and Control in Science and Industry. (Symposium held in New York City, November, 1939, under the auspices of the American Institute of Physics with the cooperation of the National Bureau of Standards and the National Research Council.) Reinhold Publishing Corporation, New York, 1941.

B1 Batcher, R. R., and Moulic, William, The Electronic Control Handbook, Caldwell-Clements, Inc., New York, 1946.

B2 Behar, M. F. (with P. R. Ewald and others), The Handbook of Measurement and Control, The Instruments Publishing Company, Inc., Pittsburgh, Pa., 1951.

B17 Blue, R. E., and Low, G. M., "Factors Affecting Laminar Boundary Layer Measurements in a Supersonic Stream," Technical Note 2891, National Advisory Committee for Aeronautics, 1953.

B18 Bridgman, P. W., Dimensional Analysis, revised edition, Yale University Press, New Haven, Conn., 1931.

C7 Carslaw, H. S., Introduction to the Mathematical Theory of the Conduction of Heat in Solids, Macmillan & Co., Ltd., London, 1921.

D10 Dahl, A. L., and Freeze, P. D., "Tests of Total Temperature Probes," Technical Report 53-251, Wright Air Development Center, Wright-Patterson Air Force Base, Ohio, June, 1953.

D11 Durand, W. F. (editor-in-chief), Aerodynamic Theory (six vols.), Julius Springer, Berlin, 1936.

E1 Eckman, D. P., Industrial Instrumentation, John Wiley & Sons, Inc., New York, 1950.

G8 Goldstein, D. L., and Scherrer, R., "Design and Calibration of a Total-Temperature Probe for Use at Supersonic Speeds," Technical Note 1885, National Advisory Committee for Aeronautics, 1949.

G9 Goldstein, S. (editor), Modern Developments in Fluid Dynamics (two vols.), Oxford at the Clarendon Press, 1938.

H2 Hague, B., Alternating Current Bridge Methods for the Measurement of Inductance, Capacitance, and Effective Resistance at Low and Telephonic Frequencies, Sir Isaac Pitman & Sons, Ltd., London, 1946.

H6 Hardy, A. C., and Perrin, F. H., The Principles of Optics, McGraw-Hill Book Company, Inc., New York, 1932.

H7 Harper, D. R., "Thermometric Lag," Scientific Paper No. 185, Bulletin of the National Bureau of Standards, Vol. 8, No. 4, pp. 659-714 (1913), Superintendent of Documents, U. S. Government Printing Office, Washington, D. C.

H8 Hendrickson, H. B., and Brombacher, W. G., "Lag of Thermometers and Thermographs for Aircraft," Monthly Weather Review, Vol. 55, pp. 72-82, 1927.

H9 Hendrickson, H. B., "Thermometric Lag of Aircraft Thermometers, Thermographs, and Barographs," Research Paper No. 222, Journal of Research of the National Bureau of Standards, Vol. 5 (September, 1930), Superintendent of Documents, U. S. Government Printing Office, Washington, D. C.

H10 Howarth, L. (editor), Modern Developments in Fluid Dynamics: High Speed Flow, Oxford at the Clarendon Press, 1953.

J4 Johnson, H. A., and Rubesin, M. W., "Aerodynamic Heating and Conductive Heat Transfer – Summary of Literature Survey," Transactions of the American Society of Mechanical Engineers, Vol. 71, pp. 447-456 (1949).

J5 Johnson, W. C., Mathematical and Physical Principles of Engineering Analysis, McGraw-Hill Book Company, Inc., New York, 1944.

K3 Kaye, J., "Survey of Friction Coefficients, Recovery Factors, and Heat Transfer Coefficients for Supersonic Flow," Journal of the Aeronautical Sciences, Vol. 21, pp. 117-130 (1954).

K4 Kleinschmidt, Von E., "Uber die Formanderung der Bourdonbarometer, der Bourdonthermometer, und der Bimetallthermometer," Bertrage Physik für Atmos., Bd 17, 1931.

L2 Lyle, Oliver, The Efficient Use of Steam, His Majesty's Stationery Office, London, 1947.

L7 Laws, F. A., Electrical Measurements, second edition, McGraw-Hill Book Company, Inc., New York, 1938.

L12 Liepmann, H. W., and Puckett, A. E., Introduction to Aerodynamics of a Compressible Fluid, John Wiley & Sons, Inc., New York, 1947.

M10 McAdams, W. H., Heat Transmission, second edition, McGraw-Hill Book Company, Inc., New York, 1942.

P6 Packer, L. S., and Box, H. C., "Vortex Free Air Thermometer," Report No. IH-775-P-2, Cornell Aeronautical Laboratory, Inc., Buffalo, N. Y., April, 1953.

P7 Page, L., and Adams, N. I., Principles of Electricity, D. Van Nostrand Company, Inc., New York, 1949.

P8 Preston, Thomas, Theory of Heat, The Macmillan Company, New York, 1929.

R1 Rhodes, T. J., Industrial Instruments for Measurement and Control, McGraw-Hill Book Company, Inc., New York, 1941.

R9 Roberts, J. K., Heat and Thermodynamics, Blackie & Son, Ltd., London and Glasgow, 1933.

S3 Sears, F. W., Principles of Physics, Vol. I: Mechanics, Heat and Sound, Vol. II: Electricity and Magnetism, second edition, Addison-Wesley Press, Inc., Cambridge, Mass., 1950.

S16 Schaefer, Clemens, Einführung in die Theoretische Physik, Walter DeGruyte and Co., Berlin and Leipzig, Vol. II: 1929; Vol. III: 1937.

S17 Schlichting, H., "Boundary Layer Theory" (lecture series), Part I "Laminar Flows," Technical Memorandum 1217; Part II "Turbulent Flows," Technical Memorandum 1218, National Advisory Council for Aeronautics, April, 1949. (W. S. 1941/42, Luftfahrtforschungsanstalt Hermann Göring Braunschweig.)

T6 Timoshenko, Stephen, "Analysis of Bimetal Thermostats," Journal of the Optical Society of America, Vol. 11, p. 233 (July-December, 1925).

W6 H. A. Wilson Company, The Blue Book of Thermometals and Electrical Contracts, Newark, N. J., 1939.

W9 Wood, W. P., and Cork, J. M., Pyrometry, McGraw-Hill Book Company, Inc., New York, 1941.

CHAPTER 32. ELECTROMECHANICAL MEASURING INSTRUMENTS

A8 American Steel & Wire Company, Manual of Spring Engineering, 71 Broadway, New York, 1941.

B8 Barnes, Wallace, Company (division of Associated Spring Corporation), "Mechanical Springs: their engineering and design," 100 Wallace Street, Briston, Conn., 1944.

B19 Bingham, E. C., Fluidity and Plasticity, McGraw-Hill Book Company, Inc., New York, 1922.

G2 General Electric Company, "Manual of Electric Instruments," Meter and Instrument Division, West Lynn, Mass., 1949.

H2 Hague, B., Alternating Current Bridge Methods for the Measurement of Inductance, Capacitance, and Effective Resistance at Low and Telephonic Frequencies, Sir Isaac Pitman & Sons, Ltd., London, 1946.

L7 Laws, F. A., Electrical Measurements, second edition, McGraw-Hill Book Company, Inc., New York, 1938.

L13 Lamb, Horace, Hydrodynamics, fifth edition, Cambridge University Press, Cambridge, Eng., 1924.

L14 Love, A. E. H., Mathematical Theory of Elasticity, Cambridge University Press, Cambridge, Eng., 1927.

O3 OSCILLOGRAPH MANUFACTURERS WHO PUBLISH CATALOG MATERIAL:
The Brush Development Company, 3405 Perkins Avenue, Cleveland 14, Ohio.
Century Geophysical Corporation, 1333 North Utica, Tulsa 6, Okla.
Consolidated Engineering Corporation, 620 North Lake, Pasadena 4, Calif.
General Electric Company, Schnectady, New York. (Bulletins on oscillograph types PM-10, PM-13, PM-17, PM-18.) See also ref. (G2).
Hathaway Instrument Company, 1315 South Clarkson Street, Denver, Colo.
Heiland Research Corporation, 130 East Fifth Avenue, Denver, Colo.
Sanborn Company, 39 Osborn Street, Cambridge 39, Mass.
William Miller Corporation, Pasadena 8, Calif.
Westinghouse Electric Corporation, Newark Plant, Newark, N. J.

P7 Page, L., and Adams, N. I., Principles of Electricity, D. Van Nostrand Company, Inc., New York, 1949.

S3 Sears, F. W., Principles of Physics; Vol. I: Mechanics, Heat and Sound, Vol. II: Electricity and Magnetism, second edition, Addison-Wesley Press, Inc., Cambridge, Mass., 1950.

T7 Timoshenko, Stephen, Theory of Elasticity, McGraw-Hill Book Company, Inc., New York, 1934.

W4 Weston Electrical Instrument Corporation, The Instrument Sketch Book, Circular E-3-C, Newark, N. J., 1951.

W10 Wickwire Spenser Steel Division of the Colorado Fuel and Iron Corp., "Springs, Wire Forms and Spring Wires" (catalog), 575 Madison Avenue, New York.

CHAPTER 33. PRESSURE-MEASURING SYSTEMS

B20 Blanchard, H. F. (editor), Motor's Auto Repair Manual, 15th edition, published by Motor, The Automotive Business Magazine, 250 W. 55th Street, New York, 1952.

D5 Den Hartog, J. P., Mechanical Vibrations, third edition, McGraw-Hill Book Company, Inc., New York, 1947.

D7 Diederichs, Herman, and Andrae, W. C., Engineering Instruments; Vol. 1: Experimental Mechanical Engineering, John Wiley & Sons, Inc., New York, 1930.

D12 DeJuhasz, K. J., The Engine Indicator, New York Instrument Publishing Company, 1934.

D13 Draper, C. S., and Li, Y. T., "New high performance engine indicator of the strain gage type," Journal of the Aeronautical Sciences, Vol. 16, pp. 593-610 (October, 1949).

G10 Geiger, F. W., Mantz, C. W., and Laporte, Otto (editors), "The shock-tube as an instrument for the investigation of transonic and supersonic flow patterns," N6-ONR-232. (Report on work done under the Office of Naval Research, April, 1947 – June, 1949.)

G11 Grinstead, C. E., Frawley, R. N., Chapman, F. W., and Schultz, H. F. (editors), "An Improved Indicator for Measuring Static and Dynamic Pressures," Society of Automotive Engineers Transactions, Vol. 52, No. 11, pp. 534-555 (November, 1944).

H11 Head, J. W., "Electronic Engine-Pressure Indicator," Electronics, Vol. 18, pp. 132-135 (January, 1945).

H12 Heldt, P. M., "Japanese Scientists Develop Simple Optical Indicator," Automotive Industries, Vol. 71, pp. 813-814 (June 30, 1934).

H13 Hildebrand, F. B., Advanced Calculus for Engineers, Prentice-Hall, Inc., New York, 1949.

I4 Iberall, A. S., "Attenuation of Oscillatory Pressures in Instrument Lines," Research Paper 2115, Journal of Research of the National Bureau of Standards, Vol. 45, No. 1 (July, 1950), Superintendent of Documents, U. S. Government Printing Office, Washington 25, D. C.

K5 Kármán, T., von, and Biot, M. A., Mathematical Methods in Engineering, McGraw-Hill Book Company, Inc., New York, 1940.

L15 Li, Y. T., "Design of Strain Gage Pressure Indicators," Proceedings of the Instrument Society of America, Vol. 7, pp. 216-221(1952).

L16 Li, Y. T., "Dynamic Pressure Measuring Systems for Jet Propulsion Research," Journal of the American Rocket Society, Vol. 23, No. 31, p. 124 (May-June, 1953).

M16 Martin, E. J., and Caris, D. F., "An Electrical Engine Indicator," The Electric Journal, Vol. 27, pp. 87-91 (February, 1930), Vol. 27, pp. 168-172 (March, 1930).

N5 Nakanishi, Ito and Kitamura, "A New High Speed Indicator for Internal Combustion Engines," Report of The Aeronautical Research Institute No. 87, pp. 161-177, Tokyo Imperial University (September, 1932).

O4 Ohman, J. (Southwest Research Institute, San Antonio, Tex.), "Vibrotron Temperature and Pressure Measurements," paper presented at the Sixth National Instrument Conference, Institute of Radio Engineers Program, Houston, Tex., September, 1951.

S18 Seamans, R. C., Jr., Blasingame, B. P., and Clementson, G. C. (editors), "The Pulse Method for the Determination of Aircraft Dynamic Performance," Journal of the Aeronautical Sciences, Vol. 17, No. 1 (January, 1950).

T8 Taylor, E. S., and Draper, C. S., "A New High-Speed Engine Indicator," Mechanical Engineering, Vol. 55, pp. 169-171 (March, 1933).

T9 Timoshenko, Stephen, Theory of Plates and Shells, McGraw-Hill Book Company, Inc., New York, 1940.

V2 Van der Pyl, L. M., "Bibliography on Bourdon Tubes and Bourdon Tube Gages," Paper 53-IRD-1, American Society of Mechanical Engineers, New York, September, 1953.

CHAPTER 34. INTEGRATORS AND DIFFERENTIATORS

A1 Ahrendt, W. R., and Taplin, J. F., Automatic Feedback Control, McGraw-Hill Book Company, Inc., New York, 1951.

A12 Ahrendt, W. R., Servomechanism Practice, McGraw-Hill Book Company, Inc., New York, 1954.

B21 Bacon, H. M., Differential and Integral Calculus, McGraw-Hill Book Company, Inc., New York, 1942.

C8 Courant, R., Differential and Integral Calculus (two volumes, translated by E. F. McShane), Blackie & Son, Ltd., London and Glasgow, 1951.

F14 Franklin, Philip, Differential and Integral Calculus, McGraw-Hill Book Company, Inc., New York, 1953.

K6 Korn, G. A., and Korn, T. M., Electronic Analog Computers, McGraw-Hill Book Company, Inc., New York, 1952.

M17 Massachusetts Institute of Technology, Servomechanisms Laboratory, "Electrical Engineering Department REAC Analog Computer Theory and Operation Manual," Report 6080-1, Cambridge, Mass., March, 1954.

N5 Navy Department, "Basic Fire Control Mechanisms," Ordnance Pamphlet No. 1140, a Bureau of Ordnance publication, Washington, D. C., September, 1944.

N6 Navy Department, "Catalog of Precision Instrument Components," Ordnance Pamphlet No. 1755, a Bureau of Ordnance publication, Washington, D. C., September, 1950.

P9 Phillips, H. B., Analytic Geometry and Calculus, second edition, John Wiley & Sons, Inc., New York, 1946.

R10 Reswick, J. B., "Scale Factors for Analog Computers," Product Engineering, March, 1954.

W11 Werner, E. F., Aircraft Instrument Maintenance, McGraw-Hill Book Company, Inc., New York, 1948.

CHAPTER 35. VIBRATION MEASUREMENT AND VIBRATION ISOLATION

A11 Allnutt, R. B., and Mintz, F., "Instruments at the David Taylor Model Basin for Measuring Vibration and Shock on Ship Structures and Machinery," Report 563, The David W. Taylor Model Basin, United States Navy, July, 1948.

B22 Ball, L. M., "Strain Gage Techniques," Proceedings of the Society for Experimental Stress Analysis, Vol. III, No. 1, pp. 1-22 (1945).

B23 Boggis, A. G., "Design of Differential Transformer Displacement Gages," Proceedings of the Society for Experimental Stress Analysis, Vol. IX, No. 2, pp. 171-184 (1952).

C9 Calidyne Instrument Company, "Model 18-D Accelerometer" (bulletin), Winchester, Mass.

C10 Consolidated Engineering Corporation, "Analytical Instruments for Science and Industry," general catalog 1948-49, Pasadena, Calif.

C11 Consolidated Engineering Corporation, "Consolidated Velocity Pickup Type 4-102" (bulletin), Pasadena, Calif.

D5 Den Hartog, J. P., Mechanical Vibrations, third edition, McGraw-Hill Book Company, Inc., New York, 1947.

D8 Draper, C. S., and Wrigley, W., "An Instrument for Measuring Low Frequency Accelerations in Flight," Journal of the Aeronautical Sciences, Vol. 7, p. 388 (July, 1940).

D14 Draper, C. S., Bentley, G. P., and Willis, H. H., "Vibration Measurement in Flight," Society of Automotive Engineers Transactions, Vol. 41, No. 3, pp. 428-436 (September, 1937).

D15 Draper, C. S., Taylor, E. S., Lancor, J. H., and Coffey, R. T., "Development of a Detonation Detector Suitable for Use in Flight," Technical Note 977, National Advisory Council for Aeronautics, December, 1944.

D16 Den Hartog, J. P., "Forced Vibrations with Combined Coulomb and Viscous Friction," Paper APM-53-9, Transactions of the American Society of Mechanical Engineers, Vol. 53 (1931).

G3 Greenwood, I. A., Jr., Holdam, J. V., Jr., and Macrae, Duncan, Jr. (editors), Electronic Instruments, Radiation Laboratory Series, 21, McGraw-Hill Book Company, Inc., New York, 1948.

G11 Grinstead, C. E., Frawley, R. N., Chapman, F. W., and Schultz, H. F., "An Improved Indicator For Measuring Static and Dynamic Pressures," Society of Automotive Engineers Transactions, Vol. 52, No. 11, pp. 534-555 (November, 1944).

H14 Hetényi, M., Handbook of Experimental Stress Analysis, John Wiley & Sons, Inc., New York, 1950.

H15 Hippel, A. van, "Ferroelectricity, Domain Structure, and Phase Transitions of Barium Titanate," Reviews of Modern Physics, Vol. 22, No. 3, pp. 221-237 (July, 1950).

L17 Lewis, R. C., "The Design and Characteristics of a High Sensitivity Direct Current Operated Accelerometer," Journal of the Acoustical Society of America, Vol. 22, No. 3, pp. 357-361 (May, 1950).

M15 Mueller, R. K., "Microsyn Electromagnetic Components," Engineering Memorandum E-224, Instrumentation Laboratory, Massachusetts Institute of Technology, Cambridge, Mass., December, 1952.

M18 Mason, W. P., Electromechanical Transducers and Wave Filters, D. Van Nostrand Co., Inc., New York, 1942.

M19 The MB Manufacturing Co., Inc., "MB Vibration Pickup," Bulletin No. 124C, New Haven, Conn.

O5 Osgood, W. F., and Graustein, W. C., Plane and Solid Analytic Geometry, The Macmillan Company, New York, 1920.

R3 Rauscher, M., Introduction to Aeronautical Dynamics, John Wiley & Sons, Inc., New York, 1953.

R11 Review of Scientific Instruments, "Errors of the Dial Gage as an Instrument for Measuring Amplitudes of Vibration," by Herbert K. Weiss, Vol. 9, No. 11, pp. 365-369 (November, 1938).

S8 Sloane, Alvin, Engineering Kinematics, The Macmillian Company, New York, 1941.

S19 Smith, F. D., and Luxford, C. A., "Stress Measurement by Magnetostriction," Proceedings of the Institution of Mechanical Engineers (London), Vol. 143, No. 1, p. 56 (April, 1940).

S20 Sperry Gyroscope Company, "Manual on Detonation Engine Testing System," pub. 23-125D (5/46), Great Neck, N. Y. (out of print).

S21 Statham, L., "Design Parameters for Linear Accelerometers," Instrument Notes, No. 9, Statham Laboratories, 12401 West Olympic Blvd., Los Angeles, Calif., January, 1952.

INDEX

A

Absorptivity, In 30-5(119)
A-c motors and generators, 126, In 30-8(143)
Acceleration, Tb 30-1(110), In 30-1(112)
  angular, Tb 30-1(110), In 30-2(113)
Acceleration recording system, 794, TR 35-4(796)
Accelerometer range, seismographic system, 606, 673, 696, Dr 35-5(699)
Accelerometers, 606, Fg 35-3(608), 643, Fg 35-7(644)
Accuracy, Df 29-3(54), 79
  measures of, Tb 29-1(84)
Accurate, 53, Df 29-3(54)
Actual indication, 71
Actual instruments, 38, 43, 46
  performance-quality-describing concepts, 47
Actuating inputs, 58, Fg 29-4(59)
Adiabatic compression, In 30-6(121)
Admittance, In 30-3(115)
Ahrendt, W. R., 27
Aircraft engines, angular vibration, 829
  vibratory torque isolation system, 840, DAS 35-1(843)
Airfoils, velocity profiles, 207
American Institute of Electrical Engineers, 22
American Society of Mechanical Engineers, 22
American Standards Association, 22
Ammeters, 218
Amplidyne generators, 126, In 30-8(142)
Amplifier coefficient multipliers, variable gain, for analog computers, Dr 34-22(545)
Amplifiers, as coducers, 5, Df 28-3(7)
  electronic, 131, In 30-9(152)
    negative feedback, 131, In 30-9(152)
  integrating, calibration, 782, TR 35-3(788)
  magnetic, In 30-8(143)
Amplitude modulation, 132
Amplitude modulators and demodulators, In 30-9(152)
Amplitude ratios, dynamic (see Dynamic amplitude ratios)
  Fourier series, spring-and-piston indicator, 353, Fg 33-5a(356), Fg 33-6a(358), Fg 33-8a(362)
Analog computer time, 539, Fg 34-31(540)
Analog computers, 538-600
  coefficient settings, 597, Dr 34-27(592)
  components, 542, Dr 34-22(543)
  "least number of components" connection, 555, Dr 34-24(556)
  numerical example, 567
  used to solve a general differential equation, 551, Dr 34-23(552), Dr 34-24(556)
  used to solve a typical positional servo system problem, 598, Dr 34-27(585)
  used to solve the (0;0, 1) differential equation, 555, Dr 34-25(561)
  used to solve the (0;0, 1, 2) differential equation, 560, Dr 34-26(568)
Analysis of error, example, 71, Df 29-5(74)
Angle resolver synchros, In 30-8(148)
Angles, 109
  approximated as vectors, 104
Angular acceleration, Tb 30-1(110), In 30-2(113)
Angular displacement, 104, In 30-2(113)
  receivers, 632, Fg 35-5(622)
Angular momentum, Tb 30-1(110), In 30-2(113)

Key: Da = *Data Summary*, DaA = *Data Analysis Summary*, Dr = *Derivation Summary*, Df = *Definition Summary*, Ds = *Description Summary*, Fg = *Figure*, In = *Information Summary*, PD = *Performance Data Summary*, Pr = *Procedure Summary*, Sp = *Specification*, SpF = *Specification Form*, Tb = *Table*, Te = *Technique Summary*, TR = *Test Report*. *For example, the entry* 39-42, Df 29-1 (40) *means* pages 39 through 42; Definition Summary 29-1, page 40.

Angular natural frequency, Tb 32-1(237)
undamped, Dr 32-1(227), 235, Tb 32-1(237)
Angular velocity, Tb 30-1(110), In 30-2(113)
receivers, 627, Fg 35-5(621)
Angular vibration, of an aircraft engine, 829
measurement using linear vibration receivers, 822, Dr 35-12(823)
Archimedes' principle, In 30-6(121)
Area, Tb 30-1(110)
Atmosphere, standard, In 30-6(122)
Attenuator coefficient multipliers, analog computer, Dr 34-22(546)
Autosyns, In 30-8(147)
Averages, as measure of uncertainty, 64, Df 29-4(67)
of indicated quantity or scale reading, associated with inaccuracy and uncertainty, 47, Fg 29-1(48)

B

Back electromotive force, 232
Band, dead, 69
pass, Df 33-1(371)
Band widths, 370, Df 33-1(371)
Behar, H. F., 27
Bellows, pressure-measuring, In 30-11(157)
Bernoulli's theorem, 107, In 30-6(123), 134
Bevel gears, In 30-7(137)
Bimetal-strip oil-pressure gage, 325, Fg 33-3(326)
Bimetal thermometers, 133, In 30-10(156), 163, Ds 31-1(164)
characteristic time, Tb 31-2(216)
Body, rigid, vibration measurement of, 819
Boundary layer, in fluid flow, 206
Bourdon tubes, pressure-measuring, In 30-11(157), 324
first-order performance functions, Dr 33-1(341)
second-order performance functions, Dr 33-2(347)
Brainerd, H. B., 102
Bridges, electrical, 132, In 30-9(153)
Brombacher, W. G., 216
Brown, G. S., 27
Buoyant force, In 30-6(121)
Butterfly valves, In 30-11(159)

C

Calibration, 43, 59
coefficients, 85
conditions, 59
error components, 71
levels, 60
of an integrating amplifier, 782, TR 35-3(788)
of a linear acceleration recording system, 794, TR 35-4(796)
of a linear vibration receiver, 751, TR 35-1(753)
of a torsional vibration receiver, 773, TR 35-2(775)
standards, primary and secondary, 60, Fg 29-5(61)
Campbell, D. P., 27
Cams, 125, In 30-7(136)
Capacitance, Tb 30-1(110), In 30-3(114)
Capacitive reactance, In 30-3(114)
Capacitor motors, 127
Capacity, heat, In 30-5(119)
Capsule, pressure-measuring, In 30-11(157)
Cathode-ray oscilloscopes, used to determine operating component dynamic response angles and sensitivities, 783, Te 35-1(784)
Cathode-ray tubes, 131, In 30-9(151)
Centrifugal tachometers, In 30-7(140)
C.g.s. (centimeter-gram-second) system, 109, Tb 30-1(111)
Characteristic time, and response time, 217
first-order, 236, 239
high damping ratio, Tb 32-1(237)
low damping ratio, Tb 32-1(237), 239
temperature receiver, Dr 31-2(177), 180
thermometric, 181, 194, Dr 31-3(195)
of different types of thermometer, Tb 31-2(216)
Characteristic time sum, high damping ratio, 236, Tb 32-1(237), 239
Charge, electric, 108, Tb 30-1(110), In 30-3(114)
Chord sensitivity, 15
Circuits, electric, 104, In 30-3(114)
Coducers, 4, Df 28-1(6), Df 28-2(6), Df 28-3(7), 131
Coefficient multipliers for analog computers, 542, Dr 34-22(543)
attenuator, Dr 34-22(546)
variable-gain-amplifier, Dr 34-22(545)
Coefficients, analog computer, 551, Dr 34-23(552)
settings of, 598, Dr 34-27(592)
performance, for moving-coil instruments, 232
second-order equation, Tb 32-1(237)
Comparison, 103
Compensation, 57
used to reduce interference effects, 410
Component analysis of a typical positional servo system, Dr 34-27(577)

Component performance of an electrical pressure-measuring system, applied to an internal combustion engine, 378, PD 33-1(379)
applied to a jet engine, 387, PD 33-2(388)
Component performance functions, for pressure receiving elements, 399
first-order characteristics, Dr 33-1(341)
second-order characteristics, Dr 33-2(347)
Components, operating, 4
analog-computer, 542, Dr 34-22(543)
combinations of (see Operating systems)
diagrams, 8, Df 28-4(9)
dynamic response angles and sensitivities, determined by a cathode-ray oscilloscope, 783, Te 35-1(784)
electromagnetic, 126, In 30-8(141)
electronic, 130, In 30-9(150)
first-order characteristics, Dr 33-1(341)
fluid, 134, In 30-11(157)
generalized performance, 18, Df 28-7(19)
ideal, 10
instrument system, 102, 125-160
measuring instruments, electromechanical, 223, Dr 32-1(225)
mechanism, 125, In 30-7(136)
names and symbols, 8
open-chain systems, 335
second-order characteristics, Dr 33-2(347)
sinusoidal performance, Df 28-8(21), Df 28-9(23)
static performance, 10, Df 28-6(14)
thermometric, 133, In 30-10(155)
Compound motors and generators, In 30-8(142)
Compression, fluid, In 30-6(121)
Computation, 103
analog (see Analog computers)
by mechanism components, magnitude conversion, 125
summing and function generating, 125
Computers (see Analog computers)
Conductance, electrical, Tb 30-1(110), In 30-3(114)
Conduction, heat, 106
Conduction heat flow, 174, Dr 31-2(177), 180
Conductivity, heat (thermal), 108, Tb 30-1(110), In 30-5(119)
Conductors, current-carrying, in magnetic fields, 105
Control elements, of a controlled system, 23
Control of temperature, 170
Control systems as coducers, 8, Df 28-3(7)
diagrams, 22-37
feedback, terminology and symbols, Df 28-10(25)
Controlled systems, 23
Convection, heat, 106
Convective heat flow, 174, 178, Dr 31-2(176)
Conversion, magnitude and physical, 103
Conversion factors, angles, 109
Converters, 29
Copper oxide diodes, In 30-9(150)
Coriolis' theorem, 104
Correct indications, 71
Correct scale readings, 47, 49
Correction coefficients, scale factor, 85
Correction components of scale reading, 70
Corrections, 38, 57
deviation, 49
scale reading, 49, 72
Coulomb damping and viscous damping combined, in seismographic systems, 659, Dr 35-1(660), 704, Dr 35-6(709)
Coulomb friction, 104, In 30-1(112), In 30-2(113), 659, Dr 35-1(660), 704, Dr 35-6(709)
equivalent damping ratio, 708, Dr 35-6(712)
Couplers, 39, Df 29-1(40), 219
electromechanical measuring systems, 223
temperature-measuring systems, 162
Crank and connecting rod linkages, 125, In 30-7(138)
Crystal diodes, In 30-9(150)
Currents, electric, 104, Tb 30-1(110), In 30-3(114)
in magnetic fields, 105
Cutoff frequencies, 370, Df 33-1(371)
Cylinder pressure of an internal combustion engine, Fg 33-5(356)
compared with pressure record from an electrical pressure-measuring system, Fg 33-11(380)
compared with pressure record from a spring-and-piston indicator, Fg 33-6(358), Fg 33-7(360), Fg 33-8(362), Fg 33-9(364)
compared with pressure record from a pressure-measuring system with inadequate low-frequency performance, Fg 33-12(382)

D

Dampers, eddy-current, 129, In 30-8(146)
moving-coil instruments, 222, Dr 32-1(225, 230), 233

Key: Da = *Data Summary*, DaA = *Data Analysis Summary*, Dr = *Derivation Summary*, Df = *Definition Summary*, Ds = *Description Summary*, Fg = *Figure*, In = *Information Summary*, PD = *Performance Data Summary*, Pt = *Procedure Summary*, Sp = *Specification*, SpF = *Specification Form*, Tb = *Table*, Te = *Technique Summary*, TR = *Test Report*. *For example, the entry* 39-42, Df 29-1 (40) *means* pages 39 through 42; Definition Summary 29-1, page 40.

Damping, 104, Tb 30-1(110), In 30-1(112), In 30-2(113)
Coulomb, 659, Dr 35-1(661), 704, Dr 35-6(709)
moving-coil instruments, 233, Dr 32-1(231)
seismograph systems, 659, Dr 35-1(661)
viscous, 659, Dr 35-1(661), 664, Dr 35-2(666)
Damping ratio, Tb 32-1(237)
determined by an optical oscillograph, 297
electromechanical measuring instruments, 235, Dr 32-1(227)
pressure receivers, determined from transient response record, 420, DA 33-1(418)
D'Arsonval galvanometer oscillographs, 385
D'Arsonval meters, In 30-8(145), 323
D-c motors and generators, 126, In 30-8(141)
Dead band, 69
Decibels, 267
Degrees (angular measurement), 109
Demodulators, In 30-9(152)
Density, Tb 30-1(110)
Dependent variable, 17
Design factors, for moving-coil instruments, 232
Design features and materials, selection of, 407
Determinate error, 57
Deviation, 56
Deviation corrections, 49
Deviation effects, dynamic, in pressure receiving elements, 403
Deviation functions of performance functions, applied to a linear vibration recording system, 811, PD 35-1(812), Tb 35-2(819)
applied to a typical recording system, 808, Dr 35-11(809), Tb 35-2(819)
for describing instrument performance, 803
Deviations, nondimensional dynamic amplitude ratio, 490, 497, Df 34-1(492)
[(0;1)-(0;0, 1)], Fg 34-27(501), Fg 34-30(507)
[(0;1)-(0;1, 2)], Fg 34-29(506)
[(0;1)-(1;1, 2)], Fg 34-30(507)
[(1;0)-(1;0, 1)], Fg 34-28(502), Fg 34-29(506)
dynamic response angle, 490, 497, Df 34-1(492)
[(0;1)-(0;0, 1)], Fg 34-30(507)
[(0;1)-(0;1, 2)], Fg 34-29(506)
[(0;1)-(1;1, 2)], Fg 34-30(507)
[(1;0)-(1;0, 1)], Fg 34-29(506)
from the ideal integrator step function response, 495
(0;0, 1) equation, Fg 34-25(498)
in measurement, 56
indicated quantity, 47
indicated scale reading, 49
Deviations (cont.)
relating function, 490
second-order from first-order response curves, 497, Fg 34-26(500), Fg 34-27(501), Fg 34-28 (502), Fg 34-29(506), Fg 34-30(507)
sinusoidal response, special voltmeter X-1, Sp 29-1(94)
step function response, [(0;1)-(0;0,1)], Fg 34-26(500)
Diagrams, measuring instruments, 10, Df 28-5(11)
operating components, 8, Df 28-4(9)
operating systems, 22-37
Dial-gage vibrometer, 643, Fg 35-7(644)
Diaphragm-piston pumps and motors, In 30-11(160)
Diaphragm-type optical engine indicator, 323, Fg 33-1(322)
Diaphragms, as pressure-measuring components, In 30-11(157)
Dictionary definitions, Df 29-3(54)
Diehlsyns, In 30-8(147)
Differential equations (see also Performance equations)
general, solution by an an analog computer, 551, Dr 34-23(552), 555, Dr 34-24(556)
(0;0,1), solution by an analog computer, 555, Dr 34-25(561)
(0;1, 2) relating function, 493, Dr 34-17(494)
(0;0, 1, 2), applied to electromechanical measuring instruments, 224, 234
parameters and equation coefficients, Tb 32-2(275)
solution by an analog computer, 560, Dr 34-26(568)
(1;1, 2) relating function, 493, Dr 34-18(496)
of electric circuits, 104
of fluid motion, 107
of heat transfer, 106
of magnetic circuits, 105
of physical systems, 102
Differentiation, 422
Differentiator performance equation forms, relating functions for, 493
Differentiators, 422, 471-489
electrical, 431, 478-489
a-c drag-cup tachometer, 431, 482, Fg 34-19 (483), Fg 34-20(484)
capacitance – amplifier – feedback-resistance, 489, Fg 34-24(490), Dr 34-16(491)
d-c tachometer, 431, 478, Fg 34-17(481), Fg 34-18(481)
resistance – amplifier – feedback-inductance, 484, Fg 34-22(486), Dr 34-14(487)
resistance-capacitance, 431, 486, Fg 34-23(488) Dr 34-15(489)
resistance-inductance, 431, 482, Fg 34-21(484), Dr 34-13(485)
rotating-magnet drag-cup tachometers, 431, 478, Fg 34-15(480), Fg 34-16(480)

Differentiators (cont.)
ideal, 427
mechanical, 431, 471-478
ball-and-disc, 431, 432, 471, Fg 34-11(472), Fg 34-12(474), Dr 34-12(475)
centrifugal tachometers, 431, 478, Fg 34-13(479), Fg 34-14(479)
performance equation forms, 489
tachometers, 473
typical, 427
Differential gears, 125, In 30-7(137)
Differential synchros, In 30-8(148)
Differential transformers, 129, In 30-8(146)
Dimensional analysis of factors controlling thermometric characteristic time, 194
Dimensional similarity factors, electromechanical measuring instruments, 235
Dimensions, 108, Tb 30-1(110)
Diodes, 130, In 30-9(150)
Direct performance analysis, 271
Displaced cosine pulse functions, 303, 832
Fourier transforms of, 304, Dr 32-3(305)
response of an aircraft engine vibration isolation system, 840, Fg 35-57(842), DaA 35-1(843)
response of a recording oscillograph, 840
used to test a recording oscillograph, 313, DaA 32-3(317)
Displaced-zero scales, 62
Displacement, relative, 659, Dr 35-1(660)
Displacement devices, 135
Displacement indicators, dial gage, 613, Fg 35-5 (618)
optical, 615, Fg 35-5(618)
Displacement meters, 607, Fg 35-3(608)
Displacement of a moving body, generalized, 601, Fg 35-1(602)
Displacement receivers, 613-636, Fg 35-5(618)
angular, E-magnet differential transformer, 632, Fg 35-5(622)
Microsyn, 632, Fg 35-5(622)
bonded resistance wire, 617, Fg 35-5(618)
concentric-coil differential coupling transformer, 635, Fg 35-5(623)
concentric-coil inductance bridge, 633, Fg 35-5 (623)
electronic tube, 624, Fg 35-5(619)
electrostatic-capacity bridge, 625, Fg 35-5(619)
electrostatic-capacity-controlled oscillator, 626, Fg 35-5(620)
Displacement receivers (cont.)
E-magnet differential transformer, 630, Fg 35-5 (622)
piezoelectric, 635, Fg 35-5(623)
unbonded resistance wire, 616, Fg 35-5(618)
Dissipated power, In 30-1(112), In 30-2(113), In 30-3(114)
Dynamic amplitude ratios, deviations, 490, 497, Df 34-1(492)
[(0;1)-(0;0, 1)], Fg 34-27(501), Fg 34-30(507)
[(0;1)-(0;1, 2)], Fg 34-29(506)
[(0;1)-(1;1, 2)], Fg 34-30(507)
[(1;0)-(1;0, 1)], Fg 34-28(502), Fg 34-29(506)
(See also Amplitude ratios and Sensitivity ratios)
Dynamic error, of a thermometer, 185
Dynamic error effects, in terms of sinusoidal response characteristics, 340
Dynamic performance parameters, determination of, 413
Dynamic response angles, components determined by a cathode-ray oscilloscope, 289, Da 32-1 (292), Fg 32-34(293), 783, Te 35-1(784)
deviations, 267, 490, Df 34-1(492), 497
(0;0, 1, 2) from unity, 267, Fg 32-21(268), Fg 32-23(270)
[(0;1)-(0;0, 1)], Fg 34-30(507)
[(0;1)-(0;1, 2)], Fg 34-29(506)
[(0;1)-(1;1, 2)], Fg 34-30(507)
[(1;0)-(1;0, 1)], Fg 34-29(506)
ideal differentiator, Dr 34-2(428)
ideal integrator, Dr 34-1(423)
open-chain systems, Pr 33-1(336), 339
performance equation, (0;0, 1, 2), 263, Fg 32-17 (262), Fg 32-19(265)
pressure-measuring system, 387, Fg 33-14b(390)
symbols and notation for, 370, Df 33-1(371)
(See also Phase angles)

E

Eckman, D. P., 27
Eddy-current dampers, 129, In 30-8(146)
Eddy-current motors, 127
Elastic element, 659, Dr 35-1(661)
Elastic forces and torques, 104
Elastic restraint, 104, Tb 30-1(110), In 30-1(112), In 30-2(113), 223
generators, Microsyn, In 30-8(149)

Key: Da = *Data Summary*, DaA = *Data Analysis Summary*, Dr = *Derivation Summary*, Df = *Definition Summary*, Ds = *Description Summary*, Fg = *Figure*, In = *Information Summary*, PD = *Performance Data Summary*, Pr = *Procedure Summary*, Sp = *Specification*, SpF = *Specification Form*, Tb = *Table*, Te = *Technique Summary*, TR = *Test Report*. *For example, the entry* 39-42, Df 29-1 (40) *means* pages 39 through 42; Definition Summary 29-1, page 40.

Elastic restraint (cont.)
moving-coil instruments, 234
performance function, Dr 32-1(226)
pressure measuring devices, In 30-11(157)
Electric charge, 108, Tb 30-1(110), In 30-3(114)
Electric circuits, 104, In 30-3(114)
Electric filtering techniques, 410
Electric quantities, Tb 30-1(110)
Electrical measuring system, internal combustion engine, cylinder-pressure records, 378
Electrical pressure-measuring systems, 323, Fg 33-1(322)
applied to an internal combustion engine, 366, Fg 33-10(366), PD 33-1(379)
applied to a jet engine, 385, Fg 33-13(386), PD 33-2(388), Fg 33-14(389)
Electrical pressure-recording systems, 361
Electrical saturation, 301
Electrical signal generating relative motion receivers, 615, Fg 35-5(618)
Electrodynamometers, 222, In 32-1(221)
Electromagnetic c.g.s. system, 109
Electromagnetic components, 126, In 30-8(141)
Electromagnetic elements of magnetic circuits, In 30-4(117)
Electromagnetic generator velocity receivers, 626, Fg 35-5(620), 651, Fg 35-7(645)
Electromagnetic permeability, 108
Electromagnets, 105
Electromechanical measuring instruments, 218-318
design of, 224
electrodynamometer, 222, In 32-1(221)
electrostatic, 222, In 32-1(221)
experimental test of, 224
functional diagrams, 219, In 32-1(220), 223, Dr 32-1(225)
moving-coil, 219, In 32-1(220), Dr 32-1(228)
moving-iron, 222, In 32-1(221)
performance equations, 234
performance functions, Dr 32-1(225)
pictorial functional diagrams, In 32-1(220)
Electromotive force, back, 232
Electronic components, 130, In 30-9(150)
saturation of, 301
Electronic-tube displacement receiver, 624, Fg 35-5(619)
Electronic-tube linear vibration receiver, 657, Fg 35-7(648)
Electronic tubes, 130, In 30-9(150)
Electrostatic capacity bridge displacement receivers, 625, Fg 35-5(619)
Electrostatic capacity velocity receivers, 625, Fg 35-5(619)
Electrostatic-capacity-controlled oscillator displacement receivers, 626, Fg 35-5(620)
Electrostatic c.g.s. system, 109
Electrostatic instruments, 222, In 32-1(221)
Electrostatic permittivity, 108
Electrostatic voltmeter, static sensitivity, Dr 32-1 (228)
Electrostriction transducers, 132, In 30-9(153)
Elements of instrument systems, 102-124
electric circuits, 104, In 30-3(114)
first-order (see First-order elements)
fluid mechanics, 107, In 30-6(123)
heat flow, 106, In 30-5(119)
integral-order (see Integral-order elements)
magnetic circuits, 105, In 30-4(116)
mechanics, 103, In 30-1(112), In 30-2(113)
second-order (see Second-order elements)
zero-order (see Zero-order elements)
E-magnet differential transformer displacement receivers, 630, 632, Fg 35-5(622)
Emissivity, In 30-5(120)
Energy, Tb 30-1(110), In 30-1(112), In 30-2(113)
heat, In 30-5(119)
Engine indicators, 323, Fg 33-1(322)
English units, 109, Tb 30-1(111)
Environment, of measuring instruments, 59
Erratic error, 56
Error, 57, Fg 29-1(48)
determinate, 57
dynamic, in terms of sinusoidal response characteristics, 340
erratic, 56
indicated quantity, 47
indication, 72
scale reading, 49, 72
Error analysis, 71

F

Feedback control systems (see Control systems, feedback)
Feedback elements, of a controlled system, 23
Filters, electrical, 132, In 30-9(154), 410
mechanical, 410
First-order elements, electromagnetic, In 30-6(118)
of electric circuits, in charge, In 30-3(114)
in current, In 30-3(115)
of fluid mechanics, In 30-6(123)

First-order elements (cont.)
rotational, In 30-2(113)
translational, In 30-1(112)
First-order profiles, 339
First-order response, of a thermometer, 180-204
of pressure-measuring system components, 339, Dr 33-1(341)
Flow (see Fluid flow)
Fluid flow components, In 30-6(123), 134, In 30-11(157)
Hagen-Poiseuille law, In 30-6(124)
high-speed, airfoil velocity profiles, 207
temperature measurement in, 204-216
through constrictions, In 30-6(124)
Fluid friction, 107
Fluid-mechanical transducers, 135
Fluid mechanics, 107, In 30-6(121)
Fluid motors, 135
Fluid pressure, 107
Fluid-pressure-coupled thermometers, 163, Ds 31-1(165)
Fluid pumps, 135
Fluids, 107
Force, 108, Tb 30-1(110)
buoyant, In 30-6(121)
Coulomb friction, In 30-1(112), In 30-2(113),663, Dr 35-1(661), 707, Dr 35-6(709)
damping, In 30-1(112), 663, Dr 35-1(661)
elastic element, 663, Dr 35-1(661)
hydrostatic, In 30-6(121)
inertia reaction, In 30-1(112), 663, Dr 35-1(661)
magnetic, In 30-4(117)
restraining, In 30-1(112)
Fourier series, used to describe input pressure to a pressure-measuring system, Dr 33-3(367)
Fourier series graphs, internal combustion engine cylinder pressure, Fg 33-5(356), Fg 33-6(358), Fg 33-8(362), Fg 33-11(380)
Fourier transforms, 105
displaced cosine pulse functions, 304, Dr 32-3(305)
rectangular pulse functions, 302, Dr 32-2(303)
Fractional deviations, sensitivity ratio, for an open-chain system, 804, Dr 35-10(805)
Free stream in fluid flow, 206
Frequency analysis techniques, 105
Frequency functions, 256, In 32-2(258)
Friction, Coulomb (see Coulomb friction)
fluid (see Fluid friction)
Friction (cont.)
viscous (see Viscous damping)
Functional diagrams, 10, Df 28-5(12)
electromechanical measuring instruments, 223, In 32-1(220), Dr 32-1(225)
indicating instruments, Df 29-1(40)
measuring instruments, Df 29-2(44)
with multiple inputs, Fg 29-4(59)
pressure-measuring systems and units, 321, Fg 33-1(322)
Functional names of operating components, 8

G

Galvanometers, 224, Dr 32-1(226)
Gas, 107
Gas constant, In 30-6(121)
Gas diodes, 130, In 30-9(150)
Gas pressure thermometers, 133, In 30-10(155)
Gas triodes, 130, In 30-9(151)
Gear pumps and motors, In 30-11(160)
Gears, 125, In 30-7(137)
Generators, a-c, 126, In 30-8(142)
induction, capacitor and split phase, In 30-8(143)
repulsion-induction, In 30-8(143)
synchronous, 127, In 30-8(144)
three-phase, In 30-8(142)
two-phase, In 30-8(142)
d-c, 126, In 30-8(141)
amplidyne, In 30-8(142)
compound, In 30-8(142)
permanent magnet, 126, In 30-8(141)
separately excited, 126, In 30-8(141)
series, In 30-8(141)
shunt, In 30-8(141)
elastic restraint, Microsyn, In 30-8(149)
signal, Microsyn, In 30-8(149)
synchro, differential, In 30-8(148)
transmitter, In 30-8(147)
torque, 218, In 32-1(220), 223, Dr 32-1(225)
Microsyn, In 30-8(149)
Grid glow tubes, In 30-9(151)
Gyroscopes, 125, In 30-7(139)
single-degree-of-freedom, 125, In 30-7(139)
Gyroscopic vertical indication, 126

Key: Da = *Data Summary*, DaA = *Data Analysis Summary*, Dr = *Derivation Summary*, Df = *Definition Summary*, Ds = *Description Summary*, Fg = *Figure*, In = *Information Summary*, PD = *Performance Data Summary*, Pr = *Procedure Summary*, Sp = *Specification*, SpF = *Specification Form*, Tb = *Table*, Te = *Technique Summary*, TR = *Test Report*. *For example, the entry* 39-42, Df 29-1 (40) *means* pages 39 through 42; Definition Summary 29-1, page 40.

H

Hagen-Poiseuille law, In 30-6(124)

Harper, D. R., 216

Heat, 106, 109, Tb 30-1(110), In 30-5(119), Dr 31-2(175)

mechanical equivalent of, In 30-6(123)

Heat capacity, 106, Tb 30-1(110), In 30-5(119)

Heat conductivity, In 30-5(119)

equivalent film coefficient of, 178

Heat energy, In 30-5(119)

Heat flow, 106, In 30-5(119), 174, Dr 31-2(175)

into a receiver, conduction, 180

convective, 178

radiation, 178

Hendrickson, H. B., 216

Hydrostatics, In 30-6(121)

Hysteresis motors, In 30-8(144)

I

Ideal differentiators, 427, Dr 34-2(428)

Ideal instruments, 38

Ideal integrators, 422, Dr 34-1(423)

step function response deviations from, 495

Ideal measuring instruments, 43, Df 29-2(45)

Ideal operating components, 10

Impedance, In 30-3(115)

Impulse function response, experimental, of a pressure-measuring system, In 33-1(415)

first-order, of a thermometer, 193

second-order, 236, Fg 32-1(238), Fg 32-2(239), Fg 32-3(240)

Impulse function strength, 193

Inaccuracy, definition, 55, Fg 29-1(48)

indicated quantity, 47, Fg 29-2(50)

measuring instruments, 47

scale reading, 47, Fg 29-2(50)

Independent variable, 17

Indicated quantities, 47, Fg 29-2(50)

inaccuracy, uncertainty, and error, Fg 29-1(48)

Indicating instrument mechanisms, representation and performance description, Df 29-1(40)

Indicating instruments, 39, Df 29-1(40)

Indicating systems, 39, Df 29-1(40), 219, Dr 32-1(226)

Indication, 39, Df 29-1(40), 219

errors and corrections, 71

Indication time, 217

second-order (-;0, 1, 2) performance equation, 244, Fg 32-8(246)

Indicator cards, from a spring-and-piston-type indicator, 352

Indicators, 39

displacement, dial gage, 613, Fg 35-5(618)

optical, 615, Fg 35-5(618)

relative motion, 613, Fg 35-5(618)

temperature, 162

for recording and control, 170

vibratory motion, 641, Fg 35-6(643)

self-contained, 642, Fg 35-7(644)

Induced voltage, In 30-4(118)

Inductance, Tb 30-1(110), In 30-3(115)

Inductance-bridge displacement receivers, 633, Fg 35-5(623)

Inductance-bridge vibration receivers, 649, 656, Fg 35-7(645)

Induction motors and generators, In 30-8(142)

Induction-repulsion motors and generators, In 30-8(143)

Inductive reactance voltage, In 30-3(115)

Inertia, 104, In 30-1(112), In 30-2(113)

Inertia reaction forces and torques, In 30-1(112), In 30-2(113)

Input current, 218

Input pressure, described in Fourier series terms, Dr 33-3(367)

Input quantity reading, 219

Input receivers, 39, Df 29-1(40)

Input receiving networks, 218, 223, Dr 32-1(225)

Input sensors, Df 29-1(40)

Input temperatures, 171

Input voltage, 218

Inputs, 4, 58

Instruments, actual, 38, 46-101

Integral-order elements, of electric circuits, in current, In 30-3(114)

Integrating amplifier, calibration, 782, Tr 35-3(788)

Integration, ideal, 422, Dr 34-1(423)

step function response deviations, 495

Integrators, 427-470

analog computer, 542, Dr 34-22(543)

electrical, eddy-current-drag-disc watt-hour-meter type, 431, 437, Fg 34-3(438), Dr 34-4(440)

motor – amplifier – feedback-tachometer, 431, 463, Fg 34-10(464), Dr 34-11(466)

resistance – amplifier – feedback-capacitance, 431, 456, Fg 34-9(460), Dr 34-10(461), 542, Dr 34-22(545)

resistance-capacitance, 431, 453, Fg 34-8(457), Dr 34-9(458)

Integrators (cont.)
electrical, viscous-shear-drag generator type, 431, 441, Fg 34-4(442), Dr 34-5(444)
ideal, 422, Dr 34-1(423)
step function response deviation, 495
liquid-flow, 431, 443, Fg 34-5(447), Dr 34-6(448)
mechanical, ball-and-disc, 431, 432, Fg 34-1(433), Fg 34-2(434), Dr 34-3(435)
performance equation forms, 489
relating functions for, 493
pneumatic pressure, 431, 450, Fg 34-7(451), Dr 34-8(454)
thermal, 431, 447, Fg 34-6(451), Dr 34-7(452)
typical, 427
Interference effects, in pressure receiving elements, 403, Dr 33-6(404)
reduction of, 398, 406, 410
Interfering inputs, 58
to pressure-measuring systems, 391
to pressure receiving elements, 391
effects on performance equations, Dr 33-4(394)
reduction of interference, 406
Internal combustion engines, as controlled systems, 29
cylinder-pressure records, 377
from an electrical measuring system, 378
Inverse performance analysis, 271
Isoelastic, 398
Isolation, of system components, 392
vibration, single-degree-of-freedom, 726, Dr 35-7(728), Dr 35-8(740)
Isolation system, vibratory force, 742, Dr 35-9 (745)
vibratory motion, for a recording oscillograph, 837
vibratory torque, for an aircraft engine, 840, DaA 35-1(843)
Isothermal compression, In 30-6(121)

K

Kaslow, Theodore, 201
Kinematic viscosity, In 30-6(123)
Kinetic energy, In 30-1(112), In 30-2(113)
Kirchoff's laws, 104, In 30-3(115)
Kleinschmidt, Von E., 163

L

Laning, J. H., Jr., 104
Laplace transforms, 105
L-C filters, In 30-9(154)
"Least number of components" connection for solving differential equations on an analog computer, 555, Dr 34-24(556)
Length, 108, Tb 30-1(110)
Levers, 125, In 30-7(136)
Li, Y. T., 319, 601
Linear acceleration (see Acceleration)
Linear displacement (see Displacement)
Linear velocity (see Velocity)
Linear vibration (see Vibration)
Linear vibration receivers used to measure angular vibration, 822, Dr 35-12(823), 829
Linkages, 125, In 30-7(138)
Liquid-filled thermometers, 133, In 30-10(155), 162, Ds 31-1(164)
characteristic time, Tb 31-2(216)
Liquid heater, 31
Liquids, 107
Logarithmic decrement, Tb 32-1(237)
Log-scale plot, graphical method for determining performance functions of open-chain systems, Pr 33-1(336)
Loru (logarithmic ratio unit), 267

M

Mach number, 108, In 30-6(123), 207, Dr 31-5(213)
Magnetic amplifiers, In 30-8(143)
Magnetic elements and circuits, 105, In 30-4(116)
Magnetic fields, In 30-4(116)
of solenoids, In 30-4(117)
Magnetic flux, 105, Tb 30-1(110), In 30-3(115), In 30-4(116), 232
Magnetic force and torque, In 30-4(117)
Magnetic moment, In 30-4(117)
Magnetic oil-pressure gages, 325, Fg 33-3(326)
Magnetic quantities, Tb 30-1(110)
Magnetomotive force, 105, Tb 30-1(110), In 30-4 (116)
of solenoids, In 30-4(117)
Magnetostriction components, 130, In 30-8(149)
Magnetostrictive linear velocity receiver, 630, Fg 35-5(621)

Key: Da = *Data Summary*, DaA = *Data Analysis Summary*, Dt = *Derivation Summary*, Df = *Definition Summary*, Ds = *Description Summary*, Fg = *Figure*, In = *Information Summary*, PD = *Performance Data Summary*, Pr = *Procedure Summary*, Sp = *Specification*, SpF = *Specification Form*, Tb = *Table*, Te = *Technique Summary*, TR = *Test Report*. *For example, the entry* 39-42, Df 29-1 (40) *means* pages 39 through 42; Definition Summary 29-1, page 40.

Magnets, 105, In 30-4(116)
Magnitude conversion, 103
Manometers, In 30-11(157), 324
Mass, 108, Tb 30-1(110), In 30-1(112)
McAdams, 178
Measurement, 38-101
Measuring instrument operation, names, symbols and defining equations, Tb 29-1(80)
Measuring instruments, 38, 42-101
actual, 43, 47-101
performance quality of, 47
diagrams, 10, Df 28-5(11), Df 29-2(44)
engineering problems associated with, 271
ideal, 43, Df 29-2(45)
perfect, 43
performance analysis, and design, 271, Tb 32-2(275)
performance description, Df 29-2(44)
response information not compatible with first- or second-order theoretical response, 284
second-order equation parameters, Tb 32-1(237)
determined from nonoscillatory transients, 277, Fg 32-28(280), Fg 32-29(283)
determined from oscillatory step function transients, 276, Fg 32-26(278), Fg 32-27(279)
determined from steady-state sinusoidal response, 282
determined from step function response, 272, Tb 32-2(275)
indication time, 244, Fg 32-8(246)
second-order performance equations, 234-283
second-order (0;0, 1, 2) performance equations, impulse function response and deviations, 236, Fg 32-1(238), Fg 32-2(239), Fg 32-3(240)
parabolic response, 252, Fg 32-14(253)
ramp-followed-by-constant response, 252, Fg 32-15(254)
ramp function response and deviations, 244, Fg 32-9(247), Fg 32-10(248), Fg 32-11(249), Fg 32-12(250), Fg 32-13(251)
sinusoidal response, 252, In 32-2(257), Fg 32-16(260), Fg 32-17(262), Fg 32-18(264), Fg 32-19(265), Fg 32-20(266)
sinusoidal response deviations, 267, Fg 32-21 (268), Fg 32-22(269), Fg 32-23(270)
step function response and deviations, 238, Fg 32-4(241), Fg 32-5(242), Fg 32-6(243), Fg 32-7(245)
specification of, 85
Measuring systems, 335-352, 365-376
component performance functions expressed as equations, 365
cutoff frequencies and band widths, 370, Df 33-1(371)
Measuring systems (cont.)
dynamic error, in terms of sinusoidal response characteristics, 340
open-chain, performance functions, 335, Pr 33-1(336), Dr 33-1(341), Dr 33-2(347)
pressure (see Pressure-measuring systems)
Mechanical elements, 103, In 30-1(112), In 30-2(113)
Mechanical equivalent of heat, In 30-6(123)
Mechanical filtering techniques, 410
Mechanical quantities, Tb 30-1(110)
Mechanics, rotational, In 30-2(113)
translational, In 30-1(112)
Mechanism components, 125, In 30-7(136)
Mechanism indication error, 71
Meters, 128, In 30-8(145)
Microsyns, 129, In 30-8(149)
angular displacement receivers, 632, Fg 35-5(622)
Mils (angular measurement), 109
M. k. s. (meter-kilogram-second) system, 109, Tb 30-1(111)
Modifying effects in pressure-measuring systems, 391
Modifying inputs, 58
effects on performance equations, 398, Dr 33-4(394)
Modulators, amplitude, 132, In 30-9(152)
Modulus of precision, 64
Moment of inertia, Tb 30-1(110), In 30-2(113)
Momentum, Tb 30-1(110), In 30-1(112), In 30-2(113)
Motors, a-c, 126, In 30-8(142)
d-c, 126, In 30-8(141)
fluid, 135, In 30-11(160)
synchro, In 30-8(147)
universal, 127
Moving-coil instruments, 219, In 32-1(220)
design factors, 232
performance equations, 232, Dr 32-1(228)
Moving-iron instruments, In 30-8(145), 222, In 32-1(221)
Mueller, R. K., 632
Multipliers, ball-and-disc, 432
coefficient, analog computer, 542, Dr 34-22(543)
Mutual inductance, In 30-3(115)

N

Names (and symbols), 8, 10, Df 28-6(14), 17, Df 28-7(19), Df 28-8(21), Df 28-9(23), Df 28-10(24), 53, Fg 29-3(52), Df 29-3(54), 63, Df 29-4(65), 72, Df 29-5(74), Tb 29-1(80), 223, Dr 32-1(225), 235, Tb 32-1(237), 370, Df 33-1(371), Fg 33-15(392)

Natural frequency, Tb 32-1(237)
angular, Tb 32-1(237)
undamped angular, Dr 32-1(227), 235, Tb 32-1(237)
undamped natural period, Tb 32-1(237)
Navier-Stokes equations, 107
Needle valves, In 30-11(159)
Negative feedback amplifiers, In 30-9(152)
Newton's law for a fluid element, 107
Newton's law of cooling, 106
Newton's laws of motion, 103, 104
Nondimensional curves, 236-271
Nondimensional equations and curves, applied to electromechanical measuring instruments, 224
Nondimensional measures of scale reading quality, Tb 29-1(83)
Nonlinear ferrous core materials, 105
Nonlinear magnetization curves, 104
Nonlinear performance equations, 284
Normal probability law, 63
Normal-zero scales, 62
Notation, (see Symbols)
Nozzles, 135, In 30-11(157)
Null, 631
Numerical example of scaling a problem for analog-computer solution, 567

O

Octaves, 267
Oil-pressure gages, 325, Fg 33-3(326)
Oldenbourg, R. C., 27
Open-chain systems, performance functions, graphical determination of, Pr 33-1(336)
graphical manipulations, 339
pressure measuring, 333
performance functions, 335
sensitivity ratio fractional deviations, 804, Dr 35-10(805)
Operating components, (see Components)
Operating frequency ranges, 370, Df 33-1(371)
Operating inputs, 59
Operating systems, (see Systems)
Optical accelerometers, 643, Fg 35-7(644)
Optical displacement indicators, 615, Fg 35-5(618)
Optical engine indicators, diaphragm-type, 323, Fg 33-1(322)
Orifice plate, fluid, 135
Oscillators, 131, In 30-9(152)
Oscillographs and oscilloscopes, 218, 284-297, 313, 385, 420, 767, 783, 795, 831
determination of performance characteristics, from aperiodic step function response, 286, DaA 32-2(288)
from displaced cosine pulse function response, 313, DaA 32-3(317)
from oscillatory step function response, 285, DaA 32-1(287)
from sinusoidal response, 289, Da 32-1(292), Da 32-2(295)
records, DaA 33-1(418), Te 35-1(785)
used to measure dynamic response angles, 783, Te 35-1(784)
vibratory motion isolation system, 837
Outputs, 4

P

Parabolic function response, first-order (0;0, 1) performance equations, ideal thermometer, 186, Fg 31-3(187)
second-order (0;0, 1, 2), performance equations, 252, Fg 32-14(253)
Parabolic plug valves, In 30-11(159)
Parameters, performance, determination of, 413
for moving-coil instruments, 232
second-order performance equations, Tb 32-1(237)
Pass band, Df 33-1(371)
Pendulums, 126, In 30-7(139)
Perfect measuring instruments, 43
Performance, generalized, 18
electrical pressure-measuring system, applied to a jet engine, PD 33-2(388)
applied to an internal combustion engine, PD 33-1(379)
indicating mechanism, Df 29-1(41)
pressure indicating mechanism, Df 29-1(42)
steady-state sinusoidal, 20
Performance analysis, direct and inverse, 271
pressure-measuring systems, 320
Performance characteristics, electromechanical measuring instruments, 234
pressure-measuring instruments, determination of, 412

Key: Da = *Data Summary*, DaA = *Data Analysis Summary*, Dr = *Derivation Summary*, Df = *Definition Summary*, Ds = *Description Summary*, Fg = *Figure*, In = *Information Summary*, PD = *Performance Data Summary* Pr = *Procedure Summary*, Sp = *Specification*, SpF = *Specification Form*, Tb = *Table*, Te = *Technique Summary*, TR = Test Report. *For example, the entry* 39-42, Df 29-1 (40) *means* pages 39 through 42; Definition Summary 29-1, page 40.

Performance coefficients, moving-coil instruments, 232

Performance-describing concepts for components, Tb 29-1(80), 85

performance function deviation function, 803

Performance-describing equations and curves, application to engineering problems, 271

Performance description, generalized operating components, 18, Df 28-7(19)

indicating instrument mechanisms, Df 29-1(40)

measuring instruments, Df 29-2(44)

sinusoidal, operating components, Df 28-8(21), Df 28-9(23)

static, operating components, Df 28-6(14)

Performance equation forms, integrators and differentiators, 489, 493

Performance equations, differentiator, ideal, Dr 34-2(428)

electromechanical measuring instruments, Dr 32-1(225)

integrator, ideal, Dr 34-1(423)

positional servo system, 596, Dr 34-27(580)

pressure-receiving elements, 393, Dr 33-4(394)

second-order parameters and coefficients, Tb 32-1(237)

second-order (0;0, 1, 2), displaced cosine function response, 307, Fg 35-42(308), Fg 35-43(309), Fg 35-44(310)

impulse function response, 236, Fg 32-1(238), Fg 32-2(239), Fg 32-3(240)

sinusoidal response forms, 255, In 32-2(257)

step function response, 238, Fg 32-4(241), Fg 32-5(242), Fg 32-6(243), Fg 32-7(245)

second-order (1,0;0, 1, 2), displaced cosine pulse function response, 832, Fg 35-52(835), Fg 35-53(836), Fg 35-54(838)

static, 13

temperature receivers, 171, Dr 31-2(175), 180

(See also Relating functions)

Performance function deviation functions, 803, 808, Dr 35-11(809), 811, PD 35-1(812), Tb 35-2(819)

Performance functions, 18

component, expressed as equations, 365

design, 271

equivalent to relating functions, 255

first-order, expressed in terms of reference frequency ratio and break point, Dr 33-1(341)

integrator, ideal, Dr 34-1(423)

measuring system, 365

open-chain systems, graphical manipulation, 339, PD 33-1(379)

pressure-receiving elements, 399, Dr 33-5(400)

profiles, logarithmic-scale, first- and second-order, 321

Performance functions (cont.)

pulse function response, evaluation of, 306, 832

second-order, expressed in terms of reference frequency ratio and break point, Dr 33-2(347)

seismographic system, viscous damping only, 664, Dr 35-2(666)

sinusoidal, 255

temperature-measuring instruments, Dr 31-1(172)

Performance parameters, moving-coil instruments, 232

pressure-measuring systems, experimental determination, 413, In 33-1(414)

Performance problems, associated with pressure-measuring systems, 334

Performance quality, measuring instruments, 47, 53, Fg 29-2(50), Fg 29-3(52), Tb 29-1(81)

Performance requirements, measuring system for internal combustion engine cylinder-pressure records, 377

Period, natural, Tb 32-1(237)

Permanent-magnet motors and generators, 126, In 30-8(141)

Permeability, electromagnetic, 108, Tb 30-1(110), In 30-4(116)

Permeance, In 30-4(116)

Permittivity, electrostatic, 108

Phototubes, 131, In 30-9(151)

Physical conversion, 103

Physical problem time, 539, Fg 34-21(541)

Physical representation terms, 13

(See also Symbols)

Pi Theorem, 196

Pickups, vibration, 607

Piezoelectric devices, 132, In 30-9(153)

Piezoelectric displacement receivers, 635, Fg 35-5(623)

Piezoelectric vibration receivers, 657, Fg 35-7(648)

Pitot tubes, 134, In 30-11(158)

Planck's radiation laws, 134, 169

Plug valves, In 30-11(159)

Potential energy, In 30-1(112), In 30-2(113), In 30-3(114, 115)

Power, Tb 30-1(110)

dissipated, In 30-1(112), In 30-2(113), In 30-3(114)

Practical factors of pressure-receiving-element design, 411

Prandtl number, 208, Dr 31-5(213)

Precision, modulus of, 64

Precision measures, scale reading quality, Tb 29-1(84)

Pressure, fluid (hydrostatic), 107, In 30-6(121)
Pressure-altitude-temperature relationships in a standard atmosphere, In 30-6(122)
Pressure gages, 10, Df 28-5(11), 38
Pressure indicators, 38, Df 29-1(41), 223
Pressure-measuring components, fluid, 134, In 30-11(157)
Pressure-measuring instruments, 38, Df 29-1(41), 324-333
high natural frequency, 416, Fg 33-17(415)
performance characteristics, 412
Pressure-measuring systems, 319-421
electrical, applied to an internal combustion engine, 361, Fg 33-10(366), 378, PD 33-1(379)
applied to a jet engine, 385, Fg 33-13(386), PD 33-2(388), Fg 33-14(389)
pressure record compared with theoretical cylinder pressure of an internal combustion engine, Fg 33-11(380)
forcing functions for experimental determination of performance parameters, In 33-1(414)
interfering and modifying effects, 391, Fg 33-15(392)
open-chain, 333
performance analysis of, 320
performance problems, 334
with inadequate low-frequency performance, Fg 33-12(382)
with input pressure described in Fourier series terms, Dr 33-3(367)
Pressure-measuring system performance requirements, for internal combustion engine cylinder-pressure records, 377
Pressure pickup, 323
Pressure receivers, Df 29-1(41), 325, Fg 33-4(328)
bellows-inductance-type, Fg 33-4(330)
catenary-diaphragm-type strain-gage, Fg 33-4(328)
design, practical features of, 411
selection of design features and materials, 407
determination of damping ratio and undamped natural frequency, DaA 33-1(418)
diaphragm piezoelectric-type, Fg 33-4(329)
flat-diaphragm capacitance-type, Fg 33-4(328)
flat-diaphragm carbon-disc, Fg 33-4(328)
magnetostriction-type rate-of-change-of-pressure, Fg 33-4(330)
tuned-ribbon-type, Fg 33-4(329)
Pressure-receiving elements, catenary diaphragm, Tb 33-1(408)
Pressure-receiving elements (cont.)
characteristics of, Tb 33-1(408)
component performance functions, 399
cylindrical, Tb 33-1(408)
design, practical factors of, 411
selection of design features and materials, 407
dynamic deviation effect, and interference effects in, 403
flat diaphragm, Tb 33-1(408)
performance functions, Dr 33-5(400)
interference effects, reduction of, 398, 406, 410
interfering inputs, Fg 33-16(393)
modifying inputs, 398
performance equations, 393, Dr 33-4(394)
spherical cap diaphragm, Tb 33-1(408)
stretched membrane, Tb 33-1(408)
Pressure-recording system, electrical, 361
Pressure records, internal combustion engine cylinder pressure, 377
Primary quantities, 108
Primary-standard instruments, 60, 325
Probability and uncertainty, 63
Process, 23
Profiles, logarithmic scale, first- and second-order, 339
Pulse functions, displaced cosine, 303, 840
Fourier transforms, 303, Dr 32-3(305)
used to test a recording oscillograph, 313, DaA 32-3(317)
rectangular, 301
Fourier transforms, 302, Dr 32-2(303)
response of a pressure-measuring system, experimental, 415, In 33-1(414)
Pulse response delay, 311
Pulse strength, 301
Pulse testing, 301
Pumps, fluid, 135, In 30-11(160)
Pyrometers, 134
optical, 169, Ds 31-1(166)
radiation, 170, Ds 31-1(167)

Q

Quality (see Performance quality)
Quantities, indicated, 47
primary, 108
Quantity of heat, Tb 30-1(110)

Key: Da = *Data Summary*, DaA = *Data Analysis Summary*, Dr = *Derivation Summary*, Df = *Definition Summary*, Ds = *Description Summary*, Fg = *Figure*, In = *Information Summary*, PD = *Performance Data Summary*, Pr = *Procedure Summary*, Sp = *Specification*, SpF = *Specification Form*, Tb = *Table*, Te = *Technique Summary*, TR = *Test Report*, *For example, the entry* 39-42, Df 29-1 (40) *means* pages 39 through 42; Definition Summary 29-1, page 40.

R

Radial pumps and motors, In 30-11(160)

Radiation, heat, 106, In 30-5(119)

Radiation heat flow, 174, Dr 31-2(176)

into a receiver, 178

Radius of gyration, In 30-2(113)

Ramp-followed-by-step-function response, second-order (0;0, 1, 2) performance equation, 252, Fg 32-15(254)

Ramp function response, first-order (0;0, 1), of a thermometer, 183, Fg 31-2(184)

second-order (0;0, 1, 2) performance equations, 244, Fg 32-9(247), Fg 32-10(248), Fg 32-11(249), Fg 32-12(250), Fg 32-13(251)

Random error, 56

Random variables, 63

Rate-of-turn indicators, 223

Rationalized systems of units, 109

R-C filters, In 30-9(154)

Receivers, 39, Df 29-1(40)

displacement (see Displacement receivers)

pressure (see Pressure receivers)

relative motion (see Relative motion receivers)

synchro motor, In 30-8(147)

temperature (see Temperature receivers)

velocity (see Velocity receivers)

vibration (see Vibration receivers)

Recording system, linear vibration, performance function in terms of component deviation functions, 811, PD 35-1(812), Tb 35-2(819)

Recording system, typical, performance function, in terms of component deviation functions, 808, Dr 35-11(809)

Rectangular pulse functions, 301

Fourier transforms, 302, Dr 32-2(303)

Rectifiers, In 30-9(150)

semiconducting, 131

Reference frequency ratios, in first-order performance functions, Dr 33-1(341)

in second-order performance functions, Dr 33-2(347)

Reference member, in vibration measurement, 602

Reference scale readings, 47

Reference voltages, 127

Reflectivity, In 30-5(119)

Relating function deviations, 490-508

Relating functions, 20, Df 28-7(19)

dimensionless, In 32-2(259)

equivalent to performance functions, 255

first-order (0;0, 1) equation, Dr 33-1(341)

Relating functions (cont.)

for integrator and differentiator performance equation forms, 493

second-order (0;0, 1, 2) equation, Dr 33-2(347)

(0;1, 2) equation, 493, Dr 34-17(494)

(1;1, 2) equation, 493, Dr 34-18(496)

(1, 0;0, 1, 2) equation, 732, Dr 35-7(728)

(2;0, 1, 2) equation, 664, Dr 35-2(666)

Relative displacement, 659, Dr 35-1(660)

Relative motion indicators, 613, Fg 35-5(618)

Relative motion receivers, 613, Fg 35-5(618)

electrical signal generating, 615, Fg 35-5(618)

electrostatic capacity, 625, Fg 35-5(619)

selection of, 637

Relative velocity receiver, electromagnetic generator, 626, Fg 35-5(620)

Reluctance, Tb 30-1(110), In 30-4(116)

Repeated observations, Fg 29-1(48)

Representation, pictorial (see Diagrams)

Repulsion-induction motors, 127

Repulsion motors, 127

Resistance, Tb 30-1(110), In 30-3(114)

Resistance-coupled thermometers, 168, Ds 31-1(165)

Resistance thermometers, 133, In 30-10(156)

characteristic time, Tb 31-2(206)

Resistance wire displacement receivers, 616, 617, Fg 35-5(618)

Resistance wire linear vibration receivers, unbonded, 648, Fg 35-7(644)

Resistivity, Tb 30-1(110), In 30-3(114)

Resolution sensitivity, 69

Response, experimental, of pressure-measuring systems, 413, In 33-1(414)

first-order (0;0, 1), of a thermometer, 181-203

second-order (0;0, 1, 2), of measuring instruments, 236-318

second-order (1, 0;0, 1, 2), of vibration isolation systems, 832

Response characteristics, for ideal thermometers, 180

Response delay, of a thermometer, 185

Response time, 217

Restraining force, In 30-1(112)

Restraining torque, In 30-2(113)

Retentivity, In 30-4(116)

Reynolds number, 107, In 30-6(123), 198, 208, Dr 31-5(213)

Rhodes, T. J., 168

Rigid body, vibration measurement of, 819

RLC series circuit, In 30-3(115)

Rotational Coulomb friction coefficient, In 30-2(113)

Rotational damping coefficient, Tb 30-1(110)

Rotational elastic restraint coefficient, Tb 30-1(110)

Rotational mechanics, In 30-2(113)

Rotational motion, 819, Fg 35-47(820)

Rotors, of a-c motors, 127

Roughness, scale reading, similar to uncertainty, 49

S

Sartorius, H., 27

Saturation, of electrical components, 301

Scalar quantities, 103

Scale characteristics, Fg 29-6(62)

Scale factor, 43, 85

Scale readings, coefficients, 85

corrections, 49, Fg 29-2(50), 70, 72, Df 29-5(74)

deviations, 49, Fg 29-2(50)

electromechanical measuring instruments, 235

inaccuracy, uncertainty, and error, 47, Fg 29-1(48), Fg 29-2(50), Tb 29-1(81)

performance quality-describing concepts, 47, Tb 29-1(81)

probable uncertainty of, 63

smoothed, 49

uncertainty measures associated with the average of a set, 78, Tb 29-1(82)

Scales, 60, Fg 29-6(62), 219, Dr 32-1(226)

Scaling for analog-computer solution, 567

Screws, 125, In 30-7(136)

Secant sensitivity, 15

Second-order elements, of electric circuits (in charge), In 30-3(115)

of fluid mechanics, In 30-6(123)

of rotational mechanics, In 30-2(113)

of translational mechanics, In 30-1(112)

Second-order equations associated with integration and differentiation, cutoff frequencies and bandwidth tolerances, 503, Tb 34-3(509), Tb 34-4(510)

deviations, 503, Tb 34-2(504)

relating functions, 493, Dr 34-17(494), Dr 34-18(496), Tb 34-1(499)

Second-order profiles, 339

Second-order response, of electromechanical measuring instruments, 234-283

of operating components, 340, Dr 33-2(347)

of seismographic systems, combined viscous and Coulomb damping, 704-739

Coulomb damping only, 736, Dr 35-8(740), Fg 35-39(743)

viscous damping only, 664-706

Seismic elements, 126, In 30-7(140)

Seismographic systems, 605, Fg 35-3(608)

as vibration receivers, 664, Dr 35-3(670)

lightly damped, vibratory frequency-receiving characteristics, 682

performance, 606, Fg 35-3(608)

in the vibratory acceleration-receiving range (accelerometer range), 696, Dr 35-5(699)

in the vibratory displacement-receiving range (vibrometer range), 678, Dr 35-3(670)

in the vibratory velocity-receiving range (velocimeter range), 688, Dr 35-4(689)

single-degree-of-freedom, generalized theory, 658, Dr 35-1(660)

with combined viscous damping and Coulomb damping, 704, 708, Dr 35-6(709), 722

with viscous damping only, 664, Dr 35-2(666), 704, Tb 35-1(706)

Selection, performed by operating components, 103

Selenium diodes, In 30-9(150)

Self-defining notation, 5

compared with other systems of notation, 36

Self inductance, In 30-3(115)

Selsyns, In 30-8(147)

Semilogarithmic plots, step function response, 193

Sensitivity, 10, 13, Df 28-6(14), 15, Fg 28-1(16), Fg 28-2(17), 256, In 32-2(257)

determined by a cathode-ray oscilloscope, measuring instruments, 291, Da 32-2(295), Fg 32-35(296)

operating components, 783, Te 35-1(784)

over-all, for measuring instruments, 256, In 32-2(257)

resolution, 69

static, 10-17, Df 28-6(15)

electromechanical measuring instruments, Dr 32-1(227)

indicating instruments, 39, Df 29-1(41)

measuring instruments, 43, Df 29-2(45)

tangent, chord, and secant, 15, Fg 28-1(16)

threshold, 69

Key: Da = *Data Summary*, DaA = *Data Analysis Summary*, Dr = *Derivation Summary*, Df = *Definition Summary*, Ds = *Description Summary*, Fg = *Figure*, In = *Information Summary*, PD = *Performance Data Summary*, Pr = *Procedure Summary*, Sp = *Specification*, SpF = *Specification Form*, Tb = *Table*, Te = *Technique Summary*, TR = *Test Report*. *For example, the entry* 39-42, Df 29-1 (40) *means* pages 39 through 42; Definition Summary 29-1, page 40.

Sensitivity deviation graphs, (0;0, 1, 2) performance equation, 267-270

Sensitivity graphs, (0;0, 1, 2) performance equation, 263-266

Sensitivity ratio fractional deviations, for an open-chain system, 804, Dr 35-10(805)

Sensitivity ratios, dimensionless, components of a pressure-measuring system, 369, Fg 33-14a(389)

symbols and notation, 370, Df 33-1(371)

Sensitivity – reference sensitivity curves, of open-chain systems, Pr 33-1(336)

Sensor, 39, Df 29-1(40)

Separately excited motors and generators, 126, In 30-8(141)

Series motors and generators, In 30-8(141)

Servomechanisms as coducers, 8, Df 28-3(7)

Servo systems, positional, with tachometric feedback, 567, Dr 34-27(577)

Shock tubes, for determining characteristics of high natural-frequency pressure-measuring instruments, 416, Fg 33-17(417)

Shunt motors and generators, In 30-8(141)

Signal generators, fluid, 134

Microsyns, In 30-8(149)

Single-degree-of-freedom gyroscopes, 125, In 30-7(139)

Single-degree-of-freedom seismographic systems, (see Seismographic systems)

Sinusoidal linkages, In 30-7(138)

Sinusoidal performance functions, steady-state (see Performance functions)

Sinusoidal relating functions, steady-state (see Relating functions)

Sinusoidal response, steady-state, 20, Df 28-8(21), Df 28-9(23)

differentiators, 427, Dr 34-2(428)

electromechanical measuring instruments, 252-270

determination of parameters from, 282

first-order (0;0, 1), of a thermometer, 188-193

special voltmeter X-1, 87, Sp 29-1(89)

integrators, 422, Dr 34-1(423)

oscillograph performance characteristics determined from, 289-297

pressure-measuring systems, 333-421

determination of performance characteristics, 412, In 33-1(414)

second-order (0;0, 1, 2) performance equations, 252-271

seismographic systems, 662

viscous damping and Coulomb damping combined, 704-726

viscous damping only, 664-706

Sinusoidal response (cont.)

temperature-measuring instruments, 188-193

Smoothing, 49

Solenoid, In 30-4(117)

Solid conduction heat flow, 174

Sound, velocity of, In 30-6(123)

Special high-damping voltmeter, designation X-1, 87, Sp 29-1(89)

Specific heat, 108, Tb 30-1(110), In 30-5(119), In 30-6(121), Dr 31-2(175)

Specification, 85

illustrative, for special high-damping voltmeter, designation X-1, 87, Sp 29-1(89)

Specification form, illustrative, SpF 29-1(86)

Split-phase motors, 127

Spool valve, balanced pressure, In 30-11(159)

Spring-and-piston, In 30-11(157)

Spring-and-piston engine indicator, 323, Fg 33-1(322)

indicator cards, 352

pressure record compared with theoretical cylinder pressure of an internal combustion engine, Fg 33-6(358), Fg 33-7(360), Fg 33-8(362), Fg 33-9(364)

Spur gears, In 30-7(137)

Squire, H. B., 214

Squirrel-cage motors, 127

Stagnation temperature, 207

Standard atmosphere, In 30-6(122)

Standard uncertainty, of scale reading, 64

Static conditions, scale readings, 47

for an operating component, 10

Static performance, 13

indicators, 39, Df 29-1(41)

measuring instruments, Df 29-2(45)

working variable symbols, 17

Static sensitivity, 39, 43

Static temperature, free-stream, 207

Steady-state sinusoidal response (see Sinusoidal response, steady-state)

Stefan-Boltzmann law of radiation, 106, 134, 169, Dr 31-2(176)

Step function response, first-order (0;0, 1), of a thermometer, 181, Fg 31-1(183)

semilogarithmic curves, 193, Dr 31-3(195)

integrators, 495, Fg 34-25(498)

[(0;1)-(0;0, 1)] deviation, Fg 34-25(498), Fg 34-26(500)

pressure-measuring system, experimental, 415, In 33-1(414)

determination of characteristic time, 194

Step function response (cont.)
second-order performance equations, 238-244
temperature-measuring instruments, 181, 193
experimental, 199, Tb 31-1(202)
Summers, analog computer, 542, Dr 34-22(544)
resistance – amplifier – feedback-resistance, Dr 34-22 (549)
resistance network, Dr 34-22(549)
Summing linkages, In 30-7(138)
Suppressed-zero scale, 62
Symbols, 4-37
comparison of, Tb 28-1(37)
dimensionless sensitivity ratio and dynamic response angle plots, Df 33-1(371)
feedback control systems, Df 28-10(24)
operating components, 8-23
generalized performance, 18, Df 28-7(19)
sinusoidal performance, Df 28-8(21), Df 28-9(23)
static performance, 10, Df 28-6(14), 17
operating systems, 22-37
self-defining, 5
working variables, 17
Synchronous motors and generators, In 30-8(144)
Synchros, 129, In 30-8(147)
System components, isolation of, 410
Systems, operating, 4
diagrams, 22-37
representation, 8
pressure-measuring (see Pressure-measuring systems)
seismographic (see Seismographic systems)
vibration isolation (see Vibration isolation systems)
vibration recording (see Vibration recording systems)

T

Tachometers, as differentiators, 431, 473, 478
centrifugal, 126, In 30-7(140), 478
used in integrators, 431, 463
Tangent sensitivity, 15
Taplin, J. F., 27
Telephone receiver, as a transducer, 5, Df 28-3(7)
Teletorques, In 30-8(147)
Temperature, 108, Tb 30-1(110), In 30-5(119), 161
absolute, In 30-6(121)
input, 171
stagnation, 207
static, free-stream, 207
Temperature gages (see Fluid-pressure-coupled thermometers, Resistance-coupled thermometers, and Thermocouple thermometers)
Temperature indicators, 162
Temperature-measuring instruments, 161-217
as indicators for recording and control, 170
essential features of, 162
high-speed fluid flow, 204-216
illustrative diagrams, Ds 31-1(164)
performance functions, Dr 31-1(172)
Temperature receivers, 162
for a moving fluid, Dr 31-2(175)
frequency functions, Dr 31-1(172)
heat flow into, 174
performance equations, 171, Dr 31-1(172), 180, Dr 31-2(175)
Terminology (see Names and symbols)
Thermal conductivity, 108, Tb 30-1(110), Dr 31-2(175)
Thermal quantities, Tb 30-1(110)
Thermocouple probe, for temperature measurement in high-speed fluid flow, 208-214, Fg 31-13(211), Fg 31-14(214)
Thermocouple thermometers, In 30-10(156), 168 Ds 31-1(166)
Thermocouples, 133, In 30-10(156)
Thermometers, 133, In 30-10(155)
air temperature, vapor-pressure type, 199-204
bimetal, 133, In 30-10(156), 163, Ds 31-1(164)
completely filled liquid, 133, In 30-10(155)
experimental response, 201
fluid-pressure-coupled, 163
for fluids, 174
for solids, 178
gas pressure, 133, In 30-10(155)
ideal response characteristics, 180-199
impulse function, 193
parabolic function, 186
ramp function, 183
sinusoidal, 188
step function, 181
liquid-in-glass, 133, In 30-10(155), 162, Ds 31-1(164)

Key: Da = *Data Summary*, DaA = *Data Analysis Summary*, Dr = *Derivation Summary*, Df = *Definition Summary*, Ds = *Description Summary*, Fg = *Figure*, In = *Information Summary*, PD = *Performance Data Summary*, Pr = *Procedure Summary*, Sp = *Specification*, SpF = *Specification Form*, Tb = *Table*, Te = *Technique Summary*, TR = *Test Report*. *For example, the entry* 39-42, Df 29-1 (40) *means* pages 39 through 42; Definition Summary 29-1, page 40.

Thermomenters (cont.)
optical pyrometers, Ds 31-1(166)
radiation meters, 174
radiation pyrometers, Ds 31-1(167)
resistance, 133, In 30-10(156)
resistance-coupled, 168, Ds 31-1(165)
thermocouple, In 30-10(156), 168, Ds 31-1(166)
vapor pressure, 133, In 30-10(156), 199-205
Thermometric characteristic time (see Characteristic time, thermometric)
Thermometric components, 133, In 30-10(155)
Threshold sensitivity, 69
Thyratrons, In 30-9(151)
Time, 108, Tb 30-1(110)
characteristic, 236, 239
Time – characteristic time ratio, 182
Timoshenko, Stephen, 163
Tolerance limits for deviations, amplitude ratio and dynamic response angle, 370, Df 33-1(371)
Torque, Tb 30-1(110)
buoyant, In 30-6(121)
Coulomb friction, In 30-2(113)
damping, In 30-2(113)
inertia reaction, In 30-2(113)
magnetic, In 30-4(117)
resistive, In 30-6(123)
restraining, In 30-2(113)
Torque generators, 218, 223
Microsyn, In 30-8(149)
moving-coil instruments, 224, Dr 32-1(225)
Torque summing members, 223
Transducers, 4, Df 28-1(6), Df 28-2(6), Df 28-3(7), 128, In 30-8(146)
fluid-mechanical, 135
magnetostriction, 130
piezoelectric or electrostriction, In 30-9(153)
Transformers, In 30-8(146)
Transients, in pressure-measuring instruments, 416, Fg 33-17(417), DaA 33-1(418)
Transistors, 131, In 30-9(151)
Translational mechanics, In 30-1(112)
Transmitters, synchro control and synchro generator, In 30-8(147)
Triodes, 130, In 30-9(150)
gas, 130, In 30-9(151)
Tubes, electronic, 130, In 30-9(150)

U

Uncertainty, 38, 47, Fg 29-1(48), 56, 63, Df 29-4(65), Tb 29-1(82)
and probability, 63
scale-reading, 47, 57
Units, 108, Tb 30-1(110)
angles, 109
for temperature receiver, performance equations, Dr 31-2(177)

V

Vacuum diodes, In 30-9(150)
Vacuum tubes, 130, In 30-9(150)
(See also Electronic tubes)
Valves, fluid, 135, In 30-11(159)
Vapor pressure thermometers, 133, In 30-10(156)
characteristic time, Tb 31-2(216)
step function response, 201
Variable-air-gap velocity receiver, 628, Fg 35-5(621)
Vectors, 103
of angles, 104
Velocimeter range, of a seismographic system, 606, Fg 35-3(608), 673, 688, Dr 35-4(689)
Velocimeters, 606, Fg 35-3(608)
Velocity, 103, Tb 30-1(110), In 30-1(112)
angular, 104, In 30-2(113)
of sound, In 30-6(123)
Velocity profiles, fluid flow, of airfoils, 207
Velocity receivers (velocimeters), 606, Fg 35-3(608), 625-630, Fg 35-5(618)
Venturi tubes, 135, In 30-11(158)
Vibrating member, 602
Vibration isolation, 726, Dr 35-7(728), Dr 35-8(740), 837-843
Vibration measurement, 601
angular, using linear vibration receivers, 822, Dr 35-12(823)
of a recording oscillograph, 837
of a rigid body, 819
of an aircraft engine, 829, 840, DaA 35-1(843)
single-degree-of-freedom, 602, Fg 35-2(604)
systems, 642, Fg 35-7(644)
Vibration receivers, 607, 641, Fg 35-6(643)
dial gage, 643, Fg 35-7(644)
electrical signal generating, 610, Fg 35-4(612)

Vibration receivers (cont.)
linear, calibration, 751, TR 35-1(753)
used to measure angular vibration, 822, Dr 35-12(823)
selection of, 658
self-contained, 610, Fg 35-4(611), 648, Fg 35-7(644)
torsional, calibration, 773, TR 35-2(775)
Vibration-receiving characteristics, of seismographic system, viscous damping only, 704, Tb 35-1(706)
Vibration recording systems, performance function in terms of component deviation functions, 808, PD 35-1(812), Tb 35-2(819)
Vibratory acceleration receivers (accelerometers), 606, Fg 35-3(608), 643, Fg 35-7(644)
Vibratory acceleration-receiving range, seismographic systems, 673, 696, Dr 35-5(699)
Vibratory displacement receivers (vibrometers), 607, Fg 35-3(608), 643, Fg 35-7(644), 664, Dr 35-3(670), 829
Vibratory displacement-receiving range, seismographic systems, 664, 669, Dr 35-3(670), 678
Vibratory force isolation system, 742, Dr 35-9(745)
Vibratory frequency-receiving characteristics, seismographic system, lightly damped, 682
Vibratory motion indicators, 641, Fg 35-6(643)
self-contained, 642, Fg 35-7(644)
Vibratory motion isolation system, recording oscillograph, 837
Vibratory motion receivers, 641, Fg 35-6(643)
self-contained, 648, Fg 35-7(644)
Vibratory torque isolation system, aircraft engine mount, 840, DaA 35-1(843)
Vibratory velocity receivers (velocimeters), 606, Fg 35-3(608)
Vibratory velocity-receiving range, seismographic systems, 673, 688, Dr 35-4(689)
Vibrometer range, seismographic systems, 664, 669, Dr 35-3(670), 678
Vibrometers, 607, Fg 35-3(608), 643, Fg 35-7(644), 664, Dr 35-3(670), 829
Viscosity, 107, Tb 30-1(110), In 30-6(123)
Viscous damping, in seismographic systems, 664, Dr 35-2(666)
coefficient, 659, Dr 35-1(661)
combined with Coulomb damping, 704, Dr 35-6(709)
Viscous flow, In 30-6(123)
external reference, 607, Fg 35-4(611)
Voltage, Tb 30-1(110)
across impedance, In 30-3(115)
capacitive reactance, In 30-3(114)
induced, In 30-4(118)
inductive reactance, In 30-3(115)
resistive, In 30-3(114)
Voltmeters, 218
electrostatic, 222, In 32-1(221)
static sensitivity, Dr 32-1(228)
special high damping, designation X-1, 87, Sp 29-1(89)
static sensitivity, Dr 32-1(227)
Volume, Tb 30-1(110)
Volume meters, 135
Vortex free-air thermometer, 214
Vortex tube, 214-216
V-port valves, In 30-11(159)

W

Wattmeters, In 30-8(145), 218
static sensitivity, Dr 32-1(227)
Webster's New Collegiate Dictionary, 53
Working variable symbols, 13, 17, Dr 28-7(19)
Worm-and-wheel gears, In 30-7(137)
Wound-rotor motors, 127

Y

Young, A. D., 214

Z

Zero-order elements, electromagnetic, In 30-4(117)
magnetic, In 30-4(116)
of electric circuits, in charge, In 30-3(114)
in current, In 30-3(114)
of fluid mechanics, In 30-6(121)
rotational mechanics, In 30-2(113)
translational mechanics, In 30-1(112)

Key: Da = *Data Summary*, DaA = *Data Analysis Summary*, Dt = *Derivation Summary*, Df = *Definition Summary*, Ds = *Description Summary*, Fg = *Figure*, In = *Information Summary*, PD = *Performance Data Summary*, Pt = *Procedure Summary*, Sp = *Specification*, SpF = *Specification Form*, Tb = *Table*, Te = *Technique Summary*, TR = *Test Report*. *For example, the entry* 39-42, Df 29-1 (40) *means* pages 39 through 42; Definition Summary 29-1, page 40.

ALLAMA IQBAL LIBRARY
22745

JAMMU & KASHMIR UNIVERSITY
LIBRARY
No. 22745
Date 12.5.58
SRINAGAR